REGULATION OF INFLAMMATION IN CHRONIC DISEASE

EDITED BY: Jixin Zhong and Guixiu Shi
PUBLISHED IN: Frontiers in Immunology

frontiers Research Topics

Frontiers Copyright Statement

© Copyright 2007-2019 Frontiers Media SA. All rights reserved.

All content included on this site, such as text, graphics, logos, button icons, images, video/audio clips, downloads, data compilations and software, is the property of or is licensed to Frontiers Media SA ("Frontiers") or its licensees and/or subcontractors. The copyright in the text of individual articles is the property of their respective authors, subject to a license granted to Frontiers.

The compilation of articles constituting this e-book, wherever published, as well as the compilation of all other content on this site, is the exclusive property of Frontiers. For the conditions for downloading and copying of e-books from Frontiers' website, please see the Terms for Website Use. If purchasing Frontiers e-books from other websites or sources, the conditions of the website concerned apply.

Images and graphics not forming part of user-contributed materials may not be downloaded or copied without permission.

Individual articles may be downloaded and reproduced in accordance with the principles of the CC-BY licence subject to any copyright or other notices. They may not be re-sold as an e-book.

As author or other contributor you grant a CC-BY licence to others to reproduce your articles, including any graphics and third-party materials supplied by you, in accordance with the Conditions for Website Use and subject to any copyright notices which you include in connection with your articles and materials.

All copyright, and all rights therein, are protected by national and international copyright laws.

The above represents a summary only. For the full conditions see the Conditions for Authors and the Conditions for Website Use.

ISSN 1664-8714
ISBN 978-2-88945-916-2
DOI 10.3389/978-2-88945-916-2

About Frontiers

Frontiers is more than just an open-access publisher of scholarly articles: it is a pioneering approach to the world of academia, radically improving the way scholarly research is managed. The grand vision of Frontiers is a world where all people have an equal opportunity to seek, share and generate knowledge. Frontiers provides immediate and permanent online open access to all its publications, but this alone is not enough to realize our grand goals.

Frontiers Journal Series

The Frontiers Journal Series is a multi-tier and interdisciplinary set of open-access, online journals, promising a paradigm shift from the current review, selection and dissemination processes in academic publishing. All Frontiers journals are driven by researchers for researchers; therefore, they constitute a service to the scholarly community. At the same time, the Frontiers Journal Series operates on a revolutionary invention, the tiered publishing system, initially addressing specific communities of scholars, and gradually climbing up to broader public understanding, thus serving the interests of the lay society, too.

Dedication to Quality

Each Frontiers article is a landmark of the highest quality, thanks to genuinely collaborative interactions between authors and review editors, who include some of the world's best academicians. Research must be certified by peers before entering a stream of knowledge that may eventually reach the public - and shape society; therefore, Frontiers only applies the most rigorous and unbiased reviews.
Frontiers revolutionizes research publishing by freely delivering the most outstanding research, evaluated with no bias from both the academic and social point of view. By applying the most advanced information technologies, Frontiers is catapulting scholarly publishing into a new generation.

What are Frontiers Research Topics?

Frontiers Research Topics are very popular trademarks of the Frontiers Journals Series: they are collections of at least ten articles, all centered on a particular subject. With their unique mix of varied contributions from Original Research to Review Articles, Frontiers Research Topics unify the most influential researchers, the latest key findings and historical advances in a hot research area! Find out more on how to host your own Frontiers Research Topic or contribute to one as an author by contacting the Frontiers Editorial Office: researchtopics@frontiersin.org

REGULATION OF INFLAMMATION IN CHRONIC DISEASE

Topic Editors:
Jixin Zhong, Case Western Reserve University, China
Guixiu Shi, Xiamen University, China

Inflammation plays a critical role in many chronic health conditions including metabolic disease, cardiovascular disease, cancer, and autoimmune disease. Images: Magic mine/Shutterstock.com and cnikola/Shutterstock.com

Citation: Zhong, J., Shi, G., eds. (2019). Regulation of Inflammation in Chronic Disease. Lausanne: Frontiers Media. doi: 10.3389/978-2-88945-916-2

Table of Contents

08 ***Editorial: Regulation of Inflammation in Chronic Disease***
Jixin Zhong and Guixiu Shi

10 ***RANTES/CCL5 Induces Collagen Degradation by Activating MMP-1 and MMP-13 Expression in Human Rheumatoid Arthritis Synovial Fibroblasts***
Solomon A. Agere, Nahid Akhtar, Jeffery M. Watson and Salahuddin Ahmed

22 ***Elevated Expression of Chemokine CXCL13 in Chronic Hepatitis B Patients Links to Immune Control During Antiviral Therapy***
Chao Liu, Xuan Huang, Melanie Werner, Ruth Broering, Jun Ge, Yongyin Li, Baolin Liao, Jian Sun, Jie Peng, Mengji Lu, Jinlin Hou and Xiaoyong Zhang

33 ***Metabolic Adaptations of CD4⁺ T Cells in Inflammatory Disease***
Cristina Dumitru, Agnieszka M. Kabat and Kevin J. Maloy

50 ***Role of Maternal Periodontitis in Preterm Birth***
Hongyu Ren and Minquan Du

60 ***Role of Anti-Osteopontin Antibodies in Multiple Sclerosis and Experimental Autoimmune Encephalomyelitis***
Nausicaa Clemente, Cristoforo Comi, Davide Raineri, Giuseppe Cappellano, Domizia Vecchio, Elisabetta Orilieri, Casimiro L. Gigliotti, Elena Boggio, Chiara Dianzani, Melissa Sorosina, Filippo Martinelli-Boneschi, Marzia Caldano, Antonio Bertolotto, Luca Ambrogio, Daniele Sblattero, Tiziana Cena, Maurizio Leone, Umberto Dianzani and Annalisa Chiocchetti

72 ***Interleukin-4 Inhibits Regulatory T Cell Differentiation Through Regulating CD103+ Dendritic Cells***
Lei Tu, Jie Chen, Hongwei Zhang and Lihua Duan

82 ***The Small Tellurium Compound AS101 Ameliorates Rat Crescentic Glomerulonephritis: Association With Inhibition of Macrophage Caspase-1 Activity* via *Very Late Antigen-4 Inactivation***
Yafit Hachmo, Yona Kalechman, Itai Skornick, Uzi Gafter, Rachel R. Caspi and Benjamin Sredni

95 ***Basophil Activation-Dependent Autoantibody and Interleukin-17 Production Exacerbate Systemic Lupus Erythematosus***
Qingjun Pan, Li Gong, Haiyan Xiao, Yongmin Feng, Lu Li, Zhenzhen Deng, Ling Ye, Jian Zheng, Carol A. Dickerson, Lin Ye, Ning An, Chen Yang and Hua-feng Liu

110 ***T Cells in Osteoarthritis: Alterations and Beyond***
Yu-sheng Li, Wei Luo, Shou-an Zhu and Guang-hua Lei

120 ***The Fos-Related Antigen 1–JUNB/Activator Protein 1 Transcription Complex, a Downstream Target of Signal Transducer and Activator of Transcription 3, Induces T Helper 17 Differentiation and Promotes Experimental Autoimmune Arthritis***
Young-Mee Moon, Seon-Yeong Lee, Seung-Ki Kwok, Seung Hoon Lee, Deokhoon Kim, Woo Kyung Kim, Yang-Mi Her, Hea-Jin Son, Eun-Kyung Kim, Jun-Geol Ryu, Hyeon-Beom Seo, Jeong-Eun Kwon, Sue-Yun Hwang, Jeehee Youn, Rho H. Seong, Dae-Myung Jue, Sung-Hwan Park, Ho-Youn Kim, Sung-Min Ahn and Mi-La Cho

131 *(–)-Epigallocatechin Gallate Targets Notch to Attenuate the Inflammatory Response in the Immediate Early Stage in Human Macrophages*
Tengfei Wang, Zemin Xiang, Ya Wang, Xi Li, Chongye Fang, Shuang Song, Chunlei Li, Haishuang Yu, Han Wang, Liang Yan, Shumei Hao, Xuanjun Wang and Jun Sheng

152 *Impact of Autoantibodies Against Glycolytic Enzymes on Pathogenicity of Autoimmune Retinopathy and Other Autoimmune Disorders*
Grazyna Adamus

163 *Corrigendum: Increased Toll-Like Receptors Activity and TLR Ligands in Patients With Autoimmune Thyroid Diseases*
Shiqiao Peng, Chenyan Li, Xinyi Wang, Xin Liu, Cheng Han, Ting Jin, Shanshan Liu, Xiaowen Zhang, Hanyi Zhang, Xue He, Xiaochen Xie, Xiaohui Yu, Chuyuan Wang, Ling Shan, Chenling Fan, Zhongyan Shan and Weiping Teng

164 *Insulin Modulates Cytokine Release, Collagen and Mucus Secretion in Lung Remodeling of Allergic Diabetic Mice*
Sabrina S. Ferreira, Fernanda P. B. Nunes, Felipe B. Casagrande and Joilson O. Martins

174 *Distinct Blood and Visceral Adipose Tissue Regulatory T Cell and Innate Lymphocyte Profiles Characterize Obesity and Colorectal Cancer*
Gloria Donninelli, Manuela Del Cornò, Marina Pierdominici, Beatrice Scazzocchio, Rosaria Varì, Barbara Varano, Ilenia Pacella, Silvia Piconese, Vincenzo Barnaba, Massimo D'Archivio, Roberta Masella, Lucia Conti and Sandra Gessani

185 *Toll-Like Receptor 4 Inhibition Improves Oxidative Stress and Mitochondrial Health in Isoproterenol-Induced Cardiac Hypertrophy in Rats*
Parmeshwar B. Katare, Pankaj K. Bagul, Amit K. Dinda and Sanjay K. Banerjee

196 *Asiatic Acid Exhibits Anti-inflammatory and Antioxidant Activities Against Lipopolysaccharide and D-Galactosamine-Induced Fulminant Hepatic Failure*
Hongming Lv, Zhimin Qi, Sisi Wang, Haihua Feng, Xuming Deng and Xinxin Ci

208 *Placental Growth Factor Contributes to Liver Inflammation, Angiogenesis, Fibrosis in Mice by Promoting Hepatic Macrophage Recruitment and Activation*
Xi Li, Qianwen Jin, Qunyan Yao, Yi Zhou, Yanting Zou, Zheng Li, Shuncai Zhang and Chuantao Tu

225 *The Extracts of* **Morinda officinalis** *and its Hairy Roots Attenuate Dextran Sodium Sulfate-Induced Chronic Ulcerative Colitis in Mice by Regulating Inflammation and Lymphocyte Apoptosis*
Jian Liang, Jiwang Liang, Hairong Hao, Huan Lin, Peng Wang, Yanfang Wu, Xiaoli Jiang, Chaodi Fu, Qian Li, Ping Ding, Huazhen Liu, Qingping Xiong, Xiaoping Lai, Lian Zhou, Shamyuen Chan and Shaozhen Hou

242 *Neutrophil Extracellular Traps and Endothelial Dysfunction in Atherosclerosis and Thrombosis*
Haozhe Qi, Shuofei Yang and Lan Zhang

251 *Dendritic Cell Subsets in Asthma: Impaired Tolerance or Exaggerated Inflammation?*
Heleen Vroman, Rudi W. Hendriks and Mirjam Kool

262 ***Inflammatory Markers for Arterial Stiffness in Cardiovascular Diseases***
Ioana Mozos, Clemens Malainer, Jarosław Horbańczuk, Cristina Gug, Dana Stoian, Constantin Tudor Luca and Atanas G. Atanasov

278 ***SIRT1/Adenosine Monophosphate-Activated Protein Kinase α Signaling Enhances Macrophage Polarization to an Anti-inflammatory Phenotype in Rheumatoid Arthritis***
So Youn Park, Sung Won Lee, Sang Yeob Lee, Ki Whan Hong, Sun Sik Bae Koanhoi Kim and Chi Dae Kim

289 ***New Insight Into the Pathogenesis of Erythema Nodosum Leprosum: The Role of Activated Memory T-Cells***
Edessa Negera, Kidist Bobosha, Stephen L. Walker, Birtukan Endale, Rawleigh Howe, Abraham Aseffa, Hazel M. Dockrell and Diana N. Lockwood

303 ***Lower Expression of MicroRNA-155 Contributes to Dysfunction of Natural Killer Cells in Patients With Chronic Hepatitis B***
Jun Ge, Zuxiong Huang, Hongyan Liu, Jiehua Chen, Zhanglian Xie, Zide Chen, Jie Peng, Jian Sun, Jinlin Hou and Xiaoyong Zhang

315 ***Immunity and Fibrogenesis: The Role of Th17/IL-17 Axis in HBV and HCV-Induced Chronic Hepatitis and Progression to Cirrhosis***
Feliciano Chanana Paquissi

331 ***Inhibition of Pro-inflammatory and Anti-apoptotic Biomarkers During Experimental Oral Cancer Chemoprevention by Dietary Black Raspberries***
Steve Oghumu, Bruce C. Casto, Jennifer Ahn-Jarvis, Logan C. Weghorst, Jim Maloney, Paul Geuy, Kyle Z. Horvath, Claire E. Bollinger, Blake M. Warner, Kurt F. Summersgill, Christopher M. Weghorst and Thomas J. Knobloch

343 ***Genes Critical for Developing Periodontitis: Lessons From Mouse Models***
Teun J. de Vries, Stefano Andreotta, Bruno G. Loos and Elena A. Nicu

359 ***Baicalin Inhibits NOD-Like Receptor Family, Pyrin Containing Domain 3 Inflammasome Activation in Murine Macrophages by Augmenting Protein Kinase A Signaling***
Chen-Guang Li, Liang Yan, Feng-Yi Mai, Zi-Jian Shi, Li-Hui Xu, Yan-Yun Jing, Qing-Bing Zha, Dong-Yun Ouyang and Xian-Hui He

374 ***Tumor Necrosis Factor-Alpha Targeting can Protect Against Arthritis With Low Sensitization to Infection***
Nadia Belmellat, Luca Semerano, Noria Segueni, Diane Damotte, Patrice Decker, Bernhard Ryffel, Valérie Quesniaux, Marie-Christophe Boissier and Eric Assier

388 ***Regulation of Neuroinflammation: What Role for the Tumor Necrosis Factor-Like Weak Inducer of Apoptosis/Fn14 Pathway?***
Audrey Boulamery and Sophie Desplat-Jégo

395 ***Inflammatory Processes Associated With Canine Intervertebral Disc Herniation***
Marie Monchaux, Simone Forterre, David Spreng, Agnieszka Karol, Franck Forterre and Karin Wuertz-Kozak

408 ***Role of Incretin Axis in Inflammatory Bowel Disease***
Lihua Duan, Xiaoquan Rao, Zachary Braunstein, Amelia C. Toomey and Jixin Zhong

415 ***Gp96 Peptide Antagonist gp96-II Confers Therapeutic Effects in Murine Intestinal Inflammation***
Claudia A. Nold-Petry, Marcel F. Nold, Ofer Levy, Yossef Kliger, Anat Oren, Itamar Borukhov, Christoph Becker, Stefan Wirtz, Manjeet K. Sandhu Markus Neurath and Charles A. Dinarello

428 ***Immunopathogenesis in Myasthenia Gravis and Neuromyelitis Optica***
Zhen Wang and Yaping Yan

442 ***Regulation of Fn14 Receptor and NF-κB Underlies Inflammation in Meniere's Disease***
Lidia Frejo, Teresa Requena, Satoshi Okawa, Alvaro Gallego-Martinez, Manuel Martinez-Bueno, Ismael Aran, Angel Batuecas-Caletrio, Jesus Benitez-Rosario, Juan M. Espinosa-Sanchez, Jesus José Fraile-Rodrigo, Ana María García-Arumi, Rocío González-Aguado, Pedro Marques, Eduardo Martin-Sanz, Nicolas Perez-Fernandez, Paz Pérez-Vázquez, Herminio Perez-Garrigues, Sofía Santos-Perez, Andres Soto-Varela, Maria C. Tapia, Gabriel Trinidad-Ruiz, Antonio del Sol, Marta E. Alarcon Riquelme and Jose A. Lopez-Escamez

457 ***Direct and Intestinal Epithelial Cell-Mediated Effects of TLR8 Triggering on Human Dendritic Cells, CD14$^+$CD16$^+$ Monocytes and γδ T Lymphocytes***
Costanza Angelini, Barbara Varano, Patrizia Puddu, Maurizio Fiori, Antonella Baldassarre, Andrea Masotti, Sandra Gessani and Lucia Conti

471 ***Type 1 Diabetes: A Chronic Anti-Self-Inflammatory Response***
Matthew Clark, Charles J. Kroger and Roland M. Tisch

481 ***The Expanding Therapeutic Perspective of CCR5 Blockade***
Luca Vangelista and Sandro Vento

488 ***Emerging Role of Immunity in Cerebral Small Vessel Disease***
Ying Fu and Yaping Yan

497 ***Bioactive Lipids and Chronic Inflammation: Managing the Fire Within***
Valerio Chiurchiù, Alessandro Leuti and Mauro Maccarrone

508 ***Proteins of TNF-α and IL6 Pathways are Elevated in Serum of Type-1 Diabetes Patients With Microalbuminuria***
Sharad Purohit, Ashok Sharma, Wenbo Zhi, Shan Bai, Diane Hopkins, Leigh Steed, Bruce Bode, Stephen W. Anderson, John Chip Reed, R. Dennis Steed and Jin-Xiong She

517 ***The Effects of Prednisolone Treatment on Cytokine Expression in Patients With Erythema Nodosum Leprosum Reactions***
Edessa Negera, Stephen L. Walker, Kidist Bobosha, Yonas Bekele, Birtukan Endale, Azeb Tarekegn, Markos Abebe, Abraham Aseffa, Hazel M. Dockrell and Diana N. Lockwood

532 ***A20/Tumor Necrosis Factor α-Induced Protein 3 in Immune Cells Controls Development of Autoinflammation and Autoimmunity: Lessons From Mouse Models***
Tridib Das, Zhongli Chen, Rudi W. Hendriks and Mirjam Kool

544 ***Sex Differences in Adipose Tissue CD8$^+$ T Cells and Regulatory T Cells in Middle-Aged Mice***
Hilda Ahnstedt, Meaghan Roy-O'Reilly, Monica S. Spychala, Alexis S. Mobley, Javiera Bravo-Alegria, Anjali Chauhan, Jaroslaw Aronowski, Sean P. Marrelli and Louise D. McCullough

554 ***Expression and Function of IL12/23 Related Cytokine Subunits (p35, p40, and p19) in Giant-Cell Arteritis Lesions: Contribution of p40 to Th1- and Th17-Mediated Inflammatory Pathways***

Georgina Espígol-Frigolé, Ester Planas-Rigol, Ester Lozano, Marc Corbera-Bellalta, Nekane Terrades-García, Sergio Prieto-González, Ana García-Martínez, Jose Hernández-Rodríguez, Josep M. Grau and Maria C. Cid

565 ***Macrophage Lamin A/C Regulates Inflammation and the Development of Obesity-Induced Insulin Resistance***

Youngjo Kim, Princess Wendy Bayona, Miri Kim, Jiyeon Chang, Sunmin Hong, Yoona Park, Andrea Budiman, Yong-Jin Kim, Chang Yong Choi, Woo Seok Kim, Jongsoon Lee and Kae Won Cho

frontiers in Immunology

EDITORIAL
published: 12 April 2019
doi: 10.3389/fimmu.2019.00737

Editorial: Regulation of Inflammation in Chronic Disease

Jixin Zhong[1]* *and Guixiu Shi*[2]

[1] Cardiovascular Research Institute, Case Western Reserve University, Cleveland, OH, United States, [2] Department of Rheumatology and Clinical Immunology, The First Affiliated Hospital of Xiamen University, Xiamen, China

Keywords: inflammation, chronic disease, immune regulation, pathogenesis, molecular mechanism

Editorial on the Research Topic

Regulation of Inflammation in Chronic Disease

Growing evidence suggests a close link between inflammation and many chronic health conditions including diabetes, metabolic syndrome, cardiovascular disease, cancer, rheumatoid arthritis, inflammatory bowel disease, asthma, and chronic obstructive lung disease. Inflammation is a normal biological defense against infection and tissue damage. Under normal circumstances, it quickly ends after the clearance of infection and injurious agents. There is precise control of the complex networks of inflammatory pathways to limit tissue damage during inflammation. Despite the recognition of the importance of inflammatory dysregulation in chronic illnesses, the mechanisms underlying the inflammatory regulation of these disorders are not fully understood. The current Research Topic issue covers a wide range of subjects in inflammatory regulation in chronic conditions such as obesity (Donninelli et al.; Kim et al.), diabetes (Clark et al.; Purohit et al.), arthritis (Agere et al.; Belmellat et al.; Li et al.; Moon et al.; Pan et al.; Park et al.) cancer (Donninelli et al.; Oghumu et al.), Meniere's disease (Frejo et al.), stroke (Fu and Yan), arteritis (Espígol-Frigolé et al.), asthma (Vroman et al.), erythema nodosum (Negera et al.), systemic lupus erythematosus (Pan et al.), autoimmune encephalomyelitis (Clemente et al.), glomerulonephritis (Hachmo et al.), myasthenia gravis (Wang and Yan), intervertebral disc herniation (Monchaux et al.), inflammatory bowel disease (Liang et al.; Nold-Petry et al.), aging (Ahnstedt et al.), periodontitis (Ren et al.), fibrosis and tissue remodeling (Agere et al.; Ferreira et al.; Li et al.; Paquissi), hepatitis (Ge et al.; Liu et al.; Paquissi), retinopathy (Adamus), and cardiovascular diseases (Katare et al.; Mozos et al.; Qi et al.).

In this Research Topic, Chiurchiù et al. summarized the cellular and molecular mechanisms of endogenous bioactive lipids in the regulation of chronic inflammation. The regulation of NF-κB inflammatory pathway by A20/TNFAIP3 and its involvement in autoimmune diseases was reviewed by Das et al. However, in many chronic conditions, the inflammatory response continues and leads to significant tissue/organ damage and abnormal repair/remodeling (Agere et al.; Ferreira et al. ; Li et al.; Paquissi). Agere et al. demonstrated in their recent work that the CC-chemokine RANTES (regulated on activation normal T-cell expressed and secreted; also called CCL5) is able to activate matrix metallopeptidase-1 (MMP-1) and MMP-13, thus inducing collagen degradation and tissue damage. In contrast, excessive production of extracellular matrix such as collagen would lead to fibrosis and abnormal remodeling, which have also been associated with inflammatory process (Ferreira et al.; Li et al.; Paquissi). Dysregulation of inflammatory response contributes broadly to the development of many chronic conditions. In chronic inflammation, immune cells become dysregulated and loss self-limiting nature. Kim and coworkers identified that macrophage lamin A/C mediates obesity-induced adipose tissue inflammation and insulin resistance by regulating NF-κB. Lamin A/C was increased in the adipose tissue macrophages (ATMs) isolated from obese humans and mice.

OPEN ACCESS

Edited and reviewed by:
Pietro Ghezzi,
Brighton and Sussex Medical School, United Kingdom

***Correspondence:**
Jixin Zhong
Jixin.Zhong@case.edu

Specialty section:
This article was submitted to Inflammation, a section of the journal Frontiers in Immunology

Received: *06 February 2019*
Accepted: *19 March 2019*
Published: *12 April 2019*

Citation:
Zhong J and Shi G (2019) Editorial: Regulation of Inflammation in Chronic Disease. Front. Immunol. 10:737. doi: 10.3389/fimmu.2019.00737

Lamin A/C overexpression spontaneously activates NF-κB, while lamin A/C deficiency ameliorated obesity-induced insulin resistance and adipose tissue inflammation (Kim et al.). A number of inflammatory cytokines such as TNF-α, IFN-γ, IL-1β, IL-6, IL-17, IL-12, IL-23, and CCL5 are involved in the pathogenesis of chronic disorders (Agere et al. ; Espígol-Frigolé et al.; Negera et al. ; Nold-Petry et al. ; Paquissi; Purohit et al.). Purohit et al. showed that the activity of TNF-α/IL-6 pathway was associated with the risk score of microalbuminuria in patients with type 1 diabetes. Patients with giant-cell arteritis have been shown to have increased levels of IL-12 and IL-23 heterodimers, which could be reduced upon glucocorticoid treatment (Espígol-Frigolé et al.). IL-12/IL-18-induced intestinal inflammation could be alleviated by blockade of heat shock protein gp96 by gp96-II peptide (Nold-Petry et al.). Metabolic reprogramming has been suggested to play an important role during this process. Dumitru et al. reviewed how CD4+ T cells metabolically adapt to different microenvironments during inflammation. Other molecules that regulating the inflammatory pathways discussed in this Research Topic include CCR5 (Vangelista and Vento), TLR (Angelini et al.; Katare et al.), NLRP3 (Li et al.), STAT3/FRA1/JUNB (Moon et al.), TWEAK/Fn14 (Boulamery and Desplat-Jégo; Frejo et al.), glucagon-like peptides (Duan et al.), IL-4 (Tu et al.).

Cortisol and anti-inflammatory natural products are able to provide protections on a number of chronic diseases (Espígol-Frigolé et al.; Lv et al.; Negera et al.; Oghumu et al.; Wang et al.). Espígol-Frigolé et al. reported that patients with giant-cell arteritis had increased levels of IL-12 and IL-23 heterodimers, which were reduced upon glucocorticoid treatment. Negera et al. reported in a case-control study that prednisolone treatment in patients with erythema nodosum leprosum significantly increased the mRNA expression of IL-10 and TGFβ and reduced the expression of TNF, IFN-γ, IL-1β, IL-6, and IL-17A in the blood and skin lesion. Studies have suggested an inverse correlation between increased fruit and vegetable consumption and improved inflammatory conditions (1–3). In this Research Topic, Oghumu et al. showed that dietary black raspberry is able to suppress pro-inflammatory pathways and inhibit oral carcinogenesis. Asiatic acid, a pentacyclic triterpene found in various vegetables and fruits, also exhibited anti-inflammatory and anti-oxidant activities in a fulminant hepatic failure disease model (Lv et al.). Wang et al. also reported that (−)-Epigallocatechin gallate, which is found in Chinese green tea and Pu'er tea, exerts its anti-inflammatory function through inhibiting Notch signaling.

As summarized above, the original research articles and review papers in this issue present a range of topics under active investigation in the area of chronic inflammatory regulation.

AUTHOR CONTRIBUTIONS

JZ and GS wrote and approved the manuscript.

FUNDING

This work was supported by grants from National Natural Science Foundation of China (81670431), National Institutes of Health (K01DK105108 and R03DK119680), American Diabetes Association (1-19-JDF-117), and American Heart Association (17GRNT33670485).

REFERENCES

1. Root MM, McGinn MC, Nieman DC, Henson DA, Heinz SA, Shanely RA, et al. Combined fruit and vegetable intake is correlated with improved inflammatory and oxidant status from a cross-sectional study in a community setting. *Nutrients.* (2012) 4:29–41. doi: 10.3390/nu4010029
2. Holt EM, Steffen LM, Moran A, Basu S, Steinberger J, Ross JA, et al. Fruit and vegetable consumption and its relation to markers of inflammation and oxidative stress in adolescents. *J Am Diet Assoc.* (2009) 109:414–21. doi: 10.1016/j.jada.2008.11.036
3. Hosseini B, Berthon BS, Saedisomeolia A, Starkey MR, Collison A, Wark PAB, et al. Effects of fruit and vegetable consumption on inflammatory biomarkers and immune cell populations: a systematic literature review and meta-analysis. *Am J Clin Nutr.* (2018) 108:136–55. doi: 10.1093/ajcn/nqy082

Conflict of Interest Statement: The authors declare that the research was conducted in the absence of any commercial or financial relationships that could be construed as a potential conflict of interest.

Copyright © 2019 Zhong and Shi. This is an open-access article distributed under the terms of the Creative Commons Attribution License (CC BY). The use, distribution or reproduction in other forums is permitted, provided the original author(s) and the copyright owner(s) are credited and that the original publication in this journal is cited, in accordance with accepted academic practice. No use, distribution or reproduction is permitted which does not comply with these terms.

frontiers in Immunology

ORIGINAL RESEARCH
published: 18 October 2017
doi: 10.3389/fimmu.2017.01341

RANTES/CCL5 Induces Collagen Degradation by Activating MMP-1 and MMP-13 Expression in Human Rheumatoid Arthritis Synovial Fibroblasts

Solomon A. Agere[1], Nahid Akhtar[1], Jeffery M. Watson[2] and Salahuddin Ahmed[1,3]†*

[1] Department of Pharmaceutical Sciences, College of Pharmacy, Washington State University, Spokane, WA, United States, [2] Department of Chemistry and Biochemistry, Gonzaga University, Spokane, WA, United States, [3] Division of Rheumatology, University of Washington School of Medicine, Seattle, WA, United States

OPEN ACCESS

Edited by:
Jixin Zhong, Case Western Reserve University, United States

Reviewed by:
Xuhui Feng, Indiana University System, United States
Junjie Zhang, University of Southern California, United States
Yinghong Hu, Emory University, United States

***Correspondence:**
Salahuddin Ahmed
salah.ahmed@wsu.edu

†Present address:
Salahuddin Ahmed, Department of Pharmaceutical Sciences, College of Pharmacy, Washington State University, Spokane, Washington, United States.

Specialty section:
This article was submitted to Inflammation, a section of the journal Frontiers in Immunology

Received: *14 July 2017*
Accepted: *03 October 2017*
Published: *18 October 2017*

Citation:
Agere SA, Akhtar N, Watson JM and Ahmed S (2017) RANTES/CCL5 Induces Collagen Degradation by Activating MMP-1 and MMP-13 Expression in Human Rheumatoid Arthritis Synovial Fibroblasts. Front. Immunol. 8:1341. doi: 10.3389/fimmu.2017.01341

Regulated on activation, normal T expressed, and secreted (RANTES)/CC ligand 5 (CCL5) participates in rheumatoid arthritis (RA) pathogenesis by facilitating leukocyte infiltration, however, its other pathological functions are not fully defined in RA. In the present study, we evaluated the effect of RANTES/CCL5 on tissue degrading enzymes matrix metalloproteinase-1 (MMP-1) and MMP-13 expression and its contribution to the progressive joint damage by RA synovial fibroblasts (RASFs). Our results showed that RANTES/CCL5 dose dependently induced MMP-1 and MMP-13 expression in monolayers and three-dimensional (3D) micromass of human RASFs, which correlated with an increase in collagenase activity. This activation by RANTES/CCL5 was observed in RASF, but not in osteoarthritis SFs (OASFs). Evaluation of the signaling events showed that RANTES/CCL5 selectively activated PKCδ, JNK, and ERK proteins to induce MMP expression in human RASFs. Pretreatment with a functional antagonist (Met-RANTES) or heparinase III [an enzyme that selectively digests heparan sulfate proteoglycans (HSPGs)] completely abrogated RANTES/CCL5-induced MMP-1 and MMP-13 expression. Interestingly, the inhibition of RANTES/CCL5 using small-interfering RNA approach reduced the ability of interleukin-1β (IL-1β) to induce MMP-1 and MMP-13 expression, asserting its mediatory role in tissue remodeling. In the inhibitor study, only the selective inhibition of HSPGs or PKCδ, ERK, and JNK markedly inhibited RANTES/CCL5-induced MMP-1 and MMP-13 production. Circular dichroism spectroscopy results demonstrated the degradation of collagen triple-helical structure upon exposure to the conditioned media from RANTES/CCL5 stimulated RASFs, which was reverted by a broad-spectrum MMP inhibitor (GM6001). These findings suggest that RANTES/CCL5 not only upregulates MMP-1 and MMP-13 expression by partly utilizing HSPGs and/or PKCδ-JNK/ERK pathways but also mediates IL-1β-induced MMP-1 and MMP-13 expression.

Keywords: rheumatoid arthritis, synovial fibroblasts, regulated on activation, normal T expressed, and secreted/CC ligand 5, matrix metalloproteinases, heparan sulfate proteoglycans

INTRODUCTION

Rheumatoid arthritis (RA) is an autoimmune disease in which activated synovial fibroblasts (SFs) produce chemokines to facilitate infiltration of inflammatory cells (1–4). Chemokines are classified in to four subfamilies (C, CC, CXC, and CX_3C) depending on the number and spacing of cysteine motif (1, 5). Chemokines exert their effect through the recruitment and retention of monocytes and T lymphocytes in the joints, leading to hyperplasia of the synovial lining, and causing the destruction of bone and articular cartilage (4, 6, 7). In response to interleukin-1β (IL-1β) and tumor necrosis factor α (TNF-α), RA synovial fibroblasts (RASFs) release chemokines that bind to their receptors to recruit inflammatory cells at the site of inflammation (8). Among these chemokines, regulated on activation, normal T expressed and secreted (RANTES)/CC ligand 5 (CCL5) is a potent CC chemokine shown to play an important role in RA pathogenesis (9); however, its role beyond chemotactic activity is not well defined in RA. RANTES/CCL5 primarily attracts lymphocytes and monocytes as well as other cell types (1, 2). RASFs produce RANTES/CCL5 upon stimulation with TNF-α, IL-1β, or interferon gamma (10).

Matrix metalloproteinases (MMPs) are matrix degrading enzymes that have high affinity to destroy or remodel extracellular matrix (ECM) (1, 11, 12). Among different MMPs, the collagenases are of particular importance as they are able to efficiently cleave collagen. MMP-1 and MMP-13 are collagenases that play a significant role in bone and cartilage degradation (13). In RA, the transformation of normal synovial lining into a hyperplastic, invasive tissue pannus utilizes MMP-1 and MMP-13 to erode joint tissue (11, 14). In particular, MMP-1 and MMP-13 are capable of degrading intact fibrillary collagen that provides strength to cartilage (11, 15).

In the present study, we evaluated the effect of RANTES/CCL5 in inducing MMP-1 and MMP-13 expression in human RASFs and its underlying mechanism of action. Furthermore, we examined the effect of RANTES/CCL5-induced MMPs on the structure of native collagen.

MATERIALS AND METHODS

Reagents and Antibodies

Recombinant human RANTES/CCL5, Met-RANTES and IL-1β, and MMP-1 ELISA Duoset were purchased from R&D systems (Minneapolis, MN, USA). MMP-13 ELISA was purchased from Ray Biotech (Norcross, GA, USA). MMP-1 and MMP-13 SYBR Green primers were purchased from Qaigen (Valencia, CA, USA). SMARTpool ON-TARGETplus RANTES small-interfering RNA (siRNA) and On-target plus non targeting siRNA (D-001810-10) control were purchased from GE Dharmacon (Lafayette, CO, USA). MMP-1, MMP-13, type I collagen, and lamin A/C antibodies were purchased from Santa Cruz Biotech (Santa Cruz, CA, USA). Rabbit monoclonal or polyclonal antibodies against p-p38 (Thr^{180}/Tyr^{182}), p-ERK (Thr^{202}/Tyr^{204}), p-JNK(Thr^{183}/Tyr^{185}), p-PKCδ (Thr^{505}), total p-38, total JNK, total ERK, p-c-Jun (Ser^{73}), and p-ATF-2 ($Thr^{69/71}$) were from Cell Signaling Technologies (Beverly, MA, USA). Rabbit polyclonal antibodies against CCR1 and CCR5 were from BioVision (Milpitas, CA) and GeneTex (Irvine, CA, USA), respectively. Heparinase III (flavobacterium heparinum derived), heparan sulfate degrading lyase was purchased from Sigma (St. Louis, MO, USA). Type I collagen was purchased from Advanced Biometrix (Carlsbad, CA, USA). Inhibitors of JNK (SP600125), ERK (PD98059), p38 (SB 02190), PKCδ (Rottlerin), and NF-κB (PDTC) were purchased from EMD Millipore (Billerica, MA, USA).

Culture of Human RASFs

Deidentified RA synovial tissues were procured under a protocol approved by the Washington State University IRB (IRB#14696) from patients with diagnosed RA or OA who had undergone total joint replacement surgery or synovectomy and in compliance with the Declaration of Helsinki. No consent was needed because investigators had access only to deidentified human materials that were not collected specifically for the purpose of this research and for which they do not have ready means to link back to living individuals. The deidentified human normal (NL), RA, or OA synovial tissues were obtained from the Cooperative Human Tissue Network (Columbus, OH, USA) and the National Disease Research Interchange (Philadelphia, PA, USA). Some RASF patient cell lines were provided by our rheumatologist collaborator Dr. David A. Fox (University of Michigan, Ann Arbor, USA). RASFs were isolated through enzymatic digestion and grown in RPMI 1640 containing 2 mM L-glutamine with 10% FBS growth medium at 37°C in a humidified atmosphere with 5% CO_2 as described earlier (16, 17). RASFs between passages 5 and 10 were used in the experiments. All treatments were performed in serum-free medium.

Treatment of RASFs

To evaluate the effect of RANTES/CCL5 on MMP-1 and MMP-13 expression, human NLSFs, RASFs or OASFs were treated with recombinant human RANTES/CCL5 (20, 50, or 100 ng/ml) for 24 h. Human RASFs were also pretreated with Met-RANTES (a functional antagonist of RANTES; 50, 100, and 200 ng/ml) for 30 min and then stimulated with RANTES/CCL5 or IL-1β for 24 h. Total RNA and conditioned media was used to study the MMP-1 and MMP-13 expression using qRT-PCR, ELISA, and Western immunoblotting, respectively. Effect of RANTES/CCL5 on the activation of NF-κB, MAPK, and PKCδ signaling pathways was determined in RASF lysates treated with RANTES/CCL5 (100 ng/ml) for 5, 15, and 30 min using Western immunoblotting. For some experiments, RASFs were pretreated with the inhibitor of p38 (SB203980; 10 μM), ERK (PD98059; 10 μM), JNK (SP600125; 10 μM), NF-KB (PDTC; 200 μM), or PKCδ (Rottlerin; 10 μM) for 2 h followed by RANTES/CCL5 treatment for 24 h. Culture supernatants were concentrated using Amicon® Ultra centrifugal filters (Millipore) and MMP-1 and MMP-13 expression was determined using Western immunoblotting.

To study the effect of Met-RANTES on IL-1β-induced signaling pathways, we pretreated RASFs with Met-RANTES (100 ng/ml) for 30 min, followed by IL-1β (10 ng/ml) stimulation for 30 min. Cell lysates were prepared to be used for the analysis of the phosphorylated proteins (p-PKCδ, p-JNK, and p-ERK).

To study the role of heparan sulfate proteoglycans (HSPGs) in RANTES/CCL5-induced MMP production, RASFs were pretreated with heparinase III (0.5 U/ml), an enzyme that recognizes HSPGs as its primary substrate, for 2 h and then stimulated with RANTES/CCL5 (100 ng/ml) for 24 h. Conditioned media was concentrated to determine MMP-1 and MMP-13 expression by Western immunoblotting.

To verify whether heparinase III affects the binding of RANTES to its receptor to inhibit the biological activity, we pretreated RASFs with heparinase III for 2 h and then stimulated with RANTES/CCL5 (100 ng/ml) for 1 h. We ran this experiment in two sets both in triplicate. In the first set, we terminated the reaction without cross-linking proteins by washing with ice-cold PBS three times. In the second set, we cross-linked proteins with 1% formaldehyde for 10 min followed by 125 mM glycine neutralization for 5 min, and then washed three times with cold PBS. Whole cell lysates were prepared using RIPA buffer and an equal amount of protein in 25 µl was used for detecting bound RANTES using a commercially available kit (R&D Systems). RANTES/CCL5 levels were normalized with per mg of cellular protein.

Human RASFs Three-Dimensional (3D) Micromass Cultures

Micromass organ cultures were constructed as described by Kiener et al. (18). Briefly, RASFs were released from the culture dish using 0.02% (weight/volume) TPCK-treated trypsin (Worthington, Lakewood, NJ, USA) in HEPES buffered saline solution (20 mM HEPES, 137 mM NaCl, and 3 mM KCl, pH 7.4) containing 2 mM $CaCl_2$. Cells were resuspended in ice-cold Matrigel Matrix (BD Biosciences) at a density of 5×10^6 cells/ml. Droplets of the cell suspension (25 µl) were placed onto 12-well culture ultralow attachment dishes (Corning, NY, USA). Thereafter, RASFs were cultured in basal culture medium (DMEM supplemented with penicillin, streptomycin, L-glutamine, nonessential amino acid solution, insulin–transferrin–selenium (BioWhittaker, Rockland, ME, USA), 0.1 mM ascorbic acid, and 10% heat-inactivated FBS). The floating 3D culture was maintained for 3 weeks; the medium was routinely replaced twice weekly. For experiments, RASFs were pretreated with Met-RANTES (200 µg/ml) for 30 min followed by stimulation with RANTES/CCL5 (100 ng/ml) for 24 h. IL-1β (10 ng/ml) for 24 h was used as a positive control. Culture supernatant were concentrated using Amicon® Ultra Centrifugal filters (Millipore) and MMP-1 and MMP-13 expression was determined using Western immunoblotting.

Transient Transfection of siRNA

To study the effect of RANTES/CCL5 knockdown on MMP-1 and MMP-13 production, RASFs were transfected with ON-TARGET plus SMART pool RANTES/CCL5 siRNA (GE Dharmacon, Lafayette, CO, USA) using Lipofectamine® RNAiMAX (Life Technologies) for 48 h and then stimulated with IL-1β (5 ng/ml) for 24 h. Conditioned media was used to study the effect of MMP-1 and MMP-13 production using ELISA.

Western Immunoblot Analyses

Western blot analysis on the cell lysates and conditioned media was performed as described in our earlier studies (16, 19). Images were analyzed using the GELDOC or Image-J software. Each band was scanned using Image lab 5.1 software and the expression values (pixels/band) were presented as mean ± SE.

In-Gel Zymography

Collagenase activity in the RANTES/CCL5-treated conditioned media was determined by the in-gel zymography method as described earlier (19). Fifteen microliter of the conditioned media was resolved under non-reducing conditions on SDS-polyacrylamide gels loaded with collagen (1 mg/ml: type A from porcine skin; Sigma, St. Louis, MO, USA) as a substrate. Following electrophoresis, the gels were washed with 2.5% Triton X-100 for 30 min with gentle shaking, followed by a 30 min or overnight wash in developing buffer (50 mM Tris–HCl, pH 8.0, 5 mM $CaCl_2$, and 0.02% NaN_3). Finally, gels were stained in Coomassie blue (R-250) and images of the digested regions representing MMPs activity were captured and analyzed using Image-J software.

Quantitative Real-time PCR Analysis

Total RNA was reverse-transcribed using SuperScript™ first Strand synthesis kit (Life Technologies, Carlsbad, CA, USA) according to the manufacturer instruction. The mRNA expression using validated primers for MMP-1 (NM_002421; Cat. No. QT00014581, Qiagen) and MMP-13 (NM_002427; Cat. No. QT00001764, Qiagen) was quantified using the power SYBR® Green PCR master mix (Life Technologies) and QuantiTect primer assay (Qiagen). GAPDH mRNA expression was used as endogenous control. Quantification of the relative expression was determined by ΔΔCt method.

Preparation of Nuclear Extracts

To study activation and nuclear translocation of p-c-Jun and p-ATF-2, RASFs were treated with RANTES/CCL5 (100 ng/ml) for 5, 15, and 30 min. Nuclear fractions were prepared as described before (1) and evaluated for p-c-Jun and p-ATF2 expression using Western immunoblotting.

In Vitro JNK/SAPK Kinase Assay

Rheumatoid arthritis synovial fibroblasts were pretreated with Met-RANTES for 30 min and stimulated with or without RANTES/CCL5 (100 ng/ml) for 30 min. Cells were washed twice with ice-cold PBS and scrapped directly into 0.25 ml of lysis buffer provided with the kinase assay kit. *In vitro* JNK/SAPK kinase assay was performed using a non-radioactive kinase assay kit according to the instruction of the manufacturer (Cell Signaling Technology) as described earlier (12).

Collagen Degradation Assay

Human RASFs were pretreated with or without GM6001 (a broad-spectrum MMP inhibitor; 20 µM) for 2 h and then stimulated with RANTES/CCL5 (100 ng/ml) or IL-1β (10 ng/ml). A modified collagen degradation assay method was followed (20) in which the conditioned media from the above experiments were added onto a 96-well plate coated with type I collagen (200 µg/well) and incubated for 24 h at 37°C. After removing the condition media, the plates were stained with Coomassie R250, washed to

remove soluble stain, and analyzed by ChemiDoc™ XRS Imager (Bio-Rad). In addition, the conditioned media (500 µl) collected after treating type I collagen was concentrated using Amicon 10K ultra 0.5 ml centrifugal filters and resolved on 7.5% SDS-PAGE using for COL1A1 detection by immunoblotting.

Circular Dichroism (CD) Spectroscopy

Condition media from RANTES/CCL5 or IL-1β stimulated RASFs was applied on collagen-coated 96-well plates in triplicate as described above for 8 and 48 h. Condition media was removed and plates were carefully washed with PBS to remove media residue. Remaining digested collagen was collected using 200 µl of 0.1% acetic acid. CD spectroscopy was performed using a Jasco J-815 spectropolarimeter outfitted with a Peltier temperature-controlled cell holder. All spectra were collected at 25°C in a 1 mm cuvette. CD signal was monitored between 200 and 250 nm wavelengths (21). Samples were normalized with 0.1% acetic acid as a blank. Native type I collagen was used as standard to compare the damage. We also performed a separate experiment to test whether there is any difference in the CD spectra when collagen is exposed to the conditioned media from untreated NLSFs and RASFs.

Statistical Analysis

Statistical analysis was performed for the protein and mRNA *in vitro* data using one-way analysis of variance test, followed by Dunnett's multiple comparison *post hoc* test with $p < 0.05$ chosen as the level of significance.

RESULTS

RANTES/CCL5 Dose Dependently Induces MMP-1 and MMP-13 Expression in Human RASFs

Human RASFs treated with RANTES/CCL5 (20, 50, and 100 ng/ml) for 24 h showed a significant increase in MMP-1 (~2.3-fold) and MMP-13 (~2.1-fold) mRNA expression when compared to the untreated control (**Figure 1A**). A similar dose-dependent increase in the MMP-1 and MMP-13 protein production was observed upon RANTES/CCL5 stimulation (**Figure 1B**). Interestingly, RANTES/CCL5 had no inducing effect on MMP-1 and MMP-13 expression in OASFs (**Figure 1C**) or in the human dermal fibroblasts (data now shown), suggesting that RANTES/CCL5 preferentially inflicts tissue damage in RA. Surprisingly, RANTES/CCL5 marginally induced MMP-1 production, but dose-dependently reduced MMP-13 production in NLSFs (**Figure 1D**). To further validate that RANTES/CCL5-induced MMP-1 and MMP-13 expression in not due to differences in the expression of its receptor CCR5, and also CCR1, we performed Western blot analysis on the whole cell lysates prepared from untreated NLSFs and RASFs. Our results showed expression levels of CCR1 in RASFs was ~20% lower than NLSFs, however, there was no significant difference observed in the expression levels of CCR5 (Figure S1 in Supplementary Material).

To further verify the effect of RANTES/CCL5 on the enzymatic activity in RASFs, collagenase activity in RANTES/CCL5-stimulated conditioned media was determined using in-gel zymography. Densitometric analysis of the developed zymograms showed that RANTES/CCL5 dose dependently induced collagenase activity in RASFs (**Figure 1E**), without affecting RASF's viability (**Figure 1F**). These findings suggest that RANTES/CCL5 selectively activates RASFs to produce MMP-1 and MMP-13 expression.

Met-RANTES Inhibits RANTES/CCL5-Induced MMP-1 and MMP-13 Expression by RASFs

To study the effect of Met-RANTES on RANTES/CCL5-induced MMP-1 and MMP-13 production, human RASFs were pretreated with Met-RANTES (50, 100, and 200 ng/ml) for 30 min prior to RANTES/CCL5 stimulation for 24 h (**Figure 2**). MMP-1 and MMP-13 expression was determined using qRT-PCR and ELISA or Western immunoblotting. Met-RANTES significantly reduced RANTES/CCL5-induced MMP-1 (~53%) and MMP-13 (~66%) mRNA expression (**Figures 2A,B**). Analysis of the conditioned media from the same treatment showed a similar decrease in MMP-1 and MMP-13 production by Met-RANTES (**Figures 2C,D**). We also developed the 3D micromass culture of RASFs (**Figure 2E**) to verify the effect of Met-RANTES on RANTES/CCL5-induced MMP-1 and MMP-13 production in a synovial tissue-like environment, which showed a similar significant reduction of MMP-1 and MMP-13 in the condition media obtained from human RASFs micromass cultures (**Figure 2F**).

RANTES/CCL5 Mediates IL-1β-Induced MMP-1 and MMP-13 Expression in RASFs

Interleukin-1β causes inflammation and tissue destruction in RA (1, 22). While IL-1β is a potent inducer of RANTES/CCL5 (22, 23), the contribution of RANTES/CCL5 in its tissue destructive property is not clear. Thus, we pretreated RASFs with Met-RANTES (50, 100, and 200 ng/ml) for 30 min, followed by IL-1β (5 ng/ml) stimulation for 24 h. Results showed that Met-RANTES markedly reduced the ability of IL-1β to produce MMP-1 (~79%) and MMP-13 (~64%) in RASFs (**Figure 3A**). Confirmation of these findings by siRNA approach showed that IL-1β-induced MMP-1 and MMP-13 production was indeed reduced by ~45% in RANTES/CCL5 siRNA-treated group when compared to their respective values in the negative control (NC) siRNA group (**Figure 3B**). We observed that siRNA targeting RANTES/CCL5 was capable of inhibiting IL-1β-induced RANTES/CCL5 production by almost 75% (**Figure 3C**).

RANTES/CCL5 Requires HSPGs to Induce MMP-1 and MMP-13 Expression in RASFs

In addition to their critical role in developing chemokine gradient around activated endothelium, HSPGs cooperate with integrins and other cell adhesion receptors to facilitate cell-ECM attachment, cell–cell interactions, and cell motility (24). To determine their possible role in RANTES/CCL5-induced MMP-1 and MMP-13 production, RASFs were pretreated with heparinase III for 2 h followed by RANTES/CCL5 stimulation for 24 h. Analysis of the conditioned media showed that heparinase III significantly inhibits RANTES/CCL5-induced MMP-1 and

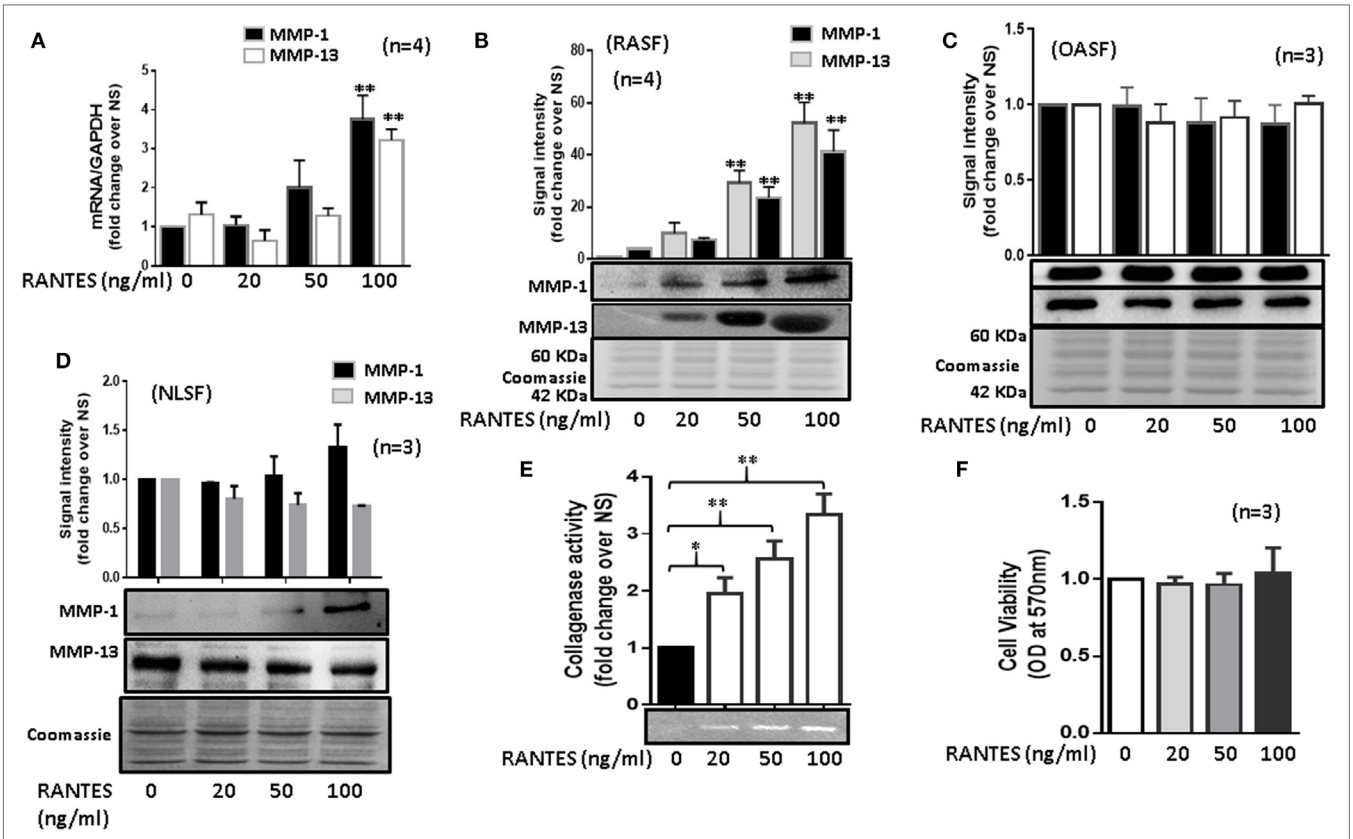

FIGURE 1 | Regulated on activation, normal T expressed, and secreted (RANTES)/CC ligand 5 (CCL5) induces matrix metalloproteinase (MMP)-1 and MMP-13 expression in rheumatoid arthritis synovial fibroblasts (RASFs). **(A)** Effect of RANTES/CCL5 on MMP-1 and MMP-13 mRNA and **(B)** protein expression was studied in RASFs. **(C,D)** Human OASFs and NLSFs were treated with different concentrations of recombinant RANTES/CCL5 (20, 50, and 100 ng/ml) and MMP-1 and MMP-13 expression was analyzed using Western immunoblotting, respectively. Gels described for **(B–D)** were stained with Commassie Blue stain to ensure equal loading of the supernatants. **(E)** Effect of RANTES/CCL5 on collagenase activity in RASFs. RASFs were treated with different concentration (20, 50, and 100 ng/ml) of RANTES/CCL5 for 24 h and conditioned media was concentrated using Amicon® Ultra Centrifugal filters (Millipore) and resolved on polyacrylamide gel loaded with collagen. Zymography image of digested regions representing MMPs activity is shown. Fold changes on developed zymograms was determined using densitometric analysis. **(F)** Effect of RANTES/CCL5 on the cell viability of RASFs was determined using MTT assay. RASFs were treated with RANTES/CCL5 (20, 50, and 100 ng/ml) for 24 h. Cell viability of cultured RASFs in the presence of RANTES/CCL5 was measured by optical densities at 570 nm. Values are represented as mean ± SE from three to four independent experiments using cells from different donors under similar conditions. $^{*}p < 0.05$; $^{**}p < 0.01$ for NS versus RANTES/CCL5 treatment.

MMP-13 expression (**Figure 3D**). To confirm whether heparinase III inhibits RANTES/CCL5 binding to the cell membrane receptor, we analyzed whole cell lysates from RASFs treated with RANTES/CCL5 (100 ng/ml) with or without heparinase III pretreatment for bound RANTES/CCL5 using ELISA kits. Our results showed that the levels of cell-membrane bound RANTES/CCL5 remained unaltered with heparinase III treatment (**Figure 3E**), suggesting that heparinase III may be able to block or interfere with RANTES/CCL5 signaling by a mechanism independent of RANTES/CCL5 binding.

RANTES/CCL5 Selectively Activates PKCδ, JNK, and ERK Pathways in Human RASFs

To study the signaling pathways involved in RANTES/CCL5-induced MMP-1 and MMP-13 production, RASFs were pretreated with the inhibitor of p38 (SB202192), ERK (PD98059), JNK (SP600125), NF-κB (PDTC), or PKCδ (Rottlerin) for 2 h, followed by RANTES/CCL5 stimulation for 24 h. The conditioned media was concentrated and used to determine MMP-1 and MMP-13 production using Western immunoblotting. Our results showed that only the inhibition of PKCδ, JNK, or ERK markedly reduced RANTES/CCL5-induced MMP-1 and MMP-13 production in RASFs (**Figure 4A**). In light of these observations, we evaluated the effect of RANTES/CCL5 (100 ng/ml) on the activation of MAPK (p38, JNK, and ERK) and PKCδ pathways at different time points (5, 15, and 30 min). Western blot analysis of the cell lysates and further densitometric analysis showed that RANTES/CCL5 selectively activates p-PKCδ, p-JNK, and p-ERK in RASFs (**Figure 4B**).

PKCδ Is an Important Upstream Mediator of RANTES/CCL5-Induced Signaling Pathways in RASFs

To determine the hierarchy of signaling proteins in RANTES/CCL5 mediated activation of PKCδ and MAPK pathways, RASFs

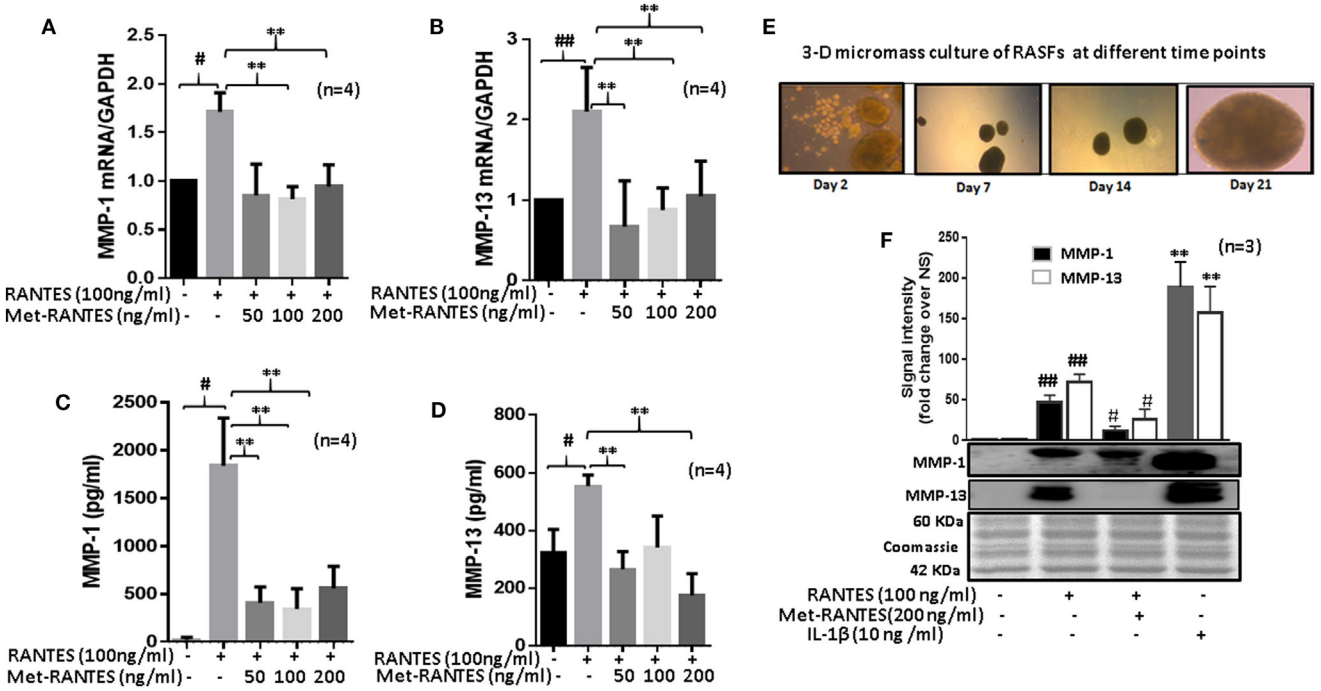

FIGURE 2 | Met-RANTES inhibits regulated on activation, normal T expressed, and secreted (RANTES)/CC ligand 5 (CCL5)-induced matrix metalloproteinase (MMP)-1 and MMP-13 expression in rheumatoid arthritis synovial fibroblasts (RASFs). **(A,B)** Effect of Met-RANTES on RANTES/CCL5-induced MMP-1 and MMP-13 mRNA and **(C,D)** at protein levels was determined using qRT-PCR and ELISA, respectively. RASFs were pretreated with Met-RANTES (50, 100, and 200 ng/ml) for 30 min followed by stimulation with RANTES/CCL5 (100 ng/ml) for 24 h. **(E,F)** Human RASFs were cultured in three-dimensional (3D) micromass for 21 days to form synovial tissue-like architect, followed by pretreatment with or without Met-RANTES for 30 min and then stimulation with RANTES (100 ng/ml) for 24 h. Interleukin (IL)-1β (10 ng/ml) 24 h stimulated RASF micromass were used as the positive control. Conditioned media was concentrated using Amicon® Ultra Centrifugal filters (Millipore) and MMP-1 and MMP-13 production was analyzed using Western immunoblotting. Densitometry was performed to determine the relative changes. Values are represented as mean ± SE from three to four independent experiments using cells from different donors. #$p < 0.05$ or ##$p < 0.01$ for NS vs. RANTES/CCL5 or IL-1β; **$p < 0.01$ for RANTES/CCL5 vs. Met-RANTES treatment. Representative figures of RASFs on 3D micromass culture (4× magnification; size 200–400 μm) are shown on days 2, 7, 14, and 21.

were pretreated with PKCδ inhibitor (Rottlerin) or JNK inhibitor (SP600125) for 2 h and then stimulated with RANTES/CCL5 (100 ng/ml) for 30 min. Cell lysates were evaluated for phosphorylation of JNK, ERK, and PKCδ. Rottlerin markedly suppressed RANTES/CCL5-induced phosphorylation of JNK, ERK, and PKCδ in RASFs (**Figure 5A**; Figure S2A in Supplementary Material). We also observed that the phosphorylation of PKCδ was partially affected by JNK inhibitor, suggesting PKCδ lies upstream of JNK/ERK in RANTES/CCL5-induced signaling cascade is RASFs (**Figure 5A**; Figure S2A in Supplementary Material).

Rheumatoid arthritis synovial fibroblasts were treated with RANTES/CCL5 for 5, 15, and 30 min and the expression of p-c-Jun and p-ATF-2 was determined in the nuclear extracts. Our results showed a time-dependent increase in the nuclear translocation of p-ATF-2 and p-c-Jun in RANTES/CCL5 stimulated RASFs (**Figure 5B**). Furthermore, we evaluated the effect of RANTES/CCL5 (100 ng/ml) alone or with Met-RANTES on SAPK/JNK *in vitro* kinase activity. Our results showed that RANTES/CCL5 significantly induced JNK kinase activity compared to the unstimulated control, which was completely inhibited by Met-RANTES pretreatment (**Figure 5C**).

To further understand the signaling mechanisms through which Met-RANTES was able to inhibit IL-1β-induced MMP-1 and MMP-13 production in RASFs (seen in **Figure 3A**), we pretreated RASFs with Met-RANTES (100 ng/ml) for 30 min, followed by IL-1β (10 ng/ml) stimulation for 30 min. Western blotting followed by the densitometric analysis of the cell lysates showed that Met-RANTES was able to inhibit p-JNK activation by roughly 30%, whereas it elicited modest inhibitory effects on p-PKCδ and p-ERK activation by IL-1β stimulation (**Figure 5D**; Figure S2B in Supplementary Material). These findings suggest that Met-RANTES inhibits IL-1β-induced MMP-1 and MMP-13 production by directly inhibiting JNK pathway in human RASFs *in vitro*.

RANTES/CCL5 Induces Collagenolytic Activity in RA

To determine the collagenolytic potential of RANTES/CCL5, RASFs were stimulated with RANTES/CCL5 (100 ng/ml) or IL-1β (10 ng/ml) for 24 h. Condition media (200 μl) was added to type I collagen coated 96-well plates and incubated for 24 h. At the time of termination, media was collected and plates were stained with Coomassie blue R250. Our results showed that collagen was

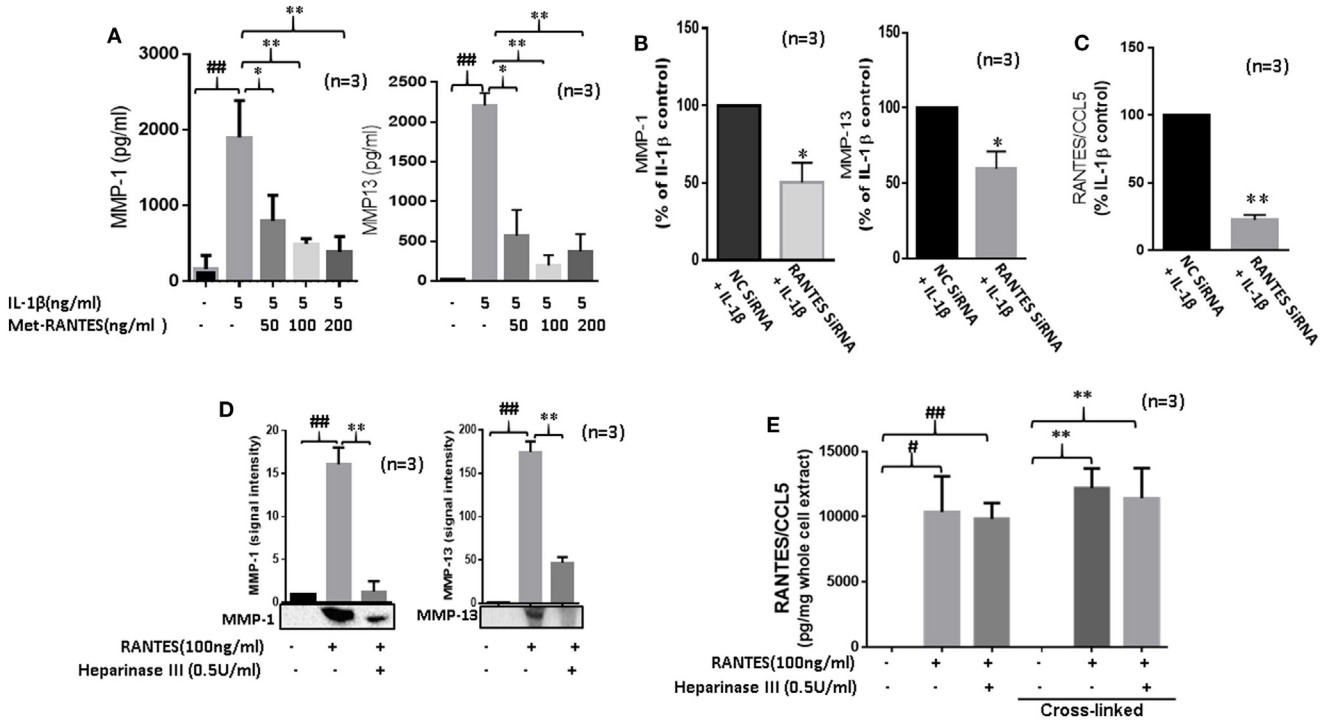

FIGURE 3 | Regulated on activation, normal T expressed, and secreted (RANTES)/CC ligand 5 (CCL5) contributes to the proinflammatory cytokine-mediated matrix metalloproteinase (MMP)-1 and MMP-13 expression in rheumatoid arthritis (RA). **(A)** Met-RANTES inhibits interleukin (IL)-1β-induced MMP-1 and MMP-13 production in rheumatoid arthritis synovial fibroblasts (RASFs). **(B)** Effect of RANTES/CCL5 knockdown on IL-1β-induced MMP-1 and MMP-13 production in RASFs. RASFs were transfected with RANTES/CCL5-specific small-interfering RNA (siRNA) for 48 h and then stimulated with IL-1β (5 ng/ml) for 24 h. Levels of MMP-1 and MMP-13 in conditioned media was quantified using ELISA and represented as percent of IL-1β-treatment control. **(C)** Conditioned media from the above treated samples were also evaluated to determine percent knockdown of RANTES/CCL5 using siRNA approach and represented as percent of IL-1β treatment control. **(D)** Degradation of heparan sulfate proteoglycans (HSPG) by heparinase III reduces RANTES/CCL5-induced MMP-1 and MMP-13 expression in RASFs. RASFs were pretreated with heparinase III (0.5 U/ml) for 2 h followed by stimulation with RANTES/CCL5 (100 ng/ml) for 24 h. Conditioned media was concentrated and used to detect MMP-1 and MMP-13 expression using Western immunoblotting. Densitometry was performed to determine the relative changes. **(E)** RASFs pretreated with heparinase III (0.5 U/ml) for 2 h followed by stimulation with RANTES/CCL5 (100 ng/ml) for 1 h were used with or without cross-linking step for the detection of RANTES/CCL5 in the whole cell lysates (25 µl). Values are represented as mean ± SE from three independent experiments performed using RASFs from different donors under similar conditions. ##$p < 0.01$ for NS vs. or RANTES/CCL5 or IL-1β. *$p < 0.05$ or **$p < 0.01$ for RANTES/CCL5 or IL-1β vs. Met-RANTES or heparinase III treatment.

digested and eroded from the wells exposed to RANTES/CCL5 or IL-1β-treated conditioned media compared to unstimulated control, indicating their collagenolytic potentials (**Figure 6A**). When these stained plates were further analyzed for absorbance at 570 nm, both RANTES/CCL5 and IL-1β-treated RASFs showed significant loss of collagen further confirming the ability of RANTES/CCL5 and IL-1β to induce collagen degradation by MMP-1 and MMP-13 production (**Figure 6B**). Western blot evaluation of the conditioned media for the digested/released collagen fragments from the coated plates for COL1A1 expression showed a marked increase in the collagen fragments, in addition to the native 220 kDa, generated in both RANTES/CCL5 and IL-1β stimulated samples (**Figure 6C**).

To further confirm collagen degradation, the conditioned media from similar experiments (8 h as early and 48 h as a late time point) were evaluated for structural changes in collagen and compared to the native collagen standard using CD spectroscopy (**Figure 6D**). Compared to the native collagen, exposure to unstimulated conditioned media, obtained from RA-affected samples, showed a marked change in the structure of collagen (**Figure 6D**). In addition, RANTES/CCL5 or IL-1β-treated conditioned media showed further conformational changes to collagen structure as evident by the loss of the characteristic collagen peaks at 200 (negative) and 225 (positive) nm (21), suggesting collagen degradation (**Figure 6D**). We also compared the untreated conditioned media from NLSFs with untreated RASFs to identify that while there were modest structural changes brought by RASF's compared to NLSF's untreated media (Figure S3 in Supplementary Material). These findings suggest that chronic activation of RASFs by RANTES/CCL5 or cytokines such as IL-1β during the disease progression leads to the subtle structural changes in the native collagen of the cartilage that eventually contribute to the tissue destruction in RA.

To verify whether this damage to collagen by RANTES/CCL5 or IL-1β were mediated by MMPs, RASFs were pretreated with a broad-spectrum MMP inhibitor (GM6001; 20 µM) for 2 h and then stimulated with RANTES/CCL5 or IL-1β for 24 h. The conditioned media was added on to type I collagen-coated plates

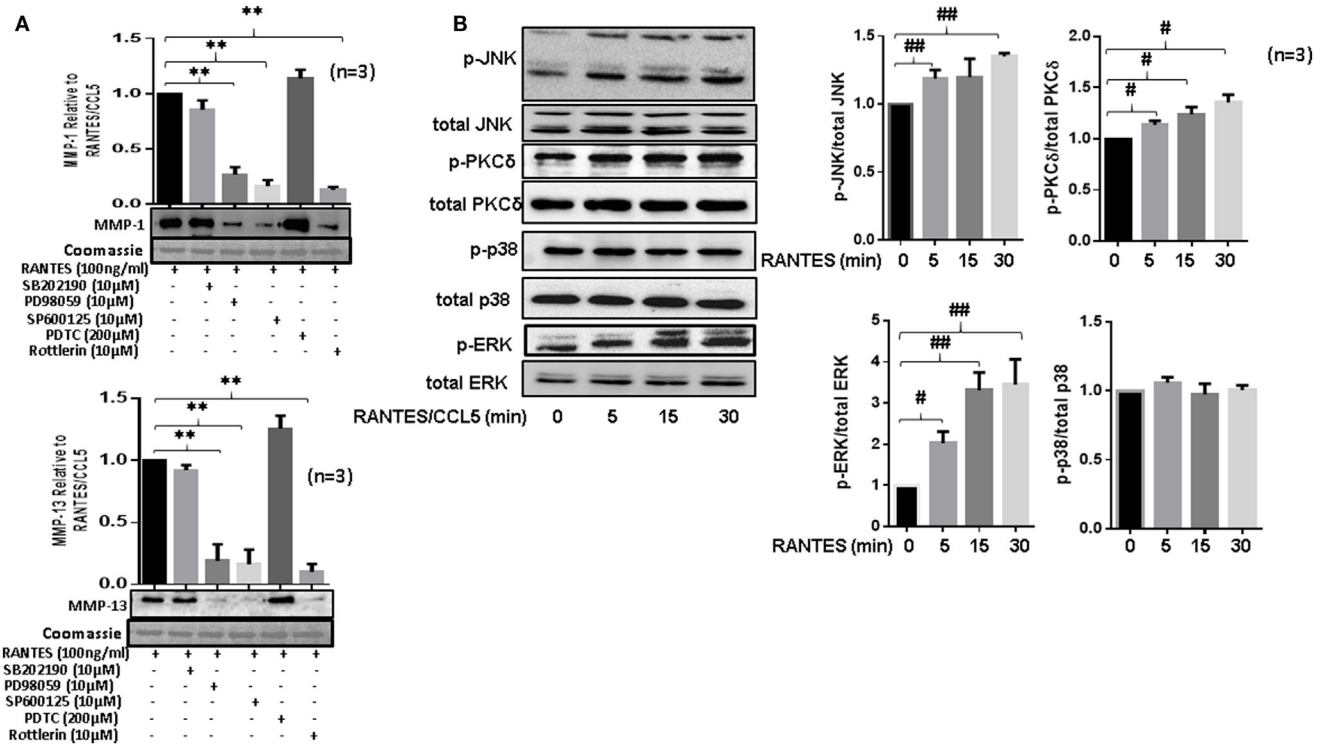

FIGURE 4 | Regulated on activation, normal T expressed, and secreted (RANTES)/CC ligand 5 (CCL5) selectively activates PKCδ and JNK pathways to induce matrix metalloproteinase (MMP)-1 and MMP-13 production in rheumatoid arthritis synovial fibroblast (RASFs). **(A)** RASFs were pretreated with p-38 inhibitor (SB203980; 10 μM), ERK inhibitor (PD98059; 10 μM), JNK inhibitor (SP600125; 10 μM), NF-KB inhibitor (PDTC; 200 μM), or PKCδ inhibitor (Rottlerin; 10 μM) for 2 h followed by stimulation with RANTES/CCL5 for 24 h. Culture supernatant were concentrated to determine MMP-1 and MMP-13 expression using Western immunoblotting. Densitometry was performed to determine the relative changes. Gels were stained with Commassie Blue R250 stain to ensure equal loading. **(B)** Effect of RANTES/CCL5 (100 ng/ml) on the MAPK (p38, JNK and ERK) and PKCδ pathways was studied in human RASFs. RASFs were treated with RANTES (100 ng/ml) for different time (5, 15, and 30 min) and effect on phosphorylation of p38, JNK, ERK, and PKCδ was determined using Western immunoblotting. Total forms of p-38, JNK, ERK, and PKCδ were used as normalizing controls, respectively. Densitometry was performed to show the relative changes. Values are represented as mean ± SE from three or more independent experiments using cells from different donors under similar conditions. $^{**}p < 0.01$ for RANTES/CCL5 vs. inhibitors; $\#p < 0.05$ or $\#\#p < 0.01$ for NS vs. RANTES/CCL5.

as described above. A significantly higher degradation of type I collagen was found in both RANTES/CCL5 or IL-1β alone treated as evidenced by the reduced Coomassie staining (**Figure 6E**). However, pretreatment with GM6001 showed a marked inhibition of collagen degradation in RANTES/CCL5 or IL-1β-treated group (**Figure 6E**). These results suggest that the effect of both RANTES/CCL5 and IL-1β on type I collagen degradation are orchestrated by MMP-1 and MMP-13 production in RASFs.

DISCUSSION

This study provides a novel mechanistic insight to the role of RANTES/CCL5 in inducing MMP-1 and MMP-13 expression in human RASFs and its damaging impact on the structure of native collagen. Furthermore, the study also showed that IL-1β-induced MMP-1 and MMP-13 is partly mediated *via* RANTES/CCL5 and there exists an opportunity to therapeutically limit the role of RANTES/CCL5 in the process of tissue destruction in RA by reducing its interaction with HSPGs found on the cell surface and ECM, or inhibiting the signaling proteins such as PKCδ in RASFs.

Regulated on activation, normal T expressed, and secreted (RANTES)/CCL5 is produced by the majority of cell types that participate in pathogenesis of RA, including SFs, endothelial cells, chondrocytes, monocyte/macrophages, and activated T cells (11, 12). RANTES/CCL5 among other CC chemokines is an established regulator of migration, cell proliferation, and leukocyte trafficking. In our previous studies, we have shown that IL-1β is a potent inducer of RANTES/CCL5 and other chemokines in human RASFs (1, 23). Administration of Met-RANTES has been shown to ameliorate experimental arthritis by reducing joint inflammation and bone destruction (25, 26). Our results showing that RANTES/CCL5 is capable of inducing MMP-1 and MMP-13 expression and collagenase activity and may also contribute to IL-1β-induced destruction further implicates RANTES/CCL5 as a potent mediator of bone and cartilage damage in RA. Whether RANTES/CCL5 acts together, in a synergistic manner, with IL-1β to exacerbate inflammation and tissue destruction by RASFs require further experiments.

An extensive joint destruction in RA, as well as OA, is mediated by an intense action of various proteinases, the most important among them being collagenases (14, 27). MMP-1 and

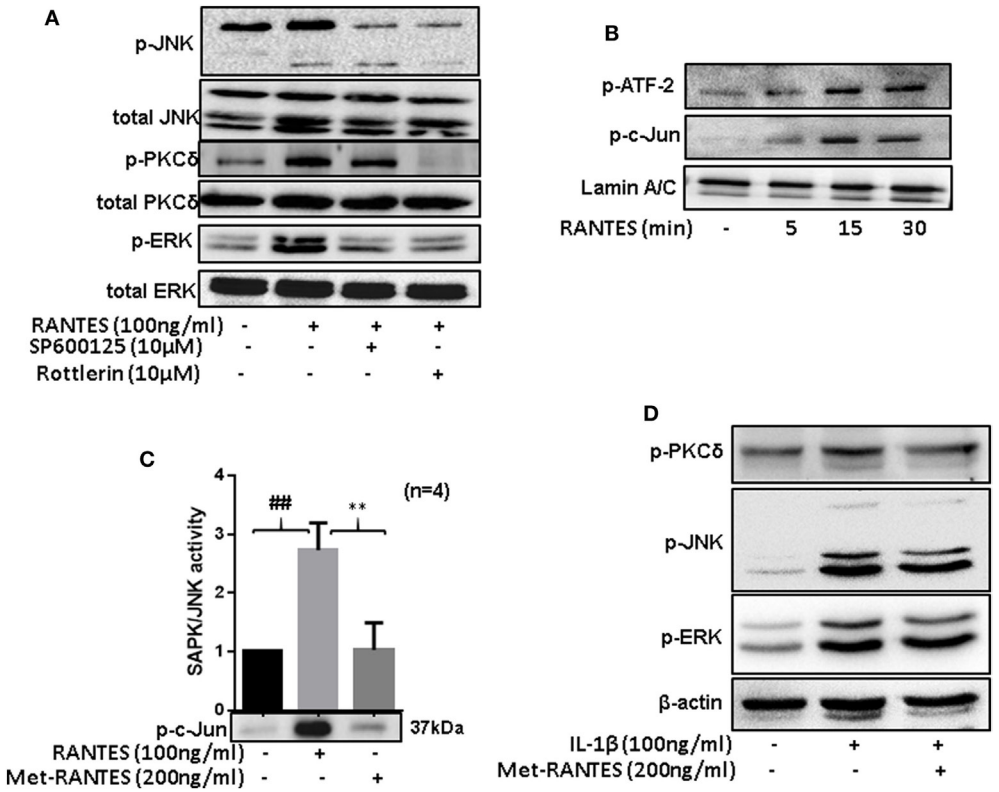

FIGURE 5 | Regulated on activation, normal T expressed, and secreted (RANTES)/CC ligand 5 (CCL5)-mediated phosphorylation of PKCδ causes JNK and ERK activation to induce matrix metalloproteinase (MMP)-1 and MMP-13 production in rheumatoid arthritis synovial fibroblasts (RASFs). **(A)** RASFs were pretreated with the inhibitor of JNK (SP 600125; 10 μM) or PKCδ (Rottlerin; 10 μM) for 2 h followed by RANTES/CCL5 stimulation (100 ng/ml) for 30 min to determine the hierarchy of signaling proteins (p-PKCδ, p-JNK, and p-ERK) in RANTES/CCL5-mediated signal transduction using Western immunoblotting. **(B)** Effect of RANTES/CCL5 on nuclear translocation of p-ATF-2 and p-c-Jun in RASFs was determined using Western immunoblotting. RASFs were stimulated with RANTES/CCL5 (100 ng/ml) for 5, 15, and 30 min and nuclear fraction were used to study the effect on p-ATF-2 and p-c-Jun. Lamin A/C was used as loading control. **(C)** Effect of Met-RANTES on RANTES/CCL5 induced SAPK/JNK activity in RASFs. RASFs were pretreated with Met-RANTES for 30 min followed by RANTES/CCL5 treatment for 30 min. Immunoprecipitation was performed using p-SAPK/JNK antibody and antagonizing effect of Met-RANTES was determined by Western immunoblotting. Densitometry was performed to show the relative changes in SAPK/JNK activity and values are represented as mean ± SE from independent experiments performed on RASFs obtained from different donors. **(D)** RASFs were pretreated with Met-RANTES for 30 min followed by IL-1β treatment for 30 min. Cell lysates were used for the detection of p-PKCδ, p-JNK, and p-ERK. ##$p < 0.01$ NS vs. RANTES/CCL5; **$p < 0.01$ RANTES vs. RANTES + Met-RANTES.

MMP-13 are produced by RASFs and their elevated levels in the synovial fluid and enhanced expression in synovial tissue biopsies from RA patients provide an evidence for their active role in tissue destruction (28, 29). Firestein et al. have demonstrated that JNK pathway mediates cytokine-induced MMP-1 and MMP-13 expression in SFs and murine inflammatory arthritis model (30, 31). The promoter region of MMP-1 and MMP-13 hosts several AP-1-binding sites, which makes it an important transcriptional regulator of these MMPs (32). In addition, IL-1β has been shown to be a more potent inducer of MMP-1 compared to TNF-α partly due to its ability to induce ERK pathway concomitantly (33), suggesting that ERK may play a supportive role in the transcriptional activation of MMP-1, and possibly MMP-13. In fact, the regulation by PKCδ of its downstream signaling proteins JNK/ERK and the inhibition of RANTES/CCL5-induced MMP-1 and MMP-13 expression by Rottlerin suggest that PKCδ might be a relevant therapeutic target in RA. This is further supported by a previous study, in which RANTES/CCL5 induced IL-6 production in human OASFs *via* PKCδ and Src pathways (27). Recent clinical studies using JAK inhibitor (tofacitinib) or anti-TNF therapy have also shown efficacy in reducing tissue destruction, in part by downregulating MMP-1 and MMP-13 expression (34, 35).

We observed the inhibition of IL-1β-induced MMP-1 and MMP-13 expression by Met-RANTES, which may partly be due to its ability to inhibit the activation of JNK pathway. While these findings are open to different interpretations, we hypothesize that Met-RANTES is effective in blocking IL-1β in a two-pronged approach: by blocking the contribution of RANTES/CCL5 produced in response to IL-1β stimulation of RASFs and by inhibiting the phosphorylation and kinase activity of JNK, thereby producing a profound decrease in MMP-1 and MMP-13 production. Our previous findings have shown PKCδ as one of the key molecules in IL-1β signaling pathway (1, 23), however, other studies suggest that the regulation of JNK activation that eventually reduces AP-1 nuclear translocation and DNA-binding activity may exhibit significant inhibition of MMP activity in

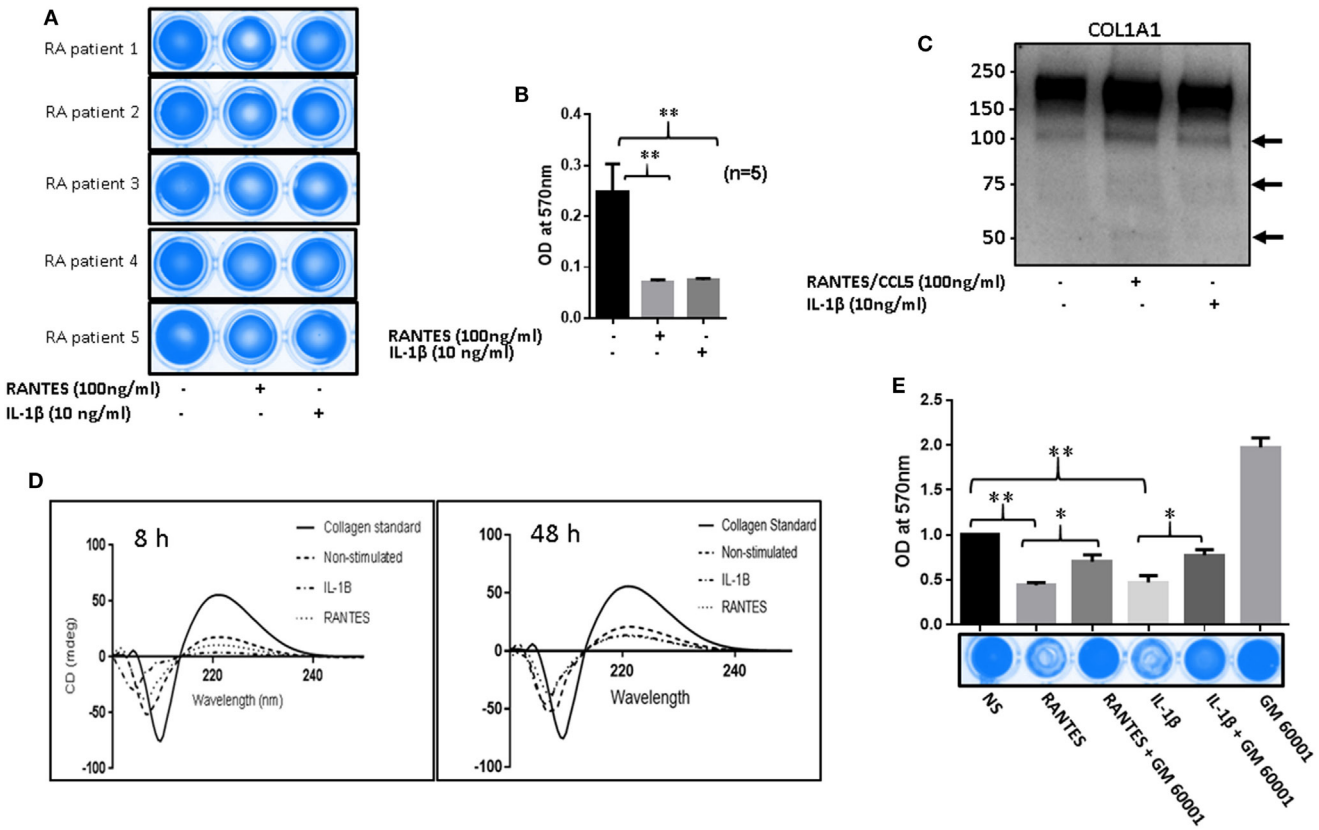

FIGURE 6 | Regulated on activation, normal T expressed, and secreted (RANTES)/CC ligand 5 (CCL5) facilitates matrix metalloproteinases (MMPs)-mediated collagen degradation in rheumatoid arthritis (RA). **(A)** RA synovial fibroblasts (RASFs) from five donors were stimulated with RANTES/CCL5 (100 ng/ml) and IL-1β (10 ng/ml) for 24 h. Condition media was placed onto a 96-well plate coated with type I collagen film and incubated for 24 h. Plates were stained with Coomassie R250 analyzed by ChemiDoc™ Imager. **(B)** Optical density (570 nm) of the RANTES/CCL5 and IL-1β-stimulated samples compared to control is shown. **(C)** Condition media from the same treatment was concentrated using Amicon 10K ultra 0.5 centrifugal filters and analyzed for type I collagen by Western blotting. **(D)** Condition media from RANTES/CCL-5 or IL-1β stimulated RASFs, was applied on collagen coated 96-well plates for 8 and 48 h. Digested collagen was collected and CD spectroscopy was performed using a Jasco J-815 spectropolarimeter. **(E)** RASFs were pretreated with GM6001 (20 μM) for 2 h and then stimulated with RANTES/CCL5 (100 ng/ml) or IL-1β (10 ng/ml). Collagen type I plates were exposed for 24 h, media aspirated, and then stained with Coomassie R250 and analyzed as described in Section "Materials and Methods." Densitometry was performed to show the relative changes. Values are represented as MEAN ± SE from experiments performed using cells from four to five donors. $^{*}p < 0.05$ or $^{**}p < 0.01$.

RASFs (30, 31, 33). Further detailed studies are warranted to confirm the effect of Met-RANTES or any other commercially available structural anatagonists of RANTES/CCL5 on cytokine signaling network in RA pathogenesis.

Heparan sulfate proteoglycans not only protect cytokines and chemokines from proteolysis, they also facilitate the formation of chemokine gradients involved in leukocyte recruitment and homing (36). Recent study showed that the selective induction of a CXCL8-binding site on endothelial syndecan-3, a transmembrane HSPG, is increased in RA synovium, which may be involved in leukocyte trafficking into RA synovial tissue (37). The syndecan family of transmembrane proteoglycans are the major source of cell surface HS in all cell types and provides complex role in inflammation (38, 39). The inhibition of RANTES/CCL5-induced MMP-1 and MMP-13 production by the depletion of HSPGs using heparinase III in RASF cultures, further confirms that in addition to CC receptor-mediated signaling, RANTES/CCL5 also utilizes HSPGs to activate signal transduction pathways in RASFs. However, our results showed that heparinase III has no effect on RANTES/CCL5 binding to the cell surface, which suggests that RANTES/CCL5 utilizes other proteoglycans present on the cell surface to bind and activate its signaling. Since RASFs are a major source of RANTES/CCL5 in the affected joints, there is a possibility that it may not rely on HSPGs to activate its signal transduction pathways. On the contrary, it can also be postulated that besides HSPGs, heparinase III may also affect other cell surface receptors by proteolytic shedding or structural modification that impairs their signaling and downstream catabolic events. These findings further warrant more elaborate study for a better therapeutic understanding of heparinase III and MMP axis. The effector molecules capable of degrading type I and II collagen within the triple helix structure are known to be attributed largely to MMPs and cysteine proteases (38). It is also known that human RASFs invade and degrade collagen rich structures associated with joints, including bone, cartilage, tendons, and ligaments

(39). Here, we demonstrated that RASFs, when stimulated with RANTES/CCL5 express MMP-1 and MMP-13 that have profound collagenase activity to directly degrade cross-linked collagen networks.

In conclusion, our results from this study suggest that RANTES/CCL5 plays a role of an active mediator, not a passive bystander, in RA pathogenesis by activating RASFs to promote MMP-1 and MMP-13 mediated ECM destruction. While the therapeutic strategies aimed at exclusively targeting RANTES/CCL5 or CCR5 were not successful in RA, these findings provide a rationale for testing HSPGs or signaling proteins as an adjunct therapeutic target to limit RASF participation in disease pathogenesis.

AUTHOR CONTRIBUTIONS

SA, NA, and SA designed this study. SA and NA performed experiments and wrote the manuscript. SA participated in writing the manuscript and provided his support to the study. JW participated in writing the manuscript and conducted and analyzed CD spectroscopy experiments. SA is the corresponding author of the manuscript.

ACKNOWLEDGMENTS

The authors thank the National Disease Research Interchange (NDRI), Philadelphia, PA, USA, and Co-operative Human Tissue Network (CHTN), Columbus, OH, USA, for providing RA synovial tissues. Authors thank Dr. David A Fox (University of Michigan) for providing some of the RASF lines developed in his lab. We would also like to thank Sharayah Riegsecker and Kelly Kopczynski for providing technical support.

FUNDING

This study was supported by the NIH grant AR063104 (SA), NIH Diversity Supplement AR063104S (SAA), and the Start-up funds from Washington State University.

SUPPLEMENTARY MATERIAL

The Supplementary Material for this article can be found online at http://www.frontiersin.org/article/10.3389/fimmu.2017.01341/full#supplementary-material.

REFERENCES

1. Ahmed S, Pakozdi A, Koch AE. Regulation of interleukin-1beta-induced chemokine production and matrix metalloproteinase 2 activation by epigallocatechin-3-gallate in rheumatoid arthritis synovial fibroblasts. *Arthritis Rheum* (2006) 54(8):2393–401. doi:10.1002/art.22023
2. Koch AE. Chemokines and their receptors in rheumatoid arthritis: future targets? *Arthritis Rheum* (2005) 52(3):710–21. doi:10.1002/art.20932
3. Katschke KJ Jr, Rottman JB, Ruth JH, Qin S, Wu L, LaRosa G, et al. Differential expression of chemokine receptors on peripheral blood, synovial fluid, and synovial tissue monocytes/macrophages in rheumatoid arthritis. *Arthritis Rheum* (2001) 44(5):1022–32. doi:10.1002/1529-0131(200105)44:5<1022:AID-ANR181>3.0.CO;2-N
4. Stievano L, Piovan E, Amadori A. C and CX3C chemokines: cell sources and physiopathological implications. *Crit Rev Immunol* (2004) 24(3):205–28. doi:10.1615/CritRevImmunol.v24.i3.40
5. Zlotnik A, Yoshie O. Chemokines: a new classification system and their role in immunity. *Immunity* (2000) 12(2):121–7. doi:10.1016/S1074-7613(00)80165-X
6. Jones BA, Riegsecker S, Rahman A, Beamer M, Aboualaiwi W, Khuder SA, et al. Role of ADAM-17, p38 MAPK, cathepsins, and the proteasome pathway in the synthesis and shedding of fractalkine/CX(3) CL1 in rheumatoid arthritis. *Arthritis Rheum* (2013) 65(11):2814–25. doi:10.1002/art.38095
7. Ludwig A, Weber C. Transmembrane chemokines: versatile 'special agents' in vascular inflammation. *Thromb Haemost* (2007) 97(5):694–703. doi:10.1160/TH07–01–0035
8. Mor A, Abramson SB, Pillinger MH. The fibroblast-like synovial cell in rheumatoid arthritis: a key player in inflammation and joint destruction. *Clin Immunol* (2005) 115(2):118–28. doi:10.1016/j.clim.2004.12.009
9. Patel DD, Zachariah JP, Whichard LP. CXCR3 and CCR5 ligands in rheumatoid arthritis synovium. *Clin Immunol* (2001) 98(1):39–45. doi:10.1006/clim.2000.4957
10. Hosaka S, Akahoshi T, Wada C, Kondo H. Expression of the chemokine superfamily in rheumatoid arthritis. *Clin Exp Immunol* (1994) 97(3):451–7. doi:10.1111/j.1365-2249.1994.tb06109.x
11. Iwamoto T, Okamoto H, Toyama Y, Momohara S. Molecular aspects of rheumatoid arthritis: chemokines in the joints of patients. *FEBS J* (2008) 275(18):4448–55. doi:10.1111/j.1742-4658.2008.06580.x
12. Ahmed S, Rahman A, Hasnain A, Goldberg VM, Haqqi TM. Phenyl N-tert-butylnitrone down-regulates interleukin-1 beta-stimulated matrix metalloproteinase-13 gene expression in human chondrocytes: suppression of c-Jun NH2-terminal kinase, p38-mitogen-activated protein kinase and activating protein-1. *J Pharmacol Exp Ther* (2003) 305(3):981–8. doi:10.1124/jpet.102.048611
13. Ishiguro N, Ito T, Oguchi T, Kojima T, Iwata H, Ionescu M, et al. Relationships of matrix metalloproteinases and their inhibitors to cartilage proteoglycan and collagen turnover and inflammation as revealed by analyses of synovial fluids from patients with rheumatoid arthritis. *Arthritis Rheum* (2001) 44(11):2503–11. doi:10.1002/1529-0131(200111)44:11<2503::AID-ART430>3.0.CO;2-P
14. Eck SM, Blackburn JS, Schmucker AC, Burrage PS, Brinckerhoff CE. Matrix metalloproteinase and G protein coupled receptors: co-conspirators in the pathogenesis of autoimmune disease and cancer. *J Autoimmun* (2009) 33(3–4):214–21. doi:10.1016/j.jaut.2009.09.011
15. Burrage PS, Mix KS, Brinckerhoff CE. Matrix metalloproteinases: role in arthritis. *Front Biosci* (2006) 11:529–43. doi:10.2741/1817
16. Singh AK, Umar S, Riegsecker S, Chourasia M, Ahmed S. Regulation of transforming growth factor beta-activated kinase activation by epigallocatechin-3-gallate in rheumatoid arthritis synovial fibroblasts: suppression of K(63)-linked autoubiquitination of tumor necrosis factor receptor-associated factor 6. *Arthritis Rheumatol* (2016) 68(2):347–58. doi:10.1002/art.39447
17. Akhtar N, Singh AK, Ahmed S. MicroRNA-17 suppresses TNF-alpha signaling by interfering with TRAF2 and cIAP2 association in rheumatoid arthritis synovial fibroblasts. *J Immunol* (2016) 197(6):2219–28. doi:10.4049/jimmunol.1600360
18. Kiener HP, Watts GF, Cui Y, Wright J, Thornhill TS, Skold M, et al. Synovial fibroblasts self-direct multicellular lining architecture and synthetic function in three-dimensional organ culture. *Arthritis Rheum* (2010) 62(3):742–52. doi:10.1002/art.27285
19. Ahmed S, Marotte H, Kwan K, Ruth JH, Campbell PL, Rabquer BJ, et al. Epigallocatechin-3-gallate inhibits IL-6 synthesis and suppresses transsignaling by enhancing soluble gp130 production. *Proc Natl Acad Sci U S A* (2008) 105(38):14692–7. doi:10.1073/pnas.0802675105
20. Sabeh F, Fox D, Weiss SJ. Membrane-type I matrix metalloproteinase-dependent regulation of rheumatoid arthritis synoviocyte function. *J Immunol* (2010) 184(11):6396–406. doi:10.4049/jimmunol.0904068
21. Jariashvili K, Madhan B, Brodsky B, Kuchava A, Namicheishvili L, Metreveli N. UV damage of collagen: insights from model collagen peptides. *Biopolymers* (2012) 97(3):189–98. doi:10.1002/bip.21725
22. Noh EM, Kim JS, Hur H, Park BH, Song EK, Han MK, et al. Cordycepin inhibits IL-1beta-induced MMP-1 and MMP-3 expression in rheumatoid

arthritis synovial fibroblasts. *Rheumatology* (2009) 48(1):45–8. doi:10.1093/rheumatology/ken417
23. Marotte H, Ruth JH, Campbell PL, Koch AE, Ahmed S. Green tea extract inhibits chemokine production, but up-regulates chemokine receptor expression, in rheumatoid arthritis synovial fibroblasts and rat adjuvant-induced arthritis. *Rheumatology* (2010) 49(3):467–79. doi:10.1093/rheumatology/kep397
24. Couchman JR. Syndecans: proteoglycan regulators of cell-surface microdomains? *Nat Rev Mol Cell Biol* (2003) 4(12):926–37. doi:10.1038/nrm1257
25. Shahrara S, Proudfoot AE, Woods JM, Ruth JH, Amin MA, Park CC, et al. Amelioration of rat adjuvant-induced arthritis by Met-RANTES. *Arthritis Rheum* (2005) 52(6):1907–19. doi:10.1002/art.21033
26. Plater-Zyberk C, Hoogewerf AJ, Proudfoot AE, Power CA, Wells TN. Effect of a CC chemokine receptor antagonist on collagen induced arthritis in DBA/1 mice. *Immunol Lett* (1997) 57(1–3):117–20. doi:10.1016/S0165-2478(97)00075-8
27. Tang CH, Hsu CJ, Fong YC. The CCL5/CCR5 axis promotes interleukin-6 production in human synovial fibroblasts. *Arthritis Rheum* (2010) 36:3615–24. doi:10.1002/art.27755
28. Yoshihara Y, Nakamura H, Obata K, Yamada H, Hayakawa T, Fujikawa K, et al. Matrix metalloproteinases and tissue inhibitors of metalloproteinases in synovial fluids from patients with rheumatoid arthritis or osteoarthritis. *Ann Rheum Dis* (2000) 59(6):455–61. doi:10.1136/ard.59.6.455
29. Miller MC, Manning HB, Jain A, Troeberg L, Dudhia J, Essex D, et al. Membrane type 1 matrix metalloproteinase is a crucial promoter of synovial invasion in human rheumatoid arthritis. *Arthritis Rheum* (2009) 60(3):686–97. doi:10.1002/art.24331
30. Han Z, Boyle DL, Aupperle KR, Bennett B, Manning AM, Firestein GS. Jun N-terminal kinase in rheumatoid arthritis. *J Pharmacol Exp Ther* (1999) 291(1):124–30.
31. Han Z, Boyle DL, Chang L, Bennett B, Karin M, Yang L, et al. c-Jun N-terminal kinase is required for metalloproteinase expression and joint destruction in inflammatory arthritis. *J Clin Invest* (2001) 108(1):73–81. doi:10.1172/JCI12466
32. Vincenti MP, Brinckerhoff CE. Transcriptional regulation of collagenase (MMP-1, MMP-13) genes in arthritis: integration of complex signaling pathways for the recruitment of gene-specific transcription factors. *Arthritis Res* (2002) 4(3):157–64. doi:10.1186/ar401
33. Barchowsky A, Frleta D, Vincenti MP. Integration of the NF-kappaB and mitogen-activated protein kinase/AP-1 pathways at the collagenase-1 promoter: divergence of IL-1 and TNF-dependent signal transduction in rabbit primary synovial fibroblasts. *Cytokine* (2000) 12(10):1469–79. doi:10.1006/cyto.2000.0743
34. Boyle DL, Soma K, Hodge J, Kavanaugh A, Mandel D, Mease P, et al. The JAK inhibitor tofacitinib suppresses synovial JAK1-STAT signalling in rheumatoid arthritis. *Ann Rheum Dis* (2015) 74(6):1311–6. doi:10.1136/annrheumdis-2014-206028
35. Catrina AI, Lampa J, Ernestam S, af Klint E, Bratt J, Klareskog L, et al. Anti-tumour necrosis factor (TNF)-alpha therapy (etanercept) down-regulates serum matrix metalloproteinase (MMP)-3 and MMP-1 in rheumatoid arthritis. *Rheumatology* (2002) 41(5):484–9. doi:10.1093/rheumatology/41.5.484
36. Sarrazin S, Lamanna WC, Esko JD. Heparan sulfate proteoglycans. *Cold Spring Harb Perspect Biol* (2011) 3(7):a004952. doi:10.1101/cshperspect.a004952
37. Patterson AM, Gardner L, Shaw J, David G, Loreau E, Aguilar L, et al. Induction of a CXCL8 binding site on endothelial syndecan-3 in rheumatoid synovium. *Arthritis Rheum* (2005) 52(8):2331–42. doi:10.1002/art.21222
38. Bernfield M, Gotte M, Park PW, Reizes O, Fitzgerald ML, Lincecum J, et al. Functions of cell surface heparan sulfate proteoglycans. *Annu Rev Biochem* (1999) 68:729–77. doi:10.1146/annurev.biochem.68.1.729
39. Severin IC, Soares A, Hantson J, Teixeira M, Sachs D, Valognes D, et al. Glycosaminoglycan analogs as a novel anti-inflammatory strategy. *Front Immunol* (2012) 3:293. doi:10.3389/fimmu.2012.00293

Conflict of Interest Statement: The authors declare that the research was conducted in the absence of any commercial or financial relationships that could be construed as a potential conflict of interest.

Copyright © 2017 Agere, Akhtar, Watson and Ahmed. This is an open-access article distributed under the terms of the Creative Commons Attribution License (CC BY). The use, distribution or reproduction in other forums is permitted, provided the original author(s) or licensor are credited and that the original publication in this journal is cited, in accordance with accepted academic practice. No use, distribution or reproduction is permitted which does not comply with these terms.

frontiers in Immunology

ORIGINAL RESEARCH
published: 23 March 2017
doi: 10.3389/fimmu.2017.00323

Elevated Expression of Chemokine CXCL13 in Chronic Hepatitis B Patients Links to Immune Control during Antiviral Therapy

Chao Liu[1†], Xuan Huang[1†], Melanie Werner[2], Ruth Broering[2], Jun Ge[1], Yongyin Li[1], Baolin Liao[3], Jian Sun[1], Jie Peng[1], Mengji Lu[4], Jinlin Hou[1] and Xiaoyong Zhang[1*]*

[1] State Key Laboratory of Organ Failure Research, Guangdong Provincial Key Laboratory of Viral Hepatitis Research, Department of Infectious Diseases, Nanfang Hospital, Southern Medical University, Guangzhou, China, [2]Department of Gastroenterology and Hepatology, Essen University Hospital, University of Duisburg-Essen, Essen, Germany, [3] Department of Infectious Disease, Guangzhou Eighth People's Hospital, Guangzhou Medical University, Guangzhou, China, [4]Institute of Virology, Essen University Hospital, University of Duisburg-Essen, Essen, Germany

C–X–C-chemokine ligand 13 (CXCL13), the ligand for C–X–C chemokine receptor type 5 (CXCR5), is a major regulator of B-cell trafficking and plays an integral role in age-dependent clearance of hepatitis B virus (HBV) in the mouse model. However, the expression and function of CXCL13 in patients with chronic hepatitis B (CHB) remain unknown. By use of liver cell subpopulations isolated from CHB patients, we found that CXCL13 mRNA was abundantly expressed in Kupffer cells (KCs), but not in primary hepatocytes, liver sinusoidal endothelial cells, and hepatic stellate cells. Interestingly, KC isolated from HBV-positive liver had much higher level of CXCL13 expression than non-HBV-infected controls. And its expression was induced by toll-like receptor 3 ligand poly I:C stimulation. Moreover, intense expression of CXCL13 protein and accumulation of $CD4^+$ T and B cells were evident in follicular-like structures in the liver tissue of CHB patients, which indicated its chemotactic effect on $CXCR5^+$ $CD4^+$ cells and B cells. Consistently, the levels of serum CXCL13 were significantly higher in the CHB patients than in healthy controls. Furthermore, CXCL13 concentration was increased in the complete response (CR) group during weeks 0–12 and did not change significantly during the course of telbivudine treatment, compared with the patients who didn't achieve CR. In conclusion, the HBV-related increase of CXCL13 production in KC and serum CXCL13 level during telbivudine treatment might be associated with immune control of chronic HBV infection.

Keywords: hepatitis B virus, chronic hepatitis B, CXCL13, Kupffer cell, hepatitis B virus e antigen seroconversion

OPEN ACCESS

Edited by:
Jixin Zhong,
Case Western Reserve University, USA

Reviewed by:
Hui Liu,
University of California, San Francisco, USA
Albrecht Piiper,
University Hospital Frankfurt, Germany
Junjie Zhang,
University of Southern California, USA

****Correspondence:***
Jinlin Hou
jlhousmu@163.com;
Xiaoyong Zhang
xiaoyzhang@smu.edu.cn

[†]These authors have contributed equally to this work.

Specialty section:
This article was submitted to Inflammation, a section of the journal Frontiers in Immunology

Received: *22 January 2017*
Accepted: *07 March 2017*
Published: *23 March 2017*

Citation:
Liu C, Huang X, Werner M, Broering R, Ge J, Li Y, Liao B, Sun J, Peng J, Lu M, Hou J and Zhang X (2017) Elevated Expression of Chemokine CXCL13 in Chronic Hepatitis B Patients Links to Immune Control during Antiviral Therapy. Front. Immunol. 8:323. doi: 10.3389/fimmu.2017.00323

Abbreviations: ALT, alanine aminotransferase; CHB, chronic hepatitis B; CR, complete response; CXCL13, C–X–C-chemokine ligand 13; CXCR5, C–X–C chemokine receptor type 5; ELISA, enzyme-linked immunosorbent assay; FDC, follicular dendritic cell; GCs, germinal centers; HBeAg, hepatitis B virus e antigen; HBV, hepatitis B virus; HC, healthy control; HCV, hepatitis C virus; HSC, hepatic stellate cell; IA, immune activation; IC, inactive carrier; IFN, interferon; IL-21, interleukin-21; IT, immune tolerance; KC, Kupffer cell; LSEC, liver sinusoidal endothelial cell; NCR, non-complete response; NPCs, non-parenchymal cells; PBMC, peripheral blood mononuclear cell; PHH, primary human hepatocyte; TBIL, total bilirubin; TFH, follicular T helper cells; TLR, toll-like receptor.

INTRODUCTION

Hepatitis B virus (HBV) is a non-cytopathic hepadnavirus that chronically infects approximate 240 million people. Every year, HBV-associated end-stage liver disease results in about 1 million patient deaths (1). It is well known that the chance of clearing HBV infection is age-dependent and relies on the host immune system. Over 95% of adult patients who acquired HBV infections have spontaneous clearance, but 90% of neonates and 30% of children 1- to 5-year olds who acquired HBV infections fail to resolve the infection and develop chronic hepatitis B (CHB) (2, 3). Generally, the natural history of chronic HBV infection can be divided into different phases, including immune tolerance (IT), immune activation (IA), inactive carrier (IC), and reactivation (4, 5). During the IA phase, the host immune system, including both innate and adaptive immune responses, were activated to clear the virus from hepatocytes. A strong, diverse, and functional adaptive immune response is considered essential for HBV clearance. However, it has been clearly shown that deletion or exhaustion of adaptive immunity leads to HBV persistence in hepatocytes (6).

Liver inflammation accompanied by elevated levels of serum alanine aminotransferase (ALT) in CHB patients are usually observed and result from immune-mediated destruction of hepatic cells. Within the inflamed liver, there is an accumulation of lymphoid and myeloid cells, including T and B cells (7). These immune cells play critical roles in the clearance of HBV-infected hepatocytes but also are involved in immune-mediated liver damage and inflammation (8). Accumulating evidence indicates that certain chemokines in the liver are necessary for providing the appropriate environment for activation and expansion of naïve lymphocytes in response to hepatitis virus infection (9). Using a mouse model of HBV infection, it was found that chemokine C–X–C-chemokine ligand 13 (CXCL13), which is involved in hepatic B-lymphocyte trafficking and lymphoid architecture and development, is expressed in an age-dependent manner in mouse hepatic macrophages and plays an integral role in facilitating an effective immune response against HBV (10).

CXCL13 is a member of CXC subtype of chemokine superfamily and is also known as a B cell—attracting chemokine 1 or B-lymphocyte chemoattractant (11). By acting through its cognate receptor C–X–C chemokine receptor type 5 (CXCR5), CXCL13 is chemotactic for mature B cells and T follicular helper (Tfh) cells (12). Importantly, CXCL13 facilitates the co-migration of B cells and Tfh cells into B cell follicles and germinal centers (GCs), where high-affinity antibody-secreting memory B and plasma cells are generated (13). Aberrant circulating CXCL13 levels have been implicated in the pathogenesis of many chronic inflammatory diseases and correlated with clinical outcomes, including various infections and autoimmune disorders associated with dysregulated humoral responses (14–16).

Previous work from our group suggested that circulating Tfh cells might have a significant role in facilitating hepatitis B virus e antigen (HBeAg) seroconversion through interleukin-21 (IL-21) secretion in patients with chronic HBV infection (17). However, the association of CXCL13 expression with the pathogenesis of CHB and clinical outcome of antiviral therapy remains unclear. The present study was designed to examine CXCL13 expression and regulation in subpopulations of hepatic cells, as well as in the serum at different phases of CHB patients. In addition, we performed an in-depth prospective analysis of the kinetics of serum CXCL13 expression of CHB patients being treated with telbivudine with different clinical outcomes.

MATERIALS AND METHODS

Study Subjects

Blood samples were obtained from 45 patients with chronic HBV infection who were recruited at Nanfang Hospital (Guangzhou, China) for a cross-sectional study. They were classified into three groups according to guidelines from the European Association for the Study of Liver Diseases: IA ($n = 20$); IT ($n = 10$), and IC ($n = 15$) (18). A total of 12 healthy controls (HCs) were enrolled for comparison. Demographic, biochemical, and virological features of the participants were listed in **Table 1**.

Fifty-five HBeAg-positive CHB subjects from Nanfang Hospital who had participated in two prospective clinical trials of telbivudine (600 mg/day, clinical trial numbers: NCT00962533

TABLE 1 | Clinical characteristics of the subjects.

Group	IA	IT	IC	HC
No. of patients	20	10	15	12
Gender (M/F)	14/6	6/4	5/10	8/4
Age (years)	28.00 (21.00–41.80)	26.50 (3.80–34.70)	36.00 (22.60–54.40)	24.00 (21.30–34.40)
Hepatitis B virus (HBV) DNA (log_{10} copies/ml)	8.40 (5.94–9.39)	7.70 (5.55–8.70)	0.00[a] (0.00–3.94)	ND
ALT (U/l)	145.00 (70.60–295.30)	22.00 (16.10–40.90)	18.00 (10.60–33.40)	15.00 (12.00–27.70)
AST (U/l)	90.50 (48.10–225.40)	24.50 (19.30–34.50)	25.00 (16.40–35.00)	22.00 (12.00–31.20)
HBsAg positive	20	10	12	0
Anti-HBs positive	0	0	1	6
Hepatitis B virus e antigen positive	20	5	5	0
Anti-Hbe positive	0	5	7	0
Anti-HBc positive	20	10	15	0
CXCL13 (pg/ml)	67.18 (46.77–180.51)	42.30 (23.92–85.69)	31.93 (17.46–98.42)	32.33 (13.69–49.90)

Data were shown as median and 10–90% percentile.

[a]*11 IC had undetectable HBV DNA.*

ALT, alanine aminotransferase; AST, aspartate aminotransferase; HC, healthy control; IA, immune activation; IC, inactive carrier; IT, immune tolerance; ND, not determined.

and CLDT600ACN07T) were also studied. According to treatment response at week 52, the participants were classified into a complete response (CR) group or a non-complete response (NCR) group (18). Subjects in the CR group had undergone ALT normalization and HBeAg seroconversion, and had achieved a serum HBV-DNA level of < 300 copies/ml by week 52; those in the NCR group had either a serum HBV-DNA level >300 copies/ml or were positive for HBeAg at week 52. All patients provided written documentation of informed consent. The study conforms to the ethical guidelines of the 1975 Declaration of Helsinki and was approved by the Ethical Committee of Nanfang Hospital.

Serological Assays and HBV-DNA Assays

The presence of HBV surface antigen, HBeAg, anti-HBs, anti-HBe, and anti-HBc was determined using ARCHITECT i2000SR system (Abbott Ireland Diagnostics Division, Sligo, Ireland) (19). HBV DNA was measured using the COBAS TaqMan HBV Test (Roche Molecular Diagnostics, Pleasanton, CA, USA) (17), which has a detection limit of 12 IU/ml (1 IU/ml = 5.82 copies/ml).

Enzyme-Linked Immunosorbent Assay (ELISA)

The concentration of CXCL13 was quantitated in duplicate wells using a commercial human CXCL13 ELISA kit (R&D Systems, Minneapolis, MN, USA) in accordance with the manufacturer's instructions.

PBMCs Isolation and Macrophage Differentiation

Peripheral blood mononuclear cells were separated on Ficoll-Histopaque (BD Biosciences, Shanghai, China) density gradients and routinely cryopreserved as previously described (17). The monocytes were isolated from PBMCs by adherence to plates coated with collagen-I (BD Biosciences, USA) at 37°C in RPMI 1640 containing 10% FBS (20). After incubation, the cells were washed by PBS for 5 min and then gently vibrated on a culture plate. The monocytes were then cultured for up to 9 days in the presence 10 ng/ml of GM-CSF (PerproTech, Rocky Hill, NJ, USA) in RPMI 1640 containing 10% FBS. This protocol resulted in more than 90% purity of the macrophages, as determined by flow cytometry analysis (FACS) using anti-CD14 APC-conjugated monoclonal antibody (BD Biosciences, USA). The differentiated macrophages were then stimulated for 6 h with 5 μg/ml of LPS or poly I:C (InvivoGen, San Diego, CA, USA).

Primary Human Hepatocytes (PHHs) and Non-Parenchymal Cells Isolation and Incubation

Liver specimens (25–100 g) were obtained from fresh tumor resections or liver transplantation donors (HBV-positive, $n = 6$; HBV-negative, $n = 6$, patients' information is in Table S1 in Supplementary Material). PHHs and non-parenchymal liver cells, including Kupffer cells (KCs), liver sinusoidal endothelial cells (LSECs), and hepatic stellate cells (HSCs), were prepared from a single human liver specimen according to a modified two-step perfusion technique, as described by our group recently (21). The study conforms to the ethical guidelines of the 1975 Declaration of Helsinki and was approved by the Institutional Review Board (ethics committee) of the medical faculty at the University of Duisburg-Essen. PHHs were seeded into collagen-I (BD Biosciences, USA) coated plates at a density of 1.25 to 2.5×10^5 viable cells per cm^2 by using DMEM/Ham's F-12 medium (Biochrome, Berlin, Germany) supplemented with 10% FBS. KCs were seeded onto plastic culture plates at a density of 4 to 6×10^5 cells per cm^2 using DMEM supplemented with 10% FBS. LSECs were cultured in coated plates with Endothelial Growth Medium 2 (PromoCell, Heidelberg, Germany) containing provided supplements. HSCs were seeded into an uncoated plastic culture flask with Stellate Cell Medium (ScienCell, Carlsbad, CA, USA) supplemented with supplied 10% FBS, 1% stellate cell growth supplement. The purities of PHH (95.5 ± 1.7%), KC (94.5 ± 1.2%), LSEC (97.8 ± 1.1%), and HSC (97.1 ± 1.5%) could be reached as determined by immunofluorescence staining with specific markers (21). These cells were stimulated using the Human toll-like receptor (TLR) 1–9 Agonist Kit (Invivogen, Toulouse, France) at recommended concentrations for 6 h. Cells were then collected for RNA extraction and CXCL13 gene expression analysis by real-time RT-PCR was performed using commercially available primer set (Qiagen, Hilden, Germany) and normalized to β-actin as previously described (22).

RNA Extraction, Reverse Transcription, and Quantitative Real-time PCR

Total cellular RNA was isolated and purified from PBMCs, stimulated macrophages or hepatic cells using the RNeasy Mini Kit (Qiagen, Hong Kong, China) according to the manufacturer's instructions. The cDNA synthesis was performed with 200 ng total RNA using the Transcriptor First Strand cDNA Synthesis Kit (Roche, Mannheim, Germany). The expression of CXCL13 genes was determined by real-time RT-PCR, which was performed using the SYBR Green I Master Kit (Roche, Switzerland) on a LightCycler 480 (Roche Diagnostics, Switzerland), as described previously (23). The expression levels of each gene are presented as values normalized against 10^6 copies of β-actin transcripts.

Immunohistochemistry

Immunohistochemistry was performed on formalin-fixed and paraffin-embedded 4-μm sections of liver tissue. Sections were incubated overnight at 4°C with appropriate concentrations of primary antibodies, including rabbit anti-CD4, mouse anti-CD19, rabbit anti-CD38, mouse anti-CD68, and mouse anti-CXCR5 (Abcam, Cambridge, MA, USA) and goat anti-CXCL13 (R&D System, USA), and then incubated with the Dako Chemate Envision Kit (Dako, Glostrup, Denmark). The reaction was visualized by CheMate™ DAB plus chromogen (Dako, Denmark). The staining was captured by light microscopy using high-power microscopic fields (400×).

Chemotaxis Assay

Chemotaxis was assessed in a two-chamber transwell cell migration system (5-μm pores, Corning, Shanghai, China) (24).

PBMCs from CHB patients (1×10^6) were purified as described above and were seeded in the upper well, and different concentrations of recombinant human CXCL13 (rh-CXCL13, PerproTech) or RPMI 1640 as controls were added to the bottom well as the chemoattractant. The cells were cultured for 2–6 h at 37°C and then collected and stained with CD19-APC, CD4-PE-Cy7, and CXCR5-PerCP-Cy5.5 (BioLegend, San Diego, CA, USA) The percentage of migrating cells was analyzed and calculated by a BD FACSCanto II flow cytometer.

Statistical Analysis

Continuous data were expressed as medians (minimum–maximum). The Mann–Whitney *U* test, Wilcoxon's signed-ranks test, and the chi-squared test were used for two-group comparisons. The Kruskal–Wallis *H* test was used when comparing more than three groups. Repeated measures analysis was used to compare changes in CXCL13 expression during treatment. The paired Student's *t*-test was used to compare individual values at different times. Receiver-operating characteristic (ROC) curves were constructed to predict a CR to LdT treatment. All statistical analyses were based on two-tailed hypothesis tests with a significance level of $p < 0.05$.

RESULTS

CXCL13 Expression in Liver Cells Is Regulated by TLR Agonists Stimulation

Previous studies in mouse model suggested that CXCL13 was predominantly expressed in liver macrophages (10). However, the expression of CXCL13 in human liver cells remains unknown. PHH and non-parenchymal liver cells composed of KC, LSEC, and HSC were isolated from fresh human liver specimens obtained from HBV-negative tumor resections of patients ($n = 6$). The CXCL13 mRNA expression in different liver cell subpopulations was examined by real-time RT-PCR. The basal expression of CXCL13 in KC, HSC, LSEC, and PHH isolated from non-HBV-infected livers was very low and had no significant difference (**Figure 1A**). Further, we investigated if CXCL13 expression was regulated by pathogen-associated molecular patterns; to do this we used various TLR1–9 agonists to stimulate the KC isolated from liver resections without HBV infection. We found that the CXCL13 mRNA expression could be induced by TLR3 agonist poly I:C for about 7.2-fold ($p = 0.03$), whereas other TLRs agonists had no significant effect (**Figure 1B**). As positive controls, interferon (IFN)-β induction was observed in poly I:C stimulation and all TLR ligands, except TLR9 ligand CPG, were able to induce IL-6 expression at different levels in KC (Figures S1A,B in Supplementary Material). Consistently, by using *in vitro* differentiated macrophages from monocytes (Figure S2A in Supplementary Material), poly I:C were able to induce CXCL13 expression at mRNA (Figure S2B in Supplementary Material) and protein levels (Figure S2C in Supplementary Material).

KC Isolated from HBV-Positive Liver Tissues Express Higher Levels of CXCL13 in Response to TLR3 Agonist Poly I:C Compared to KC with HBV-Negative Origin

To assess whether HBV infection could influence CXCL13 expression, we compared the basal and TLR3 agonist-induced expression of CXCL13 in liver cell subpopulations between HBV-positive and HBV-negative patients ($n = 6$ for each group). Interestingly, the KC isolated from HBV-positive patients had much higher level of CXCL13 expression than non-HBV patients (about 45-fold, $p < 0.001$, **Figure 2A**). Upon poly I:C stimulation, the induced CXCL13 expression in KC isolated

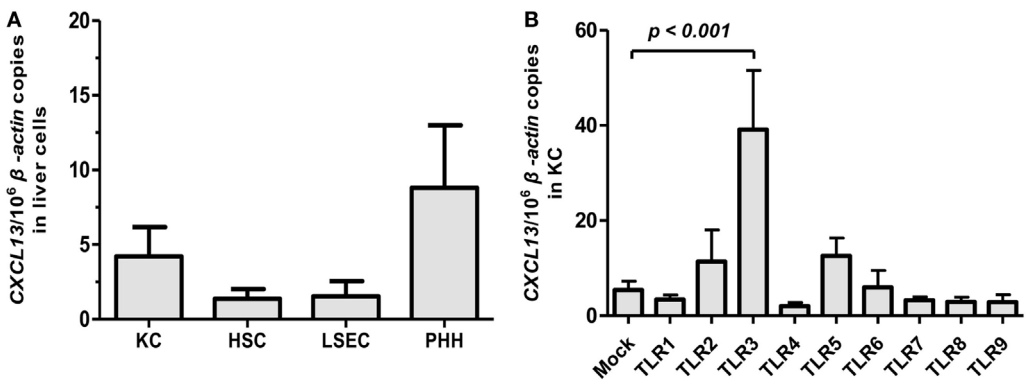

FIGURE 1 | CXCL13 expression in subpopulation of liver cells and its regulation by toll-like receptor (TLR) ligands. **(A)** Comparison of CXCL13 mRNA expression in Kupffer cell (KC), hepatic stellate cell (HSC), liver sinusoidal endothelial cell (LSEC), and primary human hepatocyte (PHH). Different subpopulation of liver cells were isolated from non-hepatitis B virus-infected livers. The total RNA of these cells was extracted and the expression of CXCL13 mRNA was determined by real-time RT-PCR. **(B)** Comparison of CXCL13 mRNA expression in KC after stimulation with TLR1–9 ligands. Isolated KC were stimulated with different TLR1–9 ligands for 6 h and then harvested for RNA extraction. CXCL13 mRNA expression was determined by real-time RT-PCR. The stimulus and concentration used as below: TLR1/2 agonist: Pam3CSK4 (4 μg/ml), TLR2 agonist: HKLM (10^8 cells/ml), TLR3 agonist: poly I:C (50 μg/ml), TLR4 agonist: LPS (30 μg/ml), TLR5 agonist: FLA (2 μg/ml), TLR6/2 agonist: FSL1 (1 μg/ml), TLR7 agonist: imiquimod (20 μg/ml), TLR8 agonist: ssRNA40 (10 μg/ml), TLR9 agonist: CpG (31.8 μg/ml). Data are representative with mean ± SEM, and determined by Mann–Whitney *U* test.

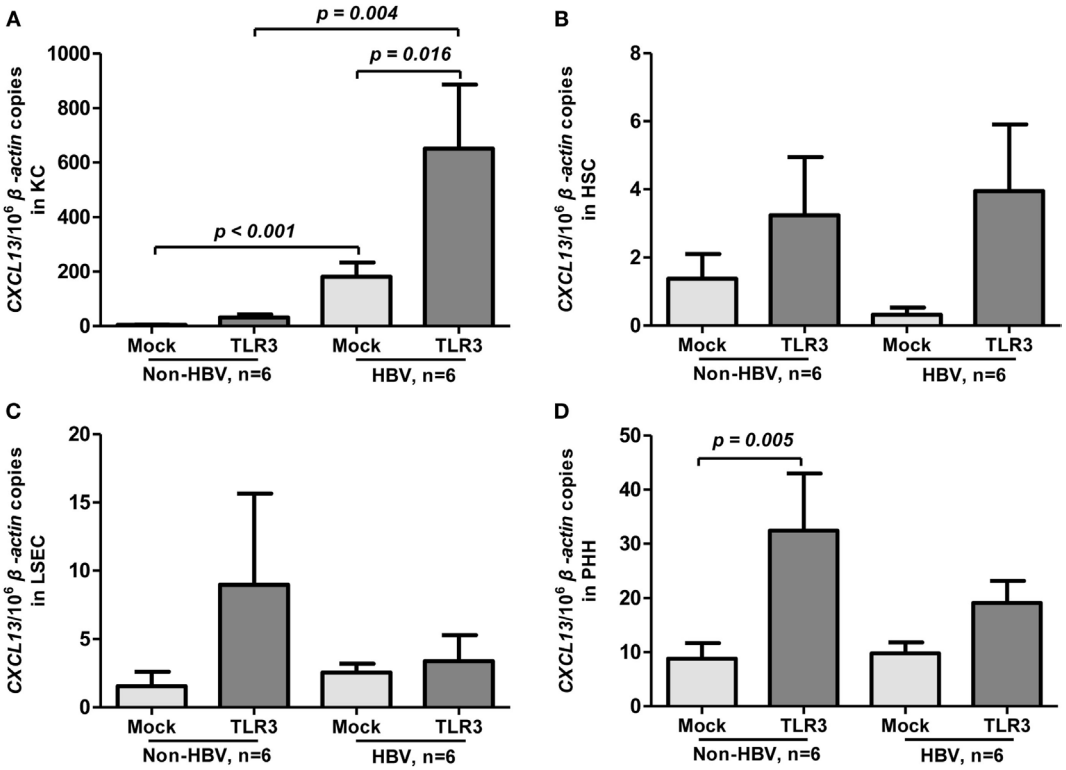

FIGURE 2 | Toll-like receptor (TLR) 3 agonist-induced expression of CXCL13 in liver cells from hepatitis B virus (HBV)-positive and non-HBV-infected patients. Comparison of the basal and TLR3 agonist-induced expression of CXCL13 in Kupffer cell (KC) **(A)**, hepatic stellate cell (HSC) **(B)**, liver sinusoidal endothelial cell (LSEC) **(C)**, and primary human hepatocyte (PHH) **(D)**. Different subpopulation of liver cells were isolated from either Non-HBV or HBV-positive subjects and stimulated with or without TLR3 agonist for 6 h. Total RNA was extracted and then the CXCL13 mRNA expression to β-actin were determined by real-time RT-PCR. Data are representative with mean ± SEM, and determined by Mann–Whitney *U* test and Wilcoxon's signed-ranks test.

from HBV-positive patients was also markedly higher than in non-HBV patients (**Figure 2A**, $p = 0.004$). However, the basal expression of CXCL13 in other cells including HSC (**Figure 2B**), LSEC (**Figure 2C**), and PHH (**Figure 2D**) had no significant difference among these two groups. Moreover, poly I:C stimulation had very weak effect on inducing CXCL13 expression in these cells, except PHH ($p = 0.005$).

Serum CXCL13 Concentrations Is Increased in the Immune-Activation Phase of Chronic HBV Infection and Negatively Correlated with HBV-DNA Levels

To elucidate whether serum CXCL13 levels in patients could also be affected by HBV infection, we examined the concentration of CXCL13 by ELISA in CHB patients. We saw that serum CXCL13 was significantly higher in CHB patients than in HCs (**Figure 3A**, $p = 0.003$). The CHB patients were further divided into three groups (IA, IT, and IC) depending on ALT levels and viral parameters. The median serum CXCL13 concentrations in the IA groups were higher compared with the IT, IC, and HC groups, and there was no significant difference among the IT, IC, and HC groups (**Figure 3A**). Serum CXCL13 concentrations were negatively and weakly correlated with serum HBV-DNA levels in CHB patients (**Figure 3B**, $r^2 = 0.077$, $p = 0.016$) but were uncorrelated with ALT levels (**Figure 3C**, $p = 0.259$). Consistent with previous data in human infant and adult samples (10), there was a weak positive correlation between serum CXCL13 concentration and age (**Figure 3D**, $r^2 = 0.051$, $p = 0.051$).

Dynamic Change of Serum CXCL13 Concentrations under Telbivudine Therapy Correlates with Treatment Outcome

To assess changes of serum CXCL13 concentrations in HBV-infected patients during nucleoside analog therapy, we studied 55 HBeAg-positive CHB patients who received 52 weeks of telbivudine treatment. During this antiviral treatment, the serum CXCL13 concentrations in all patients gradually decreased from 0 to 52 weeks of therapy, while the serum CXCL13 concentrations at baseline and 12 weeks were higher than at 24 and 52 weeks (**Figure 4A**). These patients were further divided into CR and NCR group as described in Section "Materials and Methods" (19). The features (age and sex, as well as serum ALT, AST, TBIL, HBV-DNA, and CXCL13 levels) of the CR group and NCR group from baseline to 52 weeks during therapy were compared (**Table 2**). Mean ALT levels of the CR group decreased

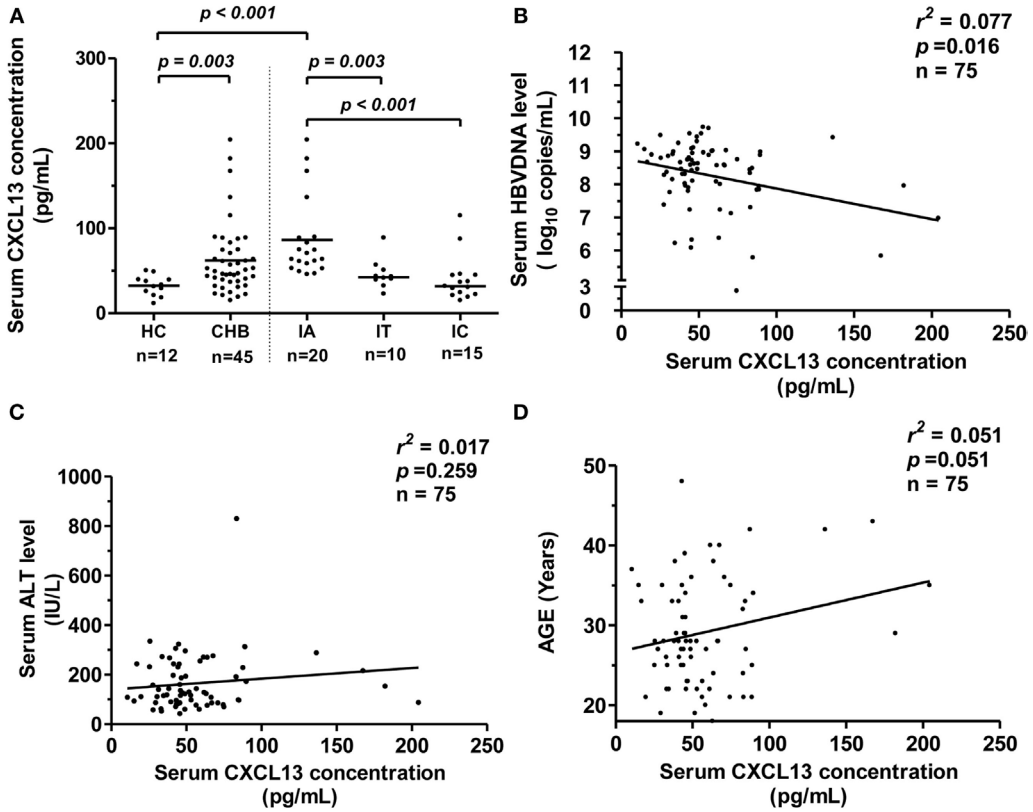

FIGURE 3 | CXCL13 expression in serum samples from chronic hepatitis B (CHB) patients and its correlation with viral parameters. **(A)** Comparison of serum CXCL13 concentration in healthy control (HC) and CHB patients with chronic hepatitis B virus (HBV) infection [divided into immune activation (IA), IT, and IC groups]. Serum CXCL13 concentrations were measured by specific enzyme-linked immunosorbent assay kit. Data are representative with median, and determined by Mann–Whitney *U* test. **(B)** The correlation between serum CXCL13 concentrations and HBV DNA (log_{10} copies/ml) in IA patients, including the baseline of CHB patients received telbivudine therapy. **(C)** The correlation between serum CXCL13 concentrations and alanine aminotransferase (ALT) levels in IA patients. **(D)** The correlation between serum CXCL13 concentrations and the age in IA patients.

to normal at week 12, and were much lower than in the NCR group at 12 weeks ($p = 0.042$). Serum HBV-DNA levels were lower in CR group than NCR group at 12, 24, and 52 weeks ($p < 0.005$). Furthermore, the serum CXCL13 was higher in the CR than the NCR group at 12 and 52 weeks (**Figure 4B**). Repeated measures analysis showed that serum CXCL13 concentration decreased in the NCR group during therapy but in the CR group it remained largely unchanged (**Figure 4C**). Finally, ROC curves were generated to assess the usefulness of 12-week CXCL13 concentrations, 0-week log_{10} HBV DNA− 12-week log_{10} HBV DNA, and combination factors between them to predict a CR at 52 weeks (**Figure 4D**). The combination factor was calculated from logistic regression analysis between CXCL13 concentrations and value of 0-week log_{10} HBV DNA− 12-week log_{10} HBV DNA. The optimal cut-off value for the 12-week CXCL13 concentration was 58.1 pg/ml. This indicated that sensitivity for detection of a CR was 42.9% with a specificity of 85.3%. The optimal cut-off value for log_{10} HBV DNA was 5.2, which provided sensitivity for detection of a CR of 47.6% and a specificity of 91.2%. The optimal cut-off value for combination factors was 0.41. This provided detection sensitivity for a CR of 76.2% and a specificity of 88.2%.

CXCL13 Is Involved in the Formation of Ectopic GC in the Liver Tissue of CHB Patients

CXCL13 is known to dictate homing and motility of $CXCR5^+$ lymphocytes, we examined the chemotaxis using CHB patient PBMCs by Transwell test (**Figure 5A**). With a concentration of 1 μg/ml CXCL13 in the bottom, the cell counting of $CXCR5^+$ lymphocytes that moved through the membrane increased significantly (**Figure 5B**). In addition, with the response time extended, an increasing number of $CXCR5^+$ lymphocytes moved through the Transwell filter membrane, and univariate *post hoc* analysis indicated that CXCL13 chemotaxis appeared to be time dependent (**Figure 5C**).

In order to verify the co-localization of CXCL13 and $CXCR5^+$ in cells, we performed immunohistochemical staining of serial sections from liver samples. The staining of CXCL13 was very low in the liver tissue of most CHB patients and all HC group patients. However, there was positive CXCL13 staining in ectopic GCs of CHB liver biopsy samples (**Figure 6A**). Interestingly, co-localization of CXCL13 with $CD68^+$ KCs could be seen in serial sections of the liver biopsies, which reflected an accumulation of

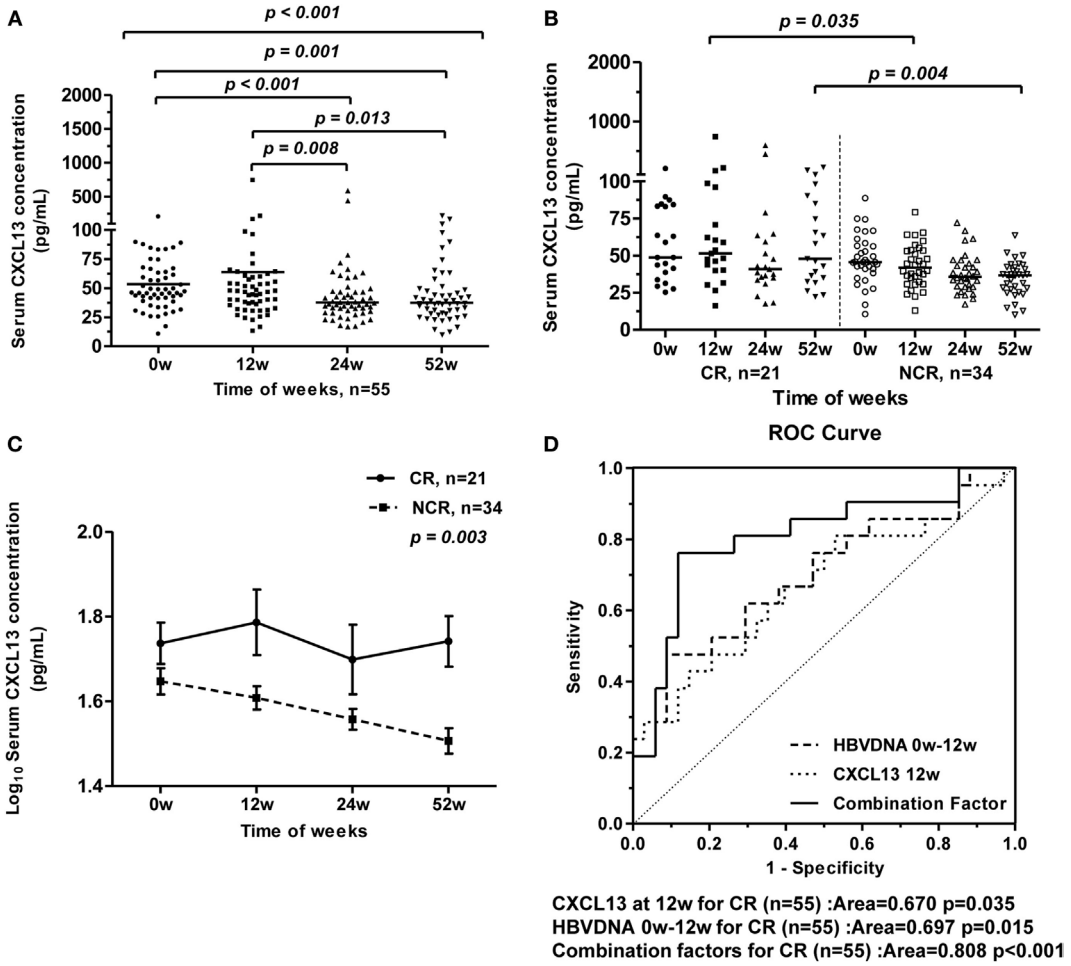

FIGURE 4 | Longitudinal analysis of serum CXCL13 concentrations of chronic hepatitis B (CHB) patients during telbivudine therapy. **(A)** Comparison of serum CXCL13 concentrations at baseline and at 12, 24, and 52 weeks after starting telbivudine therapy in all 55 hepatitis B virus e antigen-positive CHB patients. Data are representative with median, and determined by Mann–Whitney *U* test and Kruskal–Wallis H test. **(B)** Comparison of serum CXCL13 concentrations between complete response (CR) group and non-complete response (NCR) group at indicated time points. Data are representative with median, and determined by Mann–Whitney *U* test. **(C)** Repeated measures analysis of temporal dynamics of serum CXCL13 concentrations between CR group and NCR group at indicated time points. The paired Student's *t*-test was used to compare individual values at different time points. **(D)** Receiver-operating characteristic (ROC) curves for prediction of CR after telbivudine therapy, including CXCL13 concentrations at week 12, $\log_{10}$ HBV DNA copies/ml of week 0 – week 12, and combination factors above.

$CXCR5^+$ $CD4^+$ T cells, and $CXCR5^+CD19^+$ B cells in the ectopic GCs in CHB liver, and $CD38^+$ cells accumulation surrounding the GCs (**Figure 6B**). These results suggest that CXCL13 was involved in the recruitment of $CXCR5^+$ lymphocytes in the liver of CHB patients.

DISCUSSION

In the present study, we examined the CXCL13 expression in different hepatic cells from CHB patients and found that CXCL13 was highly expressed and induced by poly I:C stimulation in KC isolated from HBV-positive livers. Serum CXCL13 concentrations were consistently increased and negatively correlated with HBV-DNA titers in immune-active CHB patients. Moreover, serum CXCL13 in CR patients was found to be significantly higher than in NCR patients beginning at 12 weeks of telbivudine treatment. This suggests a role for CXCL13 in predicting CR to antiviral therapy. The findings presented here provide further evidence to support CXCL13 as an important chemokine for immune control of HBV infection.

Chronic hepatitis B has been associated with chronic inflammation mediated by immune cells, inflammatory cytokines, and chemokines (25). KCs are tissue-resident macrophages and are crucial cellular components of the intrahepatic innate immune system (26). Based on their localization, KCs are likely to interact with HBV. However, the role of KCs in inducing immunity toward HBV is poorly understood (27). As we found with results from the HBV transgenic mice model, we confirmed that KCs from HBV-positive patients had higher level of CXCL13 expression. It is likely that HBV infection could

TABLE 2 | Univariate analysis of routine markers possibly associated with hepatitis B virus e antigen seroconversion.

Variable	TW	Complete response	Non-complete response	$\chi^2/t/Z$	*p*
No. of patients		21	34		
Male (*n*, %)[a]		16 (76.2%)	28 (82.6%)	0.308	0.579
Age (years)[b]		27.00 (19.40–37.40)	28.00 (21.00–35.50)	0.110	0.913
ALT (U/l)[b]	0	174.00 (85.40–313.80)	115.50 (59.00–301.00)	1.841	0.071
	12	28.00 (16.00–85.20)	50.00 (17.00–125.00)	−2.088	0.042[#]
	24	20.00 (12.40–28.80)	24.00 (13.50–63.00)	−1.944	0.057
	52	20.00 (12.20–35.00)	19.00 (11.50–42.00)	−0.654	0.516
AST (U/l)[b]	0	105.00 (48.20–152.40)	86.00 (43.00–179.50)	0.695	0.490
	12	31.00 (21.40–46.60)	38.00 (25.00–58.50)	−1.803	0.077
	24	25.00 (19.20–36.40)	26.00 (20.50–39.50)	−1.324	0.191
	52	30.00 (18.60–76.40)	30.50 (19.50–51.50)	1.218	0.229
TBIL (μmol/ml)[b]	0	15.20 (8.72–25.26)	13.60 (8.45–22.10)	0.471	0.640
	12	11.30 (7.34–19.56)	13.20 (8.65–20.60)	−1.298	0.200
	24	12.10 (6.56–24.74)	13.35 (7.60–23.65)	−1.174	0.246
	52	13.00 (7.94–21.94)	12.10 (8.15–22.45)	−0.369	0.714
Hepatitis B virus DNA (log_{10} copies/ml)[b]	0	8.37 (6.49–9.41)	8.66 (7.11–9.53)	−0.699	0.487
	12	3.27 (2.14–4.70)	4.14 (3.11–5.55)	−4.430	0.000[#]
	24	2.34 (1.82–3.73)	3.36 (2.29–5.35)	−4.212	0.000[#]
	52	1.84 (1.81–2.46)	2.19 (1.81–5.97)	−3.306	0.002[#]
CXCL13 (pg/ml)[c]	0	48.77 (27.87–89.09)	45.51 (26.67–70.97)	−1.109	0.268
	12	51.42 (27.19–203.65)	41.80 (24.55–63.96)	−2.105	0.035[#]
	24	40.90 (19.14–374.20)	35.61 (23.37–60.83)	−1.516	0.130
	52	47.88 (24.10–160.68)	36.77 (15.71–49.50)	−2.876	0.004[#]

Data were shown as median and 10–90% percentile.

[a]*Chi-square test.*

[b]*Independent samples test.*

[c]*Mann–Whitney test.*

TW, treatment week; IL, interleukin; TBIL, total bilirubin; ULN, upper limit of normal.

[#]$p < 0.05$.

stimulate CXCL13 expression, as we observed that only TLR3 ligand poly I:C stimulation induced robust CXCL13 production. Although it is unlikely that HBV replicates in KC, activation of KC by HBV, and its proteins has been demonstrated. Hösel et al. (28) showed that HBV particles and HBsAg induce IL-1β, IL-6, CXCL8, and TNF-α production in human KC *via* NF-κB activation. Boltjes et al. (29) demonstrated that a direct interaction between HBsAg and KC resulted in HBsAg uptake, induction of cytokine production, and the induction of IFN-γ production by NK cells. Alternatively, phagocytosis of HBV itself or -infected hepatocytes by KC may allow intracellular TLR3 exposure to viral RNA (30, 31).

Additionally, CXCL13 expression in KC may be induced by the ongoing hepatic inflammation, which maintains the pathologic process in the tissue by attracting additional lymphocytes and leading to chronic damage. Under chronic HBV infection, serum CXCL13 levels were found to be elevated in CHB patients compared with HCs. The highest levels occurred in immune-active patients. It can be interpreted that the high serum levels of CXCL13 may be a consequence of high local production. In our study, CXCL13 was highly expressed in the ectopic GC of CHB liver, co-localized with KC, Tfh cells, and B cells, indicating that KC-expressed CXCL13 served as a critical regulator for the recruitment of $CXCR5^+$ lymphocytes in CHB patients. Previously, the immunohistochemical findings in liver biopsies suggested a major role for B-cells in the pathogenesis of CHB, which appeared to be driven by increased $CD20^+$ B-cells (32). In addition, we also completed a comprehensive gene-chip analysis of intrahepatic gene expression in patients at different phases of HBV infection. Consistently, CHB patients had significantly elevated expression of CXCL13 in liver tissues compared to the IT and IC groups (data not shown). However, no direct correlation between CXCL13 serum levels and ALT was detected in our study. Although these findings may indicate a lack of a direct effect of CXCL13 on liver inflammation, they do highlight the *in situ* relation between CXCL13 and $CXCR5^+$ lymphocytes.

The role of CXCL13 expression has already investigated in other types of chronic hepatitis (15, 16). Our group reported before that the levels of serum CXCL13 were significantly higher in primary biliary cirrhosis patients compared to HC. And there was a significantly higher mRNA expression of intrahepatic CXCL13 relative to HC and it suggested that CXCL13 promoted intrahepatic $CXCR5^+$ lymphocyte homing and aberrant B cell immune responses in PBC (15). We also compared the serum CXCL13 levels and liver CXCL13 expression in PBC and CHB patients. It was noted that the levels of serum CXCL13 were significantly higher in PBC than CHB. *In situ* staining revealed significantly higher expression of CXCL13 within the portal tracts in PBC than CHB (Figures

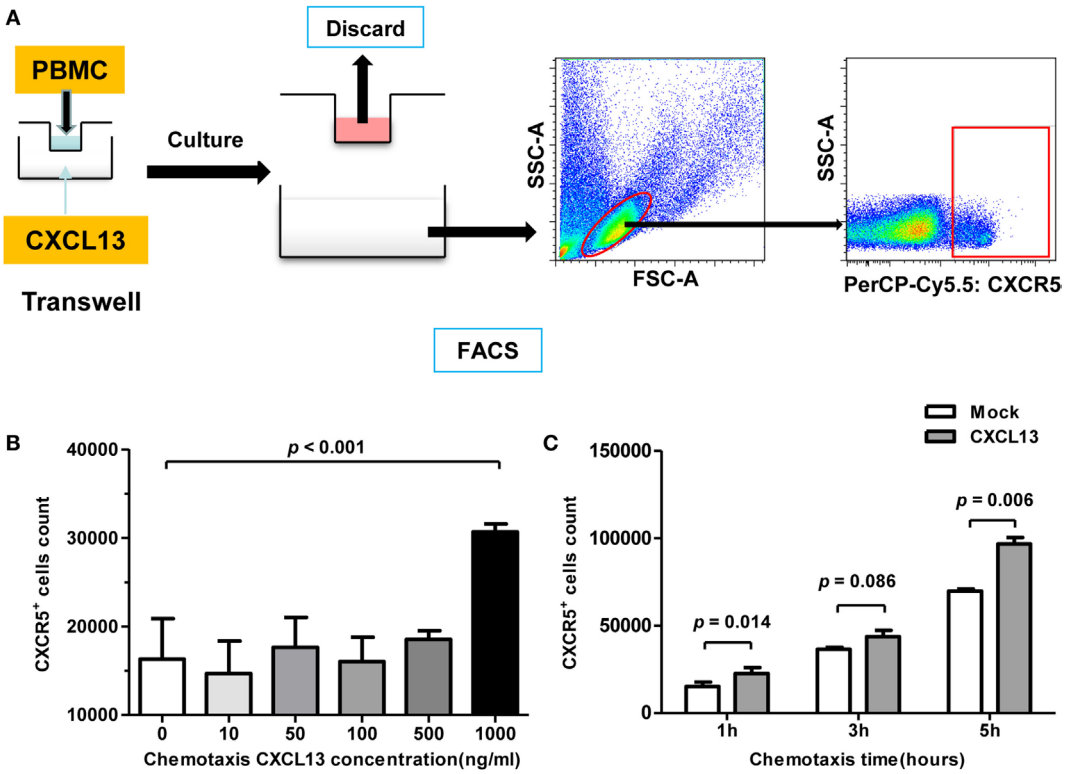

FIGURE 5 | CXCL13-mediated chemotaxis effect on CXCR5⁺ cells *in vitro*. (A) Schematic diagram of chemotaxis assay. A 1×10^6 fresh-isolated peripheral blood mononuclear cells were added into the upper chamber, and different concentration of rh-CXCL13 or median alone was added into lower chamber. After 2–6 h, the cells in the lower chamber were harvested and analyzed. **(B)** Comparison of the numbers of CXCR5⁺ cell counting in chronic hepatitis B (CHB) patients with different CXCL13 concentration in Transwell assay. Data are representative with mean ± SEM, and determined by Mann–Whitney *U* test. **(C)** Comparison of the numbers of CXCR5⁺ cell counting in CHB patients with different incubation time in Transwell assay. Data are representative with mean ± SEM, and determined by paired Student's *t*-test.

S3A,B in Supplementary Material). Additionally, serum CXCL13 levels were found to be elevated in chronic hepatitis C virus infection compared with HC and expression of CXCL13 protein was evident in inflammatory cells within portal tracts and strongly correlated with CD20⁺ B-cell numbers (16, 33). Thus, further studies are necessary to focus and identify the relationships and contributions of CXCL13 to patients with chronic hepatitis at different stages of inflammatory index of liver histology.

To establish whether CXCL13 changes contributed to the success of antiviral therapy, serum levels of this chemokine were monitored serially throughout the course of telbivudine treatment. CXCL13 levels did not change after CR to antiviral therapy. On the contrary, CXCL13 significantly declined in NCR group during the treatment. ROC curves of the serum CXCL13 concentrations at 12 weeks were generated to predict a CR at 52 weeks, but the sensitivity and specificity for detection of a CR were not as satisfactory as HBV-DNA levels. Of note, a negative correlation between CXCL13 serum levels and circulating viral load was noted. Although the combination of weeks 0–12, HBV-DNA level and serum CXCL13 concentration showed an optimal index to predict the CR, the predication value of the ROC curve may hard to be applied for clinical guidance due to the limited sample size of the patients in this study. In addition, as CXCL13 expression might be induced by the ongoing hepatic inflammation, the amelioration of liver inflammation with normalization of ALT levels explanted the decrease of CXCL13 expression during therapy. However, the higher level of CXCL13 in CR group referred to the activation of local anti-HBV immune response to contribute to viral control. Related results in our group showed the similar tendency of these immune factors during the antiviral treatment (17, 19). It was showed serum IL-21 concentration and the frequency of circulating Tfh cells were significantly higher in CR group compared with NCR group. The significant difference between CR and NCR was observed at treatment 12 weeks, the time when an increase in the IL-21-secreting Tfh cells that are associated with HBeAg seroconversion can be detected (17, 19). It could be assumed that Tfh cells and B cells would be attracted by CXCL13 and migrate to the liver, where the Tfh cells would secrete IL-21 and promote B cell maturation and production of antibodies.

In conclusion, we have observed that patients with chronic HBV infection have increased serum levels of CXCL13, possibly as the result of augmented production in the liver by

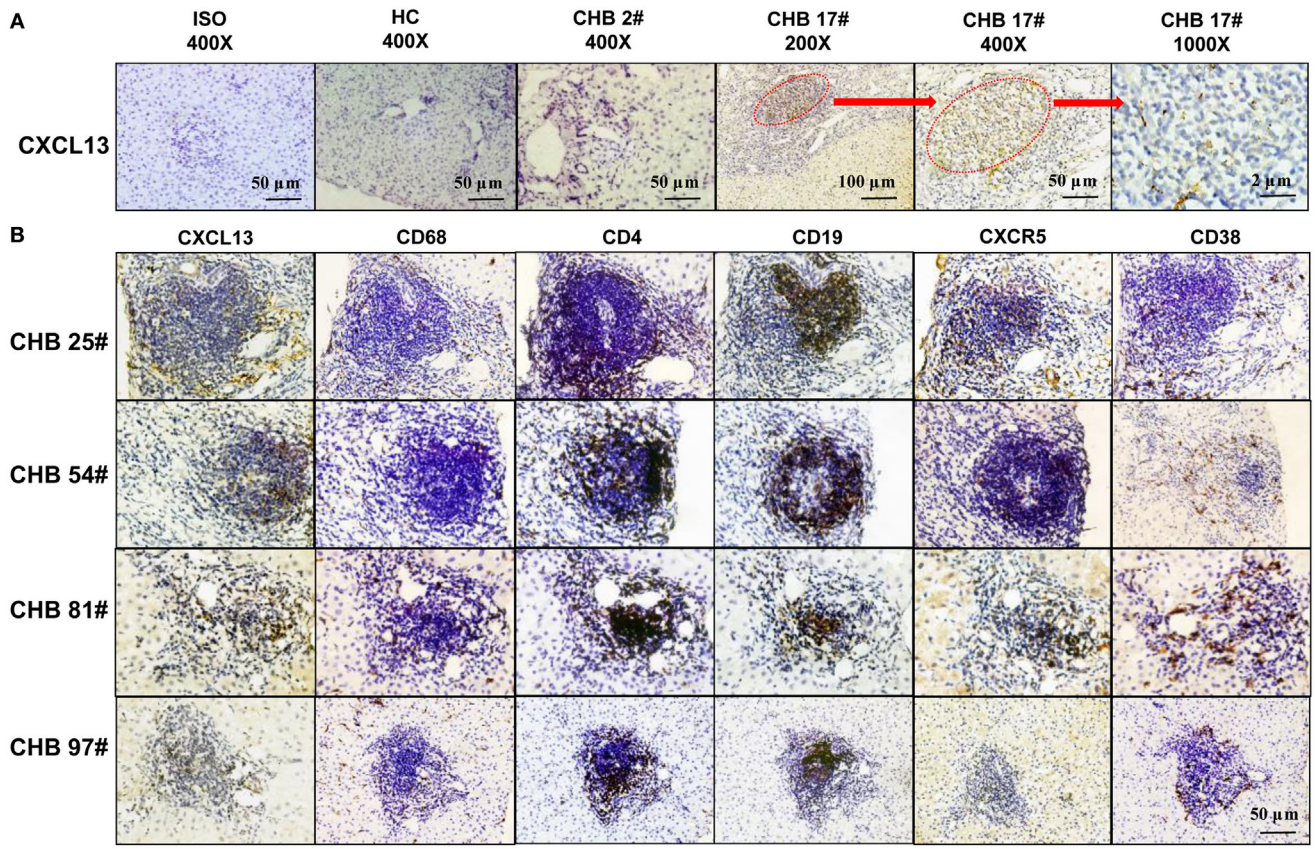

FIGURE 6 | *In situ* expression of CXCL13 in the ectopic germinal center (GC) of liver tissue from chronic hepatitis B (CHB) patients. (A) Immunohistochemical staining of CXCL13 expression in liver tissue samples with or without ectopic GC from CHB patients and healthy control (HC). Representative slides were shown with different magnifications as indicated. **(B)** Immunohistochemical staining of $CXCL13^+$, $CD4^+$, $CD19^+$, $CXCR5^+$, $CD38^+$, and $CD68^+$ cells in serial sections of liver tissue samples with ectopic GC from four representative CHB patients. Co-localization of CXCL13 expression was observed with $CD68^+$ KCs, $CXCR5^+$ $CD4^+$ T cells, and $CXCR5^+CD19^+$ B cells in the ectopic GC (magnification ×400, plotting scale equal to 50 μm).

KC. In CHB patients, CXCL13 contributes to lymphocyte migration to the liver by creating local microenvironments supportive of focal B-cell aggregations that have structural features remarkably similar to ectopic lymphoid follicles. Higher CXCL13 production seems to be involved in viral control during antiviral treatment, which suggests the possible use of serum CXCL13 monitoring to follow the treatment response to antiviral therapy and the prognosis. Future studies are also needed to determine whether TLR agonists that activate CXCL13 expression represent potential therapeutic agents for HBV infections.

AUTHOR CONTRIBUTIONS

XZ and JH conceived and designed the study. CL, XH, MW, RB, JG, YL, and BL performed the experiments and analyzed the data. XZ and CL wrote the manuscript with additional input and suggestions from JS, JP, and ML. All authors reviewed and approved the manuscript.

FUNDING

XZ was supported by grants from the National Natural Science Foundation of China (81471952, 81301434, 81641173), the Pearl River Nova Program of Guangzhou (2014J2200024), the Research Fund for the Doctoral Program of Higher Education of China (20134433120001), and Provincial Natural Science Foundation of Guangdong (2014A030313299). JH was supported by grants from the Key Clinical Specialty Discipline Construction Program and the Major Science and Technology Special Project of China (2012ZX10002003). XH was supported by grants from the Provincial Natural Science Foundation of Guangdong (2014A030310048).

SUPPLEMENTARY MATERIAL

The Supplementary Material for this article can be found online at http://journal.frontiersin.org/article/10.3389/fimmu.2017.00323/full#supplementary-material.

REFERENCES

1. Ott JJ, Stevens GA, Groeger J, Wiersma ST. Global epidemiology of hepatitis B virus infection: new estimates of age-specific HBsAg seroprevalence and endemicity. *Vaccine* (2012) 30(12):2212–9. doi:10.1016/j.vaccine.2011.12.116
2. Ganem D, Prince AM. Hepatitis B virus infection – natural history and clinical consequences. *N Engl J Med* (2004) 350(11):1118–29. doi:10.1056/NEJMra031087
3. Liang TJ. Hepatitis B: the virus and disease. *Hepatology* (2009) 49(5 Suppl):S13–21. doi:10.1002/hep.22881
4. McMahon BJ. The natural history of chronic hepatitis B virus infection. *Hepatology* (2009) 49(5 Suppl):S45–55. doi:10.1002/hep.22898
5. Yim HJ, Lok AS. Natural history of chronic hepatitis B virus infection: what we knew in 1981 and what we know in 2005. *Hepatology* (2006) 43(2 Suppl 1):S173–81. doi:10.1002/hep.20956
6. Chisari FV, Isogawa M, Wieland SF. Pathogenesis of hepatitis B virus infection. *Pathol Biol* (2010) 58(4):258–66. doi:10.1016/j.patbio.2009.11.001
7. Montano L, Aranguibel F, Boffill M, Goodall AH, Janossy G, Thomas HC. An analysis of the composition of the inflammatory infiltrate in autoimmune and hepatitis B virus-induced chronic liver disease. *Hepatology* (1983) 3(3):292–6. doi:10.1002/hep.1840030303
8. Rehermann B. Interaction between the hepatitis C virus and the immune system. *Semin Liver Dis* (2000) 20(2):127–41. doi:10.1055/s-2000-9946
9. Rot A, von Andrian UH. Chemokines in innate and adaptive host defense: basic chemokinese grammar for immune cells. *Annu Rev Immunol* (2004) 22:891–928. doi:10.1146/annurev.immunol.22.012703.104543
10. Publicover J, Gaggar A, Nishimura S, Van Horn CM, Goodsell A, Muench MO, et al. Age-dependent hepatic lymphoid organization directs successful immunity to hepatitis B. *J Clin Invest* (2013) 123(9):3728–39. doi:10.1172/JCI68182
11. Gunn MD, Ngo VN, Ansel KM, Ekland EH, Cyster JG, Williams LT. A B-cell-homing chemokine made in lymphoid follicles activates Burkitt's lymphoma receptor-1. *Nature* (1998) 391(6669):799–803. doi:10.1038/35876
12. Legler DF, Loetscher M, Roos RS, Clark-Lewis I, Baggiolini M, Moser B. B cell-attracting chemokine 1, a human CXC chemokine expressed in lymphoid tissues, selectively attracts B lymphocytes via BLR1/CXCR5. *J Exp Med* (1998) 187(4):655–60. doi:10.1084/jem.187.4.655
13. Ansel KM, Ngo VN, Hyman PL, Luther SA, Forster R, Sedgwick JD, et al. A chemokine-driven positive feedback loop organizes lymphoid follicles. *Nature* (2000) 406(6793):309–14. doi:10.1038/35018581
14. Cohen KW, Dugast AS, Alter G, McElrath MJ, Stamatatos L. HIV-1 single-stranded RNA induces CXCL13 secretion in human monocytes via TLR7 activation and plasmacytoid dendritic cell-derived type I IFN. *J Immunol* (2015) 194(6):2769–75. doi:10.4049/jimmunol.1400952
15. Li Y, Wang W, Tang L, He X, Yan X, Zhang X, et al. Chemokine (C-X-C motif) ligand 13 promotes intrahepatic chemokine (C-X-C motif) receptor 5+ lymphocyte homing and aberrant B-cell immune responses in primary biliary cirrhosis. *Hepatology* (2015) 61(6):1998–2007. doi:10.1002/hep.27725
16. Sansonno D, Tucci FA, Troiani L, Lauletta G, Montrone M, Conteduca V, et al. Increased serum levels of the chemokine CXCL13 and up-regulation of its gene expression are distinctive features of HCV-related cryoglobulinemia and correlate with active cutaneous vasculitis. *Blood* (2008) 112(5):1620–7. doi:10.1182/blood-2008-02-137455
17. Li Y, Ma S, Tang L, Li Y, Wang W, Huang X, et al. Circulating chemokine (C-X-C Motif) receptor 5(+) CD4(+) T cells benefit hepatitis B e antigen seroconversion through IL-21 in patients with chronic hepatitis B virus infection. *Hepatology* (2013) 58(4):1277–86. doi:10.1002/hep.26489
18. European Association for the Study of the Liver. EASL clinical practice guidelines: management of chronic hepatitis B virus infection. *J Hepatol* (2012) 57(1):167–85. doi:10.1016/j.jhep.2012.02.010
19. Ma SW, Huang X, Li YY, Tang LB, Sun XF, Jiang XT, et al. High serum IL-21 levels after 12 weeks of antiviral therapy predict HBeAg seroconversion in chronic hepatitis B. *J Hepatol* (2012) 56(4):775–81. doi:10.1016/j.jhep.2011.10.020
20. Gesser B, Leffers H, Jinquan T, Vestergaard C, Kirstein N, Sindet-Pedersen S, et al. Identification of functional domains on human interleukin 10. *Proc Natl Acad Sci U S A* (1997) 94(26):14620–5. doi:10.1073/pnas.94.26.14620
21. Werner M, Driftmann S, Kleinehr K, Kaiser GM, Mathe Z, Treckmann JW, et al. All-in-one: advanced preparation of human parenchymal and non-parenchymal liver cells. *PLoS One* (2015) 10(9):e0138655. doi:10.1371/journal.pone.0138655
22. Broering R, Lutterbeck M, Trippler M, Kleinehr K, Poggenpohl L, Paul A, et al. Long-term stimulation of toll-like receptor 3 in primary human hepatocytes leads to sensitization for antiviral responses induced by poly I:C treatment. *J Viral Hepat* (2014) 21(7):480–90. doi:10.1111/jvh.12174
23. Zhang X, Meng Z, Qiu S, Xu Y, Yang D, Schlaak JF, et al. Lipopolysaccharide-induced innate immune responses in primary hepatocytes downregulates woodchuck hepatitis virus replication via interferon-independent pathways. *Cell Microbiol* (2009) 11(11):1624–37. doi:10.1111/j.1462-5822.2009.01353.x
24. Kobayashi S, Murata K, Shibuya H, Morita M, Ishikawa M, Furu M, et al. A distinct human CD4+ T cell subset that secretes CXCL13 in rheumatoid synovium. *Arthritis Rheum* (2013) 65(12):3063–72. doi:10.1002/art.38173
25. Seeger C, Mason WS. HBV replication, pathobiology and therapy: unanswered questions. *J Hepatol* (2016) 64(1 Suppl):S1–3. doi:10.1016/j.jhep.2016.01.006
26. Crispe IN. The liver as a lymphoid organ. *Annu Rev Immunol* (2009) 27:147–63. doi:10.1146/annurev.immunol.021908.132629
27. Boltjes A, Movita D, Boonstra A, Woltman AM. The role of Kupffer cells in hepatitis B and hepatitis C virus infections. *J Hepatol* (2014) 61(3):660–71. doi:10.1016/j.jhep.2014.04.026
28. Hösel M, Quasdorff M, Wiegmann K, Webb D, Zedler U, Broxtermann M, et al. Not interferon, but interleukin-6 controls early gene expression in hepatitis B virus infection. *Hepatology* (2009) 50(6):1773–82. doi:10.1002/hep.23226
29. Boltjes A, van Montfoort N, Biesta PJ, Op den Brouw ML, Kwekkeboom J, van der Laan LJ, et al. Kupffer cells interact with hepatitis B surface antigen in vivo and in vitro, leading to proinflammatory cytokine production and natural killer cell function. *J Infect Dis* (2015) 211(8):1268–78. doi:10.1093/infdis/jiu599
30. Broering R, Trippler M, Werner M, Real CI, Megger DA, Bracht T, et al. Hepatic expression of proteasome subunit alpha type-6 is upregulated during viral hepatitis and putatively regulates the expression of ISG15 ubiquitin-like modifier, a proviral host gene in hepatitis C virus infection. *J Viral Hepat* (2016) 23(5):375–86. doi:10.1111/jvh.12508
31. Real CI, Lu M, Liu J, Huang X, Trippler M, Hossbach M, et al. Hepatitis B virus genome replication triggers toll-like receptor 3-dependent interferon responses in the absence of hepatitis B surface antigen. *Sci Rep* (2016) 6:24865. doi:10.1038/srep24865
32. Mohamadkhani A, Naderi E, Sotoudeh M, Katoonizadeh A, Montazeri G, Poustchi H. Clinical feature of intrahepatic B-lymphocytes in chronic hepatitis B. *Int J Inflam* (2014) 2014:896864. doi:10.1155/2014/896864
33. Nguyen N, de Esch C, Cameron B, Kumar RK, Zekry A, Lloyd AR. Positioning of leukocyte subsets in the portal and lobular compartments of hepatitis C virus-infected liver correlates with local chemokine expression. *J Gastroenterol Hepatol* (2014) 29(4):860–9. doi:10.1111/jgh.12462

Conflict of Interest Statement: The authors have nothing to disclose with respect to funding and no conflicts of interest with respect to this manuscript.

Copyright © 2017 Liu, Huang, Werner, Broering, Ge, Li, Liao, Sun, Peng, Lu, Hou and Zhang. This is an open-access article distributed under the terms of the Creative Commons Attribution License (CC BY). The use, distribution or reproduction in other forums is permitted, provided the original author(s) or licensor are credited and that the original publication in this journal is cited, in accordance with accepted academic practice. No use, distribution or reproduction is permitted which does not comply with these terms.

frontiers in Immunology

REVIEW
published: 15 March 2018
doi: 10.3389/fimmu.2018.00540

Metabolic Adaptations of CD4+ T Cells in Inflammatory Disease

*Cristina Dumitru[1], Agnieszka M. Kabat[2] and Kevin J. Maloy[1]**

[1] Sir William Dunn School of Pathology, University of Oxford, Oxford, United Kingdom, [2] Max Planck Institute of Immunobiology and Epigenetics, Freiburg im Breisgau, Germany

A controlled and self-limiting inflammatory reaction generally results in removal of the injurious agent and repair of the damaged tissue. However, in chronic inflammation, immune responses become dysregulated and prolonged, leading to tissue destruction. The role of metabolic reprogramming in orchestrating appropriate immune responses has gained increasing attention in recent years. Proliferation and differentiation of the T cell subsets that are needed to address homeostatic imbalance is accompanied by a series of metabolic adaptations, as T cells traveling from nutrient-rich secondary lymphoid tissues to sites of inflammation experience a dramatic shift in microenvironment conditions. How T cells integrate information about the local environment, such as nutrient availability or oxygen levels, and transfer these signals to functional pathways remains to be fully understood. In this review, we discuss how distinct subsets of CD4+ T cells metabolically adapt to the conditions of inflammation and whether these insights may pave the way to new treatments for human inflammatory diseases.

Keywords: Th cells, inflammation, metabolism, microenvironment, Th1 cells, Th17 cells, Th2 cells, regulatory T cells

OPEN ACCESS

Edited by:
Guixiu Shi,
Xiamen University,
China

Reviewed by:
Behdad Afzali,
King's College London,
United Kingdom
Wendy Watford,
University of Georgia,
United States

***Correspondence:**
Kevin J. Maloy
kevin.maloy@path.ox.ac.uk

Specialty section:
This article was submitted to Inflammation, a section of the journal Frontiers in Immunology

Received: *03 December 2017*
Accepted: *02 March 2018*
Published: *15 March 2018*

Citation:
Dumitru C, Kabat AM and Maloy KJ (2018) Metabolic Adaptations of CD4+ T Cells in Inflammatory Disease. Front. Immunol. 9:540. doi: 10.3389/fimmu.2018.00540

THE INFLAMMATORY MICROENVIRONMENT

It has long been appreciated that leukocytes need to adapt their metabolism to survive and proliferate in the hostile inflammatory environment. However, in recent years, there has been a growing understanding of the complex relationship between the T cell metabolic machinery and their immune function. Metabolic adaptations of T cells go beyond facilitating survival—they are also critical for T cell differentiation and immune effector function (1–4). The complicated interplay between local environment, T cell metabolism, and immune functions remains incompletely understood. In this review, we discuss how CD4+ T cells adapt to conditions of inflammation. We first consider how metabolic conditions in inflammatory microenvironments differ from those present in healthy tissues and lymphoid organs. We then summarize the metabolic pathways involved in T-cell activation, followed by discussion of recent studies examining the role of nutrients, oxygen, and temperature on CD4+ T cell differentiation and function during inflammation. We further explore how dysregulation of catabolic processes, such as autophagy, can alter the availability of nutrients and lead to aberrant immune responses. Finally, we look at how understanding the metabolic adaptations of CD4+ T cells in response to environmental factors may pave the way to new treatments for human inflammatory diseases.

A controlled and self-limiting acute inflammatory reaction is largely beneficial; however, in chronic inflammation, the response becomes dysregulated and prolonged, leading to excessive tissue destruction (5). Chronic inflammation can also develop as an independent response with entirely different pathogenesis, time-course, and clinical manifestations (6). This persistent type of inflammation is associated with many diseases, including rheumatoid arthritis (RA), asthma, celiac disease,

or inflammatory bowel disease (IBD). Moreover, several chronic conditions, including obesity, diabetes, cardiovascular disease, or cancer, are known to have inflammatory components (7).

Sites of inflammation are characterized by extensive recruitment of innate inflammatory cells and high proliferation rates of lymphocytes (8). The inflammatory responses often promote edema, which increases the distance between the parenchymal cells and blood vessels, creating a local microenvironment that is depleted of nutrients and oxygen (8). Thus, T cells traveling from nutrient-rich secondary lymphoid tissues to sites of inflammation have to adapt their metabolism to support anabolic growth and maintain their function at the low oxygen and nutrient levels characteristic of inflammatory lesions (**Figure 1**) (9). Although the characteristics of the chronic inflammatory site differ according to the tissue in which the disease unfolds, some shared features of inflammatory microenvironments include: low nutrient levels (glucose and glutamine); increased lactate production; decreased pH; and hypoxia and high concentration of reactive oxygen species (ROS) (10).

Inflammatory sites have long been described to harbor reduced glucose concentrations, which may be partly caused by proliferation of recruited leukocytes and invading pathogens (11–13). Activated T cells upregulate glucose metabolism to fuel macromolecular synthesis pathways and promote proliferation (3, 14, 15). Indeed, glycolysis is essential for T cell division, as T cells have decreased proliferation rates in glucose-deficient media, even in the presence of high levels of alternative energy sources like glutamine (16). Proliferating leukocytes are also ravenous glutamine consumers (17) and, although few studies have examined glutamine concentrations at inflamed sites, it seems likely that glutamine would decrease in the same manner as glucose. For example, in septic patients, plasma and skeletal muscle glutamine levels are decreased compared with healthy controls, and low glutamine concentrations are associated with poor prognosis (18–20). In addition, in a small study of patients receiving artificial nutrition, those with elevated markers of inflammatory stress had significantly lower concentrations of glutamine in plasma and gut mucosa (21). Similarly, patients with Crohn's disease have lower

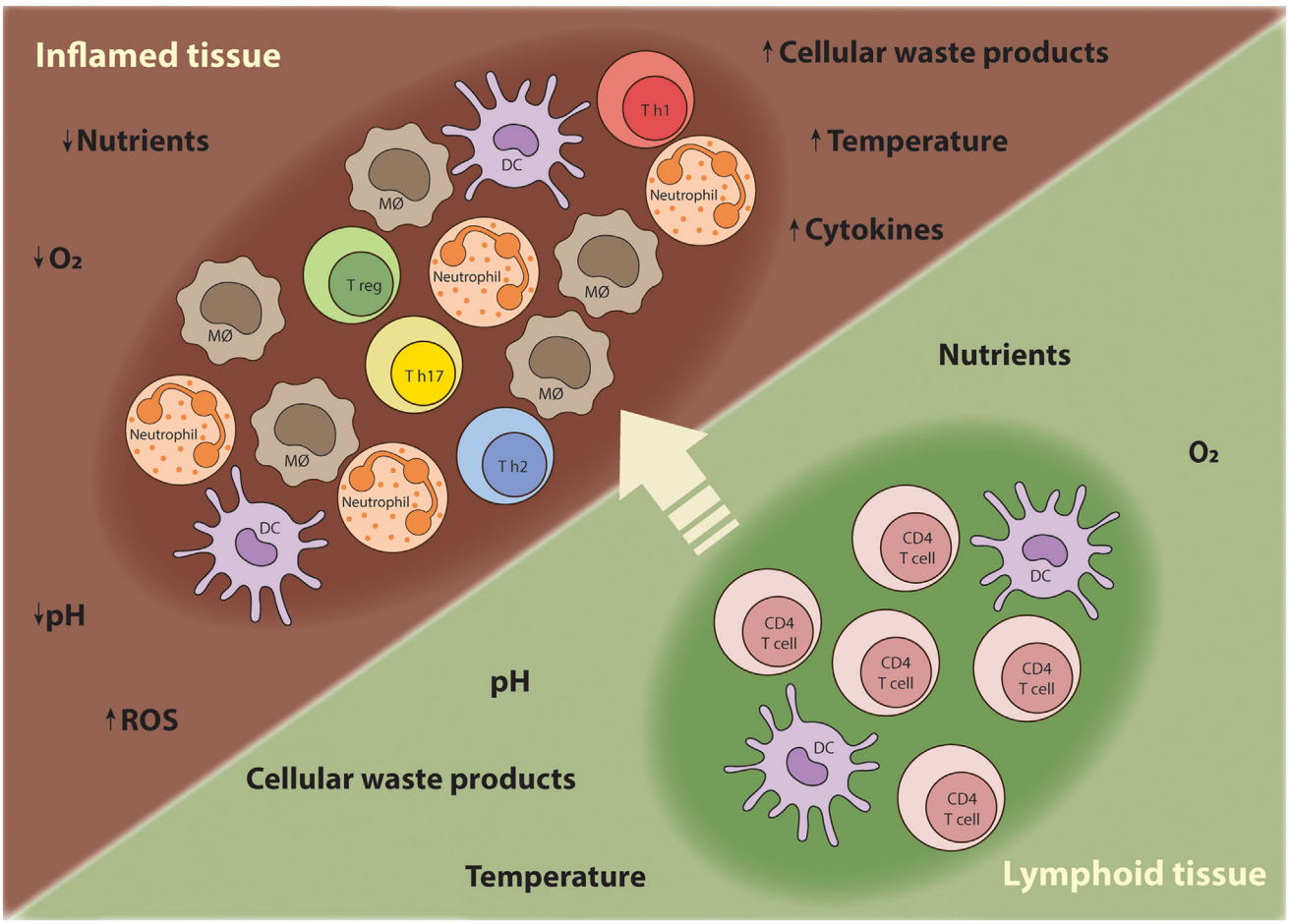

FIGURE 1 | T cells require metabolic flexibility to adapt to the chronic inflammatory environment. As T cells mature during an immune response, they migrate from nutrient-rich secondary lymphoid tissues to sites of inflammation where nutrients, oxygen, and other growth promoting factors become limited. Moreover, other innate inflammatory cells are recruited to the inflamed tissue and compete for nutrients. Thus, T cells have to metabolically adapt to these harsh conditions in order survive, proliferate, and perform their effector functions.

levels of glutamine in inflamed mucosal tissues compared with non-inflamed mucosal tissues (22). Therefore, metabolic flexibility may be necessary to sustain T cell proliferation and effector function in chronic inflammatory environments.

Physiological lactate concentration in healthy tissues or blood is normally kept at 1.5–3 mM, but this can increase to as much as 10 mM in inflammatory environments such as atherosclerotic plaques or rheumatic synovial fluid (23). Lactic acid is a by-product of glucose metabolism and lactate accumulation can also be used as an indirect reporter of another inflammatory hallmark, decreased extracellular pH (24). Extracellular lactate and acidic conditions (low pH) have been shown to reduce the proliferation and function of human and mouse cytotoxic T cells due to decreased activation and inhibition of glycolysis (25–28), while restoration of pH to physiological levels rescues T cell function (25, 29). However, a recent study reported that $CD4^+$ T cells sense lactate *via* the SLC5A12 transporter, and this interaction inhibits T cell motility, which might lead to T cells becoming entrapped at inflammatory sites, where they perpetuate the chronic inflammatory process (23).

Reactive oxygen species are key signaling molecules that play diverse roles in cellular function including cell signaling, differentiation, proliferation, and apoptosis. However, at high concentrations, they can act as mediators of inflammation due to their capacity to oxidize cellular constituents and damage DNA (30). Most ROS are generated as by-products of cellular metabolism *via* the electron transport chain (ETC), through partial reduction of the oxygen molecule during oxidative phosphorylation (OXPHOS) in mitochondria. Superoxide anion $\left(O_2^{\bullet-}\right)$, the hydroxyl radical ($^{\bullet}OH$), and hydrogen peroxide (H_2O_2) can all be generated in this way (31). ROS are abundant at inflammatory sites (32) and affect T cell functions (33, 34). For example, the presence of high levels of ROS in the environment has been reported to favor $CD4^+$ T cell differentiation toward a Th2 phenotype, but the mechanisms involved remain unclear (35, 36).

Tissue hypoxia is characteristic of various chronic inflammatory diseases such as atherosclerosis, RA, and IBD, with oxygen levels considerably lower (<2%, equivalent to 2.026 kPa) than in healthy tissues (<5%, equivalent to 5.056 kPa) (37). However, even in healthy tissues, T cells can be exposed to varying oxygen concentrations ranging between 3 and 19% (3.039–19.247 kPa) as they migrate between blood and different tissues (38). The upper airways have the highest oxygen concentration (39), while lymphoid tissues have markedly lower oxygen concentrations; e.g., 6.5% (equivalent to 6.585 kPa) in bone marrow (40) and 3–4% (3.039–4.052 kPa) in the spleen (41, 42). Several studies have shown that $CD4^+$ T cells have a reduced rate of proliferation and survival under hypoxic conditions (37, 43). When exposed to hypoxic environments, T cells upregulate the oxygen-sensitive transcription factor, hypoxia-inducible factor (HIF)-1α. HIF-1α modulates T cell differentiation and metabolism by promoting anaerobic glycolysis through increased expression of the glucose transporter Glut1, as well as induction of several glycolytic enzymes (4, 44, 45). Of note, in activated T cells HIF-1α can also be upregulated under normoxia to sustain the expression of glycolytic enzymes during Th cell differentiation (4, 46, 47).

Increasing sodium conditions *in vitro* by approximately 40 mM boosts T cell proliferation (48). In addition, secondary lymphoid tissues have higher osmolality than serum, suggesting that a high-salt environment *in vivo* favors T cell proliferation (49). There is some evidence to suggest that inflamed tissues could harbor high levels of salt. For example, excessive salt intake has been associated with enhanced induction of experimental autoimmune encephalomyelitis in mice (50, 51), worsening of disease activity in multiple sclerosis patients (52) and exacerbation of tissue damage in cardiovascular disease (53). Recent evidence suggests that high-salt environments favor T cell skewing toward a Th17 pro-inflammatory phenotype and impairs the suppressive functions of regulatory T (Treg) cells (50, 51, 54). Moreover, dietary supplementation with NaCl in a mouse model of graft-versus-host disease (GVHD) inhibited Treg function and aggravated clinical outcomes (54). Although these studies suggest that reducing salt concentrations could be beneficial for limiting pathological T cell responses in inflamed tissues, there are circumstances where reducing tissue salt concentrations may have deleterious effects. For example, a recent study found that regional hypersalinity in the renal medulla drives the recruitment and antibacterial functions of mononuclear phagocytes that prevent urinary tract infections spreading to the kidney (55). Moreover, further studies are required to determine the impact of high-salt environments on T cell metabolic processes.

The temperature gradients across the body are affected by inflammation in different ways. While internal organs such as the spleen and gut are subject to fluctuations of core body temperature during episodes of fever (37–39°C), the skin and muscles are subjected to a wider range of temperature gradients (29–37°C) (56). In addition, the normal core temperature of 37°C of both humans and mice oscillates throughout the day by approximately 1.7°C (57). Thus, lymphocytes circulating between these changing thermal compartments are required to function at various temperatures. The effects of hyperthermia on T cell function has been the subject of a few studies, and febrile temperatures are known to enhance T cell proliferation in response to mitogens (58, 59). More recently, febrile temperature was shown to induce changes in membrane fluidity in $CD4^+$ T cells leading to macromolecular clusters that reduced the requirement for CD28 costimulation (60). Presently, little is known about whether the local increase in temperature during inflammation alters T cell metabolism. Of note, mice are generally housed at a temperature comfortable for clothed humans, 19–22°C, but the thermoneutral zone for mice is around 30–32°C (61). Some studies argue that mice housed under laboratory conditions are chronically cold-stressed and have a different metabolic and thermal phenotype than mice raised at thermoneutrality (62, 63). Thus, housing temperature of mice may be a variable that requires more consideration in immunometabolism studies.

Next to daily oscillations of core body temperature, other daily rhythms can influence immune cell function. Circadian rhythms, the body's autonomous internal clock based on intricate transcriptional and translational feedback loops, anticipate and allow organisms to adapt to environmental changes by controlling a wide array of physiological and metabolic processes (64). Lifestyles that disrupt the inherent biological clock, such as

shift work, have been associated with increased systemic levels of inflammatory markers (65, 66) as well as increased incidence of cardiovascular disease (67), metabolic disorders (68, 69), and cancer (70, 71). Interestingly, trafficking and migration of immune cells, including T cells, is also regulated by circadian rhythms (72) although the exact impact of these fluctuations on T cell function remains to be fully elucidated (73, 74). The circadian clock can also influence feeding schedules and therefore could indirectly affect the availability of nutrients (69, 75). For example, the levels of several intracellular micronutrients, including magnesium, have been shown to fluctuate rhythmically in two eukaryotic cell lines (76). As ATP needs to be bound to magnesium to elicit its biological function, fluctuations in intracellular magnesium levels could affect all cell processes that require ATP for energy (77). Moreover, manipulation of magnesium levels also leads to changes of the circadian period suggesting that magnesium acts as a "meta-regulator" of the cellular clock (76). Indeed, it has been proposed that the mechanistic target of rapamycin (mTOR) pathway, which controls protein synthesis associated with proliferative signals, is highly sensitive to Mg-ATP fluctuations (76, 78, 79). Nevertheless, whether daily fluctuations in availability of magnesium influence T cell function remains to be established.

METABOLIC REPROGRAMMING IN CD4+ T CELL ACTIVATION

To drive the proliferation and differentiation of the appropriate leukocyte subsets needed to combat pathogenic infection, the immune system engages a series of coordinated growth and proliferative signals, including signals that modulate cellular metabolic processes (9) (**Figure 2**). Naïve, quiescent CD4+ T cells are characterized by a metabolic program that favors energy production over biosynthesis and generally rely on mitochondrial oxidative pathways, fueled by fatty acid or amino acid oxidation (80). Activation of CD4+ T cells triggers a dynamic network of transcriptional and translational changes which go hand in hand with metabolic adaptations to match the bioenergetic demands of the proliferating cells (80). During the initial phase after activation, oxidative metabolism is downregulated, while biosynthetic pathways are increased (81).

CD28 is one of the best characterized costimulatory receptors on naïve T cells, it promotes cell proliferation by activating different signaling pathways that sustain the bioenergetic demands associated with T cell activation (82). For example, CD28 costimulation has been described to upregulate glucose utilization allowing T cells to meet the biosynthetic demands associated with activation (83, 84). Furthermore, metabolic alterations driven by CD28 costimulation were recently shown to be important for recall of CD8+ T cell memory (T_m) responses (85). The authors found that T cells primed *in vitro* with CD28 had tighter mitochondrial cristae (inner mitochondrial folds) and used the mitochondrial fatty acid oxidation (FAO) pathway significantly more than T cells primed without CD28 (85). Using an adoptive transfer model, they showed that T cells primed without CD28 were unable to prevent tumor outgrowth, suggesting that CD8+ T_m cell responses were impaired (85).

One critical signaling pathway for the transduction of the TCR/CD28 signal in activated T cells is the PI3K–Akt pathway, which promotes entry into the cell cycle and resistance to apoptosis; however, its role in the metabolic reprogramming of T cells is debated, since the requirement for Akt activation in promoting glycolytic metabolism in activated T cells is unclear (86). T cell activation also leads to the induction of the mechanistic target of rapamycin (mTOR) pathway, either through the PI3K–Akt pathway or independently. mTOR is a conserved serine/threonine kinase that integrates signals from various stimuli, including growth factors, glucose, amino acids, and oxygen levels, to regulate growth, survival, and proliferation (87) (**Figure 2**). In mammals, mTOR forms two functionally distinct complexes, mTORC1 and mTORC2, each with specific downstream targets and functions (87). mTORC1 is characterized by the presence of the scaffolding protein Raptor (regulatory-associated protein of mTOR), while mTORC2 is characterized by the presence of the Rictor (Rapamycin-insensitive companion of mTOR) protein (87). mTOR plays a pivotal role in regulating cellular metabolic pathways such as glycolysis, lipid synthesis, and amino acid metabolism.

During T cell activation, the glycolytic program is activated by transcription factors, such as c-Myc and HIF-1α, which orchestrate the expression of glycolytic enzymes and glucose transporters that facilitate increased uptake and catabolism of glucose (87). Once in the cytoplasm, glucose can be metabolized to yield two units of pyruvate, which are further processed according to the availability of oxygen. In aerobic conditions, pyruvate is further degraded to the acetyl group of acetyl-CoA and fed into the citric acid cycle, also known as the tricarboxylic acid (TCA) or Krebs cycle, which occurs in the inner layer of the mitochondria (88). The NADH and $FADH_2$ produced at each turn of the cycle donate electrons to the ETC, a series of membrane-bound carriers, called complexes I–IV, located in the inner mitochondrial membrane (**Figure 2**). The large amount of energy released during the course of the electron transfer fuels the production of over 30 molecules of ATP through OXPHOS (88, 89).

By contrast, under low oxygen conditions, pyruvate is reduced to lactate *via* glycolysis, generating only two molecules of ATP per one unit of glucose (90). However, some cells, including activated T cells, convert glucose to lactate even when oxygen is not limiting. This aerobic glycolysis was first described by the German biochemist Otto Warburg for tumor cells, and it is thus known as the "Warburg effect" (91). Quiescent T cells generate most of their energy through OXPHOS, but T cell activation induces metabolic remodeling toward a program of anabolic growth and enhanced protein synthesis, necessitating greater uptake of nutrients. T cell activation is not merely a switch from OXPHOS to aerobic glycolysis, indeed both pathways are upregulated and cooperate to meet energetic demands, but glycolysis undergoes a marked increase and becomes the dominant metabolic pathway (90). Since ATP production *via* aerobic glycolysis is much less efficient than *via* OXPHOS, it seems counterintuitive that this pathway would dominate in proliferating T cells. However, increased glycolytic flux leads to increased production of NADH, which is used as a cofactor by numerous metabolic enzymes, as well as increased levels of glycolysis intermediates that are directed into

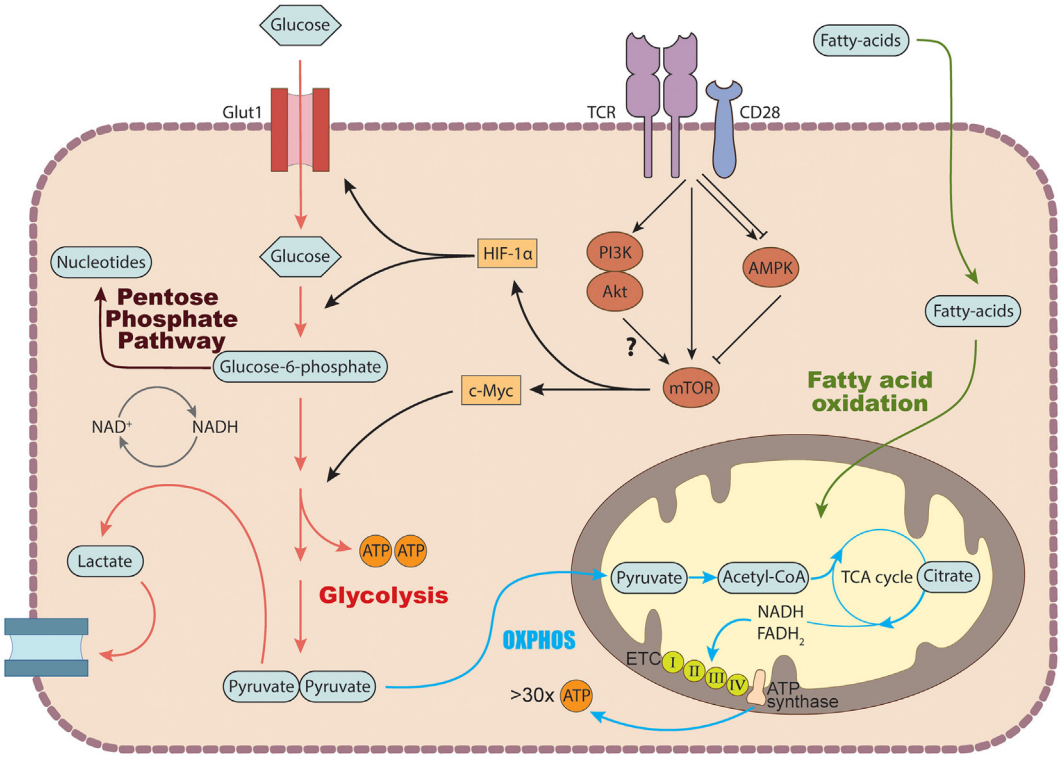

FIGURE 2 | Basic metabolic pathways in T cells. In the cytosol, glucose is converted into pyruvate *via* glycolysis. Pyruvate can either be further metabolized into lactate and secreted or enter the tricarboxylic acid (TCA) cycle to generate NADH and FADH2 which get fed into the electron transport chain (ETC) to generate ATP *via* the process of oxidative phosphorylation. Glucose breakdown intermediates produced during glycolysis can be metabolized *via* the pentose phosphate pathway donating important building blocks for nucleotide and amino acid synthesis. TCR stimulation induces the expression of several genes involved in glucose transport and metabolism by recruiting the transcription factors c-Myc and hypoxia inducible factor (HIF-1) α *via* activation of the mechanistic target of rapamycin (mTOR) machinery. In addition to glucose, T cells can also use fatty acids as a source of energy by degrading fatty acids through fatty acid oxidation.

anabolic pathways for the production of nucleotides, fatty acids, and amino acid precursors (92).

The amino acid glutamine is another critical substrate used by T cells during activation (17). Following stimulation, glutaminolytic enzymes and the glutamine antiporter CD98 are induced in a Myc-dependent fashion (93), and elimination of glutamine from the culture media decreases lymphocyte proliferation (94, 95). Glutamine is metabolized by glutaminolysis, and the intermediates produced in this process can enter the TCA cycle (17). Glutamine also acts as a nitrogen donor for the synthesis of purine and pyrimidines and is therefore able to facilitate the synthesis of nucleotides during cell proliferation (96).

Under harsh environmental conditions, cell survival is also determined by the capacity to recycle cellular nutrients as well as sense extracellular stimuli. The mTOR and adenosine monophosphate-activated protein kinase (AMPK) pathways play important roles in tailoring the metabolic adaptations of CD4+ T cell subsets during conditions where nutrients and oxygen are scarce. AMPK is a serine/threonine kinase that modulates cellular energy status in response to nutrient variations or physiological stress (97). Increases in cytoplasmic AMP-to-ATP concentrations activate the AMPK sensor. When activated, AMPK initiates metabolic reprogramming by switching on ATP-producing pathways (oxidation of glucose and fatty acids) and switching off ATP-consuming anabolic pathways (fatty acid or protein synthesis) (98). AMPK can also activate autophagy, directly or indirectly, to initiate metabolic reprogramming toward catabolic reactions (99). Autophagy is a cellular process in which the cell breaks down large cytoplasmic components such as organelles (also known as macroautophagy) to ensure sufficient metabolites when nutrients are low (100). AMPK can directly phosphorylate the autophagy proteins Ulk1/2 at multiple sites (99) and can also activate autophagy indirectly through suppression of mTORC1 signaling (99).

HOW NUTRIENT AVAILABILITY SHAPES CD4+ T CELL METABOLISM AND IMMUNE RESPONSES

The balance between protective immunity and chronic inflammation requires that T cells appropriately differentiate into the effector or regulatory lineages. In addition to multiple cues from the microenvironment, such as the presence of key cytokines, distinct metabolic programs also support the differentiation of CD4+ T cells into their separate functional subsets (2). For example, it is largely accepted that Th1, Th17, and Th2 effector

cells utilize higher rates of glycolysis, while Tregs preferentially use FAO (3). In addition, as immune responses are terminated, most effector CD4+ T cells undergo apoptosis, but some become memory T cells and revert back to OXPHOS and FAO. These memory T cells provide long-term protective immunity and do not rapidly proliferate in the absence of antigen rechallenge, and thus do not require high rates of glycolytic metabolism (2).

Effector T Cell Responses Are Dynamic Processes

Th1 Cell Function Is Highly Dependent on Environmental Levels of Nutrients

Th1 cells are considered highly glycolytic and glutaminolytic cells and rely on these pathways to support their growth and proliferation (3). Depriving naïve CD4+ T cells of glutamine during TCR stimulation results in generation of Foxp3+ Treg cells, even in the presence of Th1-polarizing conditions (101). The breakdown product of glutaminolysis, α-ketoglutarate, may act as a metabolic regulator for Th1 differentiation and proliferation by promoting the expression of T-bet and enhancing mTORC1 signaling (101). Therefore, although environmental depletion of glutamine might promote resolution of inflammation by favoring Treg cells, under other circumstances impaired Th1 responses could enhance pathogen spread, leading to aggravated tissue damage.

T cell activation and differentiation also depend on the availability of other amino acids. For example, LAT1, an L-type amino acid transporter responsible for the uptake of phenylalanine, tyrosine, leucine, arginine, and tryptophan, is required for proliferation and differentiation into Th1 and Th17 cells *in vitro* (102). Furthermore, a recent study linked the complement system to regulation of amino acid and glucose uptake in human Th1 cells (103). Signaling through CD46, a key costimulatory molecule and complement regulator expressed on human CD4+ T cells, was important for effective Th1 cell differentiation by potentiating TCR-driven Glut1 expression. Mechanistically, TCR/CD28 signaling induced the production of complement C3b that activated CD46 in an autocrine manner, resulting in the nuclear translocation of its cytoplasmic tail isoform CYT-1 (103). Nuclear CYT-1 induced transcription of LAMTOR5, which mediated upregulation of Glut1 and LAT1 and also activated mTORC1. These events were crucial for human Th1 cell differentiation as siRNA knockdown of CD46 or LAMTOR5 resulted in selective suppression of Th1 cells (103).

Glucose uptake and aerobic glycolysis is essential for IFNγ production in Th1 cells (104–106). Two mechanisms have been put forward to explain this observation. Chang et al. reported that the cytokine production is limited by the binding of the glycolytic enzyme GAPDH to the 3′ UTR of *ifng* mRNA, but this inhibition is diminished when GAPDH is engaged in its enzymatic function during glycolysis (104). More recently, Peng et al. proposed an epigenetic mechanism through which glycolysis promotes IFNγ production in Th1 cells (106). They found that expression of lactate dehydrogenase A (LDHA) in activated T cells was required to sustain aerobic glycolysis and support Th1 differentiation and that this was not dependent on the *ifng* 3′ UTR (106). Instead, LDHA-deficient T cells had severely reduced histone H3K9 acetylation (a marker associated with active transcription) at the *ifng* locus (106). Mechanistically, deletion of LDHA abrogated lactate production, thus shunting pyruvate into the mitochondria, which enhanced OXPHOS, but reduced citrate export out of the mitochondria leading to decreased cytosolic acetyl-CoA levels—the critical substrate needed for histone acetylation of gene loci through histone acetyltransferase (106). The importance of this pathway for Th1 responses *in vivo* was shown by their observations that conditional deletion of LDHA in T cells protected susceptible mice from Th1-mediated lethal auto-inflammatory disease (106). These studies suggest that when Th1 cells migrate to a glucose-deprived inflammatory environment, the reduced glucose availability will lead to a drop in glycolysis and decreased IFNγ production, possibly representing intrinsic negative feedback mechanisms to inhibit excessive Th1-mediated immune pathology.

Cellular Lipid Metabolism Supports Th17 Differentiation and Function

Th17 cells are largely confined to barrier sites such as the intestine, lungs, or skin, where they play a key role in defense from opportunistic pathogens and maintenance of epithelial barrier function (107, 108). However, it is also evident that their aberrant production of inflammatory cytokines is important in driving a number of autoimmune diseases (109, 110). Recent evidence suggests that lipid metabolic pathways play a role in regulating the dichotomous function of Th17 cells under normal and pathogenic conditions (111–113).

Lipogenic pathways are a crucial part of T cell metabolic reprogramming, as proliferating T cells require fatty acids for membrane synthesis and also for a plethora of other cellular processes, such as signaling and energy production. Activated T cells rapidly augment fatty acid synthesis (FAS) while concomitantly decreasing FAO (93). Of note, free fatty acids have been found to be highly enriched in the inflamed tissues of conditions associated with excess fat deposits, such as obesity and atherosclerosis (10). FAS takes place in the cytosol and commences with ATP consumption through the carboxylation of acetyl-CoA to malonyl-CoA, a reaction catalyzed by acetyl-CoA carboxylase 1 (ACC1) (114). By contrast, FAO occurs mainly in the mitochondria and involves generation of acetyl-CoA, which can be directly shuttled into the TCA cycle and further oxidized to generate ATP *via* OXPHOS. The enzyme acetyl-CoA carboxylase 2 is located in the inner mitochondrial membrane and promotes mitochondrial FAO (111).

These fatty acid metabolic pathways have emerged as important regulators of Th17 function. ACC1 can regulate the balance between Th17 and Treg cells, as pharmacological or genetic blockade of ACC1 impaired differentiation of human and mouse Th17 cells but favored the induction of Foxp3+ Treg cells (111). The authors proposed that Th17 cells use ACC1-driven FAS to produce phospholipids for cellular membranes, while Treg cells actively take up exogenous fatty acids to sustain their proliferation (111). Consistent with these results, in a GVHD model, mice adoptively transferred with ACC1-deficient T cells showed reduced mortality and also higher frequencies of Treg cells in

the colon in comparison with mice that received WT T cells (115). In addition, the intracellular levels of different fatty acid species may affect the pathogenicity of Th17 cells by modulating their cytokine responses. Single-cell RNA-sequencing of Th17 cells generated under pathogenic or non-pathogenic polarizing conditions implicated expression of *Cd5l*, encoding CD5 antigen-like (CD5L) protein (also known as AIM), as a regulator of Th17 cell pathogenicity (112). CD5L is a member of the scavenger receptor cysteine-rich superfamily involved in lipid metabolism, specifically in inhibition of fatty acid synthase (116). Although the mechanism remains incompletely understood, CD5L seemed to alter the intracellular balance between polyunsaturated and saturated fatty acids, thus affecting the function of two metabolic genes—*cyp51* and *sc4mol*—that synthesize ligands for RORγt, a Th17 master transcription factor (112, 113). This in turn might lead to increased RORγt binding at the anti-inflammatory genes (*IL-10)* and reduced binding at the *IL-17* and *IL-23r* loci (pro-inflammatory genes) in Th17 cells (113).

Another cell-intrinsic metabolic pathway that has been associated with a pathogenic Th17 phenotype is mTORC1. Sasaki et al. reported that deletion of *p70S6KI* (which encodes a serine/threonine kinase that is downstream from mTORC1) resulted in decreased expression of Th17-associated genes, including *il17a*, *il17f*, and *il23r* (117). By contrast, differentiation into Treg, Th1, or Th2 cells was not altered in the absence of *p70S6KI*, suggesting that it plays a selective role in the differentiation of Th17 cells (117). Consistent with these findings, *p70S6KI*-knockout mice exhibited delayed development of EAE (117).

Given the low oxygen availability at inflammatory sites, it is perhaps unsurprising that HIF-1α also plays a crucial role in adapting the T cell metabolic program to the hypoxic conditions and skewing the balance between Th17 inflammatory cells and Treg immunosuppressive cells. HIF-1α promotes glycolysis and increases the expression of RORγt while targeting Foxp3 for proteasomal degradation (4, 46). Indeed, deletion of HIF-1α in CD4+ T cells abrogated Th17 development and promoted Treg cell differentiation, even under Th17 culture conditions (4, 46). Further evidence that the hypoxic environment influences Th17 function comes from a study in which human Th17 cells differentiated *in vitro* under hypoxic conditions (1% O_2) had increased secretion of the anti-inflammatory cytokine IL-10 (118).

Furthermore, another recent study reported that *in vitro* differentiated Th17 cells use both OXPHOS and glycolysis, whereas Th17 cells isolated from steady state and inflamed tissues rely on OXPHOS to generate the energy required for cytokine production (119). Consistent with these findings, administration of the OXPHOS inhibitor oligomycin reduced inflammatory Th17 cytokine production *in vivo* and decreased pathology in a mouse model of colitis (119). Higher expression of pyruvate dehydrogenase kinase 1 (PDK1) by *in vitro*-generated Th17 cells correlated with their enhanced glycolytic metabolism (119), consistent with a previous report that PDK1 was essential for Th17 differentiation *in vitro* (120). *In vitro* differentiation of T-helper cell subsets is widely used to generate large numbers of effector cells for analyses. However, these findings regarding Th17 cells indicate that the *in vitro* differentiation conditions may affect the metabolic phenotype of the cells, which in turn could endow them with slightly different functional characteristics than their *in vivo* counterparts.

Th2 and Th9 Cells Depend on mTOR Function and Glycolytic Metabolism

Several inflammatory pathologies are associated with a Th2 cell component, including diseases associated with IgE and type 2 cytokine secretion (IL-4, IL-5, and IL-13), such as allergy, chronic asthma, and atopic dermatitis (121).

Physiological type 2 immune responses seem associated with an oxidative metabolism, as Th2 cytokines (IL-4 and IL-13) activated an STAT6-dependent program of oxidative metabolism involving peroxisome proliferator activated receptors γ and δ (PPARγ and PPARδ) in macrophages (122). Interestingly, several recent studies have also implicated PPARγ in effector Th2 function (123–125). For example, activation of the TCR/CD28-mTORC1 pathway facilitated complete activation and proliferation of Th1 and Th2 cells by promoting fatty acid uptake through increased expression of PPARγ (123). In addition, PPARγ was critical for Th2 cell responses to house dust mite and *Heligmosomoides polygyrus* antigens, as mice lacking PPARγ failed to generate IL-5- and IL-13-producing Th2 cells (124, 125). Mechanistically, PPARγ was necessary for the upregulation of the IL-33 receptor on differentiating Th2 cells in the lung, thereby promoting full Th2 effector responses. This may suggest that oxidative metabolism may have a role in the effector function of Th2 cells and promotion of pathogenic responses. However, it is important to point out that *in vitro*-polarized murine Th2 cells exhibited high glycolytic rates, similar to Th1 and Th17 cells (3, 4).

Although mTORC1 signaling is needed for Th2 lineage commitment (126), multiple studies support a role for mTORC2 as a preferential signaling pathway in the differentiation, function, and metabolism of Th2 cells (127, 128). For example, Rheb-deficient mice have impaired mTORC1 function and fail to generate Th1 and Th17 cells but are able to differentiate Th2 cells (128). Conversely, T cells from Rictor-deficient mice, in which mTORC2 activation is impaired, fail to differentiate into Th2 cells but are able to generate Th1 and Th17 cells (128). In addition, SGK1, another downstream target of mTORC2, was shown to promote commitment to the Th2 cell lineage while simultaneously blocking differentiation into the Th1 lineage (129). SGK1 prevents degradation of JunB (129), which was previously described as a Th2 cell-specific transcription factor that regulates the Th2 cytokine program (130). Moreover, genetic deletion of the GTPase RhoA, a downstream target of mTORC2, decreased glycolysis and impaired IL-4 production in murine Th2 cells, and protected mice against airway inflammation in an OVA-induced model of allergic asthma (131). Consistent with these observations, a recent genome-wide transcriptional profiling study of human Th2 cells isolated from allergic asthma patients found a positive correlation between c-Myc expression and disease status (132), again pointing toward glycolysis as a marker of Th2 cell pathogenicity. Although it seems difficult to reconcile these reports with the studies above that implicated FAO in Th2 function, it may be that metabolic flexibility is important for optimal differentiation and function of Th2 cells. Thus, while mTORC2-driven glycolysis might be primarily required for differentiation and proliferation

of Th2 cells, a mixed metabolic profile, incorporating both FAO and glycolytic activity, may be important to sustain effector Th2 cells in peripheral tissues.

Th9, characterized by the production of IL-9, are closely linked to Th2 cells (133). Th9 effector cells develop from naïve CD4+ T cells in the presence transforming growth factor-β (TGF-β) and IL-4, secrete IL-9 in large amounts, are also known to produce IL-10 and IL-21, and have been implicated in some inflammatory allergic processes, such as asthma (134). A recent study shed some light on the metabolic properties of Th9 cells. Wang et al. reported that *in vitro* differentiated Th9 cells were highly glycolytic in comparison with Th1, Th2, Th17, or Treg cells (47) and identified SIRT1 (sirtuin-1) as a negative regulator of Th9 cells. SIRT1 is an NAD^+-dependent enzyme that can deacetylate histone residues on chromatin, but it has also been proposed to act as an NAD^+-dependent metabolic sensor (135). SIRT1 was shown to inhibit Th9 cell differentiation *in vitro* and mice harboring a T cell-specific deletion of SIRT1 exhibited exacerbated airway inflammation in an OVA-induced allergy model (47). Further investigations linked TAK1 (TGF-β activated kinase), an important mediator of TGFβ signaling, with active suppression of SIRT1 in Th9 cells. The study proposed that TAK1 suppression of SIRT1, coupled with an increased mTORC1-driven glycolytic metabolism, was crucial for Th9 cell differentiation (47).

T Follicular Helper (Tfh) Cells Are Metabolically Adapted to the Germinal-Center (GC) Environment

T follicular helper cells are characterized by the expression of the chemokine receptor CXCR5, the inducible T cell costimulator ICOS, the transcription factor Bcl-6, and the production of IL-21 (136). They have a critical role in the formation and maintenance of GCs that promote the generation of affinity matured B cells (136). Several studies have linked dysregulated Tfh cell responses with autoimmune disease (137), and inflammatory sites often develop lymphoid aggregates, termed ectopic lymphoid structures (ELS), which act like functional GCs and comprise B cells and Tfh-like cells (138). The conditions within the ELS present at the inflammatory sites remain unknown; however, one could speculate that they would resemble those present in GCs.

German centers are restricted microenvironments where antigen-activated B cells undergo clonal expansion and introduce point mutations into the hypervariable regions of the BCR genes to allow for affinity maturation (139). GCs are organized into two distinct zones (termed light and dark) and B cells repeatedly cycle through the zones as they mature (139). The dark zone is associated with rapid B cell proliferation, while the light zone is traditionally associated with B cell affinity maturation and class switching, requiring help from Tfh cells (136). Cho et al. showed that mouse GC light zones are hypoxic environments with increased levels of HIFs which limit the proliferation and survival of GC B cells (140). Although this hypoxic environment may seem detrimental for B cell development, it may act as a threshold for B cell selection, reducing the risk of abnormal B lymphocyte development (140). An independent study confirmed the hypoxic nature of the GC microenvironment and showed that reversing hypoxia by placing mice in chambers containing 60% O_2 resulted in a decreased frequency of Tfh cells, reduced GC formation and impaired class switching following immunization (141). Thus, the hypoxic environment sustains the GC reaction and positively impacts on Tfh function.

Moreover, given that GCs are sites of constant proliferation it is likely that the availability of glucose and of other nutrients might be limited. Precisely how Tfh cells adapt to the metabolic demands of the GC microenvironment is not completely understood, but some studies have postulated that a restriction in mTORC1 activation may be involved. It was reported that hypoxia inhibits mTORC1 activation in GC B lymphoblasts through an HIF-1-dependent mechanism that limits the expression of amino acid transporters (140). Whether the same mechanism operates in Tfh cells is unclear, but decreased mTORC1 activity was reported to favor Tfh cell differentiation at the expense of Th1 and T-bet expression (142). Using an acute viral infection model, Ray et al. showed that shRNA silencing of mTOR or Raptor promoted Tfh cell differentiation, while silencing of Rictor had minimal effects on Tfh cells and instead promoted Th1 development (142). In addition, they found that Tfh cells were less glycolytic than Th1 cells and instead relied mainly on mitochondrial respiration (142). The authors suggested that this might be driven by Bcl-6, as overexpression of Bcl-6 in naïve CD4+ T cells recapitulated the metabolic characteristics observed in Tfh cells (142). This suggestion is consistent with previous reports in which Bcl-6 was described to downregulated genes associated with glycolysis (143, 144). Overall, these findings suggested that inhibition of mTORC1 signaling and glycolytic metabolism play an important role in the Tfh cell adaptation to the GC environment. However, recent studies using a CD4-Cre approach to drive T cell-specific deletion of Raptor or Rictor highlighted a requirement for both mTORC1 and mTORC2 in Tfh differentiation (145, 146). Thus, deletion of Raptor (mTORC1) or Rictor (mTORC2) in T cells led to decreased GC formation and Tfh differentiation upon antigen immunization or viral challenge (145, 146). Furthermore, Zeng et al. observed that *in vitro* differentiated Tfh-like cells expressed elevated levels of Glut1 in comparison with activated non-Tfh cells. Similarly, Glut1 expression was higher on Tfh cells than non-Tfh cells isolated from Peyer's patches (PP), both at steady state and upon foreign antigen challenge (146). Given that mTORC1 is required for T cell quiescence exit, Zeng et al. also explored the effects of conditional deletion of Raptor or Rictor in mature peripheral CD4+ T cells using an OX40-Cre driver. They found that conditional deletion of Raptor or Rictor in activated CD4+ T cells led to severely reduced GC formation and Tfh cell responses in PP, both at steady state and upon viral infection (146). Thus, these studies argue for positive and non-redundant roles for mTORC1 and mTORC2 in Tfh cell differentiation.

The contradicting results reporting positive or negative effects of mTORC1 and mTORC2 activation in Tfh responses are difficult to reconcile, but some of the differences might be due to the approaches used to delete or silence components of the mTOR-signaling pathway, as well as the potential differences between *in vitro* or *in vivo* generated Tfh cells. It may be that while both mTORC1 and mTORC2 are required for Tfh generation, tempering the levels of mTORC1 activation may facilitate optimal Tfh responses in GC.

Foxp3+ Treg Cells Are Endowed With Metabolic Flexibility

$CD4^+Foxp3^+$ Treg cells produce immunosuppressive cytokines such as IL-10 and TGF-β and are critical for maintaining immune tolerance and preventing deleterious inflammatory responses (147). Treg cells have distinct metabolic requirements and have been described to preferentially rely on OXPHOS driven by lipid oxidation, rather than glucose, for ATP production (3). However, recently it has been suggested that metabolic adaptations of Treg cells are context dependent and are influenced by factors such as Treg cell origin or anatomical distribution (148), although, it still remains largely undetermined how distinct subpopulations of Tregs, i.e., thymic derived (tTregs), peripherally induced (pTregs), and *in vitro* generated iTregs, differ metabolically.

The transcription factor Foxp3, which is indispensable for Treg development, function, and maintenance, was recently demonstrated to also play a major role in regulating their metabolism. It was found that Foxp3 expression was sufficient for the increased OXPHOS activity observed in mouse $Foxp3^+$ iTreg cells generated *in vitro* and that Foxp3 increased expression of ETC protein complexes that may influence Treg suppressive abilities (149, 150). In addition, Foxp3 may decrease glycolysis by inhibiting c-Myc expression through binding to the TATA box of the *Myc* gene (149). In some circumstances, aberrant increases in glycolytic activity in $Foxp3^+$ Treg cells have been associated with their dysfunction and consequent inflammation (151, 152). Murine iTregs express low levels of the glucose transporter Glut1 in comparison with effector T cells, but comparable levels to naïve T cells (3) and in human Treg cells, Glut1 expression is thought to be limited by Foxp3 through inhibition of Akt (153). Consistent with these findings, murine Treg cells overexpressing a transgenic Glut1 receptor had reduced CD25 and Foxp3 expression and could not suppress colitis in an adoptive transfer model (154).

However, it appears that increased mTORC1 activity and glycolytic metabolism might be necessary to ensure adequate Treg cell proliferation under inflammatory conditions. Evidence suggests that inflammatory stimuli and Foxp3 have opposing effects on Treg proliferation and function by differentially regulating mTORC1 and glucose metabolism. Thus, treatment of activated Treg cells with a TLR1/TLR2 agonist enhanced activation of mTORC1 and increased their proliferation but impaired their suppressive function (154). By contrast, Foxp3 expression in Treg inhibits mTORC1 signaling and glycolysis but promotes oxidative metabolism and slows their proliferation (154). These findings are consistent with previous studies showing that excessive mTORC1 activity impairs Treg function (1, 155) and with the recent discovery that Treg cells engage the serine–threonine phosphatase PP2A to suppress mTORC1 activity (156). However, other work reported that the induction and suppressive function of human iTreg cells, generated by suboptimal TCR stimulation, was tightly dependent on glycolysis (157). Mechanistically, the authors proposed that glycolysis controls the expression of the full-length *FOXP3* containing exon 2 splice variant (Foxp3-E2), responsible for the suppressive activity of Treg cells, through the glycolytic function of enolase-1 enzyme (157). Of note, human Tregs are highly proliferative *in vivo* but are hyporesponsive to TCR stimulation *in vitro* (158). Thus, it is likely that they engage glycolysis in certain contexts. Indeed, comparative proteomic analyses of human Treg and Tconv cells found that freshly isolated human Treg cells were highly glycolytic and proliferative, while *in vitro* proliferating human Tregs engaged glycolysis, but also FAO (158). In comparison, Tconv cells switched from OXPHOS to aerobic glycolysis upon *in vitro* activation (158). This again underscores that the metabolic phenotype of T cells is heavily influenced by their environmental differentiation conditions.

Overall, one could speculate that at the beginning of inflammatory process, when glucose is still available for proliferating T cells, Treg cells use glycolytic metabolism to increase their numbers, while during chronic inflammation when glucose is scarce their reliance on OXPHOS and FAO might enable them to perform suppressor functions in the effort to resolve the inflammatory process. In addition, it is also conceivable that the utilization of glucose by proliferating Treg cells could be another mechanism of immunosuppression, by depriving effector T cells of this nutrient.

Nutrient-Depleted Environments Support Immunosuppressive Responses

As detailed in Section "The Inflammatory Microenvironment," the inflammatory site is characterized by high concentrations of lactate and low-glucose levels. Previous reports have shown that L-lactate strongly suppresses effector T cells (26, 29, 159) (Scharping) and that T cells do not proliferate in glucose-deficient media (16). However, a recent study suggested that high concentrations of L-lactate do not affect Treg proliferation or their suppressive function under conditions of reduced glucose supply (149). The authors proposed that the metabolic advantage of Tregs in high lactate environments could be based on resistance to NAD^+ depletion. Teff cells rely on aerobic glycolysis to proliferate and reduce NAD^+ to NADH during the breakdown of glucose to pyruvate. Lactate dehydrogenase (LDH) further catalyzes the reduction of pyruvate into lactate (149). However, in a high lactate environment, LDH favors the reverse reaction, converting lactate to pyruvate while using NAD^+ as a cofactor. Thus, Teff cells face a redox imbalance when insufficient NAD^+ is present and glycolysis cannot proceed (149). By contrast, in Treg cells, Foxp3 inhibits glycolysis and promotes OXPHOS, which allows the cells to generate NAD^+ by oxidation in the TCA cycle (149). In addition, another recent report showed that Tregs may have developed a preference for FAO metabolism to avoid fatty acid-induced cell death (150). Long-chain fatty acids, such as palmitate, are known to have proapoptotic effects through various mechanisms, including depolarization of the mitochondrial action potential and generation of ROS (160). This study showed that Foxp3 endows Treg cells with an increased ability to utilize fatty acids as fuel for OXPHOS by upregulating the enzymes involved in FAO, thus increasing resistance to long-chain fatty acid-induced apoptosis (150).

Regulatory T cells also seem to have enhanced resistance to amino acids deprivation. For example, depriving $CD4^+$ T cells of glutamine during activation results in generation of $Foxp3^+$ Treg cells, even in the presence of Th1-polarizing conditions (101). Similarly, deficiencies in the amino acid transporters Slc7a5 and Slc1a5 (ASCT2) impaired glutamine uptake and decreased

Teff cell differentiation without affecting the generation of Treg cells (102, 161). Moreover, Treg cells can stimulate dendritic cells to express enzymes that catabolize essential amino acids, thus reducing their availability in the local microenvironment. Consequently, this limits Teff cell differentiation and further promotes the expression of Foxp3 cells by CD4+ T cells (162).

Thus, Tregs show a high degree of flexibility in fuel choice, and the ability to increase their OXPHOS capacity might represent a survival advantage in conditions of low nutrients. In addition, their adaptations to nutrient-deplete environments might give them a survival advantage at the inflammatory site and thus the ability to outlive the Teff cells and trigger the resolution of the inflammatory process.

Treg Cells Adapt to the Tissue Environment by Promoting Autophagy and Nutrient Recycling

It is also worth considering that inhibition of catabolic processes, such as autophagy, can alter the availability of nutrients thus leading to dysregulations in cell metabolism. Two recent studies described a crucial role for autophagy in regulating cellular metabolism of peripheral Treg cells. Kabat et al. generated mice in which the essential autophagy gene *Atg16l1* was selectively deleted in Foxp3+ Treg cells and found that these animals developed severe spontaneous multiorgan inflammation by 5 months of age (151). This was characterized by an accumulation of Th effector subsets and a drastic depletion of Foxp3+ Treg (151). Further analyses revealed that *Atg16l1*-deficient Treg cells had higher expression of glycolytic genes than Treg cells from control mice, whereas genes involved in FAS/FAO were markedly decreased (151). These metabolic differences were much more pronounced in Treg cells originating from the colonic lamina propria than from the spleen (151). Consistent with these findings, a parallel study reported that mice with selective deletion of the essential autophagy genes Atg7 or Atg5 in FoxP3+ Treg cells developed severe multiorgan inflammation by 5 months of age (152). *Atg7*-deficient Treg cells from these animals had aberrant mTORC1 activity, associated with increased c-Myc expression and heightened glycolytic metabolism (152). Although precisely how autophagy deficiency in Treg cell impairs their survival remains to be elucidated, these studies suggest that autophagy is important for Treg metabolic flexibility, particularly required for adaptations in peripheral tissues (151).

THERAPEUTIC PERSPECTIVES

As we have described so far, different CD4+ Th subsets are associated with overlapping but distinct metabolic profiles. This leads to the attractive hypothesis that targeting metabolic pathways could underpin new therapeutic strategies for immune and inflammatory diseases. Several studies have attempted to manipulate the effector function of lineage-committed T cells through interventions directed at metabolic pathways. For example, targeting PDK1 with dichloroacetate selectively inhibited the survival, function, and proliferation of Th17 cells and diminished inflammation in models of colitis and EAE (120). Similarly, blocking the ACC enzymes involved in *de novo* FAS with Soraphen A was shown to bias T cell differentiation away from Th17 cell development and toward a Treg fate (111). Therapeutic strategies like these could be exploited in autoimmune diseases with a strong Th17 component, such as multiple sclerosis. Also, depending on the setting, T cells may use distinct metabolic phenotypes to adapt to their environment, in nutrient scarce inflammatory environments, CD4+ T cells have to compete for nutrients with other leukocytes, as well as parenchymal and stromal cells. Therefore, another potential way to interfere with T cell metabolism is by blocking nutrient transporters on the cell surface. The solute-carrier (SLC) receptor superfamily are membrane-bound transporters that carry various molecules, including glucose and amino acids, across the cell membrane (163). Transporter families often have multiple isoforms with distinct substrate specificities and different expression levels between different cell populations, suggesting that developing a selective therapy that targets only a particular Th cell subset might be possible. For example, L-type amino acid transporter 1 (LAT1 or SLC7A5) is the main large neutral amino acid transport in activated T cells and genetic deletion of this transporter prevented the proliferation of CD4+ T cells, but their ability to differentiate into Treg cells was preserved (102). Moreover, pharmacological inhibitors of SLC7A5 were shown to constrain the inflammatory function of cytotoxic T cells (102).

Given the multitude of roles that the mTOR signaling pathways play in CD4+ T cell differentiation and function it is not surprising that mTOR inhibition has been sought as a potential therapy for chronic inflammatory conditions. The first known pharmacological inhibitor of mTOR, rapamycin, was originally developed as an immunosuppressive agent for organ transplant rejection, and mTOR was subsequently identified as its molecular target (164). The observations that the mTOR pathway differentially modulates Treg cells compared with effector Th1/Th17 cells provided additional rationale for pharmaceutical targeting of mTOR in human disease (1). In addition, overactivation of mTOR signaling through deletion of TSC1, an upstream negative regulator of mTOR, leads to reduced Treg suppressive activity in a mouse model of colitis (165). Another study showed that pharmacological inhibition of mTORC1 ameliorated DSS-induced colitis through reduced differentiation of both Th1 and Th17 cells (166). Consistent with these differential effects on Teff cells and Treg cells, mTORC1 inhibitors have been used as adjuncts during *ex vivo* expansion of human iTregs, to stabilize Foxp3 expression and function, while preventing outgrowth of Teff cells (167). These human iTregs maintained their suppressive activity after transfer into immunodeficient mice, suggesting that therapeutic Treg regimes may be enhanced by inhibiting mTORC1 (167).

It is clear that modulating metabolism *via* mTOR has potent effects on CD4+ T cells. However, mTOR plays a role in many different cells, and non-selective manipulation of this pathway has a high potential for deleterious side effects. Indeed, a wide range of adverse effects are associated with rapamycin treatment, including metabolic abnormalities (hyperlipidemia), skin reactions, and increased opportunistic infections (164).

Therapies aimed at other molecular targets within metabolic pathways are under development. Considering the capacity of AMPK to halt anabolic metabolism it is possible that targeting AMPK activation could lead to regulation of inflammatory T cell

function. A few studies have already examined the effects of pharmacological activators of AMPK in T cells. Metformin is a widely used drug in the management of type 2 diabetes due to its benefits in relation to glucose metabolism (168). However, several studies have suggested additional beneficial roles for metformin in cardiovascular protection, cancer targeting, or aging (169). Although the mechanism of action of metformin is incompletely understood, it is thought that metformin suppresses glucose production in the liver. At the cellular level, it is largely accepted that metformin inhibits mitochondrial respiration, but how this is transduced to the health promoting effects of metformin remains unclear, and metformin has been described to act *via* both AMPK-dependent and AMPK-independent mechanisms (168). By blocking mitochondrial respiration, metformin prevents ATP production and thus leads to an increased cytoplasmic ratios of ADP:ATP and AMP:ATP, leading to activation of AMPK (170). Activated AMPK inhibits FAS and instead promotes FAO, reducing hepatic lipid stores and enhancing insulin sensitivity. It was recently shown that metformin's mechanism of action relies on the nuclear pore complex (NPC) and the enzyme acyl-CoA dehydrogenase family member-10 (ACAD10) (171). By suppressing mitochondrial respiratory capacity, metformin reduces cellular ATP, restricting transit of the GTPase RagA/RagC heterodimer through the NPC, thus preventing activation of mTORC1. This subsequently enhances the transcriptional induction of ACAD10 and both the NPC and ACAD10 are required for the functional effects of metformin (171).

Treating mice with metformin has shown positive effects in several inflammatory disease models, including experimental autoimmune encephalomyelitis (172), IBD (173, 174), and GVHD (174). These studies associated metformin treatment *in vivo* with a reduction in Th17 cells and a rise in Treg cells (172–174). However, Gualdoni et al. recently compared the impact of metformin and AICAR (5-aminoimidazole-4-carboxamide ribonucleoside—a direct pharmacological activator of AMPK) and showed that only AICAR could boost Treg cell differentiation and inhibit Th17 differentiation *in vitro* (175). Combination treatments with metformin have also been trailed in preclinical models of inflammatory disease. For example, Yin et al. reported that $CD4^+$ T cells isolated from systemic lupus erythematosus (SLE) patients displayed increased glycolysis and OXPHOS. Simultaneous blockade of these two pathways with 2-deoxyglucose (2DG) and metformin normalized T-cell metabolism and reversed disease biomarkers in a mouse model of SLE (176). In addition, wild-type mice treated with 2DG and metformin did not show signs of toxicity and maintained normal immune function (176).

As previously mentioned, low plasma and tissue glutamine concentrations have been associated with inflammatory conditions, including sepsis and Crohn's disease. In addition, glutamine has been shown to have beneficial effects on intestinal barrier integrity by enhancing enterocyte proliferation and protecting against enterocyte apoptosis (177). These observations led to the hypothesis that glutamine supplementation may be beneficial for inflammatory conditions, particularly in those disease relating to impaired gut function. However, the clinical benefit of glutamine supplementation remains controversial, and a meta-analysis of clinical trials in critically ill patients failed to identify a significant positive effect of glutamine supplementation (178). Moreover, a glutamine-enriched diet in pediatric patients with Crohn's disease even leads to increased disease activity in some of the subjects (179). Given that the glutamine metabolite α-ketoglutarate was shown to promote Th1 differentiation (101), the potential benefits of glutamine on promoting mucosal barrier health may be negated by the immune-enhancing effects of glutamine on Teff cells.

The therapeutic strategies mentioned earlier illustrate the immunomodulatory potential of targeting metabolic pathways. However, it remains to be explored how targeting T cell metabolism will affect the function of other immune subsets, such as B cells and innate immune cells, which also play a key role in driving chronic inflammatory diseases.

CONCLUDING REMARKS

In chronic inflammatory diseases, T cells infiltrate and are retained at the affected site where they drive the destruction of the surrounding tissues. The inflammatory environment is a site of active leukocyte proliferation; however, here, the cells are exposed to numerous restrictive factors: hypoxic conditions, high lactate, low pH, decreased glucose and amino acids concentrations as well as increased levels of ROS. Nutrient deprivation might actually be a mechanism through which the environment regulates T cell function. The evidence presented in this review promotes the concept that Treg cells seem better equipped than Teff cells to handle nutrient starvation. The active recruitment and proliferation of leukocytes at the inflamed tissue may also contribute to the limited availability of nutrients, allowing the balance to be tilted toward Treg activity that could temper the inflammatory response.

Although we do not have much data on how nutrient availability is altered in inflamed human tissues, we can obtain some useful information by metabolic profiling of biologic samples, such as serum or urine. A recent study performed a large-scale profiling of the urine metabolome from patients with six different common inflammatory diseases: RA, psoriatic arthritis, psoriasis, SLE, Crohn's disease, and ulcerative colitis (180). They found that decreased concentrations of urine citrate, an intermediate in the TCA cycle, correlated with high disease activity in patients compared with controls (180). Several studies looking at sera samples from RA patients highlighted distinct metabolic features, including decreased levels of amino acids and glucose, along with increased levels of fatty acids and cholesterol (181–183). Moreover, metabolomic studies of the serum of MS patients revealed an excess of ROS and reactive nitrogen species (184, 185), and recent studies reported that increased glucose metabolites in the cerebrospinal fluid and serum of MS patients were positively correlated with disease progression and activity (186, 187).

A key question that arises from the studies presented in this review is how closely do *in vitro* culture models recapitulate the *in vivo* microenvironment conditions present at inflammatory sites? The vast majority of *in vitro* assays are performed at nutrient and oxygen levels that are higher than those observed in tissue. Thus, the metabolic influence that the inflammatory environment exerts on T cell function *in vivo* may account for

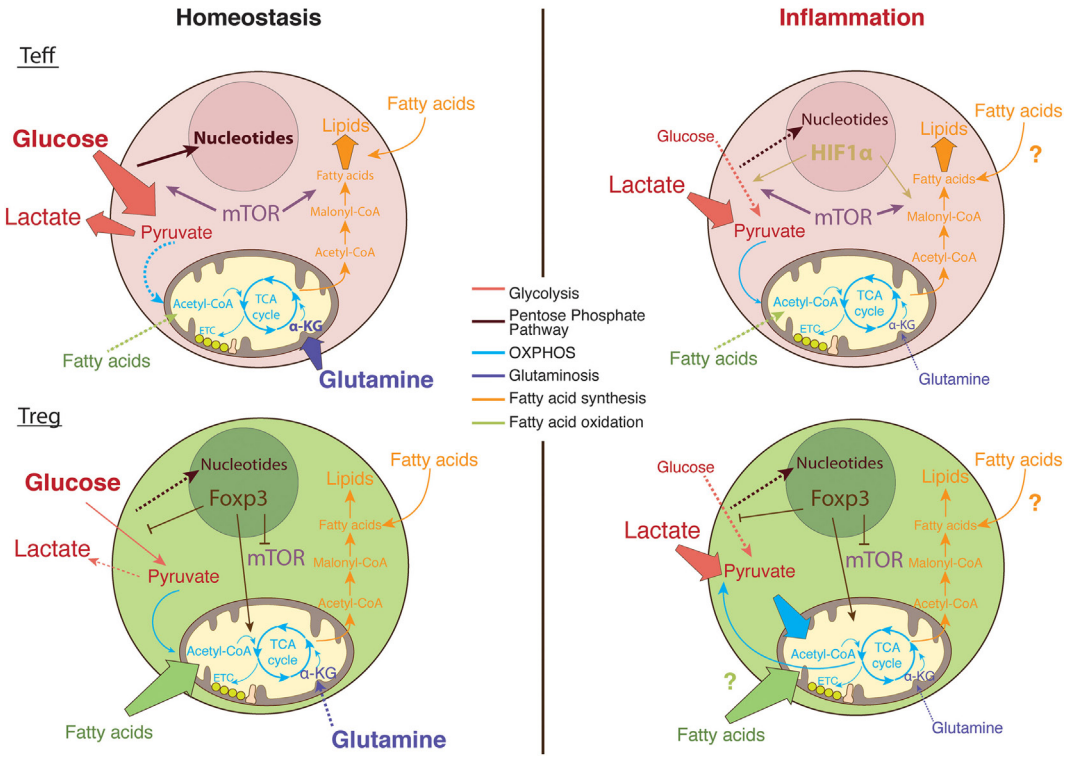

FIGURE 3 | The metabolic pathways utilized by T cells in nutrient replete versus metabolically challenging environments. Under homeostatic conditions, glucose enters the cytosol of activated T cells and is converted into pyruvate *via* glycolysis (89). Pyruvate can either be further metabolized into lactate and secreted or entered into the tricarboxylic acid (TCA) cycle to generate ATP *via* the electron transport chain (ETC) in the process of oxidative phosphorylation (OXPHOS) (120). Moreover, the glucose breakdown intermediates produced during glycolysis can be metabolized *via* the pentose phosphate pathway donating important building blocks for nucleotide and amino acid synthesis (89). Activated Teff cells rapidly augment fatty acid synthesis while concomitantly decreasing fatty acid oxidation (FAO). In comparison, regulatory T (Treg) cells actively take up exogenous fatty acids to sustain their proliferation through FAO (111). In addition, Teff cells rely on glycolysis and glutaminolysis to proliferate and obtain the necessary cofactors for survival while Tregs differentiation is enhanced in glutamine-deprived environments (3, 101). Foxp3 plays a major role in regulating the metabolic pathways necessary for Treg cells function by upregulating OXPHOS activity (149, 150), blocking mechanistic target of rapamycin (mTOR) signaling (156), and glycolysis (149). In the inflamed tissue, in low oxygen conditions, Teff cells upregulate survival mechanisms including the oxygen-sensitive transcription factor, hypoxia-inducible factor (HIF)-1α. HIF-1α promotes anaerobic metabolism through increased expression of glucose transporters, as well as induction of glycolytic enzymes (4, 45). However, glucose supply is limited in the inflamed tissue while lactate is abundant; therefore, T cells favor the conversation of lactate to pyruvate. Tregs are able to sustain the use of lactate-derived pyruvate as a source of energy through the generation of NAD^+ during OXPHOS (149).

experimental inconsistencies observed between T cell responses *in vitro* and in animal models. In addition, studies often assess the impact of single factors on T cell function, for example, either hypoxia or glucose depletion. However, these factors should also be analyzed in combination to establish a better understanding of the dynamic and synergistic effects, the inflammatory landscape plays on T cells. As discussed earlier, many metabolic activities are regulated to some extent by circadian rhythms, and several experimental studies have shown that immune parameters, including T cell responses, can vary based on the time of day procedures are performed (73, 188, 189). These observations suggest that such metabolic fluctuations could impact on the reproducibility of immunological data across experiments, and this should be considered during experimental design, particularly for *in vivo* experiments in rodents.

It remains to be fully determined how the complex T cell metabolic machinery handles the microenvironment at the inflamed site and how this shapes T cell intracellular signaling pathways and gene transcription (**Figure 3**). Understanding how the metabolic pathways that fuel T cell function and proliferation differ within the inflammatory environment may lead to targeted therapeutic strategies for chronic inflammatory diseases, with a few of these therapies already shown promising preliminary results.

AUTHOR CONTRIBUTIONS

CD, AK, and KM all contributed to the writing of this review.

FUNDING

KM is funded by a Wellcome Trust Investigator Award (102972) and by an MRC project grant (MR/N02379X/1). CD is supported by a Heatley-Merck, Sharp and Dohme studentship. AK is supported by a Humboldt Foundation postdoctoral fellowship.

REFERENCES

1. Delgoffe GM, Kole TP, Zheng Y, Zarek PE, Matthews KL, Xiao B, et al. The mTOR kinase differentially regulates effector and regulatory T cell lineage commitment. *Immunity* (2009) 30:832–44. doi:10.1016/j.immuni.2009.04.014
2. Buck MD, O'Sullivan D, Pearce EL. T cell metabolism drives immunity. *J Exp Med* (2015) 212(9):1345–60. doi:10.1084/jem.20151159
3. Michalek RD, Gerriets VA, Jacobs SR, Macintyre AN, MacIver NJ, Mason EF, et al. Cutting edge: distinct glycolytic and lipid oxidative metabolic programs are essential for effector and regulatory CD4(+) T cell subsets. *J Immunol* (2011) 186:3299–303. doi:10.4049/jimmunol.1003613
4. Shi LZ, Wang R, Huang G, Vogel P, Neale G, Green DR, et al. HIF1α-dependent glycolytic pathway orchestrates a metabolic checkpoint for the differentiation of Th17 and Treg cells. *J Exp Med* (2011) 208:1367–76. doi:10.1084/jem.20110278
5. Ashley NT, Weil ZM, Nelson RJ. Inflammation: mechanisms, costs, and natural variation. *Annu Rev Ecol Evol Syst* (2012) 43:385–406. doi:10.1146/annurev-ecolsys-040212-092530
6. Serhan CN, Ward PA, Gilroy DW. *Fundamentals of Inflammation*. Cambridge: Cambridge University Press (2010).
7. Schmid-Schönbein GW. Analysis of inflammation. *Ann Rev Biomed Eng* (2006) 8:93–151. doi:10.1146/annurev.bioeng.8.061505.095708
8. Medzhitov R. Origin and physiological roles of inflammation. *Nature* (2008) 454:428–35. doi:10.1038/nature07201
9. Kominsky DJ, Campbell EL, Colgan SP. Metabolic shifts in immunity and inflammation. *J Immunol* (2010) 184:4062–8. doi:10.4049/jimmunol.0903002
10. Haas R, Marelli-Berg F, Mauro C. In the eye of the storm: T cell behavior in the inflammatory microenvironment. *Am J Clin Exp Immunol* (2013) 2:146–55.
11. Thomas DPP, Dingle JTM. In vitro studies of rheumatoid synovium – preliminary metabolic comparison between synovial membrane and villi. *Br J Exp Pathol* (1955) 36:195–8.
12. Treuhaft PS, Mccarty DJ. Synovial fluid pH, lactate, oxygen and carbon dioxide partial pressure in various joint diseases. *Arthritis Rheum* (1971) 14:475–&. doi:10.1002/art.1780140407
13. Yang XY, Zheng KD, Lin K, Zheng GF, Zou H, Wang JM, et al. Energy metabolism disorder as a contributing factor of rheumatoid arthritis: a comparative proteomic and metabolomic study. *PLoS One* (2015) 10:e0132695. doi:10.1371/journal.pone.0132695
14. Buck MD, Sowell RT, Kaech SM, Pearce EL. Metabolic instruction of immunity. *Cell* (2017) 169:570–86. doi:10.1016/j.cell.2017.04.004
15. Pearce EL. Metabolism in T cell activation and differentiation. *Curr Opin Immunol* (2010) 22:314–20. doi:10.1016/j.coi.2010.01.018
16. Greiner EF, Guppy M, Brand K. Glucose is essential for proliferation and the glycolytic enzyme induction that provokes a transition to glycolytic energy production. *J Biol Chem* (1994) 269:31484–90.
17. Chang CH, Pearce EL. Emerging concepts of T cell metabolism as a target of immunotherapy. *Nat Immunol* (2016) 17:364–8. doi:10.1038/ni.3415
18. Askanazi J, Carpentier YA, Michelsen CB, Elwyn DH, Furst P, Kantrowitz LR, et al. Muscle and plasma amino-acids following injury – influence of intercurrent infection. *Ann Surg* (1980) 192:78–85. doi:10.1097/00000658-198007000-00014
19. Karinch AM, Pan M, Lin CM, Strange R, Souba WW. Glutamine metabolism in sepsis and infection. *J Nutr* (2001) 131:2535s–8s. doi:10.1093/jn/131.9.2535S
20. Oudemans-van Straaten HM, Bosman RJ, Treskes M, van der Spoel HJI, Zandstra DF. Plasma glutamine depletion and patient outcome in acute ICU admissions. *Intensive Care Med* (2001) 27:84–90. doi:10.1007/s001340000703
21. Hulsewe KWE, van der Hulst RWWJ, van Acker BAC, von Meyenfeldt MF, Soeters PB. Inflammation rather than nutritional depletion determines glutamine concentrations and intestinal permeability. *Clin Nutr* (2004) 23:1209–16. doi:10.1016/j.clnu.2004.04.001
22. Sido B, Seel C, Hochlelmert A, Breitkreutz R, Droge W. Low intestinal glutamine level and low glutaminase activity in Crohn's disease: a rational for glutamine supplementation? *Dig Dis Sci* (2006) 51:2170–9. doi:10.1007/s10620-006-9473-x
23. Haas R, Smith J, Rocher-Ros V, Nadkarni S, Montero-Melendez T, D'Acquisto F, et al. Lactate regulates metabolic and proinflammatory circuits in control of T cell migration and effector functions. *PLoS Biol* (2015) 13:e1002202. doi:10.1371/journal.pbio.1002202
24. Robergs RA, Ghiasvand F, Parker D. Biochemistry of exercise-induced metabolic acidosis. *Am J Physiol Regul Integr Comp Physiol* (2004) 287:R502–16. doi:10.1152/ajpregu.00114.2004
25. Brand A, Singer K, Koehl GE, Kolitzus M, Schoenhammer G, Thiel A, et al. LDHA-associated lactic acid production blunts tumor immunosurveillance by T and NK cells. *Cell Metab* (2016) 24:657–71. doi:10.1016/j.cmet.2016.08.011
26. Fischer K, Hoffmann P, Voelkl S, Meidenbauer N, Ammer J, Edinger M, et al. Inhibitory effect of tumor cell-derived lactic acid on human T cells. *Blood* (2007) 109:3812–9. doi:10.1182/blood-2006-07-035972
27. Masson D, Peters PJ, Geuze HJ, Borst J, Tschopp J. Interaction of chondroitin sulfate with perforin and granzymes of cytolytic T-cells is dependent on Ph. *Biochemistry* (1990) 29:11229–35. doi:10.1021/bi00503a011
28. Mendler AN, Hu B, Prinz PU, Kreutz M, Gottfried E, Noessner E. Tumor lactic acidosis suppresses CTL function by inhibition of p38 and JNK/c-Jun activation. *Int J Cancer* (2012) 131:633–40. doi:10.1002/ijc.26410
29. Calcinotto A, Filipazzi P, Grioni M, Iero M, De Milito A, Ricupito A, et al. Modulation of microenvironment acidity reverses anergy in human and murine tumor-infiltrating T lymphocytes. *Cancer Res* (2012) 72:2746–56. doi:10.1158/0008-5472.CAN-11-1272
30. Mittal M, Siddiqui MR, Tran K, Reddy SP, Malik AB. Reactive oxygen species in inflammation and tissue injury. *Antioxid Redox Signal* (2014) 20:1126–67. doi:10.1089/ars.2012.5149
31. Li XY, Fang P, Mai JT, Choi ET, Wang H, Yang XF. Targeting mitochondrial reactive oxygen species as novel therapy for inflammatory diseases and cancers. *J Hematol Oncol* (2013) 6:19. doi:10.1186/1756-8722-6-19
32. Kundu S, Ghosh P, Datta S, Ghosh A, Chattopadhyay S, Chatterjee M. Oxidative stress as a potential biomarker for determining disease activity in patients with rheumatoid arthritis. *Free Radic Res* (2012) 46:1482–9. doi:10.3109/10715762.2012.727991
33. Valko M, Leibfritz D, Moncol J, Cronin MTD, Mazur M, Telser J. Free radicals and antioxidants in normal physiological functions and human disease. *Int J Biochem Cell Biol* (2007) 39:44–84. doi:10.1016/j.biocel.2006.07.001
34. Griffiths Helen R, Dunston Christopher R, Bennett Stuart J, Grant Melissa M, Phillips Darren C, Kitas George D. Free radicals and redox signalling in T-cells during chronic inflammation and ageing. *Biochem Soc Trans* (2011) 39:1273. doi:10.1042/BST0391273
35. King MR, Ismail AS, Davis LS, Karp DR. Oxidative stress promotes polarization of human T cell differentiation toward a T helper 2 phenotype. *J Immunol* (2006) 176:2765–72. doi:10.4049/jimmunol.176.5.2765
36. Moghaddam AE, Gartlan KH, Kong L, Sattentau QJ. Reactive carbonyls are a major Th2-inducing damage-associated molecular pattern generated by oxidative stress. *J Immunol* (2011) 187:1626–33. doi:10.4049/jimmunol.1003906
37. Gaber T, Tran CL, Schellmann S, Hahne M, Strehl C, Hoff P, et al. Pathophysiological hypoxia affects the redox state and IL-2 signalling of human CD4+ T cells and concomitantly impairs survival and proliferation. *Eur J Immunol* (2013) 43:1588–97. doi:10.1002/eji.201242754
38. Zenewicz LA. Oxygen levels and immunological studies. *Front Immunol* (2017) 8:324. doi:10.3389/fimmu.2017.00324
39. Le QT, Chen E, Salim A, Cao H, Kong CS, Whyte R, et al. An evaluation of tumor oxygenation and gene expression in patients with early stage non-small cell lung cancers. *Clin Cancer Res* (2006) 12:1507–14. doi:10.1158/1078-0432.CCR-05-2049
40. Harrison JS, Rameshwar P, Chang V, Bandari P. Oxygen saturation in the bone marrow of healthy volunteers. *Blood* (2002) 99:394. doi:10.1182/blood.V99.1.394
41. Caldwell CC, Kojima H, Lukashev D, Armstrong J, Farber M, Apasov SG, et al. Differential effects of physiologically relevant hypoxic conditions on T lymphocyte development and effector functions. *J Immunol* (2001) 167:6140. doi:10.4049/jimmunol.167.11.6140
42. Carreau A, El Hafny-Rahbi B, Matejuk A, Grillon C, Kieda C. Why is the partial oxygen pressure of human tissues a crucial parameter? Small molecules and hypoxia. *J Cell Mol Med* (2011) 15:1239–53. doi:10.1111/j.1582-4934.2011.01258.x
43. Westendorf AM, Skibbe K, Adamczyk A, Buer J, Geffers R, Hansen W, et al. Hypoxia enhances immunosuppression by inhibiting CD4+ effector

T cell function and promoting Treg activity. *Cell Physiol Biochem* (2017) 41:1271–84. doi:10.1159/000464429
44. Finlay DK, Rosenzweig E, Sinclair LV, Feijoo-Carnero C, Hukelmann JL, Rolf J, et al. PDK1 regulation of mTOR and hypoxia-inducible factor 1 integrate metabolism and migration of CD8(+) T cells. *J Exp Med* (2012) 209:2441–53. doi:10.1084/jem.20112607
45. Lum JJ, Bui T, Gruber M, Gordan JD, DeBerardinis RJ, Covello KL, et al. The transcription factor HIF-1α plays a critical role in the growth factor-dependent regulation of both aerobic and anaerobic glycolysis. *Genes Dev* (2007) 21:1037–49. doi:10.1101/gad.1529107
46. Dang EV, Barbi J, Yang HY, Jinasena D, Yu H, Zheng Y, et al. Control of T(H)17/T(reg) balance by hypoxia-inducible factor 1. *Cell* (2011) 146: 772–84. doi:10.1016/j.cell.2011.07.033
47. Wang Y, Bi Y, Chen X, Li C, Li Y, Zhang Z, et al. Histone deacetylase SIRT1 negatively regulates the differentiation of interleukin-9-producing CD4+ T cells. *Immunity* (2016) 44:1337–49. doi:10.1016/j.immuni.2016.05.009
48. Junger WG, Liu FC, Loomis WH, Hoyt DB. Hypertonic saline enhances cellular immune function. *Circ Shock* (1994) 42:190–6.
49. Go WY, Liu XB, Roti MA, Liu F, Ho SN. NFAT5/TonEBP mutant mice define osmotic stress as a critical feature of the lymphoid microenvironment. *Proc Natl Acad Sci U S A* (2004) 101:10673–8. doi:10.1073/pnas.0403139101
50. Kleinewietfeld M, Manzel A, Titze J, Kvakan H, Yosef N, Linker RA, et al. Sodium chloride drives autoimmune disease by the induction of pathogenic TH17 cells. *Nature* (2013) 496:518–22. doi:10.1038/nature11868
51. Wu C, Yosef N, Thalhamer T, Zhu C, Xiao S, Kishi Y, et al. Induction of pathogenic TH17 cells by inducible salt-sensing kinase SGK1. *Nature* (2013) 496:513–7. doi:10.1038/nature11984
52. Farez MF, Fiol MP, Gaitan MI, Quintana FJ, Correale J. Sodium intake is associated with increased disease activity in multiple sclerosis. *J Neurol Neurosurg Psychiatry* (2015) 86:26–31. doi:10.1136/jnnp-2014-307928
53. Yilmaz R, Akoglu H, Altun B, Yildirim T, Arici M, Erdem Y. Dietary salt intake is related to inflammation and albuminuria in primary hypertensive patients. *Eur J Clin Nutr* (2012) 66:1214–8. doi:10.1038/ejcn.2012.110
54. Hernandez AL, Kitz A, Wu C, Lowther DE, Rodriguez DM, Vudattu N, et al. Sodium chloride inhibits the suppressive function of FOXP3+ regulatory T cells. *J Clin Invest* (2015) 125:4212–22. doi:10.1172/JCI81151
55. Berry MR, Mathews RJ, Ferdinand JR, Jing C, Loudon KW, Wlodek E, et al. Renal sodium gradient orchestrates a dynamic antibacterial defense zone. *Cell* (2017) 170:860–874e19. doi:10.1016/j.cell.2017.07.022
56. Hanson DF. Fever and the immune response. The effects of physiological temperatures on primary murine splenic T-cell responses in vitro. *J Immunol* (1993) 151:436–48.
57. Refinetti R. The circadian rhythm of body temperature. *Front Biosci* (2010) 15:564–94. doi:10.2741/3634
58. Roberts NJ Jr, Steigbigel RT. Hyperthermia and human leukocyte functions: effects on response of lymphocytes to mitogen and antigen and bactericidal capacity of monocytes and neutrophils. *Infect Immun* (1977) 18:673–9.
59. Smith JB, Knowlton RP, Agarwal SS. Human lymphocyte responses are enhanced by culture at 40 degrees C. *J Immunol* (1978) 121:691–4.
60. Zynda ER, Grimm MJ, Yuan M, Zhong L, Mace TA, Capitano M, et al. A role for the thermal environment in defining co-stimulation requirements for CD4(+) T cell activation. *Cell Cycle* (2015) 14:2340–54. doi:10.1080/15384101.2015.1049782
61. Gordon CJ. *Temperature Regulation in Laboratory Rodents*. Cambridge: Cambridge University Press (1993).
62. Karp CL. Unstressing intemperate models: how cold stress undermines mouse modeling. *J Exp Med* (2012) 209:1069–74. doi:10.1084/jem.20120988
63. Maloney SK, Fuller A, Mitchell D, Gordon C, Overton JM. Translating animal model research: does it matter that our rodents are cold? *Physiology* (2014) 29:413–20. doi:10.1152/physiol.00029.2014
64. Asher G, Sassone-Corsi P. Time for food: the intimate interplay between nutrition, metabolism, and the circadian clock. *Cell* (2015) 161:84–92. doi:10.1016/j.cell.2015.03.015
65. Kim SW, Jang EC, Kwon SC, Han W, Kang MS, Nam YH, et al. Night shift work and inflammatory markers in male workers aged 20-39 in a display manufacturing company. *Ann Occup Environ Med* (2016) 28:48. doi:10.1186/s40557-016-0135-y
66. Puttonen S, Viitasalo K, Harma M. Effect of shiftwork on systemic markers of inflammation. *Chronobiol Int* (2011) 28:528–35. doi:10.3109/07420528.2011.580869
67. Boggild H, Knutsson A. Shift work, risk factors and cardiovascular disease. *Scand J Work Environ Health* (1999) 25:85–99. doi:10.5271/sjweh.410
68. Antunes LC, Levandovski R, Dantas G, Caumo W, Hidalgo MP. Obesity and shift work: chronobiological aspects. *Nutr Res Rev* (2010) 23:155–68. doi:10.1017/S0954422410000016
69. Qian J, Scheer FA. Circadian system and glucose metabolism: implications for physiology and disease. *Trends Endocrinol Metab* (2016) 27:282–93. doi:10.1016/j.tem.2016.03.005
70. Davis S, Mirick DK, Stevens RG. Night shift work, light at night, and risk of breast cancer. *J Natl Cancer Inst* (2001) 93:1557–62. doi:10.1093/jnci/93.20.1557
71. Hansen J. Increased breast cancer risk among women who work predominantly at night. *Epidemiology* (2001) 12:74–7. doi:10.1097/00001648-200109000-00024
72. Scheiermann C, Kunisaki Y, Frenette PS. Circadian control of the immune system. *Nat Rev Immunol* (2013) 13:190–8. doi:10.1038/nri3386
73. Druzd D, Matveeva O, Ince L, Harrison U, He WY, Schmal C, et al. Lymphocyte circadian clocks control lymph node trafficking and adaptive immune responses. *Immunity* (2017) 46:120–32. doi:10.1016/j.immuni.2016.12.011
74. Hemmers S, Rudensky AY. The cell-intrinsic circadian clock is dispensable for lymphocyte differentiation and function. *Cell Rep* (2015) 11:1339–49. doi:10.1016/j.celrep.2015.04.058
75. Froy O. The relationship between nutrition and circadian rhythms in mammals. *Front Neuroendocrinol* (2007) 28:61–71. doi:10.1016/j.yfrne.2007.03.001
76. Feeney KA, Hansen LL, Putker M, Olivares-Yanez C, Day J, Eades LJ, et al. Daily magnesium fluxes regulate cellular timekeeping and energy balance. *Nature* (2016) 532:375–9. doi:10.1038/nature17407
77. Dunlap JC, Loros JJ. Yes, circadian rhythms actually do affect almost everything. *Cell Res* (2016) 26:759–60. doi:10.1038/cr.2016.65
78. Rubin H. The logic of the membrane, magnesium, mitosis (MMM) model for the regulation of animal cell proliferation. *Arch Biochem Biophys* (2007) 458:16–23. doi:10.1016/j.abb.2006.03.026
79. Sahni J, Tamura R, Sweet IR, Scharenberg AM. TRPM7 regulates quiescent/proliferative metabolic transitions in lymphocytes. *Cell Cycle* (2010) 9:3565–74. doi:10.4161/cc.9.17.12798
80. MacIver NJ, Michalek RD, Rathmell JC. Metabolic regulation of T lymphocytes. *Annu Rev Immunol* (2013) 31:259–83. doi:10.1146/annurev-immunol-032712-095956
81. Wang R, Green DR. Metabolic checkpoints in activated T cells. *Nat Immunol* (2012) 13:907–15. doi:10.1038/ni.2386
82. Smith-Garvin JE, Koretzky GA, Jordan MS. T cell activation. *Annu Rev Immunol* (2009) 27:591–619. doi:10.1146/annurev.immunol.021908.132706
83. Frauwirth KA, Riley JL, Harris MH, Parry RV, Rathmell JC, Plas DR, et al. The CD28 signaling pathway regulates glucose metabolism. *Immunity* (2002) 16:769–77. doi:10.1016/S1074-7613(02)00323-0
84. Jacobs SR, Herman CE, MacIver NJ, Wofford JA, Wieman HL, Hammen JJ, et al. Glucose uptake is limiting in T cell activation and requires CD28-mediated akt-dependent and independent pathways. *J Immunol* (2008) 180:4476. doi:10.4049/jimmunol.180.7.4476
85. Klein Geltink RI, O'Sullivan D, Corrado M, Bremser A, Buck MD, Buescher JM, et al. Mitochondrial priming by CD28. *Cell* (2017) 171(385–397):e311. doi:10.1016/j.cell.2017.08.018
86. Finlay D, Cantrell DA. Metabolism, migration and memory in cytotoxic T cells. *Nat Rev Immunol* (2011) 11:109–17. doi:10.1038/nri2888
87. Yang K, Chi HB. mTOR and metabolic pathways in T cell quiescence and functional activation. *Semin Immunol* (2012) 24:421–8. doi:10.1016/j.smim.2012.12.004
88. Nelson DL, Lehninger AL, Cox MM. *Lehninger Principles of Biochemistry*. New York: W.H. Freeman (2013).
89. Gerriets VA, Rathmell JC. Metabolic pathways in T cell fate and function. *Trends Immunol* (2012) 33:168–73. doi:10.1016/j.it.2012.01.010
90. Fracchia KM, Walsh CM. Metabolic mysteries of the inflammatory response: T cell polarization and plasticity. *Int Rev Immunol* (2015) 34:3–18. doi:10.3109/08830185.2014.974748

91. Warburg O, Wind F, Negelein E. The metabolism of tumors in the body. *J Gen Physiol* (1927) 8:519–30. doi:10.1085/jgp.8.6.519
92. Heiden MGV, Cantley LC, Thompson CB. Understanding the Warburg effect: the metabolic requirements of cell proliferation. *Science* (2009) 324:1029–33. doi:10.1126/science.1160809
93. Wang R, Dillon CP, Shi LZ, Milasta S, Carter R, Finkelstein D, et al. The transcription factor Myc controls metabolic reprogramming upon T lymphocyte activation. *Immunity* (2011) 35:871–82. doi:10.1016/j.immuni.2011.09.021
94. Ardawi MS, Newsholme EA. Glutamine metabolism in lymphocytes of the rat. *Biochem J* (1983) 212:835–42. doi:10.1042/bj2120835
95. Yaqoob P, Calder PC. Glutamine requirement of proliferating T lymphocytes. *Nutrition* (1997) 13:646–51. doi:10.1016/S0899-9007(97)83008-0
96. DeBerardinis RJ, Cheng T. Q's next: the diverse functions of glutamine in metabolism, cell biology and cancer. *Oncogene* (2010) 29:313–24. doi:10.1038/onc.2009.358
97. Andris F, Leo O. AMPK in lymphocyte metabolism and function. *Int Rev Immunol* (2015) 34:67–81. doi:10.3109/08830185.2014.969422
98. Almeida L, Lochner M, Berod L, Sparwasser T. Metabolic pathways in T cell activation and lineage differentiation. *Semin Immunol* (2016) 28:514–24. doi:10.1016/j.smim.2016.10.009
99. Mihaylova MM, Shaw RJ. The AMPK signalling pathway coordinates cell growth, autophagy and metabolism. *Nat Cell Biol* (2011) 13:1016–23. doi:10.1038/ncb2329
100. Levine B, Mizushima N, Virgin HW. Autophagy in immunity and inflammation. *Nature* (2011) 469:323–35. doi:10.1038/nature09782
101. Klysz D, Tai XG, Robert PA, Craveiro M, Cretenet G, Oburoglu L, et al. Glutamine-dependent alpha-ketoglutarate production regulates the balance between T helper 1 cell and regulatory T cell generation. *Sci Signal* (2015) 8:ra97. doi:10.1126/scisignal.aab2610
102. Sinclair LV, Rolf J, Emslie E, Shi YB, Taylor PM, Cantrell DA. Control of amino-acid transport by antigen receptors coordinates the metabolic reprogramming essential for T cell differentiation. *Nat Immunol* (2013) 14:500–8. doi:10.1038/ni.2556
103. Kolev M, Dimeloe S, Le Friec G, Navarini A, Arbore G, Povoleri GA, et al. Complement regulates nutrient influx and metabolic reprogramming during Th1 cell responses. *Immunity* (2015) 42:1033–47. doi:10.1016/j.immuni.2015.05.024
104. Chang CH, Curtis JD, Maggi LB, Faubert B, Villarino AV, O'Sullivan D, et al. Posttranscriptional control of T cell effector function by aerobic glycolysis. *Cell* (2013) 153:1239–51. doi:10.1016/j.cell.2013.05.016
105. Macintyre AN, Gerriets VA, Nichols AG, Michalek RD, Rudolph MC, Deoliveira D, et al. The glucose transporter Glut1 is selectively essential for CD4 T cell activation and effector function. *Cell Metab* (2014) 20:61–72. doi:10.1016/j.cmet.2014.05.004
106. Peng M, Yin N, Chhangawala S, Xu K, Leslie CS, Li MO. Aerobic glycolysis promotes T helper 1 cell differentiation through an epigenetic mechanism. *Science* (2016) 354:481–4. doi:10.1126/science.aaf6284
107. Ishigame H, Kakuta S, Nagai T, Kadoki M, Nambu A, Komiyama Y, et al. Differential roles of interleukin-17A and -17F in host defense against mucoepithelial bacterial infection and allergic responses. *Immunity* (2009) 30:108–19. doi:10.1016/j.immuni.2008.11.009
108. Ivanov II, Frutos Rde L, Manel N, Yoshinaga K, Rifkin DB, Sartor RB, et al. Specific microbiota direct the differentiation of IL-17-producing T-helper cells in the mucosa of the small intestine. *Cell Host Microbe* (2008) 4:337–49. doi:10.1016/j.chom.2008.09.009
109. Harrington LE, Hatton RD, Mangan PR, Turner H, Murphy TL, Murphy KM, et al. Interleukin 17-producing CD4+ effector T cells develop via a lineage distinct from the T helper type 1 and 2 lineages. *Nat Immunol* (2005) 6:1123–32. doi:10.1038/ni1254
110. Park H, Li Z, Yang XO, Chang SH, Nurieva R, Wang YH, et al. A distinct lineage of CD4 T cells regulates tissue inflammation by producing interleukin 17. *Nat Immunol* (2005) 6:1133–41. doi:10.1038/ni1261
111. Berod L, Friedrich C, Nandan A, Freitag J, Hagemann S, Harmrolfs K, et al. De novo fatty acid synthesis controls the fate between regulatory T and T helper 17 cells. *Nat Med* (2014) 20:1327–33. doi:10.1038/nm.3704
112. Gaublomme JT, Yosef N, Lee Y, Gertner RS, Yang LV, Wu C, et al. Single-cell genomics unveils critical regulators of Th17 cell pathogenicity. *Cell* (2015) 163:1400–12. doi:10.1016/j.cell.2015.11.009
113. Wang C, Yosef N, Gaublomme J, Wu C, Lee Y, Clish Clary B, et al. CD5L/AIM regulates lipid biosynthesis and restrains Th17 cell pathogenicity. *Cell* (2015) 163:1413–27. doi:10.1016/j.cell.2015.10.068
114. Lochner M, Berod L, Sparwasser T. Fatty acid metabolism in the regulation of T cell function. *Trends Immunol* (2015) 36:81–91. doi:10.1016/j.it.2014.12.005
115. Raha S, Raud B, Oberdorfer L, Castro CN, Schreder A, Freitag J, et al. Disruption of de novo fatty acid synthesis via acetyl-CoA carboxylase 1 inhibition prevents acute graft-versus-host disease. *Eur J Immunol* (2016) 46:2233–8. doi:10.1002/eji.201546152
116. Kurokawa J, Arai S, Nakashima K, Nagano H, Nishijima A, Miyata K, et al. Macrophage-derived AIM is endocytosed into adipocytes and decreases lipid droplets via inhibition of fatty acid synthase activity. *Cell Metab* (2010) 11:479–92. doi:10.1016/j.cmet.2010.04.013
117. Sasaki CY, Chen G, Munk R, Eitan E, Martindale J, Longo DL, et al. p(70S6K1) in the TORC1 pathway is essential for the differentiation of Th17 Cells, but not Th1, Th2, or Treg cells in mice. *Eur J Immunol* (2016) 46:212–22. doi:10.1002/eji.201445422
118. Volchenkov R, Nygaard V, Sener Z, Skalhegg BS. Th17 polarization under hypoxia results in increased IL-10 production in a pathogen-independent manner. *Front Immunol* (2017) 8:698. doi:10.3389/fimmu.2017.00698
119. Franchi L, Monteleone I, Hao LY, Spahr MA, Zhao W, Liu X, et al. Inhibiting oxidative phosphorylation in vivo restrains Th17 effector responses and ameliorates murine colitis. *J Immunol* (2017) 198:2735–46. doi:10.4049/jimmunol.1600810
120. Gerriets VA, Kishton RJ, Nichols AG, Macintyre AN, Inoue M, Ilkayeva O, et al. Metabolic programming and PDHK1 control CD4+ T cell subsets and inflammation. *J Clin Invest* (2015) 125:194–207. doi:10.1172/JCI76012
121. Bieber T. Atopic dermatitis. *N Engl J Med* (2008) 358:1483–94. doi:10.1056/NEJMra074081
122. Odegaard JI, Chawla A. Alternative macrophage activation and metabolism. *Annu Rev Pathol* (2011) 6:275–97. doi:10.1146/annurev-pathol-011110-130138
123. Angela M, Endo Y, Asou HK, Yamamoto T, Tumes DJ, Tokuyama H, et al. Fatty acid metabolic reprogramming via mTOR-mediated inductions of PPAR gamma directs early activation of T cells. *Nat Commun* (2016) 7:13683. doi:10.1038/ncomms13683
124. Chen T, Tibbitt CA, Feng X, Stark JM, Rohrbeck L, Rausch L, et al. PPAR-γ promotes type 2 immune responses in allergy and nematode infection. *Sci Immunol* (2017) 2:eaal5196. doi:10.1126/sciimmunol.aal5196
125. Nobs SP, Natali S, Pohlmeier L, Okreglicka K, Schneider C, Kurrer M, et al. PPAR gamma in dendritic cells and T cells drives pathogenic type-2 effector responses in lung inflammation. *J Exp Med* (2017) 214:3015–35. doi:10.1084/jem.20162069
126. Yang K, Shrestha S, Zeng H, Karmaus PWF, Neale G, Vogel P, et al. T Cell Exit from quiescence and differentiation into Th2 cells depend on raptor-mTORC1-mediated metabolic reprogramming. *Immunity* (2013) 39:1043–56. doi:10.1016/j.immuni.2013.09.015
127. Chapman NM, Chi HB. mTOR signaling, Tregs and immune modulation. *Immunotherapy* (2014) 6:1295–311. doi:10.2217/imt.14.84
128. Delgoffe GM, Pollizzi KN, Waickman AT, Heikamp E, Meyers DJ, Horton MR, et al. The kinase mTOR regulates the differentiation of helper T cells through the selective activation of signaling by mTORC1 and mTORC2. *Nat Immunol* (2011) 12:295–303. doi:10.1038/ni.2005
129. Heikamp EB, Patel CH, Collins S, Waickman A, Oh MH, Sun IH, et al. The AGC kinase SGK1 regulates TH1 and TH2 differentiation downstream of the mTORC2 complex. *Nat Immunol* (2014) 15:457–64. doi:10.1038/ni.2867
130. Li B, Tournier C, Davis RJ, Flavell RA. Regulation of IL-4 expression by the transcription factor JunB during T helper cell differentiation. *Embo J* (1999) 18:420–32. doi:10.1093/emboj/18.2.420
131. Yang JQ, Kalim KW, Li Y, Zhang S, Hinge A, Filippi MD, et al. RhoA orchestrates glycolysis for TH2 cell differentiation and allergic airway inflammation. *J Allergy Clin Immunol* (2016) 137(231–245):e234. doi:10.1016/j.jaci.2015.05.004
132. Seumois G, Zapardiel-Gonzalo J, White B, Singh D, Schulten V, Dillon M, et al. Transcriptional profiling of Th2 cells identifies pathogenic features associated with asthma. *J Immunol* (2016) 197:655–64. doi:10.4049/jimmunol.1600397
133. Veldhoen M, Uyttenhove C, van Snick J, Helmby H, Westendorf A, Buer J, et al. Transforming growth factor-beta 'reprograms' the differentiation of

T helper 2 cells and promotes an interleukin 9-producing subset. *Nat Immunol* (2008) 9:1341–6. doi:10.1038/ni.1659
134. Rojas-Zuleta WG, Vásquez G. Th9 lymphocytes: a recent history from IL-9 to its potential role in rheumatic diseases. *Autoimmun Rev* (2016) 15:649–55. doi:10.1016/j.autrev.2016.02.020
135. Chang HC, Guarente L. SIRT1 and other sirtuins in metabolism. *Trends Endocrinol Metab* (2014) 25:138–45. doi:10.1016/j.tem.2013.12.001
136. Crotty S. Follicular helper CD4 T cells (TFH). *Annu Rev Immunol* (2011) 29: 621–63. doi:10.1146/annurev-immunol-031210-101400
137. Ueno H, Banchereau J, Vinuesa CG. Pathophysiology of T follicular helper cells in humans and mice. *Nat Immunol* (2015) 16:142–52. doi:10.1038/ni.3054
138. Pitzalis C, Kelly S, Humby F. New learnings on the pathophysiology of RA from synovial biopsies. *Curr Opin Rheumatol* (2013) 25:334–44. doi:10.1097/BOR.0b013e32835fd8eb
139. Klein U, Dalla-Favera R. Germinal centres: role in B-cell physiology and malignancy. *Nat Rev Immunol* (2008) 8:22–33. doi:10.1038/nri2217
140. Cho SH, Raybuck AL, Stengel K, Wei M, Beck TC, Volanakis E, et al. Germinal centre hypoxia and regulation of antibody qualities by a hypoxia response system. *Nature* (2016) 537:234–8. doi:10.1038/nature19334
141. Abbott RK, Thayer M, Labuda J, Silva M, Philbrook P, Cain DW, et al. Germinal center hypoxia potentiates immunoglobulin class switch recombination. *J Immunol* (2016) 197:4014–20. doi:10.4049/jimmunol.1601401
142. Ray JP, Staron MM, Shyer JA, Ho PC, Marshall HD, Gray SM, et al. The interleukin-2-mTORc1 kinase axis defines the signaling, differentiation, and metabolism of T helper 1 and follicular b helper T cells. *Immunity* (2015) 43:690–702. doi:10.1016/j.immuni.2015.08.017
143. Oestreich KJ, Read KA, Gilbertson SE, Hough KP, McDonald PW, Krishnamoorthy V, et al. Bcl-6 directly represses the gene program of the glycolysis pathway. *Nat Immunol* (2014) 15:957–64. doi:10.1038/ni.2985
144. Nurieva RI, Chung Y, Martinez GJ, Yang XO, Tanaka S, Matskevitch TD, et al. Bcl6 mediates the development of T follicular helper cells. *Science* (2009) 325:1001–5. doi:10.1126/science.1176676
145. Yang J, Lin X, Pan Y, Wang J, Chen P, Huang H, et al. Critical roles of mTOR Complex 1 and 2 for T follicular helper cell differentiation and germinal center responses. *eLife* (2016) 5:e17936.
146. Zeng H, Cohen S, Guy C, Shrestha S, Neale G, Brown SA, et al. mTORC1 and mTORC2 kinase signaling and glucose metabolism drive follicular helper T cell differentiation. *Immunity* (2016) 45:540–54. doi:10.1016/j.immuni.2016.08.017
147. Fontenot JD, Gavin MA, Rudensky AY. Foxp3 programs the development and function of $CD4^+CD25^+$ regulatory T cells. *Nat Immunol* (2003) 4:330–6. doi:10.1038/ni904
148. Newton R, Priyadharshini B, Turka LA. Immunometabolism of regulatory T cells. *Nat Immunol* (2016) 17:618–25. doi:10.1038/ni.3466
149. Angelin A, Gil-de-Gómez L, Dahiya S, Jiao J, Guo L, Levine MH, et al. Foxp3 reprograms T cell metabolism to function in low-glucose, high-lactate environments. *Cell Metab* (2017) 25:1282.e–93.e. doi:10.1016/j.cmet.2016.12.018
150. Howie D, Cobbold SP, Adams E, Ten Bokum A, Necula AS, Zhang W, et al. Foxp3 drives oxidative phosphorylation and protection from lipotoxicity. *JCI Insight* (2017) 2:e89160. doi:10.1172/jci.insight.89160
151. Kabat AM, Harrison OJ, Riffelmacher T, Moghaddam AE, Pearson CF, Laing A, et al. The autophagy gene Atg16I1 differentially regulates T-reg and T(H)2 cells to control intestinal inflammation. *Elife* (2016) 5:e12444. doi:10.7554/eLife.12444
152. Wei J, Long L, Yang K, Guy C, Shrestha S, Chen Z, et al. Autophagy enforces functional integrity of regulatory T cells by coupling environmental cues and metabolic homeostasis. *Nat Immunol* (2016) 17:277–85. doi:10.1038/ni.3365
153. Basu S, Hubbard B, Shevach EM. Foxp3-mediated inhibition of Akt inhibits Glut1 (glucose transporter 1) expression in human T regulatory cells. *J Leukoc Biol* (2015) 97:279–83. doi:10.1189/jlb.2AB0514-273RR
154. Gerriets VA, Kishton RJ, Johnson MO, Cohen S, Siska PJ, Nichols AG, et al. Foxp3 and toll-like receptor signaling balance Treg cell anabolic metabolism for suppression. *Nat Immunol* (2016) 17:1459–66. doi:10.1038/ni.3577
155. Kopf H, de la Rosa GM, Howard OM, Chen X. Rapamycin inhibits differentiation of Th17 cells and promotes generation of $FoxP3^+$ T regulatory cells. *Int Immunopharmacol* (2007) 7:1819–24. doi:10.1016/j.intimp.2007.08.027
156. Apostolidis SA, Rodriguez-Rodriguez N, Suarez-Fueyo A, Dioufa N, Ozcan E, Crispin JC, et al. Phosphatase PP2A is requisite for the function of regulatory T cells. *Nat Immunol* (2016) 17:556–64. doi:10.1038/ni.3390
157. De Rosa V, Galgani M, Porcellini A, Colamatteo A, Santopaolo M, Zuchegna C, et al. Glycolysis controls the induction of human regulatory T cells by modulating the expression of FOXP3 exon 2 splicing variants. *Nat Immunol* (2015) 16:1174–84. doi:10.1038/ni.3269
158. Procaccini C, Carbone F, Di Silvestre D, Brambilla F, De Rosa V, Galgani M, et al. The Proteomic landscape of human ex vivo regulatory and conventional T cells reveals specific metabolic requirements. *Immunity* (2016) 44:712. doi:10.1016/j.immuni.2016.01.028
159. Scharping NE, Menk AV, Moreci RS, Whetstone RD, Dadey RE, Watkins SC, et al. The tumor microenvironment represses T cell mitochondrial biogenesis to drive intratumoral T cell metabolic insufficiency and dysfunction. *Immunity* (2016) 45:374–88. doi:10.1016/j.immuni.2016.07.009
160. Xu S, Nam SM, Kim JH, Das R, Choi SK, Nguyen TT, et al. Palmitate induces ER calcium depletion and apoptosis in mouse podocytes subsequent to mitochondrial oxidative stress. *Cell Death Dis* (2015) 6:e1976. doi:10.1038/cddis.2015.331
161. Nakaya M, Xiao YC, Zhou XF, Chang JH, Chang M, Cheng XH, et al. Inflammatory T cell responses rely on amino acid transporter ASCT2 facilitation of glutamine uptake and mTORC1 kinase activation. *Immunity* (2014) 40:692–705. doi:10.1016/j.immuni.2014.04.007
162. Cobbold SP, Adams E, Farquhar CA, Nolan KF, Howie D, Lui KO, et al. Infectious tolerance via the consumption of essential amino acids and mTOR signaling. *Proc Natl Acad Sci U S A* (2009) 106:12055–60. doi:10.1073/pnas.0903919106
163. He L, Vasiliou K, Nebert DW. Analysis and update of the human solute carrier (SLC) gene superfamily. *Hum Genomics* (2009) 3:195–206. doi:10.1186/1479-7364-3-2-195
164. Saunders RN, Metcalfe MS, Nicholson ML. Rapamycin in transplantation: a review of the evidence. *Kidney Int* (2001) 59:3–16. doi:10.1046/j.1523-1755.2001.00460.x
165. Park Y, Jin HS, Lopez J, Elly C, Kim G, Murai M, et al. TSC1 regulates the balance between effector and regulatory T cells. *J Clin Invest* (2013) 123:5165–78. doi:10.1172/JCI69751
166. Wu X, Dou YN, Yang Y, Bian DF, Tuo JQ, Tong B, et al. Arctigenin exerts anti-colitis efficacy through inhibiting the differentiation of Th1 and Th17 cells via an mTORC1-dependent pathway. *Biochem Pharmacol* (2015) 96:323–36. doi:10.1016/j.bcp.2015.06.008
167. Tresoldi E, Dell'Albani I, Stabilini A, Jofra T, Valle A, Gagliani N, et al. Stability of human rapamycin-expanded $CD4^+CD25^+$ T regulatory cells. *Haematologica* (2011) 96:1357–65. doi:10.3324/haematol.2011.041483
168. Rena G, Hardie DG, Pearson ER. The mechanisms of action of metformin. *Diabetologia* (2017) 60:1577–85. doi:10.1007/s00125-017-4342-z
169. Wang YW, He SJ, Feng X, Cheng J, Luo YT, Tian L, et al. Metformin: a review of its potential indications. *Drug Des Devel Ther* (2017) 11:2421–9. doi:10.2147/DDDT.S141675
170. Hawley SA, Ross FA, Chevtzoff C, Green KA, Evans A, Fogarty S, et al. Use of cells expressing gamma subunit variants to identify diverse mechanisms of AMPK activation. *Cell Metab* (2010) 11:554–65. doi:10.1016/j.cmet.2010.04.001
171. Wu L, Zhou B, Oshiro-Rapley N, Li M, Paulo JA, Webster CM, et al. An ancient, unified mechanism for metformin growth inhibition in *C. elegans* and cancer. *Cell* (2016) 167:1705.e–18.e. doi:10.1016/j.cell.2016.11.055
172. Sun YF, Tian T, Gao J, Liu XQ, Hou HQ, Cao RJ, et al. Metformin ameliorates the development of experimental autoimmune encephalomyelitis by regulating T helper 17 and regulatory T cells in mice. *J Neuroimmunol* (2016) 292: 58–67. doi:10.1016/j.jneuroim.2016.01.014
173. Lee SY, Lee SH, Kim EK, Kim JK, Shin DY, Cho ML. Metformin ameliorates inflammatory bowel disease by suppression of STAT3 signaling pathway and regulation of the Th17/Treg balance. *J Immunol* (2015) 10(9):e0135858. doi:10.1371/journal.pone.0135858
174. Park MJ, Lee SY, Moon SJ, Son HJ, Lee SH, Kim EK, et al. Metformin attenuates graft-versus-host disease via restricting mammalian target of rapamycin/signal transducer and activator of transcription 3 and promoting adenosine monophosphate-activated protein kinase-autophagy for the balance between T helper 17 and Tregs. *Transl Res* (2016) 173:115–30. doi:10.1016/j.trsl.2016.03.006

175. Gualdoni GA, Mayer KA, Goschl L, Boucheron N, Ellmeier W, Zlabinger GJ. The AMP analog AICAR modulates the T-reg/T(h)17 axis through enhancement of fatty acid oxidation. *FASEB J* (2016) 30:3800–9. doi:10.1096/fj.201600522R
176. Yin YM, Choi SC, Xu ZW, Perry DJ, Seay H, Croker BP, et al. Normalization of CD4(+) T cell metabolism reverses lupus. *Sci Transl Med* (2015) 7:274ra18. doi:10.1126/scitranslmed.aaa0835
177. Kim MH, Kim H. The roles of glutamine in the intestine and its implication in intestinal diseases. *Int J Mol Sci* (2017) 18:E1051. doi:10.3390/ijms18051051
178. Novak F, Heyland DK, Avenell A, Drover JW, Su XY. Glutamine supplementation in serious illness: a systematic review of the evidence. *Crit Care Med* (2002) 30:2022–9. doi:10.1097/00003246-200209000-00011
179. Akobeng AK, Miller V, Stanton J, Elbadri AM, Thomas AG. Double-blind randomized controlled trial of glutamine-enriched polymeric diet in the treatment of active Crohn's disease. *J Pediatr Gastroenterol Nutr* (2000) 30:78–84. doi:10.1097/00005176-200001000-00022
180. Alonso A, Julià A, Vinaixa M, Domènech E, Fernández-Nebro A, Cañete JD, et al. Urine metabolome profiling of immune-mediated inflammatory diseases. *BMC Med* (2016) 14:133. doi:10.1186/s12916-016-0681-8
181. Lauridsen MB, Bliddal H, Christensen R, Danneskiold-Samsoe B, Bennett R, Keun H, et al. H-1 NMR spectroscopy-based interventional metabolic phenotyping: a cohort study of rheumatoid arthritis patients. *J Proteome Res* (2010) 9:4545–53. doi:10.1021/pr1002774
182. Zabek A, Swierkot J, Malak A, Zawadzka I, Deja S, Bogunia-Kubik K, et al. Application of H-1 NMR-based serum metabolomic studies for monitoring female patients with rheumatoid arthritis. *J Pharm Biomed Anal* (2016) 117:544–50. doi:10.1016/j.jpba.2015.10.007
183. Zhou J, Chen J, Hu CF, Xie ZJ, Li HC, Wei SS, et al. Exploration of the serum metabolite signature in patients with rheumatoid arthritis using gas chromatography-mass spectrometry. *J Pharm Biomed Anal* (2016) 127:60–7. doi:10.1016/j.jpba.2016.02.004
184. Acar G, Idiman F, Idiman E, Kirkali G, Cakmakci H, Ozakbas S. Nitric oxide as an activity marker in multiple sclerosis. *J Neurol* (2003) 250:588–92. doi:10.1007/s00415-003-1041-0
185. Gilgun-Sherki Y, Melamed E, Offen D. The role of oxidative stress in the pathogenesis of multiple sclerosis: the need for effective antioxidant therapy. *J Neurol* (2004) 251:261–8. doi:10.1007/s00415-004-0348-9
186. Albanese M, Zagaglia S, Landi D, Boffa L, Nicoletti CG, Marciani MG, et al. Cerebrospinal fluid lactate is associated with multiple sclerosis disease progression. *J Neuroinflammation* (2016) 13:36. doi:10.1186/s12974-016-0502-1
187. Amorini AM, Nociti V, Petzold A, Gasperini C, Quartuccio E, Lazzarino G, et al. Serum lactate as a novel potential biomarker in multiple sclerosis. *Biochim Biophys Acta* (2014) 1842:1137–43. doi:10.1016/j.bbadis.2014.04.005
188. Haspel JA, Chettimada S, Shaik RS, Chu JH, Raby BA, Cernadas M, et al. Circadian rhythm reprogramming during lung inflammation. *Nat Commun* (2014) 5:4753. doi:10.1038/ncomms5753
189. Nguyen KD, Fentress SJ, Qiu Y, Yun K, Cox JS, Chawla A. Circadian gene Bmal1 regulates diurnal oscillations of Ly6C(hi) inflammatory monocytes. *Science* (2013) 341:1483–8. doi:10.1126/science.1240636

Conflict of Interest Statement: The authors declare that the research was conducted in the absence of any commercial or financial relationships that could be construed as a potential conflict of interest.

Copyright © 2018 Dumitru, Kabat and Maloy. This is an open-access article distributed under the terms of the Creative Commons Attribution License (CC BY). The use, distribution or reproduction in other forums is permitted, provided the original author(s) and the copyright owner are credited and that the original publication in this journal is cited, in accordance with accepted academic practice. No use, distribution or reproduction is permitted which does not comply with these terms.

frontiers in Immunology

REVIEW
published: 13 February 2017
doi: 10.3389/fimmu.2017.00139

Role of Maternal Periodontitis in Preterm Birth

*Hongyu Ren and Minquan Du**

MOST KLOS and KLOBM, School and Hospital of Stomatology, Wuhan University, Wuhan, China

In the last two decades, many studies have focused on whether periodontitis is a risk factor for preterm birth (PTB). However, both epidemiological investigation and intervention trials have reached contradictory results from different studies. What explains the different findings, and how should future studies be conducted to better assess this risk factor? This article reviews recent epidemiological, animal, and *in vitro* studies as well as intervention trials that evaluate the link between periodontitis and PTB. Periodontitis may act as a distant reservoir of microbes and inflammatory mediators and contribute to the induction of PTB. Animal studies revealed that maternal infections with periodontal pathogens increase levels of circulating IL-1β, IL-6, IL-8, IL-17, and TNF-α and induce PTB. *In vitro* models showed that periodontal pathogens/byproducts induce COX-2, IL-8, IFN-γ, and TNF-α secretion and/or apoptosis in placental tissues/cells. The effectiveness of periodontal treatment to prevent PTB is influenced by the diagnostic criteria of periodontitis, microbial community composition, severity of periodontitis, treatment strategy, treatment efficiency, and the period of treatment during pregnancy. Although intervention trials reported contradictory results, oral health maintenance is an important part of preventive care that is both effective and safe throughout pregnancy and should be supported before and during pregnancy. As contradictory epidemiological and intervention studies continue to be published, two new ideas are proposed here: (1) severe and/or generalized periodontitis promotes PTB and (2) periodontitis only promotes PTB for pregnant women who are young or HIV-infected or have preeclampsia, pre-pregnancy obesity, or susceptible genotypes.

Keywords: periodontitis, pregnancy, preterm birth, low birth weight, risk factor

OPEN ACCESS

Edited by:
Jixin Zhong,
Case Western Reserve University, USA

Reviewed by:
Yonglin Chen,
Yale University, USA
Xuhui Feng,
Indiana University, USA

***Correspondence:**
Minquan Du
duminquan@whu.edu.cn

Specialty section:
This article was submitted to Inflammation, a section of the journal Frontiers in Immunology

Received: *25 December 2016*
Accepted: *26 January 2017*
Published: *13 February 2017*

Citation:
Ren H and Du M (2017) Role of Maternal Periodontitis in Preterm Birth. Front. Immunol. 8:139. doi: 10.3389/fimmu.2017.00139

INTRODUCTION

Each year, about 15 million infants worldwide are born preterm (before 37 weeks of gestation), and these preterm babies typically have low birth weight (LBW, <2,500 g) (1). Preterm birth (PTB) is the leading cause of neonatal mortality, morbidity, and developmental loss (2). Advances in obstetric care have not altered the rates of PTB, and it is estimated that 9.6% of worldwide births are preterm (3). The highest rates of PTB are in Africa (11.9%) and North America (10.6%), and the lowest rates are in Europe (6.2%) (3). However, the underlying causes of PTB are still not entirely clear, thus an accurate identification of risk factors for PTB that are amenable to intervention would have far-reaching and long-lasting impact.

Of the multiple risk factors for PTB, maternal infection is identified consistently. Periodontal disease is a highly prevalent infectious and inflammatory disease of tooth-supporting tissues and if untreated can lead to oral disabilities (**Figure 1A**) (4). Periodontal disease is caused mainly

by gram-negative microaerophilic and anaerobic bacteria that colonize the subgingival area and produce significant amounts of proinflammatory mediators (5). Periodontal disease includes gingivitis and periodontitis. Gingivitis is the presence of gingival inflammation without loss of connective tissue attachment. Periodontitis is the presence of gingival inflammation at sites where there has been apical migration of the epithelial attachment onto the root surfaces accompanied by the loss of connective tissue and alveolar bone (**Figure 1B**) (6). In the last two decades, many studies have examined the relationship between periodontitis and PTB. Periodontitis may be a risk factor for PTB due to the presence in the bloodstream of bacteria and proinflammatory cytokines during infection that can affect distant organs (7). However, epidemiological studies and intervention trials have reached contradictory conclusions about the relationship between periodontitis and PTB. The aim of this review is to summarize the current evidence from epidemiological, animal, and *in vitro* studies, as well as intervention trials and to propose new ideas about the link between periodontitis and PTB.

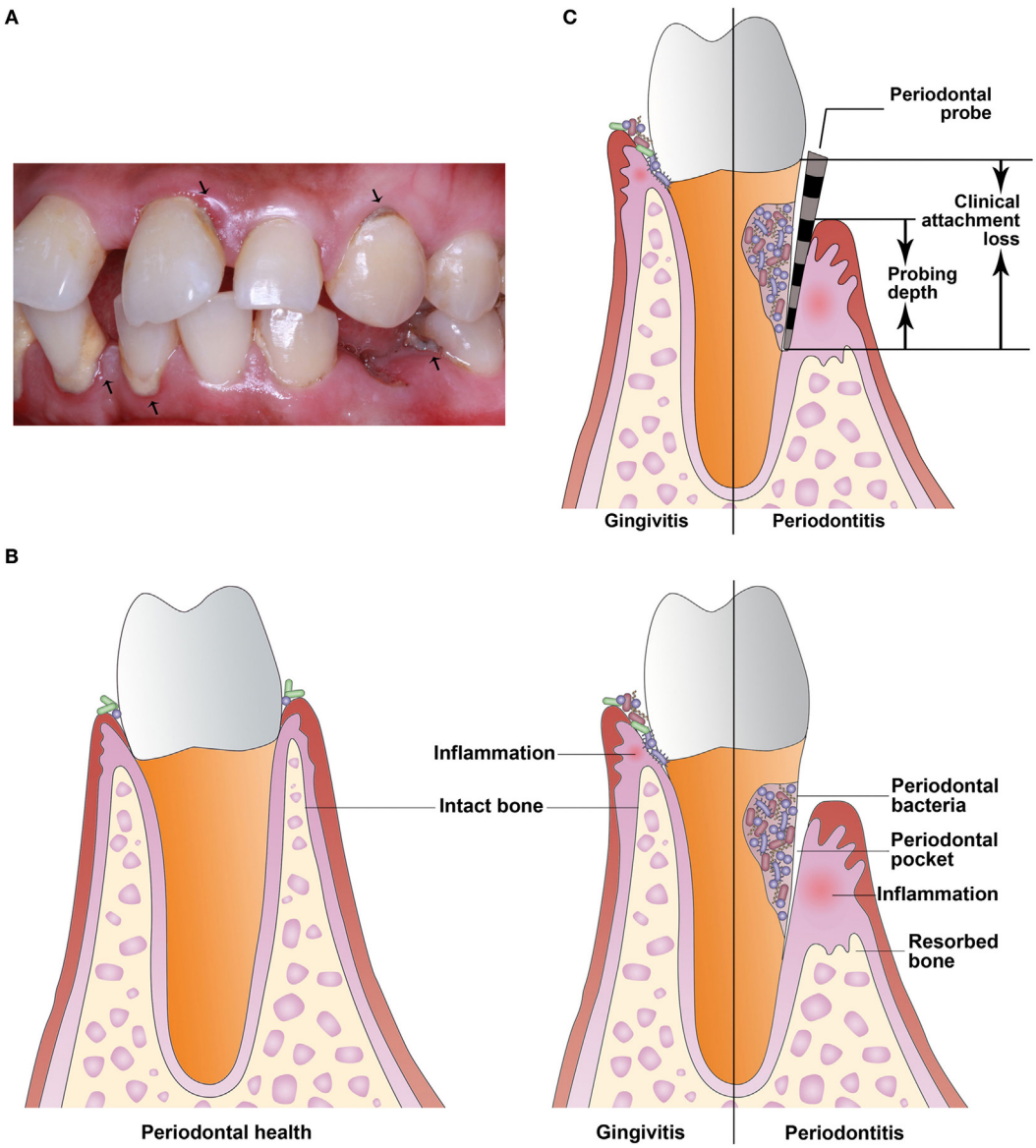

FIGURE 1 | **Periodontal disease is a highly prevalent infectious and inflammatory disease of tooth-supporting tissues**. **(A)** The arrowheads indicate periodontal disease. **(B)** Periodontal disease includes gingivitis and periodontitis. Gingivitis is the presence of gingival inflammation without loss of connective tissue attachment. Periodontitis is the presence of gingival inflammation at sites where there has been apical migration of the epithelial attachment onto the root surfaces accompanied by the loss of connective tissue and alveolar bone. **(C)** Clinical attachment loss is measured with a periodontal probe and is the distance from the base of the probeable crevice to the cementoenamel junction. Probing depth is defined as the distance between the bottom of the periodontal pocket and the gingival margin.

EPIDEMIOLOGICAL RESULTS

About one-third of all PTB are caused by preterm labor (uterine contraction) and one-third are due to the premature rupture of membranes (PROM); the remaining cases are due to other pregnancy complications such as induced labor (of which preeclampsia is the major indication) (8). In the last two decades, numerous epidemiological studies have examined the link between periodontitis and PTB, including cross-sectional, case–control, and cohort studies.

In a cross-sectional study, or census, data are collected at a defined time and is used to assess the prevalence of chronic or acute conditions, the results of intervention, or the causes of disease. In the last 5 years, several cross-sectional studies (9–11) reported a correlation between periodontitis and PTB/LBW. In a study published in 2016 (9), women with PTB were found to have worse periodontal parameters and significantly increased gingival crevicular fluid (GCF) levels of IL-6 and prostaglandin E_2 (PGE_2) compared with women who experienced full-term birth. Based on significant correlations between serum PGE_2 level and probing depth, clinical attachment loss (CAL, **Figure 1C**), and GCF TNF-α in PTB, periodontitis may increase the risk of labor triggers and hence contribute to preterm labor onset. However, in 2016 Martinez-Martinez et al. (12) suggested that PTB is a multifactorial condition and that periodontitis and the presence of periodontal pathogens are not sufficient to trigger PTB.

In case–control studies, mothers with PTB are identified and their periodontitis history is determined and compared with that of healthy control subjects. Of the 14 case–control studies published in the last 5 years, 12 (13–24) reported an association between periodontitis and PTB, LBW, or preterm LBW (PLBW), and 2 (25, 26) found no association. In a study published in 2015 (23), mothers in the periodontitis group with single delivery had an eightfold higher chance of delivering a LBW infant compared to those in the control group. The mothers in the periodontitis group with multiple deliveries delivered PTB infants with an eightfold higher frequency and LBW infants at a 10-fold higher frequency compared to the mothers in the control group.

In cohort studies, investigators monitor pregnant women to determine if those with periodontitis demonstrate a higher incidence of PTB than those without periodontitis. Of the 11 published cohort studies in the last 5 years, 7 (27–33) reported an association between periodontitis and PTB, LBW, or PLBW, and 4 (34–37) revealed no association. A hospital-based prospective study published in 2016 (33) comprising 790 pregnant women found that periodontitis was a risk factor for PTB and an independent risk factor for LBW. Recently periodontitis was also found to be associated with preeclampsia (38) and PROM (39, 40), common causes of PTB.

In the last 5 years, most literature and systematic reviews reported an association between periodontitis and PTB (41–46). A meta-analysis published in 2016 (41) assessed case–control studies reporting periodontal status and pregnancy outcomes. The computed risk ratio for periodontitis was 1.61 for PTB using data from 16 studies, the risk for LBW was 1.65 based on 10 studies, and the risk for PLBW was 3.44 based on 4 studies. A systematic and evidence-based review in 2012 (46) focused on the association of periodontitis and PTB and LBW and found 62 relevant studies that suggested that periodontitis may be a potential risk factor for PTB and LBW.

Different epidemiological data may have reached different conclusions due to the following reasons: (1) many studies used different definitions of periodontitis and adverse pregnancy outcomes, for instance the use of PLBW as a composite outcome, or PTB versus LBW, terms that reflect different disease severities and pathologic entities. (2) The risk factors of PTB may be similar to the risk factors for periodontitis (ethnicity, tobacco use, and socioeconomic and educational levels) and thus may confound the association between periodontitis and PTB. In a prospective case–control study (47), PTB was associated with periodontitis when the USA (48), but not the European (49), definitions were used. Therefore, future studies should employ both continuous and categorical assessment of periodontal status and control for confounding factors. Additionally, the further use of the composite outcome PLBW is not encouraged.

BIOLOGICAL HYPOTHESES

Periodontitis is one of the most common chronic infectious diseases and is caused mainly by gram-negative microaerophilic and anaerobic bacteria that colonize the subgingival area and produce significant amounts of proinflammatory mediators, mainly IL-1β, IL-6, PGE_2, and TNF-α (4). Periodontitis may act as a distant reservoir of both microbes and inflammatory mediators that may influence pregnancy and contribute to induction of PTB (**Figure 2**). These two potential mechanisms for how periodontitis can affect PTB are described more fully below.

Bacterial Spreading

Periodontal microorganisms can act as pathogens not only in the oral cavity but also in other body areas. This is due to the following characteristics of bacteria: (1) the ability to rapidly colonize, (2) the ability to elude the host's defense mechanisms, and (3) the ability to produce substances that directly contribute to the destruction of tissue. Periodontal pathogens/byproducts may reach the placenta and enter the amniotic fluid and fetal circulation, serving to activate inflammatory signaling pathways.

Porphyromonas gingivalis has been detected in human placenta tissues (50). Interestingly, one study reported that *P. gingivalis* was only detected within the villous mesenchyme in the preterm cohort, but not the term group (51). Thus, the detection of *P. gingivalis* in the placenta may be related to PTB (52, 53).

The *Fusobacterium nucleatum* subsp. *polymorphum* strain was not detected in vaginal samples, but was found in both neonatal gastric aspirates and oral samples from mothers with PTB and localized periodontal pockets, which strongly indicated that *F. nucleatum* subsp. *polymorphum* of oral origin may relate to PTB (54). Bohrer et al. (55) reported a case of acute chorioamnionitis caused by *F. nucleatum* that progressed to maternal sepsis in a term patient with intact membranes. Cassini et al. (56) reported that the presence of periodontal pathogen *Treponema denticola* in the vagina, regardless of the levels, increased risk of PTB.

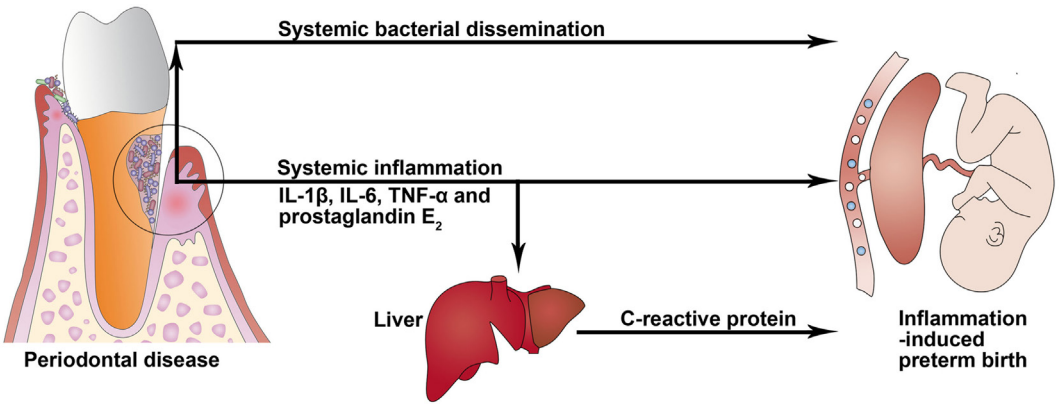

FIGURE 2 | Potential biological mechanisms linking periodontal disease to preterm birth. In periodontitis, gingival ulceration in the periodontal pocket enables egress and systemic bacterial dissemination, and locally produced proinflammatory cytokines can enter systemic circulation and induce an acute-phase response in the liver that is characterized by an increased level of C-reactive protein.

Levels of *P. gingivalis*, *F. nucleatum*, *Actinomyces actinomycetemcomitans*, *Tannerella forsythia*, *T. denticola*, *Eikenella corrodens*, and *Capnocytophaga* spp. have been reported at significantly higher levels in preterm deliveries as compared to term births (37, 52, 57). In one study (58), when *Prevotella intermedia* and/or *Aggregatibacter actinomycetemcomitans* were not detected in maternal periodontal pockets, the infants were more than 129% likely to have a normal birth weight.

The above findings suggest that periodontal bacteria may be normally present in the placenta. However, the levels of certain periodontal pathogens in the placenta may be dependent on the maternal periodontal state (59). Further studies are needed to elucidate the role of microbial load and maternal immune responses in PTB.

Hematogenous Dissemination of Inflammatory Products

Clinical attachment loss, as the main periodontal measure, is associated with plasma levels of IL-1β and TNF-α in pregnant women (60), which may promote labor activation through placental and chorion–amnion production of PGE_2 (61). Women with PTB demonstrated significantly increased GCF levels of IL-6 and PGE_2 compared with those who had full-term births (9). A systematic review in 2013 (62) reported an association between GCF inflammatory mediator levels and adverse pregnancy outcomes. In a subset of patients with severe periodontitis, locally produced proinflammatory mediators—such as IL-1β, IL-6, and TNF-α—can enter systemic circulation and induce an acute-phase response in the liver that is characterized by an increased level of C-reactive protein (CRP) (63, 64). Serum CRP level was reported to be elevated in subjects with periodontitis (65). An increased CRP level can enhance the risk of cardiovascular disease, cerebrovascular accidents, and PLBW infants (65).

Clinical studies support the association between increased levels of circulating proinflammatory mediators and PTB (66, 67) and have implicated IL-1β and IL-6 as major players in the onset of PTB (68, 69). Moreover, polymorphisms in proinflammatory genes, including the above-mentioned cytokines, have been associated with PTB (70, 71). In addition, elevated amniotic fluid level of IL-6 in the second trimester was associated with the initiation and timing of PTB (72, 73). Therefore, the potential link between periodontitis and PTB may be explained by the following mechanisms. First, periodontal pathogens/byproducts can disseminate toward the placental and fetal tissues. Immune/inflammatory reactions within the placental tissues of the pregnant woman may occur, and the release of proinflammatory mediators in the amniotic fluid may increase and further contribute to PTB. Second, systemic inflammatory changes induced by periodontitis can exacerbate local inflammatory responses within the fetoplacental unit to increase the risk for PTB.

EXPERIMENTAL ANIMAL MODELS

The possible roles of periodontitis in PTB have also been explored using experimental animal models. In separate studies, periodontal bacteria were injected into a small chamber in pregnant animals, allowing the establishment of a site of infection distant to the fetal–placental unit to mimic a periodontal infection in a reproducible and simplified manner. These results revealed that maternal infections with periodontal pathogens increase pregnancy complications.

Dental infection of mice with *P. gingivalis* significantly increased levels of circulating IL-1β, IL-6, IL-17, and TNF-α (74). Defects in the placental tissues of *P. gingivalis*-infected mice included degenerative changes in endothelial and trophoblast cells, increased placental detachment, and PROM, and *P. gingivalis* was detected in placental tissues by PCR and immunohistochemistry (74). The *P. gingivalis*-infected group delivered at gestational day (gd) 18.25 versus gd 20.45 for the non-infected control group ($p < 0.01$), with pups exhibiting LBW compared to controls ($p < 0.01$) (74). In another study (75), mice with periodontitis induced by using an inoculum of

P. gingivalis and *F. nucleatum* exhibited increased circulating levels of IL-6 and IL-8. Similarly, Miyoshi et al. (76) found high levels of contractile-associated proteins and ion channels in the myometrium of PTB model mice with chronic odontogenic *P. gingivalis* infection. In murine models, *F. nucleatum* translocated and caused intrauterine infections (77) and *Campylobacter rectus* significantly decreased fetoplacental weight (78). In a baboon model, a significantly greater frequency of the periodontitis group neonates had decreased gestational age and LBW (79). Spontaneous abortion/stillbirth/fetal demise was increased in the periodontitis group versus the control group (79). Also, combined oral infection of mice with *P. gingivalis* and *C. rectus* significantly reduced overall fecundity compared to controls (80). Overall, most animal studies reported a harmful impact of periodontitis on pregnancy outcome. However, a study performed by Fogacci et al. (81) found no increased risk for PTB or LBW in Wistar rats with induced periodontitis.

IN VITRO MODELS

In addition to the data from animal studies, *in vitro* experiments have been conducted to explore the molecular mechanisms underlying periodontitis-induced PTB. In most *in vitro* models, periodontal pathogens/byproducts were used to infect placental tissues or trophoblast cells/cell lines. These experiments were designed to mimic an *in vitro* periodontal infection in a simplified and reproducible manner to allow investigation of the interaction between periodontal pathogens and placental tissues/cells.

Riewe et al. (82) investigated the transcriptional responses after infection with *P. gingivalis* in extravillous trophoblast (HTR8) cells derived from the human placenta, and found that over 2,000 genes were differentially regulated. *P. gingivalis* induced IL-8 and IFN-γ secretion (83), apoptosis, and arrest in the G(1) phase of the cell cycle (84, 85) in HTR8 cells. Increased IFN-γ secretion and Fas expression occurred in *P. gingivalis*-induced apoptosis of HTR8 cells *via* the ERK1/2 pathway (86). In normal human term fetal membrane explants, *P. gingivalis* may significantly increase TLR7 expression (87).

Porphyromonas gingivalis has bioactive components on the cell surface, including lipopolysaccharide, capsules, and fimbriae. *P. gingivalis* lipopolysaccharide induces the production of IL-6 and IL-8 *via* TLR2 in chorion-derived cells (50) and increases expression levels of IL-8, TNF-α, and COX-2 in HTR8 cells in an NF-κB-dependent manner (74). Interestingly, Komine-Aizawa et al. (88) reported that although there is limited direct pathogenic effect of *P. gingivalis* lipopolysaccharide on trophoblast invasion, concurrent smoking reduces trophoblast invasion into the myometrium and thus inhibits maternal vascular reconstruction.

In human placental trophoblast-like BeWo cells, the presence of *A. actinomycetemcomitans* lipopolysaccharide led to increased levels of cytochrome *c*, caspase-2, caspase-3, caspase-9, and BCL2-antagonist/killer 1 mRNA and decreased levels of B-cell CLL/lymphoma 2, BCL2-like 1, and catalase mRNA, consistent with the activation of the mitochondria-dependent apoptotic pathway (89). Additionally, *C. rectus* was reported to effectively invade BeWo cells and upregulate both mRNA and protein levels of IL-6 and TNF-α in a dose-dependent manner (78). Therefore, there is significant evidence that periodontal pathogens and byproducts can induce inflammation and/or apoptosis in placental tissues and cells.

EFFECT OF PERIODONTAL TREATMENT ON PTB INCIDENCE

Periodontal treatment usually refers to non-surgical periodontal therapy that can improve periodontal health and is defined as plaque removal, plaque control, supragingival and subgingival scaling, root surface debridement, and the adjunctive use of chemical agents. To evaluate periodontitis as a risk factor for PTB, intervention studies were conducted to evaluate the effect of periodontal treatment on the risk of PTB. In these studies, women with preexisting periodontitis were randomly divided into two groups. One received periodontal treatment during or before pregnancy, and the other did not. In this type of study, the researchers could assess if periodontitis was an independent risk factor for PTB by determining if periodontal treatment decreased the incidence of PTB.

In a study published in 2015 (90), the mean gestational age in the periodontal treatment group (treatment performed during the second trimester of the gestational period) was 35.57 ± 2.40 versus 34.17 ± 2.92 weeks in the non-treated group ($p < 0.05$). The treatment group showed a statistically significant reduction in mean CRP levels after delivery compared to baseline values; the control group showed no significant reduction in CRP levels. Another study (91) suggested that periodontal treatment during pregnancy is not only safe for both the child and the mother, but also provides beneficial effects for pregnancy and embryo-fetal development, leading to reduced morbidity and mortality in PTB infants. Macedo et al. (92) also reported an association between a low number of daily tooth brushings and PTB. However, in other recent studies (93–96), periodontal treatment performed on pregnant women was not found to be efficacious in reducing PTB or LBW.

Data from recent systematic reviews are also contradictory. Several reviews (97–99) reported that the risks of perinatal outcomes could be potentially reduced by periodontal treatment in pregnant women, but other reviews (100–103) suggested that periodontal treatment during pregnancy was not an efficient way to reduce the incidence of PTB. However, the evidence was not conclusive due to confounding effects and risks of random errors and bias. Thus, further randomized clinical trials are still necessary.

The preventive effectiveness of periodontal treatment for PTB has still not been established, because it is influenced by many factors such as the diagnostic criteria of periodontitis, microbial community composition, severity of disease, treatment strategy, treatment efficiency, and the timing of treatment during pregnancy (the pre-pregnancy period or during the first or second trimester). Jeffcoat et al. (104) confirmed that decreased PTB may depend on the success of periodontal treatment. In this

study of 322 pregnant women with periodontitis, 162 were randomly assigned to receive only oral hygiene instruction and served as the untreated control group, whereas the remaining 160 received scaling and root planing treatment as well as oral hygiene instruction. No significant difference was found between the incidence of PTB in the periodontal treatment group and the control group. However, a logistic regression analysis showed a significant and strong relationship between successful periodontal treatment and full-term birth. Subjects refractory to periodontal treatment were significantly more likely to have PTB. Similarly, in another study (105), periodontal treatment during pregnancy reduced the levels of IL-1β, IL-6, IL-10, and IL-12 in GCF and improved dental parameters. Additionally, the severity of periodontitis was significantly associated with an increased risk of babies born small for gestational age, but no changes in pregnancy-related outcomes were observed following periodontal treatment. These studies suggest the need for the next randomized controlled trials to standardize methodological criteria and utilize a more precise definition of periodontitis. Additionally, for better statistical power, studies should preferably be performed as multicenter studies, and include a large number of participants. Finally, the resulting success or failure of periodontal treatment must be considered.

Preterm birth is the leading cause of infant morbidity and mortality, but classical risk factors explain only one-third of PTB cases, and current intervention strategies have not led to an appreciable reduction of PTB. Therefore, it is necessary to explore mechanisms of causality and generate new hypotheses using an integrated approach. This should be done with increased collaboration among research groups, and using more comprehensive theoretical–methodological approaches to formulate more effective intervention strategies and to detect new risk factors. Although intervention during pregnancy has not consistently been correlated with a reduction in PTB rates, oral health maintenance is an important part of preventive care that is both effective and safe throughout pregnancy and should be supported before and during pregnancy.

TWO NEW IDEAS ABOUT THE ROLE OF PERIODONTITIS IN PTB

Severe and/or Generalized Periodontitis Promotes PTB

The severity of periodontitis can be categorized based on CAL as follows: mild = 1–2 mm, moderate = 3–4 mm, and severe ≥5 mm (106). CAL is measured with a periodontal probe and is the distance from the base of the probeable crevice to the cementoenamel junction (107). In a case–control study (92), periodontitis that met definition 1 (four or more teeth with at least one site showing CAL of ≥3 mm and probing depth of ≥4 mm) was not associated with fewer weeks of gestation. However, a significant association was found between PTB and periodontitis that was classified according to definition 2 (four or more teeth with at least one site showing CAL of ≥4 mm and probing depth of ≥4 mm). A cohort study (108) of preeclamptic women showed that 49.3% of patients with mild periodontitis and 82.6% of patients with moderate to severe periodontitis delivered preterm. Several studies (47, 109–111) found a highly significant association between PTB and moderate to severe periodontitis. Other studies (112, 113) also suggested that the strength of the association between periodontitis and PTB incidence is higher with increased severity of periodontitis.

Periodontitis can also be defined according to the extent of the disease. Generalized periodontitis is defined as CAL ≥3 mm and probing depth ≥4 mm on four or more teeth and localized periodontitis is defined as CAL ≥3 mm and probing depth ≥4 mm on two or three teeth (6). In a case–control multi-center study (114) of singleton live births, periodontal examinations after delivery identified generalized and localized periodontitis. Generalized periodontitis was identified in 13.4% of PTB women and in 10.8% of control women, and localized periodontitis was identified in 11.6 and 10.8%, respectively (114). A significant association was observed between generalized periodontitis and PTB (114). A case–control study (115) confirmed that only the presence of gingival recession for more than two teeth increased the risk of PTB. In addition, several studies (108, 111, 116) reported greater risk for PTB for mothers if periodontitis progressed during pregnancy.

Periodontitis Only Promotes PTB for Pregnant Women Who Are Young or HIV-Infected or Have Preeclampsia, Pre-Pregnancy Obesity, or Susceptible Genotypes

Usin et al. (58) reported that the presence of periodontal pathogens in periodontal pockets from pregnant women with different periodontal status was only associated with PLBW infants for young mothers. Pattrapornnan et al. (117) also found a positive risk of PTB, LBW, and PLBW in HIV-infected pregnant women with periodontitis. Nabet et al. (114) demonstrated a significant association between periodontitis and PTB for preeclampsia. Riche et al. (108) and Pattanashetti et al. (118) confirmed that pregnant women with preeclampsia exhibited a greater risk for PTB if periodontitis was present or progressed during pregnancy. Interestingly, Lee et al. (119) reported that pregnant women with periodontitis were 5.56 times more likely to have PTB with preeclampsia than women without periodontitis and that the association was much stronger (odds ratio 15.94) in women with both periodontitis and obesity. In fact, there is a strong association between pre-pregnancy obesity and periodontitis in pregnant females (120).

Genetic factors involved in altered immune response against bacterial infections may also influence the effect of periodontitis in pregnancy. Periodontitis induced by *P. gingivalis* was found to drive periodontal microbiota dysbiosis and cause systemic disease *via* an impaired adaptive immune response in mice (121). Jeffcoat et al. (122) reported a significant relation between a specific polymorphism of prostaglandin E receptor 3 (a gene associated with inflammatory response) and both periodontitis treatment failure and spontaneous PTB.

CONCLUSION

Here, for the first time, we describe four possible models of periodontitis in PTB: (1) periodontitis is an independent risk factor for PTB; (2) severe and/or generalized periodontitis promotes PTB; (3) periodontitis only promotes PTB for pregnant women who are young or HIV-infected or have preeclampsia, pre-pregnancy obesity, or susceptible genotypes; and (4) periodontitis has no significant effect on PTB. Because contradictory epidemiological data continue to emerge (model 1 versus 4), future studies should try to test the second and third models, which may, to some extent, explain the conflicting epidemiological data. Although intervention during pregnancy has not consistently been correlated with a reduction in PTB rates, oral health maintenance is an important part of preventive care that is both effective and safe throughout pregnancy and should be supported before and during pregnancy.

AUTHOR CONTRIBUTIONS

HR contributed to the literature search, interpretation, writing, and proofreading of the manuscript. MD designed the study and made the ultimate decision on the manuscript.

FUNDING

This work was supported by the National Natural Science Foundation of China (NSFC Grant No. 81371145).

REFERENCES

1. Zi MY, Longo PL, Bueno-Silva B, Mayer MP. Mechanisms involved in the association between periodontitis and complications in pregnancy. *Front Public Health* (2014) 2:290. doi:10.3389/fpubh.2014.00290
2. Goldenberg RL, Culhane JF, Iams JD, Romero R. Epidemiology and causes of preterm birth. *Lancet* (2008) 371(9606):75–84. doi:10.1016/S0140-6736(08)60074-4
3. Beck S, Wojdyla D, Say L, Betran AP, Merialdi M, Requejo JH, et al. The worldwide incidence of preterm birth: a systematic review of maternal mortality and morbidity. *Bull World Health Organ* (2010) 88(1):31–8. doi:10.2471/BLT.08.062554
4. Pihlstrom BL, Michalowicz BS, Johnson NW. Periodontal diseases. *Lancet* (2005) 366(9499):1809–20. doi:10.1016/S0140-6736(05)67728-8
5. Graves D. Cytokines that promote periodontal tissue destruction. *J Periodontol* (2008) 79(8 Suppl):1585–91. doi:10.1902/jop.2008.080183
6. Armitage GC. Periodontal diagnoses and classification of periodontal diseases. *Periodontol 2000* (2004) 34:9–21. doi:10.1046/j.0906-6713.2002.003421.x
7. Seymour GJ, Ford PJ, Cullinan MP, Leishman S, Yamazaki K. Relationship between periodontal infections and systemic disease. *Clin Microbiol Infect* (2007) 13(Suppl 4):3–10. doi:10.1111/j.1469-0691.2007.01798.x
8. Bobetsis YA, Barros SP, Offenbacher S. Exploring the relationship between periodontal disease and pregnancy complications. *J Am Dent Assoc* (2006) 137:7S–13S. doi:10.14219/jada.archive.2006.0403
9. Perunovic N, Rakic MM, Nikolic LI, Jankovic SM, Aleksic ZM, Plecas DV, et al. The association between periodontal inflammation and labor triggers (elevated cytokine levels) in preterm birth: a cross-sectional study. *J Periodontol* (2016) 87(3):248–56. doi:10.1902/jop.2015.150364
10. Muwazi L, Rwenyonyi CM, Nkamba M, Kutesa A, Kagawa M, Mugyenyi G, et al. Periodontal conditions, low birth weight and preterm birth among postpartum mothers in two tertiary health facilities in Uganda. *BMC Oral Health* (2014) 14(1):42. doi:10.1186/1472-6831-14-42
11. Takeuchi N, Ekuni D, Irie K, Furuta M, Tomofuji T, Morita M, et al. Relationship between periodontal inflammation and fetal growth in pregnant women: a cross-sectional study. *Arch Gynecol Obstet* (2013) 287(5):951–7. doi:10.1007/s00404-012-2660-4
12. Martinez-Martinez RE, Moreno-Castillo DF, Loyola-Rodriguez JP, Sanchez-Medrano AG, Miguel-Hernandez JH, Olvera-Delgado JH, et al. Association between periodontitis, periodontopathogens and preterm birth: is it real? *Arch Gynecol Obstet* (2016) 294(1):47–54. doi:10.1007/s00404-015-3945-1
13. Chakki BA, Ealla KR, Hunsingi P, Kumar A, Manidanappanavar P. Influence of maternal periodontal disease as a risk factor for low birth weight infants in Indian population. *J Contemp Dent Pract* (2012) 13(5):676–80. doi:10.5005/jp-journals-10024-1208
14. Khadem N, Rahmani ME, Sanaei A, Afiat M. Association between preterm and low-birth weight with periodontal disease: a case-control study. *Iran J Reprod Med* (2012) 10(6):561–6.
15. Piscoya MD, Ximenes RA, Silva GM, Jamelli SR, Coutinho SB. Maternal periodontitis as a risk factor for prematurity. *Pediatr Int* (2012) 54(1):68–75. doi:10.1111/j.1442-200X.2011.03502.x
16. Baig SA, Khan N, Baqai T, Fatima A, Karim SA, Aziz S. Preterm birth and its associated risk factors. A study at tertiary care hospitals of Karachi, Pakistan. *J Pak Med Assoc* (2013) 63(3):414–8.
17. Mesa F, Pozo E, Blanc V, Puertas A, Bravo M, O'Valle F. Are periodontal bacterial profiles and placental inflammatory infiltrate in pregnancy related to birth outcomes? *J Periodontol* (2013) 84(9):1327–36. doi:10.1902/jop.2012.120462
18. Jacob PS, Nath S. Periodontitis among poor rural Indian mothers increases the risk of low birth weight babies: a hospital-based case control study. *J Periodontal Implant Sci* (2014) 44(2):85–93. doi:10.5051/jpis.2014.44.2.85
19. Govindaraju P, Venugopal S, Shivakumar MA, Sethuraman S, Ramaiah SK, Mukundan S. Maternal periodontal disease and preterm birth: a case-control study. *J Indian Soc Periodontol* (2015) 19(5):512–5. doi:10.4103/0972-124X.164751
20. Kayar NA, Alptekin NO, Erdal ME. Interleukin-1 receptor antagonist gene polymorphism, adverse pregnancy outcome and periodontitis in Turkish women. *Arch Oral Biol* (2015) 60(12):1777–83. doi:10.1016/j.archoralbio.2015.09.013
21. Kayar NA, Alptekin NO, Haliloglu S. Interleukin-1 receptor antagonist levels in gingival crevicular fluid and serum in nonsmoking women with preterm low birth weight and intrauterine growth retardation. *Eur J Dent* (2015) 9(1):109–16. doi:10.4103/1305-7456.149655
22. Leal AS, de Oliveira AE, Brito LM, Lopes FF, Rodrigues VP, Lima KF, et al. Association between chronic apical periodontitis and low-birth-weight preterm births. *J Endod* (2015) 41(3):353–7. doi:10.1016/j.joen.2014.11.018
23. Reza KM, Hamissi JH, Naeini SR, Karimi M. The relationship between maternal periodontal status of and preterm and low birth weight infants in Iran: a case control study. *Glob J Health Sci* (2015) 8(5):184–8. doi:10.5539/gjhs.v8n5p184
24. Pozo E, Mesa F, Ikram MH, Puertas A, Torrecillas-Martinez L, Ortega-Oller I, et al. Preterm birth and/or low birth weight are associated with periodontal disease and the increased placental immunohistochemical expression of inflammatory markers. *Histol Histopathol* (2016) 31(2):231–7. doi:10.14670/HH-11-671
25. Sugita N, Kobayashi T, Kikuchi A, Shimada Y, Hirano E, Sasahara J, et al. Immunoregulatory gene polymorphisms in Japanese women with preterm births and periodontitis. *J Reprod Immunol* (2012) 93(2):94–101. doi:10.1016/j.jri.2012.01.005
26. Abati S, Villa A, Cetin I, Dessole S, Luglie PF, Strohmenger L, et al. Lack of association between maternal periodontal status and adverse pregnancy outcomes: a multicentric epidemiologic study. *J Matern Fetal Neonatal Med* (2013) 26(4):369–72. doi:10.3109/14767058.2012.733776
27. Al HR, Khader YS, Jabali OA, Alchalabi H. Prediction of preterm and low birth weight delivery by maternal periodontal parameters: receiver

operating characteristic (ROC) curve analysis. *Matern Child Health J* (2013) 17(2):299–306. doi:10.1007/s10995-012-0974-2
28. Alchalabi HA, Al HR, Jabali OA, Khader YS. Association between periodontal disease and adverse pregnancy outcomes in a cohort of pregnant women in Jordan. *Clin Exp Obstet Gynecol* (2013) 40(3):399–402.
29. Kumar A, Basra M, Begum N, Rani V, Prasad S, Lamba AK, et al. Association of maternal periodontal health with adverse pregnancy outcome. *J Obstet Gynaecol Res* (2013) 39(1):40–5. doi:10.1111/j.1447-0756.2012.01957.x
30. Wang YL, Liou JD, Pan WL. Association between maternal periodontal disease and preterm delivery and low birth weight. *Taiwan J Obstet Gynecol* (2013) 52(1):71–6. doi:10.1016/j.tjog.2013.01.011
31. Basha S, Shivalinga SH, Noor MR. Maternal periodontitis as a possible risk factor for preterm birth and low birth weight – a prospective study. *Oral Health Prev Dent* (2015) 13(6):537–44. doi:10.3290/j.ohpd.a34053
32. Soroye M, Ayanbadejo P, Savage K, Oluwole A. Association between periodontal disease and pregnancy outcomes. *Odontostomatol Trop* (2015) 38(152):5–16.
33. Tellapragada C, Eshwara VK, Bhat P, Acharya S, Kamath A, Bhat S, et al. Risk factors for preterm birth and low birth weight among pregnant Indian women: a hospital-based prospective study. *J Prev Med Public Health* (2016) 49(3):165–75. doi:10.3961/jpmph.16.022
34. Ali TB, Abidin KZ. Relationship of periodontal disease to pre-term low birth weight infants in a selected population – a prospective study. *Community Dent Health* (2012) 29(1):100–5.
35. Harper LM, Parry S, Stamilio DM, Odibo AO, Cahill AG, Strauss JR, et al. The interaction effect of bacterial vaginosis and periodontal disease on the risk of preterm delivery. *Am J Perinatol* (2012) 29(5):347–52. doi:10.1055/s-0031-1295644
36. Schenkein HA, Koertge TE, Sabatini R, Brooks CN, Gunsolley JC. Birth weight of infants of mothers with aggressive periodontitis. *J Periodontol* (2012) 83(3):279–86. doi:10.1902/jop.2011.110192
37. Santa CI, Herrera D, Martin C, Herrero A, Sanz M. Association between periodontal status and pre-term and/or low-birth weight in Spain: clinical and microbiological parameters. *J Periodontal Res* (2013) 48(4):443–51. doi:10.1111/jre.12024
38. Soucy-Giguere L, Tetu A, Gauthier S, Morand M, Chandad F, Giguere Y, et al. Periodontal disease and adverse pregnancy outcomes: a prospective study in a low-risk population. *J Obstet Gynaecol Can* (2016) 38(4):346–50. doi:10.1016/j.jogc.2016.02.012
39. Lauren M, Minire A, Maldi X, Mirton M, Aferdita M. The impact of periodontitis in the preterm birth and body size of newborns. *Mater Sociomed* (2012) 24(1):44–7. doi:10.5455/msm.2012.24.44-47
40. Stadelmann PF, Eick S, Salvi GE, Surbek D, Mohr S, Burgin W, et al. Increased periodontal inflammation in women with preterm premature rupture of membranes. *Clin Oral Investig* (2015) 19(6):1537–46. doi:10.1007/s00784-014-1371-6
41. Corbella S, Taschieri S, Del FM, Francetti L, Weinstein R, Ferrazzi E. Adverse pregnancy outcomes and periodontitis: a systematic review and meta-analysis exploring potential association. *Quintessence Int* (2016) 47(3):193–204. doi:10.3290/j.qi.a34980
42. Ide M, Papapanou PN. Epidemiology of association between maternal periodontal disease and adverse pregnancy outcomes – systematic review. *J Clin Periodontol* (2013) 40(Suppl 14):S181–94. doi:10.1111/jcpe.12063
43. Baskaradoss JK, Geevarghese A, Al DA. Causes of adverse pregnancy outcomes and the role of maternal periodontal status – a review of the literature. *Open Dent J* (2012) 6:79–84. doi:10.2174/1874210601206010079
44. Corbella S, Taschieri S, Francetti L, De Siena F, Del FM. Periodontal disease as a risk factor for adverse pregnancy outcomes: a systematic review and meta-analysis of case-control studies. *Odontology* (2012) 100(2):232–40. doi:10.1007/s10266-011-0036-z
45. Konopka T, Paradowska-Stolarz A. Periodontitis and risk of preterm birth and low birthweight – a meta-analysis. *Ginekol Pol* (2012) 83(6):446–53.
46. Shanthi V, Vanka A, Bhambal A, Saxena V, Saxena S, Kumar SS. Association of pregnant women periodontal status to preterm and low-birth weight babies: a systematic and evidence-based review. *Dent Res J (Isfahan)* (2012) 9(4):368–80.
47. Martinez DTB, Gayet-Ageron A, Combescure C, Irion O, Baehni P. Association between early preterm birth and periodontitis according to USA and European consensus definitions. *J Matern Fetal Neonatal Med* (2012) 25(11):2160–6. doi:10.3109/14767058.2012.663827
48. Page RC, Eke PI. Case definitions for use in population-based surveillance of periodontitis. *J Periodontol* (2007) 78(7 Suppl):1387–99. doi:10.1902/jop.2007.060264
49. Tonetti MS, Claffey N. Advances in the progression of periodontitis and proposal of definitions of a periodontitis case and disease progression for use in risk factor research. Group C consensus report of the 5th European Workshop in Periodontology. *J Clin Periodontol* (2005) 32(Suppl 6):210–3. doi:10.1111/j.1600-051X.2005.00822.x
50. Hasegawa-Nakamura K, Tateishi F, Nakamura T, Nakajima Y, Kawamata K, Douchi T, et al. The possible mechanism of preterm birth associated with periodontopathic *Porphyromonas gingivalis*. *J Periodontal Res* (2011) 46(4):497–504. doi:10.1111/j.1600-0765.2011.01366.x
51. Vanterpool SF, Been JV, Houben ML, Nikkels PG, De Krijger RR, Zimmermann LJ, et al. *Porphyromonas gingivalis* within placental villous mesenchyme and umbilical cord stroma is associated with adverse pregnancy outcome. *PLoS One* (2016) 11(1):e146157. doi:10.1371/journal.pone.0146157
52. Chen ZB, He L, Kang J, Huang Z, Sha YQ, Zhu WF, et al. [Relationship between the preterm low birth weight infant and the periodontal pathogen bacteria in maternal saliva]. *Beijing Da Xue Xue Bao* (2012) 44(1):29–33.
53. Ye C, Katagiri S, Miyasaka N, Bharti P, Kobayashi H, Takeuchi Y, et al. The anti-phospholipid antibody-dependent and independent effects of periodontopathic bacteria on threatened preterm labor and preterm birth. *Arch Gynecol Obstet* (2013) 288(1):65–72. doi:10.1007/s00404-013-2741-z
54. Gonzales-Marin C, Spratt DA, Allaker RP. Maternal oral origin of *Fusobacterium nucleatum* in adverse pregnancy outcomes as determined using the 16S-23S rRNA gene intergenic transcribed spacer region. *J Med Microbiol* (2013) 62(Pt 1):133–44. doi:10.1099/jmm.0.049452-0
55. Bohrer JC, Kamemoto LE, Almeida PG, Ogasawara KK. Acute chorioamnionitis at term caused by the oral pathogen *Fusobacterium nucleatum*. *Hawaii J Med Public Health* (2012) 71(10):280–1.
56. Cassini MA, Pilloni A, Condo SG, Vitali LA, Pasquantonio G, Cerroni L. Periodontal bacteria in the genital tract: are they related to adverse pregnancy outcome? *Int J Immunopathol Pharmacol* (2013) 26(4):931–9. doi:10.1177/039463201302600411
57. Andonova I, Iliev V, Zivkovic N, Susic E, Bego I, Kotevska V. Can oral anaerobic bacteria cause adverse pregnancy outcomes? *Pril (Makedon Akad Nauk Umet Odd Med Nauki)* (2015) 36(1):137–43.
58. Usin MM, Menso J, Rodriguez VI, Gonzalez A, Tabares S, Parodi R, et al. Association between maternal periodontitis and preterm and/or low birth weight infants in normal pregnancies. *J Matern Fetal Neonatal Med* (2016) 29(1):115–9. doi:10.3109/14767058.2014.987751
59. Blanc V, O'Valle F, Pozo E, Puertas A, Leon R, Mesa F. Oral bacteria in placental tissues: increased molecular detection in pregnant periodontitis patients. *Oral Dis* (2015) 21(7):905–12. doi:10.1111/odi.12364
60. Mesa F, Pozo E, O'Valle F, Puertas A, Magan-Fernandez A, Rosel E, et al. Relationship between periodontal parameters and plasma cytokine profiles in pregnant woman with preterm birth or low birth weight. *Clin Oral Investig* (2016) 20(4):669–74. doi:10.1007/s00784-015-1553-x
61. Cetin I, Pileri P, Villa A, Calabrese S, Ottolenghi L, Abati S. Pathogenic mechanisms linking periodontal diseases with adverse pregnancy outcomes. *Reprod Sci* (2012) 19(6):633–41. doi:10.1177/1933719111432871
62. Stadelmann P, Alessandri R, Eick S, Salvi GE, Surbek D, Sculean A. The potential association between gingival crevicular fluid inflammatory mediators and adverse pregnancy outcomes: a systematic review. *Clin Oral Investig* (2013) 17(6):1453–63. doi:10.1007/s00784-013-0952-0
63. Genco RJ, Van Dyke TE. Prevention: reducing the risk of CVD in patients with periodontitis. *Nat Rev Cardiol* (2010) 7(9):479–80. doi:10.1038/nrcardio.2010.120
64. Tonetti MS. Periodontitis and risk for atherosclerosis: an update on intervention trials. *J Clin Periodontol* (2009) 36(Suppl 10):15–9. doi:10.1111/j.1600-051X.2009.01417.x
65. Patil VA, Desai MH. Effect of periodontal therapy on serum C-reactive protein levels in patients with gingivitis and chronic periodontitis: a clinico-biochemical study. *J Contemp Dent Pract* (2013) 14(2):233–7. doi:10.5005/jp-journals-10024-1305

66. Lyon D, Cheng CY, Howland L, Rattican D, Jallo N, Pickler R, et al. Integrated review of cytokines in maternal, cord, and newborn blood: part I – associations with preterm birth. *Biol Res Nurs* (2010) 11(4):371–6. doi:10.1177/1099800409344620
67. Malaeb S, Dammann O. Fetal inflammatory response and brain injury in the preterm newborn. *J Child Neurol* (2009) 24(9):1119–26. doi:10.1177/0883073809338066
68. Tanaka Y, Narahara H, Takai N, Yoshimatsu J, Anai T, Miyakawa I. Interleukin-1beta and interleukin-8 in cervicovaginal fluid during pregnancy. *Am J Obstet Gynecol* (1998) 179(3 Pt 1):644–9. doi:10.1016/S0002-9378(98)70058-4
69. Jun JK, Yoon BH, Romero R, Kim M, Moon JB, Ki SH, et al. Interleukin 6 determinations in cervical fluid have diagnostic and prognostic value in preterm premature rupture of membranes. *Am J Obstet Gynecol* (2000) 183(4):868–73. doi:10.1067/mob.2000.109034
70. Annells MF, Hart PH, Mullighan CG, Heatley SL, Robinson JS, Bardy P, et al. Interleukins-1, -4, -6, -10, tumor necrosis factor, transforming growth factor-beta, FAS, and mannose-binding protein C gene polymorphisms in Australian women: risk of preterm birth. *Am J Obstet Gynecol* (2004) 191(6):2056–67. doi:10.1016/j.ajog.2004.04.021
71. Moura E, Mattar R, de Souza E, Torloni MR, Goncalves-Primo A, Daher S. Inflammatory cytokine gene polymorphisms and spontaneous preterm birth. *J Reprod Immunol* (2009) 80(1–2):115–21. doi:10.1016/j.jri.2008.11.007
72. Romero R, Espinoza J, Kusanovic JP, Gotsch F, Hassan S, Erez O, et al. The preterm parturition syndrome. *BJOG* (2006) 113(Suppl 3):17–42. doi:10.1111/j.1471-0528.2006.01120.x
73. Goepfert AR, Goldenberg RL, Andrews WW, Hauth JC, Mercer B, Iams J, et al. The preterm prediction study: association between cervical interleukin 6 concentration and spontaneous preterm birth. National Institute of Child Health and Human Development Maternal-Fetal Medicine Units Network. *Am J Obstet Gynecol* (2001) 184(3):483–8. doi:10.1067/mob.2001.109653
74. Ao M, Miyauchi M, Furusho H, Inubushi T, Kitagawa M, Nagasaki A, et al. Dental infection of *Porphyromonas gingivalis* induces preterm birth in mice. *PLoS One* (2015) 10(8):e137249. doi:10.1371/journal.pone.0137249
75. Stockham S, Stamford JE, Roberts CT, Fitzsimmons TR, Marchant C, Bartold PM, et al. Abnormal pregnancy outcomes in mice using an induced periodontitis model and the haematogenous migration of *Fusobacterium nucleatum* sub-species to the murine placenta. *PLoS One* (2015) 10(3):e120050. doi:10.1371/journal.pone.0120050
76. Miyoshi H, Konishi H, Teraoka Y, Urabe S, Furusho H, Miyauchi M, et al. Enhanced expression of contractile-associated proteins and ion channels in preterm delivery model mice with chronic odontogenic *Porphyromonas gingivalis* infection. *Reprod Sci* (2016) 23(7):838–46. doi:10.1177/1933719115620497
77. Coppenhagen-Glazer S, Sol A, Abed J, Naor R, Zhang X, Han YW, et al. Fap2 of *Fusobacterium nucleatum* is a galactose-inhibitable adhesin involved in coaggregation, cell adhesion, and preterm birth. *Infect Immun* (2015) 83(3):1104–13. doi:10.1128/IAI.02838-14
78. Arce RM, Diaz PI, Barros SP, Galloway P, Bobetsis Y, Threadgill D, et al. Characterization of the invasive and inflammatory traits of oral *Campylobacter rectus* in a murine model of fetoplacental growth restriction and in trophoblast cultures. *J Reprod Immunol* (2010) 84(2):145–53. doi:10.1016/j.jri.2009.11.003
79. Ebersole JL, Holt SC, Cappelli D. Periodontitis in pregnant baboons: systemic inflammation and adaptive immune responses and pregnancy outcomes in a baboon model. *J Periodontal Res* (2014) 49(2):226–36. doi:10.1111/jre.12099
80. Arce RM, Barros SP, Wacker B, Peters B, Moss K, Offenbacher S. Increased TLR4 expression in murine placentas after oral infection with periodontal pathogens. *Placenta* (2009) 30(2):156–62. doi:10.1016/j.placenta.2008.11.017
81. Fogacci MF, Barbirato DS, Amaral CS, Da SP, Coelho MO, Bertozi G, et al. No association between periodontitis, preterm birth, or intrauterine growth restriction: experimental study in Wistar rats. *Am J Obstet Gynecol* (2016) 214(6):741–9. doi:10.1016/j.ajog.2015.12.008
82. Riewe SD, Mans JJ, Hirano T, Katz J, Shiverick KT, Brown TA, et al. Human trophoblast responses to *Porphyromonas gingivalis* infection. *Mol Oral Microbiol* (2010) 25(4):252–9. doi:10.1111/j.2041-1014.2010.00573.x
83. Ren H, Li Y, Jiang H, Du M. *Porphyromonas gingivalis* induces IL-8 and IFN-gamma secretion and apoptosis in human extravillous trophoblast derived HTR8/SVneo cells via activation of ERK1/2 and p38 signaling pathways. *Placenta* (2016) 45:8–15. doi:10.1016/j.placenta.2016.06.010
84. Inaba H, Kuboniwa M, Bainbridge B, Yilmaz O, Katz J, Shiverick KT, et al. *Porphyromonas gingivalis* invades human trophoblasts and inhibits proliferation by inducing G1 arrest and apoptosis. *Cell Microbiol* (2009) 11(10):1517–32. doi:10.1111/j.1462-5822.2009.01344.x
85. Inaba H, Kuboniwa M, Sugita H, Lamont RJ, Amano A. Identification of signaling pathways mediating cell cycle arrest and apoptosis induced by *Porphyromonas gingivalis* in human trophoblasts. *Infect Immun* (2012) 80(8):2847–57. doi:10.1128/IAI.00258-12
86. Ren H, Li Y, Jiang H, Du M. Interferon-gamma and Fas are involved in *Porphyromonas gingivalis*-induced apoptosis of human extravillous trophoblast-derived HTR8/SVneo cells via extracellular signal-regulated kinase 1/2 pathway. *J Periodontol* (2016) 87(11):e192–9. doi:10.1902/jop.2016.160259
87. Abrahams VM, Potter JA, Bhat G, Peltier MR, Saade G, Menon R. Bacterial modulation of human fetal membrane toll-like receptor expression. *Am J Reprod Immunol* (2013) 69(1):33–40. doi:10.1111/aji.12016
88. Komine-Aizawa S, Hirohata N, Aizawa S, Abiko Y, Hayakawa S. *Porphyromonas gingivalis* lipopolysaccharide inhibits trophoblast invasion in the presence of nicotine. *Placenta* (2015) 36(1):27–33. doi:10.1016/j.placenta.2014.10.015
89. Li Y, Shibata Y, Zhang L, Kuboyama N, Abiko Y. Periodontal pathogen *Aggregatibacter actinomycetemcomitans* LPS induces mitochondria-dependent-apoptosis in human placental trophoblasts. *Placenta* (2011) 32(1):11–9. doi:10.1016/j.placenta.2010.10.007
90. Khairnar MS, Pawar BR, Marawar PP, Khairnar DM. Estimation of changes in C-reactive protein level and pregnancy outcome after nonsurgical supportive periodontal therapy in women affected with periodontitis in a rural set up of India. *Contemp Clin Dent* (2015) 6(Suppl 1):S5–11. doi:10.4103/0976-237X.152930
91. Bilinska M, Osmola K. [Active periodontitis as a potential risk factor of preterm delivery]. *Ginekol Pol* (2014) 85(5):382–5.
92. Macedo JF, Ribeiro RA, Machado FC, Assis NM, Alves RT, Oliveira AS, et al. Periodontal disease and oral health-related behavior as factors associated with preterm birth: a case-control study in south-eastern Brazil. *J Periodontal Res* (2014) 49(4):458–64. doi:10.1111/jre.12124
93. Fiorini T, Susin C, Da RJ, Weidlich P, Vianna P, Moreira CH, et al. Effect of nonsurgical periodontal therapy on serum and gingival crevicular fluid cytokine levels during pregnancy and postpartum. *J Periodontal Res* (2013) 48(1):126–33. doi:10.1111/j.1600-0765.2012.01513.x
94. Pirie M, Linden G, Irwin C. Intrapregnancy non-surgical periodontal treatment and pregnancy outcome: a randomized controlled trial. *J Periodontol* (2013) 84(10):1391–400. doi:10.1902/jop.2012.120572
95. Weidlich P, Moreira CH, Fiorini T, Musskopf ML, Da RJ, Oppermann ML, et al. Effect of nonsurgical periodontal therapy and strict plaque control on preterm/low birth weight: a randomized controlled clinical trial. *Clin Oral Investig* (2013) 17(1):37–44. doi:10.1007/s00784-012-0679-3
96. Dasanayake AP. Scaling and root planing performed on pregnant women with mild to moderate periodontal disease is not efficacious in reducing preterm birth, low birth weight, or other poor pregnancy outcomes. *J Evid Based Dent Pract* (2012) 12(3):135–7. doi:10.1016/j.jebdp.2012.06.007
97. Kim AJ, Lo AJ, Pullin DA, Thornton-Johnson DS, Karimbux NY. Scaling and root planing treatment for periodontitis to reduce preterm birth and low birth weight: a systematic review and meta-analysis of randomized controlled trials. *J Periodontol* (2012) 83(12):1508–19. doi:10.1902/jop.2012.110636
98. Shah M, Muley A, Muley P. Effect of nonsurgical periodontal therapy during gestation period on adverse pregnancy outcome: a systematic review. *J Matern Fetal Neonatal Med* (2013) 26(17):1691–5. doi:10.3109/14767058.2013.799662

99. Schwendicke F, Karimbux N, Allareddy V, Gluud C. Periodontal treatment for preventing adverse pregnancy outcomes: a meta- and trial sequential analysis. *PLoS One* (2015) 10(6):e129060. doi:10.1371/journal.pone.0129060
100. Boutin A, Demers S, Roberge S, Roy-Morency A, Chandad F, Bujold E. Treatment of periodontal disease and prevention of preterm birth: systematic review and meta-analysis. *Am J Perinatol* (2013) 30(7):537–44. doi:10.1055/s-0032-1329687
101. Condylis B, Le Borgne H, Demoersman J, Campard G, Philippe HJ, Soueidan A. [Interest of periodontitis screening and treatment in pregnancy: systematic review]. *J Gynecol Obstet Biol Reprod (Paris)* (2013) 42(6):511–7. doi:10.1016/j.jgyn.2012.05.012
102. Michalowicz BS, Gustafsson A, Thumbigere-Math V, Buhlin K. The effects of periodontal treatment on pregnancy outcomes. *J Clin Periodontol* (2013) 40(Suppl 14):S195–208. doi:10.1111/jcpe.12081
103. Rosa MI, Pires PD, Medeiros LR, Edelweiss MI, Martinez-Mesa J. Periodontal disease treatment and risk of preterm birth: a systematic review and meta-analysis. *Cad Saude Publica* (2012) 28(10):1823–33. doi:10.1590/S0102-311X2012001000002
104. Jeffcoat M, Parry S, Sammel M, Clothier B, Catlin A, Macones G. Periodontal infection and preterm birth: successful periodontal therapy reduces the risk of preterm birth. *BJOG* (2011) 118(2):250–6. doi:10.1111/j.1471-0528.2010.02713.x
105. Penova-Veselinovic B, Keelan JA, Wang CA, Newnham JP, Pennell CE. Changes in inflammatory mediators in gingival crevicular fluid following periodontal disease treatment in pregnancy: relationship to adverse pregnancy outcome. *J Reprod Immunol* (2015) 112:1–10. doi:10.1016/j.jri.2015.05.002
106. Armitage GC. Development of a classification system for periodontal diseases and conditions. *Ann Periodontol* (1999) 4(1):1–6. doi:10.1902/annals.1999.4.1.1
107. Armitage GC. Clinical evaluation of periodontal diseases. *Periodontol 2000* (1995) 7:39–53. doi:10.1111/j.1600-0757.1995.tb00035.x
108. Riche EL, Boggess KA, Lieff S, Murtha AP, Auten RL, Beck JD, et al. Periodontal disease increases the risk of preterm delivery among preeclamptic women. *Ann Periodontol* (2002) 7(1):95–101. doi:10.1902/annals.2002.7.1.95
109. Sharma R, Maimanuku LR, Morse Z, Pack AR. Preterm low birth weights associated with periodontal disease in the Fiji Islands. *Int Dent J* (2007) 57(4):257–60. doi:10.1111/j.1875-595X.2007.tb00129.x
110. Offenbacher S, Boggess KA, Murtha AP, Jared HL, Lieff S, McKaig RG, et al. Progressive periodontal disease and risk of very preterm delivery. *Obstet Gynecol* (2006) 107(1):29–36. doi:10.1097/01.AOG.0000190212.87012.96
111. Kazmierczak W, Fiegler P, Wegrzyn P, Fiegler-Mecik H, Przybylek B, Kaminski K. [Risk assessment for preterm delivery in pregnant women with active periodontitis]. *Ginekol Pol* (2005) 76(8):632–8.
112. Gomes-Filho IS, Cruz SS, Rezende EJ, Dos SC, Soledade KR, Magalhaes MA, et al. Exposure measurement in the association between periodontal disease and prematurity/low birth weight. *J Clin Periodontol* (2007) 34(11):957–63. doi:10.1111/j.1600-051X.2007.01141.x
113. Manau C, Echeverria A, Agueda A, Guerrero A, Echeverria JJ. Periodontal disease definition may determine the association between periodontitis and pregnancy outcomes. *J Clin Periodontol* (2008) 35(5):385–97. doi:10.1111/j.1600-051X.2008.01222.x
114. Nabet C, Lelong N, Colombier ML, Sixou M, Musset AM, Goffinet F, et al. Maternal periodontitis and the causes of preterm birth: the case-control Epipap study. *J Clin Periodontol* (2010) 37(1):37–45. doi:10.1111/j.1600-051X.2009.01503.x
115. Resende M, Pinto E, Pinto M, Montenegro N. [Periodontal disease, tobacco and preterm delivery]. *Acta Med Port* (2011) 24(Suppl 2):419–30.
116. Kazmierczak W, Fiegler P, Fiegler-Mecik H, Mecik TJ, Przybylek B. [Influence of the prevention of maternal periodontitis on the risk of preterm delivery]. *Wiad Lek* (2004) 57(Suppl 1):148–51.
117. Pattrapornnan P, DeRouen TA, Songpaisan Y. Increased risks of preterm birth and a low-birth-weight baby in Thai human immunodeficiency virus-positive pregnant women with periodontitis. *J Periodontol* (2012) 83(11):1372–81. doi:10.1902/jop.2012.110500
118. Pattanashetti JI, Nagathan VM, Rao SM. Evaluation of periodontitis as a risk for preterm birth among preeclamptic and non-preeclamptic pregnant women – a case control study. *J Clin Diagn Res* (2013) 7(8):1776–8. doi:10.7860/JCDR/2013/6497.3308
119. Lee HJ, Ha JE, Bae KH. Synergistic effect of maternal obesity and periodontitis on preterm birth in women with pre-eclampsia: a prospective study. *J Clin Periodontol* (2016) 43(8):646–51. doi:10.1111/jcpe.12574
120. Lee HJ, Jun JK, Lee SM, Ha JE, Paik DI, Bae KH. Association between obesity and periodontitis in pregnant females. *J Periodontol* (2014) 85(7):e224–31. doi:10.1902/jop.2014.130578
121. Blasco-Baque V, Garidou L, Pomie C, Escoula Q, Loubieres P, Le Gall-David S, et al. Periodontitis induced by *Porphyromonas gingivalis* drives periodontal microbiota dysbiosis and insulin resistance via an impaired adaptive immune response. *Gut* (2016). doi:10.1136/gutjnl-2015-309897
122. Jeffcoat MK, Jeffcoat RL, Tanna N, Parry SH. Association of a common genetic factor, PTGER3, with outcome of periodontal therapy and preterm birth. *J Periodontol* (2014) 85(3):446–54. doi:10.1902/jop.2013.130006

Conflict of Interest Statement: The authors declare that the research was conducted in the absence of any commercial or financial relationships that could be construed as a potential conflict of interest.

Copyright © 2017 Ren and Du. This is an open-access article distributed under the terms of the Creative Commons Attribution License (CC BY). The use, distribution or reproduction in other forums is permitted, provided the original author(s) or licensor are credited and that the original publication in this journal is cited, in accordance with accepted academic practice. No use, distribution or reproduction is permitted which does not comply with these terms.

frontiers in Immunology

ORIGINAL RESEARCH
published: 23 March 2017
doi: 10.3389/fimmu.2017.00321

Role of Anti-Osteopontin Antibodies in Multiple Sclerosis and Experimental Autoimmune Encephalomyelitis

Nausicaa Clemente[1], Cristoforo Comi[2], Davide Raineri[1], Giuseppe Cappellano[3], Domizia Vecchio[2], Elisabetta Orilieri[1], Casimiro L. Gigliotti[1], Elena Boggio[1], Chiara Dianzani[4], Melissa Sorosina[5], Filippo Martinelli-Boneschi[5], Marzia Caldano[6], Antonio Bertolotto[6], Luca Ambrogio[7], Daniele Sblattero[8], Tiziana Cena[9], Maurizio Leone[10], Umberto Dianzani[1] and Annalisa Chiocchetti[1]*

[1] Department of Health Sciences, Interdisciplinary Research Center of Autoimmune Diseases (IRCAD), University of Piemonte Orientale (UPO), Novara, Italy, [2] Department of Translational Medicine, IRCAD, Neurology Unit, University of Piemonte Orientale (UPO), Novara, Italy, [3] Division for Experimental Pathophysiology and Immunology, Biocenter, Medical University of Innsbruck, Innsbruck, Austria, [4] Department of Drug Science and Technology, University of Turin, Torino, Italy, [5] Laboratory of Human Genetics of Neurological Disorders, CNS Inflammatory Unit, Division of Neuroscience, Institute of Experimental Neurology (INSPE), San Raffaele Scientific Institute, Milano, Italy, [6] Neurology Unit 2, Centro Riferimento Regionale Sclerosi Multipla (CRESM), Azienda Ospedaliero-Universitaria San Luigi, Orbassano, Italy, [7] ASO Neurologia, Azienda Ospedaliera S. Croce e Carle, Cuneo, Italy, [8] Department of Life Science, University of Trieste, Trieste, Italy, [9] Department of Translational Medicine, Medical Statistics Unit, University of Piemonte Orientale (UPO), Novara, Italy, [10] IRCAD, Neurology Unit, Scientific Institute, Hospital "Casa Sollievo della Sofferenza", San Giovanni Rotondo, Italy

OPEN ACCESS

Edited by:
Jixin Zhong, Case Western Reserve University, USA

Reviewed by:
Rui Li, Montreal Neurological Institute and Hospital, Canada
Qingfeng Chen, University of Texas Southwestern Medical Center, USA
Liman Zhang, Harvard Medical School, USA

***Correspondence:**
Umberto Dianzani
umberto.dianzani@med.uniupo.it

Specialty section:
This article was submitted to Inflammation, a section of the journal Frontiers in Immunology

Received: *27 January 2017*
Accepted: *07 March 2017*
Published: *23 March 2017*

Citation:
Clemente N, Comi C, Raineri D, Cappellano G, Vecchio D, Orilieri E, Gigliotti CL, Boggio E, Dianzani C, Sorosina M, Martinelli-Boneschi F, Caldano M, Bertolotto A, Ambrogio L, Sblattero D, Cena T, Leone M, Dianzani U and Chiocchetti A (2017) Role of Anti-Osteopontin Antibodies in Multiple Sclerosis and Experimental Autoimmune Encephalomyelitis. Front. Immunol. 8:321. doi: 10.3389/fimmu.2017.00321

Osteopontin (OPN) is highly expressed in demyelinating lesions in multiple sclerosis (MS) and experimental autoimmune encephalomyelitis (EAE). OPN is cleaved by thrombin into N- (OPN-N) and C-terminal (OPN-C) fragments with different ligands and functions. In EAE, administering recombinant OPN induces relapses, whereas treatment with anti-OPN antibodies ameliorates the disease. Anti-OPN autoantibodies (autoAbs) are spontaneously produced during EAE but have never been detected in MS. The aim of the study was to evaluate anti-OPN autoAbs in the serum of MS patients, correlate them with disease course, and recapitulate the human findings in EAE. We performed ELISA in the serum of 122 patients collected cross-sectionally, and 50 patients with relapsing–remitting (RR) disease collected at diagnosis and followed longitudinally for 10 years. In the cross-sectional patients, the autoAb levels were higher in the RR patients than in the primary- and secondary-progressive MS and healthy control groups, and they were highest in the initial stages of the disease. In the longitudinal group, the levels at diagnosis directly correlated with the number of relapses during the following 10 years. Moreover, in patients with active disease, who underwent disease-modifying treatments, autoAbs were higher than in untreated patients and were associated with low MS severity score. The autoAb displayed neutralizing activity and mainly recognized OPN-C rather than OPN-N. To confirm the clinical effect of these autoAbs *in vivo*, EAE was induced using myelin oligodendrocyte glycoprotein $MOG_{35–55}$ in C57BL/6 mice pre-vaccinated with ovalbumin (OVA)-linked OPN or OVA alone. We then evaluated the titer of antibodies to OPN, the clinical scores and *in vitro* cytokine secretion by spleen

lymphocytes. Vaccination significantly induced antibodies against OPN during EAE, decreased disease severity, and the protective effect was correlated with decreased T cell secretion of interleukin 17 and interferon-γ *ex vivo*. The best effect was obtained with OPN-C, which induced significantly faster and more complete remission than other OPN vaccines. In conclusion, these data suggest that production of anti-OPN autoAbs may favor remission in both MS and EAE. Novel strategies boosting their levels, such as vaccination or passive immunization, may be proposed as a future strategy in personalized MS therapy.

Keywords: osteopontin, multiple sclerosis, autoantibodies, experimental autoimmune encephalomyelitis, vaccination

INTRODUCTION

Multiple sclerosis (MS) is an inflammatory disease of the central nervous system (CNS) characterized by an autoimmune attack against the myelin sheaths and axons resulting in demyelination and axonal loss (1). MS patients display variable clinical courses; at onset, approximately 15% of patients display a primary-progressive (PP) form, whereas the remainder start out with a relapsing–remitting (RR) form, and most of those patients switch to a secondary-progressive (SP) form within 10–30 years (2). An increasing number of disease-modifying treatments (DMTs) are available for RR MS, and a key challenge in therapeutic decision-making is effective treatment stratification, given uncertain prognoses (3).

Data obtained in animal models and humans strongly suggest that osteopontin (OPN) plays a role in the pathogenesis of MS (4). OPN is a 60 kDa secreted phosphoprotein functioning as a free cytokine in body fluids or as an immobilized extracellular matrix molecule in mineralized tissue (5). Its expression is increased in the sera of patients with several autoimmune diseases, including MS (6–9), and it may influence the development of autoimmunity through its immunoregulatory and pro-inflammatory effects. The OPN transcript is abundant in plaques dissected from the brains of MS patients, whereas it is absent in control brain tissue (10). A similar finding has been obtained in experimental autoimmune encephalomyelitis (EAE), an animal model of MS (10, 11). In blood and cerebrospinal fluid of MS patients, OPN levels are increased and correlate with the clinical stage because higher levels have been detected in RR-MS patients than in PP-MS and SP-MS patients (6). Moreover, in RR-MS patients, OPN levels increase during relapses and decrease in the remission phase without substantial influence by interferon (IFN)-β treatment (12).

Genetic analyses have associated variations of the *OPN* gene with MS (6). In this context, we found variants of the *OPN* gene that were associated with (i) increased risk for MS (an approximately 1.5-fold increase); (ii) severe disease course, with fast switching from a RR to a SP form and evolution of disability; and (iii) production of high levels of OPN because of increased stability of the encoded mRNA (6, 13).

In MS lesions, high OPN levels are present in the perivascular cuff, which surrounds the inflamed blood vessels, contains inflammatory lymphocytes, and is delimited by the endothelium and the basement membrane. At this site, OPN may play a role in lymphocyte recruitment into the MS lesion, which involves α4β1 integrin, the target of natalizumab, an established DMT. During inflammation, thrombin acts on a cleavage site located in the middle of the OPN sequence, near to an arginine–glycine–aspartate (RGD) motif involved in binding several integrins (14), to generate two OPN fragments, one N-terminal (OPN-N) and one C-terminal (OPN-C). OPN-C contains the CD44-binding site involved in the downregulation of interleukin (IL)-10 expression and inhibition of lymphocyte apoptosis (15). OPN-N contains the RGD motif and two cryptic α4β1 integrin-binding sites unmasked by thrombin cleavage, and it is involved in the induction of IFN-γ secretion in T cells (14, 16). The functional activity of the two fragments has been mostly distinguished *in vitro* (17), but the observation that, in carotid plaques of patients with hypertension, levels of OPN-N are higher than those of OPN-C suggests that the two fragments may play different roles also in pathologic conditions *in vivo* (16).

Chabas et al. showed that $OPN^{-/-}$ mice were resistant to progressive EAE and had frequent remission; notably, myelin-reactive T cells produce more IL-10 and less IFN-γ in these mice than in their wild-type counterparts (10). Moreover, treatment with OPN exacerbated EAE in both wild-type and, to a greater extent, $OPN^{-/-}$ mice. In $OPN^{-/-}$ mice, daily administration of OPN during the spontaneous recovery of EAE counteracted the ongoing remission and induced a relapse followed by a progressive severe disease, leading to death (18).

We have recently shown that thrombin-mediated cleavage of OPN plays a role in OPN-mediated relapse induction, since a recombinant OPN-mutant resistant to thrombin-mediated cleavage was less effective than wild-type OPN in inducing the EAE relapse, and OPN-C was more effective than OPN-N (17).

Steinman et al. showed that EAE induction triggered the production of anti-OPN autoantibodies (autoAbs), and remission occurred when their titers peaked (19). Moreover, DNA vaccination with a plasmid encoding OPN before EAE induction boosted the production of these autoAbs and ameliorated the chronic course of the disease. In humans, autoAbs against OPN have been reported in rheumatoid arthritis and osteoarthritis, and their serum level was inversely correlated with markers of disease activity (20). Moreover, passive immunization with antibodies against the cryptic epitope of OPN-N exerted beneficial effects in mouse and primate models of rheumatoid arthritis (21). These

data are in accordance with reports showing the production of autoAbs against inflammatory cytokines in several autoimmune diseases and suggesting that they may play a role in counteracting the pathological response (22).

The aim of the research reported here was to evaluate anti-OPN autoAbs in the serum of MS patients, to determine their correlation with the disease course, and to perform preclinical studies assessing the possible use of anti-OPN immunization in MS therapy. The results showed that high levels of anti-OPN autoAbs are displayed by RR-MS patients, especially in the remission phase, and may have a prognostic value at diagnosis. These autoAbs displayed neutralizing activity, mainly recognized OPN-C, and decreased disease severity in EAE.

MATERIALS AND METHODS

Patients

We enrolled two groups of MS patients diagnosed according to the 2001 McDonald criteria (23):

i) a cross-sectional group of 122 patients (73 females, 49 males, mean age 43 ± SD 11 years). Seventy-two patients had RR-, 29 PP-, and 21 SP-MS course. Patients were enrolled from the MS Centers of the Maggiore University Hospital (Novara), San Luigi Hospital (Orbassano, Turin), and San Raffaele Hospital (Milano). Patients and controls were Caucasian, Italian, and unrelated. Healthy controls (HCs, $n = 40$) did not differ in age and gender from the patients.

ii) a longitudinal group of 50 bout-onset patients, recruited during a prospective study aimed at identifying predictors of disease progression (24). We included patients still on regular follow-up 10 years after diagnosis, and of whom we stored serum at time of diagnosis. Clinical data collected in the prospective cohort included age at onset, expanded disability status score, number of relapses updated at 10 years, and any DMTs. We also calculated the Multiple Sclerosis Severity Score (MSSS) at 10 years for each patient (25). DMTs included both first line (beta-IFN and glatiramer acetate) and second line treatments (azathioprine, natalizumab, and fingolimod). Clinical features of the longitudinal cohort are shown in **Table 1**. Patients were enrolled from the MS Centers of the Maggiore University Hospital (Novara) and Santa Croce e Carle Hospital (Cuneo).

Written informed consent was obtained from all subjects, and analyses were conducted according to the Declaration of Helsinki and approved by the ethical committee of University Hospital of Novara (reference no. CE1804).

TABLE 1 | Clinical variables in multiple sclerosis (MS) patients followed for at least 10 years.

	MS patients with 10-year follow-up ($n = 50$)
Female, *n* (%)	28 (56)
Follow-up, years, mean (±SD)	12.0 (±1.2)
Age of onset, years, mean (±SD)	32.0 (±9.9)
Osteopontin (OPN) levels, pg/ml, mean (±SD)	4,952 (±3,441)
OPN autoantibody levels, optical density, mean (±SD)	0.4860 (±0.3415)
Mono-symptomatic onset, *n* (%)	24 (48)
Expanded disability status score (EDSS) at first relapse, median (min–max)	2.5 (1–7.5)
EDSS at last visit, median (min–max)	2 (0–9)
Multiple Sclerosis Severity Score, mean (±SD)	2.7 (±2.4)
N relapses at 5 years, median (min–max)	3 (1–14)
N relapses at 10 years, median (min–max)	5 (1–23)
MS course at 10 years, *n* (%)	
– Relapsing–remitting	45 (90)
– Secondary progressive	5 (10)
Disease-modifying treatment, *n* (%)	32 (64)

Cloning and Production of OPN Recombinant Proteins

cDNA coding for the human and murine OPN full-length (OPN-FL), OPN-N, and OPN-C were cloned by PCR into a pUCOE expression vector as previously described (17) and stably transfected in Chinese hamster ovary cells (CHOs). Cell supernatants were collected, and the recombinant proteins were purified on a nickel-nitrilotriacetic agarose resin (Qiagen, Limburg, Netherlands) and characterized by Western blotting using either an antibody directed against the His tag (Tetra-His Antibody, Qiagen, Valencia, CA, USA) or an anti-OPN antibody directed against an epitope located in the N- or C-terminal half of the molecule: SPP1 polyclonal antibody (Invitrogen) and polyclonal anti-osteopontin antibody (Millipore, Billerica, MA, USA), respectively (17).

Detection of Anti-OPN AutoAbs by ELISA

Serum anti-OPN autoAbs were assessed by a custom-made immunoenzymatic assay (ELISA). Briefly, polystyrene ELISA Maxi-Sorp plates (Nunc, Roskilde, Denmark) were coated by overnight incubation at 4°C with 2 µg/ml of the FL-, N-, or C-OPN (recombinant OPN) as capture protein. Non-specific binding was blocked by 1 h incubation with 0.3 ml of 0.05% Tween 20 in phosphate buffered saline (PBS), pH 7.4. Each serum sample (0.1 ml diluted 1:100 in 0.05% Tween 20 in PBS, pH 7.4) was added in duplicate and incubated for 2 h at 37°C. After 10 washes with 0.05% Tween 20 in PBS, antibody binding was revealed by peroxidase-conjugated goat anti-human immunoglobulin (Ig)G (dilution 1:4.500) (Dako, Glostrup, Denmark). The results were expressed as optical density at 450 nm.

Immune Complexes Dissociation

Heat-mediated dissociation of immune complex was obtained by boiling diluted serum samples and each point of the OPN standard curve for 5 min. After 4 min chill on ice, samples were loaded into a 96-well plate for ELISA evaluation, and the results were compared to non-boiled samples. Concentration of OPN was measured by commercial ELISA according to the manufacturers (R&D system, Minneapolis, MN, USA). Absorbance was detected with a microplate reader (Bio-Rad, Hercules, CA, USA), and the I-smart program was used to calculate the standard curve.

Activation-Induced Cell Death (AICD)

Activation-induced cell death was evaluated on T cell lines obtained by activating PBMC with phytohemagglutinin (PHA) at days 0 (1 μg/ml) and cultured in RPMI 1640 medium + 10% FBS + IL-2 (2 U/ml) (Sigma, Saint Louis, MO, USA) for 6 days. In the AICD assay, cells (5×10^4/well) were cultured in wells coated with anti-CD3 mAb (OKT3, 10 μg/ml) with RPMI + 5% FBS + IL-2 (1 U/ml) in the presence or absence of recombinant OPN (1 μg/ml). AICD was performed also in the presence of IgG purified (10 μg/ml), with protein G sepharose resin (Ge Healthcare, Piscataway, NJ, USA), from three patients displaying high levels of anti-OPN autoAbs. The control was done by using a commercial goat anti-OPN-neutralizing Ab (R&D system). Live cells were then counted in each well using the trypan blue exclusion test. Assays were performed in triplicate and results were expressed as relative cell survival % calculated as follows: (total live cell count in the assay well/total live cell count in the respective control well) × 100.

Mouse Vaccination and EAE Induction

Mouse OPN-FL, OPN-N, and OPN-C were cross-linked to ovalbumin (OVA) (Sigma) with glutaraldehyde (Sigma) as reported (26).

The experimental protocol and animal handling were approved by the ethical committee of the University of Piemonte Orientale (reference no. 10821, 10/2013), Novara, Italy. Four-week-old female C57BL/6 mice ($n = 8/10$ each group) were anesthetized with isoflurane and immunized weekly intra-peritoneally for 4 weeks with 10 μg of OPN-FL/OVA, 5 μg of OPN-N/OVA or OPN-C/OVA or 10 μg of OVA in 50 μl glycine buffer, 0.15 M, pH 5.7, and 50 μl of incomplete Freund adjuvant (Sigma). EAE was induced 1 week after the last immunization with 200 μg of $MOG_{35–55}$ peptide (Espikem, Florence, Italy) and scored as reported (22).

Mouse splenocytes were purified and cultured in the presence or absence of 10 μg/ml $MOG_{35–55}$ as reported. After 5 days, levels of IFN-γ, IL-10, IL-4, and IL-17 were evaluated by ELISA (Biolegend, San Diego, CA, USA) in the supernatants and cell proliferation by incorporation of [^{3}H] thymidine (27).

Recombinant mAb Production

OPN full-length was used as a target for selecting antibodies from a phage display Ab library as previously described (28). The selection was performed in immuno tubes coated with recombinant protein incubated overnight at 4°C in PBS. The panning procedure was repeated twice. In total, 96 random clones were selected, and a specific positive clone to OPN-C was identified using phage ELISA. The positive scFv clone was converted into the human scFv–Fc format by subcloning into the pMB-SV5 (29) vector containing the human hinge–CH2–CH3 domain. For antibody production, CHOs cell lines were transfected and stable clones obtained through selection with hygromicin B (500 μg/ml, Invitrogen). The scFv–Fc molecules were purified from cell culture supernatant using a HiTrap protein G column (GE Healthcare). After elution, the preparations of purified scFv–Fc were dialyzed in BupHTM phosphate buffer (Thermo Fisher Scientific, Waltham, MA, USA), aliquoted, and stored at −80°C. The selected mAb was tested by ELISA for its capacity to bind both human and mouse OPN-C and OPN-FL. The mAb was also tested during EAE in a passive immunization protocol.

Statistical Analysis

The non-parametric Mann–Whitney *U*-test was used to compare autoAb levels in the different groups of subjects; the Pearson correlation coefficient was used to test correlations. The Wilcoxon test was used to compare autoAbs to OPN-C and OPN-N in each subject; the Friedman ANOVA test for repeated measures followed by Dunn's multiple comparison was used to compare the daily clinical EAE score (GraphPad Software, San Diego, CA, USA). p Values below 0.05 were considered statistically significant. The statistical analyses were performed with GraphPad Instat software (GraphPad Software).

RESULTS

Detection of Anti-OPN AutoAbs in MS Patients

Serum anti-OPN autoAbs were evaluated in 122 cross-sectional MS patients (72 RR, 29 PP, 21 SP) and 40 HCs by ELISA using OPN-FL. Anti-OPN autoAbs were detected in the serum of both patients and controls, but the titer was significantly higher in patients than in the controls (0.278 vs 0.147, $p < 0.0001$; **Figure 1A**). Analysis of the different MS clinical forms showed that autoAb levels were significantly higher in RR patients in relapse or remission than in SP and PP patients and HCs (0.289 vs 0.168 vs 0.169 vs 0.147; **Figure 1A**). By contrast, no differences were detected among SP and PP patients and HCs. Moreover, in RR-MS patients, the autoAb levels were higher in those in remission than in those in relapse (0.368 vs 0.237; $p < 0.01$), and they displayed an inverse correlation with disease duration at the time of blood withdrawal, which was not evident in the other disease courses (**Figure 1B**). These data suggest that the inflammatory phase of the disease, displaying high levels of OPN, drives production of anti-OPN autoAbs.

Anti-OPN-FL AutoAbs at Diagnosis and Clinical Outcome

The second cohort of patients comprised 50 consecutive bout-onset patients followed up for more than 10 years whose serum was withdrawn at diagnosis. In these patients, we evaluated the serum levels of anti-OPN autoAbs and determined their correlation with the clinical outcome after 10 years. The results showed a direct correlation between autoAb levels at diagnosis and the number of relapses occurring in the following 10 years ($r = 0.542$, $p < 0.0001$; **Figure 2A**). By contrast, no correlation was found with the MSSS after 10 years ($r = -0.029$, $p = 0.837$). Moreover, the autoAb levels were higher in patients who subsequently received DMTs ($n = 31$) than in those who remained untreated ($n = 19$, $p < 0.0001$; **Figure 2B**). Accordingly, all patients subsequently treated ($n = 31$) displayed levels higher than the 75th percentile of HC values, whereas most untreated patients ($n = 12/19$, 63%) displayed levels lower than this cutoff. Using the 75th percentile of HC values as a cutoff in untreated patients, we found that the MSSS

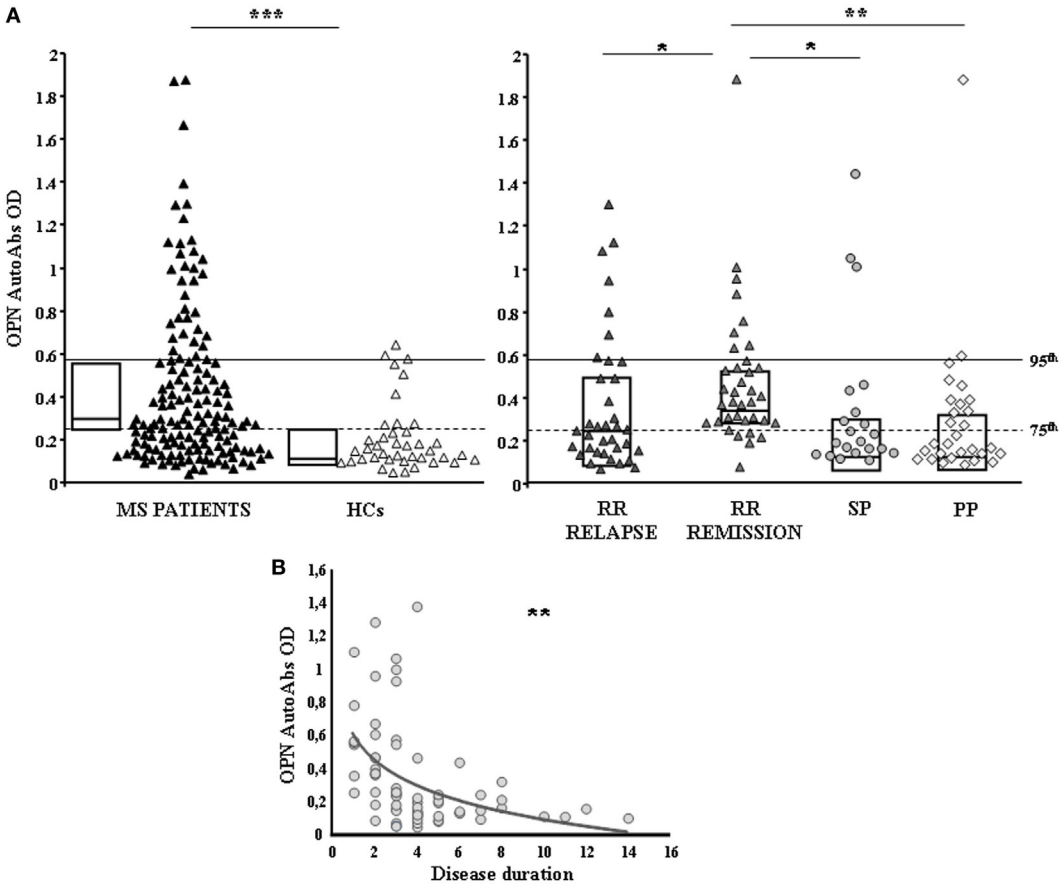

FIGURE 1 | Anti-OPN autoantibodies (autoAbs) are increased in relapsing–remitting (RR) patients compared with secondary-progressive (SP) and primary-progressive (PP) patients and healthy controls (HCs). **(A)** AutoAbs to osteopontin (OPN) in multiple sclerosis (MS) patients and HCs. AutoAbs detected by ELISA using OPN full-length as the capture protein. In the left panel, black triangles mark MS patients and white triangles the HCs. In the right panel, patients are stratified according to their clinical form at the time of blood withdrawal. Dark gray triangles: RR-relapse MS patients; light gray triangles: RR-remission MS patients; gray circles: SP-MS patients; gray diamonds: PP-MS patients; boxes: interquartile range with medians. *p* Values were calculated with the Mann–Whitney *U*-test. The horizontal lines indicate the 75th (dashed line) and 95th (continuous line) percentiles of the HCs. **(B)** Inverse correlation between autoAbs to OPN and disease duration in RR patients (Pearson correlation test) (*$p < 0.01$, **$p < 0.001$, ***$p < 0.0001$).

after 10 years was significantly lower in patients with low autoAb levels ($n = 12$) than in those with high levels ($n = 7$) (median 1.01, range 0.64–1.53 vs 3.25, 1.90–4.3, $p = 0.020$; **Figure 2C**). By contrast, when the cutoff was set at the 95th percentile of HC values in treated patients, the MSSS after 10 years was lower in those with high autoAb levels at diagnosis ($n = 15$) than in those with low levels ($n = 16$) (median 1.70, range 0.96–2.78 vs 2.54, 2.09–6.18, $p = 0.030$; **Figure 2C**). Consistently, we found that autoAb levels and the MSSS displayed a significant inverse correlation in treated patients ($r = -0.374$, $p = 0.038$; **Figure 2D**). Finally, no difference in number of relapses at 10 years was found on comparing both treated and untreated patients with different autoAb levels (data not shown).

In Vitro AutoAbs Characterization

Since serum contains both OPN and anti-OPN autoAbs, these may react to form immune complexes *in vivo*, thus blocking the cytokine activity and facilitating its removal from the bloodstream. To assess this possibility, we evaluated the amount of OPN in the sera before and after heat-mediated immune complexes dissociation. The results showed that heat increased the amount of OPN detected in all of the tested sera (**Figure 3A**). This was not ascribable to unmasking of cryptic epitopes by heat, since boiling did not increase the amount of OPN detected in the standard curve by our ELISA (data not shown).

Since we had previously demonstrated that OPN inhibits AICD (17), we used this test to investigate the autoAbs-neutralizing properties on OPN biological activity. AICD was induced in PHA-activated PBMC from healthy donors in the presence and absence of OPN-FL and each of three preparations of IgG purified from patients displaying high levels of anti-OPN autoAbs (>75th percentile of the controls). Anti-human OPN polyclonal antibodies were used as positive control of OPN-neutralizing antibodies. The results showed that all IgG preparations were able to neutralize the protective effect of OPN-FL on AICD at the same level as the anti-OPN-neutralizing Ab (**Figure 3B**).

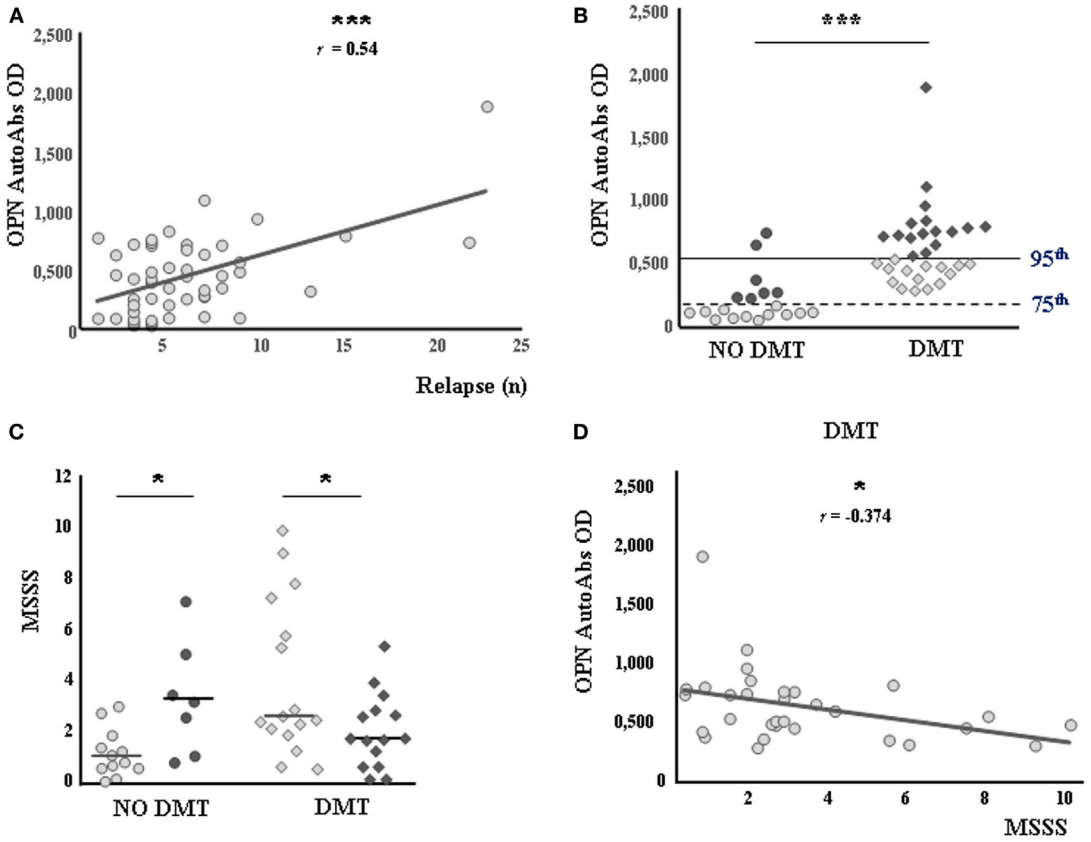

FIGURE 2 | Autoantibodies (autoAbs) to osteopontin (OPN) at diagnosis predict therapeutic benefits and a reduced Multiple Sclerosis Severity Score (MSSS). **(A)** Direct correlation between anti-OPN autoAbs and the number of relapses occurring over 10 years (Pearson correlation test). **(B)** Anti-OPN autoAbs in patients not receiving (circles) or receiving (diamonds) disease-modifying treatments (DMTs). The horizontal lines indicate the 75th (dashed line) and 95th (continuous line) percentiles of the healthy controls. Low expressors and high expressors of each group are shown in pale color and in dark color, respectively. **(C)** MSSS in patients with or without DMTs. Low expressors are shown in pale color; high expressors are shown in dark color, as in the previous panel. **(D)** Negative correlation between autoAbs to OPN and the MSSS in the treated group (Pearson correlation test) (*$p < 0.05$, ***$p < 0.0001$).

AutoAbs to OPN-C Are Higher than Those to OPN-N in MS Sera

To map the epitopes recognized by the autoAbs, we selected sera from 30 RR, 10 PP, and 10 SP patients displaying high levels (>75th percentile of the controls) of anti-OPN autoAbs and used the appropriate ELISA to compare their ability to recognize either OPN-C or OPN-N. **Figure 4** shows that all sera recognized both OPN-N and OPN-C, but the latter was always more highly recognized than the former. Moreover, the levels of autoAbs against OPN-C were higher in RR than in PP and SP, whereas those against OPN-N were higher in RR and SP than in PP (**Figure 4**).

Active Immunization against OPN-C Protects Mice from EAE

To assess the effect of the anti-OPN response *in vivo*, C57BL/6 mice were immunized four times with 10 μg of either mouse OPN-FL or OPN-N or OPN-C cross-linked to OVA. Then, EAE was induced with $MOG_{35–55}$ 1 week after the last immunization.

The serum levels of anti-OPN autoAbs were evaluated by ELISA using mouse OPN-FL immediately before the first immunization (−T32), at each immunization point (−T24, −T16, −T8), immediately before EAE induction (T0), at three points during the relapse (T16, T23, T29), and in the remission phase (T41). **Figure 5A** shows that all OPN vaccinations induced anti-OPN autoAbs detectable at the time of the fourth immunization (−T8) but, after 1 week (T0), these autoAbs remained at low levels in the mice vaccinated with OPN-N, while in those vaccinated with either OPN-FL or OPN-C, they increased to a maximum at the peak of disease (T29) and then decreased during the remission phase (T41).

Analysis of the course of EAE showed that the onset of the disease was delayed and its severity reduced by all OPN vaccinations, because the mean clinical score was 1.64 ± 0.14 (mean ± SE) in control mice vaccinated with OVA, compared to 1.04 ± 0.1 ($p < 0.001$), 1.13 ± 0.11 ($p < 0.001$), and 0.81 ± 0.09 ($p < 0.001$) in those vaccinated with OPN-FL, OPN-N, and OPN-C, respectively. Moreover, mice vaccinated with OPN-C displayed faster and more complete remission than those in the other groups (**Figure 5B**).

To analyze the effect of OPN immunization on the anti-$MOG_{35–55}$ T cells response, spleen lymphocytes were obtained at

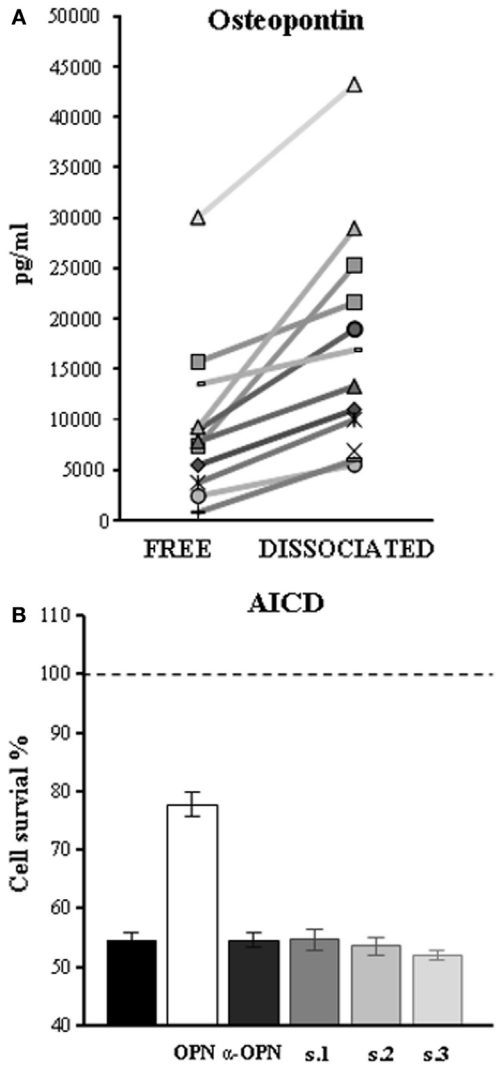

FIGURE 3 | Autoantibodies (autoAbs) to osteopontin (OPN) in serum of multiple sclerosis (MS) patients form immune complexes and neutralize OPN activities. **(A)** Heat-mediated dissociation of immune complexes increases the amount of OPN in the sera of MS patients as detected by ELISA. Each symbol represents serum from a different patient. **(B)** AutoAbs to OPN reverse inhibition of activation-induced cell death (AICD) mediated by OPN, by neutralizing its effect. AICD was induced by treating phytohemagglutinin-activated PBMC cell cultures with anti-CD3 mAb (black histogram) and cell survival detected 18 h later; results are expressed as relative cell survival % by setting 100% on the cultures performed in the absence of the anti-CD3 mAb and their means (dashed line). Histograms represent AICD in the presence of recombinant OPN (white), a commercial-neutralizing antibody to OPN (dark gray), or serum of three high-expressor patients (s1, s2, and s3).

T29 and cultured for 5 days in the presence of $MOG_{35–55}$. Cell proliferation was then assessed by [^{3}H] thymidine uptake, and levels of IFN-γ, IL-4, IL-17A, and IL-10 were evaluated in the culture supernatants by ELISA. Cells from mice vaccinated with either OPN-FL or OPN-C produced lower amounts of IL-17A and IFN-γ than those vaccinated with either OPN-N or OVA (**Figure 5C**). By contrast, proliferation (**Figure 5C**) and secretion of IL-10 and IL-4 were not significantly different in the different groups of mice (data not shown).

Passive Immunization with an Anti-OPN-C mAb Reduces Disability in EAE

To assess the *in vivo* effect of the human anti-OPN autoAbs, we produced a human recombinant mAb that was selected according to its capacity to bind human or mouse OPN-C, but not OPN-N (**Figure 6A**), and to neutralize the human OPN-mediated inhibition of AICD (**Figure 6B**). The anti-OPN-C mAb or control human IgG were injected i.p. in mice at T5, T7, and T9 after EAE induction. Analysis of the disease scores showed that disability was substantially lower in the mice treated with the mAb than in the control mice in the initial disease phases until T9 (**Figure 6C**). Subsequently, in the mAb-treated mice, the scores increased abruptly, almost reaching the scores of the control mice from T10 to T13. We then performed another set of four injections of the mAb (or IgG in the control mice) at T13, T14, T15, and T16. In the mice treated with the mAb, the treatment was followed by a decrease of the disease scores until T18, after which the scores again gradually increased and almost reached those of the control mice at T21. Subsequently, both groups of mice developed a similar remission (**Figure 6C**).

To assess whether the short-lasting effect of the mAb was due to production of antibodies against its human determinants, we searched for these reactive antibodies in the serum of the mice at T4, T12, and T24 using ELISA plates absorbed with the mAb. Results showed that the anti-mAb response was detectable at T12 and T24, and it was higher in the mice treated with the mAb than in those treated with human IgG (**Figure 6D**; $p < 0.05$).

DISCUSSION

This study has shown that patients with RR MS display high levels of anti-OPN autoAbs, and these levels are more elevated in remission than in relapse phase. By contrast, these increased levels are not detected in patients with progressive forms of MS, i.e., PP and SP (**Figure 1**). Moreover, in mouse EAE, vaccination with OPN, boosting production of anti-OPN autoAbs, ameliorates the disease course (**Figure 5**). These data suggest that production of anti-OPN autoAbs may favor remission in both MS and EAE.

We analyzed correlations between the anti-OPN autoAb levels evaluated at diagnosis and MS clinical course in a prospective cohort of RR patients (24). We found opposite behaviors of OPN autoAbs in patients receiving or not DMTs: a lower disability over 10 years was correlated with high anti-OPN autoAb levels at diagnosis in the former and with low levels in the latter group (**Figure 2**). Altogether, these findings may have two different, albeit not conflicting, explanations.

First, anti-OPN autoAbs may mark the inflammatory phase of MS. In fact, anti-OPN autoAb levels not only showed an inverse correlation with disease duration but were also higher (0.46 vs 0.26, $p = 0.0074$) in longitudinal RR patients at diagnosis than in cross-sectional RR patients, a portion of whom were tested long after diagnosis, when relapses are less frequent. In cross-sectional RR patients, the autoAb levels were higher during remission

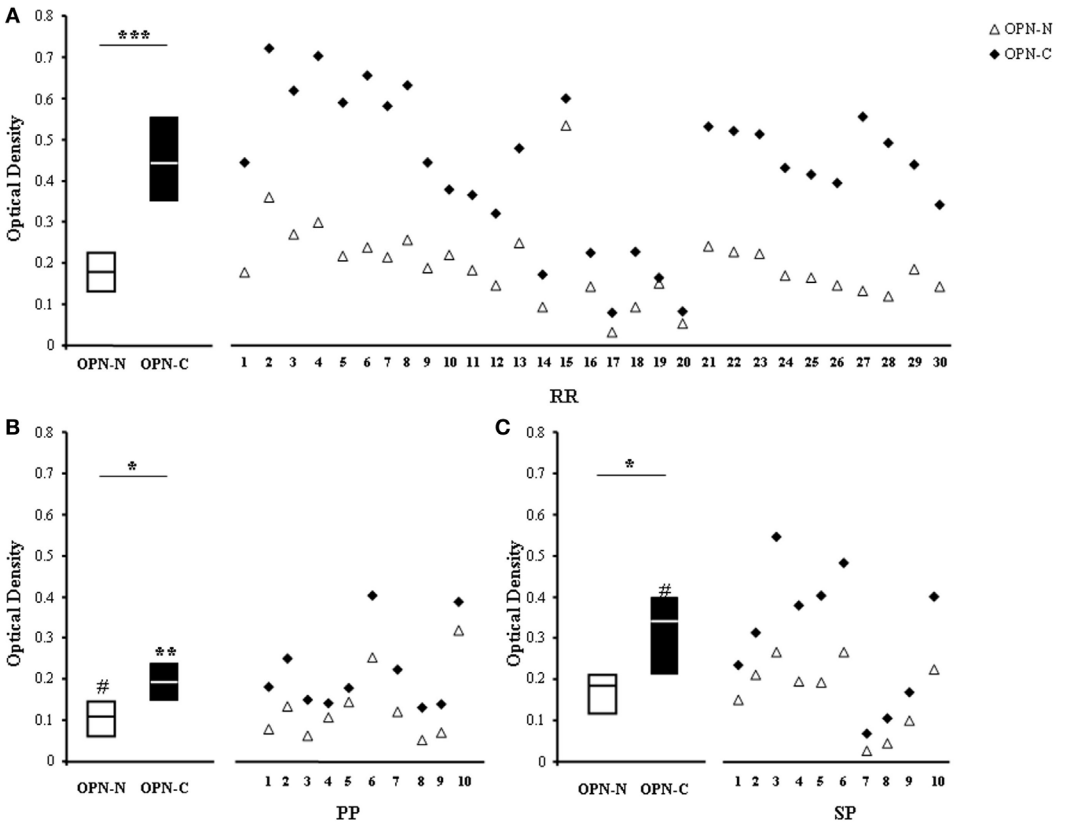

FIGURE 4 | Autoantibodies (autoAbs) to OPN-N and OPN-C fragments in multiple sclerosis (MS) patients with different clinical forms. AutoAbs detected by ELISA using either OPN-N (white triangles) or OPN-C (black diamonds) as the capture protein in 30 relapsing–remitting (RR) **(A)**, 10 primary-progressive (PP) **(B)**, and 10 secondary-progressive (SP) **(C)** MS patients. Boxes: interquartile ranges and medians (Wilcoxon test) [$^{*}p < 0.05$, $^{**}p < 0.001$, $^{***}p < 0.0001$, $^{\#}p < 0.05$ vs RR patients (Mann–Whitney *U*-test)].

than during relapse, thus suggesting that anti-OPN autoAbs are increased by the OPN peak that occurs during relapse. Indeed, high levels were detected in active patients, i.e., both longitudinal RR patients who had subsequently undergone DMTs and those who had not received treatments despite the unfavorable long-term outcome. By contrast, patients with less active disease, i.e., patients not starting DMTs and showing lower MSSS at 10 years, displayed lower antibodies at diagnosis (**Figure 2**). Overall, these data suggest that high levels of anti-OPN autoAbs at diagnosis may help in identifying active patients requiring DMTs.

Second, in patients with active disease, anti-OPN autoAbs may antagonize deleterious activities of OPN involved in MS pathogenesis and cooperate with DMTs to counteract disease progression. These data are in line with those in EAE in which vaccination with OPN, boosting production of anti-OPN autoAbs, ameliorates the disease course and improves remission, as shown also by Steinman et al. (19). Thus, the production of anti-OPN autoAbs may favor remission in both MS and EAE. This model is summarized in **Figure 7**.

Because the anti-OPN autoAbs were also detected at low levels in the controls, they may be a physiologic response intended to downmodulate the immune response, which is a mechanism that may be shared by other inflammatory cytokines (22). In line with this possibility, we show that the anti-OPN autoAbs are able to neutralize the OPN biologic activity, as detected by their ability to inhibit the OPN-mediated protection on lymphocyte AICD (**Figure 3**) (17). This neutralization may partly depend on OPN sequestration into immune complexes which may prevent OPN from binding to its cellular receptors and promote OPN removal from the inflamed tissue/bloodstream through the activity of the immune complexes clearing system. However, since the anti-OPN response is polyclonal, it is also possible that some autoAbs have direct blocking effects on the several OPN-binding sites for cellular receptors. Discriminating the role of these binding sites and of molecular and cellular interactions is crucial for designing a specific therapy to target the portion performing the pathogenic function while preserving the physiologic activity of the others.

The notion of the protective effect of autoAbs in autoimmune diseases is also supported by clinical experience with B-cell-depleting treatments. While use of anti-CD20 antibodies, such as rituximab and ocrelizumab, is considered an important therapeutic strategy in MS (30), two randomized controlled clinical trials with atacicept in MS and optic neuritis were discontinued for significant disease worsening in the treatment compared to the placebo arms (31, 32). A possible explanation for this discrepancy between the two B-cell-depleting treatments is that anti-CD20

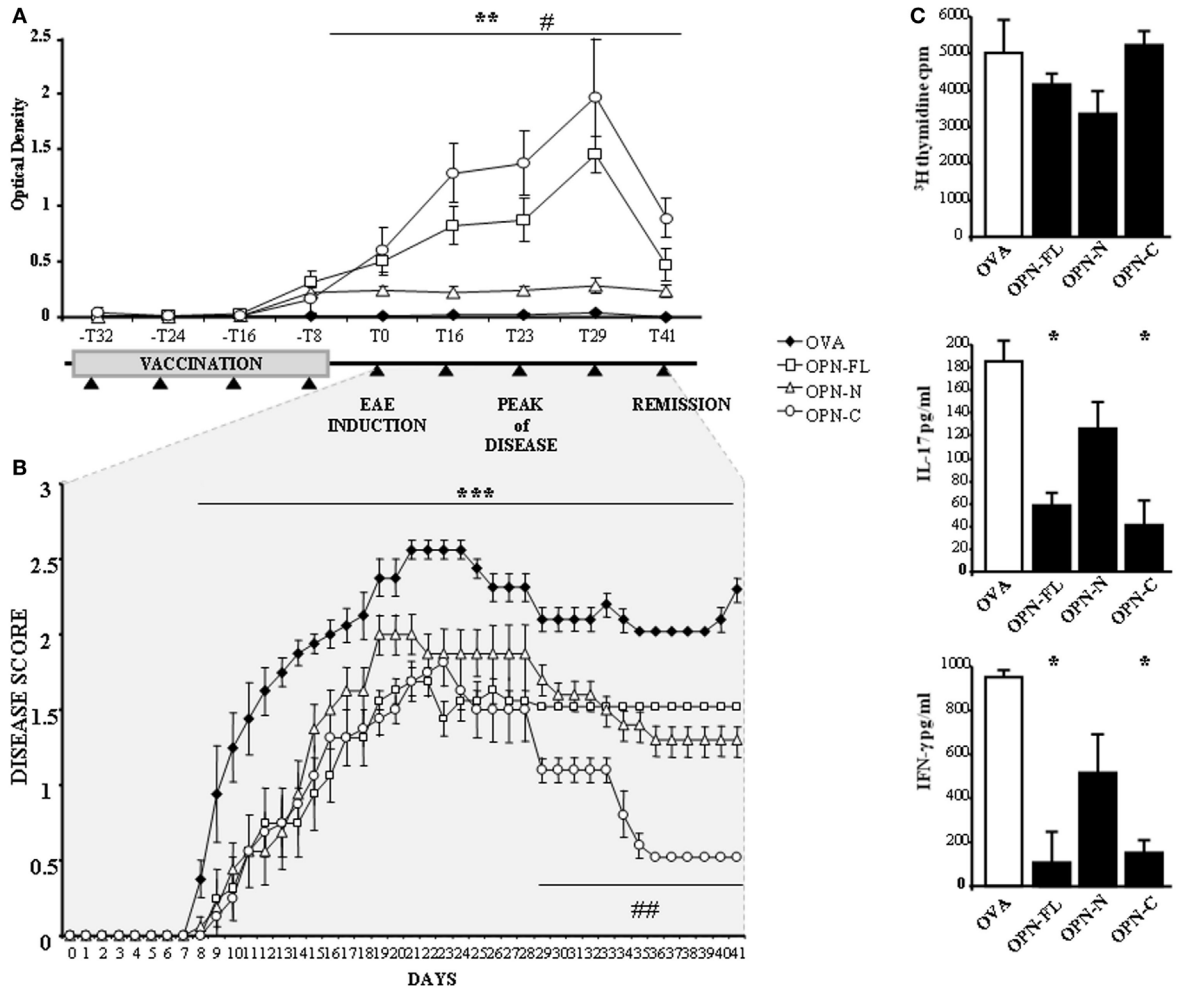

FIGURE 5 | Vaccination against osteopontin (OPN) induce autoantibodies (autoAbs) to OPN and protects mice from experimental autoimmune encephalomyelitis (EAE). **(A)** Anti-OPN autoAb levels in vaccinated EAE mice and scheme of the vaccination protocol. Four-week-old female C57BL/6 mice were immunized once a week for 4 weeks with either OPN full-length (OPN-FL) (white squares), OPN-N (white triangles), and OPN-C (white circles) cross-linked to ovalbumin (OVA) or OVA alone as a control (black diamonds). EAE was induced with MOG_{35-55} 1 week after the last immunization. Black triangles indicate blood draws to evaluate OPN autoAbs. The error bars represent the SE for each point [$^{**}p < 0.01$ OPN-FL and OPN-C vs OVA; $^{\#}p < 0.01$ OPN-FL and OPN-C vs OPN-N (Mann–Whitney *U*-test)]. **(B)** Clinical scores of EAE in mice vaccinated as described in panel **(A)**. The error bars represent the SE for each point. A non-parametric ANOVA test was used to compare the clinical scores ($^{***}p < 0.001$ OPNs vs OVA; $^{\#\#}p < 0.001$ OPN-C vs OVA, OPN-FL, OPN-N). **(C)** *In vitro* response to MOG_{35-55} of spleen lymphocytes from EAE mice vaccinated with OPNs. T cell proliferation, interleukin (IL)-17, and interferon (IFN)-γ secretion were measured in spleen lymphocyte cultures stimulated with MOG_{35-55}. Spleen lymphocytes were obtained at day 29 after EAE induction, from mice vaccinated with either OVA or OPN-FL, OPN-N, or OPN-C. Histograms represent the mean ± SE from six mice [$^{*}p < 0.05$ vs OVA (Mann–Whitney *U*-test)].

antibodies relatively spear plasma cells, thus allowing the production of protective antibodies. On the contrary, atacicept significantly reduces serum Ig concentrations, mature B cells but also plasma cells (33).

A major objective at MS diagnosis is to act at the early inflammatory stage, delaying disease progression and development of disability. Patients with RR MS may benefit from DMTs showing different degrees of both efficacy and side effects. Personalized treatment is a key challenge in decision-making with regard to MS because of the shortage of reliable markers of individual disease prognosis. Therefore, OPN and anti-OPN autoAbs might be valuable tools in this scenario. OPN levels have been analyzed extensively in MS, as biomarkers of disease activity and DMTs effectiveness (34, 35), and displaying correlations with clinical outcome. These findings have been useful to depict the immunopathological role of OPN in MS, but not to evaluate MS prognosis because of the wide variability of the OPN levels in different clinical conditions and experimental settings (36, 37). These inconsistencies may be related to the numerous clinical conditions that may influence OPN levels, the difficulty of detecting the different OPN forms (depending on glycosylation, phosphorylation, and proteolytic cleavage), and the variable amount of OPN included in the immune complexes with its autoAbs. Similarly, also detection of anti-OPN autoAbs may be misleading because they may be part of the immune complexes and vary in their ability to neutralize the multiple functions of

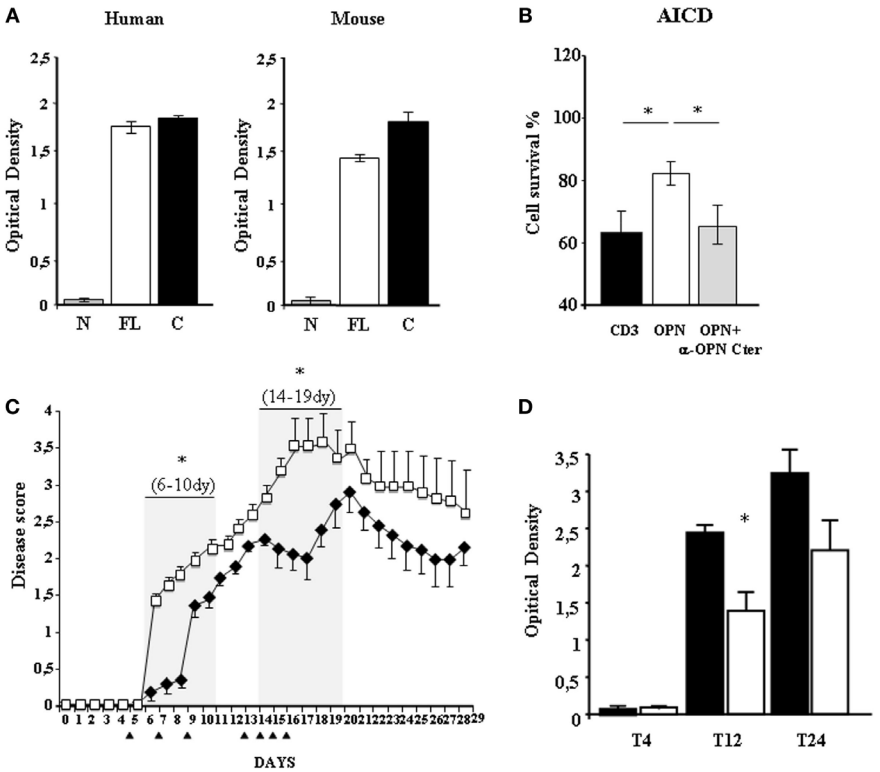

FIGURE 6 | **Passive immunization using an anti-OPN mAb reduces disability in experimental autoimmune encephalomyelitis (EAE)**. **(A)** ELISA testing of the selected mAb, showing its capacity to bind to both human and murine OPN-C, OPN-FL but not to OPN-N. **(B)** The selected mAb neutralizes osteopontin (OPN)-mediated protection from activation-induced cell death (AICD). AICD was induced as described in the legend of **Figure 3**. The white histogram represents AICD in the presence of recombinant OPN and the gray histogram AICD in the presence of both OPN and the selected mAb, neutralizing it. **(C)** Clinical scores of EAE in mice treated with the selected mAb (black diamonds) or with a control immunoglobulin (Ig)G (white squares). The error bars represent the SE for each point. Black triangles mark the days of treatment and gray boxes the significantly protected days. A non-parametric ANOVA test was used to compare the clinical scores. **(D)** ELISA detecting antibodies against the human determinants of the selected mAb (black) or its isotype control (white), in the serum of treated mice. The anti-mAb response was detectable at T12 and T24 and it was higher in the mice treated with the mAb than in those treated with human IgG [$*p < 0.05$ (Mann–Whitney *U*-test)].

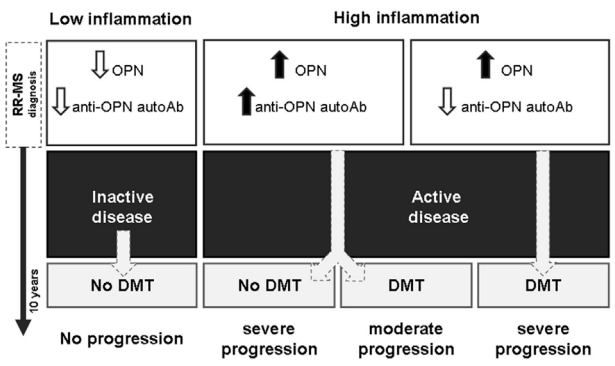

FIGURE 7 | **High anti-OPN autoantibodies (autoAbs) levels in relapsing–remitting (RR) multiple sclerosis (MS) at diagnosis mark active disease and support the efficacy of disease-modifying treatments (DMTs)**. High levels of autoAbs are displayed by patients with active disease including both those who received DMTs and those who did not, despite the subsequent disease progression, which might be associated with the high inflammation and high osteopontin (OPN) levels. However, in the treated patients, the autoAbs may cooperate with DMTs to slow down progression, whereas they are not sufficient to control the disease in the untreated patients.

OPN. It is possible that the best approach would be the parallel evaluation of both free and immune complexes-bound OPN and anti-OPN autoAbs.

Intriguingly, the anti-OPN response recognized OPN-C better than OPN-N in all patients, which may mark both quantitative (i.e., different amounts) and qualitative (i.e., different affinities) differences of the autoAbs produced against the two fragments (**Figure 4**). The focus on OPN-C was further noted by the EAE experiments because vaccination with OPN-C resulted in the greatest induction of anti-OPN autoAbs, ameliorating disease progression, particularly in terms of inducing disease remission and decreasing the autoantigen-driven production of IFN-γ and IL-17 (**Figure 5**). Moreover, passive immunization with the human anti-OPN-C recombinant antibody ameliorated the disease course (**Figure 6**). These data identified a role for the CD44-binding site displayed by OPN-C, which is intriguing because CD44 is involved in EAE by favoring the homing and survival of the autoimmune T cells, and by increasing IL-17A and IFN-γ production and decreasing IL-10 production (34–42). Moreover, data in the literature show that OPN stimulates IL-17A and IFN-γ production and inhibits IL-10 production in EAE and MS (15).

The critical role of OPN-C is surprising because the presence of the binding sites for α4β1 would instead direct the attention to OPN-N because α4β1 is involved in the CNS homing of T cells and is the target of the anti-MS drug natalizumab. However, it is noteworthy that our data indicate that OPN-N also plays a role in EAE, because vaccination with OPN-N ameliorated disease progression. Moreover, when we analyzed the autoAbs to OPN-C and OPN-N in the longitudinal group of RR-MS patients at diagnosis, we could not confirm the clinical correlations detected on the total anti-OPN autoAbs, which highlights the importance of the global response to OPN (data not shown).

In the EAE experiments, we used a prophylactic vaccination protocol in which immunization was performed before EAE induction. This procedure would be of limited benefit in humans, who would instead benefit from a therapeutic vaccination performed after the onset of disease. However, even a therapeutic vaccination would be problematic in humans because of the concern about inducing an uncontrollable anti-OPN response. By contrast, a possible approach would be to use anti-OPN-neutralizing antibodies, since we show that they can ameliorate EAE disability when administered in different phases of the disease. In our model, the effect was short-lasting, but this was probably due to the high anti-drug response elicited by the human mAb used in these experiments.

Osteopontin has pleiotropic activities in the immune response because it acts as a chemoattractant for inflammatory cells, supports differentiation of proinflammatory T cells and antibody production by B cells, and increases survival of activated lymphocytes and inflammatory cells (4, 39, 40, 43, 44). Discriminating the role of each fragment in these functions and in MS pathogenesis is crucial for designing a specific therapy to counteract only the most pathogenic fragment and function while preserving the physiologic activity of the others. This work is a proof of concept that drugs targeting OPN-C may be proposed for MS therapy.

We have shown that anti-OPN autoAbs are found at high levels in RR-MS patients during the remission, and that they influence MS evolution and prognosis in association with DMTs. Novel strategies boosting their levels, such as vaccination or passive immunization, may be proposed as a future strategy in personalized MS therapy.

AUTHOR CONTRIBUTIONS

NC, DR, GC, EO, CG, EB, and CD performed the experiments and analyzed the data. DS performed the phage display screening experiments; MS, FM-B, MC, AB, LA, ML, CC, and DV provided the patient samples and clinical data; TC performed the statistical analysis; CC, UD, and AC designed the study and wrote the manuscript.

FUNDING

This work was supported by Fondazione Italiana Sclerosi Multipla (FISM, Genova 2010/R/12-2011/R/11), Associazione Italiana Ricerca sul Cancro (IG 10237, AIRC, Milano), Fondazione Amici di Jean (Torino), and Fondazione Cassa di Risparmio di Cuneo (Cuneo).

REFERENCES

1. Zettl UK, Stüve O, Patejdl R. Immune-mediated CNS diseases: a review on nosological classification and clinical features. *Autoimmun Rev* (2012) 11(3):167–73. doi:10.1016/j.autrev.2011.05.008
2. Weinshenker BG. The natural history of multiple sclerosis. *Neurol Clin* (1995) 13(1):119–46.
3. Harris VK, Sadiq SA. Biomarkers of therapeutic response in multiple sclerosis: current status. *Mol Diagn Ther* (2014) 18(6):605–17. doi:10.1007/s40291-014-0117-0
4. Carecchio M, Comi C. The role of osteopontin in neurodegenerative diseases. *J Alzheimers Dis* (2011) 25(2):179–85. doi:10.3233/JAD-2011-102151
5. Gravallese EM. Osteopontin: a bridge between bone and the immune system. *J Clin Invest* (2003) 112(2):147–9. doi:10.3233/JAD-2011-102151
6. Chiocchetti A, Comi C, Indelicato M, Castelli L, Mesturini R, Bensi T, et al. Osteopontin gene haplotypes correlate with multiple sclerosis development and progression. *J Neuroimmunol* (2005) 163(1–2):172–8. doi:10.1016/j.jneuroim.2005.02.020
7. Sennels H, Sørensen S, Ostergaard M, Knudsen L, Hansen M, Skjødt H, et al. Circulating levels of osteopontin, osteoprotegerin, total soluble receptor activator of nuclear factor-kappa B ligand, and high-sensitivity C-reactive protein in patients with active rheumatoid arthritis randomized to etanercept alone or in combination with methotrexate. *Scand J Rheumatol* (2008) 37(4):241–7. doi:10.1080/03009740801910320
8. D'Alfonso S, Barizzone N, Giordano M, Chiocchetti A, Magnani C, Castelli L, et al. Two single-nucleotide polymorphisms in the 5' and 3' ends of the osteopontin gene contribute to susceptibility to systemic lupus erythematosus. *Arthritis Rheum* (2005) 52(2):539–47. doi:10.1002/art.20808
9. Mishima R, Takeshima F, Sawai T, Ohba K, Ohnita K, Isomoto H, et al. High plasma osteopontin levels in patients with inflammatory bowel disease. *J Clin Gastroenterol* (2007) 41(2):167–72. doi:10.1097/MCG.0b013e31802d6268
10. Chabas D, Baranzini SE, Mitchell D, Bernard CC, Rittling SR, Denhardt DT, et al. The influence of the proinflammatory cytokine, osteopontin, on autoimmune demyelinating disease. *Science* (2001) 294(5547):1731–5. doi:10.1126/science.1062960
11. Braitch M, Constantinescu CS. The role of osteopontin in experimental autoimmune encephalomyelitis (EAE) and multiple sclerosis (MS). *Inflamm Allergy Drug Targets* (2010) 9(4):249–56. doi:10.2174/187152810793358778
12. Comabella M, Pericot I, Goertsches R, Nos C, Castillo M, Blas Navarro J, et al. Plasma osteopontin levels in multiple sclerosis. *J Neuroimmunol* (2005) 158(1–2):231–9. doi:10.1016/j.jneuroim.2004.09.004
13. Comi C, Cappellano G, Chiocchetti A, Orilieri E, Buttini S, Ghezzi L, et al. The impact of osteopontin gene variations on multiple sclerosis development and progression. *Clin Dev Immunol* (2012) 2012:212893. doi:10.1155/2012/212893
14. Yokosaki Y, Matsuura N, Sasaki T, Murakami I, Schneider H, Higashiyama S, et al. The integrin alpha(9)beta(1) binds to a novel recognition sequence (SVVYGLR) in the thrombin-cleaved amino-terminal fragment of osteopontin. *J Biol Chem* (1999) 274(51):36328–34. doi:10.1074/jbc.274.51.36328
15. Murugaiyan G, Mittal A, Weiner HL. Increased osteopontin expression in dendritic cells amplifies IL-17 production by CD4+ T cells in experimental autoimmune encephalomyelitis and in multiple sclerosis. *J Immunol* (2008) 181(11):7480–8. doi:10.4049/jimmunol.181.11.7480
16. Wolak T, Sion-Vardi N, Novack V, Greenberg G, Szendro G, Tarnovscki T, et al. N-terminal rather than full-length osteopontin orits C-terminal fragment is associated with carotid-plaque inflammation inhypertensive patients. *Am J Hypertens* (2013) 26(3):326–33. doi:10.1093/ajh/hps043
17. Boggio E, Dianzani C, Gigliotti CL, Soluri MF, Clemente N, Cappellano G, et al. Thrombin cleavage of osteopontin modulates its activities in human cells in vitro and mouse experimental autoimmune encephalomyelitis in vivo. *J Immunol Res* (2016) 2016:9345495. doi:10.1155/2016/9345495
18. Hur EM, Youssef S, Haws ME, Zhang SY, Sobel RA, Steinman L. Osteopontin-induced relapse and progression of autoimmune brain disease through

enhanced survival of activated T cells. *Nat Immunol* (2007) 8(1):74–83. doi:10.1038/ni1415
19. Steinman L, Youssef S, Van Venrooij N, Chabas D, Baranzini SE, Rittling S, et al. Response to comment on "the influence of the proinflammatory cytokine, osteopontin, on autoimmune demyelinating disease". *Science* (2003) 299(5614):1845. doi:10.1126/science.1080223
20. Sakata M, Tsuruha JI, Masuko-Hongo K, Nakamura H, Matsui T, Sudo A, et al. Autoantibodies to osteopontin in patients with osteoarthritis and rheumatoid arthritis. *J Rheumatol* (2001) 28(7):1492–5.
21. Fan K, Dai J, Wang H, Wei H, Cao Z, Hou S, et al. Treatment of collagen-induced arthritis with ananti-osteopontin monoclonal antibody through promotion of apoptosis of both murine and human activated T cells. *Arthritis Rheum* (2008) 58(7):2041–52. doi:10.1002/art.23490
22. Cappellano G, Orilieri E, Woldetsadik AD, Boggio E, Soluri MF, Comi C, et al. Anti-cytokine autoantibodies in autoimmune diseases. *Am J Clin Exp Immunol* (2012) 1(2):136–46.
23. McDonald WI, Compston A, Edan G, Goodkin D, Hartung HP, Lublin FD, et al. Recommended diagnostic criteria for multiple sclerosis: guidelines from the international panel on the diagnosis of multiple sclerosis. *Ann Neurol* (2001) 50(1):121–7. doi:10.1002/ana.1032
24. Leone MA, Bonissoni S, Collimedaglia L, Tesser F, Calzoni S, Stecco A, et al. Factors predicting incomplete recovery from relapses in multiple sclerosis: a prospective study. *Mult Scler* (2008) 14(4):485–93. doi:10.1177/1352458507084650
25. Roxburgh RH, Seaman SR, Masterman T, Hensiek AE, Sawcer SJ, Vukusic S, et al. Multiple sclerosis severity score: using disability and disease duration torate disease severity. *Neurology* (2005) 64(7):1144–51. doi:10.1212/01.WNL.0000156155.19270.F8
26. Uyttenhove C, Van Snick J. Development of an anti-IL-17A auto-vaccine that prevents experimental auto-immune encephalomyelitis. *Eur J Immunol* (2006) 36(11):2868–74. doi:10.1002/eji.200636662
27. Cappellano G, Woldetsadik AD, Orilieri E, Shivakumar Y, Rizzi M, Carniato F, et al. Subcutaneous inverse vaccination with PLGA particles loaded with a MOG peptide and IL-10 decreases the severity of experimental autoimmune encephalomyelitis. *Vaccine* (2014) 32(43):5681–9. doi:10.1016/j.vaccine.2014.08.016
28. Sblattero D, Bradbury A. Exploiting recombination in single bacteria to make large phage antibody libraries. *Nat Biotechnol* (2000) 18(1):75–80. doi:10.1038/71958
29. Di Niro R, Ziller F, Florian F, Crovella S, Stebel M, Bestagno M, et al. Construction of miniantibodies for the in vivo study of human autoimmune diseases in animal models. *BMC Biotechnol* (2007) 7:46. doi:10.1186/1472-6750-7-46
30. Milo R. Therapeutic strategies targeting B-cells in multiple sclerosis. *Autoimmun Rev* (2016) 15(7):714–8. doi:10.1016/j.autrev.2016.03.006
31. Kappos L, Hartung HP, Freedman MS, Boyko A, Radü EW, Mikol DD, et al. Atacicept in multiple sclerosis (ATAMS): a randomised, placebo-controlled, double-blind, phase 2 trial. *Lancet Neurol* (2014) 13(4):353–63. doi:10.1016/S1474-4422(14)70028-6
32. Sergott RC, Bennett JL, Rieckmann P, Montalban X, Mikol D, Freudensprung U, et al. ATON: results from a phase II randomized trial of the B-cell-targeting agent atacicept in patients with optic neuritis. *J Neurol Sci* (2015) 351(1–2):174–8. doi:10.1016/j.jns.2015.02.019
33. Nestorov I, Munafo A, Papasouliotis O, Visich J. Pharmacokinetics and biological activity of atacicept in patients with rheumatoid arthritis. *J Clin Pharmacol* (2008) 48(4):406–17. doi:10.1177/0091270008315312
34. Iaffaldano P, Ruggieri M, Viterbo RG, Mastrapasqua M, Trojano M. The improvement of cognitive functions is associated with a decrease of plasma osteopontin levels in natalizumab treated relapsing multiple sclerosis. *Brain Behav Immun* (2014) 35:96–101. doi:10.1016/j.bbi.2013.08.009
35. Shimizu Y, Ota K, Ikeguchi R, Kubo S, Kabasawa C, Uchiyama S. Plasma osteopontin levels are associated with disease activity in the patients with multiple sclerosis and neuromyelitis optica. *J Neuroimmunol* (2013) 263(1–2):148–51. doi:10.1016/j.jneuroim.2013.07.005
36. Kivisäkk P, Healy BC, Francois K, Gandhi R, Gholipour T, Egorova S, et al. Evaluation of circulating osteopontin levels in an unselected cohort of patients with multiple sclerosis: relevance for biomarker development. *Mult Scler* (2014) 20(4):438–44. doi:10.1177/1352458513503052
37. Runia TF, van Meurs M, Nasserinejad K, Hintzen RQ. No evidence for an association of osteopontin plasma levels with disease activity in multiple sclerosis. *Mult Scler* (2014) 20(12):1670–1. doi:10.1177/1352458514528765
38. Guan H, Nagarkatti PS, Nagarkatti M. CD44 reciprocally regulates the differentiation of encephalitogenic Th1/Th17 and Th2/regulatory T cells through epigenetic modulation involving DNA methylation of cytokine gene promoters, thereby controlling the development of experimental autoimmune encephalomyelitis. *J Immunol* (2011) 186(12):6955–64. doi:10.4049/jimmunol.1004043
39. Winkler CW, Foster SC, Matsumoto SG, Preston MA, Xing R, Bebo BF, et al. Hyaluronan anchored to activated CD44 on central nervous system vascular endothelial cells promotes lymphocyte extravasation in experimental autoimmune encephalomyelitis. *J Biol Chem* (2012) 287(40):33237–51. doi:10.1074/jbc.M112.356287
40. Flynn KM, Michaud M, Madri JA. CD44 deficiency contributes to enhanced experimental autoimmune encephalomyelitis: a role in immune cells and vascular cells of the blood-brain barrier. *Am J Pathol* (2013) 182(4):1322–36. doi:10.1016/j.ajpath.2013.01.003
41. Deboux C, Ladraa S, Cazaubon S, Ghribi-Mallah S, Weiss N, Chaverot N, et al. Overexpression of CD44 in neural precursor cells improves trans-endothelial migration and facilitates their invasion of perivascular tissues in vivo. *PLoS One* (2013) 8(2):e57430. doi:10.1371/journal.pone.0057430
42. Ghazi-Visser L, Laman JD, Nagel S, van Meurs M, van Riel D, Tzankov A, et al. CD44 variant isoforms control experimental autoimmune encephalomyelitis by affecting the lifespan of the pathogenic T cells. *FASEB J* (2013) 27(9):3683–701. doi:10.1096/fj.13-228809
43. Comi C, Fleetwood T, Dianzani U. The role of T cell apoptosis in nervous system autoimmunity. *Autoimmun Rev* (2012) 12(2):150–6. doi:10.1016/j.autrev.2011.08.011
44. Wang KX, Denhardt DT. Osteopontin: role in immune regulation and stress responses. *Cytokine Growth Factor Rev* (2008) 19(5–6):333–45. doi:10.1016/j.cytogfr.2008.08.001

Conflict of Interest Statement: The authors declare that the research was conducted in the absence of any commercial or financial relationships that could be construed as a potential conflict of interest.

Copyright © 2017 Clemente, Comi, Raineri, Cappellano, Vecchio, Orilieri, Gigliotti, Boggio, Dianzani, Sorosina, Martinelli-Boneschi, Caldano, Bertolotto, Ambrogio, Sblattero, Cena, Leone, Dianzani and Chiocchetti. This is an open-access article distributed under the terms of the Creative Commons Attribution License (CC BY). The use, distribution or reproduction in other forums is permitted, provided the original author(s) or licensor are credited and that the original publication in this journal is cited, in accordance with accepted academic practice. No use, distribution or reproduction is permitted which does not comply with these terms.

frontiers in Immunology

ORIGINAL RESEARCH
published: 03 March 2017
doi: 10.3389/fimmu.2017.00214

Interleukin-4 Inhibits Regulatory T Cell Differentiation through Regulating CD103+ Dendritic Cells

Lei Tu[1†], Jie Chen[2†], Hongwei Zhang[3] and Lihua Duan[4]*

[1] Division of Gastroenterology, Union Hospital, Tongji Medical College, Huazhong University of Science and Technology, Wuhan, China, [2] Medical College, Xiamen University, Xiamen, China, [3] Laboratory of Clinical Immunology, Wuhan No. 1 Hospital, Tongji Medical College, Huazhong University of Science and Technology, Wuhan, China, [4] Department of Rheumatology and Clinical Immunology, The First Affiliated Hospital of Xiamen University, Xiamen, China

CD103+ dendritic cells (DCs) have been shown to play a crucial role in the pathogenesis of inflammatory bowel diseases (IBDs) through educating regulatory T (Treg) cells differentiation. However, the mechanism of CD103+ DCs subsets differentiation remains elusive. Interleukin (IL)-4 is a pleiotropic cytokine that is upregulated in certain types of inflammation, including IBDs and especially ulcerative colitis. However, the precise role of IL-4 in the differentiation of CD103+ DCs subpopulation remains unknown. In this study, we observed a repressive role of IL-4 on the CD103+ DCs differentiation in both mouse and human. High-dose IL-4 inhibited the CD103+ DC differentiation. In comparison to CD103− DCs, CD103+ DCs expressed high levels of the co-stimulatory molecules and indoleamine 2,3-dioxygenase (IDO). Interestingly, IL-4 diminished IDO expression on DCs in a dose-dependent manner. Besides, high-dose IL-4-induced bone marrow-derived DCs, and monocyte-derived DCs revealed mature DCs profiles, characterized by increased co-stimulatory molecules and decreased pinocytotic function. Furthermore, DCs generated under low concentrations of IL-4 favored Treg cells differentiation, which depend on IDO produced by CD103+ DCs. Consistently, IL-4 also reduced the frequency of CD103+ DC *in vivo*. Thus, we here demonstrated that the cytokine IL-4 involved in certain types of inflammatory diseases by orchestrating the functional phenotype of CD103+ DCs subsets.

Keywords: IL-4, dendritic cells, CD103, Treg, indoleamine 2,3-dioxygenase, inflammatory bowel diseases

OPEN ACCESS

Edited by:
Jixin Zhong,
Case Western Reserve University, USA

Reviewed by:
Yan Yang,
Wuhan Institute of Virology (CAS), China
Gengqing Song,
Cleveland Clinic Lerner College of Medicine, USA

****Correspondence:***
Lihua Duan
lh-duan@163.com

†These authors have contributed equally to this work.

Specialty section:
This article was submitted to Inflammation, a section of the journal Frontiers in Immunology

Received: *31 December 2016*
Accepted: *15 February 2017*
Published: *03 March 2017*

Citation:
Tu L, Chen J, Zhang H and Duan L (2017) Interleukin-4 Inhibits Regulatory T Cell Differentiation through Regulating CD103+ Dendritic Cells. Front. Immunol. 8:214. doi: 10.3389/fimmu.2017.00214

INTRODUCTION

Dendritic cells (DCs) is well known as the professional antigen-presenting cells, uptaking and processing pathogenic substance, and presenting the antigen to T cells through peptide–MHC complex (1). In addition to antigens presentation, DCs also play a crucial role in regulating immune response by the co-stimulatory molecules interaction, which provides the second signal in the process of T cell activation and proliferation (2). A number of studies have shown that inhibition or depletion of costimulatory molecules on DCs can improve activity of inflammatory diseases (3–6). Beyond that, there are increasing evidences indicating that DCs also have the capability to induce regulatory T (Treg) cells differentiation, which harness the immune homeostasis (7, 8).

Interleukin (IL)-4, the best-characterized member of the type 2 immune response cytokines, was produced by various types of cells including CD4+ T cells, natural killer T cells, eosinophils, and activated mast cells (9). In the meantime, the function of IL-4 is not yet fully known as the extremely broad distribution of IL-4 receptors (10). Previous studies have shown that IL-4 is the key pro-inflammatory cytokine in the pathological progression of atopic dermatitis, allergic rhinitis, COPD, and cancer (11). Besides, IL-4 has also been implicated in inflammatory bowel diseases (IBDs) (12, 13). Numerous studies have shown that the alteration of T cell polarization could ameliorate the development of disease. It has previously been demonstrated that the development of atherosclerosis and allograft rejection, resulting from Th1 immune response, can be reduced by promoting Th2 differentiation (14). However, the abnormally upregulated Th1 and Th2 immune responses can be observed simultaneously in IBDs (12, 15). Until now, the mechanism in this immune dysfunction remains elusive. Recently, it has been shown that the presence of IL-4 in the initial DCs activation could lead to a dominant Th1 immune response, which had a protective effect in *Leishmania*-infected mice (16). In addition, neutralization of IL-4 abrogated IL-12 secretion in a coculture system of human DCs and Th2 cell (17). Furthermore, high IL-12 and low IL-10 expressions were observed in DCs generated under high concentrations of IL-4 (18). The DCs function altered by IL-4 might explain the mixed Th1/Th2 immune response in IBDs.

CD103+ DCs play a crucial role in alleviating the pathological progression of IBDs through promoting the *de novo* generation of Treg cells by a indoleamine 2,3-dioxygenase (IDO) mechanism (19, 20). IDO is a cytoplasmic rate-limiting enzyme involved in the catabolism and utilization of tryptophan, which converts tryptophan into *N*-formylkynurenine and subsequently kynurenine (21). Recent studies revealed that IDO produced by DCs play a critical role in immune tolerance (22, 23). Our previous study also demonstrated that the protective effect of IL-33 is predominantly dependent on Treg cell expansion, which was closely associated with upregulation of CD103+IDO+ DCs (24). Epithelium cell-derived TGF-β and retinoic acid (RA) were found to be required for CD103+ DC tolerogenic phenotype conversion, and epithelium cell from IBDs patients showed an impaired function in CD103+ DC conversion (20), which result in a diminishment of CD103+ DCs in IBDs (25, 26). Although abnormalities in both Th1 and Th2 immune responses were detected in ulcerative colitis (UC) patients, the Th2 immune response is considered to play a predominant role (15). However, very little is known about the exact role of Th2 immune response in the DCs conditioning during the development of UC. Here, we presented evidence that IL-4 revealed suppressive role on CD103+ DCs conversion. Under high IL-4 circumstance, diminishment of CD103+ DCs was observed in mice bone marrow-derived DCs (BMDCs) and human monocyte-derived DCs (MoDCs), which also showed a weaken potency to simulate Treg cells differentiation. Thus, in addition to impaired intestinal epithelium function in CD103+ DCs conversion, the inflammatory IL-4 also inhibits CD103+ DCs induction, which retard Treg cells differentiation and exacerbate the progress of disease.

MATERIALS AND METHODS

Animals and Human Subjects

Female C57BL/6 mice of 6–8 weeks old were purchased from the Animal Center of Xiamen University (Fujian, China). The mice were housed in the specific pathogen-free facility at the Animal Center of Xiamen University for at least 1 week before inclusion in experiments. All experimental procedures involving mice were approved by the Animal Care and Use Committee of Xiamen University and were carried out in accordance with the recommendations of Animal Care and Use Committee of Xiamen University. Written informed consent was obtained from healthy volunteers ($n = 10$) in accordance with the Declaration of Helsinki. The study protocol was approved by the Ethics Committee, Tongji Medical College, Huazhong University of Science and Technology. The methods were carried out in accordance with the approved guidelines.

Induction of Colitis

Dextran sulfate sodium (DSS)-induced colitis was induced in C57BL/6 mice as described elsewhere (27). Briefly, the mice were fed DSS (mol wt. ~40,000; Sigma) 2% (wt/vol) dissolved in sterile distilled water for 7 days, followed by a period of 10 days of water without DSS. Mice received four cycles of DSS treatment, and animals were sacrificed. The serum and mesenteric lymph nodes were harvested and analyzed.

Reagents

All recombinant cytokines in *in vitro* experiments were obtained from Peprotech (London, UK). The antibodies in this study were purchased from commercial companies. Anti-mouse CD4, anti-mouse IFN-γ, anti-mouse CD25, anti-mouse Foxp3, anti-mouse CD11c, anti-mouse CD80, anti-mouse CD86, anti-mouse MHC-II, anti-mouse CD103, anti-human CD4, anti-human IFN-γ, anti-human CD25, anti-human Foxp3, anti-human CD11c, anti-human CD80, anti-human CD86, anti-human CD83, and anti-human CD103 were obtained from ebioscience (CA, USA). Anti-mouse IDO and anti-human IDO were purchased from Biolegend (CA, USA) and R&D (MN, USA), respectively.

Mouse BMDCs and Human MoDCs Generation

Bone marrow-derived DCs (BMDCs) were generated from the mice bone marrow cells as described previously (28). Briefly, BMDCs were propagated from C57BL/6 mouse at 5×10^5/ml cells in the presence of GM-CSF (10 ng/ml) and various concentration of IL-4 (2, 5, and 10 ng/ml). Half of the supernatant was replaced by same volume of fresh medium containing amount of GM-CSF and IL-4 at days 3 and 5. BMDCs were harvested at day 7 for further study. Peripheral blood samples were collected in anticoagulant tubes from healthy volunteers, and then peripheral blood mononuclear cells (PBMCs) were isolated by standard Ficoll-Hypaque density-gradient centrifugation. CD14+ monocytes were purified from PBMCs using positive selection with CD14+ Cell Isolation Kit human (Miltenyi Biotec, Bergisch Gladbach, Germany). The purity of T cells was >95% as

determined using flow cytometry. MoDCs were propagated from CD14+ monocytes under GM-CSF (50 ng/ml) and at various concentration of IL-4 (5, 10, and ng/ml). MoDCs were collected after 6 days of culture.

T Cells and DCs Coculture

Naïve CD4+ T cells were isolated from splenic cells of normal mice and PBMCs of healthy volunteers by naïve CD4+ T cells negative selection (Miltenyi Biotech, Bergisch Gladbach, Germany). Then the naïve CD4+ T cells were labeled with CFSE and then were cocultured with BMDCs or MoDC. A soluble anti-mouse CD3 or anti-human CD3 (0.5 μg/ml) antibody was added to the T cells/DCs cultural medium. The cells and supernatants were harvested after 5 days and followed by proliferation assay by flow cytometry. The Th1 and Treg cells differentiation were analyzed by intracellular flow cytometry analysis. The 1-MT (25 μM) purchased from Sigma-Aldrich (Shanghai, China) was added to some culture medium for inhibiting the IDO activity. CD103− DCs were isolated from DCs generated under low concentration of IL-4 by negative magnetic beads by the following steps. Biotin-conjugated anti-CD103 antibody was used, then anti-biotin-beads (Miltenyi Biotech, Bergisch Gladbach, Germany) were performed in accordance with manufactory instructions.

Pinocytosis Assay

The pinocytotic activities of BMDCs and MoDC were measured as described previously (29). Briefly, BMDCs and MoDCs (2 × 105/ml) were incubated with FITC-dextran (1,000 μg/ml) (Sigma-Aldrich, Shanghai, China) for 3 h at 37°C, and then the DCs were washed twice with PBS. Cells were collected and analyzed by flow cytometry on Coulter Beckman. The mean fluorescence intensity of cells incubated with FITC-dextran at 4°C was set as a fluorescence background.

Flow Cytometry

After propagation, the BMDCs and MoDCs were collected for surface co-stimulatory molecules staining. The IDO staining was performed after DCs treated by Fix/Perm Buffer Set (ebioscience, CA, USA). For cytokines intracellular staining, the cells were obtained from the coculture medium and were stimulated with 20 ng/ml PMA and 1 μg/ml ionomycin (Sigma-Aldrich, Shanghai, China) plus 2 μm of Monesin (Sigma-Aldrich, Shanghai, China) for 4 h following fluorescence-conjugated anti-CD4 antibody staining. IFN-γ and Foxp3 staining was performed in accordance with the manufacturer's instructions (ebioscience, CA, USA).

ELISA Assay

Blood samples were collected by cardiac puncture and placed at room temperature for 30 min before centrifugation. The serum was stored at −80°C until analyzed. The levels of IL-4 were determined by ELISA kits (ebioscience) according to the manufacturer's instructions.

Western Blots Assay

Total proteins extracted from BMDCs or MoDCs were performed to immunoblot assay conducted as described previously (24). The primary antibody anti-IDO (Abcam, MA, USA) and anti-β-actin (Santa Cruz Biotechnology, Santa Cruz, CA, USA) were used to probe the blots. After incubating with secondary antibody-conjugated horseradish peroxidase, the immunoreactivity was detected by an ECL system (Thermofisher, MA, USA).

Statistical Analysis

All data were analyzed in GraphPad Prism5. The data are presented as means ± SD. Statistical differences were determined by Student's *t*-test. Two-sided $p < 0.05$ was considered as significant.

RESULTS

High Concentration of IL-4 Promotes a Mature DCs Phenotype from Precursor Cells

Th2 immune response plays a crucial role in the pathogenesis of many diseases. It is well known that IL-4, the core cytokine in Th2 immunity, is essential for DCs differentiation. To mimic the inflammatory milieu, different concentrations of IL-4 were used in these experiments. There were no significant differences in the yield of BMDCs and MoDCs generation (**Figure 1**). In comparison to DCs generated under high IL-4 concentrations, DCs generated from low IL-4 concentrations displayed an immature phenotype. Co-stimulatory molecules on BMDCs and MoDCs were markedly higher in high-dose group, when compared with low dose of IL-4 treatment (**Figures 2A,B**; **Table 1**). Furthermore, under the condition of low IL-4 concentration, the BMDCs and MoDCs exhibited an increased pinocytotic ability

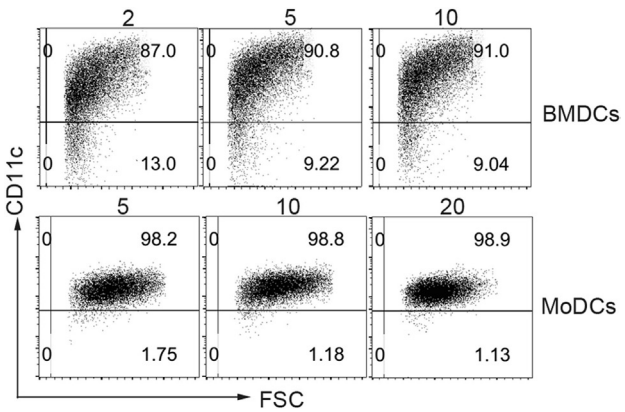

FIGURE 1 | No difference in CD11c+ dendritic cells (DCs) differentiation from precursor cells by various interleukin (IL)-4 concentrations. To determine the different dose of IL-4 in bone marrow-derived DCs (BMDCs) and monocyte-derived DCs (MoDCs) differentiation, BMDCs and MoDCs were propagated in various IL-4 concentrations (nanograms per milliliter) as described in Section "Materials and Methods." After 7 days of BMDCs and 6 days of MoDCs culture, the cells were harvested for CD11c staining, which were analyzed by flow cytometry. The CD11c+ DC were gated for analyzing. Data are representative of three independent experiments.

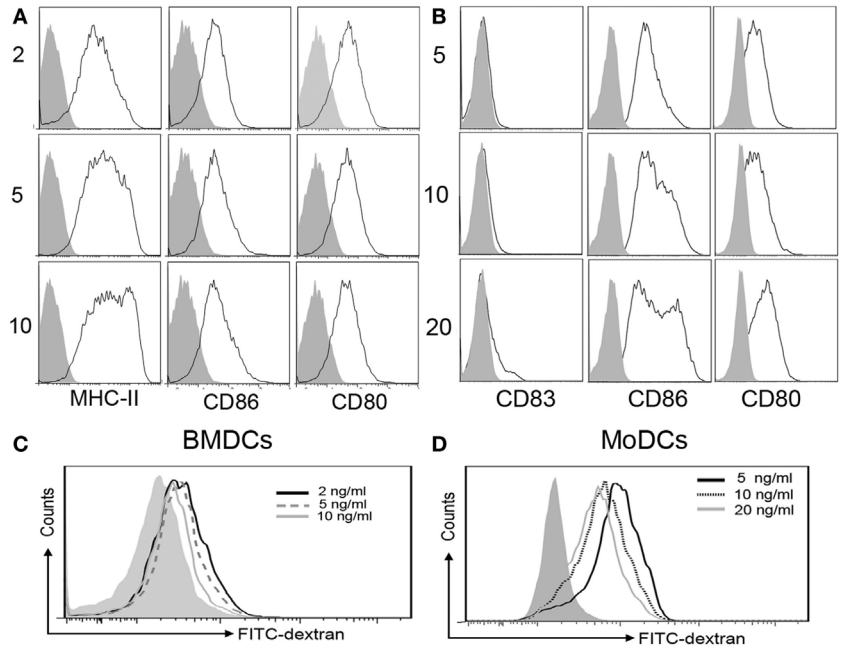

FIGURE 2 | High interleukin (IL)-4 concentration promotes a mature dendritic cells (DCs) phenotype from precursor cells. DCs were propagation under various concentration of IL-4 as described in Section "Materials and Methods," and then the cells were harvested for costimulatory molecules expression analysis by flow cytometry. **(A)** The surface expression of CD80, CD86, and MHC-II on the bone marrow-derived DCs (BMDCs) differentiated from IL-4 (2, 5, and 10 ng/ml, respectively) were plotted in histograms. **(B)** CD80, CD86, and CD83 expressions on monocyte-derived DCs (MoDCs) generated from IL-4 (5, 10, and 20 ng/ml, respectively) were detected. **(C,D)** Pinocytotic activities of BMDCs and MoDCs, which are generated from various IL-4 concentrations as shown above, were represented by mean fluorescence intensity of cells incubated with FITC-dextran. The plots shown were obtained from CD11c+ gate. Data are representative of three independent experiments.

TABLE 1 | Analysis of markers expression of dendritic cells (DCs) generated under various concentration of interleukin (IL)-4.

	Mean fluorescence intensity (MFI)			
Monocyte-derived DCs (MoDCs) (ng/ml)	**CD83**	**CD86**	**CD80**	**FITC-dextran**
5	5.97 ± 0.49	135.7 ± 18	41.9 ± 8.3	1,205.3 ± 11.0
10	6.93 ± 0.47[a]	175.0 ± 23.9[a]	38.7 ± 4.6	708.3 ± 17.5[b]
20	9.47 ± 0.75[b]	337.3 ± 53.4[b]	65.6 ± 8.3[a]	583.6 ± 4[b]
Bone marrow-derived DCs (BMDCs) (ng/ml)	**MHC-II**	**CD86**	**CD80**	**FITC-dextran**
2	277.3 ± 22.5	44.6 ± 0.7	68.2 ± 4.9	388 ± 14.6
5	375.7 ± 63.5	66.3 ± 1.5[a]	62.6 ± 4.5	348.2 ± 10
10	478.7 ± 17.8[b]	84.9 ± 2.6[b]	70.2 ± 1.0	308 ± 14.8[b]

The BMDCs and MoDCs were generated under GM-CSF and at different concentrations of IL-4 as indicated, which was detailed in **Figure 2**. *MFI of costimulatory molecules was obtained by flow cytometry analysis. The FITC-dextran by DCs pinocytosis was also analyzed by flow cytometry and present as MFI. Data from three independent experiments are presented as mean ± SD. The low concentration of IL-4 was compared with intermediate and high IL-4 groups.*

[a]*p < 0.05.*

[b]*p < 0.01.*

(**Figures 2C,D**; **Table 1**), which is a character of immature DCs. These data suggest a crucial role of IL-4 in the development of DCs from precursor cells.

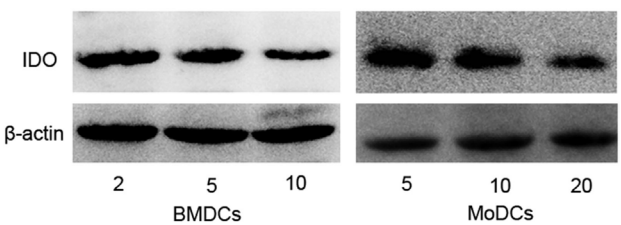

FIGURE 3 | Interleukin (IL)-4 inhibits indoleamine 2,3-dioxygenase (IDO) expression during dendritic cells differentiation. Bone marrow-derived DCs (BMDCs) were propagated from bone marrow cells in GM-CSF (10 ng/ml) and different dose of IL-4 (2, 5, and 10 ng/ml) until day 7. Monocyte-derived DCs (MoDCs) were generated from CD14+ monocytes in GM-CSF (50 ng/ml) and various dose of IL-4 (5, 10, and 20 ng/ml) until day 6. After differentiation, total protein from BMDCs and MoDCs were extracted and subjected to assess IDO expression by immunoblot. All data are representative of one of the three independent experiments.

IL-4 Promotes T Cells Activation through Regulating IDO Expression in DCs

Interestingly, previous studies have demonstrated that high concentration of IL-4 augmented IL-12 production and diminished IL-10 expression in DCs, which led to a Th1 immune response (17, 18). IDO secreted by DCs can degrade the amino acid tryptophan, which is essential for T cells proliferation, and exert an inhibitory role in T cells activation (23). However, the effect

of IL-4 on IDO expression in DCs was not clearly elucidated. In this study, we observed that IDO expressions in DCs were significantly decreased under the high concentration of IL-4 when compared with low IL-4 (**Figure 3**). To further explore the role of IDO+ DCs regulated by IL-4 in T cell immune response, the DCs were cocultured with T cells, and the proliferation was investigated. Flow cytometry analysis revealed a high proportion of dividing T cells in DCs differentiated under high-dose IL-4. Conversely, BMDCs and MoDCs differentiated under low-dose IL-4 exerts a gentle action on T cells division (**Figures 4A,B**). As expected, the neutralization of IDO enzymic activity of low-dose educated DCs by 1-MT led to a markedly enhanced capability in T cells proliferation (**Figure 4A**). What's more, when compared with that in high IL-4 group, low-dose IL-4-generated DCs showed a weaker effect on priming naïve T cells to Th1 expansion. This effect was also obviously enhanced by IDO inhibitor 1-MT (**Figures 4C,D**). These results revealed that IL-4 can regulate IDO expression and suggested that an IL-4-dominated inflammatory cytokine milieu was instructive for immune responses activation through regulating DCs functions.

IL-4 Retards CD103+ DCs Differentiation

Studies have shown that CD103+ DCs in the gut showed a high IDO expression (19). In line with increased IL-4 expression in IBDs described by other reports (12, 30), we also observed an increased IL-4 expression in DSS-induced colitis (**Figure 5A**). Besides, the CD103+ DCs subpopulation was also deceased in colitis mice (**Figure 5B**). Although above data suggested IDO expression can be regulated by IL-4 and loss of CD103+ DCs during colonic inflammation, the role of elevated IL-4 in the development of gut-associated tolerogenic CD103+ DCs remains unknown. To our expectation, high concentration IL-4 significantly reduced CD103+ DCs proportion in BMDCs and MoDCs (**Figure 5C**). In parallel with gut CD103+ DCs, the IDO expression was considerably higher in CD103+ DCs when compared with CD103− DCs from BMDCs induced by IL-4 and GM-CSF *ex vivo*. Similarly, a higher expression of IDO was also observed in CD103+ DCs from human MoDCs (**Figure 5D**). These data indicated that IL-4 involved in the process of CD103+IDO+ DCs education, suggesting that elevated IL-4 expression in IBDs might contribute to pathogenesis of colonic inflammation. However, in contrast to low expression of costimulatory molecules on CD103− DCs, CD103+ DCs highly expressed costimulatory molecules, especially in BMDCs (**Figures 6A,B**). Although costimulatory molecules commonly facilitated immune response, CD80 and CD86 are also essential for Treg cells development and proliferation in obese mice and humans, which revealed a protective effect on adipose inflammation (7, 8). Notably, CD103+ DCs derived from precursor cells *in vitro* displayed an immature character, as evidenced by a strong pinocytotic ability (**Figures 6C,D**).

Impaired Treg Cells Differentiation in DCs Generated in a Low IL-4 Environment due to the Loss of CD103+ DCs

Numerous studies revealed that CD103+ DCs exert a critical role in immune tolerance through promoting Treg cells expansion in gut immunity, and above results showed that IL-4 affected CD103+ DCs induction and Treg cells *in vitro*. However, the Treg cells expanded by DCs differentiated under various concentrations of IL-4 and CD103+ DCs *in vitro* were still elusive. The sorted naïve CD4+ T cells were cocultured with DCs differentiated under low or high IL-4 concentrations and then analyzed by flow cytometry. Both mouse BMDCs and human MoDCs were capable of priming naïve T cells to Treg cells. In contrast to DCs propagated from high-dose IL-4, DCs differentiated at a low concentration of IL-4 exerted a strong preference for expanding Treg cells (**Figures 7A,C**). Next,

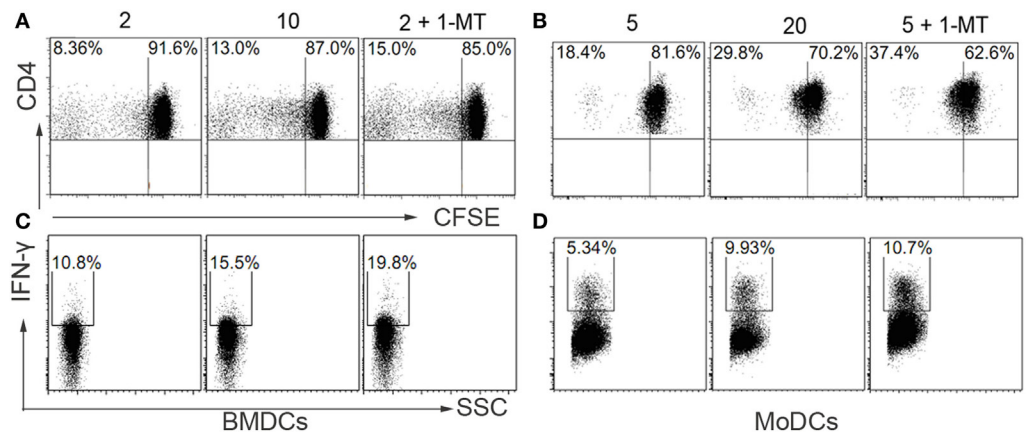

FIGURE 4 | Interleukin (IL)-4 affects the capability of dendritic cells (DCs) in T cell activation through regulating indoleamine 2,3-dioxygenase (IDO) activity. Bone marrow-derived DCs (BMDCs) and monocyte-derived DCs (MoDCs) were generated under various concentration of IL-4 (nanograms per milliliter). Then the BMDCs and MoDCs were cocultured with CFSE-labeled naïve CD4+ T cells from normal C57/BL6 mice or healthy volunteers, respectively, with or without the presence of IDO inhibitor (25 μM). After 5 days, the cells were harvested and analyzed by flow cytometry. **(A,B)** The CD4+ T cells proliferation was evaluated by cell division. Results are represented as mean ± SD. **(C,D)** The CD4+ T cells were also collected and analyzed for type 1 cytokines IFN-γ expression by flow cytometry. Results are represented as mean ± SD. The data shown are representative one of the three separate experiments.

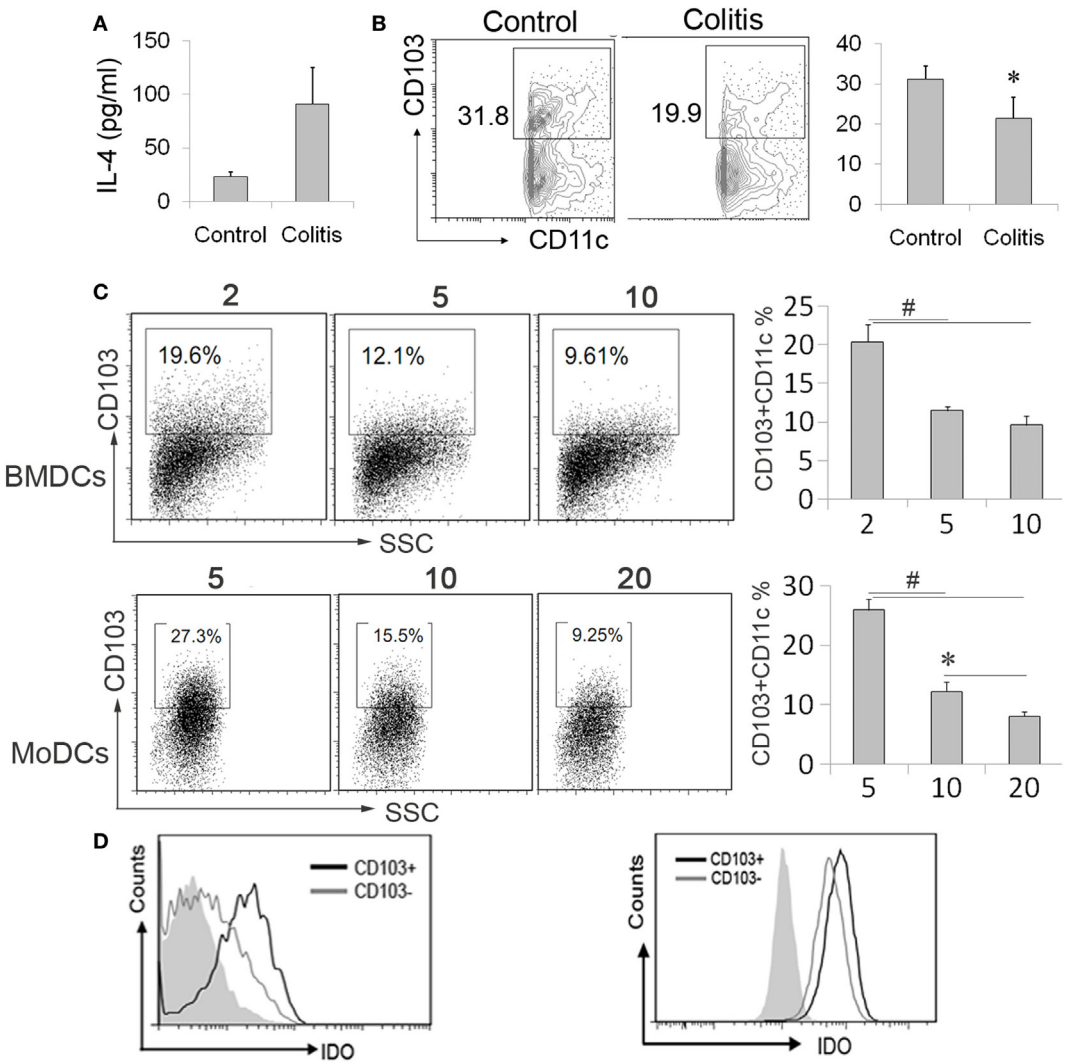

FIGURE 5 | CD103+IDO+ dendritic cells (DCs) differentiation was affected by interleukin (IL)-4. **(A,B)** Mesenteric lymph nodes (MLN) cells and serum were collected from the colitis mice after administration of DSS water or normal mice. The interleukin (IL)-4 levels in sera were detected by ELISA assay. **(A)**. MLN cells were analyzed by flow cytometry for CD103+ DCs. The data are presented as the percentage of CD11c+ gate **(B)**. The data represent mean ± SD (n = 4–6/group). **(C,D)** The differentiated bone marrow-derived DCs (BMDCs) and monocyte-derived DCs (MoDCs) from precursor cells in the presence of different IL-4 concentrations (nanograms per milliliter), followed by flow cytometry analysis of CD103 expression **(C)**. The expression of indoleamine 2,3-dioxygenase (IDO) in the subpopulation of BMDCs and MoDCs by CD103 was determined by flow cytometry. The CD11c positive gate was analyzed **(D)**. Data are from one experiment representative of three. Results are represent as mean ± SD. $^{*}p < 0.05$, $^{\#}p < 0.01$.

to explore whether the low-dose IL-4-educated DCs in Treg cells expansion was contingent on the high propagation of CD103+ DCs, the CD103− DCs generated under low-dose IL-4 were cocultured with T cells. Expectedly, compared with total DCs generated under low dose of IL-4, CD103 DCs exhibited a significant diminishment of the Treg cells differentiation in both humans and mice experiment (**Figures 7B,C**). These data clearly demonstrate that the concentration of IL-4 present during differentiation of DC precursors is crucial for the CD103+ DCs development in IBDs.

DISCUSSION

Type 2 immune response exhibits a strong preference in gut immunity by conferring protection against helminthic infection (31). Beyond that, type 2 immune response is also involved in the process of wound healing in the gut (32, 33). Nevertheless, dysregulated and overreactive Th2 immunity may lead to detrimental inflammation. Th2-induced fibrogenesis can lead to a deleterious consequence by augmenting mucosal and transmural fibrotic process, a prototypic manifestation of IBDs (15, 33). It is well known that IL-4, the core signature of Th2 responses, is highly expressed in certain types of inflammation and also exerts pleiotropic functions due to extremely broad distribution of IL-4 receptors (10). Enormous reports have also provided evidences that IL-4 participates in the pathogenesis of IBDs (34, 35). Oxazolone-induced colitis, resembling the human UC, shows a bias of type 2 immune response. It is noteworthy that oxazolone-induced colitis in mice lacking IL-4Ra or STAT6 was significantly

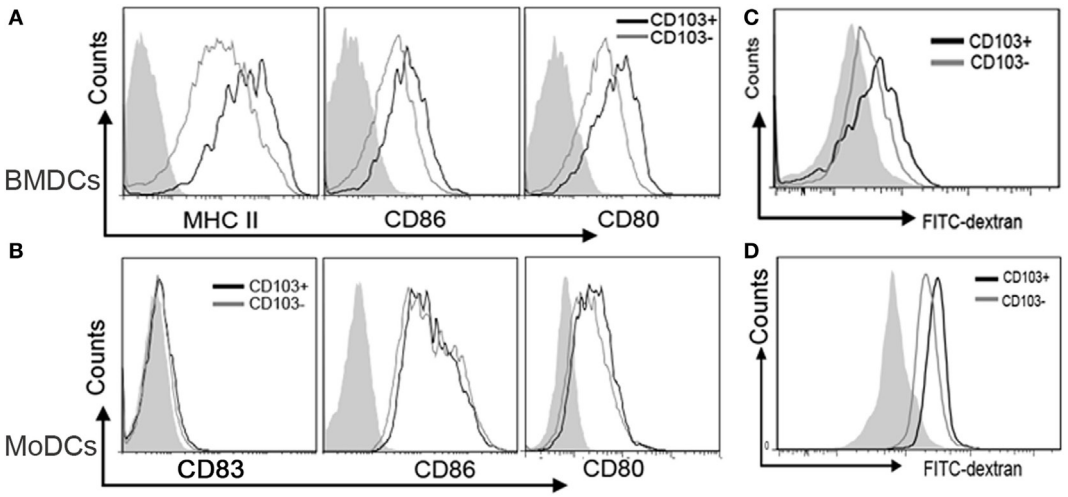

FIGURE 6 | The phenotype of CD103+ dendritic cells (DCs) differentiated from precursor cells. DCs were propagation under 2 ng/ml interleukin (IL)-4 for bone marrow-derived DCs (BMDCs) and 5 ng/ml IL-4 for monocyte-derived DCs (MoDCs) in the presence of GM-CSF as described in Section "Materials and Methods," and then the cells were harvested and analyzed by flow cytometry. **(A)** The surface expressions of CD80, CD86, and MHC-II on the CD103− and CD103+ BMDCs were detected and plotted in histograms. **(B)** CD80, CD86, and CD83 expressions on CD103− and CD103+ MoDCs were analyzed. **(C,D)** Pinocytotic activities of CD103− and CD103+ of BMDCs and MoDCs were represented by mean fluorescence intensity (MFI) of cells incubated with FITC-dextran. Data are representative of three independent experiments.

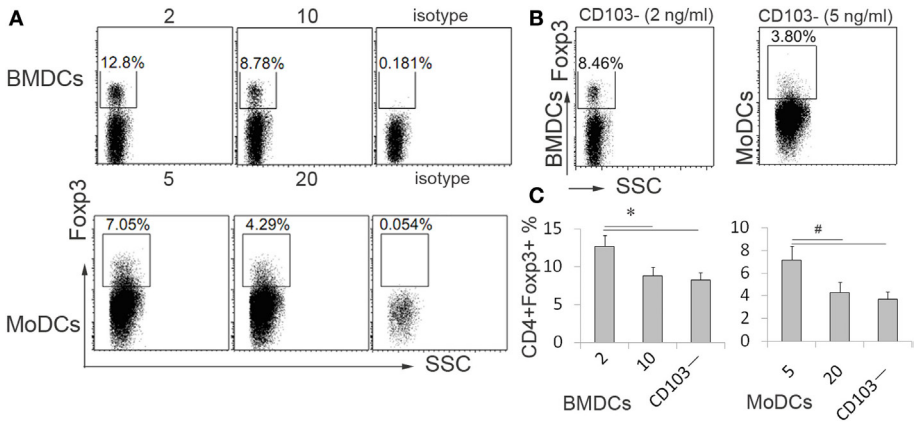

FIGURE 7 | The potential of dendritic cells (DCs) generated under low concentration of interleukin (IL)-4 in regulatory T cells differentiation depend on CD103+ DCs. BMDCs and MoDCs were generated under low (BMDC, 2 ng/ml; MoDCs, 5 ng/ml) and high (BMDC, 10 ng/ml; MoDCs, 20 ng/ml) concentration of IL-4 **(A)**. The CD103− DCs were sorted from DCs which generated under low concentration of IL-4 **(B)**. Then these DCs were subjected to cocultured with naïve CD4+ T cells for 5 days in the presence of anti-CD3 (0.5 μg/ml), respectively. Then the cells were collected for analyzing CD4+CD25+Foxp3+ differentiation by flow cytometry. Results are represented as means ± SD **(C)**. The data shown are representative of one of the three separate experiments. $^{*}p < 0.05$, $^{\#}p < 0.01$.

improved (36, 37). Consistently, blockade of IL-4 cytokine activity by IL-4 antibody administration exhibited a protective effect in oxazolone-induced colitis (38, 39). In accordance with previous studies (12, 15), our data also showed that there was an increased IL-4 level in DSS-induced colitis (data not shown). Furthermore, the importance of IL-4 in DSS-induced colitis model was confirmed by using IL-4 knockout mice (40). However, the mechanism of IL-4 in colitis remains to be defined. Robust data have indicated a crucial role for DCs in the pathogenesis (41). In this study, we demonstrate a novel function of IL-4 in regulating the CD103+ DCs differentiation. CD103+ DCs, a critical DCs subset in the gut immune homeostasis and the primary source of IDO, play a preponderant role in IBDs through promoting Treg cells differentiation (42). Our previous study also demonstrated that the administration of rIL-33 favors Treg cells function through upregulation of CD103+ DCs in animal experimental colitis (24). A tendency of decreased number of Treg cells was observed here (data not shown). The number of Treg cells was not significantly changed, which might be due to the Treg cells differentiation affected by many factors *in vivo*. However, their

suppressor activity may be abrogated *in vivo* or they are unable to counterbalance the chronic mucosal inflammation in UC (43).

Enormous progress has pinpointed that CD103+ DCs are an crucial character in the development of IBDs through promoting Treg cells differentiation. Furthermore, epithelium cells gained attention owing to its role in secretion of TGF-β and RA, which are required for CD103+ DCs tolerogenic phenotype conversion (20). Indeed, rIL-33 administration resulted in an increased ALDH1A1 and TSLP expression in intestine epithelium cells, resulting in an increased conversion of CD103+ DCs (24). Moreover, in accordance with other reports (25, 26), we also observed loss of CD103+ DCs during colonic inflammation in DSS-induced colitis (data not shown). Notably, epithelium cell from IBDs patients, which were damaged during the abnormal immune response, showed an impaired function in CD103+ DCs propagation (20). Due to the defect in Treg cell differentiation, an impaired conversion of CD103+ DCs in epithelial injury might be an important mechanism for the progression of colitis. In spite of the critical role of CD103+ DCs in the gut immune homeostasis, the understanding of CD103+ DCs conditioning during the process of abnormal immune response in IBDs is yet little to known. Although the beneficial effects of epithelium cells on CD103+ DCs conversion was impaired in the development of IBDs (20), a question remained to be addressed is that whether the epithelium injury is the cause or a consequence of CD103+ DCs loss.

Heretofore, enormous progress has been made in understanding the role of IL-4 in the pathogenesis of IBDs, and the precise mechanism of this cytokine in IBDs is still unclear and needs to be further studied (33). Until now, many cytokines exhibit a strong preference for educating DCs. IL-10-treated DCs followed by LPS stimulation suppressed alloreactive T cells during allograft rejection (44). Furthermore, IL-17 neutralization led to alteration of phenotype and function of DCs and diminishment of Th1 type immune response in the mouse chlamydial lung infection and allograft transplantation (45, 46). Not only that, in a human DCs and Th2 cell coculture system, inhibition of IL-4 activity abrogated IL-12 production (17). Moreover, DCs generated under high concentrations of IL-4 produced high amounts of IL-12 and low IL-10 DCs (18). Although IL-4 acts a crucial role in the pathogenesis of IBDs (33), very little information about its action in DCs education is available. Here, our study presented the evidence that IL-4 exerts a regulatory role in CD103+ DCs differentiation. Moreover, there was a dose-dependent effect for IL-4 in the inhibition of CD103+ DCs differentiation. These data might provide explanation why CD103+ DCs were decreased in DSS-induced colitis, where IL-4 was upregulated. Furthermore, following the loss of CD103+ DCs, Treg cell differentiation was causally defective. Our study also provided an evidence that the suppressive effect of low-concentration IL-4-generated DCs primarily depends on IDO, the key regulator of gut CD103+ DCs (19). To our surprise, the costimulatory molecules on CD103+ DCs were significantly increased when compared with CD103− DC. The costimulatory molecules play critical role in initiating the immune response (2), and B7/CD28 interaction provides the important second signal for T cell activation (47–49). Nevertheless, CD80/CD86 is also essential for Treg cells development and proliferation in obese mice and humans and inhibits adipose macrophage inflammation (7). Thus, the concrete function of upregulated costimulatory molecules on CD103+ DCs needs to be further explored.

In conclusion, we provided novel insights into the loss of CD103+ DCs in IBDs, which might be a result of elevated IL-4 expression. Beyond that, our study supported a new relationship among IL-4, CD103+ DCs, and epithelial cells in the pathogenesis of IBDs: in the initial phase of colitis, abnormal Th2 type immune response causes an increased IL-4 expression that leads to loss of tolerogenic CD103+ DC and Treg cells dysfunction. Furthermore, the injury of epithelium resulted from abnormal immune response, in turn, worsens the abnormal immune response due to impaired capability to induce CD103+ DCs conversion. Therefore, IL-4 plays a crucial in the development of colitis.

AUTHOR CONTRIBUTIONS

LD conceived the project, designed and carried out some experiments, analyzed all data, and wrote the paper; JC were responsible for design and performance of experiments and analyzed data and wrote the paper; LT performed all the experiments, analyzed all data, generated figures of the data, and performed statistical analysis; HZ performed all the experiments, analyzed all data, and generated figures of the data. All the authors read, critically revised, and agreed to be accountable for the content of manuscript.

ACKNOWLEDGMENTS

The authors are extremely grateful to all the volunteers who took part in this study.

FUNDING

This work was supported by the National Natural Science Foundation of China (NSFC 81671544, 81302564, to LD, NSFC 81301786 to JC), Fujian Province health planning of young outstanding talents training project no. 2016-ZQN-82 to LD, and Natural Science Foundation of Fujian Provincial Department of Science and Technology 2017J01356.

REFERENCES

1. Smith-Garvin JE, Koretzky GA, Jordan MS. T cell activation. *Annu Rev Immunol* (2009) 27:591–619. doi:10.1146/annurev.immunol.021908.132706
2. Chen L, Flies DB. Molecular mechanisms of T cell co-stimulation and co-inhibition. *Nat Rev Immunol* (2013) 13(4):227–42. doi:10.1038/nri3405
3. Lu L, Thomson AW. Manipulation of dendritic cells for tolerance induction in transplantation and autoimmune disease. *Transplantation* (2002) 73(1 Suppl):S19–22. doi:10.1097/00007890-200201151-00008
4. Shin DS, Ribas A. The evolution of checkpoint blockade as a cancer therapy: what's here, what's next? *Curr Opin Immunol* (2015) 33:23–35. doi:10.1016/j.coi.2015.01.006

5. Seijkens T, Kusters P, Chatzigeorgiou A, Chavakis T, Lutgens E. Immune cell crosstalk in obesity: a key role for costimulation? *Diabetes* (2014) 63(12):3982–91. doi:10.2337/db14-0272
6. Ceeraz S, Nowak EC, Burns CM, Noelle RJ. Immune checkpoint receptors in regulating immune reactivity in rheumatic disease. *Arthritis Res Ther* (2014) 16(5):469. doi:10.1186/s13075-014-0469-1
7. Zhong J, Rao X, Braunstein Z, Taylor A, Narula V, Hazey J, et al. T-cell costimulation protects obesity-induced adipose inflammation and insulin resistance. *Diabetes* (2014) 63(4):1289–302. doi:10.2337/db13-1094
8. Bour-Jordan H, Bluestone JA. Regulating the regulators: costimulatory signals control the homeostasis and function of regulatory T cells. *Immunol Rev* (2009) 229(1):41–66. doi:10.1111/j.1600-065X.2009.00775.x
9. Wynn TA. Type 2 cytokines: mechanisms and therapeutic strategies. *Nat Rev Immunol* (2015) 15(5):271–82. doi:10.1038/nri3831
10. May RD, Fung M. Strategies targeting the IL-4/IL-13 axes in disease. *Cytokine* (2015) 75(1):89–116. doi:10.1016/j.cyto.2015.05.018
11. Paul WE. History of interleukin-4. *Cytokine* (2015) 75(1):3–7. doi:10.1016/j.cyto.2015.01.038
12. Alex P, Zachos NC, Nguyen T, Gonzales L, Chen TE, Conklin LS, et al. Distinct cytokine patterns identified from multiplex profiles of murine DSS and TNBS-induced colitis. *Inflamm Bowel Dis* (2009) 15(3):341–52. doi:10.1002/ibd.20753
13. Pushparaj PN, Li D, Komai-Koma M, Guabiraba R, Alexander J, McSharry C, et al. Interleukin-33 exacerbates acute colitis via interleukin-4 in mice. *Immunology* (2013) 140(1):70–7. doi:10.1111/imm.12111
14. Miller AM, Xu D, Asquith DL, Denby L, Li Y, Sattar N, et al. IL-33 reduces the development of atherosclerosis. *J Exp Med* (2008) 205(2):339–46. doi:10.1084/jem.20071868
15. Baumgart DC, Carding SR. Inflammatory bowel disease: cause and immunobiology. *Lancet* (2007) 369(9573):1627–40. doi:10.1016/S0140-6736(07)60750-8
16. Liu D, Kebaier C, Pakpour N, Capul AA, Beverley SM, Scott P, et al. *Leishmania major* phosphoglycans influence the host early immune response by modulating dendritic cell functions. *Infect Immun* (2009) 77(8):3272–83. doi:10.1128/IAI.01447-08
17. Kalinski P, Smits HH, Schuitemaker JH, Vieira PL, van Eijk M, de Jong EC, et al. IL-4 is a mediator of IL-12p70 induction by human Th2 cells: reversal of polarized Th2 phenotype by dendritic cells. *J Immunol* (2000) 165(4):1877–81. doi:10.4049/jimmunol.165.4.1877
18. Guenova E, Volz T, Sauer K, Kaesler S, Muller MR, Wolbing F, et al. IL-4-mediated fine tuning of IL-12p70 production by human DC. *Eur J Immunol* (2008) 38(11):3138–49. doi:10.1002/eji.200838463
19. Matteoli G, Mazzini E, Iliev ID, Mileti E, Fallarino F, Puccetti P, et al. Gut CD103+ dendritic cells express indoleamine 2,3-dioxygenase which influences T regulatory/T effector cell balance and oral tolerance induction. *Gut* (2010) 59(5):595–604. doi:10.1136/gut.2009.185108
20. Iliev ID, Spadoni I, Mileti E, Matteoli G, Sonzogni A, Sampietro GM, et al. Human intestinal epithelial cells promote the differentiation of tolerogenic dendritic cells. *Gut* (2009) 58(11):1481–9. doi:10.1136/gut.2008.175166
21. Ball HJ, Jusof FF, Bakmiwewa SM, Hunt NH, Yuasa HJ. Tryptophan-catabolizing enzymes – party of three. *Front Immunol* (2014) 5:485. doi:10.3389/fimmu.2014.00485
22. Yu G, Dai H, Chen J, Duan L, Gong M, Liu L, et al. Gene delivery of indoleamine 2,3-dioxygenase prolongs cardiac allograft survival by shaping the types of T-cell responses. *J Gene Med* (2008) 10(7):754–61. doi:10.1002/jgm.1201
23. Harden JL, Egilmez NK. Indoleamine 2,3-dioxygenase and dendritic cell tolerogenicity. *Immunol Invest* (2012) 41(6–7):738–64. doi:10.3109/08820139.2012.676122
24. Duan L, Chen J, Zhang H, Yang H, Zhu P, Xiong A, et al. Interleukin-33 ameliorates experimental colitis through promoting Th2/Foxp3(+) regulatory T-cell responses in mice. *Mol Med* (2012) 18:753–61. doi:10.2119/molmed.2011.00428
25. Strauch UG, Grunwald N, Obermeier F, Gurster S, Rath HC. Loss of CD103+ intestinal dendritic cells during colonic inflammation. *World J Gastroenterol* (2010) 16(1):21–9. doi:10.3748/wjg.v16.i1.21
26. Cheng L, Jin H, Qiang Y, Wu S, Yan C, Han M, et al. High fat diet exacerbates dextran sulfate sodium induced colitis through disturbing mucosal dendritic cell homeostasis. *Int Immunopharmacol* (2016) 40:1–10. doi:10.1016/j.intimp.2016.08.018
27. Wirtz S, Neufert C, Weigmann B, Neurath MF. Chemically induced mouse models of intestinal inflammation. *Nat Protoc* (2007) 2(3):541–6. doi:10.1038/nprot.2007.41
28. Duan L, Wang CY, Chen J, Gong Q, Zhu P, Zheng F, et al. High-mobility group box 1 promotes early acute allograft rejection by enhancing IL-6-dependent Th17 alloreactive response. *Lab Invest* (2011) 91(1):43–53. doi:10.1038/labinvest.2010.141
29. Yan Y, Ding Y, Ming B, Du W, Kong X, Tian L, et al. Increase in hypotonic stress-induced endocytic activity in macrophages via ClC-3. *Mol Cells* (2014) 37(5):418–25. doi:10.14348/molcells.2014.0031
30. Da Silva AP, Pollett A, Rittling SR, Denhardt DT, Sodek J, Zohar R. Exacerbated tissue destruction in DSS-induced acute colitis of OPN-null mice is associated with downregulation of TNF-alpha expression and non-programmed cell death. *J Cell Physiol* (2006) 208(3):629–39. doi:10.1002/jcp.20701
31. Grencis RK. Immunity to helminths: resistance, regulation, and susceptibility to gastrointestinal nematodes. *Annu Rev Immunol* (2015) 33:201–25. doi:10.1146/annurev-immunol-032713-120218
32. Gause WC, Wynn TA, Allen JE. Type 2 immunity and wound healing: evolutionary refinement of adaptive immunity by helminths. *Nat Rev Immunol* (2013) 13(8):607–14. doi:10.1038/nri3476
33. Bamias G, Cominelli F. Role of type 2 immunity in intestinal inflammation. *Curr Opin Gastroenterol* (2015) 31(6):471–6. doi:10.1097/MOG.0000000000000212
34. Chinen T, Kobayashi T, Ogata H, Takaesu G, Takaki H, Hashimoto M, et al. Suppressor of cytokine signaling-1 regulates inflammatory bowel disease in which both IFNgamma and IL-4 are involved. *Gastroenterology* (2006) 130(2):373–88. doi:10.1053/j.gastro.2005.10.051
35. Ruckert Y, Schindler U, Heinig T, Nikolaus S, Raedler A, Schreiber S. IL-4 signaling mechanisms in inflammatory bowel disease mononuclear phagocytes. *Inflamm Bowel Dis* (1996) 2(4):244–52. doi:10.1002/ibd.3780020404
36. Rosen MJ, Chaturvedi R, Washington MK, Kuhnhein LA, Moore PD, Coggeshall SS, et al. STAT6 deficiency ameliorates severity of oxazolone colitis by decreasing expression of claudin-2 and Th2-inducing cytokines. *J Immunol* (2013) 190(4):1849–58. doi:10.4049/jimmunol.1201373
37. Hoving JC, Kirstein F, Nieuwenhuizen NE, Fick LC, Hobeika E, Reth M, et al. B cells that produce immunoglobulin E mediate colitis in BALB/c mice. *Gastroenterology* (2012) 142(1):96–108. doi:10.1053/j.gastro.2011.09.044
38. Kasaian MT, Page KM, Fish S, Brennan A, Cook TA, Moreira K, et al. Therapeutic activity of an interleukin-4/interleukin-13 dual antagonist on oxazolone-induced colitis in mice. *Immunology* (2014) 143(3):416–27. doi:10.1111/imm.12319
39. Boirivant M, Fuss IJ, Chu A, Strober W. Oxazolone colitis: a murine model of T helper cell type 2 colitis treatable with antibodies to interleukin 4. *J Exp Med* (1998) 188(10):1929–39. doi:10.1084/jem.188.10.1929
40. Stevceva L, Pavli P, Husband A, Ramsay A, Doe WF. Dextran sulphate sodium-induced colitis is ameliorated in interleukin 4 deficient mice. *Genes Immun* (2001) 2(6):309–16. doi:10.1038/sj.gene.6363782
41. Steinbach EC, Plevy SE. The role of macrophages and dendritic cells in the initiation of inflammation in IBD. *Inflamm Bowel Dis* (2014) 20(1):166–75. doi:10.1097/MIB.0b013e3182a69dca
42. Scott CL, Aumeunier AM, Mowat AM. Intestinal CD103+ dendritic cells: master regulators of tolerance? *Trends Immunol* (2011) 32(9):412–9. doi:10.1016/j.it.2011.06.003
43. Yu QT, Saruta M, Avanesyan A, Fleshner PR, Banham AH, Papadakis KA. Expression and functional characterization of FOXP3+ CD4+ regulatory T cells in ulcerative colitis. *Inflamm Bowel Dis* (2007) 13(2):191–9. doi:10.1002/ibd.20053
44. Dai H, Zhu H, Lei P, Yagita H, Liu J, Wen X, et al. Programmed death-1 signaling is essential for the skin allograft protection by alternatively activated dendritic cell infusion in mice. *Transplantation* (2009) 88(7):864–73. doi:10.1097/TP.0b013e3181b6ea74
45. Antonysamy MA, Fanslow WC, Fu F, Li W, Qian S, Troutt AB, et al. Evidence for a role of IL-17 in organ allograft rejection: IL-17 promotes the functional differentiation of dendritic cell progenitors. *J Immunol* (1999) 162(1):577–84.
46. Duan L, Chen J, Xia Q, Chen L, Fan K, Sigdel KR, et al. IL-17 promotes Type 1 T cell response through modulating dendritic cell function in acute

allograft rejection. *Int Immunopharmacol* (2014) 20(2):290–7. doi:10.1016/j.intimp.2014.03.010

47. McAdam AJ, Schweitzer AN, Sharpe AH. The role of B7 co-stimulation in activation and differentiation of CD4+ and CD8+ T cells. *Immunol Rev* (1998) 165:231–47. doi:10.1111/j.1600-065X.1998.tb01242.x
48. Harris NL, Ronchese F. The role of B7 costimulation in T-cell immunity. *Immunol Cell Biol* (1999) 77(4):304–11. doi:10.1046/j.1440-1711.1999.00835.x
49. Lenschow DJ, Walunas TL, Bluestone JA. CD28/B7 system of T cell costimulation. *Annu Rev Immunol* (1996) 14:233–58. doi:10.1146/annurev.immunol.14.1.233

Conflict of Interest Statement: The authors declare that the research was conducted in the absence of any commercial or financial relationships that could be construed as a potential conflict of interest.

Copyright © 2017 Tu, Chen, Zhang and Duan. This is an open-access article distributed under the terms of the Creative Commons Attribution License (CC BY). The use, distribution or reproduction in other forums is permitted, provided the original author(s) or licensor are credited and that the original publication in this journal is cited, in accordance with accepted academic practice. No use, distribution or reproduction is permitted which does not comply with these terms.

frontiers in Immunology

ORIGINAL RESEARCH
published: 07 March 2017
doi: 10.3389/fimmu.2017.00240

The Small Tellurium Compound AS101 Ameliorates Rat Crescentic Glomerulonephritis: Association with Inhibition of Macrophage Caspase-1 Activity *via* Very Late Antigen-4 Inactivation

Yafit Hachmo[1], Yona Kalechman[1], Itai Skornick[1], Uzi Gafter[2,3], Rachel R. Caspi[4†] and Benjamin Sredni[1†]*

[1] C.A.I.R. Institute, The Safdiè AIDS and Immunology Research Center, The Mina & Everard Goodman Faculty of Life Sciences, Bar-Ilan University, Ramat Gan, Israel, [2] Laboratory of Nephrology and Transplant Immunology, Rabin Medical Center, Petah-Tikva, Israel, [3] Tel Aviv University, Tel Aviv, Israel, [4] Laboratory of Immunology, National Eye Institute, National Institutes of Health, Bethesda, MD, USA

OPEN ACCESS

Edited by:
Guixiu Shi,
Xiamen University, China

Reviewed by:
Rui Li,
Montreal Neurological Institute and Hospital, Canada
Hao Wu,
Amgen, USA

***Correspondence:**
Benjamin Sredni
srednib@mail.biu.ac.il

[†]These authors have contributed equally to this work.

Specialty section:
This article was submitted to Inflammation, a section of the journal Frontiers in Immunology

Received: 08 December 2016
Accepted: 20 February 2017
Published: 07 March 2017

Citation:
Hachmo Y, Kalechman Y, Skornick I, Gafter U, Caspi RR and Sredni B (2017) The Small Tellurium Compound AS101 Ameliorates Rat Crescentic Glomerulonephritis: Association with Inhibition of Macrophage Caspase-1 Activity via Very Late Antigen-4 Inactivation. Front. Immunol. 8:240. doi: 10.3389/fimmu.2017.00240

Crescentic glomerulonephritis (CGN) is the most aggressive form of GN and, if untreated, patients can progress to end-stage renal failure within weeks of presentation. The α4β1 integrin very late antigen-4 (VLA-4) is an adhesion molecule of fundamental importance to the recruitment of leukocytes in inflammation. We addressed the role of VLA-4 in mediating progressive renal injury in a rat model of CGN using a small tellurium compound. AS101 [ammonium trichloro(dioxoethylene-*o*,*o*′)tellurate]. This compound has been previously shown to uniquely inhibit VLA-4 activity by redox inactivation of adjacent thiols in the exofacial domain of VLA-4. The study shows that administration of AS101 either before or after glomerular basement membrane antiserum injection ameliorates crescent formation or preserves renal function. This was associated with profound inhibition of critical inflammatory mediators, accompanied by decreased glomerular infiltration of macrophages. Mechanistic studies demonstrated vla-4 inactivation on glomerular macrophages both *in vitro* and *in vivo* as well as inhibition of caspase-1 activity. Importantly, this cysteine protease activity modification was dependent on VLA-4 inactivation and was associated with the anti-inflammatory activity of AS101. We propose that inactivation of macrophage VLA-4 by AS101 *in vivo* results in a decrease of inflammatory cytokines and chemokines produced in the glomeruli of diseased rats, resulting in decreased further macrophage recruitment and decreased extracellular matrix expansion. Thus, AS101, which is currently in clinical trials for other indications, might be beneficial for treatment of CGN.

Keywords: glomerulonephritis, cytokines, integrin, caspase-1, AS101, inflammation

INTRODUCTION

The hallmark of human anti-glomerular basement membrane (GBM) disease is the production of autoantibodies targeting the non-collagenous (NC1) domain of the α3 chain of type IV collagen found in the GBM (1) leading to crescent formation and crescentic glomerulonephritis (CGN). CGN is the most aggressive form of glomerular inflammation, which presents clinically

as rapidly progressive glomerulonephritis. It is characterized by disruption of the GBM, which leads to infiltration and proliferation of inflammatory cells such as macrophages in Bowman's space (2).

The glomerulonephritis is associated with interstitial nephritis in many patients with anti-GBM disease and in animal models of CGN as well (3, 4). The inflammatory process gives way to glomerulosclerosis, interstitial fibrosis, tubular atrophy, and renal failure.

Although the pathogenesis of CGN is incompletely understood and likely involves several convergent pathways, there is general agreement that circulating mononuclear phagocytes play a central role. Administration of nephrotoxic serum to rodents results in a severe proliferative and necrotizing GN that is characterized by glomerular crescent formation and accumulation of leukocytes (2–4). It is thought that infiltrating cells release inflammatory mediators that influence the behavior of glomerular, tubular, and interstitial cells. This interaction between infiltrating and resident cells leads to cellular proliferation, matrix expansion, and may ultimately lead to glomerular sclerosis and interstitial fibrosis. Monocytes and macrophages appear to have a critical role, as ablation of macrophages in murine CGN reduced glomerular injury and improved renal function (5). Infiltrating glomerular macrophages are the major source of IL-1 (6) and tumor necrosis factor (TNF) (7). TNFα was shown to promote VCAM-1 and ICAM-1 glomerular expression and the recruitment of PMNs and lymphocytes were markedly reduced in TNF-deficient mice in experimental GN induced by anti-GBM antibody (8). Thus, strategies that reduce monocyte macrophage infiltration could be a promising avenue for complementary therapy of CGN.

Another strategy to prevent leukocyte infiltration in the kidney could be to interrupt the interaction between endothelial molecules involved in cell adhesion and their ligands on circulating inflammatory cells. The α4β1 integrin or very late antigen-4 (VLA-4) is expressed mainly on monocytes, lymphocytes, and eosinophils (9). AS101 is a potent *in vitro* and *in vivo* tellurium immunomodulator, with a wealth of potential therapeutic applications (10, 11). The compound is non-toxic and is currently in phase II/III studies in patients with cervical tumors and in phase I/II studies in patients with aging macular degeneration. From a mechanistic point of view, much of the biological activity of AS101 is directly related to its chemical redox interactions with vicinal thiols in the exofacial domain of VLA-4 (12), enabling the compound to mediate such diverse effects as abrogation of the acquired drug resistance of acute myelogenous leukemia (12) and amelioration of experimental autoimmune encephalomyelitis (13). The specific redox-modulating activities of AS101 result in a variety of beneficial biological effects in diverse preclinical and clinical studies (14). The anti-inflammatory properties were found crucial for the clinical activities of AS101, including the protective effects of AS101 in autoimmune diseases (15, 16) and in septic mice (17). The same thiol–redox interactions of AS101 enabled it to exert beneficial effects in a variety of tumor models in mice and humans where AS101 had clear antitumor effects (18, 19). Importantly, as part of its activity, AS101 exerts nephroprotective effects. It was able to reduce the level of immune complex deposition in the glomeruli, reduce proteinuria, prevent glomerular hypercellularity and mesangial expansion, and reduce the mean glomerular volume in a murine model of systemic lupus erythematosus (16) and prevent kidney damage in a murine model of septic peritonitis (17).

The anti-inflammatory properties of AS101 coupled with its unique mode of VLA-4 inactivation prompted us to evaluate its potential beneficial activities in CGN and determine the role of VLA-4 inactivation in these effects. In the present study, we demonstrate that administration of AS101 both before and after induction of CGN by αGBM injection ameliorates damage to the glomeruli and preserves renal function. This was associated with profound inhibition of inflammatory mediators and a decreased infiltration of macrophages. Mechanistic studies demonstrated that these effects were associated with vla-4 inactivation on macrophages and inhibition of caspase-1 activity in a VLA-4-dependent fashion. These data suggest that AS101 could have clinical potential as a therapeutic approach to glomerulonephritis.

MATERIALS AND METHODS

Reagents

The reagents were as follows: fibronectin (FN) (Sigma; Rehovot, Israel) VCAM-1(R&D Biosystems, Minneapolis, MN, USA); BSA (Sigma); XTT cell proliferation kit (Biological Industries, Bet Haemek, Israel); FAM FLICA Caspase-3,7 and caspase-1 detection kit (Immunochemistry Technologies LLC, MN, USA); anti Cd49d, anti cd49e (Serotec, NC, USA); *Staphylococcus aureus* Cowan I (SAC) (Calbiochem-Behring Corp., La Jolla, CA, USA). LPS (Sigma); mouse anti-rat CD68 (ED1) (Serotec); rabbit anti-rat FN (Cedarlane, Burlington, ON, Canada); anti-mouse IL-18 (R&D Biosystems); anti-mouse IL-1β (Santa Cruz, Santa Cruz, CA, USA); anti αTubulin (Santa Cruz); anti-rat Thy-1.1(Cederlane); sheep anti-rat GBM (Probetex, San Antonio, TX, USA); rat IL-1β, IL-18, and TNFα ELISA kits (BiosourceThermo Fisher, Waltham, MA, USA); rat connective tissue growth factor (CTGF) and monocyte chemoattractant protein-1 (MCP-1) ELISA kits (MyBiosource, San Diego CA, USA). Creatinine and albumin assay kits (Abcam, San Francisco, CA, USA); AS101 (supplied by M. Albeck, Bar-Ilan University, Ramat Gan, Israel).

Animals

Male Sprague-Dawley rats (180–200 g) were housed in individual metabolic cages with unlimited access to food and water. Experiments conformed to approved institutional protocols and were approved by the Institutional Animal Care and Use Committee.

Experimental CGN

Rats were presensitized on day −5 by a subcutaneous injection of 6.25 mg sheep IgG in 0.5 ml emulsion (1:1 v/v) with Freund's complete adjuvant. Glomerulonephritis was induced on day 0 by a single intravenous injection of 105 mg/kg sheep anti-rat GBM (αGBM). Experimental groups were as follows: daily i.p. injection with PBS without αGBM administration (negative PBS control); daily injection with PBS of αGBM-induced rats (positive control)

and three treatment groups of daily i.p. injections with AS101 (100 μg/rat): starting 1 day before, 3 days after, or 6 days after αGBM administration.

Isolation of Glomeruli

Glomeruli were isolated from the renal cortex of rats using the differential sieving method (20). The purity of glomeruli was >95%.

Isolation and Culture of Glomerular Mesangial Cells

Isolated glomeruli were cultured in Dulbecco's modified Eagle's medium containing 5.5 mM D-(+)-glucose; 20% fetal bovine serum, 100 μg/ml streptomycin, 100 μg/ml penicillin, and 2 mM L-glutamine, at 37°C in 5% CO_2. After 10 days, the cells had the typical appearance of spindle-shaped bundles, and no polygonal endothelial or epithelial cells could be detected. Cells stained positive with a rabbit polyclonal anti-rat Thy-1.1 antibody (mesangial cell marker).

Isolation and Culture of Glomerular Macrophages

Glomeruli were cultured in Eagle's MEM, containing 10% FCS at 37°C in a 5% CO_2/air atmosphere for 3 days. Glomeruli were removed by decanting the medium after vigorous agitation. Adherent macrophages were removed by incubation for 3 min with trypsin–versene solution. Cells harvested were used immediately. These cells were 90% positive for ED1.

Western Blot Analysis

Isolated glomeruli were lysed with lysis buffer [1 M Tris (pH = 7.4), 1.5 M NaCl, 1% Triton-X, 10% glycerol, 50 mM EDTA (pH = 8), 0.1 M sodium vanadate, 0.1 M PMSF, 0.1% protease inhibitor cocktail]. Samples were boiled for 5 min, electrophoresed on 15% or SDS-PAGE, transferred to nitrocellulose, and immunoblotted with specific antibodies (IL1β, IL-18). Blots were developed using horseradish peroxidase-conjugated secondary Abs and the ECL detection system.

Quantitation of Caspase Activity

Isolated glomerular extracts were prepared in Tris/acetate buffer (pH 7.5) at 30°C. The extracts were centrifuged at 12,000 × *g* for 10 min, and the supernatant was collected. A volume of supernatant equivalent to 100 μg of protein was assayed for caspase-1 or caspase-3 activity using the colorimetric caspase-1 and -3 assay kits.

Quantitation of Cytokine Levels

IL-1β, TNF-α, CTGF, MCP-1, and IL-18 ELISA kits were used for the quantitative measurement of these cytokines either in rat sera or urine, in supernatants of cultured cells or in glomerular lysates.

Attachment Assay for Evaluation of VLA-4 Activity

96-well plates were coated with 80 μL of FN, VCAM-1, or BSA. Cells were incubated in the wells for 1 h with or without AS101 and were washed three times. The attached cells were tested by the colorimetric XTT (2,3-bis[2-methoxy-4-nitro-S-sulfophenynl] H-tetrazolium-5-carboxanilide inner salt) assay at 450 nm.

Renal Histology

Resected kidneys were cut by a coronal section through the mid portion of the kidney. One-half was fixed in 10% buffered formalin. Paraffin blocks were prepared, 3 μM sections were cut from each block and stained with hematoxylin-eosin and periodic acid Schiff stains for detection of crescent formation.

Immunohistochemistry

For ED-1 staining, fixed paraffin embedded kidney sections were incubated for 1 h with mouse anti-ED-1 (1:100) followed by horse anti-mouse Biotin-conjugated (1:500) antibodies. After incubation with secondary antibodies, the sections were incubated with HRP-streptavidin followed by DAB for an additional, washed and exposed to hematoxylin. Glomerular macrophages were counted under light microscope. One hundred glomeruli were counted/sample. For FN staining, the sections were incubated with rabbit anti-rat FN (1:100) followed by horse anti-rabbit Biotin-conjugated (1:500) antibodies. The sections were then incubated with HRP-streptavidin followed by DAB, washed, and exposed to hematoxylin. FN expansion was scored in 100 glomeruli/sample as follows: grade 0—no staining; grade 1—staining occupying up to 25% of glomerular surface area; grade 2—staining occupying 25–50% of glomerular surface area; grade 3—staining occupying more than 50% of glomerular surface area.

Fluorescence-Activated Cell Sorter (FACS) Analysis

Rats were treated with anti-GBM and PBS or with anti-GBM and AS101 (+3). At 2 weeks after anti-GBM administration, macrophages were isolated from glomeruli of rats and evaluated for VLA-4 expression by FACS analysis. VLA-4 expression on isolated glomerular macrophages was determined after incubation with FITC Mouse Anti-Rat CD49d (serotec) by FACS [FACStar plus (Becton Dickinson) flow cytometer] using The Flow Jo software.

Statistical Analysis

Data are presented as mean ± SE. For comparisons between groups in the *in vivo* and *in vitro* studies, we used the one- or two-way ANOVA. Linear correlation analysis (Pearson correlation) was applied to determine the correlation and association between parameters. Two-tailed $p < 0.05$ was considered statistically significant. The software used for all statistical analysis was IBM SPSS Statistics 21.

RESULTS

Administration of AS101 Ameliorates Crescent Formation and Preserves Renal Function in Experimental CGM

Rats were induced for CGM as described in Section "Materials and Methods." Daily i.p. injections of AS101 (100 μg/rat) preserved renal function (**Figure 1**) as evidenced by decreased

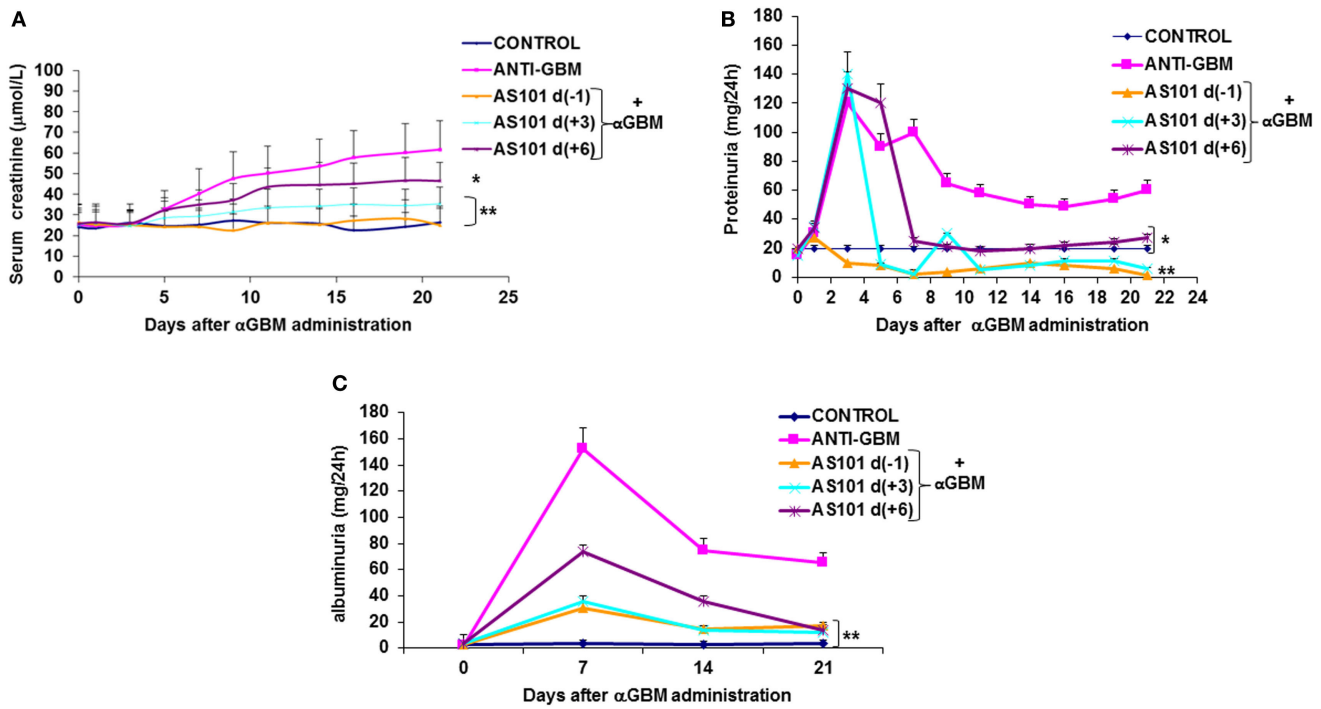

FIGURE 1 | Treatment with AS101 preserves kidney function in crescentic glomerulonephritis. GN was induced by a single intravenous injection of αGBM [sheep anti-rat glomerular basement membrane (GBM)] in rats presensitized 5 days earlier with sheep IgG, as described in Section "Materials and Methods." Experimental groups were as follows: daily i.p. injection with PBS without αGBM administration (negative control); daily injection with PBS of αGBM-induced rats (positive control) and three treatment groups of daily i.p. injections with AS101 (100 μg/rat) starting 1 day before (−1), 3 days after (+3), or 6 days after (+6) the αGBM administration. Serum creatinine **(A)** and proteinuria **(B)** were recorded on days 0, 1, 3, 5, 7, 9, 11, 14, 16, 19, and 21. Albuminuria **(C)** was recorded on days 0, 7, 14, and 21. Data are presented as mean ± SE of eight rats/group for each time point. *$p < 0.05$ decrease vs. αGBM. **$p < 0.01$ decrease vs. αGBM; the two-way ANOVA was used.

serum creatinine levels (**Figure 1A**) and decreased proteinuria (**Figure 1B**) and albuminuria (**Figure 1C**). These effects were marked and significant when treatment started 1 day before αGBM administration [AS101(−1)] or 3 days after αGBM administration [AS101(+3)]. Starting treatment 6 days after αGBM administration [AS101(+6)] still significantly improved renal function, although the effect was more modest.

Crescent formation in some rats was already evident 1 week after αGBM administration. This pathology was increased in the subsequent weeks (**Figure 2**). Treatment with AS101 before or after αGBM administration significantly ameliorated crescent formation at all time points (**Figure 2B**).

AS101 Regulates IL-18, IL-1β, and Caspase-1 Activity and Ameliorates Kidney Pathology

It is well established that in experimental CGN IL-18 and IL-1β contribute to crescent formation and inflammatory cell recruitment (21, 22). For cytokine evaluation, we chose the 2 weeks' time point in order to allow a reasonable time for the AS101(+6) protocol to be effective. IL-18 levels in both serum and urine were significantly increased 2 weeks after αGBM administration (**Figures 3A,B**). Treatment with AS101 either before or after αGBM administration significantly decreased IL-18 levels in serum as well as in urine. Moreover, glomerular IL-18 protein expression was also considerably decreased in treated rats (**Figure 3C**). This decrease was significant in all three regimens of AS101 administration. Importantly, the regulation of IL-18 by AS101 was positively and significantly correlated with disease severity (proteinuria) as analyzed by Pearson correlation test (Figure S1A in Supplementary Material).

IL-18 is synthesized as an inactive precursor that lacks a secretion signal sequence and is proteolytically activated by Caspase-1 (23). We therefore evaluated the effect of AS101 on caspase-1 activity in glomeruli of treated rats. **Figure 3D** shows a significant increase in glomerular caspase-1 activity at 2 weeks post αGBM administration, which was dramatically and significantly decreased by all three AS101 treatment regimens.

These results prompted us to evaluate levels of IL-1β, an inflammatory cytokine also proteolytically activated by caspase-1 (24–26). **Figure 4** shows that similar to IL-18, serum and urine levels of IL-1β were substantially and significantly increased 2 weeks after αGBM administration. Again, all three AS101 treatment regimens significantly decreased IL-1β detectable in serum and in urine at 2 weeks post αGBM administration (**Figures 4A,B**). Similarly, glomerular IL-1β protein was significantly decreased following AS101 treatment

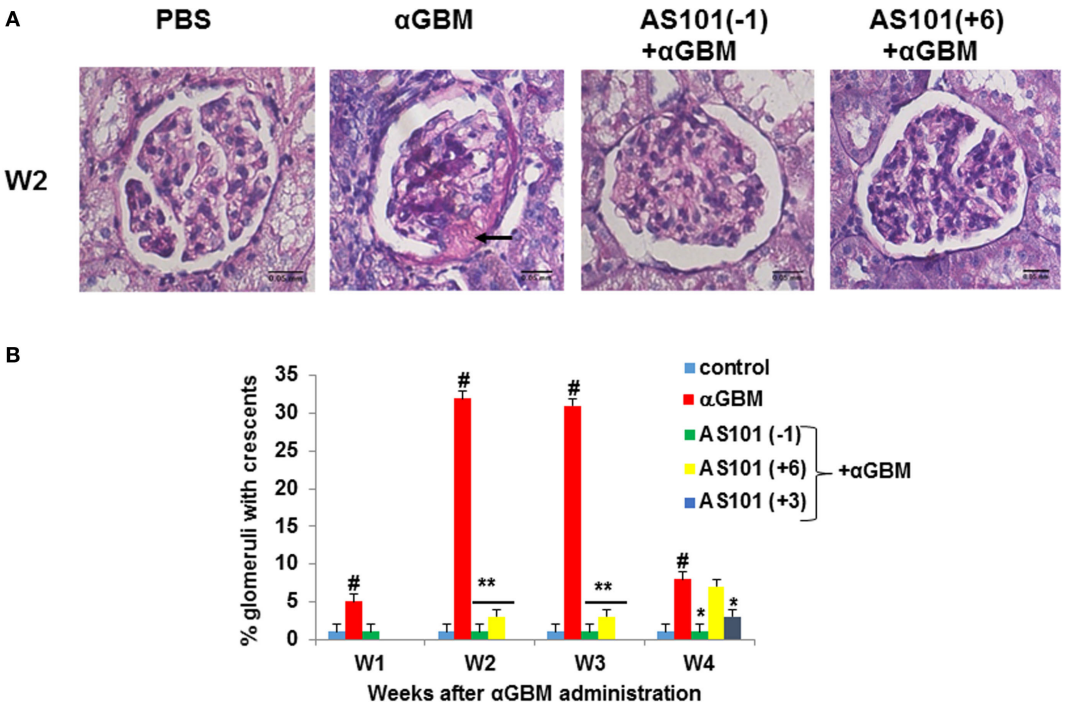

FIGURE 2 | Treatment with AS101 decreases crescent formation in crescentic glomerulonephritis. Treatment protocol was as described in **Figure 1** with one modification. Experimental groups were as follows: daily i.p. injection with PBS without αGBM administration (control); daily injection with PBS of αGBM-induced rats (αGBM only) and two treatment groups of αGBM-induced rats with daily i.p. injections of AS101 (100 μg/rat) starting 1 day before (–1), or 6 days after (+6) the αGBM administration. Groups were tested weekly until week 4. Treatment starting at day 3 (+3) was tested only at week 4. Renal Histology was performed on kidney sections for detection of crescents formation on week 2 **(A)**. The percentage of glomeruli with crescents was evaluated in 100 glomeruli/rat on weeks 1, 2, 3, and 4 after αGBM administration **(B)**. Data are presented as mean ± SE of 8 rats/group for each time point. $^{\#}p < 0.01$ increase vs. control; $^{*}p < 0.05$ decrease vs. αGBM. $^{**}p < 0.01$ decrease vs. αGBM. The two-way ANOVA was used.

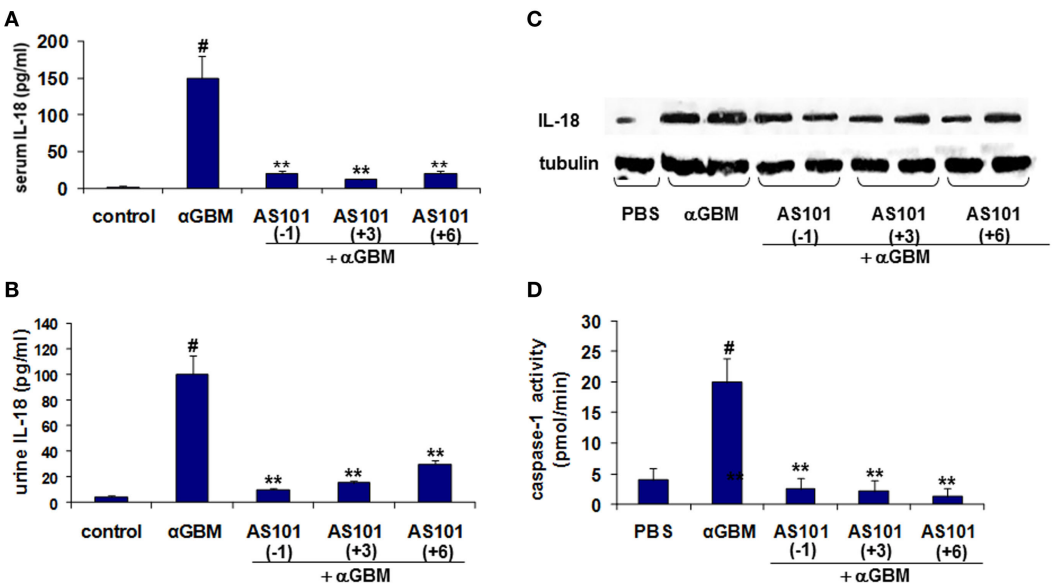

FIGURE 3 | Treatment with AS101 decreases IL-18 protein levels and glomerular caspase-1 activity in crescentic glomerulonephritis. Treatment protocol was as described in **Figure 2**. Serum **(A)**, urine **(B)**, and glomerular **(C)**. IL-18 expression was evaluated 2 weeks after αGBM administration. Glomerular caspase-1 activity **(D)** was evaluated 2 weeks after αGBM administration. Data are presented as mean ± SE of 7–8 rats/group. Healthy controls ($N = 3$). $^{\#}p < 0.01$ increase vs. control; $^{**}p < 0.01$ decrease vs. αGBM. The one-way ANOVA was used.

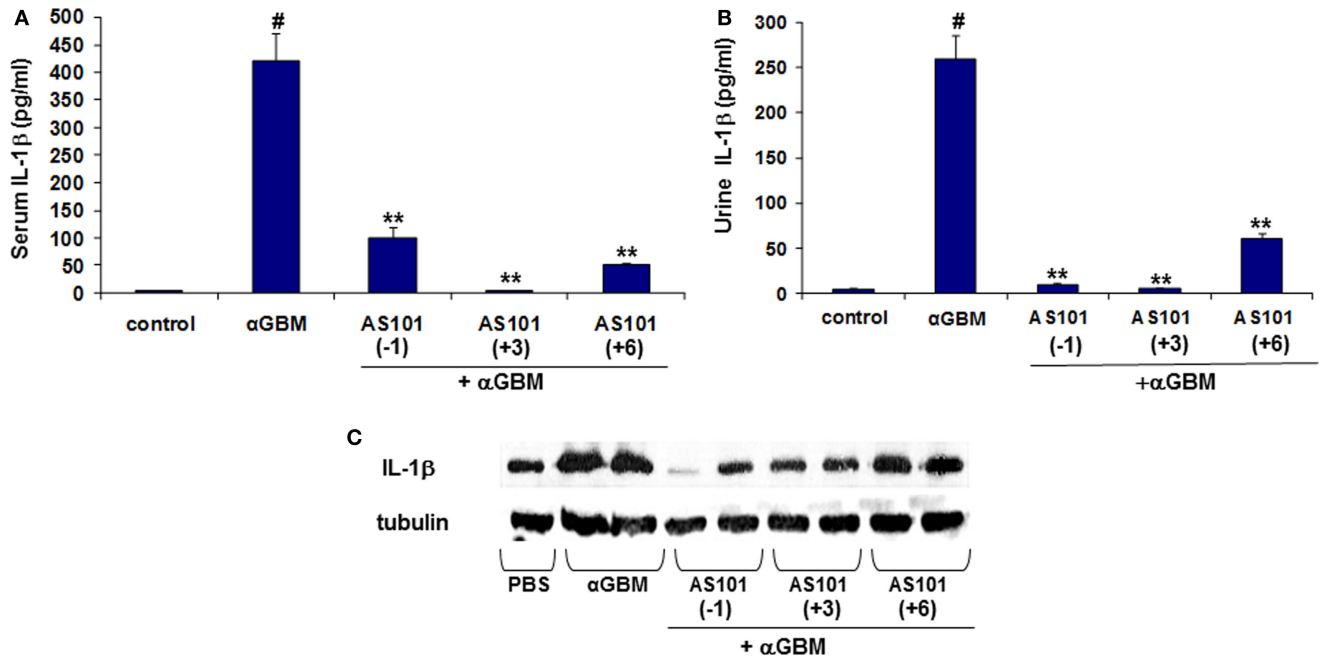

FIGURE 4 | Treatment with AS101 decreases IL-1β protein levels in crescentic glomerulonephritis. Treatment protocol was as described in **Figure 2**. Serum **(A)**, urine **(B)** and glomerular **(C)** IL-1β expression were evaluated 2 weeks after αGBM administration. Data are presented as mean ± SE of 7–9 rats/group. Healthy controls ($N = 3$). $^{\#}p < 0.01$ increase vs. control; $^{**}p < 0.01$ decrease vs. αGBM. The one-way ANOVA was used.

(**Figure 4C**). Importantly, both serum and urine IL-β levels were positively and significantly correlated with % glomeruli with crescent formation and with proteinuria (Figures S1B,C in Supplementary Material).

Regulation of TNFα Expression and Caspase-3 Activity

IL-18 is known to induce production of proinflammatory cytokines like TNFα and IL-1β (27). Furthermore, neutralization of endogenous IL-18 and TNF-α has been reported to reduce crescent formation, and tubulointerstitial scarring, with preservation of renal function (8, 21). **Figure 5A** shows that TNFα levels were strongly elevated in diseased rats, and there was a significant reduction in serum TNFα levels by all three AS101 treatment regimens. Moreover, there was a significant positive correlation between serum and urine IL-18 and IL-1β and TNFα (Figure S1D in Supplementary Material). TNFα can promote apoptosis following ligation of its receptor (28). Glomerular caspase-3 activity, the hallmark of apoptosis, was significantly increased in diseased rats and was decreased by AS101 in all treatment regimens (**Figure 5B**). A strong positive correlation between serum TNFα levels and glomerular caspase-3 activity supports a connection between these two parameters (Figure S1E in Supplementary Material).

AS101 Reduces FN Accumulation in the Glomeruli

Fibronectin is a multifunctional matrix protein that increases during glomerular injury. During inflammation, both glomerular accumulation and increased synthesis of FN have been reported (29).

Figures 5C,D show a dramatic increase in FN accumulation in glomeruli of diseased rats. Treatment with AS101 significantly inhibited this process irrespective of whether AS101 was administered starting before or after αGBM administration. A strong positive correlation was found between FN accumulation and proteinuria.

AS101 Regulates Macrophage Infiltration into the Glomeruli

Monocyte/Macrophages play an important role in the induction of CGN and glomerular injury (5). Their accumulation has been associated with increased IL-1β and IL-18 levels in various inflammatory states (30). Immunohistochemical analysis of kidneys from αGBM-induced rats showed a significant decrease in infiltrating ED1+ cells at all time points examined, by all three regimens of AS101 administration (**Figures 6A,B**). Furthermore, a positive and significant correlation was found between glomerular macrophage accumulation and levels of serum and urine IL-1β (Figure S2A in Supplementary Material) and IL-18 (Figure S2B in Supplementary Material). These results are in line with the known role of these inflammatory cytokines in macrophage accumulation and suggest that AS101 might reduce glomerular macrophage accumulation by inhibiting IL-1β and IL-18 production.

We also examined CTGF and MCP-1, two factors involved in monocytes recruitment to inflammatory sites (31, 32) and implicated in the pathogenesis of CGN (33, 34). Both CTGF and

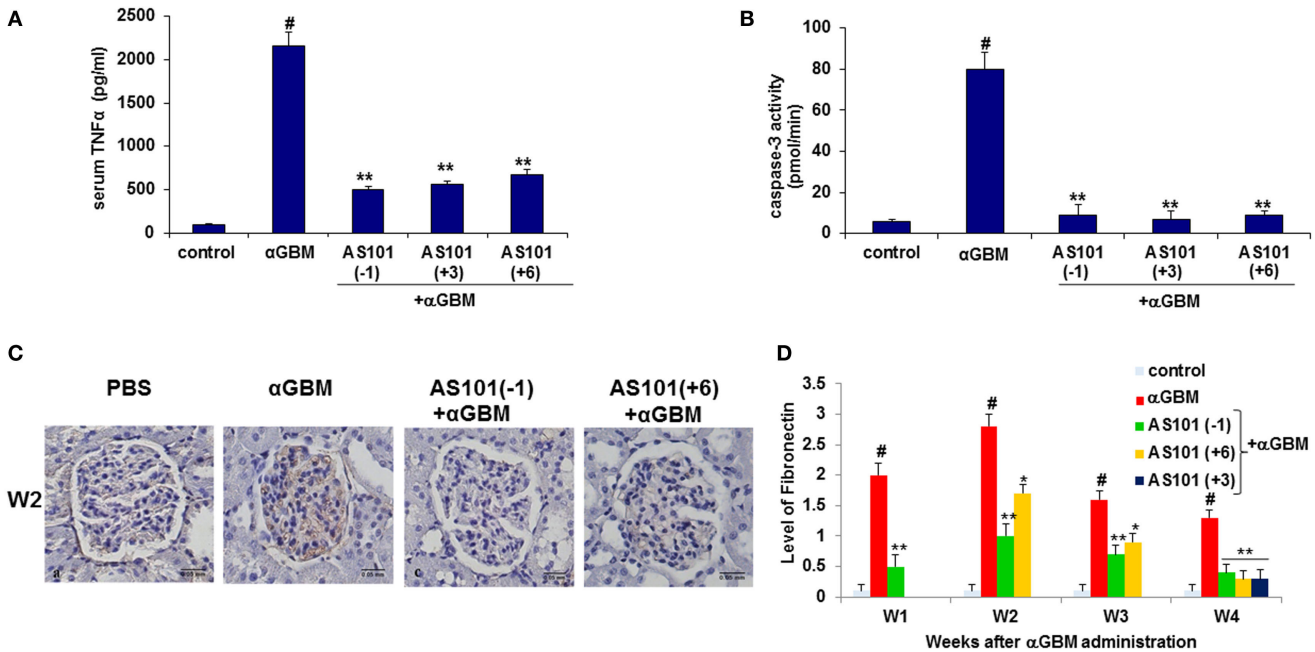

FIGURE 5 | Treatment with AS101 decreases TNFα protein levels and glomerular caspase-3 activity in crescentic glomerulonephritis. Treatment protocol was as described in **Figure 2**. Serum TNFα **(A)** and glomerular caspase-3 activity **(B)** were evaluated 2 weeks after αGBM administration ($N = 3$/group). $^{\#}p < 0.01$ increase vs. control; $^{**}p < 0.01$ decrease vs. αGBM. The one-way ANOVA was used. Immunohistochemistry was performed on kidney sections for detection of fibronectin (FN) on week 2 **(C)**. FN expansion was evaluated on weeks 1, 2, 3, and 4 and was scored in 100 glomeruli/sample as follows: grade 0 no staining; grade 1 staining occupying up to 25% of glomerular surface area; grade 2 staining occupying 25–50% of glomerular surface area; grade 3 staining occupying more than 50% of glomerular surface area **(D)**. Data are presented as mean ± SE of five rats/group for each time point. $^{\#}p < 0.01$ increase vs. control; $^{*}p < 0.01$ decrease vs. αGBM. $^{*}p < 0.05$ decrease vs. αGBM. The two-way ANOVA was used.

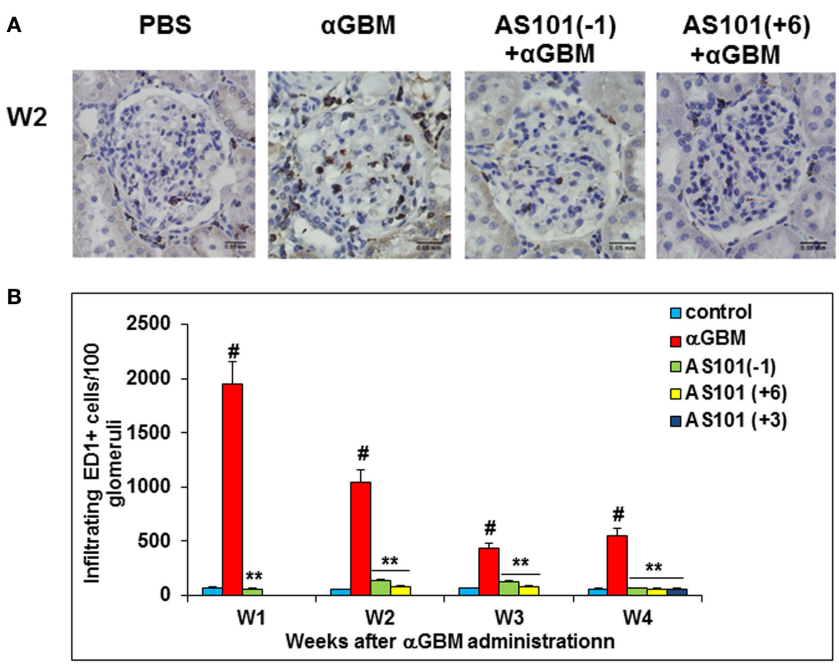

FIGURE 6 | Treatment with AS101 decreases glomerular macrophage accumulation in crescentic glomerulonephritis. Treatment protocol was as described in **Figure 2**. Immunohistochemistry was performed on kidney sections for detection of glomerular ED-1 positive accumulation on week 2 **(A)**. Glomerular macrophages were counted under light microscope. One hundred glomeruli were counted/sample. Treatment starting at day 3 was examined only at week 4 **(B)**. Data are presented as mean ± SE of five rats/group for each time point. $^{\#}p < 0.01$ increase vs. control; $^{**}p < 0.01$ decrease vs. αGBM. The two-way ANOVA was used.

MCP-1 were elevated in glomeruli of αGBM-induced rats at all time points examined, and both were significantly downregulated by AS101 treatment (**Figures 7A,B**). Expression of CTGF and MCP1 in glomeruli and their regulation by AS101 were at least in part intrinsic to the glomerular mesangial cells, as AS101 reduced production of these factors in mesangial cell cultures in a dose-dependent fashion (**Figures 7C,D**).

Inactivation of VLA-4 Is Involved in the Anti-inflammatory Activity of AS101 in CGN

Very Late Antigen-4, or α4β1 integrin, is expressed mainly on monocytes, lymphocytes, and eosinophils. Blockade of VLA-4 has been shown to prevent progression of experimental CGN, but the mechanisms involved in the beneficial effects of such blockade were not elucidated. We recently showed that AS101 inactivates the VLA-4 integrin by redox modulation of vicinal thiols within the exofacial membranal side (12). Recently, another integrin, α5β1 (VLA-5), was identified as a cell membrane receptor for a parasite-associated protein in human monocytes/macrophages, leading to activation of caspase-1and IL-1β transcription and indicating that integrin engagement can lead to inflammasome activation (35). We therefore hypothesized that VLA-4 might have a role in regulating caspase-1 activity and that inactivation of VLA-4 might underlie the beneficial activity of AS101 in CGN.

To elucidate the role of VLA-4 inactivation by AS101 in GCN and to determine whether this activity mediates the anti-inflammatory activities of AS101, we first performed *in vitro* studies involving cultured glomerular macrophages. **Figure 8** shows that glomerular macrophages secrete substantial amounts of IL-1β in response to SAC stimulation and in parallel, their caspase-1 activity is also elevated (**Figures 8A,B**). AS101 significantly inhibited both these activities in a dose-dependent manner. Glomerular macrophage VLA-4 activity was then evaluated by attachment to the VLA-4-specific ligand VCAM-1 and to FN while BSA served as a global negative control for cell attachment. Treatment with AS101 significantly inhibited macrophage attachment to both VCAM-1 and FN in a dose-dependent manner, implying that AS101 inhibits VLA-4 activity in macrophages (**Figure 8C**). Finally, we examined the role of VLA-4 and VLA-5 on caspase-1 activation and the effects of AS101 on this process. **Figure 8D** shows that both anti VLA-4- and VLA-5-neutralizing antibodies

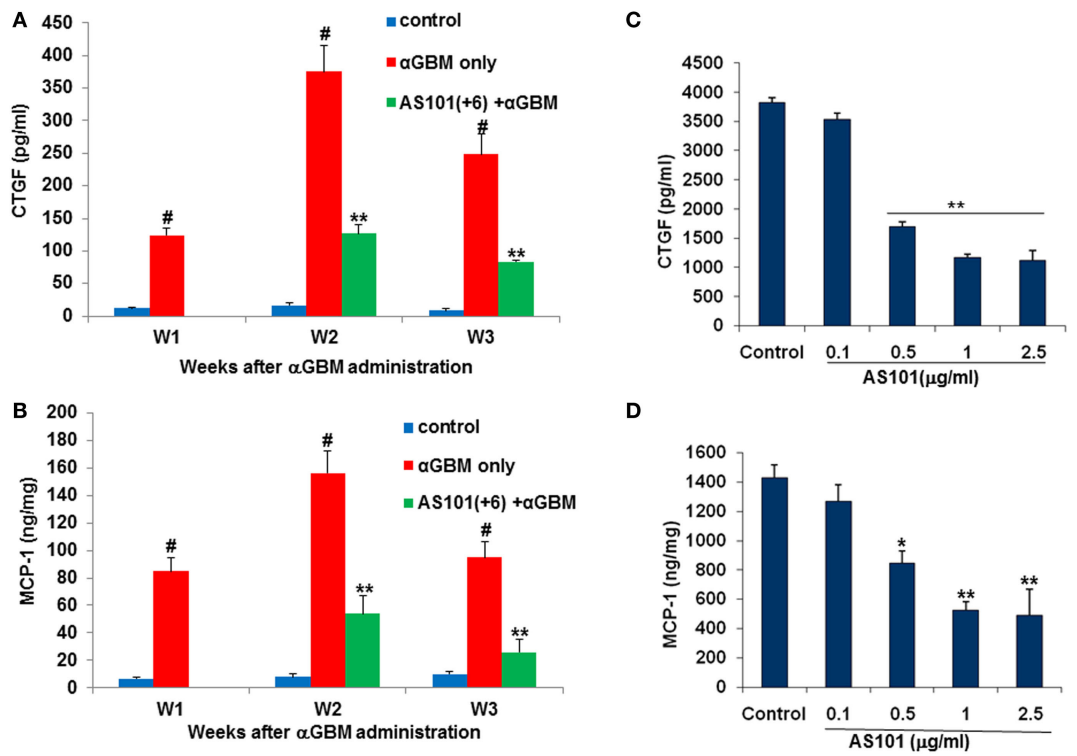

FIGURE 7 | Treatment with AS101 decreases glomerular connective tissue growth factor (CTGF) and monocyte chemoattractant protein-1 (MCP-1) protein expression in crescentic glomerulonephritis and *in vitro*. Rats were treated as follows: daily i.p. injection with PBS with no αGBM administration (control); daily injection with PBS after αGBM injection (αGBM); daily i.p. injection with AS101 (100 μg/rat) starting 6 days after αGBM administration (AS101(+6) + αGBM); Glomerular CTGF **(A)** or MCP-1 **(B)** protein expression were evaluated on weeks 1, 2, and 3 after αGBM administration. Data are presented as mean ± SE of 5 rats/group for each time point. $^{\#}p < 0.01$ increase vs. control; $^{**}p < 0.01$ decrease vs. αGBM. The two-way ANOVA was used. Glomerular mesangial cells were cultured on fibronectin-coated plates with or without various doses of AS101 and 10 μg/ml LPS for 48 h. Supernatants were collected and assayed for CTGF **(C)** and MCP-1 **(D)** content by ELISA. Results represent mean ± SE of three experiments. $^{*}p < 0.05$ decrease vs. control; $^{**}p < 0.01$ decrease vs. control. The one-way ANOVA was used.

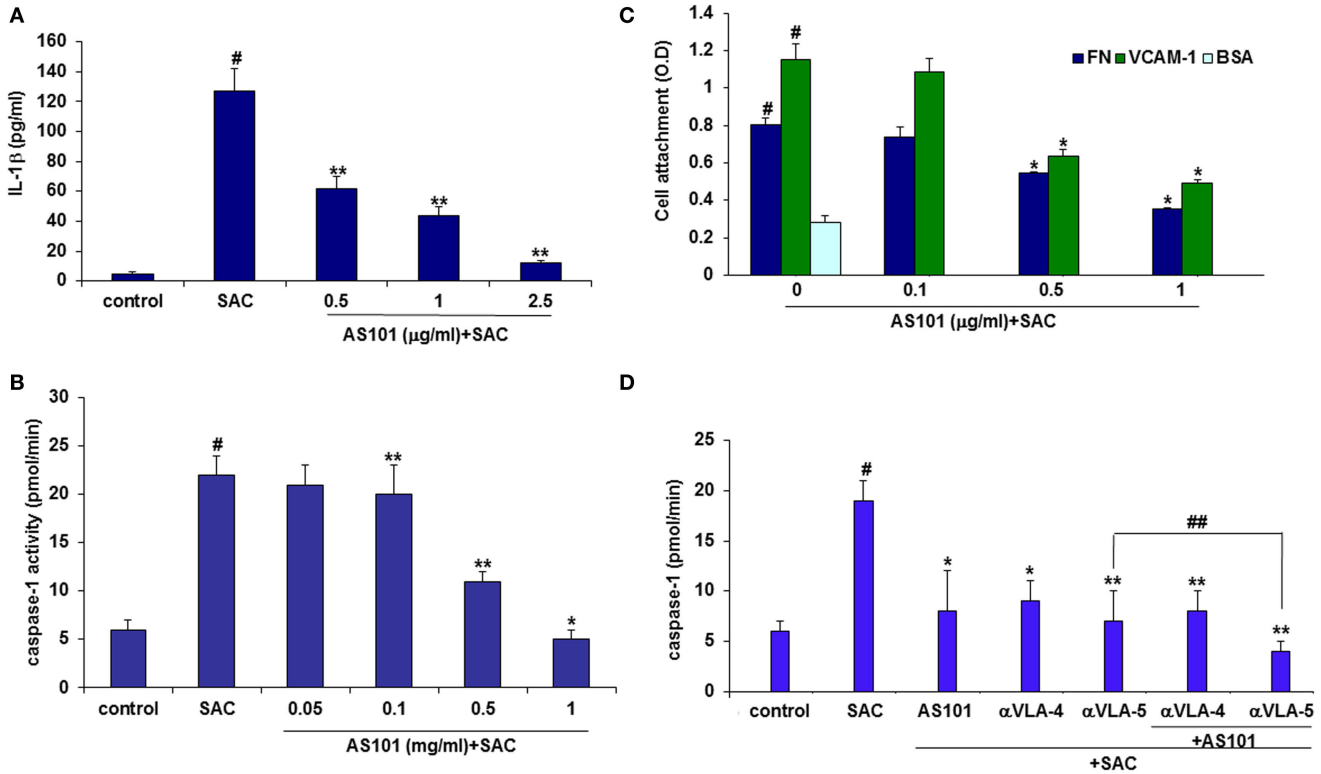

FIGURE 8 | AS101 decreases glomerular caspase-1 activity and glomerular macrophages. IL-1β secretion *in vitro*. Caspase-1 activity is very late antigen-4 (VLA-4) dependent. Isolated glomerular macrophages were treated with or without *Staphylococcus aureus* Cowan I (SAC) (5 μg/ml) and various concentrations of AS101 at 10^6/ml for 24 h. IL-1β **(A)** and caspase-1 activity **(B)** were evaluated. $^{\#}p < 0.01$ increase vs. control, $^{*}p < 0.01$ decrease vs. SAC. The one-way ANOVA was used 96-well plates were coated with VCAM-1 or fibronectin (FN) or BSA. Isolated glomerular macrophages were cultured with SAC (5 μg/ml) for 24 h. Cells were detached and cultured at 10^4/well in triplicates in the presence or absence of various AS101 concentrations for 1 h. Non-attached cells were washed out and attached cells were quantitated by XTT **(C)**. $^{\#}p < 0.01$ increase vs. BSA; $^{*}p < 0.05$ decrease vs. AS101 zero (VCAM-1 or FN). The two-way ANOVA was used. Isolated glomerular macrophages were cultured as described in **(B)** in the presence or absence of AS101 (1 μg/ml), αVLA-4 (5 μg/ml), αVLA-5 (5 μg/ml), or their combinations, with or without SAC for 24 h. Caspase-1 activity was evaluated **(D)**. $^{\#}p < 0.01$ increase vs. control; $^{**}p < 0.01$ decrease vs. SAC; $^{*}p < 0.05$ decrease vs. SAC; $^{\#\#}p < 0.05$ decrease vs. αVLA-5 without AS101. Data are presented as mean ± SE from four different experiments. The one-way ANOVA was used.

reduce caspase-1 activity in macrophages, implying the involvement of both integrins in caspase activation. Combined treatment of macrophages with AS101 and anti VLA-4 antibodies did not increase the extent of inhibition compared to AS101 and anti VLA-4 individually, suggesting that they both may share the same target site. In contrast, combined treatment of macrophages with anti VLA-5 antibodies and AS101 increased the extent of inhibition compared to each one individually, suggesting that they use a different binding site. Collectively, these data suggest that inhibition of VLA-4 activity by AS101 in macrophages plays an important role in caspase-1 inactivation.

Attenuation of CGN by AS101 Is Associated with Inactivation of VLA-4 in Glomerular Macrophages

Experiments designed to measure attachment of macrophages isolated from glomeruli of CGN vs. control rats to VCAM-1 or FN revealed CGN macrophages attach more strongly to the VLA-4 ligands than do macrophages from healthy rats, suggesting a very high VLA-4 activity (**Figure 9A**). Treatment of rats with AS101 starting 3 days after αGBM administration (+3), significantly decreased macrophage VLA-4 activity as expressed by a prompt decrease in macrophage attachment to VCAM-1 (**Figure 9A**). Furthermore, the decrease in VLA-4 activity in infiltrating macrophages from AS101-treated rats derives from direct inhibition of VLA-4 activity and not merely from suppression of VLA-4 expression (**Figure 9B**).

These data collectively imply that inactivation of glomerular macrophage VLA-4 activity by AS101 and the consequent inactivation of VLA-induced caspase-1 activation could be causally connected to attenuation of CGN by the compound.

DISCUSSION

In this study, we present data showing that administration of the non-toxic small molecule tellurium compound, AS101, ameliorates crescent formation and preserves renal function in a rat model of CGN induced by anti-GBM antibodies. Our data reveal that AS101 acts by exerting antiapoptotic and VLA-4-mediated

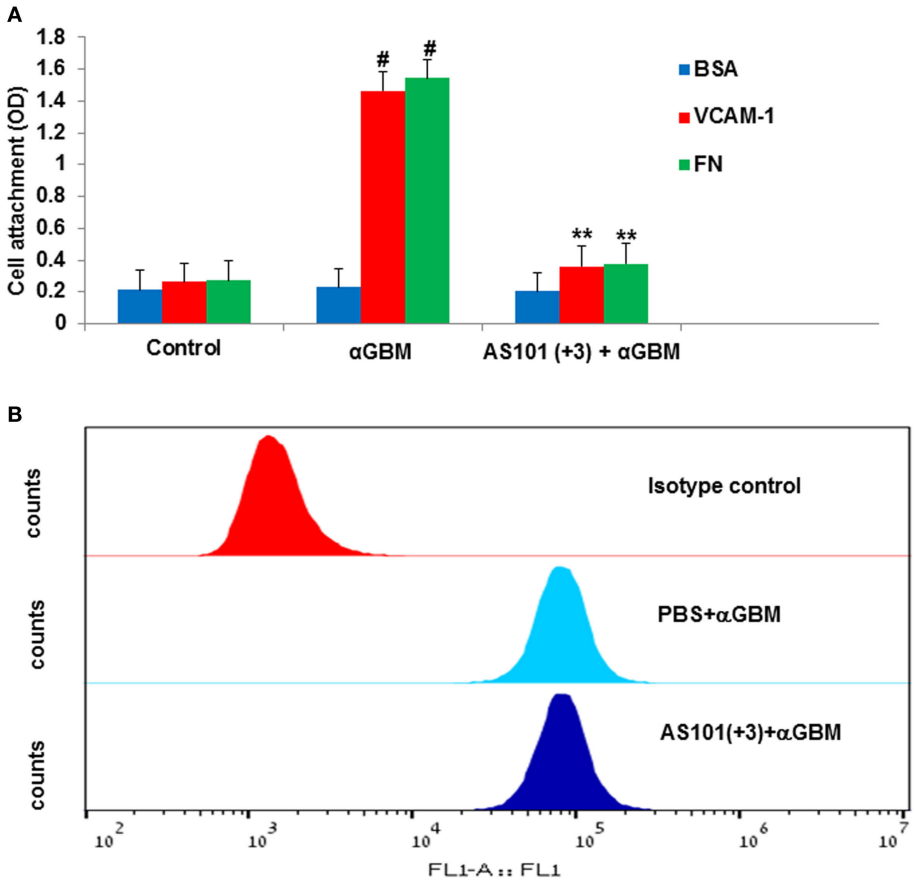

FIGURE 9 | Treatment with AS101 decreases very late antigen-4 (VLA-4) activity on glomerular macrophages. Rats were treated as follows: daily i.p. injection with PBS with no αGBM administration (control); daily injection with PBS of αGBM-induced rats (aGBM); daily i.p. injection with AS101 (100 μg/rat) starting 3 days after αGBM administration (AS101 (+3) + αGBM); At day 14 after αGBM administration, macrophages were isolated from glomeruli of treated rats and cultured on VCAM-1, fibronectin, or BSA-coated microwells at 10^4/well in triplicates for 1 h. Non-attached cells were washed out and the extent of the remaining attached cells was evaluated by XTT **(A)**. Data are presented as mean ± SE from four rats/group. $^{\#}p < 0.01$ increase vs. control; $^{**}p < 0.01$ decrease vs. αGBM. The two-way ANOVA was used **(A)**. Rats were treated with anti-glomerular basement membrane (anti-GBM) and PBS or with anti-GBM and AS101(+3). At 2 weeks after anti-GBM administration, macrophages were isolated from glomeruli of rats and evaluated for VLA-4 expression by fluorescence-activated cell sorter analysis. **(B)** Results show one representative experiment of four rats/group analyzed.

anti-inflammatory effects both *in vitro* and *in vivo* through a novel mechanism of action.

The rat model of CGN is characterized by clinical deterioration of kidney function as a result of excessive inflammatory processes followed by glomerular crescents formation and eventually glomerulosclerosis.

Apart from the role of humoral immunity in CGN, the involvement of T cells and macrophages has been long been recognized (33, 36, 37), suggesting an additional contribution of cell-mediated immunity in the pathology of the disease. Although VLA-4 inactivation by AS101 might also affect adaptive immune responses, the study focuses on the role of glomerular macrophage VLA-4 deactivation by AS101 in AS101's beneficial effects in this disease. This is in light of numerous reports showing that macrophages are key effectors of disease progression in crescentic GN.

Our study establishes that administration of AS101 either before or after induction of CGN ameliorates renal function and crescent formation. This was associated with profound inhibition of inflammatory mediators including active caspase-1, IL-1β, IL-18, MCP-1, and CTGF, and with inhibition of FN glomerular expansion. These were accompanied by decreased glomerular infiltration of macrophages. Monocytes/macrophages play an important role in the induction of CGN and glomerular injury (5). Their accumulation has been associated with increased IL-1β and IL-18 levels in various inflammatory states (30). Moreover, IL-18 and IL-1β contribute to crescent formation and inflammatory cell recruitment (21, 22). IL-18 is known to induce the production of proinflammatory cytokines like TNFα and IL-1β (27). Importantly, neutralization of endogenous IL-18 and TNF-α has been reported to reduce crescent formation, and tubulointerstitial scarring, with preservation of renal function, in experimental CGN (8, 21). Our study shows positive and significant correlations between the decrease of these inflammatory mediators by AS101 and the amelioration increscent formation, kidney function, and macrophage recruitment. Notably,

CTGF and MCP-1, which are downregulated in glomeruli of AS101-treated rats, were shown to be implicated in monocyte recruitment to inflammatory sites (9, 11) and in the pathogenesis of CGN (33, 34). The study shows a dramatic increase in FN expansion in glomeruli of diseased rats. During inflammation, both glomerular accumulation and synthesis of FN has been reported (32). Treatment with AS101 significantly inhibited this process irrespective of whether AS101 was administered starting before or after αGBM administration. There is increasing evidence that cytokines such as TNFα, IL-1β, and IL-18 play a central role in modulating endothelial function, cellular infiltration and proliferation, and extracellular matrix production (38). Furthermore, abnormal ECM accumulation plays a role in modulating the pattern of synthesis of MCP-1 by glomerular mesangial cells (39). Matrix accumulation might also play a role in maintaining monocyte infiltration after the development of ECM expansion in the subsequent phase of glomerular diseases. Expansion of ECM might be involved in the progression of glomerular diseases by manipulating the number of infiltrating monocytes and stimulation of cytokine gene expression through the induction of MCP-1 expression (39). Monocytes are involved not only in acute inflammation but also in glomerulosclerosis, a feature common to both immune and non-immune forms of progressive renal disease (40). Collectively, these data are in line with reports showing increased MCP-1 production and FN accumulation by CTGF (41, 42).

Previously, VLA-4 has been shown by two studies to prevent progression of experimental CGN (43, 44). The mechanisms of its beneficial effects were not elucidated. Nevertheless, both studies concluded that inhibition of VLA-4 activity does not affect leukocytes recruitment to the glomeruli. Our results suggest otherwise. We have recently shown that AS101 inactivates the VLA-4 integrin by specific redox modulation (12), driving a variety of beneficial biological effects in diverse preclinical and clinical studies (14). Our current study demonstrates that AS101 deactivates macrophage VLA-4 both *in vitro* and *in vivo* and presents evidence that inhibition of caspase-1 activity, associated with the anti-inflammatory activity of AS101, is dependent on VLA-4 inactivation. We speculate that the apparent discrepancy between our data and those of others, who failed to see an effect of VLA-4 blockade on macrophage recruitment, results from the unique mode of VLA-4 inactivation by AS101 as compared to neutralizing VLA-4 antibodies used by others. In fact, the possibility remains that similarly to the known phenomenon that activation of an integrin by two different ligands may exert different outcomes, its inhibition by diverse mechanisms may differentially affect cell functions. Although VCAM-1 and FN are both ligands for VLA-4, they interact with VLA-4 by a totally different mechanism (45), which might result in distinct functions. For example, the interaction between VLA on AML cells and FN results in the resistance of leukemic cells to chemotherapy, while the interaction of VLA-4 on the same cells with VCAM-1 does not (12, 46). Alternatively reduction of infiltrating macrophage could not solely depend on blocking the function of VLA-4, but may be caused by the overall anti-inflammatory effect of AS101, since AS101 can profoundly inhibit several inflammatory cytokines.

Our study is not the first demonstration that an integrin can trigger processes leading to production of inflammatory mediators. Recently, activation of the α5β1 integrin was shown to trigger macrophages to produce an extracellular burst of ATP through opening surface pannexin-1 channels that were activated by α5β1 integrin signaling in the setting of a pathogen stimulus. Subsequently, ATP delivered a critical stimulus to activate the NLRP3 inflammasome (35). Furthermore, β1 integrins have been reported to function as pathogen recognition receptors on intestinal epithelial cells to rapidly induce inflammasome-derived IL-18-mediated responses (47). Our results support and expand on these studies, and suggest for the first time that caspase-1 activity is dependent on active VLA-4. Similarly, integrins have been previously shown to induce expression of MCP-1 *via* focal adhesion kinase in mesangial cells (39). Cell adhesion to FN induced phosphorylation of FAK and MCP-1 mRNA expression. Our *in vitro* data similarly show MCP-1 and CTGF downregulation in mesangial cells cultured on FN-coated plates in the presence of AS101. In the aggregate, our data strongly support the interpretation that inactivation of VLA-4 by AS101 leads to decreased caspase-1 activity, which brings about a prompt decrease in the level of inflammatory cytokines and chemokines produced in the glomeruli of diseased rats. This in turn results in decreased ECM expansion, reducing macrophage accumulation in the glomeruli and ameliorating glomerular cell death and glomerular fibrosis, which results in preservation of kidney function.

Besides our prototype tellurium compound AS101, the investigation of therapeutic activities of other tellurium (IV) compounds is scarce in the literature, although tellurium is the fourth most abundant trace element in the human body. Our integrated results show that amelioration of the clinical status of rats with CGN can be achieved by inhibition of VLA-4 on glomerular macrophages leading to decreased caspase-1 activity followed by a significant decrease in inflammation. This regulation may be achieved using AS101, currently being tested in clinical trials and might be beneficial in the treatment of patients with CGN.

AUTHOR CONTRIBUTIONS

YH performed and analyzed the experiments. IS provided technical assistance and contributed to the preparation of the figures. YK, RC, and BS designed the study, discussed the results, and wrote the paper. UG provided technical assistance. All the authors discussed the results and commented on the manuscript.

FUNDING

This work was supported by grants from the U.S.-Israel Binational Science Foundation (BSF), 2013–2014, no. 2013481 and by The Safdie' Institute for AIDS and Immunology Research and The Dr. Tovi Comet-Walerstein Cancer Research Chair.

SUPPLEMENTARY MATERIAL

The Supplementary Material for this article can be found online at http://journal.frontiersin.org/article/10.3389/fimmu.2017.00240/full#supplementary-material.

REFERENCES

1. Saus J, Wieslander J, Langeveld JP, Quinones S, Hudson BG. Identification of the Goodpasture antigen as the alpha 3(IV) chain of collagen IV. *J Biol Chem* (1988) 263:13374–80.
2. Tarzi RM, Cook HT, Pusey CD. Crescentic glomerulonephritis: new aspects of pathogenesis. *Semin Nephrol* (2011) 31:361–8. doi:10.1016/j.semnephrol.2011.06.007
3. Andres G, Brentjens J, Kohli R, Anthone R, Anthone S, Baliah T, et al. Histology of human tubulo-interstitial nephritis associated with antibodies to renal basement membranes. *Kidney Int* (1978) 13:480–91. doi:10.1038/ki.1978.71
4. Tam FW, Smith J, Morel D, Karkar AM, Thompson EM, Cook HT, et al. Development of scarring and renal failure in a rat model of crescentic glomerulonephritis. *Nephrol Dial Transplant* (1999) 14:1658–66. doi:10.1093/ndt/14.7.1658
5. Duffield JS, Tipping PG, Kipari T, Cailhier JF, Clay S, Lang R, et al. Conditional ablation of macrophages halts progression of crescentic glomerulonephritis. *Am J Pathol* (2005) 167:1207–19. doi:10.1016/S0002-9440(10)61209-6
6. Tipping PG, Lowe MG, Holdsworth SR. Glomerular interleukin 1 production is dependent on macrophage infiltration in anti-GBM glomerulonephritis. *Kidney Int* (1991) 39:103–10. doi:10.1038/ki.1991.13
7. Tipping PG, Leong TW, Holdsworth SR. Tumor necrosis factor production by glomerular macrophages in anti-glomerular basement membrane glomerulonephritis in rabbits. *Lab Invest* (1991) 65:272–9.
8. Le Hir M, Haas C, Marino M, Ryffel B. Prevention of crescentic glomerulonephritis induced by anti-glomerular membrane antibody in tumor necrosis factor-deficient mice. *Lab Invest* (1998) 78:1625–31.
9. El Nemer W, Wautier MP, Rahuel C, Gane P, Hermand P, Galacteros F, et al. Endothelial Lu/BCAM glycoproteins are novel ligands for red blood cell alpha4beta1 integrin: role in adhesion of sickle red blood cells to endothelial cells. *Blood* (2007) 109:3544–51. doi:10.1182/blood-2006-07-035139
10. Sredni B, Caspi RR, Klein A, Kalechman Y, Danziger Y, Ben Ya'akov M, et al. A new immunomodulating compound (AS-101) with potential therapeutic application. *Nature* (1987) 330:173–6. doi:10.1038/330173a0
11. Sredni B, Xu RH, Albeck M, Gafter U, Gal R, Shani A, et al. The protective role of the immunomodulator AS101 against chemotherapy-induced alopecia studies on human and animal models. *Int J Cancer* (1996) 65:97–103. doi:10.1002/(SICI)1097-0215(19960103)65:1<97::AID-IJC17>3.0.CO;2-F
12. Layani-Bazar A, Skornick I, Berrebi A, Pauker MH, Noy E, Silberman A, et al. Redox modulation of adjacent thiols in VLA-4 by AS101 converts myeloid leukemia cells from a drug-resistant to drug-sensitive state. *Cancer Res* (2014) 74:3092–103. doi:10.1158/0008-5472.CAN-13-2159
13. Lee JH, Halperin-Sheinfeld M, Baatar D, Mughal MR, Tae HJ, Kim JW, et al. Tellurium compound AS101 ameliorates experimental autoimmune encephalomyelitis by VLA-4 inhibition and suppression of monocyte and T cell infiltration into the CNS. *Neuromolecular Med* (2014) 16:292–307. doi:10.1007/s12017-013-8277-3
14. Sredni B. Immunomodulating tellurium compounds as anti-cancer agents. *Semin Cancer Biol* (2012) 22:60–9. doi:10.1016/j.semcancer.2011.12.003
15. Halpert G, Eitan T, Voronov E, Apte RN, Rath-Wolfson L, Albeck M, et al. Multifunctional activity of a small tellurium redox immunomodulator compound, AS101, on dextran sodium sulfate-induced murine colitis. *J Biol Chem* (2014) 289:17215–27. doi:10.1074/jbc.M113.536664
16. Kalechman Y, Gafter U, Da JP, Albeck M, Alarcon-Segovia D, Sredni B. Delay in the onset of systemic lupus erythematosus following treatment with the immunomodulator AS101: association with IL-10 inhibition and increase in TNF-alpha levels. *J Immunol* (1997) 159:2658–67.
17. Kalechman Y, Gafter U, Gal R, Rushkin G, Yan D, Albeck M, et al. Anti-IL-10 therapeutic strategy using the immunomodulator AS101 in protecting mice from sepsis-induced death: dependence on timing of immunomodulating intervention. *J Immunol* (2002) 169:384–92. doi:10.4049/jimmunol.169.1.384
18. Danoch H, Kalechman Y, Albeck M, Longo DL, Sredni B. Sensitizing B- and T- cell lymphoma cells to paclitaxel/abraxane-induced death by AS101 via inhibition of the VLA-4-IL10-survivin axis. *Mol Cancer Res* (2015) 13:411–22. doi:10.1158/1541-7786.MCR-14-0459
19. Sredni B, Weil M, Khomenok G, Lebenthal I, Teitz S, Mardor Y, et al. Ammonium trichloro(dioxoethylene-o,o')tellurate (AS101) sensitizes tumors to chemotherapy by inhibiting the tumor interleukin 10 autocrine loop. *Cancer Res* (2004) 64:1843–52. doi:10.1158/0008-5472.CAN-03-3179
20. Spiro RG. The structure of the disaccharide unit of the renal glomerular basement membrane. *J Biol Chem* (1967) 242:4813–23.
21. Kitching AR, Turner AL, Wilson GR, Semple T, Odobasic D, Timoshanko JR, et al. IL-12p40 and IL-18 in crescentic glomerulonephritis: IL-12p40 is the key Th1-defining cytokine chain, whereas IL-18 promotes local inflammation and leukocyte recruitment. *J Am Soc Nephrol* (2005) 16:2023–33. doi:10.1681/ASN.2004121075
22. Schreiber A, Pham CT, Hu Y, Schneider W, Luft FC, Kettritz R. Neutrophil serine proteases promote IL-1beta generation and injury in necrotizing crescentic glomerulonephritis. *J Am Soc Nephrol* (2012) 23:470–82. doi:10.1681/ASN.2010080892
23. Gu Y, Kuida K, Tsutsui H, Ku G, Hsiao K, Fleming MA, et al. Activation of interferon-gamma inducing factor mediated by interleukin-1beta converting enzyme. *Science* (1997) 275:206–9. doi:10.1126/science.275.5297.206
24. Takeuchi O, Akira S. Pattern recognition receptors and inflammation. *Cell* (2010) 140:805–20. doi:10.1016/j.cell.2010.01.022
25. Chen GY, Nunez G. Sterile inflammation: sensing and reacting to damage. *Nat Rev Immunol* (2010) 10:826–37. doi:10.1038/nri2873
26. Howard AD, Kostura MJ, Thornberry N, Ding GJ, Limjuco G, Weidner J, et al. IL-1-converting enzyme requires aspartic acid residues for processing of the IL-1 beta precursor at two distinct sites and does not cleave 31-kDa IL-1 alpha. *J Immunol* (1991) 147:2964–9.
27. Puren AJ, Fantuzzi G, Gu Y, Su MS, Dinarello CA. Interleukin-18 (IFNgamma-inducing factor) induces IL-8 and IL-1beta via TNFalpha production from non-CD14+ human blood mononuclear cells. *J Clin Invest* (1998) 101:711–21. doi:10.1172/JCI1379
28. Guo YL, Kang B, Yang LJ, Williamson JR. Tumor necrosis factor-alpha and ceramide induce cell death through different mechanisms in rat mesangial cells. *Am J Physiol* (1999) 276:F390–7.
29. Sady SP, Goyal M, Thomas PE, Wharram BL, Wiggins RC. Fibronectin mRNA in the developing glomerular crescent in rabbit antiglomerular basement membrane disease. *J Am Soc Nephrol* (1995) 5:2087–90.
30. Arango Duque G, Descoteaux M. Macrophage cytokines: involvement in immunity and infectious diseases. *Front Immunol* (2014) 5(491):2014. doi:10.3389/fimmu.2014.00491
31. Sanchez-Lopez E, Rayego S, Rodrigues-Diez R, Rodriguez JS, Rodrigues-Diez R, Rodriguez-Vita J, et al. CTGF promotes inflammatory cell infiltration of the renal interstitium by activating NF-kappaB. *J Am Soc Nephrol* (2009) 20:1513–26. doi:10.1681/ASN.2008090999
32. Valente AJ, Rozek MM, Sprague EA, Schwartz CJ. Mechanisms in intimal monocyte-macrophage recruitment. A special role for monocyte chemotactic protein-1. *Circulation* (1992) 86:III20–5.
33. Lloyd CM, Minto AW, Dorf ME, Proudfoot A, Wells TN, Salant DJ, et al. RANTES and monocyte chemoattractant protein-1 (MCP-1) play an important role in the inflammatory phase of crescentic nephritis, but only MCP-1 is involved in crescent formation and interstitial fibrosis. *J Exp Med* (1997) 185:1371–80. doi:10.1084/jem.185.7.1371
34. Kanemoto K, Usui J, Tomari S, Yokoi H, Mukoyama M, Aten J, et al. Connective tissue growth factor participates in scar formation of crescentic glomerulonephritis. *Lab Invest* (2003) 83:1615–25. doi:10.1097/01.LAB.0000096711.58115.46
35. Mortimer L, Moreau F, Cornick S, Chadee K. The NLRP3 inflammasome is a pathogen sensor for invasive *Entamoeba histolytica* via activation of alpha5beta1 integrin at the macrophage-amebae intercellular junction. *PLoS Pathog* (2015) 11:e1004887. doi:10.1371/journal.ppat.1004887
36. Bhan AK, Schneeberger EE, Collins AB, McCluskey RT. Evidence for a pathogenic role of a cell-mediated immune mechanism in experimental glomerulonephritis. *J Exp Med* (1978) 148:246–60. doi:10.1084/jem.148.1.246
37. Nikolic-Paterson DJ, Atkins RC. The role of macrophages in glomerulonephritis. *Nephrol Dial Transplant* (2001) 16(Suppl 5):3–7. doi:10.1093/ndt/16.suppl_5.3
38. Kolinska J, Lisa V, Clark JA, Kozakova H, Zakostelecka M, Khailova L, et al. Constitutive expression of IL-18 and IL-18R in differentiated IEC-6

cells: effect of TNF-alpha and IFN-gamma treatment. *J Interferon Cytokine Res* (2008) 28:287–96. doi:10.1089/jir.2006.0130
39. Watanabe Y, Tamura M, Osajima A, Anai H, Kabashima N, Serino R, et al. Integrins induce expression of monocyte chemoattractant protein-1 via focal adhesion kinase in mesangial cells. *Kidney Int* (2003) 64:431–40. doi:10.1046/j.1523-1755.2003.00122.x
40. Nikolic-Paterson DJ, Lan HY, Atkins RC. Macrophages in immune renal injury. In: NeilsonEG, CouserWG, editors. *Immunologic Renal Diseases*. Philadelphia: Lippincott-Raven (1997). p. 575–92.
41. Wu SH, Lu C, Dong L, Chen ZQ. Signal transduction involved in CTGF-induced production of chemokines in mesangial cells. *Growth Factors* (2008) 26:192–200. doi:10.1080/08977190802227828
42. Zhu L, Zhao S, Liu S, Liu Q, Li F, Hao J. PTEN regulates renal extracellular matrix deposit via increased CTGF in diabetes mellitus. *J Cell Biochem* (2016) 117:1187–98. doi:10.1002/jcb.25402
43. Khan SB, Allen AR, Bhangal G, Smith J, Lobb RR, Cook HT, et al. Blocking VLA-4 prevents progression of experimental crescentic glomerulonephritis. *Nephron Exp Nephrol* (2003) 95:e100–10. doi:10.1159/000074326
44. Allen AR, McHale J, Smith J, Cook HT, Karkar A, Haskard DO, et al. Endothelial expression of VCAM-1 in experimental crescentic nephritis and effect of antibodies to very late antigen-4 or VCAM-1 on glomerular injury. *J Immunol* (1999) 162:5519–27.
45. Elices MJ, Osborn L, Takada Y, Crouse C, Luhowskyj S, Hemler ME, et al. VCAM-1 on activated endothelium interacts with the leukocyte integrin VLA-4 at a site distinct from the VLA-4/fibronectin binding site. *Cell* (1990) 60:577–84. doi:10.1016/0092-8674(90)90661-W
46. Matsunaga T, Takemoto N, Sato T, Takimoto R, Tanaka I, Fujimi A, et al. Interaction between leukemic-cell VLA-4 and stromal fibronectin is a decisive factor for minimal residual disease of acute myelogenous leukemia. *Nat Med* (2003) 9:1158–65. doi:10.1038/nm909
47. Thinwa J, Segovia JA, Bose S, Dube PH. Integrin-mediated first signal for inflammasome activation in intestinal epithelial cells. *J Immunol* (2014) 193:1373–82. doi:10.4049/jimmunol.1400145

Conflict of Interest Statement: We hereby declare that no author has relationships with companies that may have a financial interest in the information contained in the manuscript. There is no interest to disclose.

Copyright © 2017 Hachmo, Kalechman, Skornick, Gafter, Caspi and Sredni. This is an open-access article distributed under the terms of the Creative Commons Attribution License (CC BY). The use, distribution or reproduction in other forums is permitted, provided the original author(s) or licensor are credited and that the original publication in this journal is cited, in accordance with accepted academic practice. No use, distribution or reproduction is permitted which does not comply with these terms.

frontiers in Immunology

ORIGINAL RESEARCH
published: 27 March 2017
doi: 10.3389/fimmu.2017.00348

Basophil Activation-Dependent Autoantibody and Interleukin-17 Production Exacerbate Systemic Lupus Erythematosus

*Qingjun Pan[1], Li Gong[2], Haiyan Xiao[3], Yongmin Feng[1], Lu Li[1], Zhenzhen Deng[1], Ling Ye[1], Jian Zheng[4], Carol A. Dickerson[3], Lin Ye[1], Ning An[1], Chen Yang[1] and Hua-feng Liu[1]**

[1] Key Laboratory of Prevention and Management of Chronic Kidney Disease of Zhanjiang City, Affiliated Hospital of Guangdong Medical University, Zhanjiang, China, [2] Department of Laboratory Animal Center, Nanfang Hospital, Southern Medical University, Guangzhou, China, [3] Department of Anesthesiology and Perioperative Medicine, Medical College of Georgia, Augusta University, Augusta, GA, USA, [4] Department of Microbiology, University of Iowa, Iowa City, IA, USA

Objective: Autoantibody and inflammatory cytokines play crucial roles in the development of systemic lupus erythematosus (SLE); however, the regulation of their production warrants further investigation. This study aimed to investigate the role of basophil activation in the development of SLE based on studies in patients with SLE and spontaneous lupus-prone MRL-*lpr/lpr* mice.

Methods: The phenotypes of peripheral basophils and the production of autoantibody and interleukin (IL)-17 in patients with SLE were determined by flow cytometry and enzyme-linked immunosorbent assay, and also their correlations were investigated by statistical analysis. Thereafter, the effect of basophils on autoantibody production by B cells and Th17 differentiation in SLE were evaluated *in vitro*. Finally, the effect of basophil depletion on the development of autoimmune disorders in spontaneous lupus-prone MRL-*lpr/lpr* mice was examined.

Results: The decreased numbers and an increased activation of peripheral basophils were found to be correlated with increased autoantibody production and disease activity in patients with SLE. Correspondingly, *in vitro* coculture studies showed that basophils obtained from patients with SLE promoted autoantibody production by SLE B cells and promoted Th17 differentiation from SLE naïve $CD4^+$ T cells. The decrease of peripheral basophils in patients with SLE might be due to their migration to lymph nodes post their activation mediated by (autoreactive) IgE as supported by their increased CD62L and CCR7 expressions and accumulation in the lymph nodes of MRL-*lpr/lpr* mice. Furthermore, an increased activation of peripheral basophils was identified in MRL-*lpr/lpr* mice. Importantly, basophil-depleted MRL-*lpr/lpr* mice exhibited an extended life span, improved renal function, and lower serum levels of autoantibodies and IL-17, while basophil-adoptive-transferred mice exhibited the opposite results.

Conclusion: These finding suggest that basophil activation-dependent autoantibody and IL-17 production may constitute a critical pathogenic mechanism in SLE.

Keywords: basophil, IgE, systemic lupus erythematosus, autoantibody, interleukin-17

OPEN ACCESS

Edited by:
Guixiu Shi,
Xiamen University, China

Reviewed by:
Valentina Canti,
San Raffaele Hospital (IRCCS), Italy
Yong-Gil Kim,
University of Ulsan College of Medicine, South Korea

****Correspondence:***
Hua-feng Liu
hf-liu@263.com

Specialty section:
This article was submitted to Inflammation, a section of the journal Frontiers in Immunology

Received: *03 January 2017*
Accepted: *10 March 2017*
Published: *27 March 2017*

Citation:
Pan Q, Gong L, Xiao H, Feng Y, Li L, Deng Z, Ye L, Zheng J, Dickerson CA, Ye L, An N, Yang C and Liu H-f (2017) Basophil Activation-Dependent Autoantibody and Interleukin-17 Production Exacerbate Systemic Lupus Erythematosus. Front. Immunol. 8:348. doi: 10.3389/fimmu.2017.00348

INTRODUCTION

Systemic lupus erythematosus (SLE) is a systemic autoimmune disease that is characterized by the production of a wide spectrum of autoantibodies and inflammatory cytokines. Several types of immune cells are considered critical players in the induction of autoantibodies and inflammatory cytokine production in the pathogenesis of SLE, including overactivated B cells, abnormally activated T cell subsets, monocytes, and dendritic cells (1–3). Of these cell types, overactivated B cells play a central role by directly producing a large quantity of autoantibodies that can lead to systemic inflammation and organ damage (1, 4). However, the regulation of B cell autoantibody production is complex, and a variety of factors, such as other immune cells, environmental triggers, and genetic susceptibility, are involved (1, 5). For abnormally activated T cell subsets, increasing evidence suggests that Th17 cells play a pivotal deleterious role in the inflammation and organ damage that occur in SLE (6, 7); thus, the regulation of Th17 differentiation in SLE warrants further investigation.

T cell-dependent B cell activation has been well characterized; however, T cell-independent B cell activation is not fully understood, particularly in autoimmune diseases (8). Basophils, one of the least abundant populations of granulocytes, are well known to be involved in allergic responses and also play critical roles in acquired immunity regulation and immunological disorders by releasing different patterns of immune modulators such as cytokines and chemokines upon activation by different stimuli (9, 10). It has been confirmed that basophils can deliver helper signals to B cells and drive their differentiation toward antibody-producing cells (11); however, the influence of basophils on autoantibody production by B cells in SLE is largely unknown.

Moreover, whether basophils promote the differentiation of Th17 cells remains controversial (12–15). Differences in the microenvironment and stimulatory conditions could be possible reasons for previous discrepant results. Th17 cells' development requires synergistic effects mediated by series of cytokines, such as interleukin (IL)-23, IL-1β, TGF-β, and another key cytokine, IL-6, to drive their differentiation (16, 17). It is well documented that murine basophils can express IL-6 under specific conditions (18–20), but the effects of basophils on Th17 differentiation remain largely unknown in the context of SLE.

In 1990s, Hibbs et al. established a Src-family protein tyrosine kinase Lyn-deficient mouse model, which develops strong, constitutive Th2 skewing in early life and exhibits symptoms of an autoimmune disease that mimics some of the features of human SLE in later life (21). Although this model is unlikely to model SLE in the majority of affected persons (22), basophils were shown to be indispensable for the development of autoimmune disease in these Lyn-deficient mice (23), which have provided the possible pathogenesis of basophils in SLE. However, the mechanistic links between basophils activation and SLE, especially its activation on autoantibody and inflammatory cytokines production in SLE, remain to be further elucidated.

This study aimed to investigate the role of basophil activation in the development of SLE based on studies in patients with SLE and spontaneous lupus-prone MRL-*lpr/lpr* mice, with a special focus on the effect of basophil activation on autoantibodies and inflammatory cytokine production in SLE.

MATERIALS AND METHODS

Patients

A total of 126 patients with SLE (107 females and 19 males) (**Table 1**) and 48 healthy controls (36 females and 12 males) with no differences with regard to age, sex, or race were enrolled into the present study at the Department of Nephrology at the Affiliated Hospital of Guangdong Medical University from

TABLE 1 | Demographic characteristics of SLE patients.

	Total SLE patients (n = 126)	Newly diagnosed SLE patients (n = 48)	Followed-up SLE patients (n = 15)
Age (mean ± SD)	28.7 ± 11.3	24.3 ± 10.5	25.9 ± 10.1
Gender [F/M, no. (%)]	107 (84.9%)/19 (15.1%)	45 (93.8%)/3 (6.2%)	14 (93.3%)/1 (0.7%)
Disease duration (mean ± SD, years)	4.7 ± 3.2		
Anti-dsDNA IgG positive: no. (%)	94 (74.6%)	43 (89.6%)	14 (93.3%)
SLEDAI score			
Mean ± SD	12.2 ± 7.0	17.2 ± 5.2	18.0 ± 5.5
Median (minimum, maximum)	12 (0, 30)	16 (11, 30)	19 (11, 27)
Treatment	Treatment / *n* (%)		Patients no. + treatment
	P 67 (53.2)		1. P + CTX / 2. P + MMF
	HCQ 32 (25.4)		3. P + AZA + TW / 4. P + TW
	MMF 4 (3.2)		5. P / 6. P + CTX + TW
	CTX 61 (48.4)		7. P + CTX / 8. P + CTX + HCQ
	AZA 7 (5.6)		9. P + CTX + TW / 10. P + CTX
	TW 54 (42.9)		11. P + CTX / 12. P + HCQ
			13. P + MMF / 14. P + HCQ
			15. P + MMF

SLE, systemic lupus erythematosus; SLEDAI, SLE disease activity index; P, prednisone; HCQ, hydroxychloroquine; MMF, mycophenolate mofetil; CTX, cyclophosphamide; AZA, azathioprine; TW, Tripterygium wilfordi.

October 2012 to October 2015. Forty-eight newly diagnosed patients with active SLE without treatment (here termed newly diagnosed SLE) (**Table 1**) from the 126 patients with SLE enrolled were the main cohort studied. Fifteen patients (**Table 1**) were followed up during a 3-month period of treatment. All patients fulfilled the SLE classification criteria of the American College of Rheumatology (Atlanta, GA, USA) (24). The disease activity of the patients with SLE was evaluated using the SLE disease activity index (SLEDAI) (25). Exclusion criteria were as follows: patients with coinfections, allergies, other serious systemic diseases, and other autoimmune disorders.

This study was approved by the Ethics Committee of the Affiliated Hospital of Guangdong Medical University, and written informed consent was received from each subject.

Mice

Female MRL-*lpr/lpr* mice were purchased from the Jackson Laboratory (Bar Harbor, ME, USA) and maintained in the pathogen-free facility of the Laboratory Animal Center of Southern Hospital with the approval of the Ethics Committee for Experimental Animals at Nanfang Hospital, Southern Medical University. All experiments were performed according to the national guidelines for animal welfare.

Flow Cytometric Analysis

Human basophils were gated on FcεRIα-FITC/CD123-PerCP/Cy5.5/CD203c-PE (BioLegend, San Diego, CA, USA) positive cells after extracellular and intracellular staining. The expression levels of CD203c-PE, CD62L-APC, FcεRIα-FITC, CCR7-APC, CD63-APC, IL-13-APC, B cell-activating factor (BAFF)-APC (BioLegend, San Diego, CA, USA), IL-4-PE-Cy7, and IL-6-APC (eBioscience, San Diego, CA, USA) in basophils were quantified and expressed as relative fluorescence units (the ratio of mean fluorescence intensity normalized to controls) or as a positive percentage of total basophils.

Mouse basophils were gated on CD49b-APC/IgE-PE (BioLegend, San Diego, CA, USA). The expression levels of the activation marker CD200R-FITC (BioLegend, San Diego, CA, USA) (26), IL-4-FITC, and IL-6-FITC (eBioscience, San Diego, CA, USA) were quantified and expressed in the same way as for human basophils. A FACScanto™ II flow cytometer (Becton Dickinson, San Jose, CA, USA) and Lysys II software (Becton Dickinson, San Jose, CA, USA) or FlowJo Software (Tree Star, San Carlos, CA, USA) were used to acquire and analyze the data.

Basophil Depletion or Adoptive Transfer in MRL-*lpr/lpr* Mice

Depletion of basophils in female MRL-*lpr/lpr* mice was performed by injection of 5 μg anti-mouse FcεRI (MAR1; eBioscience, San Diego, CA, USA) twice daily intraperitoneally for 3 days (18, 27), and control group (non-depleted) mice were treated with an isotype control antibody (eBioscience, San Diego, CA, USA). For basophil-adoptive-transfer, basophils were isolated from the peripheral blood of age-matched MRL-*lpr/lpr* mice using magnetic microbeads against $CD49b^+$ (Miltenyi Biotec GmbH, Germany), and $FcεRI^+$ and $FcεRI^{++}$ basophils were further isolated by FACS-sorting (Becton Dickinson, San Jose, CA, USA) (27) to yield a purity of greater than 90%. Then, 1×10^4 basophils per mouse were adoptively transferred through the tail vein. The cumulative survival to 36 weeks was monitored. Blood was obtained by puncture of the orbital venous plexus, and serum, urine, lymph nodes, and renal samples were collected at the indicated time points.

Serum and Urine Analysis

Serum levels of IL-17 in humans and IL-17 and INF-γ in mice were measured using enzyme-linked immunosorbent assay (ELISA) kits (Life Technologies, Grand Island, New York, NY, USA). Serum levels of antinuclear IgG in humans (Zeus Scientific, Inc., Branchburg, NJ, USA) or mice (Cusabio Biotech, Wuhan, China) were measured using ELISA kits. To test for anti-dsDNA IgE in human or antinuclear IgE in mice, an anti-dsDNA IgG ELISA kit (Fuchun Kexin Biotech, Shanghai, China) or an antinuclear IgG ELISA kit (Cusabio Biotech, Wuhan, China) was modified by using HRP-anti-human IgE or HRP-anti-mouse IgE as the secondary antibody, respectively, and the serum samples were diluted at 1:25. The results are expressed as standard units (international units per milliliters, units per milliliters, or microgram per milliliters) or as the absorbance measured at 450 nm following a chromogenic (TMB) reaction (BioLegend, San Diego, CA, USA). Human serum IgE levels were determined using a chemiluminescence immunoassay (Elecsys 2010 analyzer, Roche Diagnostics Ltd., Switzerland).

To test for antinuclear IgE in humans, a line-blot method using the ANA Euroline Profile 3 kit (Euroimmun, Lübeck, Germany) was modified by using AP-anti-human IgE (Thermo Fisher Scientific, San Jose, CA, USA) as the secondary antibody, and the serum samples were diluted at 1:10.

For western blot detection of circulating immune complexes (CICs) containing IgE (IgE-CIC), PEG6000 (Sigma-Aldrich, St. Louis, MO, USA) (3.75%)-precipitated circulating CICs were prepared (28); then, HRP-anti-human IgE (Abcam Inc., Cambridge, MA, USA) was used for detection.

Twenty-four-hour urine was collected from metabolic cages to determine the levels of serum creatinine, C3 (Alpha Diagnostic Intl. Inc., San Antonio, TX, USA), blood urea nitrogen (StressMarq Biosciences Inc., Victoria, BC, Canada), and urinary proteins (Bradford method, Bio-Rad protein assay reagent).

Tissue Analysis

Immunofluorescence analysis was conducted to measure immunoglobulin deposition in human and mouse kidneys (29). FITC anti-human IgG (Sigma-Aldrich, St. Louis, MO, USA) and human IgE (eBioscience, San Diego, CA, USA), as well as FITC anti-mouse IgG (Santa Cruz Biotechnology, CA, USA) and IgE (eBioscience, San Diego, CA, USA) were employed. For human biopsy, the fluorescence intensity of glomerular staining was graded on a scale from 0 to ++++ in increments of 0.5+. Images were recorded under a TCS SP5 II confocal microscope (Leica Microsystems, Mannheim, Germany).

Isolation and Activation Assays of Human Basophils

An EasySep™ human basophil enrichment kit (Stemcell Technologies, Vancouver, BC, Canada) was used to negatively purify human basophils to obtain a purity of greater than 90% using flow cytometry (30).

For activation analysis, human basophils isolated from healthy controls were aliquoted at 4,000 cells/well in a total volume of 200 µl medium containing IL-3 (2 ng/ml, PeproTech., London, UK); to these were added the AB serum of healthy controls (20% of a total volume) or newly diagnosed patients with SLE (20% of a total volume), or CICs that were precipitated by PEG 6000 (3.75%) from the serum of newly diagnosed patients with SLE (31), or serum from newly diagnosed SLE patients that flow through a Sepharose 4B™ column (GE Healthcare, Uppsala, Sweden) coupled with anti-IgE antibody to depletion of IgE (32), or anti-IgE antibody (0.5 µg/ml; positive control) (Abcam Inc., Cambridge, MA, USA) at 37°C for 15 min (CD203c detection) or 24 h (CD62L, CCR7, and IL-4-positive detection) (33).

Autoantibody Production Assay

B cells were isolated from newly diagnosed patients with SLE using an EasySep™ Human B Cell Enrichment kit (Stemcell Technologies, Vancouver, BC, Canada) (34). Then, for the measurement of autoantibody production, B cells (1×10^5 cells/well) were cultured for 12 days with polyclonally activated $CD4^+$ T cells (1×10^5 cells/well) from healthy controls using anti-CD3 (0.5 mg/ml) (Miltenyi Biotec GmbH, Germany); or negatively purified basophils (5×10^4 cells/well) from healthy control or newly diagnosed patients with SLE. Cells were cultured in DMEM (300 µl) (10% FBS), IL-2 (10 ng/ml) and IL-3 (10 ng/ml) (PeproTech) (18, 35), as well as nuclear extracts of Hep-2 cells (10 µg/ml) isolated with a Nuclear and Cytoplasmic Extraction Kit (Thermo Fisher) as a stimulator for the first 3 days (36). Levels of antinuclear IgG (Zeus Scientific) and IgE (as described in serum and urine analysis, and culture supernatant samples were diluted 1:4), anti-nucleosomes IgG (ELISA) (Euroimmun, Lübeck, Germany) and IgE, and anti-tetanus IgG (ELISA) (ZhengZhou Etebio Technology Co., Ltd., Zhengzhou, China, approved by SFDA) and IgE in the culture supernatants were measured using ELISA kits.

Th17 Differentiation Assay

Naïve $CD4^+$ T cells from newly diagnosed patients with SLE using an EasySep™ Human Naïve $CD4^+$ T Cell Enrichment Kit (Stemcell technologies) were stimulated with anti-CD2/CD3/CD28 T cell activation beads (Miltenyi Biotec) at a bead-to-cell ratio of 1:2 for 3 days, followed by incubation for 4 days in the presence of a Th17 differentiation cytokine mixture (IL-2, 20 ng/ml; IL-6, 20 ng/ml; IL-23, 20 ng/ml; IL-1β, 20 ng/ml; TGF-β1, 5 ng/ml; anti-IL-4, 5 µg/ml; anti-IL-12, 5 µg/ml; anti-IFN-γ. 1 µg/ml; PeproTech., London, UK), or culturing in the Th17 differentiation cytokine mixture (excluding IL-6) with negatively isolated basophils (2×10^4 cells/well) from healthy controls, or from newly diagnosed patients with SLE in the absence or presence of anti-IL-6 (5 µg/ml, PeproTech., London, UK), respectively.

Statistics

All statistical analysis was performed using SPSS 16.0 (SPSS, Inc., Chicago, IL, USA). Two-group comparisons were performed using unpaired two-tailed Student's *t*-test. Multiple-group comparisons were performed using one-way analysis of variance (ANOVA) followed by the Bonferroni or Dunnett *post hoc* tests. Survival curves were analyzed using the non-parametric *Kaplan–Meier method*. Spearman's rank correlation was used to detect correlations among different study parameters. A *P*-value of <0.05 was considered to indicate statistical significance. Each symbol represents an individual patient, one mouse, or one sample. The data are presented as scatter plots and are expressed as means.

RESULTS

Decreased Numbers and Increased Activity of Peripheral Basophils Are Correlated with Disease Activity and Increased Autoantibody Production in Patients with SLE

To assess whether basophils play a role in SLE, the numbers and activation of peripheral basophils and their correlations with disease activity (SLEDAI score) were evaluated in patients with SLE. The results showed that the number (**Figure 1A**—a) and percentage (**Figure 1A**—b) of peripheral basophils in newly diagnosed patients with SLE were significantly decreased compared with healthy controls. However, these basophils were activated and exhibited higher expression levels of activation makers such as CD203c and CD63 (**Figure 1A**—c and d) compared with those from healthy controls. The representative data of FACS for basophil frequency, CD203c, and $CD63^+$ were also shown (Figure S1 in Supplementary Material) The higher expression of CD203c on basophils correlated with disease activity, as assessed by the SLEDAI score, not only in the newly diagnosed SLE patients (**Figure 1B**—a) but also in the total group of patients with SLE (**Figure 1B**—b). Additionally, the higher expression of CD203c on basophils correlated with the serum levels of antinuclear IgG and IgE (**Figure 1B**—c and d) along with the deposition of IgG and IgE in kidney biopsies (**Figure 1C**) in the total group of patients with SLE. Furthermore, a follow-up study showed that after treatment with immunosuppressants and other drugs, newly diagnosed patients with SLE who experienced effective treatment (defined as a decrease in the SLEDAI score of more than 6 and the absence of damage to the heart, lungs, brain, blood, intestines, or any other vital organs) showed an increased level of peripheral basophils and decreased basophil activity as indicated by the expression of CD203c (**Figure 1D**, nos.1–13); in contrast, patients who did not experience effective treatment did not show any of these signs (**Figure 1D**, nos.14 and 15). Also, patients with SLE who treated with *Tripterygium wilfordi* have been shown apart (Figure S2 in Supplementary Material). These findings indicate that peripheral basophil activation may play an important role in SLE.

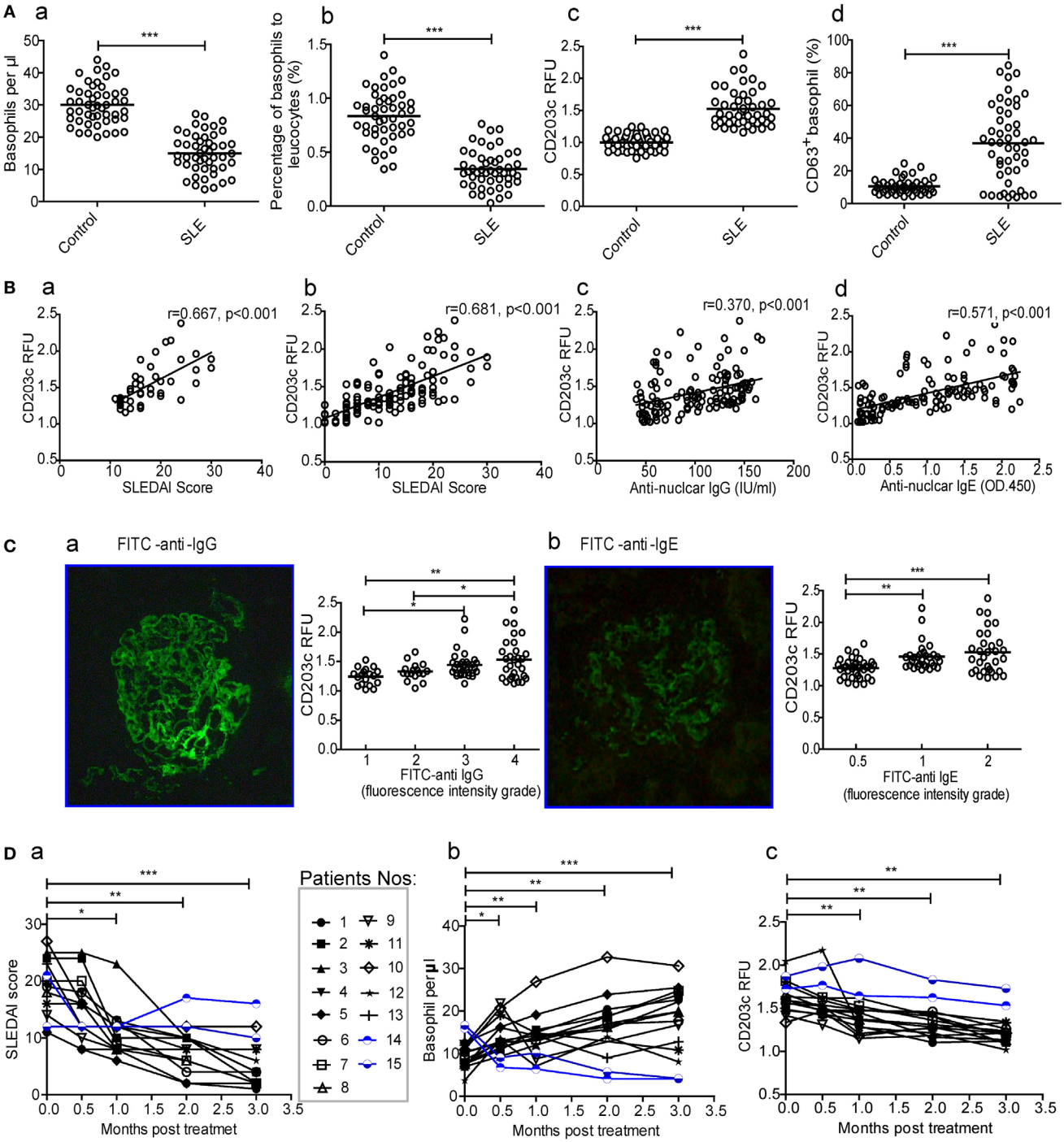

FIGURE 1 | **Numbers and activation of peripheral basophils and their correlations with disease activity and autoantibody production in patients with systemic lupus erythematosus (SLE).** **(A)** The number (a, b) and activation (CD203c expression and CD63 positive percentage) (c, d) of peripheral basophils in newly diagnosed patients with SLE (n = 48) and healthy controls (n = 48) were detected using flow cytometry. **(B)** Correlations between the activation (CD203c expression) of peripheral basophils and disease activity [SLE disease activity index (SLEDAI) score] of newly diagnosed patients with SLE (n = 48) (a), or total patients with SLE (n = 126) (b), levels of their serum antinuclear IgG (n = 126) (c), and IgE (n = 126) (d) were analyzed. **(C)** The association between the activation (CD203c expression) of peripheral basophils in patients with SLE (n = 97) who received renal biopsy and the deposition of IgG (a) and IgE (b) evaluated by fluorescence intensity grade in biopsied kidneys. **(D)** Changes in the SLEDAI score (a), the numbers (b), and activation (CD203c expression) (c) of peripheral basophils in patients with SLE (n = 15) who were followed up for 3 months posttreatment. *P < 0.05, **P < 0.01, ***P < 0.001. Data were analyzed *via* Student's t-test **(A,D)**, Spearman's rank correlation **(B)**, or one-way analysis of variance **(C)** and presented as scatter plots and are expressed as means.

(Autoreactive) IgE-Mediated Basophil Activation in Patients with SLE

Since peripheral basophils in patients with SLE were in an activated state, we next examined the mechanisms mediating their activation by looking into the potential involvement of IgE, a key inducer of basophil activation. The results showed that serum levels of anti-dsDNA IgE, antinuclear IgE and total IgE (**Figure 2A**), IgE-CIC (**Figure 2D**) in newly diagnosed patients with SLE were significantly higher than those in healthy controls, which was reconfirmed by the higher expression of the high-affinity receptor for IgE (FcεRIα) on basophils (**Figure 2B**). In addition, antinuclear IgE specific for auto-antigens, including nRNP/sm, Sm, SS-A, Ro-52, dsDNA, nucleosomes, rib-Prot, etc., can be detected in patients with SLE ($n = 36$) but not in healthy controls ($n = 36$) (**Figure 2C**). In an *in vitro* study, we found that peripheral basophils that were negatively isolated from healthy controls (**Figure 2E**) could be activated by the upregulation of CD203c expression (**Figure 2F**—a) and that the percentage of IL-4-positive cells (**Figure 2F**—b) could be increased by culturing with serum obtained from newly diagnosed patients with SLE, and IgE-CICs (**Figure 2D**) precipitated by PEG from the sera of newly diagnosed patients with SLE, but not by the serum of healthy controls or serum obtained from newly diagnosed patients with SLE by depletion of IgE. Basophils were activated with anti-IgE stimulation as a positive control (**Figure 2F**). These findings indicate that the presence of IgE, especially autoreactive IgE, mediate basophil activation in SLE.

Basophils Promote Autoantibody Production by B Cells and Th17 Differentiation in SLE

To clarify the triggers that decrease basophil counts in patients with SLE, we investigated the homing of basophils to the lymph nodes and the mechanisms that mediate this process. Our results showed that CD62L and CCR7, which are important for the homing of T cells to lymphoid tissues (37, 38), were upregulated on basophils obtained from newly diagnosed patients with SLE compared with those obtained from healthy controls (**Figure 3A**). Additionally, the expression levels of CD62L and CCR7 (**Figure 3B**) on peripheral basophils that were negatively isolated from healthy controls were increased by culturing with serum obtained from newly diagnosed patients with SLE but not by culturing with serum obtained from healthy controls.

We then examined the role of activated basophils from patients with SLE in autoantibody production by B cells from patients with SLE *in vitro*. The results showed that the percentages of IL-4-, IL-6-, IL-13-, and BAFF-positive peripheral basophils in newly diagnosed patients with SLE were significantly higher than those in healthy controls (**Figure 3C**). Moreover, basophils obtained from patients with SLE promoted antinuclear IgG and IgE production by B cells obtained from patients with SLE *in vitro*, but not those from healthy controls (**Figure 3D**—a and b). Also, anti-nucleosome IgG and IgE production has the same tendency (**Figure 3D**—c and d), while anti-tetanus IgG and IgE were not detected (data not shown). The coculture of activated T cells with B cells obtained from patients with SLE was used to produce autoantibodies as a positive control (**Figure 3D**). These findings demonstrate that basophils can amplify autoantibody production by B cells in SLE.

Next, we investigated the role of activated basophils from patients with SLE on Th17 differentiation from naïve $CD4^+$ T cells from patients with SLE *in vitro*. Similar to what was observed with B cells, the results showed that isolated basophils from newly diagnosed patients with SLE significantly promoted Th17 differentiation compared to those obtained from healthy controls in the presence of a cytokine mixture (excluding IL-6) to induce Th17 differentiation (**Figure 3E**—a and b), and this effect could be suppressed by adding anti-IL-6 antibodies (**Figure 3E**—b), which was consistent with the finding that newly diagnosed patients with SLE had a higher percentage of IL-6-positive peripheral basophils (**Figure 3C**—b) and higher serum IL-17 levels (**Figure 3E**—c) than healthy controls. These findings demonstrate that basophils can promote Th17 differentiation in SLE.

Activated Basophils Exacerbate Disease Progression in MRL-*lpr/lpr* Mice

Because clinical data and *in vitro* studies have indicated that activated basophils can promote autoantibody and IL-17 production and may exacerbate SLE, a lupus-prone MRL-*lpr/lpr* mice model that reflects the pathologies of human SLE (39) was employed to further investigate the role of basophils in SLE.

Compared to those in 6-week-old MRL-*lpr*/*lpr* mice, the expression levels of basophil activation markers, including CD200R (26), IL-4, and IL-6, were upregulated in 10- and 14-week-old mice (**Figure 4A**). Additionally, basophils were first detected in the lymph nodes of 10-week-old MRL-*lpr/lpr* mice and increased slightly in number as the mice aged (**Figure 4D**), a finding that is consistent with the upregulated expression of the homing receptors CD62L and CCR7 on basophils obtained from patients with SLE (**Figure 3A**).

We next evaluated the effects of basophil depletion and adoptive transfer on the development of autoimmune disorders in MRL-*lpr/lpr* mice. The experimental design and timelines was shown in **Figure 4B**. The results showed that one time of basophil depletion led to a significant decrease in the percentage of basophils in the peripheral blood (**Figure 4C**), lymph nodes (**Figure 4D**), and spleen (data not shown) of MRL-*lpr/lpr* mice and that this decrease lasted for more than 10 days. When basophils were depleted five times from 6 to 14 weeks of age, the survival of MRL-*lpr/lpr* mice was significantly prolonged compared with that of control and basophil-adoptive-transferred mice (**Figure 4E**).

In addition, basophil-depleted MRL-*lpr/lpr* mice exhibited a significant decrease in the ratio of spleen weight to body weight (**Figure 4F**) and the levels of serum antinuclear IgG and IgE at 20 weeks (**Figure 5A**), and an increase in the serum levels of C3 (**Figure 5C**) at 15 and 20 weeks compared with controls and basophil-adoptive-transferred mice. Basophil-depleted MRL-*lpr/lpr* mice exhibited significant decreases in the levels of

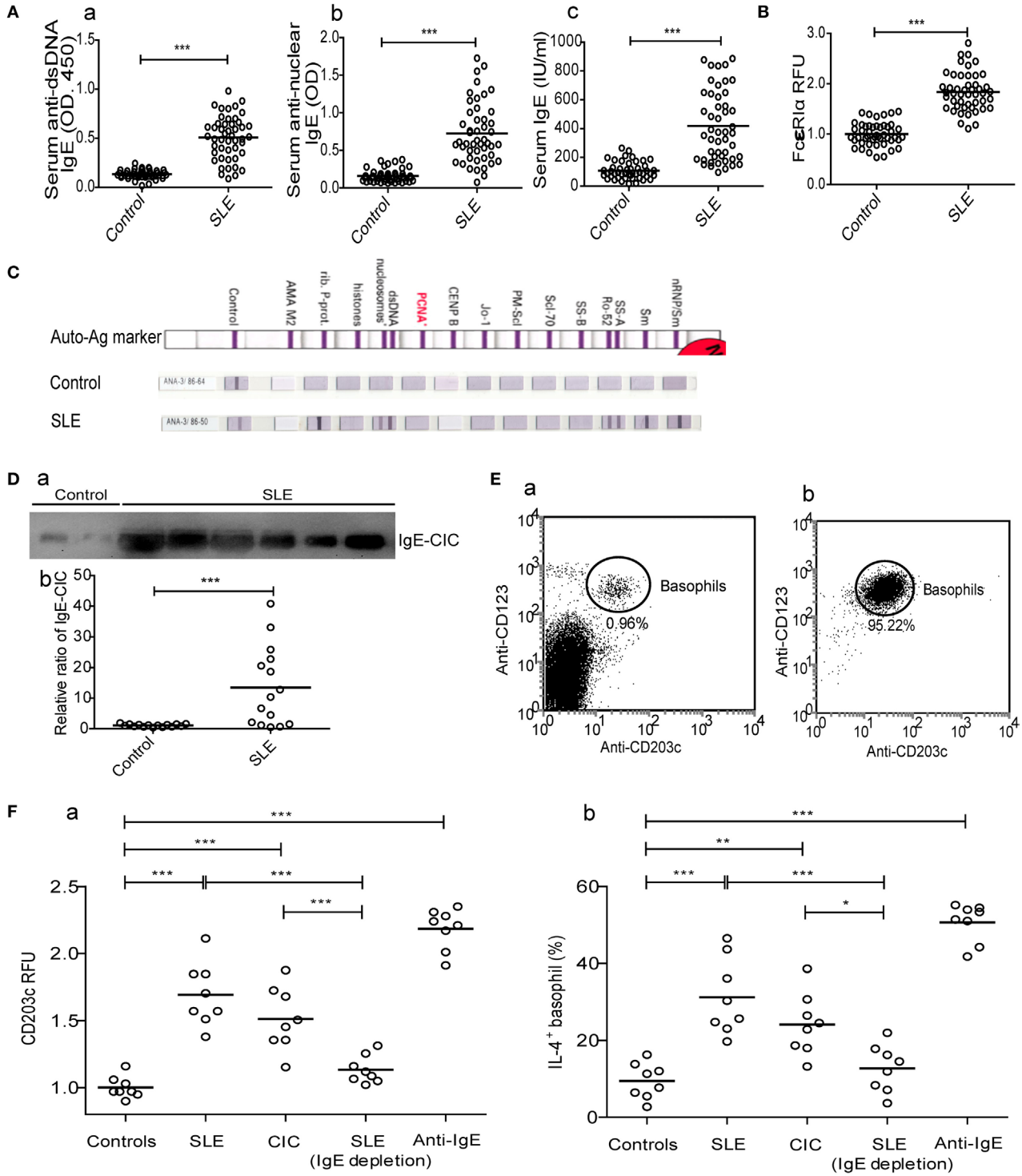

FIGURE 2 | **Mechanism of peripheral basophil activation in patients with systemic lupus erythematosus (SLE)**. **(A)** Serum levels of anti-dsDNA IgE, antinuclear IgE, and total IgE ($n = 48$); **(B)** levels of FcεRIα expression on peripheral basophils ($n = 48$); **(C)** antinuclear IgE profile ($n = 36$) (shown as representative images); and **(D)** the relative ratio of IgE-circulating immune complexes (CICs) ($n = 15$) in newly diagnosed patients with SLE and the same number of healthy controls. **(E)** Representative FCM dot-plot of peripheral basophils in PBMC of healthy controls ($n = 6$) (a) and post negatively isolated (b). **(F)** Activation [CD203c expression and interleukin (IL)-4 positive percentage] of basophils from healthy controls ($n = 8$) after stimulation with serum (20% of a total volume) of healthy control or newly diagnosed patients with SLE, CICs of newly diagnosed patients with SLE, serum (20% of a total volume) of newly diagnosed patients with SLE by depletion of IgE, or anti-IgE. $^*P < 0.05$, $^{**}P < 0.01$, $^{***}P < 0.001$. Data were analyzed *via* Student's *t*-test **(A,B,D)** or one-way analysis of variance **(F)** and presented as scatter plots and are expressed as means.

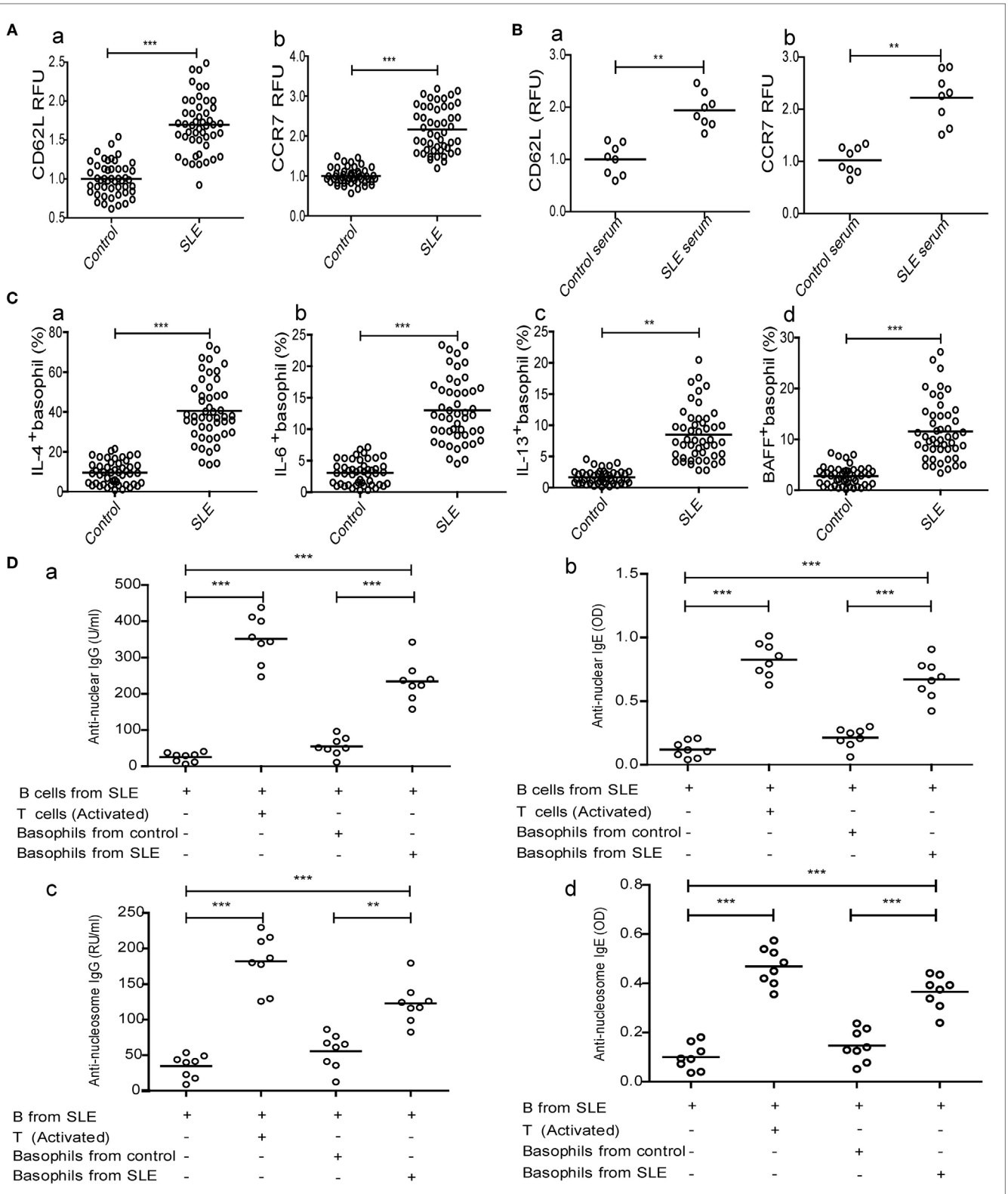

FIGURE 3 | **Continued**

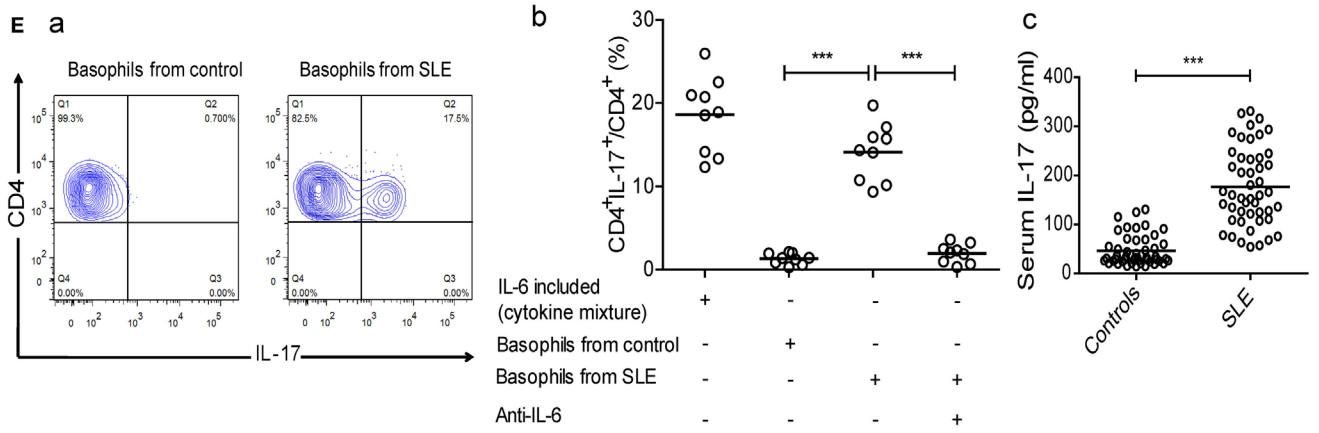

FIGURE 3 | Analysis of homing receptors expression on basophils and the effect of basophils on autoantibody production by B cells and Th17 differentiation in systemic lupus erythematosus (SLE). The expression of homing receptors (CD62L and CCR7) on **(A)** peripheral basophils of healthy controls ($n = 48$) and newly diagnosed patients with SLE ($n = 48$) and **(B)** basophils from healthy controls after stimulation with serum (20% of a total volume) of healthy control ($n = 8$) and newly diagnosed patients with SLE ($n = 8$) for 24 h. **(C)** The percentages of interleukin (IL)-4$^-$ (a), IL-6$^-$ (b), IL-13$^-$ (c), and BAFF-positive (d) peripheral basophils in newly diagnosed patients with SLE and healthy controls ($n = 48$). **(D)** Antinuclear IgG (a), antinuclear IgE (b), anti-nucleosome IgG (c), and anti-nucleosome IgE (d) produced by SLE B cells post-coculturing with basophils from healthy controls or newly diagnosed patients with SLE and activated T cells for 12 days ($n = 6$). **(E)** The proportions of Th17 differentiation from SLE naïve CD4$^+$ T cells post-coculturing in Th17 differentiation cytokines mixture (IL-6 included), or post-coculturing in Th17 differentiation cytokine mixture (excluding IL-6) with basophils from healthy controls (a, left, representative FCM plots), or basophils from newly diagnosed patients with SLE (a, right) in the absence or presence of anti-IL-6, respectively, and the statistical data ($n = 9$) (b), and serum levels of IL-17 in newly diagnosed patients with SLE ($n = 48$) and healthy controls ($n = 48$) (c). $^*P < 0.05$, $^{**}P < 0.01$, $^{***}P < 0.001$. Data were analyzed *via* Student's *t*-test **(A–C—e)** or one-way analysis of variance **(D,E—b)** and presented as scatter plots and are expressed as means.

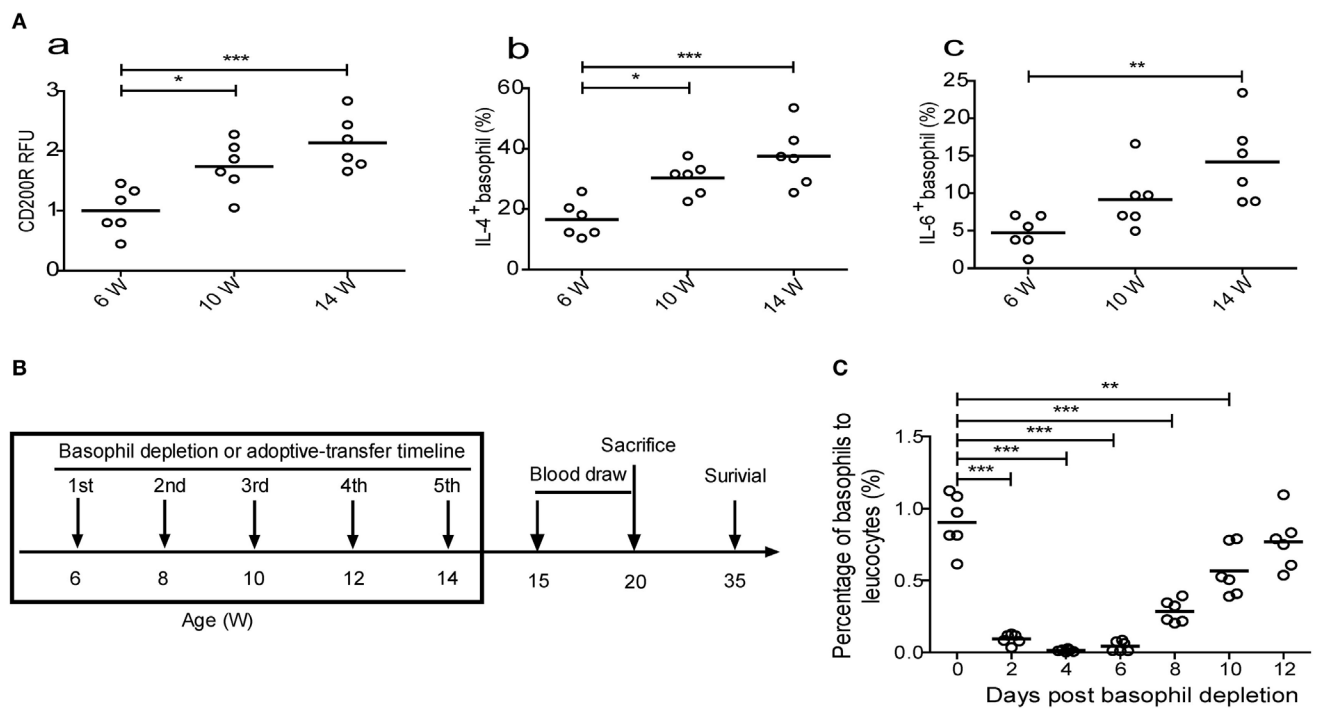

FIGURE 4 | Continued

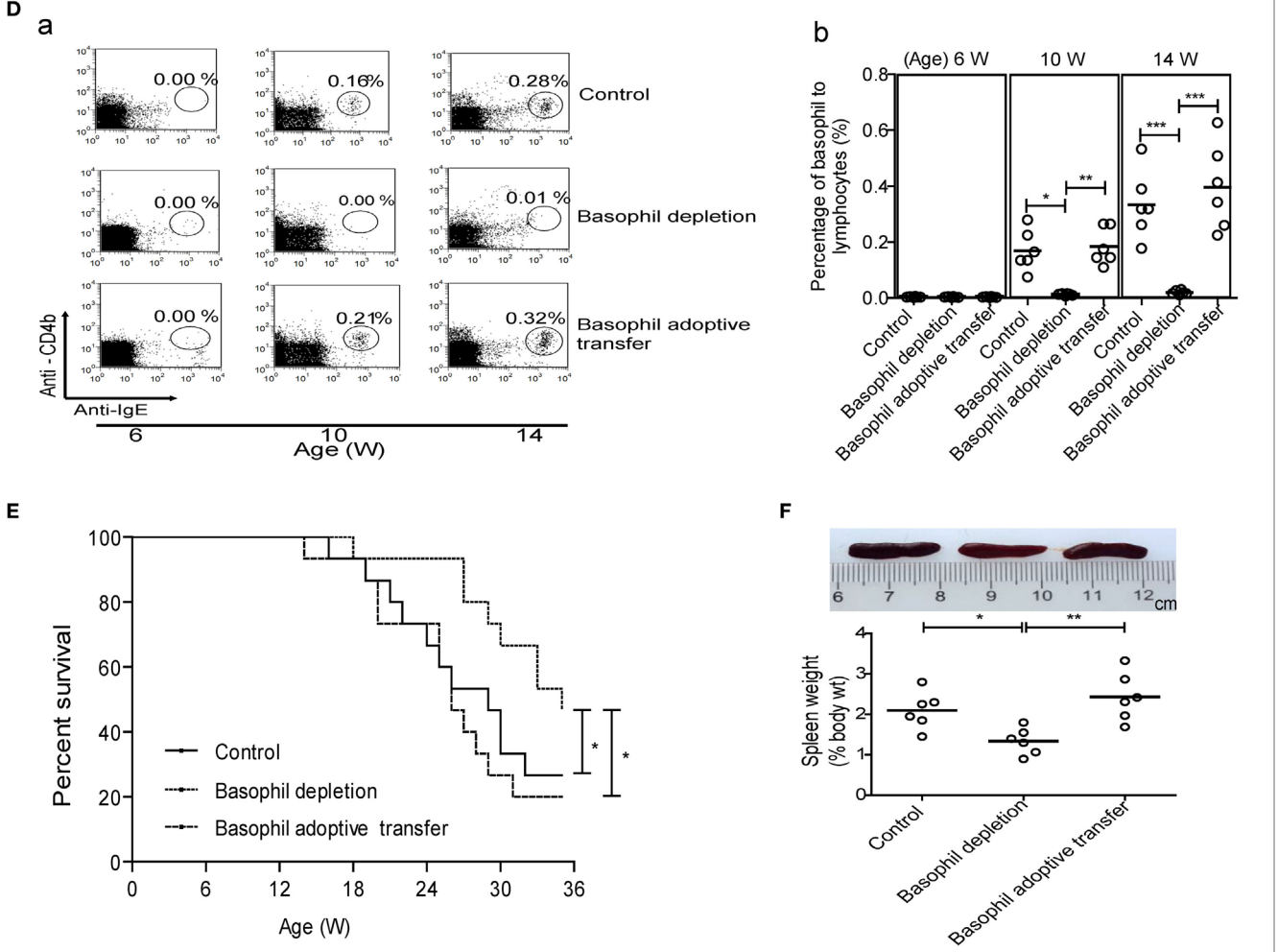

FIGURE 4 | **Effect of basophil depletion or adoptive transfer on the survival of MRL-*lpr/lpr* mice**. **(A)** CD200R expression (a) on peripheral basophils and the percentages of interleukin (IL)-4$^+$ (b) and IL-6-positive (c) peripheral basophils in MRL-*lpr/lpr* mice ($n = 6$). **(B)** Experimental design and time lines. **(C)** The changes of percentages of peripheral basophils to leukocytes in MRL-*lpr/lpr* mice ($n = 6$) after basophil depletion. **(D)** The changes of percentages of basophils to lymphocytes in the lymph nodes of control, basophil–depleted, and basophil-adoptive-transferred MRL-*lpr/lpr* mice ($n = 6$) (a) and statistical data (b). **(E)** The cumulative survival of three groups of MRL-*lpr/lpr* mice ($n = 12$) was monitored using the *Kaplan–Meier method*. **(F)** Representative images of the spleens of control, basophil–depleted, and basophil-adoptive-transferred MRL-*lpr/lpr* mice (from left to right) (a) and statistical data of the percentage of spleen weight to body weight of them (b) ($n = 6$). $^*P < 0.05$, $^{**}P < 0.01$, $^{***}P < 0.001$. Data were analyzed *via* one-way analysis of variance **(A,D,F)** and Student's *t*-test **(C)** and presented as scatter plots and are expressed as means.

serum IL-17, but not IFN-γ, at 20 weeks compared with control and basophil-adoptive-transferred mice (**Figure 5B**).

The influence of basophil depletion on renal injury in MRL-*lpr/lpr* mice was also assessed. Serum levels of creatinine, blood urea nitrogen, and urinary proteins were significantly decreased in basophil-depleted MRL-*lpr/lpr* mice at 20 weeks of age (**Figure 5D**). Basophil-depleted MRL-*lpr/lpr* mice exhibited decreased levels of IgG and IgE deposition in the glomeruli compared with the control and basophil-adoptive-transferred mice (**Figure 5E**—a). Additionally, the renal histopathology (including enlarged glomeruli, glomerular cell proliferation, and increased mesangial matrix) of basophil-depleted MRL-*lpr/lpr* mice was improved at 20 weeks compared with that of the controls (**Figure 5E**—b); however, basophil (from age-matched-MRL-*lpr/lpr* mice) adoptive-transferred MRL-*lpr/lpr* mice showed more severe glomerulonephritis than the controls (**Figure 5E**).

DISCUSSION

In this study, we used negatively isolated human basophils together with patient information and a lupus-prone mouse model to demonstrate that activated basophils amplify autoantibody and IL-17 production, thereby contributing to the pathogenesis of SLE.

Because basophils need to be activated to fulfill their biological functions (40, 41), we first demonstrated that basophils obtained from patients with SLE and MRL-*lpr/lpr* mice were activated due to higher expression of a series of activation markers and that

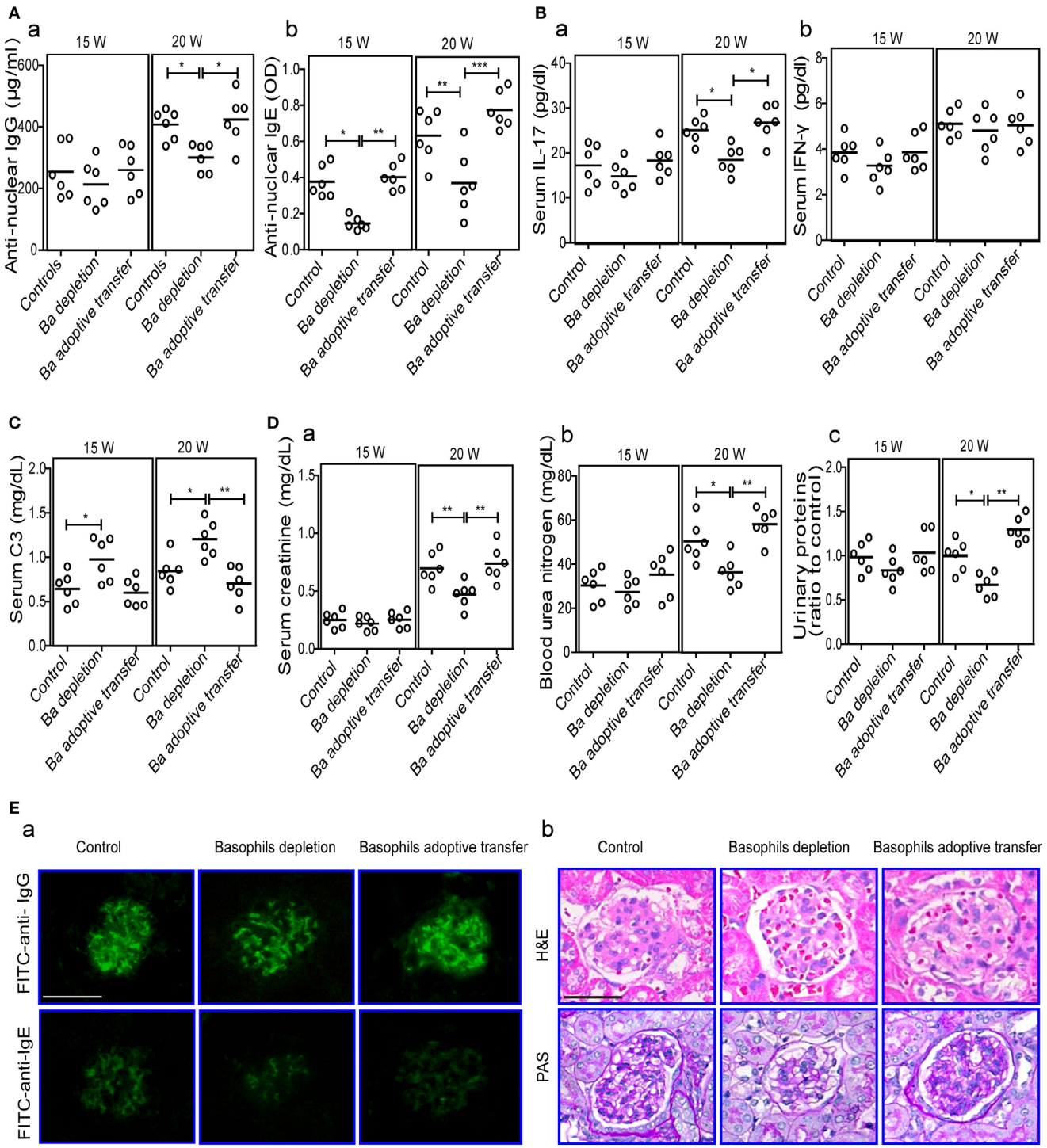

FIGURE 5 | **Effects of basophil depletion or adoptive transfer on autoantibodies and inflammatory cytokines production and renal pathology of MRL-*lpr/lpr* mice**. Serum levels of antinuclear IgG and IgE **(A)**, interleukin (IL)-17 and IFN-γ **(B)**, C3 **(C)**, and **(D)** serum creatinine (a), blood urea nitrogen (b), and urinary proteins (c) in control, basophil–depleted, and basophil-adoptive-transferred MRL-*lpr/lpr* mice ($n = 6$). **(E)** Representative images of the fluorescence microscopy examination of IgG and IgE deposition **(E**—a**)**; and the light microscopy examination of the histopathology of glomerulonephritis using H&E and PAS staining **(E**—b**)** in control, basophil–depleted, and basophil-adoptive-transferred MRL-*lpr/lpr* mice ($n = 6$) at 20 weeks of age (scale bars, 50 μm). Ba, basophil. $^{*}P < 0.05$, $^{**}P < 0.01$, $^{***}P < 0.001$. Data were analyzed *via* one-way analysis of variance **(A–D)** and presented as scatter plots and are expressed as means.

some of these also correlated with disease activity in SLE. Then, we found that IgE, especially autoreactive IgE, mediated basophil activation in SLE, based on the detection of abundant total IgE, autoreactive IgE, and the higher expression of the high-affinity receptor for IgE (FcεRIα) on basophils in patients with SLE, and *in vitro* experiments including isolated basophils cocultured with the serum of patients with SLE and PEG precipitation CIC (containing IgE). The prevalence of autoreactive IgE in SLE was also observed by others (23, 42, 43).

In addition to activation, we simultaneously found that the numbers of peripheral basophils were decreased in patients with SLE. Thus, we evaluated where the basophils trafficked to following their activation. We found that basophils were initially detected in the lymph nodes in 10-week-old MRL-*lpr/lpr* mice, and this number increased slightly as the mice aged, which confirmed the results of a previous study showing that basophils were detected in the lymph nodes and spleen in two patients with SLE (23). These findings demonstrate the homing of basophils to lymph nodes in SLE. A subsequent study indicated that basophil migration to lymphoid tissues might mediated by CD62L and CCR7, based on the higher expression of these two homing receptors on basophils in patients with SLE as well as an *in vitro* experiment. Higher expression of CD62L by basophils of patients with SLE was also was also observed by others (23). Above all, homing to lymphoid tissues after basophil activation may contribute to decreased peripheral basophil numbers in SLE.

In this study, we mainly focused on the effects of activated basophils after homing to lymphoid tissues in SLE. The first key issue to clarify was the effect of activated basophils on autoantibody production by B cells in SLE. It has been confirmed that basophils can directly interact with B cells and provide helper signals to them through IL-4, IL-13, BAFF, and CD40L, driving their differentiation to antibody-producing cells (11). Our *in vitro* study showed that basophils from patients with SLE have the ability to promote autoantibodies including antinuclear and antinucleosome IgG and IgE production by B cells. For the immunological basis, this effect was possibly mediated by a synergistic effect of IL-4, IL-6, IL-13, and BAFF, together with the constitutive expression of CD40L (35, 44), as confirmed by our observation of a high expression level of these effectors by basophils of SLE patients (**Figure 3C**). This is consistent with the finding that basophil activation was correlated with the serum levels of antinuclear antibodies and with the deposition of immunoglobulins in the glomeruli of patients with SLE. Correspondingly, our *in vivo* study also showed that basophil-depleted MRL-*lpr/lpr* mice exhibited markedly decreased levels of serum autoantibodies and immunoglobulin deposition in glomeruli. However, anti-tetanus IgG/IgE in the culture supernatants was not detected (data not shown). For the next step, we plan to investigate which effectors play key roles in the synergistic effect of them in the context of SLE.

We next investigated another key issue: the effect of activated basophils on Th17 differentiation in SLE. Our *in vitro* study first showed that activated basophils obtained from patients with SLE could promote Th17 differentiation. Furthermore, basophil-depleted MRL-*lpr/lpr* mice exhibited significant decreases in their serum IL-17 levels. The finding that activated basophils enhance IL-17 production has also been reported in another autoimmune disease, inflammatory bowel disease (12). Further analysis showed that IL-6, which is also defined as a Th17-inducing cytokine (20) due to its role in the regulation of Th17 differentiation (45), was necessary for promoting Th17 differentiation and IL-17 production by activated basophils in patients with SLE, as further confirmed by our observation that basophils obtained from patients with SLE and aged MRL-*lpr/lpr* mice both exhibited a higher expression of IL-6.

Moreover, to directly verify the role of basophils in SLE progression, a selective basophil-depletion murine model was successfully established, as reported previously (18, 46). Our results showed that basophils were activated along with aging, and the homing of basophils to lymph nodes was significantly inhibited after depletion of basophils in MRL-*lpr/lpr* mice. Consequently, the basophil-depleted mice exhibited benefits on renal function and attenuated the progression of glomerulonephritis, finally led to the extension of life span, which was accompanied with significant decreases in autoantibody and IL-17 production. However, basophil-adoptive-transferred MRL-*lpr/lpr* mice exhibited the opposite tendency, although the results were not significant possibly because the peripheral basophils were sufficient for migration, which is consistent with the observation that basophils were not significantly increased in the lymph nodes of the basophil-adoptive-transferred mice. In addition, we also used the antibody anti-CD200R3 (Ba103; Hycult, Uden, The Netherlands) for basophil depletion (47), and the results showed the same tendency (data not shown). In another study, basophils were found to be necessary for the development of autoimmune disease in Lyn-deficient mice (23). We noted that due to the induction of antibodies to basophil-depletion antibodies, the prolonged use of them *in vivo* was limited, and also the efficiency of basophil depletion in MRL-*lpr/lpr* mice was decreased for the fifth basophil depletion compared with the first time even it can led to a significant decrease in the percentage of basophils in the peripheral blood lasted for more than 6 days. Recently, several kinds of basophil ablation mouse models, Tg mouse, have been generated (48, 49), which will help us to further study the critical roles of basophils in SLE in the future. These findings demonstrate that activated basophils exacerbate disease progression in MRL-*lpr/lpr* mice.

CONCLUSION

This study demonstrates that basophils can exacerbate SLE through activation-dependent autoantibody and IL-17 production (**Figure 6**). These findings provide novel insights into the pathogenesis of SLE and may lead to the development of new therapeutic strategies for treating SLE.

AUTHOR CONTRIBUTIONS

QP and H-fL conceived and designed the experiments. QP, LG, HX, YF, LL, ZD, and LingY performed the experiments. QP and H-fL analyzed the data. YF, LL, ZD, LingY, NA, and CY contributed reagents/materials/analysis tools. QP, JZ, CD, LinY, and H-fL contributed to the writing of the manuscript. All the authors reviewed and approved the final manuscript.

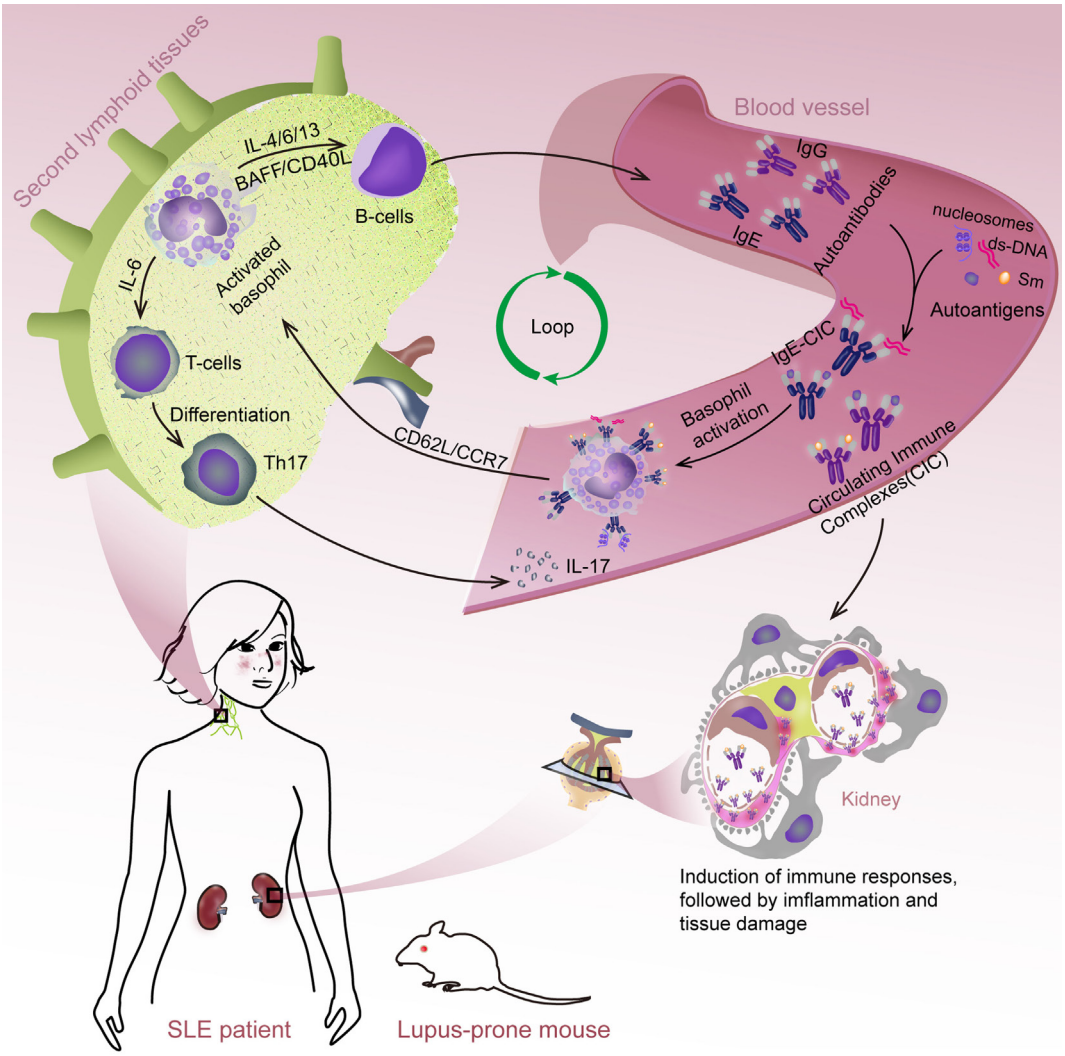

FIGURE 6 | Schematic representation of systemic lupus erythematosus (SLE) exacerbation by basophil activation-dependent autoantibody and interleukin (IL)-17 production. During the progress of SLE, peripheral basophils could migrate to secondary lymphoid tissues in response to the increased expression of CD62L/CCR7 post their activation mediated by (autoreactive) IgE. At these sites, basophils could exacerbate SLE by promoting autoantibody production possibly mediated by a synergistic effect of IL-4, IL-6, IL-13, BAFF, and CD40L, and Th17 differentiation by IL-6 resulted in the exacerbating of disease.

FUNDING

This study was supported by National Natural Science Foundation of China (no. 81202346 and no. 81471530).

SUPPLEMENTARY MATERIAL

The Supplementary Material for this article can be found online at http://journal.frontiersin.org/article/10.3389/fimmu.2017.00348/full#supplementary-material.

FIGURE S1 | Representative data of FACS for basophil frequency, CD203c, and CD63⁺ basophil. Gate 1 (①) isolates the peripheral leukocytes, and gate 2 (②) detects the low side-scatter (SSC), FcεRIα⁺ population of cells. Then, with a double gating strategy, gate 3 (③) detects $CD123^{+}CD203c^{+}$ basophil population. For $CD63^{+}$ basophil, a followed gate 4 (④) detects the low SSC, $Fc\varepsilon RI\alpha^{+}CD123^{+}CD203c^{+}CD63^{+}$ population of basophil. Gates were set according to isotype controls antibodies, respectively. The results were analyzed with FlowJo Software in a pseudocolor dot-plot.

FIGURE S2 | Numbers and activation of peripheral basophils and their correlations with disease activity and autoantibody production in patients with systemic lupus erythematosus (SLE) treated with *Tripterygium wilfordii*. (A) Correlations between the activation (CD203c expression) of peripheral basophils and disease activity [SLE disease activity index (SLEDAI) score] (a), and levels of their serum antinuclear IgG (b) or IgE (c) of patients with SLE treated with *T. wilfordi* ($n = 54$) were analyzed. **(B)** Changes in the SLEDAI score (d), the numbers (e), and activation (CD203c expression) (f) of peripheral basophils in patients with SLE treated with *T. wilfordi* ($n = 4$) who were followed up for 3 months posttreatment. $^{*}P < 0.05$, $^{**}P < 0.01$, $^{***}P < 0.001$. Data were analyzed *via* Spearman's rank correlation **(A)** or one-way analysis of variance (B) and presented as scatter plots and are expressed as means.

REFERENCES

1. Sanz I, Lee FE. B cells as therapeutic targets in SLE. *Nat Rev Rheumatol* (2010) 6(6):326–37. doi:10.1038/nrrheum.2010.68
2. Crispin JC, Kyttaris VC, Terhorst C, Tsokos GC. T cells as therapeutic targets in SLE. *Nat Rev Rheumatol* (2010) 6(6):317–25. doi:10.1038/nrrheum.2010.60
3. Ramanujam M, Davidson A. Targeting of the immune system in systemic lupus erythematosus. *Expert Rev Mol Med* (2008) 10:e2. doi:10.1017/S1462399408000562
4. Bird AK, Meednu N, Anolik JH. New insights into B cell biology in systemic lupus erythematosus and Sjogren's syndrome. *Curr Opin Rheumatol* (2015) 27(5):461–7. doi:10.1097/BOR.0000000000000201
5. Dorner T, Giesecke C, Lipsky PE. Mechanisms of B cell autoimmunity in SLE. *Arthritis Res Ther* (2011) 13(5):243. doi:10.1186/ar3433
6. Martin JC, Baeten DL, Josien R. Emerging role of IL-17 and Th17 cells in systemic lupus erythematosus. *Clin Immunol* (2014) 154(1):1–12. doi:10.1016/j.clim.2014.05.004
7. Burkett PR, Meyer zu Horste G, Kuchroo VK. Pouring fuel on the fire: Th17 cells, the environment, and autoimmunity. *J Clin Invest* (2015) 125(6):2211–9. doi:10.1172/JCI78085
8. Nutt SL, Hodgkin PD, Tarlinton DM, Corcoran LM. The generation of antibody-secreting plasma cells. *Nat Rev Immunol* (2015) 15(3):160–71. doi:10.1038/nri3795
9. Voehringer D. Protective and pathological roles of mast cells and basophils. *Nat Rev Immunol* (2013) 13(5):362–75. doi:10.1038/nri3427
10. Siracusa MC, Perrigoue JG, Comeau MR, Artis D. New paradigms in basophil development, regulation and function. *Immunol Cell Biol* (2010) 88(3):275–84. doi:10.1038/icb.2010.1
11. Merluzzi S, Betto E, Ceccaroni AA, Magris R, Giunta M, Mion F. Mast cells, basophils and B cell connection network. *Mol Immunol* (2015) 63(1):94–103. doi:10.1016/j.molimm.2014.02.016
12. Wakahara K, Baba N, Van VQ, Begin P, Rubio M, Ferraro P, et al. Human basophils interact with memory T cells to augment Th17 responses. *Blood* (2012) 120(24):4761–71. doi:10.1182/blood-2012-04-424226
13. Elias KM, Laurence A, Davidson TS, Stephens G, Kanno Y, Shevach EM, et al. Retinoic acid inhibits Th17 polarization and enhances FoxP3 expression through a Stat-3/Stat-5 independent signaling pathway. *Blood* (2008) 111(3):1013–20. doi:10.1182/blood-2007-06-096438
14. Spiegl N, Didichenko S, McCaffery P, Langen H, Dahinden CA. Human basophils activated by mast cell-derived IL-3 express retinaldehyde dehydrogenase-II and produce the immunoregulatory mediator retinoic acid. *Blood* (2008) 112(9):3762–71. doi:10.1182/blood-2008-01-135251
15. Sharma M, Stephen-Victor E, Poncet P, Kaveri SV, Bayry J. Basophils are inept at promoting human Th17 responses. *Hum Immunol* (2015) 76(2–3):176–80. doi:10.1016/j.humimm.2014.12.015
16. Dong C. TH17 cells in development: an updated view of their molecular identity and genetic programming. *Nat Rev Immunol* (2008) 8(5):337–48. doi:10.1038/nri2295
17. Noack M, Miossec P. Th17 and regulatory T cell balance in autoimmune and inflammatory diseases. *Autoimmun Rev* (2014) 13(6):668–77. doi:10.1016/j.autrev.2013.12.004
18. Denzel A, Maus UA, Rodriguez Gomez M, Moll C, Niedermeier M, Winter C, et al. Basophils enhance immunological memory responses. *Nat Immunol* (2008) 9(7):733–42. doi:10.1038/ni.1621
19. Chen K, Xu W, Wilson M, He B, Miller NW, Bengten E, et al. Immunoglobulin D enhances immune surveillance by activating antimicrobial, proinflammatory and B cell-stimulating programs in basophils. *Nat Immunol* (2009) 10(8):889–98. doi:10.1038/ni.1748
20. Yoshimoto T, Yasuda K, Tanaka H, Nakahira M, Imai Y, Fujimori Y, et al. Basophils contribute to T(H)2-IgE responses in vivo via IL-4 production and presentation of peptide-MHC class II complexes to CD4+ T cells. *Nat Immunol* (2009) 10(7):706–12. doi:10.1038/ni.1737
21. Hibbs ML, Tarlinton DM, Armes J, Grail D, Hodgson G, Maglitto R, et al. Multiple defects in the immune system of Lyn-deficient mice, culminating in autoimmune disease. *Cell* (1995) 83(2):301–11. doi:10.1016/0092-8674(95)90171-X
22. Kaveri SV, Mouthon L, Bayry J. Basophils and nephritis in lupus. *N Engl J Med* (2010) 363(11):1080–2. doi:10.1056/NEJMcibr1006936
23. Charles N, Hardwick D, Daugas E, Illei GG, Rivera J. Basophils and the T helper 2 environment can promote the development of lupus nephritis. *Nat Med* (2010) 16(6):701–7. doi:10.1038/nm.2159
24. Hochberg MC. Updating the American College of Rheumatology revised criteria for the classification of systemic lupus erythematosus. *Arthritis Rheum* (1997) 40(9):1725. doi:10.1002/art.1780400928
25. Gladman DD, Ibanez D, Urowitz MB. Systemic lupus erythematosus disease activity index 2000. *J Rheumatol* (2002) 29(2):288–91.
26. Torrero MN, Larson D, Hubner MP, Mitre E. CD200R surface expression as a marker of murine basophil activation. *Clin Exp Allergy* (2009) 39(3):361–9. doi:10.1111/j.1365-2222.2008.03154.x
27. Gomez MR, Talke Y, Hofmann C, Ketelsen I, Hermann F, Reich B, et al. Basophils control T-cell responses and limit disease activity in experimental murine colitis. *Mucosal Immunol* (2014) 7(1):188–99. doi:10.1038/mi.2013.38
28. Meretey K, Bohm U, Falus A, Bozsoky S. Radioimmune double PEG precipitation technique for detecting complexed IgE. *J Immunol Methods* (1979) 26(3):223–8. doi:10.1016/0022-1759(79)90247-3
29. Haas M. IgG subclass deposits in glomeruli of lupus and nonlupus membranous nephropathies. *Am J Kidney Dis* (1994) 23(3):358–64. doi:10.1016/S0272-6386(12)80997-8
30. Sharma M, Hegde P, Aimanianda V, Beau R, Maddur MS, Senechal H, et al. Circulating human basophils lack the features of professional antigen presenting cells. *Sci Rep* (2013) 3:1188. doi:10.1038/srep01188
31. Kabakov AE, Tertov VV, Saenko VA, Poverenny AM, Orekhov AN. The atherogenic effect of lupus sera: systemic lupus erythematosus-derived immune complexes stimulate the accumulation of cholesterol in cultured smooth muscle cells from human aorta. *Clin Immunol Immunopathol* (1992) 63(3):214–20. doi:10.1016/0090-1229(92)90225-D
32. Laffer S, Lupinek C, Rauter I, Kneidinger M, Drescher A, Jordan JH, et al. A high-affinity monoclonal anti-IgE antibody for depletion of IgE and IgE-bearing cells. *Allergy* (2008) 63(6):695–702. doi:10.1111/j.1398-9995.2008.01664.x
33. Ennis M. Basophil models of homeopathy: a sceptical view. *Homeopathy* (2010) 99(1):51–6. doi:10.1016/j.homp.2009.11.005
34. Allan LL, Hoefl K, Zheng DJ, Chung BK, Kozak FK, Tan R, et al. Apolipoprotein-mediated lipid antigen presentation in B cells provides a pathway for innate help by NKT cells. *Blood* (2009) 114(12):2411–6. doi:10.1182/blood-2009-04-211417
35. Gauchat JF, Henchoz S, Mazzei G, Aubry JP, Brunner T, Blasey H, et al. Induction of human IgE synthesis in B cells by mast cells and basophils. *Nature* (1993) 365(6444):340–3. doi:10.1038/365340a0
36. Gauld SB, Dal Porto JM, Cambier JC. B cell antigen receptor signaling: roles in cell development and disease. *Science* (2002) 296(5573):1641–2. doi:10.1126/science.1071546
37. Warnock RA, Askari S, Butcher EC, von Andrian UH. Molecular mechanisms of lymphocyte homing to peripheral lymph nodes. *J Exp Med* (1998) 187(2):205–16. doi:10.1084/jem.187.2.205
38. Lim LH, Burdick MM, Hudson SA, Mustafa FB, Konstantopoulos K, Bochner BS. Stimulation of human endothelium with IL-3 induces selective basophil accumulation in vitro. *J Immunol* (2006) 176(9):5346–53. doi:10.4049/jimmunol.176.9.5346
39. Perry D, Sang A, Yin Y, Zheng YY, Morel L. Murine models of systemic lupus erythematosus. *J Biomed Biotechnol* (2011) 2011:271694. doi:10.1155/2011/271694
40. Karasuyama H, Mukai K, Tsujimura Y, Obata K. Newly discovered roles for basophils: a neglected minority gains new respect. *Nat Rev Immunol* (2009) 9(1):9–13. doi:10.1038/nri2458
41. MacGlashan D Jr. IgE receptor and signal transduction in mast cells and basophils. *Curr Opin Immunol* (2008) 20(6):717–23. doi:10.1016/j.coi.2008.08.004
42. Dema B, Pellefigues C, Hasni S, Gault N, Jiang C, Ricks TK, et al. Autoreactive IgE is prevalent in systemic lupus erythematosus and is associated with increased disease activity and nephritis. *PLoS One* (2014) 9(2):e90424. doi:10.1371/journal.pone.0090424
43. Atta AM, Santiago MB, Guerra FG, Pereira MM, Sousa Atta ML. Autoimmune response of IgE antibodies to cellular self-antigens in systemic lupus erythematosus. *Int Arch Allergy Immunol* (2010) 152(4):401–6. doi:10.1159/000288293

44. Yanagihara Y, Kajiwara K, Basaki Y, Ikizawa K, Ebisawa M, Ra C, et al. Cultured basophils but not cultured mast cells induce human IgE synthesis in B cells after immunologic stimulation. *Clin Exp Immunol* (1998) 111(1):136–43. doi:10.1046/j.1365-2249.1998.00474.x
45. Dienz O, Rincon M. The effects of IL-6 on CD4 T cell responses. *Clin Immunol* (2009) 130(1):27–33. doi:10.1016/j.clim.2008.08.018
46. Sokol CL, Barton GM, Farr AG, Medzhitov R. A mechanism for the initiation of allergen-induced T helper type 2 responses. *Nat Immunol* (2008) 9(3):310–8. doi:10.1038/ni1558
47. Obata K, Mukai K, Tsujimura Y, Ishiwata K, Kawano Y, Minegishi Y, et al. Basophils are essential initiators of a novel type of chronic allergic inflammation. *Blood* (2007) 110(3):913–20. doi:10.1182/blood-2007-01-068718
48. Matsuoka K, Shitara H, Taya C, Kohno K, Kikkawa Y, Yonekawa H. Novel basophil- or eosinophil-depleted mouse models for functional analyses of allergic inflammation. *PLoS One* (2013) 8(4):e60958. doi:10.1371/journal.pone.0060958
49. Wada T, Ishiwata K, Koseki H, Ishikura T, Ugajin T, Ohnuma N, et al. Selective ablation of basophils in mice reveals their nonredundant role in acquired immunity against ticks. *J Clin Invest* (2010) 120(8):2867–75. doi:10.1172/JCI42680

Conflict of Interest Statement: The authors declare that this study was conducted in the absence of any commercial or financial relationships that could be construed as a potential conflict of interest.

Copyright © 2017 Pan, Gong, Xiao, Feng, Li, Deng, Ye, Zheng, Dickerson, Ye, An, Yang and Liu. This is an open-access article distributed under the terms of the Creative Commons Attribution License (CC BY). The use, distribution or reproduction in other forums is permitted, provided the original author(s) or licensor are credited and that the original publication in this journal is cited, in accordance with accepted academic practice. No use, distribution or reproduction is permitted which does not comply with these terms.

frontiers in Immunology

REVIEW
published: 30 March 2017
doi: 10.3389/fimmu.2017.00356

T Cells in Osteoarthritis: Alterations and Beyond

*Yu-sheng Li[1,2], Wei Luo[1], Shou-an Zhu[3] and Guang-hua Lei[1]**

[1] Department of Orthopaedics, Xiangya Hospital of Central South University, Changsha, China, [2] Department of Orthopaedic Surgery, School of Medicine, Johns Hopkins University, Baltimore, MD, USA, [3] Aging and Metabolism Research Program, Oklahoma Medical Research Foundation, Oklahoma City, OK, USA

Although osteoarthritis (OA) has been traditionally regarded as a non-inflammatory disease, reports increasingly suggest that it is inflammatory, at least in certain patients. OA patients often exhibit inflammatory infiltration of synovial membranes by macrophages, T cells, mast cells, B cells, plasma cells, natural killer cells, dendritic cells, granulocytes, etc. Although previous reviews have summarized the knowledge of inflammation in the pathogenesis of OA, as far as we know, no report review our current understanding about T cells, especially, each T cell subtype, in the biology of OA. This review highlights the current understanding of the role of T cells in the pathogenesis of OA, with attention to Th1 cells, Th2 cells, Th9 cells, Th17 cells, Th22 cells, regulatory T cells, follicular helper T cells, cytotoxic T cells, T memory cells, and even unconventional T cells (e.g., γδ T cells and cluster of differentiation 1 restricted T cells). The findings highlight the importance of T cells to the development and progression of OA and suggest new therapeutic approaches for OA patients based on the manipulation of T-cell responses.

Keywords: inflammation, inflammatory diseases, osteoarthritis, T cells, Th17 cells

OPEN ACCESS

Edited by:
Jixin Zhong,
Case Western Reserve University, USA

Reviewed by:
Chang Chen,
University of Illinois at Chicago, USA
Xiaojing Yue,
La Jolla Institute for Allergy and Immunology, USA
Yanlin He,
Baylor College of Medicine, USA

****Correspondence:***
Guang-hua Lei
lgh9640@sina.cn

Specialty section:
This article was submitted to Inflammation, a section of the journal Frontiers in Immunology

Received: *09 February 2017*
Accepted: *13 March 2017*
Published: *30 March 2017*

Citation:
Li Y-s, Luo W, Zhu S-a and Lei G-h (2017) T Cells in Osteoarthritis: Alterations and Beyond. Front. Immunol. 8:356. doi: 10.3389/fimmu.2017.00356

INTRODUCTION

Affecting approximately 3.8% (95% CI: 3.6–4.1) of the global population, osteoarthritis (OA) is regarded as a prevalent cause of morbidity and disability worldwide (1). OA shows many disease characteristics, such as cartilage degradation, moderate synovial inflammation, pain, alteration of bony structure, and impaired mobility (2). However, despite the severity of the disease, relatively little is known about its exact etiology. Recent compelling investigations have attributed the onset of OA to various person-level factors such as age, sex, obesity, and diet and joint-level factors such as injury, malalignment, and abnormal joint loading (3–5). Although more and more researchers have recently presented hypotheses concerning the involvement of these factors in OA, especially for person-level factors, few of their hypotheses have been demonstrated experimentally, and some have even been challenged by the latest observational studies and clinical trials (4, 6, 7).

Of the several factors potentially involved in the pathogenesis of OA, T cell-mediated immune responses and their influence on the biology of OA are the focus of this review (8–11). The scientific community once understood OA to be induced by mechanical stress in the form of cartilage destruction, with minimal if any involvement of immune responses. Thus, OA was regarded as a non-inflammatory disease, in contrast with rheumatoid arthritis (RA), an inflammatory disease (4, 7, 12, 13). However, recent studies suggest that at least in certain patients, OA is an inflammatory disease; patients have frequently been found to exhibit inflammatory infiltration of synovial membranes (9–11). Most recent studies have shown that the number of inflammatory cells in the

synovial tissue is lower in patients with OA than in patients with RA, but higher than that in healthy subjects (14–18). Indeed, little difference has been found in the percentages of T cells, B cells, and natural killer cells in the peripheral blood between patients with OA and RA (19). Leheita et al. (19) reflected on the similarity of the immune cell profiles of RA and OA and suggested that abnormalities in T cells may also contribute to the pathogenesis of OA. Further experiments indicated that inflammation in OA is anatomically restricted and varies in intensity. The synovial membranes in regions rimming the cartilage of OA patients, which contain T cells bordered by B lymphocytes and plasma cells (20), showed a pronounced inflammatory response. In contrast, only a few infiltrating lymphocytes were observed in the synovial membranes taken from macroscopically non-inflamed areas in OA patients (20). This may explain the suggestion made by some researchers that immune responses are not involved in the pathogenesis of OA. When synovial samples from patients with knee OA were analyzed, the synovial lining cells showed strong immunoreactivity and phagocytic potential with cluster of differentiation (CD) 68 antibodies (8). These findings suggested that macrophages may be associated with the pathogenesis of knee OA. Of 20 osteoarthritic synovial membranes, 5 showed lymphoid follicles containing T cells, B cells, and macrophages, and 10 (including the latter five) displayed a diffuse cellular infiltrate containing T and B cells, macrophages, and granulocytes (21). These results suggested that B cells and granulocytes may also be involved in the pathogenesis of knee OA.

To date, various immune cells have been identified in the synovial membranes of OA patients, such as macrophages, T cells, mast cells, B cells, plasma cells, natural killer cells, dendritic cells, and granulocytes (8, 10, 22–27). For a detailed description of the infiltration of synovial tissues by immune cells, a recent review of this subject should be consulted (10). Of these inflammatory cells, macrophages and T cells most abundantly infiltrate the synovial tissues of OA patients. For example, macrophages represent approximately 65% of the immune cells that infiltrate the synovial tissues of patients with OA, and T cells make up 22% of the infiltrate (17). Although previous reviews have summarized the knowledge of inflammation in the pathogenesis of OA, as far as we know, no report reviews our current understanding about T cells, especially, each T cell subtype, in the biology of OA (9, 10, 28). More importantly, the scientific community has recently contributed to the growing literature on the involvement of T cells in the pathogenesis of OA with some interesting findings regarding the alteration of T cells during OA. Thus, this review focuses on our current understanding of the significance of T cells to OA biology.

T CELLS AND OA

Analysis of enzyme-linked immunosorbent assay (ELISA) data has shown that compared with age-matched healthy controls, patients with OA show higher levels of the soluble form of CD4 (sCD4) in their serum. This suggests that peripheral T helper (Th) cells are involved in the pathogenesis of OA (29). Similarly, when stimulated with phorbol myristate acetate (PMA) and ionomycin, peripheral mononuclear cells from OA patients showed a higher expression of CD4 and CD8 markers than their counterparts from healthy controls (30). Indeed, the ratio of $CD4^+/CD8^+$ in the blood of OA patients is higher than that in the blood of healthy controls, although healthy controls and OA patients have fairly similar numbers of $CD4^+$ and $CD8^+$ T cells in their blood (31). Further evidence of the involvement of peripheral T cells in the pathogenesis of OA was provided by the discovery that the response to autologous chondrocytes of peripheral T cells isolated from OA patients is greater than of peripheral T cells isolated from controls and that this response is partially blocked by antibodies against human leukocyte antigen (HLA) classes I and II, CD4, and CD8 (32). Interestingly, T cells in a subset of OA patients were found to recognize the peptides representing amino acid regions 16–39 and 263–282 of human cartilage proteoglycan aggrecan (PG), and peripheral blood mononuclear cells from these PG-reactive OA patients showed an increased production of pro-inflammatory cytokines/chemokines in response to PG peptide stimulation (33). Based on these compelling findings, the autoimmune responses of peripheral T cells may aid understanding of immune-mediated mechanisms in OA.

Enzyme-linked immunosorbent assay analysis revealed higher levels of sCD4 not only in the peripheral blood but also in the synovial fluid of patients with OA, compared with age-matched healthy controls, which suggests that Th cells in the synovial fluid are involved in the pathogenesis of OA (29). When stimulated with PMA and ionomycin, mononuclear cells from the synovial fluid of OA patients showed a high expression of CD4 and CD8 markers (30). These compelling results suggested that T cells in the synovial fluid are associated with the pathogenesis of OA. This conclusion was supported by subsequent investigations. For example, the percentage of T cells in the synovial fluid of OA patients was found to be significantly higher than that in their peripheral blood (34), and T cells in the synovial fluid of OA patients expressed class II HLA (an indicator of activated T cells) (35). The percentages of $CD4^+$ and $CD8^+$ cells in the synovial fluid of OA patients were even similar to those found in RA patients (31).

T cells are the major constituents of synovial infiltrates in the membranes of OA patients, and both $CD4^+$ T cells and $CD8^+$ T cells have been found within synovial aggregates (35). For example, synovial tissue extracted from OA patients displayed perivascular $CD3^+$ T cell infiltration at an early stage (36). Similarly, using immunohistochemical analysis, $CD3^+$, $CD4^+$, and $CD8^+$ T cells were detected predominantly in the sublining layer and more limitedly in the deep layer of the synovium of patients with OA, whereas the presence of $CD4^+$ T cells in the synovial sublining layer was detected more strongly in OA patients than in normal subjects (15). $CD4^+$ T cells were found to be predominant among the T-cell infiltrates in the synovial tissue, and the number of $CD4^+$ T cells was higher in the synovial sublining layer of patients with OA than in that of normal subjects. Indeed, the medial synovium of patients with knee OA has been shown to contain more $CD4^+$ T cells than the lateral synovium (8). Interestingly, synovial aggregates from OA patients express CD80, an inducible costimulatory ligand involved in T-cell activation (35, 37), suggesting that synovial aggregates in OA patients are areas of antigen recognition and T-cell activation. Similarly, researchers

investigating 30 patients with OA found $CD3^+$ T cell aggregates in the synovial membrane in 65% of the patients, and the activation antigens CD69, CD25, CD38, CD43, CD45RO, and HLA class II were also found in the synovial membrane (38). In addition, HLA-antigen D-related (DR)-expressing T cells were found in the synovial membranes of OA patients using immunohistochemical analysis, although to a lesser degree than in RA patients (39). The conclusion that activated T cells are aggregated in the synovial membranes of OA patients was further supported by the discovery that virtually all T cells in OA joints express activation markers, such as HLA-DR and CD69 (40). Interestingly, OA patients older than 75 have higher percentages of $CD3^+$, $CD4^+$, and $CD8^+$ cells in their synovial membranes than OA patients younger than 75 (41). This may suggest that age is among the risk factors for OA.

Collectively, significant abnormalities in the T-cell profile have been found in the peripheral blood, synovial fluid, and synovial membranes of OA patients. Based on these findings, T cells are assumed to be associated with the pathogenesis of OA.

Th1 and OA

Under the stimulation of interleukin (IL)-12, naïve $CD4^+$ T cells differentiate into Th1 cells, which produce IL-2, interferon (IFN)-γ, tumor necrosis factor (TNF)-α, lymphotoxins, and granulocyte-macrophage colony-stimulating factor (42–44). Most current evidence indicates that Th1 cells do not alter significantly on entering the peripheral blood of OA patients. For example, flow cytometry analysis has shown that there is little difference in the percentage of circulating Th1 cells ($CD4^+IFN\text{-}\gamma^+$ T cells) between OA patients and healthy controls (45). Similarly, no variation in either the percentage or the absolute number of circulating Th1 cells ($CD4^+IFN\text{-}\gamma^+$ T cells) has been found between patients with OA and healthy controls (46). However, in a study with 25 OA patients and 13 healthy controls, the number of circulating Th1 cells ($IFN\text{-}\gamma^+CD4^+CD8^-$ T cells) and the level of serum IFN-γ were found to be significantly higher in patients with OA than in healthy controls (47). The difference in the markers ($CD4^+IFN\text{-}\gamma^+$ vs. $IFN\text{-}\gamma^+CD4^+CD8^-$) used in the two studies to define Th1 cells may account for this discrepancy. Another explanation may lie in the variation between OA patients, such as differences between the stages of OA. The alteration of the Th1 cell profile in the peripheral blood of OA patients thus requires further investigation.

In contrast with the findings for peripheral blood, the synovial fluid of OA patients shows an increase in Th1 cells. Although early experiments suggested that the concentrations of IL-2, IFN-γ, and TNF-β in the synovial fluid of OA patients are below the limit of detection by ELISA analysis (48), reverse transcription polymerase chain reaction (RT-PCR) analysis has since revealed that cells from the synovial fluid of OA patients express IL-2 and IFN-γ when stimulated with PHA and ionomycin (35). Indeed, intracellular IFN-γ has been detected at higher levels in both $CD4^+$ and $CD8^+$ cells from the synovial fluid than in the peripheral blood of OA patients (30). In addition, high concentrations of IL-1β and TNF-α have been observed in the synovial fluid of patients with OA, whereas these markers are below the limit of detection in healthy subjects (31).

Th1 cells can also be found in the synovial membranes of OA patients. For example, IL-2, IFN-γ, and their receptors are usually detected in the synovial membranes of OA patients (38, 49). Similarly, $INF\text{-}\gamma^+$ cells have been detected in the synovial membranes of patients with OA, predominantly in the sublining layer of the synovium, although to a lesser degree than in RA patients (15). In a mouse model of OA induced by anterior cruciate ligament transection (ACLT), the expression of IFN-γ increased during OA onset (30 days after ACLT) and then decreased at a later stage of OA (90 days after ACLT) (50). Most importantly, a well-designed study showed that Th1 cells are predominant in both OA and RA joints (40). Indeed, the number of $IFN\text{-}\gamma^+$ cells in the synovium of patients with OA is approximately five times greater than that of $IL\text{-}4^+$ cells (15).

In summary, although the profile of Th1 cells in the peripheral blood requires further analysis, Th1 cells have been shown to accumulate in the synovial fluid and synovial membranes of OA patients, which suggests that Th1 cells play important roles in the pathogenesis of OA. In addition, Th1 cell responses in the synovial fluid and synovial membranes of OA patients may be a marker of OA disease activity.

Th2 and OA

When stimulated by IL-4, naïve $CD4^+$ T cells differentiate into Th2 cells (44). Through the production of IL-4, IL-5, IL-10, and IL-13, Th2 cells affect the function of B cells, dendritic cells, eosinophils, etc. and play important roles in the host's defense against multicellular parasites and in the pathogenesis of allergies (42, 43, 51–54). Most recent studies have shown that Th2 cells undergo limited alteration in the peripheral blood, synovial fluid, and synovial membranes of OA patients. For example, in a study of 18 OA patients, the IL-10 transcript was found in nearly all of the patients using competitive PCR analysis, whereas IL-4 and IL-5 were not detected in the synovial membranes of any of the patients (38). Similarly, the concentrations of IL-4 and IL-10 in the synovial fluid were below the limit of detection by ELISA analysis (48). Using flow cytometry analysis, low concentrations of Th2 cytokines such as IL-4 and IL-10 were detected in both the synovial fluid and the peripheral blood of OA patients (30). Although cells from the synovial fluid of OA patients stimulated with PHA and ionomycin expressed IL-10 at 48 h poststimulation, no signal for IL-4 was detected by RT-PCR analysis (35). The observed expression of IL-10 in OA patients' synovial membranes or synovial fluid cells may come from other cells, such as regulatory T cells (Treg cells).

Together, although these compelling findings suggest that Th2 responses play only a limited role in the pathogenesis of OA, further strong evidence is needed to support this hypothesis.

Th9 and OA

Th9 cells, recently defined as subsets of Th cells, preferentially produce IL-9 (44, 55–57). Th9 cells facilitate immune responses against melanoma and intestinal worms and are closely associated with the immunopathology of allergic and autoimmune responses, such as systemic lupus erythematosus (SLE), experimental autoimmune encephalitis, and systemic sclerosis (55–57).

Th9 cells are also involved in the pathogenesis of arthritis. For example, a high level of IL-9 has been detected in the peripheral blood and synovial fluid of patients with RA and patients with psoriatic arthritis (PsA), and the level of IL-9 in the synovial fluid is higher than that in the peripheral blood for RA and PsA patients (58). Similarly, activated $CD3^+$ T cells from the peripheral blood and synovial fluid of patients with PsA or RA produce high levels of IL-9 (58). These results suggest that Th9 cells play critical roles in the pathogenesis of RA and PsA. Indeed, Th9 responses have also been observed in OA. For example, a high level of IL-9 has been detected in the peripheral blood and synovial fluid of OA patients, and the activation of purified $CD3^+$ cells from the peripheral blood and synovial fluid of patients with OA produces a high level of IL-9, although lower than that observed in RA or PsA patients (58). Even more importantly, in a study with 25 OA patients and 13 healthy controls, the number of circulating Th9 cells and serum IL-9 level were found to be significantly higher in OA patients than in healthy controls (47). This study also found that the number of circulating Th9 cells was positively associated with the level of C-reactive protein in OA patients and that both the number of Th9 cells and the level of serum IL-9 were positively correlated with OA index (47).

In summary, these well-designed experiments lead to the conclusion that Th9 cells significantly shape the pathogenesis of OA, as well as that of RA and PsA; however, the Th9 response in the synovial membranes of OA patients needs further investigation. In addition, serum IL-9 or the number of circulating Th9 cells may be a marker of OA disease activity.

Th17 and OA

Th17 cells secrete IL-17A (also known as IL-17), IL-17F, IL-21, and IL-22. Transform growth factor (TGF)-β, IL-6, IL-1β, and IL-23 have been reported to promote the differentiation of Th17 cells (44, 59–63). Th17 cells provide protection against bacterial infection and are associated with the development of autoimmune diseases *via* the recruitment of cells in the granulocyte lineage, especially neutrophils (64–67). Early investigations indicated that neither the percentages of circulating pure Th17 cells ($CD4^+$ IFN-γ^-IL-22^-IL-17^+ T cells) and Th17 cells ($CD4^+$IL-17^+ T cells) nor the level of serum IL-17 differed significantly between OA patients and healthy controls (45). Similarly, no variation in the percentage or absolute number of circulating Th17 cells or the IL-17 plasma level was found between patients with OA and healthy controls (46). These findings indicated that little alteration occurs in the Th17 cell profile in the peripheral blood of OA patients. However, later observations suggested otherwise. In a rat model of OA induced by the injection of papain and L-cysteine into the right knee joint, the OA rats were found to have a higher serum IL-17 level than the control rats (68). In addition, in a study with 25 OA patients and 13 healthy controls, the number of circulating Th17 cells and the level of serum IL-17 were found to be significantly higher in patients with OA than in healthy controls (47). As in the case of Th1 cells, variation in the markers used to define Th17 cells ($CD4^+$IL-17^+ vs. IL-$17^+CD4^+CD8^-$) and the patients selected for investigation (e.g., diagnosis standard, disease index, patients' background) may account for this discrepancy. These controversial findings regarding Th17 cell profile in the peripheral blood of OA patients suggest that the roles of circulating Th17 cells in the pathogenesis of OA need further investigation. Nevertheless, it is widely accepted that Th17 cells are present in the synovial fluid and synovial membranes of OA patients. For example, in addition to the strong expression of IL-17 mRNA in the synovial membranes of OA patients (69), a high level of IL-17 has been measured in the synovial fluid of OA patients, whereas both are below the limit of detection in healthy subjects (31, 70). In addition, Th17 cells have been detected in the joints of OA patients, albeit in smaller numbers than in RA joints (40).

Collectively, these interesting results demonstrate the accumulation of Th17 cells in the synovial fluid and synovial tissue of OA patients; however, the exact role of Th17 cell response in the biology of OA needs further investigation.

Th22 and OA

Originally, IL-22 was regarded as a product of Th17 cells; however, recent evidence has indicated that a distinct subset of human skin $CD4^+$ T cells (Th22) produces IL-22 but not IL-17 or IFN-γ (71). Increasing evidence has been provided for the involvement of Th22 cells in the biology of RA. For example, the percentage of Th22 cells is higher in RA patients than in healthy controls, and the percentage of Th22 cells is positively correlated with IL-22 expression in RA patients (45). In addition, the percentage of Th22 cells is positively correlated with both C-reactive protein levels and joint disease activity scores in RA patients (45). These compelling discoveries indicate that Th22 response is associated with the pathogenesis of RA and that blocking IL-22 expression may be a reasonable therapeutic strategy for RA. Th22 cells are also involved in the biology of ankylosing spondylitis. Similar to the results for RA, the percentage and absolute number of circulating Th22 cells were found to be elevated in patients with ankylosing spondylitis compared with healthy controls (46). Similarly, ELISA analysis revealed that the level of IL-22 in the plasma was higher in patients with ankylosing spondylitis than in healthy controls (46). However, Th22 cells seem to play a limited role in the pathogenesis of OA. For example, compared with healthy controls, OA patients show no change in the percentage of circulating Th22 cells ($CD4^+$ IFN-γ^-IL-17^-IL-22^+ T cells) and the level of IL-22 in the plasma (45). Similarly, another independent experiment revealed that neither the percentage nor the absolute number of circulating Th22 cells, nor the plasma level of IL-22, differ between patients with OA and healthy controls (46).

Collectively, unlike RA and ankylosing spondylitis, OA involves only a limited alteration of Th22 response in the peripheral blood; however, we lack data on the Th22 profile in the synovial fluid and synovial tissue of OA patients.

Treg Cells and OA

Under the influence of TGF-β, naïve T cells differentiate into Treg cells, which produce IL-10 and TGF-β (43, 72–74). Treg cells are important immunoregulators in many inflammatory and autoimmune diseases, as they modulate the secretion of anti-inflammatory cytokines and the expression of receptors for cytokines (75). For example, RA patients have a lower

percentage of Treg cells at sites of synovial inflammation and in the peripheral blood (76), which may induce the downregulation of T-cell tolerance and exacerbate the inflammatory process. Increasing evidence has been provided that the profile of Treg cells in the peripheral blood, synovial fluid, and synovial membranes of OA patients is similar to that of RA patients. For example, the percentage and absolute number of Treg cells ($CD4^+CD25^{+/high}CD127^{-/low}$) in the peripheral blood, synovial fluid, and synovial membranes are similar in RA patients and OA patients, and Treg cells in both cases show greater accumulation in the synovial fluid and synovial membranes than in the peripheral blood (77). In addition, Treg cells in the peripheral blood, synovial fluid, and synovial membranes of both OA patients and RA patients display a memory phenotype ($CD45RO^+RA^-$) (77). Neither does the activation status (CD69 and CD62L) nor the expression of markers associated with Treg function (CD152, CD154, CD274, CD279, and GITR) in the peripheral blood, synovial fluid, or synovial membranes differ between OA patients and RA patients (77). Those compelling results indicate that as in the case of RA, a decrease in Treg-cell responses is involved in the pathogenesis of OA. Indeed, Ponchel et al. (11) analyzed blood from 121 healthy controls and 114 OA patients and found that the OA patients had fewer Treg cells than the healthy controls after adjusting for age (11). Although the frequency of $CD4^+CD25^+Foxp3^+$ Treg cells has been found to be elevated in the blood of OA patients, OA patients show lower IL-10 secretion from Treg cells and fewer Tim-3^+ Treg cells in the blood (78). Similarly, in a rat model of OA induced by the injection of papain and L-cysteine into the right knee joint, the percentage of $CD4^+CD25^+Foxp3^+$ Treg cells in the peripheral blood was significantly lower in the OA rats than in the control rats (68).

In summary, a decrease in Treg-cell response may be involved in the pathogenesis of OA; however, the alteration of Treg-cell responses in the peripheral blood, synovial fluid, and synovial membranes of OA patients requires more comparative investigation with age-matched healthy controls.

Follicular Helper T (Tfh) Cells and OA

Follicular helper T cells, located in the follicles of lymphoid tissue, induce B cells to produce immunoglobulins (79). Tfh cells express various distinguishing genes, such as CXCR5, PD-1, ICOS, CD40L, Bcl-6, and IL-21 (80). Increasing evidence has been provided for the influence of Tfh cells on the severity of autoimmune diseases, such as SLE and RA. For example, the number of circulating Tfh cells ($CXCR5^+ICOS^+CD4^+$ cells or $CXCR5^+PD\text{-}1^+CD4^+$ cells) has been shown to increase in a subset of SLE patients in line with the diversity and concentration of autoantibodies and SLE severity (81). Similarly, immunohistochemistry analysis has revealed specific staining for CD4, CXCR5, and ICOS on infiltrating immune cells in the synovial tissues of RA patients, and the presence of Tfh cells ($CD4^+CXCR5^+ICOS^+$ T cells) in the synovial tissues of RA patients has been verified using both triple-fluorescence immunostaining and confocal laser scanning (82). This study provided evidence of the presence of Tfh cells in both SLE and RA patients, indicating the potentially important roles played by Tfh cells in the pathogenesis and progression of both diseases. However, the results of immunohistochemistry analysis, triple-fluorescence immunostaining, and confocal laser scanning revealed that Tfh cells are absent from the synovial tissues of OA patients (82). Yet, a recent investigation demonstrated the importance of Tfh cells to the pathogenesis and progression of OA. In the latter study, the frequency of $ICOS^+$, PD-1^+, and IL-21^+ $CXCR5^+CD4^+$ T cells in the peripheral blood of 40 patients with OA and 13 healthy controls was examined by flow cytometry, and the concentration of serum IL–21 was also determined. Compared with the healthy controls, the OA patients showed higher percentages of $CXCR5^+CD4^+$, PD-$1^+CXCR5^+CD4^+$, $ICOS^+CXCR5^+CD4^+$, and IL-$21^+CXCR5^+CD4^+$ T cells (83). Shan et al. (83) also found that OA patients exhibited higher levels of serum IL-21 than healthy controls and, even more importantly, that the expression of IL-21^+Tfh cells in OA patients was positively correlated with the disease activity of OA (83). The latter study suggests that Tfh cells play a critical role in the pathogenesis and progression of OA. However, further well-designed research is needed to characterize Tfh cell profile in the peripheral blood, synovial fluid, and synovial membranes of OA patients.

Cytotoxic T Cells and OA

The peripheral blood of OA patients has been analyzed using flow cytometry, revealing that patients with OA have significantly fewer $CD8^+$ T cells and a higher $CD4^+$:$CD8^+$ ratio than healthy subjects (84). However, patients with OA have normal proportions of $CD8^+CD45RA^+$, $CD8^+CD29^+$, and $CD8^+S6F1^+$ cells in both their peripheral blood and their synovial fluid (85). These results indicate the alteration of peripheral $CD8^+$ T cells in OA patients. Although $CD8^+$ T cells can be found in the synovial membranes of OA patients, the major component of the T-cell infiltrate cannot. Most of the T cells found in the synovial membranes of patients with OA are helper T cells, whereas cytotoxic T cells occur sparsely in patients with OA (39, 86). Similarly, fewer $CD8^+$ T cells than $CD4^+$ T cells have been found in the lining, the sublining, and even the deep layer of the synovium of patients with OA (15). In addition, although both $CD4^+$ and $CD8^+$ T cells have been found in the synovial aggregates of OA patients, the aggregates contain a larger proportion of $CD4^+$ T cells than of $CD8^+$ T cells, and the $CD8^+$ T cells are often located toward the periphery of the aggregates (35). $CD8^+$ T cells play an important role in the pathogenesis of OA, although they are not the predominant T-cell type found in the synovial aggregates of OA patients. In mice with ACLT-induced OA, $CD8^+$ T cells were activated once OA had been initiated, and the percentage of activated $CD8^+$ T cells was significantly higher in the ACLT group than in the sham group during OA progression (87). In addition, the number of $CD8^+$ T cells expressing tissue inhibitor of metalloproteinase-1 (TIMP-1) was found to be correlated with OA severity and inhibiting the expression of TIMP-1 in the joints retarded the progression of OA (87). Cartilage degeneration occurred more slowly in $CD8^+$ T cell knockout mice than in wild-type mice (87).

In summary, a significant alteration to $CD8^+$ T cells has been observed in the peripheral blood, the synovial fluid, and the synovial membranes, and $CD8^+$ T cells have been found to significantly shape the pathogenesis of OA, although they do not play the most important role in the process.

T Memory (Tm) Cells and OA

Once activated, most T cells undergo apoptosis; however, a minority persist as Tm cells. An increasing number of researchers have begun to investigate the profile of Tm cells in the pathogenesis of OA. For example, although healthy individuals showed no difference in the percentages of $CD45RO^+CD4^+$ T cells and $CD45RA^+CD4^+$ T cells in the peripheral blood, more $CD45RO^+$ cells than $CD45RA^+$ cells were found in the peripheral blood of patients with OA (88). In patients with OA, the majority of $CD4^+$ T cells in the synovial fluid and synovial tissue are $CD45RO^+$ and $CD45RA^-$, suggesting that an accumulation of $CD45RO^+$ memory $CD4^+$ T cells is a generalized phenomenon in OA joints (88). Similarly, a study with 25 OA patients and 13 healthy controls revealed that the number of circulating $CD4^+CD45RO^+$ T cells was significantly higher in patients with OA than in healthy controls (47). Other evidence for the possible involvement of Tm cells in the pathogenesis of OA includes the detection of the regulated on activation, normal T cell expressed, and secreted chemokine (a potent chemoattractant for leukocytes, such as $CD45RO^+$ memory T cells) and CD29 (a 1 integrin expressed by Tm cells) in the synovial fluid of OA patients (35, 37, 89).

In summary, $CD45RO^+$ memory $CD4^+$ T cells seem to be critical to the biology of OA, yet their exact roles in the pathogenesis of OA have yet to be determined.

Unconventional T Cells and OA

Recent investigations have also highlighted the involvement of unconventional T cells in the pathogenesis of OA. For example, more and more evidence has been provided that γδ T cells are involved in the pathogenesis of RA. For example, the number of γδ T cells has been found to increase in the synovial membranes of RA patients (90–93), and γδ T cells in the synovial membranes have more and/or more avid Fc receptors for immunoglobulin G IgG in patients with RA compared with controls (90). Further research has shown that the majority of synovial γδ T cells in RA patients do not express Vγ9, Vδ2, or Vδ1-Jγδ1 (91). However, most recent studies have indicated that the number of γδ T cells in the synovial membranes of patients with OA does not increase (91–93). Immunohistochemical staining of synovial tissue with early-stage OA shows T-cell infiltration in the perivascular area, with the clonality of restricted T cell receptor usage in the V beta chain (36), which also indicates the minimal alteration of γδ T cells in OA patients. Recent studies have shown that the synovial membranes of OA patients express CD1 (94), which presents non-protein antigens to NKT cells, suggesting that CD1-restricted T cells may play a role in the pathogenesis of OA.

Overall, although numerous studies of the involvement of conventional T cells in OA have been conducted, it will be useful to determine the importance to OA of unconventional T cells such as CD1-restricted T cells, MR1-restricted mucosal-associated invariant T cells, major histocompatibility complex class Ib-reactive T cells, and γδ T cells (95).

CONCLUSION

Various risk factors for OA have been proposed, ranging from person-level factors such as age, sex, and obesity, to joint-level factors such as injury, malalignment, and abnormal loading of

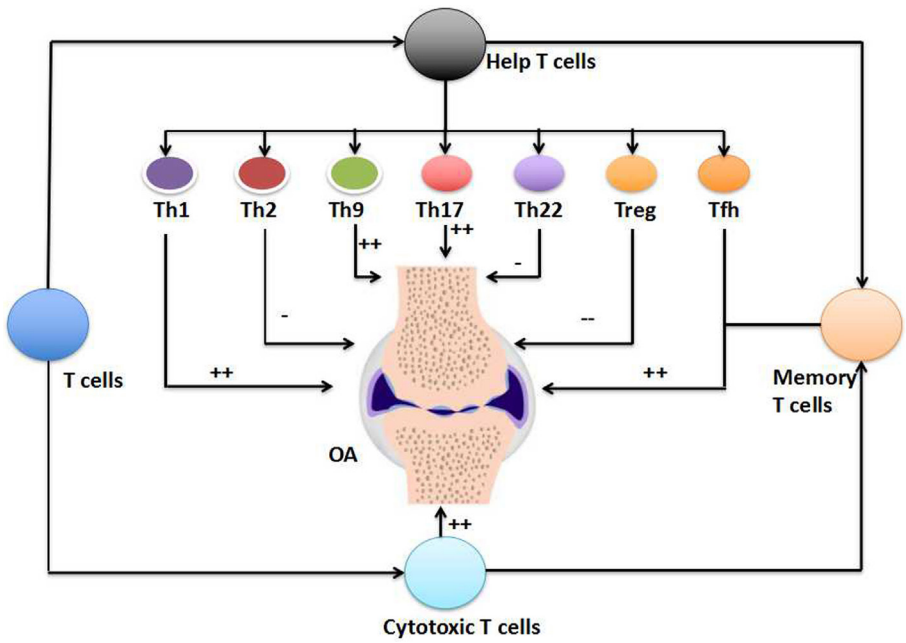

FIGURE 1 | The involvement of T cells in the pathogenesis of osteoarthritis (OA). T cells, including the T helper (Th) cells, cytotoxic T cells, and T memory (Tm) cells, have critical importance in the pathogenesis of OA (++). The involvement of unconventional T cells in the pathogenesis of OA is not shown here. Within T helper (Th) cells, Th1 cells, Th9 cells, Th17 cells, and follicular helper T (Tfh) cells increase in the peripheral blood, synovial fluid, or synovial membranes of OA patients (++). The numbers of cytotoxic T cells and Tm cells also increase in the OA. However, the numbers of Th2 cells and Th22 cells show limited alteration in the pathogenesis of OA (–), but the number of Treg cells decrease during the OA (––).

TABLE 1 | The alteration of Th subset cells in OA.

T cells	Cytokines produced by T cells	Alterations in the OA		Reference
Th1 cells	IL-2, IFN-γ, TNF-α	Peripheral blood	No	(45, 46)
		Synovial fluid	Increase	(30, 31, 35)
		Synovial membrane	Increase	(15, 38, 40, 49, 50)
Th2 cells	IL-4, IL-5, IL-10, IL-13	Peripheral blood	No	(30)
		Synovial fluid	No	(30, 35, 48)
		Synovial membrane	No	(38)
Th9 cells	IL-9	Peripheral blood	Increase	(47, 58)
		Synovial fluid	Increase	(58)
		Synovial membrane	–	
Th17 cells	IL-17A, IL-17F, IL-21, IL-22	Peripheral blood	No	(45, 46)
			Increase	(47, 68)
		Synovial fluid	Increase	(31, 70)
		Synovial membrane	Increase	(40, 69)
Th22 cells	IL-22	Peripheral blood	No	(45, 46)
		Synovial fluid	–	
		Synovial membrane	–	
Treg cells	IL-10, TGF-β	Peripheral blood	Decrease	(11, 68, 78)
		Synovial fluid	–	
		Synovial membrane	–	
Follicular Helper T cells	CXCR5, PD-1, CD40L, Bcl-6, IL-21	Peripheral blood	Increase	(83)
		Synovial fluid	–	
		Synovial membrane	No	(82)
Cytotoxic T cells		Peripheral blood	Decrease	(84)
			No[a]	(85)
		Synovial fluid	No[a]	(85)
		Synovial membrane	Increase	(15, 35, 39, 86)

IL, interleukin; IFN, interferon; TNF, tumor necrosis factor; TGF, transform growth factor; CXCR5, C-X-C chemokine receptor type 5; PD-1, programmed death 1; –, further investigations are needed; OA, osteoarthritis; Th, T helper; Treg, regulatory T.
[a]$CD8^+CD45RA^+$, $CD8^+CD29^+$, and $CD8^+S6F1^+$ cells.

joints (3–5). Increasing evidence has also been provided that inflammation is associated with the development and progression of OA, at least in certain patients. OA patients often exhibit the infiltration of synovial membranes by inflammatory cells such as macrophages, T cells, mast cells, B cells, plasma cells, natural killer cells, dendritic cells, and granulocytes (8–11). Several scholars have investigated the alteration of T cells during the pathogenesis of OA, with reference to Th1 cells, Th2 cells, Th9 cells, Th17 cells, Th22 cells, Treg cells, Tfh cells, cytotoxic T cells, Tm cells, and even unconventional T cells (e.g., γδ T cells and CD1-restricted T cells). To date, it has been widely accepted that a significant alteration occurs in the profiles of Th1 cells, Th9 cells, Th17 cells, Treg cells, cytotoxic T cells, and Tm cells in the peripheral blood, synovial fluid, and synovial membranes of OA patients (**Figure 1**; **Table 1**). However, the involvement of Th2 cells, Th22 cells, Tfh cells, and unconventional T cells in the pathogenesis of OA needs further investigation (**Figure 1**; **Table 1**). In addition, the causal relationship between the alteration of T-cell responses and the development and progression of OA has yet to be identified. Various factors such as extracellular stimulation (e.g., antigens), intracellular signaling [e.g., mTOR complex 1 (mTORC1)], and cell metabolism (e.g., amino acid metabolism) are significant determinants of the fate of T cells (54, 66, 96–100). Therefore, it will be interesting to manipulate these factors to determine their precise effects on the development and progression of OA. For example, mTORC1 is known to regulate Th17 differentiation and IL-17 expression through several pathways, including STAT3, HIF-1α, S6K1, and S6K2, which raises the possibility of regulating the pathogenesis of OA through mTORC1 signaling (66). Indeed, the great importance of mTORC1 signaling to the pathogenesis of OA has recently been highlighted (101). The metabolism and transportation of amino acids also have a remarkable influence on T-cell activation and differentiation, especially for Th1 and Th17 cells, suggesting that amino acid metabolism also affects the pathogenesis of OA. Indeed, the establishment and development of OA are associated with alterations in the metabolism and profile of amino acids such as those of the glutamate and arginine families, as well as their related metabolites (e.g., creatinine, hydroxyproline, γ-aminobutyrate, dimethylarginines, and homoarginine) (4). Furthermore, intestinal microbiota have vital roles in T-cell responses, especially those of Th17 cells (102, 103), indicating the critical functions of intestinal microbiota in the pathogenesis of OA. Indeed, intestinal microbiota have been proposed as a risk factor in the development and progression of OA (7, 104). Understanding the significance of the altered T-cell profile to the pathogenesis of OA will open up novel directions for preventing and treating OA by modulating T-cell responses.

AUTHOR CONTRIBUTIONS

Y-sL and G-hL conceived this study. Y-sL wrote the manuscript. WL and S-aZ provided critical discussion in manuscript preparation. G-hL revised the manuscript.

ACKNOWLEDGMENTS

We thank Prof. Ping Yu (Department of Immunology, Xiangya School of Medicine, Central South University) for her constructive comments. This work was supported by the National Natural Science Foundation of China (No. 814721308, 81402224, and 81401838), the Provincial Science Foundation of Hunan (No. 2015JJ3139), the Key Research and Development Program of Hunan Province (2016JC2038), the Health and Family Planning Commission of Hunan Province (B2014-12), the Administration of Traditional Chinese Medicine of Hunan Province (No.2015116), and the China Scholarship Council (student ID: 201606375101).

REFERENCES

1. Cross M, Smith E, Hoy D, Nolte S, Ackerman I, Fransen M, et al. The global burden of hip and knee osteoarthritis: estimates from the global burden of disease 2010 study. *Ann Rheum Dis* (2014) 73(7):1323–30. doi:10.1136/annrheumdis-2013-204763

2. Bingham CO III, Buckland-Wright JC, Garnero P, Cohen SB, Dougados M, Adami S, et al. Risedronate decreases biochemical markers of cartilage degradation but does not decrease symptoms or slow radiographic progression in patients with medial compartment osteoarthritis of the knee: results of the two-year multinational knee osteoarthritis structural arthritis study. *Arthritis Rheum* (2006) 54(11):3494–507. doi:10.1002/art.22160

3. Felson DT, Lawrence RC, Dieppe PA, Hirsch R, Helmick CG, Jordan JM, et al. Osteoarthritis: new insights. Part 1: the disease and its risk factors. *Ann Intern Med* (2000) 133(8):635–46. doi:10.7326/0003-4819-133-8-200010170-00016
4. Li Y, Xiao W, Luo W, Zeng C, Deng Z, Ren W, et al. Alterations of amino acid metabolism in osteoarthritis: its implications for nutrition and health. *Amino Acids* (2016) 48(4):907–14. doi:10.1007/s00726-015-2168-x
5. Malfait AM. Osteoarthritis year in review 2015: biology. *Osteoarthritis Cartilage* (2016) 24(1):21–6. doi:10.1016/j.joca.2015.09.010
6. Zhang F, Luo W, Li Y, Gao S, Lei G. Role of osteopontin in rheumatoid arthritis. *Rheumatol Int* (2015) 35(4):589–95. doi:10.1007/s00296-014-3122-z
7. Li Y, Luo W, Deng Z, Lei G. Diet-intestinal microbiota axis in osteoarthritis: a possible role. *Mediators Inflamm* (2016) 2016:3495173. doi:10.1155/2016/3495173
8. Saito I, Koshino T, Nakashima K, Uesugi M, Saito T. Increased cellular infiltrate in inflammatory synovia of osteoarthritic knees. *Osteoarthritis Cartilage* (2002) 10(2):156–62. doi:10.1053/joca.2001.0494
9. Sakkas LI, Platsoucas CD. The role of T cells in the pathogenesis of osteoarthritis. *Arthritis Rheum* (2007) 56(2):409–24. doi:10.1002/art.22369
10. de Lange-Brokaar BJ, Ioan-Facsinay A, van Osch GJ, Zuurmond AM, Schoones J, Toes RE, et al. Synovial inflammation, immune cells and their cytokines in osteoarthritis: a review. *Osteoarthritis Cartilage* (2012) 20(12):1484–99. doi:10.1016/j.joca.2012.08.027
11. Ponchel F, Burska AN, Hensor EM, Raja R, Campbell M, Emery P, et al. Changes in peripheral blood immune cell composition in osteoarthritis. *Osteoarthritis Cartilage* (2015) 23(11):1870–8. doi:10.1016/j.joca.2015.06.018
12. Hugle T, Geurts J. What drives osteoarthritis? – synovial versus subchondral bone pathology. *Rheumatology (Oxford)* (2016). doi:10.1093/rheumatology/kew389
13. Withrow J, Murphy C, Liu Y, Hunter M, Fulzele S, Hamrick MW. Extracellular vesicles in the pathogenesis of rheumatoid arthritis and osteoarthritis. *Arthritis Res Ther* (2016) 18(1):286. doi:10.1186/s13075-016-1178-8
14. Fonseca JE, Edwards JC, Blades S, Goulding NJ. Macrophage subpopulations in rheumatoid synovium: reduced CD163 expression in CD4+ T lymphocyte-rich microenvironments. *Arthritis Rheum* (2002) 46(5):1210–6. doi:10.1002/art.10207
15. Ishii H, Tanaka H, Katoh K, Nakamura H, Nagashima M, Yoshino S. Characterization of infiltrating T cells and Th1/Th2-type cytokines in the synovium of patients with osteoarthritis. *Osteoarthritis Cartilage* (2002) 10(4):277–81. doi:10.1053/joca.2001.0509
16. Diaz-Torne C, Schumacher HR, Yu X, Gomez-Vaquero C, Dai L, Chen LX, et al. Absence of histologic evidence of synovitis in patients with Gulf War veterans' illness with joint pain. *Arthritis Rheum* (2007) 57(7):1316–23. doi:10.1002/art.23006
17. Pessler F, Chen LX, Dai L, Gomez-Vaquero C, Diaz-Torne C, Paessler ME, et al. A histomorphometric analysis of synovial biopsies from individuals with Gulf War Veterans' Illness and joint pain compared to normal and osteoarthritis synovium. *Clin Rheumatol* (2008) 27(9):1127–34. doi:10.1007/s10067-008-0878-0
18. Rollin R, Marco F, Jover JA, Garcia-Asenjo JA, Rodriguez L, Lopez-Duran L, et al. Early lymphocyte activation in the synovial microenvironment in patients with osteoarthritis: comparison with rheumatoid arthritis patients and healthy controls. *Rheumatol Int* (2008) 28(8):757–64. doi:10.1007/s00296-008-0518-7
19. Leheita O, Abed Elrazek NY, Younes S, Mahmoud AZ. Lymphocytes subsets in osteoarthritis versus rheumatoid arthritis. *Egypt J Immunol* (2005) 12(2):113–24.
20. Lindblad S, Hedfors E. Arthroscopic and immunohistologic characterization of knee joint synovitis in osteoarthritis. *Arthritis Rheum* (1987) 30(10):1081–8. doi:10.1002/art.1780301001
21. Revell PA, Mayston V, Lalor P, Mapp P. The synovial membrane in osteoarthritis: a histological study including the characterisation of the cellular infiltrate present in inflammatory osteoarthritis using monoclonal antibodies. *Ann Rheum Dis* (1988) 47(4):300–7. doi:10.1136/ard.47.4.300
22. Kummer JA, Tak PP, Brinkman BM, van Tilborg AA, Kamp AM, Verweij CL, et al. Expression of granzymes A and B in synovial tissue from patients with rheumatoid arthritis and osteoarthritis. *Clin Immunol Immunopathol* (1994) 73(1):88–95. doi:10.1006/clin.1994.1173
23. Pettit AR, Ahern MJ, Zehntner S, Smith MD, Thomas R. Comparison of differentiated dendritic cell infiltration of autoimmune and osteoarthritis synovial tissue. *Arthritis Rheum* (2001) 44(1):105–10. doi:10.1002/1529-0131(200101)44:1<105:AID-ANR14>3.0.CO;2-3
24. Benito MJ, Veale DJ, FitzGerald O, van den Berg WB, Bresnihan B. Synovial tissue inflammation in early and late osteoarthritis. *Ann Rheum Dis* (2005) 64(9):1263–7. doi:10.1136/ard.2004.025270
25. Da RR, Qin Y, Baeten D, Zhang Y. B cell clonal expansion and somatic hypermutation of Ig variable heavy chain genes in the synovial membrane of patients with osteoarthritis. *J Immunol* (2007) 178(1):557–65. doi:10.4049/jimmunol.178.1.557
26. Nakano S, Mishiro T, Takahara S, Yokoi H, Hamada D, Yukata K, et al. Distinct expression of mast cell tryptase and protease activated receptor-2 in synovia of rheumatoid arthritis and osteoarthritis. *Clin Rheumatol* (2007) 26(8):1284–92. doi:10.1007/s10067-006-0495-8
27. Lebre MC, Jongbloed SL, Tas SW, Smeets TJ, McInnes IB, Tak PP. Rheumatoid arthritis synovium contains two subsets of CD83-DC-LAMP- dendritic cells with distinct cytokine profiles. *Am J Pathol* (2008) 172(4):940–50. doi:10.2353/ajpath.2008.070703
28. Sakkas LI, Platsoucas CD. Role of T cells in the pathogenesis of osteoarthritis. *Arthritis Rheum* (2002) 46(11):3112–3. doi:10.1002/art.10483
29. Symons JA, McCulloch JF, Wood NC, Duff GW. Soluble CD4 in patients with rheumatoid arthritis and osteoarthritis. *Clin Immunol Immunopathol* (1991) 60(1):72–82. doi:10.1016/0090-1229(91)90113-O
30. Dolganiuc A, Stavaru C, Anghel M, Georgescu E, Chichos B, Olinescu A. Shift toward T lymphocytes with Th1 and Tc1 cytokine-secterion profile in the joints of patients with osteoarthritis. *Roum Arch Microbiol Immunol* (1999) 58(3–4):249–58.
31. Hussein MR, Fathi NA, El-Din AM, Hassan HI, Abdullah F, Al-Hakeem E, et al. Alterations of the CD4(+), CD8 (+) T cell subsets, interleukins-1beta, IL-10, IL-17, tumor necrosis factor-alpha and soluble intercellular adhesion molecule-1 in rheumatoid arthritis and osteoarthritis: preliminary observations. *Pathol Oncol Res* (2008) 14(3):321–8. doi:10.1007/s12253-008-9016-1
32. Sakata M, Masuko-Hongo K, Nakamura H, Onuma H, Tsuruha JI, Aoki H, et al. Osteoarthritic articular chondrocytes stimulate autologous T cell responses in vitro. *Clin Exp Rheumatol* (2003) 21(6):704–10.
33. de Jong H, Berlo SE, Hombrink P, Otten HG, van Eden W, Lafeber FP, et al. Cartilage proteoglycan aggrecan epitopes induce proinflammatory autoreactive T-cell responses in rheumatoid arthritis and osteoarthritis. *Ann Rheum Dis* (2010) 69(1):255–62. doi:10.1136/ard.2008.103978
34. van de Putte LB, Meijer CJ, Lafeber GJ, Kleinjan R, Cats A. Lymphocytes in rheumatoid and nonrheumatoid synovial fluids. Nonspecificity of high T-cell and low B-cell percentages. *Ann Rheum Dis* (1975) 35(5):451–5. doi:10.1136/ard.35.5.451
35. Haynes MK, Hume EL, Smith JB. Phenotypic characterization of inflammatory cells from osteoarthritic synovium and synovial fluids. *Clin Immunol* (2002) 105(3):315–25. doi:10.1006/clim.2002.5283
36. Nakamura H, Yoshino S, Kato T, Tsuruha J, Nishioka K. T-cell mediated inflammatory pathway in osteoarthritis. *Osteoarthritis Cartilage* (1999) 7(4):401–2. doi:10.1053/joca.1998.0224
37. Sanders ME, Makgoba MW, Sharrow SO, Stephany D, Springer TA, Young HA, et al. Human memory T lymphocytes express increased levels of three cell adhesion molecules (LFA-3, CD2, and LFA-1) and three other molecules (UCHL1, CDw29, and Pgp-1) and have enhanced IFN-gamma production. *J Immunol* (1988) 140(5):1401–7.
38. Sakkas LI, Scanzello C, Johanson N, Burkholder J, Mitra A, Salgame P, et al. T cells and T-cell cytokine transcripts in the synovial membrane in patients with osteoarthritis. *Clin Diagn Lab Immunol* (1998) 5(4):430–7.
39. Johnell O, Hulth A, Henricson A. T-lymphocyte subsets and HLA-DR-expressing cells in the osteoarthritic synovialis. *Scand J Rheumatol* (1985) 14(3):259–64. doi:10.3109/03009748509100403
40. Yamada H, Nakashima Y, Okazaki K, Mawatari T, Fukushi J, Oyamada A, et al. Preferential accumulation of activated Th1 cells not only in rheumatoid arthritis but also in osteoarthritis joints. *J Rheumatol* (2011) 38(8):1569–75. doi:10.3899/jrheum.101355
41. Pawlowska J, Mikosik A, Soroczynska-Cybula M, Jozwik A, Luczkiewicz P, Mazurkiewicz S, et al. Different distribution of CD4 and CD8 T cells in synovial membrane and peripheral blood of rheumatoid arthritis and

osteoarthritis patients. *Folia Histochem Cytobiol* (2009) 47(4):627–32. doi:10.2478/v10042-009-0117-9
42. Chen K, Kolls JK. T cell-mediated host immune defenses in the lung. *Annu Rev Immunol* (2013) 31:605–33. doi:10.1146/annurev-immunol-032712-100019
43. Raphael I, Nalawade S, Eagar TN, Forsthuber TG. T cell subsets and their signature cytokines in autoimmune and inflammatory diseases. *Cytokine* (2014) 74:5–17. doi:10.1016/j.cyto.2014.09.011
44. Ren W, Liu G, Chen S, Yin J, Wang J, Tan B, et al. Melatonin signaling in T cells: functions and applications. *J Pineal Res* (2017) 62(3):e12394. doi:10.1111/jpi.12394
45. Zhang L, Li JM, Liu XG, Ma DX, Hu NW, Li YG, et al. Elevated Th22 cells correlated with Th17 cells in patients with rheumatoid arthritis. *J Clin Immunol* (2011) 31(4):606–14. doi:10.1007/s10875-011-9540-8
46. Zhang L, Li YG, Li YH, Qi L, Liu XG, Yuan CZ, et al. Increased frequencies of Th22 cells as well as Th17 cells in the peripheral blood of patients with ankylosing spondylitis and rheumatoid arthritis. *PLoS One* (2012) 7(4):e31000. doi:10.1371/journal.pone.0031000
47. Qi C, Shan Y, Wang J, Ding F, Zhao D, Yang T, et al. Circulating T helper 9 cells and increased serum interleukin-9 levels in patients with knee osteoarthritis. *Clin Exp Pharmacol Physiol* (2016) 43(5):528–34. doi:10.1111/1440-1681.12567
48. Partsch G, Wagner E, Leeb BF, Broll H, Dunky A, Smolen JS. T cell derived cytokines in psoriatic arthritis synovial fluids. *Ann Rheum Dis* (1998) 57(11):691–3. doi:10.1136/ard.57.11.691
49. Dolhain RJ, ter Haar NT, Hoefakker S, Tak PP, de Ley M, Claassen E, et al. Increased expression of interferon (IFN)-gamma together with IFN-gamma receptor in the rheumatoid synovial membrane compared with synovium of patients with osteoarthritis. *Br J Rheumatol* (1996) 35(1):24–32. doi:10.1093/rheumatology/35.1.24
50. Shen PC, Wu CL, Jou IM, Lee CH, Juan HY, Lee PJ, et al. T helper cells promote disease progression of osteoarthritis by inducing macrophage inflammatory protein-1gamma. *Osteoarthritis Cartilage* (2011) 19(6):728–36. doi:10.1016/j.joca.2011.02.014
51. Chapoval S, Dasgupta P, Dorsey NJ, Keegan AD. Regulation of the T helper cell type 2 (Th2)/T regulatory cell (Treg) balance by IL-4 and STAT6. *J Leukoc Biol* (2010) 87(6):1011–8. doi:10.1189/jlb.1209772
52. Vahedi G, Poholek AC, Hand TW, Laurence A, Kanno Y, O'Shea JJ, et al. Helper T-cell identity and evolution of differential transcriptomes and epigenomes. *Immunol Rev* (2013) 252(1):24–40. doi:10.1111/imr.12037
53. Ren W, Wang K, Yin J, Chen S, Liu G, Tan B, et al. Glutamine-induced secretion of intestinal secretory immunoglobulin A: a mechanistic perspective. *Front Immunol* (2016) 7:503. doi:10.3389/fimmu.2016.00503
54. Wu M, Xiao H, Liu G, Chen S, Tan B, Ren W, et al. Glutamine promotes intestinal SIgA secretion through intestinal microbiota and IL-13. *Mol Nutr Food Res* (2016) 60(7):1637–48. doi:10.1002/mnfr.201600026
55. Pan HF, Leng RX, Li XP, Zheng SG, Ye DQ. Targeting T-helper 9 cells and interleukin-9 in autoimmune diseases. *Cytokine Growth Factor Rev* (2013) 24(6):515–22. doi:10.1016/j.cytogfr.2013.09.001
56. Zhao P, Xiao X, Ghobrial RM, Li XC. IL-9 and Th9 cells: progress and challenges. *Int Immunol* (2013) 25(10):547–51. doi:10.1093/intimm/dxt039
57. Schmitt E, Klein M, Bopp T. Th9 cells, new players in adaptive immunity. *Trends Immunol* (2014) 35(2):61–8. doi:10.1016/j.it.2013.10.004
58. Kundu-Raychaudhuri S, Abria C, Raychaudhuri SP. IL-9, a local growth factor for synovial T cells in inflammatory arthritis. *Cytokine* (2016) 79:45–51. doi:10.1016/j.cyto.2015.12.020
59. Ivanov II, Zhou L, Littman DR. Transcriptional regulation of Th17 cell differentiation. *Semin Immunol* (2007) 19(6):409–17. doi:10.1016/j.smim.2007.10.011
60. Wilson NJ, Boniface K, Chan JR, McKenzie BS, Blumenschein WM, Mattson JD, et al. Development, cytokine profile and function of human interleukin 17-producing helper T cells. *Nat Immunol* (2007) 8(9):950–7. doi:10.1038/ni1497
61. McGeachy MJ, Cua DJ. Th17 cell differentiation: the long and winding road. *Immunity* (2008) 28(4):445–53. doi:10.1016/j.immuni.2008.03.001
62. Shabgah AG, Fattahi E, Shahneh FZ. Interleukin-17 in human inflammatory diseases. *Postepy Dermatol Alergol* (2014) 31(4):256–61. doi:10.5114/pdia.2014.40954
63. Floss DM, Schroder J, Franke M, Scheller J. Insights into IL-23 biology: from structure to function. *Cytokine Growth Factor Rev* (2015) 26(5):569–78. doi:10.1016/j.cytogfr.2015.07.005
64. Miossec P, Kolls JK. Targeting IL-17 and TH17 cells in chronic inflammation. *Nat Rev Drug Discov* (2012) 11(10):763–76. doi:10.1038/nrd3794
65. Ren W, Chen S, Zhang L, Liu G, Hussain T, Hao X, et al. Interferon tau affects mouse intestinal microbiota and expression of IL-17. *Mediators Inflamm* (2016) 2016:2839232. doi:10.1155/2016/2839232
66. Ren W, Yin J, Duan J, Liu G, Tan B, Yang G, et al. mTORC1 signaling and IL-17 expression: defining pathways and possible therapeutic targets. *Eur J Immunol* (2016) 46(2):291–9. doi:10.1002/eji.201545886
67. Xiao DF, Ren WK, Bin P, Chen S, Yin J, Gao W, et al. Chitosan lowers body weight through intestinal microbiota and reduces IL-17 expression via mTOR signalling. *J Funct Foods* (2016) 22:166–76. doi:10.1016/j.jff.2016.01.009
68. Guo SY, Ding YJ, Li L, Zhang T, Zhang ZZ, Zhang ES. Correlation of CD(4)(+) CD(2)(5)(+) Foxp(3)(+) Treg with the recovery of joint function after total knee replacement in rats with osteoarthritis. *Genet Mol Res* (2015) 14(3):7290–6. doi:10.4238/2015.July.3.4
69. Chabaud M, Durand JM, Buchs N, Fossiez F, Page G, Frappart L, et al. Human interleukin-17: a T cell-derived proinflammatory cytokine produced by the rheumatoid synovium. *Arthritis Rheum* (1999) 42(5):963–70. doi:10.1002/1529-0131(199905)42:5<963:AID-ANR15>3.0.CO;2-E
70. Sarkar S, Justa S, Brucks M, Endres J, Fox DA, Zhou X, et al. Interleukin (IL)-17A, F and AF in inflammation: a study in collagen-induced arthritis and rheumatoid arthritis. *Clin Exp Immunol* (2014) 177(3):652–61. doi:10.1111/cei.12376
71. Trifari S, Kaplan CD, Tran EH, Crellin NK, Spits H. Identification of a human helper T cell population that has abundant production of interleukin 22 and is distinct from T(H)-17, T(H)1 and T(H)2 cells. *Nat Immunol* (2009) 10(8):864–71. doi:10.1038/ni.1770
72. Hori S, Nomura T, Sakaguchi S. Control of regulatory T cell development by the transcription factor Foxp3. *Science* (2003) 299(5609):1057–61. doi:10.1126/science.1079490
73. Bommireddy R, Doetschman T. TGFbeta1 and Treg cells: alliance for tolerance. *Trends Mol Med* (2007) 13(11):492–501. doi:10.1016/j.molmed.2007.08.005
74. Carrier Y, Yuan J, Kuchroo VK, Weiner HL. Th3 cells in peripheral tolerance. I. Induction of Foxp3-positive regulatory T cells by Th3 cells derived from TGF-beta T cell-transgenic mice. *J Immunol* (2007) 178(1):179–85. doi:10.4049/jimmunol.178.1.179
75. Miyara M, Sakaguchi S. Natural regulatory T cells: mechanisms of suppression. *Trends Mol Med* (2007) 13(3):108–16. doi:10.1016/j.molmed.2007.01.003
76. Yudoh K, Matsuno H, Nakazawa F, Yonezawa T, Kimura T. Reduced expression of the regulatory CD4+ T cell subset is related to Th1/Th2 balance and disease severity in rheumatoid arthritis. *Arthritis Rheum* (2000) 43(3):617–27. doi:10.1002/1529-0131(200003)43:3<617:AID-ANR19>3.0.CO;2-B
77. Moradi B, Schnatzer P, Hagmann S, Rosshirt N, Gotterbarm T, Kretzer JP, et al. CD4(+)CD25(+)/highCD127low/(-) regulatory T cells are enriched in rheumatoid arthritis and osteoarthritis joints – analysis of frequency and phenotype in synovial membrane, synovial fluid and peripheral blood. *Arthritis Res Ther* (2014) 16(2):R97. doi:10.1186/ar4545
78. Li S, Wan J, Anderson W, Sun H, Zhang H, Peng X, et al. Downregulation of IL-10 secretion by Treg cells in osteoarthritis is associated with a reduction in Tim-3 expression. *Biomed Pharmacother* (2016) 79:159–65. doi:10.1016/j.biopha.2016.01.036
79. Ueno H, Banchereau J, Vinuesa CG. Pathophysiology of T follicular helper cells in humans and mice. *Nat Immunol* (2015) 16(2):142–52. doi:10.1038/ni.3054
80. Crotty S. Follicular helper CD4 T cells (TFH). *Annu Rev Immunol* (2011) 29:621–63. doi:10.1146/annurev-immunol-031210-101400
81. Simpson N, Gatenby PA, Wilson A, Malik S, Fulcher DA, Tangye SG, et al. Expansion of circulating T cells resembling follicular helper T cells is a fixed phenotype that identifies a subset of severe systemic lupus erythematosus. *Arthritis Rheum* (2010) 62(1):234–44. doi:10.1002/art.25032
82. Chu Y, Wang F, Zhou M, Chen L, Lu Y. A preliminary study on the characterization of follicular helper T (Tfh) cells in rheumatoid arthritis synovium. *Acta Histochem* (2014) 116(3):539–43. doi:10.1016/j.acthis.2013.10.009

83. Shan Y, Qi C, Liu Y, Gao H, Zhao D, Jiang Y. Increased frequency of peripheral blood follicular helper T cells and elevated serum IL21 levels in patients with knee osteoarthritis. *Mol Med Rep* (2017) 15(3):1095–102. doi:10.3892/mmr.2017.6132
84. Kuryliszyn-Moskal A. Comparison of blood and synovial fluid lymphocyte subsets in rheumatoid arthritis and osteoarthritis. *Clin Rheumatol* (1995) 14(1):43–50. doi:10.1007/BF02208083
85. Sohen S, Romain PL, Rothstein DM, Yamane T, Tanaka S, Anderson P, et al. Phenotypic abnormalities in CD8+ T lymphocyte subsets in patients with rheumatoid arthritis. *J Rheumatol* (1991) 18(11):1649–54.
86. Reidbord HE, Osial TA Jr. Synovial lymphocyte subsets in rheumatoid arthritis and degenerative joint disease. *J Rheumatol* (1987) 14(6):1089–94.
87. Hsieh JL, Shiau AL, Lee CH, Yang SJ, Lee BO, Jou IM, et al. CD8+ T cell-induced expression of tissue inhibitor of metalloproteinses-1 exacerbated osteoarthritis. *Int J Mol Sci* (2013) 14(10):19951–70. doi:10.3390/ijms141019951
88. Ezawa K, Yamamura M, Matsui H, Ota Z, Makino H. Comparative analysis of CD45RA- and CD45RO-positive CD4+T cells in peripheral blood, synovial fluid, and synovial tissue in patients with rheumatoid arthritis and osteoarthritis. *Acta Med Okayama* (1997) 51(1):25–31.
89. Volin MV, Shah MR, Tokuhira M, Haines GK, Woods JM, Koch AE. RANTES expression and contribution to monocyte chemotaxis in arthritis. *Clin Immunol Immunopathol* (1998) 89(1):44–53. doi:10.1006/clin.1998.4590
90. Mathieu A, Mereu MC, Pisano L. T gamma lymphocytes of peripheral blood and synovial fluid in rheumatoid arthritis: quantitative determination and qualitative analysis. *Arthritis Rheum* (1981) 24(5):658–61. doi:10.1002/art.1780240505
91. Andreu JL, Trujillo A, Alonso JM, Mulero J, Martinez C. Selective expansion of T cells bearing the gamma/delta receptor and expressing an unusual repertoire in the synovial membrane of patients with rheumatoid arthritis. *Arthritis Rheum* (1991) 34(7):808–14. doi:10.1002/art.1780340705
92. Jacobs MR, Haynes BF. Increase in TCR gamma delta T lymphocytes in synovia from rheumatoid arthritis patients with active synovitis. *J Clin Immunol* (1992) 12(2):130–8. doi:10.1007/BF00918143
93. Meliconi R, Uguccioni M, D'Errico A, Cassisa A, Frizziero L, Facchini A. T-cell receptor gamma-delta positive lymphocytes in synovial membrane. *Br J Rheumatol* (1992) 31(1):59–61. doi:10.1093/rheumatology/31.1.59
94. Cauli A, Pitzalis C, Yanni G, Awad M, Panayi GS. CD1 expression in psoriatic and rheumatoid arthritis. *Rheumatology (Oxford)* (2000) 39(6):666–73. doi:10.1093/rheumatology/39.6.666
95. Godfrey DI, Uldrich AP, McCluskey J, Rossjohn J, Moody DB. The burgeoning family of unconventional T cells. *Nat Immunol* (2015) 16(11):1114–23. doi:10.1038/ni.3298
96. Ren W, Chen S, Yin J, Duan J, Li T, Liu G, et al. Dietary arginine supplementation of mice alters the microbial population and activates intestinal innate immunity. *J Nutr* (2014) 144(6):988–95. doi:10.3945/jn.114.192120
97. Ren W, Duan J, Yin J, Liu G, Cao Z, Xiong X, et al. Dietary L-glutamine supplementation modulates microbial community and activates innate immunity in the mouse intestine. *Amino Acids* (2014) 46(10):2403–13. doi:10.1007/s00726-014-1793-0
98. Ren W, Yin J, Duan J, Liu G, Zhu X, Chen S, et al. Mouse intestinal innate immune responses altered by enterotoxigenic *Escherichia coli* (ETEC) infection. *Microbes Infect* (2014) 16(11):954–61. doi:10.1016/j.micinf.2014.09.005
99. Ren W, Yin J, Wu M, Liu G, Yang G, Xion Y, et al. Serum amino acids profile and the beneficial effects of L-arginine or L-glutamine supplementation in dextran sulfate sodium colitis. *PLoS One* (2014) 9(2):e88335. doi:10.1371/journal.pone.0088335
100. Ren W, Yin J, Chen S, Duan J, Liu G, Li T, et al. Proteome analysis for the global proteins in the jejunum tissues of enterotoxigenic *Escherichia coli* -infected piglets. *Sci Rep* (2016) 6:25640. doi:10.1038/srep25640
101. Perl A. Activation of mTOR (mechanistic target of rapamycin) in rheumatic diseases. *Nat Rev Rheumatol* (2016) 12(3):169–82. doi:10.1038/nrrheum.2015.172
102. Honda K, Littman DR. The microbiota in adaptive immune homeostasis and disease. *Nature* (2016) 535(7610):75–84. doi:10.1038/nature18848
103. Thaiss CA, Zmora N, Levy M, Elinav E. The microbiome and innate immunity. *Nature* (2016) 535(7610):65–74. doi:10.1038/nature18847
104. Huang Z, Kraus VB. Does lipopolysaccharide-mediated inflammation have a role in OA? *Nat Rev Rheumatol* (2016) 12(2):123–9. doi:10.1038/nrrheum.2015.158

Conflict of Interest Statement: The authors declare that the research was conducted in the absence of any commercial or financial relationships that could be construed as a potential conflict of interest.

Copyright © 2017 Li, Luo, Zhu and Lei. This is an open-access article distributed under the terms of the Creative Commons Attribution License (CC BY). The use, distribution or reproduction in other forums is permitted, provided the original author(s) or licensor are credited and that the original publication in this journal is cited, in accordance with accepted academic practice. No use, distribution or reproduction is permitted which does not comply with these terms.

frontiers in Immunology

ORIGINAL RESEARCH
published: 18 December 2017
doi: 10.3389/fimmu.2017.01793

The Fos-Related Antigen 1–JUNB/Activator Protein 1 Transcription Complex, a Downstream Target of Signal Transducer and Activator of Transcription 3, Induces T Helper 17 Differentiation and Promotes Experimental Autoimmune Arthritis

Young-Mee Moon[1†], Seon-Yeong Lee[1†], Seung-Ki Kwok[2†], Seung Hoon Lee[1†], Deokhoon Kim[3,4], Woo Kyung Kim[5], Yang-Mi Her[1], Hea-Jin Son[1], Eun-Kyung Kim[1], Jun-Geol Ryu[1], Hyeon-Beom Seo[1], Jeong-Eun Kwon[1], Sue-Yun Hwang[6], Jeehee Youn[7], Rho H. Seong[8], Dae-Myung Jue[9], Sung-Hwan Park[2], Ho-Youn Kim[2], Sung-Min Ahn[10†] and Mi-La Cho[1*†]*

[1]Laboratory of Immune Network, The Rheumatism Research Center, College of Medicine, Catholic Research Institute of Medical Science, The Catholic University of Korea, Seoul, South Korea, [2]Center for Rheumatic Disease, Division of Rheumatology, Department of Internal Medicine, Seoul St. Mary's Hospital, College of Medicine, The Catholic University of Korea, Seoul, South Korea, [3]Asan Institute for Life Sciences, University of Ulsan College of Medicine, Asan Medical Center, Seoul, South Korea, [4]Department of Pathology, Asan Medical Center, University of Ulsan College of Medicine, Seoul, South Korea, [5]Department of Developmental Biology, Washington University School of Medicine, St. Louis, MO, United States, [6]Department of Chemical Engineering, Hankyong National University, Anseong, South Korea, [7]Department of Biomedical Sciences, College of Medicine, Hanyang University, Seoul, South Korea, [8]Department of Biological Sciences, Institute of Molecular Biology and Genetics, Research Center for Functional Cellulomics, Seoul National University, Seoul, South Korea, [9]Department of Biochemistry, College of Medicine, The Catholic University of Korea, Seoul, South Korea, [10]Department of Hemato-oncology, Bioinformatics, Cancer Research, Systems Biology, Gachon University, Seongnam, South Korea

Dysfunction of T helper 17 (Th17) cells leads to chronic inflammatory disorders. Signal transducer and activator of transcription 3 (STAT3) orchestrates the expression of proinflammatory cytokines and pathogenic cell differentiation from interleukin (IL)-17-producing Th17 cells. However, the pathways mediated by STAT3 signaling are not fully understood. Here, we observed that Fos-related antigen 1 (FRA1) and JUNB are directly involved in STAT3 binding to sites in the promoters of *Fosl1* and *Junb*. Promoter binding increased expression of IL-17 and the development of Th17 cells. Overexpression of *Fra1* and *Junb* in mice resulted in susceptibility to collagen-induced arthritis and an increase in Th17 cell numbers and inflammatory cytokine production. In patients with rheumatoid arthritis, FRA1 and JUNB were colocalized with STAT3 in the inflamed synovium. These observations suggest that FRA1 and JUNB are associated closely with STAT3 activation, and that this activation leads to Th17 cell differentiation in autoimmune diseases and inflammation.

Keywords: Fos-related antigen 1-JUNB, signal transducer and activator of transcription 3, T helper 17, autoimmune arthritis, inflammation

OPEN ACCESS

Edited by:
Guixiu Shi,
Xiamen University, China

Reviewed by:
Yebin Zhou,
MedImmune, United States
Yinghong Hu,
Emory University, United States

****Correspondence:***
Sung-Min Ahn
smahn@gachon.ac.kr;
Mi-La Cho
iammila@catholic.ac.kr

[†]These authors have contributed equally to this work.

Specialty section:
This article was submitted to Inflammation, a section of the journal Frontiers in Immunology

Received: *11 September 2017*
Accepted: *30 November 2017*
Published: *18 December 2017*

Citation:
Moon Y-M, Lee S-Y, Kwok S-K, Lee SH, Kim D, Kim WK, Her Y-M, Son H-J, Kim E-K, Ryu J-G, Seo H-B, Kwon J-E, Hwang S-Y, Youn J, Seong RH, Jue D-M, Park S-H, Kim H-Y, Ahn S-M and Cho M-L (2017) The Fos-Related Antigen 1–JUNB/Activator Protein 1 Transcription Complex, a Downstream Target of Signal Transducer and Activator of Transcription 3, Induces T Helper 17 Differentiation and Promotes Experimental Autoimmune Arthritis. Front. Immunol. 8:1793. doi: 10.3389/fimmu.2017.01793

INTRODUCTION

T helper 17 (Th17) cells are a pathogenic subset of T helper lymphocytes that play a key role in inflammatory disorders leading to a severe chronic immune inflammatory response. Th17 cells release several proinflammatory cytokines including interleukin (IL)-17A, IL-21, and IL-22 (1). IL-17A is an inflammatory cytokine produced predominantly by Th17 cells with strong effects on stromal cells. IL-17A induces inflammatory cytokine production and leukocyte recruitment, which act to link the innate and adaptive branches of immunity (2). Both IL-17A and Th17 cells are highly involved in the pathogenesis of several autoimmune diseases, including rheumatoid arthritis (RA) (3, 4), while playing a significant role in autoimmune disorders mediated by excessive inflammation.

Signal transducer and activator of transcription 3 (STAT3) is an important transcription factor with DNA-binding properties whose activity is paramount to the inflammatory response. It has been suggested that STAT3 activation upregulates IL-17 production *via* Th17 cell proliferation (5, 6). Several transcription factors including STAT3 regulate Th17 cell differentiation (7–12); however, STAT3 also plays a key role in the immune inflammatory response. There is a general consensus that STAT3 is essential for Th17 cell differentiation (13). Moreover, STAT3 modulates the production of several cytokines including IL-17A and activates downstream transcription factors, such as RAR-related orphan receptor gamma isoform 2 (RORγt), which is responsible for the Th17 phenotype (14, 15).

The activator protein 1 (AP-1) family is a group of structurally and functionally related JUN (c-JUN, JUNB, and JUND) and FOS [c-FOS, FOSB, Fos-related antigen 1 (FRA1), and FRA2] transcription factors. AP-1 heterodimers are involved in a variety of biological processes including cell proliferation, differentiation, apoptosis, and inflammation (16, 17). It has been suggested that AP-1 proteins are involved in several pathological conditions (18–21), while JUN and FOS proteins are also associated with the immune inflammatory response. Modulation of c-FOS and c-JUN expression is critical for inhibition of IL-17 production (22) and the maintenance of suppressive regulatory T-cell function (23). Additionally, production of FRA1, a member of the FOS protein family, is increased by B cell stimulation (24). Furthermore, JUNB modulates the proliferation of B cells (25). This evidence suggests that FRA1 and JUNB may be involved in regulating the inflammatory immune response.

We hypothesized that FRA1 and JUNB modulate the Th17 cell-mediated inflammatory response. The aim of this study was to elucidate whether FRA1 and JUNB regulate autoimmune arthritis *via* Th17 cell differentiation and factors downstream of STAT3. We used *in vitro* models, *in vivo* animal models, and clinical specimens from patients with RA to investigate the biological importance of this pathway.

MATERIALS AND METHODS

Mice

Collagen-induced arthritis (CIA) was induced in 6–8-week-old male DBA/1J, BALB/c, and C57BL/6 mice (Orient, Korea). To generate *Fra1/Junb* Tg mice, a pcDNA3.1+HA (Invitrogen, CA, USA) vector containing the FRA1 and JUNB proteins coupled to a linker peptide (3 × GGGGS) was constructed. The *Fra1/Junb* fragment was synthesized by GenScript Corporation (NJ, USA), with codon optimization for expression in mammalian cells. *Fra1/Junb* Tg mice were bred from the C57BL/6 line and maintained in facilities at Macrogen Laboratories (Seoul, Korea). All mice were maintained under specific-pathogen-free conditions at the Institute of Medical Science, The Catholic University of Korea. The presence of the transgene in the founders was confirmed by PCR of genomic DNA extracted from the tail samples. Genotyping was performed by PCR analysis of genomic DNA obtained from mice at 3 weeks of age. All experimental procedures were examined and approved by the Animal Research Ethics Committee at the Catholic University of Korea.

Accession Codes

Raw RNA-seq data have been deposited in the NCBI Sequence Read Archive (SRR6320798 and SRR6320799).

A detailed description of all other experimental procedures and the statistical analysis is provided in the Section "Supplementary Materials and Methods" in Data Sheet S1 in Supplementary Material.

RESULTS

STAT3 Target Genes Are Differentially Expressed in Mouse Th17 Cells

Potential STAT3-binding sites were identified using publicly available chromatin immunoprecipitation sequencing (ChIP-Seq) data cross-referenced with differentially expressed genes in Th17 cells (14). We sequenced mRNA obtained from Th17 cells and naïve T cells and compared the results with potential STAT3-binding targets identified by ChIP-Seq to identify STAT3-regulated genes involved in Th17 cell differentiation. The literature was systematically reviewed for downstream STAT3 targets in humans and mice in multiple biological contexts. By combining these three datasets, we searched for genes with STAT3-binding sites that are upregulated during Th17 cell differentiation (**Figure 1A**; Table S1 in Supplementary Material). RNA-Seq was performed to identify genes differentially expressed between Th17 cells and naïve T cells. This integrated approach suggested that *Fosl1* (the gene locus of *Fra1*) and *Junb* are Th17 cell differentiation factors downstream of STAT3. As shown in **Figures 1B–F** and Table S2 in Supplementary Material, *Fos* and *Jun* were the predominant AP-1 subtypes expressed in naïve ($CD4^+CD62L^+$) T cells, whereas *Fosl1* and *Junb* were the predominant subtypes in Th17 cells. Other AP-1 subtypes were downregulated, suggesting that *Fosl1* and *Junb* AP-1 subtypes play an important role in Th17 cell differentiation.

Fra1 and *Junb* Are Highly Expressed in Th17 Cells, and Their Expression Is Regulated Directly by STAT3 in Mice

Quantitative real-time reverse transcription PCR (qRT-PCR) and immunoblot analyzes were used to confirm *Fra1* and *Junb*

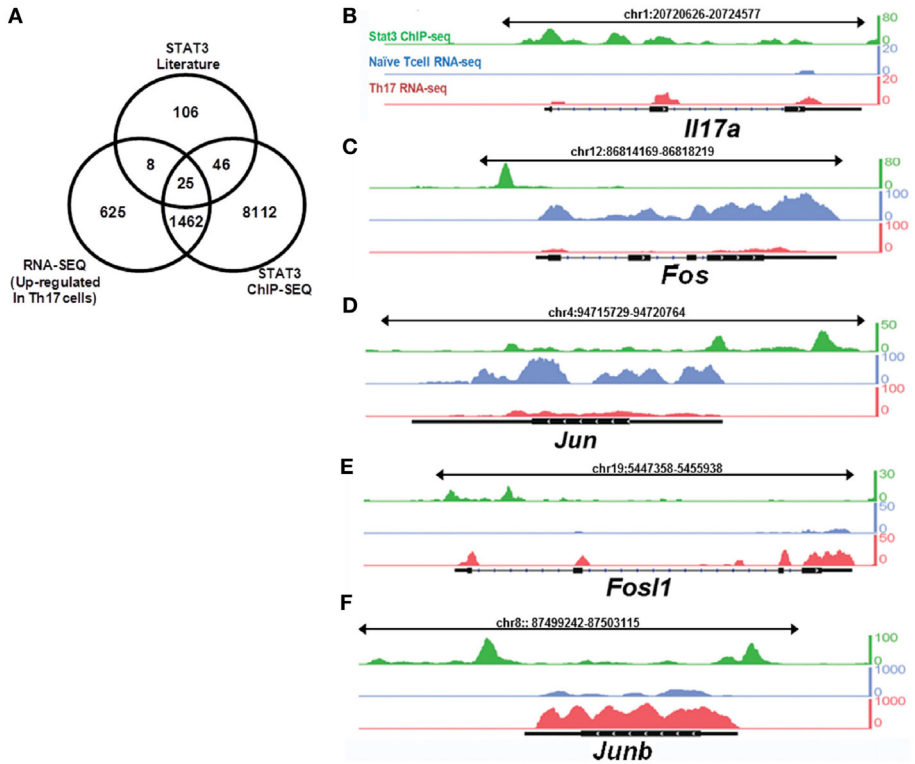

FIGURE 1 | Signal transducer and activator of transcription 3 (STAT3) target genes are differentially expressed in naïve and T helper 17 (Th17) cells. Naïve T cells ($CD4^+CD62L^+$) were isolated from 6-week-old mice ($n = 3$), stimulated under Th17-polarizing conditions for 3 days, and then sorted for $CD4^+CD62L^-$ expression. RNA was sequenced using the Illumina GA IIx. STAT3 chromatin immunoprecipitation sequencing (ChIP-Seq) data for $CD4^+$ T cells were downloaded from the NCBI Sequence Read Archive (SRP002451). **(A)** A comparison of differentially expressed genes identified by RNA-Seq, STAT3-binding target genes identified by ChIP-Seq, and the downstream targets of STAT3. The expression of **(B)** *Il17a* and **(C–F)** activator protein 1 transcription factor target genes [**(C)** *Fos*, **(D)** *Jun*, **(E)** *Fosl1*, and **(F)** *Junb*] was compared between naïve T cells and Th17 cells, with reference to STAT3-binding target genes (obtained from STAT3 ChIP-Seq data in Th17 cells). The peak profiles are color-coded as follows: naïve T cells (RNA-Seq: blue), Th17 cells (RNA-Seq: red), and STAT3-binding genes (ChIP-Seq: green).

expression. Among the various AP-1 subtypes, only *Fra1* and *Junb* mRNA levels were significantly increased in Th17 cells compared with naive T cells (**Figures 2A,B**). These findings supported the RNA-Seq results. Immunoblot analysis also showed high levels of FRA1 and JUNB expression in Th17 cells (**Figure 2C**). Co-immunoprecipitation studies were performed using antibodies against Jun family proteins (i.e., JUNB and c-JUN), followed by immunoblotting using antibodies against FOS family proteins (i.e., FRA1, c-FOS, and FOSB) to determine whether FRA1 and JUNB form a heterodimeric AP-1 complex. It was found that FRA1 forms a complex with JUNB, but not with c-JUN (**Figure 2D**).

Next, we investigated the functional association between the FRA1–JUNB complex and STAT3. The STAT3 signaling pathway was inhibited using genetically engineered STAT3-deficient $CD4^+$ T cells and STA-21, which blocks the DNA-binding activity of STAT3 (26). As shown in **Figure 3A**, $CD4^+$ T cells harboring *Stat3*$^{fl/fl}$*Cd4*-Cre had markedly decreased levels of *Fra1* and *Junb* mRNA under both neutral and Th17-polarizing conditions. Treatment with STA-21 profoundly decreased the expression of FRA1, JUNB, and STAT3 (**Figure 3B**). Moreover, STA-21 decreased the levels of STAT3 phosphorylation under Th17-polarizing conditions (**Figure 3C**). STAT3 overexpression increased the relative levels of *Fra1* and *Junb* mRNA (**Figure 3D**), while *in vitro* treatment with IL-6 upregulated *Fra1* and *Junb* mRNA (**Figure 3E**).

Co-immunoprecipitation studies were performed using anti-FRA1 and anti-JUNB antibodies followed by immunoblotting with antibodies against STAT3 to determine whether FRA1 and JUNB physically interact with STAT3. Both FRA1 and JUNB were found to form a complex with STAT3 (**Figure 3F**). We performed ChIP and qPCR to examine whether STAT3 binds directly to the promoter regions of *Fosl1* and *Junb*. The ChIP-qPCR results were compared with publicly available ChIP-Seq data from Th17 cells. We found that STAT3 binds to the predicted recognition sites upstream of *Fosl1* and *Junb*, suggesting that it regulates their expression by binding directly to their promoters (**Figure 3G**). Using confocal microscopy, we found that FRA1 and JUNB were colocalized with phosphorylated STAT3 in $CD4^+$ splenic T cells and Th17 cells from arthritic mice (**Figures 3H,I**). These findings suggest that STAT3 signaling is critical for the expression and activation of FRA1 and JUNB during Th17 cell differentiation.

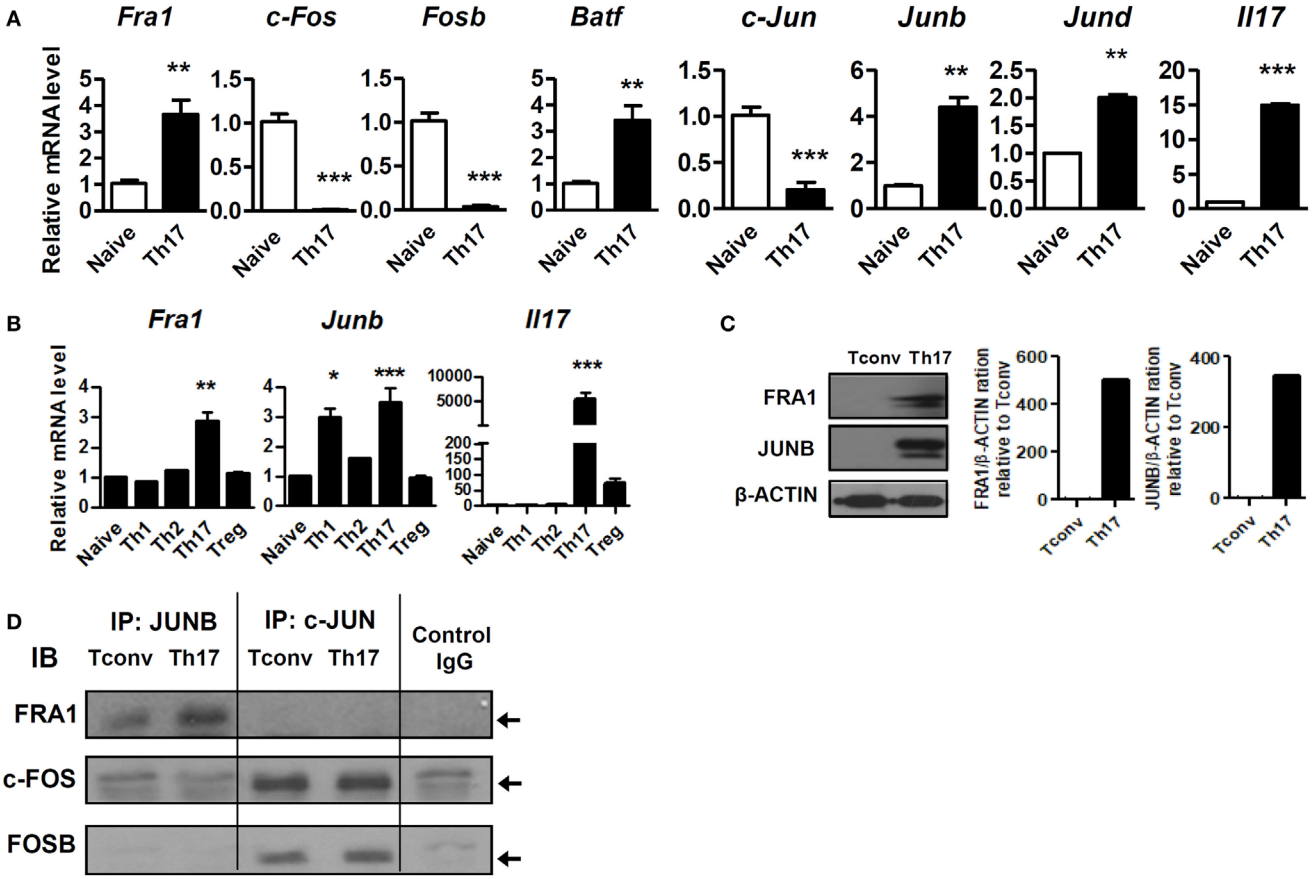

FIGURE 2 | Both Fos-related antigen 1 (FRA1) and JUNB are highly expressed in T helper 17 (Th17) cells. **(A,B)** Naïve T cells ($CD4^+CD62L^+$) were isolated from 6-week-old C57BL/6 mice ($n = 3$) and cultured for 3 days under the indicated promoters. Relative mRNA levels were measured by qRT-PCR. **(C)** Protein extracts were prepared from $CD4^+$ T cells (Tconv) and $CD4^+$ T cells cultured for 3 days under Th17-polarizing conditions (Th17). FRA1 and JUNB protein levels were evaluated by immunoblotting. **(D)** $CD4^+$ T cells cultured under Th17-polarizing conditions were lysed, and the cell lysates were subjected to co-immunoprecipitation with anti-JUNB and anti-c-JUN antibodies and immunoblotting with anti-FRA1, anti-c-FOS, and anti-FOSB antibodies. Data are representative of three **(A–C)** or two **(D)** independent experiments, each performed in triplicate **(A,B)**. The data were analyzed using an unpaired *t*-test or one-way ANOVA with Bonferroni's *post hoc* test. Error bars show the SEM. $^*p < 0.05$, $^{**}p < 0.005$, and $^{***}p < 0.0005$.

Expression of IL-17 Is Directly Regulated by the FRA1–JUNB Complex

The AP-1 family plays a versatile role in T-cell development (27). Levels of IL-17 were measured in *Fra1*- and *Junb*-overexpressing and silenced cells. The relative levels of *Il17* mRNA were significantly increased in cells overexpressing *Fra1* and *Junb*. The relative mRNA levels of other genes associated with Th17 cells, such as *Il21*, *Il22*, and *Rorc* (the RORγt gene locus), were also increased (**Figures 4A,B**). $CD4^+IL\text{-}17^+$ cells and *Il17* mRNA levels were significantly decreased when *Fra1* and *Junb* were silenced under Th17-polarizing conditions (**Figures 4C,D**). By contrast, when *c-Fos* and *c-Jun*, the dominant AP-1 subtypes in naïve T cells, were overexpressed, *Il17* mRNA levels were decreased significantly (**Figures 4E,F**). These findings support the specificity of the role of the FRA1–JUNB complex in Th17 cell differentiation.

We next investigated whether the FRA1–JUNB complex directly regulates IL-17 expression by binding to the *Il17a* promoter. The interaction between the FRA1–JUNB complex and the AP-1-binding motif within the *Il17a* promoter region was examined by electrophoretic mobility shift assay. The anti-FRA1 and anti-JUNB antibodies caused a super shift of the labeled DNA probe, indicating that the AP-1-binding motif interacts specifically with FRA1 and JUNB (**Figure 4G**). This finding was confirmed by an analysis of the *Il17a* promoter using a luciferase reporter system. Overexpression of both FRA1 and JUNB increased luciferase activity in EL4 cells. Simultaneous overexpression of FRA1 and JUNB caused luciferase activity to increase twofold (**Figure 4H**). Silencing of *Fra1* and *Junb* caused a greater than twofold reduction in luciferase activity. Simultaneous overexpression of c-FOS and c-JUN caused a significant decrease in the luciferase activity induced by the *Il17a* promoter (**Figure 4I**). ChIP-qPCR analyses showed that FRA1 and JUNB bind directly to the *Il17a* gene loci and to gene loci encoding other Th17 cell differentiation activators, such as *Il21*, *Il22*, and *Rorc* (**Figure 4J**). These findings indicate that the FRA1–JUNB complex binds to

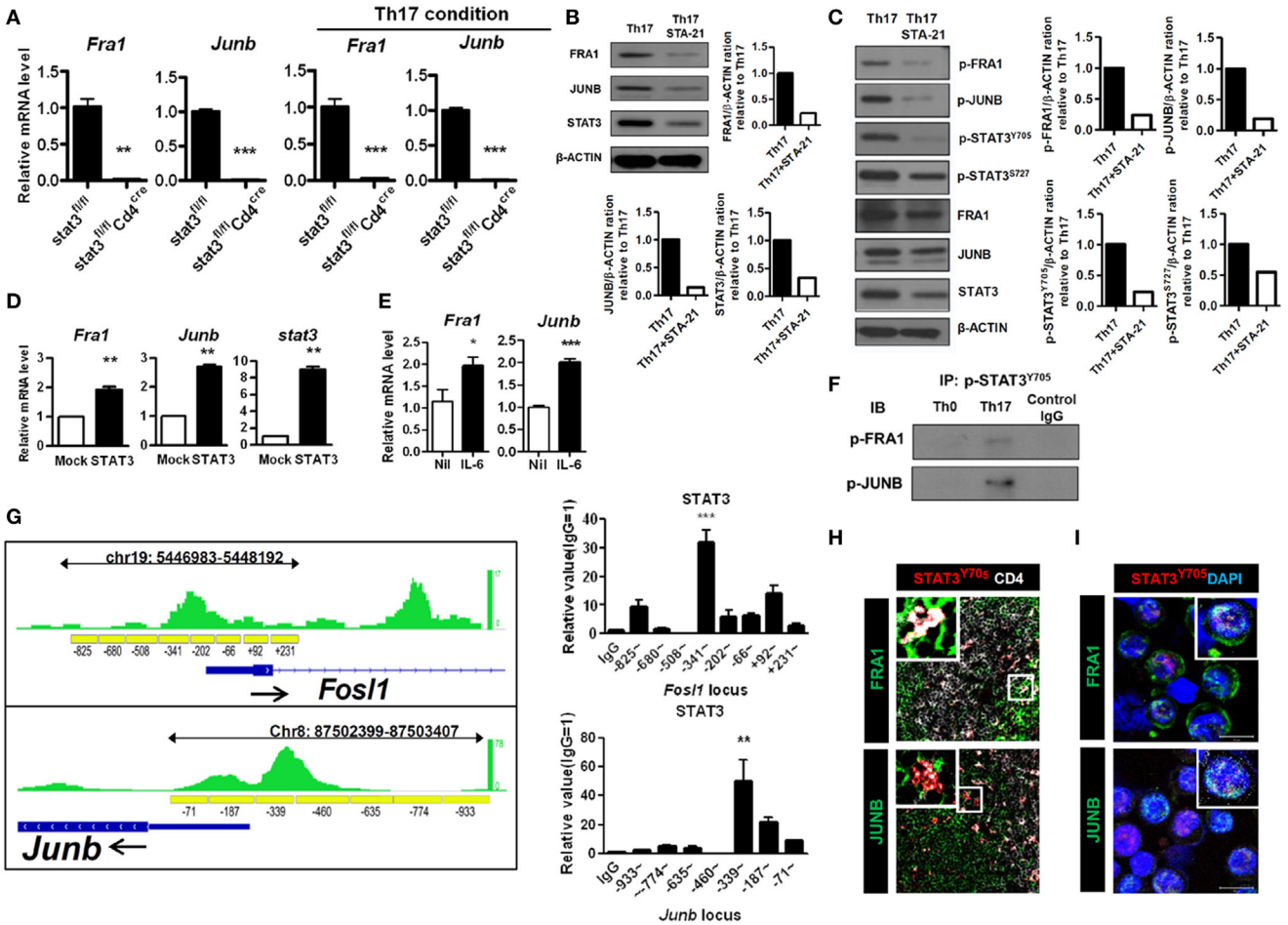

FIGURE 3 | Signal transducer and activator of transcription 3 (STAT3)-mediated activation of Fos-related antigen 1 (FRA1) and JUNB in T helper 17 (Th17) cells. **(A)** CD4+ T cells from *Stat3*$^{fl/fl}$ and *Stat3*$^{fl/fl}$Cd4-Cre were isolated (left panel) or cultured under Th17-polarizing conditions for 3 days (right panel). **(B,C)** CD4+ T cells were pretreated with STA-21 for 1 day, cultured under Th17-polarizing conditions for a further 3 days, and then treated with interleukin (IL)-6 for 2 h **(C)** before harvesting and lysing. **(D)** LBRM cells were transfected with a STAT3 expression vector, and the cells were cultured for 3 weeks in the presence of neomycin (10 μg/ml). **(E)** CD4+ T cells were cultured in the presence of IL-6 for 16 h. **(F)** CD4+ T cells were cultured under Th0- or Th17-polarizing conditions for 3 days and the lysed. The cell lysates were subjected to immunoprecipitation with an anti-phospho-STAT3^{Y705} antibody and immunoblotting with anti-phospho-FRA1 or anti-phospho-JUNB antibodies. **(G)** The STAT3-binding region (green) detected by STAT3 chromatin immunoprecipitation (ChIP) sequencing in Th17 cells is shown along with the *Fosl1* and *Junb* loci, including the primer sites (yellow boxes) (left panel). The negative control cyclophilin showed no enrichment (data not shown). CD4+ T cells were cultured under Th17-polarizing conditions for 3 days. ChIP-qPCR analysis was performed using an anti-STAT3 antibody and primers specific for *Fosl1* and *Junb* (right panel). **(H,I)** Splenic tissue was collected from collagen-induced arthritis mice. CD4+ splenic T cells and Th17 cells from arthritic mice were stained for CD4 (white), FRA1, JUNB (green), and phospho-STAT3^{Y705} **(H)** or DAPI **(I)** (blue). Data are representative of three **(B–I)** and two **(A)** independent experiments, each performed in triplicate **(A,D,E,G)**. The data were analyzed using an unpaired *t*-test; error bars show the SEM. **p* < 0.05, ***p* < 0.005, and ****p* < 0.0005.

the *IL17a* promoter region, and that this binding activates *IL17* gene transcription.

FRA1 and JUNB Are Critical for the Pathogenesis of CIA

T helper 17 cells and IL-17 contribute significantly to the development of RA (28, 29). To examine the *in vivo* role of the FRA1–JUNB complex in rheumatoid inflammation, *Fra1* and *Junb* were silenced in CIA mice by injecting *Fra1* and *Junb* short hairpin RNA vectors. This markedly reduced the incidence of arthritis and decreased the arthritis score (**Figure 5A**). The numbers of FRA1+, JUNB+, and IL-17+ cells were significantly lower within the joint tissues (**Figure 5B**). Histological examination showed that the ankle joints of *Fra1/Junb*-silenced mice had less inflammation and cartilage damage (**Figure 5C**). Inhibition of *Fra1/Junb* also reduced the expression of Th17 cytokines such as IL-6, IL-17, IL-1β, and tumor necrosis factor-α in joint tissue. Other mediators of joint destruction such as vascular endothelial growth factor and receptor activator of nuclear factor κB ligand (RANKL) were also downregulated (Figure S1A in Supplementary Material). In CIA mice, disease severity was correlated with the level of type II collagen (CII)-specific IgG antibodies (30). Silencing of *Fra1* and *Junb* reduced T-cell proliferation and CII-specific antibody production (Figures S1B,C in Supplementary Material). It also

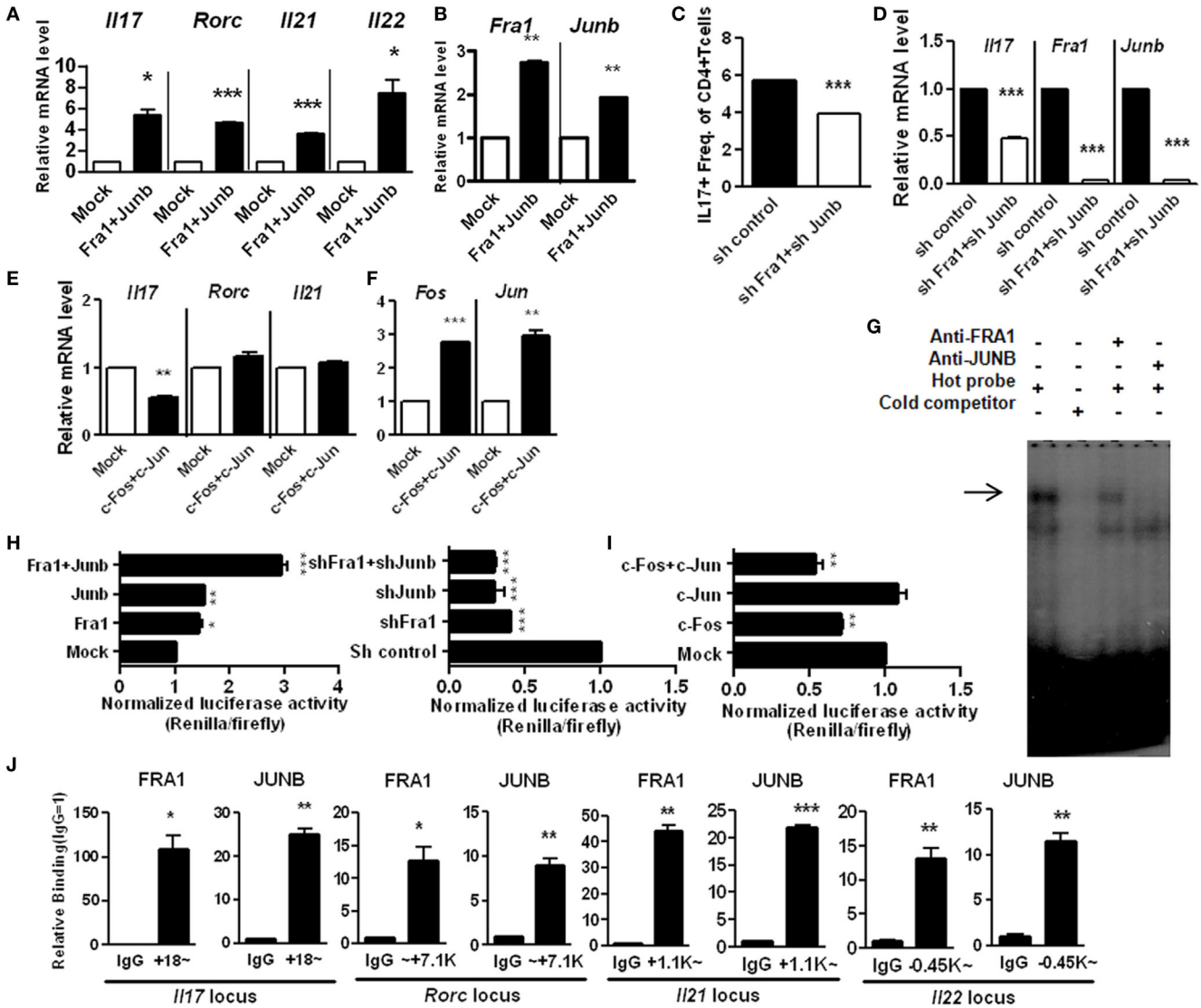

FIGURE 4 | Expression of interleukin (IL)-17 is directly mediated by the Fos-related antigen 1 (FRA1)–JUNB complex in T helper 17 (Th17) cells. LBRM cells were transfected with vectors and cultured for 3 weeks with neomycin (10 μg/ml) **(A,B,E,F)**. **(A,B)** The relative mRNA levels of each gene were measured by qRT-PCR. **(C,D)** CD4+ T cells were infected with lentiviruses harboring constructs designed to knockdown *Fra1* and *Junb*. Cells were then cultured under Th17-polarizing conditions for 3 days. $CD4^+IL\text{-}17^+$ T cells were identified by flow cytometry, and relative mRNA levels were measured by qRT-PCR. **(E,F)** The relative mRNA level of each gene was measured by qRT-PCR. **(G)** Nuclear extracts from Th17 cells were analyzed by electrophoretic mobility shift assay incorporating a radiolabeled probe derived from the activator protein 1-binding site of the *IL17a* locus and antibodies specific for FRA1 or JUNB. **(H,I)** EL4 cells were transiently transfected with expression vectors and *IL17a* promoter constructs with a CNS2 enhancer region. Luciferase activity was measured using a dual-luciferase reporter assay system. **(J)** CD4+ T cells were cultured under Th17-polarizing conditions. Chromatin immunoprecipitation-qPCR was performed using anti-FRA1 or anti-JUNB antibodies with primers specific for each gene locus. Data are representative of at least three independent experiments, performed in triplicate. Data were analyzed using an unpaired *t*-test; error bars show the SEM. $^*p < 0.05$, $^{**}p < 0.005$, and $^{***}p < 0.0005$.

substantially reduced the population of IL-17-producing $CD4^+$ T cells, considered to be Th17 cells, in the spleen and draining lymph nodes (Figure S1D in Supplementary Material).

$CD4^+$ T cells in *Fra1*/*Junb* Tg mice had different proportions of Th1 and Th17 cells (Figure S2 in Supplementary Material). CIA was induced in *Fra1*/*Junb* transgenic mice to investigate the *in vivo* effects of *Fra1* and *Junb* overexpression. Splenocytes were examined for HA-tagged FRA1/JUNB transgene by immunoblotting (**Figure 5D**). The incidence of arthritis and the arthritis score were significantly increased (**Figures 5E,F**). There was a marked increase in the levels of IL-17, FRA1, and JUNB in the spleen (**Figure 5G**). The relative mRNA level of the osteoclastogenic marker tartrate-resistant acid phosphatase was significantly higher (**Figure 5H**), while CII-specific T-cell proliferation and IgG production were also increased (**Figures 5I–K**). Overexpression of FRA1/JUNB profoundly increased CIA

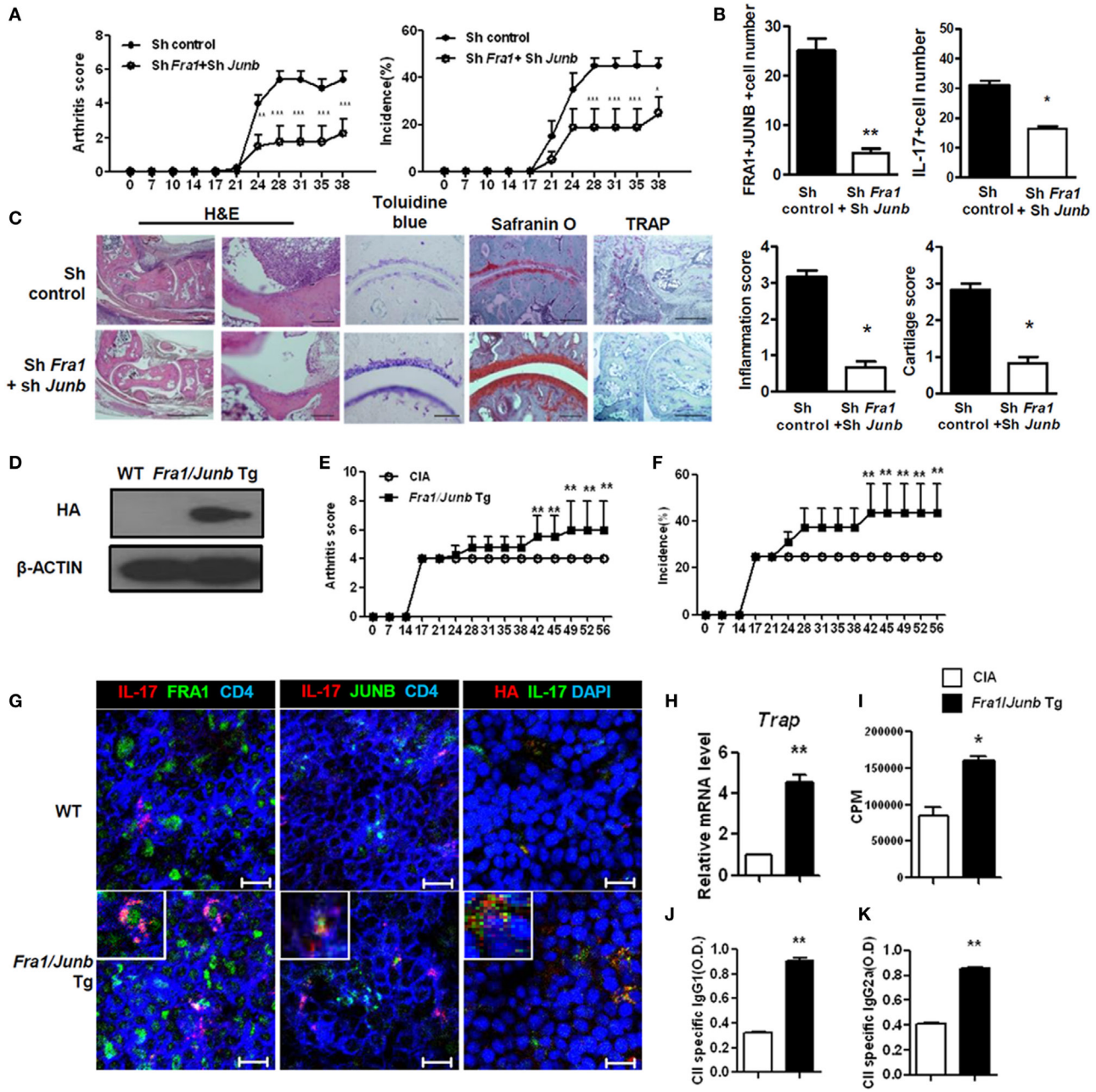

FIGURE 5 | Fos-related antigen 1 (FRA1) and JUNB are involved in the pathogenesis of collagen-induced arthritis, T helper 17 cell differentiation, and rheumatoid inflammation in mice. Arthritis was induced in mice, and shRNA control or shRNA*Fra1*/shRNA*Junb* vectors were injected on days 7 and 14 ($n = 5–7$). **(A)** Arthritis severity was measured using the incidence and mean arthritis score. **(B)** Splenic tissue from each mouse was stained. Positively stained cells were counted visually by four individuals from high-magnification images projected onto a screen, and the mean values are presented as a histogram. **(C)** On day 30 after immunization, tissues were sampled from the ankle joints and stained with toluidine blue, Safranin O (scale bar = 100 μm), H&E [scale bar = 500 μm (left); 100 μm (right)], or tartrate-resistant acid phosphatase (TRAP) (scale bar = 200 μm). The inflammation and cartilage scores are shown in bar graphs (right panel). **(D)** Splenocytes were examined for the HA-tagged FRA1/JUNB transgene by immunoblotting. **(E,F)** Disease severity was recorded using the incidence and mean arthritis score. **(G)** Splenic tissue from each mouse was stained for FRA1, JUNB, and interleukin-17 in $CD4^+$ T cells and examined by laser confocal microscopy. **(H)** The relative levels of TRAP mRNA in cells from the ankle joints were measured by qRT-PCR. **(I)** T-cell proliferation was analyzed using a mixed-lymphocyte reaction. **(J,K)** The levels of IgG1 and IgG2a antibodies specific to type II collagen were measured in serum. Data are representative of more than two independent experiments. Data were analyzed using an unpaired *t*-test or two-way ANOVA with Bonferroni's *post hoc* test; error bars show the SEM. $^*p < 0.05$, $^{**}p < 0.005$, and $^{***}p < 0.0005$.

joint pathology (Figure S3A in Supplementary Material). Immunostaining showed that the expression of various proinflammatory cytokines and RANKL, a mediator of osteoclastogenesis, was significantly greater in the joint tissues of transgenic mice with CIA (Figure S3B in Supplementary Material). IL-17 mRNA levels and Th17 cell numbers were increased markedly (Figures

S3C,D in Supplementary Material). These findings suggest that the FRA1–JUNB complex plays a major role in the development of CIA, likely through the induction of Th17 cell differentiation.

Expression and Potential Functions of FRA1 and JUNB in RA Patients

We demonstrated *in vivo* roles of FRA1 and JUNB in mice with CIA, an animal disease model for RA. To confirm the roles of FRA1 and JUNB in patients with RA, FRA1 was overexpressed in $CD4^+$ T cells isolated from healthy controls. FRA1 overexpression increased the proportion of IL-17-producing $CD4^+$ T cells during Th17 polarization (**Figure 6A**). These cells produced significantly higher levels of *Il17a* mRNA and cytokines (**Figure 6B**). *Fra1* silencing decreased *Il17a* mRNA levels and IL-17 secretion (**Figure 6C**). There were significantly increased the transcription levels of *Fra1* and *Junb* among peripheral blood mononuclear cells (PBMCs) and synovial fluid mononuclear cells (SFMCs) from RA patients compared with PBMCs from healthy controls (**Figure 6D**). *Junb* was also upregulated in RA patients. When *Fra1* was silenced in $CD4^+$ T cells isolated from SFMCs of RA patients, IL-17 secretion was decreased during Th17 polarization (**Figure 6E**). The expression of both FRA1 and JUNB was particularly high in the inflamed synovium of RA patients, a region enriched with inflammatory immune cells (**Figure 6F**). Of note, FRA1, JUNB, and phosphorylated STAT3 were colocalized in the inflamed synovium, which further supported our *in vitro* experimental results. A schematic illustration of the inflammatory signaling pathway induced by FRA1/JUNB is shown in **Figure 6G**. Th17 conditioning induces an inflammatory signal by promoting FRA1/JUNB. The inflammatory response is mediated by activation of STAT3, which regulates genes involved in Th17 cell differentiation. This cascade induces excessive inflammation and autoimmunity resulting in RA.

DISCUSSION

Although FRA1 and JUNB may have modulatory activity in the immune inflammatory response (18, 19), there is currently no

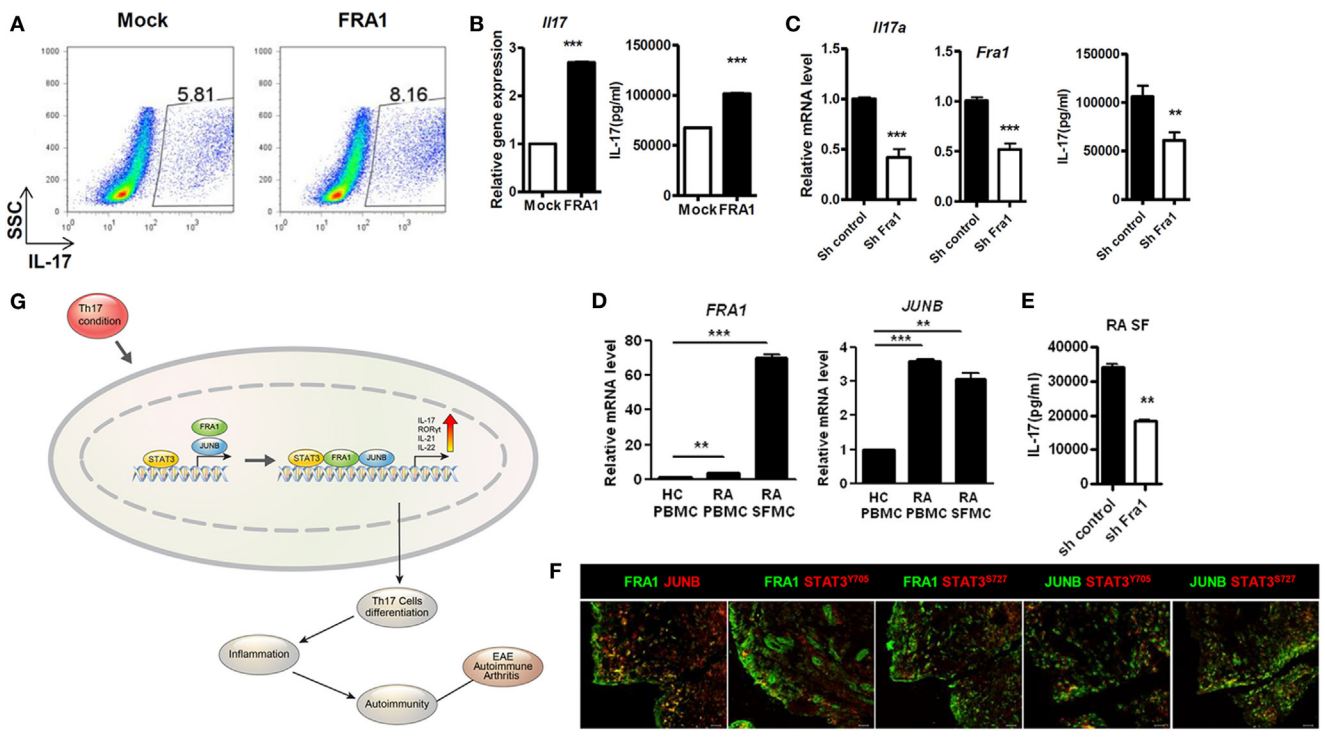

FIGURE 6 | Expression and potential function of Fos-related antigen 1 (FRA1) and JUNB in rheumatoid arthritis (RA) patients. **(A,B)** Flow cytometry, qRT-PCR, and ELISA. $CD4^+$ T cells were isolated from healthy peripheral blood mononuclear cells (PBMCs) and infected with retroviruses containing FRA1 on day 1. The infected cells were then cultured under T helper 17 (Th17)-polarizing conditions for 3 days and analyzed. **(C)** qRT-PCR and ELISA. $CD4^+$ T cells from healthy controls were infected with lentiviruses harboring constructs designed to knockdown *Fra1*. Cells were then cultured under Th17-polarizing conditions for 3 days. **(D)** qRT-PCR analysis. Total RNA was extracted from PBMCs isolated from healthy controls and from PBMCs and synovial fluid mononuclear cells (SFMCs) from RA patients. **(E)** ELISA. $CD4^+$ T cells in SFMCs from RA patients were infected with lentiviruses harboring constructs designed to knockdown *Fra1*. Cells were then cultured under Th17-polarizing conditions for 3 days. **(F)** Synovial tissue obtained from RA patients. Sections were immunostained. Data are representative of three **(A–C,F)** and two **(D,E)** independent experiments, each performed in triplicate. **(G)** A schematic illustration of the inflammatory signaling pathway mediated by FRA1/JUNB. **(B–E)** Data are representative of more than three independent experiments. Data were analyzed using an unpaired *t*-test; error bars show the SEM. $^*p < 0.05$, $^{**}p < 0.005$, and $^{***}p < 0.0005$.

evidence in the literature to support this notion in autoimmune disorders mediated by STAT3 and Th17 cells. In this study, we found evidence of previously unidentified functions of FRA1 and JUNB in Th17 cell differentiation and autoimmune disease. We investigated the modulatory function and underlying mechanisms of FRA1 and JUNB in a murine model of inflammatory arthritis. The predominant conclusion from this study was that FRA1 and JUNB exacerbate inflammation *via* the induction of Th17 cells. To our knowledge, this is the first study to implicate FRA1 and JUNB directly in STAT3 activation and regulation of Th17 cell proliferation. These observations suggest a previously unidentified function of these factors in autoimmune disease.

Activator protein 1 is comprised of dimers of FOS and JUN protein family members (31, 32). The diverse functions of AP-1 family members result from heterodimer formation between the FOS and JUN proteins (33). AP-1 is also involved in cell functions including proliferation, differentiation, and apoptosis. For example, the FRA2–JUND complex is involved in the terminal differentiation of granulosa cells into luteal cells (34) and T-cell activation (35). Additionally, AP-1 factors may play important roles in autoimmune disease and Th17 cell differentiation. It was suggested that basic leucine zipper transcription factor, ATF-like (BATF), an AP-1 protein, leads to increased Th17 cell differentiation, whereas BATF deficiency results in IL-17 downregulation (12). Loss of the AP-1 family member Fosl2 in T cells improved EAE severity *via* suppression of Th17 cell plasticity (36). We performed an integrative analysis using RNA-Seq and ChIP-Seq data to identify key factors downstream of STAT3 involved in Th17 cell differentiation. This integrative analysis suggested that upregulation of *Fra1* and *Junb* drives and promotes Th17 cell differentiation.

Signal transducer and activator of transcription 3-mediated IL-17 expression and Th17 cell differentiation involve AP-1 family proteins. Previous studies have shown a biological link between the STAT3 signaling pathway and the AP-1 family of transcription factors (12, 37, 38). In particular, STAT3-mediated expression of BATF, an AP-1 subfamily member, is associated with Th17 cell differentiation (12). In this study, RNA-Seq analysis showed that the expression of *cFos* and *cJun* was higher in naïve T cells. This suggests that AP-1 subtype switching from c-FOS–c-JUN to FRA1/JUNB is essential for Th17 cell differentiation. It can also be postulated that activation of c-FOS–c-JUN must be suppressed in parallel with activation of FRA1/JUNB by STAT3 during polarization toward the Th17 subtype. The present study identified an AP-1 complex comprising FRA1 and JUNB, which appears to function as a key factor downstream of STAT3 in Th17 cell differentiation. It appears that AP-1 subtype switching, particularly from c-FOS, FOSB, and c-JUN to FRA1 and JUNB, is required for STAT3-mediated Th17 cell differentiation.

The AP-1 family includes the c-JUN and c-FOS proteins, which play important roles in IL-17 expression and Th17 cell functions. It has been demonstrated that BATF binds to intergenic components in the *IL17a* locus and to *IL17* promoters, both of which are essential for Th17 differentiation (12). Additionally, the BATF–JUNB and BATF–JUND complexes have been shown to cooperate with IRF4 in Th17 cells to promote transcription of *IL17* (39). The c-JUN transcription factor that heterodimerizes with c-FOS to generate the AP-1 transcription factor complex is involved in suppression of IL-17 production in developing Th17 cells (16, 22). FRA2 is also a negative regulator of IL-17 (36). We observed that overexpression of FRA2 decreased the expression of *IL17a* in a promoter-fused luciferase reporter assay (data not shown). We also found that expression levels of *c-Fos* and *c-Jun* were significantly reduced, whereas *Batf* expression was increased in Th17 cells compared with naïve T cells. Overexpression of *c-Fos* and *c-Jun* significantly decreased *IL17* mRNA levels. The FRA1–JUNB complex directly activates expression of IL-17, a cytokine produced by Th17 cells. This complex plays a role in promoting the expression of other cytokines associated with Th17 cells, such as IL-21 and IL-22, by directly binding to their promoter regions. These results suggest that FRA1 and JUNB are involved in IL-17 production and Th17 cell differentiation.

Although FRA1/JUNB and c-FOS/c-JUN compete for the same AP-1-binding sites within the *IL17a* promoter, we found in this study that *IL17a* promoter activity was increased by FRA1 and JUNB overexpression but decreased by c-FOS and c-JUN overexpression. We observed an interaction between p-STAT3 and p-FRA1 or p-JUNB in Th17 cells; therefore, FRA1/JUNB and c-FOS/c-JUN may be involved in AP-1 subtype switching. Additionally, p-FRA1 binds to p-JUNB in Th17 cells. Further study is needed to confirm the AP-1 subtype switching factors involved and the mechanism of interaction between p-FRA1 and p-JUNB in Th17 cells.

This study has certain limitations. One is that the animal studies were conducted using FRA1/JUNB-1 overexpression and knockdown vectors. Adoptive transfer studies in conditional overexpression and knockout mice are required to confirm that FRA1/JUNB-1 regulates $CD4^+$ T cells, leading to autoimmune arthritis. Nonetheless, this study is the first to demonstrate functions of FRA1/JUNB-1 in Th17 cell differentiation and autoimmune arthritis. Future studies using adoptive transfer models with $CD4^+$ T cells differentially expressing FRA1/JUNB-1 are required to validate our data more precisely.

Uncontrolled Th17 cell activation is responsible for the onset of several autoimmune diseases. Th17 cells cause tissue injury *via* production of IL-17, as observed in CIA mouse models of disease. The present study showed that the FRA1–JUNB complex plays a central role in the development of RA, which is a Th17-mediated autoimmune disease. The FRA1–JUNB complex may be clinically relevant as it functions as a Th17 cell-specific regulator of proinflammatory cytokine production in CIA mouse models and hence RA. In the RA mouse model used in this study, FRA1/JUNB overexpression resulted in the development of severe inflammatory symptoms and augmented expression of IL-17 in mice. Notably, this has fueled interest in the genetic importance of FRA1/JUNB in human RA in the context of promoted STAT3 activity. FRA1 overexpression activated Th17 cell differentiation in PBMCs from healthy controls; however, FRA1 silencing downregulated IL-17 production in SFMCs from RA patients. This may indicate the potential of the FRA1–JUNB complex as a therapeutic target in human autoimmune disease. In conclusion, our results suggest a previously unidentified function of FRA1/JUNB in T-cell-mediated autoimmune diseases. FRA1/JUNB directly modulates STAT3 activation and Th17 cell differentiation. Our

identification of the involvement of FRA1/JUNB in T-cell development provides a potential therapeutic target for the treatment of autoimmune diseases.

ETHICS STATEMENT

The Animal Care Committee of The Catholic University of Korea approved the experimental protocol. All experimental procedures were evaluated and carried out in accordance with the protocols approved by the Animal Research Ethics Committee at the Catholic University of Korea (CMCU-2012-0156-01). All procedures performed followed the ethical guidelines on animal use. Approval by the ethics committee of Seoul St. Mary's Hospital (Seoul, Republic of Korea) was obtained for all procedures. All human experimental procedures were approved by the Ethics Committee of Seoul St. Mary's Hospital (Seoul, Republic of Korea, KC13TISE0032).

AUTHOR CONTRIBUTIONS

Y-MM, S-YL, S-KK, SL, S-MA, and M-LC designed the experiments and analyzed the data. Y-MM, S-YL, S-KK, and SL wrote the manuscript along with input from DK, WK, Y-MH, H-JS, E-KK, J-GR, H-BS, J-EK, S-YH, and JY. Y-MM and S-YL performed all *in vitro* assays with help from S-KK, SL, DK, WK, and H-BS. S-YL, H-JS, and J-GR performed the animal experiments. E-KK conducted all immunohistochemistry experiments. Y-MM, S-YL, S-KK, SL, RS, D-MJ, H-YK, S-HP, S-MA, and M-LC discussed and developed the study concept. All authors critically reviewed and approved the final form of the manuscript.

FUNDING

This study was supported by a grant of the Korean Health Technology R&D Project, Ministry for Health & Welfare, Republic of Korea (grant no. HI14C3417), by the Basic Science Research Program from the National Research Foundation of Korea funded by the Ministry of Education, Science and Technology (grant no. 2012-0006135), and by a grant of the Korea Health Technology R&D Project through the Korea Health Industry Development Institute, funded by the Ministry of Health & Welfare, Republic of Korea (grant no. HI15C3062).

SUPPLEMENTARY MATERIAL

The Supplementary Material for this article can be found online at http://www.frontiersin.org/articles/10.3389/fimmu.2017.01793/full#supplementary-material.

FIGURE S1 | Knockdown of FRA1/JUNB Decreases Th17 Cell Differentiation and Attenuates Rheumatoid Inflammation in Mice.

FIGURE S2 | T cell proportion of $CD4^+$Tcells in Fra1/Junb Tg mice.

FIGURE S3 | Overexpression of FRA1/JUNB Causes Th17 Cell Differentiation and Increases CIA Disease Severity.

REFERENCES

1. Harrington LE, Hatton RD, Mangan PR, Turner H, Murphy TL, Murphy KM, et al. Interleukin 17-producing CD4+ effector T cells develop via a lineage distinct from the T helper type 1 and 2 lineages. *Nat Immunol* (2005) 6:1123–32. doi:10.1038/ni1254
2. Iwakura Y, Nakae S, Saijo S, Ishigame H. The roles of IL-17A in inflammatory immune responses and host defense against pathogens. *Immunol Rev* (2008) 226:57–79. doi:10.1111/j.1600-065X.2008.00699.x
3. Komiyama Y, Nakae S, Matsuki T, Nambu A, Ishigame H, Kakuta S, et al. IL-17 plays an important role in the development of experimental autoimmune encephalomyelitis. *J Immunol* (2006) 177:566–73. doi:10.4049/jimmunol.177.1.566
4. Kotake S, Udagawa N, Takahashi N, Matsuzaki K, Itoh K, Ishiyama S, et al. IL-17 in synovial fluids from patients with rheumatoid arthritis is a potent stimulator of osteoclastogenesis. *J Clin Invest* (1999) 103:1345–52. doi:10.1172/JCI5703
5. Mathur AN, Chang HC, Zisoulis DG, Stritesky GL, Yu Q, O'Malley JT, et al. STAT3 and STAT4 direct development of IL-17-secreting Th cells. *J Immunol* (2007) 178:4901–7. doi:10.4049/jimmunol.178.8.4901
6. O'Shea JJ, Paul WE. Mechanisms underlying lineage commitment and plasticity of helper CD4+ T cells. *Science* (2010) 327:1098–102. doi:10.1126/science.1178334
7. Ivanov II, McKenzie BS, Zhou L, Tadokoro CE, Lepelley A, Lafaille JJ, et al. The orphan nuclear receptor RORgammat directs the differentiation program of proinflammatory IL-17+ T helper cells. *Cell* (2006) 126:1121–33. doi:10.1016/j.cell.2006.07.035
8. Chaudhry A, Rudra D, Treuting P, Samstein RM, Liang Y, Kas A, et al. CD4+ regulatory T cells control Th17 responses in a STAT3-dependent manner. *Science* (2009) 326:986–91. doi:10.1126/science.1172702
9. Yang XO, Panopoulos AD, Nurieva R, Chang SH, Wang D, Watowich SS, et al. STAT3 regulates cytokine-mediated generation of inflammatory helper T cells. *J Biol Chem* (2007) 282:9358–63. doi:10.1074/jbc.C600321200
10. Pan F, Ye Z, Cheng L, Liu JO. Myocyte enhancer factor 2 mediates calcium-dependent transcription of the interleukin-2 gene in T lymphocytes: a calcium signaling module that is distinct from but collaborates with the nuclear factor of activated T cells (NFAT). *J Biol Chem* (2004) 279:14477–80. doi:10.1074/jbc.C300487200
11. Zhang F, Meng G, Strober W. Interactions among the transcription factors Runx1, RORgammat and Foxp3 regulate the differentiation of interleukin 17-producing T cells. *Nat Immunol* (2008) 9:1297–306. doi:10.1038/ni.1663
12. Schraml BU, Hildner K, Ise W, Lee WL, Smith WA, Solomon B, et al. The AP-1 transcription factor BATF controls T(H)17 differentiation. *Nature* (2009) 460:405–9. doi:10.1038/nature08114
13. Chen Z, Laurence A, Kanno Y, Pacher-Zavisin M, Zhu BM, Tato C, et al. Selective regulatory function of Socs3 in the formation of IL-17-secreting T cells. *Proc Natl Acad Sci U S A* (2006) 103:8137–42. doi:10.1073/pnas.0600666103
14. Durant L, Watford WT, Ramos HL, Laurence A, Vahedi G, Wei L, et al. Diverse targets of the transcription factor STAT3 contribute to T cell pathogenicity and homeostasis. *Immunity* (2010) 32:605–15. doi:10.1016/j.immuni.2010.05.003
15. Bi Y, Liu G, Yang R. Th17 cell induction and immune regulatory effects. *J Cell Physiol* (2007) 211:273–8. doi:10.1002/jcp.20973
16. Hess J, Angel P, Schorpp-Kistner M. AP-1 subunits: quarrel and harmony among siblings. *J Cell Sci* (2004) 117:5965–73. doi:10.1242/jcs.01589
17. Thomsen MK, Bakiri L, Hasenfuss SC, Hamacher R, Martinez L, Wagner EF. JUNB/AP-1 controls IFN-gamma during inflammatory liver disease. *J Clin Invest* (2013) 123:5258–68. doi:10.1172/JCI70405
18. Pirusian ES, Nikol'skaia TA, Abdeev RM, Bruskin SA. Transcription factor AP-1 components as a psoriasis candidate genes. *Mol Biol (Mosk)* (2007) 41:1069–80.
19. Sabatakos G, Rowe GC, Kveiborg M, Wu M, Neff L, Chiusaroli R, et al. Doubly truncated FosB isoform (Delta2DeltaFosB) induces osteosclerosis in transgenic mice and modulates expression and phosphorylation of Smads in osteoblasts independent of intrinsic AP-1 activity. *J Bone Miner Res* (2008) 23:584–95. doi:10.1359/jbmr.080110

20. Eferl R, Hasselblatt P, Rath M, Popper H, Zenz R, Komnenovic V, et al. Development of pulmonary fibrosis through a pathway involving the transcription factor FRA-2/AP-1. *Proc Natl Acad Sci U S A* (2008) 105:10525–30. doi:10.1073/pnas.0801414105
21. Min L, Ji Y, Bakiri L, Qiu Z, Cen J, Chen X, et al. Liver cancer initiation is controlled by AP-1 through SIRT6-dependent inhibition of survivin. *Nat Cell Biol* (2012) 14:1203–11. doi:10.1038/ncb2590
22. Coquet JM, Middendorp S, van der Horst G, Kind J, Veraar EA, Xiao Y, et al. The CD27 and CD70 costimulatory pathway inhibits effector function of T helper 17 cells and attenuates associated autoimmunity. *Immunity* (2013) 38:53–65. doi:10.1016/j.immuni.2012.09.009
23. Lee SM, Gao B, Fang D. FoxP3 maintains Treg unresponsiveness by selectively inhibiting the promoter DNA-binding activity of AP-1. *Blood* (2008) 111:3599–606. doi:10.1182/blood-2007-09-115014
24. Huo L, Rothstein TL. Isolation and characterization of murine FRA-1: induction mediated by CD40 and surface Ig is protein kinase C dependent. *J Immunol* (1996) 157:3812–8.
25. Szremska AP, Kenner L, Weisz E, Ott RG, Passegue E, Artwohl M, et al. JUNB inhibits proliferation and transformation in B-lymphoid cells. *Blood* (2003) 102:4159–65. doi:10.1182/blood-2003-03-0915
26. Song H, Wang R, Wang S, Lin J. A low-molecular-weight compound discovered through virtual database screening inhibits STAT3 function in breast cancer cells. *Proc Natl Acad Sci U S A* (2005) 102:4700–5. doi:10.1073/pnas.0409894102
27. Jochum W, Passegue E, Wagner EF. AP-1 in mouse development and tumorigenesis. *Oncogene* (2001) 20:2401–12. doi:10.1038/sj.onc.1204389
28. Lundy SK, Sarkar S, Tesmer LA, Fox DA. Cells of the synovium in rheumatoid arthritis. T lymphocytes. *Arthritis Res Ther* (2007) 9:202. doi:10.1186/ar2107
29. Tesmer LA, Lundy SK, Sarkar S, Fox DA. Th17 cells in human disease. *Immunol Rev* (2008) 223:87–113. doi:10.1111/j.1600-065X.2008.00628.x
30. Hietala MA, Jonsson IM, Tarkowski A, Kleinau S, Pekna M. Complement deficiency ameliorates collagen-induced arthritis in mice. *J Immunol* (2002) 169:454–9. doi:10.4049/jimmunol.169.1.454
31. Jariel-Encontre I, Salvat C, Steff AM, Pariat M, Acquaviva C, Furstoss O, et al. Complex mechanisms for c-FOS and c-JUN degradation. *Mol Biol Rep* (1997) 24:51–6. doi:10.1023/A:1006804723722
32. Stancovski I, Gonen H, Orian A, Schwartz AL, Ciechanover A. Degradation of the proto-oncogene product c-FOS by the ubiquitin proteolytic system in vivo and in vitro: identification and characterization of the conjugating enzymes. *Mol Cell Biol* (1995) 15:7106–16. doi:10.1128/MCB.15.12.7106
33. Bakiri L, Matsuo K, Wisniewska M, Wagner EF, Yaniv M. Promoter specificity and biological activity of tethered AP-1 dimers. *Mol Cell Biol* (2002) 22:4952–64. doi:10.1128/MCB.22.13.4952-4964.2002
34. Sharma SC, Richards JS. Regulation of AP1 (JUN/FOS) factor expression and activation in ovarian granulosa cells. Relation of JUND and FRA2 to terminal differentiation. *J Biol Chem* (2000) 275:33718–28. doi:10.1074/jbc.M003555200
35. Boise LH, Petryniak B, Mao X, June CH, Wang CY, Lindsten T, et al. The NFAT-1 DNA binding complex in activated T cells contains FRA-1 and JUNB. *Mol Cell Biol* (1993) 13:1911–9. doi:10.1128/MCB.13.3.1911
36. Ciofani M, Madar A, Galan C, Sellars M, Mace K, Pauli F, et al. A validated regulatory network for Th17 cell specification. *Cell* (2012) 151:289–303. doi:10.1016/j.cell.2012.09.016
37. Leu JI, Crissey MA, Leu JP, Ciliberto G, Taub R. Interleukin-6-induced STAT3 and AP-1 amplify hepatocyte nuclear factor 1-mediated transactivation of hepatic genes, an adaptive response to liver injury. *Mol Cell Biol* (2001) 21:414–24. doi:10.1128/MCB.21.2.414-424.2001
38. Song Y, Qian L, Song S, Chen L, Zhang Y, Yuan G, et al. FRA-1 and STAT3 synergistically regulate activation of human MMP-9 gene. *Mol Immunol* (2008) 45:137–43. doi:10.1016/j.molimm.2007.04.031
39. Li P, Spolski R, Liao W, Wang L, Murphy TL, Murphy KM, et al. BATF-JUN is critical for IRF4-mediated transcription in T cells. *Nature* (2012) 490:543–6. doi:10.1038/nature11530

Conflict of Interest Statement: The authors declare that the research was conducted in the absence of any commercial or financial relationships that could be construed as a potential conflict of interest.

Copyright © 2017 Moon, Lee, Kwok, Lee, Kim, Kim, Her, Son, Kim, Ryu, Seo, Kwon, Hwang, Youn, Seong, Jue, Park, Kim, Ahn and Cho. This is an open-access article distributed under the terms of the Creative Commons Attribution License (CC BY). The use, distribution or reproduction in other forums is permitted, provided the original author(s) or licensor are credited and that the original publication in this journal is cited, in accordance with accepted academic practice. No use, distribution or reproduction is permitted which does not comply with these terms.

frontiers in Immunology

ORIGINAL RESEARCH
published: 10 April 2017
doi: 10.3389/fimmu.2017.00433

(–)-Epigallocatechin Gallate Targets Notch to Attenuate the Inflammatory Response in the Immediate Early Stage in Human Macrophages

Tengfei Wang[1,2], Zemin Xiang[2,3], Ya Wang[2], Xi Li[2], Chongye Fang[2], Shuang Song[2], Chunlei Li[2], Haishuang Yu[2], Han Wang[2], Liang Yan[4], Shumei Hao[3], Xuanjun Wang[2,3]* and Jun Sheng[2,3]**

[1] College of Life Science, Jilin University, Changchun, China, [2] Key Laboratory of Pu-er Tea Science, Ministry of Education, Yunnan Agricultural University, Kunming, China, [3] State Key Laboratory for Conservation and Utilization of Bio-Resources in Yunnan, Kunming, China, [4] Pu'er Institute of Pu-erh Tea, Pu'er, Yunnan, China

OPEN ACCESS

Edited by:
Jixin Zhong,
Case Western Reserve University, USA

Reviewed by:
Yanlin He,
Baylor College of Medicine, USA
Xuhui Feng,
Indiana University, USA
Yonglin Chen,
Yale University, USA
Penghua Yang,
University of Maryland School of Medicine, USA

***Correspondence:**
Shumei Hao
haosm@sina.com;
Xuanjun Wang
wangxuanjun@gmail.com;
Jun Sheng
shengj@ynau.edu.cn

Specialty section:
This article was submitted to Inflammation, a section of the journal Frontiers in Immunology

Received: 26 January 2017
Accepted: 28 March 2017
Published: 10 April 2017

Citation:
Wang T, Xiang Z, Wang Y, Li X, Fang C, Song S, Li C, Yu H, Wang H, Yan L, Hao S, Wang X and Sheng J (2017) (–)-Epigallocatechin Gallate Targets Notch to Attenuate the Inflammatory Response in the Immediate Early Stage in Human Macrophages. Front. Immunol. 8:433. doi: 10.3389/fimmu.2017.00433

Inflammation plays important roles at different stages of diabetes mellitus, tumorigenesis, and cardiovascular diseases. (–)-Epigallocatechin gallate (EGCG) can attenuate inflammatory responses effectively. However, the immediate early mechanism of EGCG in inflammation remains unclear. Here, we showed that EGCG attenuated the inflammatory response in the immediate early stage of EGCG treatment by shutting off Notch signaling and that the effect did not involve the 67-kDa laminin receptor, the common receptor for EGCG. EGCG eliminated mature Notch from the cell membrane and the nuclear Notch intercellular domain, the active form of Notch, within 2 min by rapid degradation *via* the proteasome pathway. Transcription of the Notch target gene was downregulated simultaneously. Knockdown of Notch 1/2 expression by RNA interference impaired the downregulation of the inflammatory response elicited by EGCG. Further study showed that EGCG inhibited lipopolysaccharide-induced inflammation and turned off Notch signaling in human primary macrophages. Taken together, our results show that EGCG targets Notch to regulate the inflammatory response in the immediate early stage.

Keywords: (–)-epigallocatechin gallate, Notch, macrophages, laminin receptor, inflammation

INTRODUCTION

The inflammatory response has an important role at different stages of diabetes mellitus (DM), tumorigenesis, and cardiovascular diseases (1, 2). The inflammatory response is common in the intestine and gut due to microbe invasion and damage to cells in epithelial barriers (3). Attenuation of the inflammatory response has been considered an important side effect in the therapy and prevention of cancer, DM, cardiovascular diseases, and Alzheimer's disease (4, 5). Compounds in food and drinks that can help to attenuate inflammation have been studied for their effects and mechanisms of action (6, 7).

(–)-Epigallocatechin gallate (EGCG) is found in Chinese green tea and Pu'er tea. It has been proposed to have strong anti-inflammatory effects (8, 9). The mechanisms of EGCG in the attenuation of inflammation have been explored. EGCG downregulates the phosphorylation of nuclear factor-kappa B (NF-κB), a key regulator of the classical pathway of the inflammation response induced by

lipopolysaccharide (LPS) (10). In addition, the 67-kDa laminin receptor (67LR), which has been proposed to be a receptor for EGCG on cell membranes, has been shown to downregulate the anti-inflammatory effects of EGCG (11). However, those studies have focused on the physiologic response of cells ≥6 h after EGCG treatment. Thus, those results may indicate that EGCG treatment interferes with mediator proteins in the signal transduction pathway, although the original mechanism of EGCG treatment is not clear. Such cells have undergone several rounds of signaling processes in ≥6 h, and cytokine release and feedback may have already occurred in those cells. To understand the detailed mechanisms of EGCG in inflammation, we examined the immediate early response of macrophages after EGCG addition and the underlying mechanisms.

The mechanisms of the inflammatory response have been studied extensively. The NF-κB molecule has been considered to be a key regulator/mediator of LPS-induced inflammation (12). The well-known mitogen-activated protein kinase (MAPK) pathway, which plays a key part in many other biologic processes, has also been confirmed to participate in the inflammatory response (13).

Notch signaling has a role in the development of multicellular organisms (14). Notch has been shown to function during development of the immune system, including the maturation of T cells (15). In recent years, the Notch signaling pathway has been found to have an essential role in regulation of the inflammatory response (16). Notch and toll-like receptor (TLR) pathways cooperate to activate canonical Notch target genes, including the transcriptional repressors hairy and enhancer of split-1 (Hes1) and hairy/enhancer of split related with YRPW motif protein 1 (Hey1), and to increase the production of the canonical TLR-induced cytokines, tumor necrosis factor (TNF), interleukin (IL)-6, and IL-12 (17–19). Cooperation of these pathways to increase expression of target genes is mediated by the Notch pathway component and transcription factor recombination signal-binding protein for immunoglobulin (Ig) kappa J region (17). Basal activation of the Notch signal is required to amplify the signal transduction from TLRs. The Jagged-1/Notch signaling pathway is considered a potential molecular mechanism underlying the EGCG attenuation of oxidized low-density lipoprotein–induced dysfunction of the vascular endothelium (20). Studies have shown that EGCG may prevent the uric acid-induced inflammatory effect in human umbilical vein endothelial cells in relation to Notch1 (21). The Notch pathway has also been proposed to be related to the effects of EGCG in the protection of cochlear hair cells from ototoxicity and inhibition of the proliferation of colorectal cancer cells (22, 23). These observations suggest a potential relationship between EGCG and the Notch pathway.

Here, we studied the immediate early mechanism of EGCG on the inflammatory response induced by LPS in human macrophages derived from THP-1 cells. We found that EGCG did not alter the phosphorylation levels of NF-κB or the phosphorylation state of the key MAPK molecules p38, extracellular signal–regulated kinase (ERK), and c-Jun-*N*-terminal kinase (JNK) during the first hour after EGCG treatment. However, EGCG suppressed Notch signaling, which is necessary for an increased inflammatory response. Knockdown of Notch1/2 expression impaired the effects of EGCG upon inflammation.

MATERIALS AND METHODS

Cell Culture and Transfection

The human monocyte cell line (THP-1) was purchased from the Cell Bank in the Chinese Academy of Sciences (Kunming). Cell lines were cultured in Roswell Park Memorial Institute (RPMI) 1640 medium supplemented with 10% (*v/v*) fetal bovine serum (Biological Industries, USA) and 50 μM β-mercaptoethanol. Infection was carried out using Notch 1 or Notch 2 short hairpin RNA (shRNA) Lentiviral Particles (Santa Cruz Biotechnologies, USA) according to manufacturer instructions.

Macrophage Differentiation

THP-1-derived macrophages were differentiated from THP-1 by propidium monoazide (PMA) treatment (24). THP-1 cells were counted to a density of 5×10^5 cell/mL, and viability was >95% as determined by exclusion of Trypan blue dye. Then cells were seeded on 60-mm culture dishes (5×10^6 per dish) in RPMI 1640 supplemented with 10% fetal bovine serum (Biological Industries) and treated with PMA (10 ng/mL) for 48 h. This was followed by incubation with serum-free buffer for a further 24 h at 37°C in a humidified incubator in an atmosphere of 5% CO_2. THP-1-derived macrophages were washed twice with warm RPMI 1640 to remove non-adherent cells.

Isolation of Peripheral Blood Mononuclear Cells (PBMCs) and Macrophage Differentiation

Peripheral blood mononuclear cell-derived macrophages were obtained from anticoagulated, pathogen-free human peripheral blood using Medium for Human Lymphocyte Separation (Solarbio, China) in accordance with the manufacturer instructions. The upper layer was retained as autologous serum, which was used to culture PBMC-derived macrophages. The mononuclear cells from PBMCs were washed twice with serum-free RPMI 1640 and resuspended in RBPI 1640 with 5% autologous serum. Then cells were cultured for 7 days with 50 ng/mL macrophage colony-stimulating factor-1 in a humidified incubator (37°C, 5% CO_2).

67LR Blockade

THP-1-derived macrophages were incubated with RPMI 1640 containing 5 μg/mL anti-67LR MLuC5 antibody (Santa Cruz Biotechnology) or isotype-matched control mouse IgM (Santa Cruz Biotechnology) at 37°C in a humidified incubator containing 5% CO_2 for 1 h before the addition of EGCG or LPS.

Assay for Inflammatory Cytokines

The concentrations of TNF-α and IL1-β were determined using enzyme-linked immunosorbent assay (ELISA) kits (Dakewe, China) according to manufacturer instructions. Inflammatory cytokines released in the medium were monitored by Inflammation Antibody Array 3 (Norcross, USA) according to

manufacturer instructions. THP-1-derived macrophages were pretreated with EGCG (50 μg/mL) for 30 min and stimulated with LPS (200 EU/mL) for a further 3 h. PBMC-derived macrophages were pretreated with EGCG (50 μg/mL) for 30 min and stimulated with LPS (200 EU/mL) for a further 3 or 6 h. Data were collected using a chemiluminescence imaging system (Fluor Chem E; ProteinSimple, USA) and analyzed using the RayBio® Human Inflammation Antibody Array 3 Analysis Tool.

Reverse Transcription Polymerase Chain Reaction (RT-PCR) and Quantitative RT-PCR

THP-1-derived macrophages were pretreated with EGCG (50 μg/mL) for 30 min and stimulated with LPS (200 EU/mL) for a further 1 h. RNA was isolated using TransZol® (Transgen, China). Reverse transcription of RNA was done using a PrimeScript™ RT Reagent kit with gDNA Eraser (TaKaRa Bio, Japan). Quantitative PCR was carried out on a 7900HT Real-Time PCR system (Applied Biosystems, USA) using primers (Table S1 in Supplementary Material) for human *actin*, *il1 beta*, *il6*, *il8*, *il10*, *mcp1*, *ccl3*, *ccl4*, *ccl5*, *tnf alpha*, *timp2*, *bhle40*, *ddit4*, *hk2*, *p4ha1*, *pfkfb3*, *rhou*, *elmo1*, *hes1*, and *hey1* using SYBR Green PCR Master Mix (TaKaRa Bio). All reactions were performed in triplicate and normalized to actin expression.

Immunoprecipitation and Posttranslation Modification Assay

For immunoprecipitation, cells were treated with indicated reagents before lysis in lysis buffer (50 mM Tris-HCl, pH 8.0; 120 mM NaCl; 0.5% NP-40) supplemented with a protease inhibitor cocktail (Sigma–Aldrich, USA) and phosphatase inhibitor cocktail (Sigma–Aldrich). After preclearing with protein A/G resin, lysates were incubated with Notch2 antibody for 24 h at 4°C with gentle rotation. Protein A/G resin was added to lysates and incubated for a further 6 h. Then protein A/G resin was spun down and washed five times with lysis buffer, and Notch2 was eluted with sodium citrate (pH 2.5). Notch2 eluates were neutralized with 1.5 M Tris–Cl (pH 8.8) and incubated at 37°C with ataxin-3 and peptide-*N*-glycosidase F (PNGase F) separately. The digested Notch2 was analyzed with a western blotting probe with the indicated antibodies.

Western Blotting

Cells were lysed in 150 μL lysis solution (Beyotime, China) containing phenylmethylsulfonyl fluoride (1 mM). Whole-cell lysate samples were separated by 8% sodium dodecyl sulfate–polyacrylamide gel electrophoresis and transferred to polyvinylidene difluoride membranes (Millipore, USA). The latter were blocked in 5% bovine serum albumin and incubated with primary antibody overnight at 4°C and incubated with horseradish peroxidase-conjugated secondary antibody for 1 h at room temperature. Antibodies against phospho-NF-κB, phospho-Erk1/2, phospho-p38 MAPK, Hes1, Actin, Notch1, and Notch2 were purchased from Cell Signaling Technology (USA). Anti-rabbit IgG and anti-rabbit IgG were purchased from R&D Systems (USA).

Notch Reporter Assays

A total of 293 cells were cotransfected transiently with 16 Notch-responsive element CSL (CBF1, Suppressor of Hairless, Lag-1, CSL)/mini-promoter firefly luciferase reporter (constructed by our research team) and constitutively expressed *Renilla* luciferase reporter (pRL-CMV; Promega, USA). EGCG was added alone or together with ligand-expressing cells (HepG2 cells) 18 h after transfection. Luciferase activities were measured 12–24 h after EGCG addition (Dual Glo Luciferase; Promega). Typically, three replicates were analyzed for each condition, and values were expressed as relative luciferase units (firefly signal divided by the *Renilla* signal).

Molecular Interaction Assay

To measure a possible direct interaction between Notch and EGCG, we prepared the human Notch negative regulation region (NRR). The NRR has been considered to have a key role in Notch activation. The binding affinity of EGCG and NRR was determined using an Octet Red96 system (ForteBio, USA). The biotinylated NRR protein was loaded on Super Streptavidin biosensors and acted with gradient concentration of EGCG in the assay buffer (phosphate-buffered saline, pH 6.5). We measured EGCG association and dissociation for 60 s each. Kinetic parameters and affinities were calculated from a non-linear global fit of the data between EGCG and NRR using Octet Data Analysis v7.0 (ForteBio).

Statistical Analyses

Data are represented as mean ± SD. Data were analyzed using Student's *t*-test with GraphPad (USA). $^{*}p < 0.05$, $^{**}p < 0.01$, and $^{***}p < 0.001$ were considered significant.

RESULTS

EGCG Attenuated the Immediate Early Inflammatory Response

To evaluate the direct effects of EGCG on inflammation, human macrophages differentiated from THP-1 cells (Figures S1 and S2 in Supplementary Material) for 48 h with PMA (10 ng/mL) were pretreated with EGCG (50 μg/mL) for 30 min and then stimulated with LPS (200 EU/mL) for an additional 6 h. Samples of the medium were collected 3 h after LPS stimulation. The concentration of major inflammatory cytokines was measured using ELISA kits.

Lipopolysaccharide stimulated the release of TNF-α (**Figure 1A**) and IL-1β (**Figure 1B**) significantly ($p < 0.001$), and EGCG attenuated release of these cytokines (**Figures 1A,B**) in human macrophages. To determine the effects of EGCG on inflammation in macrophages, we examined expression of inflammatory cytokines in human macrophages in culture supernatants collected 3 h post-LPS treatment under identical experimental conditions using a human inflammation antibody array (RayBio). Expression of all inflammatory cytokines was increased significantly ($p < 0.05$, $p < 0.01$, or $p < 0.001$) by LPS stimulation, as well as by TNF-α and IL-1β (**Figures 1C,D**). Expression of 24 of 40 inflammatory factors induced by LPS

was reduced significantly ($p < 0.05$, $p < 0.01$, or $p < 0.001$) by EGCG, including IL-1β, IL-6, IL-8, IL-10, monocyte chemotactic protein 1 (MCP-1), macrophage inflammatory protein 1-alpha (MIP-1α), MIP-1β, IL-12-p70, regulated on activation, normal T cell expressed and secreted, TNF-α, and TIMP-2 (**Figures 1C,D**; Table S2 in Supplementary Material). With regard to expression of the other 16 cytokines, the EGCG-treated sample showed downregulation, but this value was not significant ($0.05 < p < 0.45$) compared with that obtained for the LPS sample (**Figures 1C,D**). These results suggested that EGCG inhibited the release of inflammatory cytokines in the medium in THP-1-derived human macrophages during the immediate early stage of inflammation induced by LPS.

(−)-Epigallocatechin gallate had been shown to downregulate the mRNA levels of inflammatory cytokines in the intermediate or longer period of treatment of cells (>6 h). To ascertain whether the mRNA level of inflammatory cytokines could be attenuated in the immediate early period of EGCG treatment, the expression of major cytokines was detected on chips 1 h after EGCG addition using real-time PCR. Results showed that the mRNA levels of all

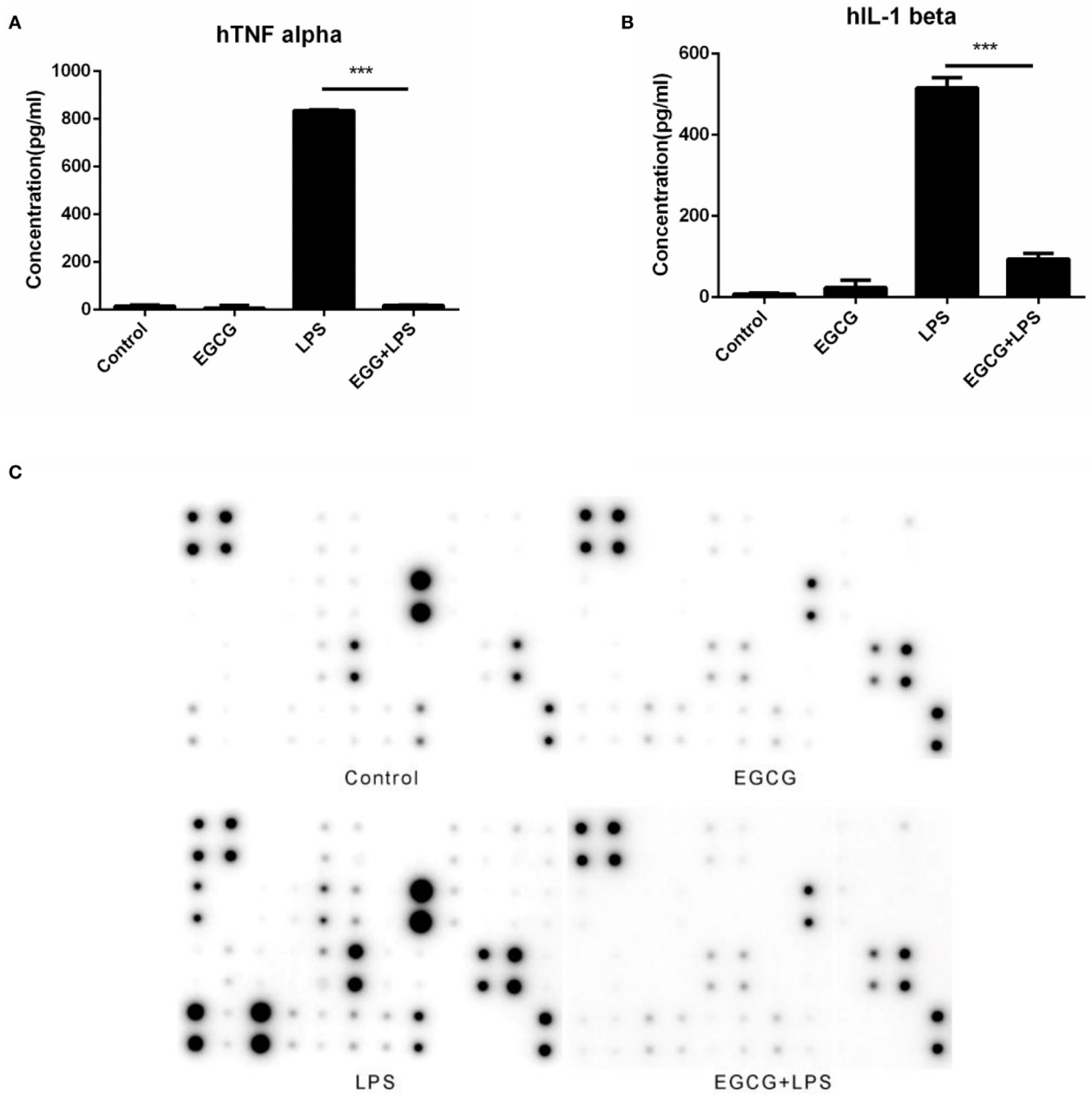

FIGURE 1 | **Continued**

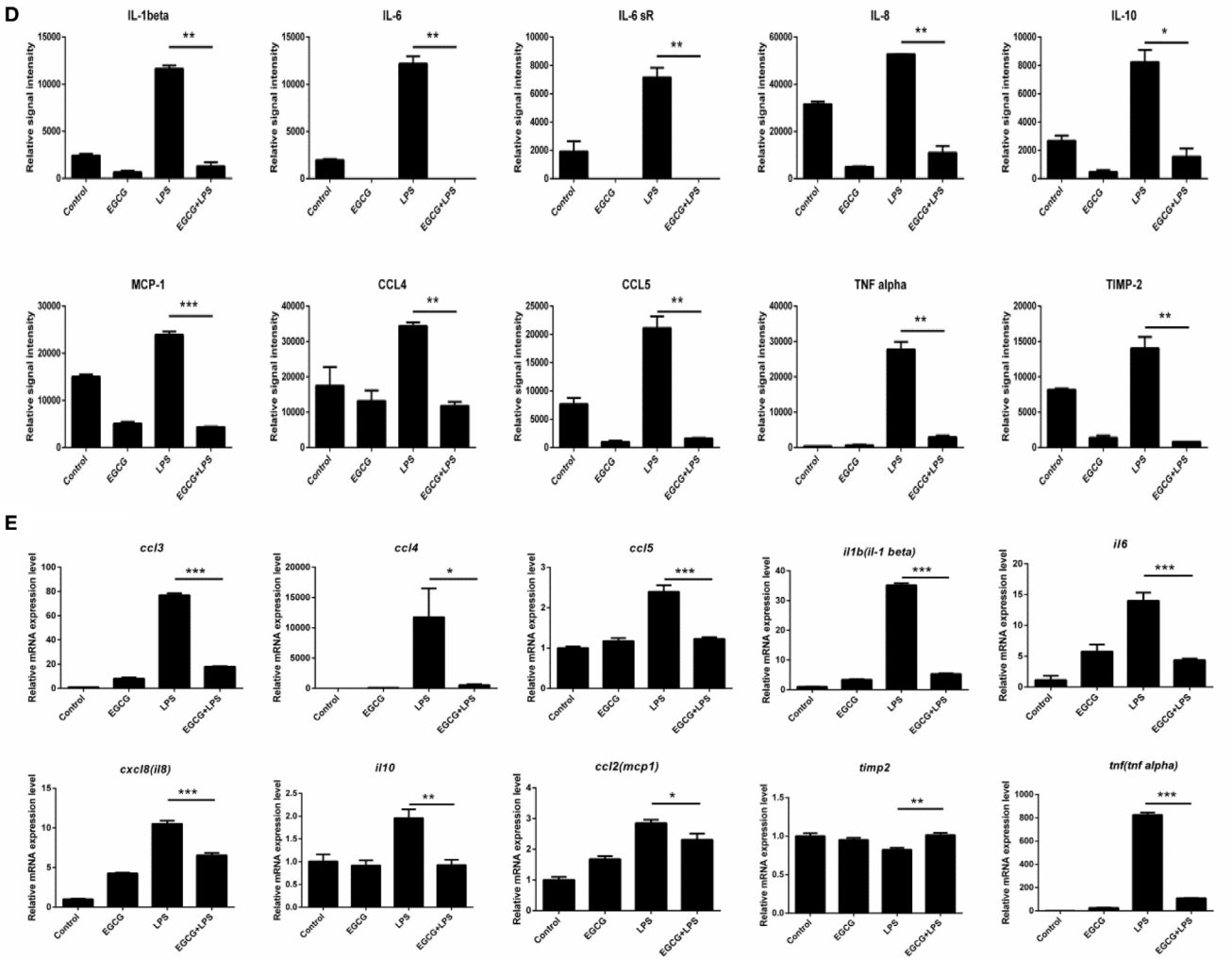

FIGURE 1 | **(–)-Epigallocatechin gallate (EGCG) attenuated the inflammatory response in the immediate early stage**. THP-1-derived macrophages were pretreated with EGCG (50 μg/mL) for 30 min before exposure to lipopolysaccharide (LPS) (200 EU/mL) for 3 h. Expression of the inflammatory cytokines in the culture medium was measured by enzyme-linked immunosorbent assay **(A,B)** and a RayBio® C-Series human inflammation antibody array **(C)**, and chips were scanned and analyzed **(D)**. mRNA levels 1 h after LPS treatment were measured by real-time polymerase chain reaction **(E)**. Data are represented as mean ± SD ($n = 3$). Differences between the two groups were assessed by two-way ANOVA using GraphPad. Representatives of three independent experiments with similar results are shown. Results are represented as mean ± SD (*$p < 0.05$, **$p < 0.01$, and ***$p < 0.001$).

measured inflammatory cytokines were decreased immediately after EGCG addition (**Figure 1E**). Taken together, these results suggested that EGCG could suppress the production of inflammatory cytokines induced by LPS in THP-1-derived human macrophages.

EGCG Attenuated Inflammation Not Involved in the Classical Immune Pathway

Classical NF-κB and MAPK pathways have been proposed as the major mechanisms underlying inflammatory signaling. These pathways have also been proposed to mediate the effects of EGCG on inflammation in the intermediate (>6 h) or longer stages (≥12 h). To ascertain whether EGCG attenuated the immediate inflammatory response *via* the same mechanism, we designed and undertook intervention studies using EGCG.

The phosphorylation of NFκB and MAPK (i.e., p42/44, p38, and JNK) in THP-1-derived human macrophages was detected by western blotting after LPS treatment for 30, 60, and 90 min. EGCG was added 30 min before LPS. In contrast to the mechanisms described for EGCG upon inflammation, the phosphorylation of NFκB (**Figure 2A**), p42/44, and JNK (**Figure 2B**) was not inhibited by EGCG within the first 60 min, and the phosphorylation of p38 increased upon EGCG addition (**Figure 2B**). Sixty minutes after EGCG addition, NFκB phosphorylation remained unchanged. Moreover, the phosphorylation of ERK (p42/44) (**Figure 2B**) also increased upon EGCG addition. Increased phosphorylation has been shown to enhance the inflammatory response, and so the

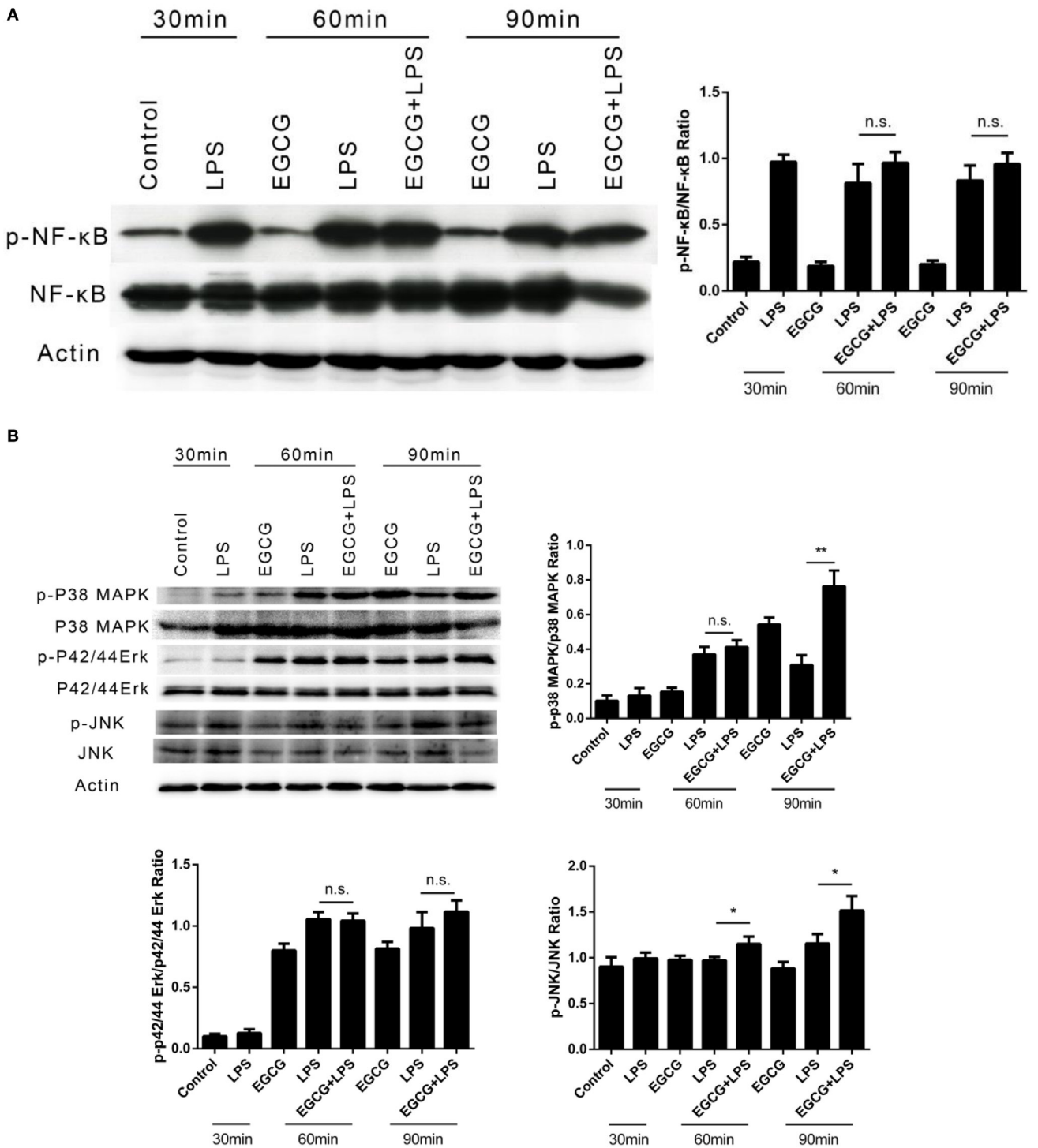

FIGURE 2 | **(–)-Epigallocatechin gallate (EGCG) attenuated inflammation not involved in the classical immune pathway**. THP-1-derived macrophages were treated with lipopolysaccharide (LPS) (200 EU/mL) for 30, 60, and 90 min by pretreated EGCG (50 μg/mL, 30 min). The major immunological pathways nuclear factor-kappa B (NF-κB) **(A)** and MAPK [p38, p42/44, and c-Jun-*N*-terminal kinase (JNK)] **(B)** were detected. n.s., not significant.

increased phosphorylation of MAPK induced by EGCG could not explain the attenuated inflammatory effects of EGCG and nor could NF-κB.

EGCG Turns-Off Notch Signaling

The Notch signaling pathway has a pivotal role in the development of multicellular organisms. Notch (specifically Notch1) is

crucial for lymphocyte development (25). Emerging evidence has shown that the Notch pathway anticipates the immune response, including inflammation (26). Basal activation of Notch1 has been shown to be necessary for enhancement of the inflammatory response (27). To ascertain whether EGCG attenuates the inflammatory response *via* the Notch pathway immediately after its addition, we examined the Notch1 and Notch2 receptors, which are expressed on the surface of human macrophages at multiple time points shortly after EGCG treatment. We found that the number of mature Notch1 and Notch2 receptors was decreased from the cell surface at all time points after EGCG treatment and that this process was not dependent on LPS stimulation (**Figure 3A**). Further studies showed that mature Notch removed the effects of EGCG in a concentration-dependent manner (**Figure 3B**) and that this decreased response was rapid (2 min) (**Figure 3C**). Simultaneously, EGCG treatment accelerated the degradation of the nuclear Notch intercellular domain (NICD), the active form of Notch, in 2 min (**Figure 3D**). In accordance with this result, a western blotting probe with a specific antibody against the new epitope formed after Notch1 cleavage showed that degradation of the active form of Notch1 was promoted by EGCG (**Figure 3E**). These results suggested that the basal signaling of Notch was turned off immediately by EGCG treatment. In accordance with these results, expression of Hes1 (a typical Notch-regulated gene) was downregulated by EGCG (**Figure 3A**). To confirm this result, expression of Notch target genes was evaluated using real-time PCR. We found that expression of some typical Notch target genes was downregulated by EGCG (**Figure 3F**), but not all of them. This finding may have been due to the complexity of gene transcription, which can be influenced by many factors. To evaluate the effects of EGCG treatment on gene expression of Notch alone, a dual luciferase reporter assay was employed. This assay involves use of the luciferase gene, which is controlled by 16×CSL, which contains 16 major Notch-regulated elements (CSL) connected in a series. Results showed that only treatment with EGCG could decrease Notch-related luciferase signaling in 293T cells and HepG2/293T cocultures (**Figure 3G**).

To understand the mechanism of Notch suppression induced by EGCG, the proteasome inhibitor MG132 was used to pretreat macrophages before EGCG addition. Notch degradation was inhibited partially by increasing (10–40 μM) concentrations of MG132 (**Figure 3H**). This result showed that MG132 inhibited the Notch degradation induced by EGCG. Western blotting demonstrated that pre-Notch1/2 accumulated immediately after EGCG treatment and that the molecular weight of pre-Notch1/2 increased over time (**Figures 3B,C**). The major change in molecular weight occurred with posttranslational modification of the protein, including glycosylation and polyubiquitination. Thus, the immunoprecipitated Notch2 from THP-1-derived macrophages was treated separately with PNGase F (which removes *N*-linked polysaccharides from the glycosylated protein) or ataxin-3 (an enzyme that removes ubiquitin from the target protein). The increased molecular weight of the accumulated precursor of Notch2 after EGCG treatment (**Figures 3B,C**) was decreased upon treatment with ataxin-3, but not PNGase F (**Figure 3I**). This result confirmed that pre-Notch was highly ubiquitinated (but not glycosylated) in EGCG-treated cells. In accordance with the MG132-based inhibition of Notch degradation induced by EGCG, the Notch mature/active form was overubiquitinated after EGCG treatment as demonstrated by an immunoprecipitation–western blotting experiment using an antibody against Notch or ubiquitin separately (**Figure 3J**). These results demonstrated that EGCG induced switching off of the Notch signal by inducing Notch degradation *via* a proteasome pathway.

Notch Is a New Target of EGCG Independent of 67LR

67-kDa laminin receptor has been proposed to be a cell surface target for EGCG to mediate its biologic activity (11). Scholars have reported that EGCG downregulates the inflammatory response in mouse macrophages *via* 67LR (28). However, those studies confirmed the effects at long time points (typically >6 h). To ascertain whether 67LR mediated the effects of EGCG on Notch and inflammation in the immediate early stage in THP-1-derived human macrophages, cells were pretreated for 1 h with the anti-67LR antibody MLuC5 (5 μg/mL), which is known to block the interaction between EGCG and 67LR. MluC5 blockade did not affect the suppression of Notch by EGCG (**Figure 4A**) or expression of the typical Notch-regulated protein Hes1 (**Figure 4A**). The effects of EGCG on the NF-κB (Figure S3A in Supplementary Material) and MAPK (Figure S3B in Supplementary Material) pathways were unaltered by MluC5 blockade 30 min after EGCG addition. To study the inflammatory effects of EGCG at the immediate early stage, MLuC5-treated macrophages were pretreated for 30 min with EGCG before LPS exposure. Production of TNF-α and IL-1β in culture supernatants from human macrophages induced by LPS was inhibited markedly by EGCG treatment in anti-67LR antibody-treated cells and control cells (**Figures 4B,C**). To determine the influence of 67LR blockade on the inflammation-attenuated effects of EGCG in human macrophages, we examined the inflammatory cytokines released in culture supernatants 3 h after LPS treatment using a human inflammation antibody array (RayBio). Expression of 27 of 40 inflammatory factors induced by LPS stimulation, as well as TNF-α and IL-1β (**Figures 4B,C**; Table S3 in Supplementary Material), was reduced significantly ($p < 0.05$, $p < 0.01$, or $p < 0.001$) by EGCG when macrophages were blocked by MluC5 (**Figures 4D,E**). These results were comparable to those of the non-blocking experiments (**Figures 1C,D**; Table S3 in Supplementary Material). The expression of major inflammatory cytokines downregulated by EGCG, such as TNF-α, IL-1β, IL-6, IL-8, IL-10, MCP-1, IL-6sR, CCL5/RANTES, and TIMP-2, was not affected by MluC5 pretreatment.

To measure a possible direct interaction between Notch and EGCG, we prepared the human NRR1. The NRR1 is located outside the cell membrane and has been considered to have a key role in Notch1 activation. Binding assays showed that NRR1 had a direct interaction with EGCG and that the affinity of EGCG to NRR1 was 2.44×10^{-6} (**Figure 4F**).

Taken together, these results demonstrated that 67LR had no influence on the inflammation-attenuated effects of EGCG at the immediate early stage. Thus, Notch is a new target of EGCG.

Knockdown of Notch 1/2 Impaired the Effects of EGCG on Inflammation

To investigate whether the effects of EGCG on cellular responses to LPS stimulation are dependent on Notch, we undertook shRNA knockdown of Notch 1/2 in THP-1 cells. THP-1 cells were infected with Notch1/2 shRNA lentiviral particles (Santa Cruz Biotechnology) and screened with puromycin (5 μg/mL) to silence expression of Notch1 or Notch2. Notch

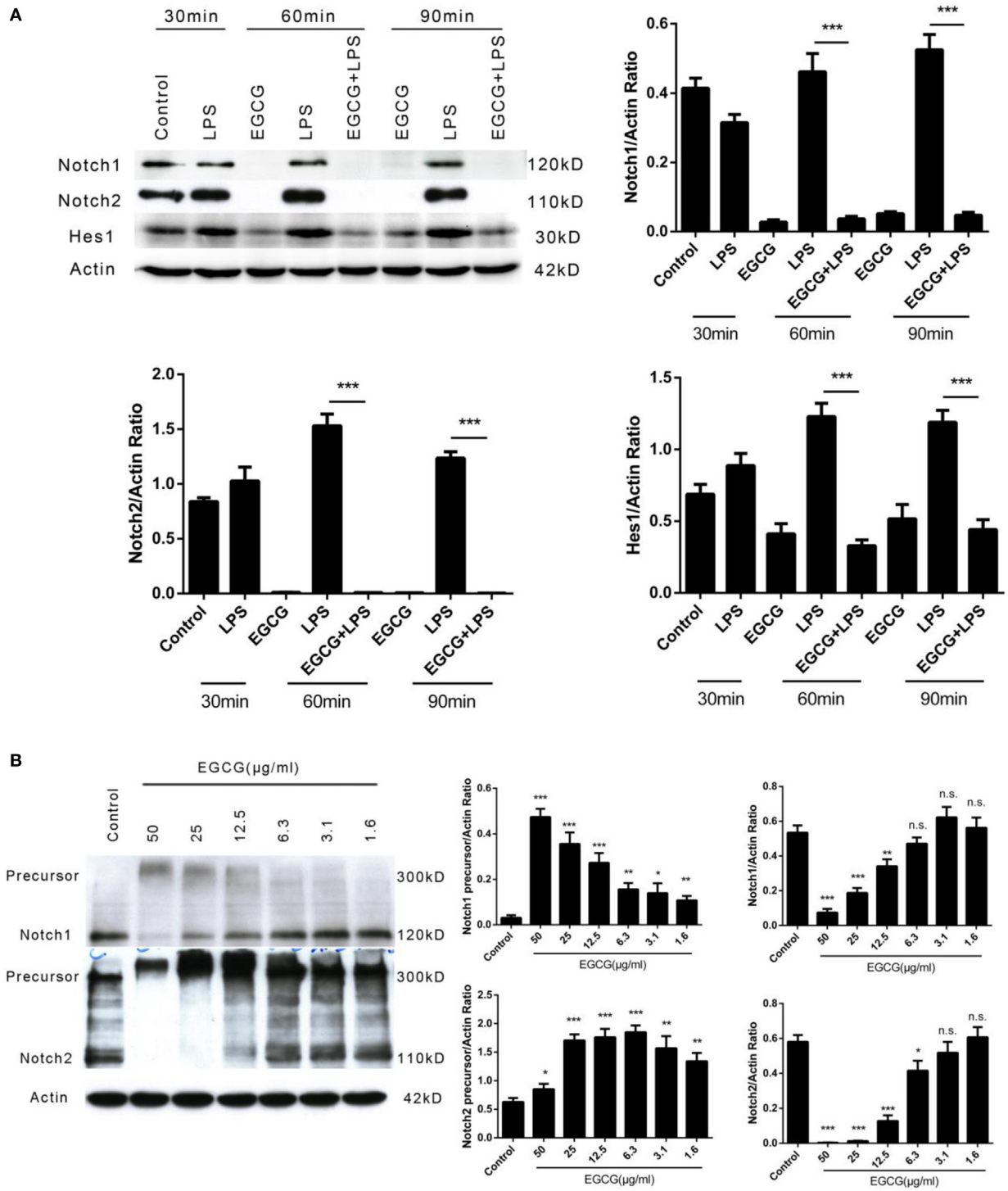

FIGURE 3 | **Continued**

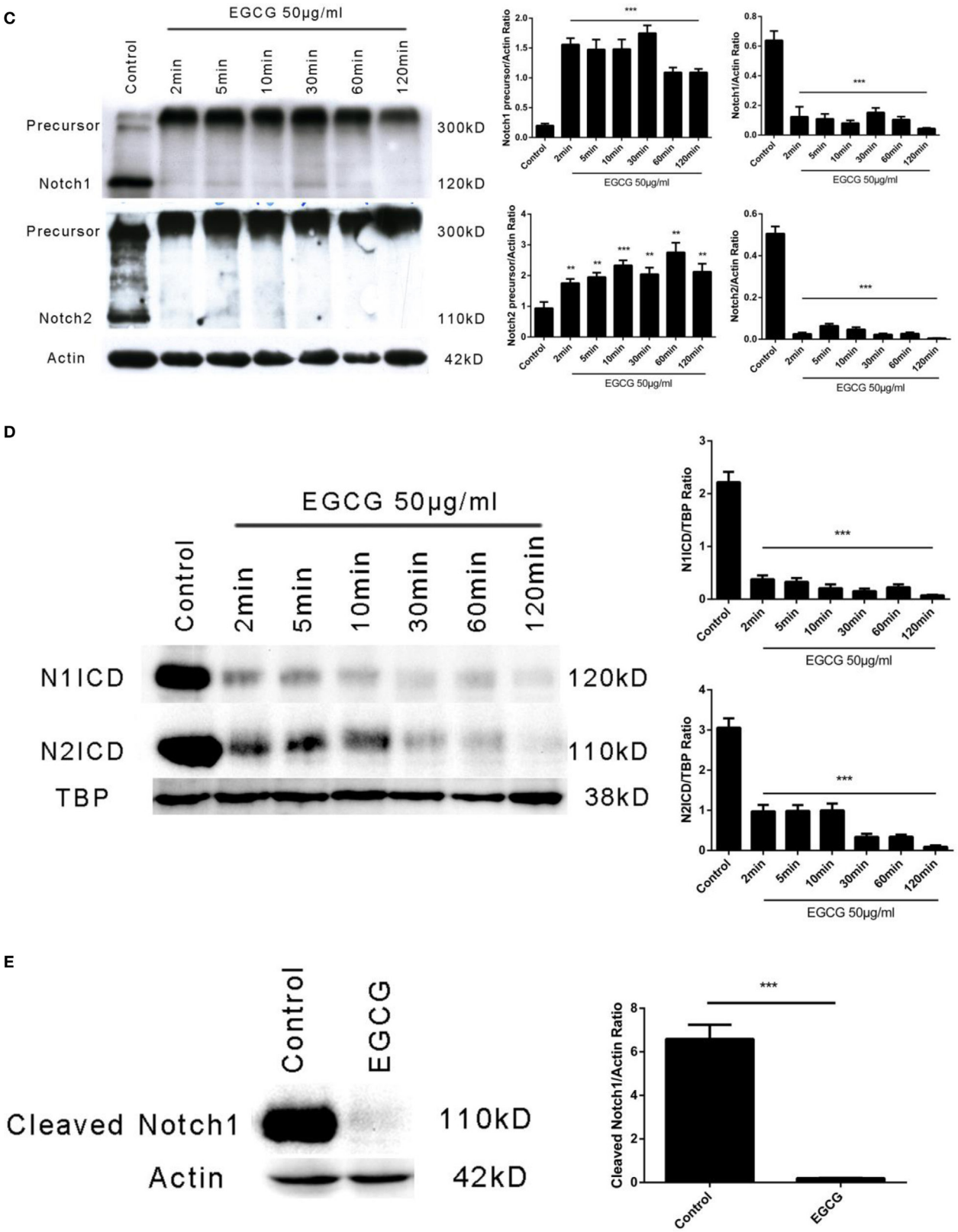

FIGURE 3 | **Continued**

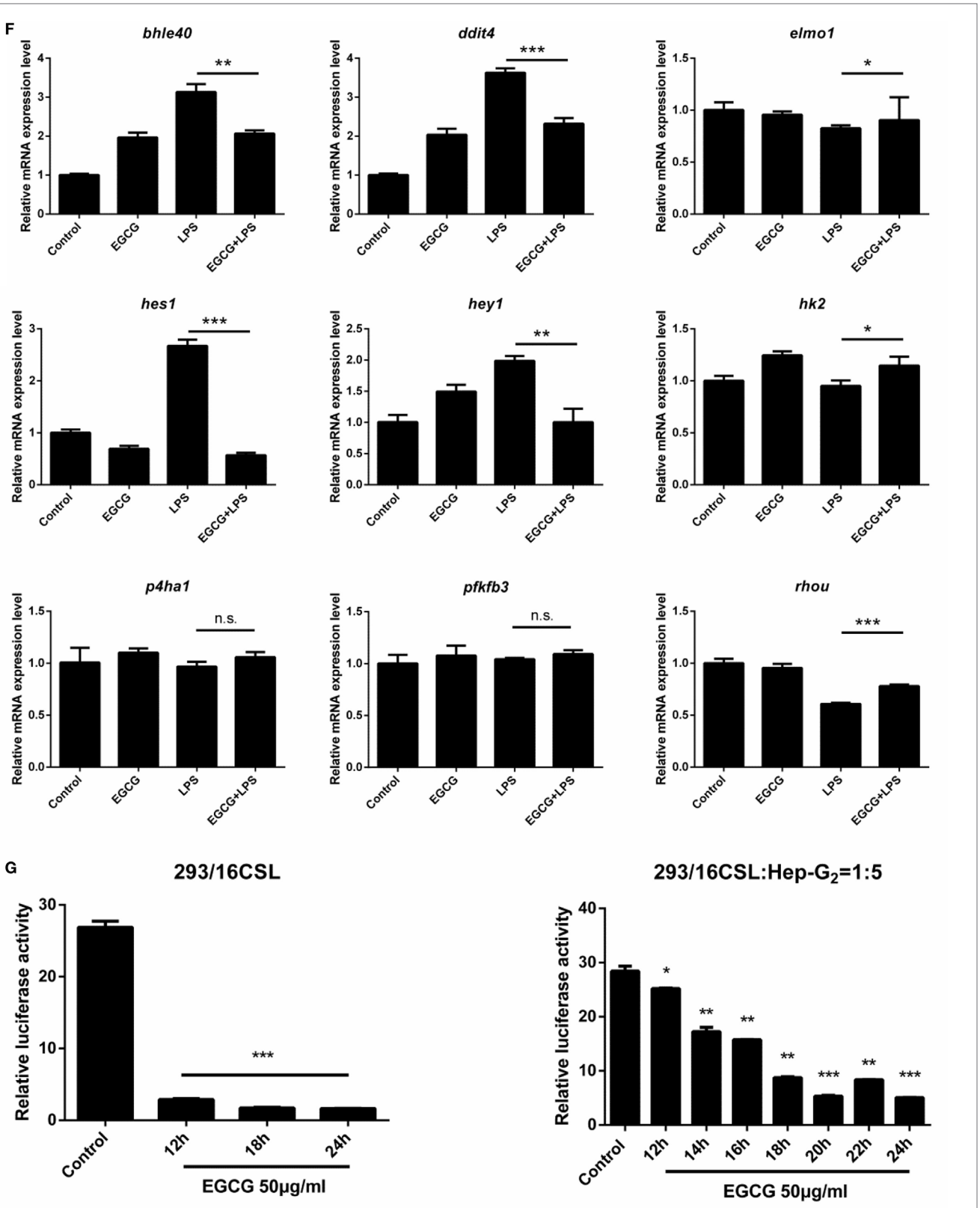

FIGURE 3 | **Continued**

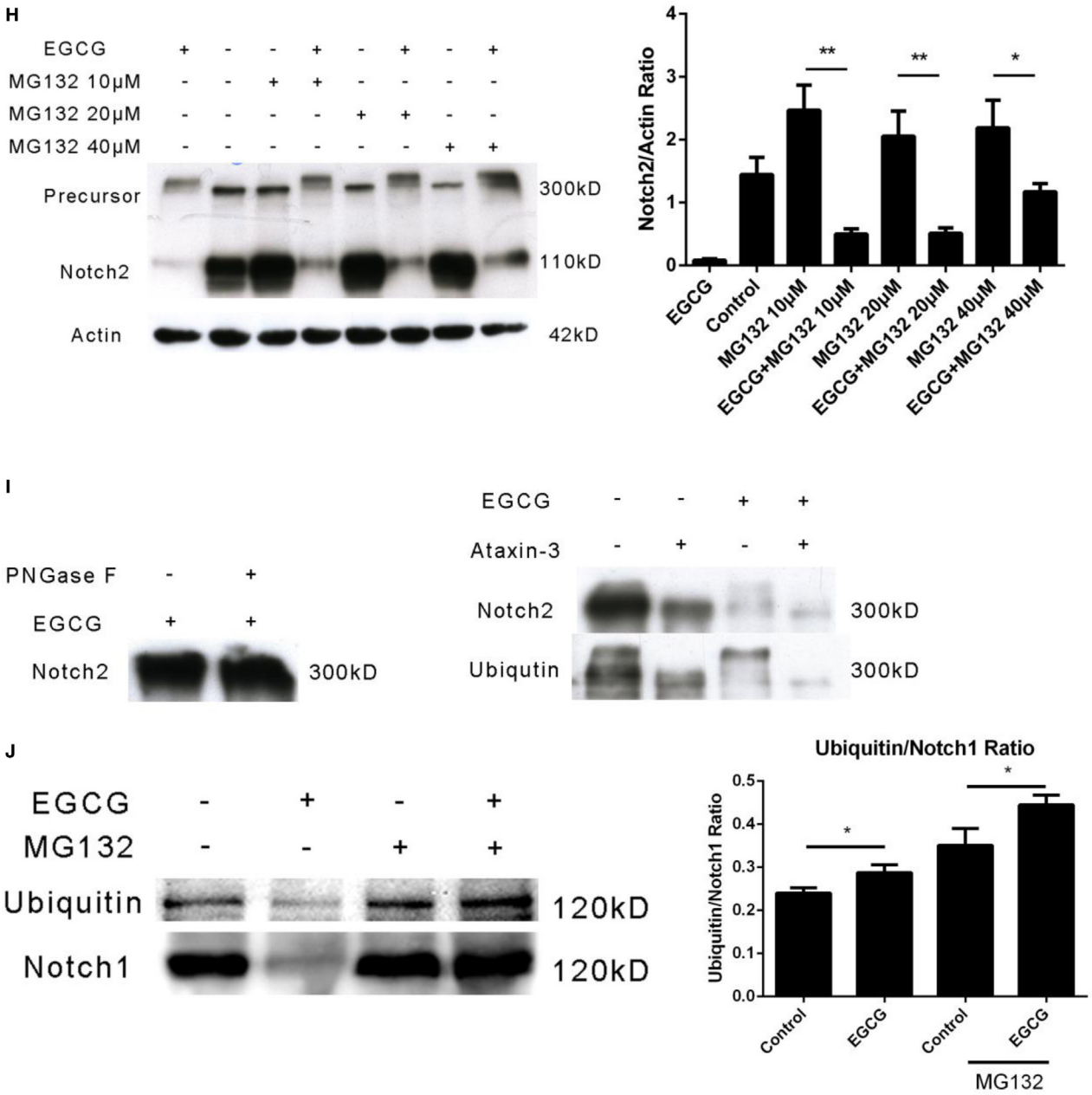

FIGURE 3 | **(–)-Epigallocatechin gallate (EGCG) shuts off the Notch signal**. **(A)** THP-1-derived macrophages were treated with lipopolysaccharide (LPS) (200 EU/mL) for 30, 60, and 90 min by pretreated EGCG (50 μg/mL, 30 min). **(B)** THP-1-derived macrophages were treated with EGCG (50, 25, 12.5, 6.3, 3.1, and 1.6 μg/mL) for 30 min. **(C)** THP-1-derived macrophages were treated with EGCG (50 μg/mL) from 2 to 120 min. **(D)** THP-1-derived macrophages were treated with EGCG (50 μg/mL) from 2 to 120 min. Notch intercellular domain (NICD) of Notch1 and Notch2 located in the nucleus was detected, with TATA-binding protein (TBP) used as the internal control. **(E)** THP-1-derived macrophages were treated with EGCG (50 μg/mL) for 30 min, and lysates were analyzed by a western blotting probe with an antibody recognizing the epitope specific for active Notch1. **(F)** THP-1-derived macrophages were pretreated with EGCG (50 μg/mL) for 30 min and exposed to LPS (200 EU/mL) for 1 h. mRNA expression was measured by real-time polymerase chain reaction. **(G)** Notch report assays: 293/16CSL alone (left) and 293/16CSL with HepG2 coculture (right). **(H)** THP-1-derived macrophages were treated with EGCG (50 μg/mL) for 30 min with or without MG132 (10, 20, and 40 μM). **(I)** Immunoprecipitation was used to pull-down Notch from macrophage cell lysates. The Notch eluate was digested with PNGase F (left) and ATX-3 (right) and probed with the appropriate antibody. **(J)** Immunoprecipitation undertaken with antibody against the *C*-terminal of Notch1. The western blotting membrane was probed with an antibody against Notch1 or ubiquitin separately. Data are represented as mean ± SD ($n = 3$). Differences between the two groups were assessed by two-way ANOVA using GraphPad. Representatives of three independent experiments with similar results are shown. Results are represented as mean ± SD (*$p < 0.05$, **$p < 0.01$, and ***$p < 0.001$). n.s., not significant.

1/2 silencing was confirmed by western blotting (**Figure 5A**). Notch 1/2-silenced THP-1 cells were treated with PMA (10 ng/mL) for 48 h to obtain macrophages that were similar to wild-type macrophages. Notch 1/2-silenced macrophages were stimulated with LPS (200 EU/mL) and pretreated (or not) for 30 min with EGCG. Expression of the inflammatory cytokines in samples 3 h after LPS addition was measured using a human inflammation antibody array (RayBio). Results showed that Notch1/2 knockdown impaired the attenuated effects of EGCG on release of inflammatory cytokines (**Figures 5B–E**). Further analyses of the inflammation array results revealed that Notch1 knockdown blocked the attenuated effects of EGCG in 30 of 40 of the inflammatory cytokines and that knockdown of Notch2 blocked the attenuated effects of EGCG in 31 of the

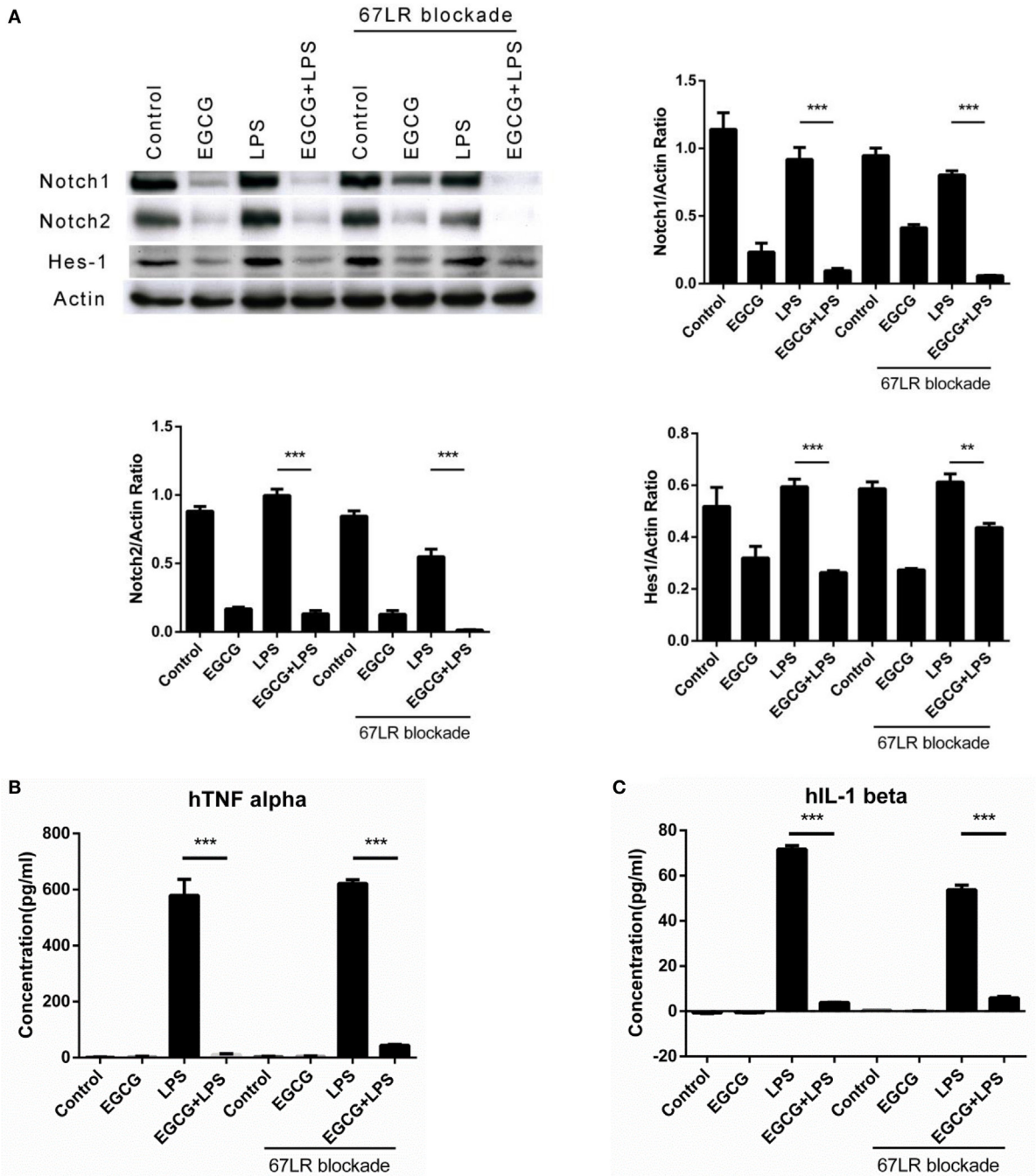

FIGURE 4 | **Continued**

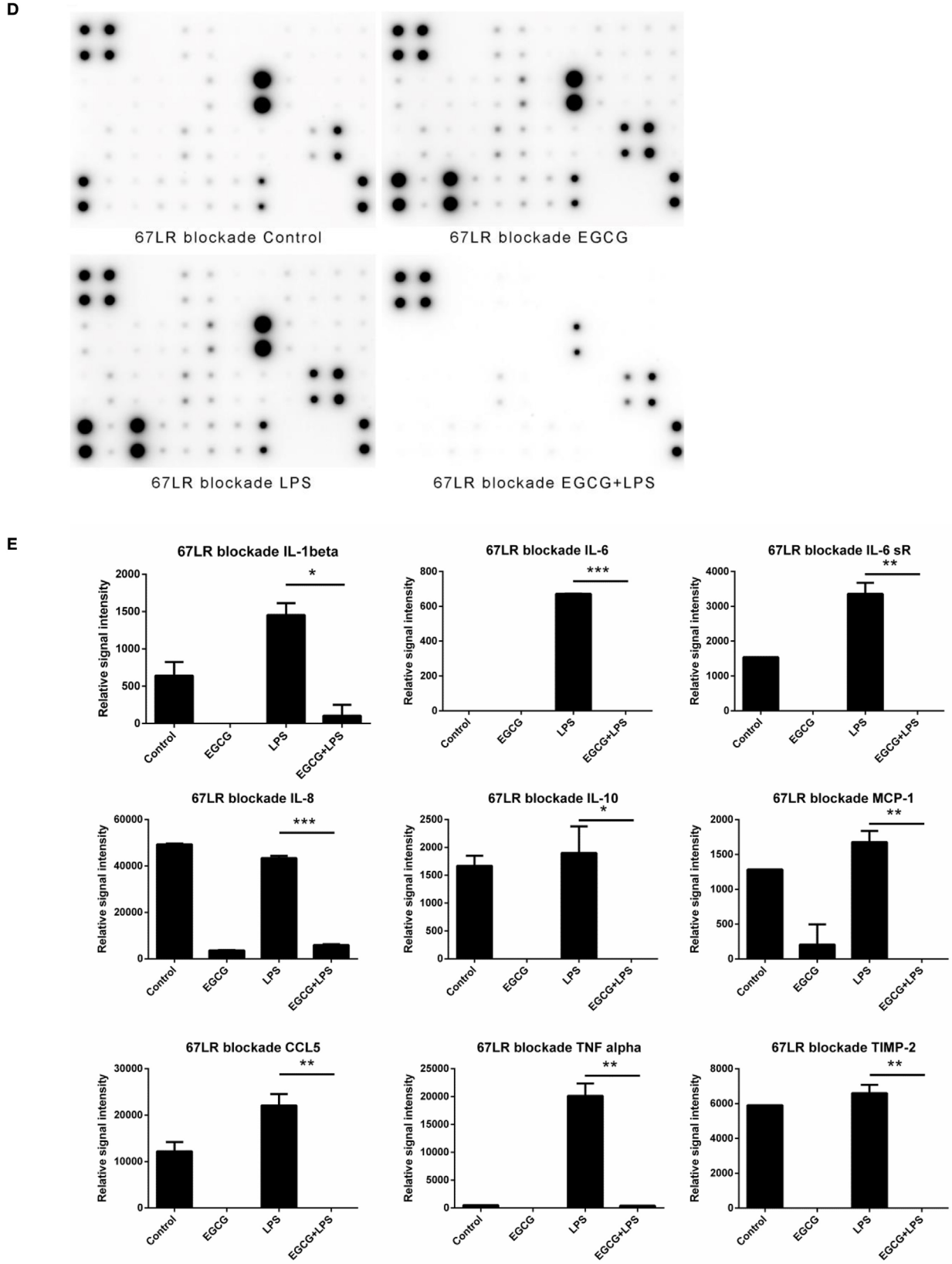

FIGURE 4 | **Continued**

F

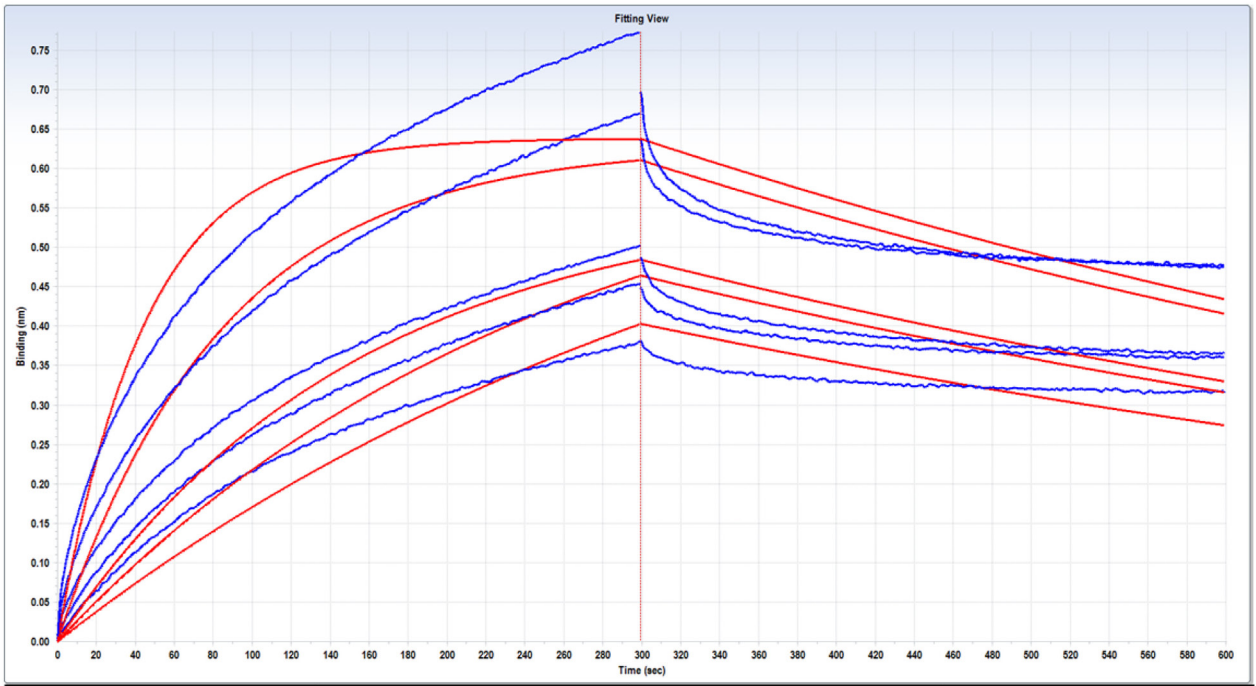

KD (M)	kon(1/Ms)	kdis(1/s)	Full R^2
2.44E-06	5.25E+02	1.28E-03	0.936015

FIGURE 4 | Notch is a new target of (−)-epigallocatechin gallate (EGCG) independent of the 67-kDa laminin receptor (67LR). THP-1-derived macrophages were preincubated with 67LR antibody (5 μg/mL) for 1 h and then treated with EGCG (50 μg/mL) for 30 min. Cell lysates were probed with Notch1/2 and hairy and enhancer of split-1 (Hes1). **(A)** THP-1-derived macrophages were pretreated with EGCG (50 μg/mL) for 30 min before exposure to lipopolysaccharide (LPS) (200 EU/mL) for 3 h. Cell lysates were probed with Notch1/2 and Hes1 **(A)**. Expression of the inflammatory cytokines in THP-1-derived macrophages in the culture medium was measured by enzyme-linked immunosorbent assay **(B,C)** and RayBio C-Series human inflammation antibody array **(D)**. Chips were scanned and analyzed **(E)**. **(F)** Interaction between EGCG and NRR1 was measured on an Octet Red96 system with association and dissociation for 300 s, respectively. The concentration of EGCG used was a double dilution starting from 40 μM. Kinetic parameters and affinities were calculated from a non-linear global fit. Data are represented as mean ± SD ($n = 3$). Differences between the two groups were assessed by two-way ANOVA using GraphPad. Representatives of three independent experiments with similar results are shown. Results are represented as mean ± SD (*$p < 0.05$, **$p < 0.01$, and ***$p < 0.001$).

40 inflammatory cytokines (**Figures 5B–E**; Tables S3 and S4 in Supplementary Material). These results demonstrated that Notch1/2 knockdown greatly impaired the inflammation-attenuated effects of EGCG and that Notch1/2 is a major target for EGCG for reduction of the inflammatory response in the early stage.

We wished to evaluate whether overexpression of the active form of Notch could impair the inflammation-attenuated effects of EGCG. Hence, NICD-green fluorescent protein, the constitutively active form of Notch1, was overexpressed in THP-1 cells by transfection, and the cells were sorted by fluorescence-activated cell sorting. However, transfection of the active form of Notch did not erase the effects of EGCG (**Figure 5F**) because EGCG treatment led to degradation of the original form and active form of Notch (**Figure 5G**). These data suggested that rapid degradation of Notch (including the basal active NICD) was induced by EGCG treatment. Such treatment also accelerated degradation of the active form of Notch (NICD-GFP).

EGCG Suppressed LPS-Induced Inflammation in Human Primary Macrophages

We demonstrated that EGCG attenuated the LPS-induced inflammation response *via* Notch1/2 in THP-1-derived macrophages. However, the THP-1 cell is derived from a patient with acute monocytic leukemia, and so it may demonstrate different mechanisms with regard to regulation of the inflammatory response. To evaluate the effects of EGCG on normal human cells, we examined the anti-inflammatory effect of EGCG on primary human macrophages differentiated from PBMCs collected from healthy human donors. Human primary macrophages cultured with 5% autologous serum were used in LPS/EGCG experiments. Similar to THP-1-derived macrophages, primary human macrophages were pretreated for 30 min with EGCG before LPS exposure. In accordance with the findings obtained in THP-1 cells, TNF-α production in the culture supernatants obtained from primary

human macrophages was increased significantly ($p < 0.001$) with LPS treatment, and LPS-induced production of inflammatory cytokines was inhibited significantly ($p < 0.001$) in EGCG-pretreated cells (**Figure 6A**). EGCG treatment also suppressed the expression of Notch1/2 and the typical Notch target protein Hes1 (**Figure 6B**). The time course in EGCG-treated human primary macrophages showed that EGCG suppressed Notch1/2 at 2 min (**Figure 6C**). Taken together, these results showed that human primary macrophages obtained from PBMCs exhibited the same effects as THP-1-derived macrophages upon EGCG treatment.

DISCUSSION

The inflammatory response, specifically that induced by LPS, can be elicited in minutes and even seconds (29, 30). The phosphorylation and nuclear translocation of the major mediators of inflammation, such as NF-κB, can be detected within 1 min (31, 32). Upregulated expression of the genes of inflammatory cytokines can be observed within several minutes using real-time PCR. Moreover, the release of the "first round" of inflammatory cytokines, such as TNF-α, can be measured by ELISA 2–3 h

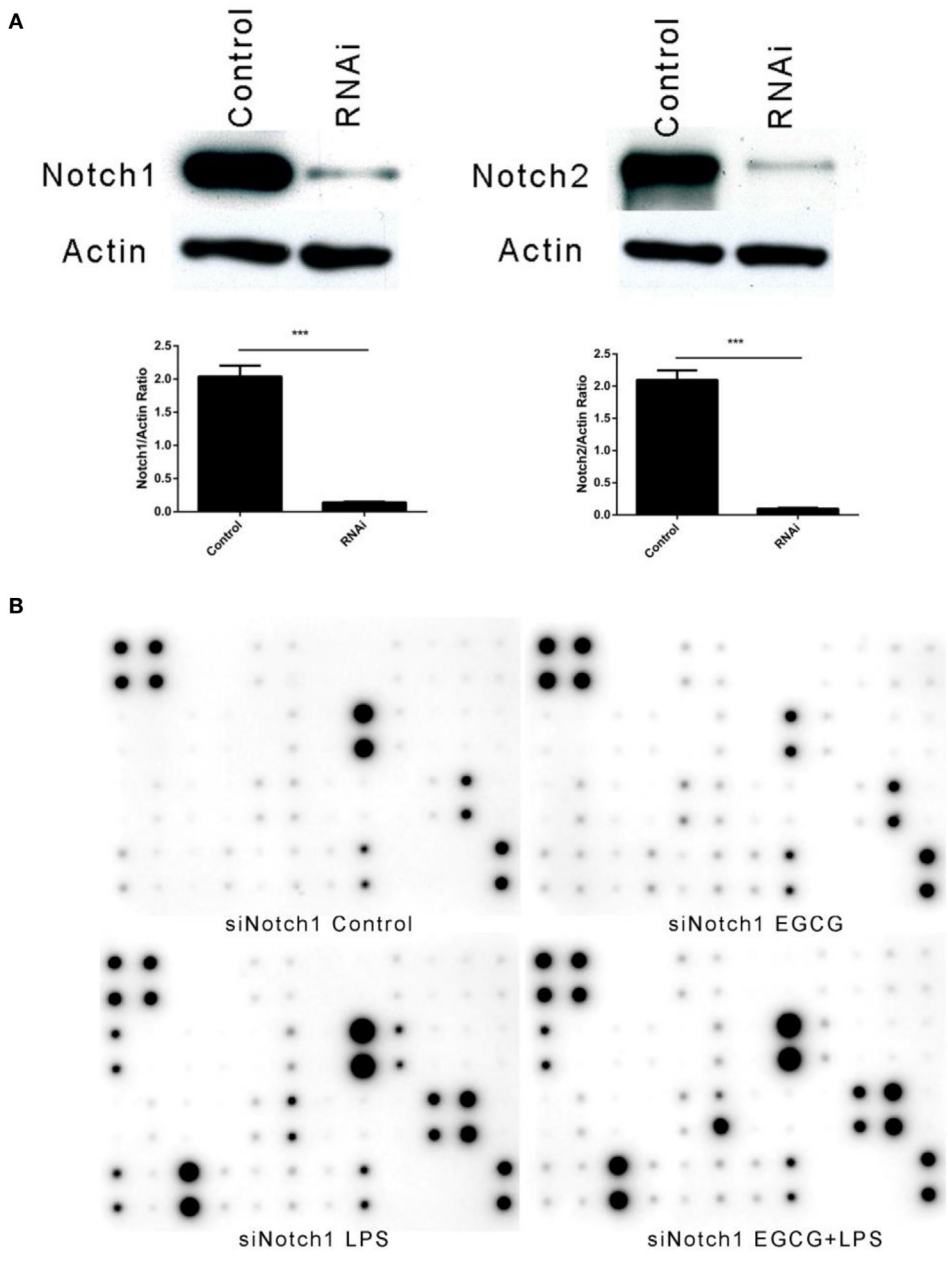

FIGURE 5 | **Continued**

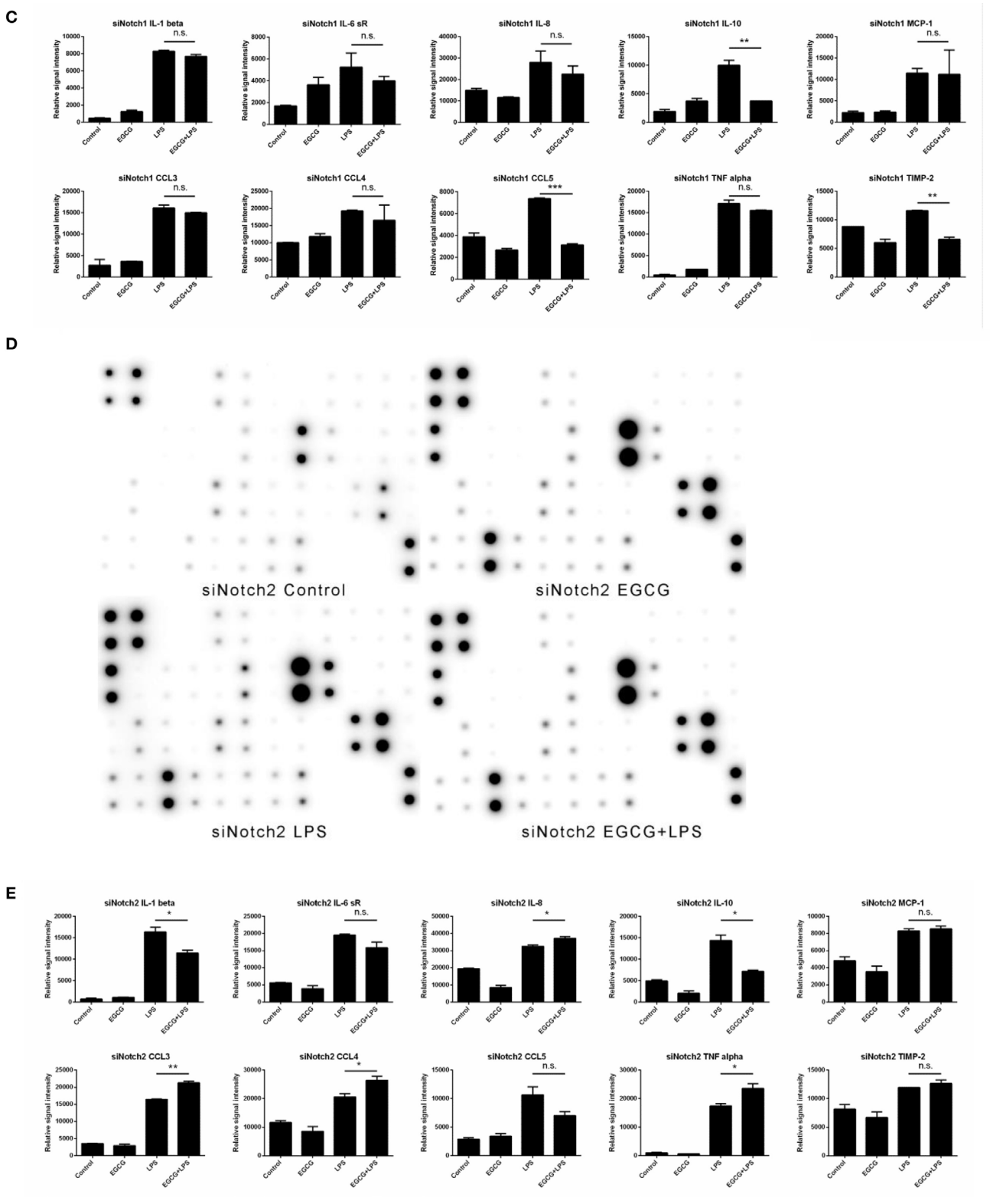

FIGURE 5 | **Continued**

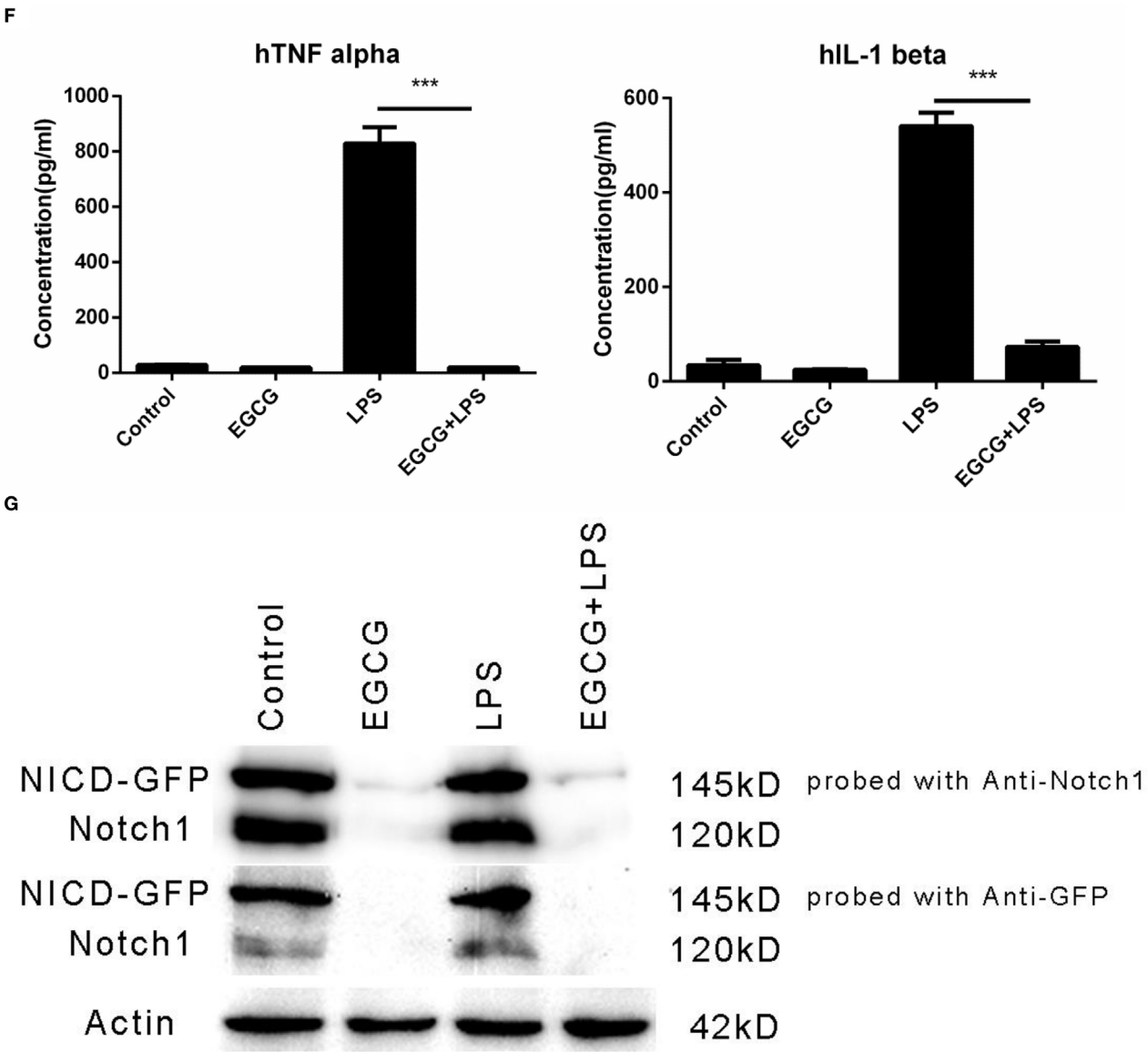

FIGURE 5 | Notch1/2 knockdown impaired the effects of (−)-epigallocatechin gallate (EGCG) on inflammation. After knockdown of Notch1 or Notch2 through infection by lentivirus particles, inflammation experiments were done the same way as for wild-type THP-1-derived macrophages. Knockdown of Notch1 or Notch2 was confirmed by western blotting **(A)**. Notch1/2 knockdown macrophages were pretreated with EGCG (50 μg/mL) for 30 min before exposure to lipopolysaccharide (LPS) (200 EU/mL) for 3 h. Expression of the inflammatory cytokines in the culture medium was measured by a RayBio C-Series human inflammation antibody array: Notch1 knockdown **(B)** and Notch2 knockdown **(D)**. Chips were scanned and analyzed: Notch1 knockdown **(C)** and Notch2 knockdown **(E)**. Notch intercellular domain (NICD)-green fluorescent protein (GFP)-overexpressed macrophages were pretreated with EGCG (50 μg/mL) for 30 min and exposed to LPS (200 EU/mL) for 3 h. Levels of tumor necrosis factor (TNF)-α and interleukin (IL)-1β in the culture medium were measured by enzyme-linked immunosorbent assay **(F)**, and cell lysates were analyzed by western blotting and a probe with antibody against Notch1 or GFP separately **(G)**. Data are represented as mean ± SD ($n = 3$). Differences between the two groups were assessed by two-way ANOVA using GraphPad. Representatives of three independent experiments with similar results are shown. Results are represented as mean ± SD (*$p < 0.05$, **$p < 0.01$, and ***$p < 0.001$). n.s., not significant.

after LPS addition. Three hours later, the released cytokines in the medium can engage with receptors on the cell membranes of cells to initiate the "second round" of the cellular response, including inflammation. Taken together, these events complicate examination of the mechanism underlying regulation of the inflammatory response and interference by special reagents. Thus, it is important to uncover the original mechanism or target in the immediate early stage.

(−)-Epigallocatechin gallate is a major bioactive compound found in Chinese green tea. It has been shown to attenuate the inflammatory response (33). The mechanisms of EGCG upon inflammation have been explored in detail. However, those

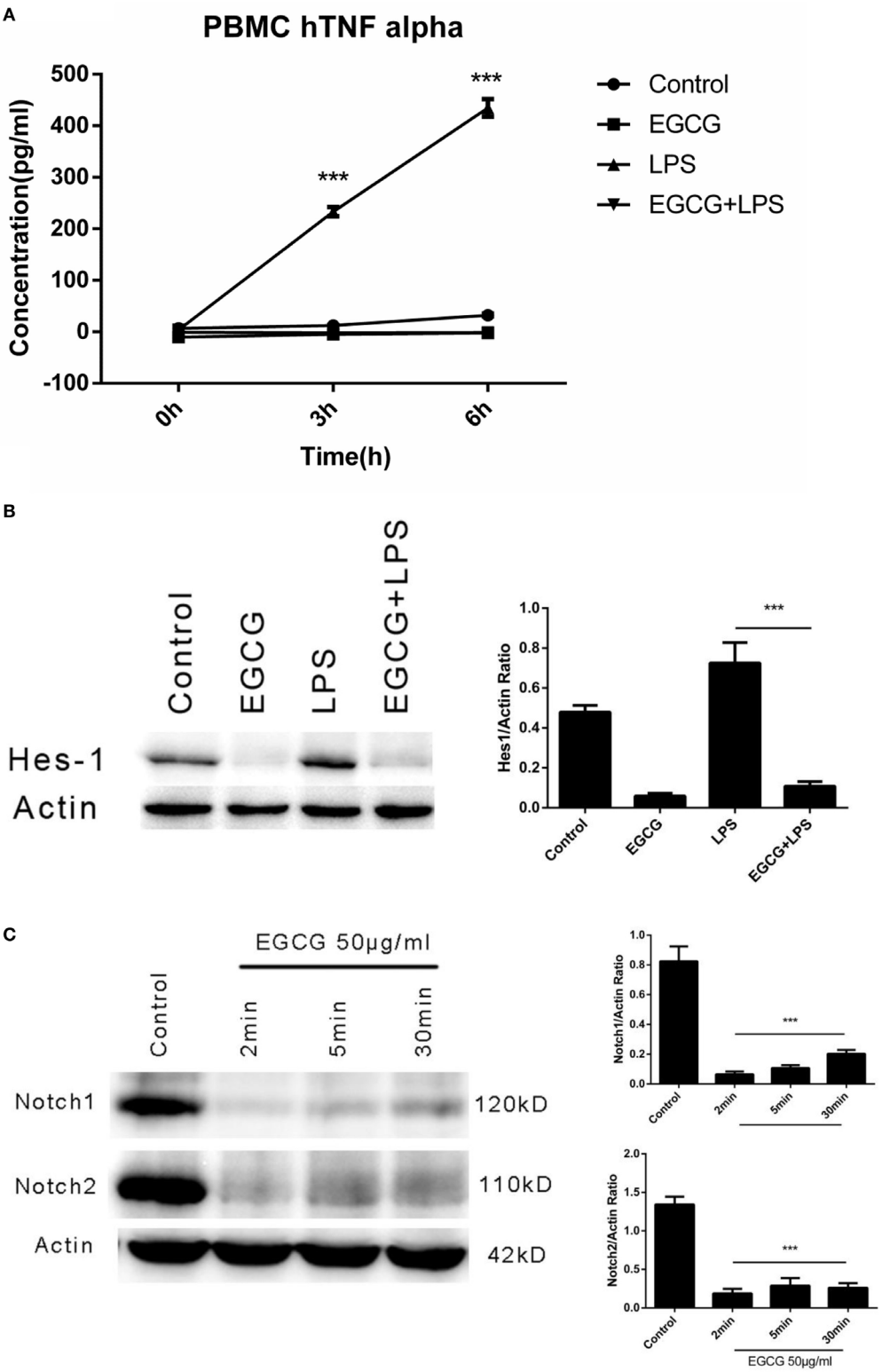

FIGURE 6 | **(–)-Epigallocatechin gallate (EGCG) suppressed lipopolysaccharide (LPS)-induced inflammation in human primary macrophages**. Human primary macrophages derived from peripheral blood mononuclear cells (PBMCs) cultured with autologous serum were pretreated with EGCG (50 μg/mL) for 30 min and exposed to LPS (200 EU/mL) for 3 h. Expression of inflammatory cytokines was measured by enzyme-linked immunosorbent assay **(A)**. Cell lysates 30 min after EGCG treatment were analyzed by western blotting and probed with hairy and enhancer of split-1 (Hes1) antibody **(B)**. Cell lysates from time course experiments of EGCG treatment were analyzed by western blotting and probed with a Notch1/2 antibody **(C)**.

studies focused on the intermediate or longer stages, which is typically >6 h or overnight, following EGCG treatment (34, 35). EGCG has been shown to downregulate the phosphorylation of key regulators of the classical pathway of the inflammatory response, such as NF-κB. In addition, 67LR (which has been proposed to be the receptor for EGCG identified from mouse cell membranes) has been shown to mediate downregulation of the anti-inflammation effects of EGCG. However, those studies also focused on the physiologic responses of cells ≥6 h after EGCG treatment. Those data suggest that EGCG treatment interferes with the mediator proteins in the signal transduction pathway, but the original mechanism of EGCG treatment is not known.

Here, we studied the immediate early response of macrophages after EGCG addition and revealed the mechanism of action of Notch. First, the inflammation-attenuated effects of EGCG in the immediate early stage were confirmed by measuring cytokine levels in the culture medium and cytokine mRNA levels in macrophages. Induction of inflammatory cytokines can be measured only 3 h after LPS addition, so ELISA and human inflammation chips were employed. EGCG reduced the expression of 24 of 40 inflammatory cytokines, and mRNA levels decreased in 9 of 10 genes 1 h after LPS addition. These results confirm that EGCG attenuates the LPS-induced inflammatory response in the immediate early stage. With regard to classical inflammation pathways, NF-κB and MAPK were examined to ascertain whether they are the major mediators of the EGCG-regulated inflammatory response in the immediate early stage. Unexpectedly, the NF-κB and MAPK pathways were not involved in reducing the anti-inflammatory effects of EGCG. However, increased phosphorylation of p38 and ERK was observed after EGCG addition (**Figure 2B**). This finding conflicts with data showing that MAPK is inhibited by EGCG (36, 37). The active form of the MAPK pathway is considered to increase the inflammatory response, even though it is a weaker regulator compared with NF-κB in macrophages. The increased activation of MAPK by EGCG in the early stage may be due to an unknown mechanism of EGCG. These data suggest the EGCG may target two signaling pathways that regulate inflammation at the early stage: activation of MAPK and shutting down Notch. In accordance with this hypothesis, EGCG treatment increased the basal inflammatory response due to MAPK activation when Notch1 was knocked down.

Based on the potential relationship between EGCG/Notch shown previously and knowledge of the role of Notch in the inflammatory process, Notch signaling was examined for mature Notch receptors and the active form of Notch, NICD (which is located in the nucleus). We found that the Notch receptor on cell membranes and the basal signal of NICD in the nucleus were erased 2 min after EGCG addition. Further study showed that the Notch signal shut-off by EGCG was concentration dependent and was not dependent on LPS treatment. Consistent with the suppression of Notch signaling, the mRNA levels of typical Notch-regulated genes were downregulated following EGCG treatment, including the protein levels of Notch target genes such as HES-1. These results demonstrate that basal Notch signaling was suppressed by EGCG. To evaluate the Notch-suppressive effect of EGCG in live cells, we undertook a Notch reporter assay in 293T cells transfected with pCMV/R-Luc and a firefly luciferase Notch reporter plasmid. We constructed them by placing the multiple NICD binding sequence (16CSL) upstream of the mini-promoter to control expression of the firefly luciferase gene. Coculture of 293T cells with HepG2 (used to provide the ligand for Notch activation) and 293T cells alone showed that Notch signaling was suppressed upon EGCG treatment. The proteasome inhibitor MG132 inhibited the Notch degradation induced by EGCG. Consistent with this result, the increase in molecular weight of pre-Notch2 induced by EGCG was confirmed due to multiple ubiquitination. Also, the ubiquitination level of mature/active Notch was increased by EGCG treatment. These results show that EGCG suppresses Notch signaling *via* a proteasome pathway.

We revealed that Notch localized on cell membranes can be a target of EGCG to attenuate the immune response in the immediate early stage. However, another surface protein, 67LR, has been shown to mediate the attenuated effect of the immune response by EGCG. To determine whether the effects of EGCG on Notch are 67LR dependent, the 67LR-blocking antibody MluC5 (which has been shown to block the 67LR-dependent effects of EGCG) was used in EGCG/Notch experiments to block the potential effects of EGCG/67LR on Notch. 67LR blockade did not impair the effects of EGCG on the immune response and Notch. These results also show that the effects of Notch by EGCG are not dependent on 67LR and that EGCG interacts with the NRR1 located outside the cell membrane of mature Notch1 at high affinity. Hence, Notch is a new target of EGCG that can modulate the immune response at the immediate early stage.

To evaluate the necessity of Notch in the immune response induced by EGCG, Notch1/2 was knocked down by infecting THP-1 cells with Notch1/2 shRNA lentiviral particles. The EGCG/Notch experiments done in macrophages derived from Notch1/2 knockdown THP-1 cells showed that knockdown of Notch1/2 lowered the strength of the immune response induced by LPS and impaired the attenuated effects of EGCG in the immediate early stage. The NICD overexpression experiment didn't show new results due to the transfected NICD is promoted to degradation by the EGCG treatment also. A basal active Notch signal is necessary for amplification of the inflammatory response, so Notch1/2 knockdown can decrease the severity of inflammation. Also, EGCG cannot lower the inflammation further if Notch1/2 has been knocked down (Figure S4 in Supplementary Material). Hence, we can conclude that Notch is the primary target of EGCG to downregulate inflammation in wild-type macrophages. Taken together, these results are consistent with previous reports on the function of Notch in the immune response and provide new information. We also carried out the EGCG/Notch experiments on primary human macrophages differentiated from PBMCs obtained from healthy donors. Those results confirmed the effects of EGCG on Notch and the immune response.

Interestingly, we showed that the Notch shut-off by EGCG is not dependent on LPS treatment and last from minutes to over 6–18 h during the EGCG treatment (Figure S5 in Supplementary Material). These results suggest that the interaction between Notch and EGCG is likely to be a conservative biochemical reaction in other types of cells, not just macrophages. Attenuation

of the inflammatory response could be just one of the effects of EGCG/Notch in macrophages. There may be diverse effects upon different cell types by EGCG due to the multiple functions of the Notch receptor (38).

In summary, we examined the immediate early mechanism of EGCG on the inflammatory response induced by LPS in human macrophages. We found that shutting off of Notch signaling is a key event in the inflammation–attenuation effects induced by EGCG in the immediate early stage.

AUTHOR CONTRIBUTIONS

JS, XW, and SH conceived and designed the experiments. TW, ZX, XL, YW, CF, SS, CL, HY, HW, and LY performed the experiments and analyzed the data. JS, XW, and SH contributed reagents/materials/analysis tools. TW and XL wrote the manuscript. All authors read and approved the final manuscript.

FUNDING

This research was supported by grants from the National Natural Science Foundation of China (31460392).

SUPPLEMENTARY MATERIAL

The Supplementary Material for this article can be found online at http://journal.frontiersin.org/article/10.3389/fimmu.2017.00433/full#supplementary-material.

REFERENCES

1. Coussens LM, Werb Z. Inflammation and cancer. *Nature* (2002) 420(6917):860–7. doi:10.1038/nature01322
2. Wellen KE, Hotamisligil GS. Inflammation, stress, and diabetes. *J Clin Invest* (2005) 115(5):1111–9. doi:10.1172/JCI25102
3. Kamada N, Seo SU, Chen GY, Nunez G. Role of the gut microbiota in immunity and inflammatory disease. *Nat Rev Immunol* (2013) 13(5):321–35. doi:10.1038/nri3430
4. Heneka MT, Carson MJ, El Khoury J, Landreth GE, Brosseron F, Feinstein DL, et al. Neuroinflammation in Alzheimer's disease. *Lancet Neurol* (2015) 14(4):388–405. doi:10.1016/S1474-4422(15)70016-5
5. Tabas I, Glass CK. Anti-inflammatory therapy in chronic disease: challenges and opportunities. *Science* (2013) 339(6116):166–72. doi:10.1126/science.1230720
6. Newman DJ, Cragg GM. Natural products as sources of new drugs over the 30 years from 1981 to 2010. *J Nat Prod* (2012) 75(3):311–35. doi:10.1021/np200906s
7. Villa FA, Gerwick L. Marine natural product drug discovery: leads for treatment of inflammation, cancer, infections, and neurological disorders. *Immunopharmacol Immunotoxicol* (2010) 32(2):228–37. doi:10.3109/08923970903296136
8. Peairs A, Dai R, Gan L, Shimp S, Rylander MN, Li L, et al. Epigallocatechin-3-gallate (EGCG) attenuates inflammation in MRL/lpr mouse mesangial cells. *Cell Mol Immunol* (2010) 7(2):123–32. doi:10.1038/cmi.2010.1
9. Zhong Y, Chiou YS, Pan MH, Shahidi F. Anti-inflammatory activity of lipophilic epigallocatechin gallate (EGCG) derivatives in LPS-stimulated murine macrophages. *Food Chem* (2012) 134(2):742–8. doi:10.1016/j.foodchem.2012.02.172
10. Syed DN, Afaq F, Kweon MH, Hadi N, Bhatia N, Spiegelman VS, et al. Green tea polyphenol EGCG suppresses cigarette smoke condensate-induced NF-kappaB activation in normal human bronchial epithelial cells. *Oncogene* (2007) 26(5):673–82. doi:10.1038/sj.onc.1209829
11. Tachibana H, Koga K, Fujimura Y, Yamada K. A receptor for green tea polyphenol EGCG. *Nat Struct Mol Biol* (2004) 11(4):380–1. doi:10.1038/nsmb743
12. Luo JL, Maeda S, Hsu LC, Yagita H, Karin M. Inhibition of NF-kappaB in cancer cells converts inflammation-induced tumor growth mediated by TNFalpha to TRAIL-mediated tumor regression. *Cancer Cell* (2004) 6(3):297–305. doi:10.1016/j.ccr.2004.08.012
13. Johnson GL, Lapadat R. Mitogen-activated protein kinase pathways mediated by ERK, JNK, and p38 protein kinases. *Science* (2002) 298(5600):1911–2. doi:10.1126/science.1072682
14. Kopan R, Ilagan MX. The canonical Notch signaling pathway: unfolding the activation mechanism. *Cell* (2009) 137(2):216–33. doi:10.1016/j.cell.2009.03.045
15. Minter LM, Turley DM, Das P, Shin HM, Joshi I, Lawlor RG, et al. Inhibitors of gamma-secretase block in vivo and in vitro T helper type 1 polarization by preventing Notch upregulation of Tbx21. *Nat Immunol* (2005) 6(7):680–8. doi:10.1038/ni1209
16. Yuan JS, Kousis PC, Suliman S, Visan I, Guidos CJ. Functions of Notch signaling in the immune system: consensus and controversies. *Annu Rev Immunol* (2010) 28:343–65. doi:10.1146/annurev.immunol.021908.132719
17. De Obaldia ME, Bell JJ, Wang X, Harly C, Yashiro-Ohtani Y, DeLong JH, et al. T cell development requires constraint of the myeloid regulator C/EBP-alpha by the Notch target and transcriptional repressor Hes1. *Nat Immunol* (2013) 14(12):1277–84. doi:10.1038/ni.2760
18. Smale ST. Selective transcription in response to an inflammatory stimulus. *Cell* (2010) 140(6):833–44. doi:10.1016/j.cell.2010.01.037
19. Takeuchi O, Akira S. Toll-like receptors; their physiological role and signal transduction system. *Int Immunopharmacol* (2001) 1(4):625–35. doi:10.1016/S1567-5769(01)00010-8
20. Yin J, Huang F, Yi Y, Yin L, Peng D. EGCG attenuates atherosclerosis through the Jagged-1/Notch pathway. *Int J Mol Med* (2016) 37(2):398–406. doi:10.3892/ijmm.2015.2422
21. Xie H, Sun J, Chen Y, Zong M, Li S, Wang Y. 2b.06: epigallocatechin-3-gallate attenuates uric acid-induced inflammatory responses and oxidative stress by modulating Notch pathway. *J Hypertens* (2015) 33(Suppl 1):e23. doi:10.1097/01.hjh.0000467411.86784.c1
22. Gu LT, Yang J, Su SZ, Liu WW, Shi ZG, Wang QR. Green tea polyphenols protects cochlear hair cells from ototoxicity by inhibiting Notch signalling. *Neurochem Res* (2015) 40(6):1211–9. doi:10.1007/s11064-015-1584-3
23. Jin H, Gong W, Zhang C, Wang S. Epigallocatechin gallate inhibits the proliferation of colorectal cancer cells by regulating Notch signaling. *Onco Targets Ther* (2013) 6:145–53. doi:10.2147/OTT.S40914
24. Park EK, Jung HS, Yang HI, Yoo MC, Kim C, Kim KS. Optimized THP-1 differentiation is required for the detection of responses to weak stimuli. *Inflamm Res* (2007) 56(1):45–50. doi:10.1007/s00011-007-6115-5
25. Allman D, Punt JA, Izon DJ, Aster JC, Pear WS. An invitation to T and more: Notch signaling in lymphopoiesis. *Cell* (2002) 109(Suppl):S1–11. doi:10.1016/S0092-8674(02)00689-X
26. Radtke F, Fasnacht N, Macdonald HR. Notch signaling in the immune system. *Immunity* (2010) 32(1):14–27. doi:10.1016/j.immuni.2010.01.004
27. Hu X, Chung AY, Wu I, Foldi J, Chen J, Ji JD, et al. Integrated regulation of toll-like receptor responses by Notch and interferon-gamma pathways. *Immunity* (2008) 29(5):691–703. doi:10.1016/j.immuni.2008.08.016
28. Hong Byun E, Fujimura Y, Yamada K, Tachibana H. TLR4 signaling inhibitory pathway induced by green tea polyphenol epigallocatechin-3-gallate through 67-kDa laminin receptor. *J Immunol* (2010) 185(1):33–45. doi:10.4049/jimmunol.0903742
29. Arai KI, Lee F, Miyajima A, Miyatake S, Arai N, Yokota T. Cytokines: coordinators of immune and inflammatory responses. *Annu Rev Biochem* (1990) 59:783–836. doi:10.1146/annurev.bi.59.070190.004031
30. Beutler B, Rietschel ET. Innate immune sensing and its roots: the story of endotoxin. *Nat Rev Immunol* (2003) 3(2):169–76. doi:10.1038/nri1004
31. Han J, Ulevitch RJ. Limiting inflammatory responses during activation of innate immunity. *Nat Immunol* (2005) 6(12):1198–205. doi:10.1038/ni1274
32. Hayden MS, Ghosh S. Signaling to NF-kappaB. *Genes Dev* (2004) 18(18):2195–224. doi:10.1101/gad.1228704

33. Chakrawarti L, Agrawal R, Dang S, Gupta S, Gabrani R. Therapeutic effects of EGCG: a patent review. *Expert Opin Ther Pat* (2016) 26(8):907–16. doi:10.1080/13543776.2016.1203419
34. Lagha AB, Grenier D. Tea polyphenols inhibit the activation of NF-kappaB and the secretion of cytokines and matrix metalloproteinases by macrophages stimulated with *Fusobacterium nucleatum*. *Sci Rep* (2016) 6:34520. doi:10.1038/srep34520
35. Wu M, Liu D, Zeng R, Xian T, Lu Y, Zeng G, et al. Epigallocatechin-3-gallate inhibits adipogenesis through down-regulation of PPARgamma and FAS expression mediated by PI3K-AKT signaling in 3T3-L1 cells. *Eur J Pharmacol* (2016) 795:134–42. doi:10.1016/j.ejphar.2016.12.006
36. Yu L, Yu H, Li X, Jin C, Zhao Y, Xu S, et al. P38 MAPK/miR-1 are involved in the protective effect of EGCG in high glucose-induced Cx43 downregulation in neonatal rat cardiomyocytes. *Cell Biol Int* (2016) 40(8):934–42. doi:10.1002/cbin.10637
37. Kim HS, Kim MH, Jeong M, Hwang YS, Lim SH, Shin BA, et al. EGCG blocks tumor promoter-induced MMP-9 expression via suppression of MAPK and AP-1 activation in human gastric AGS cells. *Anticancer Res* (2004) 24(2B):747–53.
38. Andersson ER, Sandberg R, Lendahl U. Notch signaling: simplicity in design, versatility in function. *Development* (2011) 138(17):3593–612. doi:10.1242/dev.063610

Conflict of Interest Statement: The authors declare that the research was conducted in the absence of any commercial or financial relationships that could be construed as a potential conflict of interest.

Copyright © 2017 Wang, Xiang, Wang, Li, Fang, Song, Li, Yu, Wang, Yan, Hao, Wang and Sheng. This is an open-access article distributed under the terms of the Creative Commons Attribution License (CC BY). The use, distribution or reproduction in other forums is permitted, provided the original author(s) or licensor are credited and that the original publication in this journal is cited, in accordance with accepted academic practice. No use, distribution or reproduction is permitted which does not comply with these terms.

frontiers in Immunology

REVIEW
published: 28 April 2017
doi: 10.3389/fimmu.2017.00505

Impact of Autoantibodies against Glycolytic Enzymes on Pathogenicity of Autoimmune Retinopathy and Other Autoimmune Disorders

*Grazyna Adamus**

School of Medicine, Casey Eye Institute, Oregon Health and Science University, Portland, OR, USA

Autoantibodies (AAbs) against glycolytic enzymes: aldolase, α-enolase, glyceraldehyde-3-phosphate dehydrogenase, and pyruvate kinase are prevalent in sera of patients with blinding retinal diseases, such as paraneoplastic [cancer-associated retinopathy (CAR)] and non-paraneoplastic autoimmune retinopathies, as well as in many other autoimmune diseases. CAR is a degenerative disease of the retina characterized by sudden vision loss in patients with cancer and serum anti-retinal AAbs. In this review, we discuss the widespread serum presence of anti-glycolytic enzyme AAbs and their significance in autoimmune diseases. There are multiple mechanisms responsible for antibody generation, including the innate anti-microbial response, anti-tumor response, or autoimmune response against released self-antigens from damaged, inflamed tissue. AAbs against enolase, GADPH, and aldolase exist in a single patient in elevated titers, suggesting their participation in pathogenicity. The lack of restriction of AAbs to one disease may be related to an increased expression of glycolytic enzymes in various metabolically active tissues that triggers an autoimmune response and generation of AAbs with the same specificity in several chronic and autoimmune conditions. In CAR, the importance of serum anti-glycolytic enzyme AAbs had been previously dismissed, but the retina may be without pathological consequence until a failure of the blood–retinal barrier function, which would then allow pathogenic AAbs access to their retinal targets, ultimately leading to damaging effects.

Keywords: autoantibodies, autoimmune diseases, retinopathy, glycolysis, enzymes characterization

OPEN ACCESS

Edited by:
Jixin Zhong,
Case Western Reserve University, USA

Reviewed by:
Fei Han,
Washington University in St. Louis, USA
Hao Wu,
Amgen, USA
Lu Huang,
Cornell University, USA

***Correspondence:**
Grazyna Adamus
adamusg@ohsu.edu

Specialty section:
This article was submitted to Inflammation, a section of the journal Frontiers in Immunology

Received: *31 January 2017*
Accepted: *12 April 2017*
Published: *28 April 2017*

Citation:
Adamus G (2017) Impact of Autoantibodies against Glycolytic Enzymes on Pathogenicity of Autoimmune Retinopathy and Other Autoimmune Disorders. Front. Immunol. 8:505. doi: 10.3389/fimmu.2017.00505

INTRODUCTION

Humans are genetically diverse, but despite their immunological differences, they often produce autoantibodies (AAbs) against similar autoantigens. In particular, a number of studies have shown that α-enolase and other glycolytic enzymes are targeted by AAbs associated with various pathological conditions, including autoimmune retinopathy (AR) (1–6). It is surprising because these enzymes play an important role in the cellular production of energy through the glycolytic pathway, which metabolizes glucose to pyruvate in a chain of enzymatic reactions to produce cellular adenosine triphosphate (ATP) (**Figure 1**). Energy needs of a given cell type depend on tissue physiology, in particular, metabolically active retinal photoreceptor cells that have great energetic requirements (7–10). Thus, blocking cellular functions of glycolytic enzymes by pathogenic AAbs could be devastating to any cells' survival.

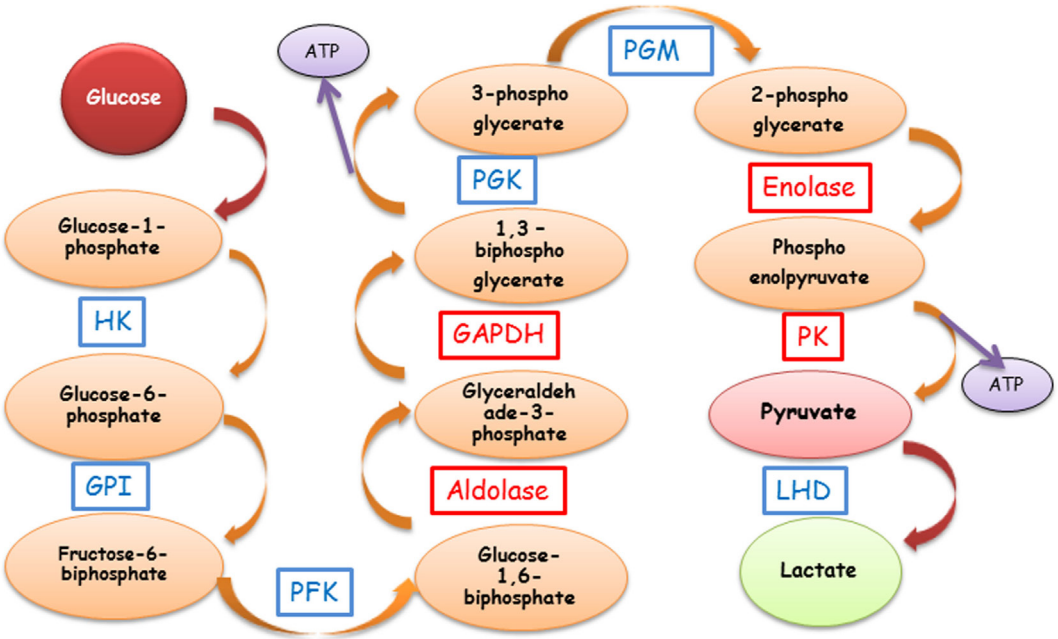

FIGURE 1 | Schematic representation of the glycolytic pathway and anti-enzymatic protein autoantibody involvement. The most common AAbs are against GAPDH, aldolase, enolase, and PK (red boxes). Abbreviations: GAPDH, glyceraldehyde-3-phosphate dehydrogenase; GPI, glucose-6-phosphate isomerase; HK, hexokinase; LDH, lactate dehydrogenase; PFK, phosphofructokinase; PGK, phosphoglycerate kinase; PGM, phosphoglycerate mutase; PK, pyruvate kinase; ATP, adenosine triphosphate; AAbs, autoantibodies.

The retina is a light-sensitive tissue located in the back of the eye, which is composed of layers of neurons such as photoreceptors, bipolar cells, and ganglion cells, supported by glial cells (Müller cells and astrocytes) (11). It is protected behind blood-ocular barriers (11). The cross-section of retinal layers is shown in **Figure 2**. The retina converts photons of light into electric signals and sends them to the brain in the process called the visual transduction cascade. This process takes place in the outer segments (OS) of the photoreceptors, including the cell membranes and pigment disk membranes of the OS. There are two types of photoreceptor cells: the rods and cones. Rods are responsible for black-and-white vision, while cones support the color vision (12). Glycolysis occurs in photoreceptor and Müller cells, providing energy to photoreceptors cells (13–15). Glucose reaches photoreceptor cells (the outer retina) from the blood, through the pigment epithelium cell layer (RPE) by glucose transmembrane transporter GLUT1 (16). Thus, RPE is important in this process by providing metabolic support to photoreceptor cells (17). In addition to energy production, the glucose metabolism may be involved in photoreceptor cell death and survival, suggesting that glycolysis and apoptosis are linked (18, 19).

Glycolytic enzymes are evolutionarily conserved proteins, have multiple functions in the cell not related to glycolysis, and are highly autoimmunogenic (19, 20). The enzymes are not only present intracellularly, but also on the cell surface, including the surface of neuronal cells; therefore, they are conceivably being exposed to the immune system (21). AAbs against four glycolytic enzymes: aldolase (ALDO), α-enolase (ENO1), glyceraldehyde-3-phosphate dehydrogenase (GAPDH), and pyruvate kinase M2 (PKM2) are particularly prevalent in sera of patients with autoimmune retinopathies, including cancer-associated retinopathy (CAR) and melanoma-associated retinopathy (MAR). Similar

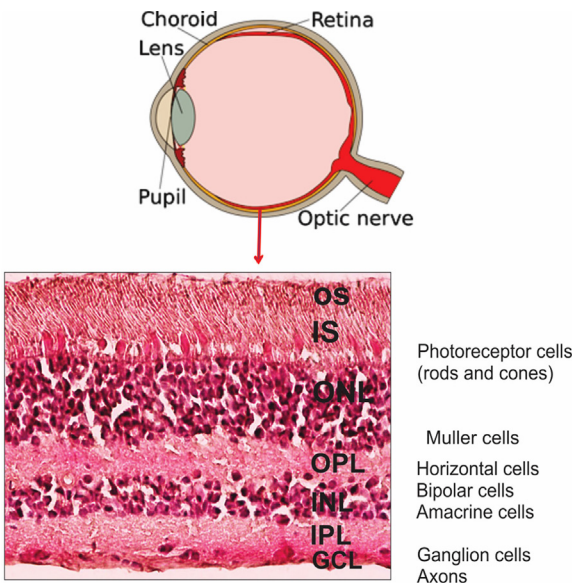

FIGURE 2 | Anatomy of human eye and retinal layers. Diagram of the eye and the organization of retinal layers and cells showing H&E staining of representative section of human retina. Abbreviations: OS, outer segments; IS, inner segments; ONL, outer nuclear layer; OPL, outer plexiform layer; INL, inner nuclear layer; IPL, inner plexiform layer; GCL, ganglion cell layer.

AAbs were also reported in autoimmune uveitis (22, 23). Although anti-enolase and other enzymes can be detected in low titers in some healthy individuals (from 0 to 10% depending on population studied), they were likely generated in response to common infections (18, 24). In contrast, AAb titers in disease are always found to be significantly higher (25).

Cancer-associated retinopathy is a rare retinal disorder, and its prevalence is unknown, but more patients with CAR or CAR-like symptoms (AR) have been identified each year (26). In CAR, patients developed a sudden loss of vision, visual field defects, photopsias, color vision loss, and dysfunction of rod and/or cone responses in the presence of a remote cancer and serum anti-retinal AAbs. These were, possibly, generated in response to antigens released from tumor, including glycolytic enzymes captured by antigen-presenting cells (27–29). To understand the role of glycolytic enzymes as target autoantigens, it is important to appreciate their biological significance in retinal disease and other autoimmune conditions. This review is an attempt to explain the high frequency of AAbs against glycolytic enzyme association in autoimmune diseases.

ENOLASE

Enolase is the most frequent autoantigen in autoimmune retinopathies, including CAR and MAR (24, 30). Of all patients with anti-retinal antibodies, over 30% have anti-α-enolase antibodies (31). Furthermore, anti-enolase AAbs have been reported in cancer, several systemic autoimmune disorders, connective tissue disorders, and inflammatory diseases, including Behçet's disease, Hashimoto's encephalopathy, ANCA-positive vasculitis, rheumatoid arthritis (RA), systemic lupus erythematosus (SLE), multiple sclerosis (MS), primary sclerosing cholangitis, and inflammatory bowel disease (3–5, 32–40).

Enolase exists as homo- or hetero-dimers of three subunits, α, β, and γ, all of which are targets of autoimmunity. α-Enolase encoded by the gene ENO1 is ubiquitous, β-enolase encoded by the gene ENO3 is as a structural protein in the lens of some species, and possibly a suppressive cytokine, and γ-enolase encoded by the gene ENO2 is a neuron-specific enolase (37, 41). This enzyme catalyzes a formation of phosphoenolpyruvate from 2-phosphoglycerate in glycolysis (**Figure 1**). Enolase-α is present throughout the retina, including OS of photoreceptor cells and Müller cells (24, 42, 43).

Enolase acts as a plasminogen receptor, modulating pericellular fibrinolytic activity, as well as other non-glycolytic functions, resulting from its subcellular and membrane localizations (44). Such a differential expression of α-enolase in tissues/organs has been linked to several pathologies, such as cancer, Alzheimer's disease (AD), and RA, among others (29, 37, 45). In addition, α-enolase has been detected on the surface of endothelial cells, hematopoietic cells (monocytes, T cells, and B cells), and neuronal cells (44). The surface expression of α-enolase in various eukaryotic cells has been found to be dependent on the pathophysiological conditions of a given cell (46). The upregulation of enolase, during metabolic processes, and its release from dying cells may also lead to its uptake by antigen-presenting cells. The subsequent B cell activation could trigger an excessive production of anti-enolase AAbs that can potentially initiate tissue injury, e.g., as a result of immune complex deposition (**Figure 2**).

In recent retinal research, remarkable findings were reported on the interaction between proteins involved in phototransduction and glycolysis. Smith et al. demonstrated a direct binding between retinal arrestin and retinal enolase, showing that arrestin slowed the catalytic activity of enolase and the light-driven translocation of arrestin modulated metabolic activity of photoreceptors (42). In contrast to arrestin, α-enolase does not change its location in the photoreceptor cell in response to light. In the dark-adapted retina, enolase was found to co-localize with arrestin in the inner segments (IS) and outer nuclear layer (ONL), but remained in the IS when arrestin translocated in response to light adaptation. These findings may explain an occasional detection of anti-enolase and anti-arrestin AAbs in the same patient with CAR or MS, suggesting that such complexes could be released from damaged photoreceptor cells, then processed by antigen-presenting cells (38, 47). Surprisingly, AAbs against arrestin and α-enolase were also reported in some patients with coronary heart disease (48). When investigators exposed cardiomyocytes to monoclonal antibody against arrestin or enolase *in vitro*, they observed decreased cell proliferation, suggesting that antibodies bound to the membrane-exposed epitopes of arrestin and enolase in living cells (48). The study suggested that these AAbs may be involved in the induction of cardiac autoimmune diseases.

Certain properties of α-enolase, especially those related to surface exposure and plasminogen-binding, suggest its role in the initiation of a disease process by modulating the pericellular and intravascular fibrinolytic system (49). Enolase is translocated from the cytoplasm to the cell surface and then serves as the plasminogen receptor on the surface of various cells and enhances pericellular plasmin production for cell invasion (50). The enolase epitope involved in the plasminogen-binding of α-enolase is located within the amino acid sequence 257–272. This binding site is different from the main pathogenic epitope in patients with CAR (the sequence 56–63), and patients with endometriosis (the sequences 53–87 and 207–238), or healthy individuals, suggesting that these disorders are not associated with disturbances of the intravascular and pericellular fibrinolytic system (1, 3, 51, 52). The linking of epitopes to specific autoimmune and inflammatory conditions is a challenge, so more research is needed to decide whether enzymatic protein epitopes would better distinguish their association with a particular disease and have a causative activity.

GLYCERALDEHYDE-3-PHOSPHATE DEHYDROGENASE

The next common autoantigen in disease is GAPDH, which catalyzes the oxidative phosphorylation of glyceraldehyde-3-phosphate to 1,3-biphosphoglycerate, leading to the reduction of nicotinamide adenine dinucleotide (NAD^+) to NADH during glycolysis (**Figure 1**). GAPDH also has various functions outside the glycolysis that are related to its localization in cytoplasm and nucleus. These functions include the cell cycle, nuclear tRNA export, DNA replication and repair, endocytosis, exocytosis,

cytoskeletal organization, iron metabolism, carcinogenesis, and cell death (53–57). It has been suggested that this functional diversity may be regulated by posttranslational GAPDH modification, by subcellular protein–protein interaction, or by protein–nucleic acid interactions (54). The first indication related to its non-glycolytic function was GAPDH association with non-glycolytic protein tubulin and its ability to bundle microtubules (58).

Autoantibodies against GADPH have been found in sera of patients with autoimmune retinopathies and optic neuropathies, including patients with paraneoplastic syndrome, and in MS as an autoimmune response to neurons and axons (59–61). In photoreceptor cells of the retina, GAPDH is distributed throughout the cell, as well as in the plasma membrane of the rod outer segments (ROS), and consists of about 2% of total ROS proteins and more than 11% of total plasma membrane proteins (62). Like α-enolase, GADPH does not translocate upon exposure of the retina to light, but it is involved in translocation of the rod phototransduction protein α-transducin from the rod inner to OS during dark adaptation (63). Both proteins GAPDH and α-transducin were also found to be antigenic targets in retinal autoimmune diseases (64, 65).

The numerous studies showed that GAPDH plays an essential role in the induction of autoimmunity, but how anti-GAPDH immune response originated in various diseases is still unknown. The autoimmune response against GAPDH might be initiated by a foreign, non-human, and GAPDH, which was found to be present on the surface of bacteria, viruses, and parasites subsequently cross-reacting with human protein (55). Cancer can also be a source of GAPDH because it was found to be overexpressed in many human cancer cells, including breast, prostate, pancreatic, lung, renal, gastric, liver, colorectal, bladder cancers, melanoma, and glioma (6, 66, 67). Those cancers are often associated with paraneoplastic syndromes, where antibody responses, initiated against tumor antigens, have adverse effects on distant tissue targets that have the same antigen or antigenic peptide (68, 69). The occurrence of AAbs specific to enolase, aldolase C, and GAPDH, was two to three times more frequent in CAR with gynecological cancers than in healthy women (59). Anti-GAPDH AAbs were also reported in 47% of patients with SLE, a chronic autoimmune disease that can damage any part of the body (skin, joints, and other organs) (55).

ALDOLASE

Aldolase C has also been identified as an important autoantigen. In glycolysis, it catalyzes the reversible conversion of fructose-1,6-bisphosphate to glyceraldehyde 3-phosphate and dihydroxyacetone phosphate (**Figure 1**). However, similar to the other enzymes, aldolase also plays several non-glycolytic roles and interacts with vacuolar-ATPase and other molecules (70). The aldolase isozyme family is composed of three members, A, B, and C, which are encoded by separate genes. The proteins are expressed in a tissue-restricted manner (71, 72). Aldolase A is expressed predominantly in muscle and brain, B in the liver, and C in the brain and retina. Neuronal expression of aldolase C has been reported in the cerebellum Purkinje cells and in all cell types of the retina (21, 72). The highest expression was shown in the ONL of the retina, where cone and rod photoreceptors are aligned, and in the inner nuclear layer (INL), consisting of the bipolar, horizontal, and amacrine neurons, as well as in Müller glia cells (72).

Aldolase C interacts with GAPDH and catalyzes GAPDH inactivation in the presence of extracellular signals, indicating that such a complex has a regulatory function (73). In addition, aldolase strongly interacts with cytoskeletal elements. Aldolase A has also been found in the nucleus of many types of tumors, and is involved in the regulation of cell proliferation (74, 75).

The occurrence of AAbs against aldolase was associated with various autoimmune diseases and cancers (4, 76, 77). Anti-aldolase A and C AAbs have been shown in CAR (59), MAR (78), and diabetic retinopathy (19). The association of serum anti-aldolase AAbs was reported in age-related macular degeneration (AMD), a degenerative disorder of the central retina (macula), suggesting that an increased presence of such antibodies could lead to the disruption of aldolase functions and inflammation in the retina (79, 80). Anti-aldolase A AAbs were also present in sera of patients with the most common human neurodegenerative disease, AD, suggesting their potential role in development of this disorder (81). They were also found in patients with hyperkinetic movement disorders and Parkinson's disease, but were not detectable in individuals with other inflammatory and non-inflammatory central nervous system diseases (82). Increased glycolytic activity and the presence of AAbs have been found to be related to tissue destruction of synovium in RA (83). Glucose phosphate isomerase, enolase, and aldolase are the key enzymes that promote RA autoimmunity by acting as target autoantigens, especially in early, untreated RA (5, 84). Ukaji et al. detected anti-aldolase A AAbs in RA patients with severe bone erosion, and suggested that a certain event may promote the production of AAbs by exposing hidden epitopes of aldolase A to the immune response, thus leading to the production of antibodies (83).

PYRUVATE KINASE (PK)

Pyruvate kinase catalyzes the last step of glycolysis and, similarly to other enzymes, is expressed in different isoforms, depending on tissue metabolism (85). PKM1 and PKM2 are expressed in cancers and normal tissues (86–88). PK is a multifunctional protein too, participating in a variety of pathways, protein–protein interactions, nuclear transport, metabolism reprogramming, gene transcription, and cell cycle progression (85). In the retina, PKM1 exists in the Müller cells and neurons, and PKM2 in glial cells and rod and cone photoreceptors, where it was found to co-localize with rhodopsin (89). PKM2 has generated a lot of interest due to its impact on changes in cellular metabolism observed in cancer, as well as in activated immune cells, by controlling activity of hypoxia-inducible factor 1-alpha and STAT3 during inflammation (90). As in other glycolytic enzymes, PKM2 was found to be an antigenic target in AR, as well as in other neurological conditions and cancers (6, 79, 80). PKM2 was targeted by AAbs in both geographic and neovascular AMD, but the level of anti-PKM2 autoantibody was best correlated with the early stages of AMD (79). PKM1 was identified as an autoimmune target in Tourette syndrome and associated neurological disorders

(91). Moreover, anti-PKM1 AAbs reacted strongly with surface antigens of infectious strains of streptococcus, and antibodies against streptococcal M proteins reacted with PK, suggesting that anti-PK antibodies originated from streptococcal infection. Furthermore, anti-PKM1 autoreactivity was significantly higher in patients who had recently acquired a streptococcal infection with exacerbated symptoms, as compared to patients with exacerbated symptoms but no evidence of a streptococcal infection (91). In spite of association of serum anti-glycolytic enzyme AAbs with many of those diseases, it is not clear whether such AAbs are the direct result of, or are made due to the released antigenic proteins from damaged cells, including failing photoreceptors in the retina during progression of macular degeneration in AMD or AR.

ANTI-GLYCOLYTIC ANTIBODIES IN CANCER—PARANEOPLASTIC SYNDROME

Autoimmune disorders associated with cancer have been described as paraneoplastic complications in a distant organ, such as the retina (92). Paraneoplastic retinopathies are rare disorders associated with cancer, not caused by cancer invasion or metastasis or are consequences of treatment. In CAR, they may result in rapid and complete blindness. It is most commonly associated with small cell carcinoma of the lung, breast, and gynecologic cancers, but associations with lymphomas, non-small cell lung, prostate, pancreatic, bladder, and colon cancers have been described (15). The generation of AAbs during tumor formation, in response to aberrant cancer antigens, is the proposed mechanism of the CAR and MAR syndromes (26, 93). CAR-like symptoms can precede the manifestations of cancer. A strong similarity or identity of autoantigens associated with AR and cancer suggests that initially, AAbs may originate against tumor antigens during tumorigenesis, and then, after crossing the blood–retinal barrier (BRB) from the circulation, and accessing retinal cells, they cross-react with remote retinal antigens (24–26, 94–96). Although healthy individuals may have AAbs against these enzymes, they are likely to be natural antibodies, primarily polyreactive IgM, which display a moderate affinity for antigens or anti-microbial antibodies lingering after infections (92, 97). Serum IgG subclass distribution and levels in patients with autoimmune diseases differs from that in healthy people (93). In AR, the target autoantigens are protein antigens, T cell-dependent antigens that can stimulate a generation of IgG1- or IgG3-AAbs. We do not know what factors (secretion of cytokines, etc.) can cause anti-retinal AAbs to become pathogenic. Moreover, the presence of an intact BRB, as well as brain–blood barriers combined with the unique microenvironment of the eye or brain, ensures that the immune attack is weakened (94). IgG might reach intra-retinal structures through breaches in the BRB or from receptor-mediated uptake. IgG is also present in the healthy eye at very low levels relative to plasma levels without harmful effects (95). In contrast, long-lasting, high-affinity AAbs of the IgG class show pathologic properties related to alterations in cell clearance, antigen-receptor signaling, or cell effector functions (96).

A common feature of solid tumors is an increased aerobic glycolysis to generate ATP (the Warburg effect) (98). The genes encoding glycolytic enzymes are overexpressed in the majority of clinically relevant cancers, particularly genes encoding ALDO, ENO1, GAPDH, and PKM2 (15, 99, 100). Moreover, these enzymatic proteins play sometimes similar cellular roles in their non-glycolytic capacity, e.g., GAPDH activates survival pathways, enolase controls transcriptional regulation, aldolase promotes epithelial mesenchymal transition, and PKM2 enhances transcription and stabilization (100, 101). As a result, differential overexpression of glycolytic enzymes and their exposure on the cell surface, cell turnover, and apoptosis, or their release into the extracellular environment, could initiate autoimmune responses and the production of specific AAbs (102).

PATHOGENIC AAbs

The highly conserved structure of glycolytic enzymes and their ubiquitous presence in all tissues support strong antigenicity (enolase, aldolase, GAPDH). Most disease-related AAbs are IgGs that are somatically mutated, suggesting that helper T cells drive the autoimmune B cell response, including anti-enolase AAbs in CAR patients (24, 103, 104). AAbs against glycolytic enzymes can also be produced in response to their mutations, misfolding, degradation, overexpression in the cell, and the protein release from damaged tissue (21). These AAbs can target any retinal cell type containing an antigen, including photoreceptor cells, ganglion cells, or bipolar cells and cause retinal dysfunction. The high sequence homology between microbial enolase, aldolase, GAPDH and PK, and human proteins was likely to facilitate the initiation and development of autoimmune reactions when these proteins are expressed on the membrane (21, 49, 105). Therefore, a *molecular mimicry* has been proposed as a mechanism of AAb formation and a contributor to the pathogenesis of autoimmune disease, for example, AAbs present in post-streptococcal infections of CNS diseases (21, 106, 107).

Anti-glycolytic enzymes AAbs were mostly studied in association with autoimmunity because their serum prevalence was *not* strictly disease-specific, many investigators dismissed their pathogenic role. However, the lack of disease restriction of the AAb response to one disease may be related to an increased expression of glycolytic proteins in various organs that triggers an autoimmune response and the occurrence of AAbs with the same specificity in several chronic and autoimmune disorders (3, 21). The presence of AAbs to distinct epitopes within an autoantigen can be a sign of disease-specific pathogenic immune activity, while the recognition of multiple epitopes within the same autoantigen may not be disease-specific (108, 109). We can speculate that the reactivity to a particular autoantigen does not necessarily cause disease, but the presence of destructive AAbs of limited epitope-specificity can ultimately spread pathogenic autoimmunity (110).

An important question is whether the widespread presence of anti-enolase, aldolase, GAPDH, and PKM2 and possibly against other enzymes like phosphoglycerate mutase, alpha-enolase, triose-phosphate isomerase, and malate dehydrogenase in various conditions is a sign of their causal role and pathogenic activity (4). In the case of anti-glycolytic protein AAbs, the induction of pathogenic effects could be a consequence of

destabilized production of energy and glucose use (2, 74, 101). The proposed pathogenic involvement of AAbs is based on several observations summarized in **Table 1**. First, the persistence of high-affinity anti-enolase, anti-aldolase, anti-GAPDH, and anti-PKM2 AAbs over the course of autoimmune and inflammatory diseases reflects their pathogenic involvement as compared to antibodies of healthy controls (4, 96). Second, specific AAbs are associated with disease progression and prognosis (36, 59, 104), e.g., PKM2 correlates with the severity and progression of AMD, suggesting their pathogenic association (79). Third, studies show that antibodies can penetrate the living cell and induce cytotoxicity *in vitro* (43). Fourth, antibodies have the ability to induce cell death by apoptosis (2). Fifth, antibodies have the capacity to induce tissue pathology *in vivo* as shown by active immunization with enzymatic antigens and by passive transfer of antibodies (111). Sixth, antibodies have the ability to inhibit the catalytic function of glycolytic enzymes. For instance, anti-enolase antibody significantly decreased the catalytic activity of enolase, which resulted in a depletion of glycolytic ATP and an increase in the intracellular calcium, leading to cell apoptosis (2). In MS patients, the percentage of anti-GAPDH AAbs in the CSF was significantly higher than in patients with other neurologic diseases (61). Such AAbs strongly inhibited the catalytic function of GADPH, which could be reversed by their pre-adsorption with immobilized enzyme (112). Thus, an increased intrathecal production of anti-GAPDH AAbs may lead to their binding of GAPDH present in axons and neurons, inhibition of GAPDH glycolytic activity, neuro-axonal apoptosis, and cytotoxicity. Also, in enzymatic assays, anti-aldolase AAbs of AD inhibited the aldolase enzymatic activity (81). All of these findings suggest that AAbs can adversely contribute to retinal and neuro-axonal degeneration.

We have identified α-enolase as a target autoantigen in CAR, MAR, and AR (24, 31, 78). Seropositive patients have a worse prognosis than seronegative patients. Patients with AAbs had more abnormalities in the rod and cone photoreceptor function, as confirmed by ERG, than seronegative patients (104). In particular, the loss of central vision was more evident and more frequent in anti-enolase seropositive patients (104). Our research showed that anti-enolase antibody played a pathogenic role in retinal cell survival and determined the molecular events occurring before and during the induction cell death induced by antibodies (1, 2, 43, 113). When anti-enolase antibodies were cultured with retinal cells *in vitro* they triggered an apoptotic cell death, as examined by morphological changes and presence of TUNEL-positive cells (1). Cytotoxic effects induced by anti-enolase autoantibody appear to be specific, since normal IgG added to the culture at the same amount did not cause cell death. This apoptotic effect is similar to the action of anti-recoverin AAbs on E1A.NR3 retinal cells (114). Internalization of anti-recoverin IgG antibody or its Fab fragments by retinal cells mediated by endocytosis leads to cytotoxicity (115).

Treatment of living retinal cells with anti-enolase antibody-induced considerable changes in the ATP production, decrease in intracellular pH, and increase in intracellular calcium levels, which led to their apoptotic death (2). Retinal cells could be protected from

TABLE 1 | Widespread occurrence of autoantibodies (AAbs) against glycolytic enzymes with pathogenic properties in autoimmune diseases.

Pathogenic potential of AAbs	Potential pathological/significance	Antigen	Reference
Association with disease	Higher levels of AAbs in patients as compared with health individuals: – Cancer-associated retinopathy – Melanoma-associated retinopathy – Non-paraneoplastic autoimmune retinopathy – Age-related macular degeneration – Glaucoma – Inflammatory bowel disease – Rheumatoid arthritis – Alzheimer's disease – Multiple sclerosis – Diabetic retinopathy – Systemic lupus erythematosus – Coronary heart disease	Enolase Aldolase glyceraldehyde-3-phosphate dehydrogenase (GAPDH) Pyruvate kinase M2 (PKM2)	(2, 4, 5, 10, 18, 23, 24, 31–33, 37, 38, 40, 49, 52, 54, 71–73, 75, 79, 83, 103)
Induction of cytotoxicity	– Intracellular antibody penetration and cytotoxicity *in vitro* – Inhibits cell proliferation	Enolase	(1, 2, 40)
Triggering cell death	Ability of antibodies to induce cell death by apoptosis	Enolase GAPDH Aldolase	(2, 19, 75, 112, 113)
In vivo functional effects	Decrease responses in electroretinogram, retinal cell dysfunction	γ-Enolase (NSE) α-Enolase	(43, 103, 110, 114)
Inhibition of enzymatic activity	– Anti-enolase AAbs inhibited catalytic function of enolase – Anti-GADPH AAbs strongly inhibited the catalytic function of enzyme – Anti-aldolase AAbs inhibited the aldolase enzymatic activity	Enolase GAPDH Aldolase	(2, 75, 99)
Overexpression in tumors	Lung, mammary gland, prostate, lymph node, cervix, cartage bone marrow, brain, colon, liver, and thyroid	Enolase Aldolase GADPH PKM2	(57, 60, 78, 86, 87)

anti-enolase antibody-induced apoptosis *in vitro* by resveratrol, a natural plant-derived drug, through multiple early molecular processes, such as reduction of intracellular calcium levels, down-regulation of Bax, upregulation of Sirt1 and Ku70 activities, and inhibition of caspase-3 activity (116). In the retina, antibodies to α-enolase mostly labeled the retinal ganglion cells and INL cells (43). Using *ex vivo* experiments and intravitreal injections, we showed that such antibodies were capable of penetrating retinal tissue and targeting the ganglion cells and INLs, and subsequently inducing their apoptotic death (43). Animal experiments have shown that an intravitreal injection of serum specific for enolase or purified anti-enolase antibody caused functional changes in the retina, showing reduced b-wave amplitudes as recorded by ERG (111, 117). Anti-α-enolase AAbs and autoantibody against γ-enolase (NSE) that were found in glaucoma, induced retinal dysfunction *in vivo* in a similar fashion to the effects induced by *N*-methyl-D-aspartate (117, 118). These findings showed that anti-enolase antibodies can play a causative role in the induction and progression of retinal degeneration in animals (30, 43, 59, 119). Antibodies that recognize and bind to cell debris in subretinal space during retinal degeneration may also trigger inflammation and synthesis of more AAbs (120). AAb binding to the cell surface-exposed enolase has led to opsonization or cell destruction, an increased inflammatory reaction, and in effect, tissue damage (121, 122). Taken together, anti-enolase AAbs have a potential to induce retinal degeneration, not only by the local formation of immune complexes but also by the direct damage to retinal cells and influence their cell function.

MANAGEMENT OF AUTOIMMUNE RETINOPATHIES

Current therapies of CAR, MAR, or AR include systemic immunosuppression with steroid, intravenous immunoglobulin (IVIg), plasmapheresis, cytotoxic medications, and rituximab. However, there is no one commonly accepted protocol, so our knowledge is limited. Early diagnosis followed by treatment of AR is important to prevent widespread retinal degeneration and permanent vision loss. Moreover, delayed initiation of treatment in the course of disease may lead to the poor visual prognosis. The most common treatment has been long-term immunosuppression with steroids (26). Short-term therapy can be done, such as intravitreal triamcinolone and subtenons depomedrol, but these do not treat the undelaying causes of this systemic autoimmune disease; thus, longer term immunosuppression may be a better approach (123).

The most common sources regarding AR treatment benefits are published case reports. For example, a brief course of oral corticosteroids in a patient with anti-enolase AAbs caused an improvement in visual fields, disappearance of enolase-α AAbs, partial recovery of the cone response, and complete recovery of the rod response as measured by ERG (124). These findings suggest a pathologic role for enolase-α AAbs in this autoimmune rod/bipolar cell dysfunction.

In another study, the authors report that anti-GADPH can cross the placenta (125). A seropositive patient with AR and severe myasthenia gravis (MG) experienced a rapid progression of vision loss from driving vision to the hand motion/light perception level over 2-year period (125). The patient then underwent weekly plasmapheresis therapy, which led to an improvement of her symptoms. She became pregnant during the course of treatment. During the time of delivery, peripheral blood was collected from mother, as well as umbilical cord blood. Both samples were seropositive for anti-GAPDH among other AAbs. Despite the presence of those AAbs in the cord blood, the 6-month old patient appeared to have developed normal visual function and no MG symptoms.

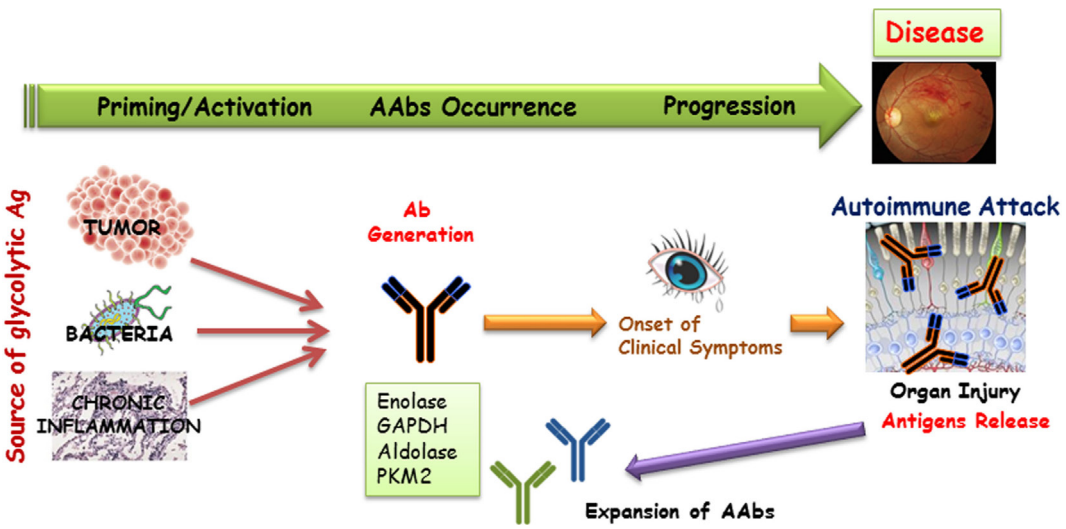

FIGURE 3 | A possible mechanism for the generation of anti-glycolytic proteins antibodies and their role in the induction of the retinal disease process. Antibodies that are generated as a result of tumor, infection, or cell turnover during inflammation may target common antigens (the same specificity antigens) in the retina. Such antibodies can be present in the serum for a long time before clinical presentation of disease occurs. Degenerating tissue can be a source of new antigens that can initiate the further expansion of autoantibodies (AAbs) production and acceleration of disease.

Intravenous immunoglobulin may be another treatment option in addition to corticosteroids or plasmapheresis that is offered to patients with paraneoplastic visual loss. IVIg infusion showed promising results in some patients. In one study of three seropositive patients with CAR, including anti-enolase AAbs treated with IVIg, some improvement in visual field and light perception was shown (126). In another case of a patient with MAR and worsening visual function, an infusion of IVIg was administered. Patient ERG responses were consistent with MAR but his antibody status was unknown [although patients with MAR may have anti-enolase AAbs (31)]. Over the course of treatment, the patient noted progressive improvement in night vision, peripheral vision, and photopsias (127).

The number of AR patients benefited from rituximab treatment (128–131). The efficacy of rituximab was studied in six patients (12 eyes) administrated as a monotherapy or in combination therapy (132). Some patients in the study had anti-enolase (three patients) and anti-aldolase (one patient) AAbs. Stabilization and/or improvement of visual acuity, visual field parameters, and electroretinography parameters were observed in 75% of patients treated with rituximab. CAR, MAR, and AR are characterized by persistently elevated levels of ant-retinal AAbs, therefore, B cell depletion therapy based on rituximab delivers promising therapy for those patients. In view of these findings, larger scale studies of should be pursued in the future.

CONCLUSION

Dissecting the possible role of anti-enzymatic protein AAbs with such a broad presence in AR and other diseases is a challenge. We propose that some specific AAbs may be unique to CAR and others may not. There are multiple mechanisms responsible for antibody generation, including the innate anti-microbial response, anti-tumor response, or autoimmune response against released self-antigens from damaged, inflamed tissue (**Figure 3**). AAbs target the same antigens as antibodies present in healthy subjects, but in low titers, lingering after infections. This suggests that at least some autoimmune diseases might emerge from a pathogenic shift in the phenotype from a normal stage to autoimmunity (109, 133). In other words, the occurrence of an autoimmune disease might not require a new autoimmunization, but rather a loss of control in the existing autoimmunity. The other possibility is that the presence of anti-glycolytic enzyme AAbs can represent a result rather than a direct cause (epiphenomenon). In such a scenario, dying photoreceptors by apoptosis, induced by some other mechanisms, produce substantial amounts of debris, containing high concentrations of the targeted antigens (glycolytic enzymatic proteins) released from OS, which could result in autoimmunization and enhanced permeability of the BRB (122). Thus, the serum presence of anti-glycolytic enzyme AAbs, whose importance had been previously dismissed, might be without pathological consequences until a failure of the BRB function, in effect allowing pathogenic AAbs access to their retinal targets, ultimately leading to damaging effects. Because of the presence of AAbs with several specificities in a single patient, this suggests that AAb arrays, rather than AAbs against a single antigen, might be responsible for degenerative processes in AR.

AUTHOR CONTRIBUTIONS

The author was totally the sole responsible for the design and writing of this review article.

FUNDING

This work was supported by grant P30 EY010572 from the National Institutes of Health (Bethesda, MD, USA) and by unrestricted departmental funding from research to prevent blindness (New York, NY, USA).

REFERENCES

1. Adamus G, Amundson D, Seigel GM, Machnicki M. Anti-enolase alpha autoantibodies in cancer-associated retinopathy: epitope mapping and cytotoxicity on retinal cells. *J Autoimmun* (1998) 11:671–7. doi:10.1006/jaut.1998.0239
2. Magrys A, Anekonda T, Ren G, Adamus G. The role of anti-alpha-enolase autoantibodies in pathogenicity of autoimmune-mediated retinopathy. *J Clin Immunol* (2007) 27:181–92. doi:10.1007/s10875-006-9065-8
3. Terrier B, Degand N, Guilpain P, Servettaz A, Guillevin L, Mouthon L. Alpha-enolase: a target of antibodies in infectious and autoimmune diseases. *Autoimmun Rev* (2007) 6:176–82. doi:10.1016/j.autrev.2006.10.004
4. Vermeulen N, Vermeire S, Arijs I, Michiels G, Ballet V, Derua R, et al. Seroreactivity against glycolytic enzymes in inflammatory bowel disease. *Inflamm Bowel Dis* (2011) 17:557–64. doi:10.1002/ibd.21388
5. Chang X, Wei C. Glycolysis and rheumatoid arthritis. *Int J Rheum Dis* (2011) 14:217–22. doi:10.1111/j.1756-185X.2011.01598.x
6. Ladd JJ, Chao T, Johnson MM, Qiu J, Chin A, Israel R, et al. Autoantibody signatures involving glycolysis and splicesome proteins precede a diagnosis of breast cancer among postmenopausal women. *Cancer Res* (2013) 73:1502–13. doi:10.1158/0008-5472.CAN-12-2560
7. Lunt SY, Vander Heiden MG. Aerobic glycolysis: meeting the metabolic requirements of cell proliferation. *Annu Rev Cell Dev Biol* (2011) 27:441–64. doi:10.1146/annurev-cellbio-092910-154237
8. Hurley JB, Lindsay KJ, Du J. Glucose, lactate, and shuttling of metabolites in vertebrate retinas. *J Neurosci Res* (2015) 93:1079–92. doi:10.1002/jnr.23583
9. Rueda EM, Johnson JE, Giddabasappa A, Swaroop A, Brooks MJ, Sigel I, et al. The cellular and compartmental profile of mouse retinal glycolysis, tricarboxylic acid cycle, oxidative phosphorylation, and ~P transferring kinases. *Mol Vis* (2016) 22:847–85.
10. Ng SK, Wood JPM, Chidlow G, Han G, Kittipassorn T, Peet DJ, et al. Cancer-like metabolism of the mammalian retina. *Clin Exp Ophthalmol* (2015) 43:367–76. doi:10.1111/ceo.12462
11. Grossniklaus HE, Geisert EE, Nickerson JM. Chapter twenty-two—introduction to the retina. In: Hejtmancik JF, John MN, editors. *Progress in Mol Biol Translat Sci*. Academic Press (2015). p. 383–96. doi:10.1016/bs.pmbts.2015.06.001
12. Koch K-W, Dell'Orco D. Protein and signaling networks in vertebrate photoreceptor cells. *Front Mol Neurosci* (2015) 8:67. doi:10.3389/fnmol.2015.00067
13. Hsu SC, Molday RS. Glucose metabolism in photoreceptor outer segments. Its role in phototransduction and in NADPH-requiring reactions. *J Biol Chem* (1994) 269:17954–9.
14. Takai Y, Ishiko S, Kagokawa H, Fukui K, Takahashi A, Yoshida A. Morphological study of acute zonal occult outer retinopathy (AZOOR) by multiplanar optical coherence tomography. *Acta Ophthalmol* (2009) 87:408–18. doi:10.1111/j.1755-3768.2008.01269.x

15. Adamus G. Latest updates on antiretinal autoantibodies associated with vision loss and breast cancer. *Invest Ophthalmol Vis Sci* (2015) 56:1680–8. doi:10.1167/iovs.14-15739
16. Gospe SM, Baker SA, Arshavsky VY. Facilitative glucose transporter Glut1 is actively excluded from rod outer segments. *J Cell Sci* (2010) 123:3639–44. doi:10.1242/jcs.072389
17. Tsacopoulos M, Poitry-Yamate CL, MacLeish PR, Poitry S. Trafficking of molecules and metabolic signals in the retina. *Prog Retin Eye Res* (1998) 17:429–42. doi:10.1016/S1350-9462(98)00010-X
18. Pratesi F, Moscato S, Sabbatini A, Chimenti D, Bombardieri S, Migliorini P. Autoantibodies specific for alpha-enolase in systemic autoimmune disorders. *J Rheumatol* (2000) 27:109–15.
19. Ahn BY, Song ES, Cho YJ, Kwon OW, Kim JK, Lee NG. Identification of an anti-aldolase autoantibody as a diagnostic marker for diabetic retinopathy by immunoproteomic analysis. *Proteomics* (2006) 6:1200–9. doi:10.1002/pmic.200500457
20. Backes C, Ludwig N, Leidinger P, Harz C, Hoffmann J, Keller A, et al. Immunogenicity of autoantigens. *BMC Genomics* (2011) 12:340. doi:10.1186/1471-2164-12-340
21. Dale RC, Candler PM, Church AJ, Wait R, Pocock JM, Giovannoni G. Neuronal surface glycolytic enzymes are autoantigen targets in post-streptococcal autoimmune CNS disease. *J Neuroimmunol* (2006) 172:187–97. doi:10.1016/j.jneuroim.2005.10.014
22. Ko AC, Brinton JP, Mahajan VB, Zimmerman B, Brinton GS, Stone EM, et al. Seroreactivity against aqueous-soluble and detergent-soluble retinal proteins in posterior uveitis. *Arch Ophthalmol* (2011) 129:415–20. doi:10.1001/archophthalmol.2011.65
23. ten Berge JCEM, Schreurs MWJ, Vermeer J, Meester-Smoor MA, Rothova A. Prevalence and clinical impact of antiretinal antibodies in uveitis. *Acta Ophthalmol* (2016) 94:282–8. doi:10.1111/aos.12939
24. Adamus G, Aptsiauri N, Guy J, Heckenlively J, Flannery J, Hargrave PA. The occurrence of serum autoantibodies against enolase in cancer-associated retinopathy. *Clin Immunol Immunopathol* (1996) 78:120–9. doi:10.1006/clin.1996.0021
25. Almqvist N, Winkler TH, Martensson IL. Autoantibodies: focus on anti-DNA antibodies. *Self Nonself* (2011) 2:11–8. doi:10.4161/self.2.1.15087
26. Heckenlively J, Ferreyra H. Autoimmune retinopathy: a review and summary. *Semin Immunopathol* (2008) 30:127–34. doi:10.1007/s00281-008-0114-7
27. Bazhin AV, Schadendorf D, Willner N, Smet CD, Heinzelmann A, Tikhomirova NK, et al. Photoreceptor proteins as cancer-retina antigens. *Int J Cancer* (2007) 120:1268–76. doi:10.1002/ijc.22458
28. Kazarian M, Laird-Offringa I. Small-cell lung cancer-associated autoantibodies: potential applications to cancer diagnosis, early detection, and therapy. *Mol Cancer* (2011) 10:33. doi:10.1186/1476-4598-10-33
29. Capello M, Ferri-Borgogno S, Cappello P, Novelli F. α-Enolase: a promising therapeutic and diagnostic tumor target. *FEBS J* (2011) 278:1064–74. doi:10.1111/j.1742-4658.2011.08025.x
30. Adamus G, Ren G, Weleber RG. Autoantibodies against retinal proteins in paraneoplastic and autoimmune retinopathy. *BMC Ophthalmol* (2004) 4:5. doi:10.1186/1471-2415-4-5
31. Adamus G. Autoantibody targets and their cancer relationship in the pathogenicity of paraneoplastic retinopathy. *Autoimmun Rev* (2009) 8:410–4. doi:10.1016/j.autrev.2009.01.002
32. Akoun GM, Scarna HM, Milleron BJ, Benichou MP, Herman DP. Serum neuron-specific enolase. A marker for disease extent and response to therapy for small-cell lung cancer. *Chest* (1985) 87:39–43. doi:10.1378/chest.87.1.39
33. Shin SJ, Kim BC, Kim TI, Lee SK, Lee KH, Kim WH. Anti-alpha-enolase antibody as a serologic marker and its correlation with disease severity in intestinal Behçet's disease. *Dig Dis Sci* (2010) 56:812–8. doi:10.1007/s10620-010-1326-y
34. Joachim S, Bruns K, Lackner K, Pfeiffer N, Grus F. Analysis of IgG antibody patterns against retinal antigens and antibodies to a-crystallin, GFAP, and a-enolase in sera of patients with "wet" age-related macular degeneration. *Graefes Arch Clin Exp Ophthalmol* (2007) 245:619–26. doi:10.1007/s00417-006-0429-9
35. Suzuki A, Iizuka A, Komiyama M, Takikawa M, Kume A, Tai S, et al. Identification of melanoma antigens using a serological proteome approach (SERPA). *Cancer Genomics Proteomics* (2010) 7:17–23.
36. Saulot V, Vittecoq O, Charlionet R, Fardellone P, Lange C, Marvin L, et al. Presence of autoantibodies to the glycolytic enzyme α-enolase in sera from patients with early rheumatoid arthritis. *Arthritis Rheum* (2002) 46:1196–201. doi:10.1002/art.10252
37. Butterfield DA, Lange MLB. Multifunctional roles of enolase in Alzheimer's disease brain: beyond altered glucose metabolism. *J Neurochem* (2009) 111:915–33. doi:10.1111/j.1471-4159.2009.06397.x
38. Forooghian F, Adamus G, Sproule M, Westall C, O'Connor P. Enolase autoantibodies and retinal function in multiple sclerosis patients. *Graefes Arch Clin Exp Ophthalmol* (2007) 245:1077–84. doi:10.1007/s00417-006-0527-8
39. Fujii A, Yoneda M, Ito T, Yamamura O, Satomi S, Higa H, et al. Autoantibodies against the amino terminal of [alpha]-enolase are a useful diagnostic marker of Hashimoto's encephalopathy. *J Neuroimmunol* (2005) 162:130–6. doi:10.1016/j.jneuroim.2005.02.004
40. Lee KH, Chung H-S, Kim HS, Oh S-H, Ha M-K, Baik J-H, et al. Human α-enolase from endothelial cells as a target antigen of anti-endothelial cell antibody in Behçet's disease. *Arthritis Rheum* (2003) 48:2025–35. doi:10.1002/art.11074
41. Shimizu A, Suzuki F, Kato K. Characterization of alpha alpha, beta beta, gamma gamma and alpha gamma human enolase isoenzymes, and preparation of hybrid enolases (alpha gamma and alpha beta) from homodimeric forms. *Biochim Biophys Acta* (1983) 748:278–84. doi:10.1016/0167-4838(83)90305-9
42. Smith WC, Bolch S, Dugger DR, Li J, Esquenazi I, Arendt A, et al. Interaction of arrestin with enolase1 in photoreceptors. *Invest Ophthalmol Vis Sci* (2011) 52:1832–40. doi:10.1167/iovs.10-5724
43. Ren G, Adamus G. Cellular targets of anti-alpha-enolase autoantibodies of patients with autoimmune retinopathy. *J Autoimmun* (2004) 23:161–7. doi:10.1016/j.jaut.2004.06.003
44. Redlitz A, Fowler BJ, Plow EF, Miles LA. The role of an enolase-related molecule in plasminogen binding to cells. *Eur J Biochem* (1995) 227:407–15. doi:10.1111/j.1432-1033.1995.tb20403.x
45. Ueta H, Nagasawa H, Oyabu-Manabe Y, Toida K, Ishimura K, Hori H. Localization of enolase in synaptic plasma membrane as an alphagamma heterodimer in rat brain. *Neurosci Res* (2004) 48:379–86. doi:10.1016/j.neures.2003.12.006
46. Díaz-Ramos À, Roig-Borrellas A, García-Melero A, López-Alemany R. α-Enolase, a multifunctional protein: its role on pathophysiological situations. *J Biomed Biotechnol* (2012) 2012:156795. doi:10.1155/2012/156795
47. Misiuk-Hojlo M, Ejma M, Gorczyca W, Szymaniec S, Witkowska D, Fortuna W, et al. Cancer-associated retinopathy in patients with breast carcinoma. *Arch Immunol Ther Exp* (2007) 55:261–5. doi:10.1007/s00005-007-0026-6
48. Mirshahi M, Le Marchand S. Co-purification of arrestin like proteins with alpha-enolase from bovine myocardial tissues and the possible role in heart diseases as an autoantigen. *Biochem Biophys Res Commun* (2015) 460:657–62. doi:10.1016/j.bbrc.2015.03.086
49. Pancholi V. Multifunctional alpha-enolase: its role in diseases. *Cell Mol Life Sci* (2001) 58:902–20. doi:10.1007/PL00000910
50. Zakrzewicz D, Didiasova M, Zakrzewicz A, Hocke AC, Uhle F, Markart P, et al. The interaction of enolase-1 with caveolae-associated proteins regulates its subcellular localization. *Biochem J* (2014) 460:295–307. doi:10.1042/BJ20130945
51. Arza B, Felez J, Lopez-Alemany R, Miles LA, Munoz-Canoves P. Identification of an epitope of alpha-enolase (a candidate plasminogen receptor) by phage display. *Thromb Haemost* (1997) 78:1097–103.
52. Walter M, Berg H, Leidenberger FA, Schweppe K-W, Northermann W. Autoreactive epitopes within the human alpha-enolase and their recognition by sera from patients with endometriosis. *J Autoimmun* (1995) 8:931–45. doi:10.1016/S0896-8411(95)80027-1
53. Sirover MA. New insights into an old protein: the functional diversity of mammalian glyceraldehyde-3-phosphate dehydrogenase. *Biochim Biophys Acta* (1999) 1432:159–84. doi:10.1016/S0167-4838(99)00119-3
54. Mazzola JL, Sirover MA. Subcellular localization of human glyceraldehyde-3-phosphate dehydrogenase is independent of its glycolytic function. *Biochim Biophys Acta* (2003) 1622:50–6. doi:10.1016/S0304-4165(03)00117-X
55. Takasaki Y, Kaneda K, Matsushita M, Yamada H, Nawata M, Matsudaira R, et al. Glyceraldehyde 3-phosphate dehydrogenase is a novel autoantigen leading autoimmune responses to proliferating cell nuclear antigen multiprotein complexes in lupus patients. *Int Immunol* (2004) 16:1295–304. doi:10.1093/intimm/dxh131

56. Nicholls C, Li H, Liu JP. GAPDH: a common enzyme with uncommon functions. *Clin Exp Pharmacol Physiol* (2012) 39:674–9. doi:10.1111/j.1440-1681.2011.05599.x
57. Nicholls C, Pinto AR, Li H, Li L, Wang L, Simpson R, et al. Glyceraldehyde-3-phosphate dehydrogenase (GAPDH) induces cancer cell senescence by interacting with telomerase RNA component. *Proc Natl Acad Sci U S A* (2012) 109:13308–13. doi:10.1073/pnas.1206672109
58. Jung DW, Kim WH, Seo S, Oh E, Yim SH, Ha HH, et al. Chemical targeting of GAPDH moonlighting function in cancer cells reveals its role in tubulin regulation. *Chem Biol* (2014) 21:1533–45. doi:10.1016/j.chembiol.2014.08.017
59. Adamus G, Choi D, Raghunath A, Schiffman J. Significance of anti-retinal autoantibodies in cancer-associated retinopathy with gynecological cancers. *J Clin Exp Ophthalmol* (2013) 4:307. doi:10.4172/2155-9570.1000307
60. Adamus G, Brown L, Schiffman J, Iannaccone A. Diversity in autoimmunity against retinal, neuronal, and axonal antigens in acquired neuro-retinopathy. *J Ophthalmic Inflamm Infect* (2011) 1:111–21. doi:10.1007/s12348-011-0028-8
61. Kolln J, Ren H-M, Da R-R, Zhang Y, Spillner E, Olek M, et al. Triosephosphate isomerase- and glyceraldehyde-3-phosphate dehydrogenase-reactive autoantibodies in the cerebrospinal fluid of patients with multiple sclerosis. *J Immunol* (2006) 177:5652–8. doi:10.4049/jimmunol.177.8.5652
62. Hsu SC, Molday RS. Glyceraldehyde-3-phosphate dehydrogenase is a major protein associated with the plasma membrane of retinal photoreceptor outer segments. *J Biol Chem* (1990) 265:13308–13.
63. Chen J, Wu M, Sezate SA, Matsumoto H, Ramsey M, McGinnis JF. Interaction of glyceraldehyde-3-phosphate dehydrogenase in the light-induced rod alpha-transducin translocation. *J Neurochem* (2008) 104: 1280–92. doi:10.1111/j.1471-4159.2007.05081.x
64. Adamus G, Brown L, Weleber RG. Molecular biomarkers for autoimmune retinopathies: significance of anti-transducin-alpha autoantibodies. *Exp Mol Pathol* (2009) 87:195–203. doi:10.1016/j.yexmp.2009.08.003
65. Joachim SC, Wuenschig D, Pfeiffer N, Grus FH. IgG antibody patterns in aqueous humor of patients with primary open angle glaucoma and pseudoexfoliation glaucoma. *Mol Vis* (2007) 13:1573–9.
66. Cerella C, Dicato M, Diederich M. Modulatory roles of glycolytic enzymes in cell death. *Biochem Pharmacol* (2014) 92:22–30. doi:10.1016/j.bcp.2014.07.005
67. Guo C, Liu S, Sun MZ. Novel insight into the role of GAPDH playing in tumor. *Clin Transl Oncol* (2013) 15:167–72. doi:10.1007/s12094-012-0924-x
68. Adamus G. Paraneoplastic retinal degeneration. In: Levin L, Albert DM, editors. *Ocular Disease: Mechanisms and Management*. Saunders Elsevier (2010). p. 599–608.
69. Chang YS, Wu W, Walsh G, Hong WK, Mao L. Enolase-alpha is frequently down-regulated in non-small cell lung cancer and predicts aggressive biological behavior. *Clin Cancer Res* (2003) 9:3641–4.
70. Lu M, Sautin YY, Holliday LS, Gluck SL. The glycolytic enzyme aldolase mediates assembly, expression, and activity of vacuolar H+-ATPase. *J Biol Chem* (2004) 279:8732–9. doi:10.1074/jbc.M303871200
71. He P, Naka T, Serada S, Fujimoto M, Tanaka T, Hashimoto S, et al. Proteomics-based identification of alpha-enolase as a tumor antigen in non-small lung cancer. *Cancer Sci* (2007) 98:1234–40. doi:10.1111/j.1349-7006.2007.00509.x
72. Fujita H, Aoki H, Ajioka I, Yamazaki M, Abe M, Oh-Nishi A, et al. Detailed expression pattern of aldolase C (Aldoc) in the cerebellum, retina and other areas of the CNS studied in Aldoc-Venus knock-in mice. *PLoS One* (2014) 9:e86679. doi:10.1371/journal.pone.0086679
73. Bulliard C, Zurbriggen R, Tornare J, Faty M, Dastoor Z, Dreyer JL. Purification of a dichlorophenol-indophenol oxidoreductase from rat and bovine synaptic membranes: tight complex association of a glyceraldehyde-3-phosphate dehydrogenase isoform, TOAD64, enolase-gamma and aldolase C. *Biochem J* (1997) 324(Pt 2):555–63. doi:10.1042/bj3240555
74. Beltran WA, Cideciyan AV, Lewin AS, Iwabe S, Khanna H, Sumaroka A, et al. Gene therapy rescues photoreceptor blindness in dogs and paves the way for treating human X-linked retinitis pigmentosa. *Proc Natl Acad Sci U S A* (2012) 109:2132–7. doi:10.1073/pnas.1118847109
75. Mamczur P, Gamian A, Kolodziej J, Dziegiel P, Rakus D. Nuclear localization of aldolase A correlates with cell proliferation. *Biochim Biophys Acta* (2013) 1833:2812–22. doi:10.1016/j.bbamcr.2013.07.013
76. Mooney CJ, Dunphy EJ, Stone B, McNeel DG. Identification of autoantibodies elicited in a patient with prostate cancer presenting as dermatomyositis. *Int J Urol* (2006) 13:211–7. doi:10.1111/j.1442-2042.2006.01263.x
77. Katayama H, Boldt C, Ladd JJ, Johnson MM, Chao T, Capello M, et al. An autoimmune response signature associated with the development of triple-negative breast cancer reflects disease pathogenesis. *Cancer Res* (2015) 75:3246–54. doi:10.1158/0008-5472.CAN-15-0248
78. Lu Y, Jia L, He S, Hurley MC, Leys MJ, Jayasundera T, et al. Melanoma-associated retinopathy: a paraneoplastic autoimmune complication. *Arch Ophthalmol* (2009) 127:1572–80. doi:10.1001/archophthalmol.2009.311
79. Morohoshi K, Ohbayashi M, Patel N, Chong V, Bird AC, Ono SJ. Identification of anti-retinal antibodies in patients with age-related macular degeneration. *Exp Mol Pathol* (2012) 93:193–9. doi:10.1016/j.yexmp.2012.03.007
80. Nita M, Grzybowski A, Ascaso FJ, Huerva V. Age-related macular degeneration in the aspect of chronic low-grade inflammation (pathophysiological parainflammation). *Mediators Inflamm* (2014) 2014:930671. doi:10.1155/2014/930671
81. Mor F, Izak M, Cohen IR. Identification of aldolase as a target antigen in Alzheimer's disease. *J Immunol* (2005) 175:3439–45. doi:10.4049/jimmunol.175.5.3439
82. Privitera D, Corti V, Alessio M, Volontè A, Lampasona V, Comi G, et al. Proteomic identification of aldolase A as an autoantibody target in patients with atypical movement disorders. *Neurol Sci* (2012) 34:313–20. doi:10.1007/s10072-012-0996-y
83. Ukaji F, Kitajima I, Kubo T, Shimizu C, Nakajima T, Maruyama I. Serum samples of patients with rheumatoid arthritis contain a specific autoantibody to "denatured" aldolase A in the osteoblast-like cell line, MG-63. *Ann Rheum Dis* (1999) 58:169–74. doi:10.1136/ard.58.3.169
84. Goëb V, Thomas-L'Otellier M, Daveau R, Charlionet R, Fardellone P, Loët X. Candidate autoantigens identified by mass spectrometry in early rheumatoid arthritis are chaperones and citrullinated glycolytic enzymes. *Arthritis Res Ther* (2009) 11:R38. doi:10.1186/ar2644
85. Gupta V, Bamezai RNK. Human pyruvate kinase M2: a multifunctional protein. *Protein Sci* (2010) 19:2031–44. doi:10.1002/pro.505
86. Bluemlein K, Gruning NM, Feichtinger RG, Lehrach H, Kofler B, Ralser M. No evidence for a shift in pyruvate kinase PKM1 to PKM2 expression during tumorigenesis. *Oncotarget* (2011) 2:393–400. doi:10.18632/oncotarget.278
87. Desai S, Ding M, Wang B, Lu Z, Zhao Q, Shaw K, et al. Tissue-specific isoform switch and DNA hypomethylation of the pyruvate kinase PKM gene in human cancers. *Oncotarget* (2014) 5:8202–10. doi:10.18632/oncotarget.1159
88. Yang W, Lu Z. Pyruvate kinase M2 at a glance. *J Cell Sci* (2015) 128:1655–60. doi:10.1242/jcs.166629
89. Casson RJ, Wood JP, Han G, Kittipassorn T, Peet DJ, Chidlow G. M-type pyruvate kinase isoforms and lactate dehydrogenase A in the mammalian retina: metabolic implications PKM1 and LDH-A in the mammalian retina. *Invest Ophthalmol Vis Sci* (2016) 57:66–80. doi:10.1167/iovs.15-17962
90. Alves-Filho JC, Palsson-McDermott EM. Pyruvate kinase M2: a potential target for regulating inflammation. *Front Immunol* (2016) 7:145. doi:10.3389/fimmu.2016.00145
91. Kansy JW, Katsovich L, McIver KS, Pick J, Zabriskie JB, Lombroso PJ, et al. Identification of pyruvate kinase as an antigen associated with Tourette syndrome. *J Neuroimmunol* (2006) 181:165–76. doi:10.1016/j.jneuroim.2006.08.007
92. Vas J, Gronwall C, Silverman GJ. Fundamental roles of the innate-like repertoire of natural antibodies in immune homeostasis. *Front Immunol* (2013) 4:4. doi:10.3389/fimmu.2013.00004
93. Zhang H, Li P, Wu D, Xu D, Hou Y, Wang Q, et al. Serum IgG subclasses in autoimmune diseases. *Medicine* (2015) 94:e387. doi:10.1097/MD.0000000000000387
94. Hu P, Pollard JD, Chan-Ling T. Breakdown of the blood-retinal barrier induced by activated T cells of nonneural specificity. *Am J Pathol* (2000) 156:1139–49. doi:10.1016/S0002-9440(10)64982-6
95. Niu N, Zhang J, Sun Y, Wang S, Sun Y, Korteweg C, et al. Expression and distribution of immunoglobulin G and its receptors in an immune privileged site: the eye. *Cell Mol Life Sci* (2011) 68:2481–92. doi:10.1007/s00018-010-0572-7
96. Elkon K, Casali P. Nature and functions of autoantibodies. *Nat Clin Pract Rheumatol* (2008) 4:491–8. doi:10.1038/ncprheum0895
97. Baumgarth N, Tung JW, Herzenberg LA. Inherent specificities in natural antibodies: a key to immune defense against pathogen invasion. *Springer Semin Immunopathol* (2005) 26:347–62. doi:10.1007/s00281-004-0182-2
98. Xu RH, Pelicano H, Zhou Y, Carew JS, Feng L, Bhalla KN, et al. Inhibition of glycolysis in cancer cells: a novel strategy to overcome drug resistance

associated with mitochondrial respiratory defect and hypoxia. *Cancer Res* (2005) 65:613–21.
99. Altenberg B, Greulich KO. Genes of glycolysis are ubiquitously overexpressed in 24 cancer classes. *Genomics* (2004) 84:1014–20. doi:10.1016/j.ygeno.2004.08.010
100. Lincet H, Icard P. How do glycolytic enzymes favour cancer cell proliferation by nonmetabolic functions? *Oncogene* (2015) 34:3751–9. doi:10.1038/onc.2014.320
101. Kim JW, Dang CV. Multifaceted roles of glycolytic enzymes. *Trends Biochem Sci* (2005) 30:142–50. doi:10.1016/j.tibs.2005.01.005
102. Ludwig N, Keller A, Leidinger P, Harz C, Backes C, Lenhof H-P, et al. Is there a general autoantibody signature for cancer? *Eur J Cancer* (2012) 48:2451–61. doi:10.1016/j.ejca.2012.01.017
103. Pillai S, Mattoo H, Cariappa A. B cells and autoimmunity. *Curr Opin Immunol* (2011) 23:721–31. doi:10.1016/j.coi.2011.10.007
104. Weleber RG, Watzke RC, Shults WT, Trzupek KM, Heckenlively JR, Egan RA, et al. Clinical and electrophysiologic characterization of paraneoplastic and autoimmune retinopathies associated with antienolase antibodies. *Am J Ophthalmol* (2005) 139:780–94. doi:10.1016/j.ajo.2004.12.104
105. Balhara V, Deshmukh SS, Kalman L, Kornblatt JA. The interaction of streptococcal enolase with canine plasminogen: the role of surfaces in complex formation. *PLoS One* (2014) 9:e88395. doi:10.1371/journal.pone.0088395
106. Oldstone MB. Molecular mimicry, microbial infection, and autoimmune disease: evolution of the concept. *Curr Top Microbiol Immunol* (2005) 296:1–17.
107. Mackay IR, Leskovsek NV, Rose NR. Cell damage and autoimmunity: a critical appraisal. *J Autoimmun* (2008) 30:5–11. doi:10.1016/j.jaut.2007.11.009
108. Herkel J, Lohse AW. Significance of autoantibodies. *Hepatology* (2008) 47:786–8. doi:10.1002/hep.22271
109. Adamus G, Yang S, Weleber RG. Unique epitopes for carbonic anhydrase II autoantibodies related to autoimmune retinopathy and cancer-associated retinopathy. *Exp Eye Res* (2016) 147:161–8. doi:10.1016/j.exer.2016.05.012
110. Lanzavecchia A. How can cryptic epitopes trigger autoimmunity? *J Exp Med* (1995) 181:1945–8. doi:10.1084/jem.181.6.1945
111. Maruyama I, Ohguro H, Ikeda Y. Retinal ganglion cells recognized by serum autoantibody against gamma-enolase found in glaucoma patients. *Invest Ophthalmol Vis Sci* (2000) 41:1657–65.
112. Kölln J, Zhang Y, Thai G, Demetriou M, Hermanowicz N, Duquette P, et al. Inhibition of glyceraldehyde-3-phosphate dehydrogenase activity by antibodies present in the cerebrospinal fluid of patients with multiple sclerosis. *J Immunol* (2010) 185:1968–75. doi:10.4049/jimmunol.0904083
113. Adamus G, Machnicki M, Elerding H, Sugden B, Blocker YS, Fox DA. Antibodies to recoverin induce apoptosis of photoreceptor and bipolar cells in vivo. *J Autoimmun* (1998) 11:523–33. doi:10.1006/jaut.1998.0221
114. Adamus G, Machnicki M, Seigel GM. Apoptotic retinal cell death induced by autoantibodies of cancer associated retinopathy. *Invest Ophthalmol Vis Sci* (1997) 38:283–91.
115. Shiraga S, Adamus G. Mechanism of CAR syndrome: anti-recoverin antibodies are the inducers of retinal cell apoptotic death via the caspase 9- and caspase 3-dependent pathway. *J Neuroimmunol* (2002) 132:72–82. doi:10.1016/S0165-5728(02)00314-4
116. Anekonda TS, Adamus G. Resveratrol prevents antibody-induced apoptotic death of retinal cells through upregulation of Sirt1 and Ku70. *BMC Res Notes* (2008) 1:122. doi:10.1186/1756-0500-1-122
117. Maruyama I, Maeda T, Okisaka S, Mizukawa A, Nakazawa M, Ohguro H. Autoantibody against neuron-specific enolase found in glaucoma patients causes retinal dysfunction in vivo. *Jpn J Ophthalmol* (2002) 46:1–12. doi:10.1016/S0021-5155(01)00453-1
118. Ikeda Y, Maruyama I, Nakazawa M, Ohguro H. Clinical significance of serum antibody against neuron-specific enolase in glaucoma patients. *Jpn J Ophthalmol* (2002) 46:13–7. doi:10.1016/S0021-5155(01)00455-5
119. Adamus G, Chew EY, Ferris FL, Klein ML. Prevalence of anti-retinal autoantibodies in different stages of age-related macular degeneration. *BMC Ophthalmol* (2014) 14:154. doi:10.1186/1471-2415-14-154
120. Kyger M, Worley A, Adamus G. Autoimmune responses against photoreceptor antigens during retinal degeneration and their role in macrophage recruitment into retinas of RCS rats. *J Neuroimmunol* (2013) 254:91–100. doi:10.1016/j.jneuroim.2012.10.007
121. Munoz LE, Lauber K, Schiller M, Manfredi AA, Herrmann M. The role of defective clearance of apoptotic cells in systemic autoimmunity. *Nat Rev Rheumatol* (2010) 6:280–9. doi:10.1038/nrrheum.2010.46
122. Nagata S, Hanayama R, Kawane K. Autoimmunity and the clearance of dead cells. *Cell* (2010) 140:619–30. doi:10.1016/j.cell.2010.02.014
123. Ferreyra HA, Jayasundera T, Khan NW, He S, Lu Y, Heckenlively JR. Management of autoimmune retinopathies with immunosuppression. *Arch Ophthalmol* (2009) 127:390–7. doi:10.1001/archophthalmol.2009.24
124. Bursztyn LL, Belrose JC, Coupland SG, Fraser JA, Proulx AA. Remission of nonparaneoplastic autoimmune retinopathy after minimal steroid treatment. *Retin Cases Brief Rep* (2015) 9:173–6. doi:10.1097/ICB.0000000000000131
125. Sierpina DI, Skale DM, Fan JT. Effect of plasmapheresis and passage of anti-retinal antibodies through the placenta in a case of non-paraneoplastic autoimmune retinopathy. *Retin Cases Brief Rep* (2017) 11(Suppl 1):S34–7. doi:10.1097/ICB.0000000000000395
126. Guy J, Aptsiauri N. Treatment of paraneoplastic visual loss with intravenous immunoglobulin: report of 3 cases. *Arch Ophthalmol* (1999) 117:471–7. doi:10.1001/archopht.117.4.471
127. Subhadra C, Dudek AZ, Rath PP, Lee MS. Improvement in visual fields in a patient with melanoma-associated retinopathy treated with intravenous immunoglobulin. *J Neuroophthalmol* (2008) 28:23–6. doi:10.1097/WNO.0b013e31816754c4
128. Mahdi N, Faia LJ, Goodwin J, Nussenblatt RB, Nida Sen H. A case of autoimmune retinopathy associated with thyroid carcinoma. *Ocul Immunol Inflamm* (2010) 18:322–3. doi:10.3109/09273941003802379
129. Fox A, Jeffrey B, Hasni S, Nussenblatt R, Sen HN. Rituximab treatment for nonparaneoplastic autoimmune retinopathy. *Can J Ophthalmol* (2015) 50:e101–4. doi:10.1016/j.jcjo.2015.08.009
130. Or C, Collins DR, Merkur AB, Wang Y, Chan CC, Forooghian F. Intravenous rituximab for the treatment of cancer-associated retinopathy. *Can J Ophthalmol* (2013) 48:e35–8. doi:10.1016/j.jcjo.2012.11.010
131. Uludag G, Onal S, Arf S, Sayman Muslubas I, Selcukbiricik F, Koc Akbay A, et al. Electroretinographic improvement after rituximab therapy in a patient with autoimmune retinopathy. *Am J Ophthalmol Case Rep* (2016) 2:4–7. doi:10.1016/j.ajoc.2016.03.007
132. Maleki A, Lamba N, Ma L, Lee S, Schmidt A, Foster CS. Rituximab as a monotherapy or in combination therapy for the treatment of non-paraneoplastic autoimmune retinopathy. *Clin Ophthalmol* (2017) 11:377–85. doi:10.2147/OPTH.S120162
133. Cohen IR. Activation of benign autoimmunity as both tumor and autoimmune disease immunotherapy: a comprehensive review. *J Autoimmun* (2014) 54:112–7. doi:10.1016/j.jaut.2014.05.002

Conflict of Interest Statement: The author declares that the research was conducted in the absence of any commercial or financial relationships that could be construed as a potential conflict of interest.

Copyright © 2017 Adamus. This is an open-access article distributed under the terms of the Creative Commons Attribution License (CC BY). The use, distribution or reproduction in other forums is permitted, provided the original author(s) or licensor are credited and that the original publication in this journal is cited, in accordance with accepted academic practice. No use, distribution or reproduction is permitted which does not comply with these terms.

frontiers in Immunology

CORRECTION
published: 15 May 2017
doi: 10.3389/fimmu.2017.00551

Corrigendum: Increased Toll-Like Receptors Activity and TLR Ligands in Patients with Autoimmune Thyroid Diseases

*Shiqiao Peng[1†], Chenyan Li[1,2†], Xinyi Wang[1,3], Xin Liu[1,4], Cheng Han[1], Ting Jin[1,5], Shanshan Liu[1,6], Xiaowen Zhang[1], Hanyi Zhang[1], Xue He[1], Xiaochen Xie[1], Xiaohui Yu[1,2], Chuyuan Wang[1,2], Ling Shan[1], Chenling Fan[1], Zhongyan Shan[1,2] and Weiping Teng[1,2]**

[1] Department of Endocrinology and Metabolism, Institute of Endocrinology, Liaoning Provincial Key Laboratory of Endocrine Diseases, The First Affiliated Hospital of China Medical University, China Medical University, Shenyang, Liaoning, China, [2] Department of Endocrinology and Metabolism, The First Hospital of China Medical University, Shenyang, China, [3] Department of Laboratory Medicine, The First Hospital of China Medical University, Shenyang, China, [4] Department of Intensive Care Unit, Affiliated Hospital of Qingdao University, Qingdao, China, [5] Department of Endocrinology, Sir Run Run Shaw Hospital, Affiliated to School of Medicine, Zhejiang University, Hangzhou, China, [6] Department of Emergency, People's Liberation Army No. 202 Hospital, Shenyang, China*

Keywords: autoimmune thyroid disease, innate immunity, toll-like receptor, signaling, pathogenesis

OPEN ACCESS

Edited and Reviewed by:
Pietro Ghezzi, Brighton and Sussex Medical School, UK

****Correspondence:***
Weiping Teng
twp@vip.163.com

[†]These authors have contributed equally to this work.

Specialty section:
This article was submitted to Inflammation, a section of the journal Frontiers in Immunology

Received: *20 March 2017*
Accepted: *25 April 2017*
Published: *15 May 2017*

Citation:
Peng S, Li C, Wang X, Liu X, Han C, Jin T, Liu S, Zhang X, Zhang H, He X, Xie X, Yu X, Wang C, Shan L, Fan C, Shan Z and Teng W (2017) Corrigendum: Increased Toll-Like Receptors Activity and TLR Ligands in Patients with Autoimmune Thyroid Diseases. Front. Immunol. 8:551. doi: 10.3389/fimmu.2017.00551

A corrigendum on

Increased Toll-Like Receptors Activity and TLR Ligands in Patients with Autoimmune Thyroid Diseases

by Peng S, Li C, Wang X, Liu X, Han C, Jin T, et al. Front Immunol (2016) 7:578. doi: 10.3389/fimmu.2016.00578

There was a mistake in the address of the author' unit 1 as published. The unit 1 in the original article was not comprehensive and did not include the affiliated hospital of China medical university. The correct address of the unit 1 should be "Department of Endocrinology and Metabolism, Institute of Endocrinology, Liaoning Provincial Key Laboratory of Endocrine Diseases, The First Affiliated Hospital of China Medical University, China Medical University, Shenyang, Liaoning, China." The correct address of author' unit 1 is below.

Address

Department of Endocrinology and Metabolism, Institute of Endocrinology, Liaoning Provincial Key Laboratory of Endocrine Diseases, The First Affiliated Hospital of China Medical University, China Medical University, Shenyang, Liaoning, China

The authors apologize for this oversight. This error does not change the scientific conclusions of the article in any way.

The original article has been updated.

Conflict of Interest Statement: The authors declare that the research was conducted in the absence of any commercial or financial relationships that could be construed as a potential conflict of interest.

Copyright © 2017 Peng, Li, Wang, Liu, Han, Jin, Liu, Zhang, Zhang, He, Xie, Yu, Wang, Shan, Fan, Shan and Teng. This is an open-access article distributed under the terms of the Creative Commons Attribution License (CC BY). The use, distribution or reproduction in other forums is permitted, provided the original author(s) or licensor are credited and that the original publication in this journal is cited, in accordance with accepted academic practice. No use, distribution or reproduction is permitted which does not comply with these terms.

frontiers in Immunology

ORIGINAL RESEARCH
published: 09 June 2017
doi: 10.3389/fimmu.2017.00633

Insulin Modulates Cytokine Release, Collagen and Mucus Secretion in Lung Remodeling of Allergic Diabetic Mice

*Sabrina S. Ferreira, Fernanda P. B. Nunes, Felipe B. Casagrande and Joilson O. Martins**

Laboratory of Immunoendocrinology, Department of Clinical and Toxicological Analyses, Faculty of Pharmaceutical Sciences of University São Paulo (FCF/USP), São Paulo, Brazil

Introduction: The role of insulin in lung remodeling in a model of asthma in healthy and diabetic mice was evaluated.

Material and methods: Diabetic male BALB/c mice (alloxan, 50 mg/kg, intravenous) and controls were sensitized by subcutaneous (s.c.) injection of ovalbumin (OA, 20 µg) in aluminum hydroxide ($Al(OH)_3$, 2 mg) 10 days after the alloxan injection and received the same dose 12 days later. Six days after the last sensitization, animals were nebulized with OA solution for 7 days. The first set of diabetic and control mice received 2 and 1 IU, respectively, of s.c. neutral protamine Hagedorn (NPH) insulin and were analyzed 8 h later. The second set of diabetic and control mice received 2 and 1 IU, respectively, of insulin 12 h before the OA challenge and half doses of insulin 2 h before each the seven OA challenges. Twenty-four hours after the last challenge, the following analyses were performed: (a) quantification of the cells in the bronchoalveolar lavage fluid (BALF), the white cell count, and blood glucose; (b) morphological analysis of lung tissues by hematoxylin and eosin staining; (c) quantification of collagen deposition in lung tissues and mucus by morphometric analysis of histological sections stained with Masson's trichrome and periodic acid-Schiff (PAS), respectively; and (d) quantification of the cytokine concentrations (IL-4, IL-5, and IL-13) in the BALF supernatant.

Results: Compared to controls, diabetic mice had significantly reduced inflammatory cells (81%) in the BALF, no eosinophils in the BALF and peripheral blood and reduced collagen deposition and mucus in the lungs. BALF concentrations of IL-4 (48%) and IL-5 (31%) decreased and IL-13 was absent. A single dose of insulin restored peripheral blood eosinophils and BALF mononuclear cells but not BALF eosinophils, collagen deposition, and mucus levels. However, multiple doses of insulin restored both total cells and eosinophils in the BALF and peripheral blood, BALF cytokines, and collagen deposition and mucus secretion into the lungs.

Conclusion: The results suggest that insulin modulates the production/release of cytokines, cell migration, deposition of collagen, and mucus secretion in lung remodeling of a mouse model of asthma.

Keywords: asthma, diabetes mellitus, insulin, remodeling, eosinophils, collagen, mucus, lung

OPEN ACCESS

Edited by:
Guixiu Shi,
Xiamen University, China

Reviewed by:
Luz Pamela Blanco,
National Institute of Health, United States
Ding Xinchun,
Indiana University—Purdue University Indianapolis, United States

***Correspondence:**
Joilson O. Martins
martinsj@usp.br

Specialty section:
This article was submitted to Inflammation, a section of the journal Frontiers in Immunology

Received: *01 March 2017*
Accepted: *12 May 2017*
Published: *09 June 2017*

Citation:
Ferreira SS, Nunes FPB, Casagrande FB and Martins JO (2017) Insulin Modulates Cytokine Release, Collagen and Mucus Secretion in Lung Remodeling of Allergic Diabetic Mice. Front. Immunol. 8:633. doi: 10.3389/fimmu.2017.00633

INTRODUCTION

Asthma is characterized by chronic inflammation of the airways and is related to exposure to allergens, infections and other factors (1). The inflammatory process in allergic asthma is predominantly characterized by increased number of eosinophils, activated mast cells, and Th2 lymphocytes (2, 3). Airway inflammation, airflow obstruction, and bronchial hyperresponsiveness are characteristic features of asthma (4–6). Airway remodeling is the result of various structural changes in the airways (7, 8). Asthma affects approximately 300 million people worldwide (9), while overall prevalence in Brazil is 10–25% (1).

Experimental and clinical studies have indicated that the inflammatory response is impaired in diabetic patients. Triggering of diabetes mellitus in asthmatic patients resulted in an improvement in the asthmatic condition and treatment with insulin restored asthma symptoms (10, 11). Insulin has been shown to modulate inflammatory components of asthmatic reactions (12, 13). Previous studies demonstrated that alloxan-induced diabetic rats present substantially reduced mast cell degranulation upon antigen challenge. Treatment of diabetic rats with insulin restored the number of degranulated mast cells, histamine release, and airway reactivity to ovalbumin (OA) (13). In addition, animals rendered diabetic by alloxan injection exhibited reduced pulmonary inflammatory infiltrate. Insulin treatment restored this condition, suggesting a major role of insulin in asthma (14). In a similar model of asthma, insulin was shown to modulate the production of cytokines, such as TNF-α and IL-1β, along with expression of adhesion molecules (P- and E-selectins) and neutrophil migration into the lungs (12). We thus examined whether insulin modulates lung remodeling in a murine model of allergic lung inflammation. This study aimed to evaluate the role of insulin in lung remodeling of a model of asthma in healthy and diabetic mice.

MATERIALS AND METHODS

Animals

We used specific pathogen-free male BALB/c mice, 8–12 weeks of age, weighing approximately 20–25 g at the beginning of the experiments. The animals were maintained at 22°C under a 12 h light–dark cycle and were allowed access to food and water *ad libitum* throughout the observation period. This study was carried out in strict accordance with the principles and guidelines adopted by the Brazilian National Council for the Control of Animal Experimentation (CONCEA) and approved by the Ethical Committee on Animal Use (CEUA) of the Faculty of Pharmaceutical Sciences (FCF) of University São Paulo (Permit Number: CEUA/FCF/340). All surgical procedures were performed under ketamine/xylazine anesthesia, and all measures were taken to minimize suffering.

Induction of Diabetes Mellitus

Diabetes mellitus was induced by intravenous injection of alloxan monohydrate (50 mg/kg; Sigma Chemical Co., St. Louis, MO, USA) dissolved in physiologic saline (SAL, 0.9% NaCl). Control mice were injected with physiologic SAL only. After 10 days, the presence of diabetes was verified by blood glucose concentrations higher than 300 mg/dL, which were determined with a blood glucose monitor (Accu-Chek Advantage II, Roche Diagnostica, São Paulo, São Paulo, Brazil), in blood samples obtained from mouse tails (15).

Induction of Allergic Asthma

Mice were sensitized on days 10 and 22 by intraperitoneal (i.p.) injection containing 20 μg of OA (Sigma, USA) and 2 mg of aluminum hydroxide [$Al(OH_3)$; Reheis Inc., USA] in PBS to a total volume of 0.2 mL. Sensitized and control mice were challenged by multiple exposures to aerosol (5% OA in PBS) from an ultrasonic nebulizer (ICEL US-800, São Paulo, Brazil), delivering particles of 0.5–10 μm diameter at approximately 0.75 cc/min for 30 min. Challenges were performed daily for 7 days (28–33 and 35). The experiments were performed 24 h after the last challenge (16).

Insulin Treatment

Diabetic and control mice were divided into two groups according to the different insulin treatments. The first set of diabetic and control mice received 2 and 1 IU, respectively, of neutral protamine Hagedorn (NPH; Eli Lilly, São Paulo, São Paulo, Brazil) insulin subcutaneously 24 h after the last challenge, and the analyses were performed 8 h after the insulin treatment (**Figure 1A**) (14). The second set of diabetic and control mice received 2 and 1 IU, respectively, of insulin subcutaneously 12 h before the OA challenges (07:00 p.m.) and half doses (07:00 a.m.) of insulin 2 h before each of the 7 OA challenges (**Figure 1B**). After 24 h, blood, lungs and bronchoalveolar lavage fluid (BALF) were collected for further analysis (17).

Kinetics of Glucose with Insulin Treatment

Glucose measurements for a kinetic curve were performed to determine when the challenges should be performed after insulin treatment. Diabetic and control mice received 2 and 1 IU, respectively, of NPH insulin subcutaneously, and glucose levels were determined at 1, 2, 3, 6, and 8 h after the insulin treatment.

Bronchoalveolar Lavage

Mice were euthanized by a lethal dose of ketamine hydrochloride (90 mg/kg) and xylazine hydrochloride (10 mg/kg). The trachea was cannulated with polyethylene tubing (24 G3/4). The lungs were then lavaged by instillation of 1 mL of PBS (pH 7.4) three times for total volume of 3 mL. The BALF was centrifuged at 1,500 rpm for 10 min, and supernatant was frozen at −70°C for later cytokine measurements. Pelleted cells were collected and resuspended in 1 mL of PBS. The total number of cells was determined using a Neubauer chamber, whereas a differential count was obtained after cells from the BALF were centrifuged.

Quantification of Cytokines in the BALF

The level of cytokines (IL-1β, IL-4, IL-5, IL-10, and IL-13) was measured in BALF supernatant samples by enzyme-linked immunosorbent assay (ELISA), using commercial kits (R&D Systems, Inc., Minneapolis, MN, USA). Assays were performed according to the manufacturer's manual.

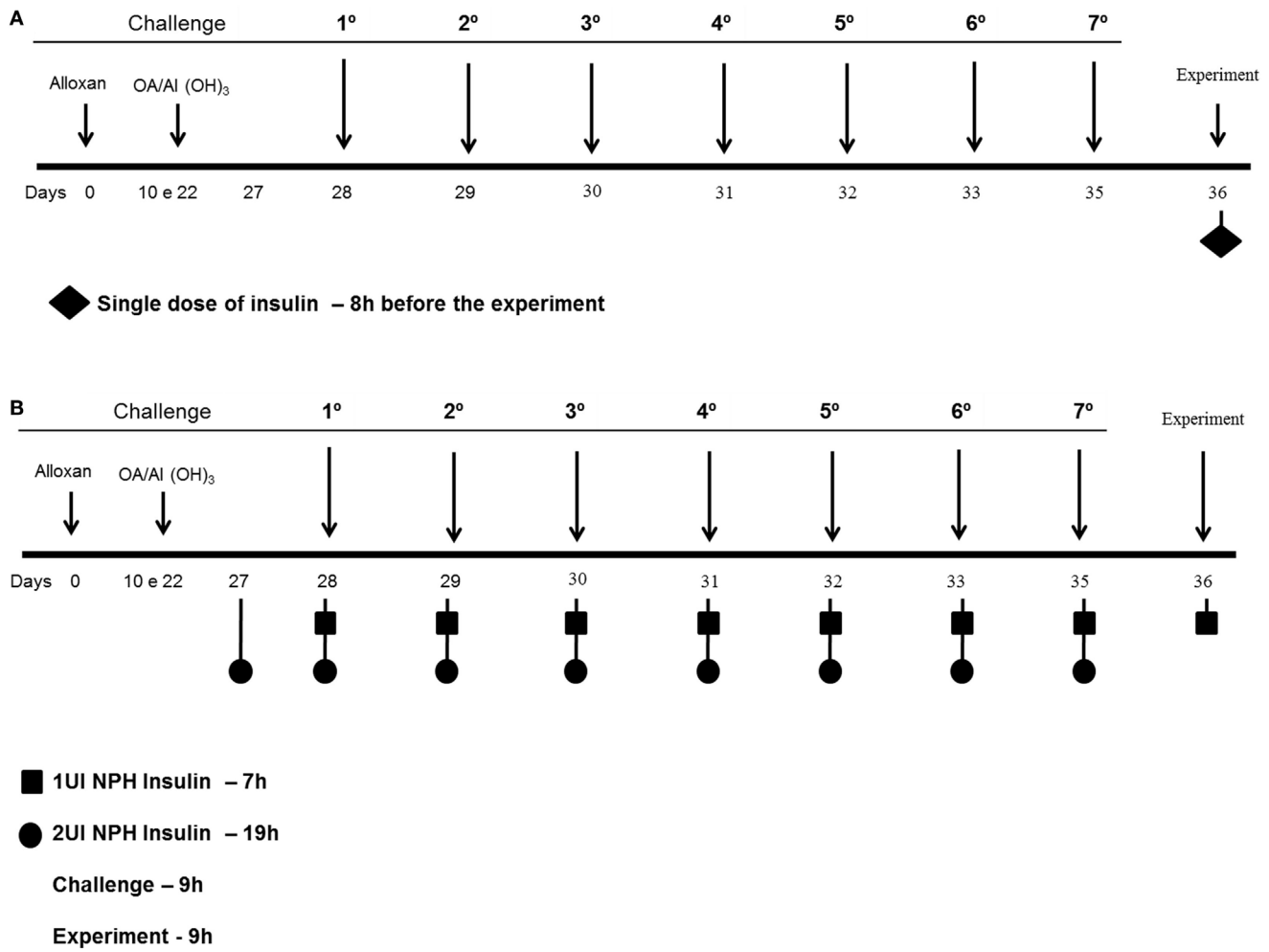

FIGURE 1 | Experimental protocols: mice were rendered diabetic by the injection of alloxan (50 mg/kg, i.v.). Ten days after, they were sensitized 2× intraperitoneal with OA and Al(OH$_3$) and then subjected to aerosol antigen challenges (7 days) with OA (5%, w/v in PBS) or PBS alone. **(A)** The first set of diabetic and control mice received 2 and 1 IU, respectively, of NPH insulin subcutaneously 24 h after the last challenge, and the analyses were performed 8 h after the insulin treatment. **(B)** The second set of diabetic and control mice received 2 and 1 IU, respectively, of insulin subcutaneously 12 h before the OA challenges (07:00 p.m.) and half doses (07:00 a.m.) of insulin 2 h before each of the 7 OA challenges; 24 h after the last challenge, blood, lungs, and BALF were collected for further analysis.

Hematological Parameters

Samples of blood collected by the intracardiac route were used for determination of the cell numbers. The total value was determined with an automated hematology counter (ABC Vet—Horiba ABX). Blood smears were stained with Rosenfeld. A total of 100 cells were counted using a conventional optic microscope (Leica Microsystems, Wetzlar, Germany).

Lung Morphology Analysis

For histological analysis, after collection of BALF, the lungs were removed and fixed in 10% formaldehyde solution, processed, and embedded in paraffin. Sections of 5 μm were cut, mounted on slides, and stained with hematoxylin and eosin (H/E) for observation of airway morphology; Masson's trichrome staining was performed for observation of collagen deposition around the airways. The collagen fibers appeared blue, the nuclei were black and the rest of the tissue (muscle, cytoplasm) stained red. Periodic acid-Schiff (PAS) histochemical staining was used to characterize the glycoprotein component of goblet cells in the respiratory epithelium (evaluation of mucus production). Slides containing the tissue were observed under a light microscope (Nikon Eclipse 80i, Tokyo, Japan) and photographed using the NIS-Elements AR 3.1 (SP3 build634) imaging software (Nikon).

Mucus Deposition Quantification and Collagen

After morphological analysis, the positive area was measured (μm^2). The maximum number of bronchioles per slide was determined. A measure of similar diameters was standardized to rule out the influence of bronchiole gage. The results are expressed as the mean total/diameter of area for each animal.

Statistical Analyses

Data were processed and analyzed by analysis of variance (ANOVA) or an unpaired *t*-test using GraphPad Prism (version 6.0 for Windows, GraphPad Software, La Jolla, CA, USA). A two-tailed *p*-value with a 95% confidence interval was acquired. Data are represented as the mean ± standard error of the mean (SEM). *p*-Values <0.05 were considered significant.

RESULTS

Body Weight Gain, Blood Glucose Levels, Insulin Treatment

Diabetes was induced by alloxan injection, and after 10 days, blood glucose levels and body weight gain were measured. Relative to controls, alloxan-treated diabetic mice exhibited a significant reduction in body weight gain (mean ± SEM; control, 1.05 g ± 0.32 g, $n = 20$; diabetic, −2.53 g ± 0.74 g, $n = 20$; $p < 0.001$) during the 10-day period and sharply elevated blood glucose levels (control, 123.14 ± 3.64 mg/dL, $n = 20$; diabetic, 559.5 ± 14.15 mg/dL, $n = 20$; $p < 0.0001$). Data collected on the 36th day showed that diabetic animals maintained insulinopenic characteristics throughout the experimental period. Diabetic animals that received daily doses of insulin for 9 days showed increases in body weight compared to that of the untreated diabetic mice. The weight increase was 50% compared to that of the non-diabetic asthmatic animals. A single dose of insulin did not rescue the body weight of the animals. Regarding the blood glucose, diabetic mice (both treated with 16 doses of insulin and not treated) showed high plasma glucose concentrations on the 36th day (**Table 1**).

Kinetics of Blood Glucose in Diabetic and Control Animals

Diabetic animals received a single dose of NPH insulin (2 UI). One hour after insulin therapy, the blood glucose of the animals was reduced to approximately half the original values, and 2 h after treatment, it increased again, as the animals displayed hyperglycemia. Similar results were observed in the control animals (1 UI). In both groups, blood glucose values were similar to pretreatment values after 6 h of insulin administration, indicating that this dose was not sufficient to normalize glycemia. Thus, we believe that the effects observed in insulin-treated mice are primarily due to the increased levels of insulin rather than to normalization of glycemia (**Table 2**).

Effect of insulin on peripheral blood cells and their migration

Relative to control (non-diabetic) OA-challenged mice, diabetic mice showed reduced leukocyte counts in the peripheral blood after OA challenge, including a reduction in the number of eosinophils. Treatment with single dose of NPH insulin 8 h before the experiment restored the impaired eosinophils to 46%. In addition, multiple doses of insulin restored the impaired eosinophils to 66%.

Relative to control (non-diabetic) OA-challenged mice, leukocyte counts in the BALF of diabetic mice were reduced after OA challenge due to an 83% reduction in the number of mononuclear cells, without the presence of eosinophils. Treatment with a single dose of insulin 8 h before the experiment restored

TABLE 1 | General characteristics of the mice.

Groups	*n*	Body weight gain (g)	Blood glucose (mg/dL)
Non-diabetic (10 days)	20	1.05 ± 0.32	123.14 ± 3.64
Diabetic (10 days)	20	−2.53 ± 0.74[#]	559.25 ± 14.15[+]
Non-diabetic + sensitized + saline (SAL) challenged (36 days)	5	1.58 ± 0.79	148.3 ± 8.83
Non-diabetic + sensitized + ovalbumin (OA) challenged (36 days)	5	1.61 ± 0.64	125 ± 5.88
Non-diabetic + sensitized + OA challenged + I1 (36 days)	5	1.78 ± 0.75	157.7 ± 7.77
Non-diabetic + sensitized + OA challenged + I16 (36 days)	5	1.78 ± 0.75	133.9 ± 8.86
Diabetic + sensitized + SAL challenged (36 days)	5	−3.9 ± 1.8	570 ± 15
Diabetic + sensitized + OA challenged (36 days)	5	−6.10 ± 2.05	551 ± 20
Diabetic + sensitized + OA challenged + I1 (36 days)	5	−5.88 ± 1.09	558.30 ± 15.79
Diabetic + sensitized + OA challenged + I16 (36 days)	5	2.88 ± 0.88[•]	467 ± 27.5

Mice were rendered diabetic by the injection of alloxan (50 mg/kg, i.v.). Ten days after, non-diabetic and diabetic mice were subjected to two sensitization procedures (20 μg OA + Al[OH$_3$]); intraperitoneal route. Twelve days after, non-diabetic and diabetic mice were subjected to OA (1% OA for 30 min) or SAL challenge (7 days). Insulin (single-dose 2 IU/diabetic mice or 1 IU/non-diabetic mice, 8 h before the experiment, s.c. 16 doses 2 IU/diabetic mice 12 h before challenge, 1 IU/diabetic mice 2 h before challenge or 1 IU/non-diabetic mice, 2 h before challenge, s.c.). Blood glucose levels were determined before insulin treatment and the experiment. Values are shown as the mean ± SEM.

[#]$p < 0.001$ compared with non-diabetic mice.

[+]$p < 0.001$ compared with non-diabetic mice.

[•]$p < 0.05$ compared with diabetic mice treated with a single dose of insulin.

Differences among the initial groups (diabetic or not) were analyzed using Student's t-test. Differences among the groups were tested with one-way analysis of variance followed by Turkey's post hoc test. A p-value <0.05 was considered statistically significant (GraphPad Prism version 6.0 for Windows, GraphPad Software, La Jolla, CA, USA).

TABLE 2 | Glucose kinetics.

Animals	Blood glucose					
	Before insulin	After insulin				
		1 h	2 h	3 h	6 h	8 h
Diabetic	500 ± 19	285 ± 38*	372 ± 20	342 ± 95	501 ± 44	568 ± 15
Non-diabetic	149 ± 11	68 ± 8[#]	67 ± 2	62 ± 2	134 ± 13	153 ± 15

The animals were treated with alloxan or saline as described above. Diabetic animals were administered 2 UI NPH insulin, and control animals received 1 UI NPH insulin. Blood samples were obtained from tail samples, and glucose was assessed with a glucometer (Accu-Check Active—Roche Diagnosis®). Values represent the mean ± SEM of blood glucose (n = 6 animals per group).

**$p < 0.05$, significantly different from pretreatment blood glucose levels with insulin.*

[#]$p < 0.05$, significantly different from pretreatment blood glucose levels with insulin.

Differences among the initial groups (diabetic or not) before and after insulin treatment were analyzed using Student's t-test.

the impaired cell migration observed in diabetic mice to values attained in control non-diabetic mice, but it did not restore the eosinophil migration. However, multiple doses of NPH insulin completely restored both total cell migration and the eosinophils in the BALF.

The morphometric analysis of lung parenchyma showed that compared to controls, the allergic reaction induced cell infiltration around blood vessels and in the lungs 24 h after the last challenge. However, diabetic mice exhibited reduced cell infiltration around the vessels and into the lungs. Treatment with a single dose of insulin 8 h before the experiment restored the amount of cells inside the blood vessels. In addition, multiple doses of insulin restored the cell migration levels around blood vessels and into the lungs (**Figure 2**).

Effect of Insulin on Cytokine Concentrations

In the BALF of non-diabetic mice, we observed an increase in the concentration of IL-1β (2.6-fold), IL-4 (2.3-fold), IL-5 (1.8-fold), and IL-13 after the OA challenge. In contrast, diabetic OA-challenged mice presented a reduction in the levels of IL-1β

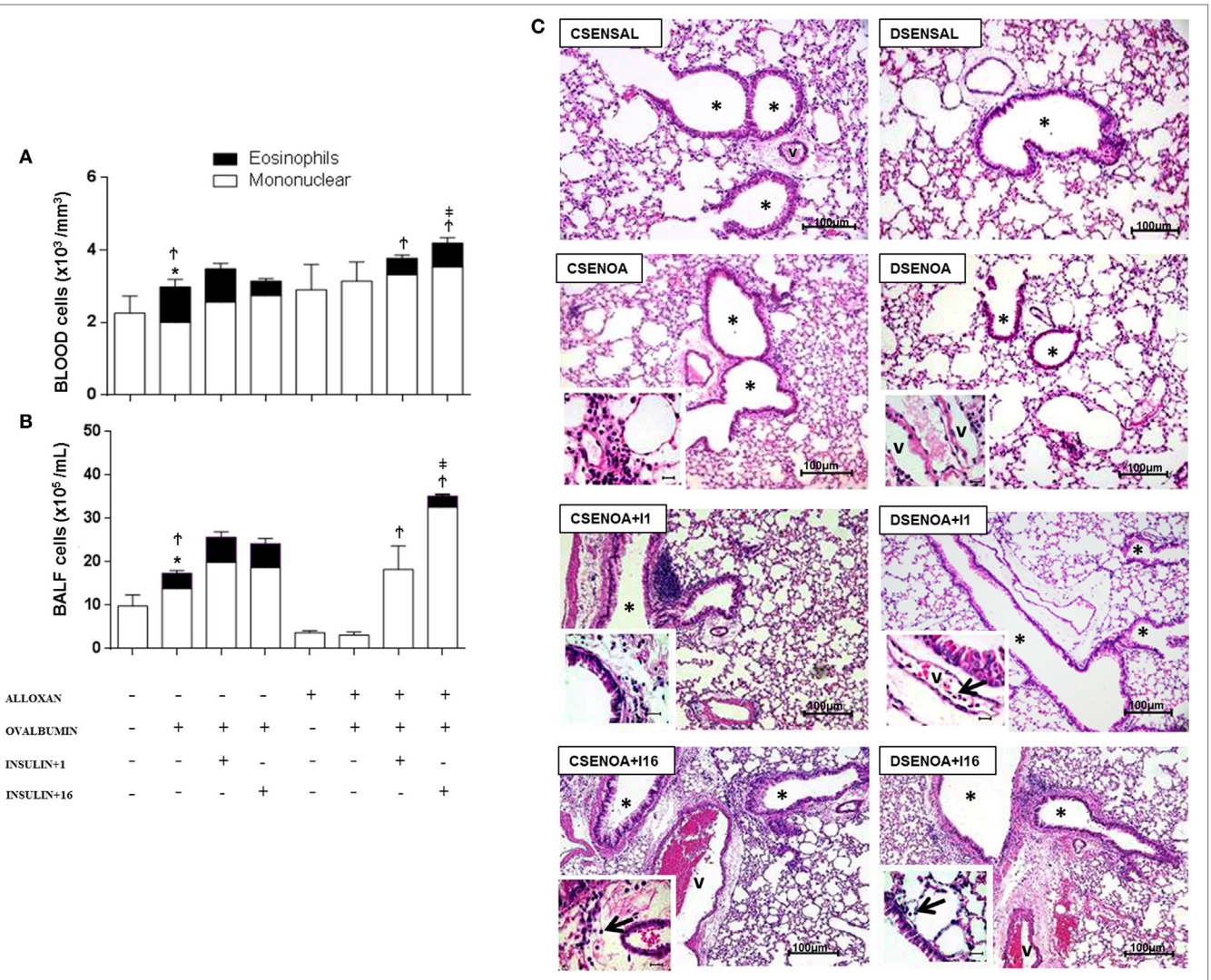

FIGURE 2 | **Role of insulin on peripheral blood cells and their migration**. **(A)** Twenty-4 hours after the last challenge in each of the groups, peripheral blood was collected to count cells; **(B)** bronchoalveolar lavage fluid was assessed 24 h thereafter. **(C)** The microphotographs of lung tissue were obtained from control non-diabetic mice sensitized and instilled with saline (CSENSAL) or sensitized and instilled with ovalbumin (OA) (CSENOA) and treated with single-dose insulin (CSENOA + I1) or treated with multiple doses of insulin (CSENOA + I16); diabetic mice sensitized and instilled with saline (DSENSAL), or sensitized and instilled with OA (DESENOA) and treated with single-dose insulin (DSENOA + I1) or treated with multiple doses of insulin (DSENOA + I16). * = bronchus; v = blood vessel; arrow: eosinophil (bars = 100 µm) H/E. Values are shown as the mean ± SEM. *$p < 0.01$ comparing OA-challenged with saline-challenged group. †$p < 0.01$ comparing OA-challenged with the diabetic OA-challenged group. ‡$p < 0.001$ comparing diabetic OA-challenged treatment to single-dose insulin. Data are representative of five animals per experimental group. Differences among the groups were tested with one-way analysis of variance followed by Tukey's *post hoc* test. A *p*-value <0.05 was considered statistically significant (GraphPad Prism version 6.0 for Windows, GraphPad Software, La Jolla, CA, USA).

(21%), IL-4 (51%), and IL-5 (68%), and IL-13 was not detected in the BALF. Treatment of diabetic mice with a single dose of insulin 8 h before the experiment restored BALF IL-4 and IL5 levels. Furthermore, multiple doses of insulin completely restored the IL-13 levels. The IL-10 levels were similar in all the studied groups, and there was no statistical difference between the groups (**Figure 3**).

Collagen Secretion: Role of Insulin

Compared to SAL-challenged mice, non-diabetic mice presented an increase (3.6-fold) in the collagen secretion of the lung parenchyma after the OA challenge. In contrast, reduced collagen secretions (82%) were observed in diabetic OA-challenged mice compared to those of the control mice. Treatment of diabetic mice with multiple doses of insulin restored collagen secretion in the lung parenchyma (**Figure 4**).

Mucus Production: Role of Insulin

Ovalbumin challenge induced mucus production in the lung parenchyma of non-diabetic mice. In contrast, mucus production was not detected in the lung parenchyma of diabetic OA-challenged mice. Treatment of diabetic mice with multiple dose of insulin restored, at least in part, mucus production in the lung parenchyma (**Figure 5**).

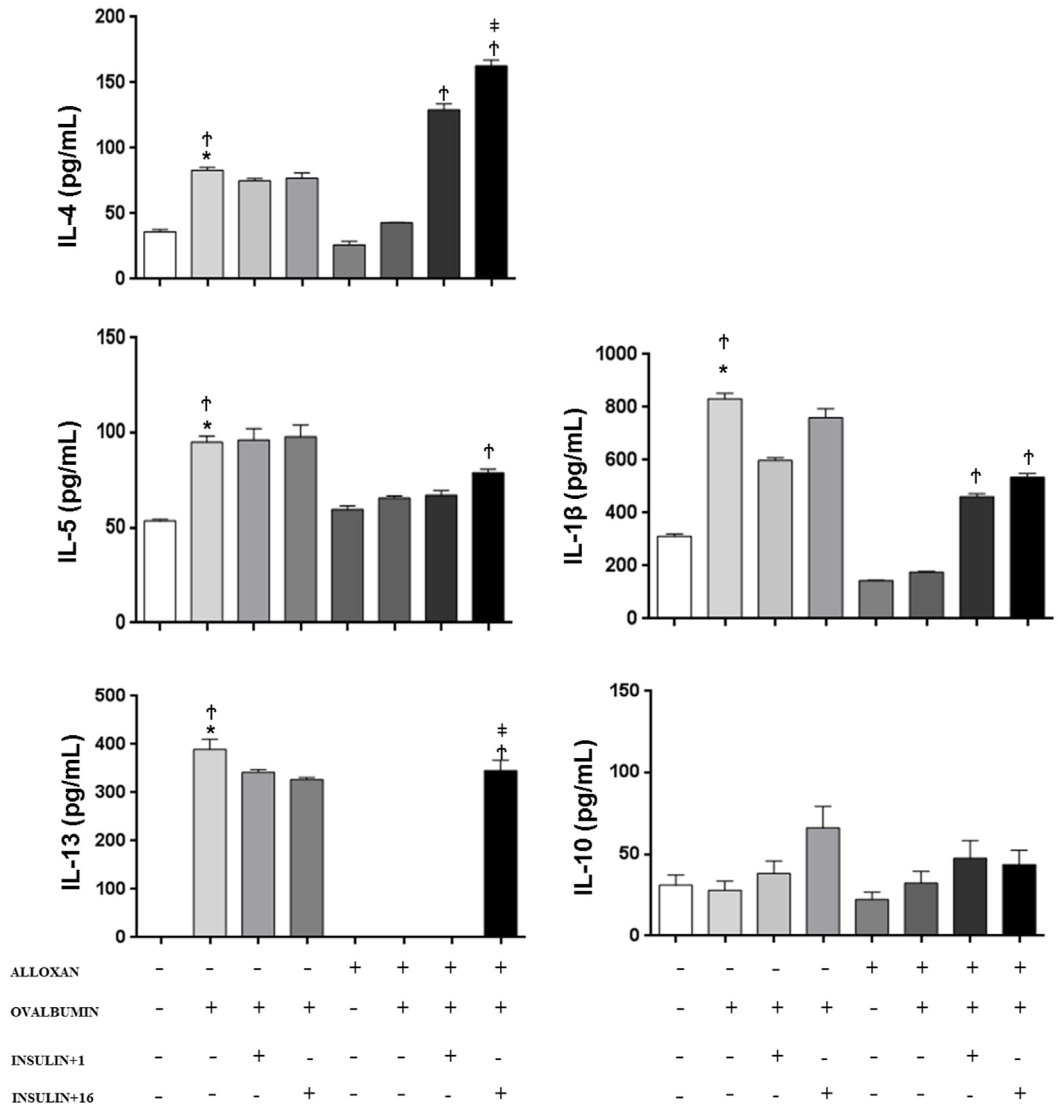

FIGURE 3 | **Effect of insulin on cytokine concentrations**. Bronchoalveolar lavage fluid was analyzed 24 h after ovalbumin (OA) sensitization of non-diabetic and diabetic mice 24 h after the last OA (experimental) or saline (control) instillation. Values are shown as the mean ± SEM. *$p < 0.01$ comparing OA-challenged with the saline-challenged group; ‡$p < 0.01$ comparing OA-challenged with the diabetic OA-challenged group. ‡$p < 0.05$ comparing diabetic OA-challenged treatment to single-dose insulin. Differences among the groups were tested with one-way analysis of variance followed by Tukey's *post hoc* test. A *p*-value <0.05 was considered statistically significant (GraphPad Prism version 6.0 for Windows, GraphPad Software, La Jolla, CA, USA).

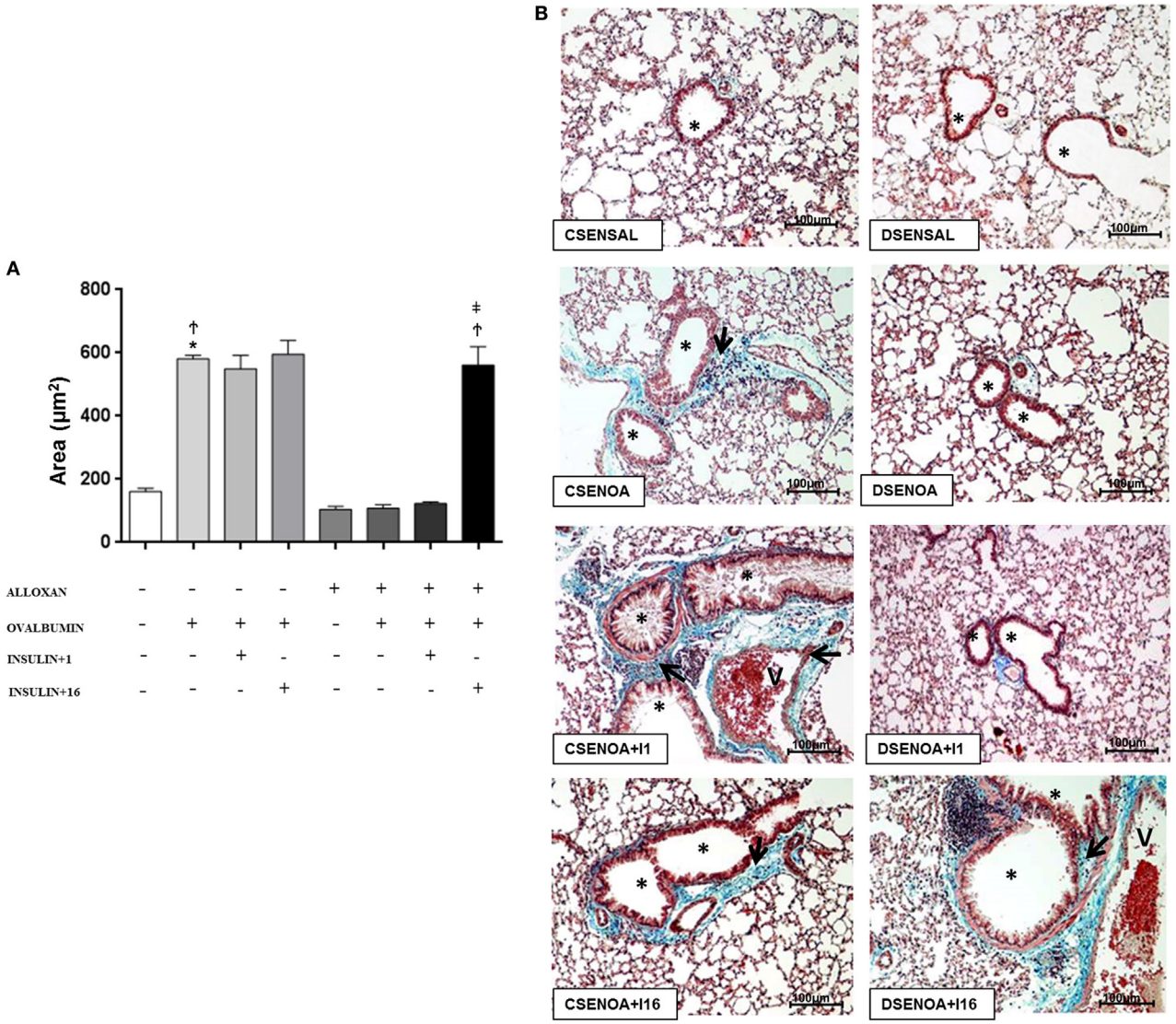

FIGURE 4 | **Collagen secretion: role of insulin**. **(A)** On average, 10 fields were photographed per slide. Quantification was performed using NIS-Elements AR software. Values represent the mean ± SEM leukocytes (n = 5 animals/group). **(B)** The microphotographs of lung tissue were obtained from control non-diabetic mice sensitized and instilled with saline (CSENSAL) or sensitized and instilled with ovalbumin (OA) (CSENOA) and treated with single-dose insulin (CSENOA + I1) or treated with consecutive doses of insulin (CSENOA + I16); diabetic mice sensitized and instilled with saline (DSENSAL) or sensitized and instilled with OA (DESENOA) and treated with single-dose insulin (DSENOA + I1) or treated with consecutive doses of insulin (DSENOA + I16). * = bronchus; v = blood vessel; arrow: collagen bars = 100 μm; Masson's trichrome. Data are representative of five animals per experimental group. Values are shown as the mean ± SEM. *$p < 0.01$ comparing OA-challenged with saline-challenged groups. †$p < 0.01$ comparing OA-challenged with diabetic OA-challenged groups. ‡$p < 0.01$ comparing diabetic OA-challenged treatment to single-dose insulin. Differences among the groups were tested with one-way analysis of variance followed by Tukey's *post hoc* test. A p-value <0.05 was considered statistically significant (GraphPad Prism version 6.0 for Windows, GraphPad Software, La Jolla, CA, USA).

DISCUSSION

The data presented here suggest that insulin modulates lung remodeling in allergic inflammatory reactions in the bronchial remodeling phase of a diabetic murine model, restoring: (a) infiltrate inflammation in the BALF; (b) eosinophilia; (c) collagen deposition around the airways; and (d) at least in part, secretion/deposition of mucus within the airways.

This asthma model is widely used and has provided important knowledge about immune and inflammatory mechanisms (18, 19). In general, this model involves sensitization of the mice by intraperitoneal injection of the allergen in combination with adjuvant material, such as $Al(OH)_3$, along with allergic exposures at the site (lung). When the animals are evaluated for asthmatic phenotypes, they present hyperresponsiveness of the airways (20), eosinophilia (21), and inflammation with Th2 profile cytokines (22, 23). After repeated exposures to the allergen, structural alterations that culminate in remodeling of the airways can occur (16, 24). This remodeling is characterized by smooth muscle hypertrophy, increased secretion of mucus, and

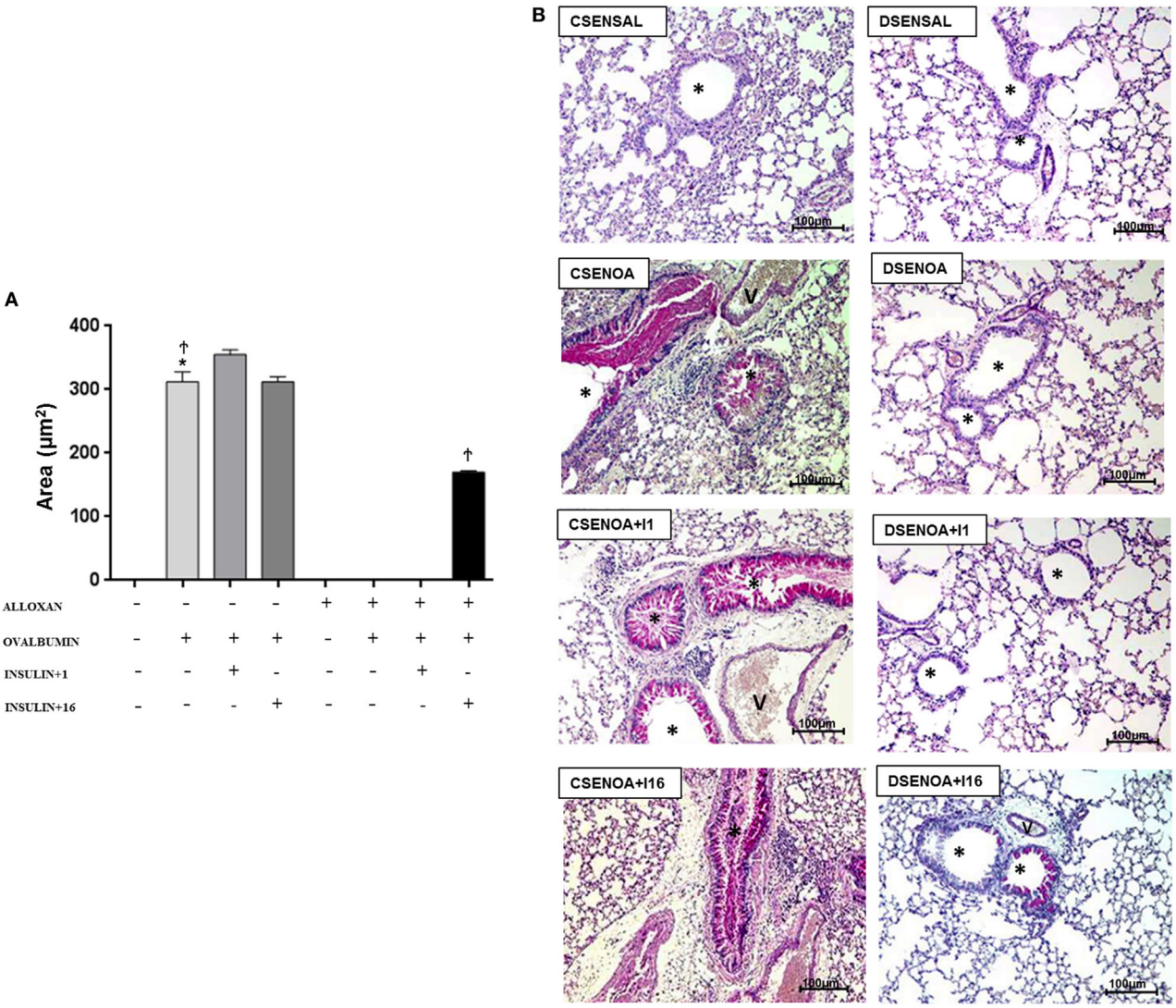

FIGURE 5 | **Mucus production: role of insulin**. **(A)** On average, 10 fields were photographed per slide. Quantification was performed using NIS-Elements AR software. Values represent the mean ± SEM leukocytes (n = 5 animals/group). **(B)** The microphotographs of lung tissue were obtained from control non-diabetic mice sensitized and instilled with saline (CSENSAL) or sensitized and instilled with ovalbumin (OA) (CSENOA) and treated with single-dose insulin (CSENOA + I1) or treated with consecutive doses of insulin (CSENOA + I16); diabetic mice sensitized and instilled with saline (DSENSAL) or sensitized and instilled with ovalbumin (OA) (DESENOA) and treated with single-dose insulin (DSENOA + I1) or treated with consecutive doses of insulin (DSENOA + I16). * = bronchus; v = blood vessel; arrow: mucus (bars = 100 µm) PAS. Data are representative of five animals per experimental group. Values are shown as the mean ± SEM. *$p < 0.001$ comparing OA-challenged with saline-challenged. †$p < 0.001$ comparing OA-challenged with the diabetic OA-challenged group. ‡$p < 0.001$ comparing diabetic OA-challenged treatment to single-dose insulin. Differences among the groups were tested with one-way analysis of variance followed by Tukey's *post hoc* test. A p-value <0.05 was considered statistically significant (GraphPad Prism version 6.0 for Windows, GraphPad Software, La Jolla, CA, USA).

deposition of collagen around the airways, which consequently result in fibrosis (24, 25).

Diabetes mellitus has high morbidity and mortality rates and results in a significant decrease in patient quality of life. One of the leading causes of death in patients with diabetes is renal failure, blindness, lower limb amputation, and cardiovascular disease (26). Additionally, diabetic patients have increased immune dysfunction and are more susceptible to infection (27). In experimental studies, diabetic mice that were infected with *Pseudomonas aeruginosa* had an increase in biofilms in their wounds, and insulin treatment increased the biofilms in the wounds of diabetic mice (28). Moreover, sensitized and OA-challenged diabetic animals exhibited reduced pulmonary inflammatory infiltrate. Treatment of these animals with insulin ameliorated this condition, suggesting that asthma symptoms are suppressed by the diabetic state (13, 29). In addition, insulin treatment amplifies the inflammatory response and hypersensitive reactions, such as tuberculin cutaneous test in rats. Animals treated with insulin, before and after skin challenges, presented gross skin reaction compared to that of untreated animals (30).

In clinical studies, triggering of diabetes mellitus in previously asthmatic patients resulted in an improvement in asthmatic

symptoms; treatment of diabetic patients with insulin aggravated asthma, and similar results were observed in non-diabetic asthmatic patients receiving insulin (10, 11). Obesity also aggravates asthma; it was reported that an increase of body mass index (BMI) and/or excess weight may increase the risk of asthma-related hospitalizations or asthma severity (31). The possible underlying mechanisms were extensively discussed by Stephanie (32) and likely include common etiologies and comorbidities between many other factors, such as adipokines, leptin, and proinflammatory cytokines. In addition, to evaluate the anti-inflammatory activity in allergic reactions induced by OA, we measured IL-10 in the BALF of the animals. In our study, IL-10 levels did not differ between groups, which suggest that the phenomenon might be linked to Th1 response polarization of diabetes mellitus type I since Han et al. (33) showed that hyperinsulinemia in obese mice results in a decrease in the production of IL-10 by regulating Treg cells. Moreover, the synergistic contribution of insulin and proinflammatory cytokines to the stimulation of the immune system has been reported. Dror et al. (34) found that insulin stimulates IL-1b secretion by resident macrophages, which could explain the mechanisms by which insulin restored IL-1β levels in our study.

In fact, previous studies by our research group using a model of pulmonary inflammation in the initial phase revealed that insulin modulates the release of cytokines, such as TNF-α and IL-1β, as well as expression of adhesion molecules, such as P and E-selectin, and consequently migration of neutrophils into the lung during the initial phase of the allergic inflammatory reaction (14). The results presented here showed decreased IL-4, IL-5, and IL-13 levels in OA-challenged diabetic mice and that single-dose insulin treatment restored levels of IL-4 and IL-5, although IL-13 was only restored by multiple doses of insulin treatment (16 doses). Although these Th2 profile cytokines play an important role in the eosinophil migration, OA-challenged diabetic mice did not present eosinophilia in both the blood and BALF. Treatment with a single dose of insulin restored eosinophilia parameters in the blood of the animals, but not in BALF, suggesting that 8 h was insufficient time for eosinophil migration to the tissue; however, with multiple doses of insulin, we observed eosinophilia in BALF. In addition, a single dose of insulin did not restore the deposition of mucus and collagen in the airways of OA-challenged diabetic mice. However, multiple doses of insulin restored the deposition of mucus and collagen in the airways, which suggests that appropriate treatment with insulin may modulate cytokine levels, cell migration, eosinophilia, and mucus and collagen deposition in lung remodeling in the murine asthma model.

The data presented here suggest that insulin regulates lung remodeling in an experimental model of allergic airway inflammation in diabetic mice by controlling cytokines, cell migration, collagen deposition, and mucus secretion into the lungs.

ETHICS STATEMENT

This study was carried out in strict accordance with the principles and guidelines adopted by the Brazilian National Council for the Control of Animal Experimentation (CONCEA) and approved by the Ethical Committee on Animal Use (CEUA) of the Faculty of Pharmaceutical Sciences (FCF) of University São Paulo (Permit Number: CEUA/FCF/340).

AUTHOR CONTRIBUTIONS

SF and JM conceived and designed the experiments; wrote the paper with the assistance of all the authors. SF, FN, and FC performed the experiments. SF, FN, and JM analyzed the data. JM contributed reagents/materials/analysis tools.

ACKNOWLEDGMENTS

The authors would like to sincerely thank Mariana C. F. Silva for the expert technical assistance. The authors are supported by grants 2010/02272-0, 2012/06617-7, 2014/05214-1, and 2017/09775-6 from São Paulo Research Foundation (FAPESP), grants 470523/2013-1 and 301617/2016-3 from National Counsel of Technological and Scientific Development (CNPq; Projeto Universal 2013 and PQ-1D), Coordenação de Aperfeiçoamento de Pessoal de Nível Superior (CAPES), and Pró-reitoria de Pesquisa da Universidade de São Paulo (PRP/USP, Projeto I and Novos Docentes), Brazil. The authors declare that there is no conflict of interest that would prejudice the impartiality of this scientific work.

REFERENCES

1. Sociedade Brasileira de Pneumonia e Tisiologia. Diretrizes da Sociedade Brasileira de Pneumologia e Tisiologia. *J Bras Pneumol* (2012) 38(1):S1–46.
2. Galli SJ, Tsai M, Piliponsky AM. The development of allergic inflammation. *Nature* (2008) 454(7203):445–54. doi:10.1038/nature07204
3. Deckers J, Madeira FB, Hammad H. Innate immune cells in asthma. *Trends Immunol* (2013) 34(11):540–7. doi:10.1016/j.it.2013.08.004
4. Holgate ST. Pathogenesis of asthma. *Clin Exp Allergy* (2008) 38(6):872–97. doi:10.1111/j.1365-2222.2008.02971.x
5. Schofield M, Calhoun KH. Immunology of asthma. *Otolaryngol Clin N Am* (2011) 44:591–601. doi:10.1016/j.otc.2011.03.002
6. Yang IV, Schwartz DA. Epigenetic mechanisms and the development of asthma. *J Clin Immunol* (2012) 130(6):1243–55. doi:10.1016/j.jaci.2012.07.052
7. Pascual RM, Peters SP. Airway remodeling contributes to the progressive loss of lung function in asthma: an overview. *J Allergy Clin Immunol* (2005) 116(3):477–86. doi:10.1016/j.jaci.2005.07.011
8. Holgate ST, Polosa R. Treatment strategies for allergy and asthma. *Nat Rev Immunol* (2008) 8:218–30. doi:10.1038/nri2262
9. GINA. *Global Initiative for Asthma*. (2016). Available from: http://ginasthma.org/
10. Helander E. Asthma and diabetes. *Acta Med Scand* (1958) 162:165–74. doi:10.1111/j.0954-6820.1958.tb01762.x
11. Douek IF, Leech NJ, Gillmor HA, Bingley PJ, Gale EAM. Children with type-1 diabetes and their unaffected siblings have fewer symptoms of asthma. *Lancet* (1999) 353:1850. doi:10.1016/S0140-6736(99)00988-5
12. Vianna ESO, Garcia-Leme J. Allergen-induced airway inflammation in rats. Role of insulin. *Am J Respir Crit Care Med* (1995) 151:809–14. doi:10.1164/ajrccm.151.3.7881676
13. Cavalher-Machado SC, De Lima WT, Damazo AS, Frias de Carvalho V, Martins MA, Silva PMR, et al. Down-regulation of mast cell activation and airway reactivity in diabetic rats: role of insulin. *Eur Respir J* (2004) 24:552–8. doi:10.1183/09031936.04.00130803
14. Martins JO, Campos CAL, Cruz JWMC, Manzolli S, Alves VAF, Vianna EO, et al. Insulin modulates cytokine release and selectin expression in the early phase of allergic airway inflammation in diabetic rats. *BMC Pulm Med* (2010) 10:39. doi:10.1186/1471-2466-10-39

15. Spiller F, Carlos D, Souto FO, de Freitas A, Soares FS, Vieira SM, et al. α1-Acid glycoprotein decreases neutrophil migration and increases susceptibility to sepsis in diabetic mice. *Diabetes* (2012) 61:1584–1584. doi:10.2337/db11-0825
16. Stumm CL, Wettlauer SH, Jancar S, Peters-Golden M. Airway remodeling in murine asthma correlates with a defect in PGE_2 synthesis by lung fibroblasts. *Am J Physiol Lung Cell Mol Physiol* (2011) 301(5):L636–44. doi:10.1152/ajplung.00158.2011
17. Di Petta A, Greco OE, Lopes FFTQS, Martins MA, Capellozi VL, Moreira LFP, et al. Insulin modulates inflammatory and repair responses to elastase-induced emphysema in diabetic rats. *Int J Exp Pathol* (2011) 92:392–9. doi:10.1111/j.1365-2613.2011.00787.x
18. Emala C, Hirshman C. Animal models of bronchial hyperreactivity. *Monogr Allergy* (1996) 33:35–52.
19. Herz U, Lumpp U, Da Palma JC, Enssle K, Takatsu K, Schonoy N, et al. The relevance of murine animal models to study the development of allergic bronchial asthma. *Immunol Cell Biol* (1996) 74:209–17. doi:10.1038/icb.1996.30
20. Barnes PJ. New drugs for asthma. *Nat Rev Drug Discov* (2004) 3:831–44. doi:10.1038/nrd1524
21. Kay AB. The role of eosinophils in the pathogenesis of asthma. *Trends Mol Med* (2005) 11:148–52. doi:10.1016/j.molmed.2005.02.002
22. Pauwels RA, Brussellee GJ, Kips JC. Cytokine manipulation in animal models of asthma. *Am J Respir Crit Care Med* (1997) 156:S78–81. doi:10.1164/ajrccm.156.4.12-tac-1
23. Manise M, Holtappels G, Crombruggen KV, Schleich F, Bachertz C, Louis R. Sputum IgE and cytokines in asthma: relationship with sputum cellular profile. *PLoS One* (2013) 8(3):e58388. doi:10.1371/journal.pone.0058388
24. Stumm CL, Halcsik E, Landgraf RG, Camara NOS, Sogayar MC, Jancar S. Lung remodeling in a mouse model of asthma involves a balance between TGF-B1 and BMP-7. *PLoS One* (2014) 9(4):e95959. doi:10.1371/journal.pone.0095959
25. Boulet L-P, Sterk PJ. Airway remodeling: the future. *Eur Respir J* (2007) 30:831–4. doi:10.1183/09031936.00110107
26. International Diabetes Federation. *IDF Diabetes Atlas*. 7th ed. Brussels: International Diabetes Federation (2015).
27. Lerco MM, Spadella CT, Machado JLM, Schellini SA, Padovani CR. Caracterização de um modelo experimental de *Diabetes mellitus,* induzido pela aloxana em ratos. *Acta Cirúrgica Brasileira* (2003) 18(2):132–42. doi:10.1590/S0102-86502003000200010
28. Watters C, Everett A, Haley C, Clinton A, Rumbaugha KP. Insulin treatment modulates the host immune system to enhance *Pseudomonas aeruginosa* wound biofilms. *Infect Immun* (2014) 82:92–100. doi:10.1128/IAI.00651-13
29. Singh S, Prakash YS, Linneberg A, Agrawal A. Insulin and the lung connecting asthma and metabolic syndrome. *J Allergy* (2013) 2013:8. doi:10.1155/2013/627384
30. Thompson GE. Enhancing effect of insulin on the tuberculin reaction in the albino rat. *Nature* (1967) 215:748–9. doi:10.1038/215748a0
31. Mossem DM, Schatz M, Magid DJ, Camargo CA. The relationship between obesity and asthma severity and control in adults. *J Allergy Clin Immunol* (2008) 122:507–11. doi:10.1016/j.jaci.2008.06.024
32. Shore SA. Obesity and asthma: lessons from animal models. *J Appl Physiol* (2007) 102:516–28. doi:10.1152/japplphysiol.00847.2006
33. Han JM, Patterson SJ, Speck M, Ehses JA, Levings MK. Insulin inhibits IL-10-mediated regulatory T cell function: implications for obesity. *J Immunol* (2014) 192:623–9. doi:10.4049/jimmunol.1302181
34. Dror E, Dalmas E, Meire DT, Wuesst S, Thévenet J, Thienel C, et al. Postprandial macrophage-derived Il-1β stimulates insulin, and both synergistically promote glucose disposal and inflammation. *Nat Immunol* (2017) 18:283–92. doi:10.1038/ni.3659

Conflict of Interest Statement: The authors declare that the research was conducted in the absence of any commercial or financial relationships that could be construed as a potential conflict of interest.

Copyright © 2017 Ferreira, Nunes, Casagrande and Martins. This is an open-access article distributed under the terms of the Creative Commons Attribution License (CC BY). The use, distribution or reproduction in other forums is permitted, provided the original author(s) or licensor are credited and that the original publication in this journal is cited, in accordance with accepted academic practice. No use, distribution or reproduction is permitted which does not comply with these terms.

frontiers in Immunology

ORIGINAL RESEARCH
published: 09 June 2017
doi: 10.3389/fimmu.2017.00643

Distinct Blood and Visceral Adipose Tissue Regulatory T Cell and Innate Lymphocyte Profiles Characterize Obesity and Colorectal Cancer

Gloria Donninelli[1†], Manuela Del Cornò[1†], Marina Pierdominici[1], Beatrice Scazzocchio[1], Rosaria Varì[1], Barbara Varano[1], Ilenia Pacella[2], Silvia Piconese[2,3], Vincenzo Barnaba[2,3], Massimo D'Archivio[1], Roberta Masella[1], Lucia Conti[1] and Sandra Gessani[1]*

[1] Center for Gender-Specific Medicine, Istituto Superiore di Sanità, Rome, Italy, [2] Dipartimento di Medicina Interna e Specialità Mediche, Sapienza Università di Roma, Rome, Italy, [3] Istituto Pasteur Italia-Fondazione Cenci Bolognetti, Rome, Italy

Visceral adipose tissue (VAT) is a main site where metabolic and immunologic processes interplay to regulate, at local and systemic level, the inflammatory status and immune response. Obesity-associated inflammation and immune dysfunctions are inextricably linked to tumor but, in spite of intense efforts, the mechanisms underpinning this association remain elusive. In this report, we characterized the profile of VAT-associated and circulating innate lymphocyte and regulatory T (T_{reg}) cell subsets underlying inflammatory conditions, such as obesity and colorectal cancer (CRC). Analysis of NK, NKT-like, γδ T, and T_{reg} cell populations in VAT and blood of healthy lean subjects revealed that $CD56^{hi}$ NK and $OX40^{+}$ T_{reg} cells are more abundant in VAT with respect to blood. Conversely, $CD56^{dim}$ NK and total T_{reg} cells are most present in the circulation, while γδ T lymphocytes are uniformly distributed in the two compartments. Interestingly, a reduced frequency of circulating activated T_{reg} cells, and a concomitant preferential enrichment of OX40-expressing T_{reg} cells in VAT, were selectively observed in obese (Ob) subjects, and directly correlated with body mass index. Likewise, CRC patients were characterized by a specific enrichment of VAT-associated NKT-like cells. In addition, Ob and CRC-affected individuals shared a significant reduction of the Vγ9Vδ2/γδ T cell ratio at systemic level. The alterations in the relative proportions of T_{reg} and NKT-like cells in VAT were found to correlate with the content of pro- and anti-inflammatory polyunsaturated fatty acids (PUFA), respectively. Overall, these results provide evidence for distinct alterations of the immune cell repertoire in the periphery with respect to the VAT microenvironment that uniquely characterize or are shared by different inflammatory conditions, such as obesity and CRC, and suggest that VAT PUFA composition may represent one of the factors that contribute to shape the immune phenotypes.

Keywords: adipose tissue, fatty acid, obesity, colorectal cancer, immune profile, regulatory T cell, γδ T lymphocyte, NKT-like cell

OPEN ACCESS

Edited by:
Jixin Zhong,
Case Western Reserve University,
United States

Reviewed by:
Fei Teng,
Weill Cornell Medical College,
United States
Rui Mao,
Augusta University,
United States
Xun Liu,
Brigham and Women's Hospital,
United States

***Correspondence:**
Lucia Conti
lucia.conti@iss.it

†These authors have contributed equally to this work.

Specialty section:
This article was submitted to Inflammation, a section of the journal Frontiers in Immunology

Received: *04 April 2017*
Accepted: *17 May 2017*
Published: *09 June 2017*

Citation:
Donninelli G, Del Cornò M, Pierdominici M, Scazzocchio B, Varì R, Varano B, Pacella I, Piconese S, Barnaba V, D'Archivio M, Masella R, Conti L and Gessani S (2017) Distinct Blood and Visceral Adipose Tissue Regulatory T Cell and Innate Lymphocyte Profiles Characterize Obesity and Colorectal Cancer. Front. Immunol. 8:643. doi: 10.3389/fimmu.2017.00643

INTRODUCTION

Obesity has become a major threat to public health because of its high global prevalence and association with an increased risk of developing chronic diseases. Obesity affects over half a billion adults worldwide, with ~3.5 million attributable deaths each year (1). Similar to gender, race, dietary habits, or smoking history, obesity is one of the risk factors for several types of cancer including colorectal cancer (CRC) (2, 3) and contributes to 3–20% of cancer deaths in western populations (4, 5). CRC is one of the most common gastrointestinal malignant tumors in the world and presents one of the highest rates of morbidity and mortality worldwide (6). Abdominal rather than total adiposity is associated with a 1.5- to 3.5-fold increased risk of developing CRC as compared to lean individuals (7).

Obesity-associated low-grade chronic inflammation is considered a main risk factor for adiposity-related pathologies including CRC (8). Indeed, a well-established link between CRC and chronic inflammation, sustained by tumor cell-extrinsic as well as -intrinsic pathways, has been recognized in multiple settings. It is generally accepted that visceral adipose tissue (VAT)-resident immune cells play a major role in the obesity-associated inflammatory status. Notably, dietary components are recognized as important modulators of inflammation, and healthy/unhealthy diets have been associated with reduced/increased CRC prevalence, respectively (9). Emerging key players in the processes leading to immune surveillance failure that may favor cancer onset in obese (Ob) subjects are the VAT and its composition in fatty acids (FA), in particular the pro-inflammatory polyunsaturated fatty acids (PUFA) (10, 11). Interestingly, dietary intake has been directly linked to PUFA composition of VAT (12) and CRC cell growth as well as tumor progression in mouse models (13). Thus, VAT might represent the initial place where PUFA-related dietary information is transferred to the immune system and contributes to regulate homeostasis.

VAT is immunologically dynamic and contains many different cell types including adipocytes and their progenitors, endothelial cells, and immune cells (14). Recent studies showed clearly that the balance between homeostasis and inflammation in adipose tissue (AT) is mainly controlled by the stromal vascular fraction (SVF) that contains, in homeostatic conditions, a unique repertoire of immune cells (15, 16), whose numbers and activation level have been reported to be altered in obesity. AT homes cells with both pro-inflammatory [M1 macrophages, neutrophils, Th1 $CD4^+$ T cells, $CD8^+$ T cells, B cells, dendritic cells (DC), and mast cells] and anti-inflammatory [M2 macrophages, regulatory T (T_{reg}) cells, Th2 $CD4^+$ T cells, eosinophils, and type 2 innate lymphoid cells, ILC2] activity. Among them, T_{reg} cells are a $CD4^+$ T cell subset specialized in immune suppression, and in maintaining immune system homeostasis (17). Furthermore, innate lymphocytes have been also recently reported to populate AT (18). In particular, NKT cells, a lineage of T lymphocytes exhibiting NK cell features (19), play beneficial or harmful roles in obesity-associated inflammation and comorbidities (20) as well as in CRC development/progression (21, 22). In addition, NK and γδ T cells are key players in immune surveillance against cancer, and impairment of their function and frequency has been observed in chronic inflammatory conditions (23, 24). Finally, recent studies have highlighted the regulatory role of ILC2 in AT metabolism and homeostasis (16). Thus, AT homeostasis is maintained through the regulation of the immune cell profile, and obesity skews this balance toward a pro-inflammatory status. The tumor-promoting effects of obesity occur not only at local level, *via* altered VAT microenvironment, but also systemically, *via* dysregulated immune cell profile and circulating inflammatory factors that mirror adipose inflammation. However, the alterations in immune cell repertoires occurring in the peripheral blood (PB), VAT, and proximal tissues deserve further investigation in order to elucidate the extent of immune dysregulation in obesity that may set the basis for cancer development.

In this study, we investigated the profile of human VAT-associated and systemic γδ T, NK, NKT-like, and T_{reg} cells in lean and obese (Ob) subjects, affected or not by CRC. We report that in healthy lean subjects innate lymphocyte subsets and T_{reg} cells exhibit a differential distribution in blood with respect to VAT. Furthermore, we identify alterations of the immune cell profile specific for Ob subjects, such as a reduced level of circulating activated T_{reg} (aT_{reg}) cells paralleling a preferential enrichment of OX40-expressing T_{reg} cells in VAT, or for CRC patients, such as an increased VAT-associated NKT-like cell frequency. In addition, obesity and CRC share a significant reduction of the Vγ9Vδ2/γδ T cell ratio at systemic level. Of note, the alterations in the relative proportions of T_{reg} and NKT-like cells in VAT correlate with the its content of pro- and anti-inflammatory PUFA, respectively, in both pathological conditions.

Overall, these results provide evidence for distinct alterations of the immune cell repertoire in the periphery with respect to the VAT microenvironment that uniquely characterize, or are shared by, obesity and CRC, and suggest a role for VAT PUFA composition in shaping immune phenotypes.

MATERIALS AND METHODS

Patients and Samples

Human VAT biopsies and blood samples from the same individual were collected from lean and Ob subjects undergoing abdominal surgery or laparoscopy for benign (i.e., gallbladder disease without icterus, umbilical hernia, and uterine fibromatosis) or CRC conditions (histologically proved primary colon adenocarcinoma, stage TNM 0–III). The exclusion criteria were as follows: clinical evidence of active infection, recent (within 14 days) use of antibiotics/anti-inflammatory drugs, pregnancy, hormonal therapies, severe mental illness, autoimmune diseases, family history of cancer, other neoplastic diseases. Subjects belonging to four groups were enrolled: normal weight (Nw), Ob, Nw with CRC (Nw/CC), and Ob with CRC (Ob/CC). In the Nw groups, the body mass index (BMI) range was 18–24.9 kg/m^2. In the Ob groups, BMI was ≥30 kg/m^2, and waist circumference ≥95 cm for men and ≥80 cm for women. For each category, the number of subjects ranged from a minimum of 6 to 16 for Nw, 4 to 15 for Ob, 6 to 13 for Nw/CC, 6 to 10 for Ob/CC. The different quantity of biological samples available for each single donor did not allow to perform all the analyses on the same number of subjects.

Blood samples were drawn at the time of obtaining peripheral vein access for surgery. Peripheral blood mononuclear cells were separated by Ficoll-Hypaque density-gradient centrifugation and collected in complete RPMI 1640 medium containing 10% FBS, 2 mM L-glutamine, penicillin/streptomycin (Euroclone). VAT biopsies were microdissected, rinsed several times in 0.9% NaCl, and digested with 5 ml of Krebs-Ringer solution (0.12 M NaCl, 4.7 M KCl, 2.5 mM $CaCl_2$, 1.2 mM $MgSO_4$, 1.2 mM KH_2PO_4) containing 20 mM HEPES pH 7.4, 3.5% fatty acid-free BSA, 200 nM adenosine, 2 mM glucose, and type 1 collagenase for 1 h (1 mg/g tissue) at 37°C in shaking water bath. VAT SVF were obtained as previously described (25). Briefly, 15–40 g of VAT biopsies were microdissected and extensively washed with sterile PBS to remove contaminating erythrocytes. The extracellular matrix was digested with 0.1% type I collagenase at 37°C, and shaken vigorously for 60 min in shaking water bath to separate the stromal cells from primary adipocytes. Dissociated tissue was filtered to remove debris, and centrifuged at 1,500 rpm for 10 min. The suspending portion containing lipid droplets was discarded and the cell pellet was resuspended, washed twice, and cultured in complete RPMI 1640.

Flow Cytometry

Peripheral blood mononuclear cells and VAT SVF cells were stained with fluorochrome-labeled antibodies CD3 (FITC), CD4 (FITC or BrilliantViolet 785), CD45RA (APC or BrilliantViolet 605), CD127 (PeCy7), γδ TCR (PE), Vδ2 (FITC), CD56 (BrillantViolet 421), OX40 (PE), CD16 (APC). Intracellular staining for FOXP3 was performed using the anti-FOXP3 (PE or PerCP-Cy5.5) mAb and FOXP3 Transcription Factor Staining Buffer Set according to manufacturer's instructions (eBioscience). At first, cells were incubated 30 min at room temperature (RT) with Fixable Viability Dye (eFluor 780, eBioscience) to stain and exclude dead cells, then staining with antibodies for surface antigens was performed for 20 min at 4°C. FOXP3 intracellular staining was performed incubating cells for 30 min at RT. Data were acquired on LSR Fortessa (Becton Dickinson) and analyzed with FlowJo software (Tree Star Inc., version 10.1r5) or on FACSCalibur flow Cytometer (BD Biosciences) and analyzed with the Cell Quest Pro software.

FA Analysis

Total lipids from VAT samples were extracted with chloroform–methanol 2:1 (v/v) and FA methyl esters prepared (26) and analyzed as previously described (10). The individual FA detected were expressed as a percent of total FA.

Statistical Analysis

GraphPad Prism 5 software was used for statistical analysis. Statistical comparison between groups was performed by the one-way analysis of variance with Newman–Keuls *post hoc* test and by the two-tailed unpaired Student's *t*-test for independent samples, as appropriate. Comparisons were expressed as means from several experiments ± SEM. Pearson's test was performed to determine simple correlations between two variables. Differences were considered significant when p values were <0.05.

RESULTS

Human Innate Lymphocytes and T_{reg} Cells Are Differentially Distributed in PB and VAT in Healthy Subjects

Several immune cell subsets populate the AT, and alterations of their relative numbers and functions have been suggested to influence obesity-associated local and systemic inflammation as well as CRC development/progression. We initially quantified the frequency of innate lymphocyte populations (γδ T, NK, NKT-like cells) and T_{reg} cells in homeostatic conditions assessing matched VAT SVF and PB samples collected from healthy lean subjects. The gating strategies and representative plots for each cell population are reported in **Figures 1A,F** and Figure S1 in Supplementary Material. As shown in **Figure 1**, no significant differences were observed in the tissue distribution of total γδ T lymphocytes (**Figure 1B**). However, the analysis of other innate cell populations revealed a preferential accumulation of the $CD56^{hi}$ NK cell subset in VAT SVF as compared to PB (**Figure 1D**), whereas the majority of circulating NK cells was $CD56^{dim}$ (**Figure 1E**). In keeping with previously published data highlighting that NKT cells are one of the AT resident cell subsets, a general enrichment of the $CD3^+CD56^+$ NKT-like cell population was found in VAT SVF (**Figure 1C**) as compared to PB. Concomitant with the accumulation of NKT-like cells, a significant decrease of T_{reg} cell ($CD4^+FOXP3^+CD127^{low}$) frequency was observed at local level as compared to PB (**Figure 1G**). Recently, different T_{reg} cell subpopulations have been described, such as aT_{reg} cells which have suppressive function, resting T_{reg} (rT_{reg}) cells which can convert to aT_{reg}, and non-suppressive T_{reg} (nsT_{reg}) cells (27). Moreover, the OX40-expressing T_{reg}, cell subset, with strong suppressive activity and high proliferative potential, has been described to be associated with tissue localization and especially cancer microenvironments (28, 29). Of note, when these cell subsets were characterized, an opposite tissue distribution was observed between aT_{reg} and OX40-expressing T_{reg} cells (**Figures 1H,I**). Specifically, a significantly higher frequency of aT_{reg} cells was detected at systemic with respect to local level (**Figure 1H**). Conversely, OX40-expressing cells were found selectively distributed in VAT SVF (**Figure 1I**), in line with the role of OX40 in imparting preferential survival to T_{reg} cells in tissues.

Obesity Is Associated with a Reduced Frequency of Circulating aT_{reg} Cells and a Preferential Enrichment of OX40-Expressing T_{reg} Cells in VAT

In chronic inflammatory diseases, such as obesity and cancer, the effector/regulatory equilibrium may be persistently perturbed, finally contributing to tumor progression by suppressing anti-tumor immunity (30). Therefore, we compared the frequency of T_{reg} cells in PB of lean and Ob subjects, affected or not by CRC. Anthropometric and clinical parameters of study subjects are shown in **Table 1**. Although no changes in the frequency of total T_{reg} cells were observed among the four donor categories studied (**Figure 2A**), a deeper analysis of T_{reg} cell subsets revealed a significantly reduced frequency of circulating aT_{reg} cells in Ob

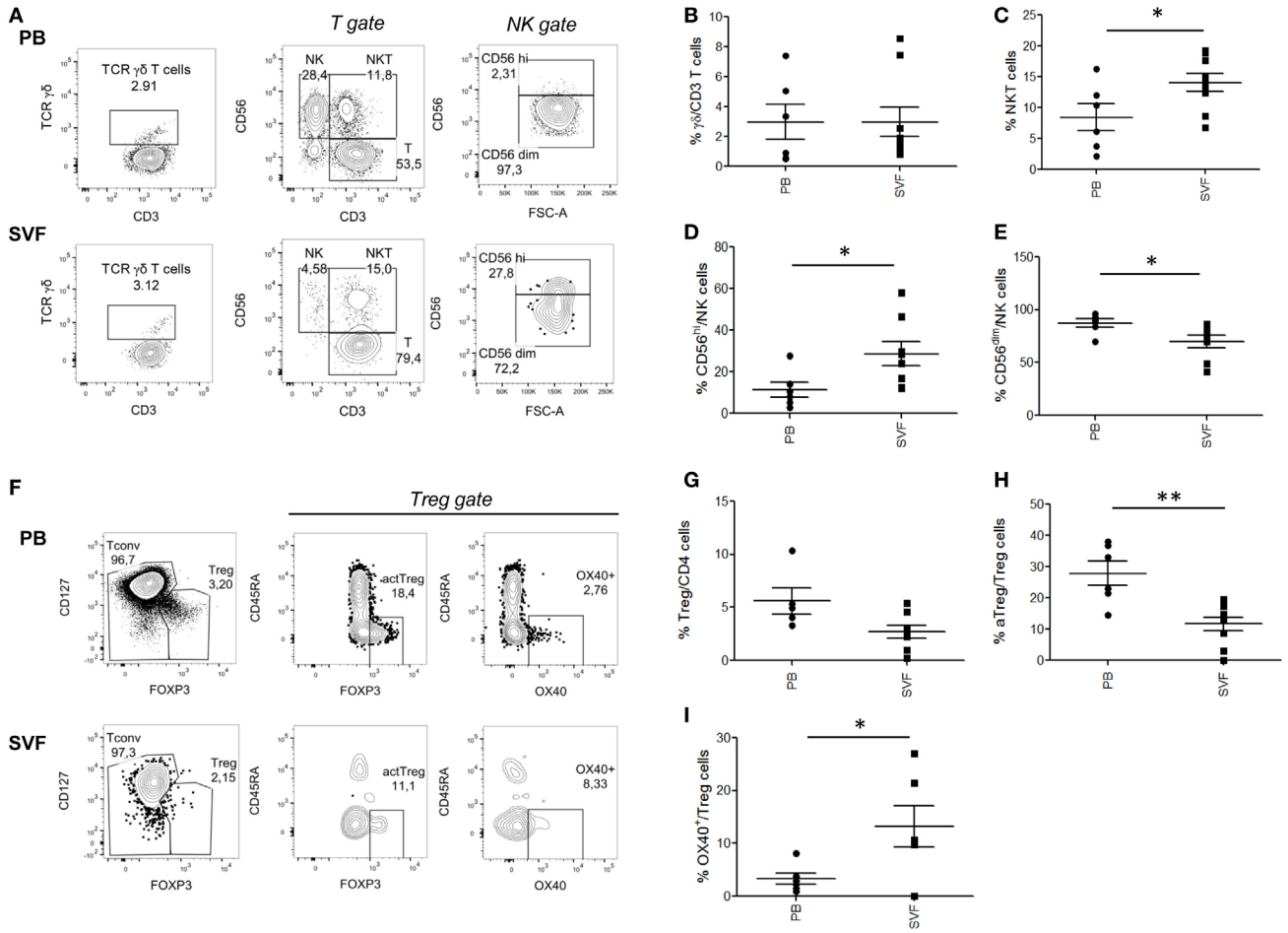

FIGURE 1 | Composition of major T lymphocyte subpopulations in visceral adipose tissue (VAT) stromal vascular fraction (SVF) versus peripheral blood (PB) of lean healthy subjects. Cell subset percentages within total PB and VAT SVF lymphocytes of nine healthy lean subjects were analyzed. Gating strategies for NK, NKT, T, and γδ T cells **(A)**, total regulatory T (T_{reg}), conventional T cells (T_{conv}), OX40$^+$ T_{reg} and activated T_{reg} cells (aT_{reg}) **(F)**, in PB and SVF from a representative donor. γδ T cells, TCRγδ$^+$CD3$^+$ **(B)**; NK cells, CD3$^-$CD56$^+$ **(D,E)**; NKT cells, CD3$^+$CD56$^+$ **(C)**; T_{reg} cells, CD4$^+$FOXP3$^+$CD127^{low} **(G)**; aT_{reg}, FOXP3^{high}CD45RA$^-$ **(H)**; OX40$^+$ T_{reg} cells **(I)**. Each dot represents an individual donor. Mean ± SEM is shown for each group. *$p < 0.05$, **$p < 0.01$, by unpaired Student's *t*-test.

TABLE 1 | Anthropometric and clinical parameters of study subjects.

Subjects	Nw	Ob	Nw/CC	Ob/CC
Number (54)	16	15	13	10
Body mass index (kg/m^2)	23.9 ± 0.78	41.22 ± 8.58	22.50 ± 1.93	32.79 ± 2.17
Age (years)	46.07 ± 12.83	32.83 ± 11.02	61.08 ± 12.85	65 ± 10.3
Sex (female/male)	8/8	7/8	9/4	3/7
Stage 0	–	–	1	1
Stage I	–	–	5	3
Stage II	–	–	3	3
Stage III	–	–	4	3

individuals, independent of CRC (**Figure 2B**). Notably, correlation analysis showed that the frequency of this subpopulation inversely correlates with BMI (**Figure 2C**). The percentage of rT_{reg} and nsT_{reg} cell subsets was not affected by obesity or CRC (Figure S2 in Supplementary Material).

The analysis of T_{reg} cells at the tissue level revealed that these cells accumulate in VAT SVF of Ob individuals, but not of CRC-affected subjects (**Figure 3A**), and that their frequency positively correlates with BMI (**Figure 3B**). Based on the pivotal role of OX40 in supporting T_{reg} cell fitness (28, 31) and on its selective expression in VAT-associated T_{reg} cells in healthy lean subjects (**Figure 1I**), we investigated whether the accumulation of this cell population observed in VAT SVF of Ob individuals was associated with a higher expression of OX40. Indeed, we found that the frequency of OX40-expressing T_{reg} cells was significantly higher in Ob subjects with respect to all other categories of individuals (**Figure 3C**). Conversely, the frequency of aT_{reg} cells remained unchanged (**Figure 3D**). Interestingly, the extent of OX40 expression in T_{reg} cells showed a positive correlation with BMI (**Figure 3E**). As shown in Figure S3 in Supplementary

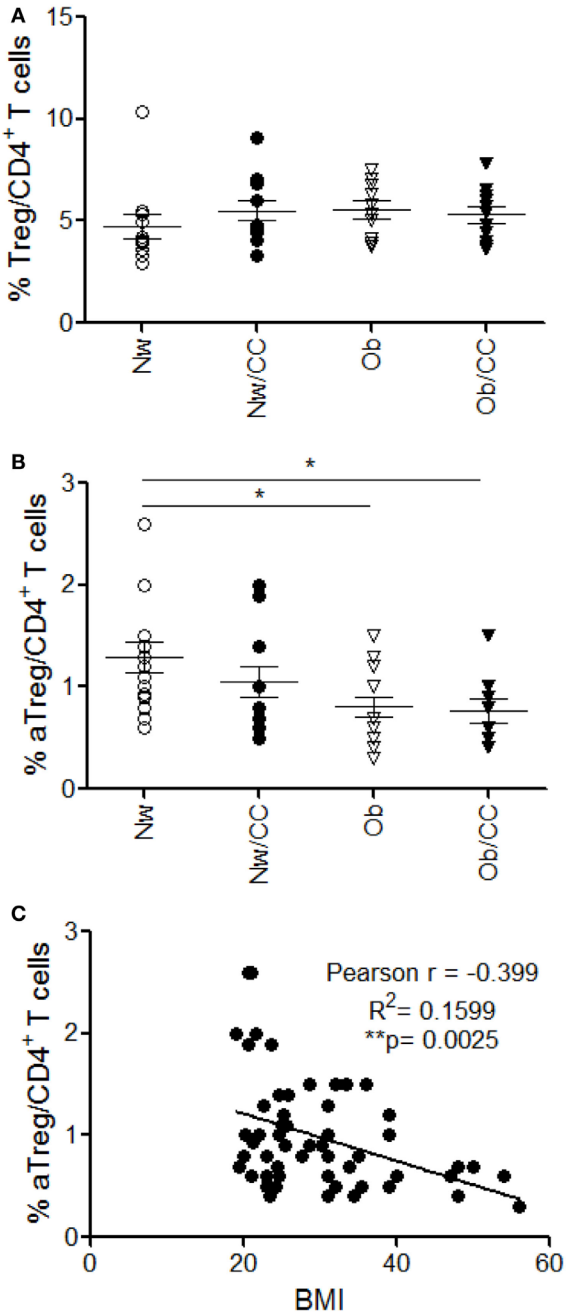

FIGURE 2 | A significant reduction of circulating CD45RA$^-$FOXP3^{hi} activated T_{reg} (aT_{reg}) cells occurs in obese (Ob) subjects: correlation with body mass index (BMI). Peripheral blood (PB) lymphocytes isolated from lean normal weight (Nw), Ob, lean affected by colorectal cancer (CRC) (Nw/CC), and Ob affected by CRC (Ob/CC) donors were analyzed by flow cytometry. Frequency of regulatory T (T_{reg}) (CD4$^+$FOXP3$^+$CD127^{low}) cells **(A)** and aT_{reg} cells (CD4$^+$FOXP3^{high} CD45RA$^-$) **(B)** was estimated in PB of the four groups. Each dot represents an individual donor. Mean ± SEM is shown for each group. *$p < 0.05$ by analysis of variance. **(C)** Pearson's correlation (r) between aT_{reg} cell frequency and BMI in all subjects (**$p < 0.01$).

Material, an increased expression of OX40 was also found in VAT-associated CD4$^+$FOXP3$^-$ conventional T cells (T_{conv}) from Ob subjects (Figure S3A in Supplementary Material); however, the frequency of OX40$^+$ T_{conv} cells did not correlate with BMI (Figure S3B in Supplementary Material). These data suggest that, in the VAT microenvironment, obesity prompts T_{reg} cell expansion, possibly as a negative feedback mechanism to counteract inflammation. Notably, this event seems disrupted in VAT of CRC patients, despite obesity.

A Selective Enrichment of VAT-Associated NKT-Like Cells Characterizes CRC Condition

To investigate whether the frequency of NK and NKT-like cells at systemic and VAT level could be affected by obesity and/or CRC, flow cytometric analysis of these subsets was also performed in the four categories of subjects. As shown in **Figure 4A**, CRC condition, rather than obesity, is characterized by an enrichment of CD3$^+$CD56$^+$ NKT-like cells. Specifically, a higher frequency of this cell population was detected in VAT SVF from CRC-affected subjects as compared to cancer-free individuals, irrespective of their BMI. Conversely, no changes in the frequency of total NK cells were observed in VAT SVF and PB among all categories of subjects (**Figure 4B**). Moreover, the tissue distribution of the CD56^{hi} and CD56^{low} NK cell subsets was not affected by obesity or CRC (data not shown).

Obesity and CRC Share a Reduced Vγ9Vδ2/γδ T Cell Ratio at Systemic Level

Among γδ T lymphocytes, the main circulating subset Vγ9Vδ2 has been involved in immunosurveillance against cancer, and impairment of its function and frequency has been observed in chronic inflammatory conditions (24). We thus investigated the distribution of γδ T cells and of the Vγ9Vδ2 subset, in PB with respect to VAT, in the four categories of subjects. Although no significant differences were observed in the frequency of VAT-associated (**Figure 5A**) and PB (**Figure 5B**) total γδ T lymphocytes (**Figure 5**), when the analysis was extended to the Vγ9Vδ2 subset, a significant reduction of the Vγ9Vδ2/γδ T cell ratio was found in the systemic compartment of Ob and CRC-affected subjects as compared to healthy lean individuals (**Figure 5C**). Of note, an inverse correlation was observed between the Vγ9Vδ2/γδ T cell ratio and BMI when Ob and lean subjects were considered (**Figure 5D**).

T_{reg} and NKT-Like Cells Are Inversely Distributed in VAT and Their Frequencies Correlate with Individual PUFA Content

An interplay between NKT and T_{reg} cells has been described in different settings. In particular, NKT cells can promote T_{reg} cell induction and, conversely, T_{reg} cells can exhibit suppressive activity on NKT cells (32, 33). Based on this knowledge and on our observation that these immune cell subsets are differently distributed in VAT SVF from Ob and CRC subjects (**Figures 3A** and **4A**), a correlation analysis between the frequencies of total T_{reg} and NKT-like cells was performed to assess the influence of obesity and CRC conditions on this relationship in human VAT. Interestingly, as shown in **Figure 6A**, we observed a significant inverse correlation between these cell populations, indicative of a potential negative interplay. This inverse relation may explain the alternate

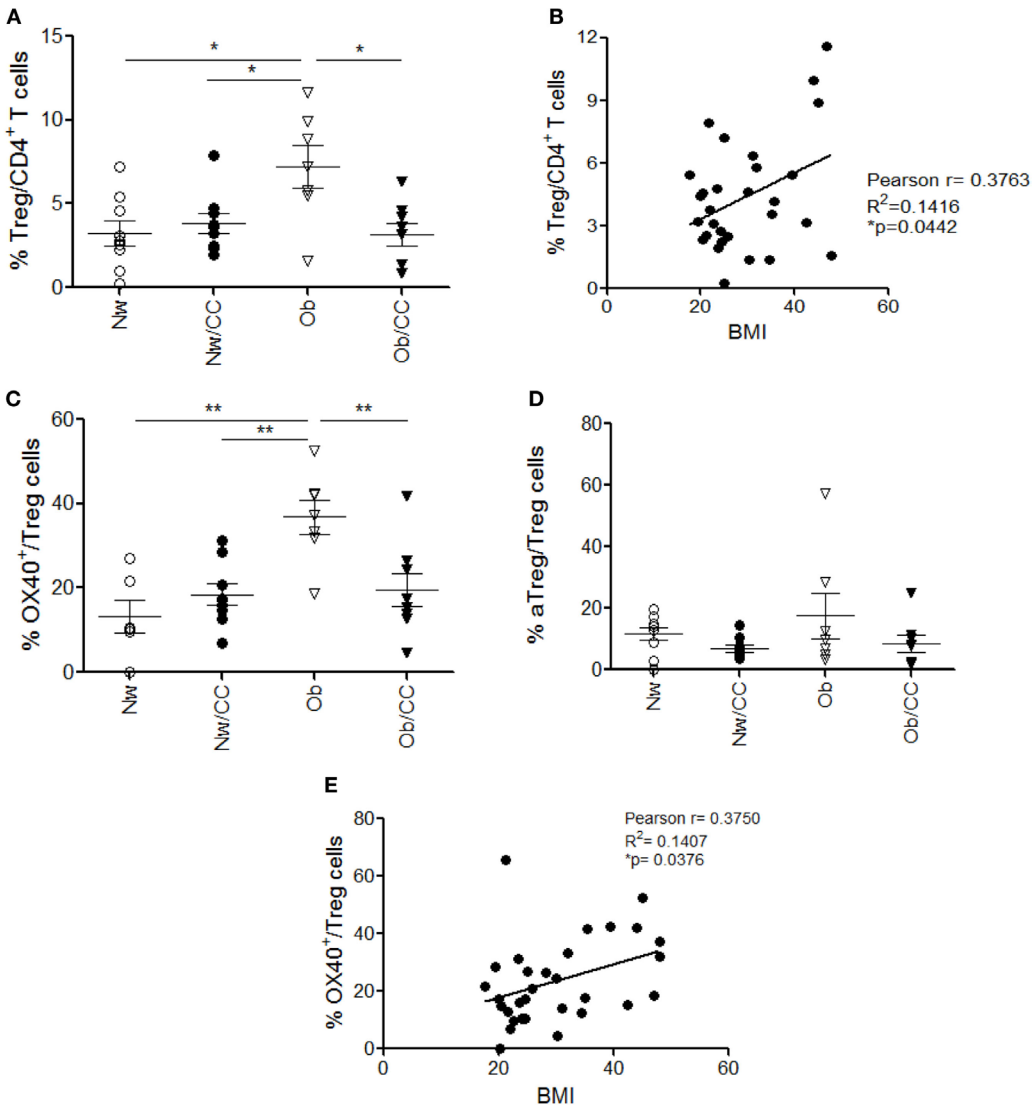

FIGURE 3 | A significant increase of total regulatory T (T_{reg}) cells and a preferential enrichment of OX40$^+$ T_{reg} cells occur in visceral adipose tissue (VAT) stromal vascular fraction (SVF) from obese (Ob) subjects: correlation with body mass index (BMI). VAT SVF lymphocytes isolated from lean normal weight (Nw), Ob, lean affected by colorectal cancer (CRC) (Nw/CC), and Ob affected by CRC (Ob/CC) donors were analyzed by flow cytometry. Frequencies of T_{reg} ($CD4^+FOXP3^+CD127^{low}$) cells **(A)**, OX40$^+$ T_{reg} cells **(C)**, and activated T_{reg} cells ($CD4^+FOXP3^{high}CD45RA^-$) **(D)** were estimated in VAT SVF of the four donor groups. Each dot represents an individual donor. Mean ± SEM is shown for each group. $^*p < 0.05$, $^{**}p < 0.01$ by analysis of variance. Pearson's correlation (r) between T_{reg} **(B)** or OX40$^+$ T_{reg} **(E)** cell frequencies and BMI, in all subjects ($^*p < 0.05$).

prevalence of NKT-like cells in VAT of CRC-affected patients, and of T_{reg} cells in VAT of CRC-free Ob subjects (**Figures 3A** and **4A**).

We have previously demonstrated a significant decrease in the ω3/ω6 PUFA ratio in Ob and CRC-affected subjects with respect to healthy lean individuals (10). Therefore, we investigated whether obesity- or cancer-associated modulation of specific immune cell subsets could be somehow related to distinct PUFA profiles, focusing on individual ω3 and ω6 PUFA. Correlation analysis showed that the T_{reg} cell frequency in VAT SVF positively correlates with ω6 PUFA arachidonic acid (AA) content when lean and Ob subjects were considered (**Figure 6B**). Likewise, the frequency of VAT-associated NKT-like cells in healthy lean and CRC subjects inversely correlated with the content of two key anti-inflammatory ω3 PUFA, docosahexaenoic (DHA) and eicosapentaenoic acid (EPA) (**Figures 6C,D**). These results suggest that PUFA composition may represent one of the factors that influence VAT microenvironment.

DISCUSSION

In this study, we performed a comparative analysis of circulating versus VAT-associated immune cell subsets unraveling not only a different distribution of specific subpopulations in PB versus VAT but also alterations in one or in another compartment that are associated with obesity or CRC condition. Specifically we observed that the frequency of circulating aT_{reg} cell subset is reduced in Ob individuals, irrespective of CRC, and inversely correlates with

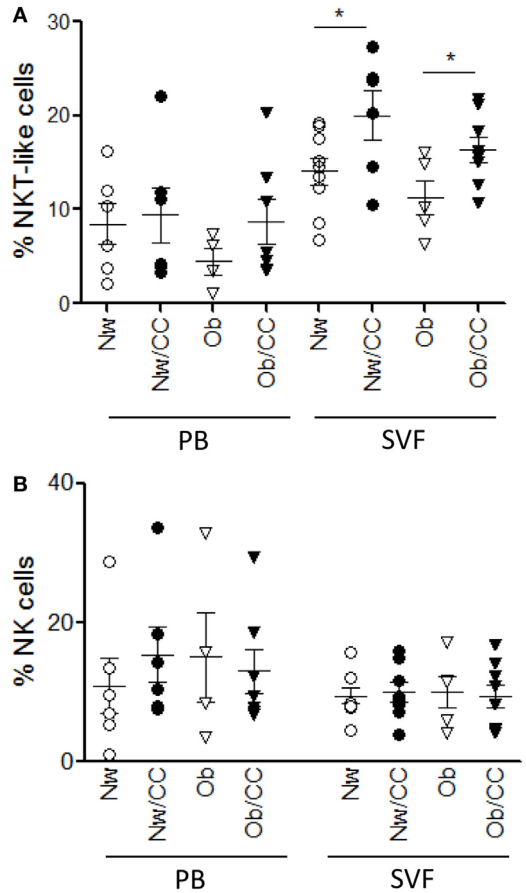

FIGURE 4 | The frequency of visceral adipose tissue (VAT)-associated NKT cells, but not NK cells, is increased in colorectal cancer (CRC)-affected subjects as compared to cancer-free donors. VAT stromal vascular fraction (SVF) and peripheral blood (PB) lymphocytes isolated from lean normal weight (Nw), obese (Ob), lean affected by CRC (Nw/CC), and Ob affected by CRC (Ob/CC) donors were analyzed by flow cytometry. Frequencies of NKT ($CD3^+CD56^+$) **(A)** and NK ($CD3^-CD56^+$) **(B)** cells were evaluated in the four categories of donors. Each dot represents an individual donor. Mean ± SEM is shown for each group. *$p < 0.05$, by analysis of variance.

BMI, likely reflecting the inflammatory status. In this respect, a previous study reported that circulating $CD4^+CD25^+FOXP3^+$ T_{reg} cells are reduced in Ob individuals and their frequency inversely correlates with biomarkers of inflammation, weight, BMI, and leptin levels (34). We did not observe a significant reduction in total T_{reg} cell frequency. However, a deeper characterization of T_{reg} cell subsets revealed, for the first time, a selective reduction of circulating aT_{reg} cells in obesity. In addition, this is the first study in which a comparative analysis between circulating and VAT-associated T_{reg} cells has been carried out in lean and Ob individuals. We found that T_{reg} cells accumulate in VAT of Ob, but not lean, subjects and this was likely due to a protective response to the inflammatory status typical of Ob subjects. In keeping with this hypothesis, we found a positive correlation between the extent of adiposity defined by BMI and the frequency of a VAT-associated T_{reg} cell population, highly expressing OX40 ($OX40^+$ T_{reg}), a marker associated with T_{reg} cell survival and suppressive function (28). Therefore, apparently, the VAT microenvironment characterizing obesity reproduces a condition that is favorable to T_{reg} cell accumulation, in particular of the $OX40^+$ subset, probably as a result of the need to counteract tissue inflammation. Contrasting results have been obtained in mouse and human models concerning the role of T_{reg} cells in regulating the inflammatory status of AT. While a clear-cut decrease of T_{reg} cells was detected in the VAT of Ob mice (35–37), inversely correlating with macrophage infiltration (36), a rather different situation was observed in humans. In keeping with our results, Zeyda and coworkers reported that systemic and AT inflammation positively correlate with T_{reg} cell abundance within the Ob group, as assessed by FOXP3 transcript expression (38). Likewise, Pereira and colleagues found a greater FOXP3 mRNA expression in VAT of Ob individuals that positively correlated with IL-6 and TNFα expression as well as BMI (39). In our study, a deeper phenotypic characterization of VAT-associated T_{reg} cells has been performed, highlighting, for the first time, the role of OX40 in driving their enrichment in VAT.

In this regard, we have previously demonstrated that $OX40^+$ T_{reg} cells, expanded in cirrhotic liver, hepatocellular carcinoma, and CRC, exhibit a phenotype ($Helios^{hi}$, $CD39^{hi}$) compatible with a strong suppressive activity, a high proliferative potential and a stable regulatory program, suggesting that CRC may take advantage from creating a favorable milieu for their accumulation (29). In this study, the lack of accumulation of T_{reg} cells in VAT of CRC-affected Ob subjects might result from their recruitment at the tumor site, an advantageous event facilitating tumor progression. Unfortunately, matched tumor tissues were not available at the time of analysis to conclusively ascertain the frequency and phenotype of T_{reg} cells at the tumor site. The role of VAT-associated T_{reg} cells in CRC has been only poorly investigated. Conversely, a number of studies have reported increased blood and tumor tissue infiltrating T_{reg} cell numbers in CRC patients (40). In particular, an increase in aT_{reg} cell number has been associated with advanced/metastatic tumor stage (41). Our failure in detecting circulating aT_{reg} cell increase in CRC-affected subjects might be explained by the fact that they have been analyzed at earlier stages of disease. Collectively, our results delineate a network of diverse T_{reg} cell subsets, differently located in blood and VAT, that contribute to obesity-associated immune dysfunctions.

NKT cells have been shown to play beneficial or harmful roles in obesity-associated inflammation and co-morbidities (20), as well as in CRC development/progression (21, 22). Accumulation of total $CD3^+CD56^+$ NKT-like cells has been reported in human VAT with a decrease of the invariant NKT cell subset associated with severe obesity and CRC (42). In keeping with this study, we found a selective enrichment of $CD3^+CD56^+$ NKT-like cells in VAT as compared to blood in healthy individuals and reported new evidence for their preferential accumulation in VAT of CRC patients, independent of BMI. Conversely, no major changes were observed in the periphery. Interestingly, we observed an opposite distribution of T_{reg} and NKT-like cells, both endowed with immunoregulatory/suppressor activity, in VAT from Ob and CRC subjects. Accordingly, when all categories of subjects were analyzed, the frequency of NKT-like cells inversely correlated with that of T_{reg} cells. In this regard, a reciprocal regulation

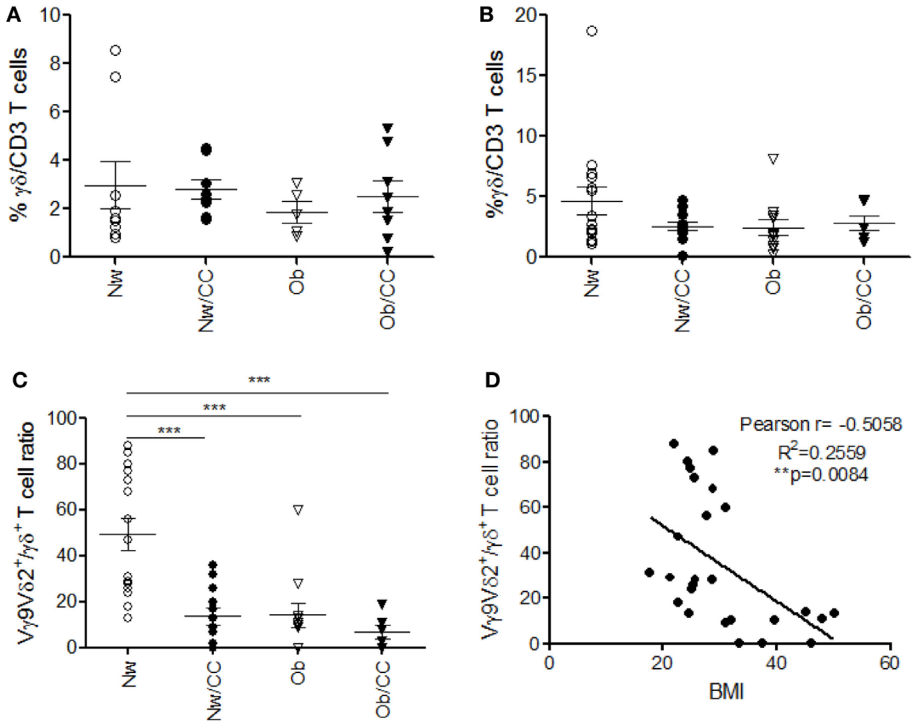

FIGURE 5 | Obese (Ob) and colorectal cancer (CRC)-affected individuals exhibit normal frequencies of peripheral blood (PB) and visceral adipose tissue (VAT)-associated total γδ T lymphocytes but a significantly reduced Vγ9Vδ2/γδ T cell ratio in PB that correlates with body mass index (BMI). VAT stromal vascular fraction (SVF) and PB lymphocytes isolated from lean normal weight (Nw), Ob, lean affected by CRC (Nw/CC), and Ob affected by CRC (Ob/CC) donors were analyzed by flow cytometry. Frequency of total γδ T cells (among $CD3^+$ T cells) was evaluated in SVF **(A)** and PB **(B)**. **(C)** Vγ9Vδ2/γδ T cell ratios (PB) were calculated in the four categories of donors. Each dot represents an individual donor. Mean ± SEM is shown for each group. ***$p < 0.001$, by analysis of variance. **(D)** Pearson's correlation (r) between the Vγ9Vδ2/γδ T cell ratio and BMI in Nw and Ob subjects (**$p < 0.01$).

between these two immune cell populations has been reported in other experimental settings (32, 33), suggesting two different scenarios: (i) a bidirectional regulation of their frequency or (ii) redundant function but different localization depending on the pathophysiological condition. Overall, we could envisage the following scenario at the level of VAT: obesity results in enrichment of T_{reg} cells as a mechanism to attenuate excessive inflammation. However, their presence could generate an immunosuppressive environment favoring tumor establishment. *Vice versa*, once the tumor has established, NKT-like cells might be recruited to the VAT. In this regard, the frequency of NKT-like cells at the tumor site has been positively correlated with significantly longer overall and disease-free survival rates, although the effector mechanisms were not identified (43).

In addition to alterations selectively associated with obesity or CRC, we demonstrate that specific innate cell subsets are affected in both pathologies. We provide herein the first evidence for a reduced Vγ9Vδ2/γδ T cell ratio in the PB of CRC-affected individuals. Moreover, such a reduction was detected in Ob subjects with respect to lean individuals, as recently reported (44) and the Vγ9Vδ2/γδ T cell ratio was found to inversely correlate with BMI. Owing to the protective role of Vγ9Vδ2 T cell-mediated responses in tumor surveillance, obesity- and CRC-induced reduction in this cell subset might be detrimental for the control of tumor development and growth. Interestingly, due to their capacity to specifically recognize and kill CRC initiating cells, γδ T lymphocytes have been proposed as a promising tool for novel immunotherapeutic strategies in patients with CRC (45). As obesity represents a risk factor for CRC and both inflammatory conditions are characterized by loss of Vγ9Vδ2 cells, we speculate that the impairment of this subset in obesity might contribute to CRC immune escape and development.

We have previously demonstrated that specific inflammatory signatures characterize the VAT of Ob and CRC subjects (10). In particular, a reduced ω3/ω6 PUFA ratio and alterations of individual ω6 PUFA profile have been observed in these subjects (10, 11). Among the different factors potentially influencing VAT microenvironment and immune cell distribution, the relative ω3/ω6 PUFA composition, which reflects their dietary intake, might play a pivotal role by virtue of the capacity of these molecules to exert anti- or pro-inflammatory activities, respectively, and to influence immune cell functions (46, 47). We demonstrate herein that the relative abundance/distribution of T_{reg} and NKT cells in VAT from Ob and CRC-affected subjects correlates with the expression of the ω6 PUFA AA and the ω3 PUFA DHA and EPA.

These results add further evidence for the presence of a regulatory/suppressive VAT microenvironment in obesity and CRC, highlighted by our previous demonstration of an increased IL-10 production, reduced immune-stimulatory properties of DC, and impaired generation of γδ T cell-mediated responses induced *ex vivo* by adipocyte microenvironment (11). In this context, the composition of VAT, in particular in FA that reflects

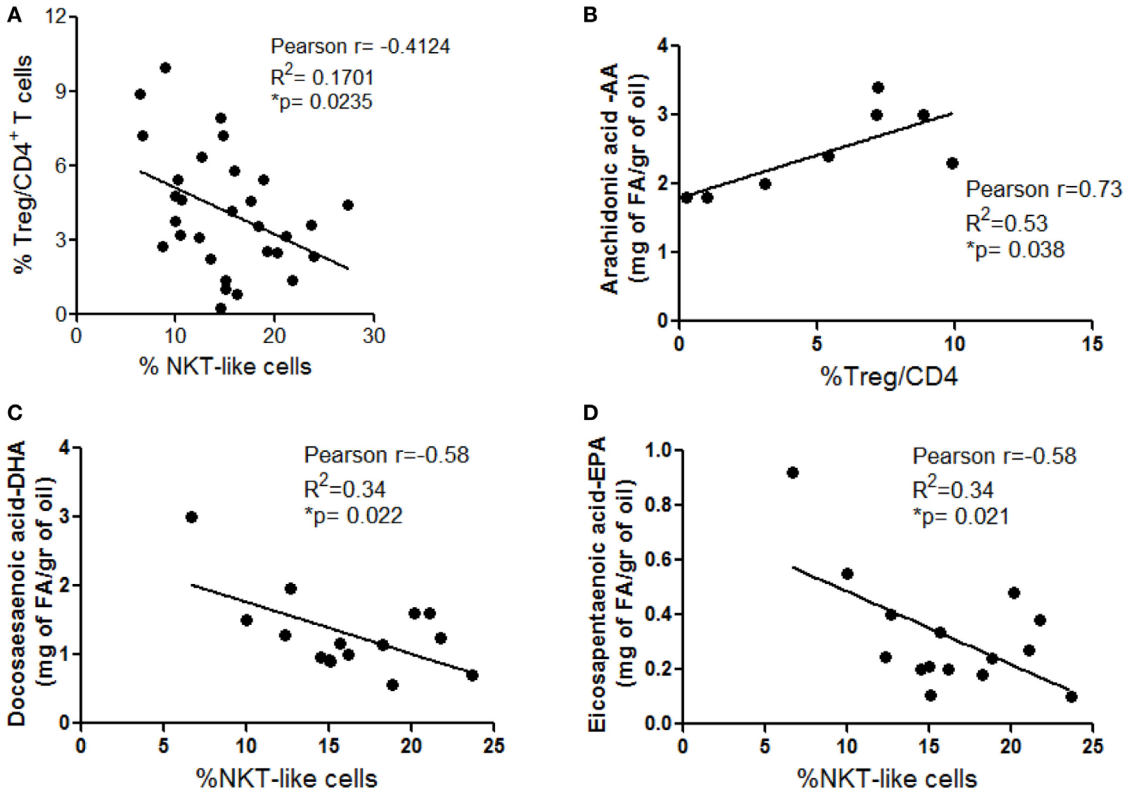

FIGURE 6 | Inverse distribution between total visceral adipose tissue (VAT) stromal vascular fraction (SVF) regulatory T (T_{reg}) and NKT-like cells and correlation with VAT polyunsaturated fatty acid content. Pearson's correlation between: total T_{reg} and NKT-like cell frequencies in VAT SVF **(A)**, arachidonic acid (AA) content, evaluated in visceral adipocytes, and T_{reg} cell frequency estimated in VAT SVF isolated from lean normal weight (Nw) and obese (Ob) donors **(B)**, and docosahexaenoic (DHA) **(C)** and eicosapentaenoic acid (EPA) **(D)** content, evaluated in visceral adipocytes, and NKT cell frequency estimated in VAT SVF isolated from lean (Nw), lean affected by colorectal cancer (CRC) (Nw/CC) and Ob affected by CRC (Ob/CC) donors.

their dietary intake, may represent an important determinant in shaping the immune cell phenotype and in influencing processes/events occurring in distal tissues that may set the basis for tumor establishment. A deep characterization of the local and systemic immune profile, allowing to distinguish between the subsets that drive pro-tumorigenic inflammation or control it, is a key issue for the comprehension of the mechanisms involved in the establishment of a tumor-favorable environment in obesity, and for the definition of more effective cancer prevention strategies based on dietary interventions.

ETHICS STATEMENT

Investigation has been conducted in accordance with the ethical standards and with the Declaration of Helsinki, and according to national and international guidelines. It was approved by the institutional review board of Istituto Superiore di Sanità. All enrolled subjects were provided with complete information about the study and asked to sign an informed consent.

AUTHOR CONTRIBUTIONS

GD, MC, MP, BV, and LC designed and performed experiments and analyzed data for the characterization of PB immune cells. BS, RV, MD, and RM contributed to VAT sample collection, processing, and metabolic evaluation. IP, SP, and VB designed and performed experiments and analyzed data for the characterization of VAT SVF immune cells. LC, SG, and MC provided important contribution to the conception of the work as well as interpretation of data and manuscript writing. MP, RM, and SP provided intellectual input throughout the study.

ACKNOWLEDGMENTS

We are indebted to Dr. S. Giammarioli for helpful advice on fatty acid analysis and Drs. F. Pennestrì, R. Persiani, G. Silecchia and A. Iacovelli for kindly providing clinical samples.

FUNDING

This work was supported by a grant of the Italian Association for Cancer Research (AIRC) (IG 2013 N14185) to SG.

SUPPLEMENTARY MATERIAL

The Supplementary Material for this article can be found online at http://journal.frontiersin.org/article/10.3389/fimmu.2017.00643/full#supplementary-material.

REFERENCES

1. WHO. *Obesity and Overweight. Fact Sheet*. (2015). Available from: http://www.who.int/mediacentre/factsheets/fs311/en/
2. Park J, Morley TS, Kim M, Clegg DJ, Scherer PE. Obesity and cancer – mechanisms underlying tumour progression and recurrence. *Nat Rev Endocrinol* (2014) 10(8):455–65. doi:10.1038/nrendo.2014.94
3. Parkin E, O'Reilly DA, Sherlock DJ, Manoharan P, Renehan AG. Excess adiposity and survival in patients with colorectal cancer: a systematic review. *Obes Rev* (2014) 15(5):434–51. doi:10.1111/obr.12140
4. Renehan AG, Roberts DL, Dive C. Obesity and cancer: pathophysiological and biological mechanisms. *Arch Physiol Biochem* (2008) 114(1):71–83. doi:10.1080/13813450801954303
5. Beddy P, Howard J, McMahon C, Knox M, de Blacam C, Ravi N, et al. Association of visceral adiposity with oesophageal and junctional adenocarcinomas. *Br J Surg* (2010) 97(7):1028–34. doi:10.1002/bjs.7100
6. Siegel RL, Miller KD, Jemal A. Cancer statistics, 2016. *CA Cancer J Clin* (2016) 66(1):7–30. doi:10.3322/caac.21332
7. Bardou M, Barkun AN, Martel M. Obesity and colorectal cancer. *Gut* (2013) 62(6):933–47. doi:10.1136/gutjnl-2013-304701
8. Gregor MF, Hotamisligil GS. Inflammatory mechanisms in obesity. *Annu Rev Immunol* (2011) 29:415–45. doi:10.1146/annurev-immunol-031210-101322
9. Turati F, Edefonti V, Bravi F, Ferraroni M, Talamini R, Giacosa A, et al. Adherence to the European food safety authority's dietary recommendations and colorectal cancer risk. *Eur J Clin Nutr* (2012) 66(4):517–22. doi:10.1038/ejcn.2011.217
10. D'Archivio M, Scazzocchio B, Giammarioli S, Fiani ML, Vari R, Santangelo C, et al. omega3-PUFAs exert anti-inflammatory activity in visceral adipocytes from colorectal cancer patients. *PLoS One* (2013) 8(10):e77432. doi:10.1371/journal.pone.0077432
11. Del Corno M, D'Archivio M, Conti L, Scazzocchio B, Vari R, Donninelli G, et al. Visceral fat adipocytes from obese and colorectal cancer subjects exhibit distinct secretory and omega6 polyunsaturated fatty acid profiles and deliver immunosuppressive signals to innate immunity cells. *Oncotarget* (2016) 7(39):63093–105. doi:10.18632/oncotarget.10998
12. Garaulet M, Perez-Llamas F, Perez-Ayala M, Martinez P, de Medina FS, Tebar FJ, et al. Site-specific differences in the fatty acid composition of abdominal adipose tissue in an obese population from a Mediterranean area: relation with dietary fatty acids, plasma lipid profile, serum insulin, and central obesity. *Am J Clin Nutr* (2001) 74(5):585–91.
13. Tsoukas MA, Ko BJ, Witte TR, Dincer F, Hardman WE, Mantzoros CS. Dietary walnut suppression of colorectal cancer in mice: mediation by miRNA patterns and fatty acid incorporation. *J Nutr Biochem* (2015) 26(7):776–83. doi:10.1016/j.jnutbio.2015.02.009
14. Lee BC, Lee J. Cellular and molecular players in adipose tissue inflammation in the development of obesity-induced insulin resistance. *Biochim Biophys Acta* (2014) 1842(3):446–62. doi:10.1016/j.bbadis.2013.05.017
15. Schipper HS, Prakken B, Kalkhoven E, Boes M. Adipose tissue-resident immune cells: key players in immunometabolism. *Trends Endocrinol Metab* (2012) 23(8):407–15. doi:10.1016/j.tem.2012.05.011
16. Cautivo KM, Molofsky AB. Regulation of metabolic health and adipose tissue function by group 2 innate lymphoid cells. *Eur J Immunol* (2016) 46(6):1315–25. doi:10.1002/eji.201545562
17. Josefowicz SZ, Lu LF, Rudensky AY. Regulatory T cells: mechanisms of differentiation and function. *Annu Rev Immunol* (2012) 30:531–64. doi:10.1146/annurev.immunol.25.022106.141623
18. Apostolopoulos V, de Courten MP, Stojanovska L, Blatch GL, Tangalakis K, de Courten B. The immunological and inflammatory network of adipose tissue in obesity. *Mol Nutr Food Res* (2016) 60(1):43–57. doi:10.1002/mnfr.201500272
19. Bendelac A, Savage PB, Teyton L. The biology of NKT cells. *Annu Rev Immunol* (2007) 25:297–336. doi:10.1146/annurev.immunol.25.022106.141711
20. Mathis D. Immunological goings-on in visceral adipose tissue. *Cell Metab* (2013) 17(6):851–9. doi:10.1016/j.cmet.2013.05.008
21. Terabe M, Berzofsky JA. The immunoregulatory role of type I and type II NKT cells in cancer and other diseases. *Cancer Immunol Immunother* (2014) 63(3):199–213. doi:10.1007/s00262-013-1509-4
22. Ni C, Wu P, Wu X, Zhang T, Wang Z, Zhang S, et al. Thymosin alpha1 enhanced cytotoxicity of iNKT cells against colon cancer via upregulating CD1d expression. *Cancer Lett* (2015) 356(2 Pt B):579–88. doi:10.1016/j.canlet.2014.10.002
23. Wensveen FM, Jelencic V, Valentic S, Sestan M, Wensveen TT, Theurich S, et al. NK cells link obesity-induced adipose stress to inflammation and insulin resistance. *Nat Immunol* (2015) 16(4):376–85. doi:10.1038/ni.3120
24. Fay NS, Larson EC, Jameson JM. Chronic Inflammation and gammadelta T Cells. *Front Immunol* (2016) 7:210. doi:10.3389/fimmu.2016.00210
25. Yang XF, He X, He J, Zhang LH, Su XJ, Dong ZY, et al. High efficient isolation and systematic identification of human adipose-derived mesenchymal stem cells. *J Biomed Sci* (2011) 18:1–9. doi:10.1186/1423-0127-18-59
26. Folch J, Lees M, Sloane Stanley GH. A simple method for the isolation and purification of total lipides from animal tissues. *J Biol Chem* (1957) 226(1):497–509.
27. Sakaguchi S, Miyara M, Costantino CM, Hafler DA. FOXP3+ regulatory T cells in the human immune system. *Nat Rev Immunol* (2010) 10(7):490–500. doi:10.1038/nri2785
28. Piconese S, Timperi E, Pacella I, Schinzari V, Tripodo C, Rossi M, et al. Human OX40 tunes the function of regulatory T cells in tumor and nontumor areas of hepatitis C virus-infected liver tissue. *Hepatology* (2014) 60(5):1494–507. doi:10.1002/hep.27188
29. Timperi E, Pacella I, Schinzari V, Focaccetti C, Sacco L, Farelli F, et al. Regulatory T cells with multiple suppressive and potentially pro-tumor activities accumulate in human colorectal cancer. *Oncoimmunology* (2016) 5(7):e1175800. doi:10.1080/2162402X.2016.1175800
30. Finn OJ. Immuno-oncology: understanding the function and dysfunction of the immune system in cancer. *Ann Oncol* (2012) 23(Suppl 8):viii6–9. doi:10.1093/annonc/mds256
31. Piconese S, Pittoni P, Burocchi A, Gorzanelli A, Care A, Tripodo C, et al. A non-redundant role for OX40 in the competitive fitness of Treg in response to IL-2. *Eur J Immunol* (2010) 40(10):2902–13. doi:10.1002/eji.201040505
32. La Cava A, Van Kaer L, Fu Dong S. CD4+CD25+ Tregs and NKT cells: regulators regulating regulators. *Trends Immunol* (2006) 27(7):322–7. doi:10.1016/j.it.2006.05.003
33. Lynch L, Michelet X, Zhang S, Brennan PJ, Moseman A, Lester C, et al. Regulatory iNKT cells lack expression of the transcription factor PLZF and control the homeostasis of T(reg) cells and macrophages in adipose tissue. *Nat Immunol* (2015) 16(1):85–95. doi:10.1038/ni.3047
34. Wagner NM, Brandhorst G, Czepluch F, Lankeit M, Eberle C, Herzberg S, et al. Circulating regulatory T cells are reduced in obesity and may identify subjects at increased metabolic and cardiovascular risk. *Obesity (Silver Spring)* (2013) 21(3):461–8. doi:10.1002/oby.20087
35. Feuerer M, Herrero L, Cipolletta D, Naaz A, Wong J, Nayer A, et al. Lean, but not obese, fat is enriched for a unique population of regulatory T cells that affect metabolic parameters. *Nat Med* (2009) 15(8):930–9. doi:10.1038/nm.2002
36. Deiuliis J, Shah Z, Shah N, Needleman B, Mikami D, Narula V, et al. Visceral adipose inflammation in obesity is associated with critical alterations in tregulatory cell numbers. *PLoS One* (2011) 6(1):e16376. doi:10.1371/journal.pone.0016376
37. Cipolletta D. Adipose tissue-resident regulatory T cells: phenotypic specialization, functions and therapeutic potential. *Immunology* (2014) 142(4):517–25. doi:10.1111/imm.12262
38. Zeyda M, Huber J, Prager G, Stulnig TM. Inflammation correlates with markers of T-cell subsets including regulatory T cells in adipose tissue from obese patients. *Obesity (Silver Spring)* (2011) 19(4):743–8. doi:10.1038/oby.2010.123
39. Pereira S, Teixeira L, Aguilar E, Oliveira M, Savassi-Rocha A, Pelaez JN, et al. Modulation of adipose tissue inflammation by FOXP3+ Treg cells, IL-10, and TGF-beta in metabolically healthy class III obese individuals. *Nutrition* (2014) 30(7–8):784–90. doi:10.1016/j.nut.2013.11.023
40. Zhang X, Kelaria S, Kerstetter J, Wang J. The functional and prognostic implications of regulatory T cells in colorectal carcinoma. *J Gastrointest Oncol* (2015) 6(3):307–13. doi:10.3978/j.issn.2078-6891.2015.017
41. Lin YC, Mahalingam J, Chiang JM, Su PJ, Chu YY, Lai HY, et al. Activated but not resting regulatory T cells accumulated in tumor microenvironment and correlated with tumor progression in patients with colorectal cancer. *Int J Cancer* (2013) 132(6):1341–50. doi:10.1002/ijc.27784
42. Lynch L, O'Shea D, Winter DC, Geoghegan J, Doherty DG, O'Farrelly C. Invariant NKT cells and CD1d(+) cells amass in human omentum and

are depleted in patients with cancer and obesity. *Eur J Immunol* (2009) 39(7):1893–901. doi:10.1002/eji.200939349
43. Tachibana T, Onodera H, Tsuruyama T, Mori A, Nagayama S, Hiai H, et al. Increased intratumor Valpha24-positive natural killer T cells: a prognostic factor for primary colorectal carcinomas. *Clin Cancer Res* (2005) 11(20):7322–7. doi:10.1158/1078-0432.CCR-05-0877
44. Costanzo AE, Taylor KR, Dutt S, Han PP, Fujioka K, Jameson JM. Obesity impairs gamma delta T cell homeostasis and antiviral function in humans. *PLoS One* (2015) 10(3):1–16. doi:10.1371/journal.pone.0120918
45. Ramutton T, Buccheri S, Dieli F, Todaro M, Stassi G, Meraviglia S. gamma delta T cells as a potential tool in colon cancer immunotherapy. *Immunotherapy* (2014) 6(9):989–99. doi:10.4155/Imt.14.59
46. Yessoufou A, Ple A, Moutairou K, Hichami A, Khan NA. Docosahexaenoic acid reduces suppressive and migratory functions of CD4+CD25+ regulatory T-cells. *J Lipid Res* (2009) 50(12):2377–88. doi:10.1194/jlr.M900101-JLR200
47. Kim W, Khan NA, McMurray DN, Prior IA, Wang N, Chapkin RS. Regulatory activity of polyunsaturated fatty acids in T-cell signaling. *Prog Lipid Res* (2010) 49(3):250–61. doi:10.1016/j.plipres.2010.01.002

Conflict of Interest Statement: The research was conducted in the absence of any commercial or financial relationships that could be construed as a potential conflict of interest.

Copyright © 2017 Donninelli, Del Cornò, Pierdominici, Scazzocchio, Varì, Varano, Pacella, Piconese, Barnaba, D'Archivio, Masella, Conti and Gessani. This is an open-access article distributed under the terms of the Creative Commons Attribution License (CC BY). The use, distribution or reproduction in other forums is permitted, provided the original author(s) or licensor are credited and that the original publication in this journal is cited, in accordance with accepted academic practice. No use, distribution or reproduction is permitted which does not comply with these terms.

frontiers in Immunology

ORIGINAL RESEARCH
published: 22 June 2017
doi: 10.3389/fimmu.2017.00719

Toll-Like Receptor 4 Inhibition Improves Oxidative Stress and Mitochondrial Health in Isoproterenol-Induced Cardiac Hypertrophy in Rats

*Parmeshwar B. Katare[1], Pankaj K. Bagul[1], Amit K. Dinda[2] and Sanjay K. Banerjee[1]**

[1] Drug Discovery Research Center (DDRC), Translational Health Science and Technology Institute (THSTI), Faridabad, India, [2] Department of Pathology, All India Institute of Medical Sciences (AIIMS), New Delhi, India

Background: Inflammation remains a crucial factor for progression of cardiac diseases and cardiac hypertrophy remains an important cause of cardiac failure over all age groups. As a key regulator of inflammation, toll-like receptor 4 (TLR4) plays an important role in pathogenesis of cardiac diseases. Being an important regulator of innate immunity, the precise pathway of TLR4-mediated cardiac complications is yet to be established. Therefore, the primary objective of the present study was to find the role of TLR4 in cardiac hypertrophy and the molecular mechanism thereof.

Methods: Cardiac hypertrophy was induced with administration of isoproterenol (5 mg/kg/day, sc). TLR4 receptor inhibitor RS-LPS (lipopolysaccharide from the photosynthetic bacterium *Rhodobacter sphaeroides*; 5 μg/day) and agonist lipopolysaccharide (LPS) (from *Escherichia coli*; 3.12 μg/day) were administered through osmotic pump along with isoproterenol. Cardiac hypertrophy as well as oxidative stress and mitochondrial parameters were evaluated.

Results: Cardiac hypertrophy was confirmed with increased heart weight/body weight ratio as well as assessment of hypertrophic markers in heart. There was a marked increase in the TLR4 expression and oxidative stress along with mitochondrial dysfunction in ISO group. TLR4 inhibition significantly decreased heart weight/body weight ratio and ANP, collagen, and β-MHC expression and restored the disturbed cellular antioxidant flux. The mitochondrial perturbations that were observed in hypertrophy heart was normalized after administration of TLR4 inhibitor but not with the agonist. TLR4 agonism further exaggerated the oxidative stress in heart and hence accelerated the disease development and progression.

Conclusion: Our data show that increased TLR4 ligand pool in cardiac hypertrophy may exaggerate the disease progression. However, inhibition of TLR4 attenuated cardiac hypertrophy through reduced cardiac redox imbalance and mitochondrial dysfunction.

Keywords: cardiac hypertrophy, isoproterenol, toll-like receptor 4, lipopolysaccharide, RS-LPS, oxidative phosphorylation

Abbreviations: TLR4, toll-like receptor 4; PRRs, pattern recognition receptors; OXPHOS, oxidative phosphorylation; PAMPs, pathogen-associated molecular patterns; DAMP, damage-associated molecular pattern; ROS, reactive oxygen species.

OPEN ACCESS

Edited by:
Jixin Zhong, Case Western Reserve University, United States

Reviewed by:
Paramananda Saikia, Cleveland Clinic, United States
Shanzhong Gong, University of Texas at Austin, United States

***Correspondence:**
Sanjay K. Banerjee
skbanerjee@thsti.res.in, banerjees74@hotmail.com

Specialty section:
This article was submitted to Inflammation, a section of the journal Frontiers in Immunology

Received: *13 April 2017*
Accepted: *06 June 2017*
Published: *22 June 2017*

Citation:
Katare PB, Bagul PK, Dinda AK and Banerjee SK (2017) Toll-Like Receptor 4 Inhibition Improves Oxidative Stress and Mitochondrial Health in Isoproterenol-Induced Cardiac Hypertrophy in Rats. Front. Immunol. 8:719. doi: 10.3389/fimmu.2017.00719

INTRODUCTION

The ability of the myocardium to successfully adapt cellular stress ultimately determines whether the heart will maintain its preserved function or decompensate and fail. Despite the importance of the myocardial response to environmental stress, very little is known with respect to the biochemical mechanisms that are responsible for mediating and integrating the stress response in the heart (1). Cardiac hypertrophy is a result of an adaptive response to pressure or volume stress. Hypertrophic growth accompanies many forms of heart disease, including ischemic disease, hypertension, heart failure, and valvular disease (2). Despite the application of state-of-the art therapy, mortality remains high at two times at 5 years after detection of the disease. Therefore, we need to seek better strategies for the treatment of cardiac hypertrophy (3–5).

Inflammation is a common phenomenon observed in case of cardiac hypertrophy. This persistent inflammation of myocardium may play a key role in disease progression. However, the underlying mechanism remains unclear. This sterile inflammation in heart is mainly regulated by toll-like receptors (TLRs). TLRs are the pattern recognition receptors (PRRs), which play an important role in innate immunity by recognizing pathogen-associated molecular patterns and damage-associated molecular patterns (DAMPs) (6). There are 13 different TLRs in mammalian cell, among which toll-like receptor 4 (TLR4) is the most studied and is a central mediator of sterile inflammation (7). TLR4 is expressed in variety of cells including cardiomyocytes (8). TLR4-mediated signaling activates NF-κB, which regulates inflammatory and immune responses, cell growth, cell survival, and cell death (9).

Apart from inflammation, TLR4 is also involved in impaired cardiac function during sepsis-induced heart failure (10, 11). The role of TLR4 activation is not only limited to septic cardiomyopathy but also plays a significant role in other cardiac diseases. It has been observed that TLR4 knockout mice are protected from ischemia reperfusion injury (12). TLR4 has been known to be involved in modulation of myocyte contractility, left ventricular hypertrophy, and ischemia reperfusion injury. Increased TLR4 expression has been reported in the myocardium from patients with heart failure and ischemia (13, 14). Inhibition of Myd88, a downstream mediator of TLR4, leads to reduced left ventricular remodeling and improved cardiac function after aortic banding (15). Studies performed by Ha et al. (16) and Ehrentraut et al. (17) had shown the protection against pressure overload cardiac hypertrophy in TLR4-deficient mice by decreased NFκB and cardiac inflammation. Similarly, TLR4 inhibitor "Iritoran" has protective effect against cardiac hypertrophy through PI3K/Akt/mTOR axis (18).

Two recent studies also have shown the improvement in cardiac function after central blockade (brain) of TLR4 through downregulation of myocardial inflammation and sympathetic activity (19, 20). All of these studies were focused to find the effect of TLR4 deficiency or inhibition on cardiac inflammation. However, in the present study, we have analyzed the effect of TLR4 modulation, i.e., both TLR4 agonist and antagonist on isoproterenol-induced rat cardiac hypertrophy focusing more on mitochondrial dysfunction.

Mitochondria are very important cellular organelles of cardiomyocytes, which need constant supply of high level of ATP for contraction. Cardiac hypertrophy is a serious health problem and progress slowly to failure heart. Mitochondrial dysfunction is a crucial event during the transition from hypertrophy to failure. It has been reported that LPS causes mitochondrial dysfunction through TLR4 activation (10, 21). Activation of TLR4-mediated signaling pathway may lead to release of many cytokines responsible for local as well as systemic inflammation. Therefore, we hypothesized that pharmacological modulation of TLR4 mitigates cardiac hypertrophy in rats, *via* attenuation of oxidative stress and mitochondrial dysfunction. The study proposes a strong rationale to investigate the potential application of TLR4 inhibitor and agonist in the treatment of cardiac hypertrophy and mitochondrial dysfunction.

MATERIALS AND METHODS

Animal Study

All experiments involving animals were undertaken with the approval of Institutional Animal Ethical Committee of Indian Institute of Chemical Technology, Hyderabad. Male Sprague-Dawley rats weighing 200–250 g were purchased from Tina lab, Hyderabad, India. Animals were housed in BIOSAFE, an animal quarantine facility of Indian Institute of Chemical Technology, Hyderabad. Animals were maintained at temperature 22 ± 2°C with relative humidity of 40 ± 15% and 12-h dark/light cycle throughout the experiment. Animals had a free access to water and diet.

Drug Solution Preparation and Dosing

Lipopolysaccharide (LPS) from *Escherichia coli* 0111:B4 strain (Invivogen) a potent TLR4 agonist and LPS from the photosynthetic bacterium *Rhodobacter sphaeroides* (RS-LPS) (Invivogen) a potent TLR4 inhibitor were used for TLR4 modulation (22). Solutions of modulators were prepared in pyrogen-free saline water and filled in the alzet pumps for sustained release. Isoproterenol (Sigma) solution was prepared in 0.4 mM ascorbate buffer immediately before dosing.

Induction of Cardiac Hypertrophy in Rat and Treatment Schedule

Animals were randomly divided into four groups: control group (CON) was administered pyrogen-free saline through s.c. route. Hypertrophy group (ISO) was administered isoproterenol 5 mg/kg/day s.c. route (23). In addition, pyrogen-free saline-filled alzet pump was implanted subcutaneously on dorsal side in both the groups. Hypertrophy + TLR4 agonist group (LPS + ISO) was administered 3.12 μg/day of LPS through alzet pump along with isoproterenol (5 mg/kg/day, sc). Hypertrophy + TLR4 antagonist group (RS + ISO) was administered 5 μg/day of RS-LPS through alzet pump along with isoproterenol (5 mg/kg/day, sc). The whole treatment schedule was followed for a period of 14 days ($N = 10$). Animals were anesthetized using a mixture of

ketamine (75 mg/kg, IP) and xylazine (5 mg/kg, IP) for surgical insertion of alzet pump. Body weight gain was monitored during the study period. At the end of study, all animals were sacrificed with high dose of anesthesia, heart was collected, and stored in −80°C or 4% formalin for downstream analysis.

Heart Weight and Body Weight Ratio

After 14 days of experiment, rats were sacrificed. Heart was removed and washed in freshly prepared phosphate buffer solution. Heart was dried on a tissue paper and weighed. Body weight of all animals was measured just before sacrificing the animals. Heart weight/body weight ratio (milligrams per gram) was used for measuring cardiac hypertrophy as described earlier (24).

Preparation of Heart Tissue Homogenate

Rat heart tissue homogenate was prepared by homogenizing 100 mg of heart tissue in 2 ml of 0.05 M phosphate buffer (pH-7.4) and centrifuging at 15,000 rpm for 30 min at 4°C. The resulting supernatant was stored at −80°C for further analysis.

TLR4 ELISA Protein Estimation

Toll-like receptor 4 protein was analyzed using ELISA assay kit from Wuhan USCN, USA. Heart tissue homogenate was used to determine the TLR4 protein expression in rat heart ($N = 4$) and estimated following manufacturers protocol. The TLR4 protein was expressed as picograms per microgram of protein.

Estimation of Antioxidant Parameters

Tissue homogenate was used for the estimation of thiobarbituric acid reactive substances (TBARS). Heart tissue homogenate supernatant was used to estimate reduced glutathione (GSH), glutathione peroxidase (GPx), glutathione reductase (GR), superoxide dismutase (SOD), reactive oxygen species (ROS), and catalase (CAT). TBARS (25) and ROS (26) were measured as markers of lipid peroxidation while GSH, SOD, CAT, GPx, and GR (27) were estimated as levels of endogenous antioxidants as described before (28).

Isolation of Mitochondria

Mitochondria were isolated from equal weight of heart tissues using mitochondria isolation kit (Pierce, Thermo Scientific, Cat No: 89801). Briefly, heart tissue was cut into small pieces and homogenized using dounce homogenizer and the homogenate was then treated according to manufacturer's protocol. The resultant mitochondrial pellet was suspended in MTP buffer containing 110 mM mannitol, 60 mM Tris HCL, 60 mM potassium chloride, 10 mM dibasic potassium phosphate, and 0.5 mM EDTA, pH-7.4. Mitochondrial purity and integrity was confirmed using Mito Tracker as described before (29).

Mitochondrial Respiratory Chain Complex Activity in Heart

The specific enzymatic activity of mitochondrial electron transport chain (ETC) complex I (NADH-ubiquinone oxidoreductase) and complex II (succinate-ubiquinone oxidoreductase) were measured in the isolated mitochondria from heart as previously described (30). β-hydroxyacyl CoA dehydrogenase activity, an important enzyme for beta oxidation and citrate synthase activity, an important enzyme of TCA cycle, were measured according to the protocol described previously (31, 32).

Electrocardiogram Recording

ECG was measured on 13th day of the experiment. Animals were anesthetized using ketamine (75 mg/kg, IP) and xylazine (5 mg/kg, IP) in a mixture and kept in supine position on homeothermic blanket to maintain the body temperature throughout the experiment. ECG was measured using PowerLab with LabChart software as described before (28) ($N = 4$). Heart rate data were used to measure the tachycardia.

Histopathology

Myocardial tissue was fixed in 4% neutral buffered formalin for 48 h. Fixed tissue was processed routinely and embedded in paraffin. Paraffin sections (5 μm) were cut and mounted on glass slides and stained with Hematoxylin and Eosin (H&E) and Masson's trichrome stains and examined under a light microscope as described previously (27, 33). Cardiomyocytes cell size was analyzed using H&E-stained sections and cardiac fibrosis was analyzed using Masson's trichrome stain with the help of ImageJ software as described before (24, 34).

Gene Expression Profiling

RNA was isolated from heart tissue of all groups ($N = 4$) using TRIzol reagent (Sigma-Aldrich) following manufacturers protocol. Quantification and quality assessment of RNA was carried out with Nano Drop spectrophotometer (Thermo Scientific) and running on 1% agarose gel prepared in DEPC-treated TBE buffer. The extracted RNA was stored in −80°C for future use. RNA was treated with DNase before cDNA synthesis. cDNA was synthesized using 2 μg RNA with superscript-III reverse transcriptase (Takara, USA). Real-time polymerase chain reaction was carried out using Step One plus (Applied Biosystems Inc., USA) and SYBR Green mix (Takara, USA). The data were normalized to the expression of reference gene, *ribosomal protein L32* (RPL32) (35). The list of primers is provided in Table S1 in Supplementary Material.

Protein Expression Profiling

Samples were processed using tissue protein extraction reagent (NE-PER kit) according to manufacturer's protocol (Thermo Scientific). After centrifugation at 16,000 × *g* for 5 min, the protein in supernatant (Cytoplasmic extract) was transferred to prechilled tube. Insoluble fraction (pellet) was suspended in ice-cold nuclear extraction reagent, vortexed, centrifuged at 16,000 × *g* for 10 min. Supernatant (nuclear extract) was transferred to prechilled tubes. Protein was quantified by BCA method (Thermo Scientific). Nuclear protein extract was used for p65 subunit of NF-κB (p65 NF-κB) and NRF2 quantification while cytoplasmic protein extract was used for SOD2 protein quantification. TLR4 was measured from total protein fraction. Protein (30 μg) was resolved in 10% SDS-polyacrylamide gel using TGX stain free kit (Bio-Rad). After electrophoresis, protein

was transferred to polyvinylidine difluoride membrane (GE Healthcare). Blocking of the membrane was performed using 3% non-fat milk in TBST containing 0.1% tween 20 at room temperature for 1 h, followed by appropriate primary antibody treatment overnight at 4°C. The membrane was washed with TBST for 5 min (three times). After washing, membrane was incubated with corresponding HRP-labeled secondary antibody at room temperature for 1 h. Membrane was washed with TBST (3 times for 5 min each) and the blot was visualized using gel doc XR system (Bio-Rad), using west dura pico (Thermo Scientific). Different antibodies used for the study are TLR4 (Abcam; Cat no. ab13444), p65 NF-kB (Abcam; Cat no. ab16502), oxidative phosphorylation (Abcam; Cat no. ab110413), NRF2 (Abcam; Cat no. ab31163), SOD2 (Abcam; Cat no. ab13533), anti-Rabbit, and anti-Mouse antibody.

Statistical Analysis

All values are expressed as the mean ± SE. One-way analysis of variance test followed by Bonferroni's correction was carried out to test for any differences between the mean values of all groups. Differences in group was assumed significant if $p < 0.05$.

RESULTS

Effect of TLR4 Modulation on Heart Weight to Body Weight Ratio and Hypertrophy Markers

Heart weight to body weight ratio (**Figure 1A**), an indicator of cardiac hypertrophy, and mRNA expression of myocardial β-MHC (**Figure 1B**), ANP (**Figure 1C**), and collagen (**Figure 1D**) were increased significantly ($p < 0.05$) in ISO group as compared to CON group. RS treatment significantly ($p < 0.05$) decreased heart weight to body weight ratio and normalized the increased ANP, β-MHC, and collagen mRNA expression. However, LPS treatment did not restore the increased heart weight to body weight ratio and hypertrophy markers (**Figure 1**).

TLR4 Inhibitor Decreased Cardiomyocyte Cell Size and Myocardial Fibrosis in Hypertrophy Heart

Cardiomyocyte size (Table S2 in Supplementary Material) and myocardial fibrosis (**Figure 2**; Figure S2 in Supplementary Material), which are hallmark of cardiac hypertrophy, were significantly ($p < 0.05$) increased in hypertrophy heart as compared to control. RS treatment significantly attenuated the increase in cardiomyocyte size and myocardial fibrosis (**Figure 2B**). LPS treatment did not change the ISO induced myocardial size but further increased myocardial fibrosis as compared to hypertrophy heart (**Figure 2**).

TLR4 Inhibitor Improved Electrocardiograph Parameters

Electrocardiogram analysis showed prolonged QT interval (Figure S1C in Supplementary Material), increased R amplitude (Figure S1B in Supplementary Material) along with increased heart rate (Figure S1A in Supplementary Material) in ISO group. All these ECG changes in the hypertrophic heart indicate the

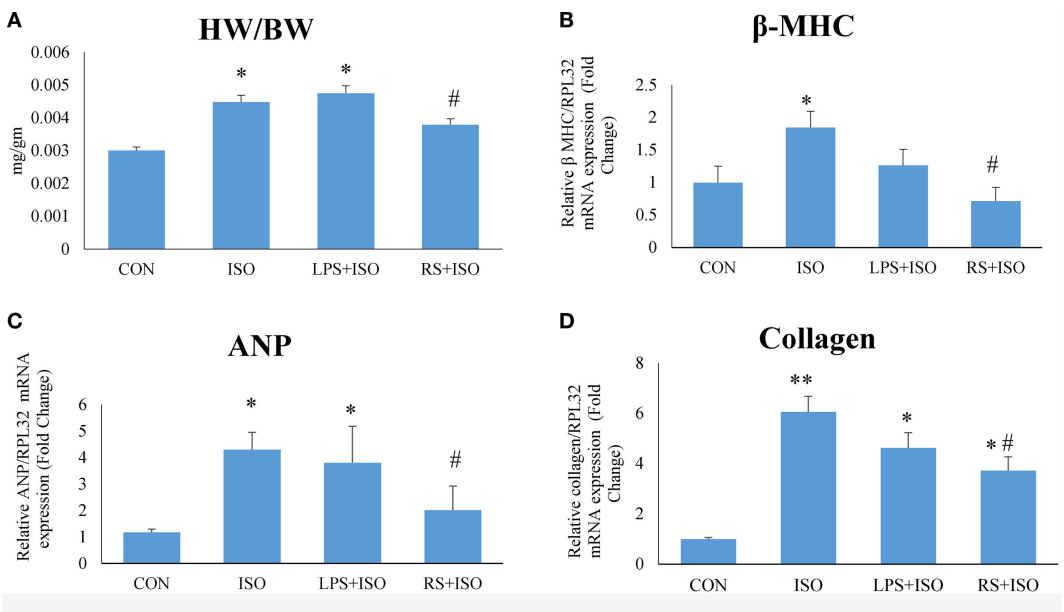

FIGURE 1 | Cardiac phenotypes and mRNA expression of hypertrophy markers. **(A)** Heart weight to body weight ratio (HW/BW) **(B)** mRNA expression of beta MHC **(C)** mRNA expression of ANP **(D)** mRNA expression of collagen. The data were normalized to the expression of reference gene, *ribosomal protein L32* (RPL32). Data shown as mean ± SEM ($N = 6$ for HW/BW, $N = 4$ for mRNA expression) $^{*}p < 0.05$, $^{**}p < 0.01$ vs CON; $^{\#}p < 0.05$, $^{\#\#}p < 0.01$ vs ISO groups.

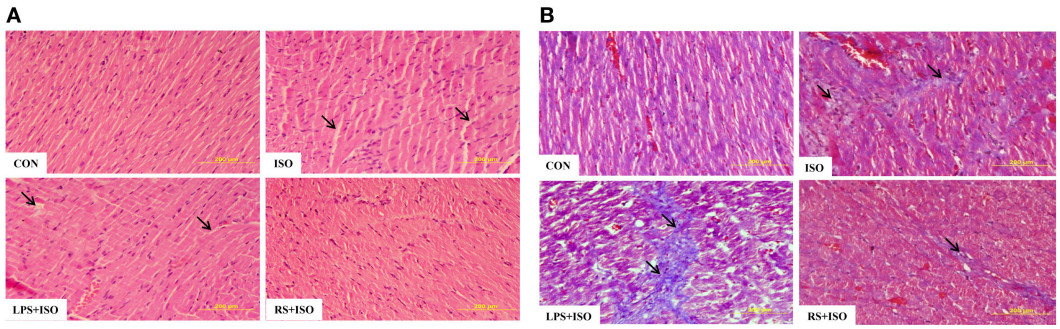

FIGURE 2 | Cardiac cell phenotypes and histopathological examination in cardiac hypertrophy and effect of toll-like receptor 4 modulation. **(A)** Hematoxylin and eosin staining of rat heart tissue. Arrows in the figure represent loss of cardiomyocytes. **(B)** Masson's trichrome staining of rat heart tissue. Arrows in figures represent the presence of fibrosis in heart tissue. Data shown as mean ± SEM, $^{*}p < 0.05$, $^{**}p < 0.01$ vs CON; $^{\#}p < 0.05$, $^{\#\#}p < 0.01$ vs ISO groups. Three sections were observed for histopathology examination and 20 cells per image were analyzed.

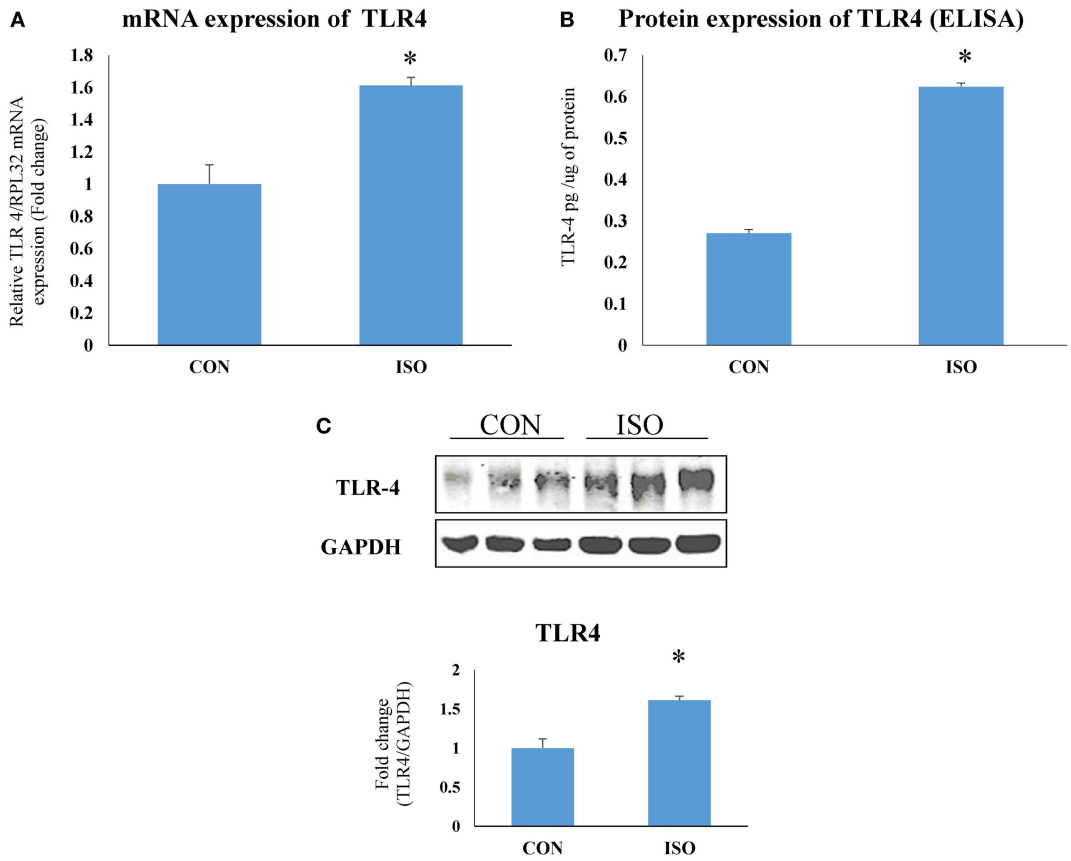

FIGURE 3 | Toll-like receptor 4 (TLR4) expression was increased in cardiac hypertrophy. **(A)** mRNA expression. The data were normalized to the expression of reference gene, *ribosomal protein L32* (RPL32), **(B)** protein expression by ELISA, and **(C)** protein expression by western blot. The data were normalized to the expression of reference gene, GAPDH. Data shown as mean ± SEM ($N = 3$ for western blot and $N = 4$ for real-time PCR and ELISA) $^{*}p < 0.05$, $^{**}p < 0.01$ vs CON.

presence of cardiac ventricular hypertrophy and tachycardia. RS (RS + ISO) administration in these rats normalized these altered electro cardiac abnormalities. LPS (LPS + ISO) treatment did not alter these perturbations in ECG (Figure S1 in Supplementary Material).

TLR4 Expression Increased in Hypertrophy Heart

Toll-like receptor 4 mRNA (**Figure 3A**) and protein (**Figures 3B,C**) expression was significantly ($p < 0.05$) increased in rat hypertrophy heart as compared to control.

TLR4 Inhibitor Attenuated Inflammatory Gene Expression in Hypertrophy Heart

Myocardial mRNA expression of inflammatory genes TNF alpha and IL-6 was significantly increased in ISO group as compared to CON group (**Figures 4A,B**). TLR4 inhibition decreased the mRNA expression of myocardial IL-6 ($p < 0.05$) as compared to ISO group. However, the level of TNF alpha was not significantly decreased by TLR4 inhibition as compared to ISO group (**Figure 4**). LPS treatment in ISO animals further increased the level of IL-6 expression ($p < 0.05$).

TLR4 Inhibitor Reduced Cardiac Oxidative Stress in Hypertrophy Heart

There was a significant ($p < 0.05$) increase in cardiac ROS (**Figure 5A**), and TBARS level (**Figure 5B**), and decrease ($p < 0.05$) in cardiac endogenous antioxidants like GR (**Figure 5C**), CAT (**Figure 5D**), GSH (**Figure 5E**), GPx (**Figure 5F**), and SOD (**Figure 5G**) in ISO group. RS treatment decreased ($p < 0.05$) cardiac ROS and TBARS level and increased endogenous antioxidants toward normal. However, we have not observed any improvement in disturbed redox balance after LPS treatment (**Figure 5**).

TLR4 Inhibitor Improved Mitochondrial ETC Complex Function in Hypertrophy Heart

Protein expression of mitochondrial complex I, III, and V (**Figures 6A,B**) was significantly ($p < 0.05$) reduced in ISO group. RS treatment restored the decreased protein expression of these mitochondrial complexes toward normal. LPS treatment found to further decrease the protein expression of these complexes in ISO group ($p < 0.05$) (**Figure 6**).

TLR4 Inhibitor Improves Mitochondrial Enzyme Activities in Hypertrophy Heart

Myocardial citrate synthase (**Figure 6C**) and 3-hydroxy-CoA dehydrogenase (**Figure 6C**) activity was significantly ($p < 0.05$) reduced in hypertrophic animals. RS treatment in ISO animals significantly ($p < 0.05$) increased citrate synthase and 3-hydroxy-CoA dehydrogenase activity. LPS treatment failed to restore the detrimental perturbations in these enzyme activities. Protein expression results of ETC complexes correlated directly with the enzyme activity. Myocardial enzyme activity of mitochondrial complex I, i.e., NADH dehydrogenase (**Figure 6C**) and complex II, i.e., succinate dehydrogenase (**Figure 6C**) were reduced in ISO animals as compared to CON group. However, these activities were normalized by RS treatment ($p < 0.05$). LPS treatment failed to increase the decreased enzyme activity of these enzymes (**Figure 6**).

TLR4 Inhibitor Attenuated Myocardial p65 NF-κB and NRF2 and Restored MnSOD Expression in Hypertrophy Heart

Myocardial p65 NF-κB and NRF2 protein expression was significantly increased in ISO group. LPS treatment further increased the expression of p65 NF-κB in hypertrophy heart. However, RS treatment reduced the increased level of P65 NF-κB and NRF2 in ISO treated rat heart (**Figures 7A–C**). Myocardial MnSOD level was significantly down in ISO animals ($p < 0.05$). LPS treatment leads to further decrease in the MnSOD level. However, RS treatment restored the decreased level of MnSOD toward normal ($p < 0.05$) (**Figures 7D,E**).

The animals with only RS-LPS treatment did not show any changes in normal physiology, whereas LPS-treated animals shown an increased cardiac fibrosis and increased oxidative stress (data not shown).

DISCUSSION

The concept that innate immunity may constitute a component of "adaptive cardiac biology" is being increasingly recognized (36). The components of the innate immunity program seem to be required to resist infectious and pressure-overload-mediated cardiac decompensation and heart failure. PRRs, part of innate immunity, play an important role in the identification of danger signals released from diseased heart (37). DAMPs released from injured cardiomyocytes acts as a danger signal (38). Recent literature shows that DAMPs released from the necrotic heart tissue alone are sufficient to induce chronic myocardial

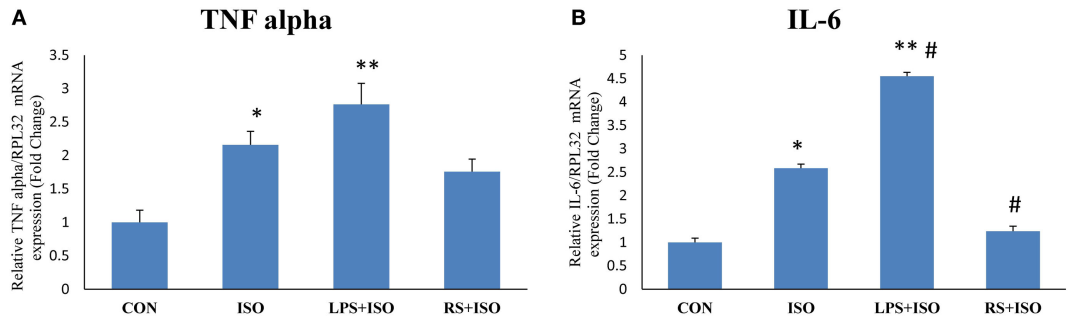

FIGURE 4 | TNF alpha and IL-6 expression in hypertrophy rat heart after toll-like receptor 4 modulation. **(A)** mRNA expression of TNF alpha **(B)** mRNA expression of IL-6. The data were normalized to the expression of reference gene, *ribosomal protein L32* (RPL32). Data shown as mean ± SEM, $^{*}p < 0.05$, $^{**}p < 0.01$ vs CON; $^{\#}p < 0.05$, $^{\#\#}p < 0.01$ vs ISO groups.

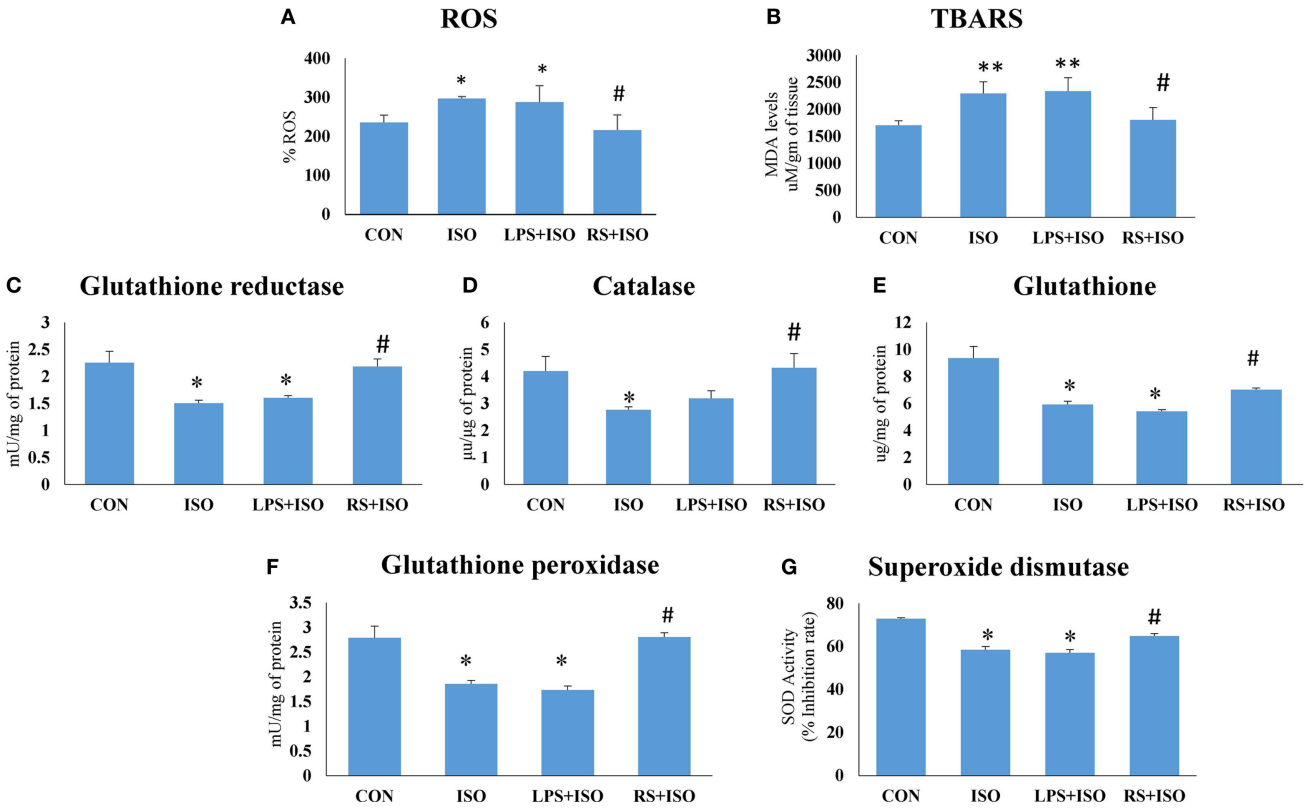

FIGURE 5 | Cardiac redox status in hypertrophic condition and effect of toll-like receptor 4 modulation on myocardial **(A)** reactive oxygen species (ROS), **(B)** thiobarbituric acid reactive substances (TBARS), **(C)** glutathione reductase activity, **(D)** catalase activity, **(E)** reduced glutathione, **(F)** glutathione peroxidase activity, and **(G)** superoxide dismutase activity. Data shown as mean ± SEM ($N = 5$) $^{*}p < 0.05$, $^{**}p < 0.01$ vs CON; $^{\#}p < 0.05$, $^{\#\#}p < 0.01$ vs ISO groups.

inflammation (39). Binding of DAMPs to PPRs on the cell surface leads to signaling *via* NF-κB and MAP kinase pathways leading to pro-inflammatory cytokine expression (IL-1, TNF-α, IL-12), chemokine secretion (IL-8, monocyte chemotactic protein-1), and thus leukocyte infiltration and inflammation (40). Recently, many studies have shown that TLR4 plays an important role in the cardiac adaptation during decompensated state of the system (41). LPS is a proven TLR4 agonist. *In vivo*, LPS activates innate immune system and evokes inflammatory responses (36). A structural analog of LPS, RS-LPS (RS), a well-known TLR4 inhibitor, has shown anti-inflammatory responses in the body. While TLR4 inhibitor may attenuate hypertrophy through inhibition of signaling pathway of TLR4, mild activation of TLR4 before injury may activate adaptive response in heart (42). Therefore, in the present study, we proposed to find the effect of TLR4 modulation on hypertrophied heart.

Toll-like receptor 4 was observed to be perturbed in many cardiac diseases including diabetic and hypertrophic cardiomyopathy (43). This dysregulation in the expression of TLR4 suggests that intact immunity of the heart is deliberately imbalanced, which may lead to increased response toward DAMPs. Protein and gene expression of TLR4 was significantly increased in cardiac hypertrophy. In the present study, we used isoproterenol-induced cardiac hypertrophy model as used in previous studies (44, 45). Isoproterenol is a sympathetic beta receptor agonist, and when administered parenterally, mimics catecholamine's action on heart. Catecholamine-induced cardiac hypertrophy is a class of "stress induced or anxiety induced hypertrophy" (46). Stress and anxiety leads to increased catecholamine's in body. Prolonged exposure to high level of catecholamine's leads to cardiac hypertrophy (47). This model is more correlated with today's stressful lifestyle. Similar to other studies, we found increased heart weight/body weight ratio, gene expression of ANP, collagen, and beta MHC, which are the markers of cardiac hypertrophy along with increased cardiomyocytes size in cardiac hypertrophy. Administration of TLR4 inhibitor (RS) attenuated most of these hypertrophy changes in heart. RS treatment in hypertrophy animals proved to be effective to revert the changes in cardiac system caused by isoproterenol. This improved cardiac health was also supported by ECG analysis. ISO administration in rats increased QT interval as well as R wave amplitude, which are the indications of left ventricular hypertrophy (48). These perturbations were restored toward normal with RS treatment. Whereas, TLR4 agonist (LPS + ISO) does not show any improvement in hypertrophy markers and ECG parameters. This indicates that TLR4 inhibitor could terminate the cardiac hypertrophy complications and its progression. However, there was no improvement of all these parameters in TLR4 agonist (LPS)-treated hypertrophy heart. Increased cardiac inflammation was successfully attenuated with RS treatment as indicated by IL-6 gene expression. LPS-treated

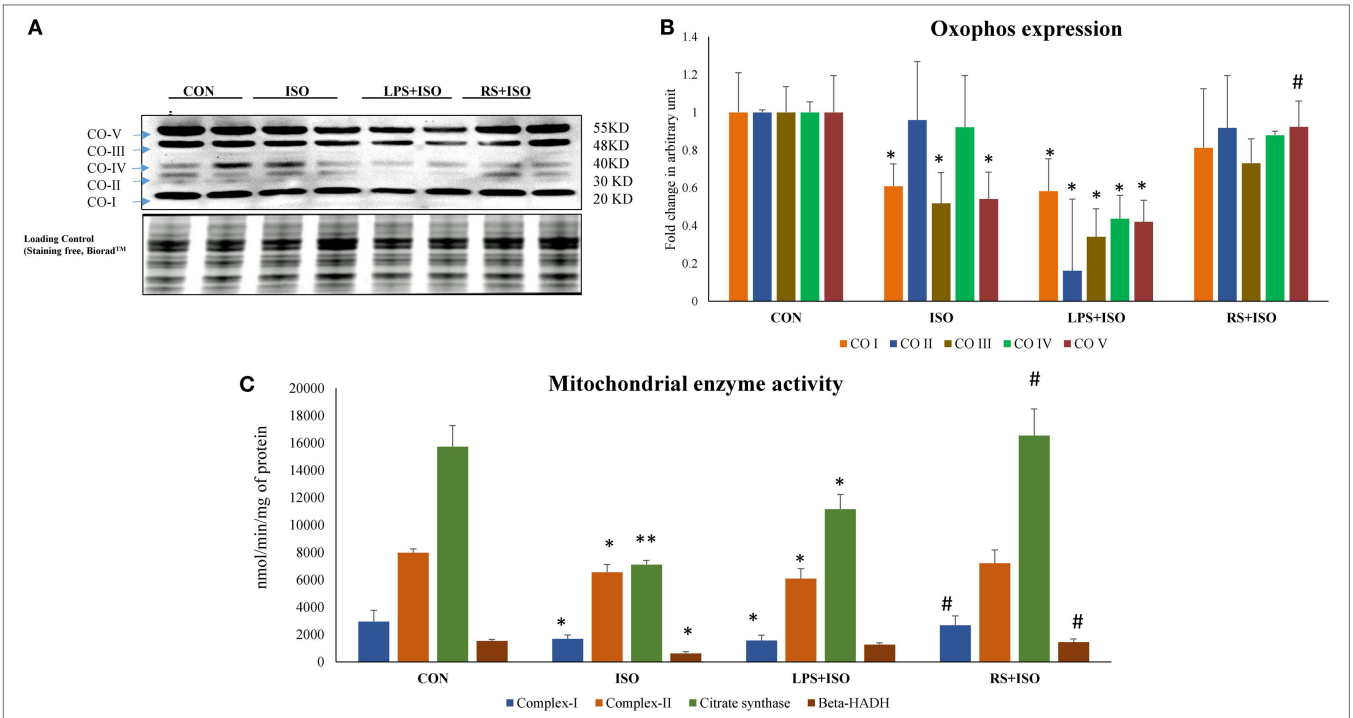

FIGURE 6 | Protein expression of mitochondrial complexes and their activity in hypertrophic rat heart and effect of toll-like receptor 4 (TLR4) modulation. **(A)** Protein expression of mitochondrial complexes, **(B)** fold change in expression of mitochondrial complexes (I–V) in all study groups. Whole gel stain was used for loading control, **(C)** mitochondrial metabolic enzymes activity in hypertrophic rat heart and effect of TLR4 modulation. (I) complex-I: NADH dehydrogenase, (II) complex-II: succinate dehydrogenase, (III) citrate synthase (IV) β-hydroxy acylcoA dehydrogenase. Data shown as mean ± SEM ($N = 4$ for activity and $N = 3$ for western blot) $^{*}p < 0.05$, $^{**}p < 0.01$ vs Con; $^{\#}p < 0.05$, $^{\#\#}p < 0.01$ vs ISO groups.

hearts were exposed to higher level of inflammation as compared to ISO- and RS-treated hearts.

Cardiac hypertrophy is often associated with alteration of cardiomyocyte redox balance. To analyze the redox system in all groups, we have measured myocardial lipid peroxidation and endogenous antioxidants like SOD, catalase, GR, and GPx activity and reduced glutathione (GSH) levels. Cardiac lipid peroxidation was found to be increased and activity of all antioxidant enzymes was decreased in ISO heart as compared to CON. RS treatment in ISO animals prevented these detrimental perturbations in redox system. However, LPS did not restore the disturbed redox balance in ISO animals.

We then assessed mitochondrial health to find out the source of redox imbalance and found wide perturbations in the ISO group, which were ameliorated with RS treatment. To confirm the role of TLR4 on mitochondrial function in cardiac hypertrophy, we have analyzed the protein expression of ETC complexes in heart of these animals. Protein expression of complex-I, III, and V was significantly decreased in ISO heart as compared to control. LPS treatment in ISO animals further reduced the mitochondrial protein expression of these complexes. RS treatment in ISO animals (RS + ISO) retained the mitochondrial complexes protein expression to normal as compared to ISO animals. Our data also suggest that mitochondrial enzyme activity is the direct outcome of TLR4 modulation. The activity of complex I and II, citrate synthase, an important enzyme from TCA cycle and 3-hydroxyacyl-CoA dehydrogenase from beta-oxidation pathway in hearts were found to be significantly decreased in ISO animals. RS treatment in hypertrophy animals (RS + ISO) preserved the activity of these enzymes. However, data suggest that LPS (TLR4 agonist) treatment did not improve the mitochondrial health and function of ETC in ISO heart and even aggravated the dysfunction in few instances. This shows the role of TLR4 in regulating mitochondrial function, which is supported with previous literature (49, 50).

Myocardial protein expression of p65 NF-κB and NRF2 were significantly increased in ISO heart. Although increased NFκB signifies increased inflammatory response in cardiomyocytes, increased level of NRF2 may signify a state of cell where defense mechanism initiated to overcome increased oxidative stress. RS treatment attenuated the oxidative stress in the cell and hence the expression of p65 NF-κB and NRF2. This indicates decreased induction of inflammation in heart due to decreased activation of TLR4. Whereas, LPS further increased the p65 NF-κB and NRF2 expression indicating further enhanced inflammation in heart. In heart, SOD is the primary defense against ROS (51). Approximately 70% SOD activity in the heart and 90% that in cardiomyocytes is contributed by MnSOD (52). The reduced level of MnSOD in hypertrophy heart is the indication of increased mitochondrial oxidative stress. Mitochondrial oxidative stress was further increased with LPS treatment in hypertrophy heart. RS treatment successfully restored decreased level of MnSOD in mitochondria. This decrease in oxidative stress could be one of the reason behind improved mitochondrial health after RS treatment in hypertrophy heart.

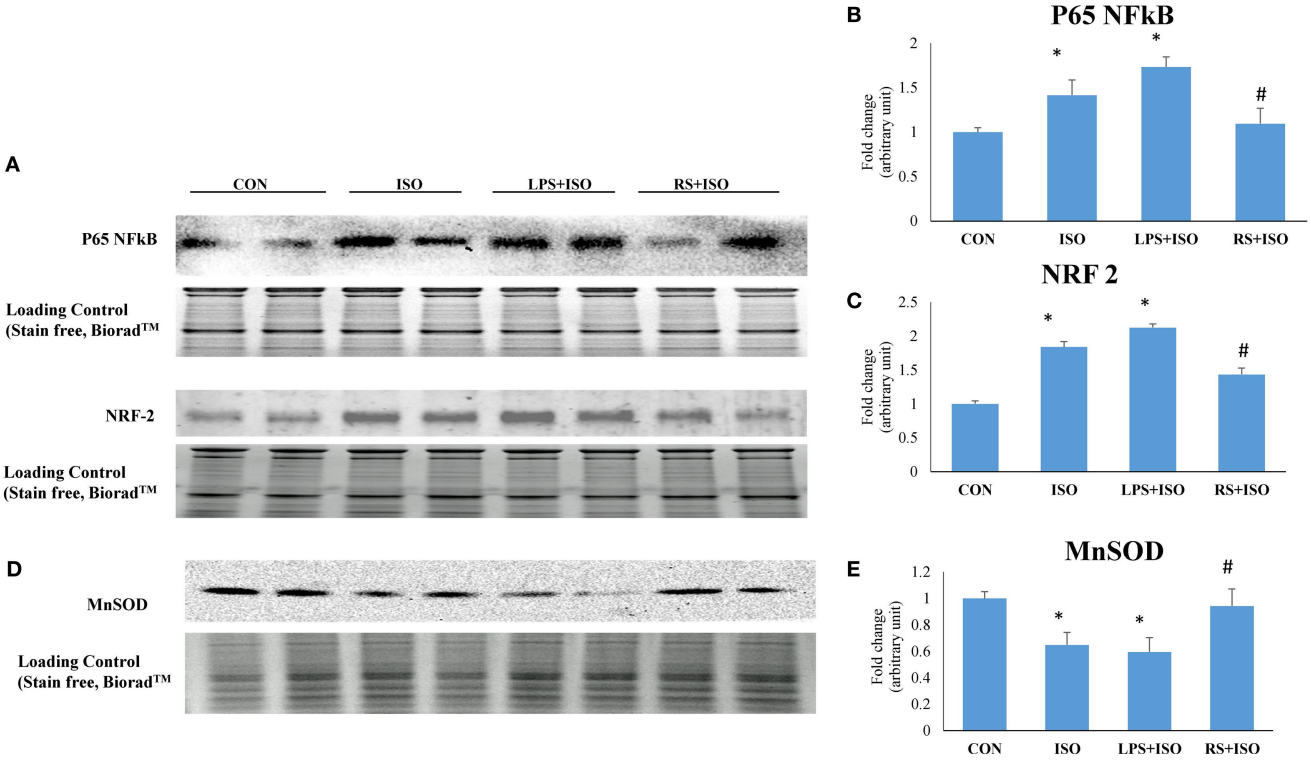

FIGURE 7 | Protein expression of p65 NF-κB, NRF2, and MnSOD in hypertrophic rat heart and effect of toll-like receptor 4 modulation. **(A)** Protein expression of p65 NF-κB and NRF2, **(B)** fold change in p65 NF-κB protein expression, **(C)** fold change in NRF2 protein expression, **(D)** protein expression of MnSOD, **(E)** fold change in MnSOD protein expression. Whole gel stain was used for loading control. Data shown as mean ± SEM ($N = 3$) $^{*}p < 0.05$, $^{**}p < 0.01$ vs CON; $^{\#}p < 0.05$, $^{\#\#}p < 0.01$ vs ISO groups.

In general, cellular damage that occurs during stress and tissue injuries is often accompanied with mitochondrial dysfunction, followed by cellular apoptosis associated with release of mitochondria-derived components (42, 53, 54). It is clear that certain amount of tissue apoptosis and cellular factors turnover occurs during normal physiology. However, the amount of TLR4 ligands pool in such cases is most likely to be below the threshold level to initiate an inflammatory cascade (55). However, during pathological state like mitochondrial dysfunction, mitochondrion releases high-affinity endogenous TLR4 ligands and induces TLR4-mediated inflammation (56). Oxidative stress induced cardiac injury, a result of mitochondrial dysfunction, may lead to the release of these endogenous TLR4 ligands that bind with TLR4 and initiate the inflammatory cascade. This increased TLR4 activation due to DAMP released from mitochondria may lead to excessive cardiomyocyte damage in a state of cardiac hypertrophy.

CONCLUSION

We found increased cardiac TLR4 expression along with increased oxidative stress and mitochondrial dysfunction in hypertrophy heart. We have demonstrated that having increased TLR4 ligand pool (LPS) during cardiac hypertrophy may accelerate the disease progression and aggravate the disease agony. Our data showed that inhibition of TLR4 in hypertrophy group attenuated cardiac hypertrophy through restoring cardiac redox balance and mitochondrial dysfunction. Further studies are required to connect the missing link between the role of TLR4 in mitochondrial dysfunction and cardiac hypertrophy.

ETHICS STATEMENT

All experiments involving animals were undertaken with the approval of Institutional Animal Ethical Committee of Indian Institute of Chemical Technology, Hyderabad.

AUTHOR CONTRIBUTIONS

PK and PB carried out animal experimentation, biochemical and molecular estimation, and statistical analysis of results. AD did the histopathological examination of heart tissue. PK and SB conceived the study, and participated in its design, coordination, and drafted the manuscript. The authors read and approved the manuscript.

ACKNOWLEDGMENTS

We thank Miss Hina Lateef Nizami for careful reading of the manuscript and thoughtful suggestions.

FUNDING

We are thankful to THSTI for providing core fund for this research. We are thankful to ICMR and CSIR for providing senior research fellowship to PK and PB, respectively.

SUPPLEMENTARY MATERIAL

The Supplementary Material for this article can be found online at http://journal.frontiersin.org/article/10.3389/fimmu.2017.00719/full#supplementary-material.

REFERENCES

1. Mann DL. Stress activated cytokines and the heart. *Cytokine Growth Factor Rev* (1996) 7(4):341–54. doi:10.1016/S1359-6101(96)00043-3
2. Frey N, Katus HA, Olson EN, Hill JA. Hypertrophy of the heart. *Circulation* (2004) 109(13):1580–9. doi:10.1161/01.CIR.0000120390.68287.BB
3. Katare BP, Banerjee SK. Repositioning of drugs in cardiometabolic disorders: importance and current scenario. *Curr Top Med Chem* (2016) 16(19): 2189–200. doi:10.2174/1568026616666160216152138
4. Levy D. Left ventricular hypertrophy. *Drugs* (1988) 35(5):1–5. doi:10.2165/00003495-198800355-00002
5. Thom T, Haase N, Rosamond W, Howard VJ, Rumsfeld J, Manolio T, et al. Heart disease and stroke statistics – 2006 update: a report from the American Heart Association statistics committee and stroke statistics subcommittee. *Circulation* (2006) 113(6):e85. doi:10.1161/CIRCULATIONAHA.105.171600
6. Takeuchi O, Akira S. Pattern recognition receptors and inflammation. *Cell* (2010) 140(6):805–20. doi:10.1016/j.cell.2010.01.022
7. Guo J, Friedman SL. Toll-like receptor 4 signaling in liver injury and hepatic fibrogenesis. *Fibrogenesis Tissue Repair* (2010) 3(1):21. doi:10.1186/1755-1536-3-21
8. Timmers L, Sluijter JP, van Keulen JK, Hoefer IE, Nederhoff MG, Goumans M-J, et al. Toll-like receptor 4 mediates maladaptive left ventricular remodeling and impairs cardiac function after myocardial infarction. *Circ Res* (2008) 102(2):257–64. doi:10.1161/CIRCRESAHA.107.158220
9. Li X, Jiang S, Tapping RI. Toll-like receptor signaling in cell proliferation and survival. *Cytokine* (2010) 49(1):1–9. doi:10.1016/j.cyto.2009.08.010
10. Tavener SA, Long EM, Robbins SM, McRae KM, Van Remmen H, Kubes P. Immune cell toll-like receptor 4 is required for cardiac myocyte impairment during endotoxemia. *Circ Res* (2004) 95(7):700–7. doi:10.1161/01.RES.0000144175.70140.8c
11. Drosatos K, Lymperopoulos A, Kennel PJ, Pollak N, Schulze PC, Goldberg IJ. Pathophysiology of sepsis-related cardiac dysfunction: driven by inflammation, energy mismanagement, or both? *Curr Heart Fail Rep* (2015) 12(2): 130–40. doi:10.1007/s11897-014-0247-z
12. Oyama J-I, Blais C, Liu X, Pu M, Kobzik L, Kelly RA, et al. Reduced myocardial ischemia-reperfusion injury in toll-like receptor 4-deficient mice. *Circulation* (2004) 109(6):784–9. doi:10.1161/01.CIR.0000112575.66565.84
13. Avlas O, Bragg A, Fuks A, Nicholson JD, Farkash A, Porat E, et al. TLR4 expression is associated with left ventricular dysfunction in patients undergoing coronary artery bypass surgery. *PLoS One* (2015) 10(6):e0120175. doi:10.1371/journal.pone.0120175
14. Kaczorowski DJ, Nakao A, McCurry KR, Billiar TR. Toll-like receptors and myocardial ischemia/reperfusion, inflammation, and injury. *Curr Cardiol Rev* (2009) 5(3):196–202. doi:10.2174/157340309788970405
15. Van Tassell BW, Seropian IM, Toldo S, Salloum FN, Smithson L, Varma A, et al. Pharmacologic inhibition of myeloid differentiation factor 88 (MyD88) prevents left ventricular dilation and hypertrophy after experimental acute myocardial infarction in the mouse. *J Cardiovasc Pharmacol* (2010) 55(4):385–90. doi:10.1097/FJC.0b013e3181d3da24
16. Ha T, Li Y, Hua F, Ma J, Gao X, Kelley J, et al. Reduced cardiac hypertrophy in toll-like receptor 4-deficient mice following pressure overload. *Cardiovasc Res* (2005) 68(2):224–34. doi:10.1016/j.cardiores.2005.05.025
17. Ehrentraut H, Ehrentraut SF, Boehm O, El Aissati S, Foltz F, Goelz L, et al. Tlr4 deficiency protects against cardiac pressure overload induced hyperinflammation. *PLoS One* (2015) 10(11):e0142921. doi:10.1371/journal.pone.0142921
18. Ehrentraut H, Weber C, Ehrentraut S, Schwederski M, Boehm O, Knuefermann P, et al. The toll-like receptor 4-antagonist eritoran reduces murine cardiac hypertrophy. *Eur J Heart Fail* (2011) 13(6):602–10. doi:10.1093/eurjhf/hfr035
19. Dange RB, Agarwal D, Teruyama R, Francis J. Toll-like receptor 4 inhibition within the paraventricular nucleus attenuates blood pressure and inflammatory response in a genetic model of hypertension. *J Neuroinflammation* (2015) 12(1):31. doi:10.1186/s12974-015-0242-7
20. Dange RB, Agarwal D, Masson GS, Vila J, Wilson B, Nair A, et al. Central blockade of TLR4 improves cardiac function and attenuates myocardial inflammation in angiotensin II-induced hypertension. *Cardiovasc Res* (2014) 103(1):17–27. doi:10.1093/cvr/cvu067
21. Vuda M, Chiusa M, Jakob S, Takala J, Zuppinger C, Djafarzadeh S. Lipopolysaccharide induces mitochondrial dysfunction in rat cardiac microvascular endothelial cells. *Crit Care* (2011) 15:1–190. doi:10.1186/cc9665
22. Lu Z, Zhang X, Li Y, Lopes-Virella MF, Huang Y. TLR4 antagonist attenuates atherogenesis in LDL receptor-deficient mice with diet-induced type 2 diabetes. *Immunobiology* (2015) 220(11):1246–54. doi:10.1016/j.imbio.2015.06.016
23. Khatua TN, Borkar RM, Mohammed SA, Dinda AK, Srinivas R, Banerjee SK. Novel sulfur metabolites of garlic attenuate cardiac hypertrophy and remodeling through induction of Na+/K+-ATPase expression. *Front Pharmacol* (2017) 8:18. doi:10.3389/fphar.2017.00018
24. Bagul PK, Dinda A, Banerjee SK. Effect of resveratrol on sirtuins expression and cardiac complications in diabetes. *Biochem Biophys Res Commun* (2015) 468(1):221–7. doi:10.1016/j.bbrc.2015.10.126
25. Ohkawa H, Ohishi N, Yagi K. Assay for lipid peroxides in animal tissues by thiobarbituric acid reaction. *Anal Biochem* (1979) 95(2):351–8. doi:10.1016/0003-2697(79)90738-3
26. Maity P, Bindu S, Dey S, Goyal M, Alam A, Pal C, et al. Indomethacin, a non-steroidal anti-inflammatory drug, develops gastropathy by inducing reactive oxygen species-mediated mitochondrial pathology and associated apoptosis in gastric mucosa a novel role of mitochondrial aconitase oxidation. *J Biol Chem* (2009) 284(5):3058–68. doi:10.1074/jbc.M805329200
27. Banerjee SK, Dinda AK, Manchanda SC, Maulik SK. Chronic garlic administration protects rat heart against oxidative stress induced by ischemic reperfusion injury. *BMC Pharmacol* (2002) 2:16. doi:10.1186/1471-2210-2-16
28. Bagul PK, Deepthi N, Sultana R, Banerjee SK. Resveratrol ameliorates cardiac oxidative stress in diabetes through deacetylation of NFkB-p65 and histone 3. *J Nutr Biochem* (2015) 26(11):1298–307. doi:10.1016/j.jnutbio.2015.06.006
29. Hoegger MJ, Lieven CJ, Levin LA. Differential production of superoxide by neuronal mitochondria. *BMC Neurosci* (2008) 9(1):4. doi:10.1186/1471-2202-9-4
30. Trounce IA, Kim YL, Jun AS, Wallace DC. [42] Assessment of mitochondrial oxidative phosphorylation in patient muscle biopsies, lymphoblasts, and transmitochondrial cell lines. *Methods Enzymol* (1996) 264:484–509. doi:10.1016/S0076-6879(96)64044-0
31. Shepherd D, Garland P. The kinetic properties of citrate synthase from rat liver mitochondria. *Biochem J* (1969) 114(3):597–610. doi:10.1042/bj1140597
32. Oppermann UC, Salim S, Tjernberg LO, Terenius L, Jörnvall H. Binding of amyloid β-peptide to mitochondrial hydroxyacyl-CoA dehydrogenase (ERAB): regulation of an SDR enzyme activity with implications for apoptosis in Alzheimer's disease. *FEBS Lett* (1999) 451(3):238–42. doi:10.1016/S0014-5793(99)00586-4
33. Bagul PK, Middela H, Matapally S, Padiya R, Bastia T, Madhusudana K, et al. Attenuation of insulin resistance, metabolic syndrome and hepatic oxidative stress by resveratrol in fructose-fed rats. *Pharmacol Res* (2012) 66(3):260–8. doi:10.1016/j.phrs.2012.05.003
34. Helms SA, Azhar G, Zuo C, Theus SA, Bartke A, Wei JY. Smaller cardiac cell size and reduced extra-cellular collagen might be beneficial for hearts of Ames dwarf mice. *Int J Biol Sci* (2010) 6(5):475–90. doi:10.7150/ijbs.6.475
35. Chowdhury D, Tangutur AD, Khatua TN, Saxena P, Banerjee SK, Bhadra MP. A proteomic view of isoproterenol induced cardiac hypertrophy: prohibitin

identified as a potential biomarker in rats. *J Transl Med* (2013) 11(1):130. doi:10.1186/1479-5876-11-130
36. Smith RM, Lecour S, Sack MN. Innate immunity and cardiac preconditioning: a putative intrinsic cardioprotective program. *Cardiovasc Res* (2002) 55(3):474–82. doi:10.1016/S0008-6363(02)00288-2
37. Suresh R, Mosser DM. Pattern recognition receptors in innate immunity, host defense, and immunopathology. *Adv Physiol Educ* (2013) 37(4):284–91. doi:10.1152/advan.00058.2013
38. De Haan J, Smeets M, Pasterkamp G, Arslan F. Danger signals in the initiation of the inflammatory response after myocardial infarction. *Mediators Inflamm* (2013) 2013:206039. doi:10.1155/2013/206039
39. Zhang W, Lavine KJ, Epelman S, Evans SA, Weinheimer CJ, Barger PM, et al. Necrotic myocardial cells release damage-associated molecular patterns that provoke fibroblast activation in vitro and trigger myocardial inflammation and fibrosis in vivo. *J Am Heart Assoc* (2015) 4(6):e001993. doi:10.1161/JAHA.115.001993
40. Srikrishna G, Freeze HH. Endogenous damage-associated molecular pattern molecules at the crossroads of inflammation and cancer. *Neoplasia* (2009) 11(7):615–28. doi:10.1593/neo.09284
41. Epelman S, Liu PP, Mann DL. Role of innate and adaptive immune mechanisms in cardiac injury and repair. *Nat Rev Immunol* (2015) 15(2):117–29. doi:10.1038/nri3800
42. Yi H, Patel AK, Sodhi CP, Hackam DJ, Hackam AS. Novel role for the innate immune receptor toll-like receptor 4 (TLR4) in the regulation of the Wnt signaling pathway and photoreceptor apoptosis. *PLoS One* (2012) 7(5):e36560. doi:10.1371/journal.pone.0036560
43. Katare P, Khatua TN, Bagul P, Adela R, Banerjee SK, editors. Expression and regulation of Tlr-4 in hypertrophic and diabetic cardiomyopathy. *Indian J Pharmacol* (2013) 45: S157–58.
44. Ennis IL, Escudero EM, Console GM, Camihort G, Dumm CG, Seidler RW, et al. Regression of isoproterenol-induced cardiac hypertrophy by Na+/H+ exchanger inhibition. *Hypertension* (2003) 41(6):1324–9. doi:10.1161/01.HYP.0000071180.12012.6E
45. Yang L, Cai X, Liu J, Jia Z, Jiao J, Zhang J, et al. CpG-ODN attenuates pathological cardiac hypertrophy and heart failure by activation of PI3Kα-Akt signaling. *PLoS One* (2013) 8(4):e62373. doi:10.1371/journal.pone.0062373
46. Banerjee S, Sood S, Dinda A, Das T, Maulik S. Chronic oral administration of raw garlic protects against isoproterenol-induced myocardial necrosis in rat. *Comp Biochem Physiol C Toxicol Pharmacol* (2003) 136(4):377–86. doi:10.1016/j.cca.2003.10.011
47. Rapacciuolo A, Esposito G, Caron K, Mao L, Thomas SA, Rockman HA. Important role of endogenous norepinephrine and epinephrine in the development of in vivo pressure-overload cardiac hypertrophy. *J Am Coll Cardiol* (2001) 38(3):876–82. doi:10.1016/S0735-1097(01)01433-4
48. Wagner GS, Macfarlane P, Wellens H, Josephson M, Gorgels A, Mirvis DM, et al. AHA/ACCF/HRS recommendations for the standardization and interpretation of the electrocardiogram. *Circulation* (2009) 119(10):e262–70. doi:10.1161/CIRCULATIONAHA.108.191098
49. Wu Y, Frisard M, Shabrokh E, Voelker K, McMilian RP, Hulver MW. The role of toll-like receptor 4 in mitochondrial function and reactive oxygen species (ROS) production in skeletal muscle. *FASEB J* (2011) 25(1 Suppl): 1051.22.
50. McMillan RP, Wu Y, Voelker K, Fundaro G, Kavanaugh J, Stevens JR, et al. Selective overexpression of toll-like receptor-4 in skeletal muscle impairs metabolic adaptation to high-fat feeding. *Am J Physiol Regul Integr Comp Physiol* (2015) 309(3):R304–13. doi:10.1152/ajpregu.00139.2015
51. Pham-Huy LA, He H, Pham-Huy C. Free radicals, antioxidants in disease and health. *Int J Biomed Sci* (2008) 4(2):89–96.
52. Sawyer DB, Siwik DA, Xiao L, Pimentel DR, Singh K, Colucci WS. Role of oxidative stress in myocardial hypertrophy and failure. *J Mol Cell Cardiol* (2002) 34(4):379–88. doi:10.1006/jmcc.2002.1526
53. Testro AG, Visvanathan K. Toll-like receptors and their role in gastrointestinal disease. *J Gastroenterol Hepatol* (2009) 24(6):943–54. doi:10.1111/j.1440-1746.2009.05854.x
54. Wang X, Sharma RK, Sikka SC, Thomas AJ, Falcone T, Agarwal A. Oxidative stress is associated with increased apoptosis leading to spermatozoa DNA damage in patients with male factor infertility. *Fertil Steril* (2003) 80(3):531–5. doi:10.1016/S0015-0282(03)00756-8
55. Rakoff-Nahoum S, Medzhitov R. Role of toll-like receptors in tissue repair and tumorigenesis. *Biochemistry (Mosc)* (2008) 73(5):555–61. doi:10.1134/S0006297908050088
56. Nicholas SA, Coughlan K, Yasinska I, Lall GS, Gibbs BF, Calzolai L, et al. Dysfunctional mitochondria contain endogenous high-affinity human toll-like receptor 4 (TLR4) ligands and induce TLR4-mediated inflammatory reactions. *Int J Biochem Cell Biol* (2011) 43(4):674–81. doi:10.1016/j.biocel.2011.01.012

Conflict of Interest Statement: The authors declare that the research was conducted in the absence of any commercial or financial relationships that could be construed as a potential conflict of interest.

Copyright © 2017 Katare, Bagul, Dinda and Banerjee. This is an open-access article distributed under the terms of the Creative Commons Attribution License (CC BY). The use, distribution or reproduction in other forums is permitted, provided the original author(s) or licensor are credited and that the original publication in this journal is cited, in accordance with accepted academic practice. No use, distribution or reproduction is permitted which does not comply with these terms.

frontiers in Immunology

ORIGINAL RESEARCH
published: 07 July 2017
doi: 10.3389/fimmu.2017.00785

Asiatic Acid Exhibits Anti-inflammatory and Antioxidant Activities against Lipopolysaccharide and D-Galactosamine-Induced Fulminant Hepatic Failure

*Hongming Lv[1,2†], Zhimin Qi[1,2†], Sisi Wang[1], Haihua Feng[1,2], Xuming Deng[1,2] and Xinxin Ci[1]**

[1] Department of Translational Medicine, The First Hospital of Jilin University, Changchun, China, [2] Key Laboratory of Zoonosis, Ministry of Education, College of Veterinary Medicine, Jilin University, Changchun, China

OPEN ACCESS

Edited by:
Jixin Zhong,
Case Western Reserve University, United States

Reviewed by:
Yonglin Chen,
Yale University, United States
Xuhui Feng,
Indiana University System, United States
Ping Chen,
Georgetown University School of Medicine, United States

***Correspondence:**
Xinxin Ci
cixinxin@jlu.edu.cn,
xinxinci520@163.com

†These authors have contributed equally to this work.

Specialty section:
This article was submitted to Inflammation, a section of the journal Frontiers in Immunology

Received: 30 March 2017
Accepted: 21 June 2017
Published: 07 July 2017

Citation:
Lv H, Qi Z, Wang S, Feng H, Deng X and Ci X (2017) Asiatic Acid Exhibits Anti-inflammatory and Antioxidant Activities against Lipopolysaccharide and D-Galactosamine-Induced Fulminant Hepatic Failure. Front. Immunol. 8:785. doi: 10.3389/fimmu.2017.00785

Inflammation and oxidative stress are essential for the pathogenesis of fulminant hepatic failure (FHF). Asiatic acid (AA), which is a pentacyclic triterpene that widely occurs in various vegetables and fruits, has been reported to possess antioxidant and anti-inflammatory properties. In this study, we investigated the protective effects of AA against lipopolysaccharide (LPS) and D-galactosamine (GalN)-induced FHF and the underlying molecular mechanisms. Our findings suggested that AA treatment effectively protected against LPS/D-GalN-induced FHF by lessening the lethality; decreasing the alanine transaminase and aspartate aminotransferase levels, interleukin (IL)-1β, IL-6, and tumor necrosis factor-α production, malondialdehyde formation, myeloperoxidase level and reactive oxygen species generation (i.e., H_2O_2, NO, and O_2^-), and increasing the glutathione and superoxide dismutase contents. Moreover, AA treatment significantly inhibited mitogen-activated protein kinase (MAPK) and nuclear factor-kappa B (NF-κB) signaling pathway activation *via* the partial induction of programmed cell death 4 (PDCD4) protein expressions, which are involved in inflammatory responses. Furthermore, AA treatment dramatically induced the expression of the glutamate-cysteine ligase modifier subunit, the glutamate-cysteine ligase catalytic subunit, heme oxygenase-1, and NAD (P) H: quinoneoxidoreductase 1 (NQO1), which are largely dependent on activation of the nuclear factor-erythroid 2-related factor 2 (Nrf2) through the induction of AMP-activated protein kinase (AMPK) and glycogen synthase kinase-3β (GSK3β) phosphorylation. Accordingly, AA exhibited protective roles against LPS/D-GalN-induced FHF by inhibiting oxidative stress and inflammation. The underlying mechanism may be associated with the inhibition of MAPK and NF-κB activation *via* the partial induction of PDCD4 and upregulation of Nrf2 in an AMPK/GSK3β pathway activation-dependent manner.

Keywords: asiatic acid, inflammation, oxidative stress, fulminant hepatic failure, AMPK/Nrf2, PDCD4

INTRODUCTION

The liver is a vital organ that is vulnerable to multiple factors, including alcohol, chemical substances, oxidative products, and the hepatitis viruses, which lead to hepatic failure (1). Fulminant hepatic failure (FHF) is a life-threatening and fatal clinical syndrome that is associated with a poor prognosis and high mortality (2). The lipopolysaccharide (LPS) and D-galactosamine

(GalN)-induced animal model of FHF is strongly relevant to human liver failure and has been widely used to investigate the mechanisms and potential therapeutic drugs for clinical FHF (3). Increasing evidence has shown that oxidative stress and inflammatory responses are two important pathogenic factors that contribute to LPS/D-GalN-induced FHF (4). Consequently, inhibiting inflammation and/or oxidative stress may be potential prevention measures for the development of FHF.

Previous abundant reports have shown that LPS/GalN-induced FHF, which is a type of toxin-induced liver injury, is dependent upon macrophage-derived inflammatory cytokines, such as interleukin (IL)-1β, IL-6, and tumor necrosis factor (TNF)-α. These cytokines are regulated by the activation of multiple signaling pathways, including toll-like receptor 4-mediated mitogen-activated protein kinase (MAPK); this pathway includes the c-Jun NH2-terminal kinase (JNK), extracellular signal-regulated kinase (ERK), p38, and nuclear factor-kappa B (NF-κB), which comprise the p50/p65 and the inhibitor of κB (IκB) protein signaling pathways (5, 6). Importantly, the tumor suppressor programmed cell death-4 (PDCD4) gene, which was initially regarded as an upregulated gene during apoptosis, is universally expressed in normal tissues, with the highest levels found in the liver (7). Additionally, PDCD4 can mediate inflammatory responses that play essential roles in the amelioration of LPS/D-GalN-induced acute liver injury *via* inhibition of MAPK and NF-κB pathway activation (8). More intriguingly, apart from inflammatory responses, the excessive accumulation of reactive oxygen species (ROS) is recognized to a possible mechanism of D-GalN/LPS-induced FHF (9). ROS overproduction not only directly triggers oxidative damage but also activates the MAPK and NF-κB signaling pathways, resulting in inflammatory responses that further stimulate inflammatory injury (10, 11). Furthermore, nuclear factor erythroid 2-related factor 2 (Nrf2), which is a key transcription factor that is required to ameliorate various oxidative stress- and inflammation-associated diseases, regulates the expression of various antioxidant genes, including heme oxygenase-1 (HO-1), NAD (P) H: quinoneoxidoreductase 1 (NQO1), and the glutamate-cysteine ligase modifier (GCLM) and glutamate-cysteine ligase catalytic (GCLC) subunit (12, 13). Previously, several reports implied that Nrf2 activation played vital roles in the pathogenesis of liver injury both *in vitro* and *in vivo* (14). To date, Nrf2 activation has been reported to be regulated by the AMP-activated protein kinase (AMPK) and subsequent inactivation of glycogen synthase kinase-3β (GSK-3β) (15, 16). Accumulating evidence has shown that various natural products, including phenols, coumarins, triterpenoid, flavonoids, and alkaloids protect against hepatic diseases through activation of the Nrf2 pathway (17, 18). Asiatic acid (AA) (**Figure 1A**) is a pentacyclic triterpene that widely occurs in many vegetables and fruits and has been reported to possess a variety of biological activities, including antioxidant and anti-inflammatory properties (19, 20). AA has been reported to reduce the pulmonary inflammation induced by cigarette smoking and inhibit liver fibrosis by blocking TGF-beta/Smad signaling *in vivo* and *in vitro* (21, 22). In this study, we explored whether AA attenuation of LPS/D-GalN-induced hepatotoxicity was associated with the induction of AMPK/GSK3β-Nrf2 and PDCD4. Our results indicated that AA treatment attenuated LPS/D-GalN-induced hepatotoxicity and inhibited inflammatory responses and oxidative stress, which possibly involved in the suppression of MAPK and NF-κB activation *via* the partial induction of PDCD4 and upregulation of Nrf2 in an AMPK/GSK3β pathway activation-dependent manner.

MATERIALS AND METHODS

Reagents and Chemical

Asiatic acid, purity >98%, was provided by the Chengdu Herbpurify Co., Ltd (Chengdu, China). LPS (*Escherichia coli* 055:B5), GalN, and dimethyl sulfoxide were purchased from Sigma-Aldrich (St. Louis, MO, USA). Inhibitors of AMPK (Compound C) was offered by Sigma-Aldrich (St. Louis, MO, USA). Fetal bovine serum, Dulbecco's modified Eagle's medium, penicillin, and streptomycin were acquired from Invitrogen-Gibco (Grand Island, NY, USA). Antibodies against Nrf2, GCLC, GCLM, HO-1, NQO1, P-AMPK, AMPK, P-PI3K, PI3K, P-AKT, AKT, P-ERK, ERK, PDCD4, P-P65, P65, IκBα, P-IκBα, and β-actin were obtained from Cell Signaling (Boston, MA, USA) or Abcam (Cambridge, MA, USA). Additionally, O_2^-, H_2O_2, NO, glutathione (GSH), superoxide dismutase (SOD), malondialdehyde (MDA), myeloperoxidase (MPO), and ROS test kits were supplied by Nanjing Jiancheng Bioengineering Institute (Nanjing, China). All other chemicals were offered by Sigma-Aldrich (St. Louis, MO, USA), if not otherwise indicated.

Animals

Female BALB/c mice (6–8 weeks), weighing approximately 18–20 g, were purchased from Liaoning Changsheng Technology Industrial Co., LTD (Certificate SCXK2010-0001; Liaoning, China). All animals were housed in a room with temperature at 24 ± 1°C, a 12 h light–dark cycle and relative humidity about 40–80%. Animals were allowed free access to tap water and normal food after feeding several days. All animal experiments were performed according to the guide for the Care and Use of Laboratory Animals, which was published by the US National Institute of Health. This study was reviewed and approved by the Animal Welfare and Research Ethics Committee at Jilin University.

Experimental Protocol

Mice were randomly divided into seven groups: control (PBS) group, AA only (25 mg/kg) group, LPS/D-GalN (L/D, 30 μg/kg and 600 mg/kg) group, and AA (6.25, 12.5, or 25 mg/kg) + (L/D) group and hemin (a HO-1 inducer as a positive group, 30 mg/kg) + (L/D) group, were administered intraperitoneally. In brief, AA (6.25, 12.5, or 25 mg/kg) or hemin (30 mg/kg) was administered intraperitoneally to mice for twice at a 12-h (interval for 12 h), followed by subjected treatment with LPS (30 μg/kg) and D-GalN (600 mg/kg), which is abbreviated as L/D. The survival rates of mice were observed for 48 h after L/D challenge. For other assays, after L/D administration for 3 and 6 h, the animals were euthanized. Subsequently, liver tissues and serum were harvested and used for hematoxylin and eosin (H&E) staining, Western blot assay, and enzyme-linked immunosorbent assay (ELISA).

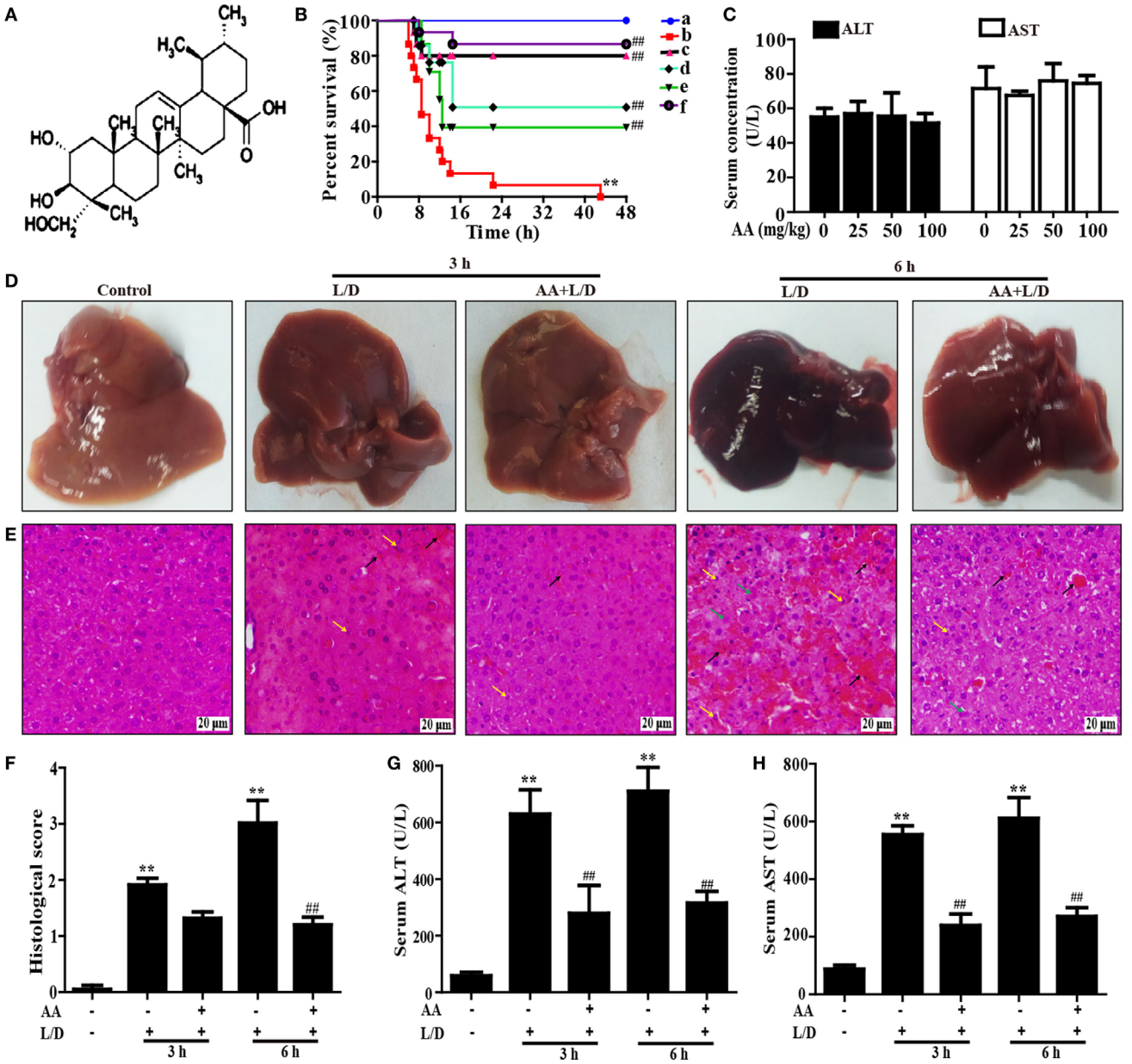

FIGURE 1 | Protective effect of AA treatment on lipopolysaccharide (LPS)/D-galactosamine (GalN)-induced fulminant hepatic failure. **(A)** The chemical structure of asiatic acid (AA). **(B)** AA (6.25, 12.5, or 25 mg/kg) or hemin (30 mg/kg) was administered intraperitoneally to mice for twice at a 12-h (interval for 12 h), followed by subjected treatment with LPS (30 μg/kg) and D-GalN (600 mg/kg), which is abbreviated as L/D. The survival rates of the mice were observed within 48 h after L/D exposure. (a) Control and AA group; (b) L/D group; (c) AA (25 mg/kg) + L/D; (d) AA (12.5 mg/kg) + L/D; (e) AA (6.25 mg/kg) + L/D; (f) hemin (30 mg/kg) + L/D. **(C)** Mice only were given an intraperitoneal injection of AA (0, 25, 50, and 100 mg/kg) and we harvested serum for the analysis of alanine transaminase (ALT) and aspartate aminotransferase (AST) levels at 6 h. **(D)** Livers ($n = 5$) from each experimental group were processed for gross examination of liver at 3 or 6 h after the L/D challenge. **(E)** Representative histological sections of the livers were stained with hematoxylin and eosin (H&E)-stained (magnification 400×, black arrows: hemorrhage; green arrows: necrotic area; yellow arrows: inflammatory cell infiltration). **(F)** The stained sections were graded using a four-point scale from 0 to 3, with 0, 1, 2, and 3 representing no damage, mild damage, moderate damage, and severe damage, respectively. Additionally, sera were collected from the mice after exposure to L/D for 3 and 6 h for measurement of the ALT and AST levels. **(G,H)** Effects of AA on the serum ALT and AST levels. Similar results were obtained from three independent experiments. All data are presented as means ± SEM ($n = 5$ in each group). $^{*}p < 0.05$ and $^{**}p < 0.01$ vs. control group; $^{\#}p < 0.05$ and $^{\#\#}p < 0.01$ vs. L/D group.

Histopathological Evaluation

Liver tissues were immersed in normal 10% neutral buffered formalin and fixed for 48 h, dehydrated in a series of graded ethanol, embedded in paraffin wax, and cut into 5-μm-thick sections. The paraffin-embedded sections were stained with hematoxylin and eosin (H&E) for pathological analysis under a light microscope. The histological changes were evaluated by a point-counting method for severity of hepatic injury using an ordinal scales in

accordance with the methods as previous described (23). Briefly, H&E-stained sections were evaluated at 400× magnification by a point-counting method for severity of hepatic injury using an ordinal scale as follows; grade 0: minimal or no evidence of injury, grade 1: mild injury consisting in cytoplasmic vacuolation and focal nuclear pyknosis, grade 2: moderate to severe injury with extensive nuclear pyknosis, cytoplasmic hypereosinophilia, and loss of intercellular borders, and grade 3: severe necrosis with disintegration of hepatic cords, hemorrhage, and neutrophil infiltration.

Biochemical Indexes Assay

All mice were euthanized at 3 or 6 h after L/D treatment, liver and blood were collected for biochemical analysis. alanine transaminase (ALT) and aspartate aminotransferase (AST) levels in serum were measured using the corresponding detection kits. In addition, mice liver tissues were homogenized and dissolved in extraction buffer to analyze the MPO, GSH, MDA, and SOD levels according to the manufacturer's instructions. All results were normalized by the total protein concentration in each sample. For other assays, all mice were sacrificed at 3 or 6 h after L/D treatment, liver tissues were collected for measurement of O_2^-, NO, H_2O_2, and ROS generation. Mice liver tissues were homogenized and dissolved in extraction buffer to analyze the O_2^-, NO, H_2O_2, and ROS levels in accordance to the manufacturer's instructions.

ELISA Assay

Blood was obtained from each sample *in vivo*, centrifuged, collected serum for measurement of the TNF-α, IL-6, and IL-1β secretion using an ELISA kit as the manufacturer's instructions (BioLegend, Inc., CA, USA), respectively. The optical density from each well was detected at 450 nm.

Western Blot Analysis

Liver tissues were collected 3 or 6 h after L/D challenge. Total protein was extracted from the liver tissues using a protein extract kit according to the manufacturer's protocol. Protein concentrations were tested by the BCA method. Equal amounts of proteins (20 μg) were separated by a 10% SDS-polyacrylamide gel and transferred onto a polyvinylidene difluoride membrane. The membrane was blocked with 5% (w/v) non-fat milk for 2 h. Then, the membrane was incubated with primary antibody and secondary antibody. Finally, the membranes were visualized by the ECL Western blotting detection system in accordance with the manufacturer's instruction and band intensities were quantified using Image J gel analysis software. All experiments were performed in triplicate.

CRISPR/Cas9 Knockout of Nrf2 Gene (24)

HepG2 cells were cultured in 12-well plates at the density of 3×10^5 cells/well for 24 h. The plasmids of expressing Cas9 with Nrf2-sgRNA and puromycin resistant gene were co-transfected into HepG2 cells using Viafect transfection reagent (Promega). At 48 h after transfection, cells were added puromycin at a concentration of 2 μg/mL and harvested for immunoblotting analysis with Nrf2 antibody. After 7 days, cells were cultured in a 96-well plates (1 cell/well).

Statistical Analysis

All data referenced above were expressed as the means ± SEM and analyzed using SPSS19.0 (IBM). Comparisons between experimental groups were conducted using one-way ANOVA, whereas multiple comparisons were made using the LSD method. Statistical significance was defined as $p < 0.05$ or $p < 0.01$.

RESULTS

AA Treatment Protected Mice against LPS/D-GalN (L/D)-Induced FHF

To investigate whether AA could protect against L/D-induced liver injury in mice, the survival rates of the mice were observed for 48 h after L/D exposure. As shown in **Figure 1B**, the mice died 7 h after L/D injection, and the survival rate was 0% at 48 h. Conversely, pretreatment with AA (25 mg/kg) effectively increased the survival rate up to 80% and no significant difference compared with hemin (a HO-1 inducer) group, a positive group. In addition, because serum AST and ALT levels were used as well-established marker of hepatic injury (25), the serum ALT and AST levels were measured. Our results indicated that no changes in serum levels of ALT and AST were induced by alone AA at various dosages ranging from 0 to 100 mg/kg, indicating that AA did not exhibit hepatotoxicity (**Figure 1C**). Meanwhile, we found that the serum ALT and AST levels were significantly increased by L/D administration compared with the control group ($p < 0.01$). However, this increase was markedly reduced by AA pretreatment, suggesting that AA treatment efficiently protected against L/D-induced FHF (**Figures 1G,H**) ($p < 0.01$). Gross and histological examinations of liver tissues were used to evaluate the protective effects of AA on L/D-induced FHF. As illustrated in **Figure 1D**, gross examination of the livers displayed apparent congestion and hemorrhage in the L/D-induced group mice 6 h after challenge, indicating severe liver injury. Similarly, histological analysis of the mouse liver sections in the L/D group showed obviously disturbed architecture, such as hepatocyte necrosis, hemorrhage, and neutrophil infiltration. However, the L/D-induced liver alterations were effectively relieved by AA treatment based on the liver injury scores (**Figures 1E,F**).

AA Treatment Reduced Inflammatory Responses in Mice with L/D-Induced FHF

The inflammatory cytokines TNF-α, IL-6, and IL-1β play vital roles in liver injury. To further explore the anti-inflammatory effects of AA, the effects of AA on TNF-α, IL-6, and IL-1β generation in the sera was measured by ELISA. As shown in **Figures 2A–C**, L/D effectively increased the secretion of TNF-α, IL-6, and IL-1β ($p < 0.01$) in the sera, whereas AA treatment inhibited the induction of inflammatory cytokine production by L/D ($p < 0.01$).

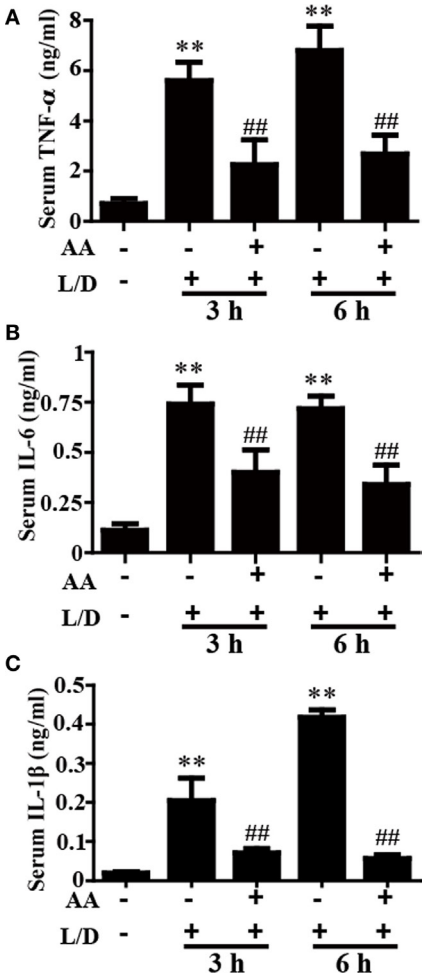

FIGURE 2 | Effect of asiatic acid (AA) treatment on inflammatory cytokines in L/D-induced fulminant hepatic failure. AA (25 mg/kg) was administered intraperitoneally to mice 1 h before L/D pretreatment. **(A–C)** Effects of AA on L/D-induced serum tumor necrosis factor (TNF)-α, interleukin (IL)-6, and IL-1β generation. Similar results were obtained from three independent experiments. All data are presented as means ± SEM ($n = 5$ in each group). $^{*}p < 0.05$ and $^{**}p < 0.01$ vs. control group; $^{\#}p < 0.05$ and $^{\#\#}p < 0.01$ vs. L/D group.

AA Treatment Inhibited the MAPK and NF-κB Activation and Induced PDCD4 Protein Expression in Mice with L/D-Induced FHF

Because the NF-κB and MAPK signaling pathways have been reported to be inflammatory pathways that play imperative roles in mice with L/D-induced FHF, we evaluated the effects of AA treatment on the L/D-induced activation of the NF-κB signaling pathway. As presented in **Figures 3A–H**, AA treatment remarkably inhibited P65, JNK, ERK, and P38 phosphorylation ($p < 0.01$) and blocked IκBα phosphorylation and degradation compared to the L/D-challenged group, suggesting the inhibition of inflammatory responses by AA might be partially responsible for blocking the activation of the NF-κB and MAPK signaling pathways.

Importantly, PDCD4 negatively or positively mediates inflammatory responses, although this topic is still controversial. Wang et al. (26) discovered that PDCD4 deficiency aggravated colitis *via* promoting the IL-6/STAT3 pathway in mice. However, Schmid et al. (27) maintained that inflammation could induce the loss of PDCD4, and Wang et al. (8) indicated that PDCD4 upregulation inhibited inflammatory responses by inhibiting NF-κB and MAPK signaling pathway activation in an LPS/D-GalN-induced mouse model. Therefore, PDCD4 may be closely associated with inflammatory responses. Indeed, we found that the PDCD4 protein expression level was dramatically reduced 3 and 6 h after L/D injection ($p < 0.05$ and $p < 0.01$, respectively) in our studies. Conversely, AA pretreatment effectively restored PDCD4 protein expression (**Figures 3I,J**), indicating that inhibition of the inflammatory responses induced by L/D challenge by AA might be partially attributed to the increased PDCD4 protein expression ($p < 0.01$).

AA Treatment Attenuated L/D-Triggered Oxidative Damage in Mice with FHF

Because oxidative damage is a major factor in mice with L/D-induced FHF, we determined whether AA pretreatment attenuated the L/D-triggered oxidative stress. As shown in **Figure 4**, L/D not only evidently increased MDA formation ($p < 0.05$ or $p < 0.01$), the MPO level ($p < 0.01$), and ROS generation (i.e., H_2O_2, NO, and O_2^- production) ($p < 0.05$ or $p < 0.01$) but also obviously decreased the SOD ($p < 0.05$) and GSH ($p < 0.01$) contents in the livers of the mice. In contrast, AA pretreatment dramatically inhibited these effects induced by L/D ($p < 0.05$ or $p < 0.01$). These observations indicated that AA treatment ameliorated hepatic injury by partially lessening L/D-triggered oxidative stress in mice.

AA Treatment Upregulated the Nrf2 and AMPK/GSK3β Signaling Pathways in Mice with L/D-Induced FHF

Increasing evidence indicates that the Nrf2-mediated signaling pathway is essential for the inhibition of oxidative stress and inflammatory responses in mice with L/D-induced FHF. Therefore, we examined whether the antioxidant and anti-inflammatory activities of AA were related to upregulation of the Nrf2-mediated signaling pathway. The inductions of GCLC, GCLM, HO-1, and NQO1, which are regulated by Nrf2 transcription, have been reported to be a key cellular protective mechanism against the inflammatory response or oxidative stress in various cell types (28, 29). As shown in **Figures 5A–F**, AA treatment remarkably enhanced Nrf2, GCLC, GCLM, HO-1, and NQO1 protein expression compared with the control group and the L/D-exposed group ($p < 0.05$ or $p < 0.01$).

Importantly, previous studies suggested that multiple signaling pathways modulated Nrf2 expression. Our previous study indicated that AA inhibited cellular damage and oxidative stress by regulating Nrf2 signaling dependent upon activation of the AKT and ERK signals in HepG2 cells (24). Accordingly, to investigate the protective mechanism of AA treatment on L/D-induced FHF, the ERK and PI3K/AKT activities were analyzed

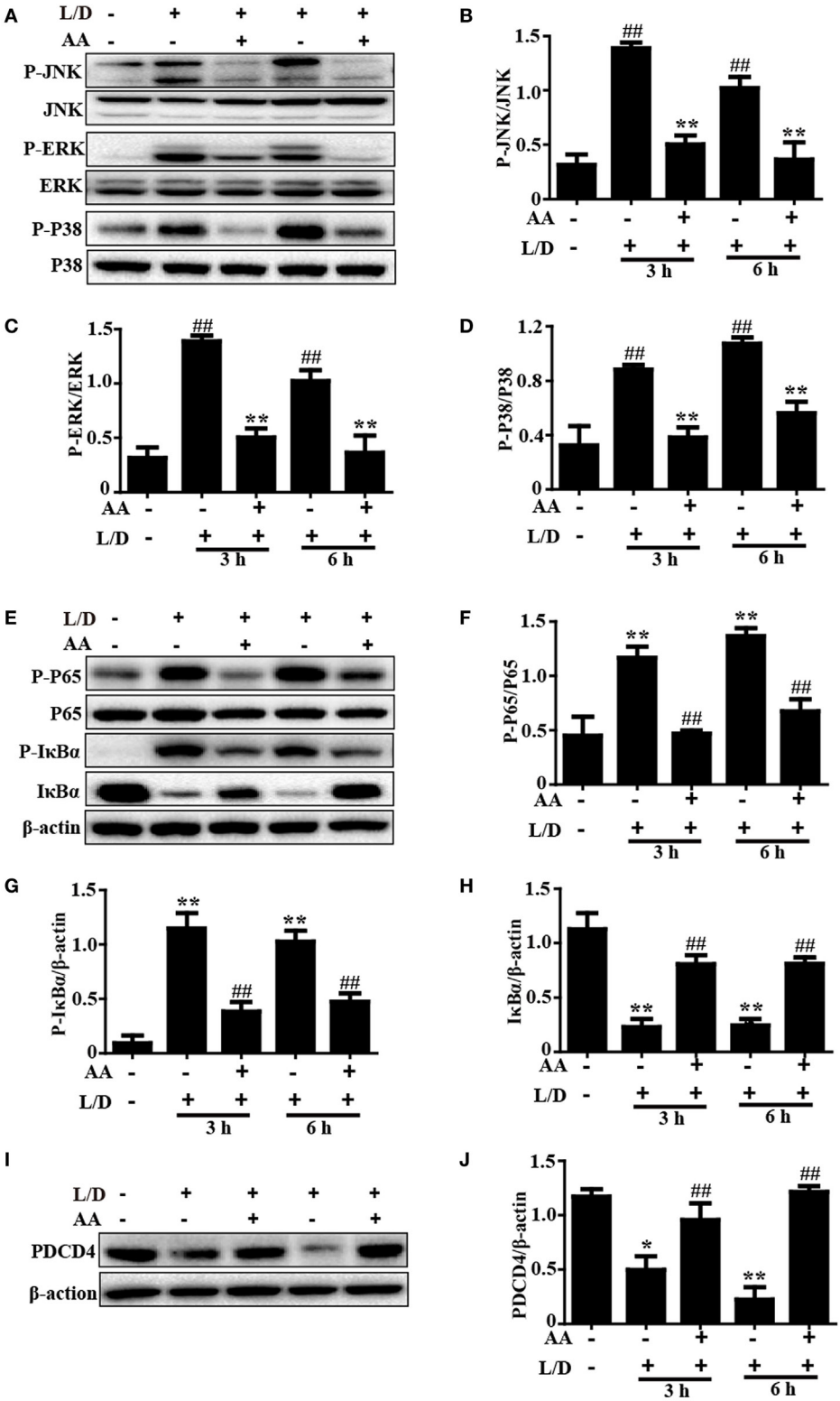

FIGURE 3 | Inhibitory effects of asiatic acid (AA) treatment on NF-κB, mitogen-activated protein kinase, and PDCD4 in L/D-induced fulminant hepatic failure. Liver tissues were collected from the mice 3 or 6 h after L/D challenge and analyzed by Western blotting. **(A,E,I)** Effects of AA on P-JNK, P-extracellular signal-regulated kinase (ERK), P-P38, P-P65, P-IκBα, IκBα, and PDCD4 expression were measured by Western blotting. **(B–D,F–H,J)** Quantification of relative protein expression was performed by densitometric analysis. Similar results were obtained from three independent experiments. All data are presented as means ± SEM ($n = 5$ in each group). $^{*}p < 0.05$ and $^{**}p < 0.01$ vs. control group; $^{\#}p < 0.05$ and $^{\#\#}p < 0.01$ vs. L/D group.

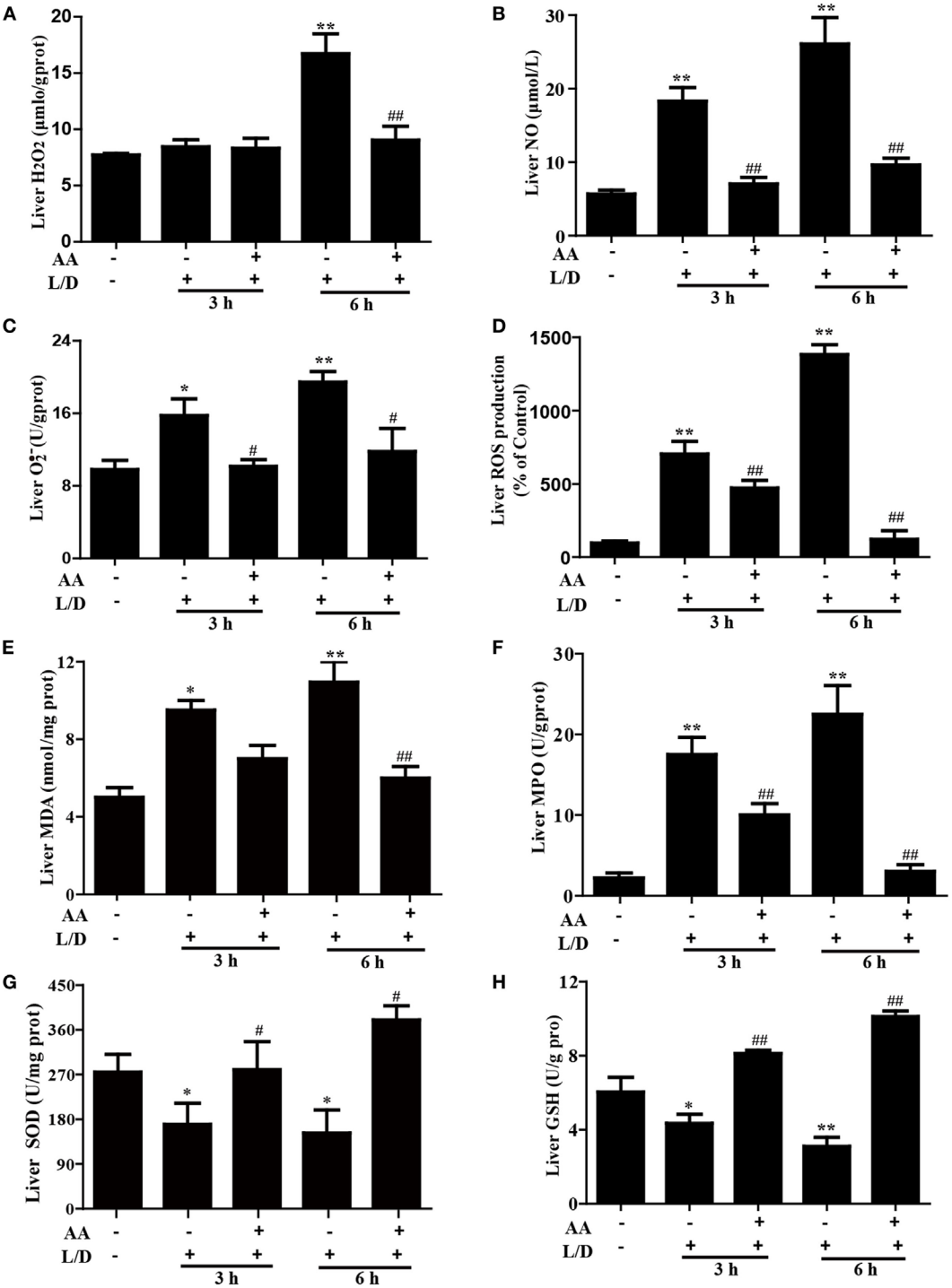

FIGURE 4 | Effects of asiatic acid (AA) treatment on the levels of oxidative markers in L/D-induced fulminant hepatic failure. Liver tissues were collected from the mice 3 or 6 h after L/D challenge for measurement of the generation of H_2O_2, NO, O_2^-, and reactive oxygen species (ROS), formation of malondialdehyde (MDA) and myeloperoxidase (MPO), and the superoxide dismutase (SOD) and glutathione (GSH) activities. **(A–D)** Effects of AA on liver H_2O_2, NO, O_2^-, and ROS production. **(E,F)** Effects of AA on the liver MDA and MPO levels. **(G,H)** Effects of AA on the liver SOD and GSH activities. Similar results were obtained from three independent experiments. All data are presented as means ± SEM ($n = 5$ in each group). $^*p < 0.05$ and $^{**}p < 0.01$ vs. control group; $^{\#}p < 0.05$ and $^{\#\#}p < 0.01$ vs. L/D group.

by Western blotting. Our results showed that AA treatment significantly inhibited L/D-induced phosphorylation of ERK, PI3K, and AKT, indicating that AA-mediated Nrf2 activation was unlikely to be associated with the ERK and PI3K/AKT signaling pathways *in vivo* (Figure S1 in Supplementary Material). However, AA treatment effectively increased AMPK and

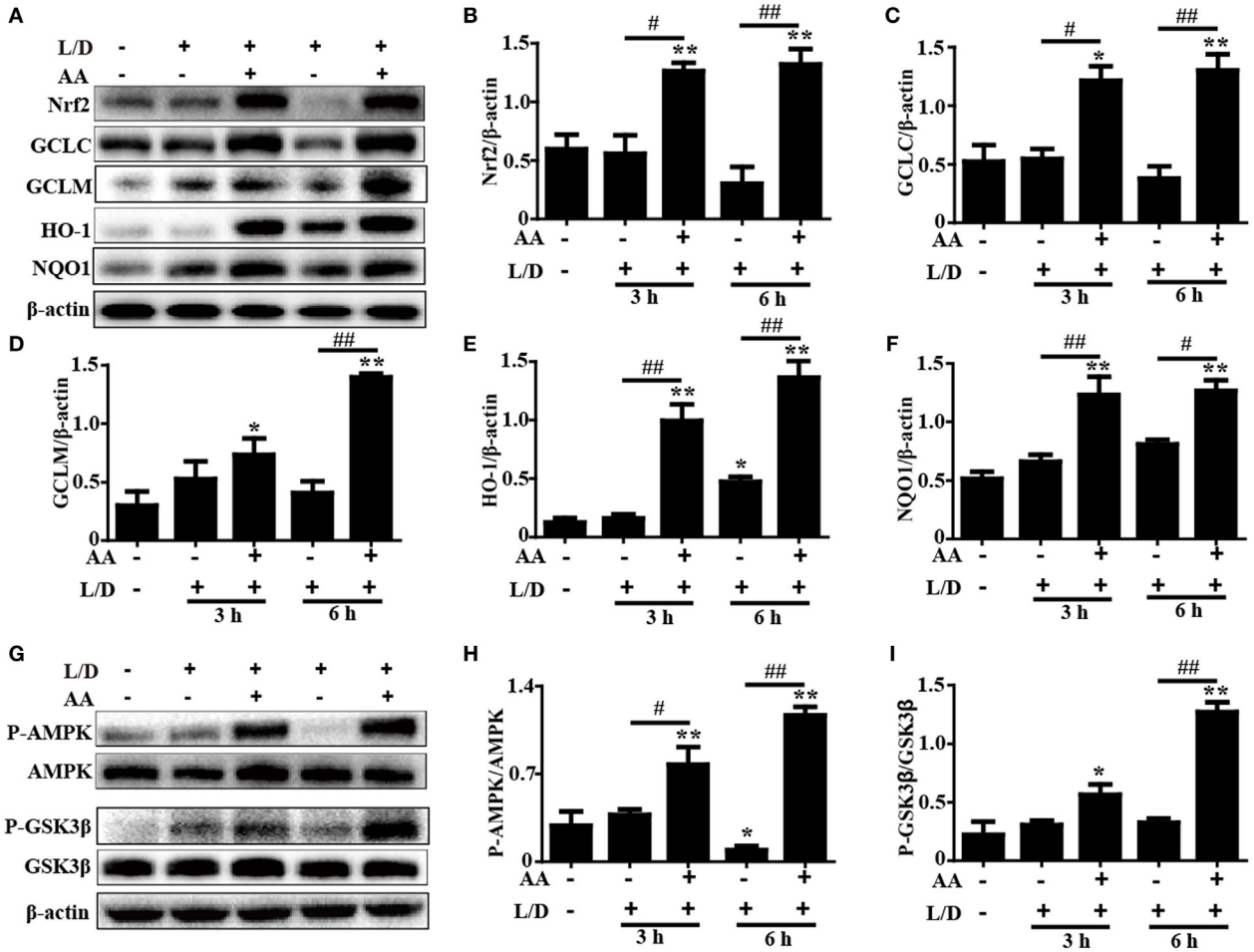

FIGURE 5 | Effects of Asiatic acid (AA) treatment on the Nrf2 and AMP-activated protein kinase (AMPK)/GSK3β signaling pathways in L/D-induced fulminant hepatic failure. Liver tissues were collected from the mice at 3 or 6 h after L/D challenge, liver tissues were collected, and analyzed by Western blotting. **(A,G)** Effects of AA on Nrf2, glutamate-cysteine ligase catalytic (GCLC), glutamate-cysteine ligase modifier (GCLM), heme oxygenase-1 (HO-1), NQO1, P-AMPK, and P-GSK3β protein expression. **(B–F,H,I)** Quantification of relative protein expression was performed by densitometric analysis. β-actin was acted used as an internal control. Similar results were obtained from three independent experiments. All data are presented as means ± SEM ($n = 5$ in each group). $^{*}p < 0.05$ and $^{**}p < 0.01$ vs. control group; $^{\#}p < 0.05$ and $^{\#\#}p < 0.01$ vs. L/D group.

GSK3β phosphorylation compared with the L/D-exposed group ($p < 0.05$ or $p < 0.01$) (**Figures 5G–I**). Furthermore, we found that AA obviously induced AMPK and GSK3β phosphorylation and Nrf2 protein expression ($p < 0.05$ or $p < 0.01$) in HepG2 cells incubated with AA (6 μM) for different times, whereas these effects were efficiently blocked by compound C (CC, an AMPK inhibitor) (Figure S2 in Supplementary Material). Together, these investigations suggest that the ability of AA to suppress inflammation and oxidative stress in L/D-induced FHF may involve upregulation of the Nrf2-medicated signaling pathway *via* activation of AMPK/GSK3β *in vivo* and *in vitro*.

AA-Induced PDCD4 Protein Expression Was Independent of Nrf2 Activation in HepG2 Cells

Based on the above outcomes, we evaluated whether the AA-induced PDCD4 expression was dependent of Nrf2 activation by using WT and $Nrf2^{-/-}$ HepG2 cells. In the present study, after exposure of HepG2 cells to AA (6 μM) for different times, we found that AA exposure for 1 h obviously enhanced PDCD4 protein expression compared to the unexposed cells ($p < 0.05$) (**Figures 6A,B**). Nrf2 protein expression induced by AA was evidently inhibited in the $Nrf2^{-/-}$ cells compared with the control cells, whereas AA-enhanced PDCD4 protein expression was not suppressed in the $Nrf2^{-/-}$HepG2 cells (**Figures 6C–H**). These results suggested that AA-induced PDCD4 protein expression is independent of Nrf2 activation in HepG2 cells.

DISCUSSION

Inflammation and oxidative stress are considered strongly interrelated biological events that are involved in the pathogenesis of various diseases, including FHF (30–32). Emerging evidence suggests that LPS/D-GalN (L/D) give rise to hepatic injuries

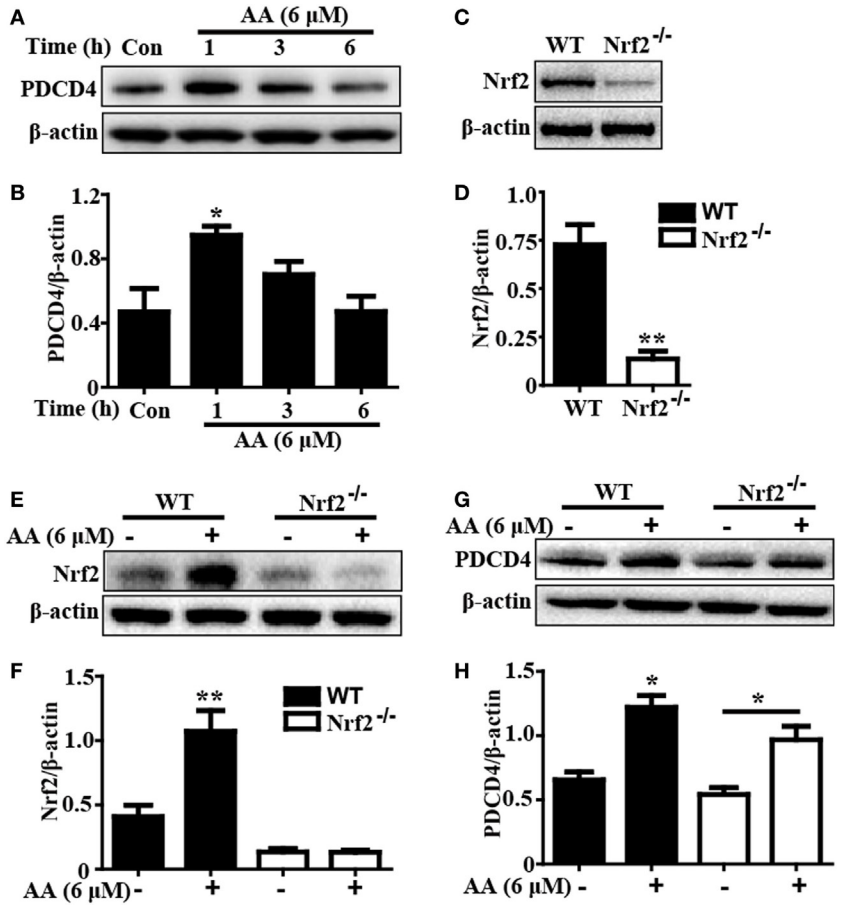

FIGURE 6 | Asiatic acid (AA)-induced PDCD4 protein expression is independent upon Nrf2 activation in HepG2 cells. **(A)** HepG2 cells were pretreated with or without AA (6 μM) for 1, 3, or 6 h. Effects of AA on PDCD4 protein expression were measured by Western blotting analysis. Additionally, **(C,E)** WT and Nrf2$^{-/-}$ HepG2 cells were pretreated with or without AA (6 μM) for 6 h. Effects of AA on Nrf2 protein expression were measured by Western blotting analysis. **(G)** WT and Nrf2$^{-/-}$ HepG2 cells were pretreated with or without AA (6 μM) for 1 h. Effects of AA on PDCD4 protein expression were measured by Western blotting analysis. **(B,D,F,H)** Quantification of relative protein expression was performed by densitometric analysis and β-actin was acted used as an internal control. Similar results were obtained from three independent experiments. All data are presented as means ± SEM ($n = 5$ in each group). *$p < 0.05$ and **$p < 0.01$ vs. control group.

resulting from oxidative stress and inflammatory responses, which parallel those of viral hepatitis (33, 34). Moreover, GalN/LPS-induced liver failure is widely accepted as a key experimental liver injury model and has contributed to investigations of the mechanisms underlying clinical liver injury and screening of some efficient hepatoprotective agents (35). Accordingly, any approach that relieves inflammatory responses and oxidative stress *in vitro* and *in vivo* may conduce to the prevention or treatment of FHF. AA has been reported to possess various biological activities, including antioxidant and anti-inflammatory properties (19, 20). Therefore, the aim of this study was to investigate whether AA played anti-inflammatory and antioxidant roles in mice with L/D-induced FHF.

Under physiological conditions, ALT and AST are mostly present in liver cells; however, these enzymes are transferred through the cell membrane into the serum when liver cells are damaged (36), which implies serious impairment of liver functions. In our studies, AA treatment effectively decreased the ALT and AST levels in sera and increased survival rate in the L/D-induced mouse model. Conversely, previous studies have indicated that L/D-induced macrophages in FHF mice provoke the release of numerous inflammatory factors, including TNF-α, IL-6, and IL-1β, by liver cells, resulting in significant damage to the live structure and functions (37, 38). Our findings demonstrated that AA pretreatment efficiently restored damage of the hepatic architecture and reduced TNF-α, IL-6, and IL-1β secretion in mice with L/D-induced FHF. Recent studies have shown that ROS, such as the superoxide radical (O_2^-), NO, and hydrogen peroxide (H_2O_2), are essential for the development of L/D-induced FHF (38, 39). Moreover, oxidative stress can increase the production of MPO and MDA formation to further result in liver tissue damage (40). In contrast, L/D-induced SOD and GSH depletion are involved in aggravating oxidative damage in mice with FHF (41). Our findings indicated that AA treatment remarkably inhibited L/D-induced ROS (O_2^-, NO, and H_2O_2) formation and increased the GSH and SOD levels, suggesting that AA treatment significantly attenuated L/D-induced oxidative damage in mice with FHF. These investigations demonstrated

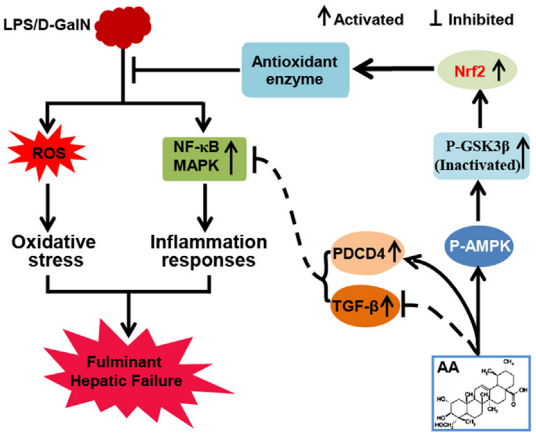

FIGURE 7 | Asiatic acid (AA)-mediated Nrf2 signaling pathway protects lipopolysaccharide (LPS)/D-galactosamine (GalN)-induced fulminant hepatic failure (FHF) *via* inhibition of oxidative stress and inflammatory responses. (AA) can induce AMP-activated protein kinase and GSK3β activation, which contributes to upregulation of the Nrf2 signaling pathway and results in the expression of abundant antioxidant genes. Furthermore, AA not only reduces LPS/D-GalN-induced reactive oxygen species overproduction but also inhibits NF-κB and mitogen-activated protein kinase (MAPK) signaling pathway activation dependent upon induction of PDCD4 protein expression. These processes play significant roles in suppressing oxidative stress and inflammatory responses to alleviate FHF.

that AA pretreatment relieved pathological changes, indicating potential for the use of AA in clinical applications for the prevention and treatment of liver injury *via* inhibition of inflammation and oxidative stress damage.

Based on the above outcomes, we investigated the protective mechanism of AA against L/D-induced inflammation and oxidative stress in mice with FHF. Increasing evidence has shown that L/D-induced activation of NF-κB and MAPK, which are associated with the regulation of cytokine generation (i.e., TNF-α, IL-1β, and IL-6 secretion), plays a pivotal role in mice with FHF (1, 42). Our results showed that AA treatment effectively inhibited L/D-induced JNK, ERK, P38, P65, and IκBα phosphorylation and blocked IκBα degradation. Moreover, PDCD4 downregulation was reported to promote LPS-stimulated secretion of proinflammatory mediators, and PDCD4 deficiency exacerbated the sensitivity of liver injury in L/D-induced mice by inducing MAPK and NF-κB pathway activation (8, 43). Our studies revealed that L/D exposure dramatically decreased PDCD4 protein expression, whereas this effect was significantly suppressed by AA pretreatment. Taken together, these results indicated that the inhibitory effects of AA pretreatment on L/D-induced inflammatory responses may be associated with suppression of NF-κB and MAPK *via* a mechanism that can partially be attributed to the induction of PDCD4 expression. Interestingly, previous reports discovered that inhibiting PDCD4 downregulation contributed to the induction of p21-dependent Nrf2 expression in HepG2 cells (44). In our study, AA-enhanced PDCD4 protein expression could not be suppressed in the $Nrf2^{-/-}$ HepG2 cells, implying that AA-induced PDCD4 protein expression was independent of Nrf2 activation in HepG2 cells. Furthermore, previous studies have suggested that Nrf2, which is a multiple signaling pathway coordinator, possesses anti-inflammatory and antioxidant properties against acute and chronic diseases, including experimental liver injury, through regulation of the expression of various antioxidant genes, such as GCLC, GCLM, NQO1, and HO-1 (45, 46). In this work, AA significantly increased Nrf2, GCLC, GCLM, NQO1, and HO-1 protein expression, which was related to the anti-inflammatory and antioxidant activities exhibited in the mice with L/D-induced FHF. Importantly, recent reports revealed that Nrf2 transcription displayed hepatoprotective involvement in the activation of the AMPK/Akt/GSK3β signaling pathway in a liver injury model (19, 30). In our study, AA pretreatment obviously promoted AMPK and GSK3β phosphorylation in both HepG2 cells and mice with FHF. Although our previous research indicated that AA-activated Nrf2 signaling was majorly dependent upon AKT and ERK activation in HepG2 cells, AA treatment effectively inhibited the activation of PI3K/AKT and ERK induced by L/D in mice. Consequently, we speculated that this discrepancy resulted from the various cell types present in the livers of the mice, which differed from the results obtained using a single cell type. Finally, to examine whether AA-mediated Nrf2 transcription was associated with AMPK/GSK3β activation, HepG2 cells were exposed to the AMPK inhibitor compound C. Our investigations found that AA-induced Nrf2 activation was blunted by the AMPK inhibitor, suggesting that AA-enhanced Nrf2 induction might be dependent on the phosphorylation of AMPK and GSK3β *in vivo* and *in vitro*.

In conclusion, as shown in **Figure 7**, the investigations of this study suggested that AA played an essential role in liver protection by inhibiting inflammatory responses and oxidative stress. The underlying mechanisms may be closely associated with the inhibition of MAPK and NF-κB activation through the partial induction of PDCD4 and upregulation of Nrf2 in an AMPK/GSK3β pathway activation-dependent manner. Accordingly, the study provides beneficial evidence for the application of AA in protecting the liver from inflammatory and oxidative stress damage during FHF.

ETHICS STATEMENT

All animal experiments were performed according to the guide for the Care and Use of Laboratory Animals, which was published by the US National Institute of Health.

AUTHOR CONTRIBUTIONS

HL wrote the paper and performed the experiments; ZQ performed the experiments; SW, HF, and XD analyzed the data; XC contributed to design the experiments.

FUNDING

This work was in part supported by the National Science Foundation of China (Grant No. 81603174), National Natural

Science Foundation of China (No. 31572347), and the General Financial Grant from the China Postdoctoral Science Foundation (Grant No. 168847).

SUPPLEMENTARY MATERIAL

The Supplementary Material for this article can be found online at http://journal.frontiersin.org/article/10.3389/fimmu.2017.00785/full#supplementary-material.

FIGURE S1 | Effects of asiatic acid treatment on PI3K/AKT signaling pathway in L/D-induced fulminant hepatic failure. Liver tissues were collected from the mice 3 or 6 h after L/D challenge and analyzed by Western blotting. **(A–C)** Quantification of relative expression of P-PI3K/PI3K and P-AKT/AKT were performed by densitometric analysis. Similar results were obtained from three independent experiments. All data are presented as means ± SEM ($n = 5$ in each group). $^{**}p < 0.01$ vs. Control group; $^{\#}p < 0.05$ and $^{\#\#}p < 0.01$ vs. L/D group.

FIGURE S2 | Effects of asiatic acid (AA) exposure on activation of the AMP-activated protein kinase (AMPK)/GSK3β/Nrf2 signaling pathways in HepG2 cells. **(A)** HepG2 cells were treated with AA (6 μM) for 1, 3, or 6 h. Western blotting analysis were used to explore phosphorylated AMPK and GSK3β expression as well as Nrf2 protein expression. **(E)** HepG2 cells were treated with compound C (CC, an AMPK inhibitor, 3 μM) for 18 h and then incubated with AA (6 μM) for another 6 h. **(B–D,F–H)** Quantification of relative protein expression was performed by densitometric analysis. β-actin was acted as an internal control. Similar results were obtained from three independent experiments. All data are presented as means ± SEM ($n = 5$ in each group). $^{*}p < 0.05$ and $^{**}p < 0.01$ vs. control group.

REFERENCES

1. Zhang X, Ding J, Gou C, Wen T, Li L, Wang X, et al. Qingchangligan formula attenuates the inflammatory response to protect the liver from acute failure induced by D-galactosamine/lipopolysaccharide in mice. *J Ethnopharmacol* (2017) 201:108–16. doi:10.1016/j.jep.2016.11.007
2. Umemura T, Tanaka E, Kiyosawa K, Kumada H, Japan de novo Hepatitis BRG. Mortality secondary to fulminant hepatic failure in patients with prior resolution of hepatitis B virus infection in Japan. *Clin Infect Dis* (2008) 5:e52–6. doi:10.1086/590968
3. Lin X, Zhang S, Huang R, Tan S, Liang S, Wu X, et al. Protective effect of tormentic acid from *Potentilla chinensis* against lipopolysaccharide/D-galactosamine induced fulminant hepatic failure in mice. *Int Immunopharmacol* (2014) 2:365–72. doi:10.1016/j.intimp.2014.02.009
4. Jaeschke H. Reactive oxygen and mechanisms of inflammatory liver injury. *J Gastroenterol Hepatol* (2000) 7:718–24. doi:10.1046/j.1440-1746.2000.02207.x
5. Zhang G, Ghosh S. Toll-like receptor-mediated NF-kappaB activation: a phylogenetically conserved paradigm in innate immunity. *J Clin Invest* (2001) 1:13–9. doi:10.1172/JCI11837
6. Wheeler MD, Yamashina S, Froh M, Rusyn I, Thurman RG. Adenoviral gene delivery can inactivate Kupffer cells: role of oxidants in NF-kappaB activation and cytokine production. *J Leukoc Biol* (2001) 4:622–30.
7. Lankat-Buttgereit B, Goke R. The tumour suppressor PDCD4: recent advances in the elucidation of function and regulation. *Biol Cell* (2009) 6:309–17. doi:10.1042/BC20080191
8. Wang X, Zhang L, Wei Z, Zhang X, Gao Q, Ma Y, et al. The inhibitory action of PDCD4 in lipopolysaccharide/D-galactosamine-induced acute liver injury. *Lab Invest* (2013) 3:291–302. doi:10.1038/labinvest.2012.174
9. Ben-Shaul V, Sofer Y, Bergman M, Zurovsky Y, Grossman S. Lipopolysaccharide-induced oxidative stress in the liver: comparison between rat and rabbit. *Shock* (1999) 4:288–93. doi:10.1097/00024382-199910000-00007
10. Hashem RM, Hassanin KM, Rashed LA, Mahmoud MO, Hassan MG. Effect of silibinin and vitamin E on the ASK1-p38 MAPK pathway in D-galactosamine/lipopolysaccharide induced hepatotoxicity. *Exp Biol Med (Maywood)* (2016) 11:1250–7. doi:10.1177/1535370216636719
11. Gloire G, Legrand-Poels S, Piette J. NF-kappaB activation by reactive oxygen species: fifteen years later. *Biochem Pharmacol* (2006) 11:1493–505. doi:10.1016/j.bcp.2006.04.011
12. Kensler TW, Wakabayashi N, Biswal S. Cell survival responses to environmental stresses via the Keap1-Nrf2-ARE pathway. *Annu Rev Pharmacol Toxicol* (2007) 47:89–116. doi:10.1146/annurev.pharmtox.46.120604.141046
13. Malhotra D, Portales-Casamar E, Singh A, Srivastava S, Arenillas D, Happel C, et al. Global mapping of binding sites for Nrf2 identifies novel targets in cell survival response through ChIP-Seq profiling and network analysis. *Nucleic Acids Res* (2010) 17:5718–34. doi:10.1093/nar/gkq212
14. Pang C, Zheng Z, Shi L, Sheng Y, Wei H, Wang Z, et al. Caffeic acid prevents acetaminophen-induced liver injury by activating the Keap1-Nrf2 antioxidative defense system. *Free Radic Biol Med* (2016) 91:236–46. doi:10.1016/j.freeradbiomed.2015.12.024
15. Shin SM, Cho IJ, Kim SG. Resveratrol protects mitochondria against oxidative stress through AMP-activated protein kinase-mediated glycogen synthase kinase-3beta inhibition downstream of poly(ADP-ribose)polymerase-LKB1 pathway. *Mol Pharmacol* (2009) 4:884–95. doi:10.1124/mol.109.058479
16. Mo C, Wang L, Zhang J, Numazawa S, Tang H, Tang X, et al. The crosstalk between Nrf2 and AMPK signal pathways is important for the anti-inflammatory effect of berberine in LPS-stimulated macrophages and endotoxin-shocked mice. *Antioxid Redox Signal* (2014) 4:574–88. doi:10.1089/ars.2012.5116
17. Emerit I, Huang CY, Serejo F, Filipe P, Fernandes A, Costa A, et al. Oxidative stress in chronic hepatitis C: a preliminary study on the protective effects of antioxidant flavonoids. *Hepatogastroenterology* (2005) 52:530–6.
18. Wang L, Zhang S, Cheng H, Lv H, Cheng G, Ci X. Nrf2-mediated liver protection by esculentoside A against acetaminophen toxicity through the AMPK/Akt/GSK3beta pathway. *Free Radic Biol Med* (2016) 101:401–12. doi:10.1016/j.freeradbiomed.2016.11.009
19. Tsao SM, Yin MC. Antioxidative and antiinflammatory activities of asiatic acid, glycyrrhizic acid, and oleanolic acid in human bronchial epithelial cells. *J Agric Food Chem* (2015) 12:3196–204. doi:10.1021/acs.jafc.5b00102
20. Pakdeechote P, Bunbupha S, Kukongviriyapan U, Prachaney P, Khrisanapant W, Kukongviriyapan V. Asiatic acid alleviates hemodynamic and metabolic alterations via restoring eNOS/iNOS expression, oxidative stress, and inflammation in diet-induced metabolic syndrome rats. *Nutrients* (2014) 1:355–70. doi:10.3390/nu6010355
21. Lee JW, Park HA, Kwon OK, Jang YG, Kim JY, Choi BK, et al. Asiatic acid inhibits pulmonary inflammation induced by cigarette smoke. *Int Immunopharmacol* (2016) 39:208–17. doi:10.1016/j.intimp.2016.07.010
22. Tang LX, He RH, Yang G, Tan JJ, Zhou L, Meng XM, et al. Asiatic acid inhibits liver fibrosis by blocking TGF-beta/Smad signaling in vivo and in vitro. *PLoS One* (2012) 2:e31350. doi:10.1371/journal.pone.0031350
23. Camargo CA Jr, Madden JF, Gao W, Selvan RS, Clavien PA. Interleukin-6 protects liver against warm ischemia/reperfusion injury and promotes hepatocyte proliferation in the rodent. *Hepatology* (1997) 6:1513–20. doi:10.1002/hep.510260619
24. Qi Z, Ci X, Huang J, Liu Q, Yu Q, Zhou J, et al. Asiatic acid enhances Nrf2 signaling to protect HepG2 cells from oxidative damage through Akt and ERK activation. *Biomed Pharmacother* (2017) 88:252–9. doi:10.1016/j.biopha.2017.01.067
25. Kim SJ, Lee SM. NLRP3 inflammasome activation in D-galactosamine and lipopolysaccharide-induced acute liver failure: role of heme oxygenase-1. *Free Radic Biol Med* (2013) 65:997–1004. doi:10.1016/j.freeradbiomed.2013.08.178
26. Wang L, Zhao M, Guo C, Wang G, Zhu F, Wang J, et al. PDCD4 deficiency aggravated colitis and colitis-associated colorectal cancer via promoting IL-6/STAT3 pathway in mice. *Inflamm Bowel Dis* (2016) 5:1107–18. doi:10.1097/MIB.0000000000000729
27. Schmid T, Bajer MM, Blees JS, Eifler LK, Milke L, Rubsamen D, et al. Inflammation-induced loss of PDCD4 is mediated by phosphorylation-dependent degradation. *Carcinogenesis* (2011) 10:1427–33. doi:10.1093/carcin/bgr131

28. Park SY, Jin ML, Ko MJ, Park G, Choi YW. Anti-neuroinflammatory effect of emodin in LPS-stimulated microglia: involvement of AMPK/Nrf2 activation. *Neurochem Res* (2016) 11:2981–92. doi:10.1007/s11064-016-2018-6
29. Li Z, Dong X, Liu H, Chen X, Shi H, Fan Y, et al. Astaxanthin protects ARPE-19 cells from oxidative stress via upregulation of Nrf2-regulated phase II enzymes through activation of PI3K/Akt. *Mol Vis* (2013) 19:1656–66.
30. Nicholls SJ. The complex intersection of inflammation and oxidation: implications for atheroprotection. *J Am Coll Cardiol* (2008) 17:1379–80. doi:10.1016/j.jacc.2008.07.037
31. Wang H, Li Y. Protective effect of bicyclol on acute hepatic failure induced by lipopolysaccharide and D-galactosamine in mice. *Eur J Pharmacol* (2006) 1-3:194–201. doi:10.1016/j.ejphar.2005.12.080
32. Nolan JP. The role of intestinal endotoxin in liver injury: a long and evolving history. *Hepatology* (2010) 5:1829–35. doi:10.1002/hep.23917
33. Tang XH, Gao L, Gao J, Fan YM, Xu LZ, Zhao XN, et al. Mechanisms of hepatoprotection of *Terminalia catappa* L. extract on D-galactosamine-induced liver damage. *Am J Chin Med* (2004) 4:509–19. doi:10.1142/S0192415X04002156
34. Endo Y, Shibazaki M, Yamaguchi K, Kai K, Sugawara S, Takada H, et al. Enhancement by galactosamine of lipopolysaccharide(LPS)-induced tumour necrosis factor production and lethality: its suppression by LPS pretreatment. *Br J Pharmacol* (1999) 1:5–12. doi:10.1038/sj.bjp.0702747
35. Nakama T, Hirono S, Moriuchi A, Hasuike S, Nagata K, Hori T, et al. Etoposide prevents apoptosis in mouse liver with D-galactosamine/lipopolysaccharide-induced fulminant hepatic failure resulting in reduction of lethality. *Hepatology* (2001) 6:1441–50. doi:10.1053/jhep.2001.24561
36. Brodsky M, Hirsh S, Albeck M, Sredni B. Resolution of inflammation-related apoptotic processes by the synthetic tellurium compound, AS101 following liver injury. *J Hepatol* (2009) 3:491–503. doi:10.1016/j.jhep.2009.04.024
37. Li J, Ge R, Zhao C, Tang L, Li J, Li Q. Farrerol regulates occludin expression in hydrogen peroxide-induced EA.hy926 cells by modulating ERK1/2 activity. *Eur J Pharmacol* (2014) 734:9–14. doi:10.1016/j.ejphar.2014.03.054
38. Xia X, Fu J, Song X, Shi Q, Su C, Song E, et al. Neohesperidin dihydrochalcone down-regulates MyD88-dependent and -independent signaling by inhibiting endotoxin-induced trafficking of TLR4 to lipid rafts. *Free Radic Biol Med* (2015) 89:522–32. doi:10.1016/j.freeradbiomed.2015.08.023
39. Takemura S, Minamiyama Y, Imaoka S, Funae Y, Hirohashi K, Inoue M, et al. Hepatic cytochrome P450 is directly inactivated by nitric oxide, not by inflammatory cytokines, in the early phase of endotoxemia. *J Hepatol* (1999) 6:1035–44. doi:10.1016/S0168-8278(99)80257-8
40. Huang H, Zhang X, Li J. Protective effect of oroxylin A against lipopolysaccharide and/or D-galactosamine-induced acute liver injury in mice. *J Surg Res* (2015) 2:522–8. doi:10.1016/j.jss.2015.01.047
41. Victor VM, Rocha M, Esplugues JV, De la Fuente M. Role of free radicals in sepsis: antioxidant therapy. *Curr Pharm Des* (2005) 24:3141–58. doi:10.2174/1381612054864894
42. Huang CC, Lin KJ, Cheng YW, Hsu CA, Yang SS, Shyur LF. Hepatoprotective effect and mechanistic insights of deoxyelephantopin, a phyto-sesquiterpene lactone, against fulminant hepatitis. *J Nutr Biochem* (2013) 3:516–30. doi:10.1016/j.jnutbio.2012.01.013
43. Yasuda M, Schmid T, Rubsamen D, Colburn NH, Irie K, Murakami A. Downregulation of programmed cell death 4 by inflammatory conditions contributes to the generation of the tumor promoting microenvironment. *Mol Carcinog* (2010) 9:837–48. doi:10.1002/mc.20660
44. Cho JH, Kim YW, Choi BY, Keum YS. Sulforaphane inhibition of TPA-mediated PDCD4 downregulation contributes to suppression of c-Jun and induction of p21-dependent Nrf2 expression. *Eur J Pharmacol* (2014) 741:247–53. doi:10.1016/j.ejphar.2014.08.007
45. Song X, Yin S, Huo Y, Liang M, Fan L, Ye M, et al. Glycycoumarin ameliorates alcohol-induced hepatotoxicity via activation of Nrf2 and autophagy. *Free Radic Biol Med* (2015) 89:135–46. doi:10.1016/j.freeradbiomed.2015.07.006
46. Jiang YM, Wang Y, Tan HS, Yu T, Fan XM, Chen P, et al. Schisandrol B protects against acetaminophen-induced acute hepatotoxicity in mice via activation of the NRF2/ARE signaling pathway. *Acta Pharmacol Sin* (2016) 3:382–9. doi:10.1038/aps.2015.120

Conflict of Interest Statement: The authors declare that the research was conducted in the absence of any commercial or financial relationships that could be construed as a potential conflict of interest.

Copyright © 2017 Lv, Qi, Wang, Feng, Deng and Ci. This is an open-access article distributed under the terms of the Creative Commons Attribution License (CC BY). The use, distribution or reproduction in other forums is permitted, provided the original author(s) or licensor are credited and that the original publication in this journal is cited, in accordance with accepted academic practice. No use, distribution or reproduction is permitted which does not comply with these terms.

frontiers in Immunology

ORIGINAL RESEARCH
published: 11 July 2017
doi: 10.3389/fimmu.2017.00801

Placental Growth Factor Contributes to Liver Inflammation, Angiogenesis, Fibrosis in Mice by Promoting Hepatic Macrophage Recruitment and Activation

*Xi Li[1], Qianwen Jin[2,3], Qunyan Yao[2,3], Yi Zhou[2,3], Yanting Zou[2,3], Zheng Li[4], Shuncai Zhang[2,3] and Chuantao Tu[2,3]**

[1] Department of Geriatrics, Zhongshan Hospital, Fudan University, Shanghai, China, [2] Department of Gastroenterology and Hepatology, Zhongshan Hospital, Fudan University, Shanghai, China, [3] Shanghai Institute of Liver Diseases, Shanghai, China, [4] Laboratory Animal Center, Zhongshan Hospital, Fudan University, Shanghai, China

OPEN ACCESS

Edited by:
Jixin Zhong,
Case Western Reserve University,
United States

Reviewed by:
Ping Wang,
Massachusetts General Hospital,
United States
Hui Liu,
University of California, San
Francisco, United States
Xiaojing Yue,
La Jolla Institute for Allergy
and Immunology, United States
Sarani Ghoshal,
Massachusetts General Hospital,
United States
Zhi-Qiang Wang,
Van Andel Institute, United States

***Correspondence:**
Chuantao Tu
tu.chuantao@zs-hospital.sh.cn,
tuchuantao@outlook.com

Specialty section:
This article was submitted
to Inflammation,
a section of the journal
Frontiers in Immunology

Received: 28 April 2017
Accepted: 26 June 2017
Published: 11 July 2017

Citation:
Li X, Jin Q, Yao Q, Zhou Y, Zou Y,
Li Z, Zhang S and Tu C (2017)
Placental Growth Factor Contributes
to Liver Inflammation, Angiogenesis,
Fibrosis in Mice by Promoting
Hepatic Macrophage Recruitment
and Activation.
Front. Immunol. 8:801.
doi: 10.3389/fimmu.2017.00801

Placental growth factor (PlGF), a member of the vascular endothelial growth factor (VEGF) family, mediates wound healing and inflammatory responses, exerting an effect on liver fibrosis and angiogenesis; however, the precise mechanism remains unclear. The aims of this study are to identify the role of PlGF in liver inflammation and fibrosis induced by bile duct ligation (BDL) in mice and to reveal the underlying molecular mechanism. PlGF small interfering RNA (siRNA) or non-targeting control siRNA was injected by tail vein starting 2 days after BDL. Liver inflammation, fibrosis, angiogenesis, macrophage infiltration, and hepatic stellate cells (HSCs) activation were examined. Our results showed that PlGF was highly expressed in fibrotic livers and mainly distributed in activated HSCs and macrophages. Furthermore, PlGF silencing strongly reduced the severity of liver inflammation and fibrosis, and inhibited the activation of HSCs. Remarkably, PlGF silencing also attenuated BDL-induced hepatic angiogenesis, as evidenced by attenuated liver endothelial cell markers CD31 and von Willebrand factor immunostaining and genes or protein expression. Interestingly, these pathological ameliorations by PlGF silencing were due to a marked reduction in the numbers of intrahepatic F4/80$^+$, CD68$^+$, and Ly6C$^+$ cell populations, which were reflected by a lower expression of these macrophage marker molecules in fibrotic livers. In addition, knockdown of PlGF by siRNA inhibited macrophages activation and substantially suppressed the expression of pro-inflammatory cytokines and chemokines in fibrotic livers. Mechanistically, evaluation of cultured RAW 264.7 cells revealed that VEGF receptor 1 (VEGFR1) mainly involved in mediating the role of PlGF in macrophages recruitment and activation, since using VEGFR1 neutralizing antibody blocking PlGF/VEGFR1 signaling axis significantly inhibited macrophages migration and inflammatory responses. Together, these findings indicate that PlGF plays an important role in liver inflammation, angiogenesis, and fibrosis by promoting hepatic macrophage recruitment and activation, and suggest that blockage of PlGF could be a promising novel therapy for chronic fibrotic liver diseases.

Keywords: placental growth factor, hepatic fibrosis, inflammation, macrophage, Kupffer cells, hepatic stellate cells, angiogenesis, small interfering RNA

INTRODUCTION

Liver fibrosis is the final common pathway of chronic liver diseases of various etiologies, which develops as a result of the sustained wound-healing process triggered by liver injury and inflammation (1–3). As chronic liver injury process, hepatic stellate cells (HSCs) become activated and transdifferentiate to myofibroblast-like cells, leading to the excess accumulation of extracellular matrix (ECM) (1–4). It has been well established that HSC activation results from the inflammatory activity of liver immune cells, predominantly macrophages (2–7). Furthermore, activated myofibroblasts can also amplify inflammatory responses by inducing the infiltration of macrophages and further secreting cytokines (4, 5). Consequently, understanding the mechanism of inflammation and fibrosis is critically important to develop treatments for chronic liver diseases (2).

Recent studies in animal models and in cirrhotic patients have provided key insights regarding the role of liver macrophages in regulating hepatic fibrogenesis and fibrosis regression (4–13). Hepatic macrophages can arise not only from proliferating resident macrophages but also from circulating monocyte that originates in the bone marrow (BM), which are recruited to the injured liver (4–6). In addition, these cells have been classified either into "pro-inflammatory" M1 or "immunoregulatory" M2 macrophages, though such binary classifications cannot represent the complex *in vivo* environment for most macrophage subsets (6, 7, 12, 13). Upon liver injury, macrophages activate and produce cytokines (TGF-β, TNF-α, and interleukin-1β), and chemokines, such as CC-chemokine ligand 2 (CCL2, also MCP-1), CCL5 (RANTES), and CXCL10 (2–8). In addition, HSCs may directly recruit Kupffer cells and circulating macrophages by the expression of adhesion molecules, such as intercellular adhesion molecule 1 (ICAM-1), vascular cell adhesion molecular-1 (VCAM-1), and E-selection (2). Therefore, chemokines and adhesion also play a pivotal role in the recruitment and differentiate of monocyte and macrophages to the sites of inflammation through receptors among the inflammatory mediators (7–10); leading to the development and progression of liver injury, inflammation, and fibrosis (3–12). Macrophages also can release large amounts of angiogenic cytokine vascular endothelial growth factor (VEGF) and induce the formation of new blood vessel growth during wound repair, inflammation, and tumor growth (9, 12–16). However, the mechanisms modulating chemokine pathways and hepatic macrophages in liver fibrogenesis are not fully understood (2–5). Therefore, elucidating the complex regulatory mechanisms by which macrophages promote inflammation and fibrosis might lead to novel therapies to suppress liver inflammation and prevent the development fibrosis (4, 5, 12).

Placental growth factor (PlGF), a member of the VEGF family, is a pleiotropic cytokine that stimulates endothelial cell (EC) growth, migration, and survival; chemoattracts macrophages and BM progenitors; and promotes pathologic angiogenesis and wound healing (17–22). Unlike VEGF, PlGF selectively binds VEGF receptor 1 (VEGFR1) and its coreceptors neurophilin-1 and -2 (17, 18). It is noteworthy that PlGF is dispensable for development and health, while blockage of PlGF pathway has been shown to reduce pathological angiogenesis without affecting healthy blood vessels (17, 18, 21). Recent reports have demonstrated that PlGF is overexpressed in cirrhotic liver and hepatocellular carcinoma (HCC) both in human and in rodent models (18, 22–26). Furthermore, we and others previously have shown that blockade of PlGF by specific antibody, small interfering RNA (siRNA), or genetic ablation suppressed liver fibrogenesis (22, 23), reduced portal hypertension (24) and inhibited HCC (18, 25, 26). Thus, PlGF signaling represents a promising target for therapy of chronic liver disease with angiogenesis (17, 22–26).

However, the mechanism underlying PlGF mediates the pathogenesis of liver fibrosis has not been fully elucidated, and identifying the novel pathological role of PlGF is very important for clinical translational research. Therefore, the aims of the study were to identify the role for PlGF in mediating liver inflammation and fibrosis and to reveal the mechanistic links of PlGF signaling between hepatic macrophages recruitment, inflammatory response, and HSC activation in the context of the fibrotic liver microenvironment.

MATERIALS AND METHODS

Chemicals and Reagents

Lipopolysaccharide (LPS), Sirius red F3B, and saturated aqueous solution of picric acid were from Sigma Chemical, Co. Ltd. (St. Louis, MO, USA). Fetal bovine serum (FBS), trypsin, Dulbecco's modified Eagle medium (DMEM), penicillin, and streptomycin were from Gibco (Carlsbad, CA, USA). Invivofectamine® 2.0 reagent, *in vivo* predesigned PlGF siRNA and *in vivo* non-targeting control (NTC) siRNA were from Life Technologies (Carlsbad, CA, USA). siRNA sequences are provided in the supporting information (Figure S1 in Supplementary Material). Recombinant mouse PlGF-2 protein was from R&D Systems Inc. (Minneapolis, MN, USA).

Animals and Experimental Design

Male BALB/c mice (8–10 weeks) were purchased from Shanghai Laboratory Animal Research Center (Shanghai, China). The experimental protocol was performed in accordance with the guiding principles for the care and use of laboratory animals approved by the Fudan University Animal Care Committee and all animals received humane care. The animals were kept in an environmentally controlled room (23 ± 2°C, 55 ± 10% humidity) with a 12-h light/dark cycle and allowed free access to food and water. Mice were subjected to bile duct ligation (BDL) to induce liver fibrosis, while controls were sham-operated (SHAM) (27, 28). Mice were randomly distributed in four groups as shown in experimental design (**Figure 1A**). To deliver each siRNA, *in vivo* ready siRNAs were mixed with Invivofectamine 2.0 regents and injected in a volume of 100 μl at a dose of 5 mg/kg for three cycles starting 2 days after BDL surgery. Six to ten mice of each group were sacrificed on days 14, 21, and 28 after BDL, respectively; and the livers were removed and cut into small pieces and either snap-frozen in liquid nitrogen for storage at −80°C or fixed in freshly prepared 4% paraformaldehyde for 24 h at 4°C. Mouse sera were isolated to assay for liver functions.

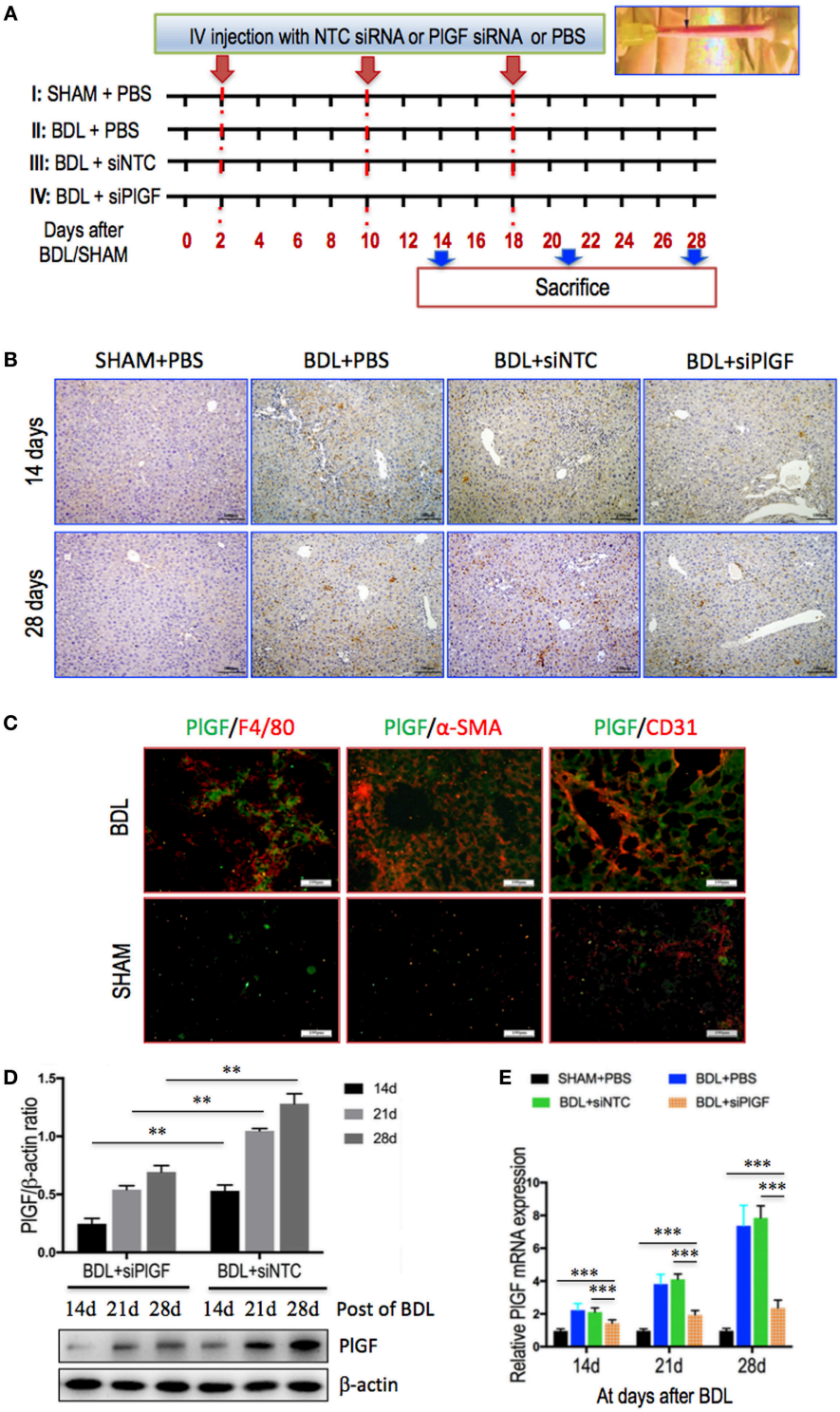

FIGURE 1 | Placental growth factor (PlGF) is highly induced in fibrotic liver and PlGF silencing robustly limits intrahepatic PlGF overexpression in bile duct ligation (BDL) mice. **(A)** Experimental study design. Mice were induced liver fibrosis by BDL for 28 days and treated with PlGF siRNA (siPlGF) or non-targeting control siRNA (siNTC) or PBS *via* tail vein injection (IV) at days 2, 10, and 18 after BDL. Six to ten mice of each group were sacrificed on days 14, 21, and 28 after BDL, respectively. Control mice were sham-operated (SHAM). **(B)** Representative microscopy images PlGF immunohistochemistry in livers from each group at days 14 and 28 after BDL or sham-operated (SHAM). Original magnification: 100×. **(C)** Immunofluorescent double staining in liver sections of BDL or SHAM mice. Livers were double stained for PlGF (green) and CD31 (endothelial cells marker), F4/80 (macrophages), or α-SMA (myofibroblasts). Original magnification: 200×. **(D)** Western blotting analysis of PlGF expression in livers from mice at day of 14, 21, and 28 after BDL. The results normalized relative to the expression of β-actin. **(E)** Quantitative RT-PCR comparing relative levels of PlGF mRNA expression in livers from mice at day of 14, 21, and 28 after BDL or SHAM. Gene expression was normalized against GAPDH and folds were fold increase over SHAM (***P* < 0.01; ****P* < 0.001).

Cells Treatment

RAW 264.7 murine cells (Sigma, St. Louis, MO, USA) were grown in 150 cm^2 flasks in DMEM supplemented with 10% FBS, 2 mM L-glutamine, 50 U/ml penicillin, and 50 μg/ml streptomycin. All incubations were performed in cells under the three or four passages. In experiments to assess the effects of PlGF on cells function, cells were transferred to 6-well plates at a density of 2.5×10^5 cells/well in serum-free medium under a humidified 5% CO_2 atmosphere at 37°C for 24 h. Then cells were washed and incubated with PBS vehicle, LPS (100 ng/ml), and recombinant mouse PlGF (rPlGF) at 50 ng/ml for 24 h at 37°C, respectively. To block the PlGF/VEGFR1 signaling, neutralizing antibody against mouse VEGFR1 (R&D Systems Inc., Minneapolis, MN, USA; 10 μg/ml) was applied where indicates. The cells were harvested for immunofluorescence analysis, RNA harvesting, and protein isolation. Staining and quantitative RT-PCR analysis were performed on three independent experiments. All measurements were performed in triplicate wells.

Cell Migration Assay

To test migration, cells were investigated using a modified Boyden chamber assay (23, 28). Briefly, RAW 264.7 cells (5×10^4 cells/well) were added to the upper chamber in DMEM without serum and exposed to rPlGF (25, 50, and 100 ng/ml) or LPS or PBS vehicle in the lower chamber. After 24 h of incubation at 37°C, cells on the upper membrane surface were removed and migratory cells on the membrane underside were fixed using 4% paraformaldehyde and stained using Crystal Violet Staining Solution (Beyotime Institute of Biotechnology, Nantong, China). Filter inserts were inverted and the number of migratory cells on the membrane underside was counted manually. The cells' migration ability was expressed as the average cell number in eight randomly chosen fields at 200× (Olympus BX45, Olympus Corporation, Tokyo, Japan).

Liver Enzymes Assays and Hydroxyproline Concentration

Serum alanine aminotransferase (ALT) and aspartate aminotransferase (AST) concentrations were determined spectrophotometrically using an automatic biochemical analyzer (Beckman, Fullerton, CA, USA). Hydroxyproline was measured in liver tissue hydrolyzates using the Hydroxyproline Assay Kit (BioVision, CA, USA) according to the manufacturer's instructions; and the results are expressed as a microgram of hydroxyproline per gram of liver tissue.

Histopathologic Evaluation, Immunohistochemistry (IHC)

In all experiments, the left liver lobe was excised and fixed with 10% neutral-buffered formalin, embedded in paraffin, and cut into 5-μm thick sections for histological analysis or IHC. Liver sections were stained with H&E and Sirius red according to standard procedures. Portal inflammation was graded with a 0–3 scale as described previously (22, 27). Fibrosis was quantified using ImageJ software 1.49 (NIH, Bethesda, MD, USA) on 10 non-contiguous Sirius red-stained sections and by the Scheuer modified histological activity index scoring system (5, 22, 27). A liver pathologist without knowledge of the treatment group examined histology. Protocol for IHC is described in detail in the supplementary experimental procedures (Figure S1 in Supplementary Material).

Immunofluorescence Staining

The dissected liver tissues retrieved were fixed in 4% paraformaldehyde solution for 30 min, washed with PBS (pH 7.4), embedded in optimum cutting temperature tissue compound (OCT compound, Sakura, Japan), and frozen at −80°C for 1 day. Then the sections (10 μm in thickness) were cut with a cryotome Cryostat (Leica, CM 1900, Germany) and placed on slides for immunofluorescence staining. Blocking was performed in PBS with 3% BSA. The slides were incubated with antibody von Willebrandfactor (vWF) (Dako North American, Inc., Carpentaria, CA, USA), F4/80, α-SMA, or CD31 (Abcam, Cambridge, CA, USA) at the dilution of 1:100 overnight at 4°C and, subsequently, incubated with antibody PlGF or VEGFR1 (Abcam, Cambridge, CA, USA) at the dilution of 1:200 for 1 h at room temperature (RT) in case of double-staining. Alexa Fluor 594 donkey anti-mouse and Alexa Fluor 488 Donkey anti-Rabbit secondary antibodies (Yeasen Biotech, Shanghai, China) were incubated at 1:200 in PBS for 1 h at RT. After washing with Tris-buffered saline for three times, the cell nuclei were counterstained with Dapi-Fluoromount-G™ (SouthernBiotech, Birmingham, AL, USA). Finally, the stained tissues were analyzed by fluorescence microscopy (BX51, Olympus, Japan).

RAW 264.7 cells plated on 24-well plates and cultured on cover glass slips were fixed and permeabilized for 10 min in 4% paraformaldehyde, 0.2% TritonX-100 in PBS. Non-specific binding was blocked with 3% BSA for 1 h at RT, and then the cells were incubated with primary antibodies for F4/80 (dilution 1:200) and VEGFR1 (dilution 1:100) overnight at 4°C. After washing twice in PBS, the cells were incubated with fluorescein-labeled secondary antibody for 1 h at RT in the dark. The nuclei were stained with DAPI in the dark for 40 min at RT. The slides were washed twice with PBS, covered with DABCO (Sigma-Aldrich, St. Louis, MO, USA), and imaged by fluorescence microscopy (IX51, Olympus, Japan).

Quantitative Analysis of Histological Markers and Angiogenesis

The number of α-SMA-, Desmin-positive cells, and the intensity of collagen III immunostaining in tissue sections were quantified using five random non-overlapping fields (100×) of each slide and determined for six animals in each group, and the area of staining was calculated as a percentage of the total area using the software NIH ImageJ 1.49 as described previously (5, 22).

For quantification of the numbers of hepatic macrophages in sections, six non-overlapping randomly selected fields of view per slide at 400× magnifications ($F4/80^+$ cells) or 200× magnifications ($CD68^+$ and $Ly6C^+$ cells) were examined and expressed as cells per fields of view; and five mice of each group were examined (22, 29, 30).

Microvascular density in the liver tissue was assessed by determining the count of CD31-labeled ECs in five areas from

each liver section at 200× magnification and is expressed as the number of CD31-positive vessels per field (22, 30). The vWF-positive cells were quantified using NIH ImageJ software; and five non-overlapping randomly selected fields of view per slide at 200× magnifications and eight mice of each group were examined (29, 30).

Western Blot Analysis

Liver samples were homogenized in RIPA lysis buffer by adding protease inhibitor Cocktail (Roche) and phosphatase inhibitors Cocktail (Sigma), and then centrifuged at 10,000 *g* at 4°C for 20 min. Protein extraction from macrophage cells was as previously described (22). The protein concentration was measured using the Bicinchoninic Acid Protein Colorimetric Assay kits (BMI, Shanghai, China) with BSA as standard. Equivalent aliquots of protein samples (40 μg) were separated by electrophoresis on 7.5–12% SDS-PAGE gels and transferred onto polyvinylidenedifluoride membranes. The membrane was then incubated in blocking buffer (5% non-fat milk powder in TBST) for 3 h followed by incubation with primary antibody in TBST overnight at 4°C with the specific primary antibodies against PlGF, α-SMA, VEGFR1, CD31, TNF-α, IL-1β, TLR4, TLR9, HIF-1α, MCP-1, VCAM-1, ICAM-1 (all from Abcam, Cambridge, CA, USA), and CXCL10 (R&D Systems Inc., Minneapolis, MN, USA) at 1:1,000 dilution. The membrane was washed with TBST and then incubated with goat anti-rabbit, anti-mouse, or anti-rat secondary antibodies (Biotech Well, Shanghai, China; 1:1,500 dilution) for 2 h at RT. GAPDH or β-actin (Cell Signaling Technology, Boston, MA, USA; 1:5,000 dilution) was used as internal control, respectively. After washing off the unbound antibody with TBST, the expression of the antibody-linked protein was determined by an ECL™ Western Blotting Detection Reagents (Amersham Pharmacia Biotech Inc., Piscataway, NJ, USA). The densitometric analysis was performed with ImageJ.

RNA Extraction and Quantitative RT-PCR

Total RNA was extracted from frozen liver tissues (caudate lobe) and cultured cells using Trizol reagent (Life Technologies, Grand Island, NY, USA) following manufacturer's protocol. RNA was extracted reverse-transcribed with random hexamers and avian myeloblastosis virus reverse transcriptase using a commercial kit (Perfect Real Time, SYBR® PrimeScriP™TaKaRa, Japan). Quantitative RT-PCR was performed for assessment of mRNA expression on an ABI Prism 7500 Sequence Detection system (Applied Biosystems, Tokyo, Japan) according to the manufacturer's protocol. Probes and primers for target genes were purchased from Sangon Biotech Co., Ltd. (Shanghai, China, Table S1 in Supplementary Material). SYBR green gene expression assays were used to quantify target genes. The relative changes normalized to GAPDH mRNA using the formula $2^{-\Delta\Delta Ct}$, where ΔΔCt represents ΔCt values normalized with the mean ΔCt of control samples.

Statistical Analysis

Data are expressed as mean ± SD. Statistical analyses were performed by using Graphpad Prism7 software (La Jolla, CA, USA). Comparisons between two independent groups were performed using a two-sample *t*-test. Comparisons between multiple groups were performed by one-way analysis of variance with *post hoc* Tukey's multiple comparison tests or by two-tailed unpaired Student's *t*-tests. A *P* value less than 0.05 was considered statistical significance.

RESULTS

PlGF Is Highly Induced in Fibrotic Liver and PlGF Silencing Robustly Limits Intrahepatic PlGF Overexpression in BDL Mice

To examine the role of PlGF in chronic liver injury and fibrosis, we have used a well-established animal model of liver fibrosis induced by BDL (**Figure 1A**). As shown in **Figure 1B**, IHC staining revealed that PlGF expression was undetectable in SHAM mice and dramatically increased in non-parenchymal cells of the fibrotic liver as fibrosis progression and minimally in hepatocytes, particularly remarkable at the portal tracts and fibrous septa at 28 days of BDL. Notably, in livers of BDL mice, PlGF immunofluorescence co-localized with α-SMA and in cells located hepatic sinusoids, suggesting that PlGF expression is upregulated in profibrotic myofibroblasts; and we also noted that PlGF slightly expressed in macrophages ($F4/80^+$) and in hepatic sinusoidal EC in sinusoids (**Figure 1C**).

To identify the role of PlGF in liver inflammation and fibrosis, we silenced PlGF *in vivo* using a chemically synthesized short, double-stranded RNA, which having well-defined structure with a phosphorylated 5′ end and hydroxylated 3′ ends with two overhanging siRNA to target hepatic PlGF expression. After 2 days of BDL, mice were injected with PlGF-specific or NTC siRNA by Invivofectamine reagent (**Figure 1A**). Efficiency of knockdown of PlGF *in vivo* by using siRNA was assessed by IHC and Western blotting; and the IHC staining signal of PlGF was obviously weak in fibrotic livers from PlGF siRNA-treated mice when compared with the livers from control and NTC siRNA-treated mice (**Figure 1B**). Consistent with our histological finding, Western blot results confirmed that targeted siRNA treatment resulted in a significant decrease in intrahepatic PlGF expression at different stages of disease progression (days 14, 21, and 28 after BDL) (**Figure 1D**). Moreover, to further ascertain the effect of siRNA-mediated suppression of PlGF expression *in vivo*, we also analyzed liver PlGF mRNA levels at 14, 21, and 28 days after BDL. Our results demonstrated that the levels of PlGF mRNA expression were gradually increased following BDL; which were significantly downregulated at their corresponding time points by PlGF siRNA administration (**Figure 1E**).

PlGF Silencing Reduces Liver Injury, Inflammation, and Fibrosis in BDL Mice

Morphological analysis by H&E staining of liver sections from BDL mice revealed distortion of the normal architecture, with a marked aggregation of lymphocytes, severe hepatocytes necrosis, and proliferation of bile ductules. Mice presented with remarkable fibrosis (stage 3 or 4) showing the characteristic pattern of extensive

portal–portal and portal–central fibrosis linkage following 4 weeks of BDL; whereas the SHAM mice shown normal architecture (**Figures 2A,B**). Impressively, however, PlGF silencing in BDL mice exhibited thinner septa, mild liver fibrosis, and more preserved hepatic parenchyma (**Figures 2A,B**). Moreover, in BDL mice, PlGF silencing decreased the severity of hepatic inflammation compared with those of NTC siRNA-treated group (1.60 ± 0.52 vs. 1.00 ± 0.47, respectively, $P = 0.021$; **Figure 2C**). This was indeed also supported by the findings that serum ALT and AST levels were decreased in BDL mice receiving PlGF siRNA (**Figure 2D**).

As revealed by the histological analysis of liver sections, there was a lower mean fibrosis score in BDL mice receiving PlGF siRNA treatment compared with those of the mice receiving NTC siRNA treatment (2.2 ± 0.8 vs. 3.2 ± 0.8, $P = 0.011$; **Figure 2E**). This was further confirmed by Sirius red-stained area analysis and hepatic hydroxyproline content, showing that PlGF silencing to BDL mice resulted in a 53.2% reduction in Sirius red-stained area ($5.64 \pm 1.21\%$ vs. $12.05 \pm 2.44\%$, $P < 0.0001$; **Figure 2F**) and a 49.5% reduction in hepatic hydroxyproline content (**Figure 2G**) compared to those animals receiving NTC siRNA. In addition, IHC evaluation showed that the deposition of collagen III was increased in the portal tracts, septa, and perisinusoidal spaces of the lobules in BDL mice, whereas PlGF siRNA treatment attenuated collagen III accumulation in livers (**Figure 2H**). These findings were supported by quantification of collagen III positive areas showing a decrease in the areas by 46.5% in fibrotic liver sections from PlGF siRNA-treated mice compared those from NTC siRNA-treated animals (**Figure 2I**). We also examined the gene expression of collagen 1α1 and collagen 3α1, suggesting the levels of both genes were significantly downregulated by siRNA-mediated PlGF knockdown in BDL mice (**Figure 2J**).

Taken together, these results suggested that PlGF silencing led to a significant reduction in BDL-induced liver inflammation and fibrogenesis in mice.

PlGF Silencing Inhibits Activation of HSCs in BDL Mice

Activated HSCs are considered central ECM-producing cells within the injured liver and also involved in the pathologic angiogenesis and vascular remodeling (22, 23). We found that PlGF silencing induced a significantly reduction in BDL-induced expression of the marker of activated HSCs, α-SMA, and Desmin as shown by IHC analysis (**Figure 3A**). Moreover, computer-assisted semiquantitative analysis demonstrated that the number of α-SMA- and Desmin-positive cells was significantly lower in livers from PlGF siRNA-treated BDL mice than those from NTC siRNA-treated BDL mice (**Figure 3B**). These findings were substantiated by quantitative RT-PCR experiments, suggesting the levels of α-SMA and Desmin mRNA transcript in fibrotic livers were correspondingly reduced following PlGF knockdown (**Figure 3C**). In addition, we also examined α-SMA protein expression by western blotting, indicating PlGF silencing with siRNA inhibited the α-SMA protein expression *in vivo* (**Figure 3D**). Collectively, these *in vivo* data indicated that PlGF silencing efficiently inhibited myofibroblastic activation of HSC during BDL-induced liver injury and fibrosis.

PlGF Silencing Attenuates Hepatic Angiogenesis in BDL Mice

To investigate the vascular changes in PlGF silencing, we conducted studies to determine hepatic neovascularization and the expression of angiogenic factors in livers. The EC marker CD31 was expressed in the endothelium of the veins and in the central veins in livers of sham-operated mice, but not along the sinusoids; and challenge mice by BDL at 28 days led to a markedly increased number of CD31-positive vessels in livers (**Figure 4A**). However, CD31-positive EC staining in BDL siPlGF liver sections was significantly less than in the BDL siNTC group as evidenced in mean microvessels density (67.9 ± 8.1 vs. 41.1 ± 6.4/per field, $P < 0.001$) (**Figure 4B**). These results were further supported by the levels of CD31 mRNA and protein expression in livers; showing that hepatic angiogenesis was inhibited by PlGF silencing in fibrotic mice (**Figures 4E,F**). Similar histologic pattern was observed in vWF staining of tissues, indicating upregulated in livers from BDL mice; however, BDL mice receiving PlGF-siRNA exhibited decrease in the intensity of vWF staining and vWF-positive vessels area in livers (**Figures 4C,D**), consistent with the decrease in vWF gene expression (**Figure 4F**). In addition, we noted a significant decrease in expression of HIF-1α in fibrotic animals treated with PlGF siRNA as shown by IHC (**Figure 4G**) and Western blot analysis for HIF-1α confirmed the morphological changes observed (Figure S1 in Supplementary Material). Similarly, hepatic HIF-1α mRNA levels in BDL mice were also significantly reduced by PlGF silencing with siRNA *in vivo* (**Figure 4H**). Together, these results indicated that PlGF silencing effectively attenuates pathologic vascular changes that occur in response to BDL.

PlGF Silencing Reduces Hepatic Macrophage Recruitment in BDL Mice

To investigate the mechanism of PlGF silencing in the pathogenesis of hepatic inflammation and fibrosis-associated angiogenesis, we explored the markers of monocytes and macrophages infiltration in fibrotic livers. Compared to the SHAM mice, IHC staining for the macrophage markers indeed revealed BDL-enhanced infiltration of $F4/80^+$ or $CD68^+$ macrophages into fibrotic livers. Remarkably, however, the increase of hepatic macrophages infiltration was significantly reduced by PlGF siRNA treatment in BDL mice when compared with those by NTC siRNA treatment mice (**Figure 5A**); and the results were further confirmed by quantification of the $F4/80^+$ or $CD68^+$ staining cells (**Figure 5B**). Moreover, these results consistent with the genes expression of F4/80 and CD68, demonstrating PlGF silencing in BDL mice strikingly decreased the upregulated F4/80 and CD68 mRNA levels (**Figure 5C**). In addition, the total number of $Ly6C^+$ cells, a marker for BM-derived circulating peripheral blood monocytes, was also significantly higher in fibrotic livers in BDL mice than normal livers from the SHAM mice. However, PlGF silencing led to reduced $Ly6C^+$ macrophage infiltration (**Figures 5A,B**). Similarly, hepatic Ly6C mRNA expression in BDL mice was also inhibited by PlGF silencing with siRNA *in vivo* (**Figure 5C**). Taken together, these results suggested that siRNA-mediated PlGF knockdown significantly reduced hepatic macrophage

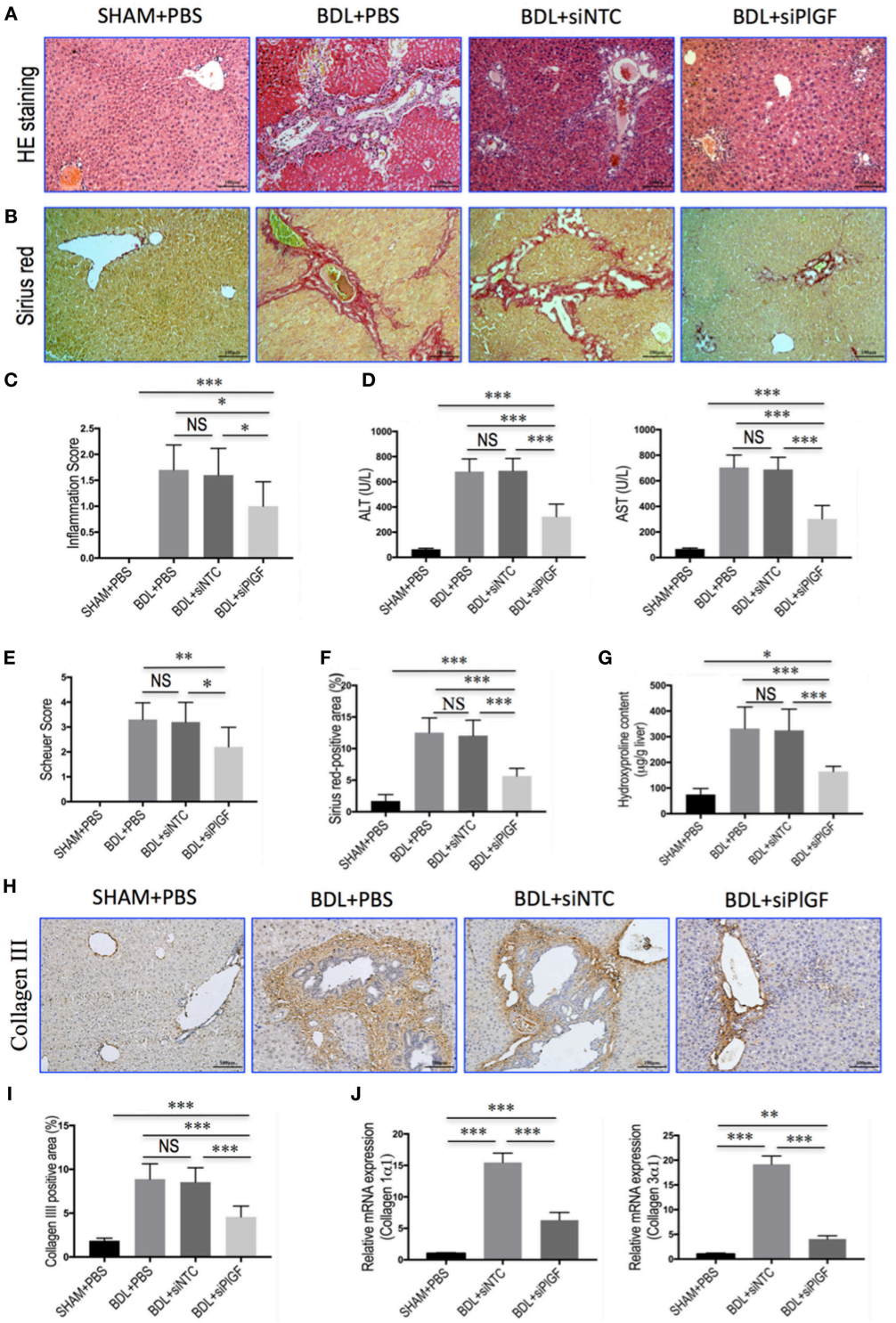

FIGURE 2 | Placental growth factor (PlGF) silencing reduces liver injury, inflammation, and fibrosis in bile duct ligation (BDL) mice. **(A)** H&E stained in liver sections (original magnification: 100×). Mice underwent SHAM or BDL surgery and received small interfering RNA or PBS and sacrifice at 28 days. **(B)** Sirius red staining of liver sections (original magnification: 100×). **(C)** Inflammation scores (n = 10/group). **(D)** Serum alanine aminotransferase (ALT) and aspartate aminotransferase (AST) concentrations in mice from each group (n = 8–10/group). **(E)** Assessment of liver fibrosis based on Scheuer's scoring system. **(F)** Hepatic fibrotic area based on Sirius red staining. **(G)** Liver hydroxyproline concentration (n = 8/group). **(H)** Representative microscopy images of collagen III immunohistochemistry (original magnification: 100×). **(I)** Quantitative analysis of collagen III positive area (n = 8/group). **(J)** Hepatic expression of collagen 1α1 and collagen 3α1 mRNA was determined by quantitative RT-PCR. Results were normalized relative to GAPDH expression and expressed as mean ± SD fold increase over SHAM control mice. $^{*}P < 0.05$; $^{**}P < 0.01$; $^{***}P < 0.001$; NS, not significant.

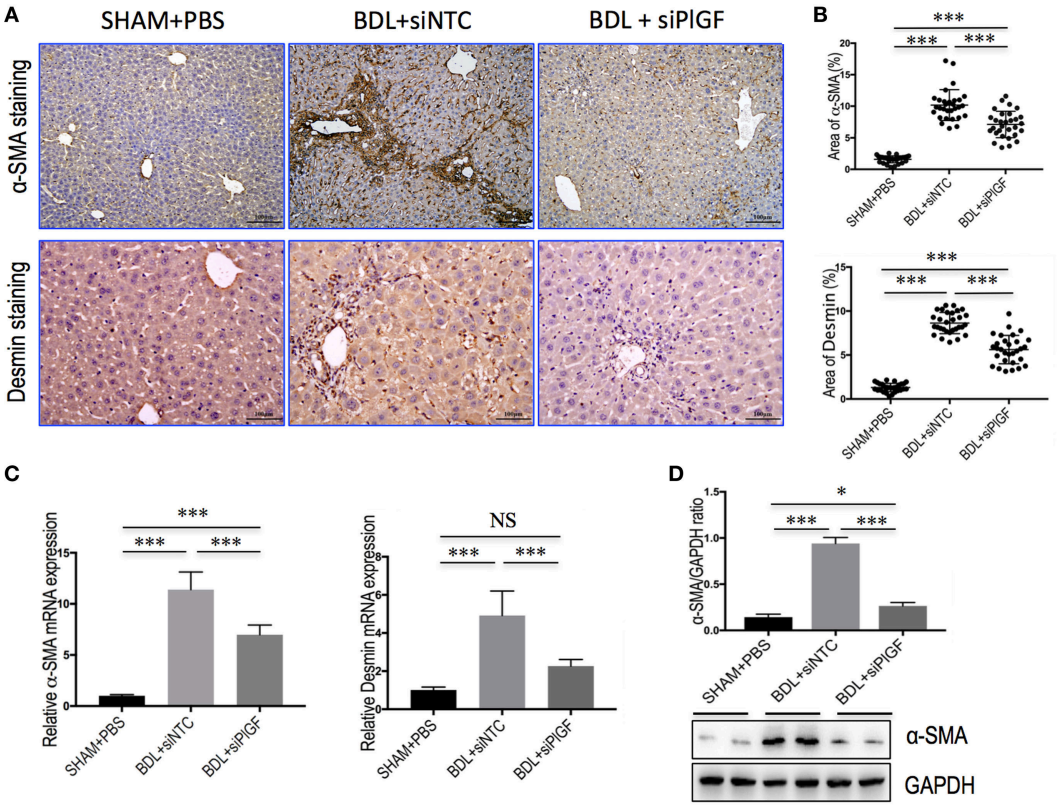

FIGURE 3 | Placental growth factor (PlGF) silencing inhibits activation of hepatic stellate cells in bile duct ligation (BDL) mice. **(A)** Representative microscopy images of α-SMA staining (original magnification: 100×) and Desmin staining (original magnification: 200×) in livers. Mice were induced liver fibrosis by BDL for 28 days and treated with small interfering RNA or PBS. **(B)** Quantification of α-SMA- and Desmin-positive area by ImageJ software (NIH). Results mean of six fields and $n = 5$/group. **(C)** Hepatic α-SMA and Desmin mRNA expression was determined by quantitative RT-PCR ($n = 5$). Results were normalized relative to GAPDH expression and expressed as mean ± SD fold change over SHAM control mice. **(D)** Western blot analysis of hepatic α-SMA expression and GAPDH as loading control. $^{*}P < 0.05$; $^{***}P < 0.001$; NS, not significant.

recruitment to the livers, which being responsible for attenuating liver inflammation and fibrosis.

PlGF Silencing Inhibits Macrophages Activation and Inflammatory Properties in BDL Mice

To investigate whether PlGF mediates liver inflammation through switching macrophages subtypes and regulating their function, we examined the expression of pro-inflammatory cytokines associated with M1 macrophages in the liver of fibrotic mice, such as TNF-α, IL-1β, and MCP-1. Our results demonstrated that hepatic expression of TNF-α, IL-1β, and MCP-1 mRNA was strongly upregulated in BDL fibrosis models. However, BDL mice receiving siPlGF reduced TNF-α, IL-1β, and MCP-1 mRNA by 6.1-fold, 7.0-fold, and 3.5-fold, respectively (**Figure 6A**). Those findings were supported by our Western blot analysis, demonstrating that the increase of these chemokines in fibrotic liver was indeed attenuated by PlGF silencing (**Figure 6B**).

In addition, we also examined the expression of TLR4 and TLR9 in livers. IHC data showed that weak constitutive expressions of TLR4 or TLR9 on sinusoidal ECs of SHAM mice livers, with hepatocytes showing no or only slight expression (**Figure 6C**). After 4 weeks BDL, increased TLR4 or TLR9 expression in livers was markedly observed in the periportal and interlobular septa, as well as increased expression on interstitial space between hepatocytes. However, giving PlGF siRNA to BDL mice resulted in moderate staining for TLR4 and TLR9 (**Figure 6C**). Consistent with these results, the expression of TLR4 and TLR9 protein was obviously upregulated in livers of BDL mice; however, siPlGF treatment to BDL mice decreased hepatic TLR4 and TLR9 expression when compared with vehicle treatment (**Figure 6D**). Similar results were seen in TLR4 and TLR9 mRNA expression, indicating PlGF silencing markedly reduced both gene expression (**Figure 6E**).

To further understand the link between PlGF knockdown and the reduction in inflammatory infiltrate, the expression of pro-inflammatory adhesive molecules, such as CXCL10, ICAM-1, and VCAM-1 in the vasculature of fibrotic mice was also analyzed. We found that the levels of CXCL10, VCAM-1, and ICAM-1 mRNA expression in livers were markedly enhanced in BDL mice received siNTC compared with SHAM mice, but these increase in livers were attenuated by PlGF siRNA treatment to BDL mice (**Figure 7A**). Meanwhile, those finding were supported by our western blotting, demonstrating that the increase of these

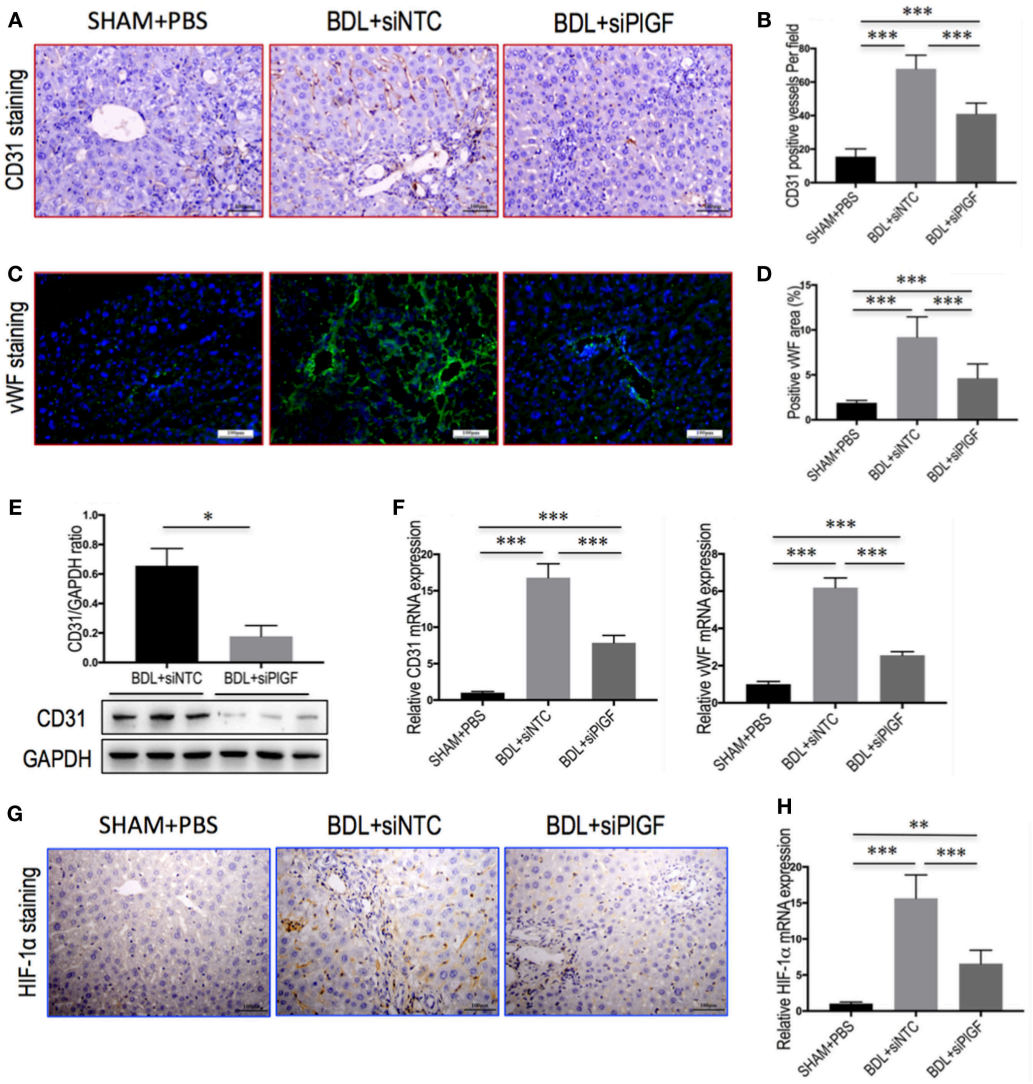

FIGURE 4 | Placental growth factor (PlGF) silencing attenuates hepatic angiogenesis in bile duct ligation (BDL) mice. Mice were induced liver fibrosis by BDL for 28 days and treated with small interfering RNA or PBS. **(A)** Representative images of intrahepatic CD31 immunohistochemistry (IHC) staining in mice from each group (original magnification: 200×). **(B)** Microvessel density was assessed by counting CD31-positive vessels (n = 8/group). **(C)** Representative images of intrahepatic von Willebrandfactor (vWF) immunofluorescence staining in mice from each group (original magnification: 200×). **(D)** Microvessel density was assessed by vWF-positive vessels area in livers (n = 8/group). **(E)** Western blot analysis of hepatic CD31 expression and GAPDH as loading control (n = 3). **(F)** Hepatic CD31 and vWF mRNA expression were determined by quantitative RT-PCR. Results were normalized relative to GAPDH expression and expressed as mean ± SD fold change over SHAM control mice (n = 5). **(G)** Representative images of intrahepatic HIF-1α IHC staining in mice from each group (original magnification: 200×). **(H)** Hepatic HIF-1α mRNA expression was determined by quantitative RT-PCR. Results were normalized relative to GAPDH expression and expressed as mean ± SD fold change over SHAM control mice (n = 5) (*P < 0.05; **P < 0.01; ***P < 0.001).

chemokines in BDL-induced fibrotic livers was indeed attenuated by PlGF silencing (**Figure 7B**).

Taken together, these results suggest that PlGF might play a key role in the activation of Kuffer cells/macrophages in liver upon chronic injury and substantially produce a variety of pro-inflammatory cytokines and chemokines.

PlGF Promotes Hepatic Macrophage Recruitment and Activation *via* VEGFR1

Placental growth factor exclusively binds to VEGFR1 and not VEGFR2 (17, 18), we, therefore, investigated whether VEGFR1 signaling in macrophages mediated the role of PlGF in liver inflammation and fibrosis *in vivo*. First, we investigated the cellular source of VEGFR1 in fibrotic livers; and our double staining of liver sections for VEGFR1 and CD31, F4/80, or α-SMA revealed obviously increased expression VEGFR1 in those non-parenchymal cells in mice of BDL, whereas there has weak expression in those cells in livers from SHAM mice (**Figure 8A**). Next, we further examined levels of VEGFR1 in fibrotic livers at 4 weeks of BDL mice by both quantitative RT-PCR and Western blot analysis, respectively. Our results showed that a marked increase in VEGFR1 mRNA and protein expression was demonstrated

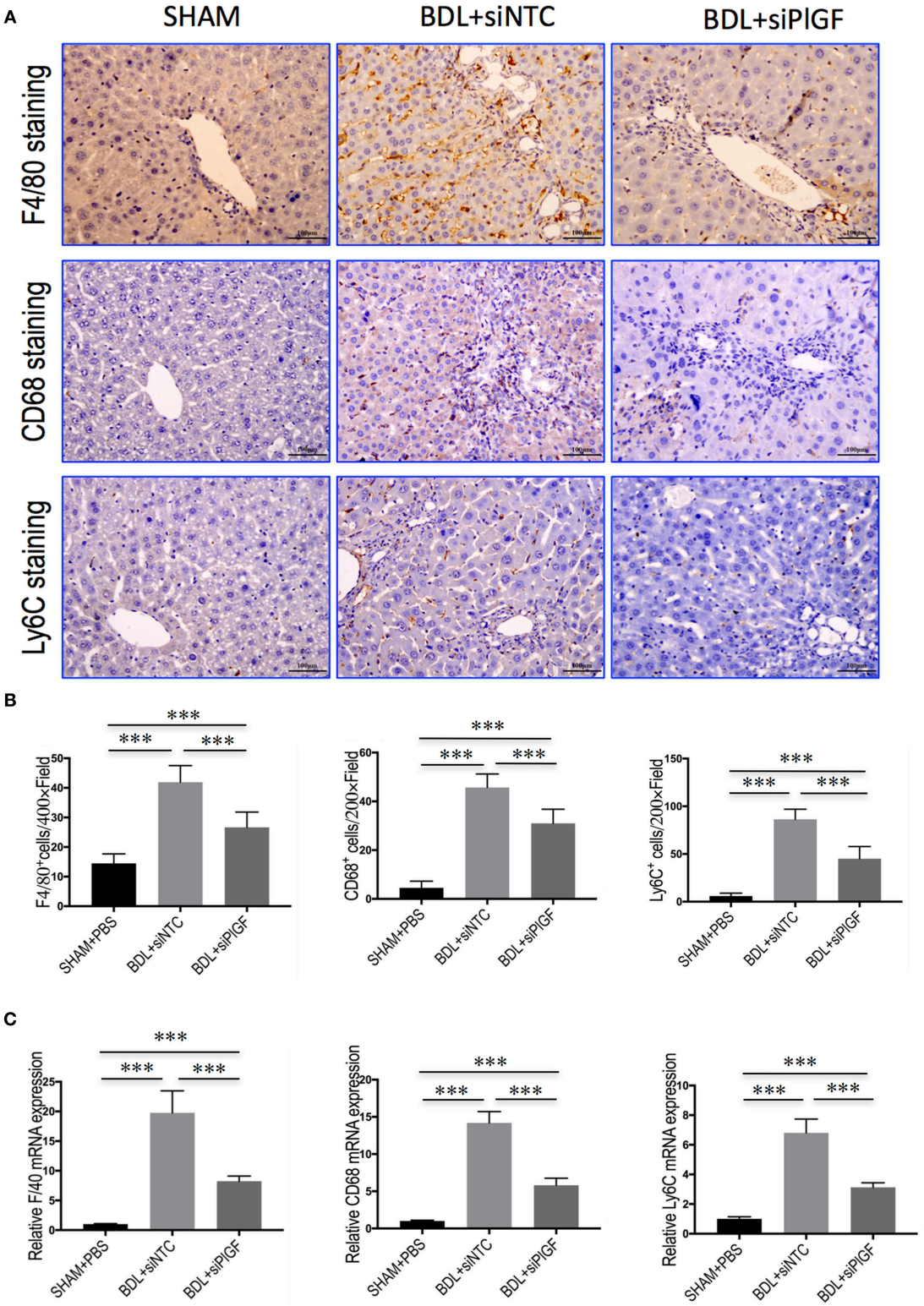

FIGURE 5 | Placental growth factor (PlGF) silencing reduces hepatic macrophage recruitment to the liver in bile duct ligation (BDL) mice. **(A)** Immunohistochemical detection of F4/80-, CD68-, and Ly6C-positive cells in liver sections (original magnification: 200×). Mice were induced liver fibrosis by BDL for 28 days and treated with small interfering RNA or PBS. **(B)** Quantization of F4/80-, CD68-, and Ly6C-positive cells in liver sections. Results mean of six fields and $n = 5$/group. **(C)** Hepatic expression of F4/80, CD68, and Ly6C mRNA was determined by quantitative RT-PCR, and the results are shown as fold change compared with sham-operated (SHAM) control and GAPDH served as loading control ($n = 5$) (***$P < 0.001$).

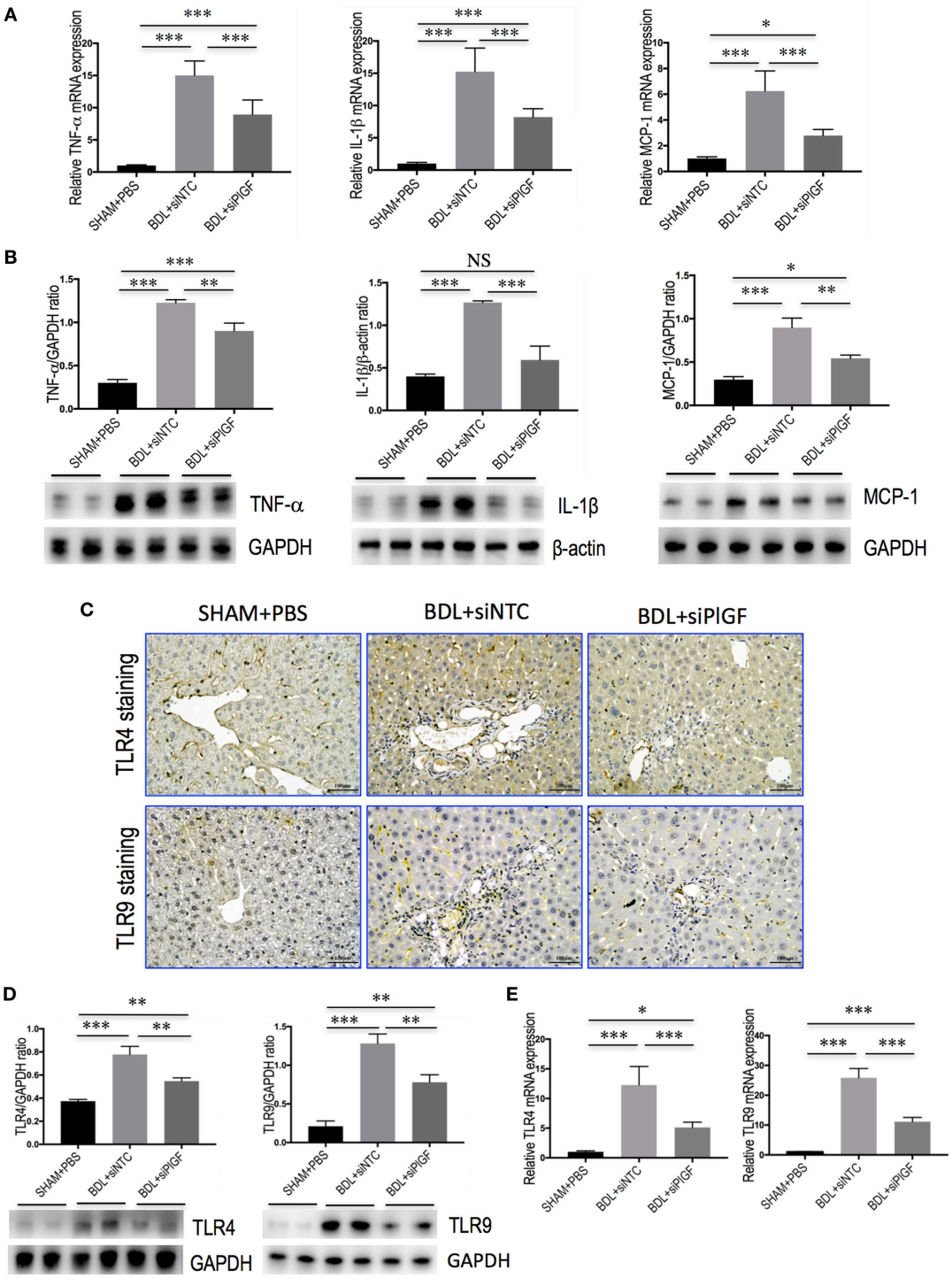

FIGURE 6 | Placental growth factor (PlGF) silencing reduces hepatic macrophages activation and inflammatory properties in bile duct ligation (BDL) mice. Mice were induced liver fibrosis by BDL for 28 days and treated with small interfering RNA or PBS. **(A)** Hepatic expression of TNF-α, IL-1β, and MCP-1 mRNA was determined by quantitative RT-PCR, and results are shown as fold change compared with sham-operated (SHAM) control and GAPDH served as loading control ($n = 5$). **(B)** Western blot analysis of hepatic TNF-α, IL-1β, and MCP-1 protein expression, with results normalized relative to the expression of GAPDH or β-actin ($n = 3$). **(C)** Immunohistochemical staining for TLR4 and TLR9 in livers (original magnification: 200×). **(D)** Western blotting analysis of hepatic TLR4 and TLR9 protein expression with results normalized relative to the expression of GAPDH ($n = 3$). **(E)** Hepatic expression of TLR4 and TLR9 mRNA was determined by quantitative RT-PCR, and the results are shown as fold change compared with SHAM control and GAPDH served as loading control ($n = 5$). $^*P < 0.05$; $^{**}P < 0.01$; $^{***}P < 0.001$; NS, not significant.

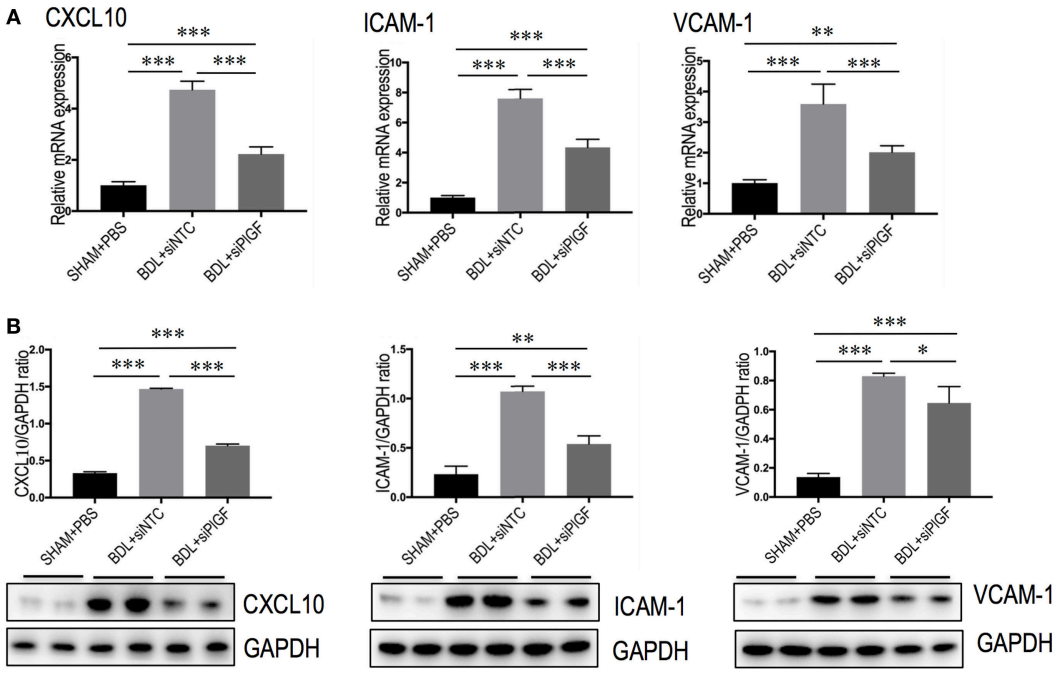

FIGURE 7 | Placental growth factor (PlGF) knockdown attenuates the expression of pro-inflammatory adhesive molecules in the vasculature of fibrotic mice. **(A)** Hepatic expression of CXCL10, intercellular adhesion molecule 1 (ICAM-1), vascular cell adhesion molecular-1 (VCAM-1) mRNA expression was determined by quantitative RT-PCR, and results are shown as fold change compared with sham-operated (SHAM) control. GAPDH served as loading control ($n = 5$). **(B)** Western blotting analysis of CXCL10, ICAM-1, and VCAM-1 protein expression in lysed liver tissue from each group mice, with results normalized relative to the expression of GAPDH ($n = 3$) (*$P < 0.05$; **$P < 0.01$; ***$P < 0.001$).

with the development of hepatic fibrosis in BDL mice compared with SHAM control (**Figures 8B,C**). However, PlGF silencing significantly downregulated the expression of VEGFR1 at gene levels and at protein levels in fibrotic livers when compared to NTC siRNA-treated fibrotic mice (**Figures 8B,C**).

To further confirm whether VEGFR1 expression on macrophages was involved in macrophages recruitment or activation upon liver injury, we tested the migratory response and inflammatory properties of mouse macrophages RAW 264.7 cell line using an *in vitro* transmigration assay with recombinant mouse PlGF (rPlGF). First, we evaluated the effect of PlGF on VEGFR1 expression from macrophages, we selected LPS as positive control since LPS is known to activate macrophages *in vitro*. Indeed, rPlGF stimulated VEGFR1 expression in RAW 264.7 cells as shown by double immunofluorescent staining (**Figure 8D**) and Western blotting (**Figure 8E**), consistent with increased expression of VGFR1 in livers from BDL mice. Similarly, the levels of VEGFR1 mRNA expression were also increased by rPlGF in a similar manner in LPS-treated (**Figure 8F**). Second, RAW 264.7 cells were treated for 24 h with rPlGF (50 ng/ml) and there was 6.98-fold increase in RAW 264.7 cell migration toward rPlGF in Boyden assays compared to cells migrating toward vehicle (**Figures 9A,B**). The 24-h incubation time and 50 ng/ml contents of PlGF were chosen on the basis of the results of a pilot studies (Figure S2 in Supplementary Material). Moreover, to determine whether PlGF could activate macrophages to generate cytokines, MCP-1, TNF-α, and IL-1β, we utilized an *in vitro* assay to mimic this situation. rPlGF treatment of RAW 264.7 cells for 24 h showed that the expression of MCP-1, TNF-α, and IL-1β mRNA were obviously increased as shown in our quantitative RT-PCR results (**Figure 9C**). Finally, to further confirm the role of PlGF in the migration and activation of macrophages, we blocked PlGF/VEGFR1 signaling axis with a specific VEGFR1 neutralizing antibody that was added to cultured cells. We found that the upregulation of inflammatory cytokines (MCP-1, TNF-α, and IL-1β) in macrophages at rPlGF challenge was reduced by VEGFR1 neutralizing antibody (**Figure 9C**), suggesting that PlGF/VEGFR1 signaling axis was strongly involved in activation of macrophages. Notably, the migratory capacity of macrophages was also significantly inhibited (52.2% reduction in mean cells number) while PlGF/VEGFR1 signaling was blocked (**Figures 9A,B**). Together, these results show clearly that PlGF promotes macrophage recruitment and activation upon liver injury *via* VEGFR1.

DISCUSSION

Currently, no effective therapy is available for liver fibrosis, and a better understanding of pathologic mechanisms regulating this disorder is urgently needed for identifying novel antifibrotic therapeutic agents (1–3). In this study, our findings lend support for the notion that PlGF plays a critical role in the pathogenesis of fibrotic liver disease and provide evidence that PlGF is a potential therapeutic target in chronic inflammatory liver diseases (22, 23).

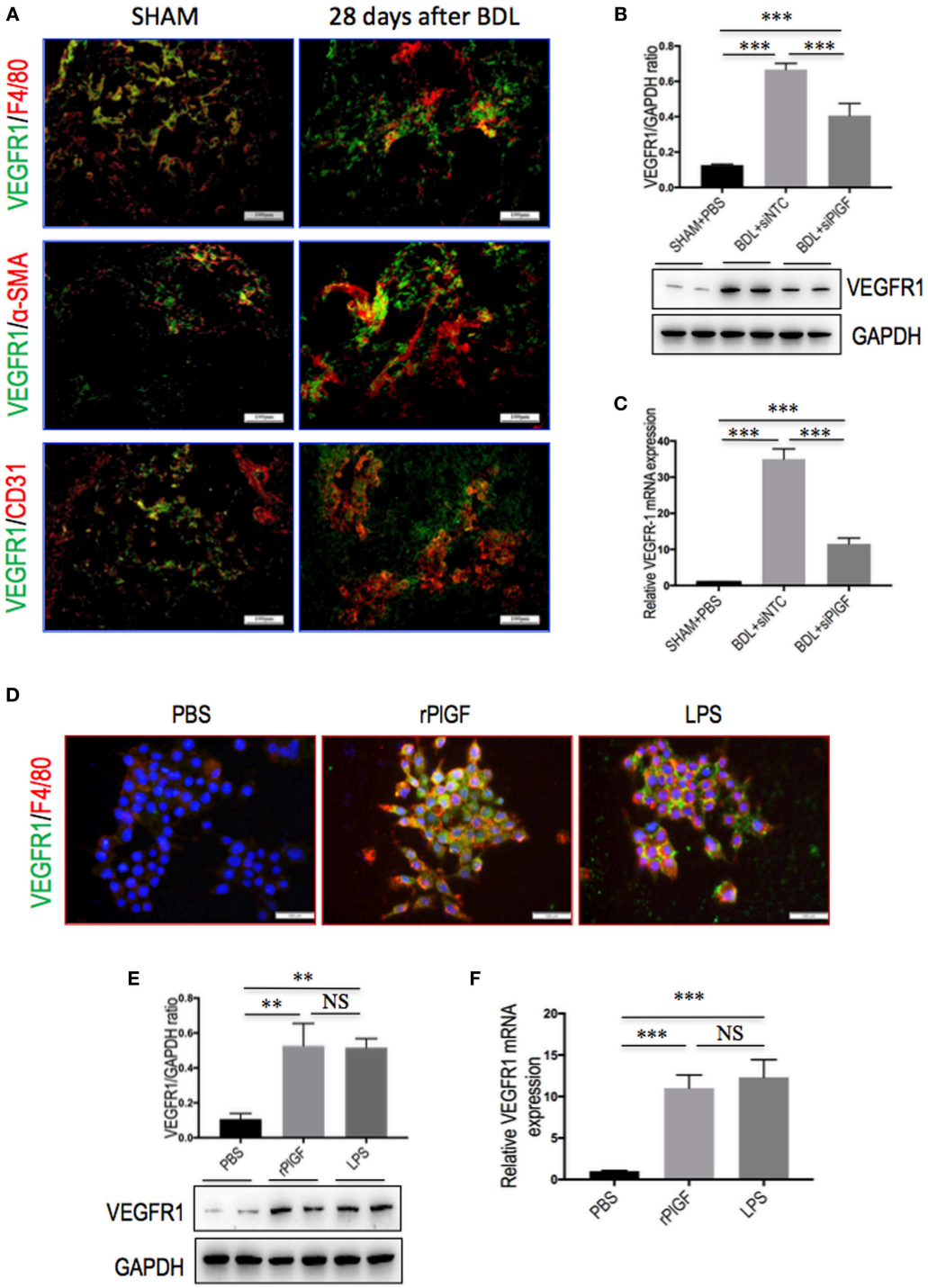

FIGURE 8 | The expression and distribution of VEGR1 in fibrotic livers and in macrophages. **(A)** Immunofluorescent double staining of vascular endothelial growth factor receptor 1 (VEGFR1) in liver sections of bile duct ligation (BDL) or sham-operated (SHAM) mice at 28 days. Livers were double stained for VEGFR1 (green) and CD31 (endothelial cells marker), F4/80 (macrophages), or α-SMA (myofibroblasts). Original magnification: 200×. **(B)** Western blotting analysis of VEGFR1 expression in lysed liver tissues, with results normalized relative to the expression of GAPDH ($n = 3$). **(C)** Hepatic VEGFR1 mRNA expression was measured by quantitative RT-PCR. Results are shown as fold change compared with SHAM control and GAPDH served as loading control ($n = 5$). **(D)** Double immunofluorescent expression of VEGFR1 (green) and macrophages marker F4/80 (red) in RAW 264.7 cell line. Cells were stimulated with rPlGF (50 ng/ml) or lipopolysaccharide (LPS) (100 ng/ml) for 24 h, respectively. DAPI as blue nuclear counterstain. Scale bar = 100 μm for each picture. **(E)** Western blot analysis for VEGFR1 in macrophages RAW 264.7 cells stimulated with rPlGF (50 ng/ml) or LPS (100 ng/ml) for 24 h. PBS and LPS serve as negative and positive controls, respectively. **(F)** The levels of VEGFR1 mRNA RT-PCR expression in RAW 264.7 cell were measured by quantitative RT-PCR. Cells stimulated with rPlGF (50 ng/ml) or LPS (100 ng/ml) for 24 h. The mRNA levels were normalized to GAPDH mRNA levels and presented as fold stimulation (mean ± SD) vs. PBS (**$P < 0.01$; ***$P < 0.001$; NS, not significant).

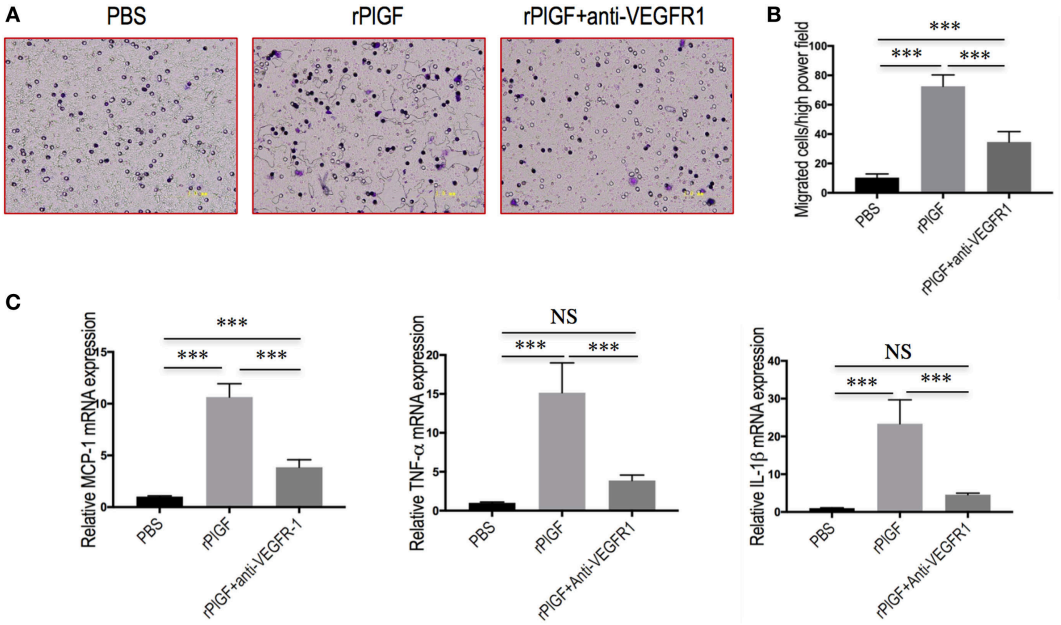

FIGURE 9 | Placental growth factor (PlGF) promotes hepatic macrophage recruitment and polarization *via* vascular endothelial growth factor receptor 1 (VEGFR1) signaling. **(A)** Migration of macrophages toward PlGF was assessed in Boyden's chamber experiments. Original magnification: 200×. **(B)** Migration of macrophages into the lower chamber was quantified 24 h after stimulation. Media only, PlGF (50 ng/ml) or PlGF + VEGFR1 blocking antibody (10 μg/ml) for 24 h. **(C)** The levels of MCP-1, TNF-1α, and IL-1β mRNA expression in RAW 264.7 cell were measured by quantitative RT-PCR. The mRNA levels were normalized to GAPDH mRNA levels and presented as fold stimulation (mean ± SD) vs. PBS. ***$P < 0.001$; NS, not significant.

Moreover, knockdown of PlGF by siRNA in BDL mice ameliorates hepatic inflammation, angiogenesis, and fibrogenesis. Most importantly, these findings have provided new insights for understanding the mechanism of PlGF contributing to liver inflammation and fibrosis through promoting recruiting hepatic macrophage to the liver and enhancing inflammatory responses.

To date, it has been widely accepted that hepatic fibrosis develops as a response to chronic liver injury and almost exclusively occurs in a pro-inflammatory environment (1–4). Recent studies indicated that hepatic macrophages play important roles in the pathogenesis of hepatic inflammation and fibrosis (9–13, 29–32). During ongoing chronic injury and the progression of fibrosis, pro-inflammatory macrophages derived from monocytes prevail in the liver (12, 13, 32–34). Both monocyte-derived macrophages and Kupffer cells have profibrogenic properties, by promoting the activation and survival of HSCs and myofibroblasts through secreting both TGF-β and PDGF (33–35). Given that inflammatory macrophages can exacerbate chronic liver disease, a deeper understanding of the mechanisms by which macrophages promote inflammation and fibrosis might lead to novel strategies to treat liver diseases (12, 31, 33).

As is well-known that PlGF is a multitasking cytokine and is involved in BM-derived cell activation, endothelial stimulation, inflammation, pathologic angiogenesis, and wound healing (17–20, 36). We demonstrated that hepatic PlGF expression was remarkably increased in the BDL model (**Figure 1**); and PlGF and its main receptor VEGFR1 were upregulated in activated HSCs and macrophages (**Figures 1** and **8**); these results agree with the findings of others and our recent reports in CCl4 animal models (22, 23). Notably, our recent *in vitro* study demonstrated that hypoxia could induce PlGF overexpression dependent on HIF-1α during liver fibrosis, then promotes HSCs activation and proliferation through modulating PI3K/Akt signaling pathway (22). Therefore, it is likely that PlGF may also induce recruitment of monocytes and macrophages to the injury livers and promote macrophages activation, contributing to liver inflammation and HSCs activation during fibrosis development. As expected, our results indeed demonstrated that PlGF silencing suppressed the activation of HSCs (**Figure 3**) and reduced the severity of liver inflammation in BDL mice (**Figure 2C**), which leads to attenuate liver fibrosis and angiogenesis.

Besides PlGF directly amplifies HSC activation, in this study, we focused particularly on the role of PlGF in interactions between macrophages and HSC as well as in activation of HSC during fibrogenesis *in vivo*. Indeed, the results of this study indicated that PlGF silencing in BDL mice remarkably inhibited the activation of macrophages (**Figures 6** and **7**) or recruitment of $CD68^+$, $F4/80^+$, and $Ly6C^+$ macrophages into the fibrotic liver (**Figure 5**), which were critically involved in the mechanism to explain the attenuated fibrosis and HSC activation observed in the treatment of PlGF silencing. Consistent with this notion, PlGF has been shown to promote monocyte infiltration in ischemic tissues, tumors, atherosclerotic plaques, and bone fractures (18, 37). Moreover, prior studies have demonstrated that inhibition of PlGF might also affect tumors by reducing TAM infiltration (18, 22–26). It also induces polarization of TAM to an M2-like proangiogenic phenotype, thereby promoting tumor vessel disorganization (17, 18, 38). In addition, the recruitment

process is also mediated by other chemokines and its receptors, such as CXCL10, ICAM-1, VCAM, and CCR2 (33, 35, 39, 40). Although mice induced by BDL significantly increased mRNA and protein expression of CXCL10, ICAM-1, and VACM-1 in livers, this increase was obviously impacted by PlGF silencing (**Figure 7**). It is noteworthy that the CXC family of chemokines also operates in pathological angiogenesis preceding/perpetuating fibrosis (39, 40).

Liver injury triggers Kupffer cell activation, leading to inflammatory cytokines and chemokines release, which exert a key role in the process of liver fibrosis and angiogenesis (31, 35, 40). In line with lower levels of intrahepatic macrophages, pro-inflammatory cytokines, such as TNF-α, IL-1β, and MCP-1 were significantly reduced in liver tissue by knockdown of PlGF by siRNA in BDL mice (**Figures 6A,B**). Several independent studies highlighted the importance of the chemokines receptor CCR2 and its main ligand, MCP-1, for monocyte/macrophage recruitment during experimental hepatic fibrosis, suggesting that inhibition of CCR2 or MCP-1 might bear therapeutic potential in chronic liver diseases (8, 9, 33, 41). In addition, macrophages also express multiple toll-like receptors (TLRs)—such as TLR4 and TLR9, and it has been reported that TLRs interact with oxDNA and microbial components, such as LPS, Hsp60, and other ligands, and result in macrophage activation and the productions of pro-inflammatory mediators (such as TNF-α and MCP-1) (32, 35, 42–44). In this study, we also found that PlGF silencing inhibited the levels of TLR4 and TLR9 gene and protein expression in fibrotic liver after 4-week BDL (**Figures 6C,E**), contributing to amelioration of liver inflammation and fibrosis (42–44). Thus, these results indicated that the interaction of HSCs with pro-inflammatory cells such as Kupffer cells was a crucial event in HSCs activation and fibrosis (6–9, 29), while chemokines and their receptors were likely to serve as important contributors to this interaction (6–9, 25, 32, 44).

In addition, fibrosis is typically associated with impaired angiogenesis and sustained development of local tissue hypoxia (6, 22). Of note, hypoxia has been shown to be a profibrotic stimulus that contributes to the development of fibrosis and angiogenesis through an HIF-mediated pathway (6, 22), we also have demonstrated that HIF-1α was increased in fibrotic livers induced by BDL (**Figure 4**; Figure S1 in Supplementary Material); however, PlGF-specific siRNA inhibited the expression of HIF-1α in fibrotic livers, thus contributing to the decreased liver fibrosis and angiogenesis. Interesting, HIF-1 is an important molecular in gene upstream of PlGF and VEGF (25, 45). Moreover, inflammatory cell infiltration has often been linked to angiogenesis (40, 44). It has been previously shown that PlGF activated and attracted macrophages, which are capable of releasing angiogenic and lymphangenic molecules mediating angiogenesis (17, 39).

Therefore, these findings suggest that PlGF is involved in hepatic macrophage infiltration and Kupffer cell activation during chronic liver injury, leading to liver fibrogenesis and promoting hepatic angiogenesis, along with HSCs activation. Our results also supported the notion that selective inactivation of Kupffer cells represents a potential mechanism aimed to disrupt the sequence of events leading to liver injury (31–35). However, it is important to mention that macrophages have divergent functions in fibrogenesis and specific populations also promote the resolution of fibrosis in liver through enhanced ECM degradation (3–6, 31, 46). This highlights that further exploring the difference activities of these various macrophages phenotypes during liver fibrosis and resolution of fibrosis are of importance therapeutically.

Mechanically, PlGF specifically binds VEGFR1 and not VEGFR2 (17, 18), activation of VEGFR1 in macrophages by VEGF or by PlGF, contributes to the exacerbation of certain pathophysiological conditions such as inflammation (17, 22, 37). Moreover, PlGF may induces VEGF release from mononuclear cells, and the binding of PlGF to VEGFR1 leads to intermolecular cross-talk between VEGFR1 and VEGFR2, which amplifies VEGFR2 signaling and consequently enhances VEGF-driven response (37, 47, 48). Therefore, the inhibition of PlGF also could suppress both VEGF-driven inflammation and angiogenesis (22, 38, 47, 48). This concept is supported by our present *in vivo* and *in vitro* studies, indicating that VEGFR1 is overexpressed on macrophages upon injury or rPlGF challenge *in vitro*; and PlGF promotes the migration and activation of macrophages into fibrotic liver dependent on VEGFR1 (**Figure 8**). Since blocking PlGF/VEGFR1 signaling axis significantly inhibits macrophages migration and reduces inflammatory gene expression *in vitro* (**Figure 9**). Recent studies also demonstrated that the PlGF/VEGFR1 signaling axis was involved in cancer-associated angiogenesis (17, 18, 38). Taken together, these observations strongly suggest that either PlGF or VEGFR1 inhibition can provide therapeutic benefit.

However, it is important to mention that our study has some limitations. Firstly, we examined the effect of PlGF on macrophages recruitment and activation in liver fibrosis by siRNA *in vivo*, as other cells in fibrotic liver, such as EC and HSC, also expression PlGF (**Figures 1B,C**), therefore, this no cell-specific siRNA delivery may also affect those cells and mediated in liver fibrosis. Second, it is worth remembering that VEGFR1 is also expressed on activated HSCs and vascular ECs in fibrotic livers (**Figure 8A**), studies focusing on the role of VEGFR1 in these cells should provide more insight into the pathogenesis of fibrosis-associated angiogenesis (45). Third, given that NRP-1 is a coreceptor of PlGF, the effect of PlGF on macrophages may also be involved in NRP-1. Finally, although this injection route delivers siRNA preferentially targeted to liver, this is a challenging process and it is necessary to administer PlGF siRNA repeatedly for the continuous knockdown of PlGF mRNA *in vivo* in order to prevent the progression of hepatic fibrosis. Therefore, further studies on the current topic will need to be undertaken.

In conclusion, our study provides evidence that PlGF mediates the pathogenesis in liver inflammation, angiogenesis, and fibrosis. PlGF is a multitasking cytokine in its ability to promote the recruitment macrophages to the liver and to induce macrophages activation during liver injury and fibrosis in BDL mice. Based on these scientific considerations, inhibiting the PlGF signaling could provide a novel therapeutic target for chronic liver diseases.

ETHICS STATEMENT

The experimental protocol was performed in accordance with the guiding principles for the care and use of laboratory animals

approved by the Fudan University Animal Care Committee and all animals received humane care.

AUTHOR CONTRIBUTIONS

XL and CT conceived the study and wrote the manuscript; XL and CT contributed to the work designing, performing, analyzing, and interpreting data from all the experiments; QY, QJ, YZhou, YZou, and SZ participated in the design, acquisition, analysis, and interpretation of data; ZL and XL carried out the surgery and all the *in vivo* animal experiments; CT and XL interpreted the data and finalized the article. All authors have critically revised and approved the final manuscript and agreed to be accountable for all aspects of the work.

ACKNOWLEDGMENTS

We thank Hongchun Liu, Lixin Li, and Jiefeng Cui for excellent assistance, and members of the laboratory for helpful discussion.

FUNDING

This work was supported by the National Natural Science Foundation of China (Grant number: 81170398).

SUPPLEMENTARY MATERIAL

The Supplementary Material for this article can be found online at http://journal.frontiersin.org/article/10.3389/fimmu.2017.00801/full#supplementary-material.

REFERENCES

1. Friedman SL. Mechanisms of hepatic fibrogenesis. *Gastroenterology* (2008) 134(6):1655–69. doi:10.1053/j.gastro.2008.03.003
2. Koyama Y, Brenner DA. Liver inflammation and fibrosis. *J Clin Invest* (2017) 127(1):55–64. doi:10.1172/JCI88881
3. Seki E, Schwabe RF. Hepatic inflammation and fibrosis: functional links and key pathways. *Hepatology* (2015) 61(3):1066–79. doi:10.1002/hep.27332
4. Pellicoro A, Ramachandran P, Iredale JP, Fallowfield JA. Liver fibrosis and repair: immune regulation of wound healing in a solid organ. *Nat Rev Immunol* (2014) 14(3):181–94. doi:10.1038/nri3623
5. Duffield JS, Forbes SJ, Constandinou CM, Clay S, Partolina M, Vuthoori S, et al. Selective depletion of macrophages reveals distinct, opposing roles during liver injury and repair. *J Clin Invest* (2005) 115(1):56–65. doi:10.1172/JCI200522675
6. Wynn TA, Vannella KM. Macrophages in tissue repair, regeneration, and fibrosis. *Immunity* (2016) 44(3):450–62. doi:10.1016/j.immuni.2016.02.015
7. Tacke F, Zimmermann HW. Macrophage heterogeneity in liver injury and fibrosis. *J Hepatol* (2014) 60(5):1090–6. doi:10.1016/j.jhep.2013.12.025
8. Seki E, de Minicis S, Inokuchi S, Taura K, Miyai K, van Rooijen N, et al. CCR2 promotes hepatic fibrosis in mice. *Hepatology* (2009) 50(1):185–97. doi:10.1002/hep.22952
9. Ehling J, Bartneck M, Wei X, Gremse F, Fech V, Möckel D, et al. CCL2-dependent infiltrating macrophages promote angiogenesis in progressive liver fibrosis. *Gut* (2014) 63(12):1960–71. doi:10.1136/gutjnl-2013-306294
10. Heymann F, Hammerich L, Storch D, Bartneck M, Huss S, Rüsseler V, et al. Hepatic macrophage migration and differentiation critical for liver fibrosis is mediated by the chemokine receptor C-C motif chemokine receptor 8 in mice. *Hepatology* (2012) 55(3):898–909. doi:10.1002/hep.24764
11. Wan J, Benkdane M, Teixeira-Clerc F, Bonnafous S, Louvet A, Lafdil F, et al. M2 Kupffer cells promote M1 Kupffer cell apoptosis: a protective mechanism against alcoholic and nonalcoholic fatty liver disease. *Hepatology* (2014) 59(1):130–42. doi:10.1002/hep.26607
12. Wynn TA, Chawla A, Pollard JW. Macrophage biology in development, homeostasis and disease. *Nature* (2013) 496(7446):445–55. doi:10.1038/nature12034
13. Beljaars L, Schippers M, Reker-Smit C, Martinez FO, Helming L, Poelstra K, et al. Hepatic localization of macrophage phenotypes during fibrogenesis and resolution of fibrosis in mice and humans. *Front Immunol* (2014) 5:430. doi:10.3389/fimmu.2014.00430
14. Kantari-Mimoun C, Castells M, Klose R, Meinecke AK, Lemberger UJ, Rautou PE, et al. Resolution of liver fibrosis requires myeloid cell-driven sinusoidal angiogenesis. *Hepatology* (2015) 61(6):2042–55. doi:10.1002/hep.27635
15. Noy R, Pollard JW. Tumor-associated macrophages: from mechanisms to therapy. *Immunity* (2014) 41(1):49–61. doi:10.1016/j.immuni.2014.09.021
16. Willenborg S, Lucas T, van Loo G, Knipper JA, Krieg T, Haase I, et al. CCR2 recruits an inflammatory macrophage subpopulation critical for angiogenesis in tissue repair. *Blood* (2012) 120(3):613–25. doi:10.1182/blood-2012-01-403386
17. Dewerchin M, Carmeliet P. PlGF: a multitasking cytokine with disease-restricted activity. *Cold Spring Harb Perspect Med* (2012) 2(8):a011056. doi:10.1101/cshperspect.a011056
18. Van de Veire S, Stalmans I, Heindryckx F, Oura H, Tijeras-Raballand A, Schmidt T, et al. Further pharmacological and genetic evidence for the efficacy of PlGF inhibition in cancer and eye disease. *Cell* (2010) 141(1):178–90. doi:10.1016/j.cell.2010.02.039
19. Fischer C, Jonckx B, Mazzone M, Zacchigna S, Loges S, Pattarini L, et al. Anti-PlGF inhibits growth of VEGF(R)-inhibitor-resistant tumors without affecting healthy vessels. *Cell* (2007) 131(3):463–75. doi:10.1016/j.cell.2007.08.038
20. Rolny C, Mazzone M, Tugues S, Laoui D, Johansson I, Coulon C, et al. HRG inhibits tumor growth and metastasis by inducing macrophage polarization and vessel normalization through downregulation of PlGF. *Cancer Cell* (2011) 19(1):31–44. doi:10.1016/j.ccr.2010.11.009
21. Fischer C, Mazzone M, Jonckx B, Carmeliet P. FLT1 and its ligands VEGFB and PlGF: drug targets for anti-angiogenic therapy? *Nat Rev Cancer* (2008) 8(12):942–56. doi:10.1038/nrc2524
22. Li X, Yao QY, Liu HC, Jin QW, Xu BL, Zhang SC, et al. Placental growth factor silencing ameliorates liver fibrosis and angiogenesis and inhibits activation of hepatic stellate cells in a murine model of chronic liver disease. *J Cell Mol Med* (2017). doi:10.1111/jcmm.13158
23. Van Steenkiste C, Ribera J, Geerts A, Pauta M, Tugues S, Casteleyn C, et al. Inhibition of placental growth factor activity reduces the severity of fibrosis, inflammation, and portal hypertension in cirrhotic mice. *Hepatology* (2011) 53(5):1629–40. doi:10.1002/hep.24238
24. Van Steenkiste C, Geerts A, Vanheule E, Van Vlierberghe H, De Vos F, Olievier K, et al. Role of placental growth factor in mesenteric neoangiogenesis in a mouse model of portal hypertension. *Gastroenterology* (2009) 137(6):2112–24. doi:10.1053/j.gastro.2009.08.068
25. Vandewynckel YP, Laukens D, Devisscher L, Bogaerts E, Paridaens A, Van den Bussche A, et al. Placental growth factor inhibition modulates the interplay between hypoxia and unfolded protein response in hepatocellular carcinoma. *BMC Cancer* (2016) 16:9. doi:10.1186/s12885-015-1990-6
26. Heindryckx F, Coulon S, Terrie E, Casteleyn C, Stassen JM, Geerts A, et al. The placental growth factor as a target against hepatocellular carcinoma in a diethylnitrosamine-induced mouse model. *J Hepatol* (2013) 58(2):319–28. doi:10.1016/j.jhep.2012.09.032
27. Jonsson JR, Clouston AD, Ando Y, Kelemen LI, Horn MJ, Adamson MD, et al. Angiotensin-converting enzyme inhibition attenuates the progression of rat hepatic fibrosis. *Gastroenterology* (2001) 121(1):148–55. doi:10.1053/gast.2001.25480
28. Seki E, De Minicis S, Gwak GY, Kluwe J, Inokuchi S, Bursill CA, et al. CCR1 and CCR5 promote hepatic fibrosis in mice. *J Clin Invest* (2009) 119(7):1858–70. doi:10.1172/JCI37444
29. Miura K, Yang L, van Rooijen N, Ohnishi H, Seki E. Hepatic recruitment of macrophages promotes nonalcoholic steatohepatitis through CCR2. *Am J Physiol Gastrointest Liver Physiol* (2012) 302(11):G1310–21. doi:10.1152/ajpgi.00365.2011

30. Sahin H, Borkham-Kamphorst E, Kuppe C, Zaldivar MM, Grouls C, Al-samman M, et al. Chemokine Cxcl9 attenuates liver fibrosis-associated angiogenesis in mice. *Hepatology* (2012) 55(5):1610–9. doi:10.1002/hep.25545
31. Tacke F. Targeting hepatic macrophages to treat liver diseases. *J Hepatol* (2017) 66(6):1300–12. doi:10.1016/j.jhep.2017.02.026
32. Karlmark KR, Weiskirchen R, Zimmermann HW, Gassler N, Ginhoux F, Weber C, et al. Hepatic recruitment of the inflammatory Gr1+ monocyte subset upon liver injury promotes hepatic fibrosis. *Hepatology* (2009) 50(1):261–74. doi:10.1002/hep.22950
33. Vannella KM, Wynn TA. Mechanisms of organ injury and repair by macrophages. *Annu Rev Physiol* (2017) 79:593–617. doi:10.1146/annurev-physiol-022516-034356
34. Ju C, Tacke F. Hepatic macrophages in homeostasis and liver diseases: from pathogenesis to novel therapeutic strategies. *Cell Mol Immunol* (2016) 13(3):316–27. doi:10.1038/cmi.2015.104
35. Krenkel O, Tacke F. Liver macrophages in tissue homeostasis and disease. *Nat Rev Immunol* (2017) 17(5):306–21. doi:10.1038/nri.2017.11
36. Snuderl M, Batista A, Kirkpatrick ND, Ruiz de Almodovar C, Riedemann L, Walsh EC, et al. Targeting placental growth factor/neuropilin 1 pathway inhibits growth and spread of medulloblastoma. *Cell* (2013) 152(5):1065–76. doi:10.1016/j.cell.2013.01.036
37. Yano K, Okada Y, Beldi G, Shih SC, Bodyak N, Okada H, et al. Elevated levels of placental growth factor represent an adaptive host response in sepsis. *J Exp Med* (2008) 205(11):2623–31. doi:10.1084/jem.20080398
38. Incio J, Tam J, Rahbari NN, Suboj P, McManus DT, Chin SM, et al. PlGF/VEGFR-1 signaling promotes macrophage polarization and accelerated tumor progression in obesity. *Clin Cancer Res* (2016) 22(12):2993–3004. doi:10.1158/1078-0432.CCR-15-1839
39. Selvaraj SK, Giri RK, Perelman N, Johnson C, Malik P, Kalra VK. Mechanism of monocyte activation and expression of proinflammatory cytochemokines by placenta growth factor. *Blood* (2003) 102:1515–24. doi:10.1182/blood-2002-11-3423
40. Marra F, Tacke F. Roles for chemokines in liver disease. *Gastroenterology* (2014) 147:577–94. doi:10.1053/j.gastro.2014.06.043
41. Baeck C, Wei X, Bartneck M, Fech V, Heymann F, Gassler N, et al. Pharmacological inhibition of the chemokine C-C motif chemokine ligand 2 (monocyte chemoattractant protein 1) accelerates liver fibrosis regression by suppressing Ly-6C (+) macrophage infiltration in mice. *Hepatology* (2014) 59(3):1060–72. doi:10.1002/hep.26783
42. Li X, Jin Q, Yao Q, Xu B, Li Z, Tu C. Quercetin attenuates the activation of hepatic stellate cells and liver fibrosis in mice through modulation of HMGB1-TLR2/4-NF-κB signaling pathways. *Toxicol Lett* (2016) 261(11):1–12. doi:10.1016/j.toxlet.2016.09.002
43. Garcia-Martinez I, Santoro N, Chen Y, Hoque R, Ouyang X, Caprio S, et al. Hepatocyte mitochondrial DNA drives nonalcoholic steatohepatitis by activation of TLR9. *J Clin Invest* (2016) 126(3):859–64. doi:10.1172/JCI83885
44. Seki E, De Minicis S, Osterreicher CH, Kluwe J, Osawa Y, Brenner DA, et al. TLR4 enhances TGF-beta signaling and hepatic fibrosis. *Nat Med* (2007) 13(11):1324–32. doi:10.1038/nm1663
45. Coulon S, Heindryckx F, Geerts A, Van Steenkiste C, Colle I, Van Vlierberghe H. Angiogenesis in chronic liver disease and its complications. *Liver Int* (2011) 31(2):146–62. doi:10.1111/j.1478-3231.2010.02369.x
46. Yang L, Kwon J, Popov Y, Gajdos GB, Ordog T, Brekken RA, et al. Vascular endothelial growth factor promotes fibrosis resolution and repair in mice. *Gastroenterology* (2014) 146(5):1339–50. doi:10.1053/j.gastro.2014.01.061
47. Carmeliet P, Moons L, Luttun A, Vincenti V, Compernolle V, De Mol M, et al. Synergism between vascular endothelial growth factor and placental growth factor contributes to angiogenesis and plasma extravasation in pathological conditions. *Nat Med* (2001) 7(5):575–83. doi:10.1038/87904
48. Kim KJ, Cho CS, Kim WU. Role of placenta growth factor in cancer and inflammation. *Exp Mol Med* (2012) 44(1):10–9. doi:10.3858/emm.2012.44.1.023

Conflict of Interest Statement: The authors declare that the research was conducted in the absence of any commercial or financial relationships that could be construed as a potential conflict of interest.

Copyright © 2017 Li, Jin, Yao, Zhou, Zou, Li, Zhang and Tu. This is an open-access article distributed under the terms of the Creative Commons Attribution License (CC BY). The use, distribution or reproduction in other forums is permitted, provided the original author(s) or licensor are credited and that the original publication in this journal is cited, in accordance with accepted academic practice. No use, distribution or reproduction is permitted which does not comply with these terms.

frontiers in Immunology

ORIGINAL RESEARCH
published: 02 August 2017
doi: 10.3389/fimmu.2017.00905

The Extracts of *Morinda officinalis* and Its Hairy Roots Attenuate Dextran Sodium Sulfate-Induced Chronic Ulcerative Colitis in Mice by Regulating Inflammation and Lymphocyte Apoptosis

Jian Liang[1†], Jiwang Liang[2†], Hairong Hao[3†], Huan Lin[1], Peng Wang[2], Yanfang Wu[1], Xiaoli Jiang[2], Chaodi Fu[2], Qian Li[1], Ping Ding[1], Huazhen Liu[4], Qingping Xiong[1], Xiaoping Lai[1], Lian Zhou[1], Shamyuen Chan[2]* and Shaozhen Hou[1]**

[1] Guangdong Provincial Key Laboratory of New Chinese Medicinals Development and Research, Guangzhou University of Chinese Medicine, Guangzhou, China, [2] Shenzhen Fan Mao Pharmaceutical Co., Limited, Shenzhen, China, [3] Affiliated Huai'an Hospital of Xuzhou Medical University, Huai'an, China, [4] Section of Immunology, Guangdong Provincial Academy of Chinese Medical Sciences, Guangdong Provincial Hospital of Chinese Medicine, Guangzhou, China

Morinda officinalis is beneficial for the treatment of inflammatory bowel disease (IBD). The hairy root with higher genetic and biochemical stability cultured from *M. officinalis* might have similar effects to treat IBD. In this study, the main chemical composition of the root extracts of *M. officinalis* (MORE) native plant and the hairy root extract of *M. officinalis* (MOHRE) was compared by quantitative HPLC. The difference of their therapeutic effects and potential mechanism was evaluated using 3% dextran sodium sulfate-induced chronic colitis in mice and T lymphocytes *in vitro.* The results found that MOHRE possesses many specific peaks unobserved in the chromatogram of native plant. The content of iridoids in the MORE (3.10%) and MOHRE (3.01%) is somewhat similar but quite different for their anthraquinones's content (0.14 and 0.66%, respectively). Despite all this, treatment with both MORE and MOHRE significantly attenuated the symptoms of colitis, including diarrhea, body weight loss, colon shortening, histological damage, and decreased inflammatory cytokine levels. In addition, they dose-dependently increased the apoptosis of T lymphocyte *in vivo* and *in vitro*. And, the differences for treatment effects on ulcerative colitis (UC) between them both in this study were mostly insignificant. The results demonstrated that the effects of MORE and MOHRE for the treatment of UC are similar, although there are a few difference on their chemical composition, indicating the hairy root cultured from *M. officinalis* might be able to replace its native plant on treatment of UC. The successful derivation of a sustainable hairy root culture provides a model system to study the synthetic pathways for bioactive metabolites, which will make the use of bioreactors to largely produce traditional medicine become reality.

Keywords: *Morinda officinalis*, hairy roots culture, ulcerative colitis, anti-inflammatory, immunoregulatory, apoptosis

OPEN ACCESS

Edited by:
Jixin Zhong,
Case Western Reserve University, United States

Reviewed by:
Xiaojing Yue,
La Jolla Institute for Allergy and Immunology, United States
Yu Zhou,
Columbia University Medical Center, United States
Ding Xinchun,
Indiana University – Purdue University Indianapolis, United States
Xun Liu,
Brigham and Women's Hospital, United States

***Correspondence:**
Lian Zhou
zl@gzucm.edu.cn;
Shamyuen Chan
samchan@phytogaa.com;
Shaozhen Hou
hsz0214@gzucm.edu.cn

†These authors have contributed equally to this work.

Specialty section:
This article was submitted to Inflammation, a section of the journal Frontiers in Immunology

Received: *26 March 2017*
Accepted: *14 July 2017*
Published: *02 August 2017*

Citation:
Liang J, Liang J, Hao H, Lin H, Wang P, Wu Y, Jiang X, Fu C, Li Q, Ding P, Liu H, Xiong Q, Lai X, Zhou L, Chan S and Hou S (2017) The Extracts of Morinda officinalis and Its Hairy Roots Attenuate Dextran Sodium Sulfate-Induced Chronic Ulcerative Colitis in Mice by Regulating Inflammation and Lymphocyte Apoptosis. Front. Immunol. 8:905. doi: 10.3389/fimmu.2017.00905

INTRODUCTION

Ulcerative colitis (UC) is a type of inflammatory bowel disease (IBD), which is characterized by chronic and repeated episodes enteropatia (1). Clinically, patients with UC often have diarrhea, abdominal pain, bloody stools, and recurrent UC, which is prone to cause colon cancer (2). The incidence of UC has been increasing annually, especially in the developed countries. Although the pathogenesis of UC is unclear, evidences have suggested that UC is closely associated with the imbalance of the immune response (3). The defect of T cell apoptosis may lead to an uncontrolled T cell activation and proliferation which is a key mechanism to cause an ultraimmune response and the inductions of proinflammatory cytokines (3). The aggressive behavior of the intestinal immune system can cause immune dysfunction, leading to the infiltration of inflammatory cells and production of a large number of proinflammatory cytokines (4), such as tumor necrosis factor α (TNF-α), interleukin-6 (IL-6), and interleukin-17 (IL-17). These proinflammatory cytokines can cause intestinal damage and further aggravate the condition of UC (5). Therefore, the medicines, which can inhibit T cells proliferation (such as steroids and calcineurin inhibitors) or induce T cells apoptosis (such as TNF-α monoclonal antibody), will exert remarkable therapeutic effects for IBD (6, 7). However, long-term use of these drugs will cause some serious adverse reactions and further aggravate the condition (8). Therefore, it is necessary to search for more effective and safe drugs or therapy to treat UC. Complementary therapies seem to have many advantages, such as lower toxicity, more safety and effectiveness, which have absorbed an increasing number of patients who want to try and use this method to treat IBD (9). Chinese herbals, as a kind of complementary therapies, contain various active components in their extracts that could show therapeutic effects on multiple targets of the body (10).

Morinda officinalis is a kind of traditional Chinese herbal medicine and natural nutritious food, as one of the four southern medicines of China. *M. officinalis* has been widely used to treat many diseases such as rheumatism, enuresis, and infertility for more than 2,000 years (11). Many studies have found that *M. officinalis* root mainly contains polysaccharides, anthraquinone, and iridoid (12). These components have extensive pharmacological activities, including anti-inflammation, antioxidant, immune-regulatory, and antitumor effect (13). Relative studies have shown that *M. officinalis* effectively reduced the levels of proinflammatory cytokines (14) (e.g., TNF-α, IL-17, IL-6, and IL-8). Accumulated evidence also suggested that *M. officinalis* could effectively treat colitis in mice induced by dextran sodium sulfate (DSS) (15). Therefore, *M. officinalis* may be working as a potential drug to treat UC. However, *M. officinalis* has a long period of cultivation, which is a time-consuming and seasonal planting, and the eradication of medicinal plants has a negative impact on the natural population of *M. officinalis*. The yield of *M. officinalis* is too low to satisfy commercial purposes. Thus, an alternative method of *M. officinalis* production is required to meet the growing demand of this medicine.

Nowadays, the role of plant tissue culture in the production of high-value secondary metabolites is on the rise. By comparing with different cultivation methods, using hairy root cultures have its benefits such as sustained growth cycle, rapid rate of growth, easy to cultivate in hormone-free medium, and obtain higher genetic and biochemical stability (16). Hairy root cultures become a useful method to produce active compound in limited and secure condition. Hairy roots can be achieved by infecting the wounded higher plants with *Agrobacterium rhizogenes* (17). *A. rhizogenes* contains Ri plasmid, which has two functional areas, namely VIR and T-DNA region. When plants were infected by *A. rhizogenes*, the T-DNA in the inhibited state was activated and integrated into the plant genome, which induced the plant cells to produce hairy roots (18).

In the present study, we used the hairy root cultures method to obtain the hairy roots of *M. officinalis*. We devoted to analyze the differences of the major chemical constituents between roots extract of *M. officinalis* (MORE) native plant and hairy roots extract of *M. officinalis* (MOHRE). Based on this, we further investigated the differences of therapeutic effect between MORE and MOHRE on DSS-induced chronic colitis. In addition, we provided a novel insight into the initial mechanism of MORE and MOHRE in chronic colitis protection.

MATERIALS AND METHODS

Drugs and Reagents

Morinda officinalis (no. 20150603) was obtained from Shenzhen Lush Pharmaceutical Co., Ltd. Positive drug mesalazin enteric-coated tablets (no. 150308) was bought from Losan Pharma GmbH (Germany). DSS was purchased from MP Biomedicals (MW; 36,000–50,000; MP Biomedicals, Solon, OH, USA). The enzyme-linked immunosorbent assay (ELISA) kits for TNF-α, IL-6, and IL-17 was bought from Huamei (Cusabio Biotech Co. Ltd., China). All plastic materials were purchased from Falcon Labware (Becton-Dickinson, Franklin Lakes, NJ, USA). RPMI Medium 1640, fetal bovine serum (FBS), and phosphate buffer saline (PBS) were obtained from GIBCO Laboratories (Grand Island, NY, USA). Penicillin G/streptomycin, MTT, and dimethyl sulfoxide (DMSO) were purchased from Sigma (St. Louis, MO, USA). Apoptosis Assay Kit was purchased from Lianke Biology Inc. (Hangzhou, China). APC antimouse CD3 antibody, PE/Cy7 antimouse CD4 antibody, and APC antimouse CD8 antibody were purchased from BioLegend (USA). All other chemicals used were analytical grade and were supplied by the Beijing Chemical Agents Company (China).

Induction of Hairy Roots of *M. Officinalis*

The stem of *M. officinalis* was used as explants for the induction of hairy roots. The excised root segments were preincubated on half-strength MS (MS/2) solid medium for 3 days before infection. *A. rhizogenes* strain MSU440 was cultivated overnight and collected the bacterial suspension of *A. rhizogenes* by centrifugated at 6,000 rpm for 5 min. The explants were soaked in the overnight grown bacterial suspension of *A. rhizogenes* strain MSU440 (OD_{600} = 0.6–0.8) for 15 min and dry blotted on sterile filter paper. The explants were cultured on 1/2 MS-based solid medium in the dark at 28 ± 1°C. After 3 days of cocultivation,

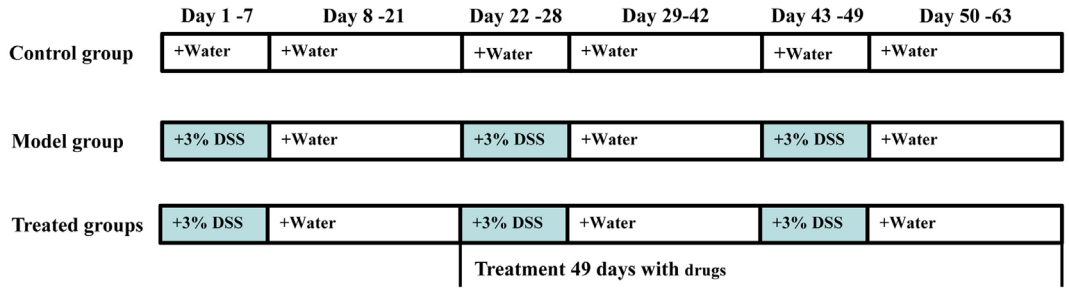

FIGURE 1 | The experimental design for 3% dextran sodium sulfate (DSS)-induced chronic ulcerative colitis (UC) in mice and administration time. Chronic colitis was induced by oral 3% DSS for three cycles. Each cycle was made up of 3% DSS for 7 days followed by 14 days of recovery with water. After the first cycle, modeled mice were randomly divided into eight groups (n = 12/group), administration of root extract of *M. officinalis* (MORE) and hairy root extract of *M. officinalis* (MOHRE) to chronic UC in mice for two cycles.

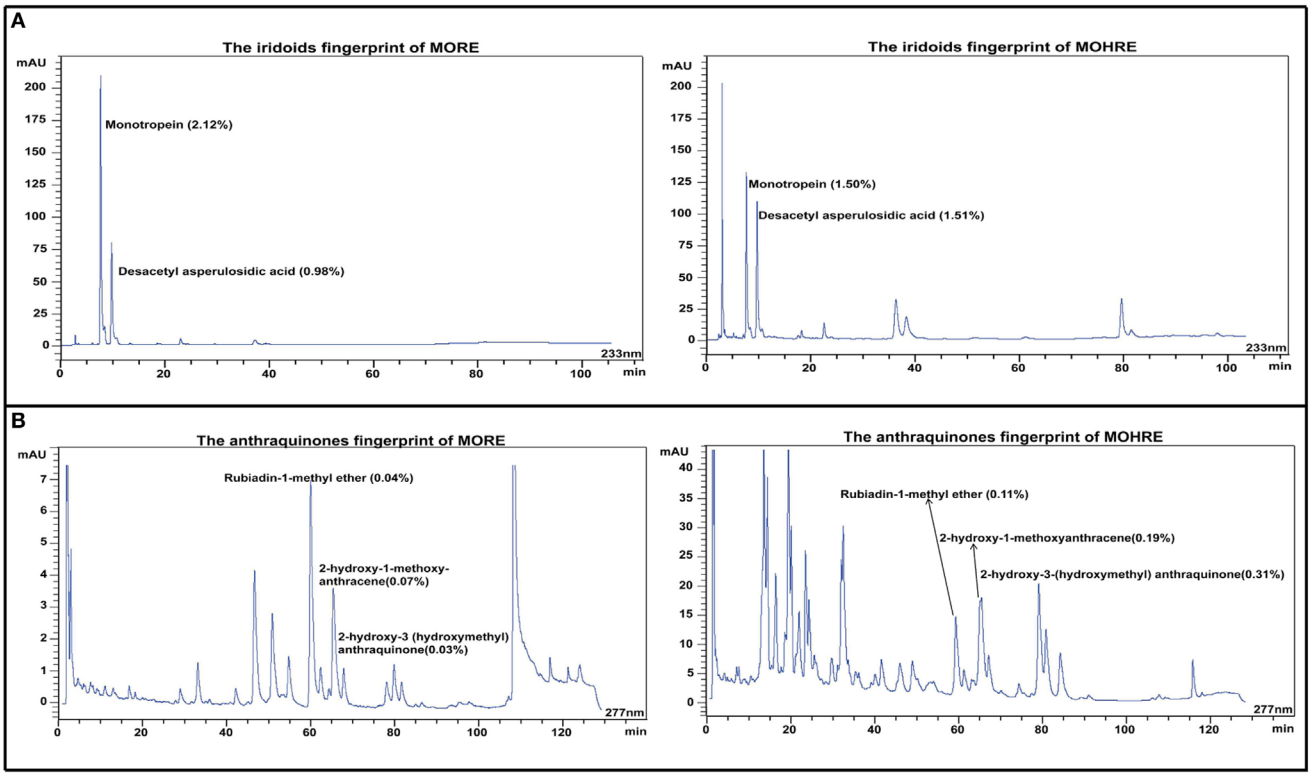

FIGURE 2 | The HPLC fingerprints derived from the roots extract of *Morinda officinalis* (MORE) and hairy roots extract of *Morinda officinalis* (MOHRE). **(A)** The HPLC fingerprints of iridoids; **(B)** The HPLC fingerprints of anthraquinones.

the explants were transferred to 1/2 MS-based solid medium of hormone free which containing sodium cefotaxim (300 mg/L) to eliminate the residual bacteria and incubated in the dark at 25 ± 1°C. The healthy hairy roots were obtained and used after once subculture every 2 weeks in this study.

Preparation of the Plant Extracts

The powder of root *M. officinalis* or hairy roots of *M. officinalis* was heated to reflux for 2 h with 8 times volume 85% alcohol. The extraction was repeated twice. The extracting solution was filtered to remove the residue. And then it was concentrated by rotary evaporator. The concentrate was freeze dried under vacuum. Dry MORE and MOHRE were used to treat mice with colitis.

HPLC Analyses

The HPLC analyses of MORE and MOHRE were performed by an Agilent 1260 High Performance Liquid Chromatograph System.

The iridoids analysis was done by using a Phenomenex Luna C18 column (250.0 × 4.6 mm, 5.0 μm). The column temperature

TABLE 1 | Effects of MORE and MOHRE in mice after acute oral administration.

Dose (g/kg)	Animals		Effects		
	Dead/total treated mice	Mortality (%)	Symptoms of toxicity	Body weight change (%)	
Control	0/6	0	None	Female	125.9 ± 0.44
				Male	130.7 ± 2.46
5 (MORE)	0/6	0	None	Female	125.1 ± 1.52
				Male	129.3 ± 3.44
5 (MOHRE)	0/6	0	None	Female	126.3 ± 0.91
				Male	130.4 ± 2.51

Values represent mean ± SEM of three animals.

was 25.00°C. The mobile phases were 0.4% H_3PO_4 solution (A) and methanol (B) with the flow rate at 1.000 mL/min. The gradient elution was 0–13 min, A 95.0%; 13–14 min, A 95.0–91.6%; 14–65 min, A 91.6–91.3%; 65–70 min, A 91.3–86.0%; 70–175 min, A 86.0–84.0%; 75–100 min, A 84.0–80.5%; 100–105 min, A 80.5–95.0%; and postrun 5.00 min. The UV detection wave length was 233 nm, and the injection volume was 10.00 μL. The quantitative analysis of iridoids was carried out by the external standard method.

The anthraquinones analysis was done with an Agilent Eclipse XDB-C18 column (150.0 mm × 4.6 mm, 5.0 μm). The column temperature was 30.00°C. The mobile phase was 0.2% H_3PO_4 solution (A) and acetonitrile (B) with the flow rate at 1.000 mL/min. The gradient elution was 0–15 min, A 90.0–80.0%; 15–50 min, A 80.0–70.0%; 50–70 min, A 70.0–60.0%; 70–100 min, A 60.0–50.0%; 100–120 min, A 50.0–20.0%; 120–125 min, A 20.0%; 125–130 min, A 20.0–90.0%; and postrun 5.00 min. The UV detection wave length was 277 nm, and the injection volume was 15.00 μL. The quantitative analysis of anthraquinones was carried out by the external standard method.

Experimental Animals

Adult male and female Kunming (KM) mice (18–22 g) were purchased from the Laboratory Animal Services Center, Guangzhou University of Chinese Medicine (Guangzhou, China). All animals were raised in accordance with the National Institutes of Health Guide for Laboratory animals' use. The study was approved by the Animal Ethics Committee of Guangzhou University of Chinese Medicine. Animals were housed under standard environment condition of temperature at 20–25°C under a 12 h dark/light cycle and allowed free access to sterilized water and standard food.

Acute Toxicity Testing

Acute oral toxicity in mice was performed by using the limit dose test of up-and-down procedure according to OECD guideline (OECD 425) (19). Healthy KM mice were randomly assigned to three groups, each group with six mice (three males and three females). A single dose of 5,000 mg/kg of extracts (MORE or MOHRE) were administered orally to each group. Each mouse was continuously observed for 4 h after the treatment. The mice were further observed once daily for 14 days and the number of deaths, body weight and toxic parameters were recorded.

Inducement of Experimental Colitis

A total of 108 male mice were included in this experiment. Chronic colitis was induced by oral administration of 3% DSS for three cycles (**Figure 1**), as described by Farkas et al. (20) and Okayasu et al. (21), with slight modification. Randomly selected 12 mice as the normal group, only received tap water every day. The others were induced by three cycles that a 7-day treatment with DSS dissolved in drinking water (3%, w/v) followed by 14 days of recovery with water. After the first cycle, according to their body weight, 96 modeled mice were randomly divided into eight groups ($n = 12$/group): DSS group, mesalazin (50 mg/kg/day) in positive control group, three groups received treatment with MORE (20, 40, and 80 mg/kg/day), the other received treatment with MOHRE (20, 40, and 80 mg/kg/day). The dose selection of extracts was based on clinical practice (usually 6,000 mg/day, 70 kg body weight). Except for the control group, the others were still administered with 3% DSS as described previously, while all drug groups were given the corresponding does of drugs. The treatment lasted for two other cycles and body weight, behavior, stool consistency, fecal occult blood (both visible and occult bleeding), disease activity index (DAI), mortality, food, and water intake of all animals were monitored daily. At the end of the experiment, animals were fasted for 12 h and then anesthetized with pentobarbital sodium (70 mg/kg, i.p.). Blood samples were collected directly from the orbit, which were transferred to 2 mL EP tubes followed by centrifuged at 3,000 rpm for 10 min at 4°C and finally stored at −80°C for biochemical assays. The spleens were weighted and the colons were quickly removed and gently rinsed with sterile and cold saline solution, then moved to cold plate for measuring the length of the colon, colon macroscopic evaluation. Subsequently the colons were divided into two parts, one was fixed in 4% paraformaldehyde for histological examination and the other was stored at −80°C for biochemical assays. Spleen was also fixed in 4% paraformaldehyde for histological examination.

Assessment of Colitis

Disease Activity Index

Disease activity index is determined according to the loss of body weight feces status and macroscopically visible blood in feces, in accordance with the method described by Cooper et al. (22) and Xiao et al. (23).

General Morphology Score

Macroscopic damage score of the colon was recorded according to the standard method of Millar et al. (24).

Histological Examination

Segments of colon and spleen were immediately fixed in 4% paraformaldehyde for 24 h, then washed with water, dehydrated with alcohol, and finally embedded in paraffin. Tissues were cut into standard sections and stained with hematoxylin–eosin (H&E) for histological examination. Segments of colon were evaluated according to the method previously reported by Boirivant et al. (25) and described as follows: 0, normal and no inflammatory cell

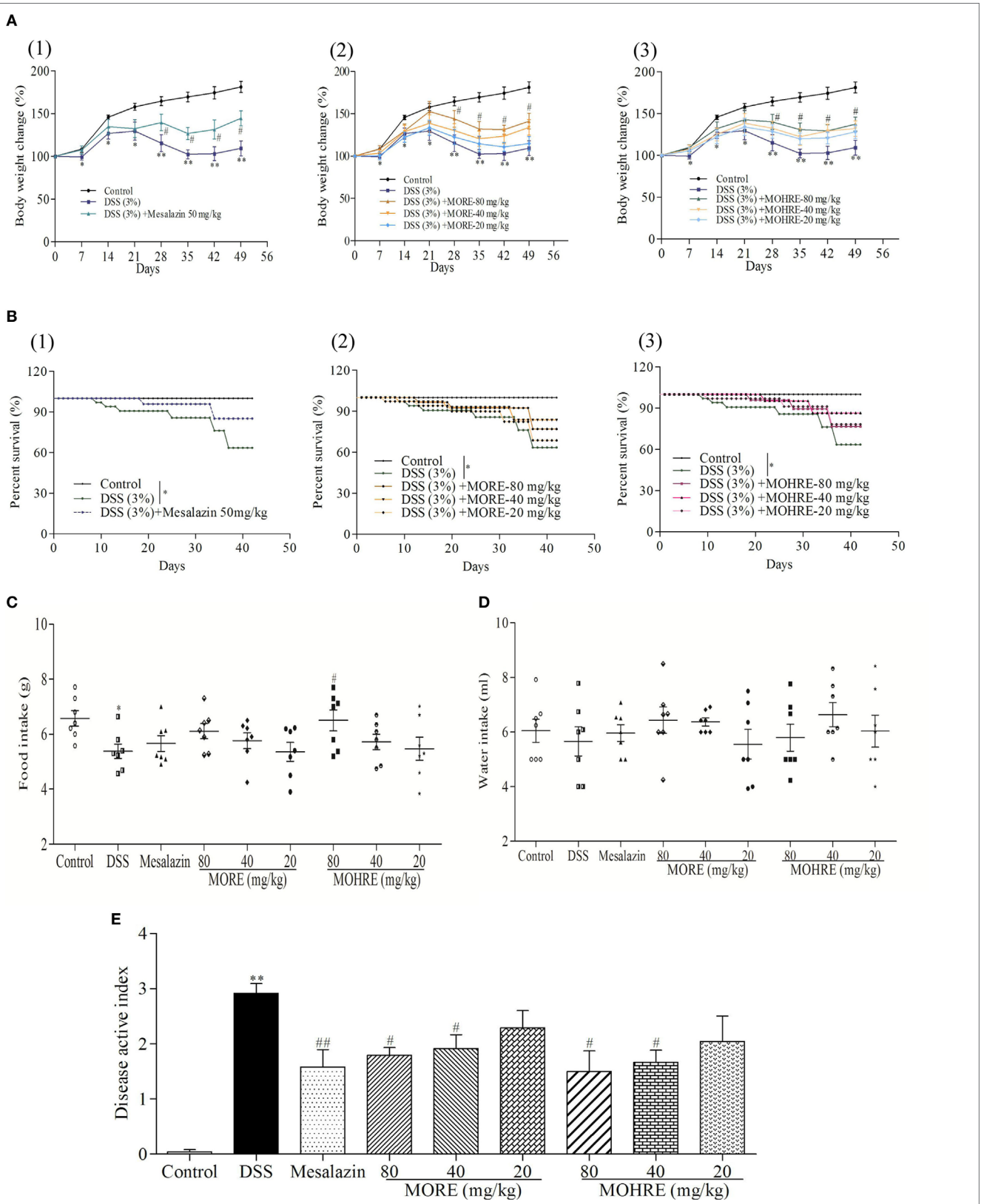

FIGURE 3 | The therapeutic effect of root extract of *Morinda officinalis* (MORE) and hairy root extract of *M. officinalis* (MOHRE) ameliorated dextran sodium sulfate (DSS)-induced chronic ulcerative colitis (UC) in mice. **(A)** Body weight. **(B)** Survival rate. **(C)** Food intake. **(D)** Water intake. **(E)** Disease active index. All data are presented as mean ± SEM of six to nine mice. $^{*}p < 0.05$. $^{**}p < 0.01$ vs. control group; $^{\#}p < 0.05$. $^{\#\#}p < 0.01$ vs. DSS group.

infiltration; 1, slight inflammatory cell infiltration and no injure in submucosal tissues; 2, moderate inflammatory cell infiltration and submucosal tissues are destroyed (damage range between 10 and 25%); 3, obvious inflammatory cell infiltration, submucosal tissues are destroyed and colonic wall thickening (damage range between 25 and 50%); and 4, serious inflammatory cell infiltration,

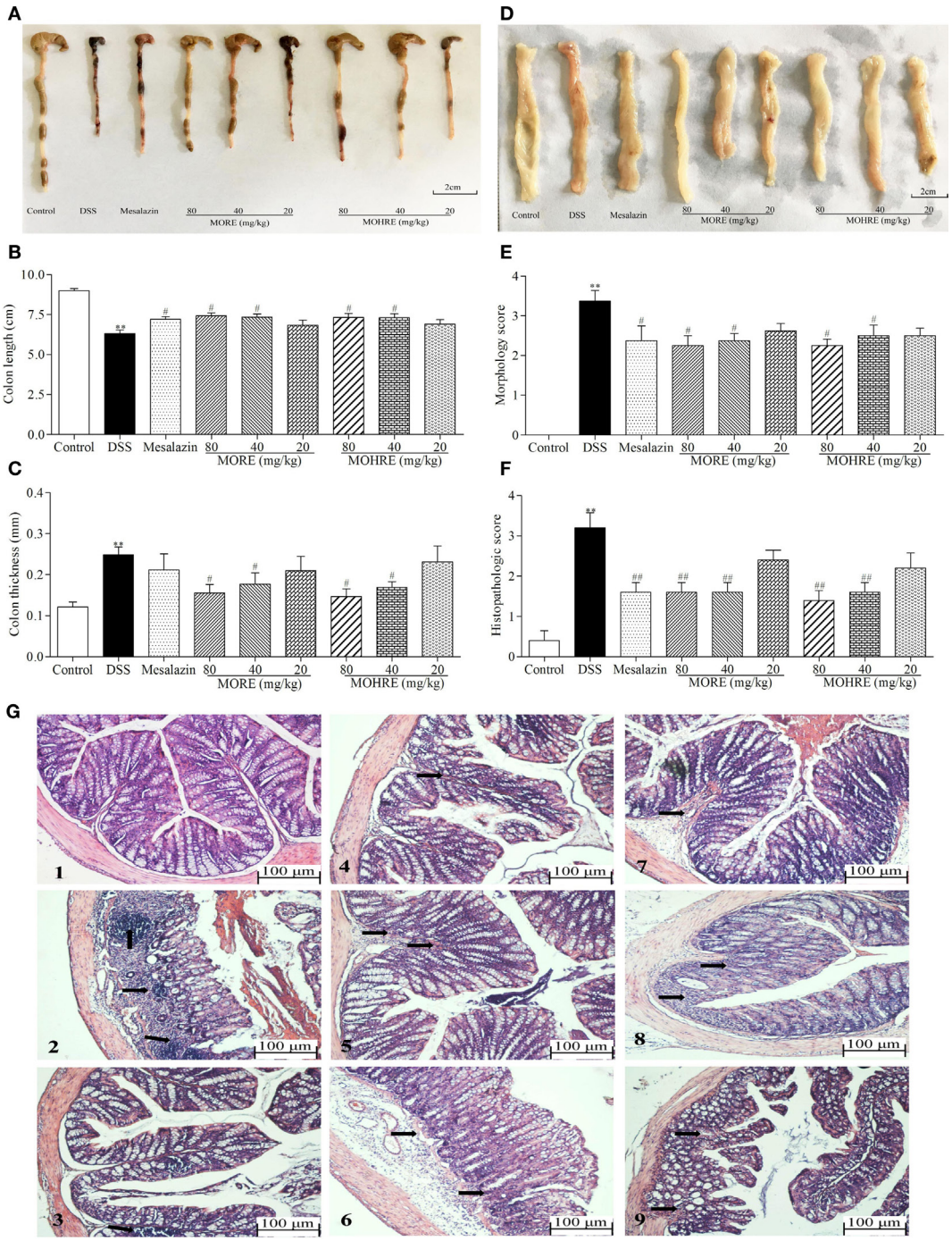

FIGURE 4 | Root extract of *Morinda officinalis* (MORE) and hairy root extract of *M. officinalis* (MOHRE) ameliorated colonic injury in dextran sodium sulfate (DSS)-induced chronic colitis mice. **(A)** Representative colon from each group. **(B)** Colon length. **(C)** Colon thickness. **(D)** The representative pictures of colon macroscopic appearances in each group. **(E)** Morphology score. **(F)** Histological score. **(G)** Representative hematoxylin–eosin (H&E) staining of colon tissues of each group (black arrows indicating inflammatory infiltration and injury), (1) Control group, (2) DSS group, (3) DSS + mesalazin (positive drug group), (4) DSS + MORE 80 mg/kg, (5) DSS + MORE 40 mg/kg, (6) DSS + MORE 20 mg/kg, (7) DSS + MOHRE 80 mg/kg, (8) DSS + MOHRE 40 mg/kg, and (9) DSS + MOHRE 20 mg/kg. All data are presented as mean ± SEM of six to nine mice. $^{*}p < 0.05$. $^{**}p < 0.01$ vs. control group; $^{\#}p < 0.05$. $^{\#\#}p < 0.01$ vs. DSS group.

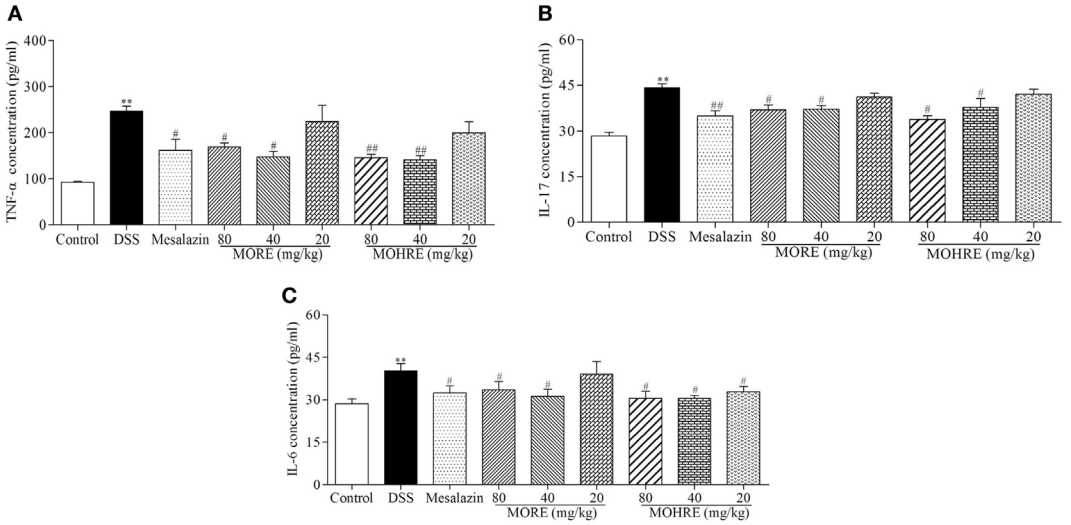

FIGURE 5 | The effect of root extract of *Morinda officinalis* (MORE) and hairy root extract of *M. officinalis* (MOHRE) on proinflammatory cytokines production in the serum of mice with dextran sodium sulfate (DSS)-induced chronic colitis. **(A)** Tumor necrosis factor α (TNF-α) concentration. **(B)** Interleukin (IL)-17 concentration. **(C)** IL-6 concentration. All data are expressed as mean ± SEM of six mice. $^{*}p < 0.05$. $^{¨}p < 0.01$ vs. control group; $^{\#}p < 0.05$. $^{\#\#}p < 0.01$ vs. DSS group.

large scale colon tissue damage (damage range > 50%) and colonic wall thickening.

Measurement of Cytokines

The systemic levels of TNF-α, IL-6, and IL-17 in the serum were measured by using a commercially available ELISA according to the manufacturer's instructions.

Apoptosis Evaluation by Annexin-V/PI *In Vivo*

At the end of the experiment, the splenocytes and peripheral blood (PB) lymphocytes were isolated from colitis mice. The method was described previously by Su et al. (26). The cells (2×10^6 cells/mL) were stained for surface markers, antimouse CD3-APC, antimouse CD4-PE/Cy7, or antimouse CD8-APC in PBS for 20 min at RT in the dark. After washing, cells apoptosis were detected by the AnnexinV/PI detection kit, according to manufacturer's instruction, briefly, cells were washed twice with precold PBS, then suspended in binding buffer and stained with 5 μL annexin V-FITC and 10 μL PI for 15 min at 25°C in the dark. Annexin V^+/PI^- cells were considered early apoptotic cells. Annexin V^+/PI^+ cells were considered late apoptotic cells. Apoptosis analysis was detected by FACS canto™ flow cytometer.

Cell Preparation

Splenocytes were isolated as described previously by Su et al. (26), with slight modification. Mice were sacrificed and the spleens were aseptically separated, washed with precold PBS. The spleens were ground and through a 70 μm strainer. After centrifuge at 300 × *g* for 5 min at 4°C, ACK Lysis Buffer was used to remove erythrocytes. Cells were collected by centrifuged at 300 × *g* for 5 min at 4°C and washed twice with PBS. Splenocytes were resuspended and cultured in RPMI1640 medium supplemented with 10% (v/v) FBS, penicillin (100 U/mL), and streptomycin (100 μg/mL) under a humidified 5% (v/v) CO_2 atmosphere at 37°C. Cells viability analysis was assessed by using trypan blue dye exclusion staining and all cases cell viability was higher than 95%.

Cytotoxicity Assay

Cytotoxicity assay was evaluated by MTT assay, 100 μL of splenocytes were seeded in 96-well plates at 3×10^6 cells/mL, treated with 100 μL MORE and MOHRE (50–400 μg/mL) for 24 h, respectively. After that, 20 μL of MTT (5 mg/mL) was added to each well and further incubated for 4 h at 37°C with 5% CO_2. 150 μL of DMSO was added into 96-well plates, and finally the plates were read at 490 nm with Multiskan Go. Without cytotoxic and optimal doses of MORE and MOHRE were selected for further apoptosis assessments. The formula was applied to calculate the cell viability (%):

$$\text{Cell viability } (\%) = \frac{(A_S - A_b)}{(A_c - A_b)} \times 100$$

where A_s, A_c, and A_b represent the absorbance of the different concentrations wells of drugs, control wells, and blank wells, respectively.

Measurement of Cell Proliferation

Splenocytes were separated and cultured by the same methods in the section cell preparation. 100 μL of splenocytes were seeded in 96-well plates at 3×10^6 cells/mL. The cells were stimulated with 5 μg/mL of Concanavalin A (ConA) and treated with 100 μL MORE and MOHRE (50, 100, and 200 μg/mL) for 24 h, the range of concentrations was optimal values according to the cytotoxicity. The formula was applied to calculate the cell proliferation by the same methods in the section Cytotoxicity Assay.

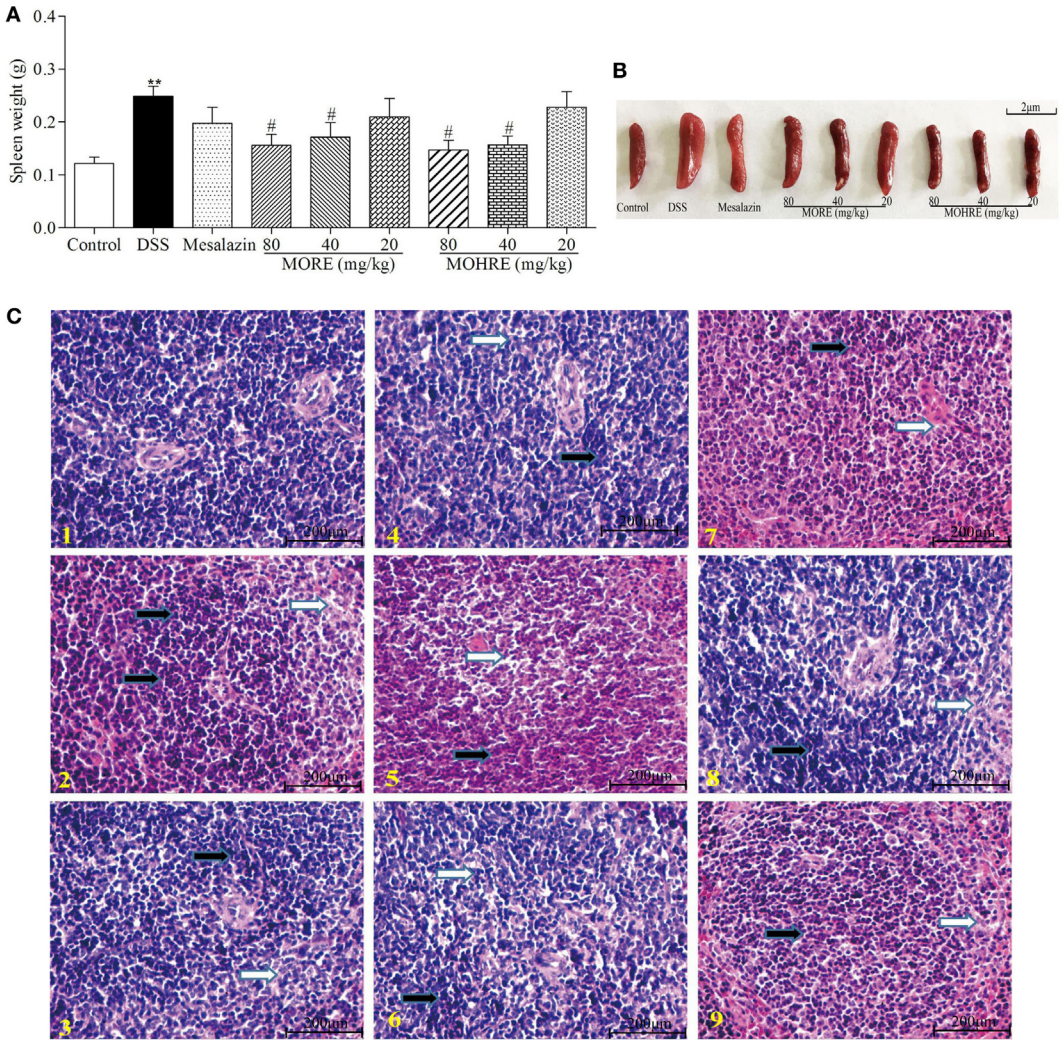

FIGURE 6 | The protective effect of root extract of *Morinda officinalis* (MORE) and hairy root extract of *M. officinalis* (MOHRE) on spleen in DSS-induced chronic colitis mice. **(A)** Spleen weight. **(B)** Representative spleen weight from each group. **(C)** Representative hematoxylin–eosin (H&E) staining of spleen tissues of each group (black arrows indicating inflammatory cell accumulation and white arrows indicating injury). (1) Control group, (2) DSS group, (3) DSS + mesalazin (positive drug group), (4) DSS + MORE 80 mg/kg, (5) DSS + MORE 40 mg/kg, (6) DSS + MORE 20 mg/kg, (7) DSS + MOHRE 80 mg/kg, (8) DSS + MOHRE 40 mg/kg, (9) DSS + MOHRE 20 mg/kg. All data are expressed as mean ± SEM of seven mice. $^{*}p < 0.05$. $^{**}p < 0.01$ vs. control group; $^{\#}p < 0.05$. $^{\#\#}p < 0.01$ vs. DSS group.

Apoptosis Analysis *In Vitro*

Splenocytes were seeded in 48-well plates at 3×10^6 cells/mL, treated with different concentrations of MORE and MOHRE (50, 100, and 200 μg/mL) for 4 h following by 5 μg/mL ConA stimulation or no stimulation with ConA for another 24 h. Apoptosis analysis was tested according to the method in section apoptosis evaluation by Annexin-V/PI *in vivo*. Apoptosis analysis was detected by FACS canto™ flow cytometer and fluorescence staining.

Statistical Analysis

Statistical analysis was performed using SPSS software (version 18.0; SPSS, Chicago, IL, USA). The analysis of survival was conducted using Kaplan–Meier method (log-rank test). All results are expressed as mean ± SEM. Results are using one-way ANOVA or Student's *t*-test when appropriate. Values of $p < 0.05$ were considered statistically significant.

RESULTS

HPLC Analysis of *M. officinalis* and Hairy Roots of *M. officinalis*

Iridoid and anthraquinones are the main active ingredients of *M. officinalis*. Here, the chromatographic peaks of hairy roots extract of *M. officinalis* (MOHRE) were more abundant than roots extract of *M. officinalis* (MORE) (**Figure 2**), suggesting that there were more secondary metabolites in the MOHRE extracts, especially anthraquinones. The content of monotropein is 2.12 and 1.50% in MORE and MOHRE, respectively, while the content of Desacetyl asperulosidic acid is 0.98% in MORE and 1.51% in

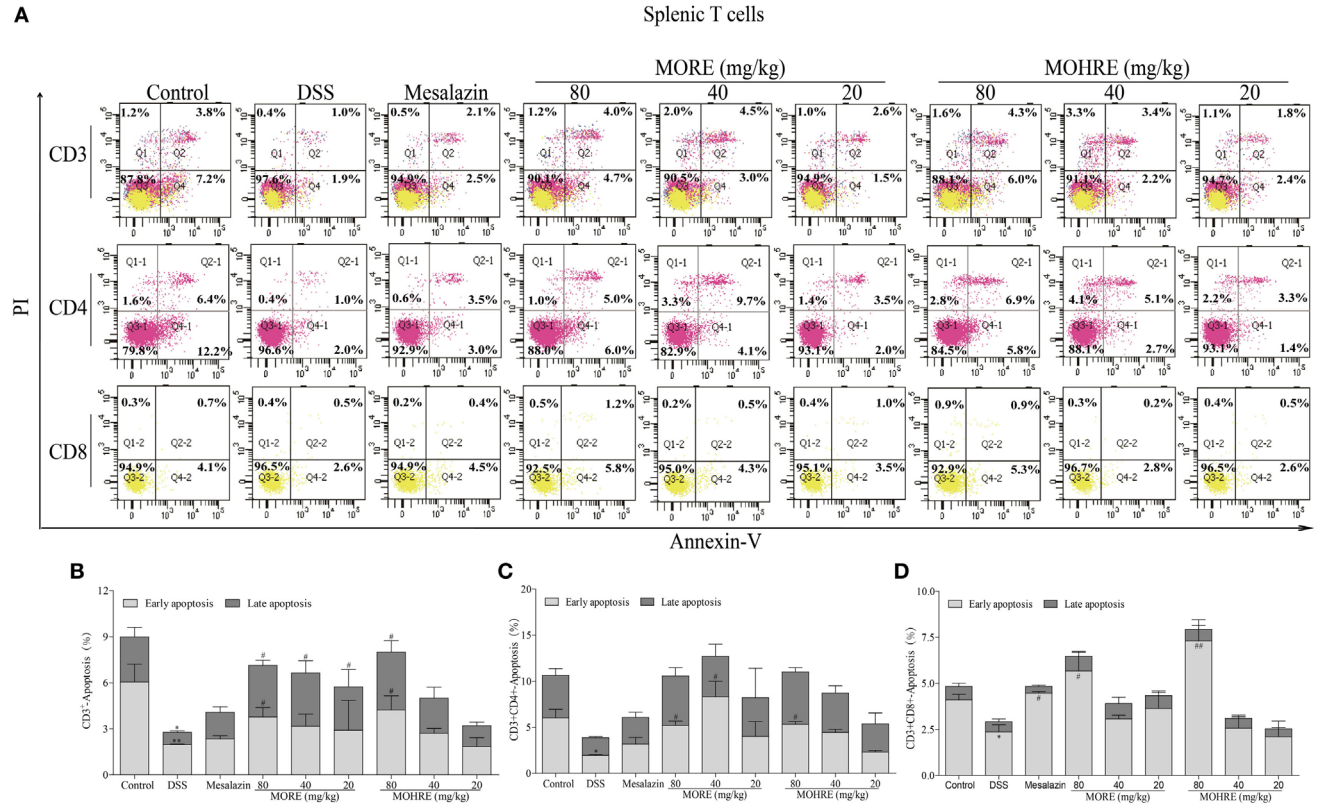

FIGURE 7 | The apoptosis effect of root extract of *Morinda officinalis* (MORE) and hairy root extract of *M. officinalis* (MOHRE) on splenic T lymphocytes in dextran sodium sulfate (DSS)-induced chronic colitis mice. **(A)** The apoptosis of $CD3^+$, $CD4^+$, and $CD8^+$ T cells was detected by Annexin V/PI staining. **(B)** The apoptosis ratio of $CD3^+$ T cells. **(C)** The apoptosis ratio of $CD3^+CD4^+$ T cells. **(D)** The apoptosis ratio of $CD3^+CD8^+$ T cells. All data are expressed as mean ± SEM of three mice. $^*p < 0.05$. $^{**}p < 0.01$ vs. control group; $^{\#}p < 0.05$. $^{\#\#}p < 0.01$ vs. DSS group.

MOHRE. In addition, the contents of rubiadin-1-methyl ether, 2-hydroxy-1-methoxy-anthracene and 2-hydroxy-3 (hydroxymethyl) anthraquinone are 0.04, 0.07, and 0.03% in MORE, as well as the contents of rubiadin-1-methyl ether, 2-hydroxy-1-methoxy-anthracene, and 2-hydroxy-3(hydroxymethyl)anthraquinone are 0.11, 0.19, and 0.31% in MOHRE. Suggesting that the content of active iridoid is similar to MORE and MOHRE, the anthraquinones are derived from the MOHRE is higher than MORE.

The Acute Toxicity Study of MORE and MOHRE

Roots extract of *Morinda officinalis* and MOHRE did not caused obvious toxic reactions and mortality with the dose of 5,000 mg/kg by oral administration. In addition, during the 14 days observation time, all animals looked bright and the body weight did not have significant change (**Table 1**).

MORE and MOHRE Attenuated DSS-Induced Murine Experimental Chronic Colitis

In this study, the body weight of colitis mice induced by DSS decreased significantly from day 7, and the animal condition continued to deteriorate until the end of the experiment in DSS group. All drug-administration groups significantly restored body weight (**Figure 3A**). The enteritis induced by DSS significantly increased the mortality of animals. Treatment with mesalazin as a positive drug, MORE, and MOHRE reduced the death of animals (**Figure 3B**). In addition, food intake and water intake also were reduced in DSS group. Treatment with mesalazin, MORE, and MOHRE could improve food intake and water intake to a certain extent (**Figures 3C,D**). DAI is a most important indicator of the effect evaluation in IBD model. In this study, the DAI score increased significantly in DSS group, indicating a severe condition of colitis. By oral administration of mesalazin, MORE, and MOHRE, the DAI scores were decreased significantly (**Figure 3E**). The roles of MORE and MOHRE revealed a dose-dependent manner. And there were not obvious differences on reversing these pathological symptoms of UC between MORE and MOHRE under the same concentration. These results showed that both MORE and MOHRE could attenuate DSS-induced experimental chronic UC with similar effect.

The colon length is inversely associated with the severity of DSS-induced colitis. Our results showed that the colon from mice in mesalazin, MORE, and MOHRE groups is longer than in the DSS group (**Figures 4A,B**). Colon thickness and

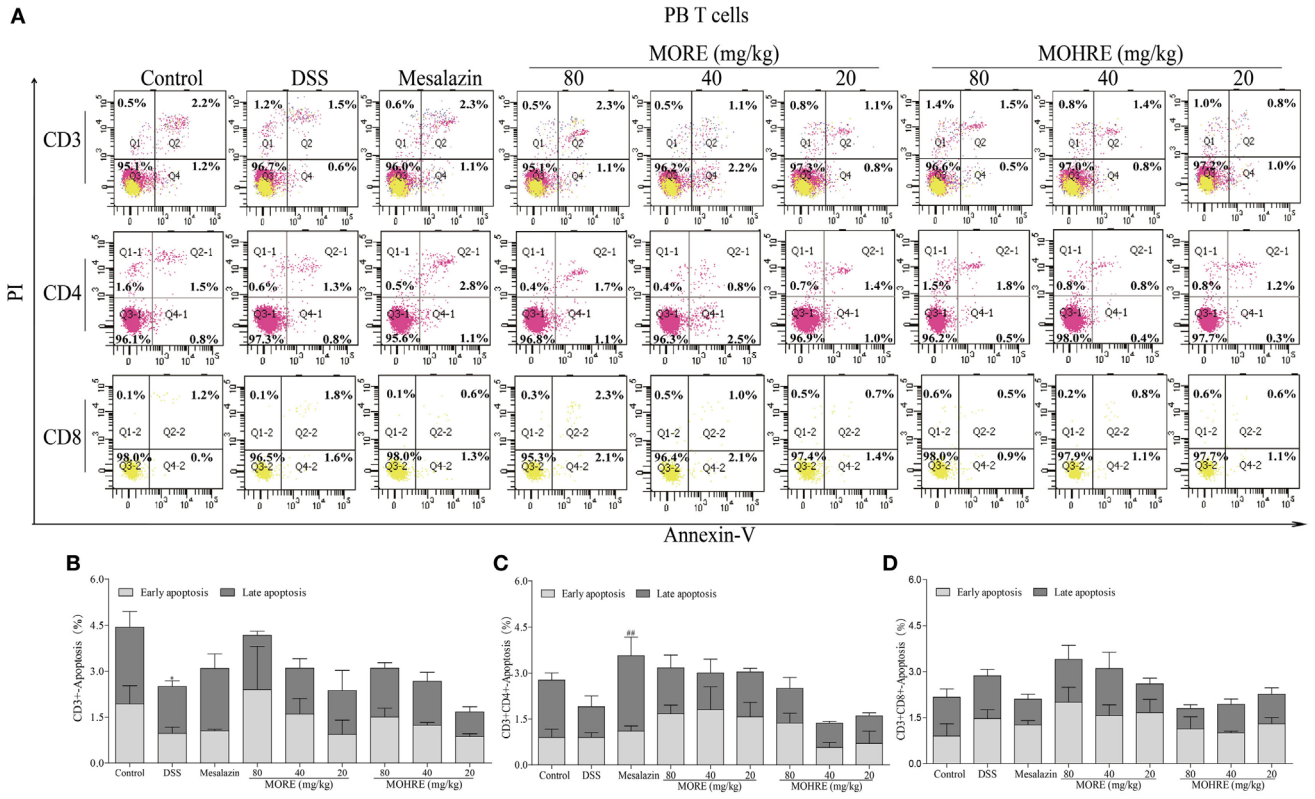

FIGURE 8 | The apoptosis effect of root extract of *Morinda officinalis* (MORE) and hairy root extract of *M. officinalis* (MOHRE) on peripheral blood (PB) T lymphocytes in dextran sodium sulfate (DSS)-induced chronic colitis mice. **(A)** The apoptosis of $CD3^+$, $CD4^+$ and $CD8^+$ T cells was detected by Annexin V/PI staining. **(B)** The apoptosis ratio of $CD3^+$ T cells. **(C)** The apoptosis ratio of $CD3^+CD4^+$ T cells. **(D)** The apoptosis ratio of $CD3^+CD8^+$ T cells. All data are expressed as mean ± SEM of three mice. $^*p < 0.05$. $^{¨}p < 0.01$ vs. control group; $^{\#}p < 0.05$. $^{\#\#}p < 0.01$ vs. DSS group.

morphology score are also the important indicators to evaluate the therapeutic effect of drug. We found that mesalazin, MORE, and MOHRE reduced colon thickness and morphology score (**Figures 4C–E**). In addition, the H&E staining of colonic tissues revealed the anti-inflammatory effects of mesalazin, MORE, and MOHRE in colon. Compared with the normal structure of the colon, DSS group showed obvious inflammatory cell infiltration, absence of epithelial cells and goblet cells. However, significant reductions in the inflammatory cell infiltration and mucous membrane ulcer were observed after treatment with mesalazin, MORE, and MOHRE (**Figures 4F,G**). Furthermore, these positive effects of MORE and MOHRE displayed a dose-dependent manner. An insignificant difference between MORE and MOHRE was observed at the same concentration. These results indicated that both MORE and MOHRE could effectively protect DSS-induced colon injury in mice.

The Effect of MORE and MOHRE on the Level of Inflammatory Cytokines in DSS-Induced Colitis

It is well known that inflammation plays an important role in the pathogenesis of UC. The abnormal activation of immune system can cause excessive secretions of proinflammatory cytokines. To understand the anti-inflammatory effect of MORE and MOHRE in DSS-induced chronic UC in mice, we measured the serum levels of proinflammatory cytokines TNF-α, IL-6, and IL-17 were significantly increased in DSS group, which were all decreased significantly in mesalazin, MORE, and MOHRE groups (**Figure 5**). There are still no significant differences between MORE and MOHRE.

The Protective Effect of MORE and MOHRE on Spleen in DSS-Induced Chronic Colitis

Chronic colitis often causes the disorder of immune function. In this study, we found that oral administration of DSS significantly increases spleen weight, and MORE and MOHRE significantly inhibited spleen swelling (**Figures 6A,B**). In addition, we analyzed the degree of spleen damage by H&E staining. We also found that DSS led to the change of spleen structure, swelling, and the accumulation of inflammatory cells. However, MORE and MOHRE could significantly effectively alleviate the injury of the spleen (**Figure 6C**). This protective effect between MORE and MOHRE was not significantly different.

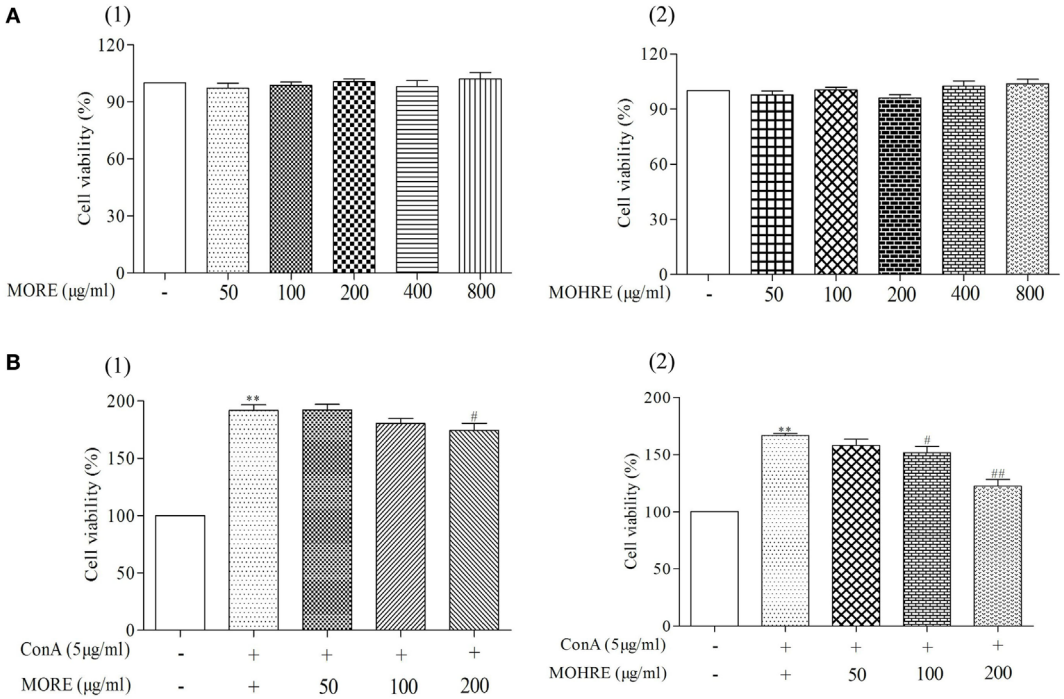

FIGURE 9 | Cytotoxic and proliferous effect of root extract of *Morinda officinalis* (MORE) and hairy root extract of *M. officinalis* (MOHRE) on lymphocytes. Cell viability was measured using MTT assay with different concentration (50–800 μg/mL) of MORE and MOHRE in the presence or absence of Concanavalin A (ConA) for 24 h. **(A)** Cytotoxicity of MORE and MOHRE on lymphocytes from normal mice in the absence of ConA for 24 h. **(B)** The proliferous effect of MORE and MOHRE on lymphocytes in the presence of ConA for 24 h. All data are expressed as mean ± SEM of three independent experiments. $^{*}p < 0.05$. $^{¨}p < 0.01$ vs. control group; $^{\#}p < 0.05$. $^{\#\#}p < 0.01$ vs. ConA group.

MORE and MOHRE Induced the Apoptosis of Splenocytes, but Not PB Lymphocytes in Colitis Mice

The apoptosis of T cells has been confirmed to be critically involved in the pathogenesis of UC. In the present study, splenocytes and PB lymphocytes from chronic colitis mice were analyzed by flow cytometry after two cycle's treatment of MORE and MOHRE. To analyze the subsets of splenic and PB T cells that suffer apoptosis following MORE and MOHRE treatment in chronic colitis mice, we applied annexin V^+/PI^+ among total T cell ($CD3^+$), helper T cells ($CD3^+CD4^+$) and cytotoxic T cell ($CD3^+CD8^+$) in spleen and PB. We found that the early and late apoptosis of splenic $CD3^+$ T were significantly decreased in DSS treated mice when compared with the control group, and early apoptosis of splenic $CD4^+$ and $CD8^+$ T cells were also significantly decreased in DSS group. Meanwhile, except PB $CD3^+$ T cells were significantly reduced in late apoptosis, the apoptosis of PB $CD4^+$ and $CD8^+$ T cells had no difference in DSS group when compared with the control group. Interestingly, MORE and MOHRE significantly induced the early and late apoptosis of splenic $CD3^+$ T cells in a dose-dependent manner *in vivo*. In addition, the early apoptosis of splenic $CD4^+$ and $CD8^+$ T cells in colitis mice were also significantly increased. However, there is no significantly difference in the induction of PB T cells apoptosis after treatment with MORE and MOHRE (**Figures 7** and **8**). The data showed that MORE and MOHRE could obviously induce the apoptosis of splenocytes, but not PB lymphocytes in chronic colitis mice. Meanwhile, the apoptosis effect of MOHRE on splenocytes or PB lymphocytes *in vivo* is similar to MORE.

The Cytotoxic and Proliferous Effect of MORE and MOHRE to Splenic Lymphocytes

According to the results from *in vivo* study, we found that splenic lymphocytes were much more sensitive to MORE- and MOHRE-induced apoptosis. Here, we further investigated the effect of MORE and MOHRE on splenic lymphocytes *in vitro*. The different concentrations of MORE and MOHRE were added into splenic lymphocytes in different 96-well plates for 24 h. The data showed that MORE and MOHRE had no toxicity to splenic lymphocytes (**Figure 9A**). However, after ConA stimulation, MORE and MOHRE inhibited the proliferation of splenic lymphocytes in a dose-dependent manner (**Figure 9B**), possessing unsignificant difference between them at the same concentration. The results revealed that MORE and MOHRE exert immunoregulatory properties for the proliferation of ConA-activated T cells *in vitro*.

The Apoptosis Assay of MORE and MOHRE on Splenic T Cells *In Vitro*

To explore the relationship between the inhibition of splenic T cells proliferation and apoptosis, we incubated splenic lymphocytes with MORE and MOHRE in the presence or absence

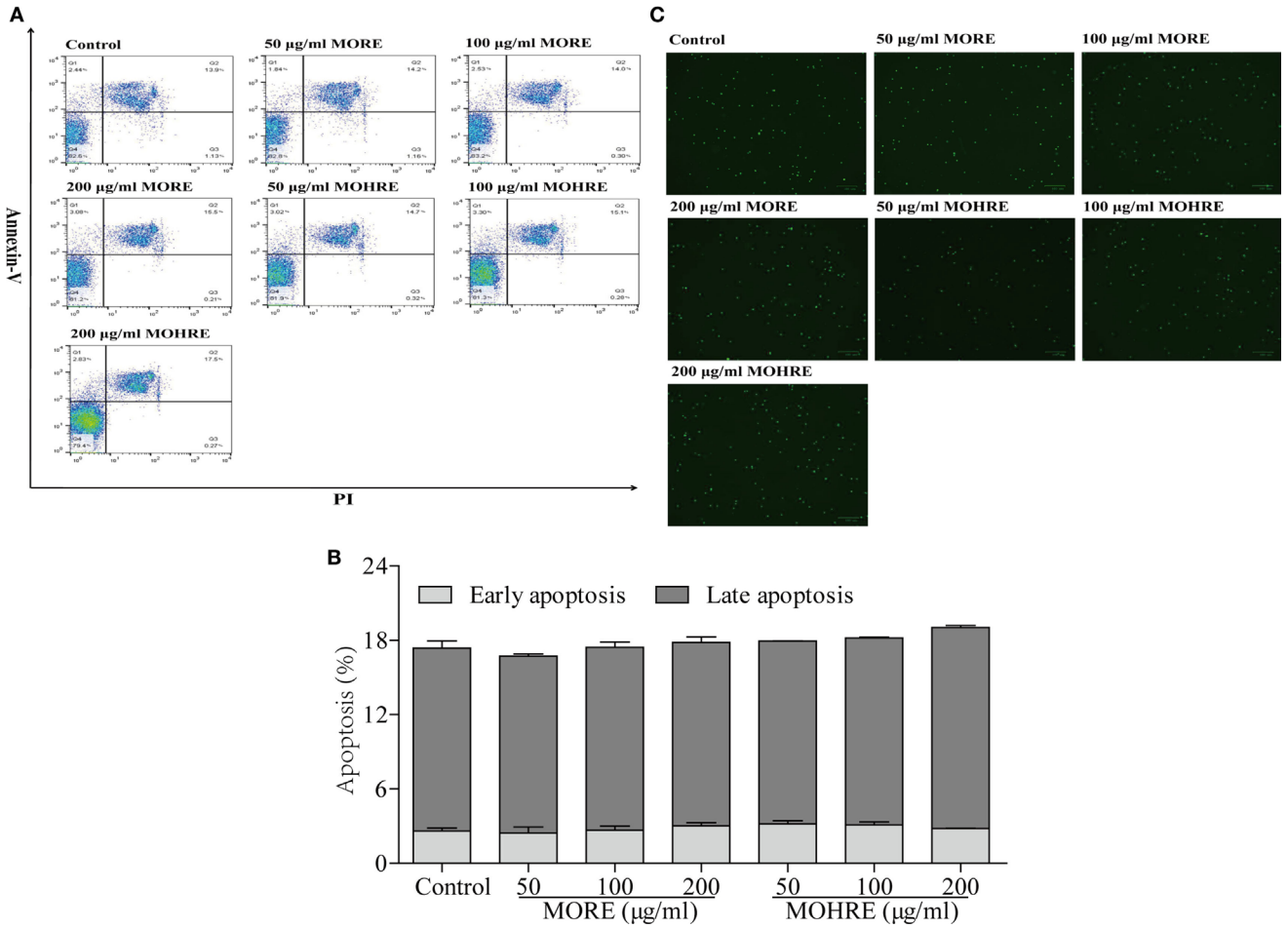

FIGURE 10 | The apoptosis effect of root extract of *Morinda officinalis* (MORE) and hairy root extract of *M. officinalis* (MOHRE) on normal splenic lymphocytes. **(A)** Representative FACS picture in each group. **(B)** Apoptosis assay. **(C)** Representative images were obtained using a fluorescence microscope (100 μm). All data are expressed as mean ± SEM of three independent experiments. *$p < 0.05$. ¨$p < 0.01$ vs. control group.

of ConA. Without ConA stimulation, MORE and MOHRE were unable to significantly induce lymphocytes apoptosis (**Figure 10**). However, after stimulation with ConA for 24 h, both MORE and MOHRE can dose-dependently induce the apoptosis of ConA-activated T lymphocytes (**Figure 11**). Meanwhile, MORE and MOHRE also could induced the early apoptosis of activated T lymphocytes at 48 in the presence of ConA stimulation (Presentation S1 in Supplementary Material). In addition, we further to explore whether $CD3^+$, $CD4^+$, and $CD8^+$ T cells population is susceptible to cause apoptosis by MORE and MOHRE in both unstimulated and Con A-stimulated lymphocyte. Our data indicated that the early and late apoptosis ratios of $CD3^+$, $CD4^+$, and $CD8^+$ T cells were no statistically differences in the unstimulated lymphocyte (**Figure 12**). However, the lymphocyte activated with ConA and exposed to MORE and MOHRE could dose-dependently increased the early and late apoptosis ratios of $CD3^+$, $CD4^+$, and $CD8^+$ T cells (**Figure 13**). The difference of these effects between MORE and MOHRE was not significant at the same concentration.

DISCUSSION

In the present study, we investigated the differences of the major chemical constituents between MORE and MOHRE. Based on this, we demonstrated the therapeutic effect of the hairy roots of *M. officinalis* on DSS-induced chronic UC in mice and investigated the apoptosis effect of *M. officinalis* and its hairy roots on T lymphocytes *in vivo* and *in vitro* for the first time. Our results showed that *M. officinalis* and its hairy roots could protect against DSS-induced chronic colitis and inhibit abnormal activation of T cells via inducing apoptosis *in vivo* and *in vitro*.

Morinda officinalis native plant contains much more polysaccharides than *M. officinalis* hairy roots (data not shown). Thus we used 85% ethanol to generate extracts without polysaccharides, the present data showed that both MORE and MOHRE are effective in treating UC mice, indicating that polysaccharides in MORE may not be an essential component in the treatment of UC mice. The content of iridoids in MORE is similar to that in MOHRE, both contain up to 3%. While the content of anthraquinones in

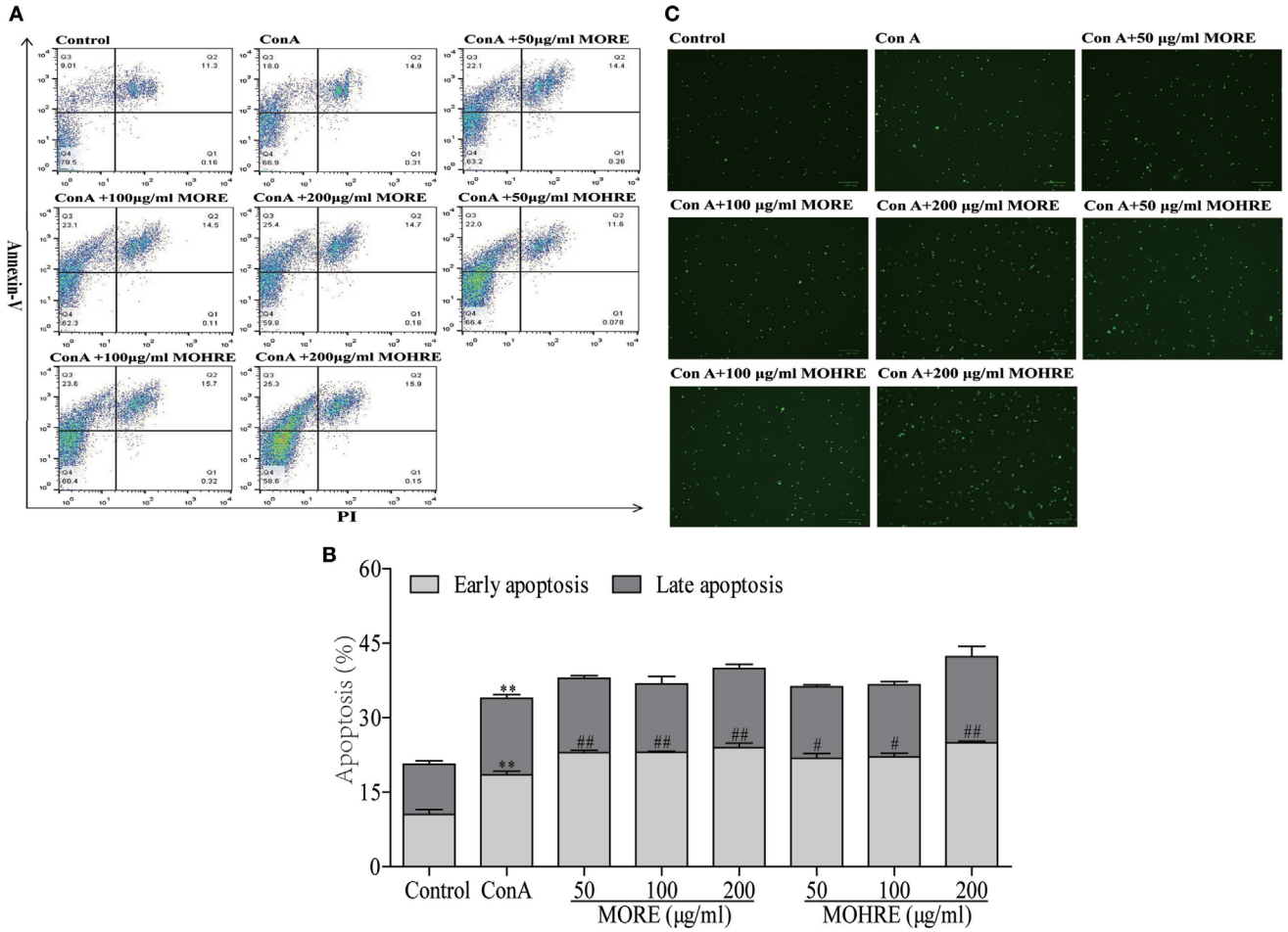

FIGURE 11 | The apoptosis effect of root extract of *Morinda officinalis* (MORE) and hairy root extract of *M. officinalis* (MOHRE) on spleen lymphocytes have been activated by Concanavalin A (ConA). **(A)** Representative FACS picture in each group. **(B)** Apoptosis assay. **(C)** Representative images were obtained using a fluorescence microscope (100 μm). All data are expressed as mean ± SEM of three independent experiments. $^{*}p < 0.05$. $^{**}p < 0.01$ vs. control group; $^{\#}p < 0.05$. $^{\#\#}p < 0.01$ vs. ConA group.

MORE is obvious less than that in MOHRE, the ratio is 0.14 vs 0.66%. Meanwhile, we found that the MOHRE exert a similar therapeutic effect on DSS-induced chronic UC in mice. Several studies have shown that these iridoids in *M. officinalis* have anti-inflammatory and immunomodulatory properties (27, 28). It also has been reported that monotropein, the main iridoid in *M. officinalis*, has therapeutic effect on DSS-induced acute colitis mice with a dose up to 200 mg/kg (15), which is much higher than the dose of MORE and MOHRE we used in our study. These data further indicated that besides monotropein, other iridoids and anthraquinone in *M. officinalis* could also exert an important role in the treatment of UC.

People with UC often have symptoms such as diarrhea, bloody stool, abdominal pain, body weight loss, and colonic shortening (29). These clinical parameters are essential to assess the severity of UC and evaluate the efficacy of the potential drugs. In this study, the results showed that oral administration of MORE and MOHRE could significantly improve body weight loss, food intake, fecal status, intestinal bleeding, and colonic tissue injury on 3% DSS-induced chronic UC in mice. In addition, DSS induced colonic mucosa injury, which led to colon edema and atrophy (30). Colonic shortening and DAI score are used as important indicators to evaluating colonic injury (31). In the present study, treatment with MORE and MOHRE significantly inhibited the colonic shortening and reduced DAI score in colitis mice. These data showed that MORE and MOHRE protected against DSS-induced chronic colitis in mice.

The DSS-induced colitis model exerted colonic mucosa injury, inflammatory cell infiltration, goblet cell loss, and colonic wall thickness (32). Many studies have demonstrated that neutrophil infiltration in the colonic mucosa tissues is one of the most remarkable histological features observed in patients with UC (33, 34). Diffuse neutrophil infiltration in the colonic mucosa tissues could aggravate inflammatory infiltration (35). Therefore, reducing the amount of neutrophil can effectively alleviate the colon injury. According to the histological analysis, oral administration of MORE and MOHRE could significantly alleviate colonic tissue damage, neutrophil infiltration, and

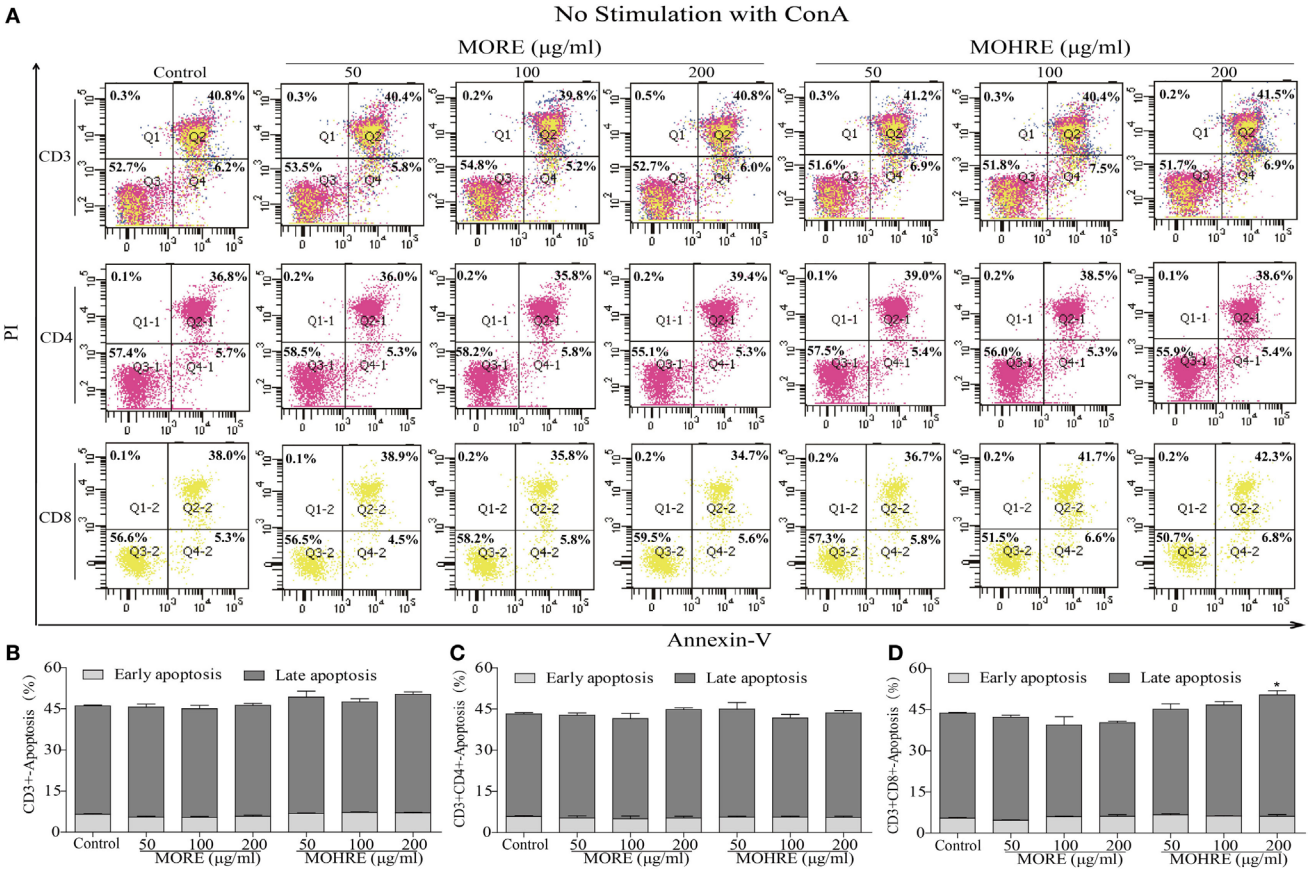

FIGURE 12 | The apoptosis effect of root extract of *Morinda officinalis* (MORE) and hairy root extract of *M. officinalis* (MOHRE) on $CD3^+$, $CD4^+$, and $CD8^+$ T cells in the absence of Concanavalin A (ConA) stimulation. **(A)** The apoptosis of $CD3^+$, $CD4^+$, and $CD8^+$ T cells was detected by Annexin V/PI staining. **(B)** The apoptosis ratio of $CD3^+$ T cells. **(C)** The apoptosis ratio of $CD3^+CD4^+$ T cells. **(D)** The apoptosis ratio of $CD3^+CD8^+$ T cells. All data are expressed as mean ± SEM of three independent experiments. $^*p < 0.05$. $^{¨}p < 0.01$ vs. control group.

promotes the repair of colonic tissue on DSS-induced colitis. The pharmacological effects may be attributed to their extracts containing iridoids and anthraquinones. Related studies have shown that these chemical compositions can downregulate NF-κB signaling pathways, indicating that a significant anti-inflammatory effect (36).

The abnormal expression of proinflammatory cytokines not only occurs in IBD patients but also appears in DSS-induced colitis model. TNF-α is a major proinflammatory cytokines, its abnormal expression is closely related to the immune dysfunction (37, 38). The aggressive release of TNF-α can activate the intestinal adaptive immune system, and recruit a large number of neutrophils and macrophages to infiltrate the colonic mucosa tissues, which in turn leads to colon injury (39). Therefore, many immunosuppressive agents have been developed to decrease the levels of TNF-α for the treatment of UC. In addition, IL-6 and IL-17 also participated in the inflammatory response of IBD and induced the production of many other proinflammatory cytokines. Overexpression of these cytokines plays an important role in the pathogenesis of IBD (40). In the present study, the levels of TNF-α, IL-6, and IL-17 were tested in colitis mice. The data show that oral administration of MORE and MOHRE can significantly decrease the serum levels of TNF-α, IL-6, and IL-17 in colitis mice, suggesting that MORE and MOHRE could suppress the production of proinflammatory cytokines and then relieve the inflammatory response.

T lymphocytes are important for immune system homeostasis and host defense, which can secrete proinflammatory and anti-inflammatory cytokines (41, 42). When the body is injured, immune cells would produce relevant cytokines to maintain immune homeostasis. However, the over expansion of activated lymphocytes can lead to a series of autoimmune diseases (43), including rheumatoid arthritis, atopic illnesses, and IBD. Many studies have indicated that the excessive proliferation of lymphocytes is closely related to the pathogenesis of IBD (44). Inhibiting the proliferation of lymphocytes or inducing lymphocytes apoptosis may provide the basis for a potential therapeutic strategy in patients with UC (45, 46). Accumulated evidences have showed that the induction of $CD4^+$ and $CD8^+$ T cells apoptosis is beneficial to treat colitis (44, 47). The data *in vivo* study indicated that MORE and MOHRE could significantly inhibit splenomegaly, improve the damage of spleen, and decrease the production of inflammatory cytokines in DSS-induced chronic colitis mice. The effects may

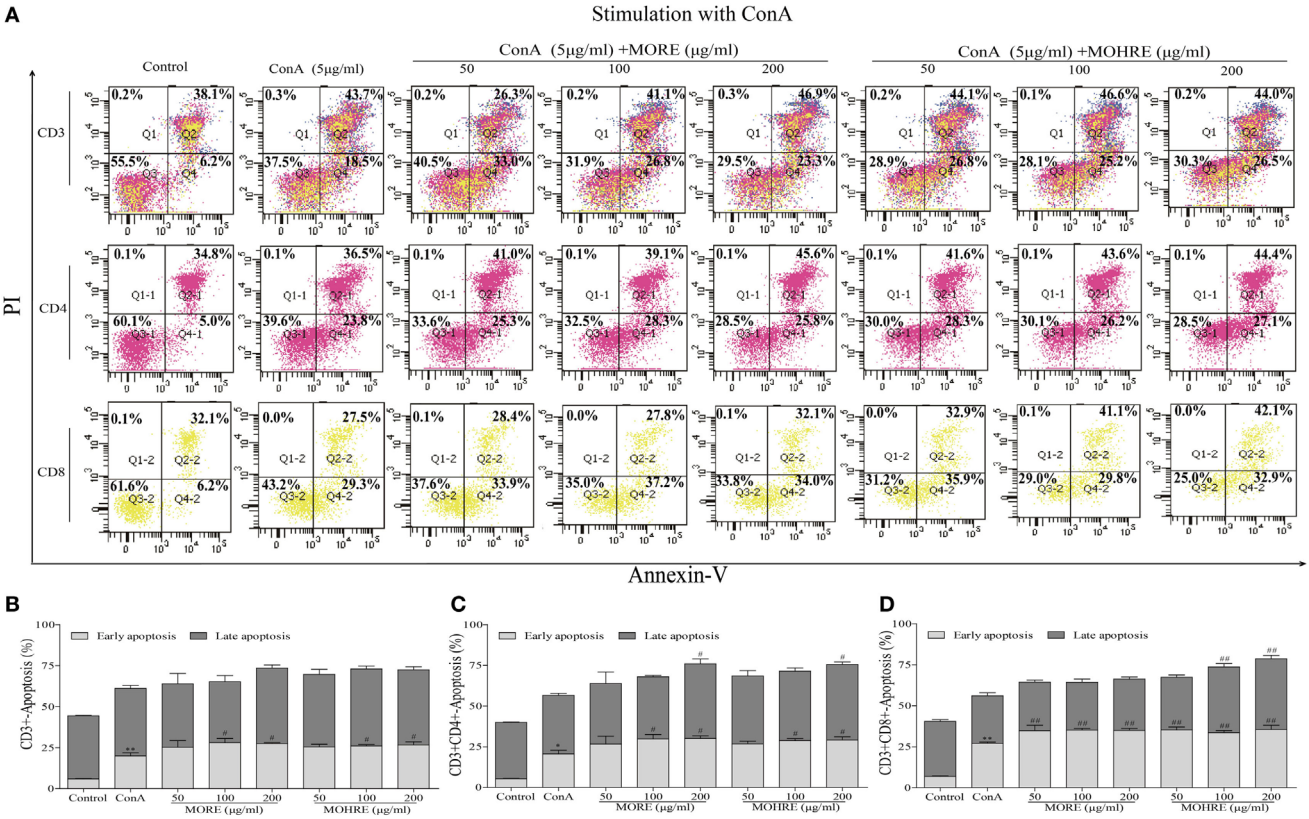

FIGURE 13 | The apoptosis effect of root extract of *Morinda officinalis* (MORE) and hairy root extract of *M. officinalis* (MOHRE) on CD3+, CD4+, and CD8+ T cells in the presence of Concanavalin A (ConA) stimulation. **(A)** The apoptosis of CD3+, CD4+, and CD8+ T cells was detected by Annexin V/PI staining. **(B)** The apoptosis ratio of CD3+ T cells. **(C)** The apoptosis ratio of CD3+CD4+ T cells. **(D)** The apoptosis ratio of CD3+CD8+ T cells. All data are expressed as mean ± SEM of three independent experiments. $^{*}p < 0.05$. $^{**}p < 0.01$ vs. control group; $^{\#}p < 0.05$. $^{\#\#}p < 0.01$ vs. ConA group.

be related to its immunomodulatory effects. The proliferation of activated T cells and malformation in cell death regulation play an important role in the pathogenesis of IBD including UC and CD. Meanwhile, many immunosuppressive agents have been used to treat IBD due to the induction of T cell apoptosis (6, 48). Based on this, we further investigated the apoptosis effects of MORE and MOHRE on splenic lymphocytes and PB lymphocytes *in vivo*. Interestingly, MORE and MOHRE significantly increased the early apoptosis of splenic CD3+, CD4+, and CD8+ T cells. The late apoptosis of splenic T cells only appeared in CD3+ T cells after treatment with MORE and MOHRE. However, the induction of T cells apoptosis in PB T cells was no significant differences. These results showed that MORE and MOHRE exert effects against activated T cells by the induction of apoptosis and the effects are more sensitive to splenic lymphocytes apoptosis.

To further confirm the apoptosis effects of MORE and MOHRE on T lymphocytes, we tested the apoptosis effects of MORE and MOHRE on T cells in the presence or absence of ConA stimulation. We found that MORE and MOHRE were non-toxic to T cells and did not induce the apoptosis of T cells in the absence of ConA stimulation. However, both MORE and MOHRE significantly inhibited the proliferation of ConA-activated T lymphocytes. Meanwhile, MORE and MOHRE dose-dependently induced activated T cells apoptosis in early and late stage. The early apoptosis of cells is a reversible course when the apoptotic stimulation is cleaned up (49). With the rise of early apoptosis, irreversible late apoptosis would gradually be accumulated. In this study, the results *in vitro* were consistent with *in vivo*. MORE and MOHRE were more sensitive to induce early apoptosis of CD3+, CD4+, and CD8+ T cell in the imbalance of immune status. These results from *in vitro* study further showed that MORE and MOHRE could exert the immunoregulatory effect by induction of T cells apoptosis only when the immune dysfunction. In this sense, it is possible that the therapeutic effects of MORE and MOHRE on DSS-induced chronic colitis may be achieved via inducing apoptosis of overactivated lymphocytes, leading to the decrease of the levels of inflammatory cytokines and the restoration of normal immune response. Based on this, it is also worth to further investigate the apoptosis effect of MORE and MOHRE on Treg or Teff cells *in vivo and in vitro*. To explore this, we should mark additional surface markers of Treg or Teff cells. Unfortunately, it was technically impossible that a 5-color flow cutometer was used in this study. However, further study along these lines should be continued.

CONCLUSION

Although the content of active chemical composition is not completely consistent, our study discovered that the hairy roots of *M. officinalis* are equally effective as the native plant in the treatment of UC in a DSS-induced chronic colitis model. Our research demonstrated three possible mechanisms of action for MORE and MOHRE, including the anti-inflammatory effect, the promotion of T lymphocyte apoptosis and the reduction of abnormal immune responses. In addition, the successful derivation of a sustainable hairy root culture provides a model platform to study the synthetic pathways for bioactive metabolites such as iridoids and anthraquinones and makes the use of bioreactors to largely produce traditional Chinese medicine a reality to treat IBD.

ETHICS STATEMENT

Adult male and female Kunming (KM) mice (18–22 g) were purchased from the Laboratory Animal Services Center, Guangzhou University of Chinese Medicine (Guangzhou, China). All animals are raised in accordance with the National Institutes of Health Guide for Laboratory animals' use. The study was approved by the Animal Ethics Committee of Guangzhou University of Chinese Medicine. Animals were housed under standard environment condition of temperature at 20–25°C under a 12 h dark/light cycle, and allowed free access to sterilized water and standard food.

AUTHOR CONTRIBUTIONS

JL, PW, HL, and JL contributed to the animal experiments, cell experiments, and data analysis. HH, YW, CF, XJ, HL, and QX contributed to the study analysis and data analysis. XL and LZ contributed to the revision of the manuscript. SC and SH contributed to the conception and design of the study.

FUNDING

This work was supported by the Guangdong Province Universities and Colleges Pearl-River Scholar Funded Scheme, the Special Funds from Central Finance of China in Support of the Development of Local Colleges and University [Educational Finance grant no. 276(2016)], Science and Technology Project Scheme of Guangdong Province (no. 2013B090800052), Innovative Development of Traditional Chinese Medicine Scientific Research Team (no. A1-AFD01515A03), and Hong Kong, Macao and Taiwan Special Science and Technology Cooperation Program (no. 2014DFH30010).

SUPPLEMENTARY MATERIAL

The Supplementary Material for this article can be found online at http://journal.frontiersin.org/article/10.3389/fimmu.2017.00905/full#supplementary-material.

REFERENCES

1. Shinzaki S, Matsuoka K, Iijima H, Mizuno S, Serada S, Fujimoto M, et al. Leucine-rich alpha-2 glycoprotein is a serum biomarker of mucosal healing in ulcerative colitis. *J Crohns Colitis* (2017) 11(1):84. doi:10.1093/ecco-jcc/jjw132
2. Witalison EE, Cui X, Causey CP, Thompson PR, Hofseth LJ. Molecular targeting of protein arginine deiminases to suppress colitis and prevent colon cancer. *Oncotarget* (2015) 6(34):36053–62. doi:10.18632/oncotarget.5937
3. Paclik D, Danese S, Berndt U, Wiedenmann B, Dignass A, Sturm A. Galectin-4 controls intestinal inflammation by selective regulation of peripheral and mucosal T cell apoptosis and cell cycle. *PLoS One* (2008) 3(7):e2629. doi:10.1371/journal.pone.0002629
4. Liu X, He H, Huang T, Lei Z, Liu F, An G, et al. Tanshinone IIA protects against dextran sulfate sodium- (DSS-) induced colitis in mice by modulation of neutrophil infiltration and activation. *Oxid Med Cell Longev* (2016) 2016(5):7916763. doi:10.1155/2016/7916763
5. He J, Liang J, Zhu S, Li J, Zhang Y, Sun W. Anti-inflammatory effects of Pulvis Fellis Suis extract in mice with ulcerative colitis. *J Ethnopharmacol* (2011) 138(1):53–9. doi:10.1016/j.jep.2011.08.019
6. Shen Y, Luo Q, Xu H, Gong F, Zhou X, Sun Y, et al. Mitochondria-dependent apoptosis of activated T lymphocytes induced by astin C, a plant cyclopeptide, for preventing murine experimental colitis. *Biochem Pharmacol* (2011) 82(3):260–8. doi:10.1016/j.bcp.2011.04.013
7. Yu QT, Saruta M, Papadakis KA. Visilizumab induces apoptosis of mucosal T lymphocytes in ulcerative colitis through activation of caspase 3 and 8 dependent pathways. *Clin Immunol* (2008) 127(3):322–9. doi:10.1016/j.clim.2008.02.009
8. Balaha M, Kandeel S, Elwan W. Garlic oil inhibits dextran sodium sulfate-induced ulcerative colitis in rats. *Life Sci* (2016) 146:40–51. doi:10.1016/j.lfs.2016.01.012
9. Yanai H, Salomon N, Lahat A. Complementary therapies in inflammatory bowel diseases. *Curr Gastroenterol Rep* (2016) 18(12):62. doi:10.1007/s11894-016-0537-6
10. Mok TS, Yeo W, Johnson PJ, Hui P, Ho WM, Lam KC, et al. A double-blind placebo-controlled randomized study of Chinese herbal medicine as complementary therapy for reduction of chemotherapy-induced toxicity. *Ann Oncol* (2007) 18(4):768–74. doi:10.1093/annonc/mdl465
11. Zhang H, Li J, Xia J, Lin S. Antioxidant activity and physicochemical properties of an acidic polysaccharide from *Morinda officinalis*. *Int J Biol Macromol* (2013) 58(7):7–12. doi:10.1016/j.ijbiomac.2013.03.031
12. Sang S, Cheng X, Zhu N, Wang M, Jhoo JW, Stark RE, et al. Iridoid glycosides from the leaves of *Morinda citrifolia*. *J Nat Prod* (2001) 64(6):799–800. doi:10.1021/np010011l
13. Bao L, Qin L, Liu L, Wu Y, Han T, Xue L, et al. Anthraquinone compounds from *Morinda officinalis* inhibit osteoclastic bone resorption in vitro. *Chem Biol Interact* (2011) 194(2–3):97–105. doi:10.1016/j.cbi.2011.08.013
14. Kim IT, Park HJ, Nam JH, Park YM, Won JH, Choi J, et al. In-vitro and in-vivo anti-inflammatory and antinociceptive effects of the methanol extract of the roots of *Morinda officinalis*. *J Pharm Pharmacol* (2005) 57(5):607–15. doi:10.1211/0022357055902
15. Shin JS, Yun KJ, Chung KS, Seo KH, Park HJ, Cho YW, et al. Monotropein isolated from the roots of *Morinda officinalis* ameliorates proinflammatory mediators in RAW 264.7 macrophages and dextran sulfate sodium (DSS)-induced colitis via NF-κB inactivation. *Food Chem Toxicol* (2013) 53:263–71. doi:10.1016/j.fct.2012.12.013
16. Banerjee S, Singh S, Ur Rahman L. Biotransformation studies using hairy root cultures – a review. *Biotechnol Adv* (2012) 30(3):461–8. doi:10.1016/j.biotechadv.2011.08.010
17. Ming Q, Su C, Zheng C, Jia M, Zhang Q, Zhang H, et al. Elicitors from the endophytic fungus *Trichoderma atroviride* promote *Salvia miltiorrhiza* hairy root growth and tanshinone biosynthesis. *J Exp Bot* (2013) 64(18):5687–94. doi:10.1093/jxb/ert342
18. Ludwig-Müller J, Jahn L, Lippert A, Püschel J, Walter A. Improvement of hairy root cultures and plants by changing biosynthetic pathways leading to pharmaceutical metabolites: strategies and applications. *Biotechnol Adv* (2014) 32(6):1168–79. doi:10.1016/j.biotechadv.2014.03.007

19. OECD. *Test No. 425: Acute Oral Toxicity: Up-and-Down Procedure*. Paris: OECD Publishing (2008).
20. Farkas S, Hornung M, Sattler C, Anthuber M, Gunthert U, Herfarth H, et al. Short-term treatment with anti-cd44v7 antibody, but not cd44v4, restores the gut mucosa in established chronic dextran sulphate sodium (DSS)-induced colitis in mice. *Clin Exp Immunol* (2005) 142(2):260–7. doi:10.1111/j.1365-2249.2005.02911.x
21. Okayasu I, Ohkusa T, Kajiura K, Kanno J, Sakamoto S. Promotion of colorectal neoplasia in experimental murine ulcerative colitis. *Gut* (1996) 39(1):87–92. doi:10.1136/gut.39.1.87
22. Cooper HS, Murthy SN, Shah RS, Sedergran DJ. Clinicopathologic study of dextran sulfate sodium experimental murine colitis. *Lab Invest* (1993) 69(2):238–49.
23. Xiao X, Kim J, Sun Q, Kim D, Park CS, Lu TS, et al. Preventive effects of cranberry products on experimental colitis induced by dextran sulphate sodium in mice. *Food Chem* (2015) 167(167):438–46. doi:10.1016/j.foodchem.2014.07.006
24. Millar AD, Rampton DS, Chander CL, Claxson AW, Blades S, Coumbe A, et al. Evaluating the antioxidant potential of new treatments for inflammatory bowel disease using a rat model of colitis. *Gut* (1996) 39(3):407–15. doi:10.1136/gut.39.3.407
25. Boirivant M, Strober W, Fuss IJ. Regulatory cells induced by feeding TNP-haptenated colonic protein cross-protect mice from colitis induced by an unrelated hapten. *Inflamm Bowel Dis* (2005) 11(1):48–55. doi:10.1097/00054725-200501000-00007
26. Su JY, Luo X, Zhang XJ, Deng XL, Su ZR, Zhou L, et al. Immunosuppressive activity of pogostone on T cells: blocking proliferation via S phase arrest. *Int Immunopharmacol* (2015) 26(2):328–37. doi:10.1016/j.intimp.2015.04.019
27. Bas E, Recio MC, Abdallah M, Máñez S, Giner RM, Cerdá-Nicolás M, et al. Inhibition of the pro-inflammatory mediators' production and anti-inflammatory effect of the iridoid scrovalentinoside. *J Ethnopharmacol* (2007) 110(3):419–27. doi:10.1016/j.jep.2006.09.038
28. Panigrahi GK, Yadav A, Mandal P, Tripathi A, Das M. Immunomodulatory potential of Rhein, an anthraquinone moiety of *Cassia occidentalis* seeds. *Toxicol Lett* (2016) 245:15–23. doi:10.1016/j.toxlet.2016.01.006
29. Goyal N, Rana A, Ahlawat A, Bijjem KR, Kumar P. Animal models of inflammatory bowel disease: a review. *Inflammopharmacology* (2014) 22(4):219–33. doi:10.1007/s10787-014-0207-y
30. Kiela PR, Laubitz D, Larmonier CB, Midura-Kiela MT, Lipko MA, Janikashvili N, et al. Changes in mucosal homeostasis predispose NHE3 knockout mice to increased susceptibility to DSS-induced epithelial injury. *Gastroenterology* (2009) 137(3):965–75. doi:10.1053/j.gastro.2009.05.043
31. Diaz-Granados N, Howe K, Lu J, Mckay DM. Dextran sulfate sodium-induced colonic histopathology, but not altered epithelial ion transport, is reduced by inhibition of phosphodiesterase activity. *Am J Pathol* (2000) 156(6):2169–77. doi:10.1016/S0002-9440(10)65087-0
32. Hu S, Chen M, Wang Y, Wang Z, Pei Y, Fan R, et al. mTOR inhibition attenuates dextran sulfate sodium-induced colitis by suppressing T cell proliferation and balancing TH1/TH17/Treg profile. *PLoS One* (2016) 11(4):e0154564. doi:10.1371/journal.pone.0154564
33. Koelink PJ, Overbeek SA, Braber S, Morgan ME, Henricks PA, Abdul Roda M, et al. Collagen degradation and neutrophilic infiltration: a vicious circle in inflammatory bowel disease. *Gut* (2014) 63(4):578–87. doi:10.1136/gutjnl-2012-303252
34. Liu W, Guo W, Hang N, Yang Y, Wu X, Shen Y, et al. MALT1 inhibitors prevent the development of DSS-induced experimental colitis in mice via inhibiting NF-κB and NLRP3 inflammasome activation. *Oncotarget* (2016) 7(21):30536–49. doi:10.18632/oncotarget.8867
35. Murphy CT, Moloney G, Hall LJ, Quinlan A, Faivre E, Casey P, et al. Use of bioluminescence imaging to track neutrophil migration and its inhibition in experimental colitis. *Clin Exp Immunol* (2010) 162(1):188–96. doi:10.1111/j.1365-2249.2010.04234.x
36. Park KS. Aucubin, a naturally occurring iridoid glycoside inhibits TNF-α-induced inflammatory responses through suppression of NF-κB activation in 3T3-L1 adipocytes. *Cytokine* (2013) 62(3):407–12. doi:10.1016/j.cyto.2013.04.005
37. Geremia A, Biancheri P, Allan P, Corazza GR, Di Sabatino A. Innate and adaptive immunity in inflammatory bowel disease. *Autoimmun Rev* (2014) 13(1):3–10. doi:10.1016/j.autrev
38. Ben-Horin S, Kopylov Y, Chowers Y. Optimizing anti-TNF treatments in inflammatory bowel disease. *Autoimmun Rev* (2014) 13(1):24–30. doi:10.1016/j.autrev.2013.06.002
39. Zindl CL, Lai JF, Lee YK, Maynard CL, Harbour SN, Ouyang W, et al. IL-22-producing neutrophils contribute to antimicrobial defense and restitution of colonic epithelial integrity during colitis. *Proc Natl Acad Sci U S A* (2013) 110(31):12768–73. doi:10.1073/pnas.1300318110
40. Strober W, Fuss IJ. Proinflammatory cytokines in the pathogenesis of inflammatory bowel diseases. *Gastroenterology* (2011) 140(6):1756–67. doi:10.1053/j.gastro.2011.02.016
41. Lenardo MJ. Molecular regulation of T lymphocyte homeostasis in the healthy and diseased immune system. *Immunol Res* (2003) 27(2):387–97. doi:10.1385/IR:27:2-3:387
42. Ten Hove T, The Olle F, Berkhout M, Bruggeman JP, Vyth-Dreese FA, Slors JF, et al. Expression of CD45RB functionally distinguishes intestinal T lymphocytes in inflammatory bowel disease. *J Leukoc Biol* (2004) 75(6):1010–5. doi:10.1189/jlb.0803400
43. Fülöp T Jr, Larbi A, Dupuis G, Pawelec G. Ageing, autoimmunity and arthritis: perturbations of TCR signal transduction pathways with ageing – a biochemical paradigm for the ageing immune system. *Arthritis Res Ther* (2003) 5(6):290–302. doi:10.1186/ar1019
44. Kotakadi VS, Jin Y, Hofseth AB, Ying L, Cui X, Volate S, et al. Ginkgo biloba extract EGb 761 has anti-inflammatory properties and ameliorates colitis in mice by driving effector T cell apoptosis. *Carcinogenesis* (2008) 29(9):1799–806. doi:10.1093/carcin/bgn143
45. Lutz C, Mozaffari M, Tosevski V, Caj M, Cippà P, McRae BL, et al. Increased lymphocyte apoptosis in mouse models of colitis upon ABT-737 treatment is dependent upon BIM expression. *Clin Exp Immunol* (2015) 181(2):343–56. doi:10.1111/cei.12635
46. Cárdeno A, Magnusson MK, Strid H, Alarcón de La Lastra C, Sánchez-Hidalgo M, Ohman L. The unsaponifiable fraction of extra virgin olive oil promotes apoptosis and attenuates activation and homing properties of T cells from patients with inflammatory bowel disease. *Food Chem* (2014) 161(11):353–60. doi:10.1016/j.foodchem.2014.04.016
47. Nancey S, Holvöet S, Graber I, Joubert G, Philippe D, Martin S, et al. CD8+ cytotoxic T cells induce relapsing colitis in normal mice. *Gastroenterology* (2006) 131(2):485–96. doi:10.1053/j.gastro.2006.05.018
48. Mudter J, Neurath MF. Apoptosis of T cells and the control of inflammatory bowel disease: therapeutic implications. *Gut* (2007) 56(2):293–303. doi:10.1136/gut.2005.090464
49. Elmore S. Apoptosis: a review of programmed cell death. *Toxicol Pathol* (2007) 35(4):495–516. doi:10.1080/01926230701320337

Conflict of Interest Statement: The authors declare that the research was conducted in the absence of any commercial or financial relationships that could be construed as a potential conflict of interest.

Copyright © 2017 Liang, Liang, Hao, Lin, Wang, Wu, Jiang, Fu, Li, Ding, Liu, Xiong, Lai, Zhou, Chan and Hou. This is an open-access article distributed under the terms of the Creative Commons Attribution License (CC BY). The use, distribution or reproduction in other forums is permitted, provided the original author(s) or licensor are credited and that the original publication in this journal is cited, in accordance with accepted academic practice. No use, distribution or reproduction is permitted which does not comply with these terms.

frontiers in Immunology

MINI REVIEW
published: 07 August 2017
doi: 10.3389/fimmu.2017.00928

Neutrophil Extracellular Traps and Endothelial Dysfunction in Atherosclerosis and Thrombosis

Haozhe Qi, Shuofei Yang† and Lan Zhang*†*

Department of Vascular Surgery, Renji Hospital, School of Medicine, Shanghai Jiao Tong University, Shanghai, China

Cardiovascular diseases are a leading cause of mortality and morbidity worldwide. Neutrophils are a component of the innate immune system which protect against pathogen invasion; however, the contribution of neutrophils to cardiovascular disease has been underestimated, despite infiltration of leukocyte subsets being a known driving force of atherosclerosis and thrombosis. In addition to their function as phagocytes, neutrophils can release their extracellular chromatin, nuclear protein, and serine proteases to form net-like fiber structures, termed neutrophil extracellular traps (NETs). NETs can entrap pathogens, induce endothelial activation, and trigger coagulation, and have been detected in atherosclerotic and thrombotic lesions in both humans and mice. Moreover, NETs can induce endothelial dysfunction and trigger proinflammatory immune responses. Overall, current data indicate that NETs are not only present in plaques and thrombi but also have causative roles in triggering formation of atherosclerotic plaques and venous thrombi. This review is focused on published findings regarding NET-associated endothelial dysfunction during atherosclerosis, atherothrombosis, and venous thrombosis pathogenesis. The NET structure is a novel discovery that will find its appropriate place in our new understanding of cardiovascular disease. In addition, NETs have high potential to be further explored toward much better treatment of atherosclerosis and venous thromboembolism in clinic.

Keywords: neutrophil extracellular traps, endothelial dysfunction, atherosclerosis, atherothrombosis, venous thromboembolism

OPEN ACCESS

Edited by:
Jixin Zhong,
Case Western Reserve University, United States

Reviewed by:
Hugo Caire Castro-Faria-Neto, Oswaldo Cruz Foundation, Brazil
Neha Dixit, DiscoveRx, United States
Shanzhong Gong, University of Texas at Austin, United States

***Correspondence:**
Shuofei Yang
yangshuofei@gmail.com;
Lan Zhang
zhanglanrjxg@gmail.com

†*These authors have contributed equally to this work.*

Specialty section:
This article was submitted to Inflammation, a section of the journal Frontiers in Immunology

Received: *08 May 2017*
Accepted: *20 July 2017*
Published: *07 August 2017*

Citation:
Qi H, Yang S and Zhang L (2017) Neutrophil Extracellular Traps and Endothelial Dysfunction in Atherosclerosis and Thrombosis. Front. Immunol. 8:928. doi: 10.3389/fimmu.2017.00928

HIGHLIGHTS

1. The NET structure, which has been clearly observed in the atherosclerotic plaque and venous thrombi, is a novel discovery that will find its appropriate place in our new understanding of cardiovascular disease.
2. This review summarizes the crosstalk mechanism between NETs and endothelial cells during the thrombosis and atherosclerosis.

Abbreviations: NETs, neutrophil extracellular traps; PMN, polymorphonuclear neutrophil; DNase, deoxyribonuclease; ECs, endothelial cells; VTE, venous thromboembolism; TLR, toll-like receptor; ROS, reactive oxygen species; NE, neutrophil elastase; PAD4, peptidyl arginine deiminase 4; G-CSF, granulocyte colony-stimulating factor; MPO, myeloperoxidase; IL, interleukin; CXCL, C-X-C motif ligand; LDL, low-density lipoprotein; DVT, deep venous thrombosis; PE, pulmonary embolism; vWF, von Willebrand factor; EDTA, ethylenediamine-tetraacetic acid.

3. NETs have high potential to be further explored to progress toward much better treatment of atherosclerosis and venous thromboembolism in clinic.

INTRODUCTION

Polymorphonuclear neutrophils (PMNs) have a significant innate immune system function in protection against pathogen invasion. In addition to classical phagocytosis, PMNs can release chromatin, nuclear proteins, and serine proteases extracellularly to form [neutrophil extracellular traps (NETs)], which comprise net-like DNA fibers containing histones and antimicrobial proteins (1). NETs can entrap pathogens to limit their dispersion, trigger coagulation, and induce endothelial injury. Since the first characterization of NETs in 2004, studies of their effects have expanded to reveal unexpected roles in sterile inflammation induced by PMNs (2, 3). Notably, the antibacterial activity of NETs is abrogated by deoxyribonuclease (DNase), which can directly degrade the chromatin fibers that comprise the backbone of NETs (2). Vascular endothelial cells (ECs) maintain the balance between anticoagulation and immune response functions. Atherosclerosis and venous thromboembolism (VTE) are two major cardiovascular diseases associated with endothelial dysfunction. Atherosclerosis and thrombosis share many common risk factors, such as obesity, diabetes, smoking, hypertension, and hyperlipidemia; however, it remains unclear whether there are specific factors involved in the pathogenesis of both atherosclerosis and VTE (4).

Neutrophil extracellular traps can be detected in both atherosclerosis and thrombosis, and the existence of these structures could be perceived as a double-edged sword in the context of disease processes, as it may both attenuate tissue injury and amplify local inflammation, leading to deterioration in disease symptoms (5). Nevertheless, no specific explanations are available for the effects of NETs on vascular endothelial function and the promotion of atherosclerosis and thrombosis. In this review, we reveal potential mechanisms underlying NET formation and endothelial dysfunction in cardiovascular disease and examine current knowledge of the potential clinical implications of these structures.

MECHANISM OF NET FORMATION

Neutrophil extracellular traps are formed during inflammation and observed *in vivo* during infections (6). The existence of NETs indicates that PMNs may undergo an alternative form of programmed cell death, termed NETosis, allowing function of these structures in innate immune defense. Depending on the different triggers involved, signaling molecule receptors and membrane integrity, NETosis is described as either "vital" or "suicidal" (7–11). In "vital" NETosis, PMNs rapidly release nuclear DNA encircled by vesicles to the extracellular space without membrane perforation, in response to stimulation by platelets *via* toll-like receptor (TLR)-4, or Gram-positive bacteria *via* TLR-2, in a reactive oxygen species (ROS)-independent manner (12). "Suicidal" NETosis is characterized by strong activation of nicotinamide adenine dinucleotide phosphate oxidase by phorbol 12-myristate 13-acetate, interleukin-8 (IL-8), or various microbial pathogens, in a ROS-dependent manner (13, 14). NETs can be released *via* neutrophil lysis or through vesicular transport of nuclear or mitochondrial DNA, without membrane rupture (12, 15). Regardless of which type of NET occurs, the molecular contents of their structures are similar, and include histones, neutrophil elastase (NE), myeloperoxidase (MPO), proteinase 3, cathepsin, and gelatinase (16, 17).

Although neutrophils are transcriptionally active cells, the majority of their DNA is transcriptionally inactive and condensed into heterochromatin. Its decondensation is mediated by peptidyl arginine deiminase 4 (PAD4), which catalyzes the conversion of histone arginines to citrullines, reducing the strong positive charge of histones, and consequently weakening histone-DNA binding (18). Spikes in intracellular Ca^{2+} can activate PAD4 to propagate NET release, and PAD4-deficient mice are unable to form NETs in response to physiological activators, such as bacteria (19, 20). NE is considered essential for histone cleavage during NETosis; accordingly, secretory leukocyte peptidase inhibitor, an endogenous elastase inhibitor, can inhibit NETosis (14, 21). The central role of elastase in NETosis is corroborated by the inability of PMNs from elastase-deficient mice to undergo this process (22).

NETs AND ATHEROSCLEROSIS

Atherosclerosis is a cardiovascular disease accompanied by chronic vascular wall inflammation, endothelial dysfunction, and smooth muscle cell proliferation (23). Given the limited lifespan of PMNs and inadequate methods for their detection, the contribution of neutrophils to atherosclerosis has been underestimated (24). Additionally, the phenotype of PMNs can alter in response to inflammation, which has also resulted in the historical neglect of the role of neutrophils in the process of atherosclerosis (**Figure 1A**) (25). Hyperlipidemia can injure ECs, promoting lipid deposition and plaque formation, and usually represents the onset of atherosclerosis. Interestingly, hyperlipidemia induces neutrophilia, which is positively associated with atherosclerotic plaque burden (24). In addition, hypercholesterolemia can induce the synthesis of granulocyte colony-stimulating factor (G-CSF), a key cytokine in the regulation of granulopoiesis, through inducing increased levels of tumor necrosis factor-α and interleukin-17 (IL-17) (26). G-CSF stimulates the proliferation of myeloid precursors and reduces bone marrow C-X-C motif ligand (CXCL)-12 levels, thereby reducing the clearance of aged PMNs (27). In addition, hypercholesterolemia can enhance serum levels of CXCL1, which promotes PMN mobilization (28). Together, these data suggest that PMNs may play a role in stimulation of atherosclerosis.

Recent studies have indicated that PMNs attach themselves to atherosclerotic plaques, primarily through NET formation (**Figure 1A**). Components of NETs, such as cathepsin G and cathelicidins, exhibit monocyte-attracting activity in atherosclerotic plaques (29, 30). The cathelicidin-related antimicrobial peptide (CRAMP) residing in neutrophil secondary granules have potent effects on recruitment and activation of immune cells, such as monocytes and dendritic cells (31). NET-derived

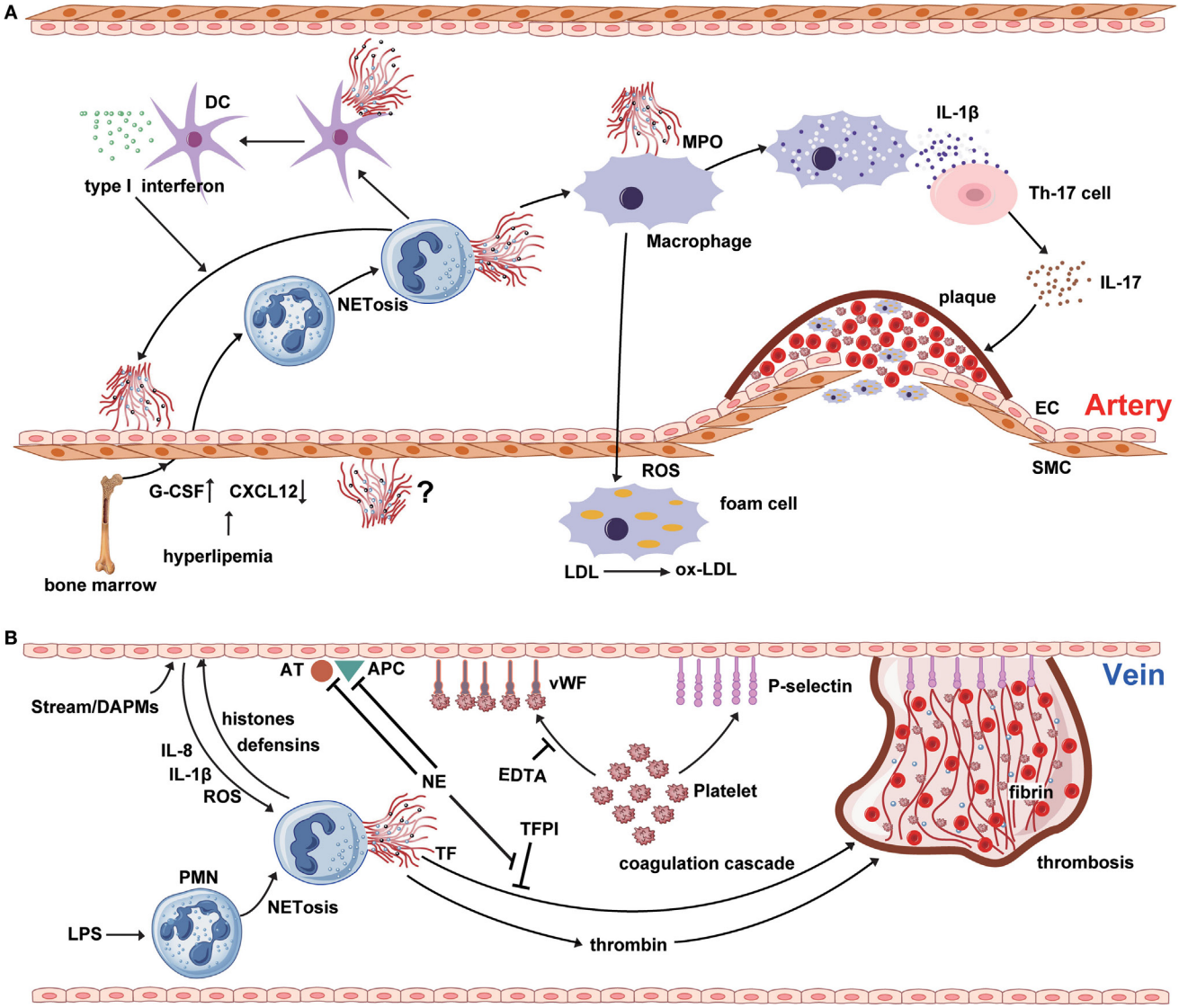

FIGURE 1 | NETosis interweaves atherosclerosis and thrombosis. **(A)** Neutrophil extracellular traps (NETs) are involved in the whole process of atherosclerosis. The myeloperoxidase from NTEs can stimulate macrophage to oxidize low-density lipoprotein (LDL) to ox-LDL and form the foam cell. The hyperlipidemia recruits neutrophil into circulation from bone marrow by upregulating the expression of granulocyte colony-stimulating factor and downregulating the level of C-X-C motif ligand -12, which is an important signal for the clearance and recruitment of aged neutrophils to the bone marrow. Cholesterol crystals can trigger the polymorphonuclear neutrophil (PMN) to release the NETs that prime the macrophages for pro-inflammatory cytokine production including IL-1β. Then IL-1β activates Th17 cell to release interleukin-17, amplifying the immune cell recruitment into the atherosclerotic plaque. As another critical source of foam cell, SMC also takes part in atherosclerosis. However, there are few reports about the interaction between NETs and SMC. **(B)** NETs are released from PMNs, which are activated by LPS or other cytokines from injured endothelial cells. NETs promote the expression of von Willebrand factor and P-selectin on the surface of venous endothelium to entrap both platelets and red blood cells, thereby creating a scaffold for fibrin deposition. Meanwhile, histones and TF from the NETs structure induce the thrombin generation and activation *via* platelet-dependent or -independent mechanism. Tissue factor pathway inhibitor (TFPI) can abrogate the function of TF. However, utrophil elastase from NETs could degrade TFPI, antithrombin, and activated protein C.

CRAMP-deleted ApoE-deficient mice develop smaller plaques than ApoE-deficient mice, suggesting that CRAMP may be involved in plaque formation (32). Moreover, NETs have been identified as a major source of CRAMP, which is deposited directly on the inflamed endothelial surface in atherosclerotic vessels. Indeed, NET-derived CRAMP anchors to ECs, where it can link with formyl-peptide receptor 2 on classical monocytes, resulting in monocyte recruitment to ECs (33). After binding to the mannose receptor of macrophages, MPO from NETs induces the release of ROS, along with other pro-inflammatory macrophage-derived cytokines (23). Furthermore, proteinases from NETs affect plaque instability, while ROS from macrophages contributes to the modification of low-density lipoprotein (LDL) to produce ox-LDL, which promotes the development of foam cells (34, 35). NETs can also regulate cytokine production from macrophages in atherosclerosis (36). More precisely, cholesterol

crystals function as danger signals, inducing interleukin-1β (IL-1β) production and triggering NET release from PMNs. Subsequently, NETs stimulate cytokine release from macrophages and activate T helper 17 cells, resulting in amplified immune cell recruitment to the atherosclerotic plaque (36).

Research has underscored the importance of NETs in the regulation of lesion size in atherosclerosis, and suggests that these structures can induce endothelial dysfunction directly by activation and damage of ECs (37). Inhibition of PAD4 using chloramidine led to decreased atherosclerotic lesion size and carotid artery thrombosis delay in a mouse model, while these effects were not observed after treatment with neutrophil-depleting antibody, or of mice lacking a functional type I interferon receptor (37). These data indicate a critical direct role for NETs in atherosclerotic lesion formation *via* type I interferon. Mixture of cell free-DNA and granule proteins can stimulate plasmacytoid dendritic cells, leading to a strong type I interferon response and a deteriorating atherosclerotic plaque burden; however, the importance of the NET-derived type I interferon response in atherogenesis has been questioned, because NETs can also regulate cytokine production by macrophages in atherosclerosis (36, 38, 39).

NETs AND ATHEROTHROMBOSIS

Atherothrombosis is the formation of a thrombus within an artery with atherosclerosis. Neutrophils as well as macrophages participate importantly in this disease process. In most cases, atherothrombosis follows rupture of atheroma, which may be triggered by NETs (8). Circulating leukocytes have a crucial role in atherothrombosis and systemic neutrophil counts are robust predictors of acute coronary events (40, 41). Moreover, complement activation can trigger PMN recruitment to the site of atherothrombosis in acute myocardial infarction (42). Coronary atherothrombosis specimens from patients with acute myocardial infarction contain numerous activated neutrophils (43–45). Sudden rupture of atherosclerotic plaques triggers platelet aggregation and fibrin deposition at the initial site of atherothrombosis to entrap circulating red blood cells. The interaction of thrombin-activated platelets with PMNs at the site of plaque rupture during acute ST-segment elevation acute myocardial infarction results in local formation of NETs (46). Elevated levels of circulating DNA and chromatin released from activated PMNs are independently associated with severe coronary atherosclerosis and the prothrombotic state (47). Interestingly, NETs are frequently found in lytic and fresh thrombus specimens, but never observed in organized thrombus (48). Hence, it can be assumed that NETs are involved at an early stage during the formation of coronary thrombus and lytic changes. A recent study involving evaluation of coronary atherothrombosis specimens demonstrated that NET burden and DNase activity in ST-elevation acute coronary syndrome are predictors of ST-segment resolution and infarct size (49).

Histological analysis of 26 thrombectomy samples from patients with acute myocardial infarction revealed that activated platelets present high-mobility group box 1 protein to PMNs, thereby inducing NET formation (50). The authors speculate that these NETs may contribute to plaque rupture and subsequent thrombus formation. In accordance with these findings, platelet-derived high-mobility group box 1 protein can facilitate NET formation and coagulation (51). Similarly, Riegger et al. analyzed 253 samples from patients with stent thrombosis after percutaneous coronary intervention (52). Approximately 23% of the thrombi specimens contained NETs; however, no differences in the number of NETs were observed according to the timing of stent thrombosis, stent type, or in comparison with samples from patients with spontaneous myocardial infarction (52). Hence, recruitment of PMNs appears to be a hallmark of stent thrombosis.

As the main initiator of coagulation, with a critical role in arterial thrombosis, tissue factor (TF) has been investigated in patients with acute ST-segment-elevation myocardial infarction (53). Local accumulation of TF-bearing NETs is observed at sites of coronary thrombosis, and PMNs release NETs, thereby exposing TF in infarct-associated, but not non-infarcted, areas (53). In addition, neutrophil islets and NETs decorated with TF were detected in thrombi obtained from infarcted regions (46). Interactions between activated platelets and PMNs at sites of plaque rupture during acute myocardial infarction result in NET formation and delivery of active TF, which together foster thrombus formation. Notably, NETs were also identified as coated with IL-17, which promotes thrombosis by enhancing platelet aggregation in coronary thrombectomy samples (48). The role of NETs has also been examined in a model of myocardial ischemia–reperfusion, and a significant cardioprotective effect of NET-inhibition treatment on myocardial ischemia–reperfusion injury was clearly demonstrated (54).

NETs AND VTE

Deep venous thrombosis (DVT) and pulmonary embolism are designated 'VTE' in the clinic. Venous thrombogenesis is usually accompanied by inflammatory reactions of ECs (55). As a key element of the inflammatory response, NETs also play an important role in venous thrombogenesis (**Figure 1B**). Unlike atherothrombosis, the onset of venous thrombosis is primarily initiated by endothelial injury, caused by disturbance of the blood stream or endothelial dysfunction, and mediated *via* damage-associated molecular patterns (56). Subsequently, Weibel–Palade bodies derived from ECs secrete massive amounts of von Willebrand factor (vWF) and P-selectin, which adhere to platelets and recruit leukocytes (57, 58). NETs predominantly form during the organizing stage of human VTE development (59). At the local lesion site, platelets interact directly with PMNs and promote the production of NETs (60). Additionally, cytokines from activated ECs (e.g., IL-1β, IL-8, and ROS) can accelerate NET formation (61). NETs, in turn, induce EC activation through NET-derived proteases; for example, histones and defensins (62). Additionally, purified histones can enhance thrombin generation through both platelet-dependent and platelet-independent mechanisms; however, platelet aggregation in response to histone H3 is inhibited by ethylenediaminetetraacetic acid (EDTA), suggesting that platelet aggregation is caused by the positive charge of histones (63–65). Intravenous administration of exogenous

histones accelerates clot formation, whereas DNase treatment significantly delays the onset of DVT (66). In addition to clinical investigations, studies in mice have identified an association between the risk of DVT and high PMN counts, supporting an important and early role for NETs in venous thrombosis (67, 68).

In the process of thrombosis propagation, circulating nucleosomes act as a platform for the degradation of tissue factor pathway inhibitor, which is mediated by NE (69). The levels of circulating nucleosomes in DVT patients are significantly elevated, and may be a useful plasma marker for NET formation (70). In addition to providing an adhesive platform for platelets, NETs also support the adhesion of red blood cells (65). NETs maintain the stability of thrombus *via* vWF, fibronectin, and fibrinogen; vWF and fibrinogen can interact with histones, and fibronectin has a DNA-binding domain (71). Heparin can remove histones, leading to the destabilization of NETs (72). *In vitro* data support the ability of NETs to stimulate the activation of coagulation cascades and platelet adhesion, and fibrin deposition colocalizes with NETs in blood clots (69). Purified histones impair thrombomodulin-dependent protein C activation to enhance plasma thrombin generation (73). Furthermore, DNA and histones interact with and trap platelets, most likely *via* electrostatic interactions or TLRs (73). Together, the findings described above indicate that NETs make a substantial contribution to maintenance of the stability of venous thrombi.

Monocytes are recruited during thrombosis and thrombolysis; however, the specific function of monocytes in dissolving NET-induced thrombus requires further investigation. NETs colocalize with fibrins and vWF in venous thrombi, and vWF and fibrins constitute the main scaffold that must be fragmented in order to destroy the integrity of the thrombus structure (**Figure 1B**) (65, 66). *In vitro*, NETs can provide a scaffold for clots to induce resistance to tPA-induced thrombolysis (65). DNase is a strong nuclease present in blood and has the power to degrade protein-free DNA; however, the ability of DNase to degrade NET-derived chromatin is limited, because their chromatin is decorated with numerous proteases and histones. Interestingly, DNase can cooperate with the plasminogen system during chromatin degradation (74). In addition, NETs may recruit plasminogen from the plasma. Histone H2B can serve as a receptor for plasminogen on the surface of human monocytes/macrophages and could potentially also serve this function in NETs (75). *In vitro* studies have shown that NET-derived NE and cathepsin G can degrade fibrin and enhance fibrinolysis in DVT (76). Plasma DNA concentrations correlate with D-dimer levels; therefore, it is plausible that circulating DNA may reflect the degradation of NETs within a thrombus (70, 77).

In immunothrombosis, NETs may function in capture of invasive pathogens, prevention of distant tissue involvement, concentration of pathogens for bactericidal killing, and recruitment of other immune cells to immune target sites (78). In models of sepsis, lipopolysaccharide can activate platelets and PMNs *via* TLR-4 to induce NETosis (50, 79). We have reported that PMNs from septic patients have significantly enhanced NET release, compared with those from healthy controls with increased risk of VTE (80). NET-associated immunothrombosis leads to more sturdy thrombi with reduced permeability and decreased susceptibility to thrombolysis, although this can be overcome with DNase treatment (81). In addition to sepsis, NETs and immunothrombosis have been implicated in other autoimmune diseases, including inflammatory bowel disease and vasculitis (82, 83).

FUTURE CHALLENGES AND CLINICAL IMPLICATIONS

Undoubtedly, more in-depth studies are needed to meticulously dissect the exact mechanisms of *in vivo* NET formation, and to clarify the importance of histone citrullination for NETosis (84). ROS generation by different types of leukocyte is a common trigger of NETosis; however, the exact mechanism of ROS-induced NETs formation and subsequent endothelial dysfunction is unclear (**Figure 1**). Moreover, how NET-derived proteases respond in atherosclerosis and thrombosis remains an open question. Movement from investigations of integrated NETs to study of more specific *in vitro* protease systems, which may better explain the phenomena associated with disease, is an interesting future prospect. NETs have been identified at each stage of cardiovascular disease. Nevertheless, whether NETs play different roles at different stages remains unknown. Additionally, it will be a challenge to explore whether NETs are involved in cross talk with smooth muscle cells, which are another major source of foam cells during atherosclerosis. Regarding DVT, it will be important to identify endogenous triggers of NET formation. Furthermore, whether the NETs involved in DVT are generated by cell lysis or a secretory process is another a critical question. A better understanding of NETosis, both with regards to structural constituents and context-specific functional decoration, will be a prerequisite to further elucidation of the role of NETs in atherosclerotic plaques and venous thrombus, and will be of paramount importance to the identification, validation, and implementation of the best molecular candidates for therapeutic targeting.

The notion that NETs represent a mechanism by which PMNs release thrombogenic signals during atherosclerosis and thrombosis may offer novel therapeutic targets (**Table 1**). Thrombolysis has become a key weapon in the arsenal against pathologic thrombosis; however, not all thrombotic events are susceptible to thrombolysis. Indeed, the addition of DNA and histones to a fibrin matrix has been shown to generate artificial thrombus more resistant to tissue plasminogen activator, and which can be partially remedied by DNase (85). Preliminary data from murine models of DVT demonstrate inhibition of thrombus formation by DNase treatment prior to model establishment (66, 67). Although DNase treatment, which likely enhances thrombolysis, appears to harbor relevant therapeutic potential, its utility and applicability to prevention of NET formation or digestion of established NETs to reduce atherosclerotic lesion growth is debatable and will remain controversial (86). Moreover, knockout of neutrophil oxidase 2, a NET component, can result in accelerating disease in a murine model of lupus; therefore, caution is required in the selection of NET-associated molecular targets. Another potential target is NET-related platelet recruitment to the endothelium (37). Specifically, blockade of

TABLE 1 | Potential targets for translation in the prevention of NET-mediated atherosclerosis and thrombosis.

Diseases	Target	Function	Clinical implications	
			Clinical therapies	Potential treatment
Atherosclerosis	cfDNA	Stimulation of plasmacytoid dendritic cells		Deoxyribonuclease (86)
	MPO	Induction of ROS		Ocimum tenuiflorum (89)
	Cathepsin G	Attraction of monocyte		Ac-Phe-Val-Thr-(4-guanidine)-Phg(P)-(OPh4-SMe)2 (90)
	Cathelicidins	Attraction of monocyte		
	IL17	Amplification of platelet aggregation		
	IL-1β	Amplification of inflammatory reaction; stimulation to Th17 cells	Rimonabant (91)	
Venous thromboembolism	Histones	Endothelial injury		Activated protein C (62)
	NE	Degradation of TFPI and fibrin		Leu89 with alanine (69)
	Cathepsin G	Degradation of fibrin and enhancement of fibrinolysis		Leu89 with alanine (69)
	P-selectin	Adherence to platelet		Anti-P-selectin aptamer; anti-P-selectin glycoprotein ligand-1 inhibitory antibody (58)
	vWF	Adherence to platelet		Anti-P-selectin glycoprotein ligand-1 inhibitory antibody (92)
	TF	Activation of coagulation cascade		TFPI (93)
	AT	Anticoagulation		
	APC	anticoagulation		
	Thrombin	Promotion of coagulation		PAR-1 antagonists (94)
	Fibrin	Promotion of coagulation	Urokinase; rtPA	

Antimicrobial proteins (1).

NETs, neutrophil extracelluar traps; cfDNA, cell-free DNA; MPO, myeloperoxidase; ROS, reactive oxygen species; IL-17, interleukin 17; IL-1β, interleukin 1β; NE, neutrophil elastase; TFPI, tissue factor pathway inhibitor; vWF, von-Willebrand factor; TF, tissue factor; AT, antithrombin; PAR, proteinase-activated receptor; APC, activated protein C; rtPA, recombinant tissue plasminogen activator.

platelet alpha-granule or endothelial Weibel–Palade body release would decrease P-selectin- and vWF-mediated platelet and PMN recruitment to the endothelium, thereby decreasing NETosis (87). Similarly, vWF degradation enzyme could be administered to prevent PMN recruitment with subsequent NETosis (88). Although these countermeasures may result in mild immunodeficiency, they could also abrogate pathologic immune-mediated thrombosis without sacrificing immune competence when administered in a controlled manner. It is noteworthy that NETs are not major role players in these diseases but may definitely exacerbate the condition and therapies may have to be combinatorial because NET formation is only one of the factors.

CONCLUSION

Neutrophil extracellular trap-structure is an important novel discovery that has potential to influence our understanding of cardiovascular disease. Functionally, NETs can induce activation of ECs, antigen-presenting cells, and platelets, and cause endothelial dysfunction, resulting in a proinflammatory immune response. As evidenced by the results of the studies discussed above, NETs can clearly contribute to the initiation and progression of atherosclerotic and thrombotic lesions. Moreover, there is evidence for an emerging role of PMNs, focused on NETosis and oxidative stress burden, in orchestrating common mechanisms involved in various forms of cardiovascular disease. Extensive future research will be required to determine the effects of NETs in endothelial dysfunction-induced cardiovascular disease; hence, the time is not yet ideal to implement therapeutic options targeting neutrophils in the context of atherosclerosis and thrombosis.

AUTHOR CONTRIBUTIONS

HQ contributed to the conception of the study, consulting literatures, and manuscript preparation; SY make the figure and modify the manuscript; LZ helped perform the analysis with constructive discussions.

ACKNOWLEDGMENTS

All authors critically revised the review for intellectual content and approved the final version.

FUNDING

This work was supported by the National Natural Science Foundation of China grants (#81670442 to LZ).

REFERENCES

1. Fuchs TA, Abed U, Goosmann C, Hurwitz R, Schulze I, Wahn V, et al. Novel cell death program leads to neutrophil extracellular traps. *J Cell Biol* (2007) 176:231–41. doi:10.1083/jcb.200606027
2. Brinkmann V, Reichard U, Goosmann C, Fauler B, Uhlemann Y, Weiss DS, et al. Neutrophil extracellular traps kill bacteria. *Science* (2004) 303:1532–5. doi:10.1126/science.1092385
3. Sorensen OE, Borregaard N. Neutrophil extracellular traps – the dark side of neutrophils. *J Clin Invest* (2016) 126:1612–20. doi:10.1172/JCI84538

4. Lowe GD. Common risk factors for both arterial and venous thrombosis. *Br J Haematol* (2008) 140:488–95. doi:10.1111/j.1365-2141.2007.06973.x
5. Jorch SK, Kubes P. An emerging role for neutrophil extracellular traps in noninfectious disease. *Nat Med* (2017) 23:279–87. doi:10.1038/nm.4294
6. Xu J, Zhang X, Pelayo R, Monestier M, Ammollo CT, Semeraro F, et al. Extracellular histones are major mediators of death in sepsis. *Nat Med* (2009) 15:1318–21. doi:10.1038/nm.2053
7. Yipp BG, Kubes P. NETosis: how vital is it? *Blood* (2013) 122:2784–94. doi:10.1182/blood-2013-04-457671
8. Doring Y, Soehnlein O, Weber C. Neutrophil extracellular traps in atherosclerosis and atherothrombosis. *Circ Res* (2017) 120:736–43. doi:10.1161/CIRCRESAHA.116.309692
9. de Buhr N, von Kockritz-Blickwede M. How neutrophil extracellular traps become visible. *J Immunol Res* (2016) 2016:4604713. doi:10.1155/2016/4604713
10. Zhao W, Fogg DK, Kaplan MJ. A novel image-based quantitative method for the characterization of NETosis. *J Immunol Methods* (2015) 423:104–10. doi:10.1016/j.jim.2015.04.027
11. Delgado-Rizo V, Martinez-Guzman MA, Iniguez-Gutierrez L, Garcia-Orozco A, Alvarado-Navarro A, Fafutis-Morris M. Neutrophil extracellular traps and its implications in inflammation: an overview. *Front Immunol* (2017) 8:81. doi:10.3389/fimmu.2017.00081
12. Pilsczek FH, Salina D, Poon KK, Fahey C, Yipp BG, Sibley CD, et al. A novel mechanism of rapid nuclear neutrophil extracellular trap formation in response to *Staphylococcus aureus*. *J Immunol* (2010) 185:7413–25. doi:10.4049/jimmunol.1000675
13. Karlsson A, Dahlgren C. Assembly and activation of the neutrophil NADPH oxidase in granule membranes. *Antioxid Redox Signal* (2002) 4:49–60. doi:10.1089/152308602753625852
14. Papayannopoulos V, Metzler KD, Hakkim A, Zychlinsky A. Neutrophil elastase and myeloperoxidase regulate the formation of neutrophil extracellular traps. *J Cell Biol* (2010) 191:677–91. doi:10.1083/jcb.201006052
15. Yousefi S, Mihalache C, Kozlowski E, Schmid I, Simon HU. Viable neutrophils release mitochondrial DNA to form neutrophil extracellular traps. *Cell Death Differ* (2009) 16:1438–44. doi:10.1038/cdd.2009.96
16. Papayannopoulos V, Zychlinsky A. NETs: a new strategy for using old weapons. *Trends Immunol* (2009) 30:513–21. doi:10.1016/j.it.2009.07.011
17. Urban CF, Ermert D, Schmid M, Abu-Abed U, Goosmann C, Nacken W, et al. Neutrophil extracellular traps contain calprotectin, a cytosolic protein complex involved in host defense against *Candida albicans*. *PLoS Pathog* (2009) 5:e1000639. doi:10.1371/journal.ppat.1000639
18. Wang Y, Li M, Stadler S, Correll S, Li P, Wang D, et al. Histone hypercitrullination mediates chromatin decondensation and neutrophil extracellular trap formation. *J Cell Biol* (2009) 184:205–13. doi:10.1083/jcb.200806072
19. Wang S, Wang Y. Peptidylarginine deiminases in citrullination, gene regulation, health and pathogenesis. *Biochim Biophys Acta* (2013) 1829:1126–35. doi:10.1016/j.bbagrm.2013.07.003
20. Li P, Li M, Lindberg MR, Kennett MJ, Xiong N, Wang Y. PAD4 is essential for antibacterial innate immunity mediated by neutrophil extracellular traps. *J Exp Med* (2010) 207:1853–62. doi:10.1084/jem.20100239
21. Zabieglo K, Majewski P, Majchrzak-Gorecka M, Wlodarczyk A, Grygier B, Zegar A, et al. The inhibitory effect of secretory leukocyte protease inhibitor (SLPI) on formation of neutrophil extracellular traps. *J Leukoc Biol* (2015) 98:99–106. doi:10.1189/jlb.4AB1114-543R
22. Rossaint J, Herter JM, Van Aken H, Napirei M, Doring Y, Weber C, et al. Synchronized integrin engagement and chemokine activation is crucial in neutrophil extracellular trap-mediated sterile inflammation. *Blood* (2014) 123:2573–84. doi:10.1182/blood-2013-07-516484
23. Hansson GK, Hermansson A. The immune system in atherosclerosis. *Nat Immunol* (2011) 12:204–12. doi:10.1038/ni.2001
24. Drechsler M, Megens RT, van Zandvoort M, Weber C, Soehnlein O. Hyperlipidemia-triggered neutrophilia promotes early atherosclerosis. *Circulation*(2010)122:1837–45.doi:10.1161/CIRCULATIONAHA.110.961714
25. Galligan C, Yoshimura T. Phenotypic and functional changes of cytokine-activated neutrophils. *Chem Immunol Allergy* (2003) 83:24–44. doi:10.1159/000071555
26. Stark MA, Huo Y, Burcin TL, Morris MA, Olson TS, Ley K. Phagocytosis of apoptotic neutrophils regulates granulopoiesis via IL-23 and IL-17. *Immunity* (2005) 22:285–94. doi:10.1016/j.immuni.2005.01.011
27. Christopher MJ, Link DC. Regulation of neutrophil homeostasis. *Curr Opin Hematol* (2007) 14:3–8. doi:10.1097/00062752-200701000-00003
28. Eash KJ, Greenbaum AM, Gopalan PK, Link DC. CXCR2 and CXCR4 antagonistically regulate neutrophil trafficking from murine bone marrow. *J Clin Invest* (2010) 120:2423–31. doi:10.1172/jci41649
29. Kougias P, Chai H, Lin PH, Yao Q, Lumsden AB, Chen C. Defensins and cathelicidins: neutrophil peptides with roles in inflammation, hyperlipidemia and atherosclerosis. *J Cell Mol Med* (2005) 9:3–10. doi:10.1111/j.1582-4934.2005.tb00332.x
30. Wang J, Sjoberg S, Tang TT, Oorni K, Wu W, Liu C, et al. Cathepsin G activity lowers plasma LDL and reduces atherosclerosis. *Biochim Biophys Acta* (2014) 1842:2174–83. doi:10.1016/j.bbadis.2014.07.026
31. Soehnlein O, Zernecke A, Eriksson EE, Rothfuchs AG, Pham CT, Herwald H, et al. Neutrophil secretion products pave the way for inflammatory monocytes. *Blood* (2008) 112:1461–71. doi:10.1182/blood-2008-02-139634
32. Doring Y, Drechsler M, Wantha S, Kemmerich K, Lievens D, Vijayan S, et al. Lack of neutrophil-derived CRAMP reduces atherosclerosis in mice. *Circ Res* (2012) 110:1052–6. doi:10.1161/circresaha.112.265868
33. Wantha S, Alard JE, Megens RT, van der Does AM, Doring Y, Drechsler M, et al. Neutrophil-derived cathelicidin promotes adhesion of classical monocytes. *Circ Res* (2013) 112:792–801. doi:10.1161/circresaha.112.300666
34. Carbone F, Mach F, Montecucco F. Update on the role of neutrophils in atherosclerotic plaque vulnerability. *Curr Drug Targets* (2015) 16:321–33. doi:10.2174/1389450115666141110093013
35. Chistiakov DA, Bobryshev YV, Orekhov AN. Neutrophil's weapons in atherosclerosis. *Exp Mol Pathol* (2015) 99:663–71. doi:10.1016/j.yexmp.2015.11.011
36. Warnatsch A, Ioannou M, Wang Q, Papayannopoulos V. Inflammation. Neutrophil extracellular traps license macrophages for cytokine production in atherosclerosis. *Science* (2015) 349:316–20. doi:10.1126/science.aaa8064
37. Knight JS, Luo W, O'Dell AA, Yalavarthi S, Zhao W, Subramanian V, et al. Peptidylarginine deiminase inhibition reduces vascular damage and modulates innate immune responses in murine models of atherosclerosis. *Circ Res* (2014) 114:947–56. doi:10.1161/CIRCRESAHA.114.303312
38. Doring Y, Manthey HD, Drechsler M, Lievens D, Megens RT, Soehnlein O, et al. Auto-antigenic protein-DNA complexes stimulate plasmacytoid dendritic cells to promote atherosclerosis. *Circulation* (2012) 125:1673–83. doi:10.1161/CIRCULATIONAHA.111.046755
39. Macritchie N, Grassia G, Sabir SR, Maddaluno M, Welsh P, Sattar N, et al. Plasmacytoid dendritic cells play a key role in promoting atherosclerosis in apolipoprotein E-deficient mice. *Arterioscler Thromb Vasc Biol* (2012) 32:2569–79. doi:10.1161/ATVBAHA.112.251314
40. Libby P, Ridker PM, Hansson GK. Progress and challenges in translating the biology of atherosclerosis. *Nature* (2011) 473:317–25. doi:10.1038/nature10146
41. Horne BD, Anderson JL, John JM, Weaver A, Bair TL, Jensen KR, et al. Which white blood cell subtypes predict increased cardiovascular risk? *J Am Coll Cardiol* (2005) 45:1638–43. doi:10.1016/j.jacc.2005.02.054
42. Distelmaier K, Adlbrecht C, Jakowitsch J, Winkler S, Dunkler D, Gerner C, et al. Local complement activation triggers neutrophil recruitment to the site of thrombus formation in acute myocardial infarction. *Thromb Haemost* (2009) 102:564–72. doi:10.1160/th09-02-0103
43. Ramaiola I, Padro T, Pena E, Juan-Babot O, Cubedo J, Martin-Yuste V, et al. Changes in thrombus composition and profilin-1 release in acute myocardial infarction. *Eur Heart J* (2015) 36:965–75. doi:10.1093/eurheartj/ehu356
44. Yunoki K, Naruko T, Sugioka K, Inaba M, Iwasa Y, Komatsu R, et al. Erythrocyte-rich thrombus aspirated from patients with ST-elevation myocardial infarction: association with oxidative stress and its impact on myocardial reperfusion. *Eur Heart J* (2012) 33:1480–90. doi:10.1093/eurheartj/ehr486
45. Silvain J, Collet JP, Nagaswami C, Beygui F, Edmondson KE, Bellemain-Appaix A, et al. Composition of coronary thrombus in acute myocardial infarction. *J Am Coll Cardiol* (2011) 57:1359–67. doi:10.1016/j.jacc.2010.09.077
46. Stakos DA, Kambas K, Konstantinidis T, Mitroulis I, Apostolidou E, Arelaki S, et al. Expression of functional tissue factor by neutrophil extracellular traps in culprit artery of acute myocardial infarction. *Eur Heart J* (2015) 36:1405–14. doi:10.1093/eurheartj/ehv007

47. Borissoff JI, Joosen IA, Versteylen MO, Brill A, Fuchs TA, Savchenko AS, et al. Elevated levels of circulating DNA and chromatin are independently associated with severe coronary atherosclerosis and a prothrombotic state. *Arterioscler Thromb Vasc Biol* (2013) 33:2032–40. doi:10.1161/ATVBAHA.113.301627
48. de Boer OJ, Li X, Teeling P, Mackaay C, Ploegmakers HJ, van der Loos CM, et al. Neutrophils, neutrophil extracellular traps and interleukin-17 associate with the organisation of thrombi in acute myocardial infarction. *Thromb Haemost* (2013) 109:290–7. doi:10.1160/TH12-06-0425
49. Mangold A, Alias S, Scherz T, Hofbauer T, Jakowitsch J, Panzenbock A, et al. Coronary neutrophil extracellular trap burden and deoxyribonuclease activity in ST-elevation acute coronary syndrome are predictors of ST-segment resolution and infarct size. *Circ Res* (2015) 116:1182–92. doi:10.1161/CIRCRESAHA.116.304944
50. Maugeri N, Campana L, Gavina M, Covino C, De Metrio M, Panciroli C, et al. Activated platelets present high mobility group box 1 to neutrophils, inducing autophagy and promoting the extrusion of neutrophil extracellular traps. *J Thromb Haemost* (2014) 12:2074–88. doi:10.1111/jth.12710
51. Stark K, Philippi V, Stockhausen S, Busse J, Antonelli A, Miller M, et al. Disulfide HMGB1 derived from platelets coordinates venous thrombosis in mice. *Blood* (2016) 128:2435–49. doi:10.1182/blood-2016-04-710632
52. Riegger J, Byrne RA, Joner M, Chandraratne S, Gershlick AH, Ten Berg JM, et al. Histopathological evaluation of thrombus in patients presenting with stent thrombosis. A multicenter European study: a report of the prevention of late stent thrombosis by an interdisciplinary global European effort consortium. *Eur Heart J* (2016) 37:1538–49. doi:10.1093/eurheartj/ehv419
53. Darbousset R, Thomas GM, Mezouar S, Frere C, Bonier R, Mackman N, et al. Tissue factor-positive neutrophils bind to injured endothelial wall and initiate thrombus formation. *Blood* (2012) 120:2133–43. doi:10.1182/blood-2012-06-437772
54. Savchenko AS, Borissoff JI, Martinod K, De Meyer SF, Gallant M, Erpenbeck L, et al. VWF-mediated leukocyte recruitment with chromatin decondensation by PAD4 increases myocardial ischemia/reperfusion injury in mice. *Blood* (2014) 123:141–8. doi:10.1182/blood-2013-07-514992
55. Di Nisio M, van Es N, Buller HR. Deep vein thrombosis and pulmonary embolism. *Lancet* (2016) 388:3060–73. doi:10.1016/S0140-6736(16)30514-1
56. Xu S, Li X, LaPenna KB, Yokota SD, Huke S, He P. New insights into shear stress-induced endothelial signaling and barrier function: cell-free fluid verses blood flow. *Cardiovasc Res* (2017) 113(5):508–18. doi:10.1093/cvr/cvx021
57. Michels A, Albanez S, Mewburn J, Nesbitt K, Gould TJ, Liaw PC, et al. Histones link inflammation and thrombosis through the induction of Weibel-Palade body exocytosis. *J Thromb Haemost* (2016) 14:2274–86. doi:10.1111/jth.13493
58. Etulain J, Martinod K, Wong SL, Cifuni SM, Schattner M, Wagner DD. P-selectin promotes neutrophil extracellular trap formation in mice. *Blood* (2015) 126:242–6. doi:10.1182/blood-2015-01-624023
59. Savchenko AS, Martinod K, Seidman MA, Wong SL, Borissoff JI, Piazza G, et al. Neutrophil extracellular traps form predominantly during the organizing stage of human venous thromboembolism development. *J Thromb Haemost* (2014) 12:860–70. doi:10.1111/jth.12571
60. Clark SR, Ma AC, Tavener SA, McDonald B, Goodarzi Z, Kelly MM, et al. Platelet TLR4 activates neutrophil extracellular traps to ensnare bacteria in septic blood. *Nat Med* (2007) 13:463–9. doi:10.1038/nm1565
61. Gupta AK, Joshi MB, Philippova M, Erne P, Hasler P, Hahn S, et al. Activated endothelial cells induce neutrophil extracellular traps and are susceptible to NETosis-mediated cell death. *FEBS Lett* (2010) 584:3193–7. doi:10.1016/j.febslet.2010.06.006
62. Saffarzadeh M, Juenemann C, Queisser MA, Lochnit G, Barreto G, Galuska SP, et al. Neutrophil extracellular traps directly induce epithelial and endothelial cell death: a predominant role of histones. *PLoS One* (2012) 7:e32366. doi:10.1371/journal.pone.0032366
63. Semeraro F, Ammollo CT, Morrissey JH, Dale GL, Friese P, Esmon NL, et al. Extracellular histones promote thrombin generation through platelet-dependent mechanisms: involvement of platelet TLR2 and TLR4. *Blood* (2011) 118:1952–61. doi:10.1182/blood-2011-03-343061
64. Gould TJ, Vu TT, Swystun LL, Dwivedi DJ, Mai SH, Weitz JI, et al. Neutrophil extracellular traps promote thrombin generation through platelet-dependent and platelet-independent mechanisms. *Arterioscler Thromb Vasc Biol* (2014) 34:1977–84. doi:10.1161/atvbaha.114.304114
65. Fuchs TA, Brill A, Duerschmied D, Schatzberg D, Monestier M, Myers DD Jr, et al. Extracellular DNA traps promote thrombosis. *Proc Natl Acad Sci U S A* (2010) 107:15880–5. doi:10.1073/pnas.1005743107
66. Brill A, Fuchs TA, Savchenko AS, Thomas GM, Martinod K, De Meyer SF, et al. Neutrophil extracellular traps promote deep vein thrombosis in mice. *J Thromb Haemost* (2012) 10:136–44. doi:10.1111/j.1538-7836.2011.04544.x
67. von Bruhl ML, Stark K, Steinhart A, Chandraratne S, Konrad I, Lorenz M, et al. Monocytes, neutrophils, and platelets cooperate to initiate and propagate venous thrombosis in mice in vivo. *J Exp Med* (2012) 209:819–35. doi:10.1084/jem.20112322
68. Ramacciotti E, Hawley AE, Farris DM, Ballard NE, Wrobleski SK, Myers DD Jr, et al. Leukocyte- and platelet-derived microparticles correlate with thrombus weight and tissue factor activity in an experimental mouse model of venous thrombosis. *Thromb Haemost* (2009) 101:748–54. doi:10.1160/TH08-09-0620
69. Massberg S, Grahl L, von Bruehl ML, Manukyan D, Pfeiler S, Goosmann C, et al. Reciprocal coupling of coagulation and innate immunity via neutrophil serine proteases. *Nat Med* (2010) 16:887–96. doi:10.1038/nm.2184
70. van Montfoort ML, Stephan F, Lauw MN, Hutten BA, Van Mierlo GJ, Solati S, et al. Circulating nucleosomes and neutrophil activation as risk factors for deep vein thrombosis. *Arterioscler Thromb Vasc Biol* (2013) 33:147–51. doi:10.1161/atvbaha.112.300498
71. Ward CM, Tetaz TJ, Andrews RK, Berndt MC. Binding of the von Willebrand factor A1 domain to histone. *Thromb Res* (1997) 86:469–77. doi:10.1016/S0049-3848(97)00096-0
72. Longstaff C, Hogwood J, Gray E, Komorowicz E, Varju I, Varga Z, et al. Neutralisation of the anti-coagulant effects of heparin by histones in blood plasma and purified systems. *Thromb Haemost* (2016) 115:591–9. doi:10.1160/th15-03-0214
73. Ammollo CT, Semeraro F, Xu J, Esmon NL, Esmon CT. Extracellular histones increase plasma thrombin generation by impairing thrombomodulin-dependent protein C activation. *J Thromb Haemost* (2011) 9:1795–803. doi:10.1111/j.1538-7836.2011.04422.x
74. Oklu R, Albadawi H, Watkins MT, Monestier M, Sillesen M, Wicky S. Detection of extracellular genomic DNA scaffold in human thrombus: implications for the use of deoxyribonuclease enzymes in thrombolysis. *J Vasc Interv Radiol* (2012) 23:712–8. doi:10.1016/j.jvir.2012.01.072
75. Das R, Burke T, Plow EF. Histone H2B as a functionally important plasminogen receptor on macrophages. *Blood* (2007) 110:3763–72. doi:10.1182/blood-2007-03-079392
76. Fuchs TA, Brill A, Wagner DD. Neutrophil extracellular trap (NET) impact on deep vein thrombosis. *Arterioscler Thromb Vasc Biol* (2012) 32:1777–83. doi:10.1161/ATVBAHA.111.242859
77. Diaz JA, Fuchs TA, Jackson TO, Kremer Hovinga JA, Lammle B, Henke PK, et al. Plasma DNA is elevated in patients with deep vein thrombosis. *J Vasc Surg Venous Lymphat Disord* (2013) 1:341–8. doi:10.1016/j.jvsv.2012.12.002
78. Engelmann B, Massberg S. Thrombosis as an intravascular effector of innate immunity. *Nat Rev Immunol* (2013) 13:34–45. doi:10.1038/nri3345
79. Ma AC, Kubes P. Platelets, neutrophils, and neutrophil extracellular traps (NETs) in sepsis. *J Thromb Haemost* (2008) 6:415–20. doi:10.1111/j.1538-7836.2007.02865.x
80. Yang S, Qi H, Kan K, Chen J, Xie H, Guo X, et al. Neutrophil extracellular traps promote hypercoagulability in patients with sepsis. *Shock* (2017) 47:132–9. doi:10.1097/shk.0000000000000741
81. Varju I, Longstaff C, Szabo L, Farkas AZ, Varga-Szabo VJ, Tanka-Salamon A, et al. DNA, histones and neutrophil extracellular traps exert anti-fibrinolytic effects in a plasma environment. *Thromb Haemost* (2015) 113:1289–98. doi:10.1160/TH14-08-0669
82. He Z, Si Y, Jiang T, Ma R, Zhang Y, Cao M, et al. Phosphotidylserine exposure and neutrophil extracellular traps enhance procoagulant activity in patients with inflammatory bowel disease. *Thromb Haemost* (2016) 115:738–51. doi:10.1160/TH15-09-0710
83. Huang YM, Wang H, Wang C, Chen M, Zhao MH. Promotion of hypercoagulability in antineutrophil cytoplasmic antibody-associated vasculitis by C5a-induced tissue factor-expressing microparticles and neutrophil

extracellular traps. *Arthritis Rheumatol* (2015) 67:2780–90. doi:10.1002/art.39239
84. Konig MF, Andrade F. A critical reappraisal of neutrophil extracellular traps and NETosis mimics based on differential requirements for protein citrullination. *Front Immunol* (2016) 7:461. doi:10.3389/fimmu.2016.00461
85. Longstaff C, Varju I, Sotonyi P, Szabo L, Krumrey M, Hoell A, et al. Mechanical stability and fibrinolytic resistance of clots containing fibrin, DNA, and histones. *J Biol Chem* (2013) 288:6946–56. doi:10.1074/jbc.M112.404301
86. Vogel B, Shinagawa H, Hofmann U, Ertl G, Frantz S. Acute DNase1 treatment improves left ventricular remodeling after myocardial infarction by disruption of free chromatin. *Basic Res Cardiol* (2015) 110:15. doi:10.1007/s00395-015-0472-y
87. Carestia A, Kaufman T, Rivadeneyra L, Landoni VI, Pozner RG, Negrotto S, et al. Mediators and molecular pathways involved in the regulation of neutrophil extracellular trap formation mediated by activated platelets. *J Leukoc Biol* (2016) 99:153–62. doi:10.1189/jlb.3A0415-161R
88. Schettert IT, Pereira AC, Lopes NH, Hueb WA, Krieger JE. Association between ADAMTS13 polymorphisms and risk of cardiovascular events in chronic coronary disease. *Thromb Res* (2010) 125:61–6. doi:10.1016/j.thromres.2009.03.008
89. Narasimhulu CA, Vardhan S. Therapeutic potential of *Ocimum tenuiflorum* as MPO inhibitor with implications for atherosclerosis prevention. *J Med Food* (2015) 18:507–15. doi:10.1089/jmf.2014.0125
90. Wang J, Sukhova GK, Liu J, Ozaki K, Lesner A, Libby P, et al. Cathepsin G deficiency reduces periaortic calcium chloride injury-induced abdominal aortic aneurysms in mice. *J Vasc Surg* (2015) 62:1615–24. doi:10.1016/j.jvs.2014.06.004
91. Dol-Gleizes F, Paumelle R, Visentin V, Mares AM, Desitter P, Hennuyer N, et al. Rimonabant, a selective cannabinoid CB1 receptor antagonist, inhibits atherosclerosis in LDL receptor-deficient mice. *Arterioscler Thromb Vasc Biol* (2009) 29:12–8. doi:10.1161/ATVBAHA.108.168757
92. Pendu R, Terraube V, Christophe OD, Gahmberg CG, de Groot PG, Lenting PJ, et al. P-selectin glycoprotein ligand 1 and beta2-integrins cooperate in the adhesion of leukocytes to von Willebrand factor. *Blood* (2006) 108:3746–52. doi:10.1182/blood-2006-03-010322
93. Osterud B. Tissue factor/TFPI and blood cells. *Thromb Res* (2012) 129:274–8. doi:10.1016/j.thromres.2011.11.049
94. Chackalamannil S, Xia Y. Thrombin receptor (PAR-1) antagonists as novel antithrombotic agents. *Expert Opin Ther Pat* (2006) 16:493–505. doi:10.1517/13543776.16.4.493

Conflict of Interest Statement: The authors declare that the research was conducted in the absence of any commercial or financial relationships that could be construed as a potential conflict of interest.

Copyright © 2017 Qi, Yang and Zhang. This is an open-access article distributed under the terms of the Creative Commons Attribution License (CC BY). The use, distribution or reproduction in other forums is permitted, provided the original author(s) or licensor are credited and that the original publication in this journal is cited, in accordance with accepted academic practice. No use, distribution or reproduction is permitted which does not comply with these terms.

frontiers in Immunology

MINI REVIEW
published: 09 August 2017
doi: 10.3389/fimmu.2017.00941

Dendritic Cell Subsets in Asthma: Impaired Tolerance or Exaggerated Inflammation?

*Heleen Vroman, Rudi W. Hendriks and Mirjam Kool**

Department of Pulmonary Medicine, Erasmus MC, Rotterdam, Netherlands

Asthma is a prevalent chronic heterogeneous inflammatory disease of the airways, leading to reversible airway obstruction, in which various inflammatory responses can be observed. Mild to moderate asthma patients often present with a Th2-mediated eosinophilic inflammation whereas in severe asthma patients, a Th17-associated neutrophilic or combined Th2 and Th17-mediated eosinophilic/neutrophilic inflammation is observed. The differentiation of these effector Th2 and Th17-cells is induced by allergen-exposed dendritic cells (DCs) that migrate toward the lung draining lymph node. The DC lineage comprises conventional DCs (cDCs) and plasmacytoid DCs (pDCs), of which the cDC lineage consists of type 1 cDCs (cDC1s) and cDC2s. During inflammation, also monocytes can differentiate into so-called monocyte-derived DCs (moDCs). These DC subsets differ both in ontogeny, localization, and in their functional properties. New identification tools and the availability of transgenic mice targeting specific DC subsets enable the investigation of how these different DC subsets contribute to or suppress asthma pathogenesis. In this review, we will discuss mechanisms used by different DC subsets to elicit or hamper the pathogenesis of both Th2-mediated eosinophilic asthma and more severe Th17-mediated neutrophilic inflammation.

Keywords: asthma, dendritic cells, Th2 cells, Th17 cells, airway inflammation

OPEN ACCESS

Edited by:
Jixin Zhong,
Case Western Reserve University,
United States

Reviewed by:
Shanzhong Gong,
University of Texas at Austin,
United States
Fei Teng,
Weill Cornell Medical College,
United States
Xiaojing Yue,
La Jolla Institute for Allergy and Immunology, United States

****Correspondence:***
Mirjam Kool
m.kool@erasmusmc.nl

Specialty section:
This article was submitted to Inflammation, a section of the journal Frontiers in Immunology

Received: *24 May 2017*
Accepted: *24 July 2017*
Published: *09 August 2017*

Citation:
Vroman H, Hendriks RW and Kool M (2017) Dendritic Cell Subsets in Asthma: Impaired Tolerance or Exaggerated Inflammation? Front. Immunol. 8:941. doi: 10.3389/fimmu.2017.00941

Allergen-activated dendritic cells (DCs) are essential not only for the induction of T helper (Th)-cell differentiation from naïve T-cells in the mediastinal lymph node (MLN) but also to drive pulmonary inflammation during continuous allergen exposure (1). Lung DCs are a heterogeneous cell population that contains two types of conventional DCs (cDCs), e.g., cDCs type 1 (cDC1s) cDC2s. Next to cDCs, the lungs also contain plasmacytoid DCs (pDCs) and under inflammatory conditions, monocyte-derived DCs (moDCs) (2–4). DCs can become activated by allergen exposure and by cytokines secreted by the airway epithelium (5, 6). Activation of DCs requires induction of

Abbreviations: AHR, airway hyperresponsiveness; BAL, bronchoalveolar lavage; BATF3, basic leucine zipper ATF-like transcription factor 3; BM, bone marrow; C, complement; CCL, chemokine ligand; CCR, chemokine receptor; cDC, conventional dendritic cell; CDP, common DC progenitor; cMoP, common monocyte progenitors; CSF-1, colony-stimulating factor 1; DC, dendritic cell; ID-2, DNA-binding protein inhibitor 2; Der p1, Dermatophagoides pteronyssinus antigen P1; DTR, diphtheria toxin; Flt3L, FMS-like tyrosine kinase 3 ligand; GM-CSF, granulocyte macrophage colony-stimulating factor; HDM, house dust mite; HLA-DR, human leukocyte antigen-D; HSC, hematopoietic stem cell; ICOSL, inducible T-cell costimulator ligand; ID2, inhibitor of DNA binding 2; IFN-α, interferon alpha; IL, interleukin; IRF, interferon regulatory factor; MDP, macrophage DC progenitor; MLN, mediastinal lymph node; mDCs, myeloid DCs; moDC, monocyte-derived DC; OVA, ovalbumin; OX-40L, OX-40 ligand; PAR-2, protease-activated receptor 2; pDC, plasmacytoid dendritic cell; PD-L1, programmed death-ligand 1; PPARγ, peroxisome proliferator-activated receptor gamma; PU.1, hematopoietic transcription factor PU.1; RA, retinoic acid; RALDH, retinal dehydrogenase; RBPJ, recombination signal-binding protein 1 for J-Kappa; RELB, v-rel avian reticuloendotheliosis viral oncogene homolog B; STAT3, signal transducer and activator of transcription 3; Th, t helper; TLR, toll like receptor; TNFAIP3, tumor necrosis factor alpha interacting protein 3; Treg, regulatory T cell; TSLP, thymic stromal lymphopoietin.

the pro-inflammatory transcription factor NF-κB, which can be negatively regulated by various proteins including the deubiquitinating enzyme tumor necrosis factor alpha interacting protein 3/A20 (7).

DC ONTOGENY

Dendritic cells originate from hematopoietic stem cells (HSCs) in the bone marrow (BM). These HSCs differentiate into the macrophage DC progenitors (MDPs) (8), which give rise to common monocyte progenitors (cMoPs) and common DC progenitors (CDPs) (**Figure 1**). Whether CDPs also develop without the intermediate MDP stage is currently unknown. CDPs give rise to pre-cDCs and pDCs (9). BM pre-cDCs contain pre-cDC1s and pre-cDC2s that are committed to cDC1 and cDC2 development. This indicates that the decision to become cDC1s or cDC2s already occurs in the BM and not in the periphery (10, 11). MoDCs develop from cMoPs (12, 13) (**Figure 1**).

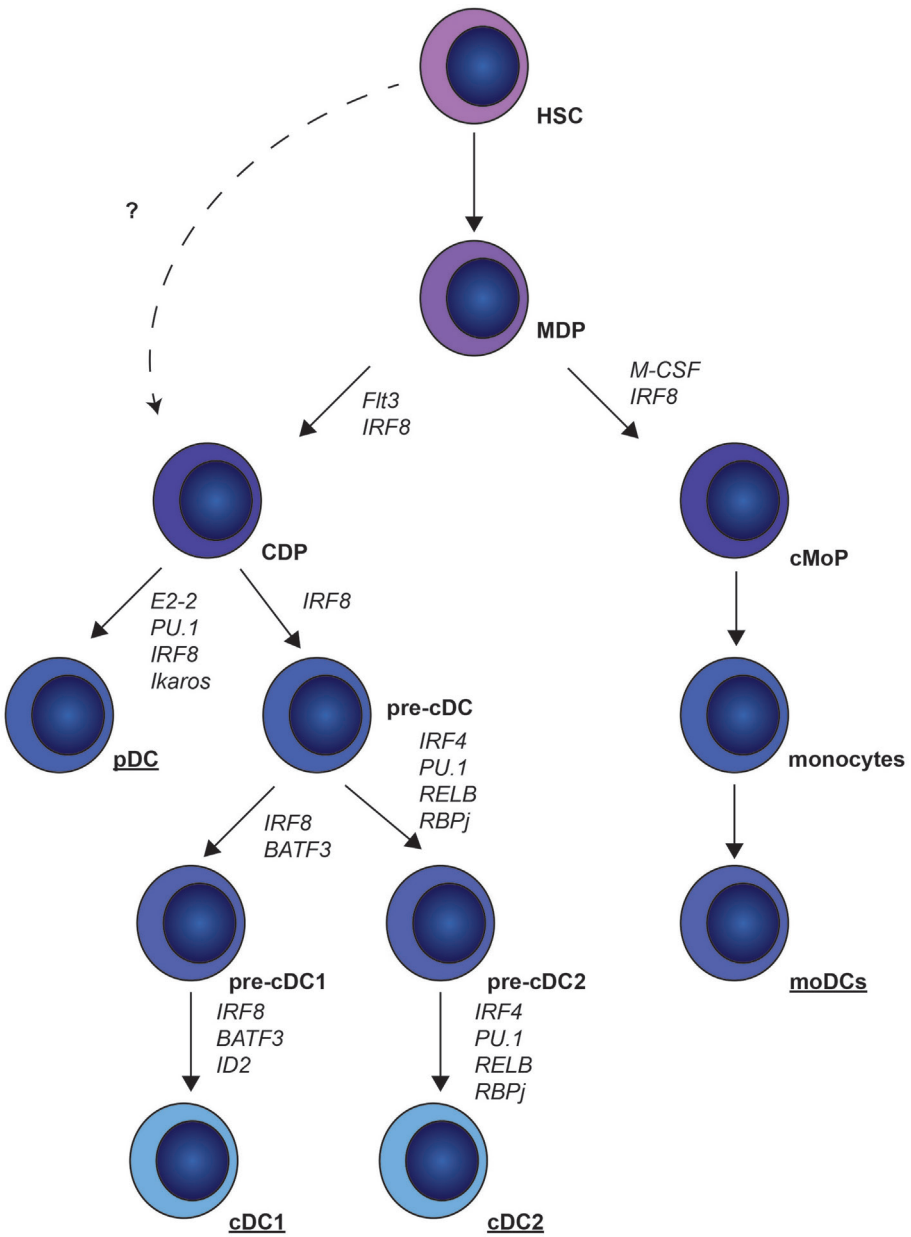

FIGURE 1 | Murine dendritic cell (DC) ontogeny. Common DC precursors (CDP) and common monocytic progenitors (cMoP) develop from myeloid-derived precursors (MDP). CDPs differentiate into plasmacytoid DCs (pDCs) under the control of E2-2, PU.1, interferon regulatory factor (IRF)8 and Ikaros, or pre-conventional DCs (cDCs) under the control of IRF8. Pre-cDCs give rise to pre-cDC1 and pre-cDC2, which finally differentiate into cDC1s and cDC2s. cMoPs give rise to monocytes that can further differentiate into monocyte-derived DCs (moDCs).

LOCATION OF PULMONARY DC SUBSETS

Because pulmonary DC numbers are low and until recently multiple markers were needed to specify DC subsets, the number of studies that investigated the location of pulmonary DC subsets during steady state is limited. It is known that cDC1s are located in close proximity of the airway epithelium, whereby their expression of CD103 (alpha integrin) and beta7 integrin (**Figure 2A**) enables interaction with E-cadherin expressed by epithelial cells. Compared to other DC subsets, cDC1s highly express tight junction proteins, which facilitate the sampling of antigen by extending their dendrites into the airway lumen. cDC1s are also found in the proximity of vascular endothelial cells (14). Most studies that investigated cDC2 localization used CD11b (14–16); however, CD11b is not exclusively expressed by cDC2s and is also highly expressed by moDCs (1). A recent study could distinguish moDCs and cDCs by crossing MacBlue mice (*Csf1r*-ECFP$^{tg/+}$) to *Itgax*-YFP or *Cx3cr1*$^{gfp/+}$ mice, in which cDCs express YFP, using Itgax-YFP mice and monocytes/macrophages express GFP, using *Cx3cr1*$^{gfp/+}$ mice. This study indicated that cDCs are located near the large airways, whereas monocytes and alveolar macrophages are localized in the alveolar space (17). Using MacBlue mice, *in situ* traveling of monocytes and monocyte-derived cells in the lungs was investigated, revealing that monocyte-derived cells are located at the interface of blood vessels and the airways (17, 18). During steady state, the majority of pulmonary pDCs are located in the alveolar interstitium (14, 19); however, pDCs are also found in pulmonary infiltrates in an ovalbumin (OVA)-mediated asthma model (19).

Currently, investigating the localization of DC subsets can be performed with fewer markers, since Guilliams et al. showed that expressions of interferon regulatory factor (IRF)4 and IRF8 are exclusive for cDC2s and cDC1s, respectively, across different organs and species (3). Combining these markers with a universal DC marker such as CD11c should visualize cDC subsets and ease localization studies.

MURINE CONVENTIONAL TYPE 1 DCs

Development of cDC1

cDC1 development is highly dependent on the transcription factor IRF8, as IRF8 drives DC precursor generation (11) and development of pre-cDCs in the BM, and promotes survival of terminally differentiated cDC1s (20). Basic leucine zipper ATF-like transcription factor 3 (BATF3) is implicated in cDC development (21), whereas inhibitor of DNA binding 2 drives terminal differentiation of cDC1s (22) (**Figure 1**). Ontogeny of cDC1s is regulated by cytokines, as FMS-like tyrosine kinase 3 ligand (Flt3L)-deficient mice completely lack cDC1s in the lungs (1, 23).

Function of cDC1s in Asthma

cDC1s are well appreciated for their superior cross-presentation of antigens to CD8$^+$ T-cells, essential for induction of virus-specific CD8$^+$ T-cells and antitumor immune responses (21, 24, 25). However, cDC1s have an inferior capacity to take up allergens compared to other DC subsets (1). Whether cDC1s are also implicated in Th2 skewing in response to allergen exposure remains controversial, as cDC1s are reported to promote, inhibit, or be redundant for Th2 immune responses (1, 26, 27). These differences may be explained by the allergen used, amount of allergen, or the mouse strain used to deplete cDC1s. Besides promoting CD8$^+$ T-cell responses, cDC1s are often associated with a tolerogenic function. cDC1s can induce differentiation of Tregs upon house dust mite (HDM) exposure through induction of retinoic acid (RA) and peroxisome proliferator-activated receptor gamma (PPARγ) (26, 28) (**Figure 2A**). During OVA or HDM-mediated airway inflammation (29) and helminth infections (30), cDC1s can limit Th2 inflammatory responses, emphasizing their tolerogenic potential. Anti-inflammatory properties of *Helicobacter pylori* treatment, which dampens allergic airway disease also depend on cDC1s (31). Furthermore, CD103-deficient mice exposed to an OVA-mediated asthma protocol containing five OVA aerosol challenges developed a more pronounced eosinophilic inflammation indicating their tolerogenic role during Th2-mediated immune responses (29). In contrast, CD103$^{-/-}$ mice that received only a single OVA challenge had decreased eosinophilic inflammation, arguing against the tolerogenic properties of cDC1s. Absence of CD103 did not affect DC migration, but decreased the percentage of allergen-loaded migratory DCs in the MLN (32). Because CD103 can be expressed on both T-cells and cDC1s (33), it is hard to determine which effects are caused by the DCs. However, it is conceivable that cDC1s are essential for allergen uptake at low antigen concentrations. This could explain the decrease in allergen-loaded DCs and the absence of Th2-cell immune responses with only a single OVA challenge. By increasing the allergen exposures, absence of cDC1s can be overcome by protease activity or passive leakage, enabling other DC subsets to access the allergens and migrate toward the MLN.

In addition to their capabilities to suppress Th2-cell differentiation, cDC1s also control Th17 immune responses upon *Aspergillus* infections through secretion of interleukin (IL)-2 (34), indicating that cDC1s maintain homeostasis in the airways. Furthermore, cDC1s are also important for the removal of apoptotic cells, because resolution of airway inflammation is reduced in CD103-deficient mice (29), and cDC1s have been shown to remove apoptotic cells (35).

As it was described that pulmonary cDC1s express Langerin (14), some studies that investigated pulmonary cDC1 function used Langerin-diphtheria toxin (DTR) mice to specifically deplete pulmonary cDC1s (1). However, flow cytometric analysis showed that only a minority of the pulmonary cDC1s expressed Langerin (36), indicating heterogeneity within the pulmonary cDC1 population.

MURINE CONVENTIONAL TYPE 2 DCs

Development of cDC2

In contrast to knowledge on cDC1 development, the transcriptional control of cDC2s is not well characterized. Differentiation of cDC2s from pre-cDCs is regulated by v-rel avian reticuloendotheliosis viral oncogene homolog B (37), PU.1 (38), recombination

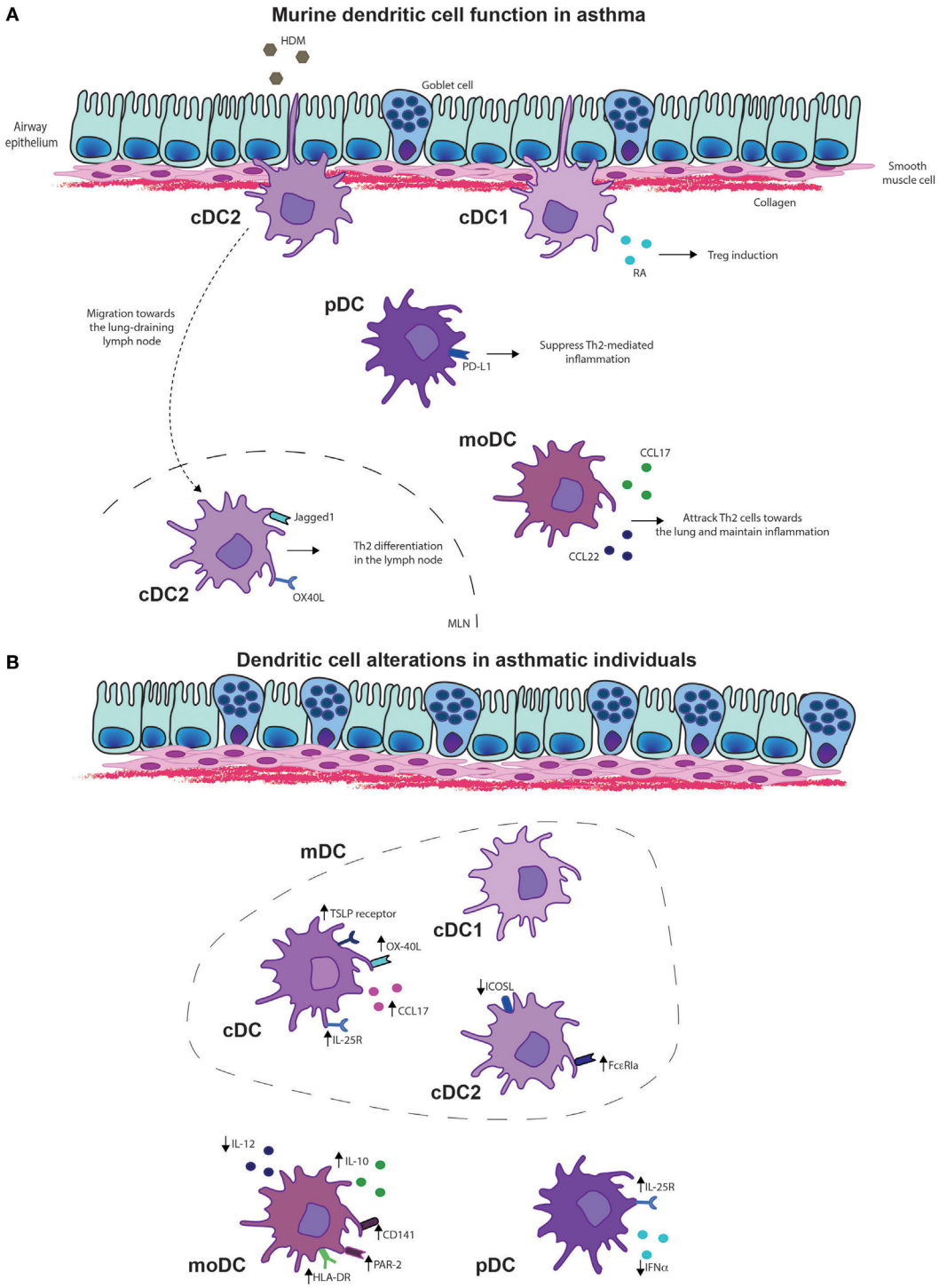

FIGURE 2 | Dendritic cell (DC) functions in asthma. **(A)** Murine DC functions in asthma. Type 2 cDCs are essential for the migration and induction of differentiation of Th2 cells in the lung draining lymph node upon allergen exposure. Monocyte-derived DCs (MoDCs) are important for the chemotaxis of effector Th2 cells toward the lungs by secretion of chemokines CCL17 and CCL22. In asthmatic disease, plasmacytoid DCs (pDCs) suppress Th2-mediated inflammation *via* programmed death-ligand 1 (PD-L1) expression, whereas cDC1s induce regulatory T cells (Tregs) *via* expression of retinoic acid (RA). **(B)** DC alterations in asthmatic individuals. Conventional DCs, including both cDC1s and cDC2s of asthma patients display higher levels of interleukin (IL)-25R, thymic stromal lymphopoietin (TSLP) receptor, OX-40 ligand (OX-40L), and secretion of CCL17. Especially inducible T-cell costimulator ligand (ICOSL) expression in cDC2s of asthmatics is reduced whereas FcεRIa expression is increased in asthmatics that display a Th2 high phenotype. MoDCs of asthmatics display increased expression of human leukocyte antigen-D (HLA-DR), CD141 and protease-activated receptor 2 (PAR-2), and the anti-inflammatory cytokine IL-10, whereas IL-12 production is reduced. pDCs of asthmatics show increased expression of the IL-25R, whereas interferon alpha (IFN-α) secretion was reduced.

signal-binding protein 1 for J-Kappa (39–41), and IRF4 (42–44). However, it is unknown during which cDC2 developmental stage these transcription factors are important (**Figure 1**). Also, the role of the cytokine Flt3L in cDC2 development is controversial, as it has been reported that cDC2 development is both dependent (1) and independent (23) of Flt3L. These differences are likely caused by different methods to distinguish cDC2s from moDCs, leading to cDC2 fractions containing moDCs that develop independent of Flt3L (1). The newly proposed universal gating strategy using IRF4 and IRF8 (3) makes the distinction between DC subsets easier and will help future studies investigating the role of specific transcription factors or cytokines in the development of DC subsets.

Function of cDC2s in Asthma

cDC2s can take up allergen very efficiently (1, 45), migrate well to the MLN, and induce proper T cell proliferation (1) (**Figure 2A**). cDC2s are essential for the induction of Th2-cell differentiation in allergen-exposed lungs (1, 45, 46) and possess the capability to induce Th17-cell differentiation in the gut (42, 47). In an HDM-mediated asthma model, cDC2s induced both Th2 and Th17 differentiation (48). HDM can be recognized by various innate receptors on the cell membrane of DCs, including C-type lectin receptors, such as Dectin-2 (49). Differentiation of both HDM-mediated Th2 and Th17 is dependent on Dectin-2-mediated recognition and/or allergen uptake, as both Th2 and Th17 cytokines are reduced in T-cells of Dectin-2-deficient mice (48). cDC2-deficient mice through IRF4 deficiency have reduced Th2 immune responses in the airways upon sensitization in the airways (50) or in the skin (51). Similarly, no eosinophilic inflammation or Th2 differentiation was induced in mice in which IRF4 was depleted in mature DCs, using a different *CD11c*Cre, which did not affect cDC2 cell development (52). This indicates the importance of cDC2s for the induction of Th2 differentiation. Dectin-1 expression on DCs appears to be important for migration, as Dectin-1-deficient cDC2s display lower levels of CCR7, and have lower numbers of migratory cDC2s in the MLN. Furthermore, Dectin-1$^{-/-}$ mice did not develop eosinophilic inflammation, nor did they show induction of Th2 or Th17 cytokines in an HDM-mediated asthma model (53). These findings indicate that Dectin-1 is required for the induction of chemokines and chemokine receptors on cDC2s, enabling migration and T-cell differentiation. cDC2s exclusively express the TNF-superfamily member OX-40 ligand (OX-40L) (54), essential for Th2 cell differentiation, indicating the importance of cDC2s for Th2 differentiation (**Figure 2A**). In neonatal mice, HDM-induced IL-33 production suppressed IL-12p35 expression and induced OX-40L in cDC2s, driving Th2 differentiation (55).

MURINE moDCs

Development of moDCs

As their name implicates and stated above, moDCs derive from monocytes. There are two types of monocytes, Ly6C^{hi} and Ly6C^{low} monocytes (56). Ly6C^{hi} monocytes migrate toward inflammatory sites and give rise to Ly6C^{hi} moDCs, Ly6C^{low} moDCs (57), and Ly6C^{low} monocytes (58). MoDCs downregulate Ly6C upon differentiation from monocytes (1). Ly6C^{low} monocytes patrol the vasculature (56, 59) and differentiate into more long-lived Ly6C^{low} moDCs (57). It is suggested that monocytes or moDCs can serve as cDC precursors, in which cDC1s arise from Ly6C^{hi} CCR2^{hi} monocytes, and cDC2s develop from Ly6C^{low} CCR2^{low} monocytes (60).

Function of moDCs in Asthma

After a primary high dose of HDM in the airways, moDCs accumulate within 48 h in the lungs and peak at 72 h in the MLN (1). HDM and other environmental factors trigger the airway epithelium to secrete chemokines and cytokines (61). Secretion of CCL2 will drive migration of monocytes toward the lungs (62), where they will differentiate into moDCs under the regulation of both CCL2 (1) and colony-stimulating factor 1 (23). MoDCs are efficient in antigen uptake; however, their capacity to drive T-cell proliferation is inferior to cDC2s. Instead, moDCs produce vast amounts of cytokines and chemokines essential for the recruitment and activation of Th2-cells upon HDM exposure (1) (**Figure 2A**). This indicates that moDCs are dispensable for Th2 differentiation but essential during the effector phase of asthma models, as depletion of CD11b^{+} myeloid cells, which includes monocytes, during allergen challenge drastically reduces eosinophilia (63). Nevertheless, with high antigen dose, moDCs migrate toward the MLN and induce Th2 differentiation in the absence of cDCs upon exposure to HDM (1) or cockroach extract (64). Depletion of migratory cDCs enhances Th2 cell-mediated immune responses in an OVA-alum model (65). Furthermore, absence of Th2-cell-mediated immunity, due to the absence of DCs, can be reverted by an adoptive transfer of monocytes that differentiate into moDCs (66). Likewise, it was shown that systemic administration of BM-derived CD11b^{+} cells efficiently induces Th2-mediated eosinophilic airway inflammation (67). This implicates that at high allergen concentration, moDCs can acquire migratory capacities, induce Th2 differentiation, and thereby drive Th2-mediated immune responses.

MURINE pDCs

Development of pDCs

Plasmacytoid DCs differentiate directly in the BM from CDPs (68). Differentiation of pDCs depends on Flt3L and signal transducer and activator of transcription 3 signaling, in combination with transcription factors, such as E2-2, IRF8, Ikaros, and PU.1, of which E2-2 is highly specific for pDC development (69–71) (**Figure 1**).

Function of pDCs in Asthma

Plasmacytoid DCs are essential for antiviral immune responses as they produce large amounts of interferon alpha (IFN-α) after Toll-like receptor (TLR7) activation (72, 73). In comparison to other DC subsets, pDCs have a limited capacity to take up and present antigens (1, 19, 74, 75). pDCs have a tolerogenic function in asthma, as pDCs induce Treg cell differentiation (76, 77), and depletion of pDCs in Siglec-H-DTR mice increased the proliferation of antigen-specific CD4^{+} T-cells (78). Increase in pDC

numbers, as induced by Flt3L treatment, alleviate eosinophilic inflammation, which is reversed upon pDC depletion (79). Programmed death-ligand 1 (PD-L1) expression on pDCs is essential for their suppressive effect, as PD-L1-deficient pDCs could not alleviate allergic airway inflammation, whereas IDO or inducible T-cell costimulator ligand (ICOSL)-deficient pDCs could do so (79) (**Figure 2A**). Development of HDM-driven allergic asthma can be inhibited by adoptive transfer of pDCs from sensitized donors (80). Different pulmonary pDC subsets have been described, e.g., $CD8\alpha^{-}\beta^{-}$, $CD8\alpha^{+}\beta^{-}$, and $CD8\alpha^{+}\beta^{+}$ pDCs (81). Only $CD8\alpha^{+}\beta^{-}$ pDCs and $CD8\alpha^{+}\beta^{+}$ pDCs have tolerogenic capacities, whereas $CD8\alpha^{-}\beta^{-}$ pDCs display more pro-inflammatory functions upon TLR7 and TLR9 stimulation (81). Specifically, $CD8\alpha^{+}\beta^{+}$ pDCs and $CD8\alpha^{+}\beta^{-}$ pDCs have increased expression of retinal dehydrogenase leading to RA production, resulting in increased Treg differentiation (81).

Plasmacytoid DCs are essential for beneficial effects observed in immunotherapy *via* complement subunit C1q. Administration of C1q reduces airway hyperresponsiveness (AHR) and eosinophilia as efficiently as dexamethasone administration. pDC depletion abrogates the protective effect of C1q (82).

Viral infections are often detected during asthma exacerbations. Viral particles activate DC subsets *via* TLR7, and its expression was decreased in pDCs by allergic inflammation. TLR7-deficient mice displayed reduced IFN secretion, increased virus replication, and increased eosinophilic inflammation and AHR, indicating that impaired TLR7 expression on pDCs by allergic inflammation exaggerates asthma exacerbations (83). Furthermore, pDCs transferred from donors with a respiratory tract syncytial virus (RSV) infection did not provide protection from Th2-mediated inflammation as transferred pDCs from naïve mice did (80). CpG-maturated pDCs are well capable of protecting from eosinophilic inflammation (79), suggesting that altered activation of pDCs affects their function.

HUMAN PULMONARY DC SUBSETS

Transcriptional Development of Human DCs

In human lungs, three different DC subsets have been described, human DC1s, which express BDCA1/CD1c, DC2s, which expresses BDCA3/CD141 and pDCs, which express BDCA2/CD123 (3, 4, 84). Gene expression profiles of human DC1s and DC2s revealed that human DC subsets resembled mouse cDC1s and cDC2s, respectively (3, 85–88). Development of human DCs is also highly dependent on Flt3L, as Flt3L injection drastically increases the number of blood DCs of healthy volunteers (89). Similar to that in mice, differentiation of human pDCs is mediated by E2-2 (90), whereas cDC1 and cDC2 differentiation is controlled by BATF3 (91) and IRF4 (92, 93), respectively.

Location of Human DC Subsets in the Lungs

$BDCA1^{+}$ cDC2s were increased in the airway epithelium of asthma patients that display a Th2 phenotype, whereas this was not observed in patients without a Th2 profile (94). DCs are increased in the outer wall of the large airways in patients who suffer from fatal asthma (95). These are likely moDCs, as they express XIIIa (95), a coagulation factor also expressed by macrophages in the skin (96). As both moDCs and macrophages are derived from monocytes this suggests an overlapping ontogeny. Unfortunately, lack of lung material containing epithelium and interstitium of both healthy controls and asthma patients complicates research on the localization of DC subset during steady state and in asthmatic lung. Recent consensus regarding universal markers that can identify DC subsets will facilitate the visualization of DC subsets in human organs (3).

Function of Human DCs in Asthma

Most studies that investigated human DC function, compared pDCs to myeloid DCs (mDCs) that include both DC1s and DC2s. Allergic asthmatics showed increased frequencies of DC1s and DC2s in peripheral blood (97), induced sputum and bronchoalveolar lavage (BAL) upon allergen inhalation compared to controls (98–100). After allergen inhalation, only DC2s migrated toward bronchial tissue (100). Allergen exposure increased the expression of thymic stromal lymphopoietin (TSLP)-receptor but not IL-33-receptor on cultured cDCs from $CD34^{+}$ BM precursors, which are implicated as Th2 instructive cytokine receptors (100). Allergen inhalation induced expression of IL-25-receptor on both cDCs and pDC (101). The costimulatory molecule OX-40L and expression of Th2 chemoattractant CCL17 was higher on cDCs of patients with mild asthma than on cDCs of healthy controls (102) (**Figure 2B**). In patients who displayed high Th2-cell numbers, a large proportion of airway mucosal DC2s expressed FcεRIa compared to Th2-cell low asthma patients (94) (**Figure 2B**). This is likely, as high IgE-levels are associated with high Th2-cell numbers, thereby suggesting that IgE increases FcεRIa expression. IgE-bound antigens are rapidly internalized, processed, and presented by DCs to antigen-specific $CD4^{+}$ T-cells (103, 104). DC2s loaded with Dermatophagoides pteronyssinus antigen P1 (Der p1) allergen-IgE immune complexes induced IL-4 and lowered IFN-γ-expression in *in vitro* cocultures with naïve T-cells (105), indicating that allergen-IgE immune complexes promote Th2 differentiation (106). CD86 expression was higher on mDCs of asthmatic children than on mDCs of atopic children. Furthermore, upon LPS stimulation IL-6 production by mDCs of asthmatic children was decreased, compared with mDCs of atopic children (107). The numbers of IL12-producing mDCs were also lower in asthmatic children (108), indicating the presence of a Th2 promoting environment in asthmatic children. cDCs of allergic asthmatics induced increased Th2 differentiation upon stimulation with TSLP and Der p compared to cDCs of controls (109). TSLP-stimulated cDCs of allergic asthmatics and not of controls, induced IL-9 production and PU.1 expression, indicative of Th9 differentiation (109). When Th2 priming capacity of DC1s and DC2s from human blood and lungs were compared, both lung and blood DC1s were superior in Th2 differentiation (110). However, in this study, live-attenuated influenza virus was used to activate DC1s and DC2s, which primarily activates DC1s, as these induce antiviral immune responses (24). The expression of CD141, a marker for DC1s, is increased in blood leukocytes during acute asthma exacerbations on moDCs,

but surprisingly not on DC1s (111). This indicates that DC1s or CD141 expression plays an important role in the pathogenesis of asthma. DC2s from allergic rhinitis patients efficiently prime Th2 differentiation (112) and express lower levels of ICOSL, compared to controls (**Figure 2B**). Blockade of ICOSL in DC2s of controls increases the production of Th2 cytokines, indicating that decreased ICOSL expression on DC2s promotes Th2 differentiation (113). Both human DC1s and DC2s induce Th2 cytokines; however, Th2 differentiation by cDC1s was observed following exposure to live-attenuated viral particles (112). This implicated that during virus infections, cDC1s in asthmatics shift from promoting Th1 immune responses or maintaining tolerance toward a Th2-promoting phenotype.

Allergen inhalation increased pDCs numbers in the airway lumen (98, 114); however, variable results exist whether circulating pDCs differ between asthmatics and healthy individuals (115, 116). In a birth cohort, circulating pDCs predicted respiratory tract infections, wheezing, and asthma diagnosis by 5 years of age (117). pDCs of severe asthmatics also produced less IFN-α following influenza infection, than pDCs of healthy controls did (118) (**Figure 2B**). Single-cell analysis revealed that characterization of pDCs based on CD123 expression included DC precursors (119, 120). Therefore, these findings need to be revisited whether they truly induced by pDCs.

House dust mite activation of cultured moDCs of HDM-allergic asthma patients expressed higher levels of human leukocyte antigen-D, induced more T-cell proliferation (121), and Th2 differentiation than control moDCs (122). When examining the frequency of $CD14^+/CD16^+$ monocytes, conflicting results exist in severe asthmatics (123, 124). Monocytes of allergic patients showed increased IL-10 and decreased IL-12 production upon HDM and Der p1 stimulation, which enhanced Th2 differentiation (125). $CD14^+/CD16^+$ monocytes of severe asthmatics display higher expression of protease activation receptor 2 (PAR-2) as compared to mild/moderate asthmatics (124) (**Figure 2B**). PAR-2-mediated activation of monocytes induces secretion of IL-1β, IL-6, and IL-8 (126), indicating that activation *via* PAR-2 facilitates secretion of cytokines important for Th17-cell differentiation and neutrophil activation and attraction, which does not occur in mild/moderate asthmatics.

CLINICAL IMPLICATIONS

In conclusion, whereas in mice the function of different DC subsets in asthma pathogenesis is becoming more and more clear, there are no studies at present that compared the Th2- or Th17-priming capacity of different human DC subsets in response to allergens. The limited number of DCs in peripheral blood and the difficulty to obtain lung or lung-draining lymph nodes hamper these studies. Current advances in single-cell analysis enable analysis of DC subsets and have already proven that more DC subsets and DC precursors can be found in peripheral blood (119, 120). Further research should provide insights into DC subset characteristics and function in asthmatics that display either a Th2, Th2/Th17, or Th17-mediated inflammation.

AUTHOR CONTRIBUTIONS

All authors listed have made a substantial, direct, and intellectual contribution to the work and approved it for publication.

ACKNOWLEDGMENTS

These studies were partly supported by Netherlands Lung Foundation (3.2.12.087, 4.2.13.054JO, and 9.2.15.065FE).

REFERENCES

1. Plantinga M, Guilliams M, Vanheerswynghels M, Deswarte K, Branco-Madeira F, Toussaint W, et al. Conventional and monocyte-derived CD11b(+) dendritic cells initiate and maintain T helper 2 cell-mediated immunity to house dust mite allergen. *Immunity* (2013) 38(2):322–35. doi:10.1016/j.immuni.2012.10.016
2. Lambrecht BN, Hammad H. Lung dendritic cells: targets for therapy in allergic disease. *Handb Exp Pharmacol* (2009) 188:99–114. doi:10.1007/978-3-540-71029-5_5
3. Guilliams M, Dutertre CA, Scott CL, McGovern N, Sichien D, Chakarov S, et al. Unsupervised high-dimensional analysis aligns dendritic cells across tissues and species. *Immunity* (2016) 45(3):669–84. doi:10.1016/j.immuni.2016.08.015
4. Guilliams M, Ginhoux F, Jakubzick C, Naik SH, Onai N, Schraml BU, et al. Dendritic cells, monocytes and macrophages: a unified nomenclature based on ontogeny. *Nat Rev Immunol* (2014) 14(8):571–8. doi:10.1038/nri3712
5. Jacquet A. Innate immune responses in house dust mite allergy. *ISRN Allergy* (2013) 2013:735031. doi:10.1155/2013/735031
6. Wang J-Y. The innate immune response in house dust mite-induced allergic inflammation. *Allergy Asthma Immunol Res* (2013) 5(2):68–74. doi:10.4168/aair.2013.5.2.68
7. Kool M, van Loo G, Waelput W, De Prijck S, Muskens F, Sze M, et al. The ubiquitin-editing protein A20 prevents dendritic cell activation, recognition of apoptotic cells, and systemic autoimmunity. *Immunity* (2011) 35(1):82–96. doi:10.1016/j.immuni.2011.05.013
8. Naik SH, Sathe P, Park HY, Metcalf D, Proietto AI, Dakic A, et al. Development of plasmacytoid and conventional dendritic cell subtypes from single precursor cells derived in vitro and in vivo. *Nat Immunol* (2007) 8(11):1217–26. doi:10.1038/ni1522
9. Belz GT, Nutt SL. Transcriptional programming of the dendritic cell network. *Nat Rev Immunol* (2012) 12(2):101–13. doi:10.1038/nri3149
10. Grajales-Reyes GE, Iwata A, Albring J, Wu X, Tussiwand R, Kc W, et al. Batf3 maintains autoactivation of Irf8 for commitment of a CD8alpha(+) conventional DC clonogenic progenitor. *Nat Immunol* (2015) 16(7):708–17. doi:10.1038/ni.3197
11. Schlitzer A, Sivakamasundari V, Chen J, Sumatoh HR, Schreuder J, Lum J, et al. Identification of cDC1- and cDC2-committed DC progenitors reveals early lineage priming at the common DC progenitor stage in the bone marrow. *Nat Immunol* (2015) 16(7):718–28. doi:10.1038/ni.3200
12. Hettinger J, Richards DM, Hansson J, Barra MM, Joschko AC, Krijgsveld J, et al. Origin of monocytes and macrophages in a committed progenitor. *Nat Immunol* (2013) 14(8):821–30. doi:10.1038/ni.2638
13. Sathe P, Metcalf D, Vremec D, Naik SH, Langdon WY, Huntington ND, et al. Lymphoid tissue and plasmacytoid dendritic cells and macrophages do not share a common macrophage-dendritic cell-restricted progenitor. *Immunity* (2014) 41(1):104–15. doi:10.1016/j.immuni.2014.05.020
14. Sung SS, Fu SM, Rose CE Jr, Gaskin F, Ju ST, Beaty SR. A major lung CD103 (alphaE)-beta7 integrin-positive epithelial dendritic cell population expressing Langerin and tight junction proteins. *J Immunol* (2006) 176(4):2161–72. doi:10.4049/jimmunol.176.4.2161
15. von Garnier C, Filgueira L, Wikstrom M, Smith M, Thomas JA, Strickland DH, et al. Anatomical location determines the distribution and function of

dendritic cells and other APCs in the respiratory tract. *J Immunol* (2005) 175(3):1609–18. doi:10.4049/jimmunol.175.3.1609
16. Thornton EE, Looney MR, Bose O, Sen D, Sheppard D, Locksley R, et al. Spatiotemporally separated antigen uptake by alveolar dendritic cells and airway presentation to T cells in the lung. *J Exp Med* (2012) 209(6):1183–99. doi:10.1084/jem.20112667
17. Rodero MP, Poupel L, Loyher PL, Hamon P, Licata F, Pessel C, et al. Immune surveillance of the lung by migrating tissue monocytes. *Elife* (2015) 4:e07847. doi:10.7554/eLife.07847
18. Sauter KA, Pridans C, Sehgal A, Bain CC, Scott C, Moffat L, et al. The MacBlue binary transgene (csf1r-gal4VP16/UAS-ECFP) provides a novel marker for visualisation of subsets of monocytes, macrophages and dendritic cells and responsiveness to CSF1 administration. *PLoS One* (2014) 9(8):e105429. doi:10.1371/journal.pone.0105429
19. de Heer HJ, Hammad H, Soullié T, Hijdra D, Vos N, Willart MA, et al. Essential role of lung plasmacytoid dendritic cells in preventing asthmatic reactions to harmless inhaled antigen. *J Exp Med* (2004) 200(1):89–98. doi:10.1084/jem.20040035
20. Sichien D, Scott CL, Martens L, Vanderkerken M, Van Gassen S, Plantinga M, et al. IRF8 transcription factor controls survival and function of terminally differentiated conventional and plasmacytoid dendritic cells, respectively. *Immunity* (2016) 45(3):626–40. doi:10.1016/j.immuni.2016.08.013
21. Hildner K, Edelson BT, Purtha WE, Diamond M, Matsushita H, Kohyama M, et al. Batf3 deficiency reveals a critical role for CD8alpha+ dendritic cells in cytotoxic T cell immunity. *Science* (2008) 322(5904):1097–100. doi:10.1126/science.1164206
22. Jackson JT, Hu Y, Liu R, Masson F, D'Amico A, Carotta S, et al. Id2 expression delineates differential checkpoints in the genetic program of CD8alpha+ and CD103+ dendritic cell lineages. *EMBO J* (2011) 30(13):2690–704. doi:10.1038/emboj.2011.163
23. Ginhoux F, Liu K, Helft J, Bogunovic M, Greter M, Hashimoto D, et al. The origin and development of nonlymphoid tissue CD103+ DCs. *J Exp Med* (2009) 206(13):3115–30. doi:10.1084/jem.20091756
24. GeurtsvanKessel CH, Willart MA, van Rijt LS, Muskens F, Kool M, Baas C, et al. Clearance of influenza virus from the lung depends on migratory langerin(+)CD11b(-) but not plasmacytoid dendritic cells. *J Exp Med* (2008) 205(7):1621–34. doi:10.1084/jem.20071365
25. Fuertes MB, Kacha AK, Kline J, Woo SR, Kranz DM, Murphy KM, et al. Host type I IFN signals are required for antitumor CD8+ T cell responses through CD8{alpha}+ dendritic cells. *J Exp Med* (2011) 208(10):2005–16. doi:10.1084/jem.20101159
26. Khare A, Krishnamoorthy N, Oriss TB, Fei M, Ray P, Ray A. Cutting edge: inhaled antigen upregulates retinaldehyde dehydrogenase in lung CD103(+) but not plasmacytoid dendritic cells to induce Foxp3 de novo in CD4(+) T cells and promote airway tolerance. *J Immunol* (2013) 191(1):25–9. doi:10.4049/jimmunol.1300193
27. Nakano H, Free ME, Whitehead GS, Maruoka S, Wilson RH, Nakano K, et al. Pulmonary CD103(+) dendritic cells prime Th2 responses to inhaled allergens. *Mucosal Immunol* (2012) 5(1):53–65. doi:10.1038/mi.2011.47
28. Khare A, Chakraborty K, Raundhal M, Ray P, Ray A. Cutting edge: dual function of PPARgamma in CD11c+ cells ensures immune tolerance in the airways. *J Immunol* (2015) 195(2):431–5. doi:10.4049/jimmunol.1500474
29. Bernatchez E, Gold MJ, Langlois A, Lemay AM, Brassard J, Flamand N, et al. Pulmonary CD103 expression regulates airway inflammation in asthma. *Am J Physiol Lung Cell Mol Physiol* (2015) 308(8):L816–26. doi:10.1152/ajplung.00319.2014
30. Everts B, Tussiwand R, Dreesen L, Fairfax KC, Huang SC, Smith AM, et al. Migratory CD103+ dendritic cells suppress helminth-driven type 2 immunity through constitutive expression of IL-12. *J Exp Med* (2016) 213(1):35–51. doi:10.1084/jem.20150235
31. Engler DB, Reuter S, van Wijck Y, Urban S, Kyburz A, Maxeiner J, et al. Effective treatment of allergic airway inflammation with *Helicobacter pylori* immunomodulators requires BATF3-dependent dendritic cells and IL-10. *Proc Natl Acad Sci U S A* (2014) 111(32):11810–5. doi:10.1073/pnas.1410579111
32. Fear VS, Lai SP, Zosky GR, Perks KL, Gorman S, Blank F, et al. A pathogenic role for the integrin CD103 in experimental allergic airways disease. *Physiol Rep* (2016) 4(21):e13021. doi:10.14814/phy2.13021
33. Agace WW, Higgins JM, Sadasivan B, Brenner MB, Parker CM. T-lymphocyte-epithelial-cell interactions: integrin alpha(E)(CD103)beta(7), LEEP-CAM and chemokines. *Curr Opin Cell Biol* (2000) 12(5):563–8. doi:10.1016/S0955-0674(00)00132-0
34. Zelante T, Wong AY, Ping TJ, Chen J, Sumatoh HR, Viganò E, et al. CD103(+) dendritic cells control Th17 cell function in the lung. *Cell Rep* (2015) 12(11):1789–801. doi:10.1016/j.celrep.2015.08.030
35. Desch AN, Randolph GJ, Murphy K, Gautier EL, Kedl RM, Lahoud MH, et al. CD103+ pulmonary dendritic cells preferentially acquire and present apoptotic cell-associated antigen. *J Exp Med* (2011) 208(9):1789–97. doi:10.1084/jem.20110538
36. Zahner SP, Kel JM, Martina CA, Brouwers-Haspels I, van Roon MA, Clausen BE. Conditional deletion of TGF-betaR1 using Langerin-Cre mice results in Langerhans cell deficiency and reduced contact hypersensitivity. *J Immunol* (2011) 187(10):5069–76. doi:10.4049/jimmunol.1101880
37. Wu L, D'Amico A, Winkel KD, Suter M, Lo D, Shortman K. RelB is essential for the development of myeloid-related CD8alpha– dendritic cells but not of lymphoid-related CD8alpha+ dendritic cells. *Immunity* (1998) 9(6):839–47. doi:10.1016/S1074-7613(00)80649-4
38. Guerriero A, Langmuir PB, Spain LM, Scott EW. PU.1 is required for myeloid-derived but not lymphoid-derived dendritic cells. *Blood* (2000) 95(3):879–85.
39. Caton ML, Smith-Raska MR, Reizis B. Notch-RBP-J signaling controls the homeostasis of CD8– dendritic cells in the spleen. *J Exp Med* (2007) 204(7):1653–64. doi:10.1084/jem.20062648
40. Lewis KL, Caton ML, Bogunovic M, Greter M, Grajkowska LT, Ng D, et al. Notch2 receptor signaling controls functional differentiation of dendritic cells in the spleen and intestine. *Immunity* (2011) 35(5):780–91. doi:10.1016/j.immuni.2011.08.013
41. Satpathy AT, Briseño CG, Lee JS, Ng D, Manieri NA, Kc W, et al. Notch2-dependent classical dendritic cells orchestrate intestinal immunity to attaching-and-effacing bacterial pathogens. *Nat Immunol* (2013) 14(9):937–48. doi:10.1038/ni.2679
42. Schlitzer A, McGovern N, Teo P, Zelante T, Atarashi K, Low D, et al. IRF4 transcription factor-dependent CD11b+ dendritic cells in human and mouse control mucosal IL-17 cytokine responses. *Immunity* (2013) 38(5):970–83. doi:10.1016/j.immuni.2013.04.011
43. Suzuki S, Honma K, Matsuyama T, Suzuki K, Toriyama K, Akitoyo I, et al. Critical roles of interferon regulatory factor 4 in CD11bhighCD8alpha– dendritic cell development. *Proc Natl Acad Sci U S A* (2004) 101(24):8981–6. doi:10.1073/pnas.0402139101
44. Tamura T, Tailor P, Yamaoka K, Kong HJ, Tsujimura H, O'Shea JJ, et al. IFN regulatory factor-4 and -8 govern dendritic cell subset development and their functional diversity. *J Immunol* (2005) 174(5):2573–81. doi:10.4049/jimmunol.174.5.2573
45. Furuhashi K, Suda T, Hasegawa H, Suzuki Y, Hashimoto D, Enomoto N, et al. Mouse lung CD103+ and CD11bhigh dendritic cells preferentially induce distinct CD4+ T-cell responses. *Am J Respir Cell Mol Biol* (2012) 46(2):165–72. doi:10.1165/rcmb.2011-0070OC
46. Raymond M, Rubio M, Fortin G, Shalaby KH, Hammad H, Lambrecht BN, et al. Selective control of SIRP-alpha-positive airway dendritic cell trafficking through CD47 is critical for the development of T(H)2-mediated allergic inflammation. *J Allergy Clin Immunol* (2009) 124(6):1333–42.e1. doi:10.1016/j.jaci.2009.07.021
47. Persson EK, Uronen-Hansson H, Semmrich M, Rivollier A, Hägerbrand K, Marsal J, et al. IRF4 transcription-factor-dependent CD103(+)CD11b(+) dendritic cells drive mucosal T helper 17 cell differentiation. *Immunity* (2013) 38(5):958–69. doi:10.1016/j.immuni.2013.03.009
48. Norimoto A, Hirose K, Iwata A, Tamachi T, Yokota M, Takahashi K, et al. Dectin-2 promotes house dust mite-induced T helper type 2 and type 17 cell differentiation and allergic airway inflammation in mice. *Am J Respir Cell Mol Biol* (2014) 51(2):201–9. doi:10.1165/rcmb.2013-0522OC
49. Barrett NA, Maekawa A, Rahman OM, Austen KF, Kanaoka Y. Dectin-2 recognition of house dust mite triggers cysteinyl leukotriene generation by dendritic cells. *J Immunol* (2009) 182(2):1119–28. doi:10.4049/jimmunol.182.2.1119
50. Gao Y, Nish SA, Jiang R, Hou L, Licona-Limón P, Weinstein JS, et al. Control of T helper 2 responses by transcription factor IRF4-dependent dendritic cells. *Immunity* (2013) 39(4):722–32. doi:10.1016/j.immuni.2013.08.028
51. Deckers J, Sichien D, Plantinga M, Van Moorleghem J, Vanheerswynghels M, Hoste E, et al. Epicutaneous sensitization to house dust mite allergen requires

IRF4-dependent dermal dendritic cells. *J Allergy Clin Immunol* (2017). doi:10.1016/j.jaci.2016.12.970
52. Williams JW, Tjota MY, Clay BS, Vander Lugt B, Bandukwala HS, Hrusch CL, et al. Transcription factor IRF4 drives dendritic cells to promote Th2 differentiation. *Nat Commun* (2013) 4:2990. doi:10.1038/ncomms3990
53. Ito T, Hirose K, Norimoto A, Tamachi T, Yokota M, Saku A, et al. Dectin-1 plays an important role in house dust mite-induced allergic airway inflammation through the activation of CD11b+ dendritic cells. *J Immunol* (2017) 198(1):61–70. doi:10.4049/jimmunol.1502393
54. Han J, Dakhama A, Jia Y, Wang M, Zeng W, Takeda K, et al. Responsiveness to respiratory syncytial virus in neonates is mediated through thymic stromal lymphopoietin and OX40 ligand. *J Allergy Clin Immunol* (2012) 130(5):1175–86.e9. doi:10.1016/j.jaci.2012.08.033
55. de Kleer IM, Kool M, de Bruijn MJ, Willart M, van Moorleghem J, Schuijs MJ, et al. Perinatal activation of the interleukin-33 pathway promotes type 2 immunity in the developing lung. *Immunity* (2016) 45(6):1285–98. doi:10.1016/j.immuni.2016.10.031
56. Geissmann F, Jung S, Littman DR. Blood monocytes consist of two principal subsets with distinct migratory properties. *Immunity* (2003) 19(1):71–82. doi:10.1016/S1074-7613(03)00174-2
57. Jakubzick C, Gautier EL, Gibbings SL, Sojka DK, Schlitzer A, Johnson TE, et al. Minimal differentiation of classical monocytes as they survey steady-state tissues and transport antigen to lymph nodes. *Immunity* (2013) 39(3):599–610. doi:10.1016/j.immuni.2013.08.007
58. Yona S, Kim KW, Wolf Y, Mildner A, Varol D, Breker M, et al. Fate mapping reveals origins and dynamics of monocytes and tissue macrophages under homeostasis. *Immunity* (2013) 38(1):79–91. doi:10.1016/j.immuni.2012.12.001
59. Auffray C, Fogg D, Garfa M, Elain G, Join-Lambert O, Kayal S, et al. Monitoring of blood vessels and tissues by a population of monocytes with patrolling behavior. *Science* (2007) 317(5838):666–70. doi:10.1126/science.1142883
60. Jakubzick C, Tacke F, Ginhoux F, Wagers AJ, van Rooijen N, Mack M, et al. Blood monocyte subsets differentially give rise to CD103+ and CD103− pulmonary dendritic cell populations. *J Immunol* (2008) 180(5):3019–27. doi:10.4049/jimmunol.180.5.3019
61. Lambrecht BN, Hammad H. The immunology of asthma. *Nat Immunol* (2015) 16(1):45–56. doi:10.1038/ni.3049
62. Robays LJ, Maes T, Lebecque S, Lira SA, Kuziel WA, Brusselle GG, et al. Chemokine receptor CCR2 but not CCR5 or CCR6 mediates the increase in pulmonary dendritic cells during allergic airway inflammation. *J Immunol* (2007) 178(8):5305–11. doi:10.4049/jimmunol.178.8.5305
63. Medoff BD, Seung E, Hong S, Thomas SY, Sandall BP, Duffield JS, et al. CD11b+ myeloid cells are the key mediators of Th2 cell homing into the airway in allergic inflammation. *J Immunol* (2009) 182(1):623–35. doi:10.4049/jimmunol.182.1.623
64. Walzer T, Brawand P, Swart D, Tocker J, De Smedt T. No defect in T-cell priming, secondary response, or tolerance induction in response to inhaled antigens in Fms-like tyrosine kinase 3 ligand-deficient mice. *J Allergy Clin Immunol* (2005) 115(1):192–9. doi:10.1016/j.jaci.2004.08.046
65. Grinnan D, Sung SS, Dougherty JA, Knowles AR, Allen MB, Rose CE III, et al. Enhanced allergen-induced airway inflammation in paucity of lymph node T cell (plt) mutant mice. *J Allergy Clin Immunol* (2006) 118(6):1234–41. doi:10.1016/j.jaci.2006.07.036
66. Kool M, Soullié T, van Nimwegen M, Willart MA, Muskens F, Jung S, et al. Alum adjuvant boosts adaptive immunity by inducing uric acid and activating inflammatory dendritic cells. *J Exp Med* (2008) 205(4):869–82. doi:10.1084/jem.20071087
67. Cruz JL, Pérez-Girón JV, Lüdtke A, Gómez-Medina S, Ruibal P, Idoyaga J, et al. Monocyte-derived dendritic cells enhance protection against secondary influenza challenge by controlling the switch in CD8+ T-cell immunodominance. *Eur J Immunol* (2017) 47(2):345–52. doi:10.1002/eji.201646523
68. Gilliet M, Boonstra A, Paturel C, Antonenko S, Xu XL, Trinchieri G, et al. The development of murine plasmacytoid dendritic cell precursors is differentially regulated by FLT3-ligand and granulocyte/macrophage colony-stimulating factor. *J Exp Med* (2002) 195(7):953–8. doi:10.1084/jem.20020045
69. Esashi E, Watowich SS. Dendritic cells: transcriptional control of plasmacytoid dendritic cell development by E2-2. *Immunol Cell Biol* (2009) 87(1):1–2. doi:10.1038/icb.2008.93
70. Li HS, Yang CY, Nallaparaju KC, Zhang H, Liu YJ, Goldrath AW, et al. The signal transducers STAT5 and STAT3 control expression of Id2 and E2-2 during dendritic cell development. *Blood* (2012) 120(22):4363–73. doi:10.1182/blood-2012-07-441311
71. Merad M, Sathe P, Helft J, Miller J, Mortha A. The dendritic cell lineage: ontogeny and function of dendritic cells and their subsets in the steady state and the inflamed setting. *Annu Rev Immunol* (2013) 31:563–604. doi:10.1146/annurev-immunol-020711-074950
72. Grayson MH, Ramos MS, Rohlfing MM, Kitchens R, Wang HD, Gould A, et al. Controls for lung dendritic cell maturation and migration during respiratory viral infection. *J Immunol* (2007) 179(3):1438–48. doi:10.4049/jimmunol.179.3.1438
73. Smit JJ, Rudd BD, Lukacs NW. Plasmacytoid dendritic cells inhibit pulmonary immunopathology and promote clearance of respiratory syncytial virus. *J Exp Med* (2006) 203(5):1153–9. doi:10.1084/jem.20052359
74. Lewkowich IP, Lajoie S, Clark JR, Herman NS, Sproles AA, Wills-Karp M. Allergen uptake, activation, and IL-23 production by pulmonary myeloid DCs drives airway hyperresponsiveness in asthma-susceptible mice. *PLoS One* (2008) 3(12):e3879. doi:10.1371/journal.pone.0003879
75. Kool M, Geurtsvankessel C, Muskens F, Madeira FB, van Nimwegen M, Kuipers H, et al. Facilitated antigen uptake and timed exposure to TLR ligands dictate the antigen-presenting potential of plasmacytoid DCs. *J Leukoc Biol* (2011) 90(6):1177–90. doi:10.1189/jlb.0610342
76. Oriss TB, Ostroukhova M, Seguin-Devaux C, Dixon-McCarthy B, Stolz DB, Watkins SC, et al. Dynamics of dendritic cell phenotype and interactions with CD4+ T cells in airway inflammation and tolerance. *J Immunol* (2005) 174(2):854–63. doi:10.4049/jimmunol.174.2.854
77. Lewkowich IP, Herman NS, Schleifer KW, Dance MP, Chen BL, Dienger KM, et al. CD4+CD25+ T cells protect against experimentally induced asthma and alter pulmonary dendritic cell phenotype and function. *J Exp Med* (2005) 202(11):1549–61. doi:10.1084/jem.20051506
78. Takagi H, Fukaya T, Eizumi K, Sato Y, Sato K, Shibazaki A, et al. Plasmacytoid dendritic cells are crucial for the initiation of inflammation and T cell immunity in vivo. *Immunity* (2011) 35(6):958–71. doi:10.1016/j.immuni.2011.10.014
79. Kool M, van Nimwegen M, Willart MA, Muskens F, Boon L, Smit JJ, et al. An anti-inflammatory role for plasmacytoid dendritic cells in allergic airway inflammation. *J Immunol* (2009) 183(2):1074–82. doi:10.4049/jimmunol.0900471
80. Tsuchida T, Matsuse H, Fukahori S, Kawano T, Tomari S, Fukushima C, et al. Effect of respiratory syncytial virus infection on plasmacytoid dendritic cell regulation of allergic airway inflammation. *Int Arch Allergy Immunol* (2012) 157(1):21–30. doi:10.1159/000324676
81. Lombardi V, Speak AO, Kerzerho J, Szely N, Akbari O. CD8alpha(+)beta(-) and CD8alpha(+)beta(+) plasmacytoid dendritic cells induce Foxp3(+) regulatory T cells and prevent the induction of airway hyper-reactivity. *Mucosal Immunol* (2012) 5(4):432–43. doi:10.1038/mi.2012.20
82. Mascarell L, Airouche S, Berjont N, Gary C, Gueguen C, Fourcade G, et al. The regulatory dendritic cell marker C1q is a potent inhibitor of allergic inflammation. *Mucosal Immunol* (2017) 10(3):695–704. doi:10.1038/mi.2016.87
83. Hatchwell L, Collison A, Girkin J, Parsons K, Li J, Zhang J, et al. Toll-like receptor 7 governs interferon and inflammatory responses to rhinovirus and is suppressed by IL-5-induced lung eosinophilia. *Thorax* (2015) 70(9):854–61. doi:10.1136/thoraxjnl-2014-205465
84. Demedts IK, Brusselle GG, Vermaelen KY, Pauwels RA. Identification and characterization of human pulmonary dendritic cells. *Am J Respir Cell Mol Biol* (2005) 32(3):177–84. doi:10.1165/rcmb.2004-0279OC
85. Robbins SH, Walzer T, Dembélé D, Thibault C, Defays A, Bessou G, et al. Novel insights into the relationships between dendritic cell subsets in human and mouse revealed by genome-wide expression profiling. *Genome Biol* (2008) 9(1):R17. doi:10.1186/gb-2008-9-1-r17
86. Haniffa M, Shin A, Bigley V, McGovern N, Teo P, See P, et al. Human tissues contain CD141hi cross-presenting dendritic cells with functional homology to mouse CD103+ nonlymphoid dendritic cells. *Immunity* (2012) 37(1):60–73. doi:10.1016/j.immuni.2012.04.012
87. Bachem A, Güttler S, Hartung E, Ebstein F, Schaefer M, Tannert A, et al. Superior antigen cross-presentation and XCR1 expression define human CD11c+CD141+ cells as homologues of mouse CD8+ dendritic cells. *J Exp Med* (2010) 207(6):1273–81. doi:10.1084/jem.20100348

88. Poulin LF, Salio M, Griessinger E, Anjos-Afonso F, Craciun L, Chen JL, et al. Characterization of human DNGR-1+ BDCA3+ leukocytes as putative equivalents of mouse CD8alpha+ dendritic cells. *J Exp Med* (2010) 207(6):1261–71. doi:10.1084/jem.20092618
89. Pulendran B, Banchereau J, Burkeholder S, Kraus E, Guinet E, Chalouni C, et al. Flt3-ligand and granulocyte colony-stimulating factor mobilize distinct human dendritic cell subsets in vivo. *J Immunol* (2000) 165(1):566–72. doi:10.4049/jimmunol.165.1.566
90. Cisse B, Caton ML, Lehner M, Maeda T, Scheu S, Locksley R, et al. Transcription factor E2-2 is an essential and specific regulator of plasmacytoid dendritic cell development. *Cell* (2008) 135(1):37–48. doi:10.1016/j.cell.2008.09.016
91. Poulin LF, Reyal Y, Uronen-Hansson H, Schraml BU, Sancho D, Murphy KM, et al. DNGR-1 is a specific and universal marker of mouse and human Batf3-dependent dendritic cells in lymphoid and nonlymphoid tissues. *Blood* (2012) 119(25):6052–62. doi:10.1182/blood-2012-01-406967
92. Schlitzer A, Ginhoux F. DNGR-ing the dendritic cell lineage. *EMBO Rep* (2013) 14(10):850–1. doi:10.1038/embor.2013.129
93. Watchmaker PB, Lahl K, Lee M, Baumjohann D, Morton J, Kim SJ, et al. Comparative transcriptional and functional profiling defines conserved programs of intestinal DC differentiation in humans and mice. *Nat Immunol* (2014) 15(1):98–108. doi:10.1038/ni.2768
94. Greer AM, Matthay MA, Kukreja J, Bhakta NR, Nguyen CP, Wolters PJ, et al. Accumulation of BDCA1(+) dendritic cells in interstitial fibrotic lung diseases and Th2-high asthma. *PLoS One* (2014) 9(6):e99084. doi:10.1371/journal.pone.0099084
95. Cagnoni EF, Ferreira DS, Ferraz da Silva LF, Nicoletti Carvalho Petry AL, Gomes dos Santos AB, Rodrigues Medeiros MC, et al. Bronchopulmonary lymph nodes and large airway cell trafficking in patients with fatal asthma. *J Allergy Clin Immunol* (2015) 135(5):e1–9. doi:10.1016/j.jaci.2014.08.021
96. Töröcsik D, Bárdos H, Hatalyák Z, Dezső B, Losonczy G, Paragh L, et al. Detection of factor XIII-A is a valuable tool for distinguishing dendritic cells and tissue macrophages in granuloma annulare and necrobiosis lipoidica. *J Eur Acad Dermatol Venereol* (2014) 28(8):1087–96. doi:10.1111/jdv.12290
97. Hayashi Y, Ishii Y, Hata-Suzuki M, Arai R, Chibana K, Takemasa A, et al. Comparative analysis of circulating dendritic cell subsets in patients with atopic diseases and sarcoidosis. *Respir Res* (2013) 14:29. doi:10.1186/1465-9921-14-29
98. Dua B, Watson RM, Gauvreau GM, O'Byrne PM. Myeloid and plasmacytoid dendritic cells in induced sputum after allergen inhalation in subjects with asthma. *J Allergy Clin Immunol* (2010) 126(1):133–9. doi:10.1016/j.jaci.2010.04.006
99. Dua B, Tang W, Watson R, Gauvreau G, O'Byrne PM. Myeloid dendritic cells type 2 after allergen inhalation in asthmatic subjects. *Clin Exp Allergy* (2014) 44(7):921–9. doi:10.1111/cea.12297
100. El-Gammal A, Oliveria JP, Howie K, Watson R, Mitchell P, Chen R, et al. Allergen-induced changes in bone marrow and airway dendritic cells in subjects with asthma. *Am J Respir Crit Care Med* (2016) 194(2):169–77. doi:10.1164/rccm.201508-1623OC
101. Tworek D, Smith SG, Salter BM, Baatjes AJ, Scime T, Watson R, et al. IL-25 receptor expression on airway dendritic cells after allergen challenge in subjects with asthma. *Am J Respir Crit Care Med* (2016) 193(9):957–64. doi:10.1164/rccm.201509-1751OC
102. Bleck B, Kazeros A, Bakal K, Garcia-Medina L, Adams A, Liu M, et al. Coexpression of type 2 immune targets in sputum-derived epithelial and dendritic cells from asthmatic subjects. *J Allergy Clin Immunol* (2015) 136(3):619–27.e5. doi:10.1016/j.jaci.2014.12.1950
103. Maurer D, Ebner C, Reininger B, Fiebiger E, Kraft D, Kinet JP, et al. The high affinity IgE receptor (Fc epsilon RI) mediates IgE-dependent allergen presentation. *J Immunol* (1995) 154(12):6285–90.
104. Maurer D, Fiebiger E, Reininger B, Ebner C, Petzelbauer P, Shi GP, et al. Fc epsilon receptor I on dendritic cells delivers IgE-bound multivalent antigens into a cathepsin S-dependent pathway of MHC class II presentation. *J Immunol* (1998) 161(6):2731–9.
105. Sharquie IK, Al-Ghouleh A, Fitton P, Clark MR, Armour KL, Sewell HF, et al. An investigation into IgE-facilitated allergen recognition and presentation by human dendritic cells. *BMC Immunol* (2013) 14:54. doi:10.1186/1471-2172-14-54
106. Shin JS, Greer AM. The role of FcepsilonRI expressed in dendritic cells and monocytes. *Cell Mol Life Sci* (2015) 72(12):2349–60. doi:10.1007/s00018-015-1870-x
107. Kaario H, Nieminen JK, Karvonen AM, Huttunen K, Schröder PC, Vaarala O, et al. Circulating dendritic cells, farm exposure and asthma at early age. *Scand J Immunol* (2016) 83(1):18–25. doi:10.1111/sji.12389
108. Hagendorens MM, Ebo DG, Bridts CH, De Clerck LS, Stevens WJ. Flow cytometrical determination of regulatory cytokines (IL-10, IL-12) and circulating dendritic cell cytokines in allergic asthmatic children. *Cytokine* (2004) 26(2):82–8. doi:10.1016/j.cyto.2004.01.001
109. Froidure A, Shen C, Gras D, Van Snick J, Chanez P, Pilette C. Myeloid dendritic cells are primed in allergic asthma for thymic stromal lymphopoietin-mediated induction of Th2 and Th9 responses. *Allergy* (2014) 69(8):1068–76. doi:10.1111/all.12435
110. Yu CI, Becker C, Metang P, Marches F, Wang Y, Toshiyuki H, et al. Human CD141+ dendritic cells induce CD4+ T cells to produce type 2 cytokines. *J Immunol* (2014) 193(9):4335–43. doi:10.4049/jimmunol.1401159
111. Yerkovich ST, Roponen M, Smith ME, McKenna K, Bosco A, Subrata LS, et al. Allergen-enhanced thrombomodulin (blood dendritic cell antigen 3, CD141) expression on dendritic cells is associated with a TH2-skewed immune response. *J Allergy Clin Immunol* (2009) 123(1):209–16.e4. doi:10.1016/j.jaci.2008.09.009
112. Pilette C, Jacobson MR, Ratajczak C, Detry B, Banfield G, VanSnick J, et al. Aberrant dendritic cell function conditions Th2-cell polarization in allergic rhinitis. *Allergy* (2013) 68(3):312–21. doi:10.1111/all.12090
113. Shen C, Hupin C, Froidure A, Detry B, Pilette C. Impaired ICOSL in human myeloid dendritic cells promotes Th2 responses in patients with allergic rhinitis and asthma. *Clin Exp Allergy* (2014) 44(6):831–41. doi:10.1111/cea.12308
114. Bratke K, Lommatzsch M, Julius P, Kuepper M, Kleine HD, Luttmann W, et al. Dendritic cell subsets in human bronchoalveolar lavage fluid after segmental allergen challenge. *Thorax* (2007) 62(2):168–75. doi:10.1136/thx.2006.067793
115. Spears M, McSharry C, Donnelly I, Jolly L, Brannigan M, Thomson J, et al. Peripheral blood dendritic cell subtypes are significantly elevated in subjects with asthma. *Clin Exp Allergy* (2011) 41(5):665–72. doi:10.1111/j.1365-2222.2010.03692.x
116. Wright AK, Mistry V, Richardson M, Shelley M, Thornton T, Terry S, et al. Toll-like receptor 9 dependent interferon-alpha release is impaired in severe asthma but is not associated with exacerbation frequency. *Immunobiology* (2015) 220(7):859–64. doi:10.1016/j.imbio.2015.01.005
117. Upham JW, Zhang G, Rate A, Yerkovich ST, Kusel M, Sly PD, et al. Plasmacytoid dendritic cells during infancy are inversely associated with childhood respiratory tract infections and wheezing. *J Allergy Clin Immunol* (2009) 124(4):707–13.e2. doi:10.1016/j.jaci.2009.07.009
118. Gill MA, Bajwa G, George TA, Dong CC, Dougherty II, Jiang N, et al. Counterregulation between the FcepsilonRI pathway and antiviral responses in human plasmacytoid dendritic cells. *J Immunol* (2010) 184(11):5999–6006. doi:10.4049/jimmunol.0901194
119. Villani AC, Satija R, Reynolds G, Sarkizova S, Shekhar K, Fletcher J, et al. Single-cell RNA-seq reveals new types of human blood dendritic cells, monocytes, and progenitors. *Science* (2017) 356(6335):eaah4573. doi:10.1126/science.aah4573
120. See P, Dutertre CA, Chen J, Günther P, McGovern N, Irac SE, et al. Mapping the human DC lineage through the integration of high-dimensional techniques. *Science* (2017) 356:eaag3009. doi:10.1126/science.aag3009
121. van den Heuvel MM, Vanhee DD, Postmus PE, Hoefsmit EC, Beelen RH. Functional and phenotypic differences of monocyte-derived dendritic cells from allergic and nonallergic patients. *J Allergy Clin Immunol* (1998) 101 (1 Pt 1):90–5. doi:10.1016/S0091-6749(98)70198-8
122. Hammad H, Charbonnier AS, Duez C, Jacquet A, Stewart GA, Tonnel AB, et al. Th2 polarization by Der p 1 – pulsed monocyte-derived dendritic cells is due to the allergic status of the donors. *Blood* (2001) 98(4):1135–41. doi:10.1182/blood.V98.4.1135
123. Moniuszko M, Bodzenta-Lukaszyk A, Kowal K, Lenczewska D, Dabrowska M. Enhanced frequencies of CD14++CD16+, but not CD14+CD16+, peripheral blood monocytes in severe asthmatic patients. *Clin Immunol* (2009) 130(3):338–46. doi:10.1016/j.clim.2008.09.011

124. Shrestha Palikhe N, Nahirney D, Laratta C, Gandhi VD, Vethanayagam D, Bhutani M, et al. Increased protease-activated receptor-2 (PAR-2) expression on CD14++CD16+ peripheral blood monocytes of patients with severe asthma. *PLoS One* (2015) 10(12):e0144500. doi:10.1371/journal.pone.0144500
125. Tomita K, Lim S, Hanazawa T, Usmani O, Stirling R, Chung KF, et al. Attenuated production of intracellular IL-10 and IL-12 in monocytes from patients with severe asthma. *Clin Immunol* (2002) 102(3):258–66. doi:10.1006/clim.2001.5176
126. Johansson U, Lawson C, Dabare M, Syndercombe-Court D, Newland AC, Howells GL, et al. Human peripheral blood monocytes express protease receptor-2 and respond to receptor activation by production of IL-6, IL-8, and IL-1{beta}. *J Leukoc Biol* (2005) 78(4):967–75. doi:10.1189/jlb.0704422

Conflict of Interest Statement: The authors declare that the research was conducted in the absence of any commercial or financial relationships that could be construed as a potential conflict of interest.

Copyright © 2017 Vroman, Hendriks and Kool. This is an open-access article distributed under the terms of the Creative Commons Attribution License (CC BY). The use, distribution or reproduction in other forums is permitted, provided the original author(s) or licensor are credited and that the original publication in this journal is cited, in accordance with accepted academic practice. No use, distribution or reproduction is permitted which does not comply with these terms.

frontiers in Immunology

REVIEW
published: 31 August 2017
doi: 10.3389/fimmu.2017.01058

Inflammatory Markers for Arterial Stiffness in Cardiovascular Diseases

Ioana Mozos[1,2], Clemens Malainer[3], Jarosław Horbańczuk[4], Cristina Gug[5], Dana Stoian[6], Constantin Tudor Luca[7] and Atanas G. Atanasov[4,8,9]**

[1] Department of Functional Sciences, "Victor Babes" University of Medicine and Pharmacy, Timisoara, Romania, [2] Center for Translational Research and Systems Medicine, "Victor Babes" University of Medicine and Pharmacy, Timisoara, Romania, [3] Independent Researcher, Vienna, Austria, [4] The Institute of Genetics and Animal Breeding, Polish Academy of Sciences, Jastrzębiec, Poland, [5] Department of Microscopic Morphology, "Victor Babes" University of Medicine and Pharmacy, Timisoara, Romania, [6] 2nd Department of Internal Medicine, "Victor Babes" University of Medicine and Pharmacy, Timisoara, Romania, [7] Department of Cardiology, "Victor Babes" University of Medicine and Pharmacy, Timisoara, Romania, [8] Department of Pharmacognosy, Faculty of Life Sciences, University of Vienna, Vienna, Austria, [9] Department of Vascular Biology and Thrombosis Research, Center for Physiology and Pharmacology, Medical University of Vienna, Vienna, Austria

OPEN ACCESS

Edited by:
Jixin Zhong,
Case Western Reserve University, United States

Reviewed by:
Xuhui Feng,
Indiana University System, United States
Ding Xinchun,
Indiana University, Purdue University Indianapolis, United States
Xiaojing Yue,
La Jolla Institute for Allergy and Immunology, United States

***Correspondence:**
Ioana Mozos
ioana_mozos@yahoo.com;
Atanas G. Atanasov
a.atanasov.mailbox@gmail.com

Specialty section:
This article was submitted to Inflammation, a section of the journal Frontiers in Immunology

Received: 20 June 2017
Accepted: 15 August 2017
Published: 31 August 2017

Citation:
Mozos I, Malainer C, Horbańczuk J, Gug C, Stoian D, Luca CT and Atanasov AG (2017) Inflammatory Markers for Arterial Stiffness in Cardiovascular Diseases. Front. Immunol. 8:1058. doi: 10.3389/fimmu.2017.01058

Arterial stiffness predicts an increased risk of cardiovascular events. Inflammation plays a major role in large arteries stiffening, related to atherosclerosis, arteriosclerosis, endothelial dysfunction, smooth muscle cell migration, vascular calcification, increased activity of metalloproteinases, extracellular matrix degradation, oxidative stress, elastolysis, and degradation of collagen. The present paper reviews main mechanisms explaining the crosstalk between inflammation and arterial stiffness and the most common inflammatory markers associated with increased arterial stiffness, considering the most recent clinical and experimental studies. Diverse studies revealed significant correlations between the severity of arterial stiffness and inflammatory markers, such as white blood cell count, neutrophil/lymphocyte ratio, adhesion molecules, fibrinogen, C-reactive protein, cytokines, microRNAs, and cyclooxygenase-2, in patients with a broad variety of diseases, such as metabolic syndrome, diabetes, coronary heart disease, peripheral arterial disease, malignant and rheumatic disorders, polycystic kidney disease, renal transplant, familial Mediterranean fever, and oral infections, and in women with preeclampsia or after menopause. There is strong evidence that inflammation plays an important and, at least, partly reversible role in the development of arterial stiffness, and inflammatory markers may be useful additional tools in the assessment of the cardiovascular risk in clinical practice. Combined assessment of arterial stiffness and inflammatory markers may improve non-invasive assessment of cardiovascular risk, enabling selection of high-risk patients for prophylactic treatment or more regular medical examination. Development of future destiffening therapies may target pro-inflammatory mechanisms.

Keywords: inflammatory markers, arterial stiffness, inflammation, cardiovascular diseases, cardiovascular risk factors

INTRODUCTION

The elasticity and distensibility of arteries maintain a relatively constant blood pressure, despite the pulsating nature of the blood flow by every heartbeat. Arteries expand by receiving blood ejected from the heart during systole and expel it to the periphery during diastole to supply the peripheral circulation with a steady flow of blood during both cardiac cycles (1). However, as a

hallmark of normal aging and apart from that also in association with many diseases compliance and distensibility of arteries decrease and the term "arterial stiffness" is used to qualitatively indicate these decreased elastic vessel wall properties (2). An increased arterial stiffness leads to a decreased buffer capacity of the arteries and an increase in pulse pressure (PP) and pulse wave velocity (PWV), causing an early return of the reflected waves and thereby an augmentation of late systolic pressure (3). As a consequence, the left ventricle has to generate an extra workload to overcome the augmented pressure, which is associated with an increased demand of oxygen and in the long-term development of left ventricular hypertrophy and heart failure (4). Insufficient arterial compliance furthermore transmits the increased pulsatile pressure deeper into the periphery and damages microvasculature of distal-end organ systems, especially in the kidney and the brain (5).

Arterial stiffness is considered a growing epidemic, associated with an increased risk of cardiovascular events (6–8). It is an early sign of structural and functional changes of the vessel wall and an independent predictor of cardiovascular disorders, that arise as a consequence of arteriosclerosis and atherosclerosis (9, 10). Several other chronic disorders may also contribute to an increase in arterial stiffness. The most important vascular changes related to increased arterial stiffness are vascular fibrosis due to collagen deposition, fragmentation of elastic fibers (elastolysis), crosslinking of collagen and elastin fibers by advanced glycation end products, and extensive vessel wall calcification (11–14). PWV and augmentation indices are commonly used measures of arterial stiffness and wave reflection.

Local inflammation is a complex non-specific protective response of vascular tissue to injury in order to eliminate its cause. Atherosclerosis is considered an inflammatory disease, because low-grade inflammation contributes to all phases of atherosclerosis development, starting with the initial phase of endothelial dysfunction, up to the formation of the mature atherosclerotic plaque, disruption of atherosclerotic injuries, precipitation of plaque rupture, and the acute thrombotic complications of atheroma (11, 15–19). Increased levels of inflammatory markers, e.g., erythrocyte sedimentation rate (ESR), C-reactive protein (CRP), and interleukin-6 (IL-6) have been associated with cardiovascular mortality and morbidity (19). As induction of experimental inflammation increases arterial stiffness, a cause–effect relationship between the two can be established, and anti-inflammatory therapy may, at least in part, reduce arterial stiffness (20, 21).

Both markers of inflammation and arterial stiffness are predictors of cardiovascular events (19). Understanding the mechanisms linking inflammation and arterial stiffness enables to apply a suitable anti-inflammatory therapy in order to reduce cardiovascular risk in several conditions.

Also, systemic inflammation has been shown to increase the risk of cardiovascular disease by accelerating atherosclerosis, destabilizing plaques, impairing endothelial function, or causing premature arterial stiffness (21–23). Considering that arterial stiffness is often the result of integrating the damage of cardiovascular risk factors on the arterial wall over a long period of time, prophylactic cardiovascular measures may open a window of opportunity to prevent the occurrence of cardiovascular disease even before first symptoms become immanent, which is an important aspect of health care in the ever-aging Western societies (10).

It is the aim of the present paper to highlight the role of inflammation on large vessels in view of arterial stiffness, review the main mechanisms explaining the crosstalk between inflammation and arterial stiffness and the most common inflammatory markers associated with an increased arterial stiffness, considering the most recent clinical and experimental studies published in biomedical research. Understanding the role of inflammation in the pathophysiology of arterial stiffness is crucial in order to enable development of new therapies by modulation of inflammatory pathways, which have been identified as major targets for the treatment of arterial stiffness.

MECHANISMS UNDERLYING THE LINK BETWEEN INFLAMMATION AND ARTERIAL STIFFNESS

Cardiovascular risk factors induce a state of inflammation able to impair vascular function (15). Activation of vascular smooth muscle cells (VSMCs) due to cardiovascular risk factors increases synthesis of the extracellular matrix and enables their migration from the vascular media to the intima (24).

Atherosclerosis is a syndrome caused due to chronic inflammatory interactions of white blood cells (WBCs) in the wall of arteries, and therefore, plasma inflammatory markers are considered potential tools for cardiovascular risk prediction (15, 25, 26). The mechanisms underlying the association between inflammation and atherosclerosis are generally complex and multifaceted (17). An increase in circulating inflammatory mediators enables WBC infiltration into arteries (27). Macrophage activation is associated with the release of inflammatory cytokines and reactive oxygen species to amplify the inflammatory reaction, and after transformation into foam cells, they undergo necrosis, further release inflammatory stimuli, and are thereby creating the necrotic core of advanced lesions (28). The onset of the inflammatory cascade, in acute and chronic inflammatory diseases and systemic subclinical low-grade inflammation, *impairs endothelial function* and the mechanical properties of the arteries (17). Endothelial cells (ECs), through reduction of bioavailability of nitric oxide (NO) and an increase of endothelin-1 due to inflammation, contribute to arterial stiffening and progressing arterial stiffing, in turn, further impairs endothelial function, thus inducing a vicious cycle (1, 3, 29). Decreased NO also promotes leukocyte adhesion (15). Additionally, endothelial dysfunction is also associated with activation of ECs which become pro-inflammatory, increasing expression of adhesion molecules, produce monocyte chemoattractant protein-1 (MCP-1) and leukocyte transmigration and activation, involving cytokines (13, 15).

Antigen-presenting cells such as dendritic cells and effector T lymphocytes play an important role in the synthesis of proatherogenic cytokines, such as IL-2, IL-18, and interferon gamma, and are therefore also important in atherosclerotic plaque progression (30). A special role among proatherogenic

cytokines has been attributed to IL-12 as its absence was shown to inhibit early, but not late, lesion development (30). In conclusion, activated endothelium contributes to the initiation and the perpetuation of vascular wall inflammation (17).

Furthermore, monocytes are attracted and recruited to the vessel wall, where they differentiate into macrophages and ingest oxidized LDL (oxLDL) *via* scavenger receptors or lectin-like oxidized low-density lipoprotein receptor 1 (LOX-1). In this context, it has been shown that overexpression of SIRT1 is able to decrease LOX-1 expression and prevent foam cell formation in a mouse model of atherogenesis regardless of serum lipid levels. The underlying mechanism for this effect was shown to rely on suppression of NFκB-signaling by deacetylating RelA/p65, thereby reducing LOX-1 expression and diminishing uptake of oxLDL and foam cell formation and consequently also arterial stiffness (31). Therefore, pharmacological activation of SIRT1 may also offer an attractive approach in the treatment of arterial stiffness. Exposure to several pro-inflammatory and proatherogenic stimuli has been shown *in vivo* to upregulate LOX-1 expression, which is the main oxLDL receptor (32), and also in humans, LOX-1 gene polymorphisms are associated with increased susceptibility to cardiovascular disease (33).

Vascular inflammation increases arterial stiffness also by *enabling vascular fibrosis and smooth muscle cell proliferation* (19). The cellular components of the arterial wall, the VSMCs, and ECs are involved in maintaining homeostatic balance of the arterial blood pressure (3). In addition, VSMC can also undergo transdifferentiation into an osteoblastic phenotype under inflammatory conditions enabling mineralization (phosphate uptake), and *calcium deposition* in the arterial media (3, 27). Inflammatory cells produce mediators such as cytokines and metalloproteinases that regulate cardiovascular remodeling (34). Activation of matrix metalloproteinases (MMPs), mediated by increased inflammatory markers, enable *degradation of elastin and collagen* of the vessel wall (18). Inflammation enables also *plaque rupture* and is thus further contributing to the occurrence of acute coronary syndromes (15).

Arteriosclerosis is the age-associated stiffening and dilation of arteries, accompanied by low-grade inflammation (35). Interestingly, in humans early signs of arterial aging (so called "fatty streaks") are already observable in children in their first decade, but it usually takes several decades for progression into a symptomatic disease (36). Arterial aging has been identified as a key mechanism enabling development and progression of cardiovascular and other chronic disorders and is heavily influenced by lifestyle factors (37). The chronic pro-inflammatory profile within aging arteries is characterized by impaired angiotensin II (AII), mineralocorticoid receptor, and endothelin-1 signaling with the result of increased activity and/or expression of downstream pro-inflammatory transcription factors, whereas levels/activity of protective factors become reduced (38). Also, the process of cellular senescence is suggested to be an important contributor to immunosenescence and "*inflamm-aging*" since senescent cells acquire a secretory phenotype, characterized by enhanced secretion of inflammatory modulators, such as monocyte chemoattractant protein-1 (MCP-1, which attracts invasion of smooth muscle cells), and cytokines, such as IL-1, IL-6, and IL-17 (39). Pro-inflammatory cytokines enable platelet and endothelial activation, which is related to an increased risk of cardiovascular events (35). Vascular aging is also associated with an increased vascular smooth muscle tone, an increased activity of the renin-angiotensin-aldosterone system, and an increase of oxidative stress, all of which contributes to arterial proinflammation and age-related arterial remodeling (13, 38). Further contributors to vascular aging are elevated levels of MMPs, calpain-1 (facilitating calcification), transforming growth factor beta-1 (increasing the production of extracellular matrix), amyloid deposition as medin, accumulation of fibronectin and cell adhesion proteins, increase of pro-inflammatory transcription factors as well as increased synthesis of advanced glycation end products, and decreased arterial expression and activity of sirtuins (13, 38). The loss of balance between oxidative and antioxidative systems results in increased production of reactive oxygen species leading to inactivation of NO and increased nitrosative stress which contributes to age-associated *endothelial dysfunction* (13, 40). The *increased degradation of elastin fibers* is mediated by activation of MMPs and serine proteinases, accompanied by a decreased activity of its endogenous inhibitor TIMP-2 (tissue inhibitor of metalloproteinases 2) (18). MMP is involved in the occurrence of *uncoiled, stiffer collagen* due to its collagenolytic activity and degradation of the basement membranes (6, 18). The increased MMPs activity is mediated by increased activity of cell adhesion molecules and cytokines (41, 42). Increased VSMC migration, proliferation and senescence, extracellular matrix deposition, matrix calcification, amyloidization and glycation, and elastin fracture disrupt the endothelium and thus, foster vascular aging (38).

Systemic subclinical low-grade inflammation is closely related to most cardiovascular risk factors, especially to hypertension and diabetes, to all stages of atherosclerosis, to arteriosclerosis and to impaired arterial elastic properties (17, 43, 44). Reduction in inflammation can decrease arterial stiffness, which was demonstrated among others in patients with rheumatoid arthritis (RA) undergoing therapy with anti-tumor necrosis factor-α (TNF-α) agents (21). Also, statins and other cholesterol-reducing agents are reported in numerous studies to have beneficial effects on wave reflection and aortic stiffness reduction in several patient groups (45, 46).

Pulse wave velocity inversely correlates with arterial distensibility, and an impaired arterial distensibility alters blood pressure, flow dynamics, increases afterload, and impairs coronary perfusion (27). Concluding, inflammation plays a major role in large artery stiffening, in the context of cardiovascular risk factors, atherosclerosis, arteriosclerosis, endothelial dysfunction, smooth muscle cell migration, vascular calcification, increased activity of metalloproteinases, extracellular matrix degradation, oxidative stress, elastolysis, degradation of collagen, and occurrence of uncoiled, stiffer collagen. Overview of relevant inflammatory markers associated with arterial stiffness and their crosstalk with other related conditions is presented in **Figure 1**.

WBCs AND ARTERIAL STIFFNESS

An increased WBC has been associated with arterial stiffness and other atherosclerotic events in multiple studies (47). Chronic

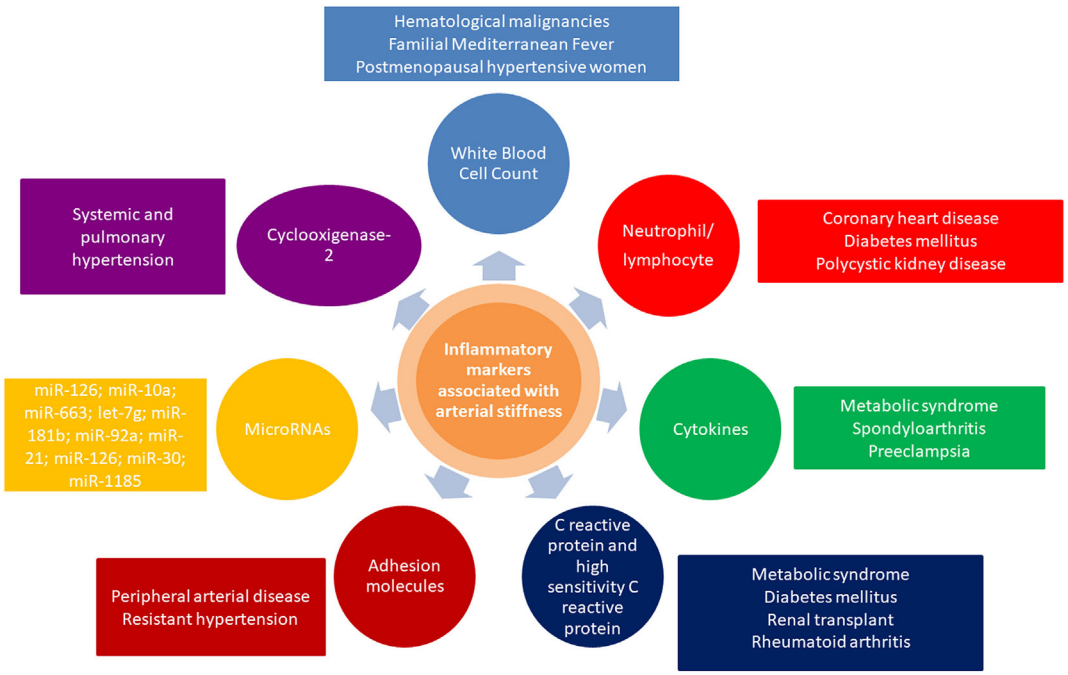

FIGURE 1 | Overview of inflammatory markers associated with arterial stiffness and their crosstalk with other related conditions.

low-grade inflammation in the arterial wall may play an important role in the initiation and progression of cardiovascular diseases, considering that stimulated WBCs adhere to the vascular endothelium and easily penetrate the intima, causing capillary leukostasis and increase in vascular resistance (19). Additionally, stimulated WBCs release some hydrolytic enzymes, cytokines, and growth factors, which have the potential to induce further vascular damage (19). Total leukocyte count enables a low cost, widely available assessment of inflammatory status (19). However, there has been a recent shift away from total WBC count toward differential white cell count as particular WBC types (e.g., neutrophils, lymphocytes, or monocytes) have been suggested to be stronger predictors of cardiovascular risk (48). This is among others because total WBC is influenced by ethnic origin and gender, which is complicating the definition of reference ranges for whole populations (49). An elevated neutrophil count, which is another marker of systemic inflammation, has been suggested as a prognostic marker of cardiovascular disease particularly in hypertensive postmenopausal women (50).

The distribution of WBC subtypes is regulated by the autonomic nervous system since lymphocytes have cholinergic receptors and granulocytes have adrenergic receptors (44, 51). Consequently, the number and function of granulocytes are stimulated by sympathetic nerves, whereby parasympathetic nerves stimulate those of lymphocytes (51). Sympathetic overactivation may be associated with endothelial dysfunction (44).

Mozos et al. found correlations and associations between arterial stiffness and neutrophil monocyte, lymphocyte, and WBC count, respectively, in patients with *hematologic malignancies* and *solid tumors* (52, 53). Increased WBC may be a consequence of the hematologic malignancy, and also a marker of systemic inflammation (47). In chronic granulocytic leukemia, significant associations were found between WBC and arterial stiffness, which are probably related to the increased blood viscosity caused by the high concentration of WBCs (54). Elevated blood viscosity increases vascular shear stress, enabling rapid growth of the atherosclerotic plaque and increasing its instability (55).

Gomez-Sanchez et al. report a positive correlation between central augmentation index (CAIx) and monocyte count only in women, and between neutrophil count and intima-media thickness (IMT) in men, in a study including 500 subjects with *intermediate risk* (56). Gender differences may be explained by higher IMT in men and higher CAIx in women, the influence of sex steroids on vascular function and the influence of anthropometric factors (e.g., differences in the distribution of body fat, average height, as well as aortic length) (56).

In patients with *familial Mediterranean fever* (FMF), which is an autosomal recessive disorder restricted to certain ethnic groups, characterized by recurrent inflammatory febrile attacks of the serosal and synovial membranes; the ongoing and recurring inflammatory state is associated with an increased cardiovascular risk and an elevated arterial stiffness (57, 58). The inflammatory process in FMF results from malfunction of the MEFV gene located on 16p and is associated with uncontrolled inflammatory reactions due to the absence of an inhibitor of C5a and excessive release of tumor necrosis factor and interleukin-1 (57, 59). The MEFV gene encodes mutated protein pyrin, essential in the innate immune system and inflammasome (59). Arterial stiffness (assessed *via* PWV) was correlated with the severity of inflammation and several inflammatory markers, including WBC, CRP,

ESR, fibrinogen, and neutrophil/lymphocyte ratio (NLR), and not to the genetic mutation (58). This is in contrast to earlier research where correlations of PWV with leukocyte count but not with CRP in patients with FMF were found (57). This discrepancy might possibly be explainable by a different dosage regime of colchicine of study participants, since colchicine is reported to alter levels of CRP in patients using the drug (60) or confounders that are not known yet or such that were not considered. Sustained inflammation functionally impairs microcirculation, which poses a reason for the increased cardiovascular risk in patients with FMF (58). The increase in the arterial stiffness during attacks might be related to the released cytokines, and subsequent inflammation-induced vasoconstriction (58). Further studies are needed to assess the relationship between arterial stiffness and interleukin-1 and TNF-α in patients with Mediterranean fever.

In conclusion, several studies report a link between arterial stiffness and WBC or leukocyte subtypes, respectively, in particular in patients with hematologic malignancies or FMF, and in postmenopausal women with hypertension (**Table 1**) (50, 52, 57, 58). It is also important to consider that arterial stiffness modulates the functional responses of WBC, as experimental studies have demonstrated that the mechanical properties of the substrate may influence migration of neutrophils: they migrate more slowly due to significantly larger traction stresses on the stiffer substrates, but more persistently, enabling movement on greater distances over time despite slower speeds (61).

Neutrophil/lymphocyte ratio, the ratio between neutrophil and lymphocyte count, is available in routine complete blood count analyses and may be used as a cost-effective biomarker of inflammation, atherosclerotic progression and systemic predictor of cardiovascular complications, especially in context of myocardial infarction and coronary heart disease (19, 62). Chronic low-grade inflammation or subclinical inflammation as indicated by the NLR plays a role in diabetes, obesity, dyslipidemia, hypertension, metabolic syndrome, and endothelial dysfunction (62–64). A higher NLR despite normal WBC shows a higher risk of atherosclerotic disease (65). NLR is a more powerful predictor of cardiovascular disease than any other leukocyte subtype (66). This might be explainable due to the fact that it is less likely to be altered by various physiological conditions (e.g., dehydration or recent exercise) and also, more importantly, that NLR is the ratio of two different, but complementary immune pathways (48).

Inflammation plays an important role in diabetes-induced cardiovascular events related to atherosclerotic injuries. NLR was correlated with aortic stiffness in patients with type 1 diabetes in a study including 76 subjects with type 1 diabetes (19) and in patients with type 2 diabetes mellitus (**Table 2**) (67).

Coronary heart disease was associated with elevations in inflammatory markers and changes in leukocyte subset distribution (68, 69). Neutrophil count and NLR are promising markers of the presence and severity of coronary heart disease (70, 71). Endothelial dysfunction in coronary arteries may result from the neutrophil–endothelium interaction, and the increased neutrophil count may accelerate endothelial abnormalities (69, 72). A higher NLR was independently associated with arterial stiffness and coronary calcium score in a large study including 849 Korean adults, revealing that higher NLR may be a useful additional measure for assessing cardiovascular risks (73). Yaman et al. evaluated 103 patients, without a previous history of coronary artery disease (CAD), who presented with STEMI without hemodynamic compromise and underwent successful primary percutaneous coronary intervention. The authors report improvement of arterial stiffness associated with a decrease in NLR (69).

TABLE 1 | White blood cell (WBC) count and arterial stiffness.

Study population	Findings	Reference
69 consecutive familial Mediterranean fever (FMF) patients and 35 controls	Pulse wave velocity (PWV) was correlated to serum C-reactive protein (CRP), WBC, erythrocyte sedimentation rate, fibrinogen, and neutrophil/lymphocyte ratio	Cakar et al. (58)
29 patients with hematologic malignancies (8 with multiple myeloma, 2 with Hodgkin's lymphoma, 11 with non-Hodgkin's lymphoma, 6 with myelodysplastic syndrome, and 2 with chronic myeloid leukemia)	An inverse correlation was found between PWV and neutrophil count (r = -0.45). Multiple regression analysis found significant associations between augmentation index (AI) and PWV, and WBC and platelet count, respectively	Mozos and Mihaescu (52)
20 patients with solid tumors (colon, lung, renal, laryngeal, pancreas, mammary and testicular cancer, and malignant melanoma) and 26 healthy controls	Significant higher values were obtained for PWV, AI and central hemodynamic variables in cancer patients compared to healthy controls. The best correlation was found between AI and neutrophil count and WBC, respectively. PWV as a measure of arterial stiffness was significantly associated with neutrophilia, monocytosis, and lymphopenia. AI was significantly associated with neutrophilia	Mozos and Mihaescu (53)
500 subjects included in the MARK study, aged 35–74 years	Monocyte count was positively correlated with central augmentation index (CAIx) in women, also after adjusting for age and other confounders	Gomez-Sanchez et al. (56)
886 postmenopausal women with hypertension	A direct relationship between neutrophil count and 24-h ambulatory pulse pressure (PP) was observed. Increased arterial stiffness, as reflected in high values of 24-h ambulatory PP, is an adverse prognostic marker in postmenopausal women with hypertension and can be used as an additional correlate for systemic inflammation	Angeli et al. (50)
23 colchicine-treated patients with FMF and 23 age- and sex-matched controls	PWV was slightly higher in colchicine-treated FMF patients than in control subjects (P = 0.05) and significantly correlated with age and leukocyte count, but no correlations between PWV and CRP levels or blood pressure could be observed PWV was furthermore found to be generally influenced by age and body mass index	Yildiz et al. (57)

TABLE 2 | Neutrophil/lymphocyte ratio (NLR) and arterial stiffness.

Study population	Findings	Reference
103 patients with STEMI who underwent successful primary percutaneous coronary intervention	Aortic velocity propagation (AVP) values improved after successful treatment in STEMI patients. The increment in AVP values was closely correlated with a decrement in NLR	Yaman et al. (69)
145 consecutive patients admitted with stable angina pectoris or acute coronary syndrome (ACS)	Augmentation index and pulse wave velocity (PWV) were positively associated with NLR. NLR might be used to risk-stratify patients, considering arterial stiffness in patients with coronary heart disease, especially in the presence of ACS	Tanindi et al. (44)
76 persons with type 1 diabetes and 36 healthy controls	The observed significant negative correlation between the NLR and markers of aortic stiffness in patients with type 1 diabetes suggests a strong association between inflammation and arterial stiffness	Ayhan et al. (19)
402 participants:133 control subjects, 138 diabetic subjects without diabetic retinopathy (DR) and 131 patients with DR	NLR and PWV were elevated both in type 2 diabetic and in DR. NLR could be independently associated with PWV	Wang et al. (67)
512 postmenopausal women with a similar socioeconomic background (204 patients with osteoporosis, 208 controls)	NLR and PWV were elevated in osteoporosis. Statistical analysis of collected data revealed a significant correlation between NLR and PWV after adjusting for confounders in osteoporosis patients, but not in the control group	Yu et al. (66)
52 autosomal dominant polycystic kidney disease patients and 25 controls	Pentraxin 3 and C-reactive protein were not correlated with arterial elasticity, while NLR was significantly negatively correlated with large artery elasticity index	Gul et al. (75)
849 Korean adults in a health examination program	A higher NLR was independently associated with arterial stiffness and coronary calcium score	Park et al. (73)

In a recent study, NLR has also been correlated with coronary artery calcium score, which is an independent risk factor for coronary artery stenosis, in asymptomatic Korean males further underlining the high predictive value of NLR in the context of arterial stiffening (62). The beta-blocker nebivolol, which is known to possess anti-inflammatory effects mediated through increased NO-release in ECs, significantly lowered NLR in hypertensive patients (74). NLR has also been associated with arterial stiffness and high coronary calcium score in several previous studies (48). Early detection of abnormal NLR levels may be helpful for detecting increased arterial stiffness in patients with coronary heart disease, type 1 and 2 diabetes mellitus, osteoporosis, and polycystic kidney disease (**Table 2**) (19, 44, 66, 67, 69, 75).

CYTOKINES AND ARTERIAL STIFFNESS

Interleukins (ILs) are a group of cytokines produced by cells of the immune system and have a pro-inflammatory effect. They trigger the acute phase reaction by continued recruitment and activation of leukocytes, and stimulate proliferation of fibroblasts (28). An increased sympathetic tone is associated with higher oxygen consumption and enhanced production of pro-inflammatory cytokines (19, 76). IL-6, IL-1, and TNF-α impair the subendothelial release of NO and increase endothelin-1 release by ECs in a dose-dependent fashion and are thus contributing to the regulation of the vascular tone (19, 77). Endothelin-1 is both a potent vasoconstrictor and mitogen for smooth muscle cells and fibroblasts and IL-6 and IL-1 were found to be the most potent and least effective stimulators of endothelin-1-release, respectively (77). Conflicting results have been obtained on the relationship IL-6-endothelial function by Cotie et al., who found that circulating IL-6 does not mediate endothelial dysfunction, considering that no relationship was observed between IL-6 levels and flow-mediated dilatation (FMD). The authors hypothesized that until there is an overt systemic inflammatory signal, such as in a disease state, no relationship exists (78). Traditional cardiovascular risk factors impair FMD, and Vita et al. found no evidence that inflammation has additional effects beyond those attributable to traditional risk factors (15). Furthermore, cytokines stimulate VSMC and interstitial cell proliferation, contributing to the development of proliferative vascular disorders (77).

Women with a history of preeclamptic pregnancies have an increased risk of cardiovascular disease, but in a recent study no relationship was found between soluble tumor necrosis factor receptor type 1 and other systemic and vascular inflammatory markers increased during *preeclamptic pregnancies* and systemic arterial properties 6 months post-partum, although those markers were increased also at term. Even at term, no general correlation between the increase of systemic and vascular inflammatory markers and systemic arterial properties could be established (79). *Metabolic syndrome*, comprising abdominal obesity, insulin resistance, dyslipidemia, and hypertension, is accompanied by abnormal regulation of cytokines and chemokines, which further underlines the importance of inflammation in the mentioned syndrome (80, 81). Higher plasma levels of IL-6 could be linked to the development of arterial stiffness and microvascular dysfunction (82).

Systemic inflammatory diseases are associated with an increased cardiovascular morbidity and mortality due to endothelial dysfunction and accelerated atherosclerosis (27). Arterial stiffness increases in accelerated atherosclerosis due to inflammation (27). An inflammatory-metabolic background is linked with increased arterial stiffness in patients with seronegative *spondyloarthritis* (SpA), as a positive correlation between PWV, augmentation indices, and ILs are reported in a single study with 108 subjects (53 patients and 55 controls) (83).

IL-18 has been previously associated with the formation, growth, progression, and vulnerability of the atherosclerotic plaque and was identified as an independent predictor of

coronary events (84). Although elevated IL-12 and IL-18 levels were not associated with arterial stiffness in patients with *chronic kidney disease* (85), IL-18 was significantly associated with arterial stiffness in patients with metabolic syndrome (86). It is hypothesized that inflammation and arterial stiffness act together in the pathogenesis and complications of metabolic syndrome and type 2 diabetes (86). The lack of association between IL-12 and IL-18 in several studies might be explained by the different effects of inflammation on large and small vessels (85).

Associations between inflammatory gene polymorphism and cardio-ankle vascular index were found only for the cluster of differentiation 14 (CD14) polymorphism among men aged 34–49 years in a study examining polymorphisms in several inflammatory genes (87). CD14 acts as a trigger in the production of cytokines (87). Targeted deletion of genes related to costimulatory factors and pro-inflammatory cytokines results in less atherosclerosis in mouse models, while interference with regulatory immunity accelerates it (30). Among other observed effects that might be beneficial in treatment and prevention of arterial stiffness, vitamin K was also shown in rat studies to suppress inflammation by decreasing expression of genes for cytokines that are associated with arterial stiffness (8, 88).

In summary, ILs and other cytokines have been associated with arterial stiffness in several disorders, such as metabolic syndrome, SpA, and preeclampsia (**Table 3**) (79, 82, 83).

CRP, HIGH-SENSITIVITY C-REACTIVE PROTEIN (hsCRP), AND ARTERIAL STIFFNESS

C-reactive protein is an acute phase reactant that predicts cardiovascular events in healthy subjects and in patients with preexisting cardiovascular disorders (89, 90). CRP is used as a marker of chronic low-grade inflammation as it is considered as a mediator of atherothrombotic disease (43, 91, 92) and is the only circulating biomarker related to vascular wall biology (10). CRP was correlated with FMD in some studies (93, 94), but no correlation was found for CRP with coronary endothelial dysfunction in patients with familial hypercholesterolemia (95, 96).

The level of CRP has been associated with indices of arterial function in several populations (7, 17, 21, 80, 97–100). However, data regarding a possible direct etiological role of CRP in arterial dysfunction and atherosclerosis are contradictory, and there are also studies reporting no significant relationship between PWV and hsCRP (17, 101). Tomiyama et al. reported that the association between CRP and arterial stiffness was not retained after adjusting for other cardiovascular risk factors (101).

A significant correlation was reported between aortic flow propagation velocity (AVP), which is a parameter of reduced arterial stiffness, assessed by transthoracic echocardiography, and high CRP levels, which is indicating a link between aortic stiffness and inflammation (7). Several other cross-sectional studies demonstrated the link between metabolic syndrome, arterial stiffness, and inflammation (97). Increased CRP levels were associated with elevated PWV in patients *after renal transplant*, and overall CRP was suggested to be a useful marker to anticipate graft survival and cardiovascular morbidity in renal transplant recipients (102).

Rheumatoid arthritis is a chronic, systemic, inflammatory disease, associated with an increased cardiovascular mortality (21). PWV correlated independently with log-transformed CRP in patients with RA, and immunomodulatory therapy with anti-TNF-α therapy reduced aortic stiffness to levels comparable to those of the healthy control group. This suggests that aortic stiffness may be reversible (21). PWV correlated with current CRP, but not with disease duration, historical inflammation or extent of radiological changes (21). Traditional assays for CRP did not have adequate sensitivity to long term predict vascular disorders, and hsCRP could represent a better predictor. hsCRP was associated with arterial stiffness in several studies (10, 18, 103, 104), but other researchers could not find an association, independent of conventional risk factors (101). Most studies used single measurements of hsCRP instead of a mean of multiple measurements, but a single assessment seems to be adequate if values of less than 10 mg/l are observed (43, 91, 92). hsCRP levels were correlated with traditional cardiovascular risk factors, such as hypertension, dyslipidemia, overweight, and obesity, but also with other inflammatory markers, including WBC, IL-6, and fibrinogen level (10).

TABLE 3 | Cytokines and arterial stiffness.

Study population	Findings	Reference
34 women with preeclampsia and 61 women with normal pregnancies	Despite increased circulating levels of systemic and vascular inflammatory markers, such as soluble tumor necrosis factor receptor type 1, monocyte chemoattractant peptide 1 pentraxin 3, and soluble vascular adhesion molecule-1 in preeclamptic pregnancies, they are not associated with proximal aortic stiffness and effective arterial elastance	Estensen et al. (79)
53 patients with spondyloarthritis (SpA) and 55 control subjects	Higher mean pulse wave velocity (PWV) and augmentation indices were obtained in patients with seronegative SpA compared to controls. Mean plasma levels of interleukin-6 (IL-6), IL-1β, and TNFα were higher in subjects with elevated PWV. Multivariate analysis revealed a significant association elevated PWV and plasma levels of IL-6, IL-1β, and tumor necrosis factor-α	Tuttolomondo et al. (83)
69 healthy volunteers, 70 chronic kidney disease (CKD) patients stage 3–4, 85 CKD stage 5	IL-12 and IL-18 were found to be elevated during the earlier stages of CKD but could NOT be associated with arterial stiffness	Yong et al. (85)
563 men, aged 64–76 years	Pulse wave propagation time of the brachial artery was independently associated with IL-18	Troseid et al. (86)

Vascular hsCRP production is stimulated by cytokines (IL-6 and IL-1) and has modulatory functions by inhibiting endothelial NO synthase and inducing the expression of adhesion molecules in ECs. hsCRP has also a major role in increasing cytokines expression and generation of reactive oxygen species by monocytes and neutrophils, promoting vasoconstriction, VSMC migration and proliferation, activation of platelets, and vascular stiffness (18, 43, 104). Increased hsCRP may be also a consequence of arterial stiffness because increased arterial stiffness is associated with higher flow reversals during diastole, which can increase the expression of adhesion molecules (43).

C-reactive protein and hsCRP were associated with arterial stiffness in patients with metabolic syndrome, renal transplant, diabetes mellitus, and RA (**Table 4**) (7, 21, 102, 104). Many interventions able to reduce cardiovascular risk have been associated with lower hsCRP values, such as weight loss, diet, exercise, smoking cessation, use of lipid-lowering drugs (statins, niacin, fibrates, gemfibrozil), aspirin, and thiazolidinediones (92).

CELL ADHESION MOLECULES AND ARTERIAL STIFFNESS

Soluble cell adhesion molecules include intercellular adhesion molecule-1 (ICAM-1), vascular cell adhesion molecule-1 (VCAM-1), the platelet (P-selectin), and endothelial selectin (E-selectin) (34). Adhesion molecules are glycoproteins involved in tissue integrity, mediation of cellular communication and interactions, and extracellular matrix contact (34). They are increased in endothelial dysfunction, vascular remodeling, and obesity. They are furthermore considered as biomarkers and mediators of cardiovascular disorders in several cardiovascular disorders, including hypertension, stroke, and coronary heart disease (34, 105, 106). They accelerate atherosclerosis by enabling attachment of circulating leukocytes to ECs (105). E-selectin and P-selectin mediate transient rolling of leukocytes along the endothelium and ICAM-1 and VCAM-1 mediate stronger attachment of leukocytes to the endothelium (106). Adhesion molecules can not only be detected on the endothelial surface but also as soluble adhesion molecules in the circulation, where they are reported as useful biomarkers to predict future fatal cardiovascular events in patients with angiographically documented CAD (107).

Selectins are C-type lectins, including L-selectin expressed on leukocytes, E-selectin expressed by cytokine-activated ECs and P-selectin which is expressed by platelets and ECs (108). E-selectin is produced exclusively by ECs and is therefore considered a superior marker of endothelial dysfunction compared to the other cell adhesion molecules, while ICAM-1 and VCAM-1 are expressed on both ECs and leukocytes (106). ICAM-1 is also expressed in hematopoietic cells and fibroblasts and was suggested to be used as a marker of low-grade inflammation (109). VCAM-1 may be a marker of plaque activity (109), but elevated VCAM-1 levels could have a protective effect from cardiovascular events in the general population (106). While Kilic et al. found no correlation between VCAM-1 and ICAM-1 and arterial stiffness, de Faria et al. reported higher VCAM-1 values in patients with increased arterial stiffness (34, 109). Further studies assessing VCAM-1 and arterial stiffness could clarify the relationship between VCAM-1 and arterial stiffness.

Kals et al. enrolled 39 patients with *peripheral arterial disease* and 34 controls and found a significantly reduced endothelial function index, an increased augmentation index (AI), estimated PWV, ICAM-1, hsCRP, myeloperoxidase, and urinary 8-iso-prostaglandin F2a (110). They found an inverse, significant

TABLE 4 | C-reactive protein (CRP), high-sensitivity C-reactive protein (hsCRP), and arterial stiffness.

Study population	Findings	Reference
100 patients with metabolic syndrome, 14 controls	There was a significant correlation between aortic flow propagation velocity (AVP), FMD (flow-mediated dilatation), and high CRP, indicating a possible link between aortic stiffness, endothelial dysfunction, and inflammation	Adel et al. (7)
150 renal transplant recipients	High (> 20 mg/L) post-transplant CRP levels predicted pulse wave velocity (PWV) and cardiovascular morbidity in a two-year time period after renal transplantation	Gurlek Demirci et al. (102)
40 patients with type 2 diabetes mellitus	hsCRP showed a moderate positive correlation with arterial stiffness in patients with type 2 diabetes mellitus	Nurizal et al. (104)
825 men (mean age: 74 years)	Arterial stiffness was found to correlate positively with circulating levels of CRP	McEniery et al. (100)
362 middle-aged and elderly men	Low-grade inflammation was shown to be independently related to increase of aortic artery stiffness over and above traditional risk factors and atherosclerosis	Nakhai-Pour et al. (43)
77 patients with rheumatoid arthritis (RA) and 142 healthy individuals	Median aortic PWV was significantly higher in RA patients than in control subjects and correlated independently with age, mean arterial pressure, and CRP	Mäki-Petäjä et al. (21)
214 asymptomatic subjects with a mean age of 59 years	CRP was related to measures of arterial wave reflection and stiffness in asymptomatic subjects	Kullo et al. (99)
866 participants above 55 years	Levels of CRP were linearly associated with PWV	Mattace-Raso et al. (98)
2,668 Japanese men (43 ± 10 years old)	PWV showed a significant correlation with the logarithm of hsCRP, but multiple linear regression analyses demonstrated that the logarithm of hsCRP was not significantly related to PWV, independent from conventional risk factors	Tomiyama et al. (101)
158 apparently healthy subjects (age range 40–65 years)	Plasma levels of hsCRP were positively correlated with AIx, central pulse pressure and central systolic blood pressure	Kampus et al. (103)

association between endothelial function index and ICAM-1 only in the controls, and significant correlations between PWV and AI, respectively, and urinary 8-iso-prostaglandin F2a in patients (110). The study demonstrated the importance of the degree of inflammation for endothelial vasomotor capacity in the subclinical condition and of oxidative stress for arterial stiffness (110).

Vascular adhesion protein-1 (VAP-1) is associated with cell membranes (in ECs, smooth muscle cells, and adipocytes) but also found as soluble VAP-1 in plasma. It serves both the function as an adhesion molecule and an amine oxidase producing aldehyde and hydrogen peroxide. It is involved in vascular injury due to its semicarbazide-sensitive amine oxidase (SSAO) activity because of releasing of formaldehyde and methylglyoxal from the breakdown of primary amines, which is responsible for direct cytotoxic damage to ECs (111, 112). VAP-1 was associated with arterial stiffness in *subjects over 60 years* after adjusting for PWV-related confounders (112). Inflammation is the main link between VAP-1 and arterial stiffness, impairing the balance between production and degradation of collagen and elastin fibers, resulting in overproduction of abnormal collagen and reducing quantities of normal elastin (6). As an adhesion molecule, VAP-1 is involved in the rolling, adhesion, and transmigration of lymphocytes, granulocytes, and monocytes from the blood into the vessel wall, and the oxidase activity of VAP-1 may have signaling effects and induce expression of E- and P-selectins and ICAM-1 in ECs (113, 114). VAP-1 is also involved in endothelial dysfunction and synthesis of advanced glycation end products that are well known to contribute to an increase in arterial stiffness. Furthermore, SSAO activity was associated with an abnormal elastin structure and production of reactive oxygen species (112).

In *systemic lupus erythematosus*, antiphospholipid antibodies bind to receptors on the endothelium to upregulate adhesion molecules such as E-selectin, ICAM-1, and VCAM-1, but the presence of the antibodies was not associated with arterial stiffness (27).

In summary, adhesion molecules were associated with arterial stiffness in patients with a peripheral arterial disease, resistant hypertension, and subjects over 60 years (**Table 5**) (34, 110).

ORAL INFECTIONS AND ARTERIAL STIFFNESS

The association between oral inflammation and the risk of major cardiovascular events, such as myocardial infarction and stroke, was described two decades ago (115, 116). Bacteria and their products from the dental plaque and crevicular fluid are involved in local destruction of gingiva and bone and they are also released to the bloodstream (117).

Periodontitis is associated with endothelial dysfunction due to periodontal pathogens, atherosclerosis, an increased risk of myocardial infarction, stroke, and peripheral arterial disease (118, 119). A 19% increase in the risk of cardiovascular disease was reported, and the risk increases in elderly patients (119, 120). Periodontitis and cardiovascular disorders share several risk factors, such as age, heredity, smoking, diabetes mellitus, hypertension, estrogen deficiency in women, a low socioeconomic status, and stress (117, 119).

Microbial pathogens associated with periodontal disease, predominantly Gram-negative bacteria, cause high levels of bacteremia after routine dental procedures and every day activities, including tooth brushing (121) and a chronic, progressive, destructive, and unresolved inflammation (122, 123). Periodontal pathogens and their noxious products gain access to the periodontal tissues and are released into the systemic circulation through the ulcerated sulcular epithelium of the gingiva, and they are a source of inflammatory mediators, which can cause insulin resistance, systemic inflammation, and explain, probably, the perio-systemic link (119, 124, 125). *Porphyromonas gingivalis* and *Treponema denticola*, bacteria causing periodontal disease, have been found in the atherosclerotic plaque (117). The levels of biomarkers such as hsCRP, TNF-α, and interleukin-6 and -1 were increased in patients with periodontitis. The autoimmune mechanism is involved in both periodontal disease and RA, which explains the significant association of both disorders associated with an increased cardiovascular risk (119). High periodontal bacteria antibodies titers were associated with atherosclerosis, regardless of smoking status (118, 126), and improvement in clinical and microbial periodontal status was associated with a decreased rate of carotid artery IMT progression (127). Probably, the atherosclerotic process is initiated or accelerated by the inflammatory periodontal reaction (128). It is also possible that a common pathway leads independently to both periodontal disease and atherosclerosis (117).

Several studies reported an increased arterial stiffness in patients with periodontitis compared to controls, suggesting that patients with periodontitis suffer from a subclinical vascular dysfunction (**Table 6**) (129–134). Future research should point out the relationship between active treatment of periodontitis

TABLE 5 | Adhesion molecules and arterial stiffness.

Study population	Findings	Reference
110 patients with resistant hypertension and 112 mild to moderate hypertensive patients	sP-selectin and sVCAM-1 were elevated in the presence of arterial stiffness and cardiac hypertrophy	de Faria et al. (34)
63 participants referred for echocardiography	No correlation was demonstrated between indices of aortic stiffness and vascular cell adhesion molecule-1 and intercellular adhesion molecule-1 levels	Kilic et al. (109)
568 Han Chinese healthy persons with an age 30 or older	Plasma vascular adhesion protein-1 (VAP-1) was associated with arterial stiffness in older individuals. VAP-1 may be important for vascular aging	Chen et al. (112)
39 patients with peripheral arterial disease and 34 controls	There was an inverse association between endothelial function index and intercellular adhesion molecule-1 in the controls, but not in the patients	Kals et al. (110)

TABLE 6 | Periodontitis and arterial stiffness.

Study population	Findings	Reference
80 volunteers and 33 pairs of periodontitis patients, matched by age and gender	An association between arterial stiffness and periodontitis was suggested by a lower degree of uniformity in the transmission of the pulse wave through the carotid arteries	Sanz-Miralles et al. (136)
57 periodontitis patients and 48 healthy controls	PWV was measured and followed up 6 months after periodontal therapy. PWV was significantly higher in periodontitis patients compared to the reference group even after adjusting for cardiovascular risk factors. Periodontal treatment did not lower significantly PWV	Houcken et al. (134)
92 patients with periodontitis and 66 matched healthy controls	Significantly higher PWV, aortic augmentation index, and central blood pressure and lower pulse pressure amplification values were found in subjects with severe or aggressive periodontitis	Jockel-Schneider et al. (132)
273 indigenous Australian adults	Arterial stiffness significantly increased with increasing extent of periodontal pocketing	Kapellas et al. (131)
532 gingivitis and 282 periodontitis cases (Asian Indians)	PWV and arterial stiffness index were elevated in periodontitis compared to gingivitis cases and in those with diabetes and hypertension	Shanker et al. (130)
1,053 Japanese subjects with 10 teeth or more	A linear, dose-dependent relationship was found between periodontal pocket depth and arterial stiffness	Hayashida et al. (129)
26 patients with refractory hypertension and generalized chronic periodontitis	Periodontal therapy significantly reduced the level of CRP, IL-6, fibrinogen, blood pressure, left ventricular mass and arterial stiffness, lowering cardiovascular risk	Vidal et al. (135)
16 periodontally healthy, 87 gingivitis, and 18 periodontitis patients with type 2 diabetes mellitus	Periodontal inflammation in patients with type 2 diabetes mellitus is associated with increased intima-media thickness and blood pressure, but not with greater arterial stiffness	Franek et al. (117)

PWV, pulse wave velocity; CRP, C-reactive proteins; IL-6, interleukin-6.

and cardiovascular benefits, because the results of the interventional studies are contradictory, especially in obese patients (117, 133, 135).

Concluding, arterial stiffness is impaired in patients with periodontitis. No study reported yet a symbiotic relationship between periodontitis and arterial stiffness or any relationship between odontogenic foci and arterial stiffness, and those could be aims of future studies.

MICRORNAs AND VASCULAR INFLAMMATION

Increasing evidence indicate that miRNAs, which are small non-coding RNAs, able to regulate gene expression and to prevent or reduce protein synthesis, have distinct profiles and play crucial roles in various physiological and pathological processes, including vascular aging and inflammation (137–140). An imbalance in the normal miRNA profile can be identified long before the onset of a disease (139, 141). MicroRNAs, such as miR-126 and miR-10a, can control vascular inflammation due to leukocyte activation and infiltration through the vascular wall (142). MicroRNA-663 specifically mediated shear stress-induced monocyte adhesion to ECs (143). Let-7g reduced, besides ECs senescence, also EC inflammation and monocyte adhesion (144). MicroRNA-181b shift macrophage polarization toward M2 anti-inflammatory phenotype, reducing macrophage accumulation and enabling tissue repair (145). Another microRNA, miR-92a, the "atheromiR candidate," upregulated by oxLDL, is a pro-inflammatory regulator in ECs by modulating inflammatory cytokines and chemokines, enabling monocyte adhesion (146). MicroRNA-92a controls also neovascularization after ischemic injury (140). MicroRNAs can also regulate adhesion molecules expression, especially miR-21 and miR-126. MicroRNA-21, highly expressed in the cardiovascular system, is the most abundant microRNA in monocytes/macrophages, related to a pro-inflammatory phenotype, control of the flow-induced inflammatory response, mediating the balance of pro- and anti-inflammatory responses, expression of adhesion molecules, polarization of macrophages and macrophage apoptosis (147). Zhou et al. demonstrated that miR-21 acts as an epigenetic mediator of the pro-inflammatory phenotype of the vascular ECs exposed to oscillatory shear stress, inhibiting expression of peroxisome proliferators-activated receptor-alpha and upregulating activator protein-1 and expression of adhesion molecules (138). A study including 95 hypertensive patients, evaluated at baseline and after 1 year of effective antihypertensive therapy, showed independent correlations between levels of miR-21 and changes of PWV, independent of blood pressure values, highlighting the significance of miR-21 in vascular remodeling (139). MicroRNA-21 enables also fibrosis in the vascular wall related to AII, promoting proliferation of interstitial fibroblasts and deposition of the extracellular matrix (139). It is also involved in regulation of VSMC phenotype and suppression of endothelial progenitor cell proliferation (139). Harris et al. showed that miR-126 inhibits VCAM-1 expression, limiting leukocyte adhesion to the vascular endothelium (137). However, miR-126 is also involved in angiogenic signaling (141). MicroRNA-30 reduces basal and TNF-α-induced expression of adhesion molecules: VCAM-1, ICAM-1, and E-selectin, impairing the expression of angiopoietin 2 and contributing to the atheroprotective effects of shear stress (148). Deng et al. enrolled 406 Chinese participants in a study and measured miR-1185, adhesion molecules levels (VCAM-1 and E-selectin), and arterial stiffness, reporting independent correlations of microRNA with PWV and adhesion molecules, respectively (149).

It is too early to consider microRNAs as diagnostic and prognostic biomarkers or therapeutic target for arterial stiffness, because there are very few studies linking vascular function and non-coding RNAs. However, miRNAs could be useful as markers of vascular remodeling and plaque instability in future studies.

CYCLOOXYGENASE-2 (COX-2), PROSTAGLANDIN SIGNALING, AND ARTERIAL STIFFNESS

During inflammation, phospholipase brakes down phospholipids of the WBC membrane into arachidonic acid, which enables synthesis of prostaglandins through the cyclooxigenase pathway, involving cyclooxygenase 1 and 2. The prostaglandins formed by the COX-2 pathway perpetuate inflammation and amplify the effects of other inflammatory mediators, due to its upregulation in monocyte-derived macrophages from the atherosclerotic lesions (150, 151). Microsomal prostaglandin E2 synthase-1 (mPGES-1) catalyzes prostaglandin E2 generation from prostaglandin H2, is primary coupled to COX-2, is strongly upregulated in inflamed tissues, and represents a key enzyme in atherosclerosis and stroke (152, 153). In atherosclerosis of the carotid arteries, both COX-2 and mPGES-1 are upregulated in the vulnerable area of the plaque and may favor plaque instability (152).

The relationship between COX-2 and vascular remodeling was described in the pulmonary circulation. Pulmonary arterial stiffness occurs early in experimental pulmonary hypertension and is an independent risk factor for mortality in pulmonary hypertension (154). COX-2 is upregulated in pulmonary artery smooth muscle cells during hypoxia, associated with upregulation of the endothelin receptor (155) and intravascular macrophage accumulation (156). The transcriptional regulator Yes-associated protein activity is increased in pulmonary hypertension in pulmonary artery smooth muscle cells and is necessary for development of stiffness-dependent remodeling phenotypes (154). However, selective COX-2 inhibition impairs the balance of vascular mediators, enables vascular hyperplasia, remodeling of the systemic vessels, platelet deposition, intravascular thrombosis, and is associated with several cardiovascular events (155).

Cyclooxygenase-2 derived prostaglandin E2, acting on EP1 receptors, is responsible for increased arterial stiffness, increased vasoconstrictor responses, extracellular matrix deposition, endothelial dysfunction, and vascular inflammation (157). AII induces expression of COX-2 and prostanoids in several vessels, and high levels of AII are expressed in vessels of hypertensive patients (157).

On the other hand, Vlachopoulos et al. demonstrated that, especially, COX-1, and also COX-2 mediate the unfavorable effects of smoking on arterial stiffness (158). Endothelial function was not improved by indomethacin or rofecoxib in patients with RA (159), and meanwhile, rofecoxib was withdrawn from the market considering the increased risk of atherothrombotic events associated with this class of drugs (150).

Despite the mechanisms linking COX-2, inflammation, and arterial stiffness, chronic COX-2 inhibition is not an effective destiffening solution, because of its prothrombotic and hypertensive undesirable effects. There is urgent need for the discovery of new effective and cardiovascular safe anti-inflammatory drugs, and mPGES-1 inhibitors may be the solution.

STUDY LIMITATIONS

Most of the studies were cross-sectional, often with only a relatively small number of participants, and sometimes with just one measurement of inflammatory markers, all of which is unfavorable for the significance of results and their interpretation. The cross-sectional design of most studies cannot establish causality, it can only establish an association (102). Relatively small numbers of study participants, which are often a specific subgroup of patients with certain morbidities does not allow to extend conclusions to the general population; therefore, the results of many studies presented here need confirmation in larger studies. Other limitations arise from an election bias due to exclusion of patients with active infections, and not considering PP amplification and the fact that arterial stiffness is not a uniform condition in all arteries (19, 98). Also, the possibility of undetected disease in study participants limits the significance of studies (57). Usually, patients with established and not early disease were studied and it is not clear if changes in arterial properties precede increase of inflammatory markers and if there is an etiological link between inflammatory markers and cardiovascular complications. It is also still not clear if old or cumulative inflammation or just acute or subacute inflammation correlate with arterial stiffness (21).

Several confounding factors may influence the level of inflammatory markers and not all of them are known currently. The level of soluble adhesion molecules is, for example, at least influenced by age, smoking status, diabetes mellitus, other inflammatory conditions, exercise, and changes in blood pressure (109). The variance of CRP due to LDL cholesterol was less than 3–5%, and values of CRP are stable over long periods, with almost no circadian variation and are not influenced by food intake (92). Major infections, trauma, and hospitalization may increase CRP 100-fold or more, and values exceeding 10 mg/l should be ignored and the test should be repeated (92).

Also, the methodologies of assessing arterial stiffness are limiting the significance of the obtained results. For example, PWV measurements have the immanent problem that it remains difficult to accurately record the femoral pressure wave in participants with peripheral artery disease, and also obesity affects the absolute value of PWV by overestimating the distance and thus yielding artificial values (160). Also, measurements of blood pressure values present a possible source of limiting significance, since blood pressure values are often derived *via* the brachial PP using a sphygmomanometer and are then converted into central PP by a transfer function. However, since vascular dimensions depend on body size and vascular properties vary with arterial pressure, age, or treatment, the premise that the characteristics of the vascular system between the two measuring sites are the same in all individuals and under all conditions is therefore not true (161). More sophisticated inflammatory markers, such as adhesion molecules and ILs, are inappropriate for routine clinical use (91, 92).

CONCLUSION

There is ample evidence of a crosstalk between arterial stiffness and systemic inflammation, and inflammation plays an important role in the development of arterial stiffness. Inflammatory markers may be useful additional tools in the assessment of the cardiovascular risk, atherosclerotic plaque remodeling, and preclinical atherosclerotic changes in clinical practice and may be used to develop risk scores for possible future cardiovascular events. This might help to close the currently existing gap between predicted cardiovascular events and their real prevalence. Most of the inflammatory markers are inexpensive and easily measurable, widely available, standardized and may be included in the annual examination of patients at risk, considering that inflammation causes a reversible increase of arterial stiffness.

Several studies revealed significant associations between arterial stiffness and inflammatory markers, such as WBC, NLR, adhesion molecules, fibrinogen, CRP, hsCRP, cytokines, microRNAs, and COX-2 in patients with metabolic syndrome, diabetes mellitus, coronary heart disease, systemic and pulmonary hypertension, peripheral arterial disease, malignant and inflammatory rheumatic disorders, polycystic kidney disease, renal transplant, FMF, in women with preeclampsia or after menopause, and in patients with severe periodontitis. Further studies are needed, in several other disorders and healthy subjects, to confirm the reversible association linking arterial stiffness and inflammatory markers and its predictive value for cardiovascular events.

Combined assessment of arterial stiffness and inflammatory markers may improve non-invasive assessment of cardiovascular risk in several disorders, enabling selection of high-risk patients for prophylactic treatment or more regular medical examination. Development of future destiffening therapies may target pro-inflammatory mechanisms, including miRNAs, enabling stabilization of the atherosclerotic plaque, control of cardiovascular risk factors, and inflamm-aging.

AUTHOR CONTRIBUTIONS

IM has written the first draft of the manuscript. CM, JH, CG, DS, CL, and AA revised and improved the first draft. All authors have seen and agreed on the finally submitted version of the manuscript.

FUNDING

The authors acknowledge the support by the Polish KNOW (Leading National Research Centre) Scientific Consortium "Healthy Animal—Safe Food," decision of Ministry of Science and Higher Education No. 05-1/KNOW2/2015.

REFERENCES

1. Shirwany NA, Zou M. Arterial stiffness: a brief review. *Acta Pharmacol Sin* (2010) 31:1267–76. doi:10.1038/aps.2010.123
2. Van Bortel LM, Struijker-Boudier H, Safar ME. Pulse pressure, arterial stiffness, and drug treatment of hypertension. *Hypertension* (2001) 38(4): 914–21. doi:10.1161/hy1001.095773
3. Avolio A, Butlin M, Liu YY, Viegas K, Avadhanam B, Lindesay G. Regulation of arterial stiffness: cellular, molecular and neurogenic mechanisms. *Artery Res* (2011) 5:122–7. doi:10.1016/j.artres.2011.10.002
4. Townsend RR. Arterial stiffness and chronic kidney disease: lessons from the chronic renal insufficiency cohort study. *Curr Opin Nephrol Hypertens* (2015) 24(1):47–53. doi:10.1097/MNH.0000000000000086
5. Hughes TM, Craft S, Lopez OL. Review of 'the potential role of arterial stiffness in the pathogenesis of Alzheimer's disease'. *Neurodegener Dis Manag* (2015) 5(2):121–35. doi:10.2217/nmt.14.53
6. Zieman SJ, Melenovsky V, Kass DA. Mechanisms, pathophysiology, and therapy of arterial stiffness. *Arterioscler Thromb Vasc Biol* (2005) 25:932–43. doi:10.1161/01.ATV.0000160548.78317.29
7. Adel M, ELSheikh A, Sameer S, Haseeb W, ELSheikh E, Kheder L. Arterial stiffness in metabolic syndrome. *J Saudi Heart Assoc* (2016) 28:249–56. doi:10.1016/j.jsha.2015.12.005
8. Mozos I, Stoian D, Luca CT. Crosstalk between vitamins A, B12, D, K, C and E status and arterial stiffness. *Dis Markers* (2017) 2017:8784971. doi:10.1155/2017/8784971
9. Erbel R, Aboyans V, Boileau C, Bartolomeo RD, Eggebrecht H, Evangelista A, et al. 2014 ESC guidelines on the diagnosis and treatment of aortic diseases. Document covering acute and chronic aortic diseases of the thoracic and abdominal aorta of the adult. *Eur Heart J* (2014) 35:2873–926. doi:10.1093/eurheartj/ehu281
10. Vlachopoulos C, Xaplanteris P, Aboyans V, Brodmann M, Cifkova R, Cosentino F, et al. The role of vascular biomarkers for primary and secondary prevention. A position paper from the European Society of Cardiology Working Group on peripheral circulation: endorsed by the Association for Research into Arterial Structure and Physiology (ARTERY) Society. *Atherosclerosis* (2015) 241:507–32. doi:10.1016/j.atherosclerosis.2015.05.007
11. Cecelja M, Chowienczyk P. Arterial stiffening: causes and consequences. *Artery Res* (2013) 7:22–7. doi:10.1016/j.artres.2012.09.001
12. Shibata T, Tsutsumi J, Hasegawa J, Sato N, Murashima E, Mori C, et al. Effects of add-on therapy consisting of a selective mineralocorticoid receptor blocker on arterial stiffness in patients with uncontrolled hypertension. *Intern Med* (2015) 54:1583–9. doi:10.2169/internalmedicine.54.3427
13. Lacolley P, Challande P, Regnault V, Lakattac EG, Wang M. Cellular and molecular determinants of arterial aging. In: Nilsson P, Olsen M, Laurent S, editors. *Early Vascular Aging*. Academic Press, Elsevier (2015). p. 7–13.
14. Smulyan H, Mookherje S, Safar ME. Two faces of hypertension: role of aortic stiffness. *J Am Soc Hypertens* (2016) 10(2):175–83. doi:10.1016/j.jash.2015.11.012
15. Vita JA, Keaney JF Jr, Larson MG, Keyes MJ, Massaro JM, Lipinska I, et al. Brachial artery vasodilator function and systemic inflammation in the Framingham Offspring Study. *Circulation* (2004) 110(23):3604–9. doi:10.1161/01.CIR.0000148821.97162.5E
16. Hansson GK. Inflammation, atherosclerosis, and coronary artery disease. *N Engl J Med* (2005) 352:1685–95. doi:10.1056/NEJMra043430
17. Aznaouridis KA, Stefanadis CI. Inflammation and arterial function. *Artery Res* (2007) 1:32–8. doi:10.1016/j.artres.2007.03.005
18. Park S, Lakatta EG. Role of inflammation in the pathogenesis of arterial stiffness. *Yonsei Med J* (2012) 53(2):258–61. doi:10.3349/ymj.2012.53.2.258
19. Ayhan H, Kasapkara HA, Aslan AN, Durmaz T, Keles T, Akcay M, et al. Relationship of neutrophil-to-lymphocyte ratio with aortic stiffness in type 1 diabetes mellitus. *Can J Diabetes* (2015) 39:317–21. doi:10.1016/j.jcjd.2015.01.004
20. Jain S, Khera R, Corrales-Medina VF, Townsend RR, Chirinos JA. Inflammation and arterial stiffness in humans. *Atherosclerosis* (2014) 237(2):381–90. doi:10.1016/j.atherosclerosis.2014.09.011
21. Mäki-Petäjä KM, Hall FC, Booth AD, Wallace SM, Yasmin, Bearcroft PW, et al. Rheumatoid arthritis is associated with increased aortic pulse-wave velocity, which is reduced by anti-tumor necrosis factor-alpha therapy. *Circulation* (2006) 114(11):1185–92. doi:10.1161/CIRCULATIONAHA.105.601641

22. Sattar N, McCarey DW, Capell H, McInnes IB. Explaining how "high-grade" systemic inflammation accelerates vascular risk in rheumatoid arthritis. *Circulation* (2003) 108:2957–63. doi:10.1161/01.CIR.0000099844.31524.05
23. Gerli R, Schillaci G, Giordano A, Bocci EB, Bistoni O, Vaudo G, et al. CD4+ CD28- T lymphocytes contribute to early atherosclerotic damage in rheumatoid arthritis patients. *Circulation* (2004) 109:2744–8. doi:10.1161/01.CIR.0000131450.66017.B3
24. Loius SF, Zahradka P. Vascular smooth muscle cell motility: from migration to invasion. *Exp Clin Cardiol* (2010) 15(4):e75–85.
25. Libby P, Ridker PM, Maseri A. Inflammation and atherosclerosis. *Circulation* (2002) 105(963):1135–43. doi:10.1161/hc0902.104353
26. Drechsler M, Megens RTA, Van Zandvoort M, Weber C, Soehnlein O. Hyperlipidemia-triggered neutrophylia promotes early atherosclerosis. *Circulation* (2010) 122(18):1837–45. doi:10.1161/CIRCULATIONAHA.110.961714
27. Yildiz M. Arterial distensibility in chronic inflammatory rheumatic disorders. *Open Cardiovasc Med J* (2010) 4:83–8. doi:10.2174/1874192401004020083
28. Jones DP, True HD, Patel J. Leukocyte trafficking in cardiovascular disease: insights from experimental models. *Mediators Inflamm* (2017) 2017:9746169. doi:10.1155/2017/9746169
29. McEniery CM, Qasem A, Schmitt M, Avolio AP, Cockcroft JR, Wilkinson IB. Endothelin-1 regulates arterial pulse wave velocity in vivo. *J Am Coll Cardiol* (2003) 42(11):1975–81. doi:10.1016/j.jacc.2003.06.016
30. Hansson GK, Hermansson A. The immune system in atherosclerosis. *Nat Immunol* (2011) 12:204–12. doi:10.1038/ni.2001
31. Stein S, Lohmann C, Schafer N, Hofmann J, Rohrer L, Besler C, et al. SIRT 1 decreases LOX-1 mediated foam cell formation in atherogenesis. *Eur Heart J* (2010) 31:2301–9. doi:10.1093/eurheartj/ehq107
32. Siti HN, Kamisah Y, Kamisah J. The role of oxidative stress, antioxidants and vascular inflammation in cardiovascular disease (a review). *Vascul Pharmacol* (2015) 71:40–56. doi:10.1016/j.vph.2015.03.005
33. Pirillo A, Norata GD, Catapano AL. LOX-1, OxLDL, and atherosclerosis. *Mediators Inflamm* (2013) 2013:152786. doi:10.1155/2013/152786
34. de Faria AP, Ritter AM, Sabbatini AR, Correa NB, Brunelli V, Modolo R, et al. Deregulation of soluble adhesion molecules in resistant hypertension and its role in cardiovascular remodeling. *Circ J* (2016) 80(5):1196–201. doi:10.1253/circj.CJ-16-0058
35. Michaud M, Balardy L, Moulis G, Gaudin C, Peyrot C, Vellas B, et al. Proinflammatory cytokines, aging and age related diseases. *J Am Med Dir Assoc* (2013) 14:877–82. doi:10.1016/j.jamda.2013.05.009
36. Mc Gill HC Jr, Mc Mahan CA, Herderick EE, Malcom GT, Tracy RE, Strong JP. Origin of atherosclerosis in childhood and adolescence. *Am J Clin Nutr* (2000) 72(5 Suppl):1307S–15S.
37. Papaioannou TG, Karatzi K, Psaltopoulou T, Tousoulis D. Arterial ageing: major nutritional and life-style effects. *Ageing Res Rev* (2017) 37:162–3. doi:10.1016/j.arr.2016.10.004
38. Wang M, Jiang L, Monticone RE, Lakatta EG. Proinflammation: the key to arterial aging. *Trends Endocrinol Metab* (2014) 25(2):72–9. doi:10.1016/j.tem.2013.10.002
39. Accardi G, Aiello A, Gambino CM, Virruso C, Caruso C, Candore G. Mediterranean nutraceutical foods: strategy to improve vascular ageing. *Mech Ageing Dev* (2016) 159:63–70. doi:10.1016/j.mad.2016.02.007
40. Mozos I, Luca CT. Crosstalk between oxidative and nitrosative stress and arterial stiffness. *Curr Vasc Pharmacol* (2017) 15:446–56. doi:10.2174/1570161115666170201115428
41. Galis ZS, Khatri JJ. Matrix metalloproteinases in vascular remodeling and atherogenesis: the good, the bad and the ugly. *Circ Res* (2002) 90:251–62. doi:10.1161/hh0302.105345
42. Wang M, Zhang J, Jiang LQ, Spinetti G, Pintus G, Monticone R, et al. Proinflammatory profile within the grossly normal aged human aortic wall. *Hypertension* (2007) 50:219–27. doi:10.1161/HYPERTENSIONAHA.107.089409
43. Nakhai-Pour HR, Grobbee DE, Bots ML, Muller M, van der Schouw YT. C-reactive protein and aortic stiffness and wave reflection in middle-aged and elderly men from the community. *J Hum Hypertens* (2007) 21(12):949–55. doi:10.1038/sj.jhh.1002255
44. Tanindi A, Erkan AF, Alhan A, Töre HF. Arterial stiffness and central arterial wave reflection are associated with serum uric acid, total bilirubin, and neutrophil-to lymphocyte ratio in patients with coronary artery disease. *Anatol J Cardiol* (2015) 15(5):396–403. doi:10.5152/akd.2014.5447
45. Mäki-Petäjä KM, Wilkinson IB. Anti-inflammatory drugs and statins for arterial stiffness reduction. *Curr Pharm Des* (2009) 15(3):290–303. doi:10.2174/138161209787354221
46. Hussein AM, Shaaya G, Arora R, Al-Khazaali A, Al-Khafaji K, Helu HK. Therapeutic modulation of aortic stiffness. *Am J Ther* (2016) 23(6):e1644–53. doi:10.1097/MJT.0000000000000408
47. Mozos I, Borzak G, Caraba A, Mihaescu R. Arterial stiffness in hematologic malignancies. *Onco Targets Ther* (2017) 10:1381–8. doi:10.2147/OTT.S126852
48. Bhat T, Teli S, Rijal J, Bhat H, Raza M, Khoueiry G, et al. Neutrophil to lymphocyte ratio and cardiovascular diseases: a review. *Expert Rev Cardiovasc Ther* (2013) 11(1):55–9. doi:10.1586/erc.12.159
49. Bain BJ. Ethnic and sex differences in the total and differential white cell count and platelet count. *J Clin Pathol* (1996) 49:664–6. doi:10.1136/jcp.49.8.664
50. Angeli F, Angeli E, Ambrosio G, Mazotta G, Cavallini C, Reboldi G, et al. Neutrophil count and ambulatory pulse pressure as predictors of cardiovascular adverse events in postmenopausal women with hypertension. *Am J Hypertens* (2011) 24(5):591–8. doi:10.1038/ajh.2011.18
51. Abo T, Kawamura T. Immunomodulation by the autonomic nervous system: therapeutic approach for cancer, collagen diseases, and inflammatory bowel diseases. *Ther Apher* (2002) 6(5):348–57. doi:10.1046/j.1526-0968.2002.00452.x
52. Mozos I, Mihaescu R. Crosstalk between arterial stiffness, arterial age and blood count in hematologic malignancies. *Jökull* (2015) 65(9):105–15.
53. Mozos I, Mihaescu R. Pulse wave velocity and central hemodynamic indices in patients with malignant solid tumors. *Jökull* (2015) 65(9):200–14.
54. Steinberg MH, Charm SE. Effect of high concentrations of leukocytes on whole blood viscosity. *Blood* (1971) 38(3):299–301.
55. Cowan AQ, Cho DJ, Rosenson RS. Importance of blood rheology in the pathophysiology of aherothrombosis. *Cardiovasc Drug Ther* (2012) 26(4):339–48. doi:10.1007/s10557-012-6402-4
56. Gomez-Sanchez L, Garcia-Ortiz L, Recio-Rodriguez JI, Patino-Alonso MC, Agudo-Conde C, Rigo F, et al. Leukocyte subtype counts and its association with vascular structure and function in adults with intermediate cardiovascular risk. MARK study. *PLoS One* (2015) 10(4):e0119963. doi:10.1371/journal.pone.0119963
57. Yildiz M, Masatlioglu S, Seymen P, Aytac E, Sahin B, Seymen HO. The carotid-femoral (aortic) pulse wave velocity as a marker of arterial stiffness in familial Mediterranean fever. *Can J Cardiol* (2006) 22(13):1127–31. doi:10.1016/S0828-282X(06)70949-7
58. Cakar M, Akhan M, Dogan T, Taskin G, Öztürk K, Cinar M, et al. Investigation of the arterial stiffness and associated factors in patients with familial Mediterranean fever. *Anatol J Cardiol* (2017) 17(2):132–8. doi:10.14744/AnatolJCardiol.2016.6985
59. Alghamdi M. Familial Mediterranean fever, review of the literature. *Clin Rheumatol* (2017) 36(8):1707–13. doi:10.1007/s10067-017-3715-5
60. Nidorf M, Thompson PL. Effect of colchicine (0.5 mg twice daily) on high-sensitivity C-reactive protein independent of aspirin and atorvastatin in patients with stable coronary artery disease. *Am J Cardiol* (2007) 99(6):805–7. doi:10.1016/j.amjcard.2006.10.039
61. Oakes PW, Patel DC, Morin NA, Zitterbart DP, Fabry B, Reichner JS, et al. Neutrophil morphology and migration are affected by substrate elasticity. *Blood* (2009) 114(7):1387–95. doi:10.1182/blood-2008-11-191445
62. Nam SH, Kang SG, Song SW. The neutrophil-lymphocyte ratio is associated with coronary artery calcification in asymptomatic Korean males: a cross-sectional study. *Biomed Res Int* (2017) 2017:1989417. doi:10.1155/2017/1989417
63. Karaman M, Balta S, Seyit Ahmet AY, Cakar M, Naharci I, Demirkol S, et al. The comparative effects of valsartan and amlodipine on vWf levels and N/L ratio in patients with newly diagnosed hypertension. *Clin Exp Hypertens* (2013) 35(7):516–22. doi:10.3109/10641963.2012.758734
64. Balta S, Kurtoglu E, Kucuk U, Demirkol S, Öztürk C. Neutrophil-lymphocyte ratio as an important assessment tool. *Expert Rev Cardiovasc Ther* (2014) 12(5):537–8. doi:10.1586/14779072.2014.902309
65. Horne BD, Anderson JL, John JM, Weaver A, Bair TL, Jensen KR, et al. Which white blood cell subtypes predict increased cardiovascular

risk? *J Am Coll Cardiol* (2005) 45(10):1638–43. doi:10.1016/j.jacc.2005.02.054
66. Yu XY, Li XS, Li Y, Liu T, Wang RT. Neutrophil-lymphocyte ratio is associated with arterial stiffness in postmenopausal women with osteoporosis. *Arch Gerontol Geriatr* (2015) 61(1):76–80. doi:10.1016/j.archger.2015.03.011
67. Wang RT, Zhang JR, Li Y, Liu T, Yu KJ. Neutrophil-lymphocyte ratio is associated with arterial stiffness in diabetic retinopathy in type 2 diabetes. *J Diabetes Complications* (2015) 29(2):245–9. doi:10.1016/j.jdiacomp.2014.11.006
68. Turkmen S, Dogdu O, Tekin K, Kucukdurmaz Z, Cagliyan CE, Sarikaya S, et al. The relationship between neutrophil/lymphocyte ratio and the TIMI flow grade in patients with STEMI undergoing primary PCI. *Eur Rev Med Pharmacol Sci* (2013) 17:2185–9.
69. Yaman M, Arslan U, Beton O, Pamukcu HE, Dogdu O. Early and late aortic propagation velocity values in STEMI patients after successful primary PCI and their relationship with neutrophil to lymphocyte ratio. *Eur Rev Med Pharmacol Sci* (2016) 20(5):912–8.
70. Arbel Y, Finkelstein A, Halkin A, Birati EY, Revivo M, Zuzut M, et al. Neutrophil/lymphocyte ratio is related to the severity of coronary artery disease and clinical outcome in patients undergoing angiography. *Atherosclerosis* (2012) 225:456–60. doi:10.1016/j.atherosclerosis.2012.09.009
71. Kalay N, Dogdu O, Koc F, Yarlioglues M, Ardic I, Akpek M, et al. Hematologic parameters and angiographic progression of coronary atherosclerosis. *Angiology* (2012) 63:213–7. doi:10.1177/0003319711412763
72. Kloner RA, Giacomelli F, Alker KJ, Hale SL, Matthews R, Bellows S. Influx of neutrophils into the walls of large epicardial coronary arteries in response to ischemia/reperfusion. *Circulation* (1991) 84:1758–72. doi:10.1161/01.CIR.84.4.1758
73. Park BJ, Shim JY, Lee HR, Lee JH, Jung DH, Kim HB, et al. Relationship of neutrophil-lymphocyte ratio with arterial stiffness and coronary calcium score. *Clin Chim Acta* (2011) 412(11–12):925–9. doi:10.1016/j.cca.2011.01.021
74. Fici F, Celik T, Balta S, Iyisoy A, Unlu M, Demitkol S, et al. Comparative effects of nebivolol and metoprolol on red cell distribution width and neutrophil/lymphocyte ratio in patients with newly diagnosed essential hypertension. *J Cardiovasc Pharmacol* (2013) 62(4):388–93. doi:10.1097/FJC.0b013e31829f716a
75. Gul CB, Yildiz A, Ersoy A, Kahvecioglu S, Asiltas B, Yildirim F, et al. Correlation between arterial stiffness and inflammatory markers in autosomal dominant polycystic kidney disease patients with preserved renal function. *Int Urol Nephrol* (2015) 47(7):1187–94. doi:10.1007/s11255-015-1022-0
76. Tracey KJ. The inflammatory reflex. *Nature* (2002) 420(691):853–9. doi:10.1038/nature01321
77. Kahaleh MB, Fan PS. Effect of cytokines on the production of endothelin by endothelial cells. *Clin Exp Rheumatol* (1997) 15(2):163–7.
78. Cotie LM, Currie KD, McGill GM, Cameron AJ, McFadden AS, Phillips SM, et al. Associations between measures of vascular structure and function and systemic circulating blood markers in humans. *Physiol Rep* (2016) 4(18):e12982. doi:10.14814/phy2.12982
79. Estensen ME, Grindheim G, Remme EW, Godang K, Henriksen T, Aukrust P, et al. Elevated inflammatory markers in preeclamptic pregnancies, but no relation to systemic arterial stiffness. *Pregnancy Hypertens* (2015) 5(4):325–9. doi:10.1016/j.preghy.2015.09.003
80. Dyck DJ, Heigenhauser GJ, Bruce CR. The role of adipokines as regulators of skeletal muscle fatty acid metabolism and insulin sensitivity. *Acta Physiol (Oxf)* (2006) 6:5–16. doi:10.1111/j.1748-1716.2005.01502.x
81. Heilbronn LK, Campbell LV. Adipose tissue macrophages, low grade inflammation and insulin resistance in human obesity. *Curr Pharm Des* (2008) 6:1225–30. doi:10.2174/138161208784246153
82. Koh KK, Han SH, Quon MJ. Inflammatory markers and the metabolic syndrome insights from therapeutic interventions. *J Am Coll Cardiol* (2005) 46:1978. doi:10.1016/j.jacc.2005.06.082
83. Tuttolomondo A, Pecoraro A, Butta C, Di Raimondo D, Ferrante A, Della Corte V, et al. Arterial stiffness indexes and serum cytokine levels in seronegative spondyloarthritis: relationships between stiffness markers and metabolic and immunoinflammatory variables. *Scand J Rheumatol* (2015) 44(6):474–9. doi:10.3109/03009742.2015.1030449
84. Blankenberg S, Luc G, Ducimetiere P, Arveiler D, Ferrières J, Amouyel P, et al. IL-18 and the risk of coronary heart disease in European men: the Prospective Epidemiological Study of Myocardial Infarction (PRIME). *Circulation* (2003) 108:2453–9. doi:10.1161/01.CIR.0000099509.76044.A2
85. Yong K, Ooi EM, Dogra G, Mannion M, Boudville N, Chan D, et al. Elevated interleukin-12 and interleukin-18 in chronic kidney disease are not associated with arterial stiffness. *Cytokine* (2013) 64(1):39–42. doi:10.1016/j.cyto.2013.05.023
86. Troseid M, Seljeflot I, Weiss TW, Klemsdal TO, Hjerkinn EM, Arnesen H. Arterial stiffness is independently associated with interleukin-18 and components of the metabolic syndrome. *Atherosclerosis* (2010) 209:337–9. doi:10.1016/j.atherosclerosis.2009.09.028
87. Kheradmand M, Niimura H, Kuwabara K, Nakahata N, Nakamura A, Ogawa S, et al. Association of inflammatory gene polymorphysms and conventional risk factors with arterial stiffness by age. *J Epidemiol* (2013) 23(6):457–65. doi:10.2188/jea.JE20130054
88. Ohsaki Y, Shirakawa H, Hiwatashi K, Furukawa Y, Mizutani T, Komai M. Vitamin K suppresses lipopolysaccharide-induced inflammation in the rat. *Biosci Biotechnol Biochem* (2006) 70(4):926–32. doi:10.1271/bbb.70.926
89. Liuzzo G, Biasucci LM, Gallimore JR, Grillo RL, Rebuzzi AG, Pepys MB, et al. The prognostic value of C-reactive protein and serum-amyloid a protein in severe unstable angina. *N Engl J Med* (1994) 331:417–24. doi:10.1056/NEJM199408183310701
90. Ridker PM, Rifai N, Rose L, Buring JE, Cook NR. Comparison of C-reactive protein and low-density lipoprotein cholesterol levels in the prediction of first cardiovascular events. *N Engl J Med* (2002) 347:1557–65. doi:10.1056/NEJMoa021993
91. Ridker PM, Buring JE, Cook NR, Rifai N. C-reactive protein, the metabolic syndrome, and risk of incident cardiovascular events: an 8-year follow-up of 14,719 initially healthy American women. *Circulation* (2003) 107:391. doi:10.1161/01.CIR.0000055014.62083.05
92. Ridker PM. Clinical application of C-reactive protein for cardiovascular disease detection and prevention. *Circulation* (2003) 107(3):363–9. doi:10.1161/01.CIR.0000053730.47739.3C
93. Tan KC, Chow WS, Tam SC, Ai VH, Lam CH, Lam KS. Atorvastatin lowers C-reactive protein and improves endothelium-dependent vasodilation in type 2 diabetes mellitus. *J Clin Endocrinol Metab* (2002) 87:563–8. doi:10.1210/jcem.87.2.8249
94. Brevetti G, Silvestro A, Di Giacomo S, Bucur R, Di Donato A, Schiano V, et al. Endothelial dysfunction in peripheral arterial disease is related to increase in plasma markers of inflammation and severity of peripheral circulatory impairment but not to classic risk factors and atherosclerotic burden. *J Vasc Surg* (2003) 38:374–9. doi:10.1016/S0741-5214(03)00124-1
95. Prasad A, Zhu J, Halcox JP, Waclawiw MA, Epstein SE, Quyyumi AA. Predisposition to atherosclerosis by infections: role of endothelial dysfunction. *Circulation* (2002) 106:184–90. doi:10.1161/01.CIR.0000021125.83697.21
96. Van Haelst PL, van Doormaal JJ, Asselbergs FW, van Roon AM, Veeger NJ, Henneman MM, et al. Correlates of endothelial function and their relationship with inflammation in patients with familial hypercholesterolaemia. *Clin Sci (Lond)* (2003) 104:627–32. doi:10.1042/CS20020293
97. Salomaa V, Riley W, Kark JD, Nardo C, Folsom AR. Noninsulin-dependent diabetes mellitus and fasting glucose and insulin concentrations are associated with arterial stiffness indexes. The ARIC Study. Atherosclerosis Risk in Communities Study. *Circulation* (1995) 91:1432–43. doi:10.1161/01.CIR.91.5.1432
98. Mattace-Raso FU, van der Cammen TJ, van der Meer IM, Schalekamp MA, Asmar R, Hofman A, et al. C-reactive protein and arterial stiffness in older adults: the Rotterdam Study. *Atherosclerosis* (2004) 176(1):111–6. doi:10.1016/j.atherosclerosis.2004.04.014
99. Kullo IJ, Seward JB, Bailey KR, Bielak LF, Grossardt BR, Sheedy PF II, et al. C-reactive protein is related to arterial wave reflection and stiffness in asymptomatic subjects from the community. *Am J Hypertens* (2005) 18(8):1123–9. doi:10.1016/j.amjhyper.2005.03.730
100. McEniery CM, Spratt M, Munnery M, Yarnell J, Lowe GD, Rumley A, et al. An analysis of prospective risk factors for aortic stiffness in men: 20-year follow-up from the Caerphilly prospective study. *Hypertension* (2010) 56:36–43. doi:10.1161/HYPERTENSIONAHA.110.150896
101. Tomiyama H, Arai T, Koji Y, Yambe M, Hirayama Y, Yamamoto Y, et al. The relationship between high-sensitive C reactive protein and pulse wave velocity in healthy Japanese men. *Atherosclerosis* (2004) 174:373–7. doi:10.1016/j.atherosclerosis.2004.01.032

102. Gurlek Demirci B, Sezer S, Colak T, Sayin CB, Tutal E, Haberal M. Post-transplant C-reactive protein predicts arterial stiffness and graft function in renal transplant recipients. *Transplant Proc* (2015) 47:1174–7. doi:10.1016/j.transproceed.2014.10.064
103. Kampus P, Kals J, Ristimäe T, Fischer K, Zilmer M, Teesalu R. High-sensitivity C-reactive protein affects central haemodynamics and augmentation index in apparently healthy persons. *J Hypertens* (2004) 22(6):1133–9. doi:10.1097/00004872-200406000-00014
104. Nurizal A, Antono D, Wijaia IP, Shatri H. Correlation between high-sensitivity C reactive protein and local arterial stiffness measured by radio frequency echotracking system in type 2 diabetic patients. *Acta Med Indones* (2014) 46(4):308–13.
105. Dörr O, Liebetrau C, Möllmann H, Gaede L, Troidl C, Rixe J, et al. Soluble fms-like tyrosine kinase-1 and endothelial adhesion molecules (intercellular cell adhesion molecule-1 and vascular cell adhesion molecule-1) as predictive markers of blood pressure reduction after renal sympathetic denervation. *Hypertension* (2014) 63:984–90. doi:10.1161/HYPERTENSIONAHA.113.02266
106. Kunutsor SK, Bakker SJL, Dullaart RPF. Soluble vascular cell adhesion molecules may be protective of future cardiovascular disease risk: findings from the PREVEND prospective cohort study. *J Atheroscler Thromb* (2017) 24:804–18. doi:10.5551/jat.38836
107. Blankenberg S, Rupprecht HJ, Bickel K, Peetz D, Hafner G, Tiret L, et al. Circulating cell adhesion molecules and death in patients with coronary artery disease. *Circulation* (2001) 104(12):1336–42. doi:10.1161/hc3701.095949
108. Preedy VR. *Adhesion Molecules*. Enfield, New Hampshire: CRC Press (2016). 534 p.
109. Kilic ID, Findikoglu G, Alihanoglu YI, Yildiz BS, Uslu S, Rota S, et al. Circulating adhesion molecules and arterial stiffness. *Cardiovasc J Afr* (2015) 26(1):21–4. doi:10.5830/CVJA-2014-060
110. Kals J, Kampus P, Kals M, Pulges A, Teesalu R, Zilmer K, et al. Inflammation and oxidative stress are associated differently with endothelial function and arterial stiffness in healthy subjects and in patients with atherosclerosis. *Scand J Clin Lab Invest* (2008) 68(7):594–601. doi:10.1080/00365510801930626
111. Boomsma F, Hut H, Bagghoe U, van der Houwen A, van den Meiracker A. Semicarbazide-sensitive amine oxidase (SSAO): from cell to circulation. *Med Sci Monit* (2005) 11(4):RA122–6.
112. Chen DW, Zhao RM, Jin Y, Zhang J, Han C, Jiang SQ, et al. Plasma soluble vascular adhesion protein-1 concentration correlates with arterial stiffness: a cross-sectional study. *Arch Gerontol Geriatr* (2015) 61:67–71. doi:10.1016/j.archger.2015.04.007
113. Merinen M, Irjala H, Salmi M, Jaakkola I, Hänninen A, Jalkanen S. Vascular adhesion protein-1 is involved in both acute and chronic inflammation in the mouse. *Am J Pathol* (2005) 166(3):793–800. doi:10.1016/S0002-9440(10)62300-0
114. Jalkanen S, Karikoski M, Mercier N, Koskinen K, Henttinen T, Elima K, et al. The oxidase activity of vascular adhesion protein-1 (VAP-1) induces endothelial E- and P-selectins and leukocyte binding. *Blood* (2007) 110(6):1864–70. doi:10.1182/blood-2007-01-069674
115. Mattila KJ, Nieminen MS, Valtonen VV, Rasi VP, Kesäniemi YA, Syrjälä SL, et al. Association between dental health and acute myocardial infarction. *BMJ* (1989) 298:779–81. doi:10.1136/bmj.298.6676.779
116. Syrjanen J, Peltola J, Valtonen V, Iivanainen M, Kaste M, Huttunen JK. Dental infections in association with cerebral infarction in young and middle-aged men. *J Intern Med* (1989) 225:179–84. doi:10.1111/j.1365-2796.1989.tb00060.x
117. Franek E, Januszkiewicz-Caulier J, Blach A, Napora M, Jedynasty K, Budlewski T, et al. Intima-media thickness and other markers of atherosclerosis in patients with type 2 diabetes and periodontal disease. *Kardiol Pol* (2012) 70(1):7–13.
118. Piepoli MF, Hoes AW, Agewall S, Albus C, Brotons C, Catapano AL, et al. 2016 European Guidelines on cardiovascular disease prevention in clinical practice: the Sixth Joint Task Force of the European Society of Cardiology and Other Societies on cardiovascular disease prevention in clinical practice (constituted by representatives of 10 societies and by invited experts) developed with the special contribution of the European Association for Cardiovascular Prevention and Rehabilitation (EACPR). *Atherosclerosis* (2016) 252:207–74. doi:10.1016/j.atherosclerosis.2016.05.037
119. Nazir MA. Prevalence of periodontal disease, its association with systemic diseases and prevention. *In J Health Sci (Qassim)* (2017) 11(2):72–80.
120. Janket SJ, Baird AE, Chuang SK, Jones JA. Meta-analysis of periodontal disease and risk of coronary heart disease and stroke. *Oral Surg Oral Med Oral Pathol Oral Radiol Endod* (2003) 95(5):559–69. doi:10.1067/moe.2003.107
121. Slocum C, Kramer C, Genco CA. Immune dysregulation mediated by the oral microbiome: potential links to chronic inflammation and atherosclerosis. *J Intern Med* (2016) 280(1):114–28. doi:10.1111/joim.12476
122. Van Dyke TE, Serhan CN. Resolution of inflammation: a new paradigm for the pathogenesis of periodontal diseases. *J Dent Res* (2003) 82(2):82–90. doi:10.1177/154405910308200202
123. Hasturk H, Kantarci A. Activation and resolution of periodontal inflammation and its systemic impact. *Periodontol 2000* (2015) 69(1):255–73. doi:10.1111/prd.12105
124. Gurav AN. The association of periodontitis and metabolic syndrome. *Dent Res J (Isfahan)* (2014) 11(1):1–10.
125. Mozos I. *Pathophysiology. Lecture Notes for Dental Medicine*. Saarbrücken, Deutschland: LAP Lambert Academic Publishing (2015). 296 p.
126. Beck JD, Eke P, Lin D, Madianos P, Couper D, Moss K, et al. Associations between IgG antibody to oral organisms and carotid intima-medial thickness in community-dwelling adults. *Atherosclerosis* (2005) 183:342–8. doi:10.1016/j.atherosclerosis.2005.03.017
127. Desvarieux M, Demmer RT, Jacobs DR, Papapanou PN, Sacco RL, Rundek T. Changes in clinical and microbiological periodontal profiles related to the progression of carotid intima-media thickness: the oral infections and vascular disease epidemiology study. *J Am Heart Assoc* (2013) 2:e000254. doi:10.1161/JAHA.113.000254
128. Zaremba M, Gorska R, Suwalski P, Kowalski J. Evaluation of the incidence of periodontitis associated bacteria in the atherosclerotic plaque of coronary blood vessels. *J Periodontol* (2007) 78:322–7. doi:10.1902/jop.2006.060081
129. Hayashida H, Saito T, Kawasaki K, Kitamura M, Furugen R, Iwasaki T, et al. Association of periodontitis with carotid artery intima-media thickness and arterial stiffness in community-dwelling people in Japan: the Nagasaki Islands study. *Atherosclerosis* (2013) 229(1):186–91. doi:10.1016/j.atherosclerosis.2013.04.002
130. Shanker J, Setty P, Arvind P, Nair J, Bhasker D, Balakrishna G, et al. Relationship between periodontal disease, *Porphyromonas gingivalis*, peripheral vascular resistance markers and coronary artery disease in Asian Indians. *Thromb Res* (2013) 132(1):e8–14. doi:10.1016/j.thromres.2013.04.023
131. Kapellas K, Jamieson LM, Do LG, Bartold PM, Wang H, Maple-Brown LJ, et al. Associations between periodontal disease and cardiovascular surrogate measures among Indigenous Australians. *Int J Cardiol* (2014) 173(2):190–6. doi:10.1016/j.ijcard.2014.02.015
132. Jockel-Schneider Y, Harks I, Haubitz I, Fickl S, Eigenthaler M, Schlagenhauf U, et al. Arterial stiffness and pulse wave reflection are increased in patients suffering from severe periodontitis. *PLoS One* (2014) 9(8):e103449. doi:10.1371/journalone.0103449
133. Schmitt A, Carra MC, Boutouyrie P, Bouchard P. Periodontitis and arterial stiffness: a systematic review and meta-analysis. *J Clin Periodontol* (2015) 42(11):977–87. doi:10.1111/jcpe.12467
134. Houcken W, Teeuw WJ, Bizzaro S, Alvarez Rodriguez E, Mulders TA, van den Born BJ, et al. Arterial stiffness in periodontitis patients and controls. A case-control and pilot intervention study. *J Hum Hypertens* (2016) 30(1):24–9. doi:10.1038/jhh.2015.41
135. Vidal F, Cordovil I, Figueredo CM, Fischer RG. Non-surgical periodontal treatment reduces cardiovascular risk in refractory hypertensive patients: a pilot study. *J Clin Periodontol* (2013) 40(7):681–7. doi:10.1111/jcpe.12110
136. Sanz-Miralles EC, Li R, Momen-Heravi F, Mendieta C, Konofagou EE, Papapanou PN. Assessment of arterial stiffness in periodontitis using a novel pulse wave imaging methodology. *J Clin Periodontol* (2017) 44(5):502–10. doi:10.1111/jcpe.12717
137. Harris TA, Yamakuchi M, Ferlito M, Mendell JT, Lowenstein CJ. MicroRNA-126 regulates endothelial expression of vascular cell adhesion molecule 1. *Proc Natl Acad Sci U S A* (2008) 105(5):1516–21. doi:10.1073/pnas.0707493105
138. Zhou J, Wang KC, Wu W, Subramaniam S, Shyy JY, Chiu JJ, et al. MicroRNA-21 targets peroxisome proliferators activated receptor-α in an autoregulatory

loop to modulate flow-induced endothelial inflammation. *Proc Natl Acad Sci U S A* (2011) 108(25):10355–60. doi:10.1073/pnas.1107052108
139. Parthenakis F, Marketou M, Kontaraki J, Patrianakos A, Nakou H, Touloupaki M, et al. Low levels of microRNA-21 are a marker of reduced arterial stiffness in well-controlled hypertension. *J Clin Hypertens (Greenwich)* (2017) 19(3):235–40. doi:10.1111/jch.12900
140. Lin X, Zhan JK, Wang YJ, Tan P, Chen YY, Deng HQ, et al. Function, role, and clinical application of microRNAs in vascular aging. *Biomed Res Int* (2016) 2016:6021394. doi:10.1155/2016/6021394
141. Fiedler J, Thum T. MicroRNAs in myocardial infarction. *Arterioscler Thromb Vasc Biol* (2013) 33(2):201–5. doi:10.1161/ATVBAHA.112.300137
142. Qin B, Yang H, Xiao B. Role of microRNAs in endothelial inflammation and senescence. *Mol Biol Rep* (2012) 39(4):4509–18. doi:10.1007/s11033-011-1241-0
143. Ni CW, Qiu H, Jo H. MicroRNA-663 upregulated by oscillatory shear stress plays a role in inflammatory response of endothelial cells. *Am J Physiol Heart Circ Physiol* (2011) 300(5):H1762–9. doi:10.1152/ajpheart.00829.2010
144. Liao YC, Wang YS, Guo YC, Lin WL, Chang MH, Juo SH. Let-7g improves multiple endothelial functions through targeting transforming growth factor-beta and SIRT-1 signaling. *J Am Coll Cardiol* (2014) 63(16):1685–94. doi:10.1016/j.jacc.2013.09.069
145. Ding Y, Sun X, Shan PF. MicroRNAs and cardiovascular disease in diabetes mellitus. *Biomed Res Int* (2017) 2017:4080364. doi:10.1155/2017/4080364
146. Loyer X, Potteaux S, Vion AC, Guérin CL, Boulkroun S, Rautou PE, et al. Inhibition of microRNA-92a prevents endothelial dysfunction and atherosclerosis in mice. *Circ Res* (2014) 114(3):434–43. doi:10.1161/CIRCRESAHA.114.302213
147. Canfran-Duque A, Rotllan N, Zhang X, Fernández-Fuertes M, Ramírez-Hidalgo C, Araldi E, et al. Macrophage deficiency of miR-21 promotes apoptosis, plaque necrosis, and vascular inflammation during atherogenesis. *EMBO Mol Med* (2017):e201607492. doi:10.15252/emmm.201607492
148. Demolli S, Doebele C, Doddaballapur A, Lang V, Fisslthaler B, Chavakis E, et al. MicroRNA-mediates anti-inflammatory effects of shear stress and KLF2 via repression of angiopoietin 2. *J Moll Cell Cardiol* (2015) 88:111–9. doi:10.1016/j.yjmcc.2015.10.009
149. Deng H, Song Z, Xu H, Deng X, Zhang Q, Chen H, et al. MicroRNA-1185 promotes arterial stiffness though modulating VCAM-1 and E-selectin. *Cell Physiol Biochem* (2017) 41(6):2183–93. doi:10.1159/000475576
150. Martinez-Gonzalez J, Badimon L. Mechanisms underlying the cardiovascular effects of COX-inhibition: benefits and risks. *Curr Pharm Des* (2007) 13(22):2215–27. doi:10.2174/138161207781368774
151. Capriotti T, Parker Frizzell J. *Pathophysiology. Introductory Concepts and Clinical Perspectives*. Philadelphia: FA Davis Company (2016). 1161 p.
152. Korotkova M, Jakobsson PJ. Characterization of microsomal prostaglandin E synthase 1 inhibitors. *Basic Clin Pharmacol Toxicol* (2014) 114(1):64–9. doi:10.1111/bcpt.12162
153. Psarra A, Nikolaou A, Kokotou MG, Limnios D, Kokotos G. Microsomal prostaglandin E2 synthase-1 inhibitors: a patent review. *Expert Opin Ther Pat* (2017) 27(9):1047–59. doi:10.1080/13543776.2017.1344218
154. Dieffenbach PB, Mallarino Haeger C, Coronata AMF, Choi KM, Varelas X, Tschumperlin DJ, et al. Arterial stiffness induces remodeling phenotypes in pulmonary artery smooth muscle cells via YAP/TAZ-mediated repression of cyclooxygenase-2. *Am J Physiol Lung Cell Mol Physiol* (2017). doi:10.1152/ajplung.00173.2017
155. Fredenburgh LE, Liang OD, Macias AA, Polte TR, Liu X, Riascos DF, et al. Absence of cyclooxigenase-2 exacerbates hypoxia-induced pulmonary hypertension and enhances contractility of vascular smooth muscle cells. *Circulation* (2008) 117(16):2114–22. doi:10.1161/CIRCULATIONAHA.107.716241
156. Liu C, Gao J, Chen B, Chen L, Belguise K, Yu W, et al. Cyclooxygenase-2 promotes pulmonary intravascular macrophage accumulation by exacerbating BMP signaling in rat experimental hepatopulmonary syndrome. *Biochem Pharmacol* (2017) 138:205–15. doi:10.1016/j.bcp.2017.06.117
157. Avendano MS, Martinez-Revelles S, Aguado A, Simões MR, González-Amor M, Palacios R, et al. Role of COX-2-derived PGE2 on vascular stiffness and function in hypertension. *Br J Pharmacol* (2016) 173(9):1541–55. doi:10.1111/bph.13457
158. Vlachopoulos C, Aznaouridis K, Bratsas A, Ioakeimidis N, Dima I, Xaplanteris P, et al. Arterial stiffening and systemic endothelial activation induced by smoking: the role of COX-1 and COX-2. *Int J Cardiol* (2015) 189:293–8. doi:10.1016/j.ijcard.2015.04.029
159. Wong M, Jiang BY, McNeill K, Farish S, Kirkham B, Chowienczyk P. Effects of selective and non-selective cyclooxygenase inhibition on endothelial function in patients with rheumatoid arthritis. *Scand J Rheumatol* (2007) 36(4):265–9. doi:10.1080/03009740701286771
160. Laurent S, Fassot C, Lacolley P, Boutouyrie P. Molecular determinants of arterial stiffness. *Artery Res* (2007) 1:26–31. doi:10.1016/j.artres.2007.03.004
161. Chen Y, Shen F, Liu J, Yang G. Arterial stiffness and stroke: de-stiffening strategy, a therapeutic target for stroke. *Stroke Vasc Neurol* (2017):e000045. doi:10.1136/svn-2016-000045

Conflict of Interest Statement: The authors declare that the research was conducted in the absence of any commercial or financial relationships that could be construed as a potential conflict of interest.

Copyright © 2017 Mozos, Malainer, Horbańczuk, Gug, Stoian, Luca and Atanasov. This is an open-access article distributed under the terms of the Creative Commons Attribution License (CC BY). The use, distribution or reproduction in other forums is permitted, provided the original author(s) or licensor are credited and that the original publication in this journal is cited, in accordance with accepted academic practice. No use, distribution or reproduction is permitted which does not comply with these terms.

frontiers in Immunology

ORIGINAL RESEARCH
published: 15 September 2017
doi: 10.3389/fimmu.2017.01135

SIRT1/Adenosine Monophosphate-Activated Protein Kinase α Signaling Enhances Macrophage Polarization to an Anti-inflammatory Phenotype in Rheumatoid Arthritis

*So Youn Park[1,2], Sung Won Lee[3], Sang Yeob Lee[3], Ki Whan Hong[2], Sun Sik Bae[1,2], Koanhoi Kim[1] and Chi Dae Kim[1,2]**

[1] Department of Pharmacology, School of Medicine, Pusan National University, Gyeongsangnam-do, South Korea, [2] Gene and Cell Therapy Research Center for Vessel-Associated Diseases, Pusan National University, Gyeongsangnam-do, South Korea, [3] Department of Internal Medicine, College of Medicine, Dong-A University, Busan, South Korea

Macrophages are crucially involved in the pathogenesis of rheumatoid arthritis (RA). Macrophages of the M1 phenotype act as pro-inflammatory mediators in synovium, whereas those of the M2 phenotype suppress inflammation and promote tissue repair. SIRT1 is a class 3 histone deacetylase with anti-inflammatory characteristics. However, the role played by SIRT1 in macrophage polarization has not been defined in RA. We investigated whether SIRT1 exerts anti-inflammatory effects by modulating M1/M2 polarization in macrophages from RA patients. In this study, SIRT1 activation promoted the phosphorylation of an adenosine monophosphate-activated protein kinase (AMPK) α/acetyl-CoA carboxylase in macrophages exposed to interleukin (IL)-4, and that this resulted in the expressions of M2 genes, including MDC, FcεRII, MrC1, and IL-10, at high levels. Furthermore, these expressions were inhibited by sirtinol (an inhibitor of SIRT1) and compound C (an inhibitor of AMPK). Moreover, SIRT1 activation downregulated LPS/interferon γ-mediated NF-κB activity by inhibiting p65 acetylation and the expression of M1 genes, such as CCL2, iNOS, IL-12 p35, and IL-12 p40. Macrophages from SIRT1 transgenic (Tg)-mice exhibited enhanced polarization of M2 phenotype macrophages and reduced polarization of M1 phenotype macrophages. In line with these observations, SIRT1-Tg mice showed less histological signs of arthritis, that is, lower TNFα and IL-1β expressions and less severe arthritis in the knee joints, compared to wild-type mice. Taken together, the study shows activation of SIRT1/AMPKα signaling exerts anti-inflammatory activities by regulating M1/M2 polarization, and thereby reduces inflammatory responses in RA. Furthermore, it suggests that SIRT1 signaling be viewed as a therapeutic target in RA.

Keywords: rheumatoid arthritis, inflammation, macrophage polarization, M1/M2 macrophages, SIRT1, adenosine monophosphate-activated protein kinase α

OPEN ACCESS

Edited by:
Guixiu Shi,
Xiamen University, China

Reviewed by:
Shanzhong Gong,
University of Texas at Austin, United States
Valerio Chiurchiù,
Università Campus Bio-Medico, Italy

***Correspondence:**
Chi Dae Kim
chidkim@pusan.ac.kr

Specialty section:
This article was submitted to Inflammation, a section of the journal Frontiers in Immunology

Received: *26 June 2017*
Accepted: *29 August 2017*
Published: *15 September 2017*

Citation:
Park SY, Lee SW, Lee SY, Hong KW, Bae SS, Kim K and Kim CD (2017) SIRT1/Adenosine Monophosphate-Activated Protein Kinase α Signaling Enhances Macrophage Polarization to an Anti-inflammatory Phenotype in Rheumatoid Arthritis. Front. Immunol. 8:1135. doi: 10.3389/fimmu.2017.01135

INTRODUCTION

Rheumatoid arthritis (RA) is a chronic inflammatory disease that can activate the immune system *via* immune cells, such as macrophages, dendritic cells, and lymphocytes. These orchestrated interactions induce the abundant productions pro-inflammatory cytokines and cellular components in RA joints, and lead to progressive joint destruction (1, 2). Macrophages in synovium exhibit

a heterogeneous phenotype, and macrophages activated by various cytokines are crucial for inflammatory processes associated with development of synovitis in RA (3). Macrophages are polarized to the classically activated M1 phenotype by Th1 cytokines [LPS, interferon (IFN)γ and interleukin (IL)-12], and this phenotype polarization results in the upregulations of pro-inflammatory mediators, including TNFα, IL-1β, and MCP-1. By contrast, macrophages are polarized to the alternative M2 phenotype by Th2 cytokines (IL-4, IL-10, and IL-13), which are associated with long-term tissue repair, immunity, and the production of anti-inflammatory cytokines (4–6). Arthritic joints display an imbalance between the M1 and M2 phenotypes (7). Furthermore, signaling pathways and the activities of transcription factors are also related to macrophage polarization, for example, NF-κB, STAT1, and SOCS1 in the M1 phenotype, and STAT6, KLF4, and PPARγ in the M2 phenotype (3). Recent findings show that synovial fluids in RA patients contain high levels of M1 macrophage-derived mediators, but low levels of M2 macrophage-derived mediators (8).

Histone/protein deacetylase SIRT1 and adenosine monophosphate-activated protein kinase (AMPK) work in tandem to control cell metabolism, transcriptional gene expression, neuroprotection, and inflammation (9, 10). AMPK activation is stimulated by SIRT1 *via* the deacetylation and activation of AMPK kinase/LKB1 (11). The N-terminal domain of SIRT1 transactivates deacetylation by interacting with endogenous SIRT1 and promoting the deacetylation of K310 of the RelA/p65 subunit, and consequently reduces the activation of NF-κB activity, leading to attenuate the expressions of pro-inflammatory cytokines (12, 13). Active AMPK participates in the suppression of inflammatory responses by inhibiting inflammatory signaling, such as, the NF-κB pathway, and conversely downregulation of AMPK activity results in increased inflammation (14). Macrophages containing constitutively active AMPKα1 blocked LPS- and fatty acid-induced inflammatory mediators through SIRT1 (15), and in AMPK $\alpha1^{-/-}$ mice pro-inflammatory states were promoted by direct phosphorylation of NF-κB (16).

Nevertheless, the function of SIRT1 in RA remains controversial. The activity and expression of SIRT1 have been shown to be diminished in the peripheral blood mononuclear cells (PBMCs) of RA patients (17). In addition, increased SIRT1 activity has been reported to alleviate arthritis by suppressing VEGF and inhibiting synovial angiogenesis (18). On the other hand, controversial results have been reported regarding the influences of sirtuins on inflammation and apoptosis (19, 20).

Given SIRT1/AMPKα signaling has an important role in regulating macrophage polarization to an anti-inflammatory M2 phenotype, and that activation of this signaling may attenuate joint inflammation in RA, we sought to establish whether SIRT1 induces AMPKα phosphorylation and subsequent NF-κB downregulation, leading to the upregulations of M2-associated cytokines and to the downregulations of the expressions of M1-associated pro-inflammatory mediators in macrophages obtained from RA patients or SIRT1-overexpressing mice. In addition, we assessed a prevention of synovial inflammation and joint destruction in SIRT1 transgenic (Tg) mice with collagen-induced arthritis (CIA).

MATERIALS AND METHODS

Materials

Resveratrol (RSV), LPS, compound C (CC), and Ficoll-Paque were purchased from Sigma-Aldrich (St. Louis, MO, USA). Recombinant human IL-4, recombinant human macrophage-colony-stimulating factor (M-CSF), and interferon (INF) γ were from Pepro Tech (Rocky Hill, NJ, USA). Sirtinol was obtained from Calbiochem (La Jolla, CA, USA). Antibodies specific for AMPKα, phosphor-AMPKα, phosphor-NF-κB p65 (Lys310), acetyl-NF-κB p65 (Lys310), acetyl-CoA carboxylase (ACC), and phosphor-ACC were from Cell Signaling (Danvers, MA, USA). Antibodies specific for SIRT1, NF-κB p65, ariginase-1, and Histone H1 were from Santa Cruz Biotechnology Inc. (Santa Cruz, CA, USA). Antibodies specific for TNFα and IL-1β were from Abcam (Cambridge, UK). Antibody specific for TRANCE/TNFSF11 was from R&D Systems (Minneapolis, MN, USA).

Patient Sample

Synovial fluid was obtained during the therapeutic arthrocentesis from the affected knees of patients with RA who fulfilled the American Rheumatism Association classification criteria (1987). All patients provided informed consent, and the study was approved the Medical Ethics Committees of the Academic Medical Center (Dong-A University Hospital, Busan, South Korea).

Cell Isolation and Cell Culture

Mononuclear cells from synovial fluid were isolated using density gradient centrifugation methods (Ficoll-Paque). Cells were incubated in RPMI with 10% FBS for 24 h, and then adherent cells were incubated in culture medium plus M-CSF (100 ng/ml) for 7 days. M1 polarization was stimulated by LPS (100 ng/ml) or INFγ (20 ng/ml), and M2 polarization was achieved by treating cells with IL-4 (20 ng/ml).

Quantitative RT-PCR

For measurement of mRNA levels, total RNA isolation and RT-PCR were performed as previously described (21). The mRNA levels were normalized to the human ribosomal 18S gene or mouse actin. Data are analyzed using LightCycler 96 software (Roche Molecular Biochemicals). Primer sequences are provided in **Table 1**.

Immunoblot Analysis

Proteins were loaded into 10% polyacrylamide gels. Protein transferred to nitrocellulose membranes, which were immunoblotted with antibodies against AMPKα, p-AMPKα, ACC, p-ACC, NF-κB p65, p-NF-κB p65, ac-NF-κB p65, and SIRT1. Protein bands were visualized using the Supersignal West Dura Chemiluminescent Substrate (Thermo Fisher Scientific Inc., Rockford, IL, USA). Signals from bands were quantified using a UN-SCAN-IT gel™ software (Silk Scientific, Orem, UT, USA).

RAN Interference Assay

For SIRT1 gene knockdown, cells were transfected with SIRT1 siRNA oligonucleotide (GenBank accession no. NM_019812.1:

TABLE 1 | Oligonucleotide sequences used for qPCR.

Human		Mouse	
Oligonucleotides, 5′–3′		**Oligonucleotides, 5′–3′**	
FcεRII	Forward: GGGAGAATCCAAGCAGGAC Reverse: GGAAGCTCCTCGATCTCTGA	Arginase-1	Forward: CCAGAAGAATGGAAGAGTCAGTGT Reverse: GCAGATATGCAGGGAGTCACC
Interleukin (IL)-10	Forward: AAGACCCAGACATCAAGGCG Reverse: AGGCATTCTTCACCTGCTCC	Fizz	Forward: TCCCAGTGAATACTGATGAGA Reverse: CCACTCTGGATCTCCCAAGA
IL-12 p35	Forward: GCCACAGGTCTGCATCCA Reverse: GACCTGGCGGGCTGAGTA	FcεRII	Forward: GGGACACAGCTCATGTTGGT Reverse: GCAGTGTCTCCCAGCTGTTT
IL-12 p40	Forward: AGCCTCCTCCTTGTGGCTA Reverse: TGGTTTTATCTTTTGTG TGTGC	IL-1β	Forward: GGTGTGTGACGTTCCCATTAG Reverse: TCGTTGCTTGGTTCTCCTTGT
iNOS	Forward: GTTCTCAAGGCACACCAGGTCTG Reverse: GCAGGTCACTTATGTCACTTATC	IL-12 p35	Forward: CTTAGCCAGTCCCGAAACCT Reverse: TTGGTCCCGTGTGATGTCT
MCP-1	Forward: GGAGCATCCACGTGTTGGC Reverse: ACAGCTTCTTTGGGACACC	IL-12 p40	Forward: GTTCAACATCAAGAGCAGTAGCA Reverse: CTGCAGACAGAGACGCCATT
MDC	Forward: GGTTGTCCTCGTCCTCCTTG Reverse: GAAGGTTAGCAACACCACGC	MCP-1	Forward: TCCCACTCACCTGCTGCTACTCA Reverse: GCTTCTTTGGGACACCTGCTG
MrC1	Forward: TCAATGGCATGAAGCGGAGA Reverse: TACTGTTCAGGGCGATCCAC	TNFα	Forward: ATGAGAAGTTCCCAAATGGC Reverse: CTCCACTTGGTGGTTTGCTA
18S	Forward: GGCCCTGTAATTGGAATGAGTC Reverse: CCAAGATCCAACTACGAGCTT	Yim-1	Forward: GGGCATACCTTTATCCTGAG Reverse: CCACTGAAGTCATCCATGTC
		Actin	Forward: GCCCTGAGGCTCTTTTCCAG Reverse: TGCCACAGGATTCCATACCC

Daejeon, South Korea) using Lipofectamine 2000 (Invitrogen, Carlsbad, CA, USA) following the manufacturer's protocol.

Luciferase Assay

Cells were transiently transfected with NF-κB luciferase reporter vector using Lipofectamine 2000 (Invitrogen) according to the manufacturer's instruction. The activity of firefly and luciferase was measured using the dual luciferase reporter assay system (Promega, Madison, WI, USA).

Mice and Cell Culture

SIRT1-Tg mice (C57BL/6N) were a generous gift from Jong-Wan Park (Seoul National University, South Korea). C57BL/6N mice were from Japan SLC (Shizuoka, Japan). All experimental procedures were approved by the Animal Experimental Committee of the College of Medicine, Pusan National University (PNU-2016-1107) and done in accordance with guidelines for animal research. Murine bone marrow cells were isolated from mouse femoral and tibial bone marrow. Bone marrow-derived macrophages (BMDMs) were prepared from bone marrow cells and cultured in RPMI with 10% FBS and M-CSF (100 ng/ml).

Induction and Monitoring of CIA

To trigger CIA, mice were sensitized by injecting 100 μg of chicken type II collagen (CII) supplemented with complete Freund's adjuvant (Sigma) intradermally at the tail base, and received a booster injection of CII supplemented with incomplete Freund's adjuvant in the same manner 14 days later by Inglis et al. (22). Mice were euthanized 38 days after initial injection, and knee joints were isolated. Arthritis severities in individual limbs were assessed by evaluating erythema, swelling, and other changes. Clinical arthritis severity and histological arthritis severity was scored using a scoring system, as previously described (23) (**Table 2**).

TABLE 2 | Arthritis severity scoring system.

Clinical arthritis severity score	
0	Normal
1	Slight erythema or swelling
2	Distinct erythematous swelling
3	Joint distortion
4	Ankylosis of the joint
Histological arthritis severity score	
0	Normal
1	Synovial inflammation—mild
	Synovial lesion—mild alteration
	Cartilage destruction—mild
	Bone erosion—mild
2	Synovial inflammation—moderate
	Synovial lesion—moderate alteration
	Cartilage destruction—moderate
	Bone erosion—moderate
3	Synovial inflammation—moderate
	Synovial lesion—severe destruction of the synovia
	Cartilage destruction—severe destruction with loss of cartilage
	Bone erosion—severe destruction, with disrupted joint architecture

Immunohistochemistry

Tissue sections were obtained from paraffin blocks and rehydrated, and then incubated with anti-TNFα, anti-IL-1β, and anti-TRANCE/TNFSF11 antibodies. Immunoreaction products were visualized using a broad-spectrum immunohistochemistry kit (Diaminobenzidine substrate kit, Vector Laboratories, Inc., Burlingame, CA, USA).

Statistical Analysis

Statistical analyses were performed using GraphPad Software (San Diego, CA, USA). Means and SDs were calculated. The parametric Student's *t*-test was used to assess the significances of differences between treated and untreated groups and considered to be significant when $P < 0.05$.

RESULTS

Upregulation of M2 Markers by SIRT1 in RA Macrophages

Macrophages were generated from synovial monocytes cultured in the presence of M-CSF for 7 days (24). When cells were treated with RSV (a pharmacological activator of SIRT1, 50 μM) for 24 or 48 h, SIRT1 protein levels were significantly elevated (Figure S1 in Supplementary Material).

To investigate the effect of SIRT1 on the M2 polarization of macrophages induced by IL-4 (20 ng/ml), we detected the mRNA levels of M2 macrophage markers, that is, MDC (macrophage-derived chemokine), FcεRII (low-affinity IgE receptors), MrC1 (C-type mannose receptor 1), and IL-10. As shown in **Figures 1A–D**, MDC, FcεRII, MrC1, and IL-10 mRNA expression levels following treatment with IL-4 (12 h) significantly increased to 2.37 ± 0.26-fold ($P < 0.001$), 3.41 ± 1.42-fold ($P < 0.05$), 3.53 ± 0.86-fold ($P < 0.05$), and 3.27 ± 1.17-fold ($P < 0.05$), respectively. When cells were pretreated with RSV (50 μM) for 24 h prior to IL-4, the mRNA expression levels of MDC, FcεRII, and MrC1 were significantly enhanced to 4.19 ± 0.52-, 10.73 ± 2.67-, and 8.10 ± 1.58-fold, respectively. IL-10 mRNA expression was only marginally increased.

Suppres sion of Expression of M1 Markers by SIRT1 in RA Macrophages

M1 phenotype macrophages are promoted by macrophage-activating factors, such as LPS and IFNγ (25). Here, we examined whether SIRT1activation affects the LPS/IFNγ-induced M1 phenotype in RA. As shown in **Figures 1E–H**, M1 macrophage markers, including MCP-1, iNOS, and IL-12 p40 mRNA levels, were significantly elevated in response to LPS (1 μg/ml), but little affected by IFNγ (20 ng/ml) alone. However, the mRNA levels of MCP-1, iNOS, IL-12 p35, and IL-12 p40 were elevated further by LPS plus IFNγ. When cells were pretreated with RSV (50 μM) for 24 h prior to exposure to LPS plus IFNγ, the mRNA expression levels of M1 macrophage markers were significantly suppressed: MCP-1 (from 7.27 ± 1.43- to 1.56 ± 0.22-fold, $P < 0.01$), iNOS (from 6.63 ± 0.86- to 2.82 ± 0.33-fold, $P < 0.01$), IL-12 p35 (from 11.56 ± 2.98- to 2.43 ± 0.44-fold, $P < 0.05$), and IL-12 p40 (from 9.63 ± 1.70- to 3.56 ± 0.69-fold, $P < 0.05$), respectively.

These results show that SIRT1 activation by RSV augments the expression of anti-inflammatory M2 macrophages and attenuates the expression of pro-inflammatory M1 macrophages.

Effects of SIRT1 Inhibition on M1/M2 Macrophages

To confirm the role of SIRT1 in RA macrophage polarization into the M2 phenotype, SIRT1 expression in macrophages was inhibited by using of siRNA against SIRT1 gene. When cells were subjected to SIRT1 gene knockdown, they showed ~60% reduction in SIRT1 protein expression. These cells did not show increase in SIRT1 protein expression in response to RSV as contrasted to the cells transfected with negative siRNA (**Figure 2A**).

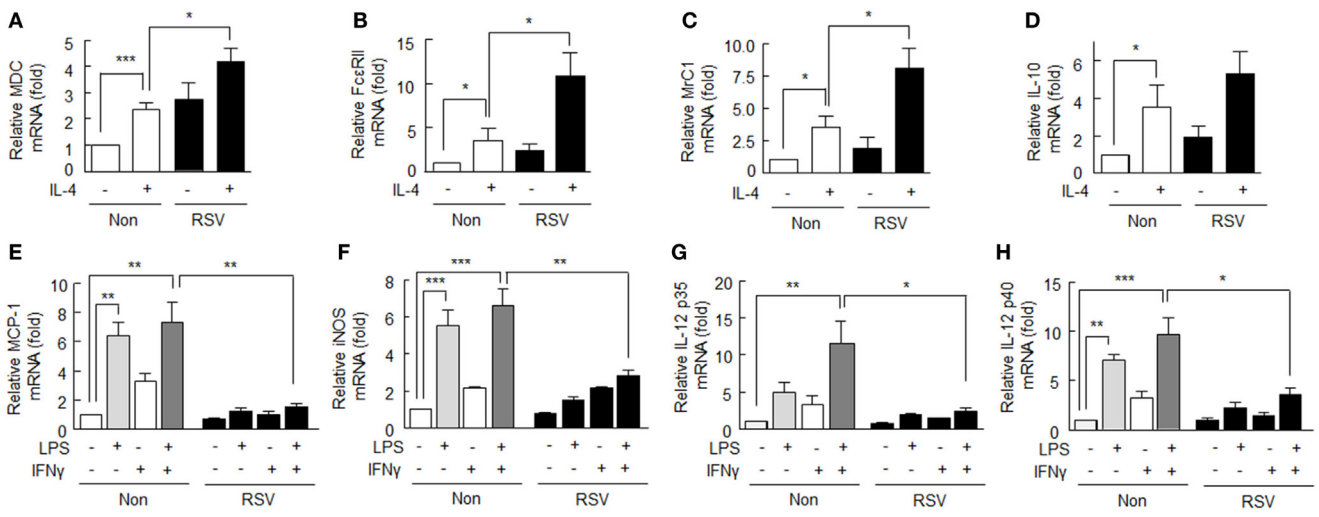

FIGURE 1 | Effects of SIRT1 activation by resveratrol (RSV) on M1 and M2 markers in rheumatoid arthritis macrophages. **(A–D)** After pretreatment with RSV (50 μM) for 24 h, cells were incubated with interleukin (IL)-4 (20 ng/ml) for 12 h. The mRNA expression levels of MDC, FcεRII, MrC1, and IL-10 were quantified by qPCR and normalized versus 18S ribosomal RNA. **(E–H)** After pretreatment with RSV (50 μM) for 24 h, cells were incubated with LPS (1 μg/ml) and/or interferon (IFN)γ (20 ng/ml) for 12 h. The mRNA expression levels of MCP-1, iNOS, IL-12 p35, and IL-12 p40 were quantified by qPCR and normalized versus 18S ribosomal RNA. Values are means ± SEMs. Results are representative of four to six independent experiments. *$P < 0.05$, **$P < 0.01$, ***$P < 0.001$ as indicated.

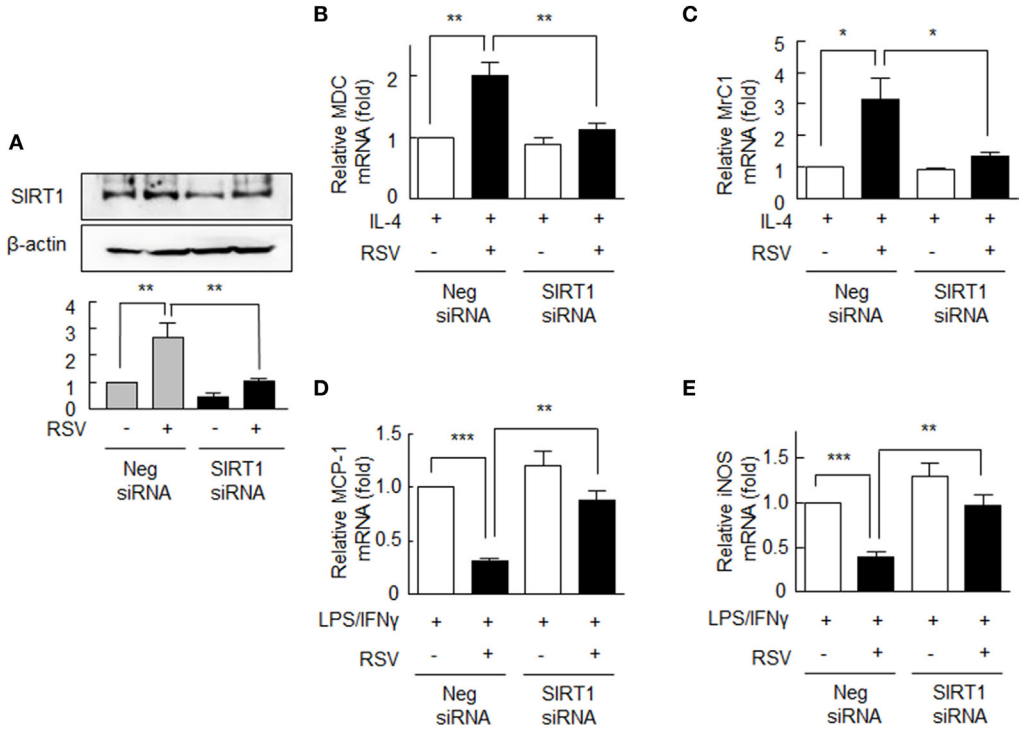

FIGURE 2 | Expression of M1/M2 polarization markers in SIRT1 siRNA-transfected rheumatoid arthritis macrophages. **(A)** Cells were either transfected with the siRNA targeting SIRT1 (200 nM) or with scrambled siRNA duplex (200 nM) for 24 h and then were treated with or without resveratrol (RSV, 50 μM) for 24 h. **(B,C)** SIRT1 gene knockdown cells were pretreated with RSV (50 μM) for 24 h and were incubated with interleukin (IL)-4 (20 ng/ml) for 12 h, and the mRNA expression levels of MDC and MrC1 were quantified by qPCR. **(D,E)** These cells were incubated with LPS (1 μg/ml) and/or interferon (IFN)γ (20 ng/ml) for 12 h**,** and then the mRNA expression levels of MCP-1 and iNOS were quantified by qPCR. These levels were normalized versus 18S ribosomal RNA. Values are means ± SEMs. Results are representative of four independent experiments. $^{*}P < 0.05$, $^{**}P < 0.01$, $^{***}P < 0.001$ as indicated.

The mRNA levels of MDC and MrC1 were not elevated by RSV in cells transfected with SIRT1 siRNA, whereas in negative control cells MDC and MrC1 mRNA levels were significantly increased (**Figures 2B,C**). By contrast, in cells transfected with SIRT1 siRNA, RSV failed to suppress the mRNA levels of MCP-1 and iNOS in response to LPS plus IFN-γ, while both were significantly suppressed by RSV in negative control cells (**Figures 2D,E**). These results further support the notion that SIRT1 modulates the macrophage phenotype differentiation in RA.

Induction of M2 Phenotype by Activation of SIRT1/AMPKα Phosphorylation

Based on a report that SIRT1 regulates AMPK signaling in attenuation of pro-inflammatory activity (10), we assessed whether the AMPK signaling activated by SIRT1 is linked to macrophage polarization to the M2 phenotype. To confirm that RSV activates AMPK in RA macrophages, we determined AMPKα phosphorylation at Thr^{172} (p-AMPKα) and ACC (a downstream target of AMPK) phosphorylation at Ser^{79} (p-ACC) (26). After treatment with RSV (50 μM for 24–48 h), p-AMPKα levels in cells were significantly increased, and similar results were obtained for p-ACC (**Figure 3A**). Furthermore, these increases were inhibited by pretreating RA macrophages with sirtinol (20 μM; a SIRT1 inhibitor) (**Figure 3B**). When cells were transfected with SIRT1 siRNA gene, RSV failed to increase the levels of p-AMPKα and p-ACC, whereas the expressions of both increased in negative control cells (**Figure 3C**).

We also investigated the involvement of the SIRT1/AMPKα signaling pathway in M2 macrophage polarization. As shown in **Figures 3D–G** IL-4 (20 ng/ml)-induced MDC, FcεRII, MrC1, and IL-10 mRNA expressions were significantly augmented by pretreating cells with RSV (50 μM). Interestingly, pretreatment with sirtinol (20 μM) or CC (1 μM, an inhibitor of AMPK) strongly prevented the RSV-induced augmentation of the expressions of MDC, FcεRII, MrC1, and IL-10 mRNAs, indicating that SIRT1/AMPKα signaling pathway leads to anti-inflammatory function of macrophages in RA.

Suppression of M1 Macrophage Polarization by SIRT1 through Downregulating NF-κB

NF-κB activation has been reported to play a key role in LPS-induced M1 macrophage polarization, and M1 macrophages are known to have κB sites in their promoter regions, including those of CCL2, iNOS, and TNFα (27). Thus, we investigated the effect of RSV on the AMPKα activation under exposure to LPS plus IFNγ in RA macrophages. After pretreatment with RSV (50 μM) for 24 h, cells were incubated with LPS (1 μg/ml) plus IFNγ (20 ng/ml) for

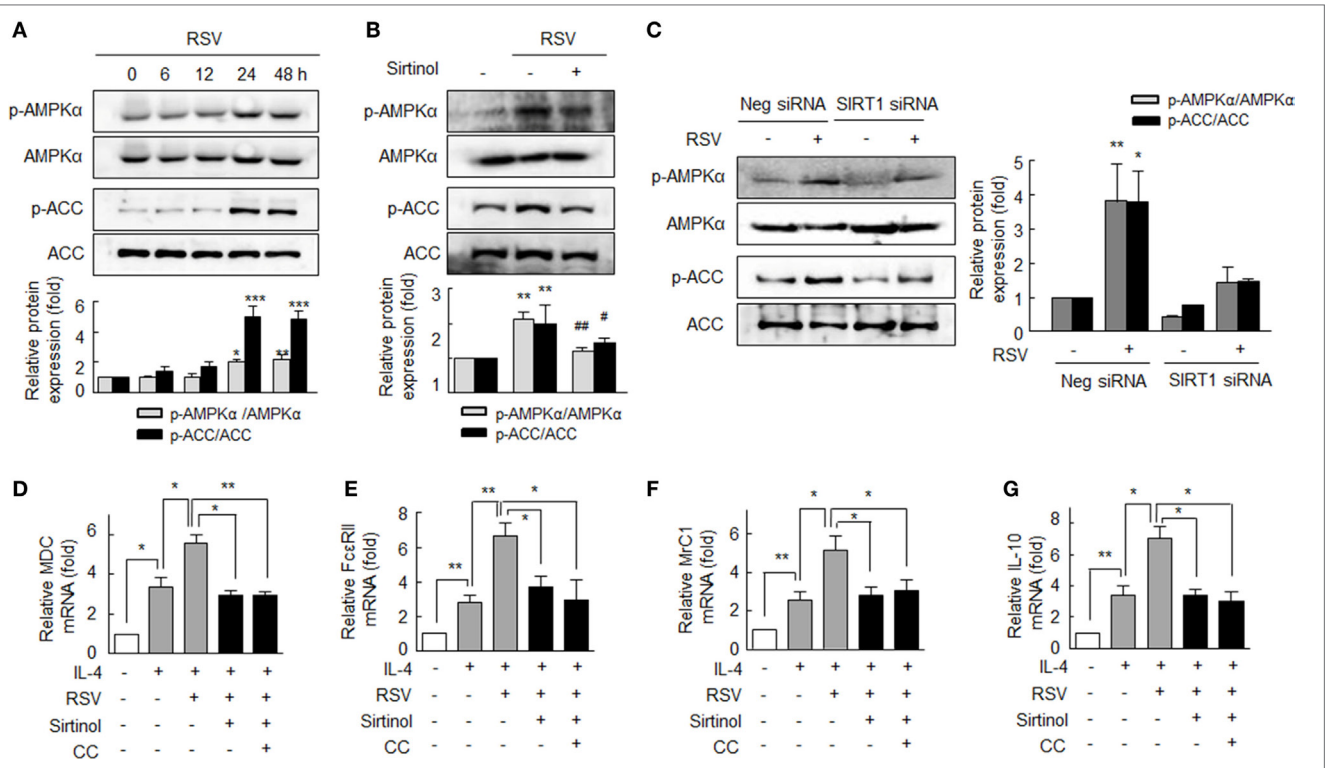

FIGURE 3 | Enhanced macrophage M2 polarization by resveratrol (RSV) by SIRT1-mediated p-adenosine monophosphate-activated protein kinase α (AMPKα) upregulation. **(A)** Effects of SIRT1 on the phosphorylations of AMPKα and acetyl-CoA carboxylase (ACC). Cells were treated with RSV (50 μM) for 0–48 h. **(B)** The antagonizing effect of sirtinol (a SIRT1 inhibitor): cells were pretreated with sirtinol (20 μM) for 30 min and then with RSV (50 μM) for 24 h. **(C)** Effect of SIRT1 gene knockdown on the phosphorylations of AMPKα and ACC. SIRT1-gene knockdown cells were treated with RSV (50 μM) for 24 h. Values are means ± SEMs. Results are representative of four independent experiments. $^{*}P < 0.05$, $^{**}P < 0.01$, $^{***}P < 0.001$ versus zero time or none; $^{\#}P < 0.05$, $^{\#\#}P < 0.01$ versus RSV alone. **(D–G)** Inhibitions of resveratrol (RSV)-induced M2 macrophages markers by sirtinol and compound C (CC). After pretreatment with RSV (50 μM) for 24 h, cells were stimulated with interleukin (IL)-4 (20 ng/ml) for 12 h with or without sirtinol (20 μM) or CC (1 μM, an AMPK inhibitor) for 30 min. The mRNA expression levels of MDC, FcεRII, MrC1, and IL-10 were quantified by qPCR and normalized versus 18S ribosomal RNA. Values are means ± SEMs. Results are representative of four to five independent experiments. $^{*}P < 0.05$, $^{**}P < 0.01$ as indicated.

0–48 h. We found intracellular levels of p-AMPKα and p-ACC had increased and that these increases were maintained after treatment for 48 h (Figure S2 in Supplementary Material).

To investigate the mechanism whereby SIRT inhibits polarization of macrophage to the M1 phenotype, we examined whether SIRT1 could inhibit NF-κB signaling. RA macrophages were pretreated with RSV (50 μM) for 24 h, and then further stimulated with LPS (1 μg/ml) plus IFNγ (20 ng/ml) for 1 h. As shown in **Figure 4A** LPS plus IFNγ significantly induced the degradation of IκBα in cytosol, whereas pretreatment of RSV resulted in prevention of the degradation of IκBα. In addition, RSV inhibited LPS plus IFNγ-induced nuclear translocation of NF-κB p65. Reportedly, NF-κB signaling is achieved through posttranslational modifications, such as phosphorylation and acetylation, which enhance the DNA-binding activity of p65 to the κB site (28–30). We then examined the effect of SIRT1 on NF-κB p65 acetylation on LPS plus IFNγ-induced M1 macrophage polarization. As shown in **Figure 4B**, increases in the levels of p65 acetylation at K310 and of p65 phosphorylation at Ser^{536} by LPS plus IFNγ were markedly inhibited by RSV pretreatment.

Furthermore, to define whether the prevention of NF-κB activity by RSV was mediated by SIRT1 activation, RA macrophages were subjected to SIRT1 knockdown by SIRT1 siRNA transfection. In the SIRT1 knockdown macrophages, the LPS plus IFNγ increased acetylation at K310 and phosphorylation of p65 at Ser^{536} were not suppressed by RSV, whereas they were significantly suppressed by RSV in negative control cells (**Figure 4C**). When cells were pretreated with RSV (50 μM) for 24 h prior to LPS plus IFN γ, increased NF-κB activity was attenuated and this reduction was prevented by sirtinol (20 μM) pretreatment (**Figure 4D**). These results suggest that SIRT1 prevents NF-κB p65 acetylation/phosphorylation, resulting in reduced M1 polarization.

Reduced M1 Polarization in BMDMs from SIRT1 Tg-Mice

To determine the phenotypic characters of macrophages, we isolated BMDMs from SIRT1 Tg-mice and determined SIRT1 protein and AMPKα phosphorylation levels in these cells.

Levels of SIRT1 protein and p-AMPKα were significantly higher in BMDMs from SIRT1 Tg-mice when compared with those from wild type (WT) mice (Figure S3 in Supplementary Material). BMDMs from SIRT1 Tg-mice were treated with IL-4 (20 ng/ml), and the mRNA levels of M2 macrophage markers,

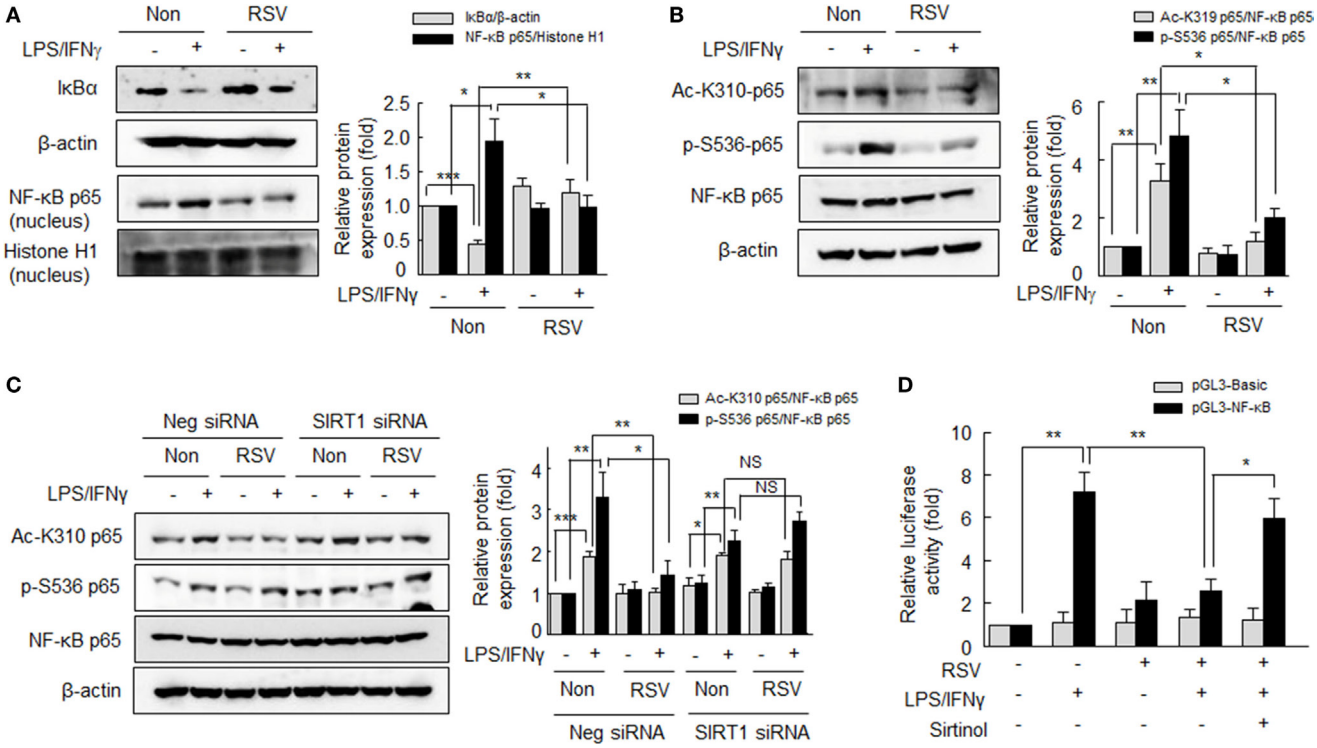

FIGURE 4 | Suppression of NF-κB signaling by resveratrol (RSV) in the LPS/interferon (IFN)γ-induced M1 macrophage polarization. **(A)** Effects of RSV on IκBα degradation and nuclear NF-κB expression. After pretreatment with RSV (50 μM) for 24 h, cells were stimulated with LPS (1 μg/ml) plus IFNγ (20 ng/ml) for 1 h. **(B)** Effects of RSV on the acetylation of p65-K310 and the phosphorylation of p65-serine 536. Cells were pretreated with RSV (50 μM) for 24 h and then with LPS (1 μg/ml) plus IFNγ (20 ng/ml) for 1 h. **(C)** Effect of SIRT1 gene knockdown on NF-κB signaling. Cells were transfected with SIRT1 siRNA or negative control siRNA at a final concentration of 200 nM. Macrophages were incubated with RSV (50 μM) for 24 h, and then exposed to LPS (1 μg/ml) plus IFNγ (20 ng/ml) for 1 h. Values are means ± SEMs. Results are representative of four to five independent experiments.*$P < 0.05$, **$P < 0.01$, ***$P < 0.001$ as indicated. **(D)** Cells were transfected with basic-pGL3-luc or NF-κB-pGL3-luc using Lipofectamine 2000. After 24 h of transfection, cells were treated with or without sirtinol (20 μM) for 30 min, and then treated with RSV (50 μM) for 24 h followed by LPS (1 μg/ml) + IFNγ (20 ng/ml) for 3 h. The firefly luciferase enzyme activity were detected in cell extracts and normalized to the *Renilla* luciferase activity. Values are means ± SEMs. Results are representative of five independent experiments. *$P < 0.05$, **$P < 0.01$ as indicated.

including ariginase-1, Fizz, Yim-1, and FcεRII were assessed. As shown in **Figures 5A–D**, the degree of expressions of ariginase-1, Fizz, Yim-1, and FcεRII mRNAs were significantly higher in response to IL-4 in macrophages obtained from SIRT1 Tg-mice than those from WT controls, suggesting increased SIRT1/AMPK levels prominently promote M2 macrophage polarization.

By contrast, when BMDMs from SIRT1 Tg-mice were incubated with LPS (1 μg/ml) plus IFNγ (20 ng/ml), mRNA levels of the M1 phenotype markers: TNF-α, IL-1β, MCP-1, IL-12 p35, and IL-12 p40 were significantly suppressed (**Figures 5E–I**), indicating that SIRT1 strongly suppressed M1 macrophage activation. These results confirm SIRT1 promotes macrophage polarization toward the M2 phenotype.

Attenuation of Inflammatory Joint Disease Induction by SIRT1 in CIA Mice

The mouse CIA model was employed because it is similar immunologically and pathologically to RA patients. SIRT1-Tg CIA mice developed less severe arthritis than WT CIA mice, as evidenced by lower scores of disease activity from days 26 to 38 (**Figure 6A**). On day 38, the mean clinical arthritis score of SIRT1 Tg-CIA mice (2.6 ± 0.4) was significantly lower than that of WT CIA mice (6.6 ± 0.68) (**Figure 6B**).

On day 38 after first injection, knee joints from SIRT1-Tg CIA and WT CIA mice were obtained for microscopic analysis. They were blindly scored for histological signs of arthritis, that is, cartilage destruction, bone erosion, and cell infiltration. Histological articular damage was significantly less severe in the knee joints of in SIRT1 Tg-CIA mice than in those of WT CIA mice (**Figure 6C**). Histological images indicated that synovial hyperplasia, bone and cartilage destruction, vascular proliferation, and inflammatory cells infiltration were markedly diminished in SIRT1-Tg CIA mice.

In addition, we assessed the expression of M2 marker arginase-1, M1 marker TNFα, and IL-1β in the knee joints by immunohistochemistry. Ariginase-1 marker in SIRT1-Tg mice was detected relatively higher in SIRT1-Tg mice than WT mice, and SIRT1 Tg-CIA mice showed less decrease in ariginase-1 expression. In contrast to ariginase-1, TNFα and IL-1β were rarely detected in SIRT1 Tg-CIA mice, compared to WT CIA mice. A similar result was obtained for RANKL expression

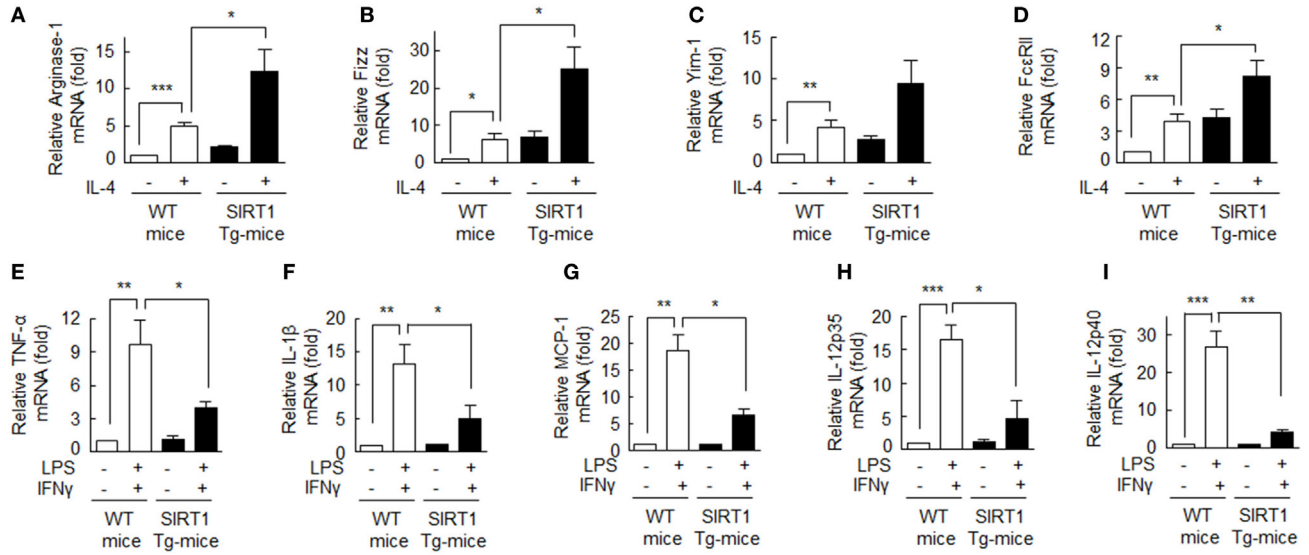

FIGURE 5 | Upregulation of the M2 phenotype and downregulation of the M1 phenotype in bone marrow-derived macrophage (BMDMs) obtained from SIRT1 transgenic (Tg)-mice. **(A–D)** Cells were incubated with interleukin (IL)-4 (20 ng/ml) for 12 h and ariginase-1, Fizz, Yim-1, and FcεRII mRNA levels were then quantified with qPCR and normalization versus 18S ribosomal RNA. **(E–I)** Cells were incubated with LPS (1 μg/ml) or interferon (IFN)γ (20 ng/ml) for 12 h and TNFα, IL-1β, MCP-1, IL-12 p35, and IL-12 p40 mRNA levels were quantified by qPCR and normalization versus 18S ribosomal RNA. Values are means ± SEMs. Results are representative of five independent experiments. *$P < 0.05$, **$P < 0.01$, ***$P < 0.001$ as indicated.

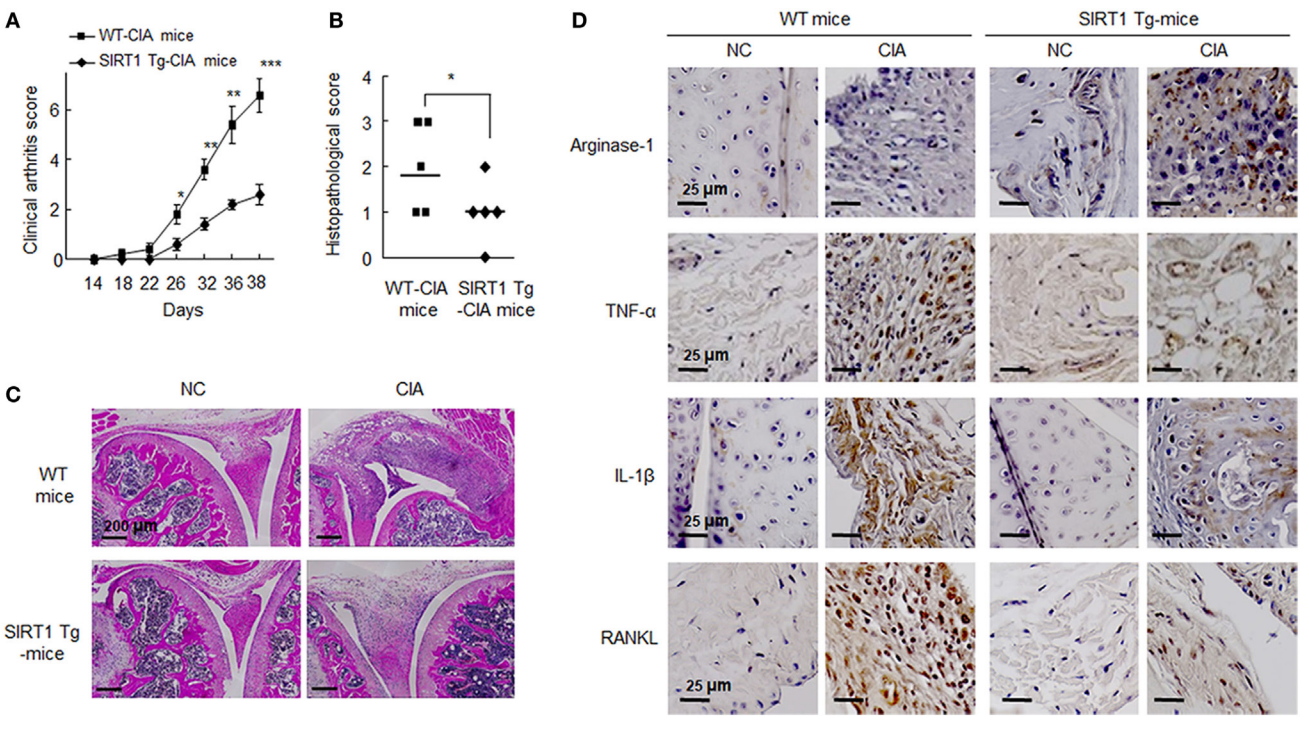

FIGURE 6 | Analysis of the pathological severity of the joints of C57BL/6N and SIRT1 transgenic (Tg) mice ($n = 5$) subjected to collagen-induced arthritis (CIA) (refer to Section "Materials and Methods" for details). **(A)** Arthritis severity scores of CIA mice were recorded after second immunization with type II collagen. **(B)** Histological scores of synovitis, pannus formation, and erosion in knee joints. Values are means ± SEMs. Results are representative of five independent experiments. *$P < 0.05$, **$P < 0.01$, ***$P < 0.001$ versus SIRT1 Tg-CIA mice. **(C)** Representative H&E staining of joints from CIA mice. Scale bar = 200 μm. **(D)** Representative sections showing staining for arginase-1, TNF-α, interleukin (IL)-1β, and RANKL, which were markedly reduced in the knee joint tissues of SIRT1 Tg-CIA mice. Tissue sections from knee joints were stained with the indicated antibodies. Staining for each antibody on each cell are shown in dark brown. Scale bars; 25 μm.

(**Figure 6D**). These results indicate the SIRT1 overexpression leads to anti-inflammatory responses in association with suppression of synovial inflammation, joint destruction in the murine CIA model.

DISCUSSION

The current study shows when RA macrophages were treated with IL-4, SIRT1 enhances macrophage polarization into the M2 phenotype by upregulating the phosphorylations of AMPKα and ACC. In line with these findings, SIRT1 significantly suppressed the M1 phenotype polarization of macrophages by inhibiting NF-κB activation. In addition, we observed that expressions of TNFα and IL-1β, the pro-inflammatory cytokines, were significantly lower in SIRT1 Tg-CIA mice than in WT CIA mice, and these reductions were associated with the suppression of synovial inflammation and bone destruction. These findings support the notion that the anti-inflammatory responses in RA are induced by activation of SIRT1/AMPKα signaling pathways.

Kennedy et al. (31) have emphasized that synovial macrophages exert a crucial role in the pathogenesis of inflammation in RA, by initiating and resolving inflammation by generating various cytokines. Macrophages populations are heterogeneous and the extents of these heterogeneities are dependent on microenvironmental signals. Dysregulation of M1/M2 polarization in macrophages was known to reflect the pathogenesis of inflammation (32). Moreover, Hah et al. (33) have advised SIRT1 as a potential therapeutic target to treat inflammatory arthritis, based on the facts that SIRT1 lack myeloid cells exacerbated inflammation due to the NF-κB hyperactivation and increased productions of cytokines associated with M1 polarization.

SIRT1 regulates the functions of several important transcription factors with anti-inflammatory effects (21, 33). However, no direct evidence supported the role of SIRT1 in macrophage polarization. In view of these situations, we focused on the negative regulatory role of SIRT1 in RA inflammation (21). M2-polarized macrophages are characterized by the upregulations of mannose receptor, CD23, CCL22, and scavenger receptor, which all have anti-inflammatory effects (34). In this study, SIRT1 activation by RSV in RA macrophages enhanced the IL-4-induced M2 phenotype, whereas treatment with SIRT1 inhibitor suppressed anti-inflammatory response. Intriguingly, the present results showed that overexpression of SIRT1 in macrophages induced an anti-inflammatory state by inducing genes encoding M2 markers, such as arginase-1, Fizz, Yim, and FcεRII. In addition, SIRT1 also inhibited M1 macrophage polarization. The expressions of M1 marker genes induced by LPS/IFNγ stimulation (a well-known means of inducing M1 polarization) were reduced in SIRT1-activated macrophages, and the high expressions of M1 markers in macrophages from WT mice treated with LPS/IFNγ were markedly lower in macrophages from SIRT1 Tg-mice. These findings suggest that SIRT1 might be useful for ameliorating RA-associated inflammation.

It has been argued SIRT1 aggravates inflammation by upregulating the expressions of pro-inflammatory cytokines in synovial fibroblasts (19) and in the synovial tissues of smokers with RA (35). Nevertheless, Wendling et al. (17) have revealed that SIRT1 expression and its activity in the cytoplasm of PBMCs from RA patients are lower than in healthy controls. Recently, we reported PMA-induced NF-κB transcriptional activation and secretions of pro-inflammatory cytokines (TNFα, IL-1β, and IL-6) were suppressed by RSV treatment, and NF-κB transcriptional activity was more largely suppressed in association with reduction in TNFα, IL-1β, and IL-6 mRNA and protein levels in the SIRT1 transgenic mice compared to the control C57BL/6 mice (21). Sag et al. (36) further emphasized that AMPK counteracts inflammatory signalings in macrophages by inhibiting LPS-induced IκBα degradation and by upregulating Akt/CREB activation. They suggested that AMPK directs signaling pathways in macrophages to suppress pro-inflammatory responses and promote macrophage polarization toward an anti-inflammatory phenotype. Similarly, in chronic kidney disease patients, the upregulation of AMPK activation leads to polarization toward the M2 phenotype in accompanying with the restoration of mitochondrial biogenesis in macrophages (37). Our present results showed SIRT1 activation by RSV increased AMPKα phosphorylation and ACC phosphorylation in RA macrophages, but not in SIRT1 gene knockdown RA macrophages. In line with these findings, the pharmacological inhibitors sirtinol (a SIRT1 inhibitor) and CC (a chemical inhibitor of AMPK) both significantly blocked SIRT1-stimulated increases in M2 macrophage polarization.

We found that SIRT1 strongly suppressed p65 acetylation at K310 and phosphorylation at Ser^{536}, and that SIRT1 increased IκBα expression in cytosol, and decreased the nuclear translocation NF-κB p65, and consequently decreased NF-κB to κB binding, which agrees with previous reports (12, 13). This result was further supported by the experiment with SIRT1 gene knockdown macrophages, in which LPS plus IFNγ increased NF-κB p65 acetylation at K310 and p65 phosphorylation at Ser^{536} were not suppressed by RSV, whereas both were significantly suppressed by RSV in negative control cells. These results are also supported by Yang et al. (15), in that AMPKα negatively regulates pro-inflammatory genes due to the deacetylation of NF-κB by SIRT1 in macrophages. These results indicate that SIRT1/AMPKα signaling enhanced M2 and suppressed M1 macrophage polarization by inhibiting NF-κB in RA macrophages.

In this study, the findings obtained from SIRT1-Tg CIA mice model supported the implication of SIRT1 in RA inflammation *in vivo*. In particular, histological articular damage was more attenuated in the knee joints of SIRT1-Tg CIA mice compared to WT CIA mice, and this reduction in articular damage was found to be associated with reduced synovial hyperplasia, bone and cartilage destruction, synovial angiogenesis, and inflammatory cell infiltration. In summary, our results show that the SIRT1/AMPKα signaling pathway is involved in the control of macrophage polarization and that SIRT1 probably acts as a negative regulator of the inflammatory processes associated with RA.

We conclude that SIRT1 modulation offers a promising strategy for treating RA inflammation.

ETHICS STATEMENT

All experimental procedures were approved by the Animal Experimental Committee of the College of Medicine, Pusan National University (PNU-2016-1107) and done in accordance with guidelines for animal research.

AUTHOR CONTRIBUTIONS

SYP designed and did the major experiments, analyzed the experimental data, and contributed to the writing. KWH and CDK designed and contributed to the writing. SWL and SYL designed the experiments and analyzed the experimental data. SSB and KK did the critical revision of the manuscript.

ACKNOWLEDGMENTS

The authors would like to thank Dr. J. W. Park (Seoul National University, Korea) for providing SIRT1-Tg mice.

FUNDING

This study was supported by the National Research Foundation of Korea (NRF-2016R1C1B2007691) and the Medical Research Center (MRC) Program through the National Research Foundation of Korea (NRF) grant funded by the Korea government (MSIP) (NRF-2015R1A5A2009656).

SUPPLEMENTARY MATERIAL

The Supplementary Material for this article can be found online at http://journal.frontiersin.org/article/10.3389/fimmu.2017.01135/full#supplementary-material.

REFERENCES

1. Tak PP, Bresnihan B. The pathogenesis and prevention of joint damage in rheumatoid arthritis: advances from synovial biopsy and tissue analysis. *Arthritis Rheum* (2000) 43:2619–33. doi:10.1002/1529-0131(200012)43:12<2619::AID-ANR1>3.0.CO;2-V
2. McInnes IB, Schett G. The pathogenesis of rheumatoid arthritis. *N Engl J Med* (2011) 365:2205–19. doi:10.1056/NEJMra1004965
3. Udalova IA, Mantovani A, Feldmann M. Macrophage heterogeneity in the context of rheumatoid arthritis. *Nat Rev Rheumatol* (2016) 12:472–85. doi:10.1038/nrrheum.2016.91
4. Gordon S. Alternative activation of macrophages. *Nat Rev Immunol* (2003) 3:23–35. doi:10.1038/nri978
5. Gordon S, Martinez FO. Alternative activation of macrophages: mechanism and functions. *Immunity* (2010) 32:593–604. doi:10.1016/j.immuni.2010.05.007
6. Mantovani A, Sica A, Sozzani S, Allavena P, Vecchi A, Locati M. The chemokine system in diverse forms of macrophage activation and polarization. *Trends Immunol* (2004) 25:677–86. doi:10.1016/j.it.2004.09.015
7. Kinne RW, Stuhlmuller B, Burmester GR. Cells of the synovium in rheumatoid arthritis. Macrophages. *Arthritis Res Ther* (2007) 9:224. doi:10.1186/ar2333
8. Vandooren B, Noordenbos T, Ambarus C, Krausz S, Cantaert T, Yeremenko N, et al. Absence of a classically activated macrophage cytokine signature in peripheral spondyloarthritis, including psoriatic arthritis. *Arthritis Rheum* (2009) 60:966–75. doi:10.1002/art.24406
9. Ruderman NB, Xu XJ, Nelson L, Cacicedo JM, Saha AK, Lan F, et al. AMPK and SIRT1: a long-standing partnership? *Am J Physiol Endocrinol Metab* (2010) 298:E751–60. doi:10.1152/ajpendo.00745.2009
10. Lan F, Cacicedo JM, Ruderman N, Ido Y. SIRT1 modulation of the acetylation status, cytosolic localization, and activity of LKB1: possible role in AMP-activated protein kinase activation. *J Biol Chem* (2008) 283:27628–35. doi:10.1074/jbc.M805711200
11. Canto C, Gerhart-Hines Z, Feige JN, Lagouge M, Noriega L, Milne JC, et al. AMPK regulates energy expenditure by modulating NAD+ metabolism and SIRT1 activity. *Nature* (2009) 458:1056–60. doi:10.1038/nature07813
12. Yeung F, Hoberg JE, Ramsey CS, Keller MD, Jones DR, Frye RA, et al. Modulation of NF-κB-dependent transcription and cell survival by the SIRT1 deacetylation. *EMBO J* (2004) 23:2369–80. doi:10.1038/sj.emboj.7600244
13. Ghisays F, Brace CS, Yackly SM, Kwon HJ, Mills KF, Kashentseva E, et al. The N-terminal domain of SIRT1 is a positive regulator of endogenous SIRT1-dependent deacetylation and transcriptional outputs. *Cell Rep* (2015) 10:1165–73. doi:10.1016/j.celrep.2015.02.036
14. O'Neill LA, Hardie DG. Metabolism of inflammation limited by AMPK and pseudo-starvation. *Nature* (2013) 493:346–55. doi:10.1038/nature11862
15. Yang Z, Kahn BB, Shi H, Xue BZ. Macrophage alpha1-AMP-activated protein kinase (alpha1 AMPK) antagonizes fatty acid-induced inflammation through SIRT1. *J Biol Chem* (2010) 285:19051–9. doi:10.1074/jbc.M110.123620
16. Zhu H, Zhang M, Liu Z, Xing J, Moriasi C, Dai X, et al. AMP-Activated protein kinase α1 in macrophages promotes collateral remodeling and arteriogenesis in mice in vivo. *Arterioscler Thromb Vasc Biol* (2011) 31:2897–908. doi:10.1161/ATVBAHA.116.307743
17. Wendling D, Abbas W, Godfrin-Valnet M, Kumar A, Guillot X, Khan KA, et al. Dysregulated serum IL-23 and SIRT1 activity in peripheral blood mononuclear cells of patients with rheumatoid arthritis. *PLoS One* (2015) 23:e0119981. doi:10.1371/journal.pone.0119981
18. Kim HY, Park SY, Lee SW, Lee HR, Lee WS, Rhim BY, et al. Inhibition of HMGB1-induced angiogenesis by cilostazol via SIRT1 activation in synovial fibroblasts from rheumatoid arthritis. *PLoS One* (2014) 15:e104743. doi:10.1371/journal.pone.0104743
19. Niederer F, Ospelt C, Brentano F, Hottiger MO, Gay RE, Gay S, et al. SIRT1 overexpression in the rheumatoid arthritis synovium contributes to proinflammatory cytokine production and apoptosis resistance. *Ann Rheum Dis* (2011) 70:1866–73. doi:10.1136/ard.2010.148957
20. Woo SJ, Lee SM, Lim HS, Hah YS, Jung ID, Park YM, et al. Myeloid deletion of SIRT1 suppresses collagen-induced arthritis in mice by modulating dendritic cell maturation. *Exp Mol Med* (2016) 48:e221. doi:10.1038/emm.2015.124
21. Park SY, Lee SW, Kim HY, Lee SY, Lee WS, Hong KW, et al. SIRT1 inhibits differentiation of monocytes to macrophages: amelioration of synovial inflammation in rheumatoid arthritis. *J Mol Med (Berl)* (2016) 94:921–31. doi:10.1007/s00109-016-1402-7
22. Inglis JJ, Simelyte E, McCann FE, Criado G, Williams RO. Protocol for the induction of arthritis in C57BL/6 mice. *Nat Protoc* (2008) 3:612–8. doi:10.1038/nprot.2008.19
23. Williams RO, Feldmann M, Maini RN. Anti-tumor necrosis factor ameliorates joint disease in murine collagen-induced arthritis. *Proc Natl Acad Sci U S A* (1992) 89:9784–8. doi:10.1073/pnas.89.20.9784
24. Zajac E, Schweighofer B, Kupriyanova TA, Juncker-Jensen A, Minder P, Quigley JP, et al. Angiogenic capacity of M1- and M2-polarized macrophages is determined by the levels of TIMP-1 complexed with their secreted proMMP-9. *Blood* (2013) 122:4054–67. doi:10.1182/blood-2013-05-501494
25. Benoit M, Desnues B, Mege JL. Macrophage polarization in bacterial infections. *J Immunol* (2008) 181:3733–9. doi:10.4049/jimmunol.181.6.3733
26. Munday MR. Regulation of mammalian acetyl-CoA carboxylase. *Biochem Soc Trans* (2002) 30:1059–64. doi:10.1042/bst030a101c
27. Tugal D, Liao X, Jain MK. Transcriptional control of macrophage polarization. *Arterioscler Thromb Vasc Biol* (2013) 33:1135–44. doi:10.1161/ATVBAHA.113.301453

28. Perkins ND. Post-translational modifications regulating the activity and function of the nuclear factor kappa B pathway. *Oncogene* (2006) 25:6717–30. doi:10.1038/sj.onc.1209937
29. Huang B, Yang XD, Lamb A, Chen LF. Posttranslational modifications of NF-κB: another layer of regulation for NF-kB signalling pathway. *Cell Signal* (2010) 22:1282–90. doi:10.1016/j.cellsig.2010.03.017
30. Chen LF, Williams SA, Mu Y, Nakano H, Duerr JM, Buckbinder L, et al. NF-κB RelA phosphorylation regulates RelA acetylation. *Mol Cell Biol* (2005) 25:7966–75. doi:10.1128/MCB.25.18.7966-7975.2005
31. Kennedy A, Fearon U, Veale DJ, Godson C. Macrophages in synovial inflammation. *Front Immunol* (2011) 10:52. doi:10.3389/fimmu.2011.00052
32. Porcheray F, Viaud S, Rimaniol AC, Léone C, Samah B, Dereuddre-Bosquet N, et al. Macrophage activation switching: an asset for the resolution of inflammation. *Clin Exp Immunol* (2005) 142:481–9. doi:10.1111/j.1365-2249.2005.02934.x
33. Hah YS, Cheon YH, Lim HS, Cho HY, Park BH, Ka SO, et al. Myeloid deletion of SIRT1 aggravates serum transfer arthritis in mice via nuclear factor-κB activation. *PLoS One* (2014) 9:e87733. doi:10.1371/journal.pone.0087733
34. Martinez FO, Helming L, Gordon S. Alternative activation of macrophages: an immunologic functional perspective. *Annu Rev Immunol* (2009) 27:451–83. doi:10.1146/annurev.immunol.021908.132532
35. Engler A, Tange C, Frank-Bertoncelj M, Gay RE, Gay S, Ospelt C. Regulation and function of SIRT1 in rheumatoid arthritis synovial fibroblasts. *J Mol Med (Berl)* (2016) 94:173–82. doi:10.1007/s00109-015-1332-9
36. Sag D, Carling D, Stout RD, Suttles J. Adenosine 5'-monophosphate-activated protein kinase promotes macrophage polarization to an anti-inflammatory functional phenotype. *J Immunol* (2008) 181:8633–41. doi:10.4049/jimmunol.181.12.8633
37. Li C, Ding XY, Xiang DM, Xu J, Huang XL, Hou FF, et al. Enhanced M1 and impaired M2 macrophage polarization and reduced mitochondrial biogenesis via inhibition of AMP kinase in chronic kidney disease. *Cell Physiol Biochem* (2015) 36:358–72. doi:10.1159/000430106

Conflict of Interest Statement: The authors declare no potential conflicts of interest.

Copyright © 2017 Park, Lee, Lee, Hong, Bae, Kim and Kim. This is an open-access article distributed under the terms of the Creative Commons Attribution License (CC BY). The use, distribution or reproduction in other forums is permitted, provided the original author(s) or licensor are credited and that the original publication in this journal is cited, in accordance with accepted academic practice. No use, distribution or reproduction is permitted which does not comply with these terms.

frontiers in Immunology

ORIGINAL RESEARCH
published: 15 September 2017
doi: 10.3389/fimmu.2017.01149

New Insight into the Pathogenesis of Erythema Nodosum Leprosum: The Role of Activated Memory T-Cells

Edessa Negera[1,2], Kidist Bobosha[2], Stephen L. Walker[1], Birtukan Endale[2], Rawleigh Howe[2], Abraham Aseffa[2], Hazel M. Dockrell[1] and Diana N. Lockwood[1]*

[1]London School of Hygiene and Tropical Medicine, Faculty of Infectious Diseases, London, United Kingdom, [2]Armauer Hansen Research Institute, Addis Ababa, Ethiopia

Memory T-cells, particularly, effector memory T cells are implicated in the pathogenesis of inflammatory diseases and may contribute to tissue injury and disease progression. Although erythema nodosum leprosum (ENL) is an inflammatory complication of leprosy, the role of memory T cell subsets has never been studied in this patient group. The aim of this study was at investigate the kinetics of memory T cell subsets in patients with ENL before and after prednisolone treatment. A case–control study design was used to recruit 35 untreated patients with ENL and 25 non-reactional lepromatous leprosy (LL) patient controls at ALERT Hospital, Ethiopia. Venous blood samples were obtained before, during, and after treatment from each patient. Peripheral blood mononuclear cells (PBMCs) were isolated and used for immunophenotyping of T cell activation and memory T-cell subsets by flow cytometry. The kinetics of these immune cells in patients with ENL before and after treatment were compared with LL patient controls as well as within ENL cases at different time points. The median percentage of $CD3^+$, $CD4^+$, and $CD8^+$ T-cells expressing activated T-cells were significantly higher in the PBMCs from patients with ENL than from LL patient controls before treatment. The median percentage of central and activated memory T-cells was significantly increased in patients with ENL compared to LL patient controls before treatment. Interestingly, patients with ENL had a lower percentage of naïve T cells (27.7%) compared to LL patient controls (59.5%) ($P < 0.0001$) before treatment. However, after prednisolone treatment, patients with ENL had a higher median percentage of naïve T-cells (43.0%) than LL controls (33.0%) ($P < 0.001$). The median percentage of activated T-cells (effector memory and effector T-cells) was significantly increased in patients with ENL (59.2%) before treatment compared to after treatment with prednisolone (33.9%) ($P < 0.005$). This is the first work which has shown T-cell activation and the different subsets of memory T cells in untreated patients with ENL. Consequently, this study delineates the role of T-cell activation in the pathogenesis of ENL reaction and challenges the long-standing dogma of immune complex as a sole etiology of ENL reaction.

Keywords: erythema nodosum leprosum, ethiopia, leprosy, memory T-cells, prednisolone, reaction

OPEN ACCESS

Edited by:
Jixin Zhong,
Case Western Reserve University,
United States

Reviewed by:
Hui Liu,
University of California, San Francisco, United States
Yanlin He,
Baylor College of Medicine,
United States

****Correspondence:***
Edessa Negera
edessan@yahoo.com

Specialty section:
This article was submitted to Inflammation, a section of the journal Frontiers in Immunology

Received: *13 July 2017*
Accepted: *31 August 2017*
Published: *15 September 2017*

Citation:
Negera E, Bobosha K, Walker SL, Endale B, Howe R, Aseffa A, Dockrell HM and Lockwood DN (2017) New Insight into the Pathogenesis of Erythema Nodosum Leprosum: The Role of Activated Memory T-Cells. Front. Immunol. 8:1149. doi: 10.3389/fimmu.2017.01149

INTRODUCTION

Leprosy is a disease caused by *Mycobacterium leprae*, an intracellular acid-fast bacillus. It mainly infects the skin and peripheral nerves. Leprosy is a disease with a five-district forms called spectrum with the localized tuberculoid leprosy (TT) and the generalized lepromatous leprosy (LL) forming the two poles of the spectrum (1).

Leprosy reactions [reversal reactions and erythema nodosum leprosum (ENL)] are immune-mediated inflammatory complications of the disease which can occur before, during, or after successful completion of multidrug treatment (2). They cause a significant morbidity and nerve damage in leprosy patients (3). ENL is an inflammatory complication of leprosy, manifesting as tender erythematous skin lesions and systemic features of disease including fever, neuritis, and bone pain (4).

Immunological memory is a characteristic of adaptive immunity. After infection, some antigen experienced T-cells generate memory T-cells which can provide life-long protection against the same infection. These memory T cells rapidly undergo clonal expansion to fight off the reoccurrence of the same infection (5). Memory is a signature of the acquired immune system. It results from antigen-specific lymphocytes clonal expansion and differentiation, which eventually persist for a lifetime (6). Memory lymphocytes ensure immediate protection in peripheral tissues and provide recall responses to antigens in secondary lymphoid organs. In the cellular immune system, these functions are carried out by distinct cell types called effector and central memory T-cells (T_{CM} cells). Protective memory is mediated by effector memory T-cells (T_{EM} cells) that roam to inflamed peripheral tissues and confer immediate effector function, whereas reactive memory is carried out by T_{CM} cells that home to T-cell areas of secondary lymphoid organs (7). T_{CM} cells proliferate and differentiate to effector cells in response to antigenic stimulation (5).

Memory T-cells are characterized into two groups based on their phenotypic and functional profiles as T_{CM} and T_{EM} cells (7). The presence or absence of lymph node homing receptors CD62L (L-selectin) and C–C chemokine receptpr-7 (CCR7) on the cell surface are used to distinguish between T_{CM} and T_{EM} cells (8). CD62L or L-selection is a glycoprotein adhesion molecule which serves as a homing receptor for lymphocytes to enter secondary lymphoid tissues through high endothelial venules. CD62L shed from the surface during T-cell activation resulting in CD62L-negative effector cells (effector cells and T_{EM} cells). Hence, effector memory T-lymphocytes do not express L-selectin, as they circulate in the periphery and have immediate effector functions upon encountering antigen. Unlike T_{EM} cells, CD62L and CCR7 are present on the surface of T_{CM} (7). Naïve (N_{TC}) and T_{CM} cells express CD62L and CCR7 for migration to secondary lymphoid organ. In the absence of CD62L and CCR7 molecules, T_{EM} and effector T cells (T_{EC}) build up in the peripheral tissues. T_{EC} cells are terminally differentiated memory T-cells. They are the relatively short-lived activated cells whose functions involve the interaction of an armed T_{EC} cell with a target cell displaying specific antigen. They neither display memory marker (CD45RO) nor the homing receptor (CD62L) (7, 8).

Central memory T-cells produce IL-2, whereas T_{EM} cells are characterized by increased secretion of effector cytokines such as IFN-γ and IL-4 (7). T_{CM} cells are moderately long-lived memory cells, capable of differentiating into shorter-lived T_{EM} cells upon antigen stimulation. In turn, T_{EM} cells differentiate into T_{EC} cells. T_{EC} cells represent terminally differentiated T_{EM} cells. Apoptotic death is the outcome of T_{EC} cells upon increased proliferation and antigen exposure (9, 10). A N_{TC} is a mature differentiated T-cell that has not encountered its cognate antigen within the periphery. N_{TC}s are usually characterized by the surface expression of L-selectin (CD62L). They do not express memory markers (CD45RO) or activation markers such as CD25, CD44, and CD69. N_{TC}s do not proliferate until they encounter their corresponding antigens. Stem memory T-cells have recently been described as sets of memory T-cells in mice and humans comprise 2–4% of $CD4^+$ and $CD8^+$ T-cells population in the periphery. It is speculated that these cells represent the earliest and long-lasting developmental stage of memory T-cells, displaying stem cell-like properties and expressing a gene profile between naïve and T_{CM} cells (10).

Few studies have intended to identify the memory T cell subsets in leprosy. One earlier study has shown that in fresh and unstimulated blood leukocytes from leprosy patients, memory T cells predominated in the PB form of the disease and correlated with IFN-γ production but such result was not observed in MB patients (11). However, the study did not use an experimental design that allowed classification of memory T cell into subsets.

The correlation between T_{CM} cell expression and pro-inflammatory cytokine production with clinical presentation of multibacillary leprosy relapse case has been investigated (12). Increased frequency of T_{CM} cells in relapsed patients was strongly correlated with the bacillary index and the number of skin lesions was reported by these authors. The study did not give attention to the memory subsets in leprosy spectrum rather they focused on relapse cases. Recently, a cross-sectional study of memory T-cells among type-1 reactions (T1R) has shown that circulating $CD4^+$ T_{EM}, $CD8^+$ T_{Ec}, and pro-inflammatory cytokines increased at the onset of T1R in BL patients (13).

Memory T-cells have not been well characterized across leprosy spectrum as well as in leprosy reactions particularly in ENL reactions. In the present study, for the first time we described memory-T cell subsets in LL and ENL reactions before and after prednisolone treatment.

MATERIALS AND METHODS

Study Design

A case–control study with follow-up for 28 weeks was used to recruit 35 patients with ENL reaction and 25 non-reactional LL patient controls between December 2014 and January 2016 at ALERT Hospital, Ethiopia.

Clinical Case Definitions

The clinical assessment of the patient was used as main diagnostic criteria for ENL cases LL patient controls (4).

Erythema Nodosum Leprosum

Erythema nodosum leprosum was clinically diagnosed when a patient had painful tender subcutaneous erythematous skin lesions with or without systemic features such as fever, neuritis, and bone pain occurring in patients with LL or borderline LL.

Lepromatous Leprosy

Lepromatous leprosy was clinically diagnosed when a patient had widely disseminated nodular lesions with ill-defined borders and BI above 2.

Acute ENL

Acute ENL was defined as an ENL episode lasting less than 24 weeks of prednisolone treatment.

Chronic ENL

Chronic ENL was defined as an ENL occurring for 24 weeks or more during which a patient has required ENL treatment either continuously or where any treatment free period has been 27 days or less.

Recurrent ENL

Recurrent ENL was defined as a second or subsequent episode of ENL occurring 28 days or more after stopping or steady decrease of steroid treatment for ENL.

ENL Recurrence or Flare-up

Erythema nodosum leprosum recurrence or flare-up was defined as the appearance of new ENL nodules after initial control, either while on treatment or after 28 days off treatment.

New ENL Case

New ENL case was defined as the occurrence of ENL for the first time in a patient with LL.

Demographic and Clinical Data Collection

Structured questionnaire were used for clinical data recording for each participant. The ENL International STudy (ENLIST) format was modified and used for clinical data recording. The data collection sheet included the demographic, clinical, and diagnostic information set following the standard guideline at each time point. The clinical information included core points such as the clinical feature, skin lesion, nerve functions, and systemic involvement.

Clinical Sample Collection

Blood samples were obtained from each patient three times: at recruitment before prednisolone administration and after 12 and 24 weeks of prednisolone treatment foe ENL cases. The 12th week was chosen since the steady decrease in prednisolone after 12th week reaches less than half of the start dose and after 24th-week prednisolone administration normally off unless the patient experiences a chronic condition. The third time-point sample (24th week) was obtained when an ENL patient completed prednisolone treatment and the free treatment period is 15 days or more.

Peripheral Blood Mononuclear Cell (PBMC) Isolation, Freezing, and Thawing

Ten milliliters of venous blood was collected in sterile BD heparinized vacutainer® tubes (BD, Franklin, Lakes, NJ, USA). PBMCs were separated by density gradient centrifugation at 800 × *g* for 25 min on Ficoll-Hypaque (Histopaque, Sigma Aldrich, UK) as described earlier (14). Cells were washed three times in sterile phosphate-buffered saline solution (1× PBS, Sigma Aldrich®, UK) and resuspended with 1 ml of Roswell Park Memorial Institute [RPMI medium 1640 (1×) + GlutaMAX™ + Pen-Strip (GIBCO™, Life technologies™, UK)]. Cell viability was determined by 0.4% sterile Trypan Blue solution (Sigma Aldrich®, UK) ranged from 94 to 98%. PBMC freezing was performed using a freezing medium composed of 20% fetal bovine serum (FBS, heat inactivated, endotoxin tested ≤ 5 EU/ml, GIBCO® Life technologies, UK), 20% dimethyl sulfoxide in RPMI medium 1640 (1×). Cells were kept at 80°C for 48–72 h and transferred to liquid nitrogen. Thomson et al. method was used for cell thawing (15). The procedure is briefly described as: cells were removed from liquid nitrogen and taken to a water bath (preadjusted to 37°C) for 30 s until thawed half way and resuspended in 10% FBS in RPMI medium 1640 (1×) at 37°C containing 1/10,000 benzonase until completely thawed, washed two times (5 min each) and counted with trypan blue. A percentage viability of above 90% was obtained. Cell concentration was adjusted to 10^6 cells/ml in RPMI. Then, 1 ml/well cell suspension was pipetted on 24-well polystyrene cell culture plate (Corning® Costar® cell culture plates) and incubated at 37°C in a 5% carbon dioxide incubator. After an overnight resting, cells were brought to flow cytometry staining room for staining with fluorochromes conjugated antibodies as described below.

Surface Staining for Flow Cytometry

About 1 × 10^6/ml cells' suspension was transferred to round-bottomed FACS tubes (Falcon®, BD, UK) followed by washing twice at 400 × g for 5 min at RT. Then, cells were resuspended in 50 µl of PBS and incubated in 1 ml of 10% human AB serum (Sigma Aldrich®, UK) for 10 min in the dark at room temperature to block non-specific Fc-mediated interactions and followed by centrifugation at 400 × *g* for 5 min. After resuspending cells in 50 µl PBS buffer, live/dead staining was performed at a concentration of 1 µl/1 ml live/dead stain (V500 Aqua, Invitrogen, Life technologies, UK) for 15 min at 4°C in the dark. Cells were washed once and stained for surface markers directed against anti-human CD3 (APC 450), anti-human CD4 (eFluoro780), anti-human CD8 (PerCp-Cy5.5), anti-human CD62L (APC), and anti-human CD45RO (PE), all from BD, Biosciences, UK. We used for each maker FMO, compensation controls, and unstained cells. Unstained cells were used to exclude the autofluorescence of cells. Cell viability was also checked before staining using 0.4% trypan blue.

Sample Acquisition and Gating Strategy

After the voltages on the photomultiplier tubes and compensation controls setting, the worksheet area was switched from the normal worksheet to the global worksheet. For inspection

purpose, the plots were produced on worksheet such as FSC-H versus FSC-A (to inspect the singlets), FSC-A versus viability marker (to inspect viable cells), and SSC-A versus FSC-A (to inspect populations such as lymphocytes, monocytes, granulocytes, etc.). The threshold for FSC was set to 5,000. For each sample, 500,000–1,000,000 cells were acquired.

Cells were gated into subpopulations with Flow Jo version 10 (Tree Star, USA) by logicle (bi-exponential) method as recommended by Mohan et al. (16) and Ehlers (17). Activated and memory T-cells were defined as $CD3^+CD62L^-$ and $CD3^+CD45RO^+$, respectively. Memory T-cells were further grouped into T_{CM} cells ($CD3^+CD45RO^+CD62L^+$) and activated memory T-cells ($CD3^+CD45RO^+CD62L^-$). T_{EC} and N_{TC}s were defined as $CD3^+CD45RO^-CD62L^-$ and $CD3^+CD45RO^-CD62L^+$, respectively (**Figure 1**). The relative percentage of each subpopulation was copied to excel for each sample and finally an excel spreadsheet electronic data were generated and used for subsequent statistical analysis.

Statistical Analysis

Differences in percentage of T-cell subsets were computed and statistically tested with two-tailed Mann–Whitney *U* test or Wilcoxon signed rank test for non-parametric distribution using STATA 14 ver. 2 (San Diego, CA, USA). Graphs were produced by GraphPad Prism version 5.01 for Windows (GraphPad Software, San Diego, CA, USA). Median and Hodges–Lehmann estimator were used for result presentation. Hodges–Lehmann is used to measure the effect size for non-parametric data (18). *P*-Value correction was applied for multiple comparisons. A statistical significance level of 0.05 was used to test the difference between cases and controls.

RESULTS

We described the median percentage of activated T-cells ($CD62L^-$), total memory T-cells ($CD45RO^+$), and the subgroups of memory T-cells before, during, and after treatment of ENL patients and compared the results with non-reactional LL patient controls as well as within ENL patients.

Increased T-Cell Activation in Untreated ENL Patients

The percentage of activated $CD3^+$ T-cells ($CD3^+CD62L^-$) was significantly increased in untreated ENL patients (59.3%) in contrast to non-reactional LL patient controls (37.7%) ($P < 0.0001$; $\Delta HL = 22.4\%$). However, after treatment statistically a significant difference was not obtained between the groups. Similarly, the median percentage of activated $CD4^+$ T-cells ($CD4^+CD62L^-$) was significantly higher (50.7%) in PBMCs of patients with ENL than in LL patient controls (27.1%) before treatment ($P < 0.0001$; $\Delta HL = 19.1\%$). However, a significant difference was not observed during and after treatment ($P > 0.05$). Nearly two-third of $CD8^+$ T-cells (71.2%) was activated ($CD8^+CD62L^-$) in untreated ENL patients while it was only 45.4% in LL patient controls ($P < 0.0001$; $\Delta HL = 27.9\%$). On the other hand, after treatment, the frequency of activated $CD8^+$ T-cells was significantly decreased to 34.5% in patients with ENL compared to 45.2% in LL patient controls ($P \leq 0.05$; $\Delta HL = 10.1\%$) (**Figure 2A**).

When the trend of T-cell activation within ENL is compared before and after treatment, it was found that the median percentage of $CD3^+$-activated T-cells before starting prednisolone treatment was higher (59.2%) than during treatment (47.0%) ($P \leq 0.05$). After treatment, the median percentage of activated $CD3^+$ T-cells was decreased to 33.9%, which was significantly lower than before treatment ($P < 0.0001$; $\Delta HL = 25.5\%$). Likewise, the median percentage of $CD4^+$-activated T-cells was significantly higher (50.7%) before treatment than during treatment (29.7%) ($P < 0.0001$; $\Delta HL = 17.75\%$). Similarly, the median percentage of activated $CD8^+$ T-cells was significantly higher (71.2%) before treatment than during (59.5%) and after (34.5%) treatment ($P \leq 0.05$) (**Figure 2B**).

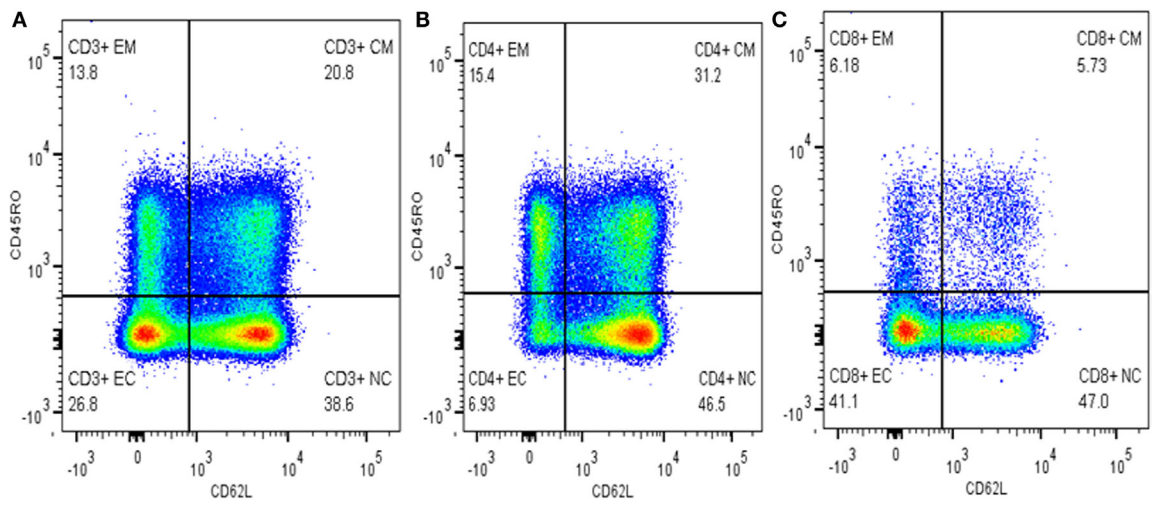

FIGURE 1 | Gating memory T-cells on different cell types. **(A)** Gated on $CD3^+$ T-cells, **(B)** gated on $CD4^+$ T-cells, and **(C)** gated on $CD8^+$ T-cells.

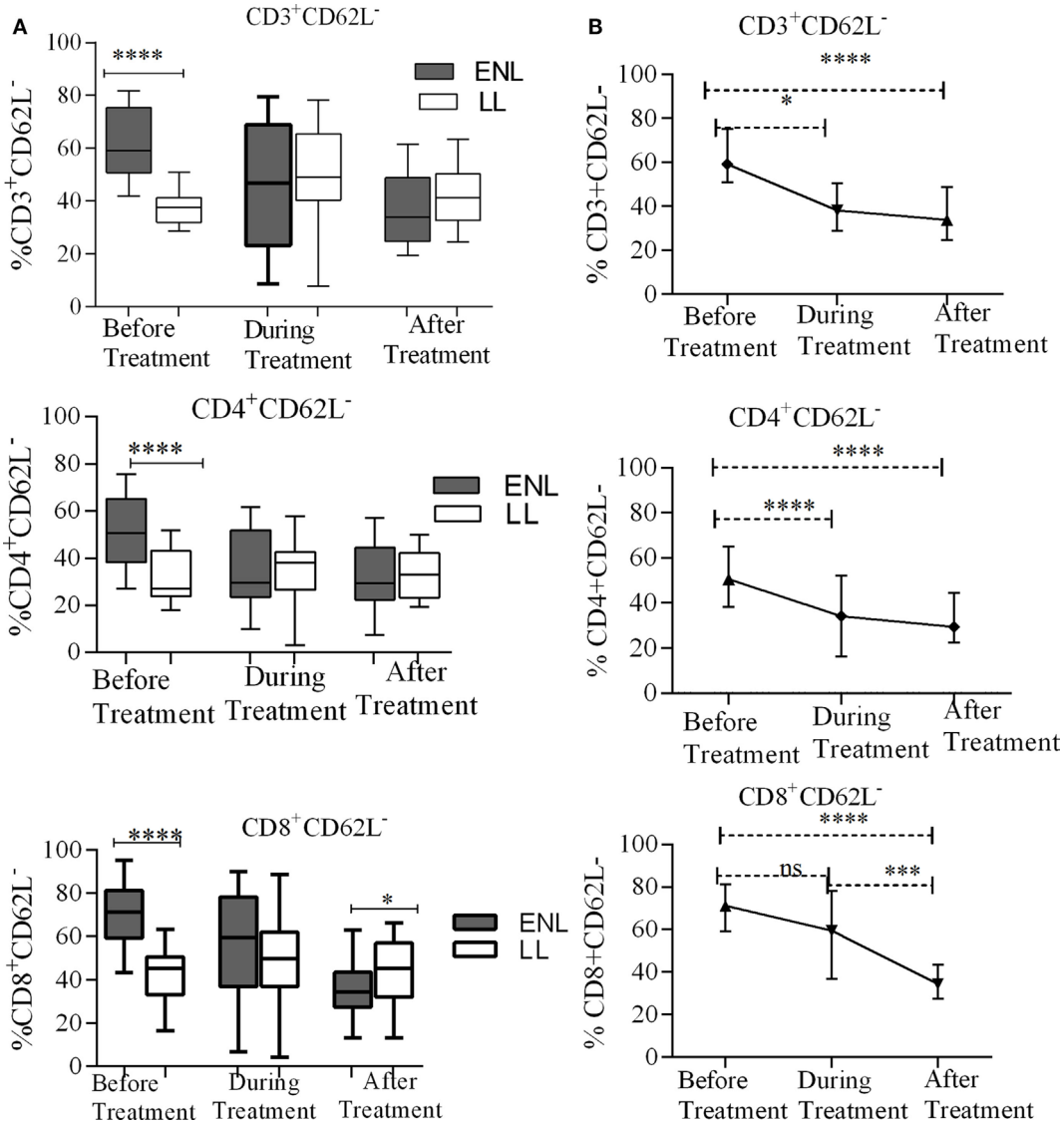

FIGURE 2 | Median percentage of total CD3+, CD4+, and CD8+ activated T-cells: **(A)** in patients with erythema nodosum leprosum (ENL) and lepromatous leprosy (LL) controls before, during, and after treatment, **(B)** within ENL patients before, during, and after treatment. *$P \leq 0.05$; ***$P < 0.001$; ****$P < 0.0001$. Box and whiskers **(A)** and error bars **(B)** show median ± interquartile range.

Increased Total Memory T-Cells in Untreated ENL Patients

Erythema nodosum leprosum patients had significantly increased $CD3^+$ total memory T-cell ($CD3^+CD45RO^+$) (40%) compared to LL patient' controls (28%) before treatment ($P \leq 0.005$; $\Delta HL = 10.5\%$). After treatment, the median percentage of $CD3^+$ total memory T-cells in ENL patients and LL controls were 31.2 and 32.7%, respectively, and the result was not statistically significantly different ($P > 0.05$). Similarly, the median percentage of $CD4^+$ total memory T-cells ($CD4^+$ $CD45RO^+$) was increased in untreated ENL patients (50%) compared to LL patient controls (30.5%) ($P < 0.0001$; $\Delta HL = 20.3\%$). After treatment, the median percentage of $CD4^+$ total memory T-cells in ENL patients (45.0%) was not significantly different compared to LL patient controls (41.8%) ($P > 0.05$). Interestingly, the median percentage of $CD8^+$ memory T-cells ($CD8^+CD45RO^+$) was not statistically significantly different between the two groups before and after treatment (**Figure 3A**).

When the median percentage of total memory T-cells was compared within ENL patients before, during, and after treatment, it was found that the median percentage of $CD3^+$ total memory T-cells was significantly higher (41.1%) before treatment than during treatment (29.2%) ($P \leq 0.001$; $\Delta HL = 11.2\%$) and after treatment (31.5%) ($P \leq 0.001$; $\Delta HL = 9.8\%$). Similarly, the median percentage of $CD4^+$ total memory T-cells was 52.3% before treatment and significantly decreased to 29.2% during treatment ($P < 0.0001$; $\Delta HL = 22.1\%$). On the other hand, unlike

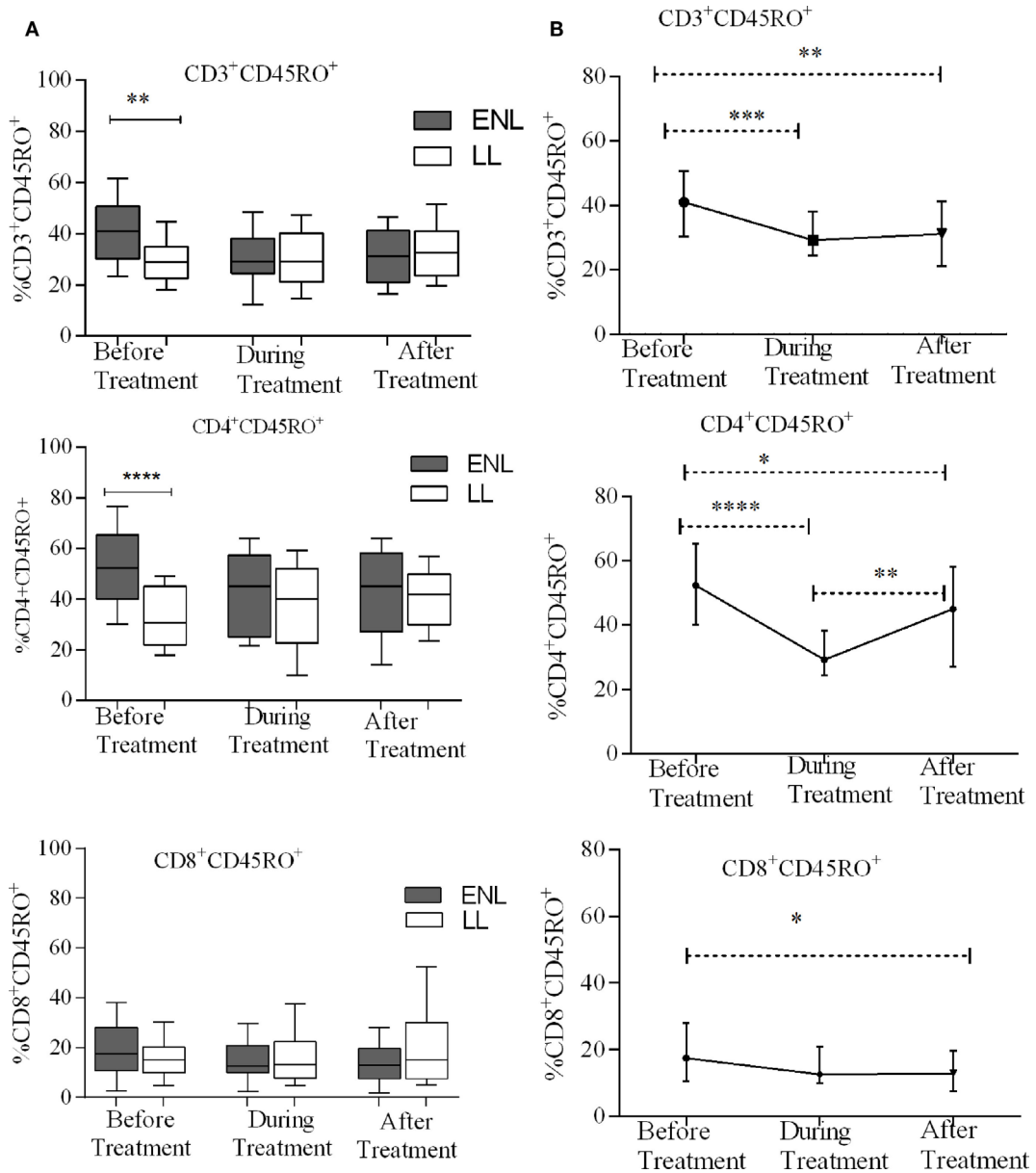

FIGURE 3 | Median percentage of total CD3+, CD4+, and CD8+ memory T-cells: **(A)** in patients with erythema nodosum leprosum (ENL) and lepromatous leprosy (LL) controls before, during, and after treatment, **(B)** within ENL patients before, during, and after treatment. *$P \leq 0.05$; **$P < 0.005$; ***$P < 0.001$; and ****$P < 0.0001$. Box and whiskers **(A)** and error bars **(B)** show median ± interquartile range.

CD3+ and CD4+ memory T-cells, the median percentage of CD8+ memory T-cells did not change within ENL patients before, during, and after treatment (**Figure 3B**).

Increased T_{EM} Cells in Patients with ENL

Effector memory T-cells are memory T-cells which have lost their CD62L expression while migrating to the tissue and progressively gain functionality with further differentiation to T_{EC} cells also called terminally differentiated T-cells (19). Measurement of T_{EM} cells is the most commonly used method to determine the extent of T-cell activation in a disease state. We measured the proportion of T_{EC} cells in unstimulated PBMCs from patients with ENL and LL controls before, during, and after treatment to prove our hypothesis that ENL is associated with increased T-cell activation.

The median percentage of CD3+ T_{EM} cells ($CD3^+CD45RO^+CD62L^-$) in the PBMCs of patients with ENL was 26.6%, which was significantly higher than in LL patient controls (8.0%) before treatment ($P < 0.0001$; $\Delta HL = 18.3\%$). Conversely, the percentage of CD3+ T_{EM} cell was found to be lower in patients with ENL (7.6%) than in LL patient controls (10.4%) after treatment ($P \leq 0.05$; $\Delta HL = 3.5\%$). Similarly, the median percentage

of CD4$^+$ T_{EM} cells (CD4$^+$CD45RO$^+$CD62L$^-$) in the PBMCs of patients with ENL was nearly three times (24.6%) higher than in the PBMCs of LL patient controls (8.9%) before treatment ($P < 0.0001$; $\Delta HL = 18.4\%$). However, unlike CD3$^+$ T_{EC} cells, the median percentage of CD4$^+$ T_{EC} cells was not significantly different between the two groups after treatment ($P > 0.05$). Likewise the median percentage of CD8$^+$ T_{EM} cells (CD8$^+$CD45RO$^+$CD62L$^-$) was significantly higher in patients with ENL (16.5%) than in LL patient controls (7.2%) before treatment ($P < 0.001$; $\Delta HL = 6.7\%$). However, after treatment, the median percentage of CD8$^+$ T_{EM} cells in patients with ENL and LL controls did not show significant difference (**Figure 4A**).

Trend analysis has shown that T_{EM} cells significantly decreased in ENL patients after prednisolone treatment. Untreated patients with ENL reactions had a higher CD3$^+$ T_{EM} cells (26.6%) than during treatment (16.8%) ($P < 0.0001$; $\Delta HL = 11.88\%$). The percentage of CD3$^+$ T-cells expressing T_{EM} cells (CD3$^+$CD45RO$^+$CD62L$^-$) was considerably decreased to 7.6% after treatment, which was substantially lower than the median percentage of CD3$^+$ T_{EM} cells before treatment ($P < 0.0001$; $\Delta HL = 20.0\%$). Likewise, the median percentage of CD4$^+$ T_{EM} (CD4$^+$CD45RO$^+$CD62L$^-$) cells was more than twofold higher (24.6%) before treatment compared to during treatment (11.4%) and the difference was statistically significant ($P < 0.0001$; $\Delta HL = 15.54\%$). The percentage of CD4$^+$ T_{EM} cells was remarkably reduced to 9.6% after treatment indicating the decreasing tendency of T-cell activation after prednisolone treatment of patients with ENL. About 16.5% of CD8$^+$ T-cells

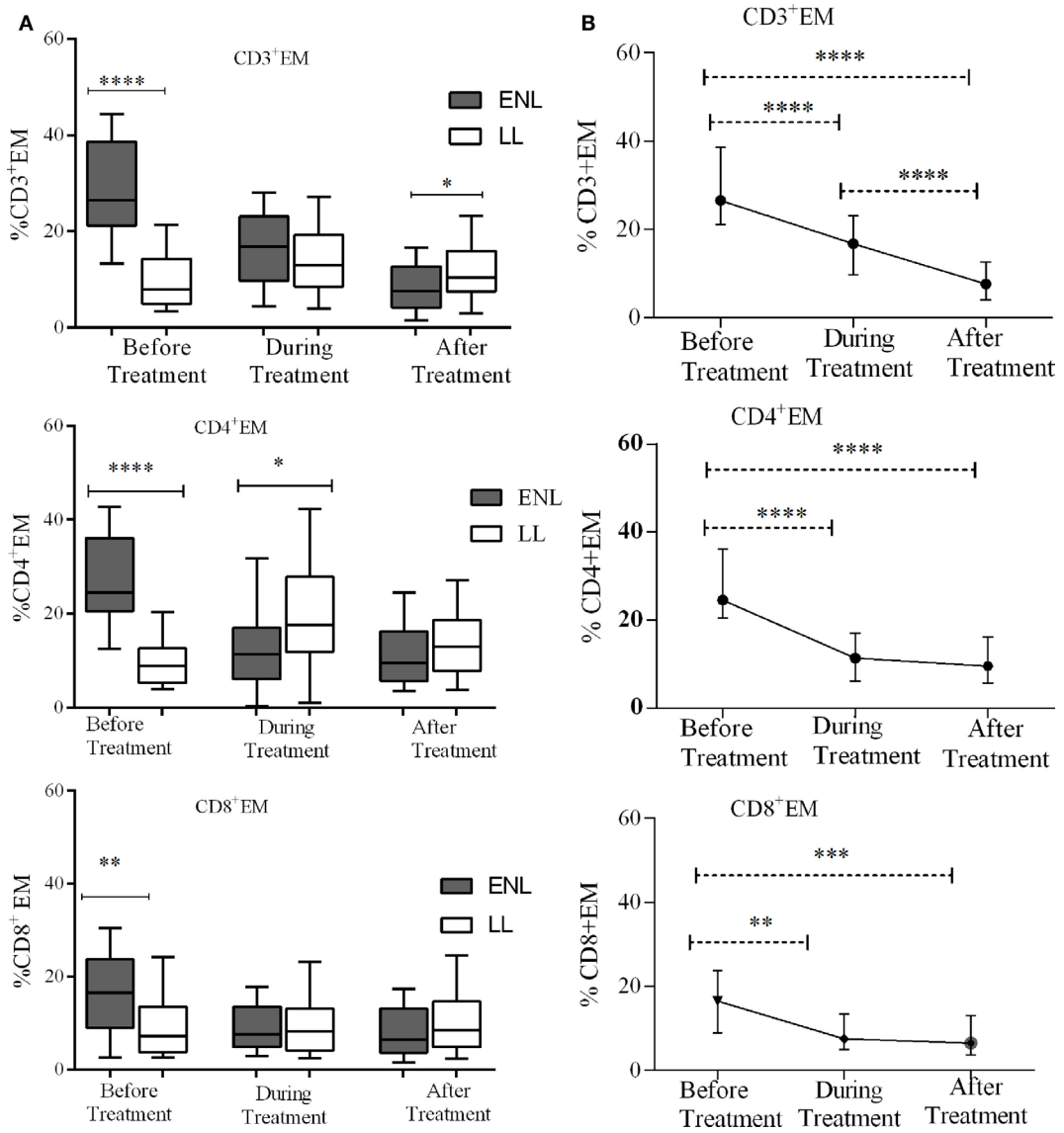

FIGURE 4 | Median percentage of CD3$^+$, CD4$^+$, and CD8$^+$ effector memory T-cells: **(A)** in patients with erythema nodosum leprosum (ENL) and lepromatous leprosy (LL) controls before, during and after treatment, **(B)** within ENL patients before, during, and after treatment. *$P \leq 0.05$; **$P < 0.005$; ***$P < 0.001$; ****$P < 0.0001$. Box and whiskers **(A)** and error bars **(B)** show median ± interquartile range.

expressed T_{EM} cells ($CD8^+CD45RO^+CD62L^-$) before treatment. During treatment, the median percentage of $CD8^+$ T-cells expressing T_{EM} cells was notably decreased to 7.5%, which was significantly low compared to before treatment ($P \leq 0.005$; $\Delta HL = 6.61\%$). However, unlike $CD4^+$ and $CD3^+$ T_{EM} cells, the proportion of $CD8^+$ T_{EM} cells did not show significant change after treatment (6.5%) (**Figure 4B**).

T_{CM} Cells Play Less Role in ENL Reaction

The median percentages of $CD3^+$ T_{CM} ($CD3^+CD62L^+CD45RO^+$) cells in patients with ENL and LL controls before, during, and after treatment were not statistically significantly different ($P > 0.05$). Unlike $CD3^+$ T_{CM}, the proportion of $CD4^+$ T_{CM} ($CD4^+CD62L^+CD45RO^+$) was significantly higher in patients with ENL (23.5%) than in LL patient controls (14.6%) before treatment ($P \leq 0.005$; $\Delta HL = 8.13\%$). However, the median percentage of $CD4^+$ T_{CM} cell was not significantly different between the two groups after treatment. Interestingly, the median percentage of $CD8^+$ T_{CM} ($CD8^+CD62L^+CD45RO^+$) cell was significantly lower in patients with ENL (1.2%) than in LL patient controls (3.5%) before treatment ($P \leq 0.0001$; $\Delta HL = 2.3\%$). After treatment, the percentage of $CD8^+$ T_{CM} cell was slightly higher in patients with ENL (2.7%) than in LL patient controls (2.0%); however, the difference was not statistically significant ($P > 0.05$) (**Figure 5A**).

Comparison within ENL has shown that the percentage of T_{CM} cells was not statistically significantly different before and after treatment (**Figure 5B**). This confirms that T_{CM} cells do not play significant role in ENL reaction unlike T_{EM} cells.

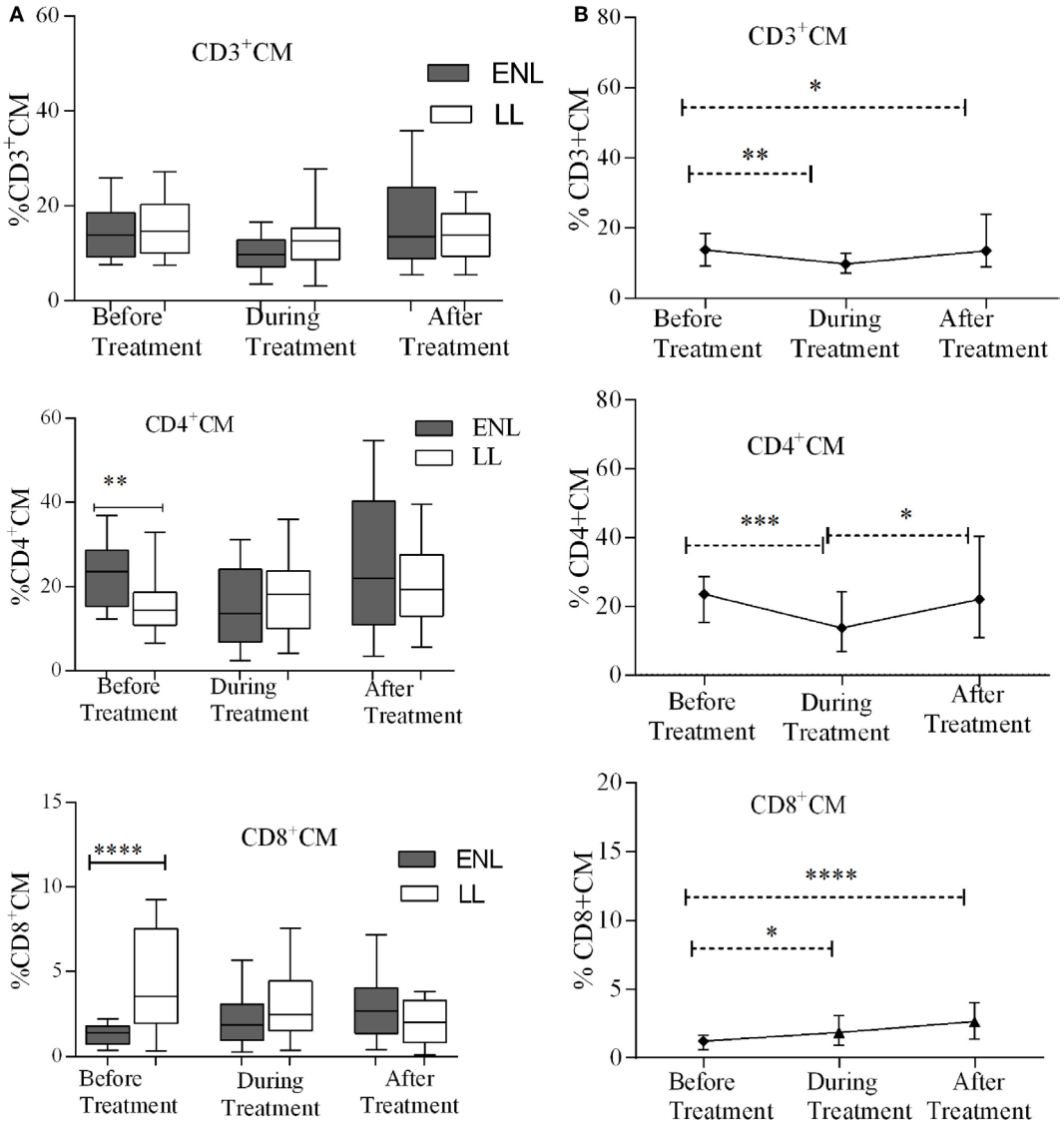

FIGURE 5 | Median percentage of $CD3^+$, $CD4^+$, and $CD8^+$ central memory T-cells: **(A)** in patients with erythema nodosum leprosum (ENL) and lepromatous leprosy (LL) controls before, during, and after treatment, **(B)** within ENL patients before, during, and after treatment. $^*P \leq 0.05$; $^{**}P < 0.005$; $^{***}P < 0.001$; $^{****}P < 0.0001$. Box and whiskers (A) and error bars (B) show median ± interquartile range.

Increased T_{EC} Cells in Untreated ENL Patients

Effector memory T-cells (T_{EC}) are short-lived unlike memory T-cells and they shortly undergo apoptosis once they meet their cognate antigens. Nearly one-third (29.3%) of $CD3^+$ T-cells were effector cells (T_{EC}) in the PBMCs of patients with ENL with the corresponding value of 20.0% in LL patient controls before treatment and the difference was statistically significant ($P \leq 0.001$; $\Delta HL = 9.0\%$). After treatment, the median percentage of $CD3^+$ T_{EC} cell was significantly decreased in patients with ENL (24.6%) compared to LL patient controls (35.3%) ($P \leq 0.05$; $\Delta HL = 8.6\%$). With regard to the median percentage of $CD4^+$ T_{EC} cell, a statistically significant difference was not obtained between the two groups before, during, or after treatment. The median percentage of T_{EC} cell expression in $CD8^+$ T-cells in patients with ENL was 62.7%, which was considerably higher than the value obtained for LL patient controls (39.5%) before treatment ($P < 0.0001$; $\Delta HL = 25.8\%$). Similar to $CD3^+$ T_{EC} cell, the proportion of $CD8^+$ T_{EC} cell in patients with ENL was significantly decreased (38.9%) compared to LL patient controls (55.2%) after treatment ($P \leq 0.005$; $\Delta HL = 14.4$) (**Figure 6A**).

The median percentage of $CD3^+$ T_{EC} cells was lower before treatment (29.3%) than during treatment (43.4%) ($P \leq 0.005$). After treatment, the percentage of these cells decreased to 24.6%. Similarly, the median percentage of $CD4^+$ T_{EC} cells was lower before treatment (14.0%) than during treatment (22.9%) ($P \leq 0.05$). After treatment, the percentage of $CD4^+$ T_{EC} cells was decreased by half (12.1%) than during treatment ($P \leq 0.05$). Like

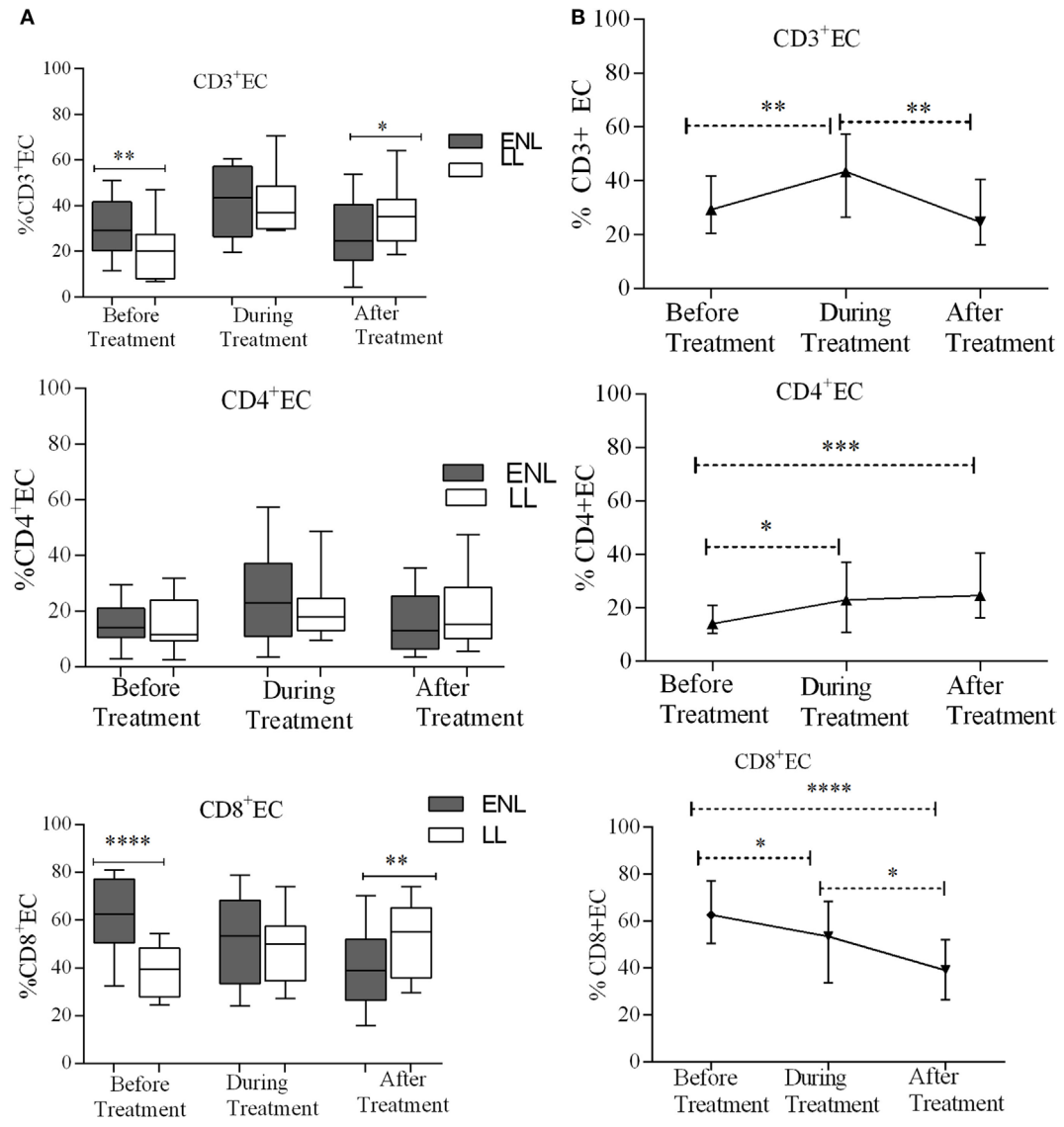

FIGURE 6 | Median percentage of $CD3^+$, $CD4^+$, and $CD8^+$ effector T-cells: **(A)** in patients with erythema nodosum leprosum (ENL) and lepromatous leprosy (LL) controls before, during, and after treatment, **(B)** within ENL patients before, during, and after treatment. *$P \leq 0.05$; **$P < 0.005$; ***$P < 0.001$; ****$P < 0.0001$. Box and whiskers **(A)** and error bars **(B)** show median ± interquartile range.

$CD3^+$ T_{EC} cells, the percentage of $CD4^+$ T_{EC} cells did not show significant difference before and after treatment. On the other hand, the median percentage of $CD8^+$ T_{EC} cells was higher (62.7%) before treatment than during treatment (53.4%) ($P \leq 0.05$). After treatment, the percentage of $CD8^+$ T_{EC} cells was considerably decreased to 38.9% compared to during treatment ($P \leq 0.05$) and before treatment ($P < 0.0001$) (**Figure 6B**).

N_{TC}s Decreased in ENL Patients Compared to Non-Reactional LL Controls

Despite the higher bacterial load in patients with LL patients, the median percentage of $CD3^+$ N_{TC}s was significantly higher (59.5%) in these patients compared to that in patients with ENL (27.7%) before treatment ($P < 0.0001$; $\Delta HL = 26.5\%$). During treatment, the median percentage of $CD3^+$ N_{TC}s significantly decreased to 32.9% in LL patient controls while in patients with ENL the percentage was slightly increased to 31.8%. After treatment, the percentage of $CD3^+$ N_{TC}s was further increased to 42.9% in patients with ENL but did not change in LL patient controls (33.0%), and the difference between the two groups was statistically significant. Similarly, the median percentage of $CD4^+$ N_{TC}s in patients with ENL (34.0%) was significantly lower than that in LL patient controls (61.5%) before treatment ($P < 0.0001$; $\Delta HL = 25.6\%$). However, during and after treatment the median percentage of $CD4^+$ N_{TC}s did not show statistically significant difference ($P > 0.05$). On the other hand, the median percentage of $CD8^+$ N_{TC}s in patients with ENL was more than three times lower (15.4%) than in LL patient controls (50.5%) before treatment ($P < 0.0001$; $\Delta HL = 31.6\%$). During treatment, while the median percentage of $CD8^+$ N_{TC}s increased to 35.5% in patients with ENL, it was decreased to 38% in LL patient controls. After treatment, the median percentage of $CD8^+$ N_{TC}s in patients with ENL and LL controls was 51.5 and 32.8%, respectively, and the difference between the two groups was statistically significant ($P \leq 0.05$; $\Delta HL = 14.4\%$) (**Figure 7A**).

Comparison within ENL has shown that the percentage of $CD3^+$ T_{NC} cell was lower (27.7%) before than after treatment (42.9%) ($P < 0.0001$). Similarly, the percentage of $CD4^+$ T_{NC} cells was lower (34.1%) before treatment than after treatment (40.4%) ($P \leq 0.005$). The percentage of $CD8^+$ T_{NC} cells was 15.4% before treatment but increased to 51.5% after treatment and it was significantly higher than before treatment ($P < 0.0001$) (**Figure 7B**).

Decreased Regulatory T-Cells (T_{reg})/T_{EM} Cells Ratio in ENL Patients Compared to LL Controls

The median percentage ratio of T_{reg} ($CD3^+CD4^+CD25^+FoxP3^+$) to T_{EM} (T_{reg}/T_{EM} cells) was significantly lower in untreated patients with ENL (0.077) than in LL controls (0.44) before treatment ($P \leq 0.0001$). However, after treatment the median percentage ratio of T_{reg}/T_{EM} cells was significantly increased in patients with ENL (0.522) compared LL controls (0.255) ($P \leq 0.005$) (**Figure 8A**).

When the ratio of T_{reg}/T_{EM} cells is compared within ENL groups, it was found that patients with ENL had a significantly lower median percentage of T_{reg}/T_{EM} cells (0.077) before treatment than after treatment (0.552) ($P < 0.0001$) (**Figure 8B**).

DISCUSSION

The ability of inflammatory cells to respond to pathogens is crucial for maintaining healthy conditions. In mammals, lymphocytes leave the circulation and migrate to secondary lymphoid organs, such as lymph nodes, where antigens are presented. When an antigen is encountered, directed release of immune cells to sites of inflammation orchestrates host defense. Both constitutive and inflammatory leukocyte trafficking is controlled by adhesion molecules. The initial tethering of leukocytes to the endothelium and to other leukocytes is assisted by selectins, particularly by L-selectins. L-selectin directs neutrophils and lymphocytes to sites of inflammation. Upon T-cell activation L-selectin is shed from the leukocyte surface (8, 20).

In this study, the status of T-cell activation and the different subtypes of memory T-cells were investigated. In leprosy, the different classes of memory T-cells have not been studied. To our knowledge, it is for the first time that the different subtypes of memory T-cells and T-cell activation are phenotypically described in patients with ENL and LL. We are the first to study the status of T-cell activation in patients with ENL. Not only T-cell activation and the different classes of memory T-cells are described but also the changes of these immune cells over time before, during, and after prednisolone treatment were investigated. Therefore, our present data will provide basic information for future studies involving T-cell activation and memory T-cells in ENL.

Increased Activation of T-Cells in Entreated ENL

In our study, patients with ENL had significantly higher percentage of $CD3^+$, $CD4^+$, and $CD8^+$ activated T-cells than LL patient controls before treatment. However, after prednisolone treatment, T-cell activation was not significantly different in patients with ENL and LL controls except for the transient activation of $CD8^+$ T-cells. This result is the evidence of T-cell activation in patients with ENL reactions. *In vitro* stimulation of PBMCs from patients with ENL reaction with *M. leprae* whole-cell sonicate has shown an increased T-cell response as assessed by IFN-γ and TNF-α production (data not shown). Excessive T-cell activation as a cause of tissue damage in several inflammatory diseases has been described in many studies (21, 22). The finding of T-cell activation in patients with ENL implies the involvement of T-cell activation in the pathogenesis of ENL.

In this study, changes in the percentage of activated T-cells were investigated before, during, and after prednisolone treatment within ENL groups. The percentages of $CD3^+$, $CD4^+$, and $CD8^+$ activated T-cells were significantly reduced during and after prednisolone treatment. The reduction of activated T-cells following prednisolone treatment may be explained by the immunosuppressive activity of prednisolone. Although studies showing the effect of prednisolone treatment on T-cell response in leprosy reactions is lacking, several studies in other

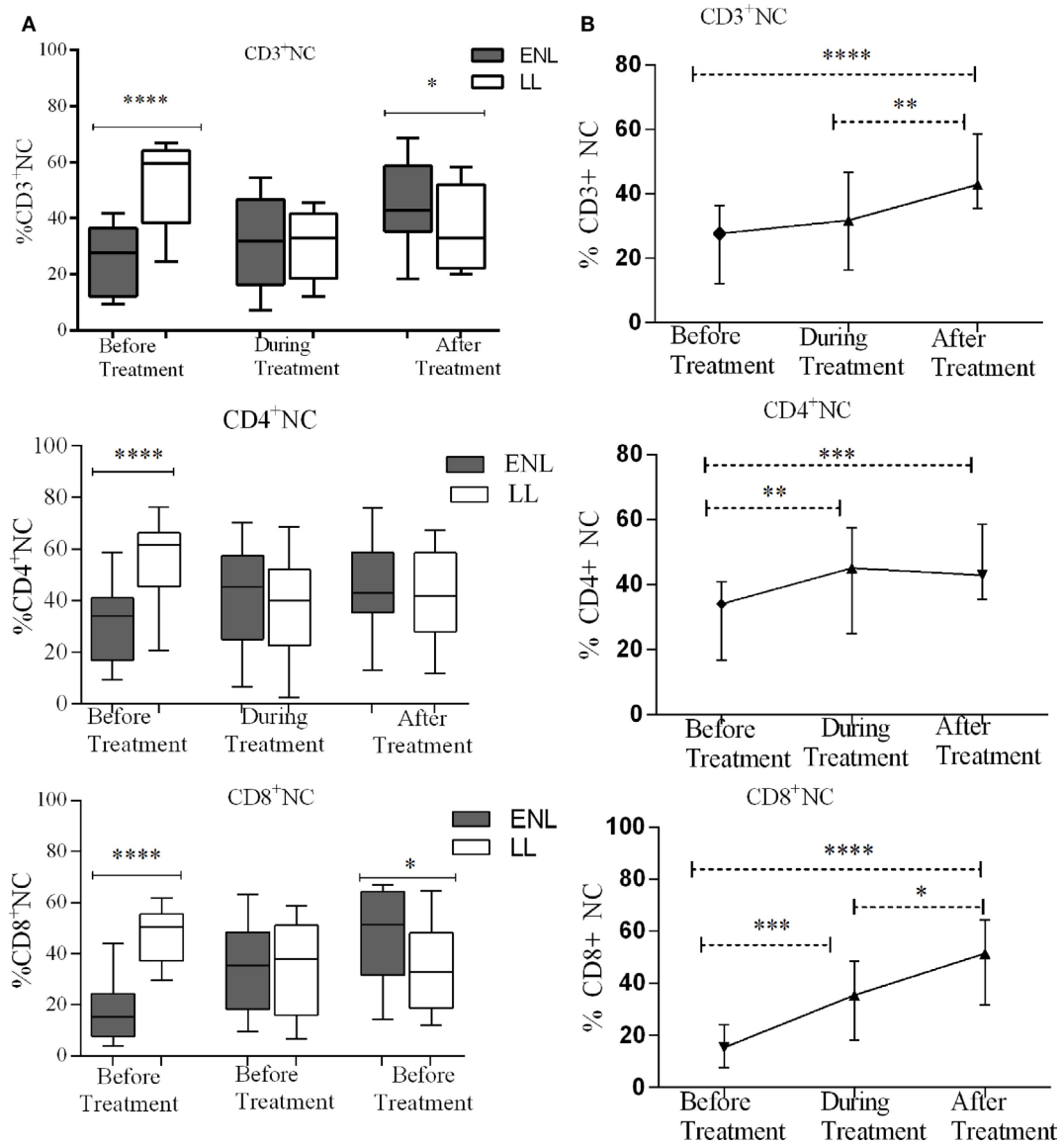

FIGURE 7 | Median percentage of CD3+, CD4+, and CD8+ naïve T-cells: **(A)** in patients with erythema nodosum leprosum (ENL) and lepromatous leprosy (LL) controls before, during, and after treatment, **(B)** within ENL patients before, during, and after treatment. *$P \leq 0.05$; **$P < 0.005$; ***$P < 0.001$; ****$P < 0.0001$. Box and whiskers **(A)** and error bars **(B)** show median ± interquartile range.

inflammatory diseases have shown the suppressive effect of prednisolone on the T-cell response (23–25). Consequently, our present findings provide evidence that the effect of prednisolone treatment of patients with ENL could be through suppressing T-cell responses.

T_{EM} Cells Significantly Increased in Untreated ENL Patients

The median percentage of CD3+, CD4+, and CD8+ T-cells expressing T_{EM} cells in the PBMCs of patients with ENL was significantly high compared to LL patient controls before treatment. Such a difference was not observed after prednisolone treatment of patients with ENL. This implies that in patients with ENL, there is a continuous activation of T-cells. This continuous T-cell activation could lead to an excess antibody–antigen complex formation but insufficient to clear bacilli from lesions (26). This means the rate of immune-complex formation is greater than the rate of immune-complex clearance, which leads to further tissue damage through recruitment of inflammatory molecules to the site of immune-complex deposition. In LL, there is high load of bacilli. The macrophages are laden with this intact bacillus but unable to process and present to T-cells for further action. LL patients are also characterized by the presence of high antibody titer although these antibodies play little or no role to protect the multiplication of *M. leprae* in these patients. Spontaneous

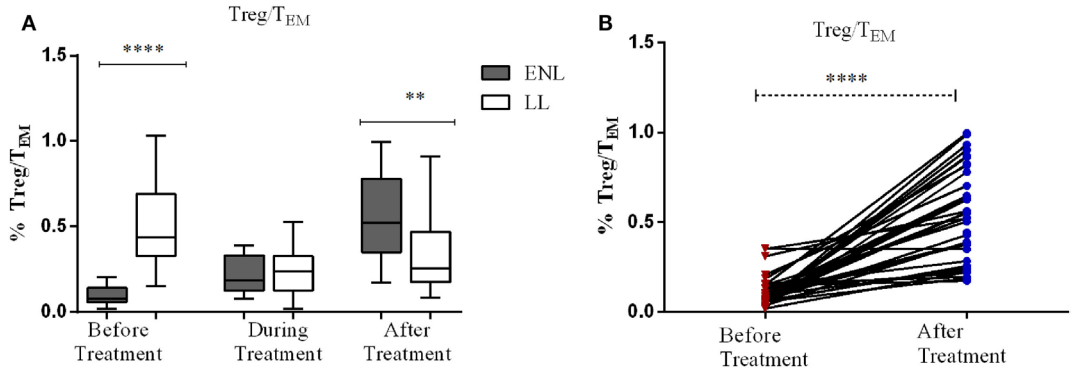

FIGURE 8 | The median percentage of regulatory T-cells (T_{reg})/effector memory T-cells (T_{EM}) cells: **(A)** in patients with erythema nodosum leprosum (ENL) and lepromatous leprosy (LL) controls before, during, and after treatment, **(B)** within ENL patients before, during, and after treatment. $^{**}P < 0.005$; $^{***}P < 0.001$; $^{****}P < 0.0001$.

activation of T-cells could lead to the macrophage activation or B-cell activation or both. Macrophage activation results in the processing of the bacilli and releasing the processed bacterial components, which further activate other immune cells. The activation of B-cells by T-cells could produce functional antibodies, which form immune-complex with the already accumulated bacterial antigens. However, this scenario is less likely to happen as it is confirmed that the different subtypes of B-cells did not significantly different in ENL and LL patients (data not shown). Whichever the activation takes place, if excess immune-complex is formed due to the presence of excess antigens in the body, it leads to more immune-complex formation than immune-complex clearance, and hence, some immune-complexes deposit in tissues and often induce inflammatory responses and can cause tissue damage. The causes of tissue damage could be due to the action of complement cleavages, which induces the release of tissue damaging granules such as histamine or the recruitment of inflammatory cells such as neutrophils and macrophages into the tissue. However, this assumption needs further study to give definitive evidence. Previous studies have suggested that human T_{EM} cells display characteristic sets of chemokine receptors and adhesion molecules that are required for homing to inflamed tissues and they have an immediate effector function (20, 27). This situation could amplify the immune response and hence further aggravate tissue damage in a vicious circle (**Figure 9**).

A kinetic analysis of the percentage of T_{EM} cells in the PBMCs from patients with ENL before, during, and after prednisolone treatment showed that the median percentage of T_{EM} cells was decreased from 27% before treatment to 8% after treatment with an effect size of 20%. It has been described in previous sections that T_{EM} cells rapidly differentiate to T_{EC} cells upon antigenic stimulation. The consequence of excessive expression of T_{EM} cells is detrimental to tissue damage (9). In apparently healthy individuals, T_{EC} cells do not express CD62L or CCR7 and hence do not home to lymph nodes (10). A breakdown in the compartmentalization of such T_{EC} cells is predicted to have unfavorable consequences for the immune system. Hence, the finding of an increased percentage of T_{EM} cells in patients with ENL before treatment suggests that T_{EC} cells take part in the process of tissue damage observed in these patients.

More T-Cells in ENL Patients Are Antigen Experienced than in LL Patients

Interestingly, the median percentage of N_{TC}s' expression in $CD3^+$, $CD4^+$, and $CD8^+$ T-cells in the PBMCs of patients with ENL was significantly low compared to LL controls before treatment implying that T-cells from patients with ENL have more antigenic exposure than those from LL. It is important to note that patients with ENL had LL before they developed ENL during which a high percentage of N_{TC}s is expected since higher percentage of N_{TC}s was investigated in this study in LL patients. Following the development of ENL, the percentage of N_{TC}s drops to below 30%. This implies that either those previously N_{TC}s became responsive and able to recognize their cognate antigen or the newly produced T-lymphocytes during the onset of ENL reactions are able to recognize and respond to the existing *M. leprae* antigens unlike in LL. It is an established fact that despite the high bacterial load in patients with LL, the cell-mediated immune response is virtually absent (28, 29). In addition to a specific loss of cell-mediated immune response against *M. leprae* in these patients, a relative impairment of the ability of lymphocytes to react *in vitro* has also been reported. Furthermore, lymph nodes from patients with LL show a deficiency of these cells in those areas associated with the development of cell-mediated immune responses (14, 28–31). Therefore, the significantly reduced median percentage of N_{TC}s in blood from patients with ENL reaction provides an evidence of T-cell responsiveness in patients with ENL. This means that unlike in LL patients, the N_{TC}s in ENL patients are primed in recognition of the *M. leprae* antigen (**Figure 9**).

The median percentage of N_{TC}s was significantly increased after prednisolone treatment within ENL groups. The percentage of N_{TC}s in untreated patients with ENL reactions was less than 30% and was increased to nearly 50% after treatment. Previous studies have shown that prednisolone treatment increases in a dose-dependent manner the percentage of N_{TC}s in experimental

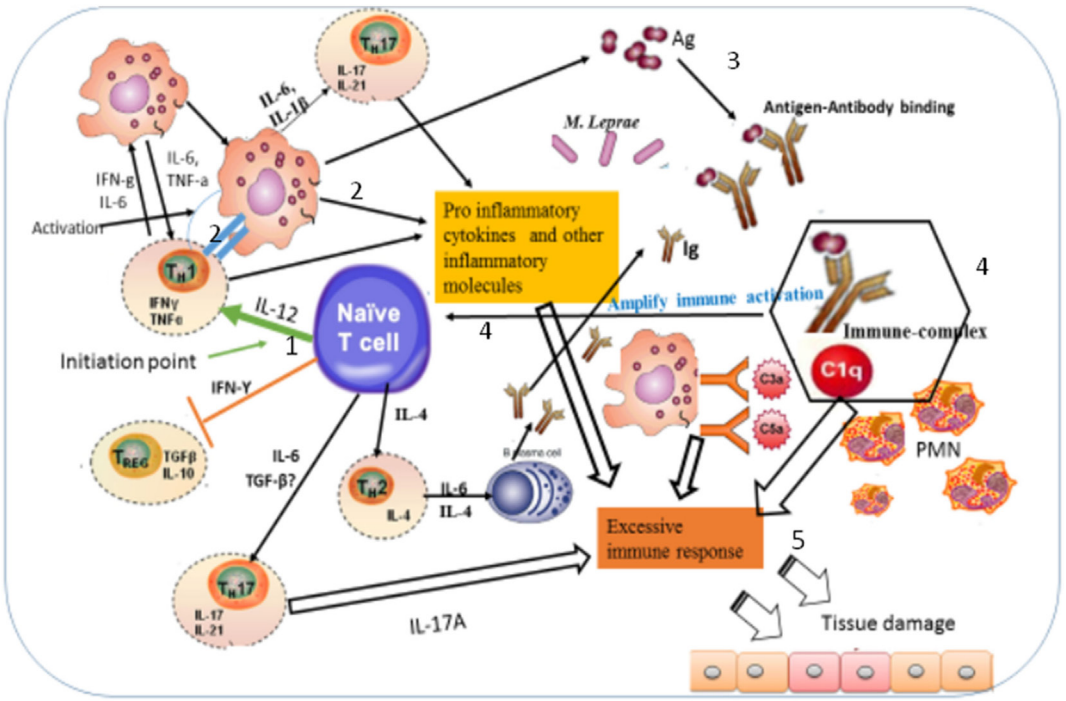

FIGURE 9 | Illustration of the possible immunopathogenesis of erythema nodosum leprosum (ENL) based on the present findings. Based on the finding of this study, the immunopathogenesis of ENL can be illustrated using the following key steps: (1) spontaneous activation of T-cells leading to activation of macrophages that are already loaded with intact *Mycobacterium leprae*. Then, the activation of macrophages produces three key events: processing *M. leprae* and releasing of the processed antigens; antigen presentation to Th1 and production of pro-inflammatory cytokines such as IFN-γ and TNF-α and other inflammatory molecules. The causes of spontaneous T-cell activation should be investigated in the future. (2) Antigen presentation to Th1 stimulates Th1 to produce chemokines, which recruits macrophages to the site of antigen deposition, pro-inflammatory cytokines (IFN-γ, TNF-α), and other inflammatory mediators that increase expression of vascular adhesion molecules. (3) The processed and released antigens bind to the presynthesized antibody leading to antigen–antibody complex formation, which in turn recruits C1q complement and hence immune-complex formation. Following the immune-complex formation, neutrophils will be recruited to the site of immune-complexes. (4) Once immune-complex is formed, it amplifies the immune response which leads to aggressive antigen presentation, immunoglobulin synthesis, and activation of other inflammatory T-cells. (5) The pro-inflammatory cytokines and other inflammatory molecules released from macrophages, Th17, and Th1 and the immune-complex formation beyond clearance lead to tissue damage as sketched above.

mice. Hence, the finding of high percentages of N_{TC}s after prednisolone treatment of patients with ENL may be explained by the fact that prednisolone resolves inflammation at least partly by increasing the percentage of N_{TC}s which concurrently reduce the percentage of activated T-cells.

In our present work, we have shown that ENL reaction is associated with increased T-cell activation. Our findings suggest that ENL reaction is a T-cell-mediated pathology. Hence, the T-cell-mediated pathology of ENL will provide further insights into disease mechanisms and will potentially result in promising new therapeutic options. Therefore, future ENL studies should consider these fertile areas to improve the treatment and management of ENL. It might also be important to think of to interfere with T-cell trafficking into tissues and thereby reducing inflammation in these patients.

ETHICS STATEMENT

Informed written consent for blood samples was obtained from patients following approval of the study by the Institutional Ethical Committee of London School of Hygiene and Tropical Medicine, UK (#6391), AHRI/ALERT, Ethiopia (P032/12), and the National Research Ethics Review Committee, Ethiopia (#310/450/06). All data have been analyzed and reported anonymously.

AUTHOR CONTRIBUTIONS

EN and DL formulated the study questions. EN, DL, HD, SW, and KB designed the study protocol. EN, BE, and KB conducted the experiment. AA, HD, and DL supervised the study. EN analyzed the data. All the authors contributed to the interpretation of the data. EN drafted the manuscript. KB, SW, BE, RH, AA, HD, and DL revised the manuscript. All the authors read and approved the final version for publication. All the authors agreed to be accountable for all aspects of the work in ensuring that questions related to the accuracy or integrity of any part of the work are appropriately investigated and resolved.

ACKNOWLEDGMENTS

We would like to thank the participants who volunteered to donate blood sample and sacrificed their time to participate

in this study. We would like to thank in particular, the study nurses Sr. Genet Amare and Sr. Haregewoin, study coordinator Mr. Fikre Mekuria, our tracer, Mr. Yilma Tesfaye, the Red Medical Clinic nurses, and Dr. Yonas Bekele for his help in the lab work. We would like to extend our sincere gratitude to Suzan Sheedy whose administrative support at LSHTM has been invaluable and AHRI staff for their unreserved support. Mr. Dawit Bogale should receive our sincere thanks for his fast and on time custom clearance of our reagents. Finally, we would like to acknowledge Homes and Hospital of St Gilles for funding the project and Armauer Hansen Research Institute for allowing us to use all laboratory facilities.

FUNDING

The study was funded by Homes and Hospitals of St Giles, UK.

REFERENCES

1. Ridley MJ, Ridley DS. The immunopathology of erythema nodosum leprosum: the role of extravascular complexes. *Lepr Rev* (1983) 54(2):95–107.
2. Lockwood DN, Vinayakumar S, Stanley JN, McAdam KP, Colston MJ. Clinical features and outcome of reversal (type 1) reactions in Hyderabad, India. *Int J Lepr Other Mycobact Dis* (1993) 61(1):8–15.
3. Walker SL, Lebas E, Doni SN, Lockwood DNJ, Lambert SM. The mortality associated with erythema nodosum leprosum in Ethiopia: a retrospective hospital-based study. *PLoS Negl Trop Dis* (2014) 8(3):e2690. doi:10.1371/journal.pntd.0002690
4. Pocaterra L, Jains S, Reddy R, Muzaffarullah S, Torres S, Suneetha S, et al. Clinical course of erythema nodosum leprosum: an 11-year chohort study in Hyderabad, India. *Am J Trop Med Hyg* (2006) 74(5):868–79. doi:10.4269/ajtmh.2006.74.868
5. Mueller SN, Gebhardt T, Carbone FR, Heath WR. Memory T cell subsets, migration patterns, and tissue residence. *Annu Rev Immunol* (2013) 31:37–61. doi:10.1146/annurev-immunol-032712-095954
6. Vita G, Lijun W. Different subsets of T cells, memory, effector functions, and CAR-T immunotherapy. *Cancers* (2016) 8(36):1–12. doi:10.3390/cancers8030036
7. Mackenziea KJ, Nowakowskaa DJ, Leecha MD, McFarlanea AJ, Wilsonc C, Fitcha PM, et al. Effector and central memory T helper 2 cells respond differently to peptide immunotherapy. *Proc Natl Acad Sci U S A* (2014) 111:E784–93. doi:10.1073/pnas.1316178111
8. Raffler NA, Rivera-Nieves J, Ley K. L-selectin in inflammation, infection and immunity. *Drug Discov Today* (2005) 2(3):213–20. doi:10.1016/j.ddstr.2005.08.012
9. Farber DL, Yudanin NA, Restifo NP. Human memory T cells: generation, compartmentalization and homeostasis. *Nat Rev Immunol* (2014) 14(1):24–35. doi:10.1038/nri3567
10. Flynn JK, Gorry PR. Stem memory T cells (TSCM)[mdash]their role in cancer and HIV immunotherapies. *Clin Trans Immunol* (2014) 3:e20. doi:10.1038/cti.2014.16
11. Mitra DK, De Rosa SC, Luke A, Balamurugan A, Khaitan BK, Tung J, et al. Differential representations of memory T cell subsets are characteristic of polarized immunity in leprosy and atopic diseases. *Int Immunol* (1999) 11(11):1801–10. doi:10.1093/intimm/11.11.1801
12. Esquenazi D, Alvim IMP, Pinheiro RO, Oliveira EB, Moreira LO, Sarno EN, et al. Correlation between central memory T cell expression and proinflammatory cytokine production with clinical presentation of multibacillary leprosy relapse. *PLoS One* (2015) 10(5):e0127416. doi:10.1371/journal.pone.0127416
13. dos Santos L, da Silva P, Alvim I, Nery J, Lara F, Sarno E, et al. Role of TEFFECTOR/MEMORY Cells, TBX21 gene expression and T-cell homing receptor on type 1 reaction in borderline lepromatous leprosy patients. *PLoS One* (2016) 11(10):e0164543. doi:10.1371/journal.pone.0164543
14. Bobosha K, Wilson L, van Meijgaarden KE, Bekele Y, Zewdie M, van der Ploeg-van Schip JJ, et al. T-cell regulation in lepromatous leprosy. *PLoS Negl Trop Dis* (2014) 8(4):e2773. doi:10.1371/journal.pntd.0002773
15. Thompson ML, Kunkel EJ, Ehrhardt RO. *Cryopreservation and Thawing of Mammalian Cells*. New York: John Wiley & Sons, Ltd (2001).
16. Mohan VP, Scanga CA, Yu K, Scott HM, Tanaka KE, Tsang E, et al. Effects of tumor necrosis factor alpha on host immune response in chronic persistent tuberculosis: possible role for limiting pathology. *Infect Immun* (2001) 69(3):1847–55. doi:10.1128/IAI.69.3.1847-1855.2001
17. Ehlers S. Tumor necrosis factor and its blockade in granulomatous infections: differential modes of action of infliximab and etanercept? *Clin Infect Dis* (2005) 41(Suppl 3):S199–203. doi:10.1086/429998
18. Gail F. Twenty nonparametric statistics and their large sample approximations. *J Mod Appl Stat Methods* (2002) 1(2):248–68. doi:10.22237/jmasm/1036110540
19. Seder RA, Darrah PA, Roederer M. T-cell quality in memory and protection: implications for vaccine design. *Nat Rev Immunol* (2008) 8(4):247–58. doi:10.1038/nri2274
20. Sallusto F, Geginat J, Lanzavecchia A. Central memory and effector memory T cell subsets: function, generation, and maintenance. *Annu Rev Immunol* (2004) 22:745–63. doi:10.1146/annurev.immunol.22.012703.104702
21. Baniyash M. TCR [zeta]-chain downregulation: curtailing an excessive inflammatory immune response. *Nat Rev Immunol* (2004) 4(9):675–87. doi:10.1038/nri1434
22. Park CO, Kupper TS. The emerging role of resident memory T cells in protective immunity and inflammatory disease. *Nat Med* (2015) 21(7):688–97. doi:10.1038/nm.3883
23. Hepburn B, Slade JD. Effect of divided daily dose prednisone therapy on circulating T cell subsets. *J Rheumatol* (1987) 14(1):19–22.
24. Shevach EM. Mechanisms of Foxp3+ T regulatory cell-mediated suppression. *Immunity* (2009) 30:636–45. doi:10.1016/j.immuni.2009.04.010
25. Kasang C, Kalluvya S, Majinge C, Kongola G, Mlewa M, Massawe I, et al. Effects of prednisolone on disease progression in antiretroviral-untreated HIV infection: a 2-year randomized, double-blind placebo-controlled clinical trial. *PLoS One* (2016) 11(1):e0146678. doi:10.1371/journal.pone.0146678
26. Cooper CL, Mueller C, Sinchaisri TA, Pirmez C, Chan J, Kaplan G, et al. Analysis of naturally occurring delayed-type hypersensitivity reactions in leprosy by in situ hybridization. *J Exp Med* (1989) 169(5):1565–81. doi:10.1084/jem.169.5.1565
27. Kaech SM, Wherry EJ, Ahmed R. Effector and memory T-cell differentiation: implications for vaccine development. *Nat Rev Immunol* (2002) 2(4):251–62. doi:10.1038/nri778
28. Godal T, Myklestad B, Samuel DR, Myrvang B. Characterization of the cellular immune defect in lepromatous leprosy: a specific lack of circulating *Mycobacterium leprae*-reactive lymphocytes. *Clin Exp Immunol* (1971) 9(6):821–31.
29. Godal T, Myrvang B, Froland SS, Shao J, Melaku G. Evidence that the mechanism of immunological tolerance ('central failure') is operative in the lack of host resistance in lepromatous leprosy. *Scand J Immunol* (1972) 1(4):311–21. doi:10.1111/j.1365-3083.1972.tb03296.x
30. Myrvang B, Godal T, Ridley DS, Fröland SS, Song YK. Immune responsiveness to *Mycobacterium leprae* and other mycobacterial antigens throughout the clinical and histopathological spectrum of leprosy. *Clin Exp Immunol* (1973) 14(4):541–53.
31. Kaplan G, Weinstein DE, Steinman RM, Levis WR, Elvers U, Patarroyo ME, et al. An analysis of in vitro T cell responsiveness in lepromatous leprosy. *J Exp Med* (1985) 162(3):917–29. doi:10.1084/jem.162.3.917

Conflict of Interest Statement: The authors declare that the research was conducted in the absence of any commercial or financial relationships that could be construed as a potential conflict of interest.

Copyright © 2017 Negera, Bobosha, Walker, Endale, Howe, Aseffa, Dockrell and Lockwood. This is an open-access article distributed under the terms of the Creative Commons Attribution License (CC BY). The use, distribution or reproduction in other forums is permitted, provided the original author(s) or licensor are credited and that the original publication in this journal is cited, in accordance with accepted academic practice. No use, distribution or reproduction is permitted which does not comply with these terms.

frontiers in Immunology

ORIGINAL RESEARCH
published: 22 September 2017
doi: 10.3389/fimmu.2017.01173

Lower Expression of MicroRNA-155 Contributes to Dysfunction of Natural Killer Cells in Patients with Chronic Hepatitis B

Jun Ge[1†], Zuxiong Huang[2,3†], Hongyan Liu[1†], Jiehua Chen[1], Zhanglian Xie[1], Zide Chen[1], Jie Peng[1], Jian Sun[1], Jinlin Hou[1] and Xiaoyong Zhang[1]*

[1] State Key Laboratory of Organ Failure Research, Guangdong Provincial Key Laboratory of Viral Hepatitis Research, Department of Infectious Diseases, Nanfang Hospital, Southern Medical University, Guangzhou, China, [2] Department of Hepatology, Mengchao Haptobiliary Hospital of Fujian Medical University, Fuzhou, China, [3] Department of Hepatology, Affiliated Infectious Disease Hospital of Fujian Medical University, Fuzhou, China

OPEN ACCESS

Edited by:
Jixin Zhong,
Case Western Reserve University,
United States

Reviewed by:
Giuseppe Sciume,
Sapienza Università di Roma,
Italy
Luz Pamela Blanco,
National Institutes of Health (NIH),
United States
Ka Man Law,
University of California,
Los Angeles, United States

***Correspondence:**
Xiaoyong Zhang
xiaoyzhang@smu.edu.cn

[†]These authors have contributed equally to this work.

Specialty section:
This article was submitted to Inflammation, a section of the journal Frontiers in Immunology

Received: 18 May 2017
Accepted: 05 September 2017
Published: 22 September 2017

Citation:
Ge J, Huang Z, Liu H, Chen J, Xie Z, Chen Z, Peng J, Sun J, Hou J and Zhang X (2017) Lower Expression of MicroRNA-155 Contributes to Dysfunction of Natural Killer Cells in Patients with Chronic Hepatitis B. Front. Immunol. 8:1173. doi: 10.3389/fimmu.2017.01173

MicroRNAs have been reported to be regulated in different ways in a variety of liver diseases. As a key modulator of cellular function in both innate and adaptive immunity, the role of miR-155 in chronic hepatitis B virus infection remains largely unknown. Here, we investigated the expression and function of miR-155 in chronic hepatitis B (CHB) patients. It was found that miR-155 expression in peripheral blood mononuclear cells (PBMCs) was lower in CHB patients than healthy controls (HC). Among CHB infection, immune-active (IA) patients with abnormal alanine aminotransferase (ALT) levels had relatively higher miR-155 expression in PBMCs and serum than immune-tolerant carriers, but were comparable to inactive carriers. Moreover, there was a positive correlation between miR-155 expression and ALT levels in CHB patients. Particularly, miR-155 expression in natural killer (NK) cells was significantly downregulated in IA patients compared with HC. Inversely, suppressor of cytokine signaling 1 (SOCS1), a target of miR-155, was upregulated in NK cells of IA patients. Overexpression of miR-155 in NK cells from IA patients led to a decrease in SOCS1 expression and an increase of IFN-γ production. Finally, accompanied by the normalization of ALT, miR-155 expression in PBMCs gradually decreased during telbivudine or peg-IFN-α-2a therapy. Interestingly, higher miR-155 expression at baseline was associated with better response to telbivudine therapy, but not peg-IFN-α-2a. In conclusion, our data suggested that miR-155 downregulation in NK cells of IA patients impaired IFN-γ production by targeting SOCS1, which may contribute to immune dysfunction during CHB infection. Additionally, baseline miR-155 expression could predict the treatment response to telbivudine therapy.

Keywords: chronic hepatitis B, miR-155, natural killer cells, suppressor of cytokine signaling 1, telbivudine

Abbreviations: ALT, alanine aminotransferase; CHB, chronic hepatitis B; CR, complete response; HBeAg, hepatitis B e antigen; HBsAg, hepatitis B surface antigen; HBV, hepatitis B virus; HC, healthy control; IA, immune activation; IC, inactive carrier; IFN, interferon; IL, interleukin; IT, immune tolerance; miRNA, microRNA; NCR, non-complete response; NK cell, nature killer cell; NSVR, non-sustained virological response; PBMC, peripheral blood mononuclear cell; peg-IFN-α-2a, pegylated interferon α-2a; SHIP1, SH2-domain containing inositol-5-phosphatase 1; SOCS1, suppressor of cytokine signaling 1; SVR, sustained virological response; TLR, toll-like receptor; TNF-α, tumor necrosis factor α.

INTRODUCTION

Hepatitis B virus (HBV) infection causes acute and chronic hepatitis and is a threat to public health across the world. It is estimated that 240 million people suffer from chronic HBV infections and are at risk of developing progressive liver diseases, such as cirrhosis, liver failure, and hepatocellular carcinoma (1). Generally, the outcome and pathogenesis of HBV infection is related to the complex interaction between viral activity and host immunity (2). MicroRNAs (miRNAs) are non-coding RNAs that regulate the expression of multiple genes at the posttranscriptional level by either translational repression or messenger RNA degradation (3). They play important roles in normal biological processes and have potential as disease biomarkers because they can indicate abnormal functions of particular organs. Many studies have reported that viral infections change host miRNAs profiles, which may affect virus–host interactions and participate in the viral life cycle and pathogenesis (4, 5). Currently, the available evidence indicates that miRNAs are involved in both the HBV life cycle and the development of HBV-associated liver diseases (6).

miR-155 is an evolutionarily conserved miRNA encoded in B-cell Integration Cluster non-coding RNA and acts as a crucial player in hematopoiesis, immune response, and inflammation (7). As miR-155 transcription is regulated by the activator protein-1 complex and the nuclear factor-κB transcription complex, the upregulation of miR-155 is often associated with increased cytokine release during the inflammatory process, particularly toll-like receptors (TLRs) signaling pathway activation (8, 9). Generally, miR-155 is involved in protective immunity when properly regulated and functions within a variety of activated immune cell types, including monocytes, natural killer (NK) cells, T cells, B cells, and dendritic cells (10). Within immune cells, miR-155 targets and represses many immune-regulatory proteins that include signaling molecules such as SH2-domain containing inositol-5-phosphatase 1 (SHIP1) (11) and suppressor of cytokine signaling 1 (SOCS1) (12), to regulate cytokines, chemokines, and transcription factors important for mounting an optimal immune response.

Because miR-155 also targets many important signaling proteins and transcription factors that govern immune processes and differentiation, it is not surprising that miR-155 has an important role during immune responses to HBV infection. Recently, Su et al. demonstrated that miR-155 could enhance innate antiviral immunity through promoting JAK/STAT signaling pathways by targeting SOCS1, and mildly inhibiting HBV replication in human hepatoma cells (13). Sarkar et al. found a positive correlation between TLR7 and miR-155 expression in HBV-infected liver biopsy and serum specimens as well as *in vitro*, which in turn modulated HBV replication (14). Yu et al. reported that expression of miR-155 was downregulated in peripheral blood mononuclear cells (PBMCs) and might correlate with the immune states of chronic hepatitis B (CHB) patients (15). However, the expression and role of miR-155 in regulating immune function during chronic HBV infection have yet to be explored.

Therefore, in the current study, we investigated the expression and function of miR-155 using (PBMCs) from CHB patients and its confirmatory expression in serum samples, as well as its alterations in PBMCs during therapy with telbivudine or pegylated interferon α-2a (peg-IFN-α-2a). The results provided new insights into the host antiviral response and the relationship between miR-155 expression and clinical outcome in patients with CHB.

MATERIALS AND METHODS

Study Subjects

In the cross-sectional study, venous blood was drawn from 73 consecutive untreated CHB patients and 21 healthy controls (HC) at Nanfang Hospital (Guangzhou, China). According to the guidelines of the European Association for the Study of Liver Diseases (16), these CHB patients were divided into three groups of study subjects: immune-tolerant (IT) carriers (IT, $n = 24$), immune activation (IA, $n = 27$), and inactive carriers (IC, $n = 22$). The characteristics of all participants, with respect to demographic, biochemical, and virological features, are listed in **Table 1**.

Forty-one HBeAg-positive CHB subjects who had participated in a prospective clinical trial of telbivudine (600 mg/day, clinical trial number: NCT00962533) (17) and another 24 patients from a prospective clinical trial of Peg-IFN-α-2a (180 μg/week, clinical trial number: NCT01086085) (18) in Nanfang Hospital were also studied.

All patients provided written documentation of informed consent to enter the study. The study protocol conformed to the ethical guidelines of the 1975 Declaration of Helsinki and was approved by the Ethical Committee of Nanfang Hospital.

Serological Assays and HBV-DNA Assays

Serum HBsAg, HBeAg, anti-HBs, anti-HBe, and anti-HBc levels were quantitatively analyzed by the ARCHITECT i2000SR system (Abbott Ireland Diagnostics Division, Sligo, Ireland). Quantification of serum HBV-DNA was assayed by the COBAS TaqMan HBV Test (Roche Molecular Diagnostics, Pleasanton, CA, USA), which has a detection limit of 12 IU/ml or 69.84 copies/ml.

PBMCs Isolation and Cell Subsets Sorting

Peripheral blood mononuclear cells were separated on Ficoll-Histopaque (BD Biosciences, Shanghai, China) density gradients and routinely cryopreserved as previously described (19). Thawed PBMCs were stained with anti-α-CD14-APC, anti-α-CD19-PE-Cy7, anti-α-CD3-APC-Cy7, and anti-α-CD56-FITC

TABLE 1 | Clinical characteristics of the subjects for cross-sectional study.

Group	HC	IT	IA	IC
n	21	24	27	22
Gender (M/F)	10/11	13/11	20/7	10/12
Age (years)	25 (22–28)	27.5 (18–38)	28 (18–38)	28 (21–45)
HBV-DNA (log_{10} copies/ml)	ND	8.01 (6.72–8.82)	8.59 (6.37–9.48)	<3
ALT (U/l)	15 (6–38)	23.8 (14–41)	113 (55–593)	16.5 (10–39)
HBeAg/anti-HBe	0/0	24/0	27/0	0/22

Values are n or median (range).

M/F, male or female; ND, not determined; ALT, alanine aminotransferase; HBeAg, hepatitis B e antigen; HBV, hepatitis B virus; HC, healthy control; IT, immune tolerance; IA, immune activation; IC, inactive carrier.

antibody (BD Biosciences, San Jose, CA, USA) for phenotype staining, while staining with 7AAD-PerCp (BD Biosciences) excluded dead cells. The stained cells were used for cell subset sorting on a BD FACSAria III (BD Biosciences). $CD56^+$ NK cells were sorted from fresh PBMCs isolated from HCs ($n = 12$) and CHB patients ($n = 12$) with CD56 MicroBeads and MACS separation columns (Miltenyi Biotech, Shanghai, China), according to the manufacturer's protocol. This purification protocol resulted in >95% purity of the selected cells, as determined by flow cytometry analysis (FACS) using anti-α-CD3-APC-Cy7 and anti-α-CD56-FITC antibody.

RNA Extraction, Reverse Transcription, and Quantitative Real-time PCR

Total cellular RNA was isolated and purified from PBMCs or cell subsets using the miRNeasy miRNA isolation kit (Qiagen, Hilden, Germany) according to the manufacturer's instructions. The cDNA synthesis was performed with 100 ng total miRNA using the miScript Reverse Transcription Kit (Qiagen). The expression of miR-155 genes was determined by real-time RT-PCR, which was performed with miScript SYBR Green PCR Kit (Qiagen) by using commercially available qPCR primer (Qiagen) on a LightCycler 480 (Roche Diagnostics International, Rotkreuz, Switzerland) according to the manufacturer's instructions. The expression levels of each gene in the PBMCs were presented as values normalized against 10^6 copies of U6 small nuclear RNA (RNU6B) transcripts. The miRNA in serum was extracted by miRNeasy Serum/Plasma Kits (Qiagen) and was synthesized as above. In addition, *C. elegans* miR-39 was added to serum samples as an internal control according to manufacturer's recommends. Then quantitative real-time RT-PCR analysis for each gene in serum was performed as it was for the PBMCs, and the results were presented as values normalized against 10^6 copies of *C. elegans* miR-39 miRNA transcripts. It was noteworthy that only 48 patients had enough corresponding serum retained to accomplish serum miR-155 detection.

Cells Surface Staining and Flow Cytometry Analysis

Natural killer cells among the PBMCs were identified by flow cytometry analysis as the $CD3^-/CD56^+$ specimens. Expression of several activating (NKG2D, NKp46) and inhibitory (NKG2A, KIR3DL1/s1, Tim3) NK receptors, as well as secondary signals required for IFN-γ production (CD16) and early activation molecules (CD69) were examined by labeling with monoclonal antibody as described above.

Cell Culture, Stimulation, and Functional Analysis

Fresh isolated NK cells were cultured at a density of 5×10^5 cells/ml in RPMI 1640 (Life Technologies-Thermo Fisher Scientific Corp, Waltham, MA, USA) supplemented with 10% fetal bovine serum (FBS, Gibco, Grand Island, New York, NY, USA), 2 mM L-glutamine (Invitrogen, Carlsbad, CA, USA) and antibiotics/penicillin–streptomycin (Life Technologies, Carlsbad, CA, USA). NK cells were stimulated with IL-12 (10 ng/ml), IL-15 (10 ng/ml), and IL-18 (100 ng/ml) for 24 h as previously described (20). After 18 h of stimulation, 10 μg/ml of brefeldin A (BD Biosciences) was added to each well and incubated for the remaining 6 h for intracellular staining, while anti-α-CD107a-PE was added at the same time. Then the cultured cells were stained with LIVE/DEAD Fixable Near-IR Dead Cell Stain kit (life Technologies) to exclude dead cells and then the remaining viable cells were exposed to anti-α-CD3-PerCp, anti-α-CD56-APC, anti-α-CD3-PE-Cy7, anti-α-CD56-PerCp, anti-α-CD16-FITC, and anti-α-IFN-γ-PE, anti-α-TNF-α-FITC anti-α-Granzyme A-PE, anti-α-Perforin-APC, anti-α-Granzyme B-APC, or isotype antibody (BD Biosciences) for phenotype or intracellular staining, while with Fix/Perm A/B (Invitrogen) fixed and broken membranes. The stained cells were analyzed on a BD Canto II flow cytometer (BD Biosciences, San Jose, CA, USA).

Transfection of NK Cells with miRNA Mimics

The hsa-miR-155-5p micrON™ miRNA mimic (miR-155 mimic) and miRNA mimic Ncontrol (miR-control) were synthesized by RiboBio (Guangzhou, China). $CD56^+$ NK cells were sorted from fresh PBMCs isolated from IA patients ($n = 6$) with CD56 MicroBeads and MACS separation columns as described above. Then 5×10^5 purified NK cells were resuspended in 0.5 ml of Gene Pulser electroporation buffer (Bio-Rad, CA, USA) with 100 nM miR-155 mimic or a miR-control, and were then transferred into Gene Pulser micropulser electroporation cuvettes (Bio-Rad). Transient transfection of the resuspended cells was performed using the Gene Pulser Xcell electroporation system (Bio-Rad), according to the manufacturer's protocol. The transfected NK cells were immediately rescued after transfection in pre-warmed complete RPMI 1640 medium in 48-well culture plates, then incubated at 37°C and 5% CO_2 for 3 days before analysis. Then the cells were stimulated and stained as above.

Cytotoxic Activity of NK Cells

The separated NK cells (effector, E) were seeded onto 96-well plates at ratios of 5:1 with 1×10^4 K562 (target cells-1, T-1), or at ratios of 2:1 with 1×10^4 HepG2.2.15 (T-2), and then incubated with IL-12 (10 ng/ml), IL-15 (10 ng/ml), and IL-18 (100 ng/ml) for 18 h. The cytolytic activity of the NK cells was determined using a Cytotoxicity LDH Assay kit-WST (Dojindo Molecular Technologies, Japan) according to the manufacturer's instructions.

Statistical Analysis

Continuous data were shown as medians (minimum-maximum). Two-group comparisons were evaluated by the Mann–Whitney *U*-test, Wilcoxon signed-rank test, Chi-squared test, and paired *t*-tests. The Kruskal–Wallis *H* test was used when comparing more than three groups. Repeated measures analysis was used to compare changes in miR-155 expression during treatment. Differences in continuous variables were evaluated by paired Student's tests. The correlations between variables were analyzed using the Spearman's rank order correlation coefficient. Receiver-operating characteristic (ROC) curves were constructed to predict a CR to telbivudine treatment. All of the tests were two-tailed

and a p-value of <0.05 calculated by SPSS Statistics 21.0 and GraphPad Prism 5.0 was considered statistically significant.

RESULTS

miR-155 Expression Was Downregulated in PBMCs with Chronic HBV Infection and It Was Positively Correlated with ALT and TLR2 Levels

For the first step, we examined the expression of miR-155 in PBMCs and serum samples from all CHB patients by real-time RT-PCR. The miR-155 levels were lower in PBMCs from CHB patients than from HCs (**Figure 1A**, $p = 0.005$). The median miR-155 levels in PBMCs were downregulated in both the IT and IC groups compared to the HC group (**Figure 1A**, HC vs IT, $p < 0.001$; HC vs IC, $p = 0.01$). Interestingly, the miR-155 expression was higher in IA patients with abnormal ALT levels (**Figure 1A**, IA vs IT, $p = 0.01$). At the same time, miR-155 serum levels during various phases of chronic HBV infection were similar to those occurring in PBMCs (**Figure 1B**, HC vs IT, $p = 0.023$; IA vs IT, $p = 0.013$). Although serum miR-155 expression in CHB patients had a tendency to be lower than in the HC group, these differences were not statistically significant (**Figure 1B**). No correlation was found between miR-155 expression in PBMCs and serum miR-155 levels (Figure S1A in Supplementary Material).

We then evaluated the association between ALT levels, HBV DNA, and miR-155 mRNA expression in PBMCs and serum of the subjects with chronic HBV infections. As shown in **Figure 1C**, Spearman analysis revealed that there was a positive correlation between miR-155 levels in PBMCs and ALT levels ($r^2 = 0.121$, $p = 0.003$), but no correlation was observed between miR-155 levels in PBMCs and HBV DNA loads (Figure S1B in Supplementary Material, $p = 0.281$). However, there was no correlation between miR-155 levels in serum and ALT (**Figure 1D**, $p = 0.269$). As TLRs had been reported to mediate miR-155 expression and function during HBV infection (14), we also examined the relationship between miR-155 and TLR2 and found there was a high positive correlation between them (Figure S1C in Supplementary Material, $r^2 = 0.305$, $p < 0.001$).

In contrast to miR-155, miR-146a is a negative modulator of innate and adaptive immunity and its upregulation in CHB causes impaired T cell function, which may contribute to immune defects and immunopathogenesis that develops during chronic HBV infection (21). We also examined the miR-146a expression in PBMCs and serum samples of CHB. Although miR-146a and miR-155 had a positive correlation in PBMCs (Figure S2A in Supplementary Material), there was no significant difference of

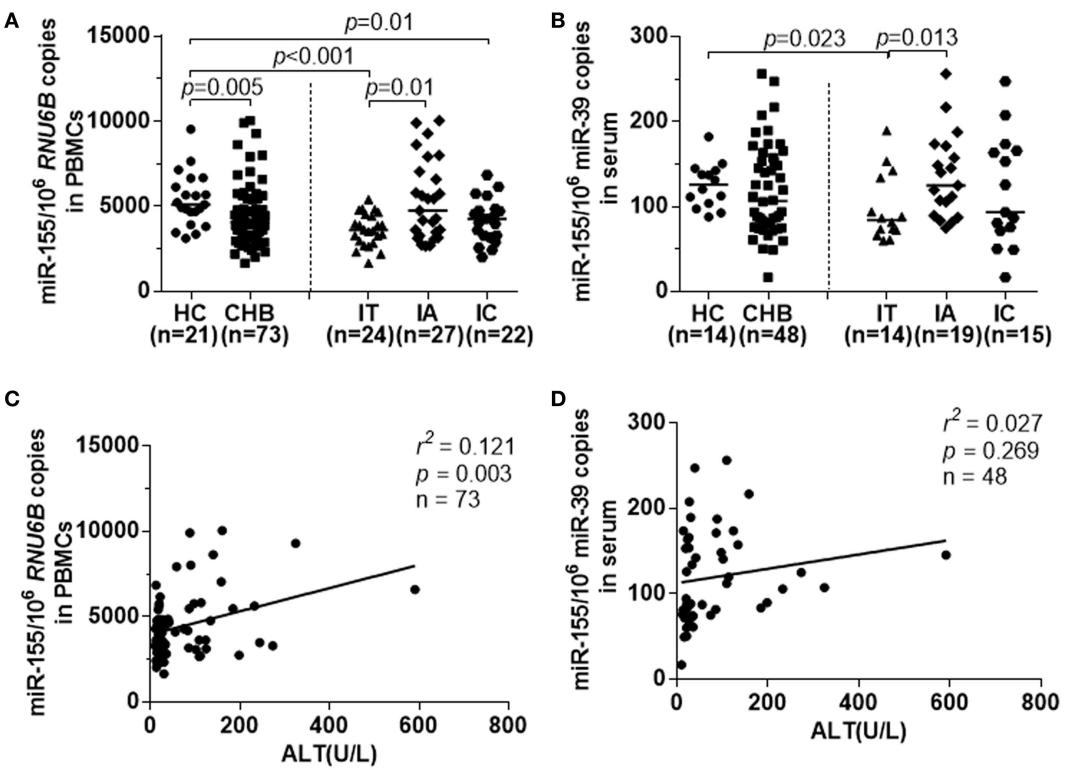

FIGURE 1 | miR-155 expression in peripheral blood mononuclear cells (PBMCs) and serum from chronically hepatitis B virus (HBV)-infected patients and HCs. miR-155 expression were examined by real-time RT-PCR. **(A)** Comparison of miR-155 mRNA levels in PBMCs among healthy controls (HC), CHB, IT, IA, and IC groups. **(B)** Comparison of serum miR-155 mRNA levels among HC, CHB, IT, IA, and IC groups. **(C)** Spearman's correlation of alanine aminotransferase (ALT) levels and miR-155 expression in PBMCs from all chronically HBV-infected patients. **(D)** Spearman's correlation of ALT levels and miR-155 expression in serum from all chronically HBV-infected patients. HC, healthy control; CHB, chronic hepatitis B; IT, immune tolerance; IA, immune activation; IC, inactive carrier.

miR-146a expression in PBMCs and serum from all CHB patients or patients with different phases of chronic HBV infection (Figures S2B,C in Supplementary Material).

Reduced miR-155 Expression Was Associated with Dysfunction of NK Cells in CHB Patients

Chronic HBV infection is a complicated process, especially in the IA phase. Abnormal ALT levels generally reflect the inflammation activity accompanied with immune activation in these patients. According to EASL guideline, under normal circumstances, only IA patients, but not IT and IC, need to be treated. However, impaired immune function in IA patients could not eliminate HBV completely, which result in HBV persistence. To further determine the effect of immune dysfunction of IA patients on miR-155 expression, we measured miR-155 levels by real-time RT-PCR in subpopulation of PBMCs from HBV-infected subjects. Compared with non-infected HCs, although the miR-155 levels of IA patients were comparable in whole PBMCs, their

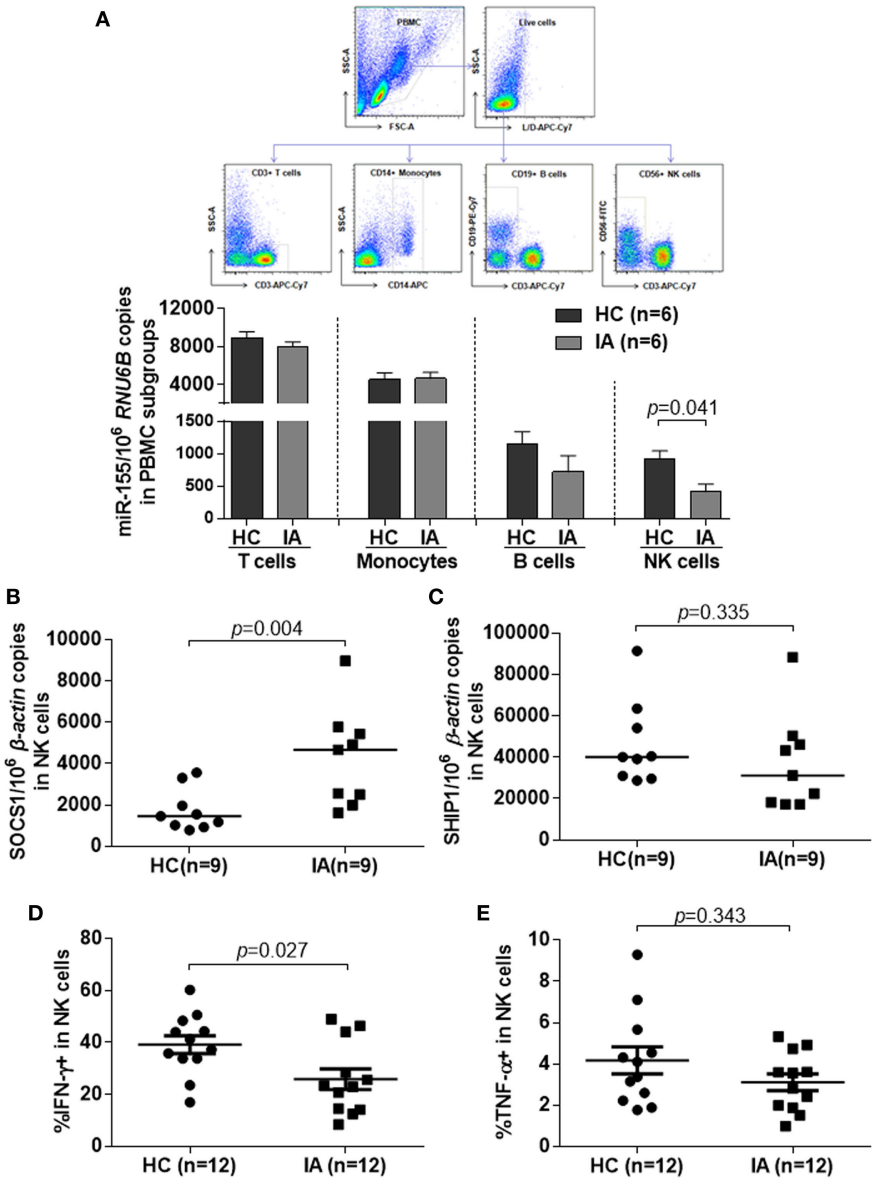

FIGURE 2 | miR-155 mRNA levels and cytokines secretion in natural killer (NK) cells was significantly downregulated in IA patients compared with HCs, while suppressor of cytokine signaling 1 (SOCS1) was upregulated in NK cells of IA group. **(A)** Purity of T, B, NK cells, and monocytes isolated from the healthy controls (HC) and IA groups by fluorescent cell sorting. miR-155 expression in different cell subsets was determined by real-time RT-PCR. **(B,C)** NK cells were isolated from peripheral blood mononuclear cells of HC and IA group by CD56 MicroBeads. SOCS1 **(B)** and SHIP1 **(C)** mRNA expression were determined by real-time RT-PCR. **(D,E)** NK cells were stimulated with IL-12 (10 ng/ml), IL-15 (10 ng/ml), and IL-18 (100 ng/ml) for 24 h. IFN-γ **(D)** and TNF-α **(E)** secretion were examined by flow cytometric analysis. HC, healthy control; IA, immune activation.

expression still were significantly decreased in $CD56^+$ NK cells ($p = 0.041$), but not in $CD3^+$ T cells, $CD14^+$ monocytes, or $CD19^+$ B cells (**Figure 2A**). As mentioned above, SOCS1 and SHIP1 are two direct targets of miR-155, validated in many cell types. We next examined the expression of these two genes in NK cells from HC and IA. The mRNA level of SOCS1 was much higher in IA patients than in HCs (**Figure 2B**, $p = 0.004$), while the mRNA levels of SHIP1 were not significantly different (**Figure 2C**). SOCS1 and SHIP1 were reported to control IFN signaling and cytokine production in NK cells. Consistently, NK cells isolated from IA patients displayed decreased IFN-γ (**Figure 2D**, $p = 0.027$) and relatively ordinary TNF-α (**Figure 2E**, $p = 0.343$) secretion compared with NK cells from HCs after stimulation with IL-12, IL-15, and IL-18. These results suggested that reduced expression of miR-155 in NK cells might contribute to lower cytokine production in activated NK cells. As defects in activation and antiviral function of NK cells having been described in patients with chronic HBV infection (22, 23), we also determined several activating (NKG2D, NKp46) and inhibitory (NKG2A, KIR3DL1/s1, Tim3) NKRs, as well as secondary signal required for IFN-γ production (CD16), early activation molecules (CD69), and cytotoxicity factors (Perforin, CD107a, Granzyme A, Granzyme B) in NK cells between IA patients and HCs. We found that there were similar lower perforin secretion (Figures S3A,B in Supplementary Material, $p = 0.009$) and NKG2D expression (Figures S3A,F,G in Supplementary Material, %, $p = 0.002$, MFI, $p = 0.001$) of NK cells in IA patients than HCs, while the secretion of CD107a, Granzyme A, and Granzyme B (Figures S3A,C–E in Supplementary Material) and the expression of NKG2A, KIR3DL1/s1, Tim3, CD16, CD69 had no significant differences in IA patients and HCs (data not shown).

Overexpression of miR-155 Led to Decrease of SOCS1 Expression and Increase of Cytokine Production in Activated NK Cells

To confirm the role of miR-155 in cytokine production in NK cells after activation, we examined the IFN-γ and TNF-α production after miR-155 overexpression in NK cells from IA patients. miR-155 mimics or miR-controls were transfected into NK cells by electronic transduction and about a threefold increase in the miR-155 level was detected by real-time RT-PCR analysis. Compared to miR-controls, electronic transduction of NK cells with the miR-155 mimics resulted in an increase of IFN-γ^+ and TNF-α^+ NK cells after stimulation with IL-12, IL-15, and IL-18 (**Figure 3A**). The frequency of IFN-γ^+ ($p = 0.033$) and TNF-α^+ ($p = 0.025$) NK cells were significantly higher in the miR-155 mimic group than in the miR-control group (**Figures 3B,C**). Moreover, miR-155 mimics transfected NK cells displayed a decrease in target gene SOCS1 expression (**Figure 3D**, $p < 0.001$). Meanwhile, to further analysis the effect of miR-155 in NK cells activity and cytotoxicity, we also determined the aforementioned factors. Regrettably, miR-155 upregulation would not increase the

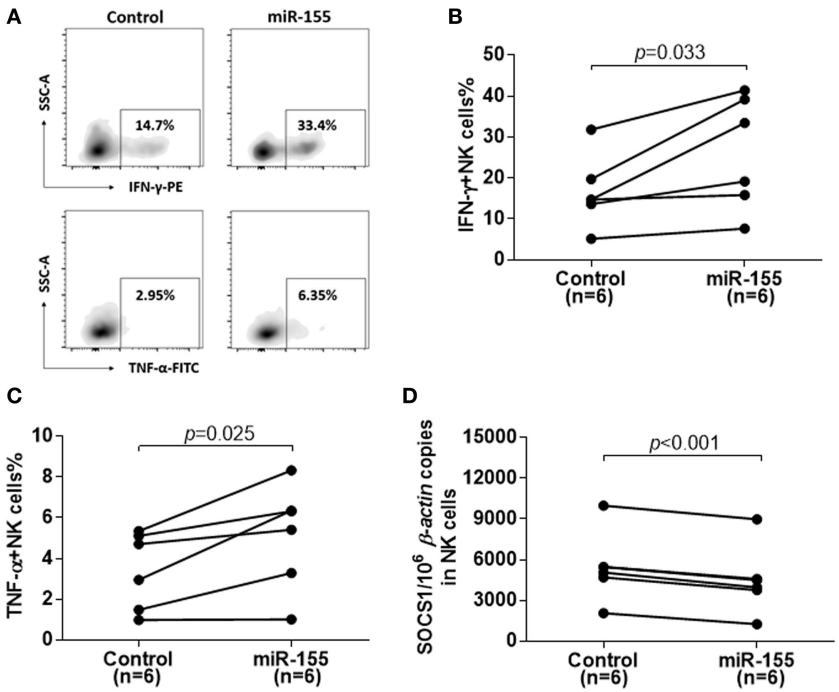

FIGURE 3 | Reconstitution of miR-155 in natural killer (NK) cells from immune-activation (IA) patients led to decreases in suppressor of cytokine signaling 1 (SOCS1) expression and increases in cytokine production. Purity of NK cells from IA patients was transfection with miR-control or miR-155-mimic for 72 h. **(A–C)** After stimulated with IL-12 (10 ng/ml), IL-15 (10 ng/ml), and IL-18 (100 ng/ml) for 24 h, IFN-γ and TNF-α secretion of isolated NK cells were detected by flow cytometric analysis. A representative pattern **(A)** and statistics analysis of IFN-γ **(B)** and TNF-α **(C)** secretion of transfected NK cells determined by flow cytometric analysis. **(D)** After 72 h transfection, SOCS1 mRNA expression in isolated NK cells was determined by real-time RT-PCR. Control, miR-control; miR-155, miR-155 mimic.

secretion of perforin (Figures S4A,C in Supplementary Material) and expression of NKG2D (Figures S4G–I in Supplementary Material) or other factors (Figures S4A,D–F in Supplementary Material) and expression of NKG2D, but only elevated the expression of CD69 after IL-12, IL-15, and IL-18 stimulation (Figures S4A,B in Supplementary Material). Consistent with the results above, overexpression of miR-155 did not promote the cytolytic activity of NK cells on K562 or HepG2.2.15 target cells (Figures S4J,K in Supplementary Material). These results suggested that miR-155 might act as a positive regulatory molecule for NK cell-mediated cytokine production, but might not have an effect on the cytotoxicity of NK cells.

Higher Baseline miR-155 Levels Was Associated with the Treatment Response to Telbivudine Therapy

Considering that miR-155 may be beneficial for cytokine-mediated antiviral function, we investigated whether miR-155 expression was associated with the antiviral response to nucleoside analog therapy. The miR-155 levels in PBMCs were examined in 41 treatment naïve HBeAg-positive IA patients who received telbivudine treatment. They were divided into complete response (CR, $n = 18$) and non-complete response (NCR, $n = 23$) groups according to their treatment outcomes at week 52. Patients in the CR group had a normalized ALT level and HBeAg seroconversion and achieved a reduction of the serum HBV DNA level to <300 copies/ml at week 52, while those in the NCR group had either a serum HBV DNA level >300 copies/ml or were positive for HBeAg at week 52 (24). The baseline clinical features of CR and NCR patients were comparable, and on-treatment HBV-DNA, HBsAg, and HBeAg were significantly lower in CR than NCR at week 12, week 24, and week 52 (**Table 2**). Interestingly, miR-155 expression in PBMCs from the CR group at the initiation of treatment was significantly higher than in those from the NCR group (**Figure 4A**, $p = 0.007$). A ROC curve was generated to assess the usefulness of baseline miR-155 levels to predict a CR at week 52. The optimal cut-off value for the miR-155 expression in PBMCs was 5,135.35/10^6 *RUN6B* copies. This indicated that sensitivity for detection of a CR was 72.2% with a specificity of 69.6% (**Figure 4B**). These results suggested that a higher level of miR-155 expression at baseline might be conducive to the immune control of HBV during nucleoside analog treatment. In the meantime, we also examined the expression of miR-146a in PBMCs between CR and NCR groups at baseline, unfortunately, there was no any differences between the two groups (Figure S5A in Supplementary Material).

We also examined the dynamic change of miR-155 expression during telbivudine therapy. Available PBMCs from 20 IA patients (including 10 CR and 10 NCR) were followed prospectively for analysis and exhibited a significant reduction of miR-155 expression at week 12 ($p = 0.032$) and week 52 ($p = 0.017$, **Figure 4C**). As analyzed separately, miR-155 expression in NCR patients showed a steady trend with no obvious decrease (**Figure 4D**). However, CR patients displayed reduced miR-155 expression but reached statistically significant differences only at week 52 (**Figure 4E**, $p = 0.003$). Moreover, we observed no significant difference of miR-146 expression after the start of therapy between the CR and NCR groups (data not shown).

TABLE 2 | Clinical characteristics of the subjects under telbivudine therapy for longitudinal study.

Group		CR	NCR	*p*-Value
N		18	23	
Gender (M/F)		15/3	21/2	0.638[a]
Age (years)		27.5 (18–42)	28 (18–40)	0.989[b]
0 weeks	HBV-DNA (log_{10} copies/ml)	8.52 (5.78–9.43)	8.63 (6.56–9.7)	0.121[b]
	ALT (U/l)	118 (60–830)	130 (55–324)	0.655[b]
	HBsAg (log_{10} IU/ml)	4.16 (2.53–4.66)	4.45 (3.24–5.07)	0.088[b]
	HBeAg (log_{10} PEIU/ml)	2.38 (0.36–3.79)	3.11 (1.33–3.93)	0.189[b]
12 weeks	HBV-DNA (log_{10} copies/ml)	3.13 (2.08–4.97)	3.99 (2.34–5.93)	0.009[b]
	ALT (U/l)	29.5 (15–160)	40 (16–211)	0.098[b]
	HBsAg (log_{10} IU/ml)	ND	ND	
	HBeAg (P/N)	12/6	23/0	0.004[a]
24 weeks	HBV-DNA (log_{10} copies/ml)	2.38 (1.84–4.09)	3.01 (1.84–5.27)	0.025[b]
	ALT (U/l)	23.5 (14–65)	25 (14–63)	0.493[b]
	HBsAg (log_{10} IU/ml)	3.24 (2.07–4.21)	3.74 (3.09–4.69)	0.009[b]
	HBeAg (P/N)	11/7	23/0	0.001[a]
52 weeks	HBV-DNA (log_{10} copies/ml)	1.84 (1.84–2.09)	1.84 (1.84–4.840)	0.006[b]
	ALT (U/l)	19.5 (13–56)	19 (12–52)	0.544[b]
	HBsAg (log_{10} IU/ml)	3.34 (1.88–4.11)	3.86 (2.90–4.76)	0.006[b]
	HbeAg (P/N)	0/18	23/0	0.000[a]

Values are n or median (range).

[a]*Chi-squared test.*

[b]*Mann–Whitney U-test.*

M/F, male or female; ND, not determined; P/N, positive or negative; CR, complete response, patients with HBeAg seroconversion at week 52; NCR, non-complete response, patients without HBeAg seroconversion at week 52; ALT, alanine aminotransferase; HBeAg, hepatitis B e antigen; HBsAg, hepatitis B surface antigen; HBV, hepatitis B virus.

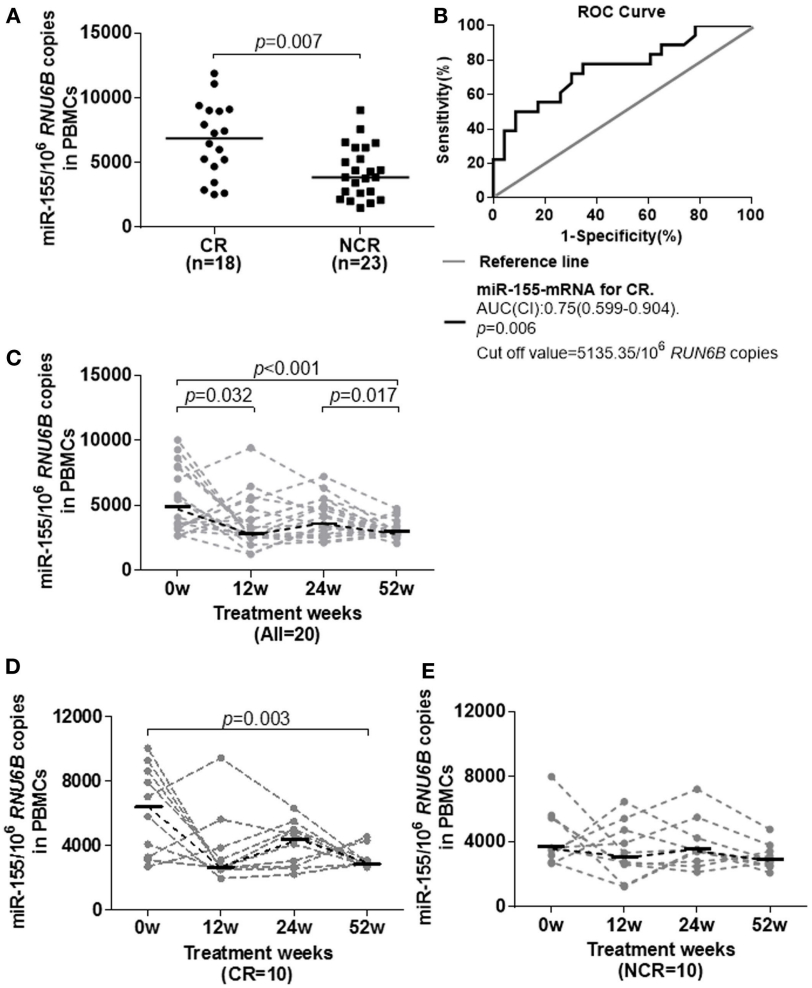

FIGURE 4 | Longitudinal analysis of miR-155 expression in peripheral blood mononuclear cells (PBMCs) of IA patients during telbivudine therapy. **(A)** miR-155 mRNA levels in PBMCs at baseline in the CR and NCR groups. **(B)** Receiver-operating characteristic (ROC) curve showed the suitability of miR-155 mRNA levels at baseline to predict a CR to telbivudine therapy. An area under the curve (AUC) of 1.0 occurs with an ideal test, whereas an AUC of <0.5 indicates a test of no diagnostic value. **(C)** Temporal dynamics of miR-155 mRNA levels in PBMCs of all patients. **(D)** Comparison of miR-155 mRNA levels among individuals in the CR group. **(E)** Comparison of miR-155 mRNA levels among individuals in the NCR group. IA, immune activation; CR, complete response; NCR, non-complete response.

Gradual Decline of miR-155 Expression in PBMCs during Peg-IFN-α-2a Antiviral Therapy

Additionally, we tested the baseline and dynamic changes of miR-155 expression in PBMCs of IA patients during peg-IFN-α-2a therapy. A total of 24 treatment naïve IA patients who received 48 weeks of peg-IFN-α-2a treatment were divided into a sustained virological response (SVR, $n = 7$) group and a non-sustained virological response (NSVR, $n = 17$) group according to their treatment responses at week 72. Subjects in the SVR group had undergone HBeAg seroconversion and had achieved a serum HBV DNA levels <1,000 copies/ml, while NSVR group had either serum HBV DNA levels >1,000 copies/ml or were positive for HBeAg. The baseline clinical features of SVR and NSVR patients were comparable, and HBV DNA and HBsAg were significantly lower in the SVR group than the NSVR group at weeks 48 and 72 (**Table 3**). However, unlike in the telbivudine treatment groups, there were no significant differences of miR-155 expression at the baseline of therapy (**Figure 5A**, $p = 0.3408$). Moreover, all the patients exhibited gradually decreasing miR-155 expression during treatment (**Figure 5B**). By comparing the SVR and NSVR groups, we found that miR-155 expression in both decreased gradually after starting treatment and showed no significant differences during the course of treatment (**Figures 5C,D**). Meanwhile, we also examined the expression of miR-146a in PBMCs between SVR and NSVR groups at baseline, but there was still no any differences between the two groups (Figure S5B in Supplementary Material), too.

DISCUSSION

In the present study, we investigated the relevance of miR-155 for impaired NK cell function during chronic HBV infection. We

TABLE 3 | Clinical characteristics of the subjects under peg-IFN-α-2a therapy for longitudinal study.

	Group	SVR	NSVR	*p*-Value
n		7	17	
Gender (M/F)		6/1	13/4	1.000[a]
Age (years)		25 (21–34)	28 (21–43)	0.349[b]
0 weeks	HBV-DNA (log_{10} copies/ml)	8.37 (5.83–9.72)	8.49 (6.00–9.94)	0.576[b]
	ALT (U/l)	249 (44–384)	172 (46–400)	0.349[b]
	HBsAg (log_{10} IU/ml)	3.38 (1.23–5.10)	4.12 (2.83–5.10)	0.166[b]
	HBeAg (log_{10} PEIU/ml)	2.52 (0.41–3.68)	3.10 (−0.52–4.01)	0.664[b]
4 weeks	HBV-DNA (log_{10} copies/ml)	6.47 (3.56–8.05)	7.50 (4.29–9.56)	0.288[b]
	ALT (U/l)	137 (55–384)	121 (22–275)	0.383[b]
	HBsAg (log_{10} IU/ml)	3.73 (1.46–4.51)	3.62 (2.18–4.92)	0.664[b]
	HBeAg (P/N)	ND	ND	
12 weeks	HBV-DNA (log_{10} copies/ml)	5.65 (2.54–6.79)	6.00 (3.31–8.80)	0.664[b]
	ALT (U/l)	84 (28–136)	46 (16–203)	0.418[b]
	HBsAg (log_{10} IU/ml)	2.97 (1.68–3.90)	3.37 (2.17–4.48)	0.099[b]
	HBeAg (P/N)	6/1	16/1	0.507[a]
24 weeks	HBV-DNA (log_{10} copies/ml)	4.77 (2.46–5.84)	4.78 (2.46–9.49)	0.383[b]
	ALT (U/l)	41 (25–85)	41 (18–129)	0.852[b]
	HBsAg (log_{10} IU/ml)	3.05 (1.64–3.86)	3.36 (1.60–4.53)	0.349[b]
	HBeAg (P/N)	5/2	16/1	0.194[a]
48 weeks	HBV-DNA (log_{10} copies/ml)	2.46 (2.46–4.70)	4.34 (2.46–8.42)	0.016[b]
	ALT (U/l)	41 (19–62)	35 (4.05–100)	0.534[b]
	HBsAg (log_{10} IU/ml)	1.79 (1.12–3.90)	3.21 (1.15–4.33)	0.047[b]
	HBeAg (P/N)	¾	15/2	0.038[a]
72 weeks	HBV-DNA (log_{10} copies/ml)	2.46 (2.46–2.79)	4.93 (2.46–9.68)	0.000[b]
	ALT (U/l)	20 (8–47)	22 (8–351)	0.494[b]
	HBsAg (log_{10} IU/ml)	2.37 (−0.33–3.85)	3.26 (1.04–5.10)	0.019[b]
	HBeAg (P/N)	0/7	15/2	0.000[a]

Values are n or median (range).

[a]*Chi-squared test.*

[b]*Mann–Whitney U-test.*

M/F, male or female; ND, not determined; P/N, positive or negative; SVR, off-treatment sustained virological response; NSVR, non- off-treatment sustained virological response; ALT, alanine aminotransferase; HBeAg, hepatitis B e antigen; HBsAg, hepatitis B surface antigen; HBV, hepatitis B virus.

found that miR-155 levels were significantly decreased in both PBMCs and serum of our subjects with chronic HBV infection, especially in the subjects who were IT or IC. However, miR-155 expression was comparable to HCs in the IA phase of CHB, which may result from chronic inflammation. Further analysis showed that lower expression of miR-155 was accompanied by a suppression of cytokine production of NK cells in IA patients. Finally, higher miR-155 expression was associated with a complete response to telbivudine therapy and a reduction of miR-155 was observed during both telbivudine and peg-IFN-α-2a therapy.

As a key modulator of the immune response and inflammation, miR-155 is dysregulated in various infectious diseases. For example, Yang et al. demonstrated the role of the TLR2/miR-155/SOCS1 signaling axis in the immunity and apoptosis of macrophages during the innate immune response to mycobacterial infections (25). Sarkar et al. reported that miR-155 was suppressed during HBV infection and a subsequent positive correlation of miR-155 with TLR7 activation (14). These findings led us to further explore the relationship between miR-155 and TLRs. We found that TLR2 had a positive correlation with miR-155 expression in PBMCs from CHB patients. Consistently, there was a positive correlation between miR-155 and liver inflammation-related abnormal ALT levels, but no correlation was observed between miR-155 and HBV DNA loads. These findings suggested that HBV infection might not influence the miR-155 expression directly, but affect the expression by mediating immune responses and inducing inflammatory cytokines (13). Unexpectedly, although miR-155 level in serum exhibited a similar expression to that in PBMCs, there was no correlation between miR-155 expression in PBMCs and serum, in parallel to the lack of relationship between miR-155 levels in serum and the ALT level. It is possible that, *in vivo*, miR-155 is ubiquitously expressed, not only in many immune cell types but also in human reproductive tissues, fibroblasts, epithelial tissues, and the central nervous system (26).

Moreover, our findings revealed that downregulation of miR-155 in NK cells resulted in the dysfunction of these cells in IA patients. Importantly, overexpression of miR-155 could lead to a decrease of SOCS1 expression and an increase of cytokine production in activated NK cells. SOCS1 was involved in negatively regulating JAK–STAT signaling (27) and mice lacking SOCS1 had increased levels of IFN-γ in the serum (28). It was also shown that endogenous SOCS1 participate in the prevention of liver diseases such as hepatitis, fibrosis, and cancers (29, 30). Recently, the H3K4me3 demethylase Kdm5a was found to be required for priming activation of NK cells by suppressing the SOCS1 epigenetically (31). NK cells play an essential role in liver immunity and act as the first line of defense against invading pathogens.

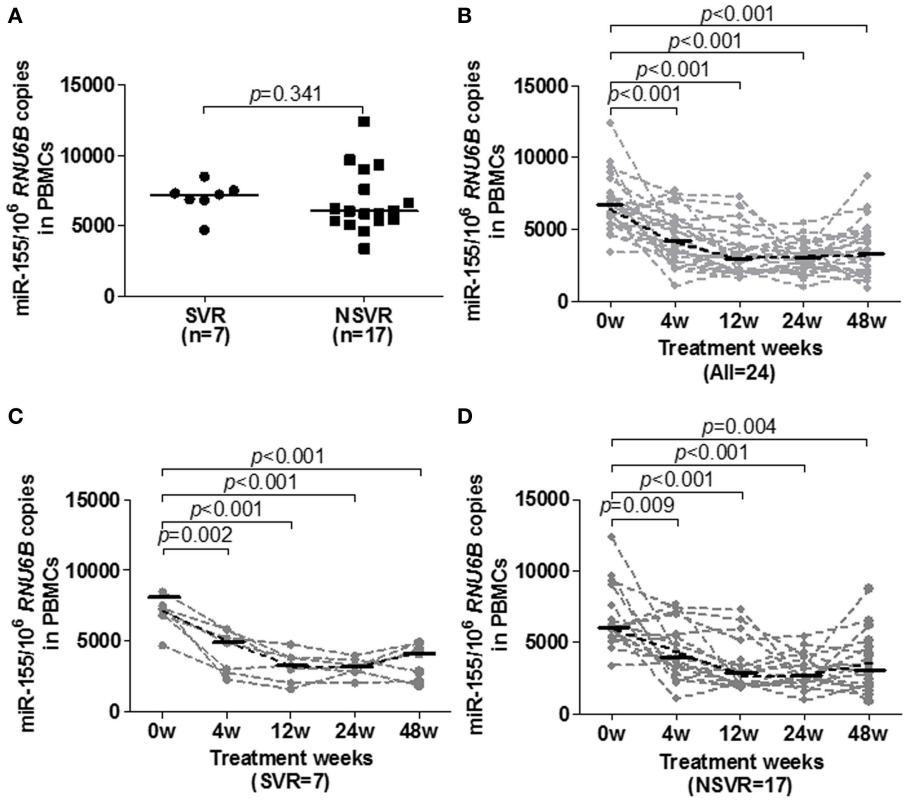

FIGURE 5 | Longitudinal analysis of miR-155 expression in peripheral blood mononuclear cells (PBMCs) of IA patients during peg-IFN-α-2a therapy. **(A)** miR-155 mRNA levels in PBMCs at baseline in the SVR and NSVR groups. **(B)** Temporal dynamics of miR-155 mRNA levels in PBMCs of all patients. **(C)** Comparison of miR-155 mRNA levels among individuals in the SVR group. **(D)** Comparison of miR-155 mRNA levels among individuals in the NSVR group. IA, immune activation; SVR, off-treatment sustained virological response; NSVR, non-off-treatment sustained virological response.

They generally become activated and eliminate HBV-infected cells directly by cytolytic killing and indirectly by secreting cytokines (32, 33). Nevertheless, the frequency, activation, and cytokine production by circulating NK cells were significantly reduced in patients with HBV infection (34). Consistent with a previous study (35), our study also documented that NK cells from IA patients produce less IFN-γ and TNF-α during stimulation with IL-12, IL-15 and IL-18, compared to that which occurs in HCs. Reconstitution of miR-155 in NK cells could lead to an increase in IFN-γ and TNF-α production. Since previous studies indicated that SHIP1 (36) and SOCS1 (37) are direct targets of miR-155, and are involved in control of cytokine production and the cytolytic function of NK cells (38). We found significantly higher expression of SOCS1 in NK cells from the IA group than in those from the HC group. Furthermore, SOCS1 expression was decreased upon overexpression of miR-155 in NK cells, which has an inverse trend with antiviral cytokine secretion. Together with two previous studies showing that ectopic expression of miR-155 in hepatoma cells mildly inhibited HBV infection by suppressing SOCS1 and subsequently upregulating the expression of several IFN-inducible antiviral genes (13, 14), our current work suggests that miR-155 might act as a positive regulator in miR-155/SOCS1/IFN-γ negative feedback loop of the innate immune system during chronic HBV infection. Regrettably, the upregulation of miR-155 seem to have no effect on NK cytotoxicity. There might be some other regulators in NK cell for its cytolytic activity.

Besides natural HBV infection, host immune status is regulated and associated with the treatment outcome of antiviral therapy (39). In both telbivudine and peg-IFN-α-2a-treated patients, there was a steady decline of miR-155 level during antiviral therapy. It was likely that the decrease and normalization of ALT level by antiviral treatment reduced the inflammation, resulted in the continuous reduction of miR-155 expression. This trend was consistent with the expression of TLR2 and TLR8 during antiviral treatment as our previous findings (24, 40). One of the important goals in the treatment of IA patients is to achieve HBeAg seroconversion, which is closely related to sustained inhibition of HBV DNA levels (41). A previous report had revealed that the profile of plasma miRNAs may predict an early virological response to IFN treatment in IA patients (42). Furthermore, miR-155 has been found to negatively correlate with viral load in patients with HCV infection and might be associated with an efficient antiviral response against HCV (43). In this study, we noted that the baseline miR-155 level in PBMCs was correlated with the treatment response to telbivudine, but not peg-IFN-α-2a. The intrinsic mechanisms for this discrepancy might be associated with the interaction of multiple immune factors that contribute to

viral pathogenesis or the different antiviral mechanisms of these two drugs (39).

In conclusion, our study indicates that chronic HBV infection may inhibit miR-155 expression and produce miR-155 dysregulation in NK cells. This may subsequently lead to suppression of NK function by targeting SOCS1. Additionally, we established a positive correlation between miR-155 expression and treatment outcomes of antiviral therapy. Given the broad function of miR-155 in both the innate and adaptive immune responses, our work provides valuable insight for functional implications of miR-155 in HBV infection, implying miR-155 may be a positive regulator contributing to the functional impairment of NK cells and viral persistence during chronic HBV infection. Understanding how miR-155 functions in the complex regulation networks involved in the immune-pathogenesis of chronic HBV infection will help us to identify novel therapeutic targets for treatment of CHB.

ETHICS STATEMENT

All patients provided written documentation of informed consent. The study conformed to the ethical guidelines of the 1975 Declaration of Helsinki and was approved by the Ethical Committee of Nanfang Hospital.

AUTHOR CONTRIBUTIONS

XZ conceived and designed the study. JG, ZH, HL, JC, ZX, and ZC performed the experiments and analyzed the data. XZ and JG wrote the manuscript with additional input and suggestions from JP, JS, and JH. All authors reviewed and approved the manuscript.

FUNDING

This work was partly supported by grants from National Natural Science Foundation of China (81301421, 81471952, 81641173, and 81670532), the Provincial Natural Science Foundation of Guangdong (2014A030313299), the Collaboration and Innovation Health Care Major Project of Guangzhou (201604020010), and the Provincial Natural Science Foundation of Fujian (2015J01361).

SUPPLEMENTARY MATERIAL

The Supplementary Material for this article can be found online at http://journal.frontiersin.org/article/10.3389/fimmu.2017.01173/full#supplementary-material.

REFERENCES

1. Ott JJ, Stevens GA, Groeger J, Wiersma ST. Global epidemiology of hepatitis B virus infection: new estimates of age-specific HBsAg seroprevalence and endemicity. *Vaccine* (2012) 30(12):2212–9. doi:10.1016/j.vaccine.2011.12.116
2. Rehermann B, Nascimbeni M. Immunology of hepatitis B virus and hepatitis C virus infection. *Nat Rev Immunol* (2005) 5(3):215–29. doi:10.1038/nri1573
3. Bartel DP. MicroRNAs: genomics, biogenesis, mechanism, and function. *Cell* (2004) 116(2):281–97. doi:10.1016/S0092-8674(04)00045-5
4. Lecellier CH, Dunoyer P, Arar K, Lehmann-Che J, Eyquem S, Himber C, et al. A cellular microRNA mediates antiviral defense in human cells. *Science* (2005) 308(5721):557–60. doi:10.1126/science.1108784
5. Scaria V, Hariharan M, Maiti S, Pillai B, Brahmachari SK. Host-virus interaction: a new role for microRNAs. *Retrovirology* (2006) 3:68. doi:10.1186/1742-4690-3-68
6. Jin WB, Wu FL, Kong D, Guo AG. HBV-encoded microRNA candidate and its target. *Comput Biol Chem* (2007) 31(2):124–6. doi:10.1016/j.compbiolchem.2007.01.005
7. Rodriguez A, Vigorito E, Clare S, Warren MV, Couttet P, Soond DR, et al. Requirement of bic/microRNA-155 for normal immune function. *Science* (2007) 316(5824):608–11. doi:10.1126/science.1139253
8. Ma X, Becker Buscaglia LE, Barker JR, Li Y. MicroRNAs in NF-kappaB signaling. *J Mol Cell Biol* (2011) 3(3):159–66. doi:10.1093/jmcb/mjr007
9. O'Neill LA, Sheedy FJ, McCoy CE. MicroRNAs: the fine-tuners of toll-like receptor signalling. *Nat Rev Immunol* (2011) 11(3):163–75. doi:10.1038/nri2957
10. Vigorito E, Kohlhaas S, Lu D, Leyland R. miR-155: an ancient regulator of the immune system. *Immunol Rev* (2013) 253(1):146–57. doi:10.1111/imr.12057
11. Trotta R, Chen L, Ciarlariello D, Josyula S, Mao C, Costinean S, et al. miR-155 regulates IFN-gamma production in natural killer cells. *Blood* (2012) 119(15):3478–85. doi:10.1182/blood-2011-12-398099
12. Wang P, Hou J, Lin L, Wang C, Liu X, Li D, et al. Inducible microRNA-155 feedback promotes type I IFN signaling in antiviral innate immunity by targeting suppressor of cytokine signaling 1. *J Immunol* (2010) 185(10):6226–33. doi:10.4049/jimmunol.1000491
13. Su C, Hou Z, Zhang C, Tian Z, Zhang J. Ectopic expression of microRNA-155 enhances innate antiviral immunity against HBV infection in human hepatoma cells. *Virol J* (2011) 8:354. doi:10.1186/1743-422x-8-354
14. Sarkar N, Panigrahi R, Pal A, Biswas A, Singh SP, Kar SK, et al. Expression of microRNA-155 correlates positively with the expression of toll-like receptor 7 and modulates hepatitis B virus via C/EBP-beta in hepatocytes. *J Viral Hepat* (2015) 22(10):817–27. doi:10.1111/jvh.12390
15. Yu SL, Deng H, Li XH, Huang YX, Xie DY, Gao ZL. Expression of microRNA-155 is downregulated in peripheral blood mononuclear cells of chronic hepatitis B patients. *Hepat Mon* (2016) 16(1):e34483. doi:10.5812/hepatmon.34483
16. European Association for the Study of the Liver. EASL clinical practice guidelines: management of chronic hepatitis B virus infection. *J Hepatol* (2012) 57(1):167–85. doi:10.1016/j.jhep.2012.02.010
17. Liu C, Huang X, Werner M, Broering R, Ge J, Li Y, et al. Elevated expression of chemokine CXCL13 in chronic hepatitis B patients links to immune control during antiviral therapy. *Front Immunol* (2017) 8:323. doi:10.3389/fimmu.2017.00323
18. Fan R, Sun J, Yuan Q, Xie Q, Bai X, Ning Q, et al. Baseline quantitative hepatitis B core antibody titre alone strongly predicts HBeAg seroconversion across chronic hepatitis B patients treated with peginterferon or nucleos(t)ide analogues. *Gut* (2016) 65(2):313–20. doi:10.1136/gutjnl-2014-308546
19. Li Y, Ma S, Tang L, Li Y, Wang W, Huang X, et al. Circulating chemokine (C-X-C Motif) receptor 5(+) CD4(+) T cells benefit hepatitis B e antigen seroconversion through IL-21 in patients with chronic hepatitis B virus infection. *Hepatology* (2013) 58(4):1277–86. doi:10.1002/hep.26489
20. Tjwa ET, van Oord GW, Hegmans JP, Janssen HL, Woltman AM. Viral load reduction improves activation and function of natural killer cells in patients with chronic hepatitis B. *J Hepatol* (2011) 54(2):209–18. doi:10.1016/j.jhep.2010.07.009
21. Wang S, Zhang X, Ju Y, Zhao B, Yan X, Hu J, et al. MicroRNA-146a feedback suppresses T cell immune function by targeting STAT1 in patients with chronic hepatitis B. *J Immunol* (2013) 191(1):293–301. doi:10.4049/jimmunol.1202100
22. Chen Y, Wei H, Gao B, Hu Z, Zheng S, Tian Z. Activation and function of hepatic NK cells in hepatitis B infection: an underinvestigated innate immune response. *J Viral Hepat* (2005) 12(1):38–45. doi:10.1111/j.1365-2893.2005.00543.x
23. Mondelli MU, Varchetta S, Oliviero B. Natural killer cells in viral hepatitis: facts and controversies. *Eur J Clin Invest* (2010) 40(9):851–63. doi:10.1111/j.1365-2362.2010.02332.x
24. Huang Z, Ge J, Pang J, Liu H, Chen J, Liao B, et al. Aberrant expression and dysfunction of TLR2 and its soluble form in chronic HBV infection and its

regulation by antiviral therapy. *Antiviral Res* (2015) 118:10–9. doi:10.1016/j.antiviral.2015.03.004
25. Yang S, Li F, Jia S, Zhang K, Jiang W, Shang Y, et al. Early secreted antigen ESAT-6 of *Mycobacterium tuberculosis* promotes apoptosis of macrophages via targeting the microRNA155-SOCS1 interaction. *Cell Physiol Biochem* (2015) 35(4):1276–88. doi:10.1159/000373950
26. Teng G, Papavasiliou FN. Shhh! Silencing by microRNA-155. *Philos Trans R Soc Lond B Biol Sci* (2009) 364(1517):631–7. doi:10.1098/rstb.2008.0209
27. Shuai K, Liu B. Regulation of JAK-STAT signalling in the immune system. *Nat Rev Immunol* (2003) 3(11):900–11. doi:10.1038/nri1226
28. Hanada T, Kobayashi T, Chinen T, Saeki K, Takaki H, Koga K, et al. IFNgamma-dependent, spontaneous development of colorectal carcinomas in SOCS1-deficient mice. *J Exp Med* (2006) 203(6):1391–7. doi:10.1084/jem.20060436
29. Naka T, Tsutsui H, Fujimoto M, Kawazoe Y, Kohzaki H, Morita Y, et al. SOCS-1/SSI-1-deficient NKT cells participate in severe hepatitis through dysregulated cross-talk inhibition of IFN-gamma and IL-4 signaling in vivo. *Immunity* (2001) 14(5):535–45. doi:10.1016/S1074-7613(01)00132-7
30. Yoshida T, Ogata H, Kamio M, Joo A, Shiraishi H, Tokunaga Y, et al. SOCS1 is a suppressor of liver fibrosis and hepatitis-induced carcinogenesis. *J Exp Med* (2004) 199(12):1701–7. doi:10.1084/jem.20031675
31. Zhao D, Zhang Q, Liu Y, Li X, Zhao K, Ding Y, et al. H3K4me3 demethylase Kdm5a is required for NK cell activation by associating with p50 to suppress SOCS1. *Cell Rep* (2016) 15(2):288–99. doi:10.1016/j.celrep.2016.03.035
32. Sun C, Sun H, Zhang C, Tian Z. NK cell receptor imbalance and NK cell dysfunction in HBV infection and hepatocellular carcinoma. *Cell Mol Immunol* (2015) 12(3):292–302. doi:10.1038/cmi.2014.91
33. Wu SF, Wang WJ, Gao YQ. Natural killer cells in hepatitis B virus infection. *Braz J Infect Dis* (2015) 19(4):417–25. doi:10.1016/j.bjid.2015.05.006
34. Lunemann S, Malone DF, Hengst J, Port K, Grabowski J, Deterding K, et al. Compromised function of natural killer cells in acute and chronic viral hepatitis. *J Infect Dis* (2014) 209(9):1362–73. doi:10.1093/infdis/jit561
35. Li Y, Wang JJ, Gao S, Liu Q, Bai J, Zhao XQ, et al. Decreased peripheral natural killer cells activity in the immune activated stage of chronic hepatitis B. *PLoS One* (2014) 9(2):e86927. doi:10.1371/journal.pone.0086927
36. Sullivan RP, Fogel LA, Leong JW, Schneider SE, Wong R, Romee R, et al. MicroRNA-155 tunes both the threshold and extent of NK cell activation via targeting of multiple signaling pathways. *J Immunol* (2013) 191(12):5904–13. doi:10.4049/jimmunol.1301950
37. Lu LF, Thai TH, Calado DP, Chaudhry A, Kubo M, Tanaka K, et al. Foxp3-dependent microRNA155 confers competitive fitness to regulatory T cells by targeting SOCS1 protein. *Immunity* (2009) 30(1):80–91. doi:10.1016/j.immuni.2008.11.010
38. Fujimoto M, Naka T. Regulation of cytokine signaling by SOCS family molecules. *Trends Immunol* (2003) 24(12):659–66. doi:10.1016/j.it.2003.10.008
39. Rehermann B, Bertoletti A. Immunological aspects of antiviral therapy of chronic hepatitis B virus and hepatitis C virus infections. *Hepatology* (2015) 61(2):712–21. doi:10.1002/hep.27323
40. Deng G, Ge J, Liu C, Pang J, Huang Z, Peng J, et al. Impaired expression and function of TLR8 in chronic HBV infection and its association with treatment responses during peg-IFN-alpha-2a antiviral therapy. *Clin Res Hepatol Gastroenterol* (2017) 41(4):386–98. doi:10.1016/j.clinre.2016.12.006
41. Lau GK, Wang FS. Uncover the immune biomarkers underlying hepatitis B e antigen (HBeAg) seroconversion: a need for more translational study. *J Hepatol* (2012) 56(4):753–5. doi:10.1016/j.jhep.2011.12.006
42. Zhang X, Chen C, Wu M, Chen L, Zhang J, Zhang X, et al. Plasma microRNA profile as a predictor of early virological response to interferon treatment in chronic hepatitis B patients. *Antivir Ther* (2012) 17(7):1243–53. doi:10.3851/imp2401
43. Jiang M, Broering R, Trippler M, Wu J, Zhang E, Zhang X, et al. MicroRNA-155 controls toll-like receptor 3- and hepatitis C virus-induced immune responses in the liver. *J Viral Hepat* (2014) 21(2):99–110. doi:10.1111/jvh.12126

Conflict of Interest Statement: The authors declare that the research was conducted in the absence of any commercial or financial relationships that could be construed as a potential conflict of interest.

Copyright © 2017 Ge, Huang, Liu, Chen, Xie, Chen, Peng, Sun, Hou and Zhang. This is an open-access article distributed under the terms of the Creative Commons Attribution License (CC BY). The use, distribution or reproduction in other forums is permitted, provided the original author(s) or licensor are credited and that the original publication in this journal is cited, in accordance with accepted academic practice. No use, distribution or reproduction is permitted which does not comply with these terms.

frontiers in Immunology

REVIEW
published: 28 September 2017
doi: 10.3389/fimmu.2017.01195

Immunity and Fibrogenesis: The Role of Th17/IL-17 Axis in HBV and HCV-induced Chronic Hepatitis and Progression to Cirrhosis

*Feliciano Chanana Paquissi**

Department of Medicine, Clínica Girassol, Luanda, Angola

Cirrhosis is a common final pathway for most chronic liver diseases; representing an increasing burden worldwide and is associated with increased morbidity and mortality. Current evidence has shown that, after an initial injury, the immune response has a significant participation in the ongoing damage, and progression from chronic viral hepatitis (CVH) to cirrhosis, driving the activation and maintenance of main fibrogenic pathways. Among immune deregulations, those related to the subtype 17 of T helper lymphocytes (Th17)/interleukin-17 (IL-17) axis have been recognized as key immunopathological and prognostic elements in patients with CVH. The Th17/IL-17 axis has been found involved in several points of fibrogenesis chain from the activation of stellate cells, increased expression of profibrotic factors as TGF-β, promotion of the myofibroblastic or epithelial–mesenchymal transition, stimulation of the synthesis of collagen, and induction of imbalance between matrix metalloproteinases and tissue inhibitors of metalloproteinases (TIMPs). It also promotes the recruitment of inflammatory cells and increases the expression of proinflammatory cytokines such as IL-6 and IL-23. So, the Th17/IL-17 axis is simultaneously the fuel and the flame of a sustained proinflammatory and profibrotic environment. This work aims to present the immunopathologic and prognostic role of the Th17/IL-17 axis and related pathways in fibrogenesis and progression to cirrhosis in patients with liver disease due to hepatitis B virus (HBV) and hepatitis C virus (HCV).

Keywords: Th17 Cells, interleukin-17, TGF-β, fibrogenesis, cirrhosis, chronic viral hepatitis, hepatitis C virus, hepatitis B virus

OPEN ACCESS

Edited by:
Guixiu Shi,
Xiamen University, China

Reviewed by:
Rui Li,
University of Pennsylvania, United States
Urs Christen,
Goethe University Frankfurt, Germany
Ankit Saxena,
National Institutes of Health (NIH), United States

***Correspondence:**
Feliciano Chanana Paquissi
fepaquissi@gmail.com

Specialty section:
This article was submitted to Inflammation, a section of the journal Frontiers in Immunology

Received: *05 July 2017*
Accepted: *11 September 2017*
Published: *28 September 2017*

Citation:
Paquissi FC (2017) Immunity and Fibrogenesis: The Role of Th17/IL-17 Axis in HBV and HCV-induced Chronic Hepatitis and Progression to Cirrhosis. Front. Immunol. 8:1195. doi: 10.3389/fimmu.2017.01195

INTRODUCTION

Liver cirrhosis is a common final pathway for most chronic liver diseases; and is increasingly becoming a major cause of global health burden, being responsive for high morbidity and mortality worldwide. Chronic viral hepatitises (CVHs) are the leading cause of cirrhosis, also with increasing burden worldwide (1). According to the report of Global Burden of Disease Study 2013, between 1990 and 2013, occurred a 63% increase in the global viral hepatitis deaths, passing from the tenth (in 1990) to seventh (in 2013) leading cause of death worldwide (1). There was also an increase in attributable years of life lost, years living with a disability (34% for each), and in the absolute burden of the disease (1). In parallel, despite significant progress in the treatment

of CVH during the last decades, the number of deaths from cirrhosis and hepatocellular carcinoma (HCC) increased in the last 20 years (2, 3).

Currently, it is known that after the initial injury, before cirrhosis is established, multiple pathways of fibrogenesis are activated as a result of continuous interaction between pathogen-related factors (4–6), the host genetic such as certain HLA haplotypes and cytokines gene polymorphisms (7–11), liver resident cells, and the immune system (9–13) (**Figure 1**). Indeed, cirrhosis is a reflection of sustained injuries and constant and exaggerated attempts of tissue repair, in which the immune system has crucial participation (14–16). The inappropriate immune response have an influence on the activation and maintenance of fibrogenic pathways and progression from CVH to cirrhosis (17–20). Multiple imbalances in immune response, either in cellular or soluble factors, have been associated with the evolution to cirrhosis in viral hepatitis (21, 22). In addition, the immune response influences on viral persistence and response to treatment (11, 23). Thus, efforts have been made in research and clinical practice, aiming to get a better comprehension of the immunological mechanisms underlying these pathways, their exploration as immune biomarkers to predict outcomes, response to treatment, as well as explore their potential as targets for adjuvant therapeutics (24–26).

Among the elements of the immune response, the subtype 17 of T helper lymphocytes (Th17) has gained space as a biomarker with noteworthy performance in the prediction of progression to cirrhosis in liver diseases, particularly in CVH (20, 28). Therefore, the cytokines secreted by Th17, particularly the interleukin-17 (IL-17), also have been implicated in the activation of fibrogenic pathways and progression to cirrhosis (13, 17). Th17 cells have a predominantly effector functional profile, being responsible for the immune surveillance, but are also involved in the pathogenesis of many autoimmune diseases and in the mechanisms of fibrosis in many organs, after the initial injury (29–31).

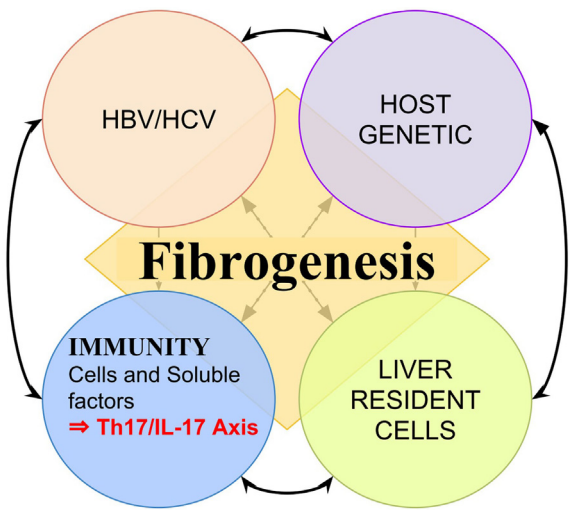

FIGURE 1 | Representation of multiple factors influencing liver fibrogenesis. Fibrogenesis is a result of continuous interaction between pathogen-related factors such as hepatitis B virus (HBV) protein X and hepatitis C virus (HCV) core antigen (4–6, 27), the host genetic such as certain HLA haplotypes (7, 8), liver resident cells, and the immune system such as certain interleukin polymorphisms (9–13, 15).

In CVH, the Th17/IL-17 axis expresses a sustained aggression, and especially a proinflammatory and profibrotic environment with recruitment and activation of other cells, promoting this way, more tissue injury and dysfunctional reparative responses (13, 17, 32, 33). This review aims to summarize the existing knowledge on the immunopathologic and prognostic role of the Th17/IL-17 axis and related pathways in fibrogenesis and progression to cirrhosis in patients with liver disease due to hepatitis B virus (HBV) and hepatitis C virus (HCV).

AN OVERVIEW OF GENERAL INFLAMMATORY BIOMARKERS AS OUTCOME PREDICTORS IN CVH

General Inflammatory biomarkers, such as C-reactive protein (CRP), and interleukin-6, have been associated with poor outcomes on viral hepatitis (11, 26, 34). High levels of interleukin-6 are related to adverse outcomes in the CVH, including greater severity (35, 36), worse response to treatment and viral persistence (11, 26), and evolution to cirrhosis, HCC, or death (35, 36). In a study including 149 patients with CHC (and 17 controls) who underwent 12 weeks' treatment with pegylated IFN-α2b and ribavirin, serum IL-6 levels were significantly higher in CHC patients than in controls, and a high pretreatment IL-6 was associated with lower rates of sustained virologic response (SVR) (52 vs. 79%; $P = 0.012$) (26). In addition, SVR was accompanied by a significant decrease in IL-6 levels (from 2.7 to 1.5 pg/ml; $P = 0.029$) at 4 weeks of treatment, remaining significantly lower in responder than in non-responder (26). In other studies, it was observed that certain polymorphisms in IL-6 or its promoter are associated with lower rate of spontaneous clearance (11), and increased risk of HCC in patients with CVH-related cirrhosis (10, 37). Many other proinflammatory cytokines, including interleukin IL-1β, IL-18, and TNF-α have been associated with increased risk of progression to cirrhosis (38–40). Certain polymorphisms in TNF-α are also associated with higher risk of becoming chronic carriers of viral infection, progression to cirrhosis and HCC (15, 40).

In addition to the soluble factors, cells of the inflammatory response as neutrophils (19, 41) and monocytes have been found associated with worse outcomes in viral hepatitis. All these elements (cells and soluble factors) are part of a context in which the Th17/IL-17 axis imbalances work as crucial elements to feed and keep this proinflammatory and profibrotic microenvironment (20, 22, 42–44), as described in the next sections.

THE TH17/IL-17 AXIS AND OUTCOME PREDICTION IN CVH

The inappropriate immune response at the level of the Th17/IL-17 axis exerts influence in maintaining the fibrogenic pathways and progression from CVH to cirrhosis (9, 44). The fibrogenic role of IL-17, the main cytokine of Th17, has been appointed in

increasing number of publications in recent years (13, 45, 46). In addition to its direct effect on fibrogenesis, the Th17/IL-17 axis is the fuel to sustain the proinflammatory environment, with the recruitment of the other cells and stimulation of the synthesis of other soluble factors (29, 33, 47–50). At the same time, Th17/IL-17 axis expresses itself, a response to a sustained proinflammatory stimulus (51, 52). So, we can understand the broad scope of the elements of this axis on the CVH, predicting outcomes in different points of the disease, from spontaneous healing (53), response to treatment (23, 54, 55), occurrence of acute decompensations (56), progression to cirrhosis (9, 28), and HCC (53), including post-transplant recurrence (57), as detailed in this section.

The Th17/IL-17 Axis and Severity of CVH

The Th17/IL-17 axis is associated with high disease severity in CVHs, as found in a study where patients with chronic hepatitis B (CHB) had higher percentage of Th17 cells in peripheral blood than healthy controls (HCs) (1.53 vs. 0.92%); and among patients there was a positive correlation between peripheral Th17 cells and serum alanine aminotransferase (ALT) (58). In another study, including 96 patients with HBV-related conditions, the serum IL-17 concentration, intrahepatic, and peripheral Th17 cells were significantly higher in both CHB and acute-on-chronic liver failure (ACLF) patients than in asymptomatic surface antigen carriers (AsC) or HCs (59). Th17 cells increased progressively as aggravated the immune inflammation from AsC, CHB, to ACLF, with a positive correlation with severity markers (INR and MELD score) (59). Compared with HCs, patients with CHC had also higher proportions of Th17 cells either circulating (1.56 vs. 0.96%) or infiltrating the liver (16.08 vs. 0.82/hpf), associated with higher serum IL-17 levels (84.86 vs. 60.52 pg/mL) (42). In these patients, both peripheral and intrahepatic Th17 cells correlated with the severity of liver inflammation and damage (28, 42).

The Th17/IL-17 Axis and Progression to Cirrhosis in CVH

Concerning the progression to cirrhosis, in a study including 173 patients with chronic liver diseases, there was a significant increase in serum IL-17 protein and IL -17 mRNA levels in chronic HBV-related conditions than in HCs ($P < 0.001$); and patients with cirrhosis exhibited the highest serum IL-17 and IL-17 mRNA in peripheral blood mononuclear cells (PBMCs) (44). In another study with 101 patients with HBV-related LC or CHB; peripheral Th17 cells increased significantly in patients with cirrhosis as increased disease severity (mean: 3.51, 3.94, and 4.46; for Child–Pugh A, B, and C, respectively) (28). In intrahepatic tissue, a study conducted among 91 patients with chronic liver diseases, there was a significant increase intrahepatic expression of IL-17 in chronic HBV-related conditions than in HCs; furthermore, intrahepatic IL-17 was mainly localized in the fibrosis region, and its level correlated strongly with the degree of fibrosis (60). Other studies have also found increased intrahepatic IL-17+ cells or IL-17 levels, which correlate positively with fibrotic staging scores and clinical progression from CHB to cirrhosis, and most IL-17+ cells located in the fibrotic area (28, 44). In addition, intrahepatic IL-17 accompanied the higher serum IL-17 protein and mRNA levels in PBMCs, being higher among patients with cirrhosis than those with CHB, or HBsAg carriers ($P < 0.01$, for both) (44). Among HCV patients, a study evaluating the effect of HCV recurrence after orthotopic liver transplantation (OLT) showed that recipients with significant HCV-induced allograft fibrosis/cirrhosis and inflammation, presented higher frequency of HCV-specific Th17 cells, as well as proinflammatory mediators (IL-17, IL-1β, IL-6, IL-8, and MCP-1) (57).

In genetic studies, it has been noted that certain polymorphisms in IL-17 genes are more often present among those who progress to LC than in CHB patients (9, 14, 53); and are associated with a significant increase in LC risk either among monozygotic patients [OR 4.1, 95% CI: 1.4–11.84 or single allele carriers (OR 1.8, 95% CI: 1.16–2.9)] (14).

The Th17/IL-17 Axis and the Response to Treatment in CVH

In CVH, the Th17/IL-17 axis status is associated with response to available treatments (23), as found in a study with 30 CHB patients, in which treatment with entecavir was associated with a significant decrease in the Th17 and Treg cell frequencies and related cytokines, in parallel to the reduction of HBV DNA load (61, 62). In other studies in CHB, the treatment either with telbivudine or with interferon-α resulted in the normalization of serum ALT and reduction or suppression of viral replication, associated with a significant decline in circulating Th17 cells and IL-17 levels (23, 54). Studies in HCV also found the same effect, as shown in a study including 27 HCV-infected patients, in which combined treatment with pegylated IFN-α and ribavirin resulted in a significant decrease in factors related to Th17 (IL-6 and IL-17), Th1 (IFN-α and MIP-1) responses, and profibrotic factors (FGF-b, VEGF); and this impact was principally in responder patients (62). In another study, Th17-related gene polymorphisms were associated with sustained responses to PEG-IFNa-2α (55).

In line with these findings, in an interventional study involving 56 cirrhotic patients allocated to autologous bone marrow mesenchymal stem cells (ABMSCs) transplantation or control group; transplantation significantly improved the liver function, accompanied by a marked decrease in Th17 cells and serum levels of proinflammatory cytokines (IL-17, TNF-α, and IL-6) (63).

The Th17/IL-17 Axis and Mortality Prediction in CVH

Beyond its effect in predicting disease severity, the Th17/IL-17 axis elements are also predictors of mortality (56). In a study including 60 HBV-infected patients (30 with CHB and 30 with ACLF), the disproportionate increase of Th17 (compared to Treg) was associated with low survival among those with ACLF (64). These results have also been found in another study including 98 patients with HBV-related conditions (70 with CHB and 28 with LC), where the low Treg/Th17 ratio was associated with low survival among patients with cirrhosis and was associated with worse Child–Pugh and MELD scores (65). In another study, including 80 HBV-infected patients (40 with ACLF and 40 with CHB), the frequency of Th17 cells in peripheral blood, as well as IL-17 mRNA level in PBMCs, was significantly higher among

ACLF patients who died than among survivors; and correlated positively with serum total bilirubin ($r = 0.392$, $P = 0.012$) and MELD score ($r = 0.383$, $P = 0.015$) (56). These findings suggest a significant contribution of this immune imbalance in disease severity and mortality.

The Role of Other IL-17 Sources and Related Imbalances in CVH Outcomes

Besides the Th17 cells, recent investigations have found other immune cells, such as mast cells, and neutrophils as important sources of IL-17 in CVH, especially in late fibrosis stages (66–68). These findings emerge in a context after many studies have shown the domain of neutrophils as a predictor of outcomes in viral hepatitis and related diseases (19, 41). Therefore, these research together bring to light the importance of the interleukin-17 in pathogenesis and progression of CVH and can be one of the ways by which neutrophils, and other immune cell populations, exercise their pathogenic and predictive effect in CVH. Other Th17-related cytokines, such as IL-6 and IL-23, are involved in the evolution of CVH, regardless of stimulation of Th17 (11, 37, 69). The IL-23 and its receptor, in particular, have been found higher among HCV-infected patients than in control (mean 24.6 vs. 20.2 pg/mL; $P = 0.005$), with a positive correlation with ALT in HCV patients (69). Concerning the IL-6, its role was described in previous sections.

Besides increased Th17 cells, CVH has been associated with decreased or disproportionate count of regulatory T lymphocytes (Treg), another T helper subset, which is the functional counterbalance of Th17 cells (70); configuring a Treg/Th17 imbalance (13, 42, 64, 71). The balance between these two T helper lymphocytes subpopulations is fundamental (21, 22), and influenced by various factors (72–74). There is a plasticity and reciprocity between the two cell subpopulations that depends on environmental factors (70, 75, 76), being the proinflammatory environment, like that of the CVH, favorable to the polarization to Th17 cells (77, 78). The Treg/Th17 imbalance has been associated with greater hepatocellular damage in CVHs (21, 71, 79) and is related to advanced stages of cirrhosis and HCC (22, 65, 79), correlating inversely with severity scores and mortality (22, 64, 65). The Treg/Th17 imbalance has also been observed in other fibrosing liver diseases, such as autoimmune liver diseases (ALD) (80), biliary atresia (81), primary biliary cirrhosis (PBC) (82–84), non-alcoholic steatohepatitis (85, 86), schistosoma-induced hepatitis (87–89), and drug-induced hepatitis (90, 91).

Table 1 summarizes the clinical studies that evaluated the role of the Th17/IL-17 axis and related imbalances as drivers and predictors of outcomes in CVH.

MECHANISMS AND PATHWAYS LINKING THE TH17/IL-17 AXIS TO FIBROGENESIS AND CIRRHOSIS IN CVH

The Th17 Differentiation and Th17-Secreted Cytokines

Overall, Th17 cells differentiate from naive T helper cells, in response to a variety of stimuli, in the presence of key cytokines, namely IL-1β, IL-6, IL-21, IL-23, and TGF-β (101–105). In viral hepatitis, the virus particles are recognized by toll-like receptor (TLR2 and TLR4) present on the surface of the antigen-presenting cells (dendritic cells, macrophages, and monocytes) that result in their activation (97, 106). These activated cells, using the nuclear factor kappa B (NF-κB) and/or mitogen-activated protein kinase (MAPK) signaling pathways, produce the proinflammatory cytokines IL-1, IL-6, IL-21, and IL-23 (38, 93, 107) that drives the Th17 differentiation (93, 104, 107, 108). In the particular case of HCV, there are two additional pathways: the first one consists in the production of the thymic stromal lymphopoietin (TSLP) by HCV-infected hepatocytes, in an NF-κB-dependent process, and is this hepatocyte-derived TSLP that enhances activated APCs to produce the IL-1, IL-6, IL-21, and IL-23 (109). The second consists in particular evidence that HCV core protein exerts a function of a toll-like receptor 2 ligand, promoting, by itself, the activation of the APCs, the production of inflammatory cytokines that favor Th17 differentiation, and the evasion of the immune system (4, 12, 27). After being differentiated, the Th17 cells secrete its cytokines (IL-17, IL-21, and IL-22), being the IL-17 the main driver of a chain of events that have in common the favoritism of the proinflammatory and profibrotic pathways (13, 47, 49).

The Role of IL-17 Axis, and Associated Signaling Pathways, in Liver Fibrogenesis and Cirrhosis

The subtype 17 of T helper lymphocyte cells is increased in almost all chronic and fibrosing liver diseases, including ALD, such as autoimmune hepatitis (AIH) (50, 110, 111), primary sclerosing cholangitis (PSC) (112, 113), PBC (16, 83, 114, 115); biliary atresia (29, 81, 116), non-alcoholic steatohepatitis (85, 117, 118), and viral hepatitis (42, 44, 58, 109). These findings reveal the pivotal role of the Th17/IL-17 axis in liver fibrogenesis. However, the stimuli that attract Th17 cells to the liver are not completely elucidated. What is known is that injured liver cells secrete a variety of chemokines, such as CXCL9, CXCL10, and CCL20 (119, 120), that drive the recruitment of Th17 cells to the liver, binding to their receptors (CXCR3 and CCR6) expressed in Th17 cells (16, 119–123). This aggregate of chemokines and their receptors seems to determine, the differential cellular recruitment (32, 123, 124), the disposition of the Th17 cells within fibrosis areas (16, 60, 119, 120); and CXCL10, in particular, has itself a profibrotic effect influencing in the number and activity of HSCs, and participating in the cross talk between hepatocytes, HSCs, and immune cells (124–126).

In the liver, Th17 cells produce their cytokines (93), with IL-17 being the most associated with the progression of cirrhosis (13, 28, 49). There are receptors for IL-17 expressed in hepatocytes, in the liver sinusoids endothelial cells, in hepatic stellate cells (HSCs), and Kupffer cells (KC) (13). The functional implication of IL-17 in liver tissue is well characterized in the activation and/or stimulation of HSCs and KC (13, 17, 127) and cholangiocytes (115, 116).

Hepatic Stellate Cells

As already said, stellate cells express receptors for IL-17 (IL-17RA and IL-17RC) on their surface (13). The stimulation with IL-17

TABLE 1 | Clinical studies on the role of the Th17/IL-17 axis and associated imbalances in predicting outcomes in chronic viral hepatitis (CVH) and cirrhosis.

Reference	Virus	Biomarker	Patients	Results
Ge et al. (58)	Hepatitis B virus (HBV)	Subtype 17 of T helper lymphocytes (Th17)	30 patients with CHB and 20 matched controls	The percentage of Th17 cells in peripheral blood of CHB patients was significantly increased than in HCs (1.53 vs. 0.92%; $P < 0.05$); and kept a positive correlation with serum ALT in CHB patients
Ye et al. (71)	HBV	Th17, Treg, interleukin-4 (IL-4), and IFN-γ	88 liver specimens from HBV-infected patients, and six samples from controls	There was an increased intrahepatic frequency of IL-17-producing cells than IFN-γ-positive, IL-4-producing, and Treg cells. These cellular imbalances were higher in patients with severe hepatocellular damage than in mild
Wang et al. (92)	HBV	IL-23/IL-17	110 HBV-infected patients (39 with ACLF and 79 with CHB) and 32 HC	The IL-23/IL-17 pathway-related proinflammatory cytokines were found significantly increased in liver tissues of patients with HBV than HC
Niu et al. (22)	HBV	IL-17+/Treg ratio	57 patients with HBV-related liver failure (26 with CLF and 31 with ACLF) and 12 controls	The frequency of liver IL-17+ T cells was significantly higher in both HBV-related liver failure (CLF and ACLF) than in HC ($P = 0.0001$). The IL-17+/Treg ratio was significantly higher in ACLF and CLF than in HC (7.00, 4.33, and 0.00, respectively). The IL17+ T cells frequency correlated positively with total bilirubin ($r = 0.579$, $P = 0.001$) and MELD score ($r = 0.367$, $P = 0.043$)
Wang et al. (93)	HBV	IL-23, Th17, and IL-17	166 HBV-infected patients (108 with CHB and 58 with ACLF) and 62 controls, who underwent liver biopsies	There was increased intrahepatic expression of both IL-23 and IL-23R in HBV-infected livers than in controls, and the primary sources of IL-23 were liver myeloid dendritic cells and macrophages. In the presence of HBsAg or HBcAg, IL-23 efficiently stimulated the differentiation of naïve T CD4+ into Th17, that shown to be the primary source of IL-17
Zhai et al. (64)	HBV	Th17 and Treg cells	60 HBV-infected patients (30 with CHB and 30 with ACLF) and 30 controls	There was an increase of both Th17 and Treg cells in peripheral blood of ACLF patients. However, IL-17A was not regulated by Treg and the last exhibited significant inhibition of IFN-γ production. Most importantly, the low Treg/Th17 ratio was associated with low survival among ACLF patients
Chang et al. (42)	HCV	Th17	50 subjects with CHC and 23 HC	Compared to healthy individuals, patients had higher proportions of Th17 cells either circulating (1.56 vs. 0.96%, $P < 0.001$) or infiltrating the liver (16.08 vs. 0.82/hpf, $P < 0.001$); associated with higher serum IL-17 levels (84.86 vs. 60.52 pg/mL, $P < 0.001$). Both (circulating and intrahepatic) Th17 cells correlated with the severity of liver inflammation and damage
Wang et al. (56)	HBV	Th17 and IL-17 mRNA	80 HBV-infected patients (40 with ACLF and 40 with CHB) and 20 HC	The frequency of Th17 cells in peripheral blood, as well as IL-17 mRNA level in PBMCs, was higher in ACLF patients than in CHB ($P = 0.045$) or HC ($P < 0.001$). In addition, Th17 cells and IL-17 mRNA level were significantly higher among ACLF patients who died than in survivors. The frequency of Th17 cells correlated positively with serum TB ($r = 0.392$, $P = 0.012$) and MELD score ($r = 0.383$, $P = 0.015$) among ACLF patients
Foster et al. (49)	HCV	IL-17 and IL-22	157 HCV-infected patients (12 with acute infection, 134 with HCV-related fibrosis, and 11 with ESLD) and 41 HC	Chronic hepatitis C patients demonstrated an expansion of IL-17 and/or IL-22-producing T cell in hepatic compartment than in peripheral blood. Acute hepatitis C was not associated with a significant difference in IL-17 and/or IL-22-producing T cells expansion
Wu et al. (18)	HBV	Th17	133 subjects, HBV-infected (40 mild CHB, 37 severe CHB, and 20 AHB) and 36 HC	Patients with AHB and severe CHB had a higher frequency of Th17 cells in peripheral blood than those with mild CHB or HC (both $P < 0.05$). The increased peripheral Th17 correlated positively with ALT levels among severe CHB patients ($r = 0.457$, $P = 0.004$)
Wang et al. (56)	HBV	IL-17	91 patients with chronic liver conditions (55 with CHB, 42 with cirrhosis, 34 with HCC, 30 AsC) and 20 matched controls	There was a significantly increased intrahepatic expression of IL-17 in HBV-related chronic liver diseases. The intrahepatic IL-17 level correlated strongly with the degree of fibrosis, and it was mainly localized in the fibrosis region
Du et al. (44)	HBV	IL-17 and IL-17 mRNA	173 patients with CHB-related conditions (47 with CHB, 49 with cirrhosis, 44 with HCC, and 33 with CLF[a])[b] and 20 matched controls	Serum IL-17 protein and mRNA levels were significantly higher in the four CHB-related conditions than in controls ($P < 0.001$). Patients with cirrhosis exhibited the highest IL-17 concentrations in the serum and IL-17 mRNA in PBMCs. In addition, the levels of IL-17 in the liver tissues was higher in patients with cirrhosis than in those with CHB; and higher in this last than in HBsAg carriers ($P < 0.01$, for both)

(*Continued*)

TABLE 1 | Continued

Reference	Virus	Biomarker	Patients	Results
Hao et al. (54)	HBV	Th17, IL-17, IL-22, and IL-23	24 CHB patients, who underwent treatment with telbivudine	Antiviral therapy was associated with a significant decline in circulating Th17 cells and IL-22 production, in parallel to the reduction of HBV DNA and normalization of serum ALT
Ashrafi Hafez et al. (69)	HCV	IL-23, and IL-27	64 patients with CHC and 37 matched controls	Serum level of IL-23 was higher in HCV-infected patients than in control group (mean 24.6 vs. 20.2 pg/mL; $P = 0.005$). There was a positive correlation between ALT and IL-23 in HCV-infected patients
Sun et al. (28)	HBV	Th17	78 patients with LC (Child A: 34; Child B: 22; Child C: 22), 23 with CHB, and 32 HC	Patients with cirrhosis had a significant increase in peripheral Th17 cells as increased disease severity (mean: 3.51, 3.94, and 4.46; for Child–Pugh A, B, and C, respectively). The plasma IL-17 concentration was significantly higher in LC patients than in HC (89.76 vs. 61.40; $P < 0.01$); and also, increased with disease severity. There was an increase in intrahepatic IL-17+ cells, which correlated positively with fibrotic staging scores and clinical progression from CHB to cirrhosis; and most IL-17+ cells were located in the fibrotic areas in the liver
Yang et al. (59)	HBV	Th17 and IL-17	96 patients with HBV-related conditions (20 AsC, 32 with CHB, 44 with ACLF), and 20 matched controls	Serum IL-17 concentration, intrahepatic, and peripheral Th17 cells were significantly higher in CHB and ACLF patients than in AsC and HCs; and increased as aggravated the immune inflammation from AsC, CHB, to ACLF. In addition, in ACLF patients, peripheral Th17 cells correlated positively with INR and MELD score
Yan et al. (94)	HBV	Th17 and Th1	150 patients with HCC (100 with HBV-related) who underwent blood and tissue samples	The levels of Th17 and Th1 cells were significantly higher in tumors of patients with HCC ($P < 0.001$) compared to corresponding non-tumor regions. The intratumoral density of IL-17-producing cells correlated inversely with OS ($r = -0.784$, $P = 0.001$); and predicted shorter DFS (median, 7.5 vs. 24.9 months, $P = 0.03$)
Yang et al. (95)	HBV	Th17, IL-17, and Treg	87 patients with HBV-associated conditions (40 with CHB, 27 with cirrhosis, and 20 with liver failure) and 20 HCs	The frequencies of Th17 in the peripheral blood were significantly higher in the patients with CHB, cirrhosis, and liver failure, compared with HC. The same trend was observed in the serum levels of IL-17. Both peripheral Th17 cells and serum IL-17 correlated positively with ALT and the prothrombin times
Feng et al. (96)	HBV	Th17 and Treg	96 HBV-infected patients, and 33 HC	Compared with controls, patients had higher Treg (6.80 vs. 4.42) and Th17 (6.15 vs. 2.66) in circulation. However, the Treg/Th17 ratio was significantly lower in patients (1.48 vs. 2.29, $P = 0.0001$); which suggests an ineffective suppression of proinflammatory response
Feng et al. (23)	HBV	Th17, IL-17, and Treg	22 CHB patients, who underwent treatment with interferon-α, and 30 HC	Compared with controls, patients had higher Th17 (3.94 vs. 2.66, $P = 0.0436$), IL-17 levels (16.88 vs. 8.59, $P = 0.004$), and Treg (5.72 vs. 4.42, $P = 0.0019$) at baseline. The suppression of viral replication induced by interferon-α was associated with a decrease in both Th17 cells, IL-17 levels, and Treg
Maggio et al. (25)	HCV	Peripheral Treg/Th17 balance	30 patients with CHC and 30 with NAFLD/NASH who underwent NLCD for 30 days	After 30 days of NLCD, CHC patients showed a significant reduction in Th17 cells frequency, and an increase in the percentage of Treg cells, thus improving Treg/Th17 balance. The decrease in Th17 cells correlated with a decline in IL-17 and IL-22 serum levels
Wang et al. (9)	HBV	IL-17A, and IL-17F gene polymorphisms	433 subjects (130 with CHB, 132 with HBV-related cirrhosis, and 71 controls)	There was a significant increase in the risk of cirrhosis among subjects carrying the IL-17A rs4711998 G allele (OR = 1.54, $P = 0.025$) and those with the IL-17A rs4711998 AG genotype (OR = 1.75, $P = 0.02$) compared with other polymorphisms
Ge et al. (14)	HBV	IL-17A and IL-17F gene polymorphisms	331 patients with HBV-related conditions (163 LC and 168 CHB) who underwent gene polymorphisms analysis	The frequency of IL-17A G197A genotype AA was significantly higher in LC that in CHB patients (42.33 vs. 27.98%, $P = 0.032$), as well as the allele A (56.34 vs. 46.15%, $P = 0.011$). There was a significant increase in LC risk either among AA genotype patients (OR 4.186, 95% CI: 1.479–11.844) or one allele carriers (OR 1.856, 95% CI: 1.161–2.967)
Tian et al. (61)	HBV	Th17, Treg, Th1, Th2, and related cytokines	30 CHB patients, who underwent treatment with Entecavir	Antiviral therapy was associated with a significant decrease in the Th17 and Treg cell frequencies and related cytokines, in parallel to the reduction of HBV DNA load. By contrast, the treatment was associated increase in the Th2 cell and related cytokines

(*Continued*)

TABLE 1 | Continued

Reference	Virus	Biomarker	Patients	Results
Zhao et al. (97)	HBV	TLR2, Th17, and IL-17	34 patients with HBV infection (10 acute and 24 CHB) and 15 matched controls	The proportion of Th17 cells among PBMCs was significantly higher in CHB (1.78%) than either AHB patients (1.28%, $P = 0.0004$) or controls (0.78%, $P = 0.0009$). After stimulation with HBV envelope peptides, the expression of TLR2 and IL-17A in T lymphocytes was remarkably increased in CHB patients than in AHB. In addition, the stimulation of PBMCs with a TLR2 agonist induced a higher frequency of Th17 cells in CHB patients than AHB patients (1.39 vs. 0.68%, $P = 0.002$); with the increased IL-17 production
Xue-Song et al. (79)	HBV	Th17, Treg, and IL-17	48 patients with chronic HBV (12 AsC, 18 CHB, and 18 ACLF), 10 with AHB, and 10 HC	Compared to HC, both AHB and ACLF patients favored the Th17 cells differentiation, accompanied by a higher proportion of peripheral Th17 cells and high level of serum IL-17A ($P < 0.01$ for both). Both Th17 frequency and plasma IL-17A levels correlated positively with ALT and TB levels among those with CHB. In asymptomatic HBV carriers, by contrast, there was a favoritism to Treg differentiation. Both CHB and ACLF had lower Treg/Th17 ratio than in HC ($P < 0.05$); and this correlated inversely with TB levels ($r = -0.41$, $P = 0.004$)
Yu et al. (65)	HBV	Treg/Th17 ratio and TGF-β1/IL-17 ratio	98 patients with HBV-related conditions (70 with CHB, 28 with LC) and 20 controls	Patients with LC, especially non-survival ones, presented a significant decrease in the Treg/Th17 ratio. The lower Treg/Th17 ratio was associated with worse Child–Pugh and MELD scores, which suggests that the dominance of Th17 over Treg has a significant contribution in disease severity
Shi et al. (98)	HBV	IL-17 and IL-17 mRNA	123 patients with HBV-related conditions (30 with CHB, 79 with LC, 14 with severe CHB), and 20 controls	IL-17 mRNA expression levels in PBMCs were significantly higher in patients with HBV-conditions than in the controls. PBMCs IL-17 mRNA and the serum IL-17 protein were significantly higher in patients in higher Child–Pugh (B or C) than in lower scores. Serum IL-17 levels correlated positively with TB, ALT, and Child score; and correlated inversely with albumin
Wang et al. (99)	HBV and HCV	Treg/Th17	38 patients with ESLD (33 due to viral cause) who underwent liver transplantation	The frequency of circulating Th17 cells was significantly increased in liver allograft recipients who developed acute rejection; whereas Tregs, and consequently the Tregs/Th17 ratio, was significantly decreased in these patients. The level of Th17 cells had a positive correlation with RAI ($r = 0.890$, $P < 0.001$).
Xu et al. (63)	HBV	Treg/Th17 balance	56 patients with LC who were randomly assigned to ABMSCs transplantation or control group	After 24-week follow-up, 20 cases and 19 controls completed the study. There was a significant increase in Treg and a marked decrease in Th17 cells in the transplantation group compared with control, leading to an increased Treg/Th17 ratio. In addition, ABMSCs transplantation improved patients' liver function and significantly decreased the serum levels of proinflammatory cytokines (IL-17, TNF-α, and IL-6)
Jimenez-Sousa et al. (62)	HCV	Th17 and Th1 factors	27 HCV-infected patients who underwent 12 weeks' treatment with pegylated IFN-α and ribavirin and 10 HC	HCV infection induced the secretion of chemokines and cytokines involved in both Th1 (like IFN-α and MIP-1) and Th17 responses (such as IL-6 and IL-17), and two profibrotic factors (FGF-b, VEGF). Compared to the control group, these increases reached significances as follow: for MIP-1 alpha (4.7-fold), TNF-α (3.0-fold), FGF-b (3.4-fold), VEGF (3.5-fold), and IL-7 (5.6-fold). The 12 weeks combined treatment resulted in a significant down-modulation of the secretion of key Th1 and Th17 proinflammatory or profibrotic factors principally in responder patients
Zhang et al. (20)	HBV	Th17	83 HBV-infected patients (66 with CHB, 23 with ACLF) and 30 HC	Patients presented higher frequency of circulating Th17 than HC; and increased with disease progression (mean, 2.42, 4.34, and 5.62% for HC, CHB, and ACLF, respectively). Both circulating and intrahepatic Th17 cells correlated positively with serum ALT, and histological activity index
Basha et al. (57)	HCV	Th17, Treg, IL-17	60 OLT recipients (51 HCV+, 9 HCV–) and, 15 HC	Recipients with recurrent HCV-induced allograft inflammation and fibrosis/cirrhosis presented a significant increase in the frequency of HCV-specific CD4+ Th17 cells; as well as proinflammatory mediators (IL-17, IL-1β, IL-6, IL-8, and MCP-1). Recurrent patients despite demonstrating increased Treg frequency, this did not inhibit HCV-specific CD4+ Th17 cells

(*Continued*)

TABLE 1 | Continued

Reference	Virus	Biomarker	Patients	Results
Hu et al. (100)	HBV	IL-21 and IL-21-secreting CD4+ T cells	79 patients with CHB (39 with ACLF, 20 with moderate, and 20 with severe disease) and 10 HC	The frequencies of IL-21-secreting CD4+ T cells were higher in ACLF (4.84%) and severe CHB (4.18%) than in moderate CHB patients (1.38%) or HC (1.10%) ($P < 0.002$ for all). Serum IL-21 levels were highest in ACLF group compared with severe or moderate CHB patients, or HC (median 96.7, 65.2, 62.3, and 50.1 pg/mL, respectively; $P < 0.001$ for all). Serum IL-21 was associated with high MELD score ($P = 0.001$) and mortality ($P = 0.038$); and recovery from ACLF was associated with a reduction in its levels ($P = 0.003$). The stimulation with rhIL-21 significantly increased the secretion of other proinflammatory cytokines (IL-1β, IL-6, and TNF-α) by PBMCs

ABMSCs, autologous bone marrow mesenchymal stem cells; ACLF, acute-on-chronic liver failure; AHB, acute hepatitis B; ALT, alanine aminotransferase; AR, acute rejection; AsC: asymptomatic surface antigen carriers; CHB, chronic hepatitis B; CLF, chronic liver failure; DFS, disease-free survival; ESLD, end-stage liver disease; FGF-b, fibroblast growth factor-basic; HC, healthy controls; Hpf, high-powered fields; INR, international normalized ratio; MIP-1, macrophage inflammatory protein-1; NLCD, normocaloric low cholesterol diet; OLT, orthotopic liver transplantation; OS, overall survival; PBMCs, peripheral blood mononuclear cells; RAI, rejection activity index; rhIL-21, recombinant human interleukin-21; TLR2, toll-like receptor 2; TB, total bilirubin; VEGF, vascular endothelial growth factor; WBC, white blood cell.

[a]*The study included liver biopsy samples obtained from CHB (n = 57) and cirrhosis (n = 31) patients.*

[b]*Control liver biopsy samples were obtained from asymptomatic HBsAg carriers (AsC, n = 35).*

induces the rapid translocation of transcription factors NF-κB and Stat3 to the cellular nucleus (13), where activate the gene transcription of proinflammatory cytokines (IL-6 and TNF-α) and profibrotic factors (TGF-β1) (17, 50). In addition, IL-17 promotes the proliferation of HSCs, the upregulation of TGF-β receptor, IL-17RA, and IL-17RC (13, 16, 127). So, the IL-17 has the property to induce the activation of HSCs and fibrogenesis, and this effect seems to be synergistic with that of IL-6 and TNF-α (13, 128).

In the liver tissue, particularly in HSCs, the IL-17 also presents the following effects: increases the genic expression of type I collagen and induces its production through TGF-β, or Stat3/SMAD2/3 signaling pathways (13, 127). In addition, IL-17 upregulates matrix metalloproteinases (MMP2, MMP3, and MMP9) expression *via* NF-κB and Stat3 signaling pathways (13, 127, 129) and increases the expression of tissue inhibitor of matrix metalloproteinase I (TIMP1) and the production of related proteins (127). The combination of these effects results in increased production of extracellular matrix and changes in its degradation. This role of IL-17 has been reinforced in experimental model where liver fibrosis was inhibited or attenuated in IL-17RA−/− mice exposed to carbon tetrachloride (CCl4) or subjected to bile duct ligation (BDL), associated with reduced mRNA expression of fibrogenic genes (collagen-α1, MMP3, TIMP1, and TGF-β1) (13, 130). The role of IL-17 on MMPs and related signaling pathway has also been found in other organs such as the heart (131).

IL-17, TGF-β, and Induction of Cellular Transition/Transdifferentiation

In addition to the direct effects, described above, the IL-17 cooperates with TGF-β1 to induce the activation of HSCs and their transition into a proliferative, contractile, and fibrogenic phenotype—the myofibroblast (13, 132, 133). These events also lead to an excessive synthesis of ECM and the contractility of myofibroblasts resulting in changes in the hepatic microarchitecture and microcirculation (134–136). The IL-17 also has the effect of inducing epithelial–mesenchymal transition (EMT) in hepatic tissue as observed in hepatocytes of patients with HCC (137) and biliary epithelial cells as seen in PBC (115). It is important to emphasize that the exposure of the hepatic tissue to IL-17 increased the expression of TGF-β in almost all liver resident cells (13, 127). Moreover, the TGF-β is well documented that induces the EMT of the hepatocytes (138–140). Therefore, we can deduce that the IL-17, through the induction of TGF-β production, is an indirect promoter of EMT in the liver (13, 132, 137, 139). This effect of IL-17 in EMT is well described in many other organs (and clinical conditions), as in the respiratory epithelium (141, 142) and prostate (143); and has been proven to be a process dependent on TGF-β or NF-κB pathways (115, 141, 142, 144).

The activation of HSCs is associated with two other Th17/IL-17 axis-related changes. The first results from the rarefaction of retinoic acid in HSCs. Under normal conditions, the quiescent HSCs have many granules containing retinoic acid (135), which acts inhibiting the Th17 and favoring the Treg cells differentiation, with a protective effect on the liver (145, 146). However, when activated HSCs undergo changes in their metabolism and retinoic acid content, which affects the differentiation of Treg cells and, consequently, the loss of the protective effect (135, 147, 148). The second results from the evidence that activated HSCs exacerbate liver fibrosis by enhancing IL-17A production by T cells, in a TLR3-dependent manner (45), that in combination with the rarefaction of retinoic acid results promoting further Treg/Th17 imbalance and fibrogenesis (45, 149).

Kupffer Cells

In KC, as well as in HSCs, stimulation with IL-17 led to the production of proinflammatory cytokines and TGF-β1, through NF-κB and Stat3 pathways (13, 150–153). It also upregulates the receptors of TGF-β, IL-17A, and IL-17C and promotes the further production of IL-17A, IL-17F (13, 127). In addition, under stress conditions, KC are involved in increased differentiation of Th17 and decreased Treg, through an IL-6-dependent mechanism, promoting further Treg/Th17 imbalance and perpetuating

the proinflammatory and fibrogenic consequences of this axis (43, 154).

The Role of IL-17 in the Systemic Circulation and Its Repercussions in the Liver Tissue

In the systemic circulation, the IL-17 sustains the proinflammatory environment, stimulating the granulopoiesis through the release of granulocyte-macrophage colony-stimulating factor (GM-CSF) (33, 155–158). On inflammatory cells (either in systemic circulation or infiltrating the liver), the IL-17 induces the release of the IL-6 (159). The elevation of the IL-6 contributes to further Th17 responses because it promotes its differentiation (104), as IL-6 receptors are expressed on the surface of CD4+ T cells (43, 51). This process also occurs using the STAT3, NF-κB, and MAPK signaling (43, 151).

The repercussion at the organic level is the liver infiltration by inflammatory cells that occurs because IL-17 promotes endothelial activation (32, 33, 47), and release of attracting chemokines such as CXCL5 and CXCL8/IL-8 (156, 160, 161) whose receptors (CXCR1 and CXCR2) are abundantly expressed neutrophils and monocytes (32, 125, 161–164). Once in the liver, neutrophils are involved in various points of the fibrogenesis chain, including the release MMP9 (165–167) and seem to affect the functioning of the TIMP-1 (168). Recent studies have shown that neutrophils released itself the IL-17, mainly in the advanced stages of fibrosis (66); and there is a sustained cross talk between neutrophils and Th17 cells (32, 164). **Figure 2** represents the chain of events from viral injury, Th17/IL-17 axis activation, to liver fibrogenesis and cirrhosis.

The Role of IL-17 Axis in Other Liver Diseases and Other Organs Fibrosis

The role of Th17/IL-17 axis in hepatic fibrosis has been found in various liver diseases such as NASH (117, 118), obstructive cholestasis (169), PSC (112), PBC (16, 114, 115), biliary atresia (29, 116), drug-induced (91, 170), protozoa-associated cirrhosis (87, 171, 172), and viral hepatitis (20, 30, 44, 173). Moreover, the role of Th17/IL-17 axis extends to related diseases such as HCC (94, 174, 175), which suggests a continuous, or at least related parts of a whole, in the pathogenesis of these conditions (53, 94, 174, 175). Additional evidence comes from

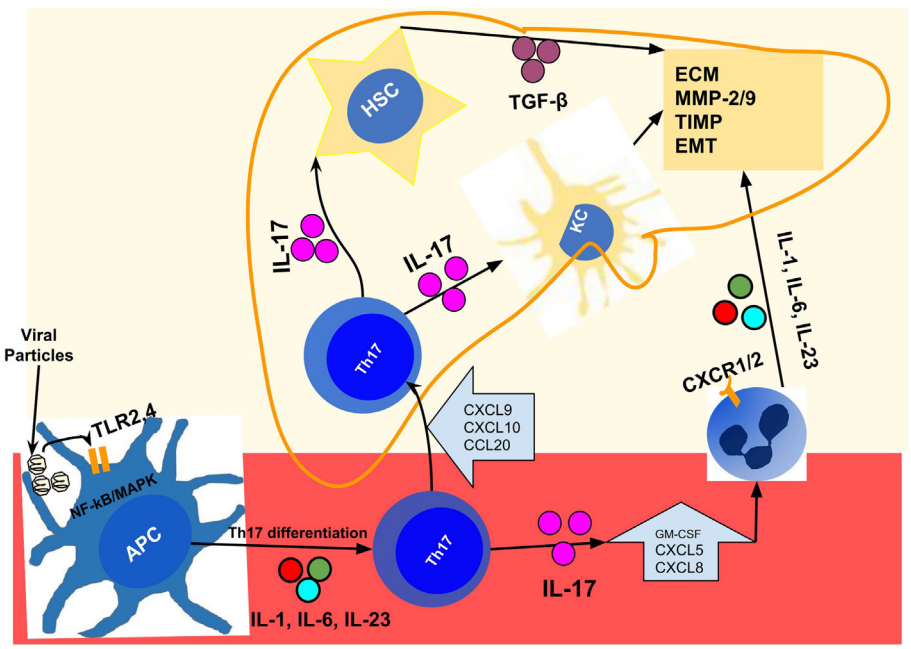

FIGURE 2 | Representation of events chain from viral injury to Th17/IL-17 axis activation, liver fibrogenesis, and cirrhosis in chronic viral hepatitis. After infection by hepatitis B virus/hepatitis C virus; distinct viral particles are recognized byTLR2 and TLR4 present on the surface of the APCs (dendritic cells, macrophages, and monocytes), which result in their activation (97, 106). These activated cells, using the NF-κB and MAPK signaling pathways, produce the proinflammatory cytokines IL-1, IL-6, IL-21, and IL-23 (38, 93, 107) that drive the Th17 differentiation and IL-17 production in peripheral blood (93, 104, 107, 108). In the liver, injured cells secrete a variety of chemokines like CXCL9, CXCL10, and CCL20 (119, 120) that drive the recruitment of Th17 cells to the liver, through binding to their receptors (CXCR3 and CCR6) expressed in Th17 cells (120–123). Intrahepatic Th17 cells and IL-17 are responsible for hepatic stellate cell activation (13, 17), increased expression of TGF-β (127), MMP (13, 127, 130), collagen synthesis (13, 127), and induction of EMT (115, 137, 142). In addition, it promotes the recruitment of other inflammatory cells (32, 160) through the release of chemokines such as CXCL5 and CXCL8/IL-8 (156, 160, 161) whose receptors (CXCR1 and CXCR2) are abundantly expressed in neutrophils, monocytes, and macrophages (32, 125, 161–164). APCs, antigen-presenting cells (dendritic cells, macrophages, and monocytes); EMT, epithelial–mesenchymal transition; HSC, hepatic stellate cell; IL-1, interleukin-1; IL-17, interleukin-17; IL-21, interleukin-21; IL-23, interleukin-23; IL-6, interleukin-6; KC, Kupffer cells; MAPK, mitogen-activated protein kinase; MMP, matrix metalloproteinases; NF-κB, nuclear factor-kappa B; TGF-β, transforming growth factor beta; Th17, T helper lymphocytes, subtype 17; TLR2, toll-like receptor 2; TLR4, toll-like receptor 4.

observational studies that have found an increased occurrence of hepatic inflammation associated with dysregulated protein/lipid metabolism, and progression to cirrhosis in clinical conditions such as psoriasis that have the Th17/IL-17 axis hyperactivation as the crucial point in their pathogenesis (48, 176).

It is worth noting that HCV infection induces the development of autoantibodies to liver autoantigens, in up to 10% of patients, in addition to previously described mechanisms, leading to an overlap between CVH and AIH (177–180). Certainly, the Th17/IL-17 axis plays a pivotal role in the progression to cirrhosis regardless of the dominant mechanism in the pathogenesis (20, 49, 111, 181, 182).

The role of the Th17/IL-17 axis has been found in other diseases with a fibrosing behavior in various organs such as intestine (31, 183), lung (184, 185), and peritoneum or kidney (46, 186); and its block has shown to prevent/mitigate the fibrosis in many pathological conditions (187–189).

Hepatoprotective Agents Targeting the Th17/IL-17 Axis, Associated Cytokines, and Signaling Pathways

As we have seen the Th7/IL-17 axis is involved in several known points of fibrogenesis chain, including the activation of HSCs (17), recruitment of inflammatory cells (32, 160), expression of proinflammatory and profibrotic cytokines (127), in stimulus to collagen synthesis, and in the imbalance between MMP and TIMPs (13, 127, 133). Added to this is the parallel evidence of being a promoter of EMT or myofibroblast transition (115, 137, 142). Therefore, the inhibition of Th17/IL-17 axis (and its signaling pathways) represents a promising strategy in the treatment of organic fibrosis.

Agents That Downregulate the Th17/IL-17 Axis or Restore the Treg/Th17 Balance

There are a variety of agents targeting these immune pathways, with the potential to slow down the CVH-induced cirrhosis. From those that downregulates the Th17/IL-17 axis to those that restore the Treg/Th17 balance. Brief citations are made about some of these agents that have shown benefit in preliminary studies, such as cannabinoid receptor 2 agonists, whose action is to counteract immune and fibrogenic responses induced by interleukin-17 (190). Another treatment that ameliorates hepatic fibrosis by regulation of Treg/Th17 cells, and downregulating the IL-17, is bone marrow-derived stem cells transplantation (63, 191). It is also worth to cite the vitamin D and analogs that inhibit the development of liver fibrosis by reducing the Th17 differentiation and IL-17 production, and activate the Treg differentiation (186, 192–194). The rapamycin demonstrated to improve hepatic fibrosis that was associated with a decrease of Th17 and expansion of Treg (91, 195). In another study, the administration of an mTOR inhibitor decreased the IL-17 production induced by IL-6; and this effect occurred through decreasing mTOR/STAT3 activation (43). Halofuginone, an inhibitor of Th17 cells differentiation (196); has shown to be a promising antifibrotic drug, and its impact in reducing liver fibrosis severity is associated with a significant reduction in Th17 cells and related cytokines (197). Another compound with protective effects in liver fibrosis is the polyphenolic molecule mongol that inhibits Th17 cells differentiation and suppresses HSCs activation (198).

Still, about Treg/Th17 balance restoration, adoptive transfer of Tregs ameliorated the severity of liver injury, accompanied by increased levels of hepatic Treg and IL-10 as shown in a model of Triptolide-induced liver injury (90). On the other hand, some drugs with use and efficiency established in viral hepatitis, such as interferon, appear to have effects that involve this axis, among its various mechanisms (24, 62, 187).

Agents Targeting the Receptors and Signaling Pathways Involved in Th17/IL-17 Axis Effects

The inhibition of the activation of HSCs is, undoubtedly, one of the most attractive strategies to slow down fibrogenesis (199). Multiple receptors and signaling pathways are involved in the chain of events of Th17/IL-17 axis-mediated HSCs activation, and can also be therapeutic targets. So, agents such as resveratrol, curcumin, Dioscin, the flavonoid quercetin, and other agents have emerged as inhibitors of the HSCs activation targeting the TLR3, TLR2/4, STAT3, and/or MAPK/NF-κB, the main receptors and pathways in Th17/IL-17 axis-mediated HSCs activation (200–207). Agents such as rosiglitazone and rapamycin demonstrated the potential to interfere with the fibrogenic pathways by reducing the expression of TGF-β (195, 208). Others such as the ruxolitinib have also shown the potential to inhibit the hepatotoxicity and fibrogenesis, after initial injury by multiple agents, by inhibiting the JAK/STAT pathway (207, 209, 210).

CONCLUSION AND FUTURE DIRECTIONS

The imbalanced immunity at Th17/IL-17 axis level plays a significant role in liver fibrogenesis after initial HCV or HBV injury. The Th17/IL-17 axis drives of a chain of events that promote a proinflammatory and profibrotic environment by recruiting neutrophils and monocytes and by inducing the expression and production of interleukin-23 and IL-6 either in the liver or peripheral cells. All resident liver cells express receptors for IL-17; and liver cells respond to the IL-17 exposition by increasing the expression of profibrotic and proinflammatory factors such as TGF-β, MMPs, and TIMP. In addition, IL-17 induces the transformation of HSCs to myofibroblasts and the EMT of the hepatocytes, promoting the synthesis of extracellular matrix, cell contractility, and all changes in the liver microstructure and microcirculation.

AUTHOR CONTRIBUTIONS

FCP: prepared the manuscript text and figures.

REFERENCES

1. Stanaway JD, Flaxman AD, Naghavi M, Fitzmaurice C, Vos T, Abubakar I, et al. The global burden of viral hepatitis from 1990 to 2013: findings from the Global Burden of Disease Study 2013. *Lancet* (2016) 388:1081–8. doi:10.1016/S0140-6736(16)30579-7
2. Mokdad AA, Lopez AD, Shahraz S, Lozano R, Mokdad AH, Stanaway J, et al. Liver cirrhosis mortality in 187 countries between 1980 and 2010: a systematic analysis. *BMC Med* (2014) 12:145. doi:10.1186/s12916-014-0145-y
3. Lozano R, Naghavi M, Foreman K, Lim S, Shibuya K, Aboyans V, et al. Global and regional mortality from 235 causes of death for 20 age groups in 1990 and 2010: a systematic analysis for the Global Burden of Disease Study 2010. *Lancet* (2012) 380:2095–128. doi:10.1016/S0140-6736(12)61728-0
4. Dolganiuc A, Oak S, Kodys K, Golenbock DT, Finberg RW, Kurt-Jones E, et al. Hepatitis C core and nonstructural 3 proteins trigger toll-like receptor 2-mediated pathways and inflammatory activation. *Gastroenterology* (2004) 127:1513–24. doi:10.1053/j.gastro.2004.08.067
5. Xiang WQ, Feng WF, Ke W, Sun Z, Chen Z, Liu W. Hepatitis B virus X protein stimulates IL-6 expression in hepatocytes via a MyD88-dependent pathway. *J Hepatol* (2011) 54:26–33. doi:10.1016/j.jhep.2010.08.006
6. Liu L, Liang H, Chen X, Zhang W, Yang S, Xu T, et al. The role of NF-kappaB in hepatitis b virus X protein-mediated upregulation of VEGF and MMPs. *Cancer Invest* (2010) 28:443–51. doi:10.3109/07357900903405959
7. Ali L, Mansoor A, Ahmad N, Siddiqi S, Mazhar K, Muazzam AG, et al. Patient HLA-DRB1* and -DQB1* allele and haplotype association with hepatitis C virus persistence and clearance. *J Gen Virol* (2010) 91:1931–8. doi:10.1099/vir.0.018119-0
8. Kamatani Y, Wattanapokayakit S, Ochi H, Kawaguchi T, Takahashi A, Hosono N, et al. A genome-wide association study identifies variants in the HLA-DP locus associated with chronic hepatitis B in Asians. *Nat Genet* (2009) 41:591–5. doi:10.1038/ng.348
9. Wang J, Liu Y, Xie L, Li S, Qin X. Association of IL-17A and IL-17F gene polymorphisms with chronic hepatitis B and hepatitis B virus-related liver cirrhosis in a Chinese population: a case-control study. *Clin Res Hepatol Gastroenterol* (2016) 40:288–96. doi:10.1016/j.clinre.2015.10.004
10. Falleti E, Fabris C, Toniutto P, Fontanini E, Cussigh A, Bitetto D, et al. Interleukin-6 polymorphisms and gender: relationship with the occurrence of hepatocellular carcinoma in patients with end-stage liver disease. *Oncology* (2009) 77:304–13. doi:10.1159/000260057
11. Barrett S, Collins M, Kenny C, Ryan E, Keane CO, Crowe J. Polymorphisms in tumour necrosis factor-alpha, transforming growth factor-beta, interleukin-10, interleukin-6, interferon-gamma, and outcome of hepatitis C virus infection. *J Med Virol* (2003) 71:212–8. doi:10.1002/jmv.10472
12. Dolganiuc A, Norkina O, Kodys K, Catalano D, Bakis G, Marshall C, et al. Viral and host factors induce macrophage activation and loss of toll-like receptor tolerance in chronic HCV infection. *Gastroenterology* (2007) 133:1627–36. doi:10.1053/j.gastro.2007.08.003
13. Meng F, Wang K, Aoyama T, Grivennikov SI, Paik Y, Scholten D, et al. Interleukin-17 signaling in inflammatory, Kupffer cells, and hepatic stellate cells exacerbates liver fibrosis in mice. *Gastroenterology* (2012) 143:765–76. doi:10.1053/j.gastro.2012.05.049
14. Ge J, Yu Y-Z, Li T, Guo Z-Y, Wu H, Tang S-C, et al. IL-17A G197A gene polymorphism contributes to susceptibility for liver cirrhosis development from patients with chronic hepatitis B infection in Chinese population. *Int J Clin Exp Med* (2015) 8:9793–8.
15. Radwan MI, Pasha HF, Mohamed RH, Hussien HI, El-Khshab MN. Influence of transforming growth factor-β1 and tumor necrosis factor-α genes polymorphisms on the development of cirrhosis and hepatocellular carcinoma in chronic hepatitis C patients. *Cytokine* (2012) 60:271–6. doi:10.1016/j.cyto.2012.05.010
16. Shi T, Zhang T, Zhang L, Yang Y, Zhang H, Zhang F. The distribution and the fibrotic role of elevated inflammatory Th17 cells in patients with primary biliary cirrhosis. *Medicine (Baltimore)* (2015) 94:e1888. doi:10.1097/MD.0000000000001888
17. Tan Z, Qian X, Jiang R, Liu Q, Wang Y, Chen C, et al. IL-17A plays a critical role in the pathogenesis of liver fibrosis through hepatic stellate cell activation. *J Immunol* (2013) 191:1835–44. doi:10.4049/jimmunol.1203013
18. Wu W, Li J, Chen F, Zhu H, Peng G, Chen Z. Circulating Th17 cells frequency is associated with the disease progression in HBV infected patients. *J Gastroenterol Hepatol* (2010) 25:750–7. doi:10.1111/j.1440-1746.2009.06154.x
19. Liu H, Zhang H, Wan G, Sang Y, Chang Y, Wang X, et al. Neutrophil-lymphocyte ratio: a novel predictor for short-term prognosis in acute-on-chronic hepatitis B liver failure. *J Viral Hepat* (2014) 21:499–507. doi:10.1111/jvh.12160
20. Zhang J-Y, Zhang Z, Lin F, Zou Z-S, Xu R-N, Jin L, et al. Interleukin-17-producing CD4(+) T cells increase with severity of liver damage in patients with chronic hepatitis B. *Hepatology* (2010) 51:81–91. doi:10.1002/hep.23273
21. Li J, Qiu S-J, She W-M, Wang F-P, Gao H, Li L, et al. Significance of the balance between regulatory T (Treg) and T helper 17 (Th17) cells during hepatitis B virus related liver fibrosis. *PLoS One* (2012) 7:e39307. doi:10.1371/journal.pone.0039307
22. Niu Y, Liu H, Yin D, Yi R, Chen T, Xue H, et al. The balance between intrahepatic IL-17(+) T cells and Foxp3(+) regulatory T cells plays an important role in HBV-related end-stage liver disease. *BMC Immunol* (2011) 12:47. doi:10.1186/1471-2172-12-47
23. Feng H, Yin J, Han Y-P, Zhou X-Y, Chen S, Yang L, et al. Sustained changes of Treg and Th17 cells during interferon-α therapy in patients with chronic hepatitis B. *Viral Immunol* (2015) 28:412–7. doi:10.1089/vim.2015.0024
24. Cui F, Meng J, Luo P, Chen P. IFN-alpha blocks IL-17 production by peripheral blood mononuclear cells in patients with chronic active hepatitis B infection. *BMC Infect Dis* (2014) 14:55. doi:10.1186/1471-2334-14-55
25. Maggio R, Viscomi C, Andreozzi P, D'Ettorre G, Viscogliosi G, Barbaro B, et al. Normocaloric low cholesterol diet modulates Th17/Treg balance in patients with chronic hepatitis C virus infection. *PLoS One* (2014) 9:e112346. doi:10.1371/journal.pone.0112346
26. Ueyama M, Nakagawa M, Sakamoto N, Onozuka I, Funaoka Y, Watanabe T, et al. Serum interleukin-6 levels correlate with resistance to treatment of chronic hepatitis C infection with pegylated-interferon-α2b plus ribavirin. *Antivir Ther* (2011) 16:1081–91. doi:10.3851/IMP1864
27. Chung H, Watanabe T, Kudo M, Chiba T. Hepatitis C virus core protein induces homotolerance and cross-tolerance to toll-like receptor ligands by activation of toll-like receptor 2. *J Infect Dis* (2010) 202:853–61. doi:10.1086/655812
28. Sun HQ, Zhang JY, Zhang H, Zou ZS, Wang FS, Jia JH. Increased Th17 cells contribute to disease progression in patients with HBV-associated liver cirrhosis. *J Viral Hepat* (2012) 19:396–403. doi:10.1111/j.1365-2893.2011.01561.x
29. Klemann C, Schröder A, Dreier A, Möhn N, Dippel S, Winterberg T, et al. Interleukin 17, produced by γδ T cells, contributes to hepatic inflammation in a mouse model of biliary atresia and is increased in livers of patients. *Gastroenterology* (2016) 150:229–41.e5. doi:10.1053/j.gastro.2015.09.008
30. Barron L, Wynn TA. Fibrosis is regulated by Th2 and Th17 responses and by dynamic interactions between fibroblasts and macrophages. *Am J Physiol Gastrointest Liver Physiol* (2011) 300:G723–8. doi:10.1152/ajpgi.00414.2010
31. Ray S, De Salvo C, Pizarro TT. Central role of IL-17/Th17 immune responses and the gut microbiota in the pathogenesis of intestinal fibrosis. *Curr Opin Gastroenterol* (2014) 30:531–8. doi:10.1097/MOG.0000000000000119
32. Griffin GK, Newton G, Tarrio ML, Bu D, Maganto-Garcia E, Azcutia V, et al. IL-17 and TNF-α sustain neutrophil recruitment during inflammation through synergistic effects on endothelial activation. *J Immunol* (2012) 188:6287–99. doi:10.4049/jimmunol.1200385
33. Yuan S, Zhang S, Zhuang Y, Zhang H, Bai J, Hou Q. Interleukin-17 stimulates STAT3-mediated endothelial cell activation for neutrophil recruitment. *Cell Physiol Biochem* (2015) 36:2340–56. doi:10.1159/000430197
34. Huang C-F, Hsieh M-Y, Yang J-F, Chen W-C, Yeh M-L, Huang C-I, et al. Serum hs-CRP was correlated with treatment response to pegylated interferon and ribavirin combination therapy in chronic hepatitis C patients. *Hepatol Int* (2010) 4:621–7. doi:10.1007/s12072-010-9200-8
35. Wong VW, Yu J, Cheng AS, Wong GL, Chan HY, Chu ES, et al. High serum interleukin-6 level predicts future hepatocellular carcinoma development in patients with chronic hepatitis B. *Int J Cancer* (2009) 124:2766–70. doi:10.1002/ijc.24281
36. Kao J-T, Lai H-C, Tsai S-M, Lin P-C, Chuang P-H, Yu C-J, et al. Rather than interleukin-27, interleukin-6 expresses positive correlation with liver severity in naïve hepatitis B infection patients. *Liver Int* (2012) 32:928–36. doi:10.1111/j.1478-3231.2011.02742.x
37. Sghaier I, Mouelhi L, Rabia NA, Alsaleh BR, Ghazoueni E, Almawi WY, et al. Genetic variants in IL-6 and IL-10 genes and susceptibility to hepatocellular

carcinoma in HCV infected patients. *Cytokine* (2017) 89:62–7. doi:10.1016/j.cyto.2016.10.004
38. Shrivastava S, Mukherjee A, Ray R, Ray RB. Hepatitis C virus induces interleukin-1β (IL-1β)/IL-18 in circulatory and resident liver macrophages. *J Virol* (2013) 87:12284–90. doi:10.1128/JVI.01962-13
39. Negash AA, Ramos HJ, Crochet N, Lau DT, Doehle B, Papic N, et al. IL-1β production through the NLRP3 inflammasome by hepatic macrophages links hepatitis C virus infection with liver inflammation and disease. *PLoS Pathog* (2013) 9:e1003330. doi:10.1371/journal.ppat.1003330
40. Gusatti Cde S, Costi C, de Medeiros RM, Halon ML, Grandi T, Medeiros AF, et al. Association between cytokine gene polymorphisms and outcome of hepatitis B virus infection in southern Brazil. *J Med Virol* (2016) 88:1759–66. doi:10.1002/jmv.24518
41. Biyik M, Ucar R, Solak Y, Gungor G, Polat I, Gaipov A, et al. Blood neutrophil-to-lymphocyte ratio independently predicts survival in patients with liver cirrhosis. *Eur J Gastroenterol Hepatol* (2013) 25:435–41. doi:10.1097/MEG.0b013e32835c2af3
42. Chang Q, Wang Y-K, Zhao Q, Wang C-Z, Hu Y-Z, Wu B-Y. Th17 cells are increased with severity of liver inflammation in patients with chronic hepatitis C. *J Gastroenterol Hepatol* (2012) 27:273–8. doi:10.1111/j.1440-1746.2011.06782.x
43. Kim HY, Jhun JY, Cho M-L, Choi JY, Byun JK, Kim E-K, et al. Interleukin-6 upregulates Th17 response via mTOR/STAT3 pathway in acute-on-chronic hepatitis B liver failure. *J Gastroenterol* (2014) 49:1264–73. doi:10.1007/s00535-013-0891-1
44. Du WJ, Zhen JH, Zeng ZQ, Zheng ZM, Xu Y, Qin LY, et al. Expression of interleukin-17 associated with disease progression and liver fibrosis with hepatitis B virus infection: IL-17 in HBV infection. *Diagn Pathol* (2013) 8:40. doi:10.1186/1746-1596-8-40
45. Seo W, Eun HS, Kim SY, Yi H-S, Lee Y-S, Park S-H, et al. Exosome-mediated activation of toll-like receptor 3 in stellate cells stimulates interleukin-17 production by γδ T cells in liver fibrosis. *Hepatology* (2016) 64:616–31. doi:10.1002/hep.28644
46. Peng X, Xiao Z, Zhang J, Li Y, Dong Y, Du J. IL-17A produced by both γδ T and Th17 cells promotes renal fibrosis via RANTES-mediated leukocyte infiltration after renal obstruction. *J Pathol* (2015) 235:79–89. doi:10.1002/path.4430
47. Roussel L, Houle F, Chan C, Yao Y, Bérubé J, Olivenstein R, et al. IL-17 promotes p38 MAPK-dependent endothelial activation enhancing neutrophil recruitment to sites of inflammation. *J Immunol* (2010) 184:4531–7. doi:10.4049/jimmunol.0903162
48. Al-Harbi NO, Nadeem A, Al-Harbi MM, Zoheir KM, Ansari MA, El-Sherbeeny AM, et al. Psoriatic inflammation causes hepatic inflammation with concomitant dysregulation in hepatic metabolism via IL-17A/IL-17 receptor signaling in a murine model. *Immunobiology* (2017) 222:128–36. doi:10.1016/j.imbio.2016.10.013
49. Foster RG, Golden-Mason L, Rutebemberwa A, Rosen HR. Interleukin (IL)-17/IL-22-producing T cells enriched within the liver of patients with chronic hepatitis C viral (HCV) infection. *Dig Dis Sci* (2012) 57:381–9. doi:10.1007/s10620-011-1997-z
50. Zhao L, Tang Y, You Z, Wang Q, Liang S, Han X, et al. Interleukin-17 contributes to the pathogenesis of autoimmune hepatitis through inducing hepatic interleukin-6 expression. *PLoS One* (2011) 6:e18909. doi:10.1371/journal.pone.0018909
51. Zhang F, Yao S, Yuan J, Zhang M, He Q, Yang G, et al. Elevated IL-6 receptor expression on CD4+ T cells contributes to the increased Th17 responses in patients with chronic hepatitis B. *Virol J* (2011) 8:270. doi:10.1186/1743-422X-8-270
52. Zhang F, Yao S, Zhang M, Yuan J, Chen X, Zhou B. Roles of circulating soluble interleukin (IL)-6 receptor and IL-6 receptor expression on CD4+ T cells in patients with chronic hepatitis B. *Int J Infect Dis* (2011) 15:e267–71. doi:10.1016/j.ijid.2010.12.008
53. Li N, Zhu Q, Li Z, Han Q, Zhang G, Chen J. IL17A gene polymorphisms, serum IL-17A and IgE levels, and hepatocellular carcinoma risk in patients with chronic hepatitis B virus infection. *Mol Carcinog* (2014) 53(6):447–57. doi:10.1002/mc.21992
54. Hao C, Wang J, Kang W, Xie Y, Zhou Y, Ma L, et al. Kinetics of Th17 cytokines during telbivudine therapy in patients with chronic hepatitis B. *Viral Immunol* (2013) 26:336–42. doi:10.1089/vim.2013.0032
55. Ju H, Liu H, Tian Z, Jiang Y, Zhang C, Liu X. Association of polymorphisms in key Th-17 immune response genes with HBeAg-positive chronic hepatitis B susceptibility and response to PEG-IFNa-2α. *Virology* (2017) 509:35–41. doi:10.1016/j.virol.2017.05.011
56. Wang L-Y, Meng Q-H, Zou Z-Q, Fan Y-C, Han J, Qi Z-X, et al. Increased frequency of circulating Th17 cells in acute-on-chronic hepatitis B liver failure. *Dig Dis Sci* (2012) 57:667–74. doi:10.1007/s10620-011-1930-5
57. Basha HI, Subramanian V, Seetharam A, Nath DS, Ramachandran S, Anderson CD, et al. Characterization of HCV-specific CD4+Th17 immunity in recurrent hepatitis C-induced liver allograft fibrosis. *Am J Transplant* (2011) 11:775–85. doi:10.1111/j.1600-6143.2011.03458.x
58. Ge J, Wang K, Meng Q-H, Qi Z-X, Meng F-L, Fan Y-C. Implication of Th17 and Th1 cells in patients with chronic active hepatitis B. *J Clin Immunol* (2010) 30:60–7. doi:10.1007/s10875-009-9328-2
59. Yang B, Wang Y, Zhao C, Yan W, Che H, Shen C, et al. Increased Th17 cells and interleukin-17 contribute to immune activation and disease aggravation in patients with chronic hepatitis B virus infection. *Immunol Lett* (2013) 149:41–9. doi:10.1016/j.imlet.2012.12.001
60. Wang L, Chen S, Xu K. IL-17 expression is correlated with hepatitis B-related liver diseases and fibrosis. *Int J Mol Med* (2011) 27:385–92. doi:10.3892/ijmm.2011.594
61. Tian Z-F, You Z-L, Yi H, Kuang X-M, Wang Y-M. Effect of entecavir on CD4+ T-cell subpopulations in patients with chronic hepatitis B. *Ann Hepatol* (2016) 15:174–82. doi:10.5604/16652681.1193705
62. Jimenez-Sousa MA, Almansa R, de la Fuente C, Caro-Paton A, Ruiz L, Sanchez-Antolín G, et al. Increased Th1, Th17 and pro-fibrotic responses in hepatitis C-infected patients are down-regulated after 12 weeks of treatment with pegylated interferon plus ribavirin. *Eur Cytokine Netw* (2010) 21:84–91. doi:10.1684/ecn.2010.0191
63. Xu L, Gong Y, Wang B, Shi K, Hou Y, Wang L, et al. A randomized trial of autologous bone marrow mesenchymal stem cells transplantation for HBV cirrhosis: regulation of Treg/Th17 cells. *J Gastroenterol Hepatol* (2014) 29:1620–8. doi:10.1111/jgh.12653
64. Zhai S, Zhang L, Dang S, Yu Y, Zhao Z, Zhao W, et al. The ratio of Th-17 to Treg cells is associated with survival of patients with acute-on-chronic hepatitis B liver failure. *Viral Immunol* (2011) 24:303–10. doi:10.1089/vim.2010.0135
65. Yu X, Guo R, Ming D, Su M, Lin C, Deng Y, et al. Ratios of regulatory T cells/T-helper 17 cells and transforming growth factor-β1/interleukin-17 to be associated with the development of hepatitis B virus-associated liver cirrhosis. *J Gastroenterol Hepatol* (2014) 29:1065–72. doi:10.1111/jgh.12459
66. Macek Jilkova Z, Afzal S, Marche H, Decaens T, Sturm N, Jouvin-Marche E, et al. Progression of fibrosis in patients with chronic viral hepatitis is associated with IL-17(+) neutrophils. *Liver Int* (2016) 36:1116–24. doi:10.1111/liv.13060
67. Taylor PR, Bonfield TL, Chmiel JF, Pearlman E. Neutrophils from F508del cystic fibrosis patients produce IL-17A and express IL-23 – dependent IL-17RC. *Clin Immunol* (2016) 170:53–60. doi:10.1016/j.clim.2016.03.016
68. Tu J-F, Pan H-Y, Ying X-H, Lou J, Ji J-S, Zou H. Mast cells comprise the major of interleukin 17-producing cells and predict a poor prognosis in hepatocellular carcinoma. *Medicine (Baltimore)* (2016) 95:e3220. doi:10.1097/MD.0000000000003220
69. Ashrafi Hafez A, Ahmadi Vasmehjani A, Baharlou R, Mousavi Nasab SD, Davami MH, Najfi A, et al. Analytical assessment of interleukin- 23 and -27 cytokines in healthy people and patients with hepatitis C virus infection (genotypes 1 and 3a). *Hepat Mon* (2014) 14:e21000. doi:10.5812/hepatmon.21000
70. Zhao L, Qiu DK, Ma X. Th17 cells: the emerging reciprocal partner of regulatory T cells in the liver. *J Dig Dis* (2010) 11:126–33. doi:10.1111/j.1751-2980.2010.00428.x
71. Ye Y, Xie X, Yu J, Zhou L, Xie H, Jiang G, et al. Involvement of Th17 and Th1 effector responses in patients with hepatitis B. *J Clin Immunol* (2010) 30:546–55. doi:10.1007/s10875-010-9416-3
72. Noack M, Miossec P. Th17 and regulatory T cell balance in autoimmune and inflammatory diseases. *Autoimmun Rev* (2014) 13:668–77. doi:10.1016/j.autrev.2013.12.004
73. O'Shea JJ, Paul WE. Mechanisms underlying lineage commitment and plasticity of helper CD4+ T cells. *Science* (2010) 327:1098–102. doi:10.1126/science.1178334
74. Kimura A, Kishimoto T. IL-6: regulator of Treg/Th17 balance. *Eur J Immunol* (2010) 40:1830–5. doi:10.1002/eji.201040391

75. Kleinewietfeld M, Hafler DA. The plasticity of human Treg and Th17 cells and its role in autoimmunity. *Semin Immunol* (2013) 25:305–12. doi:10.1016/j.smim.2013.10.009
76. Zhou L, Chong MM, Littman DR. Plasticity of CD4+ T cell lineage differentiation. *Immunity* (2009) 30:646–55. doi:10.1016/j.immuni.2009.05.001
77. Veldhoen M, Hocking RJ, Atkins CJ, Locksley RM, Stockinger B. TGFbeta in the context of an inflammatory cytokine milieu supports de novo differentiation of IL-17-producing T cells. *Immunity* (2006) 24:179–89. doi:10.1016/j.immuni.2006.01.001
78. Maddur MS, Miossec P, Kaveri SV, Bayry J. Th17 cells: biology, pathogenesis of autoimmune and inflammatory diseases, and therapeutic strategies. *Am J Pathol* (2012) 181:8–18. doi:10.1016/j.ajpath.2012.03.044
79. Xue-Song L, Cheng-Zhong L, Ying Z, Mo-Bin W. Changes of Treg and Th17 cells balance in the development of acute and chronic hepatitis B virus infection. *BMC Gastroenterol* (2012) 12:43. doi:10.1186/1471-230X-12-43
80. Mitra S, Anand S, Das A, Thapa B, Chawla YK, Minz RW. A molecular marker of disease activity in autoimmune liver diseases with histopathological correlation; FoXp3/RORγt ratio. *APMIS* (2015) 123:935–44. doi:10.1111/apm.12457
81. Yang Y, Liu YJ, Tang ST, Yang L, Yang J, Cao GQ, et al. Elevated Th17 cells accompanied by decreased regulatory T cells and cytokine environment in infants with biliary atresia. *Pediatr Surg Int* (2013) 29:1249–60. doi:10.1007/s00383-013-3421-6
82. Rong G, Zhou Y, Xiong Y, Zhou L, Geng H, Jiang T, et al. Imbalance between T helper type 17 and T regulatory cells in patients with primary biliary cirrhosis: the serum cytokine profile and peripheral cell population. *Clin Exp Immunol* (2009) 156:217–25. doi:10.1111/j.1365-2249.2009.03898.x
83. Fenoglio D, Bernuzzi F, Battaglia F, Parodi A, Kalli F, Negrini S, et al. Th17 and regulatory T lymphocytes in primary biliary cirrhosis and systemic sclerosis as models of autoimmune fibrotic diseases. *Autoimmun Rev* (2012) 12:300–4. doi:10.1016/j.autrev.2012.05.004
84. Zhong YM, Wu XR, Wang Q, Yu MF, Lu T, Zhao MY. [Changes in peripheral blood 25 – hydroxyvitamin D3, Th17 cells, and CD4(+) regulatory T cells and their clinical significance in patients with primary biliary cirrhosis]. *Zhonghua Gan Zang Bing Za Zhi* (2016) 24:829–33. doi:10.3760/cma.j.issn.1007-3418.2016.11.007
85. Rau M, Schilling A-K, Meertens J, Hering I, Weiss J, Jurowich C, et al. Progression from nonalcoholic fatty liver to nonalcoholic steatohepatitis is marked by a higher frequency of Th17 cells in the liver and an increased Th17/resting regulatory T cell ratio in peripheral blood and in the liver. *J Immunol* (2016) 196:97–105. doi:10.4049/jimmunol.1501175
86. Rolla S, Alchera E, Imarisio C, Bardina V, Valente G, Cappello P, et al. The balance between IL-17 and IL-22 produced by liver-infiltrating T-helper cells critically controls NASH development in mice. *Clin Sci (Lond)* (2016) 130:193–203. doi:10.1042/CS20150405
87. Chen D, Luo X, Xie H, Gao Z, Fang H, Huang J. Characteristics of IL-17 induction by *Schistosoma japonicum* infection in C57BL/6 mouse liver. *Immunology* (2013) 139:523–32. doi:10.1111/imm.12105
88. Tian F, Hu X, Xian K, Zong D, Liu H, Wei H, et al. B10 cells induced by *Schistosoma japonicum* soluble egg antigens modulated regulatory T cells and cytokine production of T cells. *Parasitol Res* (2015) 114:3827–34. doi:10.1007/s00436-015-4613-x
89. Shainheit MG, Lasocki KW, Finger E, Larkin BM, Smith PM, Sharpe AH, et al. The pathogenic Th17 cell response to major schistosome egg antigen is sequentially dependent on IL-23 and IL-1β. *J Immunol* (2011) 187:5328–35. doi:10.4049/jimmunol.1101445
90. Wang X, Sun L, Zhang L, Jiang Z. Effect of adoptive transfer or depletion of regulatory T cells on triptolide-induced liver injury. *Front Pharmacol* (2016) 7:99. doi:10.3389/fphar.2016.00099
91. Gu L, Deng W-S, Sun X-F, Zhou H, Xu Q. Rapamycin ameliorates CCl4-induced liver fibrosis in mice through reciprocal regulation of the Th17/Treg cell balance. *Mol Med Rep* (2016) 14:1153–61. doi:10.3892/mmr.2016.5392
92. Wang Q, Zheng Y, Huang Z, Tian Y, Zhou J, Mao Q, et al. Activated IL-23/IL-17 pathway closely correlates with increased Foxp3 expression in livers of chronic hepatitis B patients. *BMC Immunol* (2011) 12:25. doi:10.1186/1471-2172-12-25
93. Wang Q, Zhou J, Zhang B, Tian Z, Tang J, Zheng Y, et al. Hepatitis B virus induces IL-23 production in antigen presenting cells and causes liver damage via the IL-23/IL-17 axis. *PLoS Pathog* (2013) 9:e1003410. doi:10.1371/journal.ppat.1003410
94. Yan J, Liu X-L, Xiao G, Li N-L, Deng Y-N, Han L-Z, et al. Prevalence and clinical relevance of T-helper cells, Th17 and Th1, in hepatitis B virus-related hepatocellular carcinoma. *PLoS One* (2014) 9:e96080. doi:10.1371/journal.pone.0096080
95. Yang C, Cui F, Chen L, Gong X, Qin B. Correlation between Th17 and nTreg cell frequencies and the stages of progression in chronic hepatitis B. *Mol Med Rep* (2015) 13:853–9. doi:10.3892/mmr.2015.4618
96. Feng H, Yin J, Han Y-P, Zhou X-Y, Chen S, Yang L, et al. Regulatory T cells and IL-17(+) T helper cells enhanced in patients with chronic hepatitis B virus infection. *Int J Clin Exp Med* (2015) 8:8674–85.
97. Zhao R-R, Yang X-F, Dong J, Zhao Y-Y, Wei X, Huang C-X, et al. Toll-like receptor 2 promotes T helper 17 cells response in hepatitis B virus infection. *Int J Clin Exp Med* (2015) 8:7315–23.
98. Shi M, Wei J, Dong J, Meng W, Ma J, Wang T, et al. Function of interleukin-17 and -35 in the blood of patients with hepatitis B-related liver cirrhosis. *Mol Med Rep* (2015) 11:121–6. doi:10.3892/mmr.2014.2681
99. Wang Y, Zhang M, Liu Z-W, Ren W-G, Shi Y-C, Sun Y-L, et al. The ratio of circulating regulatory T cells (Tregs)/Th17 cells is associated with acute allograft rejection in liver transplantation. *PLoS One* (2014) 9:e112135. doi:10.1371/journal.pone.0112135
100. Hu X, Ma S, Huang X, Jiang X, Zhu X, Gao H, et al. Interleukin-21 is upregulated in hepatitis B-related acute-on-chronic liver failure and associated with severity of liver disease. *J Viral Hepat* (2011) 18:458–67. doi:10.1111/j.1365-2893.2011.01475.x
101. Yang L, Anderson DE, Baecher-Allan C, Hastings WD, Bettelli E, Oukka M, et al. IL-21 and TGF-β are required for differentiation of human TH17 cells. *Nature* (2008) 454:350–2. doi:10.1038/nature07021
102. Chung Y, Chang SH, Martinez GJ, Yang XO, Nurieva R, Kang HS, et al. Critical regulation of early Th17 cell differentiation by interleukin-1 signaling. *Immunity* (2009) 30:576–87. doi:10.1016/j.immuni.2009.02.007
103. Sutton CE, Lalor SJ, Sweeney CM, Brereton CF, Lavelle EC, Mills KH. Interleukin-1 and IL-23 induce innate IL-17 production from gammadelta T cells, amplifying Th17 responses and autoimmunity. *Immunity* (2009) 31:331–41. doi:10.1016/j.immuni.2009.08.001
104. Zhou L, Ivanov II, Spolski R, Min R, Shenderov K, Egawa T, et al. IL-6 programs TH-17 cell differentiation by promoting sequential engagement of the IL-21 and IL-23 pathways. *Nat Immunol* (2007) 8:967–74. doi:10.1038/ni1488
105. Acosta-Rodriguez EV, Napolitani G, Lanzavecchia A, Sallusto F. Interleukins 1beta and 6 but not transforming growth factor-beta are essential for the differentiation of interleukin 17-producing human T helper cells. *Nat Immunol* (2007) 8:942–9. doi:10.1038/ni1496
106. Lu X, Xu Q, Bu X, Ma X, Zhang F, Deng Q, et al. Relationship between expression of toll-like receptors 2/4 in dendritic cells and chronic hepatitis B virus infection. *Int J Clin Exp Pathol* (2014) 7:6048–55.
107. Benwell RK, Lee DR. Essential and synergistic roles of IL1 and IL6 in human Th17 differentiation directed by TLR ligand-activated dendritic cells. *Clin Immunol* (2010) 134:178–87. doi:10.1016/j.clim.2009.09.013
108. Korn T, Bettelli E, Gao W, Awasthi A, Jäger A, Strom TB, et al. IL-21 initiates an alternative pathway to induce proinflammatory TH17 cells. *Nature* (2007) 448:484–7. doi:10.1038/nature05970
109. Lee H-C, Sung S-SJ, Krueger PD, Jo Y-A, Rosen HR, Ziegler SF, et al. Hepatitis C virus promotes t-helper (Th)17 responses through thymic stromal lymphopoietin production by infected hepatocytes. *Hepatology* (2013) 57:1314–24. doi:10.1002/hep.26128
110. Yu H, Huang J, Liu Y, Ai G, Yan W, Wang X, et al. IL-17 contributes to autoimmune hepatitis. *J Huazhong Univ Sci Technolog Med Sci* (2010) 30:443–6. doi:10.1007/s11596-010-0446-0
111. Longhi MS, Liberal R, Holder B, Robson SC, Ma Y, Mieli-Vergani G, et al. Inhibition of interleukin-17 promotes differentiation of $CD25^-$ cells into stable T regulatory cells in patients with autoimmune hepatitis. *Gastroenterology* (2012) 142:1526–35.e6. doi:10.1053/j.gastro.2012.02.041
112. Katt J, Schwinge D, Schoknecht T, Quaas A, Sobottka I, Burandt E, et al. Increased T helper type 17 response to pathogen stimulation in patients with primary sclerosing cholangitis. *Hepatology* (2013) 58:1084–93. doi:10.1002/hep.26447
113. Kunzmann L, Schoknecht T, Stein S, Ehlken H, Hartl J, Pannicke N, et al. Increased in vivo and in vitro TH17 differentiation in patients with primary

sclerosing cholangitis. *Z Gastroenterol* (2016) 54:1343–404. doi:10.1055/s-0036-1597393
114. Yang CY, Ma X, Tsuneyama K, Huang S, Takahashi T, Chalasani NP, et al. IL-12/Th1 and IL-23/Th17 biliary microenvironment in primary biliary cirrhosis: implications for therapy. *Hepatology* (2014) 59:1944–53. doi:10.1002/hep.26979
115. Huang Q, Chu S, Yin X, Yu X, Kang C, Li X, et al. Interleukin-17A-induced epithelial-mesenchymal transition of human intrahepatic biliary epithelial cells: implications for primary biliary cirrhosis. *Tohoku J Exp Med* (2016) 240:269–75. doi:10.1620/tjem.240.269
116. Lages CS, Simmons J, Maddox A, Jones K, Karns R, Sheridan R, et al. The dendritic cell-T helper 17-macrophage axis controls cholangiocyte injury and disease progression in murine and human biliary atresia. *Hepatology* (2017) 65:174–88. doi:10.1002/hep.28851
117. Paquissi FC. Immune imbalances in non-alcoholic fatty liver disease: from general biomarkers and neutrophils to interleukin-17 axis activation and new therapeutic targets. *Front Immunol* (2016) 7:490. doi:10.3389/fimmu.2016.00490
118. Giles DA, Moreno-Fernandez ME, Stankiewicz TE, Cappelletti M, Huppert SS, Iwakura Y, et al. Regulation of inflammation by IL-17A and IL-17F modulates non-alcoholic fatty liver disease pathogenesis. *PLoS One* (2016) 11:e0149783. doi:10.1371/journal.pone.0149783
119. Zhao J, Zhang Z, Luan Y, Zou Z, Sun Y, Li Y, et al. Pathological functions of interleukin-22 in chronic liver inflammation and fibrosis with hepatitis B virus infection by promoting T helper 17 cell recruitment. *Hepatology* (2014) 59:1331–42. doi:10.1002/hep.26916
120. Oo YH, Banz V, Kavanagh D, Liaskou E, Withers DR, Humphreys E, et al. CXCR3-dependent recruitment and CCR6-mediated positioning of Th-17 cells in the inflamed liver. *J Hepatol* (2012) 57:1044–51. doi:10.1016/j.jhep.2012.07.008
121. Xu Z, Zhang X, Lau J, Yu J. C-X-C motif chemokine 10 in non-alcoholic steatohepatitis: role as a pro-inflammatory factor and clinical implication. *Expert Rev Mol Med* (2016) 18:e16. doi:10.1017/erm.2016.16
122. Zhang X, Han J, Man K, Li X, Du J, Chu ES, et al. CXC chemokine receptor 3 promotes steatohepatitis in mice through mediating inflammatory cytokines, macrophages and autophagy. *J Hepatol* (2016) 64:160–70. doi:10.1016/j.jhep.2015.09.005
123. Arsent'eva NA, Semenov AV, Lyubimova NE, Ostankov YV, Elezo DS, Kudryavtsev IV, et al. Chemokine receptors CXCR3 and CCR6 and their ligands in the liver and blood of patients with chronic hepatitis C. *Bull Exp Biol Med* (2015) 160:252–5. doi:10.1007/s10517-015-3142-z
124. Hintermann E, Bayer M, Pfeilschifter JM, Luster AD, Christen U. CXCL10 promotes liver fibrosis by prevention of NK cell mediated hepatic stellate cell inactivation. *J Autoimmun* (2010) 35:424–35. doi:10.1016/j.jaut.2010.09.003
125. Marra F, Tacke F. Roles for chemokines in liver disease. *Gastroenterology* (2014) 147:577–94.e1. doi:10.1053/j.gastro.2014.06.043
126. Seki E, Schwabe RF. Hepatic inflammation and fibrosis: functional links and key pathways. *Hepatology* (2015) 61:1066–79. doi:10.1002/hep.27332
127. Fabre T, Kared H, Friedman SL, Shoukry NH. IL-17A enhances the expression of profibrotic genes through upregulation of the TGF-β receptor on hepatic stellate cells in a JNK-dependent manner. *J Immunol* (2014) 193:3925–33. doi:10.4049/jimmunol.1400861
128. Amara S, Lopez K, Banan B, Brown S-K, Whalen M, Myles E, et al. Synergistic effect of pro-inflammatory TNFα and IL-17 in periostin mediated collagen deposition: potential role in liver fibrosis. *Mol Immunol* (2015) 64:26–35. doi:10.1016/j.molimm.2014.10.021
129. Li XL, Dou YC, Liu Y, Shi CW, Cao LL, Zhang XQ, et al. Atorvastatin ameliorates experimental autoimmune neuritis by decreased Th1/Th17 cytokines and up-regulated T regulatory cells. *Cell Immunol* (2011) 271:455–61. doi:10.1016/j.cellimm.2011.08.015
130. Li J, Lau GK-K, Chen L, Dong S, Lan H-Y, Huang X-R, et al. Interleukin 17A promotes hepatocellular carcinoma metastasis via NF-kB induced matrix metalloproteinases 2 and 9 expression. *PLoS One* (2011) 6:e21816. doi:10.1371/journal.pone.0021816
131. Cortez DM, Feldman MD, Mummidi S, Valente AJ, Steffensen B, Vincenti M, et al. IL-17 stimulates MMP-1 expression in primary human cardiac fibroblasts via p38 MAPK- and ERK1/2-dependent C/EBP-beta, NF-kappaB, and AP-1 activation. *Am J Physiol Heart Circ Physiol* (2007) 293:H3356–65. doi:10.1152/ajpheart.00928.2007
132. Bi W-R, Yang C-Q, Shi Q. Transforming growth factor-β1 induced epithelial-mesenchymal transition in hepatic fibrosis. *Hepatogastroenterology* (2012) 59:1960–3. doi:10.5754/hge11750
133. Hara M, Kono H, Furuya S, Hirayama K, Tsuchiya M, Fujii H. Interleukin-17A plays a pivotal role in cholestatic liver fibrosis in mice. *J Surg Res* (2013) 183:574–82. doi:10.1016/j.jss.2013.03.025
134. Sørensen KK, Simon-Santamaria J, McCuskey RS, Smedsrød B. Liver sinusoidal endothelial cells. *Compr Physiol* (2015) 5:1751–74. doi:10.1002/cphy.c140078
135. Puche JE, Saiman Y, Friedman SL. Hepatic stellate cells and liver fibrosis. *Compr Physiol* (2013) 3:1473–92. doi:10.1002/cphy.c120035
136. Hernandez-Gea V, Friedman SL. Pathogenesis of liver fibrosis. *Annu Rev Pathol* (2011) 6:425–56. doi:10.1146/annurev-pathol-011110-130246
137. Xu J, Wang J, Hu Y, Cheng L, Yu H. [Associations between interleukin-17A expression and epithelial-mesenchymal transition in patients with hepatocellular carcinoma]. *Zhonghua Zhong Liu Za Zhi* (2015) 37:585–90.
138. Kaimori A, Potter J, Kaimori J, Wang C, Mezey E, Koteish A. Transforming growth factor-beta1 induces an epithelial-to-mesenchymal transition state in mouse hepatocytes *in vitro*. *J Biol Chem* (2007) 282:22089–101. doi:10.1074/jbc.M700998200
139. Kaimori A, Potter JJ, Choti M, Ding Z, Mezey E, Koteish AA. Histone deacetylase inhibition suppresses the transforming growth factor β1-induced epithelial-to-mesenchymal transition in hepatocytes. *Hepatology* (2010) 52:1033–45. doi:10.1002/hep.23765
140. Chen Y-L, Lv J, Ye X-L, Sun M-Y, Xu Q, Liu C-H, et al. Sorafenib inhibits transforming growth factor β1-mediated epithelial-mesenchymal transition and apoptosis in mouse hepatocytes. *Hepatology* (2011) 53:1708–18. doi:10.1002/hep.24254
141. Ji X, Li J, Xu L, Wang W, Luo M, Luo S, et al. IL4 and IL-17A provide a Th2/Th17-polarized inflammatory milieu in favor of TGF-β1 to induce bronchial epithelial-mesenchymal transition (EMT). *Int J Clin Exp Pathol* (2013) 6:1481–92.
142. Vittal R, Fan L, Greenspan DS, Mickler EA, Gopalakrishnan B, Gu H, et al. IL-17 induces type V collagen overexpression and EMT via TGF-β-dependent pathways in obliterative bronchiolitis. *Am J Physiol Lung Cell Mol Physiol* (2013) 304:L401–14. doi:10.1152/ajplung.00080.2012
143. Zhang Q, Liu S, Parajuli KR, Zhang W, Zhang K, Mo Z, et al. Interleukin-17 promotes prostate cancer via MMP7-induced epithelial-to-mesenchymal transition. *Oncogene* (2017) 36:687–99. doi:10.1038/onc.2016.240
144. Gu K, Li M-M, Shen J, Liu F, Cao J-Y, Jin S, et al. Interleukin-17-induced EMT promotes lung cancer cell migration and invasion via NF-κB/ZEB1 signal pathway. *Am J Cancer Res* (2015) 5:1169–79.
145. Xiao S, Jin H, Korn T, Liu SM, Oukka M, Lim B, et al. Retinoic acid increases Foxp3+ regulatory T cells and inhibits development of Th17 cells by enhancing TGF-beta-driven Smad3 signaling and inhibiting IL-6 and IL-23 receptor expression. *J Immunol* (2008) 181:2277–84. doi:10.4049/jimmunol.181.4.2277
146. Dunham RM, Thapa M, Velazquez VM, Elrod EJ, Denning TL, Pulendran B, et al. Hepatic stellate cells preferentially induce Foxp3+ regulatory T cells by production of retinoic acid. *J Immunol* (2013) 190:2009–16. doi:10.4049/jimmunol.1201937
147. Lee Y-S, Jeong W-I. Retinoic acids and hepatic stellate cells in liver disease. *J Gastroenterol Hepatol* (2012) 27:75–9. doi:10.1111/j.1440-1746.2011.07007.x
148. Ichikawa S, Mucida D, Tyznik AJ, Kronenberg M, Cheroutre H. Hepatic stellate cells function as regulatory bystanders. *J Immunol* (2011) 186:5549–55. doi:10.4049/jimmunol.1003917
149. Seki E, De Minicis S, Osterreicher CH, Kluwe J, Osawa Y, Brenner DA, et al. TLR4 enhances TGF-beta signaling and hepatic fibrosis. *Nat Med* (2007) 13:1324–32. doi:10.1038/nm1663
150. Xu R, Tao A, Zhang S, Zhang M. Neutralization of interleukin-17 attenuates high fat diet-induced non-alcoholic fatty liver disease in mice. *Acta Biochim Biophys Sin (Shanghai)* (2013) 45:726–33. doi:10.1093/abbs/gmt065
151. Chen J, Liao M, Gao X, Zhong Q, Tang T, Yu X, et al. IL-17A induces pro-inflammatory cytokines production in macrophages via MAPKinases, NF-κB and AP-1. *Cell Physiol Biochem* (2013) 32:1265–74. doi:10.1159/000354525
152. Kono H, Fujii H, Ogiku M, Hosomura N, Amemiya H, Tsuchiya M, et al. Role of IL-17A in neutrophil recruitment and hepatic injury after warm ischemia-reperfusion mice. *J Immunol* (2011) 187:4818–25. doi:10.4049/jimmunol.1100490

153. Luedde T, Schwabe RF. NF-κB in the liver – linking injury, fibrosis and hepatocellular carcinoma. *Nat Rev Gastroenterol Hepatol* (2011) 8:108–18. doi:10.1038/nrgastro.2010.213
154. Gao J, Jiang Z, Wang S, Zhou Y, Shi X, Feng M. Endoplasmic reticulum stress of Kupffer cells involved in the conversion of natural regulatory T cells to Th17 cells in liver ischemia-reperfusion injury. *J Gastroenterol Hepatol* (2016) 31:883–9. doi:10.1111/jgh.13163
155. McAllister F, Henry A, Kreindler JL, Dubin PJ, Ulrich L, Steele C, et al. Role of IL-17A, IL-17F, and the IL-17 receptor in regulating growth-related oncogene-alpha and granulocyte colony-stimulating factor in bronchial epithelium: implications for airway inflammation in cystic fibrosis. *J Immunol* (2005) 175:404–12. doi:10.4049/jimmunol.175.1.404
156. Jones CE, Chan K. Interleukin-17 stimulates the expression of interleukin-8, growth-related oncogene-alpha, and granulocyte-colony-stimulating factor by human airway epithelial cells. *Am J Respir Cell Mol Biol* (2002) 26:748–53. doi:10.1165/ajrcmb.26.6.4757
157. Liu B, Tan W, Barsoum A, Gu X, Chen K, Huang W, et al. IL-17 is a potent synergistic factor with GM-CSF in mice in stimulating myelopoiesis, dendritic cell expansion, proliferation, and functional enhancement. *Exp Hematol* (2010) 38:877–84.e1. doi:10.1016/j.exphem.2010.06.004
158. Ko H-J, Brady JL, Ryg-Cornejo V, Hansen DS, Vremec D, Shortman K, et al. GM-CSF-responsive monocyte-derived dendritic cells are pivotal in Th17 pathogenesis. *J Immunol* (2014) 192:2202–9. doi:10.4049/jimmunol.1302040
159. Gu Y, Hu X, Liu C, Qv X, Xu C. Interleukin (IL)-17 promotes macrophages to produce IL-8, IL-6 and tumour necrosis factor-alpha in aplastic anaemia. *Br J Haematol* (2008) 142:109–14. doi:10.1111/j.1365-2141.2008.07161.x
160. Dragon S, Rahman MS, Yang J, Unruh H, Halayko AJ, Gounni AS. IL-17 enhances IL-1beta-mediated CXCL-8 release from human airway smooth muscle cells. *Am J Physiol Lung Cell Mol Physiol* (2006) 292:L1023–9. doi:10.1152/ajplung.00306.2006
161. Mei J, Liu Y, Dai N, Hoffmann C, Hudock KM, Zhang P, et al. Cxcr2 and Cxcl5 regulate the IL-17/G-CSF axis and neutrophil homeostasis in mice. *J Clin Invest* (2012) 122:974–86. doi:10.1172/JCI60588
162. Khanam A, Trehanpati N, Riese P, Rastogi A, Guzman CA, Sarin SK. Blockade of neutrophil's chemokine receptors CXCR1/2 abrogate liver damage in acute-on-chronic liver failure. *Front Immunol* (2017) 8:464. doi:10.3389/fimmu.2017.00464
163. Mizutani N, Nabe T, Yoshino S. IL-17A promotes the exacerbation of IL-33-induced airway hyperresponsiveness by enhancing neutrophilic inflammation via CXCR2 signaling in mice. *J Immunol* (2014) 192:1372–84. doi:10.4049/jimmunol.1301538
164. Pelletier M, Maggi L, Micheletti A, Lazzeri E, Tamassia N, Costantini C, et al. Evidence for a cross-talk between human neutrophils and Th17 cells. *Blood* (2010) 115:335–43. doi:10.1182/blood-2009-04-216085
165. Chakrabarti S, Patel KD. Regulation of matrix metalloproteinase-9 release from IL-8-stimulated human neutrophils. *J Leukoc Biol* (2005) 78:279–88. doi:10.1189/jlb.1004612
166. Chakrabarti S, Zee JM, Patel KD. Regulation of matrix metalloproteinase-9 (MMP-9) in TNF-stimulated neutrophils: novel pathways for tertiary granule release. *J Leukoc Biol* (2006) 79:214–22. doi:10.1189/jlb.0605353
167. Ohashi N, Hori T, Chen F, Jermanus S, Nakao A, Uemoto S, et al. Matrix metalloproteinase-9 in the initial injury after hepatectomy in mice. *World J Gastroenterol* (2013) 19:3027–42. doi:10.3748/wjg.v19.i20.3027
168. Seubert B, Grünwald B, Kobuch J, Cui H, Schelter F, Schaten S, et al. Tissue inhibitor of metalloproteinases (TIMP)-1 creates a premetastatic niche in the liver through SDF-1/CXCR4-dependent neutrophil recruitment in mice. *Hepatology* (2015) 61:238–48. doi:10.1002/hep.27378
169. O'Brien KM, Allen KM, Rockwell CE, Towery K, Luyendyk JP, Copple BL. IL-17A synergistically enhances bile acid-induced inflammation during obstructive cholestasis. *Am J Pathol* (2013) 183:1498–507. doi:10.1016/j.ajpath.2013.07.019
170. Liao C-C, Day Y-J, Lee H-C, Liou J-T, Chou A-H, Liu F-C. Baicalin attenuates IL-17-mediated acetaminophen-induced liver injury in a mouse model. *PLoS One* (2016) 11:e0166856. doi:10.1371/journal.pone.0166856
171. Zhang Y, Huang D, Gao W, Yan J, Zhou W, Hou X, et al. Lack of IL-17 signaling decreases liver fibrosis in murine schistosomiasis japonica. *Int Immunol* (2015) 27:317–25. doi:10.1093/intimm/dxv017
172. Zhang Y, Chen L, Gao W, Hou X, Gu Y, Gui L, et al. IL-17 neutralization significantly ameliorates hepatic granulomatous inflammation and liver damage in *Schistosoma japonicum* infected mice. *Eur J Immunol* (2012) 42:1523–35. doi:10.1002/eji.201141933
173. Xu L, Chen S, Xu K. IL-17 expression is correlated with hepatitis B-related liver diseases and fibrosis. *Int J Mol Med* (2011) 27:385–92. doi:10.3892/ijmm.2011.594
174. Liao R, Sun J, Wu H, Yi Y, Wang J-X, He H-W, et al. High expression of IL-17 and IL-17RE associate with poor prognosis of hepatocellular carcinoma. *J Exp Clin Cancer Res* (2013) 32:3. doi:10.1186/1756-9966-32-3
175. Zhang J-P, Yan J, Xu J, Pang X-H, Chen M-S, Li L, et al. Increased intratumoral IL-17-producing cells correlate with poor survival in hepatocellular carcinoma patients. *J Hepatol* (2009) 50:980–9. doi:10.1016/j.jhep.2008.12.033
176. Xu X, Su L, Gao Y, Ding Y. The prevalence of nonalcoholic fatty liver disease and related metabolic comorbidities was associated with age at onset of moderate to severe plaque psoriasis: a cross-sectional study. *PLoS One* (2017) 12:e0169952. doi:10.1371/journal.pone.0169952
177. Dalekos GN, Obermayer-Straub P, Bartels M, Maeda T, Kayser A, Braun S, et al. Cytochrome P450 2A6: a new hepatic autoantigen in patients with chronic hepatitis C virus infection. *J Hepatol* (2003) 39:800–6. doi:10.1016/S0168-8278(03)00356-8
178. Dalekos GN, Makri E, Loges S, Obermayer-Straub P, Zachou K, Tsikrikas T, et al. Increased incidence of anti-LKM autoantibodies in a consecutive cohort of hepatitis C patients from central Greece. *Eur J Gastroenterol Hepatol* (2002) 14:35–42. doi:10.1097/00042737-200201000-00007
179. Holdener M, Hintermann E, Bayer M, Rhode A, Rodrigo E, Hintereder G, et al. Breaking tolerance to the natural human liver autoantigen cytochrome P450 2D6 by virus infection. *J Exp Med* (2008) 205:1409–22. doi:10.1084/jem.20071859
180. Kitazawa E, Igarashi T, Kawaguchi N, Matsushima H, Kawashima Y, Hankins RW, et al. Differences in anti-LKM-1 autoantibody immunoreactivity to CYP2D6 antigenic sites between hepatitis C virus-negative and -positive patients. *J Autoimmun* (2001) 17:243–9. doi:10.1006/jaut.2001.0565
181. Hammerich L, Heymann F, Tacke F. Role of IL-17 and Th17 cells in liver diseases. *Clin Dev Immunol* (2011) 2011:345803. doi:10.1155/2011/345803
182. Grant CR, Liberal R, Holder BS, Cardone J, Ma Y, Robson SC, et al. Dysfunctional CD39(POS) regulatory T cells and aberrant control of T-helper type 17 cells in autoimmune hepatitis. *Hepatology* (2014) 59:1007–15. doi:10.1002/hep.26583
183. Biancheri P, Pender SL, Ammoscato F, Giuffrida P, Sampietro G, Ardizzone S, et al. The role of interleukin 17 in Crohn's disease-associated intestinal fibrosis. *Fibrogenesis Tissue Repair* (2013) 6:13. doi:10.1186/1755-1536-6-13
184. Geng J, Zhang K, Chen L, Miao J, Yao M, Ren Y, et al. Enhancement of CD147 on M1 macrophages induces differentiation of Th17 cells in the lung interstitial fibrosis. *Biochim Biophys Acta* (2014) 1842:1770–82. doi:10.1016/j.bbadis.2014.06.008
185. Bozinovski S, Seow HJ, Chan SP, Anthony D, McQualter J, Hansen M, et al. Innate cellular sources of interleukin-17A regulate macrophage accumulation in cigarette-smoke-induced lung inflammation in mice. *Clin Sci (Lond)* (2015) 129:785–96. doi:10.1042/CS20140703
186. González-Mateo GT, Fernández-Míllara V, Bellón T, Liappas G, Ruiz-Ortega M, López-Cabrera M, et al. Paricalcitol reduces peritoneal fibrosis in mice through the activation of regulatory T cells and reduction in IL-17 production. *PLoS One* (2014) 9:e108477. doi:10.1371/journal.pone.0108477
187. Lee J, Lee J, Park M-K, Lim M-A, Park E-M, Kim E-K, et al. Interferon gamma suppresses collagen-induced arthritis by regulation of Th17 through the induction of indoleamine-2,3-deoxygenase. *PLoS One* (2013) 8:e60900. doi:10.1371/journal.pone.0060900
188. Zhang S, Huang D, Weng J, Huang Y, Liu S, Zhang Q, et al. Neutralization of interleukin-17 attenuates cholestatic liver fibrosis in mice. *Scand J Immunol* (2016) 83:102–8. doi:10.1111/sji.12395
189. Mi S, Li Z, Yang H-Z, Liu H-Z, Wang J-P, Ma Y-G, et al. Blocking IL-17A promotes the resolution of pulmonary inflammation and fibrosis via TGF-beta1-dependent and -independent mechanisms. *J Immunol* (2011) 187:3003–14. doi:10.4049/jimmunol.1004081
190. Guillot A, Hamdaoui N, Bizy A, Zoltani K, Souktani R, Zafrani E-S, et al. Cannabinoid receptor 2 counteracts interleukin-17-induced immune and

fibrogenic responses in mouse liver. *Hepatology* (2014) 59:296–306. doi:10.1002/hep.26598
191. Zheng L, Chu J, Shi Y, Zhou X, Tan L, Li Q, et al. Bone marrow-derived stem cells ameliorate hepatic fibrosis by down-regulating interleukin-17. *Cell Biosci* (2013) 3:46. doi:10.1186/2045-3701-3-46
192. Tian A, Ma H, Cao X, Zhang R, Wang X, Wu B. Vitamin D improves cognitive function and modulates Th17/T reg cell balance after hepatectomy in mice. *Inflammation* (2015) 38:500–9. doi:10.1007/s10753-014-9956-4
193. Ikeda U, Wakita D, Ohkuri T, Chamoto K, Kitamura H, Iwakura Y, et al. 1α,25-Dihydroxyvitamin D3 and all-trans retinoic acid synergistically inhibit the differentiation and expansion of Th17 cells. *Immunol Lett* (2010) 134:7–16. doi:10.1016/j.imlet.2010.07.002
194. Abramovitch S, Sharvit E, Weisman Y, Bentov A, Brazowski E, Cohen G, et al. Vitamin D inhibits development of liver fibrosis in an animal model but cannot ameliorate established cirrhosis. *Am J Physiol Gastrointest Liver Physiol* (2015) 308:G112–20. doi:10.1152/ajpgi.00132.2013
195. Li WW, Sun P, Chen DD, Wang WQ, Jiao GH, Wang YJ, et al. [Preventive and therapeutic effects of rapamycin against autoimmune hepatitis and liver fibrosis and possible mechanisms]. *Zhonghua Gan Zang Bing Za Zhi* (2016) 24:368–74. doi:10.3760/cma.j.issn.1007-3418.2016.05.011
196. Sundrud MS, Koralov SB, Feuerer M, Calado DP, Kozhaya AE, Rhule-Smith A, et al. Halofuginone inhibits TH17 cell differentiation by activating the amino acid starvation response. *Science* (2009) 324:1334–8. doi:10.1126/science.1172638
197. Liang J, Zhang B, Shen R-W, Liu J-B, Gao M-H, Geng X, et al. The effect of antifibrotic drug halofugine on Th17 cells in concanavalin A-induced liver fibrosis. *Scand J Immunol* (2014) 79:163–72. doi:10.1111/sji.12144
198. Zhang H, Ju B, Zhang X, Zhu Y, Nie Y, Xu Y, et al. Magnolol attenuates concanavalin A-induced hepatic fibrosis, inhibits CD4(+) T helper 17 (Th17) cell differentiation and suppresses hepatic stellate cell activation: blockade of Smad3/Smad4 signalling. *Basic Clin Pharmacol Toxicol* (2017) 120:560–70. doi:10.1111/bcpt.12749
199. Schon H-T, Bartneck M, Borkham-Kamphorst E, Nattermann J, Lammers T, Tacke F, et al. Pharmacological intervention in hepatic stellate cell activation and hepatic fibrosis. *Front Pharmacol* (2016) 7:33. doi:10.3389/fphar.2016.00033
200. Li X, Jin Q, Yao Q, Xu B, Li Z, Tu C. Quercetin attenuates the activation of hepatic stellate cells and liver fibrosis in mice through modulation of HMGB1-TLR2/4-NF-κB signaling pathways. *Toxicol Lett* (2016) 261:1–12. doi:10.1016/j.toxlet.2016.09.002
201. Ma J-Q, Li Z, Xie W-R, Liu C-M, Liu S-S. Quercetin protects mouse liver against CCl4-induced inflammation by the TLR2/4 and MAPK/NF-κB pathway. *Int Immunopharmacol* (2015) 28:531–9. doi:10.1016/j.intimp.2015.06.036
202. Shu J-C, He Y-J, Lv X, Ye G-R, Wang L-X. Curcumin prevents liver fibrosis by inducing apoptosis and suppressing activation of hepatic stellate cells. *J Nat Med* (2009) 63:415–20. doi:10.1007/s11418-009-0347-3
203. Liu M, Xu Y, Han X, Yin L, Xu L, Qi Y, et al. Dioscin alleviates alcoholic liver fibrosis by attenuating hepatic stellate cell activation via the TLR4/MyD88/NF-κB signaling pathway. *Sci Rep* (2015) 5:18038. doi:10.1038/srep18038
204. Samuhasaneeto S, Thong-Ngam D, Kulaputana O, Suyasunanont D, Klaikeaw N. Curcumin decreased oxidative stress, inhibited NF-kappaB activation, and improved liver pathology in ethanol-induced liver injury in rats. *J Biomed Biotechnol* (2009) 2009:981963. doi:10.1155/2009/981963
205. Zhang H, Sun Q, Xu T, Hong L, Fu R, Wu J, et al. Resveratrol attenuates the progress of liver fibrosis via the Akt/nuclear factor-κB pathways. *Mol Med Rep* (2015) 13:224–30. doi:10.3892/mmr.2015.4497
206. Nunez Lopez O, Bohanon FJ, Wang X, Ye N, Corsello T, Rojas-Khalil Y, et al. STAT3 inhibition suppresses hepatic stellate cell fibrogenesis: HJC0123, a potential therapeutic agent for liver fibrosis. *RSC Adv* (2016) 6:100652–63. doi:10.1039/C6RA17459K
207. Gu Y-J, Sun W-Y, Zhang S, Li X-R, Wei W. Targeted blockade of JAK/STAT3 signaling inhibits proliferation, migration and collagen production as well as inducing the apoptosis of hepatic stellate cells. *Int J Mol Med* (2016) 38:903–11. doi:10.3892/ijmm.2016.2692
208. Lee SJ, Yang EK, Kim SG. Peroxisome proliferator-activated receptor-gamma and retinoic acid X receptor alpha represses the TGFbeta1 gene via PTEN-mediated p70 ribosomal S6 kinase-1 inhibition: role for Zf9 dephosphorylation. *Mol Pharmacol* (2006) 70:415–25. doi:10.1124/mol.106.022954
209. Hazem SH, Shaker ME, Ashamallah SA, Ibrahim TM. The novel Janus kinase inhibitor ruxolitinib confers protection against carbon tetrachloride-induced hepatotoxicity via multiple mechanisms. *Chem Biol Interact* (2014) 220:116–27. doi:10.1016/j.cbi.2014.06.017
210. Shaker ME, Hazem SH, Ashamallah SA. Inhibition of the JAK/STAT pathway by ruxolitinib ameliorates thioacetamide-induced hepatotoxicity. *Food Chem Toxicol* (2016) 96:290–301. doi:10.1016/j.fct.2016.08.018

Conflict of Interest Statement: The author declares that the research was conducted in the absence of any commercial or financial relationships that could be construed as a potential conflict of interest.

Copyright © 2017 Paquissi. This is an open-access article distributed under the terms of the Creative Commons Attribution License (CC BY). The use, distribution or reproduction in other forums is permitted, provided the original author(s) or licensor are credited and that the original publication in this journal is cited, in accordance with accepted academic practice. No use, distribution or reproduction is permitted which does not comply with these terms.

frontiers in Immunology

ORIGINAL RESEARCH
published: 23 October 2017
doi: 10.3389/fimmu.2017.01325

Inhibition of Pro-inflammatory and Anti-apoptotic Biomarkers during Experimental Oral Cancer Chemoprevention by Dietary Black Raspberries

Steve Oghumu[1,2], Bruce C. Casto[1,2], Jennifer Ahn-Jarvis[1], Logan C. Weghorst[1], Jim Maloney[1], Paul Geuy[1], Kyle Z. Horvath[1], Claire E. Bollinger[1], Blake M. Warner[3], Kurt F. Summersgill[3], Christopher M. Weghorst[1,2,4]* and Thomas J. Knobloch[1,2]**

[1] Division of Environmental Health Sciences, College of Public Health, The Ohio State University Columbus, Columbus, OH, United States, [2] Comprehensive Cancer Center, The Ohio State University Columbus, Columbus, OH, United States, [3] School of Dental Medicine, University of Pittsburgh, Pittsburgh, PA, United States, [4] Department of Otolaryngology, College of Medicine, The Ohio State University Columbus, Columbus, OH, United States

OPEN ACCESS

Edited by:
Jixin Zhong,
Case Western Reserve University,
United States

Reviewed by:
Penghua Yang,
University of Maryland,
United States
Xiaojing Yue,
La Jolla Institute for Allergy and Immunology, United States

***Correspondence:**
Steve Oghumu
oghumu.1@osu.edu;
Christopher M. Weghorst
weghorst.2@osu.edu;
Thomas J. Knobloch
knobloch.1@osu.edu

Specialty section:
This article was submitted to Inflammation, a section of the journal Frontiers in Immunology

Received: 09 August 2017
Accepted: 29 September 2017
Published: 23 October 2017

Citation:
Oghumu S, Casto BC, Ahn-Jarvis J, Weghorst LC, Maloney J, Geuy P, Horvath KZ, Bollinger CE, Warner BM, Summersgill KF, Weghorst CM and Knobloch TJ (2017) Inhibition of Pro-inflammatory and Anti-apoptotic Biomarkers during Experimental Oral Cancer Chemoprevention by Dietary Black Raspberries. Front. Immunol. 8:1325. doi: 10.3389/fimmu.2017.01325

Oral cancer continues to be a significant public health problem worldwide. Recently conducted clinical trials demonstrate the ability of black raspberries (BRBs) to modulate biomarkers of molecular efficacy that supports a chemopreventive strategy against oral cancer. However, it is essential that a preclinical animal model of black raspberry (BRB) chemoprevention which recapitulates human oral carcinogenesis be developed, so that we can validate biomarkers and evaluate potential mechanisms of action. We therefore established the ability of BRBs to inhibit oral lesion formation in a carcinogen-induced rat oral cancer model and examined potential mechanisms. F344 rats were administered 4-nitroquinoline 1-oxide (4NQO) (20 μg/ml) in drinking water for 14 weeks followed by regular drinking water for 6 weeks. At week 14, rats were fed a diet containing either 5 or 10% BRB, or 0.4% ellagic acid (EA), a BRB phytochemical. Dietary administration of 5 and 10% BRB reduced oral lesion incidence and multiplicity by 39.3 and 28.6%, respectively. Histopathological analyses demonstrate the ability of BRBs and, to a lesser extent EA, to inhibit the progression of oral cancer. Oral lesion inhibition by BRBs was associated with a reduction in the mRNA expression of pro-inflammatory biomarkers *Cxcl1*, *Mif*, and *Nfe2l2* as well as the anti-apoptotic and cell cycle associated markers *Birc5, Aurka, Ccna1*, and *Ccna2.* Cellular proliferation (Ki-67 staining) in tongue lesions was inhibited by BRBs and EA. Our study demonstrates that, in the rat 4NQO oral cancer model, dietary administration of BRBs inhibits oral carcinogenesis via inhibition of pro-inflammatory and anti-apoptotic pathways.

Keywords: oral cancer, black raspberry, chemoprevention, pro-inflammatory, biomarker

INTRODUCTION

It is estimated that there are about 48,330 new cases and 9,570 deaths due to oral cancer in the US annually (1). This amounts to greater than one person every hour every day that dies from oral cancer. Worldwide, about 300,000 cases and 145,000 deaths are reported annually (2). Due to epithelial field defects associated with oral carcinogenesis, tumor recurrence and second primary tumor incidence

are common. Despite advances in oral cancer treatment strategies, survival rates have not significantly improved over the past three decades. Consequently, new and effective approaches to oral cancer prevention and therapy are needed, and it is essential that these strategies be developed and tested in preclinical models that reflect essential features of human oral carcinogenesis.

As the molecular mechanisms that drive the multistep process of oral carcinogenesis are becoming better understood, inhibitors that target oncogenic pathways have been used in oral cancer chemoprevention and treatment. Agents used in oral cancer preclinical and clinical chemoprevention studies include inhibitors of cyclooxygenase 2 (Cox-2) (3, 4) and epidermal growth factor receptor (EGFR) (5). However, toxicity associated with molecular targeted therapeutic approaches are common.

Epidemiologic and case–control studies demonstrate a consistent inverse correlation between increased fruit and vegetable consumption and decreased oral cancer risk (6, 7). In support of these data, recent preclinical studies have clearly demonstrated the remarkable ability of black raspberries (BRBs) to prevent tumor development in oral cancer cells *in vitro* (8, 9), as well as in animal models of oral cancer in hamsters (10, 11), and esophageal and colon cancers in rats (12–14). BRBs possess a number of bioactive phytochemicals such as anthocyanins, ellagitannins, ellagic acid (EA), and others which may act in an additive or synergistic manner to inhibit cancer development. Recent clinical studies conducted by our group demonstrate the ability of dietary black raspberry (BRB) administration to modulate molecular biomarkers within the oral cavity in a manner that supports a chemopreventive strategy for oral cancer (15). These biomarkers include genes affecting inflammatory and apoptotic pathways which are crucial for oral cancer initiation, promotion, and progression (15). To translate clinically derived molecular signature of BRB responsive biomarkers into defined mechanisms of action, an appropriate experimental system of oral carcinogenesis is needed.

One of the most common animal models of oral cancer chemoprevention is the 7,12-dimethlybenz(a)anthracene (DMBA) induced hamster cheek pouch model which reflects elements characterizing human oral carcinogenesis. We have previously published on the chemopreventive efficacy of BRBs using this model (10, 11). However, this model lacks the curated and annotated genomic infrastructure necessary for the interrogation of human-relevant molecular biomarkers and the elucidation of cellular and molecular mechanisms of action. An animal model which recapitulates fundamental features of human oral carcinogenesis, is amenable to chemopreventive intervention, and has established tools for cellular, molecular, and systems biology interrogation is required for evaluation of oral cancer chemoprevention mechanistic studies. The carcinogen-induced rat oral cancer model fulfills these criteria and was therefore used in this study.

The objective of this study was to (i) establish and validate a preclinical model of oral cancer chemoprevention by BRBs which recapitulates the clinical and molecular features of human disease and (ii) define primary mechanisms of action of oral chemoprevention by the bioactive phytochemicals in BRBs using this preclinical model. To accomplish these objectives, we used 4-nitroquinoline 1-oxide (4NQO) to initiate oral carcinogenesis in F344 rats, a model that has been widely used in experimental oral carcinogenesis and chemoprevention studies (16–18). Our results demonstrate that experimental rat oral carcinogenesis represents an essential tool for the extended investigation of BRB-mediated oral chemoprevention, and validate the involvement of inflammatory, apoptotic, and cell cycle associated pathways in the oral cancer inhibitory activity of BRBs.

MATERIALS AND METHODS

Animals

Male F344 rats, 6–7 weeks old were obtained from Harlan Laboratories (Indianapolis, IN, USA) and housed at an HEPA-filtered animal facility at The Ohio State University according to animal protocols and regulations of the University Laboratory Animal Resources (PHS Animal Welfare Assurance #A3261-01 and Association for Assessment and Accreditation of Laboratory Animal Care International #0028). All experiments with rats were approved by The Ohio State University Institutional Animal Care and Use Committee (Protocol #2010A00000085) and Institutional Biosafety Committee.

Chemicals

The carcinogen 4NQO was purchased from Sigma-Aldrich (St. Louis, MO, USA; #N8141) and stored in foil-wrapped containers at −20°C. Fresh 4NQO solutions (20 μg/ml in drinking water) were prepared twice weekly for administration to rats for 14 weeks. BRBs (*Rubus occidentalis* "Jewel variety") were obtained from the Stokes Berry Farm (Wilmington, OH, USA) and shipped frozen to Van Drunen Farms (Momence, IL, USA) for freeze drying. BRB powder was stored at −20°C until incorporated into custom purified AIN-76A animal diet pellets at 5 and 10% w/w concentrations (Dyets, Inc., Bethlehem, PA, USA). EA was purchased from Sigma-Aldrich (St. Louis, MO, USA; #E2250, ≥95% HPLC) and incorporated into AIN-76A pellets at 0.4%, proportionally matched to the amount present in 10% lyophilized BRBs (Oregon Raspberry & Blackberry Commission; Corvallis, OR, USA).

Rat Oral Carcinogenesis and Chemoprevention

A control sentinel group (Group 1, $N = 20$) received regular drinking water without carcinogen (4NQO) and fed unmodified AIN-76A diet. Rats belonging to experimental groups were administered 4NQO in drinking water for 14 weeks, then randomized into four groups (Groups 2–5, $N = 35$ per group) for 6 weeks of chemopreventive agent administration (**Figure 1A**). Group 2 (carcinogen control group) received unmodified AIN-76A diet without chemopreventive agent, Group 3 received AIN-76A diet containing 5% BRB, Group 4 received AIN-76A diet containing 10% BRB, and Group 5 received AIN-76A diet containing 0.4% EA. After a 14-week carcinogen exposure and 6-week chemopreventive agent administration (20-week protocol), animals were sacrificed. Rat tongues were harvested and gross lesions were counted, categorized, and recorded. Tongue tissues were fixed in 10% neutral buffered formalin, paraffin embedded, and sectioned

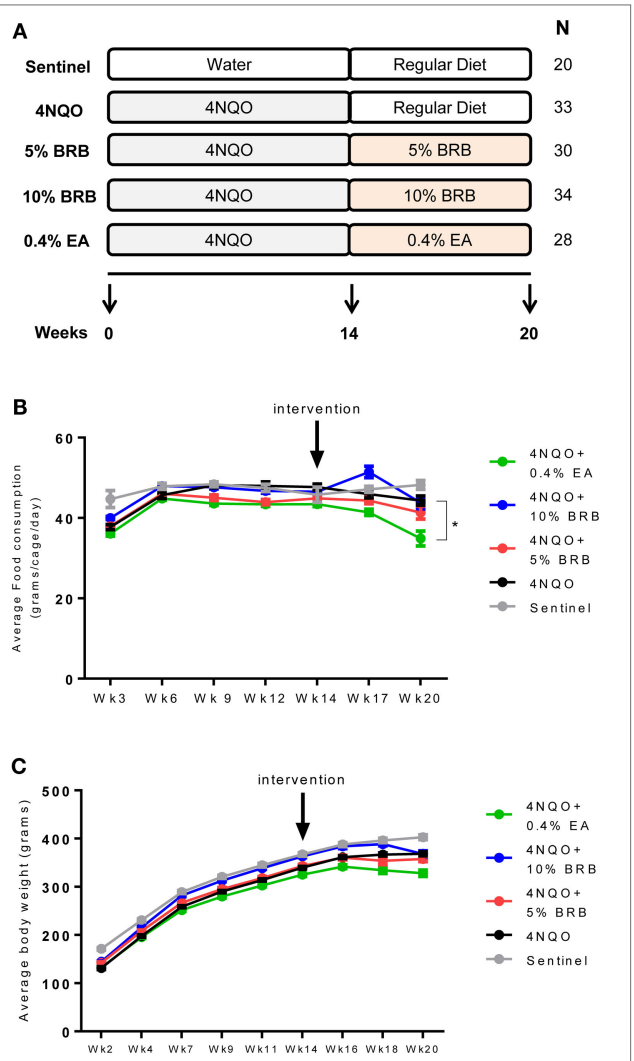

FIGURE 1 | **(A)** Scheme of rat oral carcinogenesis and chemoprevention. Rats were exposed to oral carcinogen 4-nitroquinoline 1-oxide (4NQO) (20 μg/ml in drinking water) for 14 weeks. Administration of dietary chemopreventive agent began at week 14 and continued for 6 weeks. Animals were sacrificed at week 20 for gross and histological analysis of tongue lesions and examination of cellular and molecular markers of carcinogenesis. *N* represents number of rats per group. **(B)** Average food consumption for the control and experimental rat groups during oral carcinogenesis and dietary intervention phases of the experimental protocol. Data are expressed as mean food consumption (grams/cage/day) ± SE in each rat cage belonging to an experimental group (three rats per cage). **p*-value < 0.05 for food intake comparison between 4NQO-only rat group and 4NQO + ellagic acid (EA) rat group using independent Student's *t*-test. **(C)** Average body weight measurements for control and experimental rat groups during the carcinogenesis and intervention phases of the experimental protocol. With the exception of the sentinel animals, all experimental animals were administered 4NQO and were on AIN-76A defined diet prior to intervention with dietary black raspberries (BRBs) or EA. Data are expressed as mean ± SE of all rats in the group.

for histopathology and immunohistochemistry (IHC). Total RNA was prepared from tongue tissues for reverse transcription quantitative PCR (RT-qPCR) analysis. Whole blood samples were obtained from each animal for enzyme-linked immunosorbent assay (ELISA).

Histopathology Calibration and Grading of Microscopic Lesions

Whole rat tongues were cut four times longitudinally into equal width sections. One half (two pieces, medial and lateral sections) of the tongues were placed on edge into tissue cassettes and fixed in formalin for 24 h. After fixation, the tissues were embedded in paraffin and three 5 μm sections of each tissue block were cut and mounted on Superfrost Plus slides (Fisher Scientific, Pittsburgh, PA, USA). Hematoxylin and eosin (H&E) stained slides were prepared from each block. Each section and level of tongue was delineated into three equal regions (anterior, middle, and posterior tongue) along the surface of the tongue epithelia using a millimeter ruler and dotting pen. Before grading the slides, a calibration set ($N = 10$) was selected from the set of H&E slides using a random number generator. The calibration set was reviewed independently by two oral and maxillofacial pathologists and the results were reviewed together at the microscope. Differences in grading were discussed and agreement was achieved. Blinded to the treatment groupings of the animals, the highest histopathological grade of each of the two pieces of tongue, within each anatomic region of the tongue (anterior, middle, posterior), for each section was graded independently by the oral and maxillofacial pathologists. As with the calibration set, differences in grading were discussed and agreement was achieved. The four histological categories used for grading were normal, low-grade dysplasia, high-grade dysplasia, or squamous cell carcinoma, as described previously (11). Low-grade dysplasia was characterized by changes in the epithelium such as basilar crowding and hyperplasia, cellular disorganization, and maturational disturbances within the lower one-third to the middle third of the epithelial thickness with little interruption of the keratin layer. High-grade dysplasia included the above parameters extending into the upper third of the epithelial thickness. Additional features included frequent mitotic figures, cellular pleomorphism, nuclear atypia, and some early disturbance of the keratin layer. Further, full thickness epithelial change with the above features, an expansion of multiple layers of cells into the suprabasal and intermediate layers, and with disturbance of the keratin layer but without penetration of the basement membrane was included in this category. Squamous cell carcinoma was defined as the above changes with invasion through the basement membrane.

Immunohistochemistry

Immunohistochemistry staining was performed on deparaffinized tongue tissue sections by The Ohio State University Comparative Pathology and Mouse Phenotyping Shared Resource, using Ki-67 antibody (1:100 primary antibody) or antibody against cleaved caspase 3 (1:180 primary antibody). Slides were counterstained with hematoxylin. For Ki-67 staining, cell proliferation was determined by amount of Ki-67 positive nuclei relative to total amount of nucleated cells in six random fields of tongue epithelium using a Zeiss Axioplan imaging microscope at 200× magnification and AxioVision Imaging software (Carl Zeiss Microscopy, LLC, Thornwood, NY, USA).

Reverse Transcription Quantitative PCR

Total RNA was extracted from rat tongue tissues using the AllPrep DNA/RNA Kit (Qiagen, Valencia, CA, USA). RNA was reverse transcribed to cDNA using the High Capacity cDNA Reverse Transcription Kit (Applied Biosystems, Foster City, CA, USA). PCR amplification was performed ($N \geq 20$ rats per group) using pre-validated rat-specific TaqMan Assays (Applied Biosystems, Foster City, CA, USA) in duplicates. Comparative Cq estimates were performed after reference gene set normalization. The reference gene normalization was determined using the qbase + real-time PCR data analysis software (19, 20) (Biogazelle, Ghent, Belgium), which selects the most stably expressed genes across all rat tongue RNA samples in all groups. For TaqMan assays, optimal reference genes were determined by qbase + geNorm software (19, 20) to be the combination of *Egfr* and *Bcl2*. In some experiments, rat primer sequences were selected using the Real-Time qPCR Assay tool (https://www.idtdna.com/scitools/Applications/RealTimePCR/) by Integrated DNA Technologies (Coralville, IA, USA), and PCR amplification was performed using SYBR Green chemistry (Qiagen, Valencia, CA, USA). For SYBR Green assays, optimal reference genes were determined by qbase + geNorm software (19, 20) to be the combination of *Gapdh* and *Tgfb*. In both cases, reference genes were calculated to be of high reference target stability. Genes targeted included interleukin 1 beta (*Il-1β),* nuclear factor kappa B subunit 1 *(Nfkb1),* arginase 1 (*Arg1),* prostaglandin-endoperoxidase synthase 1 (*Ptgs1),* Prostaglandin-endoperoxidase synthase 2 (*Ptgs2*), C-X-C motif chemokine ligand 1 (*Cxcl1*), macrophage migration inhibitory factor (*Mif)*, nuclear factor, erythroid 2 like 2 (*Nfe2l2),* baculoviral IAP repeat containing 5 (*Birc5),* aurora kinase A (*Aurka*), cyclin A1 (*Ccna1*), cyclin A2 (*Ccna2*), caspase 14 (*Casp14)*.

Enzyme-Linked Immunosorbent Assay

Quantitative detection of PTGS1/COX-1 in Rat serum was performed using Rat PTGS1/COX1 Sandwich ELISA Kit (#LS-F12318, LifeSpan Biosciences; Seattle, WA, USA). Detection of PTGS2/COX-2 was performed using the Rat COX-2 Competitive ELISA Kit (#RC0087, NeoScientific, Cambridge, MA, USA). Plates were read at an absorbance of 450 nm using Spectramax M3 microplate reader (Molecular Devices LLC, Downingtown, PA, USA) and concentrations were determined by extrapolation from standard curves generated by the Softmax Pro software (Molecular Devices LLC, Downingtown, PA, USA) using the COX-1 and COX-2 standards provided by each respective kit.

Statistical Analysis

Statistical evaluation was performed using IBM SPSS software Version 24 (Chicago, IL, USA), or Prism 5 (GraphPad Software; San Diego, CA, USA) and p-values ≤ 0.05 were considered to be significant. Mean ± SEM was used to report findings. Significant differences (p-value < 0.05) between 4NQO and treatment groups (5% BRB, 10% BRB, and 0.4% EA) were discriminated using a Student's independent t-test for lesion endpoint, ELISA, and Ki-67 immunohistochemical analyses. An analysis of variance was used to model the gene expression data with respect to treatment using qbase + real-time PCR data analysis software (19) (Biogazelle, Ghent, Belgium). If discriminant differences were found, the Tukey–Kramer *post hoc* test was used.

RESULTS

Effect of BRB Consumption on Food Intake, Weight, and Overall Survival of Carcinogen-Induced Rats

Following exposure to 4NQO in drinking water and subsequent administration of control or experimental diet (**Figure 1A**), food consumption and body weight measurements were determined for the various groups during the carcinogenesis and intervention phase of our study. Food consumption analysis during the carcinogenesis phase compared sentinel non-exposed animals with all animals that were exposed to the carcinogen 4NQO. No significant changes in food consumption were observed between rats administered 4NQO and non-4NQO sentinel animals (**Figure 1B**). During the intervention phase, food consumption analysis for each dietary group compared to 4NQO-only control group showed no significant differences in animals fed with 5 and 10% BRB diets. However, a significant reduction in average food consumption was observed in animals fed with 0.4% EA compared to the 4NQO control group (**Figure 1B**). Average body weights were also recorded for each animal group over the course of the study. We observed no significant changes in body weight between the sentinel group and the pooled group of animals exposed to 4NQO (**Figure 1C**). However, body weight comparisons between the 4NQO-only control group with the other treatment groups during the intervention phase revealed a significant reduction in body weight in 0.4% EA treated animals compared to 4NQO control animals but no significant body weight changes between 4NQO-only group and 10% BRB treatment group (**Figure 1C**). Taken together, while there appears to be slightly reduced preference for the 0.4% EA diet, our data demonstrate the negligible effects of whole BRB diet on overall food consumption and body weight of oral carcinogen-induced rats, which suggests that BRB-mediated chemopreventive approaches to oral cancer management are relatively safe with minimal side effects. This agrees with other studies demonstrating that BRB exerts minimal effects on normal oral tissue (21, 22).

Dietary Administration of BRBs Reduces Oral Lesion Incidence and Multiplicity in 4NQO-Induced Rats

Next, we examined effects of BRB administration on oral tumor incidence and multiplicity as well as total oral lesion incidence and multiplicity following 4NQO-induced rat oral carcinogenesis. Rats from all experimental groups were sacrificed and characterized for gross lesions, which included premalignant lesions (leukoplakia, erythroplakia), and malignant lesions (overt tumors). These data are summarized in **Table 1**. Our results indicate that the freeze-dried whole BRB supplemented diets significantly inhibited oral carcinogenesis as evidenced by reduced numbers of tumors as well as combined oral lesions (**Figures 2A–C**). These effects manifested as reductions in tumor and collective lesion incidence/multiplicity and correspond to 39.3 and 28.6%

TABLE 1 | Analysis of gross lesions in tongues of rats induced with the oral carcinogen 4-nitroquinoline 1-oxide (4NQO), with or without dietary administration of chemopreventive agent.

Group	Survival	Tumor incidence	Tumor multiplicity	Lesion incidence	Lesion multiplicity
4NQO	33/35 (94.3%)	6/33 (18.2%)	0.18	30/33 (90.9%)	3.39
4NQO + 5% black raspberries (BRB)	30/35 (85.7%)	1/30 (3.3%)	0.03	23/30 (76.7%)	2.27
4NQO + 10% BRB	34/35 (97.1%)	1/34 (2.9%)	0.03	28/34 (82.4%)	2.35
4NQO + 0.4% ellagic acid	28/35 (80.0%)	1/28 (3.6%)	0.03	24/28 (85.7%)	4.18

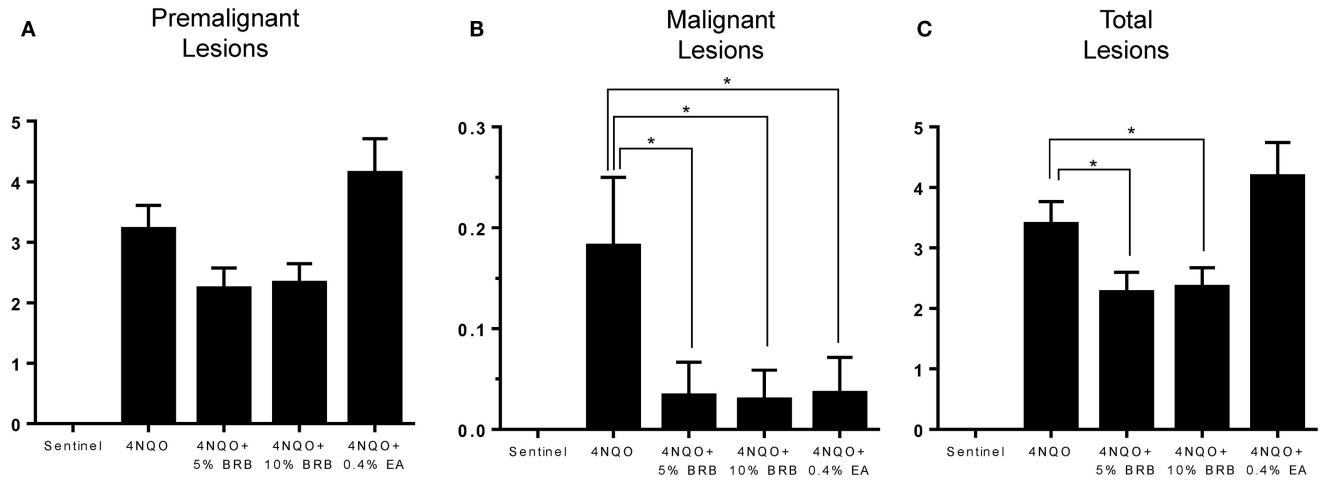

FIGURE 2 | **(A–C)** Average number of **(A)** premalignant, **(B)** malignant, and **(C)** total lesions in 4-nitroquinoline 1-oxide (4NQO)-induced rat tongues fed control diet (4NQO group) or diet supplemented with 5% black raspberry (BRB) (4NQO + 5% BRB group), 10% BRB (4NQO + 10% BRB group), or 0.4% ellagic acid (EA) (4NQO + 0.4% EA group). Data are expressed as mean ± SE of all rats in the group. *p-value < 0.05 for group comparisons using independent Student's t-test.

inhibition of gross lesions with 5 and 10% BRB diets, respectively. Further, both the 5% BRB and 10% BRB groups demonstrated the greatest number of lesion-free animals following 4NQO exposure and intervention, and all dietary interventions showed greater than fivefold decrease in tumor incidence.

Histopathological analysis of tongue sections from 4NQO-induced rats further demonstrates the chemopreventive effect of BRB diet against oral carcinogenesis (**Figures 3A–E**). 5% BRBs significantly reduced the progression of tongue lesions to squamous cell carcinomas as determined by histological grading (**Figure 3C**). It appears from our data that BRB administration delays the progression of tongue lesions beyond high-grade dysplasia, which is probably associated with the time of administration of chemopreventive agent, which began 14 weeks after 4NQO exposure. It is likely that an earlier intervention with BRBs would result in an even greater inhibition of dysplastic lesions and SCCs.

Comparisons of BRB efficacy between the 5 and 10% BRB diets further demonstrated that 5% BRB administration was more effective than 10% BRB in inhibiting gross lesion incidence and multiplicity. Total numbers of oral premalignant lesions were fewer in 5% BRB administered rats compared to 10% BRB administered rats (**Table 1**). Similarly, histopathological analysis demonstrated the increased efficacy of 5% BRB compared to 10% BRB at inhibiting SCC development during rat oral carcinogenesis (**Figures 3B–D**).

Inhibition of Oral Lesions by BRB Is Associated with Reduction in Pro-inflammatory Markers of Oral Carcinogenesis

Oral carcinogenesis is characterized by a chronic pro-inflammatory microenvironment, favoring tumor initiation and progression (23, 24). Chronic inflammation is an important underlying factor which promotes carcinogenesis (25). A recent short-term Phase 0 clinical study conducted by our group demonstrated the ability of a BRB troche to inhibit gene expression of pro-inflammatory biomarkers in oral cancer patients (15). We therefore evaluated the ability of BRBs to inhibit pro-inflammatory gene expression profiles in experimental rat oral carcinogenesis induced by 4NQO. Gene expression of the pro-inflammatory biomarkers *Cxcl1*, *Mif*, and *Nfe2l2* were downregulated in carcinogen-induced rats fed with 5 or 10% BRB diet (**Figure 4A**). These genes have been shown to play a role in oral carcinogenesis in preclinical models as well as in human oral cancer (26, 27). Prostaglandin-endoperoxidase synthase, a key enzyme in prostaglandin biosynthesis, is especially critical in mediating the pathologic consequences of chronic inflammation in OSCC (23). We therefore examined oral epithelia mRNA expression levels of *Ptgs1* and *Ptgs2*, as well as serum levels of Cox1/Ptgs1 and Cox2/Ptgs2 in normal rats, and in carcinogen-induced rats fed with regular diet, 5 or 10% BRB supplemented diets. However,

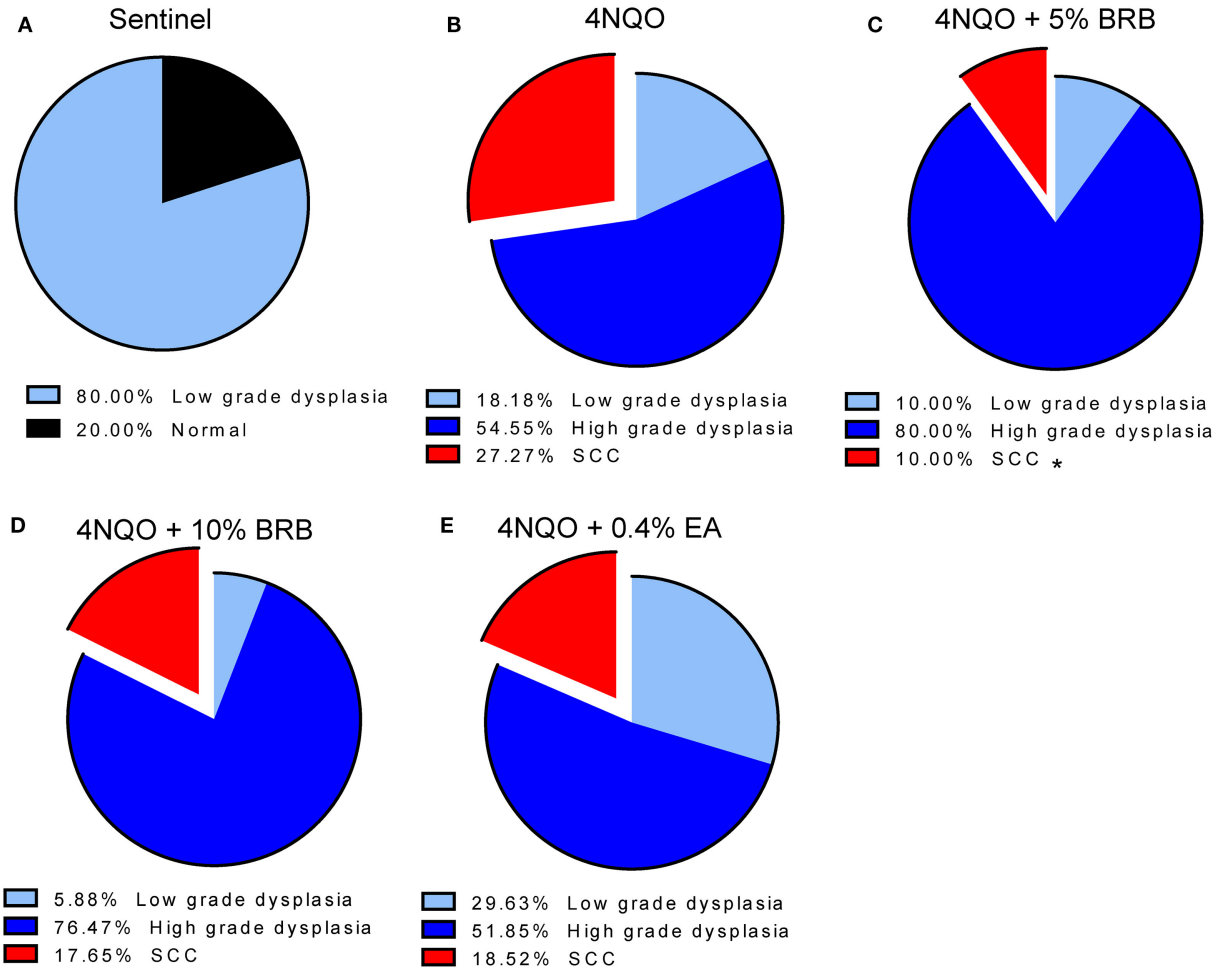

FIGURE 3 | **(A–E)** Histopathological analysis of tongue tissues from untreated and treated carcinogen-induced rats. Distribution of the histopathological grades (normal, low-grade dysplasia, high-grade dysplasia, and SCC) in tongue epithelia of **(A)** sentinel rats, **(B)** 4-nitroquinoline 1-oxide (4NQO)-induced rats fed control diet, **(C)** 4NQO-induced rats fed diet supplemented with 5% black raspberry (BRB), **(D)** 4NQO-induced rats fed diet supplemented with 10% BRB, and **(E)** 4NQO-induced rats fed diet supplemented with 0.4% ellagic acid (EA). Note the significantly reduced percentage of SCCs in 4NQO exposed rats treated with 5% BRB. *p-value < 0.05 for SCC incidence comparison between 4NQO-only exposed rats and 4NQO + 5% BRB rats, using independent Student's t-test.

we observed no significant differences in gene expression levels in rat tongue (**Figure 4A**) or protein expression levels in rat serum (**Figure 4B**) of Ptgs1 and Ptgs2 in BRB administered carcinogen-induced rats compared to untreated carcinogen-induced rats. Taken together, our data suggest that a potential mechanism of oral cancer chemoprevention by BRB phytochemicals is the inhibition of specific pro-inflammatory signaling pathways.

BRBs Inhibit Anti-apoptotic and Proliferative Pathways in 4NQO-Induced Rat Oral Carcinogenesis

Previous studies demonstrate the ability of BRB phytochemicals to inhibit cancer cell proliferation and promote apoptotic pathways in oral cancer cells *in vitro* (8, 9). These results are supported by transcriptional analysis of proliferative and apoptotic genes in clinical trials of oral cancer patients (15, 21, 28). We therefore analyzed the effects of dietary administration of BRBs on proliferative and apoptotic pathways during experimental oral carcinogenesis in our rat model. To characterize BRB-mediated effects on proliferative pathways, we analyzed the expression of Ki-67 (a proliferation marker) in tongue lesions using IHC. Proliferative indices were significantly reduced in carcinogen exposed mice that received 5 or 10% BRBs (**Figures 5A,B**). Further analysis of proliferative biomarkers by RT-qPCR analysis of rat tongues demonstrated a reduction in gene expression of the cell cycle regulated kinase *Aurka* which has been shown to play a role in tumor development and progression (**Figure 5C**). Other cell cycle associated genes inhibited by BRBs include *Ccna1,* which was inhibited by 5% BRBs and *Ccna2,* which was inhibited by 5 and 10% BRBs (**Figure 5C**). Our results demonstrate that dietary administration of BRBs

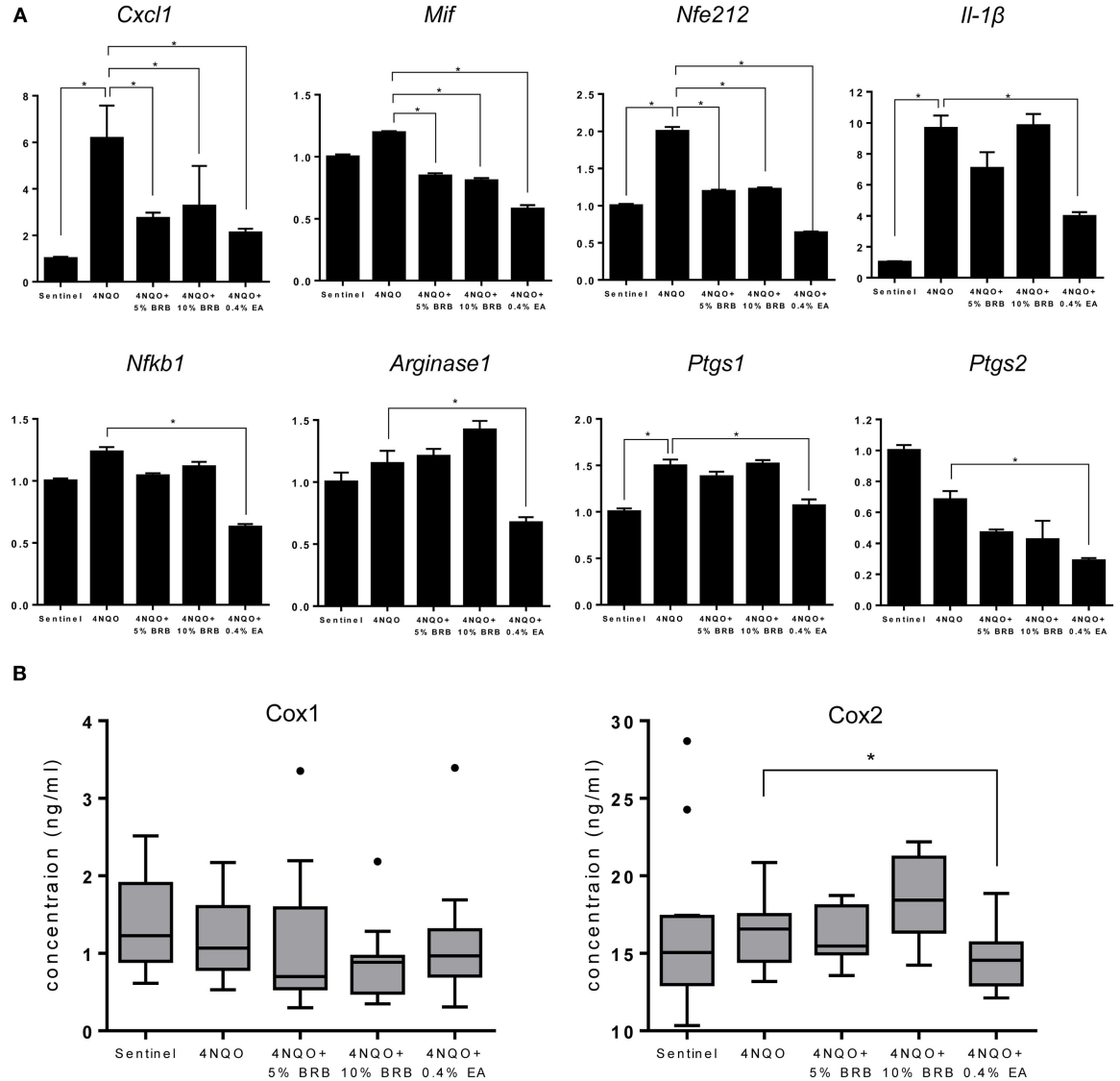

FIGURE 4 | **(A)** Gene expression profiles of the pro-inflammatory markers *Cxcl1, Mif, Nfe212, Il-1β, Nfkb1, Arg1, Ptgs1*, and *Ptgs2* during 4-nitroquinoline 1-oxide (4NQO)-induced oral carcinogenesis determined by reverse transcription quantitative PCR. Data are presented as mean fold induction over sentinels ± SE. **p*-value < 0.05 for each group ($N \geq 20$) comparison using analysis of variance analysis. **(B)** Serum concentrations of cyclooxygenase 1 (Cox-1) and Cox-2 in randomly selected rats from each experimental group ($N = 15$) during 4NQO-induced oral carcinogenesis as determined by enzyme-linked immunosorbent assay. Data are presented as mean ± SE. **p*-value < 0.05 for each respective group comparison using independent Student's *t*-test.

inhibits cellular proliferation in tongue lesions during 4NQO-induced oral carcinogenesis.

Next, we determined the effect of BRB administration on apoptotic pathways during oral carcinogenesis. Gene expression analysis by RT-qPCR demonstrated that *Birc5* (survivin), a member of the inhibitor of apoptosis (IAP) family, was downregulated by BRB treatment (**Figure 6A**). *Birc5,* which is transcriptionally upregulated during squamous cell carcinomas, exerts its function by inhibiting caspase activation, thereby blocking apoptosis (29). Targeting *Birc5* is therefore a promising strategy for oral cancer therapy. Inhibition of *Birc5* gene expression by BRB, led us to examine its effect on its downstream target caspase-3. We therefore examined cleaved caspase 3 protein expression in tongue tissues of 4NQO-treated and BRB-treated rats by IHC. Our results show that in squamous cell carcinomas, cleaved caspase 3 expression is increased in BRB-treated tissues (**Figure 6B**). We also observed that gene expression of *Casp14*, an apoptotic and keratinocyte senescence biomarker, was slightly upregulated in 10% BRB-treated rat tongues (**Figure 6A**). Taken together, our molecular analysis of experimental rat oral carcinogenesis suggests that modulation of apoptotic pathways is a mechanism of BRB-mediated oral cancer chemoprevention.

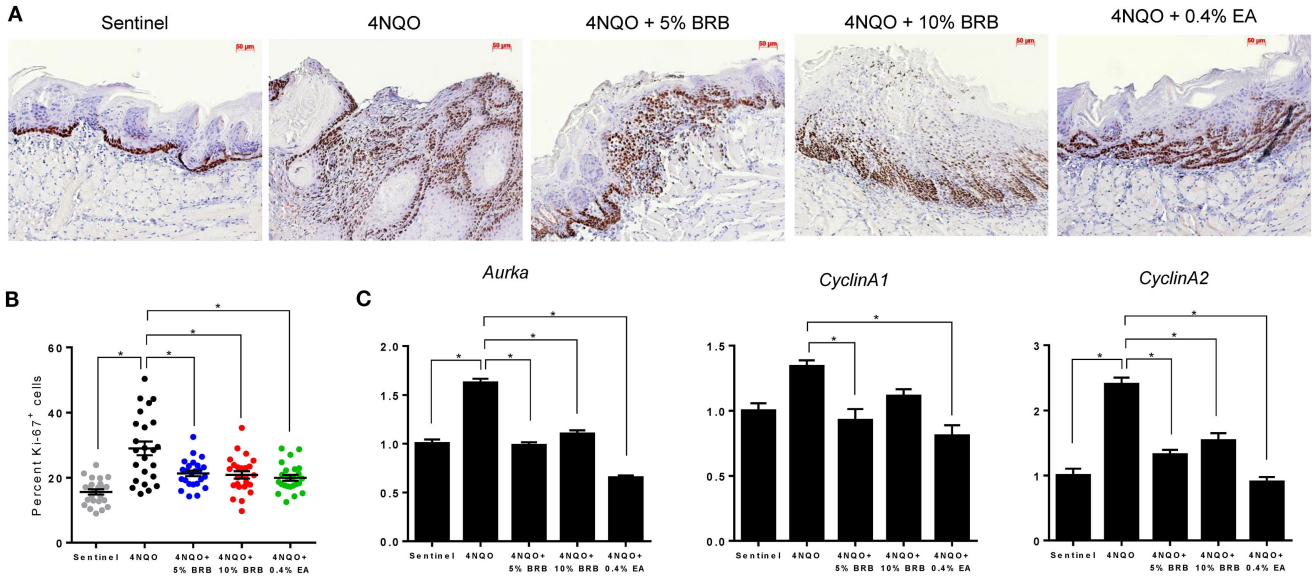

FIGURE 5 | **(A)** Representative microscopic images (×200) of tongue tissues from sentinel rats and 4-nitroquinoline 1-oxide (4NQO) exposed rats fed control diet, 5% black raspberry (BRB), 10% BRB, or 0.4% ellagic acid (EA). Paraffin sections were stained with anti-Ki-67 antibody and counterstained with hematoxylin. **(B)** Quantitation of Ki-67 positive cells in tongue epithelial tissue from sentinel rats as well as 4NQO exposed rats fed with control diet, 5% BRB, 10% BRB, or 0.4% EA. Graphic representation of percent Ki-67 positive nuclei relative to total nucleated cells in six random fields of tongue epithelium from selected rats from each experimental group. Data are expressed as percent cells ± SE. *p-value < 0.05 for each group comparison using independent Student's t-test. **(C)** Gene expression profiles of the cell cycle associated biomarkers *Aurka, Ccna1*, and *Ccna2* during 4NQO-induced oral carcinogenesis as determined by reverse transcription quantitative PCR. Data are presented as mean fold induction over sentinels ± SE. *p-value < 0.05 for each group ($N \geq 20$) comparison using analysis of variance analysis.

EA Inhibits Tumor Incidence but Does Not Reduce the Formation of Premalignant Lesions

Ellagic acid, a bioactive component of BRBs as well as other fruits, nuts, and vegetables, is a naturally occurring antioxidant and anti-proliferative polyphenolic compound known for its anticancer activities in preclinical studies (17, 30, 31). We used this compound as a control bioactive substance to compare to the oral cancer inhibitory activities of BRBs in our rat 4NQO oral cancer model. Surprisingly, as shown in **Table 1**, although EA reduced tumor incidence (0.03 EA vs 0.18 4NQO), multiplicity of premalignant lesions in EA treated rats were higher compared to 4NQO-only induced rats (4.18 EA vs 3.39 4NQO).

Gene expression profiles of 4NQO exposed EA treated rats demonstrate a reduction of genes associated with inflammation (*Il-1β, Cxcl1, Mif, Nfkb1, Arg1, Ptgs1,* and *Ptgs2*) (**Figure 4A**), cell proliferation (*Aurka, Ccna1,* and *Ccna2*) (**Figure 5C**), and apoptosis (*Birc5*) (**Figure 6A**). Serum levels of Cox2 (**Figure 4B**), and Ki-67-based cellular proliferation (**Figure 5B**) were also reduced in EA treated rats. Taken together, our data show that although EA inhibited the formation of malignant lesions in the rat tongue and modulated biomarkers of molecular efficacy, it is not as effective as BRBs in preventing the development of premalignant lesions during experimental rat oral carcinogenesis. Nevertheless, the potential of EA in adjuvant or complementary therapeutic applications against oral carcinogenesis is clearly demonstrated by the anti-oral cancer effects of EA observed in this study.

DISCUSSION

Oral squamous cell carcinoma is the resultant endpoint of an accumulation of genetic alterations that permit sequential transition from phenotypically normal cells to varying grades of dysplasia and invasive disease. The exposure of the entirety of the oral cavity by carcinogens initiates a field of epithelia with genetic defects at risk for progression to malignancy, vis-à-vis field cancerization. This presents a wide range of opportunities for chemoprevention by BRBs as previous preclinical and clinical studies have demonstrated. However, in order to extend the application of BRB phytochemicals in oral cancer chemoprevention, a suitable animal model that recapitulates the fundamental features of human oral cancer and facilitates the characterization of the cellular and molecular changes associated with BRB-mediated oral chemoprevention is essential. Although the hamster model sufficiently demonstrates the efficacy of BRBs in the chemoprevention of oral carcinogenesis (10, 11), extended investigation on the specific mechanisms of oral chemoprevention presents challenges due to the limited availability of molecular resources using this model. The rat 4NQO model of oral carcinogenesis and chemoprevention by BRBs, as described in this study, represents an essential model for demonstrating the molecular efficacy of BRBs in inhibiting oral carcinogenesis, and for determining mechanisms of BRB-mediated oral cancer prevention.

The molecular changes observed during rat 4NQO oral carcinogenesis and BRB-mediated oral chemoprevention very well

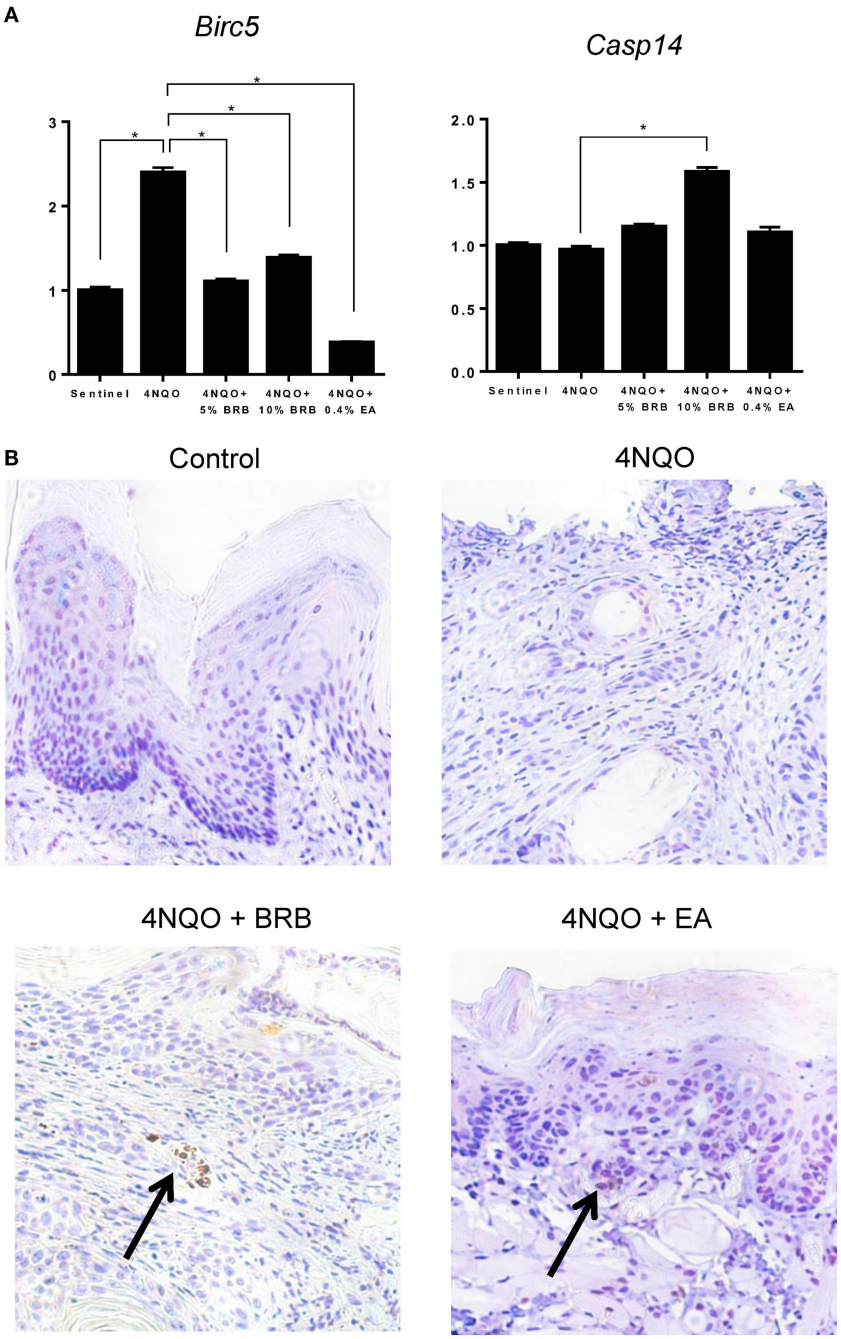

FIGURE 6 | **(A)** Gene expression profiles of the apoptotic biomarkers *Birc5* and *Casp14* during 4-nitroquinoline 1-oxide (4NQO)-induced oral carcinogenesis as determined by reverse transcription quantitative PCR. Data are presented as mean fold induction over sentinels ± SE. *p-value < 0.05 for each group ($N \geq 20$) comparison using analysis of variance analysis. **(B)** Representative immunohistochemistry stained microscopic images (×100) of tongue tissues from sentinel rats and 4NQO exposed rats fed control diet, black raspberry (BRB) supplemented diet, or ellagic acid (EA) supplemented diet. Paraffin sections were stained with antibodies against cleaved caspase 3 and counterstained with hematoxylin. In 4NQO-exposed sections, regions of dysplasia or squamous cell carcinomas are shown. Arrow points to positively stained (apoptotic) cells.

mimic those observed during an oral cancer chemoprevention trial using a BRB phytochemical-rich troche (15). Key molecular pathways modified by BRB phytochemical intervention in this recent chemoprevention clinical trial include genes regulating inflammation (*NFKB1* and *PTGS2)* and cell survival (*AURKA* and *BIRC5*). In a similar manner, these genes were significantly reduced by BRB administration in our rat model. Therefore, we can reasonably conclude that this model validates the BRB-mediated transcriptional signature in human oral squamous cell carcinomas (15).

Our results identify pro-inflammatory pathways as a major target of BRBs during oral cancer chemoprevention. A chronic pro-inflammatory microenvironment is essential to the establishment and progression of oral cancer. Inflammation contributes to oral carcinogenesis by causing the release of factors that promote cell growth, proliferation, angiogenesis and invasion (25). Furthermore, the release of inflammatory by-products, such as reactive oxygen species, accelerates mutagenic events that contribute to malignancy. Not surprisingly, therapeutic strategies that target pro-inflammatory pathways in oral cancer are the focus of extensive research efforts. Pro-inflammatory mediators which were inhibited by BRB phytochemicals during experimental rat oral carcinogenesis in our study include *Nfkb1, Ptgs2, Il-1β, Cxcl1, Mif,* and *Nfe2l2*. Similar to our previous Phase 0 BRB oral chemoprevention trial, expression of *Nfkb1* was inhibited by 5% BRB and 0.4% EA administration to oral cancer induced rats. *Nfkb1* mediates a chronic pro-inflammatory tumor microenvironment and constitutes a missing link between inflammation and cancer (32, 33). Inhibition of NF-κB signaling has been associated with reduction of inflammation-associated cancers (33). The effect of BRBs on NF-κB inhibition is especially relevant to human oral carcinogenesis, given that major risk factors for oral cancer (tobacco smoking, alcohol consumption, and HPV infection) are linked to chronic inflammation. *Ptgs2* is a major enzyme in the prostaglandin biosynthesis pathway and an inflammatory biomarker that is known to contribute to oral carcinogenesis. Although *Ptgs2* expression was inhibited in tongues of oral cancer induced rats administered 5% BRB or 0.4% EA, we did not observe any differences in the levels of Cox-2 in the sera of these rats. This suggests that the main effects of BRBs are localized to the oral epithelia of these rats and that systemic effects are limited. Although some BRB metabolites are detectable systemically (34), it is likely that the major anti-inflammatory effects of the bioactive compounds in BRBs are localized to the tissues of administration (mucosa), which makes this chemopreventive agent most impactful against cancers of the oral and gastro-intestinal mucosae (11, 12, 15, 35).

We recently demonstrated that genetic deletion of *Mif*, another pro-inflammatory mediator linking inflammation and cancer, inhibits experimental oral carcinogenesis (26). *Mif* signals through the ERK1/2 MAP kinase signaling pathway, leading to the expression of other pro-inflammatory cytokines such as *Il-1β* and *Cxcl1*. We therefore investigated the impact of BRBs on *Mif* expression and targets of this signaling pathway. Our data established that *Mif, Il-1β*, and *Cxcl1* expression were inhibited by bioactive components in BRBs, including EA. These pro-inflammatory mediators are crucial to the recruitment of innate immune cells to the oral tumor microenvironment, where they contribute to oral tumor progression.

Inhibition of apoptosis is a common strategy that enables cancer cell survival and progression (25). Increased expression of the anti-apoptotic regulator Birc5 (survivin) is one mechanism by which oral cancer cells resist apoptosis (29). In our study, there was a significantly increased expression of *Birc5* mRNA in untreated, 4NQO exposed rats. BRB administration significantly inhibited *Birc5* gene expression. Further, we demonstrated a concomitant increase in cleaved caspase-3 protein expression in oral lesions of BRB-treated rats. Our analyses of the molecular events that occur during BRB-mediated chemoprevention of experimental oral carcinogenesis demonstrate that targeting of the apoptotic pathway through inhibition of *Birc5* gene expression is a potential anticancer mechanism of BRBs.

Evidence for inhibition of proliferative signaling as a mechanism of BRB-mediated chemoprevention of oral cancer is demonstrated by the downregulation of cell cycle associated genes that are typically associated with oral carcinogenesis: *Aurka*, *Ccna1, Ccna2,* and *Ccnd1* (15, 27). This is further supported by the reduction in the expression of the proliferative marker Ki-67 in BRB-treated, carcinogen-induced rats. Of particular interest is *Aurka*, a serine/threonine kinase which plays an important role during G2 to M phase transition, is involved in various mitotic events such as centrosome maturation and separation, mitotic entry, spindle assembly, and chromosome alignment (36). Selective inhibitors of AURKA have been developed for the treatment of solid tumors and have been tested in preclinical studies against oral cancer (37). The observed effects of BRBs on this key mitotic regulator as well as in other cell cycle associated pathways demonstrates the efficacy of BRBs as a whole-food additive or synergistic mixture of complementary phytochemicals targeting multiple oncogenic pathways in oral cancer chemoprevention and therapy.

It is noteworthy that in our study 5% BRBs was more effective than 10% BRBs in inhibiting oral lesion development as well as in reducing molecular biomarkers of oral carcinogenesis. This is not entirely surprising given that similar results were observed in the hamster check pouch model of oral carcinogenesis (10) as well as rat models of esophageal and colon carcinogenesis (38). It does underscore the importance of dosage in the application of BRB-mediated oral cancer chemoprevention strategies. The complex mixture of phytochemicals in BRBs participates in a complex network of interactions within the tumor microenvironment, which ultimately affects the optimal dosage for oral chemopreventive efficacy. Future studies should address this complex network of interactions between BRB phytochemicals and the oral tumor environment, as well as the effect of phytochemical combinations on the chemopreventive efficacy of BRB. This will provide essential knowledge that will be useful in the design and implementation of future clinical trials on BRB oral cancer chemoprevention.

A major bioactive component of BRBs with demonstrable anticancer activity is EA. Numerous studies demonstrate the anticancer activity of this dietary polyphenol using *in vitro* (39) and *in vivo* (17, 30, 31) oral cancer models through mechanisms involving apoptotic (31), angiogenic (30), and proliferative (39) signaling pathways. We also found evidence for the modulation of some of these pathways in our transcriptional analysis. However, an interesting finding from our study was that while EA significantly inhibited malignant lesion development, premalignant lesions were not inhibited in EA-treated rats compared to untreated rats. Surprisingly, the incidence of gross premalignant lesions (erythroplakia and leukoplakia) was higher in EA treated rats compared to untreated rats. Taken together, these observations suggest that, in addition to pro-inflammatory, anti-apoptotic, and cell cycle associated pathways, other mechanisms

are involved in BRB-mediated inhibition of oral carcinogenesis. This is not surprising, since BRB contains a complex mixture of phytochemicals that could target other oral cancer pathways that are not described in this study. Interestingly, a previous study by Tanaka et al. showed that in 4NQO-induced rats oral carcinogenesis, 0.4% EA administration significantly inhibited the development of tongue tumors as well as hyperplastic and dysplastic lesions (17). It should be noted that in the Tanaka et al. study, rats were given 4NQO for 5 weeks and EA administration began one week prior to 4NQO exposure and continued until 1 week after 4NQO exposure. In our study, rats were exposed to 4NQO for 14 weeks and EA administration began after 4NQO exposure. This difference in the sequence and length of 4NQO exposure coupled with the differences in the time of administration of EA likely accounts for the substantive difference between these studies. While the chemoprevention model employed by Tanaka et al. is adequate for screening biologically active compounds, it has only minimal relevance to the exposure-risk reduction paradigm required for human chemoprevention studies. It is evident that the protective effect of EA depends on where along the multistep process of oral carcinogenesis intervention begins; a factor that must be considered in determining the most appropriate approach to oral cancer chemoprevention. We believe that our animal model more accurately recapitulates the exposure-cancer progression paradigm with chemopreventive strategy initiated after identification of individuals at high risk for the development of oral cancer. Furthermore, it is not surprising that BRB administration was more effective than EA in reducing the development of premalignant lesions in our model due to the complex milieu of bioactive phytochemicals that may act in an additive or synergistic manner to inhibit oral cancer development. This supports the notion that a combination of bioactive compounds, such as is found in whole foods, is potentially more effective against oral cancer.

In summary, we show that dietary administration of BRBs inhibits gross and histopathological lesion formation during 4NQO-induced rat oral carcinogenesis. This was associated with a reduction in pro-inflammatory, anti-apoptotic, and proliferative molecular biomarkers. Our results also recapitulate the predictive biomarker signature observed in a human oral cancer chemoprevention clinical trial using BRB troches (15). Further, our experimental oral cancer model shows that modulation of pro-inflammatory, apoptotic and cell cycle associated pathways are potential mechanisms of BRB-mediated oral cancer chemoprevention. Combined with data from previous studies, our results demonstrate that the incorporation of BRB phytochemicals in oral cancer chemoprevention and complementary therapy is a potentially viable strategy for oral cancer prevention and treatment.

ETHICS STATEMENT

This study was carried out in accordance with the recommendations of Ohio State University Laboratory Animal Resources guidelines, Ohio State University Institutional Animal Care and Use Committee. The protocol was approved by The Ohio State University Institutional Animal Care and Use Committee.

AUTHOR CONTRIBUTIONS

SO, CW, and TK designed the study. SO, TK, BC, LW, JM, PG, KH, CB, BW, KS, and TK performed experiments and acquired data. SO, JA-J, CW, and TK analyzed and interpreted data. SO and TK drafted the manuscript. All authors critically revised and approved the final manuscript.

FUNDING

This project was supported in part by grants K01CA207599 [SO], R21CA175836 [CW, TK], U01CA18825002S1 [SO, CW], and P30CA016058 from the National Cancer Institute; grant T32DE014320 from the National Institute of Dental and Craniofacial Research; and grant UL1TR001070 from the National Center for Advancing Translational Sciences. The content is solely the responsibility of the authors and does not necessarily represent the official views of the NCI, NIDCR, or NCATS.

REFERENCES

1. Siegel RL, Miller KD, Jemal A. Cancer statistics, 2016. *CA Cancer J Clin* (2016) 66:7–30. doi:10.3322/caac.21332
2. Ferlay J, Soerjomataram I, Dikshit R, Eser S, Mathers C, Rebelo M, et al. Cancer incidence and mortality worldwide: sources, methods and major patterns in GLOBOCAN 2012. *Int J Cancer* (2015) 136:E359–86. doi:10.1002/ijc.29210
3. McCormick DL, Phillips JM, Horn TL, Johnson WD, Steele VE, Lubet RA. Overexpression of cyclooxygenase-2 in rat oral cancers and prevention of oral carcinogenesis in rats by selective and nonselective COX inhibitors. *Cancer Prev Res (Phila)* (2010) 3:73–81. doi:10.1158/1940-6207.CAPR-09-0151
4. Mestre JR, Chan G, Zhang F, Yang EK, Sacks PG, Boyle JO, et al. Inhibition of cyclooxygenase-2 expression. An approach to preventing head and neck cancer. *Ann N Y Acad Sci* (1999) 889:62–71. doi:10.1111/j.1749-6632.1999.tb08724.x
5. Choe MS, Zhang X, Shin HJ, Shin DM, Chen ZG. Interaction between epidermal growth factor receptor- and cyclooxygenase 2-mediated pathways and its implications for the chemoprevention of head and neck cancer. *Mol Cancer Ther* (2005) 4:1448–55. doi:10.1158/1535-7163.MCT-04-0251
6. Steinmetz KA, Potter JD. Vegetables, fruit, and cancer prevention: a review. *J Am Diet Assoc* (1996) 96:1027–39. doi:10.1016/S0002-8223(96)00273-8
7. Key TJ. Fruit and vegetables and cancer risk. *Br J Cancer* (2011) 104:6–11. doi:10.1038/sj.bjc.6606032
8. Rodrigo KA, Rawal Y, Renner RJ, Schwartz SJ, Tian Q, Larsen PE, et al. Suppression of the tumorigenic phenotype in human oral squamous cell carcinoma cells by an ethanol extract derived from freeze-dried black raspberries. *Nutr Cancer* (2006) 54:58–68. doi:10.1207/s15327914nc5401_7
9. Han C, Ding H, Casto B, Stoner GD, D'Ambrosio SM. Inhibition of the growth of premalignant and malignant human oral cell lines by extracts and components of black raspberries. *Nutr Cancer* (2005) 51:207–17. doi:10.1207/s15327914nc5102_11
10. Casto BC, Kresty LA, Kraly CL, Pearl DK, Knobloch TJ, Schut HA, et al. Chemoprevention of oral cancer by black raspberries. *Anticancer Res* (2002) 22:4005–15.
11. Warner BM, Casto BC, Knobloch TJ, Accurso BT, Weghorst CM. Chemoprevention of oral cancer by topical application of black raspberries on high at-risk mucosa. *Oral Surg Oral Med Oral Pathol Oral Radiol* (2014) 118:674–83. doi:10.1016/j.oooo.2014.09.005

12. Kresty LA, Morse MA, Morgan C, Carlton PS, Lu J, Gupta A, et al. Chemoprevention of esophageal tumorigenesis by dietary administration of lyophilized black raspberries. *Cancer Res* (2001) 61:6112–9.
13. Harris GK, Gupta A, Nines RG, Kresty LA, Habib SG, Frankel WL, et al. Effects of lyophilized black raspberries on azoxymethane-induced colon cancer and 8-hydroxy-2'-deoxyguanosine levels in the Fischer 344 rat. *Nutr Cancer* (2001) 40:125–33. doi:10.1207/S15327914NC402_8
14. Peiffer DS, Wang LS, Zimmerman NP, Ransom BW, Carmella SG, Kuo CT, et al. Dietary consumption of black raspberries or their anthocyanin constituents alters innate immune cell trafficking in esophageal cancer. *Cancer Immunol Res* (2016) 4:72–82. doi:10.1158/2326-6066.CIR-15-0091
15. Knobloch TJ, Uhrig LK, Pearl DK, Casto BC, Warner BM, Clinton SK, et al. Suppression of proinflammatory and prosurvival biomarkers in oral cancer patients consuming a black raspberry phytochemical-rich troche. *Cancer Prev Res (Phila)* (2016) 9:159–71. doi:10.1158/1940-6207.CAPR-15-0187
16. Steele VE, Lubet RA. The use of animal models for cancer chemoprevention drug development. *Semin Oncol* (2010) 37:327–38. doi:10.1053/j.seminoncol.2010.05.010
17. Tanaka T, Kojima T, Kawamori T, Wang A, Suzui M, Okamoto K, et al. Inhibition of 4-nitroquinoline-1-oxide-induced rat tongue carcinogenesis by the naturally occurring plant phenolics caffeic, ellagic, chlorogenic and ferulic acids. *Carcinogenesis* (1993) 14:1321–5. doi:10.1093/carcin/14.7.1321
18. Kanojia D, Vaidya MM. 4-nitroquinoline-1-oxide induced experimental oral carcinogenesis. *Oral Oncol* (2006) 42:655–67. doi:10.1016/j.oraloncology.2005.10.013
19. Hellemans J, Mortier G, De Paepe A, Speleman F, Vandesompele J. qBase relative quantification framework and software for management and automated analysis of real-time quantitative PCR data. *Genome Biol* (2007) 8:R19. doi:10.1186/gb-2007-8-2-r19
20. Vandesompele J, De Preter K, Pattyn F, Poppe B, Van Roy N, De Paepe A, et al. Accurate normalization of real-time quantitative RT-PCR data by geometric averaging of multiple internal control genes. *Genome Biol* (2002) 3:RESEARCH0034. doi:10.1186/gb-2002-3-7-research0034
21. Kresty LA, Mallery SR, Stoner GD. Black raspberries in cancer clinical trials: past, present and future. *J Berry Res* (2016) 6:251–61. doi:10.3233/JBR-160125
22. Shumway BS, Kresty LA, Larsen PE, Zwick JC, Lu B, Fields HW, et al. Effects of a topically applied bioadhesive berry gel on loss of heterozygosity indices in premalignant oral lesions. *Clin Cancer Res* (2008) 14:2421–30. doi:10.1158/1078-0432.CCR-07-4096
23. Perez-Sayans M, Somoza-Martin JM, Barros-Angueira F, Reboiras-Lopez MD, Gandara Rey JM, Garcia-Garcia A. Genetic and molecular alterations associated with oral squamous cell cancer (review). *Oncol Rep* (2009) 22:1277–82. doi:10.3892/or_00000565
24. Feller L, Altini M, Lemmer J. Inflammation in the context of oral cancer. *Oral Oncol* (2013) 49:887–92. doi:10.1016/j.oraloncology.2013.07.003
25. Hanahan D, Weinberg RA. Hallmarks of cancer: the next generation. *Cell* (2011) 144:646–74. doi:10.1016/j.cell.2011.02.013
26. Oghumu S, Knobloch TJ, Terrazas C, Varikuti S, Ahn-Jarvis J, Bollinger CE, et al. Deletion of macrophage migration inhibitory factor inhibits murine oral carcinogenesis: potential role for chronic pro-inflammatory immune mediators. *Int J Cancer* (2016) 139:1379–90. doi:10.1002/ijc.30177
27. Ge S, Zhang J, Du Y, Hu B, Zhou Z, Lou J. Dynamic changes in the gene expression profile during rat oral carcinogenesis induced by 4-nitroquinoline 1-oxide. *Mol Med Rep* (2016) 13:2561–9. doi:10.3892/mmr.2016.4883
28. Mallery SR, Tong M, Shumway BS, Curran AE, Larsen PE, Ness GM, et al. Topical application of a mucoadhesive freeze-dried black raspberry gel induces clinical and histologic regression and reduces loss of heterozygosity events in premalignant oral intraepithelial lesions: results from a multicentered, placebo-controlled clinical trial. *Clin Cancer Res* (2014) 20:1910–24. doi:10.1158/1078-0432.CCR-13-3159
29. Khan Z, Khan AA, Yadav H, Prasad G, Bisen PS. Survivin, a molecular target for therapeutic interventions in squamous cell carcinoma. *Cell Mol Biol Lett* (2017) 22:8. doi:10.1186/s11658-017-0038-0
30. Kowshik J, Giri H, Kishore TK, Kesavan R, Vankudavath RN, Reddy GB, et al. Ellagic acid inhibits VEGF/VEGFR2, PI3K/Akt and MAPK signaling cascades in the hamster cheek pouch carcinogenesis model. *Anticancer Agents Med Chem* (2014) 14:1249–60. doi:10.2174/1871520614666140723114217
31. Anitha P, Priyadarsini RV, Kavitha K, Thiyagarajan P, Nagini S. Ellagic acid coordinately attenuates Wnt/beta-catenin and NF-kappaB signaling pathways to induce intrinsic apoptosis in an animal model of oral oncogenesis. *Eur J Nutr* (2013) 52:75–84. doi:10.1007/s00394-011-0288-y
32. Karin M, Greten FR. NF-kappaB: linking inflammation and immunity to cancer development and progression. *Nat Rev Immunol* (2005) 5:749–59. doi:10.1038/nri1703
33. Pikarsky E, Porat RM, Stein I, Abramovitch R, Amit S, Kasem S, et al. NF-kappaB functions as a tumour promoter in inflammation-associated cancer. *Nature* (2004) 431:461–6. doi:10.1038/nature02924
34. Gonzalez-Barrio R, Edwards CA, Crozier A. Colonic catabolism of ellagitannins, ellagic acid, and raspberry anthocyanins: in vivo and in vitro studies. *Drug Metab Dispos* (2011) 39:1680–8. doi:10.1124/dmd.111.039651
35. Peiffer DS, Zimmerman NP, Wang LS, Ransom BW, Carmella SG, Kuo CT, et al. Chemoprevention of esophageal cancer with black raspberries, their component anthocyanins, and a major anthocyanin metabolite, protocatechuic acid. *Cancer Prev Res (Phila)* (2014) 7:574–84. doi:10.1158/1940-6207.CAPR-14-0003
36. Pérez Fidalgo JA, Roda D, Roselló S, Rodríguez-Braun E, Cervantes A. Aurora kinase inhibitors: a new class of drugs targeting the regulatory mitotic system. *Clin Transl Oncol* (2009) 11:787. doi:10.1007/s12094-009-0447-2
37. Tanaka H, Nakashiro K-I, Iwamoto K, Tokuzen N, Fujita Y, Shirakawa R, et al. Targeting aurora kinase A suppresses the growth of human oral squamous cell carcinoma cells in vitro and in vivo. *Oral Oncol* (2013) 49:551–9. doi:10.1016/j.oraloncology.2013.02.002
38. Stoner GD, Chen T, Kresty LA, Aziz RM, Reinemann T, Nines R. Protection against esophageal cancer in rodents with lyophilized berries: potential mechanisms. *Nutr Cancer* (2006) 54:33–46. doi:10.1207/s15327914nc5401_5
39. Weisburg JH, Schuck AG, Reiss SE, Wolf BJ, Fertel SR, Zuckerbraun HL, et al. Ellagic acid, a dietary polyphenol, selectively cytotoxic to HSC-2 oral carcinoma cells. *Anticancer Res* (2013) 33:1829–36.

Conflict of Interest Statement: The authors declare that the research was conducted in the absence of any commercial or financial relationships that could be construed as a potential conflict of interest.

Copyright © 2017 Oghumu, Casto, Ahn-Jarvis, Weghorst, Maloney, Geuy, Horvath, Bollinger, Warner, Summersgill, Weghorst and Knobloch. This is an open-access article distributed under the terms of the Creative Commons Attribution License (CC BY). The use, distribution or reproduction in other forums is permitted, provided the original author(s) or licensor are credited and that the original publication in this journal is cited, in accordance with accepted academic practice. No use, distribution or reproduction is permitted which does not comply with these terms.

frontiers in Immunology

REVIEW
published: 27 October 2017
doi: 10.3389/fimmu.2017.01395

Genes Critical for Developing Periodontitis: Lessons from Mouse Models

Teun J. de Vries[1]†, Stefano Andreotta[1†], Bruno G. Loos[1] and Elena A. Nicu[1,2]*

[1] Department of Periodontology, Academic Centre for Dentistry Amsterdam (ACTA), University of Amsterdam, VU University Amsterdam, Amsterdam, Netherlands, [2] Opris Dent SRL, Sibiu, Sibiu, Romania

Since the etiology of periodontitis in humans is not fully understood, genetic mouse models may pinpoint indispensable genes for optimal immunological protection of the periodontium against tissue destruction. This review describes the current knowledge of genes that are involved for a proper maintenance of a healthy periodontium in mice. Null mutations of genes required for leukocyte cell–cell recognition and extravasation (e.g., *Icam-1, P-selectin, Beta2-integrin/Cd18*), for pathogen recognition and killing (e.g., *Tlr2*, *Tlr4*, *Lamp-2*), immune modulatory molecules (e.g., *Cxcr2*, *Ccr4*, *IL-10*, *Opg*, *IL1RA*, *Tnf-α receptor*, *IL-17 receptor*, *Socs3*, *Foxo1*), and proteolytic enzymes (e.g., *Mmp8*, *Plasmin*) cause periodontitis, most likely due to an inefficient clearance of bacteria and bacterial products. Several mechanisms resulting in periodontitis can be recognized: (1) inefficient bacterial control by the polymorphonuclear neutrophils (defective migration, killing), (2) inadequate antigen presentation by dendritic cells, or (3) exaggerated production of pro-inflammatory cytokines. In all these cases, the local immune reaction is skewed toward a Th1/Th17 (and insufficient activation of the Th2/Treg) with subsequent osteoclast activation. Finally, genotypes are described that protect the mice from periodontitis: the SCID mouse, and mice lacking *Tlr2/Tlr4*, the *Ccr1/Ccr5*, the *Tnf-α receptor p55*, and *Cathepsin K* by attenuating the inflammatory reaction and the osteoclastogenic response.

Keywords: periodontitis, mouse models, immune modulation, osteoclast, bone resorption, chronic periodontitis, knockout mouse, transgenic mice

OPEN ACCESS

Edited by:
Jixin Zhong, Case Western Reserve University, United States

Reviewed by:
Ping Chen, Georgetown University School of Medicine, United States
Yinghong Hu, Emory University, United States
Xiaoxuan Lyu, California Institute for Biomedical Research, United States

****Correspondence:***
Teun J. de Vries
teun.devries@acta.nl

†These authors have contributed equally to this work.

Specialty section:
This article was submitted to Inflammation, a section of the journal Frontiers in Immunology

Received: *07 August 2017*
Accepted: *09 October 2017*
Published: *27 October 2017*

Citation:
de Vries TJ, Andreotta S, Loos BG and Nicu EA (2017) Genes Critical for Developing Periodontitis: Lessons from Mouse Models. Front. Immunol. 8:1395. doi: 10.3389/fimmu.2017.01395

INTRODUCTION

Periodontitis is a destructive bacterial-induced chronic inflammatory disease of the tooth-supporting tissues that leads to tooth loss due to resorption of the tooth surrounding connective tissues and alveolar bone if not properly and timely treated. The biological complexity of human periodontitis is highly comparable to other chronic immune disorders (CIDs) where multiple factors determine the resultant immune fitness (1). In this way, periodontitis is related to an aberrant immune response to the bacterial biofilm on the teeth and tooth roots that border the periodontal tissues (2, 3). Most people live in symbiosis with their oral microbiome and specifically with a thin layer of dental plaque on the teeth. These individuals present some sort of immunological tolerance. The most prominent immune cell that is constantly present in the gingival dental plaque interface is the PMN, with about 30,000 of them per minute extravasating into the gingival crevices around the teeth. They have a tolerant and non-hyperreactive phenotype, not producing pro-inflammatory signals, resulting in maintenance of periodontal health in the potentially "dangerous" oral environment

harboring billions of bacteria, including low level (dormant) potential bacterial pathogens. Moreover, dendritic cells home to lymphoid organs and nodes for "training" the host in tolerance, but also preparing for adaptive immunity when needed. In fact, the dendritic cells steer the development of T regulatory cell (Treg), to be found in the gingiva. Inside the gingival tissues one can appreciate also a tolerance of B cells (again modulated by Treg), macrophages, as well as fibroblasts, having all the non-reactive host defense imprint. We could compare this state of health or "normality" of the mucosal immunity in the gingiva with that of the other mucosal surfaces, like intestinal mucosal linings, normally not reacting with overt inflammation to bacterial products and food-related antigens (1, 4).

A clear limitation of studying periodontitis in humans is the complexity of the disease, involving interactions between genes, life styles, and the tooth-related microbiome composition. In order to exclude this "noise" between individuals, one can make advantage of mouse models, where inbred strains overcome genetic variations.

Wild-type mice are relatively well protected against periodontitis. Apart from a few reports (5), spontaneous or bacteria-induced periodontitis is scarcely reported. This review describes the emerging field of genetically modified mouse models that develop periodontitis. Since single gene null mutations may already cause periodontitis, mouse knockout models are advantageous in identifying genes that are essential in the protection against periodontitis. Although a challenge with periodontitis-associated bacteria such as *Aggregatibacter actinomycetemcomitans* or *Porphyromonas gingivalis* is often required for periodontitis induction in mice, periodontitis can also occur without exogenous inoculation but in the presence of naturally present bacteria, such as described by Beertsen et al. (6) or even under sterile conditions, such as described by Sheng et al. (7). All ligature-induced periodontitis mouse models are excluded from this review, since we regard this *a priori* wounding of the periodontium as an artificial model that does not reflect natural periodontitis initiation and progression. Where possible, the mouse model findings will be related to human "naturally occurring" genetic mutations.

MOUSE PERIODONTIUM, MOUSE PERIODONTITIS

The two soft tissue components of the periodontium (From Greek, peri = around, odontos = tooth) are the gingiva and the periodontal ligament. A major difference between the human and mouse dentition is the orientation of the four continuously erupting incisors that are located underneath the mandibular or superior to the maxillary molar arch. Apart from the four incisors, mice have three molars (M1–M3) per quadrant, decreasing in size from front to back. Under normal conditions, the attachment point of the junctional epithelium (i.e., the deeper part of the epithelium that connects gingiva to teeth) is terminating at the cementum-enamel-junction (CEJ) of the teeth.

In periodontitis, typically, apical migration of junctional epithelium occurs, concomitant with invasion of inflammatory cells in the gingiva and the epithelial layer and finally recruitment of osteoclasts that degrade underlying alveolar bone. A recent study (8) has refined the sequential influxes of immune cells during periodontitis progression in mice (**Figure 1A**). Upon an exogenous challenge with periodontitis-associated bacteria, a first line of defense invasion of polymorphonuclear neutrophils (PMNs) will inactivate most bacteria. This is followed by primarily T helper (Th) 1 and Th17 cells, which are replaced gradually by Th2 and Tregs. Ultimately, osteoclasts are expanding at the alveolar bone crest where alveolar bone is been degraded in the end stage of periodontitis (**Figure 1A**). The widely used objective criterion for the diagnosis of periodontitis, both for men and mice, is the pathologically increased distance between the cementum-enamel-junction (CEJ) and the tip of the alveolar bone. In mice, this distance is measured only at the molar block and increases during periodontitis progression, eventually leading to tooth loss (**Figure 1B**). It should be emphasized at this stage, that many genes and cell types discussed here, may play a dual role. For instance, PMNs can both prevent periodontitis initiation and progression by timely eliminating bacteria. Alternatively, when not effective, the presence of PMNs can be detrimental for the periodontal tissues, since endured cytokine expression may evoke soft and hard tissue degradation by fibroblasts or inflammatory cells and osteoclasts, respectively.

MOUSE STRAINS AND PERIODONTITIS SUSCEPTIBILITY—EARLY OBSERVATIONS

Periodontitis and subsequent tooth loss, can occur spontaneously in mice; however, this is a rare phenomenon. Nevertheless, periodontitis can be induced experimentally *via* oral lavage with microbial species that are strongly associated with the development of periodontitis in human [e.g., Ref. (9)] or can be a result of genetic mutations, either or not using bacterial pressure to induce it [e.g., Ref. (10)]. Baker et al. (11) showed that the various mouse strains differ in their susceptibility to develop experimentally induced periodontitis. In these experiments, mice were pre-treated with antibiotics before being infected with viable *P. gingivalis*. Even under a high exposure to *P. gingivalis*, five out of nine inbred strains that were analyzed (A/J, A/HEJ, 129/J, SJL/J, C57BL/6J) were resistant to alveolar bone loss (measured as the distance AC-CEJ, see **Figure 1B** for explanation) and four were susceptible (AKR/J, DBA/2J, BALB/cByJ, BALB/cJ). In a recent study, this was confirmed by Shusterman et al. (12), who found BALB/c mice to be susceptible for periodontitis and not DBA/2J, C57BL/6J, and A/J mice. This could well explain why until recently periodontitis in mice was hardly encountered, since most genetically modified mice described in this paper originated from the relatively resistant C57BL/6J mice.

PERIODONTITIS IN MICE THAT LACK DEFINED SUBSETS OF IMMUNE CELLS

B and T Cells

In periodontal research, the first immune-deficient murine model was introduced by Baker and coworkers in 1994 (13)

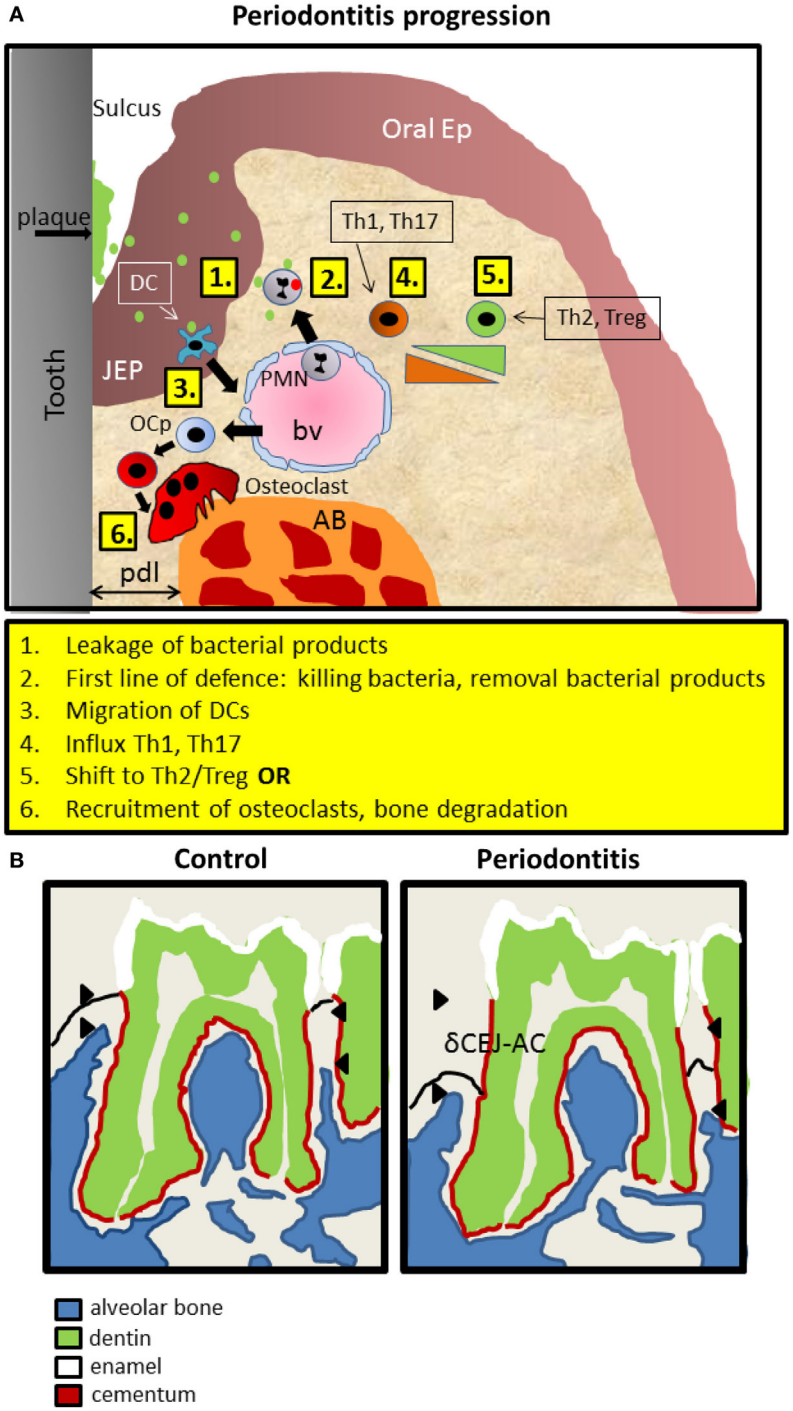

FIGURE 1 | Introduction into mouse periodontitis. **(A)** The sequence of events leading to periodontitis. **1**. Bacterial pressure (green; red inactivated) colonizing the tooth area (plaque) and present in the space between the tooth surface and the epithelium (sulcus), causes the JEP to thicken and retract. 2. First line of defense such as polymorphonuclear neutrophils (PMNs) are attracted to the infection, extravasate out of blood vessels (bv) into the tissue, and kill bacteria and remove bacterial products. 3. Langerhans cells, special dendritic cells within epithelium (ep), recognize bacterial products, migrate away and elicit a Th1 response that is present during early inflammation, coincidental with inflammatory mediators such as IL1, TNF-α, and IL-6. 4. Gradually, in a sustained inflammation, this shifts toward a Th2 phenotype with more anti-inflammatory mediators. Experimental evidence for this sequence was demonstrated by Araujo-Pires et al. (8), Arizon et al. (17), and Bittner-Eddy et al. (18). 5. Finally, and archetypal for periodontitis, precursor cells of osteoclasts (OCp) migrate to the alveolar bone (AB) and differentiate into bone degrading multinucleated osteoclasts (OC). pdl, periodontal ligament; JEP, junctional epithelium; Ep, epithelium; bv, blood vessel. **(B)** Schematic drawing of mouse periodontitis with emphasis on the hard tissues. Redrawn from a microCT image taken from the study by Koide et al. (60). Shown are the full first and part of the second of the three mouse molars of a mandible. The distance between the cementum-enamel-junction and the AB crest (δCEJ-AC) is an objective criterion for establishing periodontitis. This distance increases in periodontitis due to the degradation of AB by OC. The imaginary epithelial border—not visible with microCT is indicated with a black line.

with the goal to evaluate the effect of *P. gingivalis* infection in "severe combined immune deficiency mice," the SCID mice. The SCID mouse lacks both T and B lymphocytes. Baker et al. compared two genetically disparate strains of immunocompetent mice, C57BL/6J and BALB/cByJ with an immunodeficient strain: C.B17-*scid*/SzDcr. A pretreatment phase with antibiotics with the attempt to suppress the commensal microflora was followed by an oral infection with *P. gingivalis via* oral lavage for 42 days. Infection with *P. gingivalis* induced alveolar bone loss in immunocompetent and immunodeficient mice, but the degree of alveolar bone loss in immunocompetent strains, BALB/cByJ, was higher than that in the genetically closely related SCID strain. This study indirectly showed that mice with intact T and B cell repertoire display more bone destruction, signifying that immune cells contribute and are necessary for the onset of periodontitis-like bone resorption. In a later report, the same group (14) investigated under the same experimental conditions the role of the T cells using β_2 m-knockout mice (deficient in $CD8^+$ and $NK1^+$ T cells), A_β-knockout mice (fail to generate $CD4^+$ T cells), interferon-γ deficient mice and interleukin-6 (IL-6) deficient mice. This study showed that $CD4^+$ T cells promote alveolar bone loss, whereas $CD8^+$ and $NK1^+$ T cells did not play a direct or indirect role in the bone resorption process. A_β-knockout mice did not demonstrate significant alveolar bone loss when infected with *P. gingivalis*. These studies suggest the possible involvement of certain immune cells, with the obvious caveat that it may not reflect the progressive stages of periodontitis, since this disease is characterized with a sequential influx of defined immune cells over time. Upon infection, and as periodontitis progresses, mouse periodontium is first invaded by Th1 T-cells, followed by Th17 and at the end stage, probably reflecting a more chronic diseased state, Th2 and Tregs invade the soft periodontium (8).

Dendritic Cells

Dendritic cells are highly specialized innate immune cells that orchestrate the adaptive immune responses. In their immature state, dendritic cells can efficiently capture and process microbial antigens, but as they mature, their phenotype changes, and mature DCs can migrate toward lymphoid organs and prime naïve T cells (15). Human and murine gingiva contains several subsets of DCs, of which the Langerhans cells present in the epithelial compartment are the most studied (16).

Arizon and coworkers employed a mouse model of Langerhans cell-ablation followed by oral inoculation of *P. gingivalis* (17). In this inducible murine *Langerin* knockout model, dendritic cell ablation led to an aggravated local inflammation in the periodontium and more alveolar bone loss. Specifically, in the absence of dendritic cells, a marked increase in the number of B cells and CD4 T cells, together with a lower number of Treg cells, was observed in the inflamed periodontium. Many of the infiltrating T cells, NK cells, or γδ cells expressed also the osteoclast-activating cytokine receptor activator of nuclear factor-κB ligand (RANKL), linking the intense inflammation with the alveolar bone loss. The interpretation of these results was recently questioned by Bittner-Eddy and coworkers, in a different model of Langerhans cell ablation (18). Their model resulted in the targeted ablation of exclusively the Langerhans cells, but left other DC types unaffected such as the $Langerin^+$ DCs and the $CD8^+$ lymphoid-resident DCs; this is unlike the murine *Langerin*-DTR model employed by Arizon et al. (17). It is this combined deficiency in Langerhans cells and $Langerin^+$ DCs that explains the more severe periodontitis in the murine Langerin-model. These mice fail to induce both Th17 and Treg cells, which pushes the phenotype toward a skewed Th1 response and IFN-γ-induced osteoclastogenesis with alveolar bone loss as consequence (18).

Dendritic cell functions are regulated by transcription factors, including forkhead box-O1, *Foxo1*. FOXO1 regulates dendritic cell migration to lymph nodes and lipopolysaccharide (LPS)-induced cytokine expression by dendritic cells. Targeted deletion of *Foxo1* in the dendritic cells has been studied in a mouse model, in which periodontitis was induced by oral inoculation with *P. gingivalis* and *Fusobacterium nucleatum* (19). *Foxo1* deletion resulted in reduced migration of dendritic cells in the epithelium and conjunctive tissue around teeth. These dendritic cells expressed less IL-12 in response to *P. gingivalis* than control mice. The alveolar bone loss was more severe in the mice with a *Foxo1* deletion, probably *via* an increased production of the pro-osteoclastogenic IL-1β, IL-17, and RANKL and insufficient stimulation of B cells by the DCs in the lymph nodes. This latter suggestion is consistent with the findings of Mkonyi et al. in their blocked lymphangiogenesis model; they report that a reduced B-cell activation leads to a compensatory increase in IL-1β and IL-17, and results in enhanced bacteria-induced bone loss (20).

Macrophages

Analysis of the role of macrophages in periodontitis revealed that the M1 macrophage accumulates and is the predominant macrophage in the periodontium of mice infected with *P. gingivalis*. This coincided with increased levels of pro-osteoclastogenic and inflammatory cytokines IL-1 and IL-6. Mice in which macrophages were depleted with clodronate containing liposomes, were protected from developing periodontitis (21). Since cells from the monocyte/macrophage lineage are also precursors for bone degrading osteoclasts, this finding could suggest that macrophage depletion in turn diminishes osteoclast precursor cells.

MOUSE MODELS OF GENES ASSOCIATED WITH THE INFLAMMATORY RESPONSE TO MICROBIAL PRESSURE

The availability of knockout mice has accelerated mouse periodontitis research. In general, oral gavage models using periodontitis-associated pathogens were needed to induce periodontitis. Apparently, in most cases, exogenous bacterial pressure in conjunction with a loss of function of a certain gene is needed to evoke periodontitis. This way, essential genes necessary for combating the bacterial pressure could be identified. These include those (i) engaged in the adhesion and subsequent extravasation of leukocytes toward the infection area such as selectins and integrins, (ii) genes that are involved in recognition and clearance of bacteria such as Toll-like receptors (*Tlr2*, *Tlr4*) and the lysosome-associated membrane proteins (*Lamps*),

and *Lactoferrin* (iii) modulatory cytokines such as *IL-17* or inflammation inhibitory cytokines. As result of an enduring inflammatory response, proteases are predominantly present in the periodontium, leading to softening of the tissue and to bone degradation. In (iv), the protease models of *Mmp-8*, *Plasminogen*, and *Cathepsin K* are discussed. In (v), periodontitis models of the structural mutations of the periodontium involving bone, cementum and dentin matrix proteins and mice lacking lymphatics are briefly discussed. Finally (vi), mouse models for periodontitis in conjunction with other inflammatory diseases such as atherosclerosis and rheumatoid arthritis are discussed.

Adhesion Molecules: Selectins and Integrins

Endothelial and leukocyte adhesion molecules are responsible for the extravasation process that occurs when leukocytes are recruited to the inflammatory site. Upon extravasation, cell–cell and cell–matrix adhesion molecules are required for the homing process of the leukocytes. Adhesion molecules are classified as either *selectins* or *integrins*. Apart from their role in leukocyte homing, integrins also play a role in maintaining the proper structure of the periodontal ligament (22). Interestingly, the epithelial integrin αvβ6 participates in homeostasis of the lungs by activating the immunosuppressive cytokine TGF-beta, and thus restraining the activation of alveolar macrophages (23). A similar effect of integrins can be expected in the periodontal environment, where a hyper-responsive inflammatory response is a key mechanism for the tissue destruction occurring in periodontitis. Selectins can be divided into three family members: *P-*, *E-*, and *L-selectin*, based on the cell type on which they were identified: platelet, endothelium, and leukocyte, respectively. They mediate leukocyte rolling in response to specific activation signals from C5a, interleukin-1β, or TNF-α. The integrins bind to endothelial intercellular adhesion molecules ICAM-1 and ICAM-2, favoring the transendothelial migration of leukocytes (24). The β_2-integrins (CD18) play a role specifically for PMNs: their extravasation, and during phagocytosis and the respiratory burst (24).

Adhesion molecule deficiencies can lead to severe infection, leukocytosis, and rapidly progressive periodontal disease in humans (25). In a study by Baker and coworkers (11), the role of adhesion molecules in the onset of alveolar bone loss was analyzed in adhesion molecule deficient mice. They used three strains of mice lacking or with severe reduction of β_2-integrin *Cd18*, *Icam-1*, and *P-selectin*. Despite the absence of an exogenous infection (e.g., *via P. gingivalis)*, both the *Icam-1* and *P-selectin*-deficient mice were more susceptible to alveolar bone loss than WT mice. A recent study using *Lfa-1/Cd18* knockout mice demonstrated that increased degradation of alveolar bone was associated with increased local production of IL-17 (26). Blocking of IL-17 or its associated IL-23 decreased periodontitis progression in *Cd18* knockout mice and caused lower levels of pro-osteoclastogenesis cytokines IL-1β and RANKL. This inhibition also dramatically influenced the composition of the inflammatory infiltrate of the periodontium: lower numbers of CD3- (general T-cell marker), CD4- (specific subset of T-cells), and CD138- (plasma cells) positive cells were observed. This study showed that the inability of PMNs to migrate into the inflamed periodontium causes an influx of other immune cells and causes Th17 reactions that lead to periodontal destruction, resembling leukocyte adhesion deficiency-I type periodontitis seen in humans (26). Interestingly, blocking of IL-17 caused a reduction in the total bacterial burden, suggesting that the IL-17-driven inflammation contributed to the microbial dysbiosis, which in turn caused more periodontal destruction. A different mouse model, a knockout of the β6 integrin, resulted in a higher presence of bacteria in the periodontium, and consequently in periodontitis upon infection with periopathogens (27).

Similarly, Niederman et al. (28), who used a bacterial induction of periodontitis, showed that *P-* and *E-selectin*$^{-/-}$ mice experienced significantly more alveolar bone loss than the WT counterpart. Bone loss occurred at an earlier age and was also accompanied by a 50-fold increase in the total gingival bacterial load in the knockout mice. Moreover, a highly significant correlation between the extent of bone loss and the total bacterial burden in the *P/E*$^{-/-}$ group was observed. These knockout mice presented with a leukocytosis that resulted from the inability of the PMNs to transmigrate from the vasculature into the tissues.

These data together show that the susceptibility of mice carrying adhesion molecule deficiency in different degrees is primarily related to the inability of the PMNs to exert their role in the initial phase of the inflammatory process, and to a secondary Th17-driven dysbiosis with exacerbated osteoclastic activity. We have summarized these events in **Figure 2**.

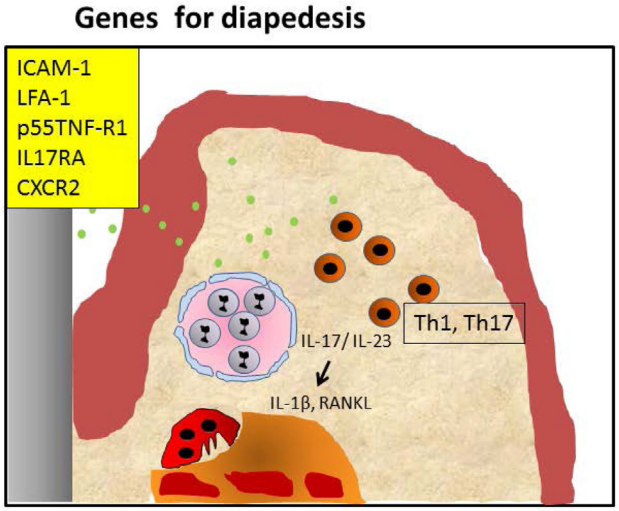

FIGURE 2 | Periodontitis caused by malfunctioning diapedesis. Knockout of leukocyte adhesion molecules such as ICAM-1, LFA-1, and P-selectin and mice with defective TNF-α receptor p55 tumor necrosis factor-α receptor (p55TNF-R1), IL-17RA, or CXCR2 mediated attraction of polymorphonuclear neutrophils (PMNs) causes a diminished penetration of PMNs in the infected periodontium, resulting in hampered clearance of periopathogens (green dots). This may lead to an accumulation of Th1/Th17 cells, both in humans and mice. IL-17 and IL-23 activate alveolar bone loss by increasing pro-osteoclastogenesis cytokines IL-1β and RANKL. This sequence of events can be blocked by anti-IL-17 (26).

Recognition and Killing of Bacteria: Toll-Like Receptors (TLR2 and TLR4), LAMP-2, and Lactoferrin

Toll-like receptors (TLRs) are pattern recognition receptors that recognize bacterial and viral compounds which stimulate innate immune responses (29). They are expressed by various cell types (epithelial cells, monocytes/macrophages, fibroblasts, and PMNs). When the TLRs interact with microbial components (e.g., LPS, fimbriae), they are activated and trigger the nuclear translocation of nuclear factor-κB (NF-κB) factor and induction of inflammation-related genes (30). In particular, this pathway leads to the production of immune mediators that initiate the inflammatory response against the microbial challenge. The TLR superfamily includes different classes of molecules and some of them have been investigated in relation to experimental periodontitis.

Burns et al. (31) analyzed the response of *Tlr2* deficient mice to a challenge with live *P. gingivalis*. The infected WT mice had more alveolar bone loss than the uninfected WT mice. Unexpectedly, the *Tlr2*$^{-/-}$ mice were protected from *P. gingivalis*-induced bone loss. Using confocal microscopy and fluorescence-activated cell sorting, they showed that clearance by PMN-mediated phagocytosis of *P. gingivalis* in the absence of TLR2 was *more* efficient compared to WT mice. Moreover, wild-type mice showed a higher inflammatory cytokine (IL-1β and TNF-α) production than the *Tlr2* knockout mice. This suggests that in the presence of TLR2, the emerging cytokine milieu is sustaining a pro-inflammatory state, resulting in a favorable ecosystem for *P. gingivalis* survival, maintaining dysbiosis thereby worsening of the periodontal condition.

The involvement of different TLR types in periodontal bone loss varies across mice strains, depending on their genetic make-up. Costalonga et al. (32), using C57BL/10J, BALB/cJ and C57BL/6J mice, showed various effects of *Tlr2* or *Tlr4* deficiency. The *Tlr4*-deficiency worsened the periodontitis in the C57BL/10J mouse, but not in the BALB/cJ mouse. In the same study, the authors showed that the C57BL/6J TLR2 knockout mice had comparable alveolar bone levels when they were either sham- or *P. gingivalis*-infected. Thus, when interpreting the studies (25, 26), one must keep in mind the variability in the cytokine response elicited by a microbial challenge in the mice studied. The BALB/c mice tend to respond with Th2 cytokines (e.g., IL-4, IL-10, IL-13) and develop more bone loss, whereas the C57BL/6J mice produce predominantly Th1 cytokines (e.g., interferon-γ, IL-2) and are protected from periodontal bone loss. Therefore, ablating TLR2 or TLR4 signaling, modifies differentially the susceptibility to develop periodontitis and dependent on mouse strain. In contrast to the findings with *P. gingivalis*, TLR2$^{-/-}$ mice that were infected with *A. actinomycetemcomitans* developed periodontitis (33). This suggests that the requirement for TLR2 to combat periodontopathogenic bacterial products depends on the specific bacterial species.

LAMP-1 and LAMP-2 are two major lysosomal membrane proteins crucial for the protection of the lysosomal membrane from the host intra-lysosomal environment. LAMP proteins, especially LAMP-2, are important regulators in successful maturation of both autophagosomes and phagosomes (34). LAMP-2 is essential for the process of fusion between phagosome and lysosome that leads to the creation of a phago-lysosome in the PMNs. The phago-lysosome formation is a prerequisite for the successful degradation of internalized pathogens (35). Beertsen and coworkers (6) used a knockout mouse model of *Lamp-2* to investigate the role of this membrane-associated protein in phagosomal maturation. *Lamp-2* knockout mice experienced more bone loss already at 7 weeks after birth than the wild-type group without any exogenous bacterial infection. The bone loss was associated with a massive plaque accumulation on the tooth surface and large infiltrated epithelial areas in *Lamp-2* deficient mice. Interestingly, inflammation completely disappeared after applying antibiotics. Electron microscopic analyses of PMN revealed that these phagocytes isolated from the *Lamp-2*$^{-/-}$ mice contained an accumulation of autophagic vacuoles due to the impossibility for the phagosomes to fuse with the lysosomes. This study underlines the importance of the PMN in functioning as the first line of defense; the PMN have the capability for oxygen-independent killing of bacteria to prevent the onset of periodontal disease and to protect against bacterial invasion and thus to avoid the generation of a pro-inflammatory state which is favorable for development of a dysbiosis.

Lactoferrin is an antimicrobial protein that has the capacity to reduce viability and pathogenicity of invading microorganisms using its properties to scavenge free iron from fluids and tissues. PMNs are the main source of lactoferrin delivery at the front of the bacterial biofilm facing periodontal tissues (36). *In vitro* studies show that lactoferrin has also the property to inhibit osteoclast differentiation (37). *Lactoferrin* knockout mice have been used to investigate the occurrence of alveolar bone loss in case of *A. actinomycetemcomitans*-induced periodontal disease (38). *Lactoferrin*-deficient mice experienced significantly more alveolar bone loss than wild-type littermates. The increased susceptibility of the *Lactoferrin*$^{-/-}$ mice was also associated with an increased tissue level of *A. actinomycetemcomitans* and increased levels of IL-1β, IL-6, TNF-α, INF-γ, and IL-12 and chemotactic cytokines like CXCL10, involved in leukocyte migration. Thus, the *Lactoferrin* knockout mouse model clearly shows that lactoferrin is important in the prevention of alveolar bone loss induced by one of the major periodontitis-associated bacteria.

Taken together, the deficiencies in *Tlr*, *Lamp-2*, and *Lactoferrin* illustrate the emerging inflammatory reactions when the innate immune mechanisms fail to effectively deal with microbial challenges. In fact, in the case of LAMP-2, the break of tolerance to naturally occurring dental biofilms is apparent. Thereby the Th1 inflammatory reaction is sustained, opening the way to chronic periodontal inflammation, a Th2 response and ultimately to bone degradation (**Figure 3**).

Immune Modulation: Chemokines, Cytokines, Growth Factors, and Transcription Factors

The host response in the periodontal tissues to the bacterial biofilm on the teeth involves the release of chemokines, cytokines,

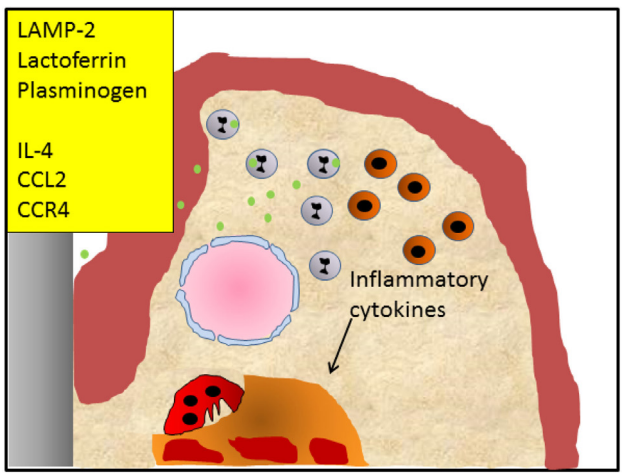

FIGURE 3 | Periodontitis caused by defective killing of bacteria. Knockout of pattern recognition receptors such as Toll-like receptors, knockout of lysosomal membrane protein LAMP-2, antimicrobial protein lactoferrin, or plasminogen causes defective clearance of bacteria, leading to activation of the Th1 signaling pathway, and initiating chronic inflammation Alternatively, knockout of genes important for the induction of the Th2 reaction and influx of T regulatory cells such as IL-4, CCL2, and CCR4 that modulate the infection, also lead to enhanced inflammation and an endured Th1 presence, such as shown by Araujo-Pires et al. (8). It can be envisaged that bacterial products accumulate due to ineffective clearance.

and growth factors that chemo-attract, activate, and/or inhibit the local cells and the immune cells. In the normal (i.e., tolerant) situation, this plethora of modulators results in a stable balance without obvious inflammation. When for some reason the host response converts to an aberrant or hyperactive state, the combined action of all modulators initiates first of all innate immune response. If this initial response is not resolved, a switch to a more acquired immune response, where a tailor made specificity by B- and T-lymphocytes is achieved. What happens in terms of periodontitis progression when one or more of these immune modulating molecules is missing, is listed below.

Suppressor of Cytokine Signaling-3

Mice with a null-mutation of *Socs-3*, the "Suppressor of Cytokine Signaling" (SOCS)-3 proteins, develop periodontitis when they are infected with *P. gingivalis*. In this specific experimental periodontitis mouse model, the investigators have noted increased expression of RANKL and an increase in osteoclast activity (39); moreover, in line with the function of *Socs-3*, they showed an increased expression of pro-inflammatory cytokines such as IL-1β and IL-6.

SMAD2 Overexpression

SMAD2 is a transcription factor of the TGF-β signaling pathway. Using a mouse model with overexpression of SMAD2 in epithelial, but not connective tissues, Alotaibi et al. (40) showed that transgenic mice were highly susceptible to alveolar bone loss, compared to their wild-type controls. The mechanisms behind this phenomena is that SMAD2 induces an increased expression of TGF-β in the gingival junctional epithelial cells, resulting in higher TNF-α and RANKL levels, and more osteoclasts in the periodontium. However, the authors note that *Smad2* transgenic mice also showed reduced proliferation of the junctional epithelium in conjunction with increased apoptotic rates, resulting in a reduced surface area of the junctional epithelium. This suggests that the observed periodontal bone destruction in the *Smad2* transgenic mice could be the result of a reduced epithelial barrier function combined with a heightened activity of the TNF-α-RANKL-osteoclast axis.

CCL3, CCR1, and CCR5

The chemokine CCL3 (also known as macrophage inflammatory protein-1α, MIP-1α) binds to the chemokine receptors CCR1 and CCR5 primarily expressed on macrophages, dendritic cells, osteoclast precursors, and Th1 lymphocytes. These interactions result in their chemoattraction, activation, and their production of cytokines. As both macrophages and Th1 cells can stimulate the formation and activity of bone resorbing osteoclasts through TNF-α and INF-γ production, the axis CCL3/CCR1/CCR5 might be relevant for periodontitis pathogenesis. Repeke and coworkers employed mouse models with target deletion of *Ccl3*, *Ccr1*, or *Ccr5* (41). When challenged by *A. actinomycetemcomitans*, the *Ccl3*$^{-/-}$ mice showed comparable periodontal destruction to the WT. The authors explained these findings by the presence of redundancy in the chemokine system, since the CCL4 and CCL5 can compensate for the lost functions of CCL3. Ablation of *Ccr1* or *Ccr5* resulted in reduced leukocyte infiltration, and this protected the mice from bone loss. Importantly, the protective effect was stronger when both receptors were knocked out simultaneously, suggesting a cooperative role for these chemokine receptors. These results suggest that an exaggerated inflammatory response is the main modulator of periodontal bone resorption.

IL-17RA, CXCR2, IL-4, and CCL22/CCR4

IL-17 is secreted by a subset of T-helper cells called Th17 cells. Its release is stimulated by TGFβ, IL-6, and IL-23 (42). IL-17 is involved in PMN recruitment and both in bone turnover, being modulatory in both bone formation and bone degradation (43), the latter especially in inflammatory diseases such as rheumatoid arthritis (44). IL-17RA is a main receptor of IL-17 and its activation by IL-17 generally results in the activation *via* the activation of NFk-B pathway to produce other pro-inflammatory cytokines (45). Yu et al. (10) investigated the role of IL-17RA in alveolar bone loss after an infection with *P. gingivalis*. With the knockout of *IL-17ra* the activity of IL-17 activity is disrupted. A morphometric analysis showed that *IL-17ra*$^{-/-}$ mice challenged with *P. gingivalis* had significant more bone loss at multiple molar sites (from 29 to 57%) in comparison with infected wild-type mice. Thus, the absence of the signal-modulating process mediated by IL-17RA results in bone loss after infection with *P. gingivalis*. Notably, alveolar bone loss was explained by an impairment in the PMN's migration toward the gingiva in *P. gingivalis*-infected

IL-17ra$^{-/-}$ mice: the PMN response at the site of gingival infection was reduced, as revealed by PMN counts in tissue sections. The failure in PMN migration is a consequence of inadequate levels of recruitment-related chemokines CXCL5 and growth related protein-α (Groα). In the same study and under the same experimental circumstances (10), *Cxcr2*$^{-/-}$ mice showed significantly more alveolar bone destruction than WT mice with an even more severe phenotype than *IL-17ra*$^{-/-}$ mice in terms of bone loss. CXCR2 is a receptor expressed on the surface of PMNs, it binds IL-17-induced chemokines like CXCL5, Groα, and macrophage inflammatory protein 2. These molecules are CXC chemokines and they play a deterministic role in the recruitment of sufficient PMN and therefore in alveolar bone conservation in the wild-type mice. We interpret the findings that most likely the chemokines regulate a normal and tolerant immune response.

Mouse models are particularly useful to shed light on the successive invasion of immune cells during periodontitis progression and the consequences for alveolar bone levels when certain immune cells cannot migrate into the periodontium. Araujo-Pires and coworkers (8) showed that when alveolar bone loss progresses rapidly after infection with a periodontal pathogen, it is accompanied by an initial influx of Th1 and Th17 cells, which leave the periodontium when the disease becomes chronic. Notably at these stages, Th2 (IL-4+) and Tregs migrate into the periodontium and slow down disease progression (**Figure 1A**). The Th2 and Treg cells express CCR4 and mice that lack this chemokine exhibit impaired influx of Tregs, accelerated bone loss accompanied with increased expression of pro-osteoclastogenic cytokines RANKL, IL-6, IL-17, and TNF-α and decreased expression of anti-osteoclastogenic cytokines osteoprotegerin (OPG), IL-10, and TGF-β. Interestingly, the rapidly progressive bone loss as well as the altered expression of pro- and anti-inflammatory cytokines could be reverted when the mice were injected with Tregs. In the same study, CCL22 could be identified as the chemokine that is important in the attraction of Th2 and Tregs. Mice treated with CCL22 neutralizing antibodies exhibited less Tregs concomitant with more alveolar bone loss. The investigators further show that CCL22 expression was severely limited in *IL-4* knockout mice. These mice were a phenocopy of the *Ccr4* null mutants: more bone loss, concomitant with more pro-osteoclastogenic cytokines. The phenotype could again be rescued by injecting Tregs (8).

The crucial experiments outlined above, showed that IL-17RA, CXCR2, IL-4, and CCL22/CCR4 are required for the natural sequences of influxes Th1, Th2, and Tregs in the periodontium. Loss of these moieties causes an enduring Th1 response by preventing Tregs to migrate into the periodontium.

p55 Tumor Necrosis Factor-α Receptor (p55TNF-R1)

TNF-α promotes recruitment of leukocytes *via* chemokine upregulation and production of matrix metalloproteinases (MMPs), needed for migration into the tissues, and mediates a wide range of inflammatory and antimicrobial effects through the TNF-α receptor p55 abbreviated as (p55TNF-R1) (46). TNF-α is recognized as an important mediator in periodontitis and its levels are increased in gingival crevicular fluid (GCF) of patients (47). The *p55Tnf-r1* knockout mice showed significantly less severe bone resorption in comparison with wild-type mice after an oral infection with *A. actinomycetemcomitans* (48). This was also accompanied by a mild inflammatory reaction given the significantly reduced number of leukocytes in the knockout group. The compromised PMN migration is dictated by the lower expression of PMNs chemoattractants (CXCL3, CXCL1, and their receptor CXCR2) in the *p55Tnf-r1* knockout mice. These chemokines are analogs of human IL-8, involved in PMN chemoattraction. Moreover, increased levels of IL-10, OPG, MMPs, and RANKL mRNA expression were seen in the *p55Tnf-r1* deficient mice in comparison to the wild-type group. The bacterial load of *A. actinomycetemcomitans* was increased in the *p55-Tnf-r1* knockout mice, indicating that this TNF-α receptor is important for proper clearance of bacteria. It is concluded by the authors that impaired TNF-α–p55TNF-R1 signaling causes protection against periodontitis through dampening of PMN invasion, hereby likely attenuating the osteoclastogenic response, despite a higher bacterial pressure.

IL-1RA

Like TNF-α, IL-1 is also a key cytokine in men and mice, and produced at any inflammatory process. It was first discovered as a bone resorbing cytokine and is known to activate osteoclasts (49). IL-1 receptor antagonist (IL-1RA) binds to the IL-1 receptor and prevents IL-1 signaling. Thus, mice lacking this regulatory protein may have a sustained activity of IL-1. Izawa et al. (50) compared periodontitis susceptibility after a challenge with *A. actinomycetemcomitans* between controls and *IL-1ra* deficient mice. Periodontitis was only established in the infected IL-1RA deficient mice, concomitant with increased formation of osteoclasts. Strikingly, no signs of periodontitis were observed in the control mice after infection, nor in the *IL-1ra* knockout mouse without bacterial infection. This indicates that a bacterial stimulus together with a sustained IL-1 signaling is needed for periodontitis progression. Expression of IL-1RA increased in *A. actinomycetemcomitans* infected WT mice increased numbers of osteoblasts, indicating that the organism activates its own negative feed-back loop after bacterial challenge.

In a different, transgenic mouse model with upregulated IL-1 signaling, the effects of IL-1α overexpression in oral epithelial cells was studied without an added bacterial challenge, just with the resident microbiome of the mice under study (51). These mice developed severe periodontitis that had all the characteristics of human periodontitis (loss of epithelial attachment, periodontal pocketing, and destruction of alveolar bone). Importantly, the total bacterial burden did not differ between the transgenic mice and their wild-type littermates. Taken together, these findings support the notion that IL-1 is a key mediator in periodontitis pathogenesis and suggest that IL-1 is certainly an important therapeutic target in human periodontitis.

IL-10, IL-12p40, and Stat3

IL-10 is one of the most important cytokines with anti-inflammatory properties (52). It is produced by activated immune

cells, especially monocytes/macrophages and T cell subsets (e.g., Th1 cells). In an autocrine fashion in monocytes/macrophages, IL-10 diminishes the production of inflammatory mediators and inhibits antigen presentation, though it enhances the uptake of antigens (53). IL-10 plays a role in the immunopathogenesis of chronic inflammatory diseases including periodontal disease (54).

When *IL-10* knockout mice were infected with *P. gingivalis via* oral lavage, *IL-10*$^{-/-}$ mice exhibited three fold more bone loss in comparison with WT mice after infection with *P. gingivalis*. This effect did not appear to be mediated *via* IL-1 since a neutralization of IL-1α, IL-1β, and IL-1RI with antibodies directed against these cytokines and receptor did not temper bone loss. This increased alveolar bone loss was not associated with an increase in the bacterial load in terms of CFUs that were grown after harvesting from the gingival crevice, and was comparable with the wild-type group. Thus, IL-10 seems to play a protective role. This is in agreement with Al-Rasheed et al. (55) who showed that a higher level of alveolar bone loss was evident in *IL-10*$^{-/-}$ mice compared with *IL-10*$^{+/+}$ mice, albeit that here, no bacterial infection had been introduced. A possible explanation of the *P. gingivalis*-induced bone loss in *IL-10*$^{-/-}$ mice can be found in the paper of Sasaki and collaborators (56), who looked at the IL-10 downstream signaling molecule Stat3. By making use of different knockout mouse models, they found that macrophages/PMN-specific *Stat3*-deficient mice exhibited more alveolar bone loss than T cell- and B cell-specific *Stat3* mice, which were resistant to alveolar bone loss. This study indicated that both the monocyte/macrophage and the granulocytic (especially the PMN) lineages are targets for the immunosuppression by IL-10. Also the *IL-12p40/IL-10* and T cell/*IL-10* double deficient mice showed resistance to alveolar bone loss in comparison to *IL-10* single knockout mice. These data strongly suggest that the T cell responses mediated *via IL-12p40* stimulate alveolar bone destruction in an *IL-10* deficient state. Interestingly, Sasaki et al. (56) showed that the prophylactic or therapeutic treatment of *IL-10*$^{-/-}$ mice with anti-inflammatory 18β-glycyrrhetinic acid (GA) can completely inhibit *P. gingivalis*-induced alveolar bone loss in mice, indicating that the anti-inflammatory mode of action of IL-10 is needed to prevent periodontitis. The *in vitro* analysis of resident peritoneal macrophages isolated from *IL-10*$^{-/-}$ mice after *E. coli* LPS challenge revealed that GA suppressed the production of IL-1β and IL-12p70 in a dose-dependent manner and also the RANKL-stimulated osteoclastogenesis was dramatically reduced by GA. The mechanism by which GA can inhibit alveolar bone loss seems to be related to its capacity to inactivate the phosphorylation of NF-κB *in vitro*.

IL-18 Overexpression

IL-18 is a member of the IL-1 family and can induce production of both Th1 and Th2 cytokines. Mice overexpressing IL-18 in the gingival tissues, develop periodontal destruction after being infected with *P. gingivalis* (57). The mechanisms of action of excess IL-18 in the gingiva appear to be T-cell mediated, as the NF-κB and RANKL levels were increased in the transgenic mice after *P. gingivalis* infection, whereas the interferon-γ was decreased.

OPG Knockout, RANKL Overexpression, and RANK Overexpression

Osteoprotegerin is the molecule expressed by osteoblast lineage cells, which inhibits osteoclast differentiation. OPG binds to RANKL complex and thus prevents the RANKL-RANK signaling to osteoclast precursor cells necessary for proper osteoclast differentiation (58). The RANKL to OPG ratio in periodontal tissue of periodontitis patients can be an indicator of alveolar bone loss (59). Koide and coworkers (60) investigated the effect on alveolar bone loss in *Opg* knockout mice. Knockout mice present with significantly more alveolar bone loss (twofold more) than the WT counterpart, occurring without any experimental bacterial application. An increased number of osteoclasts was observed in the alveolar bone compartment. In the same study, also the effect of RANKL overexpression on periodontitis development was assessed using a *Rankl* transgenic mouse. Remarkably, these mice did not develop periodontitis, but a lower bone density of alveolar bone was apparent (60). These observations indicate that disturbance of the naturally high levels of OPG relative to RANKL that normally prevail in the periodontium (59) results in destruction of alveolar bone.

Apart from knocking-out *Opg*, a similar interference with the RANKL-RANK-OPG balance can be achieved by overexpressing RANK. Mice that lack *Rank* are osteopetrotic with an overall lack of osteoclasts (61). Recently, it was shown that *Rank* transgenic mice develop periodontitis in the absence of external bacteriological pressure, likely due to an exuberant RANK-RANKL signaling (62). Apart from the apparent alveolar bone loss, these mice also display root resorption, thickening of the junctional epithelium and significantly more rests of Malassez, epithelial groups of cells within the periodontal ligament (62).

NF-κB Inhibition in Osteoblasts

Inflammatory cytokines and TLR signaling activate NF-κB, which in turn affects the function of osteoblasts and osteoclasts. Pacios et al. tested the NF-κB inhibition and bacteria-induced periodontitis in inhibitor of Kappa B kinase (*Ikk*) transgenic mice (63). Transgenic mice that express a dominant negative mutant of *Ikk*, which inhibits NF- κB in osteoblast lineage cells, are protected from alveolar bone loss in response to oral inoculation with *P. gingivalis* and *F. nucleatum,* in contrast to their wild-type counterparts. This effect was mainly due to enhanced bone formation by osteoblasts and reduced osteoclast numbers and activation, as the development of an inflammatory infiltrate containing PMNs and monocytes with consequent loss of connective tissue attachment were unaffected by the genetic manipulation. This study demonstrates that during inflammation, in addition to lymphocytes and monocytes/macrophages, osteoblasts are also a relevant source of RANKL, and thus are important in alveolar bone resorption.

Proteases

A variety of proteolytic enzymes are involved in many processes. Relevant here are their involvement in the normal homeostatic remodeling of the periodontal supportive tissues including

normal turnover and pathological degradation of alveolar bone. Proteases are also found in the systems that degrade bacteria and their pathogenic components. In the case of periodontitis, periodontal ligament and alveolar bone degradation can be excessive and can cause progressive breakdown of periodontal supportive tissue. Below we summarize the observations in three different protease knockout mouse models, those with the following genes knocked out: *Mmp-8*, *Cathepsin K*, and *plasminogen* in periodontitis mouse models.

MMP-8

MMP-8 (collagenase 2) as a collagenolytic enzyme is responsible for the pathological degradation of type I collagen, which is the predominant collagen type in the periodontal structures. Levels of MMP-8 are elevated in gingival tissue, GCF and saliva in periodontitis patients (64). MMP-8, highly expressed in neutrophils, also possesses anti-inflammatory properties because it is able to cut and thus inactivate anti-inflammatory chemokines and cytokines (65).

In a study by Kuula and coworkers (66), the role of MMP-8 in periodontitis was investigated using an *Mmp-8* knockout mouse model infected with *P. gingivalis*. *Mmp-8*$^{-/-}$ mice were infected with *P. gingivalis via* oral lavage to induce marginal periodontitis. A histological analysis showed that bone loss was significantly increased in the *P. gingivalis*-infected *Mmp-8*$^{-/-}$ group compared to the *P. gingivalis*-infected WT group. The authors conclude that MMP-8 plays a protective role in alveolar bone loss during periodontal infection, possibly by inactivating pro-inflammatory cytokines. These findings are in agreement with research conducted by Hernández et al. (67) using the same *Mmp-8* knockout under *P. gingivalis* bacterial pressure. Furthermore, these latter authors showed that the expression in the gingival papilla of LPS-induced CXC chemokine LIX/CXCL5, a potent PMN chemoattractant, was significantly higher in the *P. gingivalis*-infected WT group compared with both infected and uninfected MMP-8 knockout groups. LIX/CXCL5 can regulate the PMN influx to periodontal tissues. In clinical dentistry, however, elevated salivary MMP-8 levels have been proposed to be diagnostic for periodontitis (68), but large-scale validation studies are needed. Moreover, these findings are opposed to the findings regarding the role of MMP8 in mouse periodontitis; it could be suggested that MMP8 facilitates the primary immune reaction by enabling the influx of the appropriate immune cells. When not present, it may lead to an enduring inflammatory response, resulting in the defective clearance of bacteriological products.

Cathepsin K

Similar to the above described *Mmp-8* knockout mice, mice that lack expression of the osteoclast-related protease cathepsin K (69) are protected from developing bacterium-induced periodontitis (70). Unexpectedly, *Cathepsin K* deficiency led to an absent TLR expression in the gingival epithelium, suggesting that Cathepsin K may somehow influence the expression of TLRs. *Cathepsin K* deficient mice were protected both for developing rheumatoid arthritis and periodontitis (70). This study further showed that both DCs and macrophages express Cathepsin K and that these cells are found at a much lower density in the periodontium of cathepsin K deficient mice that were infected with a cocktail of periodontopathogenic bacteria. Likewise, the number of T-cells did not increase in the periodontium after an infection. *In vitro* cultured dendritic cells from *Cathepsin K* deficient mice had a tempered reactivity when triggered with typical TLR triggers LPS and the nucleic acid sequence CpG. Thus, these studies propose a new role for cathepsin K, i.e., as a modulator of the immune response. In a pre-clinical study, the same group has exploited this model by treating wild-type infected mice with odonacatib, an inhibitor of cathepsin K. Thus, they could pharmacologically achieve inactivity of cathepsin K. It was shown that odonacatib—a Cathepin K inhibitor that was withdrawn from the market due to side effects—treated mice were also protected against periodontitis (71). From these studies, it can be deduced that cathepsin K plays both an immune modulatory role in dendritic cells and macrophages and a role in resorption in ostoclasts. Compounds that inhibit cathepsin K activity could be potential drugs to be further explored in the treatment or prevention of periodontitis.

Plasminogen

Plasminogen is an inactive proenzyme that is synthesized mainly in the liver (72). It is activated after cleavage into the serine protease plasmin. The activation can occur either *via* tissue-type plasminogen activator (tPA) or urokinase-type PA (uPA) (73). Plasmin also plays an important role in ECM remodeling because it degrades ECM components (e.g., laminin, fibronectin, proteoglycans) and activates MMPs (74). Plasmin may be important for host defense against infection (75). Indeed plasminogen deficiency has been associated to the onset of a destructive form of periodontal disease in humans named ligneous gingivitis/periodontitis (76). In a study by Sulniute and coworkers (77), the role of plasminogen in periodontitis was investigated using a *Plasminogen* knockout mouse model. Without additional bacterial infection, both the *tPa/uPa* double knockout—that cannot convert plasminogen into plasmin—and the plasminogen-deficient mutant mice, showed to develop periodontitis, as evidenced by alveolar bone loss: the plasminogen-deficient mice showed at any time point significantly more alveolar bone loss that increased with age up to 20 weeks compatible with a clinical picture of spontaneously developing periodontitis. At the histological level, this was associated with a massive PMN accumulation. Microbial analysis revealed a 100-fold increase in bacterial accumulation in plasminogen-deficient mice. One possible explanation is that phagocytic function of PMNs may be impaired in the absence of plasminogen (78). Interestingly, the systemic supplementation of human plasminogen in *Plasminogen*-deficient mice led to complete regeneration of soft periodontal tissues and significant regrowth of the alveolar bone. These results show that plasminogen is essential for a normal and tolerant host response in the periodontal tissues and prevents an aberrant, intolerant response to normal indigenous bacteria on teeth. Interestingly, genetic variants in the human plasminogen gene have not only been associated with atherosclerotic cardiovascular diseases, but were also associated with aggressive periodontitis in Northern European study populations (79).

Mouse Periodontitis Models Involving Structural Alterations of the Periodontium

Alterations in formation and maturation of different compartments of the dental tissues have been linked to early-onset periodontitis in humans (80). This has been confirmed in several mouse models describing structural alterations in the periodontium and their associated periodontal destruction. Below, it is reiterated in all the mentioned studies that loss of integrity of the attachment of teeth to bone caused by loss of an important cementum or bone matrix protein, causes periodontitis.

Bone Sialoprotein (Bsp) Null Mice

Bone sialoprotein is an ECM protein present in bone, cellular, and acellular cementum (81). *Bsp*$^{-/-}$ mice feature delayed bone and cementum growth and mineralization, but also progressive loss of periodontal tissues at later ages (82). The periodontal ligament in these mice loses its typical parallel and oblique fiber bundle orientation from root to alveolar bone and sparse periodontal ligament inserted in cementum. These results on the one hand reduced resistance to "pressure" from the epithelium allowing apical migration of the epithelium. Extensive root and alveolar bone resorption occurred in these mice, concomitant with increased RANKL expression. Likely, the disorganized fiber organization without tensile strength gives rise to RANKL expression and hence resorption. As reviewed by Sokos et al., the periodontal ligament usually protects against osteoclast formation by high OPG and low RANKL expression (59).

Dentin Matrix Protein 1 (DMP1) Null Mice

Dentin Matrix Protein 1 is another ECM protein, and is found in dentin, bone, cartilage, and cementum. *Dmp1*$^{-/-}$ mice have, in addition to tooth abnormalities (enlarged pulp chambers, reduced dentin thickness) (83), also porous, hypomineralized alveolar bone and cementum, and a poorly organized PDL. As a result, *Dmp1*$^{-/-}$ mice develop spontaneous early-onset periodontal breakdown, already when they are 3 months of age (84). Interestingly, the interdental bone shows mainly vertical defects, reminding of the localized early-onset (juvenile) periodontitis in humans. No attempt was made to control the outgrowth of microbiota in these mice, so a bacterial contribution to the observed periodontitis cannot be excluded, especially in older animals (up to 12 months). However, the authors noted that the vertical bone loss had occurred in the *Dmp1*$^{-/-}$ mice as early as 3 months in the absence of overt signs of bacterial infection or inflammatory response.

Periostin

Periostin is a cell adhesion molecule and favors the cell–cell adhesion of pre-osteoblast attachment and spreading during bone formation (85). *Periostin*$^{-/-}$ mice develop alterations of the PDL structure already at 4 weeks of age and later, at 3 months, they show radiographic signs of alveolar bone destruction coupled with a significant increase in osteoclast activity. The inflammatory response caused a replacement of periodontal ligament by granulation tissue as shown by the increased expression of collagen type III in the null mice (86). The apparent loss of cell–cell contact between periodontal ligament cells may alter the phenotype of these cells in the null mice into a more bone catabolic phenotype or compromise the barrier function of the periodontal ligament. The mice were maintained under specific pathogen-free conditions; however, they were not completely germ-free. The loss of the periodontal ligament barrier function might have created the conditions for a dysbiotic shift in the resident microflora of the *Periostin*$^{-/-}$ mice, which might explain the massive PMN infiltrate in the affected periodontal tissues. Since Rios and coworkers (86) did not analyze the total bacterial burden in WT vs. null mice, a microbial pressure of resident species emerging in a dysbiotic state cannot be excluded as one of the contributing factors to the periodontitis that develops in the Periostin$^{-/-}$ mice.

Dentin Sialophosphoprotein (DSPP)

Dentin sialophosphoprotein is expressed in dentin, bone, and cementum. DSPP mutations are associated with dentinogenesis imperfecta in humans. The corresponding murine model of dentinogenesis imperfecta is the *Dspp* knockout mouse. The *Dspp*$^{-/-}$ mice have dental defects such as decreased cementum deposition (87). These mice show spontaneously alveolar bone loss as they age, comparable to periodontitis. Interestingly, mice that overexpress the NH_2-terminal fragment of DSPP induces an even more severe periodontal phenotype in *Dspp*$^{-/-}$ mice (88), indicating that this fragment has an inhibitory effect on the formation and mineralization of the hard tissues of the periodontium.

Ribosomal S6 Kinase

Coffin-Lowry is an X-linked genetic syndrome, characterized by mental and psychomotor retardation, skeletal and dental abnormalities. It is caused by mutations in the Ribosomal S6 kinase (RSK2), leading to complete inactivation of this enzyme. Dental abnormalities in humans include delayed eruption, hypodontia, and premature tooth loss. There is evidence from Rsk2-deficient mice, showing that the skeletal and dental defects are caused by impaired bone and cementum formation, respectively (89). At 4 months, the Rsk2-deficient mice showed hypoplastic and hypomineralized cementum, detachment of the PDL, apical migration of junctional and pocket epithelium concomitant with pocket formation and loss of alveolar bone. It was concluded that the premature tooth loss in Coffin-Lowry syndrome is most likely a consequence of defective cementum formation.

K14-VEGF Receptor 3-Ig (K14) Mice That Lack Lymphatic Vessels in Gingiva

In the gingiva, lymphatic vessels are normally found in the connective tissue layer below the oral and the junctional epithelium. These vessels widen during a bacterial challenge of the periodontium (90). The *K14-vegf receptor 3-Ig* transgenic mice lack overall lymphatics, including the gingiva. In response to oral inoculation with *P. gingivalis* develop alveolar bone loss than their WT littermates (91). The absence of lymphatics in the gingiva leads to a massive influx of macrophages around the alveolar bone, concomitant with an increased number of osteoclasts degrading the alveolar bone. A weaker activation of B cell-antibody production was also characteristic of this model. Levels of inflammatory

cytokines were only increased in the infected *K14-vegf receptor 3-Ig* transgenic mice, suggesting that here periodontitis arose due to an enduring inflammatory response.

Models on the Association between Periodontitis and Systemic Diseases

In humans, periodontitis often arises together with other inflammation-related diseases, so-called comorbidities. Development of genetic mouse variants that display both periodontitis and atherosclerosis or rheumatoid arthritis are useful in elucidating common denominators of these diseases. Here, we briefly review periodontitis/atherosclerosis and periodontitis/rheumatoid arthritis mouse.

Atherosclerosis

Periodontitis is linked to atherosclerotic cardiovascular diseases; in the last 20 years, hundreds of papers have emerged on this association (92) and plausible pathobiological mechanisms have been described (93). In addition to many epidemiological studies, also evidence on this association has been generated employing mouse models. The hyperlipidemic apolipoprotein (Apo) E-null mice have been used in a series of studies (27, 94, 95). By applying oral mono- or polymicrobial infections with *P. gingivalis*, *F. nucleatum*, *Treponema denticola*, and *Tannerella forsythia,* the authors showed that the ApoE$^{-/-}$ mice develop not only destructive periodontitis, but also progressive atherosclerosis. The mechanisms involve systemic dissemination of periodontal bacteria, aortic bacterial colonization, skewed T cell polarization in the spleen, altered cytokine, and lipid profiles in mouse serum. Important to note, the emerging phenotype in polymicrobial infections was not the sum of responses to monoinfection with each microorganism, raising the issue of microbial synergism in periodontitis and pointing at microbe–microbe interactions as modifiers of microbe–host interactions.

The β6 integrin model knockout model is relevant to further strengthen the periodontitis–atherosclerosis relationship. Upon infection with periodontopathogens, these mice developed periodontitis simultaneously with atherosclerosis (27), as measured by lipid vesicle content of blood and of aortic wall. Several indicators were elevated, only in the infected knockout mice. This study shows that effects of periodontitis on the development of atherosclerosis have been neglected in nearly all periodontitis models described in this review.

Rheumatoid Arthritis

Hao et al. used a combined transgenic mouse model, the human transgenic *Tnf*-α- and *Cathepsin K*-deficient mice to study common pathogenic processes involved in rheumatoid arthritis and periodontitis (70). *Cathepsin K* deficiency was protective against both diseases, and the authors attribute that to the dampened inflammatory reactivity, with less TLR expression, less dendritic cells and less cytokines produced in the arthritis and periodontitis lesions. This hypothesis of the shared hyper-inflammatory phenotype in periodontitis and arthritis has been confirmed by Trombone and coworkers, in a model using the acute inflammatory reactivity maximum AIRmax and minimal AIRmin mice (96). The parallel induction of arthritis and experimental periodontitis with periopathogens (*A. actinomycetemcomitans* and *P. gingivalis)* in the inflammation-prone AIRmax mice resulted in a more severe phenotype: higher leukocyte infiltration, higher local levels of IL-1β, TNF-α, RANKL, IFN-γ, and IL-17, skewed T cell polarization toward Th1 and Th17, and more periodontal destruction. Interestingly, in this study, the presence of normal oral microbiota was essential for the induction of periodontitis. This finding identifies the exaggerated inflammatory phenotype as the enabler of the ecological shift from a commensal microbiota, which in standard homeostatic condition would not be harmful to the host, to a dysbiotic biofilm, incompatible with periodontal health, even in the absence of classic periodontopathogens.

CONCLUDING REMARKS

Mouse Models of Periodontitis—Mouse Models Human Periodontitis

When interpreting the diverse mouse models, it becomes apparent that single gene deletions can give rise to periodontitis. Some KO or transgenic mouse models show periodontitis developing with a normal resident oral microbiome, while most need an exogenous bacterial infection. These observations underscore the delicate balance of immune reactions that are needed in a sequential and efficient way to combat an infection. As indicated, one could classify mutations that give rise to periodontitis due to a malfunctioning infiltration or transmigration of immune cells such as PMNs into the periodontium challenged by bacteria in the sulcus (*LFA-1, ICAM-1, P-Selectin*). Likewise, infections can endure when Tregs are unable to migrate into the periodontium and modulate the infection due to critical modulators such as *IL-4, CCL2,* and *CCR4* (**Figures 2** and **3**). The second category is the defected clearance of bacteria or bacterial products of infiltrated but dysfunctional immune cells such as PMNs that are deficient in *LAMP-2, TLRs, lactoferrin,* or *plasminogen* (**Figure 3**).

Periodontitis: A Second Hit Disease?

In many of the studies reviewed here, no periodontitis occurred in wild-type mice, not even after an infection with periodontopathogens. This was the case for 9 out of 12 studies where the fourfold comparison (wild-type; wild-type infected; knockout; knockout infected) was studied. Likewise, many of the knockout mice did not develop periodontitis in the absence of periodontopathogenic pressure (10 out of 11). Apparently, analogous to Bert Vogelstein's famous second hit hypothesis for developing colorectal cancer (97), where two hits are required to develop disease (colorectal cancer), one could thus postulate that both an underlying genetic defect and a bacterial challenge are required for developing periodontitis. For seven genes: *IL17-ra* (10), *IL1-ra* (50), *Socs-3* (39), *IL-10* as well as its downstream modulator *Stat3* (55) and adhesion molecules *Icam-1* (11) and *Beta6 integrin* (27), only the combination of functional loss with bacterial pressure resulted in periodontitis.

Though this "second hit" hypothesis applies to the above models, where the combination of a genetic defect with periodontopathogenic pressure is required, it should be noticed that many models described here do not need this exogenous pressure to

develop periodontitis. Examples are the *Lamp-2* (6), *Plasminogen* (77), *Opg* (60), *Rank* transgene (62). Peculiarly, it seems that this external pressure is not required in themutations that affect the structural integrity of the periodontium, such as *Bsp* (82), *Dmp1* (84), *Periostin* (86), and *Dspp* (87). Some of these mutations resemble genetic predisposition for developing periodontitis, such as seen in humans. We could thus make the distinction between genetic models that do require periodontopathogenic pressure and models where the mere genetic defect is enough to initiate periodontitis.

Mouse Models Can Be Valuable for Developing Treatment Strategies

Genetic models for periodontitis may shed light on new treatment modalities. An intriguing example could be the lessons learned from the periodontitis resistant Cathepsin K knockout mouse. Apparently, interference with osteoclast function can prevent alveolar bone degradation. Besides that, the Cathepsin K knockout shed new light on the role of dendritic cells and subsequent immune cell influx, thereby modulation severity of the infection. Previously, it was shown that the periodontal status of rheumatoid arthritis patients receiving anti-TNF-α treatment (98) stabilized as a side-effect of treatment. A second example could be patients with defective CD11a/CD18 that are genetically prone to develop periodontitis. Moutsopoulos et al. have shown that mice and humans with this genetic defect have a highly enhanced presence and activity of Th17 cells in the periodontium. Mice with this defect develop periodontitis, which is blocked when treating these mice with anti- IL-17 antibodies (26). Treatment modalities interfering with IL-17 activity may thus be beneficial for the periodontal status of these patients.

AUTHOR NOTE

Teun J. de Vries is a member of the Euroclast consortium (www.euroclast.eu), a Marie Curie Initial Training Network (ITN).

AUTHOR CONTRIBUTIONS

TV initiated the writing of this review. He wrote a large part of the manuscript and interpreted, summarized, and edited parts written by SA. TV made all the figures that interpret and summarize the literature. SA collected literature and did initial writing. BL contributed to two pre-final versions. He is the head of the department and a clinical periodontologist. His focus in this review was to further link mouse models and the clinic. EN has expertise in the field of granulocytes and wrote sections on DCs and other disease models that are comorbidities to periodontitis.

ACKNOWLEDGMENTS

We thank Vincent Everts for his valuable suggestions to the manuscript.

REFERENCES

1. Te Velde AA, Bezema T, van Kampen AH, Kraneveld AD, t Hart BA, van Middendorp H, et al. Embracing complexity beyond systems medicine: a new approach to chronic immune disorders. *Front Immunol* (2016) 7:587. doi:10.3389/fimmu.2016.00587
2. Loos BG, Papantonopoulos G, Jepsen S, Laine ML. What is the contribution of genetics to periodontal risk? *Dent Clin North Am* (2015) 59:761–80. doi:10.1016/j.cden.2015.06.005
3. Pihlstrom BL, Michalowicz BS, Johnson NW. Periodontal diseases. *Lancet* (2005) 366:1809–20. doi:10.1016/S0140-6736(05)67728-8
4. Brandtzaeg P. Homeostatic impact of indigenous microbiota and secretory immunity. *Benef Microbes* (2010) 1:211–27. doi:10.3920/BM2010.0009
5. Baker PJ, Roopenian DC. Genetic susceptibility to chronic periodontal disease. *Microbes Infect* (2002) 4:1157–67. doi:10.1016/S1286-4579(02)01642-8
6. Beertsen W, Willenborg M, Everts V, Zirogianni A, Podschun R, Schroder B, et al. Impaired phagosomal maturation in neutrophils leads to periodontitis in lysosomal associated membrane protein-2 (LAMP-2) knockout mice. *J Immunol* (2008) 180:475–82. doi:10.4049/jimmunol.180.1.475
7. Sheng ZF, Xu K, Ma YL, Liu JH, Dai RC, Zhang YH, et al. Zoledronate reverses mandibular bone loss in osteoprotegerin-deficient mice. *Osteoporos Int* (2009) 20:151–9. doi:10.1007/s00198-008-0640-0
8. Araujo-Pires AC, Vieira AE, Francisconi CF, Biguetti CC, Glowacki A, Yoshizawa S, et al. IL-4/CCL22/CCR4 axis controls regulatory T-cell migration that suppresses inflammatory bone loss in murine experimental periodontitis. *J Bone Miner Res* (2015) 30:412–22. doi:10.1002/jbmr.2376
9. Polak D, Wilensky A, Shapira L, Halabi A, Goldstein D, Weiss EI, et al. Mouse model of experimental periodontitis induced by *Porphyromonas gingivalis*/*Fusobacterium nucleatum* infection: bone loss and host response. *J Clin Periodontol* (2009) 36:406–10. doi:10.1111/j.1600-051X.2009.01393.x
10. Yu JJ, Ruddy MJ, Wong GC, Sfintescu C, Baker PJ, Smith JB, et al. An essential role for IL-17 in preventing pathogen-initiated bone destruction: recruitment of neutrophils to inflamed bone requires IL-17 receptor-dependent signals. *Blood* (2007) 109:3794–802. doi:10.1182/blood-2005-09-010116
11. Baker PJ, DuFour L, Dixon M, Roopenian DC. Adhesion molecule deficiencies increase *Porphyromonas gingivalis*-induced alveolar bone loss in mice. *Infect Immun* (2000) 68:3103–7. doi:10.1128/IAI.68.10.5864-5868.2000
12. Shusterman A, Salyma Y, Nashef A, Soller M, Wilensky A, Mott R, et al. Genotype is an important determinant factor of host susceptibility to periodontitis in the collaborative cross and inbred mouse populations. *BMC Genet* (2013) 14:68. doi:10.1186/1471-2156-14-68
13. Baker PJ, Evans RT, Roopenian DC. Oral infection with *Porphyromonas gingivalis* and induced alveolar bone loss in immunocompetent and severe combined immunodeficient mice. *Arch Oral Biol* (1994) 39:1035–40. doi:10.1016/0003-9969(94)90055-8
14. Baker PJ, Dixon M, Evans RT, DuFour L, Johnson E, Roopenian DC. CD4(+) T cells and the proinflammatory cytokines gamma interferon and interleukin-6 contribute to alveolar bone loss in mice. *Infect Immun* (1999) 67:2804–9.
15. Banchereau J, Steinman RM. Dendritic cells and the control of immunity. *Nature* (1998) 392:245–52. doi:10.1038/32588
16. Alcantara O, Reddy SV, Roodman GD, Boldt DH. Transcriptional regulation of the tartrate-resistant acid phosphatase (TRAP) gene by iron. *Biochem J* (1994) 298(Pt 2):421–5. doi:10.1042/bj2980421
17. Arizon M, Nudel I, Segev H, Mizraji G, Elnekave M, Furmanov K, et al. Langerhans cells down-regulate inflammation-driven alveolar bone loss. *Proc Natl Acad Sci U S A* (2012) 109:7043–8. doi:10.1073/pnas.1116770109
18. Bittner-Eddy PD, Fischer LA, Kaplan DH, Thieu K, Costalonga M. Mucosal langerhans cells promote differentiation of Th17 cells in a murine model of periodontitis but are not required for *Porphyromonas gingivalis*-driven alveolar bone destruction. *J Immunol* (2016) 197:1435–46. doi:10.4049/jimmunol.1502693

19. Mentaverri R, Kamel S, Wattel A, Prouillet C, Sevenet N, Petit JP, et al. Regulation of bone resorption and osteoclast survival by nitric oxide: possible involvement of NMDA-receptor. *J Cell Biochem* (2003) 88:1145–56. doi:10.1002/jcb.10463
20. Mkonyi LE, Bakken V, Sovik JB, Mauland EK, Fristad I, Barczyk MM, et al. Lymphangiogenesis is induced during development of periodontal disease. *J Dent Res* (2012) 91:71–7. doi:10.1177/0022034511424747
21. Lam RS, O'Brien-Simpson NM, Lenzo JC, Holden JA, Brammar GC, Walsh KA, et al. Macrophage depletion abates *Porphyromonas gingivalis*-induced alveolar bone resorption in mice. *J Immunol* (2014) 193:2349–62. doi:10.4049/jimmunol.1400853
22. Larjava H, Koivisto L, Heino J, Hakkinen L. Integrins in periodontal disease. *Exp Cell Res* (2014) 325:104–10. doi:10.1016/j.yexcr.2014.03.010
23. Morris DG, Huang X, Kaminski N, Wang Y, Shapiro SD, Dolganov G, et al. Loss of integrin alpha(v)beta6-mediated TGF-beta activation causes Mmp12-dependent emphysema. *Nature* (2003) 422:169–73. doi:10.1038/nature01413
24. Herter J, Zarbock A. Integrin regulation during leukocyte recruitment. *J Immunol* (2013) 190:4451–7. doi:10.4049/jimmunol.1203179
25. von Andrian UH, Berger EM, Ramezani L, Chambers JD, Ochs HD, Harlan JM, et al. *In vivo* behavior of neutrophils from two patients with distinct inherited leukocyte adhesion deficiency syndromes. *J Clin Invest* (1993) 91:2893–7. doi:10.1172/JCI116535
26. Moutsopoulos NM, Konkel J, Sarmadi M, Eskan MA, Wild T, Dutzan N, et al. Defective neutrophil recruitment in leukocyte adhesion deficiency type I disease causes local IL-17-driven inflammatory bone loss. *Sci Transl Med* (2014) 6:229ra40. doi:10.1126/scitranslmed.3007696
27. Velsko IM, Chukkapalli SS, Rivera-Kweh MF, Zheng D, Aukhil I, Lucas AR, et al. Periodontal pathogens invade gingiva and aortic adventitia and elicit inflammasome activation in alphavbeta6 integrin-deficient mice. *Infect Immun* (2015) 83:4582–93. doi:10.1128/IAI.01077-15
28. Niederman R, Westernoff T, Lee C, Mark LL, Kawashima N, Ullman-Culler M, et al. Infection-mediated early-onset periodontal disease in P/E-selectin-deficient mice. *J Clin Periodontol* (2001) 28:569–75. doi:10.1034/j.1600-051x.2001.028006569.x
29. Dixon DR, Bainbridge BW, Darveau RP. Modulation of the innate immune response within the periodontium. *Periodontol 2000* (2004) 35:53–74. doi:10.1111/j.0906-6713.2004.003556.x
30. Mori Y, Yoshimura A, Ukai T, Lien E, Espevik T, Hara Y. Immunohistochemical localization of toll-like receptors 2 and 4 in gingival tissue from patients with periodontitis. *Oral Microbiol Immunol* (2003) 18:54–8. doi:10.1034/j.1399-302X.2003.180109.x
31. Burns E, Bachrach G, Shapira L, Nussbaum G. Cutting edge: TLR2 is required for the innate response to *Porphyromonas gingivalis*: activation leads to bacterial persistence and TLR2 deficiency attenuates induced alveolar bone resorption. *J Immunol* (2006) 177:8296–300. doi:10.4049/jimmunol.177.12.8296
32. Costalonga M, Batas L, Reich BJ. Effects of toll-like receptor 4 on *Porphyromonas gingivalis*-induced bone loss in mice. *J Periodontal Res* (2009) 44:537–42. doi:10.1111/j.1600-0765.2008.01152.x
33. Gelani V, Fernandes AP, Gasparoto TH, Garlet TP, Cestari TM, Lima HR, et al. The role of toll-like receptor 2 in the recognition of *Aggregatibacter actinomycetemcomitans*. *J Periodontol* (2009) 80:2010–9. doi:10.1902/jop.2009.090198
34. Saftig P, Beertsen W, Eskelinen EL. LAMP-2: a control step for phagosome and autophagosome maturation. *Autophagy* (2008) 4:510–2. doi:10.4161/auto.5724
35. Tanaka Y, Guhde G, Suter A, Eskelinen EL, Hartmann D, Lullmann-Rauch R, et al. Accumulation of autophagic vacuoles and cardiomyopathy in LAMP-2-deficient mice. *Nature* (2000) 406:902–6. doi:10.1038/35022595
36. Ward PP, Conneely OM. Lactoferrin: role in iron homeostasis and host defense against microbial infection. *Biometals* (2004) 17:203–8. doi:10.1023/B:BIOM.0000027693.60932.26
37. Cornish J, Palmano K, Callon KE, Watson M, Lin JM, Valenti P, et al. Lactoferrin and bone; structure-activity relationships. *Biochem Cell Biol* (2006) 84:297–302. doi:10.1139/o06-057
38. Velusamy SK, Ganeshnarayan K, Markowitz K, Schreiner H, Furgang D, Fine DH, et al. Lactoferrin knockout mice demonstrates greater susceptibility to *Aggregatibacter actinomycetemcomitans*-induced periodontal disease. *J Periodontol* (2013) 84:1690–701. doi:10.1902/jop.2013.120587
39. Papathanasiou E, Kantarci A, Konstantinidis A, Gao H, Van Dyke TE. SOCS-3 regulates alveolar bone loss in experimental periodontitis. *J Dent Res* (2016) 95:1018–25. doi:10.1177/0022034516645332
40. Alotaibi MK, Kitase Y, Shuler CF. Smad2 overexpression induces alveolar bone loss and up regulates TNF-alpha, and RANKL. *Arch Oral Biol* (2016) 71:38–45. doi:10.1016/j.archoralbio.2016.06.023
41. Repeke CE, Ferreira SB Jr, Claudino M, Silveira EM, de Assis GF, Avila-Campos MJ, et al. Evidences of the cooperative role of the chemokines CCL3, CCL4 and CCL5 and its receptors CCR1+ and CCR5+ in RANKL+ cell migration throughout experimental periodontitis in mice. *Bone* (2010) 46(4):1122–30. doi:10.1016/j.bone.2009.12.030
42. Weaver CT, Harrington LE, Mangan PR, Gavrieli M, Murphy KM. Th17: an effector CD4 T cell lineage with regulatory T cell ties. *Immunity* (2006) 24:677–88. doi:10.1016/j.immuni.2006.06.002
43. Linden A, Adachi M. Neutrophilic airway inflammation and IL-17. *Allergy* (2002) 57:769–75. doi:10.1034/j.1398-9995.2002.02164.x
44. Lubberts E, Koenders MI, van Den Berg WB. The role of T-cell interleukin-17 in conducting destructive arthritis: lessons from animal models. *Arthritis Res Ther* (2005) 7:29–37. doi:10.1186/ar1550
45. Moseley TA, Haudenschild DR, Rose L, Reddi AH. Interleukin-17 family and IL-17 receptors. *Cytokine Growth Factor Rev* (2003) 14:155–74. doi:10.1016/S1359-6101(03)00002-9
46. Graves DT, Cochran D. The contribution of interleukin-1 and tumor necrosis factor to periodontal tissue destruction. *J Periodontol* (2003) 74:391–401. doi:10.1902/jop.2003.74.3.391
47. Engebretson SP, Lamster IB, Herrera-Abreu M, Celenti RS, Timms JM, Chaudhary AG, et al. The influence of interleukin gene polymorphism on expression of interleukin-1beta and tumor necrosis factor-alpha in periodontal tissue and gingival crevicular fluid. *J Periodontol* (1999) 70:567–73. doi:10.1902/jop.1999.70.6.567
48. Garlet GP, Cardoso CR, Campanelli AP, Ferreira BR, Avila-Campos MJ, Cunha FQ, et al. The dual role of p55 tumour necrosis factor-alpha receptor in *Actinobacillus actinomycetemcomitans*-induced experimental periodontitis: host protection and tissue destruction. *Clin Exp Immunol* (2007) 147:128–38. doi:10.1111/j.1365-2249.2006.03260.x
49. Cao Y, Jansen ID, Sprangers S, Stap J, Leenen PJ, Everts V, et al. IL-1beta differently stimulates proliferation and multinucleation of distinct mouse bone marrow osteoclast precursor subsets. *J Leukoc Biol* (2016) 100:513–23. doi:10.1189/jlb.1A1215-543R
50. Izawa A, Ishihara Y, Mizutani H, Kobayashi S, Goto H, Okabe E, et al. Inflammatory bone loss in experimental periodontitis induced by *Aggregatibacter actinomycetemcomitans* in interleukin-1 receptor antagonist knockout mice. *Infect Immun* (2014) 82:1904–13. doi:10.1128/IAI.01618-13
51. Dayan S, Stashenko P, Niederman R, Kupper TS. Oral epithelial overexpression of IL-1alpha causes periodontal disease. *J Dent Res* (2004) 83:786–90. doi:10.1177/154405910408301010
52. O'Farrell AM, Liu Y, Moore KW, Mui AL. IL-10 inhibits macrophage activation and proliferation by distinct signaling mechanisms: evidence for Stat3-dependent and -independent pathways. *EMBO J* (1998) 17:1006–18. doi:10.1093/emboj/17.4.1006
53. Sabat R, Grutz G, Warszawska K, Kirsch S, Witte E, Wolk K, et al. Biology of interleukin-10. *Cytokine Growth Factor Rev* (2010) 21:331–44. doi:10.1016/j.cytogfr.2010.09.002
54. Cullinan MP, Westerman B, Hamlet SM, Palmer JE, Faddy MJ, Seymour GJ, et al. Progression of periodontal disease and interleukin-10 gene polymorphism. *J Periodontal Res* (2008) 43:328–33. doi:10.1111/j.1600-0765.2007.01034.x
55. Al-Rasheed A, Scheerens H, Rennick DM, Fletcher HM, Tatakis DN. Accelerated alveolar bone loss in mice lacking interleukin-10. *J Dent Res* (2003) 82:632–5. doi:10.1177/154405910308200812
56. Sasaki H, Suzuki N, Kent R Jr, Kawashima N, Takeda J, Stashenko P. T cell response mediated by myeloid cell-derived IL-12 is responsible for *Porphyromonas gingivalis*-induced periodontitis in IL-10-deficient mice. *J Immunol* (2008) 180:6193–8. doi:10.4049/jimmunol.180.9.6193
57. Yoshinaka K, Shoji N, Nishioka T, Sugawara Y, Hoshino T, Sugawara S, et al. Increased interleukin-18 in the gingival tissues evokes chronic periodontitis after bacterial infection. *Tohoku J Exp Med* (2014) 232:215–22. doi:10.1620/tjem.232.215

58. Yasuda H, Shima N, Nakagawa N, Mochizuki SI, Yano K, Fujise N, et al. Identity of osteoclastogenesis inhibitory factor (OCIF) and osteoprotegerin (OPG): a mechanism by which OPG/OCIF inhibits osteoclastogenesis *in vitro*. *Endocrinology* (1998) 139:1329–37. doi:10.1210/endo.139.3.5837
59. Sokos D, Everts V, De Vries TJ. Role of periodontal ligament fibroblasts in osteoclastogenesis: a review. *J Periodontal Res* (2015) 50:152–9. doi:10.1111/jre.12197
60. Koide M, Kobayashi Y, Ninomiya T, Nakamura M, Yasuda H, Arai Y, et al. Osteoprotegerin-deficient male mice as a model for severe alveolar bone loss: comparison with RANKL-overexpressing transgenic male mice. *Endocrinology* (2013) 154:773–82. doi:10.1210/en.2012-1928
61. Dougall WC, Glaccum M, Charrier K, Rohrbach K, Brasel K, De Smedt T, et al. RANK is essential for osteoclast and lymph node development. *Genes Dev* (1999) 13:2412–24. doi:10.1101/gad.13.18.2412
62. Sojod B, Chateau D, Mueller CG, Babajko S, Berdal A, Lezot F, et al. RANK/RANKL/OPG signalization implication in periodontitis: new evidence from a RANK transgenic mouse model. *Front Physiol* (2017) 8:338. doi:10.3389/fphys.2017.00338
63. Pacios S, Xiao W, Mattos M, Lim J, Tarapore RS, Alsadun S, et al. Osteoblast lineage cells play an essential role in periodontal bone loss through activation of nuclear factor-kappa B. *Sci Rep* (2015) 5:16694. doi:10.1038/srep16694
64. Sorsa T, Golub LM. Is the excessive inhibition of matrix metalloproteinases (MMPs) by potent synthetic MMP inhibitors (MMPIs) desirable in periodontitis and other inflammatory diseases? That is: 'Leaky' MMPIs vs excessively efficient drugs. *Oral Dis* (2005) 11:408–9. doi:10.1111/j.1601-0825.2005.01160.x
65. Gueders MM, Balbin M, Rocks N, Foidart JM, Gosset P, Louis R, et al. Matrix metalloproteinase-8 deficiency promotes granulocytic allergen-induced airway inflammation. *J Immunol* (2005) 175:2589–97. doi:10.4049/jimmunol.175.4.2589
66. Kuula H, Salo T, Pirila E, Tuomainen AM, Jauhiainen M, Uitto VJ, et al. Local and systemic responses in matrix metalloproteinase 8-deficient mice during *Porphyromonas gingivalis*-induced periodontitis. *Infect Immun* (2009) 77:850–9. doi:10.1128/IAI.00873-08
67. Hernández M, Gamonal J, Salo T, Tervahartiala T, Hukkanen M, Tjaderhane L, et al. Reduced expression of lipopolysaccharide-induced CXC chemokine in *Porphyromonas gingivalis*-induced experimental periodontitis in matrix metalloproteinase-8 null mice. *J Periodontal Res* (2011) 46:58–66. doi:10.1111/j.1600-0765.2010.01310.x
68. Sorsa T, Gursoy UK, Nwhator S, Hernandez M, Tervahartiala T, Leppilahti J, et al. Analysis of matrix metalloproteinases, especially MMP-8, in gingival creviclular fluid, mouthrinse and saliva for monitoring periodontal diseases. *Periodontology* (2000) 70(2016):142–63. doi:10.1111/prd.12101
69. Saftig P, Hunziker E, Everts V, Jones S, Boyde A, Wehmeyer O, et al. Functions of cathepsin K in bone resorption. Lessons from cathepsin K deficient mice [In Process Citation]. *Adv Exp Med Biol* (2000) 477:293–303. doi:10.1007/0-306-46826-3_32
70. Hao L, Zhu G, Lu Y, Wang M, Jules J, Zhou X, et al. Deficiency of cathepsin K prevents inflammation and bone erosion in rheumatoid arthritis and periodontitis and reveals its shared osteoimmune role. *FEBS Lett* (2015) 589:1331–9. doi:10.1016/j.febslet.2015.04.008
71. Hao L, Chen J, Zhu Z, Reddy MS, Mountz JD, Chen W, et al. Cathepsin K-specific inhibitor, inhibits inflammation and bone loss caused by periodontal diseases. *J Periodontol* (2015) 86:972–83. doi:10.1902/jop.2015.140643
72. Zhang L, Seiffert D, Fowler BJ, Jenkins GR, Thinnes TC, Loskutoff DJ, et al. Plasminogen has a broad extrahepatic distribution. *Thromb Haemost* (2002) 87:493–501.
73. De Vries TJ, Van Muijen GNP, Ruiter DJ. The plasminogen activation system in tumour invasion and metastasis. *Pathol Res Pract* (1996) 192:718–33. doi:10.1016/S0344-0338(96)80094-X
74. Rifkin DB, Mazzieri R, Munger JS, Noguera I, Sung J. Proteolytic control of growth factor availability. *APMIS* (1999) 107:80–5. doi:10.1111/j.1699-0463.1999.tb01529.x
75. Syrovets T, Simmet T. Novel aspects and new roles for the serine protease plasmin. *Cell Mol Life Sci* (2004) 61:873–85. doi:10.1007/s00018-003-3348-5
76. Gunhan O, Gunhan M, Berker E, Gurgan CA, Yildirim H. Destructive membranous periodontal disease (ligneous periodontitis). *J Periodontol* (1999) 70:919–25. doi:10.1902/jop.1999.70.8.919
77. Sulniute R, Lindh T, Wilczynska M, Li J, Ny T. Plasmin is essential in preventing periodontitis in mice. *Am J Pathol* (2011) 179:819–28. doi:10.1016/j.ajpath.2011.05.003
78. Herren T, Burke TA, Jardi M, Felez J, Plow EF. Regulation of plasminogen binding to neutrophils. *Blood* (2001) 97:1070–8. doi:10.1182/blood.V97.4.1070
79. Schaefer AS, Bochenek G, Jochens A, Ellinghaus D, Dommisch H, Guzeldemir-Akcakanat E, et al. Genetic evidence for PLASMINOGEN as a shared genetic risk factor of coronary artery disease and periodontitis. *Circ Cardiovasc Genet* (2015) 8:159–67. doi:10.1161/CIRCGENETICS.114.000554
80. Hartsfield JK, Hall BD, Grix AW, Kousseff BG, Salazar JF, Haufe SMW. Pleiotropy in Coffin-Lowry syndrome: sensorineural hearing deficit and premature tooth loss as early manifestations. *Am J Med Genet* (1993) 45:552–7. doi:10.1002/ajmg.1320450505
81. Chellaiah MA, Hruska KA. The integrin avb3 and CD44 regulate the actions of osteopontin on osteoclast motility. *Calcif Tissue Int* (2002) 72:197–205. doi:10.1007/s00223-002-1025-6
82. Foster BL, Soenjaya Y, Nociti FH Jr, Holm E, Zerfas PM, Wimer HF, et al. Deficiency in acellular cementum and periodontal attachment in BSP null mice. *J Dent Res* (2013) 92:166–72. doi:10.1177/0022034512469026
83. Luchin A, Purdom G, Murphy K, Clark MY, Angel N, Cassady AI, et al. The microphthalmia transcription factor regulates expression of the tartrate-resistant acid phosphatase gene during terminal differentiation of osteoclasts. *J Bone Miner Res* (2000) 15:451–60. doi:10.1359/jbmr.2000.15.3.451
84. Ye L, Zhang S, Ke H, Bonewald LF, Feng JQ. Periodontal breakdown in the Dmp1 null mouse model of hypophosphatemic rickets. *J Dent Res* (2008) 87:624–9. doi:10.1177/154405910808700708
85. Kruzynska-Frejtag A, Wang J, Maeda M, Rogers R, Krug E, Hoffman S, et al. Periostin is expressed within the developing teeth at the sites of epithelial-mesenchymal interaction. *Dev Dyn* (2004) 229:857–68. doi:10.1002/dvdy.10453
86. Rios H, Koushik SV, Wang H, Wang J, Zhou HM, Lindsley A, et al. Periostin null mice exhibit dwarfism, incisor enamel defects, and an early-onset periodontal disease-like phenotype. *Mol Cell Biol* (2005) 25:11131–11144.
87. Gibson MP, Zhu Q, Liu Q, D'Souza RN, Feng JQ, Qin C. Loss of dentin sialophosphoprotein leads to periodontal diseases in mice. *J Periodontal Res* (2013) 48:221–7. doi:10.1111/j.1600-0765.2012.01523.x
88. Gibson MP, Jani P, Wang X, Lu Y, Qin C. Overexpressing the NH2-terminal fragment of dentin sialophosphoprotein (DSPP) aggravates the periodontal defects in Dspp knockout mice. *J Oral Biosci* (2014) 56:143–8. doi:10.1016/j.job.2014.06.003
89. Koehne T, Jeschke A, Petermann F, Seitz S, Neven M, Peters S, et al. Rsk2, the kinase mutated in Coffin-Lowry syndrome, controls cementum formation. *J Dent Res* (2016) 95:752–60. doi:10.1177/0022034516634329
90. Ashkar S, Weber GF, Panoutsakopoulou V, Sanchirico ME, Jansson M, Zawaideh S, et al. Eta-1 (osteopontin): an early component of type-1 (cell-mediated) immunity. *Science* (2000) 287:860–4. doi:10.1126/science.287.5454.860
91. Mkonyi LE, Bletsa A, Bolstad AI, Bakken V, Wiig H, Berggreen E. Gingival lymphatic drainage protects against *Porphyromonas gingivalis*-induced bone loss in mice. *Am J Pathol* (2012) 181:907–16. doi:10.1016/j.ajpath.2012.05.027
92. Lockhart PB, Bolger AF, Papapanou PN, Osinbowale O, Trevisan M, Levison ME, et al. Periodontal disease and atherosclerotic vascular disease: does the evidence support an independent association? A scientific statement from the American Heart Association. *Circulation* (2012) 125:2520–44. doi:10.1161/CIR.0b013e31825719f3
93. Schenkein HA, Loos BG. Inflammatory mechanisms linking periodontal diseases to cardiovascular diseases. *J Periodontol* (2013) 84:S51–69. doi:10.1902/jop.2013.134006
94. Chukkapalli SS, Velsko IM, Rivera-Kweh MF, Zheng D, Lucas AR, Kesavalu L. Polymicrobial oral infection with four periodontal bacteria orchestrates a distinct inflammatory response and atherosclerosis in ApoE null mice. *PLoS One* (2015) 10:e0143291. doi:10.1371/journal.pone.0143291
95. Velsko IM, Chukkapalli SS, Rivera MF, Lee JY, Chen H, Zheng D, et al. Active invasion of oral and aortic tissues by *Porphyromonas gingivalis* in mice causally links periodontitis and atherosclerosis. *PLoS One* (2014) 9:e97811. doi:10.1371/journal.pone.0097811

96. Trombone AP, Claudino M, Colavite P, de Assis GF, Avila-Campos MJ, Silva JS, et al. Periodontitis and arthritis interaction in mice involves a shared hyper-inflammatory genotype and functional immunological interferences. *Genes Immun* (2010) 11:479–89. doi:10.1038/gene.2010.13
97. Vogelstein B, Fearon ER, Hamilton SR, Kern SE, Preisinger AC, Leppert M, et al. Genetic alterations during colorectal-tumor development. *N Engl J Med* (1988) 319:525–32. doi:10.1056/NEJM198809013190901
98. Mayer Y, Balbir-Gurman A, Machtei EE. Anti-tumor necrosis factor-alpha therapy and periodontal parameters in patients with rheumatoid arthritis. *J Periodontol* (2009) 80:1414–20. doi:10.1902/jop.2009.090015

Conflict of Interest Statement: The authors declare that the research was conducted in the absence of any commercial or financial relationships that could be construed as a potential conflict of interest.

Copyright © 2017 de Vries, Andreotta, Loos and Nicu. This is an open-access article distributed under the terms of the Creative Commons Attribution License (CC BY). The use, distribution or reproduction in other forums is permitted, provided the original author(s) or licensor are credited and that the original publication in this journal is cited, in accordance with accepted academic practice. No use, distribution or reproduction is permitted which does not comply with these terms.

frontiers in Immunology

ORIGINAL RESEARCH
published: 27 October 2017
doi: 10.3389/fimmu.2017.01409

Baicalin Inhibits NOD-Like Receptor Family, Pyrin Containing Domain 3 Inflammasome Activation in Murine Macrophages by Augmenting Protein Kinase A Signaling

Chen-Guang Li[1†], Liang Yan[1†], Feng-Yi Mai[1†], Zi-Jian Shi[2], Li-Hui Xu[3], Yan-Yun Jing[1], Qing-Bing Zha[2], Dong-Yun Ouyang[1] and Xian-Hui He[1]*

[1] Department of Immunobiology, College of Life Science and Technology, Jinan University, Guangzhou, China, [2] Department of Fetal Medicine, The First Affiliated Hospital of Jinan University, Guangzhou, China, [3] Department of Cell Biology, College of Life Science and Technology, Jinan University, Guangzhou, China

The flavonoid baicalin has been reported to possess potent anti-inflammatory activities by suppressing inflammatory signaling pathways. However, whether baicalin can suppress the activation of NOD-like receptor (NLR) family, pyrin containing domain 3 (NLRP3) inflammasome in macrophages is largely unknown. Here, we showed that baicalin treatment dose-dependently inhibited adenosine triphosphate (ATP) or nigericin-induced NLRP3 inflammasome activation, as revealed by the decreased release of mature interleukin (IL)-1β, active caspase-1p10, and high-mobility group box-1 protein from lipopolysaccharide (LPS)-primed bone marrow-derived macrophages. The formation of ASC specks, a critical marker of NLRP3 inflammasome assembly, was robustly inhibited by baicalin in the macrophages upon ATP or nigericin stimulation. All these inhibitory effects of baicalin could be partly reversed by MDL12330A or H89, both of which are inhibitors of the protein kinase A (PKA) signaling pathway. Consistent with this, baicalin strongly enhanced PKA-mediated phosphorylation of NLRP3, which has been suggested to prevent ASC recruitment into the inflammasome. Of note, the PKA inhibitor H89 could block baicalin-induced NLRP3 phosphorylation on PKA-specific sites, further supporting PKA's role in this process. In addition, we showed that when administered pre and post exposure to *Escherichia coli* infection baicalin treatment significantly improved mouse survival in bacterial sepsis. Baicalin administration also significantly reduced IL-1β levels in the sera of bacterial infected mice. Altogether, our results revealed that baicalin inhibited NLRP3 inflammasome activation at least partly through augmenting PKA signaling, highlighting its therapeutic potential for the treatment of NLRP3-related inflammatory diseases.

Keywords: baicalin, NOD-like receptor (NLR) family, pyrin containing domain 3 inflammasome, interleukin-1β, protein kinase A, macrophages

OPEN ACCESS

Edited by:
Guixiu Shi,
Xiamen University, China

Reviewed by:
Charlotte M. Vines,
University of Texas at El Paso, United States
Nicolas Riteau,
National Institutes of Health (NIH), United States
Carlos De Torre,
IMIB-Arrixaca, Spain
Krzysztof Guzik,
Jagiellonian University, Poland
Luz Pamela Blanco,
National Institutes of Health (NIH), United States

****Correspondence:***
Xian-Hui He
thexh@jnu.edu.cn

[†]These authors have contributed equally to this work.

Specialty section:
This article was submitted to Inflammation, a section of the journal Frontiers in Immunology

Received: *27 July 2017*
Accepted: *11 October 2017*
Published: *27 October 2017*

Citation:
Li C-G, Yan L, Mai F-Y, Shi Z-J, Xu L-H, Jing Y-Y, Zha Q-B, Ouyang D-Y and He X-H (2017) Baicalin Inhibits NOD-Like Receptor Family, Pyrin Containing Domain 3 Inflammasome Activation in Murine Macrophages by Augmenting Protein Kinase A Signaling. Front. Immunol. 8:1409. doi: 10.3389/fimmu.2017.01409

INTRODUCTION

The NOD-like receptor (NLR) family, pyrin containing domain 3 (NLRP3) is an intracellular sensing protein that can be activated by diverse factors from pathogens, environments, and hosts (1, 2). When pathogen-associated molecular patterns (PAMPs) are bound to and recognized by the pattern recognition receptors, the nuclear factor (NF)-κB pathway is activated leading to the expression of pro-interleukin (IL)-1β, pro-IL-18, and NLRP3 (2, 3). NLRP3 can be further triggered by a variety of danger-associated molecular patterns (DAMPs), including adenosine triphosphate (ATP) derived from bacterial and host cells (4–6). Subsequently, NLRP3 recruits the adaptor molecule ASC (apoptosis-associated speck-like protein containing a caspase recruitment domain) which in turn interacts with pro-caspase-1 to form a large multi-protein complex called inflammasome. This culminates in the activation of caspase-1, thus converting pro-IL-1β and pro-IL-18 to their mature forms (1–3). Concomitantly, the active caspase-1 also cleaves gasdermin D protein to release its active N-terminal fragment, the latter of which forms pores in the plasma membrane leading to an inflammatory form of cell death named pyroptosis (7–13). Interestingly, recent studies indicated that the release of mature IL-1β is dependent on pyroptosis in macrophages (7, 11). As released IL-1β and high-mobility group box-1 (HMGB1) can further intensify the innate immunity, NLRP3 inflammasome activation constitutes a first line of defense against pathogenic infections (14, 15).

Although NLRP3 inflammasome has critical roles in combating pathogens, excessive or constitutive activation of NLRP3 inflammasome has been implicated in many inflammatory diseases in the contexts of infections, sterile tissue damages, and metabolic dysfunctions (16, 17). This is partially due to the excessive secretion of inflammatory cytokines like IL-1β upon NLRP3 inflammasome activation (18). These cytokines in turn enhance pyroptosis leading to multiple organ damage and septic death during bacterial infections (19, 20). Consistent with this notion, hyperactive NLRP3 due to conditional NLRP3 mutant knock-in resulted in hepatocyte pyroptosis, liver injury, and shortened survival of the experimental mice (19). On the contrary, blocking pyroptosis by *caspase-1/-11* or *gasdermin D* gene deletion confers the mice resistance to endotoxin-induced sepsis (20, 21). Furthermore, emerging evidence indicates that NLRP3 hyperactivation contributes to diseases of the central nervous system and lungs (22). NLRP3 inflammasome has also been implicated in the pathogenesis of metabolic disorders such as type 2 diabetes, obesity, atherosclerosis, and gout (16). In addition, the gain-of-function mutations in NLRP3 have been identified as the cause of the inherited cryopyrin-associated periodic syndrome Muckle–Wells syndrome, familial cold autoinflammatory syndrome, and neonatal-onset multisystem inflammatory disease (16, 23). Therefore, controlling NLRP3 inflammasome activation is a promising therapy for the treatment of inflammatory diseases such as bacterial infections, neurological disorders, and metabolic disorders (16).

Baicalin is a flavonoid isolated from the root of *Scutellaria baicalensis* Georgi, a well-known Chinese medicinal plant used to treat fevers (24). It has been demonstrated that baicalin possesses many bioactivities and pharmacological effects, including hepatoprotective, antioxidant, antibacterial, antiviral, and anti-inflammatory activities (24–26). Over past decades, the anti-inflammatory effects of baicalin have been intensively investigated. An early study showed that baicalin could markedly inhibit carrageenan-induced rat paw edema (27). It has also been shown to improve survival in murine model of polymicrobial sepsis induced by cecal ligation and puncture (CLP) (28–30) as well as in the model of endotoxemic shock (31). Several studies have indicated that the antiseptic and anti-inflammatory effects of baicalin are due to inhibition of inflammatory responses *via* downregulating the NF-κB signaling (31–34). There is evidence showing that baicalin may attenuate CLP-induced sepsis by inhibiting the release of HMGB1 and other cytokines including IL-1β (29). Recently, baicalin has been shown to suppress the expression of NLRP3 in LPS-stimulated piglet mononuclear phagocytes by suppressing the NF-κB pathway (35, 36).

Although those studies have revealed that baicalin exhibits potent anti-inflammatory activity likely through inhibiting NF-κB signaling, it is still elusive whether baicalin can affect NLRP3 inflammasome activation by canonical activators including ATP and nigericin. In this study, we found that baicalin robustly suppressed NLRP3 inflammasome activation in LPS-primed macrophages upon ATP or nigericin stimulation. Mechanistically, baicalin blocked ASC recruitment and speck formation in part by augmenting protein kinase A (PKA)-mediated phosphorylation of NLRP3, which has been reported to prevent NLRP3 inflammasome assembly (37, 38). Our results highlight baicalin as an agent for the treatment of NLRP3-related inflammatory diseases by promoting PKA signaling.

MATERIALS AND METHODS

Reagents and Antibodies

Baicalin (572667), MDL12330A (M182), disuccinimidyl suberate (S1885), Hoechst 33342 (B2261), propidium iodide (PI) (P4170), ATP (A6419), lipopolysaccharide (LPS) (*Escherichia coli* O111:B4) (L4391), dimethyl sulfoxide (DMSO) (D8418), Tween-80 (P8074), and Tween-20 (P1379) were bought from Sigma-Aldrich (St. Louis, MO, USA). Baicalin was dissolved in DMSO at 100 mM and stored at −20°C. H89 (S1643), cell lysis buffer for Western and IP (P0013), and phenylmethanesulfonyl fluoride (PMSF) (ST505) were obtained from Beyotime (Haimen, China). Nigericin (#tlrl-nig) was purchased from InvivoGen (San Diego, CA, USA). Dulbecco's Modified Eagle's Medium (DMEM) medium with high glucose, fetal bovine serum (FBS), streptomycin, and penicillin, Opti-MEM were products of Thermo Fisher/Gibco (Carlsbad, CA, USA). The anti-NLRP3 antibody (AG-20B-0014) was purchased from Adipogen AG (Liestal, Switzerland). The antibody against caspase-1p10 (M-20) (sc-514) was purchased from Santa Cruz Biotechnology (Dallas, TX, USA). The antibodies against phospho-(Ser/Thr) PKA substrate (#9621), IL-1β (#12242), ASC (#67824), HMGB1 (#3935), β-tubulin (#2128), and horse-radish peroxidase (HRP)-linked horse anti-mouse IgG (#7076), HRP-linked goat anti-rabbit IgG (#7074), and protein G agarose beads (#37478)

were purchased from Cell Signaling Technology (Danvers, MA, USA). CF568 goat-anti-rabbit IgG (H + L), highly cross-adsorbed (#20103) and CF488A-conjugated goat-anti-mouse IgG, and highly cross-adsorbed (#20018) were obtained from Biotium (Hayward, CA, USA).

Experimental Animals

Female C57BL/6 mice (6–8 weeks of age) were bought from the Experimental Animal Center of Southern Medical University (Guangzhou, China). All animals were acclimatized for 1 week before experiments under 12 h dark/12 h light cycle condition. Animal experiments were performed according to the guidelines for the care and use of animals approved by the Committee on the Ethics of Animal Experiments of Jinan University.

Bone Marrow-Derived Macrophage (BMDM) Culture

Mouse BMDMs were differentiated as reported previously (21, 39). Briefly, mice were sacrificed and bone marrows were collected from the femurs. Bone marrow cells were re-suspended in BM-Mac medium (80% DMEM medium containing 10% FBS plus 20% M-CSF-conditioned medium from L929 cells). Subsequently cells were seeded in 10-cm Petri dish with 10 ml BM-Mac medium and cultured at 37°C in a humidified incubator of 5% CO_2. BMDMs were ready for experiments after 6 days.

Cell Death Assay

Cell death was measured by PI incorporation as described previously (39, 40). Cells were cultured in 24-well plates and primed with 500 ng/ml LPS in Opti-MEM for 4 h. Subsequently, cells were treated with indicated concentrations of baicalin in Opti-MEM for 1 h followed by stimulation with ATP (3 mM) for 30 min or nigericin (10 μM) for 1 h. The cells were stained with PI solution (2 μg/ml PI plus 5 μg/ml Hoechst 33342) for 10 min at room temperature and observed immediately by live imaging using Zeiss Axio Observer D1 microscope equipped with a Zeiss LD Plan-Neofluar 20×/0.4 Korr M27 objective lens (Carl Zeiss MicroImaging GmbH, Göttingen, Germany). Fluorescence images were captured with a Zeiss AxioCam MR R3 cooled CCD camera controlled with ZEN software (Carl Zeiss).

Fluorescence Microscopy

Immunofluorescence analysis was performed as previously described (41, 42). In brief, BMDMs were seeded in glass-bottomed dishes (5×10^5 cells/dish) and cultured at 37°C overnight. Cells were primed with 500 ng/ml LPS in Opti-MEM for 4 h. Then the cells were treated with baicalin for 1 h, followed by treatment with ATP (3 mM) for 30 min or nigericin (10 μM) for 1 h in Opti-MEM. After fixation, permeabilization and blocking, cells were incubated with rabbit anti-ASC antibody (1:300) and mouse anti-NLRP3 antibody (1:300), followed by staining with CF568-conjugated goat-anti-rabbit IgG and CF488A-conjugated goat-anti-mouse IgG. After staining with Hoechst 33342 solution (5 μg/ml in PBS) to reveal the nuclei, the cells were observed under a Zeiss Axio Observer D1 microscope with a Zeiss LD Plan-Neofluar 40×/0.6 Korr M27 objective (Carl Zeiss MicroImaging GmbH, Göttingen, Germany). Fluorescence images were captured by a Zeiss AxioCam MR R3 cooled CCD camera controlled with ZEN software (Carl Zeiss).

ASC Oligomer Cross-linking

The cross-linking of ASC oligomers was performed as previously described (43, 44). In brief, cells were seeded in 6-well plates at 1.0×10^6 cells/well. After indicated treatments, cells were lysed with cold PBS containing 0.5% Triton-X 100, and the cell lysates were centrifuged at 6,000 × *g* for 15 min at 4°C. The pellets were washed twice with PBS and then re-suspended in 200 μl PBS. 2 mM disuccinimidyl suberate was added to the resuspended pellets, and the suspension was incubated at room temperature for 30 min with rotation. The cross-linked pellets were spun down at 6,000 × *g* for 15 min at 4°C and redissolved in 20 μl of 1× sodium dodecyl sulfate-polyacrylamide gel electrophoresis (SDS-PAGE) sample loading buffer. Samples were boiled for 5 min and analyzed by Western blotting.

Immunoprecipitation

Cells were rinsed once with ice-cold PBS and lyzed with 0.5 ml ice-cold cell lysis buffer for Western blot and IP (containing 1 mM PMSF). The cell lysates were centrifuged at 13,000 × *g* for 10 min at 4°C, precleared with a 10% volume of Protein G agarose beads for 30 min at 4°C with gentle agitation, and then incubated with anti-NLRP3 antibody (0.5 μg antibody for 100 μg cell lysate) overnight at 4°C with gentle shaking. The antibody-NLRP3 complexes were collected with a 10% volume of Protein G agarose beads for 2 h at 4°C with gentle shaking. The beads were washed five times with cell lysis buffer, boiled for 5 min in 3× SDS-PAGE sample loading buffer, and resolved by Western blot analysis.

Detection of Soluble IL-1β

Soluble IL-1β in culture supernatants and sera was determined by cytometric bead array (CBA) mouse IL-1β Flex Set (BD Biosciences, San Jose, CA, USA) according to the manufacturer's instructions. Data were acquired on a flow cytometer (FACSCalibur; Becton Dickinson, Mountain View, CA, USA) equipped with CELLQuest software (Becton Dickinson).

Precipitation of Soluble Proteins in Supernatants

Soluble protein in culture supernatants was precipitated as previously described (21, 39). The precipitated proteins were dissolved in equal volume of 1× SDS-PAGE sample loading buffer and subjected to Western blot analysis of secreted mature IL-1β, caspase-1p10, and HMGB1.

Western Blot Analysis

Western blotting was performed essentially as previously described (39). Briefly, total proteins were separated by SDS-PAGE and electro-transferred to PVDF membranes (#03010040001; Roche Diagnostics GmbH, Mannheim, Germany). The membranes were blocked by blocking buffer (PBS containing 3% FBS and 0.1% Tween-20) for 1 h and incubated with indicated primary antibody overnight at 4°C, followed by incubation with

appropriate HRP-linked secondary antibody (horse anti-mouse or goat anti-rabbit IgG). Bands were revealed with an enhanced chemiluminescence kit (BeyoECL Plus; Beyotime, Haimen, China) and recorded by X-ray films (Carestream, Xiamen, China). The blot images were captured by FluorChem8000 imaging system (AlphaInnotech, San Leandro, CA, USA). The gray values were analyzed by AlphaEaseFC 4.0.

Bacterial Infection

The mouse model of bacterial sepsis was established as previously described (5, 42). *E. coli* (DH5α strain) was grown in Luria Broth (LB) media at 37°C overnight, and then reinoculated into fresh LB media and grown for 4 h at 37°C. The viable bacteria were collected by centrifugation at 2,600 × *g* for 10 min, washed with PBS, and then resuspended in appropriate volume of PBS. Bacterial density was measured by using an ultraviolet-visible spectrophotometer (NanoDrop2000, Thermo Scientific), and the corresponding colony-forming units (CFUs) were determined on LB agar plates. All mice were acclimated for 1 week, randomly divided into three groups, and intragastrically administered once with baicalin solution (100 or 200 mg/kg body weight) or vehicle (2% Tween-80 in PBS). Three hours later, viable *E. coli* cells (2×10^9 CFU/mouse) in 0.5 ml of PBS were injected into the peritoneal cavity of each mouse. Mice were intragastrically administered once again with baicalin solution or vehicle 1 h after bacterial infection. Mouse survival was monitored every 6 h for five consecutive days. In another experiment, mice were treated similarly and were sacrificed at 4 and 8 h post bacterial infection. Their sera were collected, and serum IL-1β levels were measured by CBA mouse IL-1β Flex Set.

Statistical Analysis

All experiments were performed three times independently, with one representative experiment shown. The data were expressed as mean ± SD and analyzed for statistical significance using GraphPad Prism 5.0 (GraphPad Software Inc., San Diego, CA, USA). One-way analysis of variance followed by Tukey *post hoc* test and unpaired Student's *t*-test were used to analyze the statistical significance among multiple groups and between two groups, respectively. Kaplan–Meier survival curves were adopted for analysis of mouse survival, and the statistical difference between two groups was determined using the log-rank (Mantel–Cox) test. *P*-values < 0.05 were considered statistically significant.

RESULTS

Baicalin Inhibits NLRP3 Inflammasome Activation in BMDMs

NOD-like receptor (NLR) family, pyrin containing domain 3 inflammasome activation in macrophages needs two signals: PAMP (including LPS) priming (signal 1) and DAMP activation (signal 2) (3). We sought to explore whether baicalin could influence the activation of NLRP3 inflammasome in BMDMs. Cells were first primed with LPS (signal 1) and then pretreated with graded doses of baicalin before stimulation with NLRP3 activator ATP (signal 2). Western blotting was used to detect the two commonly used markers of inflammasome activation: the enzymatically active p10 subunit of caspase-1 (caspase-1p10) and mature IL-1β (17 kDa) in the culture supernatants. Consistent with previous reports (45), our data showed that both pro-IL-1β and NLRP3 proteins were highly induced by LPS, whereas pro-caspase-1 and ASC were constitutively expressed in macrophages irrespective of LPS priming (**Figure 1A**). Upon ATP treatment, both active caspase-1p10 (indicative of caspase-1 activation) and mature IL-1β were released into the culture supernatants. However, baicalin robustly suppressed the release of activated caspase-1p10 and mature IL-1β into the culture supernatant (**Figures 1A–C**). Notably, without ATP treatment, baicalin alone neither changed the constitutive expression nor the induced expression (by LPS) of the inflammasome related proteins (**Figure 1A**). Besides, bead-based immunoassay (CBA) was also used to detect mature IL-1β in culture supernatants. As expected, baicalin reduced ATP-induced secretion of mature IL-1β (**Figure 1D**), confirming the result of Western blot analysis of IL-1β (**Figure 1A**).

Further, we tested whether baicalin could affect NLRP3 inflammasome activation by another NLRP3 activator nigericin (a microbial toxin derived from *Streptomyces hygroscopicus*, acting as a potassium ionophore). In line with the results derived from ATP stimulation, baicalin also markedly reduced caspase-1 activation and mature IL-1β secretion in a dose-dependent manner upon nigericin stimulation (**Figures 2A–D**), indicating the suppression of NLRP3 activation. Taken together, these results indicated that baicalin inhibited NLRP3 inflammasome activation in macrophages upon ATP or nigericin stimulation.

Baicalin Inhibits ATP- or Nigericin-Induced Cell Death in LPS-Primed BMDMs

NOD-like receptor (NLR) family, pyrin containing domain 3 inflammasome triggering leads to the activation of caspase-1 rapidly culminating in an inflammatory form of cell death—pyroptosis (7, 8), which can be detected either by PI staining (40) or by measuring released cellular components including HMGB1 in the culture supernatants (46, 47). We thus explored whether baicalin inhibited ATP- or nigericin-induced cell death in BMDMs. LPS-primed cells were treated with ATP, and cell death was monitored by using fluorescence microscopy. As shown in **Figure 3A**, PI staining showed that cell death was rapidly induced by ATP. The proportion of ATP-induced cell death was ~45% (**Figure 3B**). Consistent with its effects on suppressing NLRP3 activation, baicalin markedly decreased the ratios of ATP-induced cell death in a dose-dependent manner (**Figure 3B**). Further supporting this, baicalin dose-dependently inhibited the release of HMGB1 into the culture supernatants (**Figures 3C,D**). Without ATP triggering, however, baicalin alone induced neither cell death nor HMGB1 release. Similarly, baicalin remarkably attenuated nigericin-induced cell death (**Figures 4A,B**) and the release of HMGB1 into the culture supernatants but left more HMGB1 in the cell lysates (**Figures 4C,D**). Taken together, these results indicated that baicalin suppressed ATP-or nigericin-induced NLRP3 inflammasome activation and cell death in macrophages.

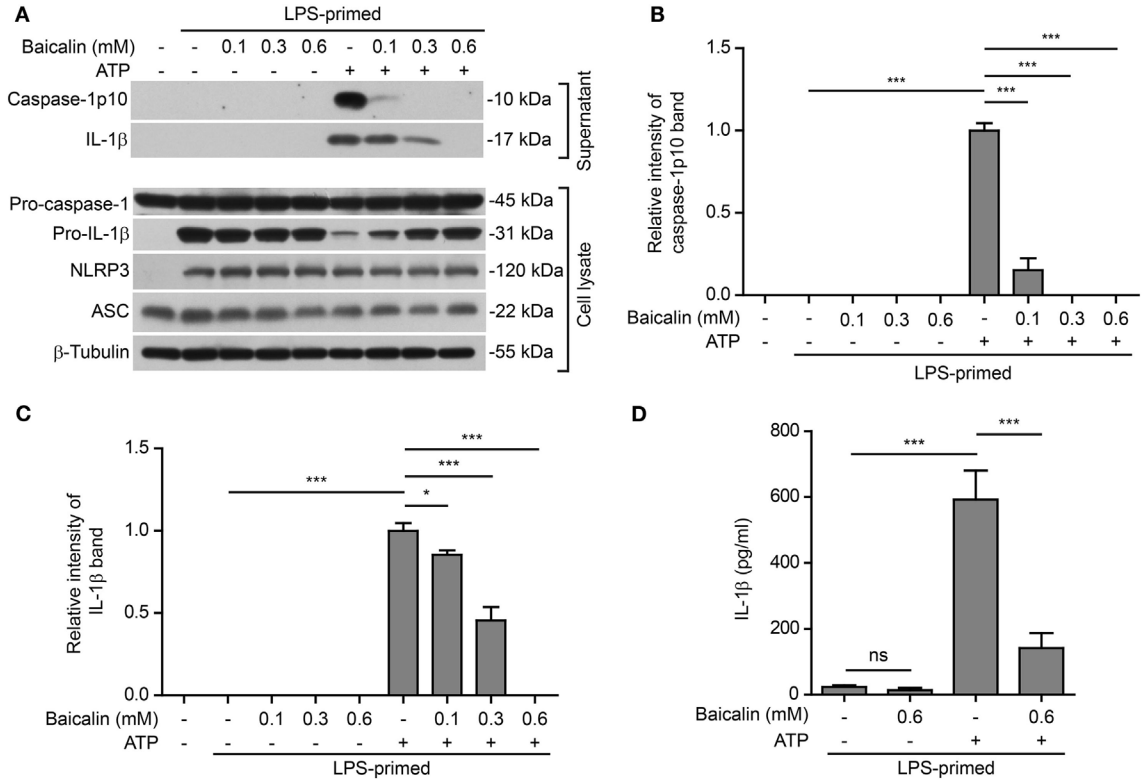

FIGURE 1 | Baicalin suppressed adenosine triphosphate (ATP)-induced activation of NOD-like receptor (NLR) family, pyrin containing domain 3 (NLRP3) inflammasome. Bone marrow-derived macrophages were first primed with LPS (500 ng/ml) for 4 h and then pretreated with graded concentrations of baicalin for 1 h, followed by incubation with ATP (3 mM) for 30 min in the absence of LPS. **(A)** Western blotting was used to assess the expression levels of indicated proteins in the cell lysates and culture supernatants, respectively. β-Tubulin was used as a loading control for cell lysates. **(B,C)** Histograms showing the relative intensity of capase-1p10 **(B)** or interleukin (IL)-1β **(C)** bands in culture supernatants in **(A)**. The intensity of capase-1p10 or IL-1β bands in ATP group was set to 1.0. The intensity of the other groups was calculated relative to the ATP group. **(D)**. Cells were treated as in panel **(A)**. The levels of soluble IL-1β were detected by cytometric bead array assay in the culture supernatants. The experiments were performed three times independently, with one representative experiment shown. Data are shown as mean ± SD ($n = 3$). *$P < 0.05$; ***$P < 0.001$; ns, not significant.

Baicalin Blocks ASC Speck Formation and Oligomerization upon NLRP3 Activation

Upon activation, NLRP3 recruits its downstream adaptor ASC to form large multi-protein complexes, which can be revealed as specks by either immunofluorescence microscopy or be evidenced as ASC oligomers by Western blotting after chemical cross-linking. We firstly analyzed the formation of ASC specks by fluorescence microscopy. Consistent with the Western blotting results (**Figures 1A** and **2A**), immunofluorescence analysis demonstrated that NLRP3 was weakly detected in unstimulated macrophages but was highly expressed in LPS-primed cells, whereas ASC expression was unaffected by LPS priming (Figure S1 in Supplementary Material). Without stimulation of NLRP3, ASC and NLRP3 were diffusely distributed in cells regardless of baicalin and/or LPS treatment, whereas ATP or nigericin treatment led to ASC speck formation in ~40 or ~30% of the cells, respectively (**Figures 5A,B** and **6A,B**). Notably, ASC specks were highly co-localized with NLRP3 dots in the cytoplasm (**Figures 5A** and **6A**), indicating the recruitment of ASC and formation of NLRP3 inflammasomes in these macrophages. Remarkably, baicalin treatment before ATP or nigericin stimulation drastically decreased the percentages of cells containing ASC specks to 3 or 1%, respectively (**Figures 5A,B** and **6A,B**), suggesting that baicalin could suppress the activation of NLRP3 inflammasome by blocking ASC speck formation.

As ASC specks formed after NLRP3 activation are insoluble in PBS containing 0.5% Triton-X 100 thus being collected as pellets and the ASC proteins within the pellets can be cross-linked by disuccinimidyl suberate to form oligomers (43), we examined the effect of baicalin on such ASC oligomerization by Western blot analysis. In LPS-primed macrophages, different ASC complexes (dimers, trimers, and higher oligomers) were observed in the samples treated with ATP or nigericin, whereas no ASC was detectable in the cells treated with vehicle or baicalin alone indicating that ASC was soluble in these cell lysates. Similar to the ASC speck assay, ATP or nigericin-induced ASC oligomerization was almost completely blocked by baicalin (**Figures 5C** and **6C**). Together, these data further confirmed that baicalin treatment inhibited NLRP3 inflammasome activation through blocking ASC recruitment into the NLRP3 inflammasome.

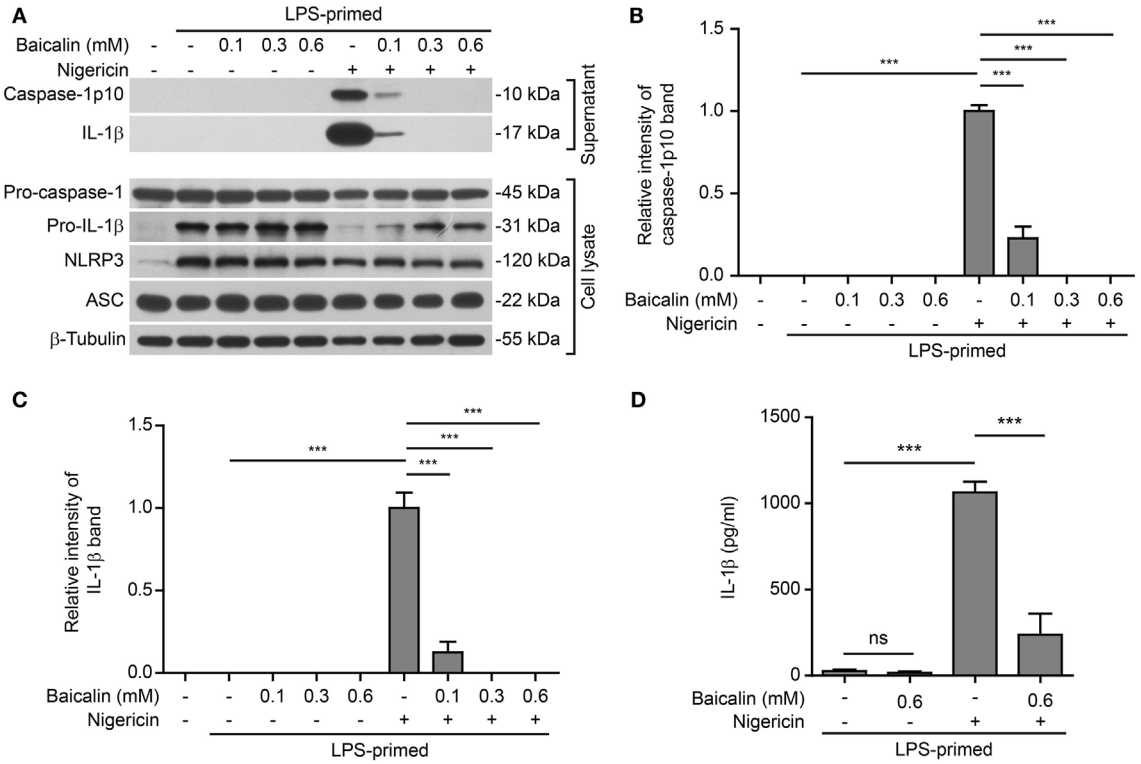

FIGURE 2 | Baicalin attenuated nigericin-induced NOD-like receptor (NLR) family, pyrin containing domain 3 (NLRP3) inflammasome activation. Bone marrow-derived macrophages were first primed with LPS (500 ng/ml) for 4 h and then pretreated with indicated doses of baicalin for 1 h, followed by incubation with nigericin (10 μM) for 1 h without LPS. **(A)** Western blot analysis was used to assess the expression and secretion of indicated proteins in the cell lysates and culture supernatants, respectively. β-Tubulin was used as a loading control for cell lysates. **(B,C)** Histograms showing the relative intensity of capase-1p10 **(B)** or interleukin (IL)-1β **(C)** bands in culture supernatants in panel **(A)**. The intensity of capase-1p10 or IL-1β bands in nigericin group was set to 1.0. The intensity of the other groups was calculated relative to the nigericin group. **(D)** The levels of soluble IL-1β were detected by cytometric bead array assay in the culture supernatants. The experiments were performed three times independently, with one representative experiment shown. Data are shown as mean ± SD ($n = 3$). ***$P < 0.001$; ns, not significant.

Baicalin-Mediated Inhibition of NLRP3 Inflammasome Activation and IL-1β Release Is Reversed by the PKA Pathway Inhibitors

In light of previous findings that the PKA negatively regulates NLRP3 activation (37, 38) and that baicalin may increase the PKA activity (48), we next explored whether baicalin suppressed the NLRP3 inflammasome activation by upregulating PKA signaling in macrophages. First, the adenyl cyclase inhibitor MDL12330A was used to block cyclic AMP (cAMP) production thus attenuating the PKA activity. As shown in **Figures 7A,B**, the effect of baicalin on suppressing mature IL-1β (17 kDa) release upon ATP stimulation was partly antagonized by MDL12330A treatment. Furthermore, MDL12330A not only increased ATP-induced cell death but also counteracted the effect of baicalin on suppressing the cell death (**Figures 7C,D**). The PKA inhibitor H89 had similar effects as MDL12330A did, counteracting the inhibitory effect of baicalin on ATP-induced cell death (**Figures 8A,B**) and IL-1β release (**Figure 8C**). Together, these results suggested that baicalin suppressed NLRP3 inflammasome activation at least in part through the PKA signaling.

Baicalin-Mediated Suppression of ASC Speck formation Is Counteracted by Blocking PKA Signaling

As baicalin could attenuate ASC speck formation upon NLRP3 activation, we next explore whether the suppression of ASC speck formation by baicalin could also be reversed by blocking the PKA activity. The PKA inhibitor H89 increased the ASC speck formation induced by ATP, and it could partly reversed the inhibitory effect of baicalin on ATP-induced ASC speck formation (**Figures 9A,B**), further confirming that PKA signaling had been involved in the action of baicalin on suppressing NLRP3 inflammasome activation.

Therefore, we next explored whether baicalin could enhance the Ser/Thr phosphorylation of NLRP3 on PKA-specific sites, which has been reported to prevent NLRP3 inflammasome activation in macrophages (37, 38). To this end, NLRP3 was immunoprecipitated, and its phosphorylation on Ser/Thr residues of PKA substrate motifs was evaluated by Western blotting. Indeed, the PKA-specific phosphorylation on Ser/Thr residues of NLRP3 was greatly increased by baicalin pretreatment. The PKA inhibitor H89 blocked such phosphorylation, further

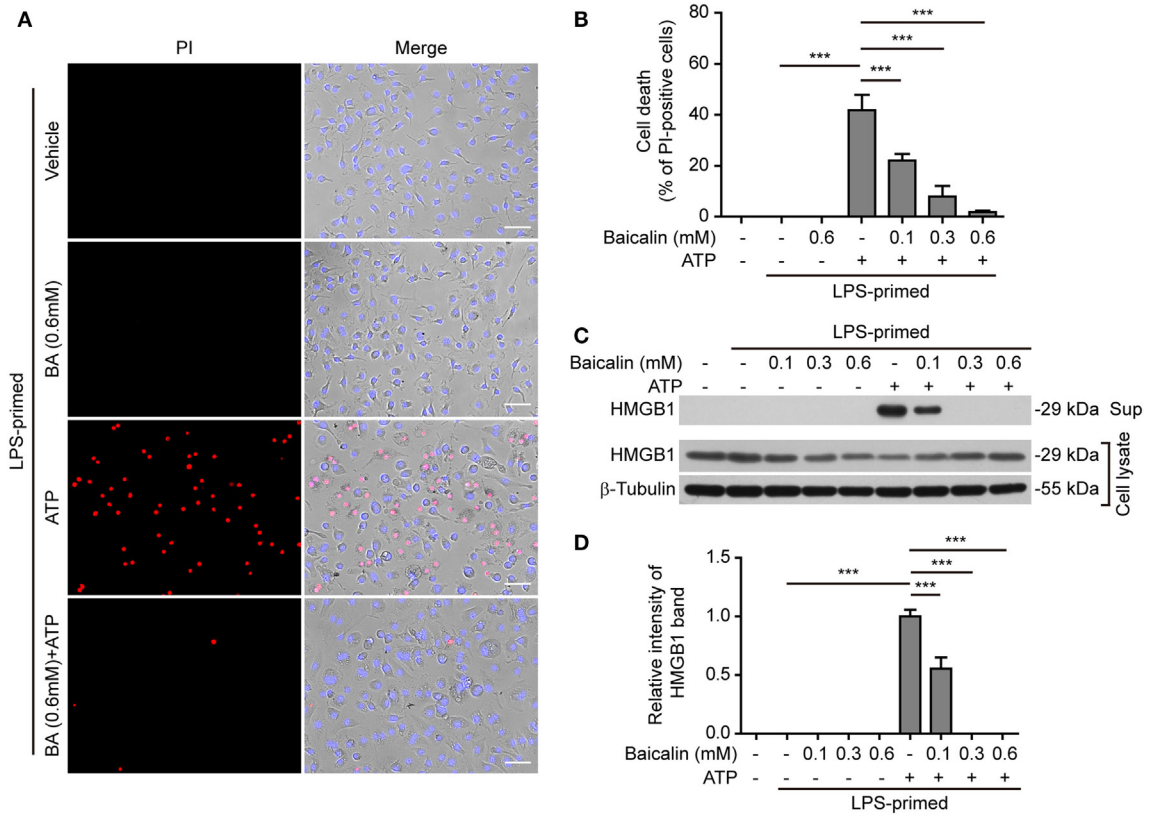

FIGURE 3 | Baicalin inhibited adenosine triphosphate (ATP)-induced cell death in macrophages. Bone marrow-derived macrophages were treatment as in **Figure 1A**. **(A)** Cell death was measured by staining with propidium iodide (PI) (red, staining dead cells) and Hoechst 33342 (blue, staining all cells) together for 10 min. All images were captured by fluorescence microscopy and showed in merge with bright-field images. One set of representative images of three independent experiments is shown. Scale bars, 50 μm. **(B)** PI-positive cells in five randomly chosen fields with each containing ~100 cells were quantified. The percentage of cell death is defined as the ratio of PI-positive cells relative to all cells (revealed by Hoechst). Data are shown as mean ± SD ($n = 5$). **(C)** Cells were treated as in panel **(A)**. Western blotting was used to assess the expression levels of indicated proteins in the cell lysates and culture supernatants, respectively. β-Tubulin was adopted as a loading control for cell lysates. **(D)** Histograms showing the relative intensity of high-mobility group box-1 (HMGB1) band in culture supernatants in panel **(C)**. The intensity of HMGB1 band in ATP group was set to 1.0 while those of the other groups were calculated relative to the ATP group. The experiments were performed three times independently, with one representative experiment shown. Data are shown as mean ± SD ($n = 3$). ***$P < 0.001$; BA, baicalin; Sup, supernatant.

verifying that baicalin-enhanced NLRP3 phosphorylation was mediated by PKA signaling (**Figures 9C,D**). Altogether, these results suggested that baicalin inhibited NLRP3 inflammasome activation at least partly through augmenting PKA signaling.

Baicalin Treatment Increases Mouse Survival in Bacterial Sepsis

As ATP-induced NLRP3 inflammasome activation has critical roles in bacterial sepsis (5), we explored whether baicalin could ameliorate sepsis in a mouse model of bacterial infection in the peritoneal cavity. Mice were administered once intragastrically with baicalin solution (100 or 200 mg/kg body weight) or vehicle 3 h before intraperitoneal injection of viable *E. coli* (2×10^9 CFU/mouse). One hour after the injection of bacteria, the mice were administered once again with baicalin or vehicle. Only 10% of mice survived the period of observation (120 h) in the vehicle group, whereas baicalin administration significantly increased their survival rates when compared with the vehicle group (**Figure 10A**). Moreover, baicalin treatment significantly decreased IL-1β levels in the sera of bacterial infected mice as compared with vehicle (**Figure 10B**), indicating that baicalin suppressed systemic inflammation in the mice, which was consistent with the *in vitro* studies showing baicalin's inhibitory effects on NLRP3 activation. Therefore, this result highlights the potential application of baicalin in the treatment of inflammatory diseases including bacterial sepsis.

DISCUSSION

In this study, we found that baicalin markedly inhibited NLRP3 inflammasome activation in LPS-primed macrophages upon ATP or nigericin triggering, thereby blocking the activation of caspase-1 and the release of mature IL-1β and HMGB1. This inhibitory action of baicalin is in part mediated by augmentation of PKA signaling as the adenyl cyclase inhibitor MDL12330A or PKA inhibitor H89 could partly reverse such an effect. Indeed,

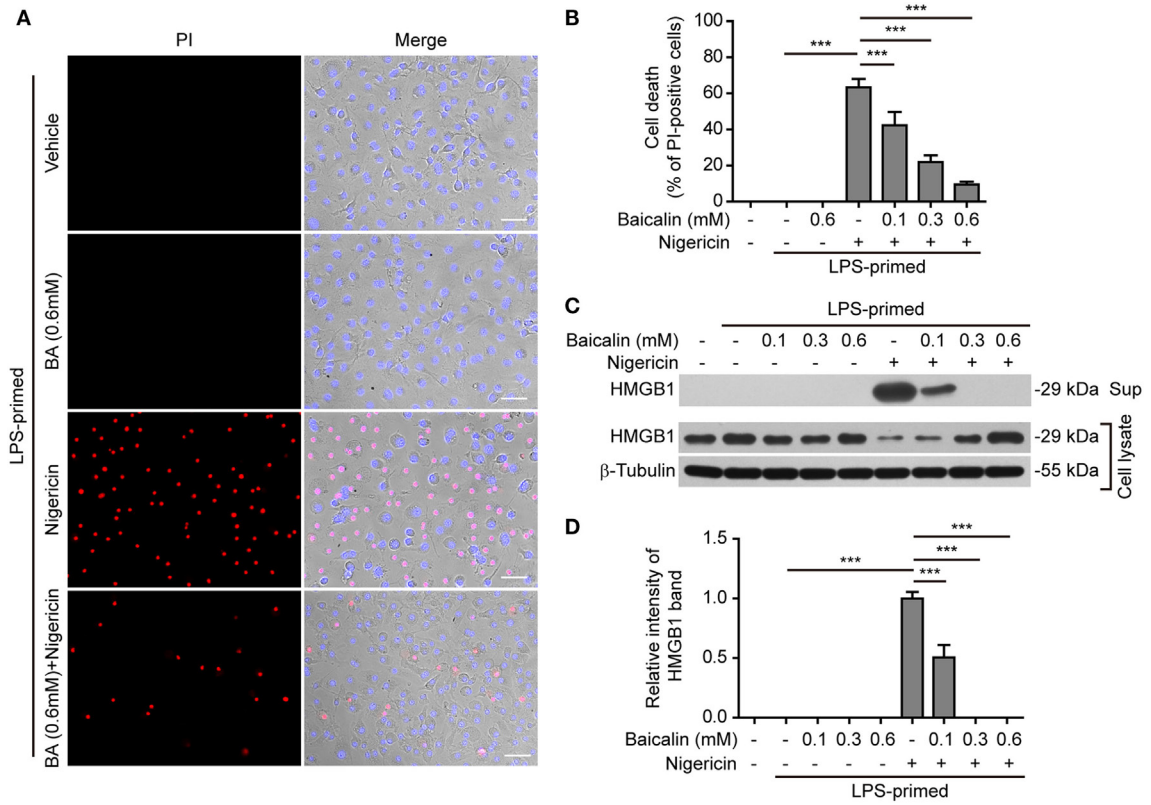

FIGURE 4 | Baicalin inhibited nigericin-induced cell death in macrophages. Bone marrow-derived macrophages were treated as indicated in **Figure 2A**. **(A)** Cell death was measured by staining with propidium iodide (PI) (red, staining dead cells) and Hoechst 33342 (blue, staining all cells) together for 10 min. All the images were captured by fluorescence microscopy and showed in merge with bright-field images. One set of representative images of three independent experiments is shown. Scale bars, 50 μm. **(B)** PI-positive cells in five randomly chosen fields each containing ~100 cells were quantified. The percentage of cell death is defined as the ratio of PI-positive cells relative to all cells (revealed by Hoechst). Data are shown as mean ± SD ($n = 5$). **(C)** Cells were treated as in panel **(A)**. Western blotting was used to assess the expression levels of indicated proteins in the cell lysates and culture supernatants, respectively. β-Tubulin was used as a loading control for cell lysates. **(D)** Histograms showing the relative intensity of high-mobility group box-1 (HMGB1) band in the culture supernatants in panel **(C)** ($n = 3$). The intensity of HMGB1 band in nigericin group was set to 1.0, and those of the other groups were calculated relative to the nigericin group. The experiments were performed three times independently, with one representative experiment shown. Data are shown as mean ± SD ($n = 3$). ***$P < 0.001$; BA, baicalin; Sup, supernatant.

baicalin enhanced PKA-mediated phosphorylation of NLRP3, thereby reducing NLRP3's capacity to recruit the adaptor ASC and the formation of ASC oligomerization. In line with the finding that baicalin inhibited NLRP3 inflammasome activation *in vitro*, baicalin administration *in vivo* significantly improved the survival of mice in bacterial sepsis.

During bacterial infection, ATP can be released either from the host's monocytes/macrophages or from bacterial cells (5, 49, 50). By acting on the purinergic P2X7 receptor on the plasma membrane, extracellular ATP can induce the efflux of K^+, thus triggering the NLRP3 inflammasome leading to the activation of caspase-1 (51–53). The activated caspase-1 further leads to pyroptosis and release of inflammatory cytokines including IL-1β and HMGB1 (7, 8, 13, 46, 47), which greatly exacerbate the inflammatory responses during bacterial infections and even leading to organ damage and septic shock (54–56). We showed in this study that baicalin markedly inhibited NLRP3 inflammasome activation in murine macrophages upon ATP stimulation, suggesting that baicalin may attenuate the severity of bacterial sepsis. Consistent with this notion, we found that baicalin could significantly improve the survival of mice in a model of bacterial sepsis. This result is in line with several previous studies showing that baicalin can prolong the survival of mice in both CLP-induced sepsis and LPS-induced endotoxemia (28–30). Consistent with our results, these previous reports showed that baicalin did reduce the levels of HMGB1 in septic mice and suppress the release of IL-1β and HMGB1 from macrophages (29), even though not clearly pointing to NLRP3 inflammasome activation. In support of our findings, two separate studies provided evidence that baicalin could suppress the NLRP3 inflammasome pathway in piglet mononuclear phagocytes in response to LPS stimulation (36) or *Haemophilus parasuis* infection (35). Those previous studies and our data indicated that baicalin robustly inhibited NLRP3 inflammasome activation to attenuate inflammatory responses during infections such as bacterial sepsis.

More recently, there is evidence indicating that PKA signaling negatively regulates NLRP3 activation. For example, bile acid induces an increase in intracellular cAMP levels through acting on its receptor TGR5, leading to PKA activation and PKA-mediated phosphorylation of NLRP3, which suppresses

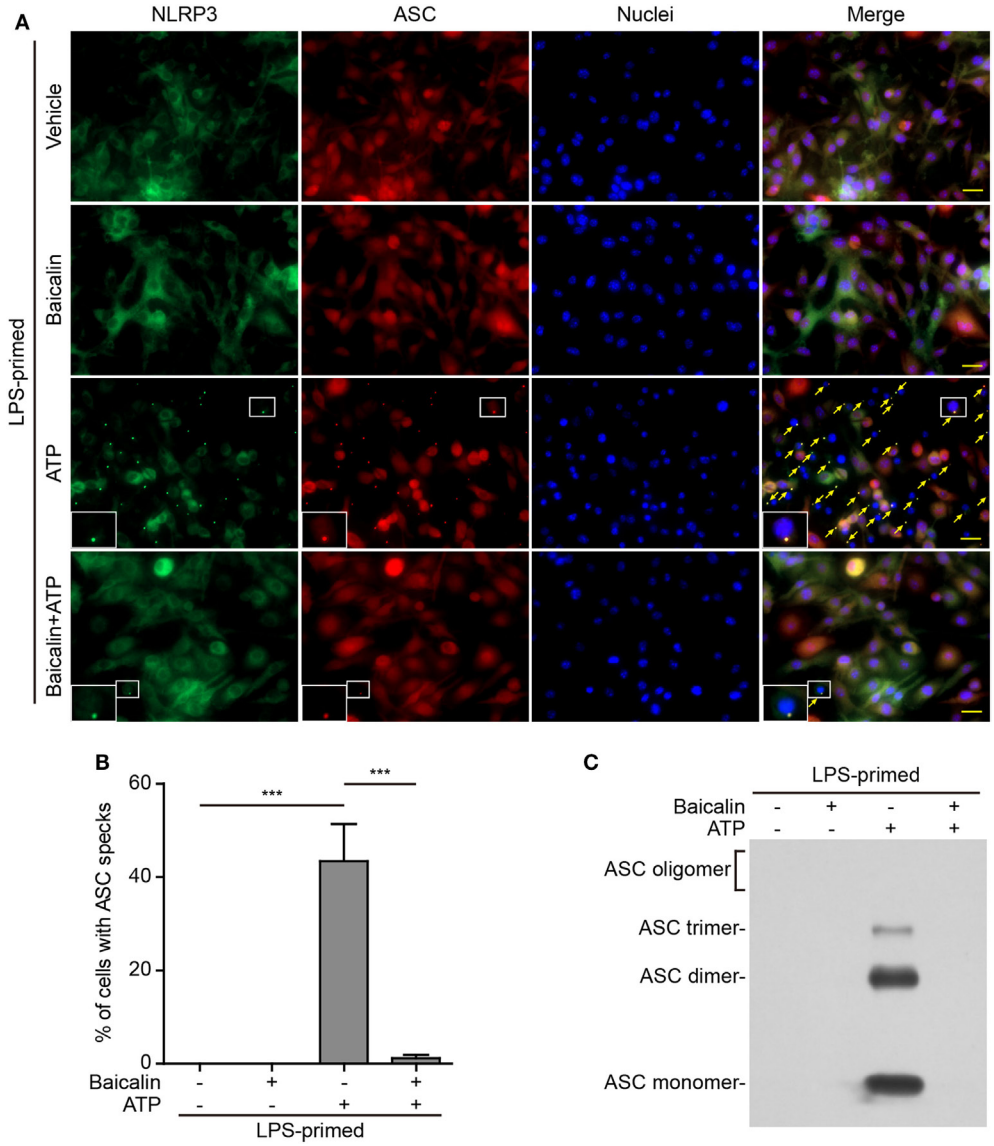

FIGURE 5 | Baicalin blocked adenosine triphosphate (ATP)-induced ASC speck formation and oligomerization. Bone marrow-derived macrophages were primed with LPS (500 ng/ml) for 4 h, pretreated with baicalin (0.6 mM) for 1 h, and triggered with ATP (3 mM) for 30 min in the absence of LPS. **(A)** Representative immunofluorescence images showing ASC (red) and NOD-like receptor (NLR) family, pyrin containing domain 3 (NLRP3) (green) subcellular distributions. Nuclei (blue) were stained with Hoechst 33342. Merged images were also presented to show the co-localization of ASC specks and NOD-like receptor (NLR) family, pyrin containing domain 3 (NLRP3) dots in the cytoplasm. Yellow arrows indicate the ASC specks, and the enlarged insets show cells with an ASC speck. Scale bars, 20 μm. **(B)** Quantification of cells with ASC specks relative to the total number of cells in five randomly chosen fields with each containing ~50 cells. **(C)** Western blot analysis for ASC in Triton-X 100 insoluble pellets cross-linked with disuccinimidyl suberate. The experiments were performed three times independently, with one representative experiment shown. Data are shown as mean ± SD ($n = 3$). ***$P < 0.001$.

NLRP3 inflammasome activation in macrophages (37). It has also been shown that prostaglandin E2 can inhibit NLRP3 inflammasome activation by inducing PKA signaling (38). In addition, dopamine negatively regulates NLRP3 inflammasome *via* a cAMP-dependent manner (57). Consistent with these studies, we in this study provided evidence that baicalin suppressed NLRP3 activation by modulating PKA activity. Baicalin greatly increased PKA-mediated Ser/Thr phosphorylation of NLRP3 and prevented ATP-induced formation of ASC specks, but these effects of baicalin could be counteracted by blocking the PKA signaling pathway with its specific inhibitors. This indicated that baicalin prevented NLRP3 inflammasome assembly by enhancing the NLRP3 phosphorylation on PKA-specific sites. In further support of this, PKA inhibitors also counteracted baicalin's effects on suppressing ATP-induced caspase-1p10 and IL-1β release. In addition, ATP-induced NLRP3 inflammasome activation was further enhanced by PKA inhibitor, which is in line with previous studies (37, 38). Collectively, these data demonstrated that

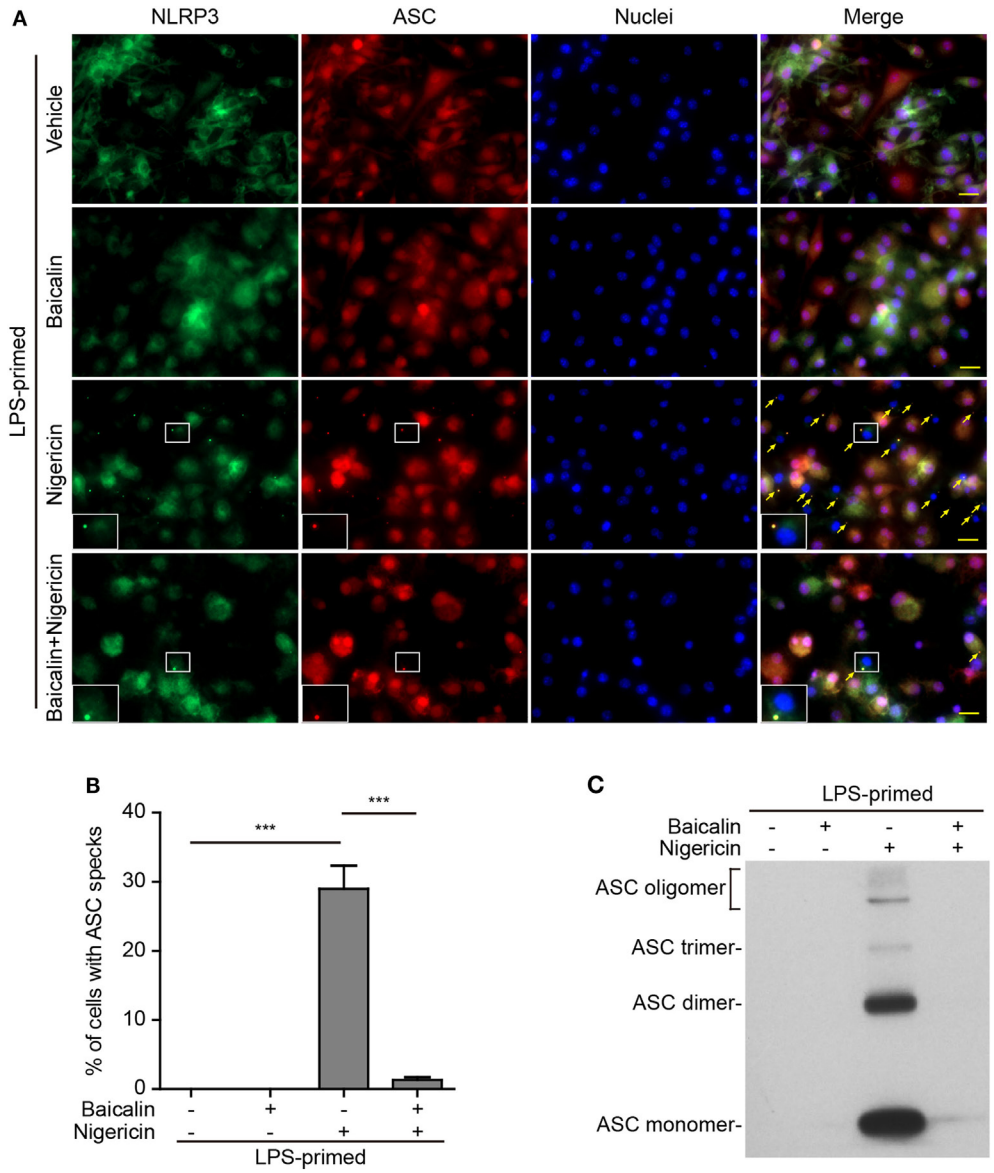

FIGURE 6 | Baicalin suppressed nigericin-induced ASC speck formation and oligomerization. Bone marrow-derived macrophages were primed with LPS (500 ng/ml) for 4 h, pretreated with baicalin (0.6 mM) for 1 h, and triggered with nigericin (10 μM) for 1 h without LPS. **(A)** Representative immunofluorescence images showing ASC (red) and NOD-like receptor (NLR) family, pyrin containing domain 3 (NLRP3) (green) subcellular distribution. Nuclei (blue) were stained with Hoechst 33342. Merged images are also presented to show the co-localization of ASC specks and NLRP3 dots in the cytoplasm. Yellow arrows indicate ASC specks, and the enlarged cell showed with an ASC speck. Scale bars, 20 μm. **(B)** Percentages of cells containing ASC specks relative to the total number of cells in five randomly chosen fields with each containing ~50 cells. **(C)** Western blot analysis for ASC in Triton-X 100 insoluble pellets cross-linked with disuccinimidyl suberate. The experiments were performed three times independently, with one representative experiment shown. Data are shown as mean ± SD ($n = 3$). ***$P < 0.001$.

baicalin can suppress NLRP3 inflammasome activation by, at least partly, modulating PKA signaling.

Furthermore, blocking cAMP formation by inhibiting the adenyl cyclase (AC) activity also significantly reversed baicalin-induced suppression of NLRP3 activation, highlighting the possibility that baicalin may modulate upstream components of PKA signaling. It was likely that baicalin might have increased cAMP levels by modulating AC activity, although we had not assayed the cAMP levels. In support of this notion, a previous study showed that baicalin administration could increase cAMP levels *in vivo* (48). However, the intracellular levels of cAMP are also regulated by its degradation enzyme phosphodiesterases (PDEs) (58). A large panel of PDEs has been shown to regulate cAMP levels thus modulating the PKA activity and NLRP3 activation. For example, the PED4 inhibitor Rolipram has been shown to inhibit NLRP3 inflammasome activation in submandibular gland cells (59). Although we had shown that AC inhibitor could reverse baicalin-mediated suppression of NLRP3, our data does not

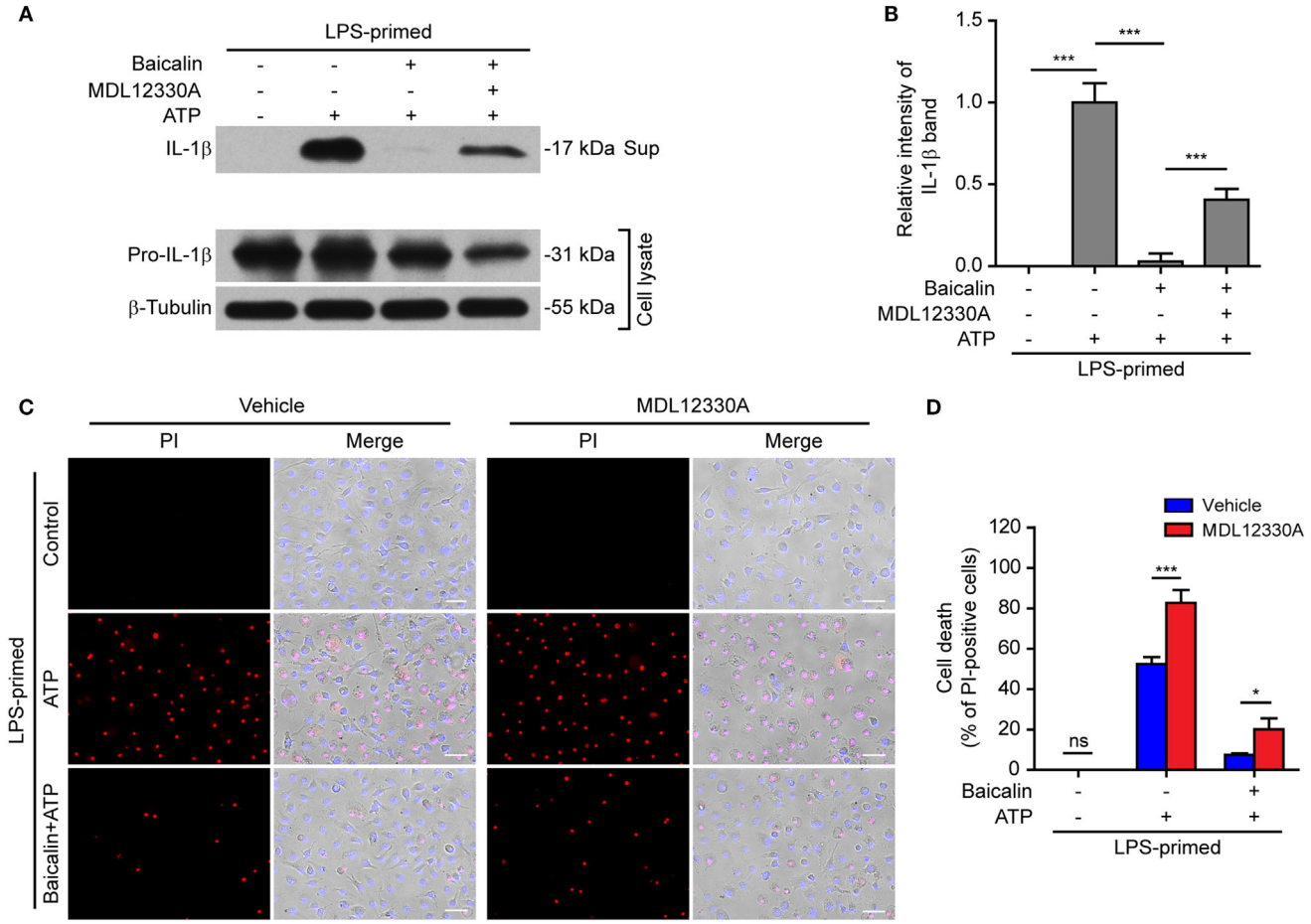

FIGURE 7 | Baicalin inhibited NOD-like receptor (NLR) family, pyrin containing domain 3 (NLRP3) inflammasome activation depending on the adenyl cyclase activity. Bone marrow-derived macrophages were primed with LPS (500 ng/ml) for 4 h, pretreated with baicalin (0.3 mM) for 30 min, and then incubated with adenyl cyclase inhibitor MDL12330A (10 μM) for 30 min, followed by co-treatment with adenosine triphosphate (ATP) (3 mM) for 30 min. **(A)** Western blot analysis was used to detect the expression and secretion of interleukin (IL)-1β in the cell lysates and culture supernatants, respectively. β-Tubulin was used as a loading control for cell lysates. **(B)**. Histograms showing the relative intensity of mature IL-1β band in panel **(A)** ($n = 3$). The intensity of IL-1β band in ATP group was set to 1.0 while those of the other groups were calculated relative to the ATP group. **(C)** Cell death was measured by staining with propidium iodide (PI) (red, staining dead cells) and Hoechst 33342 (blue, staining all nuclei) together for 10 min. All images were captured by fluorescence microscopy and showed in merge with bright-field images. One set of representative images of three independent experiments is shown. Scale bars, 50 μm. **(D)** PI-positive cells in five randomly chosen fields each containing ~100 cells were quantified. The percentage of cell death is defined as the ratio of PI-positive cells relative to all cells (revealed by Hoechst). Data are shown as mean ± SD ($n = 5$). *$P < 0.05$; ***$P < 0.001$; ns, not significant; Sup, supernatant.

exclude the possibility that baicalin may regulate PKA signaling by affecting the activity of PDEs. Recently, it has been shown that the phosphorylation of NLRP3 on Ser 3 (in mouse, which corresponds Ser 5 in human) has a critical role in modulating NLRP3 activation and that the protein phosphatase PP2A is involved in dephosphorylation and activation of NLRP3 inflammasome (60). As the motif surrounding Ser 3 (MTS*) is different from the PKA substrate motif [(K/R)(K/R)XS*/T*], it is still unknown whether Ser/Thr phosphorylation of NLRP3 on PKA-specific sites is regulated by PP2A. Besides, although H89 did inhibit the action of PKA on NLRP3 as revealed by abrogating the phosphorylation on PKA-specific sites, it should be noted that H89 may have other action targets beyond PKA (61). Therefore, further investigation is warranted to elucidate the precise mechanism by which baicalin modulates the cAMP/PKA signaling pathway.

As aforementioned, NLRP3 inflammasome activation requires two signals: the priming (first signal by LPS, etc.) and triggering (second signal by ATP or nigericin, etc.) (3, 62). Baicalin has been shown to exhibit anti-inflammatory activity by suppressing the NF-κB pathway, thus suppressing the expression of inflammatory cytokines and NLRP3 inflammasome components under various circumstances (31–36). It is worth noting that in those studies such inhibitory effects of baicalin appear to be attributed to the first signal (priming) of NLRP3 inflammasome (35, 36), thus leading to the downregulation of NLRP3 activation since the full activation of this inflammasome is relying on a marked upregulation of this key protein. However, it was unclear whether baicalin could inhibit NLRP3 inflammasome activation at the triggering step (second signal). In this study, we found that baicalin had minimal effect on the expression of

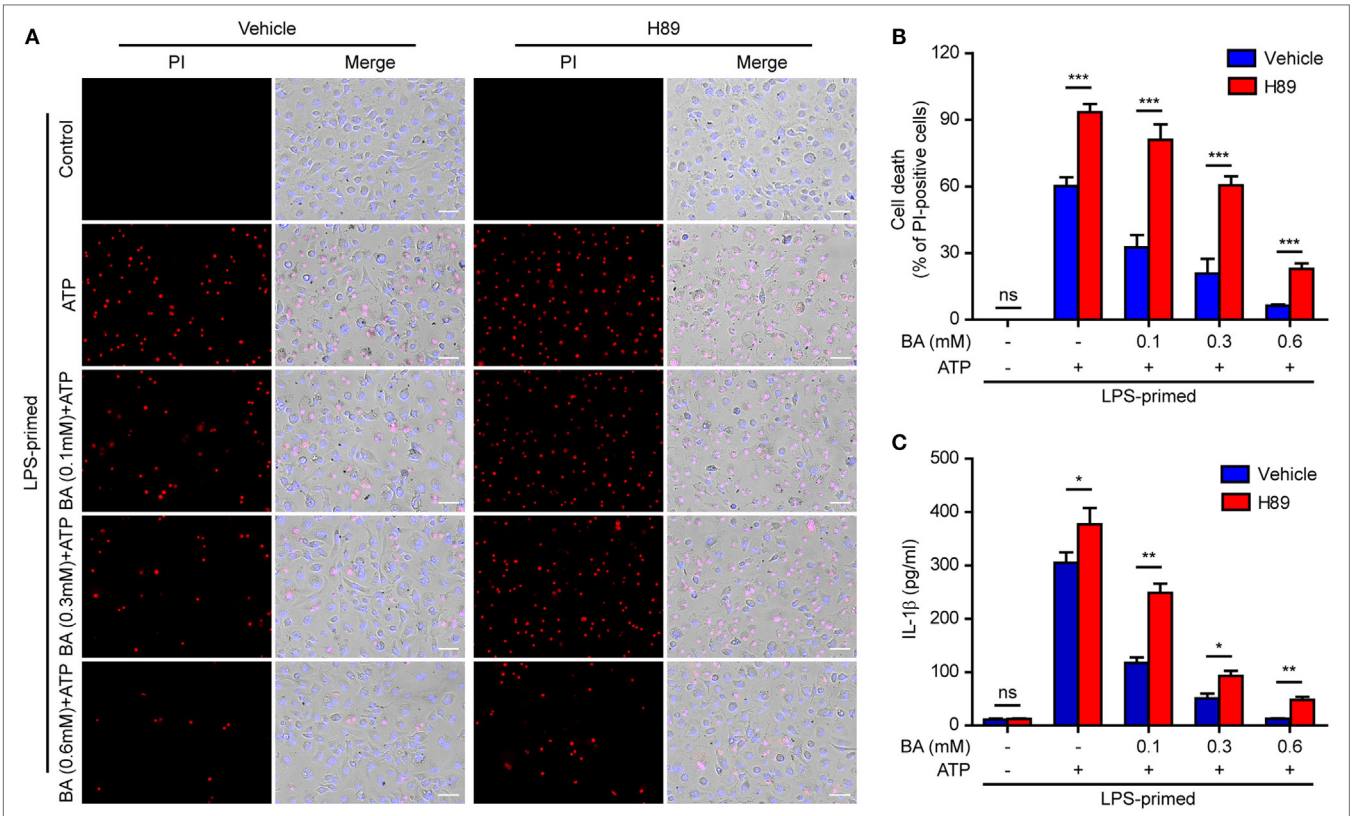

FIGURE 8 | Baicalin inhibited cell death in macrophages depending on protein kinase A (PKA) signaling. LPS-primed bone marrow-derived macrophages were pretreated with the PKA inhibitor H89 (20 μM) for 30 min and then incubated with graded doses of baicalin for 1 h, followed by stimulated with adenosine triphosphate (ATP) (3 mM) for 30 min. **(A)** Cell death was assay by propidium iodide (PI) (red) and Hoechst 33342 (blue) co-staining for 10 min. The images were captured by fluorescence microscopy. One set of representative images of three independent experiments is shown. Scale bars, 50 μm. **(B)** PI-positive cells in five randomly chosen fields each containing ~100 cells were quantified. The percentage of cell death is defined as the ratio of PI-positive cells relative to all cells (revealed by Hoechst). Data are shown as mean ± SD ($n = 5$). **(C)** Cells were treated as in panel **(A)**. The levels of soluble interleukin (IL)-1β in culture supernatants were measured by cytometric bead array assay. Data are shown as mean ± SD ($n = 3$). $^*P < 0.05$; $^{**}P < 0.01$; $^{***}P < 0.001$; ns, not significant; BA, baicalin.

NLRP3 inflammasome components, including the constitutive expression of ASC and pro-caspase-1 as well as induced expression of NLRP3 and pro-IL-1β in LPS-primed macrophages. Instead, baicalin could block NLRP3 inflammasome activation upon ATP or nigericin triggering, indicative of its action on the second signal for this inflammasome. Such inhibitory effects of baicalin are likely mediated by augmenting the PKA signaling leading to increased phosphorylation of NLRP3 on PKA-specific sites, which in turn prevents the adaptor ASC recruitment into the inflammasome. Therefore, apart from its inhibitory effects on NLRP3 transcription as revealed by previous studies (36, 37), baicalin can also inhibit NLRP3 inflammasome activation in macrophages upon ATP or nigericin triggering.

Adenosine triphosphate and nigericin have been widely used as activators to stimulate NLRP3 inflammasome activation in LPS-primed macrophages (6, 37, 38, 44), accompanied by caspase-1-dependent cell death, which is regarded as pyroptotic cell death (2, 3). Supporting this, one recent study elegantly showed that gasdermin D, NLRP3, and caspase-1 are all needed for nigericin to induce cell death and IL-1β secretion in LPS-primed RAW 264.7 cells expressing ASC, indicating that nigericin does induce pyroptosis in LPS-primed macrophages (11). However, it has been found that a diverse array of NLRP3 activators, including ATP and nigericin, induced necrosis in human THP-1 cells irrespective of LPS stimulation (63). One possible explanation for this discrepancy is that the cell death types induced by NLRP3 activators may be dependent on experimental settings (such as incubation time and stimulator concentrations). For example, in most of studies (6, 37, 38, 44), ATP (2–5 mM) and nigericin (10 μM) were incubated for 0.5–1 h to activate the NLRP3 inflammasome, respectively. But longer nigericin incubation time (4–6 h) and higher ATP concentrations (≥30 mM for 4–6 h) had been shown to trigger necrosis (63). In this study, we used nigericin stimulation for 1 h and found that baicalin significantly inhibited nigericin-induced inflammasome activation and cell death in LPS-primed macrophages, suggesting that baicalin could inhibit NLRP3-mediated pyroptosis. Similarly, as LPS plus ATP treatment induced caspase-1 activation and IL-1β release, it was likely that the accompanied cell death was pyroptosis. Further studies are warranted to uncover whether baicalin inhibits ATP- or nigericin-induced necrosis under the condition without LPS priming.

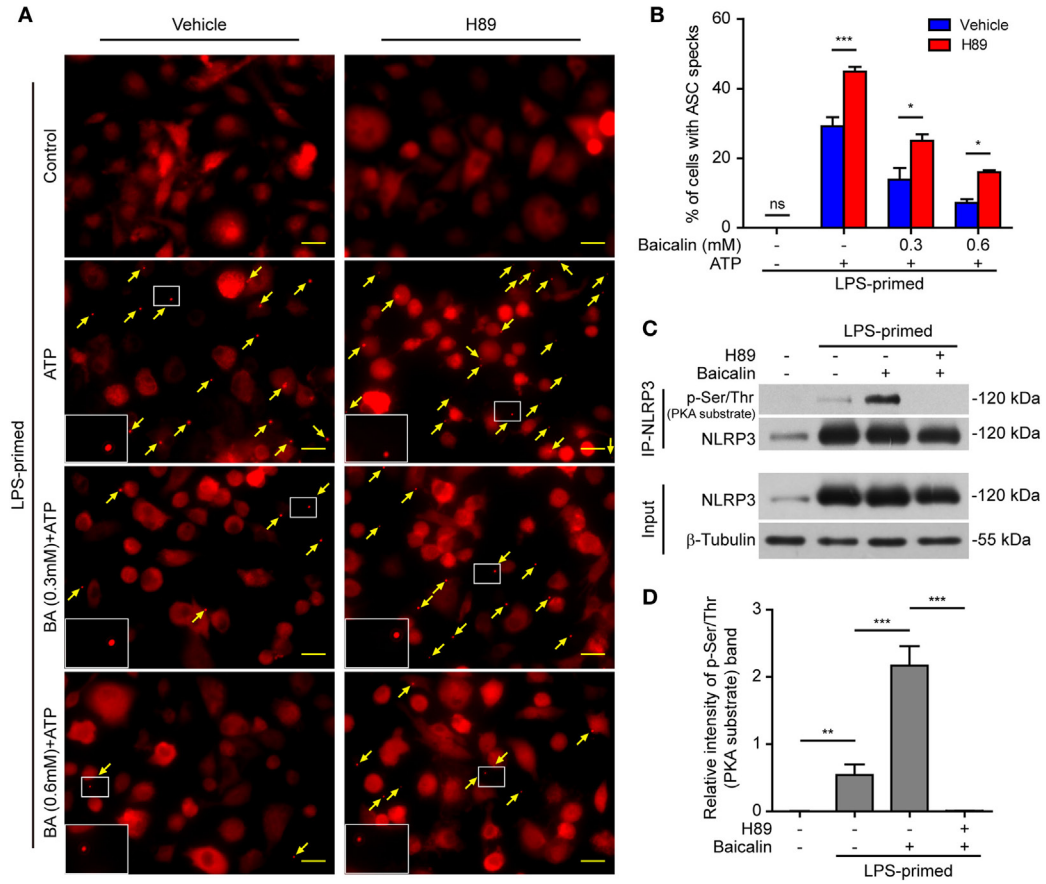

FIGURE 9 | Baicalin inhibited ASC speck formation by upregulating protein kinase A (PKA) signaling. Bone marrow-derived macrophages (BMDMs) were treated as described in **Figure 8**. **(A)** Representative immunofluorescence images showing ASC subcellular distribution. Yellow arrows indicate ASC specks. The enlarged insets showed cells with an ASC speck. Scale bars, 20 μm. **(B)** The ASC speck formation was quantified by the cells with ASC specks relative to the total cells from five random fields each containing ~50 cells. **(C)** LPS-primed BMDMs were incubated with the PKA inhibitor H89 (20 μM) for 30 min and then treated with baicalin (0.6 mM) for 1 h without adenosine triphosphate (ATP) treatment. NOD-like receptor (NLR) family, pyrin containing domain 3 (NLRP3) immunoprecipitation was analyzed for phosphorylation on PKA-specific sites (p-Ser/Thr PKA substrate). **(D)** The intensity of p-Ser/Thr phosphorylation on PKA-specific sites of NLRP3 was quantified relative to total NLRP3 in panel **(C)**. *$P < 0.05$; **$P < 0.01$; ***$P < 0.001$; ns, not significant; BA, baicalin.

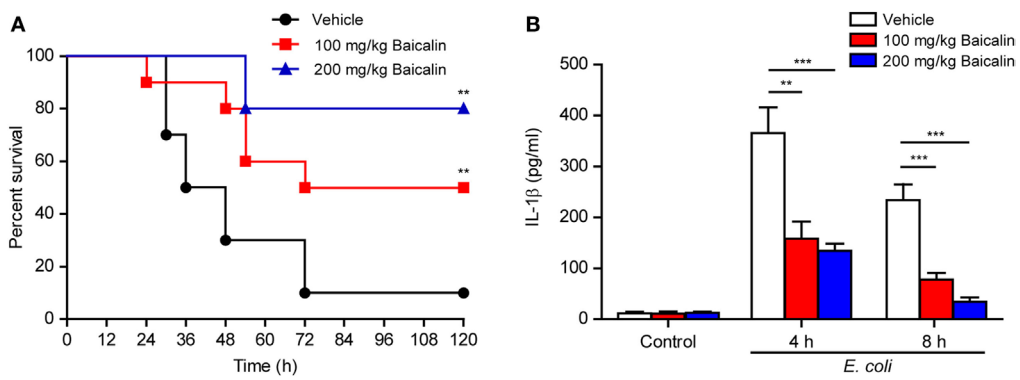

FIGURE 10 | Baicalin administration prolonged mouse survival in bacterial sepsis. **(A)** C57BL/6 mice were administered (intragastrically) with baicalin (100 or 200 mg/kg body weight) or vehicle (2% Tween-80 in PBS) once 3 h before peritoneal injection with viable *Escherichia coli* (2×10^9 CFU/mouse). One hour after the bacterial injection, mice were intragastrically administered with baicalin or vehicle once again. Mouse survival was monitored every 6 h for five consecutive days. Kaplan–Meier survival curves were used to analyze the data (10 mice per group). The significance was evaluated by the log-rank (Mantel–Cox) test. **(B)** Mice were treated as in panel **(A)**. The serum levels of interleukin (IL)-1β at 4 and 8 h post bacterial infection were measured by cytometric bead array assay (five mice per group). **$P < 0.01$; ***$P < 0.001$.

In conclusion, we found that baicalin robustly inhibited ATP or nigericin-induced NLRP3 inflammasome activation in mouse macrophages, at least partly *via* augmenting PKA signaling. Furthermore, we also showed that baicalin administration significantly prolonged mouse survival in a model of bacterial sepsis, suggestive of suppression of systemic inflammation. Although future research is warranted to unravel the precise mechanism of baicalin's action on the PKA pathway and investigations in human macrophages may provide more informative data, our studies highlight that baicalin can be used for the treatment of NLRP3-related inflammatory diseases including bacterial sepsis.

ETHICS STATEMENT

All animal experiments were performed according to the guidelines for the care and use of animals approved by the Committee on the Ethics of Animal Experiments of Jinan University.

AUTHOR CONTRIBUTIONS

C-GL, LY, F-YM, and Y-YJ performed *in vitro* studies; L-HX, Z-JS, and Q-BZ conducted animal studies; C-GL, LY, and Z-JS analyzed the data; D-YO and X-HH supervised the study; X-HH, D-YO, and C-GL wrote the paper.

FUNDING

This work was supported by the grants from the National Natural Science Foundation of China (No. 81773965, No. 81673664 and No. 81373423).

SUPPLEMENTARY MATERIAL

The Supplementary Material for this article can be found online at http://www.frontiersin.org/article/10.3389/fimmu.2017.01409/full#supplementary-material.

REFERENCES

1. Broz P, Dixit VM. Inflammasomes: mechanism of assembly, regulation and signalling. *Nat Rev Immunol* (2016) 16:407–20. doi:10.1038/nri.2016.58
2. Jo EK, Kim JK, Shin DM, Sasakawa C. Molecular mechanisms regulating NLRP3 inflammasome activation. *Cell Mol Immunol* (2016) 13:148–59. doi:10.1038/cmi.2015.95
3. He Y, Hara H, Nunez G. Mechanism and regulation of NLRP3 inflammasome activation. *Trends Biochem Sci* (2016) 41:1012–21. doi:10.1016/j.tibs.2016.09.002
4. Piccini A, Carta S, Tassi S, Lasiglie D, Fossati G, Rubartelli A. ATP is released by monocytes stimulated with pathogen-sensing receptor ligands and induces IL-1beta and IL-18 secretion in an autocrine way. *Proc Natl Acad Sci U S A* (2008) 105:8067–72. doi:10.1073/pnas.0709684105
5. Wegiel B, Larsen R, Gallo D, Chin BY, Harris C, Mannam P, et al. Macrophages sense and kill bacteria through carbon monoxide-dependent inflammasome activation. *J Clin Invest* (2014) 124:4926–40. doi:10.1172/jci72853
6. Mariathasan S, Weiss DS, Newton K, McBride J, O'Rourke K, Roose-Girma M, et al. Cryopyrin activates the inflammasome in response to toxins and ATP. *Nature* (2006) 440:228–32. doi:10.1038/nature04515
7. Liu X, Zhang Z, Ruan J, Pan Y, Magupalli VG, Wu H, et al. Inflammasome-activated gasdermin D causes pyroptosis by forming membrane pores. *Nature* (2016) 535:153–8. doi:10.1038/nature18629
8. Ding J, Wang K, Liu W, She Y, Sun Q, Shi J, et al. Pore-forming activity and structural autoinhibition of the gasdermin family. *Nature* (2016) 535:111–6. doi:10.1038/nature18590
9. Miao EA, Rajan JV, Aderem A. Caspase-1-induced pyroptotic cell death. *Immunol Rev* (2011) 243:206–14. doi:10.1111/j.1600-065X.2011.01044.x
10. Shi J, Zhao Y, Wang K, Shi X, Wang Y, Huang H, et al. Cleavage of GSDMD by inflammatory caspases determines pyroptotic cell death. *Nature* (2015) 526:660–5. doi:10.1038/nature15514
11. He WT, Wan H, Hu L, Chen P, Wang X, Huang Z, et al. Gasdermin D is an executor of pyroptosis and required for interleukin-1beta secretion. *Cell Res* (2015) 25:1285–98. doi:10.1038/cr.2015.139
12. Chen X, He WT, Hu L, Li J, Fang Y, Wang X, et al. Pyroptosis is driven by non-selective gasdermin-D pore and its morphology is different from MLKL channel-mediated necroptosis. *Cell Res* (2016) 26:1007–20. doi:10.1038/cr.2016.100
13. Sborgi L, Ruhl S, Mulvihill E, Pipercevic J, Heilig R, Stahlberg H, et al. GSDMD membrane pore formation constitutes the mechanism of pyroptotic cell death. *EMBO J* (2016) 35:1766–78. doi:10.15252/embj.201694696
14. Lamkanfi M, Dixit VM. Mechanisms and functions of inflammasomes. *Cell* (2014) 157:1013–22. doi:10.1016/j.cell.2014.04.007
15. Man SM, Karki R, Kanneganti TD. Molecular mechanisms and functions of pyroptosis, inflammatory caspases and inflammasomes in infectious diseases. *Immunol Rev* (2017) 277:61–75. doi:10.1111/imr.12534
16. Guo H, Callaway JB, Ting JP. Inflammasomes: mechanism of action, role in disease, and therapeutics. *Nat Med* (2015) 21:677–87. doi:10.1038/nm.3893
17. Prochnicki T, Latz E. Inflammasomes on the crossroads of innate immune recognition and metabolic control. *Cell Metab* (2017) 26:71–93. doi:10.1016/j.cmet.2017.06.018
18. Rathinam VA, Fitzgerald KA. Inflammasome complexes: emerging mechanisms and effector functions. *Cell* (2016) 165:792–800. doi:10.1016/j.cell.2016.03.046
19. Wree A, Eguchi A, McGeough MD, Pena CA, Johnson CD, Canbay A, et al. NLRP3 inflammasome activation results in hepatocyte pyroptosis, liver inflammation, and fibrosis in mice. *Hepatology* (2014) 59:898–910. doi:10.1002/hep.26592
20. Kayagaki N, Stowe IB, Lee BL, O'Rourke K, Anderson K, Warming S, et al. Caspase-11 cleaves gasdermin D for non-canonical inflammasome signalling. *Nature* (2015) 526:666–71. doi:10.1038/nature15541
21. Kayagaki N, Warming S, Lamkanfi M, Vande Walle L, Louie S, Dong J, et al. Non-canonical inflammasome activation targets caspase-11. *Nature* (2011) 479:117–21. doi:10.1038/nature10558
22. De Nardo D, De Nardo CM, Latz E. New insights into mechanisms controlling the NLRP3 inflammasome and its role in lung disease. *Am J Pathol* (2014) 184:42–54. doi:10.1016/j.ajpath.2013.09.007
23. de Torre-Minguela C, Mesa Del Castillo P, Pelegrin P. The NLRP3 and pyrin inflammasomes: implications in the pathophysiology of autoinflammatory diseases. *Front Immunol* (2017) 8:43. doi:10.3389/fimmu.2017.00043
24. Zhao Q, Chen XY, Martin C. *Scutellaria baicalensis*, the golden herb from the garden of Chinese medicinal plants. *Sci Bull (Beijing)* (2016) 61:1391–8. doi:10.1007/s11434-016-1136-5
25. Dinda B, Dinda S, DasSharma S, Banik R, Chakraborty A, Dinda M. Therapeutic potentials of baicalin and its aglycone, baicalein against inflammatory disorders. *Eur J Med Chem* (2017) 131:68–80. doi:10.1016/j.ejmech.2017.03.004
26. Xiao JR, Do CW, To CH. Potential therapeutic effects of baicalein, baicalin, and wogonin in ocular disorders. *J Ocul Pharmacol Ther* (2014) 30:605–14. doi:10.1089/jop.2014.0074
27. Chou TC, Chang LP, Li CY, Wong CS, Yang SP. The antiinflammatory and analgesic effects of baicalin in carrageenan-evoked thermal hyperalgesia. *Anesth Analg* (2003) 97:1724–9. doi:10.1213/01.ANE.0000087066.71572.3F
28. Hu X, Miao P, Yu R, Zheng H. The immunoprotective activity of baicalin in mouse model of cecal ligation and puncture-induced sepsis. *Cell Biochem Biophys* (2015) 71:543–7. doi:10.1007/s12013-014-0232-x

29. Wang H, Liu D. Baicalin inhibits high-mobility group box 1 release and improves survival in experimental sepsis. *Shock* (2014) 41:324–30. doi:10.1097/SHK.0000000000000122
30. Zhu J, Wang J, Sheng Y, Zou Y, Bo L, Wang F, et al. Baicalin improves survival in a murine model of polymicrobial sepsis via suppressing inflammatory response and lymphocyte apoptosis. *PLoS One* (2012) 7:e35523. doi:10.1371/journal.pone.0035523
31. Liu LL, Gong LK, Wang H, Xiao Y, Wu XF, Zhang YH, et al. Baicalin inhibits macrophage activation by lipopolysaccharide and protects mice from endotoxin shock. *Biochem Pharmacol* (2008) 75:914–22. doi:10.1016/j.bcp.2007.10.009
32. Yang W, Li H, Cong X, Wang X, Jiang Z, Zhang Q, et al. Baicalin attenuates lipopolysaccharide induced inflammation and apoptosis of cow mammary epithelial cells by regulating NF-kappaB and HSP72. *Int Immunopharmacol* (2016) 40:139–45. doi:10.1016/j.intimp.2016.08.032
33. Shin JM, Kang JH, Lee SA, Park IH, Lee HM. Baicalin down-regulates IL-1beta-stimulated extracellular matrix production in nasal fibroblasts. *PLoS One* (2016) 11:e0168195. doi:10.1371/journal.pone.0168195
34. Liu J, Wei Y, Luo Q, Xu F, Zhao Z, Zhang H, et al. Baicalin attenuates inflammation in mice with OVA-induced asthma by inhibiting NF-kappaB and suppressing CCR7/CCL19/CCL21. *Int J Mol Med* (2016) 38:1541–8. doi:10.3892/ijmm.2016.2743
35. Fu S, Xu L, Li S, Qiu Y, Liu Y, Wu Z, et al. Baicalin suppresses NLRP3 inflammasome and nuclear factor-kappa B (NF-kappaB) signaling during *Haemophilus parasuis* infection. *Vet Res* (2016) 47:80. doi:10.1186/s13567-016-0359-4
36. Ye C, Li S, Yao W, Xu L, Qiu Y, Liu Y, et al. The anti-inflammatory effects of baicalin through suppression of NLRP3 inflammasome pathway in LPS-challenged piglet mononuclear phagocytes. *Innate Immun* (2016) 22:196–204. doi:10.1177/1753425916631032
37. Guo C, Xie S, Chi Z, Zhang J, Liu Y, Zhang L, et al. Bile acids control inflammation and metabolic disorder through inhibition of NLRP3 inflammasome. *Immunity* (2016) 45:802–16. doi:10.1016/j.immuni.2016.09.008
38. Mortimer L, Moreau F, MacDonald JA, Chadee K. NLRP3 inflammasome inhibition is disrupted in a group of auto-inflammatory disease CAPS mutations. *Nat Immunol* (2016) 17:1176–86. doi:10.1038/ni.3538
39. Li CG, Yan L, Jing YY, Xu LH, Liang YD, Wei HX, et al. Berberine augments ATP-induced inflammasome activation in macrophages by enhancing AMPK signaling. *Oncotarget* (2017) 8:95–109. doi:10.18632/oncotarget.13921
40. Py BF, Jin M, Desai BN, Penumaka A, Zhu H, Kober M, et al. Caspase-11 controls interleukin-1beta release through degradation of TRPC1. *Cell Rep* (2014) 6:1122–8. doi:10.1016/j.celrep.2014.02.015
41. Zhao GX, Xu LH, Pan H, Lin QR, Huang MY, Cai JY, et al. The BH3-mimetic gossypol and noncytotoxic doses of valproic acid induce apoptosis by suppressing cyclin-A2/Akt/FOXO3a signaling. *Oncotarget* (2015) 6:38952–66. doi:10.18632/oncotarget.5731
42. Zha QB, Wei HX, Li CG, Liang YD, Xu LH, Bai WJ, et al. ATP-induced inflammasome activation and pyroptosis is regulated by AMP-activated protein kinase in macrophages. *Front Immunol* (2016) 7:597. doi:10.3389/fimmu.2016.00597
43. He Y, Varadarajan S, Munoz-Planillo R, Burberry A, Nakamura Y, Nunez G. 3,4-methylenedioxy-beta-nitrostyrene inhibits NLRP3 inflammasome activation by blocking assembly of the inflammasome. *J Biol Chem* (2014) 289:1142–50. doi:10.1074/jbc.M113.515080
44. Coll RC, Robertson AA, Chae JJ, Higgins SC, Munoz-Planillo R, Inserra MC, et al. A small-molecule inhibitor of the NLRP3 inflammasome for the treatment of inflammatory diseases. *Nat Med* (2015) 21:248–55. doi:10.1038/nm.3806
45. Kayagaki N, Wong MT, Stowe IB, Ramani SR, Gonzalez LC, Akashi-Takamura S, et al. Noncanonical inflammasome activation by intracellular LPS independent of TLR4. *Science* (2013) 341:1246–9. doi:10.1126/science.1240248
46. de Souza AW, Westra J, Limburg PC, Bijl M, Kallenberg CG. HMGB1 in vascular diseases: its role in vascular inflammation and atherosclerosis. *Autoimmun Rev* (2012) 11:909–17. doi:10.1016/j.autrev.2012.03.007
47. Gdynia G, Sauer SW, Kopitz J, Fuchs D, Duglova K, Ruppert T, et al. The HMGB1 protein induces a metabolic type of tumour cell death by blocking aerobic respiration. *Nat Commun* (2016) 7:10764. doi:10.1038/ncomms10764
48. Deng J, Wang DX, Liang AL, Tang J, Xiang DK. Effects of baicalin on alveolar fluid clearance and alpha-ENaC expression in rats with LPS-induced acute lung injury. *Can J Physiol Pharmacol* (2017) 95:122–8. doi:10.1139/cjpp-2016-0212
49. Ren H, Teng Y, Tan B, Zhang X, Jiang W, Liu M, et al. Toll-like receptor-triggered calcium mobilization protects mice against bacterial infection through extracellular ATP release. *Infect Immun* (2014) 82:5076–85. doi:10.1128/IAI.02546-14
50. Mempin R, Tran H, Chen C, Gong H, Kim Ho K, Lu S. Release of extracellular ATP by bacteria during growth. *BMC Microbiol* (2013) 13:301. doi:10.1186/1471-2180-13-301
51. Franceschini A, Capece M, Chiozzi P, Falzoni S, Sanz JM, Sarti AC, et al. The P2X7 receptor directly interacts with the NLRP3 inflammasome scaffold protein. *FASEB J* (2015) 29:2450–61. doi:10.1096/fj.14-268714
52. Pelegrin P, Surprenant A. Pannexin-1 mediates large pore formation and interleukin-1beta release by the ATP-gated P2X7 receptor. *EMBO J* (2006) 25:5071–82. doi:10.1038/sj.emboj.7601378
53. Yang D, He Y, Munoz-Planillo R, Liu Q, Nunez G. Caspase-11 requires the pannexin-1 channel and the purinergic P2X7 pore to mediate pyroptosis and endotoxic shock. *Immunity* (2015) 43:923–32. doi:10.1016/j.immuni.2015.10.009
54. Kamo N, Ke B, Ghaffari AA, Shen XD, Busuttil RW, Cheng G, et al. ASC/caspase-1/IL-1beta signaling triggers inflammatory responses by promoting HMGB1 induction in liver ischemia/reperfusion injury. *Hepatology* (2013) 58:351–62. doi:10.1002/hep.26320
55. Wang H, Yang H, Tracey KJ. Extracellular role of HMGB1 in inflammation and sepsis. *J Intern Med* (2004) 255:320–31. doi:10.1111/j.1365-2796.2003.01302.x
56. Dinarello CA, Simon A, van der Meer JW. Treating inflammation by blocking interleukin-1 in a broad spectrum of diseases. *Nat Rev Drug Discov* (2012) 11:633–52. doi:10.1038/nrd3800
57. Yan Y, Jiang W, Liu L, Wang X, Ding C, Tian Z, et al. Dopamine controls systemic inflammation through inhibition of NLRP3 inflammasome. *Cell* (2015) 160:62–73. doi:10.1016/j.cell.2014.11.047
58. Azevedo MF, Faucz FR, Bimpaki E, Horvath A, Levy I, de Alexandre RB, et al. Clinical and molecular genetics of the phosphodiesterases (PDEs). *Endocr Rev* (2014) 35:195–233. doi:10.1210/er.2013-1053
59. Lee DU, Shin DM, Hong JH. The regulatory role of rolipram on inflammatory mediators and cholinergic/adrenergic stimulation-induced signals in isolated primary mouse submandibular gland cells. *Mediators Inflamm* (2016) 2016:3745961. doi:10.1155/2016/3745961
60. Stutz A, Kolbe CC, Stahl R, Horvath GL, Franklin BS, van Ray O, et al. NLRP3 inflammasome assembly is regulated by phosphorylation of the pyrin domain. *J Exp Med* (2017) 214:1725–36. doi:10.1084/jem.20160933
61. Murray AJ. Pharmacological PKA inhibition: all may not be what it seems. *Sci Signal* (2008) 1:re4. doi:10.1126/scisignal.122re4
62. Man SM, Kanneganti TD. Regulation of inflammasome activation. *Immunol Rev* (2015) 265:6–21. doi:10.1111/imr.12296
63. Cullen SP, Kearney CJ, Clancy DM, Martin SJ. Diverse activators of the NLRP3 inflammasome promote IL-1beta secretion by triggering necrosis. *Cell Rep* (2015) 11:1535–48. doi:10.1016/j.celrep.2015.05.003

Conflict of Interest Statement: The authors declare that the research was conducted in the absence of any commercial or financial relationships that could be construed as a potential conflict of interest.

Copyright © 2017 Li, Yan, Mai, Shi, Xu, Jing, Zha, Ouyang and He. This is an open-access article distributed under the terms of the Creative Commons Attribution License (CC BY). The use, distribution or reproduction in other forums is permitted, provided the original author(s) or licensor are credited and that the original publication in this journal is cited, in accordance with accepted academic practice. No use, distribution or reproduction is permitted which does not comply with these terms.

frontiers in Immunology

ORIGINAL RESEARCH
published: 14 November 2017
doi: 10.3389/fimmu.2017.01533

Tumor Necrosis Factor-Alpha Targeting Can Protect against Arthritis with Low Sensitization to Infection

Nadia Belmellat[1,2], Luca Semerano[1,2,3], Noria Segueni[4], Diane Damotte[5], Patrice Decker[1,2], Bernhard Ryffel[4,6], Valérie Quesniaux[4], Marie-Christophe Boissier[1,2,3] and Eric Assier[1,2]*

[1] UMR 1125 INSERM, Bobigny, France, [2] Sorbonne Paris Cité Université Paris 13, Bobigny, France, [3] Service de Rhumatologie, Groupe Hospitalier Avicenne—Jean Verdier—René Muret, APHP, Bobigny, France, [4] INEM UMR7355, CNRS, University of Orléans, Orléans, France, [5] Service de pathologie Hôpitaux Universitaires Paris Centre, APHP, Université Paris Descartes, Paris, France, [6] IDM, University of Cape Town, Cape Town, South Africa

Tumor necrosis factor-alpha (TNF-α) blockade is an effective treatment for rheumatoid arthritis (RA) and other inflammatory diseases, but in patients, it is associated with reduced resistance to the infectious agents *Mycobacterium tuberculosis* and *Listeria monocytogenes*, among others. Our goal was to model infection and arthritis in mice and to compare etanercept, a currently used anti-TNF-α inhibitor, to an anti-TNF-α vaccine. We developed a murine surrogate of the TNF-α kinoid and produced an anti-murine TNF-α vaccine (TNFKi) composed of keyhole limpet hemocyanin conjugated to TNF-α, which resulted in anti-TNF-α antibody production in mice. We also used etanercept (a soluble receptor of TNF commonly used to treat RA) as a control of TNF neutralization. In a mouse model of collagen-induced arthritis, TNFKi protected against inflammation similar to etanercept. In a mouse model of acute *L. monocytogenes* infection, all TNFKi-treated mice showed cleared bacterial infection and survived, whereas etanercept-treated mice showed large liver granulomas and quickly died. Moreover, TNFKi mice infected with the virulent H37Rv *M. tuberculosis* showed resistance to infection, in contrast with etanercept-treated mice or controls. Depending on the TNF-α blockade strategy, treating arthritis with a TNF-α inhibitor could result in a different profile of infection suceptibility. Our TNFKi vaccine allowed for a better remaining host defense than did etanercept.

Keywords: tumor necrosis factor, vaccine, rheumatoid arthritis, infection, host-defense

OPEN ACCESS

Edited by:
Guixiu Shi,
Xiamen University, China

Reviewed by:
Dipyaman Ganguly,
Indian Institute of Chemical Biology (CSIR), India
Dong Li,
Jilin University, China

****Correspondence:***
Marie-Christophe Boissier
marie-christophe.boissier@aphp.fr

Specialty section:
This article was submitted to Inflammation, a section of the journal Frontiers in Immunology

Received: *01 August 2017*
Accepted: *27 October 2017*
Published: *14 November 2017*

Citation:
Belmellat N, Semerano L, Segueni N, Damotte D, Decker P, Ryffel B, Quesniaux V, Boissier M-C and Assier E (2017) Tumor Necrosis Factor-Alpha Targeting Can Protect against Arthritis with Low Sensitization to Infection. Front. Immunol. 8:1533. doi: 10.3389/fimmu.2017.01533

INTRODUCTION

Tumor necrosis factor-α (TNF-α) is a central mediator of inflammation, tumor growth control, autoimmunity, and immune response to infection (1). In rheumatoid arthritis (RA) and spondyloarthritis, two frequent and severe diseases (2), TNF-α mediates a wide variety of effector functions, including the production of pro-inflammatory cytokines and chemokines, activation of immune cells and angiogenesis.

Two types of TNF-α antagonists are used for treating rheumatic diseases, including RA and spondyloarthritides: the soluble TNF-α receptor 2 etanercept and monoclonal antibodies such as infliximab, adalimumab, golimumab, or pegylated-IgG-Fc fragments such as certolizumab. Anti-TNF-α

drugs have greatly changed the treatment of RA in terms of clinical control and articular damage prevention. However, these treatments have limitations, such as high cost, frequent therapeutic failures (only 20% of RA patients achieve sustained remission) (3), and increased risk of serious infections, such as reactivation of pulmonary and extrapulmonary tuberculosis (4, 5).

Recently, we developed an alternative strategy of TNF neutralization by a vaccination approach. A human TNF-α vaccine (hTNF-K) was obtained by chemically coupling the human cytokine to the carrier protein keyhole limpet hemocyanin (KLH) (6). Preclinical studies showed that vaccination with hTNF-K reduced arthritis development in a human TNF-α transgenic mouse (TTG) model, with a dose effect depending on level of anti-TNF-α antibody production (7–9). Anti-TNF-α antibody production was reversible and could not be stimulated by TNF-α administration, because this approach did not induce any cellular-mediated immunity against TNF-α (10). A first clinical trial was conducted with RA patients resistant to TNF antagonists and showed promising results (11).

In previous studies, we demonstrated that anti-human TNF-α vaccination activates resting autoreactive B cells to produce anti-TNF-α antibodies. The carrier protein (KLH) possesses the T epitopes able to activate T cells, thereby providing the necessary help for anti-TNF-α antibody production. No T cell being directly sensitized to TNF-α has two major consequences. First the antibody production is self-limited, with serum antibody titers showing a bell-shaped curve, with peak concentration around day 50 in mice and between day 112 and 140 in humans. Second, any increase in self-produced TNF-α (e.g., during infection) does not elicit any anti-TNF-α antibody response in immunized subjects. However, the risk of infection with the hTNF-K treatment could not be easily studied in the TTG mice because antihuman TNF-α antibodies are usually species-specific and do not cross-react with murine TNF-α.

To evaluate the risk of infection using anti-TNF-α strategies, we compared a vaccine directed against murine TNF-α we developed by coupling murine TNF-α to KLH (TNFKi) and etanercept, the anti-TNF-α treatment associated with the lowest occurrence of infections, namely iatrogenic tuberculosis (12, 13). Our data reveal the protective effect of TNFKi in two mouse models of arthritis. Furthermore, we show that, in contrast to etanercept, TNFKi had limited effects on the host resistance to *Listeria monocytogenes* and *Mycobacterium tuberculosis* infection, as reflected by a differential local immune response to the pathogens. Hence, depending on the anti-TNF-α inhibition strategy, TNF-α inhibition could control chronic inflammation without modifying the pathogen-induced immune response and, therefore, have no deleterious effect.

MATERIALS AND METHODS

Vaccine Design

Murine TNF-α was from PeproTech (315-01A-1000UG, PeproTech France). KLH (77600, Thermo Scientific Pierce), GMBS (N-[g-maleimidobutyryloxy]), succinimide ester (22309 Pierce), and SATA [*N*-succinimidyl *S*-acetylthioacetate (26102 Pierce)] were from Thermo Scientific Pierce, France. TNFKi resulted from the chemical coupling of murine TNF-α to the carrier protein KLH, by using heterobifunctional cross-linkers that react with primary amines. TNFKi was prepared as follows: 4 mg murine TNF-α was derivatized with 1.2 mg SATA for 2 h at room temperature. In parallel, 20 mg KLH was derivatized with 1.76 mg GMBS for 30 min. Cross-linker quantities were calculated to modify half of the lysine residues. For coupling, 1 mol KLH-GMBS was incubated with 20 mol TNF-SATA for 2 h at room temperature in the presence of 5 mM hydroxylamide (23225 Thermo Scientific Pierce). The heterocomplex (TNF-KLH) was dialyzed overnight against phosphate-buffered saline (PBS) by use of a Microcon tube (YM100 Millipore). TNFKi was sterilized by centrifugation in an Ultrafree-CL 0.22-µm tube (FC40GV 0S Millipore), then stored at 4°C. Three batches were prepared successively for different experiments. They were validated biochemically by ELISA and western blot analysis. Batches were systematically tested *in vivo* in the collagen-induced arthritis (CIA) model.

Mice

For CIA, 36 DBA/1 male mice (6 weeks old) were used, and for collagen antibody-induced arthritis (CAIA), 24 C57Bl/6 male mice (6 weeks old) were used, all purchased from Janvier Laboratory (France). Mice were randomly assigned to treatment groups and randomly distributed to cages. Body weight was monitored weekly. *L. monocytogenes* (LM) infection experiments involved 40 C57Bl/6 female mice (8 weeks old, Janvier Laboratory) and 10 TNF-α$^{-/-}$ mice (TNF$^{-/-}$) (14) backcrossed at least 8–10 times on a C57BL/6 genetic background, bred, and housed in the Transgenose Institute animal facility (CNRS UPS44, Orleans, France). *M. tuberculosis* (Mt) infection experiments involved 60 C57Bl/6 female mice (8 weeks old, Janvier Laboratory) and 7 TNF$^{-/-}$ mice. Mice were kept in isolators in a biohazard animal unit. Infected mice were monitored every day for clinical status and weighed twice weekly. Mice were randomly assigned to treatment groups and randomly distributed to cages (except for naïve uninfected mice).

Arthritis Models

DBA/1 mice used for CIA were injected with a 1:1 emulsion of bovine type II collagen (CIIb, 50 µg/mice) and complete Freund's adjuvant (Difco, France) on day 0 (total volume injected in the tail: 100 µl). A boost was given on day 21 with 100 µl of a 1:1 emulsion of CIIb (50 µg/mice) and incomplete Freund's adjuvant (IFA, Difco, France). Arthritis onset occurs at about 30–35 days after the first collagen injection (15).

C57Bl/6 mice used for CAIA were intraperitoneally injected with 5 mg of a cocktail of five monoclonal anti-collagen antibodies on day 0 (53100 Arthrogen-CIA Arthritogenic Monoclonal Antibody, Gentaur, Belgium) and lipopolysaccharide (50 µg, *E. coli* 0111:B4 strain) on day 3. Arthritis onset occurs at about 3–4 days after anti-collagen antibody injection and peaks at about day 7–10 (16).

Clinical signs of arthritis were evaluated with blinding to treatment three times per week. Arthritis was monitored in all four paws. For each mouse, the clinical severity of arthritis was scored as 0, normal; 1, erythema; 2, swelling; 3, deformity; and

4, ankylosis in 10 joints or groups of joints: three joints of the two hind limbs (toes, tarsus, ankle) and two joints of the two forelimbs (digits, wrist). The maximum score for each of the 10 joints was 4, so the maximum individual arthritis clinical score on a given day was 40 (17). The mean arthritic score on each day of clinical observation was calculated for each treatment group.

For histology, both left hind limbs of each mouse were collected, fixed, decalcified, dehydrated, and transferred to paraffin blocks. Slides of 7 µm thickness were stained with hematoxylin and eosin before optical microscopy observation. At least 10 fields per section were evaluated with blinding to treatment. In each joint, two variables were separately assessed on a 4-point scale (0–3, 0 indicating a normal joint, and 3, maximally severe arthritis). The first variable was inflammation, as reflected by synovial membrane thickness (synovial proliferation) and inflammatory cell infiltration. Inflammation was scored as 0, no synovial proliferation and no inflammatory cell infiltration; 1, limited or absent synovial proliferation with inflammatory cells infiltrating ≤5% of synovial membrane; 2, synovial proliferation with inflammatory cells infiltrating between 5 and 50% of synovial membrane; and 3, massive synovial proliferation with inflammatory cells infiltrating >50% of synovial membrane. The second variable was joint destruction (bone erosions, cartilage thickness, and cartilage unevenness). Joint destruction was quantified as 0, no bone erosion, smooth cartilage surface with conserved thickness; 1, presence of cartilage erosion or unevenness or thinning involving ≤50% of cartilage surface with absent or single bone erosion; 2, multiple cartilage erosions or cartilage thinning involving >50% of cartilage surface and/or >1 bone erosions involving ≤50% of articular surface; and 3, complete derangement of articular structure. For determining prevalence, histological inflammation or destruction was defined as inflammation or destruction score ≥0.5 (17).

For clinical and histological evaluation of arthritis, blinding was ensured by a random distribution of treatments inside cages, limited by the need to have each treatment group represented, and by the use of tables including only cages and mouse numbers.

Anti-TNF Immunization in CIA Model

Immunization involved the anti-mouse TNF-α vaccine (TNFKi) emulsified in IFA. DBA/1 mice ($n = 6$) were vaccinated intramuscularly with different doses of TNFKi (20, 10, or 5 µg) on days −21, −7, and 7. In the same experiment, one group of mice ($n = 6$) were intraperitoneally injected three times/week with 30 mg/kg etanercept (PAA0252P1, Pfizer) from day 22. Negative controls were mice receiving intraperitoneal injections of PBS or intramuscular injections of KLH (10 µg) emulsified in IFA. KLH and PBS were administered on the same time schedule as TNFKi or etanercept treatment, respectively.

Infection Protocols

Listeria monocytogenes (L028) was grown in BHI medium (Brain Heart Infusion, Difco Laboratories). Aliquots of *M. tuberculosis* H37Rv kept frozen at −80°C were thawed, diluted in sterile saline containing 0.05% Tween 20, and clumping was disrupted by 30 repeated aspirations through a 26-G needle (Omnican, Braun, Germany). Pulmonary infection involved delivering 2250 colony formation units (CFU) of *M. tuberculosis* H37Rv/lung into nasal cavities of mice under xylazine–ketamine anesthesia, as verified by determining bacterial load in the lungs on day 1 postinfection.

Mice were vaccinated before infection with four TNFKi intramuscular injections (10 µg) on days −44, −31, −17, and −4. One group of mice ($n = 10$) received intraperitoneal injections of etanercept (30 mg/kg) twice a week from days −4 to day 52 before and during infection. Controls were untreated (naïve) mice, vaccinated with KLH, or received intraperitoneal injections of PBS. All groups comprised 10 mice per group except for $TNF^{-/-}$ mice ($n = 7$). On day 25 postinfection for all $TNF^{-/-}$ mice or on day 28 for other groups, 5 animals were killed; lung, livers, and spleens were harvested; and the number of viable bacteria in organ homogenates was determined by plating serial dilutions in duplicate onto Middlebrook 7H11 (Difco) agar plates containing 10% OADC and incubating at 37°C. Colonies were counted at 3 weeks and results are expressed as $\log_{10}$ CFU per organ. Similar analyses were performed on day 56 (established infection) with the remaining mice.

A similar vaccination schedule was used before *L. monocytogenes* infection, and one group of mice ($n = 9$) received intraperitoneal injection of etanercept (30 mg/kg) on days −4, −2, 0, and 3 before and after infection. Controls were treated with KLH ($n = 9$ mice) or PBS ($n = 10$) on the same time schedule as TNFKi vaccination or etanercept treatment, respectively. All groups and $TNF^{-/-}$ mice ($n = 10$) underwent intraperitoneal injection on day 0 with 10^4 CFU *L. monocytogenes*. On day 4 postinfection, four mice/group were killed, then livers and spleens were harvested and the number of viable bacteria in organ homogenates was determined by plating serial dilutions on trypticase soy broth agar plates (Biovalley) and incubating overnight at 37°C, followed by counting CFU. Survival during infection was evaluated until day 11 ($n = 5$–6 mice/group of treatment).

ELISA for Anti-KLH and Anti-TNF Antibodies in Serum

Blood samples were collected at different times in accordance with the duration of experiments: 19 and 41 days after the third TNFKi vaccination in the CIA study; 7 days after the third and fourth TNFKi vaccination in the *Listeria* study; 7 days after the third and 32 days after the fourth TNFKi vaccination in the *Mycobacterium* study. Serum was obtained and tested for anti-KLH and anti-TNF-α antibody content. Specific anti-mTNF-α and anti-KLH antibody content was determined by direct ELISA. Precoated ELISA plates with 50 ng per well mTNF-α (PeproTech) or KLH (Sigma) were incubated with serial dilutions of serum from immunized and control mice. Specific antibodies were detected by using phosphatase alkaline-conjugated rabbit anti-mouse IgG (IgG-PA; Sigma-Aldrich A1902). Substrate PNP (Sigma-Aldrich) was added for 40 min. The optical density was measured at 405 nm.

Tissue Preparation for Histology and Immunohistochemistry

Lungs and livers from *M. tuberculosis*-infected mice collected on days 25–28 and 56 were fixed in 4% buffered formalin and

paraffin-embedded, and 4 μm sections were stained with hematoxylin and eosin (H&E) or underwent the Ziehl–Neelsen coloration. Sections were observed by light microscopy at 400× magnification with a Zeiss Observer D1 microscope equipped with a motorized stage connected to Histolab and Archimed software (Microvision, Les Ulis, France). The number and size of granulomas were quantified by using Archimed.

For immunohistochemistry, lung and liver sections were fixed in acetone–ethanol (5 min), and endogenous peroxidase activity was blocked with PBS and 3% H_2O_2. Endogenous biotin in the liver was blocked by using an avidin-biotin kit (Vector Laboratories, SP-2001). Tissue sections were incubated for 2 h at room temperature or overnight at 4°C with the primary antibody CD45R (AbD Serotec, MCA1258G) or inducible nitric oxide synthase (iNOS; Abcam, 15323). Sections were then incubated for 30 min at 37°C with the appropriate biotinylated secondary antibody. Avidine biotin peroxidase complexes were added to the sections for 30 min (ABC Vector kit; Vector Laboratories, PK-6100), then incubated with diaminobenzidine substrate (Imm PACT DAB, Vector: SK-4105, Biovalley). After a rinsing in water, sections were counterstained with hematoxylin before mounting and examined by use of a Zeiss Observer D1 microscope as described previously.

For *Listeria* infection, four mice per group were euthanized on day 4 postinfection. Livers were treated as described previously; H&E-stained sections were observed by light microscopy and images were obtained by using a nanozoomer. The number and size of microabcesses were assessed by using NDPview (Hamamatsu, Japan). Immunohistology of livers, macrophages (F4/80, AbD Serotec, MCA497GA), and neutrophils (Ly6G, Abcam, 25377) infiltration was performed as described for CD45R and iNOS staining.

Statistics

For arthritis studies, serial measurements of clinical variables were analyzed by the area under the receiver operating characteristic curve for each mouse as a summary measure, then as raw data for inter-group comparisons (ANOVA). Differences in arthritis onset were analyzed by ANOVA. Posttest data were compared by data distribution (Student–Newman–Keuls). For *Listeria* infection studies, evaluation of survival involved the Kaplan–Meier method (log-rank test), and bacterial burden data were analyzed by one-way ANOVA with Newman–Keuls posttest. $p < 0.05$ was considered statistically significant.

Study Approval

All applicable international, national, and/or institutional guidelines for the care and use of animals were followed. For arthritis models, all procedures were approved by the Animal Care and Use Committee of the University of Paris 13 (ethical approval ID: Ce5/2010/036). Infectious protocols were approved by the Ethics Committee for Animal Experimentation of CNRS Campus Orleans (CCO) (no. CLE CCO 2015-1071). We were particularly concerned by a strict application of the 3R rules (18).

RESULTS

TNFKi Reduced Clinical and Histological Signs of Arthritis

To investigate the anti-inflammatory effect of TNFKi *in vivo*, we used the CIA model with DBA/1 mice. Mice were vaccinated three times with 5, 10, or 20 μg/mice TNFKi (TNFKi-5, TNFKi-10, and TNFKi-20 groups). Control groups were vaccinated with KLH or PBS. Etanercept was a positive control. The first signs of arthritis appeared in all control groups at 33 ± 2 days, as expected, but in TNFKi groups at 38 ± 2 days and in the etanercept group at 41 ± 3 days. All anti-TNF treatments resulted in significantly lower clinical arthritis scores as compared with controls (**Figure 1A**).

Maximal clinical arthritis index (Amax) was significantly lower for mice with 10 μg TNFKi or etanercept treatment than other mice (Table S1 in Supplementary Material). Despite this, the incidence and onset of arthritis were not significantly delayed with TNFKi or etanercept treatment as compared with KLH and PBS controls (Table S1 in Supplementary Material). The weights of TNFKi-vaccinated mice were comparable to that of PBS and KLH controls during the experiment (data not shown).

Histology of paws of PBS and KLH control mice showed significant inflammation, with cell infiltration associated with cartilage destruction (**Figures 1B–E**). By contrast, TNFKi-10 or etanercept treatment significantly reduced the inflammatory signs of arthritis (**Figure 1F**). TNFKi-10 or etanercept treatment protected against joint destruction (**Figure 1G**). In addition, histology showed protection of joints with TNFKi vaccination in the CAIA arthritis model in C57Bl/6 mice (Figure S1 in Supplementary Material).

Thus, TNFKi was effective in protecting against TNF-mediated arthritis in mice.

TNFKi Did Not Impair Defense to *L. monocytogenes* as Compared with Etanercept

Mice were vaccinated on days −44, −31, −17, and −4 with TNFKi or intraperitoneally injected with etanercept on days −4, −2, 0, and 3 before (or after) infection with *L. monocytogenes*. Controls received PBS or KLH, and $TNF^{-/-}$ mice were a genetic control. All mice were injected intraperitoneally with *L. monocytogenes* (10^4 CFU) on day 0. Blood was collected before (day −10) and during infection (day 3) to evaluate anti-TNF-α antibody levels. ELISA revealed the production of anti-TNF-α and anti-KLH antibodies in serum from mice with TNFKi vaccination, with an increase in level in responder mice between day −10 and day 3 (Figure S2 in Supplementary Material).

Survival of mice was monitored for 11 days postinfection. All $TNF^{-/-}$ mice died within 5 days, and 80% of mice with etanercept treatment died by day 6, as expected; by contrast, mice vaccinated with TNFKi did not die due to infection during this period (**Figure 2A**). Hence, unlike etanercept, TNF-α neutralization with TNFKi protected against death due to *L. monocytogenes* infection, with a clear survival benefit. The increase in bacterial load in the liver and spleen homogenates seen on day 4 in

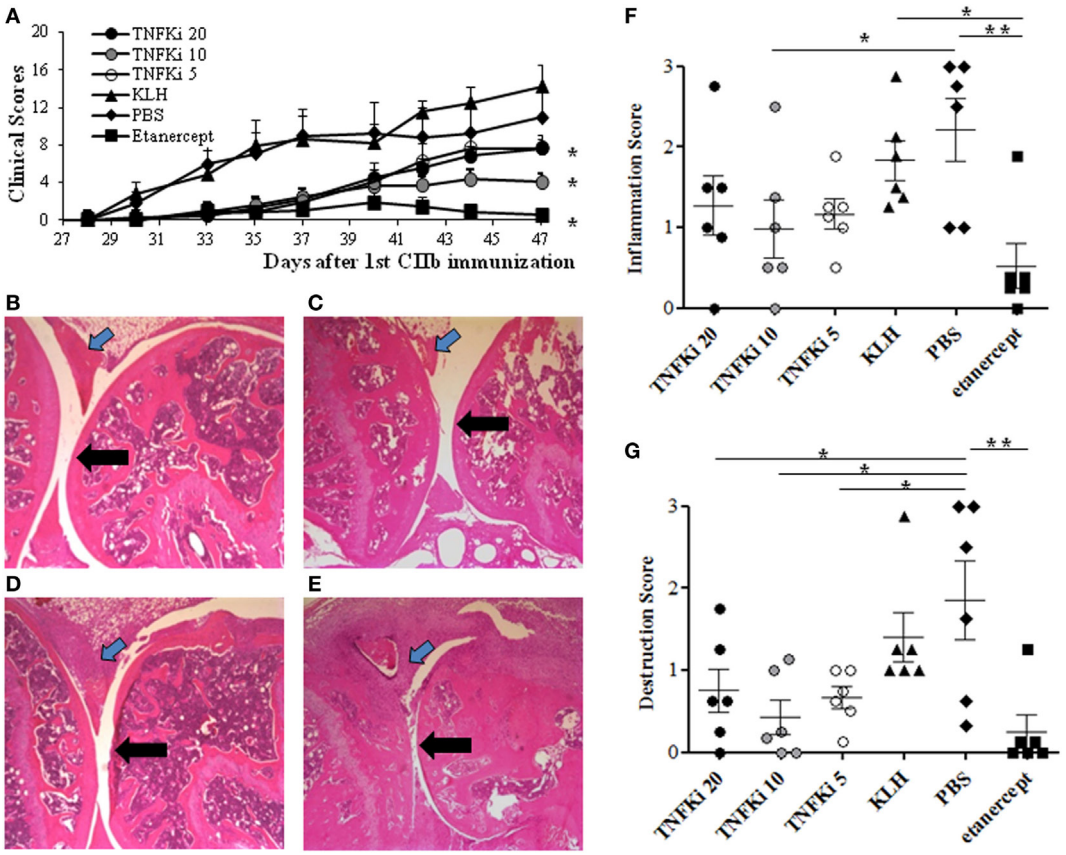

FIGURE 1 | TNFKi protects mice against clinical and histological arthritis. DBA/1 mice were vaccinated three times with keyhole limpet hemocyanin (KLH) or differents doses of TNFKi (20, 10, 5 μg) at days −21, −7, 7 before and during collagen-induced arthritis (CIA) induced by two injections of CIIb (50 μg/mice; day 0 and 21). Treatment with etanercept (30 mg/kg, two times/week) or phosphate-buffered saline (PBS) began from day 22. **(A)** Clinical arthritis was measured by using the sum of arthritis scores (0–4) from four paws (n = 6/group). Data are mean ± SEM. *$p < 0.05$ vs. both PBS and KLH during the whole experiment by ANOVA. The area under the curve (AUC) of clinical scores for each animal are the raw value. **(B–E)** Histology of paws for treatment groups. **(B)** TNFKi-20, **(C)** TNFKi-10, **(D)** TNFKi-5 (20, 10, 5 μg, respectively), **(E)** KLH shows inflammatory synovitis (blue arrow) and articular surface (black arrow). **(F)** Histological inflammation score and **(G)** joint destruction in treatment groups. Horizontal bar is mean, outer bars are SEM, and whiskers are range. *$p < 0.05$ for TNFKi and **$p < 0.01$ for etanercept vs PBS (Newman–Keuls test with subsequent *post hoc* comparisons). CIA inhibition with TNFKi was observed in three independent experiments.

TNF$^{-/-}$ mice and those with etanercept treatment was not present in either organ of TNFKi-vaccinated mice or in KLH or PBS controls (**Figures 2B,C**).

We further investigated histological changes in mouse livers on day 4 postinfection (**Figures 2D–H**). Etanercept-treated and TNF$^{-/-}$ mice showed typical and abundant hepatic microabscesses (**Figures 2E,F**) characterized by diffuse infiltration and necrotic areas, whereas liver microabscesses in mice vaccinated with TNFKi appeared smaller and similar to those from KLH and PBS control mice (**Figures 2D,G,H**). Hepatic microabscesses were significantly larger for TNF$^{-/-}$ mice than other groups, except with etanercept treatment (**Figure 2J**). In addition, the number of microabcesses was significantly larger in TNF$^{-/-}$ mice (**Figure 2I**), with no difference among TNFKi, KLH, and PBS groups.

Immunohistochemistry of liver sections to investigate the cellular composition of microabcesses after 4 days of infection revealed an increased accumulation of neutrophils (Ly6G) in TNF$^{-/-}$ and etanercept-treated mice but not TNFKi, KLH, and PBS mice (**Figure 3A**). Macrophage staining (F4/80) appeared more dispersed and less localized inside microabcesses in etanercept-treated and TNF$^{-/-}$ mice as compared with TNFKi, KLH, and PBS treatment (**Figure 3B**).

TNFKi Did Not Affect the Defense against *M. tuberculosis* Infection

We assessed the consequences of TNFKi vaccination during early and established *M. infection*. Mice were vaccinated on days −44, −31, −17, and −4 with TNFKi (10 μg/mice) or treated with etanercept (30 mg/kg twice a week from day −4 to day 52 before or after infection). Control groups were mice with KLH vaccination or PBS treatment. TNF$^{-/-}$ mice, which are very sensitive to virulent *M. tuberculosis* H37Rv infection, were used as a positive control of total infection in the absence of functional TNF. Except for five naïve mice, all mice were infected on day 0 by intranasal instillation of *M. tuberculosis* H37Rv (2,250 CFU). TNF$^{-/-}$ mice lost weight rapidly and had to be euthanized on day

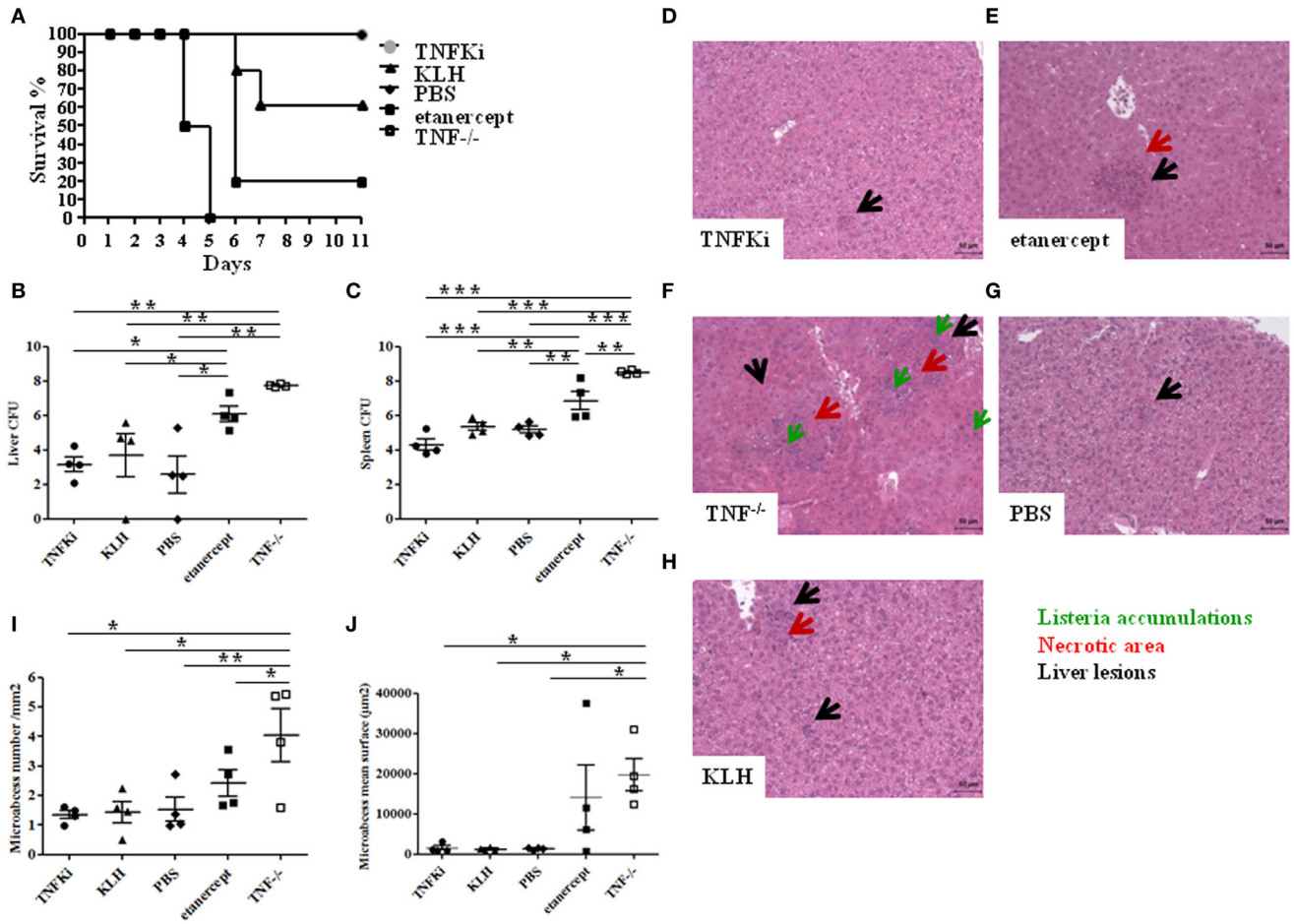

FIGURE 2 | TNFKi vaccination does not alter survival, organ infiltration, and liver lesions during *Listeria monocytogenes* infection. Mice ($n = 10$ per group) were treated with TNFKi or keyhole limpet hemocyanin (KLH) (at days −44, −31, −17, −4) or given phosphate-buffered saline (PBS) or 30 mg/kg etanercept (days −4, −2, 0, and 3). TNF$^{-/-}$ mice were a genetic control. All mice were infected with 10^4 colony forming units (CFU) *Listeria* at day 0. 4 mice per group were euthanized for bacterial burden and histological analysis at day 4. Survival was evaluated for 11 days postinfection with the remaining mice **(A)**. All TNF$^{-/-}$ mice ($n = 6$) died at 5 days postinfection. Four etanercept-treated mice died on day 6 ($n = 5$) and two mice treated with KLH ($n = 5$). All mice treated with TNFKi ($n = 6$) and PBS ($n = 6$) survived during this period. Survival of TNF$^{-/-}$ and etanercept groups was significantly reduced as compared with PBS, TNFKi, and KLH mice (*Logrank test for trend*, $p < 0.0001$). Colony-forming units (CFUs) evaluated in liver **(B)** and spleen **(C)** 4 days after infection in mice (*$p < 0.05$; **$p < 0.01$, ***$p < 0.001$, ANOVA). Liver lesions were studied 4 days after infection with *Listeria* after staining sections with hematoxylin-eosin. Liver sections **(D–H)** showing size and number of lesions (black arrow), with necrotic areas (red arrow) and *Listeria* accumulation (green arrow). Quantification of hepatic lesion number **(I)** and surface area **(j)** in slides involved use of NDPview software (Hamamatsu, Japan) (*$p < 0.05$, **$p < 0.01$, ANOVA).

25 postinfection, but the other mice did not experience body weight loss (data not shown) and were euthanized during early infection (day 28) or established infection (day 56).

Blood was collected before (day −10) and during infection (day 28) to evaluate levels of anti-TNF-α antibodies. As expected, ELISA revealed a sustained serum production of anti-TNF-α antibodies in mice vaccinated with TNFKi (Figures S3A,B in Supplementary Material).

At euthanasia, weights of lungs, spleens, and livers were evaluated as indicators of inflammation. During early infection, all TNF$^{-/-}$ mouse organs showed a marked increase in weight as compared with the other groups, with the exception of lung and spleen of etanercept-treated mice (**Figures 4A–C**). At day 56, established infection, organ weights were similar between all infected mice (**Figures 4D–F**).

Liver and lung bacterial loads were then assessed in vaccinated and TNF$^{-/-}$ and etanercept-treated mice. During early infection, total CFU were greatly increased in organs of TNF$^{-/-}$ mice as compared with all other groups ($^{\$}p < 0.001$ TNF$^{-/-}$ vs all groups in lung and liver, ANOVA) (**Figures 5A,B**). At the same time, CFU per organ were similar between TNFKi, etanercept, and control groups (KLH and PBS). At day 56, established infection, total CFU were similar in lungs of all infected mice (**Figure 5C**).

To determine the effect of TNFKi on organ integrity during early and established infection, we investigated histological changes in mouse lung and liver. Indeed, during early infection, TNF$^{-/-}$ mice showed inability to control *M. tuberculosis* infection, with rapid, exacerbated lung inflammation, and many granulomas with large necrotic areas (**Figure 6D**). In the lungs of TNFKi, KLH, and PBS groups, granulomas were more discrete, with the typical

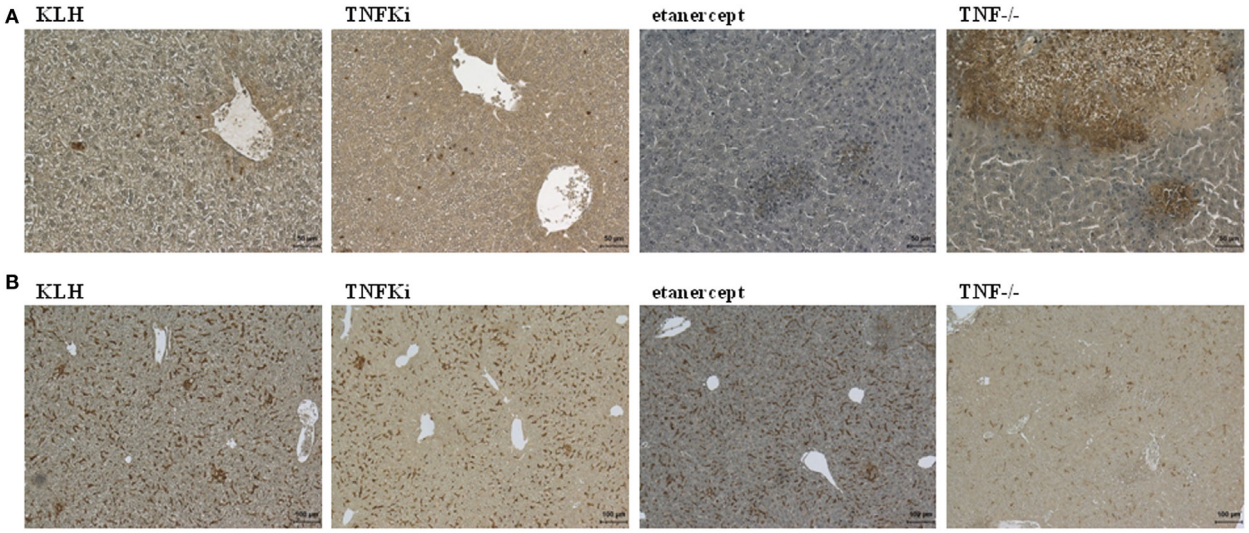

FIGURE 3 | TNFKi vaccination does not alter neutrophils and macrophages infiltration of livers during *Listeria monocytogenes* infection. Immunohistochemical staining of neutrophils expressing Ly6G **(A)** and macrophages expressing F4/80 **(B)** after 4 days of infection [scale bar **(A)** 50 µm; scale bar **(B)** 100 µm].

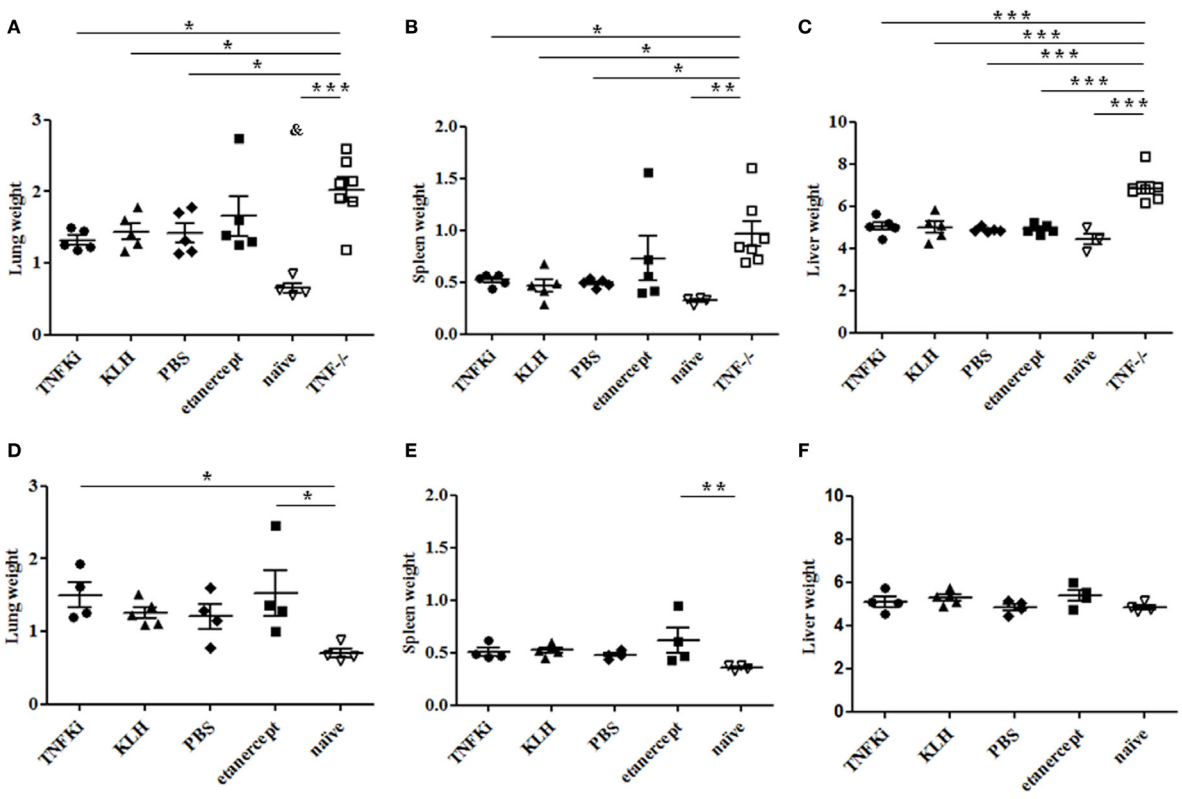

FIGURE 4 | Organ weights during early and established *M. tuberculosis* infection. C57Bl/6 mice were vaccinated with keyhole limpet hemocyanin (KLH) ($n = 10$) or 10 µg TNFKi ($n = 10$) at days −44, −31, −17, and −4 before infection. One group of mice received 30 mg/kg of etanercept ($n = 10$) twice a week from day 4 to day 52. Except for naïve mice ($n = 5$), all treated mice and TNF$^{-/-}$ mice ($n = 7$) were infected intranasally with 2,250 CFU of *M. tuberculosis* on day 0. Five mice per treatment (day 28) and all TNF$^{-/-}$ mice (day 25) were euthanized and lung, spleen, and liver were weighed. Survival was monitored until day 56 (4–5 mice/group) and organs were weighed at euthanasia. Relative organ weights were calculated as the ratio of absolute organ weights to body weights. Organ weights of mice during early infection **(A–C)** and established infection **(D–F)**. Organ weights were expressed as % of body weight. Horizontal bar is mean, outer bars are SEM, and whiskers are range. *$p < 0.05$ vs TNFKi, KLH, phosphate-buffered saline (PBS), ***$p < 0.001$ vs naïve mice; Newman–Keuls test with *post hoc* comparisons. $^{\&}p < 0.05$ naïve vs TNFKi, KLH, PBS, and etanercept.

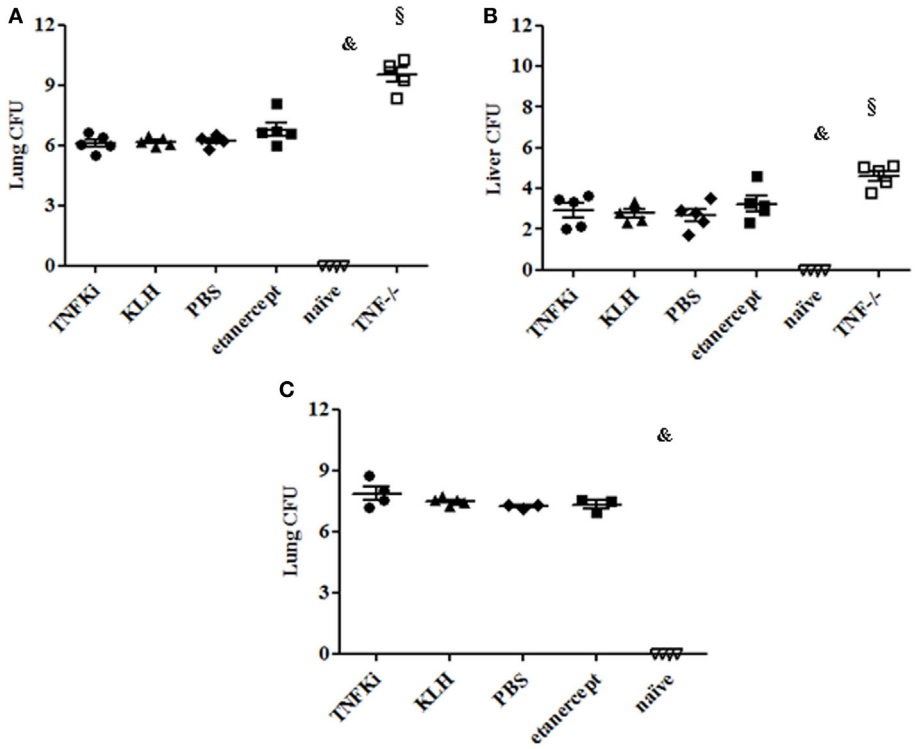

FIGURE 5 | TNFKi did not increase bacterial loads in lung and liver of *Mycobacterium tuberculosis*-infected mice. Vaccination schedule described previously. During early **(A,B)** and established infection **(C)**, a part of lungs and liver were weighted and used after lysis for bacterial culture and colony formation units (CFU) evaluation. Results are expressed as Log_{10} of CFU count per organ. CFU number in organs of mice during early infection **(A,B)** and lung during established **(C)** infection. Horizontal bar is mean, outer bars are SEM, and whiskers are range ($^{\S}p < 0.001$ $TNF^{-/-}$ vs all groups; Newman–Keuls test with subsequent *post hoc* comparisons).

granuloma structure at day 56 (**Figures 6A–H**). Etanercept-treated mice showed granulomas on day 28, but these were more developed and less structured by day 56 (**Figures 6C,G**). With Archimed software quantification, during early infection, the lung granuloma surface area was increased but not significantly in $TNF^{-/-}$ and etanercept-treated mice (**Figure 6I**). At day 56, the granuloma surface area of TNFKi- and KLH-vaccinated mice appeared decreased, contrary to etanercept treatment ($^{*}p < 0.05$ vs etanercept group, ANOVA) (**Figure 6J**). Granuloma numbers were similar between mouse groups at both phases (data not shown). During both early and established infection, all infected mice showed less free alveolar space as compared with naïve mice (**Figures 6K,L**), which was most prominent with etanercept treatment on day 56 (**Figure 6L**).

Histology of the liver at the early phase of infection (**Figures 7A–F**) revealed that granuloma surface area was significantly larger for $TNF^{-/-}$ and etanercept-treated mice than other mice (**Figure 7G**) ($^{*}p < 0.05$ vs TNFKi).

$TNF^{-/-}$ and etanercept-treated groups showed a higher number of granulomas, although not significantly (data not shown). At day 56, liver granuloma surface area was larger for etanercept-treated mice than other groups (**Figure 7H**). Hence, histology of both lungs and livers suggested that mice vaccinated with TNFKi, similar to KLH or PBS, effectively controlled the infection during the progression of the disease as compared with etanercept.

To confirm mycobacterial infiltration in granulomas, we used Ziehl–Neelsen coloration and semiquantitative evaluation of bacterial staining in mouse lungs (**Figure 8**). Microscopy revealed $TNF^{-/-}$ and etanercept-treated mice with greater mycobacteria infiltration than other groups during early and established infection (**Figures 8B,C**, $^{*}p < 0.05$ for etanercept and $^{***}p < 0.001$ for $TNF^{-/-}$ mice vs TNFKi, KLH, PBS, ANOVA).

We used immunohistochemistry of mouse lung sections to investigate the relationship between cellular infiltration or activation status and TNF-α neutralization. During early infection, iNOS was expressed in granulomas of all mouse groups (Figure S4A in Supplementary Material). Histology revealed lesions in TNFKi, KLH, and PBS lungs characterized by macrophage infiltration and a very low number of neutrophils. Conversely, in $TNF^{-/-}$ and etanercept-treated lungs, iNOS expression in macrophages co-localized with microabscesses containing altered neutrophil number. Etanercept-treated lungs showed more macrophage infiltration, higher number of foamy histiocytes expressing iNOS, and fewer neutrophils during established than early infection (Figures S4A,B and S5 in Supplementary Material). Lesions of PBS-treated lungs showed few neutrophils, and iNOS was expressed in macrophages and foamy histiocytes. Lesions of mouse lungs with KLH or TNFKi vaccination showed similar cellular infiltration as for PBS-treated lungs but a lower number of foamy histiocytes. Thus, macrophages within the granuloma

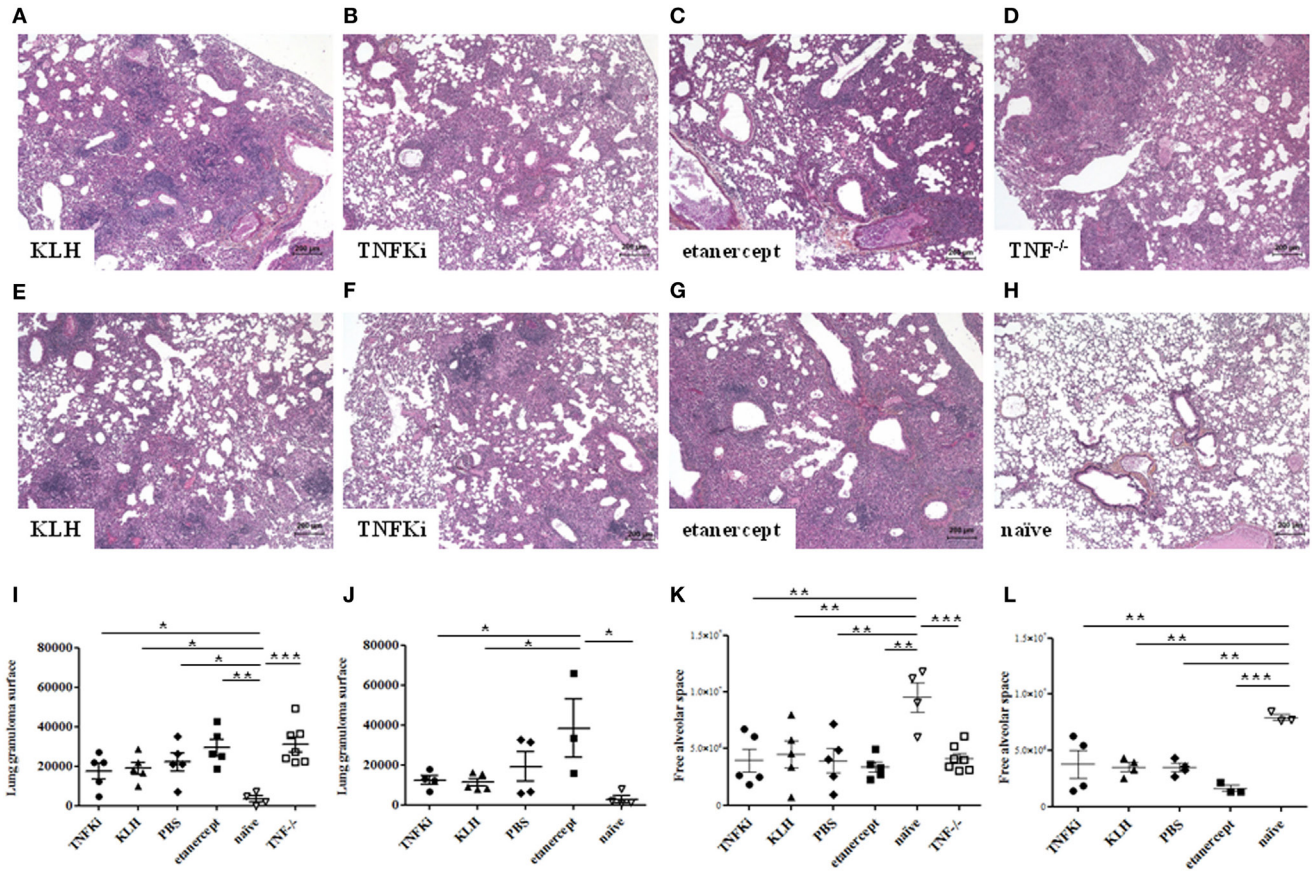

FIGURE 6 | Limited effects of TNFKi on lung granuloma formation during *Mycobacterium tuberculosis* infection. Granulomas were assessed during early **(A–D)** and established (**E–H**) infection. Lung sections were stained with hematoxylin-eosin (n = 3–7 per group). Granulomas in lungs during early infection **(A–D)** and established infection **(E–H)**. Quantification of lung granuloma surface area during early **(I)** and established infection **(J)** and alveolar space of lungs during early **(K)** and established infection **(L)**. Horizontal bar is mean, outer bars are SEM, and whiskers are range (*$p < 0.05$, **$p < 0.01$, ***$p < 0.001$, ANOVA).

of TNFKi-vaccinated lungs retained the bactericidal function controlling infection.

We explored the effect of the TNFKi on lung infiltration by B lymphocytes during *M. tuberculosis* infection (**Figure 9**). During early infection, anti-CD45R staining revealed a massive infiltration of B lymphocytes in lungs of TNFKi- and KLH-vaccinated mice, lower infiltration with PBS, and a near absence of B lymphocytes in $TNF^{-/-}$ or etanercept-treated mice. Immunostaining revealed a higher perivascular accumulation of B cells with TNFKi or KLH vaccination. During late infection, with TNFKi or KLH vaccination, pulmonary granulomas were well organized, characterized by many pulmonary nodules and accumulation of B lymphocytes. The phenotype for PBS lungs was similar to that for vaccinated lungs but with fewer B lymphocytes. By contrast, etanercept treatment resulted in massive macrophage infiltration with a large necrotic area, without typical granulomas and few B lymphocytes (**Figure 9**).

Thus, TNFKi vaccination did not impair the host control of *M. tuberculosis* infection in terms of lung and liver bacterial burden, granuloma formation or inflammatory response as compared with TNF neutralization with etanercept.

DISCUSSION

Here, by using a surrogate of human TNF-α vaccine, mouse TNFKi, we validated the anti-inflammatory effect of the vaccine in an experimental model of RA while documenting the little perturbed control of infection in TNFKi-treated mice in two models of infection, with *L monocytogenes* and *M. tuberculosis*.

A major concern of anti-TNF-α treatments is an increased risk of serious bacterial, viral, and fungal infections. Tuberculosis is the most common opportunistic infection and, to a lesser extent, bacterial infections, such as listeriosis (19–21). Anti-TNF-α vaccination has been widely explored in mice (22–24). Clinical trials in humans were promising in the early phases of development of TNF-α vaccination with a TNF-Kinoid (11), although not considered effective at 6 months in a larger study with a single low dose of vaccine that did not result in significant production of anti-TNF-α auto-antibodies (Neovacs.fr/products/tnf-kinoid/, NCT01911234). The TNFKi vaccine used in the present study consisted of mouse TNF-α linked to the KLH carrier protein. TNFKi induced the production of anti-TNF-α polyclonal antibodies and alleviated arthritis in two experimental

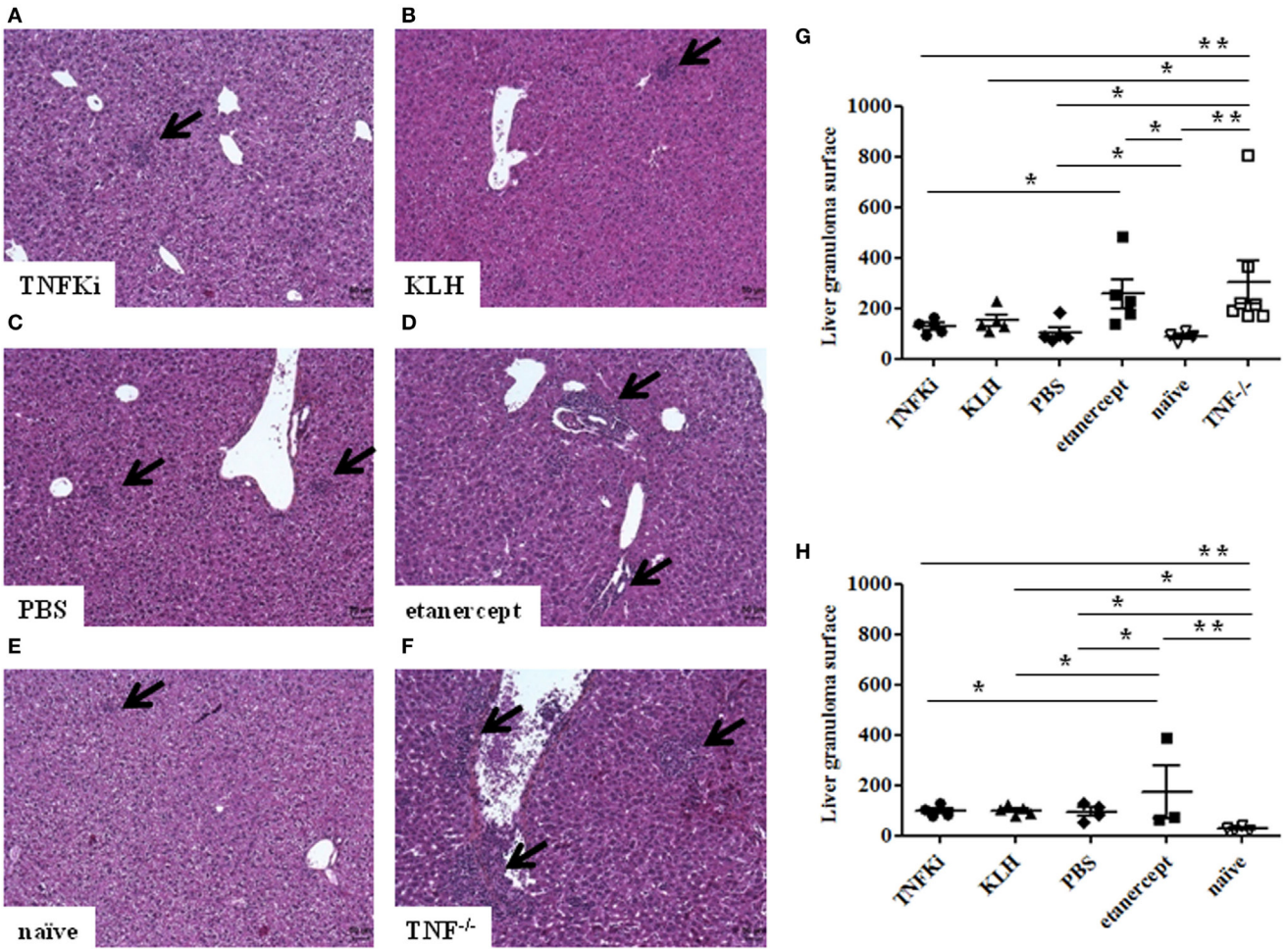

FIGURE 7 | TNFKi did not induce larger granuloma formation in liver of *Mycobacterium tuberculosis*-infected mice. Histology of granulomas (arrows) in liver sections stained with hematoxylin-eosin (n = 3–7 per group) during early infection **(A–F)**. Quantification of hepatic granuloma surface area during early **(G)** and established infection **(H)**. Horizontal bar is mean, outer bars are SEM, and whiskers are range (*$p < 0.05$, **$p < 0.01$, ANOVA).

models of arthritis, CIA and CAIA, which confirms the effective neutralization of TNF-α.

To assess to what extent this novel anti-TNF strategy would affect immunity against infectious agents, we used two experimental models of infection, with *L monocytogenes* and *M. tuberculosis*. In both cases, we compared the effect of TNFKi to that of complete lack of TNF-α ($TNF^{-/-}$ mice) and a current anti-TNF-α treatment (etanercept). Etanercept is considered the safest anti-TNF inhibitor in terms of the possible risk of serious infection (notably tuberculosis reactivation). It is a pharmacological reference for anti-TNF-α blockade in animal models of infection (25). With *L. monocytogenes* infection, anti-TNF-α polyclonal antibody production induced by TNFKi did not impair immunity to the bacterium, and all mice survived. However, TNF-α neutralization with etanercept enhanced the susceptibility to infection and $TNF^{-/-}$ mice did not show resistance to infection. TNFKi-vaccinated mice showed the same bacterial clearance in liver and spleen as immunocompetent mice (PBS and KLH controls), whereas etanercept-treated mice showed increased bacterial load. In agreement, the size and number of liver microabcesses were similar between TNFKi and control mice at day 4 postinfection. In contrast, $TNF^{-/-}$ mice showed increased number of lesions and large lesions characterized by necrotic areas. Immunization with TNFKi did not alter immune cell migration into the liver during *Listeria* infection, whereas etanercept-treated and $TNF^{-/-}$ mice exhibited neutrophil accumulation and reduced macrophage recruitment in lesions.

With the model of *M. tuberculosis* infection, TNF neutralization by TNFKi vaccination did not increase the sensitivity to the pathogen, but $TNF^{-/-}$ mice died during the early phase of infection. Previously, mice treated with a murine homolog of etanercept died due to *M. tuberculosis* infection (26). We did not observe such a drastic effect on survival with etanercept treatment; however, Zielh–Neelssen staining revealed higher bacteria loads in lungs from $TNF^{-/-}$ and etanercept-treated mice than TNFKi-vaccinated mice.

We reported previously and confirm here the striking lung inflammation in $TNF^{-/-}$ mice, including large necrotic

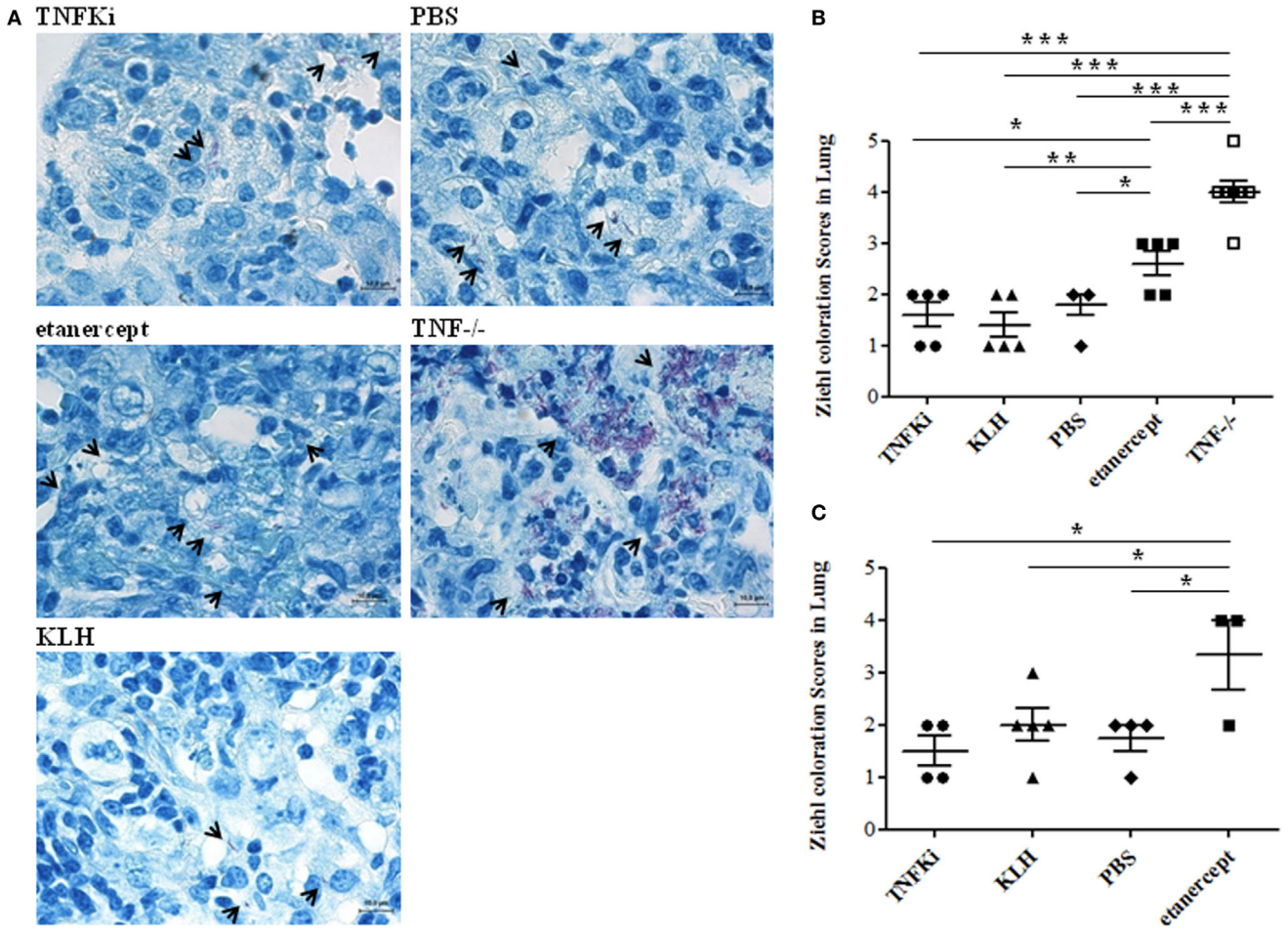

FIGURE 8 | TNFKi did not increase bacterial load in lungs of *Mycobacterium tuberculosis*-infected mice. Ziehl–Neelsen coloration showing direct recognition of mycobacteria in lung sections. *M. tuberculosis* appeared as red bacilli (arrowheads). Examples of images at early phase of infection **(A)**. Quantification of mycobacteria during the early **(B)** and established infection **(C)** after blinded observations of three fields per mice (n = 3–7 mice per group) (*$p < 0.05$ ANOVA). Scale bar, 10 µm.

granulomas (27), which were not observed in the other groups in our study. Granuloma formation and organization in lungs was not altered with established *M. tuberculosis* infection and TNFKi vaccination as compared with etanercept treatment. In addition, granulomas observed in TNFKi-vaccinated livers were similar to those in control livers. In both $TNF^{-/-}$ and etanercept-treated mice, liver granulomas were significantly larger.

The protective role of iNOS in infection led us to study its expression during the anti-*M. tuberculosis* response. Indeed, mice deficient in iNOS die due to tuberculosis infection within 33–45 days, and iNOS inhibition aggravates the course of murine tuberculosis (28, 29). We found that iNOS was expressed exclusively by macrophages within granulomas during the early phase of infection and by macrophages and foamy histiocytes during established infection. Strikingly, recruitment of macrophages and neutrophils seemed altered by etanercept treatment, because numerous neutrophils and few macrophages infiltrated lungs in the acute phase as compared with numerous macrophages and foamy histiocytes infiltrating lungs in the established phase. With TNFKi treatment, neutrophilic infiltration was rare, and few foamy histiocytes were observed during established infection. The adaptive immune response to *M. tuberculosis* is also mediated by B lymphocytes. Despite low risk of tuberculosis reactivation for RA patients receiving rituximab to deplete B cells (30), a recent study showed that in *M. tuberculosis*-infected macaques, rituximab altered local granulomatous response during acute infection (31). Furthermore, another study showed that TNF-α secreted by B lymphocytes is important for aggregation (32). In our study, contrary to etanercept, TNFKi vaccination did not impair B-cell recruitment. At day 56 postinfection, B cells formed nodules in lungs of all mouse groups, except with etanercept treatment. TNFKi allowed for B-cell recruitment in infected tissues and effective granuloma formation and maintenance during both early and established infection.

Why TNF-α neutralization with anti-TNF vaccination preserved the immune response against infection remains speculative. The risk of infection depends on the nature of the TNF-α blockers. Several studies have shown increased risk of reactivation

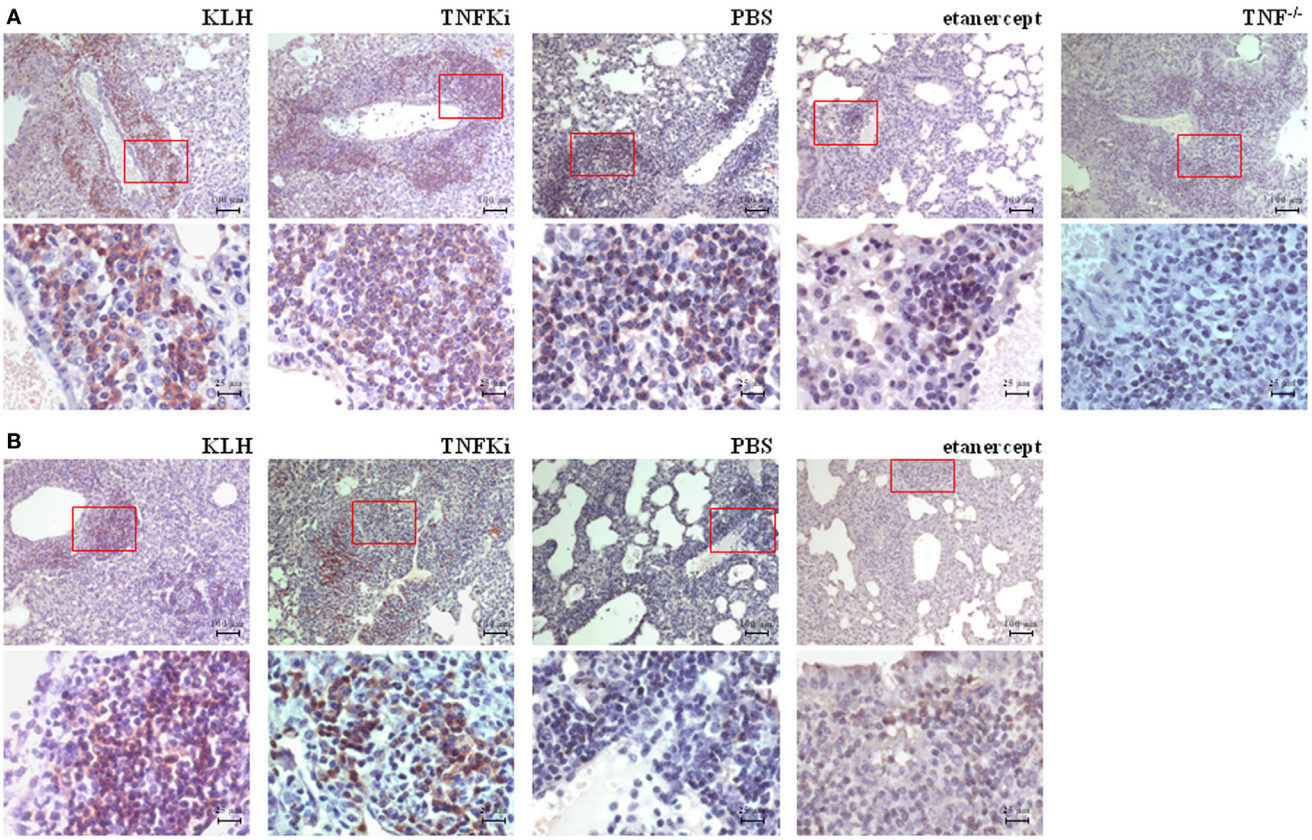

FIGURE 9 | TNFKi favored B-lymphocyte infiltration in lungs of *Mycobacterium tuberculosis*-infected mice. Immunohistochemical staining of B lymphocytes expressing CD45R. During early infection **(A)** and established infection **(B)**, perivascular accumulation of B lymphocytes in lungs of mice. Representative images of 3–7 mice per group. Scale bar, 100 µm. 4× magnification of red boxes below original picture (scale bar, 25 µm).

of latent tuberculosis with infliximab and adalimumab monoclonal antibody therapy than with the recombinant soluble TNF-α receptor etanercept (33, 34). The safety profile with both types of treatments may differ in part due to their TNF-α binding property. Infliximab forms stable complexes with soluble TNF-α and TNF-α expressed at cell membranes, whereas etanercept interacts with soluble TNF-α and only weakly and reversibly with the transmembrane form (35).

Although the importance of soluble versus membrane TNF-α has not been investigated in detail in the CIA model, the role of both forms of TNF-α were well investigated in infectious models. Indeed, mice lacking the soluble form of TNF-α but expressing a transmembrane form or expressing uncleavable membrane TNF showed control of *M. tuberculosis* infection, at least during the acute phase (36–38) or during *L. monocytogenes* infection (39). These latter mice could still form compact granulomas, which prevented bacterial spreading, whereas mice completely lacking TNF-α were severely impaired in granuloma formation. Expression of a functional transmembrane form of TNF-α also confers partial protection against *L. monocytogenes* infection (40), but TNF-α- or TNF-R1-deficient mice are highly susceptible (41).

Low levels of TNF present at the site of infection might be sufficient to control mycobacteria infection. Indeed, in TNF-deficient mice, which usually rapidly die after *Mycobacterium bovis* bacillus Calmette–Guérin (BCG) infection, the antimycobacterial immune response was restored by infection with a TNF-α-secreting recombinant *M. bovis* BCG, effectively protecting these highly susceptible mice (42).

There are some limitations to this work that warrant further studies. The exact mechanisms by which the two different anti-TNF strategies affect the immune response to infectious agents need to be further dissected. Another issue is the extrapolation of the results obtained in the animal model to humans, which is not the aim of the present study. Although we used validated models of arthritis (CIA) and infection, these models only partially mimic human disease. Moreover, differences between the human and murine immune system both in response to vaccination and infection may lead to deep discrepancies that warrant caution. No safety issues or increased risk of infection were reported when anti-TNF vaccination was administered in humans (Crohn's disease: NCT00808262; RA: NCT01040715). Nevertheless, the samples of those trials were limited and no specific studies on response to infection were performed.

In summary, arthritis improvement when targeting TNF-α does not result in a constant and uniform alteration of the host defense against infection. This alteration is variable depending

on the strategies used for targeting TNF-α. TNFKi may allow for maintenance of the host defense against *M. tuberculosis* and *L. monocytogenes* infection in mice. This is a major point for the safety features of therapeutic TNF vaccination in chronic inflammatory diseases. Pathogenic levels of TNF-α might be neutralized efficiently while maintaining the minimal levels needed to control host resistance to bacterial infection.

ETHICS STATEMENT

All applicable international, national, and/or institutional guidelines for the care and use of animals were followed. For arthritis models, all procedures were approved by the Animal Care and Use Committee of the University of Paris 13 (ethical approval ID: Ce5/2010/036). Infectious protocols were approved by the Ethics Committee for Animal Experimentation of CNRS Campus Orleans (CCO) (no. CLE CCO 2015-1071). We were particularly concerned by a strict application of the 3R rules.

AUTHOR CONTRIBUTIONS

NB performed mice immunization, evaluated clinical arthritis, performed immunoassay, *Listeria* infection, and immuno-histological analysis and helped draft the manuscript. LS performed statistical analysis, drafted and revised the manuscript. NS performed *Mycobacteria* infection, bacterial burden, and organ weight evaluations. DD participated in the immuno-histological analysis, analysis of the data, and helped to draft the manuscript. PD helped coordinate the study and helped draft the manuscript. BR and VQ established and validated the experimental infectious models and conceived a part of the *Listeria* and *Mycobacteria* infection study, participated in coordination and analysis of the data, and helped draft the manuscript. M-CB conceived of the study, analyzed the data, and helped to draft the manuscript. EA conceived of the study, performed coupling of TNF vaccine, participated in coordination of the study, analyzed the data, and drafted the manuscript.

ACKNOWLEDGMENTS

We thank Sonia Varela (animal facilities, Paris 13 University), Béatrice Marmey, Delphine Lemeiter, and Roxane Hervé for technical contributions. We also thank Matthieu Ribon, Julie Mussard, and Marjorie Bénéteau de la Prairie for their help in the project.

FUNDING

The pathophysiology, target, and therapies of RA laboratory received unrestricted grants from University of Paris 13 (BQR), Agence Nationale de la Recherche (ANR CYTOVAC project), INSERM (ProA), Direction Générale de l'Armement, Société Française de Rhumatologie, and Pfizer (Passerelle Grant).

SUPPLEMENTARY MATERIAL

The Supplementary Material for this article can be found online at http://www.frontiersin.org/article/10.3389/fimmu.2017.01533/full#supplementary-material.

REFERENCES

1. Winsauer C, Kruglov AA, Chashchina AA, Drutskaya MS, Nedospasov SA. Cellular sources of pathogenic and protective TNF and experimental strategies based on utilization of TNF humanized mice. *Cytokine Growth Factor Rev* (2014) 25(2):115–23. doi:10.1016/j.cytogfr.2013.12.005
2. Minichiello E, Semerano L, Boissier MC. Time trends in the incidence, prevalence, and severity of rheumatoid arthritis: a systematic literature review. *Joint Bone Spine* (2016) 83(6):625–30. doi:10.1016/j.jbspin.2016.07.007
3. Singh JA, Christensen R, Wells GA, Suarez-Almazor ME, Buchbinder R, Lopez-Olivo MA, et al. A network meta-analysis of randomized controlled trials of biologics for rheumatoid arthritis: a Cochrane overview. *CMAJ* (2009) 181(11):787–96. doi:10.1503/cmaj.091391
4. Wallis RS. Infectious complications of tumor necrosis factor blockade. *Curr Opin Infect Dis* (2009) 22(4):403–9. doi:10.1097/QCO.0b013e32832dda55
5. Keane J, Gershon S, Wise RP, Mirabile-Levens E, Kasznica J, Schwieterman WD, et al. Tuberculosis associated with infliximab, a tumor necrosis factor-α-neutralizing agent. *N Engl J Med* (2001) 345(15):1098–104. doi:10.1056/NEJMoa011110
6. Le Buanec H, Delavallée L, Bessis N, Paturance S, Bizzini B, Gallo R, et al. TNFalpha kinoid vaccination-induced neutralizing antibodies to TNFalpha protect mice from autologous TNFalpha-driven chronic and acute inflammation. *Proc Natl Acad Sci U S A* (2006) 103(51):19442–7. doi:10.1073/pnas.0604827103
7. Delavallée L, Le Buanec H, Bessis N, Assier E, Denys A, Bizzini B, et al. Early and long-lasting protection from arthritis in tumour necrosis factor alpha (TNFalpha) transgenic mice vaccinated against TNFalpha. *Ann Rheum Dis* (2008) 67(9):1332–8. doi:10.1136/ard.2007.079137
8. Assier E, Semerano L, Duvallet E, Delavallée L, Bernier E, Laborie M, et al. Modulation of anti-tumor necrosis factor alpha (TNF-α) antibody secretion in mice immunized with TNF-α kinoid. *Clin Vaccine Immunol* (2012) 19(5):699–703. doi:10.1128/CVI.05649-11
9. Semerano L, Biton J, Delavallée L, Duvallet E, Assier E, Bessis N, et al. Protection from articular damage by passive or active anti-tumour necrosis factor (TNF)-α immunotherapy in human TNF-α transgenic mice depends on anti-TNF-α antibody levels. *Clin Exp Immunol* (2013) 172(1):54–62. doi:10.1111/cei.12040
10. Delavallée L, Semerano L, Assier E, Vogel G, Vuagniaux G, Laborie M, et al. Active immunization to tumor necrosis factor-alpha is effective in treating chronic established inflammatory disease: a long-term study in a transgenic model of arthritis. *Arthritis Res Ther* (2009) 11(6):R195. doi:10.1186/ar2897
11. Durez P, Vandepapeliere P, Miranda P, Toncheva A, Berman A, Kehler T, et al. Therapeutic vaccination with TNF-kinoid in TNF antagonist-resistant rheumatoid arthritis: a phase II randomized, controlled clinical trial. *PLoS One* (2014) 9(12):e113465. doi:10.1371/journal.pone.0113465
12. Wallis RS, Broder M, Wong J, Lee A, Hoq L. Reactivation of latent granulomatous infections by infliximab. *Clin Infect Dis* (2005) 41(Suppl 3):S194–8. doi:10.1086/429996
13. Liao H, Zhong Z, Liu Z, Zou X. Comparison of the risk of infections in different anti-TNF agents: a meta-analysis. *Int J Rheum Dis* (2017) 20(2):161–8. doi:10.1111/1756-185X.12970
14. Marino MW, Dunn A, Grail D, Inglese M, Noguchi Y, Richards E, et al. Characterization of tumor necrosis factor-deficient mice. *Proc Natl Acad Sci U S A* (1997) 94(15):8093–8. doi:10.1073/pnas.94.15.8093
15. Ratsimandresey RA, Duvallet E, Assier E, Semerano L, Delavallée L, Bessis N, et al. Active immunization against IL-23p19 improves experimental arthritis. *Vaccine* (2011) 29(50):9329–36. doi:10.1016/j.vaccine.2011.09.134
16. Hutamekalin P, Saito T, Yamaki K, Mizutani N, Brand DD, Waritani T, et al. Collagen antibody-induced arthritis in mice: development of a new

arthritogenic 5-clone cocktail of monoclonal anti-type II collagen antibodies. *J Immunol Methods* (2009) 343(1):49–55. doi:10.1016/j.jim.2009
17. Semerano L, Duvallet E, Belmellat N, Marival N, Schall N, Monteil M, et al. Targeting VEGF-A with a vaccine decreases inflammation and joint destruction in experimental arthritis. *Angiogenesis* (2016) 19(1):39–52. doi:10.1007/s10456-015-9487-0
18. Boissier MC, Bessis N. Do we need animal models to advance research on inflammatory joint disease? *Joint Bone Spine* (2017) 84(4):381–3. doi:10.1016/j.jbspin.2017.04.005
19. Hage CA, Bowyer S, Tarvin SE, Helper D, Kleiman MB, Wheat LJ. Recognition, diagnosis, and treatment of histoplasmosis complicating tumor necrosis factor blocker therapy. *Clin Infect Dis* (2010) 50(1):85–92. doi:10.1086/648724
20. Peña-Sagredo JL, Hernández MV, Fernandez-Llanio N, Giménez-Ubeda E, Muñoz-Fernandez S, Ortiz A, et al. *Listeria monocytogenes* infection in patients with rheumatic diseases on TNF-alpha antagonist therapy: the Spanish Study Group experience. *Clin Exp Rheumatol* (2008) 26(5):854–9.
21. Che H, Lukas C, Morel J, Combe B. Risk of herpes/herpes zoster during anti-tumor necrosis factor therapy in patients with rheumatoid arthritis. Systematic review and meta-analysis. *Joint Bone Spine* (2014) 81(3):215–21. doi:10.1016/j.jbspin.2013.07.009
22. Spohn G, Guler R, Johansen P, Keller I, Jacobs M, Beck M, et al. A virus-like particle-based vaccine selectively targeting soluble TNF-alpha protects from arthritis without inducing reactivation of latent tuberculosis. *J Immunol* (2007) 178(11):7450–7. doi:10.4049/jimmunol.178.11.7450
23. Wan Y, Yuan S, Xue X, Li M, Qin X, Zhang C, et al. The preventive effect of adjuvant-free administration of TNF-PADRE autovaccine on collagen-II-induced rheumatoid arthritis in mice. *Cell Immunol* (2009) 258(1):72–7. doi:10.1016/j.cellimm.2009.03.014
24. Zhang L, Wang J, Xu A, Zhong C, Lu W, Deng L, et al. A rationally designed TNF-α epitope-scaffold immunogen induces sustained antibody response and alleviates collagen-induced arthritis in mice. *PLoS One* (2016) 11(9):e0163080. doi:10.1371/journal.pone.0163080
25. Wallis RS, Ehlers S. Tumor necrosis factor and granuloma biology: explaining the differential infection risk of etanercept and infliximab. *Semin Arthritis Rheum* (2005) 34(5 Supl1):34–8. doi:10.1016/j.semarthrit.2005.01.009
26. Plessner HL, Lin PL, Kohno T, Louie JS, Kirschner D, Chan J, et al. Neutralization of tumor necrosis factor (TNF) by antibody but not TNF receptor fusion molecule exacerbates chronic murine tuberculosis. *J Infect Dis* (2007) 195(11):1643–50. doi:10.1086/517519
27. Bourigault ML, Segueni N, Rose S, Court N, Vacher R, Vasseur V, et al. Relative contribution of IL-1α, IL-1β and TNF to the host response to *Mycobacterium tuberculosis* and attenuated *M. bovis* BCG. *Immun Inflamm Dis* (2013) 1(1):47–62. doi:10.1002/iid3.9
28. MacMicking JD, North RJ, LaCourse R, Mudgett JS, Shah SK, Nathan CF. Identification of nitric oxide synthase as a protective locus against tuberculosis. *Proc Natl Acad Sci U S A* (1997) 94(10):5243–8. doi:10.1073/pnas.94.10.5243
29. Flynn JL, Scanga CA, Tanaka KE, Chan J. Effects of aminoguanidine on latent murine tuberculosis. *J Immunol* (1998) 160(4):1796–803.
30. Liao TL, Lin CH, Chen YM, Chang CL, Chen HH, Chen DY. Different risk of tuberculosis and efficacy of isoniazid prophylaxis in rheumatoid arthritis patients with biologic therapy: a nationwide retrospective cohort study in Taiwan. *PLoS One* (2016) 11(4):e0153217. doi:10.1371/journal.pone.0153217
31. Phuah J, Wong EA, Gideon HP, Maiello P, Coleman MT, Hendricks MR, et al. Effects of B cell depletion on early *Mycobacterium tuberculosis* infection in cynomolgus macaques. *Infect Immun* (2016) 84(5):1301–11. doi:10.1128/IAI.00083-16
32. Kondratieva TK, Linge IA, Kondratieva EV, Dyatlov AV, Drutskaya MS, Zvartsev RV, et al. Formation of compact aggregates of B-lymphocytes in lung tissue during mycobacterial infection in mice depends on TNF production by these cells and is not an element of the host's immunological protection. *Biochemistry (Mosc)* (2014) 79(12):1358–62. doi:10.1134/S0006297914120098
33. Wallis RS. Tumour necrosis factor antagonists: structure, function, and tuberculosis risks. *Lancet Infect Dis* (2008) 8(10):601–11. doi:10.1016/S1473-3099(08)70227-5
34. Harris J, Keane J. How tumour necrosis factor blockers interfere with tuberculosis immunity. *Clin Exp Immunol* (2010) 161(1):1–9. doi:10.1111/j.1365-2249.2010.04146.x
35. Scallon B, Cai A, Solowski N, Rosenberg A, Song XY, Shealy D, et al. Binding and functional comparisons of two types of tumor necrosis factor antagonists. *J Pharmacol Exp Ther* (2002) 301(2):418–26. doi:10.1124/jpet.301.2.418
36. Olleros ML, Guler R, Corazza N, Vesin D, Eugster HP, Marchal G, et al. Transmembrane TNF induces an efficient cell-mediated immunity and resistance to *Mycobacterium bovis* bacillus Calmette-Guérin infection in the absence of secreted TNF and lymphotoxin-alpha. *J Immunol* (2002) 168(7):3394–401. doi:10.4049/jimmunol.168.7.3394
37. Fremond C, Allie N, Dambuza I, Grivennikov SI, Yeremeev V, Quesniaux V, et al. Membrane TNF confers protection to acute mycobacterial infection. *Respir Res* (2005) 6:136. doi:10.1186/1465-9921-6-136
38. Dambuza I, Allie N, Fick L, Johnston N, Fremond C, Mitchell J, et al. Efficacy of membrane TNF mediated host resistance is dependent on mycobacterial virulence. *Tuberculosis (Edinb)* (2008) 88(3):221–34. doi:10.1016/j.tube.2007.08.011
39. Torres D, Janot L, Quesniaux VF, Grivennikov SI, Maillet I, Sedgwick JD, et al. Membrane tumor necrosis factor confers partial protection to *Listeria* infection. *Am J Pathol* (2005) 167(6):1677–87. doi:10.1016/S0002-9440(10)61250-3
40. Musicki K, Briscoe H, Tran S, Britton WJ, Saunders BM. Differential requirements for soluble and transmembrane tumor necrosis factor in the immunological control of primary and secondary *Listeria monocytogenes* infection. *Infect Immun* (2006) 74(6):3180–9. doi:10.1128/IAI.02004-05
41. Rothe J, Lesslauer W, Lötscher H, Lang Y, Koebel P, Köntgen F, et al. Mice lacking the tumour necrosis factor receptor 1 are resistant to TNF-mediated toxicity but highly susceptible to infection by *Listeria monocytogenes*. *Nature* (1993) 364(6440):798–802. doi:10.1038/364798a0
42. Bekker LG, Moreira AL, Bergtold A, Freeman S, Ryffel B, Kaplan G. Immunopathologic effects of tumor necrosis factor alpha in murine mycobacterial infection are dose dependent. *Infect Immun* (2000) 68(12):6954–61. doi:10.1128/IAI.68.12.6954-6961.2000

Conflict of Interest Statement: BR, DD, EA, LS, M-CB, NB, NS, PD, and VQ declare no conflict of interest.

Copyright © 2017 Belmellat, Semerano, Segueni, Damotte, Decker, Ryffel, Quesniaux, Boissier and Assier. This is an open-access article distributed under the terms of the Creative Commons Attribution License (CC BY). The use, distribution or reproduction in other forums is permitted, provided the original author(s) or licensor are credited and that the original publication in this journal is cited, in accordance with accepted academic practice. No use, distribution or reproduction is permitted which does not comply with these terms.

frontiers in Immunology

MINI REVIEW
published: 16 November 2017
doi: 10.3389/fimmu.2017.01534

Regulation of Neuroinflammation: What Role for the Tumor Necrosis Factor-Like Weak Inducer of Apoptosis/Fn14 Pathway?

*Audrey Boulamery[1,2] and Sophie Desplat-Jégo[1,3]**

[1] Aix-Marseille University, CNRS, NICN, Marseille, France, [2] AP-HM, Hôpital Sainte-Marguerite, Centre Antipoison et de Toxicovigilance, Marseille, France, [3] Service d'Immunologie, Hôpital de la Conception, Marseille, France

Observed in many central nervous system diseases, neuroinflammation (NI) proceeds from peripheral immune cell infiltration into the parenchyma, from cytokine secretion and from oxidative stress. Astrocytes and microglia also get activated and proliferate. NI manifestations and consequences depend on its context and on the acute or chronic aspect of the disease. The tumor necrosis factor-like weak inducer of apoptosis (TWEAK)/Fn14 pathway has been involved in chronic human inflammatory pathologies such as neurodegenerative, autoimmune, or malignant diseases. New data now describe its regulatory effects in tissues or fluids from patients with neurological diseases. In this mini-review, we aim to highlight the role of TWEAK/Fn14 in modulating NI in multiple sclerosis, neuropsychiatric systemic lupus erythematosus, stroke, or glioma. TWEAK/Fn14 can modulate NI by activating canonical and non-canonical nuclear factor-κB pathways but also by stimulating mitogen-activated protein kinase signaling. These downstream activations are associated with (i) inflammatory cytokine, chemokine and adhesion molecule expression or release, involved in NI propagation, (ii) matrix-metalloproteinase 9 secretion, implicated in blood–brain barrier disruption and tissue remodeling, (iii) astrogliosis and microgliosis, and (iv) migration of tumor cells in glioma. In addition, we report several animal and human studies pointing to TWEAK as an attractive therapeutic target.

Keywords: tumor necrosis factor-like weak inducer of apoptosis, Fn14, central nervous system, neuroinflammation, multiple sclerosis, neuropsychiatric systemic lupus erythematosus, stroke, glioma

OPEN ACCESS

Edited by:
Jixin Zhong,
Case Western Reserve University, United States

Reviewed by:
Yumin Xia,
Second Affiliated Hospital of Xi'an Jiaotong University, China
Lu Huang,
University of Texas MD Anderson Cancer Center, United States

****Correspondence:***
Sophie Desplat-Jégo
sophie.desplat@ap-hm.fr

Specialty section:
This article was submitted to Inflammation, a section of the journal Frontiers in Immunology

Received: *21 August 2017*
Accepted: *27 October 2017*
Published: *16 November 2017*

Citation:
Boulamery A and Desplat-Jégo S (2017) Regulation of Neuroinflammation: What Role for the Tumor Necrosis Factor-Like Weak Inducer of Apoptosis/Fn14 Pathway? Front. Immunol. 8:1534. doi: 10.3389/fimmu.2017.01534

INTRODUCTION

Initially described as an accumulation of leukocytes in multiple sclerosis (MS) brain, neuroinflammation (NI) now also applies to other central nervous system (CNS) diseases (1). Among others factors, it results from peripheral immune cell infiltration through the brain barriers, from cytokine secretion and from oxidative stress (2). NI is based upon and is regulated by bidirectional communication pathways involving especially cytokines that connect the CNS and immune system (3). However, using the generic term "NI" for such a multifaceted process could be inaccurate (1). NI features depend on disease-specific conditions and differ in CNS infection, ischemia, and malignant or autoimmune diseases. Whether NI is acute or chronic is a major point to consider. In fact, transient NI is usually beneficial and must be preserved, while chronic NI is preferentially associated with diseases resulting in neurodegeneration (4, 5).

Neuroinflammation highly involves cellular components of the neurovascular unit (6, 7), which consists in microvascular endothelial cells surrounded by basal lamina, astrocytic end-feet, pericytes, and neurons. It underlies the concept of a blood–brain barrier (BBB) actively separating the parenchyma from the circulation. Resident CNS cells such as astrocytes and microglia are also involved in regulating NI and respond to CNS insults by a proliferation and an abnormal activation, respectively called astrogliosis and microgliosis. This response is not always a harmful process, it can also be a beneficial and crucial process involved in CNS repair (8–10). During NI, immune cells, microglia, and astrocytes release soluble proteins, called cytokines, which mediate cell–cell communication (11). Among them, the tumor necrosis factor (TNF)-like weak inducer of apoptosis (TWEAK) plays a dual role in the physiological versus inflammatory pathological responses of tissues, including the CNS (12–15).

Tumor necrosis factor-like weak inducer of apoptosis is a member of TNF superfamily initially shown to induce apoptosis of malignant cells (16). It is synthesized as a transmembrane protein form (mTWEAK) and proteolytically processed as a soluble cytokine (sTWEAK). Monocytes/macrophages are the main source of sTWEAK in inflammatory tissues. Until now, mTWEAK has only been described on freshly isolated monocytes (17, 18). Unlike TNF-α, TWEAK curtails the innate immune response and attenuates the transition to adaptive Th1 immunity (19). Moreover, TWEAK inhibits TNF receptor-1 signaling that promotes inflammation (20). TWEAK signaling mainly requires binding to fibroblast growth factor inducible 14 (Fn14), a member of the TNF receptor superfamily. Although Fn14 is poorly expressed in healthy endothelial cells, neurons, astrocytes, microglia, and progenitor cells, it is highly inducible in these cells. TWEAK interaction with its Fn14 receptor induces multiple molecular events and biological responses depending on cell type and microenvironment. These downstream signaling pathways have been compiled from the literature in 2012 by Bhattacharjee et al. (21), who cataloged 46 proteins and 28 induced genes. Thus, Fn14 engagement primarily activates nuclear factor-κB (NF-κB) and mitogen-activated protein kinase (MAPK) *via* interaction with intracellular TNF-receptor-associated-factors (21, 22). mTWEAK seems to activate more efficiently the canonical NF-κB pathway while both membrane and soluble TWEAK can induce the non-canonical NF-κB pathway (23). Secondary TWEAK signaling pathways have also been described, such as the phosphatidylinositol 3-kinase/Akt pathway (14).

In the CNS, TWEAK targets endothelial cells, astrocytes, and neurons. Interestingly, in murine and human astrocytes, the TWEAK/Fn14 pathway can stimulate reactivity, i.e., when cells proliferate, are activated and produce inflammation factors (24, 25). This associated mitogenic potency is mediated by the TWEAK-induced MAPK signaling pathway (26). Besides, in an *in vitro* model of human BBB, TWEAK induced microvascular cerebral endothelial cells to display an inflammatory profile: they increased (i) their secretion of proinflammatory cytokines, (ii) their production and activation of matrix-metalloproteinase 9 (MMP-9) involved in BBB disruption, and (iii) their expression of intercellular adhesion molecule-1 implicated in leukocyte adhesion to endothelium (27).

Here, we aimed to review TWEAK role in NI modulation in neurodegenerative, autoimmune, ischemic, and malignant CNS inflammatory diseases. Considering available data about TWEAK involvement in their pathogenesis, we will successively focus on MS, neuropsychiatric systemic lupus erythematosus (NPSLE), cerebral ischemia, glioma, amyotrophic lateral sclerosis (ALS), Parkinson's disease, and schizophrenia (**Table 1**).

THE TWEAK/Fn14 PATHWAY CONTRIBUTES TO TISSUE INJURY IN MS

Multiple sclerosis is a multifactorial disease involving autoimmunity against myelin components, NI, BBB disruption, tissue remodeling, and demyelination/remyelination (28).

TWEAK and Fn14 Are Upregulated in MS

Serafini et al. showed that both TWEAK and Fn14 were upregulated in postmortem MS brain sections (29). Furthermore, this increase was related to the degree of inflammation and demyelination. Perivascular and intrameningeal macrophages, microglia, and astrocytes were the main sources of TWEAK, with a different contribution according to lesion location and degree of inflammation. Fn14 was expressed by neurons and astrocytes in the cortex of highly infiltrated MS brains (29). The absence of TWEAK/Fn14 expression in healthy brain reinforces the idea that TWEAK/Fn 14 pathway could play a role in MS pathogeny. In blood, Desplat-Jégo et al. demonstrated that mTWEAK was expressed at the cell surface of monocytes derived from MS patients but not from non-MS patients (18). In MS, such mTWEAK-expressing monocytes could represent immune cells that infiltrate CNS by interacting with Fn14 molecules at the membrane of BBB endothelial cells. In the same study, sTWEAK serum and cerebrospinal fluid levels were similar in MS and non-MS patients (18), suggesting that sTWEAK is not a reliable diagnosis MS biomarker.

Myelin oligodendrocyte glycoprotein-induced experimental autoimmune encephalomyelitis (EAE) is the best-characterized animal model of MS. In chronic EAE induced in C57Bl/6 mice, TWEAK transcript levels increased in the spinal cord (24). Moreover, transgenic mice overexpressing sTWEAK developed a more severe EAE than wild-type mice (24). Besides, in cuprizone-treated mice, a model of demyelination/remyelination, TWEAK and Fn14 transcription were upregulated during both demyelination and remyelination phases (30).

Blocking the TWEAK/Fn14 Pathway Is Effective for Treating an MS Model

Treated with cuprizone TWEAK-knock-out mice displayed a significant delay in microglia accumulation and in demyelination phases (30). Reinforcing the role of TWEAK/Fn14 in MS, our team showed that EAE severity and CNS leukocyte infiltration were reduced in mice treated with blocking monoclonal anti-TWEAK antibody after the priming phase (31). Moreover, an Fn14-TNF-related apoptosis-inducing ligand (TRAIL) fusion protein was designed to simultaneously block endogenous TWEAK and mediate TRAIL inhibitory signals on activated

TABLE 1 | Mechanisms underlying the role of tumor necrosis factor-like weak inducer of apoptosis (TWEAK) in neuroinflammation regulation.

Mechanisms	Model	References
Stimulation of immune cell recruitment in central nervous system	Murine model of MS; murine model of NPSLE; murine model of cerebral ischemia	(31, 40, 47)
Stimulation of astrogliosis and microgliosis	Murine model of ALS; astrocytes culture; murine model of NPSLE	(15, 26, 40)
Attenuation of transition from innate to adaptative immunity with Th1 helper decrease	Murine model of TWEAK-KO	(19)
Cellular death	Neuronal *in vitro* model of ischemia; murine model of ALS; postmortem MS brains; murine model of NPSLE	(13, 15, 29, 40)
Downstream activation of canonical and non-canonical NF-κB pathways	Murine model of TWEAK-KO; *in vitro* model of BBB; murine model of NF-κB p50-KO; human astrocytoma cell cultures	(19, 22, 23, 45, 51, 55)
Downstream activation of MAPK pathway	Astrocyte cultures; *in vitro* model of BBB	(26, 27)
Downstream activation of Rac1 pathway	Human astrocytoma cell cultures	(51, 53)
Increase in VCAM-1 and ICAM-1 production	*In vitro* model of BBB; murine model of NPSLE	(27, 40)
Increase in MMP-9 production and activity	*In vitro* model of BBB; murine model of NF-κB p50-KO; murine model of cerebral ischemia; glioma cell cultures	(27, 45, 46, 55)
Decrease in ZO-1 expression	*In vitro* model of BBB	(27)
Increase in synthesis of pro-inflammatory mediators Il-6, Il-8, RANTES, and CCL-2	Murine model of ALS; *in vitro* model of BBB; murine model of NPSLE; murine model of cerebral ischemia	(15, 27, 37, 39, 40, 46, 47)
Cerebral Ig G deposition, increase in albumin quotient and decrease in aquaporin-4 expression	Murine model of NPSLE	(37, 39, 40)
Activation of complement and iNOS	Murine model of NPSLE	(37, 39, 40)

ALS, amyotrophic lateral sclerosis; BBB, blood–brain barrier; CCL-2, chemokine ligand 2; ICAM-1, intercellular adhesion molecule-1; Il, interleukin; Ig, immunoglobulin; Inos, inducible form of nitric-oxide synthase; KO, knock-out; MAPK, mitogen-activated protein kinase; MMP-9, matrix-metalloproteinase 9; MS, multiple sclerosis; NF-κB, nuclear factor-κB; NPSLE, neuropsychiatric systemic lupus erythematosus; Rac1, Ras-related C3 botulinum toxin substrate 1; RANTES, regulated on activation, normal T Cell expressed and secreted; VCAM-1, vascular cell adhesion molecule-1; ZO-1, zonula occludens-1.

T cells (32). Injected in EAE-mice, this protein reduced EAE severity (32, 33). Additionally, vaccinating mice or rats with TWEAK extracellular domain or with Fn14 induced the production of specific inhibitory antibodies. Such treatment was associated with reduced inflammatory spinal cord infiltration and with clinical amelioration during EAE (34). However, in humans, a raising question is the relevance of targeting TWEAK in MS when anti-TNF-α has failed to improve disease status (35). One could argue that the TWEAK/Fn14 pathway could also play a role in neuroprotection. In this way, Iocca et al. observed a modest but significant delay in remyelination of TWEAK-knock-out mice treated with cuprizone. However, this marginal delay did not result in prolonged defect in remyelination (30). Later, Echeverry et al. described a TNF-α-dependent neuroprotective effect of TWEAK in another NI model (13), but data in MS are lacking. Further studies are then needed to definitively establish that TWEAK is a relevant therapeutic target in MS.

THE TWEAK/Fn14 PATHWAY CONTRIBUTES TO NPSLE

Neuropsychiatric systemic lupus erythematosus is an autoimmune disease underlied by hyperactivation of B and T lymphocytes, leading to overproduction of autoantibodies, tissue deposition of immune complexes, and increase in proinflammatory cytokines. This inflammatory state potentially targets all the organs, with marked joint, renal, hematologic and skin damages. In a significant number of patients, neuropsychiatric manifestations can also occur and thus define NPSLE. A pathogenic role of TWEAK was shown in lupus nephritis, a renal manifestation of the disease (36). Besides, evidences of TWEAK involvement in NPSLE are growing.

TWEAK/Fn14 Interaction Compromises the BBB in NPSLE Mouse Model

Putterman et al. observed an increased expression of TWEAK and Fn14 in the cerebral cortex of the MRL/lpr mouse strain with NPSLE (37, 38). Furthermore, knocking out Fn14 in this strain (i) significantly improved cognitive function and (ii) decreased depression and anhedonia in comparison with MRL/lpr wild-type mice. These clinical parameters were associated with decreased levels of proinflammatory cytokines and preserved BBB integrity (37). Further, CNS anatomopathological studies in these mice showed (i) a reduction of fibronectin deposition and inducible form of nitric-oxyde synthase (iNOS) production, (ii) a diminution of immune infiltrates, and (iii) a decrease of IgG deposition and complement activation (39). Finally, reduced cortex neuronal degeneration, apoptosis, and gliosis were associated with improved cognitive functions in such mice (40).

TWEAK Mediates Symptoms Observed in NPSLE

These results were consolidated by intracerebroventricular injection of Fc-TWEAK in non-autoimmune mice. Just like MRL/lpr strain, these mice developed NPSLE symptoms,

associated with high levels of TWEAK pathway downstream components, complement and iNOS activation, IgG brain deposition, neurodegeneration, and apoptosis (39). Trysberg et al. suggested that NPSLE could be associated with high levels of MMP-9 and sTWEAK in cerebrospinal fluid (41, 42). They also found a significant correlation between intrathecal MMP-9 and levels of tau (a neuronal degeneration marker) and glial fibrillary acidic protein (an astrocytic degeneration marker) (41). These results suggest that TWEAK/Fn14 interaction might be involved in brain damages during NPSLE since it promotes synthesis and activation of MMP-9 in CNS (27). Nevertheless, a recent study concluded that TWEAK levels in serum and cerebro-spinal fluid did not seem relevant biomarkers for NPSLE (43).

Finally, these findings highly support the involvement of TWEAK/Fn14 interaction in NPSLE pathogenesis and symptom occurrence.

TWEAK DISPLAYS A DUAL ROLE IN CEREBRAL ISCHEMIA

Cerebral ischemia or stroke is the second cause of mortality in the world. The onset of cerebral ischemia is followed by inflammatory events that affect neurological patient's outcome. Several studies implicate TWEAK in stroke.

TWEAK/Fn14 Interaction Increases the Volume of the Ischemic Zone in Stroke

Experimental focal cerebral ischemia was associated with an increase in TWEAK and Fn14 mRNA levels (44) and with BBB disruption (45, 46). In this context, TWEAK-induced NF-κB activation resulted in both astrocytic chemokine (C-C motif) ligand-2 (CCL-2) expression, leading to polynuclear neutrophil recruitment into the damaged zone, and in upregulation of MMP-9 activity (45–47). The effective inhibition of this neuroinflammatory process by Fn14-Fc decoy injections (46, 48) was associated with a reduced ischemic zone and hastened motor function recovery (46). Stroke patients displayed significantly elevated TWEAK serum levels and, in postmortem stroke human brains, elevated Fn14 mRNA levels were associated with upregulated Fn14 immunostaining in the ischemic zone (49).

The TWEAK/Fn14 Signaling Contributes to the Protective Effect of Hypoxic Preconditioning

Hypoxic-preconditioning of mice or cultured neurons promotes neuron survival and reduces ischemic lesion volume. In this context, TWEAK and Fn14 levels increase. Moreover, the protective effect of hypoxic preconditioning was abrogated in TWEAK or Fn14 KO mice and restored in cultured neurons after addition of TWEAK (13). This suggests that the TWEAK/Fn14 pathway contributes to the protective effect of hypoxic preconditioning. This is likely mediated by neuronal TNF-α and the activation of the MAPK pathway, resulting in the inactivation of the Bcl-2-associated death promoter protein (13).

These results suggest that a relevant therapeutic strategy would be administration of TWEAK in order to protect the brain in patients at high risk of stroke.

TWEAK ACTIVATES CANONICAL AND NON-CANONICAL NF-κB PATHWAYS IN GLIOBLASTOMA

Glioblastoma, the most common primary brain tumor, is associated with a high mortality related to its high local invasiveness, angiogenesis, and immunosuppressive potency. The initiation and development of tumors are associated with repetitive tissue damage and are tightly linked to chronic inflammatory processes. Tumor cell migration is essential in glioblastoma malignancy progression and depends on its inflammatory microenvironment.

TWEAK/Fn14 Promotes Glioblastoma Cell Migration and Invasion

Tumor necrosis factor-like weak inducer of apoptosis upregulates Fn14 in migrating glioblastoma cells. This overexpression correlates with tumor aggressiveness and poor outcome (50, 51). In this way, Fn14 expression may help classifying glioma histological subtype (52). Moreover, canonical NF-κB pathway, stimulated by TWEAK, promotes Rac1 and Cdc42 expression, key mediators in the regulation of glioblastoma cell migration and invasion (51, 53, 54). Interestingly, Cherry et al. showed that MMP-9 inhibition abolished TWEAK-induced glioma invasion (55).

Targeting Fn14 Is Promising for Treating Glioblastoma

Therapeutic strategies targeting Fn14 in malignant cells have been evaluated. In these preclinical studies, manipulating Fn14 expression levels or suppressing TWEAK-Fn14-NFκB-dependent signaling decreased glioblastoma cell invasion capacity (56, 57). However, further experiments are needed to evaluate whether these strategies can significantly impact patients' survival.

THE TWEAK/Fn14 PATHWAY IS INVOLVED IN NI-ASSOCIATED NEURODEGENERATION IN ALS

Amyotrophic lateral sclerosis is a fatal neurodegenerative disease affecting motor neurons in the brain and spinal cord, and associated with NI hallmark (astrogliosis and microgliosis) and skeletal muscle atrophy. Mutations within the superoxide dismutase 1 (SOD1) are sometimes found in familial or sporadic cases. Mutant SOD1 expression was associated with inflammatory astrocytes and microglia and with skeletal muscle atrophy (58).

TWEAK/CD163 Interaction Induces Motor Neuron Death in a Mouse Model of ALS

Bowerman et al. used a model of transgenic mice overexpressing human mutant SOD1 and recapitulating the main traits of ALS to study TWEAK/Fn14 involvement in ALS (15). In this model, mTWEAK was upregulated in the spinal cord and it

induced astrocyte proliferation and IL-6 release. TWEAK and Fn14 were also found in skeletal muscle with different patterns of expression linked to disease development. In this study, the authors demonstrated a TWEAK induced-motor neuron death (15). Surprisingly, it was mediated by TWEAK interaction with CD163, a putative alternative TWEAK receptor. This neuronal death involved caspase-3 activation and was totally independent of Fn14. This work is the first implicating CD163 in mediating TWEAK effects in an inflammatory neurological disease. CD163 is a member of the scavenger receptors and is exclusively expressed by monocytes and macrophages. Increasing *in vivo* and *in vitro* evidences suggest that the interaction between TWEAK and CD163 may affect the development of atherosclerosis and related diseases (59).

TWEAK Promotes Astrogliosis and Microgliosis in ALS

Tumor necrosis factor-like weak inducer of apoptosis deletion reduced astrogliosis and microgliosis in the spinal cord, which substantiated the implication of the TWEAK pathway in ALS. However, muscle pathology was only partially reduced and TWEAK deletion did not prevent motor deterioration nor increase life span. In the same way, anti-TWEAK antibodies injected in ALS mice decreased microgliosis without improving motor functions. Bowerman et al. thus proposed a model combining the action of peripheral and central TWEAK, which could both contribute to the sustained activation of microglia in ALS (15).

This work suggests that blocking TWEAK in ALS is interesting but not sufficient and requires being included in a combinatory therapeutic approach.

TWEAK CONTRIBUTION TO PARKINSON'S DISEASE AND PSYCHIATRIC DISEASES NEEDS CONFIRMATION

Anti-TWEAK Antibodies Improve a Murine Model of Parkinson's Disease

Parkinson's disease is a neurodegenerative pathology characterized by movement impairment due to dopaminergic loss in the nigrostriatal pathway. It may also have a neuroinflammatory component, where NF-κB may play a dual role, both promoting and protecting against neurodegeneration (60). The role of TWEAK itself has been studied in the 1-methyl-4-phenyl-1,2,3,6-tetrahydropyridine (MPTP) murine model and in Parkinson's disease human brain samples (61). There was no difference in substantia nigra TWEAK concentration between MPTP mice, Parkinson's disease patients, and controls. While TWEAK or Fn14-KO failed to prevent MPTP toxicity, anti-TWEAK antibodies treatment attenuated the MPTP-induced death of dopaminergic neurons (61). These apparently conflicting results could be explained in part by existing compensatory systems, including the TNF-α pathway, since TNF is expressed in microglia of Parkinson's disease patients.

TWEAK Plasma Levels in Schizophrenia and Bipolar Disorders Are Not Conclusive

Neuroinflammation is highly suspected to be involved in psychiatric pathologies like schizophrenia or bipolar disorder. Recently, TWEAK plasma levels of patients suffering from schizophrenia were compared with controls. Although no difference was shown globally, TWEAK levels in male patients were significantly lower than in male controls, suggesting TWEAK involvement in subgroups of schizophrenia patients (62). In bipolar disorder, conflicting results were observed, perhaps due to the heterogeneity in patients' groups: Cingi et al. measured lower TWEAK plasma levels compared to healthy controls (63), while Barbosa et al. described increased concentrations, regardless of the mood (64). Nevertheless, as the interest for studying TWEAK/Fn14 pathway in psychiatric diseases is very recent, further studies will certainly be available soon.

This mini-review reveals that the TWEAK/Fn14 pathway modulates NI in neurodegenerative, immune, ischemic, and malignant CNS inflammatory diseases. In fact, as supported by both animal and human *in vitro* and *in vivo* studies, TWEAK/Fn14 can modulate NI by activating canonical and non-canonical NF-κB pathways but also MAPK signaling. Then, expression or release of inflammatory cytokines, chemokines, and adhesion molecules are upregulated and astrogliosis and microgliosis occur. Additionally, MMP-9 secretion is stimulated and reinforces BBB disruption and tissue remodeling. Note that monoclonal anti-TWEAK antibodies have been injected in patients in phase I clinical studies. In healthy volunteers or patients with solid tumors or rheumatoid arthritis, they (i) displayed a classical therapeutic antibody pharmacokinetic pattern, (ii) were associated with a favorable safety profile, and (iii) induced a decrease in circulating TWEAK serum level (65–68). Additionally, in these studies, TWEAK/Fn14 pathway inhibition yielded encouraging results, such as reduced clinical and biological inflammatory markers, including sTWEAK. All these data support the concept that the TWEAK/Fn14 axis represents a promising therapeutic target for modulating inflammation, including NI.

AUTHOR CONTRIBUTIONS

AB and SD-J both collected the publications and wrote the manuscript.

ACKNOWLEDGMENTS

We thank Nicolas Simon for reading and critical review of this paper, and Isabelle Virard for proofreading it.

FUNDING

This work was supported by Aix-Marseille University, CNRS, and AP-HM.

REFERENCES

1. Masgrau R, Guaza C, Ransohoff RM, Galea E. Should we stop saying 'glia' and 'neuroinflammation'? *Trends Mol Med* (2017) 23(6):486–500. doi:10.1016/j.molmed.2017.04.005
2. Schwartz M, Deczkowska A. Neurological disease as a failure of brain-immune crosstalk: the multiple faces of neuroinflammation. *Trends Immunol* (2016) 37(10):668–79. doi:10.1016/j.it.2016.08.001
3. Kempuraj D, Thangavel R, Selvakumar G, Zaheer S, Ahmed M, Raikwar P, et al. Brain and peripheral atypical inflammatory mediators potentiate neuroinflammation and neurodegeneration. *Front Cell Neurosci* (2017) 11:216. doi:10.3389/fncel.2017.00216
4. Lyman M, Lloyd DG, Ji X, Vizcaychipi MP, Ma D. Neuroinflammation: the role and consequences. *Neurosci Res* (2014) 79:1–12. doi:10.1016/j.neures.2013.10.004
5. Kielian T. Multifaceted roles of neuroinflammation: the need to consider both sides of the coin. *J Neurochem* (2016) 136(Suppl 1):5–9. doi:10.1111/jnc.13530
6. Wohleb ES, Godbout JP. Basic aspects of the immunology of neuroinflammation. *Mod Trends Pharmacopsychiatry* (2013) 28:1–19. doi:10.1159/000343964
7. Yepes M. TWEAK and Fn14 in the neurovascular unit. *Front Immunol* (2013) 4:367. doi:10.3389/fimmu.2013.00367
8. Pekny M, Wilhelmsson U, Pekna M. The dual role of astrocyte activation and reactive gliosis. *Neurosci Lett* (2014) 565:30–8. doi:10.1016/j.neulet.2013.12.071
9. Lopes Pinheiro MA, Kooij G, Mizee MR, Kamermans A, Enzmann G, Lyck R, et al. Immune cell trafficking across the barriers of the central nervous system in multiple sclerosis and stroke. *Biochim Biophys Acta* (2016) 1862(3):461–71. doi:10.1016/j.bbadis.2015.10.018
10. Rustenhoven J, Jansson D, Smyth LC, Dragunow M. Brain pericytes as mediators of neuroinflammation. *Trends Pharmacol Sci* (2017) 38(3):291–304. doi:10.1016/j.tips.2016.12.001
11. Becher B, Spath S, Goverman J. Cytokine networks in neuroinflammation. *Nat Rev Immunol* (2017) 17(1):49–59. doi:10.1038/nri.2016.123
12. Burkly LC, Michaelson JS, Hahm K, Jakubowski A, Zheng TS. TWEAKing tissue remodeling by a multifunctional cytokine: role of TWEAK/Fn14 pathway in health and disease. *Cytokine* (2007) 40(1):1–16. doi:10.1016/j.cyto.2007.09.007
13. Echeverry R, Wu F, Haile WB, Wu J, Yepes M. The cytokine tumor necrosis factor-like weak inducer of apoptosis and its receptor fibroblast growth factor-inducible 14 have a neuroprotective effect in the central nervous system. *J Neuroinflammation* (2012) 9:45. doi:10.1186/1742-2094-9-45
14. Burkly LC. TWEAK/Fn14 axis: the current paradigm of tissue injury-inducible function in the midst of complexities. *Semin Immunol* (2014) 26(3):229–36. doi:10.1016/j.smim.2014.02.006
15. Bowerman M, Salsac C, Coque E, Eiselt É, Deschaumes RG, Brodovitch A, et al. Tweak regulates astrogliosis, microgliosis and skeletal muscle atrophy in a mouse model of amyotrophic lateral sclerosis. *Hum Mol Genet* (2015) 24(12):3440–56. doi:10.1093/hmg/ddv094
16. Chicheportiche Y, Bourdon PR, Xu H, Hsu YM, Scott H, Hession C, et al. TWEAK, a new secreted ligand in the tumor necrosis factor family that weakly induces apoptosis. *J Biol Chem* (1997) 272(51):32401–10. doi:10.1074/jbc.272.51.32401
17. Nakayama M, Kayagaki N, Yamaguchi N, Okumura K, Yagita H. Involvement of TWEAK in interferon gamma-stimulated monocyte cytotoxicity. *J Exp Med* (2000) 192(9):1373–80. doi:10.1084/jem.192.9.1373
18. Desplat-Jégo S, Feuillet L, Creidy R, Malikova I, Rance R, Khrestchatisky M, et al. TWEAK is expressed at the cell surface of monocytes during multiple sclerosis. *J Leukoc Biol* (2009) 85(1):132–5. doi:10.1189/jlb.0608347
19. Maecker H, Varfolomeev E, Kischkel F, Lawrence D, LeBlanc H, Lee W, et al. TWEAK attenuates the transition from innate to adaptive immunity. *Cell* (2005) 123(5):931–44. doi:10.1016/j.cell.2005.09.022
20. Wicovsky A, Salzmann S, Roos C, Ehrenschwender M, Rosenthal T, Siegmund D, et al. TNF-like weak inducer of apoptosis inhibits proinflammatory TNF receptor-1 signaling. *Cell Death Differ* (2009) 16(11):1445–59. doi:10.1038/cdd.2009.80
21. Bhattacharjee M, Raju R, Radhakrishnan A, Nanjappa V, Muthusamy B, Singh K, et al. A bioinformatics resource for TWEAK-Fn14 signaling pathway. *J Signal Transduct* (2012) 2012:376470. doi:10.1155/2012/376470
22. Burkly LC. Regulation of tissue responses: the TWEAK/Fn14 pathway and other TNF/TNFR superfamily members that activate non-canonical NFκB signaling. *Front Immunol* (2015) 6:92. doi:10.3389/fimmu.2015.00092
23. Roos C, Wicovsky A, Müller N, Salzmann S, Rosenthal T, Kalthoff H, et al. Soluble and transmembrane TNF-like weak inducer of apoptosis differentially activate the classical and noncanonical NF-kappa B pathway. *J Immunol* (2010) 185(3):1593–605. doi:10.4049/jimmunol.0903555
24. Desplat-Jégo S, Varriale S, Creidy R, Terra R, Bernard D, Khrestchatisky M, et al. TWEAK is expressed by glial cells, induces astrocyte proliferation and increases EAE severity. *J Neuroimmunol* (2002) 133(1–2):116–23. doi:10.1016/S0165-5728(02)00368-5
25. Saas P, Boucraut J, Walker PR, Quiquerez AL, Billot M, Desplat-Jego S, et al. TWEAK stimulation of astrocytes and the proinflammatory consequences. *Glia* (2000) 32(1):102–7. doi:10.1002/1098-1136(200010)32:1<102::AID-GLIA100>3.0.CO;2-U
26. Rousselet E, Traver S, Monnet Y, Perrin A, Mandjee N, Hild A, et al. Tumor necrosis factor-like weak inducer of apoptosis induces astrocyte proliferation through the activation of transforming-growth factor-α/epidermal growth factor receptor signaling pathway. *Mol Pharmacol* (2012) 82(5):948–57. doi:10.1124/mol.112.079608
27. Stephan D, Sbai O, Wen J, Couraud PO, Putterman C, Khrestchatisky M, et al. TWEAK/Fn14 pathway modulates properties of a human microvascular endothelial cell model of blood brain barrier. *J Neuroinflammation* (2013) 10:9. doi:10.1186/1742-2094-10-9
28. Nazeri A, Heydarpour P, Sadaghiani S, Sahraian MA, Burkly LC, Bar-Or A. A further TWEAK to multiple sclerosis pathophysiology. *Mol Neurobiol* (2014) 49(1):78–87. doi:10.1007/s12035-013-8490-y
29. Serafini B, Magliozzi R, Rosicarelli B, Reynolds R, Zheng TS, Aloisi F. Expression of TWEAK and its receptor Fn14 in the multiple sclerosis brain: implications for inflammatory tissue injury. *J Neuropathol Exp Neurol* (2008) 67(12):1137–48. doi:10.1097/NEN.0b013e31818dab90
30. Iocca HA, Plant SR, Wang Y, Runkel L, O'Connor BP, Lundsmith ET, et al. TNF superfamily member TWEAK exacerbates inflammation and demyelination in the cuprizone-induced model. *J Neuroimmunol* (2008) 194(1–2):97–106. doi:10.1016/j.jneuroim.2007.12.003
31. Desplat-Jégo S, Creidy R, Varriale S, Allaire N, Luo Y, Bernard D, et al. Anti-TWEAK monoclonal antibodies reduce immune cell infiltration in the central nervous system and severity of experimental autoimmune encephalomyelitis. *Clin Immunol* (2005) 117(1):15–23. doi:10.1016/j.clim.2005.06.005
32. Razmara M, Hilliard B, Ziarani AK, Murali R, Yellayi S, Ghazanfar M, et al. Fn14-TRAIL, a chimeric intercellular signal exchanger, attenuates experimental autoimmune encephalomyelitis. *Am J Pathol* (2009) 174(2):460–74. doi:10.2353/ajpath.2009.080462
33. Prinz-Hadad H, Mizrachi T, Irony-Tur-Sinai M, Prigozhina TB, Aronin A, Brenner T, et al. Amelioration of autoimmune neuroinflammation by the fusion molecule Fn14·TRAIL. *J Neuroinflammation* (2013) 10:36. doi:10.1186/1742-2094-10-36
34. Mueller AM, Pedré X, Kleiter I, Hornberg M, Steinbrecher A, Giegerich G. Targeting fibroblast growth factor-inducible-14 signaling protects from chronic relapsing experimental autoimmune encephalomyelitis. *J Neuroimmunol* (2005) 159(1–2):55–65. doi:10.1016/j.jneuroim.2004.10.001
35. Van Oosten BW, Barkhof F, Truyen L, Boringa JB, Bertelsmann FW, von Blomberg BM, et al. Increased MRI activity and immune activation in two multiple sclerosis patients treated with the monoclonal anti-tumor necrosis factor antibody cA2. *Neurology* (1996) 47(6):1531–4. doi:10.1212/WNL.47.6.1531
36. Chen J, Wei L, Xia Y. Roles of tumour necrosis factor-related weak inducer of apoptosis/fibroblast growth factor-inducible 14 pathway in lupus nephritis. *Nephrology (Carlton)* (2017) 22(2):101–6. doi:10.1111/nep.12957
37. Wen J, Xia Y, Stock A, Michaelson JS, Burkly LC, Gulinello M, et al. Neuropsychiatric disease in murine lupus is dependent on the TWEAK/Fn14 pathway. *J Autoimmun* (2013) 43:44–54. doi:10.1016/j.jaut.2013.03.002
38. Stock AD, Wen J, Putterman C. Neuropsychiatric lupus, the blood brain barrier, and the TWEAK/Fn14 pathway. *Front Immunol* (2013) 4:484. doi:10.3389/fimmu.2013.00484
39. Wen J, Chen CH, Stock A, Doerner J, Gulinello M, Putterman C. Intracerebroventricular administration of TNF-like weak inducer of apoptosis induces depression-like behavior and cognitive dysfunction in

non-autoimmune mice. *Brain Behav Immun* (2016) 54:27–37. doi:10.1016/j.bbi.2015.12.017
40. Wen J, Doerner J, Weidenheim K, Xia Y, Stock A, Michaelson JS, et al. TNF-like weak inducer of apoptosis promotes blood brain barrier disruption and increases neuronal cell death in MRL/lpr mice. *J Autoimmun* (2015) 60:40–50. doi:10.1016/j.jaut.2015.03.005
41. Trysberg E, Blennow K, Zachrisson O, Tarkowski A. Intrathecal levels of matrix metalloproteinases in systemic lupus erythematosus with central nervous system engagement. *Arthritis Res Ther* (2004) 6(6):R551–6. doi:10.1186/ar1228
42. Trysberg EBL, Su L, Michaelson J, Putterman C. Cerebrospinal fluid (CSF) TWEAK: a novel biomarker for neuropsychiatric SLE? *Arthritis Rheum* (2007) 56:S750.
43. Fragoso-Loyo H, Atisha-Fregoso Y, Nuñez-Alvarez CA, Llorente L. Utility of TWEAK to assess neuropsychiatric disease activity in systemic lupus erythematosus. *Lupus* (2016) 25(4):364–9. doi:10.1177/0961203315610206
44. Potrovita I, Zhang W, Burkly L, Hahm K, Lincecum J, Wang MZ, et al. Tumor necrosis factor-like weak inducer of apoptosis-induced neurodegeneration. *J Neurosci* (2004) 24(38):8237–44. doi:10.1523/JNeurosc.1089-04.2004
45. Polavarapu R, Gongora MC, Winkles JA, Yepes M. Tumor necrosis factor-like weak inducer of apoptosis increases the permeability of the neurovascular unit through nuclear factor-kappa B pathway activation. *J Neurosci* (2005) 25(44):10094–100. doi:10.1523/JNEUROSCI.3382-05.2005
46. Zhang X, Winkles JA, Gongora MC, Polavarapu R, Michaelson JS, Hahm K, et al. TWEAK-Fn14 pathway inhibition protects the integrity of the neurovascular unit during cerebral ischemia. *J Cereb Blood Flow Metab* (2007) 27(3):534–44. doi:10.1038/sj.jcbfm.9600368
47. Haile WB, Echeverry R, Wu J, Yepes M. The interaction between tumor necrosis factor-like weak inducer of apoptosis and its receptor fibroblast growth factor-inducible 14 promotes the recruitment of neutrophils into the ischemic brain. *J Cereb Blood Flow Metab* (2010) 30(6):1147–56. doi:10.1038/jcbfm.2009.280
48. Yepes M, Brown S, Moore E, Smith E, Lawrence D, Winkles J. A soluble Fn14-Fc decoy receptor reduces infarct volume in a murine model of cerebral ischemia. *Am J Pathol* (2005) 166(2):511–20. doi:10.1016/S0002-9440(10)62273-0
49. Inta I, Frauenknecht K, Dörr H, Kohlhof P, Rabsilber T, Auffarth GU, et al. Induction of the cytokine TWEAK and its receptor Fn14 in ischemic stroke. *J Neurol Sci* (2008) 275(1–2):117–20. doi:10.1016/j.jns.2008.08.005
50. Tran NL, McDonough WS, Donohue PJ, Winkles JA, Berens TJ, Ross KR, et al. The human Fn14 receptor gene is up-regulated in migrating glioma cells in vitro and overexpressed in advanced glial tumors. *Am J Pathol* (2003) 162(4):1313–21. doi:10.1016/S0002-9440(10)63927-2
51. Tran NL, McDonough WS, Savitch BA, Fortin SP, Winkles JA, Symons M, et al. Increased fibroblast growth factor-inducible 14 expression levels promote glioma cell invasion via Rac1 and nuclear factor-kappaB and correlate with poor patient outcome. *Cancer Res* (2006) 66(19):9535–42. doi:10.1158/0008-5472.CAN-06-0418
52. Pelekanou V, Notas G, Kampa M, Tsentelierou E, Stathopoulos EN, Tsapis A, et al. BAFF, APRIL, TWEAK, BCMA, TACI and Fn14 proteins are related to human glioma tumor grade: immunohistochemistry and public microarray data meta-analysis. *PLoS One* (2013) 8(12):e83250. doi:10.1371/journal.pone.0083250
53. Fortin SP, Ennis MJ, Schumacher CA, Zylstra-Diegel CR, Williams BO, Ross JT, et al. Cdc42 and the guanine nucleotide exchange factors Ect2 and trio mediate Fn14-induced migration and invasion of glioblastoma cells. *Mol Cancer Res* (2012) 10(7):958–68. doi:10.1158/1541-7786.MCR-11-0616
54. Dhruv HD, Whitsett TG, Jameson NM, Patel F, Winkles JA, Berens ME, et al. Tumor necrosis factor-like weak inducer of apoptosis (TWEAK) promotes glioblastoma cell chemotaxis via Lyn activation. *Carcinogenesis* (2014) 35(1):218–26. doi:10.1093/carcin/bgt289
55. Cherry EM, Lee DW, Jung JU, Sitcheran R. Tumor necrosis factor-like weak inducer of apoptosis (TWEAK) promotes glioma cell invasion through induction of NF-κB-inducing kinase (NIK) and noncanonical NF-κB signaling. *Mol Cancer* (2015) 14:9. doi:10.1186/s12943-014-0273-1
56. Perez JG, Tran NL, Rosenblum MG, Schneider CS, Connolly NP, Kim AJ, et al. The TWEAK receptor Fn14 is a potential cell surface portal for targeted delivery of glioblastoma therapeutics. *Oncogene* (2016) 35(17):2145–55. doi:10.1038/onc.2015.310
57. Roos A, Dhruv HD, Mathews IT, Inge LJ, Tuncali S, Hartman LK, et al. Identification of aurintricarboxylic acid as a selective inhibitor of the TWEAK-Fn14 signaling pathway in glioblastoma cells. *Oncotarget* (2017) 8(7):12234–46. doi:10.18632/oncotarget.14685
58. Glass CK, Saijo K, Winner B, Marchetto MC, Gage FH. Mechanisms underlying inflammation in neurodegeneration. *Cell* (2010) 140(6):918–34. doi:10.1016/j.cell.2010.02.016
59. Liu H, Lin D, Xiang H, Chen W, Zhao S, Peng H, et al. The role of tumor necrosis factor-like weak inducer of apoptosis in atherosclerosis via its two different receptors. *Exp Ther Med* (2017) 14(2):891–7. doi:10.3892/etm.2017.4600
60. Baiguera C, Alghisi M, Pinna A, Bellucci A, De Luca MA, Frau L, et al. Late-onset parkinsonism in NFκB/c-Rel-deficient mice. *Brain* (2012) 135(Pt 9):2750–65. doi:10.1093/brain/aws193
61. Mustafa S, Martin HL, Burkly L, Costa A, Martins ML, Schwaninger M, et al. The role of TWEAK/Fn14 signaling in the MPTP-model of Parkinson's disease. *Neuroscience* (2016) 319:116–22. doi:10.1016/j.neuroscience.2016.01.034
62. Tatlıdil Yaylacı E, Yüksel RN, Ünal K, Altunsoy N, Cingi M, Yalçın Şahiner Ş, et al. TNF-related weak inducer of apoptosis (TWEAK) levels in schizophrenia. *Psychiatry Res* (2015) 229(3):755–9. doi:10.1016/j.psychres.2015.08.006
63. Cingi Yirün M, Yirün O, Ünal K, Yüksel RN, Altunsoy N, Tatlidil Yaylaci E, et al. Serum TNF-related weak inducer of apoptosis (TWEAK) and TNF-related apoptosis-inducing ligand (TRAIL) levels of patients with bipolar disorder in manic episode, in remission and healthy controls. *Psychiatry Res* (2017) 257:338–45. doi:10.1016/j.psychres.2017.07.067
64. Barbosa IG, Vaz GN, Rocha NP, Machado-Vieira R, Ventura MRD, Huguet RB, et al. Plasma levels of tumor necrosis factor superfamily molecules are increased in bipolar disorder. *Clin Psychopharmacol Neurosci* (2017) 15(3):269–75. doi:10.9758/cpn.2017.15.3.269
65. Cheng E, Armstrong CL, Galisteo R, Winkles JA. TWEAK/Fn14 axis-targeted therapeutics: moving basic science discoveries to the clinic. *Front Immunol* (2013) 4:473. doi:10.3389/fimmu.2013.00473
66. Wisniacki N, Amaravadi L, Galluppi GR, Zheng TS, Zhang R, Kong J, et al. Safety, tolerability, pharmacokinetics, and pharmacodynamics of anti-TWEAK monoclonal antibody in patients with rheumatoid arthritis. *Clin Ther* (2013) 35(8):1137–49. doi:10.1016/j.clinthera.2013.06.008
67. Galluppi GR, Wisniacki N, Stebbins C. Population pharmacokinetic and pharmacodynamic analysis of BIIB023, an anti-TNF-like weak inducer of apoptosis (anti-TWEAK) monoclonal antibody. *Br J Clin Pharmacol* (2016) 82(1):118–28. doi:10.1111/bcp.12914
68. Lassen UN, Meulendijks D, Siu LL, Karanikas V, Mau-Sorensen M, Schellens JH, et al. A phase I monotherapy study of RG7212, a first-in-class monoclonal antibody targeting TWEAK signaling in patients with advanced cancers. *Clin Cancer Res* (2015) 21(2):258–66. doi:10.1158/1078-0432.CCR-14-1334

Conflict of Interest Statement: The authors declare that the research was conducted in the absence of any commercial or financial relationship that could be construed as a potential conflict of interest.

Copyright © 2017 Boulamery and Desplat-Jégo. This is an open-access article distributed under the terms of the Creative Commons Attribution License (CC BY). The use, distribution or reproduction in other forums is permitted, provided the original author(s) or licensor are credited and that the original publication in this journal is cited, in accordance with accepted academic practice. No use, distribution or reproduction is permitted which does not comply with these terms.

frontiers in Immunology

ORIGINAL RESEARCH
published: 04 December 2017
doi: 10.3389/fimmu.2017.01681

Inflammatory Processes Associated with Canine Intervertebral Disc Herniation

Marie Monchaux[1], Simone Forterre[1], David Spreng[1,2], Agnieszka Karol[3], Franck Forterre[1,2†] and Karin Wuertz-Kozak[2,4,5,6,7†]*

[1] Vetsuisse Faculty, Department of Clinical Veterinary Science, University of Bern, Bern, Switzerland, [2] Competence Center of Applied Biotechnology and Molecular Medicine (CABMM), University of Zurich, Zurich, Switzerland, [3] Vetsuisse Faculty, Institute of Veterinary Pathology, University of Zurich, Zurich, Switzerland, [4] Department of Health Sciences and Technology, Institute for Biomechanics, ETH Zurich, Zurich, Switzerland, [5] Schön Clinic Munich, Harlaching, Munich, Germany, [6] Spine Research Institute, Paracelsus Medical University, Salzburg, Austria, [7] Department of Health Sciences, University of Postdam, Postdam, Germany

Intervertebral disc herniation (IVDH) is an important pathology in humans and also in dogs. While the molecular disease mechanisms are well investigated in humans, little is known about the inflammatory mediators in naturally occurring canine IVDH. The objective of this study was to investigate whether the involved proinflammatory cytokines in human IVDH are also key cytokines in canine IVDH and thus to elucidate the suitability of the dog as a model for human trials. 59 samples from 25 dogs with surgically confirmed thoracolumbar IVDH were collected and classified in three subgroups: herniated (H), affected non-herniated (NH) disc, and adjacent non-affected (NA) disc. Discs from 11 healthy dogs acted as controls (C). Samples were analyzed for IL-1, IL-6, IL-8, and TNF-α expression (qPCR/ELISA) as well as cell infiltration and activation of the MAP kinase pathways (immunohistochemistry). Gene and protein expression of all key cytokines could be detected in IVDH affected dogs. Canine IVDH was significantly associated with a higher gene expression of IL-6 (H > C, NH > C) and TNF-α (H > C, NH > C, NA > C) and a significant down-regulation of IL-1β (H < C). Dogs with spontaneous pain had significantly higher IL-6 mRNA compared to those with pain arising only upon palpation. An inter-donor comparison (H and HN relative to NA) revealed a significant increase of IL-6 gene expression (H > NA, NH > NA). IL-8 (H > C, NA > C) and TNF-α (NH > C) protein levels were significantly increased in diseased dogs while inversely, IL-6 protein levels were significantly higher in patients with better clinical outcome. Aside from resident IVD cells, mostly monocytes and macrophages were found in extruded material, with concomitant activation of extracellular signal-regulated kinase p38 in the majority of samples. Dogs with spontaneous IVDH might provide a useful model for human disc diseases. Although the expression of key cytokines found in human IVDH was also demonstrated in canine tissue, the inflammatory mechanisms accompanying canine IVDH diverges partially from humans, which will require further investigations in the future. In dogs, IL-6 seems to play an important pathological role and may represent a new potential therapeutic target for canine patients.

Keywords: intervertebral disc herniation, inflammatory mediators, IL-1β, IL-6, IL-8, TNF-α, MAP kinase pathway, canine animal model

OPEN ACCESS

Edited by:
Jixin Zhong,
Case Western Reserve University,
United States

Reviewed by:
Vineesh Vimala Raveendran,
King Faisal Specialist Hospital & Research Centre, Saudi Arabia
Oreste Gualillo,
Servicio Gallego de Salud, Spain

***Correspondence:**
Karin Wuertz-Kozak
kwuertz@ethz.ch

†These authors have shared senior authorship.

Specialty section:
This article was submitted to Inflammation, a section of the journal Frontiers in Immunology

Received: *03 August 2017*
Accepted: *15 November 2017*
Published: *04 December 2017*

Citation:
Monchaux M, Forterre S, Spreng D, Karol A, Forterre F and Wuertz-Kozak K (2017) Inflammatory Processes Associated with Canine Intervertebral Disc Herniation. Front. Immunol. 8:1681. doi: 10.3389/fimmu.2017.01681

INTRODUCTION

Intervertebral disc degeneration (IVDD) and intervertebral disc herniation (IVDH) are considered a major cause of acute and chronic low back pain, resulting in a tremendous economic burden worldwide (1–4). IVDD is characterized by progressive structural and functional changes, including a loss of hydrostatic properties of the normally highly hydrated nucleus pulposus (NP) (5), as well as increased vascular and neuronal ingrowth that is associated with chronic back pain (6). Recent human studies have identified proinflammatory cytokines, specifically IL-1β, IL-6, IL-8, and TNF-α, as pivotal contributors in the course of the pathophysiologic inflammatory cascade of intervertebral disc diseases and the development of neuropathic pain through irritation of ingrowing nerves (7–28). A herniated disc, presented as protrusion, extrusion, or sequestration, is a localized displacement of disc tissue in the epidural space (29), resulting in mechanical compression and chemical irritation of spinal nerves, which contribute to ischemia, radicular symptoms, and stimulation of the inflammatory cascade (30–39). Alongside of heredity (40, 41), multiple factors such as age and smoking are involved in the ethiopathogenesis of human IVDD and IVDH as well as in the initiation of an inflammatory cascade (42–45). Furthermore, obesity was highlighted as an important contributor to disc pathologies as it not only increases the load on the IVD (46–48), but also promotes inflammation *via* cytokine-release from adipocytes and recruited macrophages (49).

Measuring cytokine levels within the diseased tissue can provide a better understanding of the pathological process. As human tissue samples for research—especially as healthy controls—are scarce, more complex pathological investigations and testing of new therapeutic approaches often require animal experiments (50). Currently established models are predominantly based on artificially induced disc pathology through mostly invasive manipulations (e.g., stab incision in rodents), which lack similarities to the human pathology (51). In contrast, animal models based on spontaneously occurring disc pathologies, such as canine IVDH, share important similarities to the clinical presentation, pathology, lesion morphology, diagnostic, treatment, and recovery with human IVDH (50, 52, 53). IVDH in dogs has an incidence of 2% of all admissions in referral clinics and occurs predominantly in chondrodystrophic breeds, such as Beagle, Dachshund, Shi-Tzu, and French Bulldog (54–59). Similar to humans, the prevalence of overweight and obesity in dogs is increasing, being as high as 34% in the US and 25% in the UK (60, 61), with a higher risk factor for disc extrusion in dogs with higher body score index (62). Despite the potential relevance of canine IVDH as a human disease model, little in depth research has been conducted to determine its pathological processes in dogs, specifically regarding the role of inflammatory mediators in disease progression and pain development. Thus far, existing data indicate that in the early phase of canine IVDH, mRNA concentration of IL-6, a possible promoter of inflammation and apoptosis of resident glial cells, was significantly upregulated, whereas returning to baseline values in later stages of the disease. In comparison, mRNA concentration of IL-8, a potent chemokine and early mediator of inflammation, was strongly upregulated in the acute and subacute onset of IVDH. A trend of higher TNF-α mRNA concentration in acute IVDH could also be shown (63). Controversially, Karli et al. demonstrated a downregulation of IL-1β, IL-6, and TNF-α mRNA concentrations over the whole course of canine IVDH, but highlighted an upregulation of IL-8 mRNA concentration in the acute stage of the disease, which decreased when treated with non-steroidal anti-inflammatory drugs (64).

Based on the conflicting data found in the current literature, the aim of this study was to identify whether the human key cytokines are expressed in canine IVDs and to determine pathological alterations in their expression by comparing normal IVDs to diseased IVDs with IVDH, with the overall goal to provide further information on the validity of the canine disc disease model. Concomitantly, we also assessed neurologic function, pain status, and clinical outcome in affected dogs.

MATERIALS AND METHODS

Patients, Controls, and Tissue Samples

Canine disc material was collected from dogs with confirmed thoracolumbar IVDH during decompressive surgical procedures at our referral institution (November 2013 to February 2015). All samples were collected from actual referred patients and not from laboratory animals. Herniated (H) and non-herniated (NH) IVD samples were both collected from the IVDH: affected level, with H = prolapsed part and NH = contained part. Non-affected (NA) IVDs were collected from an adjacent spinal level (prophylactic disc fenestration). Inclusion criteria for IVDH patients: well-documented records of onset of clinical signs and pretreatment, neurologic findings, diagnosis, course of the disease, ethical approval, and signed owner consent.

In addition, healthy control IVDs (C) were collected from dogs included in an unrelated animal study or patients without any history or signs of spinal disease and without any anti-inflammatory pretreatment euthanized for other health reasons. These samples were directly surgically collected after euthanasia within 15 min to avoid potential artifacts in measurements of the cytokines (65–67).

In the patient group, breed, age, gender, duration of neurologic signs, pretreatment, neurologic grade, severity of pain, localization of IVD extrusion, and outcome were recorded. Duration of neurologic signs were defined as the time between the onset of clinical signs and surgery and was grouped as follows: decompression within the first 24 h after onset of clinical signs (acute), between 24 h and 7 days of onset (subacute), or after more than 7 days (chronic) (68, 69). A complete neurological examination was performed at the time of admission, maximally 12 h before surgery, at the time at discharge, and at a follow up examination between 2 and 4 weeks after discharge. The neurologic condition and pain were graded as shown in **Table 1** (64, 70, 71).

Diagnostic Imaging and Surgical Treatment

Anesthesia and analgesia were conducted under a standard clinical protocol for each patient (44). Magnetic resonance imaging (MRI) of the thoracolumbar spine was performed (Philips

TABLE 1 | Clinical scoring system.

Grade	Neurological condition	Pain
Zero		Neither spontaneous pain (vocalization, reluctance to move) nor pain on palpation of the spine
One	Spinal hyperesthesia only	No spontaneous pain, but discomfort (licking, withdrawal) on palpation of the spine
Two	Ambulatory paraparesis	Spontaneous pain and excessive pain (vocalization, aggressive behavior) on palpation of the spine
Three	Non-ambulatory paraparesis	
Four	Paraplegia with intact nociception	
Five	Paraplegia without nociception	

Panorama HFO, 1.0-T open system, Philips Medical Systems Nederland B.V., The Netherlands) to define the IVD extrusion site. Immediately after MRI, patients underwent surgery for discogenic back pain and to decompress the spinal cord. A standard hemilaminectomy at the site of extrusion, fenestration of the affected and one of the adjacent discs (cranial or caudal) were performed, allowing to take three samples of disc material (H, NH, and NA). For cytokine identification, removed disc material was collected under sterile conditions, snap frozen directly within 15 s in liquid nitrogen and stored at −80°C until sample preparation. For immunohistochemical and histological analysis, the tissue was fixed in 10% buffered formalin (1–5 days), embedded in paraffin, and cut into 5 µm sections.

Real-time PCR (RT-PCR)

For RNA isolation, each frozen disc sample was transferred into a precooled custom-made mortar, filled with liquid nitrogen and manually grinded under RNAse free conditions. The frozen tissue powder was transferred into 500 µl Trizol (Life Technologies, Van Alben Way, CA, USA), homogenized three times for 30 s (Polytron PT 2500 E, Kinematica, Luzern, Switzerland), incubated for 5 min at RT and centrifuged at 12,000 *g* for 10 min at 4°C.

The supernatant was mixed with 250 µl chloroform, vortexed for 30 s, incubated at RT for 15 min, centrifuged at 12,000 *g* for 15 min at 4°C and the aqueous phase recovered. RNA was precipitated by adding 125 µl isopropanol and 125 µl of high salt precipitation solution (0.8 M sodium citrate, 1.2 M sodium chloride), washed with 500 µl of 75% ethanol and dissolved in 25 µl RNase free water after complete removal of ethanol. The quantity of the isolated RNA was determined spectroscopically (NanoDrop® Lite, Thermo Fisher Scientific, Wilmington, DE, USA) and the quality confirmed by the sample's OD 260/280 (1.8–2.0; samples with lower quality were excluded from further analyses). cDNA was prepared using the TaqMan Reverse Transcription kit (TaqMan® Reverse Transcription Reagent, Life Technologies, Van Alben Way, CA, USA) according to the manufacturer's instruction. RT-qPCR was conducted on the CFX96 Touch qPCR Machine (Bio-Rad Laboratories, Hercules, CA, USA) as previously described (46, 47), by mixing 5 µl of TaqMan® Fast Advanced Master Mix (Life Technologies, Van Alben Way, CA, USA) with 10 ng cDNA in RNAse free water (4.5 µl in total) and 0.5 µl of canine TaqMan primers/probes (TaqMan® Gene Expression Assays, Life Technologies, Van Alben Way, CA, USA) (**Table 2**).

TABLE 2 | TaqMan primers/probes and sequence accession number.

Target gene	Assay number	Accession number
IL-1β	Cf02671951_g1	NM_001037971.1
IL-6	Cf02624282_m1	NM_001003301.1
IL-8	Cf02624283_m1	NM_001003200.1
TNF-α	Cf02624261_m1	NM_001003244.4
TATA box-binding protein (TBP)	Cf02637232_m1	XM_005627735.2

Each sample was run in duplicate for each gene, the CT value means were calculated and the comparative CT method was used for data evaluation [relative quantification (RQ)]. Samples with gene expression lower than the detection limit were attributed an artificial maximal CT value of 43, using the selection of the median as aggregation method between samples with the same experimental condition to avoid statistical and mathematical issues (72).

For group comparisons between H, NH, NA, and C, results were calculated as $2^{-\Delta CT}$ values, i.e., the expression of each target gene was normalized relative to the expression of the house keeping gene [canine TATA box-binding protein (TBP)], using the classical ΔCT method and the following algorithm:

$$RQ = 2^{-(Ct(H)_{TargetGene} - Ct(H)_{TBP})} \text{(identically for NH, NA, C).}$$

For interdonor calculations, an additional normalization step (ΔΔCT) was performed (ΔCT of H or NH minus ΔCT of NA, of the same animal). Results were calculated as $2^{-\Delta\Delta CT}$ values and shown as fold change in expression between affected discs (H, NH) and internal control discs (NA). The following algorithm was used:

$$RQ = 2^{-[(Ct(H)_{TargetGene} - Ct(H)_{TBP}) - (Ct(NA)_{TargetGene} - Ct(NA)_{TBP})]} \text{(identically for NH).}$$

The intra-assay CV was 0.74% ($n = 131$).

Total Protein and ELISA

ELISA samples were weighed and pulverized as described above, but with immersion in T-PER reagent (Tissue Protein Extraction Reagent, Thermo Fisher Scientific, Wilmington, DE, USA) at a ratio of 100 µl T-PER reagent per 10 mg tissue. The lysates were homogenized and purified following a standardized protocol. Briefly, samples were centrifuged at 12,000 *g* at 4°C for 10 min, the supernatant was collected and total protein was determined by the Bradford assay (Bio-Rad Protein Assay Dye Reagent Concentrate, Bio-Rad Laboratories, Hercules, CA, USA), with absorbance measurement at 585 nm (Infinite® 200 Pro, Tecan Group Ltd., Männedorf, Switzerland). The protein levels of IL-1β, IL-6, IL-8, and TNF-α were detected with canine specific ELISAs (MyBioSource, San Diego, CA, USA for IL-1β, IL-6, IL-8, and Quantikine ELISA Kit, R&D Systems Inc., Minneapolis, MN, USA, for TNF-α) according to the manufacturer's instructions, with a sensitivity of 1 pg/ml for IL-1β, IL-6, and IL-8 kit and

4.2 pg/ml for TNF-α. Sample concentration was calculated based on a standard curve and normalized to total protein content. Results are demonstrated either as group comparisons (H, NH, NA, C: cytokine content/total protein in pg/mg) or as interdonor comparisons (H and NH relative to NA: fold change). The median intra-assay CV is 9.0% (range 5.3–15%) and the median interassay CV 10.8% (range 9.3–15%), as provided by the supplier.

Immunohistochemistry

Serial sections were deparaffinized, heat-mediated antigen retrieval was conducted (95°C, 20 min) and sections were incubated with primary antibodies (RT, overnight) identifying infiltrating cells (polymorphonuclear, mononuclear, macrophages, multinucleated giant cells) and MAP kinase (MAPK) pathway activation (**Table 3**). Subsequently, sections were treated with an appropriate primary antibody (Marker) and washed 3× with Tris buffer before the secondary antimouse IgG was applied (1:200 dilution, 30 min). The amino-9-ethyl-carbazole substrate kit (Dako) was employed as a chromogen. Finally, the sections were counter-stained with Gill's hematoxylin for 3 min, and cover-slipped with an aqueous mounting media (Glicerine, Sigma-Aldrich).

All slides were examined and semiquantitatively evaluated independently by two investigators for infiltrating cell types in the extruded NP as well as activation of the MAPK pathway [c-Jun NH2-terminal kinase (JNK), p38 isoforms of MAPK (p-38), extracellular signal-regulated kinases (ERKs)]. The following grades were used: (−) negative; (±) weakly (less than 5% of cells positive); (+) moderately (5–25% of cells positive); (++) strongly (more than 25% of cells positive).

Statistical Analysis

For all results, an outlier calculation was performed and outliers removed before statistical analysis (MedCalc 16.8/2016, http://www.medcalc.org). Summary statistics were performed and normality assessed using D'Agostino-Pearson tests. As data were versatile regarding its distribution, nonparametric statistics were additionally used except for the interdonor comparison. A Kruskal–Wallis test was used to identify any association between gene and protein expression of cytokines with location of IVDH, duration of clinical signs, neurologic grade, pretreatment and outcome. Differences in gene or protein expression of cytokines between the samples of affected and control animals were evaluated using a Mann–Whitney *U*-test. The subgroup comparison was carried out stepwise by a Wilcoxon signed-rank test. The Bonferoni *p*-value adjustment was used to control for multiple comparisons. For inter-donor comparisons of gene and protein expression, an independent sample *t*-test and a Mann–Whitney *U*-test was performed, respectively. A Spearman's rank correlation was used to examine the relationship between gene expression and protein level. Threshold value for statistical significance was set up to $p < 0.05$ and data are presented as boxplots, with median and 95% confidential interval (CI) unless otherwise stated.

TABLE 3 | Detailed antibody information.

Marker	Provider	Order nr.	Dilution	Read-out
CD18	P. Moore	CA16.3C10	1:10	Cell infiltration
CD3	Dako	A0452	1:600	
vWF8	Dako	M0616	1:400	
p-JNK	Cell Signaling Technologies	PA5-21343	1:50	MAP kinase activation
p-p38	Cell Signaling Technologies	ab32142	1:50	
p-ERK1/2	Cell Signaling Technologies	MAI-13041	1:50	

RESULTS

Clinical Data

Twenty-five dogs with surgically confirmed thoracolumbar IVDH were included in the study. All canine patients (25 of 25 cases) were small and medium-breed dogs (<20 kg) with a median body weight at admission of 9.0 kg (range 3.6–19.0 kg). The dogs were classified as chondrodystrophic breeds with the Dachshund ($n = 5$), Cocker Spaniel, Coton de Tuléar and the French Bulldog (each $n = 2$) and the Bichon Frisé, Cavalier King Charles Spaniel, Jack Russel Terrier, Pekingese, Miniature Poodle, Pug Dog, Shi-Tzu, and the Yorkshire Terrier (each $n = 1$) or as non-chondrodystrophic or mixed breeds with the Border Collie ($n = 1$) and the Mixed Breed Dog ($n = 5$) (57, 73, 74). The median age was 5 years (range 3–13 years). Sixteen dogs were male intact, four were female intact, three were female spayed, and two were male castrated. The median duration of clinical signs until surgery was 3 days (range 1–365 days). When classified into three groups, there were 3 acute, 14 subacute, and 8 chronic cases. Ten dogs were referred without pretreatment, five had been pretreated with steroids, seven with NSAIDs, and three with a combination of both, pooled together as pretreated dogs. The neurologic status before surgery was Grade 2 in 11, Grade 3 in 6, Grade 4 in 5, and Grade 5 in 5 dogs. Pain score revealed 2 dogs with Grade 0, 14 dogs with Grade 1, and 9 animals with Grade 2. The spinal level of IVDH in the affected dogs were L2–L3 in eight dogs, Th12–Th13 in six dogs, Th11-Th12, L1–L2, L3–L4 in each three dogs, and Th10–Th11, Th13–L1 in each one dog. Fifteen dogs had a good outcome, six showed an improvement, but were not ambulatory, and four showed no improvement within 1 month after surgery. In the latter case, two of them were euthanized because of poor prognosis, a follow-up call unveiled that the other two dogs are still in physiotherapy treatment showing no improvement in the last 7 and 9 months.

Eleven euthanized dogs without signs of IVDH were included as control group. The median age of the control group was 4.5 years (2–11 years). Ten dogs were female spayed and one dog was female intact. There were 10 beagles and 1 was a mixed breed dog.

Diagnostic Imaging and Surgical Treatment

All 25 affected dogs underwent surgical decompression of the spinal cord immediately after diagnostic imaging, including the collection of the samples. Three different samples (H, NH, and NA) were collected in 14 dogs, two different samples (H,

NH) in 6 dogs, and one sample (H) in 5 dogs, resulting in a total of 59 samples. The median sample weight was 30.62 mg (range 1.7–112.3 mg). Six disc samples were excluded: four NHs and one H were excluded due to very small size and one NH sample demonstrated inconsistent housekeeping gene expression and out of range protein values. From the remaining 53 samples, 11 tissue samples weighting more than 50 mg were equally divided in samples for PCR and ELISA testing. 18 smaller samples were solely assigned to PCR testing and 24 smaller samples solely to ELISA testing. In the C group, we collected 11 samples in 11 dogs in the Th13–L1–L2 IVD space, with a median sample weight of 60.87 mg (range 30.3–133 mg). One dog was completely omitted because of RNA impurity. From the 10 remaining control samples, 4 samples weighting more than 50 mg were equally split into samples for PCR and ELISA. Three samples each were solely assigned to PCR and ELISA testing.

Cytokine Detectability

We could demonstrate gene and protein expression of the selected proinflammatory cytokines IL-1β, IL-6, IL-8, and TNF-α in IVDH in dogs.

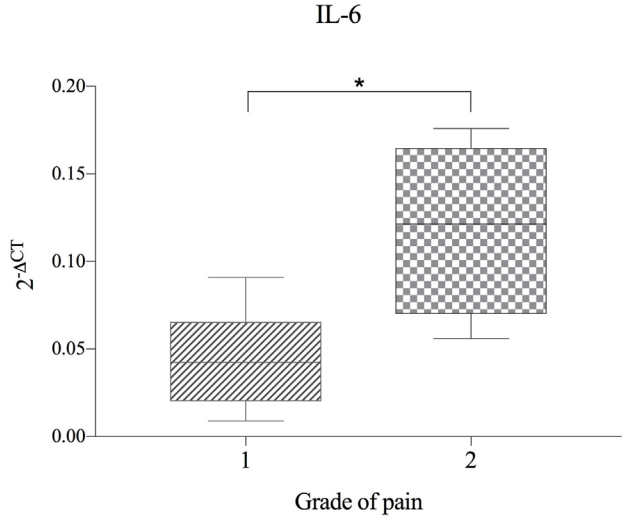

FIGURE 1 | Gene expression of IL-6 in herniated disc material, compared between dogs with differing grade of pain ($n = 11$) and shown as $2^{-\Delta CT}$. Grade 1 = no spontaneous pain, but discomfort upon palpation of the spine. Grade 2 = spontaneous pain and excessive pain upon palpation of the spine. Asterisks indicate statistical significance between groups at $p < 0.05$ (*).

Gene Expression

No significant correlation between IVDH location, duration of clinical signs or outcome, and the genes of interest was demonstrated, but the gene expression of IL-6 was significantly higher ($p = 0.043$) in pain grade 2 compared to grade 1 (**Figure 1**). Pooled results of all dogs in the respective groups (C, H, NH, NA) showed a significant downregulation of IL-1β in H compared to C, but no difference between NH or NA and C was found. IL-6 expression was significantly higher in H and NH compared to C, but not in NA. TNF-α expression showed significantly higher levels in H, NA, and NH compared to C. Gene expression of IL-8 showed no significant difference among the groups. All results are shown in **Table 4** and **Figure 2**.

As patients demonstrated differences in their basal cytokine levels, hence resulting in high donor–donor variations in subgroup comparisons, an interdonor comparison was conducted (H and HN relative to NA = internal control for each patient). A significant increase of IL-6 was observed for H and NH compared to NA. In contrast, gene expression of IL-1β, IL-8, and TNF-α were either unchanged or reduced in diseased compared to NA IVDs. All results are shown in **Table 5** and **Figure 3**.

Protein Expression

There were no significant correlations between cytokine protein levels and IVDH location, severity of pain, pretreatment or outcome and concentration of cytokines, but IL-6 was found to be significant higher in the clinical outcome group 2 compared to group 1 (**Figure 4**).

No significant differences of IL-1β or IL-6 protein expression were observed between the various groups. The concentration of IL-8 was significantly higher in H and NA compared to C, but no difference was found between NH and C. TNF-α showed significantly higher protein levels in NH compared to C, but not for H or NA. Results are shown in **Table 6** and **Figure 5**.

Like for gene expression, an additional inter-donor comparison was conducted, with NA as the internal control. However, no statistical differences were found between diseased (H, NH) and NA IVDs due to a level of variability and low sample numbers (data not shown).

No significant relationship was found between gene expression and corresponding protein concentration (IL-1β $rs = 0.02$; 95% CI, −0.66–0.67, $p = 0.97$; *IL-6* $rs = 0.30$; 95% CI, −0.41–0.78; $p = 0.41$; IL-8 $rs = -0.25$, 95% CI, −0.85–0.62, $p = 0.59$; TNF-α $rs = -0.51$, 95% CI, −0.86–0.18, $p = 0.13$). Interestingly, a significant association in gene expression between IL-6 and IL-8 ($rs = 0.79$, 95% CI 0.08–0.97, $p = 0.036$) was found in the control

TABLE 4 | Statistical results of gene expression data (subgroup comparison, independent samples).

Cytokine	Control IVD	Median (95% CI)	Comparative IVD	Median (95% CI)	*p*-Value
IL-1β	C	10.556 (5.927–27.650)	H	1.798 (0.329–7.156)	0.018
IL-6	C	0.012 (0.004–0.052)	H	0.057 (0.034–0.139)	0.013
			NH	0.178 (0.045–1.114)	0.006
TNF-α	C	0.007 (0.001–0.022)	H	0.112 (0.036–0.230)	0.008
			NA	0.087 (0.024–0.186)	0.008
			NH	0.060 (0.019–0.080)	0.007

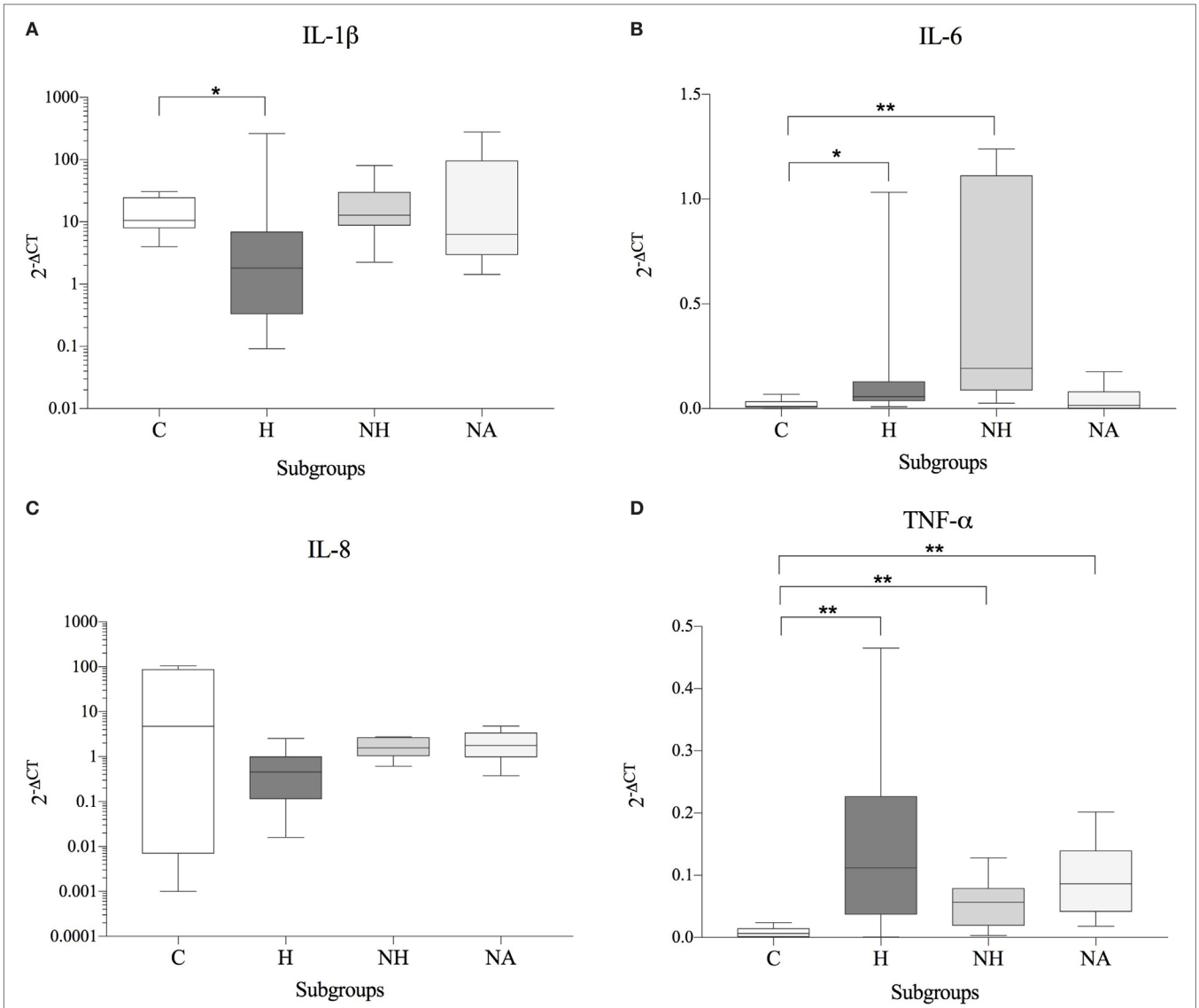

FIGURE 2 | Gene expression data (subgroup comparison, independent samples, $n \geq 6$ per subgroup) of **(A)** IL-1β, **(B)** IL-6, **(C)** IL-8, and **(D)** TNF-α, compared between herniated (H), non-herniated (NH), non-affected (NA) as well as healthy control (C) intervertebral disc material. Data are shown as $2^{-\Delta CT}$. Asterisks indicate statistical significance between groups at $p < 0.05$ (*) and $p < 0.01$ (**).

TABLE 5 | Statistical results of interdonor gene expression data (subgroup comparison, dependent samples).

Cytokine	Control IVD	Comparative IVD	Median (95% CI)	*p*-Value
IL-6	NA	H	498.625 (3.722–20,901.118)	0.031
		NH	2,473.292 (158.129–43,724.429)	0.031

group. In herniated samples, IL-1β protein correlated with IL-6 ($rs = 0.71$; 95% CI, 0.36–0.88, $p = 0.001$), IL-8 ($rs = 0.54$; 95% CI, 0.09–0.80, $p = 0.02$) as well as TNF-α concentrations ($rs = 0.55$; 95% CI, 0.11–0.81, $p = 0.02$) measured by ELISA.

Immunohistochemistry

Monocytes and macrophages were the most infiltrating cell population encountered in canine herniated IVD material. Sporadically, giant cells resembling notochordal cells were observed. CD 18 was highly expressed (++) in all samples, whereas detection of CD3 and vWF8 detection was semi-intractable and error-prone, hence not being shown. Expression of activated (phosphorylated) ERK (++) (**Figure 6**) and p38 (+/++) could be detected in most of the examined slides, whereas pJNK (−/+) was only sporadically detectable (not shown).

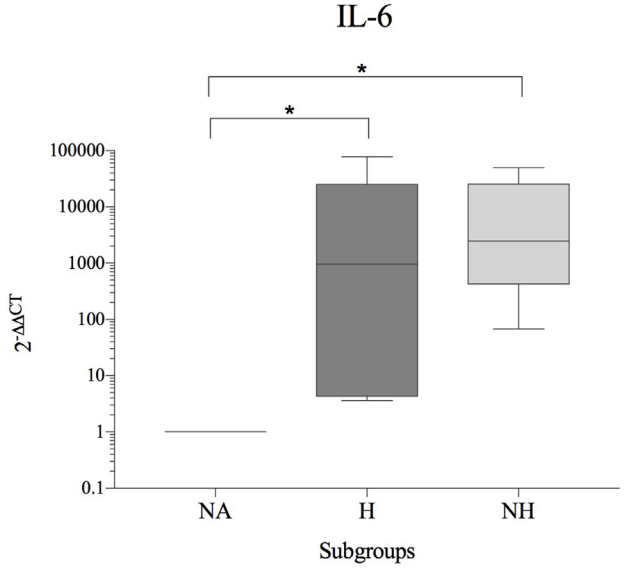

FIGURE 3 | Fold change in IL-6 gene expression (interdonor comparison, $n = 6$ per subgroup) between each dog's non-affected IVD material (NA) and the same dog's herniated (H) or non-herniated (NH) intervertebral disc material. Data are shown as $2^{-\Delta\Delta CT}$. Asterisks indicate statistical significance between groups at $p < 0.05$ (*).

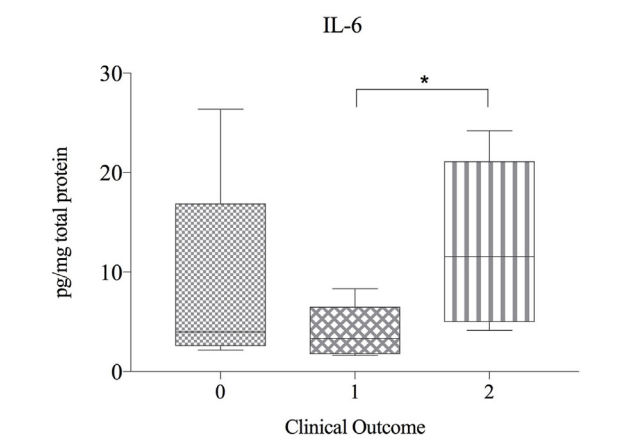

FIGURE 4 | Protein expression of IL-6 in herniated disc material, compared betwen dogs with differing clinical outcome ($n = 20$) and shown as picogram of IL-6 per milligram total protein. Grade 0 = lack of improvement. Grade 1 = improvement of neurologic status, but not able to walk. Grade 2 = recovery of ambulation or at least one grade in neurologic grades 1 and 2. Asterisks indicate statistical significance between groups at $p < 0.05$ (*).

DISCUSSION

Previous research on human IVD tissue has demonstrated that degeneration and herniation coincides with increased levels of inflammatory mediators, such as IL-1β, IL-6, IL-8, and TNF-α (8). In the present study, a comparison between diseased (herniated IVDs = H; NH) and control (C) IVDs of dogs demonstrated that disc disease was associated with significantly higher gene expression of IL-6 (H vs. C, NH vs. C) and TNF-α (H vs. C, NH vs. C). On the protein level, a significant increase of IL-8 and TNF-α in IVDs of diseased dogs compared to controls was found. A patient-specific comparison between the diseased (H, NH) and the IVDs excised from an adjacent level (NA) of the same dog revealed a pronounced pathological elevation of IL-6 (H vs. NA, NH vs. NA). In contrast, mRNA levels of IL-1β, IL-8, and TNF-α were either unchanged or reduced in diseased compared to NA IVDs of patients.

Previous studies on canine disc disease found IL-1β to be either undetectable or downregulated in dogs, which contrasts human disc pathology (64, 75). This was confirmed by our findings, showing a significant downregulation of the gene expression of IL-1β in herniated disc material (H) compared to controls, a downregulation in the affected disc material (H, NH) of the paired samples and no significant findings on the protein level.

In human IVDH, higher protein levels of the proinflammatory cytokine IL-6 were detected in different studies (10, 23, 25, 76), hence being discussed as a prognostic factor and therapeutic target. Thus far, results on IL-6 expression during canine disc disease are contradictory (63, 64, 75, 77). According to our findings, IL-6 seems to have a pivotal role, with its gene expression being significantly upregulated in the affected disc material (H, NH) of the independent and paired samples, unrelated to the duration of the clinical signs. Interestingly, we noticed a correlation between IL-6 mRNA levels and the severity of pain, with mRNA expression being significantly higher in those canine patients with basal pain than in those with pain arising only upon palpation. To the authors' knowledge, this has not been described before in canine IVDH, but might be in accordance with recent research in humans that has increasingly pointed toward IL-6 being a crucial factor in pain development (78, 79). However, IL-6 is not only a proinflammatory cytokine with significance in inflammation and diseases, but is also known to have regenerative or anti-inflammatory properties (80). Our results indicated that canine patients showing higher concentration of IL-6 protein levels in their IVD had a better outcome and were more likely to regain ambulation. This contrasting finding might be explained by the dual function of IL-6, suggesting that with time, IL-6 might control inflammation by acting as an anti-inflammatory cytokine (81, 82). IL-6 originates directly from

TABLE 6 | Statistical results of protein expression data (subgroup comparison, independent samples).

Cytokine	Control IVD	Median (95% CI)	Comparative IVD	Median (95% CI)	*p*-Value
IL-8	C	0.00001 (0.00001–0.00001)	H	3.925 (0.00001–17.823)	0.012
			NA sufficient	126.294 (13.728–187.946)	0.035
TNF-α	C	0.00001 (0.00001–0.00001)	NH sufficient	0.00001 (0.00001–9.924)	0.042

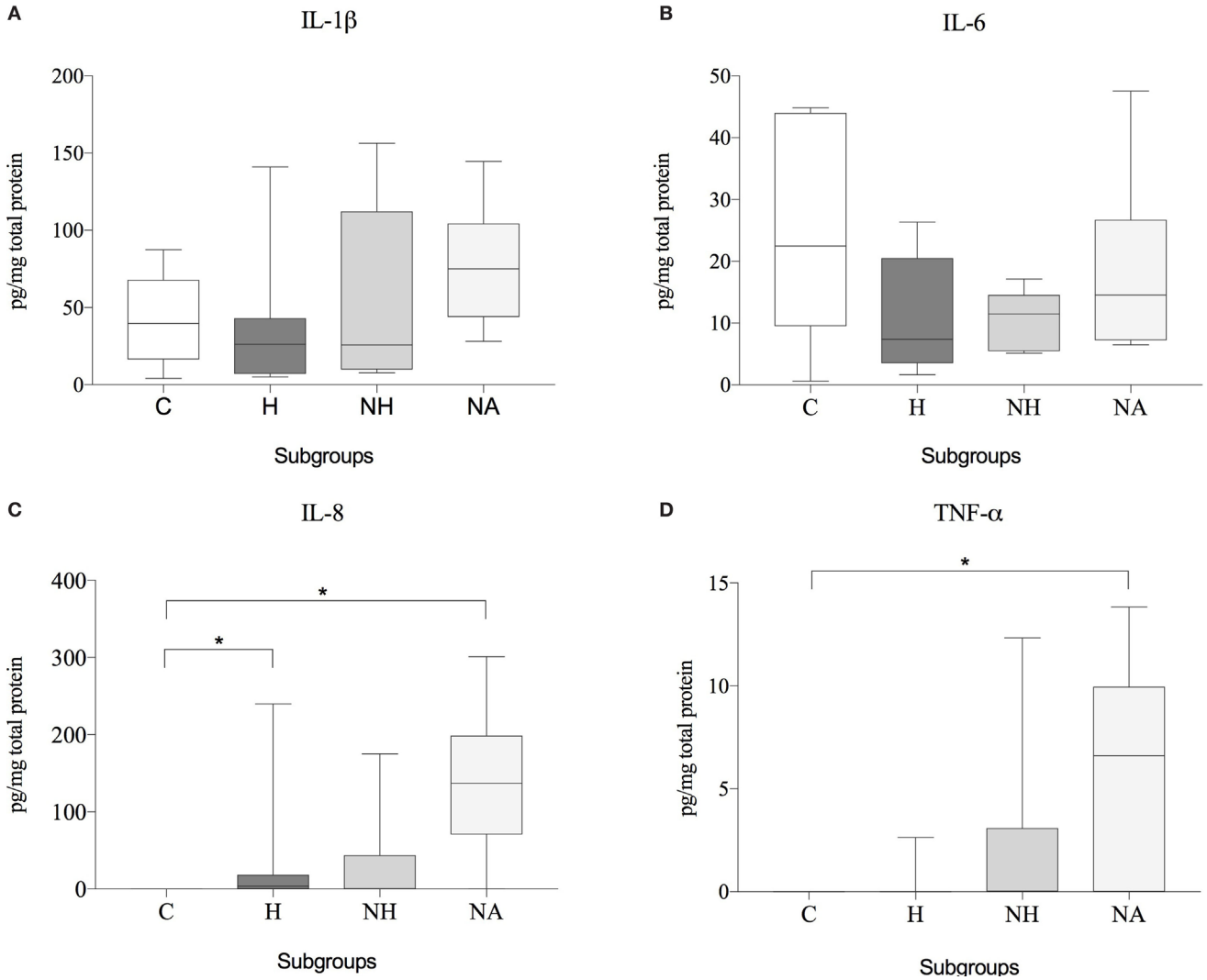

FIGURE 5 | Protein expression data (subgroup comparison, independent samples, $n \geq 6$ per subgroup) of **(A)** IL-1β, **(B)** IL-6, **(C)** IL-8, and **(D)** TNF-α, compared between herniated (H), non-herniated (NH), non-affected (NA) as well as healthy control (C) intervertebral disc material. Data are shown as picogram of each cytokine per milligram total protein. Asterisks indicate statistical significance between groups at $p < 0.05$ (*).

IVD cells (76) and also from T-cells and macrophages (83–86), the latter constituting the main cell population of the inflammatory infiltrates in the epidural space after IVD extrusion in our samples. Based on our findings, IL-6 could potentially have also a beneficial role in the late onset of the inflammatory cascade of canine IVDH. Therefore, therapeutic blockage for IL-6 should be carefully considered.

In this study, we also analyzed the expression of IL-8, which has previously been shown to be strongly upregulated in the acute phase of canine IVDH (63, 64, 77), yet with a negative correlation between its expression and the duration of spinal cord injury secondary to IVDH (77). As IL-8 is thus thought to be an early disease marker with time-dependent expression and as our patients were mostly seen for treatment at a late stage of the disease, it explains why we could not demonstrate a significant upregulation of IL-8 mRNA, but of IL-8 protein in diseased discs. Interestingly, a significant upregulation of the protein level of IL-8 in independent samples could as also be demonstrated in NA disc material, suggesting a possible secretion of IL-8 in canine disc material before the effective herniation of the affected IVD and hence further supporting a possible early stage inflammation as a trigger for IVDH.

Together with IL-1β, TNF-α is likely the most studied cytokine in human IVDD (11, 17, 28, 87, 88), inducing matrix degrading enzyme expression and upregulation of nerve growth factor. TNF-α is hence suggested to be have an important role in the development of hyperalgesia and chronic pain after IVDH in humans (7, 16, 28, 89–92). Contradictory results have been found on TNF-α expression in canine IVDH, ranging from non-detectability (64, 75, 77) to disease-related elevation (albeit non-significant) (63). In accordance with Spitzbart et al. (63), as well as with human studies, we could demonstrate a significant

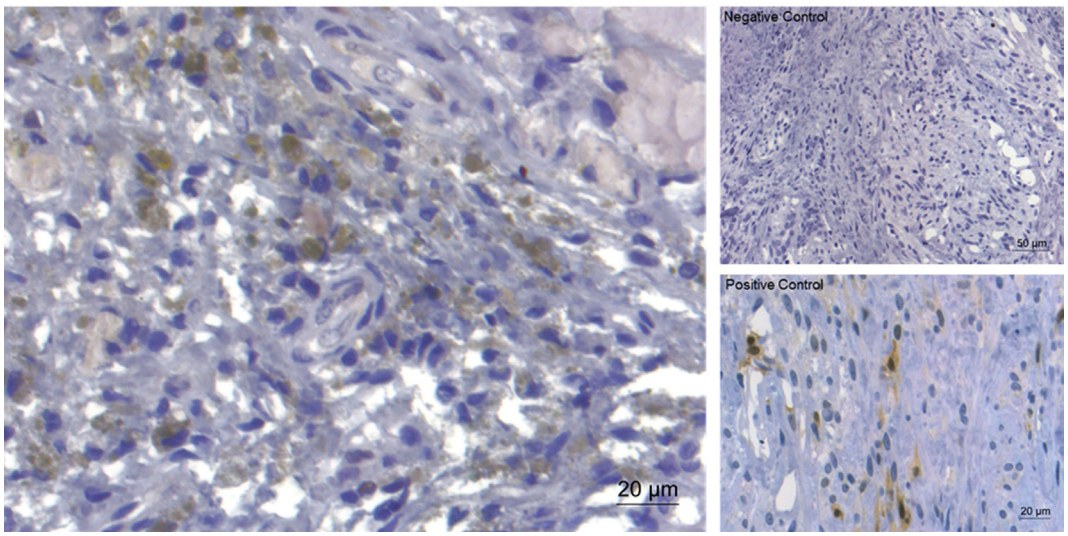

FIGURE 6 | Immunohistochemical staining for extracellular signal-regulated kinase (ERK)1/2 of extruded canine intervertebral disc material (left). Expression of ERK (brownish coloration) was detected in the majority of the examined slides. On the right, negative control and positive control (canine mammar carcinoma) are depicted.

upregulation of TNF-α on the gene expression level (H, NH) and the protein expression level (NH). Furthermore, and also similar to human NP samples in which TNF-α is known to be continuously expressed at basal levels (93), TNF-α could also be detected in adjacent discs (NA) suggesting to be a possible trigger of an early stage inflammation for IVDH.

Histological investigations demonstrated that most herniated IVDs exhibited an epidural inflammatory response, ranging from acute invasion of neutrophils to formation of chronic granulation tissue. Histological analysis of underlying inflammatory pathways demonstrated activation of the MAPKs ERK and p38 in most samples, whereas pJNK was rarely detected. MAPKs are signal transduction pathways that are activated by a multitude of stimuli, ranging from environmental, mechanical and osmotic stress to growth factors, cytokines and reactive oxygen species, with ERK and p38 controlling inflammation, catabolism as well as cell growth, differentiation and viability/death (27). The fact that the MAPKs pathways are shared between the cytokines might explain the correlation on the protein level in herniated samples of IL-1β with IL-6, IL-8, and TNF-α (94).

In accordance with our results, *in vitro* cell culture studies and rodent *in vivo* studies have previously demonstrated that p38 and ERK are activated in inflammatory environments (95–100), controlling a variety of metabolic functions associated with disc pathology, including proteoglycan degradation (96, 97). Furthermore, the decrease in osmotic pressure observed during herniation in our canine patients may also play a causative role in MAPK activation as previously demonstrated for bovine IVDs and the ERK pathway (101). Importantly, activation of p38 and ERK in our canine samples may not only induce downstream expression of additional inflammatory mediators and matrix degrading enzymes and hence play an important role in disease progression [reviewed in Ref. (27)], but may furthermore be a means to initiate resorption of non-contained herniated disc tissue (102–104).

Despite providing interesting new findings on the inflammation in canine IVDH, the present study has several limitations that should be considered. The dog size as well as the morphologic size of the herniated disc tissue imposed limitations on the number of performed tests. The quantity of surgically excised canine disc material is smaller than specimens collected in humans. Therefore, we could not divide all samples equally for PCR and ELISA testing as planned in the study design, resulting in variations in group size. Due to the non-predictable onset of canine IVDH, the group could neither be age nor gender matched, possibly influencing the results. Furthermore, most of our patients were presented at a late stage of the disease, which may explain why we might have missed the peak expression of some cytokines in the acute stage of the disease.

CONCLUSION

Inflammation in the epidural compartment plays a central role in the pathophysiology of canine IVD herniation and significantly influences the course and outcome of the disease. Working with a clinical canine model not only provides the possibility to overcome animal experimentation, but furthermore allows (different from human studies) the analysis of adjacent, NA discs. Although expression of key cytokines found in human IVDs could also be demonstrated in canine tissue, the inflammatory mechanisms accompanying IVDH in dogs partially diverge from humans. These differences need to be considered when using dogs as a model for human medicine. In dogs, IL-6 seems to play an important pathological role, but further investigations on IL-6 as a potential therapeutic target in canine patients will be needed, especially when considering its likely ambivalent role.

ETHICS STATEMENT

This study was carried out in accordance with the recommendations of "Animal Research Committee: Tierversuchsbewilligung BE 14/12, Switzerland." The protocol was approved by the "Animal Research Committee: Tierversuchsbewilligung BE 14/12, Switzerland." Furthermore, all patient-owners signed an owner consent form.

AUTHOR CONTRIBUTIONS

MM contributed to the conception and design, acquisition and data, analysis and interpretation of data, drafting of the manuscript, critical revision of the manuscript for important intellectual content, and statistical analysis. SF contributed to the analysis and interpretation of data, drafting of the manuscript, critical revision of the manuscript for important intellectual content, and the statistical analysis. DS contributed to the conception and design, critical revision of the manuscript and intellectual content, funding, and final approval of the version to be published. AK contributed to acquisition and data, interpretation and analysis of data, critical revision and administrative, technical, or material support. FF and KW-K contributed equally to the conception and design, analysis and interpretation of data, drafting of the manuscript, critical revision of the manuscript for important intellectual content, obtaining funding, administrative, technical or material support, supervision, and final approval of the version to be published. All authors agreed to be accountable for all aspects of the work in ensuring that questions related to the accuracy or integrity of any part of the work are appropriately investigated and resolved. We thank Prof. Dr. Michael Stoffel (Vetsuisse Bern, Veterinary Anatomy) for his support with histology.

FUNDING

The study was funded and supported with 37,500 $ by The Competence Center for Applied Biotechnology and Molecular Medicine Start-up Grant of the University of Zurich, Switzerland. Heel GmbH financially supported the salary of MM.

REFERENCES

1. Hoy D, March L, Brooks P, Blyth F, Woolf A, Bain C, et al. The global burden of low back pain: estimates from the Global Burden of Disease 2010 study. *Ann Rheum Dis* (2014) 73:968–74. doi:10.1136/annrheumdis-2013-204428
2. Luoma K, Riihimäki H, Luukkonen R, Raininko R, Viikari-Juntura E, Lamminen A. Low back pain in relation to lumbar disc degeneration. *Spine (Phila Pa 1976)* (2000) 25:487–92. doi:10.1097/00007632-200002150-00016
3. Kaapa E, Vanharanta H. Intervertebral disk degeneration – a central cause of back problems. *Duodecim* (1991) 107:1603–11.
4. Vanharanta H, Guyer RD, Ohnmeiss DD, Stith WJ, Sachs BL, Aprill C, et al. Disc deterioration in low-back syndromes. A prospective, multi-center CT/discography study. *Spine (Phila Pa 1976)* (1988) 13:1349–51. doi:10.1097/00007632-198812000-00003
5. Lyons G, Eisenstein SM, Sweet MB. Biochemical changes in intervertebral disc degeneration. *Biochim Biophys Acta* (1981) 673:443–53. doi:10.1016/0304-4165(81)90476-1
6. Freemont AJ, Peacock TE, Goupille P, Hoyland JA, O'Brien J, Jayson MIV. Nerve ingrowth into diseased intervertebral disc in chronic back pain. *Lancet* (1997) 350:178–81. doi:10.1016/S0140-6736(97)02135-1
7. Kepler CK, Markova DZ, Hilibrand AS, Vaccaro AR, Risbud MV, Albert TJ, et al. Substance P stimulates production of inflammatory cytokines in human disc cells. *Spine (Phila Pa 1976)* (2013) 38:E1291–9. doi:10.1097/BRS.0b013e3182a42bc2
8. Wuertz K, Haglund L. Inflammatory mediators in intervertebral disk degeneration and discogenic pain. *Global Spine J* (2013) 3:175–84. doi:10.1055/s-0033-1347299
9. Kepler CK, Markova DZ, Dibra F, Yadla S, Vaccaro AR, Risbud MV, et al. Expression and relationship of proinflammatory chemokine RANTES/CCL5 and cytokine IL-1β in painful human intervertebral discs. *Spine (Phila Pa 1976)* (2013) 38:873–80. doi:10.1097/BRS.0b013e318285ae08
10. Andrade P, Hoogland G, Garcia MA, Steinbusch HW, Daemen MA, Visser-Vandewalle V. Elevated IL-1b and IL-6 levels in lumbar herniated discs in patients with sciatic pain. *Eur Spine J* (2013) 22:714–20. doi:10.1007/s00586-012-2502-x
11. Cuéllar JM, Borges PM, Cuéllar VG, Yoo A, Scuderi GJ, Yeomans DC. Cytokine expression in the epidural space: a model of noncompressive disc herniation-induced inflammation. *Spine (Phila Pa 1976)* (2013) 38:17–23. doi:10.1097/BRS.0b013e3182604baa
12. De Souza Grava AL, Ferrari LF, Defino HLA. Cytokine inhibition and time-related influence of inflammatory stimuli on the hyperalgesia induced by the nucleus pulposus. *Eur Spine J* (2012) 21:537–45. doi:10.1007/s00586-011-2027-8
13. Studer RK, Vo N, Sowa G, Ondeck C, Kang J. Human nucleus pulposus cells react to IL-6: independent actions and amplification of response to IL-1 and TNF-α. *Spine (Phila Pa 1976)* (2011) 36:593–9. doi:10.1097/BRS.0b013e3181da38d5
14. Vo NV, Sowa GA, Kang JD, Seidel C, Studer RK. Prostaglandin E2 and prostaglandin F2alpha differentially modulate matrix metabolism of human nucleus pulposus cells. *J Orthop Res* (2010) 28:1259–66. doi:10.1002/jor.21157
15. Kim JH, Studer RK, Sowa GA, Vo NV, Kang JD. Activated macrophage-like THP-1 cells modulate anulus fibrosus cell production of inflammatory mediators in response to cytokines. *Spine (Phila Pa 1976)* (2008) 33:2253–9. doi:10.1097/BRS.0b013e318182c35f
16. Abe Y, Akeda K, An HS, Aoki Y, Pichika R, Muehleman C, et al. Proinflammatory cytokines stimulate the expression of nerve growth factor by human intervertebral disc cells. *Spine (Phila Pa 1976)* (2007) 32:635–42. doi:10.1097/01.brs.0000257556.90850.53
17. Le Maitre CL, Hoyland JA, Freemont AJ. Catabolic cytokine expression in degenerate and herniated human intervertebral discs: IL-1beta and TNFalpha expression profile. *Arthritis Res Ther* (2007) 9:R77. doi:10.1186/ar2275
18. Yoshida M, Nakamura T, Sei A, Kikuchi T, Takagi K, Matsukawa A. Intervertebral disc cells produce tumor necrosis factor alpha, interleukin-1beta, and monocyte chemoattractant protein-1 immediately after herniation: an experimental study using a new hernia model. *Spine (Phila Pa 1976)* (2005) 30:55–61. doi:10.1097/01.brs.0000149194.17891.bf
19. Ahn S-H, Cho Y-W, Ahn M-W, Jang S-H, Sohn Y-K, Kim H-S. mRNA expression of cytokines and chemokines in herniated lumbar intervertebral discs. *Spine (Phila Pa 1976)* (2002) 27:911–7. doi:10.1097/00007632-200205010-00005
20. Miyamoto H, Saura R, Harada T, Doita M, Mizuno K. The role of cyclooxygenase-2 and inflammatory cytokines in pain induction of herniated lumbar intervertebral disc. *Kobe J Med Sci* (2000) 46(1–2):13–28.
21. Nygaard OP, Mellgren SI, Osterud B. The inflammatory properties of contained and noncontained lumbar disc herniation. *Spine (Phila Pa 1976)* (1997) 22:2484–8. doi:10.1097/00007632-199711010-00004
22. Takahashi H, Suguro T, Okazima Y, Motegi M, Okada Y, Kakiuchi T. Inflammatory cytokines in the herniated disc of the lumbar spine. *Spine (Phila Pa 1976)* (1996) 21:218–24. doi:10.1097/00007632-199601150-00011
23. Kang JD, Georgescu HI, McIntyre-Larkin L, Stefanovic-Racic M, Donaldson WF, Evans CH. Herniated lumbar intervertebral discs spontaneously produce matrix metalloproteinases, nitric oxide, interleukin-6, and prostaglandin E2. *Spine (Phila Pa 1976)* (1996) 21:271–7. doi:10.1097/00007632-199602010-00004

24. Popovich PG, Jones TB. Manipulating neuroinflammatory reactions in the injured spinal cord: back to basics. *Trends Pharmacol Sci* (2003) 24:13–7. doi:10.1016/S0165-6147(02)00006-8
25. Igarashi A, Kikuchi S, Konno S, Olmarker K. Inflammatory cytokines released from the facet joint tissue in degenerative lumbar spinal disorders. *Spine (Phila Pa 1976)* (2004) 29:2091–5. doi:10.1097/01.brs.0000141265.55411.30
26. Igarashi A, Kikuchi SI, Konno SI. Correlation between inflammatory cytokines released from the lumbar facet joint tissue and symptoms in degenerative lumbar spinal disorders. *J Orthop Sci* (2007) 12:154–60. doi:10.1007/s00776-006-1105-y
27. Wuertz K, Vo N, Kletsas D, Boos N. Inflammatory and catabolic signalling in intervertebral discs: the roles of NF-KB and map kinases. *Eur Cell Mater* (2012) 23:103–20. doi:10.22203/eCM.v023a08
28. Le Maitre CL, Freemont AJ, Hoyland JA. The role of interleukin-1 in the pathogenesis of human intervertebral disc degeneration. *Arthritis Res Ther* (2005) 7:R732–45. doi:10.1186/ar1732
29. Fardon DF, Milette PC. Nomenclature and classification of lumbar disc pathology. *Spine (Phila Pa 1976)* (2001) 26:E93–113. doi:10.1016/j.spinee.2014.04.022
30. Doita M, Kanatani T, Harada T, Mizuno K. Immunohistologic study of the ruptured intervertebral disc of the lumbar spine. *Spine (Phila Pa 1976)* (1996) 21:235–41. doi:10.1097/00007632-199601150-00015
31. Doita M, Kanatani T, Ozaki T, Matsui N, Kurosaka M, Yoshiya S. Influence of macrophage infiltration of herniated disc tissue on the production of matrix metalloproteinases leading to disc resorption. *Spine (Phila Pa 1976)* (2001) 26:1522–7. doi:10.1097/00007632-200107150-00004
32. Genevay S, Finckh A, Payer M, Mezin F, Tessitore E, Gabay C, et al. Elevated levels of tumor necrosis factor-alpha in periradicular fat tissue in patients with radiculopathy from herniated disc. *Spine (Phila Pa 1976)* (2008) 33:2041–6. doi:10.1097/BRS.0b013e318183bb86
33. Kawaguchi S, Yamashita T, Katahira G, Yokozawa H, Torigoe T, Sato N. Chemokine profile of herniated intervertebral discs infiltrated with monocytes and macrophages. *Spine (Phila Pa 1976)* (2002) 27:1511–6. doi:10.1097/00007632-200207150-00006
34. Kawaguchi S, Yamashita T, Yokogushi K, Murakami T, Ohwada O, Sato N. Immunophenotypic analysis of the inflammatory infiltrates in herniated intervertebral discs. *Spine (Phila Pa 1976)* (2001) 26:1209–14. doi:10.1097/00007632-200106010-00008
35. Minamide A, Hashizume H, Yoshida M, Kawakami M, Hayashi N, Tamaki T. Effects of basic fibroblast growth factor on spontaneous resorption of herniated intervertebral discs. An experimental study in the rabbit. *Spine (Phila Pa 1976)* (1999) 24:940–5. doi:10.1097/00007632-199905150-00003
36. Yamashita M, Ohtori S, Koshi T, Inoue G, Yamauchi K, Suzuki M, et al. Tumor necrosis factor-alpha in the nucleus pulposus mediates radicular pain, but not increase of inflammatory peptide, associated with nerve damage in mice. *Spine (Phila Pa 1976)* (2008) 33:1836–42. doi:10.1097/BRS.0b013e31817bab2a
37. Zhou G, Dai L, Jiang X, Ma Z, Ping J, Li J, et al. Effects of human midkine on spontaneous resorption of herniated intervertebral discs. *Int Orthop* (2010) 34:103–8. doi:10.1007/s00264-009-0740-2
38. Schroeder GD, Guyre CA, Vaccaro AR. The epidemiology and pathophysiology of lumbar disc herniations. *Semin Spine Surg* (2016) 28:2–7. doi:10.1053/j.semss.2015.08.003
39. Goupille P, Jayson MIV, Valat JP, Freemont AJ. The role of inflammation in disk herniation-associated radiculopathy. *Semin Arthritis Rheum* (1998) 28:60–71. doi:10.1016/S0049-0172(98)80029-2
40. Kalb S, Martirosyan NL, Kalani MYS, Broc GG, Theodore N. Genetics of the degenerated intervertebral disc. *World Neurosurg* (2012) 77:491–501. doi:10.1016/j.wneu.2011.07.014
41. Yu-Ping Kao P, Chan D, Samartzis D, Sham PC, Song YQ. Genetics of lumbar disk degeneration: technology, study designs, and risk factors. *Orthop Clin North Am* (2011) 42:479–86. doi:10.1016/j.ocl.2011.07.011
42. Bachmeier BE, Nerlich AG, Weiler C, Paesold G, Jochum M, Boos N. Analysis of tissue distribution of TNF-alpha, TNF-alpha-receptors, and the activating TNF-alpha-converting enzyme suggests activation of the TNF-alpha system in the aging intervertebral disc. *Ann N Y Acad Sci* (2007) 1096:44–54. doi:10.1196/annals.1397.069
43. Di Virgilio F. New pathways for reactive oxygen species generation in inflammation and potential novel pharmacological targets. *Curr Pharm Des* (2004) 10:1647–52. doi:10.2174/1381612043384727
44. Finkel T, Holbrook NJ. Oxidants, oxidative stress and the biology of ageing. *Nature* (2000) 408:239–47. doi:10.1038/35041687
45. Ogawa T, Matsuzaki H, Uei H, Nakajima S, Tokuhashi Y, Esumi M. Alteration of gene expression in intervertebral disc degeneration of passive cigarette-smoking rats: separate quantitation in separated nucleus pulposus and annulus fibrosus. *Pathobiology* (2005) 72:146–51. doi:10.1159/000084118
46. Liuke M, Solovieva S, Lamminen A, Luoma K, Leino-Arjas P, Luukkonen R, et al. Disc degeneration of the lumbar spine in relation to overweight. *Int J Obes* (2005) 29:903–8. doi:10.1038/sj.ijo.0802974
47. Samartzis D, Karppinen J, Chan D, Luk KDK, Cheung KMC. The association of lumbar intervertebral disc degeneration on magnetic resonance imaging with body mass index in overweight and obese adults: a population-based study. *Arthritis Rheum* (2012) 64:1488–96. doi:10.1002/art.33462
48. Takatalo J, Karppinen J, Taimela S, Niinimäki J, Laitinen J, Sequeiros RB, et al. Association of abdominal obesity with lumbar disc degeneration – a magnetic resonance imaging study. *PLoS One* (2013) 8:e56244. doi:10.1371/journal.pone.0056244
49. Hamminga EA, van der Lely AJ, Neumann HAM, Thio HB. Chronic inflammation in psoriasis and obesity: implications for therapy. *Med Hypotheses* (2006) 67:768–73. doi:10.1016/j.mehy.2005.11.050
50. Singh K, Masuda K, An HS. Animal models for human disc degeneration. *Spine J* (2005) 5:267S–79S. doi:10.1016/j.spinee.2005.02.016
51. Yamada K. The dynamics of experimental posture. Experimental study of intervertebral disc herniation in bipedal animals. *Tokushima J Exp Med* (1962) 8:350–61.
52. Bergknut N, Rutges JPHJ, Kranenburg H-JC, Smolders LA, Hagman R, Smidt H-J, et al. The dog as an animal model for intervertebral disc degeneration? *Spine (Phila Pa 1976)* (2012) 37:351–8. doi:10.1097/BRS.0b013e31821e5665
53. Levine JM, Levine GJ, Porter BF, Topp K, Noble-Haeusslein LJ. Naturally occurring disk herniation in dogs: an opportunity for pre-clinical spinal cord injury research. *J Neurotrauma* (2011) 28:675–88. doi:10.1089/neu.2010.1645
54. Bergknut N, Egenvall A, Hagman R, Gustås P, Hazewinkel HAW, Meij BP, et al. Incidence of intervertebral disk degeneration-related diseases and associated mortality rates in dogs. *J Am Vet Med Assoc* (2012) 240:1300–9. doi:10.2460/javma.240.11.1300
55. Bray J, Burbidge H. The canine intervertebral disk: part one: structure and function. *J Am Anim Hosp Assoc* (1998) 34:55–63. doi:10.5326/15473317-34-1-55
56. Priester WA. Canine intervertebral disc disease – occurrence by age, breed, and sex among 8,117 cases. *Theriogenology* (1976) 6:293–303. doi:10.1016/0093-691X(76)90021-2
57. Smolders LA, Bergknut N, Grinwis GCM, Hagman R, Lagerstedt AS, Hazewinkel HAW, et al. Intervertebral disc degeneration in the dog. Part 2: chondrodystrophic and non-chondrodystrophic breeds. *Vet J* (2013) 195:292–9. doi:10.1016/j.tvjl.2012.10.011
58. Bray J, Burbidge H. The canine intervertebral disk. Part two: degenerative changes – nonchondrodystrophoid versus chondrodystrophoid disks. *J Am Anim Hosp Assoc* (1998) 34:135–44. doi:10.5326/15473317-34-2-135
59. Hansen H. A pathologic-anatomical interpretation of disc degeneration in dogs. *Acta Orthop Scand* (1951) 20:280–93. doi:10.3109/17453675108991175
60. Lund EM, Armstrong PJ, Kirk CA, Klausner JS. Prevalence and risk factors for obesity in adult dogs from private US veterinary practices. *J Appl Res Vet Med* (2006) 4:177–86.
61. Edney AT, Smith PM. Study of obesity in dogs visiting veterinary practices in the United Kingdom. *Vet Rec* (1986) 118:391–6. doi:10.1136/vr.118.14.391
62. Packer RMA, Hendricks A, Volk HA, Shihab NK, Burn CC. How long and low can you go? Effect of conformation on the risk of thoracolumbar intervertebral disc extrusion in domestic dogs. *PLoS One* (2013) 8:e69650. doi:10.1371/journal.pone.0069650
63. Spitzbarth I, Bock P, Haist V, Stein VM, Tipold A, Wewetzer K, et al. Prominent microglial activation in the early proinflammatory immune response in naturally occurring canine spinal cord injury. *J Neuropathol Exp Neurol* (2011) 70:703–14. doi:10.1097/NEN.0b013e3182270f8e
64. Karli P, Martlé V, Bossens K, Summerfield A, Doherr MG, Turner P, et al. Dominance of chemokine ligand 2 and matrix metalloproteinase-2 and -9 and suppression of pro-inflammatory cytokines in the epidural compartment after

intervertebral disc extrusion in a canine model. *Spine J* (2014) 14:2976–84. doi:10.1016/j.spinee.2014.05.021
65. Skogstrand K, Ekelund CK, Thorsen P, Vogel I, Jacobsson B, Nørgaard-Pedersen B, et al. Effects of blood sample handling procedures on measurable inflammatory markers in plasma, serum and dried blood spot samples. *J Immunol Methods* (2008) 336:78–84. doi:10.1016/j.jim.2008.04.006
66. Riches P, Gooding R, Millar BC, Rowbottom AW. Influence of collection and separation of blood samples on plasma IL-1, IL-6 and TNF-α concentrations. *J Immunol Methods* (1992) 153:125–31. doi:10.1016/0022-1759(92)90314-J
67. Keustermans GCE, Hoeks SBE, Meerding JM, Prakken BJ, de Jager W. Cytokine assays: an assessment of the preparation and treatment of blood and tissue samples. *Methods* (2013) 61:10–7. doi:10.1016/j.ymeth.2013.04.005
68. Hooper R. Extradural haemorrhages of the posterior fossa. *Br J Surg* (1954) 42:19. doi:10.1002/bjs.18004217103
69. Su T-M, Lee T-H, Lee T-C, Cheng C-H, Lu C-H. Acute clinical deterioration of posterior fossa epidural hematoma: clinical features, risk factors and outcome. *Chang Gung Med J* (2012) 35(3):271–80.
70. Fadda A, Oevermann A, Vandevelde M, Doherr MG, Forterre F, Henke D. Clinical and pathological analysis of epidural inflammation in intervertebral disk extrusion in dogs. *J Vet Intern Med* (2013) 27:924–34. doi:10.1111/jvim.12095
71. Penning V, Platt SR, Dennis R, Cappello R, Adams V. Association of spinal cord compression seen on magnetic resonance imaging with clinical outcome in 67 dogs with thoracolumbar intervertebral disc extrusion. *J Small Anim Pract* (2006) 47:644–50. doi:10.1111/j.1748-5827.2006.00252.x
72. Goni R, García P, Foissac S. The qPCR data statistical analysis. *Integromics White Pap* (2009) 1:1–9.
73. Bergknut N, Auriemma E, Wijsman S, Voorhout G, Hagman R, Lagerstedt AS, et al. Evaluation of intervertebral disk degeneration in chondrodystrophic and nonchondrodystrophic dogs by use of Pfirrmann grading of images obtained with low-field magnetic resonance imaging. *Am J Vet Res* (2011) 72:893–8. doi:10.2460/ajvr.72.7.893
74. Kranenburg HC, Grinwis GCM, Bergknut N, Gahrmann N, Voorhout G, Hazewinkel HAW, et al. Intervertebral disc disease in dogs – part 2: comparison of clinical, magnetic resonance imaging, and histological findings in 74 surgically treated dogs. *Vet J* (2013) 195:164–71. doi:10.1016/j.tvjl.2012.06.001
75. Willems N, Tellegen AR, Bergknut N, Creemers LB, Wolfswinkel J, Freudigmann C, et al. Inflammatory profiles in canine intervertebral disc degeneration. *BMC Vet Res* (2016) 12:10. doi:10.1186/s12917-016-0635-6
76. Burke JG, Watson RW, McCormack D, Dowling FE, Walsh MG, Fitzpatrick JM. Intervertebral discs which cause low back pain secrete high levels of proinflammatory mediators. *J Bone Joint Surg Br* (2002) 84:196–201. doi:10.1302/0301-620X.84B2.12511
77. Taylor AR, Welsh CJ, Young C, Spoor E, Kerwin SC, Griffin JF, et al. Cerebrospinal fluid inflammatory cytokines and chemokines in naturally occurring canine spinal cord injury. *J Neurotrauma* (2014) 31:1561–9. doi:10.1089/neu.2014.3405
78. Takada T, Nishida K, Doita M, Miyamoto H, Kurosaka M. Interleukin-6 production is upregulated by interaction between disc tissue and macrophages. *Spine (Phila Pa 1976)* (2004) 29:1089–92; discussion 1093. doi:10.1097/00007632-200405150-00007
79. Altun I. Cytokine profile in degenerated painful intervertebral disc: variability with respect to duration of symptoms and type of disease. *Spine J* (2016) 16:857–61. doi:10.1016/j.spinee.2016.03.019
80. Scheller J, Chalaris A, Schmidt-Arras D, Rose-John S. The pro- and anti-inflammatory properties of the cytokine interleukin-6. *Biochim Biophys Acta* (2011) 1813:878–88. doi:10.1016/j.bbamcr.2011.01.034
81. Watkins LR, Maier SF, Goehler LE. Immune activation: the role of pro-inflammatory cytokines in inflammation, illness responses and pathological pain states. *Pain* (1995) 63:289–302. doi:10.1016/0304-3959(95)00186-7
82. Xing Z, Gauldie J, Cox G, Baumann H, Jordana M, Lei XF, et al. IL-6 is an antiinflammatory cytokine required for controlling local or systemic acute inflammatory responses. *J Clin Invest* (1998) 101:311–20. doi:10.1172/JCI1368
83. Kishimoto T. IL-6: from its discovery to clinical applications. *Int Immunol* (2010) 22:347–52. doi:10.1093/intimm/dxq030
84. Ray A, Tatter SB, May LT, Sehgal PB. Activation of the human "beta 2-interferon/hepatocyte-stimulating factor/interleukin 6" promoter by cytokines, viruses, and second messenger agonists. *Proc Natl Acad Sci U S A* (1988) 85:6701–5. doi:10.1073/pnas.85.18.6701
85. Zhang XG, Klein B, Bataille R. Interleukin-6 is a potent myeloma-cell growth factor in patients with aggressive multiple myeloma. *Blood* (1989) 74:11–3.
86. Navarro S, Debili N, Bernaudin JF, Vainchenker W, Doly J. Regulation of the expression of IL-6 in human monocytes. *J Immunol* (1989) 142:4339–45.
87. Shamji MF, Setton LA, Jarvis W, So S, Chen J, Jing L, et al. Proinflammatory cytokine expression profile in degenerated and herniated human intervertebral disc tissues. *Arthritis Rheum* (2010) 62:1974–82. doi:10.1002/art.27444
88. Séguin CA, Pilliar RM, Roughley PJ, Kandel RA. Tumor necrosis factor-alpha modulates matrix production and catabolism in nucleus pulposus tissue. *Spine (Phila Pa 1976)* (2005) 30:1940–8. doi:10.1097/01.brs.0000176188.40263.f9
89. Le Maitre CL, Hoyland JA, Freemont AJ. Interleukin-1 receptor antagonist delivered directly and by gene therapy inhibits matrix degradation in the intact degenerate human intervertebral disc: an in situ zymographic and gene therapy study. *Arthritis Res Ther* (2007) 9:R83. doi:10.1186/ar2282
90. Wang J, Markova D, Anderson DG, Zheng Z, Shapiro IM, Risbud MV. TNF-alpha and IL-1beta promote a disintegrin-like and metalloprotease with thrombospondin type I motif-5-mediated aggrecan degradation through syndecan-4 in intervertebral disc. *J Biol Chem* (2011) 286:39738–49. doi:10.1074/jbc.M111.264549
91. Purmessur D, Freemont AJ, Hoyland JA. Expression and regulation of neurotrophins in the nondegenerate and degenerate human intervertebral disc. *Arthritis Res Ther* (2008) 10:R99. doi:10.1186/ar2487
92. Freemont AJ, Watkins A, Le Maitre C, Baird P, Jeziorska M, Knight MT, et al. Nerve growth factor expression and innervation of the painful intervertebral disc. *J Pathol* (2002) 197:286–92. doi:10.1002/path.1108
93. Olmarker K, Larsson K. Tumor necrosis factor alpha and nucleus-pulposus-induced nerve root injury. *Spine (Phila Pa 1976)* (1998) 23:2538–44. doi:10.1097/00007632-199812010-00008
94. Kaminska B. MAPK signalling pathways as molecular targets for anti-inflammatory therapy – from molecular mechanisms to therapeutic benefits. *Biochim Biophys Acta* (2005) 1754:253–62. doi:10.1016/j.bbapap.2005.08.017
95. Ulrich JA, Liebenberg EC, Thuillier DU, Lotz JC. ISSLS prize winner: repeated disc injury causes persistent inflammation. *Spine (Phila Pa 1976)* (2007) 32:2812–9. doi:10.1097/BRS.0b013e31815b9850
96. Séguin CA, Bojarski M, Pilliar RM, Roughley PJ, Kandel RA. Differential regulation of matrix degrading enzymes in a TNFα-induced model of nucleus pulposus tissue degeneration. *Matrix Biol* (2006) 25:409–18. doi:10.1016/j.matbio.2006.07.002
97. Studer RK, Gilbertson LG, Georgescu H, Sowa G, Vo N, Kang JD. p38 MAPK inhibition modulates rabbit nucleus pulposus cell response to IL-1. *J Orthop Res* (2008) 26:991–8. doi:10.1002/jor.20604
98. Klawitter M, Quero L, Klasen J, Liebscher T, Nerlich A, Boos N, et al. Triptolide exhibits anti-inflammatory, anti-catabolic as well as anabolic effects and suppresses TLR expression and MAPK activity in IL-1beta treated human intervertebral disc cells. *Eur Spine J* (2012) 21:850–9. doi:10.1007/s00586-011-1919-y
99. Wuertz K, Quero L, Sekiguchi M, Klawitter M, Nerlich A, Konno S-I, et al. The red wine polyphenol resveratrol shows promising potential for the treatment of nucleus pulposus-mediated pain in vitro and in vivo. *Spine (Phila Pa 1976)* (2011) 36:E1373–84. doi:10.1097/BRS.0b013e318221e655
100. Wang J, Chen H, Cao P, Wu X, Zang F, Shi L, et al. Inflammatory cytokines induce caveolin-1/β-catenin signalling in rat nucleus pulposus cell apoptosis through the p38 MAPK pathway. *Cell Prolif* (2016) 49:362–72. doi:10.1111/cpr.12254
101. Mavrogonatou E, Kletsas D. Effect of varying osmotic conditions on the response of bovine nucleus pulposus cells to growth factors and the activation of the ERK and Akt pathways. *J Orthop Res* (2010) 28:1276–82. doi:10.1002/jor.21140
102. Zhu Y, Liu JT, Yang LY, Du WP, Li XC, Qian X, et al. P38 mitogen-activated protein kinase inhibition modulates nucleus pulposus cell apoptosis in spontaneous resorption of herniated intervertebral discs: an experimental study in rats. *Mol Med Rep* (2016) 13:4001–6. doi:10.3892/mmr.2016.5039
103. Yang C, Cao P, Gao Y, Wu M, Lin Y, Tian Y, et al. Differential expression of p38 MAPK alpha, beta, gamma, delta isoforms in nucleus pulposus modulates

macrophage polarization in intervertebral disc degeneration. *Sci Rep* (2016) 6:22182. doi:10.1038/srep22182

104. Park JJ, Moon HJ, Park JH, Kwon TH, Park Y-K, Kim JH. Induction of proinflammatory cytokine production in intervertebral disc cells by macrophage-like THP-1 cells requires mitogen-activated protein kinase activity. *J Neurosurg Spine* (2016) 24:167–75. doi:10.3171/2015.3.SPINE14729

Conflict of Interest Statement: KW-K (08/03/2017) Relationships Pertaining to Submitted Manuscript—Money payed to the institution: 37.500 $ (CABMM Start-up Grant) Relevant financial activities outside the submitted work—Consulting Money payed to you: 85.000 $ (Schön Clinic Group). All other authors declare that the research was conducted in the absence of any commercial or financial relationships that could be construed as a potential conflict of interest.

Copyright © 2017 Monchaux, Forterre, Spreng, Karol, Forterre and Wuertz-Kozak. This is an open-access article distributed under the terms of the Creative Commons Attribution License (CC BY). The use, distribution or reproduction in other forums is permitted, provided the original author(s) or licensor are credited and that the original publication in this journal is cited, in accordance with accepted academic practice. No use, distribution or reproduction is permitted which does not comply with these terms.

frontiers in Immunology

REVIEW
published: 06 December 2017
doi: 10.3389/fimmu.2017.01734

Role of Incretin Axis in Inflammatory Bowel Disease

*Lihua Duan[1], Xiaoquan Rao[2], Zachary Braunstein[3], Amelia C. Toomey[4] and Jixin Zhong[2]**

[1] Department of Rheumatology and Clinical Immunology, The First Affiliated Hospital of Xiamen University, Xiamen, China, [2] Cardiovascular Research Institute, Case Western Reserve University, Cleveland, OH, United States, [3] Boonshoft School of Medicine, Wright State University, Dayton, OH, United States, [4] Department of Health Sciences, University of Missouri, Columbia, MO, United States

The inflammatory bowel diseases (IBDs), including Crohn's disease (CD) and ulcerative colitis (UC), are chronic inflammatory conditions of the gastrointestinal tract and involve a complicated reciprocity of environmental, genetic, and immunologic factors. Despite substantial advances in the foundational understanding of the immunological pathogenesis of IBD, the detailed mechanism of the pathological progression in IBD remains unknown. In addition to Th1/Th2 cells, whose role in IBD has been previously well defined, recent evidence indicates that Th17 cells and Tregs also play a crucial role in the development of IBD. Diets which contain excess sugars, salt, and fat may also be important actors in the pathogenesis of IBD, which may be the cause of high IBD incidence in western developed and industrialized countries. Up until now, the reason for the variance in prevalence of IBD between developed and developing countries has been unknown. This is partly due to the increasing popularity of western diets in developing countries, which makes the data harder to interpret. The enterocrinins glucagon-like peptides (GLPs), including GLP-1 and GLP-2, exhibit notable benefits on lipid metabolism, atherosclerosis formation, plasma glucose levels, and maintenance of gastric mucosa integrity. In addition to the regulation of nutrient metabolism, the emerging role of GLPs and their degrading enzyme dipeptidyl peptidase-4 (DPP-4) in gastrointestinal diseases has gained increasing attention. Therefore, here we review the function of the DPP-4/GLP axis in IBD.

Keywords: incretin, inflammatory bowel diseases, dipeptidyl peptidase-4, glucagon-like peptide-1, liraglutide

OPEN ACCESS

Edited by:
Kai Fang,
University of California, Los Angeles, United States

Reviewed by:
Maria Angela Sortino,
Università degli Studi di Catania, Italy
Andrew S. Day,
University of Otago, New Zealand

****Correspondence:***
Jixin Zhong
jixin.zhong@case.edu

Specialty section:
This article was submitted to Inflammation, a section of the journal Frontiers in Immunology

Received: *25 September 2017*
Accepted: *23 November 2017*
Published: *06 December 2017*

Citation:
Duan L, Rao X, Braunstein Z, Toomey AC and Zhong J (2017) Role of Incretin Axis in Inflammatory Bowel Disease. Front. Immunol. 8:1734. doi: 10.3389/fimmu.2017.01734

INTRODUCTION

Inflammatory bowel diseases (IBDs), including Crohn's disease (CD) and ulcerative colitis (UC), are chronic intestinal inflammatory conditions that might be caused by environmental, genetic, and immunological imbalances (1–3). The clinical treatments for these diseases are very limited and inefficient (4, 5). To develop novel therapeutic strategies for IBD, enormous research has been focused on exploring the detailed mechanism of IBD pathophysiology. Animal models, including trinitrobenzene sulfonic acid (TNBS)-induced experimental colitis, dextran sulfate salt (DSS)-induced colitis, and a number of genetic mouse models (such as IL-$10^{-/-}$), have been established to study the underlying mechanisms (6).

It is well accepted that dysregulated immune response plays a critical role in colitis (7–10). Tumor necrosis factor-α (TNF-α) is a well-studied cytokine that is implicated in the pathological progression of human IBD. Inhibition of TNF-α activity by anti-TNF-α antibody has been widely

used as a clinical treatment for IBD. Studies also indicate a profound role of the Th17/Treg axis in the pathogenesis of IBD (11, 12). Therefore, the immune suppressive drugs which can inhibit the effector T cells immune response and promoting Treg expansion are also being used in IBD patients. However, not all patients exhibit an effective response to this therapy (13, 14). In addition, serious side effects, including infection, anaphylaxis, and malignancy, have been observed during these treatments (15). Therefore, alternative therapeutics are imperative for the treatment of IBD.

Glucagon-like peptides (GLPs), including GLP-1 and GLP-2, are secreted by the endocrine cells in the gut up on nutrient uptake (16–18). Through stimulating the islet β cells to secret insulin, inhibiting gastric emptying, and reducing food ingestion, GLP-1 plays a crucial role in lowering blood glucose and controlling body weight (19, 20). Therefore, GLP-1 was used in human subjects with type 2 diabetes, especially in obese patients with type 2 diabetes (21, 22). In contrast, GLP-2 is used as a therapy for intestinal injury and short bowel syndrome due to its effects of promoting mucosal epithelium expansion, and crypt cell proliferation and improving intestinal adaptation and nutrient absorption (23–27). Because GLPs are degraded by dipeptidyl peptidase-4 (DPP-4) very quickly, resulting in very short half-lives (minutes) *in vivo* (28–31), the DPP-4 inhibitors have recently gained increasing attention (19, 21).

The role of incretin hormones in bowel disease has not been demonstrated until recently (32, 33). In DSS-induced colitis, the severity of intestinal injury was increased in GLP-1R$^{-/-}$ mice (34). In consistency with this, administration of GLP-2 led to significant improvements in animal weight loss and intestinal inflammation in IL-10-deficient mice, a spontaneous colitis mouse model (35). Here, we will discuss in-depth the actions of DPP-4/GLP axis in IBD.

OVERVIEW OF GLP FUNCTION

Glucagon-like peptide-1 exerts pleiotropic function through binding to the GLP-1 receptor and is involved in the development and progression of many diseases (17, 18). The GLP-1 receptor is widely expressed in many organs and tissues, including the endocrine pancreas, gastrointestinal tract, heart, and central nervous system. More recent work has shown that a defect in cellular response to GLP-1, akin to insulin resistance, in combination with a diminishment of GLP-1, has a predominant role in the pathogenesis of patients with T2DM. Exogenous administration of pharmacological doses of GLP-1 receptor agonists have been shown to restore β-cell sensitivity to insulin and induce the secretion of insulin. Impaired incretin response is associated with insulin resistance in both non-diabetic and diabetic individuals (36, 37).

The first two amino-acid residues in the *N*-terminus of GLP-1 are His–Ala, which causes its susceptibility to DPP-4 degradation. The *N*-terminal His–Ala residues of GLP-1 are rapidly cleaved by DPP-4 expressed on surrounding tissues, resulting in the inactivation of GLP-1 (38). Exenatide, liraglutide, dulaglutide, albiglutide, and lixisenatide are structurally modified GLP-1 analogs used in the clinical setting, exhibiting relative resistance to the cleavage by DPP-4, and a long-circulating half-life (39). Exogenous GLP-1 administration potently inhibits gastric emptying in rodent and human studies, which favors body weight loss (40). Diabetic patients are prone to develop cardiac disorders; the actions of GLP-1 on cardiac function were investigated (41). Since GLP-1 receptor is widely expressed in the brain, the role of GLP-1 in central nervous system, beyond its regulatory function on glycemic control, was explored (42, 43). Expectedly, GLP-1 possesses a protective effect on neuronal damage by reducing ibotenic acid-induced depletion of choline acetyltransferase immunoreactivity (44). GLP-1 receptor-deficient mice were shown to have defects in cognitive function (45), synaptic plasticity, and memory formation (46), which are recovered by transferring the GLP-1R gene in the hippocampus (47). These data reveal that GLP-1 may have pleiotropic functions in a multitude of diseases. The actions of GLP-1 in IBD will be discussed below.

Glucagon-like peptide-2 is a 33 amino-acid peptide and that is cleaved by DPP-4 in rodents and humans, but with a half-life that is slightly longer than GLP-1 (17). Unlike GLP-1, which plays a role in glucose homeostasis, GLP-2 primarily exerts a potential effect in intestinal weight gain, mucosal development, and intestinal integrity (17, 27). In view of the above-mentioned effects, GLP-2 treatment reduced intestinal inflammation and improved intestinal healing after injury (48, 49). In addition to the benefits in improving intestinal integrity, GLP-2 also exhibits antimicrobial effects by regulating the synthesis and activity of Paneth cell-produced antimicrobial peptides (50). In addition, GLP-2 reduces bacterial invasion by promoting secretory immunoglobulin A (IgA) expression (51). Because GLP-2 receptor is widely expressed on many tissues and cells, physiological effects of GLP-2 beyond the gut have also been reported. Like GLP-1, GLP-2 also regulates the function of central nervous system (52). Activation of GLP-2 receptors can reduce stress-induced depression (53, 54) and improve memory in animal experiments (55). It also plays a substantial role in bone metabolism *via* reducing bone reabsorption and improving bone mineral density (56). GLP-2 has been shown to improve liver regeneration and enhance lung recovery in mice (57, 58). Thus, GLP-2 reveals potential effects in and out of the gastrointestinal tract.

THE ROLE OF GLPs IN IMMUNE REGULATION

Recent studies have demonstrated that GLPs exert inflammation regulatory functions in metabolic disease. Administration of GLP-1 markedly reduced the macrophage infiltration and the production of inflammatory cytokines in the adipose tissue in ob/ob mice (59). GLP-1 has also been shown to regulate invariant natural killer T cells (iNKT) and macrophage function in humans (60, 61). Animal study carried out in Glp1r$^{-/-}$ mice suggested that GLP-1 may play a role in maintaining peripheral Treg numbers and suppressing lymphocyte hyperproliferation (62). Although GLP-2 can also blunt inflammatory cytokine production *via* inhibition of NF-κB activity and ERK phosphorylation (63), enhanced macrophage accumulation was observed in the colon of colitic mice (35). A recent study reported that GLP-1 controls of gut immunity by regulating the intestinal

intraepithelial lymphocyte function, leading to a protective role in the DSS-induced colitis (34). In consistency, GLP-2 treatment also reduced pro-inflammatory cytokine protein levels in the IL-10-deficient mouse model of colitis (35). Taken together, GLPs play a crucial role in inflammation regulation and gut disorders.

PHYSIOLOGICAL ROLE OF DPP-4 FUNCTION

Dipeptidyl peptidase-4, a type-II integral transmembrane glycoprotein, is best known for its catalytic function. A soluble form of DPP-4, which lacks the cytoplasmic and transmembrane domain, with preserved catalytic activity is also detected in the plasma (38, 64). Although the mechanism of regulation of DPP-4 expression remains unclear, TNF-α has been implicated (65, 66). The primary substrates for DPP-4 are enterocrinins, such as GLP-1, GIP, and GLP-2, which are responsible for glucose metabolism (17, 39, 67). DPP-4 gene-deficient mice show improved postprandial glucose control and are resistant to the progression of obesity and hyperinsulinemia. Inhibition of DPP-4 enzymatic activity with pharmacological agent administration improves glucose tolerance in wild-type mice, but not in DPP-4 knockout mice (68).

In addition to enterocrinins, some chemokines and cytokines could also be cleaved by DPP-4, such as stromal cell-derived factor-1 (SDF-1, also known as CXCL12), G-CSF, IL-3, GM-CSF, and erythropoietin, thereby allowing DPP-4 to regulate immune responses (69). DPP-4 also exerts non-catalytic functions *via* interacting with adenosine deaminase (ADA), caveolin-1, fibronectin, and CXCR4 (70, 71). The best-known non-catalytic function is the interaction between DPP-4 and ADA, which can act as a co-stimulatory dyad to promote T-cell activation. Our previous work has demonstrated a role of DPP-4 non-enzymatic function in regulating dendritic cell (DC)/macrophage-mediated adipose tissue inflammation in obesity (64). We also showed that long-term DDP-4 inhibition reduces atherosclerosis and inflammation *via* effects on macrophage migration ($CD11b^+$, $CD11c^+$, and $Ly6C^{hi}$) (72, 73). Furthermore, in non-obese diabetic (NOD) mice, DPP-4 inhibitors significantly increased the TGF-β levels and Treg expansion (74). Beyond that, our recent study, as well as others, demonstrated that DPP-4 plays a role in the infection of Middle Eastern respiratory syndrome (MERS) virus (75).

EFFECTS OF GLP-1 ON IBD

BP-lowering and anti-atherosclerotic effects of GLP-1R agonists have been well demonstrated, while the gastrointestinal effects of GLPs are underappreciated. Here, we will discuss the relationship between GLP-1 and inflammation in the gastrointestinal tract. UC patients with colectomy showed a slower release of GLP-1 in response to intake of glucose (76). Consistently, postprandial GLP-1 response was also impaired in patients with ileostomy (77). Yet it was not known whether the colectomy or inflammatory state affects the GLP-1 release in IBD. Subsequent studies demonstrated that although GLP-1r mRNA levels was reduced in samples harvested from inflamed sites of IBD patients and colitis mice (78), GLP-1 levels were increased in sera of IBD patients when compared with healthy controls (79, 80). The defective GLP-1 release in IBD patients with colectomy might be caused by the loss of the colonic endocrine tissue.

Therefore, these data reveal a link between gut inflammation and GLP-1 expression and brings up an emerging question that how GLP-1 is implicated in IBD. To explore this question, some studies were conducted in experimental animal colitis. In T-cell adoptive transfer-induced colitis, the GLP-1 expression in colonic tissue was significantly diminished in SCID mice with adoptive transfer of $CD4^+$ T cell when compared with control mice (81). Furthermore, in DSS-induced colitis, a considerable increase of GLP-1 was detected in colitic mice with DPP-4 inhibitor treatment (82). Notwithstanding alteration of GLP-1 expression in colitis, the exact role of GLP-1in the development of colitis remains unknown, in terms of being beneficial or detrimental. A recent study showed that the GLP-1 analog liraglutide exerts a significant improvement of disease activity endpoints, including colonic tissues histological changes and colon weight/length ratio, which might be due to its role in reducing inflammatory cytokines and chemokines, such as chemokine (C–C motif) ligand 20 (CCL20), IL-33, and IL-22 (78). As has been previously established, CCL20 is a key chemokine for CCR6 + Th17 cells (83), while IL-33 and IL-22 are the representative cytokines for Th2 and Th17 immune responses, respectively (84, 85). In line with above results, GLP-1 in sterically stabilized phospholipid micelles (GLP-1-SSM), showing a long half-life and resistant to DPP-4, markedly alleviated the development of DSS-induced mice colitis by reducing the expression of pro-inflammatory cytokine IL-1β (86). Moreover, intestinal epithelial architecture in a colitis model with GLP-1-SSM administration was significantly improved. In conclusion, GLP-1 might act as a novel therapeutic tool in ameliorating colonic inflammation.

THE INFLAMMATORY REGULATION OF GLP-2 ON IBD

Regarding the inhibition of enterocyte apoptosis and stimulation of crypt cell proliferation, GLP-2 is thought to be associated with tissue repair during injury or infection (17, 23). Therefore, in chemically induced enteritis (48) or vascular-ischemia reperfusion injury (87–89), GLP-2 shows a protective effect based on reducing epithelial barrier damage and lowering bacterial infection. It stands to reason that GLP-2 might be a potential therapeutic target in IBD, a condition characterized by destruction of the gastrointestinal epithelium. In an adoptive $CD4^+$ T-cell transfer model of colitis, the amount of GLP-2 in colon tissue was also further decreased compared with that in normal mice or SCID mice without $CD4^+$ T-cell adoptive transfer (81). However, these results were not duplicated in human IBD samples. A study showed no changes of GLP-2 levels in fasting plasma between IBD patients and controls, which pinpoints L-cell secretion is not altered in the pathogenesis of IBD (90). Nevertheless, the circulating levels of bioactive GLP-2 (1–33) were markedly increased in CD and UC patients (91). The alteration of GLP-2 (1–33) might be due to an adoptive response to intestinal injury,

which promotes mucosal epithelium restoration in a self-repair mechanism. The discrepant data might be the causal agent of the different inflammatory conditions, because an increase in GLP-2-immunoreactive L cells was found in remissive status of colitis. Another reason is probably due to the detection reagent which detects all GLP-2 or bioactive GLP-2 (1–33).

Beyond the promotion of crypt cell proliferation and mucosal integrity, GLP-2 also exerts a distinct role in anti-inflammatory actions. To mimic anti-inflammatory therapeutic approaches in humans, a combination of GLP-2 with aminosalicylates (ASAs) or corticosteroids were administrated into mice with DSS-induced colitis, while no synergistic effect was observed. Interestingly, corticosteroid administration prevented the intestinal weight increase when the mice were treated with corticosteroids and GLP-2 (92), while these treatments exhibited a similar anti-inflammatory effect in colonic tissues. However, in TNBS-induced ileitis and DSS-induced colitis, GLP-2 treatment downregulated expression of inflammatory cytokines, including IFN-γ, TNF-α, and IL-1β, while the anti-inflammatory cytokine IL-10 was increased (93). Another report also showed that GLP-2 alleviates the development of colitis through reducing the pro-inflammatory cytokines in IL-10-deficient mouse model. The level of inducible nitric oxide synthase (iNOS), a marker for classically activated macrophage, was reduced in GLP-2-treated mice (35). This suggests that GLP-2 might alter macrophage polarization.

It is noteworthy that chronic colitis is a risk factor for colon cancer. Interestingly, a few reports have shown that exogenous and endogenous GLP-2 is a potential cancer promoter in mice models, although reduced inflammation was also observed (94, 95). This might be resulted from the strong preference of GLP-2 for epithelium proliferation. Therefore, the surveillance of dysplasia and colon cancer must be vigilant in GLP-2 treatment.

INHIBITION OF DPP-4 FUNCTION IN IBD

Regarding a catalytic function of DPP-4 on GLP-1 and GLP-2, previous studies have demonstrated that DPP-4 can act as an immune regulator *via* its expression on immune cells and the ability to cleave biologically active chemokines and cytokines. Hence, DPP-4 involvement in the pathogenesis of colitis has been proposed (96). The involvement of DPP-4 might depend on two major pathways: the catalytic function and non-catalytic function (38, 73, 97). Like GLP-2, DPP-4 inhibitors have a proliferative effect on the colonic epithelium (98). It has also been demonstrated that the protective effects of DPP-4 inhibitors in IBD might be a result of increased levels of GLP-1 (82). Notably, plasma GLP-2 levels were increased in response to DPP-4 inhibitor. Thus, the effect on epithelium expansion induced by DPP-4 inhibitor probably relies on the indirect elevation of GLP-2 expression (99). To investigate the influence of DPP-4 in the pathogenesis of DSS-induced colitis, DPP-4-deficient mice were used in DSS treatment, and an increase of myeloperoxidase (MPO) activity and expression of NF-κB p65 subunit in the colonic tissues was observed. Furthermore, an increase in the percentage of splenic $CD8^+$ cells and NKT cells in CD26-deficient mice was observed (100). In keeping with GLP-2-treated mice, DPP-4-deficient mice also showed a significant increase in macrophages when compared with wild-type mice (101). These data reveal a detrimental role of DPP-4 during the development of colitis. Conversely, DPP-4-deficient rats reveal an apparent diminished disease activity index (DAI) in the low-dose DSS-induced colitis, especially in 1% DSS-induced colitis (102). A similar effect was also investigated in DPP-4 inhibitor anagliptin- and ER-319711-treated mice with DSS-induced colitis (98). In addition to ER-319711, anagliptin administration ameliorated the body weight loss and DAI. Additionally, a significantly lower histological score was observed in the anagliptin-treated group (103), which suggests that inhibition of the DPP-4 activity can facilitate the resolution of mucosal damage. Taken together, these findings suggest a complex and dichotomous biology during the development of IBD, which might be due to its multifunction.

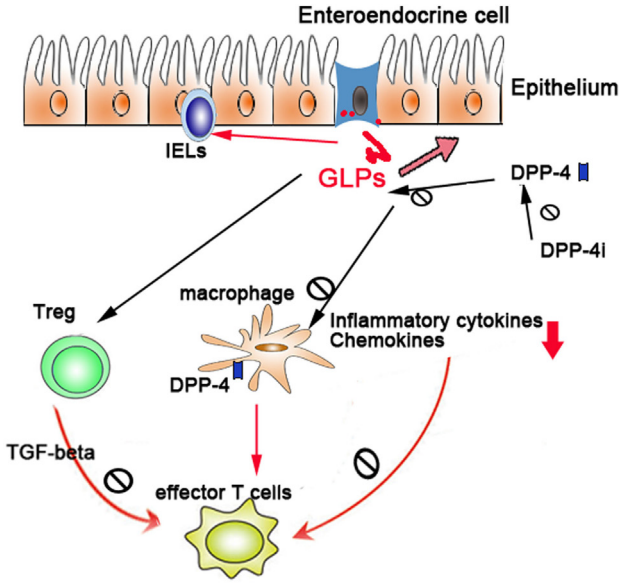

FIGURE 1 | The regulatory role of dipeptidyl peptidase-4 (DPP-4)/glucagon-like peptides (GLPs) in gut immunity: DPP-4/GLP axis regulates gut inflammation through (1) promoting the tissue repair of injured epithelium, (2) regulating the differentiation and functions of Treg and intraepithelial lymphocytes, and (3) regulating the function of macrophages and dendritic cells.

CONCLUSION

Due to the vital role of GLPs in intestinal healing and anti-inflammatory function, a sound understanding of the production, regulation, and function of GLPs and their degrading enzyme DPP-4 will facilitate the treatment of colitis. The potential mechanisms (**Figure 1**) of DPP-4/GLP axis in the IBD may include the following: (1) GLPs promote the tissue repair of injured epithelium; (2) GLPs regulate T-cell differentiation and functions (e.g., Treg, effector T cells, and intraepithelial lymphocytes); (3) GLPs and DPP-4 regulate the function of innate immune cells such as macrophages and DCs; and (4) suppression of DPP-4 enzymatic activities by pharmacological inhibitors preserves GLP function.

Although most studies in this area mainly were carried out on animal models and there are limited clinical trials, a phase-II clinical trial of teduglutide (a GLP-2 analog) observed a remission rate of 55.6% in CD patients (104). To what extent GLPs and DPP-4 contributes to IBD in humans requires further investigation.

AUTHOR CONTRIBUTIONS

LD and XR reviewed the literature and wrote the first draft. ZB, AT, and JZ reviewed the literature and finalized the manuscript. All authors have read and approved the final manuscript.

FUNDING

This work was supported by grants from NIH (K01 DK105108), American Heart Association (17GRNT33670485), American Association of Immunologists (CIIF-8745), Boehringer Ingelheim (IIS2015-10485), and National Natural Science Foundation of China (81670431 and 81671544).

REFERENCES

1. Gensollen T, Iyer SS, Kasper DL, Blumberg RS. How colonization by microbiota in early life shapes the immune system. *Science* (2016) 352(6285):539–44. doi:10.1126/science.aad9378
2. Uniken Venema WT, Voskuil MD, Dijkstra G, Weersma RK, Festen EA. The genetic background of inflammatory bowel disease: from correlation to causality. *J Pathol* (2017) 241(2):146–58. doi:10.1002/path.4817
3. Huang Y, Chen Z. Inflammatory bowel disease related innate immunity and adaptive immunity. *Am J Transl Res* (2016) 8(6):2490–7.
4. Coskun M, Vermeire S, Nielsen OH. Novel targeted therapies for inflammatory bowel disease. *Trends Pharmacol Sci* (2017) 38(2):127–42. doi:10.1016/j.tips.2016.10.014
5. Korzenik JR, Podolsky DK. Evolving knowledge and therapy of inflammatory bowel disease. *Nat Rev Drug Discov* (2006) 5(3):197–209. doi:10.1038/nrd1986
6. Elson CO, Sartor RB, Tennyson GS, Riddell RH. Experimental models of inflammatory bowel disease. *Gastroenterology* (1995) 109(4):1344–67. doi:10.1016/0016-5085(95)90599-5
7. te Velde AA, de Kort F, Sterrenburg E, Pronk I, ten Kate FJ, Hommes DW, et al. Comparative analysis of colonic gene expression of three experimental colitis models mimicking inflammatory bowel disease. *Inflamm Bowel Dis* (2007) 13(3):325–30. doi:10.1002/ibd.20079
8. Bhan AK, Mizoguchi E, Smith RN, Mizoguchi A. Lessons for human inflammatory bowel disease from experimental models. *Curr Opin Gastroenterol* (1999) 15(4):285–90. doi:10.1097/00001574-199907000-00002
9. Bouma G, Strober W. The immunological and genetic basis of inflammatory bowel disease. *Nat Rev Immunol* (2003) 3(7):521–33. doi:10.1038/nri1132
10. Neurath MF, Finotto S, Glimcher LH. The role of Th1/Th2 polarization in mucosal immunity. *Nat Med* (2002) 8(6):567–73. doi:10.1038/nm0602-567
11. Siakavellas SI, Bamias G. Role of the IL-23/IL-17 axis in Crohn's disease. *Discov Med* (2012) 14(77):253–62.
12. Omenetti S, Pizarro TT. The Treg/Th17 Axis: a dynamic balance regulated by the gut microbiome. *Front Immunol* (2015) 6:639. doi:10.3389/fimmu.2015.00639
13. Levin AD, Wildenberg ME, van den Brink GR. Mechanism of action of anti-TNF therapy in inflammatory bowel disease. *J Crohns Colitis* (2016) 10(8):989–97. doi:10.1093/ecco-jcc/jjw053
14. Palladino MA, Bahjat FR, Theodorakis EA, Moldawer LL. Anti-TNF-alpha therapies: the next generation. *Nat Rev Drug Discov* (2003) 2(9):736–46. doi:10.1038/nrd1175
15. Gisbert JP, Marin AC, Chaparro M. The risk of relapse after anti-TNF discontinuation in inflammatory bowel disease: systematic review and meta-analysis. *Am J Gastroenterol* (2016) 111(5):632–47. doi:10.1038/ajg.2016.54
16. Brubaker PL, Drucker DJ. Structure-function of the glucagon receptor family of G protein-coupled receptors: the glucagon, GIP, GLP-1, and GLP-2 receptors. *Receptors Channels* (2002) 8(3–4):179–88. doi:10.1080/10606820213687
17. Drucker DJ. Biological actions and therapeutic potential of the glucagon-like peptides. *Gastroenterology* (2002) 122(2):531–44. doi:10.1053/gast.2002.31068
18. Marathe CS, Rayner CK, Jones KL, Horowitz M. Glucagon-like peptides 1 and 2 in health and disease: a review. *Peptides* (2013) 44:75–86. doi:10.1016/j.peptides.2013.01.014
19. Gallwitz B. Glucagon-like peptide-1-based therapies for the treatment of type 2 diabetes mellitus. *Treat Endocrinol* (2005) 4(6):361–70. doi:10.2165/00024677-200504060-00005
20. Young A. Inhibition of gastric emptying. *Adv Pharmacol* (2005) 52:99–121. doi:10.1016/S1054-3589(05)52006-4
21. Gutzwiller JP, Drewe J, Goke B, Schmidt H, Rohrer B, Lareida J, et al. Glucagon-like peptide-1 promotes satiety and reduces food intake in patients with diabetes mellitus type 2. *Am J Physiol* (1999) 276(5 Pt 2):R1541–4.
22. Flint A, Raben A, Astrup A, Holst JJ. Glucagon-like peptide 1 promotes satiety and suppresses energy intake in humans. *J Clin Invest* (1998) 101(3):515–20. doi:10.1172/JCI990
23. Drucker DJ. Glucagon-like peptides: regulators of cell proliferation, differentiation, and apoptosis. *Mol Endocrinol* (2003) 17(2):161–71. doi:10.1210/me.2002-0306
24. Suri M, Turner JM, Sigalet DL, Wizzard PR, Nation PN, Ball RO, et al. Exogenous glucagon-like peptide-2 improves outcomes of intestinal adaptation in a distal-intestinal resection neonatal piglet model of short bowel syndrome. *Pediatr Res* (2014) 76(4):370–7. doi:10.1038/pr.2014.97
25. Jeppesen PB, Sanguinetti EL, Buchman A, Howard L, Scolapio JS, Ziegler TR, et al. Teduglutide (ALX-0600), a dipeptidyl peptidase IV resistant glucagon-like peptide 2 analogue, improves intestinal function in short bowel syndrome patients. *Gut* (2005) 54(9):1224–31. doi:10.1136/gut.2004.061440
26. Jeppesen PB. Clinical significance of GLP-2 in short-bowel syndrome. *J Nutr* (2003) 133(11):3721–4.
27. Martin GR, Wallace LE, Hartmann B, Holst JJ, Demchyshyn L, Toney K, et al. Nutrient-stimulated GLP-2 release and crypt cell proliferation in experimental short bowel syndrome. *Am J Physiol Gastrointest Liver Physiol* (2005) 288(3):G431–8. doi:10.1152/ajpgi.00242.2004
28. Mentlein R, Gallwitz B, Schmidt WE. Dipeptidyl-peptidase IV hydrolyses gastric inhibitory polypeptide, glucagon-like peptide-1(7-36)amide, peptide histidine methionine and is responsible for their degradation in human serum. *Eur J Biochem* (1993) 214(3):829–35. doi:10.1111/j.1432-1033.1993.tb17986.x
29. Deacon CF, Nauck MA, Toft-Nielsen M, Pridal L, Willms B, Holst JJ. Both subcutaneously and intravenously administered glucagon-like peptide I are rapidly degraded from the NH2-terminus in type II diabetic patients and in healthy subjects. *Diabetes* (1995) 44(9):1126–31. doi:10.2337/diab.44.9.1126
30. Brubaker PL, Crivici A, Izzo A, Ehrlich P, Tsai CH, Drucker DJ. Circulating and tissue forms of the intestinal growth factor, glucagon-like peptide-2. *Endocrinology* (1997) 138(11):4837–43. doi:10.1210/endo.138.11.5482
31. Hartmann B, Harr MB, Jeppesen PB, Wojdemann M, Deacon CF, Mortensen PB, et al. In vivo and in vitro degradation of glucagon-like peptide-2 in humans. *J Clin Endocrinol Metab* (2000) 85(8):2884–8. doi:10.1210/jcem.85.8.6717
32. Zietek T, Waldschmitt N, Rath E. Role of incretin hormones in bowel diseases. *Endocr Dev* (2017) 32:49–73. doi:10.1159/000475731
33. Zietek T, Rath E. Inflammation meets metabolic disease: gut feeling mediated by GLP-1. *Front Immunol* (2016) 7:154. doi:10.3389/fimmu.2016.00154
34. Yusta B, Baggio LL, Koehler J, Holland D, Cao X, Pinnell LJ, et al. GLP-1R agonists modulate enteric immune responses through the intestinal intraepithelial lymphocyte GLP-1R. *Diabetes* (2015) 64(7):2537–49. doi:10.2337/db14-1577
35. Ivory CP, Wallace LE, McCafferty DM, Sigalet DL. Interleukin-10-independent anti-inflammatory actions of glucagon-like peptide 2.

Am J Physiol Gastrointest Liver Physiol (2008) 295(6):G1202–10. doi:10.1152/ajpgi.90494.2008
36. Rask E, Olsson T, Soderberg S, Johnson O, Seckl J, Holst JJ, et al. Impaired incretin response after a mixed meal is associated with insulin resistance in nondiabetic men. *Diabetes Care* (2001) 24(9):1640–5. doi:10.2337/diacare.24.9.1640
37. Holst JJ, Knop FK, Vilsboll T, Krarup T, Madsbad S. Loss of incretin effect is a specific, important, and early characteristic of type 2 diabetes. *Diabetes Care* (2011) 34(Suppl 2):S251–7. doi:10.2337/dc11-s227
38. Zhong J, Maiseyeu A, Davis SN, Rajagopalan S. DPP4 in cardiometabolic disease: recent insights from the laboratory and clinical trials of DPP4 inhibition. *Circ Res* (2015) 116(8):1491–504. doi:10.1161/CIRCRESAHA.116.305665
39. Gupta A, Jelinek HF, Al-Aubaidy H. Glucagon like peptide-1 and its receptor agonists: their roles in management of Type 2 diabetes mellitus. *Diabetes Metab Syndr* (2017) 11(3):225–30. doi:10.1016/j.dsx.2016.09.003
40. Burcelin R, Gourdy P. Harnessing glucagon-like peptide-1 receptor agonists for the pharmacological treatment of overweight and obesity. *Obes Rev* (2017) 18(1):86–98. doi:10.1111/obr.12465
41. Waldrop G, Zhong J, Peters M, Rajagopalan S. Incretin-based therapy for diabetes: what a cardiologist needs to know. *J Am Coll Cardiol* (2016) 67(12):1488–96. doi:10.1016/j.jacc.2015.12.058
42. Muscogiuri G, DeFronzo RA, Gastaldelli A, Holst JJ. Glucagon-like peptide-1 and the central/peripheral nervous system: crosstalk in diabetes. *Trends Endocrinol Metab* (2017) 28(2):88–103. doi:10.1016/j.tem.2016.10.001
43. Holt MK, Trapp S. The physiological role of the brain GLP-1 system in stress. *Cogent Biol* (2016) 2(1):1229086. doi:10.1080/23312025.2016.1229086
44. Perry T, Haughey NJ, Mattson MP, Egan JM, Greig NH. Protection and reversal of excitotoxic neuronal damage by glucagon-like peptide-1 and exendin-4. *J Pharmacol Exp Ther* (2002) 302(3):881–8. doi:10.1124/jpet.102.037481
45. Li PC, Liu LF, Jou MJ, Wang HK. The GLP-1 receptor agonists exendin-4 and liraglutide alleviate oxidative stress and cognitive and micturition deficits induced by middle cerebral artery occlusion in diabetic mice. *BMC Neurosci* (2016) 17(1):37. doi:10.1186/s12868-016-0272-9
46. Cai HY, Wang ZJ, Holscher C, Yuan L, Zhang J, Sun P, et al. Lixisenatide attenuates the detrimental effects of amyloid beta protein on spatial working memory and hippocampal neurons in rats. *Behav Brain Res* (2017) 318:28–35. doi:10.1016/j.bbr.2016.10.033
47. During MJ, Cao L, Zuzga DS, Francis JS, Fitzsimons HL, Jiao X, et al. Glucagon-like peptide-1 receptor is involved in learning and neuroprotection. *Nat Med* (2003) 9(9):1173–9. doi:10.1038/nm919
48. Boushey RP, Yusta B, Drucker DJ. Glucagon-like peptide 2 decreases mortality and reduces the severity of indomethacin-induced murine enteritis. *Am J Physiol* (1999) 277(5 Pt 1):E937–47.
49. Bulut K, Meier JJ, Ansorge N, Felderbauer P, Schmitz F, Hoffmann P, et al. Glucagon-like peptide 2 improves intestinal wound healing through induction of epithelial cell migration in vitro-evidence for a TGF-beta-mediated effect. *Regul Pept* (2004) 121(1–3):137–43. doi:10.1016/j.regpep.2004.04.014
50. Lee SJ, Lee J, Li KK, Holland D, Maughan H, Guttman DS, et al. Disruption of the murine Glp2r impairs Paneth cell function and increases susceptibility to small bowel enteritis. *Endocrinology* (2012) 153(3):1141–51. doi:10.1210/en.2011-1954
51. Chen J, Dong JT, Li XJ, Gu Y, Cheng ZJ, Cai YK. Glucagon-like peptide-2 protects impaired intestinal mucosal barriers in obstructive jaundice rats. *World J Gastroenterol* (2015) 21(2):484–90. doi:10.3748/wjg.v21.i2.484
52. Brubaker PL, Drucker DJ. Minireview: glucagon-like peptides regulate cell proliferation and apoptosis in the pancreas, gut, and central nervous system. *Endocrinology* (2004) 145(6):2653–9. doi:10.1210/en.2004-0015
53. Sasaki-Hamada S, Nakamura R, Nakao Y, Akimoto T, Sanai E, Nagai M, et al. Antidepressant-like effects exerted by the intranasal administration of a glucagon-like peptide-2 derivative containing cell-penetrating peptides and a penetration-accelerating sequence in mice. *Peptides* (2016) 87:64–70. doi:10.1016/j.peptides.2016.11.013
54. Sasaki-Hamada S, Yuri Y, Hoshi M, Oka JI. Immunohistochemical determination of the site of antidepressant-like effects of glucagon-like peptide-2 in ACTH-treated mice. *Neuroscience* (2015) 294:156–65. doi:10.1016/j.neuroscience.2015.03.010
55. Iwai T, Jin K, Ohnuki T, Sasaki-Hamada S, Nakamura M, Saitoh A, et al. Glucagon-like peptide-2-induced memory improvement and anxiolytic effects in mice. *Neuropeptides* (2015) 49:7–14. doi:10.1016/j.npep.2014.11.001
56. Henriksen DB, Alexandersen P, Hartmann B, Adrian CL, Byrjalsen I, Bone HG, et al. Four-month treatment with GLP-2 significantly increases hip BMD: a randomized, placebo-controlled, dose-ranging study in postmenopausal women with low BMD. *Bone* (2009) 45(5):833–42. doi:10.1016/j.bone.2009.07.008
57. El-Jamal N, Erdual E, Neunlist M, Koriche D, Dubuquoy C, Maggiotto F, et al. Glugacon-like peptide-2: broad receptor expression, limited therapeutic effect on intestinal inflammation and novel role in liver regeneration. *Am J Physiol Gastrointest Liver Physiol* (2014) 307(3):G274–85. doi:10.1152/ajpgi.00389.2012
58. Arda-Pirincci P, Oztay F, Bayrak BB, Yanardag R, Bolkent S. Teduglutide, a glucagon-like peptide 2 analogue: a novel protective agent with anti-apoptotic and anti-oxidant properties in mice with lung injury. *Peptides* (2012) 38(2):238–47. doi:10.1016/j.peptides.2012.09.030
59. Lee YS, Park MS, Choung JS, Kim SS, Oh HH, Choi CS, et al. Glucagon-like peptide-1 inhibits adipose tissue macrophage infiltration and inflammation in an obese mouse model of diabetes. *Diabetologia* (2012) 55(9):2456–68. doi:10.1007/s00125-012-2592-3
60. Lynch L, Hogan AE, Duquette D, Lester C, Banks A, LeClair K, et al. iNKT cells induce FGF21 for thermogenesis and are required for maximal weight loss in GLP1 therapy. *Cell Metab* (2016) 24(3):510–9. doi:10.1016/j.cmet.2016.08.003
61. Ebinger M, Jehle DR, Fussgaenger RD, Fehmann HC, Jehle PM. Glucagon-like peptide-1 improves insulin and proinsulin binding on RINm5F cells and human monocytes. *Am J Physiol Endocrinol Metab* (2000) 279(1):E88–94.
62. Hadjiyanni I, Siminovitch KA, Danska JS, Drucker DJ. Glucagon-like peptide-1 receptor signalling selectively regulates murine lymphocyte proliferation and maintenance of peripheral regulatory T cells. *Diabetologia* (2010) 53(4):730–40. doi:10.1007/s00125-009-1643-x
63. Xie S, Liu B, Fu S, Wang W, Yin Y, Li N, et al. GLP-2 suppresses LPS-induced inflammation in macrophages by inhibiting ERK phosphorylation and NF-kappaB activation. *Cell Physiol Biochem* (2014) 34(2):590–602. doi:10.1159/000363025
64. Zhong J, Rao X, Deiuliis J, Braunstein Z, Narula V, Hazey J, et al. A potential role for dendritic cell/macrophage-expressing DPP4 in obesity-induced visceral inflammation. *Diabetes* (2013) 62(1):149–57. doi:10.2337/db12-0230
65. Duvnjak L, Blaslov K, Perkovic MN, Cuca JK. Dipeptidyl peptidase-4 activity might be a link between tumour necrosis factor alpha and insulin resistance in type 1 diabetes. *Endocrine* (2016) 53(2):453–8. doi:10.1007/s12020-016-0899-4
66. Salgado FJ, Vela E, Martin M, Franco R, Nogueira M, Cordero OJ. Mechanisms of CD26/dipeptidyl peptidase IV cytokine-dependent regulation on human activated lymphocytes. *Cytokine* (2000) 12(7):1136–41. doi:10.1006/cyto.1999.0643
67. Zhong J, Rao X, Rajagopalan S. An emerging role of dipeptidyl peptidase 4 (DPP4) beyond glucose control: potential implications in cardiovascular disease. *Atherosclerosis* (2013) 226(2):305–14. doi:10.1016/j.atherosclerosis.2012.09.012
68. Marguet D, Baggio L, Kobayashi T, Bernard AM, Pierres M, Nielsen PF, et al. Enhanced insulin secretion and improved glucose tolerance in mice lacking CD26. *Proc Natl Acad Sci U S A* (2000) 97(12):6874–9. doi:10.1073/pnas.120069197
69. Broxmeyer HE, Hoggatt J, O'Leary HA, Mantel C, Chitteti BR, Cooper S, et al. Dipeptidylpeptidase 4 negatively regulates colony-stimulating factor activity and stress hematopoiesis. *Nat Med* (2012) 18(12):1786–96. doi:10.1038/nm.2991
70. Kameoka J, Tanaka T, Nojima Y, Schlossman SF, Morimoto C. Direct association of adenosine deaminase with a T cell activation antigen, CD26. *Science* (1993) 261(5120):466–9. doi:10.1126/science.8101391
71. Wagner L, Klemann C, Stephan M, von Horsten S. Unravelling the immunological roles of dipeptidyl peptidase 4 (DPP4) activity and/or structure homologue (DASH) proteins. *Clin Exp Immunol* (2016) 184(3):265–83. doi:10.1111/cei.12757
72. Shah Z, Kampfrath T, Deiuliis JA, Zhong J, Pineda C, Ying Z, et al. Long-term dipeptidyl-peptidase 4 inhibition reduces atherosclerosis and inflammation via effects on monocyte recruitment and chemotaxis. *Circulation* (2011) 124(21):2338–49. doi:10.1161/CIRCULATIONAHA.111.041418

73. Zhong J, Rajagopalan S. Dipeptidyl peptidase-4 regulation of SDF-1/CXCR4 axis: implications for cardiovascular disease. *Front Immunol* (2015) 6:477. doi:10.3389/fimmu.2015.00477
74. Tian L, Gao J, Hao J, Zhang Y, Yi H, O'Brien TD, et al. Reversal of new-onset diabetes through modulating inflammation and stimulating beta-cell replication in nonobese diabetic mice by a dipeptidyl peptidase IV inhibitor. *Endocrinology* (2010) 151(7):3049–60. doi:10.1210/en.2010-0068
75. Coleman CM, Sisk JM, Halasz G, Zhong J, Beck SE, Matthews KL, et al. CD8+ T cells and macrophages regulate pathogenesis in a mouse model of MERS-CoV disease. *J Virol* (2016) 91(1). doi:10.1128/JVI.01825-16
76. Palnaes Hansen C, Andreasen JJ, Holst JJ. The release of gastric inhibitory peptide, glucagon-like peptide-I, and insulin after oral glucose test in colectomized subjects. *Scand J Gastroenterol* (1997) 32(5):473–7. doi:10.3109/00365529709025084
77. Robertson MD, Livesey G, Morgan LM, Hampton SM, Mathers JC. The influence of the colon on postprandial glucagon-like peptide 1 (7-36) amide concentration in man. *J Endocrinol* (1999) 161(1):25–31. doi:10.1677/joe.0.1610025
78. Bang-Berthelsen CH, Holm TL, Pyke C, Simonsen L, Sokilde R, Pociot F, et al. GLP-1 induces Barrier protective expression in Brunner's glands and regulates colonic inflammation. *Inflamm Bowel Dis* (2016) 22(9):2078–97. doi:10.1097/MIB.0000000000000847
79. Keller J, Beglinger C, Holst JJ, Andresen V, Layer P. Mechanisms of gastric emptying disturbances in chronic and acute inflammation of the distal gastrointestinal tract. *Am J Physiol Gastrointest Liver Physiol* (2009) 297(5):G861–8. doi:10.1152/ajpgi.00145.2009
80. Keller J, Binnewies U, Rosch M, Juul Holst J, Beglinger C, Andresen V, et al. Gastric emptying and disease activity in inflammatory bowel disease. *Eur J Clin Invest* (2015) 45(12):1234–42. doi:10.1111/eci.12542
81. Schmidt PT, Hartmann B, Bregenholt S, Hoist JJ, Claesson MH. Deficiency of the intestinal growth factor, glucagon-like peptide 2, in the colon of SCID mice with inflammatory bowel disease induced by transplantation of CD4+ T cells. *Scand J Gastroenterol* (2000) 35(5):522–7. doi:10.1080/003655200750023796
82. Yazbeck R, Sulda ML, Howarth GS, Bleich A, Raber K, von Horsten S, et al. Dipeptidyl peptidase expression during experimental colitis in mice. *Inflamm Bowel Dis* (2010) 16(8):1340–51. doi:10.1002/ibd.21241
83. Hirota K, Yoshitomi H, Hashimoto M, Maeda S, Teradaira S, Sugimoto N, et al. Preferential recruitment of CCR6-expressing Th17 cells to inflamed joints via CCL20 in rheumatoid arthritis and its animal model. *J Exp Med* (2007) 204(12):2803–12. doi:10.1084/jem.20071397
84. Duan L, Chen J, Zhang H, Yang H, Zhu P, Xiong A, et al. Interleukin-33 ameliorates experimental colitis through promoting Th2/Foxp3(+) regulatory T-cell responses in mice. *Mol Med* (2012) 18:753–61. doi:10.2119/molmed.2011.00428
85. Duan L, Chen J, Gong F, Shi G. The role of IL-33 in rheumatic diseases. *Clin Dev Immunol* (2013) 2013:924363. doi:10.1155/2013/924363
86. Anbazhagan AN, Thaqi M, Priyamvada S, Jayawardena D, Kumar A, Gujral T, et al. GLP-1 nanomedicine alleviates gut inflammation. *Nanomedicine* (2017) 13(2):659–65. doi:10.1016/j.nano.2016.08.004
87. Guan L, Gong D, Tian N, Zou Y. Uncoupling protein 2 involved in protection of glucagon-like peptide 2 in small intestine with ischemia-reperfusion injury in mice. *Dig Dis Sci* (2005) 50(3):554–60. doi:10.1007/s10620-005-2474-3
88. Zhang W, Zhu W, Zhang J, Li N, Li J. Protective effects of glucagon-like peptide 2 on intestinal ischemia-reperfusion rats. *Microsurgery* (2008) 28(4):285–90. doi:10.1002/micr.20491
89. Rajeevprasad R, Alavi K, Schwartz MZ. Glucagonlike peptide-2 analogue enhances intestinal mucosal mass and absorptive function after ischemia-reperfusion injury. *J Pediatr Surg* (2000) 35(11):1537–9. doi:10.1053/jpsu.2000.18301
90. Schmidt PT, Ljung T, Hartmann B, Hare KJ, Holst JJ, Hellstrom PM. Tissue levels and post-prandial secretion of the intestinal growth factor, glucagon-like peptide-2, in controls and inflammatory bowel disease: comparison with peptide YY. *Eur J Gastroenterol Hepatol* (2005) 17(2):207–12. doi:10.1097/00042737-200502000-00012
91. Xiao Q, Boushey RP, Cino M, Drucker DJ, Brubaker PL. Circulating levels of glucagon-like peptide-2 in human subjects with inflammatory bowel disease. *Am J Physiol Regul Integr Comp Physiol* (2000) 278(4):R1057–63.
92. L'Heureux MC, Brubaker PL. Glucagon-like peptide-2 and common therapeutics in a murine model of ulcerative colitis. *J Pharmacol Exp Ther* (2003) 306(1):347–54. doi:10.1124/jpet.103.051771
93. Sigalet DL, Wallace LE, Holst JJ, Martin GR, Kaji T, Tanaka H, et al. Enteric neural pathways mediate the anti-inflammatory actions of glucagon-like peptide 2. *Am J Physiol Gastrointest Liver Physiol* (2007) 293(1):G211–21. doi:10.1152/ajpgi.00530.2006
94. Trivedi S, Wiber SC, El-Zimaity HM, Brubaker PL. Glucagon-like peptide-2 increases dysplasia in rodent models of colon cancer. *Am J Physiol Gastrointest Liver Physiol* (2012) 302(8):G840–9. doi:10.1152/ajpgi.00505.2011
95. Iakoubov R, Lauffer LM, Trivedi S, Kim YI, Brubaker PL. Carcinogenic effects of exogenous and endogenous glucagon-like peptide-2 in azoxymethane-treated mice. *Endocrinology* (2009) 150(9):4033–43. doi:10.1210/en.2009-0295
96. Pucar LB, Detel D, Varljen J. [Dipeptidyl peptidase IV in inflammatory bowel diseases (DPP IV/CD26)]. *Arh Hig Rada Toksikol* (2012) 63(1):75–100. doi:10.2478/10004-1254-63-2012-2185
97. Fatima S, Ruter J, Niess JH, Klapp BF, Arck PC, Hildebrandt M. CD26-/DPP IV-positive lymphocytes in murine acute experimental colitis. *Adv Exp Med Biol* (2003) 524:345–50. doi:10.1007/0-306-47920-6_41
98. Ban H, Bamba S, Imaeda H, Inatomi O, Kobori A, Sasaki M, et al. The DPP-IV inhibitor ER-319711 has a proliferative effect on the colonic epithelium and a minimal effect in the amelioration of colitis. *Oncol Rep* (2011) 25(6):1699–703. doi:10.3892/or.2011.1223
99. Sakanaka T, Inoue T, Yorifuji N, Iguchi M, Fujiwara K, Narabayashi K, et al. The effects of a TGR5 agonist and a dipeptidyl peptidase IV inhibitor on dextran sulfate sodium-induced colitis in mice. *J Gastroenterol Hepatol* (2015) 30(Suppl 1):60–5. doi:10.1111/jgh.12740
100. Detel D, Buljevic S, Pucar LB, Kucic N, Pugel EP, Varljen J. Influence of CD26/dipeptidyl peptidase IV deficiency on immunophenotypic changes during colitis development and resolution. *J Physiol Biochem* (2016) 72(3):405–19. doi:10.1007/s13105-016-0491-7
101. Detel D, Pugel EP, Pucar LB, Buljevic S, Varljen J. Development and resolution of colitis in mice with target deletion of dipeptidyl peptidase IV. *Exp Physiol* (2012) 97(4):486–96. doi:10.1113/expphysiol.2011.061143
102. Iwaya H, Fujii N, Hagio M, Hara H, Ishizuka S. Contribution of dipeptidyl peptidase IV to the severity of dextran sulfate sodium-induced colitis in the early phase. *Biosci Biotechnol Biochem* (2013) 77(7):1461–6. doi:10.1271/bbb.130105
103. Mimura S, Ando T, Ishiguro K, Maeda O, Watanabe O, Ujihara M, et al. Dipeptidyl peptidase-4 inhibitor anagliptin facilitates restoration of dextran sulfate sodium-induced colitis. *Scand J Gastroenterol* (2013) 48(10):1152–9. doi:10.3109/00365521.2013.832366
104. Yazbeck R. Teduglutide, a glucagon-like peptide-2 analog for the treatment of gastrointestinal diseases, including short bowel syndrome. *Curr Opin Mol Ther* (2010) 12(6):798–809.

Conflict of Interest Statement: JZ is currently receiving a grant from Boehringer Ingelheim (IIS2015-10485). The remaining authors have no conflicts of interest.

Copyright © 2017 Duan, Rao, Braunstein, Toomey and Zhong. This is an open-access article distributed under the terms of the Creative Commons Attribution License (CC BY). The use, distribution or reproduction in other forums is permitted, provided the original author(s) or licensor are credited and that the original publication in this journal is cited, in accordance with accepted academic practice. No use, distribution or reproduction is permitted which does not comply with these terms.

frontiers in Immunology

ORIGINAL RESEARCH
published: 11 December 2017
doi: 10.3389/fimmu.2017.01531

Gp96 Peptide Antagonist gp96-II Confers Therapeutic Effects in Murine Intestinal Inflammation

Claudia A. Nold-Petry[1,2], Marcel F. Nold[1,2], Ofer Levy[3], Yossef Kliger[3], Anat Oren[3], Itamar Borukhov[3], Christoph Becker[4], Stefan Wirtz[4], Manjeet K. Sandhu[1,5], Markus Neurath[4] and Charles A. Dinarello[6]*

[1] Ritchie Centre, Hudson Institute of Medical Research, Clayton, VIC, Australia, [2] Department of Paediatrics, Monash University, Melbourne, VIC, Australia, [3] Compugen Ltd., Holon, Israel, [4] Medical Clinic 1, Friedrich Alexander University Erlangen-Nuremberg, Erlangen, Germany, [5] Department of Gastroenterology, Monash Health, Clayton, VIC, Australia, [6] Department of Medicine, University of Colorado Denver, Aurora, CO, United States

OPEN ACCESS

Edited by:
Guixiu Shi,
Xiamen University, China

Reviewed by:
Ka Man Law,
University of California, Los Angeles, United States
Bo-Zong Shao,
Second Military Medical University, China
Dipyaman Ganguly,
Indian Institute of Chemical Biology (CSIR), India

***Correspondence:**
Claudia A. Nold-Petry
claudia.nold@hudson.org.au

Specialty section:
This article was submitted to Inflammation, a section of the journal Frontiers in Immunology

Received: 14 July 2017
Accepted: 27 October 2017
Published: 11 December 2017

Citation:
Nold-Petry CA, Nold MF, Levy O, Kliger Y, Oren A, Borukhov I, Becker C, Wirtz S, Sandhu MK, Neurath M and Dinarello CA (2017) Gp96 Peptide Antagonist gp96-II Confers Therapeutic Effects in Murine Intestinal Inflammation. Front. Immunol. 8:1531. doi: 10.3389/fimmu.2017.01531

Background: The expression of heat shock protein gp96 is strongly correlated with the degree of tissue inflammation in ulcerative colitis and Crohn's disease, thereby leading us to the hypothesis that inhibition of expression *via* gp96-II peptide prevents intestinal inflammation.

Methods: We employed daily injections of gp96-II peptide in two murine models of intestinal inflammation, the first resulting from five daily injections of IL-12/IL-18, the second *via* a single intrarectal application of TNBS (2,4,6-trinitrobenzenesulfonic acid). We also assessed the effectiveness of gp96-II peptide in murine and human primary cell culture.

Results: In the IL-12/IL-18 model, all gp96-II peptide-treated animals survived until day 5, whereas 80% of placebo-injected animals died. gp96-II peptide reduced IL-12/IL-18-induced plasma IFNγ by 89%, IL-1β by 63%, IL-6 by 43% and tumor necrosis factor (TNF) by 70% compared to controls. The clinical assessment Disease Activity Index of intestinal inflammation severity was found to be significantly lower in the gp96-II-treated animals when compared to vehicle-injected mice. gp96-II peptide treatment in the TNBS model limited weight loss to 5% on day 7 compared with prednisolone treatment, whereas placebo-treated animals suffered a 20% weight loss. Histological disease severity was reduced equally by prednisolone (by 40%) and gp96-II peptide (35%). Mice treated with either gp96-II peptide or prednisolone exhibited improved endoscopic scores compared with vehicle-treated control mice: vascularity, fibrin, granularity, and translucency scores were reduced by up to 49% by prednisolone and by up to 30% by gp96-II peptide. *In vitro*, gp96-II peptide reduced TLR2-, TLR4- and IL-12/IL-18-induced cytokine expression in murine splenocytes, with declines in constitutive IL-6 (54%), lipopolysaccharide-induced TNF (48%), IL-6 (81%) and in *Staphylococcus epidermidis*-induced TNF (67%) and IL-6 (81%), as well as IL-12/IL-18-induced IFNγ (75%). gp96-II peptide reduced IL–1β, IL-6, TNF and GM-CSF in human peripheral blood mononuclear cells to a similar degree without affecting cell viability, whereas RANTES, IL-25 and MIF were twofold to threefold increased.

Conclusion: gp96-II peptide protects against murine intestinal inflammation by regulating inflammation *in vivo* and *in vitro*, pointing to its promise as a novel treatment for inflammatory bowel disease.

Keywords: Gp96, cytokines and inflammation, biologics, therapeutics, immunemodulatory, anti-inflammatory agent, intestinal inflammation, inflammatory bowel disease

INTRODUCTION

Inflammatory bowel disease (IBD), which includes Crohn's disease (CD) and ulcerative colitis (UC), is characterized by intense and chronic inflammation of the intestinal tract that damages the epithelium and allows penetration of bacteria across the gut epithelial barrier. Subsequently, T cells infiltrate (1) and release alarmins or damage-associated molecular patterns (DAMPs) such as gp96.

Gp96 is a multifunctional eukaryotic endoplasmic reticulum (ER) heat shock protein (HSP) that is expressed constitutively in virtually all cell types and its synthesis is increased in conditions causing ER stress (2). gp96 plays a chaperone role for most of the toll-like receptors (TLRs) (3, 4) that are essential for the innate immune response recognizing microbial products. In addition to its role in innate immunity, gp96 activates the adaptive immune pathways. After tissue damage or viral infection, gp96 is released into the extracellular space and exerts immune-stimulatory effects such as $CD8^+$ cytotoxic T lymphocyte responses. After receptor-mediated endocytosis by antigen-presenting cells (APC), peptide-loaded gp96 is presented on major histocompatibility complex class I molecules to T cells, which leads to APC activation and increased production of tumor necrosis factor (TNF) and IL-12 (5–7). Extracellular gp96 also induces TLR 4-dependent IL-12 production in dendritic cells (8). Type 1 cytokines, including interleukin (IL)-12 and IL-18, are known to play a key role in human IBD (9–14) and in murine intestinal inflammation (15–17) through their synergistic induction of IFNγ synthesis (18).

To elucidate the critical role of gp96 in promoting T-helper 1 (Th1)-mediated intestinal inflammation we applied two different models of murine inflammation. First, we injected mice daily with IL-12/IL-18, which led to murine intestinal inflammation (15, 19, 20). In order to make our preclinical study more generalizable, we chose TNBS (2,4,6-trinitrobenzenesulfonic acid) as our second model. TNBS represents a model of chemical induced intestinal inflammation and is commonly used to mimic a transmural Th-1 cell-dependent colitis, which causes epithelial injury of the colon (17) and has been widely used to study cytokine secretion patterns and effects of immunotherapies (21). We then tested blocking gp96 in both models of disease by injecting a gp96-blocking peptide (gp96-II).

As we have shown previously, gp96-II is a synthetic peptide that binds to and antagonizes gp96-mediated lipopolysaccharide (LPS)-induced cytokine production in freshly isolated human peripheral blood mononuclear cells (PBMCs) and in a murine LPS-induced endotoxin model (22). Others have shown that peptide-based inhibitors to gp96 can block the HSP90–LPS interaction (23) and that the gp96-II peptide inhibits endogenous gp96 in an allogeneic islet transplantation model by improving islet graft function (24).

Our study here shows that gp96-II peptide has actions beyond blockade of TLR pathways, notably by reducing IL-12/IL-18-, IL–1β- and anti-CD3-induced cytokine production *in vivo* and *in vitro*. Thus gp96 is a highly prospective target for the development of broad-spectrum therapies against multifactorial diseases such as IBD.

MATERIALS AND METHODS

Reagents

RPMI 1640, phosphate-buffered saline (PBS, i.e., vehicle), fetal calf serum (FCS) and penicillin/streptomycin were purchased from Cellgro, Herndon, VA, USA. Pooled human serum was acquired from MP Biomedicals, Solon, OH, USA. LPS (O55:B5), anti-CD3 mAb and Ficoll Hypaque were from Sigma-Aldrich, St. Louis, MO, USA. Canine gp96 protein (Cat # G3057-41, US Biological, Swampscott, MA, USA). We purchased the detection kit for lactate dehydrogenase (LDH) from BioVision (Mountain View, CA, USA). *Staphylococcus epidermidis* (St. epi.) was obtained from the American Type Culture Collection (strain 49134), grown overnight in suspension cultures in LB medium (Difco, Detroit, MI, USA), centrifuged, washed in pyrogen-free vehicle and a small sample was removed for determination of number of organisms by pour plate cultures. The suspension was boiled for 30 min and then remained at room temperature for 24 h. The boiled suspension was diluted in pyrogen-free vehicle to 10 million organisms per milliliter and frozen in small aliquots at −70°C. Recombinant human IL–1β, human and murine IL-12 were obtained from Peprotech, Rocky Hill, NJ, USA, and human and murine IL-18 from MBL International, Woburn, MA, USA. The gp96-II peptide is not commercially available and was provided by Compugen, Tel-Aviv, Israel. Peptide designation residues: gp96-II (active) 444–480 LNVSRETLQQHKLLKVIRKKLVRKTLDMIKKIADDKY.

Isolation of Splenocytes, PBMC and Cell Culture

Spleens of each mouse strain were aseptically removed, macerated and passed through a 70-μm cell strainer. Splenocytes were washed with PBS twice, centrifuged and re-suspended in RPMI with 5% FCS and cultured at 5×10^6/ml in a 24-well flat bottom plate and stimulated as indicated. After 24 h, the supernatant medium was removed for measuring secreted cytokines.

The Colorado Multiple Institutional Review Board approved experiments involving human blood. After informed consent was obtained, PBMCs were isolated from peripheral venous blood of

healthy volunteers by Ficoll Hypaque density gradient centrifugation. After isolation, cells were counted and examined for viability by trypan blue exclusion. For experiments on PBMC, these cells were used without further treatment. Thereafter, 0.5×10^6 cells were resuspended in 0.3 ml fresh RPMI containing 1% human serum and primocin and plated into 48-well flat bottom polystyrene plates. Cells were then either stimulated or remained untreated as controls. After 1 day at 37°C and 5% CO_2, supernatants were taken and the cells were lysed in lysis buffer (50 mM Tris, pH 7.4, 150 mM NaCl, 2 mM EDTA, 2 mM EGTA, 10% glycerol, 1% Triton X-100, 40 mM β-glycerophosphate, 50 mM sodium fluoride, 200 µM sodium vanadate, 10 µg/ml leupeptin, 10 µg/ml aprotinin, 1 µM pepstatin A and 1 mM phenylmethylsulfonyl fluoride) and frozen at −80°C. Before assay, the lysates were clarified by centrifugation at 20,000 × *g* for 10 min and the pellet discarded.

Animal Studies

IL-12/IL-18-Induced Murine Intestinal Inflammation

Animals—8 to 12-week-old C57BL/6 mice were purchased from The Jackson Laboratory (Bar Harbor, ME, USA), housed five per cage and kept on a 12-h light–dark cycle. The University of Colorado Institutional Animal Care and Use Committee approved all experiments.

After daily intraperitoneal (i.p.) injection of male C57BL/6 (3 months, 20–21 g) with 1 µg/mouse of IL-12 and IL-18, mice exhibited chronic intestinal inflammation and a type 1 immune response, causing weight loss and increased serum cytokine levels similar to that described in Ref. (15, 20). For experiments, animals were injected with IL-12/IL-18 in combination with 60 µg/mouse gp96-II peptide (22) and a control group with vehicle. On day 5, mice were anesthetized by using the Open-Drop exposure to isoflurane and plasma was obtained by orbital bleeding into tubes which contained heparin. Animals were then humanely killed by cervical dislocation and spleens were harvested for splenocyte isolation. A small aliquot of the blood was taken for white blood cell counts.

Clinical Assessment of IL-12/IL-18 Induced Murine Intestinal Inflammation

Clinical assessment of IL-12/IL-18 induced intestinal inflammation was performed in all animals at day 2 after treatment, before the vehicle animals started to die at day 3. A combinational index of disease was determined by scoring (research staff blinded to treatment) the change in body weight (%), stool consistency and occult/gross blood stools (**Table 1**) (25). The Disease Activity Index (DAI) was then calculated as the average of the three values.

Induction of TNBS (2,4,6-Trinitrobenzenesulfonic Acid) Colitis in Mice

Eight week old C57BL/6 mice were obtained from the in-house breeding stock at the University of Mainz, Germany. The University of Mainz Animal Care and Use Committee approved all experiments. A total of 60 animals were allocated to 6 groups. The model employs the use of TNBS colitis by administering a total volume of 100 µl of 2 mg TNBS intrarectally at day 0. After day 1, animals were injected intraperitoneally once daily with either placebo or with corticosteroid (prednisolone: 1 g/mouse, which we used as a positive control in this setting) or with 60 µg/mouse of gp96-II peptide twice daily, over a period of 7 days and weight was monitored daily. On day 7, the animals were humanely killed by cervical dislocation.

TABLE 1 | Scoring system for Disease Activity Index (DAI).

Score	Weight loss (%)	Stool consistency	Occult/gross blood in stools
0	None	Normal stool	No blood
1	1–5	Slightly loose	Slightly bloody
2	6–10	Loose stool	Positive blood
3	>10	Diarrhea	Gross bleeding

The degrees of body weight loss, stool consistency and occult/gross blood in stools were quantified as described. The DAI was calculated as the sum of the three scores (25).

Stool consistency: normal stool, stool with an appearance of well-formed pellets; slightly loose stool, loose stool with pasty, semi-formed, soft materials that do not adhere to anal fur; diarrhea, liquid stool that adheres to anal fur. Gross bleeding, an appearance of visible blood adhering to anal fur.

Whole Blood Assay

To investigate the long-term protective effects of gp96-II peptide, we performed *ex vivo* whole blood assays. Whole blood of animals from the IL-12/IL-18 ± gp96-II intestinal inflammation model was challenged *in vitro* with a "second hit" (i.e., stimulation with a TLR2-, TLR4-agonist or IL-1β) without further *in vitro* gp96-II peptide treatment. Blood was obtained by orbital bleeding after a 5-day injection series. A small aliquot was taken for white blood cell counts. The remaining whole blood was diluted 1:5 in RPMI and stimulated for 20 h. After this incubation, cultures were lysed with Triton X-100 (final concentration of 0.5%) and underwent a freeze–thaw cycle before cytokine determination.

Electrochemiluminescence (ECL) Assays and Enzyme-linked Immunosorbent Assay (ELISA)

Human IL-1α, IL–1β, IL-6, IFNγ and TNF as well as murine IL-6, IL-1α, IL–1β and TNF were measured using specific antibody pairs and an Origen Analyzer (Wellstat Diagnostics, Gaithersburg, MD, USA) as described (26). Antibody pairs for all cytokines were obtained from R&D Systems with the exception of the purchase of IFNγ from Fitzgerald Industries International (Concord, MA, USA). Murine IFNγ was determined by ELISA (R&D Systems) according to the manufacturer's instructions. Recombinant cytokines for ECL or ELISA standards were obtained from R&D Systems or Peprotech (Rocky Hill, NJ, USA).

Cytokine Arrays

Equal volumes of cell culture supernatants or equal protein concentrations from lysates were incubated with the precoated Human Cytokine Antibody Array membranes (Proteome Profiler Arrays™, R&D Systems) according to the manufacturer's instructions. Equal loading of protein was ascertained by densitometry of the positive control spots on the dot blot as well as by measuring total protein; differences in cell death were excluded

by LDH measurements. Analysis was performed as previously described (26).

Luminex Analysis: *In Vitro* Study of gp96 Peptide Variants

Peripheral blood mononuclear cells from three healthy human donors were incubated with nine gp96 peptide variants (30 μg/ml). After addition of 1 μg/ml of LPS for 24 h, or of anti-CD3 mAb (Sigma, St. Louis, MO, USA) for 48 h, the concentrations of several cytokines were measured in the supernatants using a Luminex analyzer (IS100, Luminex Corporation) and bead-based reagents (Upstate Biotechnology).

Reverse Transcription Quantitative Real-time Polymerase Chain Reaction (RT-PCR)

After 4 h of LPS stimulation, PBMC cell cultures were spun down and supernatants were analyzed for LDH and human TNF. Total RNA containing miRNAs was extracted from the cell pellet according to the manufacturer's instructions using the mirVana miRNA Isolation kit (Ambion, Austin TX, USA). Primer pair: 18S RNA: Hs99999901_s1 and hTNF Hs99999043_m1 (Applied Biosystems, Foster City, CA, USA).

For mRNA quantification, cDNA was synthesized from isolated RNA using a High Capacity cDNA Reverse Transcription kit (Invitrogen) according to the manufacturer's instructions. Reverse transcription quantitative real-time polymerase chain reaction (RT-qPCR) was performed using an Applied Biosystems 7900HT Fast Real-Time PCR System. Human TNF DNA levels were determined by RT-qPCR with the Taqman® Gene Expression Master Mix by Applied Biosystems (Applied Biosystems, Foster City, CA USA). Fold changes in expression were calculated by the $2^{-\Delta\Delta Cq}$ (C_q = quantification cycle) using the RQ Manager 1.2 and 18S FAM as reference gene. The primer/probe sets targeted human TNF. Total DNA content was quantified with a NanoDrop (Thermo Fisher Scientific); each sample was measured in triplicate.

Histology

The distal colon was taken at necroscopy on day 7, processed, embedded and stained with H&E as previously described in Ref. (21). An experienced gastroenterologist blinded to the treatment performed scoring. A combined score ranging from 0 to 6 was used to quantify colitis. Inflammatory cell infiltration was scored from 0 to 3 and tissue damage was scored from 0 to 3. Absence or occasional inflammatory infiltrate in the lamina propria was scored as 0, increased numbers of inflammatory cells restricted to the lamina propria was scored as 1, inflammatory infiltrates reaching the submucosa was scored as 2 and transmural cell infiltration was scored as 3. The subscore for tissue damage took into account epithelial lesions with no mucosal damage scored as 0, focal crypt lesions scored as 1, surface mucosal erosions or focal ulceration scored as 2 and extensive mucosal damage affecting the submucosa was scored as 3. The combined inflammatory and histological score resulted in the overall score ranging from 0 (no changes) to 6 (severe inflammatory infiltrate and mucosal damage).

Statistical Analysis

Data sets (raw data) were first tested for normality and equal variance (P value to reject = 0.05) with Sigma Plot 12.5 (Systat software). Thereafter, the appropriate statistical test was applied, which included paired or unpaired Student's t-test and/or by the Mann–Whitney rank sum or the Wilcoxon signed rank tests on raw data and one-way analysis of variance (ANOVA) or one-way ANOVA on ranks. All data that underwent statistical analysis are presented either as means of absolute cytokine concentrations, means of normalized cytokine concentrations, or means of percent change ± SEM.

Ethical Considerations

This study and protocol were carried out in accordance with the recommendations and approval by the Colorado Multiple Institutional Human Review Board. All subjects gave written informed consent in accordance with the Declaration of Helsinki. The animal studies and protocols were carried out in accordance with the recommendations of the Animal Review Board of the University of Colorado Denver and the Animal Review Board of the University of Mainz.

RESULTS

gp96-II Peptide Is Protective in Two Murine Models of Intestinal Disease

Daily injection with IL-12 and IL-18 led to severe acute intestinal inflammation, thereby resulting in symptoms such as bloody diarrhea and fever. IL-12/IL-18-treated mice received either a daily dose of gp96-II peptide or were injected with identical volumes of vehicle. **Figure 1A** demonstrates the protection afforded by gp96-II peptide against the IL-12/IL-18-triggered intestinal inflammation. After 5 days, 80% of the vehicle-injected mice had died, whereas in the gp96-II peptide-treated group, all mice survived. gp96-II peptide also markedly attenuated the IL-12/IL-18-induced weight loss (**Figure 1B**) and reduced the severity of diarrhea compared with the control group (data not shown). To determine the clinical presentation of IL-12/IL-18-induced intestinal inflammation on all animals, an assessment was performed on day 2, just before vehicle-treated control animals began to perish. The vehicle group presented with diarrhea and bloody stools, which were infrequent or not evident in the gp-96-II-treated group. No gross bleeding was observed in any of the animal groups. The clinical assessment DAI of intestinal inflammation severity was found to be significantly lower in the gp96-II-treated animals when compared to vehicle-injected mice (**Figure 1C**; Table S1 in Supplementary Material).

Next, we investigated plasma cytokine abundance in the surviving mice on day 5. As shown in **Figure 1D**, daily gp96-II peptide injections reduced IL-12/IL-18-induced plasma IFNγ by 89% compared to controls and inhibited plasma cytokine levels of IL-1β by 63%, IL-6 by 43% and TNF by 70% (**Figures 1E–G**). White blood cell counts showed no significant difference between the groups.

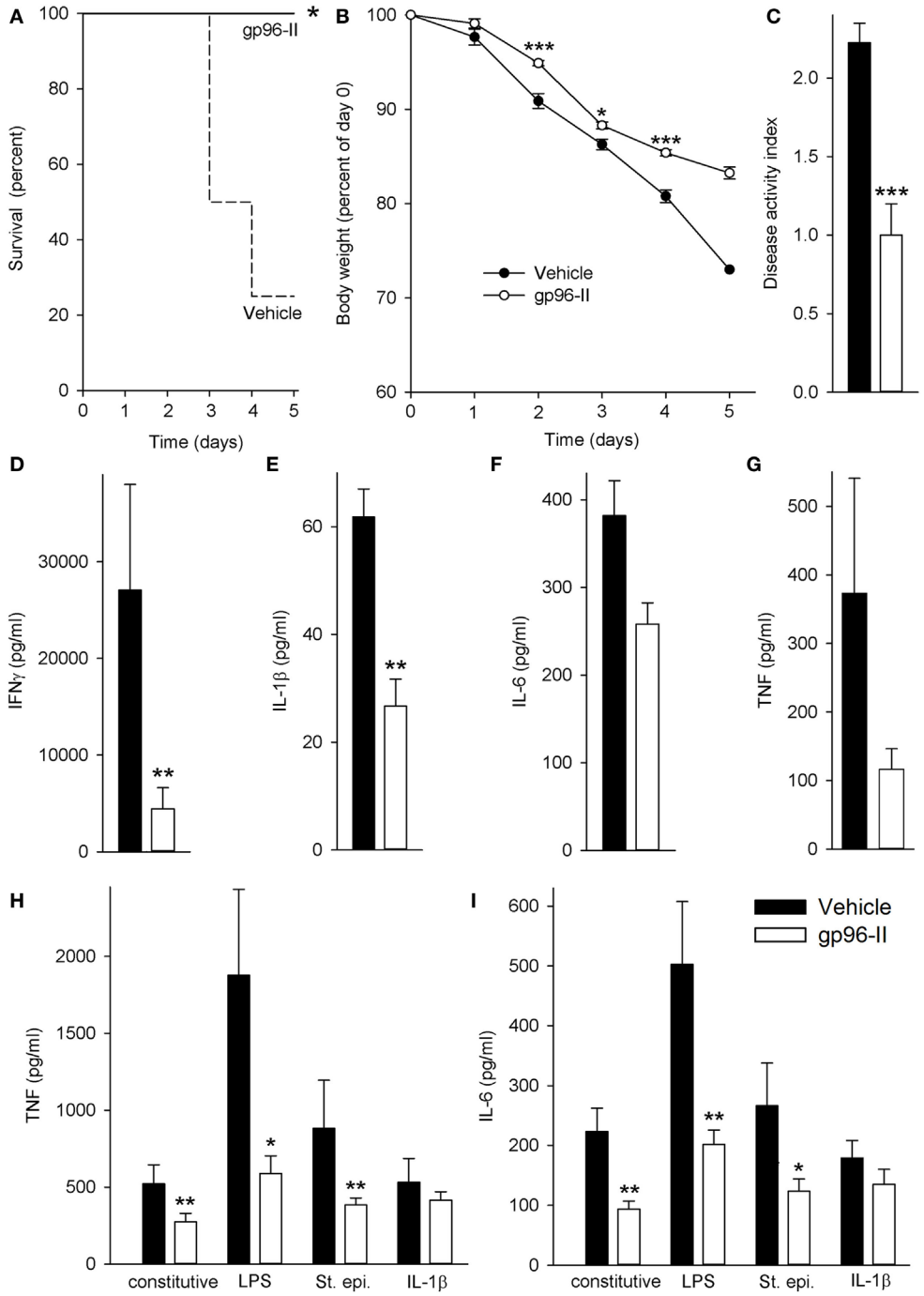

FIGURE 1 | Amelioration of IL-12/IL-18-induced intestinal inflammation by gp96-II peptide *in vivo*. C57BL/6 mice were injected daily intraperitoneally with either vehicle or gp96-II peptide (60 μg) and with IL-12 (1 μg) and IL-18 (1 μg). **(A)** Kaplan–Meier analysis of survival of vehicle-treated mice (dashed line) vs. gp96-II peptide-injected mice (solid line). $n = 10$ mice per group; $^{*}P < 0.05$ for vehicle vs. gp96-II peptide. **(B)** Means of percent changes in body weight ± SEM of surviving mice injected with IL-12/IL-18 + vehicle (filled symbols) or IL–12/IL–18 + gp96-II peptide (open symbols). $n = 10$ mice per group, identical animals to those in panel **(A)**; $^{*}P < 0.05$ and $^{***}P < 0.001$ for gp96-II peptide vs. vehicle. No statistics on last data point as only two survivors in the vehicle group. **(C)** Disease Activity Index analysis, IL-12/IL-18 + vehicle-injected mice (filled bars) and in animals treated with IL–12/IL-18 + gp96-II peptide (open bars) on day 2. $n = 9$–10 mice per group; $^{***}P < 0.001$ for gp96-II peptide vs. vehicle. **(D–G)** Concentrations of plasma IFNγ, IL-1β, IL-6 and tumor necrosis factor (TNF) ± SEM in IL-12/IL-18 + vehicle injected mice (filled bars) and in animals treated with IL–12/IL-18 + gp96-II peptide (open bars) on day 5. $n = 6$ mice per group; $^{**}P < 0.01$ for vehicle vs. gp96-II peptide treatment. **(H,I)** Comparison of cytokine abundance in *ex vivo* whole blood assays from mice that had received daily injections with IL–12/IL-18 + vehicle (filled bars) or IL-12/IL-18 + gp96-II peptide (open bars) for 5 days. Whole blood was then challenged *in vitro* for 24 h with lipopolysaccharide (1 μg/ml), *Staphylococcus epidermidis* (1:1,000), or IL-1β (25 ng/ml). The graphs show means of cytokine concentrations ± SEM; $n = 6$; $^{*}P < 0.05$ and $^{**}P < 0.01$ for vehicle vs. gp96-II peptide, absence of a symbol indicates a non-significant difference.

Having thus demonstrated that gp96-II peptide is a potent inhibitor of IL-12/IL-18-induced pro-inflammatory cytokines *in vivo*, we questioned whether residual gp96-II peptide afforded extended protection by performing *ex vivo* whole blood assays. We studied surviving mice that had either received daily injections with IL–12/IL-18 + vehicle or IL-12/IL-18 + gp96-II peptide. The mice were bled at day 5 and whole blood was challenged immediately *in vitro* for 24 h with TLR4-agonist LPS, TLR2-agonist St. epi. or the pro-inflammatory cytokine IL-1β, without any addition of gp96-II peptide to the cultures. As shown in **Figures 1H,I**, residual gp96-II peptide from the *in vivo* injections inhibited constitutive expression of TNF by 48% and IL-6 by 58%. Comparing whole blood from gp96-II and vehicle-treated mice; we found TNF was reduced by 69% when the second *in vitro* hit was LPS, 56% when it was St. epi. and 22% when it was IL-1β. Likewise, IL-6 expression was 60, 53 and 25% lower in response to all "second hit" conditions.

Our second model inducing colitis caused by intrarectal instillation of TNBS in 50% ethanol triggered mucosal inflammation mediated by a Th1 response with excessive pro-inflammatory cytokine production (17). The mice were also treated once daily with vehicle as a control, with 1 g of the corticosteroid prednisolone or twice daily with 60 μg of gp96-II peptide. The vehicle-treated group exhibited the highest mortality (**Figure 2A**) and most pronounced weight loss (**Figure 2B**); both prednisolone and gp96-II peptide completely protected the mice from the deleterious effects of TNBS (**Figures 2A,B**).

To assess tissue damage, the distal colon of each animal was obtained at necroscopy and sections were H&E stained and scored, with the assessor blinded to treatment. Prednisolone and gp96-II peptide were equally potent in reducing histological disease severity scores by 40 and 35%, respectively (**Figure 2C**).

Endoscopy on anesthetized animals on day 3 of the experiment (27) showed that mice treated with gp96-II peptide or with prednisolone had improved endoscopic scores compared with vehicle-treated control mice: vascularity, fibrin, granularity and translucency scores were reduced by up to 49% by prednisolone and by up to 30% by gp96-II peptide (**Figures 2D–G**). As shown in **Figure 2H**, mice exposed to TNBS displayed changes in intestinal morphology as characterized by edema and infiltration by inflammatory cells in the mucosal and sub-mucosal layers and tissue damage. Daily injections of gp96-II peptide or prednisolone almost completely prevented these morphological changes as shown by significantly ameliorated histological disease severity scores (**Figure 1C**).

gp96-II Peptide Reduces Cytokines in Freshly Isolated Murine Splenocytes

gp96-II peptide had an inhibitory effect in freshly isolated murine splenocytes as shown by its action in markedly reducing constitutive IL-6 by 54%, LPS-induced TNF and IL-6 by 48 and 81% respectively and St. epi.-induced TNF and IL-6 by 67 and 81% respectively (**Figures 3A,B**). gp96-II peptide inhibited IL-12 + IL-18-induced IFNγ secretion by 75% at a concentration of 60 μg/ml (**Figure 3C**).

Inhibition of LPS-Induced *TNF* mRNA by gp96-II in PBMC Does Not Affect Cell Viability

Treatment of PBMC with 30 μg/ml gp96-II peptide decreased *TNF* mRNA expression at 4 h, under steady-state conditions by 80% and after LPS stimulation by 52% (**Figure 4A**). Accordingly, protein abundance of LPS-induced TNF was also decreased (**Figure 4B**) by up to 53%. Ruling out the possibility that the anti-inflammatory effects of gp96-II peptide were attributable to cell death, we found no increase in LDH in the culture supernatants of PBMC treated with 15, 30, 60 and 120 μg/ml of gp96-II peptide for 4 h compared to vehicle; in fact, gp96-II peptide negated the small increase in LDH induced by LPS in PBMC (not shown). We also performed flow cytometry to investigate the effect of gp96-II peptide on specific subpopulations of PBMC. In cells treated with vehicle, LPS alone or LPS + gp96-II peptide (30 μg/ml) for 20 h, we found no differences in overall viability, in the percentage of lymphocytes and macrophages among live cells or in the percentage of $CD3^+$ T-cells and $CD19^+$ B-cells among lymphocytes (not shown).

Anti-inflammatory Activity Screening of Nine gp96 Peptide Variants

To determine the best anti-inflammatory gp96 peptide variant, we tested nine different gp96 peptide variants, termed gp96-I to -IX, in PBMC at a concentration of 30 μM. As shown in Figures S1A,B in Supplementary Material, peptide gp96-II (CGEN-25007) reduced LPS-induced IL-6 by 91%, IL-8 by 93%, MIP-1α by 73%, IL-1β by 93% and TNF by 60% compared to the other peptides and even outperformed the inhibitory effects of dexamethasone. Reduction of anti-CD3-induced cytokine production by gp96-II peptide was comparable for IL-1β, IL-12p40, IL-12p70 and TNF, whereas IL-1α, GM-CSF and IL-2 were not affected (Figures S1C,D in Supplementary Material). These data confirm that gp96-II peptide (CGEN-25007) is the peptide with most potent anti-inflammatory activity in LPS- as well as anti-CD3-stimulated PBMC.

gp96-II Peptide Abrogates Production of Pro-inflammatory Cytokines in Human PBMC

To investigate the clinical relevance of gp96-II peptide on inhibition of TLR2/4- or IL-1b-triggered inflammatory responses in primary human cells, we isolated fresh PBMCs and stimulated them with gp96-II peptide, either alone or in combination with LPS, or with heat-killed St. epi. or IL-1β. We found that gp96-II peptide effectively blocked the production of pro-inflammatory cytokines in PBMC. For example, 60 and 120 μg/ml gp96-II peptide decreased the concentrations of LPS-induced IL-1α (by 50 and 98%, respectively), IL–1β (by 72 and 99%, respectively), IL-6 (by 70 and 94%, respectively) and TNF (by 70 and 94%, respectively) compared with LPS alone (**Figures 5A–D**). Inhibition of the induction of pro-inflammatory cytokines by St. epi. was similar.

We also tested IL-1β as a pro-inflammatory stimulus and observed that 30 μg/ml of gp96-II peptide was sufficient to

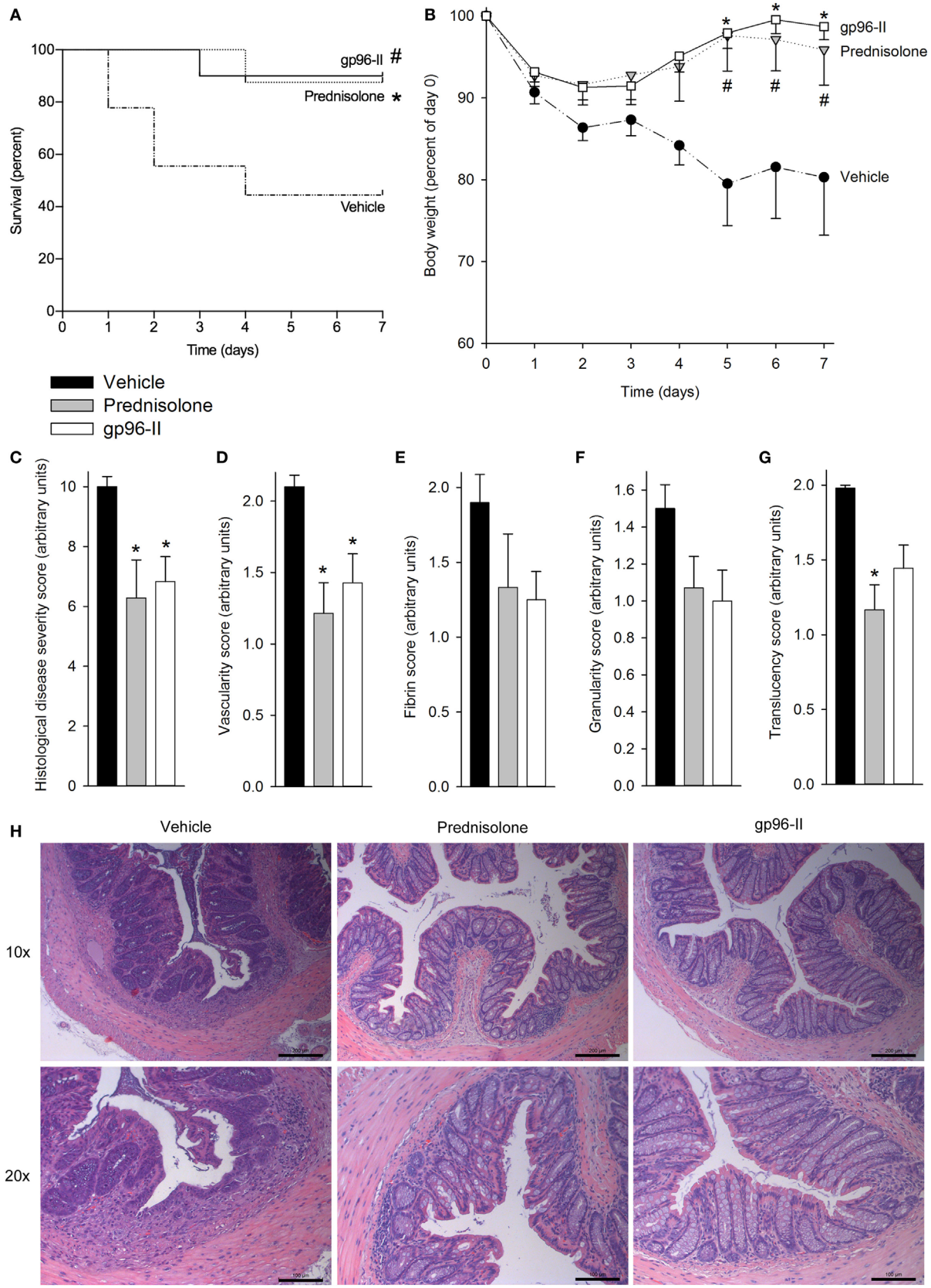

FIGURE 2 | Continued

FIGURE 2 | Continued
Amelioration of TNBS-induced colitis by gp96-II peptide. Colitis was induced by intrarectal application of TNBS on day 0. Male C57BL/6 mice either received twice daily intraperitoneal injections of vehicle or gp96-II peptide (60 μg), or were administered prednisolone (1 g) once daily for 7 days. **(A)** Kaplan–Meier analysis of survival of vehicle-treated mice (dashed line) vs. gp96-II peptide-injected mice (solid line) or vs. prednisolone injected mice (dotted line). $n = 10$ mice per group; $^{\#}P < 0.05$ for vehicle vs. gp96-II peptide, $^{*}P < 0.05$ for vehicle vs. prednisolone. **(B)** Bodyweight in percent of day 0 ± SEM is shown for the gp96-II peptide (open squares) ($n = 10$), prednisolone (gray triangles) ($n = 8$) and vehicle (solid circles) groups ($n = 9$); $^{*}P < 0.05$ for gp96-II peptide vs. vehicle; $^{\#}P < 0.05$ for prednisolone versus vehicle. **(C)** Postmortem histological disease severity scores of the colons (arbitrary units; see Materials and Methods) on day 7 ± SEM. **(D–G)** Endoscopy was performed on anesthetized mice on day 3 of the experiment and vascularity, fibrin, granularity and translucency scores (arbitrary units ± SEM) were obtained. $n = 7$ in the vehicle (filled bars) and prednisolone (gray bars) groups, $n = 9$ in the gp96-II peptide group (open bars); $^{*}P < 0.05$ for gp96-II peptide or prednisolone vs. vehicle, absence of a symbol indicates a non-significant difference. **(H)** Intestinal sections were H&E stained and analyzed on day 7, $n = 7$–9 per group. One representative image per treatment group depicting the colon at a low (10×) and high (20×) magnification. Scale bars: 200 μm for 10× magnification and 100 μm for 20× magnification.

inhibit production of IL-1α (**Figure 5A**), an unexpected result as 30 μg/ml did not reduce TLR-induced cytokines (**Figure 5D**). However, IL-1β-induced IL-6 and TNF remained unaffected by 30 and 60 μg/ml of gp96-II peptide. In addition, we investigated the effect of gp96-II peptide on IL-12/IL-18-induced IFNγ in human PBMC (**Figure 5E**). gp96-II peptide inhibited IL-12/IL-18-induced IFNγ secretion in human PBMC at a concentration of 30 μg/ml (by 20%) and at 60 μg/ml (by 61%) after 24 h and by 82% after 48 h (**Figure 5E**). Compared to TLR ligands, induction of IL-1β, IL-6, IL-1α and TNF was moderate; however, the magnitude of the reduction in IL-1α by gp96-II peptide at 60 μg/ml was 50% (not shown). To rule out unspecific effects of the gp96-II peptide, we showed that mutated nonsense peptides had no effect on any of the parameters we assessed (not shown).

Having observed that gp96-II peptide was highly effective in reducing TNF, IL-1β, IL-6 and IL-1α, we further investigated the effect of gp96-II peptide in LPS-stimulated PBMC using an array of 40 human mediators of inflammation. **Figure 6A** shows the increase in cytokine abundance and **Figure 6B** shows the decrease in cytokine abundance. In addition to confirming the results described above, the array revealed decreases in the abundance of GM-CSF and IL-1Ra, as well as increases in RANTES (threefold), IL-25 and MIF (twofold to threefold), whereas IL-10, IL-4 and IL-5 were measured but were undetectable in all conditions.

DISCUSSION

Inflammatory bowel disease, which encompasses UC and CD, is a chronic disorder characterized by severe intestinal inflammation. Our aim was to advance the prospects for anti-inflammatory agents by focusing on the role of the DAMP molecule gp96 in IBD. The data we present here provide new mechanistic insights into the role of gp96 in IBD. Our major findings are that the synthetic molecule gp96-II peptide binds to and thereby blocks the pro-inflammatory activities of HSP gp96 *via* inhibition of TLR signaling and amelioration of intestinal inflammation. Furthermore, our study shows that the inhibitory functions of gp96-II peptide protect against cytokine-induced inflammation in PBMC from healthy human donors and primary murine cells. Our detailed analysis of gp96-II peptide provides new insights into the broad mechanistic functions of gp96 and highlights the value of gp96-II peptide as a starting point in the design of small molecule inhibitors for inflammatory diseases of the intestine.

Before performing any *in vivo* testing in murine models of intestinal disease, we first screened nine different gp96-IIs *in vitro* to assess their inhibitory properties. We found that the peptide gp96-II provided the most potent and versatile inhibition. Thus, we demonstrated that inflammation induced by T cell activation *via* CD3 ligation in PBMC is reduced with gp96-II peptide to a similar degree compared with its inhibitory effects on LPS-induced inflammation. gp96-II peptide thus acts as a multifunctional immune blocking agent, adding to earlier evidence that gp96-II peptide inhibits TLR2- and TLR4-induced pro-inflammatory (27) response in PBMC and murine splenocytes (22).

Our efforts in this study were directed at a more detailed analysis of the inhibitory effects of gp96-II peptide on pro-inflammatory cytokines and the associated immunobiology. The choice of IL-12/IL-18 for the creation of an inflammatory condition to model IBD was based on several studies. Among the pro-inflammatory cytokines, the IL-1 family member IL-18 plays an important role in a range of immune-mediated pathologies. For example, in 1999, three groups independently reported the pathological role of IL-18 in IBD patients (10–12). Subsequent studies confirmed that IL-18 has a role in the pathogenesis of human IBD as well as in murine intestinal inflammation (15, 16, 28–30). The high level of IL-18 that is generated in the inflamed gut causes further damage of the intestinal epithelium, thereby promoting penetration of gut bacteria across the compromised mucosa and later infiltration of T cells (1). Subsequently, alarmins and DAMP factors such as gp96 are released.

Extracellular gp96 then activates TLR2 and TLR4 and increases synthesis of pro-inflammatory cytokines (8), including vigorous IFNγ production by T cells, profound inflammatory responses and IBD pathology (9). In addition, gp96 is overexpressed in ileal epithelial cells in biopsies from patients with CD and promotes mucosal invasion of bacteria such as *Escherichia coli* (31). Tissues from CD patients are known to have elevated IL-12 transcripts and their lamina propria mononuclear cells produce higher levels of IL-12 compared to healthy subjects (13). Moreover, gp96 activates dendritic cells *via* the TLR2 and TLR4 pathways (8), and dendritic cells and macrophages produce more IL-12 in patients with CD, leading to a prototypical activation of APC and a shift toward Th1 differentiation (32). These findings support a strong pathological association of gp96, IL-12 and IL-18 in inflammatory diseases of the gut and highlights the importance of gp96 as a key-signaling player in intestinal type 1 immune responses.

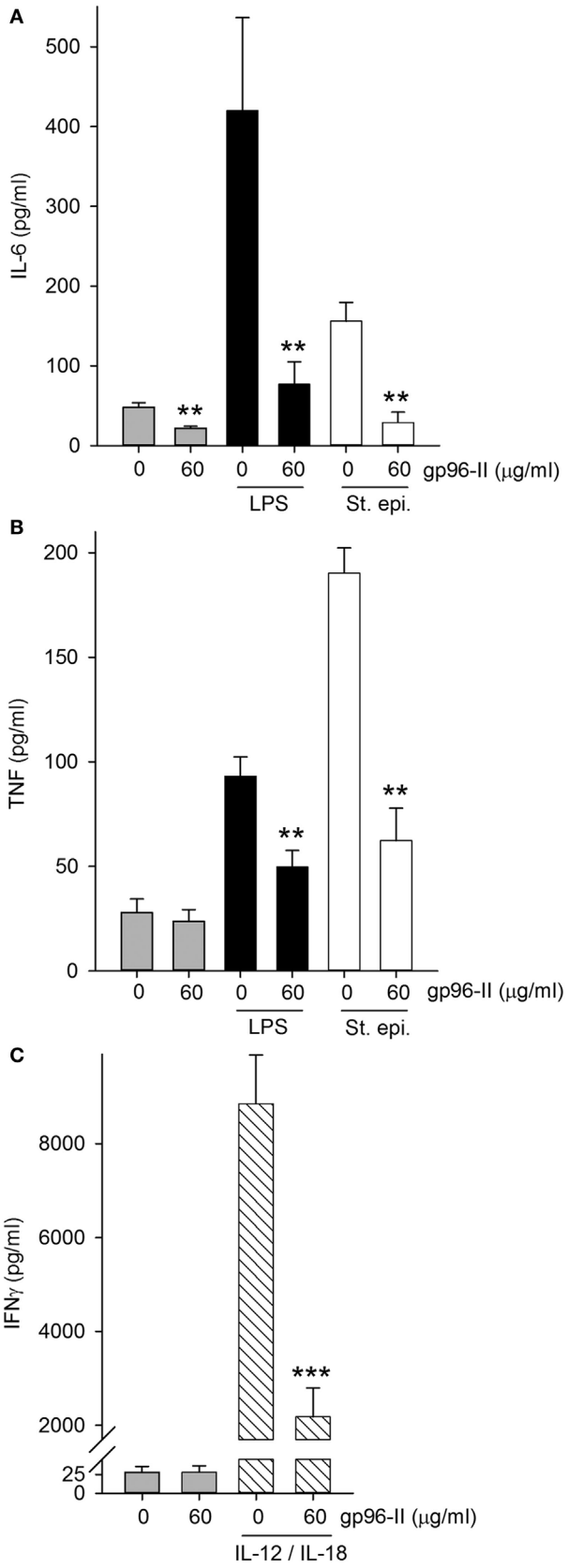

FIGURE 3 | Continued

FIGURE 3 | Continued
Effect of gp96-II peptide on TLR- or IL-12/IL-18-induced cytokine production in murine splenocytes. **(A,B)** Cells were incubated for 24 h with vehicle, lipopolysaccharide (LPS) (100 ng/ml), or *Staphylococcus epidermidis* (St. epi.) (1:4,000) in the presence or absence of gp96-II peptide (60 μg/ml). The graphs display means of absolute cytokine abundance ± SEM. **(C)** IFNγ protein abundance in cells stimulated for 24 h with either vehicle or IL-12 (20 ng/ml) + IL-18 (50 ng/ml) in the presence or absence of 60 μg/ml of gp96-II peptide. $n = 6$; $^{**}P < 0.01$ and $^{***}P < 0.001$ for LPS, St. epi. or IL-12/IL-18 alone vs. stimulus + gp96-II peptide.

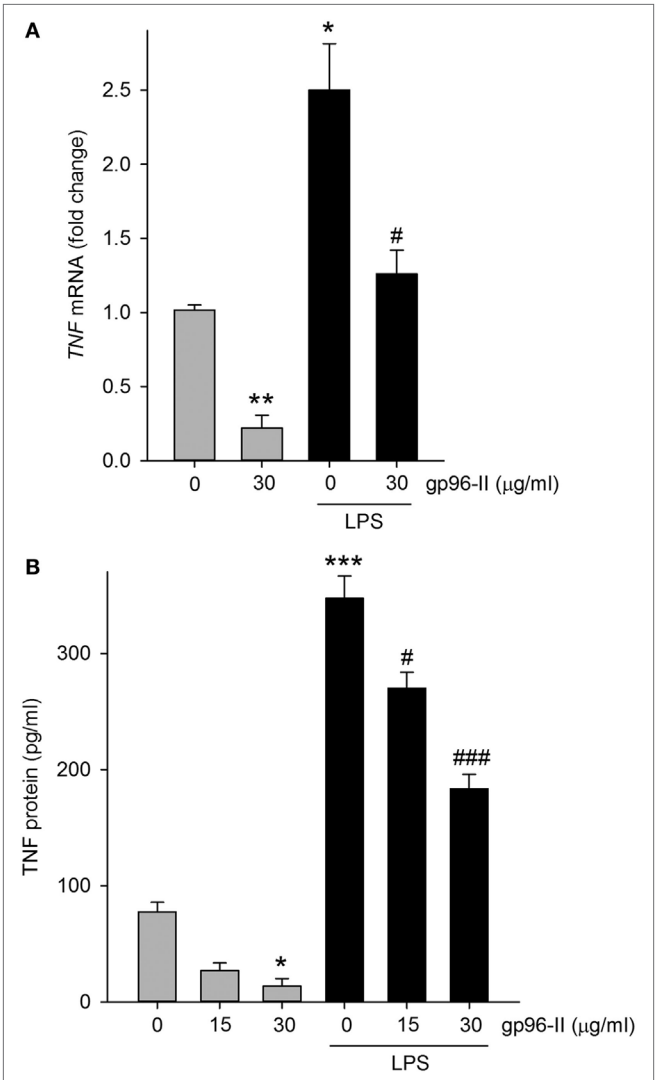

FIGURE 4 | Tumor necrosis factor (*TNF*) mRNA and protein in lipopolysaccharide (LPS)-stimulated peripheral blood mononuclear cells with and without gp96-II peptide. Cells were incubated with or without LPS in combination with gp96-II peptide (30 μg/ml) for 4 h. **(A)** Fold change in *TNF* mRNA ± SEM; **(B)** TNF protein abundance ± SEM. $n = 5$; $^{*}P < 0.05$; $^{**}P < 0.01$; and $^{***}P < 0.001$ for control vs. stimulation with LPS or gp96-II peptide alone; $^{\#}P < 0.05$ and $^{\#\#\#}P < 0.001$ for LPS plus gp96-II peptide vs. LPS alone.

Another important function exerted by IL-12 and IL-18 in synergy is a potent induction of IFNγ *in vivo* and *in vitro* (15, 19, 20, 33, 34), especially in IBD. One particular focus of our

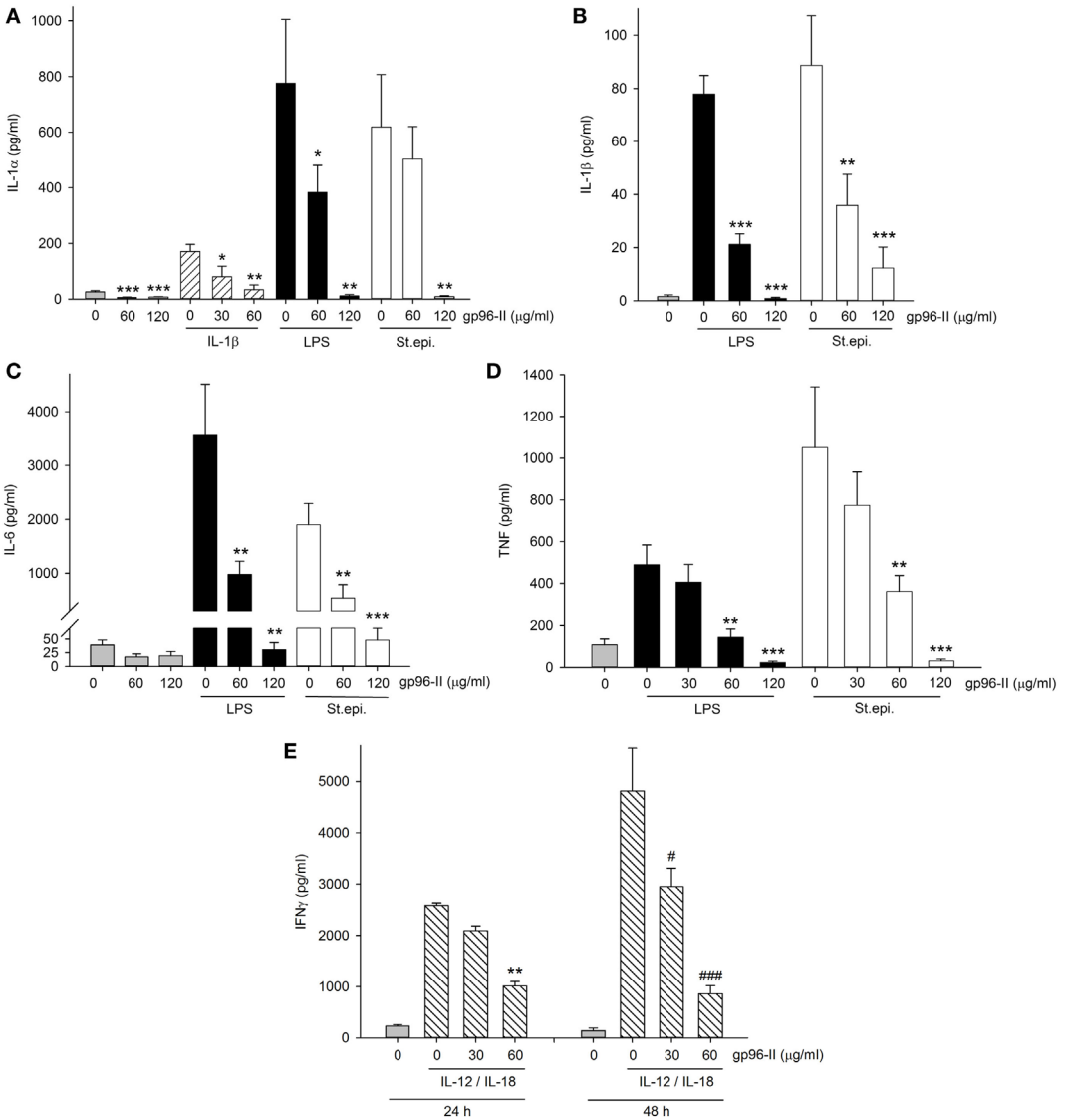

FIGURE 5 | Effect of gp96-II peptide on TLR- and cytokine-induced cytokine production in human peripheral blood mononuclear cells (PBMC). **(A–D)** Cells were incubated with lipopolysaccharide (LPS) (100 ng/ml), IL-1β (10 ng/ml), *Staphylococcus epidermidis* (St. epi.) (1:4,000) or vehicle, alone or in combination with gp96-II peptide for 24 h. The concentrations of gp96-II peptide in micrograms per milliliter are indicated. Lysates **(A)** or supernatants **(B–D)** were analyzed for cytokine abundance. The panels depict means of absolute concentrations of cytokines ± SEM, $n = 4$; $^{*}P < 0.05$; $^{**}P < 0.01$; $^{***}P < 0.001$ for IL-1β-, LPS-, or St. epi.-stimulated cells + gp96-II peptide vs. stimulated cells alone. **(E)** PBMC from four donors were incubated for the indicated periods of time in the presence or absence of IL-12 (20 ng/ml) + IL-18 (25 ng/ml) with or without gp96-II peptide at the indicated concentrations in micrograms per milliliter. $^{**}P < 0.01$ for IL-12/IL-18 vs. IL-12/IL-18 + gp96-II peptide at 24 h; $^{\#}P < 0.05$ and $^{\#\#\#}P < 0.001$ for IL-12/IL-18 vs. IL-12/IL-18 + gp96-II peptide at 48 h. Absence of a symbol indicates a non-significant difference.

study was therefore to investigate the inhibitory effect of gp96-II on IFNγ, as it has previously been shown that gp96 protein expression is dose- and time dependently increased *in vitro* by IFNγ in lymphoid and epithelial cancer cells (7, 35). We show that inhibition of gp96 with gp96-II peptide significantly inhibits IL-12/IL-18-induced INFγ induction *in vitro* in PBMC as well as in murine splenocytes. To confirm the pivotal inhibitory effect of gp96-II peptide on IL-12/IL-18-induced inflammation *in vivo*, we utilized a chronic intestinal inflammation model in which a daily i.p. co-administration of IL-18 and IL-12 induces a severe systemic toxicity and type 1 immune response in mice, causing weight loss and increased serum cytokine levels (15, 19, 20). Strikingly, animals treated with daily i.p. gp96-II peptide injections were exempt from all severe symptoms induced by daily IL-12/IL-18 injections and also suffered significantly less from systemic inflammation than control mice.

We investigated the longevity of the protective effects of gp96-II peptide *via ex vivo* whole blood experiments. Our data presented here show that cells obtained from mice injected daily with IL-12/IL-18 and treated *in vivo* with gp96-II peptide exhibited

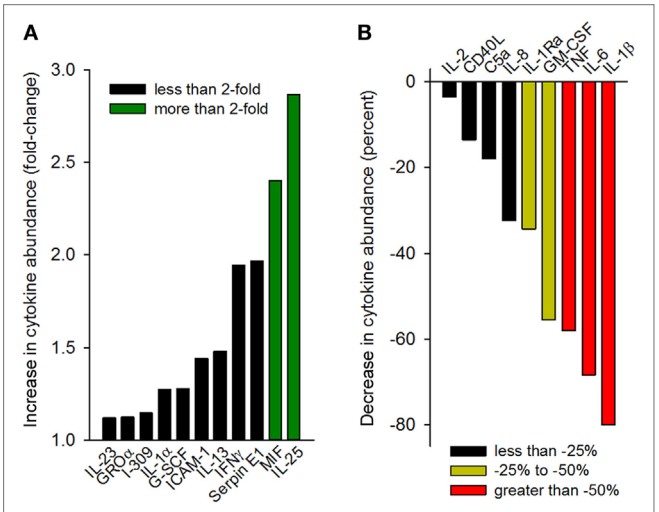

FIGURE 6 | Cytokine array analysis of supernatants of peripheral blood mononuclear cell cultures (two donors) treated with 100 ng/ml lipopolysaccharide with or without gp96-II peptide (30 μg/ml) for 24 h. Densitometric analysis of the blots is depicted as normalized density per square millimeter. Panel **(A)** describes the increase in cytokine abundance (fold change) and panel **(B)** describes the decrease in cytokine abundance in percent.

a reduced pro-inflammatory cytokine expression when exposed to a "second hit" involving stimulation with a TLR2- or TLR4-agonist or IL-1β when compared to vehicle-treated animals. Collectively, these findings suggest that gp96 has a prominent role in cytokine regulation of intestinal inflammation and that gp96-II peptide strongly and lastingly inhibits key cytokines such as IL-1β, IFNγ, TNF and IL-6, thereby improving the outcome of murine intestinal inflammation (36).

To complement these investigations, we chose TNBS as our second model of murine intestinal inflammation, as the inflammation induced by TNBS is T cell driven and associated with elevated IFNγ, which causes epithelial injury of the colon. This model has been widely used to study cytokine secretion patterns and the effect of immunotherapies (17, 21). Elevated IFNγ production is an invariable feature of IBD pathogenesis, as reviewed in detail in Ref. (37). In this context, it is relevant that TNBS colitis can be treated with antibodies to IL-12, one of the key inducers of IFNγ (17). We therefore considered that TNBS-induced colitis is a model that is well-suited for testing the impact of continuous treatment with gp96-II peptide. Our study shows that TNBS-challenged mice, if treated with gp96-II, benefit from reduced weight loss, improved endoscopic scores and present with fewer morphological changes in the colon. Indeed, our data show that the inhibitor gp96-II peptide has anti-inflammatory properties as strong as those of prednisolone, which we used as a positive control in this setting. Clinically, corticosteroids are one of the mainstay therapies for IBD in human patients.

We can speculate that gp96-II peptide exerts its mechanistic effects by reducing the pro-inflammatory cytokines IL-1β, IL-6, TNF, and IFNγ in murine samples and in PBMC induced by different triggers. Interestingly the type 2-polarizing cytokine IL-25 was increased in PBMC, whereas IL-23, G-CSF, ICAM-1, IL-13, IL-2, CD40L, C5a and IL-8 showed little or no change. Thus, gp96-II may act *via* induction of IL-25, which is well known to have protective effects in IBD (25). In this context, we note that IL-25 inhibits IL-12 and Th-1 cell-driven inflammation in colonic samples from patients and experimental colitis (38).

Several attempts have been made to introduce cytokine-based therapies for patients with IBD. However, to date, anti-inflammatory cytokines such as IFNβ (34), IL-10 (39–41) and IL-11 (42) have failed to show benefit in patients with CD. A trial with a neutralizing antibody against IFNγ (fontolizumab) was stopped despite showing some beneficial effect (43), while anti-IL-17A (secukinumab) aggravated CD (44). Initial results with the anti-TNF antibody infliximab in patients with CD (45, 46) and other anti-TNF therapies such as adalimumab and certolizumab, pointed to improved outcome of many patients with IBD (CD and UC), but within 1 year only a third maintained remission (47).

Our study was motivated by the clear need for novel targets and therapies for human intestinal inflammatory disease. That gp96 has multiple and potent pro-inflammatory effects is already well documented, including dendritic cell activation, type 1 immune polarization and downregulation of its own receptors in a negative feedback loop (5). These actions, in combination with the therapeutic benefits we report on its synthetic inhibitor gp96-II peptide, makes gp96 a promising target for the development of therapies to restore intestinal homeostasis in IBD.

ETHICS STATEMENT

This study and protocol were carried out in accordance with the recommendations and approval by the Colorado Multiple Institutional Human Review Board. All subjects gave written informed consent in accordance with the Declaration of Helsinki. The animal studies and protocols were carried out in accordance with the recommendations of the Animal Review Board of the University of Colorado Denver and The University of Mainz Animal Care and Use Committee.

AUTHOR CONTRIBUTIONS

All authors were involved in drafting the article or revising it critically for important intellectual content, and all authors approved the final version to be published. CAD and CAN-P had full access to all of the data in the study and take responsibility for the integrity of the data and the accuracy of the data analysis. Study conception and design: CAD, CAN-P, CB, SW, and MN. Acquisition of data: CAN-P, MFN, OL, YK, AO, IB, CB, SW, and MN. Analysis and interpretation of data: CAN-P, MFN, OL, YK, AO, IB, MKS, CB, SW and MN.

ACKNOWLEDGMENTS

This study was supported by research grants from the Interleukin Foundation (to MFN and CAN-P), The Blair Ritchie Fellowship (CAN-P), R&D Systems, a Fellowship by the Deutsche Forschungsgemeinschaft (to MFN), the Larkins Fellowship from Monash University (to MFN), the Victorian Government's

Operational Infrastructure Support Program and a Future Leader Fellowship to CAN-P from the National Heart Foundation of Australia CF14/3517.

SUPPLEMENTARY MATERIAL

The Supplementary Material for this article can be found online at http://www.frontiersin.org/article/10.3389/fimmu.2017.01531/full#supplementary-material.

FIGURE S1 | Anti-inflammatory activity of nine gp96-II peptides. gp96-II peptide (30 μM, open symbols) inhibits the production of cytokines from human peripheral blood mononuclear cells in response to a 24-h treatment with 1 μg/ml lipopolysaccharide (LPS) **(A,B)** or 48 h with 30 μg/ml anti-CD3 **(C,D)** in comparison to peptides gp96-I and III-X (30 μM, solid symbols) and dexamethasone. Individual cytokine abundance is depicted with each symbol representing one biological replicate. Horizontal lines show means.

TABLE S1 | Stool consistency: normal stool, stool with an appearance of well-formed pellets; slightly loose stool, loose stool with pasty, semi-formed, soft materials that do not adhere to anal fur; diarrhea, liquid stool that adheres to anal fur. Gross bleeding, an appearance of visible blood adhering to anal fur.

REFERENCES

1. Marsal J, Agace WW. Targeting T-cell migration in inflammatory bowel disease. *J Intern Med* (2012) 272(5):411–29. doi:10.1111/j.1365-2796.2012.02588.x
2. Multhoff G. Heat shock proteins in immunity. *Handb Exp Pharmacol* (2006) 172:279–304. doi:10.1007/3-540-29717-0_12
3. Yang Y, Liu B, Dai J, Srivastava PK, Zammit DJ, Lefrancois L, et al. Heat shock protein gp96 is a master chaperone for toll-like receptors and is important in the innate function of macrophages. *Immunity* (2007) 26(2):215–26. doi:10.1016/j.immuni.2006.12.005
4. Staron M, Yang Y, Liu B, Li J, Shen Y, Zuniga-Pflucker JC, et al. gp96, an endoplasmic reticulum master chaperone for integrins and toll-like receptors, selectively regulates early T and B lymphopoiesis. *Blood* (2010) 115(12): 2380–90. doi:10.1182/blood-2009-07-233031
5. Singh-Jasuja H, Scherer HU, Hilf N, Arnold-Schild D, Rammensee HG, Toes RE, et al. The heat shock protein gp96 induces maturation of dendritic cells and down-regulation of its receptor. *Eur J Immunol* (2000) 30(8):2211–5. doi:10.1002/1521-4141(2000)30:8<2211::AID-IMMU2211>3.0.CO;2-0
6. Singh-Jasuja H, Toes RE, Spee P, Munz C, Hilf N, Schoenberger SP, et al. Cross-presentation of glycoprotein 96-associated antigens on major histocompatibility complex class I molecules requires receptor-mediated endocytosis. *J Exp Med* (2000) 191(11):1965–74. doi:10.1084/jem.191.11.1965
7. Anderson SL, Shen T, Lou J, Xing L, Blachere NE, Srivastava PK, et al. The endoplasmic reticular heat shock protein gp96 is transcriptionally upregulated in interferon-treated cells. *J Exp Med* (1994) 180(4):1565–9. doi:10.1084/jem.180.4.1565
8. Vabulas RM, Braedel S, Hilf N, Singh-Jasuja H, Herter S, Ahmad-Nejad P, et al. The endoplasmic reticulum-resident heat shock protein Gp96 activates dendritic cells via the toll-like receptor 2/4 pathway. *J Biol Chem* (2002) 277(23):20847–53. doi:10.1074/jbc.M200425200
9. Ito R, Shin-Ya M, Kishida T, Urano A, Takada R, Sakagami J, et al. Interferon-gamma is causatively involved in experimental inflammatory bowel disease in mice. *Clin Exp Immunol* (2006) 146(2):330–8. doi:10.1111/j.1365-2249.2006.03214.x
10. Pizarro TT, Michie MH, Bentz M, Woraratanadharm J, Smith MF Jr, Foley E, et al. IL-18, a novel immunoregulatory cytokine, is up-regulated in Crohn's disease: expression and localization in intestinal mucosal cells. *J Immunol* (1999) 162(11):6829–35.
11. Monteleone G, Trapasso F, Parrello T, Biancone L, Stella A, Iuliano R, et al. Bioactive IL-18 expression is up-regulated in Crohn's disease. *J Immunol* (1999) 163(1):143–7.
12. Kanai T, Watanabe M, Okazawa A, Nakamaru K, Okamoto M, Naganuma M, et al. Interleukin 18 is a potent proliferative factor for intestinal mucosal lymphocytes in Crohn's disease. *Gastroenterology* (2000) 119(6):1514–23. doi:10.1053/gast.2000.20260
13. Monteleone G, Biancone L, Marasco R, Morrone G, Marasco O, Luzza F, et al. Interleukin 12 is expressed and actively released by Crohn's disease intestinal lamina propria mononuclear cells. *Gastroenterology* (1997) 112(4):1169–78. doi:10.1016/S0016-5085(97)70128-8
14. Parronchi P, Romagnani P, Annunziato F, Sampognaro S, Becchio A, Giannarini L, et al. Type 1 T-helper cell predominance and interleukin-12 expression in the gut of patients with Crohn's disease. *Am J Pathol* (1997) 150(3):823–32.
15. Chikano S, Sawada K, Shimoyama T, Kashiwamura SI, Sugihara A, Sekikawa K, et al. IL-18 and IL-12 induce intestinal inflammation and fatty liver in mice in an IFN-gamma dependent manner. *Gut* (2000) 47(6):779–86. doi:10.1136/gut.47.6.779
16. Ishikura T, Kanai T, Uraushihara K, Iiyama R, Makita S, Totsuka T, et al. Interleukin-18 overproduction exacerbates the development of colitis with markedly infiltrated macrophages in interleukin-18 transgenic mice. *J Gastroenterol Hepatol* (2003) 18(8):960–9. doi:10.1046/j.1440-1746.2003.03097.x
17. Neurath MF, Fuss I, Kelsall BL, Stuber E, Strober W. Antibodies to interleukin 12 abrogate established experimental colitis in mice. *J Exp Med* (1995) 182(5):1281–90. doi:10.1084/jem.182.5.1281
18. Okamura H, Tsutsi H, Komatsu T, Yutsudo M, Hakura A, Tanimoto T, et al. Cloning of a new cytokine that induces IFN-gamma production by T cells. *Nature* (1995) 378(6552):88–91. doi:10.1038/378088a0
19. Okamura H, Kashiwamura S, Tsutsui H, Yoshimoto T, Nakanishi K. Regulation of interferon-gamma production by IL-12 and IL-18. *Curr Opin Immunol* (1998) 10(3):259–64. doi:10.1016/S0952-7915(98)80163-5
20. Carson WE, Dierksheide JE, Jabbour S, Anghelina M, Bouchard P, Ku G, et al. Coadministration of interleukin-18 and interleukin-12 induces a fatal inflammatory response in mice: critical role of natural killer cell interferon-gamma production and STAT-mediated signal transduction. *Blood* (2000) 96(4):1465–73.
21. Wirtz S, Popp V, Kindermann M, Gerlach K, Weigmann B, Fichtner-Feigl S, et al. Chemically induced mouse models of acute and chronic intestinal inflammation. *Nat Protoc* (2017) 12(7):1295–309. doi:10.1038/nprot.2017.044
22. Kliger Y, Levy O, Oren A, Ashkenazy H, Tiran Z, Novik A, et al. Peptides modulating conformational changes in secreted chaperones: from in silico design to preclinical proof of concept. *Proc Natl Acad Sci U S A* (2009) 106(33):13797–801. doi:10.1073/pnas.0906514106
23. Wu S, Dole K, Hong F, Noman AS, Issacs J, Liu B, et al. Chaperone gp96-independent inhibition of endotoxin response by chaperone-based peptide inhibitors. *J Biol Chem* (2012) 287(24):19896–903. doi:10.1074/jbc.M112.343848
24. Ochayon DE, Mizrahi M, Shahaf G, Baranovski BM, Lewis EC. Human alpha1-antitrypsin binds to heat-shock protein gp96 and protects from endogenous gp96-mediated injury in vivo. *Front Immunol* (2013) 4:320. doi:10.3389/fimmu.2013.00320
25. McHenga SS, Wang D, Li C, Shan F, Lu C. Inhibitory effect of recombinant IL-25 on the development of dextran sulfate sodium-induced experimental colitis in mice. *Cell Mol Immunol* (2008) 5(6):425–31. doi:10.1038/cmi.2008.53
26. Nold MF, Nold-Petry CA, Zepp JA, Palmer BE, Bufler P, Dinarello CA. IL-37 is a fundamental inhibitor of innate immunity. *Nat Immunol* (2010) 11(11):1014–22. doi:10.1038/ni.1944
27. Becker C, Fantini MC, Wirtz S, Nikolaev A, Kiesslich R, Lehr HA, et al. In vivo imaging of colitis and colon cancer development in mice using high resolution chromoendoscopy. *Gut* (2005) 54(7):950–4. doi:10.1136/gut.2004.061283
28. Kanai T, Watanabe M, Okazawa A, Sato T, Yamazaki M, Okamoto S, et al. Macrophage-derived IL-18-mediated intestinal inflammation in the murine model of Crohn's disease. *Gastroenterology* (2001) 121(4):875–88. doi:10.1053/gast.2001.28021
29. Siegmund B, Fantuzzi G, Rieder F, Gamboni-Robertson F, Lehr HA, Hartmann G, et al. Neutralization of interleukin-18 reduces severity in murine colitis and intestinal IFN-gamma and TNF-alpha production. *Am J Physiol Regul Integr Comp Physiol* (2001) 281(4):R1264–73.
30. Wirtz S, Becker C, Blumberg R, Galle PR, Neurath MF. Treatment of T cell-dependent experimental colitis in SCID mice by local administration of an adenovirus expressing IL-18 antisense mRNA. *J Immunol* (2002) 168(1): 411–20. doi:10.4049/jimmunol.168.1.411

31. Rolhion N, Barnich N, Bringer MA, Glasser AL, Ranc J, Hebuterne X, et al. Abnormally expressed ER stress response chaperone Gp96 in CD favours adherent-invasive *Escherichia coli* invasion. *Gut* (2010) 59(10):1355–62. doi:10.1136/gut.2010.207456
32. Ng SC, Benjamin JL, McCarthy NE, Hedin CR, Koutsoumpas A, Plamondon S, et al. Relationship between human intestinal dendritic cells, gut microbiota, and disease activity in Crohn's disease. *Inflamm Bowel Dis* (2011) 17(10):2027–37. doi:10.1002/ibd.21590
33. Fantuzzi G, Puren AJ, Harding MW, Livingston DJ, Dinarello CA. Interleukin-18 regulation of interferon gamma production and cell proliferation as shown in interleukin-1beta-converting enzyme (caspase-1)-deficient mice. *Blood* (1998) 91(6):2118–25.
34. Pena Rossi C, Hanauer SB, Tomasevic R, Hunter JO, Shafran I, Graffner H. Interferon beta-1a for the maintenance of remission in patients with Crohn's disease: results of a phase II dose-finding study. *BMC Gastroenterol* (2009) 9:22. doi:10.1186/1471-230X-9-22
35. Chen YG, Ashok BT, Liu X, Garikapaty VP, Mittelman A, Tiwari RK. Induction of heat shock protein gp96 by immune cytokines. *Cell Stress Chaperones* (2003) 8(3):242–8. doi:10.1379/1466-1268(2003)008<0242:IOHSPG>2.0.CO;2
36. Neurath MF. Cytokines in inflammatory bowel disease. *Nat Rev Immunol* (2014) 14(5):329–42. doi:10.1038/nri3661
37. Strober W, Fuss IJ. Proinflammatory cytokines in the pathogenesis of inflammatory bowel diseases. *Gastroenterology* (2011) 140(6):1756–67. doi:10.1053/j.gastro.2011.02.016
38. Caruso R, Sarra M, Stolfi C, Rizzo A, Fina D, Fantini MC, et al. Interleukin-25 inhibits interleukin-12 production and Th1 cell-driven inflammation in the gut. *Gastroenterology* (2009) 136(7):2270–9. doi:10.1053/j.gastro.2009.02.049
39. Colombel JF, Rutgeerts P, Malchow H, Jacyna M, Nielsen OH, Rask-Madsen J, et al. Interleukin 10 (Tenovil) in the prevention of postoperative recurrence of Crohn's disease. *Gut* (2001) 49(1):42–6. doi:10.1136/gut.49.1.42
40. Schreiber S, Fedorak RN, Nielsen OH, Wild G, Williams CN, Nikolaus S, et al. Safety and efficacy of recombinant human interleukin 10 in chronic active Crohn's disease. Crohn's Disease IL-10 Cooperative Study Group. *Gastroenterology* (2000) 119(6):1461–72. doi:10.1053/gast.2000.20196
41. Fedorak RN, Gangl A, Elson CO, Rutgeerts P, Schreiber S, Wild G, et al. Recombinant human interleukin 10 in the treatment of patients with mild to moderately active Crohn's disease. The Interleukin 10 Inflammatory Bowel Disease Cooperative Study Group. *Gastroenterology* (2000) 119(6):1473–82. doi:10.1053/gast.2000.20229
42. Herrlinger KR, Witthoeft T, Raedler A, Bokemeyer B, Krummenerl T, Schulzke JD, et al. Randomized, double blind controlled trial of subcutaneous recombinant human interleukin-11 versus prednisolone in active Crohn's disease. *Am J Gastroenterol* (2006) 101(4):793–7. doi:10.1111/j.1572-0241.2005.00356.x
43. Reinisch W, Hommes DW, Van Assche G, Colombel JF, Gendre JP, Oldenburg B, et al. A dose escalating, placebo controlled, double blind, single dose and multidose, safety and tolerability study of fontolizumab, a humanised anti-interferon gamma antibody, in patients with moderate to severe Crohn's disease. *Gut* (2006) 55(8):1138–44. doi:10.1136/gut.2005.079434
44. Hueber W, Sands BE, Lewitzky S, Vandemeulebroecke M, Reinisch W, Higgins PD, et al. Secukinumab, a human anti-IL-17A monoclonal antibody, for moderate to severe Crohn's disease: unexpected results of a randomised, double-blind placebo-controlled trial. *Gut* (2012) 61(12):1693–700. doi:10.1136/gutjnl-2011-301668
45. Derkx B, Taminiau J, Radema S, Stronkhorst A, Wortel C, Tytgat G, et al. Tumour-necrosis-factor antibody treatment in Crohn's disease. *Lancet* (1993) 342(8864):173–4. doi:10.1016/0140-6736(93)91375-V
46. van Dullemen HM, van Deventer SJ, Hommes DW, Bijl HA, Jansen J, Tytgat GN, et al. Treatment of Crohn's disease with anti-tumor necrosis factor chimeric monoclonal antibody (cA2). *Gastroenterology* (1995) 109(1):129–35. doi:10.1016/0016-5085(95)90277-5
47. Peyrin-Biroulet L, Lemann M. Review article: remission rates achievable by current therapies for inflammatory bowel disease. *Aliment Pharmacol Ther* (2011) 33(8):870–9. doi:10.1111/j.1365-2036.2011.04599.x

Conflict of Interest Statement: The authors declare that the research was conducted in the absence of any commercial of financial interest that could be considered as a potential conflict of interest. Gp96-II was an in kind contribution from Compugen Ltd., 26 Harokmim Street, Holon 5885800, Israel.

Copyright © 2017 Nold-Petry, Nold, Levy, Kliger, Oren, Borukhov, Becker, Wirtz, Sandhu, Neurath and Dinarello. This is an open-access article distributed under the terms of the Creative Commons Attribution License (CC BY). The use, distribution or reproduction in other forums is permitted, provided the original author(s) or licensor are credited and that the original publication in this journal is cited, in accordance with accepted academic practice. No use, distribution or reproduction is permitted which does not comply with these terms.

frontiers in Immunology

REVIEW
published: 12 December 2017
doi: 10.3389/fimmu.2017.01785

Immunopathogenesis in Myasthenia Gravis and Neuromyelitis Optica

*Zhen Wang[1,2] and Yaping Yan[1]**

[1] Key Laboratory of the Ministry of Education for Medicinal Resources and Natural Pharmaceutical Chemistry, National Engineering Laboratory for Resource Development of Endangered Crude Drugs in Northwest China, College of Life Sciences, Shaanxi Normal University, Xi'an, China, [2] Tianjin Medical University General Hospital, Tianjin Neurological Institute, Tianjin, China

Myasthenia gravis (MG) and neuromyelitis optica (NMO) are autoimmune channelopathies of the peripheral neuromuscular junction (NMJ) and central nervous system (CNS) that are mainly mediated by humoral immunity against the acetylcholine receptor (AChR) and aquaporin-4 (AQP4), respectively. The diseases share some common features, including genetic predispositions, environmental factors, the breakdown of tolerance, the collaboration of T cells and B cells, imbalances in T helper 1 (Th1)/Th2/Th17/regulatory T cells, aberrant cytokine and antibody secretion, and complement system activation. However, some aspects of the immune mechanisms are unique. Both targets (AChR and AQP4) are expressed in the periphery and CNS, but MG mainly affects the NMJ in the periphery outside of CNS, whereas NMO preferentially involves the CNS. Inflammatory cells, including B cells and macrophages, often infiltrate the thymus but not the target—muscle in MG, whereas the infiltration of inflammatory cells, mainly polymorphonuclear leukocytes and macrophages, in NMO, is always observed in the target organ—the spinal cord. A review of the common and discrepant characteristics of these two autoimmune channelopathies may expand our understanding of the pathogenic mechanism of both disorders and assist in the development of proper treatments in the future.

Keywords: neuromyelitis optica spectrum disorders, myasthenia gravis, channelopathy, humoral immunity, inflammation

OPEN ACCESS

Edited by:
Lisa Mullen,
Brighton and Sussex Medical School, United Kingdom

Reviewed by:
Yolande Richard,
Institut National de la Santé et de la Recherche Médicale, France
Rui Li,
University of Pennsylvania, United States
Ankit Saxena,
National Institutes of Health (NIH), United States
Sergio Iván Valdés-Ferrer,
Instituto Nacional de Ciencias Médicas y Nutrición Salvador Zubirán, Mexico
Sermin Genc,
Dokuz Eylül University, Turkey

****Correspondence:***
Yaping Yan
yaping.yan@snnu.edu.cn

Specialty section:
This article was submitted to Inflammation, a section of the journal Frontiers in Immunology

Received: *30 September 2017*
Accepted: *29 November 2017*
Published: *12 December 2017*

Citation:
Wang Z and Yan Y (2017) Immunopathogenesis in Myasthenia Gravis and Neuromyelitis Optica. Front. Immunol. 8:1785. doi: 10.3389/fimmu.2017.01785

INTRODUCTION

Myasthenia gravis (MG) is an autoimmune disease in which antibodies target postsynaptic membrane components at the neuromuscular junction (NMJ) and is characterized by fluctuating muscle weakness and fatigue (1–3). MG involves specific skeletal muscles, frequently including ocular, bulbar, and proximal extremity muscles but also affects respiratory muscles in severe cases (4, 5). The disease begins with an acute or subacute onset, improves with spontaneous remission or treatment, and relapses after variable intervals (6, 7). As the most important biomarkers in diagnosis, antibodies comprise a series of immunoglobulins (Igs) binding to acetylcholine receptors (AChR)—an ion channel protein, muscle-specific kinase (MuSK), and lipoprotein receptor-related protein 4 (LRP4) or other postsynaptic proteins (4). Based on the antibody profile, clinical presentation, age of onset, and thymic pathology, patients can be divided into several subtypes: MG with anti-AChR antibodies (AChR-MG) of early-onset, late-onset or with thymoma; MG with anti-MuSK antibodies (MuSK-MG); MG with anti-LRP4 antibodies (LRP4-MG); ocular MG; and seronegative MG (1, 4). MG has a prevalence of 15–25 cases per 100,000 individuals and an annual incidence of 0.8–1 cases per 100,000 individuals (1, 8), and AChR-MG constitutes approximately 80% of all MG

cases (4, 5). The age of onset and the female-to-male ratio varies between different subtypes (2, 4, 5). The disease is usually well controlled by immunosuppressive, symptomatic, supportive, or surgical treatment in most patients; however, only a few patients (22.2% of AChR-MG, 3.6% of MuSK-MG, and 21.9% of others) obtain full remission (1, 4, 9).

Neuromyelitis optica (NMO) is a severe, idiopathic, demyelinating disorder of the central nervous system (CNS) that has recently been recognized to be distinct from the classic demyelinating disease—multiple sclerosis (MS). NMO preferentially affects the optic nerve and spinal cord, but relatively spares the brain (10). With the discovery of the diagnostic biomarker—NMO-IgG (11), a better understanding of the pathogenesis of the disease was obtained and the clinical entity evolved. In 2015, the diagnostic criteria adopted the term neuromyelitis optica spectrum disorders (NMOSD) to incorporate inaugural or limited forms of NMO (idiopathic single or recurrent longitudinally extensive myelitis or recurrent or simultaneous bilateral optic neuritis), the involvement of the brain, coexistence with other autoimmune disorders, and Asian opticospinal MS (12). Most patients are seropositive for Ig G against aquaporin-4 (AQP4-IgG) (13–16), which is the most abundant water channel protein in astrocytes throughout the CNS (17, 18). Approximately 5–10% of patients are seropositive for antibodies against myelin oligodendrocyte glycoprotein (MOG-IgG) (19–21), and a few patients are dual-positive for both antibodies (22, 23). The prevalence and incidence of NMO/NMOSD are approximately 3.9–10 and 0.07–0.73 per 100,000, respectively, the median age of onset is 35–37 years and the female-to-male ratio is approximately 8–9:1 (24). Most patients have a relapsing course, with the interval between attacks ranging from months to years; the subsequent accumulation of disability leads to a poor prognosis despite the use of immunosuppressive treatment (10, 16, 25).

As autoimmune channelopathies in the periphery and CNS, MG and NMO share many similarities: (i) they develop based on a synergy between genetic factors and environmental effects (26, 27), (ii) the common female dominance in the prevalence of some major subtypes suggests an influence of gender on both diseases (28, 29), (iii) both depend on T cell-mediated, B cell-dependent immunopathology and the effects of antibodies and complements (30, 31), (iv) patients with the two disorders display similar relapsing courses and require chronic immunomodulatory management (1, 7, 10), (v) the disorders frequently coexist with other systemic or organ-specific autoimmune disorders (32, 33), and (vi) AChR-IgG and AQP4-IgG have been co-detected in patients with MG and NMOSD in a few studies (16, 33). MG and NMO may share similar pathogenic mechanisms; however, some discrepancies exist. AChR and AQP4 are expressed in the periphery and CNS (18, 34), whereas MG mainly affects the NMJ in the periphery outside of CNS (35), and NMO preferentially involves the CNS (36, 37). Inflammatory cells, including B cells and macrophages, often infiltrate the thymus but not the target—muscle in MG (38), whereas infiltration of inflammatory cells, mainly polymorphonuclear leukocytes and macrophages, in NMO, is always observed in the target organ—the spinal cord (39). A comparison of the pathogenesis, particularly the immune regulation, between MG and NMO is compelling, and will expand our understanding of the pathogenesis and assist in the future development of appropriate treatments.

INHERITED SUSCEPTIBILITY

The prevalence of familial and monozygotic patients has helped to explain the role of hereditary factors in pathogenesis. The frequency of familial MG in general patients is approximately 3–4% (40, 41), and the concordance between monozygotic MG twins is approximately 35% (42), both of these values are higher than the prevalence of 15–25/100,000 in the general population. Similarly, two studies reported a frequency of familial occurrence of NMOSD of approximately 3% (43, 44), which is greater than the prevalence of 0.52–4.4/100,000 in the general population. Based on these findings, genetic factors are likely to be involved in the susceptibility to both MG and NMOSD. However, the concordance of only 35% in monozygotic MG twins and rare reports of monozygotic NMOSD twins support the important role of environmental factors in the etiology (42, 45).

Human leukocyte antigen (HLA) genes are always strongly associated with many autoimmune diseases (46, 47). The AH8.1 haplotype has been reported to be linked to early-onset MG in a Caucasian population (48). Recently, a genome-wide association study in Turkey found that HLA-B*08:01 and HLA-C*07:01 are associated with early-onset AChR-MG; HLA-DQA1 and HLA-DQB1 are associated with late-onset AChR-MG; and HLA-DQB1*05:02 is associated with MuSK-MG (49). However, another North American and Italian study identified a link between HLA-DQA1 and both subtypes through different variants (50). According to two studies from China, the DQ9 haplotype and HLA-DRB1*09 alleles occur more frequently in a southern Han population with ocular MG and in northern Han patients with MG than in controls, respectively (51, 52). Several studies from different populations have together identified an association of DQ*5 alleles with MuSK-MG (53–56). In addition, some associated non-HLA loci have also been identified, such as cytotoxic T lymphocyte-associated protein 4, tumor necrosis factor receptor superfamily 11A (TNFRSF11A), zinc finger and BTB domain-containing 10 (ZBTB10), protein tyrosine phosphatase nonreceptor type 22 (PTPN22), tumor necrosis factor alpha-induced protein 3-interacting protein 1 (TNIP1), and receptor activator of nuclear factor κB ligand (50, 57, 58). Finally, the polymorphisms in CHRAN1 and CHRND encoding the subunits of AChR were found to confer an increased risk of MG (59, 60), suggesting that an aberrant AChR structure might contribute to autoimmunity.

An association between NMOSD and HLA has also been reported in different populations, although this notion was refuted in one study (61). DPB1*1501 has been reported to be associated with opticospinal forms of MS—a subgroup of NMOSD in Japan, despite its presence in 60% of the general population (62). DPB1*0501 was also shown to correlate with AQP4-IgG-positive NMO/NMOSD in southern Han Chinese and Japanese populations (63, 64). In a Spanish cohort, DRB1*03 was not only more frequent in patients with NMO than in healthy controls but was also associated with AQP4-IgG seropositivity (65). This allele was also confirmed in Afro-Caribbean, Brazilian, and south Indian

patients with NMO (66–68). Similar to MG, some non-HLA loci are also likely related to NMO/NMOSD pathogenesis, such as the T cell receptor, cluster of differentiation 6, TNFRSF1A, CD58, interleukin (IL)-17A and IL-17F, and the CYP7A1 promoter (69–73). However, PTPN22, which is associated with MG and other autoimmune diseases, was not correlated with NMO (74). Unlike polymorphisms in the AChR gene in MG, polymorphisms in AQP4 are not associated with NMO susceptibility (75).

The obvious association between HLA and MG/NMO suggests that antigen-presenting cells (APCs) and lymphocytes might play important roles in transferring signals from the activated innate immune system into specific adaptive autoimmune responses and establishing long-lived memory autoimmunity. In addition, the polymorphisms in non-HLA genes involved in immune signaling might cumulatively contribute to the pathogenesis of MG and NMO by overcoming or lowering the thresholds for immune signaling.

EPIGENETIC MECHANISMS

Epigenetic mechanisms link the environmental factors and genetics in disease, which include microRNA, DNA methylation, and histone acetylation (38). Many aberrant microRNAs expression has been reported to be involved in MG, including miR-320a, miR-155, miR-146a, and let-7c in immune cells and miR-150 and miR-21 in sera (26, 38). Mamrut et al. recently studied the profile of transcriptome and methylome in MG and found extremely high similarity at the transcription and the DNA methylation levels not only between discordant twins but also between the healthy discordant twins and the whole MG patients group, which indicated the high importance of genetic predisposition in the pathogenesis of MG (76). In addition, many differentially expressed genes and methylated CpGs in peripheral monocytes were detected between MG patients and controls, which suggested numerous small changes at gene or methylation levels might together contribute to MG development (76). In NMO patients, a recent study found 17 microRNAs was upregulated and 25 microRNAs was downregulated compared with healthy controls (77). Interestingly, the downregulated expression of miR-150 and miR-21 in serum of NMO patients is different from the upregulated expression in whole blood of MG patients, which may be a result of different methods.

ENVIRONMENTAL FACTORS

Many environmental factors contribute to the onset and severity of autoimmune diseases as predisposing factors, such as diet, vitamin D, and microbiota, or lead to relapse as triggering factors, such as infections, pollutants, and pharmacological molecules (38).

Vitamin D deficiency has been found to be correlated with the prevalence of many autoimmune diseases, such as type I diabetes mellitus, MS, rheumatoid arthritis (RA), systemic lupus erythematosus (SLE), and inflammatory bowel diseases (78). Vitamin D contributes to the regulation of the immune system through multiple mechanisms, including regulation of the activation and differentiation of CD4 lymphocytes, the suppression of differentiation of monocytes into dendritic cells, the reduction of cytokine production, and stimulation of natural killer T cells (38). In patients with MG, vitamin D levels are decreased, and vitamin D improves the autoimmune response and fatigue (79). As shown in the study by Alahgholi-Hajibehzad et al., vitamin D significantly increases the function of regulatory T cells (Treg) derived from patients with MG *in vitro* (80), and complete remission of severe refractory MG was reported after treatment with a massive-dose of vitamin D; however, this finding remains to be confirmed by additional high-quality clinical trials (81). According to Mealy et al., vitamin D levels are significantly lower in patients with recurrent spinal cord disease, mainly including NMO/NMOSD (82); the finding was reproducible in other NMO/NMOSD studies (83–86). Among these studies, a group from south China found that vitamin D levels were inversely correlated with disease-related disability, clinical activity, and prognosis (83); however, Thai, Turkish, and Korean groups did not observe a correlation (84–86). Additional studies are needed to clarify whether low vitamin D levels are a predisposing factor for or a secondary consequence of NMO.

The gut microbiota consists of trillions of microorganisms that colonize the intestine and regulate the maturation and function of the host immune system (87). When the host changes his or her diet or lifestyle or overuses antibiotics, the susceptibility to autoimmune disorders may increase due to the altered symbiotic relationship between the host immune system and the microbiota (88). Despite considerable research on the relationship between the gut microbiota and other autoimmune diseases, studies of the microbiota in patients with MG are scarce. A mixture of probiotics was recently shown to reduce the clinical symptoms of experimental autoimmune MG by suppressing AChR-reactive lymphocytes and generating regulatory dendritic cells and Tregs (89). An investigation of the gut microbiota in patients with NMO revealed the overrepresentation of *Clostridium perfringens*, and the *C. perfringens* adenosine triphosphate-binding cassette transporter (ABC), shared a homologous sequence with AQP4 that could cross-react with T cells from patients with NMO (90, 91). This result provides a new cue for the pathogenesis of NMO, but further studies, including the establishment of appropriate animal models, are warranted.

Viral infections, particularly with Epstein–Barr virus (EBV), have been correlated with the pathogenesis of many autoimmune diseases in seroepidemiological and immunological studies (92). EBV-infected B cells have been detected in the target organs in many autoimmune diseases; similarly, these cells were also detected in the hyperplastic thymus of patients with MG (38, 93). High levels of antibodies against the type 1 nuclear antigen of EBV were recently shown to be more common in patients with MG (94). The virus might induce persistent inflammation in the thymus and initiate autoantigen sensitization, leading to the subsequent autoimmune response (92). However, this finding was not confirmed by two other studies (95). Antibodies against EBV were more frequently detected in the serum and cerebrospinal fluid (CSF) of patients with NMO than in controls, suggesting that EBV might be involved in NMO pathogenesis (96). In addition, a peptide derived from the TAX1BP1 protein of human T cell leukemia virus type 1 virus (HTLV-1), was used

to immunize mice and induced the production of antibodies against the peptide and homologous AQP4 epitope without any brain lesions, suggesting that HTLV might also be implicated in the pathogenesis of NMO (97), although a previous clinical study argued against this view (98).

GENDER BIAS

Most autoimmune diseases exhibit a higher incidence in females (99). Gonadal hormones and direct X-chromosome effects have been proposed to contribute to the sex bias (99). Compared with males, females have many differences in innate immunity and adaptive immunity (100). Females were revealed to have higher expression of some genes involved in toll-like receptor (TLR) pathways and stronger type I interferon (IFN) responses by transcriptional analyses (100, 101). In addition, females display higher phagocytic activities of neutrophils and macrophages, more efficient APCs and dysregulation of innate lymphoid cells (100, 102, 103). Females also have higher $CD4^+$ T cell counts, higher CD4/CD8 ratios, higher basal Ig levels, and higher B cell numbers, as well as lower Treg counts (100, 104, 105). Moreover, peripheral blood mononuclear cells (PBMCs) produce more activated $CD4^+$ T cells (100). Estrogens may play a major role in this effect as they can favor the follicular helper T cells (Tfh) response and affect B cell maturation, selection, and antibody secretion (29, 106). Furthermore, at specific doses, time points, and microenvironments, estrogens allow autoreactive B cells to escape from the normal tolerance mechanisms and to accumulate in sufficient numbers to induce autoimmunity (38, 107).

Obvious female dominance was observed in patients with early-onset AChR-MG, MuSK-MG, and LRP4-MG, with female: male ratios of 9:1, 4:1, and 2:1, respectively, indicating that sex may affect the pathogenesis of some subtypes (10, 38). The clinical severity is modulated by menstruation, which is abolished by thymectomy, and aggravation occurs during pregnancy and the postpartum period (108, 109). The increased estrogen receptor expression in thymocytes and PBMCs in patients with MG induced by the inflammatory environment suggests that estrogens potentially contribute to the MG autoimmune process by affecting cytokine production and B cell activity (29, 110).

A similar female: male distribution (8–9:1) was also observed in patients with NMO/NMOSD in a new comparative population-based study (24), and the ratio has been shown to reach 23:1 in AQP4-IgG-positive patients during fertile periods (28). Moreover, some researchers have reported a more frequent relapse rate in female patients with NMOSD during pregnancy and the postpartum period and an earlier age of NMOSD onset in patients treated with systemic hormone therapy (111, 112). Based on these findings, gender may affect NMO pathogenesis through female hormones, and genetic or epigenetic factors. Estrogen has been postulated to promote autoreactive B cell development with increasing INF I and B-cell-activating factor (BAFF) generation, to decrease autoreactive B cell apoptosis with upregulation of antiapoptotic molecules, to facilitate antibodies production and affect antibodies glycosylation, and to contribute to the pathogenesis of NMO in females (111).

INNATE IMMUNITY IN THE INITIATION OF AUTOIMMUNITY

Adaptive immunity plays a major role in both MG and NMO, but requires the innate immune system to initiate pathogenesis (93). However, the exact mechanism by which the immune system initiates autoimmunity in both diseases, particularly NMO, remains largely unknown due the lack of ideal animal models.

In early-onset AChR-MG, the pathogenic link between innate immunity and autoimmunity in the thymus is well recognized (92). Obvious IFN and TLR imprinting has been observed in the hyperplastic thymus, which potentially upregulates the α-AChR expression in epithelial and myoid cells (92). In the context of the genetics of susceptibility and predisposing environmental factors, the aberrant innate response to thymic inflammation may induce AChR sensitization and lead to adaptive immunity (92). In a recent study, an intraperitoneal injection of polyinosinic–polycytidylic acid, a mimic of double-stranded RNA, upregulated TLR3 and IFN-β expression, and stimulated α-AChR overexpression in thymic epithelial cells (TEC), specifically triggering the proliferation of B cells, the generation of anti-AChR antibodies and the presentation of MG-like clinical signs (113). In another study, EBV infection was observed in B cells and plasma cells (PCs) in the thymus of patients with MG (93). Taken together, these findings provide a possible theoretical basis for the mechanism by which innate immunity induces autoimmunity in MG.

Due to the limited data available, researchers have not clearly determined whether the initiation of autoimmunity occurs in the CNS or the periphery in patients with NMO. Levy et al. speculated that astrocyte death induced by an unknown cause might lead to the activation of microglia and the release of inflammatory mediators, thereby disrupting the blood–brain barrier (BBB) and recruiting immunocompetent cells from the periphery. APCs phagocytose cell debris, process the AQP4 antigen, present the linearized determinants to $CD4^+$ T cells, and initiate adaptive immunity (114). However, this hypothesis does not explain why AQP4 expressed in peripheral organs does not elicit autoimmunity. In the study by Zamvil et al., *C. perfringens* was overrepresented in the gut microbiome of patients with NMO compared with that of controls and the ABC protein on the bacteria reacted with AQP4 p61–80-specific T cells obtained from patients with NMO and induced Th17 polarization (90, 91). Based on this observation, a molecular mimicry mechanism in the periphery might initiate autoimmunity in patients with NMO (91), a process that must involve the innate immune system. In fact, monocytes derived from the PBMCs of patients with NMO produce more IL-6 for Th17 polarization when stimulated *in vitro* (91).

ADAPTIVE IMMUNITY

T Cells

T helper 1 (Th1)/Th2/Th17 Cells

T helper 1 cells, Th2 cells, and Th17 cells are important subtypes of $CD4^+$ T cells characterized by the different patterns of cytokines

they secrete. Th1 cells produce IFN-γ and are responsible for the defense against intracellular pathogens; Th2 cells produce IL-4, IL-5, and IL-13 and are involved in the response to parasitic infections; and Th17 cells produce IL-17 and defend against extracellular pathogens (115). Under pathological conditions, Th1 and Th17 cells are associated with autoimmunity, and Th2 cells are implicated in allergic responses (115).

Patients with MG display increased numbers of IFN-γ or IL-4-expressing cells in PBMCs, suggesting that both Th1 and Th2 cells are involved in MG (29, 116). However, in a recent study, the percentage of Th1 cells among $CD4^+$ T cells was higher than the percentage of Th2 cells, and the Th1/Th2 ratio correlated positively with clinical severity in the glucocorticoid-treated group (117). Increased numbers of Th17 cells and serum IL-17 levels were observed in patients with MG complicated with thymoma, and a correlation was observed between the percentage of Th17 cells and the AChR antibody titer (118, 119). In addition, a Th1/Th17/follicular Tfh signature was revealed in an analysis of the transcriptomes of purified thymic T cells obtained from patients with MG, most of whose thymus glands bore germinal centers (GCs) (120). However, in a heterogeneous group of patients with AChR-MG, the serum IL-17 levels were comparable to those of normal controls (121). Increased frequencies of Th1 and Th17 cytokines were detected in patients with MuSK-MG (122), although another study revealed that similar polarization was detected in PBMCs only after stimulation *in vitro* (123).

Some debate exists about the roles of Th1/Th2 cells in NMOSD. Using flow cytometry to analyze T cell subsets in PBMCs, Uzawa et al. observed a higher Th1/Th2 ratio in patients with MS but not in patients with NMOSD (124). In contrast, Shimizu et al. reported a higher Th1/Th2 ratio in patients with NMOSD than in patients with MS (125). However, it is generally accepted that Th17-related cytokine and chemokine levels are frequently elevated in the serum and CSF of patients with NMOSD (126–129). Among these cytokines, IL-6 is secreted by macrophages, dendritic cells, and B cells, induces B cells to synthesize antibodies, and facilitates the differentiation of naïve T cells into Th17 cells (127). Several studies have reported elevated serum and CSF IL-6 levels and a strong correlation between CSF IL-6 levels with clinical signs in patients with NMO (128), and IL-6 receptor blockade results in a decreased relapse rate (130). Levels of granulocyte colony-stimulating factor, which is responsible for the survival, proliferation, and differentiation of neutrophils, and IL-8, which is responsible for neutrophil recruitment, were also increased in the CSF of patients with NMO (127). Taken together, these observations suggest the important roles of Th17 cells in NMO.

Treg Cells

$CD4^+CD25^+FoxP3^+$ Treg cells form a special subgroup of $CD4^+$ T cells that are involved in the induction and maintenance of immune homeostasis and tolerance (131). Treg cells can suppress activated T cells and B cells by secreting transforming growth factor-β (TGF-β), IL-10, and IL-35 (131). Defective function of Tregs with reduced FoxP3 expression has been observed in the thymus and PBMCs of patients with AChR-MG (132, 133), but the normal Treg numbers in this study contradict the reduced Treg numbers in PBMCs found in another study (134). It remains unclear whether the Tregs number is abnormal or not in patients with NMO.

Tfh Cells

Helper T cells comprise a group of effector T cells that are characterized by the expression of transcription factor B cell lymphoma 6 and the surface marker CD4, C–X–C motif chemokine receptor 5 (CXCR5) and programmed cell death protein 1 (PD-1), which promote B cell maturation and antibody production (135). In our previous study, patients with generalized MG displayed significantly increased numbers of circulating Tfh cells and reduced numbers of follicular Tregs in PBMCs, and the numbers of Tfh cells were strongly correlated with the plasma cell frequency and AChR antibody titers (136). In addition, B cells produced antibodies in an IL-21 signaling-dependent manner when cocultured with Tfh cells (136). As in patients with MG, the Tfh cell frequency was higher in patients with NMOSD than in healthy controls and was higher in relapsing patients than in remitting patients (137). In addition, treatment with methylprednisolone decreased the numbers of Tfh cells in patients with NMOSD (137). Interestingly, in another report, the numbers of circulating memory Tfh cells were increased in patients with NMOSD and were positively correlated with the clinical severity and AQP4 antibody levels (138). Based on these findings, Tfh cells might contribute to the development of MG and NMO through an effect on autoreactive B cells.

B Cells

B Cells, Plasmablasts (PBs), PCs and Memory B Cells (MB)

Both MG and NMOSD are humoral immunity-mediated autoimmune diseases, and B cells play an important role in the pathogenesis of both disorders. PBs and PCs secrete antibodies, and MBs produce proinflammatory cytokines and exacerbate autoimmunity (111). The survival, maturation, and differentiation of B cells is regulated by BAFF (139).

In patients with MG, B cells proliferation is not detected in the peripheral blood, but GCs are observed in the hyperplastic thymus (38), in which B cells encounter the antigen, interact with Tfh, and differentiate into short-lived or long-lived PCs, IgD^-CD27^- B cells (DN), and MBs (140). Higher titers of AChR antibodies are produced by PBs or PCs in the thymus than in peripheral blood cells *in vitro*, but extra-thymic PCs also contribute to serum AChR antibody titers, based on the observation of persistent antibody generation after thymectomy (140). MBs are also involved in MG pathogenesis. In a recent case study of a patient with AChR-MG, relapse occurred after the discontinuation of rituximab and other drugs, with the repopulation of DNs and IgD^-CD27^+ MBs (141). The serum BAFF levels in patients with MG were significantly elevated, although the levels were not correlated with the clinical severity (140).

In patients with NMO, the numbers of $CD19^{int}CD27^{high}CD38^{high}CD180^-$ B cell PBs are selectively elevated in the peripheral blood and further expanded during

relapse; these cells are responsible for the generation of AQP4 antibodies in an IL-6-dependent manner (142). Rituximab was also reported to control clinical activity by reducing the number of $CD27^+$ MBs but not by inducing changes in AQP4 antibody levels, which indicates the role of MBs in the development of NMO (143, 144). The serum and CSF BAFF levels were significantly elevated in patients with NMO and the serum BAFF levels were reduced after treatment with rituximab (111).

Regulatory B Cells (Breg)

Regulatory B cells comprise a specific group of B cell subsets characterized by production of anti-inflammatory cytokines, such as TGF-β, IL-10, and IL-35, which downregulate excessive immune and inflammatory responses (145). Several studies have observed impaired Bregs in patients with MG. The frequency of $CD19^+CD1d^{high}CD5^+$ and $CD19^+CD24^{high}CD38^{high}$ subsets and IL-10-producing B cells (B10) was decreased in patients with MG, and that was correlated with clinical severity (146). In another report, the production of IL-10 and TGF-β1 was lower in patients with MG than in healthy controls (147). Similarly, Quan et al. observed a decreased frequency of $CD19^+CD24^{high}CD38^{high}$ subsets and B10 in patients with NMO compared with those in patients with MS and controls, and the frequency was even lower in patients with AQP4-IgG-positive NMO (148).

ANTIBODIES

Increasing numbers of antibodies have been discovered in patients with MG, including MuSK antibodies, LRP4 antibodies, agrin antibodies, titin antibodies, potassium voltage-gated channel subfamily A member 4 ($K_V1.4$) antibodies, ryanodine receptor antibodies, and others (4). However, AChR antibodies remain the most important antibodies in MG and are present in approximately 80% of patients (4). As the earliest recognized antibody in MG, its pathogenic mechanism has been clarified. (i) Antibodies binding to AChR can accelerate the degradation of AChR by cross-linking the receptors; (ii) AChR is blocked by steric hindrance; and (iii) the complement cascade is activated to form membrane attack complex (MAC) and induces damage to postsynaptic membranes by complement-dependent cytotoxicity (CDC) (149).

Aquaporin-4 antibodies are detected in more than 75% of patients with NMO (11), and MOG and AQP1 antibodies have also been discovered in both AQP4-IgG-positive and -negative patients (13, 23). First, AQP4 antibodies mainly comprising the IgG1 isotypes promote complement cascade activation to form the MAC in the end-feet and lead to cell death by CDC after binding to AQP4 on astrocyte (18). The released inflammatory medium, such as complement protein 3a (C3a) and C5a, together with other cytokines, recruit granulocytes and macrophages, which induce secondary oligodendrocyte damage, demyelination, and neuronal death through antibody-dependent cell-mediated cytotoxicity (ADCC) (150, 151). This mechanism provides an explanation for the typical necrotic lesions observed in the spinal cord, which are characterized by the extensive loss of AQP4 and glial fibrillary acidic protein (GFAP), the perivascular deposition of Igs and activated complement, and the massive infiltration of macrophages and polymorphonuclear leukocytes (39, 152, 153). However, vascular fibrosis and hyalinization in both active and inactive lesions has not been well explained, and a recent finding of glucose-regulated protein 78 (GRP78) autoantibodies targeting endothelial cells in the serum of patients with NMO may provide a new explanation for the vascular involvement and disruption of the BBB (154). Second, an alternative lesion pattern with prominent loss of AQP4 and GFAP but variable absent complement deposition was observed in the area postrema (155). Internalization of AQP4 caused by AQP4-IgG observed *in vitro* was examined in an attempt to decipher the lesion pattern (156), but this was debated because it does not occur *in vivo* (18).

AUTOIMMUNE COMORBIDITIES

Several studies have investigated autoimmune comorbidities in patients with MG. Approximately 15% of patients with MG are also diagnosed with another autoimmune disorder, which most frequently afflicts patients with early-onset AChR-MG (1). Among these disorders, autoimmune thyroid disease (ATD) is the most common in 10% of patients with MG, followed by SLE (1–8%) and RA (4%) (33), and the most common antibodies comprise antithyroid peroxidase antibodies, antithyroglobulin antibodies, antinuclear antibodies, and rheumatoid factor (157). Interestingly, patients with thymoma MG are more susceptible to autoimmune disorders after thymectomy than before surgery, probably due to an altered T cell repertoire (33).

Associations between NMOSD and other autoimmune diseases have also been recognized. Up to 30% of patients with NMOSD are diagnosed with a coexisting autoimmune disease, and 40% of NMOSD patients present other autoantibodies without an obvious accompanying disease (13). The most common diseases, include SLE, SS, MG, ATD, and antiphospholipid syndrome, whereas the most common antibodies comprise anti-extractable nuclear antigens antibodies, anti-SSA and anti-SSB autoantibodies, and rheumatoid factor (13). In most reported cases, the onset of SLE preceded NMOSD by several years, whereas NMOSD symptoms preceded SS by a few years (158).

Regarding the mechanisms of the associated comorbidities in patients with NMOSD, the common genetic and environmental factors have been postulated to facilitate autoimmunity, and the autoimmune comorbidities might partially contribute to the immunopathogenesis of NMOSD (32). Similar mechanisms might also apply to the comorbidities in patients with MG.

Of all the abovementioned coexisting diseases, the co-occurrence of MG and NMOSD in patients arouses much particular interest in researchers, because this is more frequent than expected in the general population (159). In one study of 117 patients with NMOSD, comorbid MG was identified in 2% of patients, and AChR antibodies were detected in 11% of patients (160). In another study of 164 patients with MG, 10–15% of patients had CNS involvement resembling an NMO-like disease, half of whom exhibited AQP4-IgG (161). MG likely has a benign course, but CNS involvement is potentially more severe when accompanied by thymomas (159, 161). AChR antibodies and AQP4 antibodies may precede the onset of the relevant symptoms, and the titers of

the two antibodies tend to be negatively correlated (159). In most cases, MG symptoms preceded the onset of NMOSD, and only a few patients developed MG after NMOSD onset (158). Most of these patients had early-onset AChR-MG, and 70% had a history of thymectomy (158). AQP4 is expressed in the thymus, and this may provide a pathogenic basis similar to that of AChR in MG (158). Additionally, the decrease in the number of Tregs following thymectomy may further contribute to NMOSD development (158). AQP4 is also expressed at the NMJ; thus, the degeneration of the postsynaptic membrane induced by AChR antibodies was postulated to initiate AQP4 sensitization in the context of the inflammatory environment in MG, and then mediate the autoimmunity against AQP4 (161).

SPECIFIC INVOLVEMENT OF DIFFERENT TARGET ORGANS

Nicotinic acetylcholine receptors (nAChRs) are expressed in both muscle and brain (34), but MG seldom involves the brain, with the exception of rare reports of cognitive impairment, epilepsy, Parkinson's disease, MS, and psychological and sleep disorders (35, 161). In addition to the major protective role of the BBB, the differences in structure between muscle and neuronal AChRs consisting of different subunits might also contribute to the brain exemption (34). In fact, antibodies from patients with MG do not bind to nAChRs in the human brain (162). In patients with AChR-MG, extraocular muscle weakness usually precedes

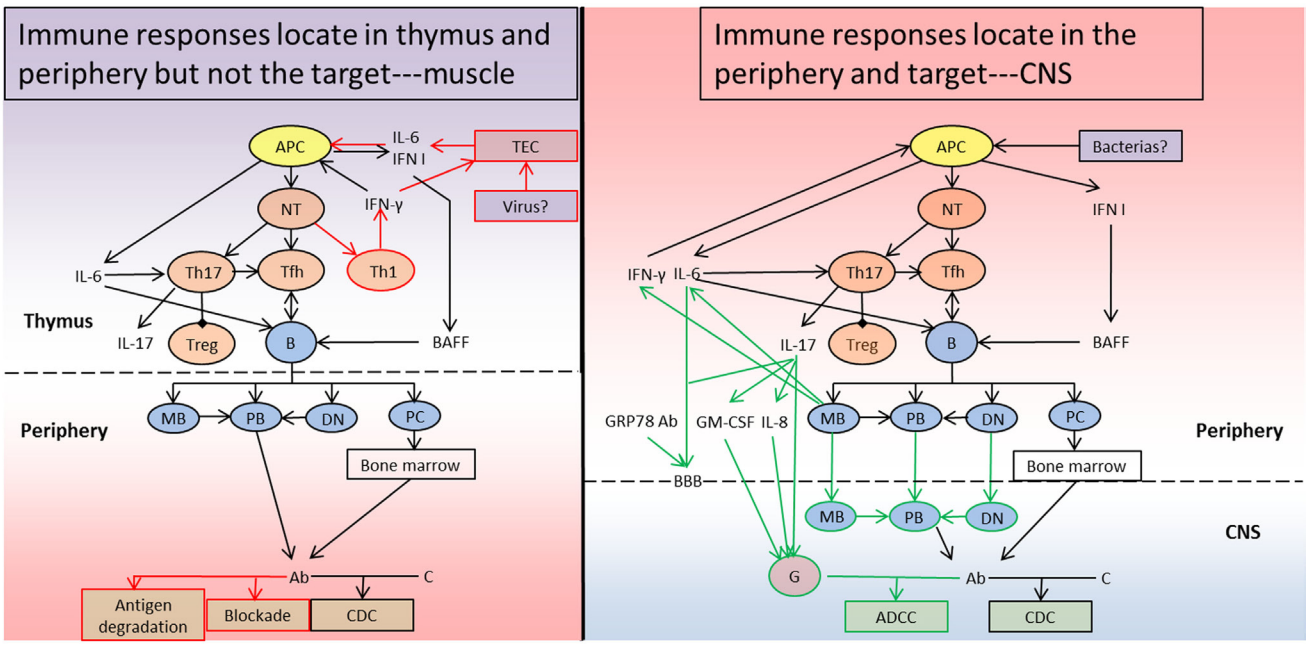

FIGURE 1 | Schematic diagram of the immunopathogenesis of myasthenia gravis (MG) and neuromyelitis optica (NMO). (Left) In the context of susceptible genetic and environmental predisposing factors in MG patients, the TECs secrete IL-6 and IFN I and upregulate acetylcholine receptor (AChR) expression after a triggering event such as viral infections. Together with the effects of the cytokines, APCs phagocytose, process, and present the AChR antigen to naïve T cells and initiate Th1, Th17, and Tfh subsets differentiation. Th1 cells and APCs generate IFN-γ, IFN I, and IL-6 to sustain and amplify the chronic inflammation. Th17 cells produce IL-17 and IL-21 to inhibit Tregs and favor Tfh development. Tfh cells interact with B cells to form germinal centers and promote B cell maturation and antibody production with the help of BAFF and IL-6. MBs, PBs, DNs, and PCs enter into the periphery from the thymus, and MBs and DNs also differentiate into PBs generating Ab, and PCs migrate into the bone marrow to produce Ab. The Ab can destroy the postsynaptic membrane by promoting antigen degradation, blocking functional sites and inducing CDC. (Right) Similar to MG, NMO also develops on the basis of susceptible genetic and environmental predisposing factors. During the priming process (for example, due to infection with particular bacteria), APCs phagocytose the pathogen and present a specific peptide to naïve T cells, which is identical with a particular peptide sequence in the aquaporin-4 (AQP4) protein. Additionally, APCs secrete IFN I to facilitate BAFF generation. The autoreactive naïve T cells then differentiate into Th17 and Tfh subsets. Th17 cells can produce IL-17 and suppress Tregs, and help Tfh development. Tfh cells promote cognate B cells maturation and differentiation into MBs, PBs, DNs, and PCs, together with BAFF. The proinflammatory MBs can further contribute to APC activation, Th17 differentiation, and B cell maturation through IL-6 and IFN-γ. IL-17 and IL-6 or GRP78 Ab can break the BBB and permit MBs, DNs, and PBs to enter into the CNS. The MBs and DNs can also progress to PB to generate Ab, which can target the AQP4 protein in astrocytes together with the antibodies produced by PCs in bone marrow. The Ab attack the astrocytes through CDC, which not only forms membrane attack complex but also generates C5a and C3a recruiting granulocytes in combination with IL-17, IL-8, and GM-CSF. The granulocytes can further aggravate the CNS lesion through ADCC. TEC, thymic epithelial cell; APC, antigen-presenting cell; NT, naïve T cell; Th1, T helper 1 cell; Th2, T helper 2 cell; Th17, T helper 17 cell; Treg, regulatory T cell; Tfh, follicular helper T cell; B, B cell; MB, memory B cell; PB, plasmablast; DN, $CD27^{-}IgD^{-}$ double negative B cell; PC, plasma cell; G, granulocyte; IL-6, interleukin 6; IL-8, interleukin 8; IL-17, interleukin 17; IFN I, type I interferon; IFN-γ, interferon γ; BAFF, B cell-activating factor; Ab, antibody; C, complement; GM-CSF, granulocyte-macrophage colony-stimulating factor; GRP78 Ab, glucose-regulated protein 78 antibody; BBB, blood–brain barrier; ADCC, antibody-dependent cell-mediated cytotoxicity; CDC, complement-dependent cytotoxicity; CNS, central nervous system. The red pathway represents the specific immune responses in MG, the green pathway refers to the unique immune responses in NMO, and the black pathway is shared by both disorders. The "periphery" means outside of thymus in MG and outside of CNS in NMO.

TABLE 1 | The comparison of immunopathogenesis between MG and NMO.

	MG	NMO
Susceptible gene	HLA (AH8.1, HLA-B*08:01, HLA-C*07:01, HLA-DQA1, HLA-DQB1, HLA-DQB1*05:02, HLA-DQA1, DQ9, HLA-DRB1*09, DQ*5); non-HLA (CTLA4, TNFRSF11A, ZBTB10, PTPN22, TNIP1, RANKL, CHNRA1, CHRND)	HLA (DPB1*1501, DPB1*0501, DRB1*03); non-HLA (TCR, CD6, TNFRSF1A, CD58, IL-17A, IL-17F, CYP7A1 promoter)
MicroRNA	miR-150 and miR-21 (↑ in sera)	miR-150 and miR-21 (↓in whole blood)
Environmental factors	Vitamin D deficiency, Epstein–Barr virus (EBV)	Vitamin D deficiency, *Clostridium perfringens*, EBV, human T cell leukemia virus type 1 virus
Gender bias	Early-onset AChR-MG, MuSK-MG, and LRP4-MG	AQP4-IgG positive patients
T helper 1 (Th1)/Th2/Th17 cells	Th1/Th2 cells (ND); Th17 cells (↑), serum Th17 cytokines (↑)	Th1/Th2 cells (ND); serum and CSF Th17 cytokines (↑)
Treg cells	FoxP3 expression (↓)	ND
Follicular T cells	Follicular helper T cells (Tfh) (↑); follicular regulatory T cells (↓)	Follicular Tfh (↑)
B cells	B cells (↑ in Thymus); memory B cells (↑ during relapse); serum BAFF levels (↑); Bregs (↓), IL-10 and TGF-β1 (↓)	Plasmablasts (↑); memory B cells (↑ during relapse); serum and CSF BAFF levels (↑); Bregs (↓)
Antibodies	AChR antibodies (80%), MuSK antibodies (1–10%), LRP4 antibodies (1–5%), agrin antibodies (minority), titin antibodies (20–30% of AChR-MG), potassium voltage-gated channel subfamily A member 4 antibodies (10–20%), ryanodine receptor antibodies (70% of MG with thymoma and 14% of late-onset AChR-MG)	AQP4 antibodies (>75%), myelin oligodendrocyte glycoprotein antibodies (5–10%), AQP1 antibodies (26%), glucose-regulated protein 78 antibodies
Autoimmune comorbidities	ATD (10%), SLE (1–8%), RA (4%); TPO antibodies (36%), TG antibodies (23%), ANA (23%), rheumatoid factor (8%), AQP4 antibodies (5–7%)	ATD (17%), SLE (2.0%), SS (2.0%), MG (2%), RA (1.3%); ANA (43%), ENA (15%), SS-A (10%), SS-B (3%); and rheumatoid factor (5%), AChR antibodies (11%)
Inflammatory infiltration	B cells and macrophages in the thymus, absent in muscle	Polymorphonuclear leukocytes and macrophages in CNS

MG, myasthenia gravis; NMO, neuromyelitis optica; HLA, human leukocyte antigen; CTLA4, cytotoxic T lymphocyte-associated protein 4; TNFRSF, tumor necrosis factor receptor superfamily; ZBTB10, zinc finger and BTB domain-containing 10; PTPN22, protein tyrosine phosphatase nonreceptor type 22; TNIP1, tumor necrosis factor alpha-induced protein 3-interacting protein 1; RANKL, receptor activator of nuclear factor κB ligand; TCR, T cell receptor; CD, cluster of differentiation; IL, interleukin; AChR, acetylcholine receptor; MuSK, muscle-specific kinase; LRP4, lipoprotein receptor-related protein 4; AQP4, aquaporin-4; Th, T helper; Treg, regulatory T; FoxP3, forkhead box P3; ND, not determined; BAFF, B-cell-activating factor; Bregs, regulatory B cells; TGF, transforming growth factor; CSF, cerebrospinal fluid; CNS, central nervous system; ENA, extractable nuclear antigen; ANA, antinuclear antibody; ATD, autoimmune thyroid disease; SLE, systemic lupus erythematosus; RA, rheumatoid arthritis.

generalized muscle weakness, and in patients with ocular MG, extraocular muscle weakness is the sole symptom, along with a lower titer of AChR antibodies (2, 163). Thus, the extraocular muscles are more susceptible to MG and many studies have attempted to explain this specificity. First, extraocular muscles have special physiological features: the neuron innervating extraocular muscles have higher firing frequencies, and the tonic fibers in extraocular muscles depend on intact AChR function, which reduces the endplate safety factor (30). Second, the expression of the complement-regulating proteins CD55 and CD59 is lower in extraocular muscles than in other muscles (164). Third, researchers are still debating whether fetal AChR expressed in extraocular muscles is a target of autoimmunity in MG (165).

The NMO target protein AQP4 is expressed not only in the CNS but also in some peripheral organs, including the kidney, skeletal muscle, stomach, and airways (166); however, the peripheral organs are relatively spared, except for a few reports of myopathy (36), even though the AQP4-IgG titer is higher in the serum than in the CSF (167). Several observations might help to explain this question: (i) AQP4 is higher expressed in CNS than in peripheral organs (168), (ii) a higher ratio of M23/M1 AQP4 isoforms with larger orthogonal arrays of particles (OAPs) of AQP4 in peripheral organs results in a higher capacity to bind to AQP4-IgG and induce CDC (168–171), (iii) the complement regulatory proteins CD46, CD55, and CD59 are expressed in AQP4-expressing cells in peripheral organs but are absent in the astrocytes, as we and others recently reported (36, 37). In addition, larger OAPs in the spinal cord and optic nerve than in the brain may also contribute to the more frequent and severer involvement of the spinal cord and optic nerve in NMO (168). Even in the brain, the typical lesions are distributed in specific location, i.e., the hypothalamic and periventricular areas (172). Higher AQP4 expression in these areas is thought to be responsible for the specific distribution (172). Recently, the involvement of the pia, ependyma, and choroid plexus was observed in 23 autopsy cases of NMO/NMOSD (173). The disruption of the blood–CSF barrier in the choroid plexus was suspected to provide a route for AQP4-IgG to enter the CNS (173), and this may offer another possible explanation for the aforementioned specific distribution in the brain—the areas may be more accessible to the penetration of AQP4-IgG from the CSF and resemble ventriculitis and leptomeningitis in patients with NMO.

THE PANORAMA OF IMMUNOPATHOGENESIS

In the abovementioned portions, we describe the profiles of the immunopathogenesis of both disorders, particularly the early-onset AChR-MG and AQP4-IgG positive NMO/NMOSD. In general, both diseases are T cell-mediated and B cell-dependent autoimmune channelopathies on the basis of the susceptible

gene and predisposing environmental factors. The schematic of immunopathogenesis in MG and NMO is shown in **Figure 1**, and the comparison between them is summarized in **Table 1**.

After triggering events such as viral infections in patients with MG, the TEC secrete IL-6 and IFN I and upregulate α-AChR expression. The APCs then phagocytose, process, and present a linear peptide of the AChR protein to naïve T cells, thus initiating Th1, Th17, and Tfh subset differentiation (29, 92). Th1 cells and APCs generate IFN-γ, IFN I, and IL-6 to sustain and amplify the chronic inflammation (29, 38). Th17 cells produce IL-17 and IL-21 to inhibit Tregs and favor Tfh development (29, 120). Tfh cells interact with B cells to form GCs and promote B cell maturation and AChR antibody production with the help of BAFF and IL-6 (120, 140). MBs, PBs, DNs, and PCs enter into the periphery from the thymus, MBs, and DNs then also differentiate into PBs to generate antibodies, and PCs migrate into the bone marrow to persistently produce antibodies (140, 141). The antibodies destroy the AChR channel on the postsynaptic membrane by promoting antigen degradation, blocking functional sites, and inducing CDC (149).

Similar to MG, during the priming process in patients with NMO (for example, with infections of some bacterias), APCs phagocytose the pathogen and present a specific peptide to naïve T cells; this peptide is identical to a peptide sequence in the AQP4 protein (91). In addtion, APCs secrete IFN I to facilitate BAFF generation (111). The autoreactive naïve T cells then differentiate into Th17 and Tfh subsets. Th17 cells can produce IL-17, suppress Tregs, and help Tfh development (126, 127). Together with BAFF, Tfh cells can promote cognate B cell maturation and differentiation into MBs, PBs, DNs, and PCs (111, 137, 174, 175). The proinflammatory MBs can further contribute to APC activation, Th17 differentiation, and B cell maturation through IL-6 and IFN-γ (111, 174). IL-17 and IL-6 or GRP78 antibodies can break the BBB and permit MBs, DNs, and PBs to enter the CNS (126, 127). The MBs and DNs can also progress to PBs to generate antibodies, which can target the AQP4 protein in astrocytes, together with the antibodies produced by PCs in bone marrow (175). The antibodies attack the astrocytes through CDC, which not only forms MAC but also generates C5a and C3a recruiting granulocytes in combination with IL-17, IL-8, and GM-CSF (111, 127, 150). The granulocytes can further aggravate the CNS lesions through ADCC (150, 176, 177).

At last, it is noteworthy that it is still in debate about the classification and the role of the DNs (178, 179). The DNs are very likely identical to the atypical memory B cells, tissue-like memory B cells, or age associated B cells (179). The conclusions are conflicting if the DNs play an immune boosting or tolerant role in autoimmune disease, such as RA or SLE, and chronic infection such as human immunodeficiency virus, malaria, or hepatitis C virus (179), which suggest the exact roles of the DNs in the development of MG and NMO should be further studied. Besides, in addition to promoting the survival and differentiation of autoreactive B cells in mature stage (139), BAFF can also facilitate the proliferation and antibody-secretion of immature-transitional B cells (180), indirectly promote the expansion of Th17 cells in RA and directly regulate the accumulation and cytokine-secretion of Tfh cells in SLE (181, 182), which is likely to be also involved in the pathogenesis of MG and NMO and deserves to be investigated.

CONCLUSION

Both of MG and NMO are developed on the basis of susceptible gene and environmental predisposing factors, which initiate the innate immunity and activate the adaptive immunity (29, 114). The autoreactive T cells cooperate with cognate B cells to generate effector and memory lymphocytes (29, 31). The autoantibodies attack NMJ together with complement in MG (29). And the autoantibodies together with complement and inflammatory cells destroy CNS after breaking BBB in NMO (114). In this review, we summarize the similarities and discrepancies between MG and NMO, including the genetics, environmental factors, gender bias, innate immunity, adaptive immunity, autoimmune comorbidities, and specific involvement. This review will help to improve our understanding of the pathogenesis, promote the mutual exchange of information in future progress regarding immune mechanisms, and facilitate the two-way communication between MG and NMO regarding new therapeutic strategies in future clinical trials. In the future, the genetic and epigenetic analysis of these patients, especially the monozygotic twins, can further unravel the pathogenic basis of both diseases; the dynamic detection of the immune cells and molecules in these patients, especially those with monoclonal antibodies therapy, will clearly decipher the pathogenic process; the development of appropriate animal models, especially in NMO, will pave the way for the drug development.

AUTHOR CONTRIBUTIONS

ZW and YY wrote and approved the final version of this manuscript.

FUNDING

YY was supported by the National Natural Science Foundation of China (81371372, 81571596) and the Fundamental Research Funds for the Central Universities (GK201701009).

REFERENCES

1. Gilhus NE. Myasthenia gravis. *N Engl J Med* (2016) 375:2570–81. doi:10.1056/NEJMra1602678
2. Gilhus NE, Verschuuren JJ. Myasthenia gravis: subgroup classification and therapeutic strategies. *Lancet Neurol* (2015) 14:1023–36. doi:10.1016/S1474-4422(15)00145-3
3. Meriggioli MN, Sanders DB. Autoimmune myasthenia gravis: emerging clinical and biological heterogeneity. *Lancet Neurol* (2009) 8:475–90. doi:10.1016/S1474-4422(09)70063-8
4. Gilhus NE, Skeie GO, Romi F, Lazaridis K, Zisimopoulou P, Tzartos S. Myasthenia gravis – autoantibody characteristics and their implications for therapy. *Nat Rev Neurol* (2016) 12:259–68. doi:10.1038/nrneurol.2016.44

5. Romi F, Hong Y, Gilhus NE. Pathophysiology and immunological profile of myasthenia gravis and its subgroups. *Curr Opin Immunol* (2017) 49:9–13. doi:10.1016/j.coi.2017.07.006
6. Vincent A, Palace J, Hilton-Jones D. Myasthenia gravis. *Lancet* (2001) 357:2122–8. doi:10.1016/S0140-6736(00)05186-2
7. Oosterhuis HJ. The natural course of myasthenia gravis: a long term follow up study. *J Neurol Neurosurg Psychiatry* (1989) 52:1121–7. doi:10.1136/jnnp.52.10.1121
8. Carr AS, Cardwell CR, McCarron PO, McConville J. A systematic review of population based epidemiological studies in myasthenia gravis. *BMC Neurol* (2010) 10:46. doi:10.1186/1471-2377-10-46
9. Baggi F, Andreetta F, Maggi L, Confalonieri P, Morandi L, Salerno F, et al. Complete stable remission and autoantibody specificity in myasthenia gravis. *Neurology* (2013) 80:188–95. doi:10.1212/WNL.0b013e31827b907b
10. Wingerchuk DM, Lennon VA, Lucchinetti CF, Pittock SJ, Weinshenker BG. The spectrum of neuromyelitis optica. *Lancet Neurol* (2007) 6:805–15. doi:10.1016/S1474-4422(07)70216-8
11. Lennon VA, Wingerchuk DM, Kryzer TJ, Pittock SJ, Lucchinetti CF, Fujihara K, et al. A serum autoantibody marker of neuromyelitis optica: distinction from multiple sclerosis. *Lancet* (2004) 364:2106–12. doi:10.1016/S0140-6736(04)17551-X
12. Wingerchuk DM, Banwell B, Bennett JL, Cabre P, Carroll W, Chitnis T, et al. International consensus diagnostic criteria for neuromyelitis optica spectrum disorders. *Neurology* (2015) 85:177–89. doi:10.1212/WNL.0000000000001729
13. Hinson SR, Lennon VA, Pittock SJ. Autoimmune AQP4 channelopathies and neuromyelitis optica spectrum disorders. *Handb Clin Neurol* (2016) 133:377–403. doi:10.1016/B978-0-444-63432-0.00021-9
14. Waters PJ, McKeon A, Leite MI, Rajasekharan S, Lennon VA, Villalobos A, et al. Serologic diagnosis of NMO: a multicenter comparison of aquaporin-4-IgG assays. *Neurology* (2012) 78:665–71; discussion 669. doi:10.1212/WNL.0b013e318248dec1
15. Fryer JP, Lennon VA, Pittock SJ, Jenkins SM, Fallier-Becker P, Clardy SL, et al. AQP4 autoantibody assay performance in clinical laboratory service. *Neurol Neuroimmunol Neuroinflamm* (2014) 1:e11. doi:10.1212/NXI.0000000000000011
16. Zekeridou A, Lennon VA. Aquaporin-4 autoimmunity. *Neurol Neuroimmunol Neuroinflamm* (2015) 2:e110. doi:10.1212/NXI.0000000000000110
17. Verkman AS. Aquaporins in clinical medicine. *Annu Rev Med* (2012) 63:303–16. doi:10.1146/annurev-med-043010-193843
18. Papadopoulos MC, Verkman AS. Aquaporin 4 and neuromyelitis optica. *Lancet Neurol* (2012) 11:535–44. doi:10.1016/S1474-4422(12)70133-3
19. Sato DK, Callegaro D, Lana-Peixoto MA, Waters PJ, de Haidar Jorge FM, Takahashi T, et al. Distinction between MOG antibody-positive and AQP4 antibody-positive NMO spectrum disorders. *Neurology* (2014) 82:474–81. doi:10.1212/WNL.0000000000000101
20. Höftberger R, Sepulveda M, Armangue T, Blanco Y, Rostásy K, Calvo AC, et al. Antibodies to MOG and AQP4 in adults with neuromyelitis optica and suspected limited forms of the disease. *Mult Scler* (2015) 21:866–74. doi:10.1177/1352458514555785
21. Hardy TA, Reddel SW, Barnett MH, Palace J, Lucchinetti CF, Weinshenker BG. Atypical inflammatory demyelinating syndromes of the CNS. *Lancet Neurol* (2016) 15:967–81. doi:10.1016/S1474-4422(16)30043-6
22. Sepúlveda M, Armangué T, Sola-Valls N, Arrambide G, Meca-Lallana JE, Oreja-Guevara C, et al. Neuromyelitis optica spectrum disorders: comparison according to the phenotype and serostatus. *Neurol Neuroimmunol Neuroinflamm* (2016) 3:e225. doi:10.1212/NXI.0000000000000225
23. Yan Y, Li Y, Fu Y, Yang L, Su L, Shi K, et al. Autoantibody to MOG suggests two distinct clinical subtypes of NMOSD. *Sci China Life Sci* (2016) 59:1270–81. doi:10.1007/s11427-015-4997-y
24. Flanagan EP, Cabre P, Weinshenker BG, St SJ, Jacobson DJ, Majed M, et al. Epidemiology of aquaporin-4 autoimmunity and neuromyelitis optica spectrum. *Ann Neurol* (2016) 79:775–83. doi:10.1002/ana.24617
25. Kitley J, Leite MI, Nakashima I, Waters P, McNeillis B, Brown R, et al. Prognostic factors and disease course in aquaporin-4 antibody-positive patients with neuromyelitis optica spectrum disorder from the United Kingdom and Japan. *Brain* (2012) 135:1834–49. doi:10.1093/brain/aws109
26. Avidan N, Le PR, Berrih-Aknin S, Miller A. Genetic basis of myasthenia gravis – a comprehensive review. *J Autoimmun* (2014) 52:146–53. doi:10.1016/j.jaut.2013.12.001
27. Pereira WL, Reiche EM, Kallaur AP, Kaimen-Maciel DR. Epidemiological, clinical, and immunological characteristics of neuromyelitis optica: a review. *J Neurol Sci* (2015) 355:7–17. doi:10.1016/j.jns.2015.05.034
28. Borisow N, Kleiter I, Gahlen A, Fischer K, Wernecke KD, Pache F, et al. Influence of female sex and fertile age on neuromyelitis optica spectrum disorders. *Mult Scler* (2017) 23:1092–103. doi:10.1177/1352458516671203
29. Berrih-Aknin S, Le PR. Myasthenia gravis: a comprehensive review of immune dysregulation and etiological mechanisms. *J Autoimmun* (2014) 52:90–100. doi:10.1016/j.jaut.2013.12.011
30. Conti-Fine BM, Diethelm-Okita B, Ostlie N, Wang W, Milani M. Immunopathogenesis of Myasthenia Gravis. In: Kaminski HJ, editor. *Myasthenia Gravis and Related Disorders. Current Clinical Neurology*. Totowa, NJ: Humana Press (2009). p. 53–91.
31. Mitsdoerffer M, Kuchroo V, Korn T. Immunology of neuromyelitis optica: a T cell-B cell collaboration. *Ann N Y Acad Sci* (2013) 1283:57–66. doi:10.1111/nyas.12118
32. Wingerchuk DM, Weinshenker BG. The emerging relationship between neuromyelitis optica and systemic rheumatologic autoimmune disease. *Mult Scler* (2012) 18:5–10. doi:10.1177/1352458511431077
33. Nacu A, Andersen JB, Lisnic V, Owe JF, Gilhus NE. Complicating autoimmune diseases in myasthenia gravis: a review. *Autoimmunity* (2015) 48:362–8. doi:10.3109/08916934.2015.1030614
34. Albuquerque EX, Pereira EF, Alkondon M, Rogers SW. Mammalian nicotinic acetylcholine receptors: from structure to function. *Physiol Rev* (2009) 89:73–120. doi:10.1152/physrev.00015.2008
35. Keesey JC. Does myasthenia gravis affect the brain. *J Neurol Sci* (1999) 170:77–89. doi:10.1016/S0022-510X(99)00205-1
36. Saadoun S, Papadopoulos MC. Role of membrane complement regulators in neuromyelitis optica. *Mult Scler* (2015) 21:1644–54. doi:10.1177/1352458515571446
37. Wang Z, Guo W, Liu Y, Gong Y, Ding X, Shi K, et al. Low expression of complement inhibitory protein CD59 contributes to humoral autoimmunity against astrocytes. *Brain Behav Immun* (2017) 65:173–82. doi:10.1016/j.bbi.2017.04.023
38. Berrih-Aknin S. Myasthenia gravis: paradox versus paradigm in autoimmunity. *J Autoimmun* (2014) 52:1–28. doi:10.1016/j.jaut.2014.05.001
39. Lucchinetti CF, Mandler RN, McGavern D, Bruck W, Gleich G, Ransohoff RM, et al. A role for humoral mechanisms in the pathogenesis of Devic's neuromyelitis optica. *Brain* (2002) 125:1450–61. doi:10.1093/brain/awf151
40. Salvado M, Canela M, Ponseti JM, Lorenzo L, Garcia C, Cazorla S, et al. Study of the prevalence of familial autoimmune myasthenia gravis in a Spanish cohort. *J Neurol Sci* (2016) 360:110–4. doi:10.1016/j.jns.2015.11.049
41. Namba T, Brunner NG, Brown SB, Muguruma M, Grob D. Familial myasthenia gravis. Report of 27 patients in 12 families and review of 164 patients in 73 families. *Arch Neurol* (1971) 25:49–60. doi:10.1001/archneur.1971.00490010059009
42. Ramanujam R, Pirskanen R, Ramanujam S, Hammarström L. Utilizing twins concordance rates to infer the predisposition to myasthenia gravis. *Twin Res Hum Genet* (2011) 14:129–36. doi:10.1375/twin.14.2.129
43. Matiello M, Kim HJ, Kim W, Brum DG, Barreira AA, Kingsbury DJ, et al. Familial neuromyelitis optica. *Neurology* (2010) 75:310–5. doi:10.1212/WNL.0b013e3181ea9f15
44. Papais-Alvarenga RM, Pereira FF, Bernardes MS, Papais-Alvarenga M, Batista E, Paiva CA, et al. Familial forms of multiple sclerosis and neuromyelitis optica at an MS center in Rio de Janeiro State, Brazil. *J Neurol Sci* (2015) 356:196–201. doi:10.1016/j.jns.2015.06.034
45. McAlpine D. Familial neuromyelitis optica: its occurrence in identical twins. *Brain* (1938) 61:430–48. doi:10.1093/brain/61.4.430
46. Jones EY, Fugger L, Strominger JL, Siebold C. MHC class II proteins and disease: a structural perspective. *Nat Rev Immunol* (2006) 6:271–82. doi:10.1038/nri1805
47. Wahren-Herlenius M, Dörner T. Immunopathogenic mechanisms of systemic autoimmune disease. *Lancet* (2013) 382:819–31. doi:10.1016/S0140-6736(13)60954-X

48. Vandiedonck C, Beaurain G, Giraud M, Hue-Beauvais C, Eymard B, Tranchant C, et al. Pleiotropic effects of the 8.1 HLA haplotype in patients with autoimmune myasthenia gravis and thymus hyperplasia. *Proc Natl Acad Sci U S A* (2004) 101:15464–9. doi:10.1073/pnas.0406756101
49. Saruhan-Direskeneli G, Hughes T, Yilmaz V, Durmus H, Adler A, Alahgholi-Hajibehzad M, et al. Genetic heterogeneity within the HLA region in three distinct clinical subgroups of myasthenia gravis. *Clin Immunol* (2016) 16(6–167):81–8. doi:10.1016/j.clim.2016.05.003
50. Renton AE, Pliner HA, Provenzano C, Evoli A, Ricciardi R, Nalls MA, et al. A genome-wide association study of myasthenia gravis. *JAMA Neurol* (2015) 72:396–404. doi:10.1001/jamaneurol.2014.4103
51. Zhu WH, Lu JH, Lin J, Xi JY, Lu J, Luo SS, et al. HLA-DQA1*03:02/DQB1*03:03:02 is strongly associated with susceptibility to childhood-onset ocular myasthenia gravis in Southern Han Chinese. *J Neuroimmunol* (2012) 247:81–5. doi:10.1016/j.jneuroim.2012.03.018
52. Xie YC, Qu Y, Sun L, Li HF, Zhang H, Shi HJ, et al. Association between HLA-DRB1 and myasthenia gravis in a northern Han Chinese population. *J Clin Neurosci* (2011) 18:1524–7. doi:10.1016/j.jocn.2011.05.002
53. Kanai T, Uzawa A, Kawaguchi N, Sakamaki T, Yoshiyama Y, Himuro K, et al. HLA-DRB1*14 and DQB1*05 are associated with Japanese anti-MuSK antibody-positive myasthenia gravis patients. *J Neurol Sci* (2016) 363:116–8. doi:10.1016/j.jns.2016.02.031
54. Ehsan S, Amirzargar A, Yekaninejad MS, Mahmoudi M, Mehravar S, Moradi B, et al. Association of HLA class II (DRB1, DQA1, DQB1) alleles and haplotypes with myasthenia gravis and its subgroups in the Iranian population. *J Neurol Sci* (2015) 359:335–42. doi:10.1016/j.jns.2015.11.021
55. Bartoccioni E, Scuderi F, Augugliaro A, Chiatamone RS, Sauchelli D, Alboino P, et al. HLA class II allele analysis in MuSK-positive myasthenia gravis suggests a role for DQ5. *Neurology* (2009) 72:195–7. doi:10.1212/01.wnl.0000339103.08830.86
56. Niks EH, Kuks JB, Roep BO, Haasnoot GW, Verduijn W, Ballieux BE, et al. Strong association of MuSK antibody-positive myasthenia gravis and HLA-DR14-DQ5. *Neurology* (2006) 66:1772–4. doi:10.1212/01.wnl.0000218159.79769.5c
57. Gregersen PK, Kosoy R, Lee AT, Lamb J, Sussman J, McKee D, et al. Risk for myasthenia gravis maps to a (151) Pro→Ala change in TNIP1 and to human leukocyte antigen-B*08. *Ann Neurol* (2012) 72:927–35. doi:10.1002/ana.23691
58. Seldin MF, Alkhairy OK, Lee AT, Lamb JA, Sussman J, Pirskanen-Matell R, et al. Genome-wide association study of late-onset myasthenia gravis: confirmation of TNFRSF11A, and identification of ZBTB10 and three distinct HLA associations. *Mol Med* (2015) 21:769–81. doi:10.2119/molmed.2015.00232
59. Giraud M, Eymard B, Tranchant C, Gajdos P, Garchon HJ. Association of the gene encoding the delta-subunit of the muscle acetylcholine receptor (CHRND) with acquired autoimmune myasthenia gravis. *Genes Immun* (2004) 5:80–3. doi:10.1038/sj.gene.6364041
60. Wilisch A, Gutsche S, Hoffacker V, Schultz A, Tzartos S, Nix W, et al. Association of acetylcholine receptor alpha-subunit gene expression in mixed thymoma with myasthenia gravis. *Neurology* (1999) 52:1460–6. doi:10.1212/WNL.52.7.1460
61. Zéphir H, Fajardy I, Outteryck O, Blanc F, Roger N, Fleury M, et al. Is neuromyelitis optica associated with human leukocyte antigen. *Mult Scler* (2009) 15:571–9. doi:10.1177/1352458508102085
62. Yamasaki K, Horiuchi I, Minohara M, Kawano Y, Ohyagi Y, Yamada T, et al. HLA-DPB1*0501-associated opticospinal multiple sclerosis: clinical, neuroimaging and immunogenetic studies. *Brain* (1999) 122(Pt 9):1689–96. doi:10.1093/brain/122.9.1689
63. Wang H, Dai Y, Qiu W, Zhong X, Wu A, Wang Y, et al. HLA-DPB1 0501 is associated with susceptibility to anti-aquaporin-4 antibodies positive neuromyelitis optica in southern Han Chinese. *J Neuroimmunol* (2011) 233:181–4. doi:10.1016/j.jneuroim.2010.11.004
64. Yoshimura S, Isobe N, Matsushita T, Yonekawa T, Masaki K, Sato S, et al. Distinct genetic and infectious profiles in Japanese neuromyelitis optica patients according to anti-aquaporin 4 antibody status. *J Neurol Neurosurg Psychiatry* (2013) 84:29–34. doi:10.1136/jnnp-2012-302925
65. Blanco Y, Ercilla-González G, Llufriu S, Casanova-Estruch B, Magraner MJ, Ramió-Torrentá L, et al. [HLA-DRB1 typing in Caucasians patients with neuromyelitis optica]. *Rev Neurol* (2011) 53:146–52.
66. Brum DG, Barreira AA, dos SAC, Kaimen-Maciel DR, Matiello M, Costa RM, et al. HLA-DRB association in neuromyelitis optica is different from that observed in multiple sclerosis. *Mult Scler* (2010) 16:21–9. doi:10.1177/1352458509350741
67. Deschamps R, Paturel L, Jeannin S, Chausson N, Olindo S, Béra O, et al. Different HLA class II (DRB1 and DQB1) alleles determine either susceptibility or resistance to NMO and multiple sclerosis among the French Afro-Caribbean population. *Mult Scler* (2011) 17:24–31. doi:10.1177/1352458510382810
68. Pandit L, Malli C, D'Cunha A, Mustafa S. Human leukocyte antigen association with neuromyelitis optica in a south Indian population. *Mult Scler* (2015) 21:1217–8. doi:10.1177/1352458515574149
69. Wang H, Zhong X, Wang K, Qiu W, Li J, Dai Y, et al. Interleukin 17 gene polymorphism is associated with anti-aquaporin 4 antibody-positive neuromyelitis optica in the Southern Han Chinese – a case control study. *J Neurol Sci* (2012) 314:26–8. doi:10.1016/j.jns.2011.11.005
70. Kim HJ, Park HY, Kim E, Lee KS, Kim KK, Choi BO, et al. Common CYP7A1 promoter polymorphism associated with risk of neuromyelitis optica. *Neurobiol Dis* (2010) 37:349–55. doi:10.1016/j.nbd.2009.10.013
71. Park TJ, Kim HJ, Kim JH, Bae JS, Cheong HS, Park BL, et al. Associations of CD6, TNFRSF1A and IRF8 polymorphisms with risk of inflammatory demyelinating diseases. *Neuropathol Appl Neurobiol* (2013) 39:519–30. doi:10.1111/j.1365-2990.2012.01304.x
72. Kim JY, Bae JS, Kim HJ, Shin HD. CD58 polymorphisms associated with the risk of neuromyelitis optica in a Korean population. *BMC Neurol* (2014) 14:57. doi:10.1186/1471-2377-14-57
73. Sato S, Yamamoto K, Matsushita T, Isobe N, Kawano Y, Iinuma K, et al. Copy number variations in multiple sclerosis and neuromyelitis optica. *Ann Neurol* (2015) 78:762–74. doi:10.1002/ana.24511
74. Asgari N, Nielsen C, Stenager E, Kyvik KO, Lillevang ST. HLA, PTPN22 and PD-1 associations as markers of autoimmunity in neuromyelitis optica. *Mult Scler* (2012) 18:23–30. doi:10.1177/1352458511417480
75. Matiello M, Schaefer-Klein JL, Hebrink DD, Kingsbury DJ, Atkinson EJ, Weinshenker BG, et al. Genetic analysis of aquaporin-4 in neuromyelitis optica. *Neurology* (2011) 77:1149–55. doi:10.1212/WNL.0b013e31822f045b
76. Mamrut S, Avidan N, Truffault F, Staun-Ram E, Sharshar T, Eymard B, et al. Methylome and transcriptome profiling in myasthenia gravis monozygotic twins. *J Autoimmun* (2017) 82:62–73. doi:10.1016/j.jaut.2017.05.005
77. Vaknin-Dembinsky A, Charbit H, Brill L, Abramsky O, Gur-Wahnon D, Ben-Dov IZ, et al. Circulating microRNAs as biomarkers for rituximab therapy, in neuromyelitis optica (NMO). *J Neuroinflammation* (2016) 13:179. doi:10.1186/s12974-016-0648-x
78. Szodoray P, Nakken B, Gaal J, Jonsson R, Szegedi A, Zold E, et al. The complex role of vitamin D in autoimmune diseases. *Scand J Immunol* (2008) 68:261–9. doi:10.1111/j.1365-3083.2008.02127.x
79. Askmark H, Haggård L, Nygren I, Punga AR. Vitamin D deficiency in patients with myasthenia gravis and improvement of fatigue after supplementation of vitamin D3: a pilot study. *Eur J Neurol* (2012) 19:1554–60. doi:10.1111/j.1468-1331.2012.03773.x
80. Alahgholi-Hajibehzad M, Oflazer P, Aysal F, Durmuş H, Gülşen-Parman Y, Marx A, et al. Regulatory function of CD4+CD25++ T cells in patients with myasthenia gravis is associated with phenotypic changes and STAT5 signaling: 1,25-Dihydroxyvitamin D3 modulates the suppressor activity. *J Neuroimmunol* (2015) 281:51–60. doi:10.1016/j.jneuroim.2015.03.008
81. Cadegiani FA. Remission of severe myasthenia gravis after massive-dose vitamin D treatment. *Am J Case Rep* (2016) 17:51–4. doi:10.12659/AJCR.894849
82. Mealy MA, Newsome S, Greenberg BM, Wingerchuk D, Calabresi P, Levy M. Low serum vitamin D levels and recurrent inflammatory spinal cord disease. *Arch Neurol* (2012) 69:352–6. doi:10.1001/archneurol.2011.1974
83. Shan Y, Tan S, Zhang L, Huang J, Sun X, Wang Y, et al. Serum 25-hydroxyvitamin D3 is associated with disease status in patients with neuromyelitis optica spectrum disorders in south China. *J Neuroimmunol* (2016) 299:118–23. doi:10.1016/j.jneuroim.2016.09.006
84. Jitprapaikulsan J, Siritho S, Prayoonwiwat N. Vitamin D level status in Thai neuromyelitis optica patients. *J Neuroimmunol* (2016) 29(5–296):75–8. doi:10.1016/j.jneuroim.2016.03.016
85. Tüzün E, Küçükhüseyin Ö, Kürtüncü M, Türkoğlu R, Yaylım İ. Reduced serum vitamin D levels in neuromyelitis optica. *Neurol Sci* (2015) 36:1701–2. doi:10.1007/s10072-015-2229-7

86. Min JH, Waters P, Vincent A, Cho HJ, Joo BE, Woo SY, et al. Low levels of vitamin D in neuromyelitis optica spectrum disorder: association with disease disability. *PLoS One* (2014) 9:e107274. doi:10.1371/journal.pone.0107274
87. Honda K, Littman DR. The microbiota in adaptive immune homeostasis and disease. *Nature* (2016) 535:75–84. doi:10.1038/nature18848
88. Okada H, Kuhn C, Feillet H, Bach JF. The 'hygiene hypothesis' for autoimmune and allergic diseases: an update. *Clin Exp Immunol* (2010) 160:1–9. doi:10.1111/j.1365-2249.2010.04139.x
89. Chae CS, Kwon HK, Hwang JS, Kim JE, Im SH. Prophylactic effect of probiotics on the development of experimental autoimmune myasthenia gravis. *PLoS One* (2012) 7:e52119. doi:10.1371/journal.pone.0052119
90. Cree BA, Spencer CM, Varrin-Doyer M, Baranzini SE, Zamvil SS. Gut microbiome analysis in neuromyelitis optica reveals overabundance of *Clostridium perfringens*. *Ann Neurol* (2016) 80:443–7. doi:10.1002/ana.24718
91. Varrin-Doyer M, Spencer CM, Schulze-Topphoff U, Nelson PA, Stroud RM, Cree BA, et al. Aquaporin 4-specific T cells in neuromyelitis optica exhibit a Th17 bias and recognize *Clostridium* ABC transporter. *Ann Neurol* (2012) 72:53–64. doi:10.1002/ana.23651
92. Cavalcante P, Cufi P, Mantegazza R, Berrih-Aknin S, Bernasconi P, Le PR. Etiology of myasthenia gravis: innate immunity signature in pathological thymus. *Autoimmun Rev* (2013) 12:863–74. doi:10.1016/j.autrev.2013.03.010
93. Cavalcante P, Serafini B, Rosicarelli B, Maggi L, Barberis M, Antozzi C, et al. Epstein-Barr virus persistence and reactivation in myasthenia gravis thymus. *Ann Neurol* (2010) 67:726–38. doi:10.1002/ana.21902
94. Csuka D, Banati M, Rozsa C, Füst G, Illes Z. High anti-EBNA-1 IgG levels are associated with early-onset myasthenia gravis. *Eur J Neurol* (2012) 19:842–6. doi:10.1111/j.1468-1331.2011.03636.x
95. Meyer M, Höls AK, Liersch B, Leistner R, Gellert K, Schalke B, et al. Lack of evidence for Epstein-Barr virus infection in myasthenia gravis thymus. *Ann Neurol* (2011) 70:515–8. doi:10.1002/ana.22522
96. Masuda S, Mori M, Arai K, Uzawa A, Muto M, Uchida T, et al. Epstein-Barr virus persistence and reactivation in neuromyelitis optica. *J Neurol Neurosurg Psychiatry* (2015) 86:1137–42. doi:10.1136/jnnp-2014-308095
97. Kampylafka EI, Alexopoulos H, El HA, Dalakas MC, Andreakos E, Tzioufas AG. Immunization of mice with a peptide derived from the HTLV-1 TAX1BP1 protein induces cross-reactive antibodies against aquaporin 4. *Autoimmunity* (2015) 48:453–9. doi:10.3109/08916934.2015.1070836
98. von GF, Jarius S, de Oliveira ACP, Brandão CO, Farias AS, Damasceno A, et al. Aquaporin-4 antibodies are not related to HTLV-1 associated myelopathy. *PLoS One* (2012) 7:e39372. doi:10.1371/journal.pone.0039372
99. Theofilopoulos AN, Kono DH, Baccala R. The multiple pathways to autoimmunity. *Nat Immunol* (2017) 18:716–24. doi:10.1038/ni.3731
100. Klein SL, Flanagan KL. Sex differences in immune responses. *Nat Rev Immunol* (2016) 16:626–38. doi:10.1038/nri.2016.90
101. Klein SL, Jedlicka A, Pekosz A. The Xs and Y of immune responses to viral vaccines. *Lancet Infect Dis* (2010) 10:338–49. doi:10.1016/S1473-3099(10)70049-9
102. Spitzer JA. Gender differences in some host defense mechanisms. *Lupus* (1999) 8:380–3. doi:10.1177/096120339900800510
103. Weinstein Y, Ran S, Segal S. Sex-associated differences in the regulation of immune responses controlled by the MHC of the mouse. *J Immunol* (1984) 132:656–61.
104. Abdullah M, Chai PS, Chong MY, Tohit ER, Ramasamy R, Pei CP, et al. Gender effect on in vitro lymphocyte subset levels of healthy individuals. *Cell Immunol* (2012) 272:214–9. doi:10.1016/j.cellimm.2011.10.009
105. Afshan G, Afzal N, Qureshi S. CD4+CD25(hi) regulatory T cells in healthy males and females mediate gender difference in the prevalence of autoimmune diseases. *Clin Lab* (2012) 58:567–71.
106. Park HJ, Park HS, Lee JU, Bothwell AL, Choi JM. Gender-specific differences in PPARγ regulation of follicular helper T cell responses with estrogen. *Sci Rep* (2016) 6:28495. doi:10.1038/srep28495
107. Straub RH. The complex role of estrogens in inflammation. *Endocr Rev* (2007) 28:521–74. doi:10.1210/er.2007-0001
108. Vijayan N, Vijayan VK, Dreyfus PM. Acetylcholinesterase activity and menstrual remissions in myasthenia gravis. *J Neurol Neurosurg Psychiatry* (1977) 40:1060–5. doi:10.1136/jnnp.40.11.1060
109. Batocchi AP, Majolini L, Evoli A, Lino MM, Minisci C, Tonali P. Course and treatment of myasthenia gravis during pregnancy. *Neurology* (1999) 52:447–52. doi:10.1212/WNL.52.3.447
110. Nancy P, Berrih-Aknin S. Differential estrogen receptor expression in autoimmune myasthenia gravis. *Endocrinology* (2005) 146:2345–53. doi:10.1210/en.2004-1003
111. Davoudi V, Keyhanian K, Bove RM, Chitnis T. Immunology of neuromyelitis optica during pregnancy. *Neurol Neuroimmunol Neuroinflamm* (2016) 3:e288. doi:10.1212/NXI.0000000000000288
112. Bove R, Elsone L, Alvarez E, Borisow N, Cortez MM, Mateen FJ, et al. Female hormonal exposures and neuromyelitis optica symptom onset in a multicenter study. *Neurol Neuroimmunol Neuroinflamm* (2017) 4:e339. doi:10.1212/NXI.0000000000000339
113. Cufi P, Dragin N, Weiss JM, Martinez-Martinez P, De Baets MH, Roussin R, et al. Implication of double-stranded RNA signaling in the etiology of autoimmune myasthenia gravis. *Ann Neurol* (2013) 73:281–93. doi:10.1002/ana.23791
114. Levy M, Wildemann B, Jarius S, Orellano B, Sasidharan S, Weber MS, et al. Immunopathogenesis of neuromyelitis optica. *Adv Immunol* (2014) 121:213–42. doi:10.1016/B978-0-12-800100-4.00006-4
115. Ziegler SF. Division of labour by CD4(+) T helper cells. *Nat Rev Immunol* (2016) 16:403. doi:10.1038/nri.2016.53
116. Link J, Navikas V, Yu M, Fredrikson S, Osterman PO, Link H. Augmented interferon-gamma, interleukin-4 and transforming growth factor-beta mRNA expression in blood mononuclear cells in myasthenia gravis. *J Neuroimmunol* (1994) 51:185–92. doi:10.1016/0165-5728(94)90080-9
117. Masuda M, Tanaka S, Nakajima K, Yamada N, Ido N, Ohtsuka T, et al. Clinical implications of the type 1/type 2 balance of helper T cells and P-glycoprotein function in peripheral T lymphocytes of myasthenia gravis patients. *Eur J Pharmacol* (2010) 627:325–31. doi:10.1016/j.ejphar.2009.10.040
118. Roche JC, Capablo JL, Larrad L, Gervas-Arruga J, Ara JR, Sánchez A, et al. Increased serum interleukin-17 levels in patients with myasthenia gravis. *Muscle Nerve* (2011) 44:278–80. doi:10.1002/mus.22070
119. Wang Z, Wang W, Chen Y, Wei D. T helper type 17 cells expand in patients with myasthenia-associated thymoma. *Scand J Immunol* (2012) 76:54–61. doi:10.1111/j.1365-3083.2012.02703.x
120. Gradolatto A, Nazzal D, Truffault F, Bismuth J, Fadel E, Foti M, et al. Both Treg cells and Tconv cells are defective in the myasthenia gravis thymus: roles of IL-17 and TNF-α. *J Autoimmun* (2014) 52:53–63. doi:10.1016/j.jaut.2013.12.015
121. Uzawa A, Kawaguchi N, Himuro K, Kanai T, Kuwabara S. Serum cytokine and chemokine profiles in patients with myasthenia gravis. *Clin Exp Immunol* (2014) 176:232–7. doi:10.1111/cei.12272
122. Yi JS, Guidon A, Sparks S, Osborne R, Juel VC, Massey JM, et al. Characterization of CD4 and CD8 T cell responses in MuSK myasthenia gravis. *J Autoimmun* (2014) 52:130–8. doi:10.1016/j.jaut.2013.12.005
123. Yilmaz V, Oflazer P, Aysal F, Durmus H, Poulas K, Yentur SP, et al. Differential cytokine changes in patients with myasthenia gravis with antibodies against AChR and MuSK. *PLoS One* (2015) 10:e0123546. doi:10.1371/journal.pone.0123546
124. Uzawa A, Mori M, Hayakawa S, Masuda S, Nomura F, Kuwabara S. Expression of chemokine receptors on peripheral blood lymphocytes in multiple sclerosis and neuromyelitis optica. *BMC Neurol* (2010) 10:113. doi:10.1186/1471-2377-10-113
125. Shimizu Y, Ota K, Kubo S, Kabasawa C, Kobayashi M, Ohashi T, et al. Association of Th1/Th2-related chemokine receptors in peripheral T cells with disease activity in patients with multiple sclerosis and neuromyelitis optica. *Eur Neurol* (2011) 66:91–7. doi:10.1159/000329576
126. Kothur K, Wienholt L, Brilot F, Dale RC. CSF cytokines/chemokines as biomarkers in neuroinflammatory CNS disorders: a systematic review. *Cytokine* (2016) 77:227–37. doi:10.1016/j.cyto.2015.10.001
127. Uzawa A, Mori M, Masahiro M, Kuwabara S. Cytokines and chemokines in neuromyelitis optica: pathogenetic and therapeutic implications. *Brain Pathol* (2014) 24:67–73. doi:10.1111/bpa.12097
128. Chang KH, Ro LS, Lyu RK, Chen CM. Biomarkers for neuromyelitis optica. *Clin Chim Acta* (2015) 440:64–71. doi:10.1016/j.cca.2014.11.004
129. Wang Y, Zhou Y, Sun X, Lu T, Wei L, Fang L, et al. Cytokine and chemokine profiles in patients with neuromyelitis optica spectrum disorder. *Neuroimmunomodulation* (2016) 23:352–8. doi:10.1159/000464135
130. Araki M, Matsuoka T, Miyamoto K, Kusunoki S, Okamoto T, Murata M, et al. Efficacy of the anti-IL-6 receptor antibody tocilizumab in

neuromyelitis optica: a pilot study. *Neurology* (2014) 82:1302–6. doi:10.1212/WNL.0000000000000317
131. Meng X, Yang J, Dong M, Zhang K, Tu E, Gao Q, et al. Regulatory T cells in cardiovascular diseases. *Nat Rev Cardiol* (2016) 13:167–79. doi:10.1038/nrcardio.2015.169
132. Thiruppathi M, Rowin J, Ganesh B, Sheng JR, Prabhakar BS, Meriggioli MN. Impaired regulatory function in circulating CD4(+)CD25(high)CD127(low/-) T cells in patients with myasthenia gravis. *Clin Immunol* (2012) 145:209–23. doi:10.1016/j.clim.2012.09.012
133. Balandina A, Lécart S, Dartevelle P, Saoudi A, Berrih-Aknin S. Functional defect of regulatory CD4(+)CD25+ T cells in the thymus of patients with autoimmune myasthenia gravis. *Blood* (2005) 105:735–41. doi:10.1182/blood-2003-11-3900
134. Masuda M, Matsumoto M, Tanaka S, Nakajima K, Yamada N, Ido N, et al. Clinical implication of peripheral CD4+CD25+ regulatory T cells and Th17 cells in myasthenia gravis patients. *J Neuroimmunol* (2010) 225:123–31. doi:10.1016/j.jneuroim.2010.03.016
135. Crotty S. Follicular helper CD4 T cells (TFH). *Annu Rev Immunol* (2011) 29:621–63. doi:10.1146/annurev-immunol-031210-101400
136. Zhang CJ, Gong Y, Zhu W, Qi Y, Yang CS, Fu Y, et al. Augmentation of circulating follicular helper T cells and their impact on autoreactive B cells in myasthenia gravis. *J Immunol* (2016) 197:2610–7. doi:10.4049/jimmunol.1500725
137. Li YJ, Zhang F, Qi Y, Chang GQ, Fu Y, Su L, et al. Association of circulating follicular helper T cells with disease course of NMO spectrum disorders. *J Neuroimmunol* (2015) 278:239–46. doi:10.1016/j.jneuroim.2014.11.011
138. Fan X, Jiang Y, Han J, Liu J, Wei Y, Jiang X, et al. Circulating memory T follicular helper cells in patients with neuromyelitis optica/neuromyelitis optica spectrum disorders. *Mediators Inflamm* (2016) 2016:3678152. doi:10.1155/2016/3678152
139. Mackay F, Browning JL. BAFF: a fundamental survival factor for B cells. *Nat Rev Immunol* (2002) 2:465–75. doi:10.1038/nri844
140. Berrihaknin S, Ragheb S, Panse RL, Lisak RP. Ectopic germinal centers, BAFF and anti-B-cell therapy in myasthenia gravis. *Autoimmun Rev* (2013) 12:885–93. doi:10.1016/j.autrev.2013.03.011
141. Muto K, Matsui N, Unai Y, Sakai W, Haji S, Udaka K, et al. Memory B cell resurgence requires repeated rituximab in myasthenia gravis. *Neuromuscul Disord* (2017) 27(10):918–22. doi:10.1016/j.nmd.2017.06.012
142. Chihara N, Aranami T, Sato W, Miyazaki Y, Miyake S, Okamoto T, et al. Interleukin 6 signaling promotes anti-aquaporin 4 autoantibody production from plasmablasts in neuromyelitis optica. *Proc Natl Acad Sci U S A* (2011) 108:3701–6. doi:10.1073/pnas.1017385108
143. Kim SH, Kim W, Li XF, Jung IJ, Kim HJ. Repeated treatment with rituximab based on the assessment of peripheral circulating memory B cells in patients with relapsing neuromyelitis optica over 2 years. *Arch Neurol* (2011) 68:1412–20. doi:10.1001/archneurol.2011.154
144. Pellkofer HL, Krumbholz M, Berthele A, Hemmer B, Gerdes LA, Havla J, et al. Long-term follow-up of patients with neuromyelitis optica after repeated therapy with rituximab. *Neurology* (2011) 76:1310–5. doi:10.1212/WNL.0b013e3182152881
145. Han J, Sun L, Fan X, Wang Z, Cheng Y, Zhu J, et al. Role of regulatory b cells in neuroimmunologic disorders. *J Neurosci Res* (2016) 94:693–701. doi:10.1002/jnr.23749
146. Sheng JR, Rezania K, Soliven B. Impaired regulatory B cells in myasthenia gravis. *J Neuroimmunol* (2016) 297:38–45. doi:10.1016/j.jneuroim.2016.05.004
147. Karim MR, Zhang HY, Yuan J, Sun Q, Wang YF. Regulatory B cells in seropositive myasthenia gravis versus healthy controls. *Front Neurol* (2017) 8:43. doi:10.3389/fneur.2017.00043
148. Quan C, Yu H, Qiao J, Xiao B, Zhao G, Wu Z, et al. Impaired regulatory function and enhanced intrathecal activation of B cells in neuromyelitis optica: distinct from multiple sclerosis. *Mult Scler* (2013) 19:289–98. doi:10.1177/1352458512454771
149. Drachman DB. Myasthenia gravis. *N Engl J Med* (1994) 330:1797–810. doi:10.1056/NEJM199406233302507
150. Ratelade J, Asavapanumas N, Ritchie AM, Wemlinger S, Bennett JL, Verkman AS. Involvement of antibody-dependent cell-mediated cytotoxicity in inflammatory demyelination in a mouse model of neuromyelitis optica. *Acta Neuropathol* (2013) 126:699–709. doi:10.1007/s00401-013-1172-z
151. Papadopoulos MC, Bennett JL, Verkman AS. Treatment of neuromyelitis optica: state-of-the-art and emerging therapies. *Nat Rev Neurol* (2014) 10:493–506. doi:10.1038/nrneurol.2014.141
152. Misu T, Fujihara K, Kakita A, Konno H, Nakamura M, Watanabe S, et al. Loss of aquaporin 4 in lesions of neuromyelitis optica: distinction from multiple sclerosis. *Brain* (2007) 130:1224–34. doi:10.1093/brain/awm047
153. Roemer SF, Parisi JE, Lennon VA, Benarroch EE, Lassmann H, Bruck W, et al. Pattern-specific loss of aquaporin-4 immunoreactivity distinguishes neuromyelitis optica from multiple sclerosis. *Brain* (2007) 130:1194–205. doi:10.1093/brain/awl371
154. Shimizu F, Schaller KL, Owens GP, Cotleur AC, Kellner D, Takeshita Y, et al. Glucose-regulated protein 78 autoantibody associates with blood-brain barrier disruption in neuromyelitis optica. *Sci Transl Med* (2017) 9:eaai9111. doi:10.1126/scitranslmed.aai9111
155. Popescu BF, Lennon VA, Parisi JE, Howe CL, Weigand SD, Cabrera-Gómez JA, et al. Neuromyelitis optica unique area postrema lesions: nausea, vomiting, and pathogenic implications. *Neurology* (2011) 76:1229–37. doi:10.1212/WNL.0b013e318214332c
156. Hinson SR, Romero MF, Popescu BF, Lucchinetti CF, Fryer JP, Wolburg H, et al. Molecular outcomes of neuromyelitis optica (NMO)-IgG binding to aquaporin-4 in astrocytes. *Proc Natl Acad Sci U S A* (2012) 109:1245–50. doi:10.1073/pnas.1109980108
157. Tamer S, Gokce GHN, Gokcal E, Yoldas TK. Coexistence of autoimmune diseases and autoantibodies in patients with myasthenia gravis. *Neurol India* (2016) 64:45–9. doi:10.4103/0028-3886.173638
158. Iyer A, Elsone L, Appleton R, Jacob A. A review of the current literature and a guide to the early diagnosis of autoimmune disorders associated with neuromyelitis optica. *Autoimmunity* (2014) 47:154–61. doi:10.3109/08916934.2014.883501
159. Leite MI, Coutinho E, Lana-Peixoto M, Apostolos S, Waters P, Sato D, et al. Myasthenia gravis and neuromyelitis optica spectrum disorder: a multicenter study of 16 patients. *Neurology* (2012) 78:1601–7. doi:10.1212/WNL.0b013e31825644ff
160. McKeon A, Lennon VA, Jacob A, Matiello M, Lucchinetti CF, Kale N, et al. Coexistence of myasthenia gravis and serological markers of neurological autoimmunity in neuromyelitis optica. *Muscle Nerve* (2009) 39:87–90. doi:10.1002/mus.21197
161. Vaknin-Dembinsky A, Abramsky O, Petrou P, Ben-Hur T, Gotkine M, Brill L, et al. Myasthenia gravis-associated neuromyelitis optica-like disease: an immunological link between the central nervous system and muscle. *Arch Neurol* (2011) 68:1557–61. doi:10.1001/archneurol.2011.200
162. Whiting PJ, Cooper J, Lindstrom JM. Antibodies in sera from patients with myasthenia gravis do not bind to nicotinic acetylcholine receptors from human brain. *J Neuroimmunol* (1987) 16:205–13. doi:10.1016/0165-5728(87)90075-0
163. Peeler CE, De Lott LB, Nagia L, Lemos J, Eggenberger ER, Cornblath WT. Clinical utility of acetylcholine receptor antibody testing in ocular myasthenia gravis. *JAMA Neurol* (2015) 72:1170–4. doi:10.1001/jamaneurol.2015.1444
164. Tüzün E, Christadoss P. Complement associated pathogenic mechanisms in myasthenia gravis. *Autoimmun Rev* (2013) 12:904–11. doi:10.1016/j.autrev.2013.03.003
165. Liu R, Xu H, Wang G, Li J, Gou L, Zhang L, et al. Extraocular muscle characteristics related to myasthenia gravis susceptibility. *PLoS One* (2013) 8:e55611. doi:10.1371/journal.pone.0055611
166. Verkman AS, Anderson MO, Papadopoulos MC. Aquaporins: important but elusive drug targets. *Nat Rev Drug Discov* (2014) 13:259–77. doi:10.1038/nrd4226
167. Takahashi T, Fujihara K, Nakashima I, Misu T, Miyazawa I, Nakamura M, et al. Anti-aquaporin-4 antibody is involved in the pathogenesis of NMO: a study on antibody titre. *Brain* (2007) 130:1235–43. doi:10.1093/brain/awm062
168. Matiello M, Schaefer-Klein J, Sun D, Weinshenker BG. Aquaporin 4 expression and tissue susceptibility to neuromyelitis optica. *JAMA Neurol* (2013) 70:1118–25. doi:10.1001/jamaneurol.2013.3124
169. Crane JM, Bennett JL, Verkman AS. Live cell analysis of aquaporin-4 m1/m23 interactions and regulated orthogonal array assembly in glial cells. *J Biol Chem* (2009) 284:35850–60. doi:10.1074/jbc.M109.071670
170. Crane JM, Lam C, Rossi A, Gupta T, Bennett JL, Verkman AS. Binding affinity and specificity of neuromyelitis optica autoantibodies to aquaporin-4

M1/M23 isoforms and orthogonal arrays. *J Biol Chem* (2011) 286:16516–24. doi:10.1074/jbc.M111.227298
171. Phuan PW, Ratelade J, Rossi A, Tradtrantip L, Verkman AS. Complement-dependent cytotoxicity in neuromyelitis optica requires aquaporin-4 protein assembly in orthogonal arrays. *J Biol Chem* (2012) 287:13829–39. doi:10.1074/jbc.M112.344325
172. Pittock SJ, Weinshenker BG, Lucchinetti CF, Wingerchuk DM, Corboy JR, Lennon VA. Neuromyelitis optica brain lesions localized at sites of high aquaporin 4 expression. *Arch Neurol* (2006) 63:964–8. doi:10.1001/archneur.63.7.964
173. Guo Y, Weigand SD, Popescu BF, Lennon VA, Parisi JE, Pittock SJ, et al. Pathogenic implications of cerebrospinal fluid barrier pathology in neuromyelitis optica. *Acta Neuropathol* (2017) 133:597–612. doi:10.1007/s00401-017-1682-1
174. Bennett JL, O'Connor KC, Bar-Or A, Zamvil SS, Hemmer B, Tedder TF, et al. B lymphocytes in neuromyelitis optica. *Neurol Neuroimmunol Neuroinflamm* (2015) 2:e104. doi:10.1212/NXI.0000000000000104
175. Kowarik MC, Astling D, Gasperi C, Wemlinger S, Schumann H, Dzieciatkowska M, et al. CNS Aquaporin-4-specific B cells connect with multiple B-cell compartments in neuromyelitis optica spectrum disorder. *Ann Clin Transl Neurol* (2017) 4:369–80. doi:10.1002/acn3.418
176. Saadoun S, Waters P, MacDonald C, Bell BA, Vincent A, Verkman AS, et al. Neutrophil protease inhibition reduces neuromyelitis optica-immunoglobulin G-induced damage in mouse brain. *Ann Neurol* (2012) 71:323–33. doi:10.1002/ana.22686
177. Zhang H, Verkman AS. Eosinophil pathogenicity mechanisms and therapeutics in neuromyelitis optica. *J Clin Invest* (2013) 123:2306–16. doi:10.1172/JCI67554
178. Pupovac A, Good-Jacobson KL. An antigen to remember: regulation of B cell memory in health and disease. *Curr Opin Immunol* (2017) 45:89–96. doi:10.1016/j.coi.2017.03.004
179. Karnell JL, Kumar V, Wang J, Wang S, Voynova E, Ettinger R. Role of CD11c(+) T-bet(+) B cells in human health and disease. *Cell Immunol* (2017). doi:10.1016/j.cellimm.2017.05.008
180. Jacobs HM, Thouvenel CD, Leach S, Arkatkar T, Metzler G, Scharping NE, et al. Cutting edge: BAFF promotes autoantibody production via TACI-dependent activation of transitional B cells. *J Immunol* (2016) 196:3525–31. doi:10.4049/jimmunol.1600017
181. Lai KLQ, King HKO, Zheng BJ, Lu L. Local BAFF gene silencing suppresses Th17-cell generation and ameliorates autoimmune arthritis. *Proc Natl Acad Sci U S A* (2008) 105:14993–8. doi:10.1073/pnas.0806044105
182. Coquery CM, Loo WM, Wade NS, Bederman AG, Tung KS, Lewis JE, et al. BAFF regulates follicular helper t cells and affects their accumulation and interferon-γ production in autoimmunity. *Arthritis Rheumatol* (2015) 67:773–84. doi:10.1002/art.38950

Conflict of Interest Statement: The authors declare that the research was conducted in the absence of any commercial or financial relationships that could be construed as a potential conflict of interest.

Copyright © 2017 Wang and Yan. This is an open-access article distributed under the terms of the Creative Commons Attribution License (CC BY). The use, distribution or reproduction in other forums is permitted, provided the original author(s) or licensor are credited and that the original publication in this journal is cited, in accordance with accepted academic practice. No use, distribution or reproduction is permitted which does not comply with these terms.

frontiers in Immunology

ORIGINAL RESEARCH
published: 13 December 2017
doi: 10.3389/fimmu.2017.01739

Regulation of Fn14 Receptor and NF-κB Underlies Inflammation in Meniere's Disease

*Lidia Frejo[1], Teresa Requena[1], Satoshi Okawa[2], Alvaro Gallego-Martinez[1], Manuel Martinez-Bueno[3], Ismael Aran[4], Angel Batuecas-Caletrio[5], Jesus Benitez-Rosario[6], Juan M. Espinosa-Sanchez[1,7], Jesus José Fraile-Rodrigo[8], Ana María García-Arumi[9], Rocío González-Aguado[10], Pedro Marques[11], Eduardo Martin-Sanz[12], Nicolas Perez-Fernandez[13], Paz Pérez-Vázquez[14], Herminio Perez-Garrigues[15], Sofía Santos-Perez[16], Andres Soto-Varela[16], Maria C. Tapia[17], Gabriel Trinidad-Ruiz[18], Antonio del Sol[2], Marta E. Alarcon Riquelme[3,19] and Jose A. Lopez-Escamez[1,7,20]**

[1] Otology and Neurotology Group CTS495, Department of Genomic Medicine – Centre for Genomics and Oncological Research – Pfizer/Universidad de Granada/Junta de Andalucía (GENYO), Granada, Spain, [2] Computational Biology Group, Luxembourg Centre for Systems Biomedicine (LCSB), Universite du Luxembourg, Belval, Luxembourg, [3] Group of Genetics of Complex Diseases, Department of Genomic Medicine – Centre for Genomics and Oncological Research – Pfizer/Universidad de Granada/Junta de Andalucía (GENYO), Granada, Spain, [4] Department of Otolaryngology, Complexo Hospitalario de Pontevedra, Pontevedra, Spain, [5] Department of Otolaryngology, Hospital Universitario Salamanca, IBSAL, Salamanca, Spain, [6] Department of Otolaryngology, Hospital Universitario de Gran Canaria Dr Negrin, Las Palmas de Gran Canaria, Las Palmas, Spain, [7] Department of Otolaryngology, Instituto de Investigación Biosanitaria ibs.GRANADA, Hospital Universitario Virgen de las Nieves, Granada, Spain, [8] Department of Otolaryngology, Hospital Miguel Servet, Zaragoza, Spain, [9] Department of Otorhinolaryngology, Hospital Universitario Vall d'Hebron, Barcelona, Spain, [10] Department of Otorhinolaryngology, Hospital Universitario Marqués de Valdecilla, Santander, Cantabria, Spain, [11] Department of Otorhinolaryngology, Centro Hospitalar de S.João, EPE, University of Porto Medical School, Porto, Portugal, [12] Department of Otolaryngology, Hospital Universitario de Getafe, Getafe, Madrid, Spain, [13] Department of Otolaryngology, Clínica Universidad de Navarra, Pamplona, Spain, [14] Department of Otorhinolaryngology, Hospital Universitario de Cabueñes, Gijón, Asturias, Spain, [15] Department of Otorhinolaryngology, Hospital La Fe, Valencia, Spain, [16] Division of Otoneurology, Department of Otorhinolaryngology, Complexo Hospitalario Universitario, Santiago de Compostela, Spain, [17] Department of Otorhinolaryngology, Instituto Antolí Candela, Madrid, Spain, [18] Division of Otoneurology, Department of Otorhinolaryngology, Complejo Hospitalario Badajoz, Badajoz, Spain, [19] Unit of Chronic Inflammatory Diseases, Institute of Environmental Medicine, Karolinska Institutet, Stockholm, Sweden, [20] Luxembourg Centre for System Biomedicine (LCSB), Universite du Luxembourg, Belval, Luxembourg

OPEN ACCESS

Edited by:
Guixiu Shi,
Xiamen University, China

Reviewed by:
Xuanjun Wang,
Yunnan Agricultural University, China
Yumin Xia,
Second Affiliated Hospital of Xi'an Jiaotong University, China

***Correspondence:**
Jose A. Lopez-Escamez
antonio.lopezescamez@genyo.es

Specialty section:
This article was submitted to Inflammation, a section of the journal Frontiers in Immunology

Received: 11 August 2017
Accepted: 23 November 2017
Published: 13 December 2017

Citation:
Frejo L, Requena T, Okawa S, Gallego-Martinez A, Martinez-Bueno M, Aran I, Batuecas-Caletrio A, Benitez-Rosario J, Espinosa-Sanchez JM, Fraile-Rodrigo JJ, García-Arumi AM, González-Aguado R, Marques P, Martin-Sanz E, Perez-Fernandez N, Pérez-Vázquez P, Perez-Garrigues H, Santos-Perez S, Soto-Varela A, Tapia MC, Trinidad-Ruiz G, del Sol A, Alarcon Riquelme ME and Lopez-Escamez JA (2017) Regulation of Fn14 Receptor and NF-κB Underlies Inflammation in Meniere's Disease. Front. Immunol. 8:1739. doi: 10.3389/fimmu.2017.01739

Meniere's disease (MD) is a rare disorder characterized by episodic vertigo, sensorineural hearing loss, tinnitus, and aural fullness. It is associated with a fluid imbalance between the secretion of endolymph in the cochlear duct and its reabsorption into the subarachnoid space, leading to an accumulation of endolymph in the inner ear. Epidemiological evidence, including familial aggregation, indicates a genetic contribution and a consistent association with autoimmune diseases (AD). We conducted a case–control study in two phases using an immune genotyping array in a total of 420 patients with bilateral MD and 1,630 controls. We have identified the first locus, at 6p21.33, suggesting an association with bilateral MD [meta-analysis leading signal rs4947296, OR = 2.089 (1.661–2.627); $p = 1.39 \times 10^{-09}$]. Gene expression profiles of homozygous genotype-selected peripheral blood mononuclear cells (PBMCs) demonstrated that this region is a *trans*-expression quantitative trait locus (eQTL) in PBMCs. Signaling analysis predicted several tumor necrosis factor-related pathways, the TWEAK/Fn14 pathway being the top candidate ($p = 2.42 \times 10^{-11}$). This pathway is involved in the modulation of inflammation in several

human AD, including multiple sclerosis, systemic lupus erythematosus, or rheumatoid arthritis. *In vitro* studies with genotype-selected lymphoblastoid cells from patients with MD suggest that this trans-eQTL may regulate cellular proliferation in lymphoid cells through the TWEAK/Fn14 pathway by increasing the translation of NF-κB. Taken together; these findings suggest that the carriers of the risk genotype may develop an NF-κB-mediated inflammatory response in MD.

Keywords: TNFRSF12A, NFKB1, TWEAK/Fn14 pathway, NF-κB signaling, vertigo, sensorineural hearing loss, Meniere's disease

INTRODUCTION

Meniere's disease [MD (MIM 156000)] is an inner ear syndrome characterized by recurrent attacks of vertigo associated with concurrent ipsilateral aural symptoms, such as fluctuating sensorineural hearing loss (SNHL), tinnitus, or aural pressure (1, 2). MD is associated with a fluid imbalance between the secretion of endolymph in the cochlear duct and the reabsorption into the subarachnoid space, leading to an accumulation of endolymph termed endolymphatic hydrops (3), but the underlying molecular mechanism remains unknown.

Epidemiological evidences support a genetic contribution in MD including: (a) a higher prevalence of MD in Caucasians over other ethnicities (4) and (b) familial clustering, as familial MD occurs in 6–10% of patients with MD in European and Asian-descent populations, respectively, and it has a high sibling recurrence risk ratio (λ_s = 24–45) (5, 6). Early case–control studies in small series using candidate genes suggested an association with HLA class II genes in different populations (7); however these studies have not been replicated (8). By contrast, a genomic approach using whole-exome sequencing in families with autosomal-dominant MD and autoimmune background has identified rare variants with potential pathogenic effects in the *FAM136A*, *DTNA*, *PRKCB*, *DPT*, and *SEMA3D* genes (9–11). Although these candidate genes for familial MD should be confirmed in sporadic and more families with MD, they start to anticipate genetic heterogeneity.

Different studies have described a MD association with several autoimmune diseases (AD), such as rheumatoid arthritis, systemic lupus erythematous (SLE), or psoriasis (12, 13). Based on the results of proteomic studies performed in small series of patients, autoimmunity has been proposed as a potential cause of MD (14, 15). However, elevated immune complexes were only found in 7% of patients with MD (16), and there is no consistent immunological biomarker for the diagnosis of MD. Therefore, the evidence to support the hypothesis of autoimmunity is limited. The TWEAK/Fn14 pathway is involved in the modulation of inflammation in several chronic AD, including multiple sclerosis, SLE, rheumatoid arthritis, or ulcerative colitis (17). However, this pathway has not been investigated in SNHL or MD.

Nuclear factor kappa B (NF-κB) is a family of transcription factors, which regulate immune and inflammatory responses. In the latent state, NF-κB is inhibited in the cytosol by IκB (inhibitor of NF-κB) proteins. Upon stimulation of innate immune receptors such as cytokines or toll-like receptors, a series of membrane proximal events lead to the activation of IκB kinases (IKK). Phosphorylation of IκBs releases NF-κB, which translocates to the nucleus to regulate gene transcription (18).

Bilateral involvement in MD (BMD) may occur in 20–47% of patients after 10 years of follow-up (19). Most patients begin with vertigo and hearing loss in one ear, and hearing loss can appear in the second ear several years later, but a significant number of individuals show simultaneous SNHL. Autoimmune inner ear disease (AIED) is a rare disorder defined by recurrent episodes of bilateral SNHL progressing over a period of several weeks or months (20). Vestibular symptoms may be present in 50% of patients and systemic autoimmune disease coexists in 30% of patients (21). This audiovestibular phenotype overlaps with BMD and it may not be possible to distinguish AIED and MD. In some cases, AIED may begin as sudden unilateral SNHL involving rapidly the second ear. Although the mechanism of AIED is not well understood, these patients show elevated levels of proinflammatory cytokines, including IL-1β and TNFα (22), and may respond to steroid therapy or anakinra (23). Furthermore, autoimmune endolymphatic hydrops was described in patients with Cogan syndrome and polyarteritis nodosa and it was found in 50% of patients with AIED.

The aim of this study was to identify susceptibility loci using the Immunochip genotyping array to define a subset of patients with MD, which may have an autoimmune dysfunction. Here, we found a locus in 6p21.33 and we demonstrated that it regulates gene expression in the tumor necrosis factor (TNF)-like weak inducer of apoptosis (TWEAK)/Fn14 pathway and induces translation of NF-κB in lymphoid cells.

MATERIALS AND METHODS

Ethics Approval Statement

The study protocol PI13/1242, with reference 01-2014, was approved by the ethic Committee for clinical research of all the recruiting centers. All participants gave written informed consent. The work was performed according to the principles of the Declaration of Helsinki of 1975 (as revised in 2013) (24).

Case Definition and Sample Population

Meniere's disease cases were diagnosed according to the clinical guidelines defined by the Committee on Hearing and Equilibrium of the American Academy of Otolaryngology Head and Neck Surgery (AAO-HNS) (25). All familial cases were excluded.

The initial cohort consisted of 681 cases of MD (492 unilateral and 189 bilateral SNHL) and 735 unrelated controls. The replication cohort was drawn from an independent group of 240 bilateral cases and 895 Iberian controls of European ancestry. The samples included in the discovery cohort were partially overlapped with a preliminary study previously published (26).

The diagnosis protocol included a complete neuro-otological evaluation including otoscopy, a pure-tone audiometry, nystagmus examination and caloric testing, and a brain MRI to exclude other possible causes of neurological symptoms. Patients were monitored with serial audiograms and the following clinical variables were studied in our series: gender, age, hearing stage, duration of the disease, bilateral SNHL, age of onset, type of headache, history of autoimmune disease, smoking, Tumarkin crisis, and the functional scale of the AAO-HNS. Hearing stage was calculated with the audiogram obtained the day of inclusion for each patient with definite MD and was defined as the mean of four-tone average of 0.5, 1, 2, and 3 kHz according to the AAO-HNS criteria: stage 1, ≤25 dB HL; stage 2, 26–40 dB HL; stage 3, 41–70 dB HL; and stage 4, >70 dB HL.

DNA and RNA Extraction

DNA was isolated from peripheral blood using the QIAamp DNA Mini Kit (Qiagen, Venlo, Netherlands), according to the manufacturer's instructions. The concentration of genomic DNA was measured using the Qubit dsDNA BR Assay Kit (Invitrogen, ThermoFisher Scientific, Waltham, MA, USA) and concentrations were standardized to 50 ng/mL for genotyping, the quality was determined by Nanodrop 2,000 C (ThermoFisher Scientific, Waltham, MA, USA).

Total RNA was obtained from peripheral blood mononuclear cells (PBMC) using the High Pure RNA Isolation Kit (Hoffmann-La Roche, Basel, Switzerland) following the manufacturer's protocols. The quantity and quality of total RNA were determined using the RNA Nano assay on the Agilent 2100 Bioanalyzer (Agilent Technologies, Waldbronn, Germany).

Genotyping and Quality Controls (QC)

DNA samples were genotyped by the Immunochip, a custom genotyping array which includes loci previously associated with 12 autoimmune disorders (27). Clusters were manually inspected and verified, and SNPs with poor clustering quality metrics were removed (call frequency <0.98, cluster separation <0.4, and GenCall scores <0.15). Further, the SNPs that did not meet the following criteria were excluded: minor allele frequency (MAF) <5%, Hardy–Weinberg equilibrium $<10^{-4}$ in controls, non-random differential missing data rate test between cases and controls $<10^{-5}$, and missing-genotype rate <0.5%. All markers in chromosome X were also excluded. After QC, 96,899 single nucleotide variants (SNVs) remained with a MAF >5% for statistical analysis.

Samples with a genotype success rate of <90% and increased heterozygosity rate (<0.18 and >0.45) were excluded from the analysis. Finally, genetic outliers determined by principal-component analysis (PCA) were removed from the analysis (>3 SD around the mean).

The genotyping of the replication cohort was performed with the TaqMan SNP assay in an ABI 7500 Fast Real-Time PCR System (Life Techonologies, Carlsbad, CA, USA). The alleles were determined using the SDS 2.2.1 software (Applied Biosystems, Foster City, CA, USA). We used PCA to identify population substructure. Furthermore, a representative sample of SNVs genotyped by the Immunochip was validated also by Taqman assays in 165 individuals. The correlation coefficient between both methods was 98%. Genotype calling was performed in all samples with the Genotyping Module (v1.8.4) of the Genome Studio Data Analysis Software. NCBI Build 36 (hg18) mapping was used (Illumina manifest file Immuno_BeadChip_11419691_B.bpm). Data were converted into the human Build hg38 using.[1]

Quality controls were performed, for each set of samples and SNVs separately, using Genome Studio Data Analysis Software and PLINK software (version 1.07) (28). After all QC, 189 patients with bilateral SNHL and 735 controls remained for further statistical analyses. We have evaluated the association between each SNV and patients with unilateral or bilateral MD.

Gene Expression Assay in PBMCs

Peripheral blood mononuclear cells were isolated from peripheral blood of patients with the main genotypes of SNVs rs4947296 by Ficoll gradients (Biowest, Nuaillé, France). After RNA extraction, gene expression levels were quantified using the Illumina HumanHT-12 v4 Expression BeadChip (Illumina Inc., San Diego, CA, USA). Probe intensity data were analyzed using Illumina's GenomeStudio software (Gene Expression Module) to determine the gene expression levels according to negative control probes for background correction and quantile normalization using negative and positive control probes. Probes with detection p-values < 0.05 in less than 10% of samples were filtered, and replicated genes were removed using the median value. Differential expression analysis between samples was performed using the R limma package. Furthermore, we evaluated if the expression of the genes located at <1 Mb distance from the locus and the MHC region were affected by rs4947296 ($p < 0.05$).

Data from the expression array can be accessed at the Gene Expression Omnibus under accession number GSE77865.

Bioinformatics Analysis

Signaling pathway analysis was performed using Ingenuity Pathways Analysis (IPA®, Qiagen, Venlo, Netherlands[2]) software. Core analysis tool was executed using the differentially expressed gene (DEG) with an adjusted p-value cutoff of 0.001. The most significant pathway was the "TWEAK Signaling pathway." Pathway enrichment analysis was performed with MetaCore (GeneGo[3]) (29), using the DEG with the enrichment p-value cutoff of 0.001. The three enriched canonical pathways "apoptosis and survival Apoptotic TNF-family pathways," "signal transduction NF-κB activation pathways," and "apoptosis and survival Anti-apoptotic TNFs-NF-κB-Bcl-2 pathway" were

[1] https://genome.ucsc.edu/cgi-bin/hgLiftOver.
[2] http://www.ingenuity.com/products/ipa.
[3] https://portal.genego.com/.

retrieved and the shortest paths from Fn14 (TNFRSF12A) to NF-κB genes were extracted. The shortest paths were visualized in Cytoscape ver. 2.7.0 (30).

Cell Culture

Peripheral blood mononuclear cells were seeded at a density of 5×10^6 cells/mL in RPMI 1640 (Thermo Fisher Scientific, Waltham, MA, USA) containing 20% Fetal Bovine Serum (FBS, Biowest, Nuaillé, France) and Epstein–Barr virus at 1:1 ratio was added to generate lymphoblasts. Cells were placed in an incubator maintained at 37°C with 7% CO_2 and cultured in RPMI 1640 supplemented with 10% FBS, non-essential amino acids, and sodium pyruvate.

Cell viability and proliferation assays were performed in lymphoblastoid cell lines (LCL) to investigate the effect of the rs4947296 homozygous conditional genotypes. Five thousand cells were plated in 96-well plates and incubated at different TWEAK (PeproTech, London, UK) concentrations to examine the effect over both cell lines (0, 50, 100, 250, and 500 ng/mL) (31). Proliferation rate was measured at 24, 48, and 72 h. At each time point, 20 μL of PrestoBlue™ (Life Technologies, Carlsbad, CA, USA) was added to each well and cultured at 37°C for 4 h. After that, the absorbance of the supernatant was measured at 570 nm in a Tecan Infinite Nanoquant M200 Pro absorbance microplate reader. Blank controls were performed for each measure using medium and PrestoBlue™ (Life Technologies, Carlsbad, CA, USA). Cell viability assay was performed using Trypan blue staining (Thermo Fisher Scientific, Waltham, MA, USA). The size of the clusters was measured using the area (μm^2) of 200 clusters for each genotype by ImageJ software (ImageJ, U. S. National Institutes of Health).

Quantitative RT-PCR (qPCR)

Quantitative RT-PCR was performed using the Brilliant III Ultra-Fast SYBR® Green qPCR Master Mix (Agilent Technologies, Santa Clara, CA, USA) and an ABI 7900 HT Fast real-time PCR Systems (Life Technologies, ThermoFisher Scientific, Waltham, MA, USA) using primers listed in **Table 1**. Hypoxanthine phosphoribosyltransferase 1 was used as housekeeping gene. Technical triplicates were performed to reduce experimental errors. The fold change for each gene was obtained using the comparative CT method (32). Statistical analyses were performed using Student's *t*-test. A p value < 0.05 was considered statistically significant.

Western Blot

Protein extraction was carried out by acetone precipitation (33). Protein concentration was determined by Bradford protein assay (Bio-Rad Laboratories, Hercules, CA, USA) and total protein was stored at −80°C. Sixty micrograms of total proteins were separated by molecular weight in a poliacrilamyde gel [Criterion™ TGX™ Precast Gels (Bio-Rad Laboratories, Hercules, CA, USA)] and transferred to a Trans-Blot® Turbo™ Midi PVDF membrane by Trans-Blot® Turbo™ Transfer System (Bio-Rad Laboratories, Hercules, CA, USA). The membrane was incubated with primary antibody against NF-κB p105/p50 (Abcam, Cambridge, UK; #ab7971, 1:400) overnight at 4°C and a chicken polyclonal antibody against GAPDH (EMD Millipore, #AB2302, 1:1,000). Then, the membrane was incubated with secondary antibodies for 1 h at room temperature. A goat anti-rabbit (R&D Systems, #HAF008, 1:3,000) and a rabbit anti-chicken (Sigma-Aldrich, #A9046-1ML, 1:9,000) were used, respectively. After that, the membrane was developed using Clarity™ Western ECL Substrate (Bio-Rad Laboratories, Hercules, CA, USA) and the images were obtained using the ImageQuant LAS4000 (GE Healthcare Life Science). ImageJ software (NIH, USA) was used for the quantification.

Confocal Image Analysis of Whole Mount LCLs

Selected LCLs were obtained from patients with MD according to the genotype. LCLs undergoing TWEAK treatment (250 ng/mL) for 48 h were fixed using fresh methanol: DMSO (4:1) and stored at −20°C until used. LCLs were then rehydrated, blocked, stained, and mounted as previously described (34). Primary antibodies were used as follows: a mouse monoclonal antibody

TABLE 1 | Primer sequences for quantitative RT-PCR.

GENE	Forward primers	Reverse primers
NFKB1	5′-GAAGCACGAATGACAGAGGC-3′	5′-GCTTGGCGGATTAGCTCTTTT-3′
TNFRSF12A	5′-CTGGCTCCAGAACAGAAAGG-3′	5′-GGGCCTAGTGTCAAGTCTGC-3′
LFA-1	5′-TTGGGGTTTGAAGAAGTCTCAG-3′	5′-GTGCCTCCCATTGAAGATGT-3′
ICAM-1	5′-GATTCTGACGAAGCCAGAGG-3′	5′-CCGGGTCTGGTTCTTGTGTA-3′
Hypoxanthine phosphoribosyltransferase 1	5′-TGACACTGGCAAAACAATGCA-3′	5′-GGTCCTTTTCACCAGCAAGCT-3′
FOS	5′-GGGGCAAGGTGGAACAGTTAT-3′	5′-CCGCTTGGAGTGTATCAGTCA-3′
BIRC3	5′-AAGCTACCTCTCAGCCTACTTT-3′	5′-CCACTGTTTTCTGTACCCGGA-3′
FADD	5′-GTGGCTGACCTGGTACAAGAG-3′	5′-GGTAGATGCGTCTGAGTTCCAT-3′
NFKBIE	5′-TCTGGCATTGAGTCTCTGCG-3′	5′-AGGAGCCATAGGTGGAATCAG-3′
CASP3	5′- GTACAGATGTCGATGCAGCAA-3′	5′- GCACACAAACAAAACTGCTCC-3′
CASP6	5′- CGATGTGCCAGTCATTCCTTT-3′	5′- GCTGCATCCACCTCAGTTATG-3′
CASP9	5′- CAGAGATTCGCAAACCAGAGG-3′	5′- CACCGACATCACCAAATCCTC-3′
APAF1	5′- GCCCTGCTCATCTGATTCATG-3′	5′- TCTCACTGACTGCACAATCCT-3′
CYCS	5′- AAGACTGGGCCAAATCTCCAT-3′	5′- TCTGCCCTTTCTTCCTTCTTCT-3′
IKBKG	5′- GATCTCAAACAGCAGCTCCAG-3′	5′- AGTCCGCCTTGTAGATATCCG-3′

against Fn14 (Santa Cruz Biotechnology, Dallas, TX, USA; #sc-56250, 1:50) and a rabbit polyclonal antibody against NF-κB p105/p50 (Abcam, Cambridge, UK; #ab7971, 1:50). As secondary antibodies, we used Alexa-555-conjugated goat anti-mouse (Life Technologies, Carlsbad, CA, USA; #A-21422, 1:500) and Alexa-633-conjugated goat anti-rabbit (Life Technologies, Carlsbad, CA, USA; #A-21071, 1:500), respectively. For nuclei staining, we used Hoechst 3342 (Life Technologies, Carlsbad, CA, USA; #H1399, 1:1,000). A laser scanning confocal microscope LSM 710 (Carl Zeiss, Oberköchen, Germany) was used for image collection and the Zeiss browser software program ZEN black edition was used to acquire and export the data. All images were taken with the same laser intensity settings on the microscope and final image processing and labeling were performed with ImageJ.

NF-κB p65 Phosphorylation Assay

Lymphoblastoid cell lines according to each genotype were plated with a density of 1×10^6cells/mL and treated with TWEAK (250 ng/mL) during 48 h at 37°C. After that time, cells were centrifuged and resuspended in an appropriate volume of HBSS containing 5% FBS (Biowest, Nuaillé, France). Cells were then lysed with Cell Lysis Buffer 5× from the NF-κB p65 (Total/phospho) Multispecies InstantOne™ ELISA Kit (Thermo Fisher Scientific, Waltham, MA, USA) and manufacturer's protocol was followed.

Statistical Analysis

We performed a descriptive statistical analysis for clinical variables, using SPSS software v.22 (SPSS Inc., Chicago, IL, USA). Data are shown as means with their SD. Quantitative variables were compared using Student's unpaired *t*-test. Qualitative variables were compared using crosstabs and Fisher's exact test. Nominal *p*-values using a 5% level to determine significance are reported. Allelic and genotypic frequencies were compared between patients and controls by logistic regression test and calculating the odds ratios (OR) and 95% confidence intervals using PLINK (version 1.07). Genotypes were imputed and implemented in IMPUTEv2 using the 1,000 Genomes Phase 3 integrated reference panel according to a previously described method (35).

Potential interactions between associated loci were also tested using the association module in PLINK v1.07. Logistic regression analyses were used to estimate the genotype-specific effects of the risk alleles.

We selected SNVs for the replication study based on the results of the discovery phase and the meta-analysis was performed by SPSS. The functional evaluation of each SNP located in candidate loci was performed *in silico* using HaploReg,[4] which provides linkage disequilibrium information (r^2 and D' measurements) and it allows us to define haplotype blocks in each chromosome used (36). Moreover, we used seeQTL[5] and RegulomeDB[6] to annotate regulatory variants of the noncoding genome such as enhancers, transcription factors binding sites, their conservation across mammals and their potential effects on regulatory motifs (37, 38).

Clinical variables were compared between patients with unilateral and BMD by unpaired *t* test for quantitative variables and χ^2 test for qualitative variables. $P < 0.05$ was considered statistically significant.

RESULTS

Bilateral MD Is Associated with a Locus in the Classical Class I Subregion of the MHC

Table 2 compares the clinical features of 1,451 patients with uni and bilateral SNHL in MD. Patients with bilateral SNHL had a longer duration of the disease ($p = 1.5 \times 10^{-6}$), worse hearing loss at diagnosis ($p = 2.5 \times 10^{-4}$), worse hearing stage ($p = 2 \times 10^{-6}$), higher frequency of AD ($p = 4 \times 10^{-3}$), and higher frequency of migraine ($p = 6 \times 10^{-3}$).

Although no significant association was found in patients with unilateral MD, two genomic regions at chromosome 2 and 6 reached confirmatory significance (*p*-values $< 10^{-6}$) in the subset of patients with BMD (**Figure 1**). To perform the replication, we selected representative TagSNVs, according to the results of the discovery phase in both regions (**Table 3**). The meta-analysis confirmed a suggestive significant association with a locus in the classical class I subregion of the MHC ~9 kb at 6p21.33 (31,081,878–31,090,401), being the leading SNV rs4947296; OR = 2.089 (1.661–2.627); $p = 1.39 \times 10^{-09}$.

TABLE 2 | Clinical features of patients with sporadic Meniere's disease.

Variables	Bilateral (*n* = 420)	Unilateral (*n* = 1,031)	*p*-Value
Age of onset, mean (SD)	45.23 (13.6)	47.24 (12.1)	0.263
Gender (% women)	59.3	57.5	0.598
Time course (years), mean (SD)	15.16 (9.1)	10.35 (±7.7)	**1.50×10^{-06}**
Affected ear (%)		Right (50.9)	
Hearing loss at diagnosis, mean (SD)	56.96 (16.7)	48.66 (19.1)	**2.47×10^{-04}**
Migraine, *n* (%)	70 (18.4)	131 (12.8)	**0.006**
History of autoimmune disease, *n* (%)	63 (19.2)	119 (12.8)	**0.004**
Smoking, *n* (%)	81 (21.3)	254 (24.3)	0.422
Hearing stage, *n* (%)			
1	7 (2.0)	117 (12.2)	**5.00×10^{-06}**
2	52 (14.9)	232 (24.2)	
3	178 (51.0)	471 (49.1)	
4	112 (32.1)	140 (14.6)	
Hearing stage, mean (SD)	3.13 (0.7)	2.66 (0.8)	**2.00×10^{-06}**
Turmakin crisis, *n* (%)	85 (29.5)	126 (16.9)	**8.00×10^{-06}**
Functional scale, *n* (%)			
1	37 (12.6)	167 (12.6)	**0.008**
2	91 (31.0)	332 (37.1)	
3	74 (25.2)	185 (20.7)	
4	46 (15.6)	126 (14.1)	
5	37 (12.6)	71 (7.9)	
6	8 (2.7)	13 (2.7)	

Numbers in bold represent significant p-values (p < 0.05).

[4]http://www.broadinstitute.org/mammals/haploreg/haploreg.php
[5]http://www.bios.unc.edu/research/genomic_software/seeQTL/.
[6]http://regulomedb.org/.

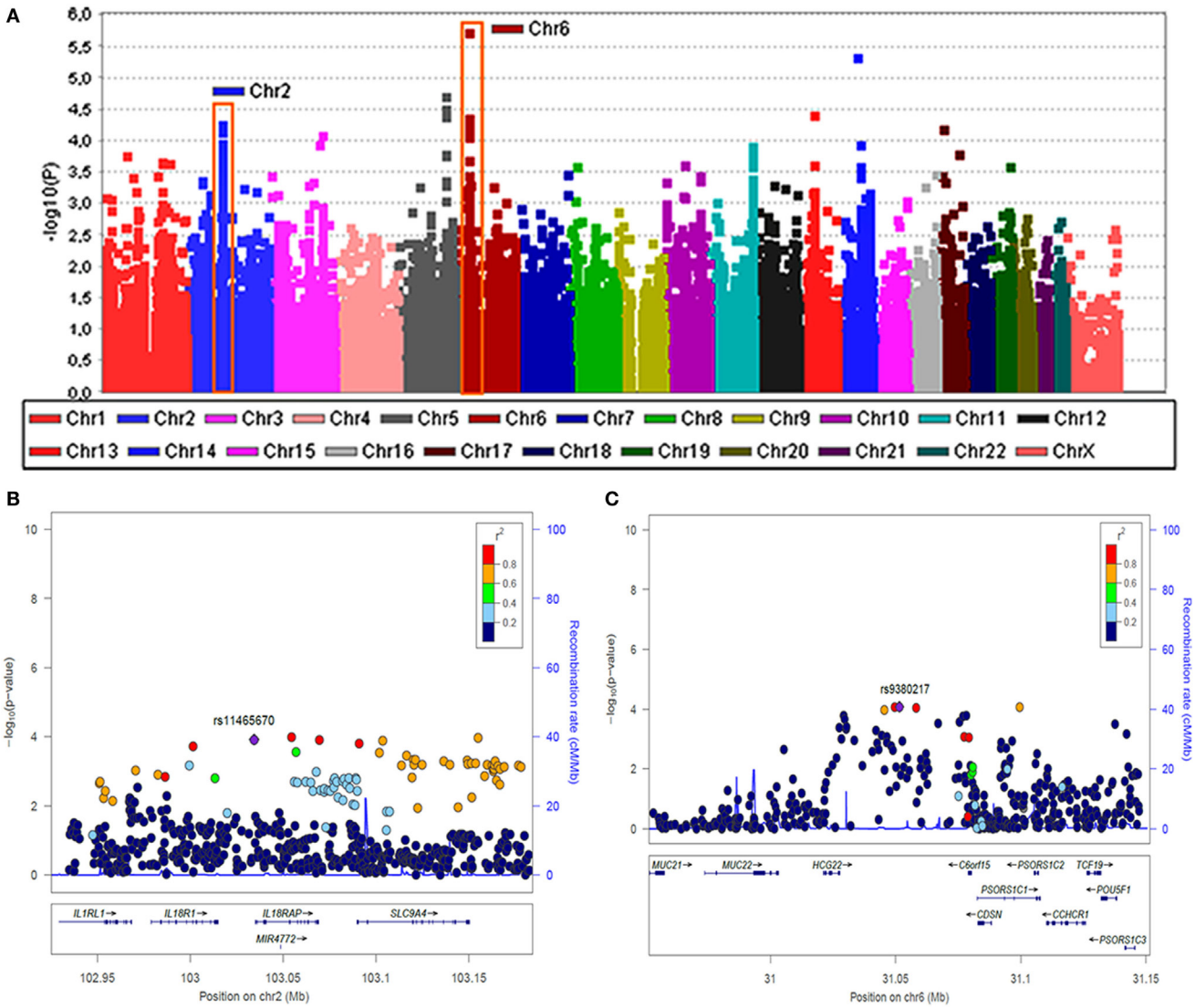

FIGURE 1 | Two loci associated with bilateral sensorineural hearing loss (SNHL). **(A)** Manhattan plot for association study findings from Immunochip genotyped bilateral cases and controls. **(B)** Association area at the region on chromosome 2 and **(C)** association area at the region on chromosome 6. Both **(B,C)** –logP values of single nucleotide variants (SNVs) associated with bilateral SNHL are shown on the left *y*-axis and the recombination rates expressed in centimorgans (cM) per Mb, are shown on the right *y*-axis. Positions in Mb are on the *x*-axis (NCBI Build GRCh38). Linkage disequilibrium for each SNV with the top SNV, displayed as a large purple diamond, is indicated by its color. The plots were drawn using LocusZoom tool (http://locuszoom.sph.umich.edu/locuszoom/).

Conditional regression analysis showed no independent associated signals in chromosome 6, and the association between this locus and BMD remained robust when it was adjusted to any variant in the region. So, according to rs4947296, we defined the homozygous risk genotype as CC and the protective genotype as TT for further studies.

The rs4947296 Regulates Gene Expression in the TWEAK/Fn14 Pathway in PBMCs

We compared the gene expression profile of PBMCs from 10 individuals according to the rs4947296 genotype (CC vs. TT). We demonstrated that this region is an expression quantitative trait locus (eQTL) in mononuclear cells, showing significant differences in the expression levels of 973 genes (adjusted $p < 0.001$, **Figure 2A**; Table S1 in Supplementary Material). Selecting those genes showing a differential expression according to the genotype, pathway analysis performed by IPA® software, predicted the activation of several candidate pathways associated with TNF (Table S2 in Supplementary Material). The TWEAK/Fn14 pathway showed 31 differentially expressed genes (DEG, 88.5%; $p = 2.42 \times 10^{-11}$). Moreover, the eQTL was also associated with the activation of the Death Receptor signaling pathway with 64 DEG (68.8%; $p = 8.45 \times 10^{-11}$); TNFR2 signaling pathway with 26 DEG (86.6%; $p = 2.97 \times 10^{-9}$), and TNRF1 signaling pathway with 37 DEG (74%; $p = 6.69 \times 10^{-9}$).

TABLE 3 | Meta-analysis of loci associated with bilateral Menière's disease.

SNV					Phase 1 (n = 189 cases; 735 controls)				Phase 2 (n = 240 cases; 895 controls)				Meta-analysis (n = 429 cases; 1,630 controls)			
Chr.	Pos.	Rs	Ref.	Alt.	RAF_C	RAF_N	OR (95%)	p-Value	RAF_C	RAF_N	OR (95%)	p-Value	RAF_C	RAF_N	OR (95%)	p-Value
2	102351615	rs4988957	C	T	0.414	0.358	1.27 (0.99–1.62)	5.24E−02	0.381	0.355	1.07 (0.93–1.23)	1.88E−01	0.406	0.351	1.16 (1.05–1.83)	2.91E−03
2	102417980	rs11465670	T	C	0.156	0.093	1.81 (1.29–2.54)	5.02E−04	0.087	0.083	1.04 (0.73–1.49)	4.41E−01	0.121	0.087	1.38 (1.10–1.73)	4.52E−03
2	102460685	rs4851589	A	G	0.337	0.279	1.32 (1.02–1.69)	3.35E−02	0.247	0.258	0.96 (0.79–1.16)	3.61E−01	0.299	0.267	1.12 (0.99–1.27)	4.53E−02
6	30814225	rs886424	C	T	0.102	0.051	2.11 (1.39–3.21)	3.55E−04	0.082	0.071	1.14 (0.81–1.62)	2.55E−01	0.095	0.067	1.41 (1.09–1.83)	7.73E−03
6	31083776	rs9380217	C	T	0.159	0.069	2.55 (1.81–3.58)	3.40E−07	0.108	0.078	1.43 (1.00–2.06)	5.52E−02	0.132	0.074	1.854 (1.465–2.347)	2.02E−07
6	31090401	**rs4947296**	T	C	0.164	0.067	2.72 (1.93–3.82)	3.15E−08	0.108	0.078	1.432 (1.024–2.004)	3.52E−02	**0.142**	**0.073**	**2.089 (1.661–2.627)**	**1.39E−09**
6	32082981	rs1150754	C	T	0.117	0.061	2.04 (1.38–3.01)	2.66E−04	0.089	0.067	1.16 (0.81–1.65)	2.35E−01	0.096	0.071	1.36 (1.05–1.77)	1.34E−02

Chr., chromosome; SNV, single nucleotide variant; Pos., genomic position; Rs, SNV identifier; Ref., reference; Alt., alternative allele on human genome reference GRCh38; RAF_C, risk allelic frequency in cases; RAF_N, risk allelic frequency in controls; OR, odds ratio.

The enrichment analysis of canonical pathways in MetaCore (adjusted $p < 0.001$) also resulted in several TNF-related pathways for apoptosis and inflammation that contained TWEAK/Fn14 sub-pathway (Table S3 in Supplementary Material). To gain insight into the possible molecular interactions that mediate TWEAK signaling to NF-κB, we extracted three enriched canonical pathways "apoptosis and survival Apoptotic TNF-family pathways," "signal transduction NF-κB activation pathways," and "apoptosis and survival Anti-apoptotic TNFs-NF-κB-Bcl-2 pathway" from MetaCore. The shortest paths from Fn14 (*TNFRSF12A*) to *NFKB1* genes were extracted (**Figure 2B**) and visualized in Cytoscape v.2.7.0 (30). These shortest paths involved several DEG, including *BIRC3* and *NFKBIE*. Although *FADD* was not among these shortest paths, it is along the *TNFRSF10A*-induced path that feeds into the TWEAK/Fn14 path, suggesting its complementary role in the TWEAK/Fn14 signaling.

We also validated the gene expression profile of *NFKB1*, *TNFRSF12A*, *BIRC3*, *FADD*, *NFKBIE*, *FOS*, *CASP3*, *CASP6*, *APAF1*, *IKBKG*, *CYCS*, and *CASP9* genes in mononuclear cells from patients by qPCR, according to the selected genotypes (**Figure 2C**).

TWEAK Induces Cluster Formation and Proliferation in Selected Lymphoblasts

Lymphoblastoid cell lines proliferate forming clusters with rosette morphology due to the expression of adhesion molecules such as LFA-1 (leukocyte function antigen 1 encoded by *ITGB2* gene) also known as CD11a/CD18 and its ligand, ICAM-1 (intercellular adhesion molecule 1, CD54) in the plasma membrane. Interestingly, the size of the clusters showed significant differences according to the genotype, being smaller for the risk genotype (CC: 30,968.88 ± 1,960.45 μm^2; TT: 103,921.33 ± 12,720.92 nm, $p = 5 \times 10^{-7}$) (**Figure 3A**).

When we treated the cells with TWEAK at a concentration of 250 ng/mL, we observed a marked increase in the size of the risk genotype clusters, which was not observed in the protective genotype (CC: 125,609.84 ± 17,502.21 μm^2, $p = 2 \times 10^{-6}$; TT: 136,132.42 ± 14,785.38 μm^2, $p = 0.02$). This experiment shows that TWEAK induces a significant aggregation of LCLs in the carriers of the risk genotype.

Next, we compared the effect of TWEAK in the proliferation of selected LCLs. So, 250 ng/mL TWEAK increased the proliferation rate after 48 h in both cell lines (CC $p = 0.017$, TT, $p = 0.013$; **Figure 3C**). This effect suggests the activation of the non-canonical NF-κB signaling *via* Fn14 receptor that we confirmed showing an increase expression of *TNFRSF12A* and *NFKB1* genes (**Figure 3B**).

To investigate if the difference in the cluster formation was related with the differential expression of cell adhesion molecule genes, we measured the mRNA levels of three cell surface markers in LCLs: the integrin LFA-1 and the adhesion molecule ICAM which binds to integrins, as well as tight-junction protein ZO-1 (*TJP1 gene*), which interacts directly with actin. We found a significant increase in the expression of *ITGB2* ($p = 5 \times 10^{-6}$; **Figure 3B**) and in *TJP1* ($p = 3.2 \times 10^{-5}$) in the risk genotype, which was not observed in the protective genotype. The differences in clusters

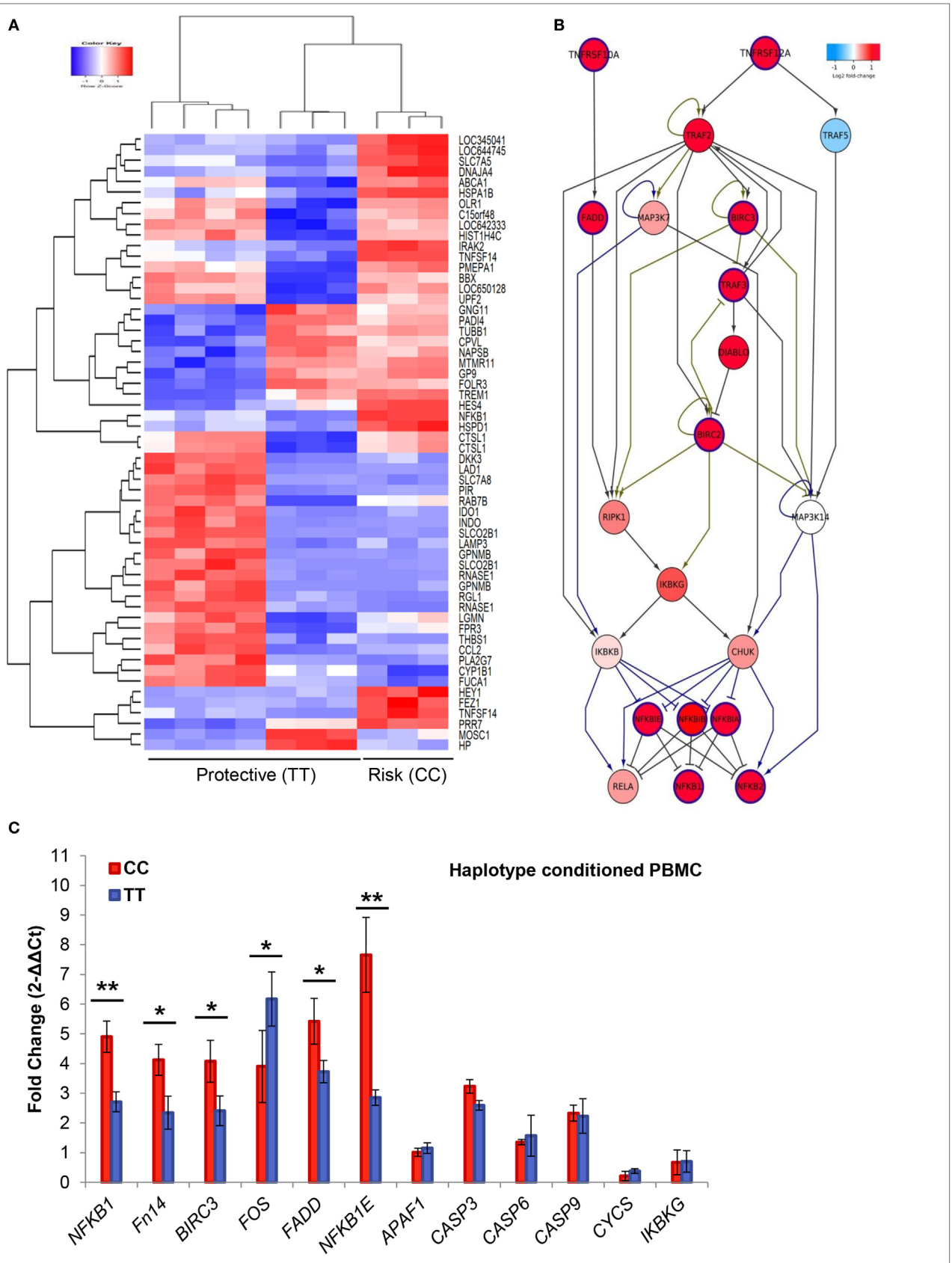

FIGURE 2 | Continued

FIGURE 2 | Continued
Gene expression in peripheral blood mononuclear cells. **(A)** Heatmap of 973 differentially expressed genes (DEG). Samples and genes (columns and rows, respectively) are reordered on the basis of the normalized expression value and give rise to groups of genes and samples with similar expression levels, according to the color key. The samples (column) were clustered into two groups according to rs4947296: three individuals with CC genotype (risk) and seven individuals with TT genotype (protective). **(B)** The shortest path from Fn14 (*TNFRSF12A*) to *NFKB* genes. DEG in mononuclear cells (adjusted $p < 0.001$), according to the homozygous genotype, were used to predict involved pathways. The network was retrieved from three MetaCore pathways ["apoptosis and survival Apoptotic tumor necrosis factor (TNF)-family pathways," "signal transduction NF-κB activation pathways," and "apoptosis and survival Anti-apoptotic TNFs-NF-κB-Bcl-2 pathway"] enriched in our pathway enrichment analysis. Log fold change is color-coded, where red nodes indicate upregulated genes, whereas blue nodes indicate downregulated genes. Activation interactions are indicated by arrow heads, whereas inhibitory interactions are indicated by blunted heads. Black edges indicate physical binding interaction, purple edges indicate phosphorylation, and brown edges indicate ubiquitination. Genes with thick purple margin are DEG. **(C)** Quantitative RT-PCR validation of genes involved in the TWEAK/Fn14 pathway (*NFKB1*, *Fn14*, *BIRC3*, *FADD*, *NFKBIE*, *FOS*, *APAF1*, *CASP3*, *CASP6*, *CASP9*, *CYCS*, and *IKBKG*) (*$p < 0.03$, **$p < 0.0005$).

size, *ITGB2* and *TJP1* expression, according to the genotype, are consistent with the hypothesis that this eQTL could regulate lymphoblasts adhesion and proliferation.

The rs4947296 May Regulate Phosphorylation in NF-κB p65 Subunit on Serine 536 in Lymphoblasts

We measured total and phosphorylated NF-κB p65 on serine 536 in conditioned LCLs to determine if the variant rs4947296 had any effect on NF-κB phosphorylation. Non-stimulated LCLs with the risk genotype (CC) showed a significantly higher amount of total NF-κB when they were compared to cells with the protective genotype (TT) at basal levels (**Figure 4A**, $p = 0.006$). Thus, when we compared risk and protective genotypes in stimulated LCLs, we also found significant differences ($p = 0.026$). However, rs4947296 did not increase phosphorylation on S536 in NF-κB p65 subunit in the risk genotype, and the stimulation with TWEAK itself, did not increase NF-κB p65 phosphorylation in LCL (**Figure 4B**, for both comparisons, $p > 0.05$).

The rs4947296 Upregulates the Translation of NF-κB in Lymphoblasts

Non-stimulated LCLs with the risk genotype (CC) showed a higher expression of *TNFRSF12A* and *NFKB1* RNA (3.6 ± 0.7 and 2.7 ± 0.7 fold higher, respectively) when they were compared to TT LCLs, confirming the previous results obtained in selected PBMC. When we stimulated both cell lines with 250 ng/mL of TWEAK, we found no significant differences for *TNFRSF12A*; however, the expression of *NFKB1* was significantly increased (CC: 10.4 ± 0.8; TT 3.7 ± 0.2, $p = 1.4 \times 10^{-4}$).

This finding was validated by western blot at protein level (**Figures 4C,D**) finding marginally significant differences when comparing risk and protective genotypes at basal levels ($p = 0.05$), but not after stimulation. When we compared each group before and after stimulation with 250 ng/mL of TWEAK, we found significant differences in the protective genotype ($p = 0.017$), but not in the risk genotype ($p = 0.49$), in accordance with the findings observed in ELISA.

We also performed immunocytochemistry to quantify *TNFRSF12A* and *NFKB1* expression at protein level in LCLs by confocal microscopy (**Figure 5**). At basal levels, we found significant differences in the translation of Fn14 between both cell lines (CC: 78.5 ± 9.6; TT 48.3 ± 3.7, $p = 10^{-3}$), but no differences were found for NF-κB (CC: 56.2 ± 4.2; TT 45.2 ± 3.3, $p = 0.06$). However, TWEAK upregulated the translation of NF-κB significantly in the risk LCLs (CC: $p = 0.01$; TT: $p = 0.04$), but it has no effect on Fn14 in neither of LCLs (CC: $p = 0.77$; TT: $p = 0.29$).

DISCUSSION

The main finding of this study is that the SNV rs4947296 is associated with bilateral MD. This variant is a trans-eQTL in lymphoid cells regulating gene expression in several genes in the TWEAK/Fn14 pathway and it activates NF-κB, probably increasing the inflammatory response in MD.

Bilateral MD Is a Heterogeneous Disorder Including Five Clinical Variants

Bilateral MD is a severe, disabling inner ear condition, whose diagnosis usually requires few years of follow-up, since it is based on clinical criteria and no biological marker is available for its diagnosis (1). Moreover, BMD is a heterogeneous disorder that includes several clinical variants. A phenotype-driven cluster analysis has defined five subgroups of patients with potentially different etiology (39). BMD type 1 and type 2 are defined by diachronic or synchronic hearing loss, respectively, without migraine or AD; BMD type 3 includes familial MD cases and we have excluded them on this study; BMD type 4 is defined by migraine as a comorbid condition without AD, and BMD type 5 includes all patients with a comorbid AD. Since the prevalence of BMD is around 25% in our cohort and BMD type 5 is found in 11% of cases, we could estimate that the prevalence of BMD type 5 will be ≈1/40,000 individuals. Our results confirm previous studies that supported a significant association between BMD, migraine and ADs (12, 13). Here, we describe a locus at 6p21.33 suggesting association with BMD, being the leading signal rs4947296.

The Variant rs4947296 Associated with BMD Is a Trans-eQTL and Regulates Several Genes in the TWEAK/Fn14 Pathway

Our results show that rs4947296 is an eQTL in mononuclear cells and it regulates the expression of 31/34 genes in the

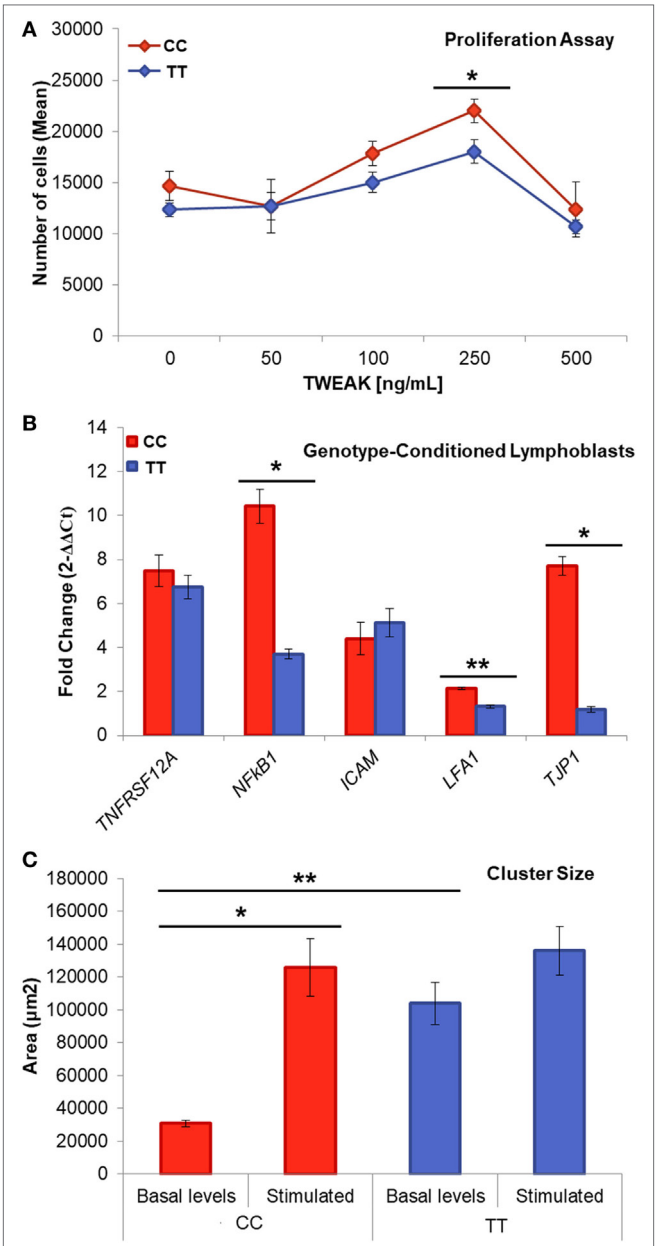

FIGURE 3 | Genotype-conditioned lymphoblastoid cell lines (LCL) for rs4947296. **(A)** Proliferation assay of homozygous LCL treated with tumor necrosis factor-like weak inducer of apoptosis (TWEAK; 0, 50, 100, 250, and 500 ng/mL) and measured using PrestoBlue™ (*$p < 0.05$). Comparisons between groups were achieved using a two-sided Student's *t*-test. **(B)** Relative gene expression according to the genotype, after treatment with 250 ng/mL of TWEAK, *p*-values: *TNFRSF12A* = 0.44; *NFKB1* = 1.36×10^{-4}; *ICAM* = 0.91; *LFA-1* = 5×10^{-6}; *TJP1* = 3.2×10^{-5} (*$p < 1 \times 10^{-4}$, **$p < 5 \times 10^{-6}$) **(C)** Cluster size within LCLs with and without stimulation (**$p = 5 \times 10^{-7}$, *$p = 0.02$). CC, risk genotype; TT, protective genotype.

TWEAK/Fn14 signaling pathway (Table S2 in Supplementary Material) and 16/51 genes in the signal transduction NF-κB activation pathways (Table S3 in Supplementary Material). The SNV rs4947296 has been previously described as one the most strongly SNV associated with Behcet's disease ($p < 10^{-12}$) in a GWAS conducted in Korean, Japanese, and Han Chinese populations (40–42), as well as associated with Graves' disease in Chinese population (43). Our study confirms that the rs4947296 is a trans-eQTL regulating gene expression in the Fn14/TWEAK pathway in lymphoid cells, and these findings support a role for an abnormal innate immune response in the pathophysiology of BMD. The TWEAK/Fn14 pathway has been involved in skin autoimmune disorders. So, TWEAK/Fn14 activation triggers Ro52-mediated photosensitization in cutaneous lupus erythematosus and involves the activation of NF-κB pathway (44). Furthermore, TWEAK/Fn14 contributes to the pathogenesis of bullous pemphigoid by reducing BP180 of hemidesmosomes and activating ERK and NF-κB pathways (45), demonstrating a pathogenic effect on the proteins of intercellular junctions.

In addition, TWEAK/Fn14 pathway could also be involved in Behcet and Graves' disease and it could be a potential target for therapy is these disorders. So, pleiotropy is a common finding in trans-eQTL for autoimmune disorders (46, 47), and SNVs in the HLA region showing trans-eQTL effects were 10-fold enriched (48).

The Variant rs4947296 Regulates NF-κB-Mediated Inflammation in Lymphoid Cells in BMD

TWEAK is a multifunctional cytokine that regulates multiple cellular responses, including angiogenesis, inflammation, cellular adhesion, proliferation, or apoptosis (49, 50). TWEAK activates signals through its receptor, Fn14, encoded by *TNFRSF12A* gene, which is highly expressed in epithelial cells and induced in several human diseases (51). High levels of TWEAK and/or Fn14 have also been found to be associated with the pathogenesis of rheumatoid arthritis (52), SLE (53), multiple sclerosis (54), or neuroinflammation (31). The binding of TWEAK to Fn14 induces both, an acute activation of the canonical NF-κB pathway and a prolonged activation of the non-canonical NF-κB pathway (49). Furthermore, the non-canonical NF-κB pathway plays a key role in immunity and immune-mediated disorders as SLE (49). Our findings using homozygous LCLs demonstrate that this eQTL upregulates the expression and translation of NF-κB in lymphoid cells and it may influence phosphorylation on S536 in the transactivation domain of NF-κB p65. Although our results were not statistically significant, they showed a trend for the risk genotype.

The non-canonical NF-κB pathway relies on the phosphorylation-induced p100 processing, which is triggered by signaling from a subset of TNFR members, including Fn14, TNFR2, BAFFR, CD40, LTβR, and RANK (55). Most of these signals are regulatory elements of the immune response and support the hypothesis that the allelic variants of genes of the immune response can modify the clinical course in MD. Previous studies have suggested that variants in *NFKB1* and *TLR10* genes are modifiers of hearing outcome in patients with uni (26) or BMD (56), but the relationship between TLR10 and NF-κB-mediated inflammation in MD is not known.

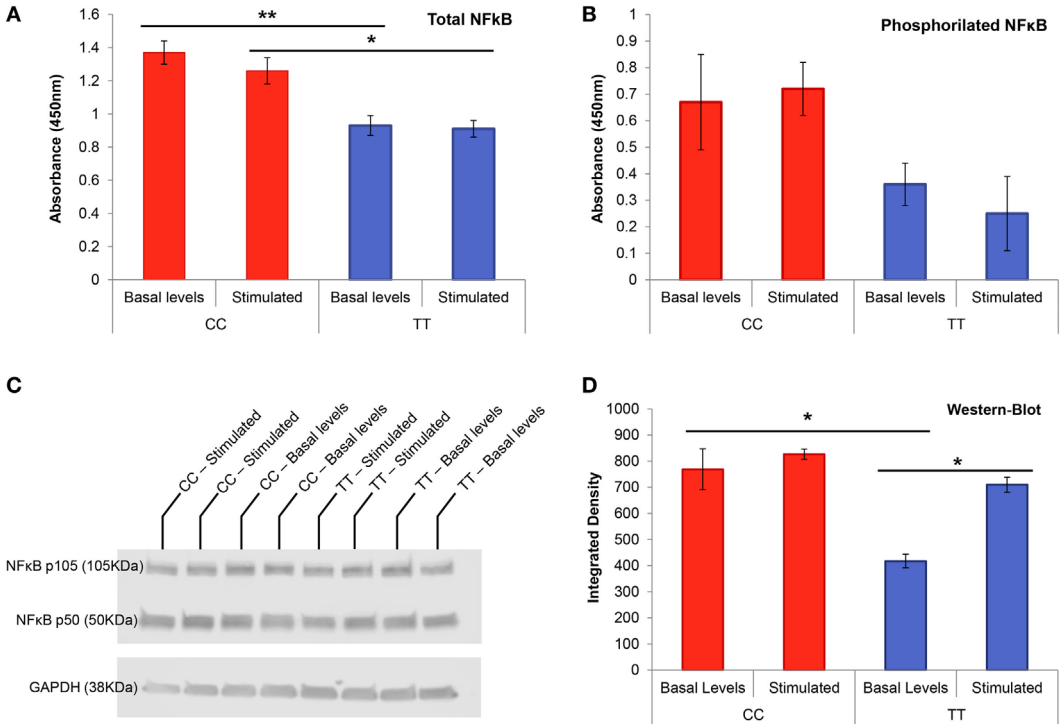

FIGURE 4 | NF-κB transcription factor protein studies in genotype-conditioned lymphoblastoid cell lines (LCLs). **(A)** Total NF-κB ELISA performed in homozygous LCL for rs4947296 at basal levels and after stimulation with TWEAK at 250 ng/mL (*$p < 0.02$, *$p < 0.006$). **(B)** Phosphorylation assay for NF-κB p65 on serine 536 in homozygous LCL at basal levels and after stimulation with TWEAK at 250 ng/mL. **(C)** Representative NF-κB western blot of homozygous LCL before and after treatment with 250 ng/mL of TWEAK. **(D)** NF-κB western blot showing significant differences between both genotype cells at basal levels as well as differences within the protective genotype cells before and after stimulation (*$p < 0.05$). CC, risk genotype; TT, protective genotype.

The Site of NF-κB-Mediated Inflammation in MD Remains to be Defined: the Blood–Labyrinth Barrier (BLB), the Endolymphatic Sac, Fibrocytes of the Spiral Ligament, or/and the Tight Junctions (TJ) at the Reticular Lamina

This study provide evidences that the risk genotype could be used as predictor for bilateral SNHL in MD and our findings support an NF-κB-mediated inflammation in MD. In addition, this signal is a trans-eQTL and it regulates TWEAK/Fn14 pathway.

Although TWEAK could induce the abnormal activation of this pathway in MD, the site of inflammation is unknown. An interesting hypothesis to explore is an inflammatory damage of the BLB, given the role of TWEAK in maintaining the blood–brain barrier (BBB) permeability and regulating the structure and function of the neurovascular unit (25) (**Figure 6**). Recent evidences suggest a role for TWEAK/Fn14 pathway in compromising the BBB in neuropsychiatric SLE (57). So, TWEAK/Fn14 interactions increase the accumulation of inflammatory cells in the choroid plexus, disorganizing BBB integrity and inducing neuronal death *in vitro* by the NF-κB signaling pathway (58, 59), but the role of TWEAK/Fn14 in the regulation of the BLB is unexplored.

A second hypothesis is that inflammation may occur in the endolymphatic sac, since proteomic studies have found a high content of immunoglobulins in the sac (15). The sac is a small organ located in the posterior cranial fossa and has a crucial role, not only in the maintenance of endolymph composition but also in the innate immune response (60). We hypothesize that, after exposure to an environmental trigger, the carriers of the risk genotype could have an abnormal NF-κB-mediated inflammatory response at the endolymphatic sac, causing an ionic imbalance in the endolymph leading to the accumulation of endolymph at the cochlear duct.

A third hypothesis will involve the increase of NF-κB in fibrocytes within the spiral ligament and the spiral limbus after a stress stimuli and the release of proinflammatory cytokines. Genetic mutations involving spiral ligament cells may lead to SNHL (61–63). Immune-mediated and acoustic trauma-mediated hearing impairment may result from the vulnerability of type I and type II fibrocytes to acoustic trauma and systemic inflammatory stress, respectively (64).

The last hypothesis affects cell adhesion molecules in the neurosensorial epithelium of the cochlea. The strict compartmentalization in the inner ear is necessary for normal hearing and is achieved by the TJs of the reticular lamina (65). An outstanding example for these interactions is established by the tight-junction proteins ZO-1, ZO-2, and ZO-3 that connect with the cytoplasmic

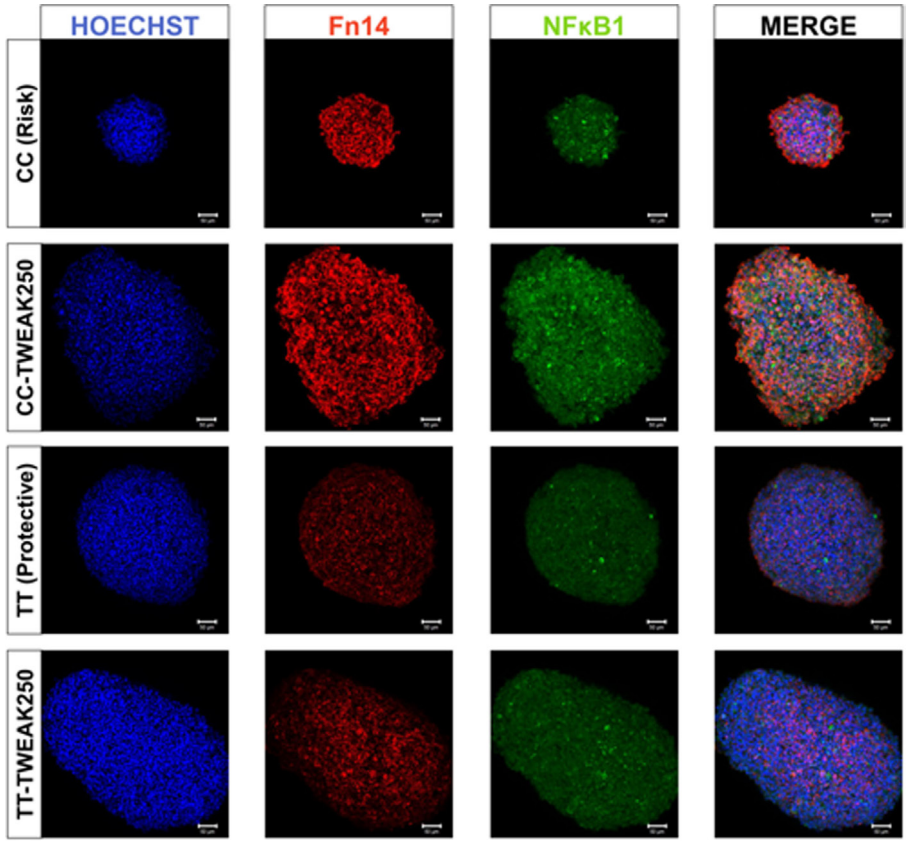

FIGURE 5 | Fn14 and NF-κB expression in homozygous lymphoblastoid cell lines (LCLs). Confocal microscopy images showing representative clusters of LCLs with Fn14 and NF-κB immunolabeling after treatment with 250 ng/mL of TWEAK. CC, risk genotype; TT, protective genotype.

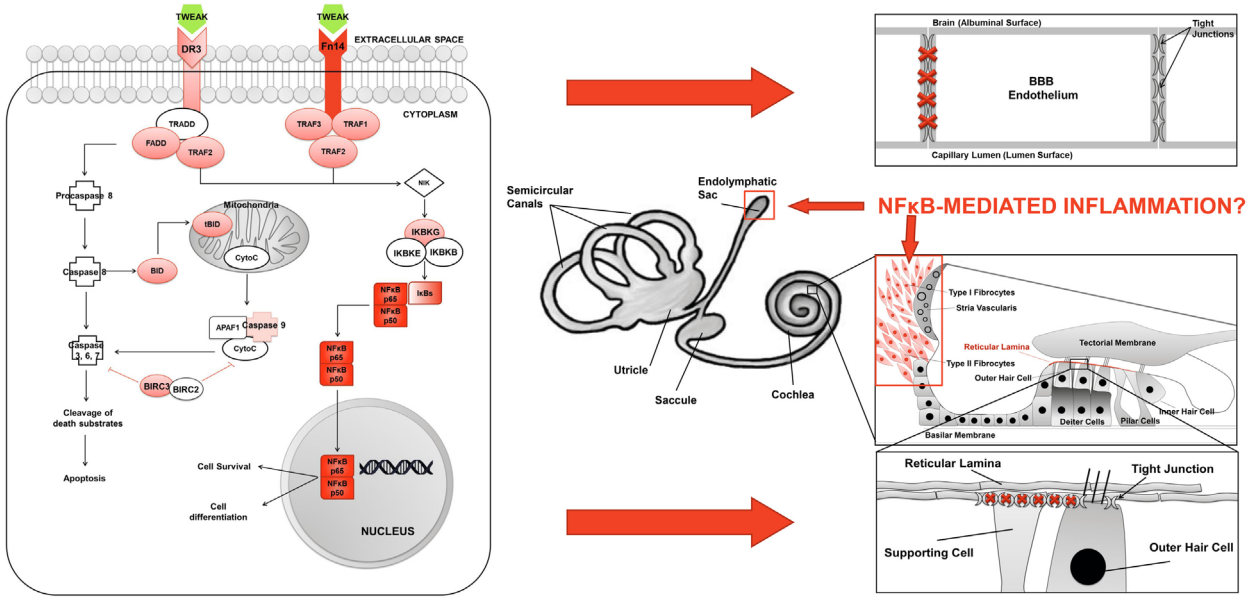

FIGURE 6 | Inflammation model in Meniere's disease (MD). **(A)** TWEAK/Fn14 pathway activates non-canonical NF-κB signaling in lymphoid cells in MD. **(B)** Potential sites of inflammatory damage are the blood–brain barrier (BBB), the endolymphatic sac, the spiral ligament, and the reticular lamina in the neurosensory epithelium of the cochlea.

domains of different integral membrane proteins such as occludins and claudins (66). TJP ZO-1 protein was shown to directly interact with F-actin, building a molecular bridge between integral membrane proteins like tricellulin (encoded by the *TRIC* gene) and the cytoskeleton, and human mutations in *TRIC* lead to deafness (67). Other members of the TJP have also been described to be involved in some types of deafness. Thus, a mutation in *TJP2* was linked to progressive NSHL DNFA51 (68). So, carriers of the risk genotype may have an abnormal expression of cell adhesion molecules, which may compromise the permeability of the reticular lamina causing an ionic imbalance.

CONCLUSION

We present experimental data showing that the rs4947296 regulates gene expression in the TWEAK/Fn14 pathway in PBMCs and LCLs. This locus is a trans-eQTL and upregulates the translation of NF-κB in LCLs, supporting a regulatory effect in immune response.

Fn14 receptor and NF-κB are potential targets for drug therapy for carriers of the risk genotype in MD. Future preclinical studies and clinical trials using inhibitors of this pathway will be needed to demonstrate any potential benefit.

PATENT

JL-E. Use of allelic variants in the locus 6p21.33 for the diagnosis, prognosis and treatment of Meniere's disease. Patent P201531458, October 9, 2015.

ETHICS STATEMENT

The study was carried out in accordance with the recommendation of the Declaration of Helsinki of 1975 (as revised in 2013). The study protocol PI13/1242 with reference number 01-2014 was approved by the Ethical Review Board in Almeria and all the ethics committees for clinical research of all the recruiting centers. All participants gave written informed consent.

AUTHOR CONTRIBUTIONS

LF, TR, and AG-M performed experimental work including genotyping and gene expression arrays, cell culture, and confocal imaging studies. LF, TR, SO, AG-M, MM-B, AS, and JL-E performed statistical and bioinformatics analyses. IA, AB-C, JBDR, JE-S, JJFR, AG-A, RG-A, PM, EM-S, NP, PP, HP-G, SS-P, AS-V, MT, GT-R, and JL-E recruited patients and obtained informed consent in all individuals. MA-R and JL-E designed the study and data interpretation. JL-E supervised all experiments and LF and JL-E drafted the manuscript. All authors revised and approved the final version of the manuscript.

ACKNOWLEDGMENTS

The authors gratefully acknowledge the contribution of patients with Meniere's disease for their participation in this study. The authors also want to specially thank to the staff of genomics and microscopy units at Genyo for the support and advice. This work was supported by Grants from Meniere's Society, UK and PI13/1242 from ISCIII by FEDER Funds from the EU. LF was a graduate student at the Biomedicine program of the University of Granada and this work has been part of her doctoral thesis.

SUPPLEMENTARY MATERIAL

The Supplementary Material for this article can be found online at http://www.frontiersin.org/articles/10.3389/fimmu.2017.01739/full#supplementary-material.

REFERENCES

1. Lopez-Escamez JA, Carey J, Chung WH, Goebel JA, Magnusson M, Mandala M, et al. Diagnostic criteria for Meniere's disease. *J Vestib Res* (2015) 25(1):1–7. doi:10.3233/ves-150549
2. Espinosa-Sanchez JM, Lopez-Escamez JA. Meniere's disease. *Handb Clin Neurol* (2016) 137:257–77. doi:10.1016/b978-0-444-63437-5.00019-4
3. Merchant SN, Adams JC, Nadol JB Jr. Pathophysiology of Meniere's syndrome: are symptoms caused by endolymphatic hydrops? *Otol Neurotol* (2005) 26(1):74–81. doi:10.1097/00129492-200501000-00013
4. Ohmen JD, White CH, Li X, Wang J, Fisher LM, Zhang H, et al. Genetic evidence for an ethnic diversity in the susceptibility to Meniere's disease. *Otol Neurotol* (2013) 34(7):1336–41. doi:10.1097/MAO.0b013e3182868818
5. Requena T, Espinosa-Sanchez JM, Cabrera S, Trinidad G, Soto-Varela A, Santos-Perez S, et al. Familial clustering and genetic heterogeneity in Meniere's disease. *Clin Genet* (2014) 85(3):245–52. doi:10.1111/cge.12150
6. Lee JM, Kim MJ, Jung J, Kim HJ, Seo YJ, Kim SH. Genetic aspects and clinical characteristics of familial Meniere's disease in a South Korean population. *Laryngoscope* (2015) 125(9):2175–80. doi:10.1002/lary.25207
7. Xenellis J, Morrison AW, McClowskey D, Festenstein H. HLA antigens in the pathogenesis of Meniere's disease. *J Laryngol Otol* (1986) 100(1):21–4. doi:10.1017/S0022215100098698
8. Hietikko E, Kotimaki J, Okuloff A, Sorri M, Mannikko M. A replication study on proposed candidate genes in Meniere's disease, and a review of the current status of genetic studies. *Int J Audiol* (2012) 51(11):841–5. doi:10.3109/14992027.2012.705900
9. Requena T, Cabrera S, Martin-Sierra C, Price SD, Lysakowski A, Lopez-Escamez JA. Identification of two novel mutations in FAM136A and DTNA genes in autosomal-dominant familial Meniere's disease. *Hum Mol Genet* (2015) 24(4):1119–26. doi:10.1093/hmg/ddu524
10. Martin-Sierra C, Requena T, Frejo L, Price SD, Gallego-Martinez A, Batuecas-Caletrio A, et al. A novel missense variant in PRKCB segregates low-frequency hearing loss in an autosomal dominant family with Meniere's disease. *Hum Mol Genet* (2016) 25(16):3407–15. doi:10.1093/hmg/ddw183
11. Martin-Sierra C, Gallego-Martinez A, Requena T, Frejo L, Batuecas-Caletrio A, Lopez-Escamez JA. Variable expressivity and genetic heterogeneity involving DPT and SEMA3D genes in autosomal dominant familial Meniere's disease. *Eur J Hum Genet* (2017) 25(2):200–7. doi:10.1038/ejhg.2016.154
12. Gazquez I, Soto-Varela A, Aran I, Santos S, Batuecas A, Trinidad G, et al. High prevalence of systemic autoimmune diseases in patients with Meniere's disease. *PLoS One* (2011) 6(10):e26759. doi:10.1371/journal.pone.0026759
13. Tyrrell JS, Whinney DJ, Ukoumunne OC, Fleming LE, Osborne NJ. Prevalence, associated factors, and comorbid conditions for Meniere's disease. *Ear Hear* (2014) 35(4):e162–9. doi:10.1097/aud.0000000000000041
14. Chiarella G, Di Domenico M, Petrolo C, Saccomanno M, Rothenberger R, Giordano A, et al. A proteomics-driven assay defines specific plasma protein signatures in different stages of Meniere's disease. *J Cell Biochem* (2014) 115(6):1097–100. doi:10.1002/jcb.24747
15. Kim SH, Kim JY, Lee HJ, Gi M, Kim BG, Choi JY. Autoimmunity as a candidate for the etiopathogenesis of Meniere's disease: detection of autoimmune reactions and diagnostic biomarker candidate. *PLoS One* (2014) 9(10):e111039. doi:10.1371/journal.pone.0111039

16. Lopez-Escamez JA, Saenz-Lopez P, Gazquez I, Moreno A, Gonzalez-Oller C, Soto-Varela A, et al. Polymorphisms of CD16A and CD32 Fcgamma receptors and circulating immune complexes in Meniere's disease: a case-control study. *BMC Med Genet* (2011) 12:2. doi:10.1186/1471-2350-12-2
17. Xu WD, Zhao Y, Liu Y. Role of the TWEAK/Fn14 pathway in autoimmune diseases. *Immunol Res* (2016) 64(1):44–50. doi:10.1007/s12026-015-8761-y
18. Napetschnig J, Wu H. Molecular basis of NF-kappaB signaling. *Annu Rev Biophys* (2013) 42:443–68. doi:10.1146/annurev-biophys-083012-130338
19. House JW, Doherty JK, Fisher LM, Derebery MJ, Berliner KI. Meniere's disease: prevalence of contralateral ear involvement. *Otol Neurotol* (2006) 27(3):355–61. doi:10.1097/00129492-200604000-00011
20. McCabe BF. Autoimmune sensorineural hearing loss. *Ann Otol Rhinol Laryngol* (1979) 88(5 Pt 1):585–9. doi:10.1177/000348947908800501
21. Ruckenstein MJ. Autoimmune inner ear disease. *Curr Opin Otolaryngol Head Neck Surg* (2004) 12(5):426–30. doi:10.1097/01.moo.0000136101.95662.aa
22. Pathak S, Goldofsky E, Vivas EX, Bonagura VR, Vambutas A. IL-1beta is overexpressed and aberrantly regulated in corticosteroid nonresponders with autoimmune inner ear disease. *J Immunol* (2011) 186(3):1870–9. doi:10.4049/jimmunol.1002275
23. Vambutas A, Lesser M, Mullooly V, Pathak S, Zahtz G, Rosen L, et al. Early efficacy trial of anakinra in corticosteroid-resistant autoimmune inner ear disease. *J Clin Invest* (2014) 124(9):4115–22. doi:10.1172/JCI76503
24. World Medical Association. World Medical Association Declaration of Helsinki: ethical principles for medical research involving human subjects. *JAMA* (2013) 310(20):2191–4. doi:10.1001/jama.2013.281053
25. Yepes M. TWEAK and Fn14 in the neurovascular unit. *Front Immunol* (2013) 4:367. doi:10.3389/fimmu.2013.00367
26. Cabrera S, Sanchez E, Requena T, Martinez-Bueno M, Benitez J, Perez N, et al. Intronic variants in the NFKB1 gene may influence hearing forecast in patients with unilateral sensorineural hearing loss in Meniere's disease. *PLoS One* (2014) 9(11):e112171. doi:10.1371/journal.pone.0112171
27. Polychronakos C. Fine points in mapping autoimmunity. *Nat Genet* (2011) 43(12):1173–4. doi:10.1038/ng.1015
28. Purcell S, Neale B, Todd-Brown K, Thomas L, Ferreira MA, Bender D, et al. PLINK: a tool set for whole-genome association and population-based linkage analyses. *Am J Hum Genet* (2007) 81(3):559–75. doi:10.1086/519795
29. Nikolsky Y, Ekins S, Nikolskaya T, Bugrim A. A novel method for generation of signature networks as biomarkers from complex high throughput data. *Toxicol Lett* (2005) 158(1):20–9. doi:10.1016/j.toxlet.2005.02.004
30. Shannon P, Markiel A, Ozier O, Baliga NS, Wang JT, Ramage D, et al. Cytoscape: a software environment for integrated models of biomolecular interaction networks. *Genome Res* (2003) 13(11):2498–504. doi:10.1101/gr.1239303
31. Stephan D, Sbai O, Wen J, Couraud PO, Putterman C, Khrestchatisky M, et al. TWEAK/Fn14 pathway modulates properties of a human microvascular endothelial cell model of blood brain barrier. *J Neuroinflammation* (2013) 10:9. doi:10.1186/1742-2094-10-9
32. Livak KJ, Schmittgen TD. Analysis of relative gene expression data using real-time quantitative PCR and the 2(-Delta Delta C(T)) method. *Methods* (2001) 25(4):402–8. doi:10.1006/meth.2001.1262
33. Pena-Llopis S, Brugarolas J. Simultaneous isolation of high-quality DNA, RNA, miRNA and proteins from tissues for genomic applications. *Nat Protoc* (2013) 8(11):2240–55. doi:10.1038/nprot.2013.141
34. Ayllon V, Bueno C, Ramos-Mejia V, Navarro-Montero O, Prieto C, Real PJ, et al. The Notch ligand DLL4 specifically marks human hematoendothelial progenitors and regulates their hematopoietic fate. *Leukemia* (2015) 29(8):1741–53. doi:10.1038/leu.2015.74
35. Howie BN, Donnelly P, Marchini J. A flexible and accurate genotype imputation method for the next generation of genome-wide association studies. *PLoS Genet* (2009) 5(6):e1000529. doi:10.1371/journal.pgen.1000529
36. Ward LD, Kellis M. HaploReg: a resource for exploring chromatin states, conservation, and regulatory motif alterations within sets of genetically linked variants. *Nucleic Acids Res* (2012) 40(Database issue):D930–4. doi:10.1093/nar/gkr917
37. Xia K, Shabalin AA, Huang S, Madar V, Zhou YH, Wang W, et al. seeQTL: a searchable database for human eQTLs. *Bioinformatics* (2012) 28(3):451–2. doi:10.1093/bioinformatics/btr678
38. Boyle AP, Hong EL, Hariharan M, Cheng Y, Schaub MA, Kasowski M, et al. Annotation of functional variation in personal genomes using RegulomeDB. *Genome Res* (2012) 22(9):1790–7. doi:10.1101/gr.137323.112
39. Frejo L, Soto-Varela A, Santos S, Aran I, Batuecas-Caletrio A, Perez-Guillen V, et al. Clinical subgroups in bilateral Meniere disease. *Front Neurol* (2016) 7:182. doi:10.3389/fneur.2016.00182
40. Hou S, Yang Z, Du L, Jiang Z, Shu Q, Chen Y, et al. Identification of a susceptibility locus in STAT4 for Behcet's disease in Han Chinese in a genome-wide association study. *Arthritis Rheum* (2012) 64(12):4104–13. doi:10.1002/art.37708
41. Mizuki N, Meguro A, Ota M, Ohno S, Shiota T, Kawagoe T, et al. Genome-wide association studies identify IL23R-IL12RB2 and IL10 as Behcet's disease susceptibility loci. *Nat Genet* (2010) 42(8):703–6. doi:10.1038/ng.624
42. Lee YJ, Horie Y, Wallace GR, Choi YS, Park JA, Choi JY, et al. Genome-wide association study identifies GIMAP as a novel susceptibility locus for Behcet's disease. *Ann Rheum Dis* (2013) 72(9):1510–6. doi:10.1136/annrheumdis-2011-200288
43. Chu X, Pan CM, Zhao SX, Liang J, Gao GQ, Zhang XM, et al. A genome-wide association study identifies two new risk loci for Graves' disease. *Nat Genet* (2011) 43(9):897–901. doi:10.1038/ng.898
44. Liu Y, Xu M, Min X, Wu K, Zhang T, Li K, et al. TWEAK/Fn14 activation participates in Ro52-mediated photosensitization in cutaneous lupus erythematosus. *Front Immunol* (2017) 8:651. doi:10.3389/fimmu.2017.00651
45. Liu Y, Peng L, Li L, Liu C, Hu X, Xiao S, et al. TWEAK/Fn14 activation contributes to the pathogenesis of bullous pemphigoid. *J Invest Dermatol* (2017) 137(7):1512–22. doi:10.1016/j.jid.2017.03.019
46. Westra HJ, Franke L. From genome to function by studying eQTLs. *Biochim Biophys Acta* (2014) 1842(10):1896–902. doi:10.1016/j.bbadis.2014.04.024
47. Heinig M, Petretto E, Wallace C, Bottolo L, Rotival M, Lu H, et al. A trans-acting locus regulates an anti-viral expression network and type 1 diabetes risk. *Nature* (2010) 467(7314):460–4. doi:10.1038/nature09386
48. Fehrmann RS, Jansen RC, Veldink JH, Westra HJ, Arends D, Bonder MJ, et al. Trans-eQTLs reveal that independent genetic variants associated with a complex phenotype converge on intermediate genes, with a major role for the HLA. *PLoS Genet* (2011) 7(8):e1002197. doi:10.1371/journal.pgen.1002197
49. Winkles JA. The TWEAK-Fn14 cytokine-receptor axis: discovery, biology and therapeutic targeting. *Nat Rev Drug Discov* (2008) 7(5):411–25. doi:10.1038/nrd2488
50. Burkly LC. Regulation of tissue responses: the TWEAK/Fn14 pathway and other TNF/TNFR superfamily members that activate non-canonical NFkappaB signaling. *Front Immunol* (2015) 6:92. doi:10.3389/fimmu.2015.00092
51. Baxter FO, Came PJ, Abell K, Kedjouar B, Huth M, Rajewsky K, et al. IKKbeta/2 induces TWEAK and apoptosis in mammary epithelial cells. *Development* (2006) 133(17):3485–94. doi:10.1242/dev.02502
52. Park JS, Kwok SK, Lim MA, Oh HJ, Kim EK, Jhun JY, et al. TWEAK promotes osteoclastogenesis in rheumatoid arthritis. *Am J Pathol* (2013) 183(3):857–67. doi:10.1016/j.ajpath.2013.05.027
53. Michaelson JS, Wisniacki N, Burkly LC, Putterman C. Role of TWEAK in lupus nephritis: a bench-to-bedside review. *J Autoimmun* (2012) 39(3):130–42. doi:10.1016/j.jaut.2012.05.003
54. Serafini B, Magliozzi R, Rosicarelli B, Reynolds R, Zheng TS, Aloisi F. Expression of TWEAK and its receptor Fn14 in the multiple sclerosis brain: implications for inflammatory tissue injury. *J Neuropathol Exp Neurol* (2008) 67(12):1137–48. doi:10.1097/NEN.0b013e31818dab90
55. Sun SC. Non-canonical NF-kappaB signaling pathway. *Cell Res* (2011) 21(1):71–85. doi:10.1038/cr.2010.177
56. Requena T, Gazquez I, Moreno A, Batuecas A, Aran I, Soto-Varela A, et al. Allelic variants in TLR10 gene may influence bilateral affectation and clinical course of Meniere's disease. *Immunogenetics* (2013) 65(5):345–55. doi:10.1007/s00251-013-0683-z
57. Stock AD, Wen J, Putterman C. Neuropsychiatric lupus, the blood brain barrier, and the TWEAK/Fn14 pathway. *Front Immunol* (2013) 4:484. doi:10.3389/fimmu.2013.00484
58. Wen J, Doerner J, Weidenheim K, Xia Y, Stock A, Michaelson JS, et al. TNF-like weak inducer of apoptosis promotes blood brain barrier disruption and increases neuronal cell death in MRL/lpr mice. *J Autoimmun* (2015) 60:40–50. doi:10.1016/j.jaut.2015.03.005
59. Haile WB, Echeverry R, Wu F, Guzman J, An J, Wu J, et al. Tumor necrosis factor-like weak inducer of apoptosis and fibroblast growth factor-inducible 14 mediate cerebral ischemia-induced poly(ADP-ribose) polymerase-1 activation

and neuronal death. *Neuroscience* (2010) 171(4):1256–64. doi:10.1016/j.neuroscience.2010.10.029
60. Moller MN, Kirkeby S, Vikesa J, Nielsen FC, Caye-Thomasen P. Gene expression demonstrates an immunological capacity of the human endolymphatic sac. *Laryngoscope* (2015) 125(8):E269–75. doi:10.1002/lary.25242
61. Minowa O, Ikeda K, Sugitani Y, Oshima T, Nakai S, Katori Y, et al. Altered cochlear fibrocytes in a mouse model of DFN3 nonsyndromic deafness. *Science* (1999) 285(5432):1408–11. doi:10.1126/science.285.5432.1408
62. Abe S, Katagiri T, Saito-Hisaminato A, Usami S, Inoue Y, Tsunoda T, et al. Identification of CRYM as a candidate responsible for nonsyndromic deafness, through cDNA microarray analysis of human cochlear and vestibular tissues. *Am J Hum Genet* (2003) 72(1):73–82. doi:10.1086/345398
63. Delprat B, Ruel J, Guitton MJ, Hamard G, Lenoir M, Pujol R, et al. Deafness and cochlear fibrocyte alterations in mice deficient for the inner ear protein otospiralin. *Mol Cell Biol* (2005) 25(2):847–53. doi:10.1128/MCB.25.2.847-853.2005
64. Adams JC, Seed B, Lu N, Landry A, Xavier RJ. Selective activation of nuclear factor kappa B in the cochlea by sensory and inflammatory stress. *Neuroscience* (2009) 160(2):530–9. doi:10.1016/j.neuroscience.2009.02.073
65. Kitajiri SI, Furuse M, Morita K, Saishin-Kiuchi Y, Kido H, Ito J, et al. Expression patterns of claudins, tight junction adhesion molecules, in the inner ear. *Hear Res* (2004) 187(1–2):25–34. doi:10.1016/S0378-5955(03)00338-1
66. Dror AA, Avraham KB. Hearing impairment: a panoply of genes and functions. *Neuron* (2010) 68(2):293–308. doi:10.1016/j.neuron.2010.10.011
67. Riazuddin S, Ahmed ZM, Fanning AS, Lagziel A, Kitajiri S, Ramzan K, et al. Tricellulin is a tight-junction protein necessary for hearing. *Am J Hum Genet* (2006) 79(6):1040–51. doi:10.1086/510022
68. Walsh T, Pierce SB, Lenz DR, Brownstein Z, Dagan-Rosenfeld O, Shahin H, et al. Genomic duplication and overexpression of TJP2/ZO-2 leads to altered expression of apoptosis genes in progressive nonsyndromic hearing loss DFNA51. *Am J Hum Genet* (2010) 87(1):101–9. doi:10.1016/j.ajhg.2010.05.011

Conflict of Interest Statement: The authors declare that the research was conducted in the absence of any commercial or financial relationships that could be construed as a potential conflict of interest.

Copyright © 2017 Frejo, Requena, Okawa, Gallego-Martinez, Martinez-Bueno, Aran, Batuecas-Caletrio, Benitez-Rosario, Espinosa-Sanchez, Fraile-Rodrigo, García-Arumi, González-Aguado, Marques, Martin-Sanz, Perez-Fernandez, Pérez-Vázquez, Perez-Garrigues, Santos-Perez, Soto-Varela, Tapia, Trinidad-Ruiz, del Sol, Alarcon Riquelme and Lopez-Escamez. This is an open-access article distributed under the terms of the Creative Commons Attribution License (CC BY). The use, distribution or reproduction in other forums is permitted, provided the original author(s) or licensor are credited and that the original publication in this journal is cited, in accordance with accepted academic practice. No use, distribution or reproduction is permitted which does not comply with these terms.

frontiers in Immunology

ORIGINAL RESEARCH
published: 22 December 2017
doi: 10.3389/fimmu.2017.01813

Direct and Intestinal Epithelial Cell-Mediated Effects of TLR8 Triggering on Human Dendritic Cells, CD14$^+$CD16$^+$ Monocytes and γδ T Lymphocytes

*Costanza Angelini[1], Barbara Varano[1,2], Patrizia Puddu[1], Maurizio Fiori[3], Antonella Baldassarre[4], Andrea Masotti[4], Sandra Gessani[1,2] and Lucia Conti[1,2]**

[1] Department of Hematology, Oncology and Molecular Medicine, Istituto Superiore di Sanità, Rome, Italy, [2] Center for Gender-Specific Medicine, Istituto Superiore di Sanità, Rome, Italy, [3] Department of Food Safety, Nutrition and Veterinary Public Health, Istituto Superiore di Sanità, Rome, Italy, [4] Bambino Gesù Children's Hospital-IRCCS, Research Laboratories, Rome, Italy

OPEN ACCESS

Edited by:
Jixin Zhong,
Case Western Reserve University,
United States

Reviewed by:
Ping Chen,
Georgetown University School of Medicine, United States
Dipyaman Ganguly,
Indian Institute of Chemical Biology (CSIR), India
David Dombrowicz,
Institut National de la Santé et de la Recherche Médicale, France

***Correspondence:**
Lucia Conti
lucia.conti@iss.it

Specialty section:
This article was submitted to Inflammation, a section of the journal Frontiers in Immunology

Received: 28 July 2017
Accepted: 01 December 2017
Published: 22 December 2017

Citation:
Angelini C, Varano B, Puddu P, Fiori M, Baldassarre A, Masotti A, Gessani S and Conti L (2017) Direct and Intestinal Epithelial Cell-Mediated Effects of TLR8 Triggering on Human Dendritic Cells, CD14$^+$CD16$^+$ Monocytes and γδ T Lymphocytes. Front. Immunol. 8:1813. doi: 10.3389/fimmu.2017.01813

Toll-like receptor (TLR)7/8 plays a crucial role in host recognition/response to viruses and its mucosal expression directly correlates with intestinal inflammation. The aim of this study was to investigate the role of TLR7/8 stimulation of intestinal epithelium in shaping the phenotype and functions of innate immunity cell subsets, and to define direct and/or epithelial cell-mediated mechanisms of the TLR7/8 agonist R848 immunomodulatory activity. We describe novel, TLR8-mediated, pro- and anti-inflammatory effects of R848 on *ex vivo* cultured human blood monocytes and γδ T lymphocytes, either induced by direct immune cell stimulation or mediated by intestinal epithelial cells (IEC). Apical stimulation with R848 led to its transport across normal polarized epithelial cell monolayer and resulted in the inhibition of monocyte differentiation toward immunostimulatory dendritic cells and Th1 type response. Furthermore, γδ T lymphocyte activation was promoted following direct exposure of these cells to the agonist. Conversely, a selective enrichment of the CD14$^+$CD16$^+$ monocyte subpopulation was observed, which required a CCL2-mediated inflammatory response of normal epithelial cells to R848. Of note, a TLR-mediated activation of control γδ T lymphocytes was promoted by inflamed intestinal epithelium from active Crohn's disease patients. This study unravels a novel regulatory mechanism linking the activation of the TLR8 pathway in IEC to the monocyte-mediated inflammatory response, and highlights the capacity of the TLR7/8 agonist R848 to directly enhance the activation of γδ T lymphocytes. Overall these results expand the range of cell targets and immune responses controlled by TLR8 triggering that may contribute to the antiviral response, to chronic inflammation, as well as to the adjuvant activity of TLR8 agonists, highlighting the role of intestinal epithelium microenvironment in shaping TLR agonist-induced responses.

Keywords: cell activation, pathogen recognition, inflammation, microenvironment, adjuvant

Abbreviations: AS, apical side; BS, basolateral side; CD, Crohn's disease; CDEIS, Crohn's Disease Endoscopic Index of Severity; CM, conditioned medium; DC, dendritic cell; IBD, inflammatory bowel disease; IEC, intestinal epithelial cells; IPP, isopentenilpyrophosphate; ODN, oligonucleotides; PRR, pattern recognition receptor; TEER, transepithelial electrical resistance; TLR, toll-like receptor; TM, transport medium; ZOL, zoledronate.

INTRODUCTION

Toll-like receptors (TLR) play a fundamental role in pathogen recognition by immune cells leading to immune response activation and pathogen clearance (1). They also control intestinal homeostasis by sensing commensal microorganisms and avoiding detrimental responses.

TLR7 and TLR8 are expressed by myeloid cells, lymphocytes and intestinal epithelial cells (IEC) (2) and recognize specific moieties in viral ssRNA. Their triggering results in viral antigen presentation and generation of protective immune response (3). Conversely, their altered expression in epithelial and lamina propria immune cells may contribute to chronic intestinal inflammation. In particular, TLR7/8 expression in colonic mucosa is increased following antibiotic-induced dysbiosis in mice (4), and abnormal TLR8 expression/signaling characterizes chronic intestinal inflammation contributing to the pathogenesis of inflammatory bowel diseases (IBD) and to inflammation-associated tumorigenesis (5). This receptor is selectively activated in inflamed colonic epithelium of IBD subjects (6, 7) and its expression directly correlates with the severity of intestinal inflammation (8). Furthermore, TLR8 expression characterizes gastrointestinal tumors and correlates with metastasis and poor prognosis (9).

The evidence that different, even opposite, effects can be elicited by TLR7/8 stimulation highlights the importance of a deeper characterization of cell types and immune functions that can be targeted when TLR7/8 agonists are used as vaccine adjuvants. In this regard, the TLR7/8 agonist R848 (also known as resiquimod, S-28463), has come to light as an effective mean of enhancing both antiviral and antitumor responses. R848 is a hydrophobic, low molecular weight synthetic compound, belonging to the imidazoquinoline family and recognizing both TLR7 and TLR8 (10). This agonist has a demonstrated potential as vaccine adjuvant and cancer therapeutic by virtue of its capacity to induce immune mediators and to directly activate dendritic cells (DC), thus preferentially triggering Th1 type responses and enhancing both humoral and cellular immunity (11, 12). However, despite its strong adjuvant properties in mice following topic and oral administration (13–15), the use of R848 in humans has been hampered by their capacity, not yet understood, to rapidly reach the bloodstream and to exert strong systemic effects, mostly dependent on cytokine storm induction (16). Nevertheless, whether and how this compound is adsorbed and/or diffuses across epithelia and tissues, and the role of the delivery route and tissue microenvironment in shaping TLR agonist-induced responses have been only poorly investigated.

The aim of this study was to identify novel cell types and/or immune functions controlled by TLR7/8 triggering of the intestinal epithelium, and to define direct and/or epithelial cell-mediated mechanisms of the R848 immunomodulatory activity. We report that R848 easily diffuses across the polarized Caco-2 cell monolayer and, through TLR8 triggering, it delivers both inflammatory and regulatory signals to monocytes and γδ T lymphocytes, either directly or through epithelial cell stimulation. Specifically, this agonist, when transported across normal epithelial cell monolayer, directly impairs the differentiation of monocytes toward immunostimulatory DC and promotes the activation of γδ T lymphocytes. Simultaneously, it drives the enrichment of the $CD14^+CD16^+$ monocyte subpopulation by stimulating inflammatory chemokine production by IEC.

These results unravel a novel regulatory mechanism linking the activation of the TLR8 pathway in IEC to the monocyte-mediated inflammatory response, and highlight the capacity of R848 to directly enhance the activation of γδ T lymphocytes. This expands the range of cell targets and immune cell responses controlled by TLR8 triggering that may contribute to the antiviral response, to chronic inflammation, as well as to the adjuvant activity of TLR8 agonists.

MATERIALS AND METHODS

Culture of Polarized Caco-2 Cells

Polarized IEC monolayer was obtained by culturing Caco-2 cells (ATCC #HTB-37, 8×10^4 cell/cm^2) on polycarbonate-coated trans-well chambers (0,4 μm pore, 24 mm diameter, Corning) in high glucose DMEM plus 10% FBS and non-essential amino acids for 21 days. Medium was changed every 2 days and IEC differentiation and integrity was monitored by measuring transepithelial electrical resistance (TEER) throughout the culture period by a Volt-meter (Millicell ERS; Millipore Co., Bedford, MA, USA). At the end of the differentiation period (TEER values >800 Ω cm^2), medium was changed, DMEM was replaced by RPMI plus 10% FBS at the basolateral side (BS), and cultures were stimulated at the apical side (AS) with R848 (Resiquimod, 5 μg/ml, kindly provided by Dr. Philippe Neuner, IRBM), CL264 (5 μg/ml, InvivoGen) or β-glucan (10 μg/ml, 1 → 3 β-glucan from baker's yeast, Sigma Aldrich) for 24 h. Agonist concentration 5-fold higher with respect to that used for immune cells was chosen to stimulate epithelial cells. Conditioned medium (CM) was then collected from the BS, filtered and stored at -80°C. IEC monolayer integrity was monitored before and at different time points after treatment by measuring TEER and phenol red transport (17). TEER variations < 10% and phenol red transport ≤ 2% were considered acceptable. Six different preparations of Caco-2 trans-well cultures, leading to comparable results, were used for the study.

HPLC Analysis of R848 Transport across Intestinal Epithelium

R848 was loaded to the IEC monolayer AS and, at different time points, CM from the BS were collected and analyzed by HPLC for agonist content. HPLC analyses were performed on HPLC system 1100 series coupled to a Diode Array Detector and autosampler (Agilent Technologies, Rome, Italy). The column was a Symmetry C18 reversed-phase (150 mm × 3.0 mm, 5 μm), connected to a Sentry Guard Column Symmetry C18 5 μm (3.9 mm × 20 mm) (Waters, Milford, MA, USA). The mobile phase was constituted by solvent A (water containing glacial acetic acid 1% v/v) and solvent B (acetonitrile).

Chromatography was carried out by linear gradient at room temperature, according to the following program: 2% B for 2 min; from 2 to 100% B in 8 min, holding on for 2 min, finally to 2% B in 2 min; the equilibrium time between analyses was 5 min. The flow rate was 0.300 ml/min and 10 µl of sample was injected onto the column. Wavelength $\lambda = 245$ nm. The extent of agonist transport was calculated by dividing the cumulative amount of molecule transported, at the different time points, into the BS CM with the original loading concentration. Caco-2 IEC monolayer was also exposed to different concentrations of R848 for 5 h, BS CM was analyzed by HPLC and the apparent permeability coefficients (Papp) were calculated as previously described (18).

Monocyte-Derived DC Generation and Culture

Monocytes were isolated from the peripheral blood of healthy donors by Ficoll/Paque density gradient centrifugation followed by immunomagnetic selection using $CD14^+$ microbeads (MACS monocyte isolation kit, Miltenyi Biotec, Auburn, CA, USA), according to the manufacturer's instructions. To obtain control immature monocyte-derived DC, monocytes were seeded at 1×10^6 cells/ml in standard medium [RPMI 1640 medium containing 10% FBS, GM-CSF (50 ng/ml, kindly provided by Schering-Plough, Dardilly, France) and IL-4 (500 U/ml, Miltenyi Biotec, Auburn, CA, USA)] and cultured for 5 days. Fresh medium plus cytokines was added at day 3 of culture. For some experiments, monocytes were cultured in standard medium and exposed to R848 (1 µg/ml), CL264 (1–2 µg/ml), or β-glucan (2 µg/ml) soon after seeding. CM-conditioned DC was generated in the same conditions by replacing standard medium with Caco-2 CM. For cytokine blocking, monocytes were seeded in CM after a 30-min pre-incubation of this latter with neutralizing Ab (2.5 µg/ml) to CCL2 (rabbit polyclonal, Sigma Aldrich) or IL-6 (mouse monoclonal, Sigma Aldrich), or with isotype control Ab (rabbit and mouse IgG, respectively). TLR blocking was performed by treating R848 CM-exposed monocytes with phosphorothioate oligonucleotides (ODN) targeting TLR7/8/9 (# 2088, TCCTGGCGGGGAAGT; 1 µM) or specific for TLR7 (# 20958, TCCTAACAAAAAAAT; 2.5 µM) soon after seeding.

γδ T Lymphocyte Isolation, Culture, and Interaction with DC

γδ T lymphocytes were isolated from cryopreserved PBMC of healthy donors by positive selection with immunomagnetic beads (Miltenyi Biotec), according to the manufacturer's instructions. Positively selected population contained >95% viable γδ T cells as assessed by flow cytometry. After an overnight culture in complete medium (RPMI plus 10% FBS), purified γδ T cells were washed, suspended in the same medium at the density of 10^6 cells/ml and exposed to R848 or CL264, or seeded, at the same density, in Caco-2 or primary IEC-derived CM. Cells were stimulated with the non-peptide phosphoantigen isopentenilpyrophosphate (IPP, 2 µg/ml, Sigma Aldrich) and cultured for 48 h.

Dendritic cell/γδ T cell co-cultures were set up by adding purified lymphocytes to autologous control or CM-generated DC (1:1 ratio) as previously described (19). Co-cultures were left untreated or stimulated with the aminobiphosphonate zoledronate (ZOL, 10 µg/ml, kindly provided by Novartis Pharma, Origgio, VA) and analyzed 48 h later.

$CD4^+$ T Cell Activation Assay

Naive $CD4^+$ T lymphocytes were isolated from PBMC of healthy donors by negative selection with immunomagnetic beads (Miltenyi Biotec), according to the manufacturer's instructions. The purity of isolated cells (≥98%) was checked by flow cytometry after labeling with anti-CD4-PE and anti-CD45 RA-FITC.

For T cell activation assay, 5-day cultured control or CM-generated DC were stimulated with LPS (10 ng/ml) for 24 h to obtain mature cells. Mature DC were washed twice in serum-free RPMI and co-cultured with freshly isolated allogeneic naive $CD4^+$ T lymphocytes (1:10 ratio), in a mixed leukocyte reaction assay, for 12 days in RPMI plus 5% human AB serum. IL-2 (50 U/ml) was added to the co-cultures at day 6. Lymphocytes were then harvested, counted, seeded in fresh medium and stimulated with PMA (50 ng/ml) and Ionomycin (1 µg/ml). 18 h later, culture medium was collected for IFNγ content determination.

Ethics Statement

Healthy donor buffy coats were obtained from Centro Trasfusionale, Sapienza University of Rome. Buffy coats were not obtained specifically for this study. Informed consent was asked to blood donors according to the Italian law n. 219 (October 21, 2005), recently revised (D.L. of the Ministry of Health, November 2, 2015). Data have been treated by Centro Trasfusionale according to the Italian law on personal data management "Codice in materia di protezione dei dati personali" (Testo unico D.L. June 30, 2003 n. 196).

Investigation including IBD patients has been conducted in accordance with the Declaration of Helsinki and, according to national and international guidelines. The study was approved by the review board of Istituto Superiore di Sanità (project identification code: CE/11/299). All the subjects included were provided with complete information about the study and asked to sign an informed consent.

Patients and Biological Samples

Endoscopic biopsies, taken from colon/ileum tissue, were obtained from patients with documented Crohn's disease (CD, $n = 8$) or age and sex matched healthy controls (HC, $n = 8$, undergoing screening colonoscopy), attending to the Digestive Endoscopy Unit (Catholic University, Rome, Italy). The exclusion criteria were: clinical evidence of active infection, recent (within 14 days) use of antibiotics, pregnancy, hormone-based therapy, and treatment with corticosteroids. Endoscopic activity was assessed according to the Crohn's Disease Endoscopic Index of Severity (remission when score <3) (20). Biopsies were kept in ice-cold PBS containing penicillin, streptomycin (50 IU/ml) and gentamycin (0.5 mg/ml) (Transport Medium, TM) before enterocyte isolation.

Isolation of Primary IEC

IEC were isolated from whole biopsies as previously described (21). Briefly, biopsies were extensively washed by shaking in TM,

and then incubated in TM containing EDTA and EGTA (1 mM) for 75 min at 21°C under soft stirring. Intestinal crypts were then allowed to detach from mucosa by vigorous shaking and cultured ON in RPMI plus 10% FBS. CM was collected, filtered, and stored at −80°C.

Determination of Soluble Immune Mediators

Caco-2 CM as well as supernatants from control and CM-generated DC, γδ T lymphocytes, and DC-T cell co-cultures were analyzed by ELISA for their content of CCL2, IL-10, PGE_2 (R&D Systems Inc., Minneapolis, MN, USA), IL-1β, IL-6, IL-12, TNFα, and IFNγ (Biolegend, San Diego, CA, USA), according to the manufacturer's instructions.

Flow Cytometry Analysis

The expression of surface markers was analyzed by flow cytometry. Briefly, cells were pre-incubated for 30 min on ice with PBS containing 10% human AB serum to block non-specific Ig binding and then incubated with the specific Abs or control isotypes for 30 min on ice, washed, and analyzed. The following Abs were used: FITC- or APC-conjugated CD14 (BD Pharmigen or eBiosciences, respectively), PE-CD1a, PE-CD206/MR, PE-CD209/DC-SIGN (BD Pharmigen), and FITC-CD16 (eBiosciences). At least 10,000 events/sample were acquired by a FACScan cytometer (BD Biosciences). Data analysis was performed by gating on the monocyte/DC populations and excluding death cells and debris.

Immunoblotting Analysis

Whole cell extracts were prepared by lysing cells in RIPA buffer [150 mM NaCl, 50 mM Tris–Cl (pH 7.5), 1% Nonidet P-40, 0.5% sodium deoxycholate, and 0.1% sodium dodecyl sulfate (SDS)] containing a cocktail of protease (Roche) and phosphatase inhibitors (Sigma-Aldrich). Cell lysates (10 μg per lane) were fractionated on 8% SDS-PAGE, transferred to a nitrocellulose membrane, and subjected to immunoblot analysis using antibodies specific for the total or tyrosine phosphorylated forms of STAT3 (Cell Signaling Technology). Equal loading of proteins was verified by blotting the same gel with antibodies to β-actin (BD Biosciences).

Real-time PCR

Total RNA was isolated from 21-day cultured polarized Caco-2 cell monolayer or freshly isolated blood monocytes and γδ T lymphocytes with Total RNA Purification Plus Kit (Norgen Biotek, Canada). RNA quality was checked on an Agilent 2100 Bioanalyzer and reverse transcribed (SuperScript™ III, ThermoFisher). Glucuronidase beta (GUSB) was used as reference gene. Primers for TLR7 (Hs.PT.58.38778009), TLR8 (Hs.PT.58.15023918.G), and GUSB (Hs.PT.39a.22214857) were purchased from Integrated DNA technologies. mRNA levels were quantified by qPCR on a QuantStudio™ 12K Flex OpenArray® (Applied Biosystems) by using the comparative $\Delta\Delta C_t$ method.

Statistical Analysis

GraphPad Prism 5 software was used for statistical analysis. Statistical comparisons were performed by the one-way analysis of variance, with Newman–Keuls *post hoc* test, for multiple groups and by the two-tailed paired Student's *t*-test for independent samples, as appropriate. Differences were considered significant when p values were <0.05.

RESULTS

R848-Conditioned IEC Affect the Differentiation of Monocyte-Derived DC and Their Capacity to Stimulate Th1 Type Responses

To assess whether TLR7/8 triggering in intestinal epithelium may transduce signals ultimately affecting the functional properties of innate immunity cells, we analyzed the effects of polarized Caco-2 cell monolayer, stimulated with R848, on the differentiation of human monocytes toward DC. Polarized IEC monolayer was left untreated or stimulated, at the AS, with R848. Human peripheral blood monocytes were induced to differentiate toward DC in the presence of control medium or CM from unstimulated or TLR-stimulated Caco-2 cells. As shown in **Figures 1A,B**, a significant proportion of monocytes exposed to CM from R848-conditioned IEC monolayer (R848 CM) did not express the DC-specific marker CD1a and retained the expression of CD14 as compared to cultures exposed to standard medium, indicative of impaired DC differentiation. Conversely, only a slight reduction in CD1a expression was detected when DC were generated in the presence of control CM (**Figures 1A,B**). Likewise, DC differentiation was not affected when monocytes were exposed to CM from Caco-2 cells stimulated with β-glucan, an immunomodulatory compound endowed with adjuvant properties, which recognizes a different family of pattern recognition receptor (PRR) (**Figures 1A,B**).

Despite the negative effect exerted by R848 CM on monocyte to DC differentiation, cells generated under these conditions expressed levels of mannose receptor (MR) and DC-SIGN comparable, or even higher, to those of cells cultured in standard medium (**Figure 1C**; MR: 98% ± 7.3 vs. 96.7% ± 6.0; DC-SIGN: 97% ± 4.9 vs. 96% ± 6.4; $n = 4$).

By contrast, when DC cultures obtained under the different conditions were analyzed for cytokine expression, significant changes in the profile of cytokines constitutively released were observed. As shown in **Figure 2A**, cells generated in R848 CM expressed higher levels of both pro-inflammatory (IL-1β, TNFα) and regulatory (IL-6, IL-10) cytokines as compared to cultures generated in control CM and standard medium, suggesting that a heterogeneous population of cells differentiated from R848 CM-stimulated monocytes.

To further investigate the nature of these cells, we analyzed the levels of phosphorylated STAT3, whose activation is induced by both IL-6 and IL-10 and has been reported in cells with regulatory/tolerogenic features. As expected, constitutive STAT3 activation was found in R848 CM-generated cells but

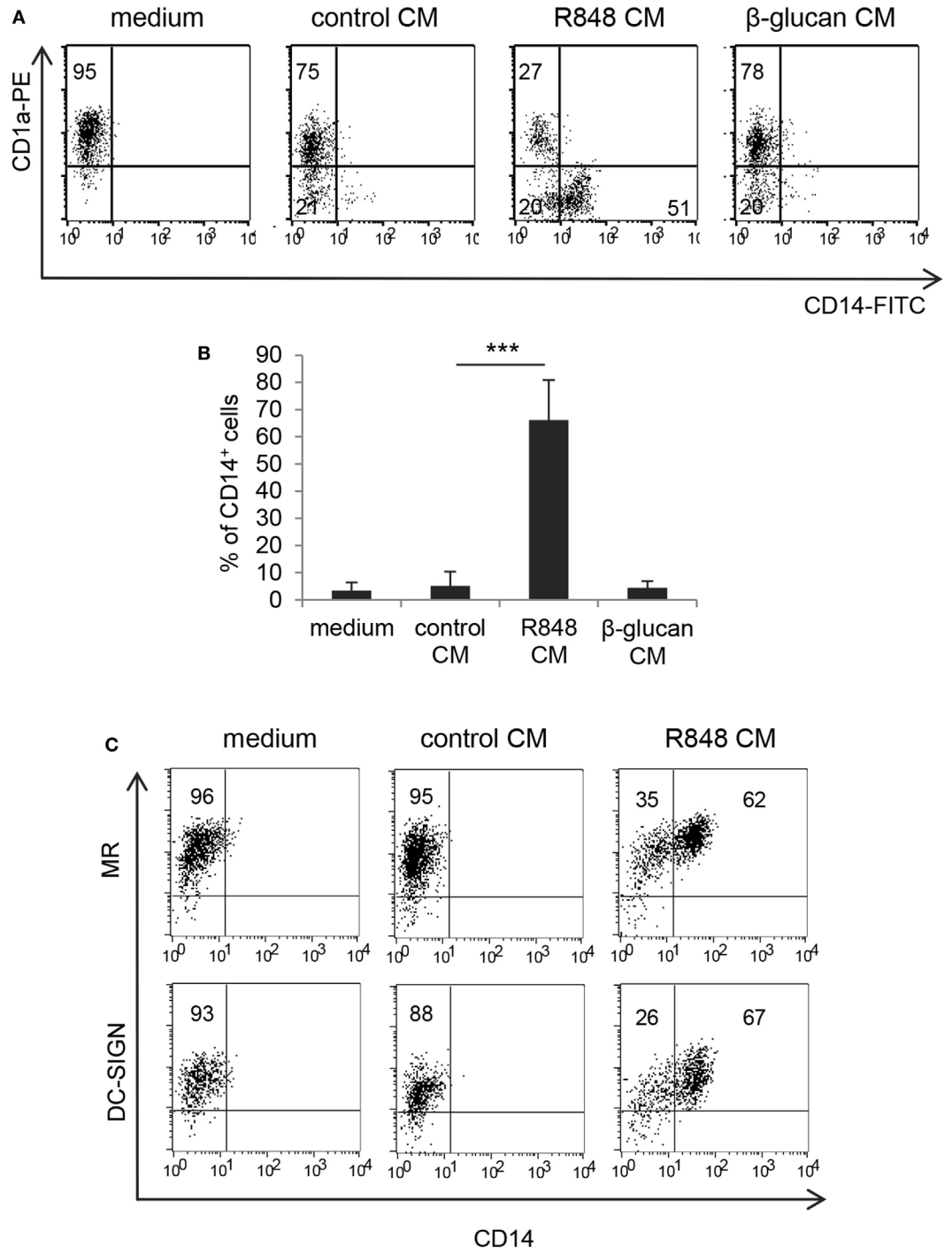

FIGURE 1 | Effects of R848-exposed intestinal epithelial cell (IEC) monolayer on dendritic cell (DC) differentiation. Peripheral blood monocytes were induced to differentiate toward DC in standard medium or in conditioned medium (CM) from Caco-2 cell-derived IEC monolayer, left untreated or stimulated with R848 **(A–C)** or β-glucan **(A,B)**. At day 5, cells were harvested and analyzed for the expression of the indicated surface markers by flow cytometry. One representative experiment out of 4 is reported in panels **(A,C)**. Numbers in quadrants indicate the percentages of positive cells. The percentage of $CD14^+$ cells is reported in panel **(B)**, mean values ± SD from 10 independent experiments are shown. $^{***}p < 0.001$.

not in cells differentiated in standard medium or control CM (**Figure 2B**). Accordingly, R848 CM-generated cells were found to impair IFNγ production in co-cultured $CD4^+$ T lymphocytes (**Figure 2C**), whereas no effect was observed on the production of IL-17 (data not shown). In line with the effect on Th1 cytokine production, a reduced secretion of the Th1-polarizing

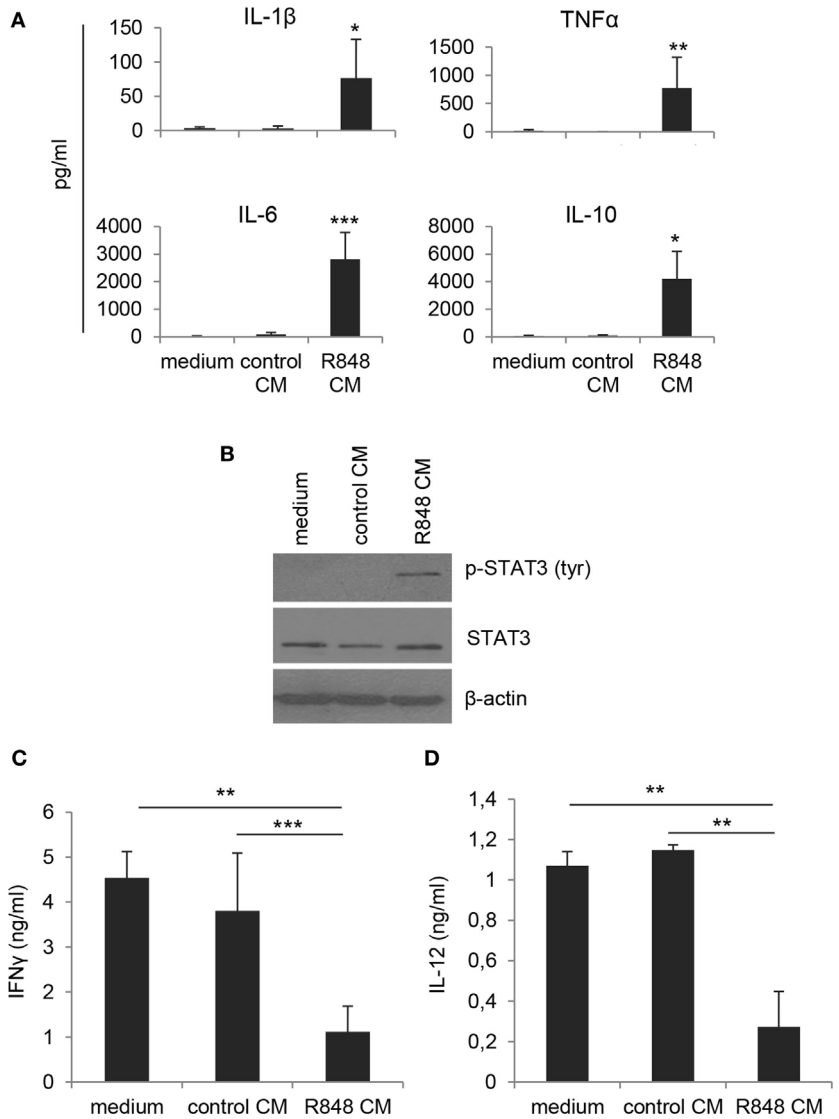

FIGURE 2 | Effects of R848-exposed IEC monolayer on DC functional properties. Monocyte-derived DC were generated as described in the legend to **Figure 1** and harvested at day 5 of culture. **(A)** Cell supernatants were analyzed for the release of the indicated cytokines by ELISA. Mean values ± SD from five independent experiments are shown. Comparisons with control CM are reported. **(B)** Western blot analysis of phospho-STAT3 (pSTAT3), total STAT3, and β-actin was performed on protein extracts. A representative blot out of four independent experiments analyzed is shown. **(C)** Cells cultured as in panels **(A,B)** were stimulated with LPS for 24 h and then co-cultured with allogeneic naive $CD4^+$ T lymphocytes (1:10 ratio). After 18 h stimulation with PMA and ionomycin, supernatants were collected and analyzed for IFNγ content. Data are shown as mean values ± SD from four independent experiments. **(D)** LPS-stimulated DC cultures were analyzed for IL-12 production by ELISA. Mean values ± SD from three independent experiments are shown. $^*p < 0.05$; $^{**}p < 0.01$; $^{***}p < 0.001$.

cytokine IL-12 was also detected in R848 CM DC-T cell co-cultures (**Figure 2D**).

Apical Exposure of Polarized Caco-2 Cells to R848 Results in Agonist Transport across the Epithelial Cell Monolayer

Given the highly hydrophobic nature and the small molecular weight of R848, as well as the rapid systemic effects observed in *in vivo* studies following its oral or intracolonic delivery, we therefore investigated whether treatment of polarized Caco-2 cells could result in agonist transport across the monolayer. To this aim, Caco-2 cell monolayer was exposed, at its AS, to R848 and CM from the BS was collected at 0.5, 2, 5, and 24 h and subject to HPLC analysis. A chromatogram of CM spiked with 5 μg/ml of R848 is shown in **Figure 3A**. A significant proportion of apically loaded R848 was found to be transported to the BS chambers already after 30 min of exposure and this proportion increased overtime, reaching more than 40% of transport at

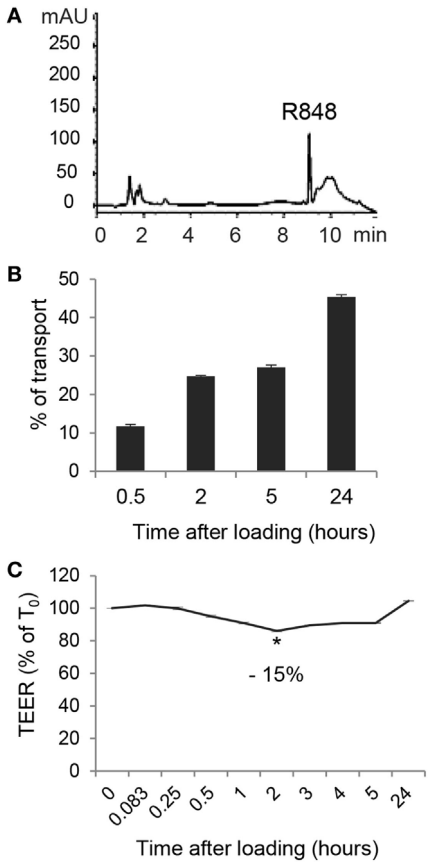

FIGURE 3 | Transport of R848 across intestinal epithelium and effect on epithelium permeability. **(A)** HPLC chromatogram of CM spiked with 5 μg/ml of R848. **(B)** R848 (5 μg/ml) was loaded to the epithelial cell monolayer apical side (AS) and, at the indicated time points, CM from the basolateral side were collected and analyzed by HPLC for agonist content. Total percent agonist transport was calculated by dividing the cumulative amount of molecule transported with the original loading concentrations. Data are expressed as mean values ± SD of triplicate samples and one representative experiment out of three is shown. **(C)** R848 (5 μg/ml) was loaded to the AS and transepithelial electrical resistance (TEER) was monitored before loading (time 0, T0) and at the indicated time points. Data are expressed as percentage of T0. Mean values ± SD of triplicate samples of one representative experiment out of three are shown. The contrast has been adjusted in the entire panel **(A)** to enhance resolution.

24 h (**Figure 3B**). To evaluate whether R848 transport could be somehow related to agonist-induced alteration of epithelial permeability, TEER was monitored before agonist loading and at different time points during treatment. As shown in **Figure 3C**, a 15% drop in TEER values was observed at 2 h post-treatment, but recovered soon after, suggesting that some reversible R848-induced perturbation of monolayer permeability could also contribute to its transport. Dose-response experiments were then performed in which Caco-2 cell monolayer was apically exposed to different R848 concentrations for 5 h and the apparent permeability was calculated (18, 22). The permeability coefficients obtained (P_{app} = 4.52 ± 0.8 × 10^{-6}, 3.5 ± 1.7 × 10^{-6}, and 3.2 ± 1.8 × 10^{-6} cm/s, with 1, 2, and 5 μg/ml apical loading, respectively) were compatible with complete agonist adsorption.

R848 CM-Induced Impairment of DC Differentiation/Activation Results from TLR8-Mediated Direct Stimulation of Monocytes by the Transported Agonist

Based on the finding that R848 is transported through IEC monolayer, we then investigated whether the effects observed with IEC CM could be reproduced after direct stimulation of immune cells by R848 or whether they required epithelial cell response to the agonist. To this aim, the exact concentration of R848 released in the BS CM at the different time points was calculated. A significant effect on the percentage of $CD14^+$ cells was only observed when CM from Caco-2 cells exposed for 24 h to 5 μg/ml of R848 was used (1 ± 0.15 μg/ml of agonist released), whereas only barely detectable changes were appreciated when CM derived from cells exposed for shorter times or lower concentrations were used (data not shown). Thus, monocytes were directly exposed to a comparable concentration of R848 (1 μg/ml) and induced to differentiate toward DC. As shown in **Figures 4A,B**, direct agonist treatment of monocytes resulted in reduced DC differentiation, as demonstrated by the high proportion of $CD14^+CD1a^-$ cells found in these cultures as compared to control cultures. The effect of the direct stimulation with the agonist on DC differentiation was comparable to that of R848 CM (**Figure 1A**). Furthermore, as observed for R848 CM-generated DC, cells differentiated following direct exposure to R848 upregulated the expression of MR and DC-SIGN and exhibited constitutive cytokine expression (data not shown). Conversely, while β-glucan CM did not exert any effect on DC differentiation (**Figure 1A**), the exogenous addition of this compound to monocytes resulted in a strong enrichment of CD14/CD1a double negative cells with respect to untreated control cultures (**Figures 4A,B**), in keeping with previously reported data (23). The biochemical properties of β-glucan might influence its transport through epithelial cells thus providing an explanation for the divergent effect of this compound with respect to R848.

As a further evidence that the effect of R848-conditioned epithelial cells on DC differentiation is dependent on the agonist released in CM, and to investigate the relative contribution of TLR7 and TLR8 to this effect, monocytes were cultured in R848 CM after pre-exposure to phosphorothioate ODN targeting TLR7/8/9 (#2088) or TLR7 (#20958). An almost complete recovery of $CD14^-CD1a^+$ DC was obtained only in the presence of the TLR7/8/9 targeting ODN, whereas the TLR7-specific ODN did not exert any significant effect (**Figures 4C,D**), thus suggesting a selective role of TLR8. In keeping with these results, monocytes were found to express significantly higher levels of TLR8 with respect to TLR7 (Figure S1 in Supplementary Material). The selective requirement of TLR8 stimulation was also confirmed in experiments in which DC differentiation was induced following monocyte exposure to the TLR7 specific ligand CL264 (**Figures 4E,F**).

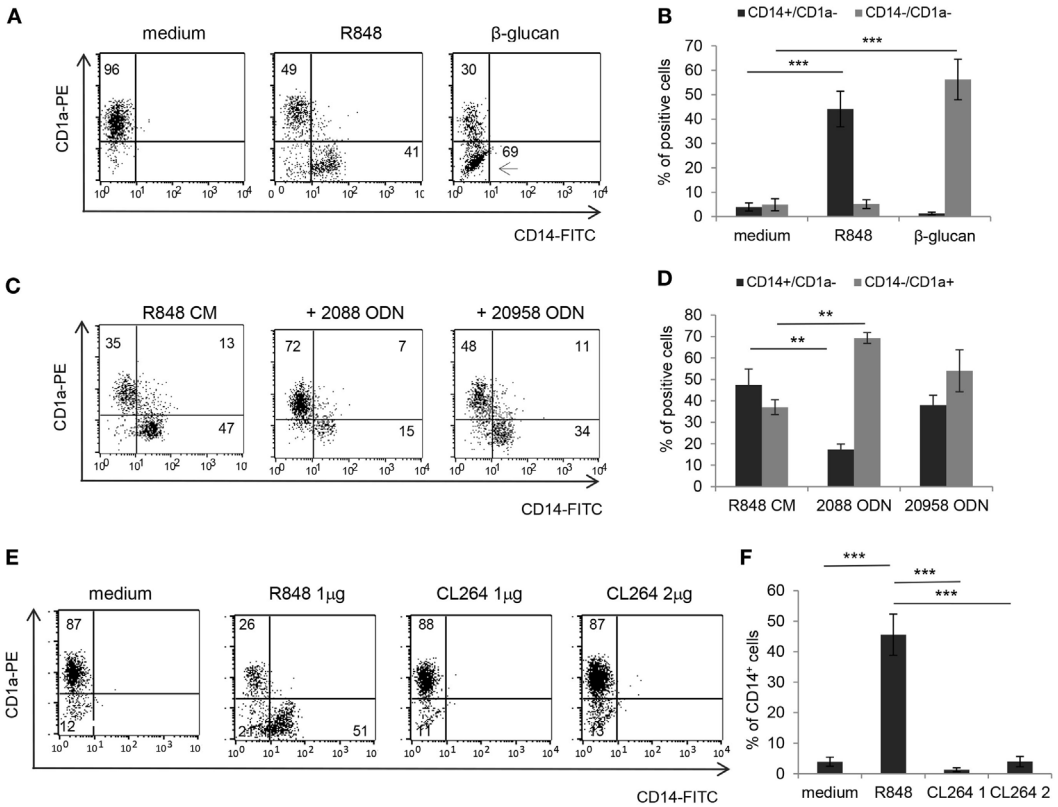

FIGURE 4 | Effects of direct R848 and CL264 stimulation of monocytes on CD14 and CD1a expression and role of TLR8. **(A,B)** Monocytes were induced to differentiate toward DC for 5 days in standard medium in the presence or in the absence of the indicated pattern recognition receptor ligands and analyzed for the expression of CD14 and CD1a by flow cytometry. One representative experiment out of five is shown in panel **(A)**. The percentages of $CD14^+CD1a^-$ and $CD14^-CD1a^-$ cells recovered is reported in panel **(B)**, mean values ± SD from five independent experiments are shown. **(C,D)** Monocytes were exposed to R848 treated Caco-2 CM and induced to differentiate toward DC following pre-incubation with TLR7/8/9 (2088) or TLR7 (20958) targeting ODN. CD14 and CD1a expression was analyzed at day 5 by flow cytometry. One representative experiment out of three is shown in panel **(C)**. The percentages of $CD14^+CD1a^-$ and $CD14^-CD1a^+$ cells obtained is reported in panel **(D)**, mean values ± SD from three independent experiments are shown. **(E,F)** Monocytes were induced to differentiate toward DC for 5 days in standard medium in the presence of R848 (1 μg/ml) or CL264 (1 or 2 μg/ml) and analyzed for CD14 and CD1a expression as in panels **(A–D)**. One representative experiment out of four is shown in panel **(E)**. The percentages of $CD14^+$ cells obtained is reported in panel **(F)** as mean values ± SD from four independent experiments. Numbers in quadrants indicate the percentages of positive cells. $^{**}p < 0.01$; $^{***}p < 0.001$.

R848-Conditioned Epithelial Cell Monolayer, but Not Direct R848 Exposure of Monocytes, Drives the Accumulation of the $CD14^+CD16^+$ Subpopulation: Role of Epithelial Cell-Derived CCL2

It has been reported that R848 injection in non-human primates results in a decrease of blood myeloid DC and concomitant enrichment of the $CD14^+CD16^+$ monocyte subpopulation, known to be associated with several inflammatory conditions (24, 25). To investigate whether R848 conditioning of IEC monolayer could affect the monocyte subset distribution, monocyte cultures exposed for 5 days to control or R848 CM were analyzed for the expression of CD14 and CD16. **Figures 5A,B** show that a proportion of the $CD14^+$ cells obtained upon monocyte exposure to R848 CM (see **Figure 1A**) indeed co-expressed CD16. As expected, cells cultured in control CM or standard medium neither expressed CD14 nor CD16 (**Figures 5A,B**). A donor-dependent variable percentage (3.1–9.8%) of CD14/CD16 double positive cells was present in the starting population of freshly isolated $CD14^+$ monocytes.

To analyze whether direct agonist exposure of monocytes could be responsible for the induction of $CD14^+CD16^+$ cells, parallel monocyte cultures were exogenously stimulated with R848 and checked for the appearance of double positive cells. In contrast to what observed with R848 CM, when monocytes were directly exposed to a comparable (1 μg/ml, **Figures 5A,B**) or even higher (up to 4 μg/ml, data not shown) concentration of the agonist, the population of CD14/CD16 double positive cells was no longer identified. Experiments with the TLR7/8 targeting ODN further confirmed that R848 CM-induced enrichment of this subset was driven by the epithelium microenvironment and not by direct stimulation of monocytes with the agonist transported across the epithelial cell monolayer (**Figure 5C**). Specifically, the addition of TLR7/8/9 ODN to monocytes completely reduced the proportion of $CD14^+CD16^-$ cells recovered (**Figure 5C**; 2.5 ± 1.7 vs.

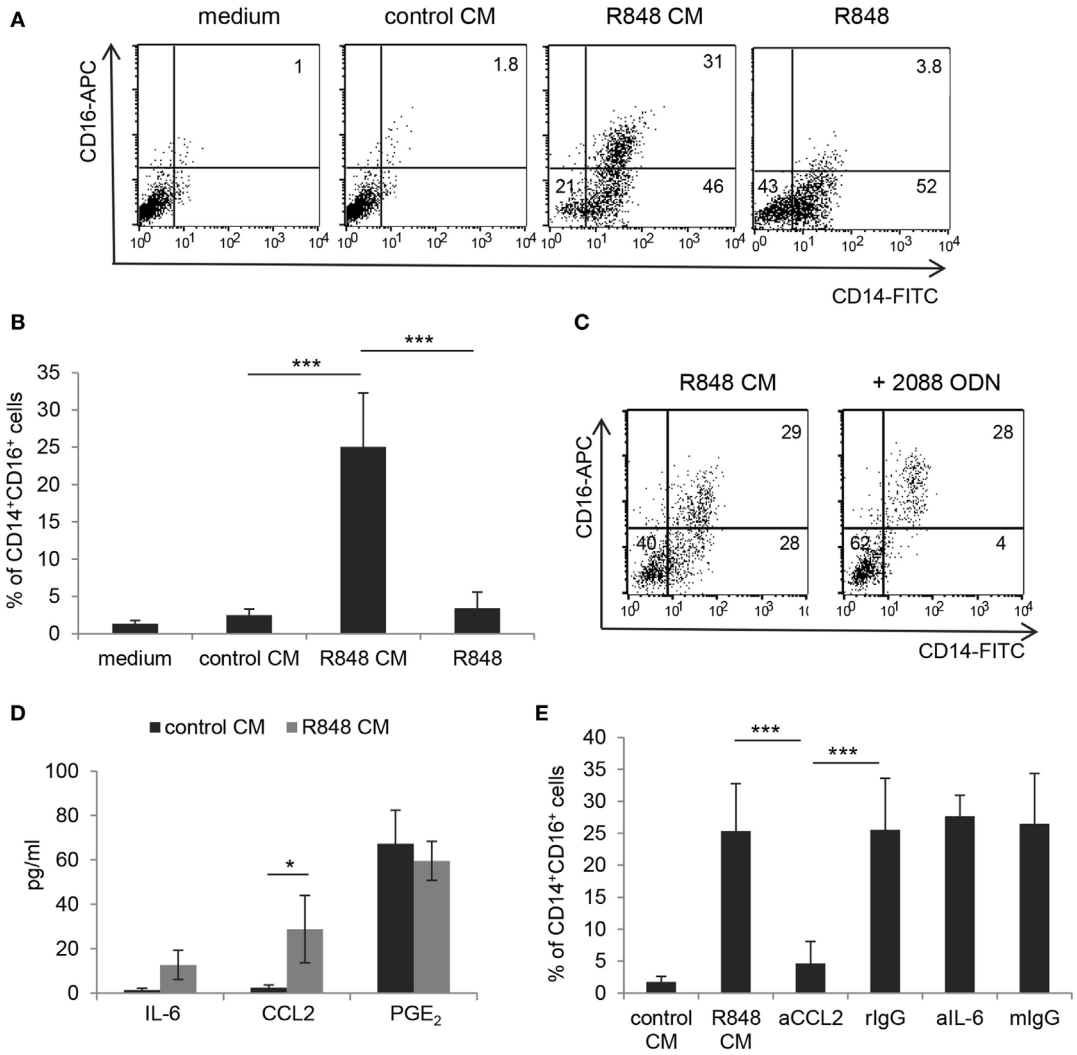

FIGURE 5 | Selective induction of CD14⁺CD16⁺ cell enrichment by R848-conditioned epithelium microenvironment and role of CCL2. **(A,B)** Monocytes were induced to differentiate toward DC by culture either in standard medium, in the presence or in the absence of R848, or in control or R848 Caco-2 CM. At day 5, cultures were analyzed for the expression of the indicated surface markers by flow cytometry. **(C)** Monocytes were cultured in R848 Caco-2 CM following pre-incubation with TLR7/8/9 targeting ODN and analyzed as in panels **(A,B)**. **(D)** Polarized Caco-2 cell monolayer was left untreated or stimulated with R848 for 24 h. CM was collected and assessed for the secretion of the indicated immune mediators. **(E)** Monocytes were exposed for 5 days to control or R848 CM, left untreated or pre-incubated with neutralizing Ab to the indicated cytokines or with isotype control Ab, and analyzed as in panels **(A,C)**. aCCL2/aIL-6 (anti-CCL2 Ab/anti-IL-6 Ab), rIgG (rabbit polyclonal IgG), and mIgG (mouse monoclonal IgG). Numbers in quadrants **(A,C)** indicate the percentages of single and double positive cells. Mean values ± SD from five, five, and four independent experiments are shown in panels **(B,D,E)**, respectively. *$p < 0.05$; ***$p < 0.001$.

35 ± 9.5%, $n = 3$, $p < 0.001$) without affecting that of the CD14/CD16 double positive cells (**Figure 5C**; 25 ± 8.7 vs. 28 ± 7.53%, $n = 3$, $p < 0.001$). No effect was exerted on this latter cell population by the TLR7-specific ODN as well (data not shown).

Notably, when monocytes were exposed to CM from Caco-2 cells stimulated with the TLR7 selective agonist CL264, the CD14⁺CD16⁺ cell enrichment was no longer observed [1.83 ± 0.9% (CL264 CM) vs. 28 ± 7.53% (R848 CM), $n = 3$, $p < 0.001$]. This suggested that the accumulation of this monocyte subpopulation induced by R848 CM requires TLR8 recognition on IEC. Accordingly, TLR8 was found to be expressed at higher levels with respect to TLR7 in Caco-2 cell monolayer (Figure S1 in Supplementary Material).

To the aim of identifying the soluble factor(s) released by R848-stimulated Caco-2 cell monolayer that could be responsible for CD14⁺CD16⁺ cell enrichment, we focused on pro-inflammatory mediators relevant for intestinal inflammation, such as IL-6, CCL2, and PGE_2. As shown in **Figure 5D**, the expression of CCL2, but not of IL-6, was significantly induced in R848-stimulated Caco-2 cell cultures as compared to unstimulated cultures. Conversely, comparable levels of PGE_2 were found in both untreated and R848-exposed epithelial cells (**Figure 5D**).

Based on this evidence, monocytes were then induced to differentiate into DC in the presence of R848 CM previously incubated with neutralizing antibodies to CCL2 or IL-6. The results of this analysis showed that CCL2 but not IL-6 blocking almost completely abolished the appearance of the $CD14^+CD16^+$ cell population (**Figure 5E**). The possible role of type I IFN was also investigated, but neutralizing Ab to these cytokines failed to affect monocyte phenotype (data not shown).

Epithelial Cell Microenvironment Impairs DC-γδ T Cell Crosstalk Independently of R848 Conditioning

In light of the negative effect on $CD4^+$ T cell-mediated IFNγ production exerted by DC generated in R848 CM (**Figure 2C**), we further analyzed the impact of these cells on the activation of γδ T lymphocytes. We previously reported that aminobiphosphonate-induced activation of γδ T cells requires the presence of DC (19). Thus, DC generated in the presence of control or R848 Caco-2 CM were co-cultured with ZOL-stimulated autologous γδ T lymphocytes, and lymphocyte activation was assessed by measuring IFNγ secretion. As shown in **Figure 6**, DC generated in Caco-2 CM, regardless of R848 stimulation, exhibited a significantly reduced capacity to activate γδ T lymphocytes, as assessed by the lower levels of IFNγ released in the co-culture medium with respect to that of control DC generated in standard medium. This suggests that signals delivered by intestinal epithelium in homeostatic conditions may negatively regulate the DC/γδ T cell cross-talk and that R848 exposure neither potentiates nor counteracts this immunosuppressive microenvironment.

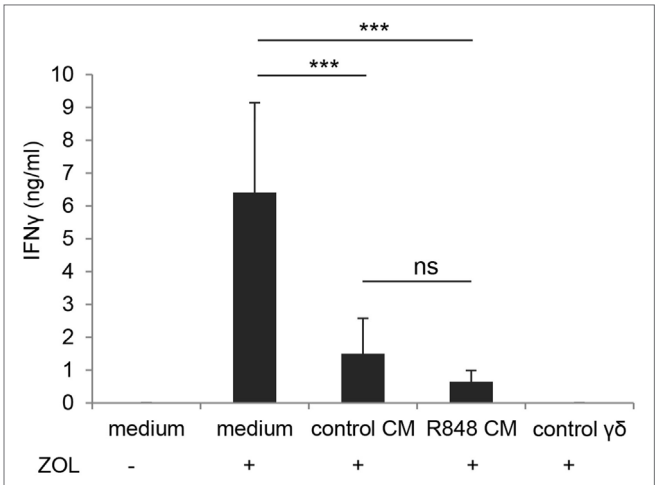

FIGURE 6 | Effect of epithelial cell microenvironment on DC-mediated activation of γδ T lymphocytes. DC generated in standard medium or in control or R848 Caco-2 CM were co-cultured with autologous γδ T lymphocytes (1:1 ratio) for 48 h in the presence (+) or in the absence (–) of zoledronate (ZOL). Co-culture medium was collected and analyzed for IFNγ content. ZOL-stimulated γδ T cells were used as a control. Data are expressed as mean values ± SD from five independent experiments. $^{***}p < 0.001$.

R848 CM and Direct R848 Exposure Potentiate Phosphoantigen-Induced Activation of γδ T Lymphocytes *via* TLR8

In order to evaluate the effect of R848-conditioned epithelial cells on the direct, DC-independent activation of γδ T cells, purified γδ T lymphocytes were stimulated with the non-peptide phosphoantigen IPP in the presence of control or R848 CM and analyzed for IFNγ secretion. As shown in **Figure 7A**, direct γδ T cell activation was not affected by their exposure to CM from unstimulated epithelial cell monolayer as comparable levels of IFNγ were released by cells cultured in control CM and standard medium. In contrast, lymphocytes cultured in R848 CM expressed significantly higher levels of this cytokine (**Figure 7A**), indicating that agonist stimulation may provide a suitable microenvironment sustaining their activation.

Based on previously reported data (26) as well as on our results (Figure S1 in Supplementary Material), showing that human circulating γδ T lymphocytes express both TLR7 and TLR8, we then assessed whether the effect of R848 CM on γδ T cell activation was due to their direct exposure to the released agonist. Thus, purified blood γδ T cell cultures were kept in standard medium and simultaneously stimulated with IPP and R848. As shown in **Figure 7B**, the agonist was *per se* able to significantly increase TCR-mediated IFNγ production at concentrations comparable to those found in Caco-2 CM, thus demonstrating that R848 transported across Caco-2 cell monolayer is responsible for γδ T lymphocyte hyper-activation. According to the higher IFNγ release, an increased proportion of CD25-positive cells was observed in γδ T cell cultures exposed to both R848 and R848 CM (data not shown).

To further investigate the relative contribution of TLR7 and TLR8 to the R848-mediated effect on γδ T lymphocytes, these cells were exposed to comparable concentrations of the TLR7 specific ligand CL264. As shown in **Figure 7C**, stimulation of lymphocytes with the TLR7 agonist did not increase IPP-induced IFNγ production, thus pointing to TLR8 as the main mediator of R848 effect. Accordingly, TLR8 was expressed at higher levels with respect to TLR7 in these cells (Figure S1 in Supplementary Material).

TLR-Mediated Activation of γδ T Lymphocytes Is Promoted by Inflamed Intestinal Epithelium from Active CD Patients

Based on our findings and data from the literature showing an increased number of activated Vδ2 T cells in intestinal mucosa from CD patients (27), we sought to investigate whether TLR/PRR activating structures likely present in inflamed intestinal microenvironment could affect the activation potential of γδ T cells. To this aim, blood γδ T lymphocytes from healthy donors were stimulated with IPP in the presence of CM of IEC, isolated from colonic biopsies of either subjects with endoscopically active CD or sex/age matched HC. As shown in **Figure 8A**, IPP-induced activation, as assessed by IFNγ production, was significantly enhanced when γδ T lymphocytes were exposed to CM of IEC from active CD patients as compared to control

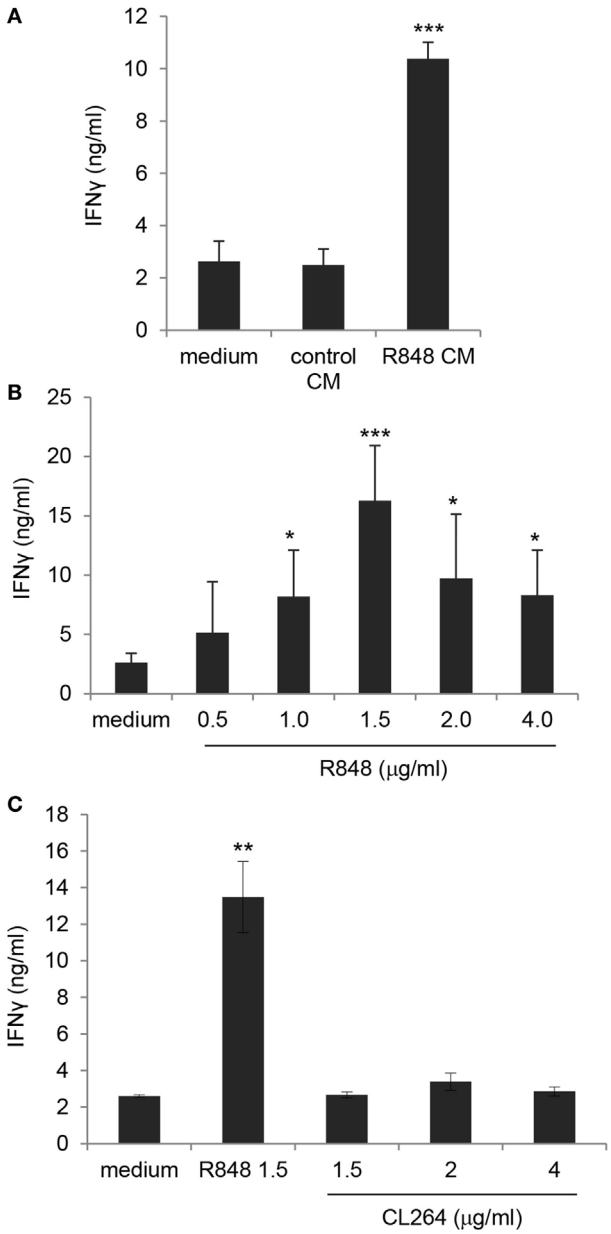

FIGURE 7 | Enhancement of γδ T lymphocyte activation by direct exposure to R848 and role of TLR8. **(A)** Positively selected blood γδ T lymphocytes were stimulated with isopentenilpyrophosphate (IPP) in the presence of standard medium or in control or R848 Caco-2 CM, and analyzed 48 h later for IFNγ production. **(B,C)** γδ T cells were stimulated with IPP in standard medium in the absence or in the presence of the indicated concentrations of R848 or CL264, and analyzed as in panel **(A)**. Data are expressed as mean values ± SD from five **(A,B)** and four **(C)** independent donors. Comparisons with medium and control CM **(A)**, with medium **(B)** and with medium and CL264 **(C)** are reported. *$p < 0.05$; **$p < 0.01$; ***$p < 0.001$.

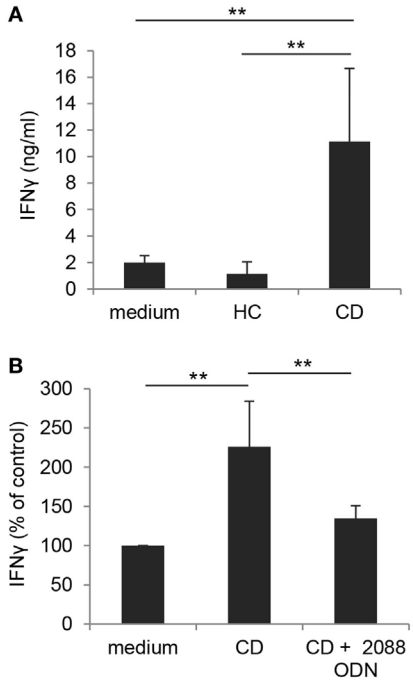

FIGURE 8 | Toll-like receptor-mediated enhancement of γδ T lymphocyte activation by CM of IEC from active Crohn's disease (CD) patients. **(A)** γδ T lymphocytes, isolated from healthy donors, were exposed to medium or to CM of IEC collected from either active CD patients or HC, stimulated with IPP and analyzed 48 h later for IFNγ production. Mean values ± SD are shown, $n = 8$. **(B)** Control γδ T lymphocytes, isolated as in panel **(A)**, were exposed to CM of IEC from active CD patients, stimulated with IPP in the presence or absence of TLR7/8/9 targeting ODN (2088), and analyzed as in panel **(A)**. Data are expressed as percentage of cytokine release relative to control medium. Mean values ± SD are shown, $n = 6$. **$p < 0.01$.

medium. Conversely, CM of IEC from HC did not significantly affect IFNγ release (**Figure 8A**). Interestingly, a significant reduction in CD CM-induced γδ T cell activation was observed when these cells were stimulated with IPP in the presence of TLR7/8/9 targeting ODN (**Figure 8B**), thus suggesting the presence of TLR targeting T cell co-activating structures in the microenvironment of patient inflamed epithelium.

DISCUSSION

The TLR7/8 agonist R848 has been extensively studied for its adjuvant activity and its effects on immune responses following either topic or oral administration. The main adjuvant activity has been so far attributed to its capacity to induce the production of immune mediators and the activation of DC, thereby leading to the enhancement of both humoral and cellular immune responses. Moreover, data from the literature suggest that most of the responses induced by oral or topic R848 delivery likely result from agonist diffusion within tissues and in the circulation thus leading to direct immune cell stimulation. The results of this study not only expand the range of cellular targets and immune responses influenced by R848 but also provide novel evidence that some of these responses might require the cooperation of agonist-conditioned tissues, such as the intestinal epithelium, thus highlighting the importance of local microenvironment in shaping immune responses.

Specifically, we demonstrate herein that R848 is easily transported across the Caco-2 cell-derived polarized IEC monolayer, showing permeability coefficients typical of completely adsorbed drugs. Consistent with our finding, previous studies performed in mice orally injected with the agonist had suggested that this molecule could easily cross the gut mucosa (14, 15). Furthermore, it was reported that, following intracolonic administration of R848 in mice, a systemic inflammatory response was induced in the absence of epithelium disruption, consistent with a rapid penetration of R848 across the intestinal wall into the draining lymphatic system (28). As a further evidence, topical R848 application was found to confer robust resistance to mice against intravenous challenge with virulent *Leishmania* strains, in keeping with a rapid and efficient transfer of the agonist into the underlying tissues and into the circulation, responsible for systemic immunization (29).

Our results also unravel the effects of TLR8 stimulation of IEC on the phenotype/function of innate immunity cells. Specifically, we report for the first time that apical exposure of polarized Caco-2 cell monolayer to R848 drives the enrichment of the inflammatory $CD14^+CD16^+$ monocyte subpopulation by inducing the production of CCL2 by epithelial cells. In keeping with this finding, data previously obtained *in vivo* in non-human primates (25) highlighted that R848 injection leads to a decrease of myeloid DC number in the blood and a concomitant enrichment of $CD14^+CD16^+$ cells, likely due to the induction of pro-inflammatory cytokines/chemokines. Interestingly, it has been shown that *in vitro* exposure of human monocytes to CCL2 results in the enrichment of the $CD14^+CD16^+$ cell subset and that this chemokine is responsible for inflammatory monocyte accumulation induced by breast cancer cell microenvironment (30). Accordingly, we demonstrate that R848-induced CCL2 in polarized Caco-2 cell monolayer strongly contributes to the accumulation of CD14/CD16 double positive cells, whereas no effect is exerted by IL-6 or type I IFN. As a further evidence that the induction of this cell population is dependent on IEC response to R848, we show that it does not occur following direct exposure of monocytes to the agonist. In this regard, although R848 was shown to regulate the expression and function of different Fcγ receptor members, with both activating and inhibitory functions, no direct effect was reported on the expression of CD16/FcγRIII (31). The enrichment of the $CD14^+CD16^+$ cell population, previously associated with chronic inflammatory conditions (32), at mucosa level might contribute to the strong inflammatory reactions that characterize R848 activity in exposed animals.

We also report that R848, either transported through the IEC monolayer or directly administered to freshly isolated γδ T cells, enhances the phosphoantigen-induced activation of these innate lymphocytes. Specifically, significantly higher levels of IFNγ are produced when the γδ TCR is triggered in the presence of R848. Although it has been shown that human γδ T lymphocytes express different TLR, including TLR7 and TLR8, to the best of our knowledge this is the first demonstration that TLR7/8 ligands can potentiate their activation. Furthermore, the selective requirement of TLR8 for this effect was also shown. Additionally, our results indicate that, at tissue level, the mechanisms of γδ T cell activation can be more complex and finely regulated. In fact we show that, although R848 transported across the IEC monolayer exerts a promoting effect on phosphoantigen-induced direct activation of γδ T lymphocytes, it does not counteract the negative control exerted by IEC microenvironment on the DC-dependent activation of these cells. This suggests that tissue microenvironment may regulate the balance between activating and inhibitory factors and ultimately dictate the type of response. In keeping with this hypothesis, and with results from other groups (33, 34), we report that this compound exerts immunosuppressive activities such as the inhibition of DC differentiation and of Th1 type response generation.

Overall, the enhancing effect of R848 on γδ T lymphocyte activation would be particularly relevant considering the key role of these cells in the first-line defense against infections and tumors (35). Notably, these unconventional T cells represent attractive effectors for cancer immunotherapy (36). On the other hand, the generation of DC characterized by a reduced capacity to induce both conventional and γδ T lymphocyte-mediated responses, would limit the inflammatory response and/or contribute to immunosuppression. The opposite, pro-inflammatory vs. regulatory, effects are consistent with the dual role of TLR7/8 agonists in driving either protective immunity or chronic inflammation/autoimmunity (3, 37). The induction of anti-inflammatory/regulatory pathways (IL-10 production and Treg cell expansion) has also been reported to limit the adjuvant activity of other TLR agonists (38). These findings highlight the complexity of effects that can be elicited by TLR agonists, depending on the target cell type, and the importance of the administration route in regulating the intensity of response and in balancing apparently opposite effects.

In addition to their relevance in the mechanism of action of R848, our data argue for an involvement of γδ T and $CD14^+CD16^+$ cell-mediated responses during natural viral infections, when TLR8 ligands are produced. In particular, expansion of these cell populations has been described in some viral infections (32, 39, 40) where they play either protective or pathogenic roles, as well as in chronic inflammatory conditions characterized by break of gut homeostasis and microbial translocation (27, 41). Notably, we show that the CM of IEC isolated from subjects with active CD strongly enhances the activation of phosphoantigen responsive control γδ T lymphocytes with respect to IEC from healthy donors. Accordingly, it has been recently reported that an increased number of activated Vδ2 T cells is detected in intestinal mucosa from CD patients (27). Although different mechanisms can be responsible for this effect, we demonstrate that TLR-activating structures released at the level of inflamed epithelium strongly contribute to γδ T lymphocyte activation induced by intestinal microenvironment of active CD patients. The response of epithelium itself to TLR stimulation might in turn potentiate, through the release of pro-inflammatory mediators, the effects of microbial products on immune cells thus enhancing/perpetuating inflammation. In this regard, TLR8 expression has been reported to be selectively activated in inflamed colonic epithelium of IBD-affected subjects (6, 7) and its mucosal expression directly correlates with the severity of intestinal inflammation (8).

Altogether, the results of this study increase our knowledge on the molecular mechanisms and cellular responses that might be

triggered by TLR8 stimulation. They also add novel information on the mechanism(s) through which R848 exerts its adjuvant activity as well as on the role that the delivery route can play in regulating TLR agonist-induced responses. A better knowledge of the mechanisms and pathways regulated through TLR stimulation as well as of the role of TLR agonist administration route in shaping immune responses might contribute to the design of more effective strategies for microbial and cancer vaccines, as well as to better understand the role of microbial molecular patterns in infectious diseases and in chronic inflammation.

ETHICS STATEMENT

This study has been conducted in accordance with the Declaration of Helsinki and, according to national and international guidelines, it was approved by the review board of Istituto Superiore di Sanità (project identification code: CE/11/299). All the subjects included were provided with complete information about the study and asked to sign an informed consent.

AUTHOR CONTRIBUTIONS

CA designed and performed the experiments; BV performed the experiments; MF performed the biochemical analyses; PP analyzed the data and provided intellectual input; AB and AM performed TLR gene expression profiles; SG provided intellectual input throughout the study; LC conceived the study, supervised work, analyzed data, and wrote the manuscript.

ACKNOWLEDGMENTS

The authors thank Centro Trasfusionale (Sapienza University of Rome) for providing blood buffycoats from healthy donors; Paola Cesaro and Cristiano Spada (Catholic University of Rome) for the enrollment and clinical characterization of patients and for biopsy collection. They are also grateful to Gloria Donninelli for her support in data analysis.

FUNDING

This work was supported by the ISS Italy-NIH USA collaborative project 11US/13 (Italian Ministry of Health) to SG.

SUPPLEMENTARY MATERIAL

The Supplementary Material for this article can be found online at http://www.frontiersin.org/articles/10.3389/fimmu.2017.01813/full#supplementary-material.

REFERENCES

1. Kawai T, Akira S. The role of pattern-recognition receptors in innate immunity: update on toll-like receptors. *Nat Immunol* (2010) 11(5):373–84. doi:10.1038/ni.1863
2. Ohto U, Tanji H, Shimizu T. Structure and function of toll-like receptor 8. *Microbes Infect* (2014) 16(4):273–82. doi:10.1016/j.micinf.2014.01.007
3. Diebold SS. Recognition of viral single-stranded RNA by toll-like receptors. *Adv Drug Deliv Rev* (2008) 60(7):813–23. doi:10.1016/j.addr.2007.11.004
4. Grasa L, Abecia L, Forcen R, Castro M, de Jalon JA, Latorre E, et al. Antibiotic-induced depletion of murine microbiota induces mild inflammation and changes in toll-like receptor patterns and intestinal motility. *Microb Ecol* (2015) 70(3):835–48. doi:10.1007/s00248-015-0613-8
5. Fukata M, Arditi M. The role of pattern recognition receptors in intestinal inflammation. *Mucosal Immunol* (2013) 6(3):451–63. doi:10.1038/mi.2013.13
6. Steenholdt C, Andresen L, Pedersen G, Hansen A, Brynskov J. Expression and function of toll-like receptor 8 and Tollip in colonic epithelial cells from patients with inflammatory bowel disease. *Scand J Gastroenterol* (2009) 44(2):195–204. doi:10.1080/00365520802495529
7. Abreu MT. Toll-like receptor signalling in the intestinal epithelium: how bacterial recognition shapes intestinal function. *Nat Rev Immunol* (2010) 10(2):131–44. doi:10.1038/nri2707
8. Sanchez-Munoz F, Fonseca-Camarillo G, Villeda-Ramirez MA, Miranda-Perez E, Mendivil EJ, Barreto-Zuniga R, et al. Transcript levels of toll-like receptors 5, 8 and 9 correlate with inflammatory activity in Ulcerative Colitis. *BMC Gastroenterol* (2011) 11:138. doi:10.1186/1471-230X-11-138
9. Helminen O, Huhta H, Lehenkari PP, Saarnio J, Karttunen TJ, Kauppila JH. Nucleic acid-sensing toll-like receptors 3, 7 and 8 in esophageal epithelium, Barrett's esophagus, dysplasia and adenocarcinoma. *Oncoimmunology* (2016) 5(5):e1127495. doi:10.1080/2162402X.2015.1127495
10. Hemmi H, Kaisho T, Takeuchi O, Sato S, Sanjo H, Hoshino K, et al. Small anti-viral compounds activate immune cells via the TLR7 MyD88-dependent signaling pathway. *Nat Immunol* (2002) 3(2):196–200. doi:10.1038/ni758
11. Ahonen CL, Gibson SJ, Smith RM, Pederson LK, Lindh JM, Tomai MA, et al. Dendritic cell maturation and subsequent enhanced T-cell stimulation induced with the novel synthetic immune response modifier R-848. *Cell Immunol* (1999) 197(1):62–72. doi:10.1006/cimm.1999.1555
12. Wagner TL, Ahonen CL, Couture AM, Gibson SJ, Miller RL, Smith RM, et al. Modulation of TH1 and TH2 cytokine production with the immune response modifiers, R-848 and imiquimod. *Cell Immunol* (1999) 191(1):10–9. doi:10.1006/cimm.1998.1406
13. Vasilakos JP, Smith RM, Gibson SJ, Lindh JM, Pederson LK, Reiter MJ, et al. Adjuvant activities of immune response modifier R-848: comparison with CpG ODN. *Cell Immunol* (2000) 204(1):64–74. doi:10.1006/cimm.2000.1689
14. Yrlid U, Cerovic V, Milling S, Jenkins CD, Klavinskis LS, MacPherson GG. A distinct subset of intestinal dendritic cells responds selectively to oral TLR7/8 stimulation. *Eur J Immunol* (2006) 36(10):2639–48. doi:10.1002/eji.200636426
15. Yrlid U, Milling SW, Miller JL, Cartland S, Jenkins CD, MacPherson GG. Regulation of intestinal dendritic cell migration and activation by plasmacytoid dendritic cells, TNF-alpha and type 1 IFNs after feeding a TLR7/8 ligand. *J Immunol* (2006) 176(9):5205–12. doi:10.4049/jimmunol.176.9.5205
16. Vasilakos JP, Tomai MA. The use of toll-like receptor 7/8 agonists as vaccine adjuvants. *Expert Rev Vaccines* (2013) 12(7):809–19. doi:10.1586/14760584.2013.811208
17. Zhang J, Lu Y, Wei J, Li L, Han L. Protective effect of carboxytmethylpachymaran on TNF-alpha-induced damage in Caco-2 cell monolayers. *Int J Biol Macromol* (2016) 93(Pt A):506–11. doi:10.1016/j.ijbiomac.2016.07.095
18. Gupta V, Doshi N, Mitragotri S. Permeation of insulin, calcitonin and exenatide across Caco-2 monolayers: measurement using a rapid, 3-day system. *PLoS One* (2013) 8(2):e57136. doi:10.1371/journal.pone.0057136
19. Conti L, Casetti R, Cardone M, Varano B, Martino A, Belardelli F, et al. Reciprocal activating interaction between dendritic cells and pamidronate-stimulated gammadelta T cells: role of CD86 and inflammatory cytokines. *J Immunol* (2005) 174(1):252–60. doi:10.4049/jimmunol.174.1.252
20. Mary JY, Modigliani R. Development and validation of an endoscopic index of the severity for Crohn's disease: a prospective multicentre study. Groupe d'Etudes Therapeutiques des Affections Inflammatoires du Tube Digestif (GETAID). *Gut* (1989) 30(7):983–9. doi:10.1136/gut.30.7.983
21. Seidelin JB, Horn T, Nielsen OH. Simple and efficient method for isolation and cultivation of endoscopically obtained human colonocytes. *Am J Physiol Gastrointest Liver Physiol* (2003) 285(6):G1122–8. doi:10.1152/ajpgi.00533.2002

22. Artursson P, Palm K, Luthman K. Caco-2 monolayers in experimental and theoretical predictions of drug transport. *Adv Drug Deliv Rev* (2001) 46(1–3):27–43. doi:10.1016/S0169-409X(00)00128-9
23. Nisini R, Torosantucci A, Romagnoli G, Chiani P, Donati S, Gagliardi MC, et al. beta-Glucan of *Candida albicans* cell wall causes the subversion of human monocyte differentiation into dendritic cells. *J Leukoc Biol* (2007) 82(5):1136–42. doi:10.1189/jlb.0307160
24. Ziegler-Heitbrock L. The CD14+ CD16+ blood monocytes: their role in infection and inflammation. *J Leukoc Biol* (2007) 81(3):584–92. doi:10.1189/jlb.0806510
25. Kwissa M, Nakaya HI, Oluoch H, Pulendran B. Distinct TLR adjuvants differentially stimulate systemic and local innate immune responses in nonhuman primates. *Blood* (2012) 119(9):2044–55. doi:10.1182/blood-2011-10-388579
26. Pietschmann K, Beetz S, Welte S, Martens I, Gruen J, Oberg HH, et al. Toll-like receptor expression and function in subsets of human gammadelta T lymphocytes. *Scand J Immunol* (2009) 70(3):245–55. doi:10.1111/j.1365-3083.2009.02290.x
27. McCarthy NE, Hedin CR, Sanders TJ, Amon P, Hoti I, Ayada I, et al. Azathioprine therapy selectively ablates human Vdelta2(+) T cells in Crohn's disease. *J Clin Invest* (2015) 125(8):3215–25. doi:10.1172/JCI80840
28. Karlsson A, Jagervall K, Utkovic H, Karlsson L, Rehnstrom E, Fredin MF, et al. Intra-colonic administration of the TLR7 agonist R-848 induces an acute local and systemic inflammation in mice. *Biochem Biophys Res Commun* (2008) 367(2):242–8. doi:10.1016/j.bbrc.2007.12.046
29. Craft N, Birnbaum R, Quanquin N, Erfe MC, Quant C, Haskell J, et al. Topical resiquimod protects against visceral infection with *Leishmania infantum* chagasi in mice. *Clin Vaccine Immunol* (2014) 21(9):1314–22. doi:10.1128/CVI.00338-14
30. Feng AL, Zhu JK, Sun JT, Yang MX, Neckenig MR, Wang XW, et al. CD16+ monocytes in breast cancer patients: expanded by monocyte chemoattractant protein-1 and may be useful for early diagnosis. *Clin Exp Immunol* (2011) 164(1):57–65. doi:10.1111/j.1365-2249.2011.04321.x
31. Butchar JP, Mehta P, Justiniano SE, Guenterberg KD, Kondadasula SV, Mo X, et al. Reciprocal regulation of activating and inhibitory Fc{gamma} receptors by TLR7/8 activation: implications for tumor immunotherapy. *Clin Cancer Res* (2010) 16(7):2065–75. doi:10.1158/1078-0432.CCR-09-2591
32. Wong KL, Yeap WH, Tai JJ, Ong SM, Dang TM, Wong SC. The three human monocyte subsets: implications for health and disease. *Immunol Res* (2012) 53(1–3):41–57. doi:10.1007/s12026-012-8297-3
33. Assier E, Marin-Esteban V, Haziot A, Maggi E, Charron D, Mooney N. TLR7/8 agonists impair monocyte-derived dendritic cell differentiation and maturation. *J Leukoc Biol* (2007) 81(1):221–8. doi:10.1189/jlb.0705385
34. Hackstein H, Knoche A, Nockher A, Poeling J, Kubin T, Jurk M, et al. The TLR7/8 ligand resiquimod targets monocyte-derived dendritic cell differentiation via TLR8 and augments functional dendritic cell generation. *Cell Immunol* (2011) 271(2):401–12. doi:10.1016/j.cellimm.2011.08.008
35. Poggi A, Zocchi MR. gammadelta T lymphocytes as a first line of immune defense: old and new ways of antigen recognition and implications for cancer immunotherapy. *Front Immunol* (2014) 5:575. doi:10.3389/fimmu.2014.00575
36. Hannani D, Ma Y, Yamazaki T, Dechanet-Merville J, Kroemer G, Zitvogel L. Harnessing gammadelta T cells in anticancer immunotherapy. *Trends Immunol* (2012) 33(5):199–206. doi:10.1016/j.it.2012.01.006
37. Yokogawa M, Takaishi M, Nakajima K, Kamijima R, Fujimoto C, Kataoka S, et al. Epicutaneous application of toll-like receptor 7 agonists leads to systemic autoimmunity in wild-type mice: a new model of systemic *Lupus erythematosus*. *Arthritis Rheumatol* (2014) 66(3):694–706. doi:10.1002/art.38298
38. Engel AL, Holt GE, Lu H. The pharmacokinetics of toll-like receptor agonists and the impact on the immune system. *Expert Rev Clin Pharmacol* (2011) 4(2):275–89. doi:10.1586/ecp.11.5
39. Latha TS, Reddy MC, Durbaka PV, Rachamallu A, Pallu R, Lomada D. gammadelta T cell-mediated immune responses in disease and therapy. *Front Immunol* (2014) 5:571. doi:10.3389/fimmu.2014.00571
40. Ahout IM, Jans J, Haroutiounian L, Simonetti ER, van der Gaast-de Jongh C, Diavatopoulos DA, et al. Reduced expression of HLA-DR on monocytes during severe respiratory syncytial virus infections. *Pediatr Infect Dis J* (2016) 35(3):e89–96. doi:10.1097/INF.0000000000001007
41. Koch S, Kucharzik T, Heidemann J, Nusrat A, Luegering A. Investigating the role of proinflammatory CD16+ monocytes in the pathogenesis of inflammatory bowel disease. *Clin Exp Immunol* (2010) 161(2):332–41. doi:10.1111/j.1365-2249.2010.04177.x

Conflict of Interest Statement: The research was conducted in the absence of any commercial or financial relationships that could be construed as a potential conflict of interest.

Copyright © 2017 Angelini, Varano, Puddu, Fiori, Baldassarre, Masotti, Gessani and Conti. This is an open-access article distributed under the terms of the Creative Commons Attribution License (CC BY). The use, distribution or reproduction in other forums is permitted, provided the original author(s) or licensor are credited and that the original publication in this journal is cited, in accordance with accepted academic practice. No use, distribution or reproduction is permitted which does not comply with these terms.

frontiers in Immunology

REVIEW
published: 22 December 2017
doi: 10.3389/fimmu.2017.01898

Type 1 Diabetes: A Chronic Anti-Self-Inflammatory Response

Matthew Clark[1†], Charles J. Kroger[1†] and Roland M. Tisch[1,2]*

[1] Department of Microbiology and Immunology, University of North Carolina at Chapel Hill, Chapel Hill, NC, United States,
[2] Lineberger Comprehensive Cancer Center, University of North Carolina at Chapel Hill, Chapel Hill, NC, United States

Inflammation is typically induced in response to a microbial infection. The release of proinflammatory cytokines enhances the stimulatory capacity of antigen-presenting cells, as well as recruits adaptive and innate immune effectors to the site of infection. Once the microbe is cleared, inflammation is resolved by various mechanisms to avoid unnecessary tissue damage. Autoimmunity arises when aberrant immune responses target self-tissues causing inflammation. In type 1 diabetes (T1D), T cells attack the insulin producing β cells in the pancreatic islets. Genetic and environmental factors increase T1D risk by in part altering central and peripheral tolerance inducing events. This results in the development and expansion of β cell-specific effector T cells (Teff) which mediate islet inflammation. Unlike protective immunity where inflammation is terminated, autoimmunity is sustained by chronic inflammation. In this review, we will highlight the key events which initiate and sustain T cell-driven pancreatic islet inflammation in nonobese diabetic mice and in human T1D. Specifically, we will discuss: (i) dysregulation of thymic selection events, (ii) the role of intrinsic and extrinsic factors that enhance the expansion and pathogenicity of Teff, (iii) defects which impair homeostasis and suppressor activity of FoxP3-expressing regulatory T cells, and (iv) properties of β cells which contribute to islet inflammation.

Keywords: autoimmunity, type 1 diabetes, immunoregulation, inflammation, T cells

OPEN ACCESS

Edited by:
Philippe Saas,
INSERM UMR1098 Interactions Hôte-Greffon-Tumeur & Ingénierie Cellulaire et Génique, France

Reviewed by:
Joanne E. Konkel,
University of Manchester, United Kingdom
Julien Diana,
Institut National de la Santé et de la Recherche Médicale, France
Thomas J. Hawke,
McMaster University, Canada
Sylvaine You,
Institut National de la Santé et de la Recherche Médicale, France

***Correspondence:**
Roland M. Tisch
rmtisch@med.unc.edu

†These authors have contributed equally to this work.

Specialty section:
This article was submitted to Inflammation, a section of the journal Frontiers in Immunology

Received: *20 October 2017*
Accepted: *12 December 2017*
Published: *22 December 2017*

Citation:
Clark M, Kroger CJ and Tisch RM (2017) Type 1 Diabetes: A Chronic Anti-Self-Inflammatory Response. Front. Immunol. 8:1898. doi: 10.3389/fimmu.2017.01898

INTRODUCTION

Type 1 diabetes (T1D) is an autoimmune disease characterized by the chronic inflammation of the pancreatic islets of Langerhans (1–4). Islet inflammation is typically marked by infiltrating adaptive and innate immune effectors. Insulitis progresses over time and when a sufficient amount of β cell mass has been rendered nonfunctional and/or destroyed, hyperglycemic blood levels are achieved, and clinical diabetes established. The immune mechanisms mediating β cell autoimmunity are heterogeneous, as reflected by the nature of the islet infiltrate and the age of clinical onset. Nevertheless, T1D is generally viewed as a T cell-driven autoimmune disease, particularly for the more prevalent and aggressive type of T1D that develops in children and adolescents versus adults (5–17). A T cell-independent subtype of T1D, however, may also exist that is thought to be largely mediated by innate immune effectors (18, 19). The events leading to the loss of β cell-specific tolerance and chronic islet inflammation are complex, and influenced by both genetic and environmental factors (20–22).

Type 1 diabetes is polygenic with more than 20 insulin-dependent diabetes mellitus (*IDDM*) genetic loci identified that are associated with increased or decreased risk for T1D (23–28). The strongest genetic association is with the human leukocyte antigen locus (*IDDM1*), and particular

class I and II haplotypes, consistent with a key role for T cells in T1D (29, 30). A number of genes regulating T, B, and innate cell immunobiology are also linked with T1D, as are genetic variants intrinsic to β cells, which deleteriously affect β cell function and/or responses to inflammation (31–37).

The identity and role of environmental factors in T1D are poorly understood. The most common hypothesis is that microbial infections initiate and/or exacerbate islet inflammation in genetically susceptible individuals (38, 39). For instance, T1D is associated with enteroviruses such as coxsackievirus B1 (40–44). Viral infection of β cells may result in direct cytolysis and/or elicit local inflammation that initiates and/or drives autoimmunity (45–47). The gut microbiota also has a profound regulatory effect on β cell autoimmunity (48, 49). In the nonobese diabetic (NOD) mouse, a spontaneous model of T1D, β cell destruction can be either promoted or prevented by changes in the composition of the gut microbiota (50, 51). Here bacterial components and metabolites are thought to impact the activation and/or differentiation status of innate and adaptive immune effectors. Longitudinal studies of at risk subjects also indicate a role for gut microbiota in human T1D (52–54).

The T cell-related events that drive chronic islet inflammation in T1D stem from dysregulation of central and peripheral tolerance, alterations in self-antigen processing, and modified β cell responses (**Figure 1**). Here, we discuss how events critical for initiating and amplifying the development of T cell-mediated islet inflammation are regulated in NOD mice and human T1D.

THYMIC ORIGINS OF DIABETOGENIC T CELLS: SETTING THE STAGE FOR ISLET INFLAMMATION

The generation of an autoreactive T cell receptor (TCR) repertoire in the periphery is established in part by inefficient negative selection of anti-self-single positive thymocytes (SP) in the thymus (55, 56). Early in ontogeny negative selection is lax, resulting in increased escape of anti-self-SP (57–59). This temporal decrease in negative selection and elevated survival of β cell-specific clonotypes may help explain the predominance of T1D onset in childhood. With time, changes in thymic structural organization and maturation of thymic antigen-presenting cells (APC) leads to more efficient negative selection and increased death of autoreactive SP (57).

Key mediators of negative selection are medullary thymic epithelial cells (mTEC) and dendritic cells (DC). Notably, mTEC

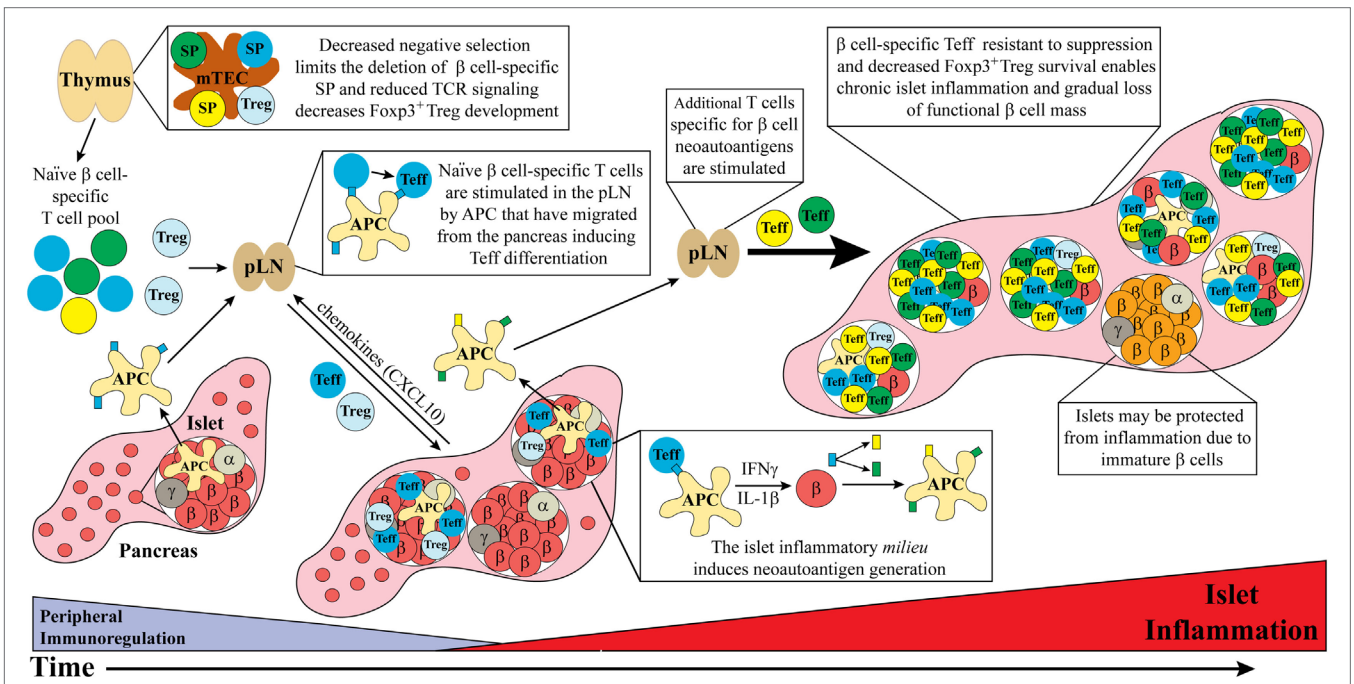

FIGURE 1 | Dysregulated thymic and peripheral events culminate in chronic islet inflammation. In general, overt diabetes results from the gradual loss of functional insulin producing β cells due to the inflammatory environment driven by infiltrating self-reactive T cells and antigen-presenting cell (APC). Although β cell-specific T cell clones are detected in both healthy and type 1 diabetes (T1D) susceptible individuals, a number of factors promote T1D development in the latter population. Decreased efficiency of negative selection in the thymus, either due to altered tissue-specific antigen expression or due to T cell receptor (TCR) signaling, allows for the increased escape of β cell-specific T cell clones into the periphery. In addition, β cell-specific Foxp3+Treg development may also be suboptimal due to dysregulation of TCR signaling. In the periphery, β cell-specific T cells are stimulated in the pancreatic lymph nodes (pLN) by APC derived from the islets, leading to effector T cell (Teff) differentiation. These pathogenic Teff then infiltrate the islets and drive inflammation leading to reduced β cell function and/or survival. Not all islets are infiltrated potentially due to an immature phenotype and reduced autoantigen expression by β cells. Ongoing islet inflammation also leads to the generation of neoautoantigens either directly in β cells or during antigen processing by APC. The presentation of neoautoantigens within the pLN promotes the activation and expansion of additional Teff pools. These events amplify and drive a chronic state of islet inflammation leading to impaired functional β cell mass and clinical onset of T1D.

express and present several tissue-specific antigens (TSA) (60–63). Recognition of MHC-self-peptide complexes with increasing avidity/affinity results in elevated TCR signaling and SP apoptosis. Dysregulation of negative selection generates a peripheral pool of anti-self-T cells displaying increased avidity/affinity, and likely an enhanced "pathogenic potential."

Parameters influencing the efficiency of negative selection both intrinsic and extrinsic to thymocytes have been linked to the development of β cell-specific T cells and T1D. Thymocyte intrinsic properties reported in NOD mice have included reduced SP sensitivity to apoptosis and altered double positive thymocyte differentiation to SP (64–67). In humans, TCR signaling needed to drive apoptosis of β cell-specific SP may be limited by a T1D-associated variant of the protein tyrosine phosphatase non-receptor 22 (*PTPN22*) gene (31, 32). PTPN22 is a negative regulator of TCR signaling, and elevated phosphatase activity by PTPN22 is predicted to reduce TCR signaling strength and diminish apoptosis induction in SP (68). An increase in PTPN22 activity may also limit thymic development of β cell-specific FoxP3-expressing regulatory $CD4^+$ T cells ($FOXP3^+$Treg), which is dependent on high(er) avidity/affinity recognition of self-peptide.

Thymocyte extrinsic factors that impact negative selection include aberrant expression of TSA in the medulla. The importance of thymic expression and presentation of TSA is readily evident in mice and humans deficient of the transcription factor autoimmune regulator (AIRE) (60, 69). Lack of AIRE, which drives expression of select TSA by mTEC, results in inefficient thymic negative selection and reduced development of tissue-specific $Foxp3^+$Treg, leading to multiorgan autoimmunity in mice (70–74). Similarly, aberrant AIRE expression and function in humans results in the development of autoimmune polyendorinology candidiasis and ectodermal dysplasia (APECD) in which a variety of organs are targeted by T cells; notably a subset of APCED patients develop T1D (75, 76). Reduced AIRE expression has been reported in NOD mice, which reflects not only T1D development but also T cell-mediated inflammation of other tissues such as the thyroid, salivary, and lacrimal glands (77).

In human T1D, a strong genetic association is linked to the insulin encoding gene *INS2* found in *IDDM2* (78). Insulin is believed to be a key autoantigen driving human T1D, which is supported by studies in NOD mice (79–81). *INS2* is preceded by a variable number of tandem repeats (VNTRs). Individuals that have 26–63 VNTRs, associated with decreased thymic *INS2* expression, have an increased risk of developing T1D. In contrast, *INS2* expression is increased with VNTRs ranging between 140 and 210, which in turn is associated with a protective phenotype (82, 83). Reduced thymic insulin expression is expected to both limit negative selection and development of insulin-specific SP and $FOXP3^+$Treg, respectively. Future studies are needed to directly demonstrate that thymic selection is dysregulated, and contributes to an expanded β cell-specific peripheral T cell pool in human T1D. Whether defects in thymic selection and development of β cell-specific T cells are necessary only early on or required throughout the disease process is another issue that needs to be tackled.

It is noteworthy that β cell-specific T cells are detected in the blood of healthy individuals, likely reflecting in part the reduced efficiency of thymic negative selection early in ontogeny. However, the phenotype of circulating β cell-specific T cells is distinct in T1D patients versus healthy subjects (84–89). The former exhibit mostly an effector/memory phenotype and expression of proinflammatory cytokines consistent with ongoing β cell autoimmunity (84–88). These findings indicate that in addition to the TCR repertoire, other factors contribute to the differentiation and expansion of diabetogenic effector T cells (Teff). For instance, the extent of tissue destruction and lethality of AIRE deficiency in mice is influenced by genotype with AIRE-deficient NOD versus C57BL/6 mice exhibiting more severe systemic autoimmunity (90, 91). Additionally, distinct TCR repertoires have been found in NOD mice in contrast to MHC matched C57BL/6 mice (92). Overall, dysregulation of thymic selection events in NOD mice acts as a precursor for islet inflammation.

EXTRINSIC AND INTRINSIC FACTORS PROMOTE PATHOGENIC EFFECTOR T CELLS IN T1D

The initiation of islet inflammation in NOD mice and humans is ill-defined. In NOD mice pancreatic remodeling shortly after birth is thought to play a key role starting the diabetogenic response (93, 94). Remodeling of the pancreas results in a wave of β cell apoptosis and release of antigens which are endocytosed by resident macrophages and DC (95). These APC then traffick to the draining pancreatic lymph nodes (pLN) to prime β cell-specific T cells and promote Teff differentiation (96, 97). Once established Teff migrate into the islets and mediate inflammation (97–99).

As alluded to above, shifts in the composition of the gut microbiota early in ontogeny are also believed to play a key role in regulating Teff differentiation in both mice and humans. Systemic release of microbiota-derived products can activate APC that in turn prime β cell-specific T cells providing an "environmental trigger" to incite T1D development (48). NOD mice in which the response to the microbiome is limited due to a deficiency in the Toll-like receptor adaptor protein MyD88, exhibit reduced β cell-specific Teff reactivity and diabetes incidence (50, 100). Strikingly, diabetes is prevented in NOD mice housed under germ-free conditions and inoculated with microbiota derived from MyD88-deficient animals (50), demonstrating that the microbiota also has a protective role in T1D. A less diverse gut microbiota in young individuals at risk for T1D is associated with progression to clinical diabetes (54). Changes in the gut microbiome have also been linked to the female bias of T1D in NOD mice (100). Interestingly, studies show that the lymphopenic environment in neonatal mice induces naïve T cells to rapidly expand and transition into a memory-like phenotype, that in turn is influenced by gut microbiota (101–104). Expansion of memory-like T cells, also seen in newborn humans, may enhance the pathogenic potential of the peripheral T cell pool and favor the development of autoimmunity in susceptible individuals.

Both CD4+ and CD8+ T cells are required for efficient β cell destruction in NOD mice (105). Islet CD8+ T cells primarily mediate β cell destruction by a cognate interaction involving perforin and granzyme B-, and Fas-Fas ligand-mediated killing (106, 107). On the other hand, islet CD4+ T cells drive β cell destruction in a bystander manner *via* secretion of proinflammatory cytokines. CD4+ and CD8+ T cells are also detected in the islets of diabetic subjects, with CD8+ T cells often predominating (6, 106). Several β cell autoantigens are recognized by the islet infiltrating T cells, and a number of these are similarly targeted in both the NOD and human diabetogenic responses including glutamic acid decarboxylase 65, proinsulin, insulin B chain, islet antigen-2, and islet-specific glucose-6-phosphatase catalytic subunit-related protein (108).

The majority of CD4+ and CD8+ T cells infiltrating the islets of NOD mice and T1D subjects exhibit a T helper 1 (Th1) effector phenotype, marked by IFNγ secretion (109). Increased Th17 cells are seen in the islets of NOD mice and the pLN of T1D subjects (109–111). The role of Th17 cells in mediating islet inflammation, however, is ill-defined. Elevated local levels of IFNγ are believed to establish a feed-forward loop that drives islet pathology. Based on NOD mouse studies, IFNγ secreted by islet CD4+ (and CD8+) Teff results in local upregulation of chemotactic cues that induce additional T, B, and innate cells to migrate into the islets, as well as promote islet retention of these effectors (109, 112). IFNγ also activates islet resident APC and stromal cells to elevate production of additional inflammatory mediators, such reactive oxygen species, which impair function and mediate β cell necrosis (107, 113, 114). Furthermore, IFNγ in the context of IL-1β and TNFα induces β cell apoptosis (113, 114).

Another proinflammatory cytokine thought to contribute to islet inflammation is IL-21 which is elevated in T1D patient serum (115). Notably, the murine IL-21 gene is located in the *Idd3* locus and IL-21 receptor (R) deficiency prevents T1D in NOD mice (116). CD4+ T follicular helper cells, which are increased in the pLN of NOD mice, are the primary source of IL-21 (112, 117–119). IL-21 has a critical role in supporting B cell development and antibody production. B cells, serving as APC, are required for efficient β cell destruction in NOD mice and likely in human T1D (117, 118, 120, 121). IL-21 also enhances maintenance of CD8+ Teff by preventing exhaustion during chronic inflammation (122, 123). Interestingly, the pathogenicity of β cell-specific CD8+ T cells is dependent on IL-21R expression (124, 125).

Defects intrinsic to Teff are also thought to facilitate chronic islet inflammation. Variants of the *CTLA4* gene are linked to T1D susceptibility in both NOD mice (*Idd5.1*) and human T1D (*IDDM12*) (33, 126). CTLA-4 which binds to the costimulatory molecules CD80 and CD86 expressed on APC, is a negative regulator of T cell activation and proliferation (34). Polymorphisms in the human *CTLA4* gene region are associated with reduced mRNA levels and a decrease in expression of the soluble (s) CTLA-4 isoform (33, 34, 126). sCTLA-4 also negatively regulates TCR signaling (33, 34, 126). Reduced expression of CTLA-4 and sCTLA-4 is expected to facilitate expansion of β cell-specific T cells. This scenario is consistent with the exacerbated β cell autoimmunity seen in NOD mice expressing a diabetogenic TCR transgene and lacking CTLA-4 expression (127). Noteworthy is that both NOD-derived and human T1D Teff also exhibit reduced sensitivity to Foxp3+Treg-mediated suppression (128, 129). In sum, the culmination of a variety of extrinsic and intrinsic factors enables Teff to expand, persist, and in turn amplify islet inflammation.

DEFECTS IN THE Foxp3+Treg POOL CONTRIBUTE TO T1D

In addition to Teff that are resistant to regulatory mechanisms that limit expansion and function, evidence indicates that the Foxp3+Treg pool is compromised in T1D (130, 131). Here, dysregulation of Foxp3+Treg homeostasis is thought to permit preferential differentiation and expansion of pathogenic β cell-specific Teff. Foxp3+Treg have an essential role in regulating immune homeostasis and reactivity to self (132–135). The lack of thymic development of Foxp3+Treg due to deficient expression or function of the FoxP3 transcription factor, results in systemic autoimmunity in both mice and humans. Foxp3+Treg mediate suppression of T cells and other immune effectors *via* multiple mechanisms including cell-contact dependent suppression, and secretion of anti-inflammatory cytokines and mediators such as IL-10, TGFβ1, and IL-35, and adenosine, respectively (136). Foxp3+Treg also function as an "IL-2 depot" to deprive Teff of IL-2 needed for expansion (136). The latter is mediated by constitutive expression of CD25, the α subunit of the IL-2R (136). Therefore, Foxp3+Treg, expressing the high affinity IL-2R, are able to out compete Teff for IL-2, which transiently express high affinity IL-2R.

IL-2 is essential for Foxp3+Treg homeostasis, expansion, and function (136). Unlike conventional T cells, Foxp3+Treg do not produce IL-2 due to FoxP3-mediated negative regulation of *Il2* transcription. Therefore, Foxp3+Treg are dependent on T cells and DC as IL-2 sources (136). This dependency is thought to enable Foxp3+Treg to more readily sense and respond to ongoing inflammation. Accordingly, defects in the IL-2/IL-2R axis have been described in the NOD model and human T1D (137–142). In NOD mice, an *Il2* variant located in *Idd3* results in reduced levels of IL-2 expression by Teff, and impaired survival and function of islet resident Foxp3+Treg (130, 143). Increased levels of proinflammatory cytokines, such as IFNγ and IL-6 that downregulate FoxP3 expression may also promote dedifferentiation of islet Foxp3+Treg into a Teff-like subsets (144, 145). These events lead to a progressive loss of islet Foxp3+Treg suppression, thereby "releasing the brakes" and favoring pathogenic Teff expansion.

The frequency of FOXP3+Treg found in blood is largely unaffected in T1D subjects (140, 141, 146–148). However, FOXP3+Treg from T1D subjects exhibit reduced suppressor function measured *in vitro* (128, 129). This aberrant activity is linked to T1D risk variants of *IL2RA* (CD25) and *PTPN2*, a phosphatase involved in IL-2R signaling (149). Notably, FOXP3+Treg expressing these variants display reduced IL-2R signaling that in turn correlates with limited suppressor activity (149, 150). Defects in IL-2R signaling have led to clinical studies testing whether low-dose IL-2 therapy enhances the FOXP3+Treg pool

in T1D subjects (149, 151). This approach has been effective in preventing and/or reversing diabetes in NOD mice by increasing the number and function of islet Foxp3$^+$Treg (149, 152). One key question not addressed is the specificity of FOXP3$^+$Treg in T1D subjects. Reduced thymic development of β cell-specific FOXP3$^+$Treg, as discussed above, would be expected to limit the "anti-diabetogenic" effects of the peripheral FOXP3$^+$Treg pool.

AMPLIFYING THE PATHOGENIC EFFECTOR T CELL RESPONSE *VIA* NEOAUTOANTIGENS

Recent findings have demonstrated that the proinflammatory *milieu* of the islets promotes processing of "neoautoantigens" (153). Importantly, these neoautoantigens are only found in the periphery so that corresponding T cell clonotypes, not deleted in the thymus and possibly expressing high affinity TCR, can be recruited into the inflammatory response. Neoautoantigens are generated *via* posttranslational modifications (PTM), such as deamidation by tissue transglutaminase (tTG) (153). PTM can occur during APC antigen processing or directly in β cells (154). tTG-dependent deamidation of a proinsulin C-peptide for instance is detected in both human DC and islets under inflammatory conditions (154). Notably the resulting modified peptide is recognized by CD4$^+$ T cells derived from T1D subjects. The MHC binding and in turn T cell stimulatory properties of peptides can also be enhanced by deamidation (155).

Neoautoantigens consisting of hybrid peptides have recently been identified. In NOD mice hybrid insulin peptides are generated *via* covalent crosslinking of a proinsulin C peptide with peptides derived from naturally occurring cleavage products produced in the β cell secretory granules (156). In addition to ongoing inflammation, PTM occurs *via* endoplasmic reticulum stress, which can be induced in β cells by the normal physiological demands associated with high levels of insulin secretion (157). Therefore, it is possible that β cell neoautoantigens in addition to amplifying inflammation, play a role in initiating the diabetogenic response. Neoautoantigens are also generated at a transcriptional level. A mutation in the open reading frame of insulin mRNA generates a neoautoantigen that stimulates CD8$^+$ T cells from T1D subjects causing β cells lysis *in vitro* (158). Alternative RNA splicing may be another mechanism leading to neoautoantigen expression, particularly since ~30% of genes in inflamed β cells undergo aberrant alternative splicing (159). In sum, β cell neoautoantigens serve as *bona fide* targets of pathogenic CD4$^+$ and CD8$^+$ T cells. The breadth of the peptidome of neoautoantigens produced and presented, and the properties of neoautoantigen-specific T cells, in terms of frequency, avidity/affinity, subset phenotype (e.g., pathogenic versus regulatory), and overall contribution to islet inflammation require further investigation.

β CELL-INTRINSIC PROPERTIES THAT REGULATE ISLET INFLAMMATION

Studies have demonstrated that intrinsic properties of β cells also influence islet inflammation. For instance, CXCL10 is produced by β cells although the role of this chemokine in disease is controversial (160). CXCL10 regulates migration of CXCR3 expressing Teff and Foxp3$^+$Treg into the islets (97–99, 161). Overexpression of CXCL10 in β cells accelerates T1D progression, and antibody blockade of CXCL10 prevents Teff migration into the islets of NOD mice (97–99, 161). On the other hand, *Cxcr3* deficiency accelerates T1D by reducing islet resident Foxp3$^+$Treg (162, 163). Therefore, depending on the context, β cells may affect inflammatory and immunoregulatory events *via* CXCL10 production. The chemokine CCL2 is also secreted by β cells, and over-expression of ectopic CCL2 recruits tolerogenic CCR2-expressing DC and blocks T1D progression in NOD mice (164). Interestingly, NOD APC shows defective migration in response to CCL2, and human T1D patients have reduced serum levels of CCL2 (164–166). Additionally, β cells produce CXCL1 and CXCL2 that recruit CXCR2-expressing neutrophils to the islets, which contribute to stimulating β cell-specific T cell reactivity (167, 168). Overall, β cell produced chemotactic cues regulate the progression of the diabetogenic response.

Along with chemokines, β cells secrete the cytokine IL-1β, which at low levels promotes β cell proliferation, and enhances production of CCL2, CXCL1, CXCL2, and insulin (169, 170). However, IL-1β also primes leukocyte effector-mediated inflammation, and as noted above, IL-1β in the context of TNFα, and/or IFN-γ induces β cell apoptosis *in vitro* (113, 114). Notably, glucagon-secreting α cells also produce IL-1β, indicating that other islet resident endocrine cells may also contribute to local inflammation (171, 172). Islet inflammation also induces upregulation of MHC class I and II on β cells to further increase β cell immunogenicity (173). Interestingly, a subpopulation of β cells have been identified which under inflammatory conditions acquires resistance to immune-mediated destruction in NOD mice (174). The latter is associated with a more immature β cell phenotype coupled with reduced expression of autoantigens and upregulation of immunomodulatory molecules such as PD-L1, an inducer of T cell exhaustion. A similar phenotype is seen for human β cells (174). Therefore, β cells not only contribute to islet inflammation but also adapt under the inflammatory conditions in order to persist. A better understanding of the events regulating this dichotomy has important implications for the treatment of T1D patients *via* β cell replacement strategies for instance.

SUMMARY

Type 1 diabetes is complex involving genetic, epigenetic and environmental factors that influence adaptive and innate effector cell populations, which ultimately culminate in pathological, chronic islet inflammation (**Figure 1**). The heterogeneity associated with human T1D and in turn the nature of islet inflammation is expected to reflect the genotype of the individual, and type of environmental insult(s) encountered (20–22). These factors dictate which immune effectors are the key drivers of pathology, the pace of disease progression, and the degree of β cell dysregulation and/or death. We propose that the rapid and aggressive T1D seen early in life is marked by a broad β cell-specific TCR repertoire with increased avidity/affinity due to insufficient

negative selection (57–59). This is coupled with β cell-specific Teff that are insensitive to peripheral tolerance inducing events, β cell-specific FOXP3$^+$Treg with impaired suppressor activity, and β cells which readily promote islet inflammation (128, 129, 147, 169, 170). Robust inflammation leads to increased β cell neoautoantigen production further amplifying the kinetics and overall inflammatory response (153, 154, 156, 158). Under these "ideal" conditions, early onset T1D develops. On the other hand, in individuals with only a partial complement of these key "disease components," islet inflammation is less robust and the kinetics of T1D onset proportionately delayed. Defining the events driving early versus late(r) T1D onset is critical for a better understanding of how islet inflammation is regulated in humans. The latter is also important for developing rational and effective immunotherapies to prevent and/or treat T1D. Devising strategies to enhance thymic negative selection early in ontogeny for instance, would be expected to purge the diabetogenic TCR repertoire to prevent T1D. Indeed, approaches are currently being studied to manipulate thymic negative selection in the context of cancer treatment by expanding the T cell repertoire specific for self-tumor antigens (175–177). Altering the gut microbiome early in life may also prove to be an effective strategy to limit expansion of the anti-self-T cell repertoire and establish robust immunoregulation in the periphery. Administration of β cell neoautoantigens may augment the efficacy of antigen-based immunotherapies to block disease progression at later stages of T1D (157). Depending on the mode of administration, β cell neoautoantigens can be used to target the corresponding clonotypes by tolerizing pathogenic Teff and/or inducing/expanding FOXP3$^+$Treg. In view of the heterogeneity in the immunopathology of T1D, it is very likely these approaches and others currently being studied will need to be combined to effectively suppress the chronic islet inflammation and β cell autoimmunity long term.

AUTHOR CONTRIBUTIONS

MC, CJK, and RMT contributed to the preparation of the review article.

FUNDING

This work was supported by National Institutes of Health grants R01DK100256 and R01DK1035486 (RMT) and T32AI007273 (MC).

REFERENCES

1. Bach JF. Insulin-dependent diabetes mellitus as an autoimmune disease. *Endocr Rev* (1994) 15(4):516–42. doi:10.1210/edrv-15-4-516
2. Tisch R, McDevitt H. Insulin-dependent diabetes mellitus. *Cell* (1996) 85(3):291–7. doi:10.1016/S0092-8674(00)81106-X
3. Eisenbarth GS. Type 1 diabetes: molecular, cellular and clinical immunology. *Adv Exp Med Biol* (2004) 552:306–10.
4. Anderson MS, Bluestone JA. The NOD mouse: a model of immune dysregulation. *Annu Rev Immunol* (2005) 23:447–85. doi:10.1146/annurev.immunol.23.021704.115643
5. Pugliese A. Autoreactive T cells in type 1 diabetes. *J Clin Invest* (2017) 127(8):2881–91. doi:10.1172/JCI94549
6. Coppieters KT, Dotta F, Amirian N, Campbell PD, Kay TW, Atkinson MA, et al. Demonstration of islet-autoreactive CD8 T cells in insulitic lesions from recent onset and long-term type 1 diabetes patients. *J Exp Med* (2012) 209(1):51–60. doi:10.1084/jem.20111187
7. Atkinson MA, von Herrath M, Powers AC, Clare-Salzler M. Current concepts on the pathogenesis of type 1 diabetes – considerations for attempts to prevent and reverse the disease. *Diabetes Care* (2015) 38(6):979–88. doi:10.2337/dc15-0144
8. Arif S, Gibson VB, Nguyen V, Bingley PJ, Todd JA, Guy C, et al. Beta-cell specific T-lymphocyte response has a distinct inflammatory phenotype in children with Type 1 diabetes compared with adults. *Diabet Med* (2017) 34(3):419–25. doi:10.1111/dme.13153
9. Heninger AK, Eugster A, Kuehn D, Buettner F, Kuhn M, Lindner A, et al. A divergent population of autoantigen-responsive CD4+ T cells in infants prior to beta cell autoimmunity. *Sci Transl Med* (2017) 9(378):eaaf8848. doi:10.1126/scitranslmed.aaf8848
10. Willcox A, Richardson SJ, Bone AJ, Foulis AK, Morgan NG. Analysis of islet inflammation in human type 1 diabetes. *Clin Exp Immunol* (2009) 155(2):173–81. doi:10.1111/j.1365-2249.2008.03860.x
11. Atkinson MA, Gianani R. The pancreas in human type 1 diabetes: providing new answers to age-old questions. *Curr Opin Endocrinol Diabetes Obes* (2009) 16(4):279–85. doi:10.1097/MED.0b013e32832e06ba
12. Coppieters KT, Roep BO, von Herrath MG. Beta cells under attack: toward a better understanding of type 1 diabetes immunopathology. *Semin Immunopathol* (2011) 33(1):1–7. doi:10.1007/s00281-010-0236-6
13. Richardson SJ, Willcox A, Bone AJ, Morgan NG, Foulis AK. Immunopathology of the human pancreas in type-I diabetes. *Semin Immunopathol* (2011) 33(1):9–21. doi:10.1007/s00281-010-0205-0
14. Campbell-Thompson M. Organ donor specimens: what can they tell us about type 1 diabetes? *Pediatr Diabetes* (2015) 16(5):320–30. doi:10.1111/pedi.12286
15. Campbell-Thompson M, Fu A, Kaddis JS, Wasserfall C, Schatz DA, Pugliese A, et al. Insulitis and beta-cell mass in the natural history of type 1 diabetes. *Diabetes* (2016) 65(3):719–31. doi:10.2337/db15-0779
16. Babon JA, DeNicola ME, Blodgett DM, Crevecoeur I, Buttrick TS, Maehr R, et al. Analysis of self-antigen specificity of islet-infiltrating T cells from human donors with type 1 diabetes. *Nat Med* (2016) 22(12):1482–7. doi:10.1038/nm.4203
17. Michels AW, Landry LG, McDaniel KA, Yu L, Campbell-Thompson M, Kwok WW, et al. Islet-derived CD4 T cells targeting proinsulin in human autoimmune diabetes. *Diabetes* (2017) 66(3):722–34. doi:10.2337/db16-1025
18. In't Veld P. Insulitis in human type 1 diabetes: the quest for an elusive lesion. *Islets* (2011) 3(4):131–8. doi:10.4161/isl.3.4.15728
19. Skog O, Korsgren S, Melhus A, Korsgren O. Revisiting the notion of type 1 diabetes being a T-cell-mediated autoimmune disease. *Curr Opin Endocrinol Diabetes Obes* (2013) 20(2):118–23. doi:10.1097/MED.0b013e32835edb89
20. van Belle TL, Coppieters KT, von Herrath MG. Type 1 diabetes: etiology, immunology, and therapeutic strategies. *Physiol Rev* (2011) 91(1):79–118. doi:10.1152/physrev.00003.2010
21. Atkinson MA. The pathogenesis and natural history of type 1 diabetes. *Cold Spring Harb Perspect Med* (2012) 2(11):a007641. doi:10.1101/cshperspect.a007641
22. Katsarou A, Gudbjornsdottir S, Rawshani A, Dabelea D, Bonifacio E, Anderson BJ, et al. Type 1 diabetes mellitus. *Nat Rev Dis Primers* (2017) 3:17016. doi:10.1038/nrdp.2017.16
23. Barrett JC, Clayton DG, Concannon P, Akolkar B, Cooper JD, Erlich HA, et al. Genome-wide association study and meta-analysis find that over 40 loci affect risk of type 1 diabetes. *Nat Genet* (2009) 41(6):703–7. doi:10.1038/ng.381
24. Concannon P, Erlich HA, Julier C, Morahan G, Nerup J, Pociot F, et al. Type 1 diabetes: evidence for susceptibility loci from four genome-wide linkage scans in 1,435 multiplex families. *Diabetes* (2005) 54(10):2995–3001. doi:10.2337/diabetes.54.10.2995
25. Pociot F, Akolkar B, Concannon P, Erlich HA, Julier C, Morahan G, et al. Genetics of type 1 diabetes: what's next? *Diabetes* (2010) 59(7):1561–71. doi:10.2337/db10-0076
26. Pociot F, McDermott MF. Genetics of type 1 diabetes mellitus. *Genes Immun* (2002) 3(5):235–49. doi:10.1038/sj.gene.6363875

27. Noble JA, Erlich HA. Genetics of type 1 diabetes. *Cold Spring Harb Perspect Med* (2012) 2(1):a007732. doi:10.1101/cshperspect.a007732
28. Onengut-Gumuscu S, Chen WM, Burren O, Cooper NJ, Quinlan AR, Mychaleckyj JC, et al. Fine mapping of type 1 diabetes susceptibility loci and evidence for colocalization of causal variants with lymphoid gene enhancers. *Nat Genet* (2015) 47(4):381–6. doi:10.1038/ng.3245
29. Singal DP, Blajchman MA. Histocompatibility (HL-A) antigens, lymphocytotoxic antibodies and tissue antibodies in patients with diabetes mellitus. *Diabetes* (1973) 22(6):429–32. doi:10.2337/diab.22.6.429
30. Nerup J, Platz P, Andersen OO, Christy M, Lyngsoe J, Poulsen JE, et al. HL-A antigens and diabetes mellitus. *Lancet* (1974) 2(7885):864–6. doi:10.1016/S0140-6736(74)91201-X
31. Bottini N, Musumeci L, Alonso A, Rahmouni S, Nika K, Rostamkhani M, et al. A functional variant of lymphoid tyrosine phosphatase is associated with type I diabetes. *Nat Genet* (2004) 36(4):337–8. doi:10.1038/ng1323
32. Smyth D, Cooper JD, Collins JE, Heward JM, Franklyn JA, Howson JM, et al. Replication of an association between the lymphoid tyrosine phosphatase locus (LYP/PTPN22) with type 1 diabetes, and evidence for its role as a general autoimmunity locus. *Diabetes* (2004) 53(11):3020–3. doi:10.2337/diabetes.53.11.3020
33. Nistico L, Buzzetti R, Pritchard LE, Van der Auwera B, Giovannini C, Bosi E, et al. The CTLA-4 gene region of chromosome 2q33 is linked to, and associated with, type 1 diabetes. Belgian Diabetes Registry. *Hum Mol Genet* (1996) 5(7):1075–80. doi:10.1093/hmg/5.7.1075
34. Ueda H, Howson JM, Esposito L, Heward J, Snook H, Chamberlain G, et al. Association of the T-cell regulatory gene CTLA4 with susceptibility to autoimmune disease. *Nature* (2003) 423(6939):506–11. doi:10.1038/nature01621
35. Field LL, Larsen Z, Pociot F, Nerup J, Tobias R, Bonnevie-Nielsen V. Evidence for a locus (IDDM16) in the immunoglobulin heavy chain region on chromosome 14q32.3 producing susceptibility to type 1 diabetes. *Genes Immun* (2002) 3(6):338–44. doi:10.1038/sj.gene.6363857
36. Morahan G, Huang D, Ymer SI, Cancilla MR, Stephen K, Dabadghao P, et al. Linkage disequilibrium of a type 1 diabetes susceptibility locus with a regulatory IL12B allele. *Nat Genet* (2001) 27(2):218–21. doi:10.1038/84872
37. Dooley J, Tian L, Schonefeldt S, Delghingaro-Augusto V, Garcia-Perez JE, Pasciuto E, et al. Genetic predisposition for beta cell fragility underlies type 1 and type 2 diabetes. *Nat Genet* (2016) 48(5):519–27. doi:10.1038/ng.3531
38. Filippi CM, von Herrath MG. Viral trigger for type 1 diabetes: pros and cons. *Diabetes* (2008) 57(11):2863–71. doi:10.2337/db07-1023
39. Op de Beeck A, Eizirik DL. Viral infections in type 1 diabetes mellitus – why the beta cells? *Nat Rev Endocrinol* (2016) 12(5):263–73. doi:10.1038/nrendo.2016.30
40. Schulte BM, Bakkers J, Lanke KH, Melchers WJ, Westerlaken C, Allebes W, et al. Detection of enterovirus RNA in peripheral blood mononuclear cells of type 1 diabetic patients beyond the stage of acute infection. *Viral Immunol* (2010) 23(1):99–104. doi:10.1089/vim.2009.0072
41. Laitinen OH, Honkanen H, Pakkanen O, Oikarinen S, Hankaniemi MM, Huhtala H, et al. Coxsackievirus B1 is associated with induction of beta-cell autoimmunity that portends type 1 diabetes. *Diabetes* (2014) 63(2):446–55. doi:10.2337/db13-0619
42. Oikarinen S, Tauriainen S, Hober D, Lucas B, Vazeou A, Sioofy-Khojine A, et al. Virus antibody survey in different European populations indicates risk association between coxsackievirus B1 and type 1 diabetes. *Diabetes* (2014) 63(2):655–62. doi:10.2337/db13-0620
43. Richardson SJ, Leete P, Dhayal S, Russell MA, Oikarinen M, Laiho JE, et al. Detection of enterovirus in the islet cells of patients with type 1 diabetes: what do we learn from immunohistochemistry? Reply to Hansson SF, Korsgren S, Ponten F et al [letter]. *Diabetologia* (2014) 57(3):647–9. doi:10.1007/s00125-014-3167-2
44. Lin HC, Wang CH, Tsai FJ, Hwang KP, Chen W, Lin CC, et al. Enterovirus infection is associated with an increased risk of childhood type 1 diabetes in Taiwan: a nationwide population-based cohort study. *Diabetologia* (2015) 58(1):79–86. doi:10.1007/s00125-014-3400-z
45. Ylipaasto P, Klingel K, Lindberg AM, Otonkoski T, Kandolf R, Hovi T, et al. Enterovirus infection in human pancreatic islet cells, islet tropism in vivo and receptor involvement in cultured islet beta cells. *Diabetologia* (2004) 47(2):225–39. doi:10.1007/s00125-003-1297-z
46. Dotta F, Censini S, van Halteren AG, Marselli L, Masini M, Dionisi S, et al. Coxsackie B4 virus infection of beta cells and natural killer cell insulitis in recent-onset type 1 diabetic patients. *Proc Natl Acad Sci U S A* (2007) 104(12):5115–20. doi:10.1073/pnas.0700442104
47. Krogvold L, Edwin B, Buanes T, Frisk G, Skog O, Anagandula M, et al. Detection of a low-grade enteroviral infection in the islets of Langerhans of living patients newly diagnosed with type 1 diabetes. *Diabetes* (2015) 64(5):1682–7. doi:10.2337/db14-1370
48. Knip M, Siljander H. The role of the intestinal microbiota in type 1 diabetes mellitus. *Nat Rev Endocrinol* (2016) 12(3):154–67. doi:10.1038/nrendo.2015.218
49. Vaarala O, Atkinson MA, Neu J. The "perfect storm" for type 1 diabetes: the complex interplay between intestinal microbiota, gut permeability, and mucosal immunity. *Diabetes* (2008) 57(10):2555–62. doi:10.2337/db08-0331
50. Wen L, Ley RE, Volchkov PY, Stranges PB, Avanesyan L, Stonebraker AC, et al. Innate immunity and intestinal microbiota in the development of type 1 diabetes. *Nature* (2008) 455(7216):1109–13. doi:10.1038/nature07336
51. Markle JG, Frank DN, Mortin-Toth S, Robertson CE, Feazel LM, Rolle-Kampczyk U, et al. Sex differences in the gut microbiome drive hormone-dependent regulation of autoimmunity. *Science* (2013) 339(6123):1084–8. doi:10.1126/science.1233521
52. de Goffau MC, Luopajarvi K, Knip M, Ilonen J, Ruohtula T, Harkonen T, et al. Fecal microbiota composition differs between children with beta-cell autoimmunity and those without. *Diabetes* (2013) 62(4):1238–44. doi:10.2337/db12-0526
53. Endesfelder D, Zu Castell W, Ardissone A, Davis-Richardson AG, Achenbach P, Hagen M, et al. Compromised gut microbiota networks in children with anti-islet cell autoimmunity. *Diabetes* (2014) 63(6):2006–14. doi:10.2337/db13-1676
54. Kostic AD, Gevers D, Siljander H, Vatanen T, Hyotylainen T, Hamalainen AM, et al. The dynamics of the human infant gut microbiome in development and in progression toward type 1 diabetes. *Cell Host Microbe* (2015) 17(2):260–73. doi:10.1016/j.chom.2015.01.001
55. Takaba H, Takayanagi H. The mechanisms of T cell selection in the thymus. *Trends Immunol* (2017) 38(11):805–16. doi:10.1016/j.it.2017.07.010
56. Klein L, Kyewski B, Allen PM, Hogquist KA. Positive and negative selection of the T cell repertoire: what thymocytes see (and don't see). *Nat Rev Immunol* (2014) 14(6):377–91. doi:10.1038/nri3667
57. He Q, Morillon YM II, Spidale NA, Kroger CJ, Liu B, Sartor RB, et al. Thymic development of autoreactive T cells in NOD mice is regulated in an age-dependent manner. *J Immunol* (2013) 191(12):5858–66. doi:10.4049/jimmunol.1302273
58. Kroger CJ, Wang B, Tisch R. Temporal increase in thymocyte negative selection parallels enhanced thymic SIRPalpha+ DC function. *Eur J Immunol* (2016) 46(10):2352–62. doi:10.1002/eji.201646354
59. Guerau-de-Arellano M, Martinic M, Benoist C, Mathis D. Neonatal tolerance revisited: a perinatal window for Aire control of autoimmunity. *J Exp Med* (2009) 206(6):1245–52. doi:10.1084/jem.20090300
60. Anderson MS, Su MA. AIRE expands: new roles in immune tolerance and beyond. *Nat Rev Immunol* (2016) 16(4):247–58. doi:10.1038/nri.2016.9
61. Anderson MS, Venanzi ES, Klein L, Chen Z, Berzins SP, Turley SJ, et al. Projection of an immunological self shadow within the thymus by the aire protein. *Science* (2002) 298(5597):1395–401. doi:10.1126/science.1075958
62. Derbinski J, Schulte A, Kyewski B, Klein L. Promiscuous gene expression in medullary thymic epithelial cells mirrors the peripheral self. *Nat Immunol* (2001) 2(11):1032–9. doi:10.1038/ni723
63. Liston A, Lesage S, Wilson J, Peltonen L, Goodnow CC. Aire regulates negative selection of organ-specific T cells. *Nat Immunol* (2003) 4(4):350–4. doi:10.1038/ni906
64. Liston A, Lesage S, Gray DH, O'Reilly LA, Strasser A, Fahrer AM, et al. Generalized resistance to thymic deletion in the NOD mouse; a polygenic trait characterized by defective induction of Bim. *Immunity* (2004) 21(6):817–30. doi:10.1016/j.immuni.2004.10.014
65. Kishimoto H, Sprent J. A defect in central tolerance in NOD mice. *Nat Immunol* (2001) 2(11):1025–31. doi:10.1038/ni726

66. Mingueneau M, Jiang W, Feuerer M, Mathis D, Benoist C. Thymic negative selection is functional in NOD mice. *J Exp Med* (2012) 209(3):623–37. doi:10.1084/jem.20112593
67. Zucchelli S, Holler P, Yamagata T, Roy M, Benoist C, Mathis D. Defective central tolerance induction in NOD mice: genomics and genetics. *Immunity* (2005) 22(3):385–96. doi:10.1016/j.immuni.2005.01.015
68. Vang T, Congia M, Macis MD, Musumeci L, Orru V, Zavattari P, et al. Autoimmune-associated lymphoid tyrosine phosphatase is a gain-of-function variant. *Nat Genet* (2005) 37(12):1317–9. doi:10.1038/ng1673
69. Abramson J, Husebye ES. Autoimmune regulator and self-tolerance – molecular and clinical aspects. *Immunol Rev* (2016) 271(1):127–40. doi:10.1111/imr.12419
70. Ramsey C, Winqvist O, Puhakka L, Halonen M, Moro A, Kampe O, et al. Aire deficient mice develop multiple features of APECED phenotype and show altered immune response. *Hum Mol Genet* (2002) 11(4):397–409. doi:10.1093/hmg/11.4.397
71. Zuklys S, Balciunaite G, Agarwal A, Fasler-Kan E, Palmer E, Hollander GA. Normal thymic architecture and negative selection are associated with Aire expression, the gene defective in the autoimmune-polyendocrinopathy-candidiasis-ectodermal dystrophy (APECED). *J Immunol* (2000) 165(4): 1976–83. doi:10.4049/jimmunol.165.4.1976
72. Yang S, Fujikado N, Kolodin D, Benoist C, Mathis D. Immune tolerance. Regulatory T cells generated early in life play a distinct role in maintaining self-tolerance. *Science* (2015) 348(6234):589–94. doi:10.1126/science.aaa7017
73. Aricha R, Feferman T, Scott HS, Souroujon MC, Berrih-Aknin S, Fuchs S. The susceptibility of Aire(-/-) mice to experimental myasthenia gravis involves alterations in regulatory T cells. *J Autoimmun* (2011) 36(1):16–24. doi:10.1016/j.jaut.2010.09.007
74. Lei Y, Ripen AM, Ishimaru N, Ohigashi I, Nagasawa T, Jeker LT, et al. Aire-dependent production of XCL1 mediates medullary accumulation of thymic dendritic cells and contributes to regulatory T cell development. *J Exp Med* (2011) 208(2):383–94. doi:10.1084/jem.20102327
75. Nagamine K, Peterson P, Scott HS, Kudoh J, Minoshima S, Heino M, et al. Positional cloning of the APECED gene. *Nat Genet* (1997) 17(4):393–8. doi:10.1038/ng1297-393
76. Finnish-German AC. An autoimmune disease, APECED, caused by mutations in a novel gene featuring two PHD-type zinc-finger domains. *Nat Genet* (1997) 17(4):399–403. doi:10.1038/ng1297-399
77. Fornari TA, Donate PB, Macedo C, Marques MM, Magalhaes DA, Passos GA. Age-related deregulation of Aire and peripheral tissue antigen genes in the thymic stroma of non-obese diabetic (NOD) mice is associated with autoimmune type 1 diabetes mellitus (DM-1). *Mol Cell Biochem* (2010) 342(1–2):21–8. doi:10.1007/s11010-010-0464-z
78. Bell GI, Horita S, Karam JH. A polymorphic locus near the human insulin gene is associated with insulin-dependent diabetes mellitus. *Diabetes* (1984) 33(2):176–83. doi:10.2337/diabetes.33.2.176
79. Unanue ER, Ferris ST, Carrero JA. The role of islet antigen presenting cells and the presentation of insulin in the initiation of autoimmune diabetes in the NOD mouse. *Immunol Rev* (2016) 272(1):183–201. doi:10.1111/imr.12430
80. Zhang L, Nakayama M, Eisenbarth GS. Insulin as an autoantigen in NOD/human diabetes. *Curr Opin Immunol* (2008) 20(1):111–8. doi:10.1016/j.coi.2007.11.005
81. Krishnamurthy B, Dudek NL, McKenzie MD, Purcell AW, Brooks AG, Gellert S, et al. Responses against islet antigens in NOD mice are prevented by tolerance to proinsulin but not IGRP. *J Clin Invest* (2006) 116(12):3258–65. doi:10.1172/JCI29602
82. Pugliese A, Zeller M, Fernandez A Jr, Zalcberg LJ, Bartlett RJ, Ricordi C, et al. The insulin gene is transcribed in the human thymus and transcription levels correlated with allelic variation at the INS VNTR-IDDM2 susceptibility locus for type 1 diabetes. *Nat Genet* (1997) 15(3):293–7. doi:10.1038/ng0397-293
83. Vafiadis P, Bennett ST, Todd JA, Nadeau J, Grabs R, Goodyer CG, et al. Insulin expression in human thymus is modulated by INS VNTR alleles at the IDDM2 locus. *Nat Genet* (1997) 15(3):289–92. doi:10.1038/ng0397-289
84. Monti P, Scirpoli M, Rigamonti A, Mayr A, Jaeger A, Bonfanti R, et al. Evidence for in vivo primed and expanded autoreactive T cells as a specific feature of patients with type 1 diabetes. *J Immunol* (2007) 179(9):5785–92. doi:10.4049/jimmunol.179.9.5785
85. Skowera A, Ladell K, McLaren JE, Dolton G, Matthews KK, Gostick E, et al. beta-cell-specific CD8 T cell phenotype in type 1 diabetes reflects chronic autoantigen exposure. *Diabetes* (2015) 64(3):916–25. doi:10.2337/db14-0332
86. Viglietta V, Kent SC, Orban T, Hafler DA. GAD65-reactive T cells are activated in patients with autoimmune type 1a diabetes. *J Clin Invest* (2002) 109(7):895–903. doi:10.1172/JCI14114
87. Arif S, Tree TI, Astill TP, Tremble JM, Bishop AJ, Dayan CM, et al. Autoreactive T cell responses show proinflammatory polarization in diabetes but a regulatory phenotype in health. *J Clin Invest* (2004) 113(3):451–63. doi:10.1172/JCI19585
88. Luce S, Lemonnier F, Briand JP, Coste J, Lahlou N, Muller S, et al. Single insulin-specific CD8+ T cells show characteristic gene expression profiles in human type 1 diabetes. *Diabetes* (2011) 60(12):3289–99. doi:10.2337/db11-0270
89. Velthuis JH, Unger WW, Abreu JR, Duinkerken G, Franken K, Peakman M, et al. Simultaneous detection of circulating autoreactive CD8+ T-cells specific for different islet cell-associated epitopes using combinatorial MHC multimers. *Diabetes* (2010) 59(7):1721–30. doi:10.2337/db09-1486
90. Chen Z, Benoist C, Mathis D. How defects in central tolerance impinge on a deficiency in regulatory T cells. *Proc Natl Acad Sci U S A* (2005) 102(41):14735–40. doi:10.1073/pnas.0507014102
91. Jiang W, Anderson MS, Bronson R, Mathis D, Benoist C. Modifier loci condition autoimmunity provoked by Aire deficiency. *J Exp Med* (2005) 202(6):805–15. doi:10.1084/jem.20050693
92. Ferreira C, Singh Y, Furmanski AL, Wong FS, Garden OA, Dyson J. Non-obese diabetic mice select a low-diversity repertoire of natural regulatory T cells. *Proc Natl Acad Sci U S A* (2009) 106(20):8320–5. doi:10.1073/pnas.0808493106
93. St-Onge L, Wehr R, Gruss P. Pancreas development and diabetes. *Curr Opin Genet Dev* (1999) 9(3):295–300. doi:10.1016/S0959-437X(99)80044-6
94. Finegood DT, Scaglia L, Bonner-Weir S. Dynamics of beta-cell mass in the growing rat pancreas. Estimation with a simple mathematical model. *Diabetes* (1995) 44(3):249–56. doi:10.2337/diabetes.44.3.249
95. Gagnerault MC, Luan JJ, Lotton C, Lepault F. Pancreatic lymph nodes are required for priming of beta cell reactive T cells in NOD mice. *J Exp Med* (2002) 196(3):369–77. doi:10.1084/jem.20011353
96. Turley S, Poirot L, Hattori M, Benoist C, Mathis D. Physiological beta cell death triggers priming of self-reactive T cells by dendritic cells in a type-1 diabetes model. *J Exp Med* (2003) 198(10):1527–37. doi:10.1084/jem.20030966
97. Rotondi M, Chiovato L, Romagnani S, Serio M, Romagnani P. Role of chemokines in endocrine autoimmune diseases. *Endocr Rev* (2007) 28(5):492–520. doi:10.1210/er.2006-0044
98. Sarkar SA, Lee CE, Victorino F, Nguyen TT, Walters JA, Burrack A, et al. Expression and regulation of chemokines in murine and human type 1 diabetes. *Diabetes* (2012) 61(2):436–46. doi:10.2337/db11-0853
99. Rhode A, Pauza ME, Barral AM, Rodrigo E, Oldstone MB, von Herrath MG, et al. Islet-specific expression of CXCL10 causes spontaneous islet infiltration and accelerates diabetes development. *J Immunol* (2005) 175(6):3516–24. doi:10.4049/jimmunol.175.6.3516
100. Yurkovetskiy L, Burrows M, Khan AA, Graham L, Volchkov P, Becker L, et al. Gender bias in autoimmunity is influenced by microbiota. *Immunity* (2013) 39(2):400–12. doi:10.1016/j.immuni.2013.08.013
101. Kawabe T, Jankovic D, Kawabe S, Huang Y, Lee PH, Yamane H, et al. Memory-phenotype CD4+ T cells spontaneously generated under steady-state conditions exert innate TH1-like effector function. *Sci Immunol* (2017) 2(12):eaam9304. doi:10.1126/sciimmunol.aam9304
102. Zhang X, Zhivaki D, Lo-Man R. Unique aspects of the perinatal immune system. *Nat Rev Immunol* (2017) 17(8):495–507. doi:10.1038/nri.2017.54
103. Jameson SC, Lee YJ, Hogquist KA. Innate memory T cells. *Adv Immunol* (2015) 126:173–213. doi:10.1016/bs.ai.2014.12.001
104. Kieper WC, Troy A, Burghardt JT, Ramsey C, Lee JY, Jiang HQ, et al. Recent immune status determines the source of antigens that drive homeostatic T cell expansion. *J Immunol* (2005) 174(6):3158–63. doi:10.4049/jimmunol.174.6.3158

105. Christianson SW, Shultz LD, Leiter EH. Adoptive transfer of diabetes into immunodeficient NOD-scid/scid mice. Relative contributions of CD4+ and CD8+ T-cells from diabetic versus prediabetic NOD. NON-Thy-1a donors. *Diabetes* (1993) 42(1):44–55. doi:10.2337/diab.42.1.44
106. Roep BO. The role of T-cells in the pathogenesis of Type 1 diabetes: from cause to cure. *Diabetologia* (2003) 46(3):305–21. doi:10.1007/s00125-003-1089-5
107. Pang S, Zhang L, Wang H, Yi Z, Li L, Gao L, et al. CD8(+) T cells specific for beta cells encounter their cognate antigens in the islets of NOD mice. *Eur J Immunol* (2009) 39(10):2716–24. doi:10.1002/eji.200939408
108. Mallone R, Brezar V, Boitard C. T cell recognition of autoantigens in human type 1 diabetes: clinical perspectives. *Clin Dev Immunol* (2011) 2011:513210. doi:10.1155/2011/513210
109. Walker LS, von Herrath M. CD4 T cell differentiation in type 1 diabetes. *Clin Exp Immunol* (2016) 183(1):16–29. doi:10.1111/cei.12672
110. Kuriya G, Uchida T, Akazawa S, Kobayashi M, Nakamura K, Satoh T, et al. Double deficiency in IL-17 and IFN-gamma signalling significantly suppresses the development of diabetes in the NOD mouse. *Diabetologia* (2013) 56(8):1773–80. doi:10.1007/s00125-013-2935-8
111. Ferraro A, Socci C, Stabilini A, Valle A, Monti P, Piemonti L, et al. Expansion of Th17 cells and functional defects in T regulatory cells are key features of the pancreatic lymph nodes in patients with type 1 diabetes. *Diabetes* (2011) 60(11):2903–13. doi:10.2337/db11-0090
112. Martin AJ, Clark M, Gojanovich G, Manzoor F, Miller K, Kline DE, et al. Anti-coreceptor therapy drives selective T cell egress by suppressing inflammation-dependent chemotactic cues. *JCI Insight* (2016) 1(17):e87636. doi:10.1172/jci.insight.87636
113. Cnop M, Welsh N, Jonas JC, Jorns A, Lenzen S, Eizirik DL. Mechanisms of pancreatic beta-cell death in type 1 and type 2 diabetes: many differences, few similarities. *Diabetes* (2005) 54(Suppl 2):S97–107. doi:10.2337/diabetes.54.suppl_2.S97
114. Yoon JW, Jun HS. Autoimmune destruction of pancreatic beta cells. *Am J Ther* (2005) 12(6):580–91. doi:10.1097/01.mjt.0000178767.67857.63
115. Ferreira RC, Simons HZ, Thompson WS, Cutler AJ, Dopico XC, Smyth DJ, et al. IL-21 production by CD4+ effector T cells and frequency of circulating follicular helper T cells are increased in type 1 diabetes patients. *Diabetologia* (2015) 58(4):781–90. doi:10.1007/s00125-015-3509-8
116. Sutherland AP, Van Belle T, Wurster AL, Suto A, Michaud M, Zhang D, et al. Interleukin-21 is required for the development of type 1 diabetes in NOD mice. *Diabetes* (2009) 58(5):1144–55. doi:10.2337/db08-0882
117. Vinuesa CG, Tangye SG, Moser B, Mackay CR. Follicular B helper T cells in antibody responses and autoimmunity. *Nat Rev Immunol* (2005) 5(11):853–65. doi:10.1038/nri1714
118. Crotty S. Follicular helper CD4 T cells (TFH). *Annu Rev Immunol* (2011) 29:621–63. doi:10.1146/annurev-immunol-031210-101400
119. Kenefeck R, Wang CJ, Kapadi T, Wardzinski L, Attridge K, Clough LE, et al. Follicular helper T cell signature in type 1 diabetes. *J Clin Invest* (2015) 125(1):292–303. doi:10.1172/JCI76238
120. Serreze DV, Chapman HD, Varnum DS, Hanson MS, Reifsnyder PC, Richard SD, et al. B lymphocytes are essential for the initiation of T cell-mediated autoimmune diabetes: analysis of a new "speed congenic" stock of NOD.Ig mu null mice. *J Exp Med* (1996) 184(5):2049–53. doi:10.1084/jem.184.5.2049
121. Noorchashm H, Lieu YK, Noorchashm N, Rostami SY, Greeley SA, Schlachterman A, et al. I-Ag7-mediated antigen presentation by B lymphocytes is critical in overcoming a checkpoint in T cell tolerance to islet beta cells of nonobese diabetic mice. *J Immunol* (1999) 163(2):743–50.
122. Frohlich A, Kisielow J, Schmitz I, Freigang S, Shamshiev AT, Weber J, et al. IL-21R on T cells is critical for sustained functionality and control of chronic viral infection. *Science* (2009) 324(5934):1576–80. doi:10.1126/science.1172815
123. Yi JS, Du M, Zajac AJ. A vital role for interleukin-21 in the control of a chronic viral infection. *Science* (2009) 324(5934):1572–6. doi:10.1126/science.1175194
124. McGuire HM, Vogelzang A, Ma CS, Hughes WE, Silveira PA, Tangye SG, et al. A subset of interleukin-21+ chemokine receptor CCR9+ T helper cells target accessory organs of the digestive system in autoimmunity. *Immunity* (2011) 34(4):602–15. doi:10.1016/j.immuni.2011.01.021
125. Sutherland AP, Joller N, Michaud M, Liu SM, Kuchroo VK, Grusby MJ. IL-21 promotes CD8+ CTL activity via the transcription factor T-bet. *J Immunol* (2013) 190(8):3977–84. doi:10.4049/jimmunol.1201730
126. Anjos S, Nguyen A, Ounissi-Benkalha H, Tessier MC, Polychronakos C. A common autoimmunity predisposing signal peptide variant of the cytotoxic T-lymphocyte antigen 4 results in inefficient glycosylation of the susceptibility allele. *J Biol Chem* (2002) 277(48):46478–86. doi:10.1074/jbc.M206894200
127. Luhder F, Chambers C, Allison JP, Benoist C, Mathis D. Pinpointing when T cell costimulatory receptor CTLA-4 must be engaged to dampen diabetogenic T cells. *Proc Natl Acad Sci U S A* (2000) 97(22):12204–9. doi:10.1073/pnas.200348397
128. Schneider A, Rieck M, Sanda S, Pihoker C, Greenbaum C, Buckner JH. The effector T cells of diabetic subjects are resistant to regulation via CD4+ FOXP3+ regulatory T cells. *J Immunol* (2008) 181(10):7350–5. doi:10.4049/jimmunol.181.10.7350
129. D'Alise AM, Auyeung V, Feuerer M, Nishio J, Fontenot J, Benoist C, et al. The defect in T-cell regulation in NOD mice is an effect on the T-cell effectors. *Proc Natl Acad Sci U S A* (2008) 105(50):19857–62. doi:10.1073/pnas.0810713105
130. Tang Q, Adams JY, Penaranda C, Melli K, Piaggio E, Sgouroudis E, et al. Central role of defective interleukin-2 production in the triggering of islet autoimmune destruction. *Immunity* (2008) 28(5):687–97. doi:10.1016/j.immuni.2008.03.016
131. Xufre C, Costa M, Roura-Mir C, Codina-Busqueta E, Usero L, Pizarro E, et al. Low frequency of GITR+ T cells in ex vivo and in vitro expanded Treg cells from type 1 diabetic patients. *Int Immunol* (2013) 25(10):563–74. doi:10.1093/intimm/dxt020
132. Brunkow ME, Jeffery EW, Hjerrild KA, Paeper B, Clark LB, Yasayko SA, et al. Disruption of a new forkhead/winged-helix protein, scurfin, results in the fatal lymphoproliferative disorder of the scurfy mouse. *Nat Genet* (2001) 27(1):68–73. doi:10.1038/83784
133. Wildin RS, Smyk-Pearson S, Filipovich AH. Clinical and molecular features of the immunodysregulation, polyendocrinopathy, enteropathy, X linked (IPEX) syndrome. *J Med Genet* (2002) 39(8):537–45. doi:10.1136/jmg.39.8.537
134. Fontenot JD, Gavin MA, Rudensky AY. Foxp3 programs the development and function of CD4+CD25+ regulatory T cells. *Nat Immunol* (2003) 4(4):330–6. doi:10.1038/ni904
135. Collison LW, Chaturvedi V, Henderson AL, Giacomin PR, Guy C, Bankoti J, et al. IL-35-mediated induction of a potent regulatory T cell population. *Nat Immunol* (2010) 11(12):1093–101. doi:10.1038/ni.1952
136. Vignali DA, Collison LW, Workman CJ. How regulatory T cells work. *Nat Rev Immunol* (2008) 8(7):523–32. doi:10.1038/nri2343
137. Lowe CE, Cooper JD, Brusko T, Walker NM, Smyth DJ, Bailey R, et al. Large-scale genetic fine mapping and genotype-phenotype associations implicate polymorphism in the IL2RA region in type 1 diabetes. *Nat Genet* (2007) 39(9):1074–82. doi:10.1038/ng2102
138. Maier LM, Anderson DE, Severson CA, Baecher-Allan C, Healy B, Liu DV, et al. Soluble IL-2RA levels in multiple sclerosis subjects and the effect of soluble IL-2RA on immune responses. *J Immunol* (2009) 182(3):1541–7. doi:10.4049/jimmunol.182.3.1541
139. Giordano C, Panto F, Caruso C, Modica MA, Zambito AM, Sapienza N, et al. Interleukin 2 and soluble interleukin 2-receptor secretion defect in vitro in newly diagnosed type I diabetic patients. *Diabetes* (1989) 38(3):310–5. doi:10.2337/diab.38.3.310
140. Brusko T, Wasserfall C, McGrail K, Schatz R, Viener HL, Schatz D, et al. No alterations in the frequency of FOXP3+ regulatory T-cells in type 1 diabetes. *Diabetes* (2007) 56(3):604–12. doi:10.2337/db06-1248
141. Brusko TM, Wasserfall CH, Clare-Salzler MJ, Schatz DA, Atkinson MA. Functional defects and the influence of age on the frequency of CD4+ CD25+ T-cells in type 1 diabetes. *Diabetes* (2005) 54(5):1407–14. doi:10.2337/diabetes.54.5.1407
142. Qu HQ, Verlaan DJ, Ge B, Lu Y, Lam KC, Grabs R, et al. A cis-acting regulatory variant in the IL2RA locus. *J Immunol* (2009) 183(8):5158–62. doi:10.4049/jimmunol.0901337
143. Denny P, Lord CJ, Hill NJ, Goy JV, Levy ER, Podolin PL, et al. Mapping of the IDDM locus Idd3 to a 0.35-cM interval containing the interleukin-2 gene. *Diabetes* (1997) 46(4):695–700. doi:10.2337/diab.46.4.695

144. Lu L, Barbi J, Pan F. The regulation of immune tolerance by FOXP3. *Nat Rev Immunol* (2017) 17(11):703–17. doi:10.1038/nri.2017.75
145. Bailey-Bucktrout SL, Bluestone JA. Regulatory T cells: stability revisited. *Trends Immunol* (2011) 32(7):301–6. doi:10.1016/j.it.2011.04.002
146. Lindley S, Dayan CM, Bishop A, Roep BO, Peakman M, Tree TI. Defective suppressor function in CD4(+)CD25(+) T-cells from patients with type 1 diabetes. *Diabetes* (2005) 54(1):92–9. doi:10.2337/diabetes.54.1.92
147. Ryba-Stanislawowska M, Rybarczyk-Kapturska K, Mysliwiec M, Mysliwska J. Elevated levels of serum IL-12 and IL-18 are associated with lower frequencies of CD4(+)CD25 (high)FOXP3 (+) regulatory t cells in young patients with type 1 diabetes. *Inflammation* (2014) 37(5):1513–20. doi:10.1007/s10753-014-9878-1
148. Haseda F, Imagawa A, Murase-Mishiba Y, Terasaki J, Hanafusa T. CD4(+) CD45RA(-) FoxP3high activated regulatory T cells are functionally impaired and related to residual insulin-secreting capacity in patients with type 1 diabetes. *Clin Exp Immunol* (2013) 173(2):207–16. doi:10.1111/cei.12116
149. Hulme MA, Wasserfall CH, Atkinson MA, Brusko TM. Central role for interleukin-2 in type 1 diabetes. *Diabetes* (2012) 61(1):14–22. doi:10.2337/db11-1213
150. Garg G, Tyler JR, Yang JH, Cutler AJ, Downes K, Pekalski M, et al. Type 1 diabetes-associated IL2RA variation lowers IL-2 signaling and contributes to diminished CD4+CD25+ regulatory T cell function. *J Immunol* (2012) 188(9):4644–53. doi:10.4049/jimmunol.1100272
151. Hartemann A, Bensimon G, Payan CA, Jacqueminet S, Bourron O, Nicolas N, et al. Low-dose interleukin 2 in patients with type 1 diabetes: a phase 1/2 randomised, double-blind, placebo-controlled trial. *Lancet Diabetes Endocrinol* (2013) 1(4):295–305. doi:10.1016/S2213-8587(13)70113-X
152. Grinberg-Bleyer Y, Baeyens A, You S, Elhage R, Fourcade G, Gregoire S, et al. IL-2 reverses established type 1 diabetes in NOD mice by a local effect on pancreatic regulatory T cells. *J Exp Med* (2010) 207(9):1871–8. doi:10.1084/jem.20100209
153. Roep BO, Kracht MJ, van Lummel M, Zaldumbide A. A roadmap of the generation of neoantigens as targets of the immune system in type 1 diabetes. *Curr Opin Immunol* (2016) 43:67–73. doi:10.1016/j.coi.2016.09.007
154. McLaughlin RJ, de Haan A, Zaldumbide A, de Koning EJ, de Ru AH, van Veelen PA, et al. Human islets and dendritic cells generate post-translationally modified islet autoantigens. *Clin Exp Immunol* (2016) 185(2):133–40. doi:10.1111/cei.12775
155. van Lummel M, Duinkerken G, van Veelen PA, de Ru A, Cordfunke R, Zaldumbide A, et al. Posttranslational modification of HLA-DQ binding islet autoantigens in type 1 diabetes. *Diabetes* (2014) 63(1):237–47. doi:10.2337/db12-1214
156. Delong T, Wiles TA, Baker RL, Bradley B, Barbour G, Reisdorph R, et al. Pathogenic CD4 T cells in type 1 diabetes recognize epitopes formed by peptide fusion. *Science* (2016) 351(6274):711–4. doi:10.1126/science.aad2791
157. Phelps EA, Cianciaruso C, Michael IP, Pasquier M, Kanaani J, Nano R, et al. Aberrant accumulation of the diabetes autoantigen GAD65 in Golgi membranes in conditions of ER stress and autoimmunity. *Diabetes* (2016) 65(9):2686–99. doi:10.2337/db16-0180
158. Kracht MJ, van Lummel M, Nikolic T, Joosten AM, Laban S, van der Slik AR, et al. Autoimmunity against a defective ribosomal insulin gene product in type 1 diabetes. *Nat Med* (2017) 23(4):501–7. doi:10.1038/nm.4289
159. Eizirik DL, Sammeth M, Bouckenooghe T, Bottu G, Sisino G, Igoillo-Esteve M, et al. The human pancreatic islet transcriptome: expression of candidate genes for type 1 diabetes and the impact of pro-inflammatory cytokines. *PLoS Genet* (2012) 8(3):e1002552. doi:10.1371/journal.pgen.1002552
160. Yoshimatsu G, Kunnathodi F, Saravanan PB, Shahbazov R, Chang C, Darden CM, et al. Pancreatic beta cell-derived IP-10/CXCL10 isletokine mediates early loss of graft function in islet cell transplantation. *Diabetes* (2017) 66(11):2857–67. doi:10.2337/db17-0578
161. Tanaka S, Nishida Y, Aida K, Maruyama T, Shimada A, Suzuki M, et al. Enterovirus infection, CXC chemokine ligand 10 (CXCL10), and CXCR3 circuit: a mechanism of accelerated beta-cell failure in fulminant type 1 diabetes. *Diabetes* (2009) 58(10):2285–91. doi:10.2337/db09-0091
162. Homann D. Back from the brink: the uses of targeting the CXCL10:CXCR3 axis in type 1 diabetes. *Diabetes* (2015) 64(12):3990–2. doi:10.2337/dbi15-0019
163. Tan TG, Mathis D, Benoist C. Singular role for T-BET+CXCR3+ regulatory T cells in protection from autoimmune diabetes. *Proc Natl Acad Sci U S A* (2016) 113(49):14103–8. doi:10.1073/pnas.1616710113
164. Kriegel MA, Rathinam C, Flavell RA. Pancreatic islet expression of chemokine CCL2 suppresses autoimmune diabetes via tolerogenic CD11c+ CD11b+ dendritic cells. *Proc Natl Acad Sci U S A* (2012) 109(9):3457–62. doi:10.1073/pnas.1115308109
165. Bouma G, Nikolic T, Coppens JM, van Helden-Meeuwsen CG, Leenen PJ, Drexhage HA, et al. NOD mice have a severely impaired ability to recruit leukocytes into sites of inflammation. *Eur J Immunol* (2005) 35(1):225–35. doi:10.1002/eji.200425513
166. Guan R, Purohit S, Wang H, Bode B, Reed JC, Steed RD, et al. Chemokine (C-C motif) ligand 2 (CCL2) in sera of patients with type 1 diabetes and diabetic complications. *PLoS One* (2011) 6(4):e17822. doi:10.1371/journal.pone.0017822
167. Diana J, Lehuen A. Macrophages and beta-cells are responsible for CXCR2-mediated neutrophil infiltration of the pancreas during autoimmune diabetes. *EMBO Mol Med* (2014) 6(8):1090–104. doi:10.15252/emmm.201404144
168. Citro A, Cantarelli E, Piemonti L. The CXCR1/2 pathway: involvement in diabetes pathophysiology and potential target for T1D interventions. *Curr Diab Rep* (2015) 15(10):68. doi:10.1007/s11892-015-0638-x
169. Maedler K, Sergeev P, Ris F, Oberholzer J, Joller-Jemelka HI, Spinas GA, et al. Glucose-induced beta cell production of IL-1beta contributes to glucotoxicity in human pancreatic islets. *J Clin Invest* (2002) 110(6):851–60. doi:10.1172/JCI15318
170. Cardozo AK, Proost P, Gysemans C, Chen MC, Mathieu C, Eizirik DL. IL-1beta and IFN-gamma induce the expression of diverse chemokines and IL-15 in human and rat pancreatic islet cells, and in islets from pre-diabetic NOD mice. *Diabetologia* (2003) 46(2):255–66. doi:10.1007/s00125-002-1017-0
171. Timper K, Dalmas E, Dror E, Rutti S, Thienel C, Sauter NS, et al. Glucose-dependent insulinotropic peptide stimulates glucagon-like peptide 1 production by pancreatic islets via interleukin 6, produced by alpha cells. *Gastroenterology* (2016) 151(1):165–79. doi:10.1053/j.gastro.2016.03.003
172. Anquetil F, Sabouri S, Thivolet C, Rodriguez-Calvo T, Zapardiel-Gonzalo J, Amirian N, et al. Alpha cells, the main source of IL-1beta in human pancreas. *J Autoimmun* (2017) 81:68–73. doi:10.1016/j.jaut.2017.03.006
173. Thomas HE, Parker JL, Schreiber RD, Kay TW. IFN-gamma action on pancreatic beta cells causes class I MHC upregulation but not diabetes. *J Clin Invest* (1998) 102(6):1249–57. doi:10.1172/JCI2899
174. Rui J, Deng S, Arazi A, Perdigoto AL, Liu Z, Herold KC. Beta cells that resist immunological attack develop during progression of autoimmune diabetes in NOD mice. *Cell Metab* (2017) 25(3):727–38. doi:10.1016/j.cmet.2017.01.005
175. Khan IS, Mouchess ML, Zhu ML, Conley B, Fasano KJ, Hou Y, et al. Enhancement of an anti-tumor immune response by transient blockade of central T cell tolerance. *J Exp Med* (2014) 211(5):761–8. doi:10.1084/jem.20131889
176. Bakhru P, Zhu ML, Wang HH, Hong LK, Khan I, Mouchess M, et al. Combination central tolerance and peripheral checkpoint blockade unleashes antimelanoma immunity. *JCI Insight* (2017) 2(18):93265. doi:10.1172/jci.insight.93265
177. Zhu ML, Bakhru P, Conley B, Nelson JS, Free M, Martin A, et al. Sex bias in CNS autoimmune disease mediated by androgen control of autoimmune regulator. *Nat Commun* (2016) 7:11350. doi:10.1038/ncomms11350

Conflict of Interest Statement: The authors have no personal, professional, or financial relationships that are considered to be a conflict of interest.

Copyright © 2017 Clark, Kroger and Tisch. This is an open-access article distributed under the terms of the Creative Commons Attribution License (CC BY). The use, distribution or reproduction in other forums is permitted, provided the original author(s) or licensor are credited and that the original publication in this journal is cited, in accordance with accepted academic practice. No use, distribution or reproduction is permitted which does not comply with these terms.

frontiers in Immunology

MINI REVIEW
published: 12 January 2018
doi: 10.3389/fimmu.2017.01981

The Expanding Therapeutic Perspective of CCR5 Blockade

Luca Vangelista[1] and Sandro Vento[2]*

[1] Department of Biomedical Sciences, Nazarbayev University School of Medicine, Astana, Kazakhstan, [2] Department of Medicine, Nazarbayev University School of Medicine and University Medical Center, Astana, Kazakhstan

CCR5 and its interaction with chemokine ligands have been crucial for understanding and tackling HIV-1 entry into target cells. However, over time, CCR5 has witnessed an impressive transition from being considered rather unimportant in physiology and pathology to becoming central in a growing number of pathophysiological conditions. It now turns out that the massive efforts devoted to combat HIV-1 entry by interfering with CCR5, and the subsequent production of chemokine ligand variants, small chemical compounds, and other molecular entities and strategies, may set the therapeutic standards for a wealth of different pathologies. Expressed on various cell types, CCR5 plays a vital role in the inflammatory response by directing cells to sites of inflammation. Aside HIV-1, CCR5 has been implicated in other infectious diseases and non-infectious diseases such as cancer, atherosclerosis, and inflammatory bowel disease. Individuals carrying the CCR5Δ32 mutation live a normal life and are warranted a natural barrier to HIV-1 infection. Therefore, CCR5 antagonism and gene-edited knockout of the receptor gained growing interest for the therapeutic role that CCR5 blockade may play in the attenuation of the severity or progression of numerous diseases.

Keywords: CCR5, CCL5, inflammation, HIV-1, cancer

OPEN ACCESS

Edited by:
Jixin Zhong,
Case Western Reserve University,
United States

Reviewed by:
Ankit Saxena,
National Institutes of Health (NIH),
United States
Elena Monica Borroni,
Humanitas Research Hospital, Italy

****Correspondence:***
Luca Vangelista
luca.vangelista@nu.edu.kz

Specialty section:
This article was submitted to Inflammation, a section of the journal Frontiers in Immunology

Received: *09 October 2017*
Accepted: *20 December 2017*
Published: *12 January 2018*

Citation:
Vangelista L and Vento S (2018) The Expanding Therapeutic Perspective of CCR5 Blockade. Front. Immunol. 8:1981. doi: 10.3389/fimmu.2017.01981

INTRODUCTION

From its discovery, CCR5 has been a key player in HIV-1 entry into target cells and, together with its chemokine ligands, helped in understanding and tackling HIV-1 infection (1, 2). CCR5 predominates among the chemokine co-receptors used by HIV-1 for cell entry, and R5-tropic HIV-1 strains are those most commonly transmitted in the early stages of infection. A 32 base pair deletion within the CCR5 gene leads to a non-functional gene product that does not reach the cell surface, and subjects with a homozygous CCR5Δ32 deletion are protected from HIV-1 infection (3).

The discovery and implication of CCR5, CXCR4, and their chemokine ligands in HIV-1 pathogenesis triggered massive research efforts that cross-fertilized many biomedical fields related to the chemokine system and regulation. In recent years, evidence has accumulated that CCR5 and its ligands may play a role in various inflammatory diseases, as cellular activation of CCR5 normally happens through chemokine binding, which then regulate intracellular trafficking and protective cellular and humoral responses. Indeed, the migration of lymphocytes to inflammatory areas is controlled by chemokine gradients (4). CCR5 may also be relevant in the development of various types of cancer, as tumor cells directly secrete or induce fibroblasts to secrete CCL5, which maintain proliferation of CCR5-positive cancer cells. Finally, CCR5 may play a role in autoimmune diseases such as rheumatoid arthritis and multiple sclerosis (MS).

In this mini-review, we describe several aspects related to the pathophysiology of CCR5, discuss its possible dispensability, and analyze its blockade as a comprehensive therapeutic perspective.

IS CCR5 A DISCARDABLE TROUBLESOME RECEPTOR?

Soon after its discovery and implication for HIV-1 entry, CCR5 has been the subject of extensive research as a possible new player in the search for preventative and therapeutic solutions to the HIV-1 infection pandemic (2). A radical approach to CCR5 targeting could be the elimination of the receptor by gene editing, in an attempt to resemble the naturally occurring Δ32 deletion (5) (**Figure 1**). This approach has its foundation on the fact that individuals homozygous for the CCR5Δ32 deletion are seemingly healthy. The proof of concept for CCR5 elimination has been provided by the so-called Berlin patient, an HIV-1 infected person who, after a double CCR5Δ32 stem cell transplant, has remained HIV free (6, 7). However, the CCR5Δ32 mutation dates thousands of years and individuals that carry it naturally may have adapted their chemokine system to physiologically balance the absence of a functional CCR5 (8). Therefore, the effect of CCR5Δ32 stem cell transplants and artificially induced CCR5 knockouts should be considered carefully, and individuals subjected to these treatments should be followed up for a long time (9). Similar caution needs to be taken when acting on CCR5 with more conventional approaches (e.g., using CCR5 antagonists), although drug discontinuation is likely to restore normal CCR5 expression and function.

Therefore, CCR5 blockade is still an open question, as well as the genetic mechanism and environmental pressure that generated the CCR5Δ32 mutation. While HIV-1 cannot be accounted for the origins of the CCR5Δ32 mutation, these have been initially attributed to selective pressure by pathogens such as *Yersinia pestis* or variola virus. However, these hypotheses have been dismissed in favor of an older selection event connected to a different pathogen (13). Indeed, the CCR5Δ32 gene has been detected in Bronze Age skeletons (14) and is estimated to have emerged ~5,000 years ago, predating the time during which smallpox and plague became widespread human pathogens (13).

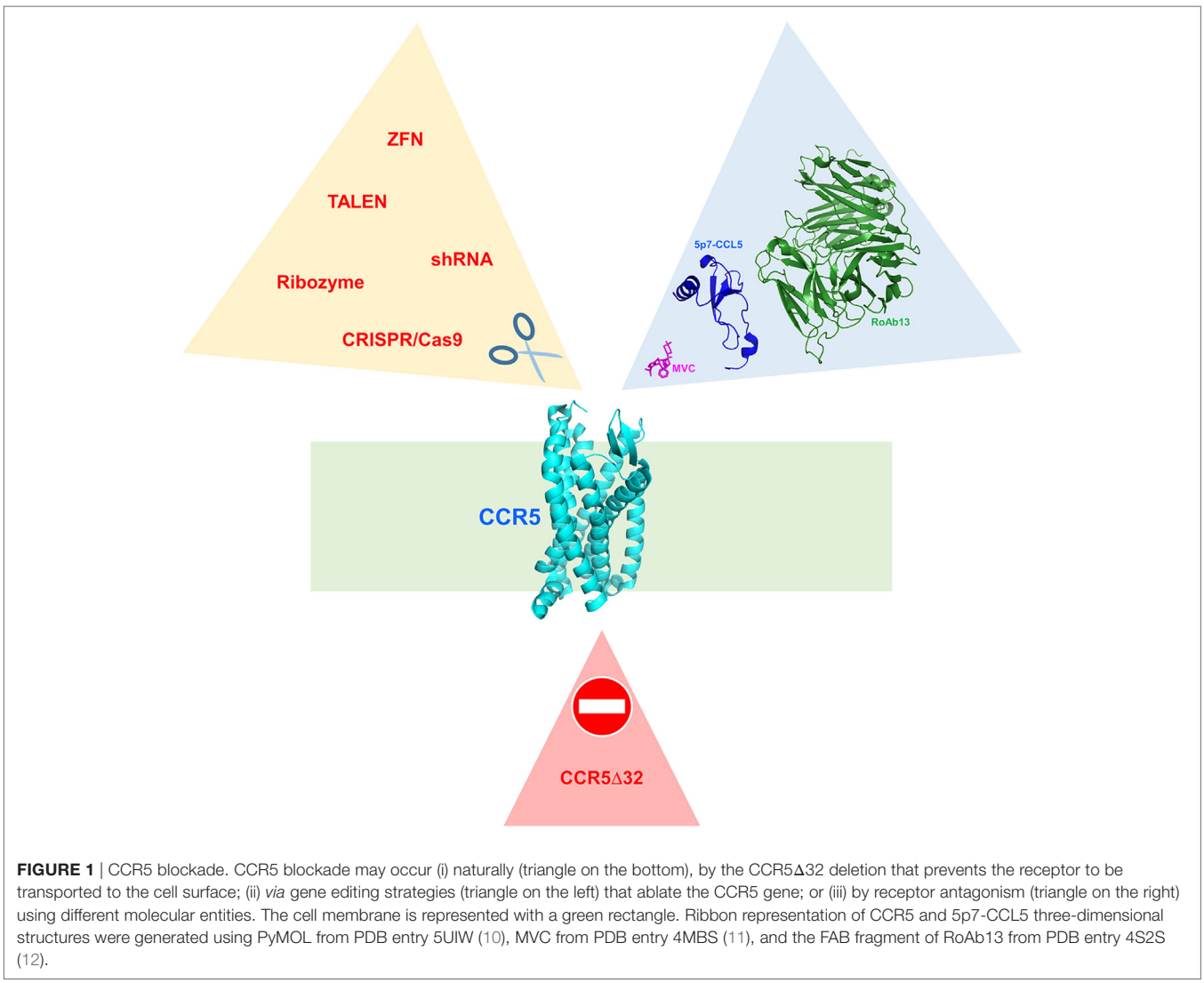

FIGURE 1 | CCR5 blockade. CCR5 blockade may occur (i) naturally (triangle on the bottom), by the CCR5Δ32 deletion that prevents the receptor to be transported to the cell surface; (ii) *via* gene editing strategies (triangle on the left) that ablate the CCR5 gene; or (iii) by receptor antagonism (triangle on the right) using different molecular entities. The cell membrane is represented with a green rectangle. Ribbon representation of CCR5 and 5p7-CCL5 three-dimensional structures were generated using PyMOL from PDB entry 5UIW (10), MVC from PDB entry 4MBS (11), and the FAB fragment of RoAb13 from PDB entry 4S2S (12).

CCR5 IN PATHOLOGY

A role for CCR5 has been suggested in numerous diseases, many involving the nervous system. CCR5 ligands are produced in the central nervous system (CNS) by microglia, astrocytes, endothelial cells, and even neurons (15, 16). The cerebrospinal fluid (CSF) of patients with relapsing-remitting MS has $CCR2^+CCR5^+$ T_H1 cells during a relapse; $CCR5^+CD8^+$ T cells and $CCR5^+$ monocytes are higher in the CSF than in the blood of patients with the disease, and CCR5 is expressed in inflammatory cells infiltrating the CNS *in vivo* (17, 18). CCR5 is also expressed on immune cells within inflammatory lesions in MS and may contribute to recruitment of these cells to the inflamed tissue or to their activation. Finally, the expression of CCR5 ligands has been shown at sites of inflammation in MS (19). Interestingly, MS can develop in people who are homozygous for the CCR5Δ32 mutation. The CCR5Δ32 allele is not associated with MS risk (20, 21), but the disease seems to be less severe in carriers of the allele (22), suggesting that CCR5 antagonists might diminish disease activity.

In contrast, homozygosity for the CCR5Δ32 allele is overrepresented in patients with symptomatic West Nile virus infection (23, 24) and is associated with severe meningoencephalitis in tick-borne encephalitis virus infections (25). Most likely, CCR5 facilitates clearance of these infections by promoting leukocyte trafficking to the CNS, a proof of its beneficial effects for human health (23). CCR5 may instead be detrimental in patients with cerebral malaria, in brain samples of whom it was found to be upregulated (26). The CCR5Δ32 allele seems to be associated with resistance to Crimean-Congo hemorrhagic fever (CCHF) virus infection, at least in the Turkish population (27). Indeed, CCL3, CCL4, and CCL5, natural ligands of CCR5, are associated with CCHF, and their levels are increased in adult patients with the infection (28).

In an emerging infectious disease, dengue virus infection, an association has been found with CCR5 expression, and the infection induces the expression of CCR5 ligands (29).

In its pathogenesis, *Toxoplasma gondii* produces a chemokine mimic that triggers CCR5, a subtle mechanism likely used to warrant *T. gondii* survival in the host (30). However, in the absence of CCR5, mice succumb to infection with uncontrolled parasite growth, altered lipid metabolism, hepatic steatosis, and widespread intestinal damage with ileum necrosis and prominent neutrophils infiltrate (31). Whether CCR5 is essential for *T. gondii* infection control in humans is unknown.

Poxviruses use chemokine receptors, including CCR5, to infect target cells; however, their molecular mechanism of receptor usage is distinct from that of HIV-1 (32). In a mouse model based on intranasal vaccinia virus infection, CCR5 expression in T cells contributes to the dissemination of the virus to the lungs and beyond; the data suggest that the role of CCR5 in vaccinia virus infection is not redundant and that CCR5 may be necessary for systemic infection *in vivo* (33).

Staphylococcus aureus is the cause of a large number of deadly infections worldwide, and the emergence of antibiotic-resistant *S. aureus* strains represents a steadily increasing global threat. The bicomponent pore-forming leukotoxin ED (LukED) is used by *S. aureus* to compromise the host immune system and cause deadly infectivity, and the gene for LukED is present in numerous clinically relevant *S. aureus* strains (34). LukE binds to human (and mouse) CCR5 on T cells, macrophages, and dendritic cells (35); subsequently, a bicomponent octamer formed by alternate LukE and LukD monomers assembles on the surface of target cells. The pores formed by LukED ultimately lead to cell death. LukED kills $CCR5^+$ cells *in vivo* in mice, and animals lacking CCR5 are protected from mortality due to *S. aureus* infection (35). Even though both LukE and gp120 target CCR5, they use different determinants on the receptor (36). Interestingly, CCR5 antagonism by maraviroc (a small chemical HIV-1 entry inhibitor) confers mice with resistance to lethal *S. aureus* infection. Maraviroc completely blocks LukED pore formation *in vitro* and therefore toxicity toward $CCR5^+$ cells (35). Therefore, the use of CCR5 antagonists to counteract *S. aureus* infection is an interesting example of antibacterial intervention, alternative or even complementary to antibiotics. In light of the debate on the emergence of the CCR5Δ32 mutation, the deadly effects of *S. aureus* infections on humankind and LukE tropism for CCR5 might have generated the ancient selection of the CCR5Δ32 allele (35).

CCR5 may also have a role in autoimmune diseases. In rheumatoid arthritis, increased levels of CCR5 ligands CCL3, CCL4, and CCL5 are found in the synovial fluid (37, 38), and the CCR5Δ32 variant seems to protect from the disease (39). However, maraviroc does not efficiently control inflammation in this setting (40).

CCR5 appears to be relevant in atherosclerosis and the development of related diseases (41). A meta-analysis of 13 studies assessed whether individuals carrying the CCR5Δ32 variant could be either protected or at risk for atherosclerosis-related cardiovascular diseases and indicated that the CCR5 Δ32-positive genotype (Δ32/Δ32 or wt/Δ32) increases the risk of atherosclerotic disease only in Asian populations (42). In a recent report, CCR5 has been described as a non-redundant, essential receptor for the homing of CD4 T cells that exacerbate atherosclerosis (43).

An increased expression of CCL5 has been detected as early as 8 days *postpartum* in a mouse model of tubulointerstitial kidney disease, an inflammatory disorder that causes progressive kidney damage and renal failure (44). It might be possible that CCL5 participates in the early cascade of event bridging the unfolded protein response (caused by an uromodulin mutation) to inflammation, although further investigations are needed (44).

CCL5 expression is increased in inflammatory bowel disease (IBD), likely pointing to a contribution by CCL5 in the progressive tissue destruction during the inflammatory processes (45). A recent investigation provided evidence that blocking CCR5 either by genetic ablation or by pharmacological inhibition with maraviroc rescued mice from colitis in both acute and chronic models (46). The latter is particularly interesting since the live microbicide strategy developed to provide vaginal *in vivo* delivery of CCL5-based HIV-1 entry inhibitors by engineered lactobacilli (47) could indeed be applied in the context of IBD, where lactobacilli are naturally resident commensal bacteria.

CCR5 has been implicated in the development of various types of cancer, including breast cancer, ovarian and cervical cancer,

prostate cancer, colon cancer, melanoma, Hodgkin lymphoma, and multiple myeloma (48). Cancer cells secrete CCL5 or induce fibroblasts to secrete CCL5, which sustain the proliferation of CCR5-positive tumor cells (48); recruit T-regulatory cells and monocytes with suppressive functions; cause osteoclast activation; and favor bone metastasis, neo-angiogenesis, and dissemination of cancer cells to distant organs (49). CCL5 has been reported to provide antitumor adjuvanticity or, conversely, to promote carcinogenesis, depending on the tumor environment (50). These opposite effects appear to be justified by the type of cancer, CCR5 expression by cancer cells, and localization of CCL5 expression. Hence, CCR5 antagonism or activation may be circumstantially tailored to provide an antitumor effect (50–53).

Finally, a multivariate analysis of unrelated HLA-matched bone marrow transplantation for hematologic malignancies conducted in Japan showed that the recipient CCR5-2086A/A genotype was significantly associated with a lower relapse rate, resulting in better disease-free and overall survival rates than other variations (54). Therefore, the recipient CCR5-2086A/A genotype affects the induction of the graft-versus-tumor effect without augmenting the development of graft-versus-host-disease (GVHD), and CCR5 genotyping in transplant recipients may be useful in determining pretransplantation risks.

In a recently published comparison of a cohort of patients enrolled in a trial of reduced-intensity allo-hematopoietic stem cell transplantation with standard GVHD prophylaxis plus maraviroc and a contemporary control cohort receiving standard GVHD prophylaxis alone, maraviroc treatment was associated with a lower incidence of acute GVHD without increased risk of disease relapse and with reduced levels of gut-specific markers (55). Maraviroc treatment increased CCR5 expression on T cells and reduced T cell activation in peripheral blood without increasing the risk of infections. These data suggest that maraviroc protects against GVHD through modulation of allo-reactive donor T cell responses.

CCR5 GENE EDITING

As discussed earlier, CCR5 knockout induced by gene therapy techniques is a strategy to reproduce the naturally occurring CCR5Δ32 deletion (56) (**Figure 1**). However, CCR5 abrogation by gene editing has been so far considered exclusively for the cure of HIV-1 (5). Zinc finger nucleases (57) have been used on CCR5 (58) and recently reviewed for their therapeutic potential and clinical trial implications (59). Other CCR5-targeted gene editing techniques include the CRISPR/Cas9 nuclease system and the transcription activator-like effector nuclease (60), as well as short hairpin RNAs (61) and ribozymes (62).

CCR5 ANTAGONISTS

In 2007, maraviroc, a negative allosteric modulator of the CCR5 receptor and therefore competitive CCR5 inhibitor, was approved for clinical use as an HIV-1 entry inhibitor that showed additional efficiency in antiretroviral-pretreated patients (63). Thus, maraviroc is far the single success story emerged from the massive pharmaceutical effort spent in the development of small chemical compounds acting as chemokine antagonists (64); many hurdles were associated with the lack of receptor specificity and the toxicity derived from it. The effect of CCR5 antagonism by maraviroc in HIV-1-infected individuals has been reported to lead to transient early treatment increase in the CD4 count and a late treatment increase in the CD8 count, which may imply a recovery of the cell-mediated immunity (65). Overall, maraviroc treatment did not seem to interfere with normal homeostasis, rather to improve it (66, 67), and ameliorate inflammatory processes in HIV-1 and beyond (68).

In the effort to attain HIV-1 entry inhibition by CCR5 blockade, CCR5 must be engaged by antagonist ligands, to avoid sustained receptor activation that could generate unwanted pro-inflammatory conditions. As described above, the participation of CCR5 in a large array of chronic inflammatory diseases makes CCR5 antagonism (or, more drastically, gene-edited CCR5 knock out) an elective therapeutic option.

Two other CCR5 antagonists have been evaluated in clinical trials in HIV-infected individuals and have failed to progress. In phase II trials in treatment-naive patients of vicriviroc, a non-competitive allosteric CCR5 antagonist (69, 70), viral rebound with continued treatment was observed (71), and in treatment-experienced patients, there was an increase in malignancies (72). Aplaviroc, a spirodiketopiperazine derivative, caused severe hepatotoxicity in infected patients in phase II clinical trials (73).

Cenicriviroc is a relatively new CCR5 antagonist presently assessed in clinical trials; it inhibits both CCR2 and CCR5 receptors and has good oral absorption (74). Cenicriviroc may offer other benefits in addition to its anti-HIV activity and is also currently in clinical trials testing its ability to reduce fibrosis in patients with non-alcoholic steatohepatitis and primary sclerosing cholangitis (75).

CCL3, CCL4, and CCL5, natural agonist ligands of CCR5, represent obvious templates for the development of protein-based CCR5 antagonists. However, CCR5 activation by these chemokines required them to be molecularly switched into antagonists. A long-lasting success story is represented by the CCL5 derivatives saga (76). Populated by several different approaches targeting the chemokine *N*-terminus, it ultimately led to highly potent variants that interact with CCR5 as antagonists (77) and are ~200-fold more potent than maraviroc in blocking HIV-1 *in vitro*.

Another protein-based approach to CCR5 antagonism is the development of monoclonal antibodies (mAbs) against CCR5 (78). PRO 140, a humanized IgG4 mAb derived from the murine mAb PA14 (79, 80), is currently in a phase III clinical trial (81). PRO 140 efficiently inhibits HIV-1 gp120 binding to CCR5 and, with lower potency, chemokines interaction with the receptor (78). Another promising anti-CCR5 mAb is CCR5mAb004, a fully human IgG4 also being tested in clinical trials (82). RoAb13 is also capable of blocking HIV-1 infection (83), and the three-dimensional structure of its Fab has been recently solved (12). Interestingly, naturally occurring anti-CCR5 antibodies have been suggested to contribute to the maintenance of homeostasis (84).

Blockade of CCR5 with antagonists is increasingly adopted to counteract inflammatory diseases and infections where this

receptor plays a relevant role. Being FDA approved and a small chemical compound, maraviroc is the CCR5 antagonist of election; however, protein-based CCR5 antagonists could be equally or even more effective. The three-dimensional structure of the complex between CCR5 and maraviroc (11) helped significantly in understanding GPCR conformational modularity and visualized the deep insertion of maraviroc in the CCR5 ligand cavity. Small chemical compounds have a relatively lower production cost and might be easier to administer, compared to protein drugs. However, last generation CCL5-based antagonists (77) provided *in vitro* anti-HIV-1 potency far superior than that of maraviroc and grant a virtually absent development of HIV-1-resistant strains (85), which is not the case for maraviroc. In a recent breakthrough in structural biology (10), the three-dimensional structure of the complex between CCR5 and 5p7-CCL5 (a potent CCR5 antagonist) (77) has been solved, revealing the extensive and deep area of CCR5 occupancy by 5p7-CCL5. This intimate molecular interaction largely justifies the impossibility for HIV-1 to generate escape mutants since gp120 occupies a similar cavity on CCR5 [modeled in Ref. (10)]; also the virus cannot generate a gp120 molecule able to circumvent the presence of 5p7-CCL5 or similar CCL5 variants. Ultimately, the high CCR5 affinity of these CCL5 variants could be exploited in the different pathological conditions where CCR5 plays a potentially crucial role.

CONCLUSION AND PERSPECTIVES

Biomedical investigations are elucidating a growing role played by CCR5 in several inflammatory diseases, and a number of microorganisms hijack CCR5 to exert their tropism. In this scenario, CCR5 blockade is conceived as a relatively harmless therapeutic option (**Figure 1**). This option is implemented either by biochemical blockade of the receptor using CCR5 antagonists or by excision of the receptor by gene editing strategies. Which of the two strategies is preferable may depend on the disease dynamics and the actual CCR5 dispensability suggested by the CCR5Δ32 allele present in individuals living a seemingly healthy life.

AUTHOR CONTRIBUTIONS

Both authors have made a substantial, direct, and intellectual contribution to the work and approved it for publication.

REFERENCES

1. Berger EA, Murphy PM, Farber JM. Chemokine receptors as HIV-1 coreceptors: roles in viral entry, tropism, and disease. *Annu Rev Immunol* (1999) 17:657–700. doi:10.1146/annurev.immunol.17.1.657
2. Lusso P. HIV and the chemokine system: 10 years later. *EMBO J* (2006) 25:447–56. doi:10.1038/sj.emboj.7600947
3. Samson M, Libert F, Doranz BJ, Rucker J, Liesnard C, Farber CM, et al. Resistance to HIV-1 infection in Caucasian individuals bearing mutant alleles of the CCR-5 chemokine receptor gene. *Nature* (1996) 382:722–5. doi:10.1038/382722a0
4. Jin T, Xu X, Hereld D. Chemotaxis, chemokine receptors and human disease. *Cytokine* (2008) 44:1–8. doi:10.1016/j.cyto.2008.06.017
5. Haworth KG, Peterson CW, Kiem HP. CCR5-edited gene therapies for HIV cure: closing the door to viral entry. *Cytotherapy* (2017) 19(11):1325–38. doi:10.1016/j.jcyt.2017.05.013
6. Hütter G, Nowak D, Mossner M, Ganepola S, Müssig A, Allers K, et al. Long-term control of HIV by CCR5 Delta32/Delta32 stem-cell transplantation. *N Engl J Med* (2009) 360:692–8. doi:10.1056/NEJMoa0802905
7. Brown TR. I am the Berlin patient: a personal reflection. *AIDS Res Hum Retroviruses* (2015) 31:2–3. doi:10.1089/AID.2014.0224
8. Barmania F, Pepper MS. C-C chemokine receptor type five (CCR5): an emerging target for the control of HIV infection. *Appl Transl Genom* (2013) 2:3–16. doi:10.1016/j.atg.2013.05.004
9. Telenti A. Safety concerns about CCR5 as an antiviral target. *Curr Opin HIV AIDS* (2009) 4:131–5. doi:10.1097/COH.0b013e3283223d76
10. Zheng Y, Han GW, Abagyan R, Wu B, Stevens RC, Cherezov V, et al. Structure of CC chemokine receptor 5 with a potent chemokine antagonist reveals mechanisms of chemokine recognition and molecular mimicry by HIV. *Immunity* (2017) 46:1005.e–17.e. doi:10.1016/j.immuni.2017.05.002
11. Tan Q, Zhu Y, Li J, Chen Z, Han GW, Kufareva I, et al. Structure of the CCR5 chemokine receptor-HIV entry inhibitor maraviroc complex. *Science* (2013) 341:1387–90. doi:10.1126/science.1241475
12. Chain B, Arnold J, Akthar S, Brandt M, Davis D, Noursadeghi M, et al. A linear epitope in the N-terminal domain of CCR5 and its interaction with antibody. *PLoS One* (2015) 10:e0128381. doi:10.1371/journal.pone.0128381
13. Hedrick PW, Verrelli BC. "Ground truth" for selection on CCR5-Delta32. *Trends Genet* (2006) 22:293–6. doi:10.1016/j.tig.2006.04.007
14. Hummel S, Schmidt D, Kremeyer B, Herrmann B, Oppermann M. Detection of the CCR5-Delta32 HIV resistance gene in Bronze Age skeletons. *Genes Immun* (2005) 6:371–4. doi:10.1038/sj.gene.6364172
15. Shukaliak JA, Dorovini-Zis K. Expression of the β chemokines RANTES and MIP 1β by human brain microvessel endothelial cells in primary culture. *J Neuropathol Exp Neurol* (2000) 59:339–52. doi:10.1093/jnen/59.5.339
16. Subileau EA, Rezaie P, Davies HA, Colyer FM, Greenwood J, Male DK, et al. Expression of chemokines and their receptors by human brain endothelium: implications for multiple sclerosis. *J Neuropathol Exp Neurol* (2009) 68:227–40. doi:10.1097/NEN.0b013e318197eca7
17. Balashov KE, Rottman JB, Weiner HL, Hancock WW. CCR5+ and CXCR3+ T cells are increased in multiple sclerosis and their ligands MIP 1α and IP 10 are expressed in demyelinating brain lesions. *Proc Natl Acad Sci U S A* (1999) 96:6873–8. doi:10.1073/pnas.96.12.6873
18. Sørensen TL, Tani M, Jensen J, Pierce V, Lucchinetti C, Folcik VA, et al. Expression of specific chemokines and chemokine receptors in the central nervous system of multiple sclerosis patients. *J Clin Invest* (1999) 103:807–15. doi:10.1172/JCI5150
19. Boven LA, Montagne L, Nottet HS, De Groot CJ. Macrophage inflammatory protein 1α (MIP 1α), MIP 1β, and RANTES mRNA semiquantification and protein expression in active demyelinating multiple sclerosis (MS) lesions. *Clin Exp Immunol* (2000) 122:257–63. doi:10.1046/j.1365-2249.2000.01334.x
20. Silversides JA, Heggarty SV, McDonnell GV, Hawkins SA, Graham CA. Influence of CCR5 δ32 polymorphism on multiple sclerosis susceptibility and disease course. *Mult Scler* (2004) 10:149–52. doi:10.1191/1352458504ms994oa
21. Kantarci OH, Morales Y, Ziemer PA, Hebrink DD, Mahad DJ, Atkinson EJ, et al. CCR5Δ32 polymorphism effects on CCR5 expression, patterns of immunopathology and disease course in multiple sclerosis. *J Neuroimmunol* (2005) 169:137–43. doi:10.1016/j.jneuroim.2005.07.025
22. van Veen T, Nielsen J, Berkhof J, Barkhof F, Kamphorst W, Bö L, et al. CCL5 and CCR5 genotypes modify clinical, radiological and pathological features of multiple sclerosis. *J Neuroimmunol* (2007) 190:157–64. doi:10.1016/j.jneuroim.2007.08.005
23. Lim JK, Glass WG, McDermott DH, Murphy PM. CCR5: no longer a "good for nothing" gene – chemokine control of West Nile virus infection. *Trends Immunol* (2006) 27:308–12. doi:10.1016/j.it.2006.05.007
24. Lim JK, Louie CY, Glaser C, Jean C, Johnson B, Johnson H, et al. Genetic deficiency of chemokine receptor CCR5 is a strong risk factor for symptomatic

West Nile virus infection: a meta-analysis of 4 cohorts in the US epidemic. *J Infect Dis* (2008) 197:262–5. doi:10.1086/524691
25. Kindberg E, Mickiene A, Ax C, Akerlind B, Vene S, Lindquist L, et al. A deletion in the chemokine receptor 5 (CCR5) gene is associated with tickborne encephalitis. *J Infect Dis* (2008) 197:266–9. doi:10.1086/524709
26. Sarfo BY, Singh S, Lillard JW Jr, Quarshie A, Gyasi RK, Armah H, et al. The cerebral-malaria-associated expression of RANTES, CCR3 and CCR5 in postmortem tissue samples. *Ann Trop Med Parasitol* (2004) 98:297–303. doi:10.1179/000349804225003271
27. Rustemoglu A, Ekinci D, Nursal AF, Barut S, Duygu F, Günal Ö. The possible role of CCR5Δ32 mutation in Crimean-Congo hemorrhagic fever infection. *J Med Virol* (2017) 89(10):1714–9. doi:10.1002/jmv.24865
28. Arasli M, Ozsurekci Y, Elaldi N, McAuley AJ, Karadag Oncel E, Tekin IO, et al. Elevated chemokine levels during adult but not pediatric Crimean-Congo hemorrhagic fever. *J Clin Virol* (2015) 66:76–82. doi:10.1016/j.jcv.2015.03.010
29. Marques RE, Guabiraba R, Del Sarto JL, Rocha RF, Queiroz AL, Cisalpino D, et al. Dengue virus requires the CC-chemokine receptor CCR5 for replication and infection development. *Immunology* (2015) 145:583–96. doi:10.1111/imm.12476
30. Aliberti J, Valenzuela JG, Carruthers VB, Hieny S, Andersen J, Charest H, et al. Molecular mimicry of a CCR5 binding-domain in the microbial activation of dendritic cells. *Nat Immunol* (2003) 4:485–90. doi:10.1038/ni915
31. Bonfá G, Benevides L, Souza Mdo C, Fonseca DM, Mineo TW, Rossi MA, et al. CCR5 controls immune and metabolic functions during *Toxoplasma gondii* infection. *PLoS One* (2014) 9:e104736. doi:10.1371/journal.pone.0104736
32. Lalani AS, Masters J, Zeng W, Barrett J, Pannu R, Everett H, et al. Use of chemokine receptors by poxviruses. *Science* (1999) 286:1968–71. doi:10.1126/science.286.5446.1968
33. Rahbar R, Murooka TT, Fish EN. Role for CCR5 in dissemination of vaccinia virus in vivo. *J Virol* (2009) 83:2226–36. doi:10.1128/JVI.01655-08
34. Vandenesch F, Naimi T, Enright MC, Lina G, Nimmo GR, Heffernan H, et al. Community-acquired methicillin-resistant *Staphylococcus aureus* carrying Panton-Valentine leukocidin genes: worldwide emergence. *Emerg Infect Dis* (2003) 9:978–84. doi:10.3201/eid0908.030089
35. Alonzo F III, Kozhaya L, Rawlings SA, Reyes-Robles T, DuMont AL, Myszka DG, et al. CCR5 is a receptor for *Staphylococcus aureus* leukotoxin ED. *Nature* (2013) 493:51–5. doi:10.1038/nature11724
36. Tam K, Schultz M, Reyes-Robles T, Vanwalscappel B, Horton J, Alonzo F III, et al. *Staphylococcus aureus* leukocidin LukED and HIV-1 gp120 target different sequence determinants on CCR5. *MBio* (2016) 7:e2024–2016. doi:10.1128/mBio.02024-16
37. Mack M, Bruhl H, Gruber R, Jaeger C, Cihak J, Eiter V, et al. Predominance of mononuclear cells expressing the chemokine receptor CCR5 in synovial effusions of patients with different forms of arthritis. *Arthritis Rheum* (1999) 42:981–8. doi:10.1002/1529-0131(199905)42:5<981::AID-ANR17>3.0.CO;2-4
38. Patel DD, Zachariah JP, Whichard LP. CXCR3 and CCR5 ligands in rheumatoid arthritis synovium. *Clin Immun* (2001) 98:39–45. doi:10.1006/clim.2000.4957
39. Pokorny V, McQueen F, Yeoman S, Merriman M, Merriman A, Harrison A, et al. Evidence for negative association of the chemokine receptor CCR5 d32 polymorphism with rheumatoid arthritis. *Ann Rheum Dis* (2005) 64:487–90. doi:10.1136/ard.2004.023333
40. Fleishaker DL, Garcia Meijide JA, Petrov A, Kohen MD, Wang X, Menon S, et al. Maraviroc, a chemokine receptor 5 antagonist, fails to demonstrate efficacy in the treatment of patients with rheumatoid arthritis in a randomized, double-blind placebo-controlled trial. *Arthritis Res Ther* (2012) 14:R11. doi:10.1186/ar3685
41. Jones KL, Maguire JJ, Davenport AP. Chemokine receptor CCR5: from AIDS to atherosclerosis. *Br J Pharmacol* (2011) 162:1453–69. doi:10.1111/j.1476-5381.2010.01147.x
42. Zhang Z, Liu J, Wang H, Wu H, Wu X, Dong J, et al. Association between chemokine receptor 5 (CCR5) delta32 gene variant and atherosclerosis: a meta-analysis of 13 studies. *Int J Clin Exp Med* (2015) 8:658–65.
43. Li J, McArdle S, Gholami A, Kimura T, Wolf D, Gerhardt T, et al. CCR5+ T-bet+FoxP3+ effector CD4 T cells drive atherosclerosis. *Circ Res* (2016) 118:1540–52. doi:10.1161/CIRCRESAHA.116.308648
44. Trudu M, Schaeffer C, Riba M, Ikehata M, Brambilla P, Messa P, et al. Early involvement of cellular stress and inflammatory signals in the pathogenesis of tubulointerstitial kidney disease due to UMOD mutations. *Sci Rep* (2017) 7:7383. doi:10.1038/s41598-017-07804-6
45. McCormack G, Moriarty D, O'Donoghue DP, McCormick PA, Sheahan K, Baird AW. Tissue cytokine and chemokine expression in inflammatory bowel disease. *Inflamm Res* (2001) 50:491–5. doi:10.1007/PL00000223
46. Mencarelli A, Cipriani S, Francisci D, Santucci L, Baldelli F, Distrutti E, et al. Highly specific blockade of CCR5 inhibits leukocyte trafficking and reduces mucosal inflammation in murine colitis. *Sci Rep* (2016) 6:30802. doi:10.1038/srep30802
47. Vangelista L, Secchi M, Liu X, Bachi A, Jia L, Xu Q, et al. Engineering of *Lactobacillus jensenii* to secrete RANTES and a CCR5 antagonist analogue as live HIV-1 blockers. *Antimicrob Agents Chemother* (2010) 54:2994–3001. doi:10.1128/AAC.01492-09
48. Aldinucci D, Colombatti A. The inflammatory chemokine CCL5 and cancer progression. *Mediators Inflamm* (2014) 2014:292376. doi:10.1155/2014/292376
49. de Oliveira CE, Oda JM, Losi Guembarovski R, de Oliveira KB, Ariza CB, Neto JS, et al. CC chemokine receptor 5: the interface of host immunity and cancer. *Dis Markers* (2014) 2014:126954. doi:10.1155/2014/126954
50. Lapteva N, Huang XF. CCL5 as an adjuvant for cancer immunotherapy. *Expert Opin Biol Ther* (2010) 10:725–33. doi:10.1517/14712591003657128
51. Velasco-Velázquez M, Xolalpa W, Pestell RG. The potential to target CCL5/CCR5 in breast cancer. *Expert Opin Ther Targets* (2014) 18:1265–75. doi:10.1517/14728222.2014.949238
52. Bronte V, Bria E. Interfering with CCL5/CCR5 at the tumor-stroma interface. *Cancer Cell* (2016) 29:437–9. doi:10.1016/j.ccell.2016.03.019
53. González-Martin A, Mira E, Mañes S. CCR5 as a potential target in cancer therapy: inhibition or stimulation? *Anticancer Agents Med Chem* (2012) 12:1045–57. doi:10.2174/187152012803529637
54. Horio T, Mizuno S, Uchino K, Mizutani M, Hanamura I, Espinoza JL, et al. The recipient CCR5 variation predicts survival outcomes after bone marrow transplantation. *Transpl Immunol* (2017) 42:34–9. doi:10.1016/j.trim.2017.05.003
55. Moy RH, Huffman AP, Richman LP, Crisalli L, Wang XK, Hoxie JA, et al. Clinical and immunologic impact of CCR5 blockade in graft-versus-host disease prophylaxis. *Blood* (2017) 129:906–16. doi:10.1182/blood-2016-08-735076
56. Hütter G, Bodor J, Ledger S, Boyd M, Millington M, Tsie M, et al. CCR5 targeted cell therapy for HIV and prevention of viral escape. *Viruses* (2015) 7:4186–203. doi:10.3390/v7082816
57. Jamieson AC, Miller JC, Pabo CO. Drug discovery with engineered zinc-finger proteins. *Nat Rev Drug Discov* (2003) 2:361–8. doi:10.1038/nrd1087
58. Perez EE, Wang J, Miller JC, Jouvenot Y, Kim KA, Liu O, et al. Establishment of HIV-1 resistance in CD4+ T cells by genome editing using zinc-finger nucleases. *Nat Biotechnol* (2008) 26:808–16. doi:10.1038/nbt1410
59. Ando D, Meyer K. Gene editing: regulatory and translation to clinic. *Hematol Oncol Clin North Am* (2017) 31:797–808. doi:10.1016/j.hoc.2017.06.002
60. Cornu TI, Mussolino C, Cathomen T. Refining strategies to translate genome editing to the clinic. *Nat Med* (2017) 23:415–23. doi:10.1038/nm.4313
61. Swamy MN, Wu H, Shankar P. Recent advances in RNAi-based strategies for therapy and prevention of HIV-1/AIDS. *Adv Drug Deliv Rev* (2016) 103:174–86. doi:10.1016/j.addr.2016.03.005
62. Scarborough RJ, Gatignol A. HIV and ribozymes. *Adv Exp Med Biol* (2015) 848:97–116. doi:10.1007/978-1-4939-2432-5_5
63. Fatkenheuer G, Nelson M, Lazzarin A, Konourina I, Hoepelman AI, Lampiris H, et al. Subgroup analyses of maraviroc in previously treated R5 HIV-1 infection. *N Engl J Med* (2008) 359:1442–55. doi:10.1056/NEJMoa0803154
64. Horuk R. Chemokine receptor antagonists: overcoming developmental hurdles. *Nat Rev Drug Discov* (2009) 8:23–33. doi:10.1038/nrd2734
65. Rusconi S, Vitiello P, Adorni F, Colella E, Focà E, Capetti A, et al. Maraviroc as intensification strategy in HIV-1 positive patients with deficient immunological response: an Italian randomized clinical trial. *PLoS One* (2013) 8:e80157. doi:10.1371/journal.pone.0080157
66. Arberas H, Guardo AC, Bargalló ME, Maleno MJ, Calvo M, Blanco JL, et al. In vitro effects of the CCR5 inhibitor maraviroc on human T cell function. *J Antimicrob Chemother* (2013) 68:577–86. doi:10.1093/jac/dks432
67. Pozo-Balado MM, Rosado-Sánchez I, Méndez-Lagares G, Rodríguez-Méndez MM, Ruiz-Mateos E, Benhnia MR, et al. Maraviroc contributes to the restoration of the homeostasis of regulatory T-cell subsets in antiretroviral-naive HIV-infected subjects. *Clin Microbiol Infect* (2016) 22:.e1–5. doi:10.1016/j.cmi.2015.12.025

68. Woollard SM, Kanmogne GD. Maraviroc: a review of its use in HIV infection and beyond. *Drug Des Devel Ther* (2015) 9:5447–68. doi:10.2147/DDDT.S90580
69. McCombie SW, Tagat JR, Vice SF, Lin SI, Steensma R, Palani A, et al. Piperazine-based CCR5 antagonists as HIV-1 inhibitors. III: synthesis, antiviral and pharmacokinetic profiles of symmetrical heteroaryl carboxamides. *Bioorg Med Chem Lett* (2003) 13:567–71. doi:10.1016/S0960-894X(02)00918-6
70. Tagat JR, McCombie SW, Nazareno D, Labroli MA, Xiao Y, Steensma RW, et al. Piperazine-based CCR5 antagonists as HIV-1 inhibitors. IV. Discovery of 1-[(4,6-dimethyl-5-pyrimidinyl)carbonyl]-4-[4-[2-methoxy-1(R)-4-(trifluoromethyl)phenyl] ethyl-3(S)-methyl-1-piperazinyl]-4-methylpiperidine (Sch-417690/Sch-D), a potent, highly selective, and orally bioavailable CCR5 antagonist. *J Med Chem* (2004) 47:2405–8. doi:10.1021/jm0304515
71. Alcom K. Second company halts CCR5 inhibitor study in another blow to new drug class. *NAM AidsMap*. (2005). Available from: www.aidsmap.com/Second-company-halts-CCR5-inhibitorstudy-in-another-blow-to-new-drug-class/page/1422234/
72. Gulick RM, Su Z, Flexner C, Hughes MD, Skolnik PR, Wilkin TJ, et al. Phase 2 study of the safety and efficacy of vicriviroc, a CCR5 inhibitor, in HIV-1-infected, treatment-experienced patients: AIDS clinical trials group 5211. *J Infect Dis* (2007) 196:304–12. doi:10.1086/518797
73. Nichols WG, Steel HM, Bonny T, Adkison K, Curtis L, Millard J, et al. Hepatotoxicity observed in clinical trials of aplaviroc (GW873140). *Antimicrob Agents Chemother* (2008) 52:858–65. doi:10.1128/AAC.00821-07
74. Seto M, Aikawa K, Miyamoto N, Aramaki Y, Kanzaki N, Takashima K, et al. Highly potent and orally active CCR5 antagonists as anti-HIV-1 agents: synthesis and biological activities of 1-benzazocine derivatives containing a sulfoxide moiety. *J Med Chem* (2006) 49:2037–48. doi:10.1021/jm0509703
75. Friedman S, Sanyal A, Goodman Z, Lefebvre E, Gottwald M, Fischer L, et al. Efficacy and safety study of cenicriviroc for the treatment of non-alcoholic steatohepatitis in adult subjects with liver fibrosis: CENTAUR phase 2b study design. *Contemp Clin Trials* (2016) 47:356–65. doi:10.1016/j.cct.2016.02.012
76. Vangelista L, Secchi M, Lusso P. Rational design of novel HIV-1 entry inhibitors by RANTES engineering. *Vaccine* (2008) 26:3008–15. doi:10.1016/j.vaccine.2007.12.023
77. Gaertner H, Cerini F, Escola JM, Kuenzi G, Melotti A, Offord R, et al. Highly potent, fully recombinant anti-HIV chemokines: reengineering a low-cost microbicide. *Proc Natl Acad Sci U S A* (2008) 105:17706–11. doi:10.1073/pnas.0805098105
78. Hutchings CJ, Koglin M, Olson WC, Marshall FH. Opportunities for therapeutic antibodies directed at G-protein-coupled receptors. *Nat Rev Drug Discov* (2017) 16(9):661. doi:10.1038/nrd.2017.91
79. Olson WC, Rabut GE, Nagashima KA, Tran DN, Anselma DJ, Monard SP, et al. Differential inhibition of human immunodeficiency virus type 1 fusion, gp120 binding, and CC-chemokine activity by monoclonal antibodies to CCR5. *J Virol* (1999) 73:4145–55.
80. Trkola A, Ketas TJ, Nagashima KA, Zhao L, Cilliers T, Morris L, et al. Potent, broad-spectrum inhibition of human immunodeficiency virus type 1 by the CCR5 monoclonal antibody PRO 140. *J Virol* (2001) 75:579–88. doi:10.1128/JVI.75.2.579-588.2001
81. Reichert JM. Antibodies to watch in 2017. *MAbs* (2017) 9:167–81. doi:10.1080/19420862.2016.1269580
82. Flego M, Ascione A, Cianfriglia M, Vella S. Clinical development of monoclonal antibody-based drugs in HIV and HCV diseases. *BMC Med* (2013) 11:4. doi:10.1186/1741-7015-11-4
83. Ji C, Brandt M, Dioszegi M, Jekle A, Schwoerer S, Challand S, et al. Novel CCR5 monoclonal antibodies with potent and broad-spectrum anti-HIV activities. *Antiviral Res* (2007) 74:125–37. doi:10.1016/j.antiviral.2006.11.003
84. Venuti A, Pastori C, Lopalco L. The role of natural antibodies to CC chemokine receptor 5 in HIV infection. *Front Immunol* (2017) 8:1358. doi:10.3389/fimmu.2017.01358
85. Nedellec R, Coetzer M, Lederman MM, Offord RE, Hartley O, Mosier DE. Resistance to the CCR5 inhibitor 5P12-RANTES requires a difficult evolution from CCR5 to CXCR4 coreceptor use. *PLoS One* (2011) 6:e22020. doi:10.1371/journal.pone.0022020

Conflict of Interest Statement: The authors declare the absence of any commercial or financial relationships that could be construed as a potential conflict of interest.

Copyright © 2018 Vangelista and Vento. This is an open-access article distributed under the terms of the Creative Commons Attribution License (CC BY). The use, distribution or reproduction in other forums is permitted, provided the original author(s) or licensor are credited and that the original publication in this journal is cited, in accordance with accepted academic practice. No use, distribution or reproduction is permitted which does not comply with these terms.

frontiers in Immunology

MINI REVIEW
published: 25 January 2018
doi: 10.3389/fimmu.2018.00067

Emerging Role of Immunity in Cerebral Small Vessel Disease

*Ying Fu and Yaping Yan**

Key Laboratory of the Ministry of Education for Medicinal Resources and Natural Pharmaceutical Chemistry, National Engineering Laboratory for Resource Development of Endangered Crude Drugs in Northwest of China, College of Life Sciences, Shaanxi Normal University, Xi'an, China

Cerebral small vessel disease (CSVD) is one of the main causes of vascular dementia in older individuals. Apart from risk containment, efforts to prevent or treat CSVD are ineffective due to the unknown pathogenesis of the disease. CSVD, a subtype of stroke, is characterized by recurrent strokes and neurodegeneration. Blood–brain barrier (BBB) impairment, chronic inflammatory responses, and leukocyte infiltration are classical pathological features of CSVD. Understanding how BBB disruption instigates inflammatory and degenerative processes may be informative for CSVD therapy. Antigens derived from the brain are found in the peripheral blood of lacunar stroke patients, and antibodies and sensitized T cells against brain antigens are also detected in patients with leukoaraiosis. These findings suggest that antigen-specific immune responses could occur in CSVD. This review describes the neurovascular unit features of CSVD, the immune responses to specific neuronal and glial processes that may be involved in a distinct mechanism of CSVD, and the current evidence of the association between mechanisms of inflammation and interventions in CSVD. We suggest that autoimmune activity should be assessed in future studies; this knowledge would benefit the development of effective therapeutic interventions in CSVD.

Keywords: cerebral small vessel disease, degeneration, pathogenesis, inflammation, autoimmune response

OPEN ACCESS

Edited by:
Niccolo Terrando,
Duke University, United States

Reviewed by:
Adonis Sfera,
Loma Linda University, United States
Alyson Anne Miller,
University of Glasgow, United Kingdom

***Correspondence:**
Yaping Yan
yaping.yan@snnu.edu.cn

Specialty section:
This article was submitted to Inflammation, a section of the journal Frontiers in Immunology

Received: *27 September 2017*
Accepted: *10 January 2018*
Published: *25 January 2018*

Citation:
Fu Y and Yan Y (2018) Emerging Role of Immunity in Cerebral Small Vessel Disease. Front. Immunol. 9:67. doi: 10.3389/fimmu.2018.00067

INTRODUCTION

Cerebral small vessel disease (CSVD) represents a diverse range of pathological changes that affect capillaries, small arteries and small veins in the brain. This disease is related to lacunar infarct, microbleeds, enlarged perivascular spaces, leukoaraiosis, and cortical atrophy. As such, CSVD causes 20% of strokes and constitutes a main source of cognitive decline, particularly in the elderly (1–4). However, apart from risk containment, efforts to prevent or to treat CSVD are ineffective (5, 6). The burdens of dementia and the cost to society imposed by CSVD are overwhelming and have incited efforts to explore new therapeutic resources (7, 8).

Immune responses have recently emerged as important elements contributing to the progression of stroke. Recent reviews in the literature have discussed the contribution of inflammatory mediators and lymphocytes to the development of brain lesions and neurological deficits that occur in acute ischemic stroke with large artery occlusion or acute cerebral hemorrhage (9–15). Recurrent minor stroke attacks in CSVD lead to blood–brain barrier (BBB) leakage (16–19), central nervous system (CNS) antigen release into the peripheral circulation and lymphocyte infiltration into brain tissue, which allow for the possibility of novel antigens deprived from the CNS to encounter the lymphocytes (20, 21). In addition to BBB disruption, blood proteins at the neurovascular unit

activate microglia to produce chemokines, which cause peripheral inflammatory cells to migrate to the CNS, create a chronic inflammatory microenvironment and encourage activated lymphocytes to encounter CNS antigens (22–28). Immune responses in CSVD are not well characterized and may contribute to the pathogenesis of CSVD injury just as to those of multiple sclerosis (MS) and neuromyelitis optica (NMO), classic autoimmune disorders of the CNS. Therefore, we will focus on identifying specific characteristics of the role of the immune system in CSVD. We will compare imaging, pathology and immune features with MS. Such comparisons will be considered in relation to the use of disease-modifying drugs and their abilities to control the progression of CSVD. We believe that the identification of the differences and similarities in the immune mechanisms involved in CSVD and MS may potentially provide valuable hints to harness the use of disease-modifying drugs for the attenuation of inflammation and to improve clinical outcomes of patients with CSVD just as those in MS. The results from proof-of-concept clinical trials with fingolimod in both acute ischemic stroke and intracerebral hemorrhage (29–32), together with natalizumab in acute ischemic stroke (33), suggest that this concept is not only reasonable but also feasible (33).

CSVD AND STROKE

Stroke comprises the following pathological types: intracerebral hemorrhage, subarachnoid hemorrhage and ischemic stroke. Lacunar-type strokes account for 20–30% of ischemic strokes (34). Moreover, small hemorrhages and microbleeds can occur in lacunar stroke (35). Although lacunas and small hemorrhages may appear after clinical attacks, most of these types of stroke develop "silently." Experiencing numerous strokes is associated with diffuse white matter hyperintensities, cerebral atrophy, and enlarged perivascular space and thus doubles the risk of dementia (1, 36, 37). This triggering of both small ischemic and hemorrhagic consequences by pathological small vessels and cerebral degeneration is collectively known as CSVD (4).

BLOOD PROTEINS AT THE NEUROVASCULAR UNIT PROMOTE IMMUNE ACTION IN THE BRAIN

Fibrin is a result of thrombin-mediated conversion of fibrinogen to an insoluble fibrin network, as the final product of the coagulation cascade. Human studies and experimental animal models provided evidence for the critical role of fibrin in inflammation (38, 39). Interactions between fibrin and microglia *via* TLR4 and CD11b/CD18 receptors were identified as direct activation pathways of the innate immune response (23, 40). Fibrin-induced activation of microglia triggers chemokine and cytokine secretion and stimulates leukocyte recruitment, thus leading to an inflammatory environment in the neurovascular unit (39). Importantly, Ryu et al. found that fibrin in the neurovascular unit of MS models was sufficient to induce the activation of myelin-specific T cells and infiltration into the CNS, demonstrating that a fibrin-induced innate immune response triggers CNS autoimmunity (23, 40). Under normal conditions, blood proteins such as plasmin and fibrinogen are not detected in the parenchyma of the brain shielded by the intact BBB. In response to BBB disruption and components from the blood entering the brain milieu, blood proteins-associated inflammation occurs in the CNS parenchyma.

Cerebral small vessel disease models, including chronic cerebral hypoperfusion and spontaneously hypertensive rats, have identified deficits in BBB integrity, which suggests a close spatial and temporal relationship between the extravasation of plasma constituents, brain tissue injury and subsequent inflammatory processes (41–45). BBB permeability has also been reported in CSVD patients. Albumin increases in the cerebrospinal fluid (CSF) of stroke patients (46, 47). Intrinsic small vessel disease results in vessel wall thickening, focal arteriolar dilatation, striking loss of normal vessel wall architecture, and extravasation of blood components into and through the wall; these findings were observed in post-mortem examinations (48–50). Neuroimaging provides considerable insights into the earliest stages of CSVD. Imaging studies revealed that BBB leakage is very subtle, persistent, and more spatially extensive in patients with CSVD (16, 18, 19); it even occurs prior to development of brain lesions (19).

Inflammatory cell infiltrations in the arteriolar wall and perivascular tissue have been noted in CSVD patients since 1902 (51–53). Moreover, clinical pathological data also demonstrated that the activation and proliferation of microglia induced the expression of MHC II and costimulatory molecules CD40 and B7-2, and the appearance of these cells in the parenchyma was accompanied by the disruption of the BBB and fibrinogen deposition, indicating that immune activation results from BBB disruption (54, 55). However, the mechanism of immune cell infiltration and activation is poorly understood in CSVD. More importantly, the contribution of immune cells to the development and progression of CSVD is also unclear.

A number of experimental studies were conducted to reveal the inflammatory pathogenesis mechanisms in CSVD (21, 56). Rosenberg et al. found that BBB disruption and MMP-9-mediated migration of T lymphocytes was related to extensive white matter abnormalities and behavioral impairments in chronically hypertensive rats. Minocycline, which has anti-inflammatory actions, including MMP-9 inhibition, effectively restored white matter integrity in SHR-SP (45). Weise et al. also showed that SHR-SP developed brain atrophy, white matter loss, BBB leakage, microglial activation with IL-1β secretion, and lymphocyte migration, suggesting a role for NK and T cells in cerebrovascular inflammation and hypertension-related cognitive decline (21).

IMMUNITY IN STROKE

Acute insults to the brain in cerebral ischemic stroke or cerebral hemorrhage cause neuronal cell death and elicit local and diffuse inflammation. Damage-associated molecular patterns trigger resident cells and initiate cellular and humoral cascades (57, 58). Such inflammatory cascades induce the overexpression of adhesion molecules and increase BBB permeability, thus favoring cumulative inflammatory cell infiltration and contributing to an increase in local and global brain damage

(13, 14, 59). Furthermore, the continuous cytokine release starts a chronic inflammatory process that allows the dynamic shift of the macrophage and microglial canonical phenotype between M1 (classical activation) and M2 (alternative activation that is presumably the result of antigen-presenting cells migrating from the periphery) (10, 60).

The presence of autoimmune responses to brain antigens in stroke patients has been reported since the early 1970s (61–64). Shortly after stroke onset, brain-derived antigens (e.g., MBP, GFAP, CK-BB, NSE, and S100) were present within the peripheral circulation (65, 66) and cervical lymph nodes (67, 68). In addition, lymphocytes traffic into the infarcted brain tissue within days after stroke (69–72), allowing for the possibility of a novel antigen to encounter the CNS (7). Concerning the systemic immune system, these antigens are essentially novel, indicating that lymphocytes encountering such an antigen could lead to the development of an autoimmune response (6).

In recent years, Becker et al. conducted a series of studies about autoimmunity in stroke, mainly the cellular immune response. Similar to other clinical studies, they found that cellular immune responses (Th1 type) to brain antigens occurred in patients with acute stroke (73–76). Furthermore, they found that the Th1 response to MBP was an independent predictor of stroke outcome, and more robust cellular responses to MBP were associated with a decreased likelihood of a good outcome (76). The same results were also found in stroke models (77, 78). At the time of stroke, animal models subjected to infections or systemic inflammatory stimuli are predisposed to develop an autoimmune response to the brain, and this response is related to poor outcomes (79–81). Accordingly, the induction of MBP-induced or MOG-induced tolerance was found to prevent CNS autoimmunity and improve outcomes in experimental stroke (82–86). Offner et al. also found that MOG-reactive cells invaded the CNS and exacerbated stoke severity, further substantiating the idea that the cellular immune response might affect stroke outcomes (87). In contrast, Meisel et al. showed that stroke-induced immunodepression might represent an adaptive mechanism that inhibited long-lasting antigen-derived brain cellular immune responses (88, 89).

The presence of antibodies to brain antigens has been described in stroke. Immunoglobulins are present in the CSF of approximately 25% of survivors in the chronic phase of stroke (90–92). Some autoantibodies to brain antigens (e.g., MBP, PLP, NF, and NR2A/2B) have been documented in individuals after stroke (93–97). In a study with 40 patients, anti-MBP antibody titers were associated with cognitive decline during the first year after stroke (98), but we still do not completely understand the pathological consequences of this humoral response. In a stroke model study, researchers found that mice with B lymphocyte infiltrates in their infarct cores developed late cognitive decline and that blocking the B cell response using a mouse analog of rituximab, an FDA-approved anti-CD20 antibody, prevented this cognitive decline. This result provides evidence that autoantibodies can interfere with neuronal function and could mediate cognitive impairment after stroke (99).

The type of immune response that develops to a particular antigen is dependent upon the microenvironment at the site of antigen encounter (100). Th1-type response, which is associated with the cellular immune response, is favored by an inflammatory microenvironment where IFN-γ is present, such as what might occur during a systemic infection; Th2-type response, which is classically associated with humoral immunity and antibody secretion, is favored by the presence of cytokines such as IL-4 (101–105). However, the cellular immune response or humoral immune response depends on the local microenvironment and the presence of costimulatory molecules. CSVD is a cerebral vascular disorder characterized by recurrent strokes with sustainable BBB disruption as well as a chronic inflammatory response at the neurovascular unit. Therefore, it is possible that immune tolerance could be damaged in stroke under certain chronic inflammatory circumstances in CSVD. As mentioned previously, blood proteins at the neurovascular unit play an important role in the communication between the brain and the immune system (**Figure 1**). However, it is still unknown whether fibrin triggers and sustains antigen-specific lymphocytes in the CNS of patients with acute brain injury in chronic phase.

UNDERSTANDING THE UNIQUE IMMUNE MECHANISMS IN CSVD IS INSTRUMENTAL FOR IMMUNE INTERVENTIONAL THERAPIES

Stroke does not systematically trigger autoimmunity; however, under certain circumstances such as pronounced microenvironment inflammation, autoreactive T cells could escape the tolerance controls and induce antigen-specific immune responses (**Figure 1**). CSVD is characterized by recurrent strokes with cumulative disabilities and vascular dementia (**Table 1**). At the onset of ischemic and hemorrhagic stroke (attack phase), emerging evidence has revealed that stroke induced a local inflammatory reaction and a plethora of innate immune responses in the brain where antigen-presenting cells became prominent; following the onset of stroke, inflammatory components (IL-4 or IFN-γ), which are produced by innate immune cells (e.g., microglia, NK cell) with the stimulation of blood proteins at the neurovascular unite, promote detrimental cellular or humoral responses and lead to diffuse neuron and oligodendrocyte damage (101–105). In chronic stages (remitting phase), the chronic inflammatory activity that is triggered by blood proteins at neurovascular units might also participate in post-stroke cognitive decline and neurodegeneration (39, 40).

The slow developments of CSVD suggest that exploring the mechanisms and interventions for its prevention or treatment will need long-term study for recurrent acute minor stroke and chronic progress neurodegeneration. A disease-modifying strategy aimed at changing the natural course of an illness is primarily applied to treat chronic diseases. In the field of neurological disorders, this concept has been used for neuroinflammatory diseases such as MS. Given the similarities in the inflammatory mechanisms and clinical characters of MS and CSVD (**Table 1**), one would ideally expect that CSVD requires a similar immunotherapeutic and preventive approach to that used for MS.

Fingolimod became the first oral drug to be FDA-approved for the treatment of relapsing-remitting MS. This drug can act

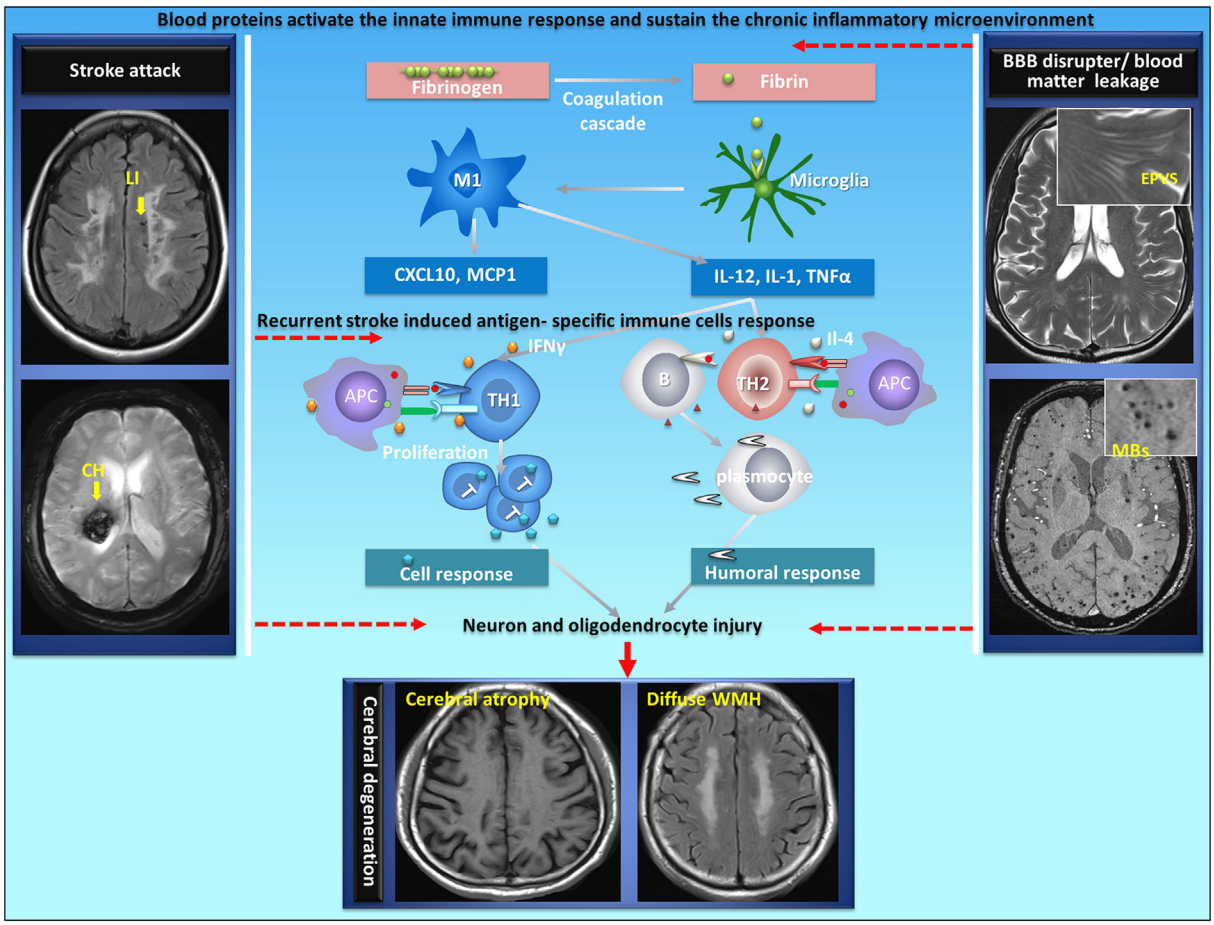

FIGURE 1 | Proposed autoimmunity mechanism in the development of neurodegeneration in CSVD. CSVD is a cerebral vascular disorder characterized by recurrent strokes with sustainable BBB disruption as well as a chronic inflammatory response at the neurovascular unit. Autoimmunity could be generated in acute stroke under certain brain chronic inflammatory circumstances with damaged immune tolerance in CSVD. Blood proteins at the neurovascular unit play an important role in the communication between the brain and the immune system. During BBB disruption, fibrinogen extravagates into the CNS and is converted to fibrin upon activation of coagulation. Fibrin, the high-affinity plasma-derived ligand for CD11b/CD18, activates CNS-resident innate immune cells (microglia and perivascular macrophages) to stimulate cytokine release, thus sustaining antigen-presenting properties by providing instructive signals (such asIL-12, IL-1, and TNFα) to promote antigen-specific (neuron or oligodendrocyte) Th1-cell or Th2-cell differentiation following a stroke. The cellular immune response or humoral immune response leads to neuron and oligodendrocyte injury. APC, antigen-presenting cells; LI, lacunar infarct; CH, cerebral hemorrhage; EPVS, enlarged perivascular space; MBs, microbleeds; CSVD, cerebral small vessel disease; BBB, blood–brain barrier. The original data were acquired in the YPY group.

on four of the five known S1P receptor subtypes (S1PR1, S1PR3, S1PR4, S1PR5) and exerts its immunomodulatory actions by affecting lymphocyte numbers, trafficking and apoptosis through S1P receptors. Specifically, fingolimod reduces circulating lymphocytes by preventing their egress from lymph nodes during stroke, and fingolimod might contribute to the prevention of the early infiltration of lymphocytes into the brain, thus reducing thromboinflammation (106–108). In our three open-label trials, patients with acute ischemic or hemorrhagic stroke were treated with oral fingolimod for 3 days after the onset of symptoms, and consequently, microvascular permeability and secondary injury were reduced in these patients (29–32). However, the action of fingolimod in acute stages involved in diffuse brain injury and cerebral degeneration is still poorly understood and needs to be elucidated (109, 110). A recent study found that fingolimod could induce VEGF expression of astrocytes by stimulating S1PR3, which plays a role in the breakdown of the BBB, a step critical to the entry of pathogenic lymphocytes into the brain (111). Of note, BBB leakage induced by fingolimod due to the activation of S1PR3 in astrocytes may limit its use, and selective S1PR1 agonist (e.g., LASW1238, RP101075) treatment should be further optimized (112, 113).

Natalizumab blocks α4-integrin, which mediates the invasion of lymphocytes (mainly T cells) into the CNS, and currently represents one of the most effective therapies for relapsing-remitting MS. The ACTION study, a randomized controlled phase IIa trial comparing the effect of a single injection of 300 mg of intravenous natalizumab and placebo within a 9-h time window after symptom onset, found no effect of natalizumab on infarct growth, but patients receiving natalizumab were more likely to have an excellent cognition outcome at 90 days. This outcome was particularly evident in subgroups of patients with smaller

TABLE 1 | Contrasting features of clinical, imaging, pathology and inflammation between CSVD and MS.

	CSVD	MS
Clinical features		
Course of disease	A chronic disease	A chronic disease
Attack events	Lacunar infarct and cerebral hemorrhage	Inflammatory demyelination activation
Disability	Accumulation	Accumulation
Neurodegeneration	Cognition, gait, neuropsychology and sleep disturbance	Cognition, gait, neuropsychology and sleep disturbance
Brain MRI		
T2/FLAIR white matter hyperintensities	Focal and diffuse	Focal and diffuse
T1 hypointensities	Transient and persistent	Transient and persistent
Microbleeds	Common	Rare
Contrast enhancing lesions	Common at stroke recurrent stage, rare at remitting stage	Common at relapse phase, rare at remitting stage
Enlarged perivascular space	Centrum semiovale and basal ganglion region	Centrum semiovale region
Cerebral atrophy	Gray matter reduced and ventricles gradually expanded	Gray matter reduced and ventricles gradually expanded
Pathology features		
Demyelinating region	Arterial watershed areas	High venule density and arterial watershed areas
Myelin	Selective loss of phospholipids and MAG with PLP preservation	Myelin loss with selective reduction of phospholipids
Axonal	Loss	Loss
Blood–brain barrier	Increased permeability and fibrin leakage	Increased permeability and fibrin leakage
Perivascular	Perivascular collagenases and inflammatory	Perivascular collagenases and inflammatory cuffs
Inflammatory cell	Microglia and astrocyte activation and lymphocytic infiltration	Microglia and astrocyte activation and lymphocytic infiltration
Inflammation features		
Triggering events for immune activation	Cell death products, microglia activation	Mostly unidentified
Location of activation signals	Brain and periphery	Periphery
Antigen specificity	Mostly antigen-specific cells and antigen-specific antibody	Mostly antigen-specific cells
Immune effector cells	Combined effects of many cells, no dominant cell type	Coordinated events dominated by T cells
Role of inflammatory mediators	Presumably many, including IFN-γ, IL-17, IL-4	Presumably many, including TNF-a, IFN-γ, IL-17
Efficacy of immune modulation	Under investigation	13 FDA-approved, disease-modifying drugs, moderate to high efficacy

infarcts. This result suggests that mitigating diffuse neuroinflammation triggered by acute stroke may additionally mitigate cerebral degeneration, especially in minor stroke. Considering the safety and efficacy of fingolimod and natalizumab in acute stroke, future preclinical animal experiments and translational clinical trials involving fingolimod and natalizumab treatment for CSVD are expected.

Dimethyl fumarate (DMF) is utilized as an oral drug to treat MS and has been demonstrated to be as potent as several other drugs but with fewer side effects (114, 115). The beneficial effects of this medication were consistent with regulation of $CD4^+$ Th1 cell differentiation. More importantly, DMF was discovered to impact the anti-oxidative stress cell machinery to promote the transcription of genes downstream of the activation of the nuclear factor Nrf2 (116, 117). It was reported that DMF might be useful for treating acute stroke. In acute stroke models, DMF prevented cerebral edema progression at the acute stage and promoted recovery at the chronic stage (118–120). Recently, an experiment using mice with bilateral common carotid artery stenosis revealed that DMF decreased microglia/macrophage activation, protected against white matter injury and improved cognition impairment (121). Multiple immunomodulatory and anti-oxidative stress actions support DMF as an appealing medication; however, its potential for impacting the degenerative aspects of CSVD remains to be explored.

Rituximab is FDA approved as a B-cell-depleting drug for rheumatoid arthritis, non-Hodgkin's lymphoma, chronic lymphocytic leukemia, and microscopic polyangiitis. Rituximab was also found to be effective in decreasing the autoantigen-specific humoral immune response or inhibiting inflammatory responses orchestrated by pathogenic B cells in patients with MS and NMO (122–127). Although both deleterious and protective regulatory roles of B lymphocytes have been increasingly recognized, translation of these roles of B lymphocytes into clinical trials in stroke has not yet occurred. However, pharmacological ablation of B lymphocytes using rituximab after 5 days of stroke prevents the appearance of delayed cognitive deficits in an animal stroke model with large vessel occlusion (99). Nevertheless, this finding suggests that rituximab treatment could be a promising therapy for CSVD, given the production of brain-reactive antibodies associated with cognitive decline in stroke patients (98).

Minocycline is a tetracycline antibiotic agent that has multiple immune-modulating properties; clinical data have shown the activity of minocycline in patients with MS or clinically isolated syndrome with a good safety profile (128–132). Minocycline also reduces infarct size in acute stroke clinical trials (132, 133). More recently, Rosenberg et al. found that minocycline decreased hypoxia-induced infiltration of leukocytes, reduced white matter damage, improved behavior, and prolonged life in CSVD models (44, 45). Since minocycline is used as an antibiotic in the clinical setting, its safety for human use has been extensively evaluated. Moreover, the multiple neuroprotective effects of minocycline in vascular injury models support its use as a potential therapeutic treatment for CSVD (134–138).

CONCLUSION AND FUTURE DIRECTIONS

Brain proteins are detected in the blood of stroke/lacunar stroke patients (64, 66). Antibodies against brain antigens develop in patients with leukoaraiosis (94), suggesting a humoral immune response to the brain injury in CSVD. Furthermore, the presence of circulating T cells sensitized against brain antigens and antigen-presenting cells carrying brain antigens in the draining lymphoid tissue of stroke patients indicate that stroke might induce antigen-specific immune responses similar to those found in MS patients. We do not know whether poststroke dementia *via* lymphocyte-mediated autoimmunity has detrimental effects; however, clinical and preclinical trials of immune modulation using lymphocyte-targeted approaches have yielded some promising results in cognitive degeneration after stroke (33, 99). Impaired tissue oxygenation, induced inflammatory responses, and induced leukocyte infiltration are classical pathological features in CSVD (**Table 1**). In theory, mitigating chronic and diffuse neuroinflammation triggered by recurrent brain injury attack to prevent cerebral degeneration could be a feasible strategy against CSVD. However, one challenge to the advancement of the field is the incomplete understanding of the complex interactions between the immune system and the brain in CSVD. Therefore, the involvement of autoimmunity in CSVD should be cautiously assessed in future studies to facilitate the development of effective therapeutic interventions for CSVD.

AUTHOR CONTRIBUTIONS

YF and YY wrote and approved the final version of this manuscript.

FUNDING

YP was supported by the National Natural Science Foundation of China (81371372, 81571596, and 81771279) and the Fundamental Research Funds for the Central Universities (GK201701009).

REFERENCES

1. Pantoni L. Cerebral small vessel disease: from pathogenesis and clinical characteristics to therapeutic challenges. *Lancet Neurol* (2010) 9:689–701. doi:10.1016/S1474-4422(10)70104-6
2. A united approach to vascular disease and neurodegeneration. *Lancet Neurol* (2012) 11:293. doi:10.1016/S1474-4422(12)70050-9
3. Wardlaw JM, Smith C, Dichgans M. Mechanisms of sporadic cerebral small vessel disease: insights from neuroimaging. *Lancet Neurol* (2013) 12:483–97. doi:10.1016/S1474-4422(13)70060-7
4. Wardlaw JM, Smith EE, Biessels GJ, Cordonnier C, Fazekas F, Frayne R, et al. Neuroimaging standards for research into small vessel disease and its contribution to ageing and neurodegeneration. *Lancet Neurol* (2013) 12:822–38. doi:10.1016/S1474-4422(13)70124-8
5. Investigators SPS, Benavente OR, Hart RG, McClure LA, Szychowski JM, Coffey CS, et al. Effects of clopidogrel added to aspirin in patients with recent lacunar stroke. *N Engl J Med* (2012) 367:817–25. doi:10.1056/NEJMoa1204133
6. Pearce LA, McClure LA, Anderson DC, Jacova C, Sharma M, Hart RG, et al. Effects of long-term blood pressure lowering and dual antiplatelet treatment on cognitive function in patients with recent lacunar stroke: a secondary analysis from the SPS3 randomised trial. *Lancet Neurol* (2014) 13:1177–85. doi:10.1016/S1474-4422(14)70224-8
7. Arboix A, Blanco-Rojas L, Marti-Vilalta JL. Advancements in understanding the mechanisms of symptomatic lacunar ischemic stroke: translation of knowledge to prevention strategies. *Expert Rev Neurother* (2014) 14:261–76. doi:10.1586/14737175.2014.884926
8. Bath PM, Wardlaw JM. Pharmacological treatment and prevention of cerebral small vessel disease: a review of potential interventions. *Int J Stroke* (2015) 10:469–78. doi:10.1111/ijs.12466
9. Macrez R, Ali C, Toutirais O, Le Mauff B, Defer G, Dirnagl U, et al. Stroke and the immune system: from pathophysiology to new therapeutic strategies. *Lancet Neurol* (2011) 10:471–80. doi:10.1016/S1474-4422(11)70066-7
10. Chamorro A, Meisel A, Planas AM, Urra X, van de Beek D, Veltkamp R. The immunology of acute stroke. *Nat Rev Neurol* (2012) 8:401–10. doi:10.1038/nrneurol.2012.98
11. Fu Y, Liu Q, Anrather J, Shi FD. Immune interventions in stroke. *Nat Rev Neurol* (2015) 11:524–35. doi:10.1038/nrneurol.2015.144
12. Wang J. Preclinical and clinical research on inflammation after intracerebral hemorrhage. *Prog Neurobiol* (2010) 92:463–77. doi:10.1016/j.pneurobio.2010.08.001
13. Mracsko E, Veltkamp R. Neuroinflammation after intracerebral hemorrhage. *Front Cell Neurosci* (2014) 8:388. doi:10.3389/fncel.2014.00388
14. Iadecola C, Anrather J. The immunology of stroke: from mechanisms to translation. *Nat Med* (2011) 17:796–808. doi:10.1038/nm.2399
15. Eltzschig HK, Carmeliet P. Hypoxia and inflammation. *N Engl J Med* (2011) 364:656–65. doi:10.1056/NEJMra0910283
16. Wardlaw JM, Doubal F, Armitage P, Chappell F, Carpenter T, Munoz Maniega S, et al. Lacunar stroke is associated with diffuse blood-brain barrier dysfunction. *Ann Neurol* (2009) 65:194–202. doi:10.1002/ana.21549
17. Wardlaw JM, Doubal FN, Valdes-Hernandez M, Wang X, Chappell FM, Shuler K, et al. Blood-brain barrier permeability and long-term clinical and imaging outcomes in cerebral small vessel disease. *Stroke* (2013) 44:525–7. doi:10.1161/STROKEAHA.112.669994
18. Huisa BN, Caprihan A, Thompson J, Prestopnik J, Qualls CR, Rosenberg GA. Long-term blood-brain barrier permeability changes in Binswanger disease. *Stroke* (2015) 46:2413–8. doi:10.1161/STROKEAHA.115.009589
19. Zhang CE, Wong SM, van de Haar HJ, Staals J, Jansen JF, Jeukens CR, et al. Blood-brain barrier leakage is more widespread in patients with cerebral small vessel disease. *Neurology* (2017) 88:426–32. doi:10.1212/WNL.0000000000003556
20. Engelhardt B, Carare RO, Bechmann I, Flugel A, Laman JD, Weller RO. Vascular, glial, and lymphatic immune gateways of the central nervous system. *Acta Neuropathol* (2016) 132:317–38. doi:10.1007/s00401-016-1606-5
21. Kaiser D, Weise G, Moller K, Scheibe J, Posel C, Baasch S, et al. Spontaneous white matter damage, cognitive decline and neuroinflammation in middle-aged hypertensive rats: an animal model of early-stage cerebral small vessel disease. *Acta Neuropathol Commun* (2014) 2:169. doi:10.1186/s40478-014-0169-8
22. Schachtrup C, Lu P, Jones LL, Lee JK, Lu J, Sachs BD, et al. Fibrinogen inhibits neurite outgrowth via beta 3 integrin-mediated phosphorylation of the EGF receptor. *Proc Natl Acad Sci U S A* (2007) 104:11814–9. doi:10.1073/pnas.0704045104
23. Ryu JK, Petersen MA, Murray SG, Baeten KM, Meyer-Franke A, Chan JP, et al. Blood coagulation protein fibrinogen promotes autoimmunity and demyelination via chemokine release and antigen presentation. *Nat Commun* (2015) 6:8164. doi:10.1038/ncomms9164
24. Bardehle S, Rafalski VA, Akassoglou K. Breaking boundaries-coagulation and fibrinolysis at the neurovascular interface. *Front Cell Neurosci* (2015) 9:354. doi:10.3389/fncel.2015.00354
25. Akassoglou K. Coagulation takes center stage in inflammation. *Blood* (2015) 125:419–20. doi:10.1182/blood-2014-11-609222
26. Cai W, Zhang K, Li P, Zhu L, Xu J, Yang B, et al. Dysfunction of the neurovascular unit in ischemic stroke and neurodegenerative diseases: an aging effect. *Ageing Res Rev* (2017) 34:77–87. doi:10.1016/j.arr.2016.09.006
27. Hu X, De Silva TM, Chen J, Faraci FM. Cerebral vascular disease and neurovascular injury in ischemic stroke. *Circ Res* (2017) 120:449–71. doi:10.1161/CIRCRESAHA.116.308427
28. Sixt M, Engelhardt B, Pausch F, Hallmann R, Wendler O, Sorokin LM. Endothelial cell laminin isoforms, laminins 8 and 10, play decisive roles

in T cell recruitment across the blood-brain barrier in experimental autoimmune encephalomyelitis. *J Cell Biol* (2001) 153:933–46. doi:10.1083/jcb.153.5.933
29. Zhu Z, Fu Y, Tian D, Sun N, Han W, Chang G, et al. Combination of the immune modulator fingolimod with alteplase in acute ischemic stroke: a pilot trial. *Circulation* (2015) 132:1104–12. doi:10.1161/CIRCULATIONAHA.115.016371
30. Fu Y, Zhang N, Ren L, Yan Y, Sun N, Li YJ, et al. Impact of an immune modulator fingolimod on acute ischemic stroke. *Proc Natl Acad Sci U S A* (2014) 111:18315–20. doi:10.1073/pnas.1416166111
31. Li YJ, Chang GQ, Liu Y, Gong Y, Yang C, Wood K, et al. Fingolimod alters inflammatory mediators and vascular permeability in intracerebral hemorrhage. *Neurosci Bull* (2015) 31:755–62. doi:10.1007/s12264-015-1532-2
32. Fu Y, Hao J, Zhang N, Ren L, Sun N, Li YJ, et al. Fingolimod for the treatment of intracerebral hemorrhage: a 2-arm proof-of-concept study. *JAMA Neurol* (2014) 71:1092–101. doi:10.1001/jamaneurol.2014.1065
33. Elkins J, Veltkamp R, Montaner J, Johnston SC, Singhal AB, Becker K, et al. Safety and efficacy of natalizumab in patients with acute ischaemic stroke (ACTION): a randomised, placebo-controlled, double-blind phase 2 trial. *Lancet Neurol* (2017) 16:217–26. doi:10.1016/S1474-4422(16)30357-X
34. Warlow C, Sudlow C, Dennis M, Wardlaw J, Sandercock P. Stroke. *Lancet* (2003) 362:1211–24. doi:10.1016/S0140-6736(03)14544-8
35. Arboix A, Garcia-Eroles L, Massons J, Oliveres M, Targa C. Hemorrhagic lacunar stroke. *Cerebrovasc Dis* (2000) 10:229–34. doi:10.1159/000016061
36. Vermeer SE, Longstreth WT Jr, Koudstaal PJ. Silent brain infarcts: a systematic review. *Lancet Neurol* (2007) 6:611–9. doi:10.1016/S1474-4422(07)70170-9
37. van Veluw SJ, Shih AY, Smith EE, Chen C, Schneider JA, Wardlaw JM, et al. Detection, risk factors, and functional consequences of cerebral microinfarcts. *Lancet Neurol* (2017) 16:730–40. doi:10.1016/S1474-4422(17)30196-5
38. Hoppe B, Dorner T. Coagulation and the fibrin network in rheumatic disease: a role beyond haemostasis. *Nat Rev Rheumatol* (2012) 8:738–46. doi:10.1038/nrrheum.2012.184
39. Davalos D, Akassoglou K. Fibrinogen as a key regulator of inflammation in disease. *Semin Immunopathol* (2012) 34:43–62. doi:10.1007/s00281-011-0290-8
40. Smiley ST, King JA, Hancock WW. Fibrinogen stimulates macrophage chemokine secretion through toll-like receptor 4. *J Immunol* (2001) 167:2887–94. doi:10.4049/jimmunol.167.5.2887
41. Holland PR, Searcy JL, Salvadores N, Scullion G, Chen G, Lawson G, et al. Gliovascular disruption and cognitive deficits in a mouse model with features of small vessel disease. *J Cereb Blood Flow Metab* (2015) 35:1005–14. doi:10.1038/jcbfm.2015.12
42. Choi JY, Cui Y, Kim BG. Interaction between hypertension and cerebral hypoperfusion in the development of cognitive dysfunction and white matter pathology in rats. *Neuroscience* (2015) 303:115–25. doi:10.1016/j.neuroscience.2015.06.056
43. Candelario-Jalil E, Thompson J, Taheri S, Grossetete M, Adair JC, Edmonds E, et al. Matrix metalloproteinases are associated with increased blood-brain barrier opening in vascular cognitive impairment. *Stroke* (2011) 42:1345–50. doi:10.1161/STROKEAHA.110.600825
44. Jalal FY, Yang Y, Thompson J, Lopez AC, Rosenberg GA. Myelin loss associated with neuroinflammation in hypertensive rats. *Stroke* (2012) 43:1115–22. doi:10.1161/STROKEAHA.111.643080
45. Jalal FY, Yang Y, Thompson JF, Roitbak T, Rosenberg GA. Hypoxia-induced neuroinflammatory white-matter injury reduced by minocycline in SHR/SP. *J Cereb Blood Flow Metab* (2015) 35:1145–53. doi:10.1038/jcbfm.2015.21
46. Skoog I, Wallin A, Fredman P, Hesse C, Aevarsson O, Karlsson I, et al. A population study on blood-brain barrier function in 85-year-olds: relation to Alzheimer's disease and vascular dementia. *Neurology* (1998) 50:966–71. doi:10.1212/WNL.50.4.966
47. Taheri S, Gasparovic C, Huisa BN, Adair JC, Edmonds E, Prestopnik J, et al. Blood-brain barrier permeability abnormalities in vascular cognitive impairment. *Stroke* (2011) 42:2158–63. doi:10.1161/STROKEAHA.110.611731
48. Fisher CM. Lacunar strokes and infarcts: a review. *Neurology* (1982) 32:871–6. doi:10.1212/WNL.32.8.871
49. Fisher CM. The arterial lesions underlying lacunes. *Acta Neuropathol* (1968) 12:1–15. doi:10.1007/BF00685305
50. Fisher CM. Capsular infarcts: the underlying vascular lesions. *Arch Neurol* (1979) 36:65–73. doi:10.1001/archneur.1979.00500380035003
51. Lu J, Moochhala S, Kaur C, Ling EA. Cellular inflammatory response associated with breakdown of the blood-brain barrier after closed head injury in rats. *J Neurotrauma* (2001) 18:399–408. doi:10.1089/089771501750170976
52. Ogata J. The arterial lesions underlying cerebral infarction. *Neuropathology* (1999) 19:112–8. doi:10.1046/j.1440-1789.1999.00216.x
53. Bailey EL, Smith C, Sudlow CL, Wardlaw JM. Pathology of lacunar ischemic stroke in humans – a systematic review. *Brain Pathol* (2012) 22:583–91. doi:10.1111/j.1750-3639.2012.00575.x
54. Simpson JE, Ince PG, Higham CE, Gelsthorpe CH, Fernando MS, Matthews F, et al. Microglial activation in white matter lesions and nonlesional white matter of ageing brains. *Neuropathol Appl Neurobiol* (2007) 33:670–83. doi:10.1111/j.1365-2990.2007.00890.x
55. Tomimoto H, Akiguchi I, Wakita H, Lin JX, Budka H. Cyclooxygenase-2 is induced in microglia during chronic cerebral ischemia in humans. *Acta Neuropathol* (2000) 99:26–30. doi:10.1007/PL00007402
56. Bailey EL, Smith C, Sudlow CL, Wardlaw JM. Is the spontaneously hypertensive stroke prone rat a pertinent model of sub cortical ischemic stroke? A systematic review. *Int J Stroke* (2011) 6:434–44. doi:10.1111/j.1747-4949.2011.00659.x
57. Liesz A, Dalpke A, Mracsko E, Antoine DJ, Roth S, Zhou W, et al. DAMP signaling is a key pathway inducing immune modulation after brain injury. *J Neurosci* (2015) 35:583–98. doi:10.1523/JNEUROSCI.2439-14.2015
58. Kono H, Rock KL. How dying cells alert the immune system to danger. *Nat Rev Immunol* (2008) 8:279–89. doi:10.1038/nri2215
59. Chen S, Yang Q, Chen G, Zhang JH. An update on inflammation in the acute phase of intracerebral hemorrhage. *Transl Stroke Res* (2015) 6:4–8. doi:10.1007/s12975-014-0384-4
60. Gliem M, Mausberg AK, Lee JI, Simiantonakis I, van Rooijen N, Hartung HP, et al. Macrophages prevent hemorrhagic infarct transformation in murine stroke models. *Ann Neurol* (2012) 71:743–52. doi:10.1002/ana.23529
61. Miro-Mur F, Urra X, Gallizioli M, Chamorro A, Planas AM. Antigen presentation after stroke. *Neurotherapeutics* (2016) 13:719–28. doi:10.1007/s13311-016-0469-8
62. Urra X, Miro F, Chamorro A, Planas AM. Antigen-specific immune reactions to ischemic stroke. *Front Cell Neurosci* (2014) 8:278. doi:10.3389/fncel.2014.00278
63. Santos Samary C, Pelosi P, Leme Silva P, Rieken Macedo Rocco P. Immunomodulation after ischemic stroke: potential mechanisms and implications for therapy. *Crit Care* (2016) 20:391. doi:10.1186/s13054-016-1573-1
64. Chiva-Blanch G, Suades R, Crespo J, Peña E, Padró T, Jiménez-Xarrié E, et al. Microparticle shedding from neural progenitor cells and vascular compartment cells is increased in ischemic stroke. *PLoS One* (2016) 11:e0148176. doi:10.1371/journal.pone.0148176
65. Jauch EC, Lindsell C, Broderick J, Fagan SC, Tilley BC, Levine SR, et al. Association of serial biochemical markers with acute ischemic stroke: the National Institute of Neurological Disorders and Stroke recombinant tissue plasminogen activator Stroke Study. *Stroke* (2006) 37:2508–13. doi:10.1161/01.STR.0000242290.01174.9e
66. Herrmann M, Vos P, Wunderlich MT, de Bruijn CH, Lamers KJ. Release of glial tissue-specific proteins after acute stroke: a comparative analysis of serum concentrations of protein S-100B and glial fibrillary acidic protein. *Stroke* (2000) 31:2670–7. doi:10.1161/01.STR.31.11.2670
67. van Zwam M, Huizinga R, Melief MJ, Wierenga-Wolf AF, van Meurs M, Voerman JS, et al. Brain antigens in functionally distinct antigen-presenting cell populations in cervical lymph nodes in MS and EAE. *J Mol Med* (2009) 87:273–86. doi:10.1007/s00109-008-0421-4
68. Planas AM, Gomez-Choco M, Urra X, Gorina R, Caballero M, Chamorro A. Brain-derived antigens in lymphoid tissue of patients with acute stroke. *J Immunol* (2012) 188:2156–63. doi:10.4049/jimmunol.1102289
69. Gelderblom M, Leypoldt F, Steinbach K, Behrens D, Choe CU, Siler DA, et al. Temporal and spatial dynamics of cerebral immune cell accumulation in stroke. *Stroke* (2009) 40:1849–57. doi:10.1161/STROKEAHA.108.534503
70. Schwab JM, Nguyen TD, Meyermann R, Schluesener HJ. Human focal cerebral infarctions induce differential lesional interleukin-16 (IL-16) expression confined to infiltrating granulocytes, CD8+ T-lymphocytes and activated microglia/macrophages. *J Neuroimmunol* (2001) 114:232–41. doi:10.1016/S0165-5728(00)00433-1
71. Zhou W, Liesz A, Bauer H, Sommer C, Lahrmann B, Valous N, et al. Postischemic brain infiltration of leukocyte subpopulations differs among

murine permanent and transient focal cerebral ischemia models. *Brain Pathol* (2013) 23:34–44. doi:10.1111/j.1750-3639.2012.00614.x
72. Mracsko E, Javidi E, Na SY, Kahn A, Liesz A, Veltkamp R. Leukocyte invasion of the brain after experimental intracerebral hemorrhage in mice. *Stroke* (2014) 45:2107–14. doi:10.1161/STROKEAHA.114.005801
73. Kallen B, Nilsson O, Thelin C. Effect of encephalitogenic protein on migration in agarose of leukoytes from patients with multiple sclerosis. A longitudinal study of patients with relapsing multiple sclerosis or with cerebral infarction. *Acta Neurol Scand* (1977) 55:47–56. doi:10.1111/j.1600-0404.1977.tb05626.x
74. Youngchaiyud U, Coates AS, Whittingham S, Mackay IR. Cellular-immune response to myelin protein: absence in multiple sclerosis and presence in cerebrovascular accidents. *Aust N Z J Med* (1974) 4:535–8. doi:10.1111/j.1445-5994.1974.tb03233.x
75. Wang WZ, Olsson T, Kostulas V, Hojeberg B, Ekre HP, Link H. Myelin antigen reactive T cells in cerebrovascular diseases. *Clin Exp Immunol* (1992) 88:157–62. doi:10.1111/j.1365-2249.1992.tb03056.x
76. Becker KJ, Kalil AJ, Tanzi P, Zierath DK, Savos AV, Gee JM, et al. Autoimmune responses to the brain after stroke are associated with worse outcome. *Stroke* (2011) 42:2763–9. doi:10.1161/STROKEAHA.111.619593
77. Zierath D, Schulze J, Kunze A, Drogomiretskiy O, Nhan D, Jaspers B, et al. The immunologic profile of adoptively transferred lymphocytes influences stroke outcome of recipients. *J Neuroimmunol* (2013) 263:28–34. doi:10.1016/j.jneuroim.2013.07.014
78. Zierath D, Kunze A, Fecteau L, Becker K. Promiscuity of autoimmune responses to MBP after stroke. *J Neuroimmunol* (2015) 285:101–5. doi:10.1016/j.jneuroim.2015.05.024
79. Becker KJ, Kindrick DL, Lester MP, Shea C, Ye ZC. Sensitization to brain antigens after stroke is augmented by lipopolysaccharide. *J Cereb Blood Flow Metab* (2005) 25:1634–44. doi:10.1038/sj.jcbfm.9600160
80. Becker KJ, Zierath D, Kunze A, Fecteau L, Lee B, Skerrett S. The contribution of antibiotics, pneumonia and the immune response to stroke outcome. *J Neuroimmunol* (2016) 29(5–296):68–74. doi:10.1016/j.jneuroim.2016.04.005
81. Zierath D, Thullbery M, Hadwin J, Gee JM, Savos A, Kalil A, et al. CNS immune responses following experimental stroke. *Neurocrit Care* (2010) 12:274–84. doi:10.1007/s12028-009-9270-4
82. Jonelis FJ, Epstein JH, Martin G. Letter: the safety of psoralens. *Arch Dermatol* (1976) 112:1036. doi:10.1001/archderm.1976.01630310082033
83. Becker K, Kindrick D, McCarron R, Hallenbeck J, Winn R. Adoptive transfer of myelin basic protein-tolerized splenocytes to naive animals reduces infarct size: a role for lymphocytes in ischemic brain injury? *Stroke* (2003) 34:1809–15. doi:10.1161/01.STR.0000078308.77727.EA
84. Gee JM, Kalil A, Thullbery M, Becker KJ. Induction of immunologic tolerance to myelin basic protein prevents central nervous system autoimmunity and improves outcome after stroke. *Stroke* (2008) 39:1575–82. doi:10.1161/STROKEAHA.107.501486
85. Gee JM, Zierath D, Hadwin J, Savos A, Kalil A, Thullbery M, et al. Long term immunologic consequences of experimental stroke and mucosal tolerance. *Exp Transl Stroke Med* (2009) 1:3. doi:10.1186/2040-7378-1-3
86. Frenkel D, Huang Z, Maron R, Koldzic DN, Hancock WW, Moskowitz MA, et al. Nasal vaccination with myelin oligodendrocyte glycoprotein reduces stroke size by inducing IL-10-producing CD4+ T cells. *J Immunol* (2003) 171:6549–55. doi:10.4049/jimmunol.171.12.6549
87. Ren X, Akiyoshi K, Grafe MR, Vandenbark AA, Hurn PD, Herson PS, et al. Myelin specific cells infiltrate MCAO lesions and exacerbate stroke severity. *Metab Brain Dis* (2012) 27:7–15. doi:10.1007/s11011-011-9267-5
88. Klehmet J, Hoffmann S, Walter G, Meisel C, Meisel A. Stroke induces specific alteration of T memory compartment controlling auto-reactive CNS antigen-specific T cell responses. *J Neurol Sci* (2016) 368:77–83. doi:10.1016/j.jns.2016.06.039
89. Romer C, Engel O, Winek K, Hochmeister S, Zhang T, Royl G, et al. Blocking stroke-induced immunodeficiency increases CNS antigen-specific autoreactivity but does not worsen functional outcome after experimental stroke. *J Neurosci* (2015) 35:7777–94. doi:10.1523/JNEUROSCI.1532-14.2015
90. Rostrom B, Link B. Oligoclonal immunoglobulins in cerebrospinal fluid in acute cerebrovascular disease. *Neurology* (1981) 31:590–6. doi:10.1212/WNL.31.5.590
91. Tsementzis SA, Chao SW, Hitchcock ER, Gill JS, Beevers DG. Oligoclonal immunoglobulin G in acute subarachnoid hemorrhage and stroke. *Neurology* (1986) 36:395–7. doi:10.1212/WNL.36.3.395
92. Pruss H, Iggena D, Baldinger T, Prinz V, Meisel A, Endres M, et al. Evidence of intrathecal immunoglobulin synthesis in stroke: a cohort study. *Arch Neurol* (2012) 69:714–7. doi:10.1001/archneurol.2011.3252
93. Arasa F. (Bioengineering). *Folia Clin Int* (1975) 25:97–103.
94. Shibata D, Cain K, Tanzi P, Zierath D, Becker K. Myelin basic protein autoantibodies, white matter disease and stroke outcome. *J Neuroimmunol* (2012) 252:106–12. doi:10.1016/j.jneuroim.2012.08.006
95. Kalev-Zylinska ML, Symes W, Little KC, Sun P, Wen D, Qiao L, et al. Stroke patients develop antibodies that react with components of N-methyl-D-aspartate receptor subunit 1 in proportion to lesion size. *Stroke* (2013) 44:2212–9. doi:10.1161/STROKEAHA.113.001235
96. Zerche M, Weissenborn K, Ott C, Dere E, Asif AR, Worthmann H, et al. Preexisting serum autoantibodies against the NMDAR subunit NR1 modulate evolution of lesion size in acute ischemic stroke. *Stroke* (2015) 46:1180–6. doi:10.1161/STROKEAHA.114.008323
97. Yan Y, Li Y, Fu Y, Yang L, Su L, Shi K, et al. Autoantibody to MOG suggests two distinct clinical subtypes of NMOSD. *Sci China Life Sci* (2016) 59:1270–81. doi:10.1007/s11427-015-4997-y
98. Becker KJ, Tanzi P, Zierath D, Buckwalter MS. Antibodies to myelin basic protein are associated with cognitive decline after stroke. *J Neuroimmunol* (2016) 29(5–296):9–11. doi:10.1016/j.jneuroim.2016.04.001
99. Doyle KP, Quach LN, Sole M, Axtell RC, Nguyen TV, Soler-Llavina GJ, et al. B-lymphocyte-mediated delayed cognitive impairment following stroke. *J Neurosci* (2015) 35:2133–45. doi:10.1523/JNEUROSCI.4098-14.2015
100. Shi K, Wang Z, Liu Y, Gong Y, Fu Y, Li S, et al. CFHR1-modified neural stem cells ameliorated brain injury in a mouse model of neuromyelitis optica spectrum disorders. *J Immunol* (2016) 197:3471–80. doi:10.4049/jimmunol.1600135
101. Weaver CT, Harrington LE, Mangan PR, Gavrieli M, Murphy KM. Th17: an effector CD4 T cell lineage with regulatory T cell ties. *Immunity* (2006) 24:677–88. doi:10.1016/j.immuni.2006.06.002
102. Zhou L, Chong MM, Littman DR. Plasticity of CD4+ T cell lineage differentiation. *Immunity* (2009) 30:646–55. doi:10.1016/j.immuni.2009.05.001
103. Zhang CJ, Gong Y, Zhu W, Qi Y, Yang CS, Fu Y, et al. Augmentation of circulating follicular helper T cells and their impact on autoreactive B cells in myasthenia gravis. *J Immunol* (2016) 197:2610–7. doi:10.4049/jimmunol.1500725
104. Wang Z, Guo W, Liu Y, Gong Y, Ding X, Shi K, et al. Low expression of complement inhibitory protein CD59 contributes to humoral autoimmunity against astrocytes. *Brain Behav Immun* (2017) 65:173–82. doi:10.1016/j.bbi.2017.04.023
105. Ding X, Yan Y, Li X, Li K, Ciric B, Yang J, et al. Silencing IFN-gamma binding/signaling in astrocytes versus microglia leads to opposite effects on central nervous system autoimmunity. *J Immunol* (2015) 194:4251–64. doi:10.4049/jimmunol.1303321
106. Liesz A, Sun L, Zhou W, Schwarting S, Mracsko E, Zorn M, et al. FTY720 reduces post-ischemic brain lymphocyte influx but does not improve outcome in permanent murine cerebral ischemia. *PLoS One* (2011) 6:e21312. doi:10.1371/journal.pone.0021312
107. Wei Y, Yemisci M, Kim HH, Yung LM, Shin HK, Hwang SK, et al. Fingolimod provides long-term protection in rodent models of cerebral ischemia. *Ann Neurol* (2011) 69:119–29. doi:10.1002/ana.22186
108. Kraft P, Gob E, Schuhmann MK, Gobel K, Deppermann C, Thielmann I, et al. FTY720 ameliorates acute ischemic stroke in mice by reducing thrombo-inflammation but not by direct neuroprotection. *Stroke* (2013) 44:3202–10. doi:10.1161/STROKEAHA.113.002880
109. Hunter SF, Bowen JD, Reder AT. The direct effects of fingolimod in the central nervous system: implications for relapsing multiple sclerosis. *CNS Drugs* (2016) 30:135–47. doi:10.1007/s40263-015-0297-0
110. Cipriani R, Chara JC, Rodriguez-Antiguedad A, Matute C. Effects of FTY720 on brain neurogenic niches in vitro and after kainic acid-induced injury. *J Neuroinflammation* (2017) 14:147. doi:10.1186/s12974-017-0922-6
111. Dusaban SS, Chun J, Rosen H, Purcell NH, Brown JH. Sphingosine 1-phosphate receptor 3 and RhoA signaling mediate inflammatory gene expression in astrocytes. *J Neuroinflammation* (2017) 14:111. doi:10.1186/s12974-017-0882-x
112. Brait VH, Tarrason G, Gavalda A, Godessart N, Planas AM. Selective sphingosine 1-phosphate receptor 1 agonist is protective against ischemia/reperfusion in mice. *Stroke* (2016) 47:3053–6. doi:10.1161/STROKEAHA.116.015371

113. Sun N, Shen Y, Han W, Shi K, Wood K, Fu Y, et al. Selective sphingosine-1-phosphate receptor 1 modulation attenuates experimental intracerebral hemorrhage. *Stroke* (2016) 47:1899–906. doi:10.1161/STROKEAHA.115.012236
114. Havrdova E, Hutchinson M, Kurukulasuriya NC, Raghupathi K, Sweetser MT, Dawson KT, et al. Oral BG-12 (dimethyl fumarate) for relapsing-remitting multiple sclerosis: a review of DEFINE and CONFIRM. Evaluation of: Gold R, Kappos L, Arnold D, et al. Placebo-controlled phase 3 study of oral BG-12 for relapsing multiple sclerosis. N Engl J Med 2012;367:1098-107; and Fox RJ, Miller DH, Phillips JT, et al. Placebo-controlled phase 3 study of oral BG-12 or glatiramer in multiple sclerosis. N Engl J Med 2012;367:1087-97. *Expert Opin Pharmacother* (2013) 14:2145–56. doi:10.1517/14656566.2013.826190
115. Fox RJ, Miller DH, Phillips JT, Hutchinson M, Havrdova E, Kita M, et al. Placebo-controlled phase 3 study of oral BG-12 or glatiramer in multiple sclerosis. *N Engl J Med* (2012) 367:1087–97. doi:10.1056/NEJMoa1206328
116. Linker RA, Lee DH, Ryan S, van Dam AM, Conrad R, Bista P, et al. Fumaric acid esters exert neuroprotective effects in neuroinflammation via activation of the Nrf2 antioxidant pathway. *Brain* (2011) 134:678–92. doi:10.1093/brain/awq386
117. Bomprezzi R. Dimethyl fumarate in the treatment of relapsing-remitting multiple sclerosis: an overview. *Ther Adv Neurol Disord* (2015) 8:20–30. doi:10.1177/1756285614564152
118. Zhao X, Sun G, Zhang J, Ting SM, Gonzales N, Aronowski J. Dimethyl fumarate protects brain from damage produced by intracerebral hemorrhage by mechanism involving Nrf2. *Stroke* (2015) 46:1923–8. doi:10.1161/STROKEAHA.115.009398
119. Yao Y, Miao W, Liu Z, Han W, Shi K, Shen Y, et al. Dimethyl fumarate and monomethyl fumarate promote post-ischemic recovery in mice. *Transl Stroke Res* (2016) 7:535–47. doi:10.1007/s12975-016-0496-0
120. Clausen BH, Lundberg L, Yli-Karjanmaa M, Martin NA, Svensson M, Alfsen MZ, et al. Fumarate decreases edema volume and improves functional outcome after experimental stroke. *Exp Neurol* (2017) 295:144–54. doi:10.1016/j.expneurol.2017.06.011
121. Fowler JH, McQueen J, Holland PR, Manso Y, Marangoni M, Scott F, et al. Dimethyl fumarate improves white matter function following severe hypoperfusion: involvement of microglia/macrophages and inflammatory mediators. *J Cereb Blood Flow Metab* (2017). doi:10.1177/0271678X17713105
122. Rommer PS, Dorner T, Freivogel K, Haas J, Kieseier BC, Kumpfel T, et al. Safety and clinical outcomes of rituximab treatment in patients with multiple sclerosis and neuromyelitis optica: experience from a National Online Registry (GRAID). *J Neuroimmune Pharmacol* (2016) 11:1–8. doi:10.1007/s11481-015-9646-5
123. He D, Guo R, Zhang F, Zhang C, Dong S, Zhou H. Rituximab for relapsing-remitting multiple sclerosis. *Cochrane Database Syst Rev* (2013):CD009130. doi:10.1002/14651858.CD009130.pub3
124. Zhang M, Zhang C, Bai P, Xue H, Wang G. Effectiveness of low dose of rituximab compared with azathioprine in Chinese patients with neuromyelitis optica: an over 2-year follow-up study. *Acta Neurol Belg* (2017) 117(3):695–702. doi:10.1007/s13760-017-0795-6
125. Annovazzi P, Capobianco M, Moiola L, Patti F, Frau J, Uccelli A, et al. Rituximab in the treatment of neuromyelitis optica: a multicentre Italian observational study. *J Neurol* (2016) 263:1727–35. doi:10.1007/s00415-016-8188-y
126. Kim SH, Huh SY, Lee SJ, Joung A, Kim HJ. A 5-year follow-up of rituximab treatment in patients with neuromyelitis optica spectrum disorder. *JAMA Neurol* (2013) 70:1110–7. doi:10.1001/jamaneurol.2013.3071
127. Yang CS, Yang L, Li T, Zhang DQ, Jin WN, Li MS, et al. Responsiveness to reduced dosage of rituximab in Chinese patients with neuromyelitis optica. *Neurology* (2013) 81:710–3. doi:10.1212/WNL.0b013e3182a1aac7
128. Yong VW, Wells J, Giuliani F, Casha S, Power C, Metz LM. The promise of minocycline in neurology. *Lancet Neurol* (2004) 3:744–51. doi:10.1016/S1474-4422(04)00937-8
129. Chen X, Ma X, Jiang Y, Pi R, Liu Y, Ma L. The prospects of minocycline in multiple sclerosis. *J Neuroimmunol* (2011) 235:1–8. doi:10.1016/j.jneuroim.2011.04.006
130. Brundula V, Rewcastle NB, Metz LM, Bernard CC, Yong VW. Targeting leukocyte MMPs and transmigration: minocycline as a potential therapy for multiple sclerosis. *Brain* (2002) 125:1297–308. doi:10.1093/brain/awf133
131. Metz LM, Li DKB, Traboulsee AL, Duquette P, Eliasziw M, Cerchiaro G, et al. Minocycline in, trial of minocycline in a clinically isolated syndrome of multiple sclerosis. *N Engl J Med* (2017) 376:2122–33. doi:10.1056/NEJMoa1608889
132. Lampl Y, Boaz M, Gilad R, Lorberboym M, Dabby R, Rapoport A, et al. Minocycline treatment in acute stroke: an open-label, evaluator-blinded study. *Neurology* (2007) 69:1404–10. doi:10.1212/01.wnl.0000277487.04281.db
133. Fagan SC, Waller JL, Nichols FT, Edwards DJ, Pettigrew LC, Clark WM, et al. Minocycline to improve neurologic outcome in stroke (MINOS): a dose-finding study. *Stroke* (2010) 41:2283–7. doi:10.1161/STROKEAHA.110.582601
134. Cai ZY, Yan Y, Sun SQ, Zhang J, Huang LG, Yan N, et al. Minocycline attenuates cognitive impairment and restrains oxidative stress in the hippocampus of rats with chronic cerebral hypoperfusion. *Neurosci Bull* (2008) 24:305–13. doi:10.1007/s12264-008-0324-y
135. Cho KO, La HO, Cho YJ, Sung KW, Kim SY. Minocycline attenuates white matter damage in a rat model of chronic cerebral hypoperfusion. *J Neurosci Res* (2006) 83:285–91. doi:10.1002/jnr.20727
136. Ma J, Zhang J, Hou WW, Wu XH, Liao RJ, Chen Y, et al. Early treatment of minocycline alleviates white matter and cognitive impairments after chronic cerebral hypoperfusion. *Sci Rep* (2015) 5:12079. doi:10.1038/srep12079
137. Fan R, Xu F, Previti ML, Davis J, Grande AM, Robinson JK, et al. Minocycline reduces microglial activation and improves behavioral deficits in a transgenic model of cerebral microvascular amyloid. *J Neurosci* (2007) 27:3057–63. doi:10.1523/JNEUROSCI.4371-06.2007
138. Manso Y, Holland PR, Kitamura A, Szymkowiak S, Duncombe J, Hennessy E, et al. Minocycline reduces microgliosis and improves subcortical white matter function in a model of cerebral vascular disease. *Glia* (2017) 66(1):34–46. doi:10.1002/glia.23190

Conflict of Interest Statement: The authors declare that the research was conducted in the absence of any commercial or financial relationships that could be construed as a potential conflict of interest.

Copyright © 2018 Fu and Yan. This is an open-access article distributed under the terms of the Creative Commons Attribution License (CC BY). The use, distribution or reproduction in other forums is permitted, provided the original author(s) or licensor are credited and that the original publication in this journal is cited, in accordance with accepted academic practice. No use, distribution or reproduction is permitted which does not comply with these terms.

frontiers in Immunology

REVIEW
published: 29 January 2018
doi: 10.3389/fimmu.2018.00038

Bioactive Lipids and Chronic Inflammation: Managing the Fire Within

Valerio Chiurchiù[1,2†], Alessandro Leuti[1,2†] and Mauro Maccarrone[1,2*†]*

[1] Department of Medicine, Campus Bio-Medico University of Rome, Rome, Italy, [2] European Center for Brain Research (CERC), Santa Lucia Foundation (IRCCS), Rome, Italy

Inflammation is an immune response that works as a contained fire that is pre-emptively sparked as a defensive process during infections or upon any kind of tissue insult, and that is spontaneously extinguished after elimination or termination of the damage. However, persistent and uncontrolled immune reactions act as a wildfire that promote chronic inflammation, unresolved tissue damage and, eventually, chronic diseases. A wide network of soluble mediators, among which endogenous bioactive lipids, governs all immune processes. They are secreted by basically all cells involved in inflammatory processes and constitute the crucial infrastructure that triggers, coordinates and confines inflammatory mechanisms. However, these molecules are also deeply involved in the detrimental transition from acute to chronic inflammation, be it for persistent or excessive action of pro-inflammatory lipids or for the impairment of the functions carried out by resolving ones. As a matter of fact, bioactive lipids have been linked, to date, to several chronic diseases, including rheumatoid arthritis, atherosclerosis, diabetes, cancer, inflammatory bowel disease, systemic lupus erythematosus, and multiple sclerosis. This review summarizes current knowledge on the involvement of the main classes of endogenous bioactive lipids—namely classical eicosanoids, pro-resolving lipid mediators, lysoglycerophospholipids/sphingolipids, and endocannabinoids—in the cellular and molecular mechanisms that lead to the pathogenesis of chronic disorders.

Keywords: eicosanoids, endocannabinoids, inflammation, resolution, specialized proresolving mediators, sphingolipids

OPEN ACCESS

Edited by:
Claudia Monaco, University of Oxford, United Kingdom

Reviewed by:
Yongsheng Li, Third Military Medical University, China
Hugo Caire Castro-Faria-Neto, Fundação Oswaldo Cruz (Fiocruz), Brazil

***Correspondence:**
Valerio Chiurchiù
v.chiurchiu@hsantalucia.it;
Mauro Maccarrone
m.maccarrone@unicampus.it

†These authors have contributed equally to this work.

Specialty section:
This article was submitted to Inflammation, a section of the journal Frontiers in Immunology

Received: *06 September 2017*
Accepted: *05 January 2018*
Published: *29 January 2018*

Citation:
Chiurchiù V, Leuti A and Maccarrone M (2018) Bioactive Lipids and Chronic Inflammation: Managing the Fire Within. Front. Immunol. 9:38. doi: 10.3389/fimmu.2018.00038

INTRODUCTION

Inflammation represents one of the best known pathophysiological processes and represents a well-conserved mechanism evolved by vertebrates as an adaptive and defensive response to tissue injury and invasion of microorganisms that might attempt to colonize the host (1, 2). Despite the apparent simplicity of its definition, inflammation is instead a rather intricate network of cellular and molecular events, at the core of which, a plethora of pre-formed or newly synthesized mediators is elegantly arranged to obtain specific temporal and spatial responses. Endogenous lipids are arguably the most important mediators not only to be implicated in all phases of inflammation, but also to be involved in the regulation and fine-tuning of its course and cessation. Indeed, lipids are not just the major constituents of cell membranes and very efficient sources of energy, but also as key pathophysiological mediators of several intercellular and intracellular processes. Thus, during the past two decades, they have been termed "bioactive lipids," due to their pivotal role

in immune regulation, inflammation, and maintenance of tissue homeostasis (3, 4). Bioactive lipids, divided into four main families according to their biochemical functions, i.e., classical eicosanoids, specialized pro-resolving mediators (SPMs), lysoglycerophospholipids/sphingolipids and endocannabinoids (eCBs), are generated from ω-6 or ω-3 essential polyunsaturated fatty acids (PUFA) precursors, that are esterified into membrane lipids and act by binding to and activating specific G protein-coupled receptors (GPRs).

BIOACTIVE LIPIDS AND INFLAMMATION

In the event of tissue insults or infections, innate immune cells, such as granulocytes and monocytes/macrophages, are recruited to the damaged site and rapidly generate classical eicosanoids, the class of lipid mediators that is responsible for acute inflammation (or angiophlogosis) characterized by the so-called "cardinal signs" of inflammation: redness, heat, swelling, pain, and loss of function (5). Classical eicosanoids are thus highly pro-inflammatory and ignite the fire during inflammation, with the aim of removing injurious stimuli, a fire that, however, needs to be self-limiting and, eventually, promptly extinguished upon cessation or elimination of the noxious stimulus. During the last process, referred to as "resolution of inflammation" or catabasis (i.e., Dante's descent into the hell), the very same innate immune cells recruited in the inflammatory milieu, where they produce classical eicosanoids, undergo a temporal lipid mediator class switch and start producing another class of bioactive lipids, the newly discovered SPMs. These lipids actively terminate inflammation and drive the restoration of full tissue homeostasis by activating the signs of resolution: removal, relief, restoration, regeneration, and remission (6, 7). When the fire of inflammation is not properly extinguished, due to impaired resolution, it turns into chronic inflammation (or histophlogosis), resulting in aberrant tissue remodeling and organ dysfunction (8). In this context, the outcome of inflammation depends also on the other two families of bioactive lipids, i.e., lysoglycerophospholipids/sphingolipids and eCBs, which regulate numerous cellular processes that are important for triggering those mechanisms that underlie cell and tissue adaption to inflammatory events (9, 10). Indeed, chronic inflammation represents often the causative agent and the main trigger of the damage associated to many pathologies, such as cancer, autoimmune, metabolic, cardiovascular, and neurodegenerative diseases (11, 12). Thus, it seems that bioactive lipids are largely involved in managing the fire of inflammation, either acting as fire-starters or as fire-fighters, or even as executives of the fire station.

CLASSICAL EICOSANOIDS

These bioactive lipids represent probably the widest and most celebrated family, and include a huge array of molecules that have the ω-6 PUFA arachidonic acid (AA) as their common biosynthetic precursor released from membrane phospholipids by phospholipase A_2 (13). AA is then used as a substrate for three different oxygen-incorporating enzymes that together synthesize over 120 heterogeneous and pleiotropic molecules: cyclooxygenases 1 and 2 (COX-1/2) drive the synthesis of prostaglandins (PGs), prostacyclins, and thromboxanes (TXs) (14–16), often referred together as prostanoids; 5-, 12-, and 15-lypooxygenases (5/12/15-LOX) produce leukotrienes (LTs) (17), hydroxyeicosatetraenoids (HETEs) (13), and lipoxins (LX) (6); P450 epoxygenase generates HETEs and epoxyeicosatrienoids (13). Even though all these bioactive lipids are involved in a plethora of physiological and homeostatic processes, including control of vascular tone, platelet aggregation, pain perception as well as ovulation, and embryo implantation (13, 18), they are mostly renowned for their ability to act as fire-starters and initiators of inflammation. Prostanoids, including PGs, such as PGD_2, PGE_2, PGI_2, and $PGF_{2\alpha}$, represent, to date, a central subject of study among eicosanoids, especially in light of the ability of non-steroidal anti-inflammatory drugs (NSAIDs) to block their synthesis by covalent inhibition of COX-1/2 (19), which in turn results in the forestall of inflammation. The fact that NSAIDs are mostly used to treat acute inflammatory symptoms, such as swelling and pain, while being essentially ineffective on chronic conditions (for which steroidal drugs are preferred as treatment), has led to the idea that prostanoids are far less involved in chronic inflammatory pathologies (13). However, recent studies conducted using knockout mice for each specific GPR of the different classical eicosanoids (e.g., EP1–4, DP1–2, IP, FP, and TP), or specific stimulation by means of selective agonists, unveiled that their role might go well beyond the acute inflammatory response. Indeed, PG signaling—especially the one mediated by PGE_2 and PGI_2—seems to be involved in the sustained inflammation that causes the transition to chronic inflammation by acting as "cytokine amplifiers" (12, 20). These observations were based on animal and cellular models of chronic inflammatory diseases, such as arthritis (21) and cancer (22), where PGs are known to be involved also in their pathogenesis. In general, PGs induce chronic inflammation through five main mechanisms: (i) enhancement of the pro-inflammatory cytokines release cascade (21); (ii) amplification of innate immunity response to pathogen- and damage-associated molecular patterns (PAMPs and DAMPs) (23); (iii) activation of specific pro-inflammatory subsets of T helper cells, e.g., T_H1 and T_H17 (24, 25); (iv) recruitment of immune cells associated with chronic inflammation (e.g., macrophages, T and B cells) by synergistically acting with chemokines (12); (v) increase of pro-inflammatory genes induced by cytokines. Consistently, many studies have reported associations between specific PG-related genes (e.g., biosynthesizing enzymes or receptors) and the susceptibility to several chronic diseases, including Crohn's disease (CD) (26), asthma (27), and multiple sclerosis (MS) (28, 29).

The main role of LTs in acute inflammation is to induce, alongside prostanoids, edema, and neutrophil influx within inflamed tissues (13). However, LTs are also central in perpetuation of inflammatory signals that lead to tissue damage in many chronic diseases. Indeed, LTs and their cysteinyl derivatives have been long known to be intimately connected to the pathogenesis of atherosclerosis, inflammatory bowel disease (IBD), psoriasis, rheumatoid arthritis (RA), as well as bronchial asthma, and MS, acting as chemoattractants for neutrophils, macrophages, eosinophils, and also T_H17 lymphocytes (30–32), thus maintaining

an ongoing and sustained inflammatory milieu. Of note, discussing the precise role of each LOX-derived eicosanoid in chronic inflammation is not an easy task, mainly due to their vast number (over 70 mediators), their differential action on cellular targets, and their complex and intermingled metabolic destiny. For instance, 5(S)-HpETE is the precursor of LTA_4, which in turn is the common precursor of all bioactive leukotrienes (33), and of LX, which instead are anti-inflammatory inasmuch as are involved in the resolution of inflammation, as discussed in the next section.

SPECIALIZED PRO-RESOLVING LIPID MEDIATORS

As mentioned above, at the peak of acute inflammation the very same cells involved in the production of pro-inflammatory lipid mediators undergo a class switch and start producing SPMs from ω-6 AA and even more from ω-3 PUFAs eicosapentaenoic acid (EPA), docosahexaenoic acid (DHA), and docosapentaenoic acid (DPA), through the stereoselective and concerted action of the same enzymes engaged in classical eicosanoids production: COXs, LOXs, and P450. To date, more than 20 different SPMs have been identified *via* sophisticated lipidomic approaches in the laboratory of Prof. Serhan, and these can be generally subdivided into six main classes: AA-derived LXs (LXA_4 and LXB_4); EPA-derived E-series resolvins ($RvE_{1–3}$); DHA-derived D-series resolvins ($RvD_{1–6}$); protectins/neuroprotectins (PD1/NPD1 and PDX); and their sulfido-conjugates (PCTRs), maresins (MaR1 and MaR2); and their conjugates (MCTR1–3), as well as the latest class to be identified, namely the DPA-derived 13-series resolvins ($RvT_{1–4}$) (6, 34, 35) (**Figure 1** summarizes the details of their respective biochemical synthesis). The lipid class switch is initiated already in the early phases of inflammation by LXA_4 and LXB_4, produced by platelets that progressively aggregate at the sites of inflammation (36). Overall, SPMs act as

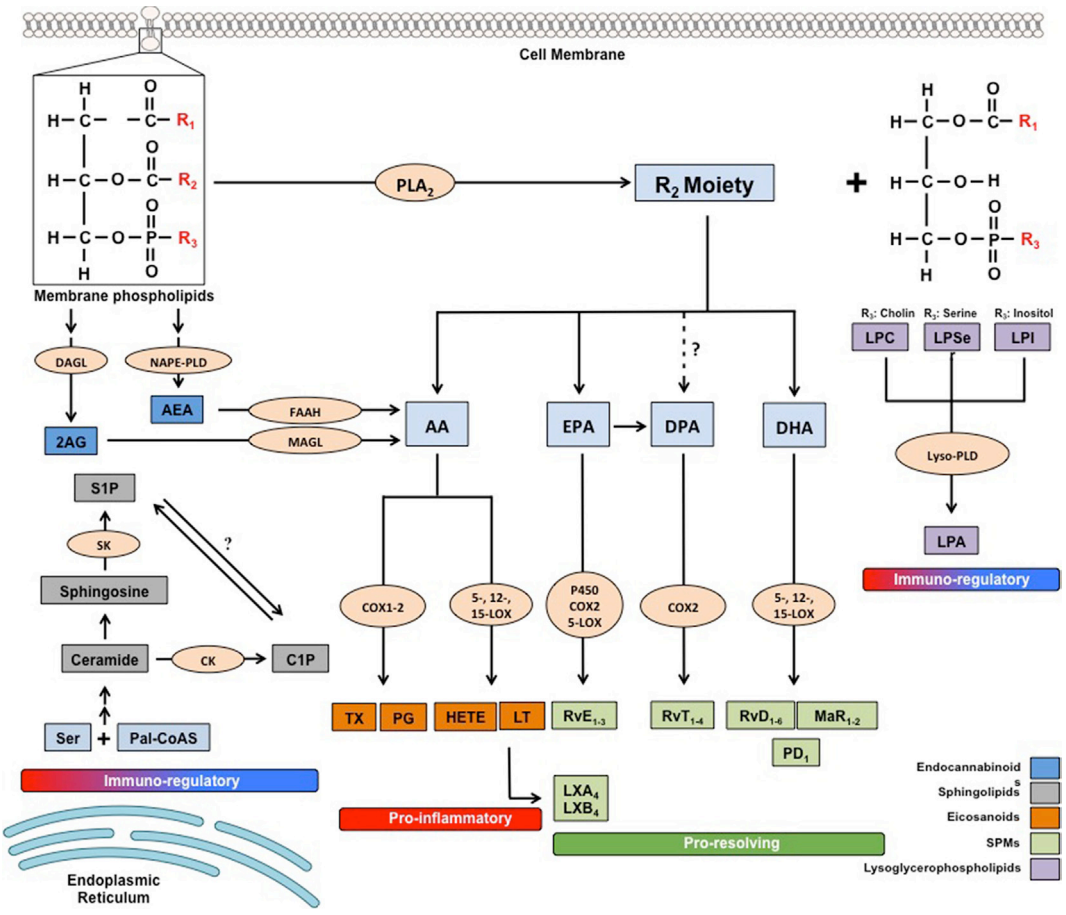

FIGURE 1 | Metabolic pathways of the main families of endogenous bioactive lipids. 2-AG, 2 arachidonoylglycerol; AA, arachidonic acid; AEA, arachidonoylethanolamide; C1P, ceramide-1-phosphate; CK, ceramide kinase; COX, cyclooxygenase; DAGL, diacylglycerol lipase; DHA, docosahexaenoic acid; DPA, docosapentaenoic acid; EPA, eicosapentaenoic acid; FAAH, fatty acid amide hydrolase; HETEs, hydroxyeicosatetraenoic acids; LOX, lipoxygenase; LPA, lysophosphatidic acid; LPC, lysophosphatidilcholine; LPI, lysophosphatidylinositol; LPSer, lysophosphatidylserine; LTs, leukotrienes; LX, lipoxin; Lyso-PLD, lyso-phospholipase D; MAGL, monoacylglycerol lipase; MaR, maresin; NAPE-PLD, *N*-arachidonoylphosphatidylethanolamide-specific phospholipase D; Pal-CoASH, palmitoyl coenzyme A; PD, protectin; PDX, protectin DX; PGs, prostaglandins; PLA_2, phospholipase A_2; Rv, resolvin; S1P, sphingosine-1-phosphate; SK, sphingosine kinase; TXs, thromboxanes.

"immunoresolvents," that is immune-pharmacological agents of resolution, as opposed to immunosuppressive agents, and they induce cessation of further leukocyte infiltration, recruitment and stimulation of nonphlogistic mononuclear cells, promote killing and clearance of pathogens and macrophage-mediated phagocytosis of apoptotic granulocytes (efferocytosis) and cellular debris, inhibit proinflammatory cytokines while inducing the production of anti-inflammatory mediators, shorten the time of resolution and activation of endogenous resolution programs, and promote tissue regeneration and healing (6, 37). Their activity is mediated by five separate GPRs, namely the formyl peptide receptor 2 (FPR2, also known as ALX), GPR32 (or DRV1), chemerin receptor 23 ChemR23 (or ERV), leukotriene B_4 receptor 1 (BLT1) and GPR18 (or DRV2), expressed in different cell tissues and with differential affinities for each SPM or other lipid mediators (38). The target receptors of most SPMs are yet to be identified and further studies will be required to characterize the signaling pathways underlying their functions.

Although most of the insight gathered so far on SPMs concerns their role in modulating acute inflammation innate components, recent investigations have reported their ability to directly modulate adaptive immune cells, such as B and T lymphocytes, which are strongly involved in chronic detrimental inflammation. Indeed, although only RvD1 has been shown to act on B cells by inducing differentiation into plasma cells and promoting IgM and IgG antibody isotype switching (39) while inhibiting IgE production (40), a growing number of studies are now reporting direct or indirect effects of several SPMs on T cells. For instance, LXA_4 and LXB_4 both inhibited TNF-α secretion from activated human T cells (41), whereby the LXA_4-induced effects were dependent on FPR2/ALX, which is expressed on T cells and their subsets (41–43). Additionally, RvE1, RvD1, and PD1 all have been shown to reduce the recruitment of $CD4^+$ and $CD8^+$ T cells (44–47), with the former SPM also limiting CD4-associated production of IFN-γ and IL-4 (45).

Of note, our group recently demonstrated that RvD1, RvD2, and MaR1 are able to hinder the production of pro-inflammatory cytokines in CD4 and CD8 T cells, as well as to inhibit *de novo* differentiation into T_H1 and T_H17, while promoting development of Treg cells without exerting any immunosuppressive and cytotoxic effect (43). Moreover, mice genetically unable to produce DHA displayed an increase in T_H1/T_H17 cells and a decrease in Treg cells (43), implying that SPMs impact on the balance between pathogenic and tolerogenic adaptive immune cells. Taken together, these findings support the view that SPMs may prevent chronicity of inflammation and/or autoimmunity and link resolution to adaptive immune cell responses. Interestingly, recent evidence indicates that pathologic conditions associated with altered SPM metabolism and function can contribute to chronicity and magnitude of persistent inflammatory conditions; as a result current research is centered on investigating the role of SPMs in chronic diseases in several mouse models and humans. Accordingly, decreased production of LX, E-, and D-series resolvins in the airways, as well as disruption of FPR2/ALX signaling have been linked to the pathogenesis of chronic obstructive pulmonary disease (COPD), and their restoration determined beneficial effects (48). Dysfunctional production of D-series resolvins and insufficient resolution has also been observed in mouse models or in human plasma samples of other typical chronic inflammatory and/or autoimmune diseases, such as (i) type-2 diabetes and obesity (49, 50); (ii) RA, in which low levels of RvD3 are associated with delayed resolution in mice and active disease in humans (51) and where RvD1 exerts protective actions on cartilage of murine model of inflammatory arthritis (52); (iii) atherosclerosis, in which evidence for impairment of resolution of vascular inflammation is governed by specific SPMs (53) and reduced RvD1 correlates with atherosclerotic plaque instability (30), and where RvD2, RvE1 and MaR1 have all been reported to have atheroprotective effects (54–57); and (iv) inflammatory bowel disease (58, 59). Accumulating evidence reveals that several neurodegenerative diseases characterized by chronic inflammation, such as MS, Alzheimer's disease (AD) and amyotrophic lateral sclerosis (ALS), also seem to be associated to failure of activating pro-resolving mechanisms, and interventions with SPMs *in vitro* or *in vivo* exert neuroprotective properties. Indeed, a dysfunctional resolution pathway in SPMs and their receptors is present in post-mortem tissues of AD patients (60, 61) and several SPMs promoted neuronal survival and β-amyloid uptake by microglia *in vitro* (61–64). Additionally, RvD1 strongly inhibited cytokine release from inflammatory macrophages in ALS spinal cord (65), and its daily administration in mouse models of MS decreased disease progression by suppressing autoreactive T cells and by inducing an M2 phenotype of monocytes/macrophages and resident brain microglial cells (66). These findings advocate the stimulation of resolution pathways as a new therapeutic strategy to prevent chronic inflammation. Topical formulation of analogs of resolvin E1 (RX-10001, RX-10008, and RX-10045) or neuroprotectin D1 (RX-20001), resistant to metabolic inactivation, are currently underway in a number of human clinical trials for several chronic conditions, such as dry eye, macular degeneration and diabetic retinopathy, as well as lung, gut and kidney inflammation (67).

LYSOPHOSPHOLIPIDS AND SPHINGOLIPIDS

These bioactive lipids comprise many compounds asymmetrically distributed in plasma membranes with glycerol or sphingosine as respective backbones, and are characterized by a great molecular diversity due to their linkage with other molecules, such as ethanolamine, choline, inositol, serine or and fatty acids (e.g., phosphoinositides, lysoglycerophospholipids, and ceramides). The detailed metabolic steps of these substances are illustrated in **Figure 1**. Biochemical interconversions between them and also into other classes of bioactive lipids, such as eicosanoids and eCBs, are also possible, thanks to the action of phospholipases, lipid kinases and lipid-phosphate phosphatases (68, 69). The most biologically active lysophospholipids, derived from membrane phospholipids by removal of one or both fatty acids, are lysophosphaditylcholine (LPC) and lysophosphatidilinositol (LPI), and their byproduct lysophosphatidic acid (LPA), which are signaling molecules involved in pivotal aspects of

cellular and tissue biology, such as plasma membrane shaping (70), cell growth and death (71), and inflammatory cascades (72). LPC and LPA modulate immune responses mostly by controlling distribution, trafficking and activation of immune cells (72–75), and their sustained activation have been suggested to be linked with several chronic inflammatory diseases, including obesity and diabetes (76, 77), cancer (74), atherosclerosis (78) and RA (79, 80).

On the other hand, the main active sphingolipids, whose peculiar chemical structure has baffled scientists for a long time (hence their name, inspired by the Egyptian Sphynx) (81), are ceramide and their byproducts ceramide 1-phosphate (C1P) and sphingosine 1-phosphate (S1P), shown in **Figure 1** (69). Sphingolipids participate in numerous inflammatory processes and are responsible for controlling intracellular trafficking and signaling, cell growth, adhesion, vascularization, survival, and apoptosis (9, 68, 82), even though specific receptors have only been identified for S1P. The role of these three sphingolipids in chronic inflammation has been extensively investigated in the past decade, and have been mostly associated with immune-dependent and vascular-related chronic inflammatory diseases, including diabetes and obesity, COPD, IBD and neuroinflammatory disorders. For instance, an excessive ceramide signaling determines adipose tissue inflammation and insulin resistance, leading to obesity and type-2 diabetes, by inducing overactive immune cells like macrophages and B cells (81–83). Of note, most of the pro-inflammatory activities of ceramide seem to be mediated through its C1P and S1P metabolites. The former enhances both acute and chronic inflammatory responses by promoting phospholipase A2-mediated eicosanoid storm and by inducing cytokine production (84, 85). However, ceramide and C1P have also been shown to negatively regulate some pro-inflammatory cytokines (86, 87), suggesting a more complex role for them in inflammation. Furthermore, C1P has also been reported to impact on insulin resistance-induced type-2 diabetes and metabolic syndrome (82), as well as to induce cell migration in several cellular models of monocytes/macrophages and endothelial cells, as reviewed in Ref. (82), implying that this bioactive lipid might be involved in chronic inflammatory diseases characterized by migration of immune cells to inappropriate sites, such as IBD, atherosclerosis, and MS. Ceramide and its metabolites are also involved in the physiological regulation of endothelial/vascular integrity and function, whereby alterations of these sphingolipids are associated with vascular dysfunctions, and thus with chronic inflammatory states (88, 89).

Sphingosine-1-phosphate is arguably the best-studied molecule of this family of bioactive lipids and its actions are mediated by five identified receptors (S1PR1–5) (90). This lipid is a key mediator for lymphocyte trafficking between lymphoid and non-lymphoid tissues, favoring the egress of effector T and B cells from lymph nodes, thymus, bone marrow, and spleen, and blocking the ability of immature dendritic cells to migrate (91, 92). This function of S1P is particularly important, since T and B cells are the fire-starters of many (if not all) chronic inflammatory conditions and autoimmune diseases, in which modulation of their function is often exploited to develop new therapeutic strategies. Accordingly, the commercially available oral drug Fingolimod was developed as a first-line disease-modifying treatment for MS due to its ability to downregulate S1PR1, and hence to sequester highly pathogenic T cells (i.e., Th1 and Th17 cells) within the lymph nodes, avoiding brain invasion and myelin damage (93, 94). Fingolimod has also been shown to reduce blood–brain barrier dysfunction, a renowned pathogenetic mechanism of MS, by attenuating the production of sphingolipids from reactive astrocytes, including ceramide (95), also because several S1P receptors are significantly upregulated in MS lesions (96, 97). Interestingly, high S1P levels have also been found in patients with IBD and asthma (81, 98) and, accordingly, these conditions were attenuated by genetic deletion of the enzyme responsible for its synthesis in rodent models of disease or by pharmacological modulation of the S1P–S1PR axis (98–100).

ENDOCANNABINOIDS

Endocannabinoids include a group of bioactive lipids endogenously produced by humans and animals that are able (although with different affinities) to bind to and activate the same receptors as the main psychoactive component of marijuana Δ^9-tetrahydrocannabinol, i.e., type-1 and type-2 cannabinoid receptors (CB_1 and CB_2). Arachidonoylethanolamide (commonly known as anandamide, AEA) and 2-arachidonoylglycerol (2-AG), both identified in the early 1990s, are the two best studied members of the eCB family, which also comprise 2-AG-ether, *O*-arachidonoylethanolamine, and palmitoylethanolamide (PEA) (10, 101). These molecules are ubiquitously produced by most tissues and immune cells, which are fully capable to metabolize them *via* a set of specific synthesizing [*N*-acyl-phosphatidylethanolamine-hydrolyzing phospholipase D (NAPE-PLD) for AEA and its congeners and diacylglycerol lipase (DAGL) for 2-AG] and degrading [fatty acid amide hydrolase FAAH for AEA and monoacylglycerol lipase (MAGL) for 2-AG] enzymes (101). Besides the aforementioned CB_1 and CB_2 receptors, eCBs also engage other molecular targets that include members of the transient receptor potential (TRP) channels, GPR55, and peroxisome proliferator-activated receptors (PPARs), differentially expressed by body districts also according to their inflammatory state (102, 103). Altogether, eCBs and their enzymes and receptors constitute the so-called "eCB system," which generally serves as a homeostatic system that controls several physiopathological states ultimately maintaining human health (104). In particular, eCBs are arguably among the most potent immunoregulatory compounds, capable of regulating the functions of several cell subsets of either innate or adaptive immunity (in particular monocytes/macrophages, dendritic cells, granulocytes, and T lymphocytes), with AEA and PEA being mostly anti-inflammatory (105–107) and 2-AG both pro- and anti-inflammatory (10, 108–111). Indeed, due to their role in the overall control of tissue homeostasis, variations in the tone of distinct eCBs within tissues, or in the expression of their metabolic enzymes or receptors have been clearly recognized as central in the pathophysiology of many chronic inflammatory diseases. Indeed, it is now clear that perturbations in all members

of the eCB system occur during every chronic inflammatory process, from cancer, metabolic, and gastrointestinal diseases to autoimmune and neuroinflammatory disorders [extensively reviewed in Ref. (112–119)]. This is because every single cell and tissue of our body produces specific eCBs (sometimes also simultaneously) "on demand" and at certain concentrations according to the stimulus and/or the need, in order to autocrinally or paracrinally orchestrate the inflammatory responses of nearby cells through complex interactions between multiple receptors or targets with different but partly overlapping activities (104). Recently, eCBs are also emerging as pro-resolving agents due to the ability of AEA and 2-AG, alongside other congeners (e.g., PEA) to boost resolution programs during neuroinflammation (120, 121), while 2-AG alone can enhance phagocytosis in human macrophages (122). Accordingly, several experimental models of chronic inflammatory diseases have been instrumental, not only to better understand the role of each member of the eCB system in their different pathogenic mechanisms, but mostly to identify in the pharmacological manipulation of either receptors or enzymes (by means of selective activation of specific receptors or inhibition of AEA, 2-AG, or PEA degrading enzymes) a promising therapeutic strategy. In line with this, modulation of the eCB system has been shown to be beneficial by attenuating inflammatory processes that include cytokine release, infiltration of leukocytes at inflamed sites, production of reactive oxygen and nitrogen species, and overall immune cell activation (123–127). These effects were particularly relevant in several neuroinflammatory and neurodegenerative diseases, such as MS and AD (119, 128–131), where chronic inflammation is indeed a hallmark and whereby targeting the eCB system seems to be a promising therapeutic approach in the near future. Interestingly, AEA and 2-AG can also be metabolized by COX-2, LOXs, and P450 into eicosanoid-like PG-ethanolamides and glyceryl esters, hydroxy-anandamides, and hydroxyeicosatetraenoyl-glycerols, respectively (132, 133). The function and biological activity of these lipids is still unclear, but it is plausible that they might play a role in chronic inflammation.

DO BIOACTIVE LIPIDS COEXIST DURING THE DIFFERENT STAGES OF INFLAMMATION?

The array of bioactive lipids that lays at the heart of tissue immune homeostasis represents a vastly intertwined network of molecules whose metabolism is rather complex, in that not only they undergo fast biosynthesis, degradation or interconversion, but also they share common metabolic enzymes, the activation or regulation of which is fascinating and still not completely unraveled. Consequently, the full elucidation of their temporal production and their role in the different phases or inflammation (from acute inflammation and its resolution to chronic inflammation) represents conceivably one of the biggest challenges of our time. To date, this has been particularly investigated for eicosanoids and SPMs in terms of their detailed temporal and spatial production and their specific role during the different inflammatory states and this is mainly due to their thorough characterization by means of lipidomics analyses performed locally in inflammatory or self-resolving tissues (i.e., edema). Indeed, both eicosanoids and SPMs are present in all phases of inflammation: the former are massively produced within the first 2–4 h and then show a reduction during the resolution phase, whereas the latter appear already at early phases of inflammation (especially LX and RvTs), usually reach their highest level at the peak of acute inflammation (6–12 h) and some specific molecules (i.e., RvD3) are produced at later stages. During chronic inflammation, as previously described, both families of bioactive lipids are present, with specific molecules being overly or inadequately produced, according to the different inflammatory diseases and tissues. Such temporal and spatial production, although less studied, is beginning to hold true also for the other families of bioactive lipids. Indeed, eCB levels raise rapidly following noxious stimuli and this is generally associated with their role in activating anti-inflammatory and protective mechanisms, although persistent inflammation usually dysregulates the eCB system in a way that their action might even become detrimental (134). On the other hand, other authors have reported diminished levels of eCBs in chronic inflammatory models, even after several days after the induction of inflammation (135). Of note, the temporal production of eCBs can only be inferred from *in vitro* studies conducted on cell lines activated with different inflammatory stimuli at different times or in tissues of patients or animal models of acute or chronic inflammatory diseases. To date, a fully detailed temporal characterization of each eCB during the different stages of inflammation, namely from an acute model of inflammation to a *bona fide* model of spontaneous resolution, is still absent and represents a future challenge. This scenario is further complicated by the fact that eCBs exist in dynamic equilibria with different other lipid-derived mediators, including eicosanoids, prostamides, and their recently identified ω-3 congeners (136).

Also sphingolipids are found during different stages of inflammation, and are likely part of the resolution machinery as suggested by the fact that apoptotic cells at the inflammation sites attract pro-resolving macrophages in a S1P-S1PR1-dependent manner (137), while neutrophil apoptosis, which is pivotal in initiating resolution, rely at least in part on the generation of ceramide (138). Furthermore, LPA might represent another brick in the resolution wall, in that it has been recently reported to be rapidly produced during the resolution phase of tissue inflammation and to recruit monocytes *via* the common pro-resolving receptor ALX/FPR2 (139). Interestingly, treatment of human fibroblasts (key cells involved in tissue healing and regeneration) with TNF-α, a cytokine that is mainly produced during acute or chronic inflammation, results in a significant increase in S1P levels, which rapidly returns to baseline within less than an hour (140), and of COX-2 expression, which can, in turn, temporally generate both eicosanoids, SPMs or even eCBs metabolites.

All these evidences not only account for a coexistence of several families of bioactive lipids during the different stages of inflammation, but also suggest that each inflammatory phase requires the concerted action of such lipid mediators, which are also likely to molecularly interact and engage in physiopathological cross talks.

TABLE 1 | Main role of bioactive lipids in chronic inflammatory diseases.

Bioactive lipid family	Bioactive lipid	Chronic inflammatory diseases	Effect
Classical eicosanoids	PGE_2, PGI_2	Rheumatoid arthritis (RA) Cancer Crohn's disease Asthma Multiple sclerosis (MS)	Cytokine amplification, enhanced innate immune responses, and recruitment of adaptive immune cells
	LTB_4	Psoriasis RA Asthma Inflammatory bowel disease (IBD) Atherosclerosis	Leukocyte chemotaxis and trafficking
Specialized pro-resolving mediators (SPMs)	LXA_4	Alzheimer's disease (AD)	Decreased production and neuroprotective effects
	RvD1	Chronic obstructive pulmonary disease Atherosclerosis Obesity/type-2 diabetes RA AD MS Amyotrophic lateral sclerosis (ALS)	Decreased production and beneficial effects Impaired metabolism and correlation with plaque instability Decrease adipose tissue and improvement of insulin sensitivity Protective on cartilage Correlation with cognitive functions and β-amyloid phagocytosis Th1/Th17 suppression and M2 induction M1 macrophages suppression
	RvD2	Obesity/type-2 diabetes Atherosclerosis	Decreased production Atheroprotective effects
	RvD3	RA	Decreased production
	PDX	AD	Decreased production and neuroprotective effects
	MaR1	AD	Decreased production and β-amyloid phagocytosis
Lysoglycero-phospholipids	Lysophosphatidic acid (LPC), lipoxygenase (LPA)	Obesity/type-2 diabetes Cancer Atherosclerosis RA	Sustained production and promotion of inflammatory cascades
Sphingolipids	Ceramide, sphingosine-1-phosphate (S1P), ceramide-1-phosphate	Type-2 diabetes Atherosclerosis IBD	Adipose tissue inflammation, insulin resistance, and activation of immune cells Leukocyte recruitment and vascular dysfunction
	S1P	MS IBD Asthma	Signaling disruption and trafficking of T and B cells from lymphoid organs Increased levels and beneficial effects
Endocannabinoids (eCBs)	Arachidonoylethanolamide, 2-arachidonoylglycerol	Cancer Metabolic diseases Gastrointestinal diseases Atherosclerosis Autoimmune diseases MS AD PD ALS Mood disorders	Differential alteration of their levels and beneficial effects when administered or upon genetical/pharmacological manipulation of a member of the eCB system
	Palmitoylethanolamide	Chronic granulomatous inflammation MS Neuropathic pain	Decreased levels and beneficial effects Increased levels and reduction of motor disability in animal models Anti-allodynic and anti-hyperalgesic effects *via* modulation of microglial and mast cell activity

CONCLUDING REMARKS

For a long time, the idea that lipids were mere constituents of cellular membranes and efficient energy sources was indisputable, but over the past two decades, not only it became clear that they actually harbor many functions in the regulation of intercellular and intracellular signaling pathways, but also that they represent bioactive molecules that are able to orchestrate a plethora of biological activities on their own, in order to maintain tissue homeostasis by governing body's defensive and healing processes like inflammation and its resolution. During these processes, several families of bioactive lipids are temporally and

spatially engaged so that the appropriate leukocytes are recruited and the noxious agent or stimulus is eliminated. Accordingly, classical eicosanoids are the fire-starters of the inflammatory processes and engage mainly cells of the innate arm of immunity that execute all possible strategies to quickly eradicate the injury. If the danger ceases or is successfully terminated, the fire of inflammation is elegantly extinguished by SPMs that recruit non-phlogistic innate immune cells and activate resolution pathways, aimed at healing the damaged tissue. On the contrary, if the injurious stimulus is either persistent or not eliminated, perhaps by failure of resolving inflammation, a wildfire of long-lasting inflammatory processes occurs and the flame of inflammation is kept alive mainly by cells of the adaptive arm of immunity, thus leading to many chronic inflammatory diseases. Under these circumstances, tissues activate several adaptation mechanisms that allow cells to cope with the changes induced by the damage, also thanks to other families of bioactive lipids like lysophospholipids, sphingolipids, and eCBs, that ultimately regulate cell growth, differentiation, and destiny with the goal of helping the body to restore homeostatic balance. Most of these bioactive lipids and several elements of their complex metabolism and signaling (i.e., enzymes and receptors) are differentially dysregulated in many chronic inflammatory diseases (**Table 1**), suggesting that managing the fire within by targeting the endogenous mechanisms involved in the spontaneous fire extinction, or in the modulation of homeostatic processes, rather than simply suppressing inflammation, could be a future and promising therapeutic strategy to be undertaken.

AUTHOR CONTRIBUTIONS

All authors listed have made a substantial, direct, and intellectual contribution to the work and approved it for publication.

ACKNOWLEDGMENTS

This work was supported by Fondazione Italiana Sclerosi Multipla (competitive FISM grant 2015/R/08 to VC) and by European Union-health EULAC (competitive EULACH16/TO 1032 grant to MM).

REFERENCES

1. Majno G, Joris I. *Cells, Tissues, and Disease. Principles of General Pathology*. II ed. Oxford: Oxford University Press (2004).
2. Kumar V, Abbas A, Aster J. *Robbins & Cotran Pathologic Basis of Disease*. IX ed. Amsterdam: Elsevier (2014).
3. Shimizu T. Lipid mediators in health and disease: enzymes and receptors as therapeutic targets for the regulation of immunity and inflammation. *Annu Rev Pharmacol Toxicol* (2009) 49:123–50. doi:10.1146/annurev.pharmtox.011008.145616
4. Chiurchiù V, Maccarrone M. Bioactive lipids as modulators of immunity, inflammation and emotions. *Curr Opin Pharmacol* (2016) 29:54–62. doi:10.1016/j.coph.2016.06.005
5. Nathan C. Points of control in inflammation. *Nature* (2002) 420:846–52. doi:10.1038/nature01320
6. Serhan CN. Pro-resolving lipid mediators are leads for resolution physiology. *Nature* (2014) 510:92–101. doi:10.1038/nature13479
7. Basil MC, Levy BD. Specialized pro-resolving mediators: endogenous regulators of infection and inflammation. *Nat Rev Immunol* (2016) 16:51–67. doi:10.1038/nri.2015.4
8. Nathan C, Ding A. Nonresolving inflammation. *Cell* (2010) 140:871–82. doi:10.1016/j.cell.2010.02.029
9. El Alwani M, Wu BX, Obeid LM, Hannun YA. Bioactive sphingolipids in the modulation of the inflammatory response. *Pharmacol Ther* (2006) 112:171–83. doi:10.1016/j.pharmthera.2006.04.004
10. Chiurchiù V, Battistini L, Maccarrone M. Endocannabinoid signalling in innate and adaptive immunity. *Immunology* (2015) 144:352–64. doi:10.1111/imm.12441
11. Fullerton JN, Gilroy DW. Resolution of inflammation: a new therapeutic frontier. *Nat Rev Drug Discov* (2016) 15:551–67. doi:10.1038/nrd.2016.39
12. Aoki T, Narumiya S. Prostaglandins and chronic inflammation. *Trends Pharmacol Sci* (2012) 33:304–11. doi:10.1016/j.tips.2012.02.004
13. Dennis EA, Norris PC. Eicosanoid storm in infection and inflammation. *Nat Rev Immunol* (2015) 15:511–23. doi:10.1038/nri3859
14. Smith WL, DeWitt DL, Garavito RM. Cyclooxygenases: structural, cellular, and molecular biology. *Annu Rev Biochem* (2000) 69:145–82. doi:10.1146/annurev.biochem.69.1.145
15. Stitham J, Midgett C, Martin KA, Hwa J. Prostacyclin: an inflammatory paradox. *Front Pharmacol* (2011) 11:517–28. doi:10.3389/fphar.2011.00024
16. Kihara Y, Gupta S, Maurya MR, Armando A, Shah I, Quehenberger O, et al. Modeling of eicosanoid fluxes reveals functional coupling between cyclooxygenases and terminal synthases. *Biophys J* (2014) 106:966–75. doi:10.1016/j.bpj.2014.01.015
17. Mandal AK, Jones PB, Bair AM, Christmas P, Miller D, Ting-ting DY, et al. The nuclear membrane organization of leukotriene synthesis. *Proc Natl Acad Sci U S A* (2008) 105:20434–9. doi:10.1073/pnas.0808211106
18. Ricciotti E, FitzGerald GA. Prostaglandins and inflammation. *Arterioscler Thromb Vasc Biol* (2011) 31:986–1000. doi:10.1161/ATVBAHA.110.207449
19. Vane JR. Biomedicine. Back to an aspirin a day? *Science* (2002) 296:474–5. doi:10.1126/science.1071702
20. Narumiya S, Furuyashiki T. Fever, inflammation, pain and beyond: prostanoid receptor research during these 25 years. *FASEB J* (2011) 25:813–8. doi:10.1096/fj.11-0302ufm
21. Honda T, Segi-Nishida E, Miyachi Y, Narumiya S. Prostacyclin-IP signaling and prostaglandin E_2-EP2/EP4 signaling both mediate joint inflammation in mouse collagen-induced arthritis. *J Exp Med* (2006) 203:325–35. doi:10.1084/jem.20051310
22. Sonoshita M, Takaku K, Sasaki N, Sugimoto Y, Ushikubi F, Narumiya S, et al. Acceleration of intestinal polyposis through prostaglandin receptor EP2 in Apc(Delta 716) knockout mice. *Nat Med* (2001) 7:1048–51. doi:10.1038/nm0901-1048
23. Hirata T, Narumiya S. Prostanoids as regulators of innate and adaptive immunity. *Adv Immunol* (2012) 116:143–74. doi:10.1016/B978-0-12-394300-2.00005-3
24. Yao C, Sakata D, Esaki Y, Li Y, Matsuoka T, Kuroiwa K, et al. Prostaglandin E2–EP4 signaling promotes immune inflammation through TH1 cell differentiation and TH17 cell expansion. *Nat Med* (2009) 15:633–40. doi:10.1038/nm.1968
25. Chen Q, Muramoto K, Masaaki N, Ding Y, Yang H, Mackey M, et al. A novel antagonist of the prostaglandin E2 EP4 receptor inhibits Th1 differentiation and Th17 expansion and is orally active in arthritis models. *Br J Pharmacol* (2010) 160:292–310. doi:10.1111/j.1476-5381.2010.00647
26. Libioulle C, Louis E, Hansoul S, Sandor C, Farnir F, Franchimont D, et al. Novel Crohn disease locus identified by genome-wide association maps to a gene desert on 5p13.1 and modulates expression of PTGER4. *PLoS Genet* (2007) 3:e58. doi:10.1371/journal.pgen.0030058
27. Oguma T, Palmer LJ, Birben E, Sonna LA, Asano K, Lilly CM. Role of prostanoid DP receptor variants in susceptibility to asthma. *N Engl J Med* (2004) 351:1752–63. doi:10.1056/NEJMoa031785
28. Tajouri L, Fernandez F, Griffiths LR. Gene expression studies in multiple sclerosis. *Curr Genomics* (2007) 8:181–9. doi:10.2174/138920207780833829
29. Sawcer S, Hellenthal G, Pirinen M, Spencer CCA, Patsopoulos NA, Moutsianas L, et al. Genetic risk and a primary role for cell-mediated immune mechanisms in multiple sclerosis. *Nature* (2011) 476:214–9. doi:10.1038/nature10251

30. Fredman G, Hellmann J, Proto JD, Kuriakose G, Colas RA, Dorweiler B, et al. An imbalance between specialized pro-resolving lipid mediators and pro-inflammatory leukotrienes promotes instability of atherosclerotic plaques. *Nat Commun* (2016) 7:12859. doi:10.1038/ncomms12859
31. De Caterina R, Zampolli A. From asthma to atherosclerosis – 5-lipoxygenase, leukotrienes, and inflammation. *N Engl J Med* (2004) 350:4–7. doi:10.1056/NEJMp038190
32. Lee W, Su Kim H, Lee GR. Leukotrienes induce the migration of Th17 cells. *Immunol Cell Biol* (2015) 93:472–9. doi:10.1038/icb.2014.104
33. Powell WS, Rokach J. Biosynthesis, biological effects, and receptors of hydroxyeicosatetraenoic acids (HETEs) and oxoeicosatetraenoic acids (oxo-ETEs) derived from arachidonic acid. *Biochim Biophys Acta* (2015) 1851:340–55. doi:10.1016/j.bbalip.2014.10.008
34. Dalli J, Chiang N, Serhan CN. Elucidation of novel 13-series resolvins that increase with atorvastatin and clear infections. *Nat Med* (2015) 21:1071–5. doi:10.1038/nm.3911
35. Serhan CN, Chiang N, Dalli J. New pro-resolving n-3 mediators bridge resolution of infectious inflammation to tissue regeneration. *Mol Aspects Med* (2017). doi:10.1016/j.mam.2017.08.002
36. Chiang N, Arita M, Serhan CN. Anti-inflammatory circuitry: lipoxin, aspirin-triggered lipoxins and their receptor ALX. *Prostaglandins Leukot Essent Fatty Acids* (2005) 73:163–77. doi:10.1016/j.plefa.2005.05.003
37. Buckley C, Gilroy D, Serhan C. Proresolving lipid mediators and mechanisms in the resolution of acute inflammation. *Immunity* (2014) 40:315–27. doi:10.1016/j.immuni.2014.02.009
38. Chiang N, Serhan CN. Structural elucidation and physiologic functions of specialized pro-resolving mediators and their receptors. *Mol Aspects Med* (2017). doi:10.1016/j.mam.2017.03.005
39. Ramon S, Gao F, Serhan CN, Phipps RP. Specialized proresolving mediators enhance human B cell differentiation to antibody-secreting cells. *J Immunol* (2012) 189:1036–42. doi:10.4049/jimmunol.1103483
40. Kim N, Ramon S, Thatcher TH, Woeller CF, Sime PJ, Phipps RP. Specialized proresolving mediators (SPMs) inhibit human B-cell IgE production. *Eur J Immunol* (2016) 46:81–91. doi:10.1002/eji.201545673
41. Ariel A, Chiang N, Arita M, Petasis NA, Serhan CN. Aspirin-triggered lipoxin A4 and B4 analogs block extracellular signal-regulated kinase-dependent TNF-alpha secretion from human T cells. *J Immunol* (2003) 170:6266–72. doi:10.4049/jimmunol.170.12.6266
42. Spurr L, Nadkarni S, Pederzoli-Ribeil M, Goulding NJ, Perretti M, D'Acquisto F. Comparative analysis of annexin A1-formyl peptide receptor 2/ALX expression in human leukocyte subsets. *Int Immunopharmacol* (2011) 11:55–66. doi:10.1016/j.intimp.2010.10.006
43. Chiurchiù V, Leuti A, Dalli J, Jacobsson A, Battistini L, Maccarrone M, et al. Proresolving lipid mediators resolvin D1, resolvin D2, and maresin 1 are critical in modulating T cell responses. *Sci Transl Med* (2016) 8:353ra111. doi:10.1126/scitranslmed.aaf7483
44. Settimio R, Clara DF, Franca F, Francesca S, Michele D. Resolvin D1 reduces the immunoinflammatory response of the rat eye following uveitis. *Mediators Inflamm* (2012) 2012:318621. doi:10.1155/2012/318621
45. Kim T-H, Kim G-D, Jin Y-H, Park YS, Park C-S. Omega-3 fatty acid-derived mediator, resolvin E1, ameliorates 2,4-dinitrofluorobenzene-induced atopic dermatitis in NC/Nga mice. *Int Immunopharmacol* (2012) 14:384–91. doi:10.1016/j.intimp.2012.08.005
46. Ariel A, Li P-L, Wang W, Tang W-X, Fredman G, Hong S, et al. The docosatriene protectin D1 is produced by TH2 skewing and promotes human T cell apoptosis via lipid raft clustering. *J Biol Chem* (2005) 280:43079–86. doi:10.1074/jbc.M509796200
47. Levy BD, Kohli P, Gotlinger K, Haworth O, Hong S, Kazani S, et al. Protectin D1 is generated in asthma and dampens airway inflammation and hyperresponsiveness. *J Immunol* (2007) 178:496–502. doi:10.4049/jimmunol.178.1.496
48. Hsiao H-M, Thatcher TH, Colas RA, Serhan CN, Phipps RP, Sime PJ. Resolvin D1 reduces emphysema and chronic inflammation. *Am J Pathol* (2015) 185:3189–201. doi:10.1016/j.ajpath.2015.08.008
49. Hellmann J, Tang Y, Kosuri M, Bhatnagar A, Spite M. Resolvin D1 decreases adipose tissue macrophage accumulation and improves insulin sensitivity in obese-diabetic mice. *FASEB J* (2011) 25:2399–407. doi:10.1096/fj.10-178657
50. Clària J, Dalli J, Yacoubian S, Gao F, Serhan CN. Resolvin D1 and resolvin D2 govern local inflammatory tone in obese fat. *J Immunol* (2012) 189:2597–605. doi:10.4049/jimmunol.1201272
51. Perretti M, Norling LV. Actions of SPM in regulating host responses in arthritis. *Mol Aspects Med* (2017) 58:57–64. doi:10.1016/j.mam.2017.04.005
52. Norling LV, Headland SE, Dalli J, Arnardottir HH, Haworth O, Jones HR, et al. Proresolving and cartilage-protective actions of resolvin D1 in inflammatory arthritis. *JCI Insight* (2016) 1:e85922. doi:10.1172/jci.insight.85922
53. Merched AJ, Ko K, Gotlinger KH, Serhan CN, Chan L. Atherosclerosis: evidence for impairment of resolution of vascular inflammation governed by specific lipid mediators. *FASEB J* (2008) 22:3595–606. doi:10.1096/fj.08-112201
54. Ho KJ, Spite M, Owens CD, Lancero H, Kroemer AHK, Pande R, et al. Aspirin-triggered lipoxin and resolvin E1 modulate vascular smooth muscle phenotype and correlate with peripheral atherosclerosis. *Am J Pathol* (2010) 177:2116–23. doi:10.2353/ajpath.2010.091082
55. Hasturk H, Abdallah R, Kantarci A, Nguyen D, Giordano N, Hamilton J, et al. Resolvin E1 (RvE1) attenuates atherosclerotic plaque formation in diet and inflammation-induced atherogenesis. *Arterioscler Thromb Vasc Biol* (2015) 35:1123–33. doi:10.1161/ATVBAHA.115.305324
56. Salic K, Morrison MC, Verschuren L, Wielinga PY, Wu L, Kleemann R, et al. Resolvin E1 attenuates atherosclerosis in absence of cholesterol-lowering effects and on top of atorvastatin. *Atherosclerosis* (2016) 250:158–65. doi:10.1016/j.atherosclerosis.2016.05.001
57. Viola JR, Lemnitzer P, Jansen Y, Csaba G, Winter C, Neideck C, et al. Resolving lipid mediators maresin 1 and resolvin D2 prevent atheroprogression in mice. *Circ Res* (2016) 119:1030–8. doi:10.1161/CIRCRESAHA.116.309492
58. Bento AF, Claudino RF, Dutra RC, Marcon R, Calixto JB. Omega-3 fatty acid-derived mediators 17(R)-hydroxy docosahexaenoic acid, aspirin-triggered resolvin D1 and resolvin D2 prevent experimental colitis in mice. *J Immunol* (2011) 187:1957–69. doi:10.4049/jimmunol.1101305
59. Schwanke RC, Marcon R, Bento AF, Calixto JB. EPA- and DHA-derived resolvins' actions in inflammatory bowel disease. *Eur J Pharmacol* (2016) 785:156–64. doi:10.1016/j.ejphar.2015.08.050
60. Wang X, Zhu M, Hjorth E, Cortés-Toro V, Eyjolfsdottir H, Graff C, et al. Resolution of inflammation is altered in Alzheimer's disease. *Alzheimers Dement* (2015) 11:40.e–50.e. doi:10.1016/j.jalz.2013.12.024
61. Zhu M, Wang X, Hjorth E, Colas RA, Schroeder L, Granholm A-C, et al. Pro-resolving lipid mediators improve neuronal survival and increase Aβ42 phagocytosis. *Mol Neurobiol* (2016) 53:2733–49. doi:10.1007/s12035-015-9544-0
62. Mizwicki MT, Liu G, Fiala M, Magpantay L, Sayre J, Siani A, et al. 1α,25-Dihydroxyvitamin D3 and resolvin D1 retune the balance between amyloid-β phagocytosis and inflammation in Alzheimer's disease patients. *J Alzheimers Dis* (2013) 34:155–70. doi:10.3233/JAD-121735
63. Fiala M, Terrando N, Dalli J. Specialized pro-resolving mediators from omega-3 fatty acids improve amyloid-β phagocytosis and regulate inflammation in patients with minor cognitive impairment. *J Alzheimers Dis* (2015) 48:293–301. doi:10.3233/JAD-150367
64. Fiala M, Halder RC, Sagong B, Ross O, Sayre J, Porter V, et al. ω-3 supplementation increases amyloid-β phagocytosis and resolvin D1 in patients with minor cognitive impairment. *FASEB J* (2015) 29:2681–9. doi:10.1096/fj.14-264218
65. Liu G, Fiala M, Mizwicki MT, Sayre J, Magpantay L, Siani A, et al. Neuronal phagocytosis by inflammatory macrophages in ALS spinal cord: inhibition of inflammation by resolvin D1. *Am J Neurodegener Dis* (2012) 1:60–74.
66. Poisson LM, Suhail H, Singh J, Datta I, Denic A, Labuzek K, et al. Untargeted plasma metabolomics identifies endogenous metabolite with drug-like properties in chronic animal model of multiple sclerosis. *J Biol Chem* (2015) 290:30697–712. doi:10.1074/jbc.M115.679068
67. Serhan CN. Discovery of specialized pro-resolving mediators marks the dawn of resolution physiology and pharmacology. *Mol Aspects Med* (2017) 2997(17):30018–30013. doi:10.1016/j.mam.2017.03.001
68. Hannun YA, Obeid LM. Principles of bioactive lipid signalling: lessons from sphingolipids. *Nat Rev Mol Cell Biol* (2008) 9:139–50. doi:10.1038/nrm2329

69. Bartke N, Hannun YA. Bioactive sphingolipids: metabolism and function. *J Lipid Res* (2009) 50:S91–6. doi:10.1194/jlr.R800080-JLR200
70. Shindou H, Hishikawa D, Harayama T, Eto M, Shimizu T. Generation of membrane diversity by lysophospholipid acyltransferases. *J Biochem* (2013) 154:21–8. doi:10.1093/jb/mvt048
71. Makide K, Kitamura H, Sato Y, Okutani M, Aoki J. Emerging lysophospholipid mediators, lysophosphatidylserine, lysophosphatidylthreonine, lysophosphatidylethanolamine and lysophosphatidylglycerol. *Prostaglandins Other Lipid Mediat* (2009) 89:135–9. doi:10.1016/j.prostaglandins.2009.04.009
72. Sevastou I, Kaffe E, Mouratis M-A, Aidinis V. Lysoglycerophospholipids in chronic inflammatory disorders: the PLA2/LPC and ATX/LPA axes. *Biochim Biophys Acta* (2013) 1831:42–60. doi:10.1016/j.bbalip.2012.07.019
73. Knowlden S, Georas SN. The autotaxin-LPA axis emerges as a novel regulator of lymphocyte homing and inflammation. *J Immunol* (2014) 192:851–7. doi:10.4049/jimmunol.1302831
74. Piñeiro R, Falasca M. Lysophosphatidylinositol signalling: new wine from an old bottle. *Biochim Biophys Acta* (2012) 1821:694–705. doi:10.1016/j.bbalip.2012.01.009
75. D'Aquilio F, Procaccini M, Izzi V, Chiurchiu' V, Giambra V, Carotenuto F, et al. Activatory properties of lysophosphatidic acid on human THP-1 cells. *Inflammation* (2007) 30:167–77. doi:10.1007/s10753-007-9034-2
76. Heimerl S, Fischer M, Baessler A, Liebisch G, Sigruener A, Wallner S, et al. Alterations of plasma lysophosphatidylcholine species in obesity and weight loss. *PLoS One* (2014) 9:e111348. doi:10.1371/journal.pone.0111348
77. Moreno-Navarrete JM, Catalan V, Whyte L, Diaz-Arteaga A, Vazquez-Martinez R, Rotellar F, et al. The L-α-lysophosphatidylinositol/GPR55 system and its potential role in human obesity. *Diabetes* (2012) 61:281–91. doi:10.2337/db11-0649
78. Lee H, Liao JJ, Graeler M, Huang MC, Goetzl EJ. Lysophospholipid regulation of mononuclear phagocytes. *Biochim Biophys Acta* (2002) 1582:175–7. doi:10.1016/S1388-1981(02)00153-1
79. Fuchs B, Schiller J, Wagner U, Häntzschel H, Arnold K. The phosphatidylcholine/lysophosphatidylcholine ratio in human plasma is an indicator of the severity of rheumatoid arthritis: investigations by 31P NMR and MALDI-TOF MS. *Clin Biochem* (2005) 38:925–33. doi:10.1016/j.clinbiochem.2005.06.006
80. Nikitopoulou I, Oikonomou N, Karouzakis E, Sevastou I, Nikolaidou-Katsaridou N, Zhao Z, et al. Autotaxin expression from synovial fibroblasts is essential for the pathogenesis of modeled arthritis. *J Exp Med* (2012) 209:925–33. doi:10.1084/jem.20112012
81. Maceyka M, Spiegel S. Sphingolipid metabolites in inflammatory disease. *Nature* (2014) 510:58–67. doi:10.1038/nature13475
82. Gomez-Muñoz A, Presa N, Gomez-Larrauri A, Rivera I-G, Trueba M, Ordoñez M. Control of inflammatory responses by ceramide, sphingosine 1-phosphate and ceramide 1-phosphate. *Prog Lipid Res* (2016) 61:51–62. doi:10.1016/j.plipres.2015.09.002
83. Vandanmagsar B, Youm Y-H, Ravussin A, Galgani JE, Stadler K, Mynatt RL, et al. The NLRP3 inflammasome instigates obesity-induced inflammation and insulin resistance. *Nat Med* (2011) 17:179–88. doi:10.1038/nm.2279
84. Pettus BJ, Bielawska A, Subramanian P, Wijesinghe DS, Maceyka M, Leslie CC, et al. Ceramide 1-phosphate is a direct activator of cytosolic phospholipase A_2. *J Biol Chem* (2004) 279:11320–6. doi:10.1074/jbc.M309262200
85. Simanshu DK, Kamlekar RK, Wijesinghe DS, Zou X, Zhai X, Mishra SK, et al. Non-vesicular trafficking by a ceramide-1-phosphate transfer protein regulates eicosanoids. *Nature* (2013) 500:463–7. doi:10.1038/nature12332
86. Józefowski S, Czerkies M, Łukasik A, Bielawska A, Bielawski J, Kwiatkowska K, et al. Ceramide and ceramide 1-phosphate are negative regulators of TNF-α production induced by lipopolysaccharide. *J Immunol* (2010) 185:6960–73. doi:10.4049/jimmunol.0902926
87. Hankins JL, Fox TE, Barth BM, Unrath KA, Kester M. Exogenous ceramide-1-phosphate reduces lipopolysaccharide (LPS)-mediated cytokine expression. *J Biol Chem* (2011) 286:44357–66. doi:10.1074/jbc.M111.264010
88. Zhang Q-J, Holland WL, Wilson L, Tanner JM, Kearns D, Cahoon JM, et al. Ceramide mediates vascular dysfunction in diet-induced obesity by PP2A-mediated dephosphorylation of the eNOS-Akt complex. *Diabetes* (2012) 61:1848–59. doi:10.2337/db11-1399
89. Camerer E, Regard JB, Cornelissen I, Srinivasan Y, Duong DN, Palmer D, et al. Sphingosine-1-phosphate in the plasma compartment regulates basal and inflammation-induced vascular leak in mice. *J Clin Invest* (2009) 119:1871–9. doi:10.1172/JCI38575
90. Spiegel S, Milstien S. The outs and the ins of sphingosine-1-phosphate in immunity. *Nat Rev Immunol* (2011) 11:403–15. doi:10.1038/nri2974
91. Cyster JG, Schwab SR. Sphingosine-1-phosphate and lymphocyte egress from lymphoid organs. *Annu Rev Immunol* (2012) 30:69–94. doi:10.1146/annurev-immunol-020711-075011
92. Kunkel GT, Maceyka M, Milstien S, Spiegel S. Targeting the sphingosine-1-phosphate axis in cancer, inflammation and beyond. *Nat Rev Drug Discov* (2013) 12:688–702. doi:10.1038/nrd4099
93. Brinkmann V, Billich A, Baumruker T, Heining P, Schmouder R, Francis G, et al. Fingolimod (FTY720): discovery and development of an oral drug to treat multiple sclerosis. *Nat Rev Drug Discov* (2010) 9:883–97. doi:10.1038/nrd3248
94. Chiurchiù V. Novel targets in multiple sclerosis: to oxidative stress and beyond. *Curr Top Med Chem* (2014) 14:2590–9. doi:10.2174/1568026614666141203143801
95. van Doorn R, Nijland PG, Dekker N, Witte ME, Lopes-Pinheiro MA, van het Hof B, et al. Fingolimod attenuates ceramide-induced blood-brain barrier dysfunction in multiple sclerosis by targeting reactive astrocytes. *Acta Neuropathol* (2012) 124:397–410. doi:10.1007/s00401-012-1014-4
96. Van Doorn R, Van Horssen J, Verzijl D, Witte M, Ronken E, Van Het Hof B, et al. Sphingosine 1-phosphate receptor 1 and 3 are upregulated in multiple sclerosis lesions. *Glia* (2010) 58:1465–76. doi:10.1002/glia.21021
97. van Doorn R, Lopes Pinheiro MA, Kooij G, Lakeman K, van het Hof B, van der Pol SMA, et al. Sphingosine 1-phosphate receptor 5 mediates the immune quiescence of the human brain endothelial barrier. *J Neuroinflammation* (2012) 9:133. doi:10.1186/1742-2094-9-133
98. Snider AJ, Kawamori T, Bradshaw SG, Orr KA, Gilkeson GS, Hannun YA, et al. A role for sphingosine kinase 1 in dextran sulfate sodium-induced colitis. *FASEB J* (2009) 23:143–52. doi:10.1096/fj.08-118109
99. Proia RL, Hla T. Emerging biology of sphingosine-1-phosphate: its role in pathogenesis and therapy. *J Clin Invest* (2015) 125:1379–87. doi:10.1172/JCI76369
100. Bamias G, Rivera-Nieves J. Targeting S1P receptors, a new mechanism of action for inflammatory bowel disease therapy. *Gastroenterology* (2016) 151:1025–7. doi:10.1053/j.gastro.2016.09.025
101. Maccarrone M, Guzmán M, Mackie K, Doherty P, Harkany T. Programming of neural cells by (endo)cannabinoids: from physiological rules to emerging therapies. *Nat Rev Neurosci* (2014) 15:786–801. doi:10.1038/nrn3846
102. Pistis M, Melis M. From surface to nuclear receptors: the endocannabinoid family extends its assets. *Curr Med Chem* (2010) 17:1450–67. doi:10.2174/092986710790980014
103. Galve-Roperh I, Chiurchiù V, Díaz-Alonso J, Bari M, Guzmán M, Maccarrone M. Cannabinoid receptor signaling in progenitor/stem cell proliferation and differentiation. *Prog Lipid Res* (2013) 52:633–50. doi:10.1016/j.plipres.2013.05.004
104. Maccarrone M, Bab I, Bíró T, Cabral GA, Dey SK, Di Marzo V, et al. Endocannabinoid signaling at the periphery: 50 years after THC. *Trends Pharmacol Sci* (2015) 36:277–96. doi:10.1016/j.tips.2015.02.008
105. Cencioni MT, Chiurchiù V, Catanzaro G, Borsellino G, Bernardi G, Battistini L, et al. Anandamide suppresses proliferation and cytokine release from primary human T-lymphocytes mainly via CB2 receptors. *PLoS One* (2010) 5:e8688. doi:10.1371/journal.pone.0008688
106. Chiurchiù V, Rapino C, Talamonti E, Leuti A, Lanuti M, Gueniche A, et al. Anandamide suppresses proinflammatory T cell responses in vitro through type-1 cannabinoid receptor-mediated mTOR inhibition in human keratinocytes. *J Immunol* (2016) 197:3545–53. doi:10.4049/jimmunol.1500546
107. Ribeiro A, Pontis S, Mengatto L, Armirotti A, Chiurchiù V, Capurro V, et al. A potent systemically active N-acylethanolamine acid amidase inhibitor that suppresses inflammation and human macrophage activation. *ACS Chem Biol* (2015) 10:1838–46. doi:10.1021/acschembio.5b00114
108. Maestroni GJM. The endogenous cannabinoid 2-arachidonoyl glycerol as in vivo chemoattractant for dendritic cells and adjuvant for Th1 response to a soluble protein. *FASEB J* (2004) 18:1914–6. doi:10.1096/fj.04-2190fje

109. Gasperi V, Evangelista D, Chiurchiù V, Florenzano F, Savini I, Oddi S, et al. 2-Arachidonoylglycerol modulates human endothelial cell/leukocyte interactions by controlling selectin expression through CB1 and CB2 receptors. *Int J Biochem Cell Biol* (2014) 51:79–88. doi:10.1016/j.biocel.2014.03.028
110. Gallily R, Breuer A, Mechoulam R. 2-Arachidonylglycerol, an endogenous cannabinoid, inhibits tumor necrosis factor-alpha production in murine macrophages, and in mice. *Eur J Pharmacol* (2000) 406:R5–7. doi:10.1016/S0014-2999(00)00653-1
111. Chang YH, Lee ST, Lin WW. Effects of cannabinoids on LPS-stimulated inflammatory mediator release from macrophages: involvement of eicosanoids. *J Cell Biochem* (2001) 81:715–23. doi:10.1002/jcb.1103
112. Velasco G, Sánchez C, Guzmán M. Endocannabinoids and cancer. *Handb Exp Pharmacol* (2015) 231:449–72. doi:10.1007/978-3-319-20825-1_16
113. Mazier W, Saucisse N, Gatta-Cherifi B, Cota D. The endocannabinoid system: pivotal orchestrator of obesity and metabolic disease. *Trends Endocrinol Metab* (2015) 26:524–37. doi:10.1016/j.tem.2015.07.007
114. Steffens S, Pacher P. The activated endocannabinoid system in atherosclerosis: driving force or protective mechanism? *Curr Drug Targets* (2015) 16:334–41. doi:10.2174/1389450115666141202113225
115. Cani PD, Plovier H, Van Hul M, Geurts L, Delzenne NM, Druart C, et al. Endocannabinoids – at the crossroads between the gut microbiota and host metabolism. *Nat Rev Endocrinol* (2016) 12:133–43. doi:10.1038/nrendo.2015.211
116. Alhouayek M, Muccioli GG. The endocannabinoid system in inflammatory bowel diseases: from pathophysiology to therapeutic opportunity. *Trends Mol Med* (2012) 18:615–25. doi:10.1016/j.molmed.2012.07.009
117. Sido JM, Nagarkatti PS, Nagarkatti M. Role of endocannabinoid activation of peripheral CB1 receptors in the regulation of autoimmune disease. *Int Rev Immunol* (2015) 34:403–14. doi:10.3109/08830185.2014.921165
118. Maccarrone M. Endocannabinoid signaling and neuroinflammatory diseases. *Curr Pharm Des* (2008) 14:2252–3. doi:10.2174/138161208785740045
119. Di Marzo V, Stella N, Zimmer A. Endocannabinoid signalling and the deteriorating brain. *Nat Rev Neurosci* (2015) 16:30–42. doi:10.1038/nrn3876
120. Mecha M, Carrillo-Salinas FJ, Feliú A, Mestre L, Guaza C. Microglia activation states and cannabinoid system: therapeutic implications. *Pharmacol Ther* (2016) 166:40–55. doi:10.1016/j.pharmthera.2016.06.011
121. Skaper SD, Facci L, Barbierato M, Zusso M, Bruschetta G, Impellizzeri D, et al. Palmitoylethanolamine and neuroinflammation: a novel therapeutic strategy of resolution. *Mol Neurobiol* (2015) 52:1034–42. doi:10.1007/s12035-015-9253-8
122. Gokoh M, Kishimoto S, Oka S, Sugiura T. 2-Arachidonoylglycerol enhances the phagocytosis of opsonized zymosan by HL-60 cells differentiated into macrophage-like cells. *Biol Pharm Bull* (2007) 30:1199–205. doi:10.1248/bpb.30.1199
123. Cabral GA, Ferreira GA, Jamerson MJ. Endocannabinoids and the immune system in health and disease. *Handb Exp Pharmacol* (2015) 231:185–211. doi:10.1007/978-3-319-20825-1_6
124. Lipina C, Hundal HS. Modulation of cellular redox homeostasis by the endocannabinoid system. *Open Biol* (2016) 6:150276. doi:10.1098/rsob.150276
125. Aizpurua-Olaizola O, Elezgarai I, Rico-Barrio I, Zarandona I, Etxebarria N, Usobiaga A. Targeting the endocannabinoid system: future therapeutic strategies. *Drug Discov Today* (2017) 22:105–10. doi:10.1016/j.drudis.2016.08.005
126. Chiurchiù V, Cencioni MT, Bisicchia E, De Bardi M, Gasperini C, Borsellino G, et al. Distinct modulation of human myeloid and plasmacytoid dendritic cells by anandamide in multiple sclerosis. *Ann Neurol* (2013) 73:626–36. doi:10.1002/ana.23875
127. Chiurchiù V, Lanuti M, Catanzaro G, Fezza F, Rapino C, Maccarrone M. Detailed characterization of the endocannabinoid system in human macrophages and foam cells, and anti-inflammatory role of type-2 cannabinoid receptor. *Atherosclerosis* (2014) 233:55–63. doi:10.1016/j.atherosclerosis.2013.12.042
128. Centonze D, Bari M, Rossi S, Prosperetti C, Furlan R, Fezza F, et al. The endocannabinoid system is dysregulated in multiple sclerosis and in experimental autoimmune encephalomyelitis. *Brain* (2007) 130:2543–53. doi:10.1093/brain/awm160
129. Centonze D, Finazzi-Agrò A, Bernardi G, Maccarrone M. The endocannabinoid system in targeting inflammatory neurodegenerative diseases. *Trends Pharmacol Sci* (2007) 28:180–7. doi:10.1016/j.tips.2007.02.004
130. Chiurchiù V, Leuti A, Maccarrone M. Cannabinoid signaling and neuroinflammatory diseases: a melting pot for the regulation of brain immune responses. *J Neuroimmune Pharmacol* (2015) 10:268–80. doi:10.1007/s11481-015-9584-2
131. Fernández-Ruiz J, Romero J, Ramos JA. Endocannabinoids and neurodegenerative disorders: Parkinson's disease, Huntington's chorea, Alzheimer's disease, and others. *Handb Exp Pharmacol* (2015) 231:233–59. doi:10.1007/978-3-319-20825-1_8
132. van der Stelt M, van Kuik JA, Bari M, van Zadelhoff G, Leeflang BR, Veldink GA, et al. Oxygenated metabolites of anandamide and 2-arachidonoylglycerol: conformational analysis and interaction with cannabinoid receptors, membrane transporter, and fatty acid amide hydrolase. *J Med Chem* (2002) 45:3709–20. doi:10.1021/jm020818q
133. Rouzer CA, Marnett LJ. Endocannabinoid oxygenation by cyclooxygenases, lipoxygenases, and cytochromes P450: cross-talk between the eicosanoid and endocannabinoid signaling pathways. *Chem Rev* (2011) 111:5899–921. doi:10.1021/cr2002799
134. Di Marzo V. Targeting the endocannabinoid system: to enhance or reduce? *Nat Rev Drug Discov* (2008) 7:438–55. doi:10.1038/nrd2553
135. De Filippis D, D'Amico A, Cipriano M, Petrosino S, Orlando P, Di Marzo V, et al. Levels of endocannabinoids and palmitoylethanolamide and their pharmacological manipulation in chronic granulomatous inflammation in rats. *Pharmacol Res* (2010) 61:321–8. doi:10.1016/j.phrs.2009.11.005
136. Witkamp R. Fatty acids, endocannabinoids and inflammation. *Eur J Pharmacol* (2016) 785:96–107. doi:10.1016/j.ejphar.2015.08.051
137. Weichand B, Weis N, Weigert A, Grossmann N, Levkau B, Brüne B. Apoptotic cells enhance sphingosine-1-phosphate receptor 1 dependent macrophage migration. *Eur J Immunol* (2013) 43:3306–13. doi:10.1002/eji.201343441
138. Scheel-Toellner D, Wang K, Craddock R, Webb PR, McGettrick HM, Assi LK, et al. Reactive oxygen species limit neutrophil life span by activating death receptor signaling. *Blood* (2004) 104:2557–64. doi:10.1182/blood-2004-01-0191
139. McArthur S, Gobbetti T, Kusters DH, Reutelingsperger CP, Flower RJ, Perretti M. Definition of a novel pathway centered on lysophosphatidic acid to recruit monocytes during the resolution phase of tissue inflammation. *J Immunol* (2015) 195:1139–51. doi:10.4049/jimmunol.1500733
140. Pettus BJ, Bielawski J, Porcelli AM, Reames DL, Johnson KR, Morrow J, et al. The sphingosine kinase 1/sphingosine-1-phosphate pathway mediates COX-2 induction and PGE2 production in response to TNF-alpha. *FASEB J* (2003) 17:1411–21. doi:10.1096/fj.02-1038com

Conflict of Interest Statement: The authors declare that the research was conducted in the absence of any commercial or financial relationships that could be construed as a potential conflict of interest.

Copyright © 2018 Chiurchiù, Leuti and Maccarrone. This is an open-access article distributed under the terms of the Creative Commons Attribution License (CC BY). The use, distribution or reproduction in other forums is permitted, provided the original author(s) and the copyright owner are credited and that the original publication in this journal is cited, in accordance with accepted academic practice. No use, distribution or reproduction is permitted which does not comply with these terms.

frontiers in Immunology

ORIGINAL RESEARCH
published: 31 January 2018
doi: 10.3389/fimmu.2018.00154

Proteins of TNF-α and IL6 Pathways Are Elevated in Serum of Type-1 Diabetes Patients with Microalbuminuria

Sharad Purohit[1,2,3†], Ashok Sharma[1†], Wenbo Zhi[1], Shan Bai[1], Diane Hopkins[1], Leigh Steed[1], Bruce Bode[4], Stephen W. Anderson[5], John Chip Reed[6], R. Dennis Steed[6] and Jin-Xiong She[1,2]*

[1] Center for Biotechnology and Genomic Medicine, Augusta University, Augusta, GA, United States, [2] Department of Obstetrics and Gynecology, Medical College of Georgia, Augusta University, Augusta, GA, United States, [3] Department of Medical Laboratory, Imaging, and Radiologic Sciences, College of Allied Health Sciences, Augusta University, Augusta, GA, United States, [4] Atlanta Diabetes Associates, Atlanta, GA, United States, [5] Pediatric Endocrine Associates, Atlanta, GA, United States, [6] Southeastern Endocrine & Diabetes, Atlanta, GA, United States

OPEN ACCESS

Edited by:
Massimo Gadina,
National Institute of Arthritis and Musculoskeletal and Skin Diseases, United States

Reviewed by:
Jun Wada,
Okayama University, Japan
Verica Paunovic,
University of Belgrade, Serbia

***Correspondence:**
Jin-Xiong She
jshe@augusta.edu

[†]These authors contributed equally to this work.

Specialty section:
This article was submitted to Inflammation, a section of the journal Frontiers in Immunology

Received: 26 September 2017
Accepted: 17 January 2018
Published: 31 January 2018

Citation:
Purohit S, Sharma A, Zhi W, Bai S, Hopkins D, Steed L, Bode B, Anderson SW, Reed JC, Steed RD and She J-X (2018) Proteins of TNF-α and IL6 Pathways Are Elevated in Serum of Type-1 Diabetes Patients with Microalbuminuria. Front. Immunol. 9:154. doi: 10.3389/fimmu.2018.00154

Soluble cytokine receptors may play an important role in development of microalbuminuria (MA) in type-1 diabetes (T1D). In this study, we measured 12 soluble receptors and ligands from TNF-α/IL6/IL2 pathways in T1D patients with MA ($n = 89$) and T1D patients without MA ($n = 483$) participating in the PAGODA study. Twelve proteins in the sera from T1D patients with and without MA were measured using multiplex Luminex assays. Ten serum proteins (sTNFR1, sTNFR2, sIL2Rα, MMP2, sgp130, sVCAM1, sIL6R, SAA, CRP, and sICAM1) were significantly elevated in T1D patients with MA. After adjusting for age, duration of diabetes, and sex in logistic regression, association remained significant for seven proteins. MA is associated with increasing concentrations of all 10 proteins, with the strongest associations observed for sTNFR1 (OR = 108.3, $P < 10^{-32}$) and sTNFR2 (OR = 65.5, $P < 10^{-37}$), followed by sIL2Rα (OR = 12.9, $P < 10^{-13}$), MMP2 (OR = 5.5, $P < 10^{-6}$), sgp130 (OR = 5.2,$P < 10^{-3}$), sIL6R (OR = 4.6, $P < 10^{-4}$), and sVCAM1 (OR = 3.3, $P < 10^{-4}$). We developed a risk score system based on the combined odds ratios associated with each quintile for each protein. The risk scores cluster MA patients into three subsets, each associated with distinct risk for MA attributable to proteins in the TNF-α/IL6 pathway (mean OR = 1, 13.5, and 126.3 for the three subsets, respectively). Our results suggest that the TNF-α/IL6 pathway is overactive in approximately 40% of the MA patients and moderately elevated in the middle 40% of the MA patients. Our results suggest the existence of distinct subsets of MA patients identifiable by their serum protein profiles.

Keywords: inflammation, cytokines, cytokine receptors, diabetes, microalbuminuria

INTRODUCTION

Chronic hyperglycemia is considered to be the main pathogenic factor involved in microalbuminuria (MA). Inflammation, increased apoptosis, and abnormal activation of the endothelium are increasingly thought to be important mechanisms for the development of MA (1). Pro-inflammatory pathways related to TNF-α and IL6 signaling can lead to enhanced deposition of extra-cellular

matrix (ECM) within kidneys as well as activation of T cells, leukocytes, and endothelial cells in diabetic patients with MA (2, 3). In addition, inflammatory protein levels in the serum have been associated with the presence of MA in type-1 diabetes (T1D) patients (4–7).

The majority of the prior studies on human patients have been limited to measurement of a single or a few serum proteins in T1D patients with MA. Inflammatory proteins such as CRP, IL6, TNF-α, and the soluble form of TNF receptors (sTNFR1 and sTNFR2) as well as adhesion molecules have been individually examined in separate studies (4–8). In the EURODIAB study, elevated plasma concentrations of inflammatory markers were highly correlated with increased levels of clinical markers of microvascular complications (7, 9). In the prospective CARE study, elevated levels of sTNFR2 and CRP were associated with early renal function loss in subjects with chronic kidney disease (CKD) (5). A report from the Multi-Ethnic Study of Atherosclerosis showed significant associations between CKD and several proteins including CRP, IL6, sTNFR1, sICAM1, fibrinogen, and factor VII (10, 11). High serum concentrations of TNF-α, IL6, CRP, osteoprotegerin, fibrinogen, sICAM1, sTNFR2, and myeloperoxidase were shown to be associated with CKD status, higher cystatin C quartiles, and higher urinary albumin-to-creatinine ratio quartiles (7, 12). Recently, serum levels of sTNFR1 and sTNFR2 in fourth quartile were found to be predictive of early renal function loss in T1D patients (13). Along with proteins of the TNF-α pathway, proteins involved in endothelial cell activation, T-cell activation, and cellular differentiation were also shown to be involved in the progression of nephropathy (14). Serum levels of these proteins have been extensively studied and their association has been established in T1D patients with MA; however, these proteins have been rarely studied in the same cohort. Secondly, the single-protein analysis has been contradictory in previous studies. Therefore, it is unknown whether and how these proteins are co-regulated and whether certain combinations of proteins can serve as better biomarkers for MA.

In the current study, we investigated 12 serum proteins related to inflammation (CRP and SAA), endothelium activation and adhesion (sICAM1 and sVCAM1), immune and cellular activation (sTNFR1, sTNFR2, sIL2Rα, sgp130, and sIL6R), and ECM modeling enzymes (MMP1, MMP2, and MMP9) in T1D patients with and without MA. We demonstrate that multiple serum proteins in the TNF-α/IL6 pathway are significantly elevated in MA patients compared with T1D patients without MA. The prime goal of the study was to identify combinations of serum proteins that are even more strongly associated with the presence of MA in the T1D patient population and can be used to define subsets of MA patients with distinct inflammation patterns.

MATERIALS AND METHODS

Study Population

All serum samples analyzed in the study were obtained from Caucasian subjects recruited into the Phenome and Genome of Diabetes Autoimmunity (PAGODA) study between 2002 and 2010. These subjects attended the Augusta University (AU) Medical Center and other endocrinology clinics in Augusta and Atlanta area of Georgia. T1D patients were screened for presence of microalbumin and creatinine in a random spot urine collection at the time of visit. Presence of MA was determined by the attending physician/endocrinologist, based on the last three microalbumin/creatinine ratio (MACR) values. We used the MACR <30 for T1D patients, and MACR values 30–300 for T1D patients with MA. Medical history, clinical, and demographic profiles for T1D subjects were captured from the medical charts (Table S1 in Supplementary Material). The research was carried out according to The Code of Ethics of the World Medical Association (Declaration of Helsinki). All study participants gave written informed consent. The study was reviewed and approved by the institutional review board at AU.

Blood samples were collected in clot activator tubes, allowed to clot at room temperature for 30 min prior to centrifugation at 3,000× *g*. Separated serum was then aliquoted into wells of 96-well plate to create a master plate. Individual daughter plates were then created by aliquoting 5–10 μL of serum from this master plate. All master and daughter plates were stored at −80°C until use.

Laboratory Measurements

We selected to measure 12 proteins (CRP, SAA, MMP1, MMP2, MMP9, sgp130, sICAM1, sVCAM1, sIL2Rα, sIL6R, sTNFR1, and sTNFR2) in our PAGODA study subjects; the selection was based on published literature on role of these proteins in inflammation and MA. Luminex assays for these 12 proteins were obtained from Millipore Inc., Billerica, MA, USA. Multiplex assays were performed according to the instructions provided with the kit. Briefly, serum samples were incubated with antibody coated microspheres, followed by biotinylated detection antibody. Detection of the proteins was accomplished by incubation with phycoerythrin-labeled streptavidin. The resultant bead immuno-complexes were then read on a FLEXMAP3D (Luminex, TX, USA) with the instrument settings recommended by the manufacturer.

Statistical Analysis

Luminex median fluorescence intensity (MFI) data were subjected to the quality control steps as described in our earlier study (15). Briefly, wells with individual bead counts <30, or bead CV >200 were flagged for exclusion. The coefficients of variation of replicate wells were also checked and wells with CV ≥25% were not included in further analyses. Concentration and MFI values for standards were log2 transformed prior to determination of the concentration using the standard curve (15). The log2-transformed data were tested for the normal distribution by plotting frequency histograms, prior to subsequent statistical analysis. The potential differences between T1D patients without any complication (T1D) and T1D patients with MA were initially examined using *t*-test. The pairwise correlation between individual protein levels was computed using Pearson correlation coefficient. The correlations between the protein levels were visualized using hierarchical clustering and presented as a heatmap. The effect of age and T1D duration on serum levels of each candidate molecule

was determined using a linear regression including age or T1D duration as covariate on data stratified by sex and disease status. To examine the relationships between MA and the serum protein levels, logistic regression was used. Age, sex, T1D duration, hypertension (HTN), and dyslipidemia were included as covariates in a stepwise manner in the logistic regression.

To assess the odds ratios (ORs) for MA at different levels of each protein. Serum level for each protein was divided into five quintiles containing 20% MA patients in each quintile (20th percentile). The cutoff protein levels from MA patients were then used to count control subjects (T1D patients without MA) and MA subjects in each quintile. The first quintile was used as reference and OR for MA was calculated for the upper four quintiles. Pearson's chi-squared test with Yates' continuity correction was used to calculate the ORs. The chi-squared test for trend in proportions was used to calculate the *p*-value of overall trend.

Risk scores (equal to OR/quintile) were assigned to each subject based on individual protein levels. Hierarchical clustering and heatmap of risk scores were used to visualize the MA patients at high, medium, and low risk, based on these risk scores. To assess the OR, using a combination of proteins, the combined risk score of each subject was calculated by simply adding risk score from multiple proteins. The combined risk score was used to calculate ORs of having MA, for upper four quintiles using the first quintile as reference.

The receiving operator characteristic (ROC) curves were used to evaluate the ability of single proteins and multiprotein models to distinguish MA patients from controls. Sensitivity values of individual and combinations of proteins at different specificity thresholds (90; 95; 99; 100%) were computed. The utility of proteins as biomarkers was assessed using the area under curve (AUC) of the ROC curves for different models.

All *p*-values were two-tailed and a $P < 0.05$ value was considered statistically significant. All statistical analyses were performed using the R language and environment for statistical computing (R version 2.15.1; R Foundation for Statistical Computing; www.r-project.org).

RESULTS

Ten Serum Proteins Significantly Elevated in MA Patients

Serum levels of 12 proteins (CRP, SAA, sICAM1, sVCAM1, MMP1, MMP2, MMP9, sIL2Rα, sIL6R, sgp130, sTNFR1, and sTNFR2) were measured in 483 T1D patients without MA (T1D) and 89 T1D patients with MA (MA) (**Figure 1A**). Comparison of the mean expression levels between T1D and MA groups revealed highly significant differences for six proteins (sTNFR1, sTNFR2, sIL2Rα, MMP2, sIL6R, and sgp130; $P < 1 \times 10^{-5}$) and moderately significant differences for four proteins (CRP, SAA, sICAM1, and sVCAM1; $P < 0.05$) (Table S1 in Supplementary Material). The remaining two proteins (MMP1 and MMP9) showed no statistically significant difference. We calculated correlations between each pair of the 12 proteins for T1D patients without complications and with MA separately. Hierarchical clustering of the correlation matrix defined four clusters of correlated proteins (**Figure 1B**). The first cluster includes sTNFR2, sIL6R, and MMP2 ($r = 0.57$–0.79); the second cluster includes sTNFR1 and sIL2Rα ($r = 0.63$); the third cluster consists of sgp130, sVCAM1, sICAM1, and MMP9 ($r = 0.4$–0.92); and the fourth cluster includes SAA and CRP ($r = 0.66$). These results indicate that a correlated group of proteins might have a common upstream regulator and correlated changes in these immunologically active proteins contribute synergistically to the pathogenesis of MA.

Influence of Covariates on Serum Protein Levels

We next examined the potential influence of various covariates on serum protein levels in T1D patients with or without MA. The only significant correlations with age were found for MMP2 (T1D: $r = 0.15$, $P = 0.0017$; MA: $r = 0.41$, $P < 1 \times 10^{-4}$) and sTNFR2 ($r = 0.09$, $P = 0.05$ vs. $r = 0.30$, $P = 0.004$). The only significant correlations with the duration of diabetes were found for MMP2 (T1D: $r = 0.23$, $P < 1 \times 10^{-5}$; MA: $r = 0.33$, $P < 0.01$) and sTNFR2 (T1D: $r = 0.17$, $P < 1 \times 10^{-3}$) (Tables S2 and S3 in Supplementary Material). Since subject age and duration of diabetes are confounded covariates, it is difficult to distinguish the effects due to age vs. duration of diabetes. A small gender difference was observed for SAA (F/M ratio = 0.7, $P < 0.01$) and sTNFR1 (F/M ratio = 1.17, $P < 0.01$) only in T1D patients (Table S4 in Supplementary Material).

Even though there was no major impact of covariates on serum protein levels, we still adjusted for these covariates in logistic regression to rule out any confounding in the protein differences observed between MA and T1D patients (**Table 1**). Logistic regression analyses were carried out using protein concentration without any covariate adjustment (Model 1), then adjusting for age (Model 2), age and duration of diabetes (Model 3), and age, duration of diabetes, and gender (Model 4). Since HTN and dyslipidemia are also risk factors for MA, we adjusted for these two variables in a separate multivariate model which included age, duration of diabetes, and gender (Model 5). In these logistic regression analyses, 7 of the 12 proteins (sTNFR1, sTNFR2, sIL2Rα, MMP2, sgp130, sVCAM1, and sIL6R) showed significant associations with MA before and after adjusting for different covariates (**Table 1**).

MA Associated with Increasing Serum Protein Levels

To examine the relationship between MA and serum proteins, we calculated the ORs for protein concentrations distributed into five quintiles. For each protein, the serum concentration in MA patients was divided into five quintiles of 20th percentile. Based on the quintile cutoff values determined from MA patients, T1D patients were also assigned to five groups. The first quintile was used as reference to calculate ORs for the second to fifth quintiles. The ORs with 95% CI and *p*-values for each protein are presented in **Figure 2A** and **Table 2**. The most important conclusion from these data is that MA is associated with increasing levels of 10/12 proteins measured in this study. The strongest association is observed with sTNFR1 ($P < 1 \times 10^{-32}$), which has an OR of 108.3 for the fifth quintile, and ORs of 36.1, 5.2, and 3.2 for the

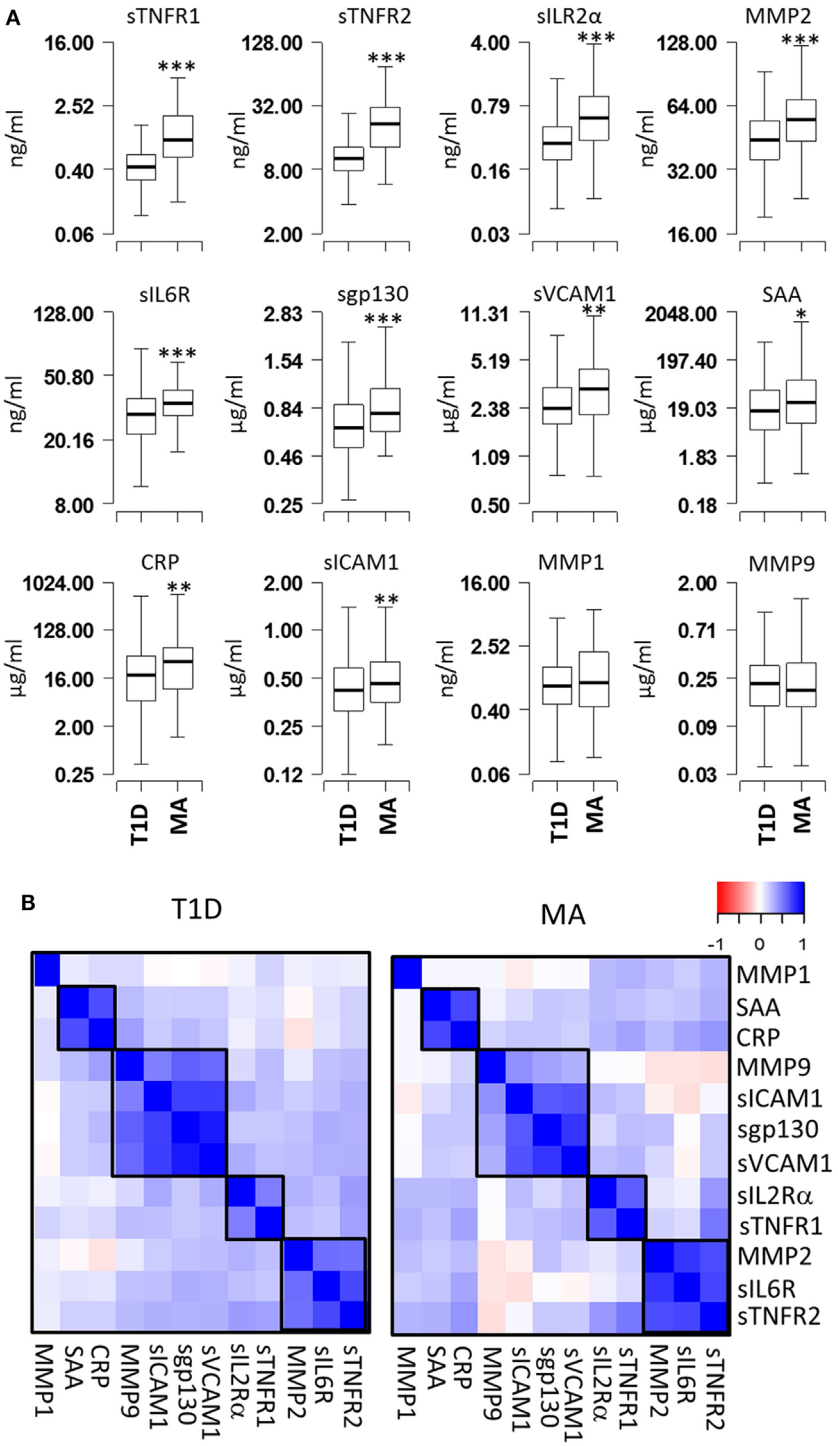

FIGURE 1 | Comparison of serum protein levels and pairwise correlations. **(A)** Box plots showing the expression levels of 12 proteins in the microalbuminuria (MA) (n = 88) and nMA (n = 482) patient groups. **(B)** Heatmaps showing the pairwise correlation coefficients in type-1 diabetes (T1D) patients with and without MA. The correlation coefficients of proteins are clustered based on the hierarchical clustering. Boxes indicate groups of proteins with higher correlations. *** $P < 0.000001$, ** $P < 0.01$, and * $P < 0.05$.

fourth, third, and second quintiles. Soluble TNFR2 has the second strongest association with ORs of 65.5 for the top quintile and ORs ranged from 3.1 to 34.7 for the second to fourth quintile (overall $P < 1 \times 10^{-37}$). Soluble IL2Rα is the third best protein with maximum OR of 12.9 ($P < 1 \times 10^{-13}$). MMP2, sgp130, sVCAM-1, and sIL6R have maximum ORs between 3 and 6 (**Figure 2A**; **Table 2**).

TABLE 1 | Odds ratios for microalbuminuria estimated using logistic regression.

Protein	Model 1	Model 2	Model 3	Model 4	Model 5
sTNFR1	5.47 (3.83–8.15)¶	4.80 (3.36–7.16)¶	4.58 (3.17–6.90)¶	4.78 (3.29–7.27)¶	4.03 (2.74–6.20)¶
sTNFR2	4.85 (3.29–7.36)¶	3.87 (2.62–5.91)¶	3.41 (2.30–5.20)¶	3.44 (2.32–5.26)¶	2.83 (1.87–4.42)¶
sIL2Rα	2.79 (2.14–3.70)¶	2.59 (1.98–3.45)¶	2.55 (1.92–3.44)¶	2.60 (1.96–3.51)¶	2.61 (1.92–3.61)¶
MMP2	2.30 (1.67–3.24)¶	1.85 (1.34–2.63)‡	1.51 (1.08–2.17)*	1.52 (1.09–2.19)*	1.56 (1.08–2.31)*
sgp130	1.87 (1.37–2.59)‡	1.83 (1.32–2.57)‡	1.77 (1.26–2.54)†	1.78 (1.26–2.56)†	1.90 (1.29–2.83)†
sVCAM1	1.69 (1.27–2.27)‡	1.61 (1.20–2.19)†	1.68 (1.23–2.33)†	1.68 (1.23–2.33)†	1.73 (1.23–2.45)†
CRP	1.52 (1.17–2.01)†	1.48 (1.12–1.98)†	1.57 (1.17–2.14)†	1.56 (1.16–2.13)†	1.33 (0.97–1.84)
sIL6R	1.72 (1.21–2.54)†	1.70 (1.17–2.55)†	1.68 (1.13–2.59)*	1.68 (1.13–2.58)*	1.58 (1.06–2.46)*
SAA	1.37 (1.07–1.77)*	1.24 (0.96–1.61)	1.39 (1.05–1.85)*	1.37 (1.04–1.83)*	1.17 (0.87–1.59)
sICAM1	1.34 (1.06–1.70)*	1.26 (0.98–1.61)	1.25 (0.96–1.62)	1.23 (0.95–1.60)	1.18 (0.90–1.56)
MMP1	1.22 (0.96–1.56)	1.11 (0.86–1.44)	1.22 (0.93–1.59)	1.22 (0.93–1.59)	1.10 (0.83–1.47)
MMP9	0.99 (0.79–1.27)	1.03 (0.81–1.35)	1.05 (0.8–1.39)	1.04 (0.80–1.39)	1.06 (0.8–1.46)

Values presented are odds ratio (95% CI). Model 1 = protein concentration only, Model 2 = protein concentration + age, Model 3 = Model 2 + duration of T1D, Model 4 = Model 3 + gender, and Model 5 = Model 4 + hypertension and dyslipidemia.
**P < 0.05, †P < 0.01, ‡P < 0.001, and ¶P < 1 × 10⁻⁵.*

Protein Combinations Defining Three Subsets of MA Patients

Since multiple serum proteins are associated with MA, we attempted to examine the combined effect of these proteins on MA. For this purpose, we calculated risk scores for each subject by adding the quintile ORs from multiple proteins and then examined association between MA and the risk scores. We first examined the risk scores based on the two best proteins, sTNFR1 and sTNFR2. The combination of sTNFR1 and sTNFR2 improved the highest OR values (OR = 135.7), suggesting an increase in proportion of MA subjects in the top quintile ($P < 1 \times 10^{-50}$) (**Figure 2B** and **Table 2**). We then examined 10 models of three-protein combinations by adding, each time, one of the remaining 10 proteins to sTNFR1 and sTNFR2. The three-protein models did not improve the maximum OR of the sTNFR1/2 model (OR = 135.7); however, the ORs associated with the fourth quintiles improved for all models and reached the levels of the fifth quintile for two models (sTNFR1/2 + sVCAM1 and sTNFR1/2 + MMP2). Subsequently, we examined two sets of four-protein models. The first set of four-protein models includes nine combinations (TNFR1/2 + sVCAM1 + one of the nine remaining) and the second set of four-protein models includes eight combinations (TNFR1/2 + sIL6R + one of the eight remaining). In general, these 17 models performed similarly as the better three-protein models (**Figure 2B**; **Table 2**).

Examination of the best three- and four-protein models suggests the existence of three subsets of MA patients. The MA patients in the top two quintiles (fourth and fifth) had extremely high risk scores (range 74.5–137.9, mean = 126.3) and the MA patients in the second and third quintiles have moderate risk score (range 5.1–21.9, mean = 13.5), while the MA patients in the bottom quintile have low risk score (reference group with OR = 1) (**Figure 2B**; **Table 2**).

Potential Utility of TNF-α/IL6 Proteins as MA Biomarkers

Receiving operator characteristic curves were used to evaluate the potential utility of these serum proteins as MA biomarkers (**Figure 2C**). The AUC for individual proteins is reasonable for two proteins (sTNFR1 = 0.82 and sTNFR2 = 0.83), but the AUC values for the other proteins are poor (<0.75). ROC curves for protein combinations were also evaluated using the combined risk scores. Combinations of three or four proteins that contain both sTNFR1 and sTNFR2 improved the AUC values to 0.87–0.89 (**Figure 2C**). These protein combinations were able to achieve 100% specificity with 14.8–18% sensitivity, 99% specificity with 37.3–39.8% sensitivity, or 95% specificity with 60.8–62.5% sensitivity (Table S5 in Supplementary Material).

DISCUSSION

This study demonstrated significant increases in 10 of the 12 examined serum proteins in MA patients compared with T1D patients without MA. Although the concentrations for two proteins (MMP2 and sTNFR2) are slightly but significantly correlated with subject age and duration of diabetes, the differences between MA and T1D patients cannot be accounted for by any of the examined covariates. The strongest associations with MA in this study were observed with the two soluble receptors of TNF-α (sTNFR1 and sTNFR2) and moderate associations were observed with several other soluble receptors (sIL2Rα, sIL6R, and sgp130) and soluble adhesion molecules (sVCAM1 and sICAM1). Using the risk score system developed in this study, combinations of these proteins allowed the definition of three subsets of MA patients with distinct patterns of the TNF-α/IL6 profiles. The identification of subsets of patients may allow the design of novel intervention strategies for different MA patients. Compared with the previous studies (16), we here show that the top 40% and the middle 40% of the MA patients have increased inflammation through the TNF-α/IL6 pathway. Blocking this pathway in these patients may ameliorate their clinical outcomes. In contrast, intervention of the TNF-α/IL6 pathway may not be effective for the bottom 20% of the patients who do not have elevated inflammation through the TNF-α/IL6 pathway. The pathogenesis in these patients may be related to the other molecules that are yet to be identified. Our risk score system may also prove to be very useful to develop biomarkers for the identification of MA patients

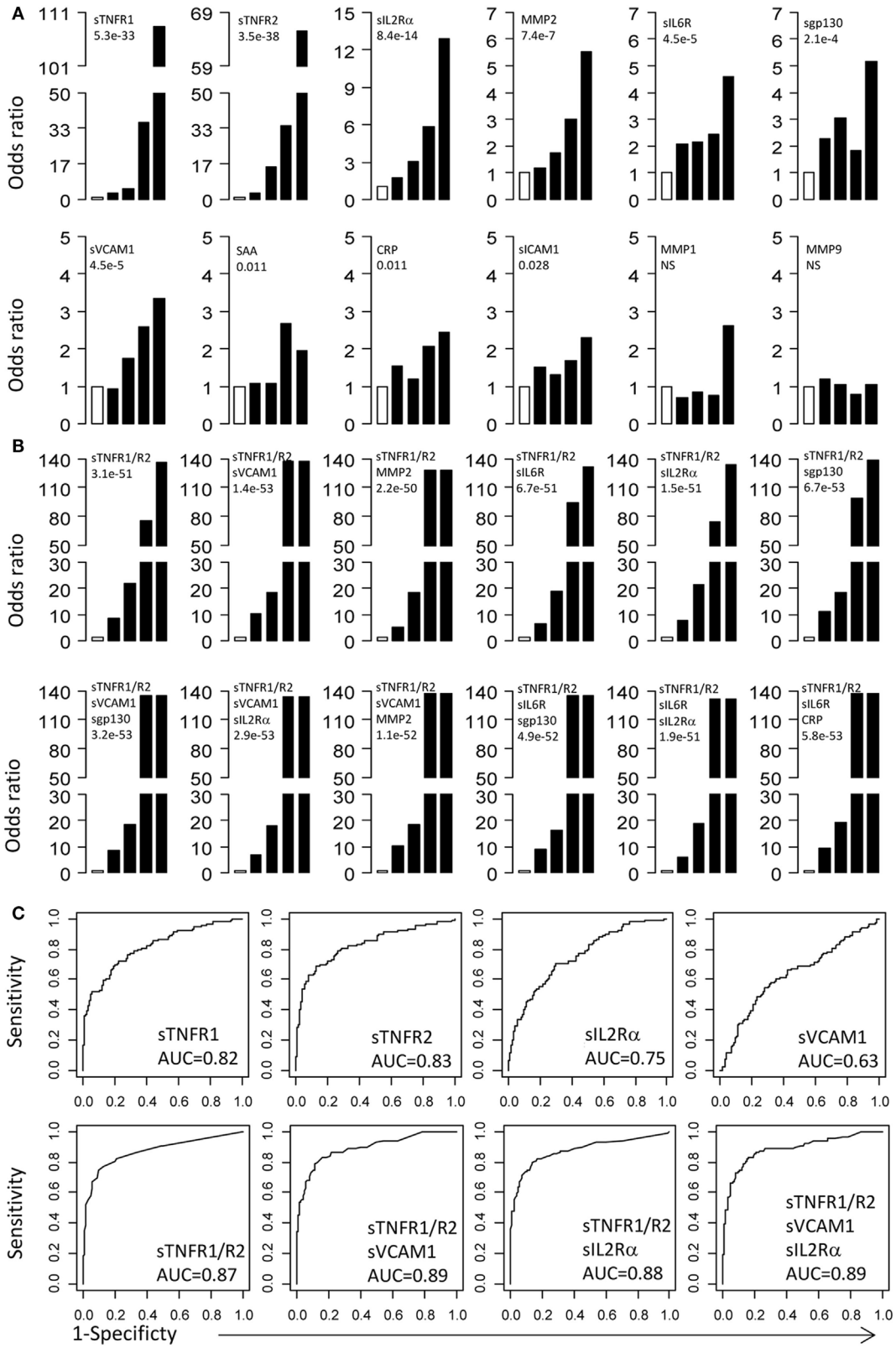

FIGURE 2 | Odds ratios (OR) and receiver operating curves (ROC). **(A)** ORs associated with each of the top four quintiles compared with the bottom first quintile for each of the 12 individual proteins. The open bar represents the first quintile as reference (OR = 1). From left to right, each of the other four solid bars represents the second to fifth quintile (20% of the MA patients). Vertical axes are ORs. **(B)** ORs associated with the risk scores calculated based on different combinations of proteins. **(C)** ROC curves for selected proteins and protein combinations.

TABLE 2 | Odds ratio (95% CI) of having microalbuminuria for each quintile.

Protein	Quintile 2 OR (95% CI)	Quintile 3 OR (95% CI)	Quintile 4 OR (95% CI)	Quintile 5 OR (95% CI)	Adj.*P*-trend
sTNFR1	3.24 (1.62–6.47)	5.16 (2.54–10.5)	36.11 (13.67–95.4)	108.34 (26.64–440.63)	5.3×10^{-33}
sTNFR2	3.12 (1.56–6.24)	15.12 (6.80–33.6)	34.69 (13.49–89.24)	65.53 (21–204.44)	3.5×10^{-38}
sIL2Rα	1.70 (0.86–3.37)	3.05 (1.51–6.16)	5.8 (2.77–12.15)	12.9 (5.64–29.49)	8.4×10^{-14}
MMP2	1.19 (0.59–2.38)	1.75 (0.87–3.54)	3.02 (1.46–6.24)	5.55 (2.57–11.97)	7.4×10^{-7}
sgp130	2.29 (1.10–4.75)	3.05 (1.45–6.41)	1.82 (0.88–3.74)	5.15 (2.37–11.19)	2.1×10^{-4}
sIL6R	2.09 (1.03–4.22)	2.14 (1.06–4.33)	2.44 (1.2–4.96)	4.59 (2.18–9.64)	4.5×10^{-5}
sVCAM1	0.94 (0.46–1.92)	1.73 (0.83–3.61)	2.59 (1.22–5.51)	3.34 (1.54–7.22)	4.5×10^{-5}
SAA	1.07 (0.52–2.21)	1.07 (0.52–2.21)	2.68 (1.25–5.74)	1.95 (0.93–4.11)	0.011
CRP	1.54 (0.74–3.19)	1.19 (0.58–2.45)	2.07 (0.99–4.34)	2.45 (1.16—5.18)	0.011
sICAM1	1.51 (0.72–3.16)	1.31 (0.63–2.73)	1.68 (0.8–3.53)	2.29 (1.08–4.87)	0.028
MMP1	0.69 (0.34–1.39)	0.85 (0.42–1.72)	0.76 (0.38–1.53)	2.63 (1.22–5.67)	NS
MMP9	1.20 (0.57–2.53)	1.05 (0.50–2.20)	0.79 (0.38–1.63)	1.04 (0.50–2.17)	NS
sTNFR1 + sTNFR2	8.59 (4.16–17.75)	21.89 (9.61–49.85)	75.39 (24.29–234.01)	135.7 (33.39–551.45)	3.1×10^{-51}
sTNFR1 + sTNFR2 + sVCAM1	10.27 (4.91–21.47)	18.6 (8.37–41.31)	137.63 (33.87–559.27)	137.63 (33.87–559.27)	1.4×10^{-53}
sTNFR1 + sTNFR2 + MMP2	5.13 (2.55–10.34)	18.33 (8.19–41.03)	128.3 (31.57–521.48)	128.3 (31.57–521.48)	2.2×10^{-50}
sTNFR1 + sTNFR2 + sIL6R	6.53 (3.21–13.30)	18.83 (8.41–42.15)	94.17 (27.37–324.04)	131.84 (32.44–535.82)	6.7×10^{-51}
sTNFR1 + sTNFR2 + sIL2Rα	7.53 (3.67–15.44)	21.63 (9.5–49.26)	74.5 (24–231.26)	134.09 (33–544.93)	1.5×10^{-51}
sTNFR1 + sTNFR2 + sgp130	11.31 (5.37–23.83)	18.64 (8.39–41.4)	98.54 (28.64–339.02)	137.96 (33.95–560.61)	6.7×10^{-53}
sTNFR1 + sTNFR2 + sVCAM1 + sgp130	10.9 (5.19–22.9)	15.97 (7.32–34.83)	137.31 (33.79–557.97)	137.31 (33.79–557.97)	3.2×10^{-53}
sTNFR1 + sTNFR2 + sVCAM1 + sIL2Rα	8.36 (4.05–17.24)	18.29 (8.23–40.63)	135.38 (33.31–550.15)	135.38 (33.31–550.15)	2.9×10^{-53}
sTNFR1 + sTNFR2 + sVCAM1 + MMP2	7.01 (3.43–14.32)	17.99 (8.1–39.97)	133.13 (32.76–541.04)	133.13 (32.76–541.04)	1.1×10^{-52}
sTNFR1 + sTNFR2 + sIL6R + sgp130	9.03 (4.35–18.72)	16.51 (7.53–36.21)	135.38 (33.31–550.15)	135.38 (33.31–550.15)	4.9×10^{-52}
sTNFR1 + sTNFR2 + sIL6R + sIL2Rα	6.13 (3.02–12.44)	18.74 (8.37–41.94)	131.2 (32.28–533.22)	131.2 (32.28–533.22)	1.9×10^{-51}
sTNFR1 + sTNFR2 + sIL6R + CRP	9.36 (4.51–19.44)	19.52 (8.72–43.68)	136.67 (33.63–555.38)	136.67 (33.63–555.38)	5.8×10^{-53}

OR, odds ratio; NS, not significant.

Quintile 1 was used as a reference. Individual protein concentrations were assigned the OR for the quintile and then summed to combine the risk scores for individual proteins.

or even identification of high-risk T1D patients for the development of MA. Indeed, serum levels of sTNFR1 and sTNFR2 in the fourth quartile have recently been found to be predictive of an early renal function loss in T1D and T2D patients (13, 16). It will be interesting to determine whether the prediction can be improved using our risk score system.

TNF-α is a pro-inflammatory cytokine, implicated in microvascular and structural changes in the kidneys of diabetic patients acting *via* TNFR1 and TNFR2 receptors. The observed elevation of the soluble TNF receptors supports the hypothesis that high concentrations of sTNFRs are pro-inflammatory by acting as the slow release reservoirs of TNF-α, which may be responsible for the chronic inflammatory state as observed in nephropathy (17). TNF-α signaling *via* TNF receptors leads to the activation of Th1-lymphocytes and endothelium by producing receptors and adhesion molecules required for abnormal migration and retention of leukocytes and lymphocytes in kidneys (18). TNFR1 is expressed ubiquitously on the surface of all cells and is directly related to the increased apoptosis *via* caspase-8 pathway (19, 20). On the other hand, TNFR2 is expressed on T-lymphocytes upon activation and is required for the cell survival and activation (21). The elevated levels of sTNFRs may reflect kidney damage *via* several mechanisms involving cell death, production of reactive oxygen species by activated leukocytes, and structural changes to renal tissues.

Elevated levels of sIL2Rα have been found in virus mediated and IgA nephropathy and Balkan nephropathy (14, 22). This is the first time that elevated levels of sIL2Rα have been reported in T1D patients with MA. Elevated levels of sIL2Rα predict the renal outcome in IgA nephropathy patients. The elevation of sIL2Rα and sTNFR2, both found on activated T cells, suggests the presence of an activated T-cell phenotype in MA patients, observed previously in patients with MA (23, 24). Influx of activated T cells in kidneys is associated with changes in glomerular structure and albumin excretion in T1D patients, as well as T1D patients with proteinuria, although the results are debatable (23, 24). The exact clinical relevance of activated T cells in kidneys of T1D patients is not very clear; it appears that damage to the kidneys occurs by activating the infiltrated macrophages. Activated macrophages in turn release reactive oxygen species, cytokines such as IL1, TNF-α, complement factors, and metalloproteinases, all of which promote renal injury (18).

The second component of the inflammatory cytokine network involves the IL6 pathway. The effect of IL6 on target cells is mediated by a complex receptor system, composed of IL6R and a signal-transducing glycoprotein (gp130). The increased concentration of soluble IL6R may be suggestive of metabolic syndrome and insulin resistance in T1D patients (25). The increase in IL6 signaling observed in T1D patients (26, 27) modulates immune response through the expansion of pathogenic Th17 cells and inhibition of generation of Foxp3 + T-regulatory cells is associated with T1D autoimmunity (28–30). It has been shown that Th17 cells contribute to inflammation during chronic kidney progression (31). The expression of IL6R is limited to the activated macrophages, lymphocytes, and leukocytes, whereas IL6 signaling in endothelial cells and other cell types occurs *via* trans-signaling through interaction of IL6/sIL6R complex with the surface bound gp130 molecule. The elevated levels of sgp130 may suggest higher

gp130 on the surface of renal endothelium and renal cells along with the activated leukocytes and lymphocytes in kidneys of MA subjects leading to increased IL6 trans-signaling and kidney injury (32, 33). Indeed, end-stage renal disease patients undergoing hemodialysis have higher expression of membrane gp130 in PBMCs, and increased spontaneous release of membrane bound gp130 (32).

Apart from the direct effect on kidneys and activation of lymphocytes, signaling *via* TNFRs and IL6R also elicits inflammatory responses by the liver and vascular endothelial cells. Under increased inflammatory stimulus, hepatic cells respond by eliciting acute phase reaction through production of CRP and SAA. Elevated levels of the acute phase proteins (CRP and SAA) are known to be deposited in the glomerular endothelium as well as in the cytoplasm of tubules. It is hypothesized that these deposits promote inflammation *via* the release of IL6, IL1, and TNF-α and chemotactic molecules by the renal cells (18, 19, 34, 35). TNF-α and CRP both upregulate the expression of ICAM1 and VCAM1 on the surface of glomerular endothelial cells (35, 36). The elevated levels of adhesion molecules (sICAM1 and sVCAM1) suggest the presence of subclinical endothelial dysfunction, which may cause increased recruitment and migration of leukocytes in the kidneys of MA patients as observed in an earlier study (19). Increased signaling *via* TNFRs and IL6R is also involved in the pathophysiology of kidneys including nephropathy *via* production of MMPs in renal tissues (37). MMP2, a zinc metalloprotease, is involved in the shedding of receptors and activation of cytokines and chemokines (38). Overexpression of MMP2 in kidneys of mice has been shown to cause structural abnormalities similar to those observed in human MA patients (39). The elevated serum levels of inflammatory, matrix metalloproteinase, and endothelial markers observed in this study reflect an increase in TNF-α and IL6-mediated secondary inflammation and endothelial dysfunction which may result in abnormal changes in renal physiology, integrity, and retention and migration of leukocytes in the kidneys of T1D patients.

In conclusion, we found significant increase in 10 serum proteins of TNF-α/IL6 pathway, which has been previously implicated in the initiation and progression of MA. Using multiple proteins and a novel risk score system, we identified three subsets of MA patients with distinct inflammatory profile. The identification of subsets may allow the design of novel intervention strategies for each subset of patients.

AUTHOR CONTRIBUTIONS

SP and J-XS were involved with conception of the project. SP was responsible for data acquisition and analysis. AS and SP were responsible for data analysis. WZ, DH, LS, BB, SA, JR, and RS contributed to clinical samples. All authors contributed to writing and editing of the manuscript.

ACKNOWLEDGMENTS

We thank a number of physicians (Andy Muir, David Brown, N. Spencer Welch, Paul Davidson, Joseph Johnson, David Robertson, Constance Baldwin, Melissa Carlucci, Mark Rappaport, Robert Schultz, and Vijayasudha Gunna) and staff members (Kim English, Jessica Leggett, Katherine Guthrie, Melanie Brown, Deana McFeely, Nellie Jenkins, JoAnn Higdon, Debbie Ellison, Tami Kinnersley, and Ann Simmonds) for their contribution in sample collection. We are very grateful to all patients and other volunteers who participated in this study.

FUNDING

This work was supported by the National Institutes of Health (grant number R21HD050196, grant number R33HD050196, and grant number 2RO1HD37800); JDRF (grant number 1-2004-661 to J-XS); and Postdoctoral Fellowship and Career Development Award from JDRF (grant number 2-2011-153 and grant number 10-2006-792 to SP, and grant number 3-2009-275 to WZ).

SUPPLEMENTARY MATERIAL

The Supplementary Material for this article can be found online at https://www.frontiersin.org/articles/10.3389/fimmu.2018.00154/full#supplementary-material.

REFERENCES

1. Caramori ML, Mauer M. Diabetes and nephropathy. *Curr Opin Nephrol Hypertens* (2003) 12:273–82. doi:10.1097/00041552-200305000-00008
2. Mohamed-Ali V, Armstrong L, Clarke D, Bolton CH, Pinkney JH. Evidence for the regulation of levels of plasma adhesion molecules by proinflammatory cytokines and their soluble receptors in type 1 diabetes. *J Intern Med* (2001) 250:415–21. doi:10.1046/j.1365-2796.2001.00900.x
3. Niewczas MA, Ficociello LH, Johnson AC, Walker W, Rosolowsky ET, Roshan B, et al. Serum concentrations of markers of TNFalpha and Fas-mediated pathways and renal function in nonproteinuric patients with type 1 diabetes. *Clin J Am Soc Nephrol* (2009) 4:62–70. doi:10.2215/CJN.03010608
4. Keller C, Katz R, Cushman M, Fried LF, Shlipak M. Association of kidney function with inflammatory and procoagulant markers in a diverse cohort: a cross-sectional analysis from the Multi-Ethnic Study of Atherosclerosis (MESA). *BMC Nephrol* (2008) 9:9. doi:10.1186/1471-2369-9-9
5. Tonelli M, Sacks F, Pfeffer M, Jhangri GS, Curhan G; Cholesterol and Recurrent Events (CARE) Trial Investigators. Biomarkers of inflammation and progression of chronic kidney disease. *Kidney Int* (2005) 68:237–45. doi:10.1111/j.1523-1755.2005.00398.x
6. Tripepi G, Mallamaci F, Zoccali C. Inflammation markers, adhesion molecules, and all-cause and cardiovascular mortality in patients with ESRD: searching for the best risk marker by multivariate modeling. *J Am Soc Nephrol* (2005) 16(Suppl 1):S83–8. doi:10.1681/ASN.2004110972
7. Upadhyay A, Larson MG, Guo CY, Vasan RS, Lipinska I, O'Donnell CJ, et al. Inflammation, kidney function and albuminuria in the Framingham Offspring cohort. *Nephrol Dial Transplant* (2011) 26:920–6. doi:10.1093/ndt/gfq471
8. Clausen P, Jacobsen P, Rossing K, Jensen JS, Parving HH, Feldt-Rasmussen B. Plasma concentrations of VCAM-1 and ICAM-1 are elevated in patients with type 1 diabetes mellitus with microalbuminuria and overt nephropathy. *Diabet Med* (2000) 17:644–9. doi:10.1046/j.1464-5491.2000.00347.x
9. Schram MT, Chaturvedi N, Schalkwijk C, Giorgino F, Ebeling P, Fuller JH, et al. Vascular risk factors and markers of endothelial function as determinants of inflammatory markers in type 1 diabetes: the EURODIAB prospective complications study. *Diabetes Care* (2003) 26:2165–73. doi:10.2337/diacare.26.7.2165
10. Fernandez-Real JM, Broch M, Ricart W, Casamitjana R, Gutierrez C, Vendrell J, et al. Plasma levels of the soluble fraction of tumor necrosis factor

receptor 2 and insulin resistance. *Diabetes* (1998) 47:1757–62. doi:10.2337/diabetes.47.11.1757
11. Lakoski SG, Cushman M, Palmas W, Blumenthal R, D'Agostino RB Jr, Herrington DM. The relationship between blood pressure and C-reactive protein in the Multi-Ethnic Study of Atherosclerosis (MESA). *J Am Coll Cardiol* (2005) 46:1869–74. doi:10.1016/j.jacc.2005.07.050
12. Mallamaci F, Tripepi G, Cutrupi S, Malatino LS, Zoccali C. Prognostic value of combined use of biomarkers of inflammation, endothelial dysfunction, and myocardiopathy in patients with ESRD. *Kidney Int* (2005) 67:2330–7. doi:10.1111/j.1523-1755.2005.00338.x
13. Gohda T, Niewczas MA, Ficociello LH, Walker WH, Skupien J, Rosetti F, et al. Circulating TNF receptors 1 and 2 predict stage 3 CKD in type 1 diabetes. *J Am Soc Nephrol* (2012) 23:516–24. doi:10.1681/ASN.2011060628
14. Lundberg S, Lundahl J, Gunnarsson I, Sundelin B, Jacobson SH. Soluble interleukin-2 receptor alfa predicts renal outcome in IgA nephropathy. *Nephrol Dial Transplant* (2012) 27:1916–23. doi:10.1093/ndt/gfr554
15. Zhi W, Sharma A, Purohit S, Miller E, Bode B, Anderson SW, et al. Discovery and validation of serum protein changes in type 1 diabetes patients using high throughput two dimensional liquid chromatography-mass spectrometry and immunoassays. *Mol Cell Proteomics* (2011) 10(11):M111.012203. doi:10.1074/mcp.M111.012203
16. Niewczas MA, Gohda T, Skupien J, Smiles AM, Walker WH, Rosetti F, et al. Circulating TNF receptors 1 and 2 predict ESRD in type 2 diabetes. *J Am Soc Nephrol* (2012) 23:507–15. doi:10.1681/ASN.2011060627
17. De Groote D, Grau GE, Dehart I, Franchimont P. Stabilisation of functional tumor necrosis factor-alpha by its soluble TNF receptors. *Eur Cytokine Netw* (1993) 4:359–62.
18. Wu CC, Sytwu HK, Lu KC, Lin YF. Role of T cells in type 2 diabetic nephropathy. *Exp Diabetes Res* (2011) 2011:514738. doi:10.1155/2011/514738
19. Lim AK, Tesch GH. Inflammation in diabetic nephropathy. *Mediators Inflamm* (2012) 2012:146154. doi:10.1155/2012/146154
20. Micheau O, Tschopp J. Induction of TNF receptor I-mediated apoptosis via two sequential signaling complexes. *Cell* (2003) 114:181–90. doi:10.1016/S0092-8674(03)00521-X
21. Tartaglia LA, Goeddel DV. Two TNF receptors. *Immunol Today* (1992) 13:151–3. doi:10.1016/0167-5699(92)90116-O
22. Voo S, Drugarin D, Margineanu F, Koreck A, Negru S, Biriescu A. The level of interleukin-2 and of soluble interleukin-2 receptor in patients with Balkan nephropathy. *Roum Arch Microbiol Immunol* (2002) 61:207–16.
23. Bending JJ, Lobo-Yeo A, Vergani D, Viberti GC. Proteinuria and activated T-lymphocytes in diabetic nephropathy. *Diabetes* (1988) 37:507–11. doi:10.2337/diabetes.37.5.507
24. Moriya R, Manivel JC, Mauer M. Juxtaglomerular apparatus T-cell infiltration affects glomerular structure in type 1 diabetic patients. *Diabetologia* (2004) 47:82–8. doi:10.1007/s00125-003-1253-y
25. Momesso DP, Bussade I, Lima GA, Fonseca LP, Russo LA, Kupfer R. Body composition, metabolic syndrome and insulin resistance in type 1 diabetes mellitus. *Arq Bras Endocrinol Metabol* (2011) 55:189–93. doi:10.1590/S0004-27302011000300003
26. Gomes KB. IL-6 and type 1 diabetes mellitus: T cell responses and increase in IL-6 receptor surface expression. *Ann Transl Med* (2017) 5:16. doi:10.21037/atm.2016.12.74
27. Hundhausen C, Roth A, Whalen E, Chen J, Schneider A, Long SA, et al. Enhanced T cell responses to IL-6 in type 1 diabetes are associated with early clinical disease and increased IL-6 receptor expression. *Sci Transl Med* (2016) 8:356ra119. doi:10.1126/scitranslmed.aad9943
28. Bellemore SM, Nikoopour E, Krougly O, Lee-Chan E, Fouser LA, Singh B. Pathogenic T helper type 17 cells contribute to type 1 diabetes independently of interleukin-22. *Clin Exp Immunol* (2016) 183:380–8. doi:10.1111/cei.12735
29. Bettelli E, Carrier Y, Gao W, Korn T, Strom TB, Oukka M, et al. Reciprocal developmental pathways for the generation of pathogenic effector TH17 and regulatory T cells. *Nature* (2006) 441:235–8. doi:10.1038/nature04753
30. Ryba-Stanislawowska M, Skrzypkowska M, Mysliwska J, Mysliwiec M. The serum IL-6 profile and Treg/Th17 peripheral cell populations in patients with type 1 diabetes. *Mediators Inflamm* (2013) 2013:205284. doi:10.1155/2013/205284
31. Mehrotra P, Collett JA, Gunst SJ, Basile DP. Th17 cells contribute to pulmonary fibrosis and inflammation during chronic kidney disease progression following acute ischemia. *Am J Physiol Regul Integr Comp Physiol* (2017). doi:10.1152/ajpregu.00147.2017
32. De La TM, Urra JM, Blanco J. Raised expression of cytokine receptor gp130 subunit on peripheral lymphocytes of patients with active lupus. A useful tool for monitoring the disease activity? *Lupus* (2009) 18:216–22. doi:10.1177/0961203308096068
33. Jostock T, Mullberg J, Ozbek S, Atreya R, Blinn G, Voltz N, et al. Soluble gp130 is the natural inhibitor of soluble interleukin-6 receptor transsignaling responses. *Eur J Biochem* (2001) 268:160–7. doi:10.1046/j.1432-1327.2001.01867.x
34. He R, Sang H, Ye RD. Serum amyloid A induces IL-8 secretion through a G protein-coupled receptor, FPRL1/LXA4R. *Blood* (2003) 101:1572–81. doi:10.1182/blood-2002-05-1431
35. Paffen E, DeMaat MP. C-reactive protein in atherosclerosis: a causal factor? *Cardiovasc Res* (2006) 71:30–9. doi:10.1016/j.cardiores.2006.03.004
36. Dember LM. Amyloidosis-associated kidney disease. *J Am Soc Nephrol* (2006) 17:3458–71. doi:10.1681/ASN.2006050460
37. Thrailkill KM, Bunn RC, Moreau CS, Cockrell GE, Simpson PM, Coleman HN, et al. Matrix metalloproteinase-2 dysregulation in type 1 diabetes. *Diabetes Care* (2007) 30:2321–6. doi:10.2337/dc07-0162
38. Catania JM, Chen G, Parrish AR. Role of matrix metalloproteinases in renal pathophysiologies. *Am J Physiol Renal Physiol* (2007) 292:F905–11. doi:10.1152/ajprenal.00421.2006
39. Cheng S, Pollock AS, Mahimkar R, Olson JL, Lovett DH. Matrix metalloproteinase 2 and basement membrane integrity: a unifying mechanism for progressive renal injury. *FASEB J* (2006) 20:1898–900. doi:10.1096/fj.06-5898fje

Conflict of Interest Statement: The authors declare that the research was conducted in the absence of any commercial or financial relationships that could be construed as a potential conflict of interest.

Copyright © 2018 Purohit, Sharma, Zhi, Bai, Hopkins, Steed, Bode, Anderson, Reed, Steed and She. This is an open-access article distributed under the terms of the Creative Commons Attribution License (CC BY). The use, distribution or reproduction in other forums is permitted, provided the original author(s) and the copyright owner are credited and that the original publication in this journal is cited, in accordance with accepted academic practice. No use, distribution or reproduction is permitted which does not comply with these terms.

frontiers in Immunology

ORIGINAL RESEARCH
published: 09 February 2018
doi: 10.3389/fimmu.2018.00189

The Effects of Prednisolone Treatment on Cytokine Expression in Patients with Erythema Nodosum Leprosum Reactions

Edessa Negera[1,2], Stephen L. Walker[1], Kidist Bobosha[2], Yonas Bekele[2], Birtukan Endale[2], Azeb Tarekegn[2], Markos Abebe[2], Abraham Aseffa[2], Hazel M. Dockrell[1] and Diana N. Lockwood[1]*

[1] Faculty of Infectious Tropical Diseases, London School of Hygiene and Tropical Medicine, London, United Kingdom, [2] Armauer Hansen Research Institute, Addis Ababa, Ethiopia

Erythema nodosum leprosum (ENL) is a systemic inflammatory complication occurring mainly in patients with lepromatous leprosy (LL) and borderline lepromatous leprosy. Prednisolone is widely used for treatment of ENL reactions but clinical improvement varies. However, there is little good *in vivo* data as to the effect of prednisolone treatment on the pro-inflammatory cytokines in patients with ENL reactions. As a result, treatment and management of reactional and post-reactional episodes of ENL often pose a therapeutic challenge. We investigated the effect of prednisolone treatment on the inflammatory cytokines TNF, IFN-γ, IL-1β, IL-6, and IL-17 and the regulatory cytokines IL-10 and TGF-β in the skin lesion and blood of patients with ENL and compared with non-reactional LL patient controls. A case–control study was employed to recruit 30 patients with ENL and 30 non-reactional LL patient controls at ALERT Hospital, Ethiopia. Blood and skin biopsy samples were obtained from each patient before and after prednisolone treatment. Peripheral blood mononuclear cells from patients with ENL cases and LL controls were cultured with *M. leprae whole-cell sonicates* (MLWCS), phytohemagglutinin or no stimulation for 6 days. The supernatants were assessed with the enzyme-linked immunosorbent assay for inflammatory and regulatory cytokines. For cytokine gene expression, mRNA was isolated from whole blood and skin lesions and then reverse transcribed into cDNA. The mRNA gene expression was quantified on a Light Cycler using real-time PCR assays specific to TNF, IFN-γ, IL-β, TGF-β, IL-17A, IL-6, IL-8, and IL-10. The *ex vivo* production of the cytokines: TNF, IFN-γ, IL-1β, and IL-17A was significantly increased in untreated patients with ENL. However, IL-10 production was significantly lower in untreated patients with ENL and significantly increased after treatment. The *ex vivo* production of IL-6 and IL-8 in patients with ENL did not show statistically significant differences before and after prednisolone treatment. The mRNA expression in blood and skin lesion for TNF, IFN-γ, IL-1β, IL-6, and IL-17A significantly reduced in patients with ENL after treatment, while mRNA expression for IL-10 and TGF-β was significantly increased both in blood and skin lesion after treatment. This is the first study examining the effect of prednisolone on the kinetics of inflammatory and regulatory cytokines in patients with ENL reactions before and after prednisolone treatment. Our findings suggest that prednisolone modulates the pro-inflammatory cytokines studied here either directly or through suppression of the immune cells producing these inflammatory cytokines.

Keywords: cytokines, erythema nodosum leprosum, leprosy, prednisolone, reaction, treatment, type-2 reaction

OPEN ACCESS

Edited by:
Manuela Mengozzi, Brighton and Sussex Medical School, United Kingdom

Reviewed by:
Danuza Esquenazi, Fundação Oswaldo Cruz (Fiocruz), Brazil
Irina Khamaganova, Pirogov Russian National Research Medical University, Russia

****Correspondence:***
Edessa Negera
edessan@yahoo.com

Specialty section:
This article was submitted to Inflammation, a section of the journal Frontiers in Immunology

Received: *18 October 2017*
Accepted: *22 January 2018*
Published: *09 February 2018*

Citation:
Negera E, Walker SL, Bobosha K, Bekele Y, Endale B, Tarekegn A, Abebe M, Aseffa A, Dockrell HM and Lockwood DN (2018) The Effects of Prednisolone Treatment on Cytokine Expression in Patients with Erythema Nodosum Leprosum Reactions. Front. Immunol. 9:189. doi: 10.3389/fimmu.2018.00189

INTRODUCTION

Leprosy is a chronic disease caused by *Mycobacterium leprae*, an acid-fast bacillus whose clinical spectrum correlates with the host immune response. It mainly infects the skin and peripheral nerves. There are five-clinical forms of leprosy called spectrum with the localized tuberculoid leprosy (TT) and the generalized lepromatous leprosy (LL) forming the two poles of the spectrum (1). Erythema nodosum leprosum (ENL) is an immune-mediated inflammatory complication causing high morbidity in affected leprosy patients (2). The clinical manifestation of ENL includes tender erythematous crops of skin lesions and systemic features of disease including fever, neuritis and bone pain (3). ENL occurs mainly in patients with LL and borderline lepromatous (BL) leprosy before, during, or after successful completion of multidrug treatment (MDT) (4).

Erythema nodosum leprosum reaction is associated reportedly with changes in cytokine profiles (5, 6). Cytokines are low molecular weight soluble proteins which mediate the cross-talk between the different cells of the immune system. They play a central role in the recruitment of the immune cells, the clonal development of the lymphocytes, the innate immune response and the effector response of most immune cells. These complex regulatory networks of cytokines often determine the clinical course of infections and the outcome (7).

In leprosy, cytokine research focused mainly on the association of different cytokine profile with the spectrum of the disease specifically with the Th1–Th2 cytokine profiles (5, 8, 9). The immune response to *M. leprae* in tuberculoid (TT) patients is associated with Th1 cytokines (IFN-γ and TNF) whereas LL patients are characterized by Th2 (IL-4, IL-5) cytokines production (6, 10–15). However, recent studies have shown that a distinct cytokine profile associated with a specific clinical form and reactions has not been attained (16–18).

The immune response to *M. leprae* is cytokine mediated, whereas the involvement of cytokines in ENL reaction is less understood. Literature reveals controversial results on the cytokines profile which are involved in ENL reaction. The presence of both Th1- and Th2-type cytokines in ENL lesions as well as in the sera of ENL patients has been reported by some authors (19–21). However, others reported that only Th1 cytokines are involved in the pathogenesis of ENL (6, 19, 22, 23). Yet other authors suggested that there is no clear association of either Th1 or Th2 cytokine secretion profile in leprosy patients with ENL reactions compared to non-reactional LL patients (8). In addition to the Th1- and Th2-driven cytokines, IL-17 has been identified as a new subset of cytokine recently reported associated with ENL reactions (24–26).

Erythema nodosum leprosum reaction is treated with prednisolone or with thalidomide. Thalidomide is not available in most leprosy endemic countries such as Ethiopia due to its severe side effects. Prednisolone is an immunosuppressor drug used for the treatment of chronic inflammatory diseases. The anti-inflammatory role of prednisolone is mainly due to its ability to suppress or inhibit the activation of transcription factors NF-kβ (27). NF-kβ regulates genes encoding for IL-1β, TNF, IL-2, and inducible nitric oxide synthase (28, 29). In leprosy reactions, although the results are conflicting, treatment of ENL with prednisolone has been correlated with downregulation of inflammatory cytokines, such as IL-1β, TNF, IFN-γ, and IL-17 (20, 22, 30). On the other hand, other studies reported the selective downregulation of regulatory cytokines after prednisolone treatment (6, 31).

Although oral prednisolone is widely used for treatment of ENL, clinical improvement varies in which more than 40% of cases do not show clinical improvement (32). High recurrent episodes and flare-ups are common in these patients. However, there is little good *in vivo* data as to the effect of prednisolone treatment on the pro-inflammatory cytokines. As a result, treatment and management of reactional and post-reactional episodes of ENL often pose a therapeutic challenge to leprologists.

We investigated the effect of prednisolone treatment on the inflammatory cytokines TNF, IFN-γ, IL-1β, IL-6, and IL-17 and the regulatory cytokines IL-10 and TGF-β in the skin lesion and blood of patients with ENL and compared with non-reactional LL patient controls. Our aim was to compare events at the local site of infection (i.e., the skin lesion) and the systemic effects of the prednisolone on the cytokine production and their gene expression before, during, and after treatment. LL patients without reactions were included as controls. We hypothesized that prednisolone treatment would downregulate the inflammatory cytokines and upregulate regulatory cytokines both locally in the skin and systemically in the blood and hence establish cytokine homeostasis.

MATERIALS AND METHODS

Study Design

A case–control study with follow-up for 28 weeks after the initiation of prednisolone treatment was used to recruit 30 patients with ENL reaction and 30 non-reactional LL patient controls between December 2014 and January 2016 at ALERT hospital, Ethiopia.

Ethical Considerations

Informed written consent for blood and skin lesion biopsies were obtained from patients following approval of the study by the Institutional Ethical Committee of London School of Hygiene and Tropical Medicine, UK (#6391), AHRI/ALERT Ethics Review Committee, Ethiopia (P032/12) and the National Research Ethics Review Committee, Ethiopia (#310/450/06). All patient data were analyzed and reported anonymously.

Patient Recruitment

Leprosy patients were recruited at ALERT Hospital, Addis Ababa, Ethiopia. The patients were classified clinically and histologically on the leprosy spectrum based on the Ridley–Jopling (RJ) classification schemes (1). ENL was clinically diagnosed when a patient with BL or LL leprosy had painful crops of tender cutaneous erythematous skin lesions (3). New ENL was defined as the occurrence of ENL for the first time in a patient with LL or BL. LL was clinically diagnosed when a patient had widely disseminated nodular lesions with ill-defined borders and BI above 2 (2).

Patients with ENL were treated according to the World Health Organization (WHO) treatment guideline with steroids that initially consisted of 40 mg oral prednisolone daily and the dose was tapered by 5 mg every fortnight for 24 weeks. All patients were received WHO-recommended leprosy MDT.

Blood and Skin Lesion Biopsy Samples

Twenty microliters of venous blood were collected into sterile BD Heparinized Vacutainer® tubes (BD, Franklin, Lakes, NJ, USA) before treatment, during treatment on week 12, and after treatment on week 24 from each patient and used for peripheral blood mononuclear cell (PBMC) isolation. In addition, 2 mL of blood was collected into PAXgene® Blood RNA Tubes (PreAnalytix, GmbH, Switzerland) before, during, and after prednisolone treatment for mRNA isolation and stored at −80°C. Six-millimeter punch biopsy was taken from each patient before and after prednisolone treatment into a Nunc® tube containing 1 mL RNAlater® solution (Thermo-Fisher Scientific) and was kept at −20°C for 48 h and then transferred to −80°C freezer. ENL and LL lesions for biopsy sample were identified and marked by a dermatologist and then biopsy samples were taken from the marked area by trained research nurses under supervision.

PBMC Isolation, Storage, and Thawing

Peripheral blood mononuclear cells were separated by density gradient centrifugation at 800 × *g* for 25 min on Ficoll–Hypaque (Histopaque, Sigma Aldrich, UK) as described earlier (33, 34). Cells were washed three times in sterile 1× phosphate-buffered saline (Sigma Aldrich®, UK) and re-suspended with 1 mL of Roswell Park Memorial Institute (RPMI medium 1640 (1×) + GlutaMAX™ + Pen-Strip GBICO™, Life technologies™, UK). Cell viability was determined by 0.4% sterile Trypan Blue solution (Sigma Aldrich®, UK), the viability was between 94 and 98%. PBMC freezing was performed using a cold freshly prepared freezing medium composed of 20% fetal bovine serum (FBS, heat inactivated, endotoxin tested ≤5 EU/ml, GIBCO® Life technologies, UK), 20% dimethyl sulfoxide in RPMI medium 1640 (1×). Cells were kept at −80°C for 2–3 days and transferred to liquid nitrogen until use. Cell thawing was done as described (35). The procedure is briefly described as follows: cells were incubated in a water bath (37°C) for 30 s until thawed half way and re-suspended in 10% FBS in RPMI medium 1640 (1×) (37°C) containing 1/10,000 benzonase until completely thawed, washed two times (5 min each), and counted. The percentage viability obtained was above 90%.

PBMC Stimulation with *M. leprae* Whole-Cell Sonicate (WCS)

Total PBMCs (200,000 cells/well) were added in triplicate into 96-well U-bottom tissue culture plates and cultured with 10 mg/mL irradiated armadillo-derived *M. leprae* WCS (kindly supplied by Dr. J. S. Spencer through the NIH/NIAID "Leprosy Research Support" Contract N01 AI-25469 from Colorado State University), 1 mg/mL phytohemagglutinin or AIM-V medium at 37°C with 5% CO_2 and 70% humidity. After 6 days, supernatants were collected and kept frozen until used in enzyme-linked immunosorbent assay (ELISA).

Cytokine Measurement by ELISA

Supernatants were tested for cytokines using a Ready-Set-Go! ® Sandwich ELISA. Capture and biotinylated detection antibodies directed against IFN-γ, TNF, IL-1β, IL-6, IL-10, IL-10, and IL-17A were purchased from eBioscience (Affymetrix, eBioscience, UK). A 96-well flat-bottom Nunc MaxiSorp® ELISA plates (Affymetrix, eBioscience, UK) were used. Standards for each cytokines were prepared by serial dilution as recommended by the supplier (Affymetrix, eBioscience, UK). Detection was performed with avidin-horseradish peroxidase (Avidin-HRP) conjugated with tetramethylbenzidine following the supplier's procedure (Affymetrix, eBioscience, UK). For all plates, the optical density (OD) at 450 nm was measured using an ELISA plate reader (Microplate reader; Bio-Rad, Richmond, CA, USA). A curve fit was applied to each standard curve according to the manufacturer's manual. Sample concentrations were interpolated from these standard curves. The assays were sensitive to over concentration ranges from 2 to 200 pg/mL for IL-6 and IL-17A, from 2 to 250 pg/mL for IL-8, from 2 to 300 pg/mL for IL-10, and from 4 to 500 pg/mL for TNF, IFN-γ, and IL-1β.

RNA Isolation and Reverse Transcription

Isolation of RNA from whole blood and skin lesion biopsies stored in RNAlater™ (Ambion, Austin, TX, USA) was performed using PAXgene Blood RNA Kit and RNeasy Fibrous Tissue Kit (QIAGEN Crawley, West Sussex, United Kingdom), respectively, according to the manufacturer's protocol. DNase I (QIAGEN) was included for all RNA preparations for DNA digestion. RNA yield was determined using a NanoDrop 2000, spectrophotometer (Thermo Scientific, Epsom, UK) and integrity was checked by agarose gel electrophoresis. For all samples, complementary DNA (cDNA was synthesized on the same day to avoid the risk of RNA degrades during storage). cDNA was synthesized from RNA (200 ng/reaction mixture) using High Capacity cDNA Reverse Transcriptase Kit (AB Applied Biosystems, UK). Reactions were incubated in an ABI9700 Programmable Thermal Cycler (Applied Biosystems, Foster City, CA, USA) for 10 min at 25°C followed by 120 min at 37°C and 5 min at 85°C and then cooling to 4°C.

Primers and Quantitative Polymerase Chain Reaction

Primers between 20 and 24 nt in length were designed across intron/exon boundaries on mRNA sequence obtained from the Nation Centre for Biotechnology Information database (NCBI) to give a product between 100–500 bp. All primer sequences were blasted on the NCBI data bank to confirm their specificity. Custom synthesis of oligonucleotide primers was performed by Sigma-life science and provided in desalted form. The nucleotide sequences of the forward and reverse primers, respectively, used in this study were as follows: for IL-10, 5′-TGAGAACCAAGACCCAGACA-3′ and 5′-TCATGGCTTTGTAGATGCCT-3′; for TNF, 5′-AGCC CATGTTGTAGCAAACC-3′ and 5′-GCTGGTTATCTCTCAG CTCCA-3′; for IL-17A, 5′-AGACCTCATTGGTGTCACTGC-3′ and 5′-CTCTCAGGGTCCTCATTG CG-3′; for Il-6, 5′-TTCGGT

CCAGTTGCCTTCTC-3′ and 5′-TACATGTCTCCTTTCTCA GGGC-3′; or IL-1β, 5′-AGCCCCAGCCAACTCAATTC-3′ and 5′-CATGGAGAACAC CACTTGTTGC-3′; for IFN-γ: 5′-GGC TTTTCAGCTCTGCATCG-3′ and 5′-TCTGTCAC TCTCCTC TTTCCA-3′; for IL-8: 5′-ACCGGAAGGAACCATCTCAC-3′ and 5′- AAAC TGCACCTTCACACAGAG-3′; for TGF-β: 5′-ACAT CAACGCAGGGTTCACT-3′ and 5′- GAAGTTGGCATGGTAG CCC-3′; for human acidic ribosomal protein (HuPO) housekeeping gene: 5′-GGACTCGTTTGTACCCGTTG-3′ and 5′-GG ACTCGTTTGTA CC CG TTG-3′.

Real-time quantitative PCR for all genes was performed on the Rotor-Gene™ 3000 programmable thermal cycler (Corbett Life Science, Qiagen, Crawley, UK) using Roter-gene® SYBR® Green PCR Kit (Qiagen, Crawley, UK). The Rotor-Gene conditions were set as follows: Initial activation step (polymerase activation) was achieved by incubating at 95°C for 15 min, 40 cycles of denaturation at 95°C for 5 s, annealing at 60°C for 10 s, extension at 72°C for 20 s, and fluorescence acquisition for 5 s at 72°C. The primer-dimer formation was checked by melting curve analysis. Melting point data were obtained by increasing the temperature from 50°C to 99°C by 1°C on each step. The interval between increases in temperature was 30 s for the first step and then 5 s for subsequent steps. An assay control was included from mRNA extraction to the amplification steps. For mRNA extraction, one assay control per batch was used. The assay control included all buffers except the sample and was processed under identical conditions with the samples. The same assay control was used during cDNA synthesis and real-time quantitative PCR (**Figure 1**).

Statistical Methods

ELISA Data

The OD of each sample for each cytokine was obtained by the ELISA reader. The OD was converted to concentration (pg/mL) by microplate manager 6. Unpaired *t*-test was used to compare the relative concentration of the cytokines production in patients with ENL and LL controls. For comparing the cytokine concentration in patients with ENL before and after treatment, paired t-test was used. Results are presented as mean ± SEM with *P*-values with a cut–off 0.05. SE was chosen since the primary objective of the study was to measure how the mean of the sample is related to the mean of the underlying population. SE takes SD and sample size into account.

Real-time Quantitative PCR

Real-time quantitative PCR for the mRNA gene expression of target genes, the relative threshold cycle value (C_T) comparison method was used. The relative gene expression was analyzed by using the $2^{-\Delta\Delta CT}$ method (36). The C_T value is the threshold number for the amplification of the target gene. Cikos et al. compared the six different methods currently used for real-time PCR data analysis and has shown that the best results were obtained with the relative standard curve (ΔC_T) method and the least coefficient

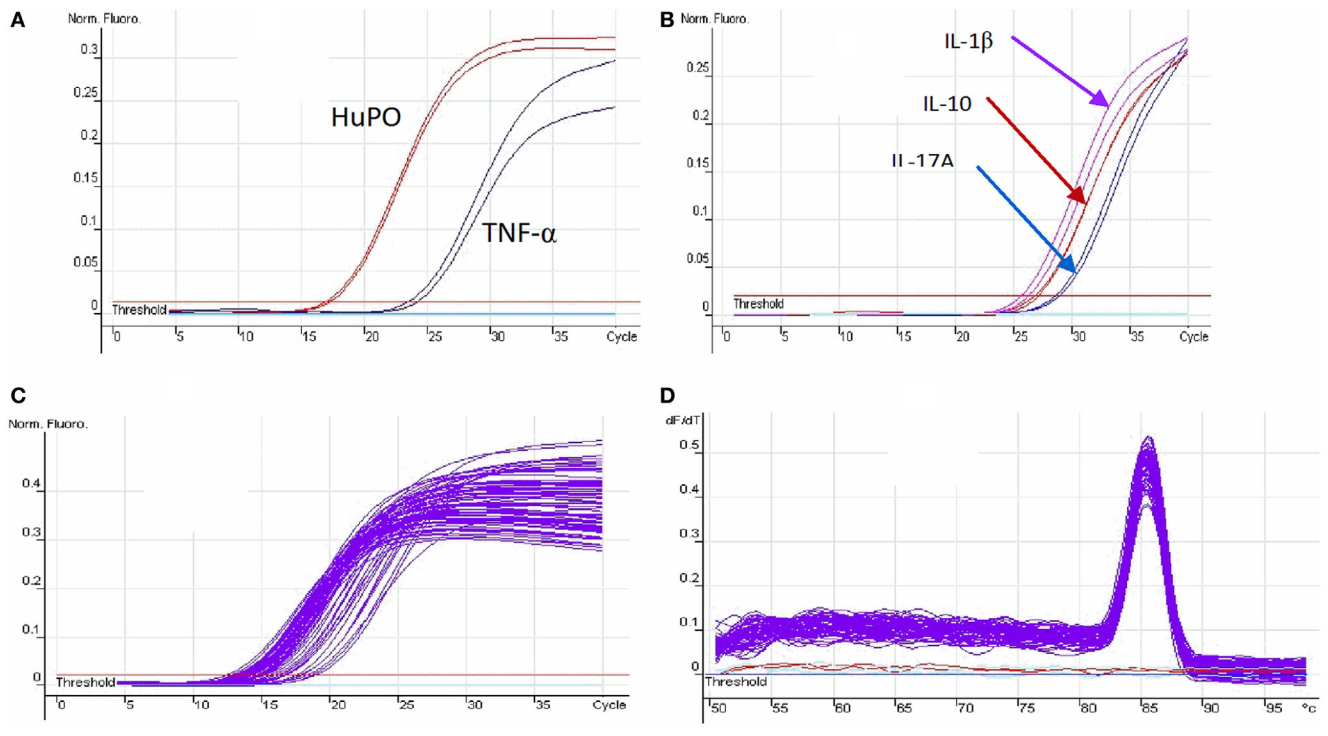

FIGURE 1 | PCR optimization: **(A)** the optimization threshold of housekeeping gene (HuPO) and TNF-α; **(B)** the optimization cycle threshold for IL-1β, IL-10, and IL-17A; **(C)** the cycle threshold of housekeeping gene for multiple samples; and **(D)** the melt curve analysis. The peak curve indicates the primer amplified the same region of all samples and primer-dimer is not detected as there is only one such peak.

of variation (ΔCV). The C_T values were obtained for the target gene and control gene (HuPO) for each patient sample at each time point. Then, the difference in C_T value was obtained by subtracting the C_T of the target gene from the C_T of the control gene and designated as ΔC_T. To compare the target gene expression in patients with ENL and LL controls, $\Delta\Delta C_T$ was obtained by subtracting the ΔC_T of LL patient control from the ΔC_T of the patient with ENL. Then, the fold change was obtained by using the formula $2^{-\Delta\Delta CT}$. similarly, for the comparison of the relative target gene expression in patients with ENL before and after treatment, $\Delta\Delta C_T$ was obtained by ΔC_T (after) minus ΔC_T (before). Then the fold change for target gene expression from the baseline (before treatment) was given by $2^{-\Delta\Delta CT}$. Unpaired *t*-test was used to compare the fold change of each target gene for patients with ENL compared to LL patient controls. To compare the expression level of the desired gene in patients with ENL before and after treatment, paired *t*-test was used.

RESULTS

Results are presented in two sections. First, we presented the results of cytokine production and then followed by the gene expressions. Within each section, we presented first the comparisons made between ENL and LL controls and then followed by the comparisons made within ENL patients at different time points.

Patient Clinical Background

Thirty LL patients with ENL reaction and 30 LL patient controls without ENL reaction were recruited between December 2014 and January 2016. The male to female ratio was 2:1 with a median age of 27.5 (range: 18–56) years in patients with ENL and 3:1 with a median age of 25.0 (range: 18–60) years in patients with non-reactional LL controls. All ENL patients were untreated with corticosteroid before recruitment. At time of recruitment, 10 ENL patients were previously untreated with MDT, 15 are on MDT and 5 were completed MDT treatment. Twenty-one LL patients were about to start MDT, 9 were on MDT at recruitment.

Increased *In Vitro* Inflammatory Cytokine Production in Untreated ENL Patients Compared to LL Controls

The mean production of TNF in response to *M. leprae* WCS stimulation was significantly higher (83.6.4 ± 18.82 pg/mL) in the culture supernatants of PBMCs from untreated ENL patients than from LL patient controls (19.4 pg/mL ± 10.44) ($P \leq 0.05$). During treatment, the level of TNF production decreased to 10.7 pg/mL in patients with ENL while it was increased to 36. 9 pg/mL in LL patient controls. After treatment, TNF production was not significantly different between the two groups (**Figure 2**).

Patients with ENL reactions had a significantly higher (1361 pg/mL ± 309.6) IFN-γ production than the LL patient controls (280.1 pg/mL ± 269.80) before treatment ($P \leq 0.05$). However, during treatment, the level of IFN-γ production was significantly decreased in patients with ENL to 304.4 pg/mL ± 119.6 while it was increased in LL patient controls to 1158.0 pg/mL ± 549.2 ($P \leq 0.05$). The level of IFN-γ production was not significantly different in both groups after treatment (**Figure 2**).

Although the amount of IL-1β production was similar in patients with ENL and LL controls before and during treatment, patients with ENL had much lower production of IL-1β than LL patient controls after treatment ($P \leq 0.05$). Higher production of IL-17A was obtained in patients with ENL cases compared to LL patient controls before treatment ($P \leq 0.005$). Although the *in vitro* production of IL-17A was considerably decreased after treatment in patients with ENL, it still remained higher than in LL patient controls ($P \leq 0.05$) (**Figure 2**).

The *in vitro* response of IL-6 production was higher in patients with ENL than in LL controls before treatment ($P \leq 0.005$). However, during and after treatment, the *in vitro* IL-6 production was not significantly different in both groups. On the other hand, the level of IL-8 production was found to be higher in patients with ENL than in LL controls throughout the study period ($P \leq 0.05$) (**Figure 2**).

The IL-10 production was considerably lower in patients with ENL (18.59 pg/mL ± 4.05) than in LL patient controls (122.6 pg/mL ± 23.18) before treatment ($P < 0.0001$). Interestingly, after treatment, the level of IL-10 production was significantly increased to 87.78 pg/mL ± 22.49 in patients with ENL while it was substantially decreased to 4.91 pg/mL ± 2.160 in LL patient controls and the difference was statistically significant ($P \leq 0.001$) (**Figure 2**).

In conclusion, the *in vitro* production of the cytokines TNF, IFN-γ, IL-17A, IL-6, and IL-8 were higher in patients with ENL than in LL patient controls before treatment while IL-10 was significantly lower in patients with ENL than in LL patient controls at recruitment.

A receiver operator characteristic (ROC) curve plot for the accuracy of a single cytokine to discriminate between patients with ENL and LL controls was produced. The most accurate cytokines that differentiate between patients with ENL and LL controls were as follows: TNF, IL-6, IL-17A, IL-1β, IL-8, IFN-γ, and IL-10 with the corresponding of area under the curves (AUCs) of 0.779, 0.763, 0.745, 0.695, 0.667, 0.557, and 0.710, respectively (**Figure 3**).

Principal Component Analysis

Principal component analysis with varimax rotation was conducted to assess the cytokine variables in order to summarize them by reducing the dimension of the dataset into principal components (**Figure 4A**). A loading score statistic was used to select the principal components most associated with the outcome variable (ENL). The assumption of independent sampling was met. The assumptions of normality, linear relationships between pairs of variables, and the variables being correlated at a moderate level were checked.

The component plot in rotated space (**Figure 4B**) shows how closely related the cytokines are to each other and to the two components. This plot of the component loadings shows that IL-6, IL-1β, and IL-8 all load highly and positively on the first component. IL-10 and TNF had near zero on the first component, but load highly on the second component. IL-17A loads moderately on the first component while IFN-γ loads moderately

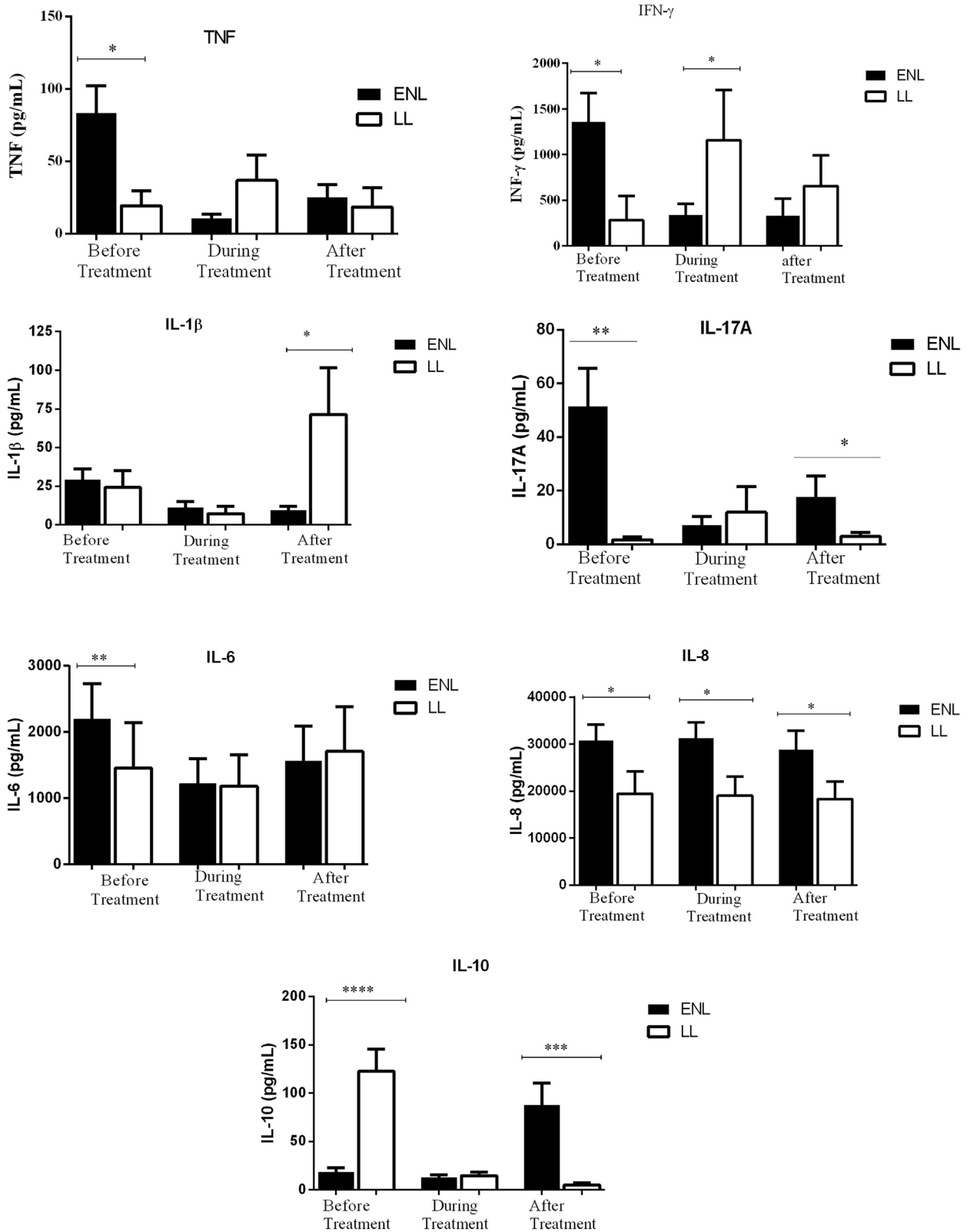

FIGURE 2 | Comparison of the levels of *in vitro* production of TNF, IFN-γ, IL-β and IL-17A, IL-6, IL-8, and LI-10 in culture supernatants of peripheral blood mononuclear cells from patients with erythema nodosum leprosum (ENL) and lepromatous leprosy (LL) controls before and after treatment. Statistical test: unpaired *t*-test, α = 0.05. *$P \leq 0.05$; ** $P \leq 0.005$. Bar graphs show mean ± SEM.

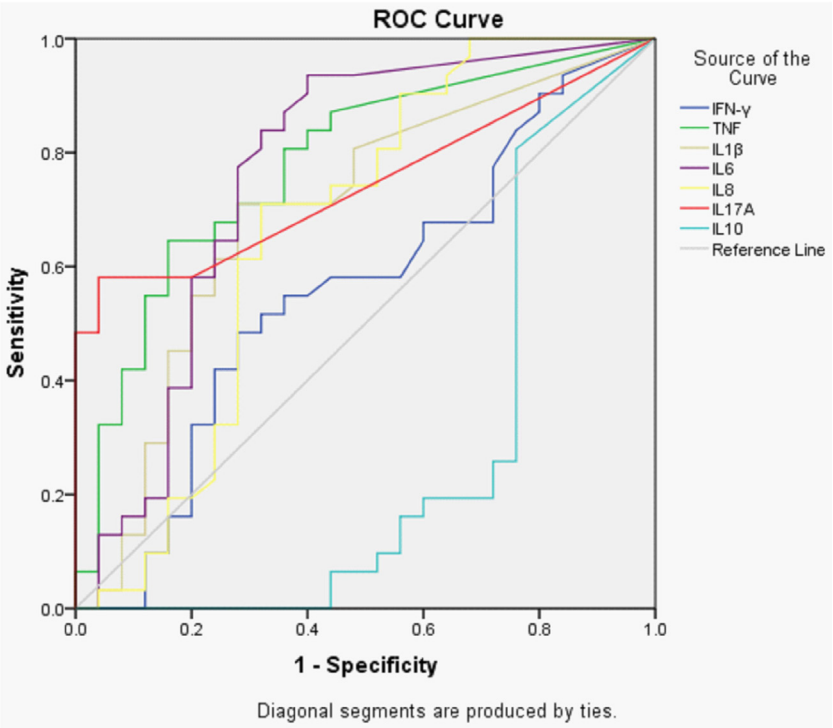

FIGURE 3 | Receiver operator characteristic (ROC) curves showing the accuracies of individual cytokines in discriminating between patients with ENL and LL controls before treatment. AUC = area under the curve.

on component 2. The cytokine levels of IL-6, IL-1β, IL-8, and IL-17 loaded together on the first component with loading coefficient of 0.860, 0.776, 0.704, and 0.472, respectively, explaining 42.274% of the total variation in the cytokine study. Component 2 is determined by three cytokines: IL-10, TNF, and IFN-γ with component loading coefficient of 0.899, 0.906, 0.120, respectively, and explaining 20.714% of the variation.

Decreased *In Vitro* Inflammatory Cytokine Production in ENL Patients after Prednisolone Treatment

The levels of IFN-γ, IL-17A, TNF, IL-6, IL-8, Il-1β, and IL-10 production in response to *M. leprae* WCS before, during, and after treatment were compared within ENL. The *in vitro* TNF production in response to *M. leprae* WCS stimulation was considerably higher (83.6 pg/mL ± 18.82) before treatment than during treatment (10.7 pg/mL ± 2.79) ($P \leq 0.001$). After treatment, it was slightly increased to 25.4 pg/mL ± 8.88 than during treatment but was still lower than the amount obtained before treatment ($P \leq 0.005$). Likewise, the *in vitro* production of IFN-γ in response to *M. leprae* WCS was considerably higher before treatment (1361.0 pg/mL ± 309.6) than during treatment (304.4 pg/mL ± 119.6) ($P \leq 0.05$) and after treatment (328.2 pg/mL ± 190.3) ($P \leq 0.05$) (**Figure 5**).

The level of IL-1β and IL-17A production were also found to be higher before treatment than during and after prednisolone treatment of patients with ENL. Although IL-6 production was appreciably decreased during treatment, it was increased after treatment and statistically a significant difference was not revealed before or after treatment. Unlike IL-6, IL-8 production did not show any significant change before, during and after treatment (**Figure 5**). On the other hand, the level of IL-10 production was very low before and during treatment but substantially increased after treatment (**Figure 5**).

In summary, the *in vitro* production of IFN-γ, IL-17A, TNF, and IL-1β to *M. leprae* WCS stimulation were higher before prednisolone treatment and have shown a significant reduction after treatment indicating the possible association of these pro-inflammatory cytokines and ENL reaction. On the other hand, the *in vitro* production of IL-10 was noticeably low before treatment and significantly increased after treatment showing its possible regulatory activity. IL-6 and IL-8 did not show significant change before and after treatment of patients with ENL.

Inflammatory Cytokines Gene Expression Upregulated in the Peripheral Blood of Untreated ENL Patients Compared to LL Controls

To investigate the cytokine gene expression in blood and skin biopsies, a fold change (FC) was used to compare the levels of these gene expressions in patients with ENL and LL controls as well as among patients with ENL before and after treatment.

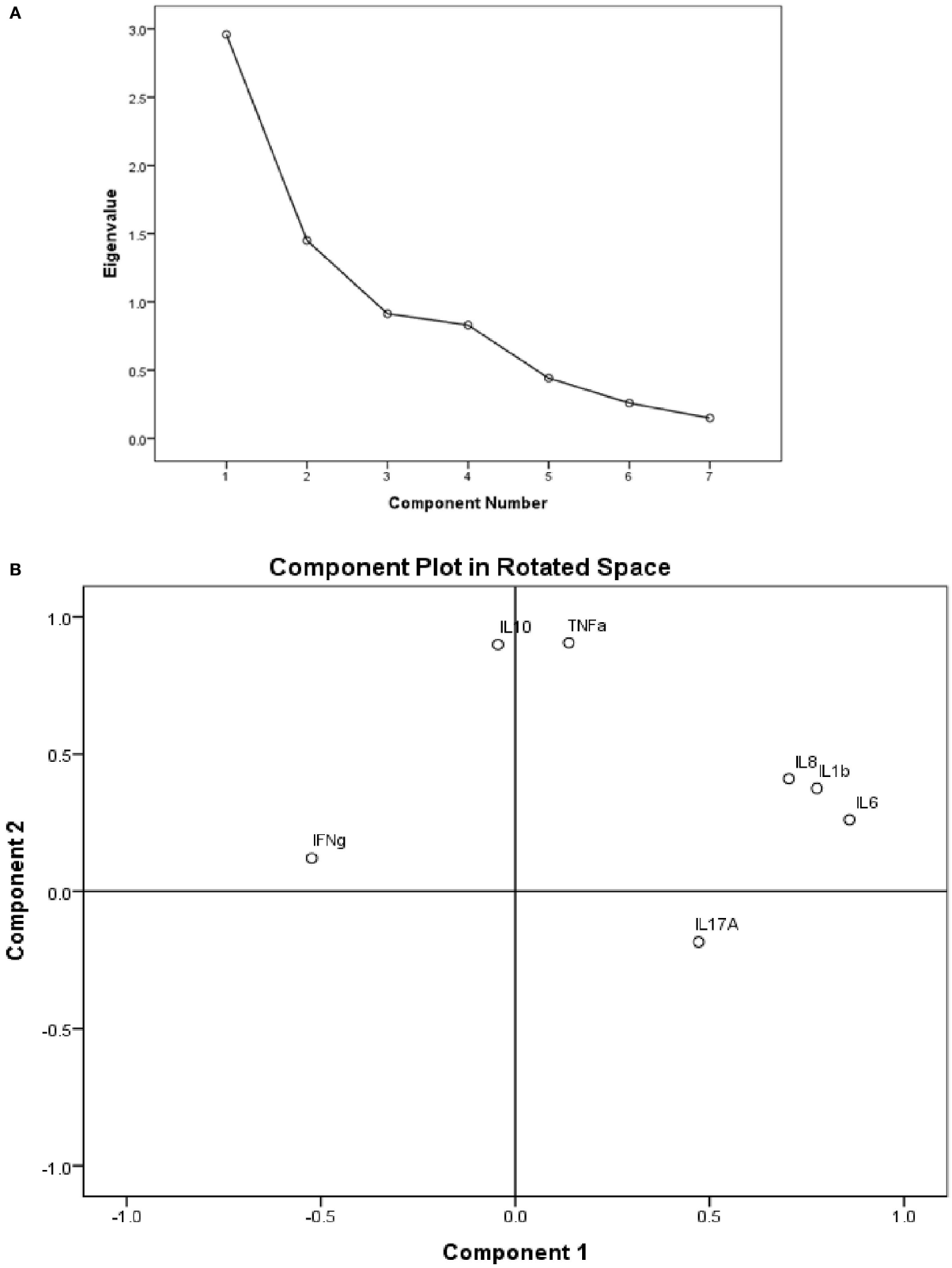

FIGURE 4 | **(A)** Scree plot showing the *in vitro* cytokine production in culture supernatants of peripheral blood mononuclear cells (PBMCs) from patients with erythema nodosum leprosum (ENL). The PCs have eigen values >1 are taken as the most significant components explaining variability in the data; **(B)** the component plot in rotated space showing visual representation of the loadings plotted in a 2-dimensional space.

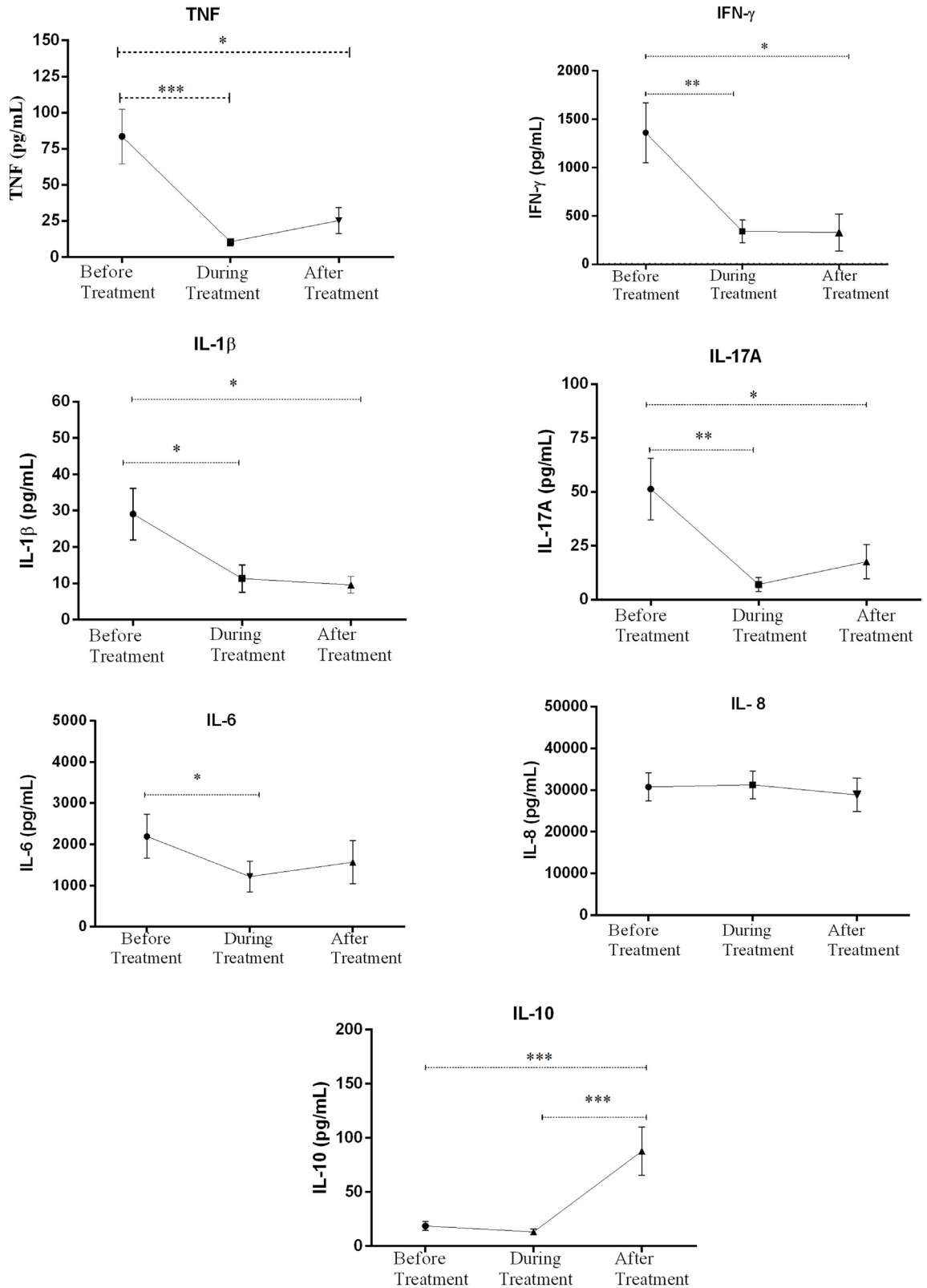

FIGURE 5 | Comparison of the levels of *in vitro* cytokine production in culture supernatants of peripheral blood mononuclear cells (PBMCs) from patients with erythema nodosum leprosum (ENL) before and after treatment. Statistical test: paired *t*-test, $\alpha = 0.05$. *$P \leq 0.05$; **$P \leq 0.005$; ***$P < 0.001$; ****$P < 0.0001$. Error bars show mean ± SEM.

The gene expression levels of TNF (FC = 3.31), IFN-γ (FC = 2.42), IL-6 (FC = 6.01), IL-8 (FC = 3.19), and IL-17A (FC = 3.58) were significantly increased in the blood samples from patients with ENL compared to LL patient controls before treatment ($P \leq 0.05$). However, after treatment, the gene expression levels of these cytokines did not reveal statistically a significant difference between ENL patients and LL controls (**Table 1**).

Although, the fold changes (FC) of mRNA gene expression for IL-1β and TGF-β were slightly increased before treatment in the blood samples from patients with ENL compared to LL patient controls, statistically a significant difference was not revealed. On the other hand, the mRNA gene expression for TGF-β was increased (FC = 4.82) in patients with ENL compared to LL patient controls after treatment ($P \leq 0.05$). The level of IL-10 gene expression was not significantly different in the two groups before and after treatment (**Table 1**).

Except IL-10, the result of mRNA gene expression of the other cytokines (TNF, IFN-γ, IL-β, TGF-β, IL-17A, IL-6, and IL-8) was found to be consistent with the result of the corresponding *in vitro* cytokine production. Unlike the IL-10 cytokine production in the culture supernatants in response to *M. leprae* WCS, its gene expression in patients with ENL did not reveal statistically significant difference compared to LL patient controls.

Comparison of Cytokine Gene Expression in Skin Biopsy Samples from Patients with ENL and LL Controls

The expression of mRNA in skin biopsies for TNF (FC = 2.04), IFN-γ (FC = 4.01), IL-1β (FC = 6.35), IL-6 (FC = 5.30), and IL-17A (FC = 2.99) were significantly higher ($P \leq 0.005$) in the biopsies from patients with ENL than in the biopsies from LL patient controls before treatment. However, except IL-6 (FC = 2.07, $P \leq 0.05$), statistically, a significant difference was not obtained in mRNA gene expression for these cytokines in patients with ENL and LL controls after treatment. The mRNA expression for IL-10 was significantly lower (FC = 0.38) in patients with ENL than in LL patient controls ($P \leq 0.0001$) before treatment but significantly increased after treatment in patients with ENL (FC = 3.5) compared to LL patient controls and the difference was statistically significant ($P \leq 0.0001$). The mRNA expression for TGF-β and IL-8 in patients with ENL and LL controls did not show statistically significant difference after treatment (**Table 2**).

Except for IL-1β and IL-10, the mRNA expression levels for most of these cytokines showed similar pattern both in blood and biopsy samples. Unlike in blood samples, the mRNA gene expression for IL-1β was significantly higher in the skin biopsies of untreated ENL patients than in LL patient controls. On the other hand, the gene mRNA expression for IL-10 was significantly lower in the biopsies of untreated ENL than in LL controls (**Table 2**).

The Kinetics of Cytokines Gene Expression in the Blood Samples within ENL Patient Group before and after Treatment

The gene expression of the cytokines was also investigated in blood samples from patients within ENL group before and after treatment. The $\Delta\Delta C_T$ of each pair was obtained by subtracting the $\Delta\Delta C_T$ before treatment from $\Delta\Delta C_T$ after treatment ($\Delta\Delta C_{T\ \text{after}} - \Delta\Delta C_{T\ \text{before}}$).

The mRNA expression for IL-8 and TGF-β did not show a statistically significant difference before and after treatment. On

TABLE 1 | Cytokine mRNA expression in the blood samples from patients with erythema nodosum leprosum and lepromatous leprosy controls before and after treatment.

Gene of interest	Before treatment			After treatment		
	$\Delta\Delta C_T$	FC	*P*-value	$\Delta\Delta C_T$	FC	*P*-value
TNF	−1.73	3.31	0.0047*	0.00	1.00	0.9989
IFN-γ	−1.27	2.42	0.0044*	0.08	0.95	0.8804
IL-1β	−1.23	2.34	0.1085	−0.24	1.18	0.7333
IL-6	−2.59	6.01	0.0003*	−0.99	1.99	0.1167
IL-8	−1.68	3.19	<0.0001*	−0.81	1.75	0.243
IL-10	0.83	0.56	0.1552	0.28	0.82	0.5882
IL-17A	−1.84	3.58	0.0002*	1.12	0.46	0.0502
TGF-β	−0.07	1.05	0.8724	−2.27	4.82	0.0119*

*Statistical test: unpaired t-test, α = 0.05, $\Delta\Delta C_T$ = delta delta C_T, FC = fold change, * = significant at α = 0.05.*

TABLE 2 | Cytokine mRNA expression in the skin biopsy samples from patients with erythema nodosum leprosum and lepromatous leprosy controls before and after treatment.

Gene of interest	Before treatment			After treatment		
	$\Delta\Delta C_T$	FC	*P*-value	$\Delta\Delta C_T$	FC	*P*-value
TNF	−1.03	2.04	0.0033*	−0.09	1.07	0.89
IFN-γ	−2.01	4.01	0.0058*	−0.32	1.25	0.5224
IL-1β	−2.67	6.35	0.0006*	−0.24	1.18	0.7333
IL-6	−2.41	5.30	0.0015*	−1.05	2.07	0.0438*
IL-8	−0.12	1.09	0.8465	−0.71	1.64	0.2333
IL-10	1.41	0.38	< 0.0001*	−1.81	3.50	<0.0001*
IL-17A	−1.58	2.99	0.0035*	−0.13	1.10	0.281
TGF-β	0.31	0.8	0.4876	−0.63	1.55	0.3598

*Statistical test: unpaired t-test, α = 0.05. $\Delta\Delta C_T$ = delta delta C_T, FC = fold change, * = significant at α = 0.05.*

TABLE 3 | Cytokine mRNA expression in the blood samples from erythema nodosum leprosum before and after treatment.

Cytokine	$\Delta\Delta C_T$	FC	*P*-value	Gene expression after treatment
TNF	1.19	0.44	0.0497*	Decreased
IFN-γ	1.61	0.33	<0.0001*	Decreased
IL-1β	1.56	0.34	0.0043*	Decreased
IL-6	1.60	0.33	<0.0001*	Decreased
IL-8	0.48	0.72	0.0790	No change
IL-10	−1.32	2.50	<0.0001*	Increased
IL-17A	2.34	0.20	<0.0001*	Decreased
TGF-β	0.24	0.85	0.7160	No change

*Statistical test: paired t-test, α = 0.05. $\Delta\Delta C_T$ = delta delta C_T; FC = fold change; * = significant at α = 0.05.*

the other hand, the gene expression levels of IFN-γ ($P < 0.0001$), IL-6 ($P \leq 0.0001$), IL-1β ($P \leq 0.005$), and TNF ($P \leq 0.05$) were significantly decreased in the blood samples from patients with ENL after treatment while it was significantly increased for IL-10 ($P \leq 0.0001$) (**Table 3**).

The Kinetics of Cytokines Gene Expression in the Skin Biopsy Samples within ENL Patient Group before and after Treatment

The mRNA expression in biopsy samples for TNF ($P \leq 0.0001$), IFN-γ ($P \leq 0.0001$), IL-1β ($P \leq 0.0005$), and IL-17A ($P \leq 0.0204$) were significantly decreased after prednisolone treatment. On the other hand, mRNA expression level for IL-10 was considerably increased after treatment ($P \leq 0.0001$). The mRNA expression for IL-6, IL-8, and TGF-β did not show statistically a significant difference before and after treatment (**Table 4**).

DISCUSSION

The *in vitro* cytokine response of PBMCs from patients with ENL and LL controls to *M. leprae* antigen and its gene expression in blood and skin biopsy samples were compared before, during, and after treatment. Some of the key findings are discussed in the following paragraphs.

The analysis of ROC curve has shown that none of these cytokines are good enough to discriminate ENL from non-reactional LL patient controls. This indicates that multiple cytokines are involved in the pathogenesis of ENL. Among the studied cytokines TNF, IL-6, and IL-7A seem more powerful to discriminate ENL from LL although the discriminating power for these cytokines is less than 80%.

TNF

The *in vitro* response of TNF to *M. leprae whole-cell sonicates* (MLWCS) in the PBMCs from patients with ENL and LL controls was investigated before and after treatment. The mean production of TNF in response to *M. leprae* antigen stimulation was significantly higher (83.6.4 ± 18.8, SE pg/mL) in the culture supernatants of PBMCs from patients with ENL than from LL patient controls (19.4 pg/mL ± 10.44) before treatment. However, TNF production was not significantly different in these groups after treatment. Similar findings have been reported by several studies (5, 37, 38). On the other hand, the detection of TNF in plasma or serum samples from patients with ENL has not been consistently reported. Some authors did not find a significant difference in patients with ENL and LL controls (39, 40). Others reported that increased TNF production occurred during corticosteroid treatment and decreased after treatment (9, 41–43). Interestingly, an upregulation of TNF production after thalidomide treatment of patients with ENL was also reported (41). These authors justified the increasing production of TNF during thalidomide treatment as an indication of immune stimulation. However, thalidomide and prednisolone may have different effect on the TNF. The variation of the results in various studies can be attributed to several factors such as experimental design, sample size, ENL definition, assay sensitivity, and assay methods.

In our study, the mRNA gene expression for TNF in blood and skin biopsies from patients with ENL was significantly upregulated compared to in LL controls before treatment. After treatment, the level of gene expression for TNF in blood and skin biopsy samples from patients with ENL was significantly decreased. Similar findings have been reported by previous studies (5, 21, 22, 38). On the other hand, the absence of any significant difference regarding the gene expression of TNF in the skin biopsies from patients with ENL and LL controls was also reported by Yamamura et al. (6).

Thus, our present kinetic study confirmed that TNF is certainly increased during ENL reactions in the same individual both *in vitro* (following stimulation of the cells with MLWCS) and *in vivo* (increased TNF gene expression *in situ*). TNF is a cell signaling cytokine involved in systemic inflammation and it is one of cytokines that contribute to the acute phase reaction (27). However, excessive production of TNF can cause tissue injury. Hence, our data imply that TNF is involved in the pathogenesis of ENL and it may be of use for the diagnosis of ENL. Investigating the sources of TNF (identifying the major immune cells producing TNF) in the pathogeneses of ENL may also be important to explore alternative therapeutics in the future.

TABLE 4 | Cytokine mRNA expression in skin biopsy samples from patients with erythema nodosum leprosum before and after treatment.

Cytokine	$\Delta\Delta C_T$	FC	*P*-value	Gene expression after treatment
TNF	2.34	0.2	<0.0001*	Decreased
IFN-γ	3.03	0.12	<0.0001*	Decreased
IL-1β	2.39	0.19	0.0005*	Decreased
IL-6	0.31	0.81	0.6451	No change
IL-8	0.16	0.90	0.7617	No change
IL-10	−1.51	2.85	<0.0001*	Increased
IL-17A	1.01	0.5	0.0204*	Decreased
TGF-β	0.09	0.94	0.8337	No change

*Statistical test: paired t-test, α = 0.05. $\Delta\Delta C_T$ = delta delta C_T, FC = fold change, * = significant at α = 0.05.*

IFN-γ

In the present study, the mean production of IFN-γ in response to *M. leprae* antigen stimulation was significantly higher (1361 pg/mL ± 309.6) in the culture supernatants of PBMCs from patients with ENL than from LL patient controls (280.1 pg/mL ± 269.8) before treatment ($P \leq 0.05$). However, IFN-γ production was not significantly different in both groups after treatment of ENL patients. Previous independent studies have also reported an increasing *in vitro* production of IFN-γ in untreated patients with ENL to the response of *M. leprae* stimulation (7, 19, 44). IFN-γ mRNA gene expression in the blood and skin biopsies from patients with ENL was significantly upregulated compared to in LL patient controls before prednisolone treatment. After treatment, the level of IFN-γ gene expression in the blood and skin biopsy samples from patients with ENL was significantly decreased. Similar findings have previously been reported by Iyer et al. (7) and Moraes et al. (20).

It should be noted that although fewer investigations have focused thus far on the role of IFN-γ, in contrast to the weight given to TNF, the results are more consistent and indicate an important role of IFN-γ in the immunopathology and occurrence of ENL. One earlier study has reported that administration of recombinant IFN-γ to patients with LL led to the development of ENL reactions in 60% of the patients over a 6- to 7-month period compared with an incidence of 15% per year with multiple drug therapy alone (45). Previous studies have demonstrated that monocyte/macrophage TNF-α production can be enhanced by the synergistic effect of IFN-γ (46). In addition, IFN-γ priming of peripheral blood monocytes from patients with leprosy has been demonstrated to enhance TNF-α production, both *in vivo* and *in vitro* (45). The mechanism by which IFN-γ induces ENL reactions in patients with leprosy is suggested to be through priming of monocytes, resulting in enhanced TNF production (47). IFN-γ is a major macrophage activator and a known inducer of macrophage TNF. It increases antigen presentation and lysosome activity of macrophages. However, over expression of INF-γ has been associated with the pathogenesis of a number of inflammatory and autoimmune diseases (48). The finding of increased INF-γ gene expression and production in untreated ENL patients in our study underlines the strong association between INF-γ and ENL reaction. Hence, IFN-γ is another candidate cytokine which may help to search for alternative effective drug for ENL treatment.

IL-6

In the present study, we found that the *in vitro* response of IL-6 production was substantially higher in patients with ENL than in LL controls before treatment. IL-6 mRNA gene expression in the blood and skin biopsy samples was also significantly upregulated in patients with ENL than in LL controls. The *in vitro* production and gene expression of this cytokine was decreased after prednisolone treatment of patients with ENL and a significant difference was not observed in the two groups after treatment. However, its gene expression in the skin samples was not appreciably decreased in patients with ENL after prednisolone treatment. This suggests that although the systemic symptoms of ENL subside after treatment, there could be an ongoing immune response locally in the skin lesions which could take a longer time to establish immune homeostasis. Similar findings have been reported by several authors (6, 20, 30, 49). IL-6 is an interleukin that acts as both a pro-inflammatory and an anti-inflammatory cytokine which is secreted by T cells and macrophages (50). It is an important cytokine-mediating fever and the acute phase response through its ability of crossing the blood–brain barrier and initiating the synthesis of prostaglandin E2 in the hypothalamus thereby changing the body's temperature set point (51). Hence, it is sensible to assume that higher levels of IL-6 production could contribute to the development of ENL reactions in non-reactional LL patients mainly owing to the potent pro-inflammatory role of IL-6 and its capacity to stimulate antibody production. The increased production of IL-6 in ENL reactions due to polymorphisms in the genes encoding the cytokine has been suggested (52). Based on the multiple effects of IL-6 on the control of innate and adaptive immune responses, its potential contribution to the immunopathogenesis of ENL reaction needs to be explored further.

IL-8

In this study, higher *in vitro* production of IL-8 to the response of PBMCs stimulation to *M. leprae* was obtained in patients with ENL than in LL controls before, during, and after prednisolone treatment. Unlike the other cytokines studied, IL-8 production did not decrease during and after prednisolone treatment of patients with ENL. The mRNA gene expression of IL-8 both in the blood and skin biopsy samples was also significantly upregulated in patients with ENL before, during, and after prednisolone treatment. Few studies have investigated the role IL-8 from serum in the immunopathogenesis of ENL by comparing its production and gene expression. IL-8 mRNA upregulation in untreated patients with ENL has been previously reported by some authors (6) and its *in vitro* production (31) and both studies are in agreement with our finding.

IL-8 (CXCL8) is a chemokine produced mainly by macrophages and plays a key role in inflammation in neutrophil recruitment and inducer of phagocytosis. Studies have shown that anti-IL-8 treatment prevent neutrophil-dependent tissue damage as well as neutrophil infiltration in several types of acute inflammatory reactions, including lipopolysaccharide (LPS)-induced dermatitis, LPS/IL-1-induced arthritis and acute immune complex-type glomerulonephritis (53).

Thus, the finding of increased IL-8 production as well as IL-8 mRNA gene expression in the blood and skin lesions from patients with ENL suggests a potential role for this chemokine in the pathogenesis of ENL. Hence, exploring the potential role of IL-8 in the immunopathogenesis of ENL may provide valuable information in the diagnosis and treatment of ENL.

IL-17

The *in vitro* production of IL-17A in PBMC samples and IL-17 mRNA gene expression in the blood and skin biopsy samples from patients with ENL was significantly increased before treatment and decreased after prednisolone treatment. IL-17A is the least studied cytokine in ENL reaction. Recently a cross-sectional study has reported that increased IL-17A production to *M. leprae* stimulation in ENL patients compared to non-reactional LL patients (26). One study has reported the upregulation of IL-17A before and after thalidomide treatment of ENL patients (24). However, the effect of thalidomide on IL-17A expression may be different from that of prednisolone. IL-17A is an immunoregulatory cytokine capable of promoting the generation of pro-inflammatory cytokines and chemokines, which leads to the attraction of neutrophils and macrophages to the inflammation site (54). The finding of increased IL-17A production and its mRNA gene expression in patients with ENL in the present study shows the involvement of IL-17A in the pathogenesis of ENL reaction. Hence, understanding the exact role of this cytokine in ENL reaction will benefit the development of novel immune modulators that reduce inflammation and thereby protect tissue damage in patients with ENL.

IL-10

The *in vitro* production of IL-10 in response to *M. leprae* stimulation in the PBMCs of patients with ENL was significantly lower than that in LL controls before treatment. After prednisolone treatment of ENL patients, IL-10 production was significantly increased and it was higher than the value obtained in LL controls. The present result is in agreement with Sampaio et al. (38). Although IL-10 mRNA gene expression in the blood samples before and after treatment in patients with ENL and LL controls did not reveal a statistically significantly different result, the longitudinal comparison in patients with ENL has shown significantly increased IL-10 mRNA gene expression after prednisolone treatment similar to the *in vitro* IL-10 production. On the other hand, unlike the blood samples, the gene expression in skin biopsy samples was significantly decreased before treatment in patients with ENL compared to LL controls and considerably increased after prednisolone treatment. Therefore, it seems that IL-10 regulates excess immune response locally in the skin than systemically in the blood. Variable and inconstant reports have been published on serum or plasma IL-10 production in patients with ENL. Increased IL-10 production in patients with ENL has been reported by some authors (9, 40). Other studies failed to detect any differences in serum IL-10 between patients with ENL and LL controls (7, 25, 43) or in IL-10 mRNA in biopsy skin specimens (22).

IL-10 is a well-known cytokine involved in downregulating macrophage functions. IL-10 has been shown to inhibit cytokine synthesis by monocytes, namely TNF-α, IL-1, IL-6, IL-8, and IL-12 (38). Thus, the finding of decreased IL-10 production as well as IL-10 gene expression in untreated patients with ENL reaction implies the loss of control over these pro-inflammatory cytokines which exacerbates ENL reactions.

In conclusion, the *in vitro* production and gene expression of the cytokines: TNF, IFN-γ, IL-6, IL-8, and IL-17A were significantly increased in untreated patients with ENL at recruitment. However, IL-10 production and gene expression was significantly lower in untreated ENL patients and significantly increased after prednisolone treatment. This is the first study examining the effect of prednisolone on the kinetics of inflammatory cytokines in patients with ENL reactions before and after treatment. Our findings suggest that prednisolone modulates the pro-inflammatory cytokines studied here either directly or through suppressing the immune cells producing these inflammatory cytokines. This needs further confirmation through identification of the immune cells producing these cytokines. Prednisolone is extensively used for treatment of ENL reactions, but clinical improvement varies, and a better understanding of the immunology of ENL is required to improve treatment for these patients. Although the immune response to *M. leprae* is cytokine mediated, the involvement of cytokines in ENL reactions is less understood. Our data clearly suggest that cytokines are involved in ENL reaction, yet the sources of these cytokines are unknown. If prednisolone effectively switch off these inflammatory cytokines, why some ENL patients do not show clinical improvement to prednisolone treatment? Therefore, cytokines may not be the only key players in the pathogenesis of ENL. There could be other factors or modulators other than cytokines which take part in the immunopathogenesis of ENL. These assumptions need to be further investigated and we need to understand how prednisolone works with cytokines which could lead us to better drugs that effectively resolve inflammation more rapidly.

ETHICS STATEMENT

Informed written consent for blood samples were obtained from patients following approval of the study by the Institutional Ethical Committee of London School of Hygiene and Tropical Medicine, UK (#6391), AHRI/ALERT, Ethiopia (P032/12) and the National Research Ethics Review Committee, Ethiopia (#310/450/06). All data have been analyzed and reported anonymously.

AUTHOR CONTRIBUTIONS

EN and DL formulated the study questions. EN, DL, HD, SW, MA, and KB designed the study protocol. EN, BE, AT, YB, and KB conducted the experiment. AA, HD, and DL supervised the study. EN analyzed the data. All authors contributed to the interpretation of the data. EN drafted the manuscript. KB, SW, BE, MA, AT, YB, AA, HD, and DL revised the manuscript. All authors read and approved the final version for publication. All authors agreed to be accountable for all aspects of the work in ensuring that questions related to the accuracy or integrity of any part of the work are appropriately investigated and resolved.

ACKNOWLEDGMENTS

We would like to thank the participants who were volunteer to donate blood sample and gave up their time to participate in this study. We would like to thank in particular, the study nurses Sr. Genet Amare and Sr. Haregewoin, study coordinator Mr. Fikre Mekuria, our tracer, Mr. Yilma Tesfaye, the Red Medical Clinic nurses. This study would have not been possible without the administrative support of Susan Sheedy at LSHTM and the AHRI staff. Mr. Dawit Bogale should receive our sincere thanks for his fast and on time custom clearance of our reagents. Finally, we would like to acknowledge Homes and Hospital of St. Gilles for funding the project and Armauer Hansen Research Institute for allowing us to use all laboratory facilities.

FUNDING

The study was funded by Homes and Hospital of St. Giles, UK.

REFERENCES

1. Ridley DS, Jopling WH. Classification of leprosy according to immmunity: five group system. *Inter J Lepr Other Micobact Dis* (1966) 34(3):355–73.
2. Walker SL, Lebas E, Doni SN, Lockwood DNJ, Lambert SM. The mortality associated with erythema nodosum leprosum in Ethiopia: a retrospective hospital-based study. *PLoS Negl Trop Dis* (2014) 8(3):e2690. doi:10.1371/journal.pntd.0002690
3. Pocaterra L, Jains S, Reddy R, Muzaffarullah S, Torres S, Suneetha S, et al. Clinical course of erythema nodosum leprosum: an 11-year chohort study in Hyderabad, India. *Am J Trop Med Hyg* (2006) 74(5):868–79. doi:10.4269/ajtmh.2006.74.868

4. Lockwood DN, Vinayakumar S, Stanley JN, McAdam KP, Colston MJ. Clinical features and outcome of reversal (type 1) reactions in Hyderabad, India. *Int J Lepr Other Mycobact Dis* (1993) 61(1):8–15.
5. Barnes PF, Chatterjee D, Brennan PJ, Rea TH, Modlin RL. Tumor necrosis factor production in patients with leprosy. *Infect Immun* (1992) 60(4):1441–6.
6. Yamamura M, Wang XH, Ohmen JD, Uyemura K, Rea TH, Bloom BR, et al. Cytokine patterns of immunologically mediated tissue damage. *J Immunol* (1992) 149(4):1470–5.
7. Iyer A, Hatta M, Usman R, Luiten S, Oskam L, Faber W, et al. Serum levels of interferon-g, tumour necrosis factor-a, soluble interleukin-6R and soluble cell activation markers for monitoring response to treatment of leprosy reactions. *Clin Exp Immunol* (2007) 150:210–6. doi:10.1111/j.1365-2249.2007.03485.x
8. Fink S, Finiasz MR, Valdez R, de la Barrera S, Sasiain MC. Evaluation of cytokine production in leprosy patients. *Medicina* (1996) 56(6):705–8.
9. Moubasher AD, Kamel NA, Zedan H, Raheem DD. Cytokines in leprosy, I. Serum cytokine profile in leprosy. *Int J Dermatol* (1998) 37(10):733–40. doi:10.1046/j.1365-4362.1998.00381.x
10. Longley J, Haregewoin A, Yemaneberhan T, Warndorff van Diepen T, Nsibami J, Knowles D, et al. In vivo responses to *Mycobacterium leprae*: antigen presentation, interleukin-2 production, and immune cell phenotypes in naturally occurring leprosy lesions. *Int J Lepr Other Mycobact Dis* (1985) 53(3):385–94.
11. Volc-Platzer B, Stemberger H, Luger T, Radaszkiewicz T, Wiedermann G. Defective intralesional interferon-gamma activity in patients with lepromatous leprosy. *Clin Exp Immunol* (1988) 71(2):235–40.
12. Arnoldi J, Gerdes J, Flad HD. Immunohistologic assessment of cytokine production of infiltrating cells in various forms of leprosy. *Am J Pathol* (1990) 137:749–53.
13. Cote-Sierra J, Foucras G, Guo T, Chiodetti L, Young AH, Hu-Li J, et al. Interleukin 2 plays a central role in Th2 differentiation. *PNAS* (2004) 101(11):3880–5. doi:10.1073/pnas.0400339101
14. Ehlers S. Tumor necrosis factor and its blockade in granulomatous infections: differential modes of action of infliximab and etanercept? *Clin Infect Dis* (2005) 41(Suppl 3):S199–203. doi:10.1086/429998
15. Mohan KH, Pai S, Rao R, Sripathi H, Prabhu S. Thechniques of immunofluorescence and thier siginificance. *Indian J Dermatol Venereol Lepr* (2008) 74(4):415–9. doi:10.4103/0378-6323.42898
16. Misra N, Murtaza A, Walker B, Narayan NP, Misra RS, Ramesh V, et al. Cytokine profile of circulating T cells of leprosy patients reflects both indiscriminate and polarized T-helper subsets: T-helper phenotype is stable and uninfluenced by related antigens of *Mycobacterium leprae*. *Immunology* (1995) 86(1):97–103.
17. Nath I, Vemuri N, Reddi AL, Jain S, Brooks P, Colston MJ, et al. The effect of antigen presenting cells on the cytokine profiles of stable and reactional lepromatous leprosy patients. *Immunol Lett* (2000) 75(1):69–76. doi:10.1016/S0165-2478(00)00271-6
18. Nath I, Saini C, Valluri VL. Immunology of leprosy and diagnostic challenges. *Clin Dermatol* (2015) 33(1):90–8. doi:10.1016/j.clindermatol.2014.07.005
19. Sreenivasan P, Misrat RS, Wilfred D, Nath I. Lepromatous leprosy patients show T helper 1-like cytokine profile with differential expression of interleukin-10 during type 1 and 2 reactions. *Immunology* (1998) 95:529–36. doi:10.1046/j.1365-2567.1998.00634.x
20. Moraes MO, Sarno EN, Teles RMB, Almeida AS, Saraiva BCC, Nery JA, et al. Anti-inflammatory drugs block cytokine mRNA accumulation in the skin and improve the clinical condition of reactional leprosy patients. *J Invest Dermatol* (2000) 115(6):935–41. doi:10.1046/j.1523-1747.2000.00158.x
21. Teles RM, Morae MO, Geraldo NTR, Salles AM, Sarno EN, Sampaio EP. Differential TNFα mRNA regulation detected in the epidermis of leprosy patients. *Arch Dermatol Res* (2002) 294(8):355–62. doi:10.1007/s00403-002-0340-0
22. Moraes MO, Sarno EN, Almeida AS, Saraiva BC, Nery JA, Martins RC, et al. Cytokine mRNA expression in leprosy: a possible role for interferon-gamma and interleukin-12 in reactions (RR and ENL). *Cand J Immunol* (1999) 50(5):541–9. doi:10.1046/j.1365-3083.1999.00622.x
23. Nath I, Vemuri N, Reddi AL, Bharadwaj M, Brooks P, Colston MJ, et al. Dysregulation of IL-4 expression in lepromatous leprosy patients with and without erythema nodosum leprosum. *Lepr Rev* (2000) 71:S130–7. doi:10.5935/0305-7518.20000084
24. Martiniuk F, Giovinazzo J, Tan AU, Shahidullah R, Haslett P, Kaplan G, et al. Lessons of leprosy: the emergence of TH17 cytokines during type II reactions (ENL) is teaching us about T-cell plasticity. *J Drugs Dermatol* (2012) 11(5):626–30.
25. Attia EA, Abdallah M, El-Khateeb E, Saad AA, Lotfi RA, Abdallah M, et al. Serum Th17 cytokines in leprosy: correlation with circulating CD4(+) CD25 (high)FoxP3 (+) T-regs cells, as well as down regulatory cytokines. *Arch Dermatol Res* (2014) 306(9):793–801. doi:10.1007/s00403-014-1486-2
26. Saini C, Siddiqui A, Ramesh V, Nath I. Leprosy reactions show increased Th17 cell activity and reduced FOXP3+ Tregs with concomitant decrease in TGF-β and increase in IL-6. *PLoS Negl Trop Dis* (2016) 10(4):e0004592. doi:10.1371/journal.pntd.0004592
27. Andersson AK, Chaduvula M, Atkinson SE, Khanolkar-Young S, Jain S, Suneetha L, et al. Effects of prednisolone treatment on cytokine expression in patients with leprosy type 1 reactions. *Infect Immun* (2005) 73:725–33. doi:10.1128/iai.73.6.3725-3733.2005
28. Gayo AL, Mozo L, Suarez A, Tunon A, Lahoz C, Gutierrez C. Glucocorticoids increase IL-10 expression in multiple sclerosis patients with acute relapse. *J Neuroimmunol* (1998) 85:122–30. doi:10.1016/S0165-5728(97)00262-2
29. Meduri GU, Tolley EA, Chrousos GP, Stentz F. Prolonged methylprednisolone treatment suppresses systemic inflammation in patients with unresolving acute respiratory distress syndrome: evidence for inadequate endogenous glucocorticoid secretion and inflammation-induced immune cell resistance to glucocorticoids. *Am J Respir Crit Care Med* (2002) 165:983–91. doi:10.1164/ajrccm.165.7.2106014
30. Moraes MO, Sampaio EP, Nery JA, Saraiva BC, Alvarenga FB, Sarno EN. Sequential erythema nodosum leprosum and reversal reaction with similar lesional cytokine mRNA patterns in a borderline leprosy patient. *Br J Dermatol* (2001) 144(1):175–81. doi:10.1046/j.1365-2133.2001.03970.x
31. Goulart IM, Mineo JR, Foss NT. Production of transforming growth factor-beta 1 (TGF-β1) by blood monocytes from patients with different clinical forms of leprosy. *Clin Exp Immunol* (2000) 122(3):330–4. doi:10.1046/j.1365-2249.2000.01376.x
32. Feuth M, Brandsma JW, Faber W, Bharadwaj M, Feuth T, Anderson AM. Erythema nodosum leprosum in Nepal: a retrospective study of clinical features and response to treatement with prednisolone or thalidomide. *Lepr Rev* (2008) 79(3):254–69.
33. Bobosha K, Wilson L, van Meijgaarden KE, Bekele Y, Zewdie M, van der Ploeg- van Schip JJ, et al. T-cell regulation in lepromatous leprosy. *PLoS Negl Trop Dis* (2014) 8(4):e2773. doi:10.1371/journal.pntd.0002773
34. Negera E, Walker SL, Bobosha K, Howe R, Aseffa A, Dockrell HM, et al. T-cell regulation in erythema nodosum leprosum. *PLoS Negl Trop Dis* (2017) 11(10):e0006001. doi:10.1371/journal.pntd.0006001
35. Thompson ML, Kunkel EJ, Ehrhardt RO. Cryopreservation and thawing of mammalian cells. *eLS*. John Wiley & Sons, Ltd (2001). doi:10.1002/9780470015902.a0002561.pub2
36. Cikos S, Bukovska A, Koppel J. Relative quantification of mRNA: comparison of methods currently used for real-time PCR data analysis. *BMC Mol Biol* (2007) 8:113. doi:10.1186/1471-2199-8-113
37. Santos DO, Suffys PN, Bonifácio K, Marques MA, Sarno EN. In vitro tumor necrosis factor production by mononuclear cells from lepromatous leprosy patients and from patients with erythema nodosum leprosum. *Clin Immunol Immunopathol* (1993) 67(3):199–203. doi:10.1006/clin.1993.1065
38. Sampaio EP, Moraes MO, Nery JAC, Santos AR, Matos HC, Sarno EN. Pentoxifylline decreases in vivo and in vitro tumour necrosis factor-alpha (TNF-α) production in lepromatous leprosy patients with erythema nodosum leprosum (ENL). *Clin Exp Immunol* (1998) 111(2):300–8. doi:10.1046/j.1365-2249.1998.00510.x
39. Lockwood DJ, Suneetha L, Sagili KD, Chaduvula MV, Mohammed I, Brakel W, et al. Cytokine and protein markers of leprosy reactions in skin and nerves: baseline results for the North Indian INFIR Cohort. *PLoS Negl Trop Dis* (2011) 5(12):e1327. doi:10.1371/journal.pntd.0001327
40. Madan N, Agrawal K, Chander R. Serum cytokine profile in leprosy and its correlation with clinico-histopathological profile. *Lepr Rev* (2011) 82:371–82.
41. Haslett PA, Roche P, Butlin CR, Macdonald M, Shrestha N, Manandhar R, et al. Effective treatment of erythema nodosum leprosum with thalidomide is associated with immune stimulation. *J Infect Dis* (2005) 192(12):2045–53. doi:10.1086/498216

42. Villahermosa LG, Fajardo TT Jr, Abalos RM, Balagon MV, Tan EV, Cellona RV, et al. A randomized, double-blind, double-dummy, controlled dose comparison of thalidomide for treatment of erythema nodosum leprosum. *Am J Trop Med Hyg* (2005) 72(5):518–26.
43. Stefani M, Guerra JG, Sousa Costa A, Sousa ALM, Costa MB, Oliveira MLW. Potential plasma markers of type 1 and type 2 leprosy reactions: a preliminary report. *BMC Infect Dis* (2009) 9:75. doi:10.1186/1471-2334-9-75
44. Cooper CL, Mueller C, Sinchaisri TA, Pirmez C, Chan J, Kaplan G, et al. Analysis of naturally occurring delayed-type hypersensitivity reactions in leprosy by in situ hybridization. *JEM* (1989) 169(5):1565–81. doi:10.1084/jem.169.5.1565
45. Sampaio EP, Moreira AL, Sarno EN, Malta AM, Kaplan G. Prolonged treatment with recombinant interferon gamma induces erythema nodosum leprosum in lepromatous leprosy patients. *J Exp Med* (1992) 175(6):1729–37. doi:10.1084/jem.175.6.1729
46. Billiau A. Interferon-gamma: biology and role in pathogenesis. *Adv Immunol* (1996) 62:61–130. doi:10.1016/S0065-2776(08)60428-9
47. Sampaio EP, Sarno EN. Expression and cytokine secretion in the states of immune reactivation in leprosy. *Braz J Med Biol Res* (1998) 31:69–76. doi:10.1590/S0100-879X1998000100009
48. Lee Sau K, Silva Diego G, Martin Jaime L, Pratama A, Hu X, Chang P-P, et al. Interferon-γ excess leads to pathogenic accumulation of follicular helper T cells and germinal centers. *Immunity* (2012) 37(5):880–92. doi:10.1016/j.immuni.2012.10.010
49. Wang L, Lin J, Zhou Z, Huo R, Shen B, Sun Y, et al. Up-regulation of Th17 cells may underlie inhibition of Treg development caused by immunization with activated syngeneic T cells. *PLoS One* (2011) 6(11):e27289. doi:10.1371/journal.pone.0027289
50. Scheller J, Chalaris A, Schmidt-Arras D, Rose-John S. The pro- and anti-inflammatory properties of the cytokine interleukin-6. *Biochim Biophys Acta* (2011) 1813(5):878–88. doi:10.1016/j.bbamcr.2011.01.034
51. Banks WA, Kastin AJ, Gutierrez EG. Penetration of interleukin-6 across the murine blood-brain barrier. *Neurosci Lett* (1994) 179(1–2):53–6. doi:10.1016/0304-3940(94)90933-4
52. Sousa AL, Fava VM, Sampaio LH, Martelli CM, Costa MB, Mira MT, et al. Genetic and immunological evidence implicates interleukin 6 as a susceptibility gene for leprosy type 2 reaction. *J Infect Dis* (2012) 205(9):1417–24. doi:10.1093/infdis/jis208
53. Harada A, Sekido N, Akahoshi T, Wada T, Mukaida N, Matsushima K. Essential involvement of interleukin-8 (IL-8) in acute inflammation. *J Leukoc Biol* (1994) 56(5):559–64. doi:10.1002/jlb.56.5.559
54. Jin W, Dong C. IL-17 cytokines in immunity and inflammation. *Emerg Microbes Infect* (2013) 2:e60. doi:10.1038/emi.2013.58

Conflict of Interest Statement: The authors declare that the research was conducted in the absence of any commercial or financial relationships that could be construed as a potential conflict of interest.

Copyright © 2018 Negera, Walker, Bobosha, Bekele, Endale, Tarekegn, Abebe, Aseffa, Dockrell and Lockwood. This is an open-access article distributed under the terms of the Creative Commons Attribution License (CC BY). The use, distribution or reproduction in other forums is permitted, provided the original author(s) and the copyright owner are credited and that the original publication in this journal is cited, in accordance with accepted academic practice. No use, distribution or reproduction is permitted which does not comply with these terms.

frontiers in Immunology

MINI REVIEW
published: 21 February 2018
doi: 10.3389/fimmu.2018.00104

A20/Tumor Necrosis Factor α-Induced Protein 3 in Immune Cells Controls Development of Autoinflammation and Autoimmunity: Lessons from Mouse Models

*Tridib Das, Zhongli Chen, Rudi W. Hendriks and Mirjam Kool**

Department of Pulmonary Medicine, Erasmus MC, Rotterdam, Netherlands

Immune cell activation is a stringently regulated process, as exaggerated innate and adaptive immune responses can lead to autoinflammatory and autoimmune diseases. Perhaps the best-characterized molecular pathway promoting cell activation is the nuclear factor-κB (NF-κB) signaling pathway. Stimulation of this pathway leads to transcription of numerous pro-inflammatory and cell-survival genes. Several mechanisms tightly control NF-κB activity, including the key regulatory zinc finger (de)ubiquitinating enzyme A20/tumor necrosis factor α-induced protein 3 (TNFAIP3). Single nucleotide polymorphisms (SNPs) in the vicinity of the *TNFAIP3* gene are associated with a spectrum of chronic systemic inflammatory diseases, indicative of its clinical relevance. Mice harboring targeted cell-specific deletions of the *Tnfaip3* gene in innate immune cells such as macrophages spontaneously develop autoinflammatory disease. When immune cells involved in the adaptive immune response, such as dendritic cells or B-cells, are targeted for A20/TNFAIP3 deletion, mice develop spontaneous inflammation that resembles human autoimmune disease. Therefore, more knowledge on A20/TNFAIP3 function in cells of the immune system is beneficial in our understanding of autoinflammation and autoimmunity. Using the aforementioned mouse models, novel A20/TNFAIP3 functions have recently been described including control of necroptosis and inflammasome activity. In this review, we discuss the function of the A20/TNFAIP3 enzyme and its critical role in various innate and adaptive immune cells. Finally, we discuss the latest findings on *TNFAIP3* SNPs in human autoinflammatory and autoimmune diseases and address that genotyping of *TNFAIP3* SNPs may guide treatment decisions.

Keywords: A20, tumor necrosis factor α-induced protein 3, NF-κB, ubiquitination, autoinflammation, autoimmune disease, mouse models, single nucleotide polymorphisms

OPEN ACCESS

Edited by:
Massimo Gadina,
National Institute of Arthritis and Musculoskeletal and Skin Diseases, United States

Reviewed by:
Michael Francis McDermott, University of Leeds, United Kingdom
Ivona Aksentijevich, National Human Genome Research Institute (NIH), United States

***Correspondence:**
Mirjam Kool
m.kool@erasmusmc.nl

Specialty section:
This article was submitted to Inflammation, a section of the journal Frontiers in Immunology

Received: *03 November 2017*
Accepted: *12 January 2018*
Published: *21 February 2018*

Citation:
Das T, Chen Z, Hendriks RW and Kool M (2018) A20/Tumor Necrosis Factor α-Induced Protein 3 in Immune Cells Controls Development of Autoinflammation and Autoimmunity: Lessons from Mouse Models. Front. Immunol. 9:104. doi: 10.3389/fimmu.2018.00104

INTRODUCTION

Autoinflammatory and autoimmune diseases share a spectrum of chronic immune system disorders (1). Autoinflammatory diseases are rare and occur due to innate immune cell dysfunction with increased cytokines such as interleukin (IL)-1β and tumor necrosis factor (TNF) α (2, 3). In contrast, autoimmune diseases are caused by adaptive immune cell dysfunction and affect millions of people

worldwide (4). Self-reactive T-cells and/or autoreactive antibodies facilitate responses against harmless tissue (5). Essential for development of these diseases is the activation status of immune cells, wherein nuclear factor-κB (NF-κB) plays a key role. NF-κB activation is tightly controlled by several mechanisms, including the key regulatory (de)ubiquitinating enzyme A20 or tumor necrosis factor α-induced protein 3 (TNFAIP3) (6). Genetic studies have demonstrated the association of *TNFAIP3* single nucleotide polymorphisms (SNPs) with multiple human diseases (7), such as systemic lupus erythematosus (SLE) (8–10), rheumatoid arthritis (RA) (9), and Crohn's disease (CD) (11, 12). A20/TNFAIP3 regulates crucial stages in immune cell homeostasis, such as NF-κB activation and apoptosis. Recently, new functions have become apparent, including the control of necroptosis and inflammasome activity (13–15). Here, we review the latest understanding of A20/TNFAIP3 as a key regulator of immune signaling and its cell-specific role in the pathogenesis of autoinflammation and autoimmunity as demonstrated in murine models.

NF-κB PATHWAY

NF-κB Activation

An important and well-characterized signaling pathway of immune cell activation is the NF-κB pathway (7), which is activated through canonical or non-canonical cascades (16). The canonical pathway is triggered by several pattern recognition receptors (PRRs), such as toll-like receptors (TLRs) and nucleotide oligomerization domain (NOD)-like receptors (NLRs) and cytokine receptors, such as TNF receptor (TNFR) and IL-1 receptor (16). PRRs are essential within the innate immune response in defense against invading pathogens. In addition, T-cell receptor (TCR) or B-cell receptor (BCR) triggering, crucial in the adaptive immune response, also leads to NF-κB activation (17). In total, five NF-κB family members have been identified thus far, termed p65 (RelA), RelB, c-Rel, NF-κB1, and NF-κB2 (18). These five members can form homo- or heterodimers and distinctive NF-κB dimers bind different DNA-binding sites, resulting in cytokine release, enhanced cell survival, proliferation, differentiation, and changes in metabolism (18, 19).

Regulation of NF-κB Activity

Several regulatory mechanisms control NF-κB signaling to maintain tissue homeostasis. One of the proteins that terminate NF-κB signaling is A20/TNFAIP3 (6). A20/TNFAIP3 regulates protein ubiquitination, an important post-translational modification (6). Ubiquitination is reversible and tightly controlled by opposing actions of ubiquitin ligases and deubiquitinases (DUBs) (20). Several ubiquitin chains are known, each having specific functions. Lysine (K)48-linked polyubiquitin chains target a protein for proteasomal degradation, whereas K63-linked or linear polyubiquitin chains stabilize protein–protein interactions important for downstream signaling molecules (16). Interestingly, A20/TNFAIP3 has both ligase and DUB activity to perform both K48 ubiquitination and K63 deubiquitination (6).

A20/TNFAIP3

A20/TNFAIP3 Protein Structure

In 1990, A20/TNFAIP3 was identified as a primary response gene after TNFα exposure in endothelial cells (21, 22). The structure of A20/TNFAIP3 reveals its dual function (**Figure 1A**). First, the N-terminal OTU domain houses the C103 catalytic cysteine site, responsible for K63 deubiquitination (6, 23). Second, the C-terminal ZnF4 domain adds K48 ubiquitin to target proteins for degradation (6). Both domains cooperate to inhibit NF-κB signaling (24). Finally, A20/TNFAIP3 ZnF7 binds linear polyubiquitin, which aids to suppress NF-κB activation (25, 26). To achieve adequate function, A20/TNFAIP3 must bind either target or accessory proteins. The OTU domain binds the target protein TNFR-associated factors (TRAF), while the C-terminus binds accessory molecules such as A20-binding protein (ABIN1 and ABIN2), Tax1 Binding Protein 1 (TAX1BP1) and NF-κB essential modulator (NEMO) (27). These accessory molecules function as adaptor proteins and localize A20/TNFAIP3 near polyubiquitin chains (28–31) [reviewed in Ref. (27, 32)].

Function of A20/TNFAIP3 in the TNFR Signaling Pathway

The multiple functions of A20/TNFAIP3 in NF-κB regulation are most apparent in the TNFR signaling pathway (**Figure 1B**). Briefly, TNFα binding to TNFR recruits receptor-interacting serine/threonine-protein kinase 1 (RIP1) and TRAF2/TRAF5 to shape the TNFR complex (33, 34). RIP1 is K63 polyubiquitinated by ubiquitin-conjugating enzyme (Ubc)13 and cellular inhibitor of apoptosis protein (cIAP)1/2. RIP1–polyubiquitin is a scaffold to recruit NEMO and transforming growth factor beta-activated kinase 1 (TAK1)-TAB2/3 complex (27). The linear ubiquitin chain assembly complex (LUBAC) produces linear polyubiquitin on NEMO, recruiting and stabilizing another IκB kinase (IKK)-NEMO complex (35, 36) (**Figure 1B**). TAK1 phosphorylates and activates IKK, containing IKK2, that finally phosphorylates IκB (37, 38). Phosphorylated IκB will be K48 polyubiquitinated and degraded (19), thereby releasing NF-κB (16) leading to its nuclear translocation.

To terminate NF-κB activation, A20/TNFAIP3 removes K63–polyubiquitin chains from RIP1 and NEMO (**Figure 1B**), thereby disrupting interactions with downstream proteins (6, 30). Furthermore, A20/TNFAIP3 adds K48 polyubiquitin chains to RIP1 and Ubc13, leading to their degradation (6, 39). A20/TNFAIP3 also destabilizes Ubc13 interaction with cIAP1/2 to prevent new K63-ubiquitinating activity (40). Finally, the ZnF7 domain of A20/TNFAIP3 binds linear ubiquitin, resulting in dissociation of LUBAC and IKK/NEMO (25, 35) and thus inhibits IKK phosphorylation (41).

Regulation of A20/TNFAIP3 Expression and Function

A20/TNFAIP3's expression and function are controlled at several levels, e.g., transcriptional, post-transcriptional, and post-translational. During steady state, A20/TNFAIP3 is minimally present in several cell types (27) due to repression by downstream

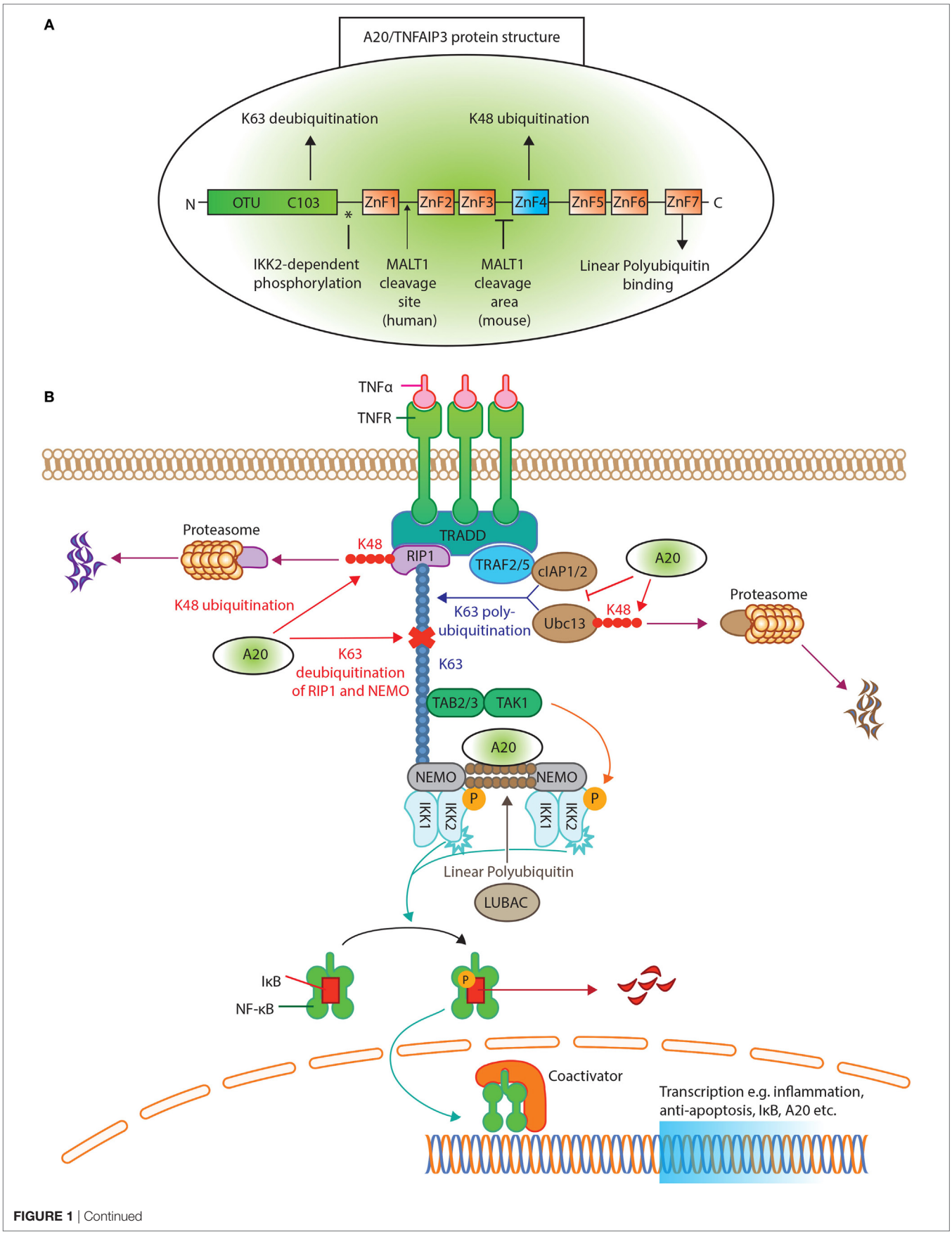

FIGURE 1 | Continued

FIGURE 1 | A20/tumor necrosis factor α-induced protein 3 (TNFAIP3) protein structure and function in tumor necrosis factor receptor (TNFR) induced NK-κB inhibition. **(A)** The protein structure of A20/TNFAIP3. The N-terminus contains the ovarian tumor (OTU) domain, with the C103 cysteine site of K63 deubiquitination. The seven zinc fingers (ZnF) are illustrated, where ZnF4 has K48-ubiquitinating activity and ZnF7 can bind linear polyubiquitin. The asterisk (*) indicates the site of IκB kinase (IKK)2-dependent phosphorylation. An arrow indicates where MALT1 cleaves human A20/TNFAIP3 (after Arginine 439), while for murine A20/TNFAIP3 it is only known that MALT1 cleaves A20/TNFAIP3 between ZnF3 and ZnF4. **(B)** TNFR activation of the NF-κB pathway. Ligand TNFα binds the TNFR receptor and allows binding of TNFR1-associated death domain protein to the TNFR. This recruits receptor-interacting serine/threonine-protein kinase 1 (RIP1) and TNFR-associated factor (TRAF)2 or TRAF5 to form the TNFR complex. RIP1 is K63 polyubiquitinated by E2-E3 ubiquitin-conjugating enzyme (Ubc)13 and cellular inhibitor of apoptosis protein (cIAP)1/2. The polyubiquitin acts as a scaffold for TAB2/TAB3 and NF-kappa-B essential modulator (NEMO) to recruit the transforming growth factor beta-activated kinase 1 (TAK1)-TAB 2/3 complex. TAK1 phosphorylates and activates the IKK, composed of IKK1(α), IKK2(β), and NEMO. The linear ubiquitin chain assembly complex (LUBAC) was shown to generate linear polyubiquitin on NEMO (and also RIP1), recruiting and stabilizing another IKK–NEMO complex. IKK2, phosphorylates IκB, allowing IκB K48 polyubiquitination and consequently degrading by proteasomes, thereby releasing NF-κB to translocate to the nucleus. A20/TNFAIP3 acts in different levels of the pathway. A20/TNFAIP3 removes K63-linked polyubiquitin chains from RIP1 and NEMO, thereby disrupting downstream signals. In addition, A20/TNFAIP3 adds K48-linked polyubiquitin chains to RIP1 and Ubc13, thus targeting them for proteasomal destruction. Beyond (de) ubiquitinating mechanisms, A20/TNFAIP3 also destabilizes Ubc13 interaction with cIAP1/2, thereby preventing new K63-ubiquitinating activity. The ZnF7 of A20/TNFAIP3 binds linear ubiquitin, thereby accelerating the dissociation of LUBAC and IKK/NEMO, resulting in NF-κB termination.

regulatory element antagonist modulator (DREAM) (42). Transcriptional activation of the *TNFAIP3* gene is facilitated by two NF-κB binding sites in the *TNFAIP3* promoter (43). *TNFAIP3* promotor activity is also controlled by regulators of cell-intrinsic energy homeostasis such as estrogen-related receptor α (ERRα) (44), linking energy homeostasis to cell activation. The stability of the *TNFAIP3* transcript is regulated by mRNA-binding proteins [e.g., ROQUIN (*Rc3h1*) (45)] and micro-(mi)RNAs, such as miR-125b, miR-19b, and miR-29c (46–48). Interestingly, one of the downstream targets of NF-κB is miR-125b, which thereby prolongs NF-κB activity (47). ROQUIN destabilizes *TNFAIP3* mRNA, leading to lower A20/TNFAIP3 protein expression (45), and mutated ROQUIN is known to induce autoimmunity in mice (49). Post-translationally, A20/TNFAIP3 protein function is improved by IKK2-dependent phosphorylation (50) (**Figure 1A**), which enhances K63 deubiquitination and K48 ubiquitination (51). Also, cell-extrinsic factors control A20/TNFAIP3 protein stability, e.g., high glucose levels target A20/TNFAIP3 for proteasomal degradation and/or reactive oxygen species (ROS) inactivate its deubiquitinating activity (52–54). Especially, the latter is important in RA, in which elevated ROS plays a pathogenic role (55, 56), possibly by inhibiting A20/TNFAIP3 function. Finally, unlike most cell types, resting T-cells constitutively express high levels of A20/TNFAIP3 protein (57), which is degraded after activation by paracaspase MALT1 to facilitate NF-κB translocation (58) (**Figure 1A**).

IMMUNE CELL-SPECIFIC DELETION OF A20/*Tnfaip3* IN MICE

A20/TNFAIP3 is critical in inflammation regulation, as mice with germ-line A20/*Tnfaip3*-deletion developed severe multi-organ inflammation and cachexia, resulting in early death (59). Conditional A20/*Tnfaip3*-floxed alleles enabled lineage-specific *Tnfaip3*-deletion and study of cell-specific contributions to autoinflammation and autoimmunity (60).

A20/TNFAIP3 Function in Myeloid Cells

To evaluate the role of A20/TNFAIP3 in myeloid cells, $Tnfaip3^{fl/fl}$ mice were crossed with lysozyme M (LysM)-cre Tg mice (61), generating $Tnfaip3^{LysM}$ mice (13, 60, 62, 63). The LysM-cre promoter is expressed in ~95–99% of macrophages and neutrophils and ~15% of splenic dendritic cells (DCs) (61). $Tnfaip3^{LysM\text{-}KO}$ mice developed enthesitis (62) and paw inflammation (63). While hallmarks of RA comprising increased Th17-cells and serum anti-collagen type II antibodies (anti-CII) were present in $Tnfaip3^{LysM\text{-}KO}$ mice, T and B cells were dispensable for paw inflammation (63). Rather, paw inflammation in $Tnfaip3^{LysM\text{-}KO}$ mice depended on IL-1β (13), suggestive of an autoinflammatory disease such as Still's disease or juvenile idiopathic arthritis. *In vitro* cultured *Tnfaip3*-deficient macrophages produced increased amounts of IL-1β, IL-6, IL-18, and TNFα compared to control macrophages (13, 63). IL-1β and IL-18 release is regulated by the NLRP3 inflammasome (64), which is pathogenic in autoinflammatory diseases such as Cryopyrin-associated autoinflammatory syndrome (CAPS) (3, 65). A20/TNFAIP3 directly controls the activity of the NLRP3 inflammasome in macrophages (13, 66).

Next, interferon (IFN)γ or IL-6-induced JAK-STAT signaling is implicated in autoinflammatory diseases (3), which is also regulated by A20/TNFAIP3 (62). *Tnfaip3*-deficient macrophages had elevated STAT1-dependent gene transcription, leading to enhanced chemokine (C–X–C motif) ligand (CXCL)9 and CXCL10 production (62). Pharmacologic JAK-STAT inhibition by tofacitinib in $Tnfaip3^{LysM\text{-}KO}$ mice resulted in reduced enthesitis (62), which is a treatment option for several autoinflammatory diseases (3).

In short, in macrophages, A20/TNFAIP3 regulates IL-1β/IL-18 release by controlling NLRP3 inflammasome activity and CXCL9/CXCL10 production through STAT1 signaling. Both pathways are essential in controlling the autoinflammatory arthritis phenotype. However, a role for neutrophils and/or DCs in the pathogenesis of arthritis cannot be excluded.

Function of A20/TNFAIP3 in DCs

DCs play a crucial role in immune homeostasis and arise in two main subsets, comprising conventional DCs type 1 or 2 (cDC1s, cDC2s) and plasmacytoid DCs (pDCs) (67). When activated, cDCs induce antigen-specific adaptive immune responses and pDCs control anti-viral responses (67). During inflammation, monocyte-derived DCs (moDCs) are recruited to inflammatory sites (68). To characterize A20/TNFAIP3 function in DCs *in vivo*, CD11c-cre-mediated (69) targeting was used in mice (70–72). $Tnfaip3^{CD11c\text{-}KO}$

mice had perturbed splenic DC homeostasis as cDC1s, cDC2s, and pDCs were drastically reduced, while moDCs were increased (71). *In vivo* loss of cDCs and pDCs in *Tnfaip3*$^{CD11c\text{-}KO}$ mice suggested that A20/TNFAIP3 supports their survival. However, *in vitro* generated granulocyte-macrophage colony-stimulating factor (GM-CSF) bone marrow-derived *Tnfaip3*-deficient DCs were more resistant to apoptosis due to upregulated anti-apoptotic molecules (71). This discrepancy might be caused by contaminating macrophages in GM-CSF cultures (73). GM-CSF-cultured DCs from *Tnfaip3*$^{CD11c\text{-}KO}$ mice exhibited an activated phenotype, shown by increased co-stimulatory molecules (e.g., CD80/CD86) and cytokine expression of IL-6, TNFα (70, 71), IL-1β, and IL-10 (71). In the pathogenesis of SLE, pDCs are pathogenic by secreting type I interferons (74), but increased type I interferon by activated pDCs was observed only *in vitro* (70).

To maintain peripheral tolerance, antigens derived from apoptotic cells are normally not presented in an immunogenic manner to T-cells (75). Strikingly, *in vitro Tnfaip3*-deficient DCs present these antigens to T-cells and induce T-cell activation (71) leading to a break of tolerance. *In vitro* apoptotic cell-pulsed DCs produce T-cell differentiating cytokines IL-12 and IL-23, leading to increased Th1-cell and Th17-cell differentiation, respectively, in *Tnfaip3*$^{CD11c\text{-}KO}$ mice (70, 71, 76). Surprisingly, three independent studies with *Tnfaip3*$^{CD11c\text{-}KO}$ mice generated different spontaneous phenotypes, i.e., inflammatory bowel disease (IBD) (70), systemic autoimmunity resembling SLE (71), and multiorgan inflammation (72). Serum IL-6 was elevated in mice developing SLE or IBD (70, 71), while both TNFα and IFNγ were significantly increased in mice with multiorgan inflammation (72). As IL-6 depletion ameliorated murine colitis and SLE development (77–80), IL-6 might directly have contributed to IBD and SLE development in *Tnfaip3*$^{CD11c\text{-}KO}$ mice. While CD is recently considered an autoinflammatory disease (81), T-cells were essential for colitis development in *Tnfaip3*$^{CD11c\text{-}KO}$ mice (70). SLE patients have increased anti-dsDNA autoantibodies (82), which were also observed in *Tnfaip3*$^{CD11c\text{-}KO}$ mice (71). The diversity of phenotypes observed in *Tnfaip3*$^{CD11c\text{-}KO}$ mice might be due to environmental differences, such as microbiota (70, 83), as antibiotics reduced IBD in *Tnfaip3*$^{CD11c\text{-}KO}$ mice (76).

Summarizing, the expression of co-stimulatory molecules, pro-inflammatory cytokines such as IL-6, and anti-apoptotic proteins in DCs is controlled by A20/TNFAIP3. A20/TNFAIP3 in DCs functions to maintain *in vivo* T-cell and B-cell homeostasis, thereby preventing spontaneous autoinflammation.

A20/TNFAIP3 Functions in T-Cells

A20/TNFAIP3 is known to regulate TCR/CD28-mediated NF-κB activation and TCR-mediated survival (84–86) and is highly expressed in naïve T-cells (57). A20/TNFAIP3's influence on T-cell homeostasis has been examined using mature T cell (maT)-cre and *Cd4*-cre mice, targeting both CD8$^+$ T-cells and CD4$^+$ T-cells (14, 15, 87). *Tnfaip3*-deletion efficiency differs between *Tnfaip3*^{maT} and *Tnfaip3*^{CD4} mice. In *Tnfaip3*$^{maT\text{-}KO}$ mice, ~80% of CD8$^+$ T-cells and ~30% of CD4$^+$ T-cells are affected (88), whereas in *Tnfaip3*$^{CD4\text{-}KO}$ mice, ~100% of both CD8$^+$ and CD4$^+$ T-cells are targeted (89). Targeted T-cells from both mouse strains showed an activated phenotype (14, 87), but only *Tnfaip3*$^{maT\text{-}KO}$ mice developed inflammatory lung and liver infiltrates with increased proportions of CD8$^+$ T-cells (87). TCR-stimulated CD8$^+$ T-cells from *Tnfaip3*$^{maT\text{-}KO}$ mice had enhanced IL-2 and IFNγ production *in vitro* which correlated with *in vivo* increased serum IFNγ (87). Serum TNFα and IL-17 were also elevated in *Tnfaip3*$^{maT\text{-}KO}$ mice (87). Since both IFNγ and TNFα are hepatotoxic factors (90–92), these cytokines likely mediated liver inflammation.

Differences in T-cell-specific *Tnfaip3* deletion between the two mouse strains could indicate that either CD8$^+$ T-cells drive inflammation in *Tnfaip3*$^{maT\text{-}KO}$ mice or CD4$^+$ T-cells have increased regulatory function in *Tnfaip3*$^{CD4\text{-}KO}$ mice. Indeed, regulatory T cell (Treg) proportions were increased in *Tnfaip3*$^{CD4\text{-}KO}$ mice, because of a reduced IL-2 dependence for their development (93). *In vitro* activated CD4$^+$ T-cells from *Tnfaip3*$^{CD4\text{-}KO}$ mice died quicker than wild-type T-cells (14, 15), due to A20/TNFAIP3's control on necroptosis (14) and autophagy (15). Necroptosis is RIPK3-dependent programmed cell death (94). Increased necroptosis in A20/*Tnfaip3*-deficient CD4$^+$ T-cells impaired Th1 and Th17-cell differentiation *in vitro* (14). Interestingly, perinatal death of *Tnfaip3*^{KO} mice was greatly delayed by RIPK3 deficiency, implying that A20/TNFAIP3 may control necroptosis in other cell types (14), such as CD8$^+$ T-cells (95). Preventing necroptosis did not fully restore survival of A20/*Tnfaip3*-deficient CD4$^+$ T-cells (14), which could be attributed to autophagy, a lysosomal degradation pathway necessary for survival after TCR stimulation (96). Autophagy is regulated by mechanistic target of rapamycin (mTOR), which is increased in *Tnfaip3*-deficient CD4$^+$ T-cells after TCR stimulation (15). Consequently, treatment with an mTOR inhibitor improves survival by enhancing autophagy (15). mTOR inhibitors are effective in murine SLE and RA (97), but should not be used in patients with A20/TNFAIP3 alterations, as it may improve pathogenic T-cell survival.

In conclusion, in CD4$^+$ T-cells, A20/TNFAIP3 regulates necroptosis and autophagy. In contrast to conventional Th-cells, Treg development is restricted by A20/TNFAIP3. In CD8$^+$ T-cells, A20/TNFAIP3 regulates necroptosis, IL-2, and IFNγ release, of which IFNγ might have contributed to a further undefined lung and liver inflammatory phenotype in *Tnfaip3*$^{maT\text{-}KO}$ mice.

A20/TNFAIP3 Function in B-Cells

B-cell homeostasis demands proper integration of TLR, BCR, and CD40-derived signals, all leading to NF-κB activation and controlled by A20/TNFAIP3 (98, 99). Using CD19-cre-driven *Tnfaip3*-ablation in mice (100–102), B-cell-specific function of A20/TNFAIP3 was examined. *In vitro* activated *Tnfaip3*-deficient B-cells exhibited exaggerated activation as assessed by CD80 and CD95 expression (101, 102) and IL-6 production (100, 102). B-cell numbers in *Tnfaip3*$^{CD19\text{-}KO}$ mice are increased in secondary lymphoid organs (100–102), most likely due to increased anti-apoptotic protein B-cell lymphoma-extra large (Bcl-x) expression (102). Already in 6-week-old *Tnfaip3*$^{CD19\text{-}KO}$ mice, elevated numbers of germinal center B-cells and plasma cells in spleen and peripheral lymph nodes were observed (100–102). *Tnfaip3*$^{CD19\text{-}KO}$ mice developed autoreactive immunoglobulins, including anti-dsDNA antibodies (100–102) and glomerular immunoglobulin deposits (102), features also observed in SLE patients. Surprisingly, no malignancies developed in

Tnfaip3$^{CD19\text{-}KO}$ mice (100, 102), which might have been expected as A20/TNFAIP3 also functions as a tumor suppressor gene in B-cell lymphomas (103–105).

Summarizing, A20/TNFAIP3 in B-cells controls co-stimulatory molecule expression, IL-6 production, and Bcl-x survival protein expression, thereby preventing autoreactive B-cells formation resulting in an autoimmune SLE phenotype.

A20/TNFAIP3 IN AUTOINFLAMMATORY AND AUTOIMMUNE PATIENTS

TNFAIP3 is one of the few genes that has been linked by genome-wide association studies (GWAS) to multiple immune diseases (106, 107). The list of common coding and non-coding variants (SNPs) in the vicinity of the *TNFAIP3* gene region associated with autoimmune conditions keeps expanding, with recently reported associations with autoimmune hepatitis (AIH) (108, 109), primary biliary cirrhosis (110) and colitis ulcerosa (111). Since a comprehensive overview of SNPs within and around the *TNFAIP3* gene has been provided elsewhere (7), we focus on a selection of SNPs with known different functional, clinical, and therapeutical consequences (**Figure 2**). We also discuss a recently described monogenic disease "Haplo-insufficiency of A20 (HA20)" (112), which clearly illustrates the importance of functional A20/TNFAIP3 protein expression levels (**Figure 2**).

TNFAIP3 SNPs and Novel Mutations Affecting A20/TNFAIP3 Expression and Function

Reduced *TNFAIP3* mRNA expression was observed in peripheral blood mononuclear cells (PBMCs) in SLE and RA patients (115–117) and in disease-affected organs, e.g., in colon or skin biopsies from CD and psoriasis patients compared to healthy tissues (118–120). In RA synovium, reduced A20/TNFAIP3 protein expression was detected compared to non-autoimmune osteoarthritic synovium (121). SNPs near the *TNFAIP3* gene can result in reduced A20/*TNFAIP3* mRNA expression and consequently protein concentrations. For instance, specific SNPs associated with SLE ("TT>A", **Figure 2H**) are situated in an enhancer region of the *TNFAIP3* gene and hamper DNA looping, resulting in reduced *TNFAIP3* mRNA expression (122) and reduced A20/TNFAIP3 protein expression in B-cells (8).

Recently, novel rare familial *TNFAIP3* mutations (**Figures 2B,G**) causing HA20 have been described (112). These mutations lead to severely reduced functional A20/TNFAIP3 protein expression (112, 123). HA20 is a dominantly inherited disease caused by high-penetrance heterozygous germ line (mostly nonsense or frameshift) mutations in *TNFAIP3* (112). Previously, A20/TNFAIP3 loss-of-function mutations were only identified as somatic variants in lymphomas (105) [reviewed in Ref. (124)]. HA20-associated mutations were first reported in seven unrelated families with an early-onset inflammatory disease resembling the common polygenic Behçet disease (112). Some patients diagnosed with Behçet-like disease were found to have similar HA20 mutations (125, 126). Recently, in a Japanese cohort the majority (59%) of HA20 patients did not fulfill the criteria of Behçet disease (127). In this study, a genotype–phenotype correlation was not observed (127). However, careful evaluation of clinical characteristics can aid diagnosing patients with HA20 or Behçet disease (128). Autoimmune diseases such as autoimmune lymphoproliferative syndrome (ALPS) and SLE were additionally recognized in HA20 patients (113, 123, 127). Excess Th17-cell differentiation was also observed in HA20 patients (127). All HA20 patients identified thus far have a strong inflammatory signature as demonstrated by elevated levels of many pro-inflammatory cytokines (e.g., IL-1β, IL-6, TNFα, IL-17, and IFNγ) and most patients respond to treatment with cytokine inhibitors (anti-TNF and anti-IL-1) (112, 127, 128). Interestingly, *Tnfaip3*$^{+/-}$ mice do not have an overt inflammatory phenotype despite elevated inflammatory cytokines (e.g., IL-1β and IL-6) in serum (129) and brain (130). Nevertheless, *Tnfaip3*$^{+/-}$ mice are more susceptible to experimental psoriasis (120) and atherosclerosis (129), but these specific symptoms are not commonly reported for HA20. Increased NLRP3 activity was detected in PBMCs of HA20 patients after LPS stimulation, leading to elevated IL-1β (112). Transfection of mutant-truncated A20/TNFAIP3 prolonged NF-κB activation due to reduced deubiquitinating function (112) (**Figure 2B**). PBMCs of a patient with HA20 also demonstrated prolonged NF-κB activation (112, 123). Mutant-truncated A20/TNFAIP3 proteins do not exert a dominant-negative effect on protein function, and this indicates that sustained NF-κB activation in HA20 is due to haploinsufficiency rather than an aberrant protein function (112). It remains unclear whether missense high penetrance mutations may have a different impact on A20/TNFAIP3 function.

Two SNPs, rs5029941 (A125V) and rs2230926 (F127C), are located in close proximity of each other near the C103 catalytic site in the OTU domain and result in non-synonymous coding changes in the A20/TNFAIP3 protein (**Figures 2D,E**). The rs2230926 (F127C) SNP, associated with multiple autoimmune diseases (**Figure 2E**), hampers A20/TNFAIP3 function after TNFα stimulation (10). The SNP location within the OTU domain (**Figure 2E**) suggests that the K63-deubiquitinating efficacy is decreased, although this was not evaluated. The A125V mutation (**Figure 2D**) results in reduced DUB activity and was shown to impair A20-mediated degradation and deubiquitination of TRAF2 (131). Although the A125V mutation was associated with protection from SLE, surprisingly the same allele was associated with increased risk of IBD (131).

In conclusion, specific SNPs functionally alter A20/TNFAIP3 expression or function, and HA20 is a disease with generalized inflammation due to severely reduced functional A20/TNFAIP3 protein expression.

TNFAIP3 SNPs Affecting Disease Progression and Treatment in Patients

Common, presumably hypomorphic, variants in *TNFAIP3* can have clinical consequences. For instance, lower *TNFAIP3* mRNA expression in PBMCs correlates with SLE disease activity as susceptibility to lupus nephritis is increased (115). SLE or SSc patients with an intron SNP (**Figure 2C**) predisposes for increased risk for either renal involvement (132) or aggravated

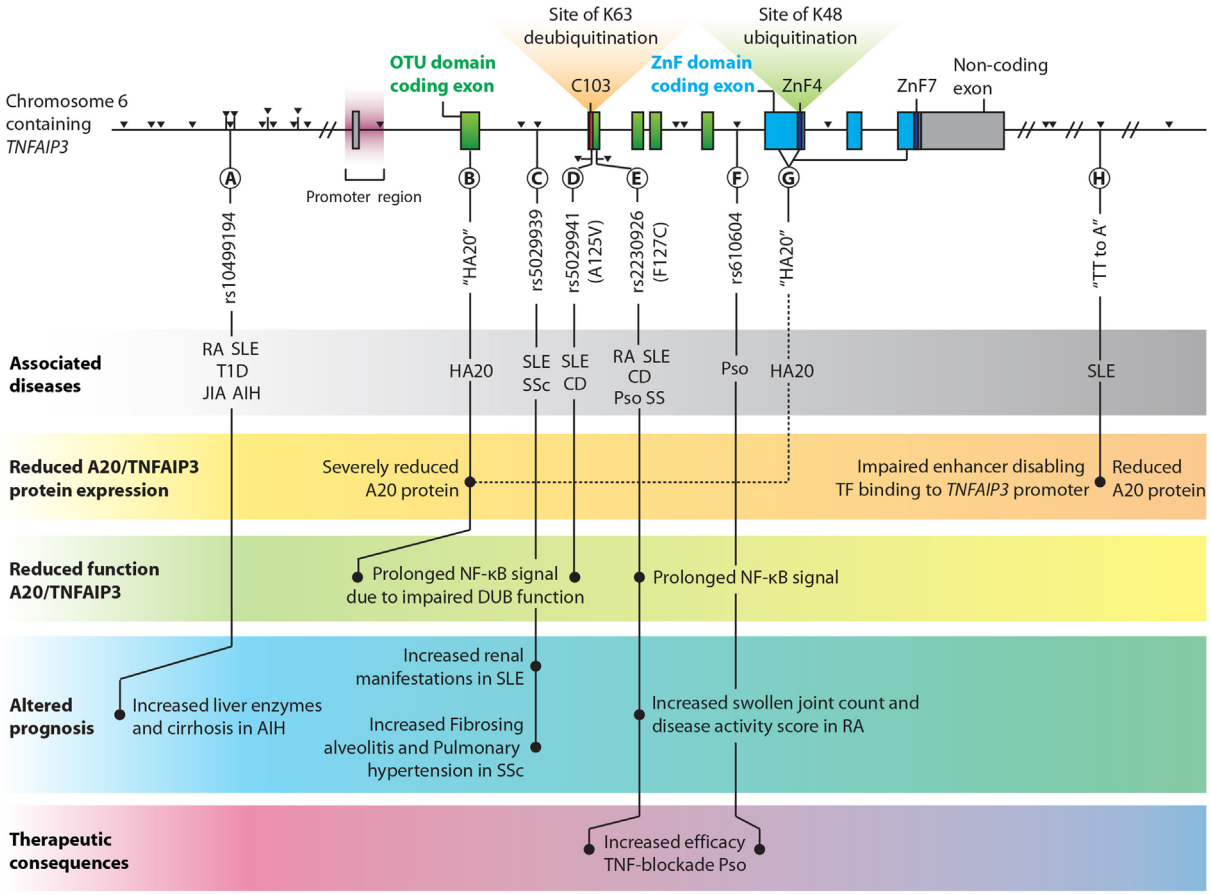

Novel mutations causing HA20				"TT to A"
Mutation	**Location**	**Mutation**	**Location**	
p.Arg45*	OTU	p.Gln415fs	ZnF1	rs148314165
p.Trp85Glyfs*11	OTU	p.Lys417Serfs*4	Between ZnF1-ZnF2	rs200820567
p.Leu227*	OTU	p.Asn449Thrfs*28	Between ZnF1-ZnF2	
p.Phe224Serfs*4	OTU	p.V489Afs*7	ZnF2	
p.Cys243Tyr	OTU	p.Ala588Valfs*80	Between ZnF3-ZnF4	
p.Arg271*	OTU	p.Thr604Argfs*93	ZnF4	
p.Tyr306*	OTU	p.His636Glufs*55	ZnF4	
p.Pro268Leufs*19	OTU	p.Phe637Glu*2	Between ZnF4-ZnF5	
		p.Gln737Serfs*79	ZnF6	

FIGURE 2 | Overview of single nucleotide polymorphisms (SNPs) and novel haplo-insufficiency of A20 (HA20) mutations in the proximity of *TNFAIP3* which are highlighted in this review. *TNFAIP3* gene SNPs, adapted with permission from: Springer Nature, Nature Reviews Immunology, A. Ma & B.A. Malynn © 2012 (7). Exons contributing to the OTU domain are depicted in green, and exons forming the zinc finger (ZnF) domains are blue. Non-coding exons are gray. The catalytic C103 site, ZnF4, and ZnF7 are highlighted. Black triangles indicate all known SNPs in the *TNFAIP3* gene with associations with autoimmune diseases. Among the various documented SNPs/novel mutations, several lead to (1) reduced A20/TNFAIP3 protein level, (2) reduced A20/TNFAIP3 efficiency, (3) altered disease prognosis, or (4) therapeutic implications and are thus highlighted in this figure **(A–H)**. Known associations with (autoinflammatory and autoimmune) diseases for SNPs are indicated in the top gray bar. Multiple novel mutations causing "HA20" and two SNPs termed "TT>A" (associated with SLE) are listed in the box in the lower left corner. The reported p.Gln415fs mutation (113) should be reported as p.Lys417Serfs*4 to stay consistent with Human Genome Variation Society nomenclature (114). Abbreviations: OTU, ovarian tumor; ZnF, zinc finger; TF, transcription factors; TNFAIP3, tumor necrosis factor α-induced protein 3; HA20, haploinsufficiency of A20; AIH, autoimmune hepatitis; SLE, systemic lupus erythematosus; SSc, systemic sclerosis; RA, rheumatoid arthritis; T1D, type 1 Diabetes; JIA, juvenile idiopathic arthritis; CD, Crohn's disease; Pso, psoriasis; SS, Sjögren syndrome.

disease with fibrosing alveolitis and pulmonary hypertension (133). Similarly, RA patients with a previously described functional SNP (**Figure 2E**) had more swollen joints and increased disease activity scores (DAS28) compared to RA patients without this SNP, indicating worse clinical prognosis (9, 117). Finally, AIH patients with an upstream SNP (**Figure 2A**) harbored increased liver enzymes and more cirrhosis at disease presentation compared to patients without this SNP (109). These findings illustrate that within autoimmune patients certain SNPs around the *TNFAIP3* gene predispose a worse clinical prognosis.

Analysis of *TNFAIP3* SNPs might guide treatment choices, e.g., with TNF-blocking therapy. For RA and CD patients, reduced *TNFAIP3* mRNA in PBMCs or colonic biopsies,

respectively, is correlated with effective TNF-blocking therapy (118, 134). Psoriasis patients harboring specific *TNFAIP3* SNPs (**Figures 2E,F**) respond more effectively to TNF blockade (135). This indicates that *TNFAIP3* SNP analysis before TNF-blocking therapy initiation is worthwhile to perform in several autoimmune diseases and may be more practical than evaluating *TNFAIP3* mRNA expression.

Treatment of Autoinflammation and Autoimmunity

Knowledge from cell-specific targeting studies in mice illustrate that loss of A20/TNFAIP3 results in either autoinflammation or autoimmunity. The pathophysiologic distinction between these conditions has therapeutic implications. Autoinflammatory diseases such as Still's disease, Behçet's disease, and most cases of HA20 are well treated with IL-1 blockade, which has only marginal effect in autoimmune diseases including RA (136). Autoinflammation may also underlie other chronic disorders such as atherosclerosis, as these patients benefit from anti-IL-1 therapy (137, 138). In contrast, autoimmune disorders (e.g., SLE) have a strong contribution of IL-6 highlighted by successful anti-IL-6 treatment (139). This is in line with mouse studies in which innate cell activation (e.g., *Tnfaip3*$^{\text{LysM-KO}}$ mice) leads to increased IL-1β (13) and adaptive immune cell activation (e.g., *Tnfaip3*$^{\text{CD19-KO}}$ mice) leads to enhanced IL-6 (70, 71, 100, 102). In line with the adaptive nature of the disease, several autoimmune diseases also improve after treatments targeting adaptive immune cells [e.g., T-cell suppression using cyclosporine (140, 141) or B-cell depletion using Rituximab] (142).

CONCLUSION

Control of immune system activation is crucial to prevent both autoinflammation and autoimmunity. A20/TNFAIP3 hereby plays an important role in several innate and adaptive immune cells. Through analysis of cell-specific deletion of A20/*Tnfaip3* in mice, it became apparent that innate myeloid cells require A20/TNFAIP3 to suppress autoinflammation, while the development of autoimmunity is primarily controlled by A20/TNFAIP3 in DCs and B-cells. In addition, novel functions of A20/TNFAIP3 on inflammasome activity and necroptosis are uncovered. It would be of great value to examine in patient material cell-specific profiles of A20/TNFAIP3 and its effector function. The direct consequence of many SNPs on A20/TNFAIP3 is yet unknown. However, it is becoming increasingly clear that specific *TNFAIP3* SNPs can alter A20/TNFAIP3 function, can affect its expression level, or are associated with poor clinical outcomes. Finally, future studies on *TNFAIP3* SNPs to predict therapeutic effectivity would greatly benefit patient health care to obtain personalized therapy.

AUTHOR CONTRIBUTIONS

All the authors listed have made a substantial, direct, and intellectual contribution to the work and approved it for publication.

FUNDING

This project was supported by grants from the Dutch Arthritis Association (12-2-410) and European Framework program 7 (FP7-MC-CIG grant 304221).

REFERENCES

1. McGonagle D, McDermott MF. A proposed classification of the immunological diseases. *PLoS Med* (2006) 3(8):e297. doi:10.1371/journal.pmed.0030297
2. McDermott MF, Aksentijevich I. The autoinflammatory syndromes. *Curr Opin Allergy Clin Immunol* (2002) 2(6):511–6. doi:10.1097/00130832-200212000-00006
3. Peckham D, Scambler T, Savic S, McDermott MF. The burgeoning field of innate immune-mediated disease and autoinflammation. *J Pathol* (2017) 241(2):123–39. doi:10.1002/path.4812
4. Ngo ST, Steyn FJ, McCombe PA. Gender differences in autoimmune disease. *Front Neuroendocrinol* (2014) 35(3):347–69. doi:10.1016/j.yfrne.2014.04.004
5. Ma WT, Chang C, Gershwin ME, Lian ZX. Development of autoantibodies precedes clinical manifestations of autoimmune diseases: a comprehensive review. *J Autoimmun* (2017) 83:95–112. doi:10.1016/j.jaut.2017.07.003
6. Wertz IE, O'Rourke KM, Zhou H, Eby M, Aravind L, Seshagiri S, et al. De-ubiquitination and ubiquitin ligase domains of A20 downregulate NF-kappaB signalling. *Nature* (2004) 430(7000):694–9. doi:10.1038/nature02794
7. Ma A, Malynn BA. A20: linking a complex regulator of ubiquitylation to immunity and human disease. *Nat Rev Immunol* (2012) 12(11):774–85. doi:10.1038/nri3313
8. Adrianto I, Wen F, Templeton A, Wiley G, King JB, Lessard CJ, et al. Association of a functional variant downstream of TNFAIP3 with systemic lupus erythematosus. *Nat Genet* (2011) 43(3):253–8. doi:10.1038/ng.766
9. Moaaz M, Mohannad N. Association of the polymorphisms of TRAF1 (rs10818488) and TNFAIP3 (rs2230926) with rheumatoid arthritis and systemic lupus erythematosus and their relationship to disease activity among Egyptian patients. *Cent Eur J Immunol* (2016) 41(2):165–75. doi:10.5114/ceji.2016.60991
10. Musone SL, Taylor KE, Lu TT, Nititham J, Ferreira RC, Ortmann W, et al. Multiple polymorphisms in the TNFAIP3 region are independently associated with systemic lupus erythematosus. *Nat Genet* (2008) 40(9):1062–4. doi:10.1038/ng.202
11. Nair RP, Duffin KC, Helms C, Ding J, Stuart PE, Goldgar D, et al. Genome-wide scan reveals association of psoriasis with IL-23 and NF-kappaB pathways. *Nat Genet* (2009) 41(2):199–204. doi:10.1038/ng.311
12. Indhumathi S, Rajappa M, Chandrashekar L, Ananthanarayanan PH, Thappa DM, Negi VS. TNFAIP3 and TNIP1 polymorphisms confer psoriasis risk in South Indian Tamils. *Br J Biomed Sci* (2015) 72(4):168–73. doi:10.1080/09674845.2015.11665748
13. Vande Walle L, Van Opdenbosch N, Jacques P, Fossoul A, Verheugen E, Vogel P, et al. Negative regulation of the NLRP3 inflammasome by A20 protects against arthritis. *Nature* (2014) 512(7512):69–73. doi:10.1038/nature13322
14. Onizawa M, Oshima S, Schulze-Topphoff U, Oses-Prieto JA, Lu T, Tavares R, et al. The ubiquitin-modifying enzyme A20 restricts ubiquitination of the kinase RIPK3 and protects cells from necroptosis. *Nat Immunol* (2015) 16(6):618–27. doi:10.1038/ni.3172
15. Matsuzawa Y, Oshima S, Takahara M, Maeyashiki C, Nemoto Y, Kobayashi M, et al. TNFAIP3 promotes survival of CD4 T cells by restricting MTOR and promoting autophagy. *Autophagy* (2015) 11(7):1052–62. doi:10.1080/15548627.2015.1055439
16. Catrysse L, Vereecke L, Beyaert R, van Loo G. A20 in inflammation and autoimmunity. *Trends Immunol* (2014) 35(1):22–31. doi:10.1016/j.it.2013.10.005
17. Siebenlist U, Brown K, Claudio E. Control of lymphocyte development by nuclear factor-kappaB. *Nat Rev Immunol* (2005) 5(6):435–45. doi:10.1038/nri1629
18. Hoesel B, Schmid JA. The complexity of NF-kappaB signaling in inflammation and cancer. *Mol Cancer* (2013) 12:86. doi:10.1186/1476-4598-12-86

19. Hayden MS, Ghosh S. NF-kappaB, the first quarter-century: remarkable progress and outstanding questions. *Genes Dev* (2012) 26(3):203–34. doi:10.1101/gad.183434.111
20. Hershko A, Ciechanover A. The ubiquitin system. *Annu Rev Biochem* (1998) 67:425–79. doi:10.1146/annurev.biochem.67.1.425
21. Opipari AW Jr, Boguski MS, Dixit VM. The A20 cDNA induced by tumor necrosis factor alpha encodes a novel type of zinc finger protein. *J Biol Chem* (1990) 265(25):14705–8.
22. Dixit VM, Green S, Sarma V, Holzman LB, Wolf FW, O'Rourke K, et al. Tumor necrosis factor-alpha induction of novel gene products in human endothelial cells including a macrophage-specific chemotaxin. *J Biol Chem* (1990) 265(5):2973–8.
23. Makarova KS, Aravind L, Koonin EV. A novel superfamily of predicted cysteine proteases from eukaryotes, viruses and *Chlamydia pneumoniae*. *Trends Biochem Sci* (2000) 25(2):50–2. doi:10.1016/S0968-0004(99)01530-3
24. Lu TT, Onizawa M, Hammer GE, Turer EE, Yin Q, Damko E, et al. Dimerization and ubiquitin mediated recruitment of A20, a complex deubiquitinating enzyme. *Immunity* (2013) 38(5):896–905. doi:10.1016/j.immuni.2013.03.008
25. Verhelst K, Carpentier I, Kreike M, Meloni L, Verstrepen L, Kensche T, et al. A20 inhibits LUBAC-mediated NF-kappaB activation by binding linear polyubiquitin chains via its zinc finger 7. *EMBO J* (2012) 31(19):3845–55. doi:10.1038/emboj.2012.240
26. Tokunaga F, Nishimasu H, Ishitani R, Goto E, Noguchi T, Mio K, et al. Specific recognition of linear polyubiquitin by A20 zinc finger 7 is involved in NF-kappaB regulation. *EMBO J* (2012) 31(19):3856–70. doi:10.1038/emboj.2012.241
27. Shembade N, Harhaj EW. Regulation of NF-kappaB signaling by the A20 deubiquitinase. *Cell Mol Immunol* (2012) 9(2):123–30. doi:10.1038/cmi.2011.59
28. Shembade N, Harhaj NS, Liebl DJ, Harhaj EW. Essential role for TAX1BP1 in the termination of TNF-alpha-, IL-1- and LPS-mediated NF-kappaB and JNK signaling. *EMBO J* (2007) 26(17):3910–22. doi:10.1038/sj.emboj.7601823
29. Oshima S, Turer EE, Callahan JA, Chai S, Advincula R, Barrera J, et al. ABIN-1 is a ubiquitin sensor that restricts cell death and sustains embryonic development. *Nature* (2009) 457(7231):906–9. doi:10.1038/nature07575
30. Mauro C, Pacifico F, Lavorgna A, Mellone S, Iannetti A, Acquaviva R, et al. ABIN-1 binds to NEMO/IKKgamma and co-operates with A20 in inhibiting NF-kappaB. *J Biol Chem* (2006) 281(27):18482–8. doi:10.1074/jbc.M601502200
31. Iha H, Peloponese JM, Verstrepen L, Zapart G, Ikeda F, Smith CD, et al. Inflammatory cardiac valvulitis in TAX1BP1-deficient mice through selective NF-kappaB activation. *EMBO J* (2008) 27(4):629–41. doi:10.1038/emboj.2008.5
32. Verstrepen L, Verhelst K, van Loo G, Carpentier I, Ley SC, Beyaert R. Expression, biological activities and mechanisms of action of A20 (TNFAIP3). *Biochem Pharmacol* (2010) 80(12):2009–20. doi:10.1016/j.bcp.2010.06.044
33. Micheau O, Tschopp J. Induction of TNF receptor I-mediated apoptosis via two sequential signaling complexes. *Cell* (2003) 114(2):181–90. doi:10.1016/S0092-8674(03)00521-X
34. Brenner D, Blaser H, Mak TW. Regulation of tumour necrosis factor signalling: live or let die. *Nat Rev Immunol* (2015) 15(6):362–74. doi:10.1038/nri3834
35. Tokunaga F. Linear ubiquitination-mediated NF-kappaB regulation and its related disorders. *J Biochem* (2013) 154(4):313–23. doi:10.1093/jb/mvt079
36. Tokunaga F, Sakata S, Saeki Y, Satomi Y, Kirisako T, Kamei K, et al. Involvement of linear polyubiquitylation of NEMO in NF-kappaB activation. *Nat Cell Biol* (2009) 11(2):123–32. doi:10.1038/ncb1821
37. Chen ZJ, Parent L, Maniatis T. Site-specific phosphorylation of IkappaBalpha by a novel ubiquitination-dependent protein kinase activity. *Cell* (1996) 84(6):853–62. doi:10.1016/S0092-8674(00)81064-8
38. Alkalay I, Yaron A, Hatzubai A, Orian A, Ciechanover A, Ben-Neriah Y. Stimulation-dependent I kappa B alpha phosphorylation marks the NF-kappa B inhibitor for degradation via the ubiquitin-proteasome pathway. *Proc Natl Acad Sci U S A* (1995) 92(23):10599–603. doi:10.1073/pnas.92.23.10599
39. Bosanac I, Wertz IE, Pan B, Yu C, Kusam S, Lam C, et al. Ubiquitin binding to A20 ZnF4 is required for modulation of NF-kappaB signaling. *Mol Cell* (2010) 40(4):548–57. doi:10.1016/j.molcel.2010.10.009
40. Shembade N, Ma A, Harhaj EW. Inhibition of NF-kappaB signaling by A20 through disruption of ubiquitin enzyme complexes. *Science* (2010) 327(5969):1135–9. doi:10.1126/science.1182364
41. Skaug B, Chen J, Du F, He J, Ma A, Chen ZJ. Direct, noncatalytic mechanism of IKK inhibition by A20. *Mol Cell* (2011) 44(4):559–71. doi:10.1016/j.molcel.2011.09.015
42. Tiruppathi C, Soni D, Wang DM, Xue J, Singh V, Thippegowda PB, et al. The transcription factor DREAM represses the deubiquitinase A20 and mediates inflammation. *Nat Immunol* (2014) 15(3):239–47. doi:10.1038/ni.2823
43. Krikos A, Laherty CD, Dixit VM. Transcriptional activation of the tumor necrosis factor alpha-inducible zinc finger protein, A20, is mediated by kappa B elements. *J Biol Chem* (1992) 267(25):17971–6.
44. Yuk JM, Kim TS, Kim SY, Lee HM, Han J, Dufour CR, et al. Orphan nuclear receptor ERRalpha controls macrophage metabolic signaling and A20 expression to negatively regulate TLR-induced inflammation. *Immunity* (2015) 43(1):80–91. doi:10.1016/j.immuni.2015.07.003
45. Murakawa Y, Hinz M, Mothes J, Schuetz A, Uhl M, Wyler E, et al. RC3H1 post-transcriptionally regulates A20 mRNA and modulates the activity of the IKK/NF-kappaB pathway. *Nat Commun* (2015) 6:7367. doi:10.1038/ncomms8367
46. Gantier MP, Stunden HJ, McCoy CE, Behlke MA, Wang D, Kaparakis-Liaskos M, et al. A miR-19 regulon that controls NF-kappaB signaling. *Nucleic Acids Res* (2012) 40(16):8048–58. doi:10.1093/nar/gks521
47. Kim SW, Ramasamy K, Bouamar H, Lin AP, Jiang D, Aguiar RC. MicroRNAs miR-125a and miR-125b constitutively activate the NF-kappaB pathway by targeting the tumor necrosis factor alpha-induced protein 3 (TNFAIP3, A20). *Proc Natl Acad Sci U S A* (2012) 109(20):7865–70. doi:10.1073/pnas.1200081109
48. Wang CM, Wang Y, Fan CG, Xu FF, Sun WS, Liu YG, et al. miR-29c targets TNFAIP3, inhibits cell proliferation and induces apoptosis in hepatitis B virus-related hepatocellular carcinoma. *Biochem Biophys Res Commun* (2011) 411(3):586–92. doi:10.1016/j.bbrc.2011.06.191
49. Vinuesa CG, Cook MC, Angelucci C, Athanasopoulos V, Rui L, Hill KM, et al. A RING-type ubiquitin ligase family member required to repress follicular helper T cells and autoimmunity. *Nature* (2005) 435(7041):452–8. doi:10.1038/nature03555
50. Hutti JE, Turk BE, Asara JM, Ma A, Cantley LC, Abbott DW. IkappaB kinase beta phosphorylates the K63 deubiquitinase A20 to cause feedback inhibition of the NF-kappaB pathway. *Mol Cell Biol* (2007) 27(21):7451–61. doi:10.1128/MCB.01101-07
51. Wertz IE, Newton K, Seshasayee D, Kusam S, Lam C, Zhang J, et al. Phosphorylation and linear ubiquitin direct A20 inhibition of inflammation. *Nature* (2015) 528(7582):370–5. doi:10.1038/nature16165
52. Kulathu Y, Garcia FJ, Mevissen TE, Busch M, Arnaudo N, Carroll KS, et al. Regulation of A20 and other OTU deubiquitinases by reversible oxidation. *Nat Commun* (2013) 4:1569. doi:10.1038/ncomms2567
53. Lee JG, Baek K, Soetandyo N, Ye Y. Reversible inactivation of deubiquitinases by reactive oxygen species in vitro and in cells. *Nat Commun* (2013) 4:1568. doi:10.1038/ncomms2532
54. Shrikhande GV, Scali ST, da Silva CG, Damrauer SM, Csizmadia E, Putheti P, et al. O-glycosylation regulates ubiquitination and degradation of the anti-inflammatory protein A20 to accelerate atherosclerosis in diabetic ApoE-null mice. *PLoS One* (2010) 5(12):e14240. doi:10.1371/journal.pone.0014240
55. Di Dalmazi G, Hirshberg J, Lyle D, Freij JB, Caturegli P. Reactive oxygen species in organ-specific autoimmunity. *Auto Immun Highlights* (2016) 7(1):11. doi:10.1007/s13317-016-0083-0
56. Kienhofer D, Boeltz S, Hoffmann MH. Reactive oxygen homeostasis – the balance for preventing autoimmunity. *Lupus* (2016) 25(8):943–54. doi:10.1177/0961203316640919
57. Tewari M, Wolf FW, Seldin MF, O'Shea KS, Dixit VM, Turka LA. Lymphoid expression and regulation of A20, an inhibitor of programmed cell death. *J Immunol* (1995) 154(4):1699–706.
58. Coornaert B, Baens M, Heyninck K, Bekaert T, Haegman M, Staal J, et al. T cell antigen receptor stimulation induces MALT1 paracaspase-mediated cleavage of the NF-kappaB inhibitor A20. *Nat Immunol* (2008) 9(3):263–71. doi:10.1038/ni1561
59. Lee EG, Boone DL, Chai S, Libby SL, Chien M, Lodolce JP, et al. Failure to regulate TNF-induced NF-kappaB and cell death responses in A20-deficient mice. *Science* (2000) 289(5488):2350–4. doi:10.1126/science.289.5488.2350
60. Maizels N. Genome engineering with Cre-loxP. *J Immunol* (2013) 191(1):5–6. doi:10.4049/jimmunol.1301241

61. Clausen BE, Burkhardt C, Reith W, Renkawitz R, Forster I. Conditional gene targeting in macrophages and granulocytes using LysMcre mice. *Transgenic Res* (1999) 8(4):265–77. doi:10.1023/A:1008942828960
62. De Wilde K, Martens A, Lambrecht S, Jacques P, Drennan MB, Debusschere K, et al. A20 inhibition of STAT1 expression in myeloid cells: a novel endogenous regulatory mechanism preventing development of enthesitis. *Ann Rheum Dis* (2016) 76(3):585–92. doi:10.1136/annrheumdis-2016-209454
63. Matmati M, Jacques P, Maelfait J, Verheugen E, Kool M, Sze M, et al. A20 (TNFAIP3) deficiency in myeloid cells triggers erosive polyarthritis resembling rheumatoid arthritis. *Nat Genet* (2011) 43(9):908–12. doi:10.1038/ng.874
64. Agostini L, Martinon F, Burns K, McDermott MF, Hawkins PN, Tschopp J. NALP3 forms an IL-1beta-processing inflammasome with increased activity in Muckle-Wells autoinflammatory disorder. *Immunity* (2004) 20(3):319–25. doi:10.1016/S1074-7613(04)00046-9
65. de Torre-Minguela C, Mesa Del Castillo P, Pelegrin P. The NLRP3 and pyrin inflammasomes: implications in the pathophysiology of autoinflammatory diseases. *Front Immunol* (2017) 8:43. doi:10.3389/fimmu.2017.00043
66. Duong BH, Onizawa M, Oses-Prieto JA, Advincula R, Burlingame A, Malynn BA, et al. A20 restricts ubiquitination of pro-interleukin-1beta protein complexes and suppresses NLRP3 inflammasome activity. *Immunity* (2015) 42(1):55–67. doi:10.1016/j.immuni.2014.12.031
67. Steinman RM, Hemmi H. Dendritic cells: translating innate to adaptive immunity. *Curr Top Microbiol Immunol* (2006) 311:17–58. doi:10.1007/3-540-32636-7_2
68. Naik SH, Metcalf D, van Nieuwenhuijze A, Wicks I, Wu L, O'Keeffe M, et al. Intrasplenic steady-state dendritic cell precursors that are distinct from monocytes. *Nat Immunol* (2006) 7(6):663–71. doi:10.1038/ni1340
69. Caton ML, Smith-Raska MR, Reizis B. Notch-RBP-J signaling controls the homeostasis of CD8- dendritic cells in the spleen. *J Exp Med* (2007) 204(7):1653–64. doi:10.1084/jem.20062648
70. Hammer GE, Turer EE, Taylor KE, Fang CJ, Advincula R, Oshima S, et al. Expression of A20 by dendritic cells preserves immune homeostasis and prevents colitis and spondyloarthritis. *Nat Immunol* (2011) 12(12):1184–93. doi:10.1038/ni.2135
71. Kool M, van Loo G, Waelput W, De Prijck S, Muskens F, Sze M, et al. The ubiquitin-editing protein A20 prevents dendritic cell activation, recognition of apoptotic cells, and systemic autoimmunity. *Immunity* (2011) 35(1):82–96. doi:10.1016/j.immuni.2011.05.013
72. Xuan NT, Wang X, Nishanth G, Waisman A, Borucki K, Isermann B, et al. A20 expression in dendritic cells protects mice from LPS-induced mortality. *Eur J Immunol* (2015) 45(3):818–28. doi:10.1002/eji.201444795
73. Helft J, Bottcher J, Chakravarty P, Zelenay S, Huotari J, Schraml BU, et al. GM-CSF mouse bone marrow cultures comprise a heterogeneous population of CD11c(+)MHCII(+) macrophages and dendritic cells. *Immunity* (2015) 42(6):1197–211. doi:10.1016/j.immuni.2015.05.018
74. Crow MK. Advances in understanding the role of type I interferons in systemic lupus erythematosus. *Curr Opin Rheumatol* (2014) 26(5):467–74. doi:10.1097/BOR.0000000000000087
75. Cummings RJ, Barbet G, Bongers G, Hartmann BM, Gettler K, Muniz L, et al. Different tissue phagocytes sample apoptotic cells to direct distinct homeostasis programs. *Nature* (2016) 539(7630):565–9. doi:10.1038/nature20138
76. Liang J, Huang HI, Benzatti FP, Karlsson AB, Zhang JJ, Youssef N, et al. Inflammatory Th1 and Th17 in the intestine are each driven by functionally specialized dendritic cells with distinct requirements for MyD88. *Cell Rep* (2016) 17(5):1330–43. doi:10.1016/j.celrep.2016.09.091
77. Cash H, Relle M, Menke J, Brochhausen C, Jones SA, Topley N, et al. Interleukin 6 (IL-6) deficiency delays lupus nephritis in MRL-Faslpr mice: the IL-6 pathway as a new therapeutic target in treatment of autoimmune kidney disease in systemic lupus erythematosus. *J Rheumatol* (2010) 37(1):60–70. doi:10.3899/jrheum.090194
78. Atreya R, Mudter J, Finotto S, Mullberg J, Jostock T, Wirtz S, et al. Blockade of interleukin 6 trans signaling suppresses T-cell resistance against apoptosis in chronic intestinal inflammation: evidence in crohn disease and experimental colitis in vivo. *Nat Med* (2000) 6(5):583–8. doi:10.1038/75068
79. Jacob N, Stohl W. Cytokine disturbances in systemic lupus erythematosus. *Arthritis Res Ther* (2011) 13(4):228. doi:10.1186/ar3349
80. Neurath MF. Current and emerging therapeutic targets for IBD. *Nat Rev Gastroenterol Hepatol* (2017) 14(5):269–78. doi:10.1038/nrgastro.2016.208
81. Ciccarelli F, De Martinis M, Ginaldi L. An update on autoinflammatory diseases. *Curr Med Chem* (2014) 21(3):261–9. doi:10.2174/09298673113206660303
82. Holman HR, Kunkel HG. Affinity between the lupus erythematosus serum factor and cell nuclei and nucleoprotein. *Science* (1957) 126(3265):162–3. doi:10.1126/science.126.3265.162
83. Hammer GE, Ma A. Molecular control of steady-state dendritic cell maturation and immune homeostasis. *Annu Rev Immunol* (2013) 31:743–91. doi:10.1146/annurev-immunol-020711-074929
84. Duwel M, Welteke V, Oeckinghaus A, Baens M, Kloo B, Ferch U, et al. A20 negatively regulates T cell receptor signaling to NF-kappaB by cleaving Malt1 ubiquitin chains. *J Immunol* (2009) 182(12):7718–28. doi:10.4049/jimmunol.0803313
85. Malewicz M, Zeller N, Yilmaz ZB, Weih F. NF kappa B controls the balance between Fas and tumor necrosis factor cell death pathways during T cell receptor-induced apoptosis via the expression of its target gene A20. *J Biol Chem* (2003) 278(35):32825–33. doi:10.1074/jbc.M304000200
86. Shi L, Chen S, Lu Y, Wang X, Xu L, Zhang F, et al. Changes in the MALT1-A20-NF-kappaB expression pattern may be related to T cell dysfunction in AML. *Cancer Cell Int* (2013) 13(1):37. doi:10.1186/1475-2867-13-37
87. Giordano M, Roncagalli R, Bourdely P, Chasson L, Buferne M, Yamasaki S, et al. The tumor necrosis factor alpha-induced protein 3 (TNFAIP3, A20) imposes a brake on antitumor activity of CD8 T cells. *Proc Natl Acad Sci U S A* (2014) 111(30):11115–20. doi:10.1073/pnas.1406259111
88. Roncagalli R, Hauri S, Fiore F, Liang Y, Chen Z, Sansoni A, et al. Quantitative proteomics analysis of signalosome dynamics in primary T cells identifies the surface receptor CD6 as a Lat adaptor-independent TCR signaling hub. *Nat Immunol* (2014) 15(4):384–92. doi:10.1038/ni.2843
89. Lee PP, Fitzpatrick DR, Beard C, Jessup HK, Lehar S, Makar KW, et al. A critical role for Dnmt1 and DNA methylation in T cell development, function, and survival. *Immunity* (2001) 15(5):763–74. doi:10.1016/S1074-7613(01)00227-8
90. Bae HR, Leung PS, Tsuneyama K, Valencia JC, Hodge DL, Kim S, et al. Chronic expression of interferon-gamma leads to murine autoimmune cholangitis with a female predominance. *Hepatology* (2016) 64(4):1189–201. doi:10.1002/hep.28641
91. Morita M, Watanabe Y, Akaike T. Protective effect of hepatocyte growth factor on interferon-gamma-induced cytotoxicity in mouse hepatocytes. *Hepatology* (1995) 21(6):1585–93. doi:10.1016/0270-9139(95)90463-8
92. Toyonaga T, Hino O, Sugai S, Wakasugi S, Abe K, Shichiri M, et al. Chronic active hepatitis in transgenic mice expressing interferon-gamma in the liver. *Proc Natl Acad Sci U S A* (1994) 91(2):614–8. doi:10.1073/pnas.91.2.614
93. Fischer JC, Otten V, Kober M, Drees C, Rosenbaum M, Schmickl M, et al. A20 restrains thymic regulatory T cell development. *J Immunol* (2017) 199(7):2356–65. doi:10.4049/jimmunol.1602102
94. He S, Wang L, Miao L, Wang T, Du F, Zhao L, et al. Receptor interacting protein kinase-3 determines cellular necrotic response to TNF-alpha. *Cell* (2009) 137(6):1100–11. doi:10.1016/j.cell.2009.05.021
95. Just S, Nishanth G, Buchbinder JH, Wang X, Naumann M, Lavrik I, et al. A20 curtails primary but augments secondary CD8+ t cell responses in intracellular bacterial infection. *Sci Rep* (2016) 6:39796. doi:10.1038/srep39796
96. McLeod IX, Jia W, He YW. The contribution of autophagy to lymphocyte survival and homeostasis. *Immunol Rev* (2012) 249(1):195–204. doi:10.1111/j.1600-065X.2012.01143.x
97. Thomson AW, Turnquist HR, Raimondi G. Immunoregulatory functions of mTOR inhibition. *Nat Rev Immunol* (2009) 9(5):324–37. doi:10.1038/nri2546
98. Bekeredjian-Ding I, Jego G. Toll-like receptors – sentries in the B-cell response. *Immunology* (2009) 128(3):311–23. doi:10.1111/j.1365-2567.2009.03173.x
99. Ferch U, Zum Buschenfelde CM, Gewies A, Wegener E, Rauser S, Peschel C, et al. MALT1 directs B cell receptor-induced canonical nuclear factor-kappaB signaling selectively to the c-Rel subunit. *Nat Immunol* (2007) 8(9):984–91. doi:10.1038/ni1493
100. Chu Y, Vahl JC, Kumar D, Heger K, Bertossi A, Wojtowicz E, et al. B cells lacking the tumor suppressor TNFAIP3/A20 display impaired differentiation and hyperactivation and cause inflammation and autoimmunity in aged mice. *Blood* (2011) 117(7):2227–36. doi:10.1182/blood-2010-09-306019

101. Hovelmeyer N, Reissig S, Xuan NT, Adams-Quack P, Lukas D, Nikolaev A, et al. A20 deficiency in B cells enhances B-cell proliferation and results in the development of autoantibodies. *Eur J Immunol* (2011) 41(3):595–601. doi:10.1002/eji.201041313
102. Tavares RM, Turer EE, Liu CL, Advincula R, Scapini P, Rhee L, et al. The ubiquitin modifying enzyme A20 restricts B cell survival and prevents autoimmunity. *Immunity* (2010) 33(2):181–91. doi:10.1016/j.immuni.2010.07.017
103. Honma K, Tsuzuki S, Nakagawa M, Tagawa H, Nakamura S, Morishima Y, et al. TNFAIP3/A20 functions as a novel tumor suppressor gene in several subtypes of non-Hodgkin lymphomas. *Blood* (2009) 114(12):2467–75. doi:10.1182/blood-2008-12-194852
104. Novak U, Rinaldi A, Kwee I, Nandula SV, Rancoita PM, Compagno M, et al. The NF-{kappa}B negative regulator TNFAIP3 (A20) is inactivated by somatic mutations and genomic deletions in marginal zone lymphomas. *Blood* (2009) 113(20):4918–21. doi:10.1182/blood-2008-08-174110
105. Schmitz R, Hansmann ML, Bohle V, Martin-Subero JI, Hartmann S, Mechtersheimer G, et al. TNFAIP3 (A20) is a tumor suppressor gene in Hodgkin lymphoma and primary mediastinal B cell lymphoma. *J Exp Med* (2009) 206(5):981–9. doi:10.1084/jem.20090528
106. Dieguez-Gonzalez R, Calaza M, Perez-Pampin E, Balsa A, Blanco FJ, Canete JD, et al. Analysis of TNFAIP3, a feedback inhibitor of nuclear factor-kappaB and the neighbor intergenic 6q23 region in rheumatoid arthritis susceptibility. *Arthritis Res Ther* (2009) 11(2):R42. doi:10.1186/ar2650
107. Vereecke L, Beyaert R, van Loo G. Genetic relationships between A20/TNFAIP3, chronic inflammation and autoimmune disease. *Biochem Soc Trans* (2011) 39(4):1086–91. doi:10.1042/BST0391086
108. de Boer YS, van Gerven NM, Zwiers A, Verwer BJ, van Hoek B, van Erpecum KJ, et al. Genome-wide association study identifies variants associated with autoimmune hepatitis type 1. *Gastroenterology* (2014) 147(2):443.e–52.e. doi:10.1053/j.gastro.2014.04.022
109. Xu E, Cao H, Lin L, Liu H. rs10499194 polymorphism in the tumor necrosis factor-alpha inducible protein 3 (TNFAIP3) gene is associated with type-1 autoimmune hepatitis risk in Chinese Han population. *PLoS One* (2017) 12(4):e0176471. doi:10.1371/journal.pone.0176471
110. Cordell HJ, Han Y, Mells GF, Li Y, Hirschfield GM, Greene CS, et al. International genome-wide meta-analysis identifies new primary biliary cirrhosis risk loci and targetable pathogenic pathways. *Nat Commun* (2015) 6:8019. doi:10.1038/ncomms9019
111. Jostins L, Ripke S, Weersma RK, Duerr RH, McGovern DP, Hui KY, et al. Host-microbe interactions have shaped the genetic architecture of inflammatory bowel disease. *Nature* (2012) 491(7422):119–24. doi:10.1038/nature11582
112. Zhou Q, Wang H, Schwartz DM, Stoffels M, Park YH, Zhang Y, et al. Loss-of-function mutations in TNFAIP3 leading to A20 haploinsufficiency cause an early-onset autoinflammatory disease. *Nat Genet* (2016) 48(1):67–73. doi:10.1038/ng.3459
113. Takagi M, Ogata S, Ueno H, Yoshida K, Yeh T, Hoshino A, et al. Haploinsufficiency of TNFAIP3 (A20) by germline mutation is involved in autoimmune lymphoproliferative syndrome. *J Allergy Clin Immunol* (2017) 139(6):1914–22. doi:10.1016/j.jaci.2016.09.038
114. Aksentijevich I, Zhou Q. NF-kappaB pathway in autoinflammatory diseases: dysregulation of protein modifications by ubiquitin defines a new category of autoinflammatory diseases. *Front Immunol* (2017) 8:399. doi:10.3389/fimmu.2017.00399
115. Li D, Wang L, Fan Y, Song L, Guo C, Zhu F, et al. Down-regulation of A20 mRNA expression in peripheral blood mononuclear cells from patients with systemic lupus erythematosus. *J Clin Immunol* (2012) 32(6):1287–91. doi:10.1007/s10875-012-9764-2
116. Wang Z, Zhang Z, Yuan J, Li LI. Altered TNFAIP3 mRNA expression in peripheral blood mononuclear cells from patients with rheumatoid arthritis. *Biomed Rep* (2015) 3(5):675–80. doi:10.3892/br.2015.486
117. Zhu L, Wang L, Wang X, Zhou L, Liao Z, Xu L, et al. Characteristics of A20 gene polymorphisms and clinical significance in patients with rheumatoid arthritis. *J Transl Med* (2015) 13:215. doi:10.1186/s12967-015-0566-1
118. Arsenescu R, Bruno ME, Rogier EW, Stefka AT, McMahan AE, Wright TB, et al. Signature biomarkers in Crohn's disease: toward a molecular classification. *Mucosal Immunol* (2008) 1(5):399–411. doi:10.1038/mi.2008.32
119. Bruno ME, Rogier EW, Arsenescu RI, Flomenhoft DR, Kurkjian CJ, Ellis GI, et al. Correlation of biomarker expression in colonic mucosa with disease phenotype in Crohn's disease and ulcerative colitis. *Dig Dis Sci* (2015) 60(10):2976–84. doi:10.1007/s10620-015-3700-2
120. Aki A, Nagasaki M, Malynn BA, Ma A, Kagari T. Hypomorphic A20 expression confers susceptibility to psoriasis. *PLoS One* (2017) 12(6):e0180481. doi:10.1371/journal.pone.0180481
121. Elsby LM, Orozco G, Denton J, Worthington J, Ray DW, Donn RP. Functional evaluation of TNFAIP3 (A20) in rheumatoid arthritis. *Clin Exp Rheumatol* (2010) 28(5):708–14.
122. Wang S, Wen F, Tessneer KL, Gaffney PM. TALEN-mediated enhancer knockout influences TNFAIP3 gene expression and mimics a molecular phenotype associated with systemic lupus erythematosus. *Genes Immun* (2016) 17(3):165–70. doi:10.1038/gene.2016.4
123. Duncan CJA, Dinnigan E, Theobald R, Grainger A, Skelton AJ, Hussain R, et al. Early-onset autoimmune disease due to a heterozygous loss-of-function mutation in TNFAIP3 (A20). *Ann Rheum Dis* (2017). doi:10.1136/annrheumdis-2016-210944
124. Malynn BA, Ma A. A20 takes on tumors: tumor suppression by an ubiquitin-editing enzyme. *J Exp Med* (2009) 206(5):977–80. doi:10.1084/jem.20090765
125. Ohnishi H, Kawamoto N, Seishima M, Ohara O, Fukao T. A Japanese family case with juvenile onset Behcet's disease caused by TNFAIP3 mutation. *Allergol Int* (2017) 66(1):146–8. doi:10.1016/j.alit.2016.06.006
126. Shigemura T, Kaneko N, Kobayashi N, Kobayashi K, Takeuchi Y, Nakano N, et al. Novel heterozygous C243Y A20/TNFAIP3 gene mutation is responsible for chronic inflammation in autosomal-dominant Behcet's disease. *RMD Open* (2016) 2(1):e000223. doi:10.1136/rmdopen-2015-000223
127. Kadowaki T, Ohnishi H, Kawamoto N, Hori T, Nishimura K, Kobayashi C, et al. Haploinsufficiency of A20 causes autoinflammatory and autoimmune disorders. *J Allergy Clin Immunol* (2017). doi:10.1016/j.jaci.2017.10.039
128. Aeschlimann FA, Batu ED, Canna SW, Go E, Gul A, Hoffmann P, et al. A20 haploinsufficiency (HA20): clinical phenotypes and disease course of patients with a newly recognised NF-kB-mediated autoinflammatory disease. *Ann Rheum Dis* (2018). doi:10.1136/annrheumdis-2017-212403
129. Wolfrum S, Teupser D, Tan M, Chen KY, Breslow JL. The protective effect of A20 on atherosclerosis in apolipoprotein E-deficient mice is associated with reduced expression of NF-kappaB target genes. *Proc Natl Acad Sci U S A* (2007) 104(47):18601–6. doi:10.1073/pnas.0709011104
130. Guedes RP, Csizmadia E, Moll HP, Ma A, Ferran C, da Silva CG. A20 deficiency causes spontaneous neuroinflammation in mice. *J Neuroinflammation* (2014) 11:122. doi:10.1186/1742-2094-11-122
131. Lodolce JP, Kolodziej LE, Rhee L, Kariuki SN, Franek BS, McGreal NM, et al. African-derived genetic polymorphisms in TNFAIP3 mediate risk for autoimmunity. *J Immunol* (2010) 184(12):7001–9. doi:10.4049/jimmunol.1000324
132. Bates JS, Lessard CJ, Leon JM, Nguyen T, Battiest LJ, Rodgers J, et al. Meta-analysis and imputation identifies a 109 kb risk haplotype spanning TNFAIP3 associated with lupus nephritis and hematologic manifestations. *Genes Immun* (2009) 10(5):470–7. doi:10.1038/gene.2009.31
133. Dieude P, Guedj M, Wipff J, Ruiz B, Riemekasten G, Matucci-Cerinic M, et al. Association of the TNFAIP3 rs5029939 variant with systemic sclerosis in the European Caucasian population. *Ann Rheum Dis* (2010) 69(11):1958–64. doi:10.1136/ard.2009.127928
134. Koczan D, Drynda S, Hecker M, Drynda A, Guthke R, Kekow J, et al. Molecular discrimination of responders and nonresponders to anti-TNF alpha therapy in rheumatoid arthritis by etanercept. *Arthritis Res Ther* (2008) 10(3):R50. doi:10.1186/ar2419
135. Tejasvi T, Stuart PE, Chandran V, Voorhees JJ, Gladman DD, Rahman P, et al. TNFAIP3 gene polymorphisms are associated with response to TNF blockade in psoriasis. *J Invest Dermatol* (2012) 132(3 Pt 1):593–600. doi:10.1038/jid.2011.376
136. Dayer JM, Oliviero F, Punzi L. A brief history of IL-1 and IL-1 Ra in rheumatology. *Front Pharmacol* (2017) 8:293. doi:10.3389/fphar.2017.00293
137. Ridker PM, Everett BM, Thuren T, MacFadyen JG, Chang WH, Ballantyne C, et al. Antiinflammatory therapy with canakinumab for atherosclerotic disease. *N Engl J Med* (2017) 377(12):1119–31. doi:10.1056/NEJMoa1707914
138. Ridker PM, MacFadyen JG, Thuren T, Everett BM, Libby P, Glynn RJ. Effect of interleukin-1beta inhibition with canakinumab on incident lung cancer in patients with atherosclerosis: exploratory results from a randomised,

double-blind, placebo-controlled trial. *Lancet* (2017) 390(10105):1833–42. doi:10.1016/S0140-6736(17)32247-X

139. Illei GG, Shirota Y, Yarboro CH, Daruwalla J, Tackey E, Takada K, et al. Tocilizumab in systemic lupus erythematosus: data on safety, preliminary efficacy, and impact on circulating plasma cells from an open-label phase I dosage-escalation study. *Arthritis Rheum* (2010) 62(2):542–52. doi:10.1002/art.27221
140. Kronke M, Leonard WJ, Depper JM, Arya SK, Wong-Staal F, Gallo RC, et al. Cyclosporin A inhibits T-cell growth factor gene expression at the level of mRNA transcription. *Proc Natl Acad Sci U S A* (1984) 81(16):5214–8. doi:10.1073/pnas.81.16.5214
141. Szamel M, Bartels F, Resch K. Cyclosporin A inhibits T cell receptor-induced interleukin-2 synthesis of human T lymphocytes by selectively preventing a transmembrane signal transduction pathway leading to sustained activation of a protein kinase C isoenzyme, protein kinase C-beta. *Eur J Immunol* (1993) 23(12):3072–81. doi:10.1002/eji.1830231205
142. Dorner T, Isenberg D, Jayne D, Wiendl H, Zillikens D, Burmester G. Current status on B-cell depletion therapy in autoimmune diseases other than rheumatoid arthritis. *Autoimmun Rev* (2009) 9(2):82–9. doi:10.1016/j.autrev.2009.08.007

Conflict of Interest Statement: The authors declare that the research was conducted in the absence of any commercial or financial relationships that could be construed as a potential conflict of interest.

Copyright © 2018 Das, Chen, Hendriks and Kool. This is an open-access article distributed under the terms of the Creative Commons Attribution License (CC BY). The use, distribution or reproduction in other forums is permitted, provided the original author(s) and the copyright owner are credited and that the original publication in this journal is cited, in accordance with accepted academic practice. No use, distribution or reproduction is permitted which does not comply with these terms.

frontiers in Immunology

ORIGINAL RESEARCH
published: 04 April 2018
doi: 10.3389/fimmu.2018.00659

Sex Differences in Adipose Tissue CD8+ T Cells and Regulatory T Cells in Middle-Aged Mice

Hilda Ahnstedt, Meaghan Roy-O'Reilly, Monica S. Spychala, Alexis S. Mobley, Javiera Bravo-Alegria, Anjali Chauhan, Jaroslaw Aronowski, Sean P. Marrelli and Louise D. McCullough*

Department of Neurology, McGovern Medical School at University of Texas Health Science Center at Houston (UTHealth), Houston, TX, United States

The prevalence of cardiovascular disease has increased among middle-aged women in the United States, yet has declined in middle-aged men. In experimental stroke, middle-aged females have larger strokes and greater inflammation than age-matched males or younger females. The mechanism underlying this shift from an "ischemia-protected" to an "ischemia-sensitive" phenotype in aging females is unknown. One potential factor is an age-related increase in systemic factors that induce inflammation. Increased abdominal fat deposition is seen in women during middle age. Adipose tissue plays a key role in obesity-induced systemic inflammation, including increased pro-inflammatory cytokines. We hypothesized that age and sex differences in adipose immune cells promote an augmented pro-inflammatory milieu in middle-aged females driven by a balance shift between pro-inflammatory and anti-inflammatory T cells. Abdominal adipose tissue immune cells from young (3–4 months) and middle-aged (15–16 months) male and female C57BL/6J mice were analyzed by flow cytometry. Plasma triglyceride (TG), high-density lipoprotein (HDL), and low-density lipoprotein (LDL) levels were determined with colorimetric assays. Middle-aged mice had higher adipose tissue mass compared to young mice. Lipid profiling showed no sex differences in TG and LDL, but middle-aged females had lower HDL (0.84 ± 0.07 μg/μl) than middle-aged males (1.35 ± 0.06 μg/μl). Flow cytometry data demonstrated an age-associated increase in adipose tissue CD8+ T cells that was augmented by female sex, with middle-aged females having a higher percentage of CD8+ cells (34.4 ± 3.2% of CD3+ T cells) than middle-aged males (24.4 ± 2.2%). This increase in CD8+ T-cell proportion was adipose tissue-specific, as this change was not observed in blood. Middle-aged females had higher numbers of activated (CD69+) CD8+ T cells than males. In addition, female CD8+ T cells produced higher levels of IFN-γ, TNF-α, and granzyme B *ex vivo*, and females had higher adipose levels of IFN-γ, RANTES and MIP-1β than middle-aged males. In parallel, females had lower levels of regulatory T cells (Tregs), an anti-inflammatory T-cell subtype, compared to age-matched males. In conclusion, middle-aged females have a detrimental combination of elevated pro-inflammatory T cells and decreased anti-inflammatory Tregs in adipose tissue, which may promote a pro-inflammatory milieu and contribute to increased cardiovascular disease burden in aging females.

Keywords: sex differences, aging, inflammation, CD8+ T cells, adipose tissue, regulatory T cells

OPEN ACCESS

Edited by:
Jixin Zhong,
Case Western Reserve University, United States

Reviewed by:
Gaurav K. Gupta,
National Institutes of Health (NIH), United States
Valerio Chiurchiù,
Università Campus Bio-Medico, Italy
Fengqian Chen,
Texas Tech University, United States

****Correspondence:***
Hilda Ahnstedt
hilda.w.ahnstedt@uth.tmc.edu

Specialty section:
This article was submitted to Inflammation, a section of the journal Frontiers in Immunology

Received: *07 October 2017*
Accepted: *16 March 2018*
Published: *04 April 2018*

Citation:
Ahnstedt H, Roy-O'Reilly M, Spychala MS, Mobley AS, Bravo-Alegria J, Chauhan A, Aronowski J, Marrelli SP and McCullough LD (2018) Sex Differences in Adipose Tissue CD8+ T Cells and Regulatory T Cells in Middle-Aged Mice. Front. Immunol. 9:659. doi: 10.3389/fimmu.2018.00659

INTRODUCTION

Aging represents the largest risk factor for cardiovascular disease. Women experience increased cardiovascular disease and elevated stroke risk in middle-age, while the prevalence in similarly aged men decreases (1, 2). Our previous studies have shown that while young female mice have smaller infarcts after an experimental stroke compared to males, this phenotype is reversed in middle-aged animals (3). The underlying mechanism behind this change from an "ischemia-protected" to an "ischemia-sensitive" phenotype in middle-aged females is unknown. One potential factor may be the age-related increase in adipose tissue in women during menopause, leading to increased adipose tissue inflammation and an enhanced systemic pro-inflammatory environment prior to the stroke. Obesity is a major health problem and a well-known predictor of cardiovascular disease in both sexes. While some cardiovascular risk factors, such as heart disease, are more prevalent in men, abdominal obesity is 2–10 times more common in women in many parts of the world (4–6). In particular, the menopausal transition is associated with a significant increase in body weight and abdominal fat in middle-aged females (7). In addition, studies suggest that abdominal obesity may contribute to a greater risk for ischemic stroke in women than in men (1, 8, 9). The reasons for the sex differences in obesity and risk of stroke in middle-aged men and women are not fully understood.

Adipose tissue is now recognized as an endocrine organ that plays a key role in obesity-induced systemic inflammation. Obesity-induced inflammation is characterized by the infiltration and retention of immune cells within the adipose tissue and the chronic release of pro-inflammatory cytokines, including TNF-α, IL-1β, IFN-γ, and IL-6 (10, 11). Infiltrating immune cells release cytokines, chemokines, metalloproteinases, and reactive oxygen species. This obesity-induced, low-grade systemic inflammation has been linked to insulin resistance, diabetes, arterial stiffness, endothelial dysfunction, and increased blood–brain barrier permeability (12–14). Aging by itself is characterized by a state of chronic inflammation, known as "inflammaging," and obesity superimposed on aging represents an additional risk factor for chronic disease and age-related complications.

Pro-inflammatory $CD8^+$ T cells and anti-inflammatory regulatory T cells (Tregs) are immune cells that normally are found in adipose tissue. The balance between these cells is believed to be an important contributor to obesity. The number of adipose $CD8^+$ effector T cells is increased in obesity and $CD8^+$ T cells have further been shown to initiate and propagate adipose inflammation by the recruitment and activation of macrophages (15, 16). Conversely, levels of anti-inflammatory Tregs are decreased in genetic- and diet-induced mouse models of obesity (17). Importantly, studies in human subjects also suggest that obesity influences adipose T-cell subset composition and activation. Compared to normal weight patients, obese human subjects have lower levels of circulating Tregs (18). In addition, increased waist circumference has been shown to influence the activation status of both $CD4^+$ and $CD8^+$ T cells (19). Furthermore, studies have shown that women may be at a greater risk for secondary health issues arising from obesity (1, 8, 9, 20).

The vast majority of experimental studies on adipose tissue inflammation and T-cell immune responses have been performed using genetic- or diet-induced obesity in young male animals. However, as age is a major driver of both obesity and risk for cardiovascular disease in humans, understanding the effects of aging on immune responses within the adipose tissue is important. Because wild-type mice tend to develop natural increases in adiposity and body weight as they age, this study utilized middle-aged mice as a translational natural model of obesity-induced adipose tissue inflammation. Here, we used young and middle-aged mice of both sexes to characterize the intersectional effects of sex and aging on adipose tissue mass, immune cell composition, pro-inflammatory responses, and lipid profile.

MATERIALS AND METHODS

Animals

Young (3–4 months) and middle-aged (15–16 months, aged in-house) C57BL/6J mice were purchased from The Jackson Laboratory (000664; Bar Harbor, ME, USA). All animals had access to chow and water *ad libitum*. Animal procedures were performed in accordance with National Institutes of Health Guidelines for the care and use of laboratory animals and approved by the Animal Welfare Committee at the University of Texas Health Science Center at Houston, TX, USA (AWC-15-0140).

Estrus Cycle Characterization in Young and Middle-Aged Female Mice

The estrus cycle in young and middle-aged female mice was monitored daily through collection of vaginal smears and examination of the types of cells present for two to three consecutive cycles as described previously (21, 22).

Tissue Harvesting

Mice were euthanized by Avertin injection and blood was collected by cardiac puncture using heparin-coated needles. For plasma collection, blood was centrifuged (10,000 × *g* for 10 min at 4°C) and the plasma supernatant was removed and stored at −80°C until use. Mice were then transcardially perfused with 60 ml cold, sterile PBS and perigonadal white adipose tissue (epididymal in males and parametrial in females, 300 mg) was carefully dissected for use in downstream applications. Uteri were collected in young and middle-aged female mice and the wet-weights recorded.

High-Density Lipoprotein (HDL), Low-Density Lipoprotein (LDL), and Triglyceride (TG) Assays

High-density lipoprotein and LDL concentrations in plasma were determined using colorimetric assays from Abcam (Cambridge, MA, USA) according to the manufacturer's instructions. Briefly, plasma was diluted 1:1 in precipitation buffer and incubated for 10 min at room temperature, followed by centrifugation (2,000 × *g* for 10 min). The supernatant containing the HDL fraction and the LDL precipitate were then incubated for 60 min at room temperature with cholesterol reaction mixture and read on a microplate reader

at OD 570 nm. For TG measurements, plasma was diluted 1:5 in TG assay buffer and TG was converted to glycerol and fatty acid by the addition of lipase. Following incubation with TG reaction mixture for 60 min at room temperature, plates were read at OD 570 nm.

Flow Cytometry

Adipose tissue was mechanically disrupted followed by digestion with collagenase II (C6885, 1 mg/ml, Sigma-Aldrich, St. Louis, MO, USA) at 37°C and 200 rpm for 45 min. EDTA (10 mM) was added during the last 5 min to facilitate dissociation of leukocytes from the adipocytes. The cell suspension was filtered through a 70-µm filter and Fc receptors were blocked with CD16/32 (BioLegend, San Diego, CA, USA) prior to staining of surface markers. Cells were stained for viability (Fixable Live/Dead Aqua Stain, Thermo Fisher Scientific, Waltham, MA, USA) for 30 min, followed by incubation with primary antibodies (CD45-BV605, CD8-BV421, and CD69-PE-Cy7 from Biolegend; and CD11b-PerCP-Cy5.5, CD4-APC, CD25-FITC, and CD3-APC-Cy7 from TONBO Biosciences, San Diego, CA, USA) for 30 min at room temperature. Subsequently, leukocytes were fixed and permeabilized with FoxP3 staining buffer set (eBioscience, Thermo Fisher Scientific) and stained with FoxP3-PE (eBioscience, Thermo Fisher Scientific) for 45 min at room temperature. Leukocytes were re-suspended in FACS buffer and count bright counting beads (Thermo Fischer Scientific) were added prior to reading in a Cytoflex S flow cytometer (Beckman-Coulter, Brea, CA, USA).

For intracellular cytokine staining, leukocytes were isolated as described above and 1×10^6 cells were incubated in complete RPMI-1640 containing Brefeldin A (Golgiplug, Thermo Fisher Scientific). Cells were then stimulated with Cell Stimulation Cocktail (eBioscience, Thermo Fisher Scientific) containing phorbol 12-myristate 13-acetate (PMA, 50 ng/ml) and ionomycin (0.95 µg/ml) or PBS (no stimulation control) and incubated for 4 h at 37°C (5% CO_2). Following Fc block and surface antigen staining (CD8-BV605, CD45-FITC, CD3 PerCP-Cy5.5, CD4-PE-Cy7, and CD11b-APC-Cy7), cells were fixed and permeabilized (BD Biosciences, San Jose, CA, USA). Cells were then stained for intracellular cytokines (IFN-γ-BV421, TNF-α-APC, granzyme B (GzmB)-PE, Biolegend) for 30 min on ice prior to flow cytometric analysis.

Multiplex Cytokine Measurement

Adipose tissue (300 mg) was homogenized in lysis buffer containing 10 mM Tris pH 7.4, 3 mM $MgCl_2$ and protease inhibitors (Roche Diagnostics, Basel, Switzerland). The homogenates were sonicated and centrifuged (1,000 × *g* for 5 min at 4°C) to separate the adipocytes, followed by a second spin at 12,000 × *g* for 15 min. Total protein concentration in the supernatants was determined with bicinchoninic acid protein assay kit (Pierce, Thermo Fisher Scientific). 50 µg of protein from each sample was loaded into a 96-well plate in duplicate and assayed according to the manufacturer's instructions using a Bio-Plex 200 system (Bio-Rad Laboratories, Hercules, CA, USA).

Analysis and Statistical Methods

For flow cytometry, leukocytes were isolated from approximately 300 mg of adipose tissue from each animal. Absolute counts were calculated by normalizing cell events to bead counts and adipose tissue weights. Statistical analysis was performed using two-way ANOVA with sex and age/treatment as the independent factors. *Post hoc* analysis was performed with Sidak's multiple comparisons test. Data from experiments using middle-aged animals only were analyzed with unpaired *t*-test or unpaired *t*-test with Welch's correction when variances were unequal. Statistical significance was considered at $p < 0.05$. All statistical analyses were performed with GraphPad Prism 7.

RESULTS

Age-Associated Increase in Adipose Tissue Mass and Shifted Lipid Profiles in Middle-Aged Females

Middle-aged mice at 15–16 months of age and young mice of 3–4 months of age were used in this study. Initially, we evaluated the translational relevance of our middle-aged male and female mice to study obesity-induced adipose tissue inflammation. A significant age-associated increase in body weight (not shown) and adipose tissue mass was observed in middle-aged males and females compared to young mice of the same sex (**Figure 1A**, two-way ANOVA, effect of age: $p < 0.001$).

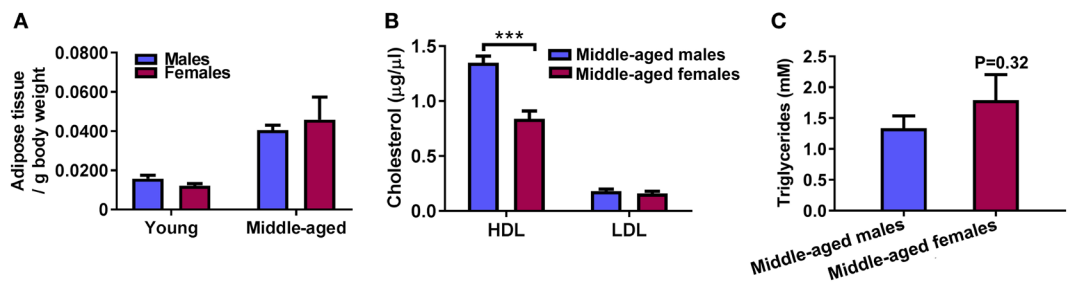

FIGURE 1 | Age-induced increase in adipose tissue mass and negatively shifted lipid profile in middle-aged females. **(A)** Perigonadal (epididymal in males and parametrial in females) adipose tissue mass normalized to body weight in young (3–4 months) and middle-aged (15–16 months) mice. Two-way ANOVA effect of age: $p < 0.001$, $n = 9$. **(B)** Plasma high-density lipoprotein (HDL) cholesterol and low-density lipoprotein cholesterol (LDL) in middle-aged mice. ***$p < 0.001$ unpaired *t*-test, $n = 10$. **(C)** Plasma triglycerides in middle-aged male and female mice. $p = 0.32$ unpaired *t*-test, $n = 9$–10.

No significant male vs female difference in body weight was seen in middle-aged mice (males: 40 ± 1 vs females: 35 ± 3 g, $n = 10$) while young males weighed more than young females (29 ± 1 vs 21 ± 1 g, $p < 0.05$, $n = 9$). Plasma TGs and HDL/LDL cholesterol levels were measured in middle-aged mice to determine the lipid profiles in these animals. Middle-aged females had lower levels of plasma HDL compared to males, a characteristic of dyslipidemia in humans (23), with no effect of sex seen on LDL cholesterol or TG levels (**Figures 1B,C**, $n = 10$). Lastly, we confirmed that middle-aged female mice used in our model were reproductively senescent. Similar to other studies, we observed an increase in uteri size in middle-aged females due to fibrosis and collagen deposition (Figure S1 in Supplementary Material) (24). We monitored the estrus cycle in young and middle-aged female mice. Vaginal smears were used to verify that young female mice were cycling while middle-aged females were acyclic and showed leukocyte-dominant diestrus-like smears (representative images in Figure S2 in Supplementary Material).

Female Sex Augments the Age-Associated Increase in Adipose Tissue CD8⁺ T Cells

Analysis of adipose tissue-derived immune cells using flow cytometry showed that there was no difference in the number of lymphoid and myeloid cells between young male and female mice (**Figure 2A**, $n = 5$). However, we found a significant increase in the lymphoid cells ($p < 0.001$), and a decrease in myeloid cells with age ($p < 0.001$), which was significantly more pronounced in females (**Figure 2A**). This change in the lymphoid-to-myeloid proportion in middle-aged females was mainly driven by a significant increase in lymphocyte cell counts (Figure S3 in Supplementary Material). There was no effect of age and sex on the lymphoid-to-myeloid cell ratio in the blood circulation, with lymphoid cells representing the dominant subset in all experimental groups (**Figure 2B**, $n = 5$).

Next, we tested whether the age-related increase in adipose tissue lymphoid cell populations was associated with changes in any specific T lymphocyte subpopulation. Flow cytometry was used to identify adipose tissue CD4⁺ and CD8⁺ T-cell populations in young and middle-aged mice of both sexes. Representative contour plots of adipose CD4⁺ and CD8⁺ T-cell populations, with outliers, from young and middle-aged mice are shown in **Figure 2C**. Middle-aged mice overall, and females especially, showed a greater age-associated increase in CD8⁺ T cells compared to young mice (% increase compared to young, females: 86 ± 5, males: 66 ± 8, $p \leq 0.05$). The proportion of adipose CD8⁺ T cells was larger in middle-aged females than in males (**Figure 2D**, $p < 0.05$). No significant age or sex differences in CD4⁺ T cells were observed (**Figure 2E**). When we measured CD8⁺ T-cell activation, we found that middle-aged females had significantly more CD8⁺ T cells that expressed CD69, a marker indicative of early T-cell activation (**Figures 2F,G**, $p < 0.001$). Analysis of CD4⁺ and CD8⁺ T-cell populations in the spleen as a comparison showed a trend toward lower levels of CD8⁺ T cells in young females that reached significance in the middle age (Figure S4A in Supplementary Material). In line with this finding, the proportion of CD4⁺ T cells was significantly higher in middle-aged females (Figure S4B in Supplementary Material).

Sex Differences in CD8⁺ T-Cell-Associated Cytokines in Adipose Tissue

Having demonstrated that middle-aged females exhibited a pronounced age-induced increase in activated CD8⁺ T cells, we characterized their phenotype. *Ex vivo* stimulation assay using PMA and ionomycin showed a strong induced production of IFN-γ in CD8⁺ T cells from middle-aged females that was significantly larger compared to middle-aged males (**Figures 3A,B**, two-way ANOVA, stim middle-aged females vs stim middle-aged males: $p < 0.001$, $n = 5$). Similar results were obtained for IFN-γ⁺ CD4⁺ T cell after stimulation (**Figure 3C**). We further measured the induced response of CD8⁺ T cells to produce TNF-α and granzyme B (GzmB), effector mechanisms of CD8⁺ T cells in mediating target cell lysis and apoptosis. Stimulation with PMA/ionomycin induced a significant increase in TNF-α⁺ CD8⁺ T cells in middle-aged females (no stim vs stim, $p < 0.001$, $n = 5$) that was significantly higher than in middle-aged males after stimulation ($p < 0.001$, **Figure 3D**). Likewise, the stimulation only led to increased GzmB production in middle-aged females and not in middle-aged males ($p < 0.05$) (**Figure 3E**).

Supporting the IFN-γ finding in our *ex vivo* studies, analysis of cytokine levels in adipose tissue homogenate showed higher levels of IFN-γ (**Figure 3F**, $p \leq 0.05$, $n = 8$–10) in female adipose tissue. Lastly, we measured the levels of RANTES (CCL5), a known CD8⁺ T-cell chemokine and ligand for the CCR5 receptor, and macrophage inflammatory protein 1β (MIP-1β, CCL4), another chemokine with specificity for the CCR5 receptor. Adipose tissue homogenates of middle-aged females showed higher levels of both RANTES and MIP-1β compared to age-matched males (**Figures 3G,H**, $p < 0.05$).

Higher Levels of Adipose Tregs in Males Compared to Age-Matched Females

Regulatory T cells is a sub-population of CD4⁺ T cells that express the T-cell activation marker CD25 and nuclear FoxP3 (gating strategy and representative contour plots in **Figures 4A,B**). In contrast to the age-associated increase in adipose CD8⁺ T cells in middle-aged females, no change in anti-inflammatory Tregs with age was observed (**Figure 4C**, $n = 9$). Independent of their age, females had significantly less adipose Tregs compared to age-matched males (two-way ANOVA, effect of sex: $p < 0.001$, **Figure 4C**). Thus, in the context of increasing pro-inflammatory CD8⁺ T cells, this lack of Treg increase in middle-aged females results in a shift in balance to the pro-inflammatory T-cell phenotype.

DISCUSSION

In the present study, we demonstrate that middle-aged mice of both sexes have significantly higher levels of adipose tissue CD8⁺ T cells than young mice. Interestingly, middle-aged female mice have a greater age-related increase in adipose CD8⁺ T cells compared to middle-aged males. No effects of sex or age were seen in

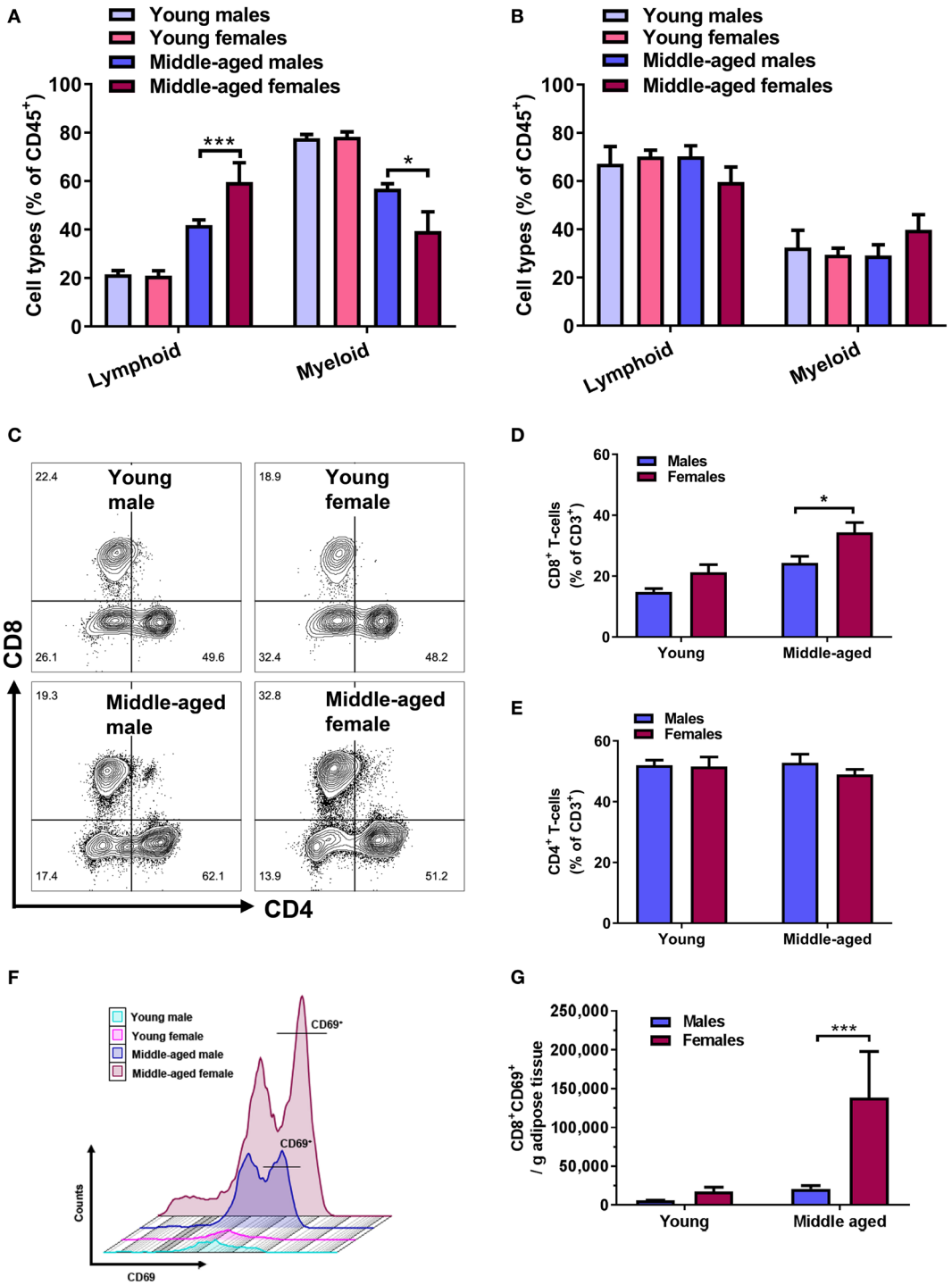

FIGURE 2 | Age-associated increases in adipose lymphoid cells and CD8⁺ T cells are pronounced in females. Flow cytometry quantification of lymphoid ($CD45^+CD11b^-$) and myeloid cell ($CD45^+CD11b^+$) percentages of **(A)** adipose tissue and **(B)** blood-derived immune cells. Two-way ANOVA lymphoid cells: effect of age $p < 0.001$, effect of sex $p < 0.01$; myeloid cells: effect of age $p < 0.001$, $^*p < 0.05$, $^{***}p < 0.001$ Sidak's multiple comparison's test, $n = 5$. **(C)** Representative contour plots of CD4⁺ and CD8⁺ T-cell populations, with outliers displayed, in adipose tissue of young and middle-aged male and female mice. **(D)** Quantification of CD8⁺ T-cell percentages ($CD3^+CD8^+$) and **(E)** CD4⁺ T cells ($CD3^+CD4^+$) in adipose tissue of young and middle-aged mice using flow cytometry. Two-way ANOVA effect of age: $p < 0.001$, sex: $p < 0.01$. $^*p < 0.05$ Sidak's multiple comparison's test, $n = 8$–9. **(F)** Representative histograms of $CD8^+CD69^+$ T cells in adipose tissue from young and middle-aged male and female mice. **(G)** Absolute number of activated CD8⁺ T cells ($CD8^+CD69^+$) normalized to bead counts and adipose tissue weights. Two-way ANOVA effect of age: $p < 0.05$, sex: $p < 0.05$, $^{***}p < 0.001$ Sidak's multiple comparison's test, $n = 5$.

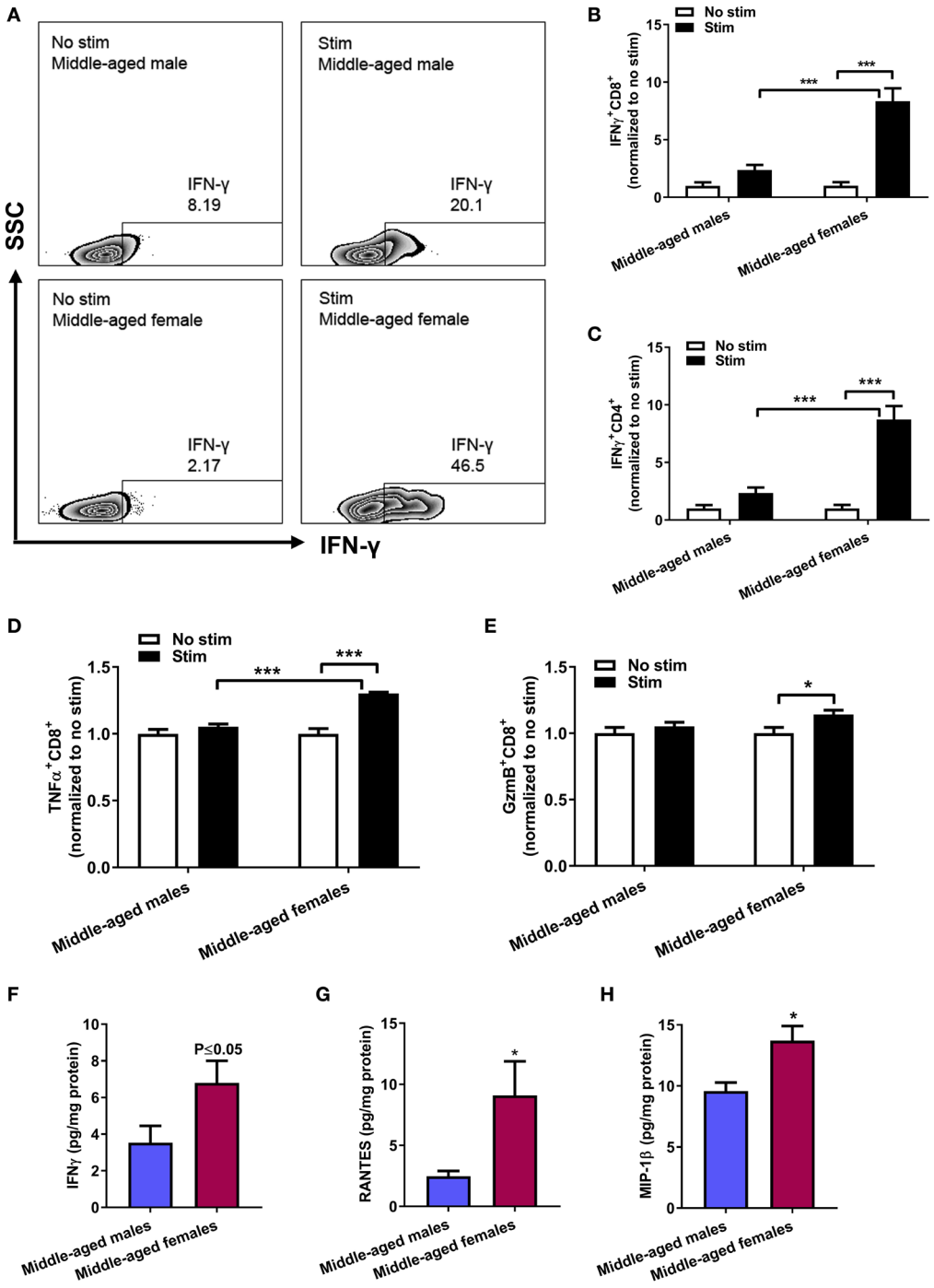

FIGURE 3 | Sex differences in adipose CD8⁺ T-cell cytokine production *ex vivo* and total adipose cytokine levels. **(A)** Representative contour plots of IFN-γ⁺CD8⁺ T cells after *ex vivo* stimulation with phorbol 12-myristate 13-acetate and ionomycin for 4 h at 37°C 5% CO_2. Quantification of **(B)** IFN-γ⁺CD8⁺ T cells, **(C)** IFN-γ⁺CD4⁺ T cells, **(D)** TNF-α⁺CD8⁺ T cells, and **(E)** Granzyme B (GzmB)⁺CD8⁺ T cells normalized to no stimulation conditions within each sex. Two-way ANOVA, $^{*}p < 0.05$, $^{***}p < 0.001$ Sidak's multiple comparison's test, $n = 5$. Total adipose levels of **(F)** IFN-γ, **(G)** RANTES, and **(H)** MIP-1β in middle-aged mice by multiplex cytokine measurement. $p \leq 0.05$ unpaired *t*-test, $^{*}p < 0.05$ unpaired *t*-test with Welch's correction, $n = 8$–10.

adipose CD4⁺ T-cell levels, suggesting that age-related adipose tissue T-cell infiltration may be subset specific.

Importantly, middle-aged females had significantly higher numbers of activated (CD69⁺) CD8⁺ T cells in adipose tissue when compared to middle-aged male mice and young mice of both sexes, suggesting that these cells are in a basally activated state. Following *ex vivo* stimulation, CD8⁺ T cells from the adipose tissue of middle-aged female mice produced significantly

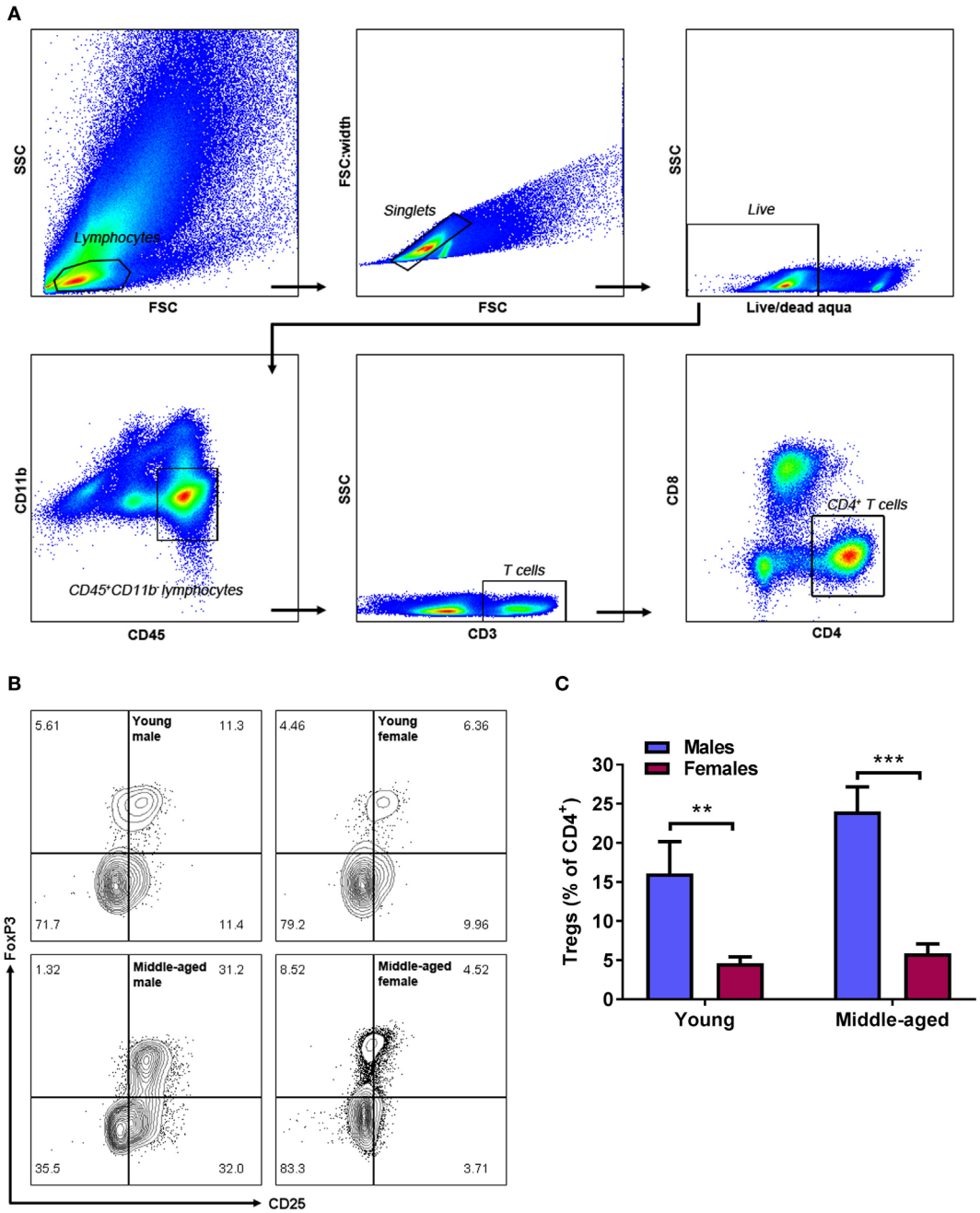

FIGURE 4 | Males have higher levels of adipose regulatory T cells (Tregs) compared to age-matched females. Gating strategy **(A)**, representative contour plots **(B)**, and quantification **(C)** of $CD4^+CD25^+FoxP3^+$ Tregs in adipose tissue from young and middle-aged male and female mice. Two-way ANOVA effect of sex: $p < 0.001$, $^{**}p < 0.01$, $^{***}p < 0.001$ Sidak's multiple comparison's test, $n = 9$.

higher levels of intracellular IFN-γ, TNF-α, and GzmB than their male counterparts confirming that these T cells have a stronger pro-inflammatory phenotype. Multiplex cytokine measurements further showed higher levels of IFN-γ, RANTES, and MIP-1β in adipose tissue harvested from females. In parallel, we demonstrate that middle-aged females have lower levels of Tregs, a pro-homeostatic immune cell that normally decreases in number in mice and humans in obesity (17, 18). The balance shift of high levels of inflammatory $CD8^+$ T cells and low levels of anti-inflammatory Tregs may promote an overall pro-inflammatory milieu in aging females (**Figure 5**) that could have adverse adipose consequences.

The rising incidence of obesity poses a major health risk worldwide and is especially a concern in the aging population (5). Almost a decade ago, a series of experimental studies suggested the importance of $CD8^+$ T cells in obesity and adipose

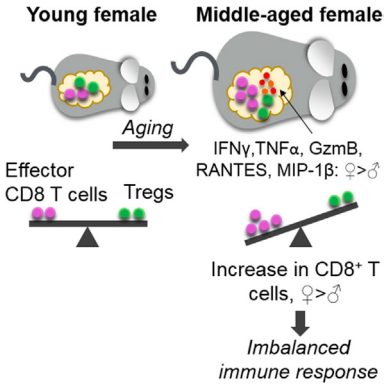

FIGURE 5 | Age-associated increase in adipose CD8+ T cells and imbalanced immune response in middle-aged females. Middle-aged females had a greater increase in adipose effector CD8+ T cells than males, without a compensatory increase in anti-inflammatory regulatory T cells (Tregs). Higher levels of the CD8+ T-cell chemokine RANTES, MIP-1β, and the pro-inflammatory cytokines IFN-γ, TNF-α, and granzyme B (GzmB) were also observed in middle-aged females. We hypothesize that this imbalance may promote a pro-inflammatory milieu and contribute to increased cardiovascular disease burden in aging females.

tissue inflammation, especially during early stages of obesity development (15–17, 25). CD8+ T-cell infiltration into adipose tissue preceded the infiltration of macrophages and was proposed to be responsible for the initiation and propagation of adipose tissue inflammation (16). It was also shown that CD8+ T cells in adipose tissue exhibit an activated phenotype, characterized by increased proliferation and augmented expression of IFN-γ (26). While most of the studies pertaining to adipose inflammation were performed in young male mice and utilized either genetic- or diet-induced models of obesity, studies comparing sex or addressing age as a factor are missing in the literature. Furthermore, it has been shown that diet-induced obesity induces different types of adipose tissue inflammation than what is observed with natural age-induced obesity (27). In addition, by using diet- or genetic-induced obesity, the body and vasculature of the animal is still young, rather than middle aged. These points are critically significant because obesity may be more common in aging women and may confer greater risk for secondary health issues such as ischemic stroke (1, 4, 5, 8, 9).

Consistent with previous studies (15, 16, 26), we confirm that increased adipose tissue mass (here, due to aging) is associated with increased number of adipose tissue lymphocytes, particularly CD8+ T cells. To our knowledge, our present studies provide the first evidence that female sex augments the age-induced increase in adipose CD8+ T-cell number and activation compared to middle-aged males. Female sex was also found to augment the pro-inflammatory T-cell phenotype in middle-aged animals, as activated CD8+ T cells harvested from the adipose tissue of female animals produced higher levels of IFN-γ, TNF-α, and GzmB when stimulated with PMA and ionomycin *ex vivo*. These cytokines and lytic enzymes are an essential part of cytotoxic CD8+ T-cell-mediated mechanisms of action. Upon recognition of antigens on the surface of target cells, the main act of cytotoxic T cells is to release specialized lytic granules containing perforin and granzymes to kill the target cells. CD8+ T cells also act by releasing cytokines IFN-γ, TNF-α, and TNF-β to recruit and activate macrophages (28). Hence, our *ex vivo* stimulation data show that the main effector mechanisms of CD8+ T cells were potentiated in middle-aged females. As further *in vivo* support for this finding, cytokine measurement in adipose tissue homogenates showed higher levels of IFN-γ in middle-aged females compared to males.

Regulatory T cells have been shown to play an important role in the downregulation of inflammation in obesity. Obese human subjects have lower levels of circulating Tregs and decreased mRNA expression of the Treg-specific FoxP3 transcript in omental adipose tissue compared to normal weight controls (17, 18). The phenomenon of decreased Treg numbers in adipose tissue has been replicated in mice using both genetic- and diet-induced obesity models (17). These earlier studies have also demonstrated that acute depletion of Tregs results in increased transcription of inflammatory genes in adipose tissue, suggesting that Tregs play an important role in suppressing obesity-related inflammation. Our data show that, independent of age, females had significantly lower number of adipose Tregs than males. The age-induced increase in activated CD8+ T cells and production of IFN-γ, TNF-α, and GzmB in females, particularly without a compensatory expansion of Tregs, may create an immune imbalance and foster a pro-inflammatory environment in the adipose tissue of middle-aged females (**Figure 5**).

The mechanisms underlying the age-induced accumulation of CD8+ T cells in adipose tissue, and the greater accumulation and pro-inflammatory activation of CD8+ T cells seen in middle-aged females, remain unknown. Our studies demonstrated increased levels of RANTES and MIP-1β in middle-aged females. These chemokines are both ligands that can bind to the CCR5 receptor, an important step in the attraction of T cells to specific tissue, and are shown to be increased in adipose tissue from obese mice and in obese humans (16, 29, 30). MIP-1β has been reported to attract NK cells (31), but our preliminary data show decreased NK cell levels with aging and did not differ between males and females (unpublished data), suggesting that the sex differences in MIP-1β levels most likely are not associated with NK cells. As MIP-1β is produced in large amounts by activated CD8+ T cells, our multiplex data are in line with our other results showing a stronger pro-inflammatory state in middle-aged female CD8+ T-cell parameters (CD69+ activation and the induced production of IFN-γ, TNF-α, and GzmB). RANTES has further been demonstrated to be specifically important for the recruitment and regulation of CD8+ T cells (32). Once recruited to adipose tissue, T cells must be activated to sustain a pro-inflammatory phenotype. Our results showing a large number of activated CD8+CD69+ T cells in adipose tissue of middle-aged females suggest that these cells have a basally active phenotype.

Few studies on obesity-related adipose tissue inflammation have investigated sex differences. In a study by Wu et al., young male and female mice were fed a high-fat diet for 24 weeks (30). The authors showed a greater accumulation of T cells in males, along with an increased expression of RANTES and CCR5, compared to females. Protection from obesity-associated inflammation in young females has been reported by others (33, 34). High-fat diet fed females showed no increase in adipose

macrophages, a lack of systemic inflammation, and an expansion of their Treg population, while the opposite effects were seen in young males (34). Estrogen likely contributes to the protection seen in young females, as ovariectomy increases adipose tissue mass and the infiltration of T cells and macrophages (35). Sex chromosomes are also important, as mice with two X chromosomes have increased adiposity and food intake independent of gonadal sex in the four core genotype model (36). Our study in middle-aged animals shows significant sex differences in obesity-related inflammation, which was characterized by an augmented age-induced accumulation of $CD8^+$ T cells in the adipose tissue of female animals, higher levels of adipose IFN-γ, TNF-α, GzmB, RANTES, and MIP-1β in female mice, and the absence of an age-related expansion of the adipose tissue Treg population in middle-aged females. The results highlight the importance of using middle-aged and aged animals of both sexes in obesity-related studies.

The shift in adipose T cells seen in middle age could be a potential contributing mechanism to the switch from an "ischemia-protected" phenotype in young female mice to an "ischemia-sensitive" phenotype in middle-aged (3). A connecting link between obesity, adipose tissue inflammation, and inflammation in the brain has been reported in mice and humans (14, 37). Future studies are needed to investigate the adipose-to-brain inflammation axis in females and middle-aged animals.

Limitations and Future Directions

In the current study, we investigated sex differences in T cells and Tregs from the abdominal adipose tissue depot as several studies show that central obesity is linked to cardiovascular disease such as ischemic stroke, and may contribute to a greater risk in women than in men (1, 8, 9). In addition, abdominal adipose tissue is one of the larger depots which made it possible for us to perform the present flow cytometry experiments and functional assays. However, a recent study suggests that other adipose tissue depots, such as epicardial adipose tissue (EAT), may also present sex differences in obesity and aging (38). It has also been shown that EAT from patients with coronary heart disease had accumulation of $CD8^+$ T cells compared to healthy patients (39). In the latter study, no sex-specific analysis was made and sex differences in age-dependent EAT inflammation and immune responses remains to be investigated.

The present study focused on lymphocytes, T cells in particular, in adipose tissue inflammation with aging as these cell populations markedly increase with age. The current study contributes to our knowledge of the established role of $CD8^+$ T cells in obesity and augments data from previous studies. However, accumulation of myeloid cells, such as macrophages, in adipose tissue is an important contributor and consequence of obesity and also warrants study. In addition, how this shift in T cells contributes to systemic inflammation and their specific contribution to the response to brain injury remains to be investigated. In particular, we plan to examine the potential causative role of adipose $CD8^+$ T cell to Treg balance on stroke outcome in middle-aged mice.

CONCLUSION

We propose that increased levels of activated adipose $CD8^+$ T cells in combination with low levels of anti-inflammatory Tregs create an imbalance in the pro/anti-inflammatory T-cell milieu and contribute to a "primed" pro-inflammatory environment in middle-aged females. This may render middle-aged females more susceptible to secondary health issues that increase in incidence with aging, such as cardiovascular disease and ischemic stroke.

ETHICS STATEMENT

Animal procedures were performed in accordance with National Institutes of Health Guidelines for the care and use of laboratory animals and approved by the Animal Welfare Committee at the University of Texas Health Science Center at Houston, Texas (AWC-15-0140).

AUTHOR CONTRIBUTIONS

HA made substantial contributions to the conception, design, and drafting of the work and performed all experiments. JA, SM, LM, and MR-O provided substantial contribution to the design of the work as well as revising for important intellectual content. MR-O, MS, AM, JB-A, and AC contributed to the flow cytometry experiments and revised the manuscript. All authors have read and approved the final version to be published.

FUNDING

This study was funded by the National Institute of Neurological Disorders and Stroke Grant R01 NS055215, NS094543, NS094280, and NS096186, American Heart Association (AHA) Postdoctoral Fellowship #17POST33660010 and postdoctoral fellowships from the Swedish Heart-Lung Foundation #20140444 and the Swedish Medical Society #SLS-404121.

SUPPLEMENTARY MATERIAL

The Supplementary Material for this article can be found online at https://www.frontiersin.org/articles/10.3389/fimmu.2018.00659/full#supplementary-material.

REFERENCES

1. Towfighi A, Saver JL, Engelhardt R, Ovbiagele B. A midlife stroke surge among women in the United States. *Neurology* (2007) 69:1898–904. doi:10.1212/01.wnl.0000268491.89956.c2
2. Towfighi A, Zheng L, Ovbiagele B. Sex-specific trends in midlife coronary heart disease risk and prevalence. *Arch Intern Med* (2009) 169:1762–6. doi:10.1001/archinternmed.2009.318
3. Manwani B, Liu F, Scranton V, Hammond MD, Sansing LH, McCullough LD. Differential effects of aging and sex on stroke induced inflammation across the lifespan. *Exp Neurol* (2013) 249:120–31. doi:10.1016/j.expneurol.2013.08.011
4. Mauvais-Jarvis F. Sex differences in metabolic homeostasis, diabetes, and obesity. *Biol Sex Differ* (2015) 6:14. doi:10.1186/s13293-015-0033-y
5. Kelly T, Yang W, Chen C-S, Reynolds K, He J. Global burden of obesity in 2005 and projections to 2030. *Int J Obes (Lond)* (2008) 32:1431–7. doi:10.1038/ijo.2008.102

6. Ford ES, Giles W, Mokdad A. Increasing prevalence of the metabolic. *Diabetes Care* (2004) 27:2444–9. doi:10.2337/diacare.27.10.2444
7. Davis SR, Castelo-Branco C, Chedraui P, Lumsden MA, Nappi RE, Shah D, et al. Understanding weight gain at menopause. *Climacteric* (2012) 15:419–29. doi:10.3109/13697137.2012.707385
8. Rodriguez-Campello A, Jimenez-Conde J, Ois A, Cuadrado-Godia E, Giralt-Steinhauer E, Vivanco RM, et al. Sex-related differences in abdominal obesity impact on ischemic stroke risk. *Eur J Neurol* (2016) 0:1–7. doi:10.1111/ene.13216
9. Zahn K, Linseisen J, Heier M, Peters A, Thorand B, Nairz F, et al. Body fat distribution and risk of incident ischemic stroke in men and women aged 50 to 74 years from the general population. The KORA Augsburg cohort study. *PLoS One* (2018) 13:e0191630. doi:10.1371/journal.pone.0191630
10. Ouchi N, Parker JL, Lugus JJ, Walsh K. Adipokines in inflammation and metabolic disease. *Nat Rev Immunol* (2011) 11:85–97. doi:10.1038/nri2921
11. Gerriets VA, MacIver NJ. Role of T cells in malnutrition and obesity. *Front Immunol* (2014) 5:379. doi:10.3389/fimmu.2014.00379
12. Frasca D, Blomberg BB, Paganelli R. Aging, obesity, and inflammatory age-related diseases. *Front Immunol* (2017) 8:1745. doi:10.3389/fimmu.2017.01745
13. Guzik TJ, Skiba DS, Touyz RM, Harrison DG. The role of infiltrating immune cells in dysfunctional adipose tissue. *Cardiovasc Res* (2017) 113:1009–23. doi:10.1093/cvr/cvx108
14. Stranahan AM, Hao S, Dey A, Yu X, Baban B. Blood-brain barrier breakdown promotes macrophage infiltration and cognitive impairment in leptin receptor-deficient mice. *J Cereb Blood Flow Metab* (2016) 36(12):2108–21. doi:10.1177/0271678X16642233
15. Winer S, Chan Y, Paltser G, Truong D, Tsui H, Bahrami J, et al. Normalization of obesity-associated insulin resistance through immunotherapy. *Nat Med* (2009) 15:921–9. doi:10.1038/nm.2001
16. Nishimura S, Manabe I, Nagasaki M, Eto K, Yamashita H, Ohsugi M, et al. CD8+ effector T cells contribute to macrophage recruitment and adipose tissue inflammation in obesity. *Nat Med* (2009) 15:914–20. doi:10.1038/nm.1964
17. Feuerer M, Herrero L, Cipolletta D, Naaz A, Wong J, Nayer A, et al. Lean, but not obese, fat is enriched for a unique population of regulatory T cells that affect metabolic parameters. *Nat Med* (2009) 15:930–9. doi:10.1038/nm.2002
18. Wagner NM, Brandhorst G, Czepluch F, Lankeit M, Eberle C, Herzberg S, et al. Circulating regulatory T cells are reduced in obesity and may identify subjects at increased metabolic and cardiovascular risk. *Obesity* (2013) 21:461–8. doi:10.1002/oby.20087
19. Travers RL, Motta AC, Betts JA, Bouloumié A, Thompson D. The impact of adiposity on adipose tissue-resident lymphocyte activation in humans. *Int J Obes (Lond)* (2015) 39(5):762–9. doi:10.1038/ijo.2014.195
20. Gami AS, Witt BJ, Howard DE, Erwin PJ, Gami LA, Somers VK, et al. Metabolic syndrome and risk of incident cardiovascular events and death. A systematic review and meta-analysis of longitudinal studies. *J Am Coll Cardiol* (2007) 49:403–14. doi:10.1016/j.jacc.2006.09.032
21. Goldman JM, Murr AS, Cooper RL. The rodent estrous cycle: characterization of vaginal cytology and its utility in toxicological studies. *Birth Defects Res B Dev Reprod Toxicol* (2007) 80:84–97. doi:10.1002/bdrb.20106
22. Marcondes FK, Bianchi F, Tanno A. Determination of the estrous cycle phases of rats: some helpful considerations. *Braz J Biol* (2002) 62:609–14. doi:10.1590/S1519-69842002000400008
23. Mooradian AD, Haas MJ, Wehmeier KR, Wong NCW. Obesity-related changes in high-density lipoprotein metabolism. *Obesity* (2008) 16:1152–60. doi:10.1038/oby.2008.202
24. Kong SB, Zhang S, Chen YJ, Wang WX, Wang BY, Chen Q, et al. Determinants of uterine aging: lessons from rodent models. *Sci China Life Sci* (2012) 55:687–93. doi:10.1007/s11427-012-4356-1
25. Rausch ME, Weisberg S, Vardhana P, Tortoriello DV. Obesity in C57BL/6J mice is characterized by adipose tissue hypoxia and cytotoxic T-cell infiltration. *Int J Obes* (2008) 32:451–63. doi:10.1038/sj.ijo.0803744
26. Jiang E, Perrard XD, Yang D, Khan IM, Perrard JL, Smith CW, et al. Essential role of CD11a in CD8+ T-cell accumulation and activation in adipose tissue. *Arterioscler Thromb Vasc Biol* (2014) 34:34–43. doi:10.1161/ATVBAHA.113.302077
27. Bapat SP, Myoung Suh J, Fang S, Liu S, Zhang Y, Cheng A, et al. Depletion of fat-resident Treg cells prevents age-associated insulin resistance. *Nature* (2015) 528:137–41. doi:10.1038/nature16151
28. Janeway CA, Travers P, Walport M, Shlomchik MJ. Immunobiology: the immune system in health and disease. *Garland Science*. New York (2001) 892 p.
29. Dalmas E, Rouault C, Abdennour M, Rovere C, Rizkalla S, Bar-Hen A, et al. Variations in circulating inflammatory factors are related to changes in calorie and carbohydrate intakes early in the course of surgery-induced weight reduction1-3. *Am J Clin Nutr* (2011) 94:450–8. doi:10.3945/ajcn.111.013771
30. Wu H, Ghosh S, Perrard XD, Feng L, Garcia GE, Perrard JL, et al. T-cell accumulation and regulated on activation, normal T cell expressed and secreted upregulation in adipose tissue in obesity. *Circulation* (2007) 115:1029–38. doi:10.1161/CIRCULATIONAHA.106.638379
31. Robertson MJ. Role of chemokines in the biology of natural killer cells. *J Leukoc Biol* (2010) 71:173–83.
32. Crawford A, Angelosanto JM, Nadwodny KL, Blackburn SD, Wherry EJ. A role for the chemokine RANTES in regulating CD8 T cell responses during chronic viral infection. *PLoS Pathog* (2011) 7:e1002098. doi:10.1371/journal.ppat.1002098
33. Singer K, Maley N, Mergian T, DelProposto J, Cho KW, Zamarron BF, et al. Differences in hematopoietic stem cells contribute to sexually dimorphic inflammatory responses to high fat diet-induced obesity. *J Biol Chem* (2015) 290:13250–62. doi:10.1074/jbc.M114.634568
34. Pettersson US, Waldén TB, Carlsson P-O, Jansson L, Phillipson M. Female mice are protected against high-fat diet induced metabolic syndrome and increase the regulatory T cell population in adipose tissue. *PLoS One* (2012) 7:e46057. doi:10.1371/journal.pone.0046057
35. Choi EK, Kim WK, Sul OJ, Park YK, Kim ES, Suh JH, et al. TNFRSF14 deficiency protects against ovariectomy-induced adipose tissue inflammation. *J Endocrinol* (2014) 220:25–33. doi:10.1530/JOE-13-0341
36. Chen X, McClusky R, Chen J, Beaven SW, Tontonoz P, Arnold AP, et al. The number of X chromosomes causes sex differences in adiposity in mice. *PLoS Genet* (2012) 8(5):e1002709. doi:10.1371/journal.pgen.1002709
37. Drake C, Boutin H, Jones MS, Denes A, McColl BW, Selvarajah JR, et al. Brain inflammation is induced by co-morbidities and risk factors for stroke. *Brain Behav Immun* (2011) 25:1113–22. doi:10.1016/j.bbi.2011.02.008
38. Kocher C, Christiansen M, Martin S, Adams C, Wehner P, Gress T, et al. Sexual dimorphism in obesity-related genes in the epicardial fat during aging. *J Physiol Biochem* (2016) 73(2):215–24. doi:10.1007/s13105-016-0542-0
39. Hirata Y, Kurobe H, Akaike M, Chikugo F, Hori T, Bando Y, et al. Enhanced inflammation in epicardial fat in patients with coronary artery disease. *Int Heart J* (2011) 52:139–42. doi:10.1536/ihj.52.139

Conflict of Interest Statement: The authors declare that the research was conducted in the absence of any commercial or financial relationships that could be construed as a potential conflict of interest.

Copyright © 2018 Ahnstedt, Roy-O'Reilly, Spychala, Mobley, Bravo-Alegria, Chauhan, Aronowski, Marrelli and McCullough. This is an open-access article distributed under the terms of the Creative Commons Attribution License (CC BY). The use, distribution or reproduction in other forums is permitted, provided the original author(s) and the copyright owner are credited and that the original publication in this journal is cited, in accordance with accepted academic practice. No use, distribution or reproduction is permitted which does not comply with these terms.

frontiers in Immunology

ORIGINAL RESEARCH
published: 20 April 2018
doi: 10.3389/fimmu.2018.00809

Expression and Function of IL12/23 Related Cytokine Subunits (p35, p40, and p19) in Giant-Cell Arteritis Lesions: Contribution of p40 to Th1- and Th17-Mediated Inflammatory Pathways

Georgina Espígol-Frigolé[1†], Ester Planas-Rigol[1†], Ester Lozano[1], Marc Corbera-Bellalta[1], Nekane Terrades-García[1], Sergio Prieto-González[1], Ana García-Martínez[2], Jose Hernández-Rodríguez[1], Josep M. Grau[3] and Maria C. Cid[1*]*

[1] Vasculitis Research Unit, Department of Autoimmune Diseases, Clinical Institute of Medicine and Dermatology, Hospital Clinic, University of Barcelona, Institut d'Investigacions Biomèdiques August Pi i Sunyer (IDIBAPS-CRB CELLEX), Barcelona, Spain, [2] Vasculitis Research Unit, Department of Emergency Medicine, Hospital Clínic, University of Barcelona, IDIBAPS, Barcelona, Spain, [3] Department of Internal Medicine, Hospital Clínic, University of Barcelona, IDIBAPS, Barcelona, Spain

Background: Giant-cell arteritis (GCA) is considered a T helper (Th)1- and Th17-mediated disease. Interleukin (IL)-12 is a heterodimeric cytokine (p35/p40) involved in Th1 differentiation. When combining with p19 subunit, p40 compose IL-23, a powerful pro-inflammatory cytokine that maintains Th17 response.

Objectives: The aims of this study were to investigate p40, p35, and p19 subunit expression in GCA lesions and their combinations to conform different cytokines, to assess the effect of glucocorticoid treatment on subunit expression, and to explore functional roles of p40 by culturing temporal artery sections with a neutralizing anti-human IL-12/IL-23p40 antibody.

Methods and results: p40 and p19 mRNA concentrations measured by real-time RT-PCR were significantly higher in temporal arteries from 50 patients compared to 20 controls (4.35 ± 4.06 vs 0.51 ± 0.75; $p < 0.0001$ and 20.32 ± 21.78 vs 4.17 ± 4.43 relative units; $p < 0.0001$, respectively). No differences were found in constitutively expressed p35 mRNA. Contrarily, p40 and p19 mRNAs were decreased in temporal arteries from 16 treated GCA patients vs those from 34 treatment-naïve GCA patients. Accordingly, dexamethasone reduced p40 and p19 expression in cultured arteries. Subunit associations to conform IL-12 and IL-23 were confirmed by proximity-ligation assay in GCA lesions. Immunofluorescence revealed widespread p19 and p35 expression by inflammatory cells, independent from p40. Blocking IL-12/IL-23p40 tended to reduce IFNγ and IL-17 mRNA production by cultured GCA arteries and tended to increase Th17 inducers IL-1β and IL-6.

Conclusion: IL-12 and IL-23 heterodimers are increased in GCA lesions and decrease with glucocorticoid treatment. p19 and p35 subunits are much more abundant than p40, indicating an independent role for these subunits or their potential association with

OPEN ACCESS

Edited by:
Jixin Zhong,
Case Western Reserve University,
United States

Reviewed by:
Paul Proost,
KU Leuven, Belgium
Christoph Baerwald,
Universitätsklinikum Leipzig,
Germany

***Correspondence:**
Georgina Espígol-Frigolé
georginaespigol@gmail.com;
Maria C. Cid
mccid@clinic.ub.es

[†]These authors have contributed equally to this work.

Specialty section:
This article was submitted to Cytokines and Soluble Mediators in Immunity, a section of the journal Frontiers in Immunology

Received: 14 December 2017
Accepted: 03 April 2018
Published: 20 April 2018

Citation:
Espígol-Frigolé G, Planas-Rigol E, Lozano E, Corbera-Bellalta M, Terrades-García N, Prieto-González S, García-Martínez A, Hernández-Rodríguez J, Grau JM and Cid MC (2018) Expression and Function of IL12/23 Related Cytokine Subunits (p35, p40, and p19) in Giant-Cell Arteritis Lesions: Contribution of p40 to Th1- and Th17-Mediated Inflammatory Pathways. Front. Immunol. 9:809. doi: 10.3389/fimmu.2018.00809

alternative subunits. The modest effect of IL-12/IL-23p40 neutralization may indicate compensation by redundant cytokines or cytokines resulting from alternative combinations.

Keywords: giant-cell arteritis, Th1/Th17 cytokines, IL-12/23 p40, IL-23p19, IL-12p35, glucocorticoid, biologic therapies

INTRODUCTION

Giant-cell arteritis (GCA) is a granulomatous vasculitis involving large and medium sized-arteries in aged individuals (1, 2). Glucocorticoids remain the cornerstone of remission-induction in GCA. However, about 40–60% of patients relapse when glucocorticoids (GC) are tapered (3–5). Recently, randomized controlled trials have indicated that inhibiting T-cell activation with abatacept (6) and, particularly, blocking interleukin (IL)-6 receptor with tocilizumab are effective in maintaining glucocorticoid-induced remission (7, 8). However, not all patients respond indicating an unmet need for a better understanding of the hierarchy and contribution of additional pathogenic pathways in GCA.

Giant-cell arteritis has been classically considered a T helper (Th)1-mediated disease based on the presence of granulomas and the expression of interferon (IFN)γ and IFNγ-induced products in the arterial lesions (9–14). However, data generated in recent years indicate that Th17-mediated mechanisms also play a significant role in GCA (14–17).

IL-12 and IL-23 are cytokines mainly produced by dendritic cells and macrophages that regulate the development of Th1 and Th17 responses, respectively. IL-12 is a heterodimeric cytokine composed by two subunits, p35 and p40, with a seminal role in Th1 differentiation and IFNγ production. The IL-12p40 subunit may also interact with p19 to conform IL-23, a crucial cytokine in maintaining and expanding Th17 differentiation (18). The observation that IL-12/23p40-deficient mice were resistant to experimentally induced autoimmune diseases suggested that IL-12 and IL-23 play a major role in triggering or maintaining chronic inflammatory diseases (19). According to these models, IL-23 might have a more prominent pro-inflammatory role since IL-12p35-deficient mice may show exacerbated disease (19–22). Currently, several therapeutic agents targeting IL-12, IL-23, or IL-17 are being tested in clinical trials for a variety of immune-mediated diseases (23).

Preliminary studies have shown that IL-12/23p40, IL-12p35, and IL-23p19 subunits are expressed in GCA lesions (24, 25), but their relative expression, combinations and functions have not been addressed. Interestingly, IL-12/23p40 but not IL-12p35 expression was increased in temporal artery biopsies from patients with relapsing GCA after 1 year of treatment (25), indicating independent functions for both subunits and suggesting a role for IL-23 in persistent disease activity (25).

The aims of this study were to investigate IL-12/23p40, IL-12p35, and IL-23p19 subunit expression in GCA lesions and their combination to conform different cytokines, to investigate the effect of glucocorticoid treatment on subunit expression, to analyze the relationship between subunit expression and glucocorticoid requirements, and to explore IL-12/23p40 function in GCA by exposing temporal artery sections to a neutralizing anti-human IL-12/IL-23p40 antibody.

MATERIALS AND METHODS

Patients

The study group consisted of 50 patients with biopsy-proven GCA diagnosed between 1997 and 2006 at our institution (Hospital Clinic, Barcelona). All patients were prospectively evaluated and treated by the authors (Georgina Espígol-Frigolé, Jose Hernández-Rodríguez, Sergio Prieto-González, and Maria C. Cid) with a predefined glucocorticoid-tapering schedule (4, 26). Patients received an initial prednisone dose of 1 mg/kg per day (up to 60 mg/day) for 1 month. Intravenous methylprednisolone pulse therapy (1 g daily for 3 days) was initially administered to patients with recent (<48 h) visual loss. Prednisone was subsequently tapered at 10 mg/week. When reaching 20 mg/day, this dose was maintained for 1–2 weeks and then reduced to 15 mg/day, which was maintained for 1 month. A further reduction to a maintenance dose of 10 mg/day was attempted. If tolerated, a reduction to 7.5 mg/day was tried after 3–6 months. A reduction to 5 mg/day was attempted approximately 3–6 months later and maintained for 1 year, after which a reduction of 1.25 mg/day was preformed every 6 months. Methotrexate at 15 mg/week was added when patients experienced ≥2 relapses or had developed GC side effects. If relapses occurred, prednisone dose was increased by 10–15 mg/day above the previous effective dose.

Clinical data recorded included disease symptoms at the time of diagnosis, number of relapses, and time to complete prednisone discontinuation with no relapse within the following 6 months. Relapse was defined as reappearance of cranial symptoms, polymyalgia rheumatica, systemic symptoms, or anemia that could not be attributed to other conditions, usually accompanied by a rebound in erythrocyte sedimentation rate (ESR) or C-reactive protein (CRP) (4, 27). Isolated fluctuations on ESR or CRP were not considered relapses.

Clinical data of the patients are displayed in Table S1 in Supplementary Material. Thirty-six patients were treatment-naïve and 14 had received prednisone (1 mg/kg/day) for a median of 7 days (range 2–12) before the performance of temporal artery biopsy. Uninvolved temporal arteries from 20 patients (14 women and 6 men) with a median of 77 years (range 64–91) in whom GCA was considered but not confirmed, served as controls. Final diagnoses of these patients are depicted in Table S2 in Supplementary Material.

This study was carried out in accordance with the recommendations of the Ethics Committee of Hospital Clínic (Barcelona), with written informed consent from all subjects. All subjects gave written informed consent in accordance with the Declaration of

Helsinki. The study was approved by the Ethics Committee of Hospital Clínic (Barcelona).

RNA Isolation and cDNA Synthesis

Temporal artery biopsies were embedded in optimal cutting temperature (OCT, Sakura, The Netherlands), snap-frozen in liquid nitrogen, and stored at −80°C. Total RNA was obtained from tissue with TRIzol Reagent (Invitrogen, Thermo Fisher Scientific, Waltham, MA, USA). RNA (1 μg) was reverse-transcribed to cDNA using the High Capacity cDNA Reverse Transcription kit (Applied Biosystems, Foster City, CA, USA).

Real-Time Quantitative PCR

cDNA was measured by quantitative real-time PCR using specific Pre-Developed TaqMan gene expression assays from Applied Biosystems using the following probes: Hs01073447_m1 (IL-12p35), Hs01011518_m1 (IL-12p40), Hs00372324_m1 (IL-23p19), Hs00989291_m1 (IFNγ), Hs00171138_m1 (CXCL11), Hs00171042_m1 (CXCL10), Hs00171065_m1 (CXCL9), Hs00174383_m1 (IL-17), Hs00174131 (IL-6), Hs01555410_m1 (IL-1β), and Hs02621508_m1 (tumor necrosis factor, TNFα). All samples were normalized to the expression of the housekeeping gene, GUSb. The comparative CT method was used to assess relative gene expression. Results were expressed as relative units.

Measurement of Circulating IL-12, IL-12p40, and IL-23p19

Plasma citrate from the 50 GCA patients was obtained at the time of diagnosis before the initiation of glucocorticoid therapy and frozen at −80°C. Plasma from 20 age- and sex-matched healthy donors was obtained for comparison. Human heterodimer IL-12 and IL-12/23p40 subunit were measured in plasma by immunoassay (Quantikine ELISA kits from R&D Systems, Minneapolis, MN, USA). To quantify plasma IL-23, Abcam kit (Cambridge, UK) detecting the IL-23p19 subunit was employed. Procedures were performed according to the manufacturer's protocol.

Immunofluorescence Staining and Confocal Microscopy

For qualitative assessment of cytokine distribution at the cellular level, immunofluorescence staining was performed in six temporal artery biopsies obtained from four patients and two controls. Temporal artery fragments were fixed in cold 4% paraformaldehyde (PFA) in phosphate-buffered saline (PBS), cryo-protected in increasing concentrations of saccharose (15 and 30%), embedded in OCT, and frozen at −80°C. Slides with 10-μm cryostat sections were further fixed with 4% paraformaldehyde for 10 min at room temperature, washed in PBS, and soaked in PBS with 0.1% Triton, 1% bovine serum albumin, and 5% donkey serum (Sigma-Aldrich, St. Louis, MO, USA) for 1 h at 4°C. Sections were incubated at 4°C overnight with the following primary antibodies: human IL-12 p35 (mouse monoclonal, Acris-Antibodies, Herford, Germany) at 1:100 dilution, human IL-23p19 (rabbit polyclonal, Abcam) and human IL-12p40 (goat polyclonal, Santa Cruz Biotechnology, Dallas, TX, USA), both at 1:50 dilution, and incubated overnight at 4°C.

Slides were washed in PBS (5 min, three times), followed by incubation with secondary antibodies (spectrally distinct Alexa Fluor-conjugated antibodies to goat, mouse and rabbit IgG; Molecular Probes, Thermo Fisher Sicentific). Nuclei were visualized with Hoechst. Slides were mounted with Prolong Gold Antifade Reagent (Molecular Probes, Thermo Fisher Sicentific) and examined using a laser scanning confocal Leica TCS SP5 microscope (Leica Microsystems, Heidelberg, Germany). Images were processed with Image J software (Wayne Rasband, Bethesda, MD, USA).

Proximity Ligation Assay (PLA)

Proximity ligation assay was used to visualize close colocalization (<40 nm) of p40 and p19 subunits (IL-23) and p40 and p35 subunits (IL-12), respectively, in temporal artery biopsies using Duolink Detection kit (Olink Bioscience). Tissues were fixed (4% PFA for 20 min at room temperature). After 1-h incubation in blocking buffer (0.1% Triton X-100, 5% FBS 1% BSA in PBS) at room temperature, slides were incubated overnight at 4°C with anti-human p19 rabbit polyclonal Ab (2 μg/ml, Sigma-Aldrich) and anti-human p40 goat polyclonal Ab (10 μg/ml, Santa Cruz Biotechnology) in blocking buffer or alternatively with anti-human p35 rabbit poyclonal Ab (5 μg/ml Atlas, Bromma, Sweden) and anti-human p40 goat polyclonal Ab (10 μg/ml Santa Cruz Biotechnology). After two washes (5 min duration) in wash buffer (0.1 M Tris–HCl pH 7.5, 0.5 M NaCl, 5% Tween-20 in ultrapure water), slides were incubated (30 min at 37°C) with PLA probe solution containing anti-rabbit MINUS and anti-goat PLUS Duolink PLA probes. After washing, circularization and ligation of the oligonucleotides in the probes, an amplification step was performed using polymerase solution (100 min at 37°C). After washing and re-fixation in 4% PFA, the slides were mounted with Duolink II Mounting medium containing DAPI and examined using a laser scanning confocal Leica TCS SP5 microscope (Leica Microsystems, Heidelberg, Germany). Images were processed with Image J software (Wayne Rasband, Bethesda, MD, USA).

Temporal Artery Culture

Temporal artery sections from 10 GCA patients and 10 controls were embedded in Matrigel to ensure prolonged survival and cultured *ex vivo* as described (10, 11, 28, 29) with or without neutralizing anti-human IL-12p40 mouse monoclonal Ab (10 μg/ml R&D Systems), or dexamethasone (DXM) (0.5 μg/ml, Sigma-Aldrich). Each condition was tested in three replicate wells. Biopsies were frozen in TRIzol reagent for RNA extraction.

Statistical Analysis

Mann–Whitney test, Spearman correlation, and Kaplan–Meier survival curves analyzed with log-rank test were used for statistical analysis using SPSS software, version PASW 18.0.

RESULTS

IL-12/23p40 and IL-23p19 Expression is Increased in Temporal Arteries From Patients With GCA

As shown in **Figures 1A,B**, IL-12/23p40 mRNA and IL-23p19 mRNA concentrations were significantly increased in temporal

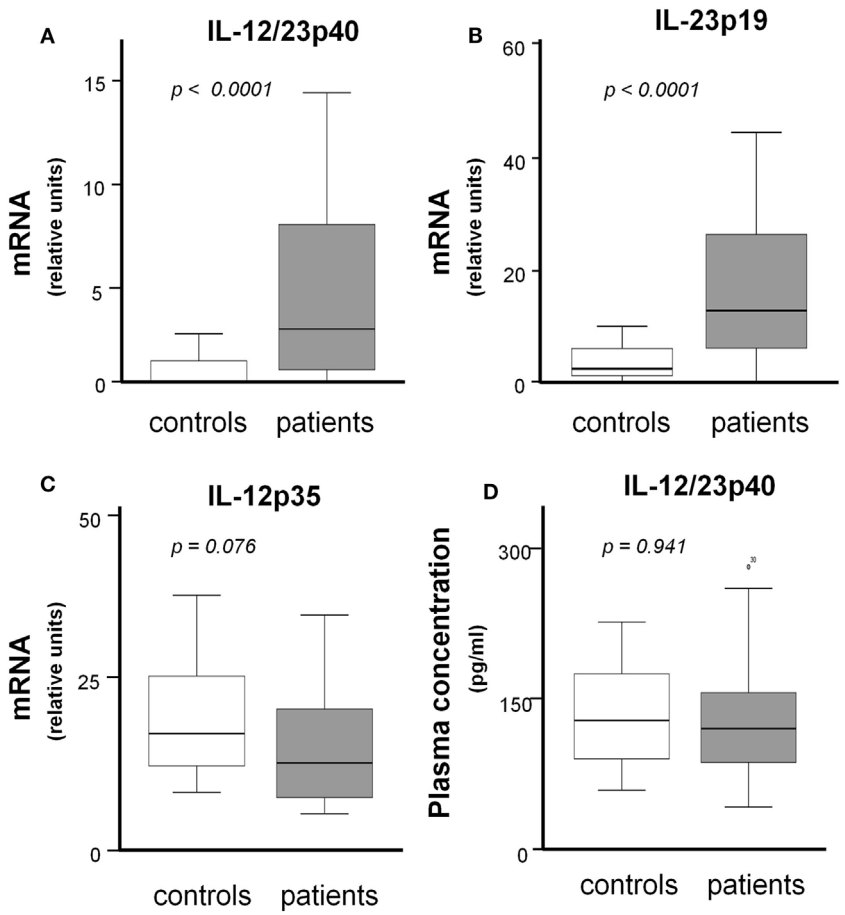

FIGURE 1 | IL-12/23p40, IL-12p35, and IL-23p19 concentrations in temporal artery biopsies (mRNA) and in serum from patients with giant-cell arteritis (GCA). **(A)** IL-12/23p40 mRNA, **(B)** IL-23p19 mRNA, and **(C)** IL-12p35 mRNA expression (relative units) in temporal artery biopsies from 36 treatment-naïve patients and 20 controls. **(D)** IL-12/23p40 concentration in sera from 36 treatment-naïve patients and 19 controls.

arteries from untreated patients compared to control arteries (4.35 ± 4.06 vs 0.51 ± 0.75 relative units; $p < 0.0001$ and 20.32 ± 21.78 vs 4.17 ± 4.43 relative units; $p < 0.0001$, respectively). By contrast, no significant differences were found in IL-12p35 mRNA expression between patients and controls (14.95 ± 8.9 vs 20.36 ± 14.93, $p = 0.076$) (**Figure 1C**). IL-12/23p40 mRNA expression in untreated GCA arteries significantly correlated with IL-12p35 ($r = 0{,}430$, $p = 0.01$) and IL-23p19 ($r = 0{,}431$, $p = 0.01$).

Plasma IL-12 and IL-23 heterodimeric cytokines were not detectable or were around the detection threshold both in patients and controls (data not shown). Although plasma IL-12/23p40 subunit was measurable, no significant differences between patients and controls were observed (130 ± 95.25 vs 115 ± 50.61 pg/ml; $p = 0.941$) (**Figure 1D**).

To assess expression of IL-12/23p40, IL-12p35, and IL-23p19 subunits at the protein level and their distribution in temporal arteries, immunofluorescence staining was performed. IL-12p35 had constitutive expression in the muscular layer from normal arteries in accordance with the remarkable IL-12p35 mRNA concentration found in control arteries (**Figure 2A**). However, IL-12p35 distribution changed in GCA-involved arteries: as the medial layer was damaged, muscular IL-12p35 decreased and it was mainly expressed by infiltrating leukocytes (**Figure 2B**). IL-12p40 and IL-23p19 protein expression was virtually undetected in normal arteries (**Figures 2C,E**) and clearly increased in GCA-affected arteries, mostly at the expenses of inflammatory cells (**Figures 2D,F**). Interestingly, intense p19 or p35 expression by inflammatory cells, independent from p40, could be observed and p19 and p35 were more abundant than p40 (**Figure 2**). Although p35 and p19 expression exceeded that of p40, association between subunits p40 and p35 or p40 and p19 to conform IL-12 and IL-23, respectively, could be confirmed by PLA in GCA lesions and barely in control arteries (**Figure 3**).

IL-12/23p40 and IL-23p19 Expression is Decreased in Temporal Arteries From Glucocorticoid-Treated GCA Patients

IL-23p19 mRNA concentrations in temporal artery biopsies from treated GCA patients were significantly lower than those found in treatment-naïve GCA patients (7.87 ± 8.04 vs 20.32 ± 21.78

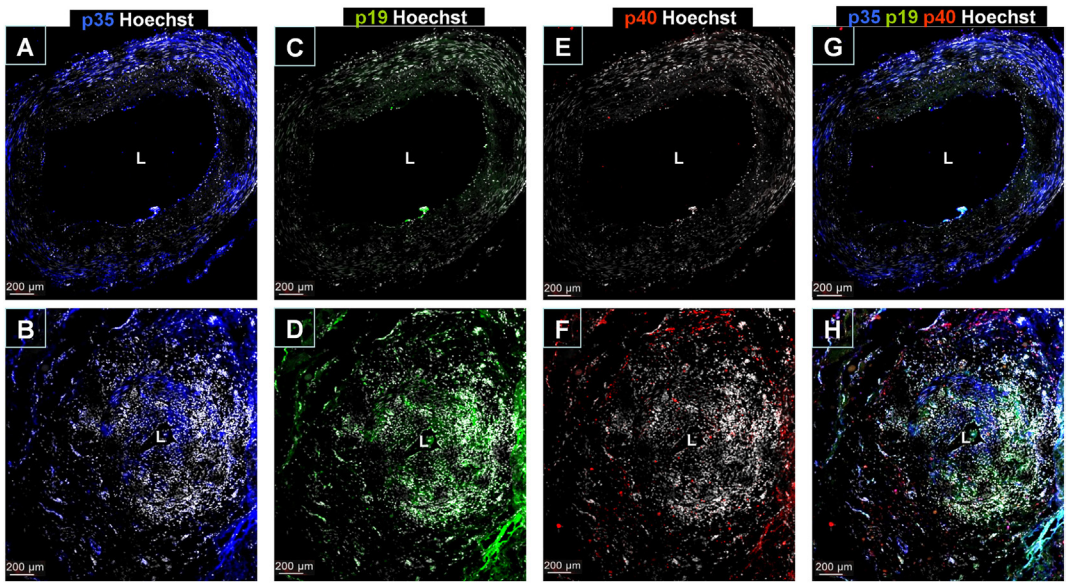

FIGURE 2 | Immunofluorescence detection of IL-12/23p40, IL-12p35, and IL-23p19 subunit expression in temporal artery lesions. **(A)** IL-12p35 staining (blue) in a temporal artery from a control individual showing almost selective expression in the media layer. Nuclei were stained with Hoechst (white). **(B)** IL-12p35 expression in GCA-involved temporal artery section, predominantly in inflammatory infiltrates. **(C,D)** Negative IL-23p19 immunostaining (green) in sections of normal temporal arteries **(C)** and intense expression in GCA samples **(D)** where IL-23p19 expression can be observed in all arterial layers especially in the most inflamed areas. **(E)** Lack of IL-12/23p40 immunostaining in a temporal artery from a control. **(F)** Detection of IL-12/23p40 expression (red) in a GCA-involved temporal artery section predominantly in the adventitial layer. **(G,H)** IL-12p35 (blue), IL-23p19 (green) and IL-12/23p40 (red) staining merge in a temporal artery section from a control and from a GCA patient, respectively. Pictures are representative of four arteries from four GCA patients and two controls, and at least three sections per sample were evaluated.

relative units; $p = 0.010$) (**Figure 4A**). IL-12/23p40 mRNA concentrations also tended to be reduced in treated patients (2.30 ± 3.39 vs 4.35 ± 4.06 relative units; $p = 0.065$) but differences did not reach statistical significance (**Figure 4B**). No differences were found in IL-12p35 mRNA between both groups (16.57 ± 8.9 vs 14.95 ± 8.9 relative units; $p = 0.183$) (**Figure 4C**).

The effect of glucocorticoids in reducing p40 and p19 expression was confirmed in cultured temporal arteries from patients with GCA. As with freshly stained arteries, IL-12/IL-23 p40 and IL-23p19 subunits tended to be more abundant in cultured arteries from patients with GCA than in those obtained from controls, although differences did not reach statistical significance, probably due to the small sample size and remarkable individual variability. DXM significantly reduced p19 mRNA and tended to decrease p40 expression (**Figures 4D,E**).

Lack of Correlation Between IL12/23p40, IL12p35, and IL23p19 mRNA Expression and GCA Clinical Findings

As shown in Table S3 in Supplementary Material, no differences in IL-12/23p40 or IL-12p35 mRNA expression according to clinical findings could be observed. A trend toward higher expression of IL23p19 mRNA was observed in patients with systemic symptoms (fever or weight loss) (41.46 ± 12.7 vs 17.79 ± 3.7 relative units, $p = 0.055$) but the difference did not reach statistical significance.

IL-12/23p40, IL-12p35, and IL-23p19 Expression and Long-Term Response to Glucocorticoid Treatment

Patients with elevated IL-12/23p40 mRNA content (above 75% percentile) in their artery lesions were able to completely withdraw prednisone earlier than patients with lower IL-12/IL-23p40mRNA levels ($p = 0.022$) (**Figure 5A**). Similarly, patients with high IL-23p19 mRNA tended to tolerate prednisone discontinuation earlier than those with lower IL-23p19 RNA values ($p = 0.104$) (**Figure 5B**). No differences were found between patients with high or low levels of IL-12p35 in terms of glucocorticoid treatment duration (**Figure 5C**). Accordingly, IL-12/IL-23p40 mRNA levels were significantly higher in patients able to completely discontinue prednisone at 3 years (7.37 ± 2.25 vs 4.29 ± 4.58 relative units; $p = 0.016$) (**Figure 5D**). No significant differences were found in IL-12p35 and IL-23p19 mRNA concentrations between patients requiring or not prednisone at 3 years (20.8 ± 10.54 vs 14.07 ± 8.74 relative units; $p = 0.065$ and 29.59 ± 25.72 vs 15.03 ± 11.25 relative units; $p = 0.084$, respectively) (**Figures 5E,F**). However, there were no significant differences in IL-12/23p40, IL-12p35, and IL-23p19 mRNA levels in temporal arteries from patients who achieved sustained remission compared with those who presented relapses (4.42 ± 4.3 vs 5.04 ± 4.21 relative units; $p = 0.516$, 15.25 ± 9.46 vs 16.63 ± 9.93 relative units; $p = 0.682$, 20.88 ± 21.59 vs 21.79 ± 22.32 relative units; $p = 0.616$, respectively) (Table S4 in Supplementary Material).

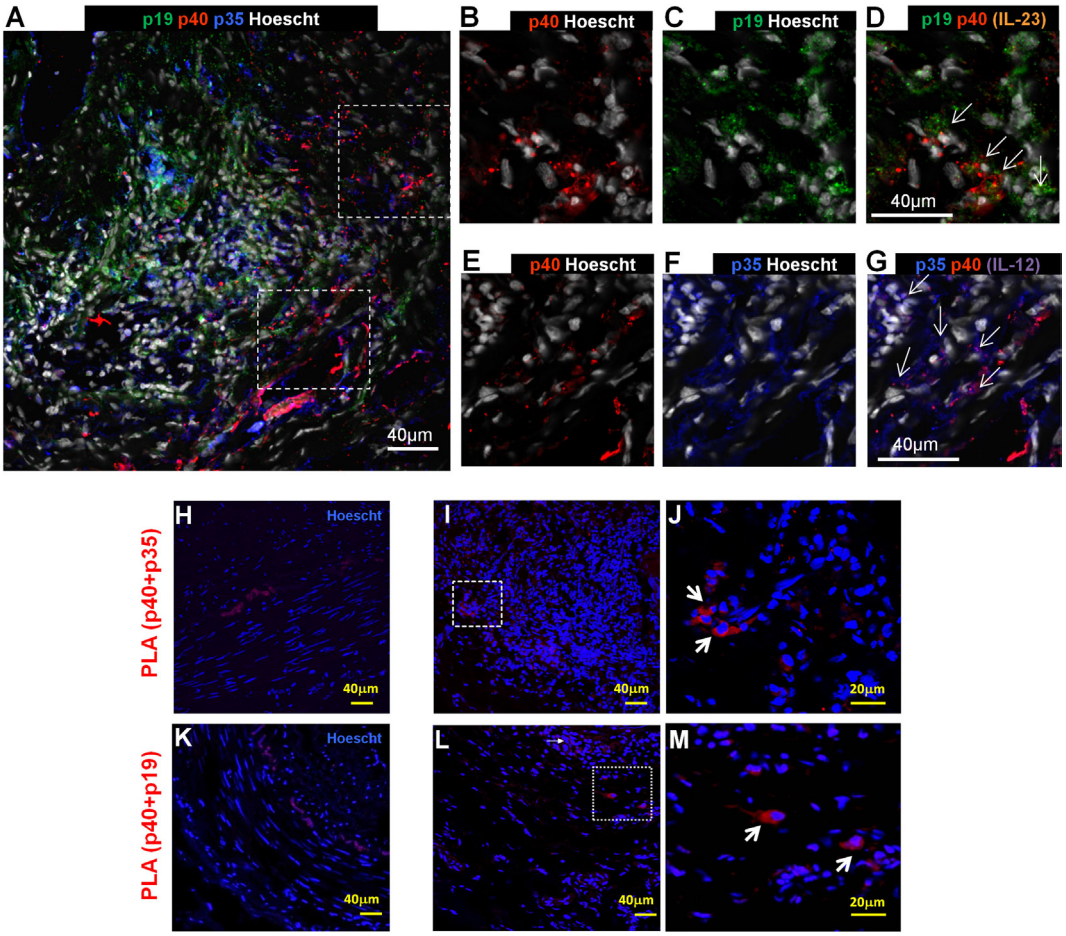

FIGURE 3 | Coexpression of subunits to conform IL-12 and IL-23 in temporal artery lesions from patients with GCA. **(A)** Close-up view of a GCA-involved artery where IL-12p35 + cells (blue) can be observed predominantly in media layer, IL-23p19 + cells (green) in all arterial layers and IL-12/23p40 + cells (red) in the adventitia. **(B)** Higher magnification of inflammatory cells expressing IL-12/23p40 (red), **(C)** IL-23p19 (green), and **(D)** merge showing expression of IL-23 (orange, indicated by arrows). **(E)** Higher magnification of inflammatory cells expressing IL-12/23p40 (red), **(F)** IL12p35 (blue), and **(G)** merge showing expression of IL-12 (purple, indicated by arrows). The temporal arteries were subjected to proximity ligation assay (PLA) to determine proximity of IL-12 and IL-23 subunits. The red staining marks the colocalization (<40 nm) of IL-12/23p40 and IL-12p35 (IL-12). Blue (Hoechst) marks the cell nuclei. **(H)** Negative PLA signalfor colocalization of IL-12/23p40 and IL-12p35 (IL-12) in a control artery. Minimal autofluorescence of the elastic lamina can be appreciated **(I)**. Positive colocalization of IL-12/23p40 and IL-12p35 (IL-12) in a GCA-affected temporal artery. The boxed area is magnified on the right **(J)**. **(K)** Negative PLA signal for colocalization of IL-12/23p40 and IL-23p19 (IL-23) in a control artery. Minimal autofluorescence of the elastic lamina can be appreciated **(L)** Colocalization of IL-12/23p40 and IL-23p19 (IL-23) in a positive GCA temporal artery. The boxed area is magnified on the right **(M)**.

Effect of Neutralizing IL-12/23p40 Subunit in Cultured Temporal Arteries From Patients With GCA

In order to elucidate potential functions of the IL-12/23p40 subunit in GCA, we investigated the effects of blocking IL-12/23p40 with a neutralizing monoclonal antibody in *ex vivo* cultured temporal artery biopsies. Several molecules related to Th1 and Th17 differentiation were investigated (9, 11, 30). Neutralization of IL-12/IL-23p40 tended to decrease IFNγ mRNA and, slightly, IFNγ-induced chemokine CXCL11 and CXCL10, but not CXCL9, mRNAs in cultured arteries. IL17 mRNA also tended to decrease and no apparent effect on TNFα expression was observed. Conversely IL-6 and IL-1β mRNA involved in Th17 differentiation tended to increase, possibly as a compensatory mechanism (**Figure 6**). As shown in the same figure, DXM significantly reduced IFNγ, CXCL10, IL-17, IL-6, and IL-1β and tended to reduce CXCL9 and TNFα.

DISCUSSION

IL-12/23p40 and IL-23p19 expression was significantly increased in GCA lesions, confirming preliminary observations obtained from small series of patients (24, 25). By contrast, IL-12p35 mRNA expression was similar between patients and controls. However, in normal arteries, IL-12p35 was primarily expressed by vascular smooth muscle cells (VSMC) whereas in GCA arteries, where substantial damage and loss of VSMC frequently occur, IL-12p35 was mostly expressed by inflammatory cells. Similar

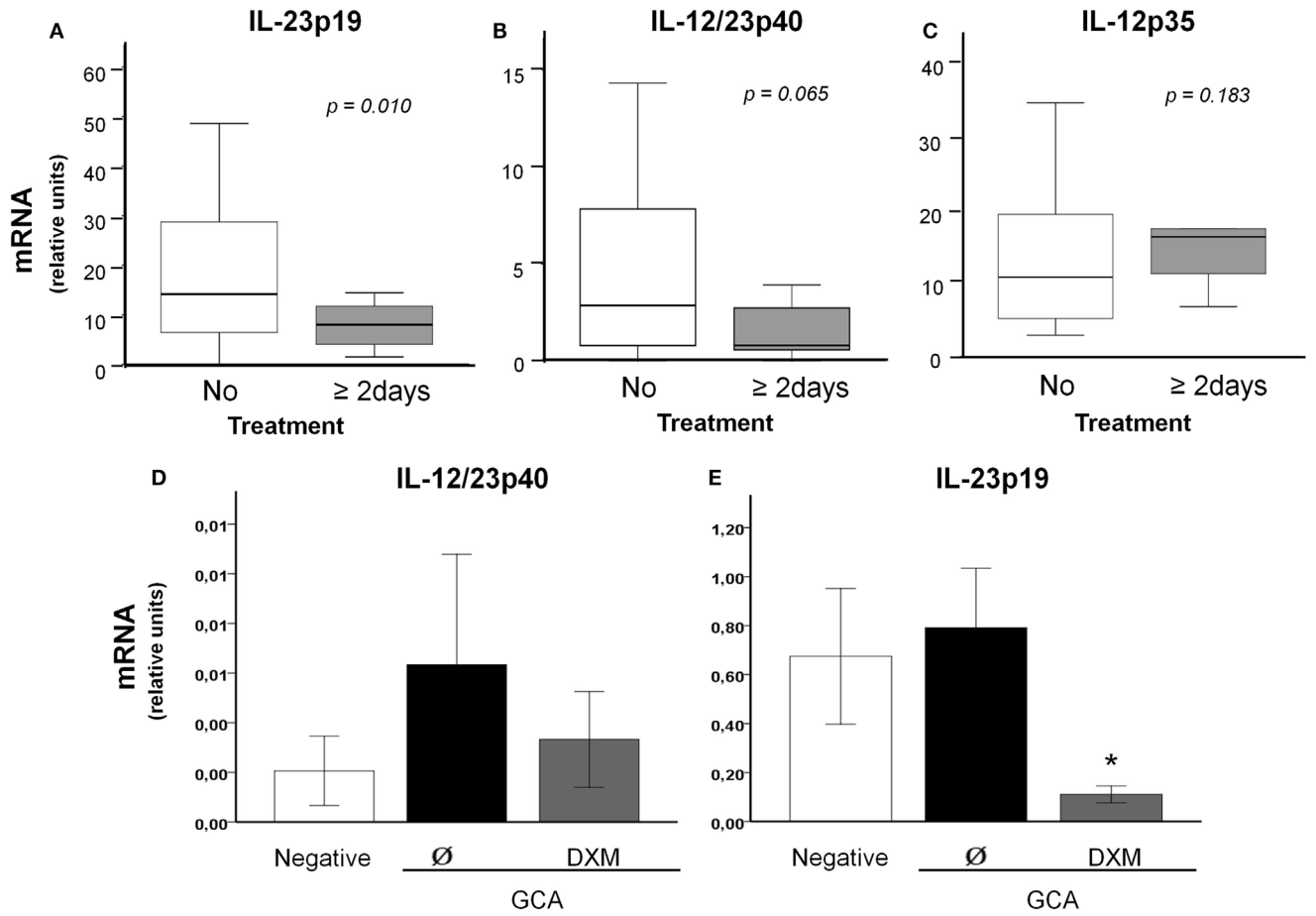

FIGURE 4 | Decreased IL-12/23p40 and IL-23p19 expression in temporal arteries from treated GCA patients. IL-23p19 **(A)**, IL-12/23p40 **(B)**, and IL-12p35 **(C)** expression (relative units) in temporal arteries from 36 treatment-naïve and 14 prednisone-treated GCA patients. **(D)** mRNA IL-12/23p40 expression and **(E)** mRNA IL-23p19 expression on cultured biopsies *(negative and GCA)*, showing the effect of dexamethasone (DXM) in GCA arteries. Bars represent mean ± SEM.

changes in distribution between normal and inflamed arteries have been observed in other molecules expressed by both VSMC and infiltrating leukocytes (29, 31). Expression of IL-12p35, IL-12/23p40, and IL-23p19 subunits suggest that IL-12 and IL-23 heterodimers are present in GCA lesions. By PLA we could demonstrate, indeed, colocalization of the IL-12/IL-23p40 and IL-12p35 subunits configuring IL-12 and colocalization of IL-12/IL-23p40 and IL-23p19 subunits conforming IL-23 in GCA, supporting the participation of both Th1 and Th17 differentiation pathways in the development of arterial inflammation. However, IL-12/23p40 expression was low, compared to its partners IL-12/p35 or IL-23p19 which were remarkably more abundant. This may explain why initial attempts using less sensitive methods concluded that there was no IL-12/23p40 expression in GCA (32). Distribution of lesions was also dissociated: while IL-23p19 and IL-12p35 subunits were detected in all arterial layers, IL-12/23p40 was mainly found in the adventitia. Consequently, our results indicate that, in GCA, p19 and p35 can be expressed independently from p40 being also part of heterodimeric cytokines other than IL-23 or IL-12, that could be also present in GCA lesions. Accordingly, increased expression of IL-23p19 exceeding the relatively low levels of bioactive IL-23 has also been detected in the rheumatoid synovium (33).

The IL-12/IL-6 family of cytokines resulting from different combinations of alpha (p28, p35, p19) and beta [p40, Ebstein-Barr induced 3 (EBi3)] subunits is currently expanding (34). Recently, a novel IL-12 family pro-inflammatory member named IL-39 composed by IL23p19 and EBi3 and secreted by lipopolysaccharide-stimulated B lymphocytes has been described (34, 35). Moreover IL-12p35 may combine with EBi3 to conform IL-35, a putatively suppressive cytokine produced by regulatory T lymphocytes (34, 36). Adding complexity, some subunits may be individually functional without interaction with partner subunits: we have recently demonstrated that IL-23p19, but not IL-12/23p40, can be expressed by endothelial cells exposed to inflammatory stimuli. Endothelial p19 has a p40-independent role as an intracellular activator of endothelial cells, by directly interacting with endothelial gp130 and leading to phosphorylation of signal transducer and activator of transcription3 (37). As observed in GCA, IL-23p19 mRNA is more abundant than

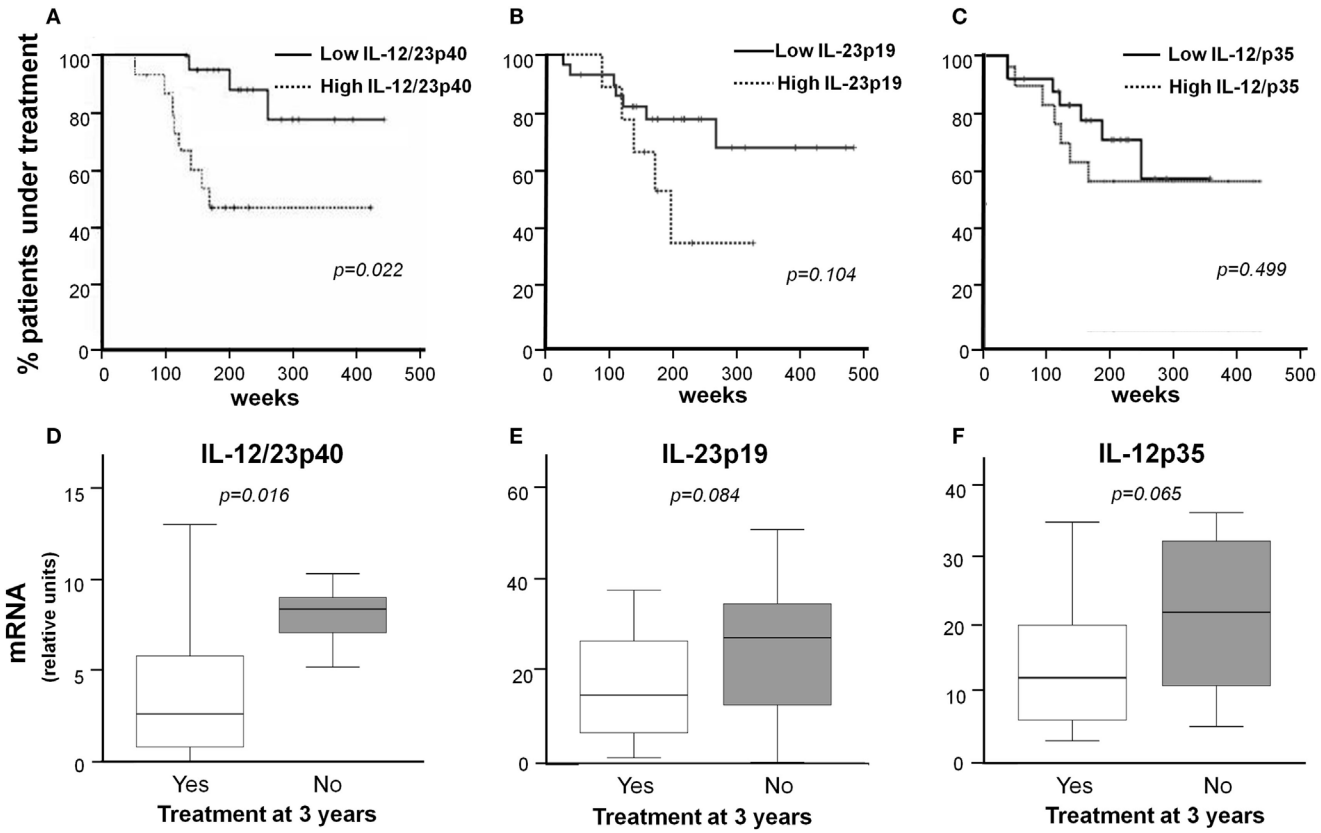

FIGURE 5 | IL-12/23p40, IL-12/23p19, and IL-12p35 mRNA expression in lesions and long-term response to therapy. Percentage of treatment-naïve GCA patients requiring prednisone treatment over time, according to the intensity of IL-12/23p40 **(A)**, IL-12/23p19 **(B)**, and IL-12p35 **(C)** mRNA expression, in temporal artery lesions. High refers to mRNA levels above the 75th percentile ($N = 26$), and low below the 75th percentile ($N = 10$). IL-12/23p40 **(D)**, IL-23p19 **(E)**, and IL-12p35 **(F)** mRNA concentrations in initial temporal artery biopsies from patients still requiring prednisone ($N = 12$) compared with patients in sustained remission ($N = 24$), 3 years after diagnosis.

IL-12/IL-23p40 mRNA in cultured macrophages (18), raising the possibility that p19 may play independent functional roles even in cells such as macrophages able to secrete mature, heterodimeric, IL-23.

Although both IL-12/and IL-23 were increased in lesions, mature IL-12 and IL-23 were barely detectable in plasma suggesting that functional activities of these cytokines are predominantly local. IL-12/23p40 subunit, which is known to form homodimers with a presumed counter-regulatory role (34, 38) was present in plasma but with no significant differences between patients and controls. Contrarily to other cytokines such as TNFα or IL-6 which have systemic effects (30), and consistent with the local paracrine effects of IL-12 and IL-23 subunits, there was no significant relationship between their tissue expression and disease manifestations.

IL-12/23p40 and, particularly, IL-23p19 were reduced in biopsies from treated patients in accordance with our previous results in a small series (25). Moreover, downregulation by glucocorticoids was confirmed in cultured arteries. Interestingly, patients with strong initial expression of IL-12/23p40 were able to discontinue prednisone treatment earlier than patients with low IL-12/23p40 expression and IL-12/23p19 followed a similar trend. Given that IL-23 is essential for the expansion and homeostasis of Th17 cells (39, 40), this finding is consistent with a previous study where we found that a strong IL-17A expression was associated with more sustained response to glucocorticoids, suggesting that patients who develop a predominantly Th17 response are more sensitive to glucocorticoid treatment (17). Downregulation of these pro-inflammatory cytokines may partially account for the therapeutic relief provided by glucocorticoids.

Although not highly expressed in lesions, IL-12/23 p40 may be relevant to vascular inflammation in large-vessel vasculitis. Recently, a meta-analysis of massive genotyping studies performed with GCA and Takayasu arteritis patients showed that a variant in close proximity to the *IL-12B* gene (encoding for IL12/23p40) is associated with increased genetic risk for both diseases, although the putative functional impact of this variant on *IL-12B* expression remains unknown (41). A recent open-label trial with ustekinumab, a monoclonal antibody neutralizing IL-12/23p40, suggests benefit in a small series of patients with refractory/relapsing GCA (42). Analysis of the peripheral blood compartment revealed reduction in both Th1 and Th17 polarization in a patient with GCA upon ustekinumab treatment (43). However, when we analyzed the effects of

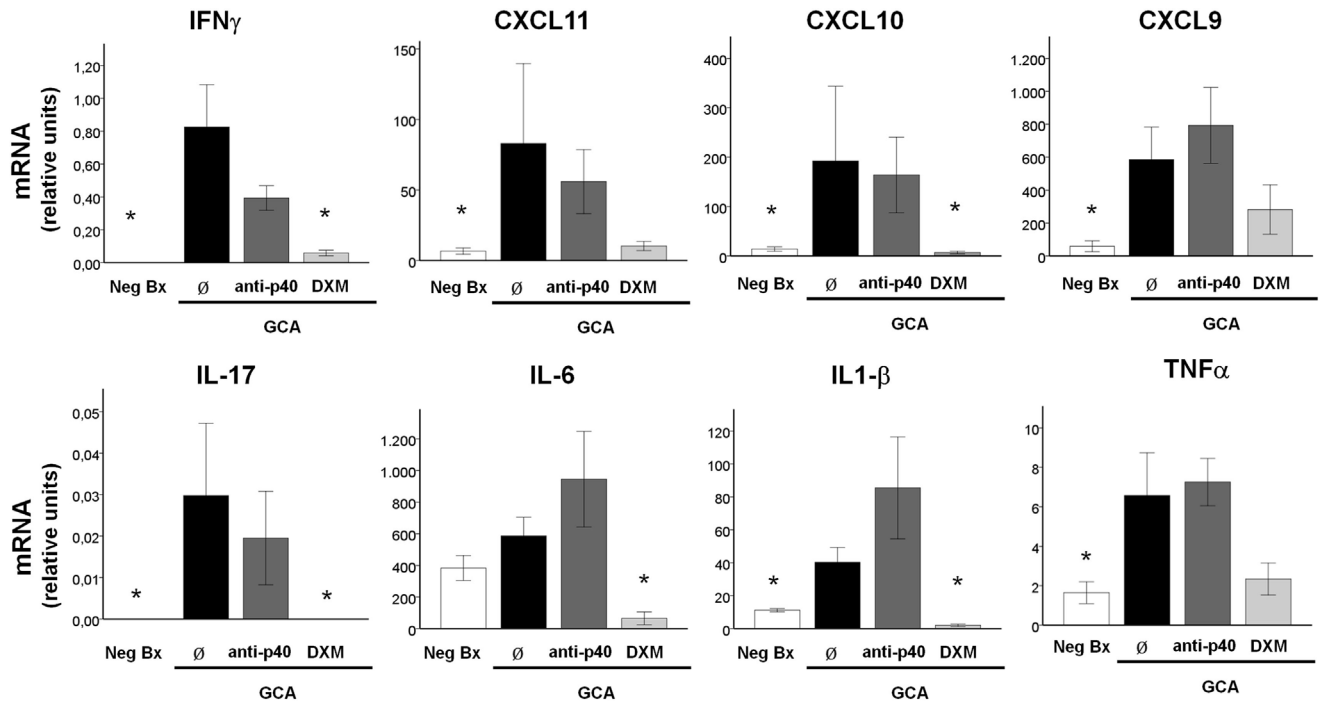

FIGURE 6 | Changes in gene expression by blocking IL-12/23p40 on cultured GCA biopsies. mRNA concentrations of IFNγ, CXCL11, CXCL10, CXCL9, IL-17, IL-6, IL-1β, and tumor necrosis factor α in 10 cultured control arteries (negative biopsies, Neg Bx) vs 10 cultured GCA-involved arteries untreated or exposed to anti-human IL-12p40 mouse monoclonal Ab (anti-p40) (10 μg/ml), or dexamethasone (DXM) (0.5 μg/ml). Statistical comparisons were performed between histologically negative and GCA-involved arteries and between GCA-involved arteries and anti-p40 treated and DXM treated. Bars represent mean ± SEM, $^*p < 0.05$.

blocking IL-12/23 p40 on involved tissue from GCA patients, only a trend, consistent with its known biology, was observed. IL-12/23p40 inhibition tended to reduce IFNγ expression as well as expression of IFNγ induced chemokines CXCL10 and 11 but not CXCL9. IL-12/23p40 blockade slightly reduced IL-17 expression although, interestingly, cytokines involved in Th17 differentiation such as IL-1β and IL-6 increased, possibly as a compensatory mechanism. Effects in tissue may be more complex than those observed in the peripheral compartment (43) and stimuli and interactions with other elements in the microenvironment may configure a protective niche. Although the inhibitory effect of the anti-IL-12/23p40 antibody used in our study may not be equivalent to that of ustekinumab, which has been generated for therapeutic purposes, recent studies suggest that neutralizing IL-12/23p19 may have more potent effects than blocking IL-12/23p40 in suppressing inflammatory activity in other diseases (44).

Our functional *ex vivo* model has some limitations such as isolation from a functional immune system or induction of changes by the culture itself in the expression of some inflammatory molecules (10). Moreover, lesions are often segmental in GCA arteries and this may have increased variability in responses. However, in spite of these limitations this model has been useful to evidence functional modifications after therapeutic intervention with various agents, including biologic agents (10, 11).

The increasingly recognized diversity of subunits configuring the IL-12/IL-6 superfamily of cytokines to which IL-12 and IL-23 belong, as well as the multiple potential partnership of subunits and receptor chains providing pro-inflammatory and anti-inflammatory stimuli depending on the specific combinations, has added an unexpected complexity to this system (34). Our results clearly indicate that additional combinations to the classical heterodimers IL-12 and IL-23 may occur in GCA and may lead to incomplete or compensated responses to the blockade of single subunits.

ETHICS STATEMENT

The study was approved by the Ethics Committee of Hospital Clínic (Barcelona). All subjects gave written informed consent in accordance with the Declaration of Helsinki.

AUTHOR CONTRIBUTIONS

GE-F, EP-R, and MC conceived experiments and interpreted data, GE-F, EP-R, and EL carried out experiments. GE-F and AG-M collected patient data. GE-F, JH-R, SP-G, and MC provided patient care. GE-F and EP-R generated figures. GE-F and MC wrote the manuscript. All authors were involved in final approval of the submitted version.

ACKNOWLEDGMENTS

This paper was supported by Instituto de Salud Carlos III (Juan Rodés program to Dr. G. Espigol-Frigolé), PI 15/00092, part of Plan Estatal de Investigación Científica y Técnica y de Innovación 2013–2016, and co-funded by ISCIII-Subdirección General de Evaluación, Fondo Europeo de Desarrollo Regional (FEDER) "Otra manera de hacer Europa," Plà Estrategic de Recerca i Innovació en Salut (PERIS), Departament de Salut de la Generalitat de Catalunya SLT002/16/00335, Ministerio de Economía, Industria y Competitividad (SAF 2014/57708-R and SAF 2017/88275-R, and CERCA program). The authors thank Mrs. Ester Tobías for her invaluable technical contribution to immunofluorescence studies and Dr. Maria Calvo and Mrs. Elisenda Coll from the Advanced Microscopy Platform from the University of Barcelona for her advice with confocal microscopy.

SUPPLEMENTARY MATERIAL

The Supplementary Material for this article can be found online at https://www.frontiersin.org/articles/10.3389/fimmu.2018.00809/full#supplementary-material.

REFERENCES

1. Jennette JC, Falk RJ, Bacon PA, Basu N, Cid MC, Ferrario F, et al. 2012 revised international Chapel Hill consensus conference nomenclature of vasculitides. *Arthritis Rheum* (2013) 65:1–11. doi:10.1002/art.37715
2. Hoffman GS. Giant-cell arteritis. *Ann Intern Med* (2016) 165:ITC65–80. doi:10.7326/AITC201611010
3. Cid MC, García-Martínez A, Lozano E, Espígol-Frigolé G, Hernández-Rodríguez J. Five clinical conundrums in the management of giant cell arteritis. *Rheum Dis Clin North Am* (2007) 33:819–34. doi:10.1016/j.rdc.2007.08.001
4. Alba MA, García-Martínez A, Prieto-González S, Tavera-Bahillo I, Corbera-Bellalta M, Planas-Rigol E, et al. Relapses in patients with giant cell arteritis: prevalence, characteristics, and associated clinical findings in a longitudinally followed cohort of 106 patients. *Medicine (Baltimore)* (2014) 93:194–201. doi:10.1097/MD.0000000000000033
5. Labarca C, Koster MJ, Crowson CS, Makol A, Ytterberg SR, Matteson EL, et al. Predictors of relapse and treatment outcomes in biopsy-proven giant cell arteritis: a retrospective cohort study. *Rheumatology* (2016) 55:347–56. doi:10.1093/rheumatology/kev348
6. Langford CA, Cuthbertson D, Ytterberg SR, Khalidi N, Monach PA, Carette S, et al. Vasculitis clinical research consortium. A randomized, double-blind trial of abatacept (CTLA-4Ig) for the treatment of giant cell arteritis. *Arthritis Rheumatol* (2017) 69:837–45. doi:10.1002/art.40044
7. Villiger PM, Adler S, Kuchen S, Wermelinger F, Dan D, Fiege V, et al. Tocilizumab for induction and maintenance of remission in giant cell arteritis: a phase 2, randomised, double-blind, placebo-controlled trial. *Lancet* (2016) 387:1921–7. doi:10.1016/S0140-6736(16)00560-2
8. Stone JH, Tuckwell K, Dimonaco S, Klearman M, Aringer M, Blockmans D, et al. Trial of tocilizumab in giant-cell arteritis. *N Engl J Med* (2017) 377:317–28. doi:10.1056/NEJMoa1613849
9. Weyand CM, Hicok KC, Hunder GG, Goronzy JJ. Tissue cytokine patterns in patients with polymyalgia rheumatica and giant cell arteritis. *Ann Intern Med* (1994) 121:484–91. doi:10.7326/0003-4819-121-7-199410010-00003
10. Corbera-Bellalta M, García-Martínez A, Lozano E, Planas-Rigol E, Tavera-Bahillo I, Alba MA, et al. Changes in biomarkers aftertherapeutic intervention in temporal arteries cultured in matrigel: a new model for preclinical studies in giant-cell arteritis. *Ann Rheum Dis* (2014) 73:616–23. doi:10.1136/annrheumdis-2012-202883
11. Corbera-Bellalta M, Planas-Rigol E, Lozano E, Terrades-García N, Alba MA, Prieto-González S, et al. Blocking interferon γ reduces expression of chemokines CXCL9, CXCL10 and CXCL11 and decreases macrophage infiltration in ex vivo cultured arteries from patients with giant cell arteritis. *Ann Rheum Dis* (2016) 75:1177–86. doi:10.1136/annrheumdis-2015-208371
12. Cid MC, Hoffman MP, Hernández-Rodríguez J, Segarra M, Elkin M, Sánchez M, et al. Association between increased CCL2 (MCP-1) expression in lesions and persistence of disease activity in giant-cell arteritis. *Rheumatology (Oxford)* (2006) 45:1356–63. doi:10.1093/rheumatology/kel128
13. Cid MC, Cebrián M, Font C, Coll-Vinent B, Hernández-Rodríguez J, Esparza J, et al. Cell adhesion molecules in the development of inflammatory infiltrates in giant cell arteritis: inflammation-induced angiogenesis as the preferential site of leukocyte-endothelial cell interactions. *Arthritis Rheum* (2000) 43:184–94. doi:10.1002/1529-0131(200001)43:1<184::AID-ANR23>3.0.CO;2-N
14. Deng J, Younge BR, Olshen RA, Goronzy JJ, Weyand CM. Th17 and Th1 T-cell responses in giant cell arteritis. *Circulation* (2010) 121:906–15. doi:10.1161/CIRCULATIONAHA.109.872903
15. Terrier B, Geri G, Chaara W, Allenbach Y, Rosenzwajg M, Costedoat-Chalumeau N, et al. Interleukin-21 modulates Th1 and Th17 responses in giant cell arteritis. *Arthritis Rheum* (2012) 64:2001–11. doi:10.1002/art.34327
16. Samson M, Audia S, Fraszczak J, Trad M, Ornetti P, Lakomy D, et al. Th1 and Th17 lymphocytes expressing CD161 are implicated in giant cell arteritis and polymyalgia rheumatica pathogenesis. *Arthritis Rheum* (2012) 64:3788–98. doi:10.1002/art.34647
17. Espígol-Frigolé G, Corbera-Bellalta M, Planas-Rigol E, Lozano E, Segarra M, García-Martínez A, et al. Increased IL-17A expression in temporal artery lesions is a predictor of sustained response to glucocorticoid treatment in patients with giant-cell arteritis. *Ann Rheum Dis* (2013) 72:1481–7. doi:10.1136/annrheumdis-2012-201836
18. Oppmann B, Lesley R, Blom B, Timans JC, Xu Y, Hunte B, et al. Novel p19 protein engages IL-12p40 to form a cytokine, IL-23, with biological activities similar as well as distinct from IL-12. *Immunity* (2000) 13:715–25. doi:10.1016/S1074-7613(00)00070-4
19. Cua DJ, Sherlock J, Chen Y, Murphy CA, Joyce B, Seymour B, et al. Interleukin-23 rather than interleukin-12 is the critical cytokine for autoimmune inflammation of the brain. *Nature* (2003) 421:744–8. doi:10.1038/nature01355
20. Yen D, Cheung J, Scheerens H, Poulet F, McClanahan T, McKenzie B, et al. IL-23 is essential for T cell-mediated colitis and promotes inflammation via IL-17 and IL-6. *J Clin Invest* (2006) 116:1310–6. doi:10.1172/JCI21404
21. Chen Y, Langrish CL, McKenzie B, Joyce-Shaikh B, Stumhofer JS, McClanahan T, et al. Anti-IL23 therapy inhibits multiple inflammatory pathways and ameliorates autoimmune encephalomyelitis. *J Clin.Invest* (2006) 116:1317–26. doi:10.1172/JCI25308
22. Mannon PJ, Fuss IJ, Mayer L, Elson CO, Sandborn WJ, Present D, et al. Anti-interleukin-12 antibody for active Crohn's disease. *N.Engl J Med* (2004) 351:2069–79. doi:10.1056/NEJMoa033402
23. Teng MW, Bowman EP, McElwee JJ, Smyth MJ, Casanova JL, Cooper AM, et al. IL-12 and IL-23 cytokines: from discovery to targeted therapies for immune-mediated inflammatory diseases. *Nat Med* (2015) 21(7):719–29. doi:10.1038/nm.3895
24. Espígol-Frigolé G, Lozano E, Garcia-Martinez A, Segarra M, Hernández-Rodriguez J, Grau J, et al. IL-12 p35, IL12/23p40 and IL-23 p19 subunit expression in giant-cell arteritis. *Ann Rheum Dis* (2007) 66(Suppl 2):140–1.
25. Visvanathan S, Rahman MU, Hoffman GS, Xu S, García-Martínez A, Segarra M, et al. Tissue and serum markers of inflammation during the follow-up of patients with giant-cell arteritis. A prospective longitudinal study. *Rheumatology (Oxford)* (2011) 50:2061–70. doi:10.1093/rheumatology/ker163
26. García-Martínez A, Hernández-Rodríguez J, Arguis P, Paredes P, Segarra M, Lozano E, et al. Development of aortic aneurysm/dilatation during the follow-up of patients with giant cell arteritis: a cross-sectional screening of fifty-four prospectively followed patients. *Arthritis Rheum* (2008) 59:422–30. doi:10.1002/art.23315
27. Hoffman GS, Cid MC, Rendt-Zagar KE, Merkel PA, Weyand CM, Stone JH, et al. Infliximab for maintenance of glucocorticosteroid-induced

remission of giant-cell arteritis. *Ann Intern Med* (2007) 146:621–30. doi:10.7326/0003-4819-146-9-200705010-00004
28. Lozano E, Segarra M, García-Martínez A, Hernández-Rodríguez J, Cid MC. Imatinib mesylate inhibits in vitro and ex vivo biological responses related to vascular occlusion in giant cell arteritis. *Ann Rheum Dis* (2008) 67(11):1581–8. doi:10.1136/ard.2007.070805
29. Planas-Rigol E, Terrades-Garcia N, Corbera-Bellalta M, Lozano E, Alba MA, Segarra M, et al. Endothelin-1 promotes vascular smooth muscle cell migration across the artery wall: a mechanism contributing to vascular remodelling and intimal hyperplasia in giant-cell arteritis. *Ann Rheum Dis* (2017) 76:1624–34. doi:10.1136/annrheumdis-2016-210792
30. Hernández-Rodríguez J, Segarra M, Vilardell C, Sánchez M, García-Martínez A, Esteban MJ, et al. Tissue production of pro-inflammatory cytokines (IL-1beta, TNFalpha and IL-6) correlates with the intensity of the systemic inflammatory response and with corticosteroid requirements in giant-cell arteritis. *Rheumatology (Oxford)* (2004) 43:294–301. doi:10.1093/rheumatology/keh058
31. Segarra M, García-Martínez A, Sánchez M, Hernández-Rodríguez J, Lozano E, Grau JM, et al. Gelatinase expression and proteolytic activity in giant-cell arteritis. *Ann Rheum Dis* (2007) 66:1429–35. doi:10.1136/ard.2006.068148
32. Krupa WM, Dewan M, Jeon MS, Kurtin PJ, Younge BR, Goronzy JJ, et al. Trapping of misdirected dendritic cells in the granulomatous lesions of giant cell arteritis. *Am J Pathol* (2002) 161(5):1815–23. doi:10.1016/S0002-9440(10)64458-6
33. Brentano F, Ospelt C, Stanczyk J, Gay RE, Gay S, Kyburz D. Abundant expression of the interleukin (IL)23 subunit p19, but low levels of bioactive IL23 in the rheumatoid synovium: differential expression and toll-like receptor-(TLR) dependent regulation of the IL23 subunits, p19 and p40, in rheumatoid arthritis. *Ann Rheum Dis* (2009) 68:143–50. doi:10.1136/ard.2007.082081
34. Hasegawa H, Mizoguchi I, Chiba Y, Ohashi M, Xu M, Yoshimoto T. Expanding diversity in molecular structures and functions of the IL-6/IL-12 heterodimeric cytokine family. *Front Immunol* (2016) 7:479 e collection. doi:10.3389/fimmu.2016.00479
35. Wang X, Wei Y, Xiao H, Liu X, Zhang Y, Han G, et al. A novel IL23-p19/Ebi3 (IL-39) cytokine mediates inflammation in lupus-like mice. *Eur J Immunol* (2016) 46:1343–50. doi:10.1002/eji.201546095
36. Collison LW, Workman CJ, Kuo TT, Boyd K, Wang Y, Vignali KM, et al. The inhibitory cytokine IL-35 contributes to regulatory T-cell function. *Nature* (2007) 450(7169):566–9. doi:10.1038/nature06306
37. Espígol-Frigolé G, Planas-Rigol E, Ohnuki H, Salvucci O, Kwak H, Ravichandran S, et al. Identification of IL-23p19 as an endothelial pro-inflammatory peptide that promotes gp130-STAT3 signaling. *Sci Signal* (2016) 9:ra28. doi:10.1126/scisignal.aad2357
38. Lee SY, Jung YO, Kim DJ, Kang CM, Moon YM, Heo YJ, et al. IL-12p40 homodimer ameliorates experimental autoimmune arthritis. *J Immunol* (2015) 195:3001–10. doi:10.4049/jimmunol.1500400
39. McGeachy MJ, Chen Y, Tato CM, Laurence A, Joyce-Shaikh B, Blumenschein WM, et al. The interleukin 23 receptor is essential for the terminal differentiation of interleukin 17-producing effector T helper cells in vivo. *Nat Immunol* (2009) 10:314–24. doi:10.1038/ni.1698
40. Haines CJ, Chen Y, Blumenschein WM, Jain R, Chang C, Joyce-Shaikh B, et al. Autoimmune memory T helper 17 cell function and expansion are dependent on interleukin-23. *Cell Rep* (2013) 3:1378–88. doi:10.1016/j.celrep.2013.03.035
41. Carmona FD, Coit P, Saruhan-Direskeneli G, Hernández-Rodríguez J, Cid MC, Solans R, et al. Analysis of the common genetic component of large-vessel vasculitides through a meta-Immunochip strategy. *Sci Rep* (2017) 7:43953. doi:10.1038/srep46012
42. Conway R, O'Neill L, O'Flynn E, Gallagher P, McCarthy GM, Murphy CC, et al. Ustekinumab for the treatment of refractory giant cell arteritis. *Ann Rheum Dis* (2016) 75(8):1578–9. doi:10.1136/annrheumdis-2016-209351
43. Samson M, Ghesquière T, Berthier S, Bonnotte B. Ustekinumab inhibits Th1 and Th17 polarisation in a patient with giant cell arteritis. *Ann Rheum Dis* (2018) 77(2):e6. doi:10.1136/annrheumdis-2017-211622
44. Papp KA, Blauvelt A, Bukhalo M, Gooderham M, Krueger JG, Lacour JP, et al. Risankizumab versus ustekinumab for moderate to severe plaque psoriasis. *N Engl J Med* (2017) 376:1551–60. doi:10.1056/NEJMoa1607017

Conflict of Interest Statement: MC has received consulting fee from Roche. All other authors declare that the research was conducted in the absence of any commercial or financial relationships that could be construed as a potential conflict of interest.

Copyright © 2018 Espígol-Frigolé, Planas-Rigol, Lozano, Corbera-Bellalta, Terrades-García, Prieto-González, García-Martínez, Hernández-Rodríguez, Grau and Cid. This is an open-access article distributed under the terms of the Creative Commons Attribution License (CC BY). The use, distribution or reproduction in other forums is permitted, provided the original author(s) and the copyright owner are credited and that the original publication in this journal is cited, in accordance with accepted academic practice. No use, distribution or reproduction is permitted which does not comply with these terms.

frontiers in Immunology

ORIGINAL RESEARCH
published: 20 April 2018
doi: 10.3389/fimmu.2018.00696

Macrophage Lamin A/C Regulates Inflammation and the Development of Obesity-Induced Insulin Resistance

Youngjo Kim[1], Princess Wendy Bayona[1], Miri Kim[1], Jiyeon Chang[1], Sunmin Hong[1], Yoona Park[1], Andrea Budiman[1], Yong-Jin Kim[2], Chang Yong Choi[3], Woo Seok Kim[4], Jongsoon Lee[5] and Kae Won Cho[1]**

[1] Soonchunhyang Institute of Medi-Bio Science (SIMS), Soonchunhyang University, Cheon-an, South Korea, [2] Department of Surgery, Soonchunhyang University Hospital, Seoul, South Korea, [3] Department of Plastic and Reconstructive Surgery, Soonchunhyang University Hospital, Gumi, South Korea, [4] Department of Surgery, Soonchunhyang University Gumi Hospital, Gumi, South Korea, [5] The Joslin Diabetes Center, Department of Medicine, Harvard Medical School, Boston, MA, United States

OPEN ACCESS

Edited by:
Jixin Zhong, Case Western Reserve University, United States

Reviewed by:
Yongsheng Li, Army Medical University, China
Jo A. Van Ginderachter, Vrije Universiteit Brussel, Belgium

***Correspondence:**
Jongsoon Lee
jongsoon.lee@joslin.harvard.edu;
Kae Won Cho
kwcho@sch.ac.kr

Specialty section:
This article was submitted to Inflammation, a section of the journal Frontiers in Immunology

Received: *11 November 2017*
Accepted: *21 March 2018*
Published: *20 April 2018*

Citation:
Kim Y, Bayona PW, Kim M, Chang J, Hong S, Park Y, Budiman A, Kim Y-J, Choi CY, Kim WS, Lee J and Cho KW (2018) Macrophage Lamin A/C Regulates Inflammation and the Development of Obesity-Induced Insulin Resistance. Front. Immunol. 9:696. doi: 10.3389/fimmu.2018.00696

Obesity-induced chronic low-grade inflammation, in particular in adipose tissue, contributes to the development of insulin resistance and type 2 diabetes. However, the mechanism by which obesity induces adipose tissue inflammation has not been completely elucidated. Recent studies suggest that alteration of the nuclear lamina is associated with age-associated chronic inflammation in humans and fly. These findings led us to investigate whether the nuclear lamina regulates obesity-mediated chronic inflammation. In this study, we show that lamin A/C mediates inflammation in macrophages. The gene and protein expression levels of lamin A/C are significantly increased in epididymal adipose tissues from obese rodent models and omental fat from obese human subjects compared to their lean controls. Flow cytometry and gene expression analyses reveal that the protein and gene expression levels of lamin A/C are increased in adipose tissue macrophages (ATMs) by obesity. We further show that ectopic overexpression of lamin A/C in macrophages spontaneously activates NF-κB, and increases the gene expression levels of proinflammatory genes, such as *Il6*, *Tnf*, *Ccl2*, and *Nos2*. Conversely, deletion of lamin A/C in macrophages reduces LPS-induced expression of these proinflammatory genes. Importantly, we find that myeloid cell-specific lamin A/C deficiency ameliorates obesity-induced insulin resistance and adipose tissue inflammation. Thus, our data suggest that lamin A/C mediates the activation of ATM inflammation by regulating NF-κB, thereby contributing to the development of obesity-induced insulin resistance.

Keywords: lamin A/C, obesity, inflammation, insulin resistance, macrophages, adipose tissue

INTRODUCTION

It has been well established that obesity-induced low-grade chronic inflammation contributes to the development of insulin resistance and type 2 diabetes in obesity. It has also been shown that white adipose tissue is the primary site for obesity-induced inflammation (1, 2), which is largely regulated by the quantitative and qualitative alterations of adipose tissue leukocytes (3–6). Adipose tissue

macrophages (ATMs) are the most abundant cell types among adipose tissue leukocytes and also considered as final effector cells to regulate adipose tissue inflammation (2, 7). ATMs are categorized as either an M1 or M2 subset, which is well established in the classical immunology field, and the polarization of M1 and M2 macrophage phenotypes is switched by obesity (4, 5). Furthermore, M1 and M2 ATM phenotypes play a critical role in the regulation of obesity-induced inflammation and insulin resistance. In lean adipose tissue, anti-inflammatory M2 macrophages (M2 ATMs) are predominant (4, 8). During obesity, another type of ATMs demarcated with CD11c is markedly accumulated in fat and functions as classically activated M1 macrophages (M1 ATMs) (5, 9). Accumulated M1 ATMs in obese adipose tissue contribute to the increased expression levels of proinflammatory cytokines, such as TNFα and IL-6, in adipose tissue, which is mechanistically linked to insulin resistance (2, 5, 9, 10). It has been shown that blockade of ATM accumulation by inhibition of monocyte trafficking during obesity prevents obesity-induced adipose tissue inflammation and glucose intolerance (11, 12). Furthermore, ablation of $CD11c^+$ ATM in obese adipose tissue attenuates adipose tissue inflammation and improves in glucose tolerance, supporting the importance of M1 ATMs in obesity-induced adipose tissue inflammation (13, 14). However, the molecular mechanism that underlies the polarization and maintenance of the proinflammatory M1 ATMs in obesity has not been fully elucidated.

The nuclear lamina is a protein meshwork that surrounds and protects the nuclear content. In addition to providing the structural scaffold of the nucleus, the nuclear lamina is involved in diverse cellular functions, including chromatin organization, DNA replication and repair, transcription, and nuclear migration (15, 16). Lamins, type V intermediate filament, are the major components of the nuclear lamina. So far, seven lamin isoforms have been reported in mammals and are grouped into A-type and B-type lamins based on their biochemical and immunological properties (17, 18). In the rodent model, alternative splicing of the single *Lmna* gene produces all A-type lamins, including lamin A, lamin C, lamin AΔ10, and lamin C3. In most somatic cells, lamin A and C are coexpressed and are the major isoforms among A-type lamins. *Lmnb1* encodes lamin B1, while *Lmnb2* expresses lamin B2 and lamin B3 through alternative splicing. Lamin A and C are rarely expressed in cells at early developmental stages and lack in some somatic cells in adulthood, whereas lamin B1 and B2 are expressed in most cells throughout development (19, 20). *Lmnb1* or *Lmnb2* knockout mice die at birth with defects in multiple tissues (21–23), whereas *Lmna* knockout mice are born apparently normal, but die 16–18 days after birth (24, 25). In humans, mutations in *LMNA* are associated with a range of diseases, including lipodystrophy, cardiomyopathy, muscular dystrophy, and progeria.

Previous studies have shown that alterations of the nuclear lamina are associated with increased immune responses and metabolic disorders in humans (26, 27). In particular, Dunningan-type lipodystrophy characterized by mutations in *LMNA* shares many features of the metabolic syndrome (28). Genome-wide association studies have identified that genetic variants in *LMNA* are linked with type 2 diabetes in several populations (29–32). Moreover, Miranda et al. found that lamin A/C expression is upregulated in adipose tissue in obese and type 2 diabetes patients (33).

Based on the importance of adipose tissue inflammation in obesity-associated metabolic dysfunction and the linkage of lamins with metabolic disorder, we hypothesize that lamins in ATMs play a role in the development of obesity-induced adipose tissue inflammation and, thereby, insulin resistance. Herein, we show that obesity increases lamin A/C expression in adipose tissue in both rodent models and human. In adipose tissue, lamin A/C is specifically upregulated in ATMs, in particular in $CD11c^+$ M1 ATMs, by obesity. We further demonstrate that overexpression of lamin A/C in macrophages promotes proinflammatory cytokine gene expression by enhancing NF-κB activity, while depletion of lamin A/C in macrophages suppresses LPS-induced inductions of proinflammatory genes. Moreover, myeloid cell-specific deletion of *Lmna* improves obesity-induced insulin resistance and adipose tissue inflammation. Hence, these data strongly suggest that lamin A/C in ATMs plays an important role in the regulation of obesity-induced inflammation and insulin resistance.

MATERIALS AND METHODS

Animal Studies

C57BL/6J male mice were purchased from Orient Bio in Korea. Mice were *ad libitum* fed with a normal diet (ND, 4.5% fat; PMI Nutrition International) or a high-fat diet (HFD) consisting of 60% fat (Research Diets) beginning 6 weeks of age for a duration of 12 weeks. *Ob/ob* and *db/db* mice were purchased from Central Laboratory Animal Inc., in Korea and were sacrificed at 10 weeks of age. Glucose tolerance tests were performed after 6 h of fasting. Mice were intraperitoneally injected with glucose (0.7 g/kg) and blood glucose levels were measured at the different time points. In $Lmna^{flox/flox}$ mice, the exon 2 of *Lmna* is cleaved upon Cre expression (25). Myeloid cell-specific *Lmna* knockout mice (hereafter referred to as MKO) were generated by crossing $Lmna^{flox/flox}$ mice with LysM-Cre mice. Cre-negative $Lmna^{flox/flox}$ littermates were used as control mice. All mouse procedures were approved by the Institutional Animal Care and Use Committee at the Soonchunhyang University (SCH16-0003, SCH17-0008).

Human Studies

The clinical studies were reviewed and approved by the Soonchunhyang University Institutional Review Board (SCH#1040875-201502-BR-009) and were carried out in accordance with the Declaration of Helsinki. Informed personal consents were obtained from all subjects. Omental white adipose tissues were obtained from patients who underwent bariatric surgery in Soonchunhyang Hospitals, Korea. The clinical and biochemical parameters are presented in Table S1 in Supplementary Material.

Flow Cytometry Analysis of Adipose Tissue Stromal Vascular Cells (SVCs)

Stromal vascular fractions (SVFs) and adipocyte fractions from adipose tissues were isolated as previously described (34). In

brief, epididymal white adipose tissues (eWAT) were minced and digested in digestion buffer (0.5% BSA, 25 mM HEPES, 50% HBSS, 50% PBS, and 1 mM EDTA) with collagenase (1 mg/ml). Suspensions were incubated at 37°C for 30 min with intermittent shaking. Then, suspensions were centrifuged at 500 × *g* for 10 min at 4°C. After centrifugation, the floating adipocyte fractions were carefully collected in separate tubes. The pellet was resuspended in RBC lysis buffer and neutralized by adding PBS. The suspension was centrifuged at 500 × *g* for 10 min at 4°C. The pellets (SVFs) were used for gene and/or protein expression analysis. For the flow cytometry analysis, cells were resuspended in staining buffer (0.1% BSA in PBS), incubated in Fc Block (Invitrogen) for 10 min on ice, and then stained with antibodies against cell-specific markers for 30 min at 4°C (Table S2 in Supplementary Material). Stained cells were washed in staining buffer and fixed in 0.1% paraformaldehyde (PFA) before analysis. For intracellular staining, cells were permeabilized and stained by using the Intracellular Fixation and Permeabilization Buffer Set (eBioscience). Cells were analyzed on a FACSCanto II Flow Cytometer (BD Biosciences) using FlowJo software (FlowJo). For sorting cells, SVFs were suspended in RPMI 1640/2% FBS and ATMs were isolated by FACSAria III (BD Bioscience).

Bone Marrow-Derived Macrophages (BMDMs) and Peritoneal Macrophages

Mouse BMDMs were derived from femoral and tibial bone marrow cells of mice. Briefly, after lysis of RBCs, bone marrow cells were differentiated in BMDM medium (RPMI 1640 containing 10% FBS, 20% L929-conditioned medium, 25 mM HEPES, and 2 mM glutamine) for 6 days. The cells were trypsinized and plated for the treatments or transfections. For the preparation of the peritoneal macrophages, mice were intraperitoneally injected with the thioglycolate solution and cells were harvested 4 days after injection by peritoneal lavage. Cells were plated in RPMI media containing 10% FBS and non-adherent cells were removed by washing with PBS. The remaining cells were used as peritoneal macrophages. For LPS treatment, a final concentration of 10 ng/ml LPS was added and incubated for 2 h.

Ectopic Expression of Lamin A/C in Macrophages

To generate lamin A/C overexpressing construct, mouse *Lmna* cDNA was amplified from IMAGE clone 4240057. The PCR product was cloned into pEGFP-C3 (Clontech) that overexpressed gene of interest fused with the EGFP gene under a CMV promoter. The resulting construct, pEGFP-C3-*Lmna*, was confirmed by DNA sequencing. pEGFP-N1 that expressed EGFP alone was used as a control. Raw 264.7 cells and BMDMs were transfected with pEGFP-C3-*Lmna* or pEGFP-N1 using Lipofectamine LTX with Plus Reagent (Thermo Fisher) and the Amaxa Nucleofector (Lonza), respectively. NF-κB activity was measured by using a Dual Luciferase Assay kit (Promega). For the luciferase assay, HEK293 cells, HeLa cells, or Raw 264.7 cells were transfected with pEGFP-C3-*Lmna* or pEGFP-N1. Ten hours after transfection, cells were re-transfected with plasmids encoding luciferase reporter gene *luc2P* containing κB binding elements in the promoter and pRL-SV40. The following day, cells were treated with 10 ng/ml LPS for 30 min and lysed and NF-κB activity was measured according to manufacturer's instructions.

Gene Expression Analysis

RNA from tissues and cells was extracted by using Trizol Reagent (Life Technologies). cDNA was synthesized from 0.5 to 1.0 μg of total RNA using the High-Capacity cDNA Reverse Transcription Kit (Applied Biosystems). PowerUp SYBR Green PCR Master Mix (Applied Biosystems) and the Step One Plus System (Applied Biosystems) were used for quantitative real-time RT-PCR (qRT-PCR). *Arbp* or 18S expression was used as an internal control for data normalization. Samples were assayed in duplicate and relative expression was determined using the $2^{-\Delta\Delta CT}$ method. PCR primers used in this study are listed in Table S3 in Supplementary Material.

Immunoblot Analysis

Cells were washed with PBS and lysed with RIPA Buffer (50 mM Tris, pH7.4, 150 mM NaCl, 1 mM EDTA, 1 mM $MgCl_2$, 1% NP-40, 1% sodium deoxycholate, 1% SDS, and 1× protease inhibitor). Proteins were separated with 10% SDS-PAGE gels and transferred onto nitrocellulose membranes. Rabbit anti-lamin A/C (Santa Cruz), goat anti-lamin B (Santa Cruz), and mouse anti-actin (Sigma) antibodies were used as primary antibodies. Anti-rabbit IgG-HRP (Life Technologies), anti-goat IgG-HRP (Jackson ImmunoResearch), and anti-mouse IgG-HRP (Life Technologies) were used as secondary antibodies. Proteins were visualized with a chemiluminescence imaging system (GE healthcare).

ELISA

Cell supernatants and blood were collected after treatment and the concentration of IL-6, MCP-1, TNFα in culture supernatants, and plasma were measured with ELISA kits (Life Tech) according to the manufacturer's instruction.

Assessment of NF-κB Nuclear Translocation

Bone marrow-derived macrophages or HeLa cells were transfected with pEGFP-C3-*Lmna* or pEGFP-N1 using the Amaxa Nucleofector (Lonza) or Lipofectamine 2000 (Life Tech), respectively. Thirty-six hours after transfection, cells were fixed with 4% PFA in PBS for 10 min at room temperature, washed twice with 0.4% Triton X-100 in PBS, and stained with rabbit anti-NF-κB antibody (Cell Signaling) and anti-rabbit IgG-Rhodamine Red-X (Jackson Immunoresearch). Nucleus was stained with 1 μg/ml Hoechst 33258 (Sigma). Fluorescence images were taken under the same condition, including the same exposure times and light intensity. For BMDMs, cells with nuclear staining were defined by both presence of a clear nuclear signal and the absence of cytoplasmic signal. For HeLa cells, the nuclear translocation index for NF-κB in a cell image was defined as average pixels in nuclear area divided by average pixels in cytoplasmic area in the same cell. Nuclear and cytoplasmic boundaries were determined by overlaying staining images of NF-κB and DNA.

Statistical Analyses

The results were expressed as mean ± SEM. Group means were compared using unpaired two-tailed *t*-test and the linear dependence between two variables was assessed by determining Pearson's correlation coefficient "*r*" values. Prims (GraphPad) was used for statistical analysis. All *P*-values of <0.05 were considered statistically significant.

RESULTS

Obesity Increases the Expression Level of Lamin A/C in Epididymal White Adipose Tissue

Since lamin A/C has been linked to type 2 diabetes (26, 32), we examined whether the expression level of lamin A/C is affected by obesity using a diet-induced obesity model. We fed C57BL/6 mice with HFD for 12 weeks. Control mice were fed with normal diet (ND) in parallel with the HFD group. As expected, body weight, adipose tissue weight, and fasting glucose levels were significantly elevated in HFD-fed mice compared to ND-fed mice (**Figures 1A,B**). HFD-fed mice also appeared to show increased liver weights compared to ND-fed mice. Furthermore, glucose tolerance test (GTT) showed markedly impaired glucose tolerance in HFD-fed mice relative to ND-fed mice (**Figure 1C**). These results indicate that HFD-fed mice successfully developed obesity and obesity-induced glucose intolerance.

Next, we examined the lamin A/C expression profiles in eWAT, inguinal white adipose tissue (iWAT), and the liver. Quantitative real-time RT-PCR (qRT-PCR) showed that HFD increased the gene expression levels of *Lmna* (gene for lamin A/C) and *Lmnb1* (gene for lamin B1) in eWAT (**Figure 1D**). The expression level of *Lmnb2* (gene for lamin B2) was not changed in eWAT of the HFD-fed mice (**Figure 1D**). There were no significant differences in the expression levels of all three lamin genes in iWAT or liver upon HFD treatments (**Figure 1D**). The expression level of *Lmna* was highest in eWAT among these tissues (Figure S1 in Supplementary Material). Immunoblot analysis confirmed the elevated protein expression of lamin A/C in eWAT of HFD-fed mice compared to ND mice (**Figure 1E**).

We then examined whether the gene expression levels of lamins were also affected in adipose tissue from genetically obese models, namely, *db*/*db* and *ob*/*ob* mice. Consistent with the diet-induced obesity model, the expression level of *Lmna* was significantly increased in both obese *db*/*db* and *ob*/*ob* mice compared to their lean controls (**Figures 1F,G**). There were no notable differences in the gene expression levels of *Lmnb1* and *Lmnb2*. These data show that obesity increases lamin A/C level specifically in the eWAT.

To delineate specific cellular compartments of eWAT with elevated lamin A/C level, we separated adipocyte and SVFs from eWAT of ND- and HFD-fed mice. The expression of the adipocyte-specific marker *Lep* was only found in the adipocyte fraction, while macrophage-specific *Emr1* expression was found in both adipocyte and SVF fractions (**Figure 1H**). The expression of *Emr1* in the adipocyte fraction was mainly due to contamination of adipose tissue immune cells, in particular ATMs that were strongly bound to the adipocytes and could not be dissociated from adipocytes during the SVF preparation (34–36). qRT-PCR revealed that HFD treatments dramatically increased the gene expression level of *Lmna* in SVFs of eWAT, whereas adipocytes showed a mild increase in *Lmna* expression by the HFD treatment (**Figure 1H**). This could be mainly due to the contamination of ATMs in the adipocyte fraction. HFD treatments also significantly increased the expression level of *Lmnb1* in SVFs, albeit to a lesser degree than *Lmna*, and showed marginal effects on adipocyte fraction (**Figure 1H**). Lamin A/C protein level was also markedly increased in SVCs of eWAT from HFD mice compared to that from ND mice (**Figure 1I**). These results indicate that adipose tissue SVCs are the major cell types that contribute to the elevated levels of lamin A/C in eWAT from obese mice.

Obesity Upregulates Lamin A/C in M1 ATMs of eWAT

Stromal vascular fraction from adipose tissue contains a variety of cell types, including ATMs, preadipocytes, dendritic cells (DCs), stem cells, T cells, and B cells (14, 37–39). To identify cellular populations responsible for obesity-induced lamin A/C upregulation in SVFs, intracellular lamin A/C staining and flow cytometry analyses were performed on SVFs from eWAT of ND- and HFD-fed mice. In lean state, only about 16% of non-ATM adipose leukocytes expressed lamin A/C, while 55% of ATMs expressed lamin A/C (**Figure 2A**). HFD treatments further decreased the frequency of lamin A/C expression in non-ATM leukocytes, whereas HFD treatment significantly increased lamin A/C expressing ATMs by about 22% (**Figure 2A**). Total protein expression levels of lamin A/C, as determined by mean fluorescence intensity (MFI), showed the similar profiles; non-ATM leukocytes expressed much lesser levels of lamin A/C than ATMs in ND mice, and HFD treatments increased lamin A/C expression in ATMs by 50% (**Figure 2B**). This was further confirmed by qRT-PCR of sorted ATMs. The expression level of *Lmna* was significantly increased over sixfold in sorted ATMs from HFD-fed mice compared to ND-fed mice (**Figure 2C**). However, the expression levels of *Lmnb1* and *Lmnb2* were not changed in ATMs from HFD-fed mice. These data together suggest that obesity-induced upregulation of lamin A/C in total adipose tissue is mainly contributed by ATMs.

Obesity changes polarization of ATMs by increasing $CD11c^+$ M1 ATMs. Hence, we next examined changes in the expression level of lamin A/C in the ATM subpopulations in obesity. Flow cytometry analysis revealed that mice fed a HFD exhibited increased the frequencies of $CD11c^+$ M1 ATMs and a decrease in the frequency of $CD11c^-$ ATMs compared to those fed with ND (**Figure 2D**). Furthermore, HFD treatment increased lamin A/C^+ ATMs in both $CD11c^+$ and $CD11c^-$ ATM populations compared to the ND-fed mice (**Figure 2E**). However, HFD treatments significantly increased the protein expression levels of lamin A/C only in $CD11c^+$ ATMs, but not in $CD11c^-$ ATMs (**Figure 2F**). These results indicate that lamin A/C is specifically upregulated in ATMs, in particular $CD11c^+$ M1 ATMs, by obesity.

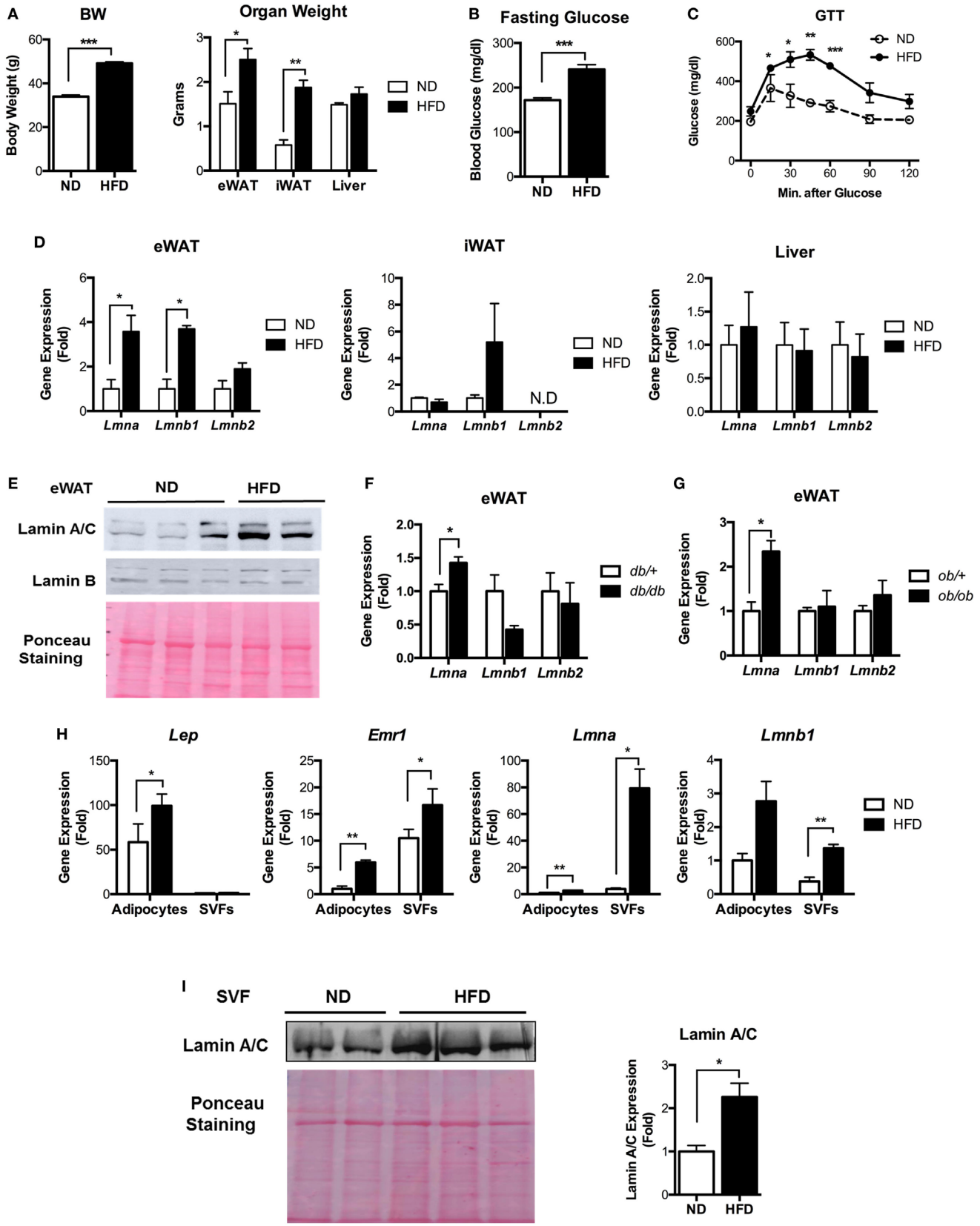

FIGURE 1 | Continued

FIGURE 1 | Lamin A/C expression is upregulated in adipose tissue from obese mice. **(A–E)** Male C57BL/6 mice were fed a normal chow diet (ND) or a high-fat diet (HFD) for 12 weeks to induce obesity ($n = 14$ per group). **(A)** Total body weights (left) and organ weights (right), **(B)** fasting blood glucose, **(C)** glucose tolerance test, and **(D)** quantitative real-time RT-PCR (qRT-PCR) analysis of *Lmna*, *Lmnb1*, and *Lmnb2* in eWAT, iWAT, and liver from ND- and HFD-fed mice. Amounts of transcripts for each gene in HFD tissues relative to those in ND tissues are presented. **(E)** Western blotting analysis of epididymal white adipose tissues (eWAT) lysate from ND- and HFD-fed mice. Lamin A/C (upper), lamin B1 (middle) protein levels are presented. Equal amount of total proteins as measured by Ponceau S staining (lower) of each lane. **(F)** qRT-PCR analysis of *Lmna, Lmnb1,* and *Lmnb2* in eWAT from *db/+* and *db/db* male mice (8 weeks, $n = 5$ per group). **(G)** qRT-PCR analysis of *Lmna, Lmnb1,* and *Lmnb2* in eWAT from *ob/+* and *ob/ob* male mice (10 weeks, $n = 4$ per group). **(H)** qRT-PCR analysis of *Lep, Emr1, Lmna,* and *Lmnb1* in adipocyte fractions and stromal vascular cell fractions from eWAT of ND and HFD mice ($n = 6$ per group). **(I)** Immunoblots of lysates from the stromal vascular fraction (SVF) of eWAT from ND and HFD mice for lamin A/C antibody (upper left), Ponceau S staining (lower left) and quantitation of lamin A/C (right) were presented. Error bars represent SEM. $^*p < 0.05$, $^{**}p < 0.01$, $^{***}p < 0.001$.

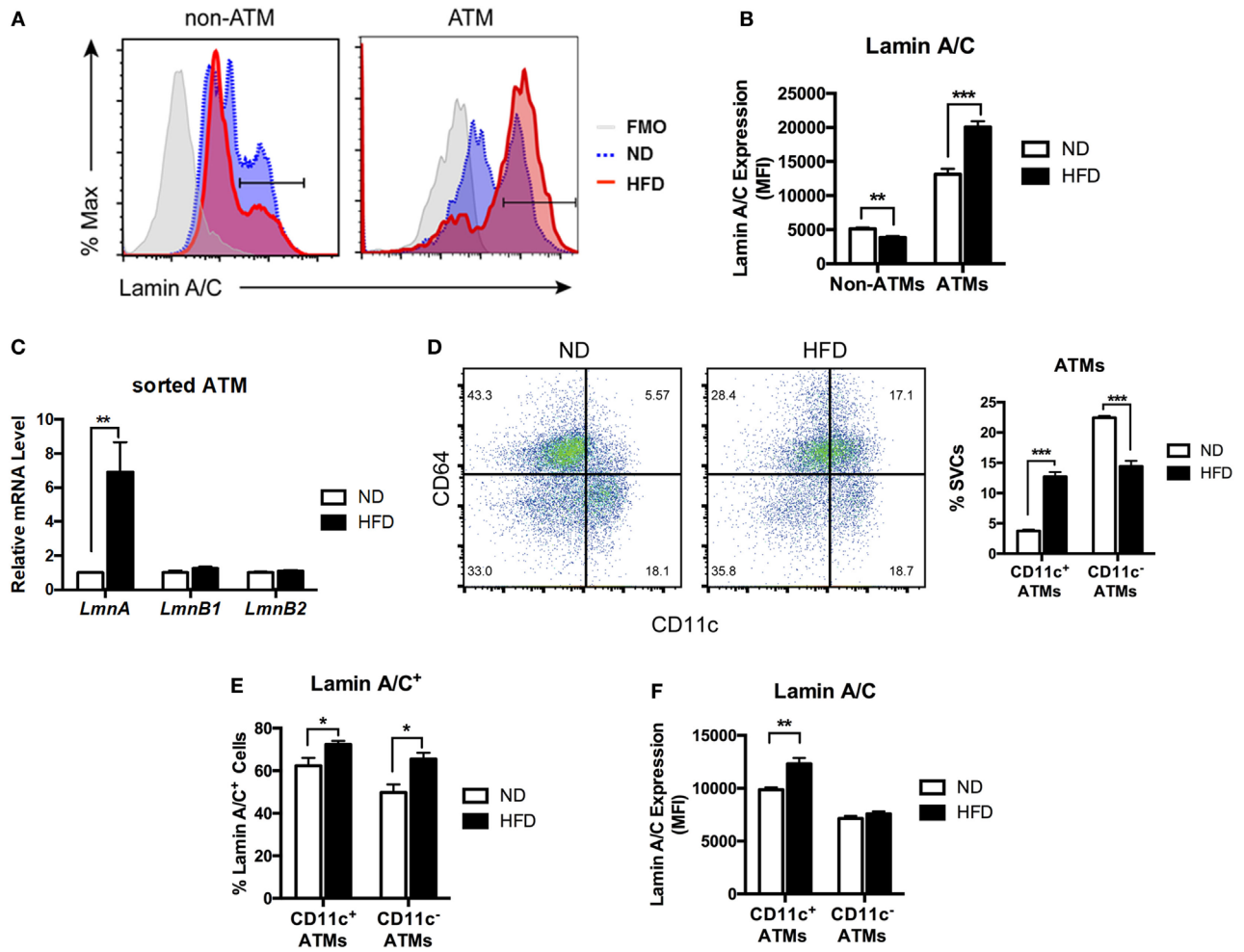

FIGURE 2 | Lamin A/C expression is elevated in adipose tissue macrophages (ATMs) from obese mice. Male C57BL/6 mice were fed a normal diet (ND) or a high-fat diet (HFD) for 12 weeks ($n = 6$ per group). **(A)** Histogram of lamin A/C in non-ATM ($CD45^+CD64^-$) and ATM ($CD45^+CD64^+$) from ND- and HFD-fed mice. **(B)** Lamin A/C expression level as determined by mean fluorescence intensity (MFI) in the non-ATM and ATM populations from epididymal white adipose tissues (eWAT) of ND and HFD mice ($n = 5$ per group). **(C)** Quantitative real-time RT-PCR analysis of *Lmna, Lmnb1,* and *Lmnb2* in sorted ATMs from eWAT of ND- and HFD-fed mice ($n = 3$ per groups). **(D)** A representative flow cytometry plot showing ATMs ($CD64^+CD11c^-$ and $CD64^+CD11c^+$) and ATDCs ($CD64^-CD11c^+$) in stromal vascular cell (left) and frequency of $CD11c^+$ ATMs and $CD11c^-$ ATMs from eWAT of ND- and HFD-fed mice (right). **(E)** The frequency of lamin A/C^+ cells in the $CD11c^+$ and $CD11c^-$ ATM populations in eWAT from ND and HFD mice. **(F)** Lamin A/C expression level as determined by MFI in the $CD11c^+$ and $CD11c^-$ ATM populations from eWAT of ND and HFD mice. Error bars represent SEM. $^*p < 0.05$, $^{**}p < 0.01$, $^{***}p < 0.001$.

Overexpression of Lamin A/C Induces Inflammation in Macrophages

Lamin A/C expression was increased in M1 ATMs by obesity, suggesting that lamin A/C could also play a role in the regulation of inflammation in macrophages. Thus, we first examined this by investigating whether ectopic overexpression of lamin A/C in Raw 264.7 macrophages regulates inflammatory responses. Transfection of GFP-*Lmna* into Raw 264.7 cells overexpressed

Lmna over the 60-fold. However, the expression level of *Lmnb1* was not affected by transfection of GFP-*Lmna* (**Figure 3A**). Interestingly, we found that overexpression of lamin A/C spontaneously increased the expression levels of proinflammatory genes, such as *Il6*, *Tnf, Ccl2,* and *Nos2* even without any stimulation (**Figure 3B**). LPS treatment further increased expression levels of *Il6*, *Ccl2*, and *Nos2* in *Lmna*-overexpressing macrophages compared to control cells (**Figure 3B**). ELISA analysis confirmed that lamin A/C overexpression increased IL6 secretion in the medium without any stimulation (**Figure 3C**). BMDMs also showed a similar pattern to Raw264.7 cells; transfection of GFP-*Lmna* into BMDMs overexpressed *Lmna* over the 140-fold, but not affecting that of *Lmnb1* (**Figure 3D**). Moreover, overexpression of lamin A/C significantly increased the expression levels of *Il6, Ccl2,* and *Nos2* (**Figure 3D**). Collectively, these results indicate that overexpression of lamin A/C increased the expression of proinflammatory genes in macrophages under both basal- and LPS-stimulated inflammatory states.

Lamin A/C Increases NF-κB Activity *via* Nuclear Translocation of Rel A

NF-κB is a master nuclear transcription factor for the genes involved in inflammatory responses. Since our data strongly suggest that lamin A/C regulates gene expression of proinflammatory responses in macrophages, we tested whether lamin A/C also mediates NF-κB functions. We first examined whether ectopic overexpression of *Lmna* changed the mRNA levels of NF-κB p105 and p65/Rel A subunits. qRT-PCR analysis revealed that overexpression of lamin A/C did not affect the gene expression levels of NF-κB p105 and p65/Rel A subunits (**Figure 4A**). We then measured NF-κB transcriptional activity by using a luciferase system. We found that transfecting *GFP-Lmna* into Raw 264.7 cells significantly increased NF-κB transcriptional activity even without any stimulation by LPS (**Figure 4B**). Increase of basal NF-κB transcriptional activity was also shown in lamin A/C overexpressing HEK293 cells and HeLa cells (Figures S2A,B in Supplementary Material). In HeLa cells, LPS

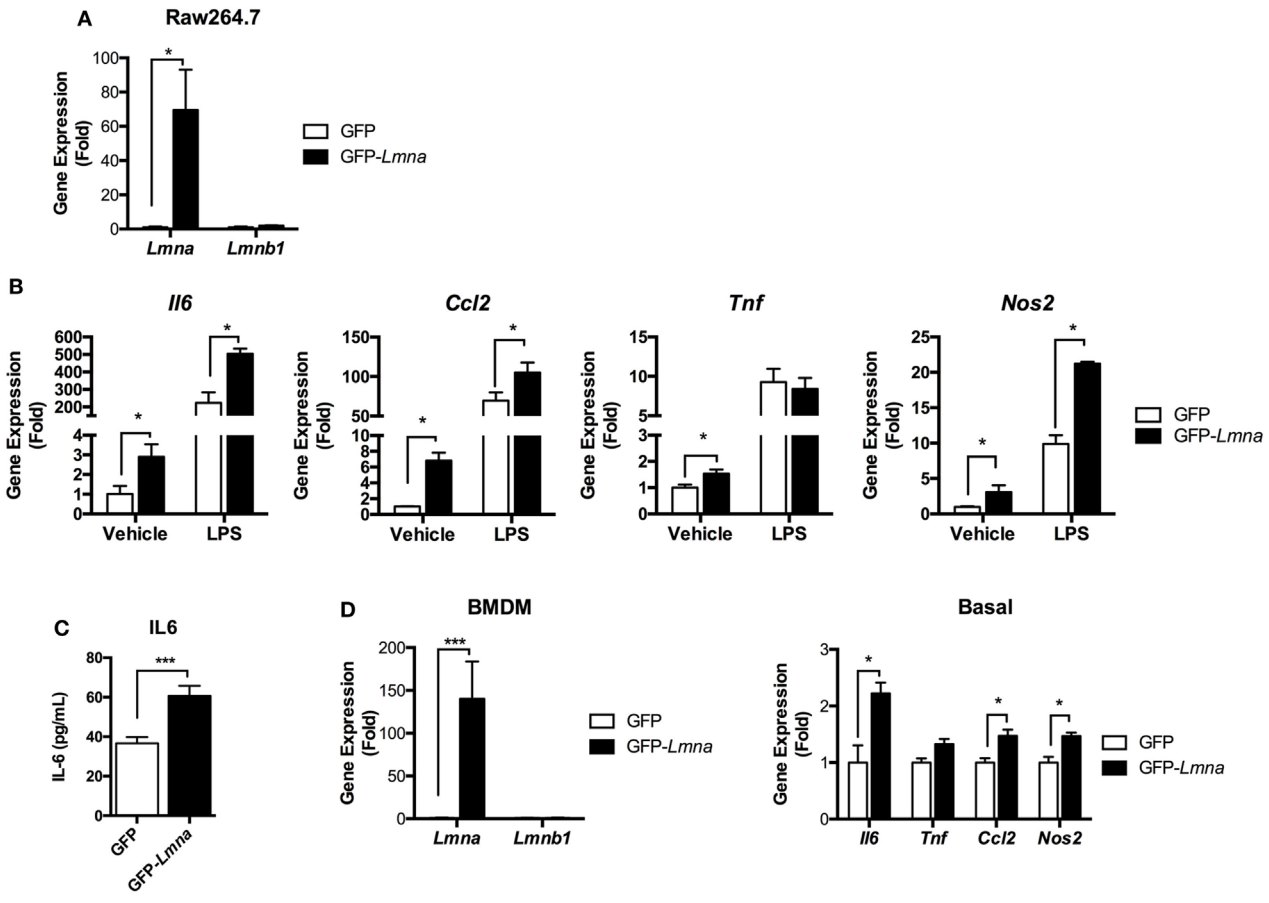

FIGURE 3 | Lamin A/C overexpression induces proinflammatory cytokine expression in macrophages. **(A–C)** Raw 264.7 cells were transfected with GFP or GFP-*Lmna*. After 24 h, transfected cells were cultured in the absence or presence of 100 ng/ml LPS for 6 h. **(A)** Quantitative real-time RT-PCR (qRT-PCR) analysis of *Lmna* and *Lmnb1* in GFP or GFP-*Lmna*-transfected cells. **(B)** qRT-PCR analysis of *Il6, Tnf, Ccl2,* and *Nos2* in GFP or GFP-*Lmna* transfected cells. **(C)** ELISA of IL-6 in supernatant of Raw 264.7 cells transfected with GFP or GFP-*Lmna* in the absence of LPS. **(D)** Characterization of bone marrow-derived macrophages (BMDMs) transfected GFP-*Lmna.* qRT-PCR analysis of *Lmna* and *Lmnb1* (left) and *Il6, Tnf, Ccl2,* and *Nos2* in GFP or GFP-*Lmna* transfected BMDMs (right). Error bars represent SEM. $^{*}p < 0.05$, $^{***}p < 0.001$.

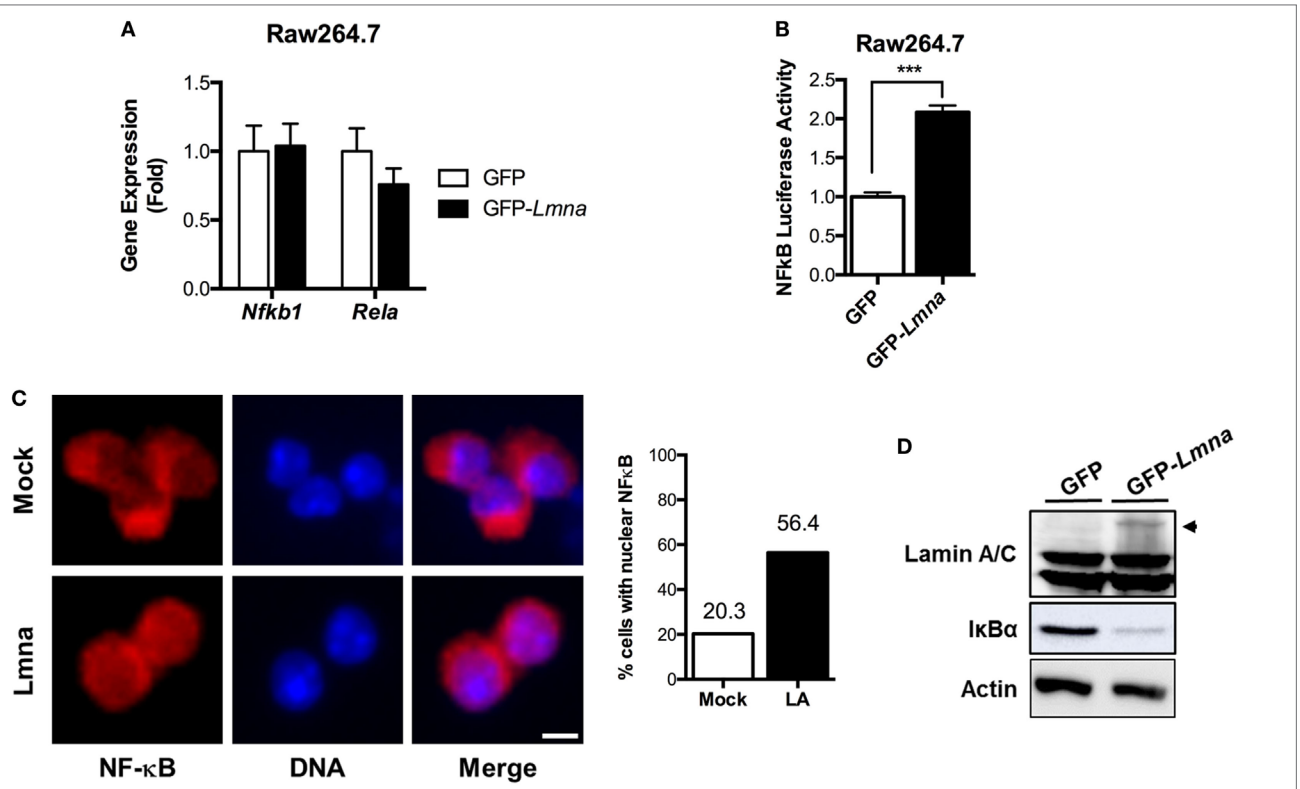

FIGURE 4 | Lamin A/C increases NF-κB activity *via* nuclear translocation of p65/Rel A, a NF-κB complex subunit. **(A)** qRT-PCR analysis of *Nfkb1* and *Rela* in Raw 264.7 cells transfected with either GFP or GFP-*Lmna*. **(B)** NF-κB luciferase activity in Raw 264.7 cells co-transfected with GFP or GFP-*Lmna* together with pNF-κB-Luc, a luciferase reporter construct that has κB responsible elements in the promoter. Luciferase activities were normalized by those in cells co-transfected with a non-reporter plasmid, pRL-SV40. **(C)** Immunofluorescence images of bone marrow-derived macrophages transfected with GFP (Mock) or GFP-*Lmna* (Lmna) and quantitation for cells with nuclear NF-κB p65/Rel A. Cells with nuclear NF-κB were defined based on the presence of nuclear signal and obvious lack of cytoplasmic signal as shown in the representative images (Scale bar: 5 μm). **(D)** Immunoblots of lysates from transfected Raw 264.7 cells with anti-Lamin A/C (top), anti-IκBα (middle), or anti-actin (bottom). Arrowhead marks GFP fusion lamin A protein size.

treatment modestly increased NF-κB activity in control cells and lamin A/C overexpression further increased NF-κB activity (Figure S2B in Supplementary Material).

We also examined nuclear translocation of endogenous Rel A in BMDM by using immunofluorescence with anti-Rel A antibody, which is another established method to determine NF-κB activation. Immunofluorescence analysis revealed that, in mock control BMDMs, Rel A signal was preferentially localized in the cytoplasm, whereas Rel A was enriched in the nucleus of BMDMs transfected with GFP-*Lmna* (**Figure 4C**). Quantitative counting of cells with nuclear Rel A staining revealed that overexpression of lamin A/C in BMDMs increased the nuclear translocation of Rel A by ~2.8-folds compared to the mock controls (**Figure 4C**). Similarly, the increase of nuclear translocation of Rel A was also observed in HeLa cells that were transfected with GFP-*Lmna* compared to control cells in both basal and TNFα-stimulated condition (Figures S2C,D in Supplementary Material). Nuclear translocation and thus activation of NF-κB are tightly regulated by the IKKβ/IκBα/NF-κB pathway. Under the basal condition, IκBα binds to NF-κB and, therefore, sequesters NF-κB in cytoplasm. However, when IKKβ is activated by stimulants, such as LPS or TNFα, IKKβ phosphorylates IκBα. Phosphorylated IκBα is poly-ubiquitinated and degraded in a proteasome-dependent way. This releases NF-κB from IκBα sequestration, and free NF-κB can be translocated into nucleus. Thus, measurements of IκBα protein amounts can be used as a surrogate marker for the activation of IKKβ. We found that overexpression of lamin A/C in BMDMs markedly decreases IκBα protein amount (**Figure 4D**), indicating that overexpression of lamin A/C activates the IKKβ/IκBα/NF-κB pathway. These data together show that lamin A/C overexpression induces NF-κB activation by activating the IKKβ/IκBα/NF-κB pathway in both basal and stimulatory conditions.

Depletion of Lamin A/C Suppresses LPS-Induced Inflammation in Macrophages

Next, we examined whether deleting *Lmna* conversely suppressed inflammatory responses in macrophages. We isolated peritoneal macrophages from control WT (CON) mice and myeloid cell-specific *Lmna* KO mice (MKO). PCR genotyping of peritoneal macrophages confirmed that $Lmna^{flox}$ alleles were cleaved in macrophages isolated from MKO mice (**Figure 5A**). $Lmna^{flox}$ alleles remained uncleaved in all other tested tissues from MKO

mice, suggesting that there was no or minimal leakage of LysM-Cre expression (data not shown). MKO mice showed almost complete depletion of *Lmna* mRNA in peritoneal macrophages without showing any compensatory increases in *Lmnb1* expression (**Figure 5B**). We then measured the IκBα protein amount to assess the activation of the IKKβ/IκBα/NF-κB pathway. We found that deletion of *Lmna* in macrophages significantly increased IκBα protein amount (**Figure 5C**), suggesting that depletion of lamin A/C inhibits IKKβ activity and, therefore, suppresses NF-κB activation. To test the role of lamin A/C in the regulation of proinflammatory gene expressions, we isolated peritoneal macrophages from CON and MKO mice and treated with LPS. We found that the basal expression levels of *Il6*, *Tnf,* and *Ccl2* were similar in both genotypes ($p > 0.05$) (**Figure 5D**). However, LPS-induced expressions of these genes were significantly lower in MKO peritoneal macrophages than those in the peritoneal macrophages from CON mice (**Figure 5D**). Secretion of IL-6 after LPS treatment was also lower in peritoneal macrophages from MKO mice than that of CON mice (**Figure 5E**). To test whether deleting *Lmna* conversely suppressed inflammatory responses *in vivo*, LPS were injected to CON and MKO mice. After 6 h injection, bloods were collected and levels of inflammatory cytokines in plasma were measured. Compared to CON, MKO lowered circulating TNFα and MCP-1 levels (**Figure 5F**). Overall, these data together demonstrate that lamin A/C regulates proinflammatory responses in macrophages.

Myeloid Cell-Specific Lamin A/C Deficiency Improves Obesity-Induced Insulin Resistance and Adipose Tissue Inflammation

Given that lamin A/C was elevated in obese adipose tissue and lamin A/C regulated inflammation in macrophages, we then

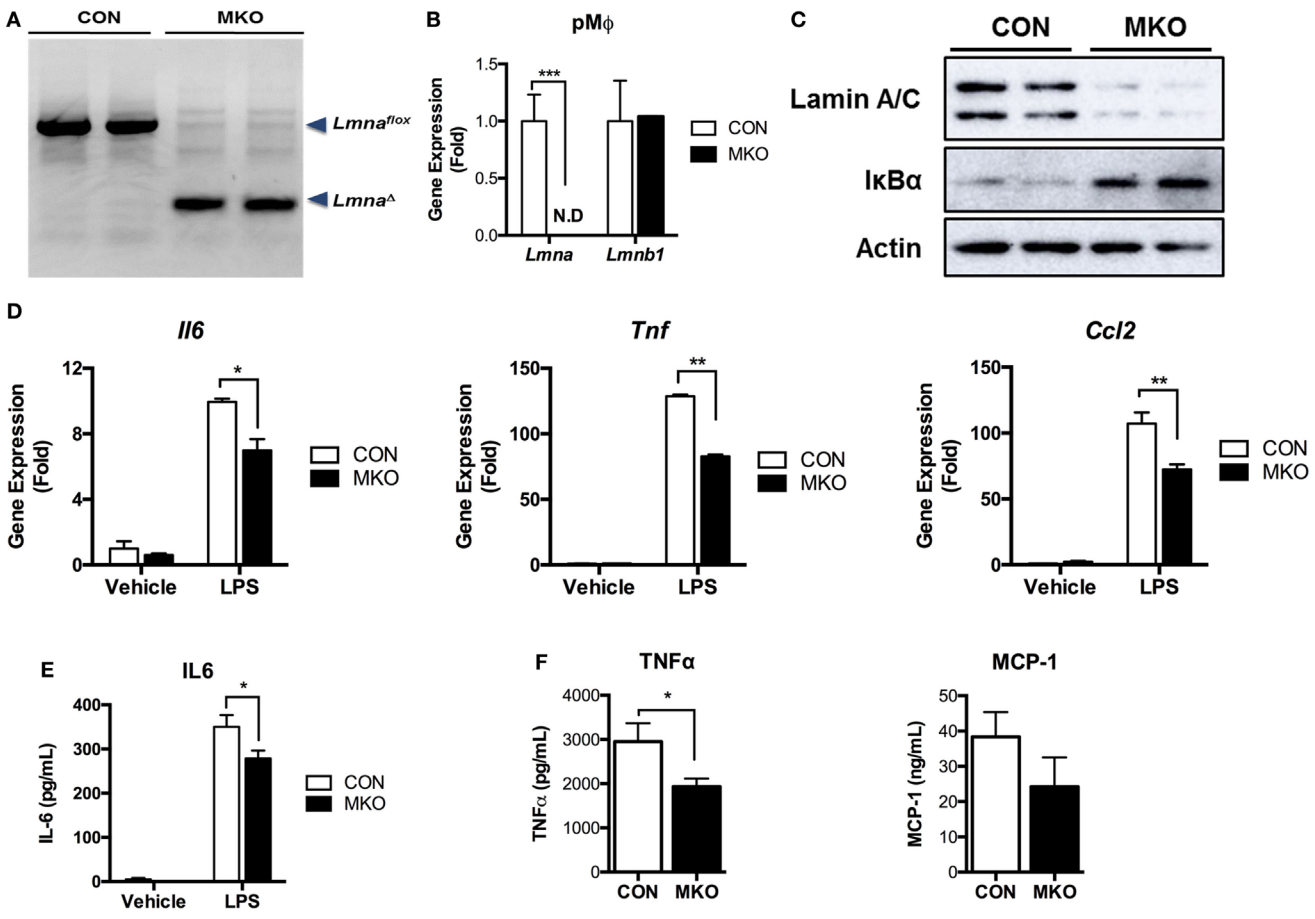

FIGURE 5 | Depletion of lamin A/C suppresses proinflammatory gene activation upon LPS treatment in macrophages. **(A–E)** Analyses of peritoneal macrophages from control and myeloid cell-specific *Lmna* KO mice (MKO) mice. **(A)** PCR genotyping of peritoneal macrophages from WT control (CON, $Lmna^{flox/flox}$) and MKO (LysM-Cre; $Lmna^{flox/flox}$) mice. Arrowheads mark $Lmna^{flox}$ (uncleaved) and $Lmna^{\Delta}$ (cleaved) alleles. **(B)** qRT-PCR analysis of *Lmna* and *Lmnb1* in peritoneal macrophages isolated from CON and MKO mice. **(C)** Immunoblots of lysates from peritoneal macrophages for lamin A/C (top), IκBα (middle), or actin (bottom). **(D,E)** Peritoneal macrophages were isolated from control and MKO mice and then treated with vehicle or 10 ng/ml LPS for 2 h. **(D)** qRT-PCR analysis of *Il6, Tnf,* and *Ccl2* in peritoneal macrophages isolated from CON and MKO mice. **(E)** Level of IL-6 in supernatant of CON and MKO peritoneal macrophages treated with vehicle or 10 ng/ml LPS for 6 h. **(F)** Plasma TNFα and MCP-1 levels after i.p. injection of LPS (20 mg/kg BW) were measured in CON and MKO mice ($n = 6$ per group). Error bars represent SEM. $^{*}p < 0.05$, $^{**}p < 0.01$.

examined the role of myeloid cell lamin A/C in the development of obesity-induced inflammation and insulin resistance. Control and MKO mice were fed with a HFD for 12 weeks. MKO mice showed similar body weight and adipose tissue weight compared to control mice (**Figures 6A,B**). However, HFD-fed MKO mice showed lower fasting glucose and insulin levels (**Figures 6C,D**) and, therefore, improved insulin resistance as determined by homeostatic model assessment for insulin resistance (HOMA-IR) (**Figure 6E**), indicating that deletion of *Lmna* in macrophages improves obesity-induced systemic insulin resistance. Gene expression analysis of total eWAT showed that deletion of *Lmna* in macrophages increased the expression levels of anti-inflammatory genes, including *Arg1* and *Il10,* and decreased the expression level of the proinflammatory gene *Nos2* (**Figure 6F**). However, *Lmna* deletion in macrophages did not affect the gene expression levels of *Emr1* and *Itgax,* which

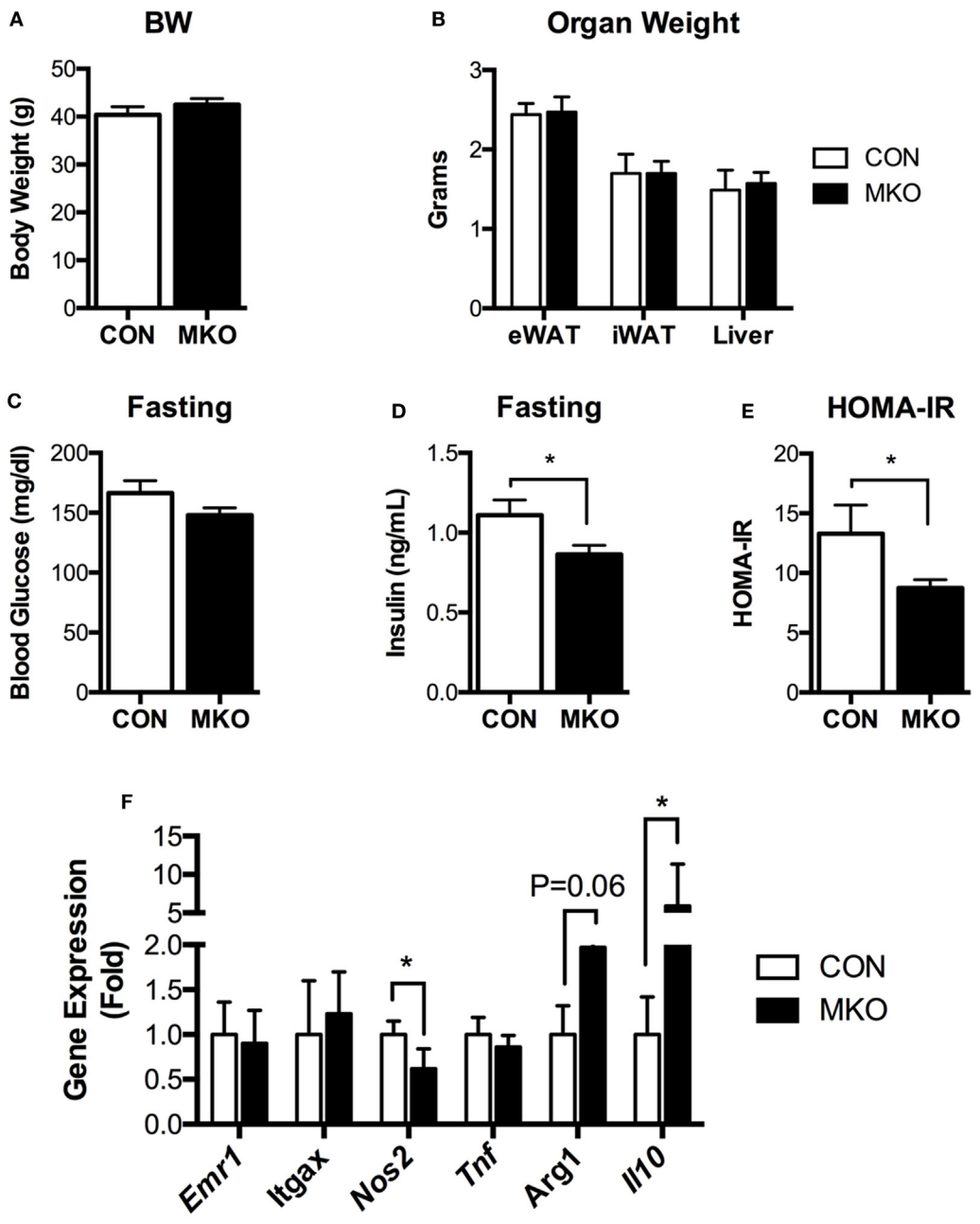

FIGURE 6 | Deletion of *Lmna* in myeloid tissues attenuates high-fat diet-induced insulin resistance in mice. CON and myeloid cell-specific *Lmna* KO mice (MKO) male mice (6 weeks) were fed a high-fat diet (HFD) for 12 weeks (CON, $n = 4$; MKO, $n = 9$). **(A)** Body weight, **(B)** organ weights of epididymal white adipose tissues (eWAT), inguinal white adipose tissue, and liver, **(C)** fasting blood glucose, **(D)** fasting plasma insulin, **(E)** homeostatic model assessment for insulin resistance index, **(F)** gene expression in eWAT from CON and MKO mice. Error bars represent SEM. $^*p < 0.05$.

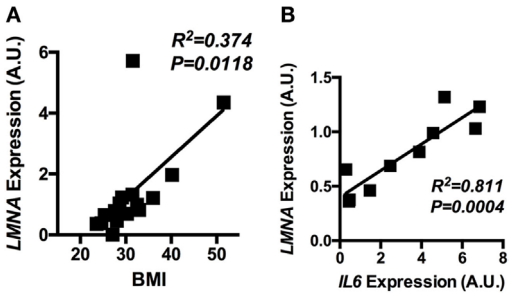

FIGURE 7 | The adipose *LMNA* expression levels correlate with BMI and *IL6* expressions in human subjects. Human omental adipose tissue samples were obtained by surgical biopsy from 30 individuals, and *LMNA* and *IL6* mRNA levels were determined by quantitative real-time RT-PCR. Linear regression analyses of *LMNA* mRNA level in human omental adipose tissue with respect to **(A)** BMI and **(B)** *IL6* mRNA levels are presented. Pearson's correlation coefficients (*r*) between *LMNA* and either BMI or *IL6* level are presented in each graph.

are macrophage-specific markers, or *Tnf* in the total adipose tissue.

The Expression Level of *LMNA* Correlates With BMI and *IL6* Gene Expression in Human Adipose Tissue

Having shown that lamin A/C was upregulated in obese WAT and had an inflammatory role in mouse macrophages, mRNA expression of lamin A/C in human visceral adipose tissue was further examined in relation to BMI. qRT-PCR analysis showed that the expression level of *LMNA* was significantly elevated in obese individuals as compared with lean or overweight subjects (data not shown). Correlation data showed that *LMNA* expression in visceral fat is positively associated with BMI ($p = 0.0118$, **Figure 7A**). We also found that *LMNA* expression was positively correlated with *IL6* expression in the same set of human adipose tissue ($p = 0.0004$, **Figure 7B**).

DISCUSSION

Adipose tissue macrophages play an important role in the regulation of adipose tissue inflammation in obesity and the development of metabolic syndromes. There has been considerable interest in identifying regulatory mechanisms to activate ATMs and maintain their proinflammatory function of ATMs in obesity. Since lamins are associated with metabolic syndromes, the goal of this study is to investigate the role of lamins in adipose tissue inflammation and systemic insulin resistance. In this study, we show that among the lamin isoforms, lamin A/C is specifically upregulated in visceral WAT of obese humans and mouse models. Importantly, lamin A/C is enhanced particularly in obese ATMs in mouse models. Furthermore, lamin A/C overexpression in macrophages leads to the upregulation of proinflammatory genes, such as *Tnf*, *Il6*, *Nos2,* and *Ccl2* by activating the IKKβ/IκBα/NF-κB pathway. Moreover, specific deletion of *Lmna* in myeloid cells not only suppresses proinflammatory responses in macrophages, but also improves obesity-induced systemic insulin resistance. These observations suggest that lamin A/C in ATMs functions as a novel regulator in obesity-induced adipose tissue inflammation and insulin resistance.

There are several studies showing the increased lamin A/C expression in adipose tissue in obesity (33, 40, 41). Miranda et al. (33) reported increased lamin A/C mRNA level in adipose tissues from obese human subjects. Independent research group also found that lamin A/C levels were elevated in adipose tissues from both obese individuals and *ob/ob* mice (41). However, these studies did not identify the cellular compartment of adipose tissue in which lamin A/C expression is elevated. In agreement with previous studies, we found that visceral adipose tissue from obese subjects and eWAT from the various obese mouse models have higher expression levels of lamin A/C. Closer examination reveals that the expression levels of lamin A/C is increased mainly in ATMs. Interestingly, induction of lamin A/C is only shown in eWAT, but not in iWAT. It has been known that visceral fat of human or eWAT of rodent models contains more inflammatory cells compared to subcutaneous fat in obese humans and rodents (42–44). Furthermore, the expression levels of proinflammatory genes are higher in eWAT than in iWAT (2). These observations suggest that the upregulation of lamin A/C in eWAT is more tightly associated with inflammation than obesity *per se*. This could explain the association of *LMNA* with *IL6* expression in human adipose tissue observed in this study.

Our results from *Lmna* gain- and loss-of-function experiments in macrophages reveal that lamin A/C is a novel regulator in the production of proinflammatory mediators, such as TNFα, IL-6, and CCL2, in line with the role of lamin A/C in immune response. In obesity, ATMs accumulate and are activated to produce high level of proinflammatory cytokines, which lead to adipose tissue inflammation and insulin resistance (5, 45). Several studies showed that inhibitions of macrophage activation and proinflammatory cytokine functions improve insulin resistance (46–48). Our results show that lamin A/C expression was upregulated in ATMs and played a role in the production of proinflammatory genes, which immediately raises a question whether lamin A/C upregulation in ATMs contributes to the development of the obesity-induced inflammation and insulin resistance. Indeed, our data with obese MKO mice showed the improvement of insulin resistance upon HFD. The notion of the immunological role of lamin A/C in chronic inflammation is consistent with recent reports showing that age-associated systemic inflammation is linked to the fluctuation of the nuclear lamina (49, 50).

NF-κB pathway has been known as a master regulator in the immune response. In this study, we homed in on the effect of lamin A/C overexpression on NF-κB activity. Since there was no change in the mRNA levels of NF-κB p105 and p65/Rel A at the basal state (**Figure 4A**) and lamin A did not directly interact with RelA (data not shown), we surmised that lamin A/C overexpression leads to increased Rel A nuclear translocation. Our studies show that NF-κB transcriptional activity

and Rel A nuclear translocation were enhanced in lamin A/C overexpressing macrophages, which was in parallel with higher levels of *Il6* and *Ccl2* in these cells. Importantly, even without any stimulation, nuclear localization of NF-κB was increased (Figures S2C,D in Supplementary Material), and this translated into the induction of NF-κB transcriptional activity and proinflammatory gene expression without any other stimulations (**Figure 3**; Figures S2A,B in Supplementary Material). The question is how lamin A/C can induce NF-κB translocation. However, we found evidence in identifying a potential molecular mechanism for this. Since IKKβ phosphorylates IκBα and this induces degradation of IκBα, we used the assessment of IκBα protein amounts as a surrogate marker for IKKβ activation. We found that overexpression of lamin A/C decreased IκBα protein amount (**Figure 4D**) and that deletion of lamin A/C conversely increased IκBα protein amount (**Figure 5C**), suggesting that lamin A/C regulates IKKβ activity. Thus one of the potential scenario how lamin A/C controls inflammation is that (1) lamin A/C activates IKKβ, and induces NF-κB nuclear translocation and activation in the basal state, (2) this, in turn, increases the expression levels of proinflammatory genes, including *Tnf*, (3) these proinflammatory cytokines then activate the IKK/IκBα/NF-κB pathway, and (4) thus this initiates the continuous vicious cycle of activation for this pathway and, therefore, induces inflammation. Supporting this is the previous study showing that accumulation of prelamin A at the nuclear lamina activates the NF-κB pathway by promoting NEMO-dependent signaling or inflammasome formation (49, 51). Another potential mechanism is the regulation of nuclear NF-κB transcriptional activity by reorganizing chromatin structure. Recent studies have been shown that the 3D genome organization undergoes dramatic changes during immune activation. A genome-wide study shows that release of immune gene loci from the nuclear periphery is important for the activation of immune responses (52). Overproduction of lamin A/C may also lead to alteration of 3D chromatin organization and/or genome interaction with the nuclear periphery causing deregulated expression of inflammatory genes. We could not also exclude the possibility for the regulation of actin dynamics by lamin A/C, since this has been identified as one mechanism by which lamin regulates the nuclear translocation and downstream signaling of transcription factor megakaryoblastic leukemia 1 (53). It is also possible that lamin A/C overexpression simply increases retention of Rel A in the nucleus in the context of obesity, which could lead to NF-κB hyperactivation, and thereby further aggravating the inflammatory cascade in already inflamed adipose tissue. Further study is needed to investigate the detailed mechanisms of lamin A/C-induced NF-κB activation and its pathophysiological relevance *in vivo*.

In summary, we show that the expression of lamin A/C, a component of nuclear lamina, is specifically upregulated in obese adipose tissue, which is largely attributed to ATMs. We also show that lamin A/C regulates proinflammatory responses *via* NF-κB activity and myeloid-specific lamin A/C deletion improves obesity-induced inflammation and insulin resistance. Thus, our data suggest that lamin A/C mediates the activation of ATM inflammation by regulating NF-κB, thereby contributing to the development of obesity-induced insulin resistance.

ETHICS STATEMENT

All mouse procedures were approved by the Institutional Animal Care and Use Committee at the Soonchunhyang University (SCH16-0003, SCH17-0008). The clinical studies were reviewed and approved by the Soonchunhyang University Institutional Review Board (SCH#1040875-201502-BR-009), and carried out in accordance with the Declaration of Helsinki. Informed personal consents were obtained from all subjects.

AUTHOR CONTRIBUTIONS

YK, JL, and KC conceived the idea. PB, JC, and YP performed animal experiments and cell culture experiments. MK and AB performed Rel A nuclear translocation and NF-κB luciferase assay experiments. SH, Y-JK, CC, and WK contributed to analysis of human studies. YK, JL, and KC interpreted the data and wrote the manuscript.

FUNDING

This work was supported by a grant of the Korea Health Technology R&D project through the Korea Health Industry Development Institute (KHDI) funded by the Ministry of Health & Welfare, Republic of Korea (grant number-HI14C2092) to KC, and the grants of Basic Science Research Program through the National Research Foundation (NRF) of Korea (grant number NRF-2014R1A1A1037106 & 2017R1D1A1B03035010) to YK and by American Diabetes Association grant 1-15-BS-111 (JL) and National Institutes of Health (NIH) grants P30 DK36836 (Joslin Diabetes Research Center).

SUPPLEMENTARY MATERIAL

The Supplementary Material for this article can be found online at https://www.frontiersin.org/articles/10.3389/fimmu.2018.00696/full#supplementary-material.

REFERENCES

1. Chiang SH, Bazuine M, Lumeng CN, Geletka LM, Mowers J, White NM, et al. The protein kinase IKKepsilon regulates energy balance in obese mice. *Cell* (2009) 138(5):961–75. doi:10.1016/j.cell.2009.06.046
2. Lee BC, Kim MS, Pae M, Yamamoto Y, Eberie D, Shimada T, et al. Adipose natural killer cells regulate adipose tissue macrophages to promote insulin resistance in obesity. *Cell Metab* (2016) 23(4):685–98. doi:10.1016/j.cmet.2016.03.002
3. Weisberg SP, McCann D, Desai M, Rosenbaum M, Leibel RL, Ferrante AW Jr. Obesity is associated with macrophage accumulation in adipose tissue. *J Clin Invest* (2003) 112(12):1796–808. doi:10.1172/JCI19246
4. Lumeng CN, Bodzin JL, Saltiel AR. Obesity induces a phenotypic switch in adipose tissue macrophage polarization. *J Clin Invest* (2007) 117(1):175–84. doi:10.1172/JCI29881
5. Lumeng CN, DelProposto JB, Westcott DJ, Saltiel AR. Phenotypic switching of adipose tissue macrophages with obesity is generated by spatiotemporal

differences in macrophage subtypes. *Diabetes* (2008) 57(12):3239–46. doi:10.2337/db08-0872
6. Xu X, Grijalva A, Skowronski A, van Eijk M, Serlie MJ, Ferrante AW Jr. Obesity activates a program of lysosomal-dependent lipid metabolism in adipose tissue macrophages independently of classic activation. *Cell Metab* (2013) 18(6):816–30. doi:10.1016/j.cmet.2013.11.001
7. Morris DL, Singer K, Lumeng CN. Adipose tissue macrophages: phenotypic plasticity and diversity in lean and obese states. *Curr Opin Clin Nutr Metab Care* (2011) 14:341–6. doi:10.1097/MCO.0b013e328347970b
8. Westcott DJ, Delproposto JB, Geletka LM, Wang T, Singer K, Saltiel AR, et al. MGL1 promotes adipose tissue inflammation and insulin resistance by regulating 7/4hi monocytes in obesity. *J Exp Med* (2009) 206(13):3143–56. doi:10.1084/jem.20091333
9. Li P, Lu M, Nguyen MT, Bae EJ, Chapman J, Feng D, et al. Functional heterogeneity of CD11c-positive adipose tissue macrophages in diet-induced obese mice. *J Biol Chem* (2010) 285(20):15333–45. doi:10.1074/jbc.M110.100263
10. Kratz M, Coats BR, Hisert KB, Hagman D, Mutskov V, Peris E, et al. Metabolic dysfunction drives a mechanistically distinct proinflammatory phenotype in adipose tissue macrophages. *Cell Metab* (2014) 20(4):614–25. doi:10.1016/j.cmet.2014.08.010
11. Kurokawa J, Nagano H, Ohara O, Kubota N, Kadowaki T, Arai S, et al. Apoptosis inhibitor of macrophage (AIM) is required for obesity-associated recruitment of inflammatory macrophages into adipose tissue. *Proc Natl Acad Sci U S A* (2011) 108(29):12072–7. doi:10.1073/pnas.1101841108
12. Ramkhelawon B, Hennessy EJ, Menager M, Ray TD, Sheedy FJ, Hutchison S, et al. Netrin-1 promotes adipose tissue macrophage retention and insulin resistance in obesity. *Nat Med* (2014) 20(4):377–84. doi:10.1038/nm.3467
13. Patsouris D, Li PP, Thapar D, Chapman J, Olefsky JM, Neels JG. Ablation of CD11c-positive cells normalizes insulin sensitivity in obese insulin resistant animals. *Cell Metab* (2008) 8(4):301–9. doi:10.1016/j.cmet.2008.08.015
14. Cho KW, Morris DL, DelProposto JL, Geletka L, Zamarron B, Martinez-Santibanez G, et al. An MHC II-dependent activation loop between adipose tissue macrophages and CD4+ T cells controls obesity-induced inflammation. *Cell Rep* (2014) 9(2):605–17. doi:10.1016/j.celrep.2014.09.004
15. Osmanagic-Myers S, Dechat T, Foisner R. Lamins at the crossroads of mechanosignaling. *Genes Dev* (2015) 29(3):225–37. doi:10.1101/gad.255968.114
16. de Leeuw R, Gruenbaum Y, Medalia O. Nuclear lamins: thin filaments with major functions. *Trends Cell Biol* (2018) 28(1):34–45. doi:10.1016/j.tcb.2017.08.004
17. Gerace L, Blobel G. The nuclear envelope lamina is reversibly depolymerized during mitosis. *Cell* (1980) 19(1):277–87. doi:10.1016/0092-8674(80)90409-2
18. Burke B, Gerace L. A cell free system to study reassembly of the nuclear envelope at the end of mitosis. *Cell* (1986) 44(4):639–52. doi:10.1016/0092-8674(86)90273-4
19. Stewart C, Burke B. Teratocarcinoma stem cells and early mouse embryos contain only a single major lamin polypeptide closely resembling lamin B. *Cell* (1987) 51(3):383–92. doi:10.1016/0092-8674(87)90634-9
20. Rober RA, Weber K, Osborn M. Differential timing of nuclear lamin A/C expression in the various organs of the mouse embryo and the young animal: a developmental study. *Development* (1989) 105(2):365–78.
21. Vergnes L, Peterfy M, Bergo MO, Young SG, Reue K. Lamin B1 is required for mouse development and nuclear integrity. *Proc Natl Acad Sci U S A* (2004) 101(28):10428–33. doi:10.1073/pnas.0401424101
22. Coffinier C, Chang SY, Nobumori C, Tu Y, Farber EA, Toth JI, et al. Abnormal development of the cerebral cortex and cerebellum in the setting of lamin B2 deficiency. *Proc Natl Acad Sci U S A* (2010) 107(11):5076–81. doi:10.1073/pnas.0908790107
23. Kim Y, Sharov AA, McDole K, Cheng M, Hao H, Fan CM, et al. Mouse B-type lamins are required for proper organogenesis but not by embryonic stem cells. *Science* (2011) 334(6063):1706–10. doi:10.1126/science.1211222
24. Kubben N, Voncken JW, Konings G, van Weeghel M, van den Hoogenhof MM, Gijbels M, et al. Post-natal myogenic and adipogenic developmental: defects and metabolic impairment upon loss of A-type lamins. *Nucleus* (2011) 2(3):195–207. doi:10.4161/nucl.2.3.15731
25. Kim Y, Zheng Y. Generation and characterization of a conditional deletion allele for Lmna in mice. *Biochem Biophys Res Commun* (2013) 440(1):8–13. doi:10.1016/j.bbrc.2013.08.082
26. Owen KR, Groves CJ, Hanson RL, Knowler WC, Shuldiner AR, Elbein SC, et al. Common variation in the LMNA gene (encoding lamin A/C) and type 2 diabetes: association analyses in 9,518 subjects. *Diabetes* (2007) 56(3):879–83. doi:10.2337/db06-0930
27. Wegner L, Andersen G, Sparso T, Grarup N, Glumer C, Borch-Johnsen K, et al. Common variation in LMNA increases susceptibility to type 2 diabetes and associates with elevated fasting glycemia and estimates of body fat and height in the general population: studies of 7,495 Danish whites. *Diabetes* (2007) 56(3):694–8. doi:10.2337/db06-0927
28. Dutour A, Roll P, Gaborit B, Courrier S, Alessi MC, Tregouet DA, et al. High prevalence of laminopathies among patients with metabolic syndrome. *Hum Mol Genet* (2011) 20(19):3779–86. doi:10.1093/hmg/ddr294
29. Elbein SC, Hoffman MD, Teng K, Leppert MF, Hasstedt SJ. A genome-wide search for type 2 diabetes susceptibility genes in Utah Caucasians. *Diabetes* (1999) 48(5):1175–82. doi:10.2337/diabetes.48.5.1175
30. Wiltshire S, Hattersley AT, Hitman GA, Walker M, Levy JC, Sampson M, et al. A genomewide scan for loci predisposing to type 2 diabetes in a U.K. population (the Diabetes UK Warren 2 Repository): analysis of 573 pedigrees provides independent replication of a susceptibility locus on chromosome 1q. *Am J Hum Genet* (2001) 69(3):553–69. doi:10.1086/323249
31. Xiang K, Wang Y, Zheng T, Jia W, Li J, Chen L, et al. Genome-wide search for type 2 diabetes/impaired glucose homeostasis susceptibility genes in the Chinese: significant linkage to chromosome 6q21-q23 and chromosome 1q21-q24. *Diabetes* (2004) 53(1):228–34. doi:10.2337/diabetes.53.1.228
32. Mesa JL, Loos RJ, Franks PW, Ong KK, Luan J, O'Rahilly S, et al. Lamin A/C polymorphisms, type 2 diabetes, and the metabolic syndrome: case-control and quantitative trait studies. *Diabetes* (2007) 56(3):884–9. doi:10.2337/db06-1055
33. Miranda M, Chacon MR, Gutierrez C, Vilarrasa N, Gomez JM, Caubet E, et al. LMNA mRNA expression is altered in human obesity and type 2 diabetes. *Obesity (Silver Spring)* (2008) 16(8):1742–8. doi:10.1038/oby.2008.276
34. Cho KW, Morris DL, Lumeng CN. Flow cytometry analyses of adipose tissue macrophages. *Methods Enzymol* (2014) 537:297–314. doi:10.1016/B978-0-12-411619-1.00016-1
35. Grant R, Youm Y, Ravussin A, Dixit VD. Quantification of adipose tissue leukocytosis in obesity. *Methods Mol Biol* (2013) 1040:195–209. doi:10.1007/978-1-62703-523-1_15
36. Ebke LA, Nestor-Kalinoski AL, Slotterbeck BD, Al-Dieri AG, Ghosh-Lester S, Russo L, et al. Tight association between macrophages and adipocytes in obesity: implications for adipocyte preparation. *Obesity (Silver Spring)* (2014) 22(5):1246–55. doi:10.1002/oby.20634
37. Nishimura S, Manabe I, Nagasaki M, Eto K, Yamashita H, Ohsugi M, et al. CD8+ effector T cells contribute to macrophage recruitment and adipose tissue inflammation in obesity. *Nat Med* (2009) 15(8):914–20. doi:10.1038/nm.1964
38. Winer DA, Winer S, Chng MH, Shen L, Engleman EG. B Lymphocytes in obesity-related adipose tissue inflammation and insulin resistance. *Cell Mol Life Sci* (2014) 71(6):1033–43. doi:10.1007/s00018-013-1486-y
39. Cho KW, Zamarron BF, Muir LA, Singer K, Porsche CE, DelProposto JB, et al. Adipose tissue dendritic cells are independent contributors to obesity-induced inflammation and insulin resistance. *J Immunol* (2016) 197(9):3650–61.
40. Nadeau M, Noel S, Laberge PY, Hurtubise J, Tchernof A. Adipose tissue lamin A/C messenger RNA expression in women. *Metabolism* (2010) 59(8):1106–14. doi:10.1016/j.metabol.2009.09.034
41. Rodriguez-Acebes S, Palacios N, Botella-Carretero JI, Olea N, Crespo L, Peromingo R, et al. Gene expression profiling of subcutaneous adipose tissue in morbid obesity using a focused microarray: distinct expression of cell-cycle- and differentiation-related genes. *BMC Med Genomics* (2010) 3:61. doi:10.1186/1755-8794-3-61
42. Fox CS, Massaro JM, Hoffmann U, Pou KM, Maurovich-Horvat P, Liu CY, et al. Abdominal visceral and subcutaneous adipose tissue compartments: association with metabolic risk factors in the Framingham Heart Study. *Circulation* (2007) 116(1):39–48. doi:10.1161/CIRCULATIONAHA.106.675355
43. Ledoux S, Queguiner I, Msika S, Calderari S, Rufat P, Gasc JM, et al. Angiogenesis associated with visceral and subcutaneous adipose tissue in severe human obesity. *Diabetes* (2008) 57(12):3247–57. doi:10.2337/db07-1812
44. Ibrahim MM. Subcutaneous and visceral adipose tissue: structural and functional differences. *Obes Rev* (2010) 11(1):11–8. doi:10.1111/j.1467-789X.2009.00623.x

45. Hotamisligil GS. Inflammation, metaflammation and immunometabolic disorders. *Nature* (2017) 542(7640):177–85. doi:10.1038/nature21363
46. Han MS, Jung DY, Morel C, Lakhani SA, Kim JK, Flavell RA, et al. JNK expression by macrophages promotes obesity-induced insulin resistance and inflammation. *Science* (2013) 339(6116):218–22. doi:10.1126/science.1227568
47. De Taeye BM, Novitskaya T, McGuinness OP, Gleaves L, Medda M, Covington JW, et al. Macrophage TNF-alpha contributes to insulin resistance and hepatic steatosis in diet-induced obesity. *Am J Physiol Endocrinol Metab* (2007) 293(3):E713–25. doi:10.1152/ajpendo.00194.2007
48. Aouadi M, Tencerova M, Vangala P, Yawe JC, Nicoloro SM, Amano SU, et al. Gene silencing in adipose tissue macrophages regulates whole-body metabolism in obese mice. *Proc Natl Acad Sci U S A* (2013) 110(20):8278–83. doi:10.1073/pnas.1300492110
49. Osorio FG, Barcena C, Soria-Valles C, Ramsay AJ, de Carlos F, Cobo J, et al. Nuclear lamina defects cause ATM-dependent NF-kappaB activation and link accelerated aging to a systemic inflammatory response. *Genes Dev* (2012) 26(20):2311–24. doi:10.1101/gad.197954.112
50. Chen H, Zheng X, Zheng Y. Age-associated loss of lamin-B leads to systemic inflammation and gut hyperplasia. *Cell* (2014) 159(4):829–43. doi:10.1016/j.cell.2014.10.028
51. Di Micco A, Frera G, Lugrin J, Jamilloux Y, Hsu ET, Tardivel A, et al. AIM2 inflammasome is activated by pharmacological disruption of nuclear envelope integrity. *Proc Natl Acad Sci U S A* (2016) 113(32):E4671–80. doi:10.1073/pnas.1602419113
52. Robson MI, de Las Heras JI, Czapiewski R, Sivakumar A, Kerr ARW, Schirmer EC. Constrained release of lamina-associated enhancers and genes from the nuclear envelope during T-cell activation facilitates their association in chromosome compartments. *Genome Res* (2017) 27(7):1126–38. doi:10.1101/gr.212308.116
53. Ho CY, Jaalouk DE, Vartiainen MK, Lammerding J. Lamin A/C and emerin regulate MKL1-SRF activity by modulating actin dynamics. *Nature* (2013) 497(7450):507–11. doi:10.1038/nature12105

Conflict of Interest Statement: The authors declare that the research was conducted in the absence of any commercial or financial relationships that could be construed as a potential conflict of interest.

Copyright © 2018 Kim, Bayona, Kim, Chang, Hong, Park, Budiman, Kim, Choi, Kim, Lee and Cho. This is an open-access article distributed under the terms of the Creative Commons Attribution License (CC BY). The use, distribution or reproduction in other forums is permitted, provided the original author(s) and the copyright owner are credited and that the original publication in this journal is cited, in accordance with accepted academic practice. No use, distribution or reproduction is permitted which does not comply with these terms.

Advantages of publishing in Frontiers

OPEN ACCESS
Articles are free to read for greatest visibility and readership

FAST PUBLICATION
Around 90 days from submission to decision

HIGH QUALITY PEER-REVIEW
Rigorous, collaborative, and constructive peer-review

TRANSPARENT PEER-REVIEW
Editors and reviewers acknowledged by name on published articles

Frontiers
Avenue du Tribunal-Fédéral 34
1005 Lausanne | Switzerland

Visit us: www.frontiersin.org
Contact us: info@frontiersin.org | +41 21 510 17 00

REPRODUCIBILITY OF RESEARCH
Support open data and methods to enhance research reproducibility

DIGITAL PUBLISHING
Articles designed for optimal readership across devices

FOLLOW US
@frontiersin

IMPACT METRICS
Advanced article metrics track visibility across digital media

EXTENSIVE PROMOTION
Marketing and promotion of impactful research

LOOP RESEARCH NETWORK
Our network increases your article's readership